

Inbred C57BL/6J and DBA/2J Mouse Strains Exhibit Constitutive Differences in Regional Brain Fatty Acid Composition

Robert K. McNamara · Jessica Able ·
Ronald Jandacek · Therese Rider · Patrick Tso

Received: 27 June 2008 / Accepted: 17 September 2008 / Published online: 16 October 2008
© AOCs 2008

Abstract Major behavioral and neurochemical features observed between inbred C57BL/6 and DBA/2 mouse strains can be reproduced within rodent strains following dietary-induced reductions in brain docosahexaenoic acid (DHA, 22:6n-3) composition. It was therefore hypothesized that C57BL/6 and DBA/2 mice exhibit constitutive differences in brain DHA composition that are independent of diet. To test this, adult C57BL/6J and DBA/2J prefrontal cortex, hippocampus, ventral striatum, and midbrain fatty acid composition was determined by gas chromatography. After correction for multiple comparisons, C57BL/6J mice exhibited significantly lower DHA composition in the hippocampus and ventral striatum, but not prefrontal cortex or midbrain, and significantly greater regional arachidonic acid (ARA, 20:4n-6):DHA ratios, relative to DBA/2J mice. C57BL/6J mice also exhibited significantly lower regional adrenic acid (ADA, 22:4n-6) composition, and a significantly smaller ADA:ARA ratio, relative to DBA/2J mice. C57BL/6J mice exhibited significantly smaller oleic acid:stearic acid ratio in the hippocampus and ventral striatum relative to DBA/2J mice. Among all mice, DHA composition was positively correlated with the ADA:ARA ratio and inversely correlated with the oleic acid:stearic acid ratio. These data demonstrate that inbred C57BL/6J and DBA/2J mouse strains exhibit constitutive

and region-specific differences in fatty acid composition independent of diet, and suggest that heritable genetic factors are an important determinant of central fatty acid composition.

Keywords Fatty acids · Docosahexaenoic acid · Prefrontal cortex · Hippocampus · Ventral striatum · Midbrain · Inbred mouse strain · C57BL/6J · DBA/2J

Introduction

Mammalian brain lipids are composed of a ratio of saturated fatty acids, monounsaturated fatty acids, and polyunsaturated fatty acids (PUFA). The principal PUFAs in the mammalian brain are the omega-6 fatty acid arachidonic acid (ARA, 20:4n-6) and the omega-3 fatty acid docosahexaenoic acid (DHA, 22:6n-3). Within brain tissues, DHA and ARA preferentially accumulate in synaptic membranes [1, 2] where they are predominantly esterified into the *sn*-2 position of phosphatidylethanolamine and phosphatidylserine phospholipids [3]. Following mobilization by different phospholipase A₂ (PLA₂) isoforms, ARA and DHA have opposing effects on second messenger [4] and inflammatory [5] signaling pathways. Dietary-induced elevations in the brain ARA:DHA ratio secondary to reduced DHA composition during perinatal development are associated with abnormalities in neurotransmitter systems including dopamine and serotonin [6] and behavior [7] in adult rodents. Moreover, significant deficits in DHA composition, and elevations in the ARA:DHA ratio, are observed in postmortem prefrontal cortex of patients with recurrent neuropsychiatric disorders, including schizophrenia [8], bipolar disorder [9], and major depression [10]. These data suggest that a

R. K. McNamara (✉) · J. Able
Department of Psychiatry, University of Cincinnati
College of Medicine, 231 Albert Sabin Way,
Cincinnati, OH 45267-0516, USA
e-mail: robert.mcnamara@psychiatry.uc.edu

R. Jandacek · T. Rider · P. Tso
Department of Pathology, University of Cincinnati,
Cincinnati, OH 45237, USA

high ARA:DHA ratio may be detrimental to normal brain development and function.

Because mammals are incapable of synthesizing omega-3 and omega-6 fatty acids *de novo*, they are entirely dependent on dietary sources to procure and maintain adequate peripheral and central tissue content. The dietary omega-3 fatty acid precursor alpha-linolenic acid (ALA, 18:3n-3) and dietary omega-6 precursor linoleic acid (LA, 18:2n-6) are converted to DHA and ARA, respectively, following a series of common and competitive microsomal desaturation-elongation reactions mediated predominantly by the liver [11]. The final synthesis of DHA requires additional metabolism within peroxisomes [12]. Stearoyl-CoA desaturase (*SCD*, delta-9 desaturase) mediates the synthesis of oleic acid from stearic acid [13], and *SCD* expression and activity is down-regulated by PUFAs including DHA [14]. Major desaturase (*FADS1*, delta-5 desaturase, *FADS2*, delta-6 desaturase), elongase (*ELOVL2/5*), peroxisome biogenesis (*PEX*), and the *SCD* gene are expressed in both liver and brain [11, 15–17]. Additionally, multiple gene products regulate cellular fatty acid transport [18]. Inherited polymorphisms in PUFA biosynthetic genes are associated with deficits in human peripheral and/or central membrane PUFA composition [19–22]. Collectively, these data indicate that heritable genetic factors are an important determinant of tissue fatty acid composition independent of diet.

C57BL/6 (C57) and DBA/2 (DBA) mice have been inbred for over 200 generations and are among the most widely used mouse strains in genetic research. Comparative studies have revealed major phenotypic differences that are independent of diet, including hippocampus protein kinase C (PKC) expression/activity [23], hippocampus-dependent learning performance [24], regional dopamine D₂ receptor binding density [25], mesocorticolimbic dopamine activity [26], locomotor response to psychostimulant drugs [27], and immobility in the forced swim test [28]. Importantly, within rodent strains dietary-induced reductions in brain DHA composition, and associated elevation in the ARA:DHA ratio, are also associated with phenotypic differences, including hippocampus PKC expression [4], hippocampus-dependent learning performance [29], regional dopamine D₂ receptor binding density [30], mesocorticolimbic dopamine neurotransmission [31], locomotor response to psychostimulant drugs [32], and immobility in the forced swim test [33]. Furthermore, we have recently found that dietary-induced deficits in brain DHA composition significantly augment behavioral sensitization in response to repeated amphetamine treatment within both adult C57 [34] and DBA [35] strains. Based on these data, it was hypothesized that C57 and DBA mice maintained on the same diet would exhibit constitutive differences in regional brain DHA composition. To test

this, we determined the fatty acid composition of the prefrontal cortex, hippocampus, ventral striatum, and midbrain of adult male C57BL/6J and DBA/2J mice maintained on the same diet.

Experimental Procedures

Animals and Diet

Adult (8 week) male inbred DBA/2J and C57BL/6J mice were purchased from Jackson Laboratories (Bar Harbor, MA). Mice were housed in groups of 4 per cage and food and water were available *ad libitum*. Mice were maintained on the same commonly used Purina LabDiet (5010) from conception until the time of sacrifice. Diet nutrient composition can be obtained at <http://www.labdiet.com/5010-head.htm>, and diet fatty acid composition is presented in Table 1 (described below). Following 2 weeks of acclimation to the animal vivarium, mice were sacrificed by decapitation (at 10 weeks), brains extracted and placed into ice-cold 0.9% NaCl for 2 min. Brains were then dissected on ice to isolate bilateral prefrontal cortex, hippocampus, ventral striatum (inc. nucleus accumbens, islands of Calleja), and midbrain (inc. ventral tegmentum, substantia nigra). The olfactory tubercle and residual striatal tissue were dissected from the prefrontal cortex. Tissues were placed in cryotubes, flash frozen in liquid nitrogen, and stored at –80 °C. All experimental procedures were approved by the University of Cincinnati Institutional Animal Care and Use Committee, and adhere to the guidelines set by the National Institutes of Health.

Table 1 Diet fatty acid composition

Fatty acid	% TTL fatty acids
8:0	–
10:0	–
12:0	–
14:0	–
16:0	19.5 ± <0.1
16:1	1.3 ± <0.1
18:0	6.5 ± <0.1
18:1n-7	1.8 ± <0.1
18:1n-9	27.5 ± 0.22
18:2n-6	39.6 ± 0.20
20:4n-6	–
18:3n-3	3.7 ± <0.1
20:5n-3	–
22:5n-3	–
22:6n-3	–

Gas Chromatography

Total (triglyceride, phospholipid, and cholesteryl ester) fatty acid composition was determined using the saponification and methylation methods originally described by Mecalfe et al. [36]. We have previously demonstrated that this method yields the same fatty acid composition as Folch (chloroform:methanol) extraction [9]. Brain samples (30–80 mg wet weight) were placed in a 20 ml glass vial into which 4 ml of 0.5 N methanolic sodium hydroxide was added, and the sample heated at 80 °C for 5 min. Following a 10 min cooling period, 3 ml of boron trifluoride in methanol was added to methylate the sample. After an additional five minutes of heating in the water bath (80 °C), the sample vial was allowed to cool, and 2 ml of a saturated solution (6.2 M) of sodium chloride and 10 ml of hexane was added. The samples were then mixed by vortex for 1 min. The hexane fraction was then transferred into a 20 ml vial containing 10 mg of sodium sulfate to dry the sample. The hexane solution was then removed for GC analysis. Samples were analyzed with a Shimadzu GC-2014 equipped with an auto-injector (Shimadzu Scientific Instruments Inc., Columbia MD). The column was a DB-23 (123–2332): 30 m (length), I.D. 0.32 mm wide bore, film thickness of 0.25 μ M (J&W Scientific, Folsom CA). The GC conditions were: column temperature ramping by holding at 120 °C for one minute followed by an increase of 5 °C/min from 120–240 °C. The temperature of the injector and flame ionization detector was 250 °C. A split (8:1) injection mode was used. The carrier gas was helium with a column flow rate of 2.5 ml/min. Fatty acid identification was determined using retention times of authenticated fatty acid methyl ester standards (Matreya LLC Inc., Pleasant Gap PA). Analysis of fatty acid methyl esters is based on areas calculated with Shimadzu Class VP 4.3 software. The mole percent (mol%) of fatty acids was calculated from the molecular weight of fatty acids and relative area percent. All samples were processed by a technician that was blind to genotype.

Statistical Analysis

Strain differences in fatty acid composition (mol%) and fatty acid ratios were analyzed with unpaired *t*-tests (two-tailed). We used Bonferroni correction with a group-wise error rate of $\alpha = 0.05$ to define significant strain differences in fatty acid composition ($n = 8$) and fatty acid ratios ($n = 3$) ($\alpha = 0.05/11 = 0.0045$). In cases of statistical significance, effect size was calculated using Cohen's *d*, with small, medium, and large effect sizes being equivalent to *d*-values of 0.30, 0.50, and 0.80, respectively. Parametric linear regression analyses were used to determine relationships between brain fatty acid composition

and fatty acid ratios within brain regions. All statistical analyses were performed using GB-STAT software (Dynamic Microsystems, Inc., Silver Springs MD).

Results

Diet Fatty Acid Composition

In the present study, mice from both strains were maintained on the same commonly used Purina LabDiet (5010), which is autoclaved prior to use in murine SPF facilities. In the present study, autoclaved pellets were randomly selected from cage hoppers for analysis by gas chromatography, and diet fatty acid composition is presented in Table 1. In this diet, ALA (18:3n-3) was the only omega-3 fatty acid, representing 3.7% of total fatty acid composition, and linoleic acid (18:2n-6) was the only omega-6 fatty acid, representing 39% of total fatty acid composition. This diet did not contain preformed DHA or ARA, or intermediate omega-3 fatty acid or omega-6 fatty acid precursors.

Regional Fatty Acid Composition

Consistent with prior mouse [37] and rat [38] studies, differential DHA composition was observed across brain regions. Specifically, DHA composition was greatest in the prefrontal cortex ($20 \pm 0.07\%$) and hippocampus ($17 \pm 0.10\%$) and lower in the ventral striatum ($15 \pm 0.10\%$) and midbrain ($13 \pm 0.09\%$). Conversely, oleic acid, which is enriched in brain white matter [39], was greatest in the ventral striatum ($20 \pm 0.13\%$) and midbrain ($25 \pm 0.13\%$), and lower in the prefrontal cortex ($15 \pm 0.07\%$) and hippocampus ($16 \pm 0.15\%$).

Strain Differences in Fatty Acid Composition

After correction for multiple comparisons, palmitic acid (16:0) (4%, DBA < C57, $P \leq 0.0001$, $d = 4.5$) was the only fatty acid that differed significantly between strains in the prefrontal cortex (Fig. 1a). In the hippocampus, there were significant strain differences observed for oleic acid (18:1n-9) (6%, DBA < C57, $P \leq 0.0001$, $d = 3.5$), adrenic acid (22:4n-6) (7%, DBA > C57, $P \leq 0.0001$, $d = 3.2$), and DHA (22:6n-3) (4%, DBA > C57, $P = 0.0003$, $d = 2.6$) compositions (Fig. 1b). In the ventral striatum, there were significant strain differences observed for *cis*-vaccenic acid (18:1n-7) (5%, DBA < C57, $P = 0.0027$, $d = 1.9$), oleic acid (18:1n-9) (4%, DBA < C57, $P = 0.0002$, $d = 2.6$), adrenic acid (22:4n-6) (18%, DBA > C57, $P \leq 0.0001$, $d = 7.0$), docosapentaenoic acid (22:5n-6) (12%, DBA > C57, $P = 0.002$, $d = 1.9$), and DHA (22:6n-3) (4%, DBA > C57, $P = 0.0002$, $d = 2.7$)

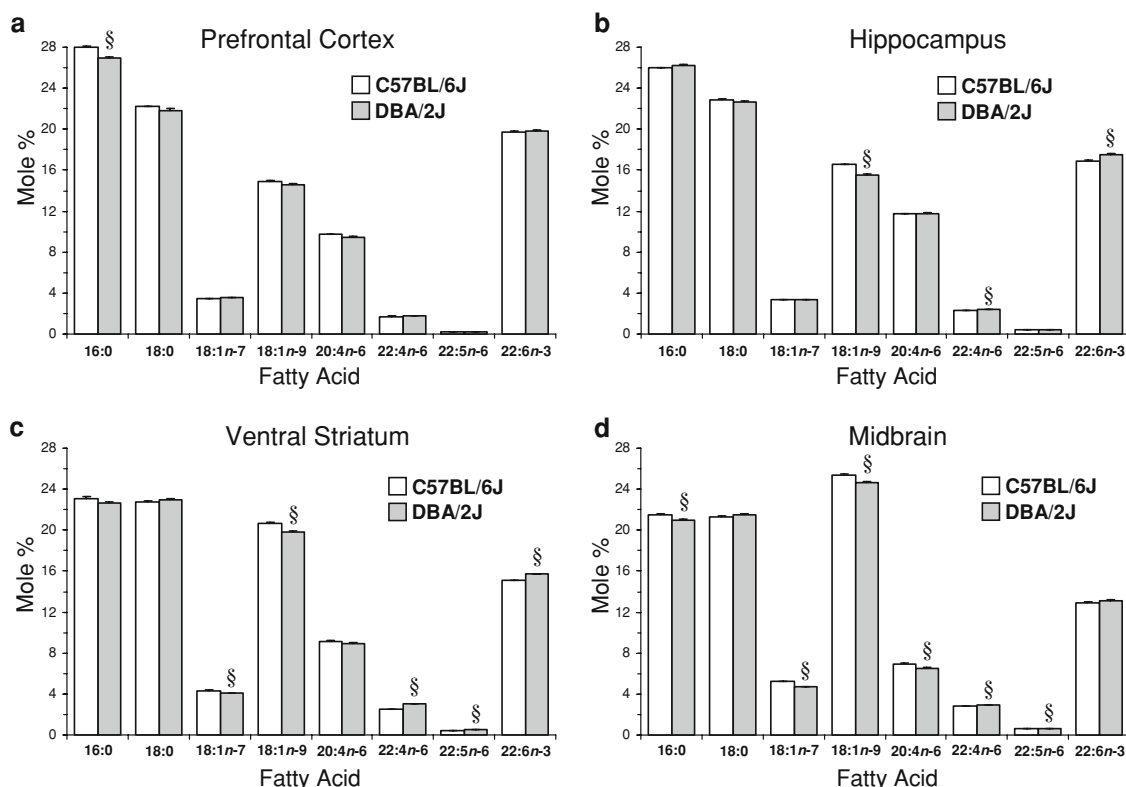


Fig. 1 Comparison of fatty acid composition (mol%) in the prefrontal cortex (a), hippocampus (b), ventral striatum (c), and midbrain (d) of adult male C57 ($n = 8$) and DBA ($n = 8$) mice. Note that significant strain differences in fatty acid composition are region-specific. 16:0, palmitic acid; 18:0, stearic acid; 18:1n-7, *cis*-vaccenic

acid; 18:1n-9, oleic acid; 20:4n-6, arachidonic acid; 22:4n-6, adrenic acid; 22:5n-6, docosapentaenoic acid; 22:6n-3, DHA. Values are means \pm SEM. § Significant at $P \leq 0.0045$ (P values and effect sizes are presented in the “Results” section)

compositions (Fig. 1c). In the midbrain, there were significant strain differences observed for palmitic acid (16:0) (3%, DBA > C57, $P \leq 0.0001$, $d = 3.5$), oleic acid (18:1n-9) (3%, DBA < C57, $P = 0.0002$, $d = 2.6$), *cis*-vaccenic acid (18:1n-7) (10%, DBA < C57, $P \leq 0.0001$, $d = 7.7$), ARA (20:4n-6) (4%, DBA < C57, $P = 0.0005$, $d = 2.4$), adrenic acid (22:4n-6) (24%, DBA > C57, $P \leq 0.0001$, $d = 13.1$), docosapentaenoic acid (22:5n-6) (12%, DBA > C57, $P = 0.0002$, $d = 2.7$), and DHA (22:6n-3) (4%, DBA > C57, $P = 0.005$, $d = 1.8$) compositions (Fig. 1d).

Strain Differences in Fatty Acid Ratios

C57 mice exhibited a greater ARA:DHA (20:4n-6/22:6n-3) ratio in the hippocampus (+5%, $P = 0.0009$, $d = 2.2$) ventral striatum (+7%, $P = 0.004$, $d = 1.8$) and midbrain (+7%, $P \leq 0.0001$, $d = 4.8$) relative to DBA mice, and there was a non-significant trend in the prefrontal cortex (+4%, $P = 0.01$, $d = 1.4$) (Fig. 2). C57 mice exhibited a smaller ADA:ARA (22:4n-6/20:4n-6) ratio, an index of elongase (*ELOVL2/5*) activity, in the hippocampus (−7%, $P \leq 0.0001$, $d = 3.0$), ventral striatum (−21%,

$P \leq 0.0001$, $d = 8.9$), and midbrain (−25%, $P \leq 0.0001$, $d = 10.7$) relative to DBA mice (Fig. 3a). C57 mice exhibited a greater oleic acid:stearic acid (18:1n-9/18:0) ratio, an index of SCD (delta-9 desaturase) activity, in the hippocampus (+6%, $P = 0.0002$, $d = 2.6$) and ventral striatum (+6%, $P = 0.0002$, $d = 2.7$) relative to DBA mice, and there was a non-significant trend in the midbrain (+4%, $P = 0.006$, $d = 1.7$) (Fig. 3b).

Correlations

Among all mice from both strains ($n = 16$), DHA composition was positively correlated with the ADA:ARA ratio in the hippocampus ($r = +0.56$, $P = 0.02$), ventral striatum ($r = +0.73$, $P = 0.001$), and midbrain ($r = +0.53$, $P = 0.03$), but not in the prefrontal cortex ($r = -0.25$, $P = 0.35$). Conversely, the ARA:DHA ratio was negatively correlated with the ADA:ARA ratio in the hippocampus ($r = -0.60$, $P = 0.01$), ventral striatum ($r = -0.72$, $P = 0.002$), and midbrain ($r = -0.87$, $P \leq 0.0001$), but not in the prefrontal cortex ($r = -0.03$, $P = 0.90$). DHA composition was negatively correlated with the oleic acid:stearic acid ratio in the prefrontal cortex

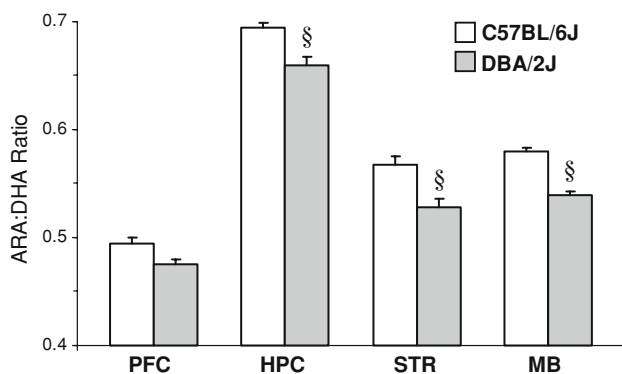


Fig. 2 Comparison of the ARA:DHA (20:4n-6/22:6n-3) ratio in the prefrontal cortex (PFC), hippocampus (HPC), ventral striatum (STR), and midbrain (MB) of adult male C57 ($n = 8$) and DBA ($n = 8$) mice. Note that DBA mice exhibit a significantly smaller ARA:DHA ratio in the hippocampus, ventral striatum, and midbrain relative to C57 mice. Values are means \pm SEM. § Significant at $P \leq 0.0045$ (P values and effect sizes are presented in the “Results” section)

($r = -0.76$, $P = 0.0007$), hippocampus ($r = -0.63$, $P = 0.008$), ventral striatum ($r = -0.63$, $P = 0.009$), and midbrain ($r = -0.80$, $P = 0.0002$).

Discussion

Based on prior findings that the prominent neurochemical and behavioral phenotypic differences observed between inbred C57 and DBA mouse strains could be reproduced within outbred rat and inbred mouse strains by dietary-induced deficits in DHA composition, we hypothesized that C57 and DBA mice maintained on the same diet would exhibit constitutive differences in regional brain DHA composition. In support of this hypothesis, C57 mice exhibited significantly lower DHA composition in the hippocampus and ventral striatum relative to DBA mice. Moreover, C57 mice exhibited a greater ARA:DHA ratio in the hippocampus, ventral striatum, and midbrain relative to DBA mice. C57 mice also exhibited significantly lower ADA composition, and a significantly smaller ADA:ARA ratio, in the hippocampus, ventral striatum, and midbrain, and lower docosapentaenoic acid (22:5n-6) composition in the ventral striatum and midbrain, relative to DBA mice. C57 mice exhibited significantly greater oleic acid (18:1n-9) composition in the hippocampus, ventral striatum, and midbrain relative to DBA mice, and a significantly smaller oleic acid:stearic acid ratio in the hippocampus and ventral striatum. Among all mice, DHA composition was positively correlated with the ADA:ARA ratio in the hippocampus, ventral striatum, and midbrain, and inversely correlated with the oleic acid:stearic acid ratio in all brain regions. Collectively, these data demonstrate that inbred C57 and DBA mice exhibit constitutive differences in

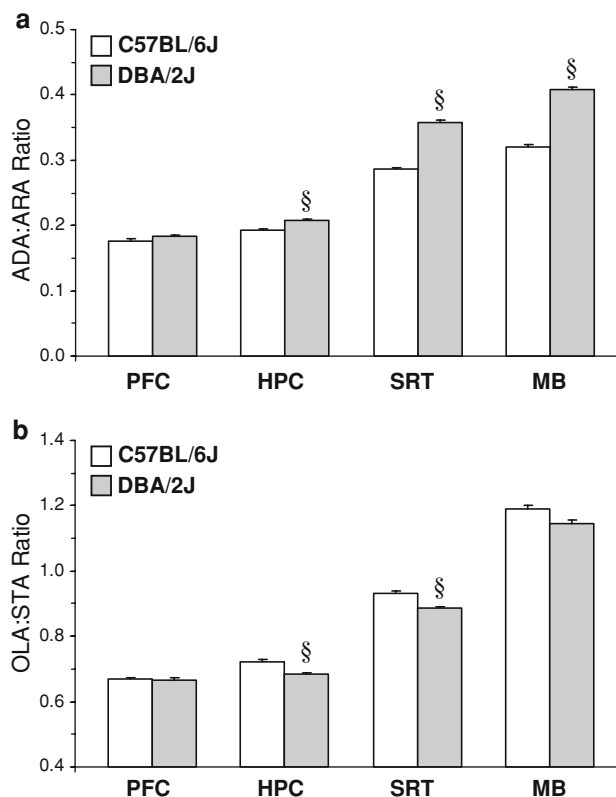


Fig. 3 Comparison of **a** the ADA:ARA (22:4n-6/20:4n-6) ratio, an index of elongase (*ELOVL2/5*) activity, and **b** the oleic acid:stearic acid (OLA:STA, 18:1n-9/18:0) ratio, an index of stearoyl-CoA desaturase (δ -9 desaturase) activity, in the prefrontal cortex (PFC), hippocampus (HPC), ventral striatum (STR), and midbrain (MB) of adult male C57 ($n = 8$) and DBA ($n = 8$) mice. Note the significant strain differences in ADA:ARA and OLA:STA ratios are region-specific. Values are means \pm SEM. § Significant at $P \leq 0.0045$ (P values and effect sizes are presented in the “Results” section)

regional brain fatty acid composition that are independent of diet.

A major finding of the present study is that C57 mice exhibited significantly lower DHA composition in the hippocampus and ventral striatum relative to DBA mice. The similarities between regional brain DHA compositions found in this study using total (triglyceride, phospholipid, and cholesteryl ester) fatty acid composition and a prior mouse study using isolated phospholipids [37] suggest that triglyceride and cholesteryl ester DHA composition comprise a relatively small percentage of total DHA composition. Although strain differences in regional brain DHA composition were small (4%), effects sizes were large (>0.8) and our prior study found that small ($\sim 10\%$) dietary-induced reductions in regional brain DHA composition were sufficient to significantly augment amphetamine-induced behavioral sensitization in adult C57 mice [34]. In the present study, prefrontal

cortex and midbrain DHA composition did not exhibit significant strain differences indicating regional-specificity. In prior studies, chronic dietary ALA depletion is associated with reductions in DHA composition in all brain regions including the prefrontal cortex and midbrain [34, 35, 37], suggesting that the present region-specific differences in DHA composition cannot be wholly attributable to strain differences in ALA-DHA biosynthesis. This is further supported by the finding that ARA composition, which is dependent upon the same biosynthetic pathway as DHA, did not exhibit significant strain differences, with the exception of the midbrain where DBA mice exhibited lower ARA composition. Moreover, dietary-induced brain DHA deficits are associated with reciprocal lower docosapentaenoic acid (22:5n-6) composition [34, 35, 37], whereas lower docosapentaenoic acid (22:5n-6) composition was observed in brain regions of C57 mice. Strain differences in regional brain DHA composition may therefore be due to region-specific differences in calcium-independent PLA₂-mediated turnover. Future investigations will be required to evaluate this and other mechanisms.

The significantly lower DHA composition, and similar or reduced ARA composition, observed in the hippocampus, ventral striatum, and midbrain of C57 mice relative to DBA mice was associated with a significantly greater ARA:DHA ratio in these regions. Because DHA inhibits, and ARA stimulates, PKC activity [4], the greater ARA:DHA ratio observed in the hippocampus of C57 mice may contribute in part to the greater PKC activity [23] and PKC-dependent synaptic plasticity [40] found in the hippocampus of C57 mice relative to DBA mice. Furthermore, elevated PKC-mediated substrate phosphorylation within the ventral striatum is associated with amphetamine-induced behavioral sensitization [41–43], and C57 mice develop significantly greater behavioral sensitization than DBA mice in response to repeated amphetamine treatment [27]. Moreover, dietary-induced reductions in regional brain DHA composition, and associated increases in the ARA:DHA ratio, significantly increase amphetamine-induced behavioral sensitization in adult DBA mice [35]. Together, these data suggest that constitutive strain differences in DHA composition and the ARA:DHA ratio may contribute to strain differences in PKC activity and associated synaptic and behavioral plasticity.

C57 mice exhibited lower ADA (22:4n-6) composition, and a significantly smaller ADA:ARA ratio, in the hippocampus, ventral striatum, and midbrain relative to DBA mice. This may reflect strain differences in elongase (*ELOVL2/5*) expression/activity, which directly mediates the synthesis of ADA from ARA [44]. The same elongases (*ELOVL2/5*) also mediate the conversion of eicosapentaenoic acid (20:5n-3) to docosapentaenoic acid (22:5n-3), a

prerequisite step in the biosynthesis of DHA from ALA. Therefore, it is possible that reduced elongase (*ELOVL2/5*) expression/activity in C57 mice may account for the lower regional brain ADA and DHA composition relative to DBA mice. Additionally or alternatively, strain differences in the ADA:ARA ratio may reflect greater shunting of ARA away from elongase-mediated fatty acid biosynthesis to cyclooxygenase-2 (COX-2)- and/or lipoxygenase-mediated prostaglandin or leukotrienes biosynthesis in C57 mice. This is supported in part by the findings that the downstream fatty acid metabolites of ARA, ADA and docosapentaenoic acid (22:5n-6), were lower in brain regions of C57 mice, and the ADA:ARA ratio was positively correlated with DHA composition. Furthermore, dietary-induced reductions in brain DHA composition are associated with elevated COX-2 expression and activity in rat brain [45]. Together, these data suggest that dietary-induced or constitutive reductions in DHA composition may promote shunting of ARA to prostaglandin biosynthesis.

DBA mice exhibited significantly lower oleic acid composition, and a smaller oleic acid:stearic acid ratio, in the hippocampus and ventral striatum relative to C57 mice, and a similar trend was observed in the midbrain. This finding is consistent with region-specific strain differences (C57 > DBA) in *SCD* (delta-9 desaturase) activity, which mediates the synthesis of oleic acid from stearic acid [13]. Consistent with the repression of *SCD* gene expression/activity by DHA [14], we also found that the oleic acid:stearic acid ratio was inversely correlated with DHA composition in all brain regions. These and our prior human postmortem findings [9, 46] suggest that DHA composition is an important determinant of brain *SCD* expression/activity. This finding may take on additional significance in view of evidence implicating *SCD* in central [47] and peripheral [48] myelin synthesis and age-related oligodendrocyte pathology [49, 50]. Moreover, we have recently found that *SCD* mRNA expression and the oleic acid:stearic acid ratio are significantly reduced, and DHA composition significantly increased, in postmortem brain tissue from patients with multiple sclerosis (McNamara et al., manuscript in preparation). Future studies will be required to determine whether strain differences in regional *SCD* expression/activity are associated with predicted differences in regional oligodendrocyte/myelin integrity.

In summary, we present evidence that inbred C57 and DBA mouse strains exhibit constitutive and region-specific differences in brain DHA composition, and associated differences in ARA:DHA, ADA:ARA, and oleic acid:stearic acid ratios, that are independent of diet. These data add to a growing body of preclinical evidence for strain differences in regional brain fatty acid composition [51, 52] and hepatic lipogenic activity [53], as well as an association between a greater brain ARA:DHA ratio and

augmented dopamine-mediated behavior [26, 27, 32, 34, 35, 52]. Furthermore, these data suggest that to-be-identified genetic factors are an important determinant of central fatty acid composition. This and prior clinical evidence for polymorphisms in lipogenic genes [19–22] suggest that genetic factors may contribute in part to the brain fatty acid composition abnormalities observed in patients with heritable psychiatric disorders including schizophrenia [8–10].

Acknowledgments This work was supported in part by National Institute of Mental Health grants MH073704 and MH074858 to R.K.M.

References

- Jones CR, Arai T, Bell JM, Rapoport SI (1996) Preferential in vivo incorporation of [³H]arachidonic acid from blood in rat brain synaptosomal fractions before and after cholinergic stimulation. *J Neurochem* 67:822–829
- Suzuki H, Manabe S, Wada O, Crawford MA (1997) Rapid incorporation of docosahexaenoic acid from dietary sources into brain microsomal, synaptosomal and mitochondrial membranes in adult mice. *Int J Vitam Nutr Res* 67:272–278
- Lee CH, Hajra AK (1991) Molecular species of diacylglycerols and phosphoglycerides and the postmortem changes in the molecular species of diacylglycerols in rat brains. *J Neurochem* 56:370–379
- McNamara RK, Ostrander M, Abplanalp W, Richtand NM, Benoit SC, Clegg DJ (2006) Modulation of phosphoinositide-protein kinase C signal transduction by omega-3 fatty acids: implications for the pathophysiology and treatment of recurrent neuropsychiatric illness. *Prostaglandins Leukot Essent Fatty Acids* 75:237–257
- Farooqui AA, Horrocks LA, Farooqui T (2007) Modulation of inflammation in brain: a matter of fat. *J Neurochem* 101:577–599
- Chalon S (2006) Omega-3 fatty acids and monoamine neurotransmission. *Prostaglandins Leukot Essent Fatty Acids* 75:259–269
- Fedorova I, Salem N Jr (2006) Omega-3 fatty acids and rodent behavior. *Prostaglandins Leukot Essent Fatty Acids* 75:271–289
- McNamara RK, Jandacek R, Rider T, Tso P, Hahn CG, Richtand NM, Stanford KE (2007) Abnormalities in the fatty acid composition of the postmortem orbitofrontal cortex of schizophrenic patients: gender differences and partial normalization with antipsychotic medications. *Schizophr Res* 91:37–50
- McNamara RK, Jandacek R, Rider T, Tso P, Stanford K, Hahn C-G, Richtand NM (2008) Deficits in docosahexaenoic acid and associated elevations in the metabolism of arachidonic acid and saturated fatty acids in the postmortem orbitofrontal cortex of patients with bipolar disorder. *Psychiatric Res* 160:285–299
- McNamara RK, Hahn CG, Jandacek R, Rider T, Tso P, Stanford KE, Richtand NM (2007) Selective deficits in the omega-3 fatty acid docosahexaenoic acid in the postmortem orbitofrontal cortex of patients with major depressive disorder. *Biol Psychiatry* 62:17–24
- Igarashi M, Ma K, Chang L, Bell JM, Rapoport SI (2007) Dietary n-3 PUFA deprivation for 15 weeks upregulates elongase and desaturase expression in rat liver but not brain. *J Lipid Res* 48:2463–2470
- Sprecher H, Chen Q, Yin FQ (1999) Regulation of the biosynthesis of 22:5n-6 and 22:6n-3: a complex intracellular process. *Lipids* 34:S153–S156
- Ntambi JM, Miyazaki M (2004) Regulation of stearoyl-CoA desaturases and role in metabolism. *Prog Lipid Res* 43:91–104
- Ntambi JM (1999) Regulation of stearoyl-CoA desaturase by polyunsaturated fatty acids and cholesterol. *J Lipid Res* 40:1549–1558
- Leonard AE, Bobik EG, Dorado J, Kroeger PE, Chuang LT, Thurmond JM, Parker-Barnes JM, Das T, Huang YS, Mukerji P (2000) Cloning of a human cDNA encoding a novel enzyme involved in the elongation of long-chain polyunsaturated fatty acids. *Biochem J* 350:765–770
- Marquardt A, Stöhr H, White K, Weber BH (2000) cDNA cloning, genomic structure, and chromosomal localization of three members of the human fatty acid desaturase family. *Genomics* 66:175–183
- Zhang L, Ge L, Parimoo S, Stenn K, Prouty SM (1999) Human stearoyl-CoA desaturase: alternative transcripts generated from a single gene by usage of tandem polyadenylation sites. *Biochem J* 340:255–264
- Hamilton JA (2007) New insights into the roles of proteins and lipids in membrane transport of fatty acids. *Prostaglandins Leukot Essent Fatty Acids* 77:355–361
- Malerba G, Schaeffer L, Xumerle L, Klopp N, Trabetti E, Biscuola M, Cavallari U, Galavotti R, Martinelli N, Guarini P, Girelli D, Olivieri O, Corrocher R, Heinrich J, Pignatti PF, Illig T (2008) SNPs of the FADS gene cluster are associated with polyunsaturated fatty acids in a cohort of patients with cardiovascular disease. *Lipids* 43:289–299
- Martinez M (1992) Abnormal profiles of polyunsaturated fatty acids in the brain, liver, kidney and retina of patients with peroxisomal disorders. *Brain Res* 583:171–182
- Matsuzono Y, Kinoshita N, Tamura S, Shimozawa N, Hamasaki M, Ghaedi K, Wanders RJ, Suzuki Y, Kondo N, Fujiki Y (1999) Human PEX19: cDNA cloning by functional complementation, mutation analysis in a patient with Zellweger syndrome, and potential role in peroxisomal membrane assembly. *Proc Natl Acad Sci USA* 96:2116–2121
- Schaeffer L, Gohlke H, Müller M, Heid IM, Palmer LJ, Kompauer I, Demmelmaier H, Illig T, Koletzko B, Heinrich J (2006) Common genetic variants of the FADS1 FADS2 gene cluster and their reconstructed haplotypes are associated with the fatty acid composition in phospholipids. *Hum Mol Genet* 15:1745–1756
- Bowers BJ, Christensen SC, Pauley JR, Paylor R, Yuva L, Dunbar SE, Wehner JM (1995) Protein and molecular characterization of hippocampal protein kinase C in C57BL/6 and DBA/2 mice. *J Neurochem* 64:2737–2746
- Paylor R, Tracy R, Wehner J, Rudy JW (1994) DBA/2 and C57BL/6 mice differ in contextual fear but not auditory fear conditioning. *Behav Neurosci* 108:810–817
- Ng GY, O'Dowd BF, George SR (1994) Genotypic differences in brain dopamine receptor functions in the DBA/2J and C57BL/6J inbred mouse strains. *Eur J Pharmacol* 269:349–364
- Ventura R, Alcaro A, Cabib S, Conversi D, Mandolesi L, Puglisi-Allegra S (2004) Dopamine in the medial prefrontal cortex controls genotype-dependent effects of amphetamine on mesoaccumbens dopamine release and locomotion. *Neuropsychopharmacology* 29:72–80
- Cabib S, Puglisi-Allegra S, Ventura R (2002) The contribution of comparative studies in inbred strains of mice to the understanding of the hyperactive phenotype. *Behav Brain Res* 130:103–109
- Lucki I, Dalvi A, Mayorga AJ (2001) Sensitivity to the effects of pharmacologically selective antidepressants in different strains of mice. *Psychopharmacology (Berl)* 155:315–322
- Moriguchi T, Salem N Jr (2003) Recovery of brain docosahexaenoate leads to recovery of spatial task performance. *J Neurochem* 87:297–309

30. Delion S, Chalon S, Guilloteau D, Besnard JC, Durand G (1996) alpha-Linolenic acid dietary deficiency alters age-related changes of dopaminergic and serotonergic neurotransmission in the rat frontal cortex. *J Neurochem* 66:1582–1591
31. Zimmer L, Vancassel S, Cantagrel S, Breton P, Delamanche S, Guilloteau D, Durand G, Chalon S (2002) The dopamine meso-corticolimbic pathway is affected by deficiency in n-3 polyunsaturated fatty acids. *Am J Clin Nutr* 75:662–667
32. Levant B, Radel JD, Carlson SE (2004) Decreased brain docosahexaenoic acid during development alters dopamine-related behaviors in adult rats that are differentially affected by dietary remediation. *Behav Brain Res* 152:49–57
33. DeMar JC Jr, Ma K, Bell JM, Igarashi M, Greenstein D, Rapoport SI (2006) One generation of n-3 polyunsaturated fatty acid deprivation increases depression and aggression test scores in rats. *J Lipid Res* 47:172–180
34. McNamara RK, Sullivan J, Richtand NM (2008) Omega-3 fatty acid deficiency augments amphetamine-induced behavioral sensitization in adult mice: prevention by chronic lithium treatment. *J Psychiatr Res* 42:458–468
35. McNamara RK, Sullivan J, Richtand NM, Jandacek R, Rider T, Tso P, Campbell N, Lipton J (2008) Omega-3 fatty acid deficiency augments amphetamine-induced behavioral sensitization in adult DBA/2J mice: Relationship with ventral striatum dopamine concentrations. *Synapse* 62:725–735
36. Metcalfe LD, Schmitz AA, Pelka JR (1966) Rapid preparation of fatty acid esters from lipids for gas chromatographic analysis. *Anal Chem* 38:514–515
37. Carrié I, Clément M, de Javel D, Francès H, Bourre JM (2000) Specific phospholipid fatty acid composition of brain regions in mice. Effects of n-3 polyunsaturated fatty acid deficiency and phospholipid supplementation. *J Lipid Res* 41:465–472
38. Xiao Y, Huang Y, Chen ZY (2005) Distribution, depletion and recovery of docosahexaenoic acid are region-specific in rat brain. *Br J Nutr* 94:544–550
39. Wilson R, Bell MV (1993) Molecular species composition of glycerophospholipids from white matter of human brain. *Lipids* 28:13–17
40. Nguyen PV, Duffy SN, Young JZ (2000) Differential maintenance and frequency-dependent tuning of LTP at hippocampal synapses of specific strains of inbred mice. *J Neurophysiol* 84:2484–2493
41. Gnegy ME, Hong P, Ferrell ST (1993) Phosphorylation of neuromodulin in rat striatum after acute and repeated, intermittent amphetamine. *Mol Brain Res* 20:289–298
42. Iwata S, Hewlett GH, Ferrell ST, Czernik AJ, Meiri KF, Gnegy ME (1996) Increased in vivo phosphorylation state of neuromodulin and synapsin I in striatum from rats treated with repeated amphetamine. *J Pharmacol Exp Ther* 278:1428–1434
43. Narita M, Akai H, Nagumo Y, Sunagawa N, Hasebe K, Nagase H, Kita T, Hara C, Suzuki T (2004) Implications of protein kinase C in the nucleus accumbens in the development of sensitization to methamphetamine in rats. *Neuroscience* 127:941–948
44. Jakobsson A, Westerberg R, Jacobsson A (2006) Fatty acid elongases in mammals: their regulation and roles in metabolism. *Prog Lipid Res* 45:237–249
45. Rao JS, Ertley RN, DeMar JC Jr, Rapoport SI, Bazinet RP, Lee HJ (2007) Dietary n-3 PUFA deprivation alters expression of enzymes of the arachidonic and docosahexaenoic acid cascades in rat frontal cortex. *Mol Psychiatry* 12:151–157
46. McNamara RK, Liu Y, Jandacek R, Rider T, Tso P (2008) The aging human orbitofrontal cortex: Decreasing polyunsaturated fatty acid composition and associated increases in lipogenic gene expression and stearoyl-CoA desaturase activity. *Prostaglandins Leukot Essent Fatty Acids* 78:293–304
47. DeWille JW, Farmer SJ (1992) Postnatal dietary fat influences mRNAs involved in myelination. *Dev Neurosci* 14:61–68
48. Garbay B, Boiron-Sargueil F, Shy M, Chbihi T, Jiang H, Kamholz J, Cassagne C (1998) Regulation of oleoyl-CoA synthesis in the peripheral nervous system: demonstration of a link with myelin synthesis. *J Neurochem* 71:1719–1726
49. Kumar VB, Vyas K, Buddhiraju M, Alshaher M, Flood JF, Morley JE (1999) Changes in membrane fatty acids and delta-9 desaturase in senescence accelerated (SAMP8) mouse hippocampus with aging. *Life Sci* 65:1657–1662
50. Tanaka J, Okuma Y, Tomobe K, Nomura Y (2005) The age-related degeneration of oligodendrocytes in the hippocampus of the senescence-accelerated mouse (SAM) P8: a quantitative immunohistochemical study. *Biol Pharm Bull* 28:615–618
51. Green P, Gispan-Herman I, Yadid G (2005) Increased arachidonic acid concentration in the brain of Flinders Sensitive Line rats, an animal model of depression. *J Lipid Res* 46:1093–1096
52. Vancassel S, Blondeau C, Lallemand S, Cador M, Linard A, Lavielle M, Dellu-Hagedorn F (2007) Hyperactivity in the rat is associated with spontaneous low level of n-3 polyunsaturated fatty acids in the frontal cortex. *Behav Brain Res* 180:119–126
53. de Antueno RJ, Elliot M, Horrobin DF (1994) Liver delta 5 and delta 6 desaturase activity differs among laboratory rat strains. *Lipids* 29:327–331

Alterations in the High Density Lipoprotein Phenotype and HDL-Associated Enzymes in Subjects with Metabolic Syndrome

K. G. Lagos · T. D. Filippatos · V. Tsimihodimos ·
I. F. Gazi · C. Rizos · A. D. Tselepis ·
D. P. Mikhailidis · Moses S. Elisaf

Received: 31 July 2008 / Accepted: 25 September 2008 / Published online: 28 October 2008
© AOCs 2008

Abstract Patients with metabolic syndrome (MetS) usually have low high density lipoprotein cholesterol (HDL-C) levels. We determined the HDL distribution profile as well as the HDL-related lipoprotein associated phospholipase A₂ (HDL-LpPLA₂) and paraoxonase-1 (PON1) activities in subjects with MetS ($n = 189$) but otherwise healthy. Age and sex-matched individuals ($n = 166$) without MetS served as controls. The lower HDL-C concentration in MetS patients was due to a reduction in both large and small HDL subclasses ($P < 0.001$ and $P < 0.05$, respectively). As the number of MetS components increased, the HDL phenotype comprised of a greater percentage of small HDL-3 and less large HDL-2 subclasses, resulting in a decreased HDL-2/HDL-3 ratio ($P < 0.001$ for all trends). Multivariate analysis revealed that HDL-2 levels and the HDL-2/HDL-3 ratio significantly and independently correlated with HDL-C (positively) and TG (negatively) levels. HDL-3 concentration significantly and independently positively correlated with HDL-C and TG levels. HDL-LpPLA₂ activity was decreased in MetS patients ($P < 0.01$), a phenomenon that may contribute to the defective antiatherogenic activity of HDL in MetS. PON1 activity did not differ between groups. We conclude that

MetS, in addition to the decrease in HDL-C concentration, is associated with alterations in the HDL phenotype, which is comprised of a greater percentage of small HDL subclasses. Furthermore, HDL-LpPLA₂ activity is decreased in MetS patients.

Keywords Metabolic syndrome · High density lipoprotein · Subclasses · Lipoprotein associated phospholipase A₂ · Paraoxonase 1 · High sensitivity C-reactive protein · Small dense low density lipoprotein cholesterol · Triglycerides

Introduction

The term metabolic syndrome (MetS) is used to describe a constellation of cardiovascular risk factors that have become a problem of epidemic proportions [1]. The diagnostic components of this syndrome involve abdominal obesity, dyslipidaemia, impaired carbohydrate metabolism and hypertension [1, 2]. Dyslipidaemia associated with MetS may substantially contribute to the increased cardiovascular disease (CVD) risk [3]. The most common lipid abnormalities associated with the MetS are elevated triglyceride (TG) and low high density lipoprotein cholesterol (HDL-C) concentrations [1, 4]. There also seems to be a preponderance of small, dense low density lipoprotein (sdLDL) subclasses [1, 4].

Numerous clinical and epidemiological studies have demonstrated the inverse and independent association between plasma HDL-C levels and the risk of coronary heart disease (CHD) [5]. It is well known that HDL does not represent a sum of identical particles but is rather comprised of discrete subfractions that differ with respect to size, density, composition, charge and other physicochemical

K. G. Lagos · V. Tsimihodimos · I. F. Gazi · C. Rizos ·
M. S. Elisaf (✉)
Department of Internal Medicine, School of Medicine,
University of Ioannina, 45 110 Ioannina, Greece
e-mail: egepi@cc.uoi.gr

T. D. Filippatos · D. P. Mikhailidis
Department of Clinical Biochemistry, Royal Free campus,
University College London (UCL), London, UK

A. D. Tselepis
Laboratory of Biochemistry, Department of Chemistry,
University of Ioannina, Ioannina, Greece

properties [6]. Of interest, the HDL subfraction distribution may have a greater predictive value for CHD events than HDL-C concentration [7–9].

HDL exhibits various anti-atherogenic, anti-oxidant, anti-inflammatory, anti-coagulant and anti-thrombotic properties [6, 9, 10]. An essential role in these beneficial functions of HDL may be played by enzymes associated with this lipoprotein, such as the lipoprotein associated phospholipase A₂ (HDL-LpPLA₂) and paraoxonase-1 (PON1) [11, 12].

The purpose of this study was to determine the distribution of HDL subclasses and the HDL-LpPLA₂ and PON1 activities in patients with and without MetS. The effects of metabolic variables on the concentration and relative distribution of HDL subclasses in this population were also assessed.

Methods

Subjects

Greek individuals ($n = 189$) who fulfilled the National Cholesterol Education Program Adult Treatment Panel III (NCEP ATP III) criteria [13] for the diagnosis of MetS but otherwise healthy were included in the study. Age and sex-matched individuals ($n = 166$) with less than three criteria for the diagnosis of MetS served as controls. Of these, 175 (105 with MetS, 70 controls) subjects participated in a previous study that assessed the LDL subclass distribution [4]. All participants gave informed written consent prior to their enrollment in the study, which was approved by the Ethics Committee of the University Hospital of Ioannina, Ioannina, Greece.

Exclusion Criteria

Individuals were excluded if they had type 2 diabetes mellitus (T2DM; fasting glucose levels >126 mg/dL; 7.0 mmol/L) or a history of CVD. In addition, patients with thyroid function abnormalities, abnormal hepatic function (aminotransferase activity >3 times the upper limit of the reference range), impaired renal function (serum creatinine levels >1.5 mg/dL; 132 μ mol/L), as well as those receiving drugs that may interfere with glucose or lipid metabolism were also excluded.

Determination of Anthropometric and Metabolic Variables

Body Weight, Waist Circumference and Blood Pressure (BP)

Body weight was determined to the nearest 0.1 kg with a calibrated beam balance and standing height was measured

to the nearest 1 cm. The body mass index (BMI) was calculated as weight (kg) divided by height squared (m^2). Waist circumference was measured midway between the lower ribs and the iliac crest. BP measurements were obtained at the same time (morning) in the sitting position, in duplicate using the right arm, following a 10-min rest and using a validated mercury sphygmomanometer (model no. FC114, Focal Corporation, Toyofuta, Kashiwa City, Chiba Pref., Japan). The appropriate cuff size was used.

General Biochemical Variables

All laboratory determinations were carried out following overnight fasting (water only allowed). Serum concentrations of fasting glucose, total cholesterol (TC) and TG were determined enzymatically on an Olympus AU600 analyzer (Olympus Diagnostica, Hamburg, Germany). HDL-C was determined by a direct assay (Olympus Diagnostica, Hamburg, Germany). Low density lipoprotein cholesterol (LDL-C) was calculated using the Friedewald formula (provided that TG were <400 mg/dL; 4.5 mmol/L) [14]; nonHDL-C was calculated as TC – HDL-C. Serum apolipoprotein (apo) AI and B levels were measured with a Behring Holding GmbH (Liederbach, Germany). Fasting serum insulin levels were measured by an AxSYM microparticle enzyme immunoassay on an AzSYM analyzer (Abbott Diagnostics, Illinois, USA). The homeostasis model assessment (HOMA) index was calculated as follows: fasting insulin (mU/L) \times fasting glucose (mg/dL)/405. Serum concentrations of high sensitivity C-reactive protein (hsCRP) were measured by the N High Sensitivity CRP method (Dade Behring Marburg GmbH, Marburg/Germany) based on particle enhanced immunonephelometry.

HDL Subclass Analysis

Analysis of the apo AI-containing lipoprotein subclasses was performed using the Lipoprint HDL System (Quantimetrix, Redondo Beach, California, USA) [15, 16]. After electrophoresis, very low density lipoprotein (VLDL) and LDL remained at the origin (Retention factor, $R_f = 0.0$), whereas albumin migrated to the front ($R_f = 1.0$). In between, up to nine bands of HDL were detected whose R_f s are 0.05, 0.10, 0.15, 0.20, 0.25, 0.29, 0.38, 0.48 and 0.53. Bands 1–3 ($R_f = 0.05$ –0.15) correspond to large HDL-2 subclasses, whereas bands 4–9 ($R_f = 0.20$ –0.53) comprised the small HDL-3 subclasses [15]. The cholesterol concentration of each HDL subclass was determined by multiplying the relative area under the curve (AUC) of each subclass by the HDL-C concentration of the sample [15].

LDL Subclass Analysis

Electrophoresis was performed using high resolution 3% polyacrylamide gel tubes and the Lipoprint LDL System (Quantimetrix, Redondo Beach, CA) according to the manufacturer's instructions [17]. LDL subclasses were estimated by the Rf between the VLDL fraction (Rf = 0.0) and the HDL fraction (Rf = 1.0). LDL is distributed as seven bands, whose Rfs are 0.32, 0.38, 0.45, 0.51, 0.56, 0.60 and 0.64 (LDL1–LDL7, respectively). LDL1 and LDL2 are defined as large, buoyant LDL, while LDL3 up to LDL7 are defined as sdLDL. Cholesterol concentration of each LDL subclass was determined by multiplying the relative AUC of each subclass by the TC concentration of the sample. Mean particle size was provided by the Lipoprint System [17, 18].

LpPLA₂ Activity

LpPLA₂ activity in total plasma as well as in HDL-rich plasma (i.e. after the precipitation of all apo B-containing lipoproteins with dextran sulfate-magnesium chloride), was determined by the trichloroacetic acid precipitation procedure using [³H]-platelet activating factor (PAF; 100 μM final concentration) as a substrate [19]. The reaction was performed for 10 min at 37 °C and LpPLA₂ activity was expressed as nmol PAF degraded per min per mL of plasma.

PON1 Activity

PON1 activity in serum was measured using paraoxon or phenylacetate as substrates, in the presence of 2 mM Ca²⁺ in 100 mM Tris-HCl buffer (pH 8.0) for paraoxon and 20 mM Tris-HCl buffer (pH 8.0) for phenyl acetate [20].

Statistical Analysis

Continuous variables were tested for normality by the Kolmogorov–Smirnov test and logarithmic transformations were performed if necessary. Data are presented as mean ± standard deviation (SD) and the median (range) for parametric and non-parametric data, respectively. An unpaired *t*-test was used for comparisons between study groups, while differences in proportions were assessed with a chi square test. One-way ANOVA or the Kruskal–Wallis test was used for comparisons between subjects with different numbers of MetS components. Analysis of covariance (ANCOVA) was used to assess the possible effect of HDL-C in the percentage of HDL subclasses in subjects with or without MetS. The relationships between study variables were investigated using the Pearson correlation coefficient (*r*), whereas correlations including at

least one non-normal distributed variable were performed using Spearman's correlation coefficient (*r_s*). Differences were considered significant at *P* < 0.05. Analyses were performed using the SPSS 15.0 statistical package for Windows (SPSS Inc., Chicago, Illinois).

Results

We enrolled 355 patients (148 men and 207 women). Of these, 189 individuals had MetS, while 166 subjects did not fulfill the criteria for this syndrome (Table 1). There were no differences in the age and sex distribution between study groups (Table 1). There was also no difference between groups in terms of smoking or menopausal status.

Anthropometric Variables

Patients with MetS had significantly greater waist circumference as well as higher BP values compared with controls (Table 1).

General Biochemical Variables

MetS patients had higher fasting glucose and insulin concentrations, as well as elevated values of the HOMA index, compared with controls (Table 1). MetS patients were characterized by an adverse lipid profile which comprised of elevated concentrations of non-HDL-C, TG and apo B, and lower levels of HDL-C and apo AI. TC levels were marginally increased in MetS patients, but LDL-C concentrations did not differ significantly between the two groups (Table 1).

Levels of hsCRP were significantly higher in MetS patients compared with controls (Table 1). There was a significant trend for elevation in the hsCRP concentration with the increase of MetS components (Kruskal–Wallis, *P* < 0.001).

HDL Subclasses

MetS patients had significantly lower cholesterol concentration in both large HDL-2 and HDL-3 subclasses (Table 2). Therefore, the decrease in HDL-C concentration in MetS patients can be attributed to the reduction of both HDL subclasses (but mainly of large HDL-2). When the cholesterol concentration of HDL-2 subclass was expressed as a percentage of HDL-C, MetS patients had significantly lower values compared with controls (Table 2). In contrast, the percentage of HDL-3 in the total HDL-C was significantly higher in MetS patients compared with controls (Table 2).

Table 1 Clinical and biochemical characteristics of the study population

	Controls	Metabolic syndrome	<i>P</i>
<i>n</i>	166	189	
<i>n</i> (males/females)	68/98	80/109	NS
Age (years)	48 ± 12	52 ± 11	NS
Smokers <i>n</i> (%)	47 (28)	56 (30)	NS
BMI (kg/m ²)	25.2 ± 4.3	28.3 ± 6.4	<0.001
Waist circumference, cm			
Men	99 ± 11	109 ± 11	<0.001
Women	88 ± 12	108 ± 13	<0.001
Systolic BP (mmHg)	123 ± 15	140 ± 16	<0.001
Diastolic BP (mmHg)	79 ± 7	89 ± 9	<0.001
Glucose (mg/dL)	91 ± 10	101 ± 15	<0.001
Insulin (mU/L)	7.4 (2–40)	12.7 (2–60)	<0.001
HOMA index	2.0 (0.4–9.6)	3.2 (0.5–9.8)	<0.001
Total cholesterol (mg/dL)	225 ± 40	236 ± 44	<0.05
Triglycerides (mg/dL)	96 (37–318)	178 (49–516)	<0.001
HDL-C (mg/dL)			
Men	51 ± 10	42 ± 8	<0.001
Women	64 ± 11	52 ± 10	<0.001
NonHDL-C (mg/dL)	167 ± 39	188 ± 39	<0.001
LDL-C (mg/dL)	147 ± 34	149 ± 39	NS
Apo AI (mg/dL)			
Men	144 ± 18	127 ± 20	<0.001
Women	163 ± 26	139 ± 27	<0.001
Apo B (mg/dL)	102 ± 25	109 ± 25	<0.05
hsCRP (mg/dL)	1.6 (0.21–8.5)	2.2 (0.2–9.0)	<0.01

Values are mean ± SD or median (range) or as stated in parentheses. To convert values for glucose to mmol/L, multiply by 0.0555. To convert total cholesterol, LDL-C and HDL-C levels from mg/dL to mmol/L, multiply by 0.0259. To convert triglyceride levels from mg/dL to mmol/L multiply by 0.0113

n number of patients; *NS* not significant; *BMI* body mass index; *BP* blood pressure; *HOMA* homeostasis model assessment; *HDL-C* high density lipoprotein cholesterol; *LDL-C* low density lipoprotein cholesterol; *apo* apolipoprotein; *hsCRP* high sensitivity C-reactive protein

There was a significant decrease in the percentage of HDL-2 as the number of MetS components increased (Kruskal–Wallis, $P < 0.001$, data not shown). In contrast, there was a significant increase in the percentage of HDL-3 as the number of MetS components increased (Kruskal–Wallis, $P < 0.001$, data not shown). Furthermore, there was a decrease in the HDL-2/HDL-3 ratio in parallel with the number of MetS components (Kruskal–Wallis, Fig. 1). The assessment of the above percentage differences with ANCOVA using the serum concentrations of HDL-C as covariate revealed same results (data not shown).

We performed multivariate analysis for the prediction of HDL-2, HDL-3 levels, as well as of the HDL-2/HDL-3 ratio, as an index of the HDL phenotype. This analysis revealed that HDL-2 levels and the HDL-2/HDL-3 ratio significantly and independently correlated with HDL-C (positively) and TG (negatively) levels (Tables 3, 4). HDL-3 levels significantly and independently positively correlated with HDL-C and TG levels (Table 3).

LpPLA₂ and PON1 Activities

Total LpPLA₂ activity was significantly increased in MetS patients compared with controls (Table 2). In contrast, HDL-LpPLA₂ was significantly decreased in MetS subjects. There was a significant trend for decrease of HDL-LpPLA₂ as the number of MetS components increased (Kruskal–Wallis, $P < 0.001$, Fig. 2). HDL-LpPLA₂ significantly negatively correlated with waist circumference, TG, VLDL-C, sdLDL-C, glucose, insulin and HOMA index, as well as with the percentage of HDL-3 (all $P < 0.05$).

PON1 activities towards both paraoxon and phenylacetate did not significantly differ between MetS subjects and controls (Table 2).

LDL Subclasses

As previously reported [4] MetS patients had significantly higher cholesterol concentrations in the VLDL and sdLDL subclasses (Table 2). When cholesterol concentrations in the sdLDL subclass were expressed as a percentage of total LDL-C, patients with MetS had significantly higher values compared with controls (Table 2). There was a significant increase in cholesterol concentrations of sdLDL subclasses as the number of MetS components increased (Kruskal–Wallis, $P < 0.001$, data not shown). The same results were obtained when cholesterol concentrations in sdLDL subclass were expressed as a percentage of total LDL-C values (Kruskal–Wallis, $P < 0.001$).

MetS patients had decreased mean LDL particle diameter compared with controls. There was a significant decrease in mean particle diameter as the number of MetS components increased (Kruskal–Wallis, $P < 0.001$, data not shown).

Discussion

The present study shows that the decrease in HDL-C concentration in patients with MetS is due to a reduction in both large and small HDL subclasses. Patients with MetS have an altered HDL phenotype comprising of an increased percentage of small HDL-3 subclass compared with

Table 2 Metabolic variables of the study population

	Controls	Metabolic syndrome	<i>P</i>
sdLDL (mg/dL)	4 (0–50)	12 (0–79)	<0.001
sdLDL (%)	3 (0–28)	9 (0–56)	<0.001
HDL-2 (mg/dL)	21 (6–44)	12 (4–37)	<0.001
HDL-2 (%)	35 (16–62)	26 (9–52)	<0.001
HDL-3 (mg/dL)	37 (18–47)	34 (14–43)	<0.05
HDL-3 (%)	66 (38–84)	74 (48–91)	<0.001
Total LpPLA ₂ activity (nmol/mL/min)	48 (22–94)	55 (25–96)	<0.001
HDL-LpPLA ₂ (nmol/mL/min)	3.4 (1.3–7.3)	2.4 (0.5–5.8)	<0.001
PON1 (paraoxon) (U/L)	60 (12–304)	60 (12–271)	NS
PON1 (phenyl acetate) (U/mL)	37 (6–78)	39 (19–88)	NS

Values are given as median (range)

To convert LDL-C and HDL-C levels from mg/dL to mmol/dL, multiply by 0.0259

sdLDL small dense low density lipoprotein cholesterol; HDL high density lipoprotein cholesterol; LpPLA₂ lipoprotein associated phospholipase A₂; PON1 paraoxonase 1; NS not significant

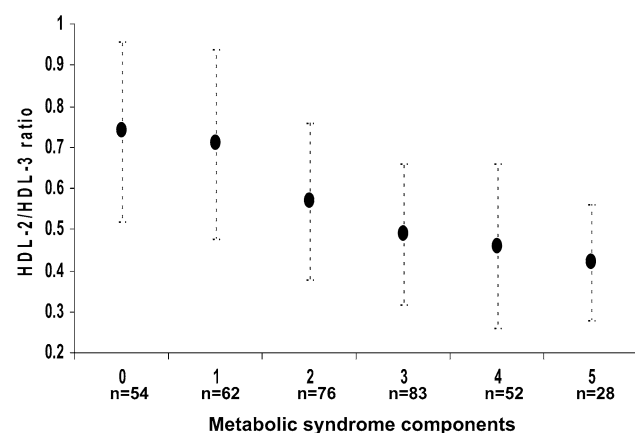


Fig. 1 Alterations of HDL-2/HDL-3 ratio according to the number of components of metabolic syndrome (Kruskal–Wallis, *P* for trend <0.001). Values are given as means \pm SD. *n* number of subjects

Table 3 Multivariate regression analysis for the prediction of HDL-2 and HDL-3 levels

Parameter	HDL-2		HDL-3	
	Beta*	<i>P</i>	Beta [†]	<i>P</i>
HDL-C	0.71	<0.001	0.83	<0.000
TG	–0.29	<0.001	0.19	<0.000

Only significant correlations are shown. Variables included in the model are those which were significantly correlated with HDL-2 and HDL-3 in univariate analysis

Beta is the standardized regression coefficient

* *R*² for the model = 70.4%

[†] *R*² for the model = 67.5%

individuals that do not fulfil the criteria for the diagnosis of the syndrome. In fact, as the number of MetS components increased, the HDL phenotype comprised of a greater

Table 4 Multivariate regression analysis for the prediction of HDL-2/HDL-3 ratio

Parameter	Beta	<i>P</i>
HDL-C	0.40	<0.001
TG	–0.24	<0.01

Beta is the standardized regression coefficient. *R*² for the model = 26.2%.

Only significant correlations are shown. Variables included in the model are those which were significantly correlated with HDL-2/HDL-3 ratio in univariate analysis

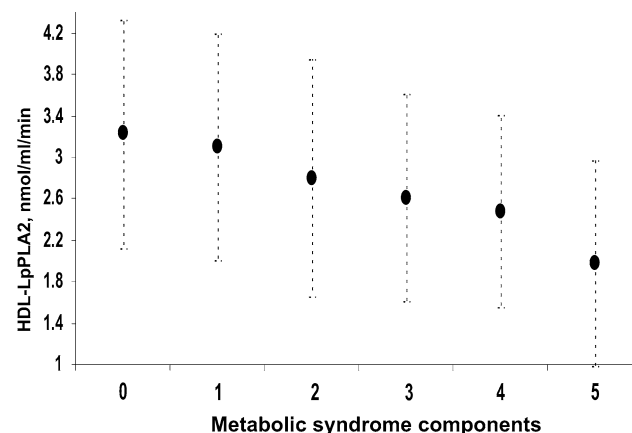


Fig. 2 Alterations of HDL-LpPLA₂ activity according to the number of components of metabolic syndrome (Kruskal–Wallis, *P* for trend <0.001). Values are given as mean \pm SD. The number of subjects is the same as for Fig. 1

percentage of small HDL-3 subclass. Furthermore, our analysis showed that the differences in the HDL phenotype are probably due to the presence of MetS and not only to lower HDL-C levels.

The HDL-C concentration independently correlated with both HDL-2 and HDL-3 levels. This suggests that the decrease in HDL-C levels affected both HDL subclasses. The HDL-2/HDL-3 ratio independently positively correlated with the HDL-C levels, suggesting that when the cholesterol content of HDL increases, this results in an increase in large HDL-2 subclass. Small HDL-3 subclass readily acquire cholesterol at cellular membranes via efflux mediated by the ATP-binding cassette transporter A1 [6, 21]. Subsequent esterification of cholesterol by the enzyme lecithin: cholesterol acyltransferase (LCAT) converts small HDL-3 to large HDL-2 [6, 21].

However, HDL-2 can be inversely converted to HDL3. This conversion occurs through several actions, including cholesteryl ester transfer protein (CETP)-mediated exchange of cholesterol esters and TGs between HDL and apoB-containing lipoproteins, selective uptake of cholesterol esters by hepatocytes mediated by scavenger receptor type BI, and phospholipid and TG hydrolysis by hepatic lipase [6, 21]. The results of multivariate analysis showing an independent positive association between TG levels and HDL-3 levels may be explained via the action of CETP. Indeed, an increase in the size of TG-rich lipoprotein pool accelerates the CETP-mediated exchange of TG and cholesterol esters between apo B-containing lipoproteins and HDL. Then, the TG in HDL are hydrolyzed by hepatic lipase, resulting in smaller HDL particles [6, 21, 22].

Our observations agree with previous studies using different HDL sub-fractionation methods. In 2,993 Framingham Heart Study participants (mean age 51 years; 53% women) without CVD, the lower HDL-C levels in MetS subjects were attributed to the decrease in all HDL particles [determined by nuclear magnetic resonance analysis (NMR)], but mainly of large HDL particles, in both men and women [23]. Other studies with small numbers of patients also showed using ultracentrifugation that HDL-C decrease in MetS is mainly due to the reduction of the light HDL-2 subfraction [24, 25]. There is no global agreement whether large or small HDL subpopulations are more anti-atherogenic. These discrepancies could be partially explained by the differences in the methodologies used for the subfractionation of HDL [6]. Epidemiological studies showed a predominance of small rather than large HDL particles among patients with CHD as compared with control subjects [7]. However, the presence of large HDL particles may have greater predictive value for imminent CHD-related events than HDL-C [7, 26, 27]. In the Veterans Affairs High Density Lipoprotein Intervention Trial (VA-HIT) the reduction of CHD events with gemfibrozil was attributed to the increase in HDL-C levels and especially the increase in NMR-deter-

mined small HDL particle numbers [28]. Nevertheless, there is evidence that low HDL-C states, as well as states with the presence of elevated inflammatory markers such as MetS and atherosclerosis, are associated with increased small HDL particles; these particles are dysfunctional, exhibiting lower anti-oxidant and anti-inflammatory activity [10, 29].

LpPLA₂ degrades PAF and oxidized phospholipids to generate lysophospholipids and oxidized fatty acids [19, 30]. Plasma LpPLA₂ activity is primarily associated with LDL, while a small proportion of the enzyme activity is associated with HDL. Although LDL-associated LpPLA₂ may exert pro-inflammatory effects, there is evidence that HDL-LpPLA₂ may have an atheroprotective role [11, 30]. The decreased HDL-LpPLA₂ activity in our MetS subjects is in agreement with previous observations that HDL in MetS has impaired antiatherogenic activity [24, 31, 32]. In fact, we observed a decrease in HDL-LpPLA₂ activity as the number of MetS components increased. In a previous study our group also found significantly decreased HDL-LpPLA₂ activity in MetS subjects [33].

PON1 is an esterase present in plasma in association with HDL [20, 34]. In vitro PON1 hydrolyzes paraoxon and phenyl acetate. In contrast, the in vivo substrates for this enzyme are considered to be phospholipid hydroperoxides and cholesteryl ester hydroperoxides, molecules that are formed during LDL oxidation [20, 35]. PON1 is able to retard LDL oxidation and to reduce the pro-inflammatory properties of oxidized LDL [20, 36, 37]. In our study, PON1 activity did not differ between MetS patients and controls. Other investigators have also shown similar PON1 activity in subjects with or without MetS [32]. However, others showed decreased PON1 activity in MetS and T2DM patients [38–44]. The impaired glucose tolerance and more marked glycaemia in T2DM, compared with MetS, may account for this difference [32, 45, 46].

MetS patients had increased concentrations of sdLDL cholesterol and hsCRP, as well as increased total plasma LpPLA₂ activity. We previously reported in a smaller study (which included some of the participants of the present study) that MetS patients have elevated sdLDL-C levels [4]. The elevation in total plasma LpPLA₂ activity in MetS has also been previously reported by another group as well as by us [17, 33, 47]. Indeed, it has been shown that higher plasma levels of total plasma LpPLA₂ activity increase the risk for incident CVD regardless of MetS [47]. This may be related to the fact that LpPLA₂ activity is a marker of the atherogenic sdLDL particles [17]. The parallel increase in hsCRP levels with the components of MetS has also been described [48]. The presence of increased sdLDL-C and hsCRP levels, as well as total

plasma LpPLA₂ activity, may aggravate the increased CVD risk of MetS patients [49–51].

Conclusions

Patients with MetS, in addition to lower HDL-C levels, have an altered HDL phenotype compared with individuals who do not have MetS. As the number of MetS components increases, the HDL phenotype comprises of a greater percentage of small HDL-3 and a lower percentage of large HDL-2 subclass. The HDL-LpPLA₂ activity is decreased in MetS patients, an effect that may contribute to the impaired anti-atherogenic activity of HDL. Furthermore, patients with MetS had increased levels of sLDL-C. Therefore, MetS, in addition to the alterations of lipoprotein quantity, is associated with changes in the quality of both LDL and HDL.

Conflict of interest statement The present study was carried out independently; no pharmaceutical company supported it financially. Some of the authors have given talks, attended conferences and participated in advisory boards and other trials sponsored by various pharmaceutical companies.

References

- Eckel RH, Grundy SM, Zimmet PZ (2005) The metabolic syndrome. *Lancet* 365:1415–1428
- Daskalopoulou SS, Mikhailidis DP, Elisaf M (2004) Prevention and treatment of the metabolic syndrome. *Angiology* 55:589–612
- Lakka HM, Laaksonen DE, Lakka TA, Niskanen LK et al (2002) The metabolic syndrome and total and cardiovascular disease mortality in middle-aged men. *JAMA* 288:2709–2716
- Gazi I, Tsimihodimos V, Filippatos T, Bairaktari E, Tselepis AD, Elisaf M (2006) Concentration and relative distribution of low-density lipoprotein subfractions in patients with metabolic syndrome defined according to the National Cholesterol Education Program criteria. *Metabolism* 55:885–891
- Chapman MJ, Assmann G, Fruchart JC, Shepherd J, Sirtori C (2004) Raising high-density lipoprotein cholesterol with reduction of cardiovascular risk: the role of nicotinic acid—a position paper developed by the European Consensus Panel on HDL-C. *Curr Med Res Opin* 20:1253–1268
- Kontush A, Chapman MJ (2006) Antiatherogenic small, dense HDL—guardian angel of the arterial wall? *Nat Clin Pract Cardiovasc Med* 3:144–153
- Asztalos BF, Cupples LA, Demissie S, Horvath KV et al (2004) High-density lipoprotein subpopulation profile and coronary heart disease prevalence in male participants of the Framingham Offspring Study. *Arterioscler Thromb Vasc Biol* 24:2181–2187
- Salonen JT, Salonen R, Seppanen K, Rauramaa R, Tuomilehto J (1991) HDL, HDL2, and HDL3 subfractions, and the risk of acute myocardial infarction. A prospective population study in eastern Finnish men. *Circulation* 84:129–139
- Link JJ, Rohatgi A, de Lemos JA (2007) HDL cholesterol: physiology, pathophysiology, and management. *Curr Probl Cardiol* 32:268–314
- Florentin M, Liberopoulos EN, Wierzbicki AS, Mikhailidis DP (2008) Multiple actions of high-density lipoprotein. *Curr Opin Cardiol* 23:370–378
- Tselepis AD, Chapman JM (2002) Inflammation, bioactive lipids and atherosclerosis: potential roles of a lipoprotein-associated phospholipase A₂, platelet activating factor-acetylhydrolase. *Atheroscler Suppl* 3:57–68
- James RW (2006) A long and winding road: defining the biological role and clinical importance of paraoxonases. *Clin Chem Lab Med* 44:1052–1059
- Grundy SM, Cleeman JI, Merz CN, Brewer HB Jr et al (2004) Implications of recent clinical trials for the National Cholesterol Education Program Adult Treatment Panel III guidelines. *J Am Coll Cardiol* 44:720–732
- Bairaktari ET, Seferiadis KI, Elisaf MS (2005) Evaluation of methods for the measurement of low-density lipoprotein cholesterol. *J Cardiovasc Pharmacol Ther* 10:45–54
- Saugos VG, Tambaki AP, Kalogirou M, Kostapanos M et al (2007) Differential effect of hypolipidemic drugs on lipoprotein-associated phospholipase A₂. *Arterioscler Thromb Vasc Biol* 27:2236–2243
- Filippatos TD, Liberopoulos EN, Kostapanos M, Gazi IF et al (2008) The effects of orlistat and fenofibrate, alone or in combination, on high-density lipoprotein subfractions and pre-beta1-HDL levels in obese patients with metabolic syndrome. *Diabetes Obes Metab* 10:476–483
- Gazi I, Lourida ES, Filippatos T, Tsimihodimos V, Elisaf M, Tselepis AD (2005) Lipoprotein-associated phospholipase A₂ activity is a marker of small, dense LDL particles in human plasma. *Clin Chem* 51:2264–2273
- Filippatos TD, Gazi IF, Liberopoulos EN, Athyros VG et al (2007) The effect of orlistat and fenofibrate, alone or in combination, on small dense LDL and lipoprotein-associated phospholipase A₂ in obese patients with metabolic syndrome. *Atherosclerosis* 193:428–437
- Tselepis AD, Dentan C, Karabina SA, Chapman MJ, Ninio E (1995) PAF-degrading acetylhydrolase is preferentially associated with dense LDL and VLDL-1 in human plasma. Catalytic characteristics and relation to the monocyte-derived enzyme. *Arterioscler Thromb Vasc Biol* 15:1764–1773
- Tsimihodimos V, Karabina SA, Tambaki AP, Bairaktari E et al (2002) Atorvastatin preferentially reduces LDL-associated platelet-activating factor acetylhydrolase activity in dyslipidemias of type IIA and type IIB. *Arterioscler Thromb Vasc Biol* 22:306–311
- von Eckardstein A, Nofer JR, Assmann G (2001) High density lipoproteins and arteriosclerosis. Role of cholesterol efflux and reverse cholesterol transport. *Arterioscler Thromb Vasc Biol* 21:13–27
- Deeb SS, Zambon A, Carr MC, Ayyobi AF, Brunzell JD (2003) Hepatic lipase and dyslipidemia: interactions among genetic variants, obesity, gender, and diet. *J Lipid Res* 44:1279–1286
- Kathiresan S, Otvos JD, Sullivan LM, Keyes MJ et al (2006) Increased small low-density lipoprotein particle number: a prominent feature of the metabolic syndrome in the Framingham Heart Study. *Circulation* 113:20–29
- de Souza JA, Vindis C, Hansel B, Negre-Salvayre A et al (2008) Metabolic syndrome features small, apolipoprotein A-I-poor, triglyceride-rich HDL3 particles with defective anti-apoptotic activity. *Atherosclerosis* 197:84–94
- Ji J, Watts GF, Johnson AG, Chan DC et al (2006) High-density lipoprotein (HDL) transport in the metabolic syndrome: application of a new model for HDL particle kinetics. *J Clin Endocrinol Metab* 91:973–979
- Asztalos BF, Collins D, Cupples LA, Demissie S et al (2005) Value of high-density lipoprotein (HDL) subpopulations in predicting

- recurrent cardiovascular events in the veterans affairs HDL intervention trial. *Arterioscler Thromb Vasc Biol* 25:2185–2191
27. Asztalos BF, Batista M, Horvath KV, Cox CE et al (2003) Change in alpha1 HDL concentration predicts progression in coronary artery stenosis. *Arterioscler Thromb Vasc Biol* 23:847–852
 28. Otvos JD, Collins D, Freedman DS, Shalaurova I et al (2006) Low-density lipoprotein and high-density lipoprotein particle subclasses predict coronary events and are favorably changed by gemfibrozil therapy in the Veterans Affairs High-Density Lipoprotein Intervention Trial. *Circulation* 113:1556–1563
 29. Athyros VG, Kakafika AI, Karagiannis A, Mikhailidis DP (2008) Do we need to consider inflammatory markers when we treat atherosclerotic disease? *Atherosclerosis* 200:1–12
 30. Elisaf M, Tselepis AD (2003) Effect of hypolipidemic drugs on lipoprotein-associated platelet activating factor acetylhydrolase. Implication for atherosclerosis. *Biochem Pharmacol* 66:2069–2073
 31. Hansel B, Kontush A, Bonnefont-Rousselot D, Bruckert E, Chapman MJ (2006) Alterations in lipoprotein defence against oxidative stress in metabolic syndrome. *Curr Atheroscler Rep* 8:501–509
 32. Hansel B, Giral P, Nobecourt E, Chantepie S et al (2004) Metabolic syndrome is associated with elevated oxidative stress and dysfunctional dense high-density lipoprotein particles displaying impaired antioxidative activity. *J Clin Endocrinol Metab* 89:4963–4971
 33. Rizos E, Tambaki AP, Gazi I, Tselepis AD, Elisaf M (2005) Lipoprotein-associated PAF-acetylhydrolase activity in subjects with the metabolic syndrome. *Prostaglandins Leukot Essent Fatty Acids* 72:203–209
 34. Mackness MI, Mackness B, Durrington PN, Connelly PW, Hegele RA (1996) Paraoxonase: biochemistry, genetics and relationship to plasma lipoproteins. *Curr Opin Lipidol* 7:69–76
 35. Mackness MI, Durrington PN (1995) HDL, its enzymes and its potential to influence lipid peroxidation. *Atherosclerosis* 115:243–253
 36. Mackness MI, Mackness B, Durrington PN (2002) Paraoxonase and coronary heart disease. *Atheroscler Suppl* 3:49–55
 37. Mackness MI, Arrol S, Abbott C, Durrington PN (1993) Protection of low-density lipoprotein against oxidative modification by high-density lipoprotein associated paraoxonase. *Atherosclerosis* 104:129–135
 38. Garin MC, Kalix B, Morabia A, James RW (2005) Small, dense lipoprotein particles and reduced paraoxonase-I in patients with the metabolic syndrome. *J Clin Endocrinol Metab* 90:2264–2269
 39. Moldoveanu E, Tanaseanu C, Tanaseanu S, Kosaka T et al (2006) Plasma markers of endothelial dysfunction in type 2 diabetics. *Eur J Intern Med* 17:38–42
 40. Mackness MI, Harty D, Bhatnagar D, Winocour PH et al (1991) Serum paraoxonase activity in familial hypercholesterolaemia and insulin-dependent diabetes mellitus. *Atherosclerosis* 86:193–199
 41. Mackness B, Durrington PN, Abuashia B, Boulton AJ, Mackness MI (2000) Low paraoxonase activity in type II diabetes mellitus complicated by retinopathy. *Clin Sci (Lond)* 98:355–363
 42. Brites FD, Verona J, Schreier LE, Fruchart JC, Castro GR, Wikinski RL (2004) Paraoxonase 1 and platelet-activating factor acetylhydrolase activities in patients with low HDL-cholesterol levels with or without primary hypertriglyceridemia. *Arch Med Res* 35:235–240
 43. Nobecourt E, Jacqueminet S, Hansel B, Chantepie S et al (2005) Defective antioxidative activity of small dense HDL3 particles in type 2 diabetes: relationship to elevated oxidative stress and hyperglycaemia. *Diabetologia* 48:529–538
 44. Kalmar T, Seres I, Balogh Z, Kaplar M, Winkler G, Paragh G (2005) Correlation between the activities of lipoprotein lipase and paraoxonase in type 2 diabetes mellitus. *Diabetes Metab* 31:574–580
 45. Hedrick CC, Thorpe SR, Fu MX, Harper CM et al (2000) Glycation impairs high-density lipoprotein function. *Diabetologia* 43:312–320
 46. Rysz J, Blaszczyk R, Banach M, Kedziora-Kornatowska K et al (2007) Evaluation of selected parameters of the antioxidative system in patients with type 2 diabetes in different periods of metabolic compensation. *Arch Immunol Ther Exp (Warsz)* 55:335–340
 47. Persson M, Hedblad B, Nelson JJ, Berglund G (2007) Elevated Lp-PLA2 levels add prognostic information to the metabolic syndrome on incidence of cardiovascular events among middle-aged nondiabetic subjects. *Arterioscler Thromb Vasc Biol* 27:1411–1416
 48. Saltevo J, Vanhala M, Kautiainen H, Kumpusalo E, Laakso M (2007) Association of C-reactive protein, interleukin-1 receptor antagonist and adiponectin with the metabolic syndrome. *Mediators Inflamm*. 2007:93573
 49. Milionis HJ, Rizos E, Goudevenos J, Seferiadis K, Mikhailidis DP, Elisaf MS (2005) Components of the metabolic syndrome and risk for first-ever acute ischemic non-embolic stroke in elderly subjects. *Stroke* 36:1372–1376
 50. Gazi IF, Tsimihodimos V, Tselepis AD, Elisaf M, Mikhailidis DP (2007) Clinical importance and therapeutic modulation of small dense low-density lipoprotein particles. *Expert Opin Biol Ther* 7:53–72
 51. Filippatos T, Tsimihodimos V, Kostapanos M, Kostara C et al (2008) Small dense LDL cholesterol and apolipoproteins C-II and C-III in non-diabetic obese subjects with metabolic syndrome. *Arch Med Sci* 4:263–269

Influence of Interesterification of a Stearic Acid-Rich Spreadable Fat on Acute Metabolic Risk Factors

Dawn M. Robinson · Natalie C. Martin ·
Lindsay E. Robinson · Latifeh Ahmadi ·
Alejandro G. Marangoni · Amanda J. Wright

Received: 27 May 2008 / Accepted: 1 October 2008 / Published online: 4 November 2008
© AOCS 2008

Abstract Chemical and enzymatic interesterification are used to create spreadable fats. However, a comparison between the two processes in terms of their acute metabolic effects has not yet been investigated. A randomised crossover study in obese (plasma TAG > 1.69 mmol/L, and BMI > 30 (BMI = kg/m²) or waist circumference > 102 cm, *n* = 11, age = 59.3 ± 1.8 years) and non-obese (plasma triacylglycerol (TAG) < 1.69 mmol/L, and BMI < 30 or waist circumference < 102 cm, *n* = 10, age = 55.8 ± 2.2 years) men was undertaken to compare the effects of chemical versus enzymatic interesterification on postprandial risk factors for type 2 diabetes (T2D) and cardiovascular disease (CVD). TAG, cholesterol, glucose, insulin and free fatty acid concentrations were measured for 6 h following consumption of 1 g fat/kg body mass of non-interesterified (NIE), chemically interesterified (CIE), enzymatically interesterified (EIE) stearic acid-rich fat spread or no fat, each with 50 g available carbohydrate from white bread. Interesterification did not affect postprandial glucose, insulin, free fatty acids or cholesterol (*P* > 0.05). Following ingestion of NIE, increases in serum oleic acid were observed, whereas both oleic and stearic acids were increased with CIE and EIE (*P* < 0.05). While postprandial TAG concentrations in non-obese subjects were not affected by fat treatment (*P* > 0.05), obese

subjects had an 85% increase in TAGs with CIE versus NIE (*P* < 0.05). The differences in TAG response between non-obese and obese subjects suggest that interesterification may affect healthy individuals differently compared to those already at risk for T2D and/or CVD.

Keywords Stearic acid · Spreadable fat · Chemical interesterification · Enzymatic interesterification · Randomisation · Postprandial · Triacylglycerol metabolism

Abbreviations

AUC	Area under the curve
BMI	Body mass index
CIE	Chemically interesterified test fat
CVD	Cardiovascular disease
DAG	Diacylglycerol
EIE	Enzymatically interesterified test fat
GC	Gas chromatography
HOMA-IR	Homeostasis model of insulin resistance
HPLC	High performance liquid chromatography
IE	Intesterification
NIE	Non-interesterified test fat
SEM	Standard error of the mean
SSS	Tristearin
T2D	Type 2 diabetes
TAG	Triacylglycerol

D. M. Robinson · N. C. Martin · L. E. Robinson ·
A. J. Wright (✉)

Department of Human Health and Nutritional Sciences,
College of Biological Sciences, University of Guelph,
Guelph, ON N1G 2W1, Canada
e-mail: ajwright@uoguelph.ca

L. Ahmadi · A. G. Marangoni
Department of Food Science, Ontario Agricultural College,
University of Guelph, Guelph, ON N1G 2W1, Canada

Introduction

Intesterification is a process used by the food industry to alter the physical properties of fats and oils and to create structured lipids for nutritional purposes. The process involves re-arrangement of the fatty acids within and between triacylglycerol (TAG) molecules. Interesterification

(IE) can be achieved by either chemical or enzymatic methods. Chemical interesterification (CIE) typically results in complete randomisation of the fatty acids present at each position on the glycerol backbone, while enzymatic interesterification (EIE) can be manipulated, primarily through enzyme selection, to achieve positional and/or fatty acid specificity for the production of desired TAGs. Because of the desire to reduce or eliminate *trans* fatty acids in processed foods, North American interest in IE has grown in recent years [1, 2], and IE fats are increasingly being used by the food industry. In particular, there is interest in interesterifying blends of hardstocks rich in saturated fatty acids with highly unsaturated oils to produce *trans* fatty acid-free fat spreads and shortenings as a strategy for chronic disease prevention [1, 3]. This trend has been fuelled by evidence that both oleic and stearic acids neither raise nor lower total cholesterol, high density lipoprotein (HDL), low density lipoprotein (LDL) or very-low density lipoprotein (VLDL)-cholesterol [4]. To date, no clinical studies have been published that directly compare the impact of chemical versus enzymatic IE methods on postprandial lipemia and glucose-related risk factors for type 2 diabetes (T2D) and cardiovascular disease (CVD). Particularly in light of the recent controversy regarding the effect of fat interesterification on CVD risk factors [5], well designed studies to address the effects of interesterification on acute and chronic risk factors are required.

TAG molecules consist of three fatty acids esterified to a glycerol backbone. The fatty acids at positions *sn*-1 and *sn*-3 are metabolized differently than the fatty acid at *sn*-2 due to the action of pancreatic lipase in the duodenum. Pancreatic lipase preferentially cleaves the fatty acids at *sn*-1 and *sn*-3, resulting in the formation of a 2-monoglyceride and two fatty acids, which are absorbed by the enterocyte [6]. Plasma cholesterol and TAG concentrations following ingestion of a fat appear to depend only on the saturation of fatty acids present at position *sn*-2, and not on the fatty acids located at *sn*-1 or *sn*-3 [7]. In this regard, the presence of saturated fatty acids, at the *sn*-2 position appears to increase absorption efficacy and result in elevated postprandial lipemia [8–11] than do corresponding monounsaturated fatty acids [12–14]. This is important since increased plasma TAG concentrations in the postprandial state may play a role in the progression of CVD just as postprandial concentrations of glucose and insulin are associated with T2D [15–17].

Since interesterification changes the positional distribution of saturated and monounsaturated fatty acids within and between TAG molecules, the process may affect postprandial metabolic risk factors implicated in T2D and CVD development and the effects may be different between chemical and enzymatic methods. However, to date, a comparison of IE methods on postprandial lipemia and glycemia following the ingestion of a highly saturated

fat with a monounsaturated-rich oil have not been evaluated. Thus, the objective of this study was to compare postprandial TAG and cholesterol concentrations, as well as glucose, insulin and free fatty acid responses in non-obese and obese men following ingestion of a NIE, CIE or EIE fat blend of a stearic acid-rich hardstock and an oleic acid-rich oil in the presence of a carbohydrate source. This study investigated both non-obese men with normal fasting TAG and obese men with elevated fasting TAG levels in order to assess the influence of existing T2D and CVD risk on the postprandial response. We hypothesized that IE of the blend would modify metabolic risk factors in the postprandial state, and that these would differ between IE methods.

Subjects and Methods

Subjects

Twenty-four male subjects between the ages of 40–70 years, who were non-smokers and not on medication to control glucose, cholesterol or TAG were recruited from the Guelph community. Subjects attended a screening visit and provided a fasting blood sample for lipid profile determination (Cholestech LDX v2.0, Hayward, CA). Non-obese subjects ($n = 12$) met the following criteria: fasting whole blood TAG < 1.69 mmol/L along with BMI < 30 and/or waist circumference < 102 cm [18]. In contrast, subjects were classified as obese ($n = 12$) if they displayed fasting whole blood TAG > 1.69 mmol/L along with BMI > 30 and/or waist circumference > 102 cm. Three subjects withdrew during the course of the study: two due to palatability of the test fats and one due to time constraints. Twenty-one subjects completed the study, of whom ten were classified as non-obese and 11 as obese. This study was approved by the University of Guelph Research Ethics Board, and informed consent was obtained from all participants.

Test Fats

A 70:30 wt% blend of high oleic sunflower oil (Vegetol 80RBD, Acatris, Minneapolis, MN, 76% oleic acid) with canola stearin (fully hydrogenated canola oil, CanAmera, Oakville, ON, 88% stearic acid) was prepared in the Guelph Food Technology Centre by heating the lipid mixture at 80 °C until all of the fat had melted and thoroughly mixing. This 70:30 (oil:stearin) physical blend constituted one of the treatments and is referred as the NIE test fat.

Samples of NIE were then interesterified by either chemical or enzymatic means, using conditions designed to

mimic industrial operations. The CIE test fat was prepared using the catalyst sodium methoxide (0.3% w/w, Sigma, St Louis, MO) and conducting the reaction at 85 °C under a nitrogen blanket for 60 min. Citric acid (2% v/w of a 20% solution, Sigma, St Louis, MO) was then added to stop the reaction and the samples were washed repeatedly with water to remove soaps and free fatty acids. Samples were then dried under vacuum using a rotary evaporator at 85 °C. Bleaching clay (1.5% w/w, courtesy of Bunge Canada, Toronto, ON) was added and the mixture was held at 85 °C for 20 min under nitrogen before being filtered, blanketed with nitrogen and stored at –20 °C until use. The EIE test fat was prepared using the non-specific *Candida antarctica* lipase immobilized on polyacrylic resin (Novozym 435, Sigma, St Louis, MO) at 5% w/w. The reaction vessel was maintained at 70 °C for 24 h in an elliptical shaking water bath. The oil was then filtered, blanketed with nitrogen, and stored at –20 °C prior to use.

To improve the sensory characteristics of the test fats, annatto (0.01% w/w, Sensient Food Colors, Kingston, ON) and butter flavour (0.4% w/w, Excellentia Flavours, Surrey, BC) were added to each spread. All fats were melted at 80 °C and portioned into individual servings corresponding to 1 g fat/kg body mass. The fats were then stored at 4 °C until the day before use when they were fully melted in a microwave to remove crystal memory and were immediately returned to 4 °C storage to solidify overnight. On the morning of each trial, the fats were spread on toasted and cooled bread, as described below.

Study Protocol

This study utilised a randomised, crossover design, with double-blinding on all fat-containing treatments but not bread alone. Postprandial responses to the test meals were measured over 6 h on four occasions, each visit separated by at least 1 week. Three-day food records were obtained from each subject before each trial and analysed using ESHA Food Processor V 9.9.0 (ESHA Research, Salem, OR) for total energy, % energy from fat, carbohydrate, dietary fibre, sugar, protein, total fat, saturated fat, *trans* fat, monounsaturated fat, polyunsaturated fat, alcohol and caffeine intake. Subjects were instructed to refrain from alcohol, strenuous exercise and caffeine for 48 h prior to each trial day and they consumed a standardised meal, containing 2,968 kJ (710 kcal), 58% energy from carbohydrate, 25% energy from fat and 17% energy from protein between 6 and 8 pm the night before followed by an overnight fast before each trial. At each visit, subjects were weighed upon arrival at the laboratory. In addition, bio-electrical impedance analysis (BodyStat 1500, Douglas, UK) was used to measure body composition at the third treatment visit.

On each of the four study days, a cannula was inserted into an antecubital vein to facilitate blood collection throughout the day. After fasting blood samples were collected, the test meal was administered. Each subject completed four treatments—a control meal of bread and water, and each fat load (either NIE, CIE, or EIE) with bread and water. Each meal consisted of three slices of toasted commercial white bread (WonderBread, Weston Bakeries, Toronto, ON, Ingredients: enriched wheat flour, water, sugar/glucose–fructose, yeast, vegetable oil (soybean and/or canola), salt, defatted soya flour, calcium propionate, stearyl-2-lactylate, monoglycerides) providing 50 g of available carbohydrate (along with 285 Calories, 3 g fat (0.6 g saturated), 1.5 g fibre, 10.5 g protein), 500 mL ambient temperature water and, if applicable, 1 g test fat/kg body mass. This approach to fat dosage is commonly used in postprandial lipid metabolism studies, especially when comparing two groups of subjects with variability in body weight and blood volume [19, 20]. Subjects consumed the test meal in less than 12 min, at which point time 0 min was set and blood samples were subsequently obtained at 15, 30, 45, 60, 90, 120, 180, 240, 300, and 360 min. Throughout each visit, subjects rested in the sitting position, were allowed to take short walks, and were permitted to consume water ad libitum throughout the day.

Serum and heparinised plasma were obtained at each time point and immediately placed on ice. Samples for glucose, insulin, TAG, total cholesterol and HDL were frozen at –20 °C prior to analysis. Serum samples for fatty acid composition analysis were stored at –80 °C until analysis.

Analytical Methods

The fatty acid and TAG composition of each test fat was determined by gas liquid chromatography (described below) and isocratic reverse phase HPLC, respectively. The Shimadzu HPLC was equipped with an Econsil C18 column and an evaporative light scattering detector (Sedex 75, Sedere, France) and used acetonitrile/chloroform (70:30 v/v) as the mobile phase. The solid fat content of NIE, CIE and EIE was measured in triplicate by pulsed nuclear magnetic resonance (American Oil Chemists' Society official method Cd 16-81) with a Bruker PC20 Series NMR analyzer (Bruker, Milton, ON).

Plasma glucose was analysed in duplicate by the glucose oxidase method (YSI 2300, YSI Incorporated, Yellow Springs, OH). Serum insulin was measured in duplicate by ¹²⁵I iodine radioimmunoassay (Diagnostic Products Corporation, Los Angeles, CA) and the homeostasis model of insulin resistance (HOMA-IR) at baseline was calculated for each subject (HOMA-IR = fasting plasma glucose × fasting

serum insulin/22.5) [21]. Serum free fatty acids were measured in duplicate using the colorimetric assay (Wako HR Series NEFA-HR [2], Wako Diagnostics, Richmond, VA).

Plasma TAG, total cholesterol and HDL-cholesterol were analysed at Guelph General Hospital (Guelph, ON) on a Uni-Cel Dx C 600i (Beckman-Coulter, Fullerton, CA) and LDL-cholesterol concentration calculated using the Friedwald method [22]. This method is not valid when TAG exceed 4.52 mmol/L, resulting in a lack of LDL data for three subjects over the course of the study. Postprandial TAG change from baseline was calculated at each time point for each subject for each treatment using the time 0 value for that day and calculating the group averages using these obtained values. This was completed to control for the observed wide inter-subject variation in fasting TAG.

Serum fatty acids were extracted by dissolving 200 μ L serum into 2 mL 2:1 chloroform/methanol and 200 μ L milli-Q water, followed by centrifugation at 780g for 10 min at 20 °C. The lipid-containing layer was dried under nitrogen, re-dissolved in 1 mL of iso-octane and fatty acids converted to fatty acid methyl esters (FAME) through the addition of 100 μ L of 2N potassium hydroxide in methanol and neutralisation with 2N hydrochloric acid. Heptadecanoic acid (17:0) was used as internal standard. The organic phase (0.8 μ L) was injected into a Shimadzu 8A-GC equipped with a flame ionisation detector and glass column (1.5 m \times 5 \times 3 mm) packed with 10% Silar 9CP on 80/100 Chromasorb WHP. Samples were injected at 230 °C and heated from 120 to 210 °C at 4 °C per min. Fatty acids present at greater than 5 wt% included palmitic, stearic, oleic and linoleic acids. The total area for these four fatty acids were summed and used to determine the relative concentration of each major fatty acid present. The change in relative serum concentration of each fatty acid was then calculated as the difference from 0 to 6 h.

Statistical Analysis

Incremental area under the curve (AUC) calculations were performed for each endpoint with GraphPad Prism (v 3.03, GraphPad Software, San Diego, CA), using the trapezoidal rule. All statistical methods used the SigmaStat statistical package (v 2.03, SigmaStat, San Jose, CA). Baseline fasting characteristics between the non-obese and obese groups were compared using a Student's *t* test while baseline fasting characteristics between the treatments and AUC responses were compared using a one-way analysis of variance. Postprandial endpoint comparisons were made using a two-way analysis of variance and Tukey's test for multiple comparisons was used for all post hoc analyses. *P*-values < 0.05 were considered significant. Data are presented as mean \pm SEM.

Results

The chemical composition and solid fat content of the test fats are shown in Table 1. Accordingly, NIE, CIE and EIE had similar fatty acid compositions, but differed extensively in both TAG composition and solid fat content. NIE contained 23% of the high melting TAG tristearin (SSS, melting temperature \sim 68 °C), compared with CIE and EIE which contained only 0.5 and 0.4% tristearin, respectively. Similarly, while NIE contained \sim 22% of OOL (melting temperature < 0 °C), CIE and EIE contained only 3.6 and 7.7% OOL, respectively. In contrast, CIE and EIE contained higher concentrations of SSO/SOS (melting temperature \sim 40 °C) and OOS/OSO (melting temperature \sim 23 °C) species. Such differences indicate that the solid

Table 1 Fatty acid and triacylglycerol composition and solid fat content of test fats

	NIE	CIE	EIE
Fatty acid composition (wt %) ^a			
16:0	5.0	5.1	5.1
18:0	28.4	30.4	29.2
18:1n-9	58.1	56.4	57.4
18:2n-6	4.7	4.7	4.7
	96.2	96.6	96.4
Triacylglycerol Species (wt %) ^{a,c}			
DAG	0.0	2.0	6.6
MLP	0.0	0.4	1.2
PLO	2.2	3.6	4.4
OOL	21.7	3.6	7.7
OOO	37.6	28.6	26.6
OPO	3.7	0.3	3.8
PPP	2.2	2.5	2.1
OOS	4.1	36.9	33.4
POS	0.0	2.5	1.2
PPS	0.0	1.4	0.7
SOS	0.0	14.8	10.7
SSP	2.2	0.1	0.1
SSS	23.3	0.5	0.4
	97.0	97.2	98.9
Solid Fat Content (%)			
25°C	20.7	14.2	13.9
30°C	19.7	9.8	9.7
37°C	18.6	5.6	5.4
45°C	17.1	2.1	2.1

DAG diacylglycerols, *M* myristic acid, *L* linoleic acid, *P* palmitic acid, *O* oleic acid, *S* stearic acid

^a Species at >1% reported

^b As determined by gas liquid chromatography

^c As determined by high performance liquid chromatography

^d As determined by pNMR

Table 2 Comparison of fasting characteristics between non-obese and obese subject groups

	Non-obese (<i>n</i> = 10)	Obese (<i>n</i> = 11)
Age (year)	55.8 ± 2.2 ^a	59.3 ± 1.8 ^a
Height (cm)	180 ± 2 ^a	176 ± 3 ^a
Weight (kg)	86.2 ± 2.4 ^a	101.8 ± 4.4 ^b
Body fat (%)	23.8 ± 5.4 ^a	31.9 ± 4.7 ^b
BMI (kg/m ²)	26.6 ± 0.8 ^a	32.9 ± 1.3 ^b
Waist circumference (cm)	94.8 ± 2.6 ^a	112.2 ± 2.5 ^b
Triacylglycerol (mmol/L)	0.89 ± 0.08 ^a	2.95 ± 0.32 ^b
Total cholesterol (mmol/L)	5.10 ± 0.26 ^a	5.84 ± 0.17 ^b
HDL-cholesterol (mmol/L)	1.24 ± 0.13 ^a	0.80 ± 0.08 ^a
LDL-cholesterol (mmol/L)	3.80 ± 0.25 ^a	3.71 ± 0.33 ^a
Plasma glucose (mmol/L)	5.08 ± 0.11 ^a	5.57 ± 0.23 ^a
Insulin (pmol/L)	39.1 ± 5.3 ^a	87.3 ± 12.2 ^b
HOMA-IR	1.2 ± 0.2 ^a	2.9 ± 0.4 ^b
Free fatty acids (mmol/L)	0.41 ± 0.04 ^a	0.52 ± 0.02 ^b

All values are mean ± SEM

Rows with different superscripts indicate $P < 0.05$

fat content of NIE around body temperature (i.e. 37 °C) was 18.6%, while only 5.4 and 5.6% solids remain in the CIE and EIE, respectively, at this temperature. There are also implications in terms of the physical functionality of the fats. For example, because of their greater variety of TAG species, compared with NIE, CIE and EIE have wider ranges of plasticity, an attribute which is required for spreadability and desired for various applications in the food industry.

By design, the non-obese and obese subject groups differed significantly in terms of BMI, waist circumference and fasting TAG. They also differed in terms of body weight, total cholesterol, insulin and HOMA-IR (Table 2). In comparing the 3-day energy and nutrient intakes leading up to each study visit, no significant differences were observed (data not shown).

Table 3 shows the change in relative serum concentrations of palmitic (16:0), stearic (18:0), oleic (18:1n-9) and linoleic (18:2n-6) acids from 0 to 6 h following ingestion of each test meal. Both the non-obese and obese subjects showed similar changes: palmitic and linoleic acid concentrations were lower following each of the NIE, CIE, and EIE meals due to the influx of exogenous stearic and oleic acids from the test fats. Stearic and oleic acid concentrations were increased after the CIE and EIE test meals, in a ratio that was similar to that in the test fats fed (approximately 2:1 oleic:stearic). In contrast, following the NIE treatment, both groups showed an increase in serum oleic, but not stearic acid concentration. As expected, ingestion of bread alone did not result in a difference in serum fatty acid content, with the exception of an increase in linoleic acid presumably from endogenous depots, as minimal fat was provided in this test meal.

Postprandial changes in plasma TAG from baseline with each treatment are shown in Fig. 1. No significant differences were observed between mean fasting TAG concentration across study days in the non-obese and obese groups ($P > 0.05$). As expected, in both subject groups, plasma TAG concentration significantly increased after consumption of each fat-containing meal as compared to

Table 3 Changes in postprandial total serum fatty acid composition (wt%) between 0 to 6 h for non-obese and obese groups following ingestion of test fats NIE, EIE, CIE with bread and bread control

	NIE	EIE	CIE	Bread
Non-obese				
Palmitic (16:0)	-3.7 ± 0.7 ^a	-6.5 ± 0.7 ^b	-5.3 ± 1.0 ^{a,b}	0.2 ± 0.2 ^c
Stearic (18:0)	-0.8 ± 0.2 ^a	3.1 ± 0.4 ^b	2.5 ± 0.5 ^b	-0.5 ± 0.1 ^a
Oleic (18:1n-9)	6.6 ± 0.9 ^a	7.5 ± 0.8 ^a	5.6 ± 1.1 ^a	-0.2 ± 0.5 ^b
Linoleic (18:2n-6)	-2.1 ± 0.5 ^a	-4.0 ± 0.4 ^a	-2.8 ± 0.7 ^a	0.4 ± 0.5 ^b
Obese				
Palmitic (16:0)	-4.6 ± 0.6 ^a	-7.6 ± 0.8 ^b	-7.0 ± 0.8 ^b	0.0 ± 0.5 ^c
Stearic (18:0)	-0.4 ± 0.3 ^a	4.8 ± 0.4 ^b	3.7 ± 0.9 ^b	-0.3 ± 0.8 ^a
Oleic (18:1n-9)	8.0 ± 1.1 ^a	7.7 ± 1.1 ^a	7.5 ± 1.1 ^a	-0.6 ± 0.6 ^b
Linoleic (18:2n-6)	-3.1 ± 0.5 ^a	-5.0 ± 0.8 ^a	-4.1 ± 1.1 ^a	0.9 ± 0.3 ^b

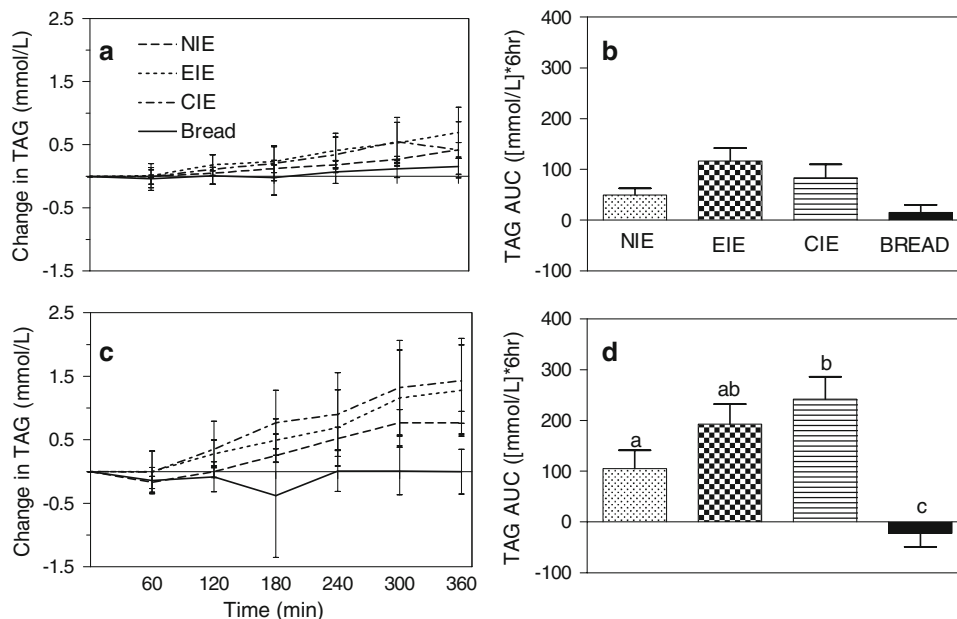
As a relative percentage of serum fatty acids

All values are mean ± SEM

Treatments across a row without common letter differ ($P < 0.05$)

Baseline serum fatty acid composition for each group (non-obese/obese); 14:0 (0.8 ± 0.1|1.1 ± 0.3), 16:0 (28.1 ± 5.4|23.6 ± 0.5), 16:1n-7 (2.9 ± 0.5|2.7 ± 0.2), 18:0 (10.8 ± 1.7|7.6 ± 0.3), 18:1n-9 (28.3 ± 5.0|27.7 ± 1.0), 18:2n-6 (25.1 ± 3.4|20.3 ± 0.5), 18:3n-3 and 20:0 (0.8 ± 0.1|1.6 ± 0.3), 20:1 (0.8 ± 0.1|1.4 ± 0.3), 20:2 (0.9 ± 0.2|1.6 ± 0.3), 20:3 (3.4 ± 0.5|1.9 ± 0.2), 20:4n-6 and 22:0 (9.5 ± 1.6|5.5 ± 0.4), 20:5n-3 (1.8 ± 0.3|1.0 ± 0.2), 24:1 (1.7 ± 0.2|1.7 ± 0.2), 22:6n-6 (3.3 ± 0.4|3.1 ± 0.4)

Fig. 1 Mean (\pm SEM) postprandial plasma TAG (triacylglycerol) concentrations from baseline during 6 h after ingestion of NIE (broken line, bar with dots), EIE (dotted line, bar with open and closed squares), CIE (dot with broken line, bar with horizontal lines) or bread-alone (solid line, filled bar) meal for non-obese (a, $n = 10$) and obese (c, $n = 11$) groups. 0–6 h incremental AUC in non-obese (b) and obese (d) subjects is also presented. Independent effects of treatment and time were observed for triacylglycerol changes ($P < 0.05$). Differences between treatments in terms of incremental AUC are indicated by different letters ($P < 0.05$)



the bread alone treatment ($P < 0.05$). In addition, AUC analysis shows that obese subjects had a greater increase in plasma TAG concentrations in response to fat-containing treatments compared with non-obese subjects (Fig. 1a vs. b). In both groups, independent effects of time and treatment on TAG response to fat-containing treatments were observed ($P < 0.05$).

Differences amongst the fat treatments were less striking. No differences were observed between NIE, CIE and EIE in the non-obese group. In the obese group, the TAG response was 85% higher following CIE compared with NIE, although there was no difference between CIE and EIE or NIE and EIE. Also, as expected, treatment had no effect on postprandial total cholesterol, HDL-cholesterol, or LDL-cholesterol between 0 and 6 h in either subject group for this acute study (data not shown).

Postprandial glucose, insulin and free fatty acid concentrations are shown in Fig. 2 (non-obese) and Fig. 3 (obese). As expected, obese subjects had higher glucose and insulin responses compared with non-obese subjects. In both groups, time and treatment significantly influenced postprandial plasma glucose concentration ($P < 0.05$). Ingestion of bread alone resulted in a significantly higher plasma glucose peak compared with when the fats were present ($P < 0.05$). However, there were no differences between the fat treatments in terms of glucose response. With respect to insulin, an elevated postprandial peak was observed in both non-obese and obese subjects with ingestion of the bread alone compared with the three fat treatments. Compared with the bread alone treatment, insulin AUC in the non-obese group was 37 and 34% lower after NIE and CIE, respectively, although neither fat load differed from EIE. Serum free fatty acids decreased sharply

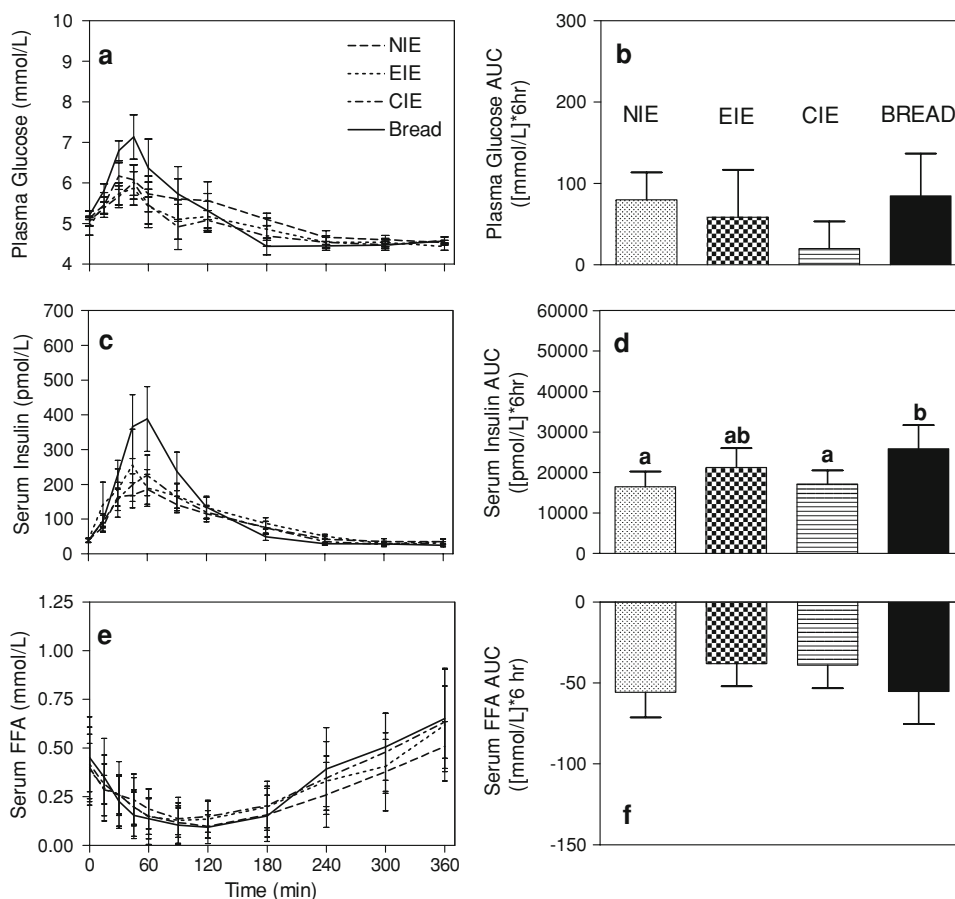
following ingestion of the test meals, and then progressively increased. There was, however, no effect of treatment or subject group with respect to serum free fatty acid response ($P > 0.05$).

Discussion

Interesterification of stearic-rich hardstocks with oleic-rich oils has been gaining popularity in the North American food industry, as this process produces a plastic fat without creating *trans* fatty acids [1, 2]. While IE can be accomplished by either chemical or enzymatic methods, a comparison of these methods on acute T2D and CVD risk factors has not yet been investigated. We sought to investigate this comparison in two subject groups which represented very different metabolic states. According to classic fasting clinical risk factors, the obese subject group was at elevated risk for T2D and CVD [23].

Analysis of serum fatty acid composition provided a means of assessing the uptake of fat with each treatment. Relative increases in stearic and oleic acids in the serum were observed with both CIE and EIE, in roughly the same proportions as in the test fats. In contrast, with NIE, no increases in serum stearic acid were observed, while oleic acid concentration increased significantly ($P < 0.05$). Although all three fat spreads had the same fatty acid composition (Table 1), the concentration of these fatty acids in the blood differed between the fats. This is likely related to the fact that the majority of stearic acid present in the NIE treatment existed as tristearin, while the stearic acid in CIE and EIE was distributed between a wider range

Fig. 2 Mean (\pm SEM) postprandial concentrations and 0–6 h incremental AUC in plasma glucose (**a**, **b**), serum insulin (**c**, **d**) and serum free fatty acids (**e**, **f**) over 6 h following ingestion of NIE (broken line, bar with dots), EIE (dotted line, bar with open and closed squares), CIE (dot with broken line, bar with horizontal lines) or bread-alone (solid line, filled bar) meal for non-obese subjects ($n = 10$). Independent effects of treatment and time were observed for glucose and insulin ($P < 0.05$). A significant effect of time was observed for serum free fatty acids ($P < 0.05$). In terms of incremental AUC, significant differences between the treatments were only observed for insulin (**d**), as indicated by different letters ($P < 0.05$)



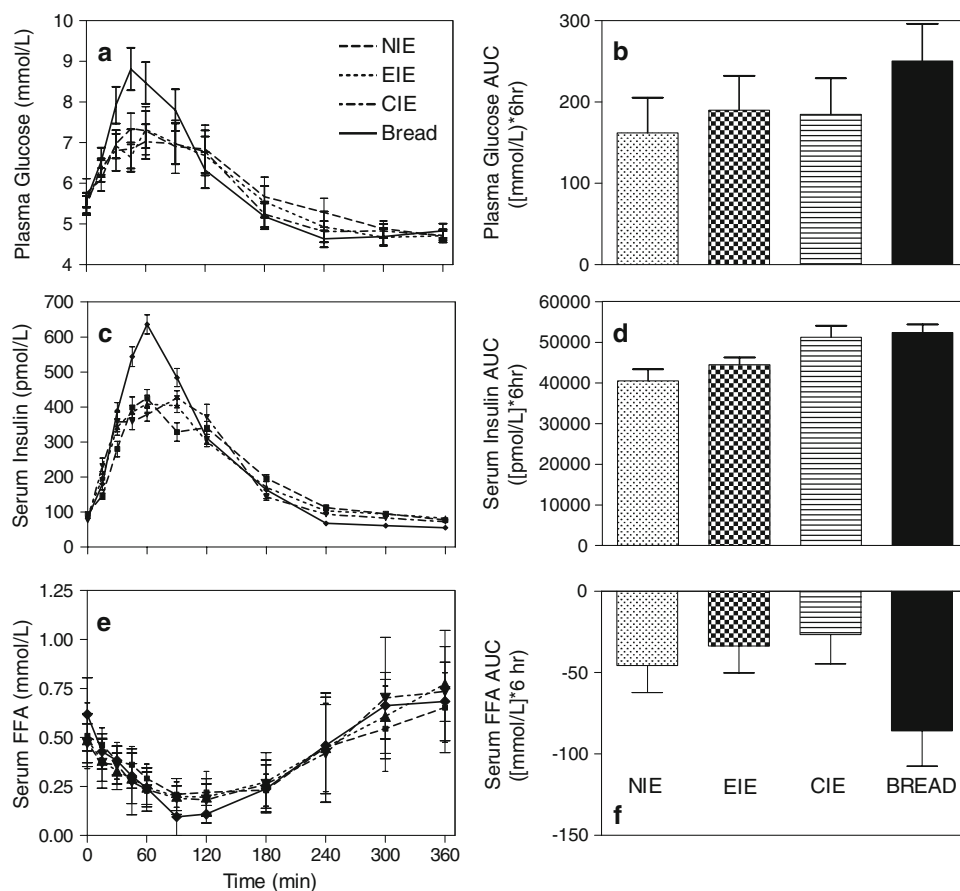
of TAG species (see Table 1). Owing to tristearin's high melting point ($\sim 68^\circ\text{C}$), this molecule is relatively unavailable for digestion by lipolysis and absorption by the enterocyte [24]. A comprehensive review of stearic acid absorption concluded that, while this fatty acid is relatively well absorbed from most TAG sources, this is not the case for tristearin for which only 15% of the stearic acid may be absorbed, due to reduced pancreatic lipase accessibility to the solid molecule [25]. Therefore, when the same amount of stearic acid is present, but is distributed amongst TAGs with lower melting temperatures (as in the CIE and EIE spreads), lipolysis and absorption are enhanced, leading to greater serum stearic acid concentrations.

As shown previously in the literature, the postprandial change in plasma TAG concentration differed between non-obese and obese subjects [19, 20]. The non-obese men showed no difference in response to any of the four treatments, suggesting they were able to effectively metabolise the fat load with minimal disturbance to blood lipid homeostasis and accumulation of plasma TAG [19]. In contrast, in the obese group, CIE resulted in a significantly increased TAG response over 6 h, compared to NIE, although neither NIE nor CIE differed significantly from EIE. Postprandial TAG metabolism can be affected by the positional distribution of the fatty acids in a test meal [7],

although the exact mechanism for this is not yet clear. Fats which differ in positional distribution have been shown to alter intestinal uptake of lipids [13] and the positional distribution of TAG in chylomicrons [26, 27], but not the clearance of TAGs by lipoprotein lipase at the adipocyte surface [27, 28]. Any of these outcomes could have affected the postprandial TAG response. In addition, the test fats had differing solid fat contents, which has been shown to affect fat absorption in the small intestine [24], and to have an effect upon postprandial lipemia [29, 30].

The reason for the apparent differences in TAG response between the NIE and CIE treatments, but not with the EIE (for the obese group only), cannot be explained by solid fat content or positional distribution arguments. Although the differences in solid fat content between the NIE and interesterification fats are consistent with the changes in serum fatty acid content, no differences were observed between the EIE and CIE samples in terms of solid fat content and therefore, the anticipated solubility during digestion would be similar. Furthermore, while the positional distribution of the test fats could not be determined, both IE reactions proceeded in a random fashion, leading to relatively similar fatty acid positional distributions in the CIE and EIE fats. Therefore, the biggest differences in positional distribution would have existed between NIE

Fig. 3 Mean (\pm SEM) postprandial concentrations and 0–6 h incremental AUC in plasma glucose (**a, b**), serum insulin (**c, d**) and serum free fatty acids (**e, f**) over 6 h following ingestion of NIE (broken line, bar with dots), EIE (dotted line, bar with open and closed squares), CIE (dot with broken line, bar with horizontal lines) or bread-alone (solid line, filled bar) meal for obese subjects ($n = 11$). Independent effects of treatment and time were observed for glucose ($P < 0.05$). There was also a significant effect of time ($P < 0.05$) and a trend to a treatment effect ($P = 0.057$) for insulin in the obese group and an effect of time for serum free fatty acids ($P < 0.05$)



and the interesterification fats, not between the interesterification fats themselves. The only difference observed between the CIE and EIE spreads, in terms of composition, is the amount of partial acylglycerols, specifically the diacylglycerols (DAG) present (see Table 1). The NIE, CIE and EIE contained 0.0, 1.2, 6.6% DAG, respectively. The consumption of DAG has been shown to affect postprandial lipemia in healthy persons, leading to an attenuated increase in serum TAGs compared to the ingestion of an equal amount of TAG of identical fatty acid composition [31]. Therefore, the greater amount of DAG in the EIE sample might explain the fact that the CIE response was greater than the NIE response, but no differences were observed between plasma EIE and NIE for the obese subjects.

The influence of fat-spread composition on the glycemic response can be assessed by considering the glucose, insulin and free fatty acid responses following each test meal. In both non-obese and obese subjects, interesterification did not result in any differences in circulating glucose, insulin or free fatty acid concentrations. This agrees with previous reports demonstrating that when carbohydrates are fed with meals that contain fats of identical mass and fatty acid composition, the fatty acid positional distribution does not influence the digestion,

absorption or clearance of glucose from the bloodstream, nor does it affect the secretion of insulin or its removal from the circulation [26, 32]. Interestingly, addition of any fat treatment (NIE, CIE or EIE) to the bread alone resulted in a significantly reduced and delayed peak and decline of glucose and insulin in both subject groups. This agrees with previous reports that even low levels of fat, when added to a carbohydrate challenge, can significantly reduce and delay the glycemic response [33]. The proposed mechanism for this effect is that the presence of fat in a meal results in a slower gastric emptying, leading to a delayed and diminished presentation of carbohydrate to the small intestine for absorption [34].

As mentioned above, differences were observed between non-obese men with relatively healthy metabolic profiles and obese men with pre-existing risk factors for T2D and CVD. Specifically, obese subjects had exaggerated plasma TAG, glucose and insulin responses to the test meals, compared with non-obese subjects. Therefore, the presence of classical fasting risk factors for T2D and CVD was associated with further dysfunctional postprandial metabolism in all test meals, agreeing with existing literature [19, 20]. Also, considering that postprandial TAG response is related to CVD risk [35] and that acute [36] and chronic [15–17] glucose and insulin control are related to

T2D and CVD progression, the postprandial impairments observed in obese subjects may be associated with further progression of chronic disease.

This study is the first to compare between the effect of CIE and EIE of a stearic-rich fat spread on acute postprandial metabolism. The data suggest that neither method of IE affects the acute glucose, insulin or free fatty acid response in the presence of carbohydrate. Interesterification had no effect on overall plasma TAG concentration in non-obese, healthy men. While both CIE and EIE of the fat spread led to alterations in the postprandial serum concentrations of stearic acid in the obese subjects, only CIE resulted in elevated postprandial TAG concentrations. This suggests that method of IE does not have an effect on relatively healthy individuals, but may affect the metabolism of people already at risk for CVD and/or T2D. Additional research to further elucidate the effect of IE on human metabolism in both the acute and chronic states is warranted.

Acknowledgments We thank the study participants for their time and commitment. We thank Mehrnoosh Kashani and Ricky Lam for their technical assistance and the Human Nutraceutical Research Unit at the University of Guelph and the Guelph Food Technology Centre for the use of their facilities. We also thank Bunge Canada for supplying the fully hydrogenated canola stearin and the Ontario Ministry of Agriculture, Food and Rural Affairs for funding.

References

- List GR, Pelloso T, Orthoefer F, Chrysam M, Mounts TL (1995) Preparation and properties of zero *trans* soybean oil margarines. *J Am Oil Chem Soc* 72:383–384
- Upritcharda JE, Zeelenberga MJ, Huizingaa H, Verschuren PM, Trautweina EA (2005) Modern fat technology: what is the potential for heart health? *Proc Nutr Soc* 64:379–386
- Sreenivasan B (1978) Interesterification of fats. *J Am Oil Chem Soc* 55:796–805
- Grundy S (1994) Influence of stearic acid on cholesterol metabolism relative to other long-chain fatty acids. *Am J Clin Nutr* 60:986S–990S
- Sundram K, Karupaiah T, and Hayes K (2007) Stearic acid-rich interesterified fat and *trans*-rich fat raise the LDL/HDL ratio and plasma glucose relative to palm olein in humans. *Nutr Metab* (serial online) 4: July 5 2007. URL: <http://www.nutritionandmetabolism.com/content/4/1/3>
- Mattson FH, Volpenhein RA (1964) The digestion and absorption of triglycerides. *J Biol Chem* 239:2772–2777
- Renaud SC, Ruf JC, Petithory D (1995) The positional distribution of fatty acids in palm oil and lard influences their biologic effects in rats. *J Nutr* 125:229–237
- Mortimer B, Kenrick MA, Holthouse DJ, Stick RV, Redgrave TG (1992) Plasma clearance of model lipoproteins containing saturated and polyunsaturated monoacylglycerols injected intravenously in the rat. *Biochem Biophys Acta* 1127:67–73
- De Fouw NJ, Kivits GAA, Quinlan PT, van Nielen WG, Wim GL (1994) Absorption of isomeric, palmitic acid-containing triacylglycerols resembling human milk fat in the adult rat. *Lipids* 29:765–770
- Redgrave TG, Kodali DR, Small DM (1998) The effect of triacyl-*sn*-glycerol structure on the metabolism of chylomicrons and triacylglycerol-rich emulsions in the rat. *J Biol Chem* 263:5118–5123
- Mortimer BC, Simmonds WJ, Joll CA, Stick RV, Redgrave TG (1988) Regulation of the metabolism of lipid emulsion model lipoproteins by a saturated acyl chain at the 2-position of triacylglycerol. *J Lipid Res* 29:713–720
- Aoe S, Yamamura J, Matsuyama H, Hase M, Shiota M, Miura S (1997) The positional distribution of dioleoyl-palmitoyl glycerol influences lymph chylomicron transport, composition and size in rats. *J Nutr* 127:1269–1273
- Brink EJ, Haddeman E (1995) Positional distribution of stearic acid and oleic acid in a triacylglycerol and dietary calcium concentration determines the apparent absorption of these fatty acids in rats. *J Nutr* 125:2379–2387
- Mattson FH, Nolen GA, Webb MR (1979) The absorbability by rats of various triglycerides of stearic and oleic acid and the effect of dietary calcium and magnesium. *J Nutr* 109:1682
- Zilvermit D (1979) Atherogenesis: a postprandial phenomenon. *Circulation* 60:473–485
- Karpe F (1997) Postprandial lipid metabolism in relation to coronary heart disease. *Proc Nutr Soc* 56:671–678
- Ceriello A, Davidson J, Hanefeld M, Leiter M, Monniere L, Owens D, Tajima N, Tuomilehto J (2006) Postprandial hyperglycaemia and cardiovascular complications of diabetes: an update. *Nutr Metab Cardiovasc Dis* 16:453–456
- Expert Panel on Detection, Evaluation, and Treatment of High Blood Cholesterol in Adults (2001) Executive summary of the third report of the national cholesterol education program (NCEP) expert panel on detection, evaluation, and treatment of high blood cholesterol in adults (adult treatment panel III). *JAMA* 285:2486–2497
- Kolovou GD, Anagnostopoulou KK, Pavlides AN, Salpea K, Iraklianiou A, Tsarpalis K, Damaskos DS, Manolis A, Cokkinos DV (2005) Postprandial lipemia in men with metabolic syndrome, hypertensives and healthy subjects. *Lipids Health Dis* 4:21–29
- Blackburn P, Lamarche B, Couillard C, Pascot A, Bergeroc N, Prud'homme D, Tremblay A, Bergeron J, Lemieux I, Despres JP (2003) Postprandial hyperlipidemia: another correlate of the "hypertriglyceridemic waist" phenotype in men. *Atherosclerosis* 171:327–336
- Matthews DR (1985) Homeostasis model assessment: insulin resistance and β -cell function from fasting plasma glucose and insulin concentrations in man. *Diabetologia* 28:412–419
- Friedewald WT, Levy RI, Fredrickson DS (1972) Estimation of the concentration of low-density lipoprotein cholesterol in plasma, without use of the preparative ultracentrifuge. *Clin Chem* 18:499–502
- National Institute of Health (1998) Clinical guidelines on the identification, evaluation and treatment of overweight and obesity in adults. *Obes Res* 6:51S–209S
- Bergstedt SE, Hayashi H, Kritchevsky D, Tso P (1990) Comparison of absorption of glycerol tristearate and glycerol trioleate by rat small intestine. *Am J Physiol Gastrointest Liver Physiol* 9:G386–G393
- Livesey G (2000) The absorption of stearic acid from triacylglycerols: an inquiry and analysis. *Nutr Res Rev* 13:185–214
- Summers LKM, Fielding BA, Herd SL, Ilic V, Clark ML, Quinlan PT, Frayn KN (1999) Use of structured triacylglycerols containing predominantly stearic and oleic acids to probe early events in metabolic processing of dietary fat. *J Lipid Res* 40:1890–1898
- Yli-Jokipii KM, Schwab US, Tahvonen RL, Kurvinen J, Mykkanen HM, Kallio HPT (2002) Triacylglycerol molecular

- weight and to a lesser extent, fatty acid positional distribution, affect chylomicron triacylglycerol composition in women. *J Nutr* 132:924–929
28. Summers LKM, Fielding BA, Ilic V, Quinlan PT, Frayn KN (1998) The effect of triacylglycerol-fatty acid positional distribution on postprandial metabolism in subcutaneous adipose tissue. *Br J Nutr* 79:141–147
 29. Yli-Jokipii K, Schwab US, Tahvonen RL, Kurvinen J, Mykkanen HM, Kallio HPT (2003) Chylomicron and VLDL TAG structures and postprandial lipid response induced by lard and modified lard. *Lipids* 38:693–703
 30. Berry SE, Miller GJ, Sanders TA (2007) The solid fat content of stearic acid-rich fats determines their postprandial effects. *Am J Clin Nutr* 85:1486–1494
 31. Taguchi H, Watanabe H, Onizawa K, Nagao T, Gotoh N, Yasukawa T, Tsushima R, Shimasaki H, Itakura H (2000) Double-blind controlled study on the effects of dietary diacylglycerol on postprandial serum and chylomicron triacylglycerol responses in healthy humans. *J Am Coll Nutr* 19:789–796
 32. Zampelas A, Williams CM, Morgan LM, Wright J, Quinlan PT (1994) The effect of triacylglycerol fatty acid positional distribution on postprandial plasma metabolite and hormone responses in normal adult men. *Br J Nutr* 71:401–410
 33. Cohen JC, Berger GM (1990) Effects of glucose ingestion on postprandial lipemia and triglyceride clearance in humans. *J Lipid Res* 31:597–602
 34. Collier G, O'Dea K (1983) The effect of coingestion of fat on the glucose, insulin, and gastric inhibitory polypeptide responses to carbohydrate and protein. *Am J Clin Nutr* 37:941–944
 35. Patsch JR, Miesenbock G, Hopferwieser T, Muhlberger B, Knapp E, Dunn JK, Gotto AM Jr, Patsch W (1992) Relation of triglyceride metabolism and coronary artery disease. Studies in the postprandial state. *Arterioscler Thromb Vasc Biol* 12:1336–1345
 36. Leiter LA, Ceriello A, Davidson JA, Hanefeld M, Monnier L, Owens DR, Tajima N, Tuomilehto J (2005) Postprandial glucose regulation: new data and new implications. *Clin Ther* 27:S42–S56

Visualization of Bile Homeostasis Using ^1H -NMR Spectroscopy as a Route for Assessing Liver Cancer

G. A. Nagana Gowda · Narasimhamurthy Shanaiah ·
Amanda Cooper · Mary Maluccio · Daniel Raftery

Received: 13 August 2008 / Accepted: 3 October 2008 / Published online: 4 November 2008
© AOCs 2008

Abstract Changes in bile synthesis by the liver or alterations in the enterohepatic circulation due to a variety of etiological conditions may represent a novel source of liver disease-specific biomarkers. Bile from patients with liver diseases exhibited significant changes in the levels of glycine- and taurine-conjugated bile acids, phospholipids, cholesterol and urea relative to non-liver disease controls. Cholangiocarcinoma and non-malignant liver diseases (NMLD) showed the most significant alterations. Further, hepatocellular carcinoma (HCC) could be differentiated from NMLD ($p = 0.02$), as well as non-liver disease controls ($p = 0.02$) based on the amounts of bile acids, phospholipids and/or cholesterol. HCC also differed with cholangiocarcinoma although not significantly. Urea increases somewhat in non-malignant liver disease relative to non-liver disease controls, while the bile acids, phospholipids and cholesterol all decrease significantly. The ratio between some major bile metabolites also distinguished NMLD ($p = 0.004$ – 0.01) from non-liver disease controls. This snapshot view of bile homeostasis, is obtainable from a simple nuclear magnetic resonance (NMR) approach and demonstrates the enormous opportunity to assess liver status, explore biomarkers for high risk diseases such as cancers and improve the understanding of normal and abnormal cellular functions.

Keywords Bile homeostasis · Liver disease · Hepatocellular carcinoma · Cholangiocarcinoma · Glycine-conjugated bile acids · Taurine-conjugated bile acids · ^1H NMR · Metabolomics

Introduction

Liver diseases remain a daunting health problem, with primary liver cancer being the most lethal. Hepatocellular carcinoma (HCC) is the leading cause of gastro-intestinal cancer deaths [1]. Clinical silence during the early stages has made early diagnosis of HCC highly challenging. Unfortunately, late diagnosis parallels high mortality rates because therapeutic options are limited and less effective. Patients with Hepatitis B and/or Hepatitis C are at particularly high-risk for the development of cancer. Cancer risk increases with the development of cirrhosis, implying that there are measurable molecular changes within the microenvironment of the liver with the progression of underlying liver disease that account for this increased risk. Targeting such molecular changes has immense potential for early disease detection. The most information-rich techniques currently employed in small molecules analyses are nuclear magnetic resonance (NMR) spectroscopy and mass spectrometry (MS) [2–5]. Recently, application of NMR spectroscopy to the detection of pancreatic, lung, ovarian, prostate and liver cancers based on small molecules is demonstrated using urine, blood or tissue samples [6–10].

A few studies have indicated the potential of metabolite detection in bile for assessing hepatobiliary diseases including cancers of the liver, pancreas and the biliary tract [11–14]. For example, the potential for screening cancer based on the alteration in phospholipid

G. A. Nagana Gowda (✉) · N. Shanaiah · D. Raftery
Department of Chemistry, Purdue University,
West Lafayette, IN 47907, USA
e-mail: ngowda@purdue.edu

A. Cooper · M. Maluccio (✉)
Department of Surgery, Indiana University,
Indianapolis, IN 46202, USA
e-mail: mmalucci@iupui.edu

content in human bile between malignant and non-malignant patients has been recently reported [14]. Monitoring the concentration of bile acids in human bile is reported to serve as a reliable indicator for liver function after hepatobiliary resection for biliary cancer [13]. Altered bile cholesterol levels have been implicated in gallstone related problems, including gallbladder cancer. Increased levels of bile acids in serum have also been reported in liver disease, indicating the altered physiology of biliary metabolites in patients with liver related problems [15–20].

Utilizing the fact that a large amount of bile fluid exists in the gallbladder (40–50 mL in humans), attempts to determine bile metabolites non-invasively using in vivo localized magnetic resonance spectroscopy have yielded encouraging results [21, 22]. However, so far no systematic studies have assessed liver diseases based on the measurement of multiple bile metabolites. Advancements in in vitro studies of bile will also benefit translational research for exploring clinical applications of bile in vivo. Therefore, methods providing a reliable snapshot of the major bile metabolites that reflect the global functional status of the liver are highly desired. From a series of comprehensive NMR studies of bile and its metabolites, we recently developed simple NMR methodologies for detecting several bile metabolites, such as individual glycine- and taurine-conjugated bile acids, phospholipids, cholesterol and urea [23–27]. Among the various bile acids, individual conjugated bile acids such as glycocholic acid, glycodeoxycholic acid, glycochenodeoxycholic acid, taurocholic acid, taurodeoxycholic acid and taurochenodeoxycholic acid have been identified, simultaneously, from a single NMR measurement. With this database of information, we can now study these major metabolites of liver origin in gallbladder bile from patients with liver diseases, and, as a result, provide a global view of liver function. Changes

in metabolite profiles due to a variety of etiologies indicate the opportunities for using metabolomics to assess disease status and obtain better insights into the cellular biochemistry of malignant and non-malignant liver diseases (NMLD).

Materials and Methods

Chemicals and Bile from Patients

Deuterated dimethylsulfoxide (DMSO), deuterium oxide (D₂O), and sodium salt of trimethylsilylpropionic acid-d₄ (TSP) were purchased from Sigma-Aldrich (Milwaukee, WI, USA).

Bile Collection

Gallbladder bile was obtained from 44 patients at the time of operation. Of these, 17 were controls (non-liver disease) which were collected from patients undergoing gallbladder procedures unrelated to liver disease. Liver diseases include both malignant, HCC ($n = 11$) and cholangiocarcinoma ($n = 7$), and non-malignant ($n = 9$) diseases. Patient profile and the sample subsets are shown in Table 1. All bile samples were collected at the commencement of the case to minimize ischemic changes, if any. A purse string suture was placed in the fundus of the gallbladder and 10 mL of bile taken via an 18 gauge needle. The bile was transferred to a 10-mL tube containing sodium azide (with a final concentration of 0.1%). The specimen was then divided into 1-mL aliquots and stored at $-80\text{ }^{\circ}\text{C}$ until analysis. An Institutional Review Board protocol, approved at both Indiana University School of Medicine and Purdue University, was in place for the collection, storage, and analysis of human bile for research purposes.

Table 1 Patient profile

Patients		Number	Gender	Mean age (years)
Liver disease (malignant)	Hepatocellular carcinoma (HCC)	11	7 male, 4 female	56.8
	Cholangio-carcinoma (CC)	7	5 male, 2 female	52.7
Liver disease (non-malignant)	Alcoholic cirrhosis (AC)	3	3 male	50.3
	Hepatitis C (HEPC)	3	2 male, 1 female	52.3
	Non-alcoholic steatohepatitis cirrhosis (NASH)	1	1 female	60
	Choledochal cyst (CHLC)	1	1 male	31
	Primary sclerosing cholangitis (PSC)	1	1 female	24
Non-liver disease (controls)	With gallstone	8	1 male, 7 female	39.8
	Without gallstone	5	2 male, 3 female	41.2
	Biliary dyskinesia	2	2 female	56.5
	Colorectal cancer	2	1 male, 1 female	52.5

NMR Experiments

All ^1H -NMR experiments were performed on a Bruker Biospin Avance 500 MHz NMR spectrometer using a 5-mm CHN inverse probehead equipped with shielded z -gradients. The temperature was kept at 25 °C for all the samples.

Spectral Analysis in Aqueous Medium

Bile solutions were prepared by diluting 100 μL of bile to 600 μL using doubly distilled water. Amide signals of individual conjugated bile acids are more accurately represented when the pH of the bile solution is in the range 6 ± 0.5 [23, 26]. Hence, the pH of each bile solution was brought to this range by the addition of 1–2 μL of 1 N hydrochloric acid. A reusable co-axial capillary tube containing TSP in D_2O was inserted into the NMR tube before recording ^1H -NMR spectra. While D_2O served as a field-frequency locking solvent, TSP served as chemical shift as well as a quantitative reference. We have observed that individual glycine- and taurine-conjugated bile acids signals are better distinguished when the coupling of their characteristic amide protons with the attached methylene protons is removed by decoupling [23]. Hence, one-dimensional ^1H spectra were obtained using a one pulse sequence incorporating both water suppression by presaturation and homonuclear decoupling of the methylene protons. Simultaneous decoupling is achieved with the decoupling frequency set at 3.65 ppm, which is between the chemical shifts of the methylene protons of conjugated taurine (3.56 ppm) and conjugated glycine (3.75 ppm). Typical parameters used were: spectral width 6,400 Hz, time domain data points 32 K, flip angle 45°, acquisition time 2.5 s, relaxation delay 6 s, number of transients 32, spectrum size 32 K points.

Spectral Analysis in Non-aqueous Medium

Well-resolved NMR signals for the bile metabolites are shown to be obtainable when the bile is mixed with an organic solvent such as DMSO. Such spectra enable distinct observation of all major metabolites such as cholesterol, lipids, total bile acids, glycine-conjugated bile acids, taurine-conjugated bile acids and urea, in addition to other metabolites using a single experiment [24]. For profiling the metabolites under these conditions, one-dimensional ^1H -NMR experiments were performed: Each bile sample (20 μL) was dissolved in 500 μL DMSO and loaded into a 5-mm NMR tube. A reusable co-axial capillary containing the TSP reference was inserted into the NMR tube and ^1H spectra were obtained using a one pulse sequence. As optimized for bile metabolites detection using

T_1 relaxation studies, 45° radiofrequency excitation pulse and a recycle delay of 6 s were used to ensure complete recovery of magnetization of all the bile metabolites as well as the TSP signal [24].

Quantitative Analysis of Bile Metabolites

Integral areas of the characteristic peaks of glycine-conjugated bile acids, taurine-conjugated bile acids, total bile acids, cholesterol, phospholipids and urea were determined for all the bile samples with reference to the TSP peak area. The bile metabolite concentrations were calculated by taking into account (1) volume of gallbladder bile used in obtaining the NMR spectra, (2) concentration of TSP reference, and (3) NMR peak areas and number of protons that contributed to the measured NMR signals for both metabolites and the reference. Although a known concentration of TSP solution was used in the capillary tube, its concentration was further calibrated from a separate ^1H -NMR experiment using a secondary reference solution of glycine. The bile metabolite quantities and their ratios were statistically compared using the unpaired t test.

Results

Proton NMR spectra of gallbladder bile in liver diseases and controls look qualitatively similar. However, the intensities of the signals greatly varied with marked differences visible between different liver diseases and control bile.

Bile in Aqueous Medium

Due to the aggregation of the amphipathic bile metabolites in an aqueous medium, the NMR signals appear relatively broad (Fig. 1). In addition, cholesterol and bile acids have a very close structural resemblance, resulting in the overlap of most of the bile acids and cholesterol signals with one another and with the phospholipid signals. With the aim of identifying individual metabolites from such complex spectra, we previously developed a library of bile acid chemical shifts by extensively analyzing one- and two-dimensional proton and carbon NMR spectra of a large number of unconjugated and glycine- and taurine-conjugated bile acids [25]. Subsequently, the analysis was extended to gallbladder bile using 1D- and 2D-NMR experiments at different field strengths (400, 700 and 800 MHz) [23]. This resulted in the detection of six conjugated bile acids in human bile (glycocholic acid, glycochenodeoxycholic acid, glycodeoxycholic acid, taurocholic acid, taurochenodeoxycholic acid and taurodeoxycholic acid). In the present study, all six of these bile

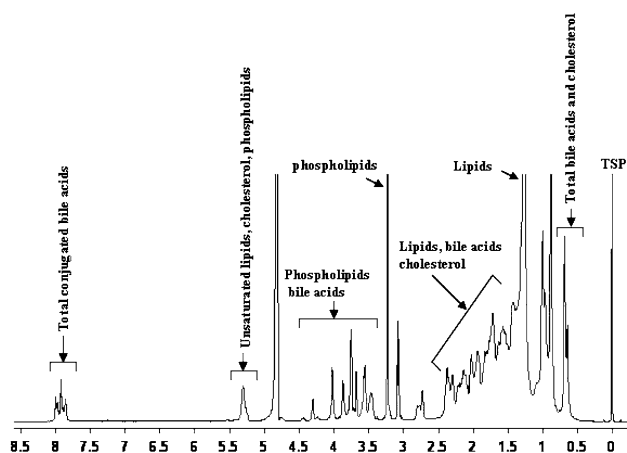


Fig. 1 $^1\text{H-NMR}$ spectrum of a representative gallbladder bile from non-liver disease controls ($n = 17$) (100 μL bile diluted to 600 μL) obtained at 500 MHz

acids were invariably detected in the control bile, and the ratio of taurine- to glycine-conjugated bile acids was observed to be nearly 1:3 (Fig. 2). In both malignant (HCC, CC) and NMLD liver disease samples, bile acids were reduced, both in their quantity and in number. Portions of typical spectra of bile from a control, a malignant- and a non-malignant liver disease are shown in Fig. 2.

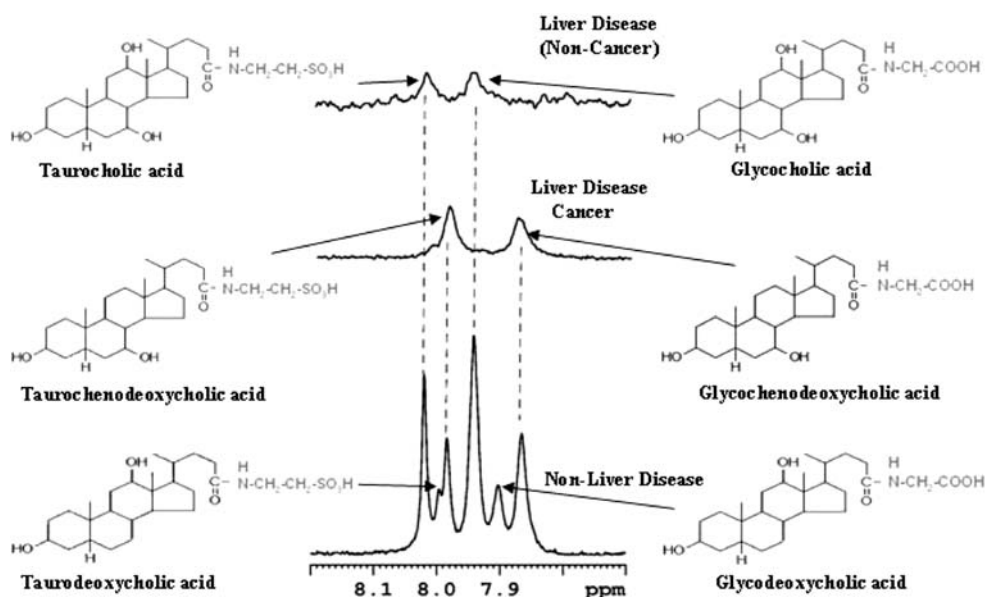
Bile in Organic Medium

The use of DMSO as a solvent provides a method for the dispersion of aggregated bile metabolites. NMR experiments performed for both liver disease and control bile using this method showed highly resolved signals, and the characteristic peaks for major bile metabolites such as total

bile acids, cholesterol, phospholipids, total glycine-conjugated bile acids, total taurine-conjugated bile acids and urea are distinctly isolated in the spectra (Fig. 3). Using the integrated areas of the characteristic marker peaks with reference to the TSP signal at 0.0 ppm, quantities of the major bile metabolites were determined (Table 2). Table 2 also provides data on the standard deviation as well as the results of unpaired t tests among the malignant and non-malignant liver disease and the controls for each of the measured bile metabolite. Portions of the bile NMR spectra that highlight altered major bile metabolite concentrations in different hepatobiliary diseases are shown in Fig. 4.

As shown in Table 2, and summarized in Fig. 5, liver diseases including hepatocellular cancer and cholangiocarcinoma exhibited significant changes in the levels of phospholipids, glycine- and taurine-conjugated bile acids, cholesterol and urea in the bile. Among the liver diseases, CC and NMLD showed most significant variation relative to the control samples. In addition, HCC patients could be differentiated from NMLD based on the amounts of phospholipids ($p = 0.02$), total bile acids ($p = 0.02$), glycine-conjugated bile acids ($p = 0.03$) and cholesterol ($p = 0.02$). Even CC could be differentiated somewhat from HCC based on bile acids ($p = 0.06$) and phospholipids ($p = 0.05$), although weakly. The differences in metabolite concentrations between CC and NMLD were not statistically significant. In benign liver disease samples (NMLD), the urea levels were increased somewhat relative to non-liver disease samples with the difference nearly significant ($p = 0.06$), while the levels of bile acids, phospholipids, and cholesterol were all significantly decreased ($p < 0.0001$) in all cases.

Fig. 2 Portions of the $^1\text{H-NMR}$ spectra for representative gallbladder bile from a control (non-liver disease, $n = 17$) and liver disease patients (malignant; $n = 18$) and non-malignant $n = 9$). One or more bile acids in the liver disease are significantly reduced or completely missing as shown in the figure



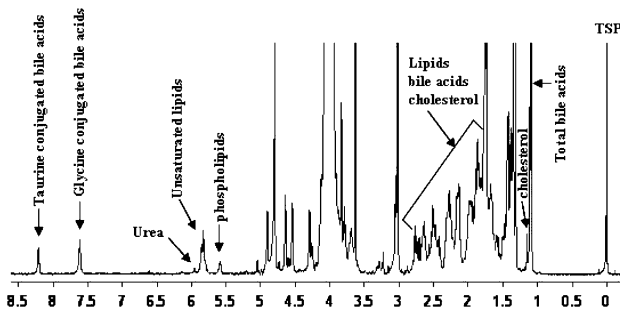


Fig. 3 $^1\text{H-NMR}$ spectrum of a representative gallbladder bile from non-liver disease controls ($n = 17$), dissolved in an organic solvent (20 μL bile dissolved in 500 μL DMSO) obtained at 500 MHz. Characteristic marker signals for all major bile components are distinctly isolated, thus enabling their quantitation in a single step

The extent of the reduction of individual bile metabolites in liver diseases varied greatly. For example, while glycine-conjugated bile acid levels were reduced to very low levels in the both malignant and NMLD, the reduction in taurine-conjugated bile acids was generally smaller (Table 2, Fig. 5). To further illustrate such compositional variations in both malignant and non-malignant diseases, ratios between some major bile metabolites were compared. As shown in Fig. 6, the ratio of glycine- to taurine-conjugated bile acids (Gly/Tau) and total bile acids to phospholipids (BA/PL) were lower ($p = 0.004$ and $p = 0.01$, respectively), and the ratio of phospholipids to cholesterol (PL/Chol) was higher ($p = 0.01$) in NMLD compared to controls.

Discussion

A key to interpreting alterations in bile metabolites for a given liver disease state is the understanding of the consequences associated with these alterations that would allow us to identify patients at high risk for disease progression. For example, underlying liver disease is the most potent correlate to the development of primary liver cancer. However, our ability to identify which patients with Hepatitis C, NASH or alcoholic cirrhosis are at most risk for the development of cancer is unknown. To determine the ability of NMR to distinguish between controls (NLD) and liver disease or liver disease and liver cancer, we evaluated bile from several unique clinical subsets: controls, patients with underlying liver disease, patients with identifiable risk factors for cancer, but no cancer at the time of bile collection and high risk patients who have gone on to develop cancer, with the bile taken after the diagnosis of cancer was made. All bile was collected at the time of surgery. Control bile was from patients undergoing surgery for non-liver related problems. Bile from patients

Table 2 Average values, along with the standard deviation, of the quantities of the bile metabolites (in mmol) determined in hepatocellular carcinoma (HCC), cholangiocarcinoma (CC), non-malignant liver diseases (NMLD) and non-liver disease controls (NLD). The errors are expressed as standard deviations; p values are from the unpaired t test between different groups; ns: non-significant

Patients	Total bile acids	Cholesterol	Phospholipids	Glycine-conjugated bile acids	Taurine-conjugated bile acids	Urea
Hepatocellular carcinoma ($n = 11$)	74.1 \pm 63.4 $p = 0.06$ vs. CC $p = 0.02$ vs. NMLD $p = 0.03$ vs. NLD	7.6 \pm 6.9 $p = \text{ns}$ vs. CC $p = 0.02$ vs. NMLD $p = 0.05$ vs. NLD	17.3 \pm 12.6 $p = 0.05$ vs. CC $p = 0.02$ vs. NMLD $p = 0.02$ vs. NLD	54.0 \pm 53.7 $p = 0.07$ vs. CC $p = 0.03$ vs. NMLD $p = 0.03$ vs. NLD	20.9 \pm 15.8 $p = \text{ns}$ vs. CC $p = \text{ns}$ vs. NMLD $p = \text{ns}$ vs. NLD	4.8 \pm 2.7 $p = \text{ns}$ vs. CC $p = \text{ns}$ vs. NMLD $p = \text{ns}$ vs. NLD
Cholangio-carcinoma ($n = 7$)	24.6 \pm 15.8 $p = \text{ns}$ vs. NMLD $p = 0.001$ vs. NLD	2.9 \pm 2.4 $p = \text{ns}$ vs. NMLD $p = 0.001$ vs. NLD	6.9 \pm 5.5 $p = \text{ns}$ vs. NMLD $p = 0.0008$ vs. NLD	15.0 \pm 12.5 $p = \text{ns}$ vs. NMLD $p = 0.0006$ vs. NLD	9.1 \pm 8.6 $p = \text{ns}$ vs. NMLD $p = 0.004$ vs. NLD	3.7 \pm 1.1 $p = \text{ns}$ vs. NMLD $p = \text{ns}$ vs. NLD
Liver disease (non-malignant) ($n = 9$)	23.5 \pm 17.8 $p = 0.0001$ vs. NLD	2.1 \pm 1.7 $p = 0.00005$ vs. NLD	6.6 \pm 4.9 $p = 0.00008$ vs. NLD	13.6 \pm 12.9 $p = 0.00005$ vs. NLD	9.8 \pm 12.1 $p = 0.006$ vs. NLD	7.9 \pm 7.9 $p = 0.06$ vs. NLD
Controls (non-liver disease) ($n = 17$)	137.7 \pm 77.8	13.0 \pm 6.9	31.3 \pm 16.0	102.7 \pm 56.4	34.9 \pm 33.3	3.9 \pm 2.6

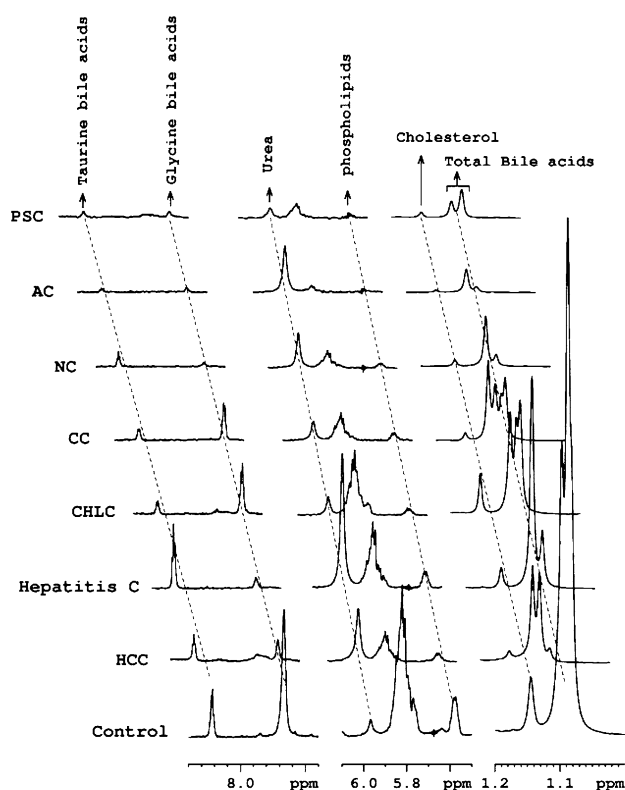


Fig. 4 Portions of typical $^1\text{H-NMR}$ spectra of gallbladder bile from liver diseases along with a non-liver disease control ($n = 17$). All spectra are plotted with identical scales for direct comparison of the relative individual metabolite quantities. *HCC* hepatocellular carcinoma ($n = 11$), *HEPC* hepatitis C ($n = 3$), *CHLC* choledochal cyst ($n = 1$), *CC* cholangiocarcinoma ($n = 7$), *NC* cirrhosis due to non-alcoholic steatohepatitis ($n = 1$), *AC* alcoholic cirrhosis ($n = 3$), *PSC* primary sclerosing cholangitis ($n = 1$)

with underlying liver disease includes patients with Hepatitis C, NASH cirrhosis, or alcoholic cirrhosis.

Bile acids, phospholipids and cholesterol are the major constituents of bile. Bile acids alone constitute a group of a large number of mainly glycine- and taurine-conjugated derivatives. Of these, conjugates of chenodeoxycholic acid and cholic acid are the primary bile acids. Primary bile acids are directly synthesized in the liver from cholesterol. Conjugates of deoxycholic acids, in contrast, are thought to be the products of bacterial deconjugation occurring during enterohepatic circulation. This pilot study using $^1\text{H-NMR}$ spectroscopy clearly shows altered bile homeostasis among different liver diseases and controls. Concentrations of major bile metabolites, including bile acids, are significantly reduced in liver disease. Importantly, apart from distinguishing from controls based on the homeostatic changes, the two malignant diseases, HCC and CC could be somewhat differentiated from each other, although weakly.

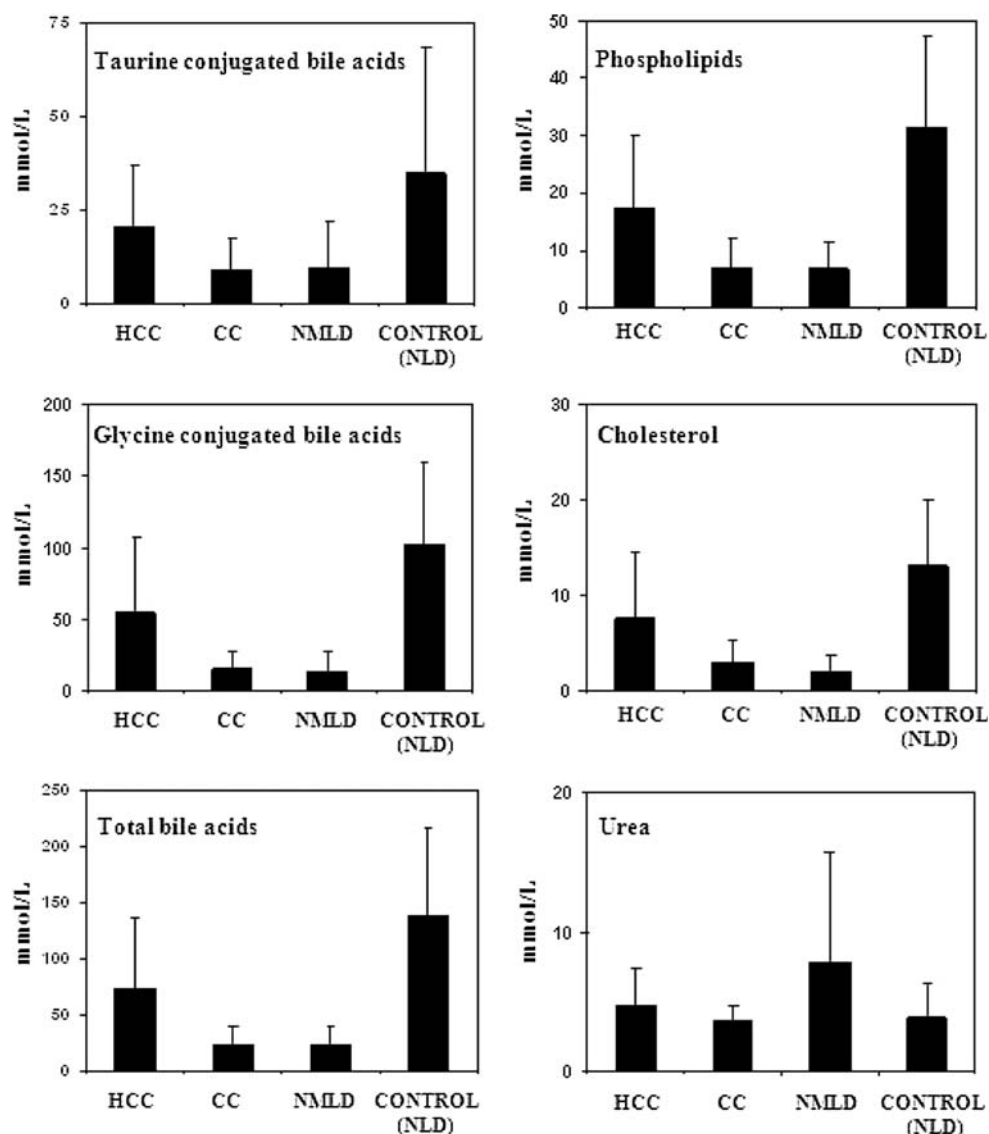
Several factors may contribute to the decreases in several major bile metabolites seen in liver diseases. These

factors may include the impairment of bile synthesis and aberrant enterohepatic circulation, arising from the obstruction of flow of biliary metabolites due to the damaged bile ducts. However, the contribution of each effect may also depend on the nature and/or the severity of the disease process. In the present study, CC and NMLD caused the highest disturbance, while HCC caused the least. Apart from the reduction in major bile metabolites in both malignant and NMLD, altered ratios of the metabolites, in some cases to a significant limit, highlight the specific etiological contributions to the bile metabolites synthesis/enterohepatic circulation (Fig. 6). Thus, metabolite ratios, together with the generally decreased absolute concentrations, may have diagnostic value in the management of different liver diseases. For bile acids, however, the possibility of changes in their concentrations due to aberrant enterohepatic circulation with no relation to liver function can not be ruled out.

In liver diseases, aberrations in enterohepatic circulation may also result in accumulation of bile metabolites in the diseased liver. A recent study on liver tissue using high resolution magic angle sample spinning NMR spectroscopy has indicated large amounts of bile acids in liver tumors compared to the non-tumor tissue [10]. Such accumulations of bile acids in the liver may also cause their elevation in circulating blood. Indeed, bile acids in blood have been shown to increase in liver disease and their measurement in serum has been reported to have diagnostic value for liver diseases including liver cancer [15–20]. A drastic reduction in several conjugated bile acids, some even to an undetectable level (Fig. 2), may indicate that depending on the nature of cellular damage, one particular conjugated bile acid synthetic pathway may be favored over the other. Such a difference in the profiles of the same bile acids between malignant and non-malignant liver disease may potentially serve as a diagnostic tool for the cancer detection. Moreover, identifying changes in specific metabolic pathways of bile acid synthesis may have implications for prognosis, similar to the finding that the patients with liver diseases with serum chenodeoxycholic acid levels exceeding $15 \mu\text{mol/L}$ are more likely to die of the disease or need liver transplantation [17].

One of the main functions of the liver is ammonia detoxification. Ammonia produced from the deamination of amino acids is converted to urea through the urea cycle and excreted through the kidney. While nearly 50% of urinary solids constitute urea, blood contains only 2.5–7.5 $\mu\text{mol/mL}$ dissolved urea. Using $^1\text{H-NMR}$ spectroscopy, we have previously shown that in a patient with non-functional liver, urea levels decrease drastically in urine [28]. In bile, we reported the observation of a urea signal using $^1\text{H-NMR}$ spectroscopy [24]. In the present investigation, we used this approach to show somewhat

Fig. 5 Comparison of differences in metabolite concentration in hepatocellular carcinoma (HCC, $n = 11$), cholangiocarcinoma (CC, $n = 7$), non-malignant liver diseases (NMLD, $n = 9$) and non-liver disease controls (NLD, $n = 17$)

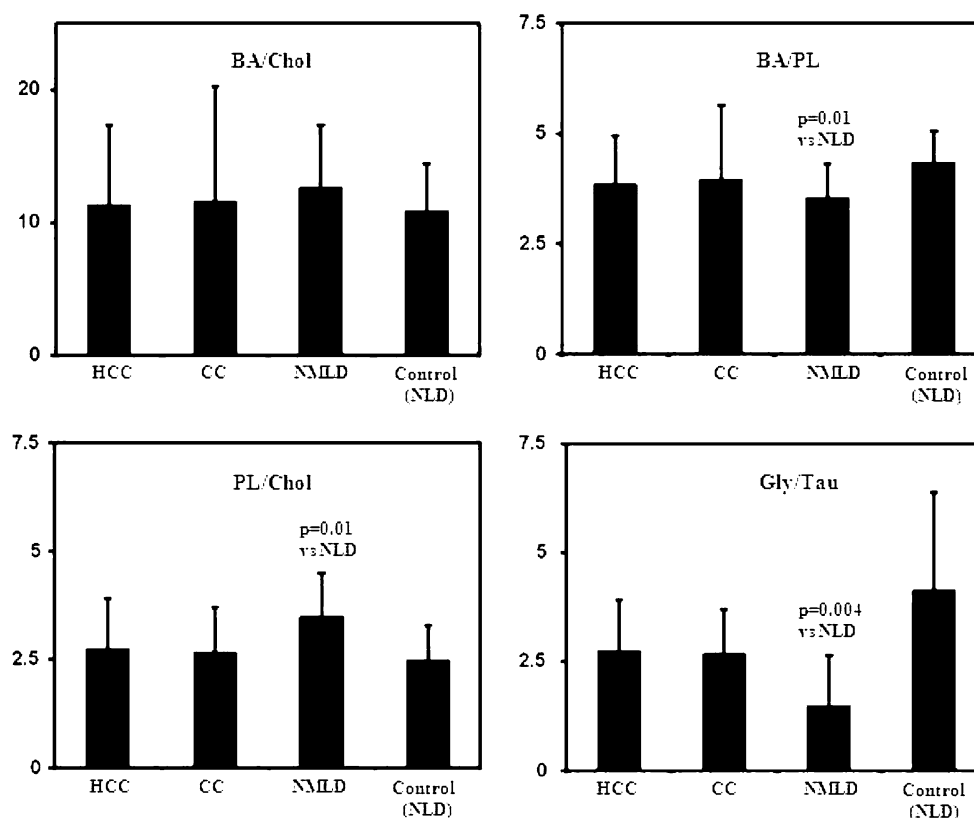


increased urea levels in benign liver diseases relative to non-liver disease controls (Table 2, Fig. 5). This is in contrast to other major bile metabolites, which decrease significantly in disease relative to controls. With the exception of a very old study reporting that urea formation and bile secretion are related [29], no definite connection between the urea and the major bile metabolites identified in this study has been documented. It remains to be seen whether the increased trend of urea levels in NMLD has anything to do with the deconjugation and deamination of taurine and/or glycine associated with bile acids. Such deconjugation has long been attributed only to gut bacterial action.

Generally, studies aimed at detecting or understanding pathological conditions are often based on the measurement of a single metabolite. For example, a decrease in the concentration of phospholipids is shown to occur in bile

from patients with HCC [14], increased cholesterol levels is shown to cause gallstone diseases, increased urea is an indicator of malfunction of the liver, and altered individual bile acids levels have been implicated in several liver diseases. In reality, the biological picture is more complex: liver synthesizes bile that has cholesterol, phospholipids, urea and several conjugated bile acids as its major constituents. Observing the status of bile homeostasis through an approach that detects such multiple metabolites quantitatively and in parallel should provide more reliable information on liver status. Analytical methods that enable visualization of these metabolites in one step thus, have far reaching implications for better understanding the specific cellular functions associated with bile synthesis and/or enterohepatic circulation under normal and disease conditions. MS, a highly sensitive analytical method, has been extensively used by a number of research groups for bile

Fig. 6 Comparison of the ratios between some major bile metabolites in different patient groups (HCC, $n = 11$; CC, $n = 7$; NMLD, $n = 9$ and NLD, $n = 17$). *BA/Chol* total bile acids to cholesterol ratio, *BA/PL* total bile acids to phospholipids ratio, *PL/Chol* phospholipids to cholesterol ratio, *Gly/Tau* glycine- to taurine-conjugated bile acids ratio. The errors are expressed as standard deviations. The p values between any two groups of patients, wherever significant are indicated



acids analysis and investigating bile acid metabolism associated with liver disease [30, 31]. A more recent review describes a number of MS approaches for the quantitative analysis of lipids in intact biological samples [32]. Utilization of such advancements in MS potentially complements and supplements the analysis of multiple metabolites in human bile using NMR spectroscopy.

Conclusions

This investigation details how changes within the bile can be visualized by use of in vitro proton magnetic resonance spectroscopy of intact gallbladder bile, a simple approach that distinctly measures several major bile metabolites simultaneously. This is the first pilot study that explores variation of several major bile metabolites using a simple one step analysis NMR method in malignant and non-malignant and, non-liver disease controls. While serum-based bile acids are shown to increase in liver diseases, this investigation on bile finds that several major bile metabolites, including bile acids, significantly decrease in various liver disease states.

Although, the study was conducted on a relatively small number of patients, significant alterations in the amounts and ratios of several major metabolites potentially indicate the immense value in the diagnosis of liver diseases. To

assess changes in the bile metabolites more accurately, we performed studies in bile after diluting and adjusting the pH or by dissolving in an organic medium. However, several major bile metabolites such as phospholipids, glycine-conjugated bile acids and taurine-conjugated bile acids can be detected in intact bile with reasonably good accuracy. These metabolites can be subjected to automated analysis using a software package when high throughput analysis is required.

In this study, the concentrations of bile metabolites were determined with no consideration of the differences in gall bladder bile concentration, if any. Studies that take into account such differences may further improve the classification of patients. Use of normalization approaches for the gallbladder bile data, when proved meaningful, and/or measurement of biliary drainage from the liver, would strengthen the findings of this study, provide better insights into the bile metabolic profile, and possibly open avenues for clinical applications.

Further, high sensitivity of bile homeostasis to liver function/disease combined with the high concentrations of major bile metabolites in gallbladder makes it convenient to assess bile using in vitro $^1\text{H-NMR}$ spectroscopy and, this may possibly provide avenues for translational research in detecting and following their dynamic variations in clinical settings using non-invasive in vivo magnetic resonance spectroscopy.

Acknowledgments This work was supported by the NIH Roadmap Initiative on Metabolomics Technology, NIH/NIDDK 3 R21 DK070290-01; the Walther Cancer Institute Multi-Institution Cancer Research Seed Project, the Purdue Oncological and Cancer Centers, and a collaborative research grant between Purdue University/Discovery Park and the Indiana University School of Medicine.

References

- Blonski W, Reddy KR (2008) Hepatitis C virus infection and hepatocellular carcinoma. *Clin Liver Dis* 12(3):661–674
- Nagana Gowda GA, Zhang S, Gu H, Asiago V, Shanaiah N, Raftery D (2008) Metabolomics-based methods for early disease diagnostics. *Expert Rev Mol Diagn* 8(5):617–633
- Pan Z, Raftery D (2007) Comparing and combining NMR spectroscopy and mass spectrometry in metabolomics. *Anal Bioanal Chem* 387(2):525–527
- van der Greef J, Smilde AK (2005) Symbiosis of chemometrics and metabolomics: past, present, and future. *J Chemometr* 19(5–7):376–386
- Pan Z, Gu H, Talaty N, Chen H, Shanaiah N, Hainline BE, Cooks RG, Raftery D (2007) Principal component analysis of urine metabolites detected by NMR and DESI-MS in patients with inborn errors of metabolism. *Anal Bioanal Chem* 387:539–549
- Chen H, Pan Z, Talaty N, Raftery D, Cooks RG (2006) Combining desorption electrospray ionization mass spectrometry and nuclear magnetic resonance for differential metabolomics without sample preparation. *Rapid Commun Mass Spectrom* 20:1577–1584
- Beger RD, Schnackenberg LK, Holland RD, Li D, Dragan Y (2006) Metabonomic models of human pancreatic cancer using 1D proton NMR spectra of lipids in plasma. *Metabolomics* 2(3):125–134
- Odunsi K, Wollman RM, Ambrosone CB, Hutson A, McCann SE, Tammela J, Geisler JP, Miller G, Sellers T, Cliby W, Qian F, Keitz B, Intengan M, Lele S, Alderfer JL (2005) Detection of epithelial ovarian cancer using H-1-NMR-based metabolomics. *Int J Cancer* 113(5):782–788
- Burns MA, He W, Wu CL, Cheng LL (2004) Quantitative pathology in tissue MR spectroscopy based human prostate metabolomics. *Technol Cancer Res Treat* 3(6):591–598
- Yang Y, Li C, Nie X, Feng X, Chen W, Yue Y, Tang H, Deng F (2007) Metabonomic studies of human hepatocellular carcinoma using high-resolution magic-angle spinning ¹H NMR spectroscopy in conjunction with multivariate data analysis. *J Proteom Res* 6:2605–2614
- Vilca Melendez H, Gilani SS, Cochrane BC, Rela M, Murphy GM, Heaton ND (1998) A validated technique for the analysis of biliary bile acid secretion in donor livers prior to transplantation. *Transpl Int* 11(3):216–222
- Cox IJ, Sharif A, Cobbold JF, Thomas HC, Taylor-Robinson SD (2006) Current and future applications of in vitro magnetic resonance spectroscopy in hepatobiliary disease. *World J Gastroenterol* 12(30):4773–4783
- Kurumiya Y, Nagino M, Nozawa K, Kamiya J, Uesaka K, Sano T, Yoshida S, Nimura Y (2003) Biliary bile acid concentration is a simple and reliable indicator for liver function after hepatobiliary resection for biliary cancer. *Surgery* 133(5):512–520
- Khan SA, Cox IJ, Thillainayagam AV, Bansil DS, Thomas HC, Taylor-Robinson SD (2005) Proton and phosphorus-31 nuclear magnetic resonance spectroscopy of human bile in hepatopancreaticobiliary cancer. *Eur J Gastroenterol Hepatol* 17(7):733–738
- Shima T, Tada H, Morimoto M, Nakagawa Y, Obata H, Sasaki T, Park H, Nakajo S, Nakashima T, Okanoue T, Kashima K (2000) Serum total bile acid level as a sensitive indicator of hepatic histological improvement in chronic hepatitis C patients responding to interferon treatment. *J Gastroenterol Hepatol* 15(3):294–299
- El-Houseini ME, Amer MA, Saad Eldin AH, El-sherbiny M, Hussein TD, Mansour O (2000) Evaluation of serum total bile acids in the diagnosis of hepatocellular carcinoma. *J Egyptian Nat Cancer Inst* 12(4):307–313
- Azer SA, Coverdale SA, Byth K, Farrell GC, Stacey NH (1996) Sequential changes in serum levels of individual bile acids in patients with chronic cholestatic liver disease. *J Gastroenterol Hepatol* 11(3):208–215
- Jönsson G, Hedenborg G, Wisén O, Norman A (1992) Serum concentrations and excretion of bile acids in cirrhosis. *Scand J Clin Lab Invest* 52(7):599–605
- Samuelson K, Aly A, Johansson C, Norman A (1982) Serum and urinary bile acids in patients with primary biliary cirrhosis. *Scand J Gastroenterol* 17(1):121–128
- Fausa O, Gjone E (1976) Serum bile acid concentrations in patients with liver disease. *Scand J Gastroenterol* 11(5):537–543
- Prescot AP, Collins DJ, Leach MO, Dzik-Jurasz AS (2003) Human gallbladder bile: noninvasive investigation in vivo with single-voxel ¹H MR spectroscopy. *Radiology* 229(2):587–592
- Künnecke B, Bruns A, von Kienlin M (2007) Non-invasive analysis of gallbladder bile composition in cynomolgus monkeys using in vivo ¹H magnetic resonance spectroscopy. *Biochim Biophys Acta* 1771(4):544–549
- Nagana Gowda GA, Ijare OB, Somashekar BS, Sharma A, Kapoor VK, Khetrpal CL (2006) Single step analysis of individual conjugated bile acids in human bile using ¹H NMR spectroscopy. *Lipids* 41:591–603
- Nagana Gowda GA, Somashekar BS, Ijare OB, Sharma A, Kapoor VK, Khetrpal CL (2006) One step analysis of major bile metabolites in human bile using ¹H NMR spectroscopy. *Lipids* 41:577–589
- Ijare OB, Somashekar BS, Jadegoud Y, Nagana Gowda GA (2005) ¹H and ¹³C NMR characterization and stereochemical assignments of bile acids in aqueous media. *Lipids* 40:1031–1041
- Ijare OB, Somashekar BS, Nagana Gowda GA, Sharma A, Kapoor VK, Khetrpal CL (2005) Quantification of glycine and taurine conjugated bile acids in human bile using ¹H NMR spectroscopy. *Magn Reson Med* 53(6):1441–1446
- Srivastava M, Jadegoud Y, Nagana Gowda GA, Sharma A, Kapoor VK, Khetrpal CL (2005) An accurate method for cholesterol analysis in bile. *Anal Lett* 38:2135–2141
- Singh HK, Yachha SK, Saxena R, Gupta A, Nagana Gowda GA, Bhandari M, Khetrpal CL (2003) Dimension of ¹H NMR spectroscopy in assessment of liver graft dysfunction. *NMR Biomed* 16:185–188
- Noël-Paton D (1886) Nature of the relationship of urea formation to bile secretion. *J Anat Physiol* 20(4):662–673
- Griffiths WJ (2003) Tandem mass spectrometry in the study of fatty acids, bile acids, and steroids. *Mass Spectrom Rev* 22(2):81–152
- Yang Y, Griffiths WJ, Nazer H, Sjøvall J (1997) Analysis of bile acids and bile alcohols in urine by capillary column liquid chromatography-mass spectrometry using fast ion atom bombardment or electrospray ionization and collision induced dissociation. *Biomed Chromatogr* 11:240–255
- Han X, Gross RW (2005) Shotgun lipidomics: electrospray ionization mass spectrometric analysis and quantitation of cellular lipidomes directly from crude extracts of biological samples. *Mass Spectrom Rev* 24(3):367–412

Effects of Rice Bran Oil Enriched with n-3 PUFA on Liver and Serum Lipids in Rats

Rajni Chopra · Kari Sambaiah

Received: 18 December 2007 / Accepted: 11 September 2008 / Published online: 22 October 2008
© AOCS 2008

Abstract Lipase-catalyzed interesterification was used to prepare different structured lipids (SL) from rice bran oil (RBO) by replacing some of the fatty acids with α -linolenic acid (ALA) from linseed oil (LSO) and n-3 long chain polyunsaturated fatty acids (PUFA) from cod liver oil (CLO). In one SL, the ALA content was 20% whereas in another the long chain n-3 PUFA content was 10%. Most of the n-3 PUFA were incorporated into the *sn*-1 and *sn*-3 positions of triacylglycerol. The influence of SL with RBO rich in ALA and EPA + DHA was studied on various lipid parameters in experimental animals. Rats fed RBO showed a decrease in total serum cholesterol by 10% when compared to groundnut oil (GNO). Similarly structured lipids with CLO and LSO significantly decreased total serum cholesterol by 19 and 22% respectively compared to rice bran oil. The serum TAGs level of rats fed SLs and blended oils were also significantly decreased by 14 and 17% respectively compared to RBO. Feeding of an n-3 PUFA rich diet resulted in the accumulation of long chain n-3 PUFA in various tissues and a reduction in the long chain n-6 PUFA. These studies indicate that the incorporation of ALA and EPA + DHA into RBO can offer health benefits.

Keywords Rice bran oil · n-3 PUFA · Linseed oil · Cod liver oil · Enzymatic acidolysis · Serum lipids · Liver lipids

Introduction

Over the past 20–30 years, intake of n-6 fatty acids (FA) has increased because of excess use of vegetable oils in our diets [1]. The fatty acid composition of our diet plays a key role in health and disease prevention [2]. Studies have shown that diet and dietary lipids have an important role to play in the prevention of risk of cardiovascular diseases [3, 4]. Clinical and epidemiological studies have shown the cardiovascular protective effects of n-3 polyunsaturated fatty acids (PUFA) [5, 6]. Based on surveys conducted on Indian dietary patterns, Ghafoorunissa [7, 8] has estimated that Indians derive 12.6 g of linoleic acid (LA) per day, equivalent to 4.8 energy % (en %) from visible and invisible fat. The requirement of LA as an essential FA is 3 en %, hence Indian diets provide adequate amounts of LA. However the intake of n-3 PUFA by Indians is in the range of 0.3 g in the rural population and 0.6 g in the urban population, equivalent to 0.2–0.3 en % [8, 9]. Dietary recommendations have been made for n-3 FA, including α -linolenic acid (ALA), eicosapentaenoic acid (EPA), and docosahexaenoic acid (DHA) to achieve nutrient adequacy in order to prevent and treat cardiovascular diseases. These recommendations are based on a large body of evidence from epidemiologic and controlled clinical studies. The n-3 FA recommendation to achieve nutritional adequacy is defined as the amount necessary to prevent deficiency symptoms and is 0.6–1.2% of energy for ALA and up to 10% of this can be provided by EPA or DHA [10]. The evidence base supports a dietary recommendation of

R. Chopra
Department of Foods and Nutrition,
Institute of Home Economics, University of Delhi,
F-4, Hauz Khas Enclave, New Delhi 110017, India

K. Sambaiah (✉)
Department of Biochemistry and Nutrition,
Central Food Technological Research Institute,
Mysore 570020, India
e-mail: sambaiah1948@yahoo.com

approximately 500 mg/day of EPA and DHA for cardiovascular disease risk reduction [11]. To achieve the recommended ALA intakes, food sources including flaxseed and flaxseed oil, walnuts and walnut oil, and canola oil are recommended. Linseed (*Linum usitatissimum*), which is rich in ALA, is an economically important oilseed crop used for edible purposes in the central and north-eastern regions of India. Green and Marshall [12] reported that linseed oil with its higher degree of unsaturation reacts immediately with oxygen to develop off flavour and rancidity and hence the shelf life of linseed oil is poor. Linseed oil is a rich source of α -linolenic acid, which is an essential fatty acid, can be utilized as a source of ALA for the synthesis of structured lipids. n-3 PUFA are considered to be anti-inflammatory, whereas the n-6 PUFA are considered to be pro-inflammatory [13]. Rice bran is a by-product of the rice milling industry. RBO obtained from rice bran is a rich source of tocopherols, tocotrienols and γ -oryzanol [14]. γ -Oryzanol has been reported to possess hypocholesterolemic and antioxidant activity [15–17]. RBO contains approximately 38% oleic acid (18:1n-6), 34% linoleic acid (18:2n-6) and 18.6% palmitic acid (16:0) [18]. However, RBO does not contain long chain n-3 PUFA, hence n-6 to n-3 ratio is high in RBO. The ratio of n-6 to n-3 fatty acid is often used to assess the balance between essential fatty acids in the diet. The WHO/FAO suggests a ratio of 5:1–10:1 [19], on the basis of proposed adequate intakes the NIH suggests a ratio of 2:3–3:1 [20]. The accretion of long chain n-3 fatty acids in tissue phospholipids may be dependent on the particular n-3 fatty acid that is provided in the diet [21]. Oily fish can provide sufficient n-3 PUFA such as EPA and DHA, however many Indians refrain from eating fish, as it is not a vegetarian food [22]. The beneficial properties of LSO and CLO have been enumerated [23–25]. LSO could be exploited as an alternate source of n-3 fatty acids. However LSO has very limited use in diet because it is oxidized rapidly due to its high level of unsaturated fatty acids. Among all unconventional edible oils, RBO seems to have great promise for use in SL and blends because of its beneficial nutritional properties due to its oryzanol, tocopherols and tocotrienol content which may confer oxidative stability to PUFA rich oil. The interest in the production of SL containing specific fatty acids have been increasing continuously because the nutritional value of triacylglycerol depends (TAG) both on fatty acid composition as well as the positional distribution of acyl groups within the TAG molecule. Therefore SL provides an opportunity for using specific end uses by improving physical and nutritional properties. Earlier investigations have revealed that SL which are enriched in n-3 PUFA may exhibit significant beneficial effects when compared to physical mixtures of oils having similar fatty acid composition. The SL may behave differently from

physical mixtures by exhibiting differences in their digestion, absorption and transport [26]. The TAG of blended oils retain their original absorption rates, whereas in SL in which the TAG are restructured have a different absorption rate [27]. Enhanced lymphatic absorption of medium chain fatty acids (MCFA) in rats was observed with a structured TAG containing MCFA (C10:0 and C8:0) in the *sn*-2 position and linoleic acid in the 1- and 3-positions compared with the physical mixture of these fats [28]. Though several groups have studied SL with respect to absorption and transport, very few studies have examined their lipidemic effects. Lee and Akoh reported that SL with n-3 PUFA like EPA and DHA when fed to mice lowered TAG and low density lipoprotein (LDL) cholesterol levels more efficiently when compared to soybean oil n-3 PUFA [29]. One of the major objectives of the present investigation was to enhance the consumption of RBO by making value added products from it. In this study the influence of SLs with RBO rich in n-3 PUFA was studied in experiment animals for their hypo-lipidemic properties.

Materials and Methods

Materials

Refined RBO, GNO and CLO were obtained from a supermarket of Mysore, Karnataka, India and LSO was purchased from Palampur, Himachal Pradesh, India. Lipozyme IM 60 was a gift from Novo Nordisk Bioindustrial Inc., (Danbury, CT, USA). Cholesterol, triolein, dipalmitoylphosphatidylcholine and thiobarbituric acid (TBA) were purchased from Sigma Chemical Co. (St Louis, MO, USA). Heparin and manganese chloride were obtained from the Sisco Research Laboratory (Mumbai, India). Digitonin was purchased from BDH Chemicals (Mumbai, India). All solvents were of analytical grade and distilled before use.

Synthesis of Structured Lipids and Preparation of Blended Oil

SLs enriched in ALA and EPA + DHA were synthesized from RBO by enzymatic acidolysis using 1,3 specific lipase, Lipozyme IM60 from *Rhizomucor miehei*. FFA obtained by alkaline hydrolysis of LSO and CLO were used as the source of ALA and EPA + DHA respectively (unpublished data). Large scale synthesis of structured lipids were prepared in stirred batch reactions. Reactions were carried out in 1-L stoppered conical flasks using optimum conditions derived for the incorporation of ALA into RBO by response surface methodology. Optimum conditions used for the preparation of SLs are as follows:

RBO and ALA were taken in 1:5.5 molar ratio, enzyme concentration (Lipozyme IM 60 from *Rhizomucor miehei*) was 1% of total substrates weight, incubated at 37.5 °C for 8 h with constant agitation. In the case of SL from RBO rich in EPA + DHA reactions were carried out using optimum conditions derived for incorporation of EPA + DHA by response surface methodology. Following optimum conditions were used: RBO and EPA + DHA were taken in 1:7.75 molar ratio, 7.75% enzyme concentration (Lipozyme IM 60 from *Rhizomucor miehei*) total substrates weight and incubated at 32.5 °C for 37 h with constant agitation. At the end of the incubations the newly synthesized SLs were purified using column chromatography and the solvent was removed by using a flash evaporator and SLs were stored under nitrogen at –20 °C.

Blended oils were prepared by physically mixing RBO and LSO in 3:2 (w/w) proportion by weight and stirring overnight under an inert atmosphere. Another blend was prepared with RBO and CLO in 1:1 (w/w) proportion under similar conditions. The ratios of blending oils were chosen in such a way that their ALA and EPA + DHA composition was similar to that of the SLs prepared.

Analysis of Fatty Acids in the *sn*-2 Position of TAG

The nature of FA in the *sn*-2 position of TAG purified through thin layer chromatography (TLC) after acidolysis was determined following the method of Luddy et al. [30]. Briefly, 1 mg of TAG was mixed with 1 mL of 1 M Tris–HCl buffer (pH 7.6), 0.25 mL of 0.05% sodium cholate, and 0.1 mL of 2.2% CaCl₂ and 1 mg of pancreatic lipase. The mixture was incubated in a water bath at 37 °C for 3 min, mixed vigorously for 1 min, centrifuged, extracted with 3 mL diethyl ether and dried over anhydrous sodium sulphate. Samples were spotted on TLC plates coated with silica gel G and developed in hexane: diethyl ether: acetic acid (50:50:1; v/v/v). The band corresponding to 2-monoacylglycerol reference standard was eluted with chloroform: methanol (2:1 v/v). The lipid was saponified with 0.5 N KOH in methanol and fatty acids were methylated with BF₃/methanol and analyzed by gas chromatography (GC) [31].

Experimental Animals

Male Wistar rats 36.0 ± 3.0 g were grouped by random selection into six dietary groups (*n* = 6 per group). They were placed in individual cages in the animal house facility of the institute and fed fresh diets daily. The animals had free access to food and water throughout the study. All the animal experiment protocols were approved by the Animal Ethical Committee of the Institute.

Diet Composition

The ingredients used in the basal diets were (g/100 g): casein 20, cellulose 5, sucrose 60, AIN-76 mineral mix 3.5, AIN 76 vitamin mix 1, methionine 0.3, choline chloride 0.2, and fat 10 [32]. Rats were fed with different diets based on groundnut oil, RBO, SL (RBO and CLO and RBO and LSO), blends of RBO + CLO and RBO + LSO.

Serum and Liver Lipid Analysis

At the end of the experimental feeding period of 60 days, rats were allowed to fast overnight and sacrificed under ether anesthesia. Blood was drawn by cardiac puncture and serum was separated by centrifugation. Liver and other tissues were removed and rinsed with ice-cold saline, blotted, weighed and stored at –80 °C until analyzed. Lipids were extracted from serum and tissues by the method of Folch et al. [33]. Serum lipid peroxides and TBA reactive substances (TBARS) in the liver were analyzed as described by Yagi [34] and Berg and Aust [35] respectively. Serum and liver cholesterol content was quantitated by the method of Searcy and Bergquist [36]. High density lipoprotein (HDL) cholesterol in serum was measured after precipitating apo B containing lipoproteins with heparin–MnCl₂ reagent [37]. LDL + VLDL cholesterol was obtained by subtracting HDL cholesterol from total cholesterol. Phospholipids were analyzed by the method of Stewart [38] using dipalmitoylphosphatidylcholine as the reference standard. TAG were estimated by the method described by Fletcher [39].

The fatty acid composition of dietary lipids, serum and tissue lipids were analyzed as methyl esters (ME) by gas chromatography (Shimadzu 14 B fitted with FID) using a fused silica capillary column 25 m × 0.25 mm (Konik Tech, Barcelona, Spain). The ME of fatty acids were prepared using BF₃/MeOH as described by Morrison and Smith [31]. The injector and detector temperatures were 230 and 240 °C, respectively. The column temperature was held isothermally at 220 °C and nitrogen was used as the carrier gas at a flow rate of 1 mL/min. Individual fatty acids were identified by comparing with retention times of standards.

Statistical Analysis

Data were expressed as mean ± SEM and analyzed by one-way analysis of variance (ANOVA) for any significance at *P* < 0.05. Mean separation was accomplished by Duncan's dunnet statistical analysis [40].

Results

Fatty Acid Composition of Dietary Lipids

Dietary lipids containing SL with LSO had 20% ALA and that with CLO had 3.7 and 5.4% EPA and DHA respectively. Blends of RBO with LSO and CLO had ALA, EPA and DHA at the same level as their SL (Table 1). Analysis of fatty acid composition at the *sn*-2 position of different dietary lipids is also given in Table 1. RBO and GNO contained only oleic acid and linoleic acid at the *sn*-2 position whereas SL with LSO contained 15% ALA and SL with CLO contained 8.1% EPA + DHA. On the other hand, a blend with LSO contained 18% ALA and a blend with CLO contained 21% of EPA + DHA.

Effect of Dietary Lipids on Growth Parameters

The influence of various dietary fats with different types of fatty acids on growth is given in Table 2. The fat content of various diets was kept constant at 10%. The amounts of diet consumed by animals in different groups were comparable except in SL with LSO and blend with CLO which showed a significant increase in food intake. There were no significant changes in body weight gain and the food efficiency

ratio except in blends with CLO where the food efficiency ratio was significantly higher compared to the other groups. Weights of heart, brain and spleen of rats fed different dietary fats were comparable. Similarly there were no changes in liver weight in any of the groups (Table 3).

Effect of Feeding Different n-3 PUFA on Serum Lipid Profile

The serum lipid profile of rats in response to different dietary lipids is given in Table 4. Rats fed RBO showed a decrease in total serum cholesterol by 10% when compared to GNO. Structured lipids with CLO and LSO significantly decreased total serum cholesterol by 19 and 22% respectively compared to rice bran oil. In the case of blends also the total cholesterol decreased significantly compared to RBO group. This reduction occurred both in the HDL and LDL fractions. There was no difference in total cholesterol content of serum in rats fed SLs and blends but HDL cholesterol was increased in blends compared to SL.

The serum TAGs level of rats fed SLs and blended oils also significantly decreased by 14 and 17% respectively compared to RBO. Serum phospholipids concentration was not altered in all n-3 PUFA fed animals except in rats fed blended oil with CLO where it was decreased. There was

Table 1 Fatty acid composition (%) of diet

Fatty acids	GNO		RBO		SL with CLO		SL with LSO		Blend with CLO		Blend with LSO		CLO	LSO
	TAG	<i>sn</i> -2 position	TAG	<i>sn</i> -2 position	TAG	<i>sn</i> -2 position	TAG	<i>sn</i> -2 position	TAG	<i>sn</i> -2 position	TAG	<i>sn</i> -2 position		
14:0	–	–	ND	–	4.9	–	ND	–	2.6	–	ND	–	–	–
16:0	11.1	ND	20.1	ND	17.2	ND	14.3	ND	17.9	ND	14.4	9.0	19.0	6.5
16:1	–	–	–	–	8.2	ND	–	–	4.4	ND	ND	–	6.0	–
18:0	2.5	ND	1.4	ND	3.4	–	2.4	–	2.7	ND	2.3	–	2.0	4.4
18:1	58.0	68.0	43.2	52.7	38.6	49.5	37.9	47.6	39.1	46.0	37.1	39.0	23.5	22.6
18:2	28.4	30.0	34.8	47.2	16.5	42.7	24.2	36.5	25.0	32.0	26.7	33.0	2.9	10.0
18:3 (ALA)	ND	–	ND	–	ND	–	20.1	15.0	ND	ND	19.4	18.0	13.2	54.6
20:4	ND	–	ND	–	0.8	–	ND	–	0.7	–	ND	–	2.1	–
20:5 (EPA)	ND	–	ND	–	3.7	3.9	ND	–	3.9	9.8	ND	–	11.8	–
22:6 (DHA)	ND	–	ND	–	5.4	4.2	ND	–	5.6	11.2	ND	–	9.2	–

Values are averages of triplicate analysis

Table 2 Effect of feeding structured lipids with rice bran oil rich in n-3 PUFA on food intake and weight gain

Values are means \pm SEM of six rats

Values not sharing a common superscript within column are statistically significant $P < 0.05$

Groups	Food intake (g/day/rat)	Body wt gained (g)	Food efficiency ratio
GNO	11.4 \pm 0.31 ^{ab}	200.6 \pm 8.2 ^a	0.36 \pm 0.01 ^a
RBO	10.5 \pm 0.44 ^a	195.8 \pm 11.3 ^a	0.37 \pm 0.01 ^{ab}
SL with CLO	11.5 \pm 0.37 ^{ab}	208.2 \pm 6.6 ^a	0.39 \pm 0.0 ^{bc}
SL with LSO	12.13 \pm 0.24 ^b	211.2 \pm 4.2 ^a	0.38 \pm 0.02 ^{ab}
Blend with CLO	11.9 \pm 0.49 ^b	217.0 \pm 7.3 ^a	0.41 \pm 0.01 ^c
Blend with LSO	11.5 \pm 0.52 ^{ab}	212.7 \pm 5.8 ^a	0.37 \pm 0.01 ^{ab}

Table 3 Effect of feeding structured lipids with rice bran oil rich in n-3 PUFA on organ weight in rats

Groups	g/100 g body wt			
	Liver	Heart	Brain	Spleen
GNO	3.23 ± 0.01 ^a	0.31 ± 0.0 ^{ab}	0.68 ± 0.03 ^{ab}	0.22 ± 0.0 ^a
RBO	3.54 ± 0.01 ^a	0.34 ± 0.01 ^{bc}	0.70 ± 0.03 ^b	0.29 ± 0.03 ^b
SL with CLO	3.55 ± .08 ^a	0.30 ± 0.02 ^{ab}	0.66 ± 0.02 ^{ab}	0.20 ± 0.01 ^a
SL with LSO	3.22 ± 0.01 ^a	0.28 ± 0.03 ^a	0.70 ± 0.01 ^b	0.24 ± 0.02 ^a
Blend with CLO	3.56 ± 0.01 ^a	0.32 ± 0.01 ^b	0.62 ± 0.01 ^a	0.24 ± 0.02 ^a
Blend with LSO	3.44 ± 0.03 ^a	0.37 ± 0.03 ^c	0.64 ± 0.01 ^{ab}	0.31 ± 0.02 ^b

Values are means ± SEM of six rats

Values not sharing a common superscript within a column are statistically significant at $P < 0.05$

Table 4 Effect of feeding structured lipids with rice bran oil rich in n-3 PUFA on the serum lipid profile in rats

Groups	Parameters mg/dL				
	Total cholesterol	HDL cholesterol	LDL + VLDL cholesterol	Phospholipids	Triacylglycerol
GNO	93.5 ± 2.29 ^c	40.6 ± 0.3 ^d	53.0 ± 2.7 ^c	135.0 ± 2.3 ^b	139.6 ± 1.8 ^c
RBO	88.8 ± 0.87 ^b	40.7 ± 0.9 ^c	48.1 ± 0.9 ^b	128.8 ± 1.2 ^b	126.9 ± 1.1 ^d
SL with CLO	72.2 ± 0.51 ^a	30.2 ± 0.3 ^a	42.0 ± 0.4 ^a	106.2 ± 1.7 ^a	108.8 ± 1.7 ^b
SL with LSO	69.6 ± 0.86 ^a	29.0 ± 0.5 ^a	40.5 ± 1.2 ^a	110.4 ± 7.7 ^a	105.8 ± 1.3 ^{ab}
Blend with CLO	72.0 ± 1.50 ^a	33.9 ± 1.1 ^b	38.2 ± 1.8 ^a	103.6 ± 1.9 ^b	99.2 ± 3.6 ^a
Blend with LSO	74.0 ± 0.59 ^a	33.2 ± 0.6 ^b	40.8 ± 1.2 ^a	111.7 ± 0.1 ^a	105.9 ± 4.0 ^{ab}

Values are means ± SEM of six rats

Values not sharing a common superscript with column are statistically significant $P < 0.05$

no difference in TAGs and phospholipids in rats fed SLs and blends.

Serum Fatty Acid Profile Rats Fed with n-3 PUFA

Significant changes were observed in SL with CLO compared to blend with CLO. The n-3 fatty acids level in rats given SLs and blends with CLO and LSO (Table 5). The ALA content was 5.4 and 4.5% in SLs and a blend with LSO respectively. A significant increase in EPA + DHA levels and arachidonic acid content significantly decreased in blends as well as in SLs both. ALA, EPA and DHA were not detected in the serum of RBO and GNO fed groups. On the other hand feeding of SLs and blends with CLO resulted

in a significant increase in the levels of all n-3 PUFA. Feeding of SLs and blends rich in n-3 PUFA significantly decreased the oleic and linoleic acid content of serum lipids.

Liver Lipid Profile of Rats Fed with n-3 PUFA

The total cholesterol content in the liver was significantly decreased in rats fed SLs with CLO and LSO compared to RBO but blends did not alter. TAG content was decreased significantly in SL with CLO and a blend with LSO compared RBO (Table 6). There was no change in TAG levels between SL and blends. Reduction in TAG content in other groups was not statistically significant compared to RBO fed group.

Table 5 Effect of feeding structured lipids with rice bran oil rich in n-3 PUFA on serum fatty acids in rats

Fatty acids	GNO	RBO	SL with CLO	SL with LSO	Blend with CLO	Blend with LSO
16:0	22.2 ± 0.2 ^{ab}	22.2 ± 0.4 ^{ab}	22.9 ± 0.3 ^{ab}	21.5 ± 0.6 ^a	22.4 ± 0.4 ^{ab}	23.8 ± 0.9 ^b
16:1	2.5 ± 0.04 ^a	2.4 ± 0.3 ^a	3.7 ± 0.4 ^b	2.5 ± 0.2 ^a	2.4 ± 0.1 ^a	2.0 ± 0.1 ^a
18:0	8.4 ± 0.4 ^a	9.1 ± 0.2 ^{ab}	8.4 ± 0.4 ^a	9.5 ± 0.3 ^{ab}	8.8 ± 0.07 ^b	9.6 ± 0.5 ^b
18:1	32.5 ± 0.3 ^c	33.2 ± 0.2 ^c	27.2 ± 0.7 ^b	27.9 ± 0.4 ^b	27.0 ± 0.5 ^b	28.7 ± 1.1 ^a
18:2	19.1 ± 0.2 ^b	17.7 ± 0.3 ^b	15.8 ± 0.5 ^a	19.2 ± 0.4 ^c	18.1 ± 0.5 ^{ab}	18.2 ± 0.5 ^{ab}
18:3	ND	ND	ND	5.4 ± 0.3 ^c	ND	4.5 ± 0.3 ^b
20:4	9.4 ± 0.4 ^c	9.6 ± 0.4 ^c	3.4 ± 0.1 ^a	4.7 ± 0.1 ^b	4.3 ± 0.2 ^{ab}	5.0 ± 0.5 ^b
20:5	ND	ND	6.0 ± 0.5 ^c	3.2 ± 0.04 ^a	5.8 ± 0.04 ^b	3.2 ± 0.05 ^a
22:6	ND	ND	2.8 ± 0.4 ^c	2.7 ± 0.04 ^{bc}	2.6 ± 0.3 ^b	2.4 ± 0.1 ^a

Values are means ± SEM of six rats

Values not sharing a common superscript within row are statistically significant at $P < 0.05$

Table 6 Effect of feeding structured lipids with rice bran oil rich in n-3 PUFA on liver lipid profile in rats

Groups	mg/g		
	Total cholesterol	Phospholipids	Triglycerides
GNO	13.4 ± 0.3 ^d	23.9 ± 0.5 ^a	16.5 ± 0.6 ^c
RBO	11.5 ± 0.3 ^c	27.0 ± 0.7 ^b	15.0 ± 0.5 ^b
SL with CLO	9.9 ± 0.6 ^b	32.6 ± 0.8 ^c	11.8 ± 0.6 ^a
SL with LSO	10.2 ± 0.2 ^{bc}	28.9 ± 1.0 ^b	13.5 ± 0.5 ^{ab}
Blend with CLO	9.8 ± 0.6 ^{ab}	32.3 ± 0.7 ^c	13.3 ± 0.4 ^{ab}
Blend with LSO	8.5 ± 0.5 ^a	33.4 ± 0.6 ^c	12.2 ± 0.6 ^a

Values are means ± SEM of six rats

Values not sharing a common superscript within column are statistically significant at $P < 0.05$

Liver Fatty Acid Profile

The fatty acid composition of the liver lipids of rats fed SLs and blended oils with CLO and LSO is given in Table 7. Feeding of SLs and blended oils with CLO resulted in a significant reduction of arachidonic acid (45%) and an

accumulation of EPA and DHA. At the same time, oleic and linoleic acids were decreased by 50 and 37% respectively, compared to the RBO fed group. On the other hand, feeding LSO either in SL or blended oils resulted in an accumulation of ALA, EPA and DHA and a reduction in the level of arachidonic acid, oleic and linoleic acids compared to the RBO fed group.

Fatty Acid Composition of Heart, Brain, Eye and Adipose Tissues

The dietary n-3 PUFA level influenced the FA composition of heart (Table 8), brain (Table 9), eye (Table 10) and adipose tissues (Table 11). The fatty acid composition of the heart was significantly influenced in rats fed n-3 PUFA containing SLs and blended oils. LSO feeding either as SLs or blended oil resulted in the significant accumulation of ALA, DHA and EPA compared to the RBO fed group. The level of DHA was significantly increased in the heart tissues of rats given SL and blends with CLO compared to RBO fed group. There was a 5.3 fold increase in the DHA

Table 7 Effect of feeding structured lipids with rice bran oil rich in n-3 PUFA on the liver fatty acid profile in rats

Fatty acids	GNO	RBO	SL with CLO	SL with LSO	Blend with CLO	Blend with LSO
16:0	19.7 ± 0.4 ^a	21.5 ± 0.3 ^{ab}	24.4 ± 0.2 ^c	21.8 ± 1.3 ^b	22.8 ± 0.8 ^{bc}	22.3 ± 0.7 ^b
16:1	3.2 ± 0.1 ^b	3.3 ± 0.4 ^b	2.5 ± 0.2 ^{ab}	2.7 ± 0.2 ^{ab}	2.0 ± 0.4 ^a	1.7 ± 0.2 ^a
18:0	10.1 ± 0.5 ^a	9.3 ± 0.4 ^a	17.6 ± 0.2 ^c	14.0 ± 1.1 ^b	14.6 ± 0.6 ^b	14.9 ± 0.7 ^b
18:1	39.0 ± 0.5 ^c	35.7 ± 1.0 ^d	17.7 ± 2.6 ^a	22.0 ± 0.6 ^b	22.1 ± 0.7 ^b	27 ± 0.8 ^c
18:2	14.0 ± 0.4 ^b	16.6 ± 0.2 ^c	10.6 ± 0.7 ^a	13.4 ± 1.1 ^b	15.5 ± 0.2 ^c	15.5 ± 0.2 ^c
18:3	ND	ND	ND	2.1 ± 0.6 ^a	ND	1.9 ± 0.6 ^a
20:4	18.4 ± 0.1 ^d	16.3 ± 0.4 ^c	9.0 ± 0.02 ^b	9.4 ± 0.1 ^b	9.6 ± 0.3 ^b	7.2 ± 0.3 ^a
20:5	ND	ND	2.4 ± 0.06 ^c	1.4 ± 0.04 ^b	2.6 ± 0.08 ^d	1.2 ± 0.01 ^a
22:6	ND	ND	10.3 ± 0.1 ^d	4.9 ± 0.06 ^a	8.4 ± 0.3 ^c	5.4 ± 0.1 ^b

Values are means ± SEM of six rats

Values not sharing a common superscript within row are statistically significant at $P < 0.05$

Table 8 Effect of feeding structured lipids with rice bran oil rich in n-3 PUFA on heart profile in rats

Fatty acids	GNO	RBO	SL with CLO	SL with LSO	Blend with CLO	Blend with LSO
16:0	15.9 ± 0.2 ^c	14.7 ± 0.1 ^b	13.1 ± 0.1 ^a	17.5 ± 0.2 ^d	13.0 ± 0.1 ^a	18.5 ± 0.4 ^c
16:1	2.1 ± 0.02 ^c	1.9 ± 0.02 ^c	3.6 ± 0.1 ^d	1.4 ± 0.02 ^b	3.9 ± 0.02 ^c	1.1 ± 0.02 ^a
18:0	27.9 ± 0.2 ^b	27.2 ± 0.2 ^b	25.6 ± 0.4 ^a	31.0 ± 0.3 ^c	26.1 ± 0.1 ^a	32.3 ± 0.4 ^d
18:1	21.7 ± 0.2 ^d	20.6 ± 0.3 ^c	18.1 ± 0.02 ^b	16.8 ± 0.1 ^a	18.7 ± 0.2 ^b	18.2 ± 0.3 ^b
18:2	14.8 ± 0.1 ^c	15.7 ± 0.3 ^d	12.2 ± 0.1 ^b	11.4 ± 0.1 ^b	13.3 ± 0.3 ^b	10.2 ± 0.1 ^a
18:3	ND	ND	ND	3.1 ± 0.02 ^a	ND	3.1 ± 0.02 ^a
20:4	17.0 ± 0.2 ^d	17.0 ± 0.3 ^d	12.3 ± 0.2 ^a	15.0 ± 0.1 ^c	13.4 ± 0.2 ^b	14.7 ± 0.3 ^c
20:5	ND	ND	2.5 ± 0.02 ^d	1.4 ± 0.02 ^a	2.3 ± 0.02 ^c	2.1 ± 0.02 ^b
22:6	2.5 ± 0.02 ^a	2.3 ± 0.02 ^a	14.5 ± 0.1 ^d	8.8 ± 0.1 ^b	12.4 ± 0.2 ^c	9.3 ± 0.3 ^b

Values are means ± SEM of six rats

Values not sharing a common superscript within row are statistically significant at $P < 0.05$

Table 9 Effect of feeding structured lipids with rice bran oil rich in n-3 PUFA on the brain fatty acid profile in rats

Fatty acids	GNO	RBO	SL with CLO	SL with LSO	Blend with CLO	Blend with LSO
16:0	21.5 ± 0.7 ^a	23.3 ± 0.3 ^b	24.6 ± 0.2 ^b	23.8 ± 0.1 ^b	24.5 ± 0.4 ^b	23.5 ± 0.3 ^b
16:1	3.8 ± 0.2 ^a	4.3 ± 0.1 ^{ab}	4.7 ± 0.4 ^b	4.3 ± 0.4 ^{ab}	4.2 ± 0.1 ^{ab}	3.8 ± 0.2 ^a
18:0	11.4 ± 0.1 ^a	11.2 ± 0.1 ^a	11.9 ± 0.1 ^{ab}	11.9 ± 0.6 ^{ab}	12.8 ± 0.2 ^{bc}	13.1 ± 0.6 ^c
18:1	37.2 ± 0.2 ^d	31.7 ± 0.7 ^c	29.7 ± 0.1 ^b	30.0 ± 0.7 ^b	31.8 ± 0.6 ^c	27.2 ± 0.4 ^a
18:2	13.1 ± 0.2 ^d	10.8 ± 0.1 ^c	8.8 ± 0.3 ^a	10.3 ± 0.2 ^{bc}	9.5 ± 0.3 ^{ab}	9.4 ± 0.2 ^a
18:3	ND	ND	ND	2.4 ± 0.1 ^b	ND	1.6 ± 0.02 ^a
20:4	7.6 ± 0.1 ^d	7.2 ± 0.3 ^d	5.0 ± 0.1 ^b	4.5 ± 0.1 ^{ab}	4.1 ± 0.2 ^a	5.3 ± 0.1 ^c
20:5	ND	ND	0.6 ± .02 ^{ab}	0.8 ± .02 ^b	0.8 ± 0.08 ^b	0.6 ± 0.05 ^{ab}
22:6	4.7 ± 0.2 ^a	4.4 ± 0.2 ^a	10.4 ± 0.1 ^e	8.1 ± 0.1 ^c	9.4 ± 0.2 ^d	7.4 ± 0.02 ^b

Values are means ± SEM of six rats

Values not sharing a common superscript within row are statistically significant at $P < 0.05$

Table 10 Effect of feeding structured lipids with rice bran oil rich in n-3 PUFA on the eye fatty acid profile in rats

Fatty acids	GNO	RBO	SL with CLO	SL with LSO	Blend with CLO	Blend with LSO
16:0	21.5 ± 0.7 ^a	22.9 ± 0.1 ^b	24.6 ± 0.4 ^c	23.8 ± 0.1 ^{bc}	24.6 ± 0.4 ^c	23.5 ± 0.3 ^{bc}
16:1	3.8 ± 0.1 ^a	4.5 ± 0.02 ^{ab}	4.6 ± 0.4 ^b	4.3 ± 0.4 ^{ab}	4.2 ± 0.1 ^{ab}	3.7 ± 0.2 ^a
18:0	11.3 ± 0.1 ^a	11.4 ± 0.1 ^a	11.9 ± 0.2 ^{ab}	11.9 ± 0.6 ^{ab}	12.8 ± 0.2 ^b	13.1 ± 0.6 ^b
18:1	35.4 ± 0.09 ^c	31.9 ± 0.7 ^b	31.0 ± 0.7 ^{bc}	29.0 ± 1.0 ^{ab}	29.3 ± 0.2 ^{ab}	27.2 ± 0.4 ^a
18:2	13.2 ± 0.2 ^d	10.7 ± 0.1 ^c	8.8 ± 0.3 ^a	10.3 ± 0.2 ^{bc}	9.5 ± 0.3 ^{ab}	9.3 ± 0.2 ^a
18:3	ND	ND	ND	2.4 ± 0.1 ^b	ND	1.7 ± 0.2 ^a
20:4	7.4 ± 0.02 ^d	7.3 ± 0.2 ^d	5.0 ± 0.1 ^{bc}	4.5 ± 0.1 ^{ab}	4.2 ± 0.2 ^a	5.3 ± 0.1 ^c
20:5	ND	ND	0.6 ± 0.02 ^a	0.8 ± 0.2 ^b	0.8 ± 0.02 ^b	0.6 ± 0.02 ^a
22:6	4.9 ± 0.2 ^a	4.7 ± 0.2 ^a	10.4 ± 0.1 ^c	7.1 ± 0.5 ^b	10.1 ± 0.3 ^c	7.5 ± 0.1 ^b

Values are means ± SEM of six rats

Values not sharing a common superscript within row are statistically significant at $P < 0.05$

Table 11 Effect of feeding structured lipids with rice bran oil rich in n-3 PUFA on the adipose tissue fatty acid profile in rats

Fatty acids	GNO	RBO	SL with CLO	SL with LSO	Blend with CLO	Blend with LSO
14:0	3.4 ± 0.2 ^a	3.4 ± 0.2 ^a	5.9 ± 0.3 ^d	4.8 ± 0.1 ^b	5.3 ± 0.2 ^c	5.0 ± 0.1 ^b
16:0	17.9 ± 0.1 ^a	22.3 ± 0.4 ^b	28.6 ± 0.8 ^d	25.2 ± 0.5 ^c	25.0 ± 0.2 ^c	20.9 ± 0.9 ^b
16:1	8.2 ± 0.1 ^{ab}	8.7 ± 0.1 ^{bc}	9.2 ± 0.3 ^c	8.0 ± 0.1 ^a	8.9 ± 0.02 ^c	7.9 ± 0.2 ^a
18:0	2.8 ± 0.2 ^{ab}	2.4 ± 0.2 ^a	3.6 ± 0.1 ^d	2.3 ± 0.1 ^a	3.5 ± 0.3 ^{cd}	3.1 ± 0.02 ^{bc}
18:1	59.6 ± 0.4 ^d	43.4 ± 0.4 ^c	39.1 ± 0.7 ^a	39.2 ± 0.5 ^a	41.4 ± 0.7 ^b	42.2 ± 0.8 ^b
18:2	19.7 ± 0.3 ^d	20.5 ± 0.3 ^d	10.8 ± 0.4 ^a	14.8 ± 0.8 ^b	16.7 ± 0.3 ^c	17.7 ± 0.4 ^c
18:3	ND	ND	ND	10.5 ± 0.6 ^a	ND	10.3 ± 0.2 ^a
20:4	0.2 ± 0.01 ^a	0.26 ± 0.02 ^a	0.2 ± 0.02 ^a	0.19 ± 0.01 ^a	0.3 ± 0.02 ^b	0.3 ± 0.02 ^b
20:5	ND	ND	1.0 ± 0.02 ^a	ND	1.0 ± 0.02 ^a	ND
22:6	ND	ND	2.7 ± 0.02 ^b	ND	1.4 ± 0.1 ^a	ND

Values are means ± SEM of six rats

Values not sharing a common superscript within row are statistically significant at $P < 0.05$

level of rats fed SL with CLO compared to RBO, whereas in rats fed SL and a blend with LSO, the increase in DHA was only 2.9 fold compared to the RBO fed group. Rats fed

SL and blends with CLO significantly decreased the levels of oleic and linoleic acids. In the brain, small amounts (2.4 and 1.6%) of ALA was detected in rats fed structured lipids

and blends with LSO respectively, whereas this fatty acid was not detected in other dietary groups. The basal level of DHA in RBO and GNO was 4.4 and 4.7% respectively of the total FAs, whereas it was increased to 10.4 and 8.1% in SL with CLO and LSO respectively compared to RBO fed group. Similarly it was increased in the case of blends up to 9.4 and 7.4% of the total FAs in the blended oil groups as compared to RBO and GNO. In the eye, the DHA content was increased significantly in all groups of animals compared to RBO. Whereas only small amounts of EPA were detected in these animals. ALA was detected only in LSO fed animals. There was a significant reduction in arachidonic acid. In the adipose tissue of rats fed structured lipids and blends with LSO had 10.5 and 10.3% of ALA respectively of the total fatty acids, whereas it was not detected in rats of other dietary groups. EPA and DHA were found only in small amounts in rats fed SL and blends with CLO.

Discussion

The present investigation was aimed at enriching rice bran oil with ALA from linseed oil and EPA + DHA from cod liver oil and studying the effect of these modified lipids on changes in the serum and hepatic lipid profiles of rats when fed as the sole source of dietary fat. The effect of SLs synthesized was also compared with that of blends of RBO with CLO and LSO with similar levels of n-3 PUFA. Even though 1, 3 positional specific lipase from *Rhizomucor miehei* [41] was used as a catalyst, amounts of ALA (15%) and EPA + DHA (8.1%) were incorporated into the SLs synthesized with LSO and CLO respectively. This indicated that most of the ALA and EPA + DHA in the modified lipids was incorporated in the 1 and 3 positions of the triacylglycerol molecule of RBO. The small increase in the ALA and EPA + DHA at the *sn*-2 position of SLs could be attributed to acyl migration and such acyl migration was reported by Xu et al. [42, 43]. In the case of blended oils, fatty acid composition was similar to that of the SL and their fatty acid content at the *sn*-2 position was similar to that of SLs. Numerous studies have shown that SLs have unique metabolic pathways and exhibit many superior metabolic benefits in comparison to that of the blended oils. Studies have shown that rats receiving SLs containing both medium chain and long chain fatty acids showed the greatest gain in body weight, enhanced skeleton muscle and liver protein synthesis as well as a marked increase in nitrogen retention over comparable groups of rats given physical mixtures of long chain TAG and medium chain TAGs [44, 45]. Even though many studies have clearly shown that there are significant differences in the mode of absorption of fatty acids based on acylglycerol

structures, very few studies have addressed the lipidemic effects of modified lipids. The SLs containing n-3 PUFA showed a significantly higher hypolipidemic effect than that of the blended oils when fed as a sole source of fat in the diet. A similar hypolipidemic effect of SL was also observed in liver. Feeding SL and blends increased the ALA and EPA + DHA levels in the liver and other tissues lipids. This also resulted in an incremental increase in the accumulation of EPA + DHA in the serum, liver and other tissues. This indicated that conversion of ALA to long chain PUFA takes place in rats. The increase in EPA and DHA was higher in rats fed fats containing these fatty acids in a preformed state. Both blended oils and SL increased the 18:3 and EPA + DHA levels in the liver and other tissues. One reason for this may be the higher levels of EPA and DHA in the diets containing modified lipids. Another reason could be due to the slow conversion of ALA to long chain n-3 PUFA (EPA and DHA). Preformed EPA + DHA was taken up by serum and liver much more efficiently than that obtained from ALA. The level of arachidonic acid in heart tissue decreased when n-3 PUFA was included in the diet. Earlier studies have shown that feeding a diet containing ALA can increase the level of this FA as well as the level of long chain metabolites, to varying degrees [46–51]. Rats fed SLs and blends with n-3 PUFA increased the amount of n-3 PUFA in the liver and heart tissue which is in agreement with the findings of Medeiros et al. [52].

The brain is a unique organ characterized by the presence of a high concentration of DHA, which influences its structure and functional properties [53]. The high level of DHA in the brain of a number of mammalian species irrespective of their size led to early speculation that this fatty acid plays a crucial role in the nervous system. Many studies using ALA deficient diets have shown a reduction in the level of DHA in the brain and loss of many cognitive functions [54]. Studies have reported that supplementation of arachidonic acid and DHA can remedy the cognitive dysfunction due to organic brain damage or aging [55]. Feeding rats with SLs and blends containing 18:3 and EPA + DHA increased the DHA levels in the brain compared to RBO and GNO fed rats. We also observed that rats fed preformed DHA in the form of SL and blend with CLO showed a higher levels of DHA in the brain as compared to those fed SL and blends with LSO. This finding is in agreement with an earlier report showing that preformed DHA is incorporated efficiently into brain tissue [50, 56]. Earlier studies have shown a small but significant increase in the 18:3 and EPA levels in brain tissue when the diet was high in n-3 FAs [56]. Studies indicated that feeding a diet high in ALA to guinea pigs increased the EPA and DHA levels in liver, heart, and adipose tissues when compared with a diet low in ALA [57–59]. However, in our study,

EPA and DHA were not detected in the adipose tissue when rats fed with SL and blends containing ALA. Similarly, other study has reported that ALA enriched diets resulted in the accumulation of ALA, but not EPA and DHA [59]. These studies may indicate that with a high intake of n-3 PUFA, ALA can accumulate in adipose tissue but its elongation to EPA and DHA is restricted. However these fatty acids can accumulate in adipose tissue when given in a preformed state. The American Heart Association recommends for those individuals without heart disease that they eat a variety of fish at least twice a week and include oils and foods rich in ALA (flaxseed, canola, and soybean oils; flaxseeds and walnuts) [60].

In conclusion, the present studies indicated that ALA and EPA + DHA were efficiently absorbed from SLs as well as from blended oils. The food intake and growth of animals also showed that the SL was as efficient as a blended oil in supporting the growth of the animals without having any adverse effects. Rice bran oil enriched with n-3 PUFA significantly lowered the serum and liver lipids which are high risk factors for cardiovascular diseases. Therefore, RBO can be enriched with ALA and EPA + DHA by lipase catalyzed interesterification reactions and these modified lipids exhibited hypocholesterolemic and hypolipidemic effects in rats when compared to unmodified RBO. Use of an immobilized enzyme for the preparation of structured lipids offers the advantage of adding desirable fatty acids at a specific position of TAG.

Acknowledgments The authors thank the Director, CFTRI Mysore, for constant encouragement. Rajni Chopra expresses her gratitude and thanks to the University Grant Commission (UGC), New Delhi for awarding her a Senior Research Fellowship.

References

1. Simopoulos AP (1999) Essential fatty acids in health and chronic diseases. *Am J Clin Nutr* 70:S560–S569
2. Simopoulos AP (2001) n-3 Fatty acids and human health: defining strategies for public policy. *Lipids* 36:S83–S89
3. Schultz MB, Hoffmann K (2006) Methodological approaches to study dietary pattern in relation to risk factors of CHD and stroke. *Br J Nutr* 95:860–869
4. Katan MB, Zock PL, Mensink RP (1995) Dietary oils, serum lipoproteins, and coronary heart disease. *Am J Clin Nutr* 61:1368S–1373S
5. Morris MC (1994) Dietary fats and blood pressure. *J Cardiovasc Risk* 1:21–30
6. Sacks FM, Hebert P, Appel LJ, Borhani NO, Applegate WB, Cohen JD, Cutler JA, Kirchner KA, Kuller LH, Roth KJ (1994) The effect of fish oil on blood pressure and high-density lipoprotein-cholesterol levels in phase I of the Trials of Hypertension Prevention. Trials of hypertension prevention collaborative research group. *J Hyperten* 12:S23–S31
7. Ghafoorunissa (1990) Availability of linoleic acid from cereal: pulse diets. *Lipids* 25:763–766
8. Ghafoorunissa (1996) Fats in Indian diets and their nutritional implications. *Lipids* 31:S287–S291
9. Achaya KT (1995) Fat intake in India: an update. *J Sci Ind Res* 54:91–97
10. COMA (1994) Cardiovascular review group. Report on health and social subjects: nutritional aspects of cardiovascular disease. London: Department of health. 46
11. Domingo JL (2007) Omega-3 fatty acids and the benefits of fish consumption: is all that glitters gold? *Environ Int* 33:993–998
12. Green AG, Marshall DR (1984) Isolation of induced mutants in linseed (*Linum usitatissimum*) having reduced linolenic acid content. *Euphytica* 33:321–328
13. Lauren WC, Robert EC, Eric JM, Jolly CA (2005) Dietary n-3 polyunsaturated fatty acids increase T-lymphocyte phospholipids mass and acyl-CoA binding protein expression. *Lipids* 40: 81–87
14. Shin T, Godber JS, Martin DF, Wells JH (1997) Hydrolytic stability and changes in E-vitamins and oryzanol of extruded rice bran during storage. *J Food Sci* 62:704–708
15. Seetharamaiah GS, Chandrasekhara N (1989) Studies on hypocholesterolemic activity of rice bran oil. *Atherosclerosis* 78:219–235
16. Sugano M, Tsuji E (1997) Rice bran oil and cholesterol metabolism. *J Nutr* 127:521S–524S
17. Wilson TA, Nicolosia JR, Woolfey B, Kritchevsky D (2007) Rice bran oil and oryzanol reduce plasma lipid and lipoprotein cholesterol concentrations and aortic cholesterol ester accumulation to a greater extent than ferulic acid in hypercholesterolemic hamsters. *J Nutr Biochem* 18:105–112
18. Rukmini C, Raghuram TC (1991) Nutritional and biochemical aspects of the hypolipidemic action of rice bran oil. *J Am Coll Nutr* 10:593–601
19. FAO and WHO joint consultation (1995) Fats and oils in human nutrition. *Nutr Rev* 53:202–205
20. Simopoulos AP, Leaf A, Salem N (1999) Workshop on the essentiality of recommended dietary intakes for omega 6 and omega 3 fatty acids. National Institute of Health, Bethesda
21. Barelo- Coblijin G, Collison LW, Jolly CA, Murphy EJ (2005) Dietary α -linolenic acid increase brain but not heart and liver docosahexaenoic acid levels. *Lipids* 40:787–798
22. Cughey GE, Mantzioris E, Gibson RA, Cleland LG, James MJ (1996) The effect of human tumor necrosis factor alpha and interleukin 1 beta production of diet enriched in n-3 fatty acid from vegetable oil or fish oil. *Am J Clin Nutr* 63:116–122
23. Cunnane SC, Ganguly S, Menaard C, Liede AC, Hamadeh MJ, Chen ZY, Woolever T (1993) High α -linolenic acid flax seed (*Linum usitatissimum*). Some nutritional properties in humans. *Br J Nutr* 69:443–453
24. Jenkins DJA, Kendall CWC, Vidgen E, Agarawal S, Rao AV, Rosenberg RS, Diamandis EP, Novokmet R, Mehling CC, Perera T (1999) Health aspects of partially defatted flaxseed, including effect on serum lipids, oxidative measures and ex vivo androgen and progestin activity: a controlled crossover trial. *Am J Clin Nutr* 69:395–402
25. Owen AJ, Peter-Przyborowska BA, Hoy AJ, McLennan PL (2004) Dietary fish oil dose—and time—response effects on cardiac phospholipids fatty acid composition. *Lipids* 39:955–961
26. Tso P, Karlstad MD, Bistran BR, DeMichele SJ (1995) Intestinal digestion, absorption and transport of structured triglycerides and cholesterol in rats. *Am J Physiol* 268:G568–G577
27. Jensen GL, McGarvey N, Taraszewski R, Wixon SK, Seidner DL, Pai T, Yeh YY, Lee TW, DeMichele SJ (1994) Lymphatic absorption of enterally fed structured triacylglycerol vs physical mix in a canine model. *Am J Clin Nutr* 60:518–524
28. Ikeda I, Tomari Y, Sugano M, Watanabe S, Nagata J (1991) Lymphatic absorption of structured glycerolipids containing

- medium-chain fatty acids and 18:2 acid and their effects on cholesterol absorption in rats. *Lipids* 26:369–373
29. Lee KT, Akoh CC (1999) Effects of structured lipid containing omega-3 and medium chain fatty acids on serum lipids and immunological variables in mice. *J Food Biochem* 23:197–208
 30. Luddy FE, Barford RA, Herb SF, Magidman P, Riemenschneider RW (1964) Pancreatic lipolysis of triglycerides by a semimicro technique. *J Am Oil Chem Soc* 41:693–696
 31. Morrison MR, Smith M (1964) Preparation of fatty acid methyl esters and dimethyl acetyls from lipids with boron fluoride-methanol. *J Lipid Res* 5:600–608
 32. Anonymous (1977) Report of the American institute of nutrition, Ad-hoc committee on standards for nutritional studies. *J Nutr* 107:1340–1348
 33. Folch J, Lees M, Sloane-Stanley GH (1957) A simple method for the isolation and purification of total lipids from animal tissues. *J Biol Chem* 226:497–509
 34. Yagi K (1984) Lipid peroxidation: assay for blood plasma or serum. *Meth Enzymol* 105:238–331
 35. Berg JA, Aust SD (1978) Microsomal lipid peroxidation. *Meth Enzymol* 52:302–310
 36. Searcy RL, Bergquist LM (1960) A new color reaction for the quantification of serum cholesterol. *Clin Chim Acta* 5:192–199
 37. Warnick GR, Albers JJ (1978) A comprehensive evaluation of the heparin manganese chloride precipitation procedure for estimating HDL cholesterol. *J Lipid Res* 19:65–76
 38. Stewart JCM (1980) Colorimetric evaluation of phospholipids with ammonium ferrothiocyanate. *Anal Biochem* 104:10–14
 39. Fletcher MJ (1968) A colorimetric method for estimating serum triglycerides. *Clin Chim Acta* 22:303–307
 40. Snedecor GW, Cochran WG (eds) *Statistical methods*. Iowa state University Press, Ames
 41. Macrae AR (1983) Lipase-catalyzed interesterification of oils and fats. *J Am Oil Chem Soc* 60:291–294
 42. Xu X, Fomuso LB, Akoh CC (2000) Modification of Menhaden oil by enzymatic acidolysis to produce structured lipids: optimization by response surface design in a packed bed reactor. *J Am Oil Chem Soc* 77:171–176
 43. Xu X, Skands ARH, Alder-Nissen J, Hoy C-E (1998) Production of specific structured lipids by enzymatic interesterification: optimization of the reaction by response surface design. *Fett/Lipids* 100:463–471
 44. DeMichele SJ, Karlstad MD, Babayan BK, Istfan N, Blackburn GL, Bistrrian BR (1988) Enhanced skeleton muscle and liver protein synthesis with structured lipids in enterally fed burned rats. *Metabolism* 37:787–795
 45. Mok KT, Maiz A, Yamazaki K, Sobrado J, Babayan BK, Moldawer LL, Bistrrian BR, Blackburn GL (1984) Structured medium-chain and long-chain triglyceride emulsions are superior to physical mixture in sparing body protein in the burned rats. *Metabolism* 33:910–915
 46. Gerster H (1998) Can adult adequately convert α -linolenic acid (18:3n-3) to eicosapentaenoic acid (20:5n-3) and docosahexaenoic acid (22:6n-3). *Intl J Vit Nutr Res* 68:159–173
 47. Mantzioris E, James MJ, Gibson RA, Cleland LG (1994) Dietary substitution with α -linolenic acid—rich vegetable oil increase eicosapentaenoic acid concentration in tissues. *Am J Clin Nutr* 59:1304–1309
 48. Bazinet RP, McMillan EG, Cunnane SC (2003) Dietary α -linolenic acid increase the n-3 PUFA content of Sow's milk and tissues of suckling piglets. *Lipids* 38:1045–1049
 49. Ramaprasad TR, Baskaran V, Sambaiah K, Lokesh BR (2004) Supplementation and delivery of n-3 fatty acids through spray-dried milk reduces serum and liver lipids in rats. *Lipids* 39:627–632
 50. Barcelo-Coblijn G, Collison LW, Jolly CA, Murphy EJ (2005) Dietary α -linolenic acid increases brain but not heart and liver docosahexaenoic acid levels. *Lipids* 40:787–797
 51. MacDonald-Wicks LK, Garg ML (2004) Incorporation of n-3 fatty acids into plasma and liver lipids into rats: importance of background dietary fat. *Lipids* 39:545–551
 52. Medeiros DM, Hampton M, Kurtzer K, Parelman M, Al-Tamimi E, Drouillard JS (2007) Feeding enriched omega-3 fatty acid beef to rats increases omega-3 fatty acid content of heart and liver membranes and decrease serum vascular cell adhesion molecule-I and cholesterol levels. *Nutr Res* 27:295–299
 53. Brenner RR (1984) Effect unsaturated fatty acids on membrane structure and kinetics. *Prog Lipid Res* 23:69–96
 54. Ahmed A, Moriguchi T, Salem NJ (2002) Decrease in neuron size in docosahexaenoic acid-deficient brain. *Pediatr Neurol* 26:210–218
 55. Kotani S, Sakaguchi E, Warashina S, Matsukawa N, Ishikura Y, Kiso Y, Sakakibara M, Yoshimoto T, Guo J, Yamashima T (2006) Dietary supplementation of arachidonic and docosahexaenoic acids improves cognitive dysfunction. *Neurosci Res* 56:159–164
 56. Kao BT, DePeters EJ, Enennaam LV (2006) Mice raised on milk transgenically enriched with n-3 PUFA have increased brain docosahexaenoic acid. *Lipids* 41:543–549
 57. Zhong F, Sinclair AJ (2000) Increased α -linolenic acid intake increase tissue α -linolenic acid content and apparent oxidation with little effect on tissue docosahexaenoic acid in the guinea pigs. *Lipids* 35:395–400
 58. Wistuba TJ, Kegely EB, Apple JK, Rule DC (2007) Feeding feedlot steers fish oil alters the fatty acid composition of adipose and muscle tissue. *Meat Sci* 77:196–203
 59. Lin DS, Connors WE (1990) Are the n-3 fatty acids from dietary fish oil deposited in the triglyceride stores of adipose tissue? *Am J Clin Nutr* 51:535–539
 60. Kris-Etherton PM, Harris WS, Appel LJ (2002) Fish consumption, fish oil, omega-3 fatty acids, and cardiovascular disease. *Circulation* 106:2747–2757

Oolichan Grease: A Unique Marine Lipid and Dietary Staple of the North Pacific Coast

Stephen D. Phinney · James A. Wortman ·
Douglas Bibus

Received: 3 April 2008 / Accepted: 16 September 2008 / Published online: 14 October 2008
© AOCS 2008

Abstract Oolichan grease, a dietary fat prepared from smelt-like fish, is highly prized by north Pacific coast aboriginal cultures. The composition of oolichan grease is unclear, with one report indicating a high 22:6n-3 content consistent with cold-water marine oils, but another reporting a much lower value. We noted that oolichan grease remains solid up to 15 °C, suggesting a low polyunsaturate content. After extracting total lipids from four fresh oolichan fish and four samples of grease, fatty acids were quantitated by high resolution gas chromatography (GC), as were additional samples of fish lipid and grease that were fractionated into triglyceride (TG), phospholipid (PL), and free fatty acids by thin-layer chromatography. In contradistinction to one prior report, we found EPA and DHA in fresh fish total lipids to be 0.9 and 2.2 wt%, respectively, while in the extracted grease, both were reduced to 0.5 wt%. Only the fresh fish PL fraction contained appreciable DHA. The bulk of the grease consisted of saturated fatty acids (30.3 wt%) and mono-unsaturates (55.0 wt%), explaining its high melting point. Excepting its very low omega-6 content (<2 wt%), oolichan grease is

quite similar in composition to human adipose TG. Its solid state at environmental temperatures and low peroxidizability index made it suitable for storage and transport, explaining its status as a preferred trade item among regional aboriginal groups.

Keywords Oolichan grease · Eulachon · Dietary fat · Low carbohydrate diet

Introduction

Dietary fat serves a host of functions, providing two classes of essential fatty acids, a vehicle for fat soluble vitamins, imparting flavor and texture, and functioning as an energy dense (and thus efficiently transportable) calorie source. Particularly among aboriginal hunting cultures, fat was highly valued, and the annual hunting/fishing cycle was often timed to yield selected animals at points of highest body fat content.

Much has been written about the “Paleolithic diet”, and it has been variously characterized as relatively high in protein with moderate fat [1] or low in protein and high in carbohydrate [2], but most researchers in the field of nutritional anthropology have avoided or ignored traditional diets providing less than 20% of energy as carbohydrate. It is also a common assumption that non-farming aboriginal cultures conformed to a primitive mixed dietary pattern until the adoption of agricultural foods. However even a cursory look at pre-Columbian North American dietary patterns reveals a great diversity food sources and nutrient mixes.

As one moves north in the area that is now the US and Canada, both the opportunity to farm and the availability of wild nuts, seeds, and fruit is decreased. At the geographic

S. D. Phinney
UC Davis (emeritus), Davis, CA, USA

J. A. Wortman
First Nations and Inuit Health Branch, Health Canada,
Vancouver, BC, Canada

D. Bibus
The Center for Spirituality and Health, The University
of Minnesota and Lipid Technologies, LLC, Austin,
MN 55912, USA

S. D. Phinney (✉)
6108 Boothbay Court, Elk Grove, CA 95758, USA
e-mail: sdphbt@comcast.net

apex of this climate-determined food pyramid, the Inuit culture evolved the tools and skills over 3,000 years necessary to live year round in the Arctic [3], where dietary carbohydrate was essentially unavailable. Based upon the observations of acculturated European explorers who lived among them, the Inuit diet consisted mostly of fat, was moderate in protein, and was virtually devoid of carbohydrate [4–6].

The experience of Stefansson [5] is particularly worthy of note, as he lived for a decade among the Inuit in the Arctic and ate their diet exclusively for periods of up to 2 years without re-supply. When challenged by the emerging nutrition establishment in the 1920s, Stefansson and another explorer consented to prove that a European could subsist on just meat and fat, doing so under observation for a year [6, 7]. Although they ate foods available in New York at the time, these explorers were effectively demonstrating a pattern of eating directly derived from the Inuit culture. And based upon proximate analysis of meals consumed, their diet consisted of 85% of energy from fat, 15% from protein, and inconsequential carbohydrate [7].

High fat, moderate protein, low carbohydrate eating patterns were not unique to Arctic cultures. Some Native American and First Nations cultures in the central continental region did not or chose not to farm, subsisting principally upon the buffalo, with a well-documented group being the Lakota/Dakota/Nakota Nation [8]. Further west, farming was not practiced on the Pacific coast north of what is now Mexico; and north of Puget Sound, the only dietary carbohydrate source was seasonal berries.

Of particular importance to the aboriginal cultures along the north Pacific coast was a small fish called the oolichan (ooligan, eulachan, candle fish—*Thaleichthys pacificus*). Along the coast from northern California to the Bering Strait, this smelt-like fish was harvested in great quantities when it spawned in the spring. It was eaten fresh, dried, and smoked; however the bulk of the harvest was fermented, mixed with water and boiled in wooden tubs, and the released fat (about 20% by weight in the fresh fish) was skimmed and saved for use throughout the year [9].

In addition to being used locally along the coast, this oolichan oil, commonly called “grease”, was a highly prized commodity of trade, being carried inland as far as 300 miles on established footpaths known as grease trails. This network of trails supported extensive trading amongst the aboriginal bands in the region; and while many other items such as copper, flint, furs, and dried meat were transported over them, they existed principally for the purpose of carrying oolichan grease inland.

In conversations with First Nations elders along the British Columbia coast, one is struck by the uniformly strong appreciation of oolichan grease as a cornerstone of their diet and culture. Now increasingly rare due to the

disappearance of the oolichan fishery, oolichan grease was a major part of the daily diet in this region up until the last generation. Discussions with elders in rural areas suggest that up to half of the daily dietary energy was supplied by oolichan grease prior to European contact.

Oolichan grease from the British Columbia coast has been previously studied for its fatty acid composition [9, 10]. The report by Kuhnlein et al. [10] indicates that it contained a relatively high DHA content (18–23%) typical of cold-water fish oils. In contrast, Iverson et al. [11] reported that fat extracted from fresh oolichan contained 1.5% EPA and 2.5% DHA. Given that oolichan grease is a semi-liquid at room temperature, the second report by Iverson is more consistent with its physical properties, as DHA has a very low melting point. To better understand its nutrient composition and the reason for the strong cultural preference for this unusual fat source, we obtained samples of oolichan fish and the extracted grease to evaluate their fatty acid compositions.

Methods

To determine the initial fatty acid composition of the oolichan fish and how the traditional extraction process (i.e., fermentation and boiling) might change the mix of fatty acids in the prepared grease, four individual fresh frozen fish from the 2006 Nass River harvest and four samples of grease (three from the 2005 harvest and one from 2006) were analyzed. All samples of fresh fish and grease were shipped frozen and stored at -80°C until analysis.

The total fatty acid composition of these eight samples (four fresh fish, four samples of grease) were determined by the methods described below. In addition, one sample each of the fish and grease was also subjected to thin-layer chromatographic separation into individual lipid fractions (triglycerides, phospholipids, and free fatty acids) and the composition of these individual fractions was also determined by high resolution gas chromatography.

Whole fish samples were weighed and homogenized in a laboratory blender in the presence of a determined amount of water. Lipids were then extracted from the homogenized fish (and also directly from the grease) according to the method of Bligh/Dyer whereby mixtures of plasma, methanol, chloroform and water were prepared such that lipids are recovered in the resulting nonpolar chloroform layer. Resulting lipid extracts were maintained under an atmosphere of nitrogen at all times following extraction and kept frozen prior to additional processing. Immediately prior to lipid class separation, lipid samples were dried under a gentle stream of nitrogen, rediluted in $50\ \mu\text{l}$ of chloroform and prepared for lipid class separation. Lipid

classes including total phospholipid (PL), free fatty acids (FFA) and triglyceride (TG) were separated on commercial available silica gel G plates (AnalTech, Newark, DE, USA). The chromatographic plates were developed in a solvent system consisting of distilled petroleum ether (b.p. 30–60°C):diethyl ether:acetic acid (80:20:1, by vol). Following development, the silica gel plates were sprayed with a methanolic solution containing 0.5% 2,7-dichlorofluorescein which was then used to visualize lipid classes under ultraviolet light. Desired corresponding lipid bands were then scraped into Teflon line screw cap tubes. The samples were then transesterified with 4% sulfuric acid in methanol in an 80 °C water bath for 90 min. Resulting fatty acid methyl esters were extracted with water and petroleum ether and stored frozen until gas chromatographic analysis was performed.

Lipid class fatty acid methyl ester compositions were determined by capillary gas chromatography. Methyl ester samples were blown to dryness under nitrogen and resuspended in hexane. Resulting fatty acid methyl esters were separated and quantified with a Shimadzu capillary gas chromatograph (GC17) utilizing a 30 m Restek free fatty acid phase (FFAP) coating. The instrument was temperature programmed from 190 to 240 °C at 7°C/min with a final hold of 10 min, separating and measuring fatty acid methyl esters ranging from 12:0 to 24:1.

Detected fatty acids were identified by comparison to authentic fatty acid standards (NuChek Prep, Elysian, MN, USA) and processed with EZChrom software (Scientific Products, CA, USA). Resulting data are expressed in percent composition by weight. Individual peaks, representing as little as 0.05% of the fatty acid methyl esters, were distinguished.

Results

Consistent with the observed high melting point, all four samples of the oolichan grease were found to have a significant component of saturated fatty acids and very low levels of the long-chain omega-3 fatty acids that are typically found in most cold-water fish oils. Specifically, both EPA and DHA were each present at approximately 0.5%, as opposed to the 10–20% contents of each in salmon, herring, and cod liver oils. The dominant fatty acid class in the oolichan grease was mono-unsaturated fat, which is typical of both olive oil and also human stored body fat [12]. Also of note was the very low level of omega-6 fatty acids, with linoleate (18:2n-6) at 0.8% and arachidonate (20:4n-6) at 0.2%.

The whole fish analysis yielded similar composition profiles to that of the grease samples, with the exception that there were two to fourfold greater proportions of EPA and DHA in the whole fish. This result is explained by the analysis of the individual lipid fractions from the fish, in which the phospholipid fraction had 10% EPA and 33% DHA. These results are shown in Table 1. The higher levels of long-chain omega-3 fatty acids in the PL fraction would be required for cell membranes to function in the frigid waters in which these fish live. However, these PL fatty acids are clearly not extracted into the oolichan grease during processing, thus making the final product less prone to peroxidation and rancidity than the whole fish from which it comes.

The oolichan grease samples were not specifically analyzed for cholesterol content but there was very little cholesteryl ester evident on the thin-layer chromatography plate, suggesting that the total cholesterol content is quite

Table 1 Fatty acid composition of oolichan fish and grease, including individual lipid fractions

Fatty acid	Oolichan fish	Fish TG	Fish PL	Fish FFA	Oolichan grease	Grease TG	Grease PL	Grease FFA
14:0	6.6 ± 0.3	4.3	0.4	1.0	7.5 ± 0.2	7.0	6.6	5.4
16:0	17.9 ± 1.6	22.2	18.3	31.8	18.8 ± 0.3	20.0	23.0	20.0
16:1n-7	5.6 ± 0.4	5.5	2.0	2.8	6.9 ± 0.5	6.1	5.9	6.7
18:0	4.7 ± 0.4	5.1	4.7	20.0	4.0 ± 0.2	4.6	7.9	3.8
18:1n-9	47.1 ± 4.8	48.7	15.0	23.5	43.4 ± 1.8	51.1	41.0	45.0
18:1n-7	3.5 ± 0.8	2.5	2.8	–	4.7 ± 0.5	–	–	–
18:2n-6	0.7 ± 0.2	0.6	0.8	0.8	0.8 ± 0.0	0.8	0.8	0.7
20:1n-7	1.3 ± 0.5	0.2	0.2	0.1	1.3 ± 0.1	2.2	–	0.2
20:4n-6	0.3 ± 0.0	0.1	2.6	0.9	0.2 ± 0.0	0.1	1.0	0.3
20:5n-3	0.9 ± 0.1	0.2	9.5	4.0	0.5 ± 0.1	0.4	0.5	0.6
22:6n-3	2.2 ± 0.7	0.8	33.6	6.5	0.5 ± 0.1	0.2	2.4	1.7
Other	9.2				11.4			

Data are means ± SD

TG triglyceride, PL phospholipid, FFA free fatty acid

low. There was, however, a large unidentified peak observed during the GC analysis, consistent with a high squalene content. Squalene is a lipid found in modest amounts in olive oil and has previously been reported to occur at high levels in the oolichan fish [13]. Squalene is found in human skin and is a valued ingredient in skin moisturizer preparations.

Discussion

The key observation of this report is the very low content of omega-3 HUFA (specifically EPA and DHA) in oolichan grease. This, along with its dominant proportions of mono-unsaturates and saturates, is consistent with its relatively high melting point. Together, these properties reduce its propensity for rancidity and improve its portability as a solid at environmental temperatures, thus explaining in part its popularity as a storable fat and desirable unit of trade.

Our results from the analysis of fresh oolichan fish are consistent with those of Iverson et al. [11], and both differ from the reported high DHA content by Kuhnlein et al. [10]. What is also apparent from our results is that the traditional process of aging and slow extraction of oolichan grease as practiced by coastal First Nations further reduced the HUFA content in the grease, thereby further raising its melting point and reducing its peroxidizability.

In addition to benefitting its portability and shelf life, this reduction in HUFA as a result of the traditional extraction procedure would not have significantly altered the nutritional benefits of the grease in the context of the local diet. For one thing, the local diet included a great deal of salmon plus the blubber and flesh of sea mammals such as seal, sea lion, and whale—all rich sources of omega-3 fatty acids. One also needs to keep in perspective the fact that the local diet was very low in carbohydrate. Because a low carbohydrate diet for humans is necessarily high in fat, the high omega-3 fatty acid content of most marine lipids (seen as a benefit when used as an occasional food or

dietary supplement) might become a liability when used as a dietary staple.

If oolichan grease were used to supply about half of an adult's daily energy intake (4–5 oz/day), the total EPA + DHA intake would be less than 2 g compared to 30 g or more if the same amount of energy was obtained from seal, whale or fish oil. While a sustained intake of EPA + DHA at 30 g per day may be tolerable for a number of months, it is probably not beneficial (as evidenced by Prof. Hugh Sinclair's [14] bleeding tendency after eating only seal meat and blubber for 100 days). Thus, given the dietary conditions of the region, oolichan grease has unique nutritional properties that would have made it the preferred fat source for the traditional diet.

It is interesting to note the similarity of the composition of oolichan grease to that of human adipose tissue (Table 2). Assuming that the composition of human adipose tissue reflects the preferred mix of fatty acids to be used when human metabolism is utilizing mostly fat for fuel (e.g., during a famine), then the composition of oolichan grease would appear to be well suited as a dietary mainstay during a low carbohydrate diet. The human fat data used in this table came from people eating an industrial diet in California [12], which explains their much higher (but not necessarily healthier) 18:2n-6 level and very low levels of EPA and DHA.

One question raised by our results is the disparity in the reported DHA contents from fresh oolichan and the extracted grease between our study and that of Kuhnlein et al. [10]. The prior study analyzed 19 samples from 5 geographic sites compared to our four samples from one site, and both studies also examined lipids extracted from fresh fish. However, in the current report we performed the additional step of thin-layer chromatographic separation of the fish and grease lipids to determine the individual compositions of the TP, PL, and TG. Of particular note on the GC runs of the crude lipid extracts of both the raw fish and the grease was a single broad peak that eluted late, shortly after the elution time for DHA. Given both its separation from the small DHA peak found in these lipid

Table 2 Comparison table of oolichan fish lipids, oolichan grease, and human adipose

Fatty acid	Oolichan fish ^a	Grease ^a	Fish (Iverson)	Grease (Kuhnlein)	Human fat (Tang)
14:0	6.6	7.5	8.6	4.6	2.4
16:0	17.8	18.8	16.7	12.1	19.1
16:1n-7	5.6	6.9	8.1	4.7	7.5
18:0	4.7	4.0	2.4	2.6	2.8
18:1n-9 + 7	50.7	48.1	36.3	32.0	45.3
18:2n-6	0.7	0.8	0.9	0.5	15.6
20:4n-6	0.3	0.2	0.2	0.5	0.4
20:5n-3	0.9	0.5	1.5	0.6	0.1
22:6n-3	2.2	0.5	2.5	18.0	0.1

Data are means

^a Data from this study, Iverson [11], Kuhnlein [10], Tang [12]

samples and its breadth, this peak was clearly not DHA. However, it would have been tempting for a chromatographer to identify it as such, particularly given the expectation of finding appreciable DHA in a cold-water marine oil sample.

There are a number of interesting conclusions that can be drawn as a result of our study. By selecting this small fish as a starting material and through its processing by fermentation and hot water extraction, First Nations cultures along the north Pacific coast developed a unique dietary lipid that is highly suited for human consumption, particularly in the context of the high fat diet that was traditional to that region. Furthermore, the low PUFA and HUFA contents afforded it both a high melting point and reduced peroxidizability, improving its ability to be stored and transported compared to other concentrated fat sources in the region. And yet, when eaten in quantity as a dietary staple (e.g., 2–4 oz per day) the 100–200 mg/day each of arachidonate and EPA/DHA would easily satisfy daily needs for these two essential fatty acid classes [15].

In conclusion, seen from the perspective of its fatty acid composition and related physical properties, oolichan grease can be appreciated as a refined fat that was uniquely suited for the needs of the regional population and their pre-contact low carbohydrate, high fat diet. Given these properties, the strong appreciation for oolichan grease throughout the region and the development of this unique fat product as a major item of pre-Columbian trade can be better appreciated.

Acknowledgments Numerous members of First Nations Bands in British Columbia contributed both samples and invaluable insight critical to the genesis of this report. We would like to especially thank Eva Dick and Barb Cranmer of the Namgis First Nation and Chester and Mary Moore, Bill Moore, CJ Martin, and Willard Martin of the Nisga'a First Nation. The authors also note the mentorship and

guidance of Prof. Ralph Holman. This project was supported in part by a grant from Health Canada.

References

1. Cordain L, Miller JB, Eaton SB et al (2000) Plant–animal subsistence ratios and macronutrient energy estimations in worldwide hunter-gatherer diets. *Am J Clin Nutr* 71:682–692
2. Blackburn GL (2008) The low fat imperative. *Obesity* 16:5–6
3. Diamond J (2005) *Collapse*. Viking Press, Penguin Group, NY, pp 257–276
4. Rae J (1953) Arctic correspondence 1844–1855. Hudson's Bay Record Society, London, p 189
5. Stefansson V (1956) *Fat of the land*. The McMillan, NY
6. McClellan WS, DuBois EF (1930) *Clinical Calorimetry XLV. Prolonged meat diets with a study of kidney function and ketosis*. *J Biol Chem* 87:651–668
7. McClellan WS, Rupp VR, Toscani V (1930) *Clinical Calorimetry XLVI. Prolonged meat diets with a study of the metabolism of nitrogen, calcium, and phosphorus*. *J Biol Chem* 87:669–680
8. Marshall JM (2006) *The day the world ended at little bighorn*. Viking Press, Penguin Group, NY
9. Moody MF (2008) *Eulachon past and present*. Masters Thesis, University of British Columbia. <http://circle.ubc.ca/handle/2429/676>
10. Kuhnlein HV, Yeboah F, Sedgemore M et al (1996) Nutritional qualities of ooligan grease: a traditional food fat of British Columbia first nations. *J Food Compos Anal* 9:18–31
11. Iverson SJ, Frost KJ, Lang SLC (2002) Fat content and fatty acid composition of forage fish and invertebrates in Prince William sound, Alaska: factors contributing to among and within species variability. *Mar Ecol Ser* 241:161–181
12. Tang AB, Nishimura KY, Phinney SD (1993) Preferential reduction in adipose tissue 18:3n-3 during very low calorie dieting despite supplementation with 18:3n-3. *Lipids* 28:987–993
13. Ackman RG, Addison RF, Eaton CA (1968) Unusual occurrence of squalene in a fish, the eulachon *Thaleichthys pacificus*. *Nature* 220:1033–1034
14. McLean A (2002) Fine wines and fish oil: the life of Hugh MacDonald Sinclair. *J R Soc Med* 95:263–264
15. <http://www.issfal.org.uk/Welcome/PolicyStatement3.asp>

Effect of Linseed Fed as Rolled Seeds, Extruded Seeds or Oil on Fatty Acid Rumen Metabolism and Intestinal Digestibility in Cows

Michel Doreau · Sophie Laverroux ·
Jérôme Normand · Guillaume Chesneau ·
Frédéric Glasser

Received: 4 July 2008 / Accepted: 23 September 2008 / Published online: 1 November 2008
© AOCS 2008

Abstract Linseed, a source of linolenic acid, is used in ruminant diets to increase polyunsaturated fatty acids (FA) in animal products. Seed processing is known to have an impact on FA rumen metabolism, but few data are available for linseed. We studied the effect of linseed lipid on ruminal metabolism and intestinal digestibility in cows. Three modes of linseed processing: rolled linseed (RL), extruded linseed (EL) and linseed oil plus linseed meal (LO), supplemented at 7.5% of DM intake, were compared to a control diet (C). Duodenal flows, intestinal digestibility and plasma composition were determined. The duodenal flow of linolenic acid was similar among diets. The sum of t10 and t11-18:1, which were coeluted, was increased with lipid-supplemented diets and represented more than 60% of *trans* 18:1 for EL and LO diets. The main 18:2 isomers were c9, c12 and t11, c15 among the non-conjugated isomers, and t11, t13 among CLA. Linseed supplementation increased the duodenal flow of unsaturated intermediates of biohydrogenation, and this effect was more pronounced for extruded seeds and oil than for rolled seeds. For most 18-carbon FA, intestinal digestibility was slightly higher for C and LO diets than for RL and EL. Plasma concentrations of non-conjugated 18:2 and linolenic acid were similar among the lipid-supplemented diets. Within diet, profiles of 18:1

isomers (except c9) remained very similar between duodenal and plasma FA.

Keywords Linseed · Extrusion · Fatty acids · Rumen metabolism · Digestion · Cow

Abbreviations

BH	Biohydrogenation
C	Control diet
CLA	Conjugated linoleic acid
DM	Dry matter
EL	Extruded linseed
FA	Fatty acid
LO	Linseed oil
RL	Rolled linseed

Introduction

Linolenic acid, along with other fatty acids (FA) of the n-3 series, is known to have positive effects on human health, particularly by decreasing the incidence of cardiovascular diseases [1]. It has been suggested that the nutritional value of milk and beef could be improved by increasing linolenic acid content in ruminant diets. The two main sources of linolenic acid are grass, both fresh and ensiled [2], and linseed. Linseed is easy to incorporate in production rations and, despite extensive biohydrogenation (BH) in the rumen; it has been demonstrated to increase linolenic acid content significantly in both milk [3, 4] and meat [5–8]. Furthermore, these authors showed that animal products following linseed intake are enriched in c9, t11-18:2, which is an isomer of conjugated linoleic acid (CLA) that may have a positive effect on human health by decreasing the

M. Doreau (✉) · S. Laverroux · F. Glasser
INRA, UR1213 Herbivores, Site de Theix,
63122 Saint-Genès-Champanelle, France
e-mail: doreau@clermont.inra.fr

J. Normand
Institut de l'Élevage, Service Viande, 5 rue Hermann Frenkel,
69364 Lyon Cedex 07, France

G. Chesneau
Valorex, 35210 Combournillé, France

incidence of cancer [9, 10]. Linseed incorporation also increases proportions of other FA such as t11-18:1 or c11, t15-18:2. These modifications in product composition arise from modifications in ruminal FA metabolism [11]. At the same time, it has been shown that moderate amounts of linseed added to rations do not impair organic matter or fiber digestion [12], whereas important amounts of linseed oil strongly reduced organic matter and fiber digestion [13].

Oilseeds can be either given as whole seeds or processed by different techniques, the most common being extrusion. In the case of linseeds, since digestion may not be optimized following the intake of whole seeds that have not been mechanically treated, it is recommended to supply them as rolled or ground seeds [7]. Theoretically, since the extrusion process breaks down plant cells, it is expected that cytosolic triglycerides are more accessible to rumen bacteria than when whole seed is given, meaning they are more rapidly available for lipolysis and BH. In two experiments recently carried out with extruded linseed, Akraim et al. [14] did not find any effect of linseed extrusion on duodenal FA composition, whereas Gonthier et al. [15] found that extrusion increased the disappearance of linolenic acid but also increased the proportion of intermediate compounds such as *trans* 18:1 FA in duodenal flow. These inconsistent data need to be verified, especially because Akraim et al. [14] did not measure duodenal flows while Gonthier et al. [15] did not determine *cis* and *trans* 18:1 composition in detail. Moreover, oil within the seed needs to be compared with free oil, firstly to evaluate the effects of oil accessibility according to its form of presentation, and secondly because published experiments have focused exclusively on either linseed oil or linseed but never the two in the same experiment and in the same amount. The aim of this study was thus (1) to investigate the consequences of a linseed supply on the changes in organic matter and fiber digestion (evaluated in a complementary paper [16]) and in the composition of absorbable FA; (2) to compare three modes of processing, i.e. rolled seeds, extruded seeds, and oil of this FA composition.

Materials and Methods

Experimental Design, Animals and Diets

All details on experimental design, animals, diets and samplings were described by Doreau et al. [16]. Briefly, four dry cows fitted with ruminal and duodenal cannulas were used in a 4 × 4 Latin square design with 5-week periods, with sampling during the last week of each period. They received four treatments: (1) control diet (C); (2) diet C supplemented with 7.5% rolled linseeds on dry matter

(DM) basis (RL); (3) diet C supplemented with 7.5% extruded linseeds on DM basis (EL); (4) diet C supplemented with 4.9% linseed oil and 2.6% linseed meal on DM basis (LO). Diets were given in limited amounts (i.e. 90% of individual voluntary intake determined in a pre-experimental period) to avoid refusals and differences in intake among diets. All diets comprised 60% corn silage, 10% hay, 14% dairy concentrate, 15% experimental concentrates, 0.5% urea and 0.5% of a concentrate mineral–vitamin premix (DM basis). Extruded linseeds were supplied as Croquelin[®] (Valorex, Combourtillé, France) which is an extruded mixture of 50% linseeds, 30% wheat bran and 20% sunflower meal (DM basis). Extrusion was performed with a one-screw extruder at 120°C after a low-temperature (72°C) preconditioning with steam for 157 min. In the RL diet, the linseeds of the same batch as that used to make Croquelin[®] were rolled with a roll crusher. Particle size, determined by dry sieving, was 22.6% > 2.0 mm, 62.0% between 0.8 and 2.0 mm; 9.4% between 0.4 and 0.8 mm, and 6.0% > 0.4 mm; the proportion of intact seeds was very low. Linseed oil was obtained by cold pressing and provided by Vandeputte (Mouscron, Belgium). Corn silage was offered in two equal portions at 9.30 a.m. and 4.30 p.m. Hay and concentrates, including oil, were offered at 9.00 a.m.

Fatty Acid Analyzes, Duodenal Flow and Intestinal Digestibility Calculations

Fatty acids in feedstuffs, duodenal digesta and feces were directly transmethylated, essentially as described by Sukhija and Palmquist [17] with modifications according to Loor et al. [11] in order to decrease isomerization of *cis*–*trans* conjugated double bonds due to too high temperature and too acidic pH. Total plasma lipids were extracted according to the method described in Folch et al. [18] using a chloroform/methanol mixture (2:1, by vol) (3 mL plasma + 20 mL mixture) and then rinsed with 6 mL distilled water and recovered in 1 mL hexane. Extracted FA were methylated with 2 mL of 0.5 N NaOCH₃ at 50°C for 45 min followed by 2 mL 5% HCl in methanol at 50°C for 45 min. After neutralization with 6% K₂CO₃ and additional hexane, a hexanoic phase containing FA methyl esters was recovered. Methyl tricosanoate was used as internal standard. Samples were injected by auto-sampler into a Varian CP-3800 gas chromatograph equipped with a flame ionization detector. Methyl esters from all samples were separated on a 100 m × 0.25 mm i.d. CP-Sil 88 fused-silica capillary column. Hydrogen was the carrier gas. Injector pressure was held constant at 23 psi. Pure methyl ester standards purchased from Supelco (Bellefont, USA), Sigma (St Louis, USA), Nu-Chek Prep (Elysian, USA), and Biovalley (Conches, France) were used to identify peaks, except for

certain *trans* and *cis* 18:1 isomers that were identified in order of elution and according to Kramer et al. [19], and t11, c15-18:2 that was identified according to Ulberth and Henninger [20].

Satisfactory separations of most *cis* and *trans* 18:1 and CLA isomers were obtained with a single chromatographic run. There was a partial coelution of different monounsaturated *cis* and *trans* 18-carbon isomers as well as c9, c11-18:2, and 21:0, as previously reported with the CP-Sil 88 100 m capillary column. In particular, due to the imperfect separation between t10 and t11-18:1 in some samples, the results give the sum of these two isomers.

Duodenal flows and intestinal digestibility of fatty acids were determined from duodenal flow of DM and fecal DM as described by Doreau et al. [16], and from FA determination in duodenal contents and feces. Rumen BH was computed as $(\text{intake} - \text{duodenal flow})/\text{intake} \times 100$.

Statistical Analyses

Statistical analyzes of fatty acid duodenal flows and digestibilities were performed as a 4×4 Latin square using the PROC MIXED procedure of the SAS statistical analysis software suite [21]. The statistical model included the effect of cow as random effect and the effects of period and treatment as fixed effects. Differences among means were determined using the Student–Newman–Keuls test. Differences at $P < 0.10$ were considered to be significant.

Results

Fatty acid intake was increased by 235 g/day on average between the C diet and the lipid-supplemented diets, with similar dry matter intakes (Table 1). This increase was mainly due to linolenic acid (+140 g/day) and, to a

lesser extent, linoleic acid (+30 g/day) and oleic acid (+40 g/day).

Duodenal Flow of Fatty Acids

Duodenal flows of total FA were similar among the three lipid-supplemented diets and higher than for the control diet (Table 2). The ratio of duodenal flow to intake of total FA was 1.18, 0.87, 0.96 and 0.98 for diets C, RL, EL and LO, respectively (SEM = 0.03), and was significantly lower for lipid-supplemented diets than for the C diet ($P < 0.01$). The difference among diets in duodenal flow of total FA was due to differences in 18-carbon FA. Duodenal flows of 18:0 and total *cis* 18:1 FA was lower for diet C than for the other 3 diets. Duodenal flows of total *trans* 18:1 and total CLA were highest with the EL and LO diets, lowest with the C diet, and intermediate with the RL diet (not significantly different from the other three diets). Duodenal flow of total non-conjugated 18:2 was higher with diets EL and LO than with diets C and RL. Duodenal flow of linolenic acid was numerically maximal with the EL diet and minimal with the C diet, but the differences were not significant due to high inter-animal variability. No significant differences were found for the other FA. Except for t5 and c9-18:1, there were between-diet differences for all the 18:1 isomers (Table 3). For t6 + t7 + t8, t9, t12, t13 + t14 + c6, c10 + t15, c12, c13, c14 + t16 and c15-18:1, the duodenal flows were similar among linseed-supplemented diets and significantly higher than with control diet. For the coelution t10 + t11 and c11-18:1, the duodenal flows were higher with EL and LO diets compared with C and RL diets. For t4-18:1, the duodenal flow was higher with EL and LO diets than with the RL diet, all three surpassing the C diet.

Among non-conjugated 18:2, the flow of linoleic acid did not differ among diets; the flow of t11, c15-18:2 was higher with the EL and LO diets than with the C and RL diets, the flow of c9, t12-18:2 was higher with the RL, EL and LO diets than with the C diet, and the flows of t9, t12 and t9, c12-18:2 were higher with the LO diet than with the C diet and intermediate with RL and EL diets (Table 3). Among CLA, t10, c12-18:2 flow did not differ among diets, the duodenal flow of the coelution of c9, t11 and t8, c10-18:2 was higher with the EL and LO diets than with the C and RL diets, the flow of the coelution of t11, c13 and c9, c11-18:2 was higher with the LO diet than with the C and RL diets, EL diet being intermediate, and the flow of t11, t13 and of other t, t-CLA was higher with the RL, EL and LO diets than with the C diet.

The BH of oleic and linoleic acids was higher with the RL diet than with the C diet, and intermediate with EL and LO diets (Table 4). The biohydrogenation of linolenic acid did not significantly differ among diets (Table 4).

Table 1 Dry matter and fatty acid intake (g/day, except dry matter in kg/day)

	Diet			
	C	RL	EL	LO
Dry matter (kg/day)	10.5	10.0	9.9	9.9
Total FA	269.4	514.8	501.2	497.7
16:0	41.6	54.0	54.0	51.7
18:0	6.6	16.6	16.0	14.9
c9 18:1	52.7	92.9	93.2	93.1
c9, c12 18:2	112.6	145.0	142.0	142.9
c9, c12, c15 18:3	40.8	188.5	179.0	175.5

C control diet, RL control diet supplemented with 7.5% rolled linseed, EL control diet supplemented with 7.5% extruded linseed, LO control diet supplemented with 4.9% of linseed oil and 2.6% linseed meal

Table 2 Duodenal flow of main fatty acids (g/day)

	Diet				SEM	Statistical level
	C	RL	EL	LO		
Total FA	317.4 a	447.6 b	472.9 b	486.6 b	14.58	$P < 0.01$
12:0	1.0	0.8	0.8	0.9	0.08	NS
14:0	2.6	2.3	2.4	2.6	0.17	NS
Iso 15:0	1.7	1.4	1.5	1.6	0.10	NS
Anteiso 15:0	3.8	3.4	3.5	3.9	0.14	NS
15:0	3.4	3.1	3.2	3.5	0.18	NS
Iso 16:0	3.1	2.6	2.5	2.9	0.22	NS
16:0	49.0	53.5	55.0	56.3	2.35	NS
17:0	2.0	1.9	1.8	2.0	0.11	NS
18:0	168.8 a	252.3 b	228.9 ab	227.9 ab	10.52	$P < 0.01$
Sum of <i>cis</i> 18:1	22.2 a	38.0 b	39.0 b	40.1 b	2.94	$P < 0.05$
Sum of <i>trans</i> 18:1	32.1 a	56.1 ab	82.4 b	93.3 b	6.16	$P < 0.01$
Sum of non-conjugated 18:2	15.2 a	17.5 a	31.6 b	33.3 b	2.69	$P < 0.01$
Sum of CLA	1.0 a	1.7 ab	2.7 b	3.0 b	0.21	$P < 0.01$
18:3n-3	2.1	5.9	7.8	4.7	1.69	NS
20:0	1.8	1.8	2.0	2.0	0.08	NS
22:0	1.2	1.2	1.4	1.4	0.056	NS
24:0	1.4	1.4	1.6	1.7	0.078	NS

C control diet, RL control diet supplemented with 7.5% rolled linseed, EL control diet supplemented with 7.5% extruded linseed, LO control diet supplemented with 4.9% linseed oil and 2.6% linseed meal

Means with different letters within a row are significantly different ($P < 0.05$)

Fatty Acid Digestibility

Intestinal digestibility of total FA was higher with the C and LO diets than with the RL diet, the EL diet being intermediate and not significantly different from the three other diets (Table 5). Digestibility of 12- to 17-carbon FA, and digestibility of linolenic acid did not differ among diets. Digestibility of *cis* and *trans* 18:1 isomers and of 18:2 isomers was highest with the LO diet and lowest with the RL diet. Considering 18:1 isomers, digestibility was the lowest with the RL diet for all 18:1 isomers, the difference being significant for most of them (Table 6). Digestibility was the highest with the LO diet for most isomers, especially those for which duodenal flow was high, i.e. t10, t11, c9 and the coelution of c10 and t15-18:1. Digestibility of t11, c15-18:2 did not differ among diets, whereas digestibility of linoleic acid was lower with the RL diet than with the other three diets. Digestibility of individual CLA isomers and minor non-conjugated 18:2 isomers was not calculated because the very low duodenal flows resulted in inaccurate measurements.

Plasma Fatty Acids

Among the saturated FA, only 14- to 16-carbon FA and 17:0 differed among diets in their plasma content, with a higher proportion for C diet compared to the others (Table 7). Among monounsaturated FA, the proportion of oleic acid ranged between 9.8 and 11.5% according to diet and did not differ significantly among diets (Table 8). The

percentage of t11-18:1, which was the main *trans* 18:1 isomer, was higher with the EL and LO diets than with the C and RL diets. There were no between-diet differences in t4, t5, t9, t10, c9, c10 + t15, c11 and c13-18:1 (Table 8). There were higher proportions of the coelution of t13, t14 and c6-18:1 with the RL and LO diets than with the C diet, the EL diet being intermediate. There was a higher proportion of c12-18:1 with the RL diet than with the C and EL diets, the LO diet being intermediate.

Conjugated linoleic acids were present in very small amounts. There was a lower proportion of c9, t11-isomer (coeluted with t8, c10) in total FA with the RL diet (0.19%) than with the LO diet (0.36%), the C (0.27%) and EL (0.34%) diets being intermediate ($P < 0.05$). Other isomers were found in some animals, but only in trace amounts.

Discussion

Duodenal Flow and Biohydrogenation

The rumen balance of total FA is consistent with the equation published in Schmidely et al. [22], with a positive balance (a net synthesis of both C12–C17 and C18 FA) in the C diet, and a slightly negative balance for the lipid-supplemented diets.

The main monounsaturated C18 isomers at duodenum for lipid-supplemented diets were found in peaks corresponding to the coelution of t10 and t11-18:1, the coelution of t13, t14 and c6-18:1, c9-18:1 and the coelution of c10

Table 3 Duodenal flow of unsaturated 18-carbon fatty acids (g/day)

	Diet				SEM	Statistical level
	C	RL	EL	LO		
18:1 isomers						
t4	0.37 a	0.57 b	0.69 c	0.72 c	0.021	$P < 0.01$
t5	0.27	0.42	0.38	0.39	0.095	NS
t6 + t7 + t8	1.48 a	2.62 b	3.25 b	3.72 b	0.208	$P < 0.01$
t9	1.13 a	1.80 b	2.07 b	2.18 b	0.174	$P < 0.05$
t10 + t11	18.22 a	23.98 a	51.58 b	59.29 b	4.720	$P < 0.01$
t12	2.87 a	5.70 b	6.66 b	7.12 b	0.405	$P < 0.01$
t13 + t14 + c6	5.80 a	17.83 b	14.77 b	17.32 b	1.344	$P < 0.01$
c9	10.74	11.44	15.47	14.70	1.643	NS
c10 + t15	5.22 a	11.79 b	10.85 b	11.46 b	0.670	$P < 0.01$
c11	2.61 a	2.79 a	3.61 b	3.70 b	0.231	$P < 0.05$
c12	2.14 a	4.42 b	3.76 b	3.73 b	0.335	$P < 0.05$
c13	0.25 a	0.59 b	0.58 b	0.64 b	0.048	$P < 0.01$
is-14 + t16	2.47 a	6.39 b	4.81 b	5.14 b	0.306	$P < 0.01$
c15	0.70 a	3.76 b	2.87 b	3.37 b	0.328	$P < 0.01$
Non-conjugated 18:2						
t9, t12	0.06 a	0.16 ab	0.20 ab	0.33 b	0.043	$P < 0.05$
c9, t12	0.46 a	0.89 b	0.78 b	0.77 b	0.033	$P < 0.01$
t9, c12	0.06 a	0.13 ab	0.11 ab	0.16 b	0.019	$P < 0.05$
t11, c15	1.49 a	4.72 a	12.50 b	14.01 b	1.374	$P < 0.01$
c9, c12	10.59	7.89	12.13	12.02	1.225	NS
Conjugated 18:2 (CLA)						
c9, t11 + t8, c10	0.22 a	0.16 a	0.57 b	0.64 b	0.084	$P < 0.05$
t10, c12 + 21:0	0.09	0.08	0.10	0.12	0.011	NS
t11, c13 + c9, c11	0.12 a	0.07 a	0.46 ab	0.59 b	0.070	$P < 0.01$
t11, t13	0.13 a	0.66 b	0.64 b	0.80 b	0.064	$P < 0.01$
Sum of other t, t-CLA	0.46 a	0.77 b	0.89 b	0.89 b	0.054	$P < 0.01$

C control diet, RL control diet supplemented with 7.5% rolled linseed, EL control diet supplemented with 7.5% extruded linseed, LO control diet supplemented with 4.9% linseed oil and 2.6% linseed meal
Means with different letters within a row are significantly different ($P < 0.05$)

Table 4 Ruminal biohydrogenation of unsaturated FA (%)

	Diet				SEM	Statistical effect
	C	RL	EL	LO		
c9-18:1	79.2 a	87.3 b	83.4 ab	84.1 ab	1.88	$P < 0.10$
c9, c12-18:2	90.7 a	94.5 b	91.5 ab	91.6 ab	0.90	$P < 0.10$
c9, c12, c15-18:3	94.9	97.0	95.8	97.3	0.91	NS

C control diet, RL control diet supplemented with 7.5% rolled linseed, EL control diet supplemented with 7.5% extruded linseed, LO control diet supplemented with 4.9% linseed oil and 2.6% linseed meal

Means with different letters within a row are significantly different ($P < 0.05$)

and t15-18:1. These data are similar to those found with linseed oil-supplemented diets [11, 23] and in vitro data [24], and these isomers most probably arise from partial BH of linolenic acid and dietary c9-18:1. The high amount of t11, c15 among non-conjugated 18:2 isomers and t11, t13 among CLA confirms the importance of carbon 13 and

carbon 15 desaturated C18 as BH intermediates of linolenic acid [24]. In all diets, the duodenal flows of total CLA represented less than 10% of the non-conjugated 18:2.

Among the different lipid-supplemented diets, RL exhibited the highest BH for oleic and linoleic acid, whereas linolenic acid BH did not seem to be affected by the supplement. The duodenal flows are consistent, since the RL diet induced a higher flow of 18:0 and lower flows of BH intermediates (*trans* 18:1 and 18:2) compared to EL and LO diets.

The most surprising result of this experiment was the numerically higher amount of linolenic acid at the duodenum with the EL diet than with the RL diet. Other data showed either a lower amount of linolenic acid with extruded linseed [15] or no variation [14]. A part of these differences among trials may be explained by differences in technological processes. In our trial, the small particle size of rolled linseeds probably results in a rapid release of oil. The extrusion process apparently shows limited

Table 5 Intestinal digestibility of main fatty acids (%)

	Diet				SEM	Statistical level
	C	RL	EL	LO		
Total FA	75.7 b	66.9 a	72.4 ab	76.3 b	2.05	$P < 0.10$
12:0	47.2	37.7	42.0	43.5	5.70	NS
14:0	45.0	38.6	47.3	43.6	5.22	NS
Iso 15:0	54.0	49.2	50.7	52.2	6.06	NS
Anteiso 15:0	63.1	56.6	59.2	60.3	4.13	NS
15:0	41.6	36.9	39.2	41.7	6.15	NS
Iso 16:0	37.0	35.4	31.2	32.8	6.67	NS
16:0	69.6	65.2	66.0	70.0	2.67	NS
17:0	31.3	17.1	17.8	18.3	8.11	NS
18:0	79.5 b	65.4 a	69.9 ab	73.8 ab	3.08	$P < 0.1$
Sum of <i>cis</i> 18:1	77.80 ab	74.5 a	76.9 ab	82.1 b	1.00	$P < 0.01$
Sum of <i>trans</i> 18:1	85.4 bc	78.6 a	81.6 ab	87.6 c	0.89	$P < 0.10$
Sum of non-conjugated 18:2	73.6 a	68.1 a	79.9 ab	85.7 b	2.74	$P < 0.05$
Sum of CLA	60.6 ab	48.2 a	60.9 ab	80.6 b	5.26	$P < 0.05$
18:3n-3	66.6	61.9	72.2	83.8	7.77	NS
20:0	69.7 b	59.7 a	66.2 b	69.1 b	2.12	$P < 0.10$
22:0	57.7 ab	52.8 a	58.6 ab	62.8 b	2.16	$P < 0.10$
24:0	58.9 ab	52.3 a	60.3 ab	63.7 b	2.17	$P < 0.05$

C control diet, RL control diet supplemented with 7.5% of rolled linseed, EL control diet supplemented with 7.5% extruded linseed, LO control diet supplemented with 4.9% linseed oil and 2.6% linseed meal
Means with different letters within a row are significantly different ($P < 0.05$)

Table 6 Intestinal digestibility of main 18:1 and 18:2 isomers (%)

	Diet				SEM	Statistical level
	C	RL	EL	LO		
18:1 isomers						
t4	80.2	77.6	82.3	83.6	2.02	NS
t5	90.8 b	85.0 a	89.5 b	91.6 b	1.20	$P < 0.05$
t6 + t7 + t8	89.3 b	83.6 a	85.5 a	89.1 b	0.85	$P < 0.01$
t9	89.1 b	84.2 a	84.1 a	88.2 b	1.08	$P < 0.05$
t10 + t11	84.2 bc	75.6 a	80.0 ab	87.9 c	1.76	$P < 0.01$
t12	86.4 ab	82.2 a	85.2 ab	88.4 b	0.81	$P < 0.01$
t13 + t14 + c6	88.5 b	82.5 a	84.6 ab	87.3 ab	1.14	$P < 0.05$
c9	70.8 ab	59.3 a	64.6 ab	74.4 b	3.03	$P < 0.05$
c10 + t15	83.3 b	75.7 a	79.7 ab	84.1b	0.92	$P < 0.01$
c11	75.7 ab	71.9 a	77.7 ab	80.6 b	1.00	$P < 0.01$
c12	88.3 a	90.1 ab	91.6 b	91.1 ab	0.45	$P < 0.01$
c13	96.3	91.9	95.2	94.4	1.73	NS
c14 + t16	86.2 b	73.8 a	77.8 ab	81.1 ab	2.28	$P < 0.05$
c15	86.5	85.4	87.6	89.1	1.16	NS
18:2 isomers						
t11, c15	74.0	65.3	78.4	92.1	6.65	NS
c9, cis12	73.4b	61.4a	78.1b	78.0b	3.53	$P < 0.05$

C control diet, RL control diet supplemented with 7.5% rolled linseed, EL control diet supplemented with 7.5% extruded linseed, LO control diet supplemented with 4.9% linseed oil and 2.6% linseed meal
Means with different letters within a row are significantly different ($P < 0.05$)

differences in temperature with processes used in other publications, but preconditioning before extrusion modifies biohydrogenation [14], due to changes in oil availability (Enjalbert, Chesneau, Troegeler-Meynadier, Nicot, unpublished data). Our finding is confirmed by a series of 6

feeding trials on bulls and steers receiving linseeds either rolled or extruded with the same process [5]: muscles contained more linolenic acid with EL than with RL. Similarly, Petit et al. [25] observed that extrusion of soybean and canola led to higher linoleic acid deposits in lamb

Table 7 Plasma content of main fatty acids (% total FA, except total FA in g/L)

	Diet				SEM	Statistical level
	C	RL	EL	LO		
Total FA (g/L)	1.114 a	1.640 b	1.614 b	1.599 b	0.127	$P < 0.10$
12:0	0.094	0.063	0.056	0.066	0.014	NS
Iso 14:0	0.086 b	0.038 a	0.036 a	0.070 ab	0.009	$P < 0.05$
14:0	0.570 b	0.364 a	0.373 a	0.373 a	0.011	$P < 0.01$
Iso 15:0	0.272 c	0.156 a	0.181 ab	0.206 b	0.011	$P < 0.05$
Anteiso 15:0	0.508 b	0.345 a	0.305 a	0.391 a	0.028	$P < 0.05$
15:0	0.639 b	0.454 a	0.441 a	0.478 a	0.022	$P < 0.01$
Iso 16:0	0.406 b	0.273 a	0.257 a	0.305 a	0.022	$P < 0.05$
16:0	13.962 b	11.951 a	11.585 a	11.648 a	0.182	$P < 0.01$
Iso 17:0	0.426	0.305	0.298	0.367	0.028	NS
17:0	0.972 b	0.718 a	0.732 a	0.762 a	0.029	$P < 0.01$
18:0	23.969	24.623	22.525	23.834	0.835	NS
Sum of <i>cis</i> 18:1	13.241	13.120	11.613	13.232	0.818	NS
Sum of <i>trans</i> 18:1	3.103 a	4.130 a	5.214 b	6.185 b	0.358	$P < 0.10$
Sum of non-conjugated 18:2	27.831	27.378	28.927	26.945	1.236	NS
Sum of CLA	0.300 ab	0.212 a	0.397 b	0.421 b	0.044	$P < 0.10$
18:3 n-3	0.364 b	0.212 ab	0.153 a	0.234 ab	0.047	$P < 0.10$
20:0	0.045	0.044	0.070	0.084	0.026	NS
22:0	0.026	0.022	0.000	0.054	0.020	NS
24:0	0.064	0.007	0.015	0.000	0.018	NS

C control diet, RL control diet supplemented with 7.5% rolled linseed, EL control diet supplemented with 7.5% extruded linseed, LO control diet supplemented with 4.9% linseed oil and 2.6% linseed meal

Means with different letters within a row are significantly different ($P < 0.05$)

Table 8 Plasma content of 18:1 isomers (% total FA)

	Diet				SEM	Statistical level
	C	RL	EL	LO		
t4	0.020	0.007	0.034	0.032	0.010	NS
t5	0.010	0.049	0.018	0.054	0.015	NS
t6 + t7 + t8	0.151 a	0.187 ab	0.206 ab	0.251 b	0.012	$P < 0.01$
t9	0.207	0.217	0.210	0.270	0.022	NS
t10	0.248	0.212	0.238	0.357	0.053	NS
t11	1.500 a	1.561 a	3.142 b	3.620 b	0.336	$P < 0.01$
t12	0.301 a	0.549 b	0.426 ab	0.460 ab	0.032	$P < 0.01$
t13 + t14 + c6	0.655 a	1.346 b	0.939 ab	1.140 b	0.018	$P < 0.05$
c9	11.487	10.737	9.798	11.184	0.764	NS
c10 + t15	0.122	0.155	0.187	0.173	0.036	NS
c11	0.672	0.502	0.500	0.501	0.047	NS
c12	0.538 a	1.006 b	0.637 a	0.762 ab	0.073	$P < 0.05$
c13	0.098	0.071	0.044	0.080	0.017	NS
c14 + t16	0.241 a	0.409 b	0.285 a	0.337 ab	0.027	$P < 0.05$
c15	0.084 a	0.249 b	0.161 ab	0.196 ab	0.027	$P < 0.05$

CL control diet, RL control diet supplemented with 7.5% rolled linseed, EL control diet supplemented with 7.5% extruded linseed, LO control diet supplemented with 4.9% linseed oil and 2.6% linseed meal

Means with different letters within a row are significantly different ($P < 0.05$)

muscle. These authors explained the protection of polyunsaturated FA in extruded oilseeds by the decrease in protein degradability following extrusion, which would protect lipid droplets against hydrogenation. However, in the present experiment, proteins were not protected by extrusion [16]. In the present experiment, measurements of the FA composition of rumen fluid [26] confirmed the fact

that lipids are rapidly released in rumen from extruded seeds, leading to a higher passage rate towards the duodenum. Under this hypothesis, a slower release of FA from rolled seeds may lead to a more complete BH, whereas a more rapid release of FA may result in a higher bypass if the rates of isomerization and hydrogenation is lower than the rate of lipolysis. This latter hypothesis is consistent

with in vitro and in vivo data [27, 28]. Isomerization and hydrogenation rates may be lowered by the toxic effect of the free polyunsaturated FA released in the rumen. The duodenal flows of most FA obtained with the EL and LO diets were very similar and not significantly different. The majority of comparisons between extruded and raw oilseeds have been made on dairy cows through comparison of milk FA profiles, giving highly inconsistent data, with some authors observing lower levels of unsaturated FA with extruded seeds compared to raw seeds (Chouinard et al. [29] on soybean) while other authors reported the opposite trend (McNamee et al. [30] on rapeseed, McGuffey and Schingoethe [31] on sunflower seed, Chouinard et al. [32] on soybeans). The effects of extrusion on 18:0 and 18:1 isomers are also very different among studies.

Intestinal Digestibility

Intestinal digestibility of total FA and differences between the main FA are consistent with the means of published data [22, 33, 34]. For 18:1 FA, *trans* isomers proved to be more digestible than *cis* isomers, which is consistent with recent data (e.g. Doreau et al. [35, 36], Loor et al. [11], review by Glasser et al. [34]). This is probably due to the stereochemical configuration of these FA. In the present experiment, oleic acid had a lower digestibility than other *cis* isomers. This has been observed only by Doreau et al. [35] with forage diets, but not by other authors with forage or mixed diets containing linseeds. A reason could be that duodenal oleic acid is still mainly dietary oleic acid and hence in the esterified form whereas the other *cis* isomers are mainly BH intermediates and hence in the unesterified form. This lower intestinal digestibility corresponds, both in Doreau et al. [35] and in the present experiment, to a high level of BH.

In the present experiment, digestibilities of oleic, linoleic and linolenic FA were always lower for the RL diet compared to the other diets. In contrast, Gonthier et al. [15] observed a lower digestibility of the control diet compared to linseed-supplemented diets, and no difference among linseed-supplemented diets. The digestibility of the control diet may differ according to the basal ration. The differences observed among the lipid-supplemented diets in the present study may be partly due to between-diet differences in the availability of intracellular oil. However, the low duodenal flow of linolenic acid ($\leq 5\%$ of intake) means that at least 95% of dietary lipids were hydrolyzed and hydrogenated, and virtually all the FA were released from their original matrix. The absence of variation of digestibility with diet for palmitic acid is explained by its origin: palmitic acid is derived mainly from dietary compounds other than linseeds, or from microbial synthesis. We observed

the same differences in digestibility between the 3 forms of linseeds (i.e. $RL \leq EL \leq LO$) for 18:1 and 18:2 isomers resulting from BH. These differences among diets can be explained by differences in FA metabolism in the large intestine and/or by differences in mechanisms of FA absorption in the small intestine. These hypotheses remain to be evaluated.

As numerical differences in digestibility were low compared to differences in duodenal flows between FA, the apparently absorbed amounts were highly correlated to duodenal flows. However, between-diet differences in duodenal flow and digestibility may be compensated for or increased when apparently absorbed amounts are considered. Absorbed amounts of linolenic acid were similar between RL, EL and LO diets (3.7, 5.6 and 4.9 g/day, respectively) whereas they were lower with RL than EL and LO for linoleic acid (4.8, 9.5 and 9.4 g/day) and oleic acid (6.8, 10.0 and 10.9 g/day), as well as for BH intermediates such as the coelution of t10 and t11-18:1 (19.1, 41.3 and 52.1 g/day) and t11, c15-18:2 (2.9, 9.8 and 13.0 g/day). These differences may result in differences in plasma and milk composition. In particular, the milk and meat contents of CLA derived from absorbed vaccenic acid may be higher when linseed is extruded or as oil than it is rolled.

Use of Plasma FA Composition as a Predictor of BH Pathways

Total plasma FA composition does not reflect FA absorption because it contains all lipoproteic fractions and is a criterion of global lipid metabolism, including lipid mobilization, organ uptake, hepatic lipid metabolism [37]. For example, plasma FA composition always shows high levels of linoleic acid whereas the absorbed amounts of this FA are very low. However, studies performed by Sinclair et al. [38] with sheep, Scislawski et al. [6] with steers and Loor et al. [23] with dairy cows have shown that diet supplementation with linseed oil results in an increased proportion of linolenic acid in plasma lipids. This was not observed in the present experiment, perhaps due to the very low increase in absorbed linolenic acid in lipid-supplemented diets compared to the control diet. We observed a global increase in total plasma FA content, mainly due to 18-carbon FA, whose proportions in total FA increased at the expense of 12- to 17-carbon FA. Non-conjugated 18:2 isomers (mainly linoleic acid) and linolenic acids were present in much higher proportions in plasma and were not linked to the absorbed amounts, reflecting an endogenous regulation of their plasma levels, independently of their dietary supply.

Similarly, there was a higher proportion of c9-18:1 in plasma FA than in duodenal flow, probably because of endogenous delta-9 desaturation of 18:0 in enterocytes and

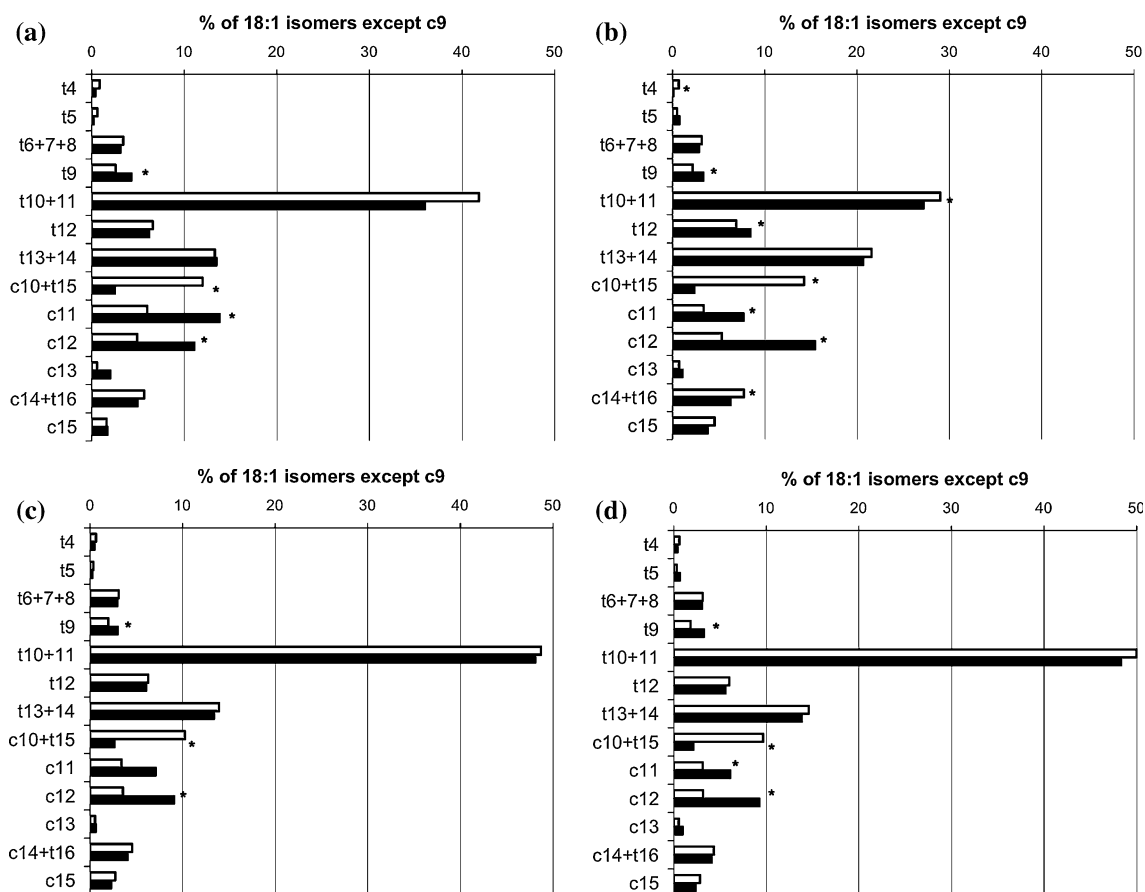


Fig. 1 Comparison of 18:1 isomers (expressed in % of total 18:1 isomers except c9-18:1) between duodenal fluid (white bars) and plasma (black bars) from cows fed a control diet (C, **a**), or a control diet supplemented with 7.5% rolled linseed (RL, **b**), 7.5% extruded

linseed (EL, **c**) or 4.9% of linseed oil and 2.6% linseed meal (LO, **d**). Asterisk a significant difference between duodenum and plasma (Paired *T* test, $P < 0.05$)

other tissues. When 18:1 isomer proportions were compared between duodenum fluid and plasma (not taking into account c9-18:1 for the above-cited reason), *trans* 18:1 profiles in plasma closely reflected the respective profiles at the duodenum, which was also observed for some but not all *cis* 18:1 isomers, as shown by Fig. 1. Unfortunately, we did not determine the t10:t11 ratio due to coelutions in duodenal samples. This profile similarity has recently been observed in experiments on dairy cows receiving either two different diets supplied with linseed oil [3, 11] or receiving three different oils [4, 23]. However, in the latter experiments, the t10:t11 ratio in duodenal contents was imperfectly predicted by plasma composition. Additional experiments are required in order to propose prediction equations. The similarity of *trans* 18:1 profiles between duodenal and plasma FA means that these isomers have similar metabolisms (no difference in organ uptake or oxidation according to the position of the double bond).

In conclusion, linseed supplementation increased the duodenal flow of unsaturated intermediates of biohydrogenation, and this effect was more pronounced for extruded

seeds and oil than for rolled seeds. Duodenal flow of linolenic acid was however similar among diets, due to its very high ruminal hydrogenation, which was not affected by linseed supplementation.

Acknowledgments This experiment was funded by the ACTA (Association pour la Coopération Technique Agricole, Paris, France). The authors thank the various INRA staff for their skills in animal care, feeding and sampling.

References

- Williams CM (2000) Dietary fatty acids and human health. *Ann Zootech* 49:165–180
- Boufaied H, Chouinard PY, Tremblay GF, Petit HV, Michaud R, Belanger G (2003) Fatty acids in forages. I. Factors affecting concentrations. *Can J Anim Sci* 83:501–511
- Loor JJ, Ferlay A, Ollier A, Doreau M, Chilliard Y (2005) Relationship among *trans* and conjugated fatty acids and bovine milk fat yield due to dietary concentrate and linseed oil. *J Dairy Sci* 88:726–740
- Loor JJ, Ferlay A, Ollier A, Ueda K, Doreau M, Chilliard Y (2005) High-concentrate diets and polyunsaturated oils alter *trans*

- and conjugated isomers in bovine rumen, blood, and milk. *J Dairy Sci* 88:3986–3999
5. Normand J, Bastien D, Bauchart D, Chaigneau F, Chesneau G, Doreau M, Farrié JP, Joulié A, Le Pichon D, Peyronnet C, Quinsac A, Renon J, Ribaud D, Turin F, Weill P (2005), Produire de la viande bovine enrichie en acides gras polyinsaturés oméga 3 à partir de graines de lin: quelles modalités d'apport du lin, quelles conséquences sur la viande ? In: Renc Rech Rum INRA-Inst. Elevage, Paris, pp 359–366
 6. Scislowski V, Bauchart D, Gruffat D, Laplaud PM, Durand D (2005) Effects of dietary n-6 or n-3 polyunsaturated fatty acids protected or not against ruminal hydrogenation on plasma lipids and their susceptibility to peroxidation in fattening steers. *J Anim Sci* 83:2162–2174
 7. Maddock TD, Bauer ML, Koch KB, Anderson VL, Maddock RJ, Barcelo-Coblijn G, Murphy EJ, Lardy GP (2006) Effect of processing flax in beef feedlot diets on performance, carcass characteristics, and trained sensory panel ratings. *J Anim Sci* 84:1544–1551
 8. Kronberg S, Barceló-Coblijn G, Shin J, Lee K, Murphy E (2006) Bovine muscle n-3 fatty acid content is increased with flaxseed feeding. *Lipids* 41:1059–1068
 9. Bauman DE, Lock AL, Corl BA, Ip C, Salter AM, Parodi PM (2005) Milk fatty acids and human health: potential role of conjugated linoleic acid and *trans* fatty acids. In: Sejrnsen K, Hvelplund T, Nielsen MO (eds) Ruminant physiology: digestion, metabolism and impact of nutrition on gene expression, immunology and stress. Wageningen Academic Publishers, Wageningen, pp 529–561
 10. Shingfield KJ, Chilliard Y, Toivonen V, Kairenius P, Givens DI (2008) Bioactive components of milk *trans* fatty acids and bioactive lipids in ruminant milk. In: Bösze Z (ed) Bioactive components of milk. Springer, New York, pp 3–65
 11. Loor JJ, Ueda K, Ferlay A, Chilliard Y, Doreau M (2004) Biohydrogenation, duodenal flow, and intestinal digestibility of *trans* fatty acids and conjugated linoleic acids in response to dietary forage: concentrate ratio and linseed oil in dairy cows. *J Dairy Sci* 87:2472–2485
 12. Ueda K, Ferlay A, Chabrot J, Loor JJ, Chilliard Y, Doreau M (2003) Effect of linseed oil supplementation on ruminal digestion in dairy cows fed diets with different forage: concentrate ratios. *J Dairy Sci* 86:3999–4007
 13. Ikwuegbu OA, Sutton JD (1982) The effect of varying the amount of linseed oil supplementation on rumen metabolism in sheep. *Br J Nutr* 48:365–375
 14. Akraim F, Nicot MC, Weill P, Enjalbert F (2006) Effects of preconditioning and extrusion of linseed on the ruminal biohydrogenation of fatty acids. 1. In vivo studies. *Anim Res* 55:83–91
 15. Gonthier C, Mustafa AF, Berthiaume R, Petit HV, Ouellet DR (2004) Feeding micronized and extruded flaxseed to dairy cows: effects on digestion and ruminal biohydrogenation of long-chain fatty acids. *Can J Anim Sci* 84:705–711
 16. Doreau M, Aurousseau E, Martin C (2008) Effects of linseed lipids fed as rolled seeds, extruded seeds or oil on organic matter and nitrogen digestion in cows. *Anim Feed Sci Technol* (in press)
 17. Sukhija PS, Palmquist DL (1988) Rapid method for determination of total fatty acid content and composition of feedstuffs and feces. *J Agric Food Chem* 36:1202–1206
 18. Folch J, Lees M, Sloane-Stanley GH (1957) A simple method for the isolation and purification of total lipids from animal tissues. *J Biol Chem* 226:497–509
 19. Kramer JKG, Blackadar CB, Zhou J (2002) Evaluation of two GC columns (60-m Supelcowax 10 and 100-m CP Sil 88) for analysis of milkfat with emphasis on CLA, 18:1, 18:2 and 18:3 isomers, and short- and long-chain FA. *Lipids* 37:823–835
 20. Ulberth F, Henninger M (1994) Quantification of *trans* fatty acids in milk fat using spectroscopic and chromatographic methods. *J Dairy Res* 61:517–527
 21. SAS Institute (2000) SAS user's guide: statistics. Version 8.1, Cary
 22. Schmidely P, Glasser F, Doreau M, Sauvant D (2008) Digestion of fatty acids in ruminants: a meta-analysis of flows and variation factors. 1. Total fatty acids. *Animal* 2:677–690
 23. Loor JJ, Ueda K, Ferlay A, Chilliard Y, Doreau M (2005) Intestinal flow and digestibility of *trans* fatty acids and conjugated linoleic acids (CLA) in dairy cows fed a high-concentrate diet supplemented with fish oil, linseed oil, or sunflower oil. *Anim Feed Sci Technol* 119:203–225
 24. Jouany JP, Lassalas B, Doreau M, Glasser F (2007) Dynamic features of the rumen metabolism of linoleic acid, linolenic acid, and linseed oil measured in vitro. *Lipids* 42:351–360
 25. Petit HV, Rioux R, D'Oliveira PS, Prado INd (1997) Performance of growing lambs fed grass silage with raw or extruded soybean or canola seeds. *Can J Anim Sci* 77:455–463
 26. Glasser F, Laverroux S, Doreau M (2006) Rumen biohydrogenation kinetics of linseed fed as crude seeds, extruded seeds or oil. In: Fourth Europe Federation lipid congress, oils, fats and lipids for a healthier future, Madrid, pp 640
 27. Beam TM, Jenkins TC, Moate PJ, Kohn RA, Palmquist DL (2000) Effects of amount and source of fat on the rates of lipolysis and biohydrogenation of fatty acids in ruminal contents. *J Dairy Sci* 83:2564–2573
 28. Hawke JC, Silcock WR (1970) The in vitro rates of lipolysis and biohydrogenation in rumen contents. *Biochim Biophys Acta* 218:201–212
 29. Chouinard PY, Levesque J, Girard V, Brisson GJ (1997) Dietary soybeans extruded at different temperatures: milk composition and in situ fatty acid reactions. *J Dairy Sci* 80:2913–2924
 30. McNamee BF, Fearon AM, Pearce J (2002) Effect of feeding oilseed supplements to dairy cows on ruminal and milk fatty acid composition. *J Sci Food Agric* 82:677–684
 31. McGuffey RK, Schingoethe DJ (1982) Whole sunflower seeds for high producing dairy cows. *J Dairy Sci* 65:1479–1483
 32. Chouinard PY, Girard V, Brisson GJ (1997) Performance and profiles of milk fatty acids of cows fed full fat, heat-treated soybeans using various processing methods. *J Dairy Sci* 80:334–342
 33. Doreau M, Ferlay A (1994) Digestion and utilisation of fatty acids by ruminants. *Anim Feed Sci Technol* 45:379–396
 34. Glasser F, Schmidely P, Sauvant D, Doreau M (2008) Digestion of fatty acids in ruminants: a meta-analysis of flows and variation factors. 2. C18 fatty acids. *Animal* 2:691–704
 35. Doreau M, Ueda K, Poncet C (2003) Fatty acid ruminal metabolism and intestinal digestibility in sheep fed ryegrass silage and hay. *Tropical subtropical agroecosyst* 3:289–293
 36. Doreau M, Rearte D, Portelli J, Peyraud JL (2007) Fatty acid ruminal metabolism and digestibility in cows fed perennial ryegrass. *Eur J Lipid Sci Technol* 109:790–798
 37. Bauchart D (1993) Lipid absorption and transport in ruminants. *J Dairy Sci* 76:3864–3881
 38. Sinclair LA, Cooper SL, Chikunya S, Wilkinson RG, Hallett KG, Enser M, Wood JD (2005) Biohydrogenation of n-3 polyunsaturated fatty acids in the rumen and their effects on microbial metabolism and plasma fatty acid concentrations in sheep. *Anim Sci* 81:239–248

Two Novel Ceramides with a Phytosphingolipid and a Tertiary Amide Structure from *Zephyranthes candida*

Zhi-ping Wu · Yu Chen · Bing Xia · Ming Wang ·
Yun-Fa Dong · Xu Feng

Received: 10 August 2008 / Accepted: 17 September 2008 / Published online: 22 October 2008
© AOCS 2008

Abstract Two novel ceramides, Candidamide A (**1**) with a phytosphingolipid structure, and Candidamide B (**2**) with a tertiary amide structure, together with 12 known compounds (**3–14**) have been isolated from the bulbs of *Zephyranthes candida*. The structures of **1** and **2** have been elucidated to be 1,3,5,6-tetrahydroxy-2-(2'-hydroxytetra-cosanoyl amino)-8-(*E*)-octadecadiene (**1**) and (2*S*,3*S*,4*R*,8*E*,2'*R*)-2-[*N*-(2'-hydroxyoctadecanoyl)-*N*-(1'',2''-dihydroxy-ethyl)-amino]-8-hexacosene-1,3,4-triol (**2**) on the basis of spectroscopic evidence including IR, MS, NMR (¹H-NMR, ¹³C-NMR, DEPT, ¹H-¹H COSY, HSQC, HMBC). The known compounds were identified as (2*S*)-3',7-dihydroxy-4'-methoxyflavan (**3**), (2*S*)-4'-hydroxy-7-methoxyflavan (**4**), (2*S*)-4',7-dihydroxyflavan (**5**), 7-hydroxy-3', 4'-methylene-dioxyflavan (**6**), ambrettolide (**7**), β -sitosterol (**8**), β -dau-costerin (**9**), rutin (**10**), pancratistatin (**11**), lycorine (**12**), haemanthidine (**13**), and haemanthamine (**14**). In the anti-microbial assay, candidamide A (**1**) and candidamide B (**2**) displayed moderate activities against bacteria *Staphylo-coccus aureus* and *Escherichia coli*, and fungi *Aspergillus niger*, *Candida albicans* and *Trichophyton rubrum*.

Keywords *Zephyranthes candida* · Amaryllidaceae · Ceramides · Phytosphingolipid · Tertiary amide · Candidamide A · Candidamide B · Antimicrobial

Abbreviations

CC	Column chromatography
COSY	Correlation spectroscopy
DEPT	Distortionless enhancement by polarization transfer
HMBC	Heteronuclear multiple bond correlation
HSQC	Heteronuclear single quantum correlation
HR	High resolution
LCB	Long chain base
FA	Fatty acid
MICs	Minimum inhibitory concentrations

Introduction

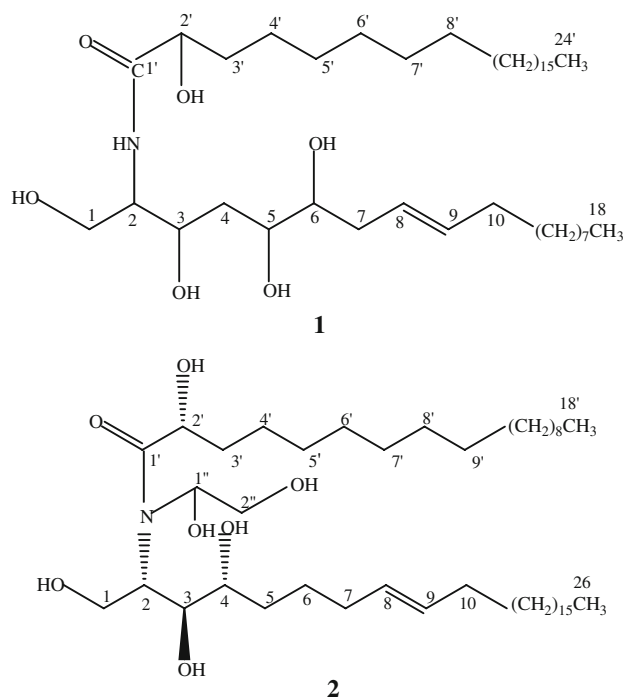
There are about 60 species in the genus *Zephyranthes*, family Amaryllidaceae [1], mainly distributed in the warm-temperate regions of Western Hemisphere. Only two species, *Zephyranthes candida* and *Z. carinata* grow in China, and *Z. candida* is used as ornamental and medicinal plant in China. Plants of this genus are well known in many countries for their pharmacological activities and are widely used in folk medicine. *Z. candida* has been employed in Africa as a treatment for diabetes mellitus and *Z. parulla* appears in a history of Peru for treating tumors, *Z. rosea* and *Z. flava* are used for variety of therapeutic purposes in India [2–5]. Previous chemical investigation of this genus mainly led to the isolation of many alkaloids with cytotoxic activity and some flavans [6–10].

Z.-p. Wu · Y. Chen · B. Xia · M. Wang · Y.-F. Dong ·
X. Feng (✉)
Jiangsu Institute of Botany, Chinese Academy of Sciences,
Nanjing Botanical Garden, Mem. Sun Yat-Sen, 210014 Nanjing,
People's Republic of China
e-mail: fengxu@mail.cnbg.net

Z.-p. Wu
College of Life Science, Nanjing Agricultural University,
210095 Nanjing, People's Republic of China
e-mail: wzhp05@126.com

Except for the isolation of a flavonoid glycoside, kaempferol-3-*O*-rhamnoglucoside [11], five alkaloids, lycorine, zephyranthine, tazettine, nerinine and haemanthidine [12], and a cytostatic alkaloid, *trans*-dihydronarci lasine [13], a more detailed chemical study of *Z. candida* has not been reported previously. In our work for a search of potent bioactive alkaloids from the plants of family Amaryllidaceae, we investigated the chemical constituents from the bulbs of *Z. candida*. Two novel ceramides (namely, candidamide A (**1**) and candidamide B (**2**), Scheme 1) with a phytosphingolipid and a tertiary amide structure, respectively, were characterized. This paper describes the isolation, structural determination and antimicrobial activity of candidamide A (**1**) and candidamide B (**2**), together with 12 known compounds, (2*S*)-3',7-dihydroxy-4'-methoxyflavan (**3**), (2*S*)-4'-hydroxy-7-methoxyflavan (**4**), (2*S*)-4',7-dihydroxyflavan (**5**), 7-hydroxy-3', 4'-methylenedioxyflavan (**6**), ambrettolide (**7**), β -sitosterol (**8**), β -daucosterin (**9**), rutin (**10**), pancratistatin (**11**), lycorine (**12**), haemanthidine (**13**), and haemanthamine (**14**) from the bulbs of *Z. candida*.

Ceramides are a unique class of secondary metabolites, and various ceramides have been isolated from a number of marine organisms, fungi, and some plants, some of which exhibit cytotoxic [14, 15], antifungal [15, 16], antimicrobial [17, 18], antileishmanial and immunomodulatory [19], and cytostatic activities [20]. Due to their scarcity in natural sources and their promising biological and pharmacological activities, they have aroused increasing research interest.



Scheme 1 Chemical structures of **1** and **2**

Experimental Procedures

Chromatographic and Instrumental Methods

Melting points were measured using a SGW X-4 micro-melting point apparatus and uncorrected. Optical rotations were measured with a JASCO P-1020 optical rotation apparatus. IR spectra were recorded on an IMPACT 400 spectrometer in KBr discs. NMR spectra were obtained on a Bruker spectrometers operating at 500 MHz (500 MHz for ¹H NMR and 125 MHz for ¹³C NMR) using TMS as internal standard and chemical shifts were recorded as δ values. Mass spectra (EI-MS and ESI-MS) were measured on Agilent 1100 LC/MSD SL mass spectrometer. HR-ESI-MS spectra were obtained on Agilent 1100 LC/MSD TOF mass spectrometer.

Materials

Silica gel for column chromatography (CC) (100–200 and 200–300 mesh) and TLC plates (10–40 μ m) were the products of Qingdao Marine Chemical Co., Ltd (Qingdao, People's Republic of China). Sephadex LH-20 was purchased from the Pharmacia Corporation. RP-18 reverse-phase silica gel was purchased from the Merck Corporation. D101 was purchased from Tianjin Chemical Factory (Tianjin, People's Republic of China).

The bulbs of *Z. candida* were collected from Nanjing Agricultural University, Jiangsu Province, People's Republic of China, in August, 2006. A voucher specimen (no. 61018/JSH) documenting the collection was authenticated at the Herbarium by Prof. Yun-Fa Dong, Phytochemist, Institute of Botany (Nanjing Botanical Garden Mem. Sun Yat-Sen), Jiangsu Province and Chinese Academy of Sciences, where it was deposited.

Extraction and Isolation

The air-dried and powdered bulbs (cut the ground parts) of *Z. candida* (2.1 kg) were extracted with 95% EtOH (10 L \times 3) at room temperature for 3 days. The aqueous EtOH phase was evaporated under reduced pressure and the residue was dried in vacuo. The resulting residue was dissolved in H₂O, basified to pH 8–9 with 10% aqueous NH₃ solvent, and extracted with CHCl₃ (3 \times) and then CHCl₃/MeOH (3:2, vol/vol). The extracts were combined and evaporated. The crude residue (126.0 g) was purified by silica gel column chromatography eluting with petroleum ether/EtOAc from 95:5 to 5:95 (vol/vol, 800 ml each) gradients, finally, EtOAc/MeOH (50:50, vol/vol, 800 ml). All fractions were collected and combined on the basis of analytical TLC, and five main crude fractions (Fr. 1–5) were yielded. Fr. 1 (23.0 g) was subjected to CC by elution with CHCl₃/MeOH (20:1; 18:1;

Table 1 ^{13}C and ^1H -NMR Data of compound **1** (125 and 500 MHz, respectively, pyridine- d_5)

Atom no.	^{13}C (DEPT)	^1H (J in Hz)	Atom no.	^{13}C (DEPT)	^1H (J in Hz)
1a,1b	62.1 (CH ₂)	4.50 (<i>dd</i> , 11.0, 4.5)	16	30.3 (CH ₂)	1.25 (<i>m</i>)
		4.40 (<i>dd</i> , 10.5, 5.0)	17	26.6 (CH ₂)	1.25 (<i>m</i>)
2	53.0 (CH)	5.08 (<i>m</i>)	18	14.3 (CH ₃)	0.85 (<i>t</i> , 6.7)
3	76.8 (CH)	4.33 (<i>m</i>)	NH	–	8.54 (<i>d</i> , 8.9)
4	34.2 (CH ₂)	2.21 (<i>m</i>)	1'	175.3 (C)	–
5	72.9 (CH)	4.25 (<i>m</i>)	2'	72.5 (CH)	4.60 (<i>m</i>)
6	73.0 (CH)	4.27 (<i>m</i>)	3'	35.7 (CH ₂)	2.04 (<i>m</i>)
7	33.3 (CH ₂)	1.93 (<i>m</i>)	4'	25.8 (CH ₂)	1.77 (<i>m</i>)
8	130.7 (CH)	5.47 (<i>dt</i> , 13.7, 4.7)	5'–21'	29.5–30.2 (CH ₂)	1.25–1.45 (<i>br s</i>)
9	130.8 (CH)	5.52 (<i>dt</i> , 13.7, 4.7)	22'	26.7 (CH ₂)	1.25 (<i>m</i>)
10	33.0 (CH ₂)	1.93 (<i>m</i>)	23'	22.9 (CH ₂)	1.25 (<i>m</i>)
11	32.1 (CH ₂)	1.25 (<i>m</i>)	24'	14.3 (CH ₃)	0.85 (<i>t</i> , 6.7)
12–15	29.5–30.2 (CH ₂)	1.25–1.45 (<i>br s</i>)			

15:1; 12:1; 9:1, vol/vol, 200 ml each) to yield compounds **3** (11 mg), **4** (8 mg), **5** (20 mg), and **6** (14 mg). Fr. 2 (21.5 g) was applied to CC by elution with $\text{CHCl}_3/\text{MeOH}$ (12:1; 10:1, vol/vol, 200 ml each) to afford compound **7** (21 mg), compound **8** (207 mg) and compound **13** (8 mg). The antimicrobial fraction (Fr. 3, 9.5 g) was separated by CC with $\text{CHCl}_3/\text{MeOH}$ (10:1; 8:1, vol/vol, 250 ml each) to give two subfractions (Fr. 3-1, 87 mg and Fr. 3-2, 38 mg) and further purified by Sephadex LH-20 eluted with $\text{CHCl}_3/\text{MeOH}$ (1:1, vol/vol, 200 ml each) to yield compounds **1** (33 mg) and **2** (28 mg), respectively. Compound **9** (52 mg) was crystallized from the petroleum ether/EtOAc (1:1, vol/vol) solution of fraction (Fr. 4, 18.0 g). Fr. 5 (25.0 g) was subjected to D101 column eluted with 25% EtOH, 40% EtOH, 55% EtOH, 70% EtOH, and 85% EtOH to give several subfractions. The 25% EtOH and 40% EtOH subfractions (210 mg) were purified by Sephadex LH-20 eluted with 60% MeOH to yield compound **10** (57 mg), and the 55% EtOH subfraction (760 mg) was successively purified by CC with $\text{CHCl}_3/\text{MeOH}$ (8:1, vol/vol, 600 ml) and RP-18 (MeOH) to afford compounds **11** (9 mg), **12** (79 mg) and **14** (22 mg).

1, 3, 5, 6-tetrahydroxy-2-(2'-hydroxytetradecanoyl amino)-8-(E)-octadecadiene (1)

White amorphous powder; m.p. 146–147 °C; $[\alpha]_{\text{D}}^{25} + 16.67$ ($c = 0.06$, pyridine). IR (KBr) ν_{max} 3,345, 3,200, 2,910, 2,830, 1,615, 1,540, 1,465, 1,270, 1,060, 1,018, 720 cm^{-1} ; ^1H - and ^{13}C -NMR data see Table 1; EIMS (70 eV) m/z (rel. int.) 697 (32), 682 (100), 570 (3), 654 (65), 482 (2), 450 (5), 426 (2), 408 (8), 360 (18), 359 (80), 337 (25), 323 (2), 277 (2), 247 (45), 241 (6), 163 (2), 128 (2); HRESIMS: m/z 720.4150 ($[\text{M} + \text{Na}]^+$; $\text{C}_{42}\text{H}_{83}\text{NO}_6 \text{Na}^+$; calc. 720.4168).

2S,3S,4R,8E,2'R)-2-[N-(2'-hydroxyoctadecanoyl)-N-(1'',2'')-dihydroxyethyl]-amino]-8-hexacosene-1, 3,4-triol (2)

White amorphous powder; m.p. 148–150 °C; $[\alpha]_{\text{D}}^{25} + 45.82$ ($c = 0.055$, pyridine). IR (KBr) ν_{max} 3,335, 2,920, 2,850, 1,640, 1,610, 1,540, 1,470, 1,070, 980, 718 cm^{-1} ; ^1H and ^{13}C -NMR data see Table 2; EIMS (70 eV) m/z (rel. int.) 734 (100), 733 (46), 697 (22), 679 (8), 514 (16), 486 (4), 468 (12), 450 (2), 432 (3), 358 (17), 239 (14), 186 (9), 171 (2), 145 (2); HRESIMS: m/z 792.3570 ($[\text{M} + \text{Na}]^+$; $\text{C}_{46}\text{H}_{91}\text{NO}_7\text{Na}^+$; calc. 792.3575).

Antimicrobial Assay

Evaluation of antimicrobial activities of fractions and pure compounds **1** and **2** was performed by using a reference agar dilution method [17].

Antibacterial activities were evaluated against a Gram positive bacterium *Staphylococcus aureus* and a Gram-negative bacterium *Escherichia coli*. Antifungal activities were evaluated against fungi *Aspergillus niger*, *Candida albicans* and *Trichophyton rubrum*. Reference drugs penicillin G and ketoconazole were used as positive controls to the growth of bacteria and fungi, respectively. The samples were dissolved in DMSO at a concentration of 0.1 mg/ml. Suitably quantified volumes of these test solutions were mixed with agar medium (20 ml) to prepare plates with a given concentration (≤ 0.1 mg/ml) of the tested material. Test bacteria were subsequently incubated in these 'drug-containing' plates. The lowest concentration in which no growth of test microbes could be discerned was accordingly defined as the minimal inhibitory concentration (MIC).

Table 2 ^{13}C - and ^1H -NMR Data of compound **2** (125 and 500 MHz, resp., pyridine- d_5)

Atom no.	^{13}C (DEPT)	^1H (J in Hz)	Atom no.	^{13}C (DEPT)	^1H (J in Hz)
1a, 1b	61.9 (CH_2)	4.41 (dd , 10.8, 4.7)	25	23.0 (CH_2)	1.25 (m)
		4.46 (dd , 10.8, 5.7)	26	14.3 (CH_3)	0.86 (t , 6.8)
2	53.1 (CH)	5.12 (m)	1'	174.0 (C)	–
3	76.8 (CH)	4.33 (dd , 6.2, 4.7)	2'	76.3 (CH)	4.73 (dd , 7.8, 4.1)
4	73.3 (CH)	4.52 (m)	3'a, 3'b	34.3 (CH_2)	2.28 (m)
5a, 5b	33.0 (CH_2)	2.05 (m)			1.87 (m)
		1.97 (m)	4'	26.7 (CH_2)	1.93 (m)
6	26.6 (CH_2)	1.63 (m)	5'–15'	29.5–30.4 (CH_2)	1.25–1.38 ($br\ s$)
7	33.9 (CH_2)	2.15 (m)	16'	32.1 (CH_2)	1.23 (m)
8	130.8 (CH)	5.52 (dt , 14.8, 5.2)	17'	23.0 (CH_2)	1.25 (m)
9	130.7 (CH)	5.50 (dt , 14.8, 5.2)	18'	14.3 (CH_3)	0.86 (t , 6.8)
10	33.3 (CH_2)	2.20 (m)	1''	73.0 (CH)	4.27 (m)
11	30.4 (CH_2)	1.25 (m)	2''a, 2''b	72.8 (CH_2)	4.26 (dd , 11.3, 5.3)
12–23	29.5–30.4 (CH_2)	1.25–1.38 ($br\ s$)			4.20 (dd , 11.3, 5.0)
24	32.1 (CH_2)	1.23 (m)			

Results and Discussion

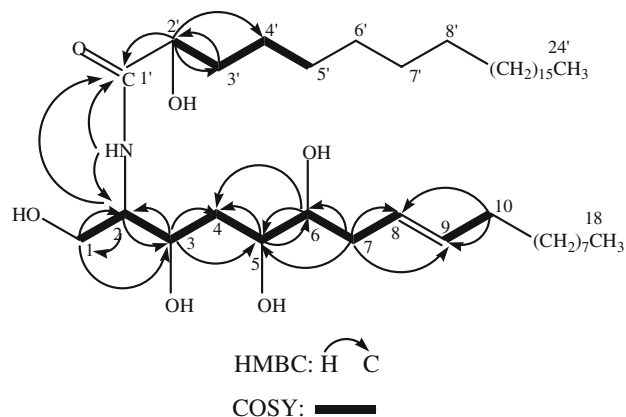
The antimicrobial fraction (Fr. 3) from the extract of the bulbs of *Z. candida* was separated by CC on silica gel to give two subfractions (Fr. 3-1 and Fr. 3-2) and further purified by Sephadex LH-20 to yield compounds **1** and **2**, respectively. Their structures were elucidated as follows.

Compound **1** was obtained as white amorphous powder, $[\alpha]_D^{25} = +16.67$ ($c = 0.06$, pyridine). The ion at m/z 698 ($[\text{M} + \text{H}]^+$) in the ESIMS was in agreement with the formula $\text{C}_{42}\text{H}_{83}\text{NO}_6$, which was confirmed by the positive HRESIMS ($[\text{M} + \text{Na}]^+$ ion at m/z 720.4150). The IR spectrum featured absorptions (3,345, 3,200, 1,615, and $1,540\text{ cm}^{-1}$) indicating the presence of hydroxyl, amide carbonyl and olefinic functions, respectively. The ^1H -NMR spectral data of **1** (Table 1) indicated the presence of two terminal methyl protons at δ_{H} 0.85 (6H, t, $J = 6.7$ Hz), methylenes protons at δ_{H} 1.25–1.45 ($br\ s$), an amide proton signal at δ_{H} 8.54 (1H, d, $J = 8.9$ Hz), signals of a *trans*-olefinic bond at δ_{H} 5.47 (1H, dt, $J = 13.7, 4.7$ Hz) and 5.52 (1H, dt, $J = 13.7, 4.7$ Hz) and six characteristic signals of geminal carbon protons to hydroxyl groups were also observed at δ_{H} 4.60 (1H, m), 4.50 (1H, dd, $J = 11.0, 4.5$ Hz), 4.40 (1H, dd, $J = 10.5, 5.0$ Hz), 4.33 (1H, m), 4.25 (1H, m), 4.27 (1H, m). Another signal at low field was observed at δ_{H} 5.08 (1H, m) for a methine proton vicinal to the nitrogen atom of an amide linkage, the data indicated a phytosphingolipid structure [21, 22].

To further confirm, ^{13}C -NMR spectral data of **1** (Table 1) showed one quaternary carbon at δ_{C} 175.3 (CONH), two olefinic methine carbon atoms at δ_{C} 130.7 and 130.8 (C=C), as well as five methines at δ_{C} 53.0 (CHNH), 76.8 (CHOH), 72.9 (CHOH), 73.0 (CHOH), 72.5 (CHOH) and one methylene at δ_{C} 62.1 (CH_2OH). The C-8,

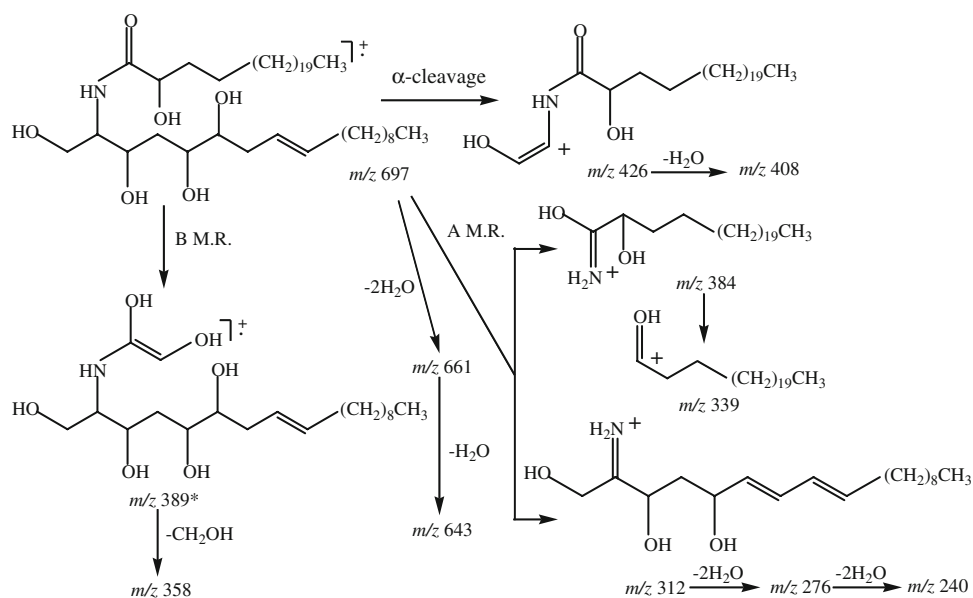
C-9 alkenyl bond was found to be *trans*, as the evidence, the geometry (*E*) of the double bond in the unsaturated long chain base (LCB) was determined on the basis of the ^{13}C -NMR chemical shifts of C-7 and C-10 (δ_{C} 33.3, 33.0) of the methylene carbon next to the olefinic carbon, which usually appears at $\delta \approx 27$ in (*Z*) isomers and at $\delta \approx 33$ in (*E*) isomers [23], and the coupling constant of H-8 and H-9 was 13.7 Hz. The structure of **1** was deduced by combined analysis of DEPT, HSQC and HMBC spectra (Scheme 2). All these spectral data revealed that **1** possessed two aliphatic long chains containing one double bond and five hydroxyl groups, and suggested it to be a phytosphingosine type ceramide.

The fragmentation pattern of compound **1** in EI mode was consistent with the pattern obtained in ESI mode. The number of carbons in the LCB and the fatty acid (FA) were determined to be 18 and 24, respectively. The negatively and positively charged ESIMS of **1** showed significant



Scheme 2 Key HMBC and ^1H - ^1H COSY correlations of **1**

Scheme 3 EI-MS fragment analysis for compound **1** (*peak not observed)



fragment ions at m/z 570 $[M-C_9H_{19}]^-$ and 163 $[LCB + H-C_{11}H_{21}]^+$ suggesting the C=C bond to be located at C-8 and C-9. This was confirmed on the basis of the typical fragment ions at m/z 128 $[LCB-CH_2OH-CH_2-CHOH-C_8H_{16}]^-$ and 247 $[M + H-C_{22}H_{45}-CHOH-C_8H_{16}]^+$ in the negatively and positively charged ESIMS which were formed by elimination of octene through McLafferty rearrangement [24, 25]. On the other hand, the presence of 2-amino and 1, 2', 3, 5, 6 pentahydroxyl groups as well as C-8 and C-9 double bond in the main chain were also able to be established from the fragments observed after McLafferty rearrangement [26] (Scheme 3).

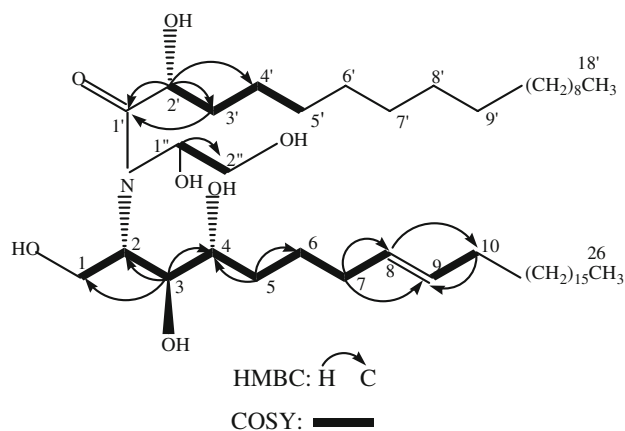
The 1H - 1H COSY spectra of **1** showed a pair of double doublets of oxygenated methylene at δ_H 4.50 (1H, dd, $J = 11.0, 4.5$ Hz) and 4.40 (1H, dd, $J = 10.5, 5.0$ Hz) coupled to the nitrogen bearing methylene signal at δ_H 5.08 (1H, m), which coupled further to the signal at δ_H 4.33 (1H, m). Olefinic protons at δ_H 5.47 (1H, dt, $J = 13.7, 4.7$ Hz) and 5.52 (1H, dt, $J = 13.7, 4.7$ Hz) showed coupling with methylene protons resonated at δ_H 1.93 (1H, m) and 1.93 (1H, m). In the HMBC spectrum of **1**, the signal at δ_H 4.60 correlated to the quaternary carbon and methylene carbon resonated at δ_C 175.3 and 35.7, respectively. The proton at δ_H 5.08 showed correlation with oxygenated methylene (δ_C 62.1) and oxygenated methines (δ_C 76.8) (Scheme 2). With these information and compared with the literature [27], the structure of compound **1** was assigned as 1,3,5,6-tetrahydroxy-2-(2'-hydroxytetracosanoyl amino)-8-(*E*)-octadecadiene, and designated to be candidamide A.

Compound **2** was also obtained as a white amorphous powder. The compound was optically active, with $[\alpha]_D^{25} = +45.82$ ($c = 0.055$, pyridine), and had the molecular

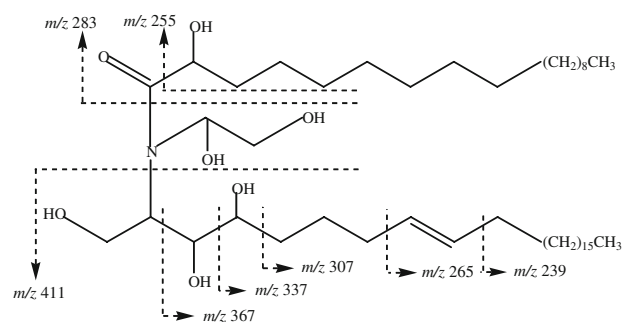
formula $C_{46}H_{91}NO_7$, as determined according to the ion peak at 792.3570 ($[M + Na]^+$; calc. 792.3575) in the positive HRESIMS. The IR spectrum showed the presence of OH groups ($3,335\text{ cm}^{-1}$), amide carbonyl ($1,610\text{ cm}^{-1}$), and aliphatic long chains (718 cm^{-1}). The 1H - and ^{13}C -NMR spectra of **2** (Table 2) indicated the presence of hydroxyl, amide groups and two aliphatic long chains. All these information suggested that compound **2** has a ceramide nature. The position and geometry of the double bond were confirmed by 1H , 1H -COSY analyses, EIMS and ESIMS fragments analyses and ^{13}C -NMR data of carbon next to the double bond.

There were six carbon atom signals bearing hydroxyl groups (δ_C 61.9, 76.8, 73.3, 76.3, 73.0 and 72.8) and one double bond (δ_C 130.8, 130.7) in the ^{13}C -NMR of compound **2**. The signal at δ_H 5.12 (H-2) showed a cross-peak with the signals at δ_H 4.41, 4.46 (H-1) and 4.33 (H-3) in 1H , 1H -COSY spectra of **2** and the latter correlated with the signal at δ_H 4.52 (H-4). The correlations were also observed in 1H - 1H COSY spectra between δ_H 4.26, 4.20 (H-2'') and 4.27 (H-1''), δ_H 2.28, 1.87 (H-3') and 4.73 (H-2'), δ_H 2.05, 1.97 (H-5) and 4.52 (H-4), δ_H 1.63 (H-6) and 2.05, 1.97 (H-5), δ_H 2.15 (H-7) and 1.63 (H-6). The structure of **2** was deduced by combined analysis of HSQC and HMBC spectra (Scheme 4). In the 1H -NMR of **2**, however, there were no signals between the δ_H 8–9, which indicated a tertiary amide may be present [28].

The length of the LCB and the fatty acid (FA), together with the presence of 2-amino and 1, 2', 3, 4 tetrahydroxyl groups as well as C-8, C-9 double bond were established due to EIMS and ESIMS fragment pattern analysis (Schemes 5, 6). The fragmentation pattern of compound **2** in EI mode was

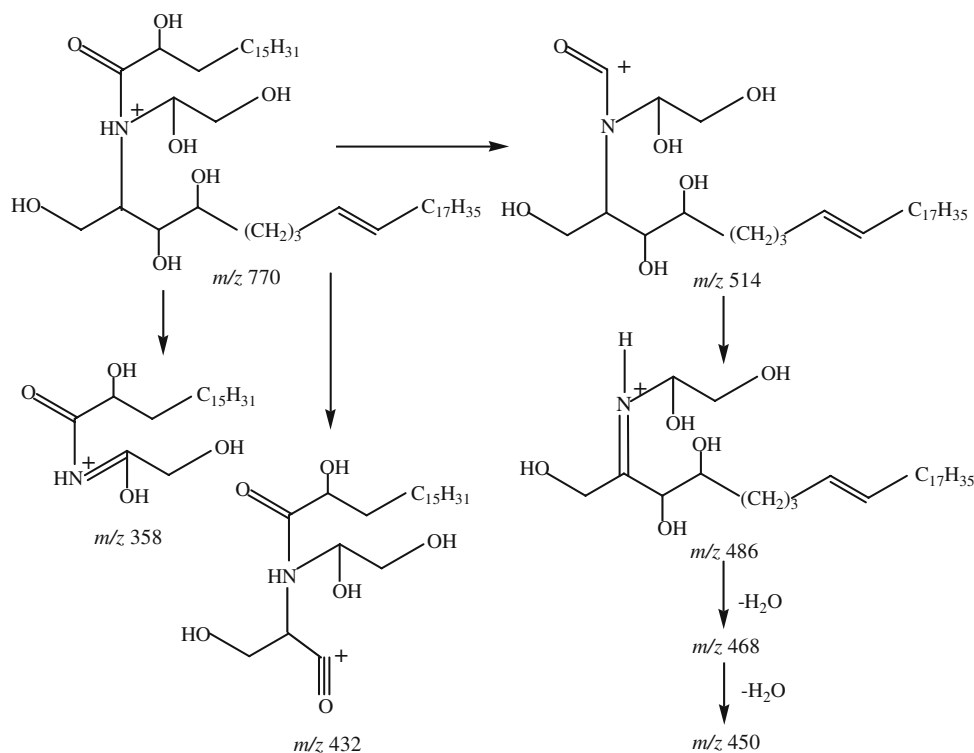


Scheme 4 Key HMBC and ^1H - ^{13}C COSY correlations of **2**



Scheme 5 EI-MS fragment analysis for compound **2**

Scheme 6 ESI-MS fragment analysis of compound **2**



consistent with the pattern obtained in ESI mode. Fragments at m/z 514, 486, 468, 450, 432, and 358 were the six significant ions of compound **2**, predicting 26 and 18 carbons in the LCB and FA, respectively, and that the double bond must be located in the LCB (Scheme 6). In addition, the fragments at m/z 486 and 358 suggested compound **2** was a tertiary amide. Further investigation of the EIMS showed two important fragment ions at m/z 265 and 239 suggesting the C=C bond to be located at C-8 and C-9. This was confirmed in the EIMS of **2** which displayed the characteristic peaks at m/z 171 [LCB-H-C₁₇H₃₅]⁺ and 145 [LCB-H-C₁₉H₃₇]⁺. Moreover, the C-8, C-9 double bond of **2** was proven by EIMS spectra, giving typical fragment ion at m/z 186 [LCB-H-C₁₆H₃₂]⁺ formed by elimination of hexadecene through McLafferty rearrangement [17, 24]. The 8, 9 alkenyl bond should be *trans* according to the chemical shifts of C-7 and C-10 (δ_{C} 33.9 and 33.3) [29, 30] and the coupling constant of H-8 and H-9 (14.8 Hz).

Regarding the stereochemistry, the formulated relative configuration of compound **2** was based on the carbon chemical shifts at δ_{C} 61.9 (C-1), 53.1 (C-2), 76.8 (C-3), 73.3 (C-4), 174.0 (C-1'), 76.3 (C-2'), which happened to be fairly close to those previously reported for (2*S*, 3*S*, 4*R*, 2'*R*) sphingosine moieties [31–33]. Including biogenetic considerations, compound **2** was determined to be (2*S*, 3*S*, 4*R*, 8*E*, 2'*R*)-2-[*N*-(2'-hydroxyoctadecanoyl)-*N*-(1'', 2''-dihydroxyethyl)-amino]-8-hexacosene-1,3,4-triol. We have named compound **2** candidamide B.

Antimicrobial activities of the fractions and the individual isolated compounds **1** and **2** against Gram positive and Gram negative bacteria and against fungi were tested using the reference agar dilution method.

In the antibacterial assay, compound **1** exhibited no activity against Gram positive bacterium *S. aureus* and Gram negative bacterium *E. coli*, while compound **2** exhibited moderate activities against *S. aureus* and *E. coli*, with minimum inhibitory concentrations (MICs) of 30 and 50 µg/ml. The MICs of the positive control penicillin G against *S. aureus* and *E. coli* were 0.46 and 0.77 µg/ml.

In the antifungal assay, the results indicated that compound **1** inhibited growth of fungi *A. niger* and *C. albicans*, with MICs of 20 and 50 µg/ml. Compound **2** inhibited growth of fungi *C. albicans* and *T. rubrum* with MICs of 50 and 40 µg/ml. The MICs of the positive control ketoconazole against *A. niger*, *C. albicans* and *T. rubrum* were 0.87, 0.92 and 1.26 µg/ml, respectively.

The 12 known compounds, (2*S*)-3',7-dihydroxy-4'-methoxyflavan (**3**) [34], (2*S*)-4'-hydroxy-7-methoxyflavan (**4**) [35], (2*S*)-4',7-dihydroxyflavan (**5**) [35], 7-hydroxy-3',4'-methylenedioxyflavan (**6**) [4], ambrettolide (**7**) [36], pancratistatin (**11**) [8], lycorine (**12**) [37], haemanthidine (**13**) [38] and haemanthamine (**14**) [38] were identified by their spectral data and by comparing their spectral data with those reported, β-sitosterol (**8**), β-daucosterin (**9**), and rutin (**10**) were identified by their spectral data and by co-TLC with authentic samples.

A literature survey revealed that compound **1** belongs to a kind of rarely occurring class of ceramide with a phytosphingolipid structure [27], and compound **2** containing a tertiary amide structure has been very uncommonly reported both for natural occurring and synthetic ones [31]. To the best of our knowledge, there has been no report on ceramide constituents to date in the genus *Zephyranthes*, and even family Amaryllidaceae. The presence of ceramides in *Z. candida* suggests a so promising biochemical research as to further obtain valuable bioactive compounds except alkaloids from the plants of genus *Zephyranthes*.

Acknowledgments This work was financially supported in part by the Natural Science Foundation of Jiangsu Province (BK2004062). The authors wish to acknowledge Professor Y.-L. Wu at State Key Laboratory of Bio-organic and Natural Products Chemistry, Shanghai Institute of Organic Chemistry, Chinese Academy of Sciences, Shanghai China, for making suggestions on this paper.

References

1. Thoibi DT, Borua PK (1997) Meiotic behaviour and pollen fertility in three species of *Zephyranthes* (Amaryllidaceae). *Biol Plant* 39:355–360
2. Pettit GR, Gaddamidi V, Cragg GM (1984) Antineoplastic agents, 105. *Zephyranthes grandiflora*. *J Nat Prod* 47:1018–1020
3. Ghosal S, Singh SK, Srivastava RS (1986) Alkaloids of *Zephyranthes flava*. *Phytochemistry* 25:1975–1978
4. Ghosal S, Singh SK, Srivastava RS (1985) Flavans from *Zephyranthes flava*. *Phytochemistry* 24:151–153
5. Ghosal S, Singh SK, Unnikrishnan G (1987) Chemical constituents of Amaryllidaceae. Part 25. Phosphatidylpyrrolophenanthridine alkaloids from *Zephyranthes flava*. *Phytochemistry* 26:823–828
6. Zaida TA, Myrna CR, Iraida SS (1989) Preliminary study of *Zephyranthes eggersiana* Urban. *Revista Cubana de Farmacia* 23:147–150
7. Iraida SS, Zaida TA (1989) Determination of the presence of lactams in the plant *Zephyranthes tubispatha* Herb, Amaryllidaceae. *Revista Cubana de Farmacia* 23(1–2):151–154
8. Kojima K, Mutsuga M, Inoue M, Ogihara Y (1998) Two alkaloids from *Zephyranthes carinata*. *Phytochemistry* 48:1199–1202
9. Mutsuga M, Kojima K, Nose M, Inoue M, Ogihara Y (2001) Cytotoxic activities of alkaloids from *Zephyranthes carinata*. *Nat Med* 55:201–204
10. Herrera MR, Machocho AK, Brun R, Viladomat F, Codina C, Bastida J (2001) Crinane and lycorane type alkaloids from *Zephyranthes citrina*. *Planta Med* 67:191–193
11. Mitsuru N, Tokunaru H, Masao T, Mitsuo M, Shuichi H (1978) Isolation of kaempferol-3-*O*-rhamnoglucoside, a flavonoid glycoside from *Zephyranthes candida*. *J Biosci* 33C:587–588
12. Ozeki S (1964) Alkaloids of *Zephyranthes candida*. I. Isolation of bases. *Yakugaku Zasshi*. 84:1194–1197
13. Pettit GR, Cragg GM, Singh SB, Duke JA, Doubek DL (1990) Antineoplastic agents, 162. *Zephyranthes candida*. *J Nat Prod* 53:176–178
14. Li X, Sun DD, Chen JW, He LW, Zhang HQ, Xu HQ (2007) New sphingolipids from the root of *Isatis indigotica* and their cytotoxic activity. *Fitoterapia* 78:490–495
15. Li HY, Matsunaga S, Fusetani N (1995) Halicyclindrosides, antifungal and cytotoxic cerebrosides from the marine sponge *Halichondria cylindroata*. *Tetrahedron* 51:2273–2280
16. Zhang Y, Wang S, Li XM, Cui CM, Feng C, Wang BG (2007) New sphingolipids with a previously unreported 9-methyl-C₂₀-sphingosine moiety from a marine alga endophytic fungus *Aspergillus niger* EN-13. *Lipids* 42:759–764
17. Chen JH, Cui GY, Liu JY, Tan RX (2003) Pinelloside, an antimicrobial cerebroside from *Pinellia ternata*. *Phytochemistry* 64:903–906
18. Cateni F, Zilic J, Falsone G, Scialino G, Banfi E (2003) New cerebrosides from *Euphorbia peplis* L.: antimicrobial activity evaluation. *Bioorg Med Chem Lett* 13:4345–4350
19. Mishra PK, Singh N, Ahmad G, Dube A, Maurya R (2005) Glycolipids and other constituents from *Desmodium gangeticum* with antileishmanial and immunomodulatory activities. *Bioorg Med Chem Lett* 15:4543–4546
20. Cateni F, Zilic J, Falsone G, Hollan F, Frausin F, Scarcia V (2003) Preliminary biological assay on cerebroside mixture from *Euphorbia nicaeensis* All. Isolation and structure determination of five glucocerebrosides. *IL Farmaco* 58:809–817
21. Natori T, Morita M, Akimoto K, Koezuka Y (1994) Agelasphins, novel antitumor and immunostimulatory cerebrosides from the marine sponge *Agelas mauritanicus*. *Tetrahedron* 50:2771–2784
22. Gao JM, Yang X, Wang CY, Liu JK (2001) Armillaramide, a new sphingolipid from the fungus *Armillaria mellea*. *Fitoterapia* 72:857–972
23. Higuchi R, Inagaki M, Togawa K, Miyamoto T, Komori T (1994) Isolation and structure of cerebrosides from the sea cucumber *Pentacta australis*. *Liebigs Ann Chem* 7:653–658
24. Ouyang MA, Liu R, Kuo YH (2005) A new cerebrosides, asperiamide A, from the marine fungus *Aspergillus* sp. *J Asian Nat Prod Res* 7:761–765

25. Simo CCF, Kouam SF, Poumale HMP, Simo IK, Ngadjui BT, Green IR, Krohn K (2008) Benjaminamide: a new ceramide and other compounds from the twigs of *Ficus benamina* (Moraceae). *Biochem Syst Ecol* 36:238–243
26. Chen XS, Wu YL, Chen DH (2002) Structure determination and synthesis of a new cerebrosides isolation from the traditional Chinese medicine *Typhonium giganteum* Engl. *Tetrahedron Lett* 43:3529–3532
27. Kumar N, Singh B, Gupta AP, Kaul VK (2006) Lonijaposides, novel cerebrosides from *Lonicera japonica*. *Tetrahedron* 62:4317–4322
28. Chen XS, Chen DH, Si JY, Guang ZT (2001) Chemical constituents of *Typhonium giganteum* Engl. *J Asian Nat Prod Res* 3:277–283
29. Su BN, Takaishi Y (1999) Morinins H-K, four novel phenylpropanol ester lipid metabolites from *Morina chinensis*. *J Nat Prod* 62:1325–1327
30. Shibuya H, Kawashima K, Sakagami M, Kawanishi H, Shimomura M, Ohashi K, Kitagawa I (1990) Sphingolipids and glycerolipids. I. Chemical structure and ionophoretic activities of soyacerebrosides I and II from soybean. *Chem Pharm Bull* 38:2933–2938
31. Liu A, Zou ZM, Xu LZ, Yang SL (2005) A new cerebroside from *Uvaria tonkinensis* var. *subglabra*. *J Asian Nat Prod Res* 7:861–865
32. Oueslati MH, Mighri Z, Jannet HB, Abreu PM (2005) New ceramides from *Rantherium suaveolens*. *Lipids* 40:1075–1079
33. Lin YP, Yan J, Qiu MH (2006) Novel imine from *Hemsleya macrocarpa* var. *clavata*. *Lipids* 41:97–99
34. Masaoud M, Ripperger H, Porzel A (1995) Flavonoids of dragon's blood from *Dracaena cinnabari*. *Phytochemistry* 38:745–749
35. Achenbach H, Stocker M, Manael AC (1988) Flavonoid and other constituents of *Bauhinia manca*. *Phytochemistry* 27:1835–1842
36. San V, Seoan E (1982) Synthesis of ambrettolide from phloionolic acid. *Perkin Trans I* 7:1837–1838
37. Likhitwitayawuid K, Angerhofer CK, Chai H, Pezzuto JM, Cordell GA (1993) Cytotoxic and antimalarial alkaloids from the bulbs of *Crinum amabile*. *J Nat Prod* 8:1331–1338
38. Kihara M, Konishi K, Xu L, Kobayashi S (1991) Alkaloidal constituents of the flowers of *Lycoris radiata* Herb (Amaryllidaceae). *Chem Pharm Bull* 39:1849–1853

Identification of Novel Acetylenic Alcohols and a New Dihydrothiopyranone from the Tropical Sponge *Reniochalina* sp.

Hyi-Seung Lee · Ji Hye Lee · Hoshik Won ·
Song-Kyu Park · Hwan Mook Kim · Hee Jae Shin ·
Heung Sik Park · Chung J. Sim · Hye-Kyeong Kim

Received: 17 May 2008 / Accepted: 23 September 2008 / Published online: 22 October 2008
© AOCS 2008

Abstract Two new acetylenic alcohols (**1–2**) and a new dihydrothiopyranone (**3**) were isolated from the tropical sponge *Reniochalina* sp. Their structures were determined by spectroscopic and chemical methods to be (3*R*)-hydroxyoctatriacont-(4*E*)-en-1-yne (**1**), 5-hydroxyheptatriacont-(3*Z*)-en-1-yne (**2**) and 2-hexadecyl-2,3-dihydrothiopyran-4-one (**3**). The acetylenic alcohol (**1**) exhibited significant growth inhibitory effect against human tumor cell lines.

Keywords Tropical sponge · *Reniochalina* sp. · Acetylenic alcohol · Dihydrothiopyranone · Growth inhibition

Abbreviations

COSY Correlation spectroscopy
DEPT Distortionless enhancement by polarization transfer
HMBC Heteronuclear multiple-bond correlation
HR High resolution
HSQC Heteronuclear single quantum coherence

Introduction

Acetylenic alcohols, a group of sponge metabolites, exhibit great structural variations in chain length and functional groups [1–18]. Most of these compounds have shown various interesting bioactivities such as brine shrimp lethality [1], cytotoxicity [2–6, 9–14], α -glucosidase inhibition [15] and HIV-1 integrase inhibition [16].

During the course of our search for biologically active constituents from tropical marine invertebrates [19], we tested a crude extract of a sponge of the genus *Reniochalina* (class Demospongiae, order Halichondria, family Axnellidae) from the Federated States of Micronesia. This extract displayed moderate growth inhibition against several human tumor cell lines. Guided by the results of ¹H-NMR analysis, fractions of the crude extracts were obtained by solvent partitioning followed by the isolation and purification of compounds using different chromatographic methods including reversed-phase vacuum flash chromatography and C₁₈ HPLC. This resulted in the isolation of two pure acetylenic alcohols (**1**, **2**) and a dihydrothiopyranone (**3**) (Fig. 1). In this paper, we describe the structural elucidation and evaluation of the bioactivities of these secondary metabolites.

H.-S. Lee · H. J. Shin · H. S. Park
Marine Natural Products Laboratory,
Korea Ocean Research & Development Institute,
Ansan 426-744, South Korea

J. H. Lee · H. Won
Department of Applied Chemistry, Hanyang University,
Ansan 425-791, South Korea

S.-K. Park · H. M. Kim
Bio-Evaluation Center, KRIBB, Taejon 305-806,
South Korea

C. J. Sim
Department of Biology, Hannam University,
Taejon 306-791, South Korea

H.-K. Kim (✉)
Department of Food Science and Nutrition,
The Catholic University of Korea, Bucheon 420-743,
South Korea
e-mail: hkyeong@catholic.ac.kr

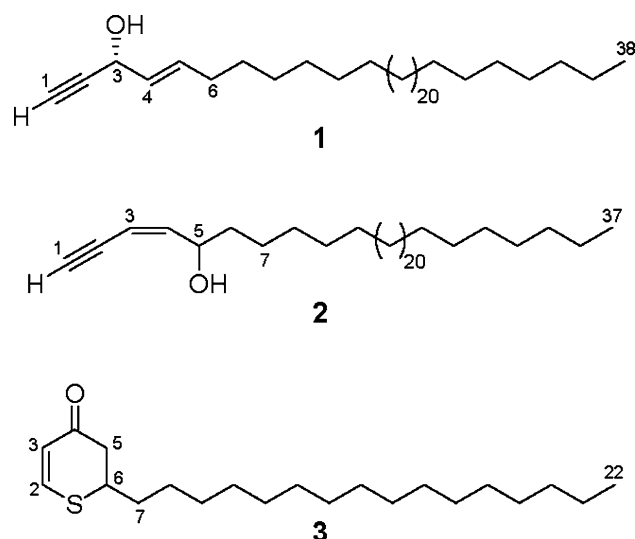


Fig. 1 Chemical structures of compounds 1–3

Materials and Methods

General Experimental Procedure

The IR spectra were recorded on a Varian 1000 FTIR spectrophotometer as thin films. Optical rotation of the samples was measured on a JASCO DIP-370 automatic polarimeter. The ^1H NMR spectra were recorded on a Varian Unity 500 spectrometer at 500 MHz and the ^{13}C NMR spectra on the same instrument at 125 MHz. Chemical shifts are expressed on a δ (ppm) scale and CDCl_3 (^1H , 7.26 ppm; ^{13}C , 77.0 ppm) and CD_3OD (^1H , 3.30 ppm; ^{13}C , 49.0 ppm) were used as internal standards. Mass spectra were obtained with a Micromass Auto Spec spectrometer.

Animal Material

The specimens of *Reniochalina* sp. (Sample No. 06CH-105) were collected by Dr. H. S. Park at a depth of 25–35 m from Chuuk Atoll, Federated States of Micronesia, in July 2006. The sponge specimen was identified by C. J. Sim on the basis of macro- and micromorphological feature analysis. A voucher specimen (Registry No. 06CH-105) is currently deposited at the Natural History Museum, Han-nam University, Korea under the curatorship of C. J. Sim.

Extraction and Isolation

The fresh sponge was frozen immediately after collection and stored at -25°C until analyzed. The specimens were lyophilized (dry wt 160.2 g) and then extracted twice with 300-mL portions of MeOH and once with 300 mL of CH_2Cl_2 . The resulting extracts were pooled, filtered and concentrated under reduced pressure to yield a residue of

30.1 g of crude extract. This residue was partitioned between H_2O and *n*-BuOH to yield 10.9 g of organic-soluble material. The *n*-BuOH phase was re-partitioned with 15% aqueous MeOH (1.93 g) and *n*-hexane (8.78 g). The residue of the aqueous MeOH layer was subjected to C_{18} reversed-phase flash chromatography using gradient mixture of MeOH and H_2O . The fraction eluted with 100% MeOH was dried (510 mg) and separated by reversed-phase HPLC (YMC ODS-A column, 1 cm \times 25 cm, 5% aqueous CH_3CN) to give 4.4 mg of compound **1** as a major products. The residue of the *n*-hexane layer was subjected to silica flash chromatography and eluted with a *n*-hexane: EtOAc gradient.

An aliquot (870 mg) of the fraction (3.88 g) eluted with *n*-hexane/EtOAc (80:20) was dried and separated by normal phase HPLC (YMC Sil column, 1 cm \times 25 cm) with a mobile phase of *n*-hexane/EtOAc (90:10). Two compounds were detected: in order of elution, compounds **3** and **2**. Further purification of these compounds was achieved by reversed-phase HPLC (YMC ODS-AQ column, 1 cm \times 25 cm, 15% aqueous CH_3CN) to give 1.5 and 11.6 mg of pure compounds **2** and **3**, respectively.

(3R)-Hydroxyoctatriacont-(4E)-en-1-yne (**1**)

IR (neat) 3,448, 1,637, 1,260, 749 cm^{-1} ; ^1H NMR (CD_3OD , 500 MHz) δ 5.84 (1H, dt, $J = 15.3, 7.2$, H-5), 5.54 (1H, dd, $J = 15.3, 6.1$, H-4), 4.73 (1H, dd, $J = 6.1, 2.0$, H-3), 2.85 (1H, d, $J = 2.0$, H-1), 2.07 (2H, m, H-6), 1.28 (62H, m, H-7 to H-37), 0.87 (3H, t, $J = 7.2$, H-38); ^{13}C NMR (CD_3OD , 125 MHz) δ 134.1 (C-5), 130.6 (C-4), 84.7 (C-2), 74.4 (C-1), 63.1 (C-3), 33.0 (C-6), 32.9 (C-7), 30.7 (29C), 23.7 (C-37), 14.1 (C-38); $[\alpha]_{\text{D}} -21.2$ ($c = 1.2$, MeOH); HRFABMS(+) m/z 567.5498 (M + Na), (calcd for $\text{C}_{38}\text{H}_{72}\text{ONa}$, m/z 567.5480)

5-Hydroxyheptatriacont-(3Z)-en-1-yne (**2**)

IR (neat) 3,446, 1,770, 1,632, 1,246, 1,055 cm^{-1} ; ^1H NMR (CDCl_3 , 500 MHz) δ 5.93 (1H, dd, $J = 10.7, 8.2$, H-4), 5.48 (1H, dd, $J = 10.7, 2.4$, H-3), 4.61 (1H, dt, $J = 8.2, 6.3$, H-5), 3.07 (1H, d, $J = 2.4$, H-1), 1.56 (2H, m, H-6), 1.22 (60H, m, H-7 to H-36), 0.82 (3H, t, $J = 6.8$, H-37); ^{13}C NMR (CDCl_3 , 125 MHz) δ 147.4 (C-4), 108.8 (C-3), 82.7 (C-1), 79.4 (C-2), 70.0 (C-5), 36.5 (C-6), 31.9 (C-7), 29.5(28C), 22.6 (C-36), 14.1 (C-37); $[\alpha]_{\text{D}} -18.3$ ($c = 0.8$, MeOH); HRFABMS(+) m/z 531.5490 (M + H), (calcd for $\text{C}_{37}\text{H}_{71}\text{O}$, m/z 531.5505).

2-Hexadecyl-2,3-dihydrothiopyran-4-one (**3**)

IR (neat) 1,770, 1,759, 1,375, 1,246, 1,054 cm^{-1} ; ^1H NMR (CDCl_3 , 500 MHz) δ 7.35 (1H, d, $J = 10.2$, H-2), 6.09 (1H,

d, $J = 10.2$, H-3), 3.42 (1H, m, H-6), 2.72 (1H, dd, $J = 16.3, 11.7$, H-5), 2.69 (1H, dd, $J = 16.3, 3.4$, H-5), 1.62 (2H, m, H-7), 1.20 (28H, m), 0.80 (3H, t, $J = 6.1$, H-22); ^{13}C NMR (CDCl_3 , 125 MHz) δ 194.7 (C-4), 145.8 (C-2), 123.3 (C-3), 44.5 (C-5), 43.0 (C-6), 33.9 (C-7), 29.5 (12C), 26.5 (C-8), 22.6 (C-21), 14.1 (C-22); $[\alpha]_{\text{D}} -14.6$ ($c = 0.9$, MeOH); HRFABMS(+) m/z 339.2713 (M + H), (calcd for $\text{C}_{21}\text{H}_{39}\text{OS}$, m/z 339.2722).

Preparation of MTPA Esters of Compound 1

(S)-MTPA Ester of 1 To a stirred solution of 3.2 mg of **1** in 0.5 mL of dry pyridine was added 30 μL of (–)-MTPA chloride. After stirring the mixture under N_2 for 3 h at room temperature, the solvent was removed by blowing with N_2 . The residue was purified with reversed-phase HPLC (YMC ODS column, 4.6 mm \times 25 cm, 5% aqueous MeOH) to yield 2.1 mg of **1S** as a colorless gum: ^1H NMR (CDCl_3 , 500 MHz) δ 7.53 (2H, m, Ar), 7.44–7.41 (3H, m, Ar), 6.07 (1H, dt, $J = 15.2, 6.6$ Hz, H-5), 6.01 (1H, br dd, $J = 6.6, 2.0$ Hz, H-3), 5.60 (1H, ddt, $J = 15.2, 6.6, 1.5$, H-4), 3.56 (3H, s, OMe), 2.59 (1H, d, $J = 2.0$ Hz, H-1), 2.08 (2H, m, H-6), 1.28 (62H, m, H-7 to H-37), 0.87 (3H, t, $J = 7.2$, H-38).

(R)-MTPA Ester of 1. Prepared as described for **1S**. From 3.1 mg of **1** and 30 μL of (+)-MTPA chloride was obtained 1.9 mg of **1R** as a colorless gum: ^1H NMR (CDCl_3 , 500 MHz) δ 7.54 (2H, m, Ar), 7.44–7.39 (3H, m, Ar), 6.04 (1H, br d, $J = 6.8$ Hz, H-3), 6.00 (1H, dt, $J = 15.1, 6.8$ Hz, H-5), 5.50 (1H, ddt, $J = 15.1, 6.8, 1.5$ Hz, H-4), 3.59 (3H, s, OMe), 2.63 (1H, d, $J = 2.0$ Hz, H-1), 2.04 (2H, m, H-6), 1.28 (62H, m, H-7 to H-37), 0.87 (3H, t, $J = 7.2$, H-38); $\Delta(\delta\mathbf{1S}-\delta\mathbf{1R})$ H-1 -20.5 Hz; H-3 -11.2 Hz; H-4 $+54.1$ Hz; H-5 $+37.5$ Hz; H-6 $+21.0$ Hz.

Oxidation of Compound 3

The sodium metaperiodate (2.4 mg, 11.2 μmol) was added to the thiopyran (**3**, 2.2 mg, 6.5 μmol) in the mixture (9:1, 3 mL) of methanol and dichloromethane solution. The resulting mixture was stirred at room temperature for 20 h and was filtered. The filtrate was concentrated under N_2 and subjected to silica HPLC (YMC silica column, 4.6 mm \times 25 cm) with *n*-hexane/EtOAc (90:10) to afford 0.3 mg of compound **4**.

2-Hexadecyl-2,3-dihydrothiopyran-1,4-dione (**4**)

^1H NMR (CD_3OD , 500 MHz) δ 7.11 (1H, d, $J = 10.9$, H-2), 6.31 (1H, d, $J = 10.9$, H-3), 3.54 (1H, dd, $J = 16.5, 3.41$, H-5), 3.30 (1H, dd, $J = 16.5, 11.7$, H-5), 2.97 (1H, m, H-6), 2.12 (2H, m, H-7), 1.50 (28H, m), 0.80 (3H, t, $J = 6.8$, H-22), ^{13}C NMR (CD_3OD , 125 MHz) δ 195.9

(C-4), 142.8 (C-2), 132.7 (C-3), 59.5 (C-6), 41.0 (C-5), 31.9 (C-7), 29.4 (12C), 26.3 (C-8), 22.6 (C-21), 14.1 (C-22); HRFABMS(+) m/z 355.2660 (M + H), (calcd for $\text{C}_{21}\text{H}_{39}\text{O}_2\text{S}$, m/z 355.2671).

Cell Culture and Growth Inhibition Assay

Human cancer cell lines of various origins, specifically, ACHN (renal), NCI-H23 (lung), MDA-MB-231 (breast), HCT-15 (colon), NUGC-3 (stomach) and PC-3 (prostate), were used for cell growth inhibition assays. The cells were cultured in RPMI 1640 medium supplemented with 5% fetal bovine serum at 37 °C in humidified air containing 5% CO_2 .

Inhibition of cell growth for an individual compound was determined with the total protein SRB assay described previously [20]. In brief, the cells were plated at a proper density in 96-well plates and incubated for 24 h. After further incubation for 48 h in the presence or absence of the compounds (at concentration of 0.1, 1, and 10 $\mu\text{g}/\text{mL}$) cells were fixed with 50% trichloroacetic acid and stained with sulforhodamine B. The absorbance was measured in quadruplicate at 540 nm using a microplate reader and the percentage of cell viability was calculated.

Results and Discussion

Frozen specimens of *Reniochalina* sp. were extracted with MeOH and CH_2Cl_2 . The combined extract was partitioned between *n*-BuOH and H_2O . The *n*-butanol layer was dissolved in 15% aqueous MeOH and extracted with hexane. Further separation of the methanolic phase by ODS flash chromatography, followed by reversed-phase HPLC, afforded an acetylenic alcohol (**1**). On the other hand, purification of the *n*-hexane layer on a silica gel column followed by reversed-phase HPLC led to the isolation of the acetylenic alcohol (**2**) and the dihydrothiopyranone (**3**).

Compound **1** was isolated as a colorless gum with the molecular formula $\text{C}_{38}\text{H}_{72}\text{O}$ determined by combined HRFABMS and ^{13}C NMR spectrometry. The characteristic features of the acetylenic alcohol appeared in the ^1H NMR spectra which exhibited signals corresponding to a terminal acetylene (δ 2.85), a oxymethine (δ 4.73) and a disubstituted double bond (δ 5.54, 5.84). The configuration of the double bond was assigned as *E* based on the vicinal coupling constant of the olefinic protons ($J = 15.3$ Hz). Corresponding carbon signals were observed at δ 74.4, 84.7 (acetylene), 63.1 (oxymethine), 130.6, 134.1 (double bond) in ^{13}C NMR spectra. In addition, DEPT data showed a quaternary carbon at δ 84.7 (C) and a methyl carbon at δ 14.1 (CH_3).

The structure of compound **1** was determined by 2D-NMR experiments. In a ^1H - ^1H -COSY experiment, the

olefinic proton signals showed correlations to an oxymethine at δ 4.73 and a methylene at δ 2.07. The signal at δ 4.73 was, in turn, correlated with a small coupling constant to the terminal acetylene proton at δ 2.85 ($J = 2.0$ Hz). A combination of the HSQC and HMBC data allowed assignment of the characteristic ^{13}C -NMR signals, and the HMBC correlations from H-3 to C-1, C-2, C-4 and C-5, from H-4 to C-2, C-3 and C-6, and from H-5 to C-3, C-6 and C-7 confirmed the location of acetylene, oxymethine, olefin, and two methylenes (Fig. 2). The number of methylenes which were overlapped at δ 30.7 in ^{13}C -NMR spectra were presumed with the integration of ^{13}C -NMR spectra and confirmed by MS data. A revision of existing literature revealed that structurally similar acetylenic alcohols had been isolated from the sponge *Cribrochalina vasculum* [1, 2]. However, compound **1** differs from other known metabolites in chain length. The absolute configuration of the asymmetric center at C-3 was determined by modified Mosher's method [21, 22]. Treatment of **1** with (–) and (+)-MTPA chloride in pyridine yielded the corresponding esters **1S** and **1R**, respectively. All of the key protons of both compounds were assigned by a combination of ^1H -NMR and ^1H -COSY data. The absolute configuration was defined as *R* by ^1H -NMR chemical shift difference values ($\delta\Delta = \delta\mathbf{1S} - \delta\mathbf{1R}$) for protons adjacent to the ester group (Fig. 3). Compound **1** is therefore (3*R*)-hydroxyoctatriacont-(4*E*)-en-1-yne.

The molecular formula of compound **2** was determined to be $\text{C}_{37}\text{H}_{70}\text{O}$ by HRFABMS. The ^1H - and ^{13}C -NMR spectra of this compound were similar to those of compound **1** except for the data from acetylenic and olefinic groups. The acetylenic proton signal in ^1H -NMR spectra was shifted to down fields (from δ 2.85 to δ 3.07) and

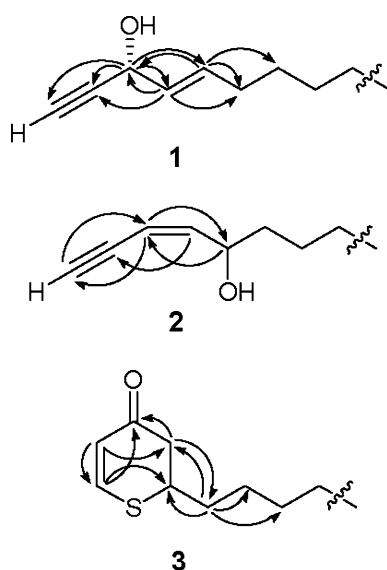


Fig. 2 Key HMBC correlations (H \rightarrow C) of compounds **1**–**3**

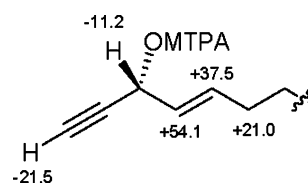


Fig. 3 Selected $\Delta(\delta\mathbf{1S} - \delta\mathbf{1R})$ of MTPA ester of compound **1**

olefinic signals in ^{13}C -NMR spectra showed large differences (from δ 130.6, 134.1 to δ 108.8, 147.4). The small coupling constant ($J = 2.4$ Hz) between the olefinic protons at δ 5.48 and the acetylenic proton δ 3.07 suggested that these were connected to each other via an acetylenic moiety. Additionally, the *Z* geometry of the double bond in compound **2** was assigned by the coupling constant of $J = 10.7$ Hz. The COSY, HSQC and HMBC experiments allowed the assignment of subunits. Important HMBC interactions of compound **2** are shown in Fig. 2. The number of methylenes in **2** had also been determined by ^{13}C -NMR spectra and MS data. Accordingly, the structure assigned to compound **2** was 5-hydroxyheptatriacont-(3*Z*)-en-1-yne which is also different to previously reported acetylenic alcohols in its chain length.

In addition to the acetylenic alcohols, a new dihydrothiopyranone (**3**) was isolated as a colorless gum. Using combined HRFABMS and ^{13}C -NMR analysis, the molecular formula for compound **3** was determined to be $\text{C}_{21}\text{H}_{38}\text{OS}$. The ^{13}C -NMR data of this compound contained signals of a quaternary carbon at δ 194.7, interpreted as a ketone, and two olefinic carbons at δ 145.8 (CH), 123.3 (CH). A further study of the molecular formula revealed that **3** had an additional degree of unsaturation, hence a cyclic framework. With this information, further 2D NMR experiments were carried out to determine the structure of **3**. According to results of the COSY and HSQC experiments, all of the proton-bearing carbons and their protons were matched except for the overlapped methylene signals at δ 1.20 (28H) in ^1H -NMR and δ 29.5 (12C) in ^{13}C -NMR spectra. The HMBC correlations between signals of the olefinic proton at δ 7.35 with carbonyl carbon δ 194.7 (C-4) and methyne carbon δ 43.0 (C-6) suggested the presence of a dihydrothiopyranone ring (Fig. 2).

For the confirmation of the presence of sulfur in the ring, mild oxidation with NaIO_4 was performed yielding the sulfoxide-form, compound **4** (Fig. 4).

With the aid of this experimental information, the structure of **3** was confirmed by comparison with literature spectral data of dihydrothiopyranone derivative [23]. The ^1H - and ^{13}C -NMR spectral data of the six-membered ring in 2-butyl-2,3-dihydrothiopyran-4-one, which was a synthetic intermediate, were similar to those of compound **3**.

The growth inhibitory activities of compounds **1**, **2**, and **3** against six human tumor cell lines including ACHN,

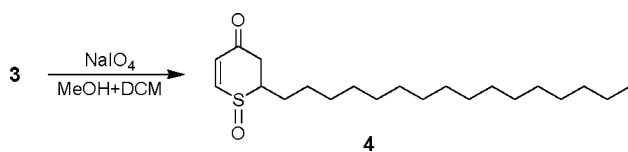


Fig. 4 Oxidation of compound **3**

Table 1 Growth inhibition (GI_{50} , $\mu\text{g/mL}$) of compounds **1–2** against human tumor cell lines

Compound	ACHN	NCI-H23	MDA-MB-231	HCT-15	NUGC-3	PC-3
1	0.156	0.117	0.386	0.345	1.493	0.732
2	>10	>10	>10	>10	>10	>10
Adriamycin	0.198	0.248	0.278	0.708	0.198	0.488

NCI-H23, MDA-MB-231, HCT 15, NUGC-3, and PC-3 were evaluated. In vitro growth inhibition activity was tested 48 h after treatment of the cells using the SRB (sulfurhodamine B) assay using adriamycin as a positive control. As can be appreciated by the results summarized in Table 1, compound **1** showed significant growth inhibition against ACHN, NCI-H23, and HCT 15 with GI_{50} values of 0.156, 0.117, and 0.345 $\mu\text{g/mL}$, respectively. In the case of compounds **2** and **3**, no cell growth inhibitory activity was observed against any of the tumor cell lines even at the highest concentration tested (10 $\mu\text{g/mL}$) thus no GI_{50} is reported.

Acknowledgments We are grateful to the Department of Marine Resources, State of Chuuk, Federated States of Micronesia, for supporting marine organism research. This research was partially supported by the Korea Ocean Research and Development Institute (PE98210, PE98220), the KRIBB Research Initiative Program, and the Ministry of Land, Transport and Maritime, Korea (PM50400).

References

- Aiello A, Fattorusso E, Menna M, Pansini M (1992) Further bioactive acetylenic compounds from the Caribbean sponge *Cribrachalina vasculum*. *J Nat Prod* 55:1275–1280
- Hallock YF, Cardellina JHII, Balaschak MS, Alexander MR, Prather TR, Shoemaker RH, Boyd MR (1995) Antitumor activity and stereochemistry of acetylenic alcohols from the sponge *Cribrachalina vasculum*. *J Nat Prod* 58:1801–1807
- Dai J-R, Hallock YF, Cardellina JHII, Boyd MR (1996) Vasculyne, a new cytotoxic acetylenic alcohol from the marine sponge *Cribrachalina vasculum*. *J Nat Prod* 59:88–89
- Dai J-R, Hallock YF, Cardellina JHII, Gray GN, Boyd MR (1996) Triangulynes A–H and triangulynic acid, new cytotoxic polyacetylenes from the marine sponge *Pellina triangulate*. *J Nat Prod* 59:860–865
- Seo Y, Cho KW, Rho J-R, Shin J, Sim CJ (1998) Petrocortynes and petrosiacetylenes, novel polyacetylenes from a sponge of the genus *Petrosia*. *Tetrahedron* 54:447–462
- Shin J, Seo Y, Cho KW, Rho J-R, Paul VJ (1998) Osirisynes A–F, highly oxygenated polyacetylenes from the sponge *Haliclona osiris*. *Tetrahedron* 54:8711–8720
- Rooney F, Capon RJ (1998) Callyspongynes A and B: new polyacetylenic lipids from a southern Australian marine sponge, *Callyspongia* sp. *Lipids* 33:639–642
- Guo Y, Gavagnin M, Salierno C, Cimino G (1998) Further petroformynes from both Atlantic and Mediterranean populations of the sponge *Petrosia ficiformis*. *J Nat Prod* 61:333–337
- Seo Y, Cho KW, Lee H-S, Rho J-R, Shin J (1999) New acetylenic enol ethers of glycerol from the sponge *Petrosia* sp. *J Nat Prod* 62:122–126
- Watanabe K, Tsuda Y, Yamane Y, Takahashi H, Iguchi K, Naoki H, Fujita T, van Soest RWM (2000) Strongylodiols A, B and C, new cytotoxic acetylenic alcohols isolated from the Okinawan marine sponge of the genus *Strongylophora* as each enantiomeric mixture with a different ratio. *Tetrahedron Lett* 41:9271–9276
- Lim YJ, Park HS, Im KS, Lee C-O, Hong J, Lee M-Y, Kim D-K, Jung JH (2001) Additional cytotoxic polyacetylenes from the marine sponge *Petrosia* species. *J Nat Prod* 64:46–53
- Lee H-S, Rho J-R, Sim CJ, Shin J (2003) New acetylenic acids from a sponge of the genus *Stelletta*. *J Nat Prod* 66:566–568
- Youssef DTA, van Soest RWM, Fusetani N (2003) Callyspongynols A–C, New cytotoxic C_{22} -polyacetylenic alcohols from a Red Sea sponge, *Callyspongia* species. *J Nat Prod* 66:679–681
- Dembitsky VM (2006) Anticancer activity of natural and synthetic acetylenic lipids. *Lipids* 41:883–924
- Nakao Y, Uehara T, Matunaga S, Fusetani N, van Soest RWM (2002) Callyspongynic acid, a polyacetylenic acid which inhibits α -Glucosidase, from the marine sponge *Callyspongia truncata*. *J Nat Prod* 65:922–924
- Lech ML, Harper MK, Faulkner DJ (2003) Brominated polyacetylenes from the Philippines sponge *Diplastrella* sp. *J Nat Prod* 66:667–670
- de Jesus RP, Faulkner DJ (2003) Chlorinated acetylenes from the San Diego sponge *Haliclona lunisimilis*. *J Nat Prod* 66:671–674
- Watanabe K, Tsuda Y, Hamada M, Omori M, Mori G, Iguchi K, Naoki H, Fujita T, van Soest RWM (2005) Acetylenic strongylodiols from a *Petrosia* (*Strongylophora*) Okinawan marine sponge. *J Nat Prod* 68:1001–1005
- Lee H-S, Lee T-H, Yang SH, Shin HJ, Shin J, Oh K-B (2007) Sesterterpene sulfates as isocitrate lyase inhibitors from tropical sponge *Hippospongia* sp. *Bioorg Med Chem Lett* 17:2483–2486
- Kuo SC, Lee HZ, Juang JP, Lin YT, Wu TS, Chang JJ, Lednicer D, Paull KD, Lin CM, Hamel E, Lee KH (1993) Synthesis and cytotoxicity of 1, 6, 7, 8-Substituted 2-(4'-Substituted phenyl)-4-quinolones and related compounds: identification as antimetabolic agents interacting with tubulin. *J Med Chem* 36:1146–1156
- Ohtani I, Kusumi T, Kashman Y, Kakisawa H (1991) A new aspect of the high-field NMR application of Mosher's method. The absolute configuration of marine triterpene siphonolol A. *J Org Chem* 56:1296–1298
- Bernart MW, Hallock YF, Cardellina JHII, Boyd MR (1994) Stereochemistry of enynols—a caveat on the exciton chirality method. *Tetrahedron Lett* 35:993–994
- Jeffery SM, Sutherland AG, Pyke SM, Powell AK, Taylor RJK (1993) Isolation of episulfones from the Ramberg–Backlund rearrangement. Part 2: X-ray molecular structure of 2, 3-epithio-8, 8-dimethyl-6, 10-dioxaspiro[4, 5]-decane S, S-dioxide and of r-6-benzyl-t-7, t-8-epithio-1, 4-dioxaspiro[4, 4]nonane S, S-dioxide. *J Chem Soc Perkin Trans* 1:2317–2327

Simultaneous Quantification of Plant Glyceroglycolipids Including Sulfoquinovosyldiacylglycerol by HPLC–ELSD with Binary Gradient Elution

Keita Yunoki · Mayumi Sato · Kazuto Seki ·
Takeshi Ohkubo · Yukihiisa Tanaka · Masao Ohnishi

Received: 22 May 2008 / Accepted: 23 September 2008 / Published online: 22 October 2008
© AOCS 2008

Abstract Membrane lipids of photosynthetic organisms consist of glycerophospholipids and glyceroglycolipids. We investigated a method for the simultaneous quantitative analysis of neutral and acidic lipids using HPLC–ELSD, and quantified monogalactosyldiacylglycerol (MGDG), digalactosyldiacylglycerol (DGDG) and sulfoquinovosyldiacylglycerol (SQDG). Ten complex lipid classes were separated with a binary gradient system consisting of chloroform and methanol–acetone–water–acetic acid (30:60:9:1, v/v/v/v) with 0.3% triethylamine (pH 4), and were eluted within 16 min. The contents of SQDG in ten edible plants ranged from 3 to 101 mg/100 g, and were positively correlated to the neutral glyceroglycolipids contents.

Keywords Glyceroglycolipid · Sulfoquinovosyldiacylglycerol · Monogalactosyldiacylglycerol · Digalactosyldiacylglycerol · Acidic lipid · Plant · Chloroplast · ELSD · Binary gradient · HPLC

Introduction

Glyceroglycolipids are major membrane lipids in photosynthetic organisms such as higher plants and algae. MGDG, DGDG and SQDG are all polar lipids particularly found in chloroplasts, and account for 90% of the total lipids in the chloroplast thylakoid membrane [1]. It has been established that SQDG, which is a negatively charged (acidic) sulfolipid present in the thylakoid membrane with phosphatidylglycerol, is important for preservation of structure and function of membranes, despite its slight amount [2, 3]. Moreover, these glycolipids have been evaluated for the functionality of their bioactive substances and are known to have various biological activities, including improving the intestinal environment [4], anti-tumor activity [5–7], anti-inflammatory activity [8, 9] and protection against cell death [7, 10]. Among them, SQDG has been identified as a new functional component because it has specific biological inhibitory activities against DNA polymerase [11–15], certain types of viruses [16–19], P-selectin receptor [20], telomerase [21], angiogenesis [22] and inflammation/proliferation [23].

People consume these glycolipids daily from plant foodstuffs. Sugawara et al. [24] analyzed the contents of neutral glycolipids in various plants using HPLC. In this way, the main neutral glycolipids in plants present no particular difficulties for analysis and are easily separated

K. Yunoki · M. Ohnishi (✉)
Department of Agricultural and Life Science,
Obihiro University of Agriculture and Veterinary Medicine,
Obihiro, Hokkaido 080-8555, Japan
e-mail: mohnishi@obihiro.ac.jp

K. Yunoki
e-mail: yunoki@obihiro.ac.jp

M. Sato · K. Seki
Hokkaido Forest Products Research Institute, Asahikawa,
Hokkaido 071-0198, Japan

M. Sato · M. Ohnishi
United Graduate School of Agriculture Sciences, Iwate
University, Morioka, Iwate 020-8550, Japan

T. Ohkubo
Functional Foods Research Laboratory, NOF Corporation,
Chidori-cho, Kawasaki-ku, Kawasaki, Kanagawa 210-0865,
Japan

Y. Tanaka
Tsukuba Corporate Research Laboratory, NOF Corporation,
Tokodai 5-chome, Tsukuba, Ibaraki 300-2635, Japan

from phospholipids by HPLC. However, since SQDG presents greater analytical problems because of its highly polar anionic (acidic) nature, the only methods that have been devised for their analysis is the TLC/densitometry method [25] and the complicated triadic gradient elution by HPLC [26]. Therefore, publications reporting SQDG contents in plants are rare. In the present study, we developed optimal HPLC conditions with a binary gradient system to separate and quantify neutral and acidic glyceroglycolipids in edible plants.

Materials and Methods

Materials

Chromatographically pure working standards of SQDG, MGDG and DGDG were prepared from spinach total lipids. Firstly, spinach TL (prepared as described below) was subjected to silicic acid column chromatography. After removing the non-polar lipids from the cartridge with chloroform, the glycolipid fraction was eluted with acetone [27]. The crude glycolipid fraction obtained was further fractionated with stepwise elution of chloroform–acetone [27]. The DGDG fraction, including SQDG, was applied to a DEAE column and separated to neutral DGDG and acidic SQDG lipid fractions as described below. Finally, each glycolipid was subjected to preparative TLC with a solvent system of chloroform–methanol–water (70:35:7, v/v/v) to give one spot. The glycolipids were dissolved in chloroform–methanol (2:1, v/v) and 0.001% butylhydroxytoluene (Wako, Japan) was added. Standard samples of cholesterol, phosphatidylethanolamine (PE), phosphatidylcholine (PC), phosphatidylglycerol (PG) from egg yolk, and phosphatidylinositol (PI) from soybeans were purchased from Sigma (St Louis, USA), and cerebroside (CE, lower spot) from bovine brain was purchased from Doosan Serdary Research Laboratories (Toronto, Canada). Commercial standards of MGDG, DGDG, acylsterylglucoside (ASG, from soybeans) and sterylglucoside (SG, from soybeans) were purchased from Funakoshi Co. (Tokyo, Japan). SQDG was purchased from Kanto Chemical Co. (Tokyo, Japan). They were used for comparing LC retention times.

Spinach (leaf, *Spinacia oleracea* L.), parsley (leaf, *Petroselinum crispum*), perilla (leaf, *Perilla frutescens*), Chinese chive (leaf, *Allium tuberosum*), green onion (leaf, *Allium cepa*), crown daisy (leaf and stem, *Chrysanthemum coronarium*), broccoli (flower and stem, *Brassica oleracea* var. *italica*), green pepper (fruit, *Capsicum annuum* cv. *grossum*), cucumber (fruit, *Cucumis sativus*) and pumpkin (fruit, *Cucurbita maxima*) were purchased at a local supermarket in Obihiro, Japan. The pumpkin fruit was cut into two pieces to remove the loose stringy pulp with seeds,

and the outer green epidermis was removed to obtain the isolated pumpkin flesh.

Extraction, Separation and Detection of Lipids

Fresh plant samples (5–50 g) were cut into pieces and heated in a microwave oven for 1 min to deactivate lipolytic enzymes and then extracted three times with chloroform–methanol (2:1, v/v) for 1 h, respectively, after homogenization (Polytron, Kinematica, Switzerland). After filtration using filter paper (Advantec No. 2, Toyo Roshi Kaisha, Japan), the extracts were combined and washed once with water in a mixture of chloroform–methanol–water (with a ratio of 8:4:3, v/v/v) [28]. After partition, the lower phase was concentrated to dryness using a rotary evaporator, and the lipids were weighed to yield the total lipids (TL).

Then, green pepper TL was separated into neutral and acidic lipid fractions by anion-exchange column chromatography. Briefly, 50 mg of TL was inserted into a diethylaminoethyl (DEAE) column (Toyopak DEAE M, Tosoh, Tokyo, Japan), and stepwise eluted with chloroform–methanol (neutral lipid fraction), followed by elution with chloroform–methanol–0.1 M ammonium acetate (20:80:0.2, v/v/v) [29]. The latter fraction was washed twice in a mixture of chloroform–methanol–water (with a ratio of 8:4:3, v/v/v), then the lower phase was concentrated to dryness to yield the acidic lipid fraction.

To detect glyceroglycolipids, TL was analyzed by silicic acid TLC (Silica gel 60, 0.25 mm, Merck, Germany) with a chloroform–acetone–methanol–acetic acid–water mixture (50:20:10:10:5, v/v/v/v/v). Glyceroglycolipid species were visualized after spraying with anthrone/sulfuric acid, followed by brief heating.

HPLC and GC Analyses

A portion of the total lipids was dissolved in chloroform–methanol (2:1, v/v) solution (1 mg/ml) and filtered (GL Chromatodisc, 0.45 μ m, GL science, Japan) for HPLC analysis. Plant TL was analyzed by a normal-phase HPLC equipped with an evaporative light scattering detector. Instrument: Shimadzu LC-10AD (Kyoto, Japan); mobile phase: solvent A, chloroform and solvent B, methanol–acetone–water–acetic acid (30:60:9:1, v/v/v/v) with 0.3% triethylamine (pH 4); gradient: Table 1; column: LiChrospher 100 Diol (column size 250 \times 4 mm i.d.; particle size 5 μ m, Merck, Germany) with an LiChroCART 4–4 guard column; flow rate: 0.9 ml/min; injection volume 10–20 μ l; column temperature 35 $^{\circ}$ C; detector ELSD (70 $^{\circ}$ C, 350 kpa, Sedex 75, Sedere, France). The amounts of SQDG, MGDG and DGDG in plant samples were calculated from the calibration curve of each standard

Table 1 Elution program for the binary gradient system

Time (min)	A (%)	B (%)
1	100	0
2	70	30
6	70	30
8	50	50
13	50	50
15	0	100
17	0	100
20	100	0

A Chloroform

B Methanol–acetone–water–acetic acid (30:60:9:1) with 0.3% triethylamine (pH 4)

component described above, since ELSD provided a curvilinear response to mass of standard lipids. All data are averages \pm SD of independent experiments from three samples.

MGDG, DGDG and SQDG from spinach leaves were methanolized with 5% HCl/methanol at 95 °C for 2 h, and fatty acid methyl esters were analyzed by GC according to our previous report [30].

Results

HPLC Analysis of Standard Lipids and Component Fatty Acids of Glyceroglycolipids

Chromatographically pure working standards were analyzed by HPLC (Fig. 1). MGDG, DGDG and SQDG prepared from spinach leaves each exhibited a single peak (Fig. 1a) and were identified by co-chromatography with commercial standards, and were used as standard compounds for their calibration curves. The correlation coefficients were from 0.9980 to 0.9998. The detection limit of SQDG was 0.1 μ g. The predominant fatty acids were α -linolenic acid (68 mol%) and oleic acid (30 mol%) for MGDG, α -linolenic acid (86 mol%) for DGDG, and palmitic acid (46 mol%) and α -linolenic acid (46 mol%) for SQDG. The glycolipids (MGDG, SQDG, DGDG, ASG, SG and CMH) and phospholipids (PC, PE, PG and PI) were completely separated from each other (Fig. 1b–e).

TLC of Plant Total Lipids

Total lipids obtained from spinach leaf, broccoli flower and stem, green pepper fruit and pumpkin fruit were analyzed by TLC (Fig. 2). Spinach TL (lane A) contained not only a significant amount of neutral glyceroglycolipids such as MGDG and DGDG but also SQDG, which was located below the DGDG spot (identified by co-chromatography

with commercial MGDG, DGDG and SQDG standards). In this TLC system, SQDG could be clearly separated, but DGDG overlapped with PC. Broccoli TL (lane B) contained a significant amount of glycerophospholipids and a small amount of glyceroglycolipids. In green pepper TL (lane C), glycolipids such as sterylglucoside (SG) and ceramide monohexoside (CMH), were found in relatively significant amounts. In pumpkin TL (lane D), two large spots of Rf values 0.01 and 0.04 with positive coloring reaction to anthrone/sulfuric acid reagent were assumed to be triglycosyldiacylglycerol (TGDG) and tetraglycosyldiacylglycerol (TeGDG), respectively [31].

HPLC Profiles of Plant Total Lipids

Lipid extracts from four plant tissues shown in Fig. 2 were analyzed by HPLC (Fig. 3). Non-polar lipids and pigments including chlorophyll were eluted within 4 min after the start of analysis. Ten complex lipid species were detected from green pepper TL (injection amount 20 μ g), and all were eluted within 16 min. These peaks were identified by analyzing the neutral and acidic lipid fractions of green pepper, and comparing them with retention times of standard components (Fig. 1). It was confirmed that peaks 4, 6 and 11 shown in the acidic lipid fraction were PG, SQDG and PI, respectively. The peak at about 4 min in acidic lipid fraction was tentatively identified as free fatty acids. Although all glyceroglycolipids and glycerophospholipids were detected in spinach TL, SG and CMH, of which the contents are low, were not detected with an injection amount of 10 μ g (within the maximum detection limit of MGDG). When 20 μ g of broccoli TL was injected the SQDG peak was very small and the PC peak exceeded the detection limit of the ELSD. In pumpkin TL, peaks 12 and 13 around 18–19 min were assumed to be TGDG and TeGDG, respectively, because the preparative isolates obtained from HPLC analysis corresponded to Rf value and color reaction by anthrone/sulfuric acid of their spots on TLC shown in Fig. 2.

Determination of Glyceroglycolipids in Plant Foodstuff

Contents of MGDG, DGDG and SQDG in ten fresh edible plants were determined (Table 2). The glyceroglycolipid profile was significantly different among the plants. Contents of SQDG ranged from 3 mg/100 g for green onion to 101 mg/100 g for parsley. Total glycolipid contents were generally low in green onion, green pepper and cucumber with low TL contents (0.17/100 g). Although the TL content (1.1/100 g) of perilla was close to that of broccoli, the glycolipid content (397 mg/100 g) of perilla was three times higher than broccoli. Green leafy vegetables, such as spinach, parsley, perilla and chive, were rich in MGDG, whereas crown daisy, green pepper and pumpkin were

Fig. 1 HPLC profiles of standard compounds. Injection: *A* 2 μ g, *B* 0.6 μ g, *C* 1 μ g, *D* 1 μ g, *E* 3 μ g. *MGDG* monogalactosyldiacylglycerol, *DGDG* digalactosyldiacylglycerol, *SQDG* sulfoquinovosyldiacylglycerol, *ASG* acylsterylglucoside, *SG* sterylglucoside, *Chol* cholesterol, *CMH* ceramide monohexoside, *PE* phosphatidylethanolamine, *PC* phosphatidylcholine, *PG* phosphatidylglycerol, *PI* phosphatidylinositol

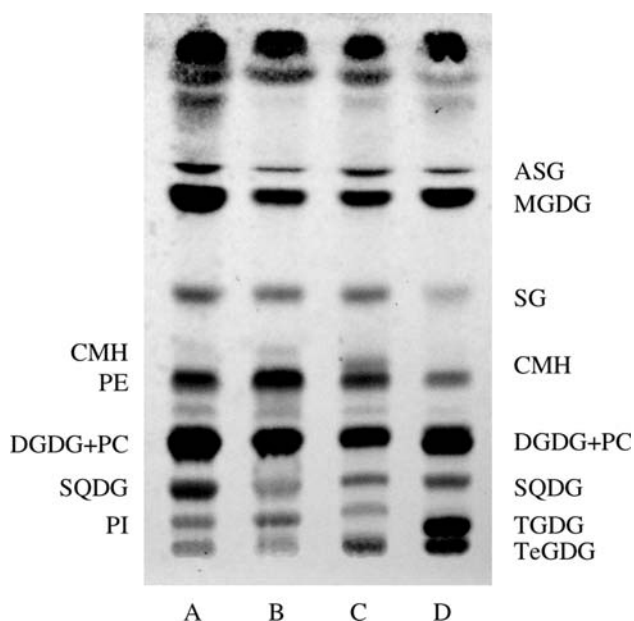
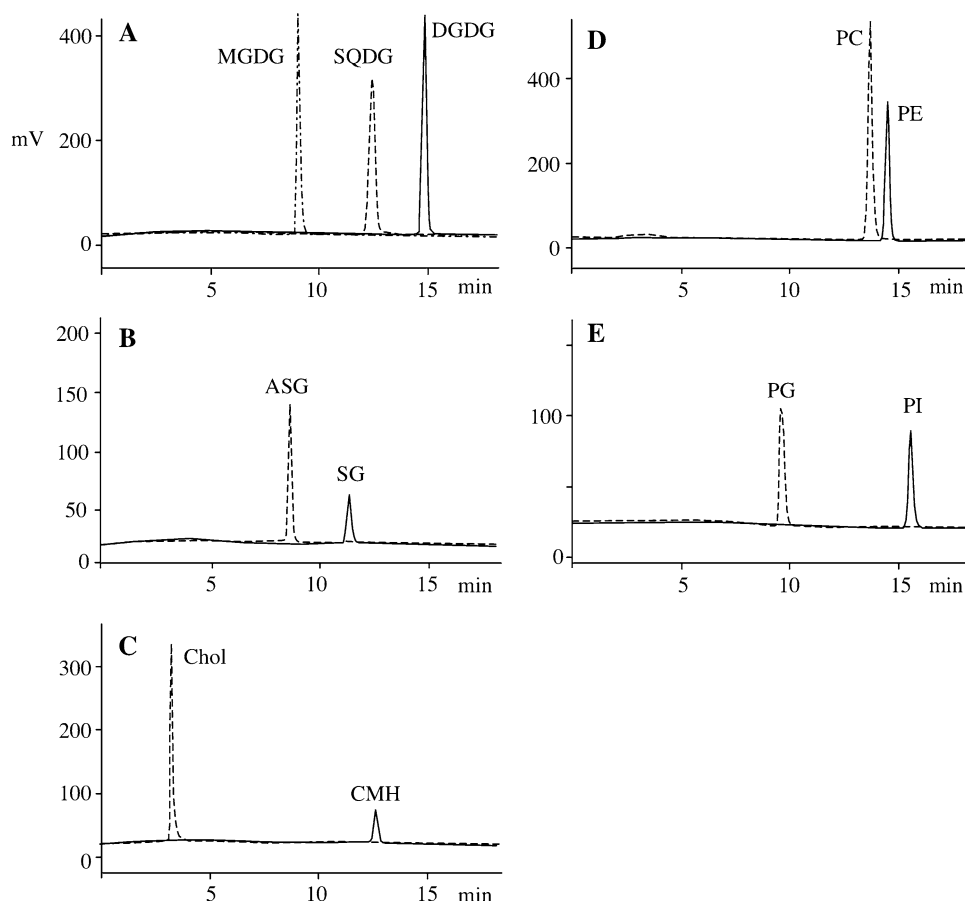


Fig. 2 TLC of total lipids prepared from plant foodstuff. *A* spinach, *B* broccoli, *C* green pepper, *D* pumpkin. Solvent chloroform–acetone–methanol–acetic acid–water (50:20:10:10:5, v/v/v/v/v), Detection anthrone–sulfuric acid followed by heating. See Fig. 1 for abbreviations. *TGDG* triglycosyldiacylglycerol, *TeGDG* tetraglycosyldiacylglycerol

relatively high in DGDG. SQDG was highest in parsley (101 mg), followed by crown daisy (48 mg) and spinach (45 mg). Also, SQDG was comparatively rich even in pumpkin (26 mg), a fruit vegetable. Relative amounts of SQDG in glyceroglycolipids were high in cucumber, pumpkin and crown daisy.

Discussion

Glyceroglycolipids are the main lipid class present in photosynthetic plant tissues and are accompanied by glycerophospholipids. Acidic glycerophospholipids and glyceroglycolipids including PG, PI and SQDG, as well as neutral glycolipids including acylsterylglucoside, CMH, MGDG and DGDG, and neutral phospholipids including PC and PE, were detected in a single HPLC run without any pretreatment such as anion-exchange column chromatography. This may have resulted from not only addition of acid (acetic acid), but also a basic substance (triethylamine), which may have improved the dissolubility of acidic lipid groups.

Since green pepper TL contained almost all of the glycolipid and phospholipid classes detected by TLC analysis

Fig. 3 Typical HPLC profiles of lipid fractions prepared from plant foodstuffs. *TL* total lipid, *NL* neutral lipid fraction, *AL* acidic lipid fraction. 1 Chol, 2 ASG, 3 MGDG, 4 PG, 5 SG, 6 SQDG, 7 CMH, 8 PC, 9 PE, 10 DGDG, 11 PI, 12 TG DG, 13 TeGDG. See Fig. 1 for abbreviations. *FFA* free fatty acids

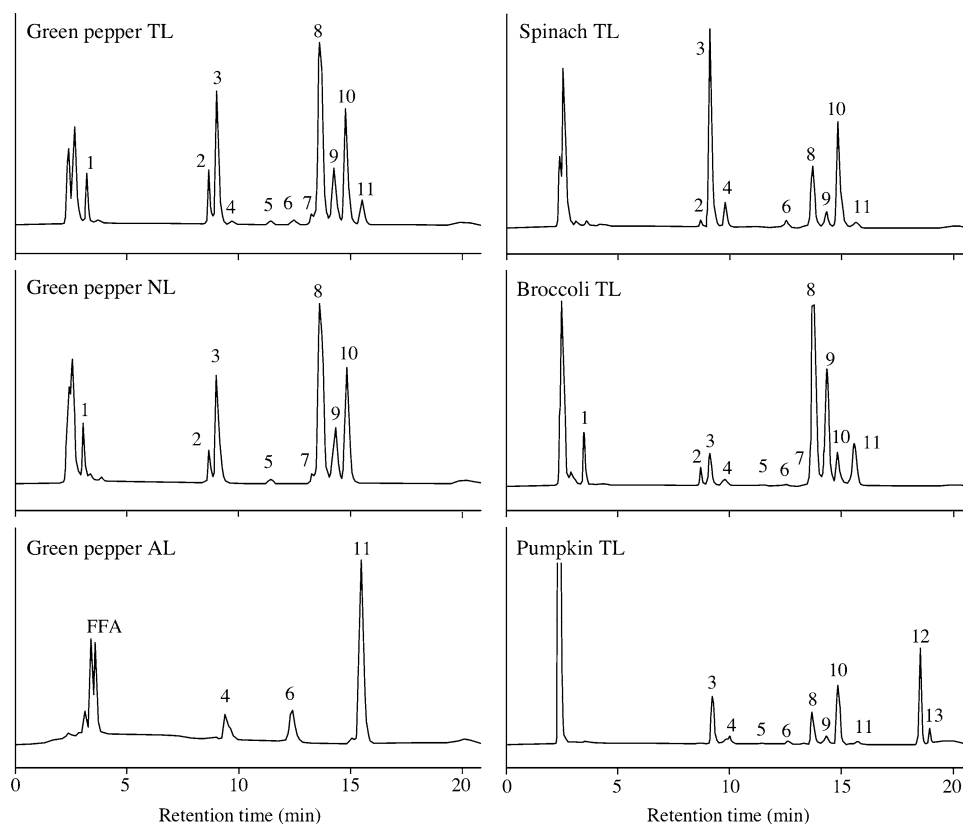


Table 2 Glyceroglycolipid contents of edible plants determined by HPLC–ELSD

Vegetables	Organ	Total lipids (g/100 g)	MGDG ^a	DGDG ^a	SQDG ^a	Total ^a	Ratio M:D:S
Spinach	Leaf	0.7 ± 0.01	243 ± 26	136 ± 10	45 ± 4	424 ± 38	57:32:11
Parsley	Leaf	1.6 ± 0.05	697 ± 51	147 ± 15	101 ± 7	945 ± 74	74:15:11
Perilla	Leaf	1.1 ± 0.08	222 ± 21	139 ± 15	36 ± 8	397 ± 36	56:35:9
Chive	Leaf	0.6 ± 0.06	158 ± 46	57 ± 19	18 ± 6	233 ± 72	68:24:8
Green onion	Leaf	0.2 ± 0.01	12 ± 3	8 ± 1	3 ± 0	23 ± 4	52:35:13
Crown daisy	Leaf and stem	0.7 ± 0.13	123 ± 22	132 ± 24	48 ± 9	303 ± 56	40:44:16
Broccoli	Flower and stem	1.0 ± 0.06	50 ± 1	39 ± 1	14 ± 1	103 ± 2	48:38:14
Green pepper	Fruit	0.2 ± 0.01	21 ± 5	23 ± 5	6 ± 1	50 ± 10	42:46:12
Cucumber	Fruit	0.2 ± 0.01	11 ± 3	8 ± 2	4 ± 0	23 ± 5	48:35:17
Pumpkin	Fruit	0.7 ± 0.01	66 ± 11	77 ± 5	26 ± 1	169 ± 12	39:46:15

M:D:S indicate the ratio of MGDG/DGDG/SQDG

Data indicate lipid content per fresh weight

^a Values are mg/100 g

(Fig. 2), it was possible to simultaneously detect both glycolipids and phospholipids from a single analytical HPLC. However, since broccoli TL was rich in glycerophospholipids, SQDG could not be detected within the detection limit of PC (Fig. 3). Moreover, since spinach TL was rich in glyceroglycolipids, SG and CMH could not be detected within the detection limit of MGDG. In these cases, in order to quantify all lipids including phospholipids, it may be necessary to analyze them repeatedly by

changing the injection volume, or to measure them separately by separating the neutral and acidic lipids using an anion-exchange column like DEAE (as shown in Fig. 3). Despite large quantitative differences in SQDG, this study revealed that plant glyceroglycolipids, including SQDG, could be simultaneously detected in all samples. Some research into the occurrence of TG DG has previously been reported in pumpkin [24, 31], but not research into TeGDG. Since TeGDG has also been identified in oat kernels

[32], further verification of these oligoglycosyl-DGs by determining the molar ratio of fatty acid/sugar or by using LC–MS will be needed.

The glycerolglycolipid levels in the various tissues (leaf, fruit, flower, and stem) of each common species were unique. The levels of MGDG were especially high in dark green leafy vegetables such as parsley, chive, and spinach. The levels of DGDG were especially high in crown daisy leaf and stem, pumpkin fruit, and were relatively high in green pepper. It was assumed that this is because the thylakoid membrane with high amount of MGDG in the chloroplasts develops in tissues with active photosynthesis, whereas non-photosynthetic tissues such as fruit, flower and stem were high in DGDG derived from the outer envelope of chloroplasts [1]. It was found that SQDG contents in vegetables were positively correlated ($R = 0.970$, $P < 0.01$) to neutral glycerolglycolipid contents (sum of MGDG and DGDG). Moreover, although sulfur compounds are present in allium including chive and green onion as allyl sulfide, and in broccoli as isothiocyanate, this was not related to the content of SQDG, which has the same sulfur component.

In the future, we plan to use this new HPLC method to compare the levels of SQDG in various agricultural by products and identify one or more of them as potential commercial sources of SQDG.

References

- Block MA, Dorne A-J, Joyard J, Douce R (2005) J Biol Chem 258:13281–13286
- Benning C (1998) Biosynthesis and function of the sulfolipid sulfoquinovosyl diacylglycerol. Annu Rev Plant Physiol Plant Mol Biol 49:53–75
- Guler S, Seeliger S, Hartel H, Render G, Benning C (1996) A null mutant of *Synechococcus* sp. PCC7942 deficient in the sulfolipid sulfoquinovosyl diacylglycerol. J Biol Chem 271:7501–7507
- Sugawara T, Miyazawa T (2001) Beneficial effect of dietary wheat glycolipids on cecum short-chain fatty acid and secondary bile acid profiles in mice. J Nutr Sci Vitaminol (Tokyo) 47:299–305
- Morimoto T, Nagatsu A, Murakami N, Sakakibara J, Tokuda H, Nishino H, Iwashima A (1995) Anti-tumour-promoting glycerolglycolipids from the green alga, *Chlorella vulgaris*. Phytochemistry 40:1433–1437
- Murakami A, Nakamura Y, Koshimizu K, Ohigashi H (1995) Glycerolglycolipids from citrus hystrix, a traditional herb in Thailand, potently inhibit the tumour-promoting activity of 12-*O*-tetradecanoylphorbol 13-acetate in mouse skin. J Agric Food Chem 43:2779–2783
- Murakami C, Kumagai T, Hada T, Kanekazu U, Nakazawa S, Kamisuki S, Maeda N, Xu X, Yoshida H, Sugawara F, Sakaguchi K, Mizushima Y (2003) Effects of glycolipids from spinach on mammalian DNA polymerases. Biochem Pharmacol 65:259–267
- Manez S, Recio MC, Gil I, Gomez C, Giner RM, Waterman PG, Rios JL (1999) A glycosyl analogue of diacylglycerol and other anti-inflammatory constituents from *Inula viscosa*. J Nat Prod 62:601–604
- Larsen E, Kharazmi A, Christensen LP, Christensen SB (2003) An antiinflammatory galactolipid from rose hip (*Rosa canina*) that inhibits chemotaxis of human peripheral blood neutrophils in vitro. J Nat Prod 66:994–995
- Matsufugi M, Nagamatsu Y, Yoshimato A (2000) Protective effects of bacterial glycerolglycolipid M874B against cell death caused by exposure to heat and hydrogen peroxide. J Biosci Bioeng 89:345–349
- Ohta K, Mizushima Y, Hirata N, Takemura M, Sugawara F, Matsukage A, Yoshida S, Sakaguchi K (1998) Sulphoquinovosyldiacylglycerol, KM043, a new potent inhibitor of eukaryotic DNA polymerases and HIV reverse transcriptase type 1 from a marine red alga, *Gigartina tenella*. Chem Pharm Bull (Tokyo) 46:684–686
- Ohta K, Mizushima Y, Hirata N, Takemura M, Sugawara F, Matsukage A, Yoshida S, Sakaguchi K (1999) Action of a new mammalian DNA polymerase inhibitor, sulphoquinovosyldiacylglycerol. Biol Pharm Bull 22:111–116
- Ohta K, Hanashima S, Mizushima Y, Yamazaki T, Saneyoshi M, Sugawara F, Sakaguchi K (2000) Studies on a novel DNA polymerase inhibitor group, synthetic sulphoquinovosyldiacylglycerols: inhibitory action on cell proliferation. Mutat Res 467:139–152
- Hanashima S, Mizushima Y, Ohta K, Yamazaki T, Sugawara F, Sakaguchi K (2000) Structure–activity relationship of a novel group of mammalian DNA polymerase inhibitors, synthetic sulphoquinovosylacylglycerols. Jpn J Cancer Res 91:1073–1083
- Murakami C, Yamazaki T, Hanashima S, Takahashi S, Ohta K, Yoshida H, Sugawara F, Sakaguchi K, Mizushima Y (2002) Structure–function relationship of synthetic sulphoquinovosylacylglycerols as mammalian DNA polymerase inhibitors. Arch Biochem Biophys 403:229–236
- Gustafson KR, Cardellina JH 2nd, Fuller RW, Weislow OS, Kiser RF, Snader KM, Patterson GM, Boyd MR (1989) AIDS-antiviral sulfolipids from cyanobacteria (blue green algae). J Natl Cancer Inst 81:1254–1258
- Gordon DM, Danishefsky SJ (1992) Synthesis of a cyanobacterial sulfolipid: confirmation of its structure, stereochemistry, and anti-HIV-1 activity. J Am Chem Soc 114:659–663
- Reshef V, Mizrahi E, Maretzki T, Silberstein C, Loya S, Hizi A, Carmeli S (1997) New acylated sulfoglycolipids and digalactolipids and related known glycolipids from cyanobacteria with a potential to inhibit the reverse transcriptase of HIV-1. J Nat Prod 60:1251–1260
- Loya S, Reshef V, Mizrahi E, Silberstein C, Rachamim Y, Carmeli S, Hizi A (1998) The inhibition of reverse transcriptase of HIV-1 by the natural sulfoglycolipids from cyanobacteria: contribution of different moieties to their high potency. J Nat Prod 61:891–895
- Golik J, Dickey JK, Todderud G, Lee D, Alford J, Huang S, Klohr S, Eustice D, Aruffo A, Agler ML (1997) Isolation and structure determination of sulfonovosyl dipalmitoyl glyceride, a P-selectin receptor inhibitor from the alga *Dictyochloris fragrans*. J Nat Prod 60:387–389
- Eitsuka T, Nakagawa K, Igarashi M, Miyazawa T (2004) Telomerase inhibition by sulfoquinovosyldiacylglycerol from edible purple laver (*Porphyra yezoensis*). Cancer Lett 212:15–20
- Matsubara K, Matsumoto H, Mizushima Y, Mori M, Nakajima N, Fuchigami M, Yoshida H, Hada T (2005) Inhibitory effect of glycolipids from spinach on in vitro and ex vivo angiogenesis. Oncol Rep 14:157–160
- Bergé JP, Debiton E, Dumay J, Durand P, Barthomeuf C (2002) In vitro anti-inflammatory and anti-proliferative activity of sulfolipids from the red alga *Porphyridium cruentum*. J Agric Food Chem 50:6227–6232

24. Sugawara T, Miyazawa T (1999) Separation and determination of glycolipids from edible plant sources by high-performance liquid chromatography and evaporative light-scattering detection. *Lipids* 34:1231–1237
25. Kuriyama I, Musumi K, Yonezawa Y, Takemura M, Maeda N, Iijima H, Hada T, Yoshida H, Mizushima Y (2005) Inhibitory effects of glycolipids fraction from spinach on mammalian DNA polymerase activity and human cancer cell proliferation. *J Nutr Biochem* 16:594–601
26. Beermann C, Green A, Mobius M, Schmitt JJ, Boehm G (2003) Lipid class separation by HPLC combined with GC FA analysis: comparison of seed lipid compositions from different *Brassica napus* L. varieties. *J Am Oil Chem Soc* 80:747–753
27. Rouser G, Kritchevsky G, Yamamoto A (1967) Column chromatographic and associated procedures for separation and determination of phosphatides and glycolipids. In: Marinetti GV (ed) *Lipid chromatographic analysis*. Marcel Dekker, New York, pp 99–161
28. Folch J, Lees M, Sloane SGH (1957) A simple method for the isolation and purification of total lipids from animal tissues. *J Biol Chem* 226:497–509
29. Galliard T (1969) The isolation and characterization of trigalactosyl diglyceride from potato tubers. *Biochem J* 115:335–339
30. Yunoki K, Yasui Y, Hirose S, Ohnishi M (2005) Fatty acids in must prepared from 11 grapes grown in Japan: comparison with wine and effect on fatty acid ethyl ester formation. *Lipids* 40:361–367
31. Ito S, Okada S, Fujino Y (1974) Glyceroglycolipids in pumpkin. *Nippon Nogeikagaku Kaishi* 48:431–436
32. Moreau RA, Doehlert DC, Welti R, Isaac G, Roth M, Tamura P, Nuñez A (2008) The identification of mono-, di-, tri-, and tetragalactosyl-diacylglycerols and their natural estolides in oat kernels. *Lipids* 43:533–548

Diversity of the Enzymatic Activity in the Lipoxygenase Gene Family of *Arabidopsis thaliana*

Gerard Bannenberg · Marta Martínez ·
Mats Hamberg · Carmen Castresana

Received: 31 July 2008 / Accepted: 18 September 2008 / Published online: 24 October 2008
© AOCs 2008

Abstract Lipoxygenases (LOX) catalyze the oxygenation of polyunsaturated fatty acids, the first step in the biosynthesis of a large group of biologically active fatty acid metabolites collectively named oxylipins. In the present study we report the characterization of the enzymatic activity of the six lipoxygenases found in the genome of the model plant *Arabidopsis thaliana*. Recombinant expressed AtLOX-1 and AtLOX-5 had comparable oxygenase activity with either linoleic acid or linolenic acid. AtLOX-2, AtLOX-3, AtLOX-4 and AtLOX-6 displayed a selective oxygenation of linolenic acid. Analyses by high-performance liquid chromatography and gas chromatography-mass spectrometry demonstrated that AtLOX-1 and AtLOX-5 are 9S-lipoxygenases, and AtLOX-2, AtLOX-3, AtLOX-4 and AtLOX-6 are 13S-lipoxygenases. None of the enzymes had dual positional specificity. The determined activities correlated with that predicted by their phylogenetic relationship to other biochemically-characterized plant lipoxygenases.

Keywords *Arabidopsis thaliana* · Fatty acid · Fatty acid hydroperoxide · Lipoxygenase · Oxylipins

Gerard Bannenberg, Marta Martínez shared first authors.

G. Bannenberg · M. Martínez · C. Castresana (✉)
Departamento de Genética Molecular de Plantas,
Centro Nacional de Biotecnología, CSIC,
Madrid, Spain
e-mail: gbannenberg@cnb.csic.es

M. Hamberg
Department of Medical Biochemistry and Biophysics,
Division of Physiological Chemistry II, Karolinska Institutet,
Stockholm, Sweden

Abbreviations

AtLOX	Lipoxygenase from <i>Arabidopsis thaliana</i>
GC-MS	Gas-liquid chromatography-mass spectrometry
HOD	Hydroxyoctadecadienoic acid
LOX	Lipoxygenase
SP-HPLC	Straight-phase HPLC

Introduction

Lipoxygenases (LOX) are non-heme iron-containing dioxygenases which catalyze the incorporation of molecular oxygen at a 1(Z),4(Z)-pentadienyl moiety of polyunsaturated fatty acids forming hydroperoxy fatty acids [1–3]. In plants, these primary products serve as precursors of a range of oxylipins which have important regulatory roles in development and in the defense towards microbial pathogens and herbivores [4–6]. Within a single plant species, distinct lipoxygenase genes are expressed in a temporal and spatial specific manner to initiate distinct biosynthetic pathways and generate specific functional derivatives. Thus, determination of the enzymatic activity catalyzed by individual isoforms is an essential requisite for assigning roles to distinct oxylipin biosynthetic pathways.

Lipoxygenases can be conveniently classified as 9- and 13-lipoxygenases, according to the position of oxygen incorporation in linoleic acid and linolenic acid, the most important substrates for LOX catalysis in plants [7, 8]. Moreover, lipoxygenases with dual 9- and 13-lipoxygenase activity have also been identified [9, 10]. Lipoxygenase reactions are further characterized by a high stereospecificity, with most lipoxygenases catalyzing the formation of (S)-configured fatty acid hydroperoxides. Specific oxylipins

that are implicated in different components of plant development include the 13-LOX-derived jasmonic acid in fertilization, and novel 9-lipoxygenase derivatives in lateral root development [11–13]. In addition, several lines of evidence indicate important roles of 9- and 13-lipoxygenases in plant defense reactions [14–17], e.g. the temporal correlation between lipoxygenase expression and different types of microbial infections of plants [18–21], the modification of the plant response to infection in mutants and transgenic lines altered in the synthesis of oxylipins [22, 23], the signaling activity of oxylipins as inducers of defense gene expression [24, 25], and the antimicrobial effect displayed by many oxylipins [26]. Among the various described lipoxygenase-derived plant lipid mediators, jasmonic acid has received most attention due to its important role in the protection of plants towards pathogens and insect pests via the activation of specific defense genes [13, 25, 27–29]. The first step in its biosynthesis is catalyzed by 13-lipoxygenase, yet it is still for the most part unknown which 13-lipoxygenase isoenzymes contribute to jasmonic acid biosynthesis under particular circumstances. Compared to 13-lipoxygenase, the function of 9-lipoxygenases and 9-lipoxygenase-derived oxylipins has not received as much attention, but its role has recently received increased appreciation [12, 30].

One of the model plant species employed extensively for the study of plant biology is *Arabidopsis thaliana*. Six predicted lipoxygenase genes are present in its genome, but the nature of their enzymatic activity has not been determined. *At-LOX* gene expression has been recently examined in *Arabidopsis* seedlings and a role for two putative 9-lipoxygenases, *AtLOX-1* and *AtLOX-5*, in lateral root development has been shown [12]. *AtLOX-1* is probably located in the cytosol and its gene expression is activated in roots, leaf senescence, pathogen infection and upon exposure to methyl jasmonate [31–33]. *AtLOX-2* is localized in the chloroplast thylakoid and envelope membrane [34], and is expressed in leaves and flowers [15]. *At-LOX-2* gene transcription is activated after exposure to methyl jasmonate [35] and green leafy volatiles [36], and is down-regulated during senescence [32]. *AtLOX-2* is essential for jasmonic acid formation upon wounding [15]. Substantially less is known about the localization, activity and function of other *Arabidopsis* lipoxygenases *At-LOX-3*, *At-LOX-4*, *At-LOX-5*, and *At-LOX-6*. The *At-LOX-3* gene is expressed in roots, and gene transcription of both *At-LOX-3* and *At-LOX-4* is known to be activated during leaf senescence [32], as well as by exogenous jasmonate [37].

Given the central regulatory roles of specific 9- and 13-lipoxygenase-derived oxylipins, a comprehensive understanding of the nature of enzymatic activity of lipoxygenases is fundamental. Biochemical characterization of a number of

lipoxygenases indicated that their catalytic activity can be predicted from their primary structure to a certain extent [7], but unequivocal assignment of regio- and stereo specificity of lipoxygenase-catalyzed fatty acid oxygenations requires direct experimental determination. In order to facilitate further studies on the role of lipoxygenases in plant development and defense, we set out to characterize biochemically the regio- and stereospecificity of the six lipoxygenases present in the *A. thaliana* genome. The presented results comprise the systematic characterization of the regio- and stereospecificity of the fatty acid oxygenations catalyzed by the complete family of lipoxygenases of *A. thaliana*.

Experimental Procedures

Cloning of *Arabidopsis* Ecotype Columbia Lipoxygenase cDNAs

LOX2, LOX4 and LOX5 cDNAs were obtained by using Protoscript^R First Strand cDNA Synthesis Kit (New England Biolabs, Ipswich, MA, USA) with RNA isolated from leaves 1 h post touching and amplified by PCR with the Expand High-Fidelity PCR System (Roche Diagnostics GmbH, Mannheim, Germany). LOX3 cDNA was obtained and amplified in only one step by RT-PCR using the Titan One Tube RT-PCR system (Roche Applied Science) with the above mentioned RNA, which was previously treated with DNase TURBO DNA-freeTM (Ambion) to remove contaminating DNA. LOX1 and LOX6 cDNAs were PCR-amplified from templates H3C1 and U15695 clones with GenBank accessions W43645 and BT010546, respectively, obtained from the *Arabidopsis* Biological Resource Center (Ohio State University, Columbus, OH, USA) by using *PfuUltra*TM High-Fidelity DNA Polymerase (Stratagene, La Jolla, CA, USA).

All amplification steps were performed with a GeneAmp PCR System 9700 thermal cycler (Applied Biosystems). Primers used and amplification products are described in Table 1. Products were initially cloned in plasmid pGEMTeasy (Promega, Madison, WI, USA), and later transferred to pFastBac1 expression vector (Life Technologies, Gaithersburg, MD, USA) by taking advantage of *SpeI* (LOX1, LOX2, LOX4, LOX5, and LOX6) or *NorI* (LOX3) restriction sites. Correctly encoded proteins were confirmed by DNA sequencing.

Heterologous Expression of *Arabidopsis thaliana* Lipoxygenases

Recombinant baculoviruses expressing *A. thaliana* *AtLOX-1*, *AtLOX-2*, *AtLOX-3*, *AtLOX-4*, *AtLOX-5*, and

Table 1 Identity of *A. thaliana* lipoxygenases, and primers used for gene amplification

Locus	Description	Upper primer		Lower primer		Amplicon length (bp)	Encoded protein length (amino acids)
		5' Position ^a	Sequence ^b	5' Position ^a	Sequence ^c		
Atlg55020	LOX1	-29	GAATCAAAA <u>ACTAGTACTTCACCCAA</u>	+2595	GAAGCGAGAGTTGTTTCAGATAG	2,624	859
Atlg45140	LOX2	-16	AGAAGAGAAAA <u>ACTAGTAGTATTGTAG</u>	+2711	TGAGAAAAGAAAATGCATAGATC	2,727	896
Atlg17420	LOX3	-3	GTGATGGCCCTTAGCTAAAGAGTTA	+2769	CCTTCTTAATATATAGATACACTATTAG	2,772	919
Atlg72520	LOX4	-16	ACTAATTCTTACTAGTATGGCCTTAG	+2792	ATTGAATAATTTCTAAATAGATACACTAT	2,808	926
Atlg22400	LOX5	-12	ACTAGTATCGCCATGATCCACACCG	+2677	GAGAGAGGGTTTATCTTTAGATTGAGAC	2,689	886
Atlg67560	LOX6	-15	CAA <u>ACTAGTGTAA</u> AAATGTTTCGTAGCA	+2757	CATCTAAATGGAAATGCTGTGTGG	2,772	917

^a From the translation start site

^b Underlined are mutated bases in order to create an *SpeI* restriction site, bold bases indicate the translation start site

^c Bold bases indicate the translation stop codon

AtLOX-6 were generated using the Bac-to-Bac baculovirus expression system (InVitrogen, Paisley, UK). The recombinant pFastBac plasmids were transferred into DH10Bac *E. coli* cells containing the baculovirus shuttle vector bMON14272 and the helper plasmid pMON7124. Recombinant bacmid DNA was prepared from galactosidase-negative and kanamycin-, gentamycin- and tetracycline-resistant bacterial clones. High titer recombinant baculovirus was obtained by lipofectamine transfection of the bacmids into High Five insect cells after one round of viral amplification. AtLOX-1, AtLOX-2, AtLOX-3, AtLOX-4, AtLOX-5, and AtLOX-6 were expressed by infecting High Five insect cell cultures, grown at 28 °C in Tc-100 medium supplemented with 10% fetal calf serum, with the recombinant baculoviruses. At 48 h after infection, cells were collected by centrifugation (5 min, 3,000g), washed twice with Dulbecco's phosphate-buffered saline (pH 7.4), divided in aliquots and pelleted by centrifugation (5 min, 3,000g). Cell pellets were snap-frozen in liquid nitrogen and stored at -80 °C. Total protein lysates of lipoxygenase-expressing High Five insect cells were prepared in sample buffer (30 mM Tris, pH 6.8, 0.5% sodium dodecyl sulfate, 0.5% β -mercaptoethanol, 5% glycerol, 1 mM EDTA, 1 \times protease inhibitor cocktail (Sigma P-2714), 0.005% bromophenol blue), and separated by sodium dodecyl sulfate/polyacrylamide gel electrophoresis (9% cross-linked gels) at 100 V for 3 h in a Bio-Rad gel electrophoresis system [38]. Proteins were stained with Coomassie Brilliant Blue. The apparent molecular weight of the recombinant proteins was determined using molecular weight marker proteins (BenchMark, InVitrogen). Total protein content was determined by the Bradford method, using cell homogenates prepared in 0.1 M Tris buffer, pH 7.4 with 0.1% Triton X-100 [39].

Oxygenase Activity

Oxygenase activity was determined by measurement of oxygen consumption during lipoxygenase-catalyzed fatty acid oxygenation by means of a Clark-type oxygen electrode (Hansatech Instruments Ltd, Norfolk, UK). For oxygenation assays insect cell homogenates were prepared by brief sonication (4 °C, 3 \times 3 s at 35 W; Labsonic U sonicator, B. Braun) in 0.1 M Tris pH 7.4 containing 1 mM PMSF, 10 μ g/ml leupeptin, 10 μ g/ml chymostatin and 10 μ g/ml pepstatin, kept on ice, and analyzed immediately thereafter. Homogenates corresponding to approximately 20 μ g total protein were added to the measuring cell containing 1.5 ml 0.1 M Tris, pH 7.4 and 100 μ M linoleic acid, linolenic acid and arachidonic acid. Oxygen consumption was recorded at room temperature, and the rate of enzyme activity calculated as

nmol oxygen consumed during the first minute per mg protein.

Enzyme Incubations and Product Identification

For the determination of lipoxygenase product formation, homogenates of lipoxygenase-expressing High Five cells ($\sim 6 \times 10^6$ cells) were prepared by a brief sonication (3 times 3 s, 10 W at 0 °C) in 0.5 ml 0.1 M Tris buffer pH 7.4. Incubations (5 ml) were carried out with linoleic acid (100 μ M) in 0.1 M Tris buffer pH 7.4 at 23 °C for 30 min, under oxygen atmosphere. AtLOX2 and AtLOX-6-containing cell preparations were found to be very sensitive to enzymatic inactivation even when sonicated briefly, and were hence incubated by directly resuspending the frozen cell pellets in the incubation buffer. At the end of the incubations, hydroperoxides were reduced to hydroxides by the addition of 100 mg SnCl₂ in 20 ml of ethanol. Products were extracted with diethyl ether and derivatized to methyl esters with diazomethane. The regio- and stereochemistry of the HOD-methyl esters were determined essentially as previously described [40]. Thus, the composition of the 9- and 13-HOD (*E,Z*) and (*E,E*) isomers was determined by straight-phase HPLC using a Thermo SpectraSeries P100 HPLC pump and a column of Nucleosil 50-5 (250 \times 4.6 mm; Macherey-Nagel, Düren, Germany). The solvent system used was 0.6% 2-propanol/hexane (v/v) at a flow rate of 2 ml/min, and detection was at 234 nm using a Thermo SpectraSeries UV100 detector. The products were identified by co-elution with standards of the methyl esters of 9-hydroxy-10(*E*),12(*Z*)-octadecadienoic acid, 9-hydroxy-10(*E*),12(*E*)-octadecadienoic acid, 13-hydroxy-9(*Z*),11(*E*)-octadecadienoic acid and 13-hydroxy-9(*E*),11(*E*)-octadecadienoic acid. For steric analysis, the HOD-methyl esters collected during straight-phase HPLC were further analyzed by chiral phase HPLC using a column of Chiralcel OB-H (250 \times 4.6 mm; Daicel Chemical Industries, Osaka, Japan) and standards of the methyl esters of 9*S*-, 9*R*-, 13*S*- and 13*R*-hydroxy-(*E,Z*)-octadecadienoic acids. Chromatographic conditions were: mobile phase, 2-propanol/hexane (1.5:98.5% v/v), flow rate 0.5 ml/min. Detection was at 234 nm. The most abundant oxygenation products were collected and converted to trimethylsilyl ether derivatives by treatment with trimethylchlorosilane/hexamethyldisilazane/pyridine (2:1:2, v/v/v) prior to analysis by GC/MS. A Hewlett-Packard model 5970B mass selective detector connected to a Hewlett-Packard model 5890 gas chromatograph equipped with a capillary column of 5% phenylmethyl siloxane (12 m, 0.33 μ m film thickness) were used for GC-MS analysis. Helium was used as the carrier gas, the inlet temperature was 200 °C, and the column temperature was raised from 120 to 300 °C at 10 °C/min.

Sequence Alignment and Phylogenetic Relationship Analysis of *Arabidopsis thaliana* Lipoxygenases with Other Enzymatically-Characterized Plant Lipoxygenases

Arabidopsis thaliana lipoxygenases were aligned with 28 enzymatically-characterized plant lipoxygenases using the Clustal W2 program [41] and subjected to phylogenetic analysis by the neighbor-joining and maximum parsimony methods using the PHYLIP package [42] through the facilities of the Mobylye platform from Institut Pasteur server (<http://mobylye.pasteur.fr/cgi-bin/MobylyePortal/portal.py>). To maximize the statistical significance of the phylogenetic trees generated by the distance and parsimony methods, 1,000 bootstrap replicates were obtained by both methods.

Results

Lipoxygenase Activity of *Arabidopsis thaliana* Lipoxygenases

Bioinformatic analysis of the *A. thaliana* genome indicates the existence of six lipoxygenase genes. No systematic study has been published which addresses the characterization of the complete *A. thaliana* lipoxygenase family. To determine if *A. thaliana* lipoxygenase-1, -2, -3, -4, -5, and -6 are authentic lipoxygenases, the corresponding full-length cDNAs were cloned and expressed in insect cells, and the regio- and stereospecificity of the oxygenase activity with fatty acids was determined. Infection of High Five insect cells with recombinant baculovirus containing the *At-LOX1-6/pFastBac* construct resulted in the expression of the six lipoxygenases at high level (Fig. 1). The molecular mass of the expressed proteins was in accordance with the calculated masses of the full-length proteins, namely 98–105 kD. Insect cells infected with baculovirus prepared from empty pFastBac vector did not express lipoxygenase (Fig. 1).

In oxygen consumption assays with linoleic acid, linolenic acid and arachidonic acid as substrate, homogenates of lipoxygenase-expressing insect cells displayed oxygenase activity (Fig. 1b). Maximal activities were measured at neutral pH for AtLOX-1, -3, -4, -5, and -6 (data not shown). AtLOX-2 displayed low oxygenase activities (≤ 10 nmol O₂ min⁻¹ mg⁻¹ protein), and no clear pH optimum could be defined. Maximal oxygenase activities were measured with AtLOX-1 using linolenic acid as substrate (554 ± 44 nmol O₂ min⁻¹ mg⁻¹ protein; mean \pm standard error, $n = 4$). A comparison of the oxygenation activities of each lipoxygenase revealed that AtLOX-1 and AtLOX-5 oxygenated both linoleic acid and

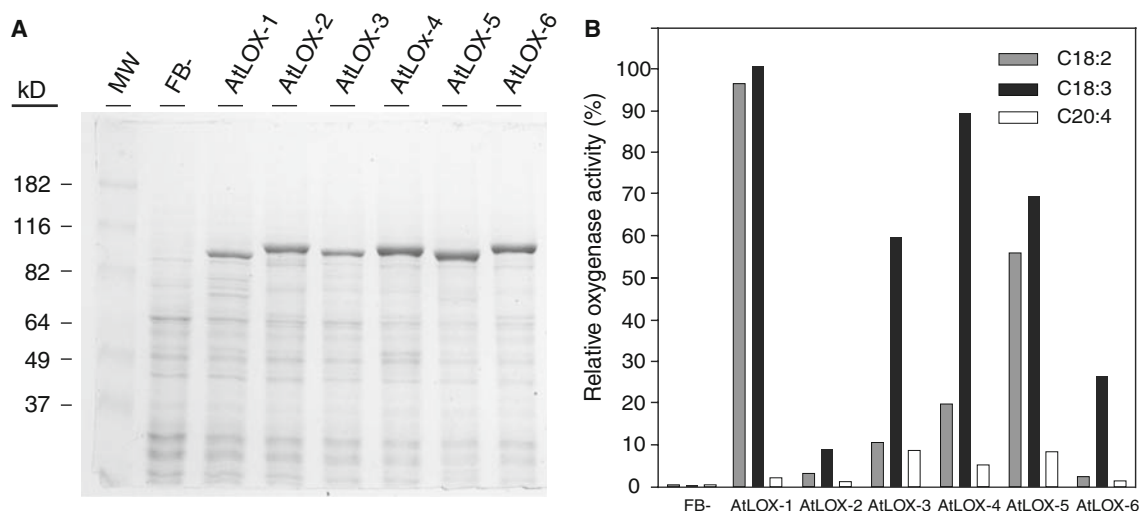


Fig. 1 Heterologous expression of *A. thaliana* lipoxygenases in insect cells. **a** SDS-polyacrylamide gel illustrating the expression of *A. thaliana* lipoxygenases in High Five insect cells infected with recombinant baculovirus. Lane 1, molecular mass markers (MW indicated in kDa); lane 2 cells infected with baculovirus without transposed gene (FB-); lanes 3–8 cells infected with recombinant pFastBac/AtLOX-1, AtLOX-2, AtLOX-3, AtLOX-4, AtLOX-5 and AtLOX-6 baculovirus, respectively, 48 h after infection. Each lane

corresponds to protein lysates derived from approximately 125,000 cells. **b** Oxygenase activity of the recombinant expressed *A. thaliana* lipoxygenases with linoleic acid (C18:2), linolenic acid (C18:3) and arachidonic acid (C20:4). Oxygenase activities are expressed as a percentage of the highest oxygenase activity measured (100% corresponds to $554 \text{ nmol O}_2 \text{ min}^{-1} \text{ mg}^{-1}$ protein for AtLOX-1 with $100 \mu\text{M}$ C18:3)

linolenic acid with similar activity (Fig. 1b). In contrast, AtLOX-2, AtLOX-3, AtLOX-4 and AtLOX-6 oxygenated linolenic acid more effectively than linoleic acid. Arachidonic acid was a relatively poor substrate for all six *A. thaliana* lipoxygenases. No oxygenase activity was detected in homogenates of insect cells infected with baculovirus devoid of lipoxygenase gene (FB-).

Straight-phase HPLC analysis of the reduced and methyl-esterified oxygenation products formed from linoleic acid established the positional specificity of the heterologously expressed lipoxygenases by co-chromatography with standards of the methyl esters of 13-HOD-*E,Z*, 13-HOD-*E,E*, 9-HOD-*E,Z* and 9-HOD-*E,E* (Fig. 2; Table 2). AtLOX-1 and AtLOX-5 were found to form exclusively 9-HOD-*E,Z*, whereas AtLOX-2, AtLOX-3, AtLOX-4 and AtLOX-6 formed 13-HOD-*E,Z*. Representative chromatograms for one 13-lipoxygenase (AtLOX-2) and one 9-lipoxygenase (AtLOX-5) are shown in Fig. 2. No enzymatic activity was detected in homogenates of insect cells infected with baculovirus devoid of lipoxygenase gene (Fig. 2, bottom panel).

The structure of the products was confirmed by gas chromatography-electron impact mass spectrometry after trimethylsilylation of methyl-esterified lipoxygenase products purified by straight-phase HPLC. Diagnostic ions for both 9-HOD-Me and 13-HOD-Me TMS derivatives were m/z 382 (M^+), m/z 311 ($(\text{CH}_3)_3\text{SiO}^+=\text{CH}-\text{CH}=\text{CH}-\text{CH}=\text{CH}-(\text{CH}_2)_7-\text{COOCH}_3$) and m/z 225 ($\text{M}^+-(\text{CH}_2)_7-\text{COOCH}_3$). The ratio of ion intensities of m/z 311/225 was

indicative of either 9-HOD-methyl ester (ratio 0.19) or 13-HOD-methyl ester (ratio 1.8), respectively (Fig. 3, lower panels). Only in the case of AtLOX-2 a low additional enzymatic activity could be confirmed mass-spectrometrically in addition to the formation of 13-HOD, namely 0.7% of the product was 9-HOD.

The stereochemistry of the lipoxygenase-catalyzed HOD acids from linoleic acid was determined by chiral phase HPLC. Steric analysis of the SP-HPLC-purified methyl esters of 9-HOD and 13-HOD demonstrated that all lipoxygenases catalyzed the incorporation of oxygen with the *S*-configuration (Fig. 3; Table 2). Representative recordings for one 13-lipoxygenase (AtLOX-2) and one 9-lipoxygenase (AtLOX-5) are shown in Fig. 3.

Sequence Alignment and Phylogenetic Relationship Analysis of *A. thaliana* Lipoxygenases with Other Enzymatically Characterized Plant Lipoxygenases

In order to determine whether the primary structure of the *A. thaliana* lipoxygenases accurately predicts the determined regiospecificity of oxygenation, a phylogenetic analysis was performed in which the extent of sequence diversification of the *A. thaliana* lipoxygenases was compared with that of 28 biochemically characterized plant lipoxygenases. The phylogenetic tree, shown in Fig. 4, displayed four main clusters, which were assigned the labels A–D. Calculation of evolutionary distances of the *A. thaliana* lipoxygenases to the other plant lipoxygenases

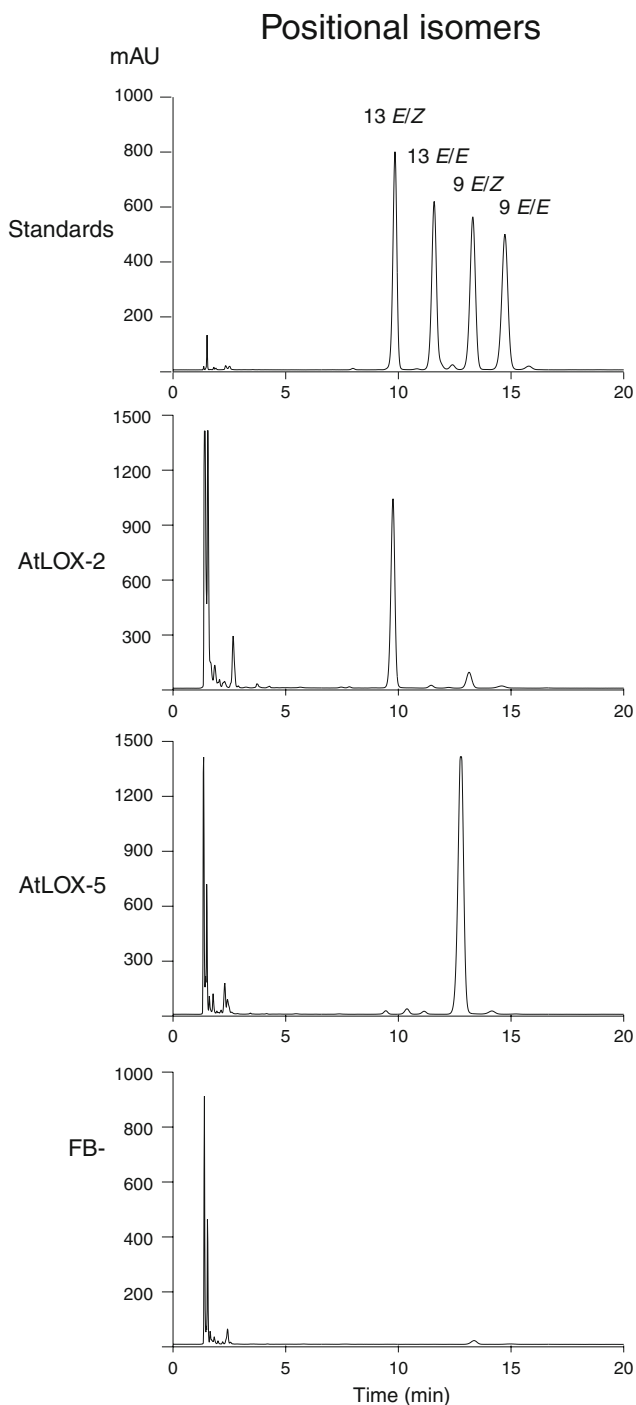


Fig. 2 Determination of positional specificity of *A. thaliana* lipoxygenases. Straight-phase HPLC analysis of 9- and 13-hydroxy-octadecadienoic acid formed by incubation of linoleic acid with homogenates of *A. thaliana* lipoxygenase-expressing insect cells. Products were identified as their methyl esters by co-elution with synthetic standards (*top panel*). Representative chromatograms are shown for the regiospecific oxygenation of linoleic acid by one *A. thaliana* 13-lipoxygenase (*AtLOX-2*), one 9-lipoxygenase (*AtLOX-5*), and homogenate of control infected insect cells (*FB-*)

indicated that AtLOX-1 and AtLOX-5, both characterized in the present study as 9*S*-lipoxygenases, grouped with several other plant 9*S*-lipoxygenases as well as with lipoxygenases with dual 9/13-specificity (Cluster C). Upon closer inspection the two *A. thaliana* 9-lipoxygenases grouped closely with 9-lipoxygenases from dicotyledonous plants (almond, tobacco, and three potato 9-lipoxygenases), whereas 9-lipoxygenases from monocotyledonous species formed a separate subgroup. All cluster D species are members of the legume family *Fabaceae*. Thus, lipoxygenase proteins in this group seem to have evolved independently of other dicotyledonous lipoxygenases. Most of the lipoxygenases in cluster D are 13-lipoxygenases although some harbor dual specificity. None of the *Arabidopsis* LOX proteins is included in this cluster. AtLOX-2, -3, -4 and -6 grouped together with plant lipoxygenases which are exclusively 13-lipoxygenases. Within this quite large group of 13-lipoxygenases from both mono- and dicotyledonous plant species, AtLOX-2 (Cluster A) appears to be distantly related to AtLOX-3, -4 and -6 (Cluster B). The latter three *Arabidopsis* lipoxygenases grouped closely together with one potato 13-lipoxygenase.

Based on their cellular localization, lipoxygenases have been classified as Type II, which contain a chloroplastic N-terminal localization peptide, and type I, including those proteins that do not show any apparent signal localization sequence [7]. Lipoxygenases grouped in Clusters A and B are Type II lipoxygenases with 13-LOX activity, whereas proteins in clusters C and D are Type I lipoxygenases of which some have known 9-LOX activity, some 13-LOX activity, and some are dual specificity lipoxygenases. In summary, the enzymatic activities of the six *A. thaliana* lipoxygenases characterized in this study correlate well with that predicted by their phylogenetic relationship to other biochemically characterized plant lipoxygenases.

Discussion

Plants have evolved elaborate signaling systems to regulate a variety of physiological responses to the environment, and to facilitate intercellular cross-talk in development and reproduction. Plant oxylipins comprise a large class of oxygenated fatty acid-derived lipid mediators that contribute to such signaling circuits [4, 43]. A variety of functions has been ascribed to different oxylipins, which encompass critical roles in plant defense against microbial pathogens and herbivorous insects, as well as in reproduction and organ development [5, 7, 12, 13, 29, 44]. The biosynthesis of plant oxylipins is initiated by primary fatty

Table 2 Measured retention times and diagnostic ions for AtLOX-1 to AtLOX-6-derived hydroxy-octadecadienoic acids, and hydroxy-octadecadienoic acid standards on straight-phase HPLC, chiral phase HPLC, and gas chromatography

Enzyme	Substrate	Straight-phase t_r (min)	Chiral phase t_r (min)	GC t_r (min)	Hydroxy acid ions	Hydroxy acid	Enzymatic activity
AtLOX-1	C18:2	13.2 (0 ^a)	48.7 (2.9 ^c)	11.66	225, 311, 382	9S-hydroxy-18:2	9S-LOX
AtLOX-2	C18:2	9.8 (0 ^b)	54.6 (0.6 ^d)	11.66	225, 311, 382	13S-hydroxy-18:2	13S-LOX
AtLOX-3	C18:2	9.8 (0 ^b)	54.8 (0.8 ^d)	11.67	225, 311, 382	13S-hydroxy-18:2	13S-LOX
AtLOX-4	C18:2	9.4 (0.4 ^b)	53.7 (0.3 ^d)	11.66	225, 311, 382	13S-hydroxy-18:2	13S-LOX
AtLOX-5	C18:2	12.9 (0.3 ^a)	48.8 (2.8 ^c)	11.68	225, 311, 382	9S-hydroxy-18:2	9S-LOX
AtLOX-6	C18:2	10.2 (0.4 ^b)	53.5 (0.5 ^d)	11.66	225, 311, 382	13S-hydroxy-18:2	13S-LOX
<i>Standards</i>							
	13-(<i>E/Z</i>)-HOD-me	9.8					
	13-(<i>E/E</i>)-HOD-me	11.7					
	9-(<i>E/Z</i>)-HOD-me	13.2					
	9-(<i>E/E</i>)-HOD-me	14.6					
	13 <i>R</i> -(<i>E/Z</i>)-HOD-me		49.5				
	13 <i>S</i> -(<i>E/Z</i>)-HOD-me		54.0				
	9 <i>S</i> -(<i>E/Z</i>)-HOD-me		51.6				
	9 <i>R</i> -(<i>E/Z</i>)-HOD-me		61.8				
	9-(<i>E/Z</i>)-HOD-me-TMS			11.67	225, 311, 382		
	13-(<i>E/Z</i>)-HOD-me-TMS			11.67	225, 311, 382		

For GC/MS analysis the hydroxy acid products were derivatized with diazomethane and trimethylchlorosilane and analyzed by GC/MS as the methyl ester/trimethylsilyl derivative. Retention time differences of the methylated enzymatic products from the nearest eluting standard are indicated between parenthesis, and are labelled with (a) 9(*E/Z*)-HOD-me, (b) 13(*E/Z*)-HOD-me, (c) 9*S*-(*E/Z*)-HOD-me, and (d) 13*S*-(*E/Z*)-HOD-me

acid oxygenases, among which the 9- and 13-lipoxygenases have been studied most intensively [45].

Six lipoxygenase genes are known to be present in the *A. thaliana* genome, yet little information is currently available on the specific function of each isoform. Lipoxygenase activity in *A. thaliana* appears to be dominant in young leaves and gradually decreases as leaves grow older [8]. Detailed studies of the six lipoxygenase genes in *A. thaliana* seedlings revealed expression in leaves of *AtLOX-1*, *At-LOX-2*, *At-LOX3* and *AtLOX-4*. *AtLOX-1*, *At-LOX-3*, *At-LOX5* were actively expressed in root initials where a 9-lipoxygenase-derived oxylipin regulates lateral root formation [12], whereas no expression of *AtLOX-6* was observed in the examined seedlings. The specific activities of lipoxygenases in other *A. thaliana* tissues has been reported in little further detail and no published information is available for allowing the assessment of functional importance of the different lipoxygenases [46]. In view of the fundamental roles for plant physiology embodied by the lipoxygenases, it is of importance to determine the biochemical properties of individual members of this

family of fatty acid oxygenases before further insight into their physiological function can be obtained.

The present study provides a comprehensive biochemical analysis of the enzymatic activity of the six heterologously expressed lipoxygenases of *A. thaliana*. The determination of enzymatic activity revealed that all six *A. thaliana* lipoxygenases are *S*-lipoxygenases. Analysis of positional specificity indicated that *AtLOX-1* and *AtLOX-5* are 9-lipoxygenases, and *AtLOX-2*, -3, -4 and -6 are 13-lipoxygenases. No mixed activity lipoxygenases were identified. Homogenates of insect cells expressing *AtLOX-2* displayed very low activity in oxygenase assays and both *AtLOX-2* and *AtLOX-6* were found to only catalyze measurable amounts of HOD product when cell pellets were not sonicated. These observations possibly point to a more labile nature of these two enzymes.

Based on the protein primary structure, the positional specificity of lipoxygenases can be predicted with relatively high confidence. Alignment studies of known lipoxygenases have unveiled several determinants allowing to predict the positional oxygenation specificity on a molecular basis,

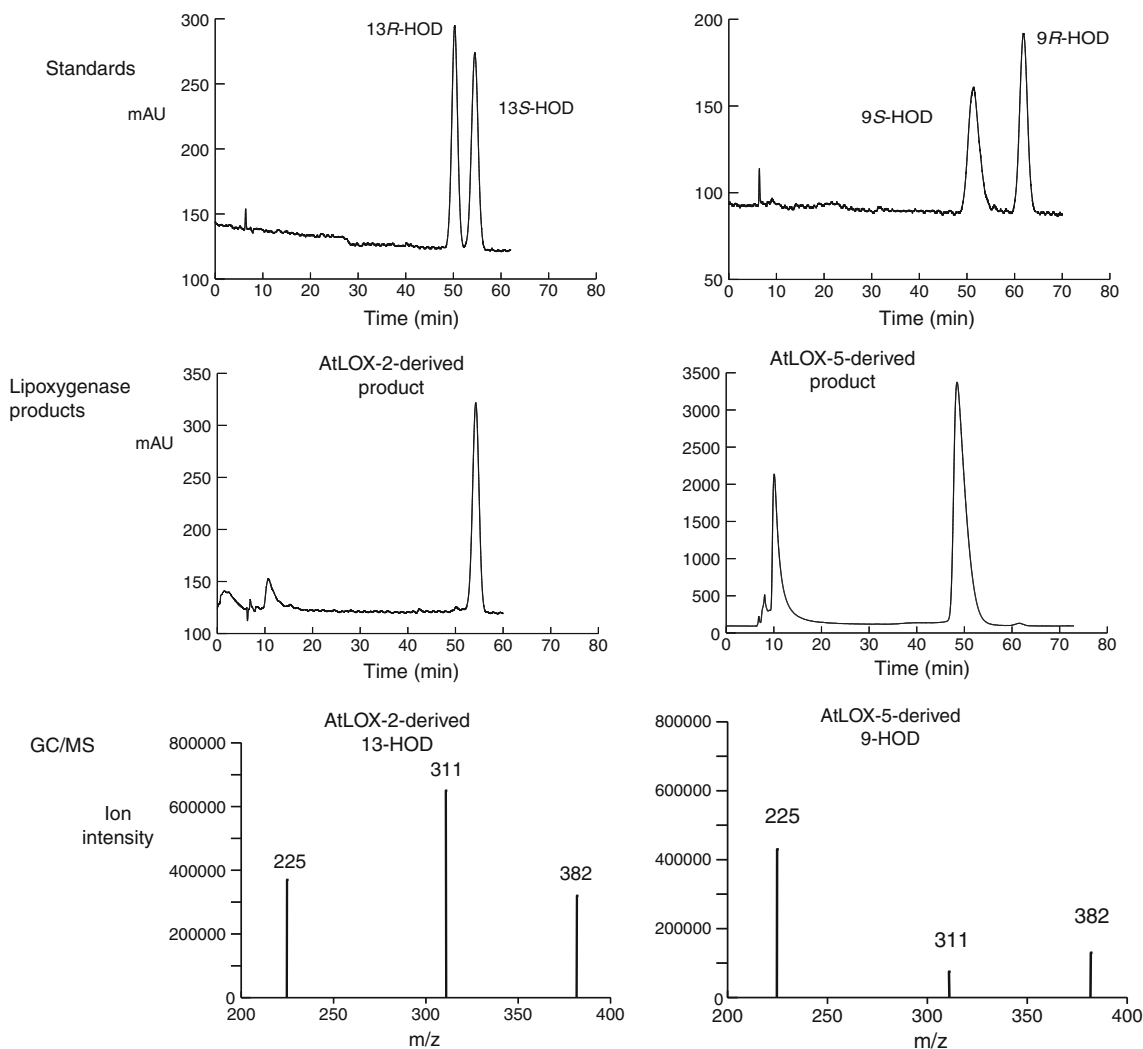


Fig. 3 Determination of stereospecificity of *A. thaliana* lipoxygenases. Steric analysis of 9- and 13-hydroxy-octadecadienoic acid formed by *A. thaliana* lipoxygenases, determined by chiral HPLC as their methyl esters, and GC/MS identification of the 9- and 13-hydroxy-octadecadienoic acid products analyzed as the methyl ester/trimethylsilyl derivative. Representative chromatograms are shown for the hydroxy-octadecadienoic acid products formed by one *A. thaliana* 13-lipoxygenase (AtLOX-2), and one 9-lipoxygenase

(AtLOX-5) (middle panels). Products were identified by co-elution with standards (top panels). Peaks collected from straight-phase HPLC were derivatized with trimethylchlorosilane and analyzed by GC-MS, as described under "Material and methods". Representative selected ion monitoring mass spectra are shown for AtLOX-2-derived 13-HOD (bottom left panel), and AtLOX-5-derived 9-HOD (bottom right panel)

including specific amino acids and surface loops which line the substrate cavity and determine substrate orientation and configuration [9, 47]. Based on their primary structure, AtLOX-1 and AtLOX-5 were predicted to be 9-lipoxygenases and AtLOX-2, AtLOX-3, AtLOX-4 and AtLOX-6 were predicted to be 13-lipoxygenases. In accordance with these predictions, our results on the biochemical characterization of the six *A. thaliana* lipoxygenases presented in this study fully confirm the activity of the distinct isoforms examined. However, prediction of enzyme activity cannot yet provide a complete understanding of catalytic behaviour for all

lipoxygenases. Thus, inspection of the phylogenetic tree indicates that protein similarity alone is not enough to fully predict lipoxygenase substrate specificity. Our phylogenetic analysis clearly shows that AtLOX-1 and AtLOX-5 group together with other biochemically-characterized 9-lipoxygenases as well as with dual specificity lipoxygenases (cluster C). Likewise, cluster D also groups both lipoxygenases with exclusively 13-LOX activity and dual specificity. Hence, results shown here illustrate that biochemical characterization remains essential to unequivocally assign enzymatic activity of plant lipoxygenases.

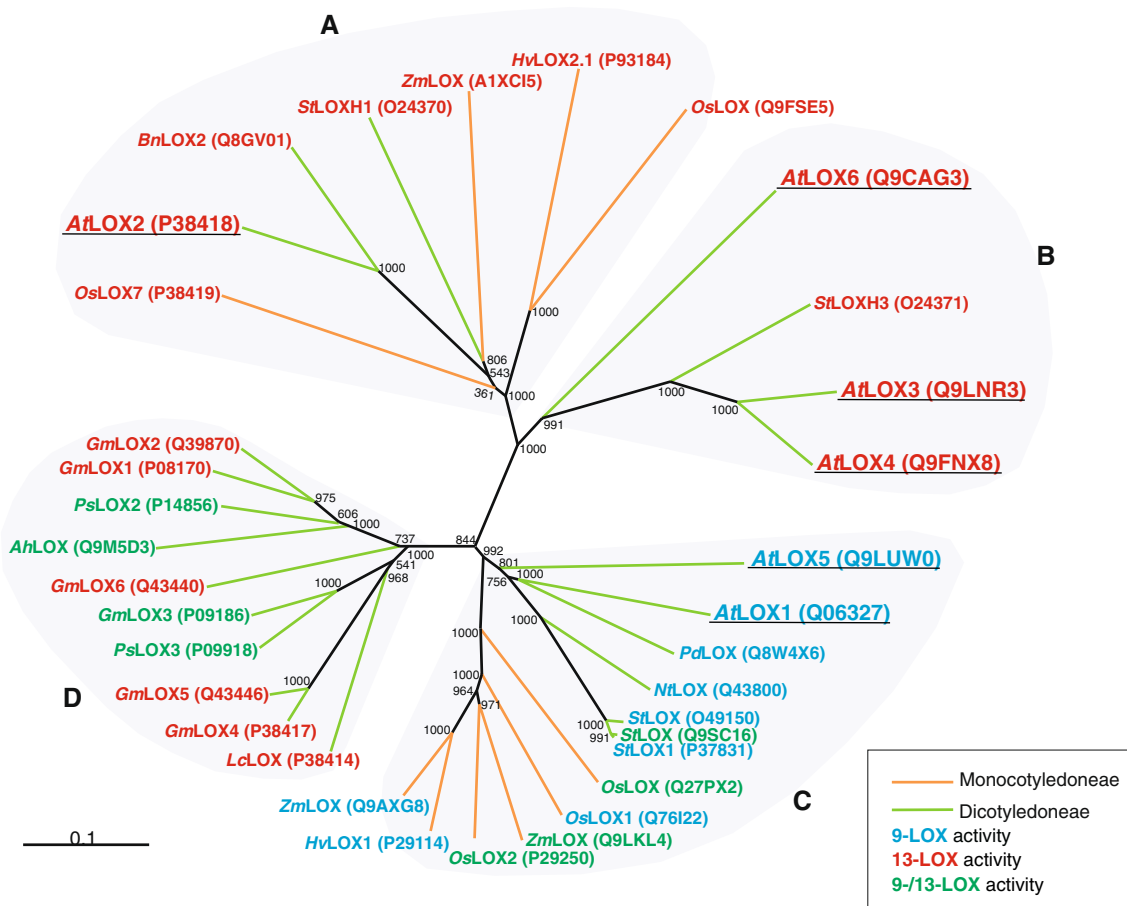


Fig. 4 Phylogenetic relationship between the characterized *A. thaliana* lipoxygenases and enzymatically characterized lipoxygenases from other plant species. Phylogenetic analysis of plant LOX proteins was carried out by using parsimony and distance methods. 1,000 bootstrap replicates were obtained by both methods, with nearly the same results, and only a single tree retrieved from the distance analysis is shown. The % reliability of each branch point of the unrooted tree, as assessed by the analysis of 1,000 trees is shown on each branch stem. Branches colored in *green* and *orange* represent lipoxygenases from monocotyledonous and dicotyledonous species, respectively. 9-Lipoxygenases are labeled in *blue*, 13-lipoxygenases in *red*, and lipoxygenases with dual specificity in *green*, and the six *A. thaliana* lipoxygenases are *underlined*. The identities of the individual lipoxygenase protein sequences are indicated by their Uniprot entry number (<http://www.pir.uniprot.org>). The scale bar corresponds to a distance of 10 changes per 100 amino acids positions. Four clusters in the phylogenetic tree have been arbitrarily assigned the names A, B, C, and D. Individual plant lipoxygenases: AtLOX1 (*Arabidopsis thaliana*; LOX1:At:1), AtLOX2 (*Arabidopsis thaliana*; LOX2:At:1), AtLOX3 (*Arabidopsis thaliana*; LOX2:At:2), AtLOX4 (*Arabidopsis*

thaliana; LOX2:At:3), AtLOX5 (*Arabidopsis thaliana*; LOX1:At:2), AtLOX6 (*Arabidopsis thaliana*; LOX2:At:4), AhLOX (*Arachis hypogaea*; LOX1:Ah:1), BnLOX2 (*Brassica napus*; LOX2:Bn:2), GmLOX1 (*Glycine max*; LOX1:Gm:1), GmLOX2 (*Glycine max*; LOX1:Gm:2), GmLOX3 (*Glycine max*; LOX1:Gm:3), GmLOX4 (*Glycine max*; LOX1:Gm:4), GmLOX5 (*Glycine max*; Q43446, LOX1:Gm:5), GmLOX6 (*Glycine max*; Q43440, LOX1:Gm:6), HvLOX1 (*Hordeum vulgare*; LOX1:Hv:1), HvLOX2.1 (*Hordeum vulgare*; LOX2:Hv:1), LcLOX (*Lens culinaris*; LOX1:Lc:1), NtLOX (*Nicotiana tabacum*; LOX1:Nt:1), OsLOX2 (*Oryza sativa*; LOX1:Os:1), OsLOX7 (*Oryza sativa*; LOX2:Os:1), OsLOX (*Oryza sativa*; Q9FSE5, LOX2:Os:2), OsLOX (*Oryza sativa*; Q27PX2, Os-lox-1), OsLOX1 (*Oryza sativa*; Q76I22, R9-lox-1), PsLOX2 (*Pisum sativum*; LOX1:Ps:2), PsLOX3 (*Pisum sativum*; LOX1:Ps:3), PnLOX (*Prunus dulcis*; LOX1:Pd:1), StLOX1 (*Solanum tuberosum*; LOX1:St:1), StLOX (*Solanum tuberosum*; LOX1:St:3), StLOXH1 (*Solanum tuberosum*; LOX2:St:1), StLOXH3 (*Solanum tuberosum*; LOX2:St:2), ZmLOX (*Zea mays*; A1XC15, LOX2:Zm:10), ZmLOX (*Zea mays*; Q9LKL4, Zm-lox.b), ZmLOX (*Zea mays*; Q9AXG8, Zm-lox-3)

The four characterized *A. thaliana* 13-lipoxygenases, AtLOX-2, AtLOX-3, AtLOX-4 and AtLOX-6 group together with so-called type II 13-lipoxygenases [7], which contain an N-terminal localization peptide which directs the lipoxygenase to the chloroplast. Both mono- and dicotyledonous 13-lipoxygenases are found in this group. The difference between the two clusters (A and B) that

make up this group could possibly reside in either differences in the sub-organellar localization of the chloroplast (thylakoid and stroma), or in their expression and functional characteristics. Two 13-LOX *S. tuberosum* proteins, LOXH1 and LOXH3, present in clusters A and B, respectively, are nearly equally present in both stroma (20%) and thylakoid (80%) but do display different

expression patterns. LOXH3 accumulates upon wounding in potato, and LOXH1 is present at constant levels in both non-wounded and wounded tissues [48]. This indicates that among the *Arabidopsis* 13-lipoxygenases, AtLOX-3, -4, and -6, present in Cluster B, could be more related to defense pathways than AtLOX-2 (Cluster A). By proteomic analysis both AtLOX-5 and AtLOX-6 have both been found to be present in chloroplasts [34]. AtLOX-5 is phylogenetically related to 9-lipoxygenases which do not contain an N-terminal localization peptide (group C), and its localization in chloroplasts is thus unexpected. This indicates that besides biochemical determination of positional specificity of oxygenase activity, biochemical characterization of subcellular localization of lipoxygenase also remains essential for confirmation of predictions based on primary sequence alone.

A comparison of the substrate specificity of the six lipoxygenases using linoleic acid, linolenic acid and arachidonic acid showed that AtLOX-1 and AtLOX-5 oxygenated both linolenic acid and linoleic acid with similar activity. In contrast, AtLOX-2, AtLOX-3, AtLOX-4 and AtLOX-6 oxygenated linolenic acid more effectively than linoleic acid. These results were obtained at high substrate concentrations (100 μ M), and future studies could aim to obtain a more detailed picture of catalytic activity. Nevertheless, the results demonstrate that linolenic acid is the preferred substrate for the *A. thaliana* 13-lipoxygenases. This observation suggests that, in plants, tissues with predominant expression of one of the 13-lipoxygenases may generate mostly 13*S*-hydroperoxyoctadecatrienoic acid, which can be used for jasmonic acid synthesis. In other tissues where 9-lipoxygenase expression is high, such as root initials [12], both 9*S*-hydroperoxyoctadecadienoic acid and 9*S*-hydroperoxyoctadecatrienoic acid are expected to be formed.

In summary, the present study concludes that AtLOX-1 and AtLOX-5 are 9*S*-lipoxygenases, and AtLOX-2, AtLOX-3, AtLOX-4 and AtLOX-6 are 13*S*-lipoxygenases. These results provide a firm basis facilitating future studies employing *A. thaliana* on the role of lipoxygenases in plant physiology and patho-physiology.

Acknowledgments The expert technical assistance by Mrs. G. Hamberg and Mr. T. Cascón is gratefully acknowledged. The authors would like to thank the Arabidopsis Biological Resource Center at Ohio State University for the kind provision of materials. This work was supported by grants from the Swedish Research Council for Environment, Agricultural Sciences and Spatial Planning (project number 2001-2553), grant QLK5-CT-2001-02445 (NODO) from the European Union, and by grant BIO2006-08581 to Carmen Castresana from the Ministry of Education and Science (Spain). Gerard Bannenbergh is a Ramón y Cajal fellow supported by the Spanish Ministry of Science and Innovation, and the Centro Nacional de Biotecnología, Consejo Superior de Investigaciones Científicas, Spain. Marta

Martínez was supported by grant BIO2006-08581 to Carmen Castresana from the Ministry of Education and Science (Spain).

References

1. Brash AR (1999) Lipoxygenases: occurrence, functions, catalysis, and acquisition of substrate. *J Biol Chem* 274:23679–23682
2. Liavonchanka A, Feussner I (2006) Lipoxygenases: occurrence, functions and catalysis. *J Plant Physiol* 163:348–357
3. Gardner HW (1991) Recent investigations into the lipoxygenase pathway of plants. *Biochim Biophys Acta* 1084:221–239
4. Weber H (2002) Fatty acid-derived signals in plants. *Trends Plant Sci* 7:217–224
5. Howe GA, Schilmiller AL (2002) Oxylinp metabolism in response to stress. *Curr Opin Plant Biol* 5:230–236
6. Chehab EW, Kaspi R, Savchenko T, Rowe H, Negre-Zakharov F, Kliebenstein D, Dehesh K (2008) Distinct roles of jasmonates and aldehydes in plant-defense responses. *PLoS ONE* 3:1–10 (e1904)
7. Feussner I, Wasternack C (2002) The lipoxygenase pathway. *Annu Rev Plant Biol* 53:275–297
8. Berger S, Weichert H, Porzel A, Wasternack C, Kühn H, Feussner I (2001) Enzymatic and non-enzymatic lipid peroxidation in leaf development. *Biochim Biophys Acta* 1533:266–276
9. Hughes RK, West SL, Hornostaj AR, Lawson DM, Fairhurst SA, Sanchez RO, Hough P, Robinson BH, Casey R (2001) Probing a novel potato lipoxygenase with dual positional specificity reveals primary determinants of substrate binding and requirements for a surface hydrophobic loop and has implications for the role of lipoxygenases in tubers. *Biochem J* 353:345–355
10. Fukushige H, Wang C, Simpson TD, Gardner HW, Hildebrand DF (2005) Purification and identification of linoleic acid hydroperoxides generated by soybean seed lipoxygenases 2 and 3. *J Agric Food Chem* 53:5691–5694
11. Vick BA, Zimmerman DC (1983) The biosynthesis of jasmonic acid: a physiological role for plant lipoxygenase. *Biochem Biophys Res Commun* 111:470–477
12. Velloso T, Martínez M, López MA, Vicente J, Cascón T, Dolan L, Hamberg M, Castresana C (2007) Oxylinps produced by the 9-lipoxygenase pathway in *Arabidopsis* regulate lateral root development and defense responses through a specific signaling cascade. *Plant Cell* 19:831–846
13. Browse J (2005) Jasmonate: an oxylinp signal with many roles in plants. *Vitam Horm* 72:431–456
14. Conconi A, Miquel M, Browse JA, Ryan CA (1996) Intracellular levels of free linolenic and linoleic acids increase in tomato leaves in response to wounding. *Plant Physiol* 111:797–803
15. Bell E, Creelman RA, Mullet JE (1995) A chloroplast lipoxygenase is required for wound-induced jasmonic acid accumulation in *Arabidopsis*. *Proc Natl Acad Sci USA* 92:8675–8679
16. Halitschke R, Baldwin IT (2003) Antisense LOX expression increases herbivore performance by decreasing defense responses and inhibiting growth-related transcriptional reorganization in *Nicotiana attenuata*. *Plant J* 40:794–807
17. Royo J, León J, Vancanney G, Albar JP, Rosahl S, Ortego F, Castanera P, Sánchez-Serrano JJ (1999) Antisense-mediated depletion of a potato lipoxygenase reduces wound induction of protein inhibitors and increases weight gain of insect pests. *Proc Natl Acad Sci USA* 96:1146–1151
18. Yamamoto H, Tani T (1986) Possible involvement of lipoxygenase in the mechanism of oat to *Puccinia coronata avenae*. *J Phytopathol* 116:329–337

19. Ohta H, Shida K, Peng Y-L, Furusawa I, Shishiyama J, Aibara S, Morita Y (1991) A lipoxygenase pathway is activated in rice after infection with the rice blast fungus *Magnaporthe grisea*. *Plant Physiol* 97:94–98
20. Brodhagen M, Tsiatsigiannis DI, Hornung E, Goebel C, Feussner I, Keller NP (2008) Reciprocal oxylipin-mediated cross-talk in the *Aspergillus*-seed pathosystem. *Mol Microbiol* 67:378–391
21. Gao X, Shim W-B, Gobel C, Kunze S, Feussner I, Meeley R, Balint-Kurti P, Kolomiets M (2007) Disruption of a maize 9-lipoxygenase results in increased resistance to fungal pathogens and reduced levels of contamination with mycotoxin fumonisin. *Mol Plant Microbe Interact* 20:922–933
22. Rance I, Fournier J, Esquerre-Tugaye M-T (1998) The incompatible interaction between *Phytophthora parasitica* var. *nicotianae* race 0 and tobacco is suppressed in transgenic plants expressing antisense lipoxygenase sequences. *Proc Natl Acad Sci USA* 95:6554–6559
23. Vijayan P, Shockey J, Lévesque CA, Cook RJ, Browse J (1998) A role for jasmonate in pathogen defense of *Arabidopsis*. *Proc Natl Acad Sci USA* 95:7209–7214
24. Glazebrook J (2001) Genes controlling expression of defense responses in *Arabidopsis*—2001 status. *Curr Opin Plant Biol* 4:301–308
25. Wasternack C (2007) Jasmonates: an update on biosynthesis, signal transduction and action in plant stress response, growth and development. *Ann Bot* 100:681–697
26. Prost I, Dhondt S, Rothe G, Vicente J, Rodriguez MJ, Kift N, Carbonne F, Griffiths G, Esquerré-Tugayé MT, Rosahl S, Castresana C, Hamberg M, Fournier J (2005) Evaluation of the antimicrobial activities of plant oxylipins supports their involvement in defense against pathogens. *Plant Physiol* 139:1902–1913
27. Chini A, Fonseca S, Fernández G, Adie B, Chico JM, Lorenzo O, García-Casado G, López-Vidriero I, Lozano FM, Ponce MR, Micol JL, Solano R (2007) The JAZ family of repressors is the missing link in jasmonate signalling. *Nature* 448:666–671
28. Thines B, Katsir L, Melotto M, Niu Y, Mandaokar A, Liu G, Nomura K, He SY, Howe GA, Browse J (2007) JAZ repressor proteins are targets of the SCF^{CO11} complex during jasmonate signalling. *Nature* 448:661–665
29. Howe GA, Jander G (2008) Plant immunity to insect herbivores. *Annu Rev Plant Biol* 59:41–66
30. Göbel C, Feussner I, Hamberg M, Rosahl S (2002) Oxylipin profiling in pathogen-infected potato leaves. *Biochim Biophys Acta* 1584:55–64
31. Melan MA, Dong X, Endara ME, Davis KR, Ausubel FM, Peterman TK (1993) An *Arabidopsis thaliana* lipoxygenase gene can be induced by pathogens, abscisic acid, and methyl jasmonate. *Plant Physiol* 101:441–450
32. He Y, Fukushige H, Hildebrand DF, Gan S (2002) Evidence supporting a role of jasmonic acid in *Arabidopsis* leaf senescence. *Plant Physiol* 128:876–884
33. Melan MA, Enriquez ALD, Peterman TK (1994) The *LOX1* gene of *Arabidopsis* is temporally and spatially regulated in germinating seedlings. *Plant Physiol* 105:385–393
34. Peltier JB, Ytterberg AJ, Sun Q, van Wijk KJ (2004) New functions of the thylakoid membrane proteome of *Arabidopsis thaliana* revealed by a simple, fast and versatile fractionation strategy. *J Biol Chem* 279:49367–49383
35. Bell E, Mullet JE (1993) Characterization of an *Arabidopsis* lipoxygenase gene responsive to methyl jasmonate and wounding. *Plant Physiol* 103:1133–1137
36. Kishimoto K, Matsui K, Ozawa R, Takabayashi J (2005) Volatile C6-aldehydes and allo-ocimene activate defense genes and induce resistance against *Botrytis cinerea* in *Arabidopsis thaliana*. *Plant Cell Physiol* 46:1093–1102
37. Chung HS, Koo AJK, Gao X, Jayanty S, Thines B, Jones AD, Howe GA (2008) Regulation and function of Arabidopsis JASMONATE ZIM-domain genes in response to wounding and herbivory. *Plant Physiol* 146:952–964
38. Laemmli UK (1970) Cleavage of structural proteins during the assembly of the head of bacteriophage T4. *Nature* 227:680–685
39. Bradford MM (1976) A rapid and sensitive method for the quantitation of microgram quantities of protein utilizing the principle of protein-dye binding. *Anal Biochem* 72:248–254
40. Hamberg M (1998) Stereochemistry of oxygenation of linoleic acid catalyzed by prostaglandin-endoperoxide H synthase-2. *Arch Biochem Biophys* 349:376–380
41. Larkin MA, Blackshields G, Brown NP, Chenna R, McGettigan PA, McWilliam H, Valentin F, Wallace IM, Wilm A, Lopez R, Thompson JD, Gibson TJ, Higgins DG (2007) ClustalW and ClustalX version 2.0. *Bioinformatics* 23:2947–2948
42. Felsenstein J (1989) PHYLIP-phylogeny inference package (version 3.2). *Cladistics* 5:164–166
43. Farmer EE, Almeras E, Krishnamurthy V (2003) Jasmonates and related oxylipins in plant responses to pathogenesis and herbivory. *Curr Opin Plant Biol* 6:372–378
44. Weiler EW, Laudert D, Stelmach BA, Hennig P, Biesgen C, Kubigsteltig I (1999) Octadecanoid and hexadecanoid signalling in plant defence. *Novartis Found Symp* 223:191–204
45. Shibata D, Axelrod B (1995) Plant lipoxygenases. *J Lipid Mediat Cell Signal* 12:213–228
46. Fritsche K, Hornung E, Hause B, Stenzel I, Wasternack C, Feussner I (2000) Isolation and characterization of lipoxygenase isozymes, Proceedings 11th international conference on arabidopsis research, University of Wisconsin, Madison, USA
47. Hornung E, Walther M, Kühn H, Feussner I (1999) Conversion of cucumber linoleate 13-lipoxygenase to a 9-lipoxygenating species by site-directed mutagenesis. *Proc Natl Acad Sci USA* 96:4192–4197
48. Farnaki T, Sanmartín M, Jiménez P, Paneque M, Sanz C, Vancanneyt G, León J, Sánchez-Serrano JJ (2007) Differential distribution of the lipoxygenase pathway enzymes within potato chloroplasts. *J Exp Botany* 58:555–568

The Depressive Effects of 5,8,11-Eicosatrienoic Acid (20:3n-9) on Osteoblasts

Tomohito Hamazaki · Nobuo Suzuki · Retno Widyowati · Tatsuro Miyahara · Shigetoshi Kadota · Hiroshi Ochiai · Kei Hamazaki

Received: 29 July 2008 / Accepted: 30 September 2008 / Published online: 22 October 2008
© AOCs 2008

Abstract In cases of essential fatty acid deficiency, 5,8,11-eicosatrienoic acid (Mead acid, 20:3n-9) is synthesized from oleic acid as a 20-carbon analog of arachidonic acid. It was reported that 20:3n-9 levels were markedly higher in human fetal cartilage than in the muscle, liver and spleen. We, therefore, hypothesized that 20:3n-9 decreased osteoblastic activity. Goldfish scales were incubated either with 20:3n-9 or with oleic acid at 15 °C for 6 and 18 h. Both osteoblastic and osteoclastic activities in the scale were assessed by measuring alkaline phosphatase (ALP) and tartrate-resistant acid phosphatase, respectively. MC3T3-E1 cells (an osteoblast cell line derived from the mouse) were incubated with 20:3n-9 or oleic acid at 37 °C for 6 and 18 h. ALP activity in cell lysate was measured. In the case of experiments with scales, 20:3n-9 (1–100 μM) significantly suppressed osteoblastic activity after 6 and 18 h of incubation, whereas oleic acid did not change this

activity. Osteoclastic activity was not affected either by 20:3n-9 or by oleic acid. In the case with the cell line, osteoblastic activity was again significantly decreased with 20:3n-9 (10–30 μM) after 6-h incubation but not after 18 h incubation. The presence of 20:3n-9 in fetal cartilage may be important for the prevention of calcification in the cartilage. 20:3n-9 could be applied to some clinical situations where bone formation should be inhibited.

Keywords Bone · Cartilage · Co-culture · Fatty acids · Goldfish scales · Osteoclasts

Abbreviations

20:3n-9	5,8,11-Eicosatrienoic acid (20:3n-9, Mead acid)
AA	Arachidonic acid
ALP	Alkaline phosphatase
TRAP	Tartrate-resistant acid phosphatase
CF	Cystic fibrosis
RANK	Receptor activator of NF-κB
RANKL	Receptor activator of NF-κB ligand
LTB ₄	Leukotriene B ₄

T. Hamazaki (✉) · K. Hamazaki
Department of Clinical Sciences,
Institute of Natural Medicine, University of Toyama,
2630 Sugitani, Toyama, Toyama 9300194, Japan
e-mail: hamazaki@inm.u-toyama.ac.jp

N. Suzuki
Noto Marine Laboratory,
Institute of Nature and Environmental Technology,
Kanazawa University, Housu-gun, Ishikawa 927-0553, Japan

R. Widyowati · S. Kadota
Department of Natural Products Chemistry,
Institute of Natural Medicine, University of Toyama,
Toyama, Japan

T. Miyahara · H. Ochiai
Department of Human Science, Faculty of Medicine,
University of Toyama, Toyama, Japan

Introduction

In cases of essential fatty acid deficiency, 5,8,11-eicosatrienoic acid (20:3n-9), sometimes also called Mead acid, is synthesized from oleic acid as a 20-carbon analog of arachidonic acid (AA). Holman suggested that the ratio of trienoic to tetraenoic acids (20:3n-9/AA) could be used as a measure of essential fatty acid status, a value of 0.4 or greater defining essential fatty acid deficiency [1].

Adkisson et al. [2] measured the fatty acid composition of various tissues of young chickens, fetal calves and

newborn pigs, and found that the cartilage had unusually high levels of 20:3n-9 and low levels of n-6 polyunsaturated fatty acids. For example, the 20:3n-9 and AA concentrations in the chicken epiphyseal plate phosphatidylethanolamine fraction were 8.2 ± 1.3 and $2.8 \pm 0.6\%$ of total fatty acids, respectively. It was also reported that the 20:3n-9 levels were markedly higher in human fetal cartilage ($2.0 \pm 0.6\%$ of total fatty acids) than in fetal muscle ($0.2 \pm 0.2\%$), liver ($0.4 \pm 0.2\%$) and spleen ($0.1 \pm 0.2\%$) [3]. Because of the absence of blood vessels in cartilage, essential fatty acids do not easily reach the tissue, which is probably a major reason of increased synthesis of 20:3n-9 in the tissue. In fact, a considerable amount of 20:3n-9 (3.2% of total fatty acids in the polar lipid fraction) was also found in the calf lens [2]. Our question was whether there was any biological consequence for such high levels of 20:3n-9 in cartilage.

Except for bone tissues, calcification usually means a pathological condition. Of all the tissues that may be calcified in pathological conditions, cartilage is probably the most sensitive tissue. If cartilage is calcified, it might not be cartilage any more; it might be called bone. For instance, complete calcification of the epiphyseal plate, which of course has a high amount of 20:3n-9 [2], in growing long bones stops its function as longitudinal-bone-growth-promoting cartilage. From these considerations, we hypothesized that unusually high concentrations of 20:3n-9 found in the cartilage might have depressive effects against osteoblasts to keep it from ossification.

The teleost scale is a calcified tissue that contains osteoblasts, osteoclasts, and bone matrix like avian and mammalian bone [4, 5]. We had been using scales of goldfish as the source of osteoblasts and osteoclasts. Alkaline phosphatase (ALP) and tartrate-resistant acid phosphatase (TRAP) activities are measurable with scales from the same fish, and used as surrogate markers of osteoblastic and osteoclastic activities, respectively [5]. We tested our hypothesis using this scale system and a different system (an osteoblast cell line).

Materials and Methods

Goldfish (*Carassius auratus*)

Our previous study [6] found that mature female goldfish were more sensitive to calcemic hormones such as calcitonin than mature males. In the present study, therefore, mature female goldfish (30–50 g) were purchased from a commercial source (Higashikawa Fish Farm, Yamatokoriyama, Nara). All experimental procedures were conducted in accordance with the Guide for the Care and Use of Laboratory Animals of Kanazawa University.

Effects of 20:3n-9 and Oleic Acid on TRAP and ALP Activities in Cultured Scales

The methods for ALP and TRAP assays with cultured scales were performed as described previously [7]. Briefly, Eagle's minimum essential medium (MEM) containing antibiotics and HEPES buffer (20 mM, pH 7.0) was used as culture medium. Scales collected from goldfish under anesthesia were incubated for 6 or 18 h in the medium supplemented with either 20:3n-9 or oleic acid (Sigma-Aldrich Corporation, St. Louis, Missouri). Those free fatty acids were separately dissolved in ethanol and diluted in the medium at 0.01–100 μ M, and their effects were compared with those with oleic acid at the same concentrations. The final concentration of ethanol in the medium was less than 0.5% and this concentration did not affect TRAP and ALP at all. After incubation, scales were fixed in 10% formalin in a 0.05 M cacodylate buffer (pH 7.4) and kept in a 0.05 M cacodylate buffer at 4 °C until analysis. The assay methods of ALP and TRAP activities have been described previously [7]. Briefly, each scale was transferred to a 96-well-microplate and incubated with *p*-nitrophenyl-phosphate, the substrate. In the case of TRAP assay, 20 mM tartrate in a 0.1 M sodium acetate buffer (pH 5.3) was used. After incubation at 20 °C for 30 min, the reaction was stopped by adding 50 μ l of a 3 N NaOH–20 mM EDTA solution, and the absorbance was measured at 405 nm. ALP activity was measured under alkaline conditions (100 mM Tris–HCl, pH 9.5; 1 mM $MgCl_2$; 0.1 mM $ZnCl_2$). Other conditions were similar to those for the measurement of TRAP activity.

Cell Culture

Osteoblastic cell line MC3T3-E1 (5×10^4 cells) were plated in wells of a 24-well plate in 1 mL of α -MEM containing 10% FBS. After 3 days of incubation, the cells were washed with serum-free medium and were cultured for 6 or 18 h in α -MEM containing 1% FBS and free fatty acids (20:3n-9 or oleic acid). Ethanol was used for dilution of fatty acids as described above. The final concentration of ethanol was 0.1% and this concentration did not affect the ALP activity of cultured cells. ALP activity was assayed according to the method of [8] with slight modifications. Briefly, at the end of incubation, the medium was discarded, and the cells were washed. The cell lysate with sodium dodecyl sulfate was stocked in microtubes at -20 °C. Cell lysate was incubated with *p*-nitrophenyl phosphate at an alkaline condition (0.1 M sodium carbonate buffer, pH 10.0) for 30 min at 37 °C. The protein content in the cell lysate was estimated by the BCA method with bovine serum albumin as standard. One unit of ALP

was defined as the activity causing the release of 1 nmol of *p*-nitrophenol/min/mg protein.

Statistics

Results from eight scales are shown as means \pm SEM. In the case of the cell line, results from six wells are shown as means \pm SEM. The effects of fatty acids were compared with results with oleic acid by the *t* test after ANOVA. Differences were considered significant at $P < 0.05$.

Results

Experiments with Goldfish Scales

The effects of fatty acids on ALP activities assayed with scales are shown in Fig. 1. ALP activities of scales were significantly depressed after 6 (panel a) and 18 h (panel b) of incubation with 20:3n-9 at 1.0–100 μ M concentrations, whereas oleic acid did not affect ALP activities at any concentrations tested, irrespective of incubation times. TRAP activities after incubation with fatty acids are shown in Fig. 2. The two fatty acids did not exert any influence on TRAP activity at all.

Experiments with MC3T3-E1 Cells

The effects of 20:3n-9 on ALP were retested with a different assay system with an osteoblastic cell line, MC3T3-E1. 20:3n-9 depressed ALP activities after 6 h of incubation (Fig. 3, panel a), but not after 18 h of incubation (Fig. 3, panel b).

Discussion

We assayed the effects of bone-affecting hormones, endocrine disruptors, heavy metals with our scale co-culture system, and found that those agents influenced osteoblastic and osteoclastic activities exactly as in the case of mammalian bones [6, 9–11]. Incubation for 64 h with 0.1 μ M cadmium, the notorious heavy metal damaging the bone and kidney leading to itai-itai byo (ouch-ouch disease) [12], decreased ALP activity by about 27% in our scale system [10]. The decrease of ALP activity by 10 μ M 20:3n-9 for 6 h (about 25% as shown in Fig. 1) was comparable with ALP-depressing effects of cadmium. Moreover, effects of 20:3n-9 appeared much faster than cadmium; in fact, no effects on ALP activity were detected at 18 or 36 h of incubation with cadmium [10].

The bone complex includes osteoblasts, osteoclasts, and the bone matrix. An interaction between osteoclasts and osteoblasts has recently been noted in mammals (for a review, see [13]). In the same *in vitro* scale assay system used in the present study, we found that melatonin depressed both osteoclastic and osteoblastic activities [14]. Actually melatonin did stimulate proliferation and differentiation of isolated (not co-cultured) mammalian osteoblasts [15, 16]. The receptor activator of NF- κ B (RANK) and the RANK ligand (RANKL) have been identified in osteoclasts and osteoblasts, respectively [17]. Osteoclasts were activated by RANKL binding to RANK, and multi-nucleated osteoclasts (active type of osteoclasts) were then induced [17]. Application of parathyroid hormone activated osteoclasts through the RANK-RANKL system in our scale system (N. Suzuki, unpublished data). Consequently, co-culture systems with both

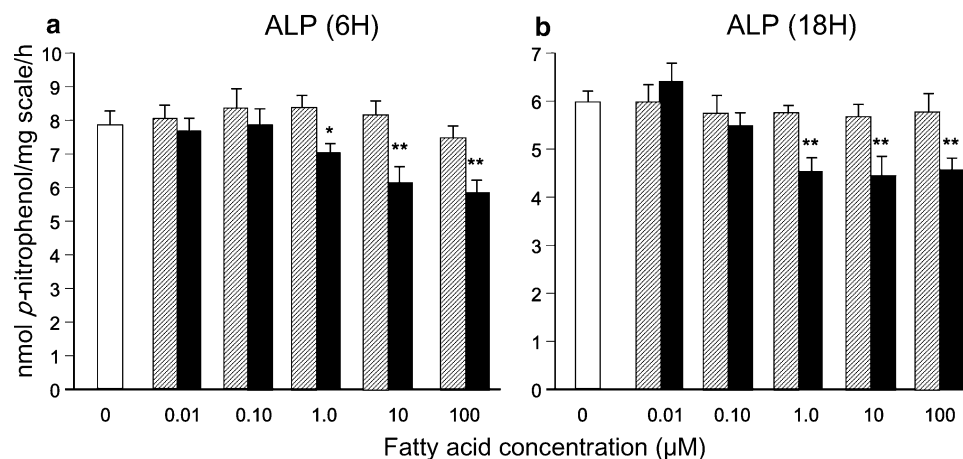


Fig. 1 The effects of 20:3n-9 and oleic acid on osteoblastic activity in goldfish scales. Goldfish scales were incubated with various amounts of 20:3n-9 and oleic acid for **a** 6 and **b** 18 h. Alkaline phosphatase (ALP) activity of scales was measured as osteoblastic

activity. ALP activities were compared with values obtained with oleic acid at the same concentrations. *Open column* activity without fatty acids, *hatched columns* those with oleic acid, *filled columns* those with 20:3n-9. $n = 8$. * $P < 0.05$, ** $P < 0.01$

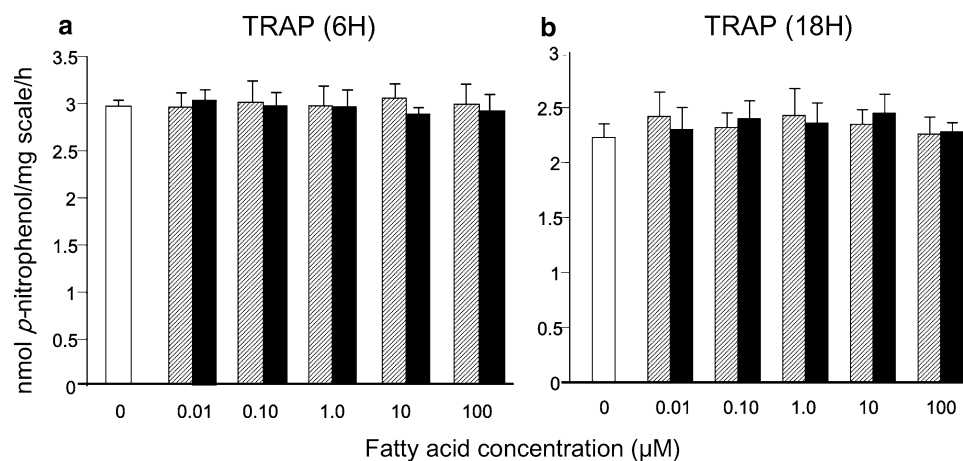
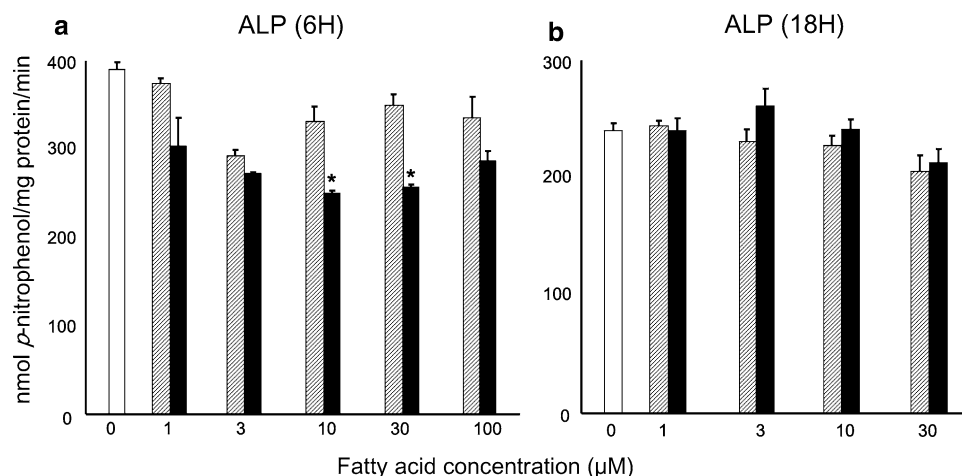


Fig. 2 The effects of 20:3n-9 and oleic acid on osteoclastic activity in goldfish scales. Goldfish scales were incubated with various amounts of 20:3n-9 and oleic acid for **a** 6 and **b** 18 h. Tartrate-resistant acid phosphatase (*TRAP*) activity of scales was measured as osteoclastic activity. *TRAP* activities were compared with values

obtained with oleic acid at the same concentrations. 20:3n-9 did not affect *TRAP* activities at all. *Open column* activity without fatty acids, *hatched columns* those with oleic acid, *filled columns* those with 20:3n-9. $n = 8$

Fig. 3 The effects of 20:3n-9 and oleic acid on osteoblastic activity in MC3T3-E1 cells (osteoblastic cell line). MC3T3-E1 cells were incubated with various amounts of 20:3n-9 and oleic acid for **a** 6 and **b** 18 h. ALP activity was measured as osteoblastic activity. ALP activities were compared with values obtained with oleic acid at the same concentrations. *Open column* activity without fatty acids, *hatched columns* those with oleic acid, *filled columns* those with 20:3n-9. $n = 3-4$. * $P < 0.05$



osteoclasts and osteoblasts are definitely required for accurate effect assessment of bioactive materials in the area of bone formation and resorption [18].

In this scale *in vitro* system, 20:3n-9 depressed only osteoblastic activity and not osteoclastic activity at all, which was different from the case of melatonin (see above). To the best of our knowledge, 20:3n-9 is the only biomaterial that depresses osteoblastic activity without affecting osteoclastic activity. In the present study we compared the effects of 20:3n-9 with those of oleic acid, the major n-9 unsaturated fatty acid. Actually the effects of a saturated fatty acid, stearic acid, were also investigated. There were no measurable effects of stearic acid at 0.01–100 μM at all (data not shown).

In order to rule out a slight possibility that the effects of 20:3n-9 on osteoblasts were observable only in fish scales, another system was employed; an osteoblastic cell line, MC3T3-E1. The results with the cell line were similar to

those obtained from scales, although the effects were detected at 6-h incubation and not at 18-h incubation. The reason why the effects disappeared after 18 h of incubation was not clear. It was possible that 20:3n-9 might be metabolized faster with MC3T3-E1 cells, which had probably more metabolically active surface areas than scales. Scales were mostly surrounded with scale pocket lining cells. The results with MC3T3-E1 cells also indicated that the depressive effects of 20:3n-9 were not mediated through osteoclastic cells.

The present study did not have any mechanistic research components, and it is difficult to speculate how 20:3n-9 exerted its effects. Owing to its analogy to AA, dietary supplementation with 20:3n-9 was shown to depress leukotriene B₄ (LTB₄) in rats [19, 20]. LTB₄ has been shown to stimulate bone resorption both *in vitro* and *in vivo* [21, 22]. Actually it was found that the bone-forming capacity of osteoblasts was impaired when cells were cultured in the

presence of 5-LO metabolites including LTB₄ [23]. Consequently, it is unlikely that the depressive effect of 20:3n-9 on LTB₄ synthesis might explain our findings. On the other hand, 20:3n-9 itself was reported to be converted to 11- and 13-hydroxyl metabolites by prostaglandin H synthase-1 and -2 [24], and also to 5-hydroxy and 5-oxo metabolites by 5-lipoxygenase [25]. However, it is not clear whether any of those metabolites might have any osteoblast-depressing effects. It might be a new interesting area of research. CB2 cannabinoid receptors are expressed by osteoblasts and osteoclasts. Their activation stimulates bone formation and suppressed bone resorption [26]. Chemically synthesized 20:3n-9 ethanolamide was found to be a potent agonist to the human CB2 receptor [27]. Consequently, it is unlikely that 20:3n-9 exerted its effects through its conversion to cannabinoid analogues.

Compared with normal controls, patients with cystic fibrosis (CF) were reported to have enhanced blood 20:3n-9 levels [28–30]. As life expectancy in CF patients increases, new clinical problems come to be noticed; osteoporosis is one of them [31]. A long list of the possible reasons was described for osteoporosis in CF [31]. Enhanced blood 20:3n-9 levels in CF patients may be filed in that list. As described in Introduction, except for the epiphyseal plate, calcification of tissues usually implies pathological conditions. For example, ossification of the posterior longitudinal ligament is a common pathological condition seen in Japan and other Asian countries [32]. The thickening of the ligament by ossification compresses the spinal cord and nerve roots. Is there any possibility that 20:3n-9 might stop or at least delay the progression of ossification? Other clinical applications might also be possible.

Our findings that 20:3n-9 depresses osteoblastic activity are very new; further research is warranted.

Acknowledgments The authors are grateful to Ms. Hiroko Hamatani for her technical assistance. This work was partly supported by Open Research Center, Kinjogakuin University, and Polyene Project, Ltd.

References

- Holman RT (1960) The ratio of trienoic:tetraenoic acids in tissue lipids as a measure of essential fatty acid requirement. *J Nutr* 70:405–410
- Adkisson HD 4th, Risener FS Jr, Zarrinkar PP, Walla MD, Christie WW, Wuthier RE (1991) Unique fatty acid composition of normal cartilage: discovery of high levels of n-9 eicosatrienoic acid and low levels of n-6 polyunsaturated fatty acids. *FASEB J* 5:344–353
- Cleland KA, James MJ, Neumann MA, Gibson RA, Cleland LG (1995) Differences in fatty acid composition of immature and mature articular cartilage in humans and sheep. *Lipids* 30:949–953
- Azuma K, Kobayashi M, Nakamura M, Suzuki N, Yashima S, Iwamuro S, Ikegame M, Yamamoto T, Hattori A (2007) Two osteoclastic markers expressed in multinucleate osteoclasts of goldfish scales. *Biochem Biophys Res Commun* 362:594–600
- Suzuki N, Kitamura K, Nemoto T, Shimizu N, Wada S, Kondo T, Tabata MJ, Sodeyama F, Ijiri K, Hattori A (2007) Effect of vibration on osteoblastic and osteoclastic activities: analysis of bone metabolism using goldfish scale as a model for bone. *Adv Space Res* 40:1711–1721
- Suzuki N, Suzuki T, Kurokawa T (2000) Suppression of osteoclastic activities by calcitonin in the scales of goldfish (freshwater teleost) and nibbler fish (seawater teleost). *Peptides* 21:115–124
- Suzuki N, Somei M, Kitamura K, Reiter RJ, Hattori A (2008) Novel bromomelatonin derivatives suppress osteoclastic activity and increase osteoblastic activity: implications for the treatment of bone diseases. *J Pineal Res* 44:326–334
- Kumegawa M, Ikeda E, Tanaka S, Haneji T, Yora T, Sakagishi Y, Minami N, Hiramatsu M (1984) The effects of prostaglandin E₂, parathyroid hormone, 1, 25-dihydroxycholecalciferol, and cyclic nucleotide analogs on alkaline phosphatase activity in osteoblastic cells. *Calcif Tissue Int* 36:72–76
- Suzuki N, Hattori A (2003) Bisphenol A suppresses osteoclastic and osteoblastic activities in the cultured scales of goldfish. *Life Sci* 73:2237–2247
- Suzuki N, Yamamoto M, Watanabe K, Kambegawa A, Hattori A (2004) Both mercury and cadmium directly influence calcium homeostasis resulting from the suppression of scale bone cells: the scale is a good model for the evaluation of heavy metals in bone metabolism. *J Bone Miner Metab* 22:439–446
- Suzuki N, Tabata MJ, Kambegawa A, Srivastav AK, Shimada A, Takeda H, Kobayashi M, Wada S, Katsumata T, Hattori A (2006) Tributyltin inhibits osteoblastic activity and disrupts calcium metabolism through an increase in plasma calcium and calcitonin levels in teleosts. *Life Sci* 78:2533–2541
- Tsuchiya K (1969) Causation of ouch-ouch disease (itai-itai byo): an introductory review. Part I: nature of the disease. *Keio J Med* 18:181–194
- Martin TJ, Sims NA (2005) Osteoclast-derived activity in the coupling of bone formation to resorption. *Trends Mol Med* 11:76–81
- Suzuki N, Hattori A (2002) Melatonin suppresses osteoclastic and osteoblastic activities in the scales of goldfish. *J Pineal Res* 33:253–258
- Roth JA, Kim B-G, Lin W-L, Cho M-I (1999) Melatonin promotes osteoblast differentiation and bone formation. *J Biol Chem* 274:22041–22047
- Nakade O, Koyama H, Arijji H, Yajima A, Kaku T (1999) Melatonin stimulates proliferation and type I collagen synthesis in human bone cell in vitro. *J Pineal Res* 27:106–110
- Teitelbaum SL (2000) Bone resorption by osteoclasts. *Science* 289:1504–1508
- Suzuki N, Somei M, Seki A, Reiter RJ, Hattori A (2008) Novel bromomelatonin derivatives as potentially effective drugs to treat bone diseases. *J Pineal Res* 45:229–234
- James MJ, Gibson RA, Neumann MA, Cleland LG (1993) Effect of dietary supplementation with n-9 eicosatrienoic acid on leukotriene B₄ synthesis in rats: a novel approach to inhibition of eicosanoid synthesis. *J Exp Med* 178:2261–2265
- Cleland LG, Gibson RA, Neumann MA, Hamazaki T, Akimoto K, James MJ (1996) Dietary (n-9) eicosatrienoic acid from a cultured fungus inhibits leukotriene B₄ synthesis in rats and the effect is modified by dietary linoleic acid. *J Nutr* 126:1534–1540
- Garcia C, Qiao M, Chen D, Kirchen M, Gallwitz W, Mundy GR, Bonewald LF (1996) Effects of synthetic peptido-leukotrienes on bone resorption in vitro. *J Bone Miner Res* 11:521–529
- Garcia C, Boyce BF, Gilles J, Dallas M, Qiao M, Mundy GR, Bonewald LF (1996) Leukotriene B₄ stimulates osteoclastic bone

- resorption both in vitro and in vivo. *J Bone Miner Res* 11: 1619–1627
23. Traianedes K, Dallas MR, Garrett IR, Mundy GR, Bonewald LF (1998) 5-Lipoxygenase metabolites inhibit bone formation in vitro. *Endocrinology* 139:3178–3184
 24. Oliw EH, Hörnsten L, Sprecher H (1997) Oxygenation of 5, 8, 11-eicosatrienoic acid by prostaglandin H synthase-2 of ovine placental cotyledons: isolation of 13-hydroxy-5, 8, 11-eicosatrienoic and 11-hydroxy-5, 8, 12-eicosatrienoic acids. *J Chromatogr B Biomed Sci Appl* 690:332–337
 25. Patel P, Cossette C, Anumolu JR, Gravel S, Lesimple A, Mamer OA, Rokach J, Powell WS (2008) Structural requirements for activation of the 5-oxo-6E, 8Z, 11Z, 14Z-eicosatetraenoic acid (5-oxo-EETE) receptor: identification of a mead acid metabolite with potent agonist activity. *J Pharmacol Exp Ther* 325:698–707
 26. Bab I, Zimmer A (2008) Cannabinoid receptors and the regulation of bone mass. *Br J Pharmacol* 153:182–188
 27. Priller J, Briley EM, Mansouri J, Devane WA, Mackie K, Felder CC (1995) Mead ethanolamide, a novel eicosanoid, is an agonist for the central (CB1) and peripheral (CB2) cannabinoid receptors. *Mol Pharmacol* 48:288–292
 28. Gronowitz E, Mellström D, Strandvik B (2006) Serum phospholipid fatty acid pattern is associated with bone mineral density in children, but not adults, with cystic fibrosis. *Br J Nutr* 95:1159–1165
 29. Van Biervliet S, Vanbillemont G, Van Biervliet JP, Declercq D, Robberecht E, Christophe A (2007) Relation between fatty acid composition and clinical status or genotype in cystic fibrosis patients. *Ann Nutr Metab* 51:541–549
 30. Coste TC, Deumer G, Reychler G, Lebecque P, Wallemacq P, Leal T (2008) Influence of pancreatic status and sex on polyunsaturated fatty acid profiles in cystic fibrosis. *Clin Chem* 54: 388–395
 31. Döring G, Conway SP (2008) Osteoporosis in cystic fibrosis. *J Pediatr (Rio J)* 84:1–3
 32. Ogata N, Kawaguchi H (2004) Ossification of the posterior longitudinal ligament of spine (OPLL). *Clin Calcium* 14:42–48 (in Japanese)

The Antiproliferative Effect of EPA in HL60 Cells is Mediated by Alterations in Calcium Homeostasis

Jens Erik Slagsvold · Caroline Hild Hakvåg Pettersen ·
Turid Follestad · Hans Einar Krokan ·
Svanhild Arentz Schönberg

Received: 7 August 2008 / Accepted: 27 October 2008 / Published online: 20 November 2008
© AOCs 2008

Abstract Studies show that n-3 polyunsaturated fatty acids (PUFA) inhibit proliferation and induce apoptosis in cancer cells. Recent reports indicate that this effect is due to activation of the unfolded protein response (UPR). However, what causes this activation has been unclear. We examined the effects of eicosapentaenoic acid (EPA) on the human leukemia cell line HL60 and the econazole (Ec) resistant HL60 clone E2R2. Ec depletes Ca^{2+} from the ER and blocks Ca^{2+} influx in mammalian cells, leading to activation of the UPR and apoptosis. EPA inhibited growth of HL60 cells strongly, while E2R2 cells were much less affected. Gene expression analysis of HL60 cells revealed extensive changes in transcripts related to the ER homeostasis, Ca^{2+} -homeostasis and cell cycle/apoptosis. Protein levels of phosphorylated eIF2 α , a selective translation

inhibitor and UPR hallmark, activating transcription factor 4 (ATF4) and sequestosome-1 were moderately increased, whereas the cell cycle/progression protein cyclin D1 was decreased in HL60. In contrast, EPA concentrations that strongly inhibited and caused activation of the UPR in HL60 cells had no effect on the expression level of these UPR markers in E2R2 cells. Given that the only known difference between these cells is Ec-resistance, our results strongly suggest that the inhibitory effect of EPA on HL60 cells is initially mediated through alterations of the Ca^{2+} -homeostasis followed by activation of the UPR.

Keywords Cancer · E2R2 · Econazole-resistant · EPA · HL60 · UPR · PUFA

J. E. Slagsvold · C. H. H. Pettersen · S. A. Schönberg
Department of Laboratory Medicine,
Children's and Women's Health,
Norwegian University of Science and Technology (NTNU),
Erling Skjalgssons gate 1, 7006 Trondheim, Norway

T. Follestad
Department of Mathematical Sciences,
Norwegian University of Science and Technology (NTNU),
7491 Trondheim, Norway

H. E. Krokan
Department of Cancer Research and Molecular Medicine,
Norwegian University of Science and Technology (NTNU),
Erling Skjalgssons gate 1, 7006 Trondheim, Norway

S. A. Schönberg (✉)
Department of Laboratory Medicine,
Children's and Women's Health,
Norwegian University of Science and Technology,
St Olav's Hospital, 7489 Trondheim, Norway
e-mail: svanhild.schonberg@ntnu.no

Abbreviations

ATF3, ATF4 and ATF6	Activating transcription factor 3, 4 and 6
CHOP	Growth arrest- and DNA damage-inducible gene 153/C/EBP-homologous protein (CHOP/Gadd153)
Ec	Econazole
EPA	Eicosapentaenoic acid (20:5n-3)
ER	Endoplasmic reticulum
ERAD	ER-associated degradation
eIF2 α	Eukaryote translation initiation factor 2 α
EIF2AK3/PERK	eIF2 α kinase 3
HMOX-1	Heme oxygenase (decycling) 1
IP3	Inositol 1,4,5-triphosphate
PUFA	Polyunsaturated fatty acids
SQSTM1	Sequestosome-1
SOC	Store-operated Ca^{2+} channels
UPR	Unfolded protein response

Introduction

Epidemiological studies indicate an inverse relationship between dietary intake of n-3 polyunsaturated fatty acids (PUFA) and cancer, especially colon, prostate and breast cancer [1–5]. However, results of such studies are not entirely consistent [6]. Substantial experimental work from in vitro and animal models has shown that n-3 PUFA inhibit cancer cell proliferation, promote cell differentiation, limit angiogenesis and induce apoptosis [7–10].

Several mechanisms have been proposed to explain this including lipid peroxidation [11], activation of peroxisome proliferator-activated receptors (PPARs) [12], activation of retinoid X receptor alpha [13], altered activation of the Ras proteins [9], as well as modulation of eicosanoid production by inhibition of the cyclooxygenase-2 (COX-2) enzyme [5, 14]. However, the molecular mechanisms behind these effects are poorly understood. Our recent studies on colon cancer cells suggest that activation of the unfolded protein response (UPR) may play a major role in mediating the growth inhibitory effect of n-3 PUFA on these cells [15]. Similar pathways have been proposed by others [16]. However, what causes this activation has been unclear. In the present study we wanted to examine whether alterations in Ca^{2+} -homeostasis may precede activation of UPR in human leukemia HL60 cells after treatment with the n-3 PUFA eicosapentaenoic acid (EPA).

The endoplasmic reticulum (ER) is site of lipid synthesis and protein maturation [17]. It serves as an important intracellular Ca^{2+} buffer, and the concentration of Ca^{2+} is several times higher than in the cytosol. ER Ca^{2+} -levels control ER homeostasis by modulating numerous enzymatic cascades, the endomembrane Ca^{2+} -uptake and activation of Ca^{2+} release through channels in ER [18]. Eukaryotic cells can increase their cytosolic Ca^{2+} levels via two mechanisms: release of Ca^{2+} from intracellular stores or influx via plasma membrane channels. Channels in the plasma membrane, like the store-operated Ca^{2+} channels (SOC), regulate the influx of Ca^{2+} into the cell. Studies have shown that the antiproliferative effect of EPA and other PUFA may be mediated through the depletion of Ca^{2+} from intracellular stores [19, 20]. EPA induces Ca^{2+} release from intracellular Ca^{2+} stores by mobilizing the inositol 1,4,5-triphosphate (IP_3) sensitive Ca^{2+} pool through an IP_3 independent route, and inhibits Ca^{2+} influx through SOC in the plasma membrane [20, 21]. Over time this leads to depletion of intracellular Ca^{2+} due to leakage through the plasma membrane causing ER stress and activation of the UPR through the PERK/eIF2 α pathway that may lead to apoptosis [19, 22]. In contrast, studies show that the monounsaturated fatty acid oleic acid did not mobilize Ca^{2+} nor cause activation of the UPR in the same manner as EPA [15, 20, 21].

Conditions interfering with the function of ER are collectively called ER stress. The stress is induced by changes in Ca^{2+} concentration, nutrient deprivation, alterations in the oxidation-reduction balance, failure of post-translational modifications, or excessive protein synthesis, and can lead to the activation of a coordinated adaptive program called the UPR [23]. This co-ordinated response halts the build-up of proteins, allows time for the elimination of unfolded proteins, and re-establishes cellular homeostasis [24]. Figure 1 gives an overview of the UPR transducers and the response initiation following ER stress. Phosphorylation of eukaryote translation initiation factor 2 α (eIF2 α) by eIF2 α kinase 3 (EIF2AK3/PERK) leads to attenuation of global protein synthesis, but promotes translation of certain mRNAs, like ER resident protein chaperones, protein foldases and activating transcription factor 4 (ATF4) mRNA [24, 25]. If the stress cannot be resolved, the cell dies by apoptosis [26].

PUFA mobilize Ca^{2+} from the same intracellular pool as that mobilized by econazole (Ec) in leukaemia cells [27]. Ec is an antifungal imidazole that depletes Ca^{2+} from the ER and blocks Ca^{2+} influx in mammalian cells [28, 29]. This results in sustained depletion of Ca^{2+} from ER stores, activation of the UPR and eventually cell death [30]. However, Ec resistant cell lines have been isolated, like the E2R2 cell line, which is a clone of the human promyelocytic cell line HL60 [31]. E2R2 cells display increased SOC influx and resistance to depletion of Ca^{2+} stores in the

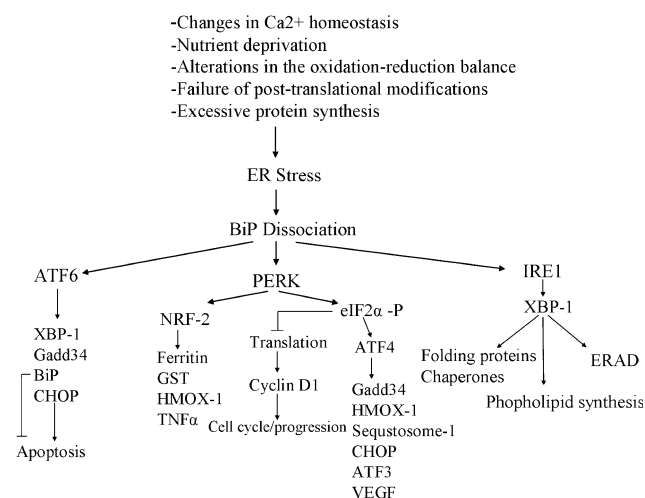


Fig. 1 Overview of the unfolded protein response. Three transmembrane proteins mediate the UPR-signal across the ER-membrane; inositol-requiring enzyme 1 (IRE1), eukaryote translation initiation factor 2 α (eIF2 α) kinase 3 (EIF2AK3/PERK) and activating transcription factor 6 (ATF6). Phosphorylation of eIF2 α by PERK leads to attenuation of global protein synthesis, but promotes translation of certain mRNAs, like activating transcription factor 4 (ATF4) mRNA. Loss of cyclin D1 during ER stress leads to G1-arrest and provides the cell with an opportunity to restore cell homeostasis. However, if the stress cannot be resolved, the cell dies by apoptosis

ER by Ec. E2R2 cells also maintain protein synthesis after treatment with Ec, as well as thapsigargin, most likely due to overexpression of ribosomal proteins. The increased SOC activity is likely to be responsible for the continuous replenishment of Ca^{2+} into the ER store, compensating for the ER Ca^{2+} store depletion caused by Ec. The HL60 cells on the other hand, do not display any of these properties and Ec treatment of these cells results in ER stress related cell death [31].

PUFA inhibit proliferation and induce apoptosis in a dose and time dependent manner in HL60 cells [32] and other leukemia cell lines [33]. In this study we wanted to investigate the role of Ca^{2+} -homeostasis in the antiproliferative effect of EPA. We therefore examined the effect of EPA on the Ec resistant HL60 clone E2R2 and HL60 cells. Cell proliferation was inhibited and several transcripts and proteins involved in the UPR were affected in HL60 cells by EPA treatment. In contrast, neither proliferation nor protein expression of key-mediators of the UPR were affected by treatment with 35 μM EPA in E2R2 cells. Altogether, these results indicate that alterations in Ca^{2+} homeostasis result in induction of ER stress and UPR response in HL60 cells after EPA treatment.

Experimental Procedures

Cell Culture and Fatty Acid Treatment

Human promyelocytic cells (HL60 cells) and E2R2 (generously provided by Zhang and Berger [31]) cells were cultured in RPMI 1640 medium supplemented with 2 mM L-glutamine (Invitrogen, Paisley, UK) and 10% (v/v) fetal bovine serum (FBS) (Euroclone, Pero, Italy) (complete growth medium) at 37 °C in an atmosphere of 5% CO_2 /air. The stock solution of EPA in ethanol (Cayman Chemical, Ann Arbor, USA) was stored at -20 °C and diluted in complete growth medium before experiments (35 μM) (final concentration of ethanol < 0.025% v/v). Cell density was determined using a Coulter Z1 counter, and 3×10^6 cells were seeded in 175-cm² cell culture flasks with 28 mL growth medium. No extra antioxidants were added to the medium as previous studies have shown that antioxidants do not influence the effect of EPA on cell proliferation and apoptosis [32, 34]. Cultures were supplemented with 20, 35 or 70 μM EPA or ethanol (control) and cell density was measured after 12, 24 and 48 h as described above.

RNA Isolation

HL60 cells were treated with EPA for 12, 24 or 48 h before centrifugation (500g, 7 min) and harvesting. Total RNA

was isolated using the High Pure RNA Isolation Kit from Roche Diagnostics (Mannheim, Germany) according to the instruction manual. RNA concentration and quality were determined using the NanoDrop1000 (NanoDrop Technologies, Wilmington, Delaware) and agarose gel electrophoresis.

Gene Expression Profiling

Synthesis of cDNA and biotinylated cRNA was performed according to the eukaryote expression manual provided by Affymetrix. In brief, 5 μg total RNA (HL60) was subjected to double-stranded cDNA synthesis using a T7-oligo(dT)₂₄-primer (Affymetrix, Santa Clara, CA) and the SuperScript™ Double-Stranded cDNA Labeling Kit (Invitrogen, Carlsbad, CA). After clean up (GeneChip Sample Clean Up Module, Affymetrix), all the prepared cDNA was used for in vitro transcription using the GeneChip® IVT Labelling Kit (Affymetrix). 20 μg fragmented cRNA were prepared for hybridization to the Human Genome U133 Plus 2.0 GeneChip (Affymetrix). Hybridization and washing/staining were performed using the Hybridization oven 640 and Fluidics Station 450 (EukGE-WS2v5 protocol). Staining was performed using Streptavidin, R-phycoerythrin conjugate (SAPE, Molecular Probes, Eugene, Oregon) and biotinylated anti-streptavidin antibody (Vector Laboratories, Burlingame, CA). The arrays were scanned using an Affymetrix GeneChip 3000 scanner controlled by GeneChip® Operating Software 1.4 (GCOS, Affymetrix). Expression profiling was performed in triplicate at all time points using total RNA isolated from independent biological replicates.

All experiments have been submitted to ArrayExpress with accession number E-MEXP-1389.

Statistical Analysis of Gene Expression Data

Statistical analysis was performed as described previously in Jakobsen et al. [15]. In short, gene expression summary measures were first computed from the raw data on the CEL-files, based on a linear statistical model for background-corrected, quantile normalized and log-transformed PM values, using the robust multiarray average (RMA) method [35]. Next, treatment effects were estimated by fitting a linear model to these RMA expression measures, and finally, tests for significant differential expression were performed using moderated *t* tests, in which variance estimates for each gene are found by borrowing strength from data on the remaining genes [36].

Differentially expressed genes were selected based on a threshold of 0.05 on adjusted *P* values, meaning that the expected proportion of genes falsely classified as differential expressed should be approximately 0.05. To account

for multiple testing, the *P* values were calculated controlling the False Discovery Rate (FDR) [37], where the estimated value of the proportion of non-differentially expressed genes was inserted [38]. Time effects in the control groups were considered negligible and omitted from the model. All statistical analyzes were performed in *R*, using the packages *limma* and *affy* from Bioconductor [39]. Annotation of differentially expressed genes was performed using the NetAffx Analysis Centre (<http://www.Affymetrix.com>) and NMC Annotation Tool/eGOn V2.0 (<http://www.GeneTools.no>).

Western Blotting

HL60 and E2R2 cells were treated with EPA for 3, 6 and 12 h before harvesting. The cells were washed in ice cold PBS-1 mM EDTA and pelleted by centrifugation (500g, 10 min at 4 °C). Nuclear extracts for detection of cyclin D1 and sequestosome-1 (SQSTM1) were prepared using a nuclear extract kit (Active Motif, Belgium) according to manufacturer's instructions. Total protein for detection of ATF4 was prepared as described by Akbari et al. [40].

To detect phosphorylated eIF2 α , pellets were lysed in 2 \times packed cell volumes of lysis buffer 20 mM HEPES, pH 7.5, 150 mM NaCl, 1% triton-X100, 10% glycerol, 1 mM EDTA, 100 mM NaF, 17.5 mM beta-glycerophosphate, protease inhibitor cocktail "Complete" (Roche), and phosphatase inhibitor cocktail 1 and 2 (Sigma-Aldrich, St. Louis, MO) on ice for 10 min. Equal amounts of protein were separated on 10% precast denaturing NuPAGE gels (Invitrogen, Carlsbad, CA) and transferred to PVDF membranes (Millipore, Billerica, MA). Membranes were blocked in PBS supplied with 5% non-fat dry milk and 0.1% Tween[®]-20 (BioRad, Herkules, CA) and further incubated overnight at 4 °C with the indicated primary antibodies; cyclin D1 (mouse monoclonal antibody, Cell Signaling Technology, Danvers, MA), SQSTM1 (rabbit polyclonal, Abcam), ATF4 (rabbit polyclonal, Santa Cruz Biotechnology, CA), phosphorylated eIF2 α (Serine 51, Cell Signaling Technology). The membranes were also probed for total eIF2 α (Cell Signaling Technology) as a control after stripping the membrane in Restore Western blot Stripping buffer (Pierce, Rockford, IL). All blots were reprobated with β -actin (mouse monoclonal, Abcam) as a loading control. For the eIF2 α antibody incubations and washing steps, TBST buffer (20 mM Tris-HCl, 137 mM NaCl, 0.1% (v/v) Tween-20) supplied with 5% non-fat dry milk was used. The blots were incubated with HRP-conjugated secondary antibodies (DAKO, Carpinteria, CA and Pierce, Rockford, IL) and detected by chemiluminescence using Super Signal West Femto Maximum Sensitivity Substrate (Pierce, Rockford, IL) and visualized by Kodak Image Station 4000R (Eastman Kodak Company, Rochester, NY).

Statistical Analysis

Statistical analysis of the effect of different concentrations of EPA on cell proliferation compared to control was carried out using a one-way ANOVA test followed by a Tukey HSD post-hoc test. The results from the western blot analysis were analyzed using a Student's *t* test. Differences were considered significant with a *P* < 0.05. The statistical analysis was performed using SPSS 15.0 for Windows.

Results

Effect of EPA on Cell Proliferation

Proliferation of HL60 cells was inhibited in a dose and time dependent manner by EPA in line with previous reports [32, 41]. EPA concentrations of 20 and 35 μ M reduced the cell number to approximately 50 and 60%, respectively, after 48 h, whereas treatment with 70 μ M abolished further proliferation (Fig. 2a). In contrast, E2R2 cells were much less affected after treatment with equal molar concentrations of EPA. EPA concentrations of 20 and 35 μ M did not affect cell proliferation, whereas treatment with 70 μ M reduced the cell number approximately 50% after 48 h (Fig. 2b).

Gene Expression Patterns and Signaling Pathways

Several complex gene networks and cell signalling pathways were affected after EPA treatment of HL60 cells. Even though the fold change value of most transcripts was modest, most of the changes in gene expression were seen already after 12 h, whereas the differences diminished with time, indicating that EPA causes early responses (Table 1). Transcripts were classified into several functional categories after annotation as shown in Table 2 and outlined below. Relevant proteins were detected by western blotting in both cell lines.

Ca²⁺ Homeostasis

PUFA have been shown to cause alterations in intracellular Ca²⁺ homeostasis [20, 21]. The mRNA level for a large number of genes involved in Ca²⁺ homeostasis was affected by EPA treatment of HL60 cells, most of them being upregulated (Table 2).

UPR

Alterations in ER Ca²⁺-homeostasis cause ER stress and activation of the UPR [23]. Several key transcripts involved in ER stress were upregulated in the HL60 cells

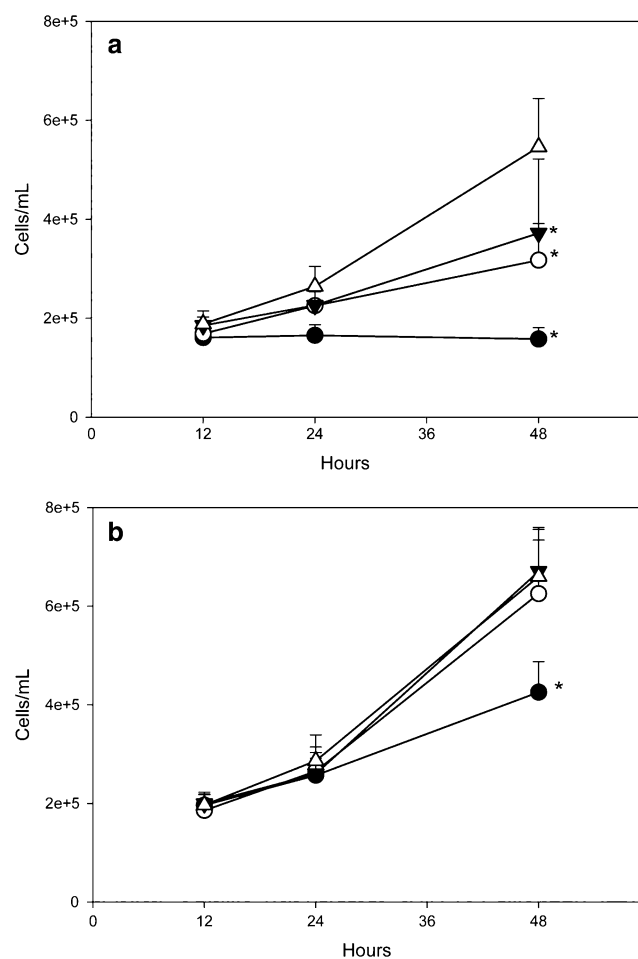


Fig. 2 Effect of EPA on cell proliferation. HL60 **a** and E2R2 **b** cells were cultured under standard conditions and treated with 20 (filled inverted triangles), 35 (open circles), 70 (closed circles) μM EPA or absolute ethanol (triangles) (control). Cell density was measured after 12, 24 and 48 h. The values represent the mean cell density + SD derived from three separate experiments. *Results analyzed by a one-way ANOVA test followed by a Tukey HSD post-hoc test and considered significant different from control ($P < 0.05$)

Table 1 Number of differently expressed genes at different time points in HL60 cells after treatment with EPA (35 μM)

Time point	Number of differently expressed genes HL60
12 (h)	2974 \uparrow 2247 \downarrow
24 (h)	908 \uparrow 138 \downarrow
48 (h)	90 \uparrow 11 \downarrow

after EPA treatment (Table 2). For example the upstream activator PERK (the eIF2 α kinase). Increased levels of phosphorylated eIF2 α were detected by western blotting as early as 3 h after EPA treatment (Fig. 3a). Phosphorylation of eIF2 α leads to attenuation of global protein synthesis, but promotes translation of certain mRNAs, like ATF4

mRNA [25, 42]. As expected from this, ATF4 was moderately upregulated at protein level after 12 h EPA treatment (Fig. 3a). Targets downstream from ATF4, like *HMOX-1*, *ATF3*, vascular endothelial growth factor (*VEGF*) and *SQSTM1* were also upregulated (Table 2). Moderately increased amount of SQSTM1 at protein level was also detected at 12 h (Fig. 3a).

Based on the results from the HL60 cells, protein expression of key-mediators of the UPR was investigated in the E2R2 cells after EPA treatment. Protein levels of phosphorylated eIF2 α , ATF4 and SQSTM1 were equally expressed in E2R2 cells treated with EPA and control cells (Fig. 3a).

Several members of the molecular chaperones, foldases and the ubiquitin/proteasome system were also upregulated at the mRNA level in HL60, indicating the presence of ER stress (Table 2).

Cell Cycle and Apoptosis

Activation of the UPR may halt cell cycle progression [24]. Gene expression studies of the HL60 cells showed 103 downregulated transcripts involved in cell cycle. Cyclin D1 is an important regulator of G1 to S phase progression and thereby cell cycle [43]. Cyclin D1 was downregulated at transcript as well as protein level in HL60 (Table 2; Fig. 3b). However, in E2R2 cells, cyclin D1 was not downregulated at protein level, but was equally expressed in treated and non-treated cells (Fig. 3b). Calcium/calmodulin-dependent protein kinase 1 (CAMK1) was downregulated in the HL60 cells. CAMK1 is important for cell cycle progression through activation of cyclin/cdk complexes [44]. This in addition to phosphorylation of eIF2 α may contribute to the inhibition of cell cycle/progression.

Activation of the UPR may trigger apoptosis mediated by several caspases. Caspase-4, -7 and -9 are among the most important mediators of ER stress-induced apoptosis [45, 46]. All of these as well as several other caspases and caspase related transcripts were upregulated at mRNA level in EPA treated HL60 cells (Table 2). The pro-apoptotic factor Tribbles homolog 3 (TRIB3), known to be induced by ER stress through the PERK-ATF4-CHOP pathway [47], was upregulated at several time points. In addition, pro-apoptotic transcripts related to Bcl-2 were upregulated (Table 2). All together 106 transcripts involved in cell death were upregulated.

Discussion

In this study we show that HL60 cells are strongly growth inhibited by EPA, while the Ec-resistant HL60 clone E2R2

Table 2 Functional categories of selected differentially expressed transcripts affected in HL60 cells treated with EPA (35 μ M) at 12, 24 and 48 h

Gene symbol	Affymetrix ID	Refseq NCBI ID	Description	HL60		
				Fold change		
				12 (h)	24 (h)	48 (h)
Ca²⁺ homeostasis						
BLVRB	202201_at	NM_000713	Biliverdin reductase B (flavin reductase (NADPH))	1.4	1.5	
CAMK1	204392_at	NM_003656	Calcium/calmodulin-dependent protein kinase 1	-1.8		
CAPN2	208683_at	NM_001748	Calpain 2, large subunit	2.3	1.8	
IP3R1	203710_at	NM_001099952	Inositol 1,4,5-triphosphate receptor, type 1	1.3		
		NM_002224				
IP3R1	211323_s_at	NM_001099952	Inositol 1,4,5-triphosphate receptor, type 1	1.2		
		NM_002222				
IP3R1	240052_at	NM_001099952	Inositol 1,4,5-triphosphate receptor, type 1	1.5	1.5	
		NM_002222				
S100A4	203186_s_at	NM_002961	S100 calcium binding protein A4		1.6	
		NM_019554				
S100A6	217728_at	NM_014624	S100 calcium binding protein A6		1.6	
S100A8	202917_s_at	NM_002964	S100 calcium binding protein A8	1.8	4.1	2.0
S100A9	203535_at	NM_002965	S100 calcium binding protein A9		2.5	
S100A11	200660_at	NM_005620	S100 calcium binding protein A11 (calgizzarin)		1.4	
S100A11	208540_x_at	NM_021039	S100 calcium binding protein A11 (calgizzarin)		1.4	
S100P	204351_at	NM_005980	S100 calcium binding protein P	1.8	2.2	2.5
ER stress response						
ATF3	202672_s_at	NM_001030287	Activating transcription factor 3	1.9	1.3	1.5
		NM_001040619				
		NM_001674				
		NM_004024				
GRP94/TRAI	200599_s_at	NM_003299	Glucose regulated protein 95 kDa/Tumor rejection antigen 1	1.2		
HMOX1	203665_at	NM_002133	Heme oxygenase (decycling) 1	1.5		
PDIA4/ERP70	208658_at	NM_004911	Protein disulfide isomerase related protein	1.3		
PERK	218696_at	NM_004836	PKR-like ER kinase	1.3		
SERP1	200971_s_at	NM_014445	Stress-associated endoplasmic reticulum protein 1	1.1		
SQSTM1	201471_s_at	NM_003900	Sequestosome 1	2	1.5	
SQSTM1	213112_s_at	NM_003900	Sequestosome 1	1.5		
SQSTM1	244804_at	NM_003900	Sequestosome 1	1.7		
ASNS	205047_s_at	NM_001673	Asparagine synthetase	1.5	1.3	1.5
		NM_133436				
		NM_183356				
VEGF	210512_s_at	NM_001025366	Vascular endothelial factor	1.4		
		NM_001025367				
		NM_001025368				
		NM_001025369				
		NM_001025370				
		NM_001033756				
		NM_0033				
VCP	208648_at	NM_007126	Valosin-containing protein	1.3		
Chaperones/Protein folding						
Clorf24	217967_s_at	NM_052966	Chromosome 1 open reading frame 24	1.4		

Table 2 continued

Gene symbol	Affymetrix ID	Refseq NCBI ID	Description	HL60		
				Fold change		
				12 (h)	24 (h)	48 (h)
DNAJB2	202500_at	NM_001039550 NM_006736	DnaJ (Hsp40) homolog, subfamily B, member B2	1.4		
DNAJB4	203810_at	NM_007034	DnaJ (Hsp40) homolog, subfamily B, member B4	2.6	1.6	
DNAJB9	202842_s_at	NM_012328	DnaJ (Hsp40) homolog, subfamily B, member B9		1.3	
DNAJB9	202843_at	NM_012328	DnaJ (Hsp40) homolog, subfamily B, member B9		1.5	
DNAJB9	1554462_a_at	NM_012328	DnaJ (Hsp40) homolog, subfamily B, member B9		1.2	
DNAJB14	222850_s_at	NM_001031723 NM_024920	DnaJ (Hsp40) homolog, subfamily B, member 14	1.4		
DNAJB14	219237_s_at	NM_001031723 NM_024920	DnaJ (Hsp40) homolog, subfamily B, member 14	1.4		
DNAJC1	218409_s_at	NM_022365	DnaJ (Hsp40) homolog, subfamily C, member 1	1.2		
DNAJC10	221781_s_at	NM_018981	DnaJ (Hsp40) homolog, subfamily C, member 10	1.2		
DNAJC10	221782_at	NM_018981	DnaJ (Hsp40) homolog, subfamily C, member 10	1.4		
DNAJC10	225174_at	NM_018981	DnaJ (Hsp40) homolog, subfamily C, member 10	1.5		
STCH	202557_at	NM_006948	Stress 70 protein chaperone, microsome-associated, 60 kDa	1.3		
CLGN	205830_at	NM_004362	Calmeqin	1.5		
Ubiquitine/proteasome						
UBE2D3	240383_at	NM_003340 NM_181886 NM_181887 NM_181888 NM_181889 NM_181890 NM_181891 NM_181892 NM_181893	Ubiquitin-conjugating enzyme E2D3		1.7	
UBE2I	208760_at	NM_003345 NM_194259 NM_194260 NM_194261	Ubiquitin-conjugating enzyme E2I		1.3	
UBE2L6	201649_at	NM_004223 NM_198183	Ubiquitin-conjugating enzyme E2L 6	1.2	1.4	
PSMA1	210759_s_at	NM_002786 NM_148976	Proteasome subunit, alpha type, 1	1.2		
PSMA1	211746_x_at	NM_002786 NM_148976	Proteasome subunit, alpha type, 1	1.2		
PSMA1	201676_x_at	NM_002786 NM_148976	Proteasome subunit, alpha type, 1	1.2		
PSMC1	204219_s_at	NM_002802	Proteasome 26S subunit, ATPase, 1	1.2		
PSMC2	201068_s_at	NM_002803	Proteasome 26S subunit, ATPase, 2	1.3		
PSMC2	201067_at	NM_002803	Proteasome 26S subunit, ATPase, 2	1.4		
PSMC2	238020_at	NM_002803	Proteasome 26S subunit, ATPase, 2	1.3		
PSMD1	201198_s_at	NM_002807	Proteasome 26S subunit, non-ATPase, 1	1.4		
PSMD1	201199_s_at	NM_002807	Proteasome 26S subunit, non-ATPase, 1	1.4		
PSMD6	202753_at	NM_014814	Proteasome 26S subunit, non-ATPase, 6	1.2		
PSMD14	212296_at	NM_005805	Proteasome 26S subunit, non-ATPase, 14	1.2		

Table 2 continued

Gene symbol	Affymetrix ID	Refseq NCBI ID	Description	HL60		
				Fold change		
				12 (h)	24 (h)	48 (h)
Cell cycle/Apoptosis						
APAF1	204859_s_at	NM_001160 NM_013229 NM_181861 NM_181868 NM_181869	Apoptotic peptidase activating factor 1	1.3		
BCL2A1	205681_at	NM_004049	BCL2-related protein A1	1.8	1.8	1.5
BCL2L13	217955_at	NM_015367	BCL2-like 13 (apoptosis facilitator)	1.3		
BCL2L13	226798_at	NM_015367	BCL2-like 13 (apoptosis facilitator)	1.2		
BNIP3L	221478_at	NM_004331	BCL2/adenovirus E1B 19 kDa interacting protein 3-like	1.3		
BNIP3L	221479_s_at	NM_004331	BCL2/adenovirus E1B 19 kDa interacting protein 3-like	1.4		
CARD12	1552553_a_at	NM_021209	Caspase recruitment domain family, member 12	1.4		
CARD6	224414_s_at	NM_032587	Caspase recruitment domain family, member 6	1.5		
CARD8	1554479_a_at	NM_014959	Caspase recruitment domain family, member 8	1.4	1.2	
CASP4	209310_s_at	NM_001225 NM_033306 NM_033307	Caspase 4, apoptosis-related cysteine peptidase	1.4		
CASP6	211464_x_at	NM_001226 NM_032992	Caspase 6, apoptosis-related cysteine peptidase	1.3		
CASP7	207181_s_at	NM_001227 NM_033338 NM_033339 NM_033340	Caspase 7, apoptosis-related cysteine peptidase	1.4		
CASP8	213373_s_at	NM_001080124 NM_001080125 NM_001228 NM_033355 NM_033356 NM_033358	Caspase 8, apoptosis-related cysteine peptidase	1.3		
CASP9	203984_s_at	NM_001229 NM_032996	Caspase 9, apoptosis-related cysteine peptidase	1.3		
CCND1	208712_at	NM_053056	Cyclin D1	-1.6		
CCND1	208711_s_at	NM_053056	Cyclin D1	-1.5		
TRIB3	218145_at	NM_021158	Tribbles homolog 3 (Drosophila)	1.5	1.3	1.4
TRIB3	1555788_a_at	NM_021158	Tribbles homolog 3 (Drosophila)	1.3		

is much less affected by the same treatment. The observed difference in EPA-sensitivity between the two cell lines is most likely mediated through alterations of Ca^{2+} -homeostasis and activation of ER stress and UPR.

Several transcripts involved in the Ca^{2+} -homeostasis were affected in the HL60 cells after EPA treatment (Table 2), indicating that EPA treatment causes alterations in intracellular Ca^{2+} levels. This is also in line with findings in our recent study on colon cancer cells showing that

DHA affects Ca^{2+} homeostasis [15], as well as several other studies on different cell lines [19–21].

Alterations in ER Ca^{2+} -homeostasis cause ER stress and activation of the UPR [23]. Several genes involved in the UPR response (Fig. 1) were affected at mRNA as well as protein level in the HL60 cells (Table 2; Fig. 3a). In particular, we found elevated levels of phosphorylated eIF2 α [48]. Altered mRNA expression of UPR transcripts and increased level of phosphorylated eIF2 α following n-3

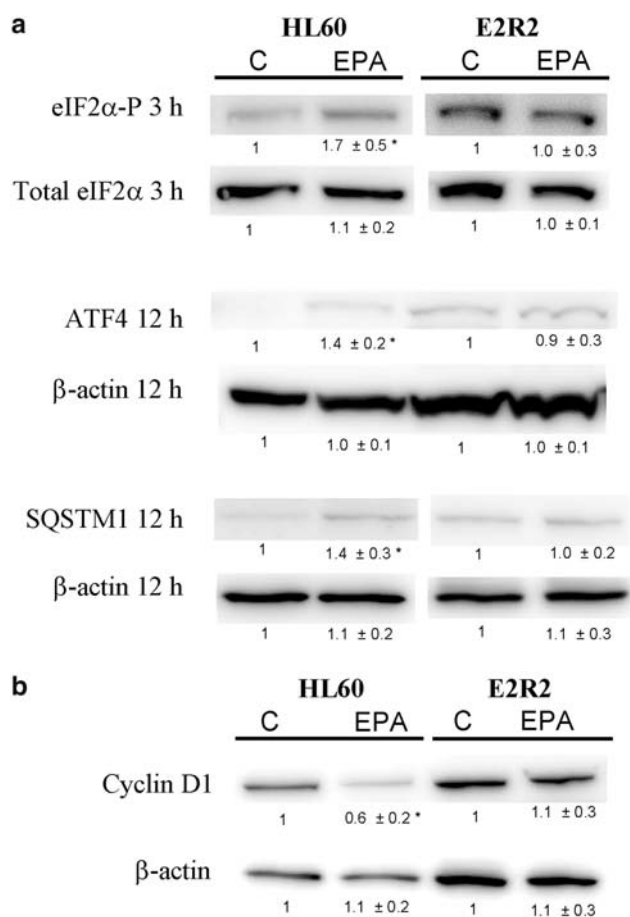


Fig. 3 ER stress signalling and UPR in response to EPA. Western blot analysis of proteins involved in the UPR pathway in HL60 and E2R2 cells cultured under standard conditions and treated with 35 μ M EPA or absolute ethanol (control C). Differences in protein levels are given as mean band signal strength ratio; EPA treated/control cells \pm SD for three or more independent experiments. One representative blot is shown. β -actin was used as a control for equal protein loading. *Results analyzed by Student's *t* test and considered significant different from control ($P \leq 0.05$). **a** eIF2 α -P and total eIF2 α : 3 h cytoplasmic extracts; ATF4: 12 h total protein extracts; SQSTM1: 12 h nuclear extracts. **b** Cyclin D1 12 h nuclear extracts

PUFA treatment are in line with previous reports on other cancer cell lines [15, 19]. Furthermore, upregulated mRNA levels of chaperones, foldases and transcripts involved in the ubiquitin/proteasome system indicate that EPA alters ER homeostasis (Table 2). Altogether, these data indicate that EPA treatment of HL60 cells causes ER stress. In contrast to the HL60 cells, EPA treatment of the E2R2 did not increase protein levels of key-mediators of the UPR like phosphorylated eIF2 α , ATF4 and SQSTM1 compared to control cells. This confirms that EPA treatment of the E2R2 cells does not result in activation of the UPR.

Loss of cyclin D1 caused by phosphorylated eIF2 α during ER stress leads to G1-arrest and provides the cell with an opportunity to restore cell homeostasis [49]. This is

in agreement with the finding that cyclin D1 was down-regulated at mRNA as well as protein level (Table 2; Fig. 3b), and in line with previous reports [15, 19]. Furthermore, this may explain why previous studies have shown that PUFA treatment of HL60 cells increase the portion of cells in the G1 phase of the cell cycle [8, 32]. In line with the same reports stating that EPA treatment inhibits cell cycle and causes apoptosis, we found several genes involved in cell cycle/progression to be downregulated, and genes involved in apoptosis to be upregulated.

Cyclin D1 has been shown to be important for the development and progression of several cancers including lymphoma, parathyroid adenoma and cancer of the breast, oesophagus, lung and bladder [50–55]. Cyclin D1 is a proto-oncogene and is an important regulator of G1 to S phase progression in many different cell types. It binds to cyclin dependent kinase 4 and 6 (CDK4 and CDK6) and forms active complexes that promote cell cycle progression by phosphorylating and inactivating the retinoblastoma protein (RB) [43]. It is also a transcriptional modulator regulating the activity of several transcription factors and histone deacetylase (HDAC3) [56]. Cyclin D1 is therefore used as a key marker of cell viability and established as an important prognostic marker in different types of cancer [57, 58]. In contrast to HL60 cells, protein level of cyclin D1 was not downregulated in response to EPA in the E2R2 cells, but equally expressed in control and EPA treated cells (Fig. 3b), indicating that cell cycle is not affected. This also confirmed the differences found in cell proliferation after EPA treatment (Fig. 2).

The only known difference between HL60 cells and E2R2 cells is that E2R2 is resistant to the imidazole Ec, which depletes Ca²⁺ from the ER and blocks Ca²⁺ influx in mammalian cells [28, 29]. Ec treatment of E2R2 cells does not cause ER stress by phosphorylation of eIF2 α or cell death [31]. The different response to EPA in these two cell lines, strongly suggests that the inhibitory effect of EPA on HL60 cells is mediated through alterations of the Ca²⁺ homeostasis, leading to activation of the ER stress response. This is to be expected, as studies have shown that PUFA mobilizes Ca²⁺ from the same intracellular pool as that mobilized by Ec [27]. E2R2 cells have been shown to display increased SOC influx compared to HL60 [31]. We therefore speculate that this is one of the main mechanisms that maintain cell viability in E2R2 cells compared to HL60 cells when exposed to EPA.

Several studies show an antiproliferative effect of EPA and other PUFA on cancer cells. However, no unified mechanism has been identified. Activation of the UPR has been suggested to mediate the inhibitory effect of PUFA on cancer, but what causes this activation has been unclear. In this study we show that EPA induces activation of the UPR in HL60 cells, but not in the Ec resistant HL60 clone E2R2.

This indicates that the antiproliferative effect of EPA is mediated through alterations in Ca^{2+} homeostasis, leading to activation of the UPR and thereby growth arrest/apoptosis.

Acknowledgments We thank Professor Stuart A. Berger, University Health Network, Toronto, Canada, for kindly providing the E2R2 cells. Thanks to Gro Leite Størvold, Hilde Bremseth, Anne Gøril Lundemo for technical assistance and Professor Kristian S. Bjerve for good support. The project was financed by The Faculty of Medicine, NTNU, The Cancer Research Fund, Trondheim University Hospital and The Research Council of Norway through grants from the Functional Genomics Program (FUGE). Microarray experiments were performed at the microarray core facility at the Norwegian Microarray Consortium (NMC), Trondheim, which is supported by FUGE, The Norwegian Research Council. Financial support was also given by the cross-disciplinary project “BIOEMIT-Prediction and modification in functional genomics: combining bioinformatical, bioethical, biomedical and biotechnological research”, NTNU.

References

1. Roynette CE, Calder PC, Dupertuis YM, Pichard C (2004) n-3 Polyunsaturated fatty acids and colon cancer prevention. *Clin Nutr* 23:139–151
2. Terry PD, Rohan TE, Wolk A (2003) Intakes of fish and marine fatty acids and the risks of cancers of the breast and prostate and of other hormone-related cancers: a review of the epidemiologic evidence. *Am J Clin Nutr* 77:532–543
3. Caygill CP, Charlett A, Hill MJ (1996) Fat, fish, fish oil and cancer. *Br J Cancer* 74:159–164
4. Sasaki S, Horacek M, Kesteloot H (1993) An ecological study of the relationship between dietary fat intake and breast cancer mortality. *Prev Med* 22:187–202
5. Berquin IM, Edwards IJ, Chen YQ (2008) Multi-targeted therapy of cancer by omega-3 fatty acids. *Cancer Lett* 49:363–377
6. MacLean CH, Newberry SJ, Mojica WA, Khanna P, Issa AM, Suttorp MJ, Lim YW, Traina SB, Hilton L, Garland R, Morton SC (2006) Effects of omega-3 fatty acids on cancer risk: a systematic review. *Jama* 295:403–415
7. Falconer JS, Ross JA, Fearon KC, Hawkins RA, O’Riordain MG, Carter DC (1994) Effect of eicosapentaenoic acid and other fatty acids on the growth in vitro of human pancreatic cancer cell lines. *Br J Cancer* 69:826–832
8. Finstad HS, Drevon CA, Kulseth MA, Synstad AV, Knudsen E, Kolset SO (1998) Cell proliferation, apoptosis and accumulation of lipid droplets in U937-1 cells incubated with eicosapentaenoic acid. *Biochem J* 336:451–459
9. Collett ED, Davidson LA, Fan YY, Lupton JR, Chapkin RS (2001) n-6 and n-3 polyunsaturated fatty acids differentially modulate oncogenic Ras activation in colonocytes. *Am J Physiol Cell Physiol* 280:C1066–C1075
10. Hardman WE, Sun L, Short N, Cameron IL (2005) Dietary omega-3 fatty acids and ionizing irradiation on human breast cancer xenograft growth and angiogenesis. *Cancer Cell Int* 5:12
11. Stoll BA (2002) n-3 fatty acids and lipid peroxidation in breast cancer inhibition. *Br J Nutr* 87:193–198
12. Chawla A, Repa JJ, Evans RM, Mangelsdorf DJ (2001) Nuclear receptors and lipid physiology: opening the X-files. *Science* 294:1866–1870
13. Fan YY, Spencer TE, Wang N, Moyer MP, Chapkin RS (2003) Chemopreventive n-3 fatty acids activate RXR α in colonocytes. *Carcinogenesis* 24:1541–1548
14. Rao CV, Hirose Y, Indranie C, Reddy BS (2001) Modulation of experimental colon tumorigenesis by types and amounts of dietary fatty acids. *Cancer Res* 61:1927–1933
15. Jakobsen CH, Størvold GL, Bremseth H, Follstad T, Sand K, Mack M, Olsen KS, Lundemo AG, Iversen JG, Krokan HE, Schonberg SM (2008) DHA induces ER stress and growth arrest in human colon cancer cells—associations with cholesterol and calcium homeostasis. *J Lipid Res* 49:2089–2100
16. Aktas H, Halperin JA (2004) Translational regulation of gene expression by omega-3 fatty acids. *J Nutr* 134:2487S–2491S
17. Zaloga GP, Marik P (2001) Lipid modulation and systemic inflammation. *Crit Care Clin* 17:201–217
18. Grolach A, Klappa P, Kietzmann T (2006) The endoplasmic reticulum: folding, calcium homeostasis, signalling, and redox control. *Antioxid Redox Signal* 8:1391–1418
19. Palakurthi SS, Fluckiger R, Aktas H, Changolkar AK, Shahsafaei A, Harneit S, Kilic E, Halperin JA (2000) Inhibition of translation initiation mediates the anticancer effect of the n-3 polyunsaturated fatty acid eicosapentaenoic acid. *Cancer Res* 60:2919–2925
20. Chow SC, Jondal M (1990) Polyunsaturated free fatty acids stimulate an increase in cytosolic Ca^{2+} by mobilizing the inositol 1, 4, 5-trisphosphate-sensitive Ca^{2+} pool in T-cells through a mechanism independent of phosphoinositide turnover. *J Biol Chem* 265:902–907
21. Calviello G, Palozza P, Di Nicuolo F, Maggiano N, Bartoli GM (2000) n-3 PUFA dietary supplementation inhibits proliferation and store-operated calcium influx in thymoma cells growing in Balb/c mice. *J Lipid Res* 41:182–189
22. Brostrom MA, Brostrom CO (2003) Calcium dynamics and endoplasmic reticular function in the regulation of protein synthesis: implications for cell growth and adaptability. *Cell Calcium* 34:345–363
23. Rutkowski DT, Kaufman RJ (2004) A trip to the ER: coping with stress. *Trends Cell Biol* 14:20–28
24. Wu J, Kaufman RJ (2006) From acute ER stress to physiological roles of the unfolded protein response. *Cell Death Differ* 13:374–384
25. Bertolotti A, Zhang Y, Hendershot LM, Harding HP, Ron D (2000) Dynamic interaction of BiP and ER stress transducers in the unfolded-protein response. *Nat Cell Biol* 2:326–332
26. Kim R, Emi M, Tanabe K, Murakami S (2006) Role of the unfolded protein response in cell death. *Apoptosis* 11:5–13
27. Gamberucci A, Fulceri R, Bygrave FL, Benedetti A (1997) Unsaturated fatty acids mobilize intracellular calcium independent of IP₃ generation and VIA insertion at the plasma membrane. *Biochem Biophys Res Commun* 241:312–316
28. Gamberucci A, Fulceri R, Benedetti A, Bygrave FL (1998) On the mechanism of action of econazole, the capacitative calcium inflow blocker. *Biochem Biophys Res Commun* 248:75–77
29. Jan CR, Ho CM, Wu SN, Tseng CJ (1999) Multiple effects of econazole on calcium signalling: depletion of thapsigargin-sensitive calcium store, activation of extracellular calcium influx, and inhibition of capacitative calcium entry. *Biochim Biophys Acta* 1448:533–542
30. Soboloff J, Berger SA (2002) Sustained ER Ca^{2+} depletion suppresses protein synthesis and induces activation-enhanced cell death in mast cells. *J Biol Chem* 277:13812–13820
31. Zhang Y, Berger SA (2004) Increased calcium influx and ribosomal content correlate with resistance to endoplasmic reticulum stress-induced cell death in mutant leukemia cell lines. *J Biol Chem* 279:6507–6516
32. Finstad HS, Kolset SO, Holme JA, Wiger R, Farrants AK, Blomhoff R, Drevon CA (1994) Effect of n-3 and n-6 fatty acids on proliferation and differentiation of promyelocytic leukemic HL-60 cells. *Blood* 84:3799–3809

33. Finstad HS, Myhrstad MC, Heimli H, Lomo J, Blomhoff HK, Kolset SO, Drevon CA (1998) Multiplication and death-type of leukemia cell lines exposed to very long-chain polyunsaturated fatty acids. *Leukemia* 12:921–929
34. Arita K, Yamamoto Y, Takehara Y, Utsumi T, Kanno T, Miyaguchi C, Akiyama J, Yoshioka T, Utsumi K (2003) Mechanisms of enhanced apoptosis in HL-60 cells by UV-irradiated n-3 and n-6 polyunsaturated fatty acids. *Free Radic Biol Med* 35:189–199
35. Irizarry RA, Bolstad BM, Collin F, Cope LM, Hobbs B, Speed TP (2003) Summaries of affymetrix genechip probe level data. *Nucleic Acids Res* 31:15
36. Smyth GK (2004) Linear models and empirical Bayes methods for assessing differential expression in microarray experiments. *Stat Appl Genet Mol Biol* 3
37. Benjamini Y, Hochberg Y (1995) Controlling the false discovery rate: a practical and powerful approach to multiple testing. *J Royal Statistical Soc B* 57:289–300
38. Langaas M, Lindqvist B, Ferkingstad E (2005) Estimating the proportion of true null hypotheses, with application to DNA microarray data. *J Royal Statistical Soc B* 67:555–572
39. Gentleman RC, Carey VJ, Bates DM, Bolstad B, Dettling M, Dudoit S, Ellis B, Gautier L, Ge Y, Gentry J, Hornik K, Hothorn T, Huber W, Iacus S, Irizarry R, Leisch FLC, Maechler M, Rossini AJ, Sawitzki G, Smith C, Smyth G, Tierney L, Yang JY, Zhang J (2004) Bioconductor: open software development for computational biology and bioinformatics. *Genome Biol* 5:R80
40. Akbari M, Otterlei M, Pena-Diaz J, Aas PA, Kavli B, Liabakk NB, Hagen L, Imai K, Durandy A, Slupphaug G, Krokan HE (2004) Repair of U/G and U/A in DNA by UNG2-associated repair complexes takes place predominantly by short-patch repair both in proliferating and growth-arrested cells. *Nucleic Acids Res* 32:5486–5498
41. Arita K, Kobuchi H, Utsumi T, Takehara Y, Akiyama J, Horton AA, Utsumi K (2001) Mechanism of apoptosis in HL-60 cells induced by n-3 and n-6 polyunsaturated fatty acids. *Biochem Pharmacol* 62:821–828
42. Harding HP, Zhang Y, Bertolotti A, Zeng H, Ron D (2000) Perk is essential for translational regulation and cell survival during the unfolded protein response. *Mol Cell* 5:897–904
43. Weinberg RA (1995) The retinoblastoma protein and cell cycle control. *Cell* 81:323–330
44. Kahl CR, Means AR (2004) Regulation of cyclin D1/Cdk4 complexes by calcium/calmodulin-dependent protein kinase I. *J Biol Chem* 279:15411–15419
45. Hitomi J, Katayama T, Eguchi Y, Kudo T, Taniguchi M, Koyama Y, Manabe T, Yamagishi S, Bando Y, Imaizumi K, Tsujimoto Y, Tohyama M (2004) Involvement of caspase-4 in endoplasmic reticulum stress-induced apoptosis and a beta-induced cell death. *J Cell Biol* 165:347–356
46. Momoi T (2004) Caspases involved in ER stress-mediated cell death. *J Chem Neuroanat* 28:101–105
47. Corcoran CA, Luo X, He Q, Jiang C, Huang Y, Sheikh MS (2005) Genotoxic and endoplasmic reticulum stresses differentially regulate TRB3 expression. *Cancer Biol Ther* 4:1063–1067
48. Kaufman RJ (2004) Regulation of mRNA translation by protein folding in the endoplasmic reticulum. *Trends Biochem Sci* 29:152–158
49. Brewer JW, Hendershot LM, Sherr CJ, Diehl JA (1999) Mammalian unfolded protein response inhibits cyclin D1 translocation and cell-cycle progression. *Proc Natl Acad Sci U S A* 96:8505–8510
50. Dai Y, Hamm TE, Dent P, Grant S (2006) Cyclin D1 overexpression increases the susceptibility of human U266 myeloma cells to CDK inhibitors through a process involving p130-, p107- and E2F-dependent S phase entry. *Cell Cycle* 5:437–446
51. Motokura T, Bloom T, Kim HG, Juppner H, Ruderman JV, Kronenberg HM, Arnold A (1991) A novel cyclin encoded by a bc11-linked candidate oncogene. *Nature* 350:512–515
52. Kehn K, Berro R, Alhaj A, Bottazzi ME, Yeh WI, Klase Z, Van Duyn R, Fu S, Kashanchi F (2007) Functional consequences of cyclin D1/BRCA1 interaction in breast cancer cells. *Oncogene* 26:5060–5069
53. Lagarde SM, ten Kate FJ, Richel DJ, Offerhaus GJ, van Lanschot JJ (2007) Molecular prognostic factors in adenocarcinoma of the esophagus and gastroesophageal junction. *Ann Surg Oncol* 14:977–991
54. Gautschi O, Ratschiller D, Gugger M, Betticher DC, Heighway J (2007) Cyclin D1 in non-small cell lung cancer: a key driver of malignant transformation. *Lung Cancer* 55:1–14
55. Yurakh AO, Ramos D, Calabuig-Farinas S, Lopez-Guerrero JA, Rubio J, Solsona E, Romanenko AM, Vozianov AF, Pellin A, Llombart-Bosch A (2006) Molecular and immunohistochemical analysis of the prognostic value of cell-cycle regulators in urothelial neoplasms of the bladder. *Eur Urol* 50:506–515
56. Coqueret O (2002) Linking cyclins to transcriptional control. *Gene* 299:35–55
57. Esteva FJ, Hortobagyi GN (2004) Prognostic molecular markers in early breast cancer. *Breast Cancer Res* 6:109–118
58. Stojadinovic A, Brennan MF, Hoos A, Omeroglu A, Leung DH, Dudas ME, Nissan A, Cordon-Cardo C, Ghossein RA (2003) Adrenocortical adenoma and carcinoma: histopathological and molecular comparative analysis. *Mod Pathol* 16:742–751

Atorvastatin Decreases Stearoyl-CoA Desaturase Gene Expression in THP-1 Macrophages Incubated with Oxidized LDL

Paula Martín-Fuentes · Angel Luis García-Otín ·
Luisa Calvo · Diego Gómez-Coronado ·
Fernando Civeira · Ana Cenarro

Received: 17 April 2008 / Accepted: 6 October 2008 / Published online: 4 November 2008
© AOCs 2008

Abstract Statins, inhibitors of HMG-CoA reductase, reduce plasma low-density lipoprotein (LDL) cholesterol levels decreasing the incidence of coronary events. However, the observed benefit of statins appears to extend beyond their lipid-lowering effects. Previous studies by our group have demonstrated that atorvastatin in oxidized LDL incubated macrophages modifies the gene expression profile of certain enzymes involved in fatty acid metabolism, mainly stearoyl-CoA desaturase (SCD). SCD is a rate-limiting enzyme in the biosynthesis of monounsaturated fatty acids and its expression is mediated by sterol regulatory element-binding protein-1 (SREBP-1). The aim of this study was to determine whether atorvastatin might affect the fatty acid composition in macrophages and if their SCD gene expression profile could explain this effect. Therefore, THP-1 macrophages were treated with atorvastatin and native or oxidized LDL, their fatty acid composition was determined by gas-chromatography, and the SCD and SREBP-1 gene expression profile was analysed using quantitative RT-PCR. We found that

atorvastatin reduces the percentage of palmitoleic and oleic acids in THP-1 cells incubated with oxLDL, which could be explained by the inhibition of SCD and SREBP-1 gene expression. The observed results were reversed when mevalonate was added to THP-1 macrophages. This would suggest that inhibition of SCD in THP-1 macrophages incubated with oxLDL and the change in fatty acid composition is an important effect of atorvastatin.

Keywords Atorvastatin · Fatty acids · Stearoyl-CoA desaturase · THP-1 · Gene expression · Cholesterol

Introduction

Statins, inhibitors of 3-hydroxy-3-methylglutaryl coenzyme A (HMG-CoA) reductase, a rate-limiting enzyme for cholesterol synthesis, have revolutionized the treatment of hypercholesterolemia reducing the incidence of coronary events and the rate of mortality in coronary patients. They inhibit HMG-CoA reductase competitively, reduce low-density lipoprotein (LDL) cholesterol levels more than other cholesterol-lowering drugs, and lower triglycerides in hypertriglyceridemic patients [1]. Several landmark clinical trials have demonstrated the benefit of lipid lowering with statins for the primary and secondary prevention of coronary heart disease (WOSCOPS, AFCAPS/TextCAPS, HS, CARE, LIPID, HPS, TNT) [2, 3]. However, the observed benefit with statin therapy was much greater than might have been expected through the reduction of cholesterol levels alone. Results in these experimental studies suggested the possibility that some antiatherosclerotic effects of statins may not be a direct consequence of their influence on LDL cholesterol concentration [4, 5]. These

P. Martín-Fuentes (✉) · A. L. García-Otín · F. Civeira ·
A. Cenarro

Laboratorio de Investigación Molecular,
Instituto Aragonés de Ciencias de la Salud (I+CS),
Hospital Universitario Miguel Servet,
Edificio de Consultas Externas,
planta 4ª, c/ Cardenal Gomá, s/n, 50009 Zaragoza, Spain
e-mail: pmartin.iacs@aragon.es

L. Calvo
Servicio de Bioquímica, Hospital Universitario Miguel Servet,
Zaragoza, Spain

D. Gómez-Coronado
Servicio de Bioquímica-Investigación, Hospital Ramón y Cajal,
Madrid, Spain

effects are known as pleiotropic effects of statins and they include improvement of endothelial dysfunction, increased nitric oxide bioavailability, antioxidant effects, anti-inflammatory properties and stabilization of atherosclerotic plaques [6, 7]. Some of the pleiotropic effects of statins may be explained by preventing the prenylation of small G proteins, including Ras and Rho proteins [8], since statins decrease availability of isoprenoids and they can not be attached to these signalling proteins [9, 10]. However, other effects may even be fully dissociated from inhibition of HMG-CoA reductase, and many take place at very low drug concentrations [6].

Previous studies in our group have demonstrated, using gene expression arrays, that atorvastatin in macrophages incubated with oxidized LDL (oxLDL) modifies the gene expression profile of certain enzymes involved in fatty acid metabolism, mainly Stearoyl-CoA desaturase (SCD), suggesting that statins could change fatty acid composition in macrophages ([11], M. Artieda, unpublished).

Stearoyl-CoA desaturase (SCD), also known as delta-9-desaturase, is an endoplasmic reticulum rate-limiting enzyme in the biosynthesis of monounsaturated fatty acids (MUFA) from saturated fatty acids and plays a central role in regulation of fatty acid metabolism [12]. SCD introduces the first *cis*-double bond in the delta-9 position (between carbons 9 and 10) in palmitic acid (16:0) and stearic acid (18:0), which are converted into palmitoleic acid (16:1) and oleic acid (18:1), respectively [13, 14]. These products are the most abundant monounsaturated fatty acids of phospholipids, triglycerides and cholesteryl esters [15]. Apart from being components of lipids, monounsaturated fatty acids also serve as mediators of signal transduction and cellular differentiation [16]. Overall, the expression of SCD can influence membrane fluidity, lipid metabolism and adiposity. Given the multiple roles of monounsaturated fatty acids, changes in SCD activity and alterations in the balance between saturated and monounsaturated fatty acids would be expected to have an effect in various diseases including cancer, diabetes, atherosclerosis and obesity [12].

The activity of SCD appears to be largely mediated by SREBP-1. It has been demonstrated that mice expressing an active form of SREBP-1 have increased expression of SCD and increased synthesis of MUFA, while knockout of SREBP-1 leads to a decrease in SCD expression [17, 18].

The aim of this study was to determine whether HMG-CoA reductase inhibitors might affect the fatty acid composition in macrophages, and if their SCD gene expression profile could be involved. In order to test our hypothesis, THP-1 macrophages were treated with atorvastatin and native or oxidized LDL, their fatty acid composition was determined by gas-chromatography, and the SCD and SREBP-1 gene expression profile was analysed using quantitative RT-PCR.

Materials and Methods

Cell Culture

THP-1 cells (European Collection of Cell Cultures, Salisbury, UK) were grown in suspension in T25 or T75 flasks (TPP) in RPMI 1640 containing 10% heat inactivated FBS (GIBCO®), 10 mM HEPES, 2 mM L-glutamine, 1 mM sodium pyruvate, 5×10^{-5} M 2- β -mercaptoethanol, non-essential amino acids, penicillin (100 U/ml), streptomycin (100 μ g/ml), and Fungizone (250 μ g/l) at 37 °C in 5% CO₂. To induce THP-1 differentiation into a macrophage phenotype, 1×10^6 cells per well were seeded in 6-well plates and stimulated with phorbol 12-myristate 13-acetate (PMA) (Sigma) at a final concentration of 10^{-7} mol/l for 48 h until they adhered to the well and exhibited macrophage-like morphology. For the experiments, the cells were allowed to reach 70–80% confluence.

Isolation and Oxidation of LDL

Low-density lipoprotein was isolated from one homozygous familial hypercholesterolemia patient who is regularly treated with dextran sulfate LDL-apheresis. The apolipoprotein B-containing lipoproteins retained by dextran sulfate were eluted from the column with 0.702 M NaCl, subjected to a single vertical spin density gradient ultracentrifugation in a VTI 50 rotor (Beckman Coulter Inc.), and dialyzed at 4 °C for 24 h against EDTA-free PBS. The protein content of LDL was determined by the Bradford method. LDL was diluted to 200 mg/l in PBS (without EDTA) to prevent its aggregation. Oxidation of LDL was performed by incubation at 37 °C with 8 μ mol/l CuCl₂ for 24 h. The reaction was stopped by adding 1 mmol/l EDTA and storing at 4 °C. Oxidation of LDL was confirmed by Sudan Black LDL staining and agarose gel electrophoresis, and conjugated diene formation assessment by spectrophotometry at 234 nm.

Experimental Design

To test the effect of atorvastatin on SCD gene expression and fatty acid composition, cells were incubated in the absence or presence of atorvastatin at a final concentration of 5 μ M. The same volume of DMSO was added to cells without atorvastatin and the total volume of DMSO added to the cell culture was under 0.1% of the total culture medium. To assess if the effects on SCD gene expression were due to atorvastatin, macrophages were incubated with 100 μ M of mevalonate (Sigma). The same volume of ethanol was added to cells without mevalonate and the total volume of ethanol added to the cell culture was under 0.1% of the total culture medium. Cells were incubated in the

absence/presence of atorvastatin and in the absence/presence of mevalonate for 1 h at 37 °C and 5% CO₂, before addition of 50 µg/ml native LDL (nLDL), oxidized LDL (oxLDL), or the same volume of PBS for control cells. Under these conditions, the cells were incubated for 18 hours at 37 °C and 5% CO₂. Atorvastatin calcium was kindly provided by Pfizer. All the experiments were run in triplicate.

Gene Expression Analysis

Total RNA was isolated from macrophage THP-1 cells using an RNeasy kit (Qiagen Inc., Valencia, CA, USA), following the manufacturer's instructions. Total RNA was quantified by spectrophotometry at 260 nm and its purity assessed by the ratio $A_{260\text{nm}}/A_{280\text{nm}}$. RNA integrity was verified by visualization of ethidium bromide-stained 1% agarose gels.

Two µg of each total RNA sample was treated with 1U DNase I (Ambion Corp., Austin, TX, USA), and it was reverse transcribed with 200 U SuperScript III RNase H⁻ Reverse Transcriptase (Invitrogen Corp.) using 150 ng of random hexamer primers (Invitrogen Corp.) to prime cDNA synthesis. Real-time RT-PCR was carried out using the ABI Prism 7000 HT Sequence Detection System, TaqMan Universal PCR Master Mix, unlabeled PCR primers and TaqMan MGB probes (FAM dye-labeled) from Assay-on-Demand (SCD, Hs00748952_s1; SREBF1, Hs01088691_m1; 18srRNA, Hs099999901_s1 and RPLP0, Hs99999902_m1) according to the manufacturer's recommendations (Applied Biosystems, Foster City, CA, USA). All samples were run in triplicate.

Sequence Detector Software (SDS) (Applied Biosystems) was used for data analysis. A threshold cycle (Ct) value was determined from each amplification plot. The relative expression ratios or fold changes of target genes were calculated using the comparative ΔCt method. Expression of target genes was normalized by the endogenous reference genes 18srRNA and RPLP0, using the geNorm method [19, 20].

Fatty Acid Analysis

Cells were washed twice with PBS, scraped from the culture wells with Versene (GIBCO®) and homogenized on ice by sonication for 10 s with a Soniprep 150 Sonicator set to maximum power. The extraction was performed with chloroform/methanol (2:1 v/v) according to the Folch method [21]. The aqueous phase was discarded and the organic phase was dried under nitrogen. The lipids extracted were subjected to methanolysis in 5% H₂SO₄ in methanol at 80 °C for 90 min [22]. The resultant fatty acid methyl esters were extracted with hexane.

Fatty acids were chromatographed as methyl esters on a 25-m fused silica column with an internal diameter of 0.20 µm. The column was wall-coated with 0.20 mm SP-2330. Analysis was performed on a Hewlett-Packard 6890 gas chromatograph equipped with a flame ionization detector of hydrogen/water. Nitrogen was used as the carrier gas. The split ratio was 17:1. The injection port temperature was 200 °C and the detector was at 250 °C. The column temperature was held at 80 °C for 5 min and this was raised in a step-wise fashion until a plateau at 220 °C. The gas chromatograph was calibrated using a standard mixture of fatty acids. ChemStation software (Hewlett-Packard) was used for the analysis of the chromatograms. Data were presented as a percentage of the fatty acid composition.

Statistical Analyses

Data are presented as means \pm standard deviation (SD). The distribution of quantitative variables was tested for normality. Differences between compared conditions were tested with the *t* test for continuous variables. Comparisons of quantitative variables without a normal distribution were made using the Mann–Whitney *U* non-parametric test. Statistical analysis was performed using the Statistical Package for the Social Sciences (SPSS Inc.) version 11.0, and a value of $P < 0.05$ was considered statistically significant for all analyses.

Results

Fatty Acid Composition

Fatty acid composition of THP-1 cells after treatment with atorvastatin in each studied condition: control, native LDL and oxidized LDL, is shown in Table 1. Saturated fatty acids, palmitic acid (16:0) and stearic acid (18:0), are the main substrates for Stearoyl CoA desaturase. Palmitoleic (16:1) and oleic (18:1) acids were the most affected by atorvastatin treatment reaching statistical differences only in the oxLDL situation.

Stearic acid (18:0) content increased significantly in the oxLDL situation after addition of atorvastatin ($19.0 \pm 2.4\%$ vs. $23.3 \pm 3.2\%$, $P = 0.026$). The percentage of stearic acid was also increased after addition of atorvastatin in the control situation and in the nLDL condition, although it was not statistically different. Its monounsaturated fatty acid, oleic acid (18:1), was significantly reduced after incubation with atorvastatin from $21.8 \pm 2.7\%$ to $17.5 \pm 3.2\%$, $P = 0.029$, in the oxLDL condition. Oleic acid content showed a tendency to diminish after addition of atorvastatin in the control

Table 1 Fatty acid composition of THP-1 cells under each condition studied

	AT-PBS+	AT+PBS+	<i>P</i>	AT-ntLDL+	AT+ntLDL+	<i>P</i>	AT-oxLDL+	AT+oxLDL+	<i>P</i>
12:0	0.5 ± 0.5	0.3 ± 0.1	NS	0.4 ± 0.5	0.3 ± 0.3	NS	0.4 ± 0.2	0.3 ± 0.3	NS
14:0	3.1 ± 0.8	3.1 ± 0.8	NS	2.5 ± 1.0	3.1 ± 0.7	NS	3.2 ± 0.4	3.0 ± 1.4	NS
16:0	28.5 ± 2.7	29.3 ± 1.7	NS	28.8 ± 5.8	30.7 ± 4.6	NS	29.3 ± 3.1	30.5 ± 4.1	NS
16:1	5.9 ± 2.4	5.6 ± 2.6	NS	4.6 ± 1.3	4.4 ± 0.8	NS	5.2 ± 1.3	4.4 ± 0.8	NS
18:0	18.8 ± 4.4	21.2 ± 4.7	NS	20.1 ± 4.4	20.3 ± 2.5	NS	19.0 ± 2.4	23.3 ± 3.2	0.026
18:1	21.8 ± 3.2	19.8 ± 1.7	NS	20.9 ± 3.0	19.5 ± 3.2	NS	21.8 ± 2.7	17.5 ± 3.2	0.029
18:2n-6	3.2 ± 1.3	2.5 ± 0.5	NS	3.7 ± 0.2	3.5 ± 1.5	NS	3.0 ± 0.4	3.1 ± 1.0	NS
18:3n-6	0.3 ± 0.1	0.3 ± 0.2	NS	0.3 ± 0.1	0.4 ± 0.1	NS	0.3 ± <0.1	0.3 ± 0.1	NS
18:3n-3	0.2 ± <0.1	0.2 ± 0.1	NS	0.3 ± 0.1	0.3 ± 0.1	NS	0.3 ± <0.1	0.2 ± 0.1	NS
18:4	0.5 ± 0.3	0.4 ± 0.5	NS	0.5 ± 0.3	0.3 ± 0.2	NS	0.2 ± 0.2	0.2 ± 0.2	NS
20:0	1.5 ± 0.7	1.2 ± 0.7	NS	1.4 ± 0.4	1.7 ± 0.5	NS	1.4 ± 0.6	1.4 ± 1.0	NS
20:1	0.5 ± 0.6	0.4 ± 0.6	NS	0.5 ± 0.6	0.3 ± 0.5	NS	0.5 ± 0.6	0.6 ± 0.6	NS
20:2	0.3 ± 0.7	0.2 ± 0.2	NS	0.3 ± 0.4	0.4 ± 0.5	NS	0.3 ± 0.3	0.8 ± 1.2	NS
20:3n-6	0.5 ± 0.2	0.5 ± <0.1	NS	0.6 ± 0.1	0.5 ± 0.2	NS	0.5 ± <0.1	0.5 ± 0.2	NS
20:4n-6	1.7 ± 0.4	1.5 ± 0.3	NS	1.9 ± 0.4	1.7 ± 0.6	NS	1.6 ± 0.1	1.6 ± 0.4	NS
20:5n-3	0.7 ± 0.5	0.5 ± 0.1	NS	0.5 ± 0.3	0.4 ± 0.2	NS	0.5 ± 0.1	0.4 ± 0.1	NS
22:0	2.0 ± 1.5	2.7 ± 1.2	NS	2.3 ± 1.2	2.8 ± 1.4	NS	2.7 ± 1.3	2.2 ± 1.2	NS
22:1	0.1 ± 0.2	0.2 ± 0.2	NS	0.1 ± 0.2	0.2 ± 0.3	NS	0.1 ± 0.2	0.1 ± 0.2	NS
22:4n-6	0.7 ± 1.3	0.1 ± 0.1	NS	0.2 ± 0.2	0.2 ± 0.2	NS	0.1 ± 0.1	0.1 ± 0.1	NS
22:5n-3	0.7 ± 0.1	0.7 ± 0.1	NS	0.8 ± 0.3	1.2 ± 0.9	NS	0.8 ± 0.1	0.8 ± 0.4	NS
24:0	2.7 ± 0.7	3.1 ± 1.0	NS	2.9 ± 0.9	2.1 ± 1.7	NS	3.2 ± 0.8	1.8 ± 1.1	0.042
22:6n-3	3.4 ± 1.8	3.6 ± 1.7	NS	3.5 ± 1.5	4.1 ± 1.6	NS	3.4 ± 1.0	5.0 ± 4.2	NS
24:1	0.5 ± 0.3	0.3 ± 0.8	NS	0.3 ± 0.3	0.3 ± 0.4	NS	0.3 ± 0.3	0.6 ± 1.0	NS
26:0	1.5 ± 0.6	1.6 ± 0.8	NS	1.5 ± 0.7	1.1 ± 0.9	NS	1.7 ± 0.5	0.9 ± 0.7	0.035

Results are expressed as a percentage of the total macrophages fatty acid content and represent the mean ± standard deviation from six replicate determinations

AT atorvastatin, ntLDL native LDL, oxLDL oxidized LDL, NS non-significant, – absence, + presence

situation and in the ntLDL condition, although it was not statistically significant.

In the same way as stearic acid, palmitic acid (16:0) content increased under all the conditions after addition of atorvastatin at the same time that palmitoleic acid (16:1) diminished after addition of atorvastatin, although the differences did not reach statistical significance. Moreover, two saturated very long chain fatty acids (VLCFA), lignoceric acid (24:0) and hexacosanoic acid (26:0), were significantly decreased by atorvastatin addition from 3.2 ± 0.8% to 1.8 ± 1.1%, $P = 0.042$, and from 1.7 ± 0.5% to 0.9 ± 0.7%, $P = 0.035$, respectively, when the culture medium was supplemented with oxLDL.

The incubation of THP-1 cells with LDL also caused changes in the fatty acid composition (Table 1). OxLDL supplementation caused a decrease in the percentage of linoleic acid (18:2n-6) with respect to the control situation (3.2 ± 1.3% vs. 3.0 ± 0.4%). The opposite effect was observed in the percentage of alpha-linolenic acid (18:3n-3), which was increased in ntLDL (0.3 ± 0.1%) and oxLDL (0.3 ± <0.1%) stimulated culture cells with respect to the

control situation (0.2 ± <0.1%) ($P = 0.041$ for ntLDL vs. control). Incubation with LDL also produced an increase in the percentages of docosanoic (22:0) and lignoceric (24:0) acids: the ntLDL situation; from 2.0 ± 1.5% to 2.3 ± 1.2%, for docosanoic; and from 2.7 ± 0.7% to 2.9 ± 0.9%, for lignoceric, and in the oxLDL situation, from 2.0 ± 1.5% to 2.7 ± 1.3%, for docosanoic; and from 2.7 ± 0.7% to 3.2 ± 0.8%, for lignoceric.

In Table 2, the same results, but grouped in content of saturated (SAT), monounsaturated (MUFA), polyunsaturated (PUFA), n-3 and n-6 fatty acids, are shown. The addition of atorvastatin significantly decreased the proportion of monounsaturated (MUFA) fatty acids in the oxLDL condition from 27.9 ± 2.9% to 23.2 ± 3.5%, $P = 0.030$. Atorvastatin also diminished MUFA content from 28.8 ± 6.0% to 26.3 ± 3.6% in the control situation; from 26.5 ± 3.9% to 24.6 ± 3.9% in the ntLDL condition, although the differences did not reach statistical significance. Inversely, atorvastatin addition showed an increasing tendency of the proportion of SAT in all conditions, although these differences were not statistically significant (Table 2).

Table 2 Percentage of saturated, monounsaturated, polyunsaturated, n-3 and n-6 fatty acids in THP-1 cells under each studied condition

	AT-PBS+	AT+PBS+	<i>P</i>	AT-ntLDL+	AT+ntLDL+	<i>P</i>	AT-oxLDL+	AT+oxLDL+	<i>P</i>
SAT	58.6 ± 3.6	62.6 ± 4.2	NS	60.1 ± 5.6	62.1 ± 5.6	NS	60.9 ± 2.8	63.5 ± 3.0	NS
MUFA	28.8 ± 6.0	26.3 ± 3.6	NS	26.5 ± 3.9	24.6 ± 3.9	NS	27.9 ± 2.9	23.2 ± 3.5	0.030
PUFA	12.3 ± 3.0	10.7 ± 1.8	NS	12.5 ± 2.0	13.1 ± 2.3	NS	11.0 ± 1.2	12.9 ± 2.9	NS
n-3	5.0 ± 2.1	5.6 ± 1.8	NS	5.1 ± 1.7	6.0 ± 2.0	NS	4.9 ± 1.0	6.4 ± 3.9	NS
n-6	6.4 ± 1.8	5.0 ± 0.7	NS	6.7 ± 0.5	6.4 ± 2.4	NS	5.6 ± 0.6	5.6 ± 1.2	NS

Results are expressed as a percentage of the total macrophages fatty acid content and represent the mean ± standard deviation of six replicate determinations

AT atorvastatin, ntLDL native LDL, oxLDL oxidized LDL, SAT saturated fatty acids, MUFA monounsaturated fatty acids, PUFA polyunsaturated fatty acids, NS non-significant, – absence, + presence

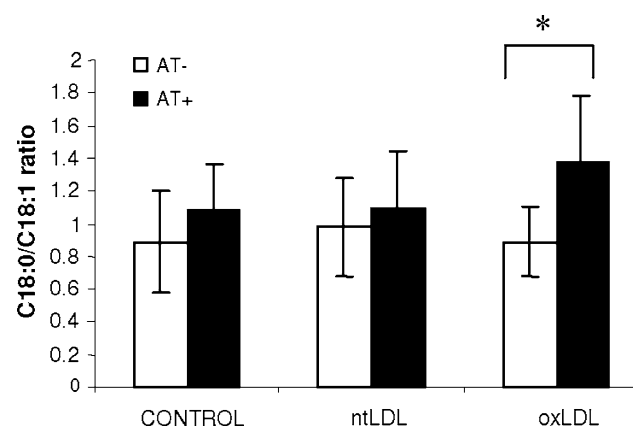


Fig. 1 Effect of atorvastatin on the saturation index (C18:0/C18:1 ratio). C18:0/C18:1 ratios from THP-1 cells without atorvastatin (white bars) and with atorvastatin (black bars) in different studied situations: control, with ntLDL, with oxLDL. Data are shown as mean ± standard deviation from six replicate determinations. **P* < 0.05 for paired-samples *t* test

Effect of Atorvastatin on the Saturation Index (C18:0/C18:1)

The ratio of C18:0 and C18:1 fatty acid percentages in THP-1 cells under each condition studied is shown in Fig. 1. This saturation index was higher in THP-1 cells with atorvastatin as compared to those without atorvastatin. The C18:0/C18:1 ratio changed from 0.9 ± 0.3 to 1.1 ± 0.3 , in the control situation and from 1.0 ± 0.3 to 1.1 ± 0.3 , in cells supplemented with ntLDL, but these differences were not statistically significant. However, the saturation index significantly increased in cells supplemented with oxLDL from 0.9 ± 0.2 to 1.4 ± 0.4 , *P* = 0.015.

Stearoyl-CoA Desaturase and SREBP-1 Gene Expression

RNA from THP-1 cells in the control situation, incubated with ntLDL and oxLDL in a culture medium without or

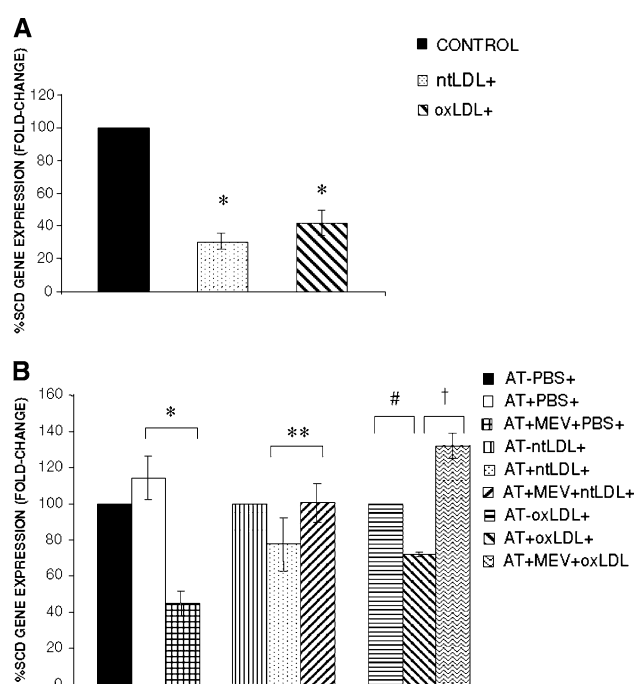


Fig. 2 Effect of atorvastatin on SCD gene expression. THP-1 cells were incubated with ntLDL or oxLDL and without or with atorvastatin. **a** The SCD gene expression results obtained after adding native LDL or oxidized LDL in the culture medium (without atorvastatin). **P* < 0.05 for paired-samples *t* test. **b** The SCD gene expression results obtained after treatment with atorvastatin under each condition studied: control, native LDL and oxidized LDL, and without or with mevalonate. Data show mean gene expression ± standard deviation for SCD gene from four replicate determinations. **P* < 0.05 (AT+PBS+ compared with AT+MEV+PBS+). ***P* < 0.05 (AT+ntLDL+ compared with AT+MEV+ntLDL+). **P* < 0.05 (AT-oxLDL+ compared with AT+oxLDL+). †*P* < 0.01 (AT+oxLDL+ compared with AT+MEV+oxLDL+). The statistics were calculated by paired-samples *t* test

with atorvastatin and without or with mevalonate was analysed using real time RT-PCR to quantify SCD and SREBP-1 gene expression. The SCD gene expression results obtained are shown in Fig. 2. In Fig. 2a, results of SCD gene expression from THP-1 cells incubated with

ntLDL or oxLDL (without atorvastatin) are shown. When ntLDL or oxLDL were added in the culture medium, SCD mRNA was significantly decreased by 70 and 60%, respectively, compared with the control situation. Fig. 2b shows the SCD gene expression results obtained after treatment with atorvastatin and mevalonate in each studied condition: control, ntLDL and oxLDL. Atorvastatin did not produce any effect in the SCD gene expression when it was added to THP-1 cells in the basal situation, whereas SCD mRNA was reduced by 23% after administration of atorvastatin in macrophages incubated with ntLDL, and it was significantly decreased by 30% when incubated with oxLDL. In the presence of atorvastatin and mevalonate, SCD gene expression level was salvaged in each studied condition. The SREBP-1 gene expression results obtained are shown in Fig. 3. In Fig. 3a, results of SREBP-1 gene expression from THP-1 cells incubated with ntLDL or oxLDL (without atorvastatin) are shown. When ntLDL or oxLDL were added to the culture medium, SREBP-1 mRNA was significantly decreased by 44 and 18%, respectively, compared with the control situation. Figure 3b shows the SREBP-1 gene expression results obtained after treatment with atorvastatin and mevalonate under each studied condition: control, ntLDL and oxLDL. SREBP-1 gene expression decreased significantly when atorvastatin was added to THP-1 cells in the basal situation and when they were incubated with oxLDL by 54 and 67%, respectively, whereas SREBP-1 mRNA was reduced by 23% after administration of atorvastatin in macrophages incubated with ntLDL. In the presence of atorvastatin and mevalonate, SREBP-1 gene expression level was salvaged in each studied condition.

Discussion

The aim of this study was to determine whether the HMG-CoA reductase inhibitor atorvastatin might affect the fatty acid composition in macrophages THP-1 and if the SCD gene expression profile could be involved.

We demonstrated that administration of atorvastatin to THP-1 cells incubated with oxLDL causes an increase in the saturated fatty acid, stearic (18:0) acid, as well as a decrease in the percentage of its monounsaturated fatty acid, oleic (18:1) acid. Our results also show that saturated very long chain fatty acids, such as lignoceric acid (24:0) and hexacosanoic acid (26:0), in THP-1 cells, were significantly reduced by the treatment with atorvastatin. These changes produced an increase in the saturation index, a well-established surrogate of SCD activity [23], and we demonstrated that these effects were probably due to the ability of atorvastatin to inhibit SCD gene expression since mevalonate treatment was able to reverse this effect. The

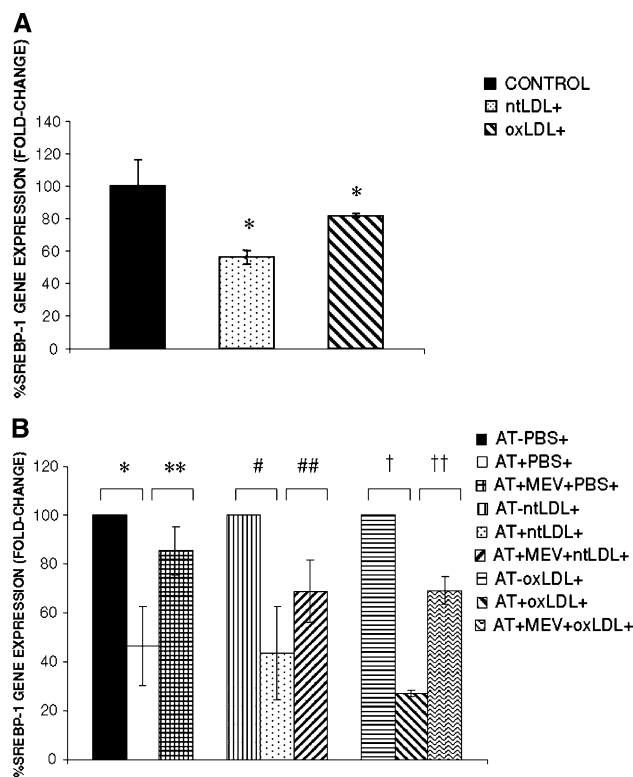


Fig. 3 Effect of atorvastatin on SREBP-1 gene expression. THP-1 cells were incubated with ntLDL or oxLDL and without or with atorvastatin. **a** The SREBP-1 gene expression results obtained after adding native LDL or oxidized LDL in the culture medium (without atorvastatin). **b** The SREBP-1 gene expression results obtained after treatment with atorvastatin in each studied condition: control, native LDL and oxidized LDL, and without or with mevalonate. Data show mean gene expression \pm standard deviation for the SREBP-1 gene from four replicate determinations. * $P < 0.05$ (AT-PBS+ compared with AT+PBS+). ** $P < 0.05$ (AT+PBS+ compared with AT+MEV+PBS+). # $P < 0.05$ (AT-ntLDL+ compared with AT+ntLDL+). ## $P < 0.05$ (AT+ntLDL+ compared with AT+MEV+ntLDL+). † $P < 0.05$ (AT-oxLDL+ compared with AT+oxLDL+). †† $P < 0.05$ (AT+oxLDL+ compared with AT+MEV+oxLDL+). Statistic was calculated by paired-samples *t* test

results of fatty acid composition obtained were very similar to those shown by other authors in THP-1 and human macrophages [24, 25].

Statins affect the production of long chain polyunsaturated fatty acids (PUFA) by increasing the conversion of linoleic acid to its derivatives through enhanced activities of the delta-5 and delta-6 desaturases [24, 26]. They also demonstrated that simvastatin decreases the production of oleic acid and delta-9 desaturase activity in THP-1 cells, whereas in HepG2 cells it is increased [24]. Our finding of lower formation of C18:1 in THP-1 cells incubated with oxLDL during treatment with atorvastatin is in agreement with this study. Moreover, we have demonstrated for the first time that atorvastatin inhibits stearyl-CoA desaturase gene expression when macrophages are exposed to oxidized LDL.

The expression of SCD is regulated by SREBP-1, which is induced by LXR/RXR ligands [27–31]. We have demonstrated that SREBP-1 and SCD gene expression was significantly decreased when native LDL and oxidized LDL were added to the incubation medium of THP-1. It is well known that PUFA and cholesterol are strong repressors of SREBP-1 activity and expression [32, 33] and that PUFA and cholesterol inhibit LXR transcriptional activity, and subsequently, SREBP-1 activity [32]. Therefore, the addition of LDL to the culture medium and its incorporation to the cells would increase the presence of PUFA and cholesterol in THP-1 cells.

Our data have also demonstrated that, when atorvastatin was added to THP-1 cells, SREBP-1 and SCD gene expression was inhibited and this effect was amplified when macrophages were incubated with oxLDL. The nuclear hormone receptor LXR/RXR serves as a sterol sensor to regulate the transcription of gene products that control intracellular cholesterol homeostasis, such as SREBP-1 [31]. SREBPs have been established as transcription factors of lipid synthetic genes, especially for cholesterol and fatty acid synthesis [34]. SREBP-1 seems to be involved in fatty acid and glucose/insulin metabolism, whereas SREBP-2 specifically regulates cholesterol synthesis [35, 36]. SREBP-1 and SREBP-2 are regulated in different ways, as demonstrated by Sheng et al. [37]. They showed that SREBP-2 protein was up regulated, while the nuclear form SREBP-1 decreased, after hamsters were treated with Colestipol and the HMG-CoA reductase inhibitor mevinolin [37]. This is consistent with another study that demonstrated that treatment with atorvastatin decreases the expression of SREBP-1, preventing fatty liver by inhibiting fatty acid synthesis, in a mouse model of type II diabetes [38]. Atorvastatin reduces the internalization of native and oxidized LDL in macrophages and endothelial cells [39, 40] diminishing the availability of oxysterols in the cells. This effect could explain the results observed in our experiments because atorvastatin could exert its action by reducing the natural ligands for LXR/RXR, subsequently reducing expression of SREBP-1, and as a consequence, inhibiting SCD gene expression. Moreover, mevalonate treatment was able to reverse SREBP-1 and SCD mRNA levels in the presence of atorvastatin, suggesting an HMG-CoA reductase dependent effect in the observed reduction of SREBP-1 and SCD gene expression.

Statins are highly effective cholesterol-lowering drugs, but such observations suggest that they may have biochemical effects beyond the simple inhibition of cholesterol synthesis. Previous works have analysed the effect of statins on fatty acid metabolism, and our findings are consistent with those showing that statins can influence desaturase enzyme activity and they can modify fatty acid composition in various cell types studied [26, 41, 42]. The

effects of statins in fatty acid composition in monocytes could explain some of the observed effects independent of changes in plasma LDL cholesterol. Inhibition of SCD gene expression in mice with targeted disruption of the SCD1 gene produces low levels of triglycerides and cholesteryl esters, and SCD activity correlates with plasma triglycerides in the mouse and humans [23]. This fact is in accordance with our results of SCD inhibition by atorvastatin, as it has been demonstrated that plasma triglycerides decrease after atorvastatin therapy in hypertriglyceridemic patients [1]. Moreover, findings that atorvastatin inhibits SCD activity and gene expression in monocytes treated with oxLDL would suggest that intracellular lipid levels might be an important factor in determining the effects of statins, as demonstrated by Zelvyte et al. [43] when analyzing the anti-inflammatory effects of statins. Further studies are required to evaluate the role of cholesterol loading on the effects of statins and to determine how relevant our observations are to arterial foam cells “in vivo”.

In conclusion, when studied “in vitro”, atorvastatin reduces the percentage of palmitoleic and oleic acids at the expense of their saturated fatty acids in THP-1 cells incubated with oxLDL, which could be explained by the induced inhibition of SCD and SREBP-1 gene expression. Moreover, these effects were reversed when mevalonate was added to THP-1 macrophages. All these data would suggest that inhibition of SCD in macrophages THP-1 would be an important effect of atorvastatin independent of plasma cholesterol lowering.

Acknowledgments This work was supported by grants from the Fondo de Investigación Sanitaria [PI061238, PI061402, PI071221 and RD06/0014/0008-0029 (RECAVA)] and Ministerio de Educación y Ciencia (SAF2005-07042).

References

- Stein E, Black D (2002) Lipoprotein changes with statins. *Curr Atheroscler Rep* 4:14–18
- Vaughan C, Gotto AJ, Basson C (2000) The evolving role of statins in the management of atherosclerosis. *J Am Coll Cardiol* 35:1–10
- Shepherd J, Barter P, Carmena R, Deedwania P, Fruchart J, Haffner S, Hsia J, Breazna A, LaRosa J, Grundy S, Waters D (2006) Effect of lowering LDL cholesterol substantially below currently recommended levels in patients with coronary heart disease and diabetes: the treating to new targets (TNT) study. *Diabetes Care* 29:1220–1226
- Yildirim A, Müderrisoğlu H (2004) Non-lipid effects of statins: emerging new indications. *Curr Vasc Pharmacol* 2:309–318
- Ray K, Cannon C, Ganz P (2006) Beyond lipid lowering: what have we learned about the benefits of statins from the acute coronary syndromes trials? *Am J Cardiol* 98:18P–25P
- Davignon J (2004) Beneficial cardiovascular pleiotropic effects of statins. *Circulation* 109:III39–III43

7. Fichtlscherer S, Schmidt-Lucke C, Bojunga S, Rössig L, Heeschen C, Dimmeler S, Zeiher A (2006) Differential effects of short-term lipid lowering with ezetimibe and statins on endothelial function in patients with CAD: clinical evidence for 'pleiotropic' functions of statin therapy. *Eur Heart J* 27:1182–1190
8. Ghittoni R, Napolitani G, Benati D, Olivieri C, Uliveri C, Patrussi L, Laghi Pasini F, Lanzavecchia A, Baldari C (2006) Simvastatin inhibits the MHC class II pathway of antigen presentation by impairing Ras superfamily GTPases. *Eur J Immunol* 36:2885–2893
9. Casey P, Seabra M (1996) Protein prenyltransferases. *J Biol Chem* 271:5289–5292
10. Bi X, Baudry M, Liu J, Yao Y, Fu L, Brucher F, Lynch G (2004) Inhibition of geranylgeranylation mediates the effects of 3-hydroxy-3-methylglutaryl (HMG)-CoA reductase inhibitors on microglia. *J Biol Chem* 279:48238–48245
11. Artieda M, Cenarro A, Junquera C, Lasiera P, Martínez-Lorenzo M, Pocoví M, Civeira C (2005) Tendon xanthomas in familial hypercholesterolemia are associated with a differential inflammatory response of macrophages to oxidized LDL. *FEBS Lett* 579:4503–4512
12. Ntambi J (1999) Regulation of stearoyl-CoA desaturase by polyunsaturated fatty acids and cholesterol. *J Lipid Res* 40:1549–1558
13. Enoch H, Catalá A, Strittmatter P (1976) Mechanism of rat liver microsomal stearoyl-CoA desaturase: studies of the substrate specificity, enzyme–substrate interactions, and the function of lipid. *J Biol Chem* 251:5095–5103
14. Ntambi J (1995) The regulation of stearoyl-CoA desaturase (SCD). *Prog Lipid Res* 34:139–150
15. Miyazaki M, Kim Y, Ntambi J (2001) A lipogenic diet in mice with a disruption of the stearoyl-CoA desaturase 1 gene reveals a stringent requirement of endogenous monounsaturated fatty acids for triglyceride synthesis. *J Lipid Res* 42:1018–1024
16. Zhang L, Mia M, Zheng C, Hossain M, Yamasaki F, Tokunaga O, Kohashi O (1999) The preventive effects of incomplete Freund's adjuvant and other vehicles on the development of adjuvant-induced arthritis in Lewis rats. *Immunology* 98:267–272
17. Shimomura I, Shimano H, Korn B, Bashmakov Y, Horton J (1998) Nuclear sterol regulatory element-binding proteins activate genes responsible for the entire program of unsaturated fatty acid biosynthesis in transgenic mouse liver. *J Biol Chem* 273:35299–35306
18. Liang G, Yang J, Horton J, Hammer R, Goldstein J, Brown M (2002) Diminished hepatic response to fasting/refeeding and liver X receptor agonists in mice with selective deficiency of sterol regulatory element-binding protein-1c. *J Biol Chem* 277:9520–9528
19. Huggett J, Dheda K, Bustin S, Zumla A (2005) Real-time RT-PCR normalisation; strategies and considerations. *Genes Immun* 6:279–284
20. Vandesompele J, De Preter K, Pattyn F, Poppe B, Van Roy N, De Paepe A, Speleman F (2002) Accurate normalization of real-time quantitative RT-PCR data by geometric averaging of multiple internal control genes. *Genome Biol* 3:1–12
21. Folch J, Lees M, Sloane Stanley GH (1957) A simple method for the isolation and purification of total lipides from animal tissues. *J Biol Chem* 226:497–509
22. Christie W, Brechany E, Johnson S, Holman R (1986) A comparison of pyrrolidide and picolinyl ester derivatives for the identification of fatty acids in natural samples by gas chromatography-mass spectrometry. *Lipids* 21:657–661
23. Attie AD, Krauss RM, Gray-Keller MP, Brownlie A, Miyazaki M, Kastelein JJ, Lusis AJ, Stalenhoef AF, Stoehr JP, Hayden MR, Ntambi JM (2002) Relationship between stearoyl-CoA desaturase activity and plasma triglycerides in human and mouse hypertriglyceridemia. *J Lipid Res* 43:1899–1907
24. Risé P, Colombo C, Galli C (1997) Effects of simvastatin on the metabolism of polyunsaturated fatty acids and on glycerolipid, cholesterol, and de novo lipid synthesis in THP-1 cells. *J Lipid Res* 38:1299–1307
25. Kew S, Banerjee T, Minihane AM, Finnegan YE, Williams CM, Calder PC (2003) Relation between the fatty acid composition of peripheral blood mononuclear cells and measures of immune cell function in healthy, free-living subjects aged 25–72 y. *Am J Clin Nutr* 77:1278–1286
26. Risé P, Ghezzi S, Priori I, Galli C (2005) Differential modulation by simvastatin of the metabolic pathways in the n-9, n-6 and n-3 fatty acid series, in human monocytic and hepatocytic cell lines. *Biochem Pharmacol* 69:1095–1100
27. Horton J (2002) Sterol regulatory element-binding proteins: transcriptional activators of lipid synthesis. *Biochem Soc Trans* 30:1091–1095
28. Tabor D, Kim J, Spiegelman B, Edwards P (1998) Transcriptional activation of the stearoyl-CoA desaturase 2 gene by sterol regulatory element-binding protein/adipocyte determination and differentiation factor 1. *J Biol Chem* 273:22052–22058
29. Tabor D, Kim J, Spiegelman B, Edwards P (1999) Identification of conserved *cis*-elements and transcription factors required for sterol-regulated transcription of stearoyl-CoA desaturase 1 and 2. *J Biol Chem* 274:20603–20610
30. Shimomura I, Bashmakov Y, Horton J (1999) Increased levels of nuclear SREBP-1c associated with fatty livers in two mouse models of diabetes mellitus. *J Biol Chem* 274:30028–30032
31. Repa JJ, Liang G, Ou J, Bashmakov Y, Lobaccaro J, Shimomura I, Shan B, Brown M, Goldstein J, Mangelsdorf D (2000) Regulation of mouse sterol regulatory element-binding protein-1c gene (SREBP-1c) by oxysterol receptors, LXRalpha and LXRbeta. *Genes Dev* 14:2819–2830
32. Yoshikawa T, Shimano H, Yahagi N, Ide T, Amemiya-Kudo M, Matsuzaka T, Nakakuki M, Tomita S, Okazaki H, Tamura Y, Iizuka Y, Ohashi K, Takahashi A, Sone H, Osuga Ji J, Gotoda T, Ishibashi S, Yamada N (2002) Polyunsaturated fatty acids suppress sterol regulatory element-binding protein 1c promoter activity by inhibition of liver X receptor (LXR) binding to LXR response elements. *J Biol Chem* 277:1705–1711
33. Bené H, Lasky D, Ntambi JM (2001) Cloning and characterization of the human stearoyl-CoA desaturase gene promoter: transcriptional activation by sterol regulatory element binding protein and repression by polyunsaturated fatty acids and cholesterol. *Biochem Biophys Res Commun* 284:1194–1198
34. Shimano H (2001) Sterol regulatory element-binding proteins (SREBPs): transcriptional regulators of lipid synthetic genes. *Prog Lipid Res* 40:439–452
35. Brown M, Goldstein J (1997) The SREBP pathway: regulation of cholesterol metabolism by proteolysis of a membrane-bound transcription factor. *Cell* 89:331–340
36. Wang X, Sato R, Brown M, Hua X, Goldstein J (1994) SREBP-1, a membrane-bound transcription factor released by sterol-regulated proteolysis. *Cell* 77:53–62
37. Sheng Z, Otani H, Brown M, Goldstein J (1995) Independent regulation of sterol regulatory element-binding proteins 1 and 2 in hamster liver. *Proc Natl Acad Sci USA* 92:935–938
38. Suzuki M, Kakuta H, Takahashi A, Shimano H, Tada-Iida K, Yokoo T, Kihara R, Yamada N (2005) Effects of atorvastatin on glucose metabolism and insulin resistance in KK/Ay mice. *J Atheroscler Thromb* 12:77–84
39. Fuhrman B, Koren L, Volkova N, Keidar S, Hayek T, Aviram M (2002) Atorvastatin therapy in hypercholesterolemic patients suppresses cellular uptake of oxidized-LDL by differentiating monocytes. *Atherosclerosis* 164:179–185

40. Li DY, Chen HJ, Mehta JL (2001) Statins inhibit oxidized-LDL-mediated LOX-1 expression, uptake of oxidized-LDL and reduction in PKB phosphorylation. *Cardiovasc Res* 52:130–135
41. Harris J, Hibbeln J, Mackey R, Muldoon M (2004) Statin treatment alters serum n-3 and n-6 fatty acids in hypercholesterolemic patients. *Prostaglandins Leukot Essent Fatty Acids* 71:263–269
42. Jula A, Marniemi J, Rönnemaa T, Virtanen A, Huupponen R (2005) Effects of diet and simvastatin on fatty acid composition in hypercholesterolemic men: a randomized controlled trial. *Arterioscler Thromb Vasc Biol* 25:1952–1959
43. Zelvyte I, Dominaitiene R, Crisby M, Janciauskiene S (2002) Modulation of inflammatory mediators and PPARgamma and NFkappaB expression by pravastatin in response to lipoproteins in human monocytes in vitro. *Pharmacol Res* 45:147–154

Effect of a Seaweed Extract on Fatty Acid Accumulation and Glycerol-3-Phosphate Dehydrogenase Activity in 3T3-L1 Adipocytes

M. L. He · Y. Wang · J. S. You · P. S. Mir ·
T. A. McAllister

Received: 4 July 2008 / Accepted: 6 October 2008 / Published online: 4 November 2008
© AOCS 2008

Abstract This study was to determine the effect of a seaweed *Ascophyllum nodosum* extract (SE) containing 220 mg g⁻¹ phlorotannins on differentiation and fatty acid accumulation in differentiating 3T3-L1 adipocytes. 3T3-L1 cells (2 × 10⁴ mL⁻¹) were seeded to 24-well plates and proliferated to reach confluence and then were treated with media containing 0, 12.5, 25, 50, 75 and 100 µg mL⁻¹ SE for 8 days. Dexamethasone, methyl-isobutylxanthine and insulin (DMI) were added to the media in the first 2 days to induce cell differentiation. On day 8 the adipocytes were harvested for measuring cellular fatty acid concentration and the activity of glycerol-3-phosphate dehydrogenase (GPDH). It was found that treatment with SE increased ($P < 0.01$, $n = 6$) cellular myristoleic acid (C14:1), palmitoleic acid (C16:1) and oleic acid (C18:1) and total monounsaturated fatty acids (MUFA) without significantly affecting the cell number and saturated fatty acid (SFA). Ratios of MUFA/SFA, C14:1/C14:0, C16:1/C16:0 and C18:1/C18:0 in cellular lipids increased ($P < 0.05$, $n = 6$) with the SE treatment in a dose dependent manner ($P < 0.001$). Treatment with 75 µg mL⁻¹ SE depressed ($P < 0.05$) cellular GPDH activity. The results indicate

that the biological factors in the SE may be involved in differentiation and MUFA accumulation in adipocytes.

Keywords 3T3-L1 cell line · Fatty acid accumulation · Glycerol-3-phosphate dehydrogenase · Adipocyte differentiation · Seaweed *Ascophyllum nodosum*

Abbreviations

DHAP	Dihydroxyacetone phosphate
DMEM	Dulbecco's modified Eagle's medium
DMI	Dexamethasone, methyl-isobutylxanthine and insulin
FA	Fatty acids
FBS	Fetal bovine serum
GPDH	Glycerol-3-phosphate dehydrogenase
MUFA	Monounsaturated fatty acids
NADH	β -Nicotinamide adenine dinucleotide, reduced form
PBS	Phosphate buffered saline
SFA	Saturated fatty acids

Introduction

Seaweeds have been used traditionally as food and feed in many countries. It was found in animal and human studies that some seaweed and their extracts had functional effects such as antitumor, antiproliferation [1, 2], antiobesity [3], immunomodulatory [4–6], antioxidation [7, 8] and antimicrobial [9].

Brown seaweed *Ascophyllum nodosum* meal or extracts have been used as natural feed additives for pigs [4], lambs [5] and beef cattle [10–12]. It was found that some extracts from the seaweed could improve animal production

M. L. He · Y. Wang · J. S. You · P. S. Mir · T. A. McAllister
Agriculture and Agri-Food Canada, Lethbridge Research Centre,
Lethbridge, AB, Canada

M. L. He (✉)
Department of Agriculture, Food and Nutritional Science,
University of Alberta, Edmonton, AB, Canada
e-mail: moro_he@yahoo.com

J. S. You
Department of Bioscience and Biotechnology,
Dalian University of Technology, Dalian,
Liaoning, China

performance, which may be attributed to their antioxidant and immunomodulatory characteristics. Recent studies found that supplementation with 2% *Ascophyllum nodosum* meal to cattle diet increased the amount of intramuscular fat, improved carcass quality and extended beef shelf life [13]. However, little information was available on the mechanism.

3T3-L1 cell lines have been used as a cell model for study on differentiation of preadipocytes to adipocytes [14] and fatty acid accumulation [15, 16]. After the 3T3-L1 cells grow to reach confluence they are able to start differentiating to adipocytes in a media with supplementation of additional dexamethasone, methyl-isobutylxanthine and insulin (DMI) [17]. The cellular glycerol-3-phosphate dehydrogenase [EC 1.1.1.8] (GPDH) is a main marker enzyme for the differentiation. The effect of biological factors on lipogenesis and adipogenesis can be estimated by determining GPDH activity and cellular fatty acid accumulation in the differentiating adipocytes [18, 19].

The object of this study was to determine effect of a seaweed extract (SE) from *Ascophyllum nodosum* on cellular fatty acid accumulation and differentiation of 3T3-L1 adipocytes. The SE with various dosages was supplemented to differentiation media during the overall differentiation period. The cell morphology, viability, cellular fatty acid accumulation and GPDH activity in the adipocytes treated with or without SE in various dosages were compared.

Materials and Methods

Preparation of Seaweed Extract

Brown seaweeds *Ascophyllum nodosum* were originally from the Atlantic coastline of Nova Scotia, Canada (Acadian Seaplants Limited, Dartmouth, NS, Canada). The seaweed extract was prepared using a procedure introduced by Wang et al. [20]. The ground seaweeds powder (diameter <500 µm) was mixed with aqueous methanol (80:100 v/v) in ratio of 1 g:25 mL. The mixture was stirred for 2 h at room temperature and then filtered through Whatman #1 filter paper. Methanol in the filtrate was then evaporated at 40 °C and the remaining aqueous fraction was freeze-dried as the seaweed extract for cell culture experiment. The SE contained 220 mg phlorotannins per g dry matter. This was determined by a method introduced by Stern et al. [21].

Cell Culture Experiment

The 3T3-L1 cell line was obtained from ATCC™ (VA, USA). The cells with a passage of five were used in the

present study. The cells were seeded to 24-well plates at a density of 2×10^4 cells per mL of Dulbecco's modified Eagle's medium (DMEM, Sigma, MO, USA) containing 10% fetal bovine serum (FBS, Sigma, MO, USA). The plates were placed in a humidified 5% CO₂ atmosphere at 37 °C for cell proliferation until they reached confluence. The cells were then treated with media containing 0, 12.5, 25, 50, 75 and 100 µg mL⁻¹ of the SE during the overall differentiation period for 8 days. An 80% ethanol water solution was used as carrier solvent for SE. It was added to the media in 1/1,000 (v/v). During the first two days all the groups were in a basal media containing 0.1 µmol L⁻¹ dexamethasone (Sigma, MO, USA), 1 mmol L⁻¹ methyl-isobutylxanthine (Sigma, MO, USA) and 0.1 µmol L⁻¹ insulin (Bovine insulin, Sigma, MO, USA) that acted as the main factors to induce initial differentiation. On day 8 at the end of culture experiment, subsets of cells were harvested for analysis of GPDH activity ($n = 6$ per treatment) and for fatty acids concentration ($n = 6$ per treatment). The remainder ($n = 4$ per treatment) of the plate was stained with Oil-Red O and then Mayer's hematoxylin (Sigma, MO, USA).

Harvesting and Counting Cells

To harvest the cells for cell counting and analysis of cellular fatty acids, cells were washed with a warm phosphate buffered saline (PBS, calcium and magnesium free, pH 7.08) and dissociated with PBS solution containing 0.25% trypsin and 100 mg L⁻¹ EDTA by incubation at 37 °C for 5 min. The cells were then counted on a haemocytometer. For preparing extract for analysis of GPDH activity, the cells were first washed with cold PBS, followed by addition of 0.5 mL Tris-EDTA (pH 7.5). The cells were collected mechanically and crushed under an ultrasonic cell disruptor (Microson™, NY, USA). After centrifugation at 12,800×g at 4 °C for 5 min the supernatant was taken for analysis of GPDH activity. All the harvested cells and extracts were stored at -80 °C for further analysis.

Staining and Photographing Cells

Briefly, 1 mL cold buffered formalin was added to the cell culture and left to stand at room temperature for 30 min. Then it was replaced with fresh 2 ml of cold buffered formalin for 1 h at room temperature to achieve fixation. Cells were then washed with deionised water and 1 ml 0.5% Oil-Red O (Sigma, MO, USA) in isopropanol:deionised water (3:2) was added to the fixed cells for 1 h to stain the oil bodies in the cells. Then the cells were washed with deionised water, and counterstained with Mayer's Hematoxylin (1 g L⁻¹, Sigma, MO, USA) for 3 min. The stained cells were washed with deionised water

again. The cell cultures were photographed using a microscope (Olympus CKX41, Olympus, Japan) with a digital camera (Moticam 2300, Motic China Group Co., Ltd. China).

GPDH [1.1.1.8] Activity and Protein Analysis

The GPDH activity was measured using the method of Wise and Green [18] with modifications. The measurement was done in 98-well micro plate. The following aliquots were added to the well in sequences: 50 μL solution (pH 7.5) that was formed by 0.5 mol L^{-1} triethanolamine, 10 mmol L^{-1} EDTA and 10 mmol L^{-1} 2-mercaptoethanol (TEA solution), 100 μL 5 mmol L^{-1} dihydroxyacetone phosphate (DHAP), 200 μL 0.5 mmol L^{-1} β -nicotinamide adenine dinucleotide with reduced form (NADH), and 50 μL of extract. The disappearance of NADH at 25 $^{\circ}\text{C}$ was measured by a spectrophotometric method at 340 nm with microplate spectrophotometer. The activity of GPDH was expressed as units per min = $[\text{NADH (100 nmol)} \times \text{change of OD}_{340}]/[1.25 \times \text{time (min)} \times \text{protein (mg)}]$. Protein content was measured with Total Protein Kit (Micro Lowry, Onishi & Barr Modification, Sigma-Aldrich Inc., MO, USA) based on the method of Lowry et al. [22].

Extraction of Cellular Lipids

The cellular lipids were extracted by using a procedure reported previously [16]. The harvested cells that had been stored in -80°C freezer were then transferred and washed into a test tube with 4 mL isopropanol. Then 4 mL hexane was added and the cells were crushed using an ultrasonic reactor for 10 min. After crushing the cells, 4 mL water was added to the mixture and the tubes were centrifuged at $2,000 \times g$ at 5 $^{\circ}\text{C}$ for 5 min. Then the upper layer was transferred to a new tube. After the hexane was evaporated under nitrogen in a 38 $^{\circ}\text{C}$ water bath, the residue was stored at -80°C for further analysis.

Methylation and Determination of Fatty Acids

A combined base/acid methylation method [23] with modifications was used. Nonadecanoic acid (C19:0) methyl ester (100 μL , 5.96 mg mL^{-1} hexane Nu-Chek Prep, Inc., MN, USA) was used as an internal standard added to the tubes containing lipids. Then 2 mL of sodium methoxide (0.5 mmol L^{-1} in methanol) was added to each tube. The tubes were flushed with nitrogen and mixed completely. They were placed in a 50 $^{\circ}\text{C}$ water bath for 10 min. After that 1 mL boron trifluoride (14% in methanol) was added and the tubes were reheated in a 50 $^{\circ}\text{C}$ water bath for another 10 min. After cooling down, 5 mL water and 2 mL hexane were added to the tube and the solution was mixed

completely. They were allowed to stand for 10 min and the upper layer (hexane) was taken into a GC vial flushed with nitrogen for fatty acid determination by gas chromatography. Fatty acid methyl esters were quantified by a gas chromatograph (Hewlett Packard GC System 5890; Mississauga, ON) equipped with a flame ionisation detector and SP-2560 fused silica capillary column (100 m with 0.2 mm film thickness; Supelco Inc., Oakville, ON). Samples were loaded on to the column via 5 μL splitless injections. The initial oven temperature (120 $^{\circ}\text{C}$) was held for 15 min and then increased at 5 $^{\circ}\text{C min}^{-1}$ to 160 $^{\circ}\text{C}$, and held for 15 min. Next the temperature was increased at 4 $^{\circ}\text{C min}^{-1}$ to 240 $^{\circ}\text{C}$ and held for 30 min. Inlet and detector temperatures were maintained at 220 and 275 $^{\circ}\text{C}$, respectively. The helium carrier gas flow rate through the column was 1.7 mL min^{-1} . Hydrogen flow to the detector was 34 mL min^{-1} , the air flow was 320 mL min^{-1} and the helium make-up gas flow rate was 29 mL min^{-1} . Peaks in the chromatograms were identified and quantified using pure methyl ester standards (Sigma-Aldrich, Oakville, ON) and reported as μg fatty acid per 10^5 cells. The recovery rates and correction factors were calculated based on the internal standard fatty acid.

Statistical Analysis

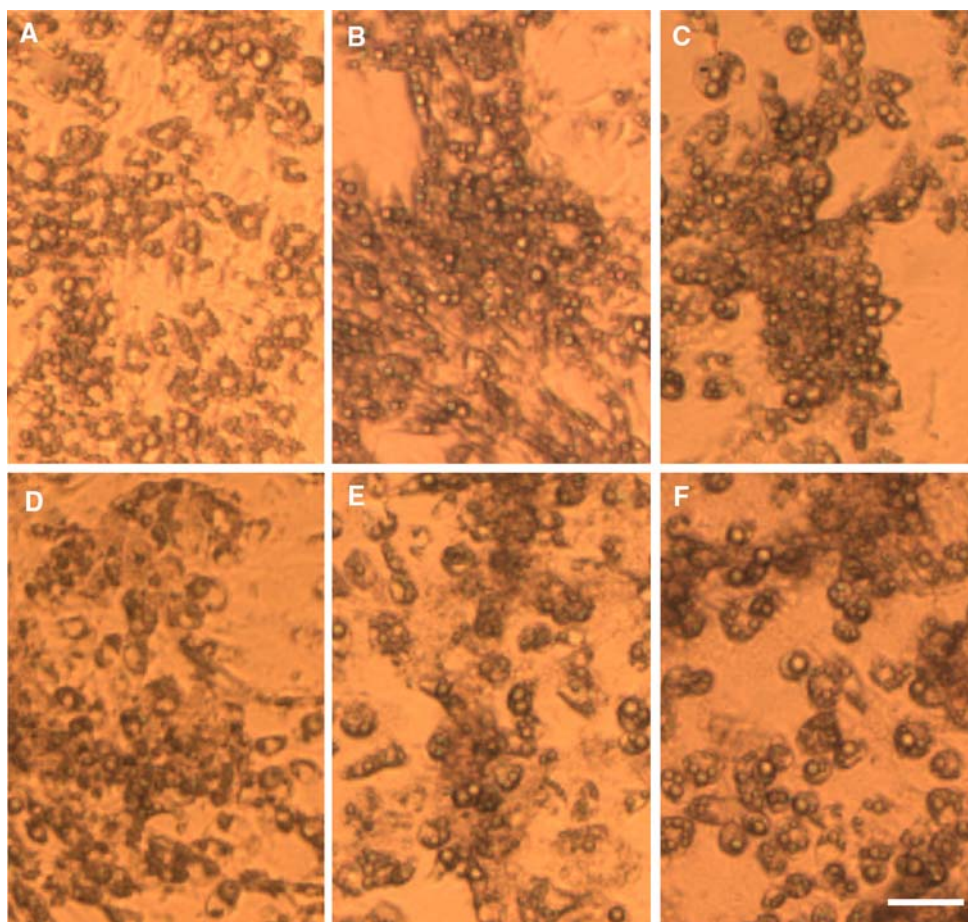
Analysis of variance (ANOVA) was conducted using SAS-PROC MIXED [24] to determine the effect of SE in various dosages on the cellular GPDH activity, fatty acids concentration and the ratio of saturated fatty acids to monounsaturated fatty acids. Tukey test was applied for multiple comparisons when a significant difference ($P \leq 0.05$) was found among the treatment groups. Pearson correlation (2-tailed) analysis was used for analysis of correlations between the ratio of MUFA/SFA and SE dosage [25].

Results

Adipocyte Morphology and Viability of the Cells

The images of the cells on day 8 and those Oil-Red O stained cells at the end of the experiment are shown in Figs. 1 and 2, respectively. The oil drops were observed in most of the cells in both the control and the treatment groups. Differences were shown in the appearance of the distribution of the cells between the control and the SE treatments. The adipocytes treated with SE especially those with 75 and 100 $\mu\text{g mL}^{-1}$ SE contained larger oil drops than those in the control (Figs. 1, 2). Also the cells in the wells treated with 12.5 and 25 $\mu\text{g mL}^{-1}$ SE were gathered to form radial scattered groups (Fig. 1). Treatment with SE

Fig. 1 Photos of 3T3-L1 adipocytes on day 8 of post-confluence treated with 0 (a), 12.5 (b), 25 (c), 50 (d), 75 (e) and 100 (f) $\mu\text{g mL}^{-1}$ seaweed extract during the experimental period. Bar = 50 μm



did not significantly affect the total number of the cells that were harvested at the end of experiment (Table 1).

GPDH Activity

The comparison on cellular GPDH activity in the adipocytes harvested at the end of experiment is shown in Fig. 3. Treatment with 75 $\mu\text{g mL}^{-1}$ SE decreased ($P < 0.05$) GPDH activity by approximately 20% (Fig. 3). Treatment with 25 $\mu\text{g mL}^{-1}$ did not significantly affect the GPDH activity although the value was relatively lower than that in the control.

Concentration of Cellular Fatty Acids

Supplementation with 12.5, 25, 50, 75 and 100 $\mu\text{g mL}^{-1}$ SE to the media significantly increased ($P < 0.05$) the amount of monounsaturated fatty acids (MUFA) in the adipocytes (Table 1). Concentration of cellular myristoleic acid (C14:1) and palmitoleic acid (C16:1) in the adipocytes treated with 12.5, 25, 50, 75 and 100 $\mu\text{g mL}^{-1}$ SE was higher ($P < 0.05$) compared to that of the control. Cellular concentration of cellular oleic acid (C18:1) in the adipocytes treated with 75 and 100 $\mu\text{g mL}^{-1}$ SE was also higher

($P < 0.05$) than that of the control. The amount of cellular total fatty acids and that of saturated fatty acids (SFA) in the adipocytes were not significantly affected by supplementation of SE to the media. Cellular concentration of palmitic acid (C16:0) and stearic acid (C18:0) were not affected by supplementation of the SE. However, cellular concentration of myristic acid (C14:0) in the adipocytes treated with the SE tended ($P = 0.07$) to be increased (Table 1).

Ratio of MUFA to SFA

The ratio of total MUFA to SFA as well as the individual ratios of C14:1/C14:0, C16:1/C16:0 and C18:1/C18:0 in adipocytes treated with 12.5, 25, 50, 75 and 100 $\mu\text{g mL}^{-1}$ SE were significantly higher ($P < 0.05$) compared to those in the control group (Table 1). The treatment with 100 $\mu\text{g mL}^{-1}$ SE had the highest ratio of total MUFA/SFA and that of C14:1/C14:0, C16:1/C16:0 and C18:1/C18:0 among the groups. There were significantly positive correlations ($P < 0.001$) between the SE dosage and the ratio of MUFA/SFA, C14:1/C14:0, C16:1/C16:0 and C18:1/C18:0 with coefficient of 0.8, 0.8, 0.6 and 0.5 respectively.

Fig. 2 Photos of fixed and Oil-Red O and Mayer's hematoxylin stained 3T3-L1 adipocytes at the end of experiment treated with 0 (a), 12.5 (b), 25 (c), 50 (d), 75 (e) and 100 (f) $\mu\text{g mL}^{-1}$ seaweed extract during the experimental period. Bar = 50 μm

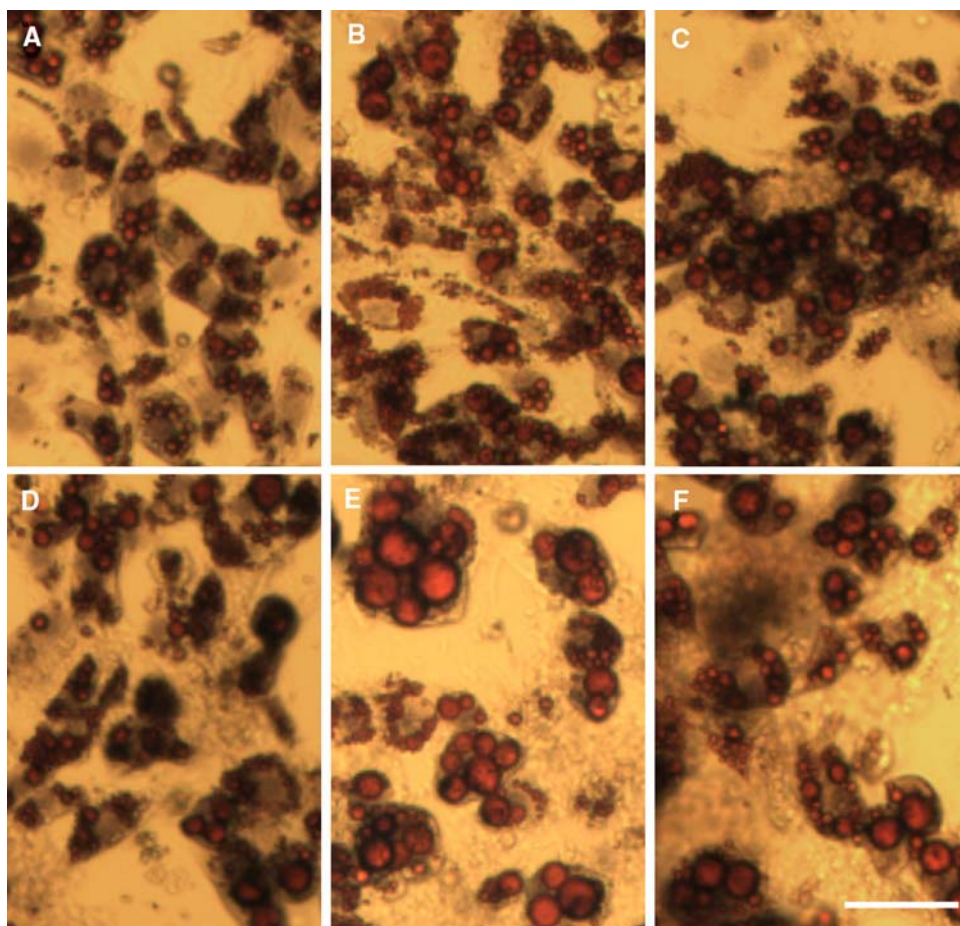


Table 1 Concentration of cellular fatty acids in the 3T3-L1 adipocytes treated with or without seaweed extract during the experimental period

	Seaweed extract treatment ($\mu\text{g mL}^{-1}$)						SEM	<i>P</i> -value
	0	12.5	25	50	75	100		
Cell number, $n \times 10^5$	3.40	3.23	3.37	3.35	3.20	3.33	0.06	0.16
Cellular FA, $\mu\text{g } 10^5 \text{ cells}^{-1}$								
C14:0	1.30	1.38	1.47	1.40	1.47	1.50	0.05	0.07
C14:1cis	0.23a	0.30b	0.30b	0.30b	0.35b	0.35b	0.02	<0.001
C16:0	12.13	12.85	12.78	11.68	12.55	11.90	0.46	0.42
C16:1cis	7.58a	9.17b	9.47b	9.02b	9.35b	9.17b	0.35	0.01
C18:0	1.43	1.27	1.28	1.27	1.38	1.32	0.08	0.71
C18:1cis-9	3.25a	3.57ab	3.62ab	3.55ab	3.92b	3.90b	0.12	0.01
SFA	14.88	15.50	15.52	14.35	15.40	14.70	0.58	0.64
MUFA	11.07a	13.03b	13.42b	12.85b	13.65b	13.43b	0.44	<0.001
Total FA	25.97	28.53	28.93	27.18	29.02	28.12	1.00	0.27
Ratio of MUFA/SFA								
C14:1/14:0	0.19a	0.22b	0.21b	0.22b	0.24b	0.24b	0.01	0.01
C16:1/16:0	0.62a	0.71b	0.74bc	0.77c	0.75bc	0.77c	0.01	<0.001
C18:1/18:0	2.33a	2.85b	2.85b	2.87b	2.87b	2.99b	0.11	<0.001
MUFA/SFA	0.74a	0.84b	0.87bc	0.90 cd	0.89 cd	0.92d	0.01	<0.001

a–d means ($n = 6$) without the same letter differ significantly ($P < 0.05$)

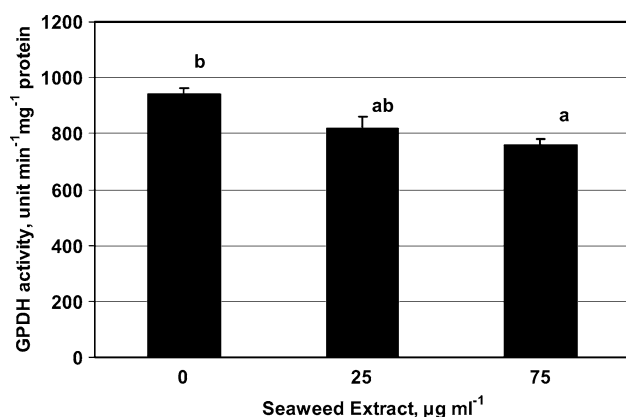


Fig. 3 Activity of glycerol-3-phosphate dehydrogenase (GPDH) in the 3T3-L1 adipocytes treated with or without seaweed extract during experimental period. a–b: means (\pm SE, $n = 6$) without the same letter differ significantly ($P < 0.05$)

Discussion

Extracts of seaweed have been tested as feed additives for improving animal health and production performance. The effects of seaweeds and their extracts may be diverse on their breed, preparation method and applied dosage. Brown seaweed *Ascophyllum nodosum* meal or extracts have been tested as feed additives for animal production [4, 5, 10, 11, 13]. Studies found that their supplementation to the diet could improve desirable intramuscular fat content in beef and extended shelf life of the meat products [13]. This may be attributed to the antioxidants and other biological components in SE which may affect the lipid accumulation and ratio of monounsaturated fatty acids in fat tissues. In the present study, it was found that supplementation of the SE increased MUFA concentration and composition in adipocytes without affecting the amount of cellular total fatty acid. The ratio of cellular MUFA/SFA increased in a dose-dependent manner only when the relative low doses (12.5, 25 and 50 $\mu\text{g mL}^{-1}$) were applied. With relative high doses (75, 100 $\mu\text{g mL}^{-1}$) the supplementation of SE did not show further improvement on the ratio of MUFA/SFA. One of the possible reasons is that not all the tannins added to the media were effective for the cells because they might form tannin-protein complexes with albumin in the media. More tannin molecules may be consumed when the relative high doses were applied.

The main biological components in the SE were phlorotannins [20], which were detected in amounts as high as 220 mg g^{-1} dry matter using a method by Stern et al. [21]. Phlorotannins from brown seaweed have been reported as possessing several biological activities such as being an antioxidant and preventing skin carcinogenesis [2, 26]. Liu et al. [27] have assessed the effect of tannic acids extracted from a banaba *Lagerstroemia speciosa* L. on

differentiation of 3T3-L1 adipocytes and found that the tannic acids inhibited the differentiation but stimulated glucose transport in 3T3-L1 cells. Similarly, in the present study, an inhibitory effect of SE on cellular GPDH activity (Fig. 3) was found and that may be attributed to the effect of phlorotannins. In animal studies Wriese and Lambert [28] observed that consumption of drinking water containing tannic acid resulted in a higher weight fat pad which may be caused by increased fatty acid accumulation through decreasing both basal and isoproterenol-stimulated lipolysis. However, Yoshikawa et al. [29] found that oral supplementation of the tannin fraction from *Salacia reticulata*, inhibited GPDH activity in epididymal fat tissue of Zucker fatty rats and therefore showed a mild antiobesity effect. The GPDH is the key enzyme catalysing conversion of dihydroxyacetone phosphate (DHAP) to glycerol-3-phosphate for further synthesis of fatty acids and triacylglycerol (TAG). Abnormal fat development was found in transgenic mice overexpressing GPDH [30]. Decline of GPDH activity indicated a slow down on de novo synthesis of fatty acids and TAG. It also reflected the inhibition on differentiation in the early differentiating preadipocytes and lipogenesis in the mature adipocytes.

Related to the results that SE improved the cellular MUFA in the adipocytes, a previous study by Cherian et al. [31] found that dietary supplementation of a sorghum Valpo Red, which contains high tannins, to broiler chicks significantly improved C16:1, C18:1 and total MUFA composition in breast muscle total lipids compared to the control and another sorghum Ruby Red which contains low tannins. All of these together with the findings in the present study suggest both terrestrial tannins and phlorotannins may be involved in the lipogenesis and adipogenesis of fat tissues.

Lipogenesis and lipolysis always concurrently exist in mature adipocytes. GPDH is the key enzyme for controlling the lipogenic synthesis rate in the cells, especially for those adipocytes in the differentiation period [19]. The inhibition on GPDH activity affects the lipogenesis and may result in a less de novo fatty acids synthesis. The previous study on effect of CLAs on the differentiation of 3T3 cells found there was a positive correlation between GPDH activity and cellular fatty acids, especially that of MUFA C16:1 and C18:1 [16]. However, in the present study, the concentration of MUFA in the cells as well as the composition in the total fatty acids were increased while the GPDH activity was decreased. It suggested that the increase of MUFA found in the present study was independent of the change in GPDH activity. The antioxidant effect of SE may contribute the most to accumulation and protection of MUFA against being oxidised and degraded.

The present study found that the cellular ratio of MUFA/SFA was increased in an SE dose dependent manner. The

ratio of MUFA/SFA such as C14:1/C14:0, C16:1/C16:0 and C18:1/C18:0 may be related to metabolic rate and physiological responses of the cells, and therefore may affect membrane fluidity of cells [32]. Changes in the ratio of MUFA to SFA may in turn affect lipogenesis and lipolysis in the adipocytes. Cellular lipid accumulation in mature adipocytes depends on both lipogenesis and lipolysis and may alter cell size and the cellular fatty acid composition. It was found [33] that in growing and fattening beef cattle the composition of cellular monounsaturated fatty acids such as C14:1, C16:1 and C18:1 had strong positive correlation with mean size of adipocytes, while that of saturated fatty acids C18:0 and C16:0 had a negative correlation with it. A similar correlation was found between the cellular fatty acids composition and adipocytes distributed in the same fat pad that excluded variations caused by animal, feed and environment [34]. In the present study the results on profiles of the adipocytes (Figs. 1, 2) show the SE groups, especially those treated with 75 and 100 $\mu\text{g mL}^{-1}$, had accumulated more large oil drops, which were also found to have a significantly higher ratio of MUFA/SFA (Table 1) compared to those in the control. These findings in the present study suggest that there is a similar correlation between the composition of fatty acids, especially the ratio of MUFA/SFA and the cell size, which is dependent on the cellular fatty acid accumulation.

Fatty acids and their composition in animal products may affect the quality, flavour and nutritional value. Diets high in saturated fatty acids may be correlated with an increased incidence of coronary heart disease [35]. Decreasing dietary SFA or increasing ratio of USFA/SFA could lower the plasma total and LDL-cholesterol [36] and this may lower the incidence of heart attack, cardiac death, heart failure or stroke [37]. The results suggest that a high-MUFA diet could also be an alternative to a low-fat diet for medical nutrition therapy in diabetes [38]. Therefore, the positive effect of the seaweed and the tannin fraction on the ratio of MUSF/SFA in the adipocytes that was found in the present study, and those in animal experiments [31] may contribute new knowledge to improve food quality and human health.

In conclusion, the present study found that supplementation of the SE from *Ascophyllum nodosum* to the medium significantly increased accumulation of cellular MUFA and the ratio of MUFA/SFA in a dose-dependent manner in differentiating 3T3-L1 adipocytes. Supplementation with a high dose of SE to the media inhibited the GPDH activity. The results suggest that SE may have diverse effects on differentiation and fatty acid accumulation in differentiating adipocytes. The biological factors in SE such as phlorotannins may be involved in lipogenesis and lipolysis, and may improve monounsaturated fatty acid accumulation in adipose tissue.

Acknowledgments M.L.H. thanks B. Pink and K. Jakober for their help in checking and revising the manuscript. The manuscript is Lethbridge Research Centre contribution #387-08046.

References

- Riou D, Collicec-Jouault S, Pinczon du Sel D, Bosch S, Siavoshian S, Le Bert V, Tomasoni C, Sinquin C, Durand P, Roussakis C (1996) Antitumor and antiproliferative effects of a fucan extracted from *Ascophyllum nodosum* against a non-small-cell bronchopulmonary carcinoma line. *Anticancer Res* 16:1213–1218
- Hwang H, Chen T, Nines RG, Shin HC, Stoner GD (2006) Photochemoprevention of UVB-induced skin carcinogenesis in SKH-1 mice by brown algae polyphenols. *Int J Cancer* 119:2742–2749
- Maeda H, Hosokawa M, Sashima T, Takahashi N, Kawada T, Miyashita K (2006) Fucoxanthin and its metabolite, fucoxanthinol, suppress adipocyte differentiation in 3T3-L1 cells. *Int J Mol Med* 18:147–152
- Turner JL, Dritz SS, Higgins JJ, Minton JE (2002) Effects of *Ascophyllum nodosum* extract on growth performance and immune function of young pigs challenged with *Salmonella typhimurium*. *J Anim Sci* 80:1947–1953
- Saker KE, Fike JH, Veit H, Ward DL (2004) Brown seaweed (TascoTM) treated conserved forage enhances antioxidant status and immune function in heat-stressed Wether lambs. *J Anim Physiol Anim Nutr (Berl)* 88:122–130
- Saker KE, Allen VG, Fontenot JP, Bagley CP, Ivy RL, Evans RR, Wester DB (2001) Tasco-forage: II. Monocyte immune cell response and performance of beef steers grazing tall fescue treated with a seaweed extract. *J Anim Sci* 79:1022–1031
- Lim SN, Cheung PCK, Ooi VEC, Ang PO (2002) Evaluation of antioxidative activity of extracts from a brown seaweed, *Sargassum siliquastrum*. *J Agric Food Chem* 50:3862–3866
- Huang HL, Wang BG (2004) Antioxidant capacity and lipophilic content of seaweeds collected from the Qingdao coastline. *J Agric Food Chem* 52:4993–4997
- Horikawa M, Noro T, Kamei Y (1999) In vitro anti-methicillin-resistant *Staphylococcus aureus* activity found in extracts of marine algae indigenous to the coastline of Japan. *J Antibiot (Tokyo)* 52:186–189
- Allen VG, Pond KR, Saker KE, Fontenot JP, Bagley CP, Ivy RL, Evans RR, Schmidt RE, Fike JH, Zhang X, Ayad JY, Brown CP, Miller MF, Montgomery JL, Wester DB, Melton C (2001) Tasco: influence of a brown seaweed on antioxidants in forages and livestock—a review. *J Anim Sci* 79:E21–E31
- Allen VG, Pond KR, Saker SE, Fontenot JP, Bagley CP, Ivy RL, Evans RR, Brown CP, Miller MF, Montgomery JL, Dettle TM, Wester DB (2001) Tasco-forage: III. Influence of a seaweed extract on performance, monocyte immune cell response, and carcass characteristics in feedlot-finished steers. *J Anim Sci* 79:1032–1040
- Fike JH, Allen VG, Schmidt RE, Zhang X, Fontenot JP, Bagley CP, Ivy RL, Evans RR, Coelho RW, Wester DB (2001) Tasco-forage: I. Influence of a seaweed extract on antioxidant activity in tall fescue and in ruminants. *J Anim Sci* 79:1011–1021
- Braden KW, Blanton JR Jr, Montgomery JL, van Santen E, Allen VG, Miller MF (2007) Tasco Supplementation: effect on carcass characteristics, sensory attributes, and retail display shelf-life. *J Anim Sci* 85:754–768
- Green H, Kehinde O (1974) An established pre-adipose cell line and its differentiation in culture. *Cell* 3:127–133
- Satory DL, Smith SB (1999) Conjugated linoleic acid inhibits proliferation but stimulates lipid filling of murine 3T3-L1 pre-adipocytes. *J Nutr* 129:92–97

16. He ML, Hnin TM, Kuwayama H, Mir PS, Okine EK, Hidari H (2006) Effect of conjugated linoleic acid type, treatment period and dosage on differentiation of 3T3 cells. *Lipids* 41:937–949
17. Ntambi JM, Kim YC (2000) Adipocyte differentiation and gene expression. *J Nutr* 130:3122S–3126S
18. Wise LS, Green H (1979) Participation of one isozyme of cytosolic glycerophosphate in adipose conversion of 3T3 cells. *J Biol Chem* 254:273–275
19. Spiegelman BM, Frank M, Green H (1983) Molecular cloning of mRNA from 3T3 adipocytes. Regulation of mRNA content for glycerophosphate dehydrogenase and other differentiation-dependent proteins during adipocyte development. *J Biol Chem* 258:10083–10089
20. Wang Y, Xu Z, Bach SJ, McAllister TA (2008) Effects of phlorotannins from *Ascophyllum nodosum* (brown seaweed) on ruminal digestion of forage and concentrate diets in vitro. *Anim Feed Sci Technol* 145:375–395
21. Stern JL, Hagerman AE, Steingerg PD, Winter FC, Estes JA (1996) A new assay for quantifying brown algal phlorotannins and comparisons to previous methods. *J Chem Ecol* 22:1273–1293
22. Lowry OH, Rosebrough NJ, Farr AL, Randall RJ (1951) Protein measurement with the folin phenol reagent. *J Biol Chem* 193:265–275
23. Kramer JKG, Fellner V, Dugan MER, Sauer FD, Mossob MM, Yurawecz MP (1997) Evaluating acid and base catalysts in the methylation of milk and rumen fatty acids with special emphasis on conjugated dienes and total *trans* fatty acids. *Lipids* 32:1219–1228
24. SAS (1997) SAS® System for Windows™ 6.12. SAS Institute, Cary
25. SPSS (1999) SPSS 10.0 for Windows. SPSS®, Chicago
26. Nakamura T, Nagayama K, Uchida K, Tanaka R (1996) Antioxidant activity of phlorotannins isolated from the brown alga *Eisenia bicyclis*. *Fisheries Sci* 62:923–926
27. Liu X, Kim JK, Li Y, Li J, Liu F, Chen X (2005) Tannic acid stimulates glucose transport and inhibits adipocyte differentiation in 3T3-L1 cells. *J Nutr* 135:165–171
28. Wisez F, Lambert B (2001) Differential long-term effects of tannic acid on adenylcyclase activity and lipolysis in rat adipocytes. *Phytomedicine* 8:292–297
29. Yoshikawa M, Shimoda H, Nishida N, Takada M, Matsuda H (2002) Salacia reticulata and its polyphenolic constituents with lipase inhibitory and lipolytic activities have mild antiobesity effects in rats. *J Nutr* 132:1819–1824
30. Kozak LP, Kozak UC, Clarke GT (1991) Abnormal brown and white fat development in transgenic mice overexpressing glycerol-3-phosphate dehydrogenase. *Genes Dev* 5:2256–2264
31. Cherian G, Selvaraj RK, Goeger MP, Stitt PA (2002) Muscle fatty acid composition and thiobarbituric acid-reactive substances of broilers fed different cultivars of sorghum. *Poult Sci* 81:1415–1420
32. Field C, Ryan E, Thomson A, Clandinin M (1997) Diet fat composition alters membrane phospholipid composition, insulin binding and glucose metabolism in adipocytes from control and diabetic animals. *J Biol Chem* 265:11143–11150
33. He ML, Roh SG, Oka H, Hidaka S, Matsunaga N, Hidari H (1997) The relationship between fatty acid composition and the size of adipocytes from subcutaneous adipose tissue of Holstein steers during the fattening period. *Anim Sci Technol (Jpn)* 68:838–842
34. He ML, Hidaka S, Matsunaga N, Hidari H (2000) Comparison of fatty acid composition among isolated bovine adipocytes with different sizes. *J Anim Physiol Anim Nutr (Berl)* 83:215–223
35. Hu FB, Stampfer MJ, Manson JE, Ascherio A, Colditz GA, Speizer FE, Hennekens CH, Willett WC (1999) Dietary saturated fats and their food sources in relation to the risk of coronary heart disease in women. *Am J Clin Nutr* 70:1001–1008
36. Abbey M, Noakes M, Belling GB, Nestel PJ (1994) Partial replacement of saturated fatty acids with almonds or walnuts lowers total plasma cholesterol and low-density-lipoprotein cholesterol. *Am J Clin Nutr* 59:995–999
37. de Lorgeril M, Salen P, Martin JL, Monjaud I, Delaye J, Mamelle N (1999) Mediterranean diet, traditional risk factors, and the rate of cardiovascular complications after myocardial infarction: final report of the Lyon diet heart study. *Circulation* 99:779–785
38. Ros E (2003) Dietary cis-monounsaturated fatty acids and metabolic control in type 2 diabetes. *Am J Clin Nutr* 78(suppl):617S–625S

Dietary Marine-Derived Tocopherol has a Higher Biological Availability in Mice Relative to Alpha-Tocopherol

Naohiro Gotoh · Hiroyuki Watanabe ·
Tomiko Oka · Daisuke Mashimo · Noriko Noguchi ·
Kazuhiko Hata · Shun Wada

Received: 21 March 2008 / Accepted: 7 October 2008 / Published online: 7 November 2008
© AOCS 2008

Abstract The biologic availability of two kinds of tococomonoenols, marine-derived tocopherol (MDT) and α -tococomonoenol, was investigated in ICR mice. Vitamin E-deficient ICR mice were fed MDT and α -tococomonoenol together with α -tocopherol, β -tocopherol, γ -tocopherol, and δ -tocopherol, and storage in liver, spleen, lung, and brain was quantified using reverse-phase high-performance liquid chromatography. The vitamin E relative biologic availability (VE-RBA) in liver was 100 for α -tocopherol, 26 ± 3 for β -tocopherol, 4 ± 2 for γ -tocopherol, not detected for δ -tocopherol, 49 ± 6 for MDT, and 30 ± 7 for α -tococomonoenol. The VE-RBA in brain was 100 for α -tocopherol, 5 ± 2 for β -tocopherol, not detected for γ -tocopherol and δ -tocopherol, 8 ± 1 for MDT, and 4 ± 1 for α -tococomonoenol. Tocopherols and tococomonoenols did not accumulate in the spleen or lung. MDT and α -tococomonoenol had high VE-RBA values. The VE-RBA value for MDT was much higher than that for β -tocopherol.

Keywords α -Tococomonoenol · Liver · Marine-derived tocopherol · Mouse · Vitamin E relative biologic availability

Abbreviations

ECD	Electrochemical detector
FL	Fluorescence detector
MDT	Marine-derived tocopherol
α -TTP	α -Tocopherol transfer protein
VEHTM	Vitamin E homologues and tococomonoenols mixture
VE-RBA	Vitamin E relative biologic availability

Introduction

Vitamin E is essential for maintaining cellular homeostasis in animals. The vitamin was originally discovered as an antisterility component in rodents [1], but this effect has not been observed in humans. It is currently recognized that the main role of vitamin E in the mammalian body is as an antioxidant [2–4]. Vitamin E is a generic term used to refer to eight homologues, α -tocopherol, β -tocopherol, γ -tocopherol, δ -tocopherol, α -tocotrienol, β -tocotrienol, γ -tocotrienol, and δ -tocotrienol. Approximately 10 years ago, however, two novel types of vitamin E were discovered in Japan [5, 6]. In 1995, α -tococomonoenol was found in rice bran and palm oil at levels of 7–14 mg/g [5]. The structure of α -tococomonoenol resembles that of α -tocopherol, except that one double bond locates between the 11' and 12' carbons of the phytyl side chain [5, 7]. Palm oil and rice bran characteristically contain α -tocotrienol. α -Tococomonoenol might be an intermediate substance formed by the metabolism of α -tocopherol to α -tocotrienol,

N. Gotoh · T. Oka · D. Mashimo · S. Wada (✉)
Department of Food Science and Technology,
Tokyo University of Marine Science and Technology,
4-5-7 Konan, Minato-ku, Tokyo 108-8477, Japan
e-mail: wada@kaiyodai.ac.jp

H. Watanabe
Department of Health Science, Kochi Women's University,
5-15, Eikokujicho, Kochi, Kochi 780-8515, Japan

N. Noguchi
Laboratory for Systems Biology and Medicine,
Research Center for Advanced Science and Technology,
University of Tokyo, 4-6-1, Meguro-ku, Tokyo 153-8904, Japan

K. Hata
Nippon Suisan Kaisha, Ltd, 559-6, Kitano-machi, Hachioji,
Tokyo 192-0906, Japan

or by α -tocotrienol to α -tocopherol, in palm and rice. The other novel vitamin E was a different kind of tocomonoenol, named “marine-derived tocopherol” (MDT). The existence of MDT was first reported in 1999 [6]. MDT was originally found in salmon roe, but its presence in a wide range of marine organisms was later confirmed [6, 8, 9]. The structure of MDT is very similar to that of α -tocomonoenol, but the position of the double bond in the phytyl side chain is different. The double bond in MDT locates at the end of the side chain. MDT levels are conventionally expressed in %MDT, $100 \times \text{MDT}/(\text{MDT} + \alpha\text{-tocopherol})$, and the values range from 0 to 38 in marine organisms. Both tocomonoenols are present in human plasma [8], likely incorporated into the body via foods.

Relative vitamin E activity is a factor indicating the relative availability of vitamin E homologues in the mammalian body [3, 4]. A wide range of values in various animals have been determined by several methods, including liver-storage bioassay [10, 11], inhibition rate of fetal resorption [12, 13], inhibition rate of erythrocyte hemolysis [14], muscular dystrophy [15], in rat [12–14], chick [10, 11], and rabbit [15]. Representative values are 100 for α -tocopherol, 2–40 for β -tocopherol, 1–11 for γ -tocopherol, 1 for δ -tocopherol, 27–29 for α -tocotrienol, and 5 for β -tocotrienol [2]. These values have been used to determine the “Recommended Daily Amounts” for humans worldwide. Importantly, however, the values have not been examined in human clinical investigations. These values are thought to be strongly related to the affinity to α -tocopherol transfer protein (α -TTP) in the liver [16, 17].

As mentioned above, novel tocomonoenols were detected in human plasma, but their relative availabilities have not yet been investigated. There is a high consumption of marine fish worldwide and MDT is found in almost all marine organisms. Therefore, we investigated the vitamin E relative biologic availability (VE-RBA) of MDT in ICR mice and comparing it with that of β -tocopherol. The VE-RBA of α -tocomonoenol was also examined in this study.

Materials and Methods

Reagents and Ingredients

α -Tocopherol, β -tocopherol, γ -tocopherol, and δ -tocopherol were a kind gift from Eisai Co., Ltd. (Tokyo, Japan). Silica Gel 60 N (spherical, neutral) for column chromatography was purchased from Kanto Chemical Co., Inc. (Tokyo, Japan). Other chemicals used in the experiments were purchased from Wako Pure Chemical Industries Ltd. (Osaka, Japan). Vitamin-free casein and AIN-93G mineral mixture were obtained from CLEA Japan, Inc. (Tokyo,

Japan). Vitamin E-free corn oil was obtained from Tama Biochemical Co., Ltd. (Tokyo, Japan). AIN-93 vitamin mixture and AIN-93 vitamin E-free vitamin mixture were purchased from Oriental Yeast Co., Ltd. (Tokyo, Japan).

Separation of Tocomonoenols from Tuna Oil Deodorization Scum

The deodorization scum formed from tuna oil was obtained from Nippon Suisan Kaisha, Ltd. (Tokyo, Japan). Deodorization scum (100 g) was mixed with 200 mL of 1 N KOH methanol solution, stirred with a magnetic stirrer for 10 min and placed in the dark for 30 min. The solution was separated into two layers and the upper layer was collected and neutralized with 12 N HCl. The neutralized solution was then separated into two layers and the upper layer was collected in a separating funnel and mixed gently with 200 mL of hexane and saturated NaCl solution. The separation funnel was placed in the dark and the upper layer was collected and evaporated with a rotary evaporator under vacuum at 40 °C. The evaporated upper layer was viscous and dark brown.

The Silica Gel 60 N was packed in a column using a mixture of hexane and ethyl acetate (95:5, v/v). The viscous dark brown substance was mixed with Silica Gel 60 N in hexane solution and dried completely with a rotary evaporator. The dried silica gel was charged onto the packed column and a mixture of hexane and ethyl acetate (95:5, v/v) was flowed onto the column continuously. Each liter of the eluted solution was collected and run on a high-performance liquid chromatography (HPLC) -fluorescence detector (FL) to evaluate the presence of vitamin Es after the solute was changed from the mixture of hexane and ethyl acetate to methanol. The HPLC system comprised a pump (L-6000, Hitachi High-Technologies Corporation, Tokyo, Japan), docosyl silyl (C22) column (DOCOSIL-B, 250 \times 4.6 mm, i.d. 5 mm, Senshu Scientific Co., Ltd, Tokyo, Japan), FL (RF-10AXL, Shimadzu Co., Kyoto, Japan), and Chromatopac integrator (C-R6A, Shimadzu Co., Kyoto, Japan). Methanol was used as an eluent; the flow rate was 1.0 mL/min and the column temperature was room temperature. The FL excitation and emission wavelengths were 298 and 325 nm, respectively. After the second fractionation, fractions containing tocopherols were collected and dried using a rotary evaporator.

The collected tocopherols were mixed with methanol and subjected to HPLC-FL for fractionation. The HPLC-FL system comprised a pump (L-6000), C22 column (DOCOSIL-B, 250 \times 10.0 mm, i.d. 5 mm), FL (FP-920, JASCO Corporation, Tokyo, Japan), and Chromatopac integrator (C-R6A). The flow rate was 3.0 mL/min. Other conditions were the same as described above. The peak

appearing before α -tocopherol was collected (Fig. 2). However, the peak really consisted of two peaks, at 32.66 and 33.70 min, and they were very difficult to fractionate separately because they were too close to each other.

Structure Analyses of Collected Tocomonoenols

The molecular weights were measured to identify the structures that gave the two peaks on the chromatogram (Fig. 2) using HPLC-Atmospheric Pressure Chemical Ionization Mass Spectrometry (Waters Alliance ZMD LC/MS system, Waters Corporation, Milford, MA) equipped with octadecyl silyl (ODS) column (Supelcosil LC-18, 150 \times 4.6 mm, i.d. 5 mm, Sigma-Aldrich Co., Bellefonte, PA). Methanol was used as an eluent; the flow rate was 1.0 mL/min and the column temperature was room temperature. Data acquisition, processing, and instrument control were performed using MassLynx software (Waters Corporation, Milford, MA). The APCI conditions of capillary voltage, positive mode cone voltage, negative mode cone voltage, heater temperature, gas flow and corona voltage were 4.0 kV, 80 V, 40 V, 400 °C, 500 L/h and 15 V, respectively. The analyses were performed in positive ion mode. Spectra were obtained over the range of m/z 250–450 with a scan time of 0.5 s.

Each of the two peaks was carefully collected and applied to HPLC-FL for fractionation. Each fraction was completely dried with a rotary evaporator at 40 °C and resolved in deuterium-labeled chloroform (CDCl_3). The CDCl_3 solution was placed into a micro-NMR sample tube (CMS-005J, Shigemi Co., Ltd., Tokyo Japan) and subjected to ^1H -NMR analyses (AVANCE 400 WB, Bruker, Karlsruhe, Germany) operated at 400 MHz. The ^1H -NMR spectra were acquired with the following conditions, temperature: 15 °C, pulse delay: 1.0 s, acquisition time: 2.0 s, data points: 32 K, pulse angle: 30°, number of scans: 512, spectra width, 20.55 ppm.

Preparation of “Vitamin E Homologues and Tocomonoenols Mixture”

The fractionated tocomonoenols were mixed with α -tocopherol, β -tocopherol, γ -tocopherol, and δ -tocopherol in ethanol, and the concentrations of MDT, α -tocopherol, β -tocopherol, γ -tocopherol, and δ -tocopherol were adjusted to be the same. Finally, the ethanol was removed from the solution and the residue was used as a “Vitamin E Homologues and Tocomonoenols Mixture (VEHTM)”. The actual ratios of the vitamin E homologues and tocomonoenols were reconfirmed using an HPLC-electrochemical detector (ECD). This HPLC system comprised a pump (PU-1580, JASCO Corporation, Tokyo, Japan), tandem-jointed octadecyl silyl columns (ODS, Supelcosil LC-18,

250 \times 4.6 mm, i.d. 5 mm), ECD (NANOSPACE SI-1, Shiseido Co., Ltd., Tokyo, Japan), and a Chromatopac integrator (C-R6A). The oxidation potential of the ECD was +600 mV (vs. Ag/AgCl) at the glassy carbon electrode. A mixture of methanol and distilled water (50/1, v/v) containing 50 mM sodium perchlorate was used for the elution and the flow rate was 1.0 mL/min. The analyses were performed under ambient conditions.

Animals and Diets

All the experiments were performed in accordance with the Kochi Women’s University Guidelines for Animal Use and Care. Four-week-old male ICR mice (Slc:ICR, Japan SLC, Inc., Shizuoka, Japan) were used in all the experiments. Twenty-four mice were fed an AIN-93G based diet without vitamin E for the first 28 days. After that, six mice were selected randomly and liver, spleen, lung, and brain were obtained from the mice. The organs were stored at -75 °C until use. The remaining mice were randomly divided into three groups of six mice. The first group was fed a normal AIN-93 based diet for next 14 days (Normal Feed Group). The second group was given an AIN-93 based diet including VEHTM for 14 days (Test Feed Group). The third group was continuously fed an AIN-93G based diet without vitamin E for 14 days (VE-free Feed Group) (Fig. 1). The composition of the respective diets is shown in Tables 1, 2, 3, 4, and 5. The mice in each group were housed in one cage under a controlled 12-h light and 12-h dark cycle at 22 ± 2 °C and $55 \pm 15\%$ relative humidity. The mice had free access to water and fed via a powder feeder apparatus daily (Rodent CAFE, Oriental Yeast Co., Ltd., Tokyo, Japan). On the last day in the morning, mice were weighed. The liver, spleen, lung, and brain were obtained from the mice and weighed. The organs were stored at -75 °C until use.

Extraction of Fat from Organs and Analyses of Vitamin E Homologues and Tocomonoenols

The removed organs were homogenized with two times their weight of normal saline. The homogenate was placed in a test tube with a screw cap and two times the volume of a chloroform and methanol mixture (2:1, v/v) was added to the homogenate. The solution was mixed vigorously with a vortex mixer and centrifuged at $700 \times g$ for 10 min. The bottom layer was carefully removed with a Pasteur pipette and placed in a new test tube to dry under a nitrogen stream. The dried sample was solved in ethanol for HPLC analysis. The ethanol solution was subjected to the HPLC-ECD system described above to analyze the ratio of the respective vitamin E homologues in each organ and tissue examined. The actual amounts of the respective vitamin E

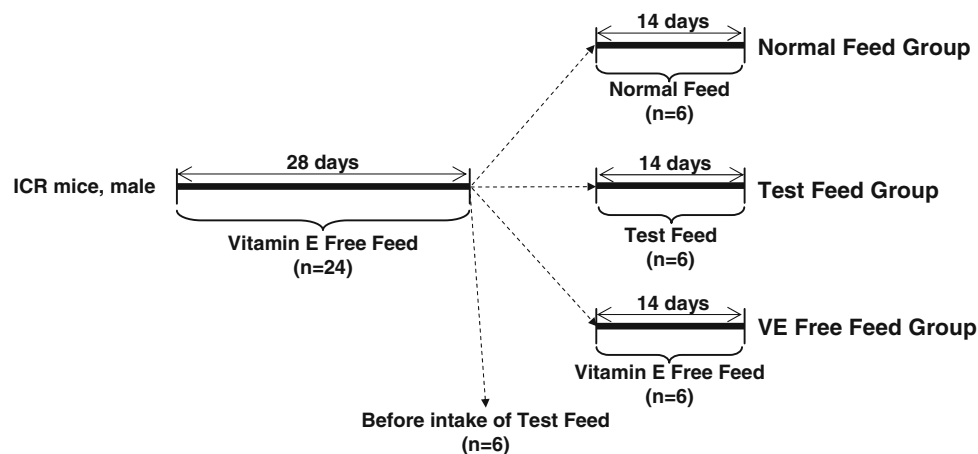


Fig. 1 Animal testing flowchart. Twenty-four mice were fed an AIN-93G diet without vitamin E for the first 28 days. After that, six mice were randomly selected to obtain liver, spleen, lung, and brain. The remaining mice were randomly divided into three groups of six mice. The first group was fed a normal AIN-93 diet for another 14 days

(Normal Feed Group); the second group was given an AIN-93 based diet that included VEHTM for another 14 days (Test Feed Group); the third group was continuously fed an AIN-93G diet without vitamin E for another 14 days (VE-free Feed Group). Finally, liver, spleen, lung, and brain of all the mice were obtained

Table 1 Basic composition of feed

Components	Relative ratio
Corn starch	62.9
Milk casein	20.0
Soybean oil	7.0
Cellulose powder	5.0
Mineral mixture ^a	3.5
Vitamin mixture ^b	1.0
Lecithin	0.3
Choline bitartrate	0.3
t-Butylhydroquinone	0.0

^a For details see Table 2

^b For details see Table 3

homologues were determined using calibration curves. The calibration curves were prepared for α -tocopherol, β -tocopherol, γ -tocopherol, and δ -tocopherol using standard solutions dissolved in ethanol. The calibration curves for α -tocopherol were also adapted for the tocomonoenols because the structure of the chroman ring of α -tocopherol is the same as that of tocomonoenol.

The VE-RBA of vitamin E homologues and tocomonoenols was calculated using the following Equation

$$\text{VE-RBA} = ([A]/[B])/([C]/[D]) \times 100$$

where [A] is the concentration of vitamin E homolog or tocomonoenol in organ (mg/g), [B] is the concentration of vitamin E homolog or tocomonoenol in VEHTM (mg/g), [C] is the concentration of α -tocopherol in organ (mg/g), and [D] is the concentration of α -tocopherol in VEHTM (mg/g).

Table 2 Composition of mineral mixture

Components	Relative ratio
CaCO ₃	35.7
KH ₂ PO ₄	19.6
K ₃ C ₆ H ₅ O ₇ ·H ₂ O	7.1
NaCl	7.4
K ₂ SO ₄	4.7
MgO	2.4
FeC ₆ H ₅ O ₇ ·H ₂ O	0.6
5ZnO·2CO ₂ ·H ₂ O	0.2
MnCO ₃	0.1
CuCO ₃ Cu(OH) ₂ ·H ₂ O	0.0
KIO ₃	0.0
Na ₂ SeO ₄	0.0
(NH ₄) ₆ Mo ₇ O ₂₄ ·4H ₂ O	0.0
Na ₂ SiO ₃ ·9H ₂ O	0.2
CrK(SO ₄) ₂ ·12H ₂ O	0.0
H ₃ BO ₃	0.0
NaF	0.0
NiCO ₃ ·2Ni(OH) ₂ ·4H ₂ O	0.0
LiCl	0.0
NH ₄ VO ₃	0.0
Sugar	22.1

Statistical Analyses

Statistical analysis was performed using one-factor ANOVA and a post hoc test (Tukey–Kramer) among the groups. Differences were considered significant when the *P* value was less than 0.05.

Table 3 Composition of vitamin mixtures

Components	Normal Feed (relative ratio)	VE-free Feed (relative ratio)	Test Feed (relative ratio)
Nicotinic acid	0.3	0.3	0.3
DL-Calcium pantothenate	0.3	0.3	0.3
Vitamin B ₆	0.1	0.1	0.1
Vitamin B ₁	0.1	0.1	0.1
Vitamin B ₂	0.1	0.1	0.1
Folic acid	0.0	0.0	0.0
D-Biotin (2%)	0.1	0.1	0.1
Vitamin B ₁₂	0.3	0.3	0.3
Vitamin E (50%)	1.5 ^c	0.0	1.5 ^d
Vitamin A (500,000 IU/g)	0.1	0.1	0.1
Vitamin D ₃ (500,000 IU/g)	0.0	0.0	0.0
Vitamin K ₁ (phyloquinone)	0.0	0.0	0.0
Sugar	97.2	98.7	97.2

^c For details see Table 4^d For details see Table 5**Table 4** Composition of vitamin E in normal feed

Components	Relative ratio
D- α -Tocopherol	69.9
D- β -Tocopherol	5.4
D- γ -Tocopherol	20.4
D- δ -Tocopherol	4.3

Table 5 Composition of vitamin E in Test Feed

Components	Relative ratio
D- α -Tocopherol	12.8
D- β -Tocopherol	15.0
D- γ -Tocopherol	13.0
D- δ -Tocopherol	12.6
MDT	12.9
α -Tocomonoenol	33.8

Results

Structure Analyses of Collected Tococomonoenols

Reverse phase HPLC-FL was used to fractionate MDT from tuna oil scum (Fig. 2). The elution order of tocopherols was δ -tocopherol, β - and γ -tocopherol, and α -tocopherol. Normally, MDT appears between the γ -tocopherol and δ -tocopherol peaks under reverse-phase HPLC conditions [8]; therefore, one of the two unidentified peaks was thought to be MDT. The two peaks were very close to each other at 32.66 and 33.70 min and it was difficult to separate each peak. Therefore, structure analyses of the compounds of each peak were conducted to identify the MDT peak and to elucidate the structure of the other compound. In the HPLC-APCI/MS, both unidentified

peaks were at m/z 428.3, corresponding to molecular ion peak $[M]^+$, and the value was within 2 of that of α -tocopherol (m/z 430.4) (Fig. 3). These results indicate that both unidentified compounds had the same molecular weight. ¹H-NMR analyses of both compounds were also performed and the results are shown in Fig. 4. One of the two peaks that appeared second in the HPLC-FL chromatogram showed characteristic triplet–quartet–quartet peaks at 5.09–5.12 ppm in ¹H-NMR spectrum (Fig. 4, right). In contrast, there was no peak around 5.10 ppm, and instead a characteristic broad singlet peak was observed at 4.69 and 4.67 ppm in the ¹H-NMR spectrum of the other compound, which appeared first in the HPLC-FL chromatogram (Fig. 4, left).

The Actual Ratio of Vitamin E Homologues in Prepared “Vitamin E Homologues and Tococomonoenols Mixture”

The prepared VEHTM was subjected to HPLC-ECD and the ratio of the respective vitamin homologues was calculated with respective calibration curves. The results are shown in Tables 1, 2, 3, 4, and 5 as “Composition of vitamin E in Test Feed”.

Biologic Availability of Tococomonoenols in Mouse

None of the mice died during the 42-day test period. The final body weight, liver weight per body weight, spleen weight per body weight, lung weight per body weight, and brain weight per body weight are shown in Table 6. Significant differences were observed in lung and brain among the groups. The contents of the vitamin E homologues and tococomonoenols in the various organs before and after

Fig. 2 HPLC-FL chromatogram of fractionated tuna oil deodorizing scum. (A) First fractionation, (B) Second fractionation

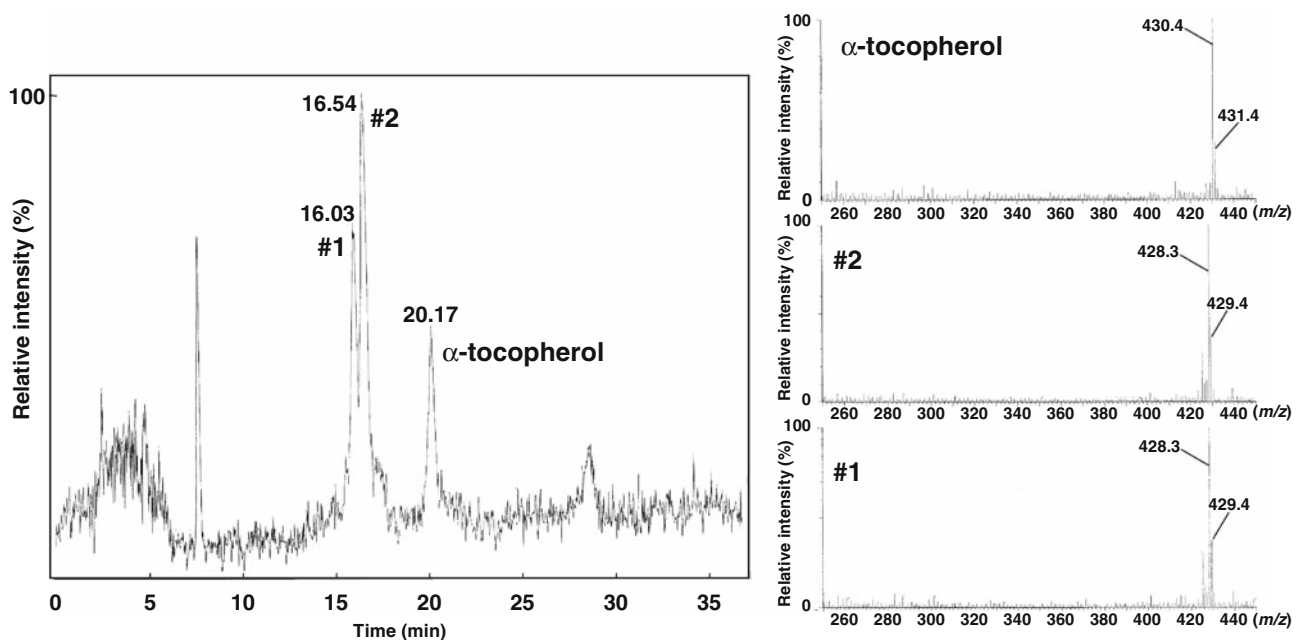
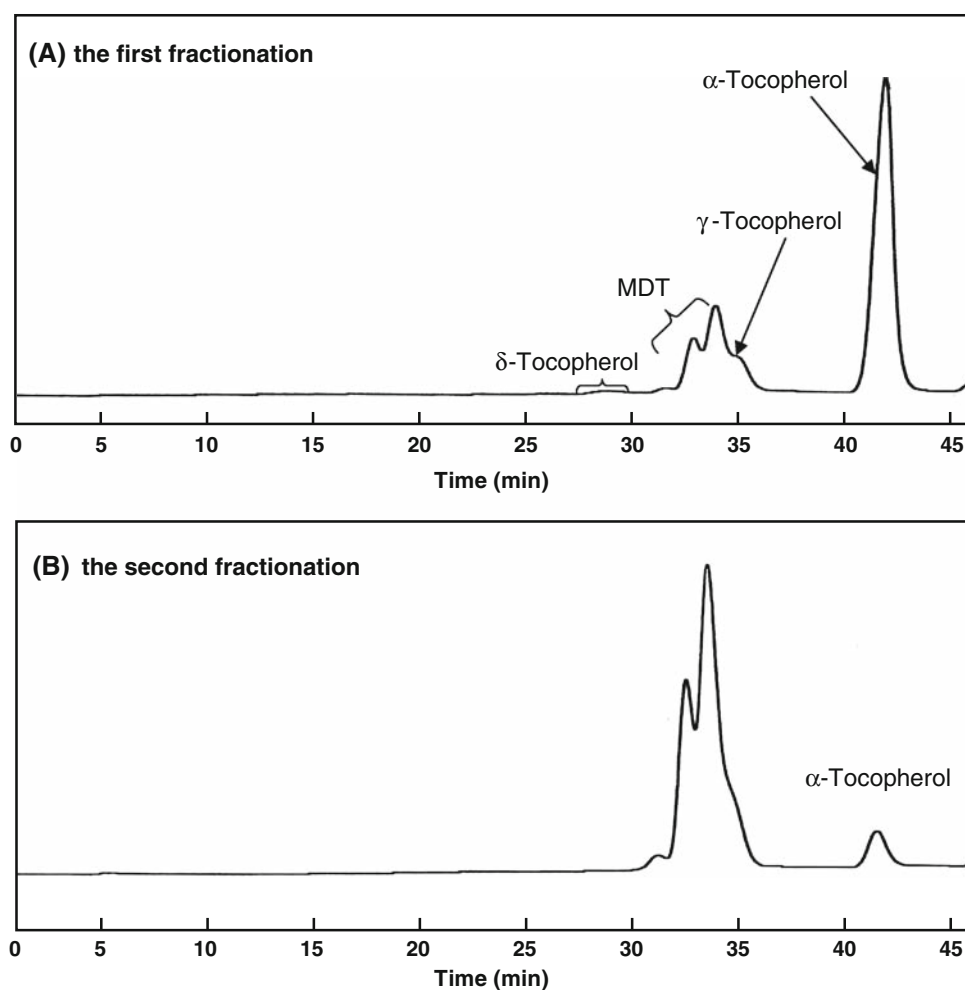


Fig. 3 LC-APCI/MS chromatogram of fractionated MDT purified from tuna oil deodorizing scum. Two peaks appeared closely at 32.66 (#1) and 33.70 (#2) min in the total ion current chromatogram (left).

The unidentified peaks were at m/z 428.3 and the value was within 2 of that of α -tocopherol (m/z 430.4) (right)

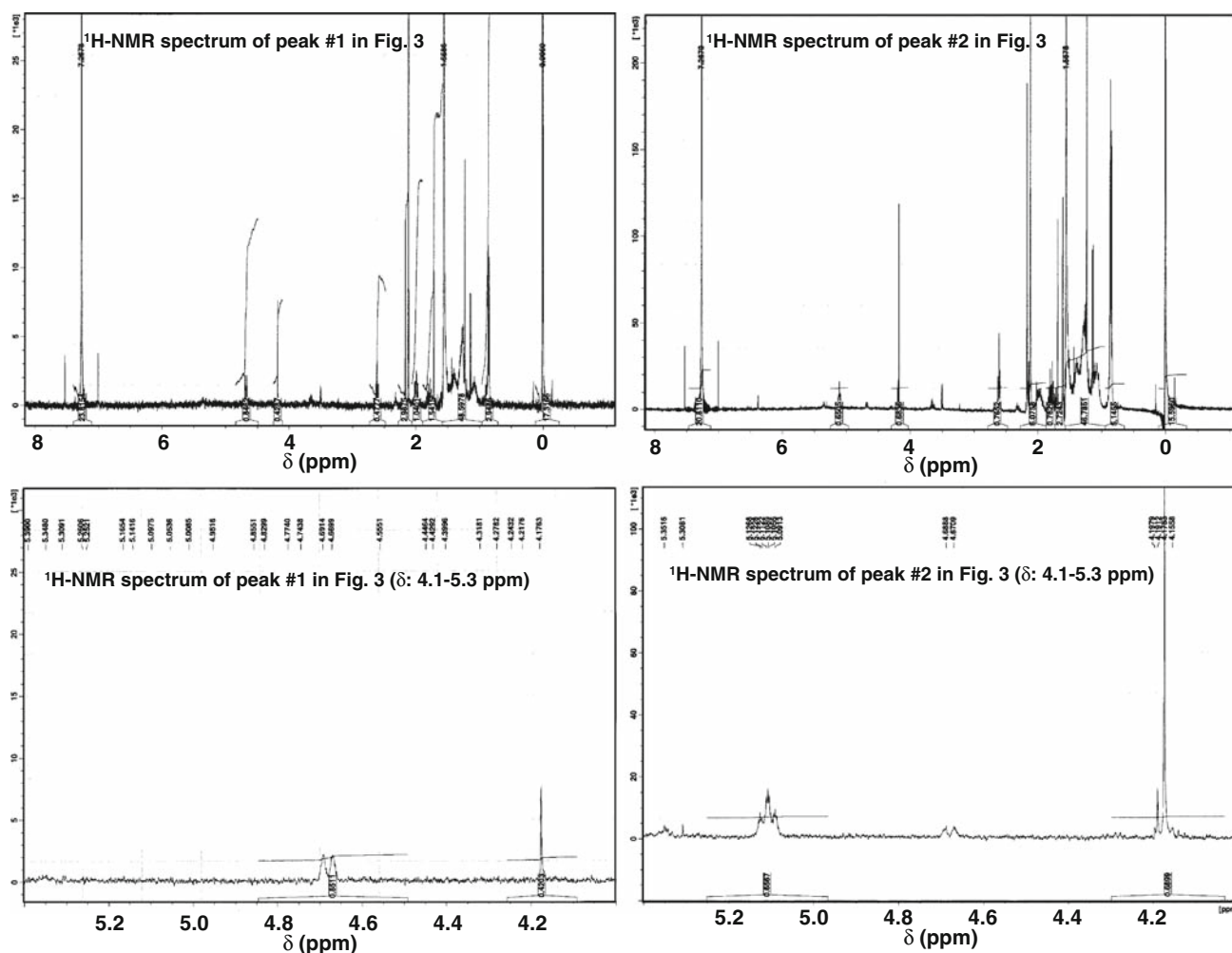


Fig. 4 $^1\text{H-NMR}$ spectra of the two unidentified compounds shown in Fig. 3. The compound that appeared second (#2) in Fig. 3 had characteristic triplet–quartet–quartet peaks at 5.09–5.12 ppm (right).

In contrast, the compound that appeared first (#1) in Fig. 3 had a characteristic broad singlet peak at 4.69 and 4.67 ppm, and no peak around 5.10 ppm (left).

Table 6 Comparison of final body weight and organ weight per body weight

	Normal Feed Group	Test Feed Group	VE-free Feed Group
Liver ^A (%)	4.8 ± 0.4	5.1 ± 0.2	4.7 ± 0.3
Lung ^A (%)	0.5 ± 0.0 ^a	0.5 ± 0.0 ^b	0.6 ± 0.1 ^{ab}
Spleen ^A (%)	0.4 ± 0.1	0.3 ± 0.0	0.3 ± 0.1
Brain ^A (%)	1.2 ± 0.1 ^{ab}	1.2 ± 0.1 ^a	1.1 ± 0.0 ^b
Body weight (g)	40.0 ± 1.8	40.4 ± 3.9	43.0 ± 1.4

Each value in the table represents the mean ± standard deviation of six samples. Mean values within each row with different superscripts are significantly different ($P < 0.05$)

^A Organ weight per body weight (%) = (Each organ weight/body weight) × 100

intake of the Test feed are summarized in Table 7. The VE-RBA of vitamin E homologues and tococomonoenols in liver and brain of the “Test Feed Group” were calculated and

are summarized in Table 8. The representative HPLC-ECD chromatograms of the liver extract are shown in Fig. 5.

Discussion

Commercially distributed natural vitamin E such as mixed tocopherol and δ -rich tocopherol are mainly prepared by molecular distillation from deodorization scum formed in the purification process of edible plant oils [18, 19]. Oil scum contains concentrated free fatty acids, sterols, and tocopherols, and therefore the deodorization scum formed from tuna oil was used as the source of MDT in the present study. MDT was present in high concentrations in the oil scum, along with the other vitamin E compounds. The molecular weights of both compounds were the same and within 2 of that of α -tocopherol (Fig. 3). This result indicates that both compounds are tococomonoenols. One of the

Table 7 Vitamin E homologue and tococomonoenol content in liver and brain before and after intake of Test Feed ($\mu\text{g/g}$ organ weight)

		α -Tocopherol	β -Tocopherol	γ -Tocopherol	δ -Tocopherol	MDT	α -Tococomonoenol
Before intake of Test Feed	Liver	Not detected	Not detected	Not detected	Not detected	Not detected	Not detected
	Brain	0.2 ± 0.3	Not detected	Not detected	Not detected	Not detected	Not detected
After intake of Test Feed	Liver	4.8 ± 2.5	0.6 ± 0.3	0.4 ± 0.2	Not detected	1.0 ± 0.5	1.7 ± 0.8
	Brain	3.2 ± 2.8	0.1 ± 0.1	Not detected	Not detected	0.3 ± 0.3	0.3 ± 0.3

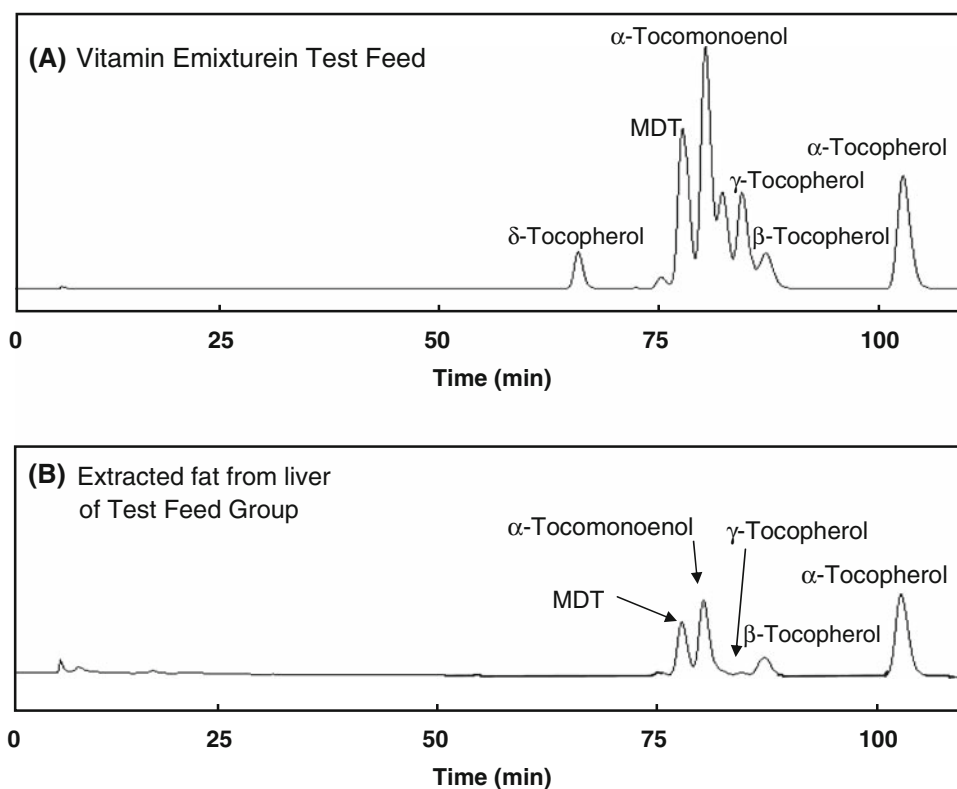
Each value in the Table represents the mean \pm standard deviation of six samples

Not detected: less than $0.1 \mu\text{g/g}$ organ weight

Table 8 Vitamin E relative biologic availability of vitamin E homologues and tococomonoenols in liver and brain

	α -Tocopherol	β -Tocopherol	γ -Tocopherol	δ -Tocopherol	MDT	α -Tococomonoenol
Liver	100 ^a	26 ± 3^b	4 ± 2^c	Not detected	49 ± 6^d	30 ± 7^b
Brain	100 ^a	5 ± 2^b	Not detected	Not detected	8 ± 1^c	4 ± 1^d

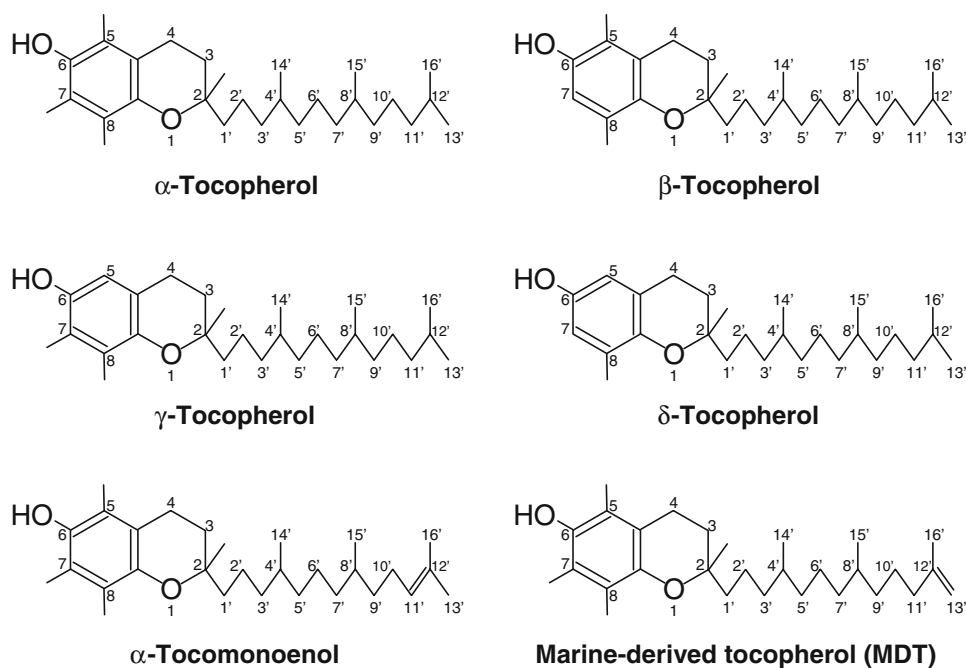
Each value in the table represents the mean \pm standard deviation of six samples. Mean values within each row with different superscripts are significantly different ($P < 0.05$)

Fig. 5 Comparison of HPLC-ECD chromatogram between (A) vitamin E mixture in Test Feed and (B) extracted fat from the liver of the Test Feed Group

two compounds that eluted afterward in two peaks had characteristic triplet–quartet–quartet peaks at 5.09–5.12 ppm in the $^1\text{H-NMR}$ spectrum (Fig. 4, right). This peak corresponds to hydrogen binding at the 11' carbon (Fig. 6). Matsumoto et al. [6] reported that α -tococomonoenol had characteristic triplet–quartet–quartet peaks at 5.12 ppm. Therefore, the compound that eluted in the second of the two peaks was thought to be α -tococomonoenol. In contrast, because the two broad singlet peaks appeared at 4.69 and 4.67 ppm corresponded to hydrogens

located at the double bond at the 13' carbon at the terminal phytol side chain, the $^1\text{H-NMR}$ spectrum of the other compound was thought to represent MDT [5]. These speculations concerning both structures is reasonable because the reverse phase HPLC-ECD chromatogram of human plasma detected α -tococomonoenol and MDT, and MDT eluted ahead of α -tococomonoenol on the chromatogram. This is a strange result because there are no reports that marine organisms contain α -tococomonoenol. Thus, α -tococomonoenol might be formed by migration of the

Fig. 6 Structures of vitamin E homologues and novel tocomonoenols



double bond in MDT. The temperature used for the deodorization of the oil is about 250°C [18], which might be sufficient to induce migration of the double bond of MDT to form α -tocomonoenol. Furthermore, the location of the double bond in α -tocomonoenol is more stable than that in MDT from a thermodynamic point of view. Consequently, the α -tocomonoenol contained in fish oil scum is thought to be formed during the deodorizing process.

The separation of α -tocomonoenol and MDT was difficult; therefore, both were fractionated at the same time and mixed with α -tocopherol, β -tocopherol, γ -tocopherol, and δ -tocopherol for preparation of the VEHTM. The objective of this study was to evaluate the VE-RBA of MDT by comparing it with that of β -tocopherol because β -tocopherol is thought to possess the highest vitamin E relative activity among vitamin E homologues with the exception of α -tocopherol [3, 4]. Therefore, the contents of the tocopherol homologues were adjusted to that of MDT. As a result, the actual ratios of tocopherols and tocomonoenols in VEHTM were not adjusted completely and the VEHTM contained a 2.5-fold greater amount of α -tocomonoenol than of the tocopherols and MDT (Tables 1, 2, 3, 4, 5). Previous studies of relative vitamin E activity for respective tocopherols demonstrated that the feeding amount of tocopherol and conditions do not affect the results [12]. Therefore, this study uses a single feeding lot. Furthermore, all the VE-RBA values of α -tocopherol, β -tocopherol, γ -tocopherol, and δ -tocopherol obtained from the liver were consistent with the previously reported values (Tables 1, 2, 3, 4, 5); therefore, the Test feeding period was thought to be appropriate.

The classical methods used to determine relative vitamin E activities of vitamin E homologues include liver-storage bioassay, inhibition rate of fetal resorption, inhibition rate of erythrocyte hemolysis, muscular dystrophy, in rat, chick, and rabbit. The relative vitamin E activities currently in use are determined by those methods. In 1991, α -TTP, which binds tocopherols and enhances its transfer between membranes, was purified from rat liver [16]. The relative affinity of vitamin E homologues for α -TTP is now considered to be the “relative vitamin E activity” value [17]. Recently, α -TTP null mice were created and used for research on the role of α -tocopherol in animals [20–22]. These mice become vitamin E-deficient, which damages the body. In the present study, ICR mice were chosen as test animals not previously used to determine the biologic availability of vitamin E using the classical methods because it is apparent that α -TTP is present in the mouse liver.

In the present study, the wash-out period for endogenous tocopherols was 28 days because Mino et al. [23] reported that endogenous tocopherols in plasma and erythrocytes were almost absent in rat after 4 weeks of continuous ingestion of a vitamin E-deficient diet. The storage level of α -tocopherol and β -tocopherol in liver of the ICR mice decreased to less than 0.10 $\mu\text{g/g}$ organ weight after ingesting a vitamin E-deficient diet for 28 days (Table 7). The objective of this experiment was to evaluate the VE-RBA of MDT in comparison with that of β -tocopherol. Therefore, α -tocopherol and β -tocopherol depletion in liver after this wash-out period was thought to be sufficient for the experiment. Storage of the tocopherol homologues and

tocomonoenol was measured in four different organs and tissues, i.e., liver, spleen, lung, and brain, because liver is the organ classically used for the determination of “relative vitamin E activity”, spleen and lung are the organs that store large amounts of α -tocopherol in rat [24], and brain tissue contains high amounts of docosahexaenoic acid, and tocopherols are thought to accumulate to prevent the oxidation of docosahexaenoic acid. There were no significant differences in relative liver and spleen weights among the groups. In contrast, there were significant differences in lung and brain, but the differences were not greater in any one group, suggesting that the mice in all groups experienced equivalent growth. After the 28-day wash-out period, the endogenous tocopherols had disappeared in all organs examined except the brain, but a fairly large amount of α -tocopherol remained in the brain (Table 7). Ingold et al. [25] and Burton et al. [26] previously reported that the turnover of α -tocopherol in the brain, testes, and spinal cord is very slow. Our result is consistent with their finding, and suggests that α -tocopherol is important for maintaining homeostasis in the brain. The tocopherol content in mouse brain in the Normal Feed and Test Feed groups was one order of magnitude higher than that in VE-free Feed group, indicating that tocopherols are transported to the brain in greater amounts, because no tocopherols were observed in spleen and lung (Table 7).

The calculated results of VE-RBA of vitamin E homologues and tocomonoenols were shown in Table 8. These VE-RBA values obtained in the present study are consistent with previously reported values [2]. The VE-RBA values for MDT and α -tocomonoenol were high. Particularly, the VE-RBA for MDT was higher than that for β -tocopherol, indicating that the two novel tocomonoenols accumulate readily in liver. On the other hand, the VE-RBA values obtained from brain were smaller than the corresponding values in the liver, likely due to the endogenous α -tocopherol remaining in the brain after the 28-day wash-out period. Nevertheless, VE-RBA for MDT was higher than that for β -tocopherol in brain. Incidentally, tocopherol and tocomonoenol accumulation was not observed in spleen and lung, even though they are representative vitamin E storage organs in rat [24]. This might be due to species-specific differences.

There is only one double bond on the phytyl side chain in MDT and α -tocomonoenol, but it is located in a different position. MDT has a double bond between the 12' and 13' carbons. The location of the double bond in α -tocomonoenol is between the 11' and 12' carbons (Fig. 6). Despite the proximity of the double bonds on the phytyl side chain, the VE-RBA for MDT and α -tocomonoenol are much different. The relative vitamin E activity for α -tocotrienol, which has the same chroman ring structure as α -tocopherol and three double bonds located on the phytyl side chain, is

reported to be 27 to 29 or 17 to 25 [2]. The relative affinity of α -tocotrienol for α -TTP is also reported to be 12.4 [17]. Therefore, it is possible that α -TTP distinguishes the structure of not only the chroman ring, but also that of the phytyl side chain. Furthermore, as the VE-RBA for MDT is significantly higher than that for α -tocomonoenol, it is also possible that α -TTP recognizes the terminal structure of the phytyl side chain.

Marine-derived tocopherol and α -tocomonoenol are contained in marine fish and rice bran, respectively. These are commonly consumed foods in Japan and are central to a macrobiotic diet. Thus, it is important to clarify the function of these tocomonoenols.

NMR Spectra of α -Tocomonoenol

^1H NMR (400 MHz, CDCl_3) δ 1.62 (d, $J = 2$ Hz, 3H, 16'-H), 1.70 (d, $J = 2$ Hz, 3H, 13'-H), 1.97 (m, 2H, 10'-H), 5.09–5.12 (tq, $J = 7, 2, 2$ Hz, 1H, 11'-H).

NMR Spectra of MDT

^1H NMR (400 MHz, CDCl_3) δ 1.72 (s, 3H, 14'-H), 1.99 (br t, $J = 7$ Hz, 2H, 11'-H), 4.67 (br s, 1H, 13'-H), 4.69 (br s, 1H, 13'-H).

Acknowledgments We thank Dr. Yasukazu Yoshida for valuable comments. This work was supported by a grant from Nippon Suisan Kaisha, Ltd., Japan.

References

- Evans HM, Bishop KS (1922) On the existence of a hitherto unrecognized dietary factor essential for reproduction. *Science* 56:650–651
- Fennema OR (1996) *Food Chemistry*, 3rd ed. Marcel Dekker, New York, pp 553–557
- Packer L, Traber MG, Kraemer K, Frei B (2002) *The antioxidant vitamin C and E*. AOCS Press, Champaign, pp 133–151
- Brigelius-Flohe R, Traber MG (1999) Vitamin E: function and metabolism. *FASEB J* 13:1145–1155
- Matsumoto A, Takahashi S, Nakano K, Kijima S (1995) Identification of new vitamin E in plant oil. *J Jpn Oil Chem Soc* 44:593–597
- Yamamoto Y, Maita N, Fujisawa A, Takashima J, Ishii Y, Dunlop WC (1999) A new vitamin E (α -tocomonoenol) from eggs of the pacific salmon. *J Nat Prod* 62:1685–1687
- Mg MH, Choo YM, Ma AN, Chuah CH, Hashim MA (2004) Separation of vitamin E (tocopherol, tocotrienol, and tocomonoenol) in palm oil. *Lipids* 39:1031–1035
- Yamamoto Y, Fujisawa A, Hara A, Dunlop WC (2001) An unusual vitamin E constituent (α -tocomonoenol) provides enhanced antioxidant protection in marine organisms adapted to cold-water environments. *Proc Natl Acad Sci USA* 98:13144–13148

9. Dunlop WC, Fujisawa A, Yamamoto Y, Moylan TJ, Sidell BD (2002) Notothenioid fish, krill and phytoplankton from Antarctica contain a vitamin E constituent (α -tocomonoenol) functionally associated with cold-water adaptation. *Comp Biochem Physiol B Biochem Mol Biol* 133:299–305
10. Dicks MW, Matterson LD (1961) Chick liver-storage bioassay of alpha-tocopherol: methods. *J Nutr* 75:165–174
11. Matterson LD, Pudalkiewicz WJ (1974) Relative potency of several forms of α -tocopherols in the chick liver storage bioassay. *J Nutr* 104:79–83
12. Leth T, Søndergaard H (1977) Biological activity of vitamin E compounds and natural materials by the resorption-gestation test, and chemical determination of the vitamin E activity in foods and feeds. *J Nutr* 107:2236–2243
13. Harris PL, Ludwig MI (1949) Relative vitamin E potency of natural and of synthetic α -tocopherol. *J Biol Chem* 179:1111–1115
14. Bunyan J, Green J, Edwin EE, Diplock AT (1960) Studies on vitamin E3. The relative activities of tocopherols and some other substances in vivo and in vitro against dilauric acid-induced haemolysis of erythrocytes. *Biochem J* 75:460–467
15. Hove EL, Harris PL (1947) Relative activity of the tocopherols in curing muscular dystrophy in rabbits. *J Nutr* 33:95–106
16. Sato Y, Hagiwara K, Arai H, Inoue K (1991) Purification and characterization of the α -tocopherol transfer protein from rat liver. *FEBS Lett* 288:41–45
17. Hosomi A, Arita M, Sato Y, Kiyose C, Ueda T, Igarashi O, Arai H, Inoue K (1997) Affinity for α -tocopherol transfer protein as a determinant of the biological activities of vitamin E analogs. *FEBS Lett* 409:105–108
18. Ghosh S, Bhattacharyya DK (1996) Isolation of tocopherol and sterol concentrate from sunflower oil deodorizer distillate. *J Am Oil Chem Soc* 73:1271–1274
19. Kim SK, Rhee JS (1982) Isolation and purification of tocopherols and sterols from soya oil deodorization. *Korean J Food Sci Technol* 14:174–178
20. Leonard OS, Terasawa Y, Farese RV Jr, Traber MG (2002) Incorporation of deuterated *RRR*- or *all-rac*- α -tocopherol in plasma and tissues of α -tocopherol transfer protein-null mice. *Am J Clin Nutr* 75:555–560
21. Vasu VT, Hobson B, Gohil K, Cross CE (2007) Genome-wide screening of alpha-tocopherol sensitive genes in heart tissue from alpha-tocopherol transfer protein null mice (ATTP^{-/-}). *FEBS Lett* 581:1572–1578
22. Tanito M, Yoshida Y, Kaidzu S, Chen ZH, Cynshi O, Jishage K, Niki E, Ohira A (2007) Acceleration of age-related changes in the retina in α -tocopherol transfer protein null mice fed vitamin E deficient diet. *Invest Ophthalmol Vis Sci* 48:396–404
23. Mino M, Kitagawa M, Nakagawa S (1981) Changes of alpha-tocopherol levels in red blood cells and plasma with respect to hemolysis induced by dialuric acid vitamin E-deficient rats. *J Nutr Sci Vitaminol* 27:199–207
24. Behrens WA, Madère R (1991) Tissue discrimination between dietary *RRR*- α - and *all-rac*- α -tocopherols in rats. *J Nutr* 121:454–459
25. Ingold KU, Burton GW, Foster DO, Hughes L, Lidsay DA, Webb A (1987) Biokinetics of and discrimination between dietary *RRR*- and *SRR*- α -tocopherols in the male rat. *Lipids* 22:163–172
26. Burton GW, Wronska U, Stone L, Foster DO, Ingold KU (1990) Biokinetics of dietary *RRR*- α -tocopherol in the male guinea pig at three dietary levels of vitamin C and two levels of vitamin E. evidence that vitamin C does not “spare” vitamin E in vivo. *Lipids* 25:199–210

Radical Scavenging Activity of Lipophilized Products from Lipase-Catalyzed Transesterification of Triolein with Cinnamic and Ferulic Acids

Wee-Sim Choo · Edward John Birch

Received: 29 July 2008 / Accepted: 16 September 2008 / Published online: 15 October 2008
© AOCS 2008

Abstract Lipase-catalyzed transesterification of triolein with cinnamic and ferulic acids using an immobilized lipase from *Candida antarctica* (E.C. 3.1.1.3) was conducted to evaluate the antioxidant activity of the lipophilized products as model systems for enhanced protection of unsaturated oil. The lipophilized products were identified using ESI-MS. Free radical scavenging activity was determined using the DPPH radical method. The polarity of the solvents proved important in determining the radical scavenging activity of the substrates. Ferulic acid showed much higher radical scavenging activity than cinnamic acid, which has limited activity. The esterification of cinnamic acid and ferulic acid with triolein resulted in significant increase and decrease in the radical scavenging activity, respectively. These opposite effects were due to the effect of addition of electron-donating alkyl groups on the predominant mechanism of reaction (hydrogen atom transfer or electron transfer) of a species with DPPH. The effect of esterification of cinnamic acid was confirmed using ethyl cinnamate which greatly enhances the radical scavenging activity. Although, compared to the lipophilized cinnamic acid product, the activity was lower. The radical scavenging activity of the main component isolated from lipophilized cinnamic acid product using solid phase extraction, monocinnamoyl dioleoyl glycerol, was as good as the unseparated mixture of lipophilized product. Based on the ratio of a substrate to

DPPH concentration, lipophilized ferulic acid was a much more efficient radical scavenger than lipophilized cinnamic acid.

Keywords Lipase-catalyzed transesterification · Cinnamic acid · Ferulic acid · Free radical scavenging activity · Antioxidant

Abbreviations

CA	Cinnamic acid
DPPH	2, 2-Diphenyl-1-picrylhydrazyl radical
EC	Ethyl cinnamate
ESI-MS	Electrospray ionization-mass spectroscopy
ESI-MS-MS	Electrospray ionization-mass spectroscopy-mass spectroscopy
ET	Electron transfer
FA	Ferulic acid
HAT	Hydrogen atom transfer
HBA	Hydrogen bond accepting
HPLC	High performance liquid chromatography
RSA	Radical scavenging activity
SPE	Solid phase extraction
TO	Triolein

Introduction

Phenolic acids are natural antioxidants that occur ubiquitously in fruits, vegetables, spices and aromatic herbs [1]. Phenolic acids are hydrophilic in character, which may reduce their antioxidant effectiveness in stabilizing fats and oils. According to Decker [2] and Massaeli et al. [3], the solubility of an antioxidant in relation to the site of oxidation is an important factor to be considered.

Presented at the 99th AOCS Annual Meeting and Expo, Seattle, Washington, USA, May 18–21, 2008.

W.-S. Choo · E. J. Birch (✉)
Department of Food Science, University of Otago, P.O. Box 56,
Dunedin 9054, New Zealand
e-mail: john.birch@stonebow.otago.ac.nz

Lipophilization of phenolic acids, which involves esterification with a lipophilic moiety is a way to utilize their antioxidative properties [4–6]. The reducing properties of phenolics as hydrogen or electron donating agents predict their potential for action as free radical scavengers [7]. Many “antioxidant” studies used 1,1-diphenyl-2-picrylhydrazyl free radical (DPPH) to describe their free radical scavenging activity [8].

Cinnamic acid, 3-phenyl-2-propenoic acid, is an unsubstituted phenylpropanoid with limited antioxidant capacity. Previous studies reported the chemical and biocatalytic synthesis of cinnamoyl esters and glycerols [9, 10]. A recent work examined the kinetics of chemical esterification of glycerol with cinnamic acid and its derivatives [11]. As cinnamic acid has the backbone structure of the phenyl propanoids or cinnamic acid derivatives group of known antioxidants, Karboune et al. [12] investigated the lipase-catalyzed transesterification of cinnamic acid with triolein and found that the resulting mixture of cinnamoylated lipids had higher radical (DPPH) scavenging activity than that of cinnamic acid. Ferulic acid, present naturally in flaxseeds, is one of the ubiquitous compounds in nature. According to Kikuzaki et al. [13], ferulic acid and its esters have been recognized as antioxidants. The radical (DPPH) scavenging activity of ferulic acid was better than that of a series of alkyl ferulates [13] and ethyl ferulate [14]. However, in an ethanol-buffer solution of linoleic acid at 40 °C in the dark, the alkyl ferulates showed better antioxidant activity than that of ferulic acid [13]. A study by Safari et al. [15] involving the lipase-catalyzed transesterification of triolein with ferulic acid showed that the radical (DPPH) scavenging activity of feruloylated lipids was lower than ferulic acid.

The main objectives of this research were to characterize the lipophilized products from lipase-catalyzed transesterification of triolein (a model triacylglycerol having no antioxidant present) with cinnamic and ferulic acids and to evaluate their free radical scavenging activity as model systems for enhancement of antioxidant activity of unsaturated oils (usually with some levels of antioxidants present). Another objective of this research was to extend the work of Karboune et al. [12] by isolating and separating the cinnamoylated lipid classes produced by lipase-catalyzed transesterification of triolein with cinnamic acid to examine their structure-enhanced-activity relationship.

Experimental Procedure

Materials

Commercially available immobilized lipase B from *Candida antarctica* [E.C. 3.1.1.3; Novozym 435, with an

activity of 10,000 propyl laurate units per solid gram (PLU)], was a gift from Novozymes (Bagsværd, Denmark). Cinnamic acid (CA), ferulic acid (FA), triolein (TO), ethyl cinnamate (EC) and 2,2-diphenyl-1-picrylhydrazyl (DPPH) were purchased from Sigma Chemicals Co. (St Louis, MO, USA). Mega Bond Elut aminopropyl disposable columns (5 g) were purchased from Varian Sample Preparation Products (Harbor City, CA, USA). All the chemicals and solvents used were of analytical or HPLC grade.

Enzymatic Transesterification

The enzymatic transesterification of TO with CA or FA was carried out according to a modified method of Karboune et al. [12]. TO (1,000 mg) was dissolved in 10 mL of *n*-hexane in a 50 mL Erlenmeyer flask. CA (167 mg) or FA (55 mg) was added to the reaction mixture followed by Novozym 435 (236 mg for CA system; 211 mg for FA system). The mol ratio of TO:CA and TO:FA was 1:1 and 4:1, respectively. The flask was incubated under nitrogen at 50 °C, with continuous shaking, in an orbital shaker at 120 rpm (Model SS70, Chiltern Scientific, Auckland, New Zealand) for 2 weeks. The enzymatic reaction was stopped by termination of contact with immobilized lipase by filtration using Whatman glass microfiber filter paper C.

Removal of Unreacted CA/FA by Aqueous Solvent Washing of Reaction Components

The above product in *n*-hexane was washed with four volumes of acetone:methanol:water (7:7:6; 6 mL). This was followed by drying the recovered hexane fraction under nitrogen at room temperature.

Hydrolysis of Lipophilized Products for Quantification

Lipophilized products free from unreacted CA or FA (2.0–7.0 mg) were weighed into a glass tube (15.0 cm × 1.3 cm with Teflon-lined screw cap). One mL of 4 N methanolic NaOH was added and the hydrolysis was carried out under nitrogen at 50 °C for 3 h, followed by acidification with concentrated HCl. Acidity was checked using Litmus paper. This solution was then evaporated to dryness. The dried sample was dissolved in 2 mL isopropanol:hexane (4:1) prior to HPLC analysis.

The conversion of CA or FA was calculated as w/w ratio of CA or FA released from the hydrolysis of lipophilized products to its initial amount. Quantification was based on an external standard method where a calibration curve [25, 50, 75, 100, 125 and 150 µg CA or FA dissolved in 1 mL of isopropanol:hexane (4:1)] was prepared.

HPLC Analysis of Reaction Components

The enzymatic reaction components were monitored by HPLC analysis, according to the method of Sabally et al. [16]. The separation of reaction components was performed on a C-18 Phenosphere-Next column (250 × 4.6 mm, 5 μm; Phenomenex, Torrance, CA, USA.) using a Varian 9010 solvent delivery system (Varian Associates, Inc., Walnut Creek, CA, USA), a SPD-M10AV diode array detector (Shimadzu, Kyoto, Japan) and an analyzing software, Shimadzu Class-M10A. Detection of reaction components was achieved at 215 and 280 nm (CA system) and 215 and 290 nm (FA system). These wavelengths, 280 and 290 nm, were selected from the absorption spectrum of CA and FA, respectively. Elution of a 20 μL injected sample was carried out with a gradient system using an acetonitrile/methanol mixture (7:5, vol/vol) as solvent A and isopropanol as solvent B; the elution was initiated by a flow of 100% solvent A for 10 min, followed by a 20 min linear gradient to 100% solvent B, which was maintained for an additional 5 min. The flow rate was 1 mL/min. Typically, a 10 min equilibration period was used between samples, requiring about 45 min/sample.

Electrospray Ionization-Mass Spectroscopy (ESI-MS) and Electrospray Ionization-Mass Spectroscopy–Mass Spectroscopy (ESI-MS–MS) Analysis of Reaction Components

The reaction components were recovered by HPLC and analyzed using an ESI-MS system, Bruker microTOFQ (Bruker Daltronics, Bremen, Germany). Samples were introduced using direct infusion into the ESI source in a positive mode with a collision energy of 10 eV. Capillary voltage of –4.5 kV and a dry gas of 99% N₂ at 180 °C were employed. Sampling was averaged for 3 min over a *m/z* range of 100–1,000 amu. The mass was calibrated using an external calibrant of sodium formate clusters. Spectra were processed using Compass software version 1.3 (Bruker Daltronics, Bremen, Germany). Selected ions that were tentatively identified were chosen to undergo

further analysis by ESI-MS–MS with collision energy between 20–40 eV.

Separation of Lipophilized Products of Lipase-Catalyzed Transesterification of TO and CA Using Solid Phase Extraction (SPE)

A method of Vaghela and Kilara [17] using an aminopropyl bonded phase to separate lipid mixtures was modified in this study to separate the lipophilized products. Two aminopropyl Mega Bond Elut columns (5 g) were used in the separation and each column was preconditioned with 2 × 20 mL of hexane before applying the sample. Sample (40 mg) was dissolved in 2 mL of hexane and applied to the first column. Then the column was sequentially eluted with 60 mL of each solvent A, B and C, eluting the respective components as indicated in Table 1. After separation, solvents from each SPE eluent were evaporated using a rotary vacuum evaporator. The fractions from solvent A and B were combined and dissolved in 2 mL of hexane before loading on a second aminopropyl column. Then the column was sequentially eluted with 30 and 60 mL of solvents D and E, respectively, eluting the indicated components (Table 1). Again, eluting solvents were removed using a rotary vacuum evaporator. All fractions were stored at –20 °C until further analysis.

Determination of Radical Scavenging Activity (%RSA)

The %RSA of compounds was measured using a modified DPPH radical method of Sabally et al. [16]. The concentration of sample and DPPH solution was modified to suit the rate of reactivities of the samples analyzed here. For the evaluation of free radical scavenging activity of the FA system, four samples were tested [TO, FA, lipophilized product including unreacted TO from lipase-catalyzed transesterification of TO and FA following aqueous solvent washing to remove unreacted FA (abbreviated as TOFA) and mixture of TO and FA]. TO and TOFA concentrations were set at 25.0 mM. The amount of FA tested was equivalent to the amount of FA esterified to the oleoyl

Table 1 Solvents required for SPE with Mega Bond Elut aminopropyl column of reaction components of lipase-catalyzed reaction of TO and CA

Name	Solvents	Amount (mL)	Components eluted
A	1% (vol/vol) Diethyl ether, 10% (vol/vol) dichloromethane in hexane	60	TO, monocinnamoyl dioleoyl glycerol and dicinnamoyl oleoyl glycerol
B	10% (vol/vol) Diethyl ether, 10% (vol/vol) dichloromethane in hexane	60	Monocinnamoyl dioleoyl glycerol and dicinnamoyl oleoyl glycerol
C	2:1 (vol/vol) Chloroform/methanol	60	Monocinnamoyl oleoyl glycerol
D	5% (vol/vol) Diethyl ether in hexane	30	TO
E	15% (vol/vol) Diethyl ether in hexane	60	Monocinnamoyl dioleoyl glycerol

glycerols of TO in TOFA. The sample for analysis was mixed with 2×10^{-4} M DPPH solution in ethanol or ethyl acetate. The ratio of a substrate to DPPH concentration was $1:8 \times 10^{-3}$. The reduction of DPPH radical was monitored spectrophotometrically at 517 nm over a period of 30 min against a blank assay. The percentage of the remaining radical was calculated as the absorbance of the sample at 517 nm, divided by that of the DPPH control at the same time, multiplied by 100.

For the evaluation of %RSA of the CA system, seven samples were tested [TO, CA, lipophilized product including unreacted TO from lipase-catalyzed transesterification of TO and CA following aqueous solvent washing to remove unreacted CA (abbreviated as TOCA), mixture of TO and CA, ethyl cinnamate (EC), monocinnamoyl dioleoyl glycerol (OOCA) and monocinnamoyl oleoyl glycerol (OCAOH)]. Due to the limited fractions of cinnamoylated lipid obtained from SPE, the sample for analysis was mixed with 5×10^{-6} M DPPH solution in dichloromethane. The concentration of the six samples containing a CA moiety or addition of CA was set at 5.5 mM of CA equivalents to examine the structure–activity relationship. TO concentration was set at 5.5 mM. The ratio of a substrate to DPPH concentration was $1:9.1 \times 10^{-4}$. The reduction of DPPH was monitored spectrophotometrically at 517 nm over a period of 30 min, against a blank assay. The percentage of the remaining radical was calculated as the absorbance of the sample at 517 nm, divided by that of the DPPH control at the same time, multiplied by 100.

Results and Discussion

Figure 1 shows a chromatogram of reaction components of lipase-catalyzed transesterification of TO and CA after aqueous solvent washing. TO was detected at 215 nm. Lipophilized products and CA were detected at both 215 nm and 280 nm. Three lipophilized products were observed at the retention times of 9.734, 15.418 and 27.029 min at 280 nm. Using an external standard of TO, TO was detected at the retention time of 32.219 min at 215 nm. The extent of conversion of CA to lipophilized products was determined most accurately by measuring the amount of CA released from the hydrolysis of reaction components (after aqueous solvent washing) using HPLC. Quantification of CA was carried out using an external standard of CA. The average percentage conversion of CA in this lipase-catalyzed transesterification of TO and CA was 45.3%.

The identification of the 3 lipophilized product peaks of lipase-catalyzed transesterification of TO with CA was determined using ESI-MS (Table 2). The first peak at

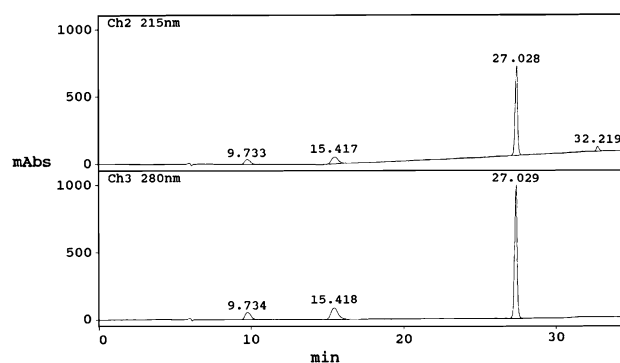


Fig. 1 HPLC chromatogram at 215 and 280 nm of reaction components of lipase-catalyzed transesterification of TO and CA after removal of enzyme followed by aqueous solvent washing. Peaks were identified as follows: monocinnamoyl oleoyl glycerol (9.734); dicinnamoyl oleoyl glycerol (15.418); monocinnamoyl dioleoyl glycerol (27.029); triolein (32.219)

9.734 min at 280 nm in Fig. 1 was found to be monocinnamoyl oleoyl glycerol, with two positions on the glycerol having acyl groups (one CA and one oleic acid) and one position having a hydroxyl group (–OH) group. Peak 15.418 and 27.029 min at 280 nm in Fig. 1 were found to be dicinnamoyl oleoyl glycerol and monocinnamoyl dioleoyl glycerol, respectively. Karboune et al. [12] reported the formation of two molecular species (monocinnamoyl oleoyl glycerol and monocinnamoyl dioleoyl glycerol) but no dicinnamoyl product. This may be due to the use of different HPLC elution solvent, wavelength of UV detection (235 nm) and evaporative light scattering detection employed by Karboune et al. [12]. Karboune et al. [12] has indicated that a minor peak obtained using HPLC with both UV and evaporative light scattering detector has the presence of a phenolic ring in its structural formula but only suggested it to be a product of side-reaction with CA.

Figure 2 shows a chromatogram of reaction components of lipase-catalyzed transesterification of TO and FA after aqueous solvent washing. TO was detected at 215 nm. Lipophilized products and FA were detected at both 215 and 290 nm. Two lipophilized products were observed at the retention times of 6.009 and 22.451 min at 290 nm. Using an external standard of TO, TO was detected at the retention time of 32.241 min at 215 nm. The average percentage conversion of FA in this lipase-catalyzed transesterification of TO and FA was 24.8%. The percentage conversion of FA was lower than that of CA. These results were in agreement with that of Guyot et al. [18] for the esterification of cinnamic and ferulic acids with fatty alcohols. The difference in the reaction conversion was due to the electronic distribution of the phenolic acids which affected the reactivity of the carboxylic function [4, 18].

The identification of the two lipophilized product peaks of lipase-catalyzed transesterification of TO with FA was

Table 2 Summary of ESI-MS and ESI-MS–MS data of lipophilized products of lipase-catalyzed transesterification of TO and CA

Lipophilized products	HPLC (280 nm) retention time (min)	Molecular weight	ESI-MS (M + 23) ⁺	ESI-MS–MS fragmentation ^a
Monocinnamoyl oleoyl glycerol	9.734	486	509	339 [–CA] 205 [–C18:1]
Dicinnamoyl oleoyl glycerol	15.418	616	639	469 [–CA] 335 [–C18:1]
Monocinnamoyl dioleoyl glycerol	27.029	750	773	603 [–CA] 469 [–C18:1]

(M + 23)⁺ represents the protonated molecular ion with a sodium (mass = 23)

^a The ESI-MS–MS fragment ions were protonated with hydrogen instead of sodium

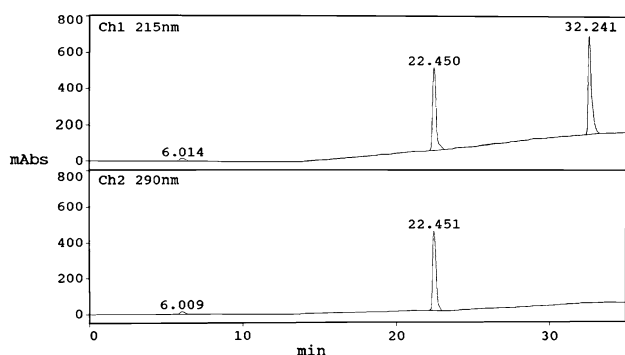


Fig. 2 HPLC chromatogram at 215 and 290 nm of reaction components of lipase-catalyzed transesterification of TO and FA after removal of enzyme followed by aqueous solvent washing. Peaks were identified as follows: monoferuloyl oleoyl glycerol (6.009); monoferuloyl dioleoyl glycerol (22.451), triolein (32.241)

determined using ESI-MS (Table 3). The first peak at 6.009 min at 290 nm in Fig. 2 was found to be monoferuloyl oleoyl glycerol, with two positions on the glycerol having acyl groups (one FA and one oleic acid) and one position having a hydroxyl (–OH) group. Peak 22.451 min at 290 nm in Fig. 2 was found to be monoferuloyl dioleoyl glycerol. Diferuloyl oleoyl glycerol was not detected in this study. These results were in agreement with the findings of Safari et al. [15].

Based on the study conducted here on the transesterification of TO with CA or FA by Novozym 435, an adaptation of the reaction scheme proposed by Safari et al. [15] is shown in Scheme 1. According to Laszlo and Compton [19], triacylglycerol could not serve as an acyl acceptor directly. Triacylglycerol must first undergo hydrolysis to generate a diacylglycerol containing a free hydroxyl group. The generated diacylglycerol then reacts with a phenolic acid to produce a phenolic lipid.

A substrate may react with DPPH via two different mechanisms: (1) a direct abstraction of a hydrogen atom by DPPH (hydrogen atom transfer, HAT reactions) and (2) an electron-transfer process to DPPH (electron transfer, ET reactions) [20]. The mechanisms for reaction of a substrate in the FA system with DPPH (adapted from Foti et al. [20] and Foti [21]) is shown in Scheme 2. The electron transfer

mechanism (k_1) would be favored in this system due to the substituted hydroxyl group on the benzene ring. Hydrogen bond accepting (HBA) solvents can favor the ET reaction (k_1) because of the stabilizing effect on the phenoxyl anion (ArO^-) and therefore accelerate the overall process but at the same time, HBA solvents can block the substrate into a hydrogen-bonded complex (k_3) making it unreactive toward the DPPH radical [21, 22]. It would be the fine balance of these opposing effects of solvation that determines the final effect of the solvent on the inhibition of free radical scavenging activity of a substrate [22]. Ethanol is the commonly used solvent in the DPPH test [23] and was the solvent used by Karboune et al. [12], Sabally et al. [16, 24, 25] and Safari et al. [15] in their investigation of free radical scavenging activity of phenolic lipids toward the stable free radical DPPH. Ethyl acetate was found by Espin et al. [26] in their characterization of the free radical capacity of vegetable oils and oil fractions using DPPH to give the best results. Other solvents investigated by Espin et al. [26] included hexane, chloroform, acetone and ether.

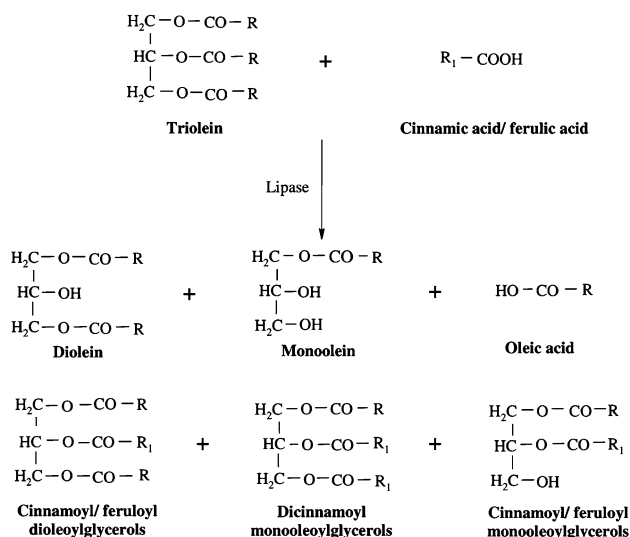
The %RSA of the FA system was tested in ethanol and ethyl acetate (Fig. 3). The HBA ability (the β^{H} parameter) of ethanol and ethyl acetate was 0.44 [27] and 0.45 [28], respectively. However, the slightly higher %RSA obtained for FA in ethanol (96.1%) than that in ethyl acetate (87.6%) indicates that the polarity of the solvent and solubility of FA may have affected its free radical scavenging activity. The relatively more polar ethanol may have increased the ET reaction rate of FA. When FA was added to TO and mixed, %RSA obtained for this mixture (TO + FA) was similar to that of FA, due to TO not having any free radical scavenging activity. TOFA underwent aqueous solvent washing to remove unreacted FA. The %RSA of washed TOFA tested in ethanol (65.9%) was lower than that in ethyl acetate (72.2%). The relatively more non-polar ethyl acetate may have increased the HAT reaction of TOFA. This reverse effect of solvent in free radical scavenging activity of TOFA as compared to that of FA again indicates that the polarity of the solvent and solubility of a substrate may have affected its free radical scavenging activity. The decrease in free radical scavenging activity after esterification of the carboxyl group of FA in this study was in

Table 3 Summary of ESI-MS data of lipophilized products of lipase-catalyzed transesterification of TO and FA

Lipophilized products	HPLC (290 nm) retention time (min)	Molecular weight	ESI-MS ($M + 23$) ⁺	ESI-MS-MS fragmentation ^a
Monoferuloyl oleoyl glycerol	6.009	532	555	339 [-FA] 251 [-C18:1]
Monoferuloyl dioleoyl glycerol	22.451	796	819	603 [-FA] 515 [-C18:1]

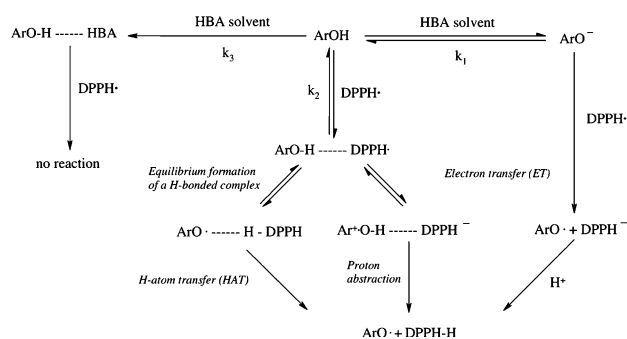
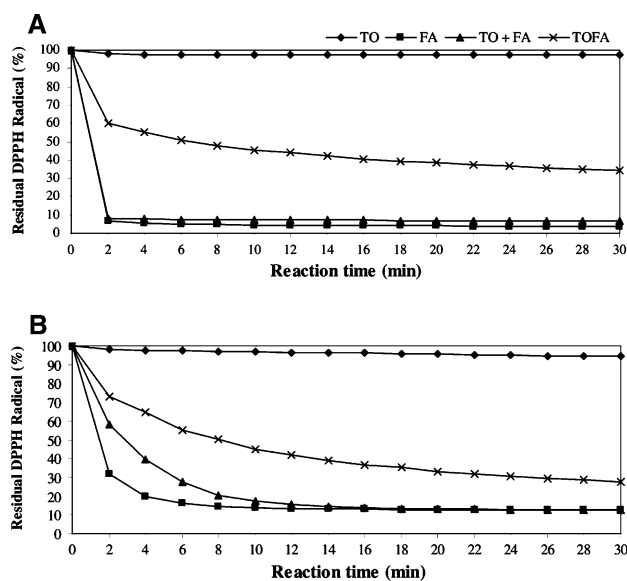
($M + 23$)⁺ represents the protonated molecular ion with a sodium (mass = 23)

^a The ESI-MS-MS fragment ions were protonated with hydrogen instead of sodium

**Scheme 1** Reaction scheme of lipase-catalyzed transesterification of TO with CA or FA. Adapted from Safari et al. [15]

agreement with the findings of Kikuzaki et al. [13] and Safari et al. [15]. These decreases are most likely due to the addition of an alkyl group to the carboxylic ethylene side chain of TOFA which may donate electrons inductively to the benzene ring and have less stabilizing effect on the ionization (k_1 in Scheme 2). The rate of ET reaction for TOFA would therefore be slower than that of FA and hence a lower free radical scavenging activity for TOFA.

The DPPH scavenging analysis carried out on TOCA using ethanol and ethyl acetate showed solvent interaction that precluded the measurement of its free radical scavenging activity. Upon mixing TOCA with DPPH, the absorbance increased and was higher than DPPH control. TOCA was then tested in ethanol and ethyl acetate without DPPH and again showed an increase in its absorbance. This interaction of TOCA with these two solvents may be due to a certain effect of solubility on the absorbance.

**Scheme 2** Mechanisms of reaction of a substrate in the FA system with DPPH. Adapted from Foti et al. [20] and Foti [21]. *ArOH* A hydroxyl-substituted phenylpropanoid substrate, *HBA* hydrogen bond accepting**Fig. 3** Time course for DPPH radical scavenging activity of FA system tested in ethanol (a) and ethyl acetate (b). Lipophilized product including unreacted TO from the lipase-catalyzed transesterification of TO and FA was abbreviated as TOFA. TOFA underwent aqueous solvent washing to remove unreacted FA. The mixture of TO and FA was abbreviated as TO + FA

The reaction pathway involving the ET mechanism was not favored in the CA system as there was no hydroxyl group substituent on the benzene ring of CA. A moderately polar aprotic solvent which cannot serve as a hydrogen-

bond donor, dichloromethane [29], was selected instead to evaluate the free radical scavenging activity of the CA system (Fig. 4). Dichloromethane was tested for any solvent interaction with TOCA and there was found to be none. In this solvent, the predominant mechanism for reaction of a substrate in the CA system with DPPH would be a HAT mechanism. No free radical scavenging activity was obtained for TO (Fig. 4). CA and the mixture (TO + CA) showed very little free radical scavenging activity. This is in accordance with the results obtained for CA in ethanol by Karboune et al. [12]. The %RSA of EC at 30 min of reaction was 45.2%. EC is more known as a compound with strong sensory properties at low threshold [30]. According to Bhatia et al. [31], EC was approved by the FDA as a flavoring agent. To the authors' best knowledge, there has not been study reporting the free radical scavenging activity of EC. The %RSA of TOCA at 30 min of reaction was 63.9%. These results indicate that esterification of the carboxyl group of CA resulted in an increase in the free radical scavenging activity and were in agreement with the findings of cinnamoylated lipids by Karboune et al. [12].

The increase in the free radical scavenging activity of TOCA and EC is most likely due to replacement of the carboxylic H at the $-\text{CH}=\text{C}-\text{COOH}$ part of the CA with an alkyl (C_2H_5) group (in the case of EC) and a larger alkyl group (in the case of TOCA). Alkyl substituents (such as CH_3) in substituted benzenes may donate electrons inductively to the benzene ring compared with a hydrogen. Electron-donating substituents thereby increase the reactivity of the benzene ring toward electrophilic substitution [32]. The addition of alkyl groups to the carboxylic

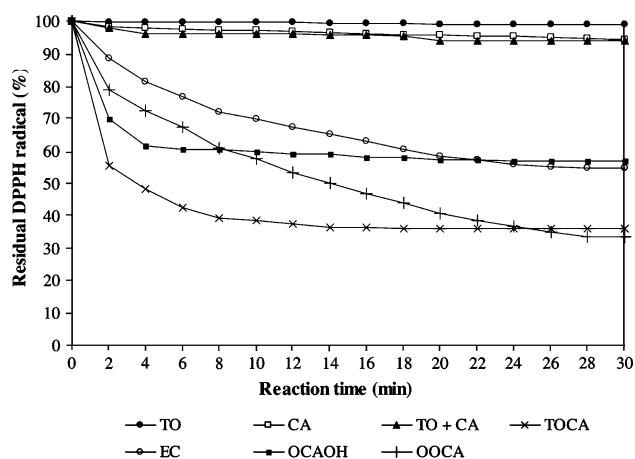


Fig. 4 Time course for DPPH radical scavenging activity of CA system tested in dichloromethane. Lipophilized product including unreacted TO from the lipase-catalyzed transesterification of TO and CA was abbreviated as TOCA. TOCA underwent aqueous solvent washing to remove unreacted CA. The mixture of TO and CA was abbreviated as TO + CA. EC Ethyl cinnamate, OOCA monocinnamoyl dioleoyl glycerol, OCAOH monocinnamoyl oleoyl glycerol

ethylene side chain of TOCA and EC may have increased the reactivity of the benzene ring towards a HAT reaction. According to Morrison and Boyd [33], the electron-donating strength of alkyl groups in carboxylic acids increases with alkyl chain length. The electron-donating strength of a longer alkyl group in TOCA may be greater than the alkyl (C_2H_5) group in EC and hence a higher rate of HAT reaction from TOCA to the DPPH than that in EC. Therefore, the rate of the HAT reaction of TOCA was faster than that of EC and very much faster than CA.

It was probable that dicinnamoyl oleoyl glycerol (OCAOCA) has free radical scavenging activity but it was not tested because it was not obtained individually by SPE. Overall, the components of TOCA, with a calculated ratio of OCAOH:OCAOCA:OOCA (1:2.1:7.7) based on CA equivalents and (1:2.6:12) on a molecular basis respectively, have each contributed to the free radical scavenging activity of TOCA. The %RSA at 30 min of reaction of OOCA was greater than that of OCAOH, which gave a similar activity to EC (Fig. 4). At 30 min of reaction, the free radical scavenging activity of TOCA was as good as OOCA. This was very likely as the main component in TOCA was OOCA on CA equivalents or molecular basis and a synergistic effect by OCAOCA and/or OCAOH on OOCA may have reinforced its individual action. This synergism was well documented for mixtures of hindered and non-hindered phenols [14].

Conclusions

The %RSA of FA was comparatively very high compared to CA, which showed limited activity. These results were in agreement with those of Velkov et al. [34]. Based on the ratio of a substrate to DPPH concentration tested, TOFA was comparatively a much better free radical scavenger than TOCA although the difference in solvents selected needs to be considered here. The choice of solvent for the DPPH assay is critical in evaluating the free radical scavenging activity of substrates of differing polarity, and support previous observations by other authors [2, 3] that the solubility of an antioxidant in relation to the site of oxidation is an important factor for consideration on the use of antioxidants. The synthesis and evaluation of the free radical scavenging activity of TOCA and TOFA in this study serves as model systems for the evaluation of free radical scavenging activity of the lipophilized products from lipase-catalyzed transesterification of unsaturated oil with cinnamic and ferulic acids under the same conditions.

Acknowledgments The funding provided by University of Otago Research and Enterprise Office to the author Wee Sim Choo for writing up this paper was greatly appreciated.

References

1. Silva FAM, Borges F, Ferreira MA (2001) Effects of phenolic propyl esters on the oxidative stability of refined sunflower oil. *J Agric Food Chem* 49:3936–3941
2. Decker EA (1998) Strategies for manipulating the prooxidative/antioxidative balance of foods to maximize oxidative stability. *Trends Food Sci Technol* 9:241–248
3. Massaeli H, Sobrattee S, Pierce GN (1999) The importance of lipid solubility in antioxidants and free radical generating systems for determining lipoprotein peroxidation. *Free Radical Biol Med* 26:1524–1530
4. Buisman GJH, van Helteren CTW, Kramer GFH, Veldsink JW, Derksen JTP, Cuperus FP (1998) Enzymatic esterifications of functionalized phenols for the synthesis of lipophilic antioxidants. *Biotechnol Lett* 20:131–136
5. Stamatis H, Sereti V, Kolisis FN (1999) Studies on the enzymatic synthesis of lipophilic derivatives of natural antioxidants. *J Am Oil Chem Soc* 76:1505–1510
6. Figueroa-Espinoza M-C, Villeneuve P (2005) Phenolic acids enzymatic lipophilization. *J Agric Food Chem* 53:2779–2787
7. Rice-Evans CA, Miller NJ, Paganga G (1997) Antioxidant properties of phenolic compounds. *Trends Plant Sci* 2:152–159
8. Hermans N, Cos P, Maes L, De Bruyne T, Berghe DV, Vlietinck AJ, Pieters L (2007) Challenges and pitfalls in antioxidant research. *Curr Med Chem* 14:417–430
9. Batovska DI, Kishimoto T, Bankova VS, Kamenarska ZG (2005) Synthesis of some phenylpropanoid monoglycerides via the Mitsunobu protocol. *Molecules* 10:552–558
10. Vosmann K, Weitkamp P, Weber N (2006) Solvent-free lipase-catalyzed preparation of long-chain alkyl phenylpropanoates and phenylpropyl alkanooates. *J Agric Food Chem* 54:2969–2976
11. Holser RA (2008) Kinetics of cinnamoyl glycerol formation. *J Am Oil Chem Soc* 85:221–225
12. Karboune S, Safari M, Lue BM, Yeboah FK, Kermasha S (2005) Lipase-catalyzed biosynthesis of cinnamoylated lipids in a selected organic solvent medium. *J Biotechnol* 119:281–290
13. Kikuzaki H, Hisamoto M, Hirose K, Akiyama K, Taniguchi H (2002) Antioxidant properties of ferulic acid and its related compounds. *J Agric Food Chem* 50:2161–2168
14. Nenadis N, Zhang HY, Tsimidou MZ (2003) Structure-antioxidant activity relationship of ferulic acid derivatives: effect of carbon side chain characteristic groups. *J Agric Food Chem* 51:1874–1879
15. Safari M, Karboune S, St-Louis R, Kermasha S (2006) Enzymatic synthesis of structured phenolic lipids by incorporation of selected phenolic acids into triolein. *Biocatal Biotransform* 24:272–279
16. Sabally K, Karboune S, St-Louis R, Kermasha S (2006) Lipase-catalyzed transesterification of trilinolein or trilinolenin with selected phenolic acids. *J Am Oil Chem Soc* 83:101–107
17. Vaghela MN, Kilara A (1995) A rapid method for extraction of total lipids from whey protein concentrates and separation of lipid classes with solid phase extraction. *J Am Oil Chem Soc* 72:1117–1121
18. Guyot B, Bosquette B, Pina M, Graille J (1997) Esterification of phenolic acids from green coffee with an immobilized lipase from *Candida antarctica* in solvent-free medium. *Biotechnol Lett* 19:529–532
19. Laszlo JA, Compton DL (2006) Enzymatic glycerolysis and transesterification of vegetable oil for enhanced production of feruloylated glycerols. *J Am Oil Chem Soc* 83:765–770
20. Foti MC, Daquino C, Geraci C (2004) Electron-transfer reaction of cinnamic acids and their methyl esters with the DPPH radical in alcoholic solutions. *J Org Chem* 69:2309–2314
21. Foti MC (2007) Antioxidant properties of phenols. *J Pharm Pharmacol* 59:1673–1685
22. Foti M, Ruberto G (2001) Kinetic solvent effects on phenolic antioxidants determined by spectrophotometric measurements. *J Agric Food Chem* 49:342–348
23. Nenadis N, Tsimidou M (2002) Observations on the estimation of scavenging activity of phenolic compounds using rapid 1, 1-diphenyl-2-picrylhydrazyl (DPPH) tests. *J Am Oil Chem Soc* 79:1191–1195
24. Sabally K, Karboune S, St-Louis R, Kermasha S (2006) Lipase-catalyzed transesterification of dihydrocaffeic acid with flaxseed oil for the synthesis of phenolic lipids. *J Biotechnol* 127:167–176
25. Sabally K, Karboune S, St-Louis R, Kermasha S (2007) Lipase-catalyzed synthesis of phenolic lipids from fish liver oil and dihydrocaffeic acid. *Biocatal Biotransform* 25:211–218
26. Espin JC, Soler-Rivas C, Wichers HJ (2000) Characterization of the total free radical scavenger capacity of vegetable oils and oil fractions using 2, 2-diphenyl-1-picrylhydrazyl radical. *J Agric Food Chem* 48:648–656
27. Abraham MH, Grellier PL, Prior DV, Morris JJ, Taylor PJ (1990) Hydrogen-bonding. 10. A scale of solute hydrogen-bond basicity using log *k* values for complexation in tetrachloromethane. *J Chem Soc-Perkin Trans* 2:521–529
28. Foti MC, Barclay LRC, Ingold KU (2002) The role of hydrogen bonding on the h-atom-donating abilities of catechols and naphthalene diols and on a previously overlooked aspect of their infrared spectra. *J Am Oil Chem Soc* 124:12881–12888
29. Brown WH, Foote CS, Iverson BL (2005) Organic chemistry. Thomson Brooks/Cole, Belmont
30. El-Massry KF, El-Ghorab AH, Farouk A (2002) Antioxidant activity and volatile components of Egyptian *Artemisia judaica* L. *Food Chem* 79:331–336
31. Bhatia SP, Wellington GA, Cocchiara J, Lalko J, Letizia CS, Api AM (2007) Fragrance Material Review on Ethyl Cinnamate. *Food Chem Toxicol* 45:S90–S94
32. Bruice PY (1998) Reactions of benzene and substituted benzenes. Organic chemistry. Prentice Hall, New Jersey
33. Morrison RT, Boyd RN (1966) Carboxylic acids. Organic chemistry. Allyn and Bacon Inc., Boston
34. Velkov ZA, Kolev MK, Tadjer AV (2007) Modeling and statistical analysis of DPPH scavenging activity of phenolics. *Collect Czech Chem Commun* 72:1461–1471

Phytosterol-Enriched Yogurt Increases LDL Affinity and Reduces CD36 Expression in Polygenic Hypercholesterolemia

Gianluca Ruii · Silvia Pinach · Fabrizio Veglia · Roberto Gambino · Saverio Marena · Barbara Uberti · Natalina Alemanno · Davina Burt · Gianfranco Pagano · Maurizio Cassader

Received: 1 May 2008 / Accepted: 14 October 2008 / Published online: 8 November 2008
© AOCs 2008

Abstract Dietary enrichment with phytosterols (plant sterols similar to cholesterol) is able to reduce plasma cholesterol levels due to reduced intestinal absorption. The aim of this study was to investigate the effect of phytosterol-enriched yogurt consumption on the major serum lipid parameters, low density lipoprotein (LDL) receptor activity, LDL-receptor affinity, and CD36 expression in hypercholesterolemic subjects. Fifteen patients affected by polygenic hypercholesterolemia were evaluated in a single-blind randomized crossover study after a 4 weeks treatment with a phytosterol-enriched yogurt containing 1.6 g esterified phytosterols (equivalent to 1.0 g free phytosterol). Lipid parameters were compared with a phytosterol-free placebo-controlled diet. The effect of the two treatments on each variable, measured as percentage change, was compared by paired samples *t* test and covariance analysis. The treatment induced a modest but significant decrease in LDL-cholesterol levels (4.3%, $P = 0.03$) and a significant increase in high density lipoprotein (HDL) 3-cholesterol (17.1%, $P = 0.01$). Phytosterol consumption had no effect on LDL-receptor activity whereas patient LDL-receptor affinity significantly increased (9.7%, $P = 0.01$) and CD36 expression showed a marked significant decrease (18.2%, $P = 0.01$) in the phytosterol-enriched yoghurt patients. Our data show that the oral administration of a phytosterol-

enriched yogurt has modest but significant effects on commonly measured lipid parameters. The improvement of LDL-receptor affinity and the reduction in CD36 expression may reflect an important antiatherogenic effect.

Keywords Phytosterols · Low-density lipoprotein receptor · Low-density lipoprotein affinity · CD36

Introduction

Changes in dietary habits represent an important action in the strategy to reduce cardiovascular risk not only in at-risk patients but also in the whole population [1].

Phytosterols, a commonly used term for plant sterols and stanols, are a complex class of compounds chemically resembling cholesterol present in vegetable and other food sources [1]. Previous studies have demonstrated that phytosterols dissolved in food fats, such as margarine or in a liquid formula, show recognized long-term cholesterol-lowering properties [2] due to their ability to reduce intestinal cholesterol absorption [3].

The lower cholesterol (Chol) flux to the liver results in a decreased Apolipoprotein (Apo) B-lipoproteins production and in a compensatory increase in low density lipoprotein (LDL) receptor activity resulting in a reduction of total and LDL-carried plasma cholesterol levels [4].

Although a lack of effect of phytosterols on lipid levels has recently been reported [5], long term studies have demonstrated the efficacy of phytosterols in reducing LDL-Chol levels with a decrease ranging from 3 to 25% [6, 7] and their use has also been recommended [8].

A beneficial effect of plant sterol ingestion on LDL particle characteristics has also been reported [9]. LDL

G. Ruii · S. Pinach · R. Gambino · S. Marena · B. Uberti · N. Alemanno · D. Burt · G. Pagano · M. Cassader (✉)
Department of Internal Medicine, University of Turin,
Corso A. M. Dogliotti 14, 10126 Turin, Italy
e-mail: maurizio.cassader@unito.it

S. Pinach
e-mail: silvia.pinach@unito.it

F. Veglia
Centro Cardiologico Monzino IRCCS, Milan, Italy

particles undergo physical–chemical alterations during their life-cycle in plasma and, instead of normal LDL-receptor uptake, these modified LDL are catabolized by CD36, a class B scavenger receptor involved in atherosclerosis [10].

The aim of this study was to examine the effect of the oral administration of single-dose phytosterol-enriched yoghurt on lipoprotein metabolism in 15 non-familial hyper-cholesterolemic patients. Lipoprotein levels, LDL-receptor activity, LDL-receptor affinity, and CD36 expression were evaluated before and after treatment.

Materials

Fetal calf serum and RPMI 1640 with L-glutamine were obtained from GibcoBRL (Life Technologies, Milan, Italy). Bovine serum albumin (BSA), 1,1'-Dioctadecyl-3,3,3',3'-tetramethyl-indocarbocyanine perchlorate (DiI), dimethyl-sulfoxide (DMSO), penicillin, streptomycin and lipoprotein deficient serum (LPDS) were obtained from Sigma (St Louis, USA). Lymphoprep was from Nycomed Pharma AS (Oslo, Norway). Millex-GV filters (pore diameter 0.22 μm) were obtained from Millipore S.A. (Molsheim, France). Conical tubes (50 mL and 15 mL), 50 and 100-mL flasks were obtained from Falcon, Becton Dickinson Labware (NY, USA). All commercially available materials were of the highest grade. OptiPrepTM was a kind gift from Axis-Shield (Sentinel, Milan, Italy). Fluorescent-labeled monoclonal antibodies PE-CD14 and FITC-CD36, nonspecific isotype matched control antibodies (PE-conjugated rat IgG2 α and FITC-conjugated rat IgG1) were from BD Pharmingen (Oxford, UK). QIAamp Blood Kit was from Qiagen-Geneco M-Medical s.r.l. (Florence, Italy). Taq DNA polymerase was obtained from Roche Diagnostic (Milan, Italy). HhaI restriction endonuclease was from New England Biolabs (Ipswich, USA). Silver staining was from Biorad (Milan, Italy).

Methods

Healthy Volunteers

Healthy unrelated volunteers were enrolled as lymphocyte and LDL donors from the staff and students of the Department of Internal Medicine, University of Turin, Italy.

Subjects and Study Design

Study subjects were 15 outpatients (10 males, 5 females), attending the Lipid Clinic of the Department of Internal Medicine at the University of Turin, affected by polygenic hypercholesterolemia. The diagnosis was made on the basis

of triglycerides levels <200 mg/dL, LDL-Cholesterol >160 mg/dL and absence of elevated blood cholesterol in first degree relatives. The patients were previously treated with statins but had discontinued the therapy due to appearance of clinical and hematological side effects.

The treatment protocol was designed to allocate patients to one of the two 4-week treatment sequences: diet + placebo or diet + phytosterols using a randomized, single-blind, crossover design. Each phase was followed by a three weeks-washout period during which the subjects consumed the diet, administered during the first phase.

A diet was designed based on the recommended nutrient intakes for Europeans to provide 2,250 kcal per 70 kg individual daily (males) and 1,800 kcal per 60 kg individual daily (females). The Harris–Benedict equation was used to estimate each patient's basal energy requirement [11], which was then multiplied for an activity factor of 1.4 to compensate for the additional energy needs of mildly to moderately active healthy adults. The nutrient content of the diet was calculated by using Winfood (Medimatica, Te, Italy). Dietary carbohydrate, fat and protein made up 55, 30 and 15% of ingested energy respectively; with a saturated fat less than 7% of total calories as suggested [8]. The diet was consumed by the patients at home without supervision. However, the patients were asked to keep an alimentary diary which was subsequently examined by the dietician during the patients visit.

Phytosterols were given as a commercially available yoghurt drink. This is semi-skimmed milk fermented with lactic acid bacteria, commonly used in the manufacture of yoghurt, with a caloric value of 69 kcal per 100 g of product and a Protein/Carbohydrate/Fat content of 3.2, 11.5 and 1.1 g, respectively. The fat content is 0.1 g of saturated fat, 0.68 g of monounsaturated fat and 0.32 g of polyunsaturated fat. The yoghurt is supplemented with 1.6 g esterified phytosterols (equivalent to 1.0 g free phytosterols) obtained from tall oil, a by-product of wood processing. The placebo drink was fermented pasteurized milk with a caloric value of 48 kcal per 100 g of product and a fat content of 1.5 g.

At recruitment, the patients had a session with a dietician who recorded their anthropometric characteristics, and gave them a controlled diet. A blood sample was drawn for plasma lipid measurement. The patients' anthropometric and biochemical characteristics are listed in Table 1. Patients were scheduled for a second visit 4–6 weeks later, when they were interviewed again by the dietician and a blood sample was drawn to measure their plasma lipid and lipoprotein values.

The patients were instructed to drink the placebo or the sterol-enriched yoghurt in the morning and all the patients completed the protocol. At the end of each treatment period, blood samples were collected from all patients.

Table 1 Anthropometric and plasma lipid baseline characteristics of the patients (Values are means \pm SD)

Age (years)	54.2 \pm 7.3
Sex (M/F)	10/5
BMI (kg/m ²)	24.3 \pm 1.7
Systolic blood pressure (mmHg)	131.5 \pm 10.3
Diastolic blood pressure (mmHg)	75.5 \pm 4.9
Smoke (Y/N)	2/13
Total cholesterol (mg/dL)	308.2 \pm 19.6
HDL cholesterol (mg/dL)	47.2 \pm 6.9
HDL2 cholesterol (mg/dL)	19.5 \pm 5.3
HDL3 cholesterol (mg/dL)	28.5 \pm 4.5
LDL cholesterol (mg/dL)	230.6 \pm 26.7
Triglycerides (mg/dL)	152.2 \pm 23.9
Blood glucose (mg/dL)	79.4 \pm 13.1
HbA1c (%)	5.3 \pm 0.6
Apolipoprotein B (mg/dL)	172.2 \pm 32.0
Apolipoprotein A1 (mg/dL)	134.7 \pm 9.3

Patients gave their informed consent and the protocol was approved by the local Ethical Commission.

To evaluate LDL metabolism, LDL-receptor activity was measured on patients' lymphocytes and LDL-receptor affinity was determined, by competitive assay, on LDL-receptors expressed by lymphocytes obtained from healthy control subjects. The receptor affinity of patients' LDL was measured after LDL isolation by self-generating gradient. LDL isolated from healthy volunteers and labeled with DiI were used to measure patients LDL-receptor activity and LDL-receptor affinity. The expression of CD36 was measured on patient CD14⁺ peripheral mononuclear cells isolated in the same analytical session.

Biochemical Measurements

Plasma total cholesterol, triglycerides (Tg), ApoAI and B were analyzed using a Hitachi 911 Automatic Autoanalyzer and commercial enzymatic kits (Sentinel, Milan, Italy). HDL-2 and HDL3-Chol were determined after precipitation of Apo B-rich lipoproteins. Plasma HDL2- and HDL3-Chol levels were determined according to Gidez et al. [12] HDL2 and HDL3 were separated after precipitation of ApoB-containing lipoproteins with heparin and manganese chloride, and HDL2 were further precipitated with dextran sulphate.

Apolipoprotein E Genotype

All the patients were typed for Apo E genotype, assessed by polymerase chain reaction (PCR) amplification of genomic DNA using specific oligonucleotide primers.

Genomic DNA was isolated from frozen EDTA whole blood using the QIAamp Blood Kit. Genomic DNA (0.5 μ g) was amplified in 25- μ l reaction mixture containing 10 mmol/L Tris-HCl (pH 8.3); 50 mmol/L KCl; 200 μ mol each of dATP, dCTP, dGTP and dTTP; 1.5 mmol/L MgCl₂; 200 pmol of each primer, and 1.8 U Taq DNA polymerase.

The amplification cycle was performed in a gene Gene Cycler (Biorad, Milan, Italy). Five minutes of denaturation at 94 °C was followed by 30 cycles of 1 min at 90 °C, 1 min at 60 °C and 2 min at 70 °C. PCR products were cleaved with 4 U of HhaI restriction endonuclease, as recommended by the manufacturer. Subsequently, the samples were electrophoresed through a 10% nondenaturing polyacrylamide gel and visualized by silver staining. The sizes of HhaI fragment were estimated by comparison with known size markers (MspI-digested pUC18 DNA).

Lymphocytes Isolation and Culture

Lymphocytes were prepared under sterile conditions, using a modified version of the method of Böyum [13] as previously described [14]. To obtain maximal receptor expression, lymphocytes were incubated for 72 h at 37 °C in a humidified carbon dioxide incubator (CO₂ 5.0%) in sterile RPMI with 10% human lipoprotein-depleted serum.

Briefly, diluted blood was layered upon lymphoprep (2:1 v/v) and centrifuged at 400 g for 30 min at 20 °C. The interface containing the lymphocytes was isolated, the cells were washed three times with sterile phosphate-buffered saline (PBS) and finally with RPMI enriched with L-glutamine (290 mg/L), penicillin (100,000 U/L), streptomycin (100 mg/L), and 10% fetal calf serum (FCS). After sedimentation the cell pellet was resuspended in the above solution in a 50-mL flask. Non-adherent cells were harvested and washed twice with cold RPMI/BSA (2 g/L). Cells were adjusted to obtain a final concentration of 0.8–1 \times 10⁶ cells/mL in each tube and used directly in the assay. Viability of the cells was >95% as assessed by the trypan blue exclusion test.

Isolation and Collection of Patients LDL with Self-Generating Gradient

Low density lipoprotein was isolated by a single-step centrifugation method using OptiPrepTM, an iodixanol self-generating gradient, as previously described [15] and outlined by the supplier (Axis Shield Reference Manual M10). In brief, a solution of plasma/OptiPrep (4:1 v/v), lower phase, was mixed in a plastic conical tube. The upper phase was made up of 0.75 parts of OptiPrep mixed with 4.25 parts of 0.14 M sodium chloride buffered to pH 7.4 with

HEPES (HBS). From the upper phase, 1.4 mL was transferred to Beckman Optiseal tubes for the TLN100 rotor; 1.4 mL of the lower phase was transferred to the bottom of the tube below the upper phase using a syringe with a long metal cannula. HBS (~0.1 mL) was carefully layered on top of the upper phase to fill the tube. The tubes were capped and centrifuged at 100,000 rpm (350,000g) for 2 h 30 min at 16 °C in the TL100 Beckman ultracentrifuge. LDL appeared as a distinct ring in the middle of the tube and was collected by piercing the tube using a syringe fitted with a large gauge needle. Purity was checked by agarose gel electrophoresis.

Isolation and Labeling of Normal LDL

Low density lipoprotein (density 1.019–1.063 g/mL) and lipoprotein deficient serum (density >1.210 g/mL) were isolated and purified by sequential preparative ultracentrifugation as described by Havel [16] and LDL was labeled with DiI (DiI-LDL) as described by Løhne et al. [17]. LDL specific activity was measured with a spectrofluorimeter. The difference in specific activity between different preparations of LDL was less than 14%.

LDL-Receptor Assay

LDL-receptor activity was determined on patient's lymphocytes incubated with normal DiI-labeled LDL as described by Løhne et al. [17] with at a final concentration of 10 µg/mL LDL protein for 2 h at 37 °C on a rotary shaker in a humidified carbon dioxide incubator (5.0% CO₂). Cells were then washed twice, resuspended in PBS and directly analyzed by flow cytometry. The final cell concentration was 0.4–0.6 × 10⁶ cells/mL. Each experiment was performed in duplicate.

LDL-Binding Assay

To assess binding, LDL from each subject was tested in a competition assay using DiI-labeled pooled human LDL as tracer. Whereas incubation at 37 °C allows binding and internalization of LDL through its own receptor, incubation at 4 °C reflects binding only [18]. Lymphocytes obtained from healthy subjects were incubated in the dark with increasing concentrations of the patient's LDL and a fixed dose of pooled DiI-LDL. The patient's LDL concentration which inhibited 50% of the binding of pooled LDL was determined by flow cytometry. The value obtained was defined as the binding or affinity of the patient's LDL, after normalization with a normal LDL competition curve and expressed as a percentage. Each experiment was performed in duplicate.

CD36 Expression

Mononuclear cells (0.5–0.6 × 10⁶ cells/mL) were isolated as above and incubated with 10 µL of fluorescent-labeled monoclonal antibodies PE-CD14 and FITC-CD36 for 20 min at room temperature in the dark. Staining with nonspecific isotype matched control antibodies (PE-conjugated rat IgG2α and FITC-conjugated rat IgG1) was performed in each experiment. Cells were washed twice with PBS and finally resuspended in 500 µL of PBS. Analysis of stained monocytes was performed on a FAC-Scan flow cytometer using the Cell Quest Software (Becton-Dickinson). For each sample 10,000 events were collected.

During analysis, monocytes were identified by their reactivity with CD14-FITC and their distinctive forward and orthogonal light scatter profile. Mean fluorescence intensity (MFI) values were used as indirect measures of antigen density after conversion from the logarithmic scale used for data acquisition to a linear scale for data analysis. MFI values derived for cells stained with isotype control antibodies were taken as indicators of autofluorescence, non-specific antibody binding or instrument noise and were subtracted from MFI values obtained by staining for CD14 or CD36.

Flow Cytometry Measurements

The uptake of DiI-LDL was measured on a FACScan flow cytometer (Becton-Dickinson, Mountainview, USA). A morphological scatter, forward-scatter FSC (cell size) and side-scatter SSC (cell granularity), for each lymphocyte or monocyte preparation was performed. DiI emission (FL2) was measured at 585 ± 21 nm using a bandpass filter from gated cell population. The fluorescence signals from 10,000 cells were routinely collected. The number of receptor-positive cells was determined setting the marker at the highest range of the unstained lymphocytes (autofluorescence) in the acquisition plot (SSC/FL2); in the following acquisition of stained lymphocytes, the fluorescence signals over the marker were expressed as percentage of positive cells out of total cells in gated region. The % value obtained (measured in duplicate) reflects the degree of DiI-LDL uptake (binding and internalization) by lymphocytes through the LDL-receptor. The mean intra-assay coefficient value was below 2.0%.

In the LDL binding assay, performed at 4 °C, the fluorescence signals over the marker reflect the concentration of the patient's LDL which inhibited the normal DiI-LDL binding to the cell surface. The concentration value which inhibited 50% binding of normal LDL was normalized to the normal LDL competition curve and expressed as a percentage.

Table 2 Effects of placebo and phytosterol-enriched yoghurt drink on plasma lipid, lipoprotein and apolipoprotein values

Variable	Placebo	$\Delta\%$	Yoghurt	$\Delta\%$	<i>P</i>
Triglycerides					
Before treatment	133.9 ± 26.8	1.5	133.3 ± 25.7	4.0	Ns
After treatment	135.0 ± 21.9		139.6 ± 25.5		
Total cholesterol					
Before treatment	309.9 ± 21.4	0.9	315.3 ± 28.3	2.4*	Ns
After treatment	312.7 ± 24.1		307.1 ± 21.0		
HDL cholesterol					
Before treatment	47.8 ± 8.4	1.4	49.5 ± 10.4	4.3*	0.01
After treatment	47.2 ± 9.4		51.6 ± 11.1		
HDL2 cholesterol					
Before treatment	19.4 ± 5.8	0.7	19.5 ± 5.8	3.0	Ns
After treatment	19.3 ± 6.1		18.4 ± 5.0		
HDL3 cholesterol					
Before treatment	28.4 ± 4.4	0.7	28.2 ± 4.3	17.1§	0.001
After treatment	28.2 ± 4.4		33.2 ± 7.5		
LDL cholesterol					
Before treatment	235.3 ± 27.5	1.2	239.1 ± 38.1	4.3§	0.03
After treatment	238.5 ± 33.2		227.6 ± 31.6		
Apolipoprotein B					
Before treatment	174.6 ± 34.7	0.5	172.6 ± 35.8	3.3	Ns
After treatment	173.6 ± 34.2		166.4 ± 36.0		
Apolipoprotein A1					
Before treatment	137.6 ± 9.3	1.1	138.6 ± 9.3	3.2	0.03
After treatment	135.9 ± 10.8		141.9 ± 10.0		

Values, mg/dL, are means ± SD. *P* indicate statistical difference evaluated by repeated measures covariance analysis, including treatment sequence in the model * *P* < 0.05, § *P* < 0.01 indicate difference before/after treatment evaluated by paired *t* test

Statistics

The effects of the two treatments on each variable were measured as percentage change (after treatment value/before treatment value × 100) and were compared by paired samples *t* test. Results were also compared by repeated measures covariance analysis (ANCOVA), including the treatment sequence in the model. All tests were two-sided and a *P* value below 0.05 was considered as statistically significant. All analyses were performed using the SAS statistical package v. 8.2 (SAS Institute, Cary, NC, USA). All data, if not specified otherwise, are means ± SD.

Results

All the patients enrolled completed the study and no adverse events were reported. The baseline anthropometric characteristics of the study subjects are presented in Table 1. During the control diet and the treatment period with phytosterols and the placebo, body mass index (BMI), blood pressure and fasting blood glucose levels showed no significant changes (data not shown).

The lipid parameters were analyzed over the 4-week phytosterol oral administration and over the placebo

period, measured as percentage change before/after treatment and compared by a paired sample *t* test. Analysis revealed the absence of significant changes after placebo treatment. By contrast, phytosterol consumption caused a reduction in LDL-Chol plasma levels (2.4%, *P* < 0.05 and 4.3%, *P* < 0.01, respectively) with a non-significant reduction in ApoB levels. In spite of a 4.3% increase of HDL-Chol (*P* < 0.05), a significant increase in HDL3-Chol (*P* < 0.01) with a non-significant reduction in HDL2-Chol levels was observed.

When the effect of the two treatments was compared by covariance analysis for repeated measures including the treatment sequence, total cholesterol became non-significant while the difference in LDL-Chol (*P* = 0.03), HDL-Chol (*P* = 0.01) and HDL3-Chol (*P* = 0.01) remained significant. Also ApoA1 levels showed a significant increase (*P* = 0.03) (Table 2).

Although the 4-week phytosterol consumption had no significant effect on LDL-receptor activity, LDL binding to LDL-receptors expressed by control lymphocytes in comparison to placebo was significantly increased (9.7%, *P* = 0.01) (Table 3).

CD36 expression measured as mean fluorescence intensity of CD14+ cells, showed a marked decrease after 4 weeks of phytosterol treatment in all patients (18%,

Table 3 LDL-receptor activity, LDL binding and CD36 expression

Variable	Placebo	$\Delta\%$	Yoghurt	$\Delta\%$	<i>P</i>
LDL uptake (%)					
Before treatment	68.6 \pm 7.3	1.7*	76.7 \pm 9.0	3.7*	Ns
After treatment	69.9 \pm 8.4		72.6 \pm 9.1		
LDL binding (%)					
Before treatment	71.6 \pm 6.7	1.6	72.1 \pm 11.6	9.7*	0.01
After treatment	72.6 \pm 6.6		78.8 \pm 13.7		
CD36 (MIF)					
Before treatment	1,904.1 \pm 411.6	2.6	2,286.5 \pm 476	18.2§	0.01
After treatment	1,849.5 \pm 410.1		1,806.3 \pm 246		

LDL uptake (%) by patients' lymphocytes is an expression of LDL-receptor activity. Throughout the paper, the terms are used as being synonymous. LDL binding (%) of the patients is the affinity of the particles to LDL-receptors expressed by normal lymphocytes. Throughout the paper the terms are used as being synonymous. Values are means \pm SD. *P* indicate statistical difference evaluated by repeated measures covariance analysis, including treatment sequence in the model

MIF mean intensity of fluorescence, expressed in arbitrary units

* *P* < 0.05, § *P* < 0.01 indicate difference before/after treatment evaluated by paired *t* test

P = 0.01). These differences retained their significance also when the treatment sequence was included in the analysis by ANCOVA.

All the patients were typed for Apo E genotype and were all homozygous for the most common ϵ 3 allele except one patient who was heterozygous for the ϵ 4 allele. Due to the low number of subjects in each Apo E genotype groups, no comparison was made between the different Apo ϵ alleles.

Discussion

The study was designed to evaluate the effect of a controlled diet supplemented with a fixed dose of phytosterols, provided as a yogurt drink, on lipoprotein metabolism in a group of patients with polygenic hypercholesterolemia. Polygenic hypercholesterolemia is the most common form of hypercholesterolemia caused by a susceptible genotype, still unknown, aggravated by excessive saturated fat, *trans* fatty acid and cholesterol intake. The patients did not exhibit any LDL-receptor defect and manifested a moderate hypercholesterolemia (240–350 mg/dL) with serum triglyceride concentrations within the reference range.

Phytosterol-consuming patients showed a statistically significant reduction in total cholesterol and LDL-Chol

levels, a significant increase in ApoA1, HDL-Chol and HDL3-Chol and a non-significant decrease in ApoB when measured as a percentage change before/after treatment and compared by paired sample *t* test. No statistically significant difference was observed after placebo treatment. When data were compared by covariance analysis the reduction of LDL-Chol remained significant (*P* = 0.03), as did the changes in HDL-Chol (*P* = 0.01), HDL3-Chol (*P* = 0.001) and ApoA1 levels (*P* = 0.03).

The decrease in LDL-Chol reported here (4.3%) agrees with the results presented in the literature. Some trials failed to lower plasma lipid levels [5, 19], but in a meta-analysis consisting of 41 stanol/sterol ester trials with the dose varying from 0.8 to 4.2 g of stanol/sterol per day, the majority of studies demonstrated an LDL-Chol decrease, although with a wide range (3–25%) [6]. As other authors [5, 19] observed, the reason for the slight changes of LDL-Chol levels in our patients may be due to the product formula and to the timing of consumption. Actually, the more significant reduction of lipid values was obtained using sterol-enriched solid food products, while recent studies on the effect of low-fat milk products on lipid profile showed a pooled 4.9% LDL-Chol difference after treatment, with a difference meal-time dependent [20]. The food product we used is a 1.6 g phytosterol-enriched yogurt and was consumed by our patients, in the morning outside mealtimes. As our patients were not ϵ 4 carriers, a determinant in cholesterol absorption [21], we speculate that the LDL-Chol decrease we obtained may be related to our study design with a reduced efficacy of phytosterol consumption as liquid products, outside of mealtimes. Thus, a reduction of LDL-Chol levels associated to an increase in HDL-Chol and HDL3-Chol represents a positive event due to phytosterol ingestion in regard to protection against atherosclerosis.

Moreover, the HDL3-Chol increase shows a generally positive effect of phytosterols on lipid metabolism: HDL3 particles exert an anti-atherogenic activity by way of antioxidative, anti-inflammatory, anti-thrombotic and anti-apoptotic actions [22].

The LDL-receptor pathway represents a key determinant in cholesterol homeostasis and normal LDL-receptor activity is a pre-requisite for normal cholesterol levels as LDL carry 60–80% of plasma cholesterol. Functional tests of LDL-receptor activity and LDL ligand function can theoretically identify defects in LDL catabolism, distinguish between receptor and ligand defects and provide useful information about pharmacological/dietetic intervention. These studies have been based classically on the use of ¹²⁵I-labeled LDL on cultured human fibroblasts [23]. Fluorescence flow cytometry represents a simple and fast technique allowing the quantification of LDL-receptor expression and LDL ligand function, also on patient's

peripheral blood mononuclear cells. Human lymphocytes, lacking scavenger receptors are a suitable and widely used model to investigate LDL metabolism both in normal and pathological states [24, 25].

The method used to measure LDL binding (which involved the use of patient's LDL in competition with normal DiI-labelled LDL for normally expressed LDL-receptor) gave information about the qualitative abnormalities in patient's LDL particle.

The reduction of LDL-Chol we observed was not associated with an increase in LDL-receptor activity, measured as LDL uptake by patient lymphocytes. Other authors reported plant stanol esters consumption led to a reduction in LDL-Chol linked to increased LDL-receptor activity [26]. Changes in LDL-receptor activity are dependent on cholesterol cell concentration, in turn to LDL-cholesterol plasma levels and cell synthesis.

Our inability to document an increase in LDL-receptor activity may be due to the small reduction in the LDL-Chol level. By contrast, LDL affinity increased significantly, with a near 10% increase after sterols consumption. The LDL particle's content and size is a major determinant in their recognition and catabolism through LDL-receptor and the role of small dense LDL in the development of atherosclerotic lesions is well known [27] and a decrease in smaller LDL particles by sterol-enriched diet was recently observed [9].

We can speculate that the increased affinity of LDL observed is related to a reduction of smaller LDL particles and, because of this, to a change in the LDL particle number, as stated by the LDL Chol and Apo B decreases. Consequently, the beneficial effect related to phytosterols results in a better catabolism of LDL.

The beneficial effect of a phytosterol supplemented diet is also the significant reduction (–18%) in CD36 expression after treatment. Class B scavenger receptor CD36 is a complex multifunctional protein that plays a critical role in the initiation of atherosclerotic lesions through its ability to bind and internalize modified LDL, facilitating the formation of lipid-engorged macrophage foam cells [10, 28, 29]. CD36 expression on the cell surface is up-regulated by oxidized LDL with a dose dependent increase [30, 31] and, as previously cited, a reduction in CD36 expression may indicate a decrease in oxidated LDL related to the phytosterol supplemented diet.

Our results confirm previous reports showing a significant decrease in plasma concentrations of oxidated LDL after a plant sterols enriched diet [32, 33].

In conclusion, our data indicate a positive effect of single-dose phytosterol-enriched yogurt on lipoprotein metabolism with a slight improvement in common lipid parameters in comparison to LDL behavior and cellular receptor expression.

Our data agree with the general consensus regarding the role of plant sterols in human cholesterol metabolism and may provide a further explanation of the mechanism of the action of phytosterols in hypercholesterolemic patients.

Acknowledgments We thank Franco De Michieli for helpful cooperation in the collection of data.

References

- Moreau RA, Whitaker MB, Hicks KB (2002) Phytosterols, phytostanols, and their conjugates in foods: structural diversity, quantitative analysis, and health-promoting uses. *Prog Lipid Res* 41:457–500. doi:10.1016/S0163-7827(02)00006-1
- Best MM, Duncan CH, Van Loon EJ, Wathen JD (1954) Lowering of serum cholesterol by the administration of a plant sterol. *Circulation* 10:201–206
- Heinemann T, Kullak-Ublick A, Pietruck B, von Bergman K (1991) Mechanism of action of plant sterols on inhibition of cholesterol absorption. *Eur J Clin Pharmacol* 40(suppl 1):59–63S
- Plat J, Mensink RP (2005) Plant stanol and sterol esters in the control of blood cholesterol levels: mechanism and safety aspects. *Am J Cardiol* 96(suppl):15D–22D. doi:10.1016/j.amjcard.2005.03.015
- AbuMweis SS, Vanstone CA, Ebine N, Kassis A, Ausman LM, Jones PJH et al (2006) Intake of a single morning dose of standard and novel plant sterol preparations for 4 weeks does not dramatically affect plasma lipid concentrations in humans. *J Nutr* 136:1012–1016
- Katan MB, Grundy SM, Jones P, Law M, Miettinen T, Paoletti R (2003) for the Stresa Workshop participants. Efficacy and safety of plant stanols and sterols in the management of blood cholesterol levels. *Mayo Clin Proc* 78:965–978
- Normen L, Frohlich J, Trautwein E et al (2004) Role of plant sterols in cholesterol lowering. In: Dutta PC (ed) *Phytosterols as functional food components and nutraceuticals*. Marcel-Dekker, Inc, New York, pp 243–315
- National Cholesterol Education Program (NCEP) Expert panel on detection, evaluation, and treatment of high blood cholesterol in adults (Adult Treatment Panel III) (2002) Third report of the National Cholesterol Education Program (NCEP) Expert Panel on Detection, Evaluation, and Treatment of High Blood Cholesterol in Adults (Adult Treatment Panel III) final report. *Circulation* 106:3143–3421
- Shrestha S, Freake HC, McGrane MM, Volek JS, Fernandez ML (2007) A combination of psyllium and plant sterols alters lipoprotein metabolism in hypercholesterolemic subjects by modifying the intravascular processing of lipoproteins and increasing LDL uptake. *J Nutr* 137(5):1165–1170
- Febbraio M, Silverstein RL (2007) CD36: Implications in cardiovascular disease. *Int J Biochem Cell Biol* 39:2012–2030. doi:10.1016/j.biocel.2007.03.012
- Harris JA, Benedict FG (1919) *A biometric study of basal metabolism in man*. Carnegie Institute of Washington, Washington
- Gidez LI, Miller GJ, Burstein M, Slagle S, Eder HA (1982) Separation and quantitation of subclasses of human plasma high density lipoproteins were performed by a simple precipitation procedure. *J Lipid Res* 23(8):1206–1223
- Böyum A (1968) Isolation of mononuclear cells and granulocytes from human blood. *Scand J Clin Lab Invest* 97:77–89
- Ruii G, Pinach S, Gambino R, Uberti B, Alemanno N, Pagano G et al (2005) Influence of cyclosporine on low-density lipoprotein

- uptake in human lymphocytes. *Metabolism* 54:1620–1625. doi:10.1016/j.metabol.2005.06.010
15. Sawle A, Higgins MK, Olivant MP, Higgins JAA (2002) A rapid single-step centrifugation method for determination of HDL LDL, and VLDL cholesterol, and TG, and identification of predominant LDL subclass. *J Lipid Res* 43:335–343
 16. Havel RJ, Eder HA, Bragdon JH (1955) The distribution and chemical composition of ultracentrifugally separated lipoproteins in human serum. *J Clin Invest* 34:1345–1353
 17. Løhne K, Urdal P, Leren TP, Tonstad S, Ose L (1995) Standardization of a flow cytometric method for measurement of low density lipoprotein receptor activity on blood mononuclear cells. *Cytometry* 20:290–295
 18. Innerarity TL, Pitas RE, Mahley RW (1986) Lipoprotein-receptor interactions. In: Albers JJ, Segrest JP (eds) *Methods in enzymology*, vol 129. Academic Press, Dublin, pp 542–565
 19. Jones PJH, Vanstone CA, Raeini-Sarjaz M, St-Onge MP (2003) Phytosterols in low- and nonfat beverages as part of a controlled diet fail to lower plasma lipid levels. *J Lipid Res* 44:1713–1719
 20. Seppo L, Jauhiainen T, Nevala R, Poussa T, Korpela R (2007) Plant stanol esters in low-fat milk products lower serum total and LDL cholesterol. *Eur J Nutr* 46:111–117
 21. Vanhanen HT, Blomqvist S, Ehnholm C (1993) Serum cholesterol, cholesterol precursors, and plant sterols in hypercholesterolemic subjects with different apoE phenotypes during dietary sitostanol ester treatment. *J Lipid Res* 34:1535–1544
 22. Barter P, Kastelein J, Nunn A, Hoobs R (2003) High density lipoproteins (HDLs) and atherosclerosis: the unanswered questions. *Atherosclerosis* 168:195–211. doi:10.1016/S0021-9150(03)00006-6
 23. Goldstein JL, Brown MS (1976) Binding and degradation of low density lipoproteins by cultured human fibroblasts. Comparison of cells from a normal subject and from a patient with homozygous familial hypercholesterolemia. *J Biol Chem* 249:5153–5162
 24. Terpstra V, van Amersfoort ES, van Velzen AG, Kuiper J, van Berkel TJC (2000) Hepatic and extrahepatic scavenger receptors: function in relation to disease. *Arterioscler Thromb Vasc Biol* 20:1860–1876
 25. Duvillard L, Gambert P, Lizard G (2004) Etude du recepteur des lipoproteins de basse densite par cytometrie en flux: interest biologiques et cliniques. *Ann Biol Clin* 62:87–91
 26. Plat J, Mensink RP (2002) Effects of plant stanol esters on LDL receptor protein expression and on LDL receptor and HMG-CoA reductase mRNA expression in mononuclear blood cells of healthy men and women. *FASEB J* 16:258–260
 27. Berneis KK, Krauss RM (2002) Metabolic origins and clinical significance of LDL heterogeneity. *J Lipid Res* 43:1363–1379
 28. Campos H, Arnold KS, Balestra ME, Innerarity TL, Krauss RM (1996) Differences in receptor binding of LDL subfractions. *Arterioscler Thromb Vasc Biol* 16:794–801
 29. Han J, Hajjar DP, Febbraio M, Nicholson AC (1997) Native and modified low density lipoproteins increase the functional expression of the macrophage class B scavenger receptor, CD36. *J Biol Chem* 272:21654–21659
 30. Viana M, Villacorta L, Bonet B, Indart A, Munteanu A, Sanchezvera I et al (2005) Effects of aldehydes on CD36 expression. *Free Radic Res* 39:973–977
 31. van Bennekum A, Werder M, Thuahnai ST, Han CH, Duong P, Williams DL et al (2005) Class B scavenger receptor-mediated intestinal absorption of dietary β -carotene and cholesterol. *Biochemistry* 44:4517–4525
 32. Hansel B, Nicolle C, Lalanne F, Tondou F, Lassel T, Donazzolo Y et al (2007) Effect of low-fat, fermented milk enriched with plant sterols on serum lipid profile and oxidative stress in moderate hypercholesterolemia. *Am J Clin Nutr* 86:790–796
 33. Homma Y, Ikeda I, Ishikawa T, Tateno M, Sugano M, Nakamura H (2003) Decrease in plasma low-density lipoprotein cholesterol, apolipoprotein B, cholesteryl ester transfer protein, and oxidized low-density lipoprotein by plant stanol ester-containing spread: a randomized, placebo-controlled trial. *Nutrition* 19:369–374

Effect of Diacylglycerol on Postprandial Serum Triacylglycerol Concentration: A Meta-analysis

Tongcheng Xu · Xia Li · Xiaohang Ma ·
Zhiguo Zhang · Tiansong Zhang · Duo Li

Received: 4 April 2008 / Accepted: 7 October 2008 / Published online: 7 November 2008
© AOCS 2008

Abstract Diacylglycerol (DAG) supplementation has been shown to be associated with the reduction of postprandial triacylglycerol (TAG) concentration, although the extent of the association is uncertain. We quantitatively examined the effect of dietary DAG on postprandial serum TAG concentration by conducting a meta-analysis of randomized controlled trials. Potential papers were initially searched for in the electronic databases of Medline, Embase and Cochrane library. Inclusion criteria required the trial to be randomized with DAG as the treatment group, and TAG as the control group. Information was extracted independently by two investigators and the effect of DAG on postprandial TAG concentration was examined in Review Manager 4.2. Seven papers were included in the statistic pooling. DAG supplementation reduced the increment of postprandial TAG concentration significantly

at postprandial 2 h (Weighted mean difference (WMD) -0.07 mmol/L; 95% CI -0.13 to 0.00 mmol/L; $P = 0.05$), 4 h (WMD -0.15 mmol/L; 95% CI -0.24 to -0.06 mmol/L; $P = 0.002$) and 6 h (WMD -0.14 mmol/L; 95% CI -0.23 to -0.05 mmol/L; $P = 0.002$). Linear regression showed that the effect of DAG was positively correlated with the daily dosage at 2 h ($P = 0.095$) and 6 h ($P = 0.053$) after lipid loading. In conclusion, compared with TAG oil, DAG reduced the postprandial serum TAG concentration at 2 h, 4 h and 6 h postprandial and was positively correlated with daily dosage.

Keywords Diacylglycerol · Triacylglycerol · Postprandial time · Daily dosage · Sensitivity analysis · Meta-analysis

Abbreviations

DAG	Diacylglycerol
TAG	Triacylglycerol
MAG	Monoacylglycerol
TRL	Triacylglycerol-rich lipoprotein
WMD	Weighted mean difference
SMD	Standard mean difference
AS	Atherosclerosis
T2DM	Type 2 diabetes mellitus
NGT	Normal glucose tolerance
IGT	Impaired glucose tolerance

Introduction

Postprandial serum triacylglycerol (TAG), mainly in the form of triacylglycerol-rich lipoprotein (TRL), has revealed itself to be an independent risk for atherosclerosis

T. Xu · Z. Zhang · D. Li (✉)
Department of Food Science and Nutrition,
Zhejiang University, 268 Kaixuan Road,
310029 Hangzhou, China
e-mail: Duoli@zju.edu.cn

X. Li
Shandong Academy of Pharmaceutical Science, Jinan, China

T. Xu
Shandong Academy of Agricultural Science,
Institute of Atomic Energy Application in Agriculture,
Jinan, China
e-mail: danceforever@live.com

X. Ma
College of Life Sciences, Zhejiang University, Hangzhou, China

T. Zhang
Department of Traditional Chinese Medicine,
Jingan District Centre Hospital, Shanghai, China

(AS) [1, 2]. Impaired postprandial serum TAG clearance has been shown to be associated with visceral obesity which is one of the strong predictors of type 2 diabetes mellitus (T2DM) [3, 4]. In fact, hypertriglyceridemia is commonly observed in patients with T2DM, and a strong correlation has also been confirmed between postprandial hypertriglyceridemia and insulin resistance [5]. Moderate hypertriglyceridemia persists even after the serum glucose was well controlled in patients with T2DM [6]. So the control of postprandial TAG concentration is important for patients with either AS or T2DM.

Some studies showed that the supplementation of dietary 1,3-diacylglycerol-rich oil (designated as DAG oil) reduced the postprandial serum TAG concentration compared with TAG oil in rats [7, 8] and humans [9, 10]. The effect of DAG was influenced by the duration of postprandial time because the increments of postprandial TAG concentration in the DAG group were not significantly smaller than those of the TAG group at all postprandial time points [9, 10]. Further, this effect might be influenced by daily dosage [9].

Meta-analysis is a statistical technique in which results of separate studies are combined to increase statistical power and clarity, and to estimate the size of treatment effects more accurately [11]. This method has some inherent weaknesses such as the sources of bias are not controlled and the heavy reliance on published studies. Despite these weaknesses, meta-analysis has still been employed in many clinical settings to evaluate efficacy and safety of a variety of therapeutic interventions due to its advantages. We therefore undertook a meta-analysis of randomized TAG-controlled trials to assess the association between DAG intake and postprandial serum TAG concentration.

Methods

Selection of Studies

Potential papers were initially searched in the electronic databases of Medline (1966–2007), Embase (1984–2007) and Cochrane library (2006–2007) using the terms in Table 1. The references of all located papers were searched for further studies.

Inclusion Criteria

The trials were included if the study was published in English as a full-length article; the study was a randomized controlled trial; the study was conducted on human subjects; DAG was the only intervention; and the study took postprandial serum TAG concentration as one of the endpoints.

Table 1 Search strategy and search terms

(1)	Diacylglycerol
(2)	Diacylglycerols
(3)	Diglyceride
(4)	Diglycerides
(5)	DAG
(6)	(1) or (2) or (3) or (4) or (5)
(7)	Postprandial
(8)	Triacylglycerol
(9)	Triacylglycerols
(10)	Triglyceride
(11)	Triglycerides
(12)	TAG
(13)	Lipid
(14)	Hyperlipidemia
(15)	(8) or (9) or (10) or (11) or (12) or (13) or (14)
(16)	(6) and (7) and (15)

Extraction of Information

The detailed information was extracted independently by two investigators (TX and XL) and differences were resolved by discussion with a third investigator (XM). Authors were contacted to provide additional information. Relevant data included the first author's name, year of publication, number of subjects, study design (Parallel or crossover; Open, single- or double-blinded), age and BMI of subjects, duration of washout, daily dosage of DAG or TAG, the mean change of serum TAG concentration from baseline at all postprandial time points along with corresponding standard deviation (SD) or standard error (SE).

Taguchi et al. [9] reported postprandial serum TAG concentrations in the form of a figure, and the author was asked for detailed data but we received no reply. So the specific data was obtained by measuring figure and sensitivity analysis was performed to determine whether the overall result was robust enough for inclusion of these studies. Data of 3 dosage groups (10, 20 and 44 g) were extracted as 3 independent studies [9, 12]. This extraction method was also used for the study conducted by He et al. [13]. Two separate cohorts from the study conducted by Joshipura et al. [14] were extracted and included as two independent trials.

Takase et al. [15] reported TAG concentration as mg/dL which was transformed to mmol/L before analysis. Ai et al. [16] examined the effect of DAG on postprandial serum TAG concentration in the normal glucose tolerance (NGT) and impaired glucose tolerance (IGT) groups independently, so the data of both groups was extracted as two independent studies. In this study, the SDs of mean increment in postprandial TAG concentration were not

reported. The author was contacted for detailed data but no reply was received. Therefore, the missing SDs were imputed using methods in the Cochrane Handbook [17].

Statistical Analysis

The validity of random design was tested by meta-analysis in advance. Then, the effect of DAG on postprandial serum TAG concentration was assessed using the software of Review Manager 4.2.2, developed by The Nordic Cochrane Center (Update Software Ltd, Oxford, England). The weighted mean difference (WMD) was taken as the effect size. The rationality of combining the results of different studies was examined with the Chi-square (χ^2) test. Values of P and I^2 were calculated in the Review Manager to assess whether there was more variation in the results of studies than would be expected by chance. It is generally regarded that if the P value is smaller than 0.1 or the I^2 value is larger than 25%, there is more variation than expected by chance, and it may not be advisable to combine these studies in meta-analysis. A fixed effect model was adopted when there was no heterogeneity among all studies and the random effect model was adopted when there was heterogeneity. Funnel plot asymmetry was used to detect any publication bias in the meta-analysis. Fail-safe number analysis was used to determine the number of studies with null effect that would have to exist to nullify the reported reduction efficacy. Sensitivity analysis was performed to test the influence of studies with imputed SDs on the overall result. The influence of daily dosage on the effect of DAG was assessed using linear regression in SPSS 12.0. Postprandial serum TAG concentration might be influenced by the altered glucose metabolism because hypertriglyceridemia is one of the complications of T2DM. Given that 3 from 7 papers involving subjects with altered glucose metabolism, the studies at each of the time points were divided into normal and abnormal glucose status groups to determine whether the DAG oil was effective in reducing the increment of postprandial serum TAG concentration in each group.

Results

Validity of Random Design

Seven papers with 151 subjects were included in the statistical pooling (Table 2). Initial fasting serum TAG concentrations were reported in five papers [10, 16, 18–20]. Meta-analysis showed that it was rational to combine them ($P = 0.91$, $I^2 = 0\%$) and there was no significant difference in fasting serum TAG concentration between DAG and TAG groups (WMD 0.00 mmol/L; 95% CI -0.15 to 0.15 mmol/L; $P = 1.00$).

Postprandial 0.5 h and 1 h

Only one study compared the postprandial 0.5-h and 1-h TAG concentrations between DAG and TAG groups [20]. There was no significant differences at 0.5 h (WMD -0.01 mmol/L; 95% CI -0.07 to 0.05 mmol/L; $P = 0.73$) and 1 h (WMD -0.03 mmol/L; 95% CI -0.13 to 0.07 mmol/L; $P = 0.56$).

Postprandial 2 h

The postprandial 2-h TAG concentrations were reported in 7 papers with 9 independent studies [9, 10, 15, 16, 18–20]. χ^2 test showed that there was no significant heterogeneity and it was rational to combine them ($P = 0.46$; $I^2 = 0\%$). Meta-analysis showed that there was significant difference between DAG and TAG groups (WMD -0.07 mmol/L; 95% CI -0.13 to 0.00 mmol/L; $P = 0.05$). The funnel plot was slightly asymmetrical for DAG suggesting a small publication bias (Fig. 1a).

Sensitivity analysis showed that the effect of DAG on postprandial serum TAG concentration was slightly reduced by removing those studies with imputed SDs (WMD -0.06 mmol/L; 95% CI -0.13 to 0.01 mmol/L; $P = 0.07$) [16]. In contrast, the removal of studies in which, the specific data was obtained by measuring the figure, increased the effect of DAG slightly (WMD -0.08 mmol/L; 95% CI -0.15 to 0.00 mmol/L; $P = 0.04$) [9]. It is noticeable that the removal of a study which distributed out of the 95% CI reduced the effect of DAG greatly (WMD -0.05 mmol/L; 95% CI -0.12 to 0.01 mmol/L; $P = 0.11$) [10].

The influence of dosage on the effect of DAG was investigated by plotting the change in TAG concentration against the dosage of DAG (g/d). The change in TAG concentration represented the difference between the increment of DAG and TAG groups from the baseline. In studies conducted by Tada et al. [10, 18], the daily dosage was reported as 30 g lipids/m² which was transformed to g/d using the Stevenson formulation of “body area = $0.0061 \times \text{height} + 0.0128 \times \text{weight} - 0.1529$ ”. Three studies were excluded from the dosage-effect analysis because they did not give detailed information about the calculation of the daily dosage in the unit g/d [15, 16]. Regression analysis showed that there was no significant correlation between dosage and the effect of DAG ($R^2 = 0.541$; $P = 0.095$) (Fig. 2a).

Sub-group analysis showed that DAG intake did not reduce the postprandial serum TAG concentration in normal subjects (WMD -0.05 mmol/L; 95% CI -0.13 to 0.03 mmol/L; $P = 0.19$) and subjects with abnormal glucose status (WMD -0.09 mmol/L; 95% CI -0.21 to 0.02 mmol/L; $P = 0.12$).

Table 2 Studies characteristics

Studies	Scores	M/F	Subjects	Age	BMI	Washout	Daily dosage
Ai et al. [16] (IGT)	5	14/0	IGT	44.00 ± 2.00	27.00 ± 1.00	1 week	17 g/m ² /d
Ai et al. [16] (NGT)	5	11/0	NGT	26.00 ± 1.00	21.60 ± 0.40	1 week	17 g/m ² /d
Saito et al. [20]	4	13/0	H	34.60 ± 5.60	23.20 ± 2.10	1 or 2 weeks	30 g/d
Tada et al. [10]	4	6/0	NR	35.50 ± 3.94	24.85 ± 1.74	1 month	30 g/m ² /d
Tada et al. [18]	4	1/5	2-DM	62.00 ± 4.00	24.42 ± 3.12	2 weeks	30 g/m ² /d
Taguchi et al. [9]	4	13/0	H	34.00 ± 4.00	22.60 ± 2.20	7 days	10 g/d
Taguchi et al. [9]	4	10/0	H	36.00 ± 6.00	23.60 ± 3.50	7 days	20 g/d
Taguchi et al. [9]	4	17/0	H	33.00 ± 8.00	23.80 ± 3.30	7 days	44 g/d
Takase et al. [15]	4	18/0	IS or IR	37.00 ± 1.00	25.20 ± 0.60	1 week	10 g/60 kg wt./d
Tomonobu et al. [19]	5	36/7	H	28–57	19.8–30.3	2 weeks	10 g/d

Studies	Postprandial time (h)								Composition of test meal
	0	0.5	1	2	3	4	6	8	
Ai et al. [16] (IGT)	NS				NS	S			DAG or TAG 33%, water 57%, protein 3%, carbohydrate 7% (wt.%)
Ai et al. [16] (NGT)	NS				NS	NS			
Saito et al. [20]	NS	NS	NS	NS		S			DAG or TAG 34.5%, sugars 52.1% and protein 14.1% of the total energy
Tada et al. [10]	NS			S	S	NS	NS	S	DAG or TAG 35%, casein sodium 2%, fatty acid sucrose polyester 0.5% lecithin from soybeans 0.36%, aspartame 0.2%, water 61.94% (wt.%)
Tada et al. [18]	NS				NS	NS	NS		DAG or TAG 35%, casein sodium 1%, fatty acid sucrose polyester 0.5% skim milk 3%, soybean lecithin 0.36%, water 60.14% (wt.%)
Taguchi et al. [9]	NS				NS	S			DAG or TAG oil 10 g, water 47.5 g, UCCade lemon 12.5 g, TORYS
Taguchi et al. [9]	NS					S	S		CONC orange 12.5 g, reduced starch hydrolysate 12.88 g and erythritol 3.32 g/100 g
Taguchi et al. [9]	NS				NS	S	NS		
Takase et al. [15]	NS				NS	NS	S		Fat 70.9% (DAG or TAG 66.3), protein 2.5%, carbohydrate 2.2% (wt.%)
Tomonobu et al. [19]	NS				NS	NS	NS	S	DAG or TAG 19%, protein 30%, carbohydrates 51% (wt.%)

3 and 2 independent studies were extracted from the paper conducted by Taguchi et al. and Ai et al. respectively

IGT Impaired glucose tolerance, NGT Normal glucose tolerance, H Healthy, NR Not reported, IS Insulin sensitive, IR Insulin resistance, 2-DM Type 2 diabetes mellitus

S and NS: There was or was not a significant difference between the DAG and TAG groups in the increment of TAG concentration. The presence of letter (S or NS) represented this time point were reported. S or NS represented the postprandial TAG concentration reaching the peak at this time point

Postprandial 3 h

Three papers reported postprandial 3 h TAG concentrations [10, 15, 19]. The χ^2 test showed that there was no significant heterogeneity ($P = 0.28$; $I^2 = 22.5\%$). Meta-analysis indicated that there was no significant difference in the increment of postprandial serum TAG concentration between DAG and TAG groups (WMD -0.12 mmol/L; 95% CI -0.26 to 0.01 mmol/L; $P = 0.06$).

Postprandial 4 h

Postprandial 4-h TAG concentrations were reported in 7 papers with 10 independent studies [9, 10, 15, 16, 18–20]. χ^2 test showed that there was no significant heterogeneity ($P = 0.81$; $I^2 = 0\%$). Meta-analysis showed that DAG decreased the increment of postprandial serum TAG

concentration significantly compared with TAG (WMD -0.15 mmol/L; 95% CI -0.24 to -0.06 mmol/L; $P = 0.002$). The funnel plot displayed good symmetry (Fig. 1b).

Sensitivity analysis showed that the removal of studies with imputed SDs did not influence the effect of DAG (WMD -0.16 mmol/L; 95% CI -0.26 to -0.06 mmol/L; $P = 0.002$) [16]. Although the removal of studies reporting TAG concentrations in the form of a figure reduced the effect of DAG greatly [9], there was still a significant difference between DAG and TAG groups (WMD -0.13 mmol/L; 95% CI -0.25 to -0.02 mmol/L; $P = 0.02$). Removal of all the above studies reduced the effect of DAG greatly too (WMD -0.15 mmol/L; 95% CI -0.29 to -0.02 mmol/L; $P = 0.02$).

Linear regression showed that there was no significant correlation between daily dosage and the effect of DAG ($R^2 = 0.101$; $P = 0.487$) (Fig. 2b).

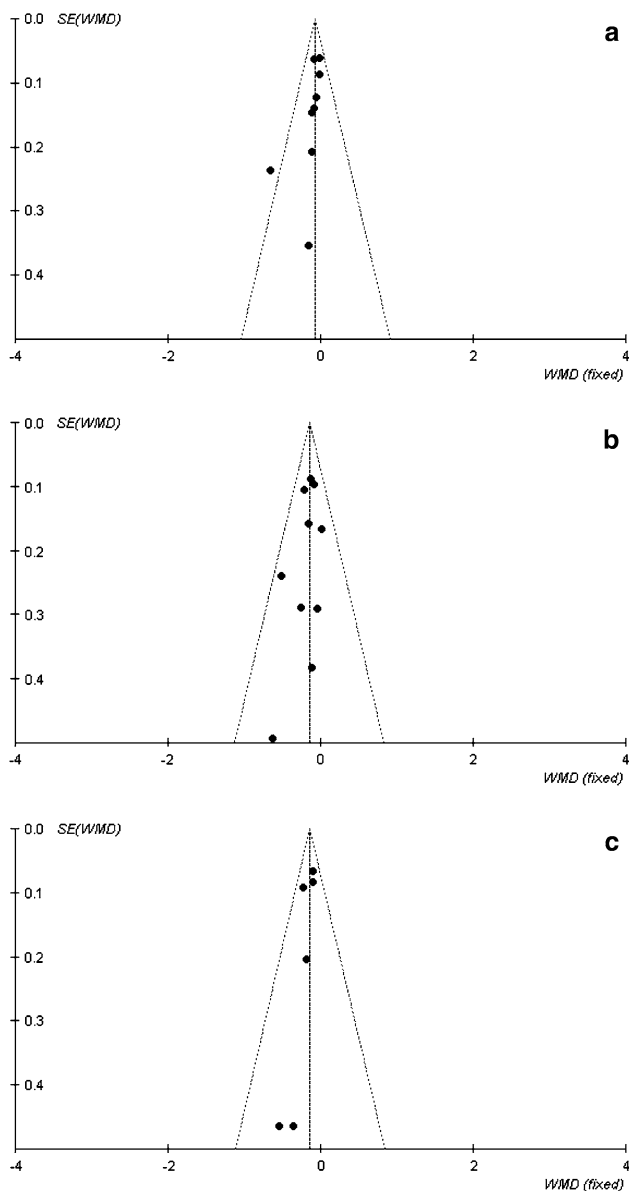


Fig. 1 Funnel plot of postprandial 2 h (a), 4 h (b) and 6 h (c)

Sub-group analysis showed that DAG intake reduced the postprandial serum TAG concentration in normal subjects (WMD -0.13 mmol/L; 95% CI -0.24 to -0.02 mmol/L; $P = 0.02$) and subjects with abnormal glucose status (WMD -0.18 mmol/L; 95% CI -0.34 to -0.01 mmol/L; $P = 0.03$).

Postprandial 6 h

Four papers with 6 independent studies reported the postprandial 6-h TAG concentrations [9, 11, 18, 19]. χ^2 test showed that it was rational to combine them ($P = 0.77$; $I^2 = 0\%$). Meta-analysis showed that DAG reduced the increment of postprandial TAG concentration significantly compared with TAG (WMD -0.14 mmol/L; 95% CI -0.23 to -0.05 mmol/L; $P = 0.002$). The funnel plot

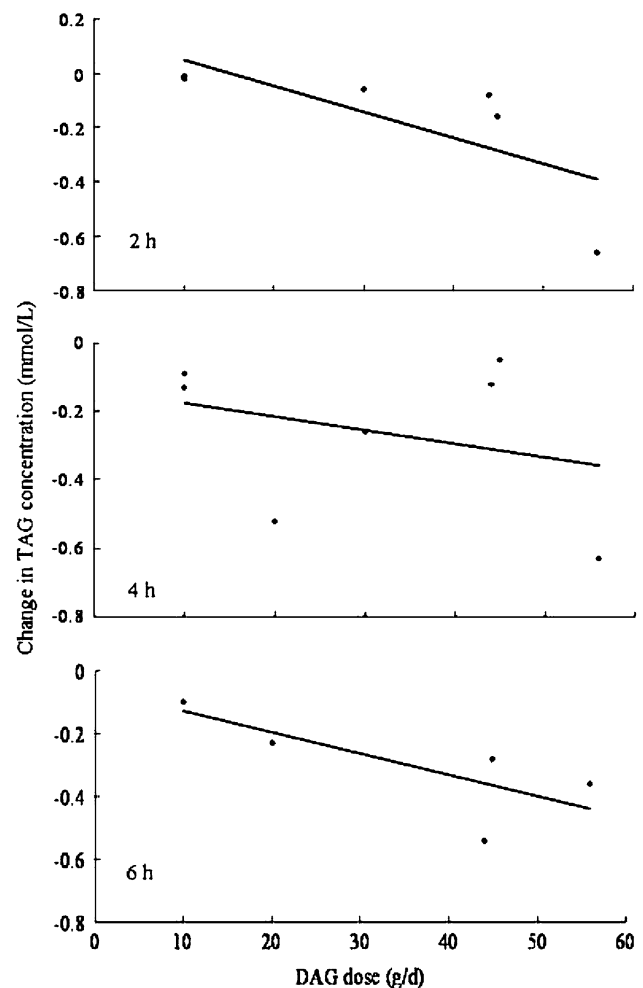


Fig. 2 Correlation between daily dosage and the effect of DAG **a** $Y = -0.0095X + 0.143$ (2 h; $R^2 = 0.541$; $P = 0.095$) **b** $Y = -0.0040X - 0.135$ (4 h; $R^2 = 0.101$; $P = 0.487$) **c** $Y = -0.0068X - 0.060$ (6 h; $R^2 = 0.650$; $P = 0.053$)

indicated a low possibility of publication bias (Fig. 1c). Sensitivity analysis showed that the removal of studies reporting data in the form of a figure reduced the effect of DAG significantly (WMD -0.12 mmol/L; 95% CI -0.27 to 0.03 mmol/L; $P = 0.12$). Linear regression showed that there was no significant correlation between daily dosage and effect ($R^2 = 0.650$; $P = 0.053$) (Fig. 2c).

Sub-group analysis showed that DAG intake could reduce the postprandial TAG concentration in normal subjects (WMD -0.14 mmol/L; 95% CI -0.23 to -0.05 mmol/L; $P = 0.002$) but not in subjects with abnormal glucose status (WMD -0.18 mmol/L; 95% CI -0.58 to 0.22 mmol/L; $P = 0.38$).

Postprandial 8 h

The 8-h postprandial TAG concentrations were reported in 2 papers with 2 independent studies [9, 11]. χ^2 test showed

that there was no significant heterogeneity between two studies ($P = 0.74$; $I^2 = 0\%$). Meta-analysis showed that there was no significant difference in the increment of postprandial serum TAG concentration between DAG and TAG groups (WMD -0.24 mmol/L; 95% CI -0.56 to 0.07 mmol/L; $P = 0.13$).

Fail-Safe Number Analysis of All Time Points

Numbers of included studies and the corresponding fail-safe numbers were 1 and 1 at 0.5 h, 1 and 1 at 1 h, 9 and 11 at 2 h, 3 and 3 at 3 h, 10 and 28 at 4 h, 6 and 19 at 6 h, 2 and 0 at 8 h. The numbers of studies included with corresponding fail-safe numbers of each of the time points are shown in Fig. 3.

Discussion

In meta-analysis of continuous outcomes, WMD and standardized mean difference (SMD) are commonly used as the effect size in determining the effect of intervention. The influences of initial values are usually not taken into account because all the studies included were randomly designed. However, some evidence showed that the initial value of some variables incidentally differed between two groups although subjects were assigned randomly [21]. The effect of intervention might be related to the initial values, such as subjects with an abundance of visceral fat area tended to achieve larger loss of visceral fat after intervention [22]. Actually, a weak but significant correlation between the initial value and the loss of visceral fat has already been observed in study conducted by Nagao et al. [21]. Therefore, the difference in the initial values of tested variables needed to be examined, especially since no published meta-analysis was available. In this study, a meta-analysis was performed to test the validity of random

design. Results showed that no significant difference in the fasting TAG concentrations was found between DAG and TAG groups. This high comparability between 2 groups might be due to the crossover design. Therefore, where studies with parallel design are concerned, the validity of random design needs to be determined.

Only one study reported the postprandial 0.5 h and 1 h TAG concentrations. Although there was no significant differences in the increment of postprandial TAG concentration between DAG and TAG groups, the P values decreased from 0.73 (0.5 h) to 0.56 (1 h) which indicated that the beneficial effect of DAG might be increased by extending the postprandial time. Meta-analysis showed that DAG could reduce the increment of TAG concentration significantly compared with TAG ($P = 0.05$) at 2 h after intervention. However, the removal of the study which did not distribute in the 95% CI reduced the effect of DAG greatly ($P = 0.11$) [11]. The effect of DAG reached a peak at postprandial 4 h ($P = 0.002$) although this effect was reduced but still was significant by the removal of 3 studies in which all data were reported in the form of a figure [9]. This large effect persisted at 6 h ($P = 0.002$) but decreased at 8 h ($P = 0.13$) after lipid loading. P values at each of the time points are displayed in Fig. 4 which provides an intuitive expression. These results indicated that the beneficial effect of DAG on postprandial TAG concentration was significantly influenced by the duration of postprandial time.

Apart from being influenced by postprandial time, the effect of DAG might be influenced by daily dosage too. Linear regression showed that the effect of DAG was obviously correlated with daily dosage at postprandial 2 h, although this correlation was not significant ($P = 0.095$). This obvious correlation indicated that the study conducted by Tada et al., in which daily dosage of 30 g lipid/m² was the largest, favored the DAG group greatly and the removal of it reduced the effect of DAG greatly in sensitivity

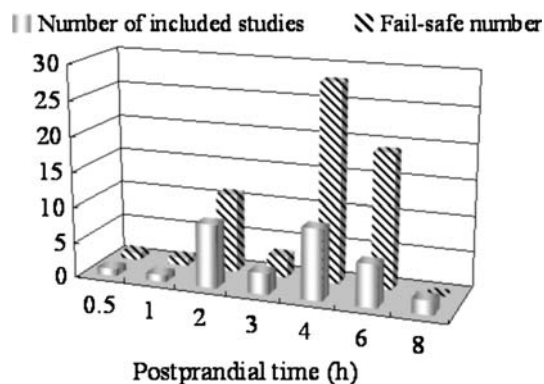


Fig. 3 Relationship between number of included studies and fail-safe number

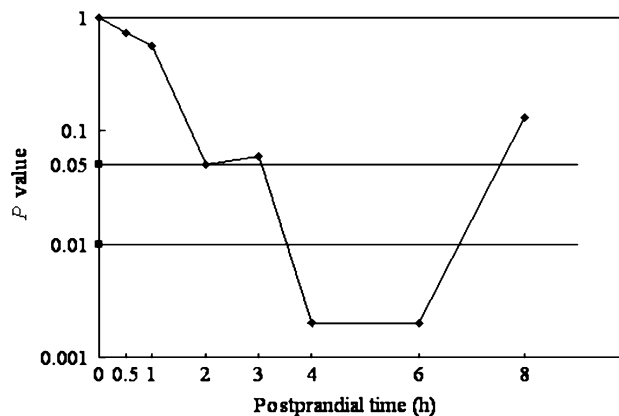


Fig. 4 Influence of postprandial time on the effect of DAG

analysis [10]. Linear regression also showed that there was a more obvious correlation between daily dosage and effect at postprandial 6 h ($P = 0.053$). This obvious correlation indicated that 2 studies with dosage of 20 g/d and 44 g/d were the most favored DAG interventions [9] and the sensitivity analysis of removing them reduced the beneficial effect greatly ($P = 0.12$). It was noticeable that the correlation at postprandial 4 h decreased greatly ($P = 0.487$). In all 10 independent studies, the number of studies in which TAG concentration reached the peak at postprandial 2 h, 3 h and 4 h was 1, 2 and 7 respectively. These results indicated that at least in 9 studies, TAG concentrations were increasing at 2 h, while in 10 studies TAG concentrations were decreasing at 6 h. This consistency in increasing or decreasing might result in these obviously positive correlations. However, TAG concentrations were rising in some studies and falling in others, and this inconsistency might result in the low correlation between daily dosage and the effect at postprandial 4 h.

Sub-group analysis (2, 4 and 6 h) showed that the WMDs of the group with abnormal glucose status were larger than those of the group with normal status which means that subjects with abnormal glucose status tended to achieve a higher reduction in the increment of postprandial TAG concentration after DAG oil supplementation. The smaller P values of abnormal glucose status groups at 2 h and 4 h also proved this trend. The larger P value of the abnormal group at 6 h compared to that of the normal group might be due to the greater 95% CI because its WMD was larger than that of the normal group. Data of the other time points was not analyzed by sub-group analysis because the number of included studies was small and it was inappropriate to split them.

There were several limitations to this study. Firstly, it was conceivable that some trials were not published although systematic efforts were made to locate and retrieve them. The distorting effects arising from publication bias and location bias have been reported repeatedly [23–25]. Secondly, necessary data for meta-analysis and linear regression were not reported in all studies. The overall results must have been affected by the use of imputed SDs although sensitivity analysis verified their rationality. Thirdly, there was some clinical heterogeneity among all studies although χ^2 tests indicated the non-existence of statistic heterogeneity. Different initial characteristics such as fasting TAG concentration ranging from 0.80 to 1.67 mmol/L [16], methodological diversity such as different washout periods ranging from 1 week [9, 15, 16] to 1 month [10], different test meal composition might influence the results of this study. Finally, although the greater fail-safe number indicated that the publication bias is not evident at the three important time points (2, 4 and 6 h), it was evident that publication bias might exist at 0.5,

1, 3 and 8 h respectively possibly due to the limited number of the studies included. The fail-safe number decreased with the decreasing number of the included studies indicating the possibility of an increased publication bias (Fig. 3).

In spite of these limitations, all papers were randomized, double-blind, TAG controlled, crossover designed which indicated high methodological quality. Funnel plots indicated the low possibility of publication bias. These results indicated the robustness of meta-analysis, demonstrating that DAG reduced the increment of postprandial TAG concentration significantly compared with TAG. This beneficial effect is most likely attributable to the different structure of DAG from TAG because its energy value and digestibility are similar to those of TAG [26]. The initial products of digested TAG are free fatty acids and 2-monooacylglycerol (MAG) and those for 1,3-DAG are free fatty acids and 1(3)-MAG [27]. The resynthesis of TAG in small intestinal epithelial cells from 2-MAG is faster than from 1(3)-MAG because the later involves the phosphatic acid pathway, a slower turnover pathway than the 2-MAG pathway. It suggests that the extent of postprandial TAG concentration increment after a single dose of DAG emulsion was less than that after a single dose of TAG emulsion.

In conclusion, compared to TAG oil, DAG reduced serum postprandial TAG concentrations significantly at postprandial 2 h, 4 h and 6 h which were positively correlated with daily dosage.

References

- Goldberg RB (2000) Hyperlipidemia and cardiovascular risk factors in patients with type 2 diabetes. *Am J Manage Care* 6:S682–S691
- Roccatagliata D, Avanzini F, Monesi L, Caimi V, Lauri D, Longoni P, Marchioli R, Tombesi M, Tognoni G, Roncaglioni MC (2006) Is global cardiovascular risk considered in current practice? Treatment and control of hypertension, hyperlipidemia, and diabetes according to patients' risk level. *Vasc Health Risk Manage* 2:507–514
- Uiterwaal CS, Grobbee DE, Witteman JC, van Stiphout WA, Krauss XH, Havekes LM, de Bruijn AM, Van Tol A, Hofman A (1994) Postprandial triglyceride response in young adult men and familial risk for coronary atherosclerosis. *Ann Intern Med* 121:576–583
- Couillard C, Bergeron N, Prud'homme D, Bergeron J, Tremblay A, Bouchard C, Mauriege P, Despres JP (1998) Postprandial triglyceride response in visceral obesity in men. *Diabetes* 47:953–960
- Jeppesen J, Hollenbeck CB, Zhou MY, Coulston AM, Jones C, Chen YD, Reaven GM (1995) Relation between insulin resistance, hyperinsulinemia, postheparin plasma lipoprotein lipase activity, and postprandial lipemia. *Arterioscler Thromb Vasc Biol* 15:320–324
- Stern MP, Mitchell BD, Haffner SM, Hazuda HP (1992) Does glycemic control of type II diabetes suffice to control diabetic

- dyslipidemia? A community perspective. *Diabetes Care* 15:638–644
7. Hara K, Onizawa K, Honda H, Otsuji K, Ide T, Murata M (1993) Dietary diacylglycerol-dependent reduction in serum triacylglycerol concentration in rats. *Ann Nutr Metab* 37:185–191
 8. Murata M, Ide T, Hara K (1997) Reciprocal responses to dietary diacylglycerol of hepatic enzymes of fatty acid synthesis and oxidation in the rat. *Br J Nutr* 77:107–121
 9. Taguchi H, Watanabe H, Onizawa K, Nagao T, Gotoh N, Yasukawa T, Tsushima R, Shimasaki H, Itakura H (2000) Double-blind controlled study on the effects of dietary diacylglycerol on postprandial serum and chylomicron triacylglycerol responses in healthy humans. *J Am Coll Nutr* 19:789–796
 10. Tada N, Watanabe H, Matsuo N, Tokimitsu I, Okazaki M (2001) Dynamics of postprandial remnant-like lipoprotein particles in serum after loading of diacylglycerols. *Clin Chim Acta* 311:109–117
 11. Gibaldi M (1993) Meta-analysis. A review of its place in therapeutic decision making. *Drugs* 46:805–818
 12. Whigham LD, Watras AC, Schoeller DA (2007) Efficacy of conjugated linoleic acid for reducing fat mass: a meta-analysis in humans. *Am J Clin Nutr* 85:1203–1211
 13. He FJ, Nowson CA, MacGregor GA (2006) Fruit and vegetable consumption and stroke: meta-analysis of cohort studies. *Lancet* 367:320–326
 14. Joshipura KJ, Ascherio A, Manson JE, Stampfer MJ, Rimm EB, Speizer FE, Hennekens CH, Spiegelman D, Willett WC (1999) Fruit and vegetable intake in relation to risk of ischemic stroke. *JAMA* 282:1233–1239
 15. Takase H, Shoji K, Hase T, Tokimitsu I (2005) Effect of diacylglycerol on postprandial lipid metabolism in non-diabetic subjects with and without insulin resistance. *Atherosclerosis* 180:197–204
 16. Ai M, Tanaka A, Shoji K, Ogita K, Hase T, Tokimitsu I, Shimokado K (2006) Suppressive effects of diacylglycerol oil on postprandial hyperlipidemia in insulin resistance and glucose intolerance. *Atherosclerosis* 195:398–403
 17. Higgins J, Green S (2006) *Cochrane handbook for systematic reviews of interventions* 4.2.6. Wiley, Chichester
 18. Tada N, Shoji K, Takeshita M, Watanabe H, Yoshida H, Hase T, Matsuo N, Tokimitsu I (2005) Effects of diacylglycerol ingestion on postprandial hyperlipidemia in diabetes. *Clin Chim Acta* 353:87–94
 19. Tomonobu K, Hase T, Tokimitsu I (2006) Dietary diacylglycerol in a typical meal suppresses postprandial increases in serum lipid levels compared with dietary triacylglycerol. *Nutrition* 22:128–135
 20. Saito S, Tomonobu K, Hase T, Tokimitsu I (2006) Effects of diacylglycerol on postprandial energy expenditure and respiratory quotient in healthy subjects. *Nutrition* 22:30–35
 21. Nagao T, Watanabe H, Goto N, Onizawa K, Taguchi H, Matsuo N, Yasukawa T, Tsushima R, Shimasaki H, Itakura H (2000) Dietary diacylglycerol suppresses accumulation of body fat compared to triacylglycerol in men in a double-blind controlled trial. *J Nutr* 130:792–797
 22. Leenen R, van Der KK, Deurenberg P, Seidell JC, Weststrate JA, Schouten FJ, Hautvast JG (1992) Visceral fat accumulation in obese subjects: relation to energy expenditure and response to weight loss. *Am J Physiol* 263:E913–E919
 23. Dickersin K (1990) The existence of publication bias and risk factors for its occurrence. *JAMA* 263:1385–1389
 24. Easterbrook PJ, Berlin JA, Gopalan R, Matthews DR (1991) Publication bias in clinical research. *Lancet* 337:867–872
 25. Egger M, Smith GD (1998) Bias in location and selection of studies. *BMJ* 316:61–66
 26. Taguchi H, Nagao T, Watanabe H, Onizawa K, Matsuo N, Tokimitsu I, Itakura H (2001) Energy value and digestibility of dietary oil containing mainly 1,3-diacylglycerol are similar to those of triacylglycerol. *Lipids* 36:379–382
 27. Kondo H, Hase T, Murase T, Tokimitsu I (2003) Digestion and assimilation features of dietary DAG in the rat small intestine. *Lipids* 38:25–30

Determination of Triacylglycerols in Butterfat by Normal-Phase HPLC and Electrospray–Tandem Mass Spectrometry

P. Kalo · A. Kemppinen · V. Ollilainen

Received: 15 April 2008 / Accepted: 11 September 2008 / Published online: 24 October 2008
© AOCS 2008

Abstract Here, we report the identification and quantification of the molecular species of long-, medium-, and short-chain triacylglycerols (TAG) in butterfat (BF), including TAG with an odd number of acyl carbons (ACN) and TAG with unidentified molecular species. In the present study, in addition to auto-MS², a large number of methods, each recording MS² for 1–4 ions, were used for identification of TAG species. For the quantification of long-chain, odd ACN TAG, and TAG with unidentified molecular species, molar correction factors (MCF) were calculated from the uncorrected mol% (area mol%) of each ACN:DB (number of double bonds) class in randomized butterfat (RBF), and the respective mol% in the calculated random composition of RBF. The butyrate, caproate, and medium-chain (C₈, C₁₀) TAG were quantified using regio- or acyl-chain-specific MCF calculated from their area mol% in RBF and mol% in the calculated random composition. These methods enabled us to identify ca. 450 TAG species in 184 quantified peaks of 88 ACN:DB classes. The proportions of saturated, monoene, diene, triene, tetraene, pentaene, and hexaene TAG were 40.0, 38.4, 16.2, 4.5, 0.6, 0.1, and 0.03 mol%, respectively. The proportions of TAG with not identified molecular species and odd ACN TAG were 11.8 and 5.7 mol%, respectively. The most abundant short-chain TAG species were

butyroyldipalmitoylglycerol + butyroylmyristoylstearyl-glycerol (5.25 mol%) and butyroylpalmitoyloleoylglycerol (4.08 mol%).

Keywords Normal-phase liquid chromatography · Ion trap · Positive electrospray ionization tandem mass spectrometry · Milk fat · Long-, medium-, short-chain, and odd acyl carbon number triacylglycerols · Quantification of triacylglycerol species · Regioisomers · Molar correction factors

Abbreviations

ACN	The number of acyl group carbons
ACN:DB	The number of acyl group carbons:the number of double bonds
APCI	Atmospheric pressure chemical ionization
BF	Butterfat
CI	Chemical ionization
DAG	Diacylglycerol(s)
EI-MS	Electron ionization mass spectrometry
ESI-MS	Electrospray mass spectrometry
ESI-MS ²	Electrospray tandem mass spectrometry
GC	Gas-liquid chromatography
HPLC	High performance liquid chromatography
ISTD	Internal standard
LC-MS	Liquid chromatography-mass spectrometry
MCF	Molar correction factor
MF	Milk fat
NP	Normal-phase
RBF	Randomized butterfat
RP	Reversed-phase
RRT	Relative retention time
SFC	Supercritical fluid chromatography
sn	Stereospecific numbering

P. Kalo (✉) · V. Ollilainen
Department of Applied Chemistry and Microbiology,
University of Helsinki, Helsinki, Finland
e-mail: paavo.kalo@helsinki.fi

A. Kemppinen
Department of Food Technology, University of Helsinki,
Helsinki, Finland

SPE	Solid phase extraction
TAG	Triacylglycerol(s)
TLC	Thin layer chromatography

Introduction

Milk fat (MF) is one of the most complex natural fats for which the expression “the marvel of Nature” is very appropriate. More than 400 different, mainly esterified fatty acids (FA) have been identified, and a high number of triacylglycerol (TAG), phospholipid, glycolipid, diacylglycerol (DAG), and free fatty acid (FFA) molecular species as well [1]. The proportion of the major lipid class, TAG is 97–98% of total milk lipids. Owing to the high number of different FA, milk fat may theoretically contain a huge number of TAG, namely n^3 (n is the number of FA), and it is expected that FA are randomly distributed. However, the distribution of FA in native milk fat is specific, and the number of TAG species is markedly lower than n^3 . Regiospecific analysis of TAG showed that short-chain FA, C_4 and C_6 are preferentially, but not exclusively, esterified in the *sn*-3 position [2–4]. Separation and identification of milk TAG have been studied by high temperature gas–liquid chromatography (GC) [5–9], supercritical fluid chromatography (SFC) [10, 11], reversed-phase high performance liquid chromatography (RP-HPLC) [12–18], and normal-phase HPLC (NP-HPLC) [19]. Gresti et al. [14] determined more than 220 molecular species of even-numbered TAG by fractionation of MF using RP-HPLC and determination of TAG and FA compositions of these fractions by capillary GC. Kemppinen and Kalo [9] determined recently more than 130 molecular species of even-numbered TAG in butterfat (BF) and randomized BF (RBF) using silver ion chromatographic fractionation into saturated, monoene, and diene and triene fractions and GC-electron ionization mass spectrometry (EI-MS).

In NP-HPLC, TAG have been shown to elute in the order of the descending number of acyl group carbons (ACN), but in the order of the ascending number of double bonds [20, 21]. In recent years, NP-HPLC has been applied in lipid class separations in several studies as reviewed by Lin [22]. The small particle size, regular columns are able to separate regioisomers of acetate and propionate TAG [23] and microbore silica gel columns are able to separate regioisomers of acetate, butyrate and caproate TAG [19, 24]. Furthermore, microbore silica gel columns have been observed to separate molecular species in several lipid classes sufficiently to allow identification by electrospray tandem mass spectrometry (ESI-MS²)

[25]. The fragmentation mechanism in the ESI-MS² of $[M + NH_4]^+$ has been investigated in a number of studies [25–29].

In the direct inlet MS, the size of molecular ions and fragment ions [30–32] and the degree of unsaturation [30, 33, 34] have been found to affect the relative yields of ions and the correction factors. Furthermore, isobaric TAG with different acyl-chains and regioisomers have been shown to have different correction factors in direct inlet MS [33] and ESI-MS [19, 24]. In direct inlet HPLC-MS, the correction factors have been calculated from the ratio of the area percentage of total ion current and calculated TAG composition [33], in negative ion tandem MS (NI-MS²) from $[RCOO]^-$ ions in the daughter ion spectra of $[M - H]^-$ ions and respective ions in the spectra of standards [34]. In RP-LC-APCI-MS, Byrdwell et al. [35, 36] determined correction factors (1) by comparisons of FA values determined for TAG by GC and the sum of areas of all DAG peaks and protonated TAG peaks in MS, and (2) by dividing the expected TAG composition (calculated based on random distribution of FA) by the TAG composition determined by LC-MS. In NP-LC-ESI-MS, correction factors have been determined for short-chain TAG regioisomers by linear calibration using the plots $n(1)/n(ISTD)$, determined for TAG species in the randomized samples of three-acid standard mixtures by GC, versus area (1)/area (ISTD) in the ESI ion chromatograms of ammonium adducts [19, 24]. In GC-EI-MS, linear calibration has been used in the determination of correction factors for $[M - RCOO]^+$ ions as well [9].

Several acetate TAG have been identified in MF [5, 19, 37–39] and their relative ratios have been estimated [19], but their content in total milk fat have not been measured. TAG with odd ACN separate from the even ACN by GC on a polarizable capillary column [5] and by RP-HPLC [13]. In the latter research their total content was estimated at 11.6–15.1%.

In the present study, our aim was to identify and quantify the molecular species of long-, medium-, and short-chain TAG in BF, including TAG with odd ACN, by NP-HPLC-ESI-MS. Our aim was also to quantify long-chain even and odd ACN TAG, and TAG with not identified molecular species, using molar correction factors (MCF) calculated from the area data of each ACN:DB class and internal standard recorded for randomized butterfat (RBF) and the calculated random composition of TAG species. Further, our aim was to quantify butyrate, caproate, and medium-chain (C_8 , C_{10}) TAG using regio- or acyl-chain-specific MCF calculated from their areas in RBF and mol% in the calculated random composition.

Materials and Methods

Materials

Anhydrous BF was purchased from Valio Ltd (Helsinki, Finland). BF was dried under vacuum, below 3.3 kPa, for 100 min at 95 °C to the water content of 55–85 ppm and heated for 30 min at 95 °C with bleaching earth (2%). Randomized BF (RBF) was prepared by interesterification of a sample of dried and bleached BF with 1% of sodium methoxide as catalyst for 1 h at 85–90 °C [9, 24]. The standard mixture GLC74 of fatty acid methyl esters was purchased from Nu-Chek Prep (Elysian, MN, USA). All solvents were purchased from Rathburn (Walkerburn, United Kingdom) and were HPLC grade. Flash column chromatography grade silica gel 60 was purchased from Merck (Darmstadt, Germany) and had the characteristics described elsewhere [19].

Determination of Randomness of RBF by Lipase Hydrolysis

Isolation of TAG

Triacylglycerols were isolated from a ca. 12 mg aliquot of raw interesterification product of BF on a 0.5 g silica gel solid phase extraction (SPE) column STRATATM-SI-1 (Phenomenex). Prior to the introduction of the sample, the column was eluted with 5 mL hexane. The sample was introduced in 0.1 mL of 22/78 (v/v) dichloromethane:hexane and sterol esters and fatty acid methyl esters were eluted with 4 mL of the same solvent mixture. TAG were eluted with 4 mL of dichloromethane and partial acylglycerols with 4 mL of 40/60 (v/v) acetone/dichloromethane. The fractionation was monitored by thin layer chromatography on a 0.25-mm plain silica gel plate, which was eluted with hexane/diethyl ether/acetic acid 50:50:1 (v/v/v). After drying, the plate was sprayed with 2,7-dichlorofluorescein.

Transesterification of TAG

In order to transesterify the TAG to fatty acid methyl esters (FAME), 0.2 µL 2 M sodium methoxide in methanol and 20 µL hexane were added to a 0.3 mg aliquot of isolated TAG in a 0.25 mL insert of an autosampler vial, mixed for 1 min in a Vortex mixer and after centrifugation with 800–1,000 rpm for 10 min, 1 µL of supernatant was injected to a Micromat gas chromatograph equipped with a 30-m HP-Innowax capillary column with 0.25 mm i.d.

Determination of Fatty Acids in the *sn*-2 Position

A fat sample was hydrolyzed by porcine pancreatic lipase, type II (Sigma, St Louis, MO, USA) according to the principles presented by Hendrikse and Harwood [40] as follows: 5.3 mg TAG sample and 150 µL TRIS buffer, pH 8, 25 µL sodium cholate (1 g/L), and 10 µL calcium chloride (2.2%) were mixed in a 1.5-mL autosampler vial, heated for 1 min at 40 °C in a water bath, and mixed for 2 min in a Vortex mixer. After cooling with tap water, 50 µL 6 M hydrochloric acid and 0.2 mL diethyl ether were added and centrifuged 800–1,000 rpm for 1 min. The supernatant diethyl ether layer was drawn off with a Pasteur pipette. The extraction with 0.2 mL diethyl ether was repeated twice. The combined ether extracts were dried with anhydrous sodium sulphate and applied as a band on a 0.25-mm plain silica gel plate. The plate was developed as described above. The monoacylglycerol (MAG) band was scraped off and MAG were extracted from sorbent twice with 1 mL of diethyl ether. After evaporation of ether extract to ca. 0.1 mL, the extract was transferred to a 0.25-mL insert and evaporated to dryness and the *sn*-2 MAG were transesterified to FAME as described above for TAG.

Fractionation by Silica Gel Solid Phase Extraction

The SPE column (5.4 × 1.5 cm) was prepared in a 15-mL Isolute filtration column tube with microbore filters (International Sorbent Technology, Hengoed, United Kingdom) using a dry packing method. The BF sample (100 mg) was fractionated as follows: prior to elution of the TAG fractions, cholesterol esters were eluted with 40 mL 22/78 dichloromethane:hexane. TAG were eluted in four fractions I, II, III, and IV on the silica gel SPE. Fraction I was eluted with 60 mL of 60:40 dichloromethane/hexane, and fractions II, III, and IV with 40 mL of 65/35, 85/15, and 100/0 dichloromethane/hexane, respectively [19]. The amounts of trinonanoin (Sigma, St Louis, MO, USA) internal standard added were: 14.766 µmol to fraction I, 3.691 µmol to fraction II, 0.886 µmol to fraction III, and 0.148 µmol to fraction IV. The solvents were evaporated to dryness from fractions I–IV and following free fatty acid, diacylglycerol, sterol, and monoacylglycerol fractions. The weighing of evaporation residues revealed total recovery of 100%. The evaporation residues of fractions I–IV were dissolved in 5.0, 2.5, 1.0, and 0.3 mL of 2/1 chloroform:methanol. The same principles were used in the fractionation of RBF. To fraction I was added 7.773, to fraction II 3.887, to fraction III 1.555, and to fraction IV 0.777 µmol trinonanoin as the internal standard. After evaporation of the solvents, fractions I–IV were dissolved in 5.0, 2.5, 1.0, and 1.0 mL of 2/1 chloroform:methanol.

The BF and RBF fractions were stored in tightly closed vials at $-18\text{ }^{\circ}\text{C}$ under argon and kept in darkness.

Normal-Phase Liquid Chromatography–Electrospray Tandem Mass Spectrometry

The TAG fractions of BF and RBF were analyzed by normal-phase HPLC (NP-HPLC) using three Phenomenex Luna 3- μm silica columns, $100 \times 2.0\text{ mm}$, and a $4 \times 2.0\text{ mm}$ guard column, in series. The same multistage binary gradient of hexane (A) and hexane/methyl-*tert*-butyl ether/acetic acid (60:40:1), by vol. (B) as in the previous study [19] with the following parameters was used (time in min/%B by vol./flow in mL/min): 0/0/0.1, 2/5/0.1, 18/18/0.1, 30/18/0.1, 31/90/0.1, 49/90/0.1, 50/99/0.1, 64/99/0.5, 65/0/0.5, and 75/0/0.5. In order to compensate for a malfunction of the chromatograph, some samples were analyzed using B (50:50:1, by vol.). A 3D ion-trap Bruker Esquire LC–MS (Bruker Daltonic, Bremen, Germany) was operated in positive ESI mode. Capillary voltage was set to 3,000 V, capillary exit offset 60 V, skimmer potential 20 V, and trap drive value 55. The reagent solvent, chloroform/methanol/ammonia water (25%) 20:10:3 (by vol.), was pumped with a flow rate of 6.0 mL/min via a 1:100 split device to the effluent flow. Full scan ESI mass spectra were recorded in duplicate or triplicate using a scan range of 50–1,000 m/z and summation of 15 spectra. Nebulizer nitrogen pressure was 275 kPa, drying gas (nitrogen) flow 8 L/min, and drying temperature $300\text{ }^{\circ}\text{C}$. Auto-MS/MS spectra of two most intense ions eluting concurrently were recorded using helium (99.996%, 0.1 kPa) as the collision gas. In addition to auto-MS/MS, 78 methods with time-windows for isolation and fragmentation of 1–4 ions were used. Prior to the analyses of the BF and RBF fractions, the linearity of detector response was studied by injecting several volumes or dilutions of these SPE fractions. The injection volume/dilution selected was the one that showed the highest peak areas without affecting the area ratio of high abundance and low abundance peaks.

Determination of Molar Correction Factors for Correction of Ion Yield

The TAG in the fractions I–IV of RBF were analyzed by NP-HPLC with the three silica columns in series and the effluent flow was conveyed to the ion source of the mass spectrometer. Then 105 different ion chromatograms for TAG ammonium adducts were extracted from the MS data recorded in duplicate. These ion chromatograms of isobaric TAG were integrated. For identification of the molecular species of isobaric TAG in these ion chromatograms auto-MS/MS, and 78 methods with time windows for isolation and collision induced decay of 1–4 ions, were applied. The

presence of a known amount of internal standard (trinonanoic acid) in the four fractions permitted the calculation of uncorrected molar amount (area mol) of each integrated peak in each ion chromatogram. And the area mol% (uncorrected mol%) could be calculated from the mean of duplicate data for the respective uncorrected molar amount (area mol) and the sum of all area moles in the four fractions.

Results

Determination of the Randomness of RBF by Lipase Hydrolysis

A sample of RBF TAG was hydrolyzed by 1.3-specific pancreatic lipase according to the principles presented by Hendrikse and Harwood [40] and the *sn*-2-MAG of hydrolysate were isolated by TLC. Samples of TAG and *sn*-2-MAG were transesterified to FAME and their compositions were determined by GC. The percentage of C-6:0, C-8:0, C-10:0, C-12:0, C-14:0, C-14:1, C-15:0, C-16:0, C-16:1, C-17:0, C-17:1, C-18:0, C-18:1, C-18:2 in the *sn*-2 position was 29.5, 32.0, 37.5, 37.1, 36.5, 22.8, 38.0, 35.8, 28.2, 38.0, 35.1, 35.0, 29.1, 23.4%, respectively (on the average 32.7%, SD 5.3). Unfortunately, owing to the small sample of TAG subjected to lipase hydrolysis, the major part of C-4:0 MAG remained on the TLC plate. In order to avoid the impairment of other percentages, the percentages of C-4:0 had to be disregarded. The presented data indicate random distribution of FA among the three positions of TAG.

Identification of Molecular Species of TAG

The four SPE fractions of BF and RBF were analyzed by HPLC–ESI–MS using three micro-bore silica gel columns in series. Ion chromatograms (EIC) were extracted from ESI–MS data for 105 ACN:DB classes of TAG in BF and RBF and MS² were recorded for each peak with sufficient intensity using auto-MS² or/and a method with time windows for the ACN:DB class in question. The collision induced decay (CID) of ammonium adducts, $[\text{M} + \text{NH}_4]^+$, generated by ESI produced abundant $[\text{DAG}]^+$ ions, $[(\text{M} + \text{NH}_4) - \text{NH}_3 - \text{FA}]^+$, and low intensity $[(\text{M} + \text{NH}_4) - \text{NH}_3]^+$ ions. The acyl-chains of TAG were deduced from $[\text{DAG}]^+$ ions. The preferential loss of acyl-chains from the primary positions of long-chain [28] and short-chain TAG [19, 24] in the CID of ESI produced $[\text{M} + \text{NH}_4]^+$ ions that enabled the identification of chromatographically separated regioisomer of short-chain (C₂–C₆) TAG, and the predominant regioisomer of medium- and long-chain TAG (Table 3).

In a previous study [19], the resolution of regioisomers of butyrate and caproate TAG, in 20 randomized mixtures of three monoacid TAG, were studied under the same chromatographic conditions as in the present paper. The regioisomers of dibutyrate TAG were resolved with baseline resolution, R_S values between 1.5 and 2.0, and those of dicaproate TAG only partially with R_S in the range 0.5–1.1. In the present study, Fig. 1 demonstrates the resolution and identification of acyl-chain- and regioisomers of TAG 26:0 in BF. In the first peak (B) separated partially from peak C were eluted 12:0/10:0/4:0 + 14:0/8:0/4:0, in the peak C 14:0/8:0/4:0, in the partially separated peaks D and E regioisomers 16:0/6:0/4:0 and 6:0/16:0/4:0, and in the peak F 18:0/4:0/4:0. In contrast to the identification of regioisomers L/4:0/4:0 and 4:0/L/4:0 in the TAG 24:0 and 26:1, the regioisomer 4:0/18:0/4:0 was not identified.

In the randomized standard mixtures [19], the regioisomers of TAG with one butyryl chain were separated to the baseline with R_S between 1.6 and 2.9. Those of saturated TAG with one caproyl chain were separated close to the baseline with R_S in the range 1.0–1.5 and those of unsaturated TAG with one caproyl chain close to the baseline or partially with R_S in the range 0.5–1.3. In the present study, Fig. 2b shows the resolution of acyl-chain isomers of TAG 36:0 and identification of acyl-chain- and regioisomers. The MS² spectra B–F indicated that in the peak B eluted trilaurin and medium-chain TAG, in the peak C 16:0/14:0/6:0, in the peak D 16:0/16:0/4:0 + (18:0/14:0/4:0), in the peak E 18:0/2:0/16:0, and in the peak F 18:0/16:0/2:0 + 16:0/18:0/2:0.

Figure 3 demonstrates the separation and identification of acyl-chain isomers of odd-numbered long-chain TAG.

From the CID of peak B of TAG 51:0 were identified 19:0/16:0/16:0 and 19:0/14:0/18:0, from that of the peak C 20:0/15:0/16:0 and 20:0/14:0/17:0, and from that of peak D 18:0/17:0/16:0 and 18:0/15:0/18:0. Figure 4 shows EIC, MS, and MS² for TAG 50:1 as an example of the resolution and identification of acyl-chain isomers of long-chain even-numbered TAG. The CID of peak E of TAG 50:1 is consistent with 20:0/12:0/18:1, 20:0/16:0/14:1 + 20:0/14:1/16:0, 20:0/14:0/16:1 and that of peak F with 18:1/16:0/16:0, 18:1/14:0/18:0 (16:0/18:0/16:1). Figure 5 reveals the resolution and identification of TAG 56:1 regioisomers. The CID of peak B indicates regioisomers 20:0/18:0/18:1 + 20:0/18:1/18:0 and that of peak C regioisomer 18:1/20:0/18:0 together with 18:1/22:0/16:0.

Quantification of Molecular Species of TAG in an Interesterified Standard Mixture

In order to test the applicability of the proposed quantification method, the MS data of equimolar interesterified mixture of tributyrin, trimyristin and triolein recorded in the previous study [19] were reanalyzed. From duplicate area data for 15 TAG species in the solution A, were calculated the uncorrected molar amount, uncorrected mol%, and the mol% according to random distribution. The MCF obtained from the ratios of calculated mol% and uncorrected mol% are shown in Table 1. Molar amounts of the TAG species in the solution B of the same interesterified mixture were calculated from the MCF and area data. Molar amounts of TAG species in the solution B were similar or very similar to those determined by GC except

Fig. 1 Identification of the TAG 26:0 molecular species from the MS² data of fraction III. **a** EIC of the ammonium adduct 26:0, $m/z = 516.7$. **b** Tandem MS at 43.6 min: 12:0/10:0/4:0 + 14:0/8:0/4:0. **c** Tandem MS at 44.0 min: 14:0/8:0/4:0. **d** Tandem MS at 44.6 min: 16:0/6:0/4:0. **e** Tandem MS at 44.9 min: 6:0/16:0/4:0. **f** Tandem MS at 46.2 min: 18:0/4:0/4:0

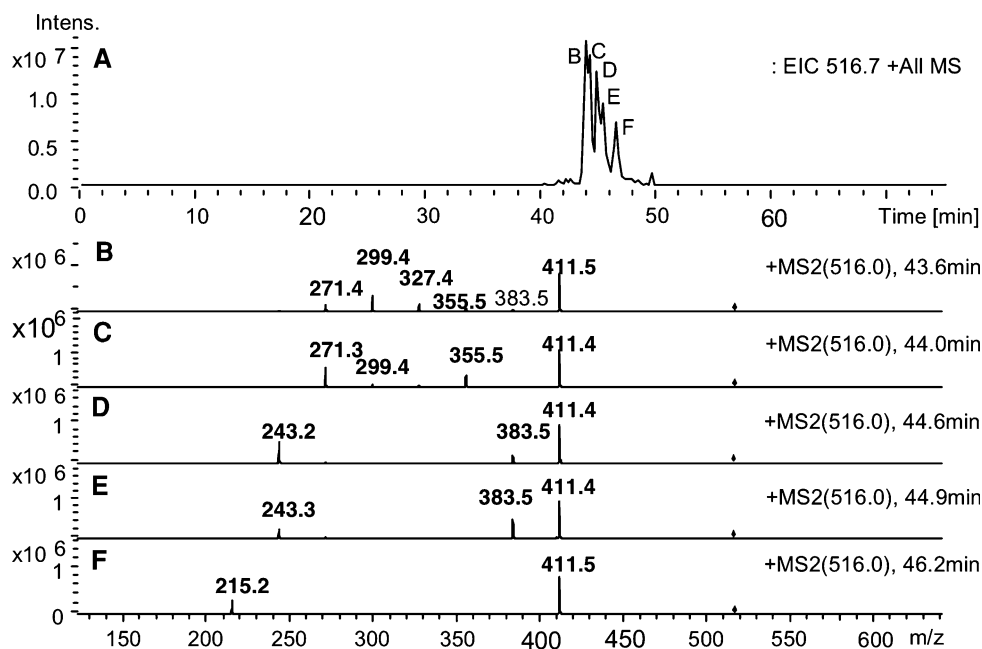
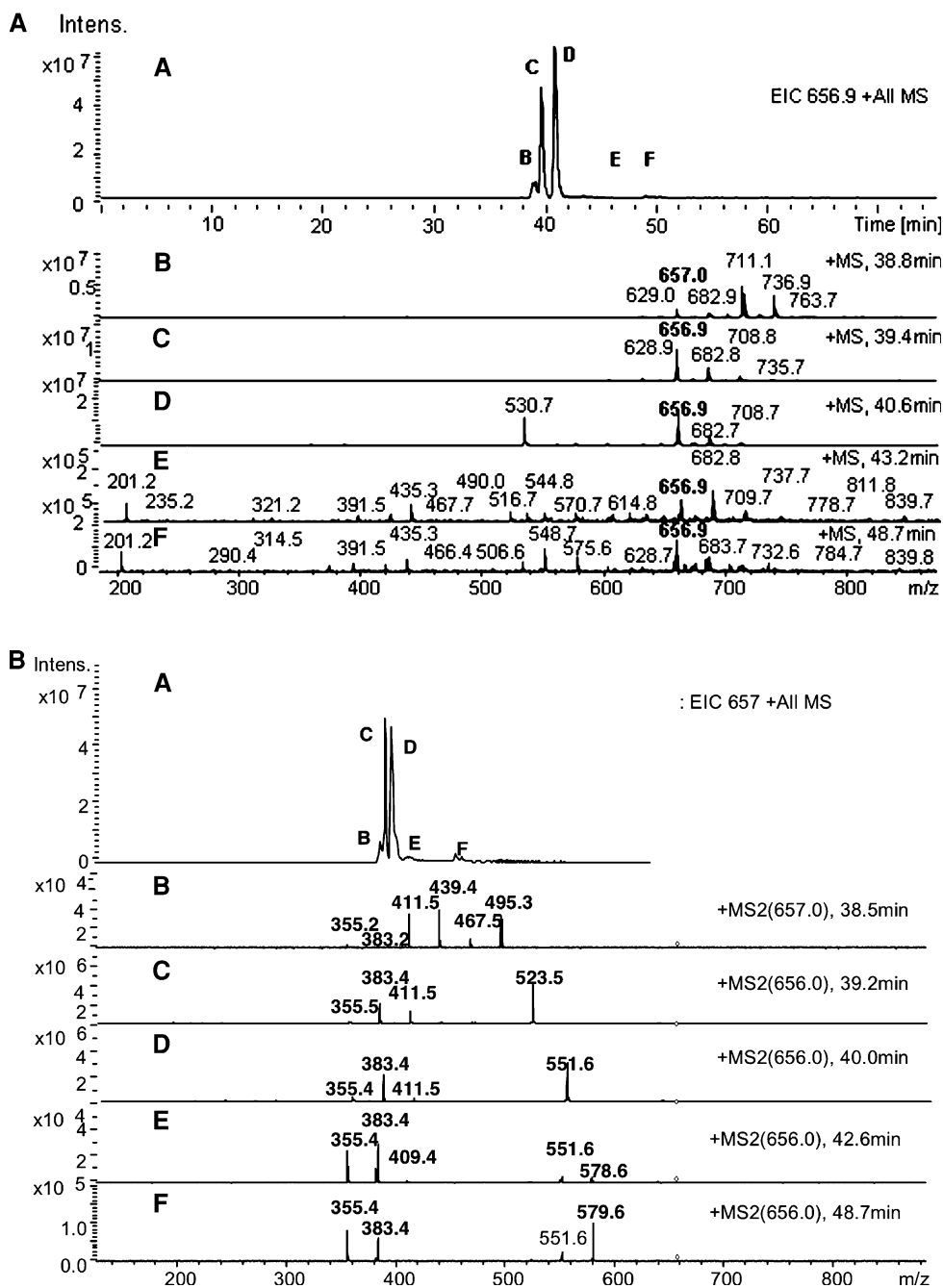


Fig. 2 a Mass spectra recorded for TAG 36:0 species in fraction II. (A) EIC of the ammonium adduct 36:0, $m/z = 656.9$. (B) MS at 38.8 min. (C) MS at 39.4 min. (D) MS at 40.6 min. (E) MS at 43.2 min. (F) MS at 48.7 min. **b** Identification of the TAG 36:0 molecular species from the MS² data of fraction II. (A) EIC of the ammonium adduct 36:0, $m/z = 656.9$. (B) Tandem MS at 38.5 min: 12:0/12:0/12:0, 14:0/10:0/12:0, 14:0/14:0/8:0, 12:0/16:0/8:0, 10:0/18:0/8:0, (10:0/16:0/10:0). (C) Tandem MS at 39.2 min: 16:0/14:0/6:0. (D) Tandem MS at 40.0 min: 16:0/16:0/4:0 (18:0/14:0/4:0). (E) Tandem MS at 42.6 min: 18:0/2:0/16:0. (F) Tandem MS at 48.7 min: 18:0/16:0/2:0 + 16:0/18:0/2:0



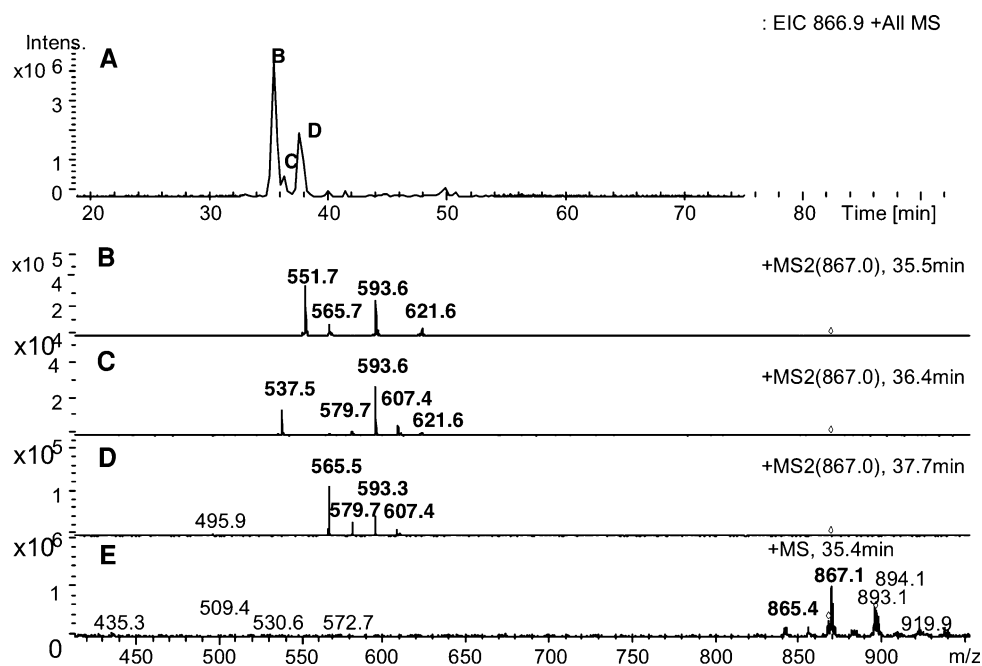
that for tributyrin. Regioisomeric ratios were on the average 0.501 (SD = 0.100, $n = 10$), as expected.

Determination of Molar Correction Factors for the Correction of the Ion Yield

For the determination of MCF, ion chromatograms for 105 ACN:DB classes were extracted from the ESI-MS data of four SPE fractions of RBF and the ion chromatograms were integrated. The TAG species in all peaks with sufficient intensity were identified from recorded HPLC-ESI-MS².

The uncorrected molar amount (area mol) was calculated from the area data and the amount of ISTD in each SPE fractions of RBF for the peaks in all EIC. The sum of all uncorrected molar amounts in the four SPE fractions for the respective peaks with similar relative retention time (RRT) and identity of TAG species was calculated. The uncorrected mol% of the TAG species in these peaks was obtained by dividing each sum of uncorrected molar amounts in the four SPE fractions with the sum of all uncorrected amounts. MCF for an ACN:DB-class was calculated by dividing the mol% of ACN:DB class calculated

Fig. 3 Identification of the TAG 51:0 molecular species from the MS² data of fraction I. **a** EIC of the ammonium adduct 51:0, $m/z = 866.9$. **b** Tandem MS at 35.5 min: 19:0/16:0/16:0, 19:0/14:0/18:0. **c** Tandem MS at 36.4 min: 20:0/15:0/16:0, 20:0/14:0/17:0. **d** Tandem MS at 37.7 min: 18:0/17:0/16:0, 18:0/15:0/18:0. **e** MS at 35.4 min



according to random distribution by the sum of all experimentally determined uncorrected mol% for all peaks except acetates and the peaks with not identified molecular species eluting after acetate peaks (Table 2). The acyl-chain- and regiospecific MCF for butyrate and caproate TAG and acyl-chain-specific for medium-chain TAG were calculated by dividing the sum of mol% of the TAG species in the composition calculated according to random distribution, which were identified in the respective peak in RBF, by the experimentally determined respective uncorrected mol% (Table 2).

Molar correction factors varied widely, because the ion yield is affected by molecular size, unsaturation, and regioisomerism. Wide variation of MCF for BF TAG can be expected, because in BF TAG all these parameters vary extensively. The specific MCF showed a few trends: the ratios of MCF for $X/4:0/4:0$ and $4:0/X/4:0$ for 24:0 and 26:1 were 1.60 and 1.40, respectively. The ratio of MCF for even-numbered $X/X/4:0$ and $X/X/6:0$ in the ACN range 28–40 varied considerably and was on the average 2.86 (SD = 1.38, $n = 13$). The ratio of MCF for even-numbered $X/X/M$ and $X/X/6:0$ varied as well. In addition, a few trends were observed in the values of MCF for even-numbered saturated TAG. MCF increased from ACN:DB 18:0 to 24:0, 26:0 to 36:0, 40:0 to 48:0, and decreased to 54:0. Those for even-numbered monoene TAG varied considerably and increased from ACN:DB 22:1 to 26:1, decreased to 30:1, increased to 36:1, decreased to 38:1, increased from 40:1 to 50:1, and decreased to 54:1. Comparison of MCF for saturated and monoene TAG with the same ACN showed that those for saturated were higher for TAG 22 and 24, those for monoene higher for TAG 26–32,

those for saturated higher for TAG 34–48, and those for monoene higher for TAG 50–54.

¹³C may have a considerable effect in quantification of TAG that has to be corrected in direct ESI–MS as shown by Han and Gross [41]. However, in the present study using NP-HPLC–ESI–MS and MCF calculated from the ratio of calculated mol% and uncorrected mol% of randomized BF corrects isotope effects as well [19]. On the other hand, the partial resolution of isologous TAG with different unsaturation diminishes the isotope errors considerably.

Quantification of Butterfat TAG

For quantification of BF TAG, ion chromatograms for 105 ACN:DB classes were extracted from ESI–MS data of four SPE fractions (in duplicate (fractions I–III) and in triplicate (fraction IV), and the EIC were integrated. The peaks with sufficient intensity were identified from recorded HPLC–ESI–MS² data. The molar amounts of integrated peaks in duplicate or triplicate ESI–MS for four SPE fractions were calculated from the area data, the amount of ISTD, and the MCF determined (Table 2). A specific MCF was used when available. If not, the respective MCF for ACN:DB was used. For acetates the MCF of the butyrate with the same ACN was used. For TAG with ACN 55–57, the MCF of TAG 54 with the same unsaturation was used. In the next step, the sums of the means of molar amounts for respective peaks, with similar RRT and identity, in the four SPE fractions were calculated. Finally the mol% was obtained from the molar amount of TAG in each peak and the sum of all molar amounts of TAG (Table 3). Relative deviation for the identified peaks higher than 1 mol%, in

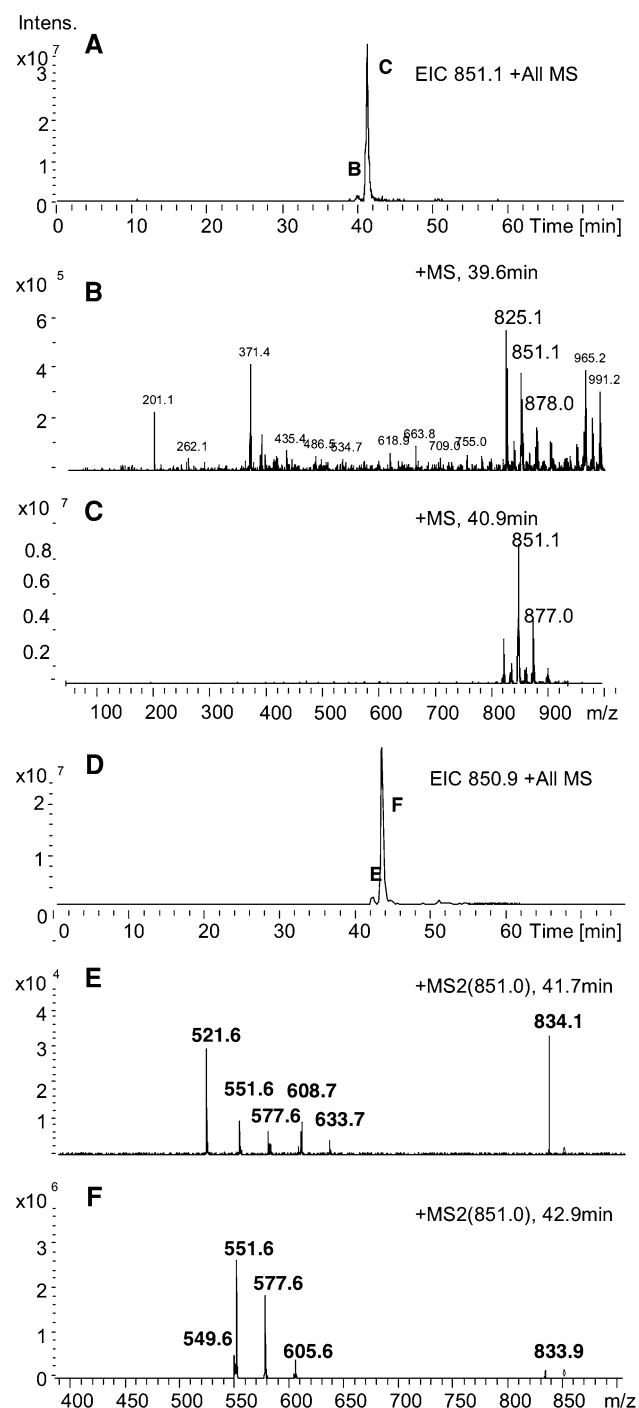


Fig. 4 Identification of the TAG 50:1 molecular species from the MS² data of fraction I. **a** EIC used for quantification of the ammonium adduct 50:1, $m/z = 851$. **b** MS at 39.6 min. **c** MS at 40.9 min. **d** EIC used for identification of TAG 50:1. **e** Tandem MS at 41.7 min: 20:0/12:0/18:1, 20:0/16:0/14:1 + 20:0/14:1/16:0, 20:0/14:0/16:1. **f** Tandem MS at 42.9 min: 18:1/16:0/16:0, 18:1/14:0/18:0, (16:0/18:0/16:1)

the range 0.1–1 mol%, and lower than 0.1 mol% was on the average 4.8, 9.1, and 10.6%, respectively. The proportions of saturated, monoene, diene, triene, tetraene, pentaene, and hexaene TAG were 40.0, 38.4, 16.2, 4.5, 0.6,

0.1, and 0.03 mol%, respectively. The proportion of TAG with not identified molecular species and odd ACN TAG were 11.8 and 5.7 mol%, respectively.

TAG Species in Butterfat

The TAG with two or three short acyl chains (C_2 , C_4 , C_6) in the ACN range 18–28 were detected predominantly in the fractions III and IV (Table 3). The total proportion of this category of TAG was 0.309 mol%. The caproates eluted before butyrates and butyrates before acetates. The regioisomers $X/S/S$ ($X/S/S'$) and $S/X/S$ ($S/X/S'$) (S denotes short acyl chain, and the structure in italics denotes chromatographically resolved regioisomer), separated from each other when present. The $L/S/S$ ($L/S/S'$) regioisomers (L denotes long-chain acyl C_{12} – C_{20}) were predominant, e.g., the molar ratios of $L/4:0/4:0$ and $4:0/L/4:0$ for ACN:DB 24:0 and 26:1 were 15.5 and 7.0, respectively. Butyrocaproates were identified in seven ACN:DB classes. In two ACN:DB classes both $L/6:0/4:0$ and $6:0/L/4:0$ regioisomers were found, in four ACN:DB classes $L/6:0/4:0$ and in one $6:0/L/4:0$ solely. Furthermore, one acetobutyrate and one acetocaproate were detected.

The even-numbered short-chain TAG (classified according to the shortest acyl-chain) with one short acyl chain in the ACN range 30–42 comprised 37.5 mol% and were found predominantly in the fraction II. All identified even-numbered butyrate and caproate TAG with one short acyl chain were $L/M/S$, $M/L/S$ or $L/L/S$ regioisomers. Acetate TAG species identified in the ACN range 22–38 comprised 0.232 mol%. The proportion of the most abundant acetate TAG, $18:0/16:0/2:0 + 16:0/18:0/2:0$ was 0.070 mol%. The $X/X/2:0$ regioisomers predominated. In four ACN:DB classes only $X/X/2:0$ regioisomers were detected, in one class only $X/2:0/X$ regioisomer, and in three classes both regioisomers with $X/X/2:0 : X/2:0/X$ ratios 2.6, 0.18, 0.56, respectively (Table 3). The most abundant peaks of short-chain TAG species were $16:0/16:0/4:0 + 18:0/14:0/4:0$ (5.25 mol%), $18:1/16:0/4:0$ (4.08 mol%), $16:0/14:0/4:0 + 18:0/12:0/4:0$ (3.34 mol%), $18:0/16:0/4:0$ (2.85 mol%), $18:1/18:0/4:0$ (1.99 mol%), and $18:1/14:0/4:0 + (16:0/16:1/4:0 + 16:1/16:0/4:0)$ (1.96 mol%).

The medium-chain TAG (C_7 , C_8 , C_{10}) eluted before caproates and comprised ca. 9.1 mol%. Those in the ACN range 30–34 were detected predominantly in SPE fraction II, and those in the range 36–46 in the fraction I. However, medium-chain TAG in the ACN range 40–46 coeluted with long-chain TAG (C_{12} or C_{14} as the shortest chain) (Table 3). Owing to the lack of chromatographic resolution of the medium-chain TAG regioisomers only the predominant regioisomer could be identified. The most abundant peak of medium-chain TAG (including one long-chain

Fig. 5 Resolution and identification of the regioisomers of TAG 56:1. **a** EIC of the ammonium adduct 56:1, $m/z = 935$. **b** Tandem MS at 40.6 min: 20:0/18:0/18:1 + 20:0/18:1/18:0. **c** Tandem MS at 41.9 min: 18:1/20:0/18:0, (18:1/22:0/16:0)

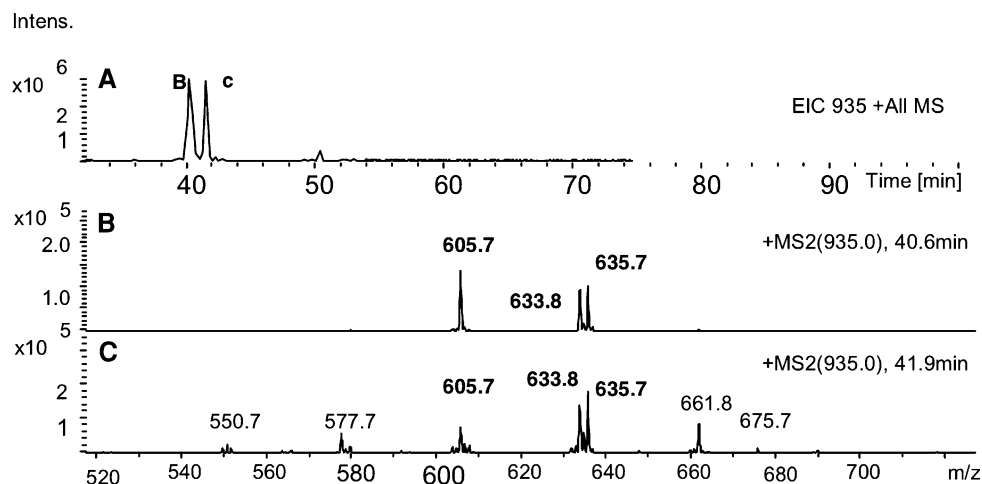


Table 1 Determination of molar amounts of triacylglycerol species in the solution B of interesterified mixture of tributyrin, trimyristin, and triolein using molar correction factors calculated from the ratio of calculated mol% and uncorrected mol% in the solution A

	TAG species	MCF ^a	Area (B1) ^b	n_i^c (B1)	Area (B2)	n_i (B2)	Average n_i	SD ^d	n_i , GC ^e
ISTD	9:0/9:0/9:0		43942247		36519280				
12:0	4:0/4:0/4:0	1.693	6220337	0.078	6492503	0.098	0.088	0.014	0.041
22:0	14:0/4:0/4:0	0.397	51230948	0.151	49167984	0.174	0.163	0.017	0.231 ^f
	4:0/14:0/4:0	0.378	26358225	0.074	22693723	0.077	0.075	0.002	
26:1	18:1/4:0/4:0	0.320	59503228	0.133	70378376	0.190	0.162	0.040	0.230 ^f
	4:0/18:1/4:0	0.443	26968523	0.089	23078894	0.091	0.090	0.002	
32:0	14:0/4:0/14:0	1.921	8252370	0.118	7109958	0.122	0.120	0.003	0.099
	14:0/14:0/4:0	0.748	34935525	0.194	25741983	0.172	0.183	0.016	0.159
36:1	18:1/4:0/14:0	1.345	19524029	0.195	15506733	0.186	0.191	0.006	0.204
	18:1/14:0/4:0 + 14:0/18:1/4:0	1.634	33312386	0.404	27167511	0.396	0.400	0.005	0.356
40:2	18:1/4:0/18:1	1.298	8819459	0.085	8028206	0.093	0.089	0.006	0.096
	18:1/18:1/4:0	1.960	15098343	0.220	13831347	0.242	0.231	0.016	0.175
42:0	14:0/14:0/14:0	1.845	8520264	0.117	6307416	0.104	0.110	0.009	0.110
46:1	14:0/14:0/18:1	2.518	14581281	0.272	9172983	0.206	0.239	0.047	0.341
50:2	14:0/18:1/18:1	3.695	15403347	0.422	12832387	0.423	0.423	0.001	0.398
54:3	18:1/18:1/18:1	3.495	5702320	0.148	4496606	0.140	0.144	0.005	0.138

^a Molar correction factor calculated from the ratio of calculated mol% and uncorrected mol% of the solution A of the interesterified mixture

^b B denotes solution B of the interesterified mixture and 1, and 2, the first and second analysis

^c Molar amount

^d Standard deviation

^e Gas chromatographic analysis on polarizable phenylmethylsilicone capillary column [8, 9]

^f The sum of regioisomers

TAG) in the ACN range 30–38 was 14:0/12:0/12:0, 16:0/12:0/10:0, 16:0/14:0/8:0, 18:0/10:0/10:0, 18:0/12:0/8:0, 14:0/14:0/10:0 (0.57 mol%) (the structure in normal font denotes the predominant regioisomer).

The odd ACN TAG species were quantified in the ACN ranges 23–25; 29–57 and the molecular species of the most abundant peaks were identified in the ACN range 33–57 (Table 3). The total content of odd ACN TAG was 5.7 mol%. The short-chain TAG with odd ACN in the ACN

range 33–43 eluted in separate peaks in the order caproate, valerate, butyrate, propionate, and were X/X/6:0, X/X/5:0 or X/X/4:0 regioisomers in the ACN range 39–43, X/X/6:0, X/X/4:0, and X/X/3:0 regioisomers in the ACN:DB class 37:0, X/6:0/X in 37:1, X/6:0/X, X/X/6:0, X/X/4:0, and X/X/3:0 in 35:0, and X/3:0/X, X/4:0/X in 35:1, X/X/4:0 and X/X/6:0 in 33:1. The long-chain TAG with odd ACN in the ACN range 45–57 eluted in two or three identified peaks (except TAG 45:1, 47:1). In the first of the two peaks

Table 2 Molar correction factors (MCF) calculated from the ratio of the mole percentage calculated according to random distribution and the uncorrected mole percentage of triacylglycerol species in randomized butterfat

ACN:DB ^a	TAG species	Area mol% ^b	Calc. mol% ^c	MCF ^d
12:0	ACN:DB	0.034	0.210	6.112
18:0	ACN:DB	0.606	0.286	0.472
20:0	ACN:DB	0.728	0.357	0.490
	6:0/10:0/4:0 ^e	0.078	0.050	0.638
22:1	ACN:DB	0.180	0.044	0.245
22:0	ACN:DB	1.367	0.779	0.570
	12:0/6:0/4:0	0.067	0.046	0.684
	14:0/4:0/4:0	0.558	0.360	0.646
23:0	ACN:DB	0.213	0.044	0.207
24:1	ACN:DB	0.295	0.099	0.336
24:0	ACN:DB	2.523	1.788	0.708
	X/X/4:0 ^f	0.284	0.144	0.506
	6:0/14:0/4:0 ^g	0.379	0.144	0.379
	16:0/4:0/4:0	0.823	0.793	0.963
	4:0/16:0/4:0	0.657	0.396	0.603
25:1	ACN:DB	0.064	0.015	0.229
25:0	ACN:DB	0.233	0.218	0.933
26:2	ACN:DB	0.310	0.084	0.269
26:1	ACN:DB	1.779	0.997	0.561
	X/X/4:0 ^f	0.129	0.039	0.299
	18:1/4:0/4:0	0.909	0.616	0.678
	4:0/18:1/4:0	0.625	0.308	0.493
26:0	ACN:DB	4.775	1.864	0.390
	X/M/4:0 ^f	0.380	0.156	0.410
	16:0/6:0/4:0	0.535	0.316	0.590
	6:0/16:0/4:0	0.535	0.316	0.590
	18:0/4:0/4:0	0.566	0.328	0.579
27:1	ACN:DB	0.076	0.012	0.154
27:0	ACN:DB	0.013	0.038	2.979
28:1	ACN:DB	1.668	0.801	0.480
	18:1/6:0/4:0	0.426	0.245	0.576
28:0	X/X/6:0 ^f	0.838	0.151	0.180
	X/X/4:0 ^f	1.559	0.748	0.647
29:1	ACN:DB	0.083	0.005	0.061
29:0	ACN:DB	0.272	0.039	0.144
30:1	ACN:DB	1.394	0.546	0.391
30:0	X/X/M ^{f,j}	0.834	0.297	0.357
	X/X/6:0 ^g	0.726	0.177	0.244
	X/X/4:0 ^f	1.535	0.583	0.380
31:1	ACN:DB	0.101	0.009	0.087
31:0	ACN:DB	0.272	0.046	0.171
32:1	X/X/4:0 ^f	1.055	0.440	0.968
	X/X/6:0 ^f	0.024	0.084	0.186
32:0	X/X/M ^f	0.331	0.090	0.273
	X/X/6:0 ^f	0.849	0.311	0.366
	X/X/4:0 ^f	1.506	0.938	0.623

Table 2 continued

ACN:DB ^a	TAG species	Area mol% ^b	Calc. mol% ^c	MCF ^d
33:1	ACN:DB	0.114	0.014	0.125
33:0	ACN:DB	0.391	0.096	0.247
	X/X/6:0 ^f	0.140	0.025	0.181
	X/X/4:0 ^f	0.194	0.051	0.261
34:1	ACN:DB	1.944	1.079	0.555
	X/X/6:0 ^f	0.675	0.166	0.246
	X/X/4:0 ^f	1.044	0.522	0.500
34:0	X/X/M ^f	0.622	0.183	0.294
	X/X/6:0 ^f	1.626	0.296	0.182
	X/X/4:0 ^f	1.812	1.542	0.851
35:1	ACN:DB	0.187	0.034	0.183
35:0	ACN:DB	0.554	0.231	0.418
	X/X/6:0	0.133	0.020	0.151
	X/X/4:0	0.198	0.112	0.563
36:2	ACN:DB	0.653	0.307	0.470
36:1	X/X/M ^e	0.440	0.100	0.227
	X/X/6:0 ^g	1.557	0.735	0.472
	X/X/4:0 ^g	1.288	1.088	0.845
36:0	X/X/M ^f	1.090	0.279	0.256
	16:0/14:0/6:0 ^h	1.417	0.543	0.383
	X/X/4:0 ^f	1.271	2.062	1.622
37:1	ACN:DB	0.468	0.196	0.419
37:0	ACN:DB	0.609	0.244	0.400
	X/X/6:0	0.129	0.067	0.515
	X/X/4:0	0.165	0.050	0.300
38:2	X/X/6:0 ^f	0.173	0.073	0.420
	X/X/4:0 ^f	0.465	0.336	0.722
38:1	ACN:DB	10.729	4.599	0.429
	X/X/6:0 ^f	1.998	0.504	0.252
	18:1/16:0/4:0	2.051	2.329	1.136
38:0	X/X/M ^f	1.332	0.398	0.299
	X/X/6:0 ^f	2.425	0.822	0.339
	18:0/16:0/4:0	1.347	1.239	0.920
39:1	ACN:DB	0.618	0.155	0.250
	X/X/6:0	0.129	0.049	0.381
	18:1/17:0/4:0	0.157	0.039	0.245
39:0	X/X/M ^f	0.132	0.057	0.433
	X/X/6:0 ^f	0.240	0.038	0.159
	18:0/17:0/4:0	0.094	0.020	0.217
40:4	ACN:DB	0.140	0.083	0.596
40:3	ACN:DB	0.553	0.335	0.605
40:2	ACN:DB	2.580	1.749	0.678
	X/X/6:0 ^g	1.366	0.586	0.429
	18:1/18:1/4:0	1.082	0.905	0.836
40:1	X/X/M ^g	1.593	0.787	0.494
	X/X/6:0 ^g	2.651	0.955	0.360
	18:1/18:0/4:0	1.300	0.963	0.741
40:0	X/X/M ^f	1.860	1.218	0.655

Table 2 continued

ACN:DB ^a	TAG species	Area mol% ^b	Calc. mol% ^c	MCF ^d
	<i>18:0/16:0/6:0</i>	<i>1.205</i>	<i>0.494</i>	<i>0.410</i>
	<i>18:0/18:0/4:0</i>	<i>0.446</i>	<i>0.256</i>	<i>0.574</i>
41:1	ACN:DB	0.416	0.072	0.172
41:0	ACN:DB	0.443	0.117	0.265
42:3	<i>18:2/18:1/6:0</i>	<i>0.121</i>	<i>0.065</i>	<i>0.540</i>
42:2	ACN:DB	1.636	0.767	0.469
	X/X/M ^g	0.401	0.113	0.283
	X/X/6:0 ^f	1.193	0.395	0.331
42:1	ACN:DB	2.839	1.963	0.692
	X/X/M + L/L/L ⁱ	1.777	1.276	0.718
42:0	X/X/M + L/L/L	1.503	1.967	1.308
	<i>18:0/18:0/6:0</i>	<i>0.114</i>	<i>0.010</i>	<i>0.087</i>
	<i>20:0/4:0/18:0</i>	0.132	0.010	0.078
43:1	ACN:DB	0.326	0.077	0.237
43:0	ACN:DB	0.247	0.136	0.548
44:2	ACN:DB	0.986	0.494	0.500
44:1	ACN:DB	1.690	2.037	1.206
44:0	ACN:DB	1.202	2.360	1.964
45:1	ACN:DB	0.227	0.105	0.463
45:0	ACN:DB	0.222	0.207	0.929
46:3	ACN:DB	0.307	0.138	0.449
46:2	ACN:DB	0.711	0.775	1.091
46:1	ACN:DB	1.090	2.519	2.312
46:0	ACN:DB	0.867	2.935	3.386
47:1	ACN:DB	0.167	0.204	1.218
47:0	ACN:DB	0.173	0.290	1.675
48:4	ACN:DB	0.077	0.026	0.341
48:3	ACN:DB	0.225	0.207	0.876
48:2	ACN:DB	0.507	1.105	2.178
48:1	ACN:DB	0.946	3.851	4.070
	<i>18:1/14:0/16:0</i>	0.926	3.003	3.243
48:0	ACN:DB	0.753	3.142	4.173
	20:0/X/X	0.033	0.017	0.533
	<i>16:0/14:0/18:0^f</i>	0.703	3.014	4.288
49:1	ACN:DB	0.175	0.382	2.182
49:0	ACN:DB	0.155	0.227	1.469
50:4	ACN:DB	0.089	0.098	1.107
50:3	ACN:DB	0.244	0.478	1.963
50:2	ACN:DB	0.527	2.039	3.865
50:1	ACN:DB	0.867	4.767	5.498
50:0	ACN:DB	0.528	2.119	4.016
	20:0/X/X	0.028	0.032	1.151
	<i>18:0/16:0/16:0^f</i>	0.454	2.087	4.594
51:1	ACN:DB	0.128	0.254	1.982
51:0	ACN:DB	0.111	0.085	0.766
52:4	ACN:DB	0.098	0.182	1.857
52:3	ACN:DB	0.203	0.688	3.392
52:2	ACN:DB	0.548	2.959	5.404

Table 2 continued

ACN:DB ^a	TAG species	Area mol% ^b	Calc. mol% ^c	MCF ^d
52:1	ACN:DB	0.665	2.794	4.198
	20:0/X/X	0.049	0.025	0.509
	18:1/18:0/16:0	0.604	2.730	4.521
52:0	ACN:DB	0.351	0.774	2.206
	20:0/X/X	0.050	0.050	1.000
	18:0/18:0/16:0	0.269	0.726	2.700
53:2	ACN:DB	0.051	0.076	1.504
53:1	ACN:DB	0.101	0.054	0.537
53:0	ACN:DB	0.116	0.012	0.104
54:6	ACN:DB	0.023	0.010	0.415
54:5	ACN:DB	0.041	0.074	1.836
54:4	ACN:DB	0.045	0.045	1.013
54:3	ACN:DB	0.172	0.871	5.054
54:2	ACN:DB	0.321	1.111	3.459
54:1	ACN:DB	0.339	0.619	1.825
54:0	ACN:DB	0.181	0.129	0.713

Italics in this table are relevant in assignments of regioisomers of short-chain (and a few other) TAG, which were chromatographically resolved and identified from MS². This enabled calculation of regio-specific MCF

- ^a The number of acyl group carbons:the number of double bonds
^b Uncorrected mol% (area mol%) of triacylglycerol species in randomized butterfat
^c Mol% of triacylglycerol species in randomized butterfat calculated according to random distribution
^d Molar correction factor MCF = calc.mol%/area mol%
^e Structure in italics indicates the regioisomer identified by MS²
^f Two or more triacylglycerol species identified
^g Included minor impurities of other identity
^h Included other regioisomer
ⁱ M denotes medium-chain acyl (C₈–C₁₀) and L long-chain acyl (C₁₂–C₂₄)
^j Structure in normal font indicates predominant regioisomer

eluted TAG with the longest odd ACN acyl (19:0) and in the second TAG with a shorter odd ACN acyl (15:0 or 17:0). When three peaks were identified, in the first eluted TAG with the longest odd ACN acyl (19:0), in the second TAG with the longest even ACN acyl (20:0), and in the third TAG with the shorter odd ACN acyl (15:0 or 17:0). In the first peak of TAG 55:1 eluted regioisomers *19:0/18:1/18:0* and *19:0/18:0/18:1*, and in the second peak regioisomer *18:1/19:0/18:0* together with 18:0/19:1/18:0. The most abundant peaks of TAG species with odd ACN were (18:1/15:0/16:0 + 18:1/16:0/15:0) + (18:1/17:0/14:0 + 18:1/14:0/17:0) + 16:0/17:1/16:0 + 16:0/16:1/17:0 (0.41 mol%), 15:0 14:0 10:0 + 12:0 17:0 10:0 + 12:0/13:0/14:0 + (15:0/16:0/8:0 + 15:0/8:0/16:0) + 16:0/16:0/7:0 + 14:0/18:0/7:0 (0.31 mol%), (18:1/16:0/17:0 + 18:1/17:0/16:0) + 18:0/17:1/16:0 + 18:1/15:0/18:0 (0.26 mol%).

Table 3 Composition of triacylglycerol species in butterfat

$[M + NH_4]^{+a}$ (m/z^b)/ ACN:DB ^c /RRT ^d	Major and (minor) molecular species	Mol% \pm SD ^e	Fr. I ^f	Fr. II	Fr. III	Fr. IV
320.4/12:0/1.23	4:0/4:0/4:0 Total 12:0	0.0692 \pm 0.0057 0.0692		0.0526	0.0166	
404.4/18:0/1.13	II, III: 6:0/6:0/6:0 NIMS ^g Total 18:0	0.0288 \pm 0.0029 0.0005 \pm 0.0002 0.0292		0.0202	0.0084	0.0002 0.0005
432.4/20:0/1.17	IV: 6:0/10:0/4:0 ^h NIMS two peaks Total 20:0	0.0022 \pm 0.0004 0.0698 \pm 0.0050 0.0720		0.0674	0.0004 0.0016	0.0018 0.0007
458.4/22:1/1.23	NIMS five peaks Total 22:1	0.0010 \pm 0.0001 0.0010		0.0008		0.0001
460.4/22:0/1.13 /1.16 /1.24	III, IV: 12:0/6:0/4:0, (8:0/8:0/6:0) IV: 14:0/4:0/4:0 NIMS two peaks IV: 4:0/16:0/2:0 Total 22:0	0.0103 \pm 0.0018 0.0027 \pm 0.0003 0.0019 \pm 0.0002 0.0019 \pm 0.0002 0.0168		0.0010	0.0054 0.0007 0.0001 0.0001	0.0049 0.0020 0.0008 0.0018
474.4/23:0	NIMS three peaks Total 23:0	0.0009 0.0009		0.0009		
486.5/24:1	NIMS six peaks Total 24:1	0.0083 \pm 0.0023 0.0083		0.0034	0.0022	0.0027
488.6/24:0 /1.09 /1.12 /1.16 /1.19 /1.21 /1.24	NIMS III, IV: 14:0/6:0/4:0, (12:0/8:0/4:0) IV: 6:0/14:0/4:0 III, IV: 16:0/4:0/4:0 IV: 4:0/16:0/4:0 NIMS IV: 16:0/6:0/2:0 NIMS three peaks Total 24:0	0.0002 \pm 0.0000 0.0148 \pm 0.0021 0.0156 \pm 0.0021 0.0217 \pm 0.0042 0.0014 \pm 0.0004 0.0003 \pm 0.0001 0.0083 \pm 0.0004 0.0003 0.0626		0.0002 0.0006 0.0003	0.0085 0.0091 0.0167 0.0010 0.0003	0.0057 0.0062 0.0050 0.0004 0.0003 0.0077
502.6/25:0	NIMS four peaks Total 25:0	0.0027 \pm 0.0010 0.0027		0.0027		
512.6/26:2	NIMS five peaks Total 26:2	0.0024 \pm 0.0003 0.0024	0.0010	0.0004	0.0003	0.0007
514.6/26:1/1.10 /1.14 /1.17	III, IV: 16:1/6:0/4:0, 12:0/10:1/4:0 III, IV: 18:1/4:0/4:0 IV: 4:0/18:1/4:0 NIMS eight peaks Total 26:1	0.0052 \pm 0.0008 0.0232 \pm 0.0039 0.0033 \pm 0.0003 0.0316 \pm 0.0062 0.0632		0.0097	0.0042 0.0122 0.0007 0.0005	0.0010 0.0109 0.0025 0.0021
516.7/26:0/1.06 /1.09 /1.12 /1.12 /1.23	II: 12:0/10:0/4:0 III; IV: 12:0/10:0/4:0, 14:0/8:0/4:0 III, IV: 16:0/6:0/4:0 III, IV: 6:0/16:0/4:0 III, IV: 18:0/4:0/4:0 NIMS two peaks NIMS acetate Total 26:0	0.0497 \pm 0.0067 0.0427 \pm 0.0079 0.0163 \pm 0.0021 0.0038 \pm 0.0009 0.0035 \pm 0.0005 0.0077 \pm 0.0002 0.1237		0.0107 0.0032	0.0372 0.0388 0.0089 0.0008 0.0011 0.016	0.0018 0.0039 0.0021 0.0030 0.0015 0.0061
530.7/27:0	NIMS five peaks Total 27:0	0.0105 0.0105				
542.7/28:1/1.03	NIMS	0.0026 \pm 0.0003		0.0026		

Table 3 continued

$[M + NH_4]^{+a}$ (m/z^b)/ ACN:DB ^c /RRT ^d	Major and (minor) molecular species	Mol% \pm SD ^e	Fr. I ^f	Fr. II	Fr. III	Fr. IV
/1.07	II: 18:1/6:0_/4:0 ^j III, IV: 18:1/6:0/4:0, (16:1/6:0/6:0, 14:0/10:1/4:0, 6:0/18:1/ 4:0, 10:1/14:0/4:0)	0.0099 \pm 0.0008		0.0049		0.0050
/1.17	NIMS Total 28:1	0.0422 \pm 0.0099 0.0548			0.0397	0.0025
544.7/28:0/1.01	II: 14:0/8:0/6:0, 10:0/8:0/10:0, 10:0/ 12:0/6:0	0.0136 \pm 0.0023		0.0136		
/1.02	II: 8:0/14:0/6:0, 8:0/12:0/8:0	0.0095 \pm 0.0018		0.0095		
/1.03	II, III, IV: 14:0/10:0/4:0, (12:0/10:0/6:0, 16:0/8:0/4:0), (12:0/12:0/4:0, 12:0/ 8:0/8:0)	0.1849 \pm 0.0156		0.1738	0.0101	0.0010
/1.05	III, IV: 16:0/8:0/4:0. (14:0/10:0/4:0)	0.0982 \pm 0.0139			0.0971	0.0012
/1.07	III, IV: 18:0/6:0/4:0, (16:0/6:0/6:0)	0.0260 \pm 0.0050			0.0252	0.0008
/1.12	III: 16:0/2:0/10:0, 18:0/2:0/8:0	0.0018 \pm 0.0003			0.0013	0.0006
/1.20	NIMS Total 28:0	0.0098 \pm 0.0012 0.3438			0.0038	0.0060
556.7/29:1	NIMS three peaks Total 29:1	0.0002 \pm 0.0001 0.0002		0.0002		
558.7/29:0	NIMS five peaks Total 29:0	0.0125 \pm 0.0006 0.0125		0.0125		
570.7/30:1/1.01	II: 18:1/6:0/6:0	0.0061 \pm 0.0000		0.0061		
/1.02	II: 14:1/8:0/8:0, 8:0/18:1/4:0	0.0239 \pm 0.0050		0.0239	0.0000	
/1.06	II: 18:1/8:0/4:0 III, IV: 18:1/8:0/4:0, 16:0/10:1/4:0, 12:1_/14:0/4:0, 14:1_ 12:0/4:0	0.0759 \pm 0.0053	0.0018	0.0432	0.0303	0.0005
	NIMS four peaks Total 30:1	0.0194 \pm 0.0026 0.1252	0.0012	0.0057	0.0101	0.0023
572.7/30:0/0.98	II: 10:0/10:0/10:0, 14:0/8:0/8:0 ⁱ	0.0345 \pm 0.0021	0.0041	0.0304		
/1.00	II: 14:0/10:0/6:0, 16:0_/8:0/6:0	0.0448 \pm 0.0003	0.0043	0.0405		
/1.01	II: 8:0/16:0/6:0, 10:0/14:0/6:0, 8:0/14:0/ 8:0	0.0076 \pm 0.0000		0.0076	0.0000	
/1.03	I, III: 16:0/10:0/4:0, 14:0_/12:0/4:0, 18:0/8:0/4:0	0.4314 \pm 0.0131	0.0054	0.3705	0.0553	0.0003
	NIMS two peaks	0.0046 \pm 0.0002	0.0046			
/1.22	III, IV: 18:0/10:0/2:0, 16:0/12:0/2:0, 14:0/14:0/2:0	0.0071 \pm 0.0008			0.0043	0.0028
	Total 30:0	0.5300				
584.8/31:1	NIMS nine peaks Total 31:1	0.0032 \pm 0.0005 0.0032		0.0032		
586.8/31:0	NIMS five peaks Total 31:0	0.0290 \pm 0.0025 0.0290		0.0290		
598.8/32:1/1.00	NIMS	0.0243 \pm 0.0010	0.0013	0.0229		
/1.03	I, II, III: 18:1/10:0/4:0, 14:1/14:0/4:0, 16:0_/12:1/4:0, 12:0_/16:1/4:0	0.6882 \pm 0.0147	0.0080	0.5929	0.0870	0.0004
	NIMS four peaks	0.0062 \pm 0.0006	0.0062			
/1.22	III: NIMS Acetate Total 32:1	0.0119 \pm 0.0014 0.7306			0.0082	0.0037
600.8/32:0/0.98	I: 14:0/8:0/10:0, 12:0/10:0/10:0 II:10:0/ 14:0/8:0, 12:0/12:0/8:0	0.1070 \pm 0.0037	0.0333	0.0736		
/0.99	I: 16:0/10:0/6:0, 12:0/12:0/8:0, 14:0/ 12:0/6:0 II: 16:0_/10:0/6:0	0.1944 \pm 0.0066	0.0259	0.1684		

Table 3 continued

[M + NH ₄] ⁺ ^a (<i>m/z</i> ^b)/ ACN:DB ^c /RRT ^d	Major and (minor) molecular species	Mol% ± SD ^e	Fr. I ^f	Fr. II	Fr. III	Fr. IV
/1.02	I, II, III: 16:0_12:0/4:0, 14:0/14:0/4:0, 18:0_10:0/4:0	1.3877 ± 0.0493	0.0241	1.3080	0.0552	0.0004
	NIMS three peaks	0.0223 ± 0.0020	0.0051		0.0133	0.0039
	Total 32:0	1.7114				
612.7/33:1	NIMS six peaks	0.0113 ± 0.0015		0.0113		
	Total 33:1	0.0113				
614.8/33:0/0.96	NIMS	0.0107 ± 0.0027	0.0048	0.0060		
/0.98	II: 17:0_10:0/6:0	0.0160 ± 0.0005	0.0029	0.0131		
	NIMS	0.0010 ± 0.0000	0.0010			
/1.01	I, II: 15:0_14:0/4:0	0.0765 ± 0.0024	0.0026	0.0739		
	NIMS four peaks	0.0129 ± 0.0008	0.0041	0.0089		
	Total 33:0	0.1172				
626.8/34:1/0.97	NIMS	0.0251 ± 0.0018	0.0251			
/0.98	I, II: 14:1 10:0 10:0, 18:1/8:0/8:0, 16:1/ 8:0/10:0	0.0962 ± 0.0060	0.0373	0.0589		
/0.99	II: 10:0/18:1/6:0, 14:1/14:0/6:0	0.1002 ± 0.0011		0.1002		
/1.01	I, II: 18:1_12:0/4:0, (16:1_14:0/4:0, 14:1_16:0/4:0)	0.6661 ± 0.0301	0.0125	0.6536		
	NIMS three peaks	0.0036	0.0036			
	Total 34:1	0.8912				
628.8/34:0/0.96	I, II: 14:0/8:0_12:0, 16:0/8:0/10:0, 10:0/ 14:0/10:0, 12:0/12:0/10:0	0.1747 ± 0.0024	0.0788	0.0959		
/0.98	I, II: 16:0/12:0/6:0, 14:0/14:0/6:0, 18:0/ 10:0/6:0	0.3605 ± 0.0415	0.1157	0.2448		
/1.01	I, II: 16:0/14:0/4:0, 18:0/12:0/4:0	3.3376 ± 0.2675	0.3551	2.9825		
	NIMS	0.0046 ± 0.0000	0.0046			
	Total 34:0	3.8773				
640.8/35:1/	NIMS two peaks	0.0117 ± 0.0012	0.0031	0.0086		
/1.01	II: 15:0/4:0/16:1, 17:1/4:0/14:0	0.0269 ± 0.0009	0.0006	0.0262		
/1.05	II: 18:1/3:0_14:0	0.0029 ± 0.0003		0.0029		
	NIMS three peaks	0.0029 ± 0.0005	0.0025	0.0004		
	Total 35:1	0.0443				
642.8/35:0/	NIMS two peaks	0.0343 ± 0.0074	0.0183	0.0160		
/0.97	I: 15:0/6:0/14:0	0.0150 ± 0.0000	0.0150			
/0.97	II: 15:0/14:0/6:0	0.0229 ± 0.0019		0.0229		
/1.00	NIMS	0.2465 ± 0.0115	0.0078	0.2387		
/1.01	I, II: 16:0_15:0/4:0	0.0015 ± 0.0000	0.0015			
/1.04	NIMS	0.0481 ± 0.0007		0.0481		
/1.13	I, II: 16:0/16:0/3:0, 18:0/14:0/3:0	0.0026 ± 0.0000	0.0026			
	Total 35:0	0.3709				
652.8/36:2/	NIMS two peaks	0.0091 ± 0.0011	0.0091			
/0.99	II: 18:1/8:0/10:1	0.0587 ± 0.0039	0.0065	0.0521		
/1.02	I, II: 18:1/14:1/4:0, 18:2/14:0/4:0	0.2859 ± 0.0100	0.0052	0.2807		
	NIMS	0.0008 ± 0.0000	0.0008			
	Total 36:2	0.3545				
654.9/36:1/0.96	I: 18:1/10:0/8:0	0.0743 ± 0.0011	0.0352	0.0390		
/0.98	I: 18:1/12:0/6:0, 16:0/14:1/6:0, 14:0/ 16:1/6:0, 14:0/10:1_12:0	0.4816 ± 0.0162	0.1420	0.3396		
/1.00	I: 18:1/14:0/4:0 (16:0_16:1/4:0)	1.9628 ± 0.0680	0.0659	1.8969		

Table 3 continued

[M + NH ₄] ⁺ ^a (<i>m/z</i> ^b)/ ACN:DB ^c /RRT ^d	Major and (minor) molecular species	Mol% ± SD ^e	Fr. I ^f	Fr. II	Fr. III	Fr. IV
/1.08	I: 16:0_18:1/2:0	0.0408 ± 0.0071	0.0025	0.0383		
/1.20	NIMS	0.0096 ± 0.0034		0.0096		
	Total 36:1	2.5690				
657.0/36:0/0.94	I, II: 12:0/12:0/12:0, 10:0/16:0/10:0, 10:0 14:0 12:0, 14:0/8:0/14:0, 16:0/8:0/12:0 10:0/18:0/8:0	0.2445 ± 0.0095	0.1417	0.1028		
/0.96	I, II: 16:0/14:0/6:0, 18:0_12:0/6:0	1.3493 ± 0.0362	0.5773	0.7720		
/0.99	I,II: 16:0/16:0/4:0, 18:0/14:0/4:0	5.2455 ± 0.2829	0.6230	4.6225		
/1.06	II: 18:0/2:0/16:0	0.0266 ± 0.0000		0.0266		
/1.19	II: 18:0_16:0/2:0	0.0704 ± 0.0466		0.0704		
	Total 36:0	6.9363				
669.0/37:1/	NIMS two peaks	0.1001 ± 0.0041	0.0425	0.0576		
/0.99	I: 18:1/6:0/13:0	0.1385 ± 0.0083	0.0064	0.1321		
/1.04	NIMS	0.0214 ± 0.0015		0.0214		
	Total 37:1	0.2601				
671.0/37:0/	NIMS two peaks	0.0378 ± 0.0000	0.0378			
/0.94	I: 14:0/8:0/15:0	0.0481 ± 0.0039	0.0284	0.0197		
/0.96	I, II: 14:0_17:0/6:0, 15:0_16:0/6:0	0.2792 ± 0.0824	0.1283	0.1509		
/0.98	NIMS	0.0338 ± 0.0000	0.0122	0.0216		
/1.00	I, II: 17:0/16:0/4:0, 18:0/15:0/4:0	0.1069 ± 0.0091	0.0302	0.0767		
/1.03	II: 18:0/16:0/3:0	0.0151 ± 0.0024		0.0151		
	Total 37:0	0.5208				
680.9/38:2/0.96	NIMS	0.0139 ± 0.0000	0.0139			
/0.98	I: 18:2_14:0/6:0, 18:1/14:1/6:0, 18:1/ 10:1/10:0, 10:0/18:2/10:0 II: 18:2/14:0/ 6:0	0.3470 ± 0.1256	0.1764	0.1707		
/1.01	I, II: 18:2/16:0/4:0, 18:1_16:1/4:0	0.6490 ± 0.0169	0.0233	0.6257		
/1.07	II: 18:1/2:0/18:1	0.0250 ± 0.0003		0.0250		
/1.20	II: 18:1/18:1/2:0	0.0044 ± 0.0000		0.0044		
	Total 38:2	1.0394				
682.9/38:1/0.94	I, II: 18:1/12:0/8:0, 18:1/10:0/10:0, 16:1_ 14:0/8:0, 14:1/16:0/8:0, 16:1/12:0/10:0	0.2889 ± 0.0164	0.1619	0.1270		
/0.97	I, II: 18:1/14:0_6:0, 16:1/16:0/6:0, 18:1/ 10:0/10:0, 12:0/14:1/12:0, 14:0/14:1/ 10:0	0.9735 ± 0.0223	0.4403	0.5332		
/0.99	I, II: 18:1/16:0/4:0	4.0781 ± 0.1684	0.9695	3.1086		
/1.06	II: 18:1/2:0/18:0	0.0290 ± 0.0033		0.0290		
/1.19	II: 18:1/18:0/2:0	0.0163 ± 0.0000		0.0163		
	Total 38:1	5.3858				
684.9/38:0/0.94	I, II: 14:0/12:0/12:0, 16:0_12:0/10:0, 16:0/14:0/8:0, 18:0/10:0/10:0, 18:0/ 12:0/8:0, 14:0/14:0/10:0	0.5656 ± 0.0125	0.3878	0.1778		
/0.96	I, II: 16:0/16:0/6:0, 18:0/14:0/6:0	1.3270 ± 0.0227	0.6754	0.6516		
/0.99	I, II: 18:0/16:0/4:0	2.8515 ± 0.1077	1.0744	1.7771		
	Total 38:0	4.7441				
697/39:1/0.94	NIMS	0.0161 ± 0.0022	0.0161			
/0.95	I: 18:1/15:0/6:0	0.0959 ± 0.0011	0.0840	0.0118		
/0.96	I: 16:0/18:1/5:0	0.0503 ± 0.0053		0.0503		
/0.98	NIMS	0.0162 ± 0.0022		0.0162		
/0.99	I: 17:0/18:1/4:0	0.0768 ± 0.0009	0.0269	0.0499		

Table 3 continued

[M + NH ₄] ⁺ ^a (<i>m/z</i>) ^b / ACN:DB ^c /RRT ^d	Major and (minor) molecular species	Mol% ± SD ^e	Fr. I ^f	Fr. II	Fr. III	Fr. IV
/1.03	NIMS	0.0061 ± 0.0007		0.0061		
	Total 39:1	0.2613				
699/39:0/0.94	I, II: 15:0 14:0 10:0, 12:0 17:0 10:0, 12:0/ 13:0/14:0, 15:0_/16:0/8:0, 16:0/16:0/ 7:0, 14:0/18:0/7:0	0.3091 ± 0.2370	0.1545	0.1545		
/0.96	I, II: 16:0/17:0/6:0, 18:0/15:0/6:0	0.0614 ± 0.0047	0.0334	0.0280		
/0.99	I, II: 18:0/17:0/4:0	0.0563 ± 0.0009	0.0236	0.0326		
	NIMS two peaks	0.0066 ± 0.0012		0.0066		
	Total 39:0	0.4333				
705/40:4/	NIMS three peaks	0.0116 ± 0.0022	0.0050	0.0066		
/1.02	II: 18:3/18:1/4:0, 18:2/18:2/4:0	0.1091 ± 0.0169	0.0020	0.1071		
	Total 40:4	0.1207				
706.9/40:3/0.97	NIMS	0.1480 ± 0.0049	0.0532	0.0948		
/1.01	II: 18:2/18:1/4:0, 18:3/18:0/4:0	0.2550 ± 0.0083	0.0132	0.2418		
	Total 40:3	0.4030				
708.9/40:2/0.94	II: 18:1/8:0/14:1, 14:1/16:1/10:0	0.1221 ± 0.0137	0.0728	0.0493		
/0.96	I, II: 18:2/16:0/6:0, 18:1/16:1/6:0, 16:1/ 14:0/10:1, 18:1/12:0/10:1, 16:1/16:1_ 8:0	0.4239 ± 0.0103	0.2061	0.2178		
/0.99	I, II: 18:1/18:1/4:0, 18:0/18:2/4:0	1.4125 ± 0.0396	0.3823	1.0302		
	Total 40:2	1.9585				
711.0/40:1/0.93	I: 18:1/14:0_/8:0, 18:1/12:0_/10:0, 18:1/ 6:0/16:0, 16:0/16:1/8:0, 16:0/14:1/10:0, 14:0/14:1/12:0, 14:0/16:1_/10:0 II: 18:1_/14:0/8:0, 18:1/6:0/16:0	0.6793 ± 0.0068	0.4795	0.1998		
/0.96	I, II: 18:1/16:0/6:0, 18:0/16:1/6:0	1.2996 ± 0.0463	0.6706	0.6290		
/0.99	I, II: 18:1_/18:0/4:0	1.9919 ± 0.0177	0.7104	1.2816		
	Total 40:1	3.9709				
712.9/40:0/0.92	NIMS	0.5323 ± 0.0263	0.5323			
/0.94	I, II: 16:0/16:0_/8:0, 14:0/18:0_/8:0, 16:0/ 14:0/10:0, 18:0/12:0/10:0, 14:0/12:0/ 14:0, 16:0/12:0/12:0	1.1329 ± 0.0285	0.7323	0.4006		
/0.95	I, II: 18:0/16:0/6:0	0.8382 ± 0.0154	0.4822	0.3559		
/0.98	I, II: 18:0/18:0/4:0	0.7203 ± 0.0192	0.3062	0.4141		
	Total 40:0	3.2236				
724.9/41:1/0.93	I: 18:1/15:0/8:0 II: 15:0/18:1/8:0, 17:0/ 16:1/8:0	0.0376 ± 0.0019	0.0268	0.0108		
/0.95	I: 17:0/18:1/6:0	0.0443 ± 0.0010	0.0245	0.0197		
	NIMS three peaks	0.0201 ± 0.0019	0.0079	0.0121		
	Total 41:1	0.1020				
726.9/41:0/0.94	NIMS	0.0182 ± 0.0030		0.0182		
/0.95	I, II: 16:0/15:0/10:0, 16:0/9:0/16:0, 15:0/ 12:0/14:0, 16:0/17:0/8:0, 14:0/17:0/ 10:0, 18:0/6:0/17:0	0.0807 ± 0.0029	0.0663	0.0145		
/0.98	I: 18:0/17:0/6:0	0.0336 ± 0.0010	0.0232	0.0104		
/1.01	I: 18:0/19:0/4:0	0.0144 ± 0.0013	0.0087	0.0058		
/1.05	NIMS	0.0018 ± 0.0000		0.0018		
	Total 41:0	0.1488				
734.9/42:3/0.96	I, II: 18:2_/18:1/6:0, (18:3_/18:0/6:0)	0.1461 ± 0.0010	0.1461	0.0000		
	Total 42:3	0.1461				

Table 3 continued

[M + NH ₄] ⁺ ^a (<i>m/z</i> ^b)/ ACN:DB ^c /RRT ^d	Major and (minor) molecular species	Mol% ± SD ^e	Fr. I ^f	Fr. II	Fr. III	Fr. IV
736.9/42:2/0.93	I: 18:1_16:1/8:0, 18:2/14:0/10:0, 18:1/ 14:1/10:0 II: 16:0/8:0/18:2, 16:1/8:0/ 18:1, 16:1/10:0/16:1, 18:1/6:0/18:1	0.1387 ± 0.0094	0.1027	0.0360		
/0.95	I, II: 18:1/18:1/6:0, 18:2_/18:0/6:0	0.5177 ± 0.0235	0.2719	0.2457		
/0.98	II: 18:1/20:1/4:0	0.0223 ± 0.0000		0.0223		
	Total 42:2	0.6787				
738.9/42:1/0.93	I:18:1/16:0/8:0, 18:1/10:0_/14:0, 14:0/ 14:1/14:0, 16:0/12:1_/14:0, 16:0/12:0/ 14:1, 18:0/14:1/10:0, II: 18:1/8:0_ 16:0, 16:0/16:1/10:0, 18:1/12:0/12:0, 14:0/16:1_/12:0	1.5021 ± 0.0377	1.1644	0.3378		
/0.95	I, II: 18:1/18:0/6:0	1.0864 ± 0.0422	0.6640	0.4225		
/0.98	I: 18:1_/20:0/4:0, 18:0/20:1/4:0	0.0654 ± 0.0041	0.0207	0.0447		
	Total 42:1	2.6539				
740.9/42:0/0.92	I: 16:0/16:0_/10:0, 16:0/12:0_/14:0, 14:0/ 14:0/14:0, 14:0_/18:0/10:0, 18:0/12:0/ 12:0 II: I + 16:0/8:0/18:0	2.7736 ± 0.0081	2.2428	0.5308		
/0.94	I, II: 18:0/18:0/6:0	0.0416 ± 0.0047	0.0261	0.0155		
/0.98	I, II: 20:0_/18:0/4:0	0.0023 ± 0.0002		0.0023		
/1.23	NIMS	0.0004 ± 0.0001		0.0004		
	Total 42:0	2.8179				
753.0/43:1/0.91	I: 15:0/18:1/10:0, 18:1/17:0/8:0, 16:1/ 17:0/10:0	0.0434 ± 0.0036	0.0434			
/0.93	I: 18:0/10:1/15:0	0.0241 ± 0.0003	0.0113	0.0129		
/0.95	NIMS	0.0033 ± 0.0008		0.0033		
/0.98	I: 23:1/16:0/4:0	0.0055 ± 0.0006	0.0037	0.0017		
	NIMS two peaks	0.0050 ± 0.0020		0.0050		
	Total 43:1	0.0813				
755.0/43:0/0.85	I: 19:0/14:0/10:0, 19:0/8:0/16:0	0.0050 ± 0.0002	0.0050			
/0.91	I: 15:0_/14:0/14:0, 15:0/12:0/16:0, 16:0/ 17:0/10:0, 14:0/17:0_/12:0, 18:0/13:0/ 12:0	0.1028 ± 0.0119	0.1028			
	NIMS six peaks	0.0562 ± 0.0021	0.0116	0.0446		
	Total 43:0	0.1641				
765.0/44:2/0.92	I, II: 18:2/18:0/8:0, 18:1/18:1_/8:0, 18:2/ 10:0/16:0, 16:0/14:1/14:1, 18:1/10:0/ 16:1, 18:1/14:1/12:0	0.3916 ± 0.0067	0.3103	0.0813		
/0.94	I, II: 18:1/18:1/8:0, 18:2/8:0_/18:0, 18:1/ 10:1_/16:0	0.1618 ± 0.0039	0.1035	0.0583		
	Total 44:2	0.5534				
767.0/44:1/0.91	I, II: 18:1/16:0_/10:0, 18:0/16:1/10:0, 18:1/14:0/12:0, 18:1/8:0/18:0, 18:0/ 14:1/12:0, 18:1/8:0/18:0, 16:0/16:1_ 12:0, 16:0/14:1/14:0, 14:0/16:1/14:0	2.1709 ± 0.1393	1.7866	0.3843		
/0.94	NIMS	0.1795 ± 0.0255	0.1302	0.0492		
	Total 44:1	2.3504				
769.0/44:0/0.90	I: 16:0/14:0/14:0, 16:0/12:0/16:0, 18:0_ 14:0_/12:0, 18:0/10:0/16:0	2.1933 ± 0.1471	2.1933			
	NIMS four peaks	0.4822 ± 0.0259		0.4822		
	Total 44:0	2.6754				
781.0/45:1/0.90	I: 18:1/10:0_/17:0, 18:1/12:0_/15:0, 18:0_/17:1/10:0, 14:0 14:0 17:1	0.0678 ± 0.0028	0.0678			

Table 3 continued

$[M + NH_4]^{+a}$ (m/z^b)/ ACN:DB ^c /RRT ^d	Major and (minor) molecular species	Mol% \pm SD ^e	Fr. I ^f	Fr. II	Fr. III	Fr. IV
783.0/45:0/0.84 /0.90	NIMS six peaks	0.0396 \pm 0.0141	0.0084	0.0312		
	Total 45:1	0.1074				
	I: 19:0/12:0/14:0, 19:0/10:0/16:0	0.0117 \pm 0.0001	0.0117			
791.0/46:3/0.92 /0.93	I: 16:0/15:0_/14:0, 16:0/17:0_/12:0, 14:0/ 17:0/14:0, (13:0/16:0/16:0, 15:0/18:0/ 12:0, 18:0/10:0/17:0)	0.1236 \pm 0.0118	0.1236			
	NIMS six peaks	0.0958 \pm 0.0081	0.0274	0.0684		
	Total 45:0	0.2311				
793.0/46:2/0.92 /0.94	NIMS	0.0898 \pm 0.0214	0.0583	0.0315		
	I: 18:1/18:1_/10:1, 18:1/18:2/10:0, 18:3/ 14:0/14:0	0.0526 \pm 0.0345	0.0526			
	Total 46:3	0.1486				
795.0/46:1/0.90	I: 18:1/14:0/14:1, 18:1/10:0/18:1, 16:1/ 16:1/14:0, 18:0/10:0/18:2	0.8833 \pm 0.0373	0.7363	0.1470		
	NIMS	0.0054 \pm 0.0014		0.0054		
	Total 46:2	0.8888				
797.0/46:0/0.88 /0.91	I: 18:1/12:0_/16:0, 16:0/16:1/14:0, 16:0/ 14:1/16:0, 18:1/10:0_/18:0, 18:1/14:0/ 14:0, 14:0/18:0_/14:1, 12:0/16:1/18:0	2.6644 \pm 0.1353	2.4547	0.2098		
	NIMS two peaks	0.3569 \pm 0.1273	0.0613	0.2956		
	Total 46:1	3.0213				
809.0/47:1/0.84 /0.89	NIMS	0.4632 \pm 0.0146	0.0809	0.3823		
	I: 16:0/16:0/14:0, 16:0/12:0/18:0, 18:0/ 14:0/14:0, 18:0/10:0/18:0	2.5632 \pm 0.0737	2.5249	0.0384		
	Total 46:0	3.1052				
811.0/47:0/0.84 /0.89	NIMS two peaks	0.0788 \pm 0.0116	0.0468	0.0320		
	I: 18:1/12:0_/17:0, 18:1/15:0_/14:0, 16:0/ 17:1/14:0	0.1776 \pm 0.0009	0.1776			
	Total 47:1	3.0301				
816.9/48:4/0.93	NIMS six peaks	0.1123 \pm 0.0124	0.0389	0.0735		
	I: 19:0/12:0/16:0, 19:0/14:0/14:0, 19:0/ 10:0/18:0	0.0265 \pm 0.0011	0.0265			
	Total 47:0	0.3741				
819.0/48:3/0.91 /0.91	I: 15:0/16:0/16:0, 15:0/18:0_/14:0, 16:0/ 17:0/14:0	0.2093 \pm 0.0085	0.2093			
	NIMS eight peaks	0.1384 \pm 0.0124	0.0501	0.0884		
	Total 48:4	0.0359				
821.1/48:2/0.90 /0.91	I: 20:4/16:0/12:0, 18:3/12:0/18:1, 18:2/ 12:1/18:1	0.0201 \pm 0.0030	0.0190	0.0011		
	NIMS four peaks	0.0158 \pm 0.0080	0.0094	0.0065		
	Total 48:3	0.2670				
821.1/48:2/0.90 /0.91	NIMS	0.1092 \pm 0.0641	0.1092			
	I: 14:1/18:1/16:1, 18:1/18:2/12:1	0.1091 \pm 0.0000	0.1091			
	Total 48:3	0.2670				
821.1/48:2/0.90 /0.91	NIMS two peaks	0.0488 \pm 0.0172	0.0000	0.0488		
	I: 18:2/14:0/16:0, 18:1/16:1/14:0, 18:1/ 14:1_/16:0, 18:1/12:0/18:1, 16:0/16:1/ 16:1	1.2499 \pm 0.0380	1.2499			
	Total 48:2	1.4481				
821.1/48:2/0.90 /0.91	NIMS	0.1982 \pm 0.0049		0.1982		
	Total 48:2	1.4481				

Table 3 continued

$[M + NH_4]^{+a}$ (m/z^b)/ ACN:DB ^c /RRT ^d	Major and (minor) molecular species	Mol% \pm SD ^e	Fr. I ^f	Fr. II	Fr. III	Fr. IV
823.0/48:1/0.86	NIMS	0.0824 \pm 0.0231	0.0824			
/0.89	I: 18:1/14:0_/16:0, 16:0/16:1/16:0	3.0842 \pm 0.2009	3.0842			
/0.91	NIMS	0.6062 \pm 0.0202		0.6062		
	Total 48:1	3.7729				
825.0/48:0/0.85	I: 20:0/14:0/14:0, 20:0/12:0/16:0, 20:0/ 10:0_/18:0	0.0277 \pm 0.0032	0.0277			
/0.89	I: 16:0/16:0/16:0, 18:0/14:0/16:0, (18:0/ 12:0/18:0)	2.3901 \pm 0.1632	2.3901			
/0.90	NIMS	0.4307 \pm 0.0199		0.4307		
	Total 48:0	2.8485				
837.0/49:1/0.84	I: 19:0/12:0/18:1, 19:0/14:1/16:0	0.0261 \pm 0.0052	0.0261			
/0.90	I: 18:1/15:0_/16:0, 18:1/17:0_/14:0, 16:0/ 17:1/16:0, 16:0/16:1/17:0	0.4121 \pm 0.0271	0.3531	0.0590		
	NIMS three peaks	0.0765 \pm 0.0107	0.0445	0.0320		
	Total 49:1	0.5147				
839.0/49:0/0.83	I: 19:0/14:0/16:0, (19:0/12:0/18:0)	0.0581 \pm 0.0063	0.0581			
/0.85	NIMS	0.0146 \pm 0.0013	0.0146			
/0.89	I: 18:0/15:0_/16:0, 16:0/16:0/17:0	0.1770 \pm 0.0185	0.1536	0.0235		
	NIMS six peaks	0.0812 \pm 0.0090	0.0379	0.0434		
	Total 49:0	0.3309				
845.0/50:4/0.92	I: 18:3/18:1_/14:0, 18:2/18:2/14:0, 18:1/ 14:1_/18:2	0.1246 \pm 0.0004	0.1048	0.0197		
	Total 50:4	0.1246				
847.0/50:3/0.90	I: 18:2_/18:1/14:0, (18:1/14:1/18:1, 18:3/ 18:0/14:0, 18:3/16:0/16:0, 18:2/18:0_ 14:1, 18:1/16:1/16:1)	0.4795 \pm 0.1023	0.4795			
	NIMS three peaks	0.0782 \pm 0.0039	0.0000	0.0782		
	Total 50:3	0.5577				
849.0/50:2/0.90	I: 18:1/14:0_/18:1, 18:1/16:1/16:0, 18:2/ 16:0/16:0, 18:2/14:0/18:0, 18:1/14:1/ 18:0, 18:0/16:1/16:1	2.7974 \pm 0.2199	2.4319	0.3654		
	Total 50:2	2.7974				
851.0/50:1/0.85	I: 20:0/12:0/18:1, 20:0/16:0_/14:1, 20:0/ 14:0/16:1	0.1869 \pm 0.0507	0.1869			
/0.88	I: 18:1/16:0/16:0, 18:1/14:0_/18:0, 16:0/ 18:0/16:1	4.7740 \pm 0.3820	4.7740			
	NIMS two peaks	1.0625 \pm 0.4519	0.0000	1.0625		
	Total 50:1	6.0234				
853.0/50:0/0.83	NIMS	0.0400 \pm 0.0000	0.0400			
/0.85	I: 20:0/14:0/16:0, (20:0/12:0/18:0)	0.0996 \pm 0.0075	0.0996			
/0.88	I: 18:0/16:0/16:0, (18:0/14:0/18:0)	2.0429 \pm 0.1615	2.0429			
/0.90	NIMS	0.2518 \pm 0.0443		0.2518		
	Total 50:0	2.4345				
865.3/51:1/	NIMS	0.0099 \pm 0.0000	0.0099			
/0.83	I: 19:0/14:0/18:1, (19:0/16:0/16:1, 19:0/ 14:1_/18:0)	0.0515 \pm 0.0034	0.0515			
/0.88	I: 18:1/16:0_/17:0, 18:0/17:1/16:0, 18:1/ 15:0/18:0	0.2612 \pm 0.0084	0.2612			
	NIMS four peaks	0.0917 \pm 0.0041	0.0210	0.0707		
	Total 51:1	0.4143				

Table 3 continued

$[M + NH_4]^{+a}$ (m/z^b)/ ACN:DB ^c /RRT ^d	Major and (minor) molecular species	Mol% \pm SD ^e	Fr. I ^f	Fr. II	Fr. III	Fr. IV
867.3/51:0/0.82	I: 19:0/16:0/16:0, 19:0/14:0/18:0	0.0378 \pm 0.0061	0.0378			
/0.84	I: 20:0/17:0/14:0, 20:0/15:0/16:0	0.0115 \pm 0.0001	0.0115			
/0.88	I: 18:0/17:0/16:0, 18:0/15:0/18:0	0.0498 \pm 0.0058	0.0498			
	NIMS eight peaks	0.0547 \pm 0.0108	0.0297	0.0250		
	Total 51:0	0.1537				
873.3/52:4/0.90	I: 20:4/16:0/16:0, 18:3/18:1/16:0, 18:2/18:2/16:0	0.2044 \pm 0.0114	0.2002	0.0041		
/0.92	NIMS	0.0337 \pm 0.0004		0.0337		
	Total 52:4	0.2380				
875.3/52:3/0.89	I: 18:2/18:1/16:0, 18:1/18:1/16:1, 18:3/18:0/16:0, 18:2/18:0/16:1	0.6485 \pm 0.4467	0.6485			
	NIMS two peaks	0.6374 \pm 0.0135	0.4980	0.1393		
	Total 52:3	1.2858				
877.3/52:2/0.85	NIMS	0.0490 \pm 0.0000	0.0490			
/0.88	I, II: 18:1/16:0/18:1, 18:2/18:0/16:0	3.7087 \pm 0.3616	3.6568	0.0519		
/0.90	NIMS	0.5242 \pm 0.0213		0.5242		
	Total 52:2	4.2819				
879.3/52:1/0.84	I: 20:0/14:0/18:1, (20:0/16:0/16:1)	0.0400 \pm 0.0007	0.0400			
/0.88	I: 18:1/16:0/18:0, (18:0/16:1/18:0)	2.7534 \pm 0.2378	2.7534			
/0.89	NIMS	0.4676 \pm 0.0348		0.4676		
	Total 52:1	3.2611				
881.3/52:0/0.83	NIMS	0.0163 \pm 0.0000	0.0163			
/0.85	I: 20:0/16:0/16:0, 20:0/14:0/18:0	0.1168 \pm 0.0069	0.1148	0.0020		
/0.87	I: 18:0/16:0/18:0	0.9151 \pm 0.0718	0.9151			
	NIMS two peaks	0.0951 \pm 0.0094		0.0951		
	Total 52:0	1.1432				
891.3/53:2/0.83	I: 19:1/16:0/18:1, 18:2/15:0/20:0	0.0091 \pm 0.0009	0.0091			
/0.85	NIMS	0.0033 \pm 0.0000	0.0033			
/0.88	I: 18:1/18:0/17:1, 18:0/18:2/17:0	0.0823 \pm 0.0137	0.0823			
	NIMS two peaks	0.0407 \pm 0.0106	0.0171	0.0236		
	Total 53:2	0.1355				
893.3/53:1/0.82	I: 19:0/16:0/18:1, (19:0/16:1/18:0, 16:0/19:1/18:0)	0.0208 \pm 0.0020	0.0208			
/0.84	I: 20:0/15:0/18:1, (20:0/16:0/17:1)	0.0081 \pm 0.0005	0.0081			
/0.87	I: 17:0/18:0/18:1	0.0369 \pm 0.0037	0.0369			
	NIMS eight peaks	0.0195 \pm 0.0021	0.0045	0.0150		
	Total 53:1	0.0853				
895.3/53:0/0.82	I: 19:0/16:0/18:0	0.0031 \pm 0.0006	0.0031			
/0.84	I: 20:0/15:0/18:0, 20:0/17:0/16:0	0.0018 \pm 0.0002	0.0018			
/0.87	I: 18:0/17:0/18:0, 18:0/19:0/16:0	0.0043 \pm 0.0003	0.0043			
	NIMS five peaks	0.0073 \pm 0.0018	0.0040	0.0033		
	Total 53:0	0.0165				
897.0/54:6/	NIMS seven peaks	0.0345 \pm 0.0040	0.0263	0.0082		
	Total 54:6	0.0345				
899.0/54:5/0.91	I: 18:1/18:2/18:2, 18:3/18:2/18:0, 18:1/18:1/18:3	0.0979 \pm 0.0144	0.0806	0.0173		
	NIMS	0.0031 \pm 0.0008		0.0031		
	Total 54:5	0.1010				

Table 3 continued

[M + NH ₄] ⁺ ^a (<i>m/z</i> ^b)/ ACN:DB ^c /RRT ^d	Major and (minor) molecular species	Mol% ± SD ^e	Fr. I ^f	Fr. II	Fr. III	Fr. IV
901.0/54:4/0.89	I: 18:1/18:2/18:1, 18:0/18:2/18:2, 18:1/ 18:3_/18:0	0.1173 ± 0.0129	0.1039	0.0134		
/0.92	NIMS	0.0117 ± 0.0077		0.0117		
	Total 54:4	0.1290				
903.0/54:3/0.89	I: 18:1/18:1/18:1, 18:1/18:2/18:0, (18:0/ 18:3/18:0)	1.5592 ± 0.0732	1.3822	0.1770		
	NIMS two peaks	0.0846 ± 0.0168	0.0000	0.0846		
	Total 54:3	1.6438				
905.0/54:2/0.84	I: 20:0/16:1/18:1, 20:0/18:2/16:0, 18:1/ 20:1/16:0	0.0653 ± 0.0002	0.0653			
/0.87	I: 18:1/18:0/18:1, (18:0/18:2/18:0)	1.3853 ± 0.0634	1.3853			
/0.89	NIMS	0.2014 ± 0.0122		0.2014		
	Total 54:2	1.6521				
907.0/54:1/0.84	I: 20:0/16:0/18:1, (20:0/16:1/18:0)	0.2096 ± 0.0099	0.2096			
/0.87	I: 18:0/18:0/18:1	0.5835 ± 0.0317	0.5835			
	NIMS three peaks	0.0762 ± 0.0063		0.0762		
	Total 54:1	0.8693				
909.0/54:0/ /0.86	NIMS two peaks I: 18:0/18:0/18:0	0.0575 ± 0.0075 0.1150 ± 0.0127	0.0575 0.1150			
	NIMS five peaks	0.0258 ± 0.0033	0.0068	0.0190		
	Total 54:0	0.1983				
921.2/55:1/0.81 /0.84 /0.87	NIMS I: 19:0/18:1_/18:0 I: 18:1/19:0/18:0, 18:0/19:1/18:0	0.0271 ± 0.0067 0.0371 ± 0.0261 0.0725 ± 0.0065	0.0271 0.0371 0.0725			
	NIMS six peaks	0.0519 ± 0.0111	0.0243	0.0276		
	Total 55:1	0.1886				
923.2/55:0/ /0.86	NIMS two peaks I: 19:0/18:0/18:0, 18:0/21:0/16:0, (20:0/ 17:0/18:0)	0.0100 ± 0.0039 0.0188 ± 0.0010	0.0100 0.0188			
	NIMS five peaks	0.0278 ± 0.0046	0.0148	0.0131		
	Total 55:0	0.0567				
933.3/56:2/0.84 /0.86	I: 20:0/18:1/18:1, (20:0/18:0_/18:2) I: 18:1/20:1/18:0	0.1552 ± 0.0211 0.1472 ± 0.0032	0.1552 0.1472			
	NIMS four peaks	0.0477 ± 0.0068	0.0080	0.0397		
	Total 56:2	0.3501				
935.3/56:1/0.84 /0.86	I: 20:0/18:0_/18:1 I: 18:1/20:0/18:0, (18:1/22:0/16:0)	0.0906 ± 0.0056 0.1004 ± 0.0027	0.0890 0.1004	0.0015		
	NIMS five peaks	0.0290 ± 0.0045	0.0041	0.0249		
	Total 56:1	0.2200				
937.3/56:0/0.83 /0.86	I: 20:0/18:0/18:0 I: 18:0/20:0/18:0, 16:0/22:0/18:0, 16:0/ 24:0/16:0	0.0160 ± 0.0004 0.0436 ± 0.0069	0.0160 0.0436			
	NIMS six peaks	0.0096 ± 0.0011	0.0016	0.0080		
	Total 56:0	0.0692				
947.3/57:2/0.87	I: 18:1/21:0/18:1, 18:1/16:0/23:1, 18:1/ 21:1_/18:0	0.0794 ± 0.0073	0.0752	0.0042		
	NIMS two peaks	0.0228 ± 0.0009	0.0118	0.0109		
	Total 57:2	0.1022				
949.3/57:1/0.84	NIMS	0.0062 ± 0.0002	0.0062			

Table 3 continued

$[M + NH_4]^+{}^a$ (m/z^b)/ ACN:DB ^c /RRT ^d	Major and (minor) molecular species	Mol% \pm SD ^e	Fr. I ^f	Fr. II	Fr. III	Fr. IV
/0.86	I: 18:0/23:1_/16:0, 18:1/23:0/16:0	0.0590 \pm 0.0044	0.0590			
	NIMS three peaks	0.0328 \pm 0.0088	0.0153	0.0176		
	Total 57:1	0.0981				
951.3/57:0/	NIMS four peaks	0.0285 \pm 0.0044	0.0205	0.0080		
	Total 57:0	0.0285				
	Total	100.0	60.4	38.8	0.6	0.1
	Saturated	40.0				
	Monoene	38.4				
	Diene	16.2				
	Triene	4.5				
	Tetraene	0.6				
	Pentaene	0.1				
	Hexaene	0.0				
	NIMS	11.8				
	Odd ACN TAG	5.7				

^a Ammonium adduct^b Mass to charge ratio^c The number of acyl group carbons:the number of double bonds^d Relative retention time. Average of two or three chromatograms. In general, the SD was $\leq \pm 0.01$ ^e Standard deviations (SD_I , SD_{II} , SD_{III} , SD_{IV}) for molar amounts in each fraction (I, II, III, and IV) were calculated. The SD for the sum of the molar amounts was calculated using equation
$$SD = \sqrt{(SD_I^2 + SD_{II}^2 + SD_{III}^2 + SD_{IV}^2)}$$
 [43]. The SD for mol% was obtained by multiplying the mol% by the ratio of SD and the sum of molar amounts in the four fractions
^f Fractions from SPE fractionation^g Not identified molecular species^h Structure in italics indicates regioisomer identified by MS²ⁱ Structure in normal font indicates predominant regioisomer^j 18:1/6:0_/4:0 indicates 18:1/6:0/4:0 + 18:1/4:0/6:0

In the ACN range 36–40 eluted 12:0/12:0/12:0, 14:0/12:0/12:0, 14:0/12:0/14:0, 14:0/14:1/12 or 16:0/12:0/12:0 with some ACN:DB class of medium-chain TAG, and in the ACN range 42–46 medium-chain and long-chain TAG eluted in the same peaks with increasing proportions of long-chain TAG (Table 3). The total content of long-chain TAG (in the ACN range 43–57) was ca. 43.2 mol%. In the first peak of saturated TAG with 48–52 and 56 ACN, monoene TAG with 50–56 ACN, and diene TAG with 52 ACN eluted TAG with acyl 20:0, and in the second peak the longest acyl was C₁₈ or C₁₆ in TAG with 48–54 ACN, and 20:0, 22:0 or 24:0 in TAG with 56 ACN. The regioisomers *20:0/18:0/18:1* and *20:0/18:1/18:0* of TAG 56:1 eluted in the first peak and the regioisomer *18:1/20:0/18:0* together with 18:1/22:0/16:0 in the second peak. The regioisomer *20:0/18:0/18:0* of TAG 56:0 eluted in the first peak and the symmetric regioisomer *18:0/20:0/18:0* together with 16:0/22:0/18:0 and 16:0/24:0/16:0 in the second peak. The most abundant peaks of long-chain TAG species were 18:1/16:0/16:0 + (18:1/14:0/18:0 + 18:1/18:0/14:0) +

16:0/18:0/16:1 (4.77 mol%), 18:1/16:0/18:1 + 18:2/18:0/16:0 (3.71 mol%), (18:1/14:0/16:0 + 18:1/16:0/14:0) + 16:0/16:1/16:0 (3.08 mol%), (18:1/14:0/18:1 + 18:1/18:1/14:0) + 18:1/16:1/16:0 + 18:2/16:0/16:0 + 18:2/14:0/18:0 + 18:1/14:1/18:0 + 18:0/16:1/16:1 (2.80 mol%), (18:1/16:0/18:0 + 18:1/18:0/16:0) + 18:0/16:1/18:0 (2.75 mol%), 16:0/16:0/14:0 + 16:0/12:0/18:0 + 18:0/14:0/14:0 + 18:0/10:0/18:0 (2.56 mol%), 16:0/16:0/16:0 + 18:0/14:0/16:0 + (18:0/12:0/18:0) (2.39 mol%).

Discussion

Resolution and Identification of TAG

The studies of Plattner and Payne-Wahl [20] and Rhodes and Netting [21] showed that NP-HPLC has a relatively high potential for separation of TAG species with different chain-lengths and different unsaturation. The major application of NP-HPLC in lipid analysis has been lipid class

separations introduced by Christie [42]. In 1999, NP-HPLC was used for the separation of short- and long-chain TAG produced by interesterification of triacetin and soybean oil [22], and in 2003 and 2004 for analysis of short-chain TAG standards produced by chemical interesterifications [24] and short-chain TAG in BF [19]. Two 100×2 mm silica columns in series separated the *L/S/S* and *S/L/S* regioisomers, and *L/S/L* and *L/L/S* butyrate regioisomers ($S = 4:0$) to the baseline, and caproate regioisomers ($S = 6:0$) close to the baseline [24]. In the present work, similarly to the previous paper [19], the regioisomers of TAG with two short acyl chains eluted in different peaks: e.g. *14:0/6:0/4:0* and *6:0/14:0/4:0*, *16:0/4:0/4:0* and *4:0/16:0/4:0*, *18:1/4:0/4:0* and *4:0/18:1/4:0*. Furthermore, the regioisomers of TAG with one short acyl chain separated to the baseline as presented in the previous paper [19]. In addition, TAG with one or two medium chain acyls (C_8 or C_{10}) separated from caproates and *sn-2* and *sn-3* acetates from butyrates. In the ACN range 32–42, in the first peak of each even-numbered ACN:DB class eluted medium-chain TAG, in the second caproates, in the third butyrates, and if identified, in the fourth *sn-2* acetates, and in the fifth *sn-3* acetates. Thus the least polar eluted first and the most polar last. Unexpectedly, probably owing to the residual polarity of the column support, the same elution order has been observed in RP-HPLC [15, 16]. The expected reverse elution order was observed in the RP-HPLC analysis by Spanos et al. [17] and by the authors (P. Kalo, A. Kemppinen, V. Ollilainen, unpublished data). Medium-chain TAG in the ACN range 40–46 coeluted with long-chain TAG. Similar coelution was reported in the ACN range 42–46 in the RP-HPLC analysis [17].

As already noted, TAG 20:0/X/X eluted in the first peak of saturated TAG with 48–52 and 56 ACN, monoene TAG with 50–56 ACN, and diene TAG with 52 ACN. Some TAG of this category have been identified by RP-HPLC among other long-chain TAG species, but not in separate peaks [17, 18]. In general, the TAG species identified in the second peak with the longest acyl C_{18} or C_{16} in the 48–54 ACN range, are similar to those identified by RP-HPLC [17] although a higher number of TAG species have been identified in the present study. To our knowledge, the resolution of regioisomers of long-chain even-numbered TAG 56:1, *20:0/18:0/18:1* + *20:0/18:1/18:0* in the first peak and *18:1/20:0/18:0* in the second, and TAG 56:0, *20:0/18:0/18:0* in the first peak and *18:0/20:0/18:0* in the second peak have not been observed before.

The regioisomers of odd ACN TAG with one short acyl chain may be separated as the elution order of 35:0 TAG shows: *15:0/6:0/14:0*, *15:0/14:0/6:0*, *16:0/15:0/4:0* + *15:0/16:0/4:0*, *16:0/16:0/3:0* + *18:0/14:0/3:0*. There are also sufficient polarity differences between molecular species of odd long-chain TAG in ACN range 45–55 for

adequate separation. The least polar TAG 19:0/X/X eluted first, followed by second least polar TAG 20:0/X/X, and most polar 18:0/X/X. The resolution of TAG 55:1 regioisomers *19:0/18:1/18:0* + *19:0/18:0/18:1* in the first peak and *18:1/19:0/18:0* in the second peak has not been reported before.

Quantification of TAG

In our previous paper [19] we quantified short-chain TAG in BF by NP-HPLC on three microbore silica gel columns in series. EIC of $[M + NH_4]^+$ of TAG were integrated and MCF, determined for molecular species of TAG in a high number of interesterified mixtures of three monoacid TAG by linear calibration, were used to correct the ion yield. The composition of short-chain TAG was calculated by normalization from the molar amounts of TAG species and their total proportion determined by GC [8]. In order to be able to quantify, in addition to the short-chain TAG, also long-chain TAG, acetate TAG, odd ACN TAG, and non-identified TAG we decided to modify applicable in NP-HPLC–ESI the method used by Byrdwell et al. [35] in LC–APCI–MS for determination of response factors based on randomized fat and calculated random composition.

The TAG species with different levels of unsaturation have different molecular geometry. Similarly isobaric TAG species with different acyl chains have different molecular structure, as well as the regioisomers of short-chain TAG. This is valid for all short-chain TAG with ACN 22 and higher. These contain at least one long-chain FA. The difference in the molecular structure appears in different polarity and in separation by NP-chromatographic analysis and may appear in the different ion yield and MCF as well.

For comparison of the TAG composition determined in this study with that calculated according to random distribution, the experimental and random data for even ACN TAG are shown in Fig. 6a and those for odd ACN TAG in Fig. 6b. Figure 6a shows two maxima for experimental values, one at ACN 38 (11.2 mol%) and another at ACN 50 (11.9 mol%). All experimental sum values of TAG with different unsaturation differed from respective values calculated according to random distribution. This indicates the specific distribution of TAG in native BF. Furthermore, the non-randomness of TAG composition of BF can be easily deduced by comparison of ACN:DB classes in the experimental and random composition. Figure 6b shows two maxima for experimental values as well, one at ACN 37 and another at ACN 49. Likewise, for even ACN TAG, comparison of experimental and calculated values of ACN or ACN:DB classes indicate specific distribution of odd ACN TAG in BF.

In the present study, molar ratios of saturated acyls and double bonds calculated from the TAG data shown in

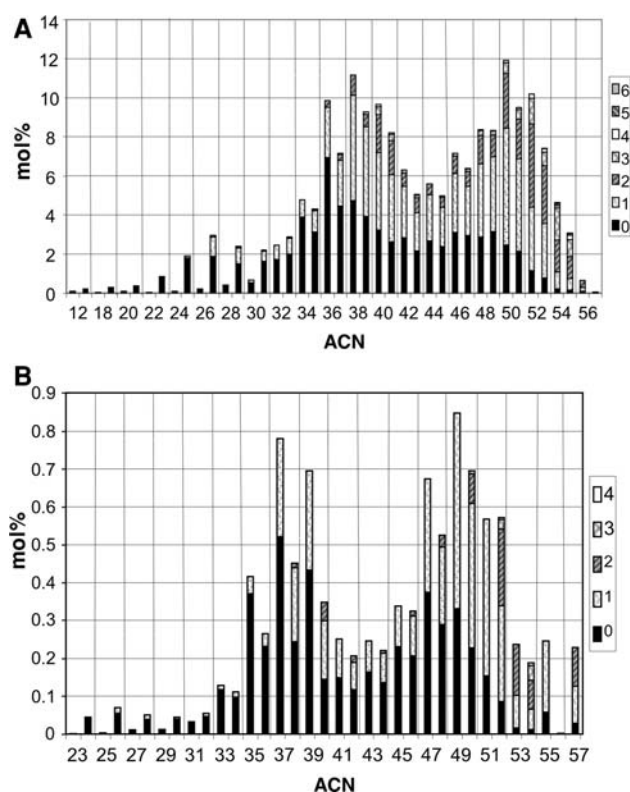


Fig. 6 Acyl carbon number:double bond (*ACN:DB*) class composition of butterfat triacylglycerols (*TAG*). In each acyl carbon number (*ACN*) class, the left column shows experimental data and the right column the *TAG* composition calculated according to the random distribution. **a** Even-numbered *TAG*. **b** Odd-numbered *TAG*. 0 Saturated, 1 monoene, 2 diene, 3 triene, 4 tetraene, 5 pentaene, 6 hexaene (at the top of *ACN* 54 a very small column) *TAG*

Table 3 and in Fig. 6a and b, and on the other hand from the FA composition, were 2.43 and 2.46, respectively. Ratios of butyrates and caproates calculated from *TAG* data and from FA composition were 2.58 and 2.51, respectively. Those of butyrates and medium-chain acyls ($C_8 + C_{10}$) 2.13 and 2.13, respectively, those of medium-chain acyls and caproates 1.22 and 1.18, respectively, and those of long-chain saturated and long-chain unsaturated 2.08 and 2.15, respectively.

Acetate *TAG*

Acetate *TAG* in milk lipids have been studied by thin layer chromatography (TLC) on plain silica gel and packed column GC [37] or capillary GC and GC–MS [5]. Investigation of the positional distribution of the acetyl group in milk fat *TAG* by chiral-phase HPLC of acetate *TAG* isolated by TLC, hydrogenated, and subjected to Grignard degradation [38] indicated that acetates are entirely in the *sn*-3 position. The regioisomeric structures of acetate *TAG* isolated by silica gel column chromatography from bovine udder were characterized by 1D- and 2D-NMR and

collision-induced dissociation tandem mass spectrometry coupled with fast atom bombardment [39], and indicated the presence of acetate in the *sn*-3 position in all molecular species of acetate *TAG*. On the contrary, determination of regioisomeric structures of acetate *TAG* in butterfat by normal-phase HPLC–ESI tandem MS [19] showed in the *ACN* range 22–30 the relative *X/X/2:0* and *X/2:0/X* regioisomer ratio 90.5:9.5. In the present study, the molar ratio of *X/X/2:0* and *X/2:0/X* regioisomers in the *ACN* range 22–38 was 1.82:1. In the present and previous study [19] the SPE fractionation ensured that *TAG* species of any size and polarity were eluted from the SPE column and were subjected to NP-HPLC–ESI–MS analysis. Thus the possible loss of *sn*-2 acetyl isomers during the fractionation step was minimized.

Odd *ACN* *TAG*

Myher et al. [5] studied the fourth most volatile 2.5% molecular distillate of milk fat by GC–MS, and found in the analysis on a polarizable capillary column that in the *ACN* range 33–41 several isobaric odd *ACN* *TAG* eluted in three peaks, which in full MS yielded the same “diacylglycerol” fragments. The three peaks were considered normal-, anteiso-, iso-odd acyl-chain *TAG*. The mol% of *TAG* species was estimated from the knowledge of the carbon number distribution and the flame ionization response in the GC. The same authors [15] identified by RP-HPLC in the most volatile 2.5% molecular distillate saturated branch- and normal-acyl-chain isomers of several odd *ACN* *TAG* species in *ACN* range 25–37. The compositions of saturated and monounsaturated *TAG* of molecular distillate were estimated by RP-HPLC from the area percentages that are derived from the sum of the diacylglycerol fragment intensities. Marai et al. [16] investigated randomized butteroil *TAG* by RP-HPLC with light-scattering and MS detection and identified saturated odd *ACN* *TAG* with 31–49 *ACN*. Only one molecular species was identified in each *ACN* class except in 37:0, where two isobaric butyrates were identified. The branched chain acyls were not shown among the identified odd *ACN* *TAG*. Uncorrected estimates of *TAG* species by HPLC–light-scattering detection and HPLC–MS were presented. Spanos et al. [17] studied milk fat *TAG* by RP-HPLC with light-scattering and desorption CI tandem MS and identified one caprylate and caproate, and two butyrate 37:0 *TAG*, and one 47:1 *TAG* species. Mottram and Evershed [18] identified in milk fat by RP-HPLC–APCI–MS one butyrate 33:0 and 35:0 *TAG*, two butyrate 37:0 *TAG* species, two long-chain (47:1 and 49:0) *TAG* species, and one 51:1 *TAG* species.

In the present study, acyl-chain- and regioisomers of short-chain odd *ACN* *TAG* were separated and the

regioisomers of the most abundant long-chain odd ACN TAG were deduced from MS² data. For quantification of abundant odd ACN TAG specific MCF were used.

Even-Numbered Butyrate and Caproate TAG

The molecular species of TAG with two or three short acyl chains in the ACN range 12–28 that were identified and quantified are more numerous here than in the GC–MS study of similar BF [9]. Even regioisomers of some butyrocaproates have been resolved in the present study. Furthermore tributyrin and tricaproin have been quantified. There is relatively good agreement with proportions of major short-chain TAG with one short acyl chain in these two studies although the ratio of saturated to monoene TAG showed different values, 40.1:38.4 in the present study and 44.9:34.1 in the GC–MS study [9]. If the same proportion of non-identified and odd ACN TAG is expected in the GC–MS as in the present study, 11.8 and 5.7 mol%, for a total of 17.5 mol%, the total mol% of identified TAG is 82.5. If the TAG determined by GC–MS are normalized to the sum of 82.5 mol%, the major TAG peaks in the present study and (in the GC–MS study [9]) are 16:0/16:0/4:0 + 18:0/14:0/4:0 : 5.25 (5.22) mol%, 18:1/16:0/4:0 : 4.08 (4.17) mol%, 16:0/14:0/4:0 + 18:0/12:0/4:0 : 3.34 (2.46) mol%, 18:0/16:0/4:0 : 2.85 (2.27) mol%, 18:1/18:0/4:0 : 1.99 (1.13) mol%, and 18:1/14:0/4:0 + (16:0/16:1/4:0 + 16:1/16:0/4:0) : 1.96 (2.51) mol%. Gresti et al. [14] studied much more unsaturated summer butterfat TAG than in the present study [13] by RP-HPLC fractionation and gas chromatographic determination of TAG and FA of fractions. Despite the difference in the degree of unsaturation of BF in the present study and in that of Gresti et al., there is relatively good accordance with the proportions of short-chain TAG containing one short-chain acyl. The major TAG species in this category in the present study and (in that by Gresti et al. [14]) were: 16:0/16:0/4:0 + 18:0/14:0/4:0 : 5.25 (4.55) mol%, 18:1/16:0/4:0 : 4.08 (4.17) mol%, 16:0/14:0/4:0 + 18:0/12:0/4:0 : 3.34 (3.41) mol%, 18:0/16:0/4:0 : 2.85 (2.47) mol%, 18:1/18:0/4:0 : 1.99 (1.58) mol%, 18:1/14:0/4:0 + (16:0/16:1/4:0 + 16:1/16:0/4:0) : 1.96 (2.21) mol%.

Medium-Chain TAG

There is also similarity in the proportions of medium-chain TAG in the present study, GC–MS [9], and in the study of Gresti et al. [14]. The proportions of the medium-chain TAG 38:0 (including one long-chain TAG) 14:0/12:0/12:0, 16:0/12:0/10:0, 16:0/14:0/8:0, 18:0/10:0/10:0, 18:0/12:0/8:0, 14:0/14:0/10:0 in the present study, in [9], and in [14] were 0.57, 0.86, and 0.91 mol%, respectively. The proportions of medium-chain TAG (including the coeluting long-chain TAG) in these three studies were: 40:0: 1.13,

2.36, 2.97; 40:1: 0.68, 0.25, 0.83; 42:0: 2.78, 3.09, 2.41; 42:1: 1.50, 1.08, 2.55; 44:0: 2.19, 2.45, 1.65; 44:1: 2.17, 1.73, 2.72; 46:0: 2.56, 2.63, 1.52; 46:1: 2.66, 2.85, 2.72 mol%, respectively.

Long-Chain TAG

There is relatively good accordance with the proportions of major unsaturated long-chain TAG in the present study and (in that reported by Gresti et al. [14]): 18:1/16:0/16:0 + (18:1/14:0/18:0 + 18:1/18:0/14:0) + 16:0/18:0/16:1: 4.77 (3.94) mol%, 18:1/16:0/18:1 + 18:2/18:0/16:0: 3.71 (2.39) mol%, (18:1/14:0/16:0 + 18:1/16:0/14:0) + 16:0/16:1/16:0: 3.08 (2.95) mol%, (18:1/14:0/18:1 + 18:1/18:1/14:0) + 18:1/16:1/16:0 + 18:2/16:0/16:0 + 18:2/14:0/18:0 + 18:1/14:1/18:0 + 18:0/16:1/16:1: 2.80 (2.18) mol%, (18:1/16:0/18:0 + 18:1/18:0/16:0) + (18:0/16:1/18:0) : 2.75 (2.39) mol%, but the higher degree of unsaturation in the BF analyzed by Gresti et al. [14], relative to our data, produced lower proportions of saturated long-chain TAG: 16:0/16:0/14:0 + 16:0/12:0/18:0 + 18:0/14:0/14:0 + 18:0/10:0/18:0: 2.56 (1.52) mol%, 16:0/16:0/16:0 + 18:0/14:0/16:0 + (18:0/12:0/18:0): 2.39 (1.09) mol%, 18:0/16:0/16:0 + 18:0/14:0/18:0: 2.04 (0.74) mol%, 18:0/16:0/18:0: 0.92 (0.43) mol%.

The methodology used in the analysis of BF TAG provides abundant information on the structures of a great number of molecular species of TAG. The ability of the NP-HPLC column used to resolve acyl-chain- and regioisomers of TAG with different polarities enabled the identification and quantification of a great number of TAG species by positive ESI–MS and –MS². Regioisomeric identification and quantification of TAG with two short acyl chains, even-numbered TAG with one short acyl chain, odd-numbered TAG with one short acyl chain, and identification and quantification of TAG species of medium-chain and long-chain even-numbered and odd-numbered TAG provide detailed structural and quantitative data of these major and minor sub classes of TAG in BF. This data may be exploited in the future in the studies of TAG absorption, metabolism, nutrition, crystallization, fractionation or modification.

Acknowledgments Financial support from the Jenny and Antti Wihuri Foundation and Finnish Society of Dairy Science is gratefully acknowledged.

References

- Jensen RG (2002) The composition of bovine milk lipids: January 1995 to December 2000. *J Dairy Sci* 85:295–350
- Breckenridge WC, Kuksis A (1968) Specific distribution of short-chain fatty acids in molecular distillates of bovine milk fat. *J Lipid Res* 9:388–393

3. Marai L, Breckenridge WC, Kuksis A (1969) Specific distribution of fatty acids in the milk fat triglycerides of goat and sheep. *Lipids* 4:562–570
4. Pitas RE, Sampugna J, Jensen RG (1967) Triglyceride structure of cows' milk fat. Preliminary observations on the fatty acid compositions of positions 1, 2, and 3. *J Dairy Sci* 50:1332–1336
5. Myher JJ, Kuksis A, Marai L, Sandra P (1988) Identification of the more complex triacylglycerols in bovine milk fat by gas chromatography–mass spectrometry using polar capillary columns. *J Chromatogr* 452:93–118
6. Kalo P, Kempainen A (1993) Mass spectrometric identification of triacylglycerols of enzymatically modified butterfat separated on a polarizable phenylmethylsilicone column. *J Am Oil Chem Soc* 70:1209–1217
7. Kempainen A, Kalo P (1993) Fractionation of the triacylglycerols of lipase-modified butter oil. *J Am Oil Chem Soc* 70:1203–1207
8. Kempainen A, Kalo P (1998) Analysis of *sn*-1(3)- and *sn*-2-short-chain acyl isomers of triacylglycerols in butteroil by gas–liquid chromatography. *J Am Oil Chem Soc* 75:91–100
9. Kempainen A, Kalo P (2006) Quantification of triacylglycerols in butterfat by gas chromatography–electron impact mass spectrometry using molar correction factors for $[M - RCOO]^+$ ions. *J Chromatogr A* 1134:260–283
10. Kallio H, Laakso P, Huopalahti R, Linko RR (1989) Analysis of butter fat triacylglycerols by supercritical fluid chromatography/electron impact mass spectrometry. *Anal Chem* 60:698–700
11. Laakso P, Manninen P (1997) Identification of milk fat triacylglycerols by capillary supercritical fluid chromatography–atmospheric pressure chemical ionization mass spectrometry. *Lipids* 32:1285–1295
12. Kuksis A, Marai L, Myher JJ (1991) Reversed-phase liquid chromatography–mass spectrometry of complex mixtures of natural triacylglycerols with chloride–attachment negative chemical ionization. *J Chromatogr* 588:73–87
13. Maniongui C, Gresti C, Bugaut M, Gauthier S, Bezard J (1991) Determination of bovine butterfat triacylglycerols by reversed-phase liquid chromatography and gas chromatography. *J Chromatogr* 543:81–103
14. Gresti J, Bugaut M, Maniongui C, Bezard J (1993) Composition of molecular species of triacylglycerols in bovine milk fat. *J Dairy Sci* 76:1850–1869
15. Myher JJ, Kuksis A, Marai L (1993) Identification of the less common isologous short-chain triacylglycerols in the most volatile 2.5% molecular distillate of butter oil. *J Am Oil Chem Soc* 70:1183–1191
16. Marai L, Kuksis A, Myher JJ (1994) Reversed-phase liquid chromatography–mass spectrometry of the uncommon triacylglycerol structures generated by randomization of butteroil. *J Chromatogr* 672:87–99
17. Spanos GA, Schwartz RB, van Breemen RB, Huang CH (1995) High-performance liquid chromatography with light-scattering detection and desorption chemical–ionization tandem mass spectrometry of milk fat triacylglycerols. *Lipids* 30:85–90
18. Mottram HR, Evershed RP (2001) Elucidation of the composition of bovine milk fat triacylglycerols using high-performance liquid chromatography–atmospheric pressure chemical ionisation mass spectrometry. *J Chromatogr* 926:239–253
19. Kalo P, Kempainen A, Ollilainen V, Kuksis A (2004) Regio-specific determination of short-chain triacylglycerols in butterfat by normal-phase HPLC with on-line electrospray–tandem mass spectrometry. *Lipids* 39:915–928
20. Plattner RD, Payne-Wahl K (1979) Separation of triglycerides by chain length and degree of unsaturation on silica HPLC columns. *Lipids* 14:152–153
21. Rhodes SH, Netting AG (1988) Normal-phase high-performance liquid chromatography of triacylglycerols. *J Chromatogr* 448:135–143
22. Lin JT (2007) HPLC separation of acyl lipid classes. *J Liq Chrom Relat Technol* 30:2005–2020
23. Mangos TJ, Jones KC, Foglia TA (1999) Normal-phase high performance liquid chromatographic separation and characterization of short- and long-chain triacylglycerols. *Chromatographia* 49:363–368
24. Kalo P, Kempainen A, Ollilainen V, Kuksis A (2003) Analysis of regioisomers of short-chain triacylglycerols by normal-phase liquid chromatography–electrospray tandem mass spectrometry. *Int J Mass Spectrom* 229:167–180
25. Kalo P, Ollilainen V, Rocha JM, Malcata FX (2006) Identification of simple lipids by normal-phase liquid chromatography–positive electrospray tandem mass spectrometry, and application of developed methods in comprehensive analysis of low erucic acid rapeseed oil lipids. *Int J Mass Spectrom* 254:106–121
26. Duffin KL, Henion JD, Shieh JJ (1991) Electrospray and tandem mass spectrometric characterization of acylglycerol mixtures that are dissolved in nonpolar solvents. *Anal Chem* 63:1781–1788
27. Cheng C, Gross ML, Pittenauer E (1998) Complete structural elucidation of triacylglycerols by tandem sector mass spectrometry. *Anal Chem* 70:4417–4426
28. Marzilli LA, Fay LB, Dionisi F, Vouros P (2003) Structural characterization of triacylglycerols using electrospray ionization–MSⁿ ion-trap MS. *J Am Oil Chem Soc* 80:195–202
29. McAnoy AM, Wu CC, Murphy RC (2005) Direct qualitative analysis of triacylglycerols by electrospray mass spectrometry using a linear ion trap. *J Am Soc Mass Spectrom* 16:1498–1509
30. Hites RA (1970) Quantitative analysis of triglyceride mixtures by mass spectrometry. *Anal Chem* 42:1736–1740
31. Lauer WM, Aasen AJ, Graff G, Holman RT (1970) Mass spectrometry of triglycerides: I. Structural effects. *Lipids* 5:861–868
32. Schulte E, Höhn M, Rapp U (1981) Mass spectrometric determination of triglyceride patterns of fats by the direct chemical ionization technique (DCI). *Fresenius Z Anal Chem* 307:115–119
33. Myher JJ, Kuksis A, Marai L, Manganaro F (1984) Quantitation of natural triacylglycerols by reversed-phase liquid chromatography with direct liquid inlet mass spectrometry. *J Chromatogr* 283:289–301
34. Kallio H, Currie G (1993) Analysis of low erucic acid turnip rapeseed oil (*Brassica campestris*) by negative ion chemical ionization tandem mass spectrometry. A method giving information on the fatty acid composition in positions *sn*-2 and *sn*-1/3 of triacylglycerols. *Lipids* 28:207–215
35. Byrdwell WC, Emken EA, Neff WE, Adlof RO (1996) Quantitative analysis of triglycerides using atmospheric pressure chemical ionization–mass spectrometry. *Lipids* 31:919–935
36. Byrdwell WC, Neff WE (1996) Analysis of genetically modified Canola varieties by atmospheric pressure chemical ionization mass spectrometric and flame ionization detection. *J Liq Chrom Relat Technol* 19:2203–2225
37. Parodi PW (1975) Detection of acetodiacylglycerols in milk fat lipids by thin-layer chromatography. *J Chromatogr* 111(1975): 223–226
38. Itabashi Y, Myher JJ, Kuksis A (1993) Determination of positional distribution of short-chain fatty acids in bovine milk fat on chiral columns. *J Am Oil Chem Soc* 70:1177–1181
39. Limb JK, Kim YH, Han SY, Jhon GJ (1999) Isolation and characterization of monoacetyldiglycerides from bovine udder. *J Lipid Res* 40:2169–2176
40. Hendrikse PW, Harwood JL (1986) Analytical methods. In: Gunstone FD, Harwood JL, Padley FB (eds) *The lipid handbook*. Chapman and Hall, London

41. Han X, Gross RW (2001) Quantitative analysis and molecular species fingerprinting of triacylglyceride molecular species directly from lipid extracts of biological samples by electrospray ionization tandem mass spectrometry. *Anal Biochem* 295:88–100
42. Christie WW (1985) Rapid separation and quantification of lipid classes by high performance liquid chromatography and mass (light scattering) detection. *J Lipid Res* 26:507–512
43. Harris DC (1987) *Quantitative chemical analysis*. W. H. Freeman and Company, New York

Comparative Analysis of Brain Lipids in Mice, Cats, and Humans with Sandhoff Disease

Rena C. Baek · Douglas R. Martin ·
Nancy R. Cox · Thomas N. Seyfried

Received: 11 September 2008 / Accepted: 29 October 2008 / Published online: 26 November 2008
© AOCS 2008

Abstract Sandhoff disease (SD) is a glycosphingolipid (GSL) storage disease that arises from an autosomal recessive mutation in the gene for the β -subunit of β -Hexosaminidase A (*Hexb* gene), which catabolizes ganglioside GM2 within lysosomes. Accumulation of GM2 and asialo-GM2 (GA2) occurs primarily in the CNS, leading to neurodegeneration and brain dysfunction. We analyzed the total lipids in the brains of SD mice, cats, and humans. GM2 and GA2 were mostly undetectable in the normal mouse, cat, and human brain. The lipid abnormalities in the SD cat brain were generally intermediate to those observed in the SD mouse and the SD human brains. GM2 comprised 38, 67, and 87% of the total brain ganglioside distribution in the SD mice, cats, and humans, respectively. The ratio of GA2–GM2 was 0.93, 0.13, and 0.27 in the SD mice, cats, and humans, respectively, suggesting that the relative storage of GA2 is greater in the SD mouse than in the SD cat or human. Finally, the myelin-enriched lipids, cerebroside and sulfatides, were significantly lower in the SD brains than in the control brains. This study is the first comparative analysis of brain lipids in mice, cats, and humans with SD and will be important for designing therapies for Sandhoff disease patients.

Keywords Sandhoff disease · β -Hexosaminidase · Gangliosides · Glycosphingolipids · GM2 · GA2 · Cerebroside · Sulfatides · Myelin

Abbreviations

CHCl ₃	Chloroform
CNS	Central nervous system
GA2	Asialo-GM2
GSL	Glycosphingolipid
HexA	β -Hexosaminidase A
HPTLC	High-performance thin-layer chromatograph
MeOH	Methanol
SD	Sandhoff disease

Introduction

Sandhoff disease (SD) is an incurable lysosomal storage disorder that arises from an autosomal recessive mutation, which causes abnormal accumulation of ganglioside GM2 leading to progressive neurodegeneration [1, 2]. GM2 is catabolized by β -hexosaminidase A (HexA), which consists of an α and a β subunit encoded by the *Hexa* and *Hexb* genes, respectively, in complex with the GM2 activator protein. GM2 accumulation can result from inherited defects in either the hexosaminidase α or β subunit, or in the GM2 activator protein, leading to Tay-Sachs disease (B variant), Sandhoff disease (O variant), or GM2 activator deficiency (AB variant), respectively. SD patients have defects in the *Hexb* gene, and as a result, they lack activity of both β -hexosaminidase isozymes A ($\alpha\beta$) and B ($\beta\beta$). Consequently, patients accumulate GM2 and its asialo derivative, GA2, and also oligosaccharides and other hexosaminidase substrates within lysosomes [1, 2]. The onset of

R. C. Baek · T. N. Seyfried (✉)
Biology Department, Boston College, Chestnut Hill,
MA 02467, USA
e-mail: thomas.seyfried@bc.edu

D. R. Martin · N. R. Cox
Scott-Ritchey Research Center and Department of Pathobiology,
College of Veterinary Medicine, Auburn University,
Auburn, AL 36849, USA

disease ranges from infancy to adulthood, and excessive CNS GM2 accumulation leads to progressive neurodegeneration, brain dysfunction, and ultimately death.

Although the biochemical defect in SD has been known for many years, there are presently no therapies. The development of mouse models of lysosomal storage disorders has provided the necessary tools for advancement in possible therapies and treatments. However, with some success in bone marrow transplantation, gene therapy, stem cell therapy, caloric restriction, non-steroidal anti-inflammatory drug therapy, and substrate reduction therapy in SD mice, there are still no treatments available for patients [3–12].

A possible disconnect from mouse studies to clinical treatments is the difference in the applicable brain size between mouse and human. The brain weight of the mouse is around 0.4 g while an infantile human brain weighs around 400 g, representing a 1,000-fold difference in size [13–15]. A naturally occurring, authentic model of SD in cats (fG_{M2} Baker) has been previously characterized and could potentially serve as an intermediate model between mouse and man [16–19]. Although the feline brain is closer in size and complexity to the human brain, it is not clear how the mouse and the cat animal models of SD compare to the human patient.

While the CNS GM2 accumulation has been reported for the mouse and cat models of SD and in the patient [11, 19–22], the comparative total lipid analysis has never been done. In particular, our objective was to analyze similar brain regions, at a similar phenotypic time-point, using the same methodology to compare the total lipid distribution between mice, cats, and humans with SD. Knowledge gained from this study could help provide the foundation to bridge the gap between the successes in mouse studies to treatment in patients.

Experimental Procedures

Mice

The SV/129 *Hexb* $-/-$ (SD) mice were obtained from Dr. Richard Proia (NIH). These mice were derived by disruption of the murine *Hexb* gene and transferring this gene into the mouse genome through homologous recombination and embryonic stem cell technology as previously described [20]. *Hexb* $-/-$ mice were derived from crosses of *Hexb* $+/-$ females with *Hexb* $-/-$ males. Genotypes of mice were determined by measuring the specific activity of total hexosaminidase using a modification of the Galjaard procedure as previously described [23, 24]. *Hexb* $+/-$ and *Hexb* $-/-$ mice were propagated in the Boston College Animal Facility and were housed in plastic cages with filter tops containing

Sani-Chip bedding (P.J. Murphy Forest Products Corp., Montville, NJ, USA). Other conditions were as we recently described [12]. The cortical brain region from normal and SD mice was collected around 4 months of age (humane end-point) and stored at -80°C . All animal experiments were carried out with ethical committee approval in accordance with the National Institutes of Health Guide for the Care and Use of Laboratory Animals and were approved by the Institutional Animal Care Committee.

Cats

The SD cats were obtained from the fG_{M2} Baker colony and have been previously described [17, 19]. Sequence analysis determined that the causative mutation in this domestic shorthair SD cat resulted from a 25-base-pair inversion at the 3' end of the *Hexb* gene [16]. Affected cats have <3% normal hexosaminidase activity in cerebral cortex and, therefore, represent an authentic model to study Sandhoff disease. Animals were euthanized by pentobarbital overdose according to recommendations of the AVMA Panel on Euthanasia, then transcatheterially perfused with heparinized, cold saline (0.9% NaCl) until jugular perfusate was clear. Cerebral cortex samples were collected from normal and SD cats around 5 months of age (humane end-point) and were frozen immediately in liquid nitrogen and stored at -80°C until use. All animal procedures were approved by the Auburn University Institutional Animal Care and Use Committee.

Human Samples

Age-matched normal and SD human cortex samples were obtained from the NICHD Brain and Tissue Bank for Developmental Disorders at the University of Maryland, Baltimore.

Lipid Isolation, Purification, and Quantitation

Total Lipid Extraction

The lipids were isolated from frontal lobe regions of the SD patients and the cats, and from the entire cortex of the SD mice. Total lipids were extracted with chloroform (CHCl₃) and methanol (MeOH) 1:1 by volume and purified from the lyophilized brain tissue using modifications of previously described procedures [12, 25, 26].

Column Chromatography

Neutral and acidic lipids were separated using DEAE-Sephadex (A-25, Pharmacia Biotech, Upsala, Sweden)

column chromatography as previously described [27]. The total lipid extract, suspended in $\text{CHCl}_3:\text{CH}_3\text{OH}:\text{dH}_2\text{O}$, 30:60:8 by volume (solvent A), was applied to a DEAE-Sephadex column (1.2 mL bed volume) that had been equilibrated prior with solvent A. The column was washed twice with 20 mL solvent A and the entire neutral lipid fraction, consisting of the initial eluent plus washes, was collected. This fraction contained cholesterol, phosphatidylcholine, phosphatidylethanolamine and plasmalogens, sphingomyelin, and neutral GSLs to include cerebrosides and asialo-GM2 (GA2). Next, acidic lipids were eluted from the column with 35 mL $\text{CHCl}_3:\text{CH}_3\text{OH}:0.8\text{ M Na acetate}$, 30:60:8 by volume.

Ganglioside Purification

The acidic lipid fraction containing gangliosides was dried by rotary evaporation and then partitioned to separate the acidic lipids into the lower organic phase and the gangliosides into the upper aqueous phase as previously described [25, 28, 29]. The amount of sialic acid in the ganglioside fraction was determined by the resorcinol assay and then the ganglioside fraction was further purified with base treatment and desalting, as previously described [24, 26].

Acidic Phospholipid Purification

After the ganglioside fraction (Folch upper phase) was transferred, the acidic phospholipid fraction (Folch lower phase) was evaporated under a stream of nitrogen and re-suspended in 10 mL of $\text{CHCl}_3:\text{CH}_3\text{OH}$ (1:1 by volume). This fraction contained fatty acids, cardiolipin, phosphatidylserine, phosphatidylinositol, and sulfatides.

Neutral Lipid Purification

Neutral lipids were dried by rotary evaporation and re-suspended in 10 mL $\text{CHCl}_3:\text{CH}_3\text{OH}$ (2:1 by volume). To further purify GA2, a 4 mL aliquot of the neutral lipid fraction was evaporated under a stream of nitrogen, base treated with 1 N NaOH, and Folch partitioned as described previously [26]. The Folch lower phase containing GA2 was evaporated under a stream of nitrogen and re-suspended in 5 mL $\text{CHCl}_3:\text{CH}_3\text{OH}$ (2:1 by volume).

High-Performance Thin-Layer Chromatography

All lipids were analyzed qualitatively by high-performance thin-layer chromatography (HPTLC) according to previously described methods [25–27, 30]. To enhance precision, an internal standard (oleoyl alcohol) was added to the neutral and acidic lipid standards and samples as

previously described [27]. Purified lipid standards were either purchased from Matreya Inc. (Pleasant Gap, PA, USA), Sigma (St Louis, MO, USA), or were a gift from Dr. Robert Yu (Medical College of Georgia, Augusta, GA, USA).

For gangliosides and GA2, the HPTLC plates were developed and visualized as previously described [26]. For neutral and acidic phospholipids, the plates were developed to a height of either 4.5 or 6 cm, respectively, with chloroform:methanol:acetic acid:formic acid:water (35:15:6:2:1 by volume), and then both were developed to the top with hexanes:diisopropyl ether:acetic acid (65:35:2 by volume) as previously described [27, 31]. Neutral and acidic phospholipids were visualized by charring with 3% cupric acetate in 8% phosphoric acid solution, followed by heating in an oven at 165 °C for 7 min. The percentage distribution and density of individual bands was determined as previously described [26]. Briefly, the HPTLC plates were scanned on a personal Densitometer SI with ImageQuant software (Molecular Dynamics) or on a ScanMaker 4800 with ScanWizard5 V 7.00 software (Microtek). The total brain ganglioside distribution was normalized to 100% and the percentage distribution values were used to calculate sialic acid concentration of individual gangliosides as we previously described [32]. The density value for GA2 was fit to a standard curve of known lipid concentration and used to calculate concentration. For the neutral and the acidic phospholipids, each lipid was normalized to an internal standard (oleyl alcohol) and its concentration was quantified using a standard curve of each respective lipid.

Statistical Analysis

All data were analyzed by the two-tailed Student's *t* test to calculate statistical significance between the normal and the SD samples using Statview 5.0 software.

Results

Our objective was to compare the lipid distribution in the cerebral cortex of mice, cats, and humans with Sandhoff disease, using our established lipid isolation procedures. The comparative lipid analysis, to include gangliosides and neutral and acidic phospholipids, was done in age-matched normal and SD mice and cats at their respective humane end-points. Although the samples were not collected at “identical” time points in disease progression, they were collected at “similar” time points. Since the SD human samples were collected during autopsy from diseased patients, we elected to collect tissue from the SD mice and

cats at a humane end-point to correlate our analysis with the human samples. The humane end point used for the mice was about 120 days [11]. The SD cat samples were collected from mid to terminal disease stage under the guidance of Auburn University's Institutional Animal Care and Use Committee. Disease progression in SD cats is stereotypical and is charted primarily by neuromuscular function. Disease onset begins at about 8 weeks with a slight head tremor, and the animal progressively loses ability to ambulate. Mid-disease is reached at about 12 weeks, when the animal has an unstable gait and falls occasionally. The humane endpoint occurs at approximately 20 weeks, when the animal can no longer walk or sit upright. Our study is the first to compare the total lipid distribution at a similar point in disease progression in mice, cats, and humans with Sandhoff disease.

The *Hexb* mutations in the mice and cats studied in this report generate similar levels of residual total hexosaminidase activity in brain, about 3% of normal levels in both models [9, 10, 19, 20]. While the mouse mutation is a targeted disruption of the *Hexb* gene after the 12th of 14 exons, the cat mutation results in a premature termination codon in exon 14. While we are uncertain whether the artificial 4MUG substrate used for enzyme assays reflects the true enzymatic activity toward native gangliosides, we consider that the mouse and cat mutations are functionally equivalent. Consequently, differences in ganglioside storage profiles are more likely due to inter-species differences in ganglioside metabolism than to differences in residual enzyme activity.

Gangliosides

The total brain ganglioside concentration in mice, cats, and humans is shown in Table 1. In general, the total brain ganglioside concentrations in the normal animals are relatively similar among species. While all of the SD brains have significantly elevated total brain ganglioside concentrations compared to normal, the percent increase in total brain ganglioside concentration was greatest in the SD human (337%), followed by the SD cat (262%), and then the SD mouse (162%). The quantitative and qualitative distribution of individual gangliosides in the mice, cats, and human with SD is shown in Fig. 1 and in Table 2. The most significant finding was that GM2 comprised 38, 67, and 87% of the total brain ganglioside distribution in the SD mice, cats, and human, respectively. While the percent distribution for GM1, GD1a, GT1a/LD1, GD1b, GT1b, and GQ1b in the SD mouse and the SD cat were significantly different than that of normal, these differences were not associated with significant changes in the concentration for each ganglioside. Although ganglioside GT1a/LD1 was not detected in the normal cats, GT1a/LD1 was present in the

Table 1 Total brain ganglioside concentration in normal and Sandhoff disease mice, cats, and humans

Species	Age (months)	N	Ganglioside content (μg sialic acid/100 mg dry weight)	% increase
Mouse				
Normal	4.0 \pm 0.1	3	531 \pm 9	
Sandhoff	4.0 \pm 0.1	3	858 \pm 30**	162
Cat				
Normal	5.6 \pm 0.8	3	499 \pm 14	
Sandhoff	4.6 \pm 0.3	4	1305 \pm 122**	262
Human				
Normal	28.3 \pm 3.1	3	484 \pm 26	
Sandhoff	23.8 \pm 9.7	2	1629 \pm 31	337

Values shown are means \pm SEM, except for the Human Sandhoff samples, where values are means \pm interquartile range

N the number of independent samples analyzed

The asterisks indicate that the value is significantly different from the normal strain at ** $P < 0.01$ as determined by the two-tailed *t* test

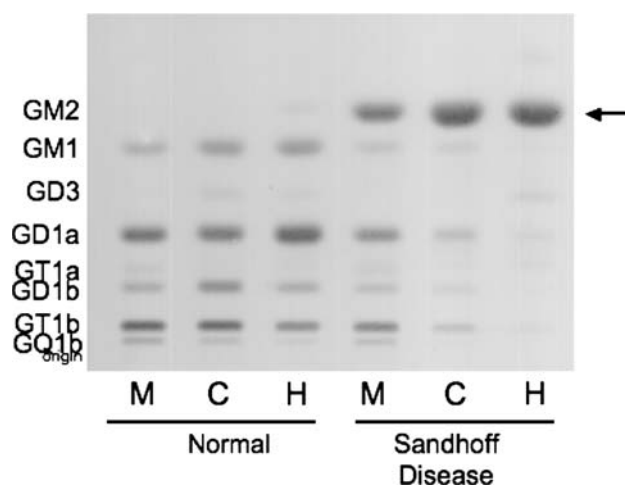


Fig. 1 HPTLC analysis of cortical gangliosides in normal and Sandhoff disease mice (M), cats (C), and humans (H). The amount of ganglioside spotted per lane was equivalent to 1.5 μg sialic acid. The plate was developed in one ascending run with chloroform:methanol:0.02% aqueous calcium chloride (55:45:10 by volume). Gangliosides were visualized with resorcinol-HCl spray

SD cat. In addition, GQ1b concentration was significantly reduced in the SD cat compared to the normal cat. The concentration of all major gangliosides (GM1, GD1a, GD1b, GT1b, and GQ1b) was reduced in the SD patient compared to the normal human, and these results are consistent with previous findings [21, 22]. In our analysis, we also observed an elevation in GD3 and GT1a/LD1 in the SD human.

While GA2 was undetectable in the normal brains, GA2 accumulated in the SD brains (Table 3). Since GA2 is derived from GM2 through the action of a sialidase, we

Table 2 Brain ganglioside distribution in normal and Sandhoff disease mice, cats, and humans

Ganglioside	Mouse		Cat		Human	
	Normal	Sandhoff	Normal	Sandhoff	Normal	Sandhoff
<i>N</i>	3	3	3	4	3	2
GM2						
Percent ^a	ND	38.1 ± 1.5	ND	67.3 ± 3.8	1.8 ± 0.4	87.1 ± 3.6
Concentration ^b	ND	327.2 ± 23.7	ND	884.4 ± 116.8	8.6 ± 1.5	1418.7 ± 84.5
GM1						
Percent	11.4 ± 0.5	6.5 ± 0.3**	20.4 ± 1.5	6.0 ± 0.8**	20.2 ± 0.7	1.7 ± 1.5
Concentration	60.7 ± 3.5	55.6 ± 1.0	101.8 ± 8.3	76.2 ± 6.9	97.4 ± 3.7	26.8 ± 26.2
GD3						
Percent	ND	ND	2.4 ± 0.4	trace	1.8 ± 0.2	2.4 ± 2.9
Concentration	ND	ND	11.8 ± 1.9	trace	8.8 ± 0.5	37.6 ± 46.4
GD1a						
Percent	38.6 ± 0.5	23.4 ± 1.2**	35.9 ± 3.9	13.3 ± 2.8**	47.2 ± 0.7	3.3 ± 0.4
Concentration	205.3 ± 5.6	200.1 ± 9.0	179.2 ± 21.6	168.1 ± 28.3	228.7 ± 15.2	53.3 ± 7.0
GT1a/LD1						
Percent	3.0 ± 0.1	2.0 ± 0.1**	ND	0.8 ± 0.1	1.4 ± 0.5	1.4 ± 0.1
Concentration	15.9 ± 0.9	16.7 ± 1.0	ND	11.4 ± 3.0	6.9 ± 2.7	21.6 ± 1.5
GD1b						
Percent	10.5 ± 0.2	5.7 ± 0.2**	16.0 ± 2.0	3.9 ± 0.4**	10.0 ± 0.4	0.9 ± 0.4
Concentration	55.7 ± 1.8	48.7 ± 0.3	79.6 ± 9.6	51.0 ± 7.8	48.7 ± 4.2	13.1 ± 6.0
GT1b						
Percent	29.1 ± 1.1	19.5 ± 1.0**	22.3 ± 2.5	7.8 ± 0.5**	16.2 ± 0.4	2.0 ± 0.2
Concentration	154.7 ± 5.0	167.6 ± 9.0	110.8 ± 12.3	102.0 ± 13.6	78.2 ± 3.2	32.7 ± 4.9
GQ1b						
Percent	7.4 ± 0.2	4.9 ± 0.6*	3.1 ± 0.6	0.6 ± 0.1**	1.5 ± 0.2	ND
Concentration	39.1 ± 0.8	42.0 ± 5.0	15.4 ± 2.8	8.5 ± 1.9**	7.0 ± 0.8	ND

Values shown are means ± SEM, except for the Human Sandhoff samples, where values are means ± interquartile range

N the number of independent samples analyzed

ND not detectable

The asterisks indicate that the value is significantly different from the normal strain at* $P < 0.05$ and at ** $P < 0.01$ as determined by the two-tailed *t* test

^a Percent distribution determined from densitometric scanning of HPTLC as shown in Fig. 1

^b Concentration expressed as µg sialic acid/100 mg dry weight

looked at the ratio of GA2–GM2 (µmol/100 mg dry weight) (Fig. 2). The ratio of GA2–GM2 was 0.93, 0.13, and 0.27 in the SD mice, cats, and humans, respectively. Interestingly, the ratio of GA2–GM2 was greatest in the SD mouse while this ratio was significantly less in the SD cat and human.

Neutral Lipids

The qualitative and quantitative distribution of the neutral brain lipids in mice, cats, and humans with Sandhoff disease (SD) is shown in Fig. 3 and Table 4. The concentration of cerebroside, (the myelin-enriched glycolipid), was significantly lower in the SD brains compared to the age-matched control brains. These findings are consistent

with previous reports of lower cerebroside in SD mice and humans [11, 21]. Although statistically significant, the reduction in cerebroside in the SD mice was less pronounced than in the SD cats and humans. No statistical differences were found between the normal and SD brains for the concentration of cholesterol, ceramide, phosphatidylethanolamine, and phosphatidylcholine. Since sphingomyelin co-migrated with GA2 in our HPTLC solvent system, we did not quantify the concentration of sphingomyelin in the SD brains.

Acidic Lipids

The qualitative and quantitative distribution of the acidic lipids in mice, cats, and human with Sandhoff disease (SD)

Table 3 Brain GM2 and GA2 concentration in normal and Sandhoff disease mice, cats, and humans

Species	<i>N</i>	GM2 Concentration (mmol/100 mg dry weight)	GA2 Concentration (mmol/100 mg dry weight)
Mouse			
Normal	3	ND	ND
Sandhoff	3	4.73 ± 0.34	4.33 ± 0.06
Cat			
Normal	3	ND	ND
Sandhoff	4	12.79 ± 1.69	1.60 ± 0.10
Human			
Normal	3	ND	ND
Sandhoff	2	20.51 ± 1.22	5.44 ± 1.02

Values shown are means ± SEM, except for the Human Sandhoff samples, where values are means ± interquartile range

N the number of independent samples analyzed

ND not detectable

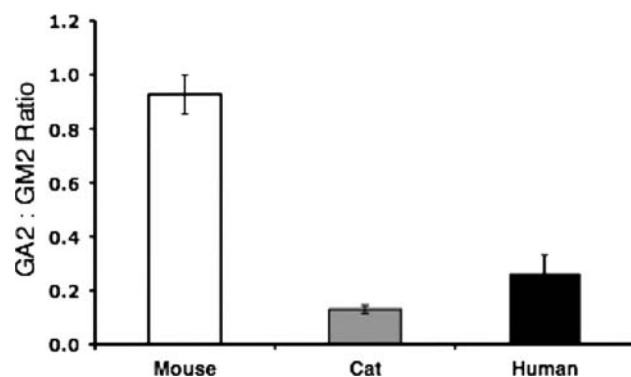


Fig. 2 Ratio of brain GA2–GM2 in Sandhoff disease mice (*N* = 3), cats (*N* = 4), and humans (*N* = 2). Values shown are means ± SEM, except for the Human Sandhoff samples, where values are means ± interquartile range

is shown in Fig. 4 and Table 4. The most noticeable difference in the acidic lipid distribution was the reduction in sulfatides, another myelin-enriched glycolipid, in the SD compared to normal. As with cerebroside, the SD cat represented an intermediate between the SD mice and the SD humans in terms of the reduction of sulfatides. The presence of some GM2 on the HPTLC plate in the SD samples resulted from lower phase carryover during isolation. No significant differences were observed between the normal and the SD groups for the distribution or content of cardiolipin, phosphatidylserine, and phosphatidylinositol. We further analyzed cerebroside and sulfatides in SD as a percent of normal (Fig. 5). The myelin lipids were present at trace levels in the SD humans compared to the normal humans, and the concentration of cerebroside and sulfatides in the SD mouse was about

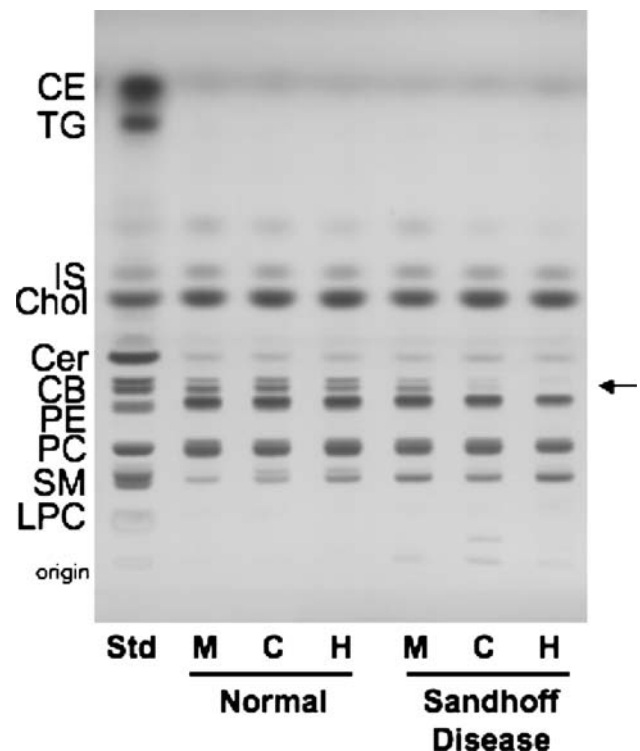


Fig. 3 HPTLC of cortical neutral lipids in normal and Sandhoff disease mice (M), cats (C), and humans (H). The amount of neutral lipids spotted per lane was equivalent to approximately 70 µg brain dry weight. The plate was developed to a height of 4.5 cm with chloroform:methanol:acetic acid:formic acid:water (35:15:6:2:1 by volume), then developed to the top with hexanes:diisopropyl ether:acetic acid (65:35:2 by volume). The bands were visualized by charring with 3% cupric acetate in 8% phosphoric acid solution. CE cholesterol esters, TG triglycerides, IS internal standard, Chol cholesterol, CM ceramide, CB cerebroside (doublet, indicated by arrow), PE phosphatidylethanolamine, PC phosphatidylcholine, SM sphingomyelin, GA2 asialo GM2, LPC lyso-phosphatidylcholine

58 and 76%, respectively, of that in the normal mouse. Interestingly, the concentration of cerebroside and sulfatides in the SD cat was about 11 and 14%, respectively, of that in the normal cat. Thus, the lipid profile in the SD cat brain is intermediate to the SD mice and the SD humans in terms of GM2 and GA2 storage, as well as the reduction in cerebroside and sulfatides.

Discussion

Our results show for the first time the comparative analysis of brain lipids in mice, cats, and humans with SD. In contrast to a previous study, which showed that GM2 was about 42% of the total brain ganglioside distribution in the SD cat, we show that GM2 accounts for 67% of the total ganglioside distribution in the SD cat [19]. The ganglioside distribution in the SD cat in the previous study was analyzed at an earlier age (11 weeks), which could account for

Table 4 Brain neutral and acidic lipid distribution in normal and Sandhoff disease mice, cats, and humans

Lipids	Concentration ($\mu\text{g}/\text{mg}$ dry weight) ^a					
	Mouse		Cat		Human	
	Normal	Sandhoff	Normal	Sandhoff	Normal	Sandhoff
<i>N</i>	3	3	3	4	3	2
Neutral lipids						
Chol ^b	64.6 \pm 0.4	58.7 \pm 3.6	79.3 \pm 8.7	70.7 \pm 5.9	66.9 \pm 1.0	61.2 \pm 4.1
CB	26.4 \pm 0.2	15.3 \pm 2.1*	41.7 \pm 8.5	4.6 \pm 3.2**	21.5 \pm 0.1	trace
PE	96.3 \pm 11.3	95.7 \pm 11.8	108.4 \pm 11.6	102.7 \pm 12.1	91.4 \pm 3.4	63.1 \pm 14.4
PC	71.7 \pm 6.7	68.4 \pm 8.2	76.1 \pm 8.2	71.0 \pm 6.3	42.0 \pm 12.3	35.9 \pm 22.3
Acidic lipids						
CL	2.5 \pm 0.2	3.8 \pm 0.7	2.1 \pm 0.3	3.7 \pm 1.1	1.8 \pm 0.2	2.7 \pm 3.9
Sulf	5.2 \pm 0.2	3.9 \pm 0.2**	7.6 \pm 1.5	1.0 \pm 0.6**	5.1 \pm 0.8	trace
PS	19.6 \pm 1.4	19.1 \pm 1.9	22.4 \pm 1.6	15.1 \pm 2.4	28.2 \pm 2.6	15.9 \pm 7.0
PI	6.2 \pm 0.4	6.6 \pm 0.6	6.1 \pm 0.2	5.0 \pm 0.9	6.2 \pm 0.6	4.4 \pm 0.8

Values shown are means \pm SEM, except for the Human Sandhoff samples, where values are means \pm interquartile range

N the number of independent samples analyzed

The asterisks indicate that the value is significantly different from the normal strain at * $P < 0.05$ and at ** $P < 0.01$ as determined by the two-tailed *t* test

^a Determined from densitometric scanning of HPTLC plates as shown in Figs. 3 and 4

^b Lipid abbreviations are as described in Figs. 3 and 4

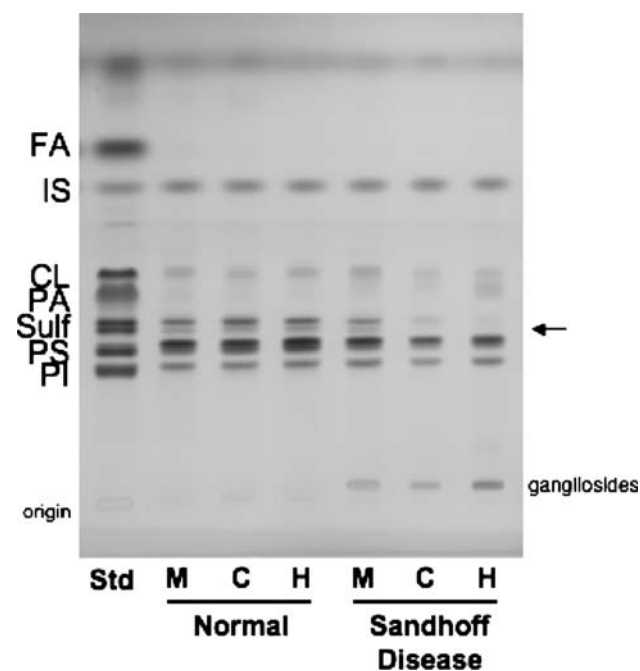


Fig. 4 HPTLC of cortical acidic lipids in normal and Sandhoff disease mice (M), cats (C), and humans (H). The amount of acidic lipids spotted per lane was equivalent to approximately 200 μg brain dry weight. The plate was developed to a height of 6 cm with chloroform:methanol:acetic acid:formic acid:water (35:15:6:2:1 by volume), then developed to the top with hexanes:diisopropyl ether:acetic acid (65:35:2 by volume). The bands were visualized by charring with 3% cupric acetate in 8% phosphoric acid solution. *FA* fatty acids, *IS* internal standard, *CL* cardiolipin, *PA* phosphatidic acid, *Sulf* sulfatides (doublet, indicated by arrow), *PS* phosphatidylserine, *PI* phosphatidylinositol

the lower GM2 distribution [19]. For our study, we analyzed the total brain ganglioside distribution at a similar time-point in disease progression in the SD mouse, cat, and human, and we showed that GM2 accumulation in the SD cat is intermediate between the SD mouse and the SD patient. In addition, we also observed an increase in GD3 in the SD human, suggesting an increase in reactive gliosis, perhaps as a result of disease progression [33]. The degree of GM2 accumulation in the SD patient compared to the SD mouse poses a major hurdle in developing therapy, and our results suggest that the SD cat is an appropriate intermediate model to study.

In addition to GM2, GA2 was also a major storage material in the SD brain of all the species [2, 11, 12, 20, 21]. The role of GA2 in disease progression is unclear. It is interesting to note, however, that GA2 is unlikely the primary cause of pathogenesis and neurodegeneration in GM2 gangliosidosis, since GA2 accumulation in Tay-Sachs disease is much less than in SD [2, 21]. Also, pathology in GM1 and GM2 retina was associated more with ganglioside accumulation than with accumulation of asialo-gangliosides [44]. The ratio of GA2–GM2 storage was greater in the SD mouse than in the SD cat or patient. Previous studies showed that sialidase activity is more active in SD mice than in humans and is able to convert significant amounts of GM2 to GA2 [20, 34–36]. Our results suggest that the activity of the feline sialidase is more similar to the human sialidase than to the mouse sialidase.

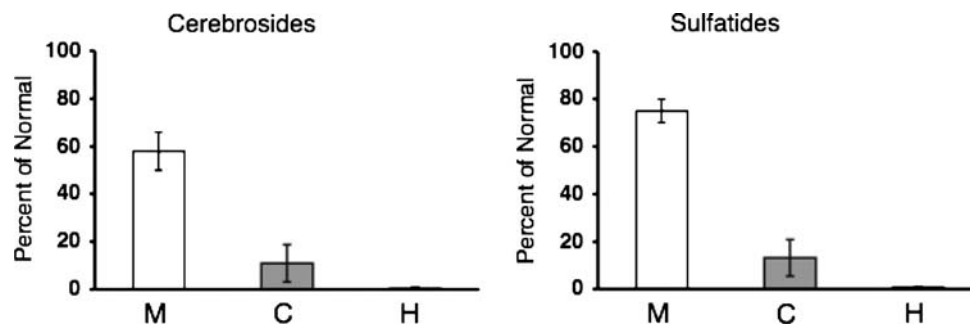


Fig. 5 Cortical concentration of cerebrosides and sulfatides as a percentage of normal in Sandhoff disease mice ($N = 3$), cats ($N = 4$), and humans ($N = 2$). Values shown are means \pm SEM, except for

the Human Sandhoff samples, where values are means \pm interquartile range. Trace amounts of cerebrosides and sulfatides were detected in the SD human samples

In addition to abnormal GSL storage, pathogenesis in lysosomal storage diseases is also associated with dysmyelination [21, 37–39]. Reductions in the myelin-enriched lipids, cerebrosides and sulfatides were shown in the SD mice and in patients with GM2 gangliosidosis [11, 21, 40]. Magnetic resonance imaging analysis also revealed significant white matter changes in the brains of patients and in animal models of GSL storage disorders [37–39, 41, 42]. Furthermore, low angle X-ray diffraction analysis showed hypomyelination in the optic nerves of SD mice [43]. These findings together suggest that the abnormal accumulation of GSLs may influence myelin and that dysmyelination may also contribute to disease progression. Our results showed that the myelin-enriched lipids, cerebrosides and sulfatides are significantly reduced in SD compared to normal. We also found that cerebrosides and sulfatides were significantly reduced in the SD cat compared to the normal cat. Like GM2 accumulation, the reductions in the myelin-enriched lipids in the SD cat were intermediate to that observed in the SD mouse and human.

It is interesting to note that disease onset and eventual death in the SD cats also occur intermediate to these milestones in the SD mice and patients. The SD mice begin to display phenotypic abnormalities at around 12 weeks of age and are humanely euthanized at 16 weeks of age [11, 20]. The onset of disease in the SD mice occurs after sexual maturation, and as a result, the SD mice are able to reproduce [11]. However, behavioral dysfunction is first detected in the SD cats at 6–8 weeks of age and in the SD patient at around 24 weeks of age [2, 19]. The SD cat and patient both succumb to the disease prior to reproduction. Our results show that GM2 storage is greater in SD humans and cats than in SD mice, but that GA2 storage is relatively greater in SD mice than in SD humans and cats. As much of the current progress has been limited to studies in mice, our results suggest that feline SD could be an important model to test and develop potential therapies for patients and could help translate the therapeutic success seen in mice to treatment in humans.

Acknowledgments We acknowledge the NICHD Brain and Tissue Bank for Developmental Disorders at the University of Maryland, Baltimore (NICHD contract # N01-HD-4-3368 and N01-HD-4-3383) for the human tissue samples. This work was supported in part from NIH grant (NS055195), the National Tay-Sachs and Allied Disease Association, and from the Lysosomal Storage Disease Research Consortium.

References

- Neufeld EF (1991) Lysosomal storage diseases. *Annu Rev Biochem* 60:257–280
- Gravel RA, Clarke JTR, Kaback MM, Mahuran D, Sandhoff K, Suzuki K (1995) The GM2 gangliosidosis. In: Scriver CR, Beaudet AL, Sly WS, Valle D (eds) *The metabolic and molecular bases of inherited disease*, 7th edn. McGraw-Hill, New York
- Chavany C, Jendoubi M (1998) Biology and potential strategies for the treatment of GM2 gangliosidosis. *Mol Med Today* 4:158–165
- Jeyakumar M, Smith DA, Williams I, Borja MC, Neville DCA, Butters TD, Dwek RA, Platt FM (2004) Anti-inflammatory and anti-oxidant therapies increase survival in the Sandhoff disease mouse: synergy with *N*-butyldeoxyjirimycin. *Ann Neurology* 56:642–649
- Jeyakumar M, Butters TD, Dwek RA, Platt FM (2002) Glycosphingolipid lysosomal storage diseases: therapy and pathogenesis. *Neuropathol Appl Neurobiol* 28:343–357
- Schiffmann R, Brady RO (2002) New prospects for the treatment of lysosomal storage diseases. *Drugs* 62:733–742
- Lee JP, Jeyakumar M, Gonzalez R, Takahashi H, Lee PJ, Baek RC, Clark D, Rose H, Fu G, Clarke J, McKercher S, Meerloo J, Muller FJ, Park KI, Butters TD, Dwek RA, Schwartz P, Tong G, Wenger D, Lipton SA, Seyfried TN, Platt FM, Snyder EY (2007) Stem cells act through multiple mechanisms to benefit mice with neurodegenerative metabolic disease. *Nat Med* 13:439–447
- Andersson U, Smith D, Jeyakumar M, Butters TD, Borja MC, Dwek RA, Platt FM (2004) Improved outcome of *N*-butyldeoxygalactonojirimycin-mediated substrate reduction therapy in a mouse model of Sandhoff disease. *Neurobiol Dis* 16:506–515
- Cachon-Gonzalez MB, Wang SZ, Lynch A, Ziegler R, Cheng SH, Cox TM (2006) Effective gene therapy in an authentic model of Tay-Sachs-related diseases. *Proc Natl Acad Sci USA* 103:10373–10378
- Norflus F, Tift CJ, McDonald MP, Goldstein G, Crawley JN, Hoffmann A, Sandhoff K, Suzuki K, Proia RL (1998) Bone marrow transplantation prolongs life span and ameliorates neurologic manifestations in Sandhoff disease mice. *J Clin Invest* 101:1881–1888

11. Denny CA, Kasperzyk JL, Gorham KN, Bronson RT, Seyfried TN (2006) Influence of caloric restriction on motor behavior, longevity, and brain lipid composition in Sandhoff disease mice. *J Neurosci Res* 83:1028–1038
12. Baek RC, Kasperzyk JL, Platt FM, Seyfried TN (2008) *N*-butyldeoxygalactonojirimycin reduces brain ganglioside and GM2 content in neonatal Sandhoff disease mice. *Neurochem Int* 52:1125–1133
13. Haug H (1987) Brain sizes, surfaces, and neuronal sizes of the cortex cerebri: a stereological investigation of man and his variability and a comparison with some mammals (primates, whales, marsupials, insectivores, and one elephant). *Am J Anat* 180:126–142
14. Roth G, Dicke U (2005) Evolution of the brain and intelligence. *Trends Cogn Sci* 9:250–257
15. Hofman MA (1984) Energy metabolism and relative brain size in human neonates from single and multiple gestations. An allometric study. *Biol Neonate* 45:157–164
16. Martin DR, Krum BK, Varadarajan GS, Hathcock TL, Smith BF, Baker HJ (2004) An inversion of 25 base pairs causes feline GM2 gangliosidosis variant. *Exp Neurol* 187:30–37
17. Baker HJ, Reynolds GD, Walkley SU, Cox NR, Baker GH (1979) The gangliosidoses: comparative features and research applications. *Vet Pathol* 16:635–649
18. Cork LC, Munnell JF, Lorenz MD (1978) The pathology of feline GM2 gangliosidosis. *Am J Pathol* 90:723–734
19. Cork LC, Munnell JF, Lorenz MD, Murphy JV, Baker HJ, Rattazzi MC (1977) GM2 ganglioside lysosomal storage disease in cats with beta-hexosaminidase deficiency. *Science* 196:1014–1017
20. Sango K, Yamanaka S, Hoffmann A, Okuda Y, Grinberg A, Westphal H, McDonald MP, Crawley JN, Sandhoff K, Suzuki K, Proia RL (1995) Mouse models of Tay-Sachs and Sandhoff diseases differ in neurologic phenotype and ganglioside metabolism. *Nat Genet* 11:170–176
21. Sandhoff K, Harzer K, Wasse W, Jatzkewitz H (1971) Enzyme alterations and lipid storage in three variants of Tay-Sachs disease. *J Neurochem* 18:2469–2489
22. Rosengren B, Mansson JE, Svennerholm L (1987) Composition of gangliosides and neutral glycosphingolipids of brain in classical Tay-Sachs and Sandhoff disease: more lyso-GM2 in Sandhoff disease? *J Neurochem* 49:834–840
23. Galjaard H (1980) Genetic metabolic disease: diagnosis and prenatal analysis. Elsevier, Amsterdam
24. Hauser EC, Kasperzyk JL, d'Azzo A, Seyfried TN (2004) Inheritance of lysosomal acid β -galactosidase activity and gangliosides in crosses of DBA/2 J and knockout mice. *Biochem Genet* 42:241–257
25. Seyfried TN, Glaser GH, Yu RK (1978) Cerebral, cerebellar, and brain stem gangliosides in mice susceptible to audiogenic seizures. *J Neurochem* 31:21–27
26. Kasperzyk JL, El-Abbadi MM, Hauser EC, D'Azzo A, Platt FM, Seyfried TN (2004) *N*-butyldeoxygalactonojirimycin reduces neonatal brain ganglioside content in a mouse model of GM1 gangliosidosis. *J Neurochem* 89:645–653
27. Macala LJ, Yu RK, Ando S (1983) Analysis of brain lipids by high performance thin-layer chromatography and densitometry. *J Lipid Res* 24:1243–1250
28. Folch J, Lees M, Sloane-Stanley GH (1957) A simple method for the isolation and purification of total lipids from animal tissues. *J Biol Chem* 226:497–509
29. Kasperzyk JL, d'Azzo A, Platt FM, Alroy J, Seyfried TN (2005) Substrate reduction reduces gangliosides in postnatal cerebrum-brainstem and cerebellum in GM1 gangliosidosis mice. *J Lipid Res* 46:744–751
30. Ando S, Chang NC, Yu RK (1978) High-performance thin-layer chromatography and densitometric determination of brain ganglioside compositions of several species. *Anal Biochem* 89:437–450
31. Seyfried TN, Bernard D, Mayeda F, Macala L, Yu RK (1984) Genetic analysis of cerebellar lipids in mice susceptible to audiogenic seizures. *Exp Neurol* 84:590–595
32. Seyfried TN, Yu RK, Miyazawa N (1982) Differential cellular enrichment of gangliosides in the mouse cerebellum: analysis using neurological mutants. *J Neurochem* 38:551–559
33. Seyfried TN, Yu RK (1985) Ganglioside GD3: structure, cellular distribution, and possible function. *Mol Cell Biochem* 68:3–10
34. Li SC, Li YT, Moriya S, Miyagi T (2001) Degradation of G(M1) and G(M2) by mammalian sialidases. *Biochem J* 360:233–237
35. Yuzyuk JA, Bertoni C, Beccari T, Orlicchio A, Wu YY, Li SC, Li YT (1998) Specificity of mouse GM2 activator protein and beta-*N*-acetylhexosaminidases A and B. Similarities and differences with their human counterparts in the catabolism of GM2. *J Biol Chem* 273:66–72
36. Bertoni C, Li YT, Li SC (1999) Catabolism of asialo-GM2 in man and mouse. Specificity of human/mouse chimeric GM2 activator proteins. *J Biol Chem* 274:28612–28618
37. Kroll RA, Pagel MA, Roman-Goldstein S, Barkovich AJ, D'Agostino AN, Neuwelt EA (1995) White matter changes associated with feline GM2 gangliosidosis (Sandhoff disease): correlation of MR findings with pathologic and ultrastructural abnormalities. *AJNR Am J Neuroradiol* 16:1219–1226
38. Folkert RD, Alroy J, Bhan I, Kaye EM (2000) Infantile G(M1) gangliosidosis: complete morphology and histochemistry of two autopsy cases, with particular reference to delayed central nervous system myelination. *Pediatr Dev Pathol* 3:73–86
39. Kaye EM, Alroy J, Raghavan SS, Schwarting GA, Adelman LS, Runge V, Gelblum D, Thalhammer JG, Zuniga G (1992) Dysmyelination in animal model of GM1 gangliosidosis. *Pediatr Neurol* 8:255–261
40. Pellkofer R, Jatzkewitz H (1974) The enzymic degradation of cerebroside and sulphatides in human demyelination due to disseminated sclerosis and encephalitis, and to Tay-Sachs disease. *Acta neuropathologica* 29:25–35
41. van der Voorn JP, Pouwels PJ, Kamphorst W, Powers JM, Lammens M, Barkhof F, van der Knaap MS (2005) Histopathologic correlates of radial stripes on MR images in lysosomal storage disorders. *AJNR Am J Neuroradiol* 26:442–446
42. Vite CH, Magnitsky S, Aleman D, O'Donnell P, Cullen K, Ding W, Pickup S, Wolfe JH, Poptani H (2007) apparent diffusion coefficient reveals gray and white matter disease, and t2 mapping detects white matter disease in the brain in feline alpha-mannosidosis. *AJNR Am J Neuroradiol*
43. McNally MA, Baek RC, Avila RL, Seyfried TN, Strichartz GR, Kirschner DA (2007) Peripheral nervous system manifestations in a Sandhoff disease mouse model: nerve conduction, myelin structure, lipid analysis. *J Negat Results Biomed* 6:8
44. Denny CA, Alroy J, Pawlyk BS, Sandberg MA, d'Azzo A, Seyfried TN (2007) Neurochemical, morphological, and neurophysiological abnormalities in retinas of Sandhoff and GM1 gangliosidosis. *J Neurochem* 101:1294–1302

On the Substrate Binding of Linoleate 9-Lipoxygenases

Alexandra-Zoi Andreou · Ellen Hornung ·
Susan Kunze · Sabine Rosahl · Ivo Feussner

Received: 21 July 2008 / Accepted: 30 October 2008 / Published online: 27 November 2008
© The Author(s) 2008. This article is published with open access at Springerlink.com

Abstract Lipoxygenases (LOX; linoleate:oxygen oxidoreductase EC 1.13.11.12) consist of a class of enzymes that catalyze the regio- and stereo specific dioxygenation of polyunsaturated fatty acids. Here we characterize two proteins that belong to the less studied class of 9-LOXs, *Solanum tuberosum* StLOX1 and *Arabidopsis thaliana* AtLOX1. The proteins were recombinantly expressed in *E. coli* and the product specificity of the enzymes was tested against different fatty acid substrates. Both enzymes showed high specificity against all tested C18 fatty acids and produced (9*S*)-hydroperoxides. However, incubation of the C20 fatty acid arachidonic acid with AtLOX1 gave a mixture of racemic hydroperoxides. On the other hand, with StLOX1 we observed the formation of a mixture of products among which the (5*S*)-hydroperoxy eicosatetraenoic acid (5*S*-H(P)ETE) was the most abundant. Esterified fatty acids were no substrates. We used site directed mutagenesis to modify a conserved valine residue in the active site of StLOX1 and examine the importance of space within the active site, which has been shown to play a role in determining the positional specificity. The Val576Phe mutant still catalyzed

the formation of (9*S*)-hydroperoxides with C18 fatty acids, while it exhibited altered specificity against arachidonic acid and produced mainly (11*S*)-H(P)ETE. These data confirm the model that in case of linoleate 9-LOX binding of the substrate takes place with the carboxyl-group first.

Keywords Lipid peroxidation · Oxylipin formation · *Solanum tuberosum*

Abbreviations

20:4(n-6)	Arachidonic acid
18:3(n-3)	α -Linolenic acid
CP-HPLC	Chiral phase-HPLC
GC	Gas chromatography
18:3(n-6)	γ -Linolenic acid
HPLC	High performance liquid chromatography
HETE	Hydroxy eicosatetraenoic acid
H(P)ETE	Hydro(pero)xy eicosatetraenoic acid
H(P)ODE	Hydro(pero)xy octadecadienoic acid
H(P)OTE	Hydro(pero)xy octadecatrienoic acid
18:2(n-6)	Linoleic acid
LOX	Lipoxygenase(s)
RP-HPLC	Reversed phase-HPLC
20:4-PC	1,2-Diarachidonoyl-sn-glycero-3-phosphatidylcholine
SP-HPLC	Straight phase-HPLC
wt	Wild type

Sequence data: The nucleotide sequences reported in this paper are annotated in the GenBank/EMBL data bank under the accession numbers Q06327 and S73865.

A.-Z. Andreou · E. Hornung · S. Kunze · I. Feussner (✉)
Department of Plant Biochemistry,
Georg-August-University of Göttingen,
Albrecht-von-Haller-Institute of Plant Sciences,
Justus-von-Liebig-Weg 11, 37085 Göttingen, Germany
e-mail: ifeussn@gwdg.de

S. Rosahl
Department of Stress and Developmental Biology,
Institute of Plant Biochemistry, Weinberg 3,
06120 Halle, Saale, Germany

Introduction

Lipoxygenases (LOX) are a family of non-heme iron containing fatty acid dioxygenases that catalyze the insertion of molecular oxygen into polyunsaturated fatty acids containing a (1*Z*,4*Z*)-pentadiene system to produce

hydroperoxides in a regio- and stereo specific manner [1]. One mode of classification of plant LOX is based on the structural features of the proteins and specifically the presence or absence of an amino-terminal plastidic transit peptide, which directs the nascent protein to the plastid. Enzymes are separated into type 1-LOX, which consist of enzymes with high sequence similarity (~75%) and no plastidic transit peptide and type 2-LOX which carry a transit peptide sequence and show only moderate sequence similarity (~35%) [2]. A second, more common way classifies the enzymes according to the positional specificity of oxygen insertion into C18 fatty acids in 9- and 13-LOX [2], while mammalian LOX may be classified

according to the oxygenation of C20 fatty acids in arachidonate 5-, 8-, 9-, 11-, 12- or 15-LOX [1] (Fig. 1).

Two models have been used in order to describe the positional specificity of LOX. Based on data from mammalian LOX, the space-related hypothesis was established, according to which, the fatty acid penetrates the active site with its methyl end first and the depth of the substrate-binding pocket determines the site of hydrogen abstraction and position of oxygen insertion [3, 4]. In the case of plant LOX, the orientation-related hypothesis has been suggested, according to which, in 13-LOX, the substrate enters the active site with the methyl end first. In this class of enzymes, a phenylalanine or a histidine aligning with the so called

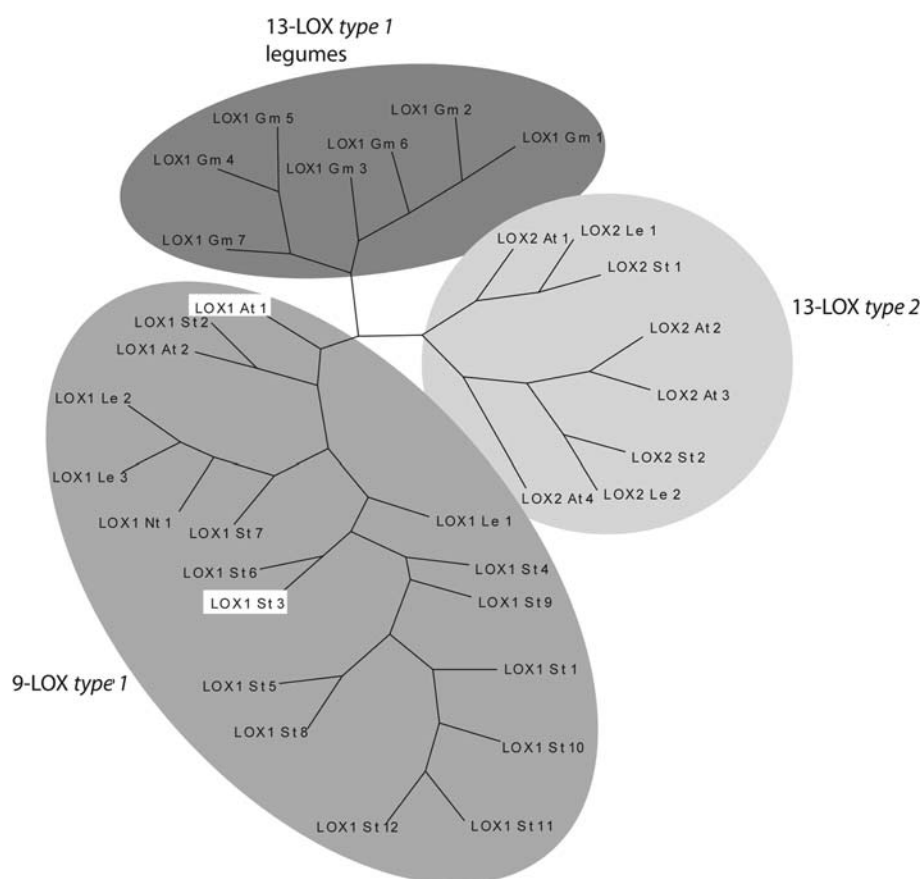


Fig. 1 Phylogenetic analysis of certain plant LOX. The circles indicate the grouping of the enzymes into subcategories. The analysis was performed with PHYLIP 3.5, and the proteins mentioned in the tree refer to the corresponding accession numbers in the gene bank. For clarification, within the tree only sequences from distinct plant species have been included and have been partially renamed according to the nomenclature of [43]: *Arabidopsis thaliana*: LOX1:At:1 (AtLOX1, Q06327), LOX2:At:1 (AtLOX2, P38418), LOX2:At:2 (AtLOX3, AAF79461), LOX2:At:3 (AtLOX4, AAF21176), LOX1:At:2 (AtLOX5, CAC19365), LOX2:At:4 (AtLOX6, AAG52309); *Glycine max*: LOX1:Gm:1 (Soybean LOX1, AAA33986), LOX1:Gm:2 (Soybean LOX2, AAA33987), LOX1:Gm:3 (Soybean LOX3, CAA31664), LOX1:Gm:4 (Soybean vlxa, BAA03101), LOX1:Gm:5 (Soybean vlxb, AAB67732),

LOX1:Gm:6 (Soybean vlxc, AAA96817), LOX1:Gm:7 (Soybean vlxd, S13381); *Lycopersicon esculentum*: LOX1:Le:1 (tom-LOXA, P38415), LOX1:Le:2 (tomLOXB, P38416), LOX1:Le:3 (tomLOX-tox, AAG21691), LOX2:Le:1 (tomLOXC, AAB65766), LOX2:Le:2 (tomLOXD, AAB65767); *Nicotiana tabacum*: LOX1:Nt:1 (NtLOX, S57964); *Solanum tuberosum*: LOX1:St:1 (SOLTULOX1, S44940), LOX1:St:2 (STLOX, AAD09202), LOX1:St:3 (StLOX1, P37831), LOX1:St:4 (CAA64766), LOX1:St:5 (CAA64765), LOX1:St:6 (POTLX-2, AAB67860) LOX1:St:7 (POTLX-3, AAB67865), LOX1:St:8 (POTLX-1, AAB67858), LOX1:St:9 (AAD04258), LOX1:St:10 (pLOX2, AAB81595), LOX1:St:11 (pLOX1, AAB81594), LOX1:St:12 (CAB65460), LOX2:St:1 (StLOXH1, CAA65268), LOX2:St:2 (St-LOXH3, CAA65269)

“Sloane determinants” controls the depth of the enzyme active site (Table 1). In 9-LOX the amino acid aligning with this position is usually a less space-filling valine residue. It is suggested that the presence of the smaller amino acid demasks a positively charged arginine residue, the so-called “Hornung determinant”, at the bottom of the substrate pocket, which can stabilize an insertion of the substrate with the carboxylic group first in the active site pocket leading to a preferable oxygen insertion in position 9 [5].

The molecular determinants of stereo specificity of the LOX reaction have been the focus of a number of recent studies [6]. These studies have highlighted the importance of a single amino acid residue, which is a conserved alanine in *S*-specific LOX and a glycine in the case of *R*-LOX. Conversion of the glycine of an *R*-LOX to an alanine and vice versa has been successful in partially switching the position of oxygenation and chirality of the product of the enzymatic reaction, for example converting a (13*S*)- into a (9*R*)-LOX enzyme [7]. Based on recent mutagenesis data obtained for a LOX from *Anabeana* sp. PCC 7120, the existing model for stereo control of the LOX reaction may be expanded for enzymes that seem to have in general a bulkier amino acid in *S*-LOX at this position that controls stereospecificity [8, 9].

Plant LOX are involved in a variety of processes of plant growth and development, e.g. through the mobilization of storage lipids during germination [10]. Furthermore, a class of these enzymes is thought to function as nitrogen storage proteins during vegetative growth [11]. Another important function of LOX secondary products, such as jasmonic acid, is their crucial role in defense responses against wounding and pathogen attack [12].

In most plant species, LOX are encoded by gene families, composed of a number of isozymes, differing in the position of substrate oxygenation, substrate specificity and kinetic parameters [13]. These enzymes are also often spatially and temporarily differentially expressed [14].

A relatively simple LOX family exists in *Arabidopsis thaliana*. It contains six putative lipoxygenase sequences

(AtLOX1-6) [2]. So far, physiological functions of four of these enzymes, AtLOX1 (*lox1:At:1*), AtLOX2 (*lox2:At:1*) AtLOX3 (*lox2:At:2*) and AtLOX4 (*lox2:At:3*) have been described, but biochemical characterization has still to take place. AtLOX1 has been previously described to be expressed in various organs of the plant and upregulated in response to pathogen attack [15], while AtLOX2 is expressed upon wounding [16]. AtLOX3 and AtLOX4 have been discussed to be involved in leaf senescence [17]. Based on sequence determinants and homology AtLOX1 (*lox1:At:1*) is postulated to harbor 9-LOX activity, whereas AtLOX2-4 may harbor 13-LOX activity (Table 1; Fig. 1).

In potato, a number of LOX cDNAs have been isolated from tubers, roots and leaves [18–24]. LOX belong to the group of genes that have been shown to be expressed early during potato tuber formation [22, 24], and LOX secondary products, such as jasmonic acid and its derivative tuberonic acid, have been shown to induce tuberization in vitro [25, 26]. Interestingly, the most abundant LOX activity detected was of 9-positional specificity and this activity increases upon wounding [27].

Our studies focus on two type 1-LOX, StLOX1 (*lox1:St:3*) and AtLOX1. StLOX1 is a LOX from potato tubers [19], which has a pH-optimum between pH 5.5 and 7.5, uses linoleic [18:2(n-6)] and α -linolenic acid [18:3(n-3)] preferentially, but can also use arachidonic acid [20:4(n-6)] as substrate. The later is converted primarily to 5-H(P)ETE. The specificity of this reaction is however lower than in the case of mammalian arachidonate 5-LOX [28]. AtLOX1 also belongs to the same class of enzymes, but its product specificity with C18 and C20 fatty acids has yet to be investigated. A comparison of the determinants of positional specificity of characterized LOX enzymes with *lox1:St:3* indicates that both enzymes carry the typical determinants of 9-LOX, namely a threonine and a valine (Table 1). In order to obtain a better insight into the factors determining the positional specificity of 9-LOX, we overexpressed the recombinant enzymes, investigated the enzymatic activity

Table 1 Alignment of amino acid residues possibly determining the positional specificity of plant and moss LOX

Enzyme	Acc. no.	Position of amino acid residues	Amino acid residues
9-LOX			
<i>Solanum tuberosum</i> StLOX1	P37831	575/576	Thr/Val
<i>Arabidopsis thaliana</i> AtLOX1	Q06327	576/577	Thr/Val
<i>Hordeum vulgare</i> LOX-A	L35931	574/575	Thr/Val
<i>Cucumis sativus</i> LOX1:Cs4	CAB83038	594/595	Thr/Val
13-LOX			
<i>Glycine max</i> sLOX-1	P08170	556/557	Thr/Phe
<i>Oryza sativa</i> LOX-1	BAA03102	678/679	Ser/Phe
<i>Arabidopsis thaliana</i> AtLOX2	P38418	611/612	Cys/Phe
<i>Physcomitrella patens</i> PpLOX	CAE47464	654/655	His/Phe

with different substrates and generated and characterized a mutant of potato tuber LOX, where the typical Val determinant of 9-LOX has been exchanged for a Phe, which alters the specificity of the enzyme against arachidonic acid.

Experimental Procedures

The chemicals used were from the following sources: standards of chiral and racemic hydroxy fatty acids from Cayman Chem. (Ann Arbor, MI, USA), trilinolein and triarachidonin from Sigma (Deisenhofen, Germany), 1,2-diarachidonoyl-*sn*-glycero-3-phosphatidylcholine from Larodan (Malmo, Sweden); methanol, hexane, 2-propanol (all HPLC grade) from Baker (Griesheim, Germany). Restriction enzymes were purchased from MBI Fermentas (St Leon-Rot, Germany).

Site-Directed Mutagenesis

As a template for site directed mutagenesis plasmid pET-stLOX1 was used, consisting of the potato tuber LOX [19] in pET3b (Novagen, Germany). Mutagenesis was carried out by using the QuikChange site-directed mutagenesis kit (Stratagene, Heidelberg, Germany). The oligonucleotides used for mutagenesis contained apart from the appropriate base changes additional conservative base exchanges which either created new restriction sites or deleted existing ones for simplified identification of mutants. The following oligonucleotides were used: stLOX-V576Fa 5'-GGTGGGGTTCTTGAGAGTACATTCTTTCCTTCGA AATTTGCCATGGAAATGTCAG-3'; stLOX-V576Fb 5'-CGTACATTTCCATGGCAAATTTTCGAAGGAAAGA ATGTACTCTCAAGAACCCACC-3'. In addition all mutations were sequenced and at least three different bacterial colonies were expressed and used for analysis of enzymatic parameters.

Protein Expression and LOX Activity Assay

For expression analysis StLOX1 containing plasmids and pBS-SK-*AtLOX1* (ABRC clone H3C1T7) were transferred into *E. coli* strain BL21(De3) Star (Novagen, Germany). Thirty millilitre cultures were grown at 37 °C to an OD₆₀₀ of 0.6, induced with 1 mM IPTG and cultivated further at 16 °C for 48 h. Cells were harvested by centrifugation at 4 °C at 4,000×*g* resuspended in 5 ml lysis buffer [50 mM Tris-HCl, pH 7, 300 mM NaCl, 10% (v/v) glycerol, 0.1% (v/v) Tween 20] and lysed by sonification. Nine-hundred microliters of lysate was incubated with 250 µg of the respective fatty acids for 30 min at RT, the resulting hydroperoxides were reduced with 2.5 mg tin(II) chloride in methanol, acidified with glacial acetic acid to pH 3 and lipids were extracted by the

method of Bligh and Dyer [29]. Analysis of the fatty acids was performed on a HPLC (see below).

The activity of StLOX1 with trilinolein or triarachidonin was measured by incubating 900 µl lysate with 1 mg of the respective substrate under constant shaking for 30 min at room temperature. In order to test activity against 20:4-PC, 0.6 mg of substrate were incubated with the enzyme in 5 ml buffer (50 mM Tris pH 7, 4 mM sodium deoxycholate) under constant stirring in RT. In both cases reduction of the hydroperoxides was carried out as described above. The lipid bound fatty acids were then converted to the corresponding methyl esters by adding 500 µl of 1% sodium methoxide solution in methanol to the dried samples after chloroform evaporation and shaken for 20 min at room temperature. Five-hundred microliters of 6 M NaCl was added to the reaction and the methyl esters were then extracted twice with 750 µl hexane. The solvent was removed by evaporation under a stream of nitrogen and the sample was dissolved in 80 µl of methanol/water/acetic acid (85:15:0.1, v/v/v).

Analytics

High performance liquid chromatography (HPLC) analysis was carried out on an Agilent (Waldbronn, Germany) 1100 HPLC system coupled to a diode array detector. Reversed phase-HPLC (RP-HPLC) of the free fatty acid derivatives was carried out on a Nucleosil C-18 column (Macherey-Nagel, Düren, FRG; 250 × 2 mm, 5 µm particle size) with a solvent system of methanol/water/acetic acid (90/10/0.1, v/v/v) and a flow rate of 0.18 ml/min. The absorbance at 234 nm (conjugated diene system of the hydroxy fatty acids) and 210 nm (polyenoic fatty acids) were recorded simultaneously. Straight phase-HPLC (SP-HPLC) of hydroxy fatty acid isomers was carried out on a Phenomenex Luna Silica column (Aschaffenburg, Germany; 50 × 4.6 mm, 3 µm particle size) with a solvent system of *n*-hexane/2-propanol/trifluoroacetic acid (100/1/0.1, v/v/v) and a flow rate of 0.2 ml/min. The enantiomer composition of the hydroxy fatty acids (C18) was analyzed by chiral phase-HPLC (CP-HPLC) on a Chiralcel OD-H column (Diacel Chem. Industries, distributed by Merck, Darmstadt, Germany; 150 × 2.1 mm, 5 µm particle size) with a solvent system of hexane/2-propanol/trifluoroacetic acid (100/5/0.1, v/v/v) and a flow rate of 0.1 ml/min. For separation of chiral isomers of 12, 15, 11 and 8 hydroxy eicosatetraenoic acid (HETE) a solvent system of hexane/2-propanol/trifluoroacetic acid (100/2/0.1, v/v/v) was used. 5-HETE stereo isomers were analyzed using a solvent system of *n*-hexane/2-propanol/trifluoroacetic acid (100/1/0.1 v/v/v) at a flow rate of 0.2 ml/min. Methyl esters were separated by RP-HPLC with a solvent system of methanol/water/acetic acid (75:25:0.1, v/v/v) at a flow rate of 0.18 ml/min.

SP-HPLC analysis was carried out with a solvent system hexane: 2-propanol: trifluoro acetic acid (100:1:0.1, v/v/v) at a flow rate of 0.1 ml/min.

Phylogenetic Analysis

Phylogenetic tree analysis was performed on deduced amino acid sequences of selected LOX by using PHYLIP3.5 (Department of Genome Sciences, University of Washington) [30] using default parameters.

Results

Our studies aim was to analyze the substrate specificity of two putative 9-LOX, StLOX1, a LOX from potato tubers [19] and AtLOX1 (*lox1:At:1*), a LOX expressed in *Arabidopsis* leaves, roots inflorescences and young seedlings [31]. In order to characterize their regio- and stereospecificity, we overexpressed the enzymes in *E. coli* and investigated the enzymatic activity with different substrates. Moreover we generated and characterized a mutant that alters the specificity of StLOX1.

Product Analysis of StLOX1 and AtLOX1

For product analysis, crude cell extracts of *E. coli* expressing StLOX1 were incubated with 250 μ g of 18:2(n-6), 18:3(n-3), γ -linolenic acid [18:3(n-6)], and 20:4(n-6), respectively, and the reduced products were analyzed by HPLC. *E. coli* cell extracts expressing AtLOX1 were likewise incubated with 18:2(n-6), 18:3(n-3) and 20:4(n-6) and products were analyzed. When 18:2(n-6) was used as substrate StLOX1 produced 9-hydro(pero)xy octadecadienoic acid [9-H(P)ODE, 98%] with almost exclusively *S* stereo configuration (Fig. 2a). Racemic 13-H(P)ODE was only a minor byproduct. Correspondingly, 94% 9-H(P)ODE of primarily *S* configuration was the main product of 18:2(n-6) incubation with AtLOX1 (Fig. 3a; Table 2). 18:3(n-3) is converted in a comparable manner to 9-hydro(pero)xy octadecatrienoic acid [9-H(P)OTE; 94%], mainly of the *S* enantiomer by both enzymes (Figs. 2b, 3b; Table 2). Racemic 12-, 13- and 16-H(P)OTE were only minor byproducts. Similarly, upon incubation of StLOX1 with 18:3(n-6), the main product was (9*S*)- γ -H(P)OTE (72%), with racemic 6-, 10- and 13- γ -H(P)OTE as secondary products (Fig. 2c). The two enzymes, however,

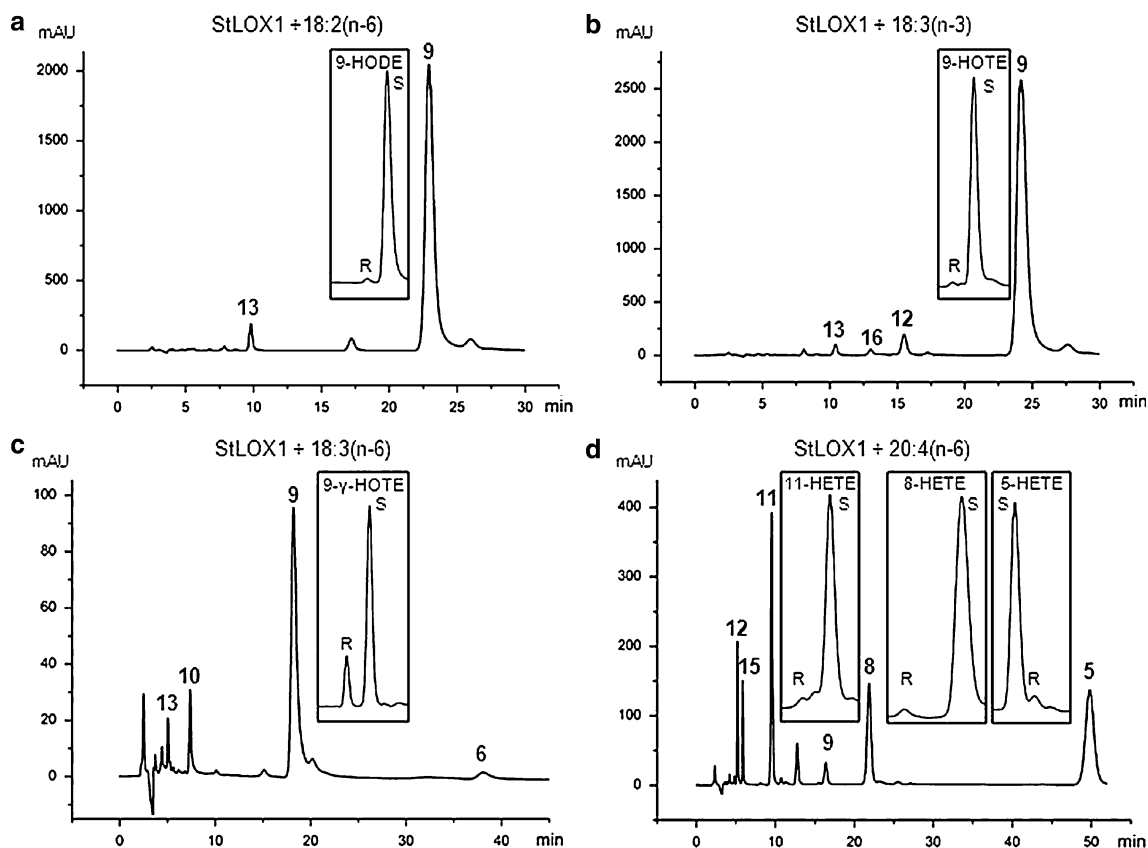


Fig. 2 SP-HPLC analysis of products formed by wt StLOX1 incubated with **a** 18:2(n-6), **b** 18:3(n-3), **c** 18:3(n-6) and **d** 20:4(n-6) (here in their reduced form). The separation of the enantiomers of

chiral products by CP-HPLC is shown in the insets. Enzyme preparations of StLOX1 were incubated with their respective substrates at pH 7

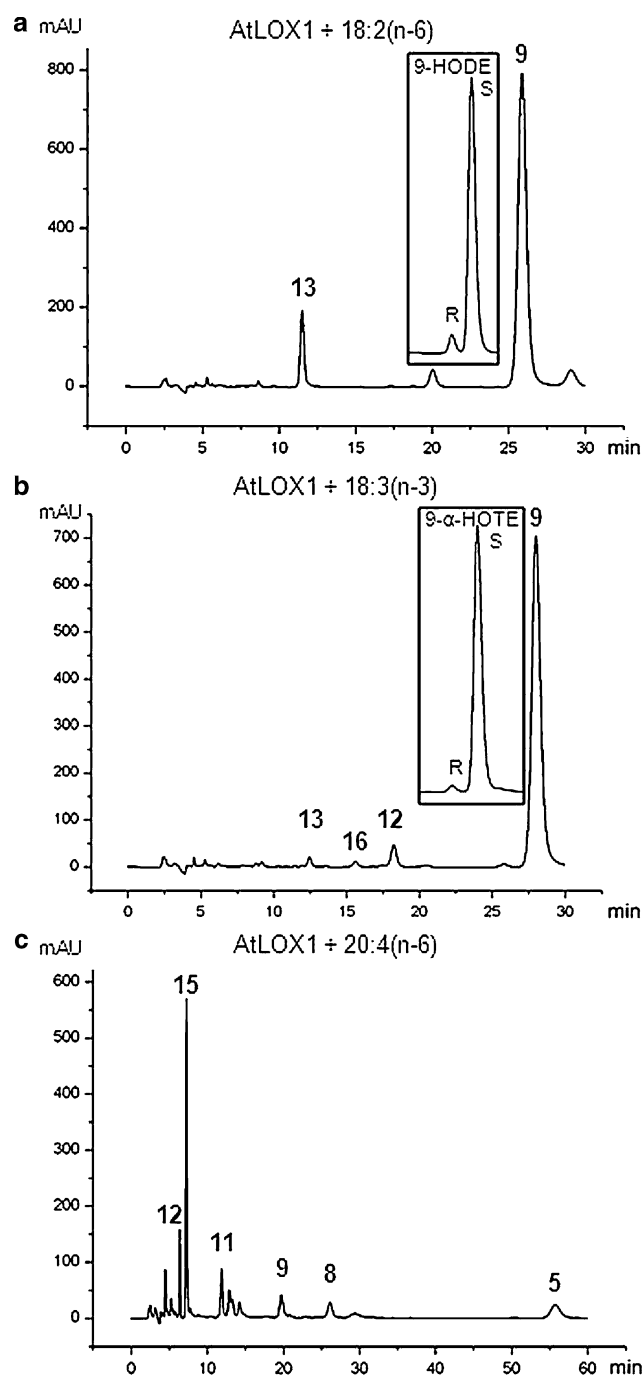


Fig. 3 SP-HPLC analysis of products formed by wt AtLOX1 incubated with **a** 18:2(n-6), **b** 18:3(n-3) and **c** 20:4(n-6) (here in their reduced form). The separation of the enantiomers of chiral products by CP-HPLC is shown in the insets. Enzyme preparations of AtLOX1 were incubated with their respective substrates at pH 7

exhibited different product specificity when 20:4(n-6) was used as substrate. AtLOX1 exhibited notably decreased enzymatic activity against 20:4(n-6) in comparison to the tested C18 substrates as estimated by RP-HPLC analysis of products formed when a mixture of substrates was applied (data not shown). In addition the C20 fatty acid was

Table 2 Products formed from the reaction of wt AtLOX1 with various fatty acid substrates

Substrate	Products	Ratio (%)	S enantiomer (%)
18:2(n-6)	13/9-HOD	10:90	49:94
18:3(n-3)	13/16/12/9-HOT	1:1:4:94	49:51:47:98
20:4(n-6)	15/12/11/9/8/5-HETE	44:11:13:9:9:14	50:53:53:50:48:NA

NA not analyzed

converted into a mixture of racemic products of comparable amounts (Fig 3c; Table 2). On the other hand, StLOX1 converted 20:4(n-6) into a mixture of three major products, 5-H(P)ETE (43%), 11-H(P)ETE (26%) and 8-H(P)ETE (23%). Chiral analysis of the fatty acid hydroperoxides by CP-HPLC revealed that the main products, 5-, 11- and 8-H(P)ETE are primarily of the typical S configuration. Minor amounts of racemic 12-H(P)ETE, 15-H(P)ETE and 9-H(P)ETE could also be detected (Fig 2d).

Additionally, we tested the activity of StLOX1 against a number of esterified fatty acids as substrates. Trilinolein and triarachidonin were used as substrates under the conditions described for the cucumber lipid body LOX, CslbLOX [5], while 1,2-diarachidonoyl-*sn*-glycero-3-phosphatidylcholine, as has been described for other LOX enzymes [8, 9]. We could not observe activity against any of the substrates, which suggests that binding of the substrate takes place with the carboxyl-group first.

Mutagenesis of Positional Determinants Identified from Other LOX Isoforms

Mutagenesis studies on LOX identified that among plant enzymes, one conserved amino acid, bulky in the case of 13-LOX and smaller in the case of 9-LOX (Table 1), plays a crucial role in determining the positional specificity of the product. In the case of StLOX1, the amino acid aligning with this residue is the widely conserved among 9-LOX valine (V576). In order to investigate the influence of these residues on StLOX1, we introduced the more space filling phenylalanine at this position. This resulted in a pair of residues, similar to the ones found in the active site of sLOX-1, a 13-LOX from soybean (Table 1). Subsequently, we tested the specificity of the mutant obtained with the same substrates as the wt. 18:2(n-6), 18:3(n-3) and 18:3(n-6) were converted, in a comparable manner as the wt, primarily into their respective 9-hydroperoxides (data not shown). Interestingly, conversion of valine to a phenylalanine resulted in a shift of the major oxygenation product specificity from 5-H(P)ETE in the wt enzyme to 11-H(P)ETE (55%) in the mutant. Significant amounts of 8-H(P)ETE, comparable to the wt, were also formed (22%), while 12-H(P)ETE, 15-H(P)ETE, 5-H(P)ETE were only

Table 3 Products formed from the reaction of wt StLOX1 and V576F mutant with 20:4(n-6)

Enzyme	Positional isomers obtained with arachidonic acid (<i>S</i> enantiomer) (%)				
	12	15	11	8	5
Wild type StLOX1	6 (45)	4 (56)	26 (99)	23 (80)	41 (97)
V576F	4 (57)	9 (53)	55 (100)	22 (92)	10 (NA)

NA not analyzed

present in smaller amounts ($\leq 10\%$; Table 3). 9-H(P)ETE could only be detected in traces. Chiral analysis of the hydroperoxides revealed chirality of 11-H(P)ETE and 8-H(P)ETE in *S* configuration while 15-H(P)ETE and 12-H(P)ETE were racemic (Fig. 4). The amounts of 5-H(P)ETE and 9H(P)ETE were too low for CP analysis.

Discussion

In this study we aimed to characterize the product specificity of two predicted 9-LOX, a LOX from potato tubers

and a LOX from *Arabidopsis*. For this purpose, we analyzed the LOX reaction products after incubation of the recombinantly expressed proteins with different fatty acid substrates. We also performed mutagenesis studies on StLOX1 and altered one of the residues, which has been reported to play a role in determining the positional specificity of LOX.

StLOX1 could convert all tested C18 fatty acids, 18:2(n-6), 18:3(n-3) and 18:3(n-6), to the corresponding (9*S*)-hydroperoxides with high specificity. Similar results have been previously observed for other analyzed potato tuber LOX [24, 32]. AtLOX1 showed comparably high specificity against the C18 fatty acids 18:2(n-6) and 18:3(n-3). These 9-hydroperoxides can be further metabolized by enzymes, such as the hydroperoxide reductase, divinyl ether synthase and epoxy alcohol synthase to yield epoxy alcohols and divinyl ethers among other products [33]. The function of the 9-LOX-derived products is still unclear, but they have been implicated in responses against biotic and abiotic stress. One possibility is that they confer resistance against pathogen attack. For example, LOX pathway products accumulate in potato leaves when they are under *P. infestans* infection [34]. Additionally, upregulation of 9-LOX transcripts has been observed upon wounding [19]. Similarly, in *Arabidopsis*, AtLOX1 has been reported to be induced by the stress-related hormones abscisic acid and methyl jasmonate and pathogen attack [31]. Another postulated function of 9-hydroperoxide derivatives is in potato that they may play a role in tuber growth regulation [35].

Additionally, we analyzed the metabolism of 20:4(n-6) by AtLOX1 and StLOX1. AtLOX1 did not demonstrate any specificity against the C20 fatty acid, since a mixture of racemic products was obtained. LOX often show decreased specificity when the protein in the reaction is in limiting amounts. However, we incubated the protein with a mixture of substrates and C18 fatty acids were converted into chiral products while C20 fatty acids were not. Therefore, this explanation seems unlikely. There are no previous reports on the product specificity of *Arabidopsis* lipoxygenases with 20:4(n-6), so it appears that this fatty acid may not be a substrate for AtLOX1. On the other hand, potato tuber LOX have been studied for many years as a model for 5-LOX activity [36, 37]. In the case of StLOX1, 5-H(P)ETE was the main reaction product, while 11-H(P)ETE and 8-H(P)ETE were also produced in

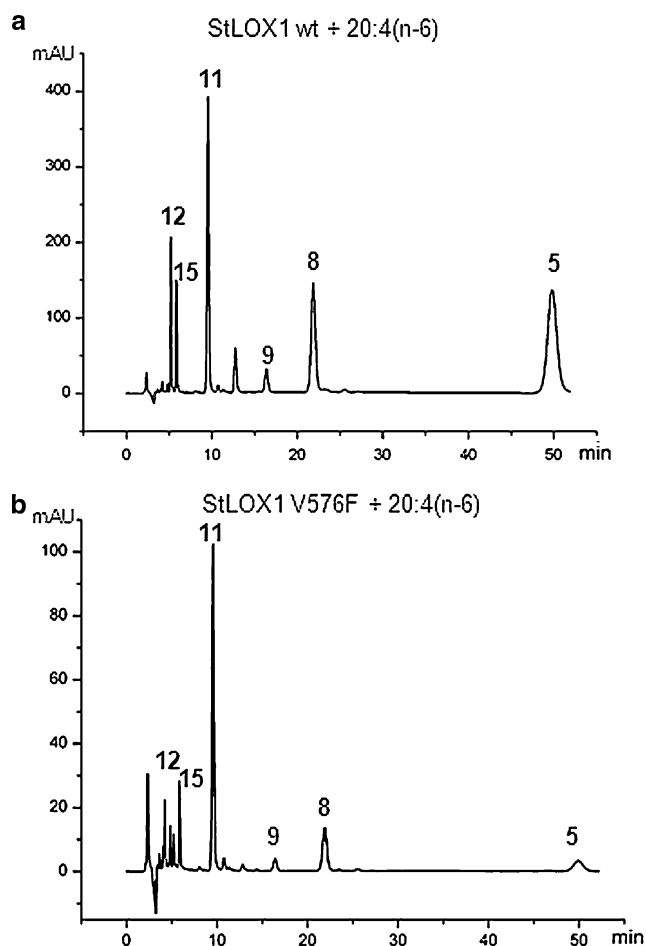


Fig. 4 SP-HPLC analysis of products formed by **a** wt StLOX1 and **b** V576F “Sloane” mutant enzyme with 20:4(n-6) as substrate (here in their reduced form for SP-HPLC analysis). Enzyme preparations of wt and Val → Phe (V576F) were incubated with 20:4(n-6) at pH 7

significant amounts. For 5-H(P)ETE production a hydrogen atom is abstracted from the C7 carbon atom of 20:4(n-6). The resulting carbon-centered radical intermediate undergoes rearrangement in the (n-2) position and in a final step, oxygen is inserted at C5. Similarly, 11-H(P)ETE and 8-H(P)ETE are the result of hydrogen abstraction at C13 and C10, respectively and a subsequent introduction of oxygen in the (n-2) position. The relatively low specificity of the first step of the LOX reaction suggests that binding of the substrate in the active site is more flexible in comparison to C18 fatty acids, allowing in the case of 20:4(n-6) abstraction of hydrogen atoms from different carbon atoms in comparison to C18 substrates, where in all cases the hydrogen atom of C11 is preferentially abstracted. The percentages of product formation are similar to the ones reported for the tomato enzyme [38]. The relative amount of 5-H(P)ETE is smaller though than the ones reported from a previously characterized potato tuber LOX [39] and a barley isozyme [40]. Chiral phase analysis showed that the hydroperoxides were of *S*-configuration. Similar results have been reported from other analyses of 5-hydroperoxides from plant enzymes [38, 40].

Regarding the substrate binding in the active site of StLOX1, the fact that no reaction products could be observed with trilinolein and triarachidonin or 1,2-di-arachidonoyl-*sn*-glycero-3-phosphatidylcholine supports that the fatty acids can only bind with their carboxyl group first. This is a similar mode of binding as has been previously suggested for 9-LOX [41, 42].

In addition the product specificity of a StLOX1 mutant in which a valine residue aligning with one of the “Sloane” determinants was exchanged against a bulkier phenylalanine was examined. Remarkably, this exchange did not influence the product specificity of the enzyme, when C18 fatty acids were used as substrates. According to the existing models, the residue in question is in close proximity to an arginine residue positioned on the bottom of the active site pocket. In 13-LOX the phenylalanine is thought to shield the positive charge of this arginine and lead to a preferential entry of the fatty acid with the methyl group first, leading to oxygenation at position C13 [5]. However, our data on StLOX1 suggest that the valine to phenylalanine exchange may not be sufficient to change the product specificity of C18 fatty acid conversion for this enzyme and therefore does not alter the favored substrate orientation in the active site of the enzyme. When the mutant enzyme, however, was incubated with 20:4(n-6) we observed an altered specificity, namely 11-H(P)ETE was the main product. This change suggests that inserting a bulky amino acid at the bottom of the active site pocket influences at least the alignment of the bulkier fatty acid 20:4(n-6) in the active site, although the substrate orientation is not altered either. In summary our data support the

previously suggested active site model that in case of 9-LOX the substrate binds with its carboxyl-group first that seem to be the natural substrates of these enzymes.

Acknowledgments The authors are grateful to Dr. Cornelia Göbel, Göttingen, for her expert technical support. A.A. is supported by the International master/Ph.D. program Molecular Biology and the Max Planck Research School Molecular Biology (Göttingen). The project is funded by IRTG 1422 Metal Sites in Biomolecules: Structures, Regulation and Mechanisms. We thank the ABRC for providing with the cDNA encoding AtLOX1.

Open Access This article is distributed under the terms of the Creative Commons Attribution Noncommercial License which permits any noncommercial use, distribution, and reproduction in any medium, provided the original author(s) and source are credited.

References

- Schneider C, Pratt DA, Porter NA, Brash AR (2007) Control of oxygenation in lipoxygenase and cyclooxygenase catalysis. *Chem Biol* 14:473–488
- Liavonchanka A, Feussner I (2006) Lipoxygenases: occurrence, functions and catalysis. *J Plant Physiol* 163:348–357
- Browner MF, Gillmor SA, Fletterick R (1998) Burying a charge. *Nat Struct Biol* 5:179
- Sloane DL, Leung R, Craik CS, Sigal E (1991) A primary determinant for lipoxygenase positional specificity. *Nature* 354:149–152
- Hornung E, Walther M, Kühn H, Feussner I (1999) Conversion of cucumber linoleate 13-lipoxygenase to a 9-lipoxygenating species by site-directed mutagenesis. *Proc Natl Acad Sci USA* 96:4192–4197
- Coffa G, Schneider C, Brash AR (2005) A comprehensive model of positional and stereo control in lipoxygenases. *Biochem Biophys Res Commun* 338:87–92
- Coffa G, Brash AR (2004) A single active site residue directs oxygenation stereospecificity in lipoxygenases: stereocontrol is linked to the position of oxygenation. *Proc Natl Acad Sci USA* 101:15579–15584
- Andreou A-Z, Vanko M, Bezakova L, Feussner I (2008) Properties of a mini 9*R*-lipoxygenase from *Nostoc* sp. PCC 7120 and its mutant forms. *Phytochemistry* 69:1832–1837
- Zheng Y, Boeglin WE, Schneider C, Brash AR (2008) A 49-kDa mini-lipoxygenase from *Anabaena* sp. PCC 7120 retains catalytically complete functionality. *J Biol Chem* 283:5138–5147
- Feussner I, Kühn H, Wasternack C (2001) The lipoxygenase dependent degradation of storage lipids. *Trends Plant Sci* 6:268–273
- Fischer AM, Dubbs WE, Baker RA, Fuller MA, Stephenson LC, Grimes HD (1999) Protein dynamics, activity and cellular localization of soybean lipoxygenases indicate distinct functional roles for individual isoforms. *Plant J* 19:543–554
- Howe GA, Jander G (2008) Plant immunity to insect herbivores. *Annu Rev Plant Biol* 59:41–66
- Feussner I, Wasternack C (2002) The lipoxygenase pathway. *Annu Rev Plant Biol* 53:275–297
- Siedow JN (1991) Plant lipoxygenase—structure and function. *Ann Rev Plant Physiol Plant Mol Biol* 42:145–188
- Bell E, Mullet JE (1993) Characterization of an Arabidopsis-lipoxygenase gene responsive to methyl jasmonate and wounding. *Plant Physiol* 103:1133–1137

16. Bell E, Creelman RA, Mullet JE (1995) A chloroplast lipoxygenase is required for wound-induced jasmonic acid accumulation in *Arabidopsis*. *Proc Natl Acad Sci USA* 92:8675–8679
17. He Y, Fukushige H, Hildebrand DF, Gan S (2002) Evidence supporting a role of jasmonic acid in *Arabidopsis* leaf senescence. *Plant Physiol* 128:876–884
18. Casey R (1995) Sequence of a cDNA clone encoding a potato (*Solanum tuberosum*) tuber lipoxygenase. *Plant Physiol* 107:265–266
19. Geerts A, Feltkamp D, Rosahl S (1994) Expression of lipoxygenase in wounded tubers of *Solanum tuberosum* L. *Plant Physiol* 105:269–277
20. Hughes RK, West SI, Hornostaj AR, Lawson DM, Fairhurst SA, Sanchez RO, Hough P, Robinson BH, Casey R (2001) Probing a novel potato lipoxygenase with dual positional specificity reveals primary determinants of substrate binding and requirements for a surface hydrophobic loop and has implications for the role of lipoxygenases in tubers. *Biochem J* 353:345–355
21. Kolomiets MV, Chen H, Gladon RJ, Braun EJ, Hannapel DJ (2000) A leaf lipoxygenase of potato induced specifically by pathogen infection. *Plant Physiol* 124:1121–1130
22. Kolomiets MV, Hannapel DJ, Gladon RJ (1996) Potato lipoxygenase genes expressed during the early stages of tuberization. *Plant Physiol* 112:446
23. Kolomiets MV, Hannapel DJ, Gladon RJ (1996) Nucleotide sequence of a cDNA clone for a lipoxygenase from abscisic acid-treated potato leaves. *Plant Physiol* 112:446
24. Royo J, Vancanneyt G, Perez AG, Sanz C, Störmann K, Rosahl S, Sanchez-Serrano JJ (1996) Characterization of three potato lipoxygenases with distinct enzymatic activities and different organ-specific and wound-regulated expression patterns. *J Biol Chem* 271:21012–21019
25. Pelacho AM, Mingo-Castel AM (1991) Jasmonic acid induces tuberization of potato stolons cultured in vitro. *Plant Physiol* 97:1253–1255
26. Koda Y, Kikuta Y, Tazaki H, Tsujino Y, Sakamura S, Yoshihara T (1991) Potato tuber-inducing activities of jasmonic acid and related compounds. *Phytochemistry* 30:1435–1438
27. Galliard T (1980) Lipid oxidation and flavor biogenesis in edible plants. *J Am Oil Chem Soc* 57:A164–A165
28. Feussner I, Kühn H (2000) Application of lipoxygenases and related enzymes for the preparation of oxygenated lipids. In: Bornscheuer UT (ed) *Enzymes in lipid modification*. Wiley-VCH, Weinheim
29. Bligh EG, Dyer WJ (1959) A rapid method of total lipid extraction and purification. *Can J Biochem Physiol* 37:911–917
30. Felsenstein J, Churchill GA (1996) A hidden Markov model approach to variation among sites in rate of evolution. *Mol Biol Evol* 13:93–104
31. Melan MA, Dong XN, Endara ME, Davis KR, Ausubel FM, Peterman TK (1993) An *Arabidopsis thaliana* lipoxygenase gene can be induced by pathogens, abscisic acid, and methyl jasmonate. *Plant Physiol* 101:441–450
32. Chen XY, Reddanna P, Reddy GR, Kidd R, Hildenbrandt G, Reddy CC (1998) Expression, purification, and characterization of a recombinant 5-lipoxygenase from potato tuber. *Biochem Biophys Res Commun* 243:438–443
33. Stumpe M, Feussner I (2006) Formation of oxylipins by CYP74 enzymes. *Phytochemistry Rev* 5:347–357
34. Weber H, Chetelat A, Caldeleri D, Farmer EE (1999) Divinyl ether fatty acid synthesis in late blight-diseased potato leaves. *Plant Cell* 11:485–493
35. Kolomiets MV, Hannapel DJ, Chen H, Tymeson M, Gladon RJ (2001) Lipoxygenase is involved in the control of potato tuber development. *Plant Cell* 13:613–626
36. Galliard T, Phillips DR (1972) The enzymic conversion of linoleic acid into 9-(nona-1', 3'-dienoxy)non-8-enoic acid, a novel unsaturated ether derivative isolated from homogenates of *Solanum tuberosum* tubers. *Biochem J* 129:743–753
37. Shimizu T, Radmark O, Samuelsson B (1984) Enzyme with dual lipoxygenase activities catalyses leukotriene A4 synthesis from arachidonic acid. *Proc Natl Acad Sci USA* 81:689–693
38. Regdel D, Kühn H, Schewe T (1994) On the reaction specificity of the lipoxygenase from tomato fruits. *Biochim Biophys Acta* 1210:297–302
39. Mulliez E, Leblanc J-P, Girerd J-J, Rigaud M, Chottard J-C (1987) 5-Lipoxygenase from potato tubers. Improved purification and physicochemical characteristics. *Biochim Biophys Acta* 916:13–23
40. van Aarle PGM, Debarse MMJ, Veldink GA, Vliegthart JFG (1991) Purification of a lipoxygenase from ungerminated barley—characterization and product formation. *FEBS Lett* 280:159–162
41. Gardner HW (1989) Soybean lipoxygenase-1 enzymatically forms both 9(S)- and 13(S)-hydroperoxides from linoleic acid by a pH-dependent mechanism. *Biochim Biophys Acta* 1001:274–281
42. Veldink G, Garssen GJ, Vliegthart JFG, Bolding J (1972) Positional specificity of corn germ lipoxygenase as a function of pH. *Biochem Biophys Res Commun* 47:22–26
43. Shibata D, Slusarenko A, Casey R, Hildebrand D, Bell E (1994) Lipoxygenases. *Plant Mol Biol Rep* 12:S41–S42

Uptake and Incorporation of Pinolenic Acid Reduces n-6 Polyunsaturated Fatty Acid and Downstream Prostaglandin Formation in Murine Macrophage

Lu-Te Chuang · Po-Jung Tsai · Chia-Long Lee · Yung-Sheng Huang

Received: 10 July 2008 / Accepted: 19 November 2008 / Published online: 8 January 2009
© AOCS 2008

Abstract Many reports have shown the beneficial effects of consumption of pine seeds and pine seed oil. However, few studies have examined the biological effect of pinolenic acid (PNA; $\Delta 5,9,12-18:3$), the main fatty acid in pine seed oil. In this study, using murine macrophage RAW264.7 cells as a model, we examined the effect of PNA on polyunsaturated fatty acid (PUFA) metabolism, prostaglandin (PG) biosynthesis and cyclooxygenase-2 (COX-2) expression. Results showed that PNA was readily taken up, incorporated and elongated to form eicosatrienoic acid (ETrA, $\Delta 7,11,14-20:3$) in macrophage cells. A small portion of this elongated metabolite was further elongated to form $\Delta 9,13,16-22:3$. The degree of incorporation of PNA and its metabolites into cellular phospholipids varied with the length of incubation time and the concentration of PNA in the medium. Incubation of PNA also modified the fatty acid profile of phospholipids: the levels of 18- and 20-carbon PUFA were significantly decreased, whereas those of 22-carbon fatty acids increased. This finding suggests that PNA enhances the elongation of 20-carbon fatty acids to 22-carbon fatty acids. The syntheses of PGE₁

from dihomo- γ -linolenic acid (DGLA, $\Delta 8,11,14-20:4$) and PGE₂ from arachidonic acid (ARA, $\Delta 5,8,11,14-20:4$) were also suppressed by the presence of PNA and its metabolite. As the expression of COX-2 was not suppressed, the inhibitory effect of PNA on PG activity was attributed in part to substrate competition between the PNA metabolite (i.e., $\Delta 7,11,14-20:3$) and DGLA (or ARA).

Keywords Non-methylene interrupted fatty acids · Sciadonic acid · Gamma-linolenic acid · Cyclooxygenase 2

Abbreviations

ADA	Adrenic acid ($\Delta 7, 10, 13, 16-22:4$)
ARA	Arachidonic acid ($\Delta 5, 8, 11, 14-20:4$)
COX-2	Cyclooxygenase 2
DGLA	Dihomo-gamma-linolenic acid ($\Delta 8, 11, 14-20:3$)
DHA	Docosahexaenoic acid (22:6)
DMEM	Dulbecco's modified Eagles medium
DMSO	Dimethyl sulfoxide
DPA	Docosapentaenoic acid (22:5)
DTrA	Docosatrienoic acid (22:3)
EDA	Eicosadienoic acid (20:2)
EPA	Eicosapentaenoic acid ($\Delta 5, 8, 11, 14, 17-20:5$)
ETA	Eicosatetraenoic acid ($\Delta 8, 11, 14, 17-20:4$)
ETrA	Eicosatrienoic acid (20:3)
FACES	Fatty acid chain elongation system
GC	Gas chromatography
GC-MS	Gas chromatograph mass spectrometry
GLA	Gamma-linolenic acid ($\Delta 6, 9, 12-18:3$)
NMIFA	Non-methylene-interrupted fatty acids
PGE	Prostaglandin E
PNA	Pinolenic acid ($\Delta 5, 9, 12-18:3$)
PSO	Pine seed oil

L.-T. Chuang · C.-L. Lee
Department of Biotechnology, Yuanpei University,
Hsinchu, Taiwan

P.-J. Tsai
Department of Human Development and Family Studies,
National Taiwan Normal University, Taipei, Taiwan

Y.-S. Huang (✉)
Department of Food Science and Biotechnology,
National Chung Hsing University, 250 Kuo-Kuang Rd,
Taichung 402, Taiwan
e-mail: yshuang@nchu.edu.tw

SDS-PAGE Sodium dodecyl sulfate-polyacrylamide gel electrophoresis

Introduction

Pine seed and pine seed oil (PSO) have been consumed for years by the general public in many parts of the world. Several animal studies have shown that PSO supplementation lowers blood lipids, reduces blood pressure and affects lipoprotein metabolism [1–4]. However, the mechanism as to how PSO exerts these beneficial effects is still not fully understood. Pinolenic acid (PNA, $\Delta 5,9,12-18:3$) is the main fatty acid present in PSO. It is a rare n-6 octadecatrienoic acid, belonging to a group of non-methylene-interrupted polyunsaturated fatty acids (NMIFAs). Its chemical structure is very similar to its positional isomer, gamma-linolenic acid (GLA; $\Delta 6,9,12-18:3$). Previously, GLA supplementation has been demonstrated to exert beneficial effects, such as lowering inflammation-related diseases [5, 6], hypertension and other chronic diseases [7, 8]. In mammals, dietary GLA is rapidly elongated to form dihomo- γ -linolenic acid (DGLA; $\Delta 8,11,14-20:3$) [9, 10], a precursor of anti-inflammatory eicosanoid, prostaglandin E_1 (PGE_1). DGLA competes with arachidonic acid (ARA; $\Delta 5,8,11,14-20:4$) as substrate for cyclooxygenase-2 (COX-2), and subsequently reduces the synthesis of pro-inflammatory prostaglandins [11]. Thus, the effect of GLA was exerted through modulation of n-6

PUFA metabolism and eicosanoid synthesis (Scheme 1, [12]). Similar to GLA, PNA can also be elongated by the fatty acid chain elongation system (FACES) in rat liver microsomes and human hepatoma HepG2 cells to form eicosatrienoic acid (ETrA, $\Delta 7,11,14-20:3$) [10, 13]. It has also been shown that ETrA, similar to its isomer DGLA ($\Delta 8,11,14-20:3$), could substitute ARA for incorporation into cellular phospholipid fractions [13]. Therefore, the present study, using murine macrophage-like RAW264.7 cells as a model, was carried out to examine whether PNA and/or its metabolites affect the polyunsaturated fatty acid (PUFA) metabolism and prostaglandin production.

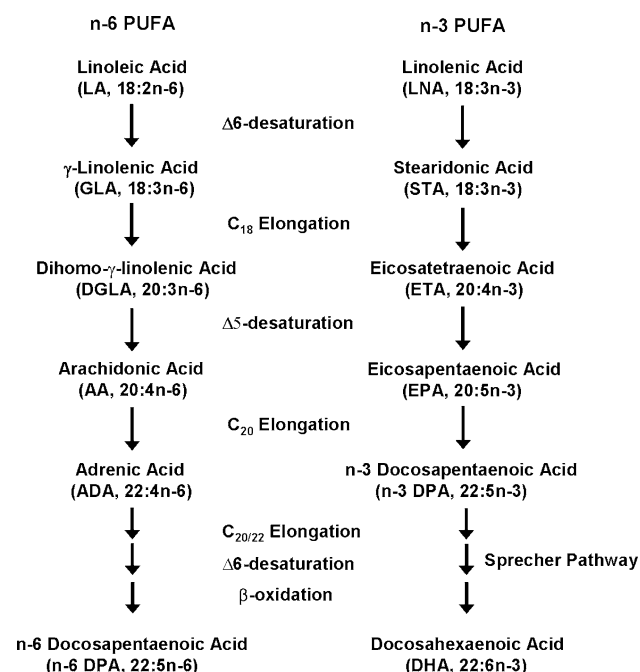
Experimental Procedures

Chemicals

Authentic fatty acids, i.e., PNA, ARA and n-3 eicosatetraenoic acid (n-3 ETA, $\Delta 8,11,14,17-20:4$) and PGE_2 assay kit were obtained from Cayman Chemicals (Ann Arbor, MI). GLC standard RL-461, triheptadecanoin, and DGLA were purchased from Nu-Chek-Prep, Inc. (Elysian, MN). Lipopolysaccharide (LPS, from *Escherichia coli* 026:B6), dimethyl sulfoxide (DMSO), cell proliferation kit, Tween-20, protease inhibitors were supplied by Sigma Chemical (St. Louis, MO). Dulbecco's modified Eagles medium (DMEM), fetal bovine serum (FBS) and phosphate-buffered saline (PBS) were obtained from Gibco (Carlsbad, CA). PGE_1 assay kit was purchased from Assay Designs, Inc. (Ann Arbor, MI). All reagent-grade organic solvents were from Burdick & Jackson (Muskegon, MI).

Cell Culture and Culture Conditions

The murine macrophage RAW 264.7 cell line was obtained from the Bioresource Collection and Research Center (Hsinchu, Taiwan). Cells were maintained in DMEM medium supplemented with 10% heated-inactivated FBS, and incubated at 37 °C and 5% CO_2 in a humidity-controlled atmosphere. Macrophage cells (5×10^5) were seeded in a 100-mm tissue culture plate, and allowed to adhere for 4 h at 37 °C. After cell adhesion, the culture medium was replaced by DMEM medium with different levels of PNA. The first study was carried out to examine the uptake and metabolism of PNA, cells were incubated in the DMEM serum medium supplemented with 50 μM PNA for 24 h. The second study was performed to examine whether the uptake of PNA was time- or dose-dependent, the same number of macrophage cells (5×10^5) were cultured in the same DMEM medium supplemented with 50 μM of PNA for 12, 24, 48 or 72 h, or with different levels of PNA (0, 10, 25, 50 or 100 μM) for 24 h. The cell



Scheme 1 n-6 and n-3 polyunsaturated fatty acid metabolism in mammalian cells [19]

viability was monitored by the methods of trypan blue dye exclusion [14] and MTT assay [15].

Lipid Extraction and Fatty Acid Analysis

After incubation, cells in plates were collected and harvested by centrifugation. The pellet was washed twice with sterile PBS. Total cellular lipids were then extracted following with minor modification the Folch method [16]. Briefly, cell pellets were extracted with 15 ml chloroform–methanol (2:1, v/v) at 4 °C for overnight. After adding 3 ml of 0.9% (w/v) NaCl solution, the mixture was vortexed and centrifuged. The chloroform phase containing the total lipid extract was then removed from the aqueous phase, and evaporated at 40°C using a stream of nitrogen. To separate the total phospholipid fraction, the lipid extracts were fractionated by thin-layer chromatography using hexane/diethyl ether/acetic acid (70:30:1, v/v/v) as the developing system. Fatty acids of the phospholipid fraction were methylated, and fatty acid methyl esters analyzed by an Agilent 6890 gas chromatography (GC) equipped with a flame-ionization detector and a fused-silica capillary column (Omegawax; 30 m × 0.32 mm, i.d., film thickness 0.25 μm, Supelco, Bellefonte, PA, USA) [17]. To separate the isomer of eicosatrienoic acid (ETrA), an HP-88 capillary column (100 m × 0.25 mm, i.d., film thickness 0.2 μm, Hewlett-Packard, Sunnyvale, CA, USA) was utilized. For quantitation of fatty acids, a known amount of triheptadecanoin was added to each lipid sample as the internal standard. The identity of PNA elongated metabolite was determined by gas chromatograph mass spectrometry (GC-MS), using a Hewlett Packard mass selective detector operating at an ionization voltage of 70 eV with a scan range of 20–500 Da.

In-Vitro Study of PGE₁ and PGE₂ Production

RAW264.7 cells were seeded in 24-well plates at 5×10^5 cells/well with complete DMEM medium containing 10% FBS. The cells were allowed to adhere for 4 h at 37 °C. After 24 h of treatment of PNA and/or other fatty acids, cells were stimulated with 0.1 μg/ml LPS for 16 h. Cell-free supernatants were collected and concentrations of both prostaglandins (PGE₁ and PGE₂) were analyzed with respective enzyme immunoassay kits.

Detection of COX-2 Expression by Western Blotting

Confluent macrophage cells (2.5×10^7) were pre-incubated with 50 μM of PNA and/or other fatty acids for 24 h and then stimulated with LPS for 16 h. Total protein was extracted from cells, and its concentration determined using the BCA Protein Assay Reagent Kit (Pierce, Rockford, IL). Denatured proteins were separated by 10% sodium dodecyl

sulfate-polyacrylamide gel electrophoresis (SDS-PAGE), and transferred on a polyvinylidene difluoride membrane. After nonspecific blocking, membranes were probed with a 1:500 dilution of anti-mouse COX-2 antibody (BD Biosciences, Franklin Lakes, NJ), washed with PBS-T (10% Tween 20), and then reacted with a 1:5,000 dilution of anti-mouse immunoglobulin-alkaline phosphatase (Sigma, St. Louis, MO, USA). Following further washing in PBS-T three times, the immuno-complexes were visualized by colorimetric blotting substrates BCIP/NBT (Sigma, St. Louis, MO, USA).

Statistical Analyses

Data were analyzed by analysis of variance (ANOVA) and Fisher's protected least significant difference (LSD) to determine differences between means of the uptake rates and between means of the conversion rates. Means differences were considered significant at $P \leq 0.05$.

Results

Uptake and Metabolism of PNA in Macrophages

To examine the uptake and metabolism of PNA by macrophage, RAW264.7 cells were incubated in the culture medium containing 50 μM of PNA for 24 h. Results from the gas chromatographic analysis (GC analysis) show that a significant level of PNA (14% by weight of cellular phospholipids) and eicosatrienoic acid (ETrA) (19% by weight of cellular phospholipids) were detected in cells incubated with PNA as compared to the control where neither PNA nor ETrA was detected (Fig. 1). Further GC analysis using the HP-88 capillary column (100 m × 0.25 mm) revealed that the ETrA peak contained two isomers (Fig. 1, inset A). Gas chromatography-mass spectrometric analysis shows that the major ETrA peak was the PNA elongation metabolite ($\Delta 7,11,14-20:3$), whereas the minor peak was DGLA (<3% of ETrA) (data not shown). A low level (2% of cellular phospholipids) of docosatrienoic acid (DTrA) was also observed. The DTrA peak has an identical retention time to n-6 docosatrienoic acid ($\Delta 10,13,16-22:3$), an elongation metabolite of DGLA (Fig. 1, inset B). As this peak could only be observed in cells incubated with PNA but not in the controls, it was tentatively identified as $\Delta 9,13,16-22:3$, a possible elongation product of $\Delta 7,11,14-20:3$.

Effect of Incubation Time and Dose Response on PNA Metabolism in Macrophages

To examine the effect of the length of the incubation time on PNA uptake and metabolism, cells were incubated with

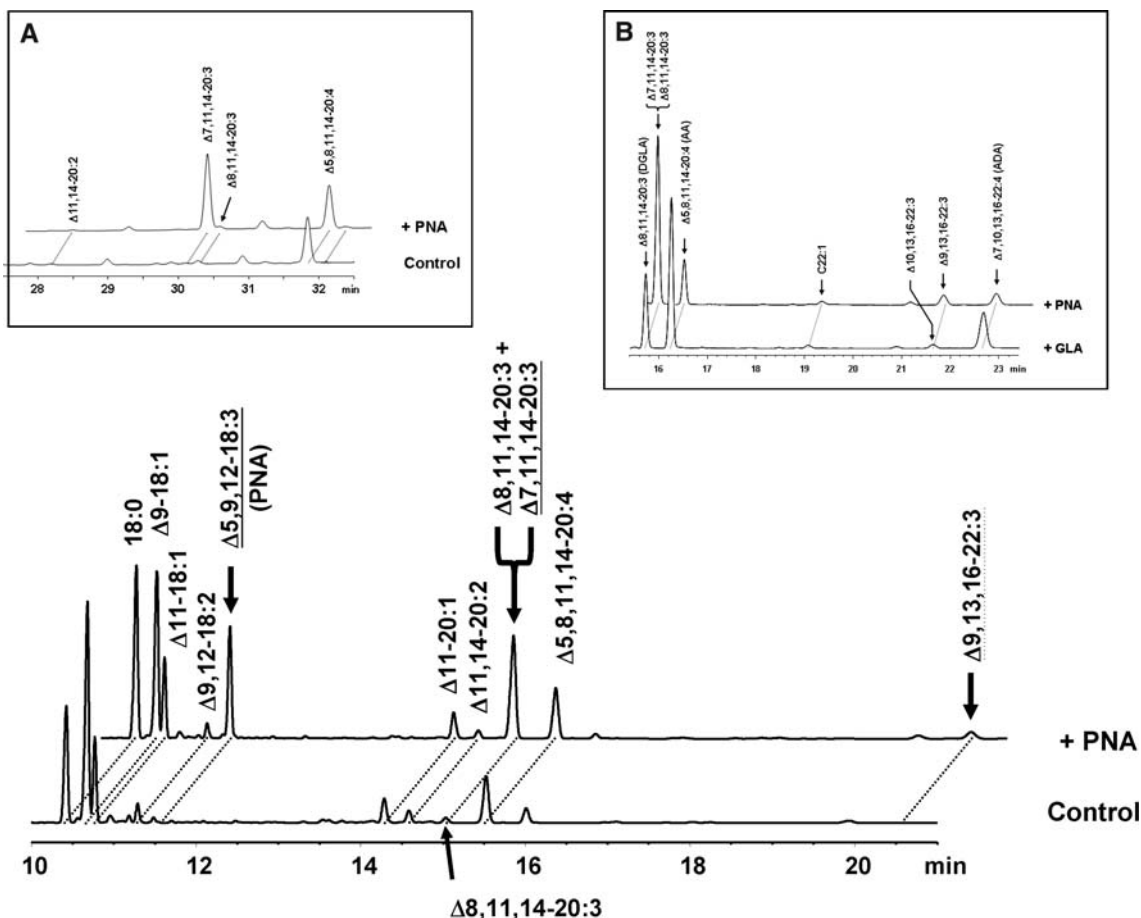
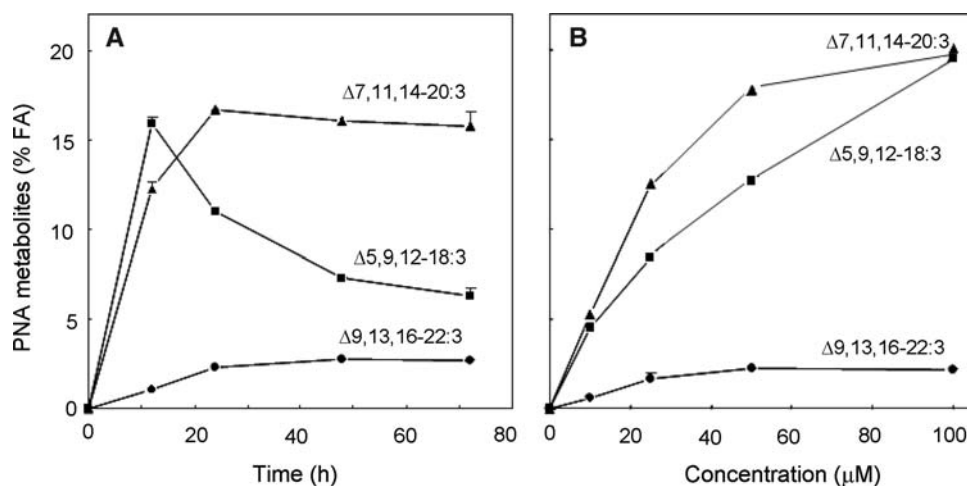


Fig. 1 Gas chromatogram of fatty acids of total lipids in the RAW264.7 cells cultured in the medium containing 50 μM of PNA. Solid arrows show the presence of pinolenic acid (PNA; $\Delta 5,9,12-18:3$), eicosatrienoic acid (ETrA; $\Delta 7,11,14-20:3$ and $\Delta 8,11,14-20:3$) and docosatrienoic acid (DTrA; $\Delta 9,13,16-22:3$), respectively. Inset A

shows the gas chromatogram of cellular phospholipids fatty acids in an HP-88 capillary column. Inset B compares gas chromatograms of fatty acids in cells incubated in medium containing either PNA or GLA

Fig. 2 Effects of different incubation times (a) and PNA concentration (b) on the levels of $\Delta 5,9,12-18:3$ (PNA) (■), $\Delta 7,11,14-20:3$ (▲) and $\Delta 9,13,16-22:3$ (●) in cellular phospholipids. RAW264.7 cells were incubated with medium containing 50 μM of PNA for 48 h, or different levels (0, 10, 25, 50, or 100 μM) of PNA for 24 h



50 μM PNA for 12, 24, 48 or 72 h. The phospholipids fatty acid composition in total cellular lipids was then analyzed. The results in Fig. 2a show that PNA was readily

incorporated into cellular phospholipids. The proportion of PNA elevated rapidly, reached the maximum at 12 h and fell thereafter. A significant portion of PNA was elongated

to $\Delta 7,11,14-20:3$. A small portion of $\Delta 7,11,14-20:3$ was further elongated to $\Delta 9,13,16-22:3$. The levels of these two PNA metabolites increased as the incubation time increased and reached a plateau after 24 h of incubation.

To examine the effect of varying PNA concentration in the medium on phospholipid fatty acid composition, the cells were incubated with 10, 25, 50 or 100 μM of PNA for 24 h. Results in Fig. 2b show that the level of PNA and its metabolites increased as the concentration of PNA in the medium increased.

Effect of PNA Incubation on Phospholipid Fatty Acid Composition

We also examined the composition of other fatty acids in cells incubated with different levels of PNA. The results in Fig. 3a show that when the levels of PNA and its metabolites in cellular phospholipids increased, those of total monounsaturated fatty acids and n-6 PUFA decreased. The effects were dose-dependent. With respect to levels of saturated fatty acids and n-3 PUFA, a significant lowering effect was observed only when the concentration of PNA in the medium exceeded 25 μM .

Among n-6 PUFA, incubation with PNA significantly lowered the levels of 18- and 20-carbon fatty acids, e.g.,

linoleic acid (LA; $\Delta 9,12-18:2$), GLA, eicosadienoic acid (EDA; $\Delta 11,14-20:2$), DGLA and ARA. In contrast, PNA incubation raised the levels of the 22-carbon fatty acids, i.e., adrenic acid (ADA; $\Delta 7,10,13,16-22:4$) and n-6 docosapentaenoic acid (n-6 DPA; $\Delta 4,7,10,13,16-22:5$). The increase reached a plateau when the concentration exceeded 50 μM .

To examine the effect of PNA incubation on n-3 fatty acid metabolism, macrophage cells were incubated with a medium containing 25 μM of n-3 eicosatetraenoic acid (n-3 ETA; $\Delta 8,11,14,17-20:4$) alone or in combination with 25 μM of PNA for 24 h. Results in Fig. 4a show that levels of the 20-carbon n-3 fatty acids (n-3 ETA and EPA) were decreased, whereas those of 22-carbon n-3 fatty acids, i.e., n-3 docosapentaenoic acid (n-3 DPA, $\Delta 7,10,13,16,19-22:5$) and docosahexaenoic acid (DHA; $\Delta 4,7,10,13,16,19-22:6$) were increased. However, the levels of total n-3 PUFA were decreased in cells incubated with PNA (Fig. 4b).

Effect of PNA on Synthesis of Prostaglandin E₁ and E₂

The results shown in Fig. 3b demonstrate that PNA incubation lowered the level of 20-carbon n-6 PUFA, i.e., DGLA and ARA in macrophage cellular phospholipids. It

Fig. 3 Effects of PNA on the level of total saturated fatty acids (SFA), total monounsaturated fatty acids (MUFA), total n-6 or n-3 polyunsaturated fatty acids (n-6 or n-3 PUFA) (a), and individual n-6 polyunsaturated fatty acids (b). RAW264.7 cells were incubated with the medium containing 0 μM (\square), 10 μM (\square), 25 μM (\square), 50 μM (\square) or 100 μM (\blacksquare) of PNA for 24 h. Each value represented the mean \pm SE of three independent experiments. In each fatty acid or group of fatty acids, values with different letters are significantly different from each other at $P < 0.05$

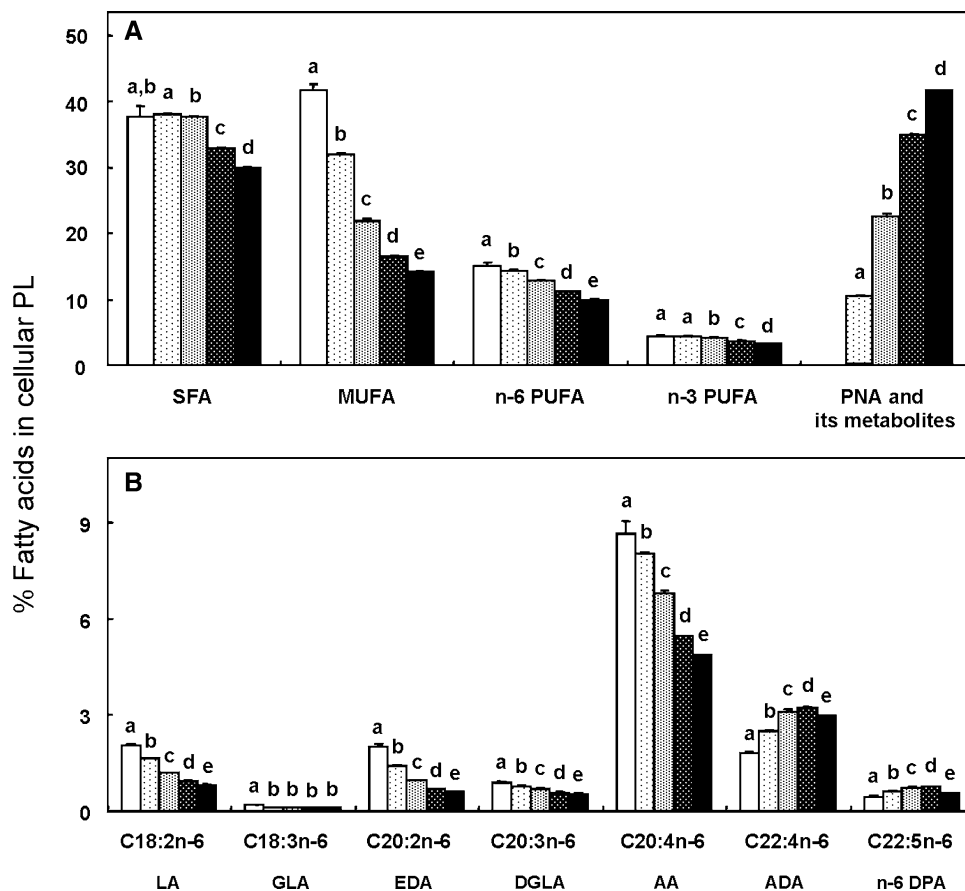
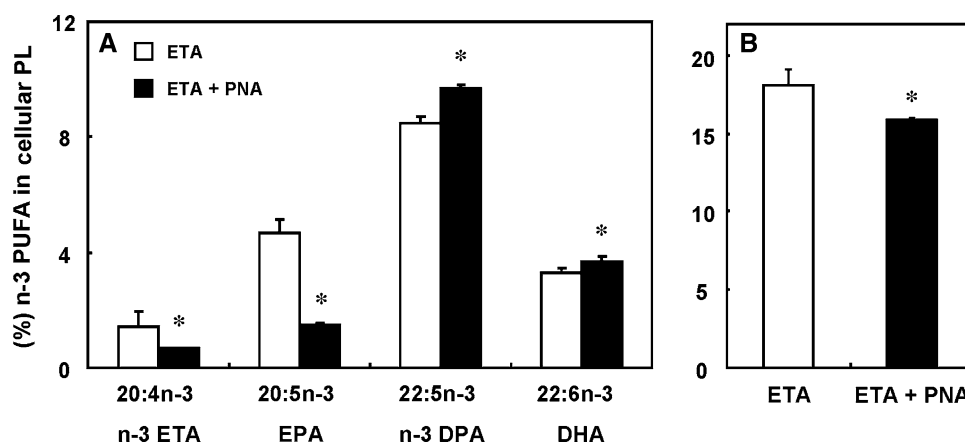


Fig. 4 Effects of PNA incubation on levels of total n-3 polyunsaturated fatty acids (n-3 PUFA) (a), and individual n-3 polyunsaturated fatty acids (b). Cells were incubated with 25 μ M of n-3 ETA alone (\square) or a combination of 25 μ M of n-3 ETA and 25 μ M of PNA (\blacksquare) for 24 h. Each value represents the mean \pm SE of three independent experiments. In each category, symbol (*) denotes the difference between 2 values is significant at $P < 0.05$



is possible that reduction of DGLA and ARA, could lead to a decrease in synthesis of PGE₁ and PGE₂, respectively. To examine this possibility, macrophage cells were incubated with varying levels of PNA (0, 12, 25, 50, and 100 μ M) for 24 h and then treated with LPS for 16 h to stimulate the prostaglandin synthesis. Results in Fig. 5 (upper panel) show that LPS stimulation increased significantly the synthesis of both PGE₁ and PGE₂. Addition of PNA in the medium decreased the levels of both PGE₁ and PGE₂. The effect was dose-dependent.

In a separated study, we examined the effect of PNA (50 μ M) on synthesis of PGE₁ or PGE₂ in macrophage cells pre-incubated with 50 μ M of DGLA or ARA. The results in Fig. 5 (lower panel) show that cells pre-treated with DGLA or ARA significantly increased the production of PGE₁ or PGE₂, respectively. However, addition of PNA into medium significantly suppressed the level of PGE₁ in cells pre-incubated with DGLA by 53%, and PGE₂ in cells pre-incubated with ARA by 22%.

Effect of PNA on Expression of COX-2 Protein

To understand the mechanism of the inhibitory effect of PNA on PGE₁ and PGE₂ activity, we examined the effect of PNA on the expression of COX-2 enzyme. Results in Fig. 6 show that expression of COX-2 in RAW264.7 cells was highly induced upon LPS simulation (Fig. 6, lane 2 vs. lane 1). When cells were treated with ARA or PNA alone, the levels of COX-2 protein in comparison with the control were increased by 18%, and 12%, respectively (lanes 3 and 5). When cells were treated with a combination of ARA and PNA, the levels of COX-2 protein were increased synergistically (26%, $P < 0.01$). In contrast, incubation with DGLA, the cellular level of COX-2 protein was decreased by 11% (lane 7). Addition of PNA in the medium eradicated the lowering effect of DGLA: the level of COX-2 protein was raised to between those in cells incubated with PNA and those with DGLA (lane 6).

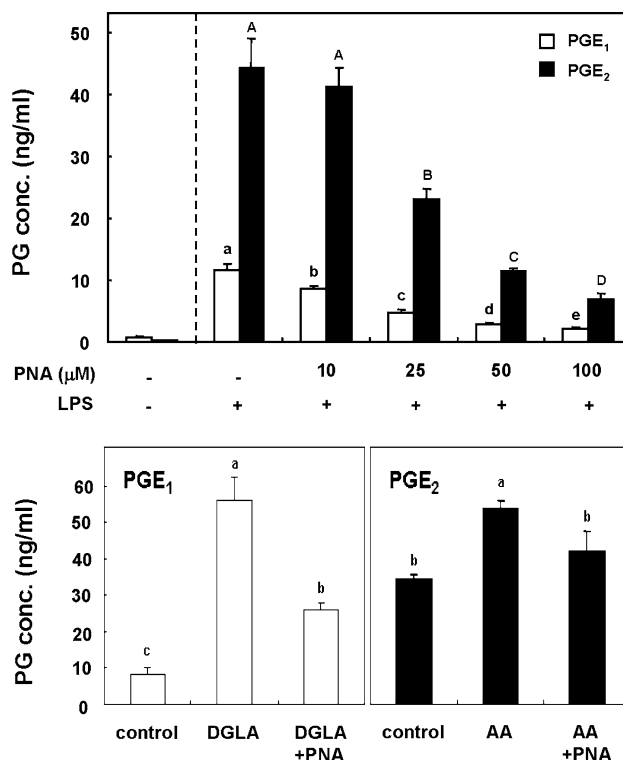


Fig. 5 Effect of PNA on formation of prostaglandin E₁ (\square) and prostaglandin E₂ (\blacksquare) in the LPS-treated RAW264.7 macrophage cells. Cells were incubated in the medium containing different levels (0, 10, 25, 50, or 100 μ M) of PNA (upper panel) for 24 h, or in the medium containing either 50 μ M of DGLA (or AA) alone or in a combination of 50 μ M of PNA and 50 μ M of DGLA (or AA) for 24 h (lower panel), followed by LPS treatment for 16 h. Each value represents the mean \pm SE of three independent experiments. In PGE₁ (\square) or PGE₂ (\blacksquare), values with different letters or numbers are significantly different from each other at $P < 0.05$

Discussion

In this study, we observed that PNA was readily taken up, incorporated and metabolized in murine RAW264.7 macrophage cells. In cells, PNA was rapidly elongated to form $\Delta 7,11,14-20:3$. A similar finding has previously been

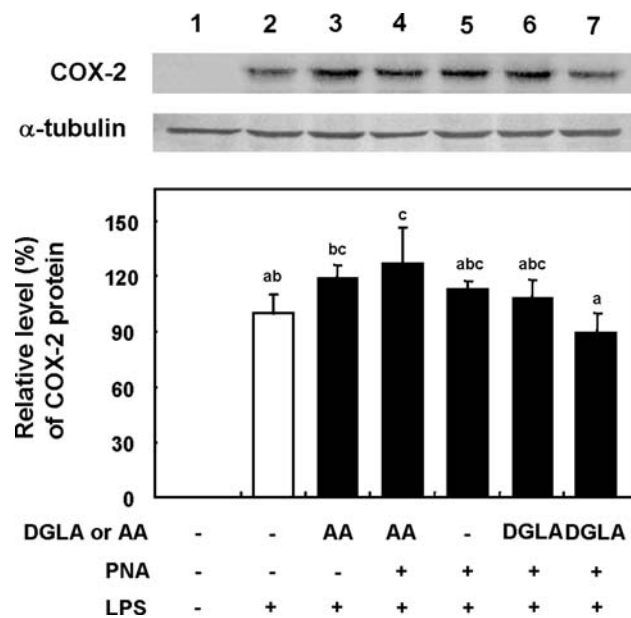


Fig. 6 Effects of PNA on the expression of COX-2 in RAW264.7 macrophage cells. Cells were incubated with only medium, or medium containing 50 μM of AA, DGLA or PNA alone, or a mixture of 50 μM AA and 50 μM PNA or 50 μM DGLA and 50 μM PNA for 24 h, followed by LPS treatment for 16 h. Cyclooxygenase-2 expression was determined by Western blot analysis. α -tubulin was used as a loading control. Each value represents the mean \pm SE of three independent experiments. Values with different letters are significantly different from each other at $P < 0.05$

reported in human hepatoma HepG2 cells [13]. We have also observed the presence of $\Delta 9,13,16-22:3$ in cellular phospholipids (Fig. 1). The level of $\Delta 9,13,16-22:3$ increased as the length of incubation time and concentration of PNA in medium increased. These findings suggest that a portion of $\Delta 7,11,14-20:3$ underwent further elongation. This reaction was probably catalyzed by the fatty acid chain elongation system (FACES) which converts specifically 20-carbon fatty acids to 22-carbon fatty acids, such as ARA to ADA, EPA to n-3 DPA [19, 20]. Chapkin and his colleague has demonstrated in macrophages the elongation of DGLA ($\Delta 8,11,14-20:3$) to n-6 docosatrienoic acid (DTrA; $\Delta 10,13,16-22:3$) by this enzyme system [18].

Incubation of PNA also modified compositions of cell membrane fatty acids in RAW264.7 cells. In cells incubated with PNA, significant portions of total n-6 PUFA, 18-carbon and 20-carbon n-6 fatty acids in phospholipids were replaced by PNA and its metabolites (Fig. 3a). In spite of this, levels of 22-carbon ADA and n-6 DPA were increased significantly in cells incubated with PNA (Fig. 3b). Similarly, PNA decreased levels of total n-3 fatty acids, n-3 ETA and EPA when n-3 ETA was supplemented into the medium, but levels of 22-carbon n-3 fatty acids (i.e., DPA and DHA) were increased (Fig. 4b). These findings suggest that the metabolism of 20-carbon fatty acids to 22-carbon

fatty acids (conversion of ARA to n-6 DPA or EPA to DHA) was enhanced in cells incubated with PNA (Scheme 1).

In this study, we observed the inhibitory effect of PNA on eicosanoid production (Fig. 5). This effect could be exerted via the competitive incorporation of PNA and $\Delta 7,11,14-20:3$ into phospholipids which reduced the level of DGLA and ARA available for formation of eicosanoids (Fig. 3b and 5a). Previously, Li and his colleagues have shown that one of conjugated linoleic acid isomers (10*t*,12*c*-CLA) reduced LPS-stimulated PGE₂ production by decreasing the level of COX-2 protein expression in RAW264.7 cells [21]. Similarly, the inhibitory effect of PNA on PGE production could be due to its ability to modulate protein production. Results in the present study showed an increase in the level of COX-2 in macrophage cells treated with PNA (Fig. 6). This finding is comparable with the report that EPA treatment induced the expression of COX-2, but suppressed the formation of PGE₂ in cultured human lung cancer A549 cells [22]. Thus, the inhibitory effect of PNA on prostaglandin production was not exerted through suppression of COX-2 expression.

It is of interest to note that sciadonic acid ($\Delta 5,11,14-20:3$), another NMIFA found in *Podocarpus nagi* (Podocarpaceae) seed oil, behaves very similarly to PNA. This acid could be taken up, incorporated into phospholipids, and reduced both levels of ARA and PGE₂ in cultured skin keratinocytes [23]. In comparison with PNA, the inhibitory effect of sciadonic acid on the level of ARA in membrane phospholipids became evident only when the concentration of sciadonic acid in the culture medium exceeded 15 μM , and inhibition on PGE₂ production was observed only when the concentration of sciadonic acid reached 100 μM [22]; while the inhibitory effects of PNA on the level of DGLA (or ARA) and its respective prostaglandin could be observed when the concentration of PNA was only 10 μM (Fig. 2b and 5a). This finding suggests that PNA as compared to sciadonic acid is more potent on suppressing the PG production. The explanation may be attributed to the difference in chemical structures between these two acids: the PNA elongation product ($\Delta 7,11,14-20:3$) is more similar to DGLA ($\Delta 8,11,14-20:3$) and ARA ($\Delta 5,8,11,14-20:4$) than is sciadonic acid ($\Delta 5,11,14-20:3$) in competing for the catalytic sites of the COX-2 enzyme. This difference in chemical structure could also explain the greater inhibitory effect of PNA on conversion of DGLA to PGE₁ (53%) than that on conversion of ARA to PGE₂ (22%).

In this study, we have clearly shown that PNA was metabolized to form $\Delta 7,11,14-20:3$ and $\Delta 9,13,16-22:3$, and they significantly modulated n-6 PUFA metabolism and PGE synthesis. However, in rats, fed PSO failed to modulate prostacyclin [1, 24]. This could be due to low incorporation of PNA into phospholipid fractions (2–4% of

total fatty acids) [1, 25], and to a lower rate of elongation of PNA to $\Delta 7,11,14-20:3$ as compared to that of GLA to DGLA [1, 10, 24].

In conclusion, by using murine RAW264.7 macrophage cells, we demonstrated that exogenous PNA could be taken up, incorporated and metabolized to form elongation products. The incorporated PNA and its metabolite modulated fatty acid compositions of cellular phospholipids and PUFA metabolism. Since DGLA (or ARA) was substituted by PNA and its metabolites, the synthesis of PGE₁ (or PGE₂) were also influenced. The inhibitory effect was not due to suppression on COX-2 protein expression at the translation level, but due to substrate competition substitution of DGLA or ARA.

Acknowledgments This work was supported in part by grants (95-2313-B-264-001- and 96-2320-B-264-001-) from the National Science Council, Taiwan.

References

- Sugano M, Ikeda I, Wakamatsu K, Oka T (1994) Influence of Korean pine (*Pinus koraiensis*)-seed oil containing *cis*-5, *cis*-9, *cis*-12-octadecatrienoic acid on polyunsaturated fatty acid metabolism, eicosanoid production and blood pressure. *Br J Nutr* 72:775–783
- Asset G, Staels B, Wolff RL, Bauge E, Madj Z, Fruchart J-C, Dallongeville J (1999) Effects of *Pinus pinaster* and *Pinus koraiensis* seed oil supplementation on lipoprotein metabolism in the rat. *Lipids* 34:39–44
- Asset G, Leroy A, Bauge E, Wolff RL, Fruchart J-C, Dallongeville J (2000) Effects of dietary maritime pine (*Pinus pinaster*)-seed oil on high-density lipoprotein levels and in vitro cholesterol efflux in mice expressing human apolipoprotein A-I. *Br J Nutr* 84:353–360
- Asset G, Bauge E, Wolff RL, Fruchart J-C, Dallongeville J (2001) Effects of dietary maritime pine seed oil on lipoprotein metabolism and atherosclerosis development in mice expressing human apolipoprotein B. *Eur J Nutr* 40:268–274
- Calder PC, Zurier RB (2001) Polyunsaturated fatty acids and rheumatoid arthritis. *Curr Opin Clin Nutr Metab Care* 4:115–121
- Kast RE (2001) Borage oil reduction of rheumatoid arthritis activity may be mediated by increased cAMP that suppresses tumor necrosis factor-alpha. *Int Immunopharmacol* 12:2197–2199
- Engler MM, Schambelan M, Engler MB, Ball DL, Goodfriend TL (1998) Effects of dietary gamma-linolenic acid on blood pressure and adrenal angiotensin receptors in hypertensive rats. *Proc Soc Exp Biol Med* 218:234–237
- Arisaka M, Arisaka O, Yamashiro Y (1991) Fatty acid and prostaglandin metabolism in children with diabetes mellitus. II. The effect of evening primrose oil supplementation on serum fatty acid and plasma prostaglandin levels. *Prostaglandins Leukot Essent Fatty Acids* 43:197–201
- Chapkin RS, Coble KJ (1991) Utilization of γ -linolenic acid by mouse peritoneal macrophages. *Biochim Biophys Acta* 1085:365–370
- Tanaka T, Hattori T, Kouchi M, Hirano K, Satouchi K (1998) Methylene-interrupted double bond in polyunsaturated fatty acid is an essential structure for metabolism by the fatty acid chain elongation system of rat liver. *Biochim Biophys Acta* 1393:299–306
- Levin G, Duffin KL, Obukowicz MG, Hummert SL, Fujiwara H, Needleman P, Raz A (2002) Differential metabolism of dihomo- γ -linolenic acid (DGLA) and arachidonic acid (AA) by cyclooxygenase-1 (COX-1) and cyclooxygenase-2 (COX-2): Implications for cellular synthesis of PGE1 and PGE2. *Biochem J* 365:489–496
- Sprecher H, Luthria DL, Mohammed BS, Baykousheva SP (1995) Reevaluation of the pathways for the biosynthesis of polyunsaturated fatty acids. *J Lipid Res* 36:2471–2477
- Tanaka T, Takimoto T, Morishige J, Kikuta Y, Sugiura T, Satouchi K (1999) Non-methylene-interrupted polyunsaturated fatty acids: effective substitute for arachidonate of phosphatidylinositol. *Biochem Biophys Res Comm* 264:683–688
- McAteer JA, Davis J (1994) Basic cell culture technique and maintenance of cell lines. In: Davis JM (ed) *Basic cell culture, a practical approach*. Oxford University Press, Oxford, pp 93–148
- Mosmann T (1983) Rapid colorimetric assay for cellular growth and survival: Application to proliferation and cytotoxicity assays. *J Immunol Meth* 65:55–63
- Folch J, Lees M, Sloane-Stanley GH (1957) A simple method for the isolation and purification of total lipids from animal tissues. *J Biol Chem* 226:497–509
- Chuang LT, Leonard AE, Liu JW, Mukerji P, Bray T, Huang YS (2001) Inhibitory effect of conjugated linoleic acid on linoleic acid elongation in transformed yeast with human elongase. *Lipids* 36:1099–1103
- Chapkin RS, Miller CC, Somers SD, Erickson KL (1998) Utilization of dihomo-gamma-linolenic acid (8, 11, 14-eicosatrienoic acid) by murine peritoneal macrophages. *Biochim Biophys Acta* 959:322–331
- Leonard AE, Bobik EG, Dorado J, Kroeger PE, Chuang LT, Thurmon JM, Parker-Barnes JM, Das T, Huang YS, Mukerji P (2000) Cloning of a human cDNA encoding a novel enzyme involved in the elongation of long-chain polyunsaturated fatty acids. *Biochem J* 350:765–770
- Leonard AE, Kelder B, Bobik EG, Chuang LT, Lewis C, Kopicchick JJ, Mukerji P, Huang YS (2002) Identification and expression of mammalian long-chain PUFA elongation enzymes. *Lipids* 37:733–740
- Li G, Barnes D, Butz D, Bjorling D, Cook ME (2005) 10t, 12c-conjugated linoleic acid inhibits lipopolysaccharide-induced cyclooxygenase expression in vitro and in vivo. *J Lipid Res* 46:2134–2142
- Yang P, Chan D, Felix E, Cartwright C, Menter DG, Madden T, Klein RD, Fischer RM, Newman RA (2004) Formation and antiproliferative effect of prostaglandin E3 from eicosapentaenoic acid in human lung cancer cells. *J Lipid Res* 45:1030–1039
- Berger A, Monnard I, Baur M, Charbonnet C, Safonova I, Jomard A (2002) Epidermal anti-inflammatory properties of 5, 11, 14 20:3: Effects on mouse ear edema, PGE2 levels in cultured keratinocytes, and PPAR activation. *Lipids Health Dis* 1:5
- Tanaka T, Hattori T, Kouchi M, Hirano K, Satouchi K (1998) Non-methylene interrupted polyenoic fatty acid: structural characterization and metabolism by fatty acid chain elongation system in rat liver. In: Riemersma RA, Armstrong R, Kelly RW, Wilson R (eds) *Essential fatty acids and eicosanoids*. American Oil Chemist Society Press, Champaign, IL, pp 229–233
- Matsuo N, Osada K, Kodama T, Lim BO, Nakao A, Yamada K, Sugano M (1996) Effect of γ -linolenic acid and its positional isomer pinolenic acid on immune parameters of Brown-Norway rats. *Prostaglandins Leukot Essent Fatty Acids* 55:223–229

Protective Effects of EPA and Deleterious Effects of DHA on eNOS Activity in Ea hy 926 Cultured with Lysophosphatidylcholine

Sylviane Tardivel · Aurélie Gousset-Dupont ·
Véronique Robert · Marie-Luce Pourci ·
Alain Grynberg · Bernard Lacour

Received: 20 June 2008 / Accepted: 7 January 2009 / Published online: 4 February 2009
© AOCs 2009

Abstract Oxidized low density lipoprotein (Ox-LDL) is a well-established risk factor in atherosclerosis and lysophosphatidylcholine (LysoPtdCho) is considered to be one of the major atherogenic component of Ox-LDL. The purpose of this work was to investigate the effects of two membrane n-3 long chain polyunsaturated fatty acids (n-3 PUFAs), EPA (eicosapentaenoic acid) and DHA (docosahexaenoic acid) compared to n-6 PUFA, ARA (arachidonic acid), on the activation of endothelial NO synthase (eNOS) by histamine in Ea hy 926 endothelial cells incubated during 24 h in the presence or the absence of LysoPtdCho. DHA (50 μ M) produced a ROS induction in cells and aggravated the LysoPtdCho-induced oxidative stress. It did not modify the basal eNOS activity but impaired the stimulation of eNOS induced by histamine and was unable to correct the deleterious effect of LysoPtdCho on histamine-stimulated eNOS activity or phosphorylation of Ser 1177. In contrast, EPA (90 μ M) did not modify the ROS level produced in the presence or absence of LysoPtdCho or basal eNOS activity and the stimulating effect of histamine on eNOS. However, it diminished the deleterious

effect of LysoPtdCho as well as on the histamine-stimulated eNOS activity on the phosphorylation on Ser 1177 of eNOS. The beneficial effect of EPA but not DHA on endothelial eNOS activity in Ea hy 926 could be also partially due to a slight decrease in membrane DHA content in EPA-treated cells. Consequently, the equilibrium between NO generated by eNOS and ROS due to oxidative stress could explain, in part, the beneficial effect of EPA on the development of cardiovascular diseases. By contrast ARA an n-6 PUFA was devoid of any effect on ROS generation or eNOS activity in the basal state or after histamine-induced stimulation. In vivo experiments should be undertaken to confirm these results.

Keywords Endothelial nitric oxide synthase · Lysophosphatidylcholine · n-3 PUFA · EPA · DHA · ARA · Eicosapentaenoic acid · Docosahexaenoic acid · Arachidonic acid · Reactive oxygen species

Introduction

The oxidation of low-density lipoproteins (LDL) is a key event in atherogenesis. One of the major deleterious component of these oxidized LDL (Ox-LDL) is considered to be lysophosphatidylcholine (LysoPtdCho), which represents up to 50% of phosphatidylcholine [1, 2]. LysoPtdCho is also present in high concentration in the atherosclerotic plaques of the artery wall [3]. Thus, LysoPtdCho is believed to play an important role in atherosclerosis by altering various functions in different cell-types, including endothelial cells, smooth muscle cells, monocytes, macrophages, and T-cells [4]. In endothelial cells, the acute effects of LysoPtdCho have been extensively reported in the literature. It has been shown that the acute addition of LysoPtdCho to endothelial

S. Tardivel (✉) · A. Gousset-Dupont · V. Robert ·
M.-L. Pourci · A. Grynberg · B. Lacour
Univ Paris-Sud 11, UMR1154, INRA-UPS,
Faculté de Pharmacie, 5 rue J-B Clément,
Châtenay-Malabry F-92296, France
e-mail: Sylviane.Tardivel@u-psud.fr

S. Tardivel · A. Gousset-Dupont · V. Robert · M.-L. Pourci ·
A. Grynberg · B. Lacour
IFR141, INRA, Châtenay-Malabry F-92296, France

S. Tardivel · B. Lacour
Ecole Pratique des Hautes Etudes, Laboratoire Nutrition
lipidique et apoptose dans le système vasculaire,
5 rue J-B Clément, Châtenay-Malabry F-92296, France

cells in culture up-regulates the expression of cell adhesion molecules (ICAM 1 and VCAM 1) [5], induces the expression of chemotactic factors on the endothelial surface [6], prevents the activation of endothelial NO synthase (eNOS) [7] and increases the apoptosis of endothelial cells [8, 9]. By contrast, only few studies concern the chronic effects of LysoPtdCho in endothelial cells. During chronic administration of LysoPtdCho, a stimulation of the generation of reactive oxygen species (ROS) via NADPH oxidase activation in endothelial cells has been reported [10, 11]. One of the best documented toxic effects of oxygen radicals is peroxidation of polyunsaturated fatty acids (PUFAs) present in membrane phospholipids. However, PUFAs and particularly arachidonic acid are used in endothelial cells to generate prostaglandins, principally PgE2 and PgI2, which are implicated together with NO in the vasodilatation of arteries in response to aggressive agents. In this context, n-3 PUFAs, especially eicosapentaenoic acid (EPA, C20:5n-3) and docosahexaenoic acid (DHA, C22:6n-3) have been shown to exert beneficial effects in the prevention of cardiovascular disease [12]. At the level of vessels, EPA has been reported to be able to increase endothelium-dependent relaxation of coronary arteries [13] and was associated with a reduced morbidity and mortality in atherosclerosis [14]. When added to the culture medium of endothelial cells for 24 h, EPA, and DHA are well incorporated into the cell membrane phospholipids [15]. However, because of their high degree of unsaturation, the incorporation of n-3 PUFAs into membrane phospholipids may also promote peroxidation and the subsequent propagation of oxygen radicals decreasing the bioavailability of NO to produce vascular relaxation.

The present study was designed to reproduce the situation of atherosclerotic arteries in Ea hy 926 endothelial cells cultured for 24 h in the presence of LysoPtdCho in order to determine: (1) the basal eNOS activity and the effect of histamine on eNOS activity in these cells; (2) the modifications of basal and histamine-stimulated eNOS activity when Ea hy 926 cells were cultured in the presence of DHA or EPA compared with cells cultured in the presence of n-6 PUFA, i.e., ARA.

Materials and Methods

Materials

Fetal bovine serum (FBS) was purchased from Biowest (Nuaille, France). Penicillin (10,000 U/mL), streptomycin (10,000 µg/mL) and D-MEM (4,500 mg/L glucose, glutamax) were obtained from Invitrogen (Cergy Pontoise, France). HAT (Hypoxanthine, Aminopterin, Thymidine) medium supplement (50X), cis-5,8,11,14,17-eicosapentaenoic acid (EPA), cis-4,7,10,13,16,19-docosahexaenoic acid

(DHA), arachidonic acid (ARA), lysophosphatidylcholine, namely 1-palmitoyl-*sn*-glycero 3 phosphocholine (LysoPtd Cho) and L-nitroarginine methyl ester (L-NAME) were purchased from Sigma (Saint Quentin Fallavier, France). The anti eNOS and anti phospho-Ser-1177 eNOS antibodies were obtained from Cell Signaling (Ozyme, Saint Quentin en Yvelines France), the secondary antibody was obtained from Sigma. The fluoroprobe 5-(and 6)-chloromethyl-2'-7'-dichlorodihydro fluorescein diacetate acetyl ester (CM-H₂DCFDA) was from Molecular Probes (Cergy Pontoise, France).

Cell Culture

Ea hy 926 is a permanent endothelial cell line derived from human umbilical vein endothelial cells that express factor VIII antigen [16], oxidatively modified human LDL receptor [17] and show calcium-dependent stimulation of endothelial nitric oxide synthase (eNOS) [18]. Cells were kindly provided by Dr Cora-Jean Edgell [16]. They were cultured in a phenol-red-free DMEM culture medium supplemented with 10% FBS, 2% HAT medium supplement (the final concentration of hypoxanthine, aminopterin, thymidine was 100 µM, 0.4 Mm, and 16 µM, respectively) and 1% penicillin/streptomycin. ARA, EPA, and DHA were linked to albumin, for 3 h at 37 °C, by mixing 1 mg free fatty acid/16 mg albumin/40 mL culture medium, as previously described [19]. The final molar ratio ARA, EPA, or DHA/albumin was close to 3.

To investigate the effect of ARA, EPA, or DHA on eNOS expression and activity, the cells were seeded (200,000 cells/well) on six-well plates and were grown until confluence. Then they were preincubated with different PUFA concentrations (25–120 µM in the culture medium) and/or different LysoPtdCho concentrations (10–100 µM) during 24 h, before acute treatment with histamine (10 µM, 10 min).

Cell Viability Assay

We used the tetrazolium salt MTT (3-[4,5-dimethylthiazol-2-yl]-2,5-diphenyltetrazolium bromide) assay to investigate the viability of cells cultured in the presence of different treatments. Briefly, the cells were seeded onto 96-well flat-bottomed culture plates at 15×10^4 cells/mL and cultured until confluence. The cells were treated with ARA, EPA, or DHA in the presence or absence of 60 µM LysoPtdCho for 24 h. MTT (0.5 mg/mL) was added to each well during the 4 last hours. The medium was discarded and 150 µL DMSO was added to each well to solubilize the formazan crystals and the absorbance of each well was measured at 540 nm using a microplate reader (ELX 800G). Mitochondrial dehydrogenase of viable cells can

reduce MTT to insoluble formazan which can be dissolved by DMSO.

eNOS Activity (Citrulline Assay)

eNOS activity in intact cells was determined by following the conversion of incorporated (^3H) L-arginine to (^3H) L-citrulline [20–22]. The cells were incubated at 37 °C for 45 min in arginine deprivation buffer (109 mM NaCl, 5.4 mM KCl, 1.8 mM CaCl_2 , 1 mM MgSO_4 , 25 mM HEPES, 5 mM glucose, pH 7.4). The reaction was started by the addition of 10 μM arginine and L-(^3H) arginine (0.5 μCi , 200 Ci/mmol). eNOS activity was evaluated in the absence or in the presence of 10 μM histamine. After 10 min, the reaction was stopped with cold buffer 1 (PBS, 5 mM L-arginine, 5 mM EDTA) and the cells were lysed with cold buffer 2 (40 mM sodium acetate, 1 mM L-citrulline, 2 mM EDTA, 2 mM EGTA). After sonication, the lysate was applied to 3-mL DOWEX 50X8-400 columns (Aldrich), pre-equilibrated in buffer 2. Citrulline was eluted with 2 mL of buffer 2, and radioactivity corresponding to [^3H] L-citrulline was quantified by liquid scintillation counting. The eNOS activity was expressed as dpm citrulline/mg of total cell protein produced in 10 min.

Measurement of Intracellular Reactive Oxygen Species (ROS)

The determination of intracellular ROS generation was based on the oxidation of the fluoroprobe CM- H_2DCFDA which is hydrolyzed to DCFH in the cell. DCFH is oxidized to highly fluorescent DCF in the presence of ROS. Cells were seeded in 96 well plates at 15×10^4 cells/mL. After confluence, cells were incubated with ARA, EPA, or DHA and/or LysoPtdCho for 24 h in phenol-red-free medium and 10 μM CM- H_2DCFDA was applied on cells during the last 30 min. Thereafter, the cells were washed in PBS, 1 mM CaCl_2 , 5 mM MgCl_2 , and 5 mM glucose. DCF fluorescence was monitored on a microplate fluorimeter reader (Tecan, Polarion, Trappes, France) using 485 nm excitation and 535 nm emission wavelengths.

Western Blot

After the different treatments, cells were washed with cold PBS and homogenized in lysis buffer (150 mM NaCl, 50 mM Tris, 1 mM EDTA, 50 mM NaF, 1 mM Na_3VO_3 , 1 mM PMSF, 1% Sigma inhibitor cocktail and 1% Nonidet P-40). The lysate was clarified by centrifugation (15 min, $12,000 \times g$, 4 °C). The protein concentration of the supernatant was determined using the Biorad Protein Assay. Cell proteins of lysates (20 μg) were separated on NuPAGE 4–12% Bis-Tris gels (Invitrogen) and transferred onto a

nitrocellulose membrane. The membranes were blocked with 5% non-fat dry milk and incubated overnight at 4 °C with primary antibodies (diluted 1/1000). Secondary specific horseradish-peroxidase linked antibodies (diluted 1/5000) were added for 1 h at room temperature. Bound antibodies were detected using the enhanced chemiluminescence system (ECL, Amersham Bioscience) with Kodak Biomax light films. The bands of immunoblots were scanned and quantified by densitometric analysis using Scion Image software (Scion Corp., Frederick, MD).

Fatty Acid Analysis

Cells were harvested in 1 mL distilled water, and lipids were extracted in a 2:1 chloroform: methanol mixture [23]. Fatty acids were trans-methylated with BF_3 -methanol. The methyl esters were analyzed by gas chromatography on an econocap EC-WAX capillary column (0.32×30 m, Alltech Associates) using heptadecanoic acid (C17:0) as internal standard, as previously described [24].

Conjugated Dienes Analysis

Conjugated dienes were measured by UV absorbance at 235 nm according to Grau et al. [25] with slight modifications. Cells from 3 wells of six-well plates were washed with cold PBS and lysed in 1 mL of 0.02% EDTA and 1.6% NaCl. The suspension was mixed with 4 mL of chloroform: methanol (2:1), homogenized for 2 min in a glass-Teflon potter and centrifuged 10 min at $400 \times g$. The chloroform phase was filtered through anhydrous sodium sulfate (Whatman number 1) which was washed with 2 mL of chloroform. The organic solvent was removed under nitrogen stream and the extracted lipid fraction was dissolved in 2 mL cyclohexane. The absorbance was determined at 235 nm in 1 cm quartz cuvette against cyclohexane.

Statistical Analysis

The results are expressed as means \pm SEM. Statistical analyses were performed by one-way analysis of variance, followed by a Bonferroni *t* test. Values of $p < 0.05$ were considered as statistically significant.

Results

Effect of LysoPtdCho on eNOS Activity

In the absence of LysoPtdCho, 10 μM histamine induced a 3.5-fold increase of arginine conversion to citrulline (Fig. 1). The addition of 1 mM L-NAME, an eNOS inhibitor, 30 min before histamine stimulation, prevented

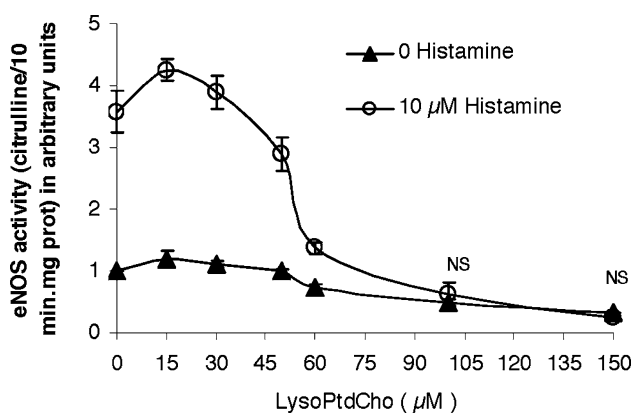


Fig. 1 Dose-effect of LysoPtdCho on histamine stimulation of eNOS activity in Ea hy 926 cells. Ea hy 926 cells were pre-incubated for 24 h with increasing concentrations of LysoPtdCho (0–150 µM). Then, the cells were incubated with 10 µM [3 H] L-arginine in the presence or absence of 10 µM histamine for 10 min. [3 H] L-citrulline production was considered as an indicator of eNOS enzyme activity. Each point represents mean \pm SEM of three or four independent experiments. All values were significantly different between groups ($p < 0.05$) except for 100 and 150 µM LysoPtdCho where they were no significantly different (NS)

citrulline formation completely. In these conditions, the stimulating effect of histamine was reduced by $99 \pm 5.2\%$. The presence of low concentration of LysoPtdCho in the incubation medium (15 or 30 µM) led to no significant modification of histamine-induced eNOS activity. By contrast, with concentrations higher than 30 µM, LysoPtdCho decreased dose-dependently the activation of eNOS induced by 10 µM histamine. The presence of LysoPtdCho was devoid of any cellular toxicity until a concentration of 80 µM in the incubation medium as evaluated by the number of living cells and MTT test (data not shown). However, when LysoPtdCho concentration was superior to 80 µM, the viability of cells was decreased. To evaluate the effects of ARA, EPA, and DHA on the impairment of eNOS activation induced by LysoPtdCho, all further experiments were performed with a concentration of 60 µM LysoPtdCho to obtain a maximal amplitude of eNOS response to PUFAs in the absence of toxicity for the cells. In our system containing 10% SVF, LysoPtdCho added in our culture media accounted for 15% of total phospholipids.

Effect of LysoPtdCho on Ser 1177 eNOS Phosphorylation

The expression of total eNOS and phospho-Ser-1177 eNOS in Ea hy 926 is presented in Fig. 2. Histamine stimulated phosphorylation of Ser 1177 eNOS in control cells in the absence of LysoPtdCho. However, a pretreatment of cells for 24 h with 60 µM LysoPtdCho abolished quite completely the phosphorylation of eNOS on Ser 1177 site. On

the other hand, increasing the doses of LysoPtdCho between 10 and 60 µM did not modify the expression of total eNOS protein. LysoPtdCho modified in a similar manner the phosphorylation of eNOS on Ser 1177 site and the protein activity as demonstrated by the similar patterns of the curves depicted in Figs. 1 and 2.

Effect of ARA, EPA, or DHA on eNOS Activity

The effects of ARA, EPA, or DHA on eNOS activity in the presence or in absence of LysoPtdCho are summarized in Table 1. The cellular eNOS activity was similarly increased by histamine in control, ARA and EPA-treated cells (90 or 120 µM). L-NAME (1 mM) blocked completely the histamine-induced eNOS stimulation as well in control cells as in all PUFAs-treated cells: the stimulating effect of histamine on eNOS was reduced by 98.2 ± 5.0 , 103.1 ± 7.8 , and $92.0 \pm 4.8\%$ when 120 µM ARA or EPA or 50 µM DHA were added to the culture medium, respectively. LysoPtdCho neither in control cells nor in ARA- and EPA- or DHA-treated cells significantly modified the basal activity of eNOS. On the other hand, when cells were incubated for 24 h with 90 or 120 µM EPA, the chronic inhibitory effect of LysoPtdCho on histamine-stimulated eNOS activity was significantly decreased. Thereby, EPA protected the cells against the deleterious effect of LysoPtdCho. The treatment of the cells with 50 µM EPA did not produce any effects on eNOS activity versus control cells whatever the experimental condition (data not shown). eNOS activity of cells incubated with 90 or 120 µM ARA was similar to that of control cells under all the incubation conditions. By contrast, the chronic incubation of cells in the presence of 25 or 50 µM DHA significantly decreased the stimulation of eNOS by histamine and failed to affect the deleterious effect of LysoPtdCho on histamine-induced eNOS activity. In these conditions, the global effect of DHA on eNOS can be considered as deleterious due to its capacity to decrease NO generation. All these effects were observed in the absence of cellular toxicity as estimated by the MTT test (Fig. 3). However, increasing DHA treatments to 90 and 120 µM, concentrations used in EPA and ARA groups, led to cell death (Fig. 3).

Effect of ARA, EPA, or DHA on Ser 1177 eNOS Phosphorylation

As shown in Fig. 4, the induction of eNOS phosphorylation on Ser 1177 by 10 µM histamine was decreased in the presence of 60 µM LysoPtdCho as expected. However, the presence of 90 µM EPA in the incubation medium of cells during 24 h abolished the LysoPtdCho-induced inhibition of phosphorylation of eNOS, outlining a protective effect

Fig. 2 Dose-effect of LysoPtdCho on Ser 1177 phosphorylation of eNOS induced by histamine in Ea hy 926 cells. Ea hy 926 cells were pre-incubated for 24 h with increasing concentrations of LysoPtdCho (0–100 μ M). Then, the cells were stimulated or not with 10 μ M histamine for 10 min. The cells were lysed and a western blot analysis was performed using anti-Ser1177 phospho-eNOS and eNOS antibodies. The presented blot is representative of four independent experiments. The graph represents the densitometric analysis (mean \pm SEM) of blots of four separate experiments. All values were significantly different between groups ($p < 0.05$) except for LysoPtdCho concentrations above or equal to 50 μ M

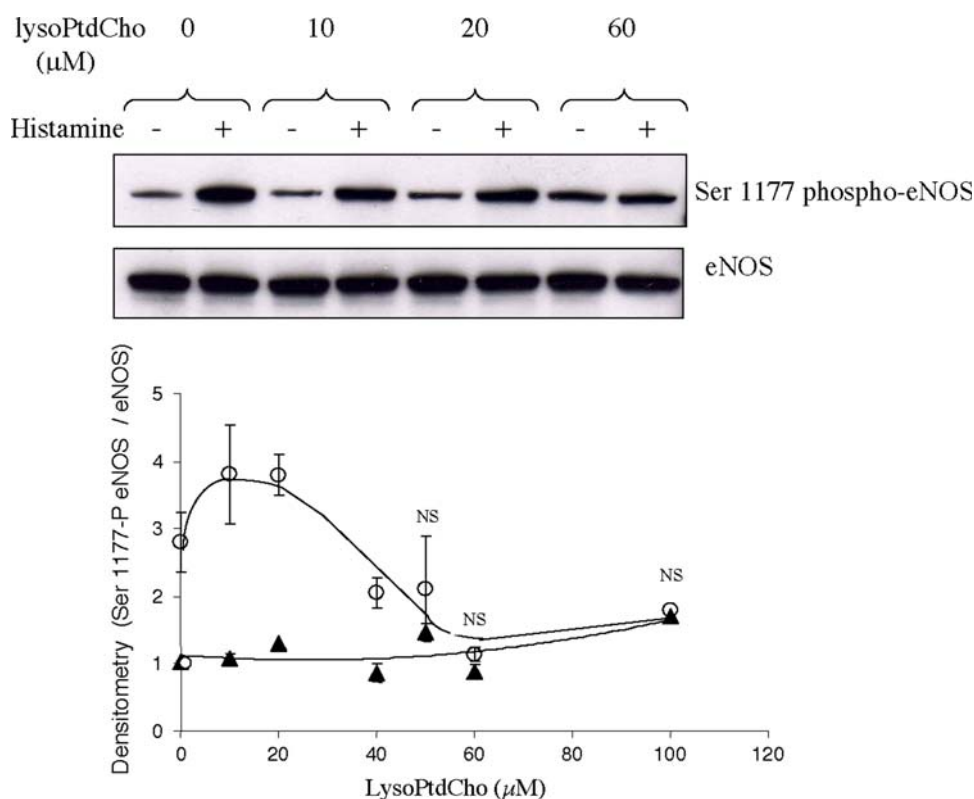


Table 1 Effect of ARA, EPA, or on eNOS activity

	Control	ARA		EPA		DHA	
		90 μ M	120 μ M	90 μ M	120 μ M	25 μ M	50 μ M
Basal activity	100	106 \pm 11	110 \pm 13	97 \pm 4	92 \pm 8	87 \pm 12	95 \pm 16
10 μ M Histamine	415 \pm 37	448 \pm 41	464 \pm 25	396 \pm 59	464 \pm 19	305 \pm 46*	197 \pm 13**
60 μ M lysoPtdCho	72 \pm 9	77 \pm 20	70 \pm 18	78 \pm 12	70 \pm 7	95 \pm 22	81 \pm 24
10 μ M Histamine	116 \pm 17	120 \pm 18	111 \pm 29	166 \pm 13*	192 \pm 8**	145 \pm 30	112 \pm 7
60 μ M lysoPtdCho							

Ea hy 926 cells were pre-incubated for 24 h in a control culture medium or in a medium containing ARA, EPA, or DHA at the indicated concentrations in the presence or not of 60 μ M LysoPtdCho. Then, the cells were incubated with 10 μ M [3H] L-arginine in the presence or absence of 10 μ M histamine for 10 min to test eNOS activity. Citrulline production was expressed as percentage of citrulline liberated in control cells. Each value represents mean \pm SEM of four independent experiments. Asterisks in the column indicate a significant difference between control cells and EPA or DHA treated cells (* $p < 0.05$; ** $p < 0.01$)

of EPA on eNOS activation. By contrast, the presence of 50 μ M DHA in the incubation medium of cells during 24 h did not restore the inhibitory effect of LysoPtdCho on phosphorylation of eNOS. Similarly, the presence of 90 μ M ARA in the incubation medium during 24 h did not protect the cells from the deleterious effect of LysoPtdCho on the phosphorylation of eNOS.

Effect of LysoPtdCho on Intracellular ROS Generation

The generation of ROS, as measured using CM-H₂DCFDA probe was investigated in cells exposed to LysoPtdCho in the

presence or absence of ARA, EPA, or DHA for 2, 4, and 24 h (Fig. 5). With LysoPtdCho alone, ROS generation was slightly, but significantly increased after 2 h, then returned to basal level at 4 h until 24 h. Treatment of cells with ARA or EPA even in the presence of LysoPtdCho did not change the level of ROS with respect to cells incubated in the control culture medium. In contrast, treatment of cells for 24 h with DHA alone led to a three-fold increase in ROS generation. When the cells were incubated in the presence of LysoPtdCho and DHA, we observed an important production of ROS after 2 and 4 h and a more higher production of ROS at 24 h (eight-fold increase versus control).

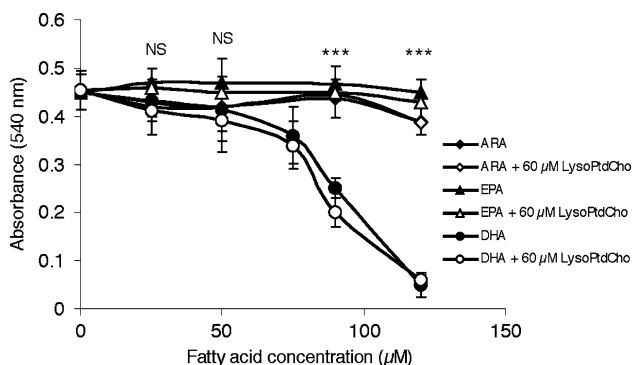


Fig. 3 Effect of LysoPtdCho and PUFAs on cell viability assessed by the MTT test in Ea hy 926 cells. Cells were incubated for 24 h in a culture medium containing the indicated concentrations of PUFAs in the presence or absence of 60 µM LysoPtdCho. The results correspond to the absorbance of formazan determined at 540 nm. Each symbol indicates mean ± SEM of three experiments (each experiment was carried out in triplicate). ***: significant difference ($p < 0.05$), ARA or EPA versus DHA group; NS: non-significant difference

Effect of ARA, EPA, or DHA on Conjugated Dienes Generation

Conjugated dienes were evaluated in Ea hy 926 cells incubated for 24 h with or without 60 µM LysoPtdCho in control or in ARA-, EPA-, or DHA-supplemented medium. As shown in Fig. 6, the conjugated dienes content of ARA-, EPA-, and DHA- enriched cells did not change as compared with control cells. The presence of 60 µM LysoPtdCho in the cells incubation medium induced no

further generation of conjugated dienes neither in control cells nor in cells grown in ARA- or EPA-supplemented medium, but significantly increased the conjugated dienes content of DHA treated cells.

Effect of ARA, EPA, or DHA Supplementation in the Incubation Medium on Fatty Acids Enrichment of Ea hy 926 Cells

Incubation of Ea hy 926 cells during 24 h with different concentrations of ARA (90 or 120 µM), EPA (50, 90, or 120 µM) or DHA (25 or 50 µM) significantly and dose-dependently increased the cell content of each added PUFA in cell phospholipids (Fig. 7d, a, c). The supplementation with EPA led also to an important dose-dependent enrichment of cells in docosapentaenoic acid (DPA, C22:5n-3) (Fig. 7b), indicating a significant elongation of EPA in DPA. By contrast, no further desaturation of DPA in DHA occurred and the DHA level in EPA-supplemented cells was even significantly decreased with 90 and 120 µM EPA (Fig. 7c). The concomitant addition of 60 µM LysoPtdCho to either ARA-, EPA-, or DHA- enriched medium did not modify the incorporation of either ARA, EPA, or DHA in cell structure in comparison with cells treated with ARA, EPA, or DHA alone (Fig. 7a, c, d). However, the presence of LysoPtdCho in EPA-treated cells significantly reduced the enrichment of the membranes in DPA in comparison with EPA-treated cells (Fig. 7b) suggesting that LysoPtdCho modifies the elongation of EPA or the structure or remodeling of phospholipids.

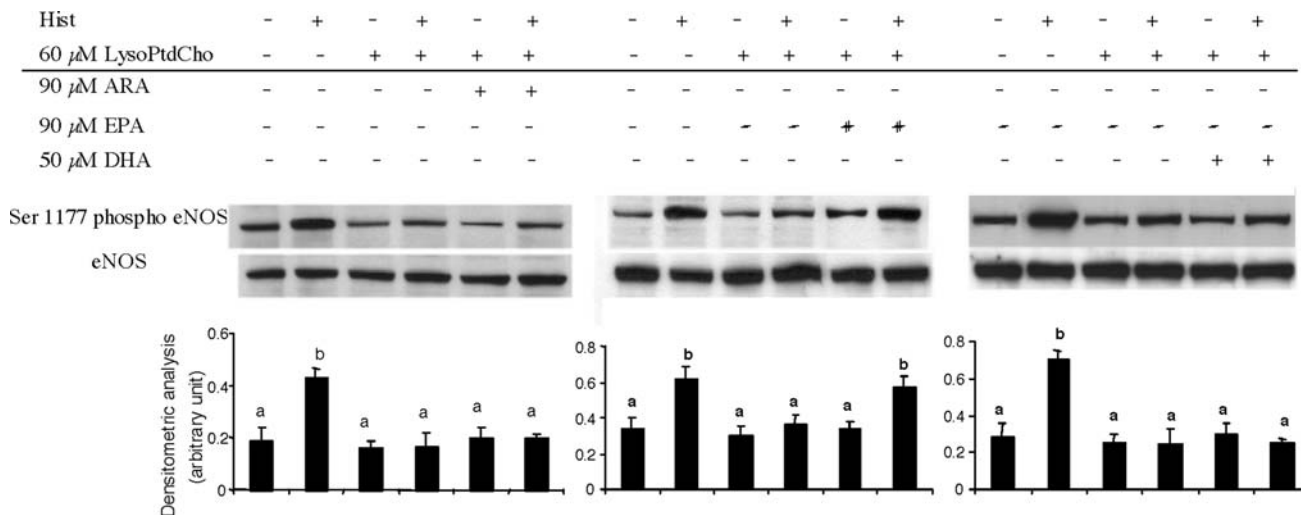


Fig. 4 Effect of ARA, EPA, or DHA on the impairment by 60 µM LysoPtdCho of histamine-induced phosphorylation of eNOS. Ea hy 926 cells were pre-incubated for 24 h with 60 µM LysoPtdCho added or not of 90 µM EPA or ARA or 50 µM DHA. Then, the cells were stimulated with 10 µM histamine for 10 min. Proteins of cell lysates were analysed by western blotting using anti-Ser1177 phospho-eNOS and eNOS antibodies. The blots presented are representative of four

independent experiments. The results of the densitometric analysis of blots (Ser 1177 P-eNOS/eNOS) are summarized at the bottom of the figure. Each column represents the mean ± SEM of 3–4 independent experiments. Different letters indicate a significant difference between groups ($p < 0.05$), the same letter indicates no significant difference between groups

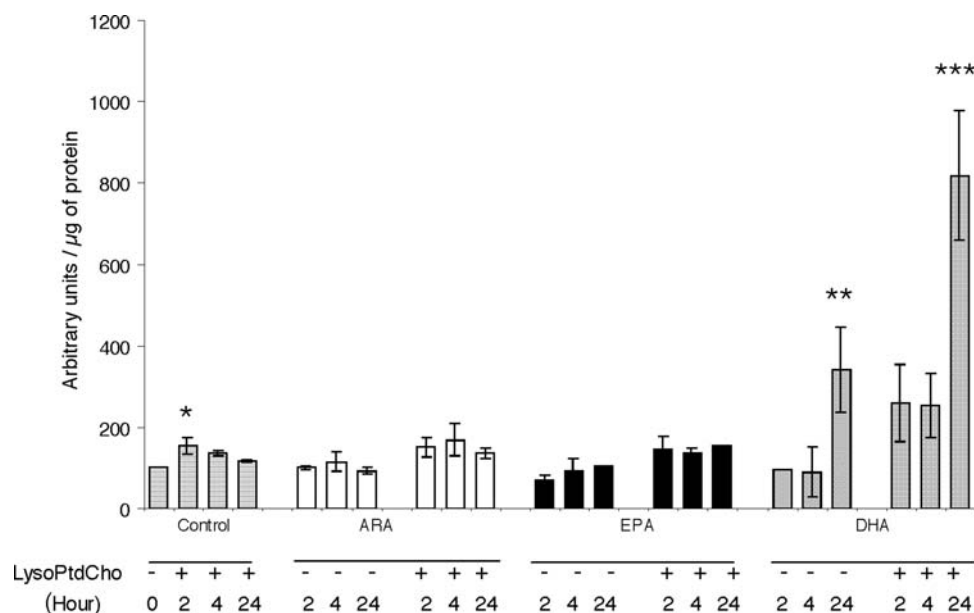


Fig. 5 Intracellular ROS generation in Ea hy 926 cells exposed to LysoPtdCho during different time periods in the presence of ARA, EPA, or DHA. Ea hy 926 cells were pre-incubated with 60 μ M LysoPtdCho in the presence or absence of 90 μ M ARA or 90 μ M EPA or 50 μ M DHA from 2 to 24 h. Then, the cells were loaded with 10 μ M CM-H₂DCFDA during 30 min. After washing, DCF

fluorescence of cells was analyzed at 485/535 nm (excitation/emission). Each column indicates the mean \pm SEM of DCF fluorescence per μ g of proteins. Asterisks indicate a significant difference between control cells without LysoPtdCho treatment and DHA treated cells (*** p < 0.001; ** p < 0.01; * p < 0.05)

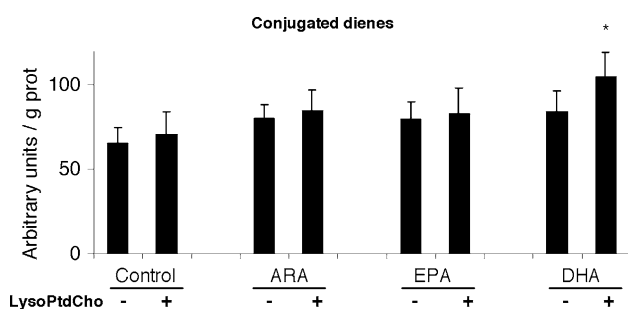


Fig. 6 Effect of ARA, EPA, or DHA on conjugated dienes content of cells. Ea hy 926 cells were incubated with 90 μ M ARA or 90 μ M EPA or 50 μ M DHA in the presence or absence of 60 μ M LysoPtdCho for 24 h. After washing, the cells were harvested in 1.6% NaCl, 0.02% EDTA. After lipid extraction in chloroform:methanol 2:1 (v:v), conjugated dienes were measured by UV absorbance at 235 nm. Each column indicates the mean \pm SEM of arbitrary units/g of proteins (n = 4 separate experiments). Asterisk indicates a significant difference with control cells (* p < 0.05)

Discussion

The present results demonstrate that the chronic incubation of Ea hy 926 endothelial cells with LysoPtdCho decreased the stimulating effect of histamine on eNOS activity. The incorporation of EPA in cell phospholipids prevented this deleterious effect of LysoPtdCho. Conversely, the presence of DHA in similar conditions displayed deleterious effects on endothelial function by decreasing histamine-induced eNOS activation and increasing the oxidative stress (ROS

generation and conjugated dienes). In contrast, ARA had no effect on either histamine-induced eNOS activation on ROS or conjugated dienes formation.

The present study was designed to simulate the pathophysiological status of endothelial cells of the arterial wall continuously exposed to oxidized LDL in vivo during the atherosclerotic process. Thus we exposed Ea hy 926 cells for 24 h to LysoPtdCho, which is a major component of oxidized LDL playing an important role in the alteration of endothelial function during atherosclerosis development. In these conditions, LysoPtdCho induced a decrease in the stimulating effect of histamine on eNOS activity and a concomitant decrease in Ser 1177 eNOS phosphorylation. This result is in agreement with the decreased endothelial release of NO by LysoPtdCho as reported in the literature [26, 27]. Several mechanisms have been proposed to explain the effect of LysoPtdCho including a decrease of arginine availability due to an inactivation of the arginine transporter [28], an increased production of asymmetric dimethyl arginine (ADMA), an endogenous eNOS inhibitor [29], or still a decrease in eNOS expression [30]. In the present work, we showed that the chronic exposition of cells to LysoPtdCho similarly impaired both the histamine-induced activity and the histamine-induced Ser 1177 phosphorylation of eNOS suggesting that a kinase signaling pathway could be involved in the impairment of eNOS activity by LysoPtdCho. In contrast, LysoPtdCho did not modify the total eNOS expression, contrary to the result

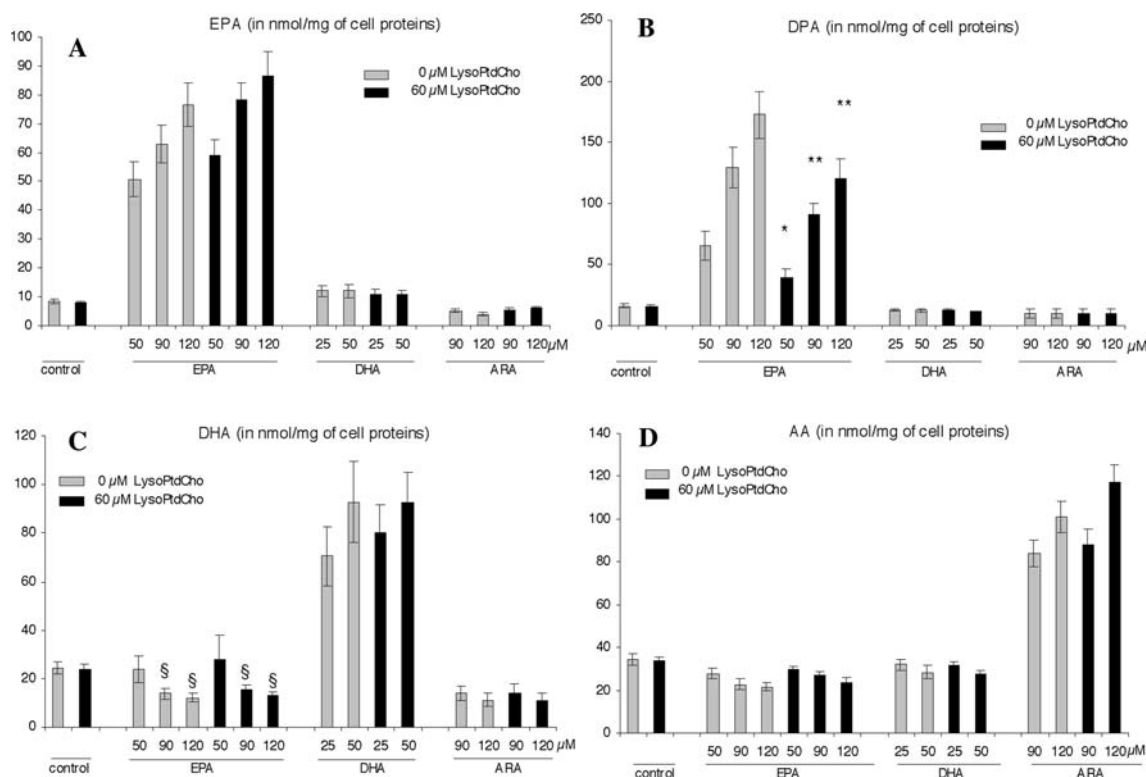


Fig. 7 Effect of the supplementation of the culture medium in ARA, EPA, or DHA in the presence or absence LysoPtdCho on the incorporation of ARA, EPA, and DHA in Ea hy 926 cells. Ea hy 926 cells were incubated with increasing concentrations of ARA, EPA, or DHA in the presence or absence of 60 μ M LysoPtdCho during 24 h. After washing, the cells were lysed in chloroform–methanol 2/1 (v/v) and fatty acids were extracted. Fatty acids were trans-methylated with BF₃-methanol and the methyl esters were analyzed by gas

chromatography. The content of cells in EPA (a), DPA (b), DHA (c), and ARA (d) was expressed in nmol/mg of cell proteins. Each column represents the mean \pm SEM of 4 separate experiments. Asterisks (*) indicate a significant difference between EPA and (EPA + LysoPtdCho)-treated cells for DPA content in the cells (* p < 0.05; ** p < 0.01). § indicate a significant difference between treated and control cells (in absence of LysoPtdCho) (§ p < 0.05)

reported in HUVEC with a very high concentration of 100 μ M LysoPtdCho often considered as a detergent [31]. Yet the 60 μ M LysoPtdCho concentration used in our culture medium is higher than the concentrations used in other studies [30, 32], but our medium contained antioxidants and albumin which is able to bind a part of LysoPtdCho as in physiological conditions.

Besides its effect on eNOS activity, LysoPtdCho can also impair NO availability by its capacity to generate superoxide anions which scavenge NO three times faster than their degradation by superoxide dismutase [33]. The stimulation by LysoPtdCho of the production of superoxide anions in endothelial cells has been attributed to a stimulation of NADPH oxidase [34, 35], or to a stimulation of the mitochondrial pathway [32]. The present study documented a significant increase of ROS generation after 2 h of exposition of Ea hy 926 cells to LysoPtdCho. However, the peak of ROS was obtained 2 h after incubation with LysoPtdCho and returned slowly to the basal level within 24 h, suggesting an adaptation of the cells to the oxidative stress by induction of antioxidant protective pathways as previously reported [36].

Concerning the chronic effects of PUFAs, we have demonstrated that the incorporation of ARA, DHA, and EPA in Ea hy 926 endothelial cells was proportional to the concentration of the three PUFAs in incubation medium, as previously reported [15]. EPA appeared more readily incorporated than DHA in Ea hy 926 phospholipids, since the cells accepted a concentration of 120 μ M EPA in the medium without apparent cellular toxicity, whereas cellular viability was impaired above 50 μ M DHA. Additionally, the conversion of DPA to DHA was not achieved in the EPA-treated cells and their DHA content was even largely decreased, probably in agreement with the human origin of the Ea hy 926 cell line characterized by their extremely low conversion of DPA to DHA as described in the literature [37].

The present study demonstrated different effects of EPA and DHA on the activation of eNOS by histamine. While EPA at a concentration of 90 or 120 μ M in the incubation medium did not modify the basal activity of eNOS nor the stimulating effect of histamine on eNOS, as reported by others [38], it decreased the deleterious effect of LysoPtdCho on the histamine-stimulated eNOS activity as well

as on the phosphorylation on Ser 1177 of eNOS. Such a protective effect was not observed in our previous study [15], when eNOS activity was measured in the presence of 25 mM glucose which is known to decrease NO production in endothelial cells [39] and when the cells were exposed to LysoPtdCho for a short time (15 min). The use of a physiological glucose concentration (5 mM) in the present study and the duration of exposure to LysoPtdCho may explain the differences between the non-similar effects of the PUFAs between the two studies. The mechanisms involved in the two conditions are probably also different. Our results were consistent with other studies which showed that EPA is able to induce eNOS translocation by dissociation from caveolin, eNOS phosphorylation, and NO synthesis in HUVECs [38]. By contrast, DHA was devoid of action on basal eNOS activity, but impaired histamine-induced eNOS activation and was unable to correct the deleterious effect of LysoPtdCho on histamine-stimulated eNOS activity or phosphorylation of Ser 1177. The difference between the two n-3 long chain PUFAs may be related to a higher membrane fluidity of endothelial cells grown in the presence of DHA than in the presence of EPA [40]. Such modifications in membrane properties may directly affect the functionality of membrane-bound proteins including eNOS or the accessibility of different membrane receptors including receptors for histamine or LysoPtdCho.

Our results also evidenced a difference between EPA and DHA in terms of ROS production and conjugated dienes formation, especially in the presence of LysoPtdCho. EPA and DPA are less unsaturated than DHA and may confer to the cells a lower sensitivity to radical attacks than DHA-enriched membranes [41]. Furthermore the incubation of cells with EPA induced a decrease of the membrane content in DHA. However, there are some discrepancies in the studies concerning the effect of DHA and EPA on lipid peroxide generation, either showing no modification [40] or showing a moderate increase of lipid peroxidation [42]. The amount of antioxidant compounds in the culture medium may partly explain these discrepancies. We also observed that the presence of LysoPtdCho in EPA-treated cells induced a decrease of DPA content in the cell membranes. Our study reported a large stimulation of ROS production at 24 h in cells cultured in the presence of DHA, especially in the presence of LysoPtdCho. This indicates probably that DHA must be incorporated in plasma membranes to become the target of free-radicals attack at their double bonds. This incorporation takes some time and explains the delayed effect of DHA on ROS production. The production of ROS was increased even more after concomitant exposure of cells to DHA and LysoPtdCho. The plasma membrane is probably modified by the presence of DHA and LysoPtdCho and the

antioxidant defense system located in plasma membranes becomes ineffective under such conditions. Similarly, oxidized LDL which contain large quantities of LysoPtdCho also induce ROS production in a time-dependent manner up to 4 days in monocytes/mononuclear cells [43].

In summary, the results of the present study show that the enrichment of Ea hy 926 cells with DHA favored ROS production in living cells, as already reported in an intestinal cell line [44] and aggravated the LysoPtdCho-induced oxidative stress. Furthermore, membrane DHA enrichment had no effect on basal eNOS activity, but impaired the stimulation of eNOS induced by histamine and was unable to correct the deleterious effect of LysoPtdCho on histamine-stimulated eNOS activity and Ser 1177 phosphorylation. By contrast, enrichment with EPA did not modify the ROS level produced in the presence or absence of LysoPtdCho, nor the basal eNOS activity and the stimulating effect of histamine on eNOS. However, it decreased the deleterious effect of LysoPtdCho on the histamine-stimulated eNOS activity as well as on the phosphorylation on Ser 1177 of eNOS. The dietary supplementation with n-3 PUFA is an increasing practice which could be justified by the beneficial role of EPA in vascular diseases. However, high intake of such fatty acids may have deleterious effects on endothelial cells, in particular those situations involving oxidative stress in which the balance between the synthesis of nitric oxide and its inactivation by oxidative stress may be unbalanced or improved by PUFAs. Oxidation susceptibility of n-3 PUFA requires to be counterbalanced by antioxidants. In-vivo human studies conducted in dyslipidemic subjects, have effectively demonstrated the positive potentials in combining n-3 PUFA dietary supplementation with vitamin E, niacin and γ -oryzanol to improve the lipid pattern, decrease serum ROS concentration and increase the total antioxidant capacity of serum together [45]. Convincing beneficial effects of a combination of vitamin E, vitamin C, and L-arginine, the natural precursor of NO, have been provided both on eNOS and oxidation-sensitive gene expression in human endothelial cells exposed to shear stress *in vitro* and *in vivo* [46]. Recently, nanomolar concentrations of DHA applied for 7 days on human coronary endothelial cells increased weak expression of eNOS in response to Akt kinase activation [47]. The effects of n-3 PUFAs remain conflicting between different experimental models and further studies will be required to confirm the real effects of DHA and EPA on atherogenesis. By contrast ARA a n-6 PUFA had no effect on ROS generation or eNOS activity in the basal state or after histamine-induced stimulation.

Acknowledgments The authors would like to thank Anne-Marie Gueugneau and Jean-Paul Macaire for their expert technical assistance and Kim NG Bonaventure for carefully reading the manuscript.

References

- Chen L, Liang B, Froese DE, Liu S, Wong JT, Tran K, Hatch GM, Mymin D, Kroeger EA, Man RY, Choy PC (1997) Oxidative modification of low density lipoprotein in normal and hyperlipidemic patients: effect of lysophosphatidylcholine composition on vascular relaxation. *J Lipid Res* 38:546–553
- Stiko A, Regnstrom J, Shah PK, Cercek B, Nilsson J (1996) Active oxygen species and lysophosphatidylcholine are involved in oxidized low density lipoprotein activation of smooth muscle cell DNA synthesis. *Arterioscler Thromb Vasc Biol* 16:194–200
- Portman OW, Alexander M (1969) Lysophosphatidylcholine concentrations and metabolism in aortic intima plus inner media: effect of nutritionally induced atherosclerosis. *J Lipid Res* 10:158–165
- Matsumoto T, Kobayashi T, Kamata K (2007) Role of lysophosphatidylcholine (LPC) in atherosclerosis. *Curr Med Chem* 14: 3209–3220
- Kume N, Cybulsky MI, Gimbrone MA Jr (1992) Lysophosphatidylcholine, a component of atherogenic lipoproteins, induces mononuclear leukocyte adhesion molecules in cultured human and rabbit arterial endothelial cells. *J Clin Invest* 90:1138–1144
- Takabe W, Kanai Y, Chairoungdua A, Shibata N, Toi S, Kobayashi M, Kodama T, Noguchi N (2004) Lysophosphatidylcholine enhances cytokine production of endothelial cells via induction of L-type amino acid transporter 1 and cell surface antigen 4F2. *Arterioscler Thromb Vasc Biol* 24:1640–1645
- Millanvoye-Van Brussel E, Topal G, Brunet A, Do Pham T, Deckert V, Rendu F, David-Dufilho M (2004) Lysophosphatidylcholine and 7-oxocholesterol modulate Ca²⁺ signals and inhibit the phosphorylation of endothelial NO synthase and cytosolic phospholipase A2. *Biochem J* 380:533–539
- Harada-Shiba M, Kinoshita M, Kamido H, Shimokado K (1998) Oxidized low density lipoprotein induces apoptosis in cultured human umbilical vein endothelial cells by common and unique mechanisms. *J Biol Chem* 273:9681–9687
- Takahashi M, Okazaki H, Ogata Y, Takeuchi K, Ikeda U, Shimada K (2002) Lysophosphatidylcholine induces apoptosis in human endothelial cells through a p38-mitogen-activated protein kinase-dependent mechanism. *Atherosclerosis* 161:387–394
- Jia SJ, Jiang DJ, Hu CP, Zhang XH, Deng HW, Li YJ (2006) Lysophosphatidylcholine-induced elevation of asymmetric dimethylarginine level by the NADPH oxidase pathway in endothelial cells. *Vascul Pharmacol* 44:143–148
- Heinloth A, Heermeier K, Raff U, Wanner C, Galle J (2000) Stimulation of NADPH oxidase by oxidized low-density lipoprotein induces proliferation of human vascular endothelial cells. *J Am Soc Nephrol* 11:1819–1825
- von Schacky C, Harris WS (2007) Cardiovascular benefits of omega-3 fatty acids. *Cardiovasc Res* 73:310–315
- Omura M, Kobayashi S, Mizukami Y, Mogami K, Todoroki-Ikeda N, Miyake T, Matsuzaki M (2001) Eicosapentaenoic acid (EPA) induces Ca²⁺-independent activation and translocation of endothelial nitric oxide synthase and endothelium-dependent vasorelaxation. *FEBS Lett* 487:361–366
- Biscione F, Pignalberi C, Totteri A, Messina F, Altamura G (2007) Cardiovascular effects of omega-3 free fatty acids. *Curr Vasc Pharmacol* 5:163–172
- Gousset-Dupont A, Robert V, Grynberg A, Lacour B, Tardivel S (2007) The effect of n-3 PUFA on eNOS activity and expression in Ea hy 926 cells. *Prostaglandins Leukot Essent Fatty Acids* 76:131–139
- Edgell CJ, McDonald CC, Graham JB (1983) Permanent cell line expressing human factor VIII-related antigen established by hybridization. *Proc Natl Acad Sci USA* 80:3734–3737
- Pech-Amsellem MA, Myara I, Storogenko M, Demuth K, Proust A, Moatti N (1996) Enhanced modifications of low-density lipoproteins (LDL) by endothelial cells from smokers: a possible mechanism of smoking-related atherosclerosis. *Cardiovasc Res* 31:975–983
- May JM, Qu ZC, Li X (2003) Ascorbic acid blunts oxidant stress due to menadione in endothelial cells. *Arch Biochem Biophys* 411:136–144
- Delerive P, Oudot F, Ponsard B, Talpin S, Sergiel JP, Cordelet C, Athias P, Grynberg A (1999) Hypoxia-reoxygenation and polyunsaturated fatty acids modulate adrenergic functions in cultured cardiomyocytes. *J Mol Cell Cardiol* 31:377–386
- Huang A, Thomas SR, Keaney JF Jr (2002) Measurements of redox control of nitric oxide bioavailability. *Methods Enzymol* 359:209–216
- Weissman BA, Gross SS (2001) Measurement of NO and NO synthase. *Curr Protoc Neurosci*, Chapter 7: Unit7.13
- Combet S, Balligand JL, Lameire N, Goffin E, Devuyst O (2000) A specific method for measurement of nitric oxide synthase enzymatic activity in peritoneal biopsies. *Kidney Int* 57:332–338
- Folch J, Lees M, Sloane Stanley GH (1957) A simple method for the isolation and purification of total lipides from animal tissues. *J Biol Chem* 226:497–509
- Rousseau D, Helies-Toussaint C, Moreau D, Raederstorff D, Grynberg A (2003) Dietary n-3 PUFAs affect the blood pressure rise and cardiac impairments in a hyperinsulinemia rat model in vivo. *Am J Physiol Heart Circ Physiol* 285:H1294–H1302
- Grau A, Guardiola F, Boatella J, Baucells MD, Codony R (2000) Evaluation of lipid ultraviolet absorption as a parameter to measure lipid oxidation in dark chicken meat. *J Agric Food Chem* 48:4128–4135
- Deng HF, Xiong Y (2005) Effect of pravastatin on impaired endothelium-dependent relaxation induced by lysophosphatidylcholine in rat aorta. *Acta Pharmacol Sin* 26:92–98
- Yokoyama M, Hirata K, Miyake R, Akita H, Ishikawa Y, Fukuzaki H (1990) Lysophosphatidylcholine: essential role in the inhibition of endothelium-dependent vasorelaxation by oxidized low density lipoprotein. *Biochem Biophys Res Commun* 168:301–308
- Dudek R, Wildhirt S, Suzuki H, Winder S, Bing RJ (1995) Intracellular translocation of endothelial nitric oxide synthase by lysophosphatidylcholine. *Pharmacology* 50:257–260
- Cooke JP (2000) Does ADMA cause endothelial dysfunction? *Arterioscler Thromb Vasc Biol* 20:2032–2037
- Safaya R, Chai H, Kougiyas P, Lin P, Lumsden A, Yao Q, Chen C (2005) Effect of lysophosphatidylcholine on vasomotor functions of porcine coronary arteries. *J Surg Res* 126:182–188
- Zembowicz A, Tang JL, Wu KK (1995) Transcriptional induction of endothelial nitric oxide synthase type III by lysophosphatidylcholine. *J Biol Chem* 270:17006–17010
- Watanabe N, Zmijewski JW, Takabe W, Umez-Goto M, Le Goffe C, Sekine A, Landar A, Watanabe A, Aoki J, Arai H, Kodama T, Murphy MP, Kalyanaraman R, Darley-Usmar VM, Noguchi N (2006) Activation of mitogen-activated protein kinases by lysophosphatidylcholine-induced mitochondrial reactive oxygen species generation in endothelial cells. *Am J Pathol* 168:1737–1748
- Thomson L, Trujillo M, Telleri R, Radi R (1995) Kinetics of cytochrome c²⁺ oxidation by peroxynitrite: implications for superoxide measurements in nitric oxide-producing biological systems. *Arch Biochem Biophys* 319:491–497
- Kugiyama K, Sugiyama S, Ogata N, Oka H, Doi H, Ota Y, Yasue H (1999) Burst production of superoxide anion in human endothelial cells by lysophosphatidylcholine. *Atherosclerosis* 143:201–204
- Takeshita S, Inoue N, Gao D, Rikitake Y, Kawashima S, Tawa R, Sakurai H, Yokoyama M (2000) Lysophosphatidylcholine enhances superoxide anions production via endothelial NADH/NADPH oxidase. *J Atheroscler Thromb* 7:238–246

36. Rossary A, Arab K, Steghens JP (2007) Polyunsaturated fatty acids modulate NOX 4 anion superoxide production in human fibroblasts. *Biochem J* 406:77–83
37. Williams CM, Burdge G (2006) Long-chain n-3 PUFA: plant v marine sources. *Proc Nutr Soc* 65:42–50
38. Li Q, Zhang Q, Wang M, Zhao S, Ma J, Luo N, Li N, Li Y, Xu G, Li J (2007) Eicosapentaenoic acid modifies lipid composition in caveolae and induces translocation of endothelial nitric oxide synthase. *Biochimie* 89:169–177
39. Cai S, Khoo J, Channon KM (2005) Augmented BH4 by gene transfer restores nitric oxide synthase function in hyperglycemic human endothelial cells. *Cardiovasc Res* 65:823–831
40. Hashimoto M, Hossain S, Yamasaki H, Yazawa K, Masumura S (1999) Effects of eicosapentaenoic acid and docosahexaenoic acid on plasma membrane fluidity of aortic endothelial cells. *Lipids* 34:1297–1304
41. Liu J, Yeo HC, Doniger SJ, Ames BN (1997) Assay of aldehydes from lipid peroxidation: gas chromatography-mass spectrometry compared to thiobarbituric acid. *Anal Biochem* 245:161–166
42. Gilbert M, Dalloz S, Maclouf J, Lagarde M (1999) Differential effects of long chain n-3 fatty acids on the expression of PGH synthase isoforms in bovine aortic endothelial cells. *Prostaglandins Leukot Essent Fatty Acids* 60:363–365
43. Chen JW, Chen YH, Lin SJ (2006) Long-term exposure to oxidized low-density lipoprotein enhances tumor necrosis factor-alpha-stimulated endothelial adhesiveness of monocytes by activating superoxide generation and redox-sensitive pathways. *Free Radic Biol Med* 40:817–826
44. Roig-Perez S, Guardiola F, Moreto M, Ferrer R (2004) Lipid peroxidation induced by DHA enrichment modifies paracellular permeability in Caco-2 cells: protective role of taurine. *J Lipid Res* 45:1418–1428
45. Accinni R, Rosina M, Bamonti F, Della Noce C, Tonini A, Bernacchi F, Campolo J, Caruso R, Novembrino C, Ghersi L, Lonati S, Grossi S, Ippolito S, Lorenzano E, Ciani A, Gorini M (2006) Effects of combined dietary supplementation on oxidative and inflammatory status in dyslipidemic subjects. *Nutr Metab Cardiovasc Dis* 16:121–127
46. de Nigris F, Lerman LO, Ignarro SW, Sica G, Lerman A, Palinski W, Ignarro LJ, Napoli C (2003) Beneficial effects of antioxidants and L-arginine on oxidation-sensitive gene expression and endothelial NO synthase activity at sites of disturbed shear stress. *Proc Natl Acad Sci USA* 100:1420–1425
47. Stebbins CL, Stice JP, Hart M, Mbai FN, Knowlton ARA (2008) Effects of dietary decosahexaenoic acid (DHA) on eNOS in human coronary artery endothelial cells. *J Cardiovasc Pharmacol Ther* 13:261–268

Early Dissimilar Fates of Liver Eicosapentaenoic Acid in Rats Fed Liposomes or Fish Oil and Gene Expression Related to Lipid Metabolism

Maud Sabine Cansell · Aurélie Battin ·
Pascal Degrace · Joseph Gresti · Pierre Clouet ·
Nicole Combe

Received: 29 August 2008 / Accepted: 18 December 2008 / Published online: 21 January 2009
© AOCS 2009

Abstract The study was undertaken to determine whether eicosapentaenoic acid (EPA, 20:5 n-3) and docosahexaenoic acid (DHA, 22:6 n-3), esterified in phospholipids (PL) as liposomes or in triglycerides (TG) as oil, exhibited comparable fates in liver lipids and whether these fates were associated with gene expressions related to fatty acid (FA) metabolism. PL and TG mixtures with close contents in EPA and DHA were administered to rats over 2 weeks. Most relevant events occurred after 3 days for both treatments. At that time, liposomes, compared with oil, increased the liver content in PL with a FA composition enriched in n-6 FA, comparable in DHA and much lower in EPA. Moreover, liposomes increased the activity and mRNA levels of carnitine palmitoyltransferase (CPT) I. In contrast, fish oil exerted opposite effects on CPT I and increased the genic expression of lipogenic enzymes. Liposomes, unlike fish oil, apparently increased the mRNA levels of acyl-CoA oxidase and the activity of the peroxisomal FA-oxidising system. Concomitantly, mRNA levels of hepatic lipoprotein receptors were increased with both diets, but intracellular proteins involved in free FA uptake and lipid synthesis were up-regulated only with liposome-treated rats. The quasi absence of EPA in hepatic PL of

liposome-treated rats on the short term could result from increased β -oxidation activities through metabolic regulations induced by more available free EPA and other PUFA.

Keywords Liposomes · Fish oil · EPA · Hepatic and plasma lipids · Mitochondrial and peroxisomal oxidation · Enzymes for lipogenesis · Proteins and enzymes for lipid transport

Abbreviations

AA	Arachidonic acid
ACC	Acetyl-CoA carboxylase
ACO	Acyl-CoA oxidase
CS	Citrate synthase
CPT	Carnitine palmitoyltransferase
CTPpct	Phosphocholine cytidylyltransferase
DAG	Diacylglycerol
DGAT	Acyl-CoA:diacylglycerol acyltransferase
DHA	Docosahexaenoic acid
EPA	Eicosapentaenoic acid
FA	Fatty acid
FAS	Fatty acid synthase
FFA	Free fatty acids
FAT/CD36	Fatty acid translocase
GC	Gas chromatography
HAD	Hydroxyacyl-CoA dehydrogenase
LDL-R	LDL-receptor
LRP	Low density lipoprotein receptor-related protein
MAO	Monoamine oxidase
MUFA	Monounsaturated fatty acids
PFAOS	Peroxisomal FA-oxidising system
PPAR α	Peroxisome proliferator activated receptor α
PL	Phospholipids

M. S. Cansell (✉) · A. Battin
Laboratoire TREFLE UMR 8508, ISTAB,
Université Bordeaux I, Avenue des Facultés,
33405 Talence Cedex, France
e-mail: maud.cansell@u-bordeaux1.fr

P. Degrace · J. Gresti · P. Clouet
UMR 866 INSERM-UB, 21000 Dijon, France

N. Combe
Unité de Nutrition & Santé, ITERG,
33405 Talence Cedex, France

PUFA	Polyunsaturated fatty acids
SFA	Saturated fatty acids
TLC	Thin layer chromatography
TG	Triglycerides

Introduction

Polyunsaturated fatty acids (PUFA) of the n-3 series, especially eicosapentaenoic acid (EPA, 20:5 n-3) and docosahexaenoic acid (DHA, 22:6 n-3), have received considerable interest since they were associated with beneficial health effects regarding atherosclerotic vascular disease [1–3] or inflammatory disease [4, 5]. In this context, there is a growing interest to increase the intake of n-3 PUFA. Different strategies have been developed consisting in using food enriched in n-3 PUFA [6, 7], diets supplemented with marine oils [8, 9], free fatty acids (FFA) [10] or ethyl-fatty acid (FA) esters [11–13]. Furthermore, some studies have focussed on the difference in the chemical form of the FA esters because it may affect the absorption, distribution and metabolic fate of long-chain PUFA, especially when these are given as triglycerides (TG) or phospholipids (PL) [14–19].

Liposomes are currently prepared from different PL sources such as egg or soybean [20]. Phospholipids extracted from marine organisms were also used as they presented nutritional interests due to their high PUFA contents [21]. In marine lipid-based liposomes, PUFA were shown to be not very sensitive to oxidation under conditions resembling those within the gastrointestinal tract [21, 22]. Besides, marine PL were actively hydrolysed by phospholipase A₂ within preformed interfaces [21, 22]. These properties made it possible to use liposomes for PUFA supplementation and, thus, to compare the intestinal fate of marine lipid-based liposomes (PL essentially) with that of fish oil (TG essentially). In rats fed any dietary lipid source presenting a close FA composition, lymphatic TG and PL amounts were similar [23] and a hypotriglyceridemic effect was observed in both cases over the 2 weeks of the trial [24]. Fish oil induced a decrease in plasma PL over the whole period but, with liposomes, plasma PL decreased only after 3 days of treatment with progressive reversion to the initial value [24]. At the end of the two dietary treatments, FA compositions of plasma lipids strongly differed presumably resulting from the alteration of the liver lipid FA compositions with possible consequences on lipid-related regulations occurring during the first 2 weeks of the trial. The aim of the present study was therefore to determine whether EPA and DHA, esterified in PL as liposomes or in TG as oil, exhibited comparable effects on liver lipid metabolism. This was performed, first, through the determination of the time course distribution of the main PUFA

in the liver and plasma lipids of rats orally injected with liposomes or fish oil over 2 weeks. Second, we investigated whether the changes in liver FA distribution resulted from altered activities involved in EPA and other PUFA β -oxidation, and whether these changes were associated with the modification of the expression of genes related to lipid transport and esterification.

Experimental Procedure

Animals and Diets

Official French regulations for the care and use of laboratory animals were followed. Five-week-old male Wistar rats weighing 250–300 g obtained from Elevage Janvier (Saint-Berthein, France) were housed in a controlled environment with constant temperature ($21 \pm 1^\circ\text{C}$) and humidity (50%). They were fed ad libitum a standard diet (AO4, UAR, Epinay, France) for 5 days, then a fat-free diet (UAR) for 2 days before and during the supplementation experiments. Every morning of the experimental period, they were injected, through a gastric cannula, with 3 g of lipids per kg of body weight as either fish oil (rich in TG) or liposome suspension (rich in PL [23, 24]). The lipid source referred to as fish oil was composed of a mixture of a n-3 PUFA rich oil derived from several fish oils (EPAX 2050 TG, Polaris, France), a commercial vegetable oil and cholesterol (Sigma, Saint Quentin Fallavier, France) to balance the lipid species and FA compositions of the liposome suspension based on a crude marine lipid extract. This allowed the accurate comparison of fates of EPA and DHA originating from fish oil and liposomes. For both diets, n-3 PUFA, n-6 PUFA and cholesterol contents were adjusted to get a final fat bulk providing $\sim 9.3\%$ of energy. In particular, EPA and DHA represented 19 and 39% of total FA in fish oil, and 15 and 37% of total FA in liposomes, respectively. Lipid classes and their FA compositions as well as liposome preparation have been previously detailed [21, 23–25]. At least four rats were killed each time: on day 0 as common controls, thereafter on days 3, 7 and 13, on both lipid treatments. The animals were killed after pentobarbital anesthesia, their livers were removed, washed with a saline solution (9% NaCl), blotted and weighed. One part of the livers was immediately used for the isolation of a mitochondrial fraction as already described [26], while the remaining part was stored at -20°C for further analysis.

Analytical Methods

Total lipids from liver samples with glyceryl triheptadecanoate and 1,2-dipentadecanoyl-*sn*-glycero-3-phosphocholine added as internal standards for further TG and PL

quantification, respectively, were extracted with 20 vol of chloroform/methanol (2:1, v/v) according to the method of Folch et al. [27]. TG and PL were separated by thin layer chromatography using hexane/ether/methanol/acetic acid (90:20:3:2 by vol) as a developing solvent. The Merck silica gel (60G) glass plates (20 × 20 cm, 0.5 mm thickness) were previously activated at 110 °C for 1 h. FA of TG and PL were transmethylated by boron trifluoride-methanol complex [28] and their methyl esters were analysed by gas chromatography (GC) separation on a Carbowax 20 M capillary column (30 m long, 0.32 mm i.d., helium as a carrier gas). The GC system was a gas chromatograph Packard (model 438) equipped with a flame ionisation detector Shimadzu CR3A. The injector and the detector were maintained at 230 °C. The column temperature was first fixed at 80 °C for 1 min, then increased from 80 to 170 °C over 3 min and from 170 to 210 °C over 10 min. The monitored FA-related peak surfaces were treated by a Shimadzu integration system. FA from Sigma France and natural extracts of known composition were used as standards for column calibration.

Hepatic Enzyme Activities

The content of liver in mitochondria was indirectly estimated through the determination of activities of monoamine oxidase (MAO) [29] and citrate synthase (CS) [30], as marker enzymes of mitochondrial outer membranes and matrix, respectively, and in peroxisomes through the determination of urate oxidase activity [31]. Carnitine palmitoyltransferase (CPT) I activity was measured on isolated mitochondrial fractions as previously detailed [26]. The measurement of CN⁻-insensitive palmitoyl-CoA-dependent NAD⁺ reduction [32], described as the peroxisomal FA-oxidising system (PFAOS), gave specific information about the peroxisomal very long chain FA β -oxidation capacity. Measurements of MAO, CS, urate oxidase and PFAOS activities were performed on crude liver homogenates and were expressed per g of liver.

Gene Expression

Total mRNA was extracted from the livers by the Tri-Reagent method adapted from the procedure of Chomczynski and Sacchi [33]. Tri-Reagent was provided by Euromedex (Souffelweyersheim, France). Total mRNA was reverse-transcribed using the Iscript cDNA kit (Bio-Rad). Real-time PCR was performed as described previously in a 96-well plate using an iCycler iQ (Bio-Rad) [34]. Primer pairs were designed using 'Primers!' software and were synthesised by MWG-Biotech AG (Ebersberg, Germany). The sequences of the forward and reverse primers used were: 5'-atcgagcaggatagag-3' and 5'-accacctgtcaagcatcttc-3'

for CPT I; 5'-aggagcgtcttgaaaacag-3' and 5'-actctcgcaaaagaatggc-3' for hydroxyacyl-CoA dehydrogenase (HAD); 5'-cgaactgtccgctacttc-3' and 5'-tgagttaccccaaatgc-3' for peroxisome proliferator activated receptor α (PPAR α); 5'-aggtggctgtaagaagagtgc-3' and 5'-ccgagatgccatattccctc-3' for acyl-CoA oxidase (ACO); 5'-gctgggggactcagaat-3' and 5'-aggaaaagcagtaccgaac-3' for acetyl-CoA carboxylase (ACC) 1; 5'-cctgatagtgcgggaaag-3' and 5'-tctgggtggtcgaataacttg-3' for fatty acid synthase (FAS); 5'-gcctacgctgtttctcacc-3' and 5'-ggcctcgccattagaatg-3' for low density lipoprotein receptor-related protein (LRP); 5'-tgggtcca taggtttctg-3' and 5'-ttgggatcaggctggtat-3' for LDL-receptor (LDL-R); 5'-tccagaaccagacaacca-3' and 5'-ccaatg ccagcacacata-3' for fatty acid translocase (FAT/CD36); 5'-tcctaccgggatgcaatct-3' and 5'-ctcgtagtgcaggtgtgcc-3' for diacylglycerol acyltransferase (DGAT1); 5'-gattgattcgtc gccat-3' and 5'-cctgctcttgatgtgctta-3' for phosphocholine cytidylyltransferase (CTPpct); 5'-tgagcttagcgttcttttg-3' and 5'-agctttcttggggtcagc-3' for HMG-CoA reductase; 5'-aga-gtaatacatgccgacg-3' and 5'-accgggtggtttgatct-3' for 18S. Data were analysed using the Bio-Rad software and Microsoft Excel. The relative gene expression quantitation was calculated from standard curves for each gene established using four dilutions (1/10–1/10,000) of cDNA positive controls and normalised with 18S.

Statistical Analysis

Differences between the two groups were tested for significance by using the ANOVA or Fisher's *t* tests and were considered significant at *P* < 0.05. Data were expressed as mean values \pm SEM.

Results

Fatty Acid Contents of Liver and Plasma Lipids

Between the common starting time (day 0) and day 13 on the diet supplemented with fish oil or liposomes, variations of very low amplitude were observed in liver TG, expressed as their contents in total FA (Fig. 1a, dotted lines). Over the 13 days, for both treatments, the amounts of total FA in TG remained under 5 mg/g of liver (Fig. 1a, dotted lines) and under 2 mg/g of liver for saturated fatty acids (SFA) (Fig. 1b, dotted lines) and monounsaturated fatty acids (MUFA) (Fig. 1c, dotted lines). Regardless of the treatment, the content of TG in the main FA of n-3 and n-6 families remained under 1 mg/g of liver (Figs. 2, 3, dotted lines). From 25 mg of total FA in PL per g of liver at the beginning of the trial period, an increase reaching 27 and 30 mg/g of liver was observed after 3 days of fish oil or liposome treatment, respectively. Over the whole period,

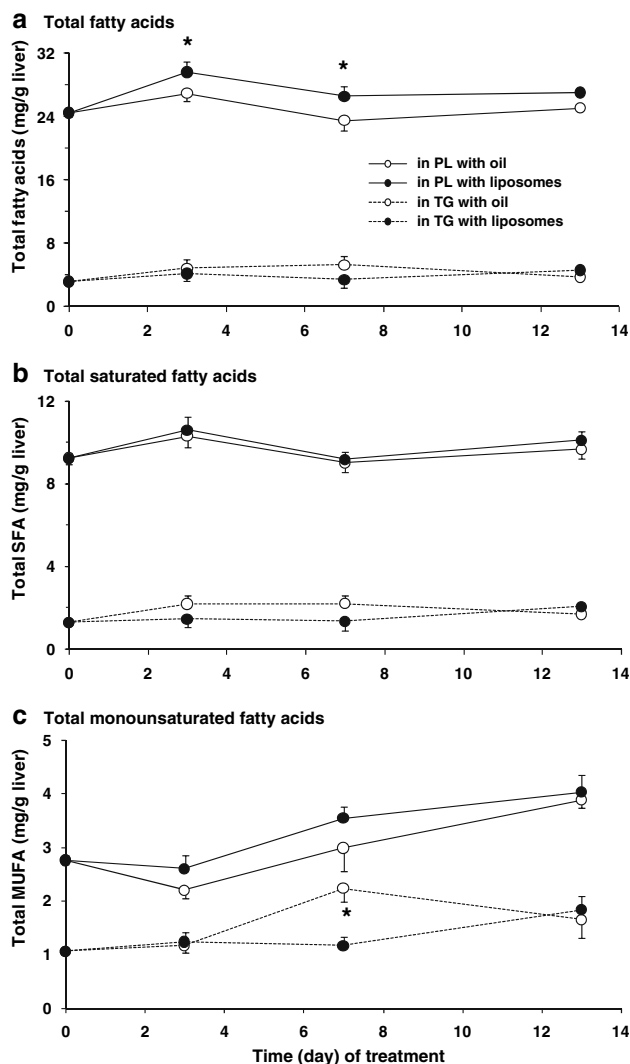


Fig. 1 Time course content in total (a), saturated (b) and monounsaturated (c) fatty acids of TG and PL in the liver of rats fed fish oil or liposomes over 13 days. Values of each point (with symbols defined in a) are means \pm SEM ($n \geq 4$ rats). Means at a time on either lipid source, given with an asterisk, differ at $P < 0.05$

the values expressed per g of liver with the liposome group were significantly greater (~ 3 mg) than with the fish oil group (Fig. 1a, continuous lines). As regards SFA and MUFA that originated from dietary source, lipogenesis, and possibly desaturation, there was no statistical difference between values obtained from fish oil and liposome groups at any time of the trial (Fig. 1b, c, continuous lines). In total FA of liver PL, 12% were n-3 PUFA, with more than 90% represented by EPA and DHA. Between days 0 and 3, DHA contents of liver PL increased nearly similarly with both diets (Fig. 2a, continuous lines), while the enrichment in EPA of PL was 4 times lower with liposomes than with fish oil (Fig. 2b, continuous lines). Concomitantly, there were significant greater contents in

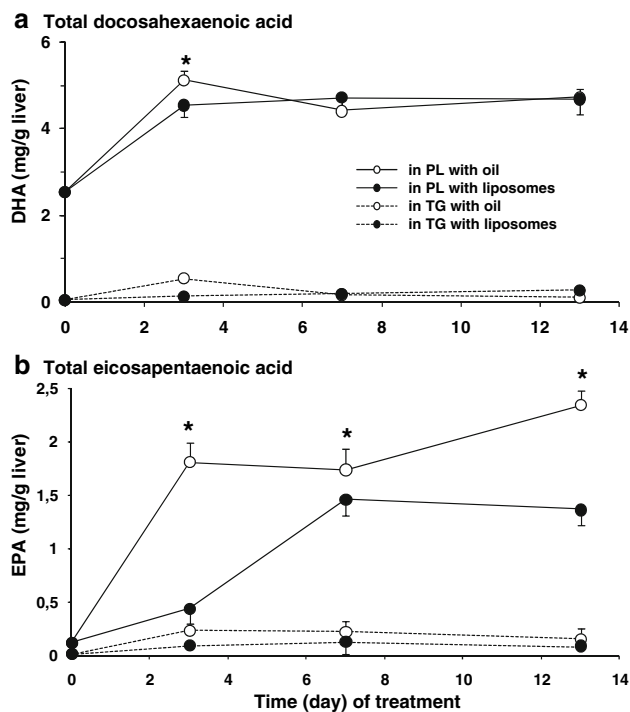


Fig. 2 Time course content in docosahexaenoic (DHA) (a) and eicosapentaenoic (EPA) (b) of TG and PL in the liver of rats fed fish oil or liposomes over 13 days. Statistical data as indicated in the legend of Fig. 1

the main two representative n-6 FA, arachidonic (AA, 20:4 n-6) and linoleic (18:2 n-6) acids in rats fed liposomes than in those fed fish oil (Fig. 3a, b, continuous lines). On the whole, giving fish oil or liposomes containing close FA contents very differently affected both the distribution and content of EPA and representative n-6 PUFA in total liver PL.

The time course content in plasma TG and PL has been previously given by Cansell et al. in [24], while the present study detailed the distribution of the main n-3 and n-6 PUFA in total plasma lipids (Fig. 4a–d). The percentage in DHA was shown to increase from day 0–3, then plateaued until day 13 with both treatments. This was not the case with EPA, whose increase with liposomes was nearly 3- and 2-times less elevated than with fish oil on days 3 and 13, respectively (Fig. 4b). Inversely, AA and linoleic acid, that initially represented 18 and 15% of total FA in plasma lipids, respectively, dropped to nearly 11 and 5% after 13 days, with no significant difference from each FA between both treatments all over the whole trial period (Fig. 4c, d).

Mitochondrial and Peroxisomal Activities

The mitochondrial content of livers was estimated through two marker enzyme activities unrelated to FA

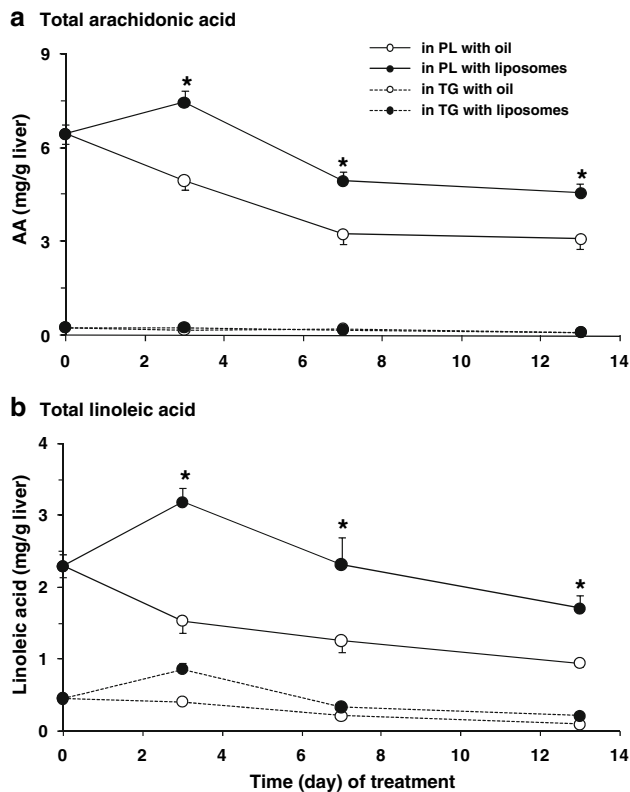


Fig. 3 Time course content in arachidonic acid (AA) (a) and linoleic acid (b) of TG and PL in the liver of rats fed fish oil or liposomes over 13 days. Statistical data as indicated in the legend of Fig. 1

oxidation, thereby unlikely to be altered by both lipid treatments, one being located in the mitochondrial outer membrane (with MAO), the other one representing a key step of the tricarboxylic acid cycle in the matrix (with CS). Figure 5a shows that there was no significant difference for enzyme activity between fish oil and liposomes, which suggested no change in the mitochondrial content of the livers of rats receiving both lipid sources. As regards the corresponding FA oxidation pathway, CPT I activity was significantly greater with the liposome treatment than with the fish oil one at all the times studied, as pointed out by an increasing activity with liposomes on day 3 and a decreasing activity with fish oil at all the times (Fig. 5b). The results with liposomes nearly paralleled the levels of mRNA found for CPT I and HAD (Fig. 5c, d), whose activities catalyse the entry of FA into mitochondria and the beginning of the β -oxidation cycle, respectively. With fish oil, the levels of mRNA for either enzyme were all decreased, except on day 3 for HAD (Fig. 5c, d).

The peroxisomal content of the livers was estimated through the activity of urate oxidase, a specific component of rat liver peroxisomes. All values were comparable with both treatments, except on day 3 (Fig. 6a), probably

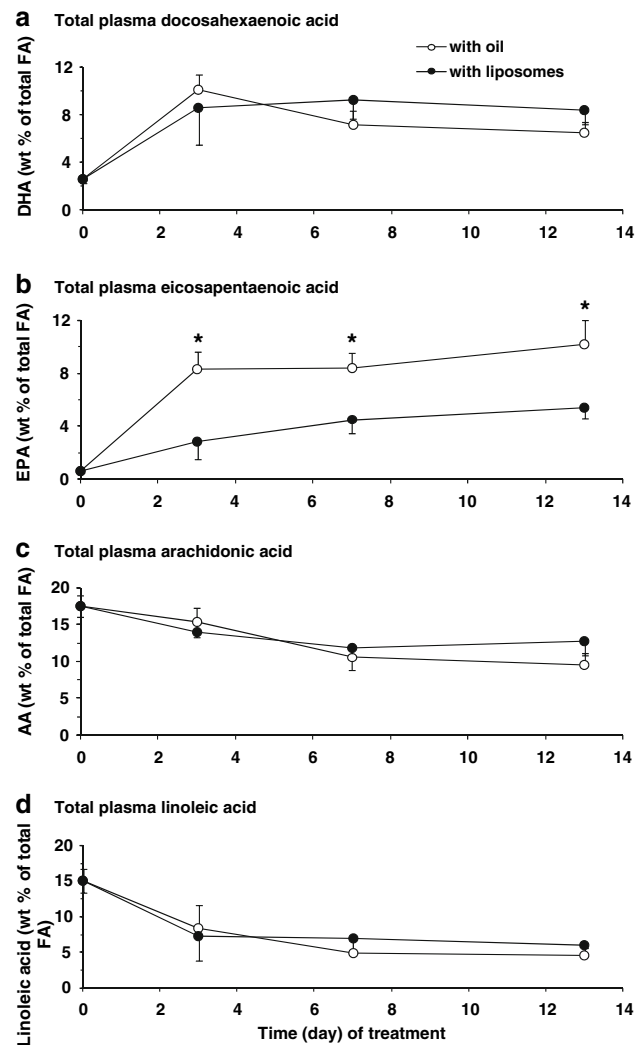
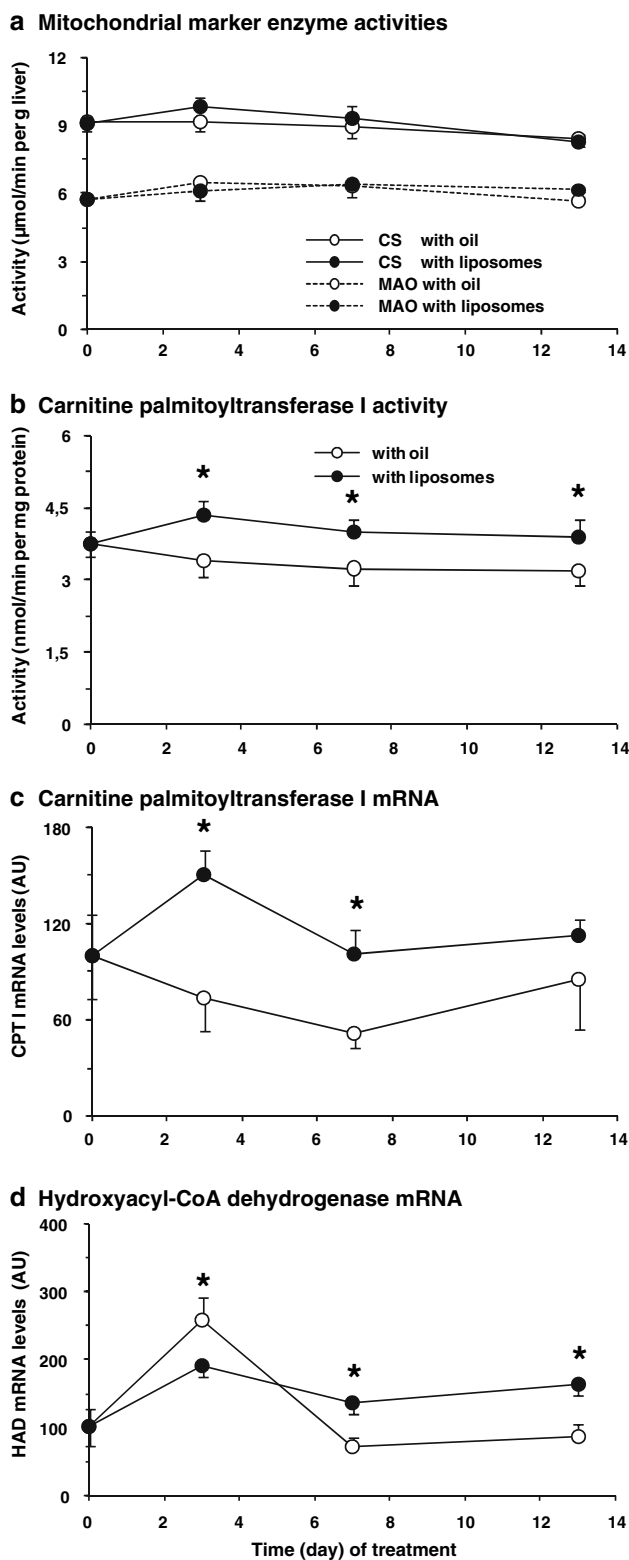


Fig. 4 Time course weight percentage of docosahexaenoic (DHA) (a), eicosapentaenoic (EPA) (b), arachidonic (AA) (c) and linoleic (d) acids in total plasma lipids of rats fed fish oil or liposomes over 13 days. Statistical data as indicated in the legend of Fig. 1

accounting for undetermined molecules interfering in the reaction. However, stable and comparable values on days 0, 7 and 13 suggested that the initial amounts of peroxisomes per g of liver were preserved in rats fed fish oil or liposomes. As regards PFAOS (a group of enzymes acting at the beginning of the peroxisomal β -oxidation cycle, particularly on long- and very-long chain FA), its activity moderately increased from day 0 to 13 with both diets (Fig. 6b), but earlier and to a greater extent in rats ingesting liposomes, especially on day 3. Over the whole trial, PPAR α mRNA levels were unaffected with any of the lipid sources, except a down-regulation on day 7 with fish oil (Fig. 6c). Expression levels of ACO, that is the first enzyme of the PFAOS sequence, are very sensitive to PPAR α activation and statistically increased at any time of



the liposome treatment (Fig. 6d). These data contrasted with the neutral or negative (on day 7) effect of fish oil on ACO mRNA levels (Fig. 6d).

Fig. 5 Time course activities of mitochondrial marker enzymes (a) and carnitine palmitoyltransferase I (CPT I) (b), and mRNA levels of CPT I (c) and hydroxyacyl-CoA dehydrogenase (HAD) (d) in the liver of rats fed fish oil or liposomes over 13 days. Activity rates of citrate synthase (CS) were given as $\mu\text{mol}/\text{min}$ per g of liver and those of monoamine oxidase (MAO) were increased 10 times to fit nearly in the middle of the graph. CPT I activity was given as nmol of palmitoyl-CoA whose palmitoyl moieties were transferred to carnitine per min and per mg of mitochondrial protein. Gene expressions are given as arbitrary units (AU) by reference to those obtained on day 0 (=100). For each gene, 18S was used for normalisation. Statistical data as indicated in the legend of Fig. 1

Gene Regulation of Enzymes and Proteins Providing Liver Cells with Lipids

From the lipogenic point of view, the levels of ACC1 mRNA increased and were almost comparable with both lipid sources over the whole trial period (Fig. 7a). The levels of FAS mRNA on day 3 were significantly more elevated with fish oil and practically unchanged with liposomes, but, on day 13, they increased only with liposomes (Fig. 7b). Concerning circulating fats, liver cell-surfaces are equipped with LRP, a property of which is to recognise chylomicron remnants via their ApoE moieties. Figure 8a shows that LRP mRNA levels dramatically and similarly increased with both fish oil and liposomes only on day 3. LDL-R of liver cell membranes have the capacity to take up LDL from blood and their expression levels reached a maximum on day 3 in rats fed fish oil, with a same though delayed increase on day 13 in rats fed liposomes (Fig. 8b). As regards FAT/CD36, a role of which is to take up/transport FFA from cell membranes to the cytoplasm through translocation mechanism, its expression levels were unchanged with fish oil over the whole trial period, but sharply increased (more than 10 times) only with liposomes on day 3 (Fig. 8c).

Expression Levels of Enzymes Involved in FA Esterification

Liver FA arising from lipogenesis and circulating lipids are β -oxidised or ascribed to TG and PL synthesis for fat deposit, membrane building and lipoprotein assembly. The expression levels of key enzymes of TG synthesis (DGAT) and of phosphatidylcholine synthesis (CTPpct) were unchanged with fish oil at any time of the trial, but with liposomes there was a significant increase in mRNA levels of DGAT and CTPpct only on day 3 (Fig. 9a, b). Cholesterol used with TG and PL for lipoprotein assembly mainly arises from internalised LDL and from the activity of HMG-CoA reductase, a key enzyme of the cholesterol synthesis whose level depends on available acetyl-CoA moieties. Figure 9c shows that there were increased levels of HMG-CoA reductase mRNA mainly on day 3 with both lipid sources, but to a nearly twice greater extent with liposomes than with fish oil.

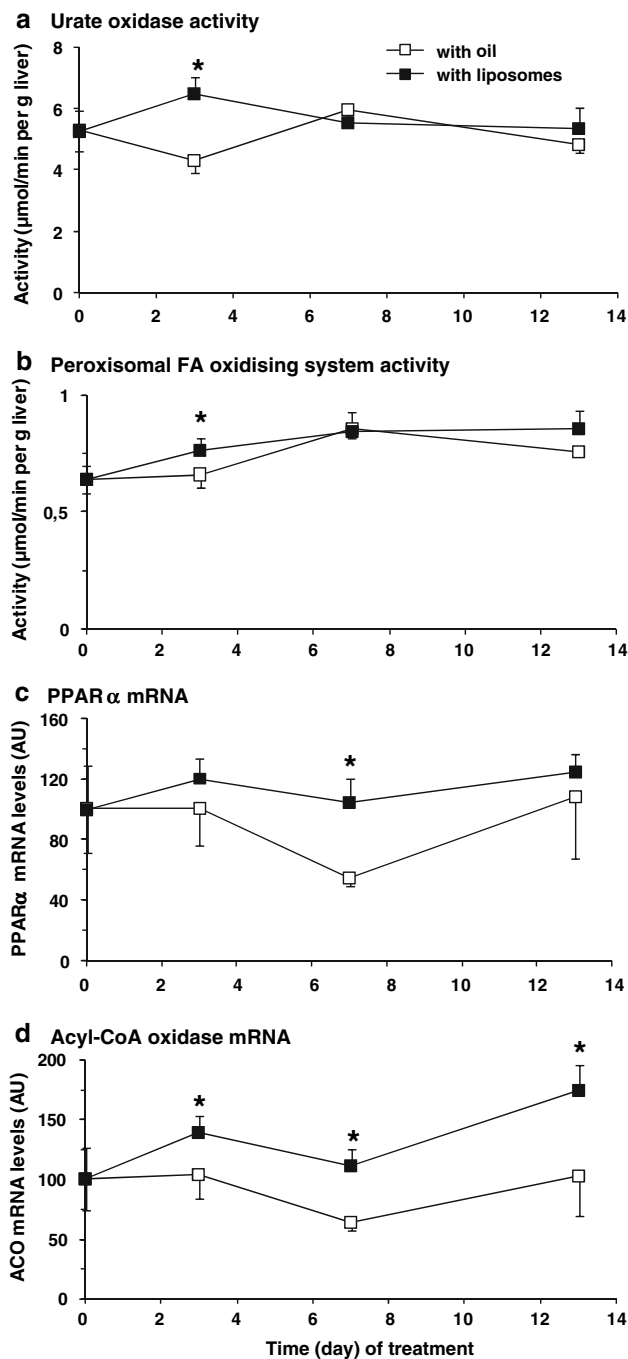


Fig. 6 Time course activities of peroxisomal urate oxidase (a) and peroxisomal FA oxidising system (b), and mRNA levels of peroxisome proliferator-activated receptor alpha (PPAR α) (c) and acyl-CoA oxidase (ACO) (d) in the liver of rats fed fish oil or liposomes over 13 days. Statistical data and gene expressions as indicated in the legends of Figs. 1 and 5, respectively

Discussion

The study shows that the administration of two marine fats essentially consisting of TG (fish oil) or PL (liposomes) with nearly identical n-3 PUFA contents resulted in early

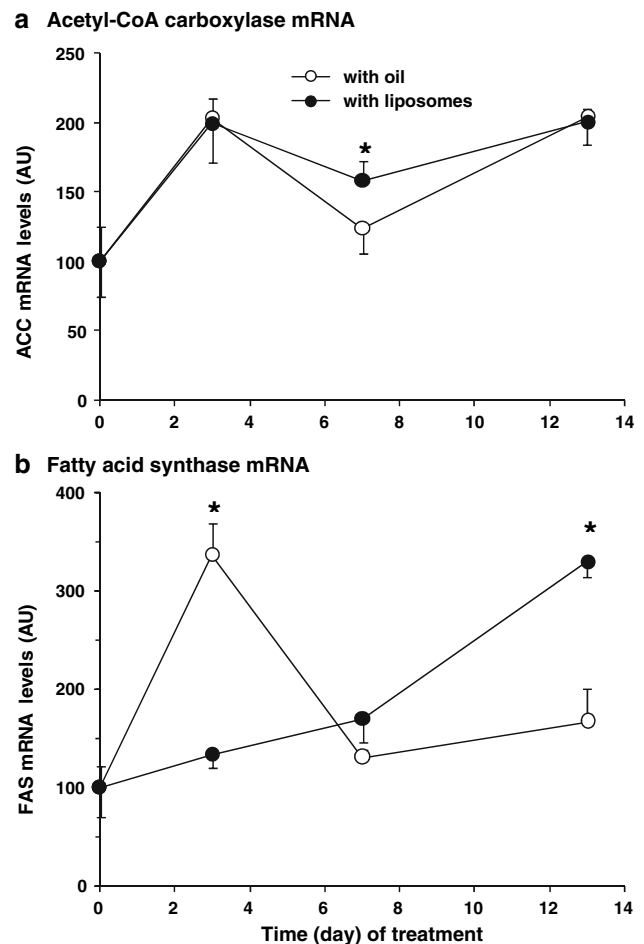


Fig. 7 Time course mRNA levels of acetyl-CoA carboxylase (ACC) (a) and fatty acid synthase (FAS) (b) in the liver of rats fed fish oil or liposomes over 13 days. Statistical data and gene expressions as indicated in the legends of Figs. 1 and 5, respectively

distinct time course fates of EPA and n-6 PUFA in liver PL. On day 3, the apparent increase of liver PL in arachidonic and linoleic acids with liposomes was particularly unexpected because these n-6 PUFA were absent from the lipid mixture ingested [24]. The amounts of PUFA of n-3 and n-6 series recovered in liver TG were too low after the administration of both lipid sources to provide any relevant information about the early events related to lipid metabolism. The changes in FA composition of liver PL were expected to depend on particular reciprocal exchanges between blood and liver lipids, and also on specifically regulated activities in hepatocytes.

Influence of Extrahepatic Fats on Liver Lipids

The rats were sacrificed 24 h after the last administration of both lipid mixtures. In the meantime, chylomicrons derived from ingested fats were partially used for the metabolic requirements of most organs and the replenishment of

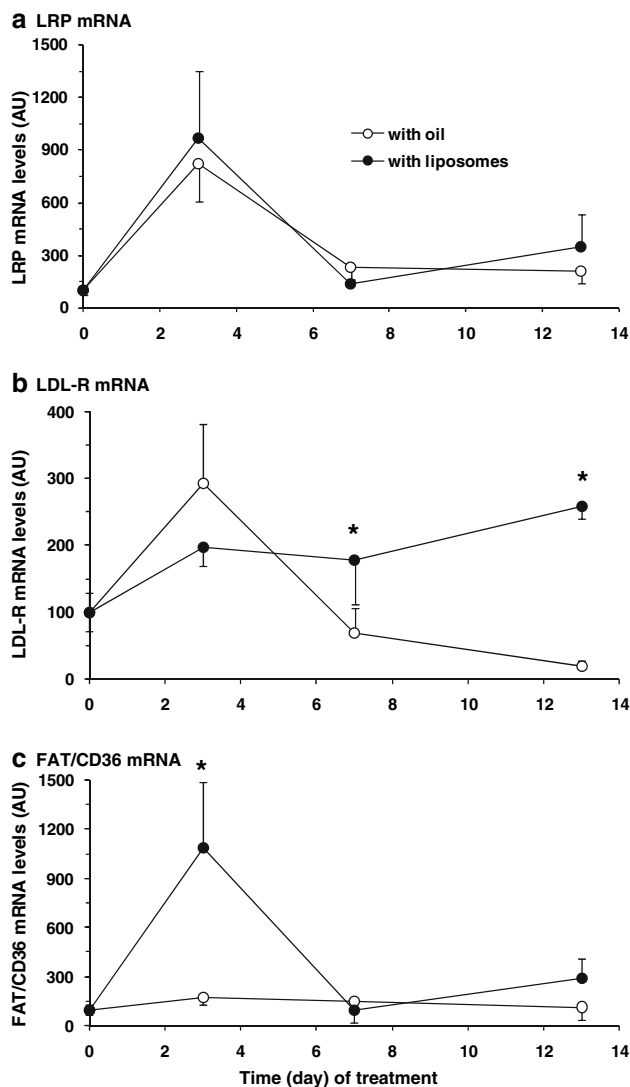


Fig. 8 Time course mRNA levels of LRP (a), LDL-R (b), and FAT/CD36 (c) in the liver of rats fed fish oil or liposomes over 13 days. Statistical data and gene expressions as indicated in the legends of Figs. 1 and 5, respectively

adipose tissues. Chylomicron remnants were then recognised, via their ApoE moieties, by LRP present on liver cell-surfaces [35] and internalised. The apparent comparable up-regulation of these receptors only on day 3 for both treatments showed that the underlying mechanisms were unrelated to the nature of the lipid source. During the time of dietary fat deprivation, VLDL secreted by the liver and used in most organs evolved as LDL that were removed from blood via LDL-R of liver membranes. These receptors were also up-regulated on day 3 with both lipid sources. However, their up- and down-regulation at the end of the trial period with liposomes and fish oil, respectively, suggested that the lipid assembly of VLDL within liver cells largely depended on the origin of ingested fats and/or on particular intrahepatic lipid-related activities. It is worth

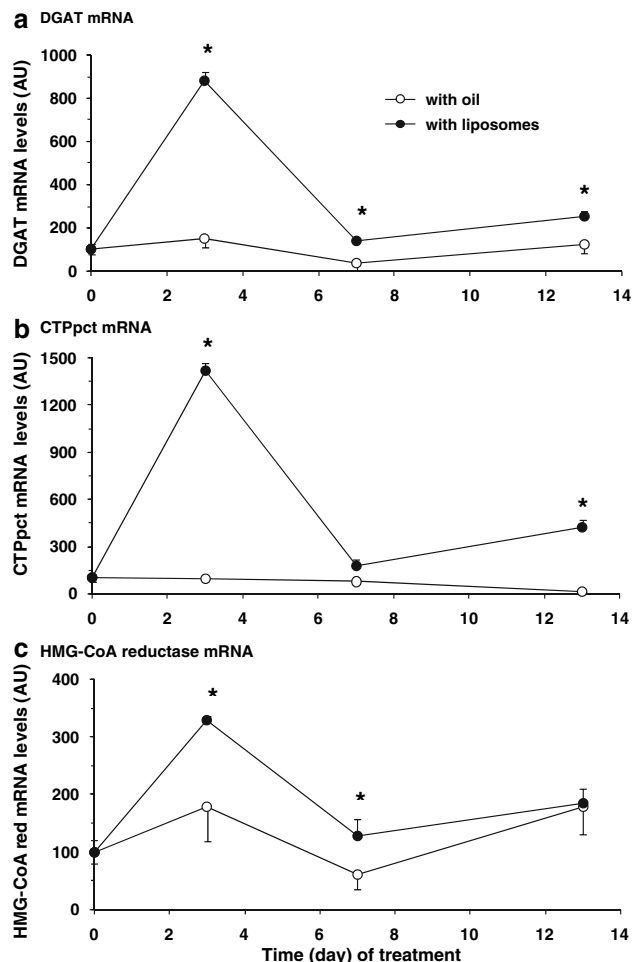


Fig. 9 Time course mRNA levels of DGAT (a), CTPpct (b) and HMG-CoA reductase (c) in the liver of rats fed fish oil or liposomes over 13 days. Statistical data and gene expressions as indicated in the legends of Figs. 1 and 5, respectively

noting that FAT/CD36 was strongly up-regulated only on day 3 with liposomes. This suggested a greater entry of FFA into liver cells, after increased extra hepatic lipolytic activities. This hypothesis could explain the punctual increase in arachidonic and linoleic acids of liver PL on day 3 with liposomes characterised by the lack of n-6 PUFA [24].

Esterification, Assembly and Secretion of Liver Lipids

The very low level of liver fats with each of our lipid sources suggested that the levels of VLDL secretion was maximum, but was not associated with excess blood fats, as this has been observed in other comparable situations [36, 37]. Yet, liposomes were shown to increase, only on day 3, the levels of expression of DGAT and CTPpct implied in TG and PL synthesis, respectively, but there was no marked difference in liver and blood lipid contents

between both treatments. VLDL assembly requires, in addition to TG and PL, cholesterol that was provided by dietary fats and endogenous synthesis. The induction of HMG-CoA reductase, only on day 3 with liposomes, could be considered as complementary of TG and PL synthesis for VLDL assembly. Yet, none of these up-regulations with liposomes appeared to be essential because fish oil exhibited comparable effects on liver and blood lipids [24]. Since EPA was reported to down-regulate lipogenic genes [38–42], the transitory up-regulation of DGAT and CTPpct on day 3 with liposomes could result from other FA released from extrahepatic tissues.

Metabolic Fates and Regulatory Effects of Liver PUFA

Dietary fats exert versatile effects in the liver through their constitutive FA, as membrane lipid building, cell energy requirement and gene regulation. The minimal amounts of EPA from liver PL and blood lipids in the very short term with liposomes, compared with fish oil, strongly suggested that EPA was largely oxidised during the first days of treatment. This n-3 PUFA was demonstrated to be oxidised both in mitochondria and peroxisomes, while DHA oxidation was shown to occur only in peroxisomes [43]. The data collected showed that the mitochondrial and peroxisomal contents of liver were unchanged no matter what the lipid source. Moreover, the increased activities and mRNA levels of key enzymes related to corresponding FA oxidation pathways after 3 days of liposome treatment could be responsible for the early oxidation of EPA. This effect should be mainly mediated through CPT I whose activity was always greater with liposomes than with fish oil. The difference in CPT I activity between both treatments might appear to be of too low amplitude considering the almost absence of EPA in PL on day 3 with liposomes, but could be much greater by taking into account the characteristic of CPT I to be more active at low malonyl-CoA concentrations. Indeed, as already mentioned, the animals were killed 24 h after the last intragastric injection of the lipid mixture, but were provided in the meantime with a fat-free diet. This diet containing carbohydrates should increase the lipogenic pathway via insulin secretion. This normal physiological answer was illustrated by the two times increase in ACC expression with both lipid sources, but was only consistent on day 3 of the fish oil treatment with FAS expression that increased 3 times. This means that, if the expression levels were equally effective on enzyme synthesis and activity, malonyl-CoA produced by the former reaction was not only used for FA synthesis, but also for CPT I inhibition [44] and thus EPA preservation. By contrast, with liposomes, malonyl-CoA formation should normally give rise to reduced CPT I activity, but that happened without any increased FAS expression. These

apparently inconsistent data might result from particular effects of PUFA on enzymes of the lipogenic pathway. Indeed, ACC was demonstrated to be activated by insulin and inactivated in the presence of PUFA through reversible enzyme conformation [45]. This means for instance that existing and newly synthesised ACC were deactivated in the presence of increased free PUFA concentration. Besides, free EPA was shown to inhibit not only ACC (as some other PUFA), but also the whole lipogenic pathway with FAS [42]. Under these latter conditions, FA synthesis might be reduced partly because of a decreased malonyl-CoA synthesis, which increased CPT I activity and consequently the mitochondrial oxidation of EPA and other PUFA. As EPA is oxidised in mitochondria to a greater extent than AA [46], it was coherent that, on day 3 with liposomes, EPA was reduced and AA increased in PL by comparison with fish oil (Figs. 2b vs. 3a). In addition, with greater ACO expression levels in liposome-fed than in fish oil-fed rats, peroxisomal oxidation was expected to target more efficiently EPA and AA. However, the increase in AA on day 3 with liposomes indicated that the peroxisomal activity was insufficient to prevent the temporary increase of PL in AA, yet absent from the lipid source. The increase in both the expression and activity of CPT I, with a nearly basal level of PPAR α expression with liposomes, might be due to a sufficient activation of existing receptors by cell PUFA as already observed [47] and to the fact that liver CPT I was also regulated by PUFA through a PPAR α -independent pathway [48].

Origin of Increased Free n-6 PUFA in the Liver of Liposome-Fed Rats

The above results implied that efficient free PUFA concentrations existed in liver cells during the first 3 days of the liposome treatment and originated from extrahepatic lipolytic activities. In vivo data show that PL or PL-derived compounds exert lipolytic effects on adipose tissues in mice [49], rabbits [50] and humans [51], but our previous studies did not reveal any significant difference in the lipid class composition of intestinal lymph between both lipid sources [23]. By contrast, direct EPA administration was shown to reduce the level of retroperitoneal adiposity through the inhibition of the adipogenic transcription factor PPAR γ gene expression [52]. Very recently, EPA was demonstrated to increase lipolysis in 3T3-L1 adipocytes through up-regulation of the lipolytic gene expression and down-regulation of the adipogenic gene expression [53]. Finally the release of EPA from blood lipids, to a greater extent with liposomes than with fish oil, appeared to be a prerequisite for the early dissimilar fates of EPA and n-6 PUFA in liver PL. The greater bioavailability of EPA in rats fed liposomes compared with fish oil might originate

from the initial distribution of PUFA in plasma lipids. Indeed, we previously showed that EPA was less abundant in the *sn*-2 position of chylomicron TG in rats fed liposomes than in those fed fish oil [23]. A similar unequal distribution was found in plasma and liver TG from rats fed diets enriched in seal oil, with more EPA in the *sn*-1 position [54]. Assuming that this latter position was more sensitive to hydrolysis than the *sn*-2 one [55], EPA might be more rapidly released and might immediately exhibit its lipolytic effect on adipose tissues. EPA and other PUFA taken up by liver cells might then act on gene regulation, resulting particularly in early mitochondrial EPA oxidation and a decrease in lipogenic activity.

This time course study underlined the importance of events occurring in rats fed marine fats for 3 days and demonstrated that EPA present in fish oil and marine liposomes did not exert comparable effects on liver lipid related-metabolic pathways with direct consequences on its own distribution in PL. Because of the beneficial effects of marine fats on health, the early specific hydrolysis of EPA as a free form from liposome-derived blood lipids deserves to be clarified further.

Acknowledgment Mireille Lamarque is gratefully acknowledged for her assistance in English.

References

1. von Schacky C (2000) n-3 Fatty acids and the prevention of coronary atherosclerosis. *Am J Clin Nutr* 71:224S–227S
2. Calder PC (2004) n-3 Fatty acids and cardiovascular disease: evidence explained and mechanisms explored. *Clin Sci (Lond)* 107:1–11
3. Schmidt EB, Arnesen H, de Caterina R, Rasmussen LH, Kristensen SD (2005) Marine n-3 polyunsaturated fatty acids and coronary heart disease. Part I. Background, epidemiology, animal data, effects on risk factors and safety. *Thromb Res* 115:163–170
4. Belluzzi A, Boschi S, Brignola C, Munarini A, Cariani G, Miglio F (2000) Polyunsaturated fatty acids and inflammatory bowel disease. *Am J Clin Nutr* 7:339S–342S
5. Ziboh VA, Miller CC, Cho Y (2000) Metabolism of polyunsaturated fatty acids by skin epidermal enzymes: generation of antiinflammatory and antiproliferative metabolites. *Am J Clin Nutr* 71:361S–366S
6. Carrero JJ, Baro L, Fonolla J, Gonzalez-Santiago M, Martinez-Ferez A, Castillo R, Jimenez J, Boza JJ, Lopez-Huertas E (2004) Cardiovascular effects of milk enriched with omega-3 polyunsaturated fatty acids, oleic acid, folic acid, and vitamins E and B6 in volunteers with mild hyperlipidemia. *Nutrition* 20:521–527
7. Sindelar CA, Scheerger SB, Plugge SL, Eskridge KM, Wander RC, Lewis NM (2004) Serum lipids of physically active adults consuming omega-3 fatty acid-enriched eggs or conventional eggs. *Nutr Res* 24:731–739
8. Berbert AA, Kondo CR, Almendra CL, Matsuo T, Dichi I (2005) Supplementation of fish oil and olive oil in patients with rheumatoid arthritis. *Nutrition* 21:131–136
9. Gaiva MH, Couto RC, Oyama LM, Couto GE, Silveira VL, Ribeiro EB, Nascimento CM (2003) Diets rich in polyunsaturated fatty acids: effect on hepatic metabolism in rats. *Nutrition* 19:144–149
10. Ikeda I, Sasaki E, Yasunami H, Nomiyama S, Nakayama M, Sugano M, Imaizumi K, Yazawa K (1995) Digestion lymphatic transport of eicosapentaenoic, docosahexaenoic acids given in the form of triacylglycerol, free acid, ethyl ester in rats. *Biochim Biophys Acta* 1259:297–304
11. Ikeda I, Cha JY, Yanagita T, Nakatani N, Oogami K, Imaizumi K, Yazawa K (1998) Effects of dietary alpha-linolenic, eicosapentaenoic and docosahexaenoic acids on hepatic lipogenesis and beta-oxidation in rats. *Biosci Biotechnol Biochem* 62:675–680
12. Hong DD, Takahashi Y, Kushiro M, Ide T (2003) Divergent effects of eicosapentaenoic and docosahexaenoic acid ethyl esters, and fish oil on hepatic fatty acid oxidation in the rat. *Biochim Biophys Acta* 1635:29–36
13. Shirai N, Suzuki H (2003) Effects of simultaneous docosahexaenoic acid and catechin intakes on the plasma and liver lipids low and high-fat diet fed mice. *Nutr Res* 23:959–969
14. Carnielli VP, Verlatto G, Pederzini F, Luijendijk I, Boerlage A, Pedrotti D, Sauer PJ (1998) Intestinal absorption of long-chain polyunsaturated fatty acids in preterm infants fed breast milk or formula. *Am J Clin Nutr* 67:97–103
15. Morgan C, Davies L, Corcoran F, Stammers J, Colley J, Spencer SA, Hull D (1998) Fatty acid balance studies in term infants fed formula milk containing long-chain polyunsaturated fatty acids. *Acta Paediatr* 87:136–142
16. Lemaitre-Delaunay D, Pachiaudi C, Laville M, Pousin J, Armstrong M, Lagarde M (1999) Blood compartmental metabolism of docosahexaenoic acid (DHA) in humans after ingestion of a single dose of [(13)C]DHA in phosphatidylcholine. *J Lipid Res* 40:1867–1874
17. Song JH, Fujimoto K, Miyazawa T (2000) Polyunsaturated (n-3) fatty acids susceptible to peroxidation are increased in plasma and tissue lipids of rats fed docosahexaenoic acid-containing oils. *J Nutr* 130:3028–3033
18. Ramirez M, Amate L, Gil A (2001) Absorption and distribution of dietary fatty acids from different sources. *Early Hum Dev* 65:S95–S101
19. Amate L, Gil A, Ramirez M (2001) Feeding infant piglets formula with long-chain polyunsaturated fatty acids as triacylglycerols or phospholipids influences the distribution of these fatty acids in plasma lipoprotein fractions. *J Nutr* 131:1250–1255
20. Lasic DD (1993) *Liposomes: from physics to applications*. Elsevier, Amsterdam
21. Nacka F, Cansell M, Gouygou JP, Gerbeaud C, Meleard P, Entressangles B (2001) Physical and chemical stability of marine lipid-based liposomes under acid conditions. *Colloids Surf B Biointerfaces* 20:257–266
22. Nacka F, Cansell M, Entressangles B (2001) In vitro behavior of marine lipid-based liposomes. Influence of pH, temperature, bile salts, and phospholipase A2. *Lipids* 36:35–42
23. Cansell M, Nacka F, Combe N (2003) Marine lipid-based liposomes increase in vivo FA bioavailability. *Lipids* 38:551–559
24. Cansell M, Moussaoui N, Petit AP, Denizot A, Combe N (2006) Feeding rats with liposomes or fish oil differently affects their lipid metabolism. *Eur J Lipid Sci Technol* 108:459–467
25. Nacka F, Cansell M, Meleard P, Combe N (2001) Incorporation of alpha-tocopherol in marine lipid-based liposomes: in vitro and in vivo studies. *Lipids* 36:1313–1320
26. Niot I, Pacot F, Bouchard P, Gresti J, Bernard A, Bezard J, Clouet P (1994) Involvement of microsomal vesicles in part of the sensitivity of carnitine palmitoyltransferase I to malonyl-CoA inhibition in mitochondrial fractions of rat liver. *Biochem J* 304:577–584

27. Folch J, Lees M, Sloane Stanley GH (1957) A simple method for the isolation and purification of total lipides from animal tissues. *J Biol Chem* 226:497–509
28. Slover HT, Lanza E (1979) Quantitative analysis of food fatty acids by capillary gas chromatography. *J Am Oil Chem Soc* 56:933–943
29. Weissbach H, Smith TE, Daly JW, Witkop B, Udenfriend S (1960) A rapid spectrophotometric assay of mono-amine oxidase based on the rate of disappearance of kynuramine. *J Biol Chem* 235:1160–1163
30. Robinson JB, Srere PA (1985) Organization of Krebs tricarboxylic acid cycle enzymes in mitochondria. *J Biol Chem* 260:10800–10805
31. Leighton F, Poole B, Beaufay H, Baudhuin P, Coffey JW, Fowler S, De Duve C (1968) The large-scale separation of peroxisomes, mitochondria, and lysosomes from the livers of rats injected with triton WR-1339. Improved isolation procedures, automated analysis, biochemical and morphological properties of fractions. *J Cell Biol* 37:482–513
32. Bronfman M, Inestrosa NC, Leighton F (1979) Fatty acid oxidation by human liver peroxisomes. *Biochem Biophys Res Commun* 88:1030–1036
33. Chomczynski P, Sacchi N (1987) Single-step method of RNA isolation by acid guanidinium thiocyanate-phenol-chloroform extraction. *Anal Biochem* 162:156–159
34. Degrace P, Moindrot B, Mohamed I, Gresti J, Du ZY, Chardigny JM, Sebedio JL, Clouet P (2006) Upregulation of liver VLDL receptor and FAT/CD36 expression in LDLR^{-/-} apoB100/100 mice fed trans-10, cis-12 conjugated linoleic acid. *J Lipid Res* 47:2647–2655
35. Hussain MM, Maxfield FR, Mas-Oliva J, Tabas I, Ji ZS, Innerarity TL, Mahley RW (1991) Clearance of chylomicron remnants by the low density lipoprotein receptor-related protein/alpha 2-macroglobulin receptor. *J Biol Chem* 266:13936–13940
36. Benner KG, Sasaki A, Gowen DR, Weaver A, Connor WE (1990) The differential effect of eicosapentaenoic acid and oleic acid on lipid synthesis and VLDL secretion in rabbit hepatocytes. *Lipids* 25:534–540
37. Berge RK, Madsen L, Vaagenes H, Tronstad KJ, Gottlicher M, Rustan AC (1999) In contrast with docosahexaenoic acid, eicosapentaenoic acid and hypolipidaemic derivatives decrease hepatic synthesis and secretion of triacylglycerol by decreased diacylglycerol acyltransferase activity and stimulation of fatty acid oxidation. *Biochem J* 343:191–197
38. Perez-Echarri N, Perez-Matute P, Marcos-Gomez B, Marti A, Martinez JA, Moreno-Aliaga MJ (2009) Down-regulation in muscle and liver lipogenic genes: EPA ethyl ester treatment in lean and overweight (high-fat-fed) rats. *J Nutr Biochem* (in press)
39. Raclot T, Oudart H (1999) Selectivity of fatty acids on lipid metabolism and gene expression. *Proc Nutr Soc* 58:633–646
40. Sampath H, Ntambi JM (2005) Polyunsaturated fatty acid regulation of genes of lipid metabolism. *Annu Rev Nutr* 25:317–340
41. Zheng X, Rivabene R, Cavallari C, Napolitano M, Avella M, Bravo E, Botham KM (2002) The effects of chylomicron remnants enriched in n-3 or n-6 polyunsaturated fatty acids on the transcription of genes regulating their uptake and metabolism by the liver: influence of cellular oxidative state. *Free Radic Biol Med* 32:1123–1131
42. Willumsen N, Skorve J, Hexeberg S, Rustan AC, Berge RK (1993) The hypotriglyceridemic effect of eicosapentaenoic acid in rats is reflected in increased mitochondrial fatty acid oxidation followed by diminished lipogenesis. *Lipids* 28:683–690
43. Madsen L, Froyland L, Dyroy E, Helland K, Berge RK (1998) Docosahexaenoic and eicosapentaenoic acids are differently metabolized in rat liver during mitochondria and peroxisome proliferation. *J Lipid Res* 39:583–593
44. Mills SE, Foster DW, McGarry JD (1983) Interaction of malonyl-CoA and related compounds with mitochondria from different rat tissues. Relationship between ligand binding and inhibition of carnitine palmitoyltransferase I. *Biochem J* 214:83–91
45. Halestrap AP, Denton RM (1973) Insulin and the regulation of adipose tissue acetyl-CoA carboxylase. *Biochem J* 132:509–517
46. Christophersen BO, Hagve TA, Christensen E, Johansen Y, Tverdal S (1986) Eicosapentaenoic- and arachidonic acid metabolism in isolated liver cells. *Scand J Clin Lab Invest* 184:55–60
47. Knight BL, Hebbachi A, Hauton D, Brown AM, Wiggins D, Patel DD, Gibbons GF (2005) A role for PPARalpha in the control of SREBP activity and lipid synthesis in the liver. *Biochem J* 389:413–421
48. Louet JF, Chatelain F, Decaux JF, Park EA, Kohl C, Pineau T, Girard J, Pegorier JP (2001) Long-chain fatty acids regulate liver carnitine palmitoyltransferase I gene (L-CPT I) expression through a peroxisome-proliferator-activated receptor alpha (PPARalpha)-independent pathway. *Biochem J* 354:189–197
49. Moriya H, Hosokawa M, Miyashita K (2007) Combination effect of herring roe lipids and proteins on plasma lipids and abdominal fat weight of mouse. *J Food Sci* 72:C231–C234
50. Rittes PG, Rittes JC, Carriel Amary MF (2006) Injection of phosphatidylcholine in fat tissue: experimental study of local action in rabbits. *Aesthetic Plast Surg* 30:474–478
51. Rose PT, Morgan M (2005) Histological changes associated with mesotherapy for fat dissolution. *J Cosmet Laser Ther* 7:17–19
52. Perez-Matute P, Perez-Echarri N, Martinez JA, Marti A, Moreno-Aliaga MJ (2007) Eicosapentaenoic acid actions on adiposity and insulin resistance in control and high-fat-fed rats: role of apoptosis, adiponectin and tumour necrosis factor-alpha. *Br J Nutr* 97:389–398
53. Lee MS, Kwun IS, Kim Y (2008) Eicosapentaenoic acid increases lipolysis through up-regulation of the lipolytic gene expression and down-regulation of the adipogenic gene expression in 3T3-L1 adipocytes. *Genes Nutr* 2:327–330
54. Yoshida H, Mawatari M, Ikeda I, Imaizumi K, Seto A, Tsuji H (1999) Effect of dietary seal and fish oils on triacylglycerol metabolism in rats. *J Nutr Sci Vitaminol (Tokyo)* 45:411–421
55. Sadou H, Leger CL, Descomps B, Barjon JN, Monnier L, Crastes de Paulet A (1995) Differential incorporation of fish-oil eicosapentaenoate and docosahexaenoate into lipids of lipoprotein fractions as related to their glyceryl esterification: a short-term (postprandial) and long-term study in healthy humans. *Am J Clin Nutr* 62:1193–1200

Inhibitory Effect of Conjugated α -Linolenic Acid from Bifidobacteria of Intestinal Origin on SW480 Cancer Cells

Mairéad Coakley · Sebastiano Banni ·
Mark C. Johnson · Susan Mills · Rosaleen Devery ·
Gerald Fitzgerald · R. Paul Ross · Catherine Stanton

Received: 14 February 2008 / Accepted: 4 November 2008 / Published online: 2 December 2008
© AOCs 2008

Abstract In this study, we assessed the ability of six strains of bifidobacteria (previously shown by us to possess the ability to convert linoleic acid to *c*9, *t*11-conjugated linoleic acid (CLA) to grow in the presence of α -linolenic acid and to generate conjugated isomers of the fatty acid substrate during fermentation for 42 h. The six strains of bifidobacteria were grown in modified MRS (mMRS) containing α -linolenic acid for 42 h at 37 °C, after which the fatty acid composition of the growth medium was assessed by gas liquid chromatography (GLC). Indeed, following fermentation of one of the strains, namely *Bifidobacterium breve* NCIMB 702258, in the presence of 0.41 mg/ml α -linolenic acid, 79.1% was converted to the conjugated isomer, C18:3 *c*9, *t*11, *c*15 conjugated α -linolenic acid (CALA). To examine the inhibitory effect of the fermented oils produced, SW480 colon cancer cells were cultured in the presence of the extracted fermented oil (10–50 μ g/ml) for 5 days. The data indicate an inhibitory effect on cell growth ($p \leq 0.001$) of CALA, with cell numbers

reduced by 85% at a concentration of 180 μ M, compared with a reduction of only 50% with α -linolenic acid ($p \leq 0.01$).

Keywords *Bifidobacterium* · α -Linolenic acid · Conjugated α -linolenic acid (CALA) · Cancer · Health promotion

Introduction

α -Linolenic acid is an essential dietary fatty acid, which has been reported to exhibit anti-carcinogenic effects in animals [1, 2]. Recently, minute concentrations of α -linolenic acid biohydrogenation intermediates, such as the *c*9, *t*11, *c*15 C18:3 isomer have been identified in milk [3]. It has been reported that a conjugated form of α -linolenic acid may be more potent in terms of health promoting benefits than the parent α -linolenic acid molecule. Indeed, the conjugated linoleic acid (CLA) isomers (in particular, *c*9, *t*11 CLA and *t*10, *c*12 CLA) have been the focus of considerable research efforts in recent years, and are now known to confer many health benefits including anti-cancer [4–7], anti-obesity [5, 8, 9] and anti-atherosclerotic [5, 10, 11] effects. Recent evidence has also highlighted health promoting properties with regard to other conjugated PUFAs [12, 13]. These include fatty acids such as *c*9, *t*11, *t*13 α -eleostearic acid (α -ESA) [14–16] demonstrating anti-cancer properties, and *c*9, *t*11, *c*13 conjugated linolenic acid which has demonstrated a hypolipidemic effect [17]. Indeed, α -ESA was shown to have a more potent anti-tumour effect than *c*9, *t*11 and *t*10, *c*12 CLA in nude mice with DLD-1 human colon cancer cells [15]. Furthermore, when conjugated α -linolenic acid (CALA) and CLA were examined separately during the initiation and promotion

M. Coakley · M. C. Johnson · S. Mills · R. Paul Ross ·
C. Stanton (✉)
Teagasc, Biotechnology Centre, Moorepark Food Research
Centre, Fermoy, Cork, Ireland
e-mail: catherine.stanton@teagasc.ie

S. Mills · G. Fitzgerald · R. Paul Ross · C. Stanton
Alimentary Pharmabiotic Centre, University College,
Cork, Ireland

R. Devery
National Institute for Cellular Biotechnology,
Dublin City University, Dublin, Ireland

S. Banni
Dipartimento di Biologia Sperimentale,
Università degli Studi di Cagliari, Cittadella Universitaria,
09042 Monserrato, Cagliari, Italy

stages of PhIP-induced mammary gland carcinogenesis in rats, both CALA and CLA retarded development of mammary tumours and decreased mammary carcinogenesis in the post-initiation period with inhibition of cell proliferation [18].

Previously, we have shown that bifidobacteria of human origin are capable of producing the biologically active *c9*, *t11* CLA and *t9*, *t11* CLA isomers from linoleic acid during fermentation [19–21]. The aim of this study was to assess the ability of a selection of CLA-producing bifidobacteria to grow in and isomerise α -linolenic acid during fermentation in MRS medium. Furthermore, the inhibitory effects of the fermented fatty acids obtained following fermentation of *B. breve* NCIMB 702258 in the presence of α -linolenic acid were assessed and compared with the unfermented α -linolenic acid control.

Materials and Methods

Bacterial Strains

The bacterial strains used in this study are detailed in Table 1, and were selected based on their ability to isomerise linoleic acid to *c9*, *t11* CLA [19]. The bifidobacteria were grown anaerobically (anaerobic jars with Anaerocult A gas packs; Merck, Darmstadt, Germany) in MRS medium (Difco Laboratories, Detroit, MI, USA) with 0.05% (w/v) L-cysteine hydrochloride (98% pure; Sigma Chemical Co., St Louis, MO, USA) (cys-MRS), at 37 °C for 24–48 h.

Bioconversion of α -Linolenic Acid by Bifidobacteria

A selection of bifidobacteria (see Table 1 for details) were grown (2% inoculum) in cys-MRS with added α -linolenic acid (C18:3 *c9*, *c12*, *c15* octadecatrienoic acid, Sigma

Chemical Co.) to assess bioconversion of this substrate by the bifidobacteria. The α -linolenic acid was added as a 30 mg/ml stock solution in distilled water containing 2% (v/v) Tween 80. The α -linolenic acid stock solution was previously filter-sterilised through a 0.45 μ m Minisart filter and stored in the dark at –20 °C. The strains were incubated anaerobically for 42 h at 37 °C. Following incubation, the fatty acid composition of the bacterial supernatant was assessed following fat extraction and gas liquid chromatography (GLC) analysis, as described in Coakley et al. [19]. The fatty acid content in samples following the bioconversion assays were corrected against the fatty acids in the cys-MRS medium.

Identification of the Fatty Acid Product from Bioconversion of α -Linolenic Acid by Bifidobacteria

The bioconversion product resulting from the growth of bifidobacteria in medium containing α -linolenic acid was identified using diode array (DAD) and mass spectrometry (MS) detectors in line, following separation by HPLC. Separation of the product was carried out with a Hewlett–Packard 1100 HPLC system (Hewlett–Packard, Palo Alto, CA, USA) equipped with a diode array detector. A C-18 Inertsil 5 ODS-2 Chrompack column (5- μ m particle size, 150 \times 4.6 mm) (Chrompack International BV, Middleburg, The Netherlands), was used with a mobile phase of CH₃CN/H₂O/CH₃COOH (70/30/0.12, v/v/v) at a flow rate of 1.5 ml/min [22]. Conjugated diene unsaturated fatty acids were detected at 234 nm. Analytes in the HPLC mobile phase displaying second derivative UV spectra characteristic of the conjugated diene chromophore were further characterised by using HPLC Agilent 1100 HPLC system (Agilent, Palo Alto, CA) equipped with a APCI-MS in ion positive mode using a mobile phase of CH₃CN/H₂O/CH₃COOH (30/70/0.12, v/v/v) at a flow rate of 1 ml/min. For the HPLC-MS analyses, the mobile phase was modified with 2 mM of NH₄O₂CCH₃, as described previously [23].

Generation of CALA Oil for Assessment of Inhibitory Activity in SW480 Colon Cancer Cells

The CALA oil for the cell culture study was generated by growing *B. breve* NCIMB 702258 in cys-MRS supplemented with α -linolenic acid (0.5 mg/ml). A control for the cell culture study was generated with cys-MRS medium supplemented with 0.5 mg/ml α -linolenic acid (no bacteria added, thus no conversion). The oil (either the α -linolenic acid (control) or CALA (experimental) was extracted from the medium, as described above and assessed by GLC prior to use in the cell culture study. The oils were stored in ethanol under nitrogen at –20 °C. Human colon cancer

Table 1 Bacterial strains used in this study

Species	Strain	Source
<i>Bifidobacterium breve</i>	NCIMB 702258	Infant intestine
	NCTC 11815	Infant intestine
	NCIMB 8815	Nursling stools
	NCIMB 8807	Nursling stools
	DPC 6035	Neonatal faeces
<i>Bifidobacterium lactis</i>	Bb12	Chr. Hansen

NCIMB National Collection of Industrial and Marine Bacteria, Aberdeen, UK; NCTC National Collection of Type Cultures, Central Public Health Laboratory, London, UK; DPC Dairy Products Research Centre Culture Collection, Teagasc, Moorepark Food Research Centre, Fermoy, Co. Cork, Ireland; Chr. Hansen, Little Island, Cork, Ireland

cells were obtained from the European Collection of Cell Cultures (ECACC, Porton Down, Salisbury, UK). Human colon cancer cells (SW480) were cultured in the presence of different concentrations of the fermented CALA oil and the unfermented α -linolenic acid control oil. Culture media and supplements were purchased from Sigma Aldrich Ireland Ltd. (Dublin, Ireland). The SW480 cells were maintained in Dulbecco's Minimum Essential Medium (DMEM) supplemented with 5% (v/v) fetal bovine serum, 0.2 mmol/L L-glutamine, 1 mmol/L HEPES and 1 unit/ml penicillin and streptomycin. SW480 cells were grown in 96 well plates and maintained at 37 °C in a humidified atmosphere. The pH of the media was maintained at 7.2–7.4 by a required flow of 95% air and 5% CO₂. Initially, 1×10^4 cells were seeded in wells and cultured for 24 h at 37 °C, allowing the cells to attach to the substratum. The medium was then replaced with media containing either of the two oils to yield CALA or α -linolenic acid concentrations ranging from 10 to 50 μ g/ml. Control flasks were supplemented with equivalent volumes of ethanol (0.5% v/v). Following incubation for 5 days, cell viability was determined using the MTS method (Promega Corporation, Madison, WI, USA), a colorimetric method for determining the number of viable cells in proliferation or cytotoxicity assays subsequent to incubation with MTS tetrazolium compound. Following incubation with MTS for 2 h, the absorbance was recorded at 492 nm with a 96-well plate reader. Cell viability (%) after treatment was expressed relative to the ethanol control which represents 100%. Three independent experiments were performed in triplicate for each treatment and the Student's *t* test was used to determine significant differences between treatments (* $p \leq 0.05$; ** $p \leq 0.01$; *** $p \leq 0.001$).

Results

Bioconversion of α -Linolenic Acid by Bifidobacteria

To assess whether the bifidobacteria in this study (Table 1) could generate a bioconversion product from α -linolenic acid, the strains were grown in the presence of the fatty acid for 42 h. While five of the *Bifidobacterium* strains assessed demonstrated the ability to convert α -linolenic acid to a modified fatty acid (based on GLC) (Fig. 1), *B. lactis* Bb12 did not exhibit the ability to modify the α -linolenic acid substrate. Furthermore, the *B. breve* strains exhibited intra-species variation in efficiency of modification of α -linolenic acid, varying from 67.6 for *B. breve* DPC 6035 to 80.7% for *B. breve* NCIMB 8807 in 0.24 mg/ml α -linolenic acid and 49.4 (*B. breve* NCTC 11815) to 79.1% (*B. breve* NCIMB 702258) in 0.41 mg/ml α -linolenic acid. All of the active *B. breve* strains were derived

from human intestinal sources (infant intestine, nursing stools and neonatal faeces).

Identification of the Bioconversion Product

The presence of conjugated double bonds in the modified fatty acid derived from fermentation of *B. breve* strains with linolenic acid was initially verified by UV spectrophotometry [24], by measuring the absorbance of the fat soluble hexane layer at a wavelength of 233 nm. Fatty acids with conjugated double bonds are characterised by an absorption peak at 233 nm.

The product resulting from the bioconversion of α -linolenic acid by *B. breve* NCIMB 702258 was subsequently identified (using DAD and MS detectors in line, following separation by HPLC) as *c9, t11, c15* CALA (data not shown). A further characterization of *c9, t11, c15* CALA was obtained by the UV and MS spectra (Fig. 2). The bioconversion product showed a mass spectrum with three signals at *m/z* 279.4, 296.4 and 301.4, which were identified as the $[M^+H]^+$, $[M^+NH_4]^+$ and $[M^+Na]^+$ quasi-molecular ions consistent with the molecular weight 278.4 Da of CALA.

Another peak on the bioconversion profile, generated at a much lower concentration than the *c9, t11, c15* CALA isomer, was tentatively identified as *t9, t11, c15* CALA (Fig. 3) by its lower max absorption with respect to the major peak attributed to *c9, t11, c15*. A similar lower max absorption was detected with *t9, t11* with respect to *c9, t11* [25]. In addition, the production of *t9, t11, c15* CALA from α -linolenic acid in combination with *c9, t11, c15* CALA also reflects the generation of *t9, t11* CLA from linoleic acid by *B. breve* NCIMB 702258, which was produced directly from *c9, t11* CLA [20]. However, future studies

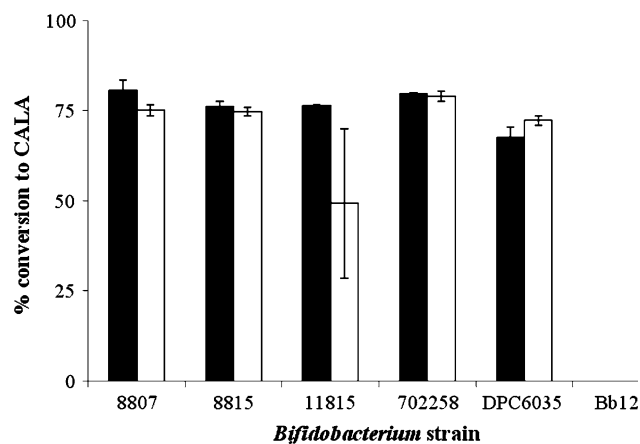


Fig. 1 Bioconversion of α -linolenic acid by a selection of bifidobacteria. The strains were grown in a medium containing 0.24 mg/ml (filled squares) and 0.41 mg/ml (open squares) α -linolenic acid. Conversion to conjugated α -linolenic acid (CALA) was assessed in the bacterial supernatant

Fig. 2 Identification of CALA by UV spectrum (a) and MS spectrum (b)

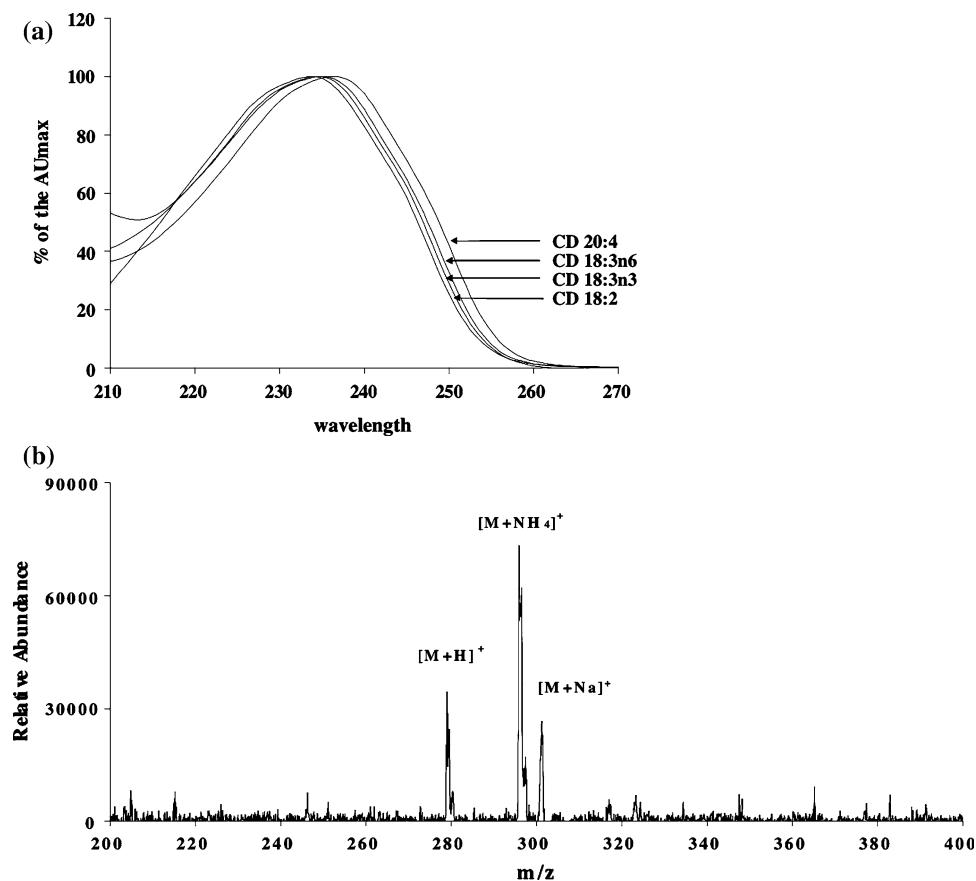
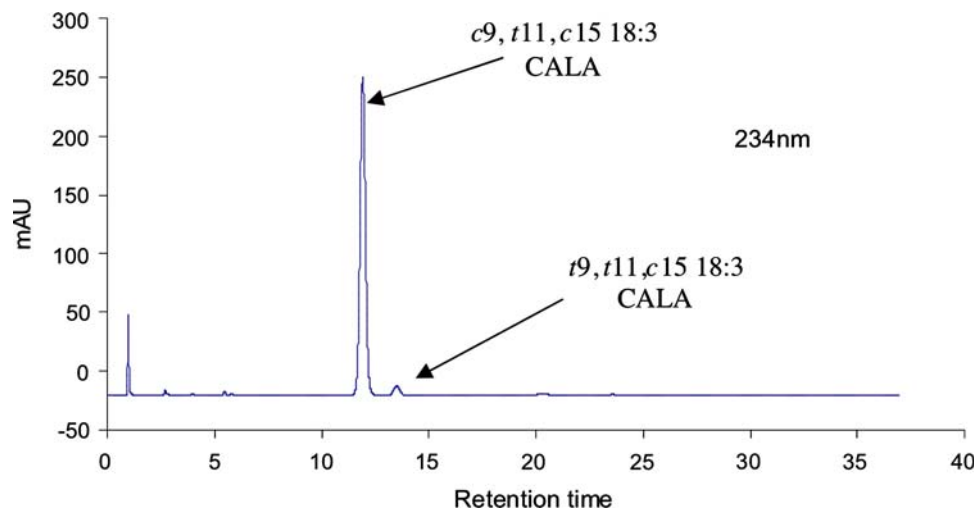


Fig. 3 HPLC separation of *c*9, *t*11, *c*15 conjugated α -linolenic acid from another CALA isomer, which has been identified as *t*9, *t*11, *c*15 CALA



will aim at a definitive identification of the geometrical isomerism by more MS sophisticated techniques.

Generation of CALA Oil and α -Linolenic Acid Oil for Inhibitory Effects on Colon Cancer Cell Growth

Small concentrations of C14:0, C16:0, C18:0, C18:1 *t*11 and linoleic acid were present in the CALA oil sample for the cell culture study. However, these fatty acids

were also present in similar quantities in the control sample (α -linolenic acid) (Table 2). The major difference between the control and CALA oils was the concentration of C18:1 oleic acid. There was 9.7% oleic acid in the control oil compared to 17.2% in the CALA oil due to the bioconversion by *B. breve* NCIMB 702258. However, at the concentrations examined, oleic acid did not have any impact on SW480 cell growth (data not shown).

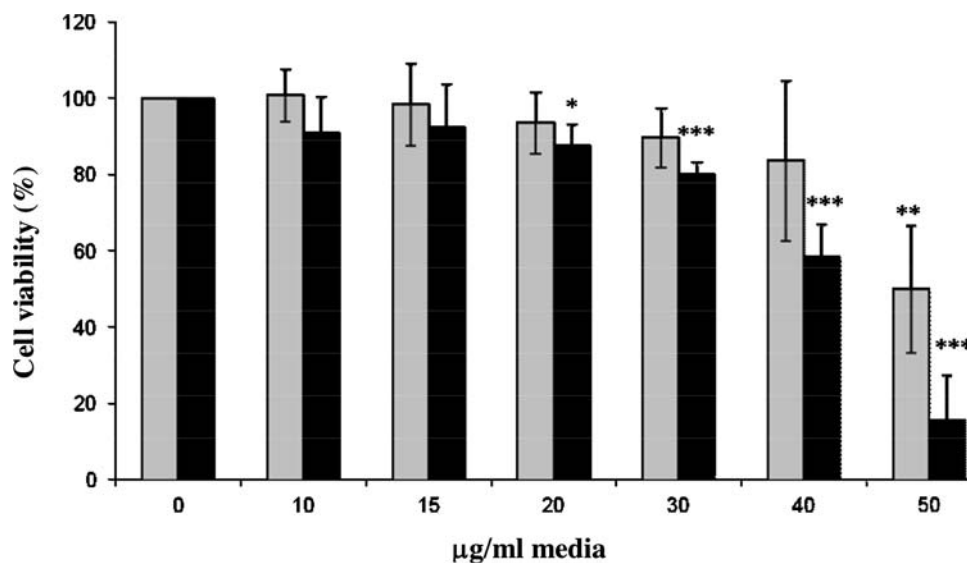
Table 2 Percent fatty acids present in control oil and CALA oil samples for cell culture studies

Fatty acids	Total fatty acids (%)	
	Control oil	Experimental oil
C14:0 Myristic acid	3.7	4.8
C16:0 Palmitic acid	1.8	2.4
C18:0 Stearic acid	2.1	3.1
C18:1- <i>t</i> 11 Vaccenic acid	0.6	1.1
C18:1 <i>c</i> 9 Oleic acid	9.7	17.2
C18:2 Linoleic acid	2.6	1.2
C18:3 Linolenic acid	61.0	5.0
CALA	4.5	55.6
Total	100	100

Biological Activity of CALA in Cell Culture

SW480 cells were incubated for 5 days in the presence of varying concentrations (10–50 $\mu\text{g/ml}$) of either CALA or α -linolenic acid, enabling the effect of both CALA and its precursor on SW480 cell viability to be examined (Fig. 4). A dose-dependent decrease in cell numbers occurred with increasing CALA concentrations with CALA being more potent in reducing cell numbers than α -linolenic acid. Maximal difference in this inhibitory effect occurred at 180 μM (50 $\mu\text{g/ml}$), resulting in an 85% reduction in cell numbers in cultures exposed to CALA, compared with a 50% reduction in cells exposed to α -linolenic acid. However, CALA did not exhibit as potent an inhibitory effect on SW480 colon cancer cells as *c*9, *t*11 CLA or *t*9, *t*11 CLA, as we have shown previously, where incubation with 10 $\mu\text{g/ml}$ of *c*9, *t*11 CLA or *t*9, *t*11 CLA caused 32 and 43% reductions in SW480 cell numbers, respectively [20].

Fig. 4 Comparison of cell viability of SW480 colon cancer cells following 5 days exposure to the same concentrations of α -linolenic acid (shaded squares) and CALA (filled squares) (Statistical analysis: * $p \leq 0.05$; ** $p \leq 0.01$; *** $p \leq 0.001$)



Discussion

In total, there are 28 different isomers of CLA, however, health benefits have mainly been associated with two of these isomers, namely, *c*9, *t*11 and *t*10, *c*12 CLA [5, 26]. It has previously been demonstrated in our laboratory that bifidobacteria, some of human intestinal origin, have the enzymatic capability to synthesise the *c*9, *t*11 and *t*9, *t*11 CLA isomers from free linoleic acid [19, 20]. Bifidobacteria are natural inhabitants of the human gastrointestinal tract and confer probiotic properties, with some having exhibited potential anti-carcinogenic effects [27, 28]. Recently, several unique biological effects have been associated with conjugated linolenic acids, which are produced as a result of isomerisation of α -linolenic acid [13–16, 29, 30]. Until recently, conjugated linolenic acids have only been produced in the laboratory from linolenic acid by alkali-isomerisation, while Ogawa et al. [31] successfully produced CALA using a strain of *Lactobacillus plantarum*.

In this study, six bifidobacteria strains were assessed for their ability to produce conjugated linolenic acid from α -linolenic acid. Interestingly, the five strains of human origin were able to perform the bioconversion. This result is significant in itself, as the ability of bifidobacteria to produce bioactive fatty acid metabolites is possibly linked to their health promoting properties and adds further weight to the anti-proliferative activities associated with intestinal bifidobacteria. While the majority of the substrate required for this conversion is likely absorbed in the small intestine, unabsorbed dietary fatty acids have been found in the colon. Indeed, Vonk et al. [32] proposed that 6–8 g of lipids enter the colon per day, while Hill [33] estimated that 5 g of long chain fatty acids enter the colon on a daily basis. In addition, considering the low levels of *c*9, *t*11, *c*15-CALA in dietary sources [3, 34], the use of CALA-

producing bifidobacteria provides a suitable method for enhancing the physiological concentration of this fatty acid. The bioconversion product produced by one of the five strains, namely, *B. breve* NCIMB 702258, which originated from an infant intestine, was further analysed and identified as *c9, t11, c15*-CALA. Furthermore, *t9, t11, c15*-CALA was identified, but at much lower concentrations.

Evaluation of the inhibitory effects of *c9, t11, c15*-CALA on SW480 colon cancer cells indicated that the presence of this conjugated fatty acid in the growth medium led to a suppressive effect on tumour cell growth. Indeed, a concentration of 180 μ M resulted in 85% reduction in cell numbers, indicating that the conjugated fatty acid was more potent than α -linolenic acid, which resulted in only a 50% reduction in cell numbers. While there are no data available on the physiological concentration of CALA, it has been reported that ALA is found in plasma at a concentration of $0.26 \pm 0.06\%$ of total fatty acids [35]. Thus, the concentrations of ALA used in the present study [10–50 μ g/ml (0.001–0.005%)] are within physiological range.

Typical species associated with the infant gastrointestinal tract are *B. breve*, *B. infantis* and *B. longum*, while *B. catenulatum*, *B. adolescentis*, *B. bifidum* and *B. pseudocatenulatum* are more generally found in adult faeces. *B. adolescentis* has been reported as the most common species in adults [36], although others have found *B. catenulatum* to predominate in adults [37]. Thus, while *B. breve* is not considered a major inhabitant of the adult intestine, it has been identified in faecal samples from adults in the region of 10^8 cells/g [38, 39]. In addition, studies from population dynamics of bifidobacteria in human faeces during raffinose administration to adults indicated that minor species such as *B. breve* proliferated [40]. Development of this strain as a supplement in a probiotic product such as yoghurt would likely increase its presence in the adult/elderly intestine thus targeting the population most at risk from diseases of the colon.

The ability of isomers of conjugated linolenic acids to inhibit cancer cell growth may be linked to a number of cellular effects. For example, to date, the inhibitory properties of isomers of CLA have been attributed to a number of mechanisms including alteration of lipid peroxidation, tissue fatty acid composition, eicosanoid metabolism, gene expression, cell cycle regulation, cell proliferation and apoptosis [41]. In the case of conjugated linolenic acid isomers, earlier studies indicated that these exerted their effects through lipid peroxidation [15]. Indeed, several studies have indicated that lipid peroxidation alone can induce suppression of growth and apoptosis [42–45]. A more recent study comparing the effects of all-*trans*-conjugated linolenic acids on human colon cancer Caco-2 cells

indicated that β -eleostearic acid (*t9, t11, t13*) and β -calendic acid (*t8, t10, t12*) have signalling pathways different from those of α -ESA and α -calendic acid (*t8, t10, c12*), and exhibit high potency for reducing the cell viability of Caco-2 cells [13]. In another study, α -ESA was found to induce apoptosis through the up-regulation of GADD45, p53 and PPAR γ in human colon cancer Caco-2 cells [14]. Yasui et al. [16] also observed an increase in the levels of PPAR γ in HT-29 cells which were treated with α -ESA. Indeed, PPAR γ is one of the target molecules in cancer prevention [46, 47]. Furthermore, the *t9, t11, c13* isomer from catalpa seed oil was shown to suppress the development of colonic aberrant crypt foci induced by azoxymethane in rats through down-regulation of cyclooxygenase-2 (COX-2) [29]. Interestingly, studies using rat intestine demonstrated that while both α -ESA and *c9, t11, c13* conjugated linolenic acid were slowly absorbed, a portion of both fatty acids was quickly converted to the biologically active isomer *c9, t11*-CLA through a Δ 13-saturation reaction [48], suggesting that in the colon the therapeutic effects of conjugated linolenic acids may also be due to the increased production of biologically active CLA isomers. Thus, it is evident that different fatty acid structures exert the same effect through different pathways. Further studies will be required to determine the biological mechanisms of the *c9, t11, c15*-CALA isomer in this study resulting in the inhibition of growth of SW480 colon cancer cells.

Conclusion

This study showed that five strains of bifidobacteria, all of human intestinal origin converted α -linolenic acid to conjugated α -linolenic acid. This microbially produced conjugated α -linolenic acid exhibited inhibitory effects on the growth of SW480 colon cancer cells, in vitro. The ability of bifidobacteria of human intestinal origin to biosynthesise biologically active lipids such as *c9, t11* CLA and conjugated α -linolenic acid may be linked to their suggested therapeutic effects.

Acknowledgments The technical assistance of Seamus Aherne is gratefully acknowledged. This work was funded by SFI funds, and in part by the Irish Government under the National Development Plan 2000–2006 and by EU Project QLK1-2002-02362.

References

1. Dupertuis YM, Meguid MM, Pichard C (2007) Colon cancer therapy: new perspectives of nutritional manipulations using polyunsaturated fatty acids. *Curr Opin Clin Nutr Metab Care* 10:427–432
2. Larsson SC, Kumlin M, Ingelman-Sundberg M, Wolk A (2004) Dietary long-chain n-3 fatty acids for the prevention of cancer: a review of potential mechanisms. *Am J Clin Nutr* 79:935–945

3. Destailats F, Trottier JP, Galvez JM, Angers P (2005) Analysis of alpha-linolenic acid biohydrogenation intermediates in milk fat with emphasis on conjugated linolenic acids. *J Dairy Sci* 88:3231–3239
4. Miller A, Stanton C, Murphy J, Devery R (2003) Conjugated linoleic acid (CLA)-enriched milk fat inhibits growth and modulates CLA-responsive biomarkers in MCF-7 and SW480 human cancer cell lines. *Br J Nutr* 90:877–885
5. Bhattacharya A, Banu J, Rahman M, Causey J, Fernandes G (2006) Biological effects of conjugated linoleic acids in health and disease. *J Nutr Biochem* 17:789–810
6. Ip C, Dong Y, Ip MM, Banni S, Carta G, Angioni G, Murru E, Spada S, Melis MP, Saebo A (2002) Conjugated linoleic acid isomers and mammary cancer prevention. *Nutr Cancer* 43:52–58
7. Belury MA (2002) Inhibition of carcinogenesis by conjugated linoleic acid: potential mechanisms of action. *J Nutr* 132:2995–2998
8. Wang YW, Jones PJ (2004) Conjugated linoleic acid and obesity control: efficacy and mechanisms. *Int J Obes Relat Metab Disord* 28:941–955
9. Terpstra AHM (2004) Effect of conjugated linoleic acid on body composition and plasma lipids in humans. *Amer J Clin Nutr* 79:352–361
10. Kritchevsky D, Tepper SA, Wright S, Tso P, Czarnecki SK (2000) Influence of conjugated linoleic acid (CLA) on establishment and progression of atherosclerosis in rabbits. *J Am Coll Nutr* 19:472S–477S
11. Nicolosi RJ, Rogers EJ, Kritchevsky D, Scimeca JA, Huth PJ (1997) Dietary conjugated linoleic acid reduces plasma lipoproteins and early aortic atherosclerosis in hypercholesterolemic hamsters. *Artery* 22:266–277
12. Nagao K, Yanagita T (2005) Conjugated fatty acids in food and their health benefits. *J Biosci Bioeng* 100:152–157
13. Yasui Y, Hosokawa M, Kohno H, Tanaka T, Myashita K (2006) Growth inhibition and apoptosis induction by all-*trans*-conjugated linolenic acids on human colon cancer cells. *Anticancer Res* 26:1855–1860
14. Yasui Y, Hosokawa M, Sahara T, Suzuki R, Ohgiya S, Kohno H, Tanaka T, Miyashita K (2005) Bitter gourd seed fatty acid rich in 9*c*, 11*t*, 13*t*-conjugated linolenic acid induces apoptosis and up-regulates the GADD45, p53 and PPAR γ in human colon cancer Caco-2 cells. *Prostaglandins Leukot Essent Fatty Acids* 73:113–119
15. Tsuzuki T, Tokuyama Y, Igarashi M, Miyazawa T (2004) Tumor growth suppression by α -eleostearic acid, a linolenic acid isomer with a conjugated triene system, via lipid peroxidation. *Carcinogenesis* 25:1417–1425
16. Yasui Y, Hosokawa M, Kohno H, Tanaka T, Miyashita K (2006) Troglitazone and 9*cis*, 11*trans*, 13*trans*-conjugated linolenic acid: comparison of their antiproliferative and apoptosis-inducing effects on different colon cancer cell lines. *Chemotherapy* 52:220–225
17. Arao K, Yotsumoto H, Han SY, Nagao K, Yanagita T (2004) The 9*cis*, 11*trans*, 13*cis* isomer of conjugated linolenic acid reduces apolipoprotein B100 secretion and triacylglycerol synthesis in HepG2 cells. *Biosci Biotechnol Biochem* 68:2643–2645
18. Futakuchi M, Cheng JL, Hirose M, Kimoto N, Cho YM, Iwata T, Kasai M, Tokudome S, Shirai T (2002) Inhibition of conjugated fatty acids derived from safflower or perilla oil of induction and development of mammary tumors in rats induced by 2-amino-1-methyl-6-phenylimidazo[4, 5-b]pyridine (PhIP). *Cancer Lett* 178:131–139
19. Coakley M, Ross RP, Nordgren M, Fitzgerald G, Devery R, Stanton C (2003) Conjugated linoleic acid biosynthesis by human-derived *Bifidobacterium* species. *J Appl Microbiol* 94:138–145
20. Coakley M, Johnson MC, McGrath E, Rahman S, Ross RP, Fitzgerald GF, Devery R, Stanton C (2006) Intestinal bifidobacteria that produce *trans*-9, *trans*-11 CLA: a fatty acid with antiproliferative activity against human colon SW480 and HT-29 cancer cells. *Nutr Cancer* 56:95–102
21. Rosberg-Cody E, Ross RP, Hussey S, Ryan CA, Murphy BP, Fitzgerald GF, Devery R, Stanton C (2004) Mining the microbiota of the neonatal gastrointestinal tract for conjugated linoleic acid-producing bifidobacteria. *Appl Environ Microbiol* 70:4635–4641
22. Melis MP, Angioni E, Carta G, Murru E, Scannu P, Spada S, Banni S (2001) Characterisation of conjugated linoleic acid and its metabolites by RP-HPLC with diode array detector. *Eur J Lipid Sci Technol* 103:617–621
23. Banni S, Day BW, Evans RW, Corongiu FP, Lombardi B (1995) Detection of conjugated diene fatty acid isomers in liver lipids of rats fed a choline devoid diet indicates that the diet does not cause lipid peroxidation. *J Nutr Biochem* 6:281–289
24. Barrett E, Ross RP, Fitzgerald GF, Stanton C (2007) Rapid screening method for analyzing the conjugated linoleic acid production capabilities of bacterial cultures. *Appl Environ Microbiol* 73:2333–2337
25. Angioni E, Lercker G, Frega NG, Carta G, Melis MP, Murru E, Spada S, Banni S (2002) UV spectral properties of lipids as a tool for their identification. *Eur J Lipid Sci Technol* 104:59–64
26. Fritsche JRR, Steinhart H (1999) Formation, contents and estimation of daily intake of conjugated linoleic acid isomers and *trans*-fatty acids in foods. *Adv Conjugated Linoleic Acid Res* 1:378–396
27. Leahy S, Higgins D, Fitzgerald GF, van Sinderen D (2005) Getting better with bifidobacteria. *J Appl Microbiol* 98:1303–1315
28. Picard C, Fioramonti J, Francois A, Robinson T, Neant F, Matuchansky C (2005) Review article: bifidobacteria as probiotic agents—physiological effects and clinical benefits. *Aliment Pharmacol Ther* 22:495–512
29. Suzuki R, Yasui Y, Kohno H, Miyamoto S, Hosokawa M, Miyashita K, Tanaka T (2006) Catalpa seed oil rich in 9*t*, 11*t*, 13*c*-conjugated linolenic acid suppresses the development of colonic aberrant crypt foci induced by azoxymethane in rats. *Oncol Rep* 16:989–996
30. Chuang C-Y, Hsu C, Chao C, Wein Y-S, Kuo Y-H, Huang C (2006) Fractionation and identification of 9*c*, 11*t*, 13*t*-conjugated linolenic acid as an activator of PPAR α in bitter melon (*Momordica charantia* L.). *J Biomed Sci* 13:763–772
31. Ogawa J, Kishino S, Ando A, Sugimoto S, Mihara K, Shimizu S (2005) Production of conjugated fatty acids by lactic acid bacteria. *J Biosci Bioeng* 100:355–364
32. Vonk RJ, Kalivianakis M, Minich DM, Buijleveld CM, Verade HJ (1997) The metabolic importance of unabsorbed dietary lipids in the colon. *Scand J Gastroenterol* 222:65–67
33. Hill MJ (1998) Composition and control of ileal contents. *Eur J Cancer Prev* 7:S75–S78
34. Plourde M, Destailats F, Chouinard PY, Angers P (2007) Conjugated alpha-linolenic acid isomers in bovine milk and muscle. *J Dairy Sci* 90:5269–5275
35. Rise P, Eligini S, Ghezzi S, Colli S, Galli C (2007) Fatty acid composition of plasma, blood cells and whole blood: relevance for the assessment of the fatty acid status in humans. *Prostaglandins Leukot Essent Fatty Acids* 76:363–369
36. Biavati B, Vescovo M, Torriani S, Bottazzi V (2000) Bifidobacteria: history, ecology, physiology and applications. *Ann Microbiol* 50:117–131
37. Matsuki T, Watanabe K, Tanaka R (2003) Genus- and species-specific PCR primers for the detection and identification of bifidobacteria. *Curr Issues Intest Microbiol* 4:61–69

38. Gueimonde M, Debor L, Tolkkio S, Jokisalo E, Salminen S (2007) Quantitative assessment of faecal bifidobacterial populations by real-time PCR using lanthanide probes. *J Appl Microbiol* 102:1116–1122
39. Barrett E, Ross RP, Fitzgerald GF, Stanton C (2007) Rapid screening method for analyzing the conjugated linoleic acid production capabilities of bacterial cultures. *Appl Environ Microbiol* 73:2333–2337
40. Dinoto A, Marques TM, Sakamoto K, Fukiya S, Watanabe J, Ito S, Yokota A (2006) Population dynamics of *Bifidobacterium* species in human feces during raffinose administration monitored by fluorescence in situ hybridization-flow cytometry. *Appl Environ Microbiol* 72:7739–7747
41. Kelley NS, Hubbard NE, Erickson KL (2007) Conjugated linoleic acid isomers and cancer. *J Nutr* 137:2599–2607
42. Esterbauer H (1993) Cytotoxicity and genotoxicity of lipid oxidation products. *Am J Clin Nutr* 57:779S–786S
43. Sandstorm PA, Tebbey PW, Van Cleave S, Buttke TM (1994) Lipid hydroperoxides induce apoptosis in T cells displaying a HIV-associated glutathione peroxidase deficiency. *J Biol Chem* 269:798–801
44. Aoshima H, Satoh T, Sakai N, Yamada M, Enokiko Y, Ikeuchi T, Hatanaka H (1997) Generation of free radicals during lipid hydroperoxide-triggered apoptosis in PC12 h cells. *Biochim Biophys Acta* 1345:35–42
45. Ji C, Rouzer CA, Marnett LJ, Pietenpol JA (1998) Induction of cell cycle arrest by the endogenous product of lipid peroxidation, malondialdehyde. *Carcinogenesis* 19:1275–1283
46. Gupta RA, Dubois RN (2002) PPAR γ as a target for treatment of colorectal cancer. *Am J Physiol* 283:G266–G269
47. Sporn MB, Suh N, Mangelsdorf DJ (2001) Prospects for prevention and treatment of cancer with selective PPAR γ modulators (SPARMS). *Trends Mol Med* 7:395–400
48. Tsuzuki T, Kawakami Y, Abe R, Nakagawa K, Koba K, Imamura J, Iwata T, Ikeda I, Miyazawa T (2006) Conjugated linolenic acid is slowly absorbed in rat intestine, but quickly converted to conjugated linoleic acid. *J Nutr* 136:2153–2159

Evaluating the *trans* Fatty Acid, CLA, PUFA and Erucic Acid Diversity in Human Milk from Five Regions in China

Jing Li · Yawei Fan · Zhiwu Zhang · Hai Yu ·
Yin An · John K. G. Kramer · Zeyuan Deng

Received: 23 October 2008 / Accepted: 4 January 2009 / Published online: 31 January 2009
© AOCS 2009

Abstract Human milk was obtained from 97 healthy lactating women from five different regions in China. Twenty-four hour dietary questionnaire identified the foods consumed that showed distinct differences in food types between cities. The southern and central regions had higher levels of total *trans* fatty acids (TFA) and conjugated linoleic acids (CLA) in human milk than the northern region. The major isomers in human milk from the northern region were vaccenic and rumenic acids, whereas the other regions had a random distribution of these isomers. This was consistent with the isomer distribution in the refined vegetable oils used and their increased formation during high temperature stir-frying. The human milk composition showed little evidence that partially hydrogenated fats were consumed, except eight mothers in Guangzhou who reported eating crackers, plus four other mothers. The TFA concentration in these human milk samples was higher (2.06–3.96%). The amount of n-6 (1.70–2.24%) and n-3 (0.60–1.47%) highly unsaturated fatty acids (HUFA) in human milk and the resultant ratio (1.43–2.95) showed all mothers in China had an adequate supply of HUFA in their

diet. Rapeseed oil was consumed evidenced by erucic acids in human milk. The levels of erucic acid were below internationally accepted limits for human consumption. The levels of undesirable TFA and CLA isomers in human milk are a concern. Efforts to decrease the practice of high temperature stir-frying using unsaturated oils, and a promotion to increase consumption of dairy and ruminant products should be considered in China.

Keywords Human milk · Survey · *trans* Fatty acid · Conjugated linoleic acid · Polyunsaturated fatty acid · Erucic acid

Abbreviations

ARA	Arachidonic acid
BCFA	Branch chain fatty acid
CLA	Conjugated linoleic acid
DHA	Docosahexaenoic acid
DUFA	Diunsaturated fatty acid
HUFA	Highly unsaturated fatty acid
FA	Fatty acid
FAME	Fatty acid methyl ester
MCFA	Medium-chain fatty acid
MUFA	Monounsaturated fatty acid
PHF	Partially hydrogenated fat
PUFA	Polyunsaturated fatty acid
SFA	Saturated fatty acid
TFA	<i>trans</i> Fatty acid
TUFA	Triunsaturated fatty acid

J. Li · Y. Fan · Z. Deng (✉)
State Key Lab of Food Science and Technology,
Institute for Advanced Study, University of Nanchang,
235, Nanjing East Road, 330047 Nanchang, Jiangxi,
People's Republic of China
e-mail: zeyuandeng@hotmail.com

Z. Zhang · Y. An
Yili Group Ltd Co., Hohhot, Inner Mongolia, China

J. Li · H. Yu · J. K. G. Kramer
Guelph Food Research Center, Agriculture and Agri-Food
Canada, Guelph, ON N1G 5C9, Canada

J. K. G. Kramer
e-mail: kramerj@agr.gc.ca

Introduction

The importance of breastfeeding is well recognized as providing infants with complete nutrition for development

and immunological protection in the first few months. The fat in human milk plays a key role in supplying energy and essential n-3 and n-6 polyunsaturated fatty acids (PUFA), and specifically the highly unsaturated fatty acids (HUFA) arachidonic (ARA 20:4n-6) and docosahexaenoic acids (DHA 22:6n-3), required for growth and optimal mental and vision development [1–4]. Infants lack the capacity to synthesize sufficient n-3 and n-6 HUFA from the linolenic (18:3n-3) and linoleic acid (18:2n-6) precursors [5, 6], and for this reason an adequate supply and balance of these HUFA are recommended in the mother's diet [3, 4, 7, 8]. The fatty acid (FA) composition of the maternal diet is known to influence the composition of human milk within 24 h of consumption [9]. Several surveys have been undertaken to assess the HUFA status of human milk in different populations [10, 11]. Studies have also been conducted to determine any detrimental effects associated with the higher consumption of n-3 HUFA by mothers, particularly fish products, a major source of DHA, which may possibly be contaminated [12].

In recent years the issue of *trans* fatty acids (TFA) in the human diet has become a major concern because of health implications [13]. Infants are equally exposed to TFA since they pass through the placenta and into the milk [14–16]. TFA generally occur in foods containing partially hydrogenated fats (PHF) and ruminant products, which differ in their *trans* isomer composition [17, 18]. Moreover, TFA can also be produced during domestic frying [19–21] and deodorization [22] with both generating a random distribution of TFA isomers. There has been a significant drop in the total TFA content in Western Europe in the 1990s as the result of voluntary discontinuation by industry of PHF production [23]. During the discussion period to introduce mandatory TFA labeling of food products in Canada [24], a decline in total TFA content in human milk has also become evident in Canada [16, 25].

Another group of FA of interest in infant development are the conjugated linoleic acids (CLA) known to provide protection against cancer [26] and other benefits [27] in experimental animals. Further research is needed to demonstrate that humans receive the same benefit [28, 29]. Possible benefit of ruminic acid for breast-fed infants needs to be examined since breast-fed infants have a higher content of *Bifidobacteria* in their gut than formula-fed infants, and these bacteria are known to synthesize vaccenic (11*t*-18:1) and ruminic acids (9*c*11*t*-18:2) from 18:2n-6 [30, 31].

A few surveys on the fat composition of human milk are currently available from China. These surveys basically focused on the DHA status and were restricted to the Beijing [32–34], the northeast coastal region [35] and one city in the west-central region of China [11, 36]. The occurrence of CLA was only reported in one of the surveys

[11]. In none of the studies was there an attempt to evaluate the TFA profile that would reflect the type of fats consumed, whether derived from ruminants, hydrogenated fat, oils after stir frying, or deodorized vegetable oils. In addition, all these studies reported the presence of erucic acid in human milk [11, 32–36]. Erucic acid was also found to be present in blood lipids of Chinese children [37].

The present study was designed to evaluate the TFA, CLA, HUFA and erucic acid content, composition and variation of human milk from five regions in China known for their distinct differences in diet and method of food preparation. We were particularly interested in determining the TFA and CLA profiles since they would provide a good indication of the dietary fat sources consumed (ruminants or partially hydrogenated products), the type of frying process used, and the occurrence of erucic acid in human milk from different regions.

Subjects and Methods

Subjects

Breast milk was collected from 97 healthy lactating women who had given birth in hospitals and were generally from the middle CLAs. Five cities in China were selected which were Guangzhou (GZ, $n = 25$) and Shanghai (SH, $n = 25$) coastal cities in the south and east, respectively, Nanchang (NC, $n = 25$) in central China, Harbin (HA, $n = 11$) in Manchuria a major cereal producing region, and Hohhot (HT, $n = 11$) in Inner Mongolia a region known for extensive dairy and beef production. Milk samples were collected between January and April (NC, SH) and August–November 2004 (GZ, HA, HT). Written informed consent was obtained from each volunteer. At the time of sample collection, all the mothers were asked to complete a 24-h dietary recall questionnaire prior to collection that identified the foods consumed at each meal and snacks. Mothers consumed self-selected diets without being given any dietary recommendations. A quantitative measurement of the amount consumed was not requested because of the difficulty of estimating each food type when meals are prepared at home that consisted of mixtures of meat, vegetables and rice. The study was approved by the Human Ethics Committee of the University of Nanchang and the Yili Company in Inner Mongolia.

Milk was obtained from each woman at 9 a.m. on each collection day; transitional milk at day 10 and 13 after delivery, and mature milk at day 21 and 25. Under the supervision of professional nurses, nursing mothers were instructed to manually express breast milk to fill a 15-mL sterile disposable polypropylene tube fitted with a cap (Zhejiang Gongdong Medical Plastic Company, Hangzhou,

China). The tubes had been previously washed with 10% HNO₃ and deionized water. All tubes were capped and frozen in domestic freezers and transported as soon as possible to medical facilities where they were frozen at -70°C . After completion of sample collections they were shipped under refrigeration to the University of Nanchang where they were stored at -70°C until analyzed.

Fatty Acid Analysis

Milk lipid samples were thawed to room temperature and thoroughly mixed to assure homogeneity. One mL of total milk was extracted by using chloroform/methanol (1:1) and the total lipids were methylated using sodium methoxide as described previously [38]. The fatty acid methyl esters (FAME) were analyzed by gas chromatography equipped with an autosampler, and a flame ionization detector (Model 6890 N, Agilent Technologies, Shanghai, China). A 100 m H 0.25 mm (ID) (0.2 μm film thickness) fused silica capillary column coated with 100% cyanopropyl polysiloxane was used (CP-Sil 88, Chrompack; Middelburg, The Netherlands). The initial temperature of the program was 45°C held for 4 min, and then increased at a rate of $13^{\circ}\text{C}/\text{min}$ to 175°C , and held for 27 min. The oven temperature was then further increased to 215°C at a rate of $4^{\circ}\text{C}/\text{min}$ and held for 35 min [38]. All peaks were identified by comparison of their retention times with a standard FAME mixture (#463) spiked with a mixture of four positional CLA isomers (#UC-59 M) and 21:0, 23:0 and 26:0. All of these FAME were obtained from Nu-Chek Prep Inc. (Elysian, MN).

Selected foods were analyzed to determine the source of certain FA in human milk. Retail bovine milk was purchased in the Nanchang area from different suppliers and production dates during the same time human milk was collected to evaluate the milk FA composition. In addition, most of the refined vegetable oils available in the market in China were analyzed for their FA composition [39]. Crackers similar to those consumed by mothers in Guangzhou were analyzed and compared to other PHF. Several vegetable oils (soybean, canola, peanut and corn oil) were locally purchased in Canada and subjected to typical wok cooking of Chinese cabbage. The oils before and after wok cooking were analyzed by GC according to published procedures [40; JKG, Kramer, unpublished data]. All the samples were analyzed using the same methods as described above.

Statistical Analysis

The FA composition data were analyzed using the GLM procedure of the statistical analysis system (SAS Release 9.1, SAS Institute Inc., Cary, NC, USA) based on a split

plot design in which cities are as main plots, time periods within cities as sub-plots, and mothers as replicates. The statistical model included city, time period, mother, and city by time period interaction. City effects were tested using the error term of mother nested within city. Least square means of FA composition were calculated using the option of LS-MEAN and statistical differences among cities and lactation periods were identified at $P < 0.05$ using the option of P-DIFF.

Results

Food Consumption Questionnaire

Based on the 24-h recall questionnaire completed each time milk was sampled (Table 1), all mothers consumed rice. Consumption of other carbohydrate sources (oats, steamed wheat buns, lotus roots, bread and cakes) was highest and most frequent in Shanghai and least in Guangzhou. All nursing mothers ate meat during lactation, but there were regional differences in the type of meat consumed. Pork consumption was much more prevalent in southern (96–100%) and central China (100%) than in the northern

Table 1 Dietary recall of food consumed by lactating women from five regions in China

Food groups	GZ	SH	NC	HA	HT
Carbohydrates (CHO)					
Only rice	80	20	72	60	55
Occasionally other CHOs	10	52	24	40	27
Regularly other CHOs	10	28	4	0	18
Crackers	32	0	0	0	0
Meats					
Pork	100	96	100	60	55
Only pork	12	8	24	10	0
Always pork	64	44	64	50	9
Pork and fowl	68	80	72	70	9
Pork, fowl and ruminants	20	12	4	10	36
Only fowl	0	4	0	10	27
Ruminants and fowl	0	0	0	0	18
Fish/shrimp	100	100	80	70	18
Other foods					
Dairy	32	64	48	20	55
Eggs	56	96	92	90	100
Vegetables and tofu	72	96	84	40	91
Fruit	60	48	32	10	18

The values are expressed as percentage of total number of mothers in each city

GZ Guangzhou, SH Shanghai, NC Nanchang, HA Harbin, HT Hohhot, *Only pork* mothers ate only pork and did not eat other meat products, *Always pork* mothers ate pork on all four collection days

regions (55–60%) where beef, sheep and poultry consumption was much higher. All mothers in Guangzhou and Shanghai consumed fish or shrimp caught in salt water, while the fish consumed in Nanchang (80%) and Harbin (70%) was mainly from fresh water. The lowest fish consumption was reported in Hohhot (18%), which agrees with rural women surveyed in Inner Mongolia [35]. Egg consumption was very prevalent during the lactation period in all regions of China (92–100%), with the exception of Guangzhou where only half of the mothers ate eggs (Table 1). Dairy consumption ranged from 20% in Harbin to 64% in Shanghai. It was surprising that dairy consumption of nursing mothers was only 55% in Hohhot, the major dairy region of China. Consumption of vegetables and tofu was a major component in most maternal diets in China (>72%), with the exception of Harbin in north east China (40%). Fruit consumption was generally found to be rather low in the northern cities of Harbin and Hohhot (10 and 18%; Table 1) despite the fact that the human milk was collected between August and November when a variety of fruits would have been available at a reasonable cost; similar results were reported in other surveys on human milk in China [33, 36]. On the other hand, fruit consumption was much higher in Guangzhou (60%) where most mothers reported eating papaya and chieh-qua that are available all year round.

Fatty Acid Composition of Human Milk

Human milk samples for each of the four collection periods were analyzed separately, but then combined into transitional (day 10 and 13) and mature milk (day 21 and 25) because of their similarity (Table 2). In general, there were significant regional differences for most of the FA in human milk, and only few differences between transitional and mature milk and between mothers within the same city; there were only few statistically significant interactions between lactation times and locations.

Saturated Fatty Acids

The total saturated fatty acids (SFA) of human milk ranged from 35 to 42% of total lipids, with palmitic acid (16:0) accounting for just over half of total SFA, followed by stearic acid (18:0) at about 6% of total FA, and the sum of the medium-chain fatty acids (MCFA; 8:0–14:0) at about 12% (Table 2). Significant differences were observed between the total SFA content of human milk from Nanchang and Harbin compared to the other three cities, due mainly to lower levels of 16:0, 14:0 and 12:0 (Table 2). Human milk also contains small amounts of branch-chain fatty acids (BCFA) that are generally derived from milk and meat of ruminants. Higher levels of BCFA were found in the

human milk fats from Hohhot, Shanghai and Guangzhou. Guangzhou also had higher levels of the long-chain SFA ($\geq 20:0$), which reflects the higher consumption of fruits and vegetables that contain these FA in the form of wax esters. Human milk from Shanghai contained the highest level of MCFA (13.62–14.57%). Consumption of high carbohydrate/low fat diets was reported to cause increased levels of MCFA in human milk [41, 42], but this was unlikely the case in Shanghai, since the level of total MCFA was about 14%, similar to that found in human milk from nursing mothers on a balanced diet in America (14%) [41]. In contrast, high MCFA were observed in human milk from Egypt (20%) [41], the Dominican Republic (45%) [42] and the Philippines (31%) [11].

cis Monounsaturated Fatty Acids

The *cis* monounsaturated fatty acids (MUFA) in human milk ranged from 31 to 38% of total lipids. The major isomer was oleic acid (9*c*-18:1) that accounted for about 85% of the total *cis*-MUFA; the highest levels were found in Nanchang and the lowest in Shanghai (Table 2). Other *cis*-MUFA included 11*c*-18:1 (2%) and 9*c*-16:1 (1.8%). Small amounts of erucic acid (13*c*-22:1) were found in all human milk samples indicating that rapeseed oil was available and consumed. There were regional differences in the amount of erucic acid found in human milk between Shanghai (0.08%) and Nanchang (0.22%), and the content of the individual human milk samples ranged from 0.00% (three in GZ and one in HA) to 0.90% (in NC).

trans Fatty Acids

Small amounts of *trans*-MUFA were present in all human milk samples ranging in content between 0.15 and 1.32% (Table 2), and the *trans*-18:1 isomers accounted for more than 96% of the total in the *trans*-MUFA in the southern and central regions, and somewhat less in the northern cities (85–96%). There were significant regional differences both in the total TFA content and the distribution of the *trans*-18:1 isomers. The two northern cities, Hohhot and Harbin, had significantly less total *trans*-18:1 than the other cities (Fig. 1, upper), but the human milk from several mothers had an isomer distribution that showed a greater similarity to ruminant fats with relatively more vaccenic acid (11*t*-18:1) (7 of 11 mothers from HT and 3 of 11 in HA). This compares with the other three cities where none of the human milk samples had this isomer distribution. Instead, all four *trans*-18:1 isomers from 6-9*t*- to 11*t*-18:1 were found to be similar in abundance. Typical representative GC separations of the 18:1 region are shown in Fig. 2 for two human milk samples with distinctly different *trans*-18:1 patterns. Human milk A was selected

Table 2 Fatty acids composition of transitional (T) and mature (M) human milk from five regions in China expressed as % of total fatty acids

City	GZ		SH		NC		HA		HT		SEM	City	Time	Mother	City × time
	T	M	T	M	T	M	T	M	T	M					
8:0	0.16	0.13	0.15	0.16	0.17	0.25	0.13	0.64	0.13	0.11	0.03	***	***	**	***
10:0	1.43	1.33	1.47	1.51	1.13	1.6	1.36	0.79	1.11	1.04	0.17	**	NS	**	**
12:0	5.69	5.02	6.54	6.21	4.22	5.49	5.25	4.89	5.35	4.60	0.60	***	NS	*	NS
14:0	5.19	4.63	6.41	5.74	3.76	4.67	4.53	4.27	5.62	4.60	0.60	***	NS	*	NS
15:0 iso	0.02	0.04	0.02	0.02	0.03	0.02	0.01	0.02	0.02	0.02	0.01	*	NS	NS	NS
15:0 anti	0.01	0.02	0.02	0.02	0.01	0.01	0.02	0.02	0.03	0.03	0.01	*	NS	NS	NS
15:0	0.17	0.17	0.15	0.15	0.08	0.11	0.11	0.12	0.15	0.14	0.01	***	NS	NS	NS
16:0 iso	0.03	0.04	0.02	0.03	0.00	0.01	0.04	0.03	0.04	0.04	0.01	***	NS	NS	NS
16:0	22.34	22.09	20.34	20.56	19.73	19.09	20.18	20.37	21.87	22.22	0.79	***	NS	**	NS
17:0 iso	0.09	0.09	0.05	0.05	0.06	0.04	0.04	0.04	0.07	0.07	0.01	***	NS	NS	NS
17:0	0.25	0.28	0.25	0.25	0.22	0.21	0.23	0.25	0.25	0.24	0.02	***	NS	NS	NS
18:0	6.41	6.52	5.67	5.99	5.42	5.51	5.72	6.61	6.15	6.79	0.32	***	NS	*	***
20:0	0.24	0.25	0.18	0.19	0.17	0.18	0.16	0.09	0.18	0.18	0.01	***	NS	NS	**
22:0	0.12	0.13	0.09	0.08	0.08	0.08	0.06	0.06	0.05	0.05	0.01	***	NS	NS	NS
23:0	0.02	0.05	0.03	0.03	0.05	0.23	0.02	0.02	0.01	0.01	0.01	***	NS	NS	***
24:0	0.08	0.06	0.09	0.05	0.05	0.05	0.03	0.03	0.02	0.01	0.02	**	NS	NS	NS
∑ SFA	42.25	40.85	41.48	41.04	35.18	37.55	37.89	38.25	41.05	40.15	1.03	***	NS	NS	NS
∑ BCFA	0.15	0.19	0.11	0.12	0.1	0.08	0.11	0.11	0.16	0.16	0.02	***	NS	NS	NS
∑ MCFA	12.47	11.11	14.57	13.62	9.28	12.01	11.27	10.59	12.21	10.35	0.74	***	NS	**	***
9c14:1	0.05	0.05	0.06	0.06	0.08	0.05	0.05	0.05	0.06	0.06	0.01	NS	NS	NS	NS
9r16:1	0.04	0.04	0.03	0.01	0.03	0.02	0.01	0.03	0.02	0.02	0.01	**	NS	NS	**
7c16:1	0.38	0.36	0.44	0.41	0.48	0.44	0.38	0.23	0.38	0.35	0.02	***	***	**	**
9c16:1	2.2	2.26	1.78	1.79	1.65	1.56	2.00	0.97	1.91	2.06	0.14	***	**	***	***
9c17:1	0.13	0.14	0.12	0.12	0.1	0.09	0.11	0.11	0.12	0.13	0.01	***	NS	NS	NS
9r18:1	0.44	0.45	0.45	0.45	0.48	0.46	0.04	0.05	0.14	0.13	0.05	***	NS	**	NS
10r18:1	0.34	0.35	0.36	0.33	0.33	0.3	0.02	0.03	0.09	0.09	0.04	***	NS	***	NS
11r18:1	0.26	0.31	0.26	0.22	0.24	0.21	0.06	0.06	0.14	0.15	0.04	***	NS	NS	NS
12r/6-8c18:1	0.17	0.17	0.17	0.16	0.14	0.13	0.02	0.03	0.06	0.06	0.02	***	NS	***	NS
9c/10c18:1	29.09	29.67	25.93	26.03	32.72	30.61	27.06	27.33	28.97	29.59	0.98	***	NS	*	NS
11c18:1	2.12	2.09	2.03	1.93	2.22	2.05	1.90	1.86	1.97	1.96	0.08	***	NS	**	NS
12c18:1	0.12	0.13	0.14	0.14	0.14	0.13	0.03	0.04	0.04	0.04	0.01	***	NS	***	NS
13c18:1	0.09	0.09	0.10	0.09	0.10	1.00	0.04	0.04	0.05	0.45	0.01	***	NS	NS	NS
14c18:1	0.05	0.06	0.04	0.04	0.05	0.05	0.01	0.01	0.01	0.01	0.01	***	NS	*	NS
15c18:1	0.06	0.06	0.05	0.05	0.05	0.05	0.01	0.05	0.01	0.01	0.01	***	**	**	***
13c22:1	0.12	0.12	0.09	0.08	0.23	0.22	0.10	0.09	0.14	0.13	0.02	***	NS	*	NS
15c24:1	0.06	0.06	0.08	0.05	0.12	0.11	0.06	0.04	0.21	0.19	0.02	***	NS	NS	NS
∑ cis MUFA	34.35	34.97	30.77	30.71	37.71	36.14	31.65	30.73	33.73	34.85	1.06	***	NS	*	NS
∑ trans MUFA	1.25	1.32	1.27	1.17	1.22	1.12	0.15	0.20	0.45	0.45	0.15	***	NS	***	NS
∑ trans-18:1	1.21	1.28	1.24	1.16	1.19	1.10	0.14	0.17	0.43	0.43	0.15	***	NS	***	NS
∑ cis18:1	31.53	32.1	28.29	28.28	35.26	32.99	29.06	29.28	31.05	31.66	1.03	***	NS	*	NS
18:2n-6	15.71	16.58	19.15	19.82	17.05	17.58	23.27	23.7	16.37	16.79	1.03	***	NS	**	NS
18:3n-6	0.01	0.01	0.01	0.02	0.01	0.04	0.13	0.16	0.11	0.13	0.01	***	**	NS	NS
20:2n-6	0.54	0.49	0.57	0.48	0.53	0.51	0.53	0.42	0.52	0.49	0.04	NS	**	NS	NS
20:3n-6	0.35	0.32	0.38	0.40	0.40	0.41	0.42	0.45	0.42	0.41	0.04	**	NS	NS	NS
20:4n-6	0.55	0.54	0.61	0.56	0.68	0.63	0.76	0.73	0.61	0.54	0.05	***	NS	**	NS
22:2n-6	0.09	0.06	0.10	0.07	0.09	0.06	0.09	0.07	0.10	0.08	0.01	NS	***	NS	NS
22:4n-6	0.01	0.07	0.15	0.13	0.17	0.17	0.17	0.16	0.18	0.14	0.02	***	NS	NS	***

Table 2 continued

City	GZ		SH		NC		HA		HT		SEM	City	Time	Mother	City × time	
	T	M	T	M	T	M	T	M	T	M						
Fatty acids																
22:5n-6	0.16	0.11	0.07	0.07	0.10	0.08	0.13	0.12	0.13	0.11	0.01	***	**	*	*	
18:3n-3	0.9	0.94	1.43	1.48	1.25	1.38	2.17	2.18	2.22	2.68	0.21	***	NS	**	NS	
18:4n-3	0.00	0.01	0.01	0.02	0.02	0.02	0.03	0.04	0.02	0.03	0.01	***	NS	*	NS	
20:3n-3	0.09	0.08	0.01	0.01	0.08	0.12	0.10	0.09	0.00	0.00	0.02	***	NS	NS	NS	
20:4n-3	0.08	0.08	0.08	0.08	0.07	0.07	0.10	0.11	0.12	0.13	0.02	***	NS	**	NS	
20:5n-3	0.04	0.09	0.10	0.06	0.04	0.04	0.58	0.06	0.04	0.03	0.02	NS	NS	NS	*	
22:5n-3	0.17	0.16	0.14	0.14	0.13	0.11	0.16	0.16	0.16	0.15	0.01	***	NS	***	NS	
22:6n-3	0.41	0.39	0.47	0.42	0.39	0.35	0.53	0.51	0.4	0.29	0.04	***	*	***	NS	
9c11t-18:2	0.08	0.09	0.11	0.11	0.09	0.07	0.08	0.09	0.09	0.10	0.01	***	NS	NS	NS	
9t11c-18:2	0.04	0.03	0.06	0.05	0.04	0.04	0.00	0.01	0.01	0.01	0.01	***	NS	NS	NS	
11t13c-18:2	0.03	0.03	0.04	0.04	0.03	0.06	0.01	0.01	0.01	0.01	0.01	***	NS	NS	**	
∑tt-CLA	0.07	0.07	0.04	0.05	0.09	0.11	0.02	0.02	0.01	0.01	0.01	***	NS	NS	NS	
∑ CLA	0.22	0.22	0.25	0.25	0.25	0.28	0.11	0.13	0.12	0.13	0.02	***	NS	NS	NS	
9c12t-18:2	0.15	0.15	0.1	0.1	0.21	0.19	0.04	0.03	0.06	0.06	0.02	***	NS	**	NS	
9t12c-18:2	0.14	0.14	0.26	0.27	0.19	0.2	0.04	0.20	0.05	0.05	0.03	***	**	**	*	
∑ trans DUFA	0.29	0.29	0.36	0.37	0.40	0.39	0.08	0.23	0.11	0.11	0.04	***	NS	***	NS	
cct-18:3	0.06	0.07	0.1	0.13	0.07	0.11	0.06	0.06	0.06	0.05	0.02	***	NS	NS	NS	
ctc-18:3	0.07	0.07	0.12	0.13	0.03	0.12	0.03	0.03	0.00	0.00	0.02	***	*	NS	***	
tcc-18:3	0.03	0.04	0.05	0.04	0.03	0.03	0.06	0.05	0.04	0.04	0.01	NS	NS	NS	NS	
∑trans TUFA	0.16	0.18	0.27	0.30	0.13	0.26	0.15	0.14	0.10	0.09	0.05	***	NS	*	NS	
∑ PUFA	19.78	21.27	24.57	24.68	21.79	22.5	29.51	29.46	21.73	22.71	1.15	***	NS	*	NS	
∑ n-6 PUFA	17.42	18.18	21.04	21.55	19.03	19.48	25.5	25.81	18.44	18.69	1.05	***	NS	**	NS	
∑ n-3 PUFA	1.69	1.75	2.24	2.21	1.98	2.09	3.67	3.15	2.96	3.31	0.22	***	NS	***	NS	
∑ n-6 HUFA	1.70	2.24	1.88	1.71	1.97	1.86	2.10	1.95	1.96	1.77	0.12	***	*	*	NS	
∑ n-3 HUFA	0.79	0.80	0.80	0.71	0.71	0.69	1.47	0.93	0.72	0.60	0.07	***	NS	***	NS	
n-6/n-3PUFA	10.31	10.76	9.39	9.75	9.61	9.32	6.95	8.19	6.23	5.65	0.78	***	NS	***	NS	
n-6/n-3HUFA	2.15	2.80	2.35	2.41	2.77	2.70	1.43	2.10	2.72	2.95	0.19	***	NS	***	NS	

GZ Guangzhou, SH Shanghai, NC Nanchang, HA Harbin, HT Hohhot, SEM standard error mean, BCFA branch chain fatty acid, CLA conjugated linoleic acid, DUFA diunsaturated fatty acid, HUFA highly unsaturated fatty acid, MCFA medium-chain fatty acid, MUFA monounsaturated fatty acid, PUFA polyunsaturated fatty acid, SFA saturated fatty acid, TFA trans fatty acid, TUFA triunsaturated fatty acid

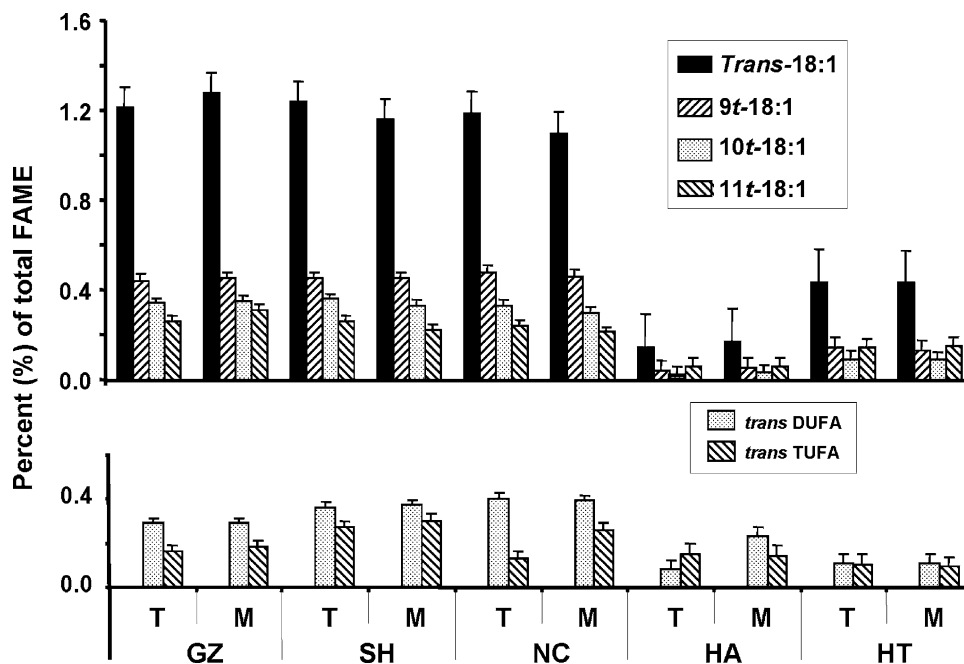
Significant differences between cities, times, mothers and city by time interaction are: NS ($P > 0.05$); * ($P < 0.05$); ** ($P < 0.01$); *** ($P < 0.001$)

from one of eight mothers in Guangzhou who reported consuming crackers. Crackers were subsequently analyzed and found to contain 20.1% TFA which suggested that this product was a possible source of TFA; see the *trans*-18:1 profile of a cracker in Fig. 2. The human milk from one of these mothers showed a higher total TFA content (3.3%) and a random distribution of *trans*-18:1 isomers (human milk A, Fig. 2). The human milk of four more mothers, three from Nanchang and one from Shanghai, had an equally high TFA content, even though they did not report consuming products that could have contained PHF. Human milk B was selected from Hohhot in which 11t-18:1 was the most prominent *trans*-18:1 isomer (Fig. 2), and the total TFA content was about 0.6% of total milk fat. The FA composition of bovine milk collected in Nanchang

in 2004 (Table 3) shows that 11t-18:1 was the prominent *trans*-18:1 isomer (Fig. 2). The final GC graph shows the *trans*-18:1 profile of fully refined soybean oil after wok cooking (Fig. 2, wok fried oil; J Kramer, unpublished data).

Diunsaturated fatty acids (DUFA, mainly 9c12t- and 9t12c-18:2) and triunsaturated fatty acids (TUFA, mainly 9t12c15c-, 9c12c15t- and 9c12t15c-18:3) containing one *trans* double bond were also detected in the human milk samples from China (Table 2). In general, the content of these isomers was lower in the two northern cities than in southern and central China (Fig. 1, lower). In addition, there were differences in the distribution of the di- and triunsaturated isomers. In the southern and central regions, DUFA predominated arising mainly from linoleic acid,

Fig. 1 Total content of *trans*-18:1 and selected *trans*-18:1 isomers (percentage of total fatty acids) of transitional (*T*) and mature (*M*) human milk from five cities in China (*GZ* Guangzhou, *SH* Shanghai, *NC* Nanchang, *HA* Harbin, *HT* Hohhot). The lower graph shows the total content of mono *trans* containing diunsaturated fatty acids (DUFA) and triunsaturated fatty acids (TUFA) from the same human milk samples



while in the two northern cities the distribution of the DUFA and TUFA was generally similar.

Conjugated Linoleic Acids

The average total CLA content in human milk ranged from 0.11% in Harbin to 0.28% in Nanchang (Table 2). There were significantly higher levels of total CLA in the cities of southern and central China than in the two northern cities of Harbin and Hohhot. However, the CLA in these three cities

consisted mainly of CLA isomers other than rumenic acid (9*c*11*t*-18:2) (Fig. 3). Rumenic acid accounted for less than 44% of total CLA in human milk from Guangzhou, Shanghai and Nanchang, but more than 70% in Harbin and Hohhot. Examining the individual human milk samples (transitional and mature human milk per mother) showed a wide range of 0.05–0.56% for total CLA and 0.02–0.25% for rumenic acid. Interestingly, neither the highest levels of total CLA or rumenic acid were associated with human milk from the northern two cities (total CLA 0.05–0.24%; rumenic acid 0.03–0.18%). The total CLA content in bovine milk available in China (0.66% of total milk fat) consisted mainly of rumenic acid (89.09 ± 2.97%) (Table 3).

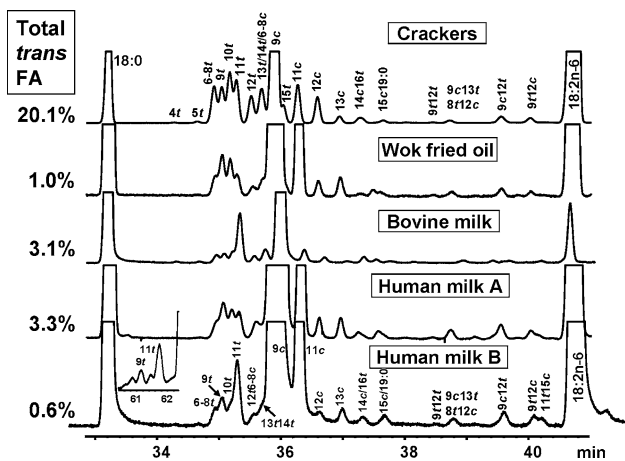


Fig. 2 Partial gas chromatographic separation of the 18:1 isomers of the fat in crackers from China, soybean oil after wok frying, bovine milk sampled in Nanchang China, and two human milk samples selected from Guangzhou (*A*) and Hohhot (*B*). The percentage of total *trans* fatty acid (*FA*) content of each of these samples is shown on the left hand side. The insert of 6*t*–8*t* to 11*t*-18:1 in human milk *B* was obtained using a GC temperature program described previously [40] to provide a better separation of these 18:1 isomers

Polyunsaturated Fatty Acids

The relative concentration of total n-6 PUFA in human milk ranged from about 17.42% of total FA in Guangzhou to about 25.81% in Harbin (Table 2). Linoleic acid (18:2*n*-6) consistently accounted for about 90% of total n-6 PUFA in all regions. On the other hand, the relative concentration of total n-3 PUFA in human milk ranged from about 1.69% in Guangzhou to about 3.67% in Harbin (Table 2). It is of interest to note that the relative proportion of linolenic acid (18:3*n*-3) to total n-3 PUFA increased with increased levels of total n-3 PUFA content in human milk from about 53% in Guangzhou to nearly 80% in Hohhot. A higher concentration of 18:2*n*-6 and 18:3*n*-3 is generally associated with the consumption of fruits, vegetables, and vegetable oils such as sunflower, soybean and rapeseed oils. The high consumption of chicken and fowl in the northern cities (Table 1) also contributed to the higher levels of 18:3*n*-3 in

Table 3 Fatty acid composition (%) of bovine milk from retail stores in Nanchang, China during time human milk was sampled

Fatty acid	Mean	SD	Fatty acid	Mean	SD	Fatty acid	Mean	SD
4:0	2.84	0.18	9 <i>c</i> -12:1	0.07	0.01	13 <i>t</i> /14 <i>t</i> -	0.57	0.04
6:0	1.81	0.07	9 <i>c</i> -14:1	0.67	0.04	16 <i>t</i> -	0.14	0.01
7:0	0.01	0.01	9 <i>c</i> -16:1	0.91	0.05	∑ <i>trans</i> MUFA	3.39	0.18
8:0	1.13	0.05	13 <i>c</i> -	0.02	0.01	∑ <i>trans</i> -18:1	3.27	0.17
9:0	0.04	0.01	11 <i>c</i> -	0.03	0.00			
10:0	2.55	0.15	13 <i>c</i> -	0.11	0.01	<i>c</i> / <i>t</i> -18:2	0.32	0.04
11:0	0.23	0.02	7 <i>c</i> -17:1	0.02	0.01			
12:0	3.03	0.19	9 <i>c</i> -	0.16	0.01	9 <i>c</i> 11 <i>t</i> -18:2	0.57	0.05
13:0	0.10	0.01	9 <i>c</i> -18:1	15.85	0.65	7 <i>t</i> 9 <i>c</i> -	0.02	0.01
13:0 iso	0.05	0.01	11 <i>c</i> -	0.34	0.03	10 <i>t</i> 12 <i>c</i> -	0.01	0.01
13:0 ai	0.08	0.00	12 <i>c</i> -	0.22	0.01	11 <i>t</i> 13 <i>c</i> -	0.02	0.01
14:0	10.75	0.47	13 <i>c</i> -	0.06	0.01	11 <i>t</i> 13 <i>t</i> -	0.02	0.00
14:0 iso	0.19	0.01	14 <i>c</i> -	0.07	0.01	9 <i>t</i> 11 <i>t</i> /10 <i>t</i> 12 <i>t</i> -	0.03	0.00
15:0	0.99	0.06	15 <i>c</i> -	0.08	0.00	∑ CLA	0.66	0.07
15:0 iso	0.30	0.03	16 <i>c</i> -	0.08	0.02	9 <i>c</i> 11 <i>t</i> -18:2/∑CLA (%)	89.09	2.97
15:0 ai	0.60	0.03	9 <i>c</i> -20:1	0.14	0.03			
16:0	29.49	1.10	11 <i>c</i> -	0.07	0.04	18:2 <i>n</i> -6	1.86	0.15
16-iso	0.35	0.01	13 <i>c</i> -22:1	0.04	0.05	18:3 <i>n</i> -6	0.03	0.00
17:0	0.62	0.03	15 <i>c</i> -24:1	0.01	0.01	20:2 <i>n</i> -6	0.01	0.01
17:0 ai	0.64	0.02	∑ <i>cis</i> MUFA	19.01	0.65	20:3 <i>n</i> -6	0.09	0.01
18:0	16.79	0.71	9 <i>t</i> -16:1	0.08	0.01	20:4 <i>n</i> -6	0.12	0.01
18:0 iso	0.08	0.01	4 <i>t</i> -18:1	0.04	0.00	22:4 <i>n</i> -6	0.03	0.00
19:0	0.12	0.01	5 <i>t</i> -	0.05	0.01	18:3 <i>n</i> -3	0.18	0.04
20:0	0.31	0.06	6 <i>t</i> -8 <i>t</i> -	0.30	0.02	20:5 <i>n</i> -3	0.02	0.00
21:0	0.05	0.01	9 <i>t</i> -	0.32	0.01	22:5 <i>n</i> -3	0.03	0.00
22:0	0.09	0.03	10 <i>t</i> -	0.29	0.03	∑ <i>n</i> -6 PUFA	2.14	0.16
24:0	0.04	0.01	11 <i>t</i> -	1.35	0.19	∑ <i>n</i> -3 PUFA	0.23	0.05
∑ SFA	73.69	0.95	12 <i>t</i> -	0.25	0.01	<i>n</i> -6/ <i>n</i> -3 PUFA	9.52	1.17

SFA Saturated fatty acids, *cis* MUFA *cis* monounsaturated fatty acids, *trans* MUFA *trans* monounsaturated fatty acids, *trans*-18:1 *trans*-18:1 isomers, CLA conjugated linoleic acids, *n*-6 PUFA *n*-6 polyunsaturated fatty acids, *n*-3 PUFA *n*-3 polyunsaturated fatty acids

this region. The *n*-6/*n*-3 ratio of total PUFA in human milk ranged from about ten in Guangzhou to about six in Hohhot (Table 2).

Several *n*-6 HUFA metabolites were present in all human milk accounting for nearly 2% of total FA, with only minor differences measured between cities (Table 2). The major *n*-6 HUFA were 20:2*n*-6, 20:3*n*-6 and ARA (20:4*n*-6). The content of ARA ranged from 0.54% in Guangzhou to 0.76% in Harbin, and showed a weak correlation ($R = 0.58$) to the content of 18:2*n*-6 in human milk. The content of ARA in all the human milk samples ranged from 0.24 to 1.19% of total milk fat.

Six *n*-3 HUFA metabolites were identified in human milk ranging in content from 0.60 to 1.47% of total FA, the highest levels were found in Harbin and the lowest in Hohhot (Table 2). DHA was the predominant *n*-3 HUFA present at 0.29 to 0.53% of total FA accounting for about half of the *n*-3

HUFA. As expected, there was no correlation of 18:3*n*-3 to DHA ($R = 0.0001$), since this conversion is known to be very low in humans [5–7]. The content of DHA in all the human milk samples (transitional and mature human milk per mother) ranged from 0.15 to 1.00% of total milk fat, but only three human milk samples had a level of less than 0.2% of total milk fat, and these were not from the same mother. Docosapentaenoic acid (22:5*n*-3), at 0.11–0.17% of total FA, was the second most abundant *n*-3 HUFA, and occurred at about 20% of total *n*-3 HUFA. On the other hand, eicosapentaenoic acid (20:5*n*-3) was only present in minor amounts (at 0.05, or 6% of total *n*-3 HUFA), and there were no significant differences between cities.

A comparison of the average *n*-6 and *n*-3 HUFA content and *n*-6/*n*-3 ratio shows that human milk from all regions investigated in this study contained at least 1.7% total *n*-6 HUFA and 0.6% *n*-3 HUFA, with a ratio of about 2.5

Fig. 3 Comparison of the average total CLA, rumenic acid (9*c*11*t*-18:2), and the combined *trans*, *trans*-CLA isomers (percentage of total fatty acids) from transitional and mature human milk of the five cities in China (GZ Guangzhou, SH Shanghai, NC Nanchang, HA Harbin, HT Hohhot) with the scale on the left side. The scale on the right side represents the percent of rumenic acid (9*c*11*t*-18:2) in total CLA (solid bars) for the five cities

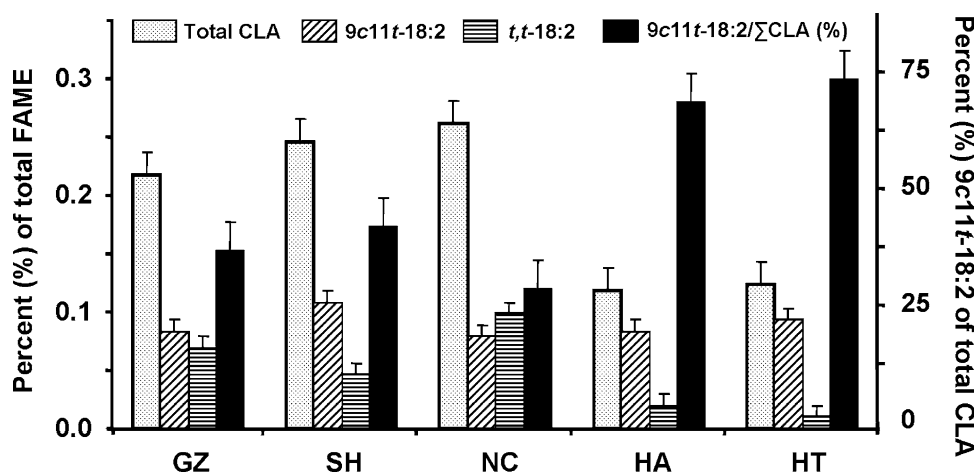
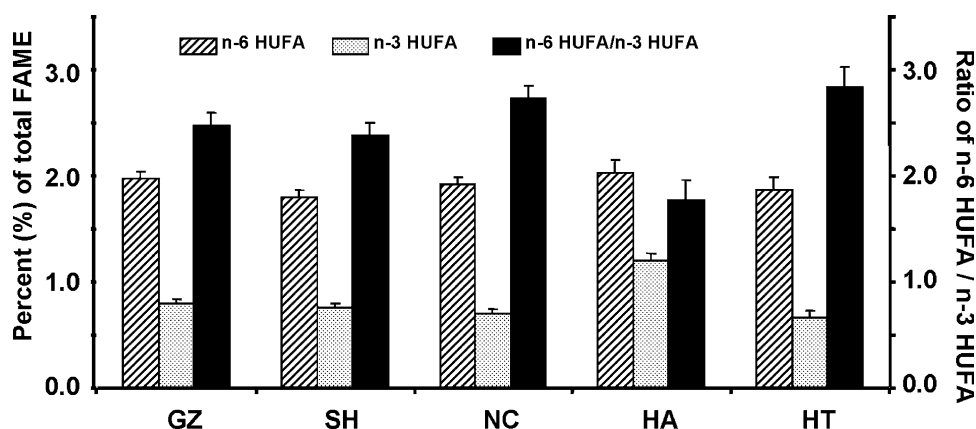


Fig. 4 Comparison of the average total n-6 HUFA and n-3 HUFA content (percentage of total fatty acids) from transitional and mature human milk of the five cities in China (GZ Guangzhou, SH Shanghai, NC Nanchang, HA Harbin, HT Hohhot) with the scale on the left side. The scale on the right side represents the ratios of n-6 HUFA to n-3 HUFA (solid bars) for the five cities



(Fig. 4). Examining all the individual human milk samples (transitional and mature human milk per mother) showed a wide range of ARA to DHA from 0.73 to 3.41%, but only 20 samples had ARA levels less than DHA, i.e., below 1.00, and 13 samples were below 0.90; the lowest ratio was 0.72.

Discussion

Today, food consumption patterns are continually changing particularly with the introduction of FA and convenient foods and greater availability of variety and packaged foods. A better transportation network and an increase of disposable income are also making these foods more accessible to the general population. In this study we wanted to expand on previous surveys conducted in China that focused mainly on DHA [11, 32–36], by investigating the TFA and CLA contents in human milk not previously addressed. We also wanted to evaluate the levels of erucic acid in human milk in the various regions since rapeseed oil is used extensively for cooking in China. The rapeseed oil still contains appreciable amounts of erucic acid. An

analysis of human milk is a good indicator of the fat sources consumed by the mothers the previous day, since dietary FA [9], including TFA and CLA, have been shown to appear in human milk within 12–36 h later [43, 44]. The amount and isomer pattern observed in the human milk will reflect the type of TFA and CLA contained in the foods consumed [17, 18].

trans Fatty Acids

Generally, the major sources of TFA in human diet are derived from products containing PHF [23, 45] or ruminant fats [46, 47]. These two fats are distinguishable by their characteristic *trans*-18:1 isomer profile [18, 38]. In industrially produced hardened fats the distribution of the *trans*-18:1 isomers is random, i.e., the isomers from 6*t*-8*t* to 11*t*-18:1 are present in approximately equal amounts [19, 20, 23], whereas in ruminant fats vaccenic acid is the most abundant isomer in [40, 45]. Our results show that the average total TFA concentration of the human milk samples in China did not exceed 2% (Fig. 1). This is in marked contrast to many Western countries that reported averages of 3.8–7.2% total TFA in human milk [16, 18, 25, 48, 49]

and with some concentrations reaching as high as 15.4% [16]. The TFA in human milk are attributed to the consumption of food products containing PHF. There has been a noticeable decline in the TFA content in human milk in Western countries [25, 50] since the adoption of mandatory labeling of TFA in food products [24], and the current negative health image of TFA. In China, there was evidence that some mothers consumed food containing industrially produced hardened fats. Eight mothers in Guangzhou (Fig. 2, human milk A), three in Nanchang and one in Shanghai had increased levels of total TFA that ranged from 2.06 to 3.96% in their human milk. All eight mothers in Guangzhou reported eating crackers, a possible source of TFA; the other mothers with a similar high level of TFA did not provide any information on their questionnaire as to the source of their TFA. Subsequent analysis of common crackers available in Guangzhou showed that they contained 20.1% TFA (Fig. 2, cracker). Unfortunately, the dietary questionnaire did not provide information as to how many crackers were consumed, so a total TFA intake from these crackers could not be calculated. A direct correlation between the amount of TFA consumed and measured in human milk could not be established by Aitchison et al. [43], but the authors did conclude that dietary TFA are extensively transferred into human milk 12–36 h after consumption. It is evident from our results that only 12 nursing mothers out of 97 in our survey consumed any TFA containing foods, even though these products are available, such as crackers. It would appear that levels greater than 2% total TFA in human milk can be accounted for by the consumption of products containing PHF, but these products do not necessarily account for the remaining TFA in human milk.

If ruminant products (meat and milk) were the major source of TFA in the diet, one would expect a TFA profile with vaccenic acid as the major *trans*-18:1 isomer (Fig. 2, human milk B). Only in the northern cities of Hohhot and Harbin was there evidence that human milk samples had *trans*-18:1 patterns similar to those seen in the bovine milk sampled and analyzed in Nanchang (Table 3; representative GC graph of bovine milk in Fig. 2), but this *trans*-18:1 pattern was not observed in human milk samples from any of the other cities. The greater availability and consumption of ruminant products in Hohhot, a region known for extensive dairy and beef production, contributed to a higher level of total *trans*-18:1 and vaccenic acid in human milk in comparison to Harbin (Table 2; Fig. 1). In their study, Chulei et al. [35] surveyed human milk from the herdswomen in Inner Mongolia and reported high dairy consumption in this group of women. It would have been interesting to compare this human milk with samples of the urban women in Hohhot collected in this study. Unfortunately, the authors [35] did not provide the TFA

content and isomer composition of the human milk. It is unlikely that TFA from ruminant fats account for much of the TFA in human milk from the southern and central cities of China, because the pattern of *trans*-18:1 isomers in the southern and central cities was random, and unlike the typical pattern observed with ruminant fats. Furthermore, it is of interest to note that the total *trans*-18:1 content in Hohhot is about one-third that found in the southern and central cities (Fig. 1; 0.43 vs 1.10–1.28%). Therefore, sources other than ruminant and partially hydrogenated fats need to be considered to explain the higher levels TFA in human milk from the southern and central regions.

Fully refined vegetable oils have been identified as another source of TFA that are formed during the deodorization step [22]. The high temperature during deodorization results in the formation of geometric isomers of 18:3n-3 (*trans*-TUFA) and 18:2n-6 (*trans*-DUFA) [21, 51], and to a lesser extent of *trans*-MUFA. The vegetable oils currently available in the urban centers in China are fully refined and deodorized and were reported to contain 1–2% *trans*-MUFA and 0.1–0.2% *trans*-DUFA [39]. Consumption of these vegetable oils would contribute to the *trans*-DUFA and *trans*-TUFA in the southern and central regions (Fig. 1). However, it would not explain the much lower levels of all TFA observed in the two northern cities in China, particularly Harbin, where presumably refined vegetable oils were also used.

Less frequently investigated is the contribution of TFA arising from using PUFA-rich oils for frying at high temperatures [19–21]. Heating PUFA rich vegetable oils at temperatures in excess of 200 °C under nitrogen was reported to result in the geometric isomerization of 18:2n-6 and 18:3n-3 to form *trans*-DUFA and *trans*-TUFA, respectively, [19, 20, 52]. Wok cooking is popular in the southern and central regions of China, and during wok cooking oil temperatures of 240–280 °C have been reported [53]. This would explain the higher levels of *trans*-DUFA and *trans*-TUFA from human milk in the southern and central regions of China compared to the northern cities (Fig. 1), since soybean, rapeseed and peanut oils [54], all vegetable oils rich in PUFA are generally used for wok frying. However, it would not explain the higher levels of *trans*-MUFA with a random distribution of *trans*-18:1 isomers from 6*t*-8*t*- to 11*t*-18:1 (Fig. 2, human milk A) if we assume that heat treatment of vegetable oils is limited to geometric isomerization [19, 20, 52]. We suspected that frying at these high temperatures in open pans might not be limited to geometric isomerization of *cis*-unsaturated double bond, but may also cause positional isomerization. We therefore undertook a small study in which five common vegetable oils (soybean, canola, peanut, corn, and sunflower oils) were purchased and each in

turn was used in wok cooking of Chinese cabbage. Analysis indeed showed that the *trans*-MUFA, *trans*-DUFA and *trans*-DUFA content increased after wok cooking, and the *trans*-18:1 profile showed a random distribution of isomers (Fig. 2, wok fried oil; J. Kramer, unpublished data). This, in part, could explain the higher levels of TFA in the human milk from the southern and central regions of China compared to the northern cities (Fig. 1), where wok cooking is generally not practiced. Similar high levels of *trans*-DUFA were previously reported in human milk surveyed from Hong Kong [0.18%; 36] where wok cooking is common.

Recent studies have shown that *trans*-DUFA may be a greater risk factor for coronary heart disease than *trans*-MUFA [55]. These TFA have also been shown to be metabolized to *trans* containing PUFA that interfere with brain and retinal function [56, 57]. Based on the analysis of human milk in this study, levels of up to 4% total TFA in human milk may not appear to be a major concern compared to the much higher levels found in other countries [16, 25, 48]. However, frying in a wok at elevated temperatures resulted in increased proportions of *trans*-DUFA and *trans*-TUFA in human milk that may pose a greater risk. Therefore, a reduction in these undesirable TFA would be prudent by reducing the temperature during frying and consuming more ruminant products higher in vaccenic acid.

Conjugated Linoleic Acids

Bovine milk is generally a major source of CLA in the diet, and therefore, an analysis of bovine milk would be a good indicator of the quality of rumenic acid available to nursing mothers. Most of the bovine milk in China is produced in the northern region, as were the samples we collected in Nanchang. This bovine milk contained 0.66% total CLA and consisted mainly of rumenic acid (89.09%; Table 3). Only in the two northern cities of Hohhot and Harbin was there evidence from the human milk results that mothers consumed appreciable amounts of such ruminant products, since more than 70% of the total CLA in the human milk samples was rumenic acid (Fig. 3). CLA is known to be absorbed by nursing mothers [44] and CLA was shown to plateau between 8 and 28 h after consumption [58]. Both the total CLA and rumenic acid content in human milk from the northern region was in marked contrast to that found in the southern and central regions of China, where the total CLA content was found to be about twice as much, but the relative abundance of rumenic acid was less than 44% (Fig. 3). In addition, that human milk contained an equal amount of *trans,trans*-CLA (Fig. 3), as well as significant amounts of 9*t*11*c*-18:2 (Table 2).

The total rumenic acid content in the human milk surveyed in this study ranged from 0.07 to 0.11% of total milk fat, which is consistent with a previous report on human milk from China [11; 0.07%], and other countries in which consumption of dairy and meat from ruminant is generally low, such as in the Philippines (0.08%) and Japan (0.13%). On the other hand, in countries where dairy and meat consumption is high, average levels of 0.20–0.43% total rumenic acid are common [11, 18, 25, 44, 48], and values as high as 0.63 [18] and 0.66% [48] have been observed.

Conjugated linoleic acid has been shown to be produced during heating of PUFA rich oils at 220 °C [59] and during the deodorization step of refining vegetable oils [59]. The CLA isomer composition produced as the result of excessive heating was shown to be a random distribution of several CLA isomers with large amounts of *trans, trans*-CLA [60], similar to what was produced during partial hydrogenation [61]. This type of CLA isomer distribution was in fact observed in the human milk from the southern and central regions of China derived presumably from both refined vegetable oils and wok-type frying (Fig. 3).

When reporting the CLA it is important to include both the amount of rumenic acid as well as total CLA content. It is well known that the different CLA isomers have diverse biological effects. Some isomers have negative effects [28, 29, 62] that may even neutralize the beneficial effects of other CLA isomers, such as the interaction of 10*t*12*c*-18:2 and rumenic acid (9*c*11*t*-18:2) [62]. In general, rumenic acid appears to have a beneficial influence in animal models [63], cell cultures [26] and humans [62, 64, 65]. It would be of interest to know whether the biological effectiveness of rumenic acid is the same whether present at 70% of total CLA (as in the northern cities) or in mixtures with other CLA isomers (less than 44% of total CLA; as in the southern and central cities). When evaluating the health benefits of rumenic acid in infants, a comparison between breast-fed to formula-fed infants should be investigated, since the former have much higher levels of *Bifidobacteria* in their intestinal tract that are known to produce rumenic and vaccenic acids [30, 31].

Polyunsaturated Fatty Acids

The human milk sampled from all regions in China were found to contain appreciable amounts of both n-3 and n-6 HUFA that could have been derived from fish, eggs, or different meats (Table 1). Similar values of DHA were reported in three previous surveys from China [11, 35, 36]; except for mothers from Zhangzi Island and Inner Mongolia who had extreme values for DHA depending on whether they consumed a high amount of fish or very little, respectively, [35]. The results reported by Xiang et al. [32, 33] appear to be from a rather atypical population in the

Beijing area, since the HUFA content and profile observed in their human milk samples were similar to those generally found in North America [11].

The average content of ARA and DHA did not appear to show great differences between the different regions of China (Fig. 4). However, an assessment of the individual mothers was of interest since it showed a fivefold difference in the total ARA, and a sevenfold difference in total DHA content between human milk samples from all parts of China; in this study separate transitional and mature milk values were reported for each mother. Based on a recent report for health-care providers, a consensus recommendation was reached that a minimum of 0.2% and a maximum of 0.5% DHA in total milk fat is recommended for optimal visual and cognitive development for the fetus and neonate [66]. Furthermore, it was recommended that the levels of ARA and DHA should be similar [66], since the n-6 and n-3 PUFA compete for the same enzymes and produce eicosanoids generally involved in opposing physiological, immunological and inflammatory pathways [1, 4]. Using this criterion, only 3 of 168 human milk samples analyzed in this study had a level below the minimum recommended level of 0.2% DHA in total milk fat, while 49 samples exceed the level of 0.5% DHA. However, it should be noted that most of the high DHA values were generally accompanied with equally high ARA values. Only 13 human milk samples had an ARA to DHA ratio of less than 0.90. The average worldwide ratio of ARA to DHA in human milk was shown to be about 1.5, which is similar to that found in our study, but a variation from 0.36 in the Dominican Republic to 10 in Rural South Africa were reported [10]. Discussions will no doubt continue on to the optimal amount and ratio of ARA to DHA for human milk.

Contamination of fish and fish products has been well publicized, which is the reason many people in Western countries choose to reduce their intake of fish or seafood. However, seafood is an important source of DHA, beneficial for human health in general, and essential for the infant's retinal and brain development [3, 7, 8]. To improve the DHA status of mothers with a low fish intake, it has been suggested that the maternal diet should be supplemented with 200 mg/day DHA from mid-pregnancy through lactation [66, 67]. Based on the results of this study it would appear that there is sufficient DHA in the human milk, and the recommended daily supplementation of 200 mg DHA for nursing mothers [66] may not be necessary in China.

Erucic Acid

In the current survey, small amounts of erucic acid were found in most human milk samples (mean values ranged from 0.08 to 0.23%; Table 2), which is consistent with previous surveys reported in 1997 (0.16 and 0.58%) [36],

1999 (0.18 and 0.32%) [32], 2005 (0.32%) [33], and in 2006 (1.21%) [11]. Erucic acid is derived from rapeseed oil, the second most consumed vegetable oil after soybean oil in China [54]. This oil was shown to contain 4.3% erucic acid [39]. This level of erucic acid in the rapeseed oil is below the previous limit of 5% set by Canada [68] and the European Commission considered to be safe for adult consumption [69], but above the level of 2% set in the United States [70]. The limit of erucic acid is 2% in the latest CODEX standard for low erucic acid rapeseed oil [71]. For infant formulas, the limit of C₂₂ monoenoic FA in Canada is 1/100 kcal [72]. This compares to the United States where canola oil is excluded for use in infant formulas [70], and Europe where there is no specific regulations for the use of low erucic acid rapeseed oils in infant formulas. In the current study, the highest value of erucic acid in the human milk was 0.90%, which would be below the Canadian regulation for infant formulas [72].

Questions about the safety of erucic acid have occasionally been raised in the popular press. These concerns are based on publications in the early 1970s that erucic acid uncoupled oxidative phosphorylation [73] and caused lipid accumulation in rat heart tissue [74]. The reason for the reduced ATP production was subsequently found to be due to inappropriate isolation of rat heart mitochondria [75], while lipid accumulation was shown to be unique to rats that naturally have a low level of peroxisomal β -oxidative activity [76, 77], and tissue specific metabolism of erucic acid [78]. Continued feeding of erucic acid to rats was shown to induce peroxisomal β -oxidation resulting in a decrease of the accumulated lipid [76, 77]. Similar effects were not observed in pigs, monkeys and humans [77]. Furthermore, no differences were found in the oxidation rates between erucic and palmitic acids in isolated perfused pig hearts measured using ³¹P NMR, indicating that the decrease in oxidation rates and ATP production observed in isolated rat mitochondria [73] were not replicated in the intact pig heart [79]. Direct evidence that energy metabolism of erucic acid was normal and similar to palmitic acid was provided by an in situ ³¹P-NMR experiment, in which perfused hearts of newborn piglets were used as a model [80]. Therefore, safety concerns about erucic acid have no scientific merit. On the contrary, erucic acid (22:1n-9) is a normal component in mammals. It is an intermediate in the chain elongation of oleic acid (18:1n-9) to nervonic acid (24:1n-9) [81]. Moreover, nervonic acid is a major FA involved in maintaining the structural integrity of sphingomyelin, a ubiquitous constituent of all nervous tissues, the myelin sheath, adrenal cortex, and most mammalian cell membranes. Feeding erucic acid to rats was shown to increase the levels of nervonic acid at the expense of the very long-chain SFA in sphingomyelin [82]. This observation was used to further reduce the level of very long-chain SFA that could not be achieved by

dietary restriction of SFA in X-linked adrenoleukodystrophy (ALD) patients suffering from a peroxisomal disorder. In these patients, the very long-chain SFA (>23:0) accumulate in sphingomyelin because ALD patients lack the ability to metabolize very long-chain SFA [83]. The combination of restricting the consumption of dietary SFA and inclusion of erucic acid in the diet (Lorenzo oil) has led to a normalization of the very long-chain SFA in the plasma lipids of ALD patients. In a 6.9 ± 2.7 year follow-up study, 74% of the patients were found to have normal neurological brain MRI results [84]. Therefore, instead of a safety concern, erucic acid appears to provide a benefit for ALD patients. The levels of <5% in the rapeseed oil in China should therefore not be of any health concern.

Conclusion

In conclusion, the results of this human milk survey from five cities in China show characteristic FA patterns associated with the type of foods consumed and ways of preparation. Despite the lack of information from the questionnaire as to the composition and amount of foods consumed, it was possible to establish how few mothers availed themselves of food products containing PHF high in TFA. If there was a trend towards westernization in eating habits in any of the five cities reported, the nursing mothers surveyed certainly did not participate in it. The cities in the southern and central regions had significantly higher levels of total TFA and CLA in their human milk than the two northern cities, but the isomer distribution in the TFA and CLA were random. This originated mainly from the use of refined and unsaturated vegetable oils used in stir-fry (wok cooking). This is in marked contrast to human milk in the northern region where the major isomers were vaccenic and rumenic acids derived mainly from dairy and ruminant products. There appears to be an adequate amount of both n-6 and n-3 HUFA in all regions of China, with very few human milk samples having less than recommended 0.2% level of DHA and a 1:1 ratio of ARA to DHA. Rapeseed oil is readily available and used for frying purposes in China evident by small amounts of erucic acid detected in almost all human milk samples. A level of less than 5% erucic acid in the rapeseed oil and up to 0.90% in human milk would appear to be safe based on scientific evidence. The energy derived from fat appears to be lower in China compared to Western countries [33], but the TFA and CLA composition in human milk consists of isomers other than vaccenic and rumenic acids for all regions, except in the northern cities. Efforts should be encouraged to reduce these TFA isomers by decreasing the frying temperature, or increasing the consumption of dairy and ruminant meat products rich in vaccenic and rumenic acids.

Acknowledgments This study was financed by Chinese National Key Technology Research and Development Program (2006BA-D27B04), the Jiangxi Innovative Funding for graduate students, and the Yili Group Ltd Co., Hohhot, Inner Mongolia. Jing Li is the recipient of a scholarship from the China Scholarship Council. We also appreciate the support from Agriculture and Agri-Food Canada (ARAFC) and the advice of Dr. Jocelyne Letarte at ARAFC.

References

- Lauritzen L, Hansen HS, Jørgensen MH, Michaelsen KF (2001) The essentiality of long chain n-3 fatty acids in relation to development and function of the brain and retina. *Prog Lipid Res* 40:1–94
- Udell T, Gibson RA, Markrides M, the PUFA Study Group (2005) The effect of α -linolenic acid and linoleic acid on the growth and development of formula-fed infants: a systematic review and meta-analysis of randomized controlled trials. *Lipids* 40:1–11
- Cetina I, Koletzko B (2008) Long-chain n-3 fatty acid supply in pregnancy and lactation. *Curr Opin Clin Nutr Metab Care* 11:297–302
- Hadders-Algra M (2008) Prenatal long-chain polyunsaturated fatty acid status: the importance of a balanced intake of docosahexaenoic acid and arachidonic acid. *J Perinat Med* 36:101–109
- Del Prado M, Villalpando S, Elizondo A, Rodríguez M, Demmelmair H, Koletzko B (2001) Contribution of dietary and newly formed arachidonic acid to human milk lipids in women eating a low-fat diet. *Am J Clin Nutr* 74:242–247
- Carnielli VP, Simonato M, Verlato G, Luijendijk I, De Curtis M, Sauer PJJ, Cogo PE (2007) Synthesis of long-chain polyunsaturated fatty acids in preterm newborns fed formula with long-chain polyunsaturated fatty acids. *Am J Clin Nutr* 86:1323–1330
- Henriksen C, Haugholt K, Lindgren M, Aurvåg AK, Rønnestad A, Grønn M, Solberg R, Moen A, Nakstad B, Berge RK, Smith L, Iversen PO, Drevon CA (2008) Improved cognitive development among preterm infants attributable to early supplementation of human milk with docosahexaenoic acid and arachidonic acid. *Pediatrics* 121:1137–1145
- Birch EE, Garfield S, Castañeda Y, Hughbanks-Wheaton D, Uauy R, Hoffman D (2007) Visual acuity and cognitive outcomes at 4 years of age in a double-blind, randomized trial of long-chain polyunsaturated fatty acid-supplemented infant formula. *Early Human Dev* 83:279–284
- Brenna JT, Varamini B, Jensen RG, Diersen-Schade DA, Boettcher JA, Arterburn LM (2007) Docosahexaenoic and arachidonic acid concentrations in human breast milk worldwide. *Am J Clin Nutr* 85:1457–1464
- Francois CA, Connor SL, Wander RC, Connor WE (1998) Acute effects of dietary fatty acids on the fatty acids of human milk. *Am J Clin Nutr* 67:301–308
- Yuhas R, Pramuk K, Lien EL (2006) Human milk fatty acid composition from nine countries varies most in DHA. *Lipids* 41:851–858
- Hibbeln JR, Davis JM, Steer C, Emmett P, Rogers I, Williams C, Golding J (2007) Maternal seafood consumption in pregnancy and neurodevelopmental outcomes in childhood (ALSPAC study): an observational cohort study. *Lancet* 369:578–585
- Mensink RP, Zock PL, Kester ADM, Katan MB (2003) Effects of dietary fatty acids and carbohydrates on the ratio of serum total to HDL cholesterol and on serum lipids and apolipoproteins: a meta-analysis of 60 controlled trials. *Am J Clin Nutr* 77:1146–1155
- Carlson SE, Clandinin MT, Cook HW, Emken EA, Filer LJ Jr (1997) *trans* Fatty acids: infant and fetal development. *Am J Clin Nutr* 66:717S–736S

15. Decsi T, Burus I, Molnár S, Minda H, Veitl V (2001) Inverse association between *trans* isomeric and long-chain polyunsaturated fatty acids in cord blood lipids of full-term infants. *Am J Clin Nutr* 74:364–368
16. Chen ZY, Pelletier G, Hollywood R, Ratnayake WMN (1995) *trans* Fatty acid isomers in Canadian human milk. *Lipids* 30:15–21
17. Precht D, Molkenkin J (1997) *Trans*-geometrical and positional isomers of linoleic acid including conjugated linoleic acid (CLA) in German milk and vegetable fats. *Fett/Lipid* 99:319–326
18. Precht D, Molketin J (1999) C18:1, C18:2 and C18:3 *trans* and *cis* fatty acid isomers including conjugated *cis* 9, *trans* 11 linoleic acid (CLA) as well as total fat composition of German human milk lipids. *Nahrung* 43:233–244
19. Martin JC, Dobarganes MC, Nour M, Marquez-Ruiz G, Christie WW, Lavillonnière F, Sébédio JL (1998) Effect of fatty acid positional distribution and triacylglycerol composition on lipid by-products formation during heat treatment: I. Polymer formation. *J Am Oil Chem Soc* 75:1065–1071
20. Sébédio JL, Catte M, Boudier MA, Prevost J, Grandgirard A (1996) Formation of fatty acid geometric isomers and cyclic fatty acid monomers during the finish frying of frozen prefried potatoes. *Food Res Int* 29:109–116
21. Sánchez-Muniz FJ, Bastida S, Márquez-Ruiz G, Dobarganes C (2008) Effect of heating and frying on oil and food fatty acids. In: Chow CK (ed) *Fatty acids in foods and their health implication*. CRC Press, Boca Raton, pp 511–543
22. Ackman RG, Hooper SN, Hooper DL (1974) Linolenic acid artifacts from deodorization of oils. *J Am Oil Chem Soc* 51:42–49
23. Wolff RL, Combe NA, Destailats F, Boué C, Precht D, Molkenkin J, Entressangles B (2000) Follow-up of the $\Delta 4$ to $\Delta 16$ *trans*-18:1 isomer profile and content in French processed foods containing partially hydrogenated vegetable oils during the period 1995–1999. Analytical and nutritional implications. *Lipids* 35:815–825
24. Ratnayake WMN, Zehaluk C (2005) *trans* Fatty acids in foods and their labeling regulations. In: Akoh CC, Lai OM (eds) *Healthful lipids*. AOCS Press, Champaign, pp 1–32
25. Friesen R, Innis SM (2006) *trans* Fatty acids in human milk in Canada declined with the introduction of *trans* fat food labeling. *J Nutr* 136:2558–2561
26. Ip MM, Masson-Welch PA, Ip C (2003) Prevention of mammary cancer with conjugated linoleic acid: role of the stroma and the epithelium. *J Mammary Gland Biol Neoplasia* 8:103–118
27. Belury MA (2002) Dietary conjugated linoleic acid in health: physiological effects and mechanisms of action. *Annu Rev Nutr* 22:505–531
28. Larsen TM, Toubro S, Astrup A (2003) Efficacy and safety of dietary supplements containing CLA for the treatment of obesity: evidence from animal and human studies. *J Lipid Res* 44:2234–2241
29. Terpstra AHM (2004) Effect of conjugated linoleic acid on body composition and plasma lipids in humans: an overview of the literature. *Am J Clin Nutr* 79:352–361
30. Coakley M, Ross RP, Nordgren M, Fitzgerald G, Devery R, Stanton C (2003) Conjugated linoleic acid biosynthesis by human-derived *Bifidobacterium* species. *J Appl Microbiol* 94:138–145
31. Harmsen HJM, Wildeboer-Veloo ACM, Grijpstra J, Knol J, Degener JE, Welling GW (2000) Development of 16S rRNA-based probes for the *Coriobacterium* group and the *Atopobium* cluster and their application for enumeration of *Coriobacteriaceae* in human feces from volunteers of different age groups. *J Appl Environ Microbiol* 66:4523–4527
32. Xiang M, Lei S, Li T, Zetterström R (1999) Composition of long chain polyunsaturated fatty acids in human milk and growth of young infants in rural areas of northern China. *Acta Paediatr* 88:126–131
33. Xiang M, Harbige LS, Zetterström R (2005) Long-chain polyunsaturated fatty acids in Chinese and Swedish mothers: diet, breast milk and infant growth. *Acta Paediatrica* 94:1543–1549
34. Xiang M, Harbige LS, Zetterström R (2007) Breast milk levels of zinc and n-6 polyunsaturated fatty acids and growth of healthy Chinese infants. *Acta Paediatrica* 96:387–390
35. Chulei R, Xiaofang L, Hongsheng M, Xiulan M, Guizheng L, Gianhong D, de Francesco CA, Connor WE (1995) Milk composition in women from five different regions of China: the great diversity of milk fatty acids. *J Nutr* 125:2993–2998
36. Chen ZY, Kwan KY, Tong KK, Ratnayake WMN, Li HQ, Leung SSF (1997) Breast milk fatty acid composition: a comparative study between Hong Kong and Chongqing Chinese. *Lipids* 32:1061–1067
37. Laryea MD, Jiang YF, Xu GL, Lombeck I (1992) Fatty acid composition of blood lipids in Chinese children consuming high erucic acid rapeseed oil. *Ann Nutr Metab* 36:273–278
38. Cruz-Hernandez C, Deng Z, Zhou J, Hill AR, Yurawecz MP, Delmonte P, Mossoba MM, Dugan MER, Kramer JKG (2004) Methods for analysis of conjugated linoleic acids and *trans*-18:1 isomers in dairy fats by using a combination of gas chromatography, silver-ion thin-layer chromatography/gas chromatography, and silver-ion liquid chromatography. *J AOAC Int* 87:545–562
39. Huang YH, Deng ZY (2007) Analysis of fatty acids content in plant oil. *Food Sci Technol* 10:248–250
40. Kramer JKG, Hernandez M, Cruz-Hernandez C, Kraft J, Dugan MER (2008) Combining results of two GC separations partly achieves determination of all *cis* and *trans* 16:1, 18:1, 18:2 and 18:3 except CLA isomers of milk fat as demonstrated using Ag-ion SPE fractionation. *Lipids* 43:259–273
41. Borschel MW, Elkin RG, Kirksey A, Story JA, Galal O, Harrison GG, Jerome NW (1986) Fatty acid composition of mature human milk of Egyptian and American women. *Am J Clin Nutr* 44:330–335
42. van Beusekom CM, Martini IA, Rutgers HM, Boersma ER, Muskiet FAJ (1990) A carbohydrate-rich diet not only leads to incorporation of medium-chain fatty acids (6:0–14:0) in milk triglycerides but also in each milk-phospholipid subCLAs. *Am J Clin Nutr* 52:326–334
43. Aitchison JM, Dunkley WL, Canolty NL, Smith LM (1977) Influence of diet on *trans* fatty acids in human milk. *Am J Clin Nutr* 30:2006–2015
44. Rist L, Mueller A, Barthel C, Snijders B, Jansen M, Simões-Wüst AP, Huber M, Kummeling I, von Mandach U, Steinhart H, Thijs C (2007) Influence of organic diet on the amount of conjugated linoleic acids in breast milk of lactating women in the Netherlands. *Br J Nutr* 97:735–743
45. Ratnayake WMN, Pelletier G (1992) Positional and geometrical isomers of linoleic acid in partially hydrogenated oils. *J Am Oil Chem Soc* 69:95–105
46. Precht D, Molkenkin J (1996) Rapid analysis of the isomers of *trans*-octadecenoic acid in milk fat. *Int Dairy J* 6:791–809
47. Jensen RG (1999) Lipids in human milk. *Lipids* 34:1243–1271
48. Mosley EE, Wright AL, McGuire MK, McGuire MA (2005) *trans* Fatty acids in milk produced by women in the United States. *Am J Clin Nutr* 82:1292–1297
49. Koletzko B, Mroczek M, Bremer HJ (1988) Fatty acid composition of mature human milk in Germany. *Am J Clin Nutr* 47:954–959
50. Szabó E, Boehm G, Beermann C, Weyermann M, Brenner H, Rothenbacher D, Decsi T (2007) *trans* Octadecenoic acid and *trans* octadecadienoic acid are inversely related to long-chain polyunsaturates in human milk: results of a large birth cohort study. *Am J Clin Nutr* 85:1320–1326

51. Wolff RL (1992) *trans*-Polyunsaturated fatty acids in French edible rapeseed and soybean oils. *J Am Oil Chem Soc* 69:106–110
52. Sebedio JL, Grandgirard A, Prevost J (1988) Linoleic acid isomers in heat treated sunflower oils. *JAOCS* 65:362–366
53. Shields PG, Xu GX, Blot WJ, Fraumeni JF, Trivers GE, Pellizzari ED, Qu YH, Gao YT, Harris CC (1995) Mutagens from heated Chinese and US cooking oils. *J Natl Cancer Inst* 87:836–841
54. USDA Foreign Agricultural Service (2007) Oilseeds: world markets and trade, circular series FOP 12-07, December 2007. <http://www.FA.usda.gov/oilseeds/circular/2007/December/oilseeds.pdf>, p 30
55. Lemaitre RN, King IB, Mozaffarian D, Sotodehnia N, Siscovick DS (2006) *trans*-Fatty acids and sudden cardiac death. *Atherosclerosis Suppl* 7:13–15
56. Grandgirard A, Bourre JM, Julliard F, Homayoun P, Dumont O, Picciotti M, Sébédio JL (1994) Incorporation of *trans* long-chain n-3 polyunsaturated fatty acids in rat brain structures and retina. *Lipids* 29:251–258
57. Acar N, Bonhomme B, Joffre C, Bron AM, Creuzot-Garcher C, Bretilon L, Doly M, Chardigny JM (2006) The retina is more susceptible than the brain and the liver to the incorporation of *trans* isomers of DHA in rats consuming *trans* isomers of alpha-linolenic acid. *Reprod Nutr* 5:515–525
58. Moutsoulis ARA, Rule DC, Murrieta CM, Bauman DE, Lock AL, Barbano DM, Carey GB (2008) Human breast milk enrichment in conjugated linoleic acid after consumption of a conjugated linoleic acid-rich food product: a pilot study. *Nutr Res* 28:437–442
59. Juanéda P, Brac de la Périère S, Sébédio JL, Grégoire S (2003) Influence of heat and refining on formation of CLA isomers in sunflower oil. *J Am Oil Chem Soc* 80:937–940
60. Juanéda P, de la Périère SB, Sébédio J-L, Grégoire S (2003) Influence of heat and refining on formation of CLA isomers in sunflower oil. *J Am Oil Chem Soc* 80:937–940
61. Azizian H, Kramer JKG (2005) A rapid method for the quantification of fatty acids in fats and oils with emphasis on *trans* fatty acids using Fourier transform near infrared spectroscopy (FT-NIR). *Lipids* 40:855–867
62. Tricon S, Burdge GC, Kew S, Banerjee T, Russell JJ, Jones EL, Grimble RF, Williams CM, Yaqoob P, Calder PC (2004) Opposing effects of *cis*-9, *trans*-11 and *trans*-10, *cis*-12 conjugated linoleic acid on blood lipids in healthy humans. *Am J Clin Nutr* 80:614–620
63. Roy A, Chardigny JM, Bauchart D, Ferlay A, Lorenz S, Durand D, Gruffat D, Faulconnier Y, Sébédio J-L, Chilliard Y (2007) Butters rich either in *trans*-10-C18:1 or in *trans*-11-C18:1 plus *cis*-9, *trans*-11 CLA differentially affect plasma lipids and aortic fatty streak in experimental atherosclerosis in rabbits. *Animal* 1:467–476
64. Larsson SC, Bergkvist L, Wolk A (2005) High-fat dairy food and conjugated linoleic acid intakes in relation to colorectal cancer incidence in the Swedish mammography cohort. *Am J Clin Nutr* 82:894–900
65. Aro A, Männistö S, Salminen I, Ovaskainen M-L, Kataja V, Uusitupa M (2000) Inverse association between dietary and serum conjugated linoleic acid and risk of breast cancer in postmenopausal women. *Nutr Cancer* 38:151–157
66. Koletzko B, Lien E, Agostoni C, Böhles H, Campoy C, Cetin I, Decsi T, Dudenhausen JW, Dupont C, Forsyth S, Hoesli I, Holzgreve W, Lapillonne A, Putet G, Secher NJ, Symonds M, Szajewska H, Willatts P, Uauy R (2008) The roles of long-chain polyunsaturated fatty acids in pregnancy, lactation and infancy: review of current knowledge and consensus recommendations. *J Perinat Med* 36:5–14
67. Jacobson JL, Jacobson SW, Muckle G, Kaplan-Estrin M, Ayotte P, Dewailly E (2008) Beneficial effects of a polyunsaturated fatty acid on infant development: evidence from the Inuit of Arctic Quebec. *J Pediatr* 152:356–364
68. Department of National Health and Welfare, B.09.022 (1978) C₂₂ monoenoic fatty acids in fats and oils. Consolidated Regulations of Canada VIII: 74
69. Council Directive of the European Communities (1976) Relating to the fixing of the maximum level of erucic acid in oils and fats intended as such for human consumption and in foodstuffs containing added oils or fats. Official Journal L 202, 28/07/1976: 0035–0037
70. United States Food and Drug Administration (1985) Direct food substance affirmed as generally recognized as safe; low erucic acid rapeseed oil. *Fed Regist* 50:3745–3755
71. CODEX standard for named vegetable oils, CODEX-STAN 210 (amended 2003, 2005)
72. Department of National Health and Welfare, B.25.052 (1982) C₂₂ monoenoic fatty acids in infant formulas. Food and Drug regulations, Minister of Supply and Services Canada 73E, 5 August 1982
73. Houtsmuller UMT, Struijk CB, Van der Beek A (1970) Decrease in rate of ATP synthesis of isolated rat heart mitochondria induced by dietary erucic acid. *Biochim Biophys Acta* 218:564–566
74. Abdellatif AMM, Vles RO (1970) Pathological effects of dietary rapeseed oil in rats. *Nutr Metab* 12:285–295
75. Dow-Walsh DS, Mahadevan S, Kramer JKG, Sauer FD (1975) Failure of dietary erucic acid to impair oxidative capacity or ATP production of rat heart mitochondria isolated under controlled conditions. *Biochim Biophys Acta* 396:125–132
76. Osmundsen H, Bremer J, Pedersen JI (1991) Metabolic aspects of peroxisomal β -oxidation. *Biochim Biophys Acta* 1085:141–158
77. Sauer FD, Kramer JKG (1983) The metabolism of docosenoic acids in the heart. In: Kramer JKG, Sauer FD, Pigden WJ (eds) High and low erucic acid rapeseed oils. Academic Press, New York, pp 335–354
78. Murphy CC, Murphy EJ, Golovko MY (2008) Erucic acid is differentially taken up and metabolized in rat liver and heart. *Lipids* 43:391–400
79. Sauer FD, Kramer JKG, Forester GV, Butler KW (1989) Palmitic and erucic acid metabolism in isolated perfused hearts from weanling pigs. *Biochim Biophys Acta* 1004:205–214
80. Stewart LC, Kramer JKG, Sauer FD, Clarke K, Wolynetz MS (1993) Lipid accumulation in isolated perfused rat hearts has no apparent effect on mechanical function or energy metabolism as measured by ³¹P NMR. *J Lipid Res* 34:1573–1581
81. Kishimoto Y, Radin NS (1963) Biosynthesis of nervonic acid and its homologues from carboxy-labelled oleic acid. *J Lipid Res* 4:444–447
82. Kramer JKG, Hulan HW, Trenholm HL, Corner AH (1979) Growth, lipid metabolism and pathology of two strains of rats fed high fat diets. *J Nutr* 109:202–213
83. Wanders RJA, van Roermund CWT, Wijland MJA, Schutgens RBH, van den Bosch H, Schram AW, Tager JM (1988) Direct demonstration that the deficient oxidation of very long chain fatty acids in X-linked adrenoleukodystrophy is due to an impaired ability of Peroxisomes to activate very long chain fatty acids. *Biochem Biophys Res Commun* 153:618–624
84. Moser HW, Raymond GV, Lu S-E, Muenz LR, Moser AB, Xu J, Jones RO, Loes DJ, Melhem ER, Dubey P, Bezman L, Brereton NH, Odono A (2005) Follow-up of 89 asymptomatic patients with adrenoleukodystrophy treated with Lorenzo's oil. *Arch Neurol* 62:1073–1080

Phytosterol Intake and Dietary Fat Reduction are Independent and Additive in their Ability to Reduce Plasma LDL Cholesterol

Shirley C. Chen · Joseph T. Judd · Matthew Kramer ·
Gert W. Meijer · Beverly A. Clevidence · David J. Baer

Received: 1 December 2008 / Accepted: 17 December 2008 / Published online: 15 January 2009
© AOCS 2009

Abstract We studied the interrelationship of diet and plant sterols (PS) on plasma lipids, lipoproteins and carotenoids. Mildly hypercholesterolemic men ($n = 13$) and postmenopausal women ($n = 9$) underwent four randomized, crossover, double-blind, controlled feeding periods of 23 days each. The design consisted of two levels of PS (0 and 3.3 g/day) and two background diets having fat content either typical of the American diet (total and saturated fat at 33.5 and 13.2% of energy, respectively), or a Step 1 type of diet (total and saturated fat at 26.4 and 7.7% of energy, respectively). Plasma total cholesterol (TC), high density lipoprotein (HDL) cholesterol, low density lipoprotein (LDL) cholesterol, Apo A1 and Apo B were 4.3, 5.3, 4.5, 2.8 and 2.5% lower, respectively ($P \leq 0.0001$; <0.0001 , 0.0016, 0.0006, and 0.0069), with the Step 1 diet than with the typical American diet. Diet had no effect on TC/HDL cholesterol ($P = 0.1062$). Plant sterol intake lowered TC, LDL cholesterol, and Apo B by 9.0, 12.4 and 6.1% and TC/HDL by 9.6% ($P \leq 0.0001$ for all), respectively,

without affecting HDL cholesterol and Apo A1 ($P = 0.2831$ and 0.732). The PS effect in lowering plasma TC and LDL cholesterol was independent of and additive to the effect due to dietary fat reduction. Responses of plasma carotenoids to PS intake were consistent with the literature.

Keywords Plant sterols · LDL cholesterol · Typical American diet · Step 1 diet

Abbreviations

Apo A1	Apolipoprotein A1
Apo B	Apolipoprotein B
BHNRC	Beltsville Human Nutrition Research Center
HDL	High density lipoprotein
HPLC	High-performance liquid chromatography
HRT	Hormone-replacement therapy
LDL	Low density lipoprotein
NCEP	National Cholesterol Education Program
PS	Plant sterols
SEM	Standard error of the mean
SFA	Saturated fatty acid
TAD	Typical American Diet
TC	Total cholesterol
TAG	Triacylglycerides
USDA	US Department of Agriculture

Mention of trade names or commercial products in this article is solely for the purpose of providing specific information and does not imply recommendation or endorsement by the US Department of Agriculture.

S. C. Chen · J. T. Judd · B. A. Clevidence · D. J. Baer (✉)
Food Components and Health Laboratory,
Beltsville Human Nutrition Research Center, USDA, ARS,
Beltsville, MD, USA
e-mail: david.baer@ars.usda.gov

M. Kramer
Biometrical Consulting Service, Agricultural Research Service,
US Department of Agriculture, Beltsville, MD, USA

G. W. Meijer
Unilever Research and Development Foods, Vlaardingen,
The Netherlands

Introduction

The landmark study by Miettinen et al. [1] reported the year-long efficacy of a margarine enriched with plant stanol-esters in reducing the low density lipoprotein (LDL) cholesterol concentrations of mildly hypercholesterolemic adults. Since then, numerous human studies on the efficacy

and safety of plant sterols (PS) and plant stanols, either in free forms or as esters, and alone or in combination with each other, have been published. The LDL cholesterol-lowering effects of PS and plant stanols are equivalent and additive to those of diet or lipid-lowering medications and the optimal daily intake is 2–2.5 g/day [2–5].

Effects of PS incorporated into different food forms [6] have been studied but not the impact of the fat level and composition of the background diet. Earlier studies have suggested that increasing saturated fat and cholesterol intakes may enhance the PS induced LDL cholesterol-lowering effect [7, 8]. A review of the literature found that the background diets in previous studies were either uncontrolled, such as free-living subjects consuming their habitual diets [1, 9, 10]; semi-controlled, such as free-living subjects receiving dietary counseling [9, 11]; or controlled but unvaried [12–14]. The only study in which fat intakes were varied by design did not quantify the effect of dietary fat [15]. A direct comparison of diets with varying fat level and composition has not been reported to date.

In the United States, the recommendation for individuals with elevated serum LDL cholesterol concentrations is to replace their customary diets with a “therapeutic lifestyle change (TLC) diet” consisting of saturated fat intake at <7% of calories, and cholesterol intake at <200 mg/day and including the use of viscous fiber and plant stanols/sterols as an initial step towards achieving the LDL cholesterol goal [16]. We designed the present study to determine the effect of three daily servings of PS in the presence of two practical background diets differing in fat level and composition on responses in lipids, lipoproteins, retinol, tocopherols, and carotenoids. These diets represent a typical American diet (TAD, relatively high in fat and saturated fat) and a TLC like diet (Step 1 diet).

Experimental Procedure

Study Design

The four dietary treatments consisted of two background diets (TAD and Step 1) in combination with two levels of PS (0 and 3.3 g/day) in a double-blind, randomized cross-over design, with each participant consuming each of the diets for 28 days. The fundamental differences between the TAD and Step 1 diets were their fat levels (33.5 vs. 26.4% of the calories for TAD and Step 1 diet, respectively) and fat composition (saturated/*cis*-monounsaturated/*cis*-polyunsaturated/*trans* fat at 13.2/11.5/6.5/2.4 for the TAD and 7.7/8.9/7.1/2.6 for the Step 1 diet). Blood samples were collected during the fourth week, after 22 days of feeding. As it

has been established that new steady states for plasma total cholesterol (TC), high density lipoprotein (HDL) cholesterol, and TAG are reached in 3–4 weeks [17], study subjects were then switched to the next diet with no washout between periods. The study protocol was approved by the Johns Hopkins University, Bloomberg School of Public Health, Committee on Human Research (Baltimore, MD). A detailed description of the subject recruitment procedures and selection criteria has been presented elsewhere [13]. Subjects were blinded to the four experimental diets. The salad dressings and margarines, with and without added PS, were prepared specifically for this study and supplied color-coded and blinded to the investigators by Unilever Foods, NA (Englewood Cliffs, NJ). Biological samples were coded and blinded to the analysts.

Diets

The four experimental diets were planned using data from the United States Department of Agriculture (USDA) National Nutrient Database for Standard Reference, Release 19 [18]. Typical American diet and Step 1 diets were composed of foods commonly eaten in the United States. Ranch salad dressing (8 g fat/serving) and a 60% fat spread (8.4 g fat/serving) were fed as part of the TAD diets, and Italian salad dressing (3.8 g fat/serving) and a 32% fat spread (4.5 g fat/serving) were fed a part of the Step 1 diets. Salad dressings and spreads were either fortified with 1.1 g PS per serving (equivalent to 1.8 g/serving of PS as esters from vegetable oil sources) and used in +PS diets, or having no added PS and used in the –PS diets. One serving of margarine was included in the breakfast, and one serving each of margarine and salad dressing were served at dinner for a total of zero (–PS) or 3.3 g/day of add PS (+PS).

A 7-day menu rotation was used. From Monday through Friday all subjects consumed breakfast and dinner at the Human Study Facility of Beltsville Human Nutrition Research Center (BHNRC) under the supervision of a dietitian. At breakfast, each subject was provided with a carry-out lunch to be consumed off-site that day. Snacks were included in the daily menu, which the subjects were allowed to eat either at dinner or later in the evening. Meals for the weekend were packaged for home consumption and were provided to the subjects, with written instructions, after dinner on Friday. Unlimited amounts of coffee, tea, and diet sodas were allowed, but all additives (sugar and milk) for coffee and tea were provided with the meals. Only foods provided by the Human Study Facility were allowed during the study.

Each weekday morning the subjects were weighed before breakfast when they arrived at the Facility. Energy intake was adjusted in 200- or 400-kcal increments to

maintain initial body weight. The subjects were fed the same items and the same proportions of each item relative to total dietary energy intake. Therefore, the relative amounts of all nutrients, other than those provided by the margarine and salad dressing, were constant for all subjects. Each day, the subjects completed a questionnaire detailing beverage intake, factors related to dietary compliance, exercise, medications, and illnesses. The questionnaires were reviewed routinely by a study investigator and all problems identified were discussed with the subject during the next meal.

During each feeding period, two composites of the 7-day menu cycle were made at two energy levels for each of the four diets. The food items were collected and prepared as though they were to be consumed. They were then homogenized in a blender with ice added to prevent heat build-up. The blended samples were freeze-dried in pre-weighed containers and weighed again after drying. The samples were then pulverized, and a weekly composite for each energy level was prepared by mixing together 15% by weight of each day's freeze-dried sample. The eight diet composites were analyzed for dry matter, crude protein, crude fat, total dietary fiber, ash, and fatty acid composition (Covance Laboratories Inc., Madison, WI) and sterol content and composition [14]. The fatty acid composition of the food composites was analyzed by using method AOCS 996.06. Carotenoid concentrations were estimated by using the US Department of Agriculture–Nutrition Coordinating Center carotenoid database for US foods [19].

Blood Collection and Analysis

Baseline (i.e., pretreatment) blood samples were collected on two separate days during the week immediately before the start of the first controlled feeding period. Blood samples were also collected on days 22 and 24 of the fourth week of each controlled feeding period. Procedures for blood sampling and processing were those described in the protocol for the Lipid Research Clinics Program [20]. Plasma concentrations of TC, HDL cholesterol, and TAG were measured enzymatically with commercial kits (Sigma Chemical Company, St Louis, MO) at the Lipid Research Clinic Laboratory at the George Washington University Medical Center, which maintains standardization with the Centers for Disease Control and Prevention, US Department of Health and Human Services. Low density lipoprotein cholesterol was calculated using the Friedewald equation [21]. Plasma concentrations of apolipoproteins A1 (Apo A1) and B (Apo B) were measured by rate nephelometry (Beckman ICS Immunochemical Analyzer; Beckman Instruments, Fullerton, CA). For each analysis, samples from an individual subject were processed in the same analytical run. Plasma concentrations of lutein, α - and β -cryptoxanthin,

lycopene, α - and β -carotene, total carotenoids, retinol, and α -, γ -, and δ -tocopherol were measured by HPLC as previously described [22, 23]. The precision and accuracy of the HDL chromatograph (HPLC) system was verified by using standard reference material 968b (National Institute of Standards and Technology, Gaithersburg, MD).

Statistical Analyses

All analyses were performed using SAS (SAS, Cary, NC) for Windows (v.9.1 2002–2003). The analytic plan was designed a priori and described a mixed-effects model for analysis of the data for repeated measurements [24]. For each variable the mean of two sample measurements taken during week 4 of each feeding period was analyzed. Individual differences were accounted for using the baseline value as a covariate, and by including a random subject effect in the model. The remaining time series (residual) correlation was modeled as one parameter autoregressive. Contrasts between diets, PS, gender and diet and/or gender and/or PS were tested by a *F*-test for differences among groups. Significant differences between baseline adjusted means (LS mean) were determined by Tukey–Kramer *t*-tests [25]. Plasma carotenoids were analyzed statistically with and without lipid standardization. A SAS Proc TTest [25] was used to compare the mean baseline values of men and women, and lipoprotein cholesterol values under baseline and TAD–PS intakes.

Results

Subjects

The characteristics of the subjects prior to the start of the intervention are shown in Table 1. Fourteen men and nine postmenopausal women (who were not using hormone replacement therapy) completed the four dietary intervention periods. Data from one male subject were dropped from the analyses because of suspicion of noncompliance. The male participants were younger on average than the female participants. At baseline, mean plasma lipid and lipoprotein cholesterol concentrations for men and women were not different. Plasma concentrations of TC and LDL cholesterol were higher at baseline than during the TAD–PS controlled dietary periods ($P = 0.0189$ and 0.018 , respectively), whereas TAG and HDL cholesterol were comparable ($P > 0.05$ for both).

Diets

The compositions of the TAD and the Step 1 diet, which were formulated by adding control or test spreads and salad

Table 1 Age, body mass index, energy intake, and baseline plasma lipids, lipoproteins, retinol, tocopherols, and carotenoids

	Men (<i>n</i> = 13)	Women (<i>n</i> = 9) ^a	All (<i>n</i> = 22)
Age (years)	47.0 ± 3.0	61.0 ± 2.4	51.7 ± 2.4
Body mass index (kg/m ²)	28.2 ± 0.8	27.8 ± 1.0	28.0 ± 0.6
Energy intake ^b (MJ/day)	12.10 ± 0.51	9.39 ± 0.39	10.99 ± 0.44
Baseline blood lipids and lipoproteins			
TAG (mmol/L)	1.46 ± 0.19	1.84 ± 0.39	1.62 ± 0.20
TC (mmol/L)	5.80 ± 0.20	5.97 ± 0.22	5.87 ± 0.14
HDL cholesterol (mmol/L)	1.34 ± 0.12	1.43 ± 0.10	1.38 ± 0.08
LDL cholesterol (mmol/L)	3.80 ± 0.16	3.71 ± 0.13	3.76 ± 0.10
TC/HDL	4.66 ± 0.34	4.30 ± 0.26	4.51 ± 0.23
Apolipoprotein A1 (g/L)	1.49 ± 0.05	1.59 ± 0.09	1.53 ± 0.06
Apolipoprotein B (g/L)	0.88 ± 0.05	0.91 ± 0.05	0.89 ± 0.04
Apo B/Apo A1	0.62 ± 0.05	0.59 ± 0.05	0.61 ± 0.04
Baseline blood carotenoids, retinol, and tocopherols			
Retinol (μmol/mmol TC)	0.45 ± 0.03	0.41 ± 0.07	0.43 ± 0.03
δ-Tocopherol (μmol/mmol TC)	0.04 ± 0.01	0.03 ± 0.01	0.04 ± 0.00
γ-Tocopherol (μmol/mmol TC)	1.17 ± 0.11	1.08 ± 0.14	1.13 ± 0.08
α-Tocopherol (μmol/mmol TC)	7.40 ± 0.41	6.82 ± 0.79	7.16 ± 0.40
Lutein (μmol/mmol TC)	0.07 ± 0.00	0.05 ± 0.01	0.06 ± 0.00
Zeaxanthin (μmol/mmol TC)	0.03 ± 0.00	0.02 ± 0.00	0.02 ± 0.00
α-Cryptoxanthin (μmol/mmol TC)	0.02 ± 0.00	0.01 ± 0.00	0.02 ± 0.00
β-Cryptoxanthin (μmol/mmol TC)	0.06 ± 0.00	0.04 ± 0.00	0.05 ± 0.00
Lycopene (μmol/mmol TC)	0.08 ± 0.01	0.07 ± 0.01	0.07 ± 0.00
α-Carotene (μmol/mmol TC)	0.03 ± 0.00	0.03 ± 0.00	0.03 ± 0.00
β-Carotene (μmol/mmol TC)	0.11 ± 0.01	0.11 ± 0.02	0.11 ± 0.01
Total carotenoids (μmol/mmol TC)	0.39 ± 0.02	0.34 ± 0.02	0.37 ± 0.01

Values are mean ± SEM

^a Women were postmenopausal and were not receiving hormone replacement therapy

^b Average daily energy intake from all four diets

dressings to a common experimental background diet, are listed in Table 2. The TAD was designed to contain 34% of energy from fat with a ratio of saturated to total monounsaturated to total polyunsaturated fatty acids (S:M:P) of 1:1:0.5. The analytical results showed that the fat energy contribution was slightly lower than planned at 33.5%, but the S:M:P ratio was achieved. The ratio of saturated to *cis*-monounsaturated to *cis*-polyunsaturated fatty acids was 1.0:0.9:0.5. The Step 1 diet was planned to have less than 30% of energy from fat, to have less than 7% of energy from saturated fat, and to have an S:M:P ratio of 1:1.5:1. The analytical results showed that fat contributed 26.4% of energy and that saturated fatty acids contributed 7.7% of energy. The target S:M:P ratio was achieved, and the ratio of saturated to *cis*-monounsaturated to *cis*-polyunsaturated fatty acids was 1.0:1.2:0.9. The *trans* fat content of both diets was close to the mean US population intake of 2.6% of energy [26]. Both diets were designed to provide less than 250 mg cholesterol/day for the average subject, and

the Step 1 diet was designed to have approximately 30% less cholesterol than the TAD. The analysis of the dietary composites showed that the TAD had a total fat content of close to those reported in the 2005–2006 NHANES [27], and a slightly higher saturated fat content. The TAD and Step 1 diets had approximately equal dietary fiber content and provided about 26 g dietary fiber per day. This amount of fiber is considerably higher than the average intake reported for the US diet of 18.0 g/day and 14.3 g/day for men and women aged 19 years and over, respectively [27], but was constant across all treatments.

Excluding the PS-enriched foods, the TAD and the Step 1 diets contained comparable amounts of dietary noncholesterol sterols, with both diets providing less than 400 mg PS/day for intake of the average subject. Sitosterol and campesterol accounted for at least 70% of the PS. The profile of noncholesterol sterols in the two +PS controlled diets reflected that of the soybean PS ester extract incorporated in the spread and dressings. From the 3.3 g/day

Table 2 Diet composition of the typical American diet (TAD) and Step 1 type diet

	TAD	Step 1
Protein (% of energy)	16.2	17.4
Carbohydrate (% of energy)	50.3	56.2
Fat (% of energy)	33.5	26.4
Saturated	13.19	7.67
12:0	2.17	0.17
14:0	1.27	0.43
16:0	4.74	3.89
18:0	3.64	2.51
<i>cis</i> -Monounsaturated	11.49	8.94
18:1	11.08	8.59
<i>cis</i> -Polyunsaturated	6.49	7.10
18:2	5.80	6.60
18:3	0.62	0.53
<i>trans</i>	2.35	2.57
18:1	1.96	2.13
18:2	0.33	0.44
Dietary fiber (g/1,000 kcal)	11.6	12.0
Cholesterol (mg/1,000 kcal)	96.3	68.7
Plant sterols ^a (mg/1,000 kcal)	145.7	143.0

^a The percentage distribution of PS in the +PS diets is brassicasterol 2.5, campesterol 24.6, campestanol 0.8, stigmasterol 18.2, β -sitosterol 47.7, β -sitostanol 1.3, D5-avenasterol 1.2; the percentage distribution of PS in the –PS diets is brassicasterol 2.2, campesterol 19.2, campestanol 1.5, stigmasterol 9.7, β -sitosterol 53.3, β -sitostanol 2.7, D5-avenasterol 3.8

intake of PS in the +PS diets, 1.56 g was sitosterol and 0.81 g was campesterol.

The carotenoid-containing foods in the four experimental diets were the same, were fed in equal amounts in proportion to energy intake, and provided α - and β -carotene intakes that exceeded those reported in the 2005–2006 NHANES [27]. The calculated carotenoid content of the common background diet contained 4.82 mg/1,000 kcal total carotenoids, 1.69 mg/1,000 kcal β -carotene, 0.39 mg/1,000 kcal α -carotene, 2.05 mg/1,000 kcal lycopene, and 0.64 mg/1,000 kcal lutein + zeaxanthin.

Responses of Plasma Lipids and Lipoproteins to PS Intake and Diet

Body mass index had no significant effect on any of the dependent variables studied. There was also no effect of sex on lipids or lipoproteins; therefore, data from both sexes were combined for analyses and reporting.

Main Effects

Independent of PS, plasma concentrations of TC, HDLC, LDLC, Apo A1 and Apo B were lower by 4.4, 5.3, 4.5, 2.8,

and 2.5%, respectively, with the Step 1 diet substituting for the TAD. Diet had no significant effect on plasma concentrations of TAG or the ratio of TC to HDLC (TC/HDLC). Independent of the type of diet, the consumption of 3.3 g PS/day reduced plasma concentrations of TC, LDLC, and TC/HDLC by 9.0, 12.4, and 9.6%, respectively. Plasma TAG, HDLC, and Apo A1 concentrations were not significantly affected by PS intake. In response to PS intake, plasma Apo B concentrations were reduced from 0.82 to 0.77 g/L, and the ratio of Apo B to Apo A1 was reduced from 0.60 to 0.55 (Table 3).

Interaction Effects

Diet \times PS interactions existed for the plasma concentration of Apo B ($P = 0.0035$) and the Apo B/Apo A1 ratio ($P = 0.0011$). When PS were not added to the diets, the plasma Apo B concentration after consumption of the TAD (0.85 g/L) was higher than that after consumption of the Step 1 diet (0.80 g/L). With PS intake, Apo B concentrations after consumption of both diets (to 0.77 g/L) were not significantly different. Without PS intake, there was no effect of diet on the ratio of Apo B–Apo A1. Subsequent to PS intake, however, the reduction in this ratio after consumption of the TAD was greater than after consumption of the Step 1 diet (Table 3).

Responses of Plasma Retinol, Tocopherols, and Carotenoids to PS Intake and Diet

The effects of diet and PS intake on the absolute and TC standardized plasma concentrations of retinol; α -, γ -, and δ -tocopherols; lutein; zeaxanthin; α - and β -cryptoxanthins; lycopene; and α - and β -carotene are presented in Table 4 with responses from each sex combined (the sex effect and the diet \times PS interaction were not significant, $P > 0.05$). Absolute plasma concentrations of all compounds except retinol and δ -tocopherol were reduced by the intake of 3.3 g PS/day. After standardization for TC, the effects of PS were limited to cryptoxanthins, lycopene, and carotenes; the reductions were 5.9% for α -cryptoxanthin, 7.8% for β -cryptoxanthin, 24.7% for lycopene, 14.3% for α -carotene, and 21.0% for β -carotene.

Diet had no effect on the absolute concentrations of retinol, α -tocopherol, β -cryptoxanthin, lycopene, and α -carotene. Concentrations of γ -tocopherol, lutein, zeaxanthin, and α -cryptoxanthin were higher, and the concentration of β -carotene was lower with a TAD background diet. Subsequent to standardization for TC, plasma concentrations of γ - and δ -tocopherols and zeaxanthin remained higher after the consumption of the TAD than after the Step 1 diet. There was no diet effect on concentrations of retinol, α -tocopherol, lutein, cryptoxanthins, and lycopene.

Table 3 Effects of diet and intake of plant sterols (PS) on plasma lipids and lipoproteins

	Treatments ¹					Diet effect		PS effect			P value (<i>F</i> test)		
	Step 1		TAD		SEM	Step 1	TAD	-PS	+PS	SEM	Diet	PS	Diet × PS
	-PS	+PS	-PS	+PS									
TAG (mmol/L)	1.53 ²	1.41	1.52	1.41	0.08	1.47	1.46	1.52	1.41	0.07	0.8739	0.0530	0.6933
TC (mmol/L)	5.31 ^c	4.83 ^a	5.55 ^d	5.06 ^b	0.10	5.07	5.30	5.43	4.94	0.10	<0.0001	<0.0001	0.9147
HDLc (mmol/L)	1.24 ^a	1.25 ^a	1.31 ^b	1.32 ^b	0.03	1.25	1.32	1.29	1.29	0.03	<0.0001	0.2831	0.5247
LDLc (mmol/L ⁴)	3.38 ^b	2.95 ^a	3.55 ^b	3.10 ^a	0.08	3.17	3.32	3.46	3.03	0.07	0.0016	<0.0001	0.7873
TC/HDLc	4.53 ^b	4.12 ^a	4.47 ^b	4.03 ^a	0.09	4.33	4.25	4.50	4.07	0.08	0.1062	<0.0001	0.7496
Apo A1 (g/L)	1.40 ^a	1.40 ^a	1.44 ^{ab}	1.45 ^b	0.02	1.40	1.44	1.42	1.42	0.02	0.0006	0.7324	0.7476
Apo B (g/L)	0.80 ^b	0.77 ^a	0.85 ^c	0.77 ^a	0.02	0.79	0.81	0.82	0.77	0.02	0.0069	<0.0001	0.0035 ³
Apo B/Apo A1	0.59 ^b	0.56 ^a	0.61 ^b	0.54 ^a	0.01	0.58	0.58	0.60	0.55	0.01	0.9814	<0.0001	0.0011 ⁴

¹ Among four treatments, values in a row with different superscripts differ, $P < 0.05$ (Tukey–Kramer)

² LS mean

³ In the presence of PS, no diet effect was detected for plasma Apo B level ($P = 0.9982$). In the absence of PS Apo B after TAD feeding was higher than that after Step 1 feeding ($P = 0.0006$)

⁴ The PS induced lowering of Apo B/Apo A1 was greater after TAD feeding (a 11.5% reduction, $P < 0.0001$) than after Step 1 feeding (a 5.1% reduction, $P = 0.0277$)

Concentrations of α - and β -carotene were lower after consumption of the TAD background diet. The higher TC-corrected plasma retinol concentration after PS intake in the present study was mainly due to the significant reduction in TC related to PS, because there was no effect of PS on the uncorrected plasma retinol concentration.

Discussion

The main objective of the study was to investigate, whether the magnitude of reduction in blood concentration of LDL cholesterol in response to PS intake is different between a diet representing what average Americans eat and a diet representing what health professionals recommend for blood cholesterol management. Within the context of the present study design, a diet effect and a PS effect were observed. Because there was no diet × PS interaction, our data demonstrate experimentally, for the first time, that the effects of PS and diet on plasma lipoprotein cholesterol concentrations are additive, at least for diets ranging in composition from the Step 1 to the TAD.

The magnitude of PS induced reduction in plasma TC and LDL cholesterol concentrations found in this study is comparable with the changes reported in the literature in which 2–3 g PS/day was consumed in conjunction with various background diets. Under Step 1 feeding alone, three servings of PS produced a 12.7% reduction in LDL cholesterol which is consistent with our prior study in which two servings of PS were fed and a 9.7% reduction in LDL cholesterol was observed [13]. Most importantly, these data show that a 16.9% reduction in plasma LDL

cholesterol concentration and a 7.8% increase in the TC/HDL cholesterol ratio were accomplished by switching from a TAD to a Step 1 +PS diet. For the reduction in LDL cholesterol, 72.7% was attributed to the PS and 27.3% to the switch from the TAD to the Step 1 diet. For the reduction in the TC/HDL cholesterol ratio, 100% was attributed to PS.

Because of the power gained from using a crossover design of this study, we were able to report for the first time a diet × PS interaction for Apo B and Apo B/Apo A1. The diet effect on Apo B was detectable only in the absence of PS which may be explained by the greater effect of PS on Apo B masking the weaker diet effect. Apo B/Apo A1 ratio has been suggested to be a better index than TC/HDL cholesterol ratio, non-HDL cholesterol/HDL cholesterol ratio, or LDL cholesterol/HDL cholesterol ratio to predict coronary risk [28]. As such, our finding of a greater PS effect on Apo B/Apo A1 ratio with TAD feeding than Step 1 feeding is of practical significance as the majority of the Americans are consuming diets closer to the TAD than the Step 1 diet [27].

Consistent with the literature, the present study found no effect of PS on plasma TAG and Apo A1 concentrations, whereas LDL cholesterol and Apo B concentrations, and thus the Apo B/Apo A1 ratio, were lowered by PS intake. The diet effects on TC, HDL cholesterol, LDL cholesterol, Apo A1, and Apo B were as expected. A diet effect on TAG was not observed possibly because the number of subjects was insufficient for such a purpose [29]. The subject sample size in this study was determined based on the detection of a significant difference in LDL cholesterol and not TAG.

Table 4 Effects of diet and intake of plant sterols (PS) on plasma retinol, tocopherols and carotenoids

Plasma concentration	Diet effect		PS effect			<i>P</i> value (<i>F</i> test)	
	Step 1	TAD	–PS	+PS	SEM	Diet	PS
Retinol							
μmol/L	2.25 ^a	2.28	2.28	2.24	0.09	0.6153	0.4965
μmol/mmol TC	0.44	0.43	0.42	0.45	0.02	0.3130	0.0062
δ-Tocopherol							
μmol/L	0.20	0.23	0.22	0.21	0.02	0.0019	0.5149
μmol/mmol TC	0.04	0.04	0.04	0.04	<0.01	0.0142	0.5034
γ-Tocopherol							
μmol/L	5.80	6.49	6.40	5.89	0.32	0.0006	0.0108
μmol/mmol TC	1.14	1.22	1.18	1.18	0.06	0.0191	0.8451
α-Tocopherol							
μmol/L	36.12	35.85	38.36	33.60	1.68	0.7908	<0.0001
μmol/mmol TC	6.95	6.72	6.95	6.72	0.25	0.1155	0.1160
Lutein							
μmol/L	0.30	0.33	0.34	0.30	0.02	0.0073	0.0011
μmol/mmol TC	0.06	0.06	0.06	0.06	<0.01	0.0592	0.2663
Zeaxanthin							
μmol/L	0.11	0.13	0.13	0.11	0.01	<0.0001	0.0013
μmol/mmol TC	0.02	0.03	0.02	0.02	<0.01	<0.0001	0.1784
α-Cryptoxanthin							
μmol/L	0.083	0.091	0.095	0.080	0.004	0.0119	<0.0001
μmol/mmol TC	0.016	0.017	0.017	0.016	0.001	0.1837	0.0104
β-Cryptoxanthin							
μmol/L	0.253	0.260	0.279	0.233	0.011	0.3198	<0.0001
μmol/mmol TC	0.049	0.048	0.051	0.047	0.002	0.5325	0.0008
Lycopene							
μmol/L	0.340	0.335	0.399	0.275	0.02	0.6653	<0.0001
μmol/mmol TC	0.066	0.063	0.073	0.055	<0.01	0.0925	<0.0001
α-Carotene							
μmol/L	0.142	0.132	0.152	0.122	0.01	0.0969	<0.0001
μmol/mmol TC	0.027	0.024	0.028	0.024	<0.01	0.0059	0.0033
β-Carotene							
μmol/L	0.501	0.438	0.545	0.394	0.02	<0.0001	<0.0001
μmol/mmol TC	0.097	0.081	0.100	0.079	0.01	<0.0001	<0.0001

^a LS mean

Qualitatively, the responses of plasma retinol, tocopherols, and carotenoids to PS intake observed in the present study were as expected. Quantitatively, the responses are consistent with those reported by us previously but greater than those reported by others in studies in which comparable amounts of PS were consumed, particularly for α - and β -carotene and lycopene. Richelle et al. [30] recently identified reductions in absorption of β -carotene and α -tocopherol as a mechanism for the PS intake-associated reductions in the circulation. We found higher plasma TC standardized concentrations of γ -tocopherols and zeaxanthin after consumption of the TAD than the Step 1 diet.

This finding is consistent with the knowledge that an increase in fat intake promotes the absorption of tocopherols and carotenoids [31]. The observation that the TAD, as compared with the Step 1 diet, produced significant reductions in TC-corrected plasma α - and β -carotene concentrations was unexpected and unexplainable, but is probably not physiologically important because the differences are insignificant in the context of their typical ranges in plasma.

In conclusion, our study is the first example of a direct comparison of the influence of diets versus the influence of PS intake on blood lipoprotein concentrations. Our findings

confirm that the LDL cholesterol-reducing effects resulting from PS intake and from switching from the TAD to the Step 1 diet are independent of each other, and that both are important but the effect of PS intake is quantitatively far greater. Our findings should not be taken as a suggestion that diet is of no consequence, because in fact the diet effect and the PS effect are additive. A limitation of the present study, as in most other published studies of PS and plant stanols, is the possible lack of generalizability because study participation was restricted to mildly hypercholesterolemic adults and, in our case, middle-aged male and non-HRT using postmenopausal female subjects. It is important to extend this study to larger and more varied groups.

Acknowledgments This paper is dedicated to our late mentor, colleague, and friend, David Kritchevsky, Ph.D. We are grateful to Elke Trautwein, Ph.D., of the Unilever Food and Health Research Institute for helpful discussions; Richard A. Muesing, Ph.D., of George Washington University for determining plasma concentrations of lipids, apoproteins, and lipoprotein cholesterols. Supported in part through a Research Support Agreement between the Agricultural Research Service, US Department of Agriculture, and Unilever US, Englewood Cliffs, NJ.

Conflict of interest statement J.T. Judd, M. Kramer, B.A. Clevidence, and D.J. Baer, no conflicts of interest. S.C. Chen was an employee of Unilever Foods, NA at the time the dietary portion of the study was conducted. G.W. Meijer is an employee of Unilever.

References

- Miettinen TA, Puska P, Gylling H, Vanhanen H, Vartiainen E (1995) Reduction of serum cholesterol with sitostanol-ester margarine in a mildly hypercholesterolemic population. *N Engl J Med* 333:1308–1312
- Katan MB, Grundy SM, Jones P, Law M, Miettinen T, Paoletti R (2003) Efficacy and safety of plant stanols and sterols in the management of blood cholesterol levels. *Mayo Clin Proc* 78:965–978
- Ostlund RE Jr (2002) Phytosterols in human nutrition. *Annu Rev Nutr* 22:533–549
- Lichtenstein AH (2002) Plant sterols and blood lipid levels. *Curr Opin Clin Nutr Metab Care* 5:147–152
- Plat J, Mensink RP (2005) Plant stanol and sterol esters in the control of blood cholesterol levels: mechanism and safety aspects. *Am J Cardiol* 96:15D–22D
- Nestel P, Cehun M, Pomeroy S, Abbey M, Weldon G (2001) Cholesterol-lowering effects of plant sterol esters and non-esterified stanols in margarine, butter and low-fat foods. *Eur J Clin Nutr* 55:1084–1090
- Miettinen TA, Vanhanen H (1994) Dietary sitostanol related to absorption, synthesis and serum level of cholesterol in different apolipoprotein E phenotypes. *Atherosclerosis* 105:217–226
- Pelletier X, Belbraouet S, Mirabel D, Mordret F, Perrin JL, Pages X, Debry G (1995) A diet moderately enriched in phytosterols lowers plasma cholesterol concentrations in normocholesterolemic humans. *Ann Nutr Metab* 39:291–295
- Hallikainen MA, Sarkkinen ES, Gylling H, Erkkila AT, Uusitupa MI (2000) Comparison of the effects of plant sterol ester and plant stanol ester-enriched margarines in lowering serum cholesterol concentrations in hypercholesterolaemic subjects on a low-fat diet. *Eur J Clin Nutr* 54:715–725
- Weststrate JA, Meijer GW (1998) Plant sterol-enriched margarines and reduction of plasma total- and LDL-cholesterol concentrations in normocholesterolaemic and mildly hypercholesterolaemic subjects. *Eur J Clin Nutr* 52:334–343
- Maki KC, Davidson MH, Umporowicz DM, Schaefer EJ, Dicklin MR, Ingram KA, Chen S, McNamara JR, Gebhart BW, Ribaya-Mercado JD, Perrone G, Robins SJ, Franke WC (2001) Lipid responses to plant-sterol-enriched reduced-fat spreads incorporated into a National Cholesterol Education Program Step I diet. *Am J Clin Nutr* 74:33–43
- Jones PJ, Ntanos FY, Raeini-Sarjaz M, Vanstone CA (1999) Cholesterol-lowering efficacy of a sitostanol-containing phytosterol mixture with a prudent diet in hyperlipidemic men. *Am J Clin Nutr* 69:1144–1150
- Judd JT, Baer DJ, Chen SC, Clevidence BA, Muesing RA, Kramer M, Meijer GW (2002) Plant sterol esters lower plasma lipids and most carotenoids in mildly hypercholesterolemic adults. *Lipids* 37:33–42
- Vanstone CA, Raeini-Sarjaz M, Parsons WE, Jones PJ (2002) Unesterified plant sterols and stanols lower LDL-cholesterol concentrations equivalently in hypercholesterolemic persons. *Am J Clin Nutr* 76:1272–1278
- Gylling H, Miettinen TA (1999) Cholesterol reduction by different plant stanol mixtures and with variable fat intake. *Metabolism* 48:575–580
- Third Report of the National Cholesterol Education Program (NCEP) Expert Panel on Detection, Evaluation, and Treatment of High Blood Cholesterol in Adults (Adult Treatment Panel III) final report (2002) *Circulation* 106:3143–3421
- Kris-Etherton PM, Dietschy J (1997) Design criteria for studies examining individual fatty acid effects on cardiovascular disease risk factors: human and animal studies. *Am J Clin Nutr* 65:1590S–1596S
- Composition of foods, agriculture handbook no. 8, sections 1–22. In: US Department of Agriculture HNIS (ed), US Government Printing Office, 1976–1990
- Holden JM, Eldridge AL, Beecher GR, Buzzard IM, Bhagwat SA, Davis CS, Douglass LW, Gebhardt SE, Haytowitz DB, Schakel S (1999) Carotenoid content of US foods: an update of the database. *J Food Comp Anal* 12:169–196
- Hainline A, Karon J, Lippel K (1982) Manual of laboratory operations: lipid and lipoprotein analysis. In: USGPO HEW (ed) Lipid research clinics program pub no. (NIH) 75–628 (rev.). National Heart Lung and Blood Institute, Bethesda
- Friedewald WT, Levy RI, Fredrickson DS (1972) Estimation of the concentration of low-density lipoprotein cholesterol in plasma, without use of the preparative ultracentrifuge. *Clin Chem* 18:499–502
- Khachik F, Beecher GR, Goli MB, Lusby WR, Smith JC Jr (1992) Separation and identification of carotenoids and their oxidation products in the extracts of human plasma. *Anal Chem* 64:2111–2122
- Bieri JG, Brown ED, Smith JC Jr (1985) Determination of individual carotenoids in human plasma by high performance liquid chromatography. *J Liq Chromatogr* 8:473–484
- Littell RC, Milliken GA, Stroup WW, Wolfinger RD (1996) SAS system for mixed models. SAS, Cary
- SAS/STAT (2003) User's guide. Version 9.1.3. Cary, NC: SAS Institute Inc.
- Allison DB, Egan SK, Barraj LM, Caughman C, Infante M, Heimbach JT (1999) Estimated intakes of *trans* fatty and other fatty acids in the US population. *J Am Diet Assoc* 99:166–174 (quiz 175–176)

27. What we eat in America, NHANES 2005–2006: documentation and data files (2008). In: US Department of Agriculture ARS (ed)
28. Walldius G, Jungner I, Aastveit AH, Holme I, Furberg CD, Sniderman AD (2004) The apoB/apoA-I ratio is better than the cholesterol ratios to estimate the balance between plasma pro-atherogenic and antiatherogenic lipoproteins and to predict coronary risk. *Clin Chem Lab Med* 42:1355–1363
29. Ginsberg HN, Kris-Etherton P, Dennis B, Elmer PJ, Ershow A, Lefevre M, Pearson T, Roheim P, Ramakrishnan R, Reed R, Stewart K, Stewart P, Phillips K, Anderson N (1998) Effects of reducing dietary saturated fatty acids on plasma lipids and lipoproteins in healthy subjects: the DELTA study, protocol 1. *Arterioscler Thromb Vasc Biol* 18:441–449
30. Richelle M, Enslen M, Hager C, Groux M, Tavazzi I, Godin JP, Berger A, Metairon S, Quaile S, Piguët-Welsch C, Sagalowicz L, Green H, Fay LB (2004) Both free and esterified plant sterols reduce cholesterol absorption and the bioavailability of beta-carotene and alpha-tocopherol in normocholesterolemic humans. *Am J Clin Nutr* 80:171–177
31. Parker RS, Swanson JE, You CS, Edwards AJ, Huang T (1999) Bioavailability of carotenoids in human subjects. *Proc Nutr Soc* 58:155–162

Shapes and Coiling of Mixed Phospholipid Vesicles

Gerardo Paredes-Quijada · Helim Aranda-Espinoza · Amir Maldonado

Received: 11 September 2008 / Accepted: 15 December 2008 / Published online: 27 January 2009
© AOCs 2009

Abstract We have studied some physical properties of mixed phosphatidylcholine (SOPC)–phosphatidylserine (SOPS) vesicles. In a previous work (Paredes et al. in *J Biol Phys* 32:177–181, 2006) it was shown that the shape of the vesicles depends on the SOPC:SOPS composition, and that coiled cylindrical vesicles exist in samples with low SOPS contents. In this work, we further studied the same system of mixed vesicles. Differential scanning calorimetry (DSC) experiments displayed peaks characteristic of lipid mixing in the liquid state, ruling out a possible phase transition as an explanation of vesicle coiling. In addition, small-angle X-ray scattering (SAXS) experiments allowed us to estimate the periodicity distance inside the vesicles. This distance is $d \approx 60 \text{ \AA}$, as revealed by the Bragg peaks observed in the experiments. Finally, the coiling transition of a cylindrical vesicle was observed under solvent flow. This observation indicates that the vesicle coiling reported previously for this system (Paredes et al. in *J Biol Phys* 32:177–181, 2006) does not depend on the SOPC:SOPS composition alone, but also on mechanical perturbations during the preparation steps.

Keywords Biological membranes · Vesicles · Phospholipids · SOPC · SOPS · Vesicle coiling

Introduction

Giant vesicles have been used as models for studying membrane properties that can be relevant in biological phenomena [1, 2]. For this reason, the development of new methods for the preparation of vesicles of controlled properties (size, shape, mono- or multilamellarity) is of current interest, as well as the understanding of the mechanisms underlying the established methods. From all these, the simplest one is the hydration method, where a dried phospholipid film is hydrated with an appropriate amount of a solvent, with the vesicles forming after shaking or stirring [3]. Regardless of its simplicity, the mechanisms that favor vesicle formation at each stage of the procedure (drying, hydration, shaking) are not fully understood so far [3].

In a previous work, we reported experimental results regarding the shapes of mixed phospholipid vesicles [4]. The aggregates were prepared by the hydration method from mixtures of phosphatidylcholine (SOPC) and phosphatidylserine (SOPS) in different proportions. Using optical microscopy, we showed that the shape of the vesicles depends on the SOPC:SOPS composition. The main results of reference [4] are summarized in Table 1. It is interesting to note that among the observed vesicle shapes, there are coiled cylindrical vesicles for SOPC:SOPS molar proportions between 90:10 and 70:30 [4]. The variety of structures was interpreted in terms of the packing parameter model [5], in which the geometry of the molecules determines the aggregate structure.

G. Paredes-Quijada (✉)
Posgrado en Polímeros y Materiales, Universidad de Sonora,
Apdo. Postal 130, 83000 Hermosillo, Sonora, México
e-mail: gtparedes@correo.fisica.uson.mx

H. Aranda-Espinoza
Fischell Bioengineering Department, University of Maryland,
3135 Kim Engineering Building, College Park, MD 20742, USA

A. Maldonado
Departamento de Física, Universidad de Sonora, Apdo.
Postal 1626, 83000 Hermosillo, Sonora, México

Table 1 Summary of the SOPC:SOPS vesicle shapes and sizes observed in [4]

SOPC:SOPS composition	Shapes of the observed vesicles	Characteristic dimensions of the observed vesicles (μm)
0:00–95:05	Spherical	$D_{\text{spheres}} = 17$
	Cylindrical	$D_{\text{cylinders}} = 5$
90:10–70:30	Spherical	$D_{\text{spheres}} = 16$
	Cylindrical	$D_{\text{cylinders}} = 5$
	Coils	See Table 2
60:40–0:100	Spherical	$D_{\text{spheres}} = 16$

In this paper we report experiments on the same system

In this work, we report further experiments in the SOPC:SOPS system. Our aim was a better characterization of the vesicles described in reference [4], as well as the coiling transition described therein. We performed differential scanning calorimetry (DSC) experiments in order to determine the phase transition temperatures of the phospholipid mixtures. Small-angle X-ray scattering (SAXS) experiments were performed in order to have an idea of the periodicity distance inside the multilayered vesicles. In addition, the same vesicles were hydrated with solutions of monovalent and divalent salts in order to screen electrostatic interactions in the membrane and to assess if electrostatic effects are relevant in the coiling of cylindrical vesicles. Finally, the coiling of a cylindrical vesicle under solvent flow was followed using optical microscopy.

Experimental Methods

Materials

Vesicles were made of 1-Stearoyl-2-Oleoyl-*sn*-Glycero-3-Phosphocholine (SOPC) and 1-Stearoyl-2-Oleoyl-*sn*-Glycero-3-Phospho-L-Serine (SOPS). The molecular weights of these lipids are 788.14 g/mol and 812.05 g/mol respectively. Both phospholipids were purchased from Polar Avanti Lipids, Inc. (Alabaster, AL) and received as 10 mg/mL chloroform solutions. Purity is greater than 99%. They were stored at $-20\text{ }^{\circ}\text{C}$. Sucrose was obtained from Sigma (St Louis, MO). Ultrapure water with a resistivity greater than $18\text{ M}\Omega\text{ cm}$ was used to prepare all solutions. For the samples hydrated with brine, we used two monovalent (NaCl, KCl) and two divalent (CaCl_2 , MgCl_2) salts, all obtained from Sigma (St Louis, MO).

Sample Preparation

The samples were prepared by vacuum drying appropriate amounts of SOPC:SOPS mixtures at room temperature (3 h); the total phospholipid mass in every sample was 200 μg . In all our experiments, the samples were hydrated with 1 ml of a 60 mM sucrose solution in glass vials. The solvent of the sucrose solution was pure water, but brine solutions were used when we studied the effect of mono and divalent salts. Hydration with higher volumes of solvent gave qualitatively the same kind of aggregates. Note that above the phospholipid concentration range 2–8 mM there is non-ideal mixing of SOPC and SOPS [6]. Thus, our samples were prepared below this range, i.e. the phospholipid concentration was 0.2 mM, in order to ensure ideal SOPC–SOPS mixing. The SOPC:SOPS proportions of our samples were the same as those of reference [4] (see also Table 1). We worked in slightly acidic conditions ($\text{pH} = 6$). This pH is above the pK of the serine group in SOPS, which is thus not protonated.

Vesicle Shape and Size

In order to observe and to take images of the vesicles, 20 μl of the vesicle suspension were transferred to an observation chamber made with microscope cover slides and sealed with vacuum grease. The aggregates were observed using a LEICA DMIL inverted optical microscope with objective lenses $20\times$ and $40\times$. From the microscopy pictures we characterized the vesicle populations and measured the aggregate dimensions by using a microscopic scale of 2 $\mu\text{l}/\text{division}$ (Edmund Industrial Optics, Barrington, NJ). The vesicle dynamics was followed using a video camera (30 frames/s). All the experiments were conducted at room temperature, well above the chain melting transition of both lipids.

DSC and SAXS Experiments

Calorimetry experiments were performed in order to know the temperature transitions of the mixtures. A volume of 700 μl of the samples was injected in a calorimeter (Provo, UT) which measured the heat flow in the interval between 5 and $30\text{ }^{\circ}\text{C}$, at a rate of $1\text{ }^{\circ}\text{C}/\text{min}$. Small-angle X-ray scattering (SAXS) experiments were also performed in order to have some information about the interbilayer distance in the samples. We use a Rigaku rotating anode source that produces the $\text{CuK}\alpha$ lines (1.54 \AA). The linear detector, with 512 channels, was placed 81 cm from the sample position. For the SAXS experiments, the samples were more concentrated in order to have a strong enough signal.

Experimental Results

In Fig. 1, we present DSC results for several SOPC:SOPS proportions. The DSC thermograms reveal a well-defined transition peak in the samples, indicating mixing of the phospholipids. The main transition for the mixtures lies between 8 and 18 °C, well below room temperature. All the transition temperatures lie between those of SOPC (≈ 6 °C) and SOPS (≈ 26 °C) [7]. This is an indication that effects related to the solid-liquid melting transition in the membranes can be ruled out. We can conclude that in our samples, the lipids are mixed in the liquid state.

Several vesicle shapes (spheres, cylinders, complex aggregates) appeared in the optical microscopy experiments, as reported in reference [4] and summarized in Table 1.

Since the vesicles were prepared by a hydration method, they should be multilayered aggregates. These vesicles can be pictured as onion-like structures, composed of layers of concentric spherical or cylindrical membranes. A representation of the vesicles is shown in Fig. 2. Due to the concentric layers, the aggregates have a local lamellar nature that should display a Bragg interference peak in scattering experiments. In order to have an idea of the

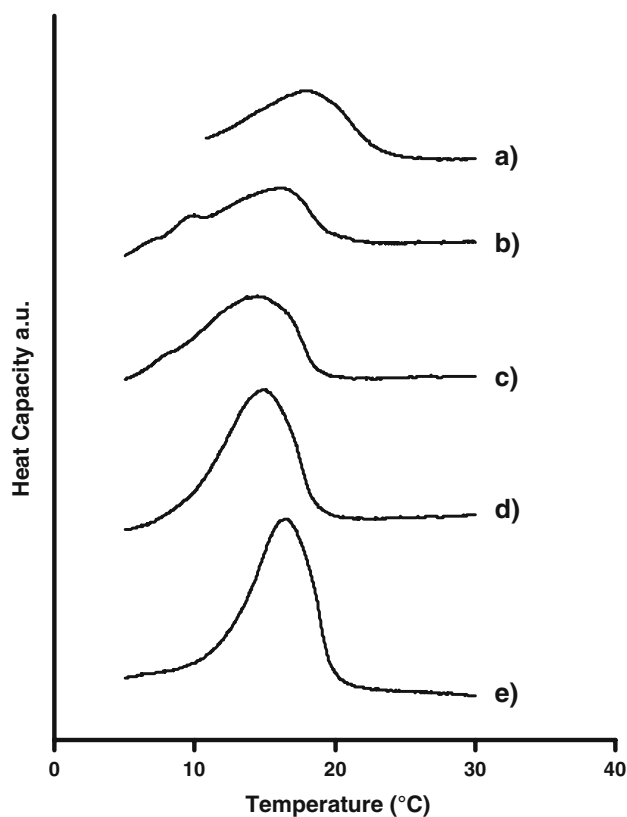


Fig. 1 DSC thermograms of SOPC:SOPS membranes with different proportions: *a* 90:10, *b* 70:30, *c* 50:50, *d* 30:70 and *e* 10:90. The transition temperatures are below room temperature

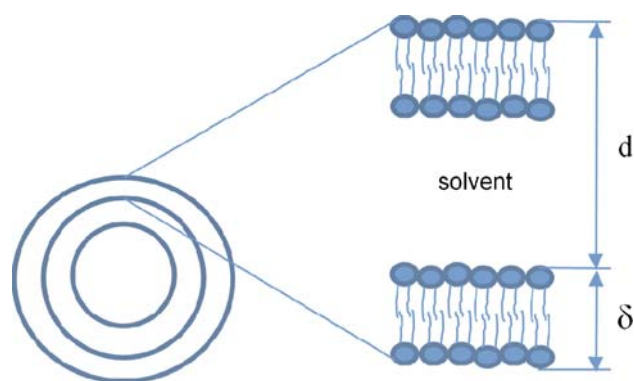


Fig. 2 Schematic representation of the vesicles prepared by the hydration method. They can be pictured as onion-like structures, composed of layers of concentric membranes. Note that the aggregates have a local lamellar nature, where d is the periodicity distance. δ is the membrane thickness. Note that the drawings are not at scale

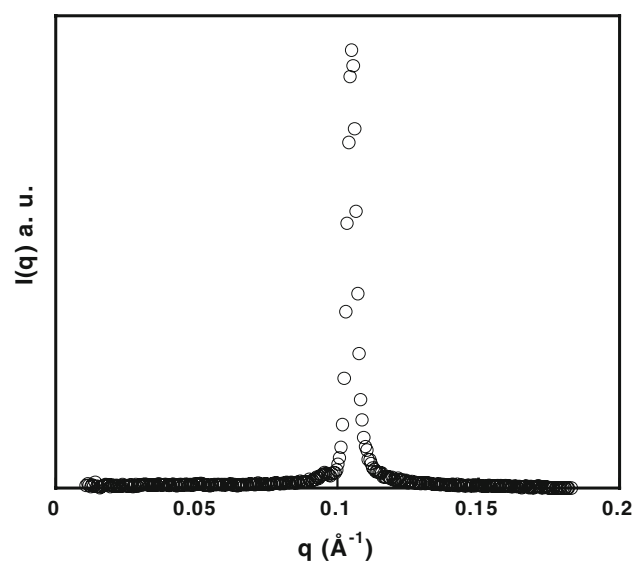
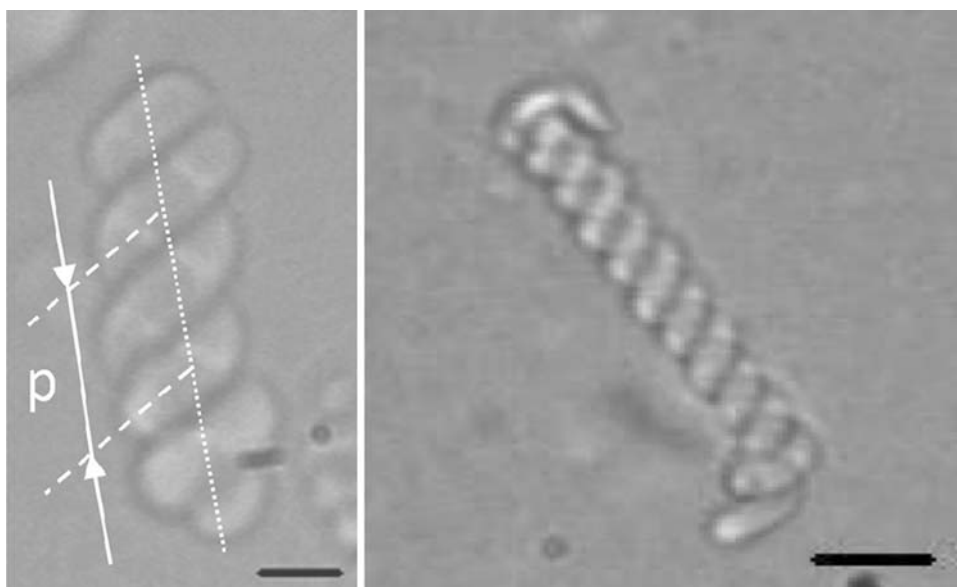


Fig. 3 SAXS spectra of a sample with 100:0 composition. The Bragg peak indicates a multilamellar structure. From the position of the peak, the periodicity distance is $d \approx 60$ Å

periodicity distance d of the lamellar structure inside the vesicles (Fig. 2), we have performed SAXS experiments. Since the scattering signal was too low with the concentrations used for the optical microscopy experiments, the samples for X-ray Scattering were more concentrated. The SAXS spectra displayed a well-defined Bragg peak (Fig. 3), indicating that the vesicles have a multilamellar structure. From the peak position we computed the periodicity distance d using the Bragg relationship, $d = 2\pi/q_{\max}$. In our vesicles, this interbilayer distance is $d \approx 60$ Å. Note that systematic SAXS experiments could be interesting in order to study properties such as the

Fig. 4 Two of the coiled vesicles observed in the 90:10–70:30 SOPC:SOPS proportion range. p is the pitch of the helical structure. The *bar* represents 10 μm



interbilayer distance and the membrane elastic constants [8] as a function of concentration, temperature and pH.

In reference [4] it was reported that a striking structure observed for some SOPC:SOPS proportions is that of coiled vesicles. In Fig. 4 we present two of such coiled aggregates. We have measured the characteristic dimensions of the coiled vesicles. These dimensions are: the length of the coiled vesicle (l), the radius of the coiled cylinder (r) and the pitch (p) of the helical structure. Note that since the coiled vesicles are double helices [4, 9], the pitch p is defined as the repetition distance (for a single cylinder) along the helical axis (Fig. 4). The measured dimensions are shown in Table 2. As the ratio between the pitch of the helix p , and the radius of the cylinder r , is an indication of the tightness (or looseness) of the coiled structure, in Fig. 5 we have plotted p as a function of r . We

Table 2 Measured length, cylinder diameter and pitch of typical coiled vesicles observed in the proportion range 90:10–70:30

Vesicle	Length l	Cylinder radius r	Pitch p
1	18.09	2.92	8.33
2	22.50	3.33	4.17
3	23.75	5.02	18.33
4	25.83	4.17	10.43
5	31.43	4.17	9.32
6	35.42	3.33	4.17
7	48.32	3.25	9.58
8	52.29	6.67	17.98
9	57.21	7.96	29.36
10	62.7	8.92	25
11	66.65	9.51	25.00

The values are given in microns

see in this picture that the pitch is linearly related to the cylinder radius. The ratio of the radius to the pitch is obtained from the slope of this curve; its value is $r/p = 0.22 \pm 0.09$. This value is very near to that of the tightly wound helices observed in the phosphatidylcholine/cardiophilin mixture in the presence of calcium ions ($r/p = 0.214$) [10]. Looser helix formation has been observed in egg-PC vesicles, where the radius/pitch ratio is $r/p = 0.175 \pm 0.015$ [11].

In order to assess if electrostatic effects, such as the charge relaxation mechanism [12], do play a role in the coiling of our vesicles, we performed experiments with different salt concentrations in the solvent. For this, we

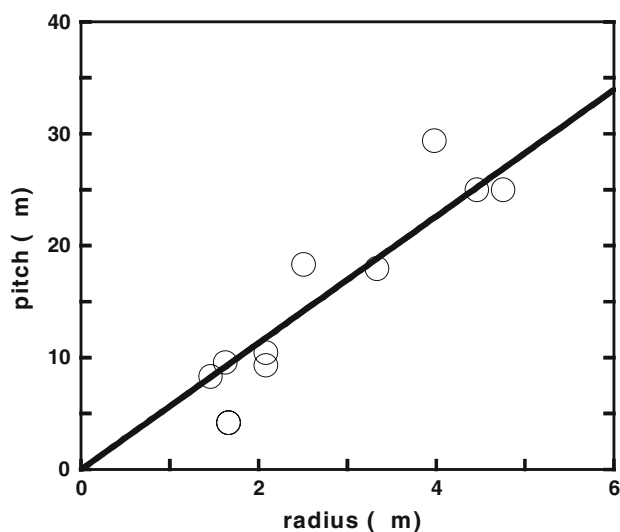


Fig. 5 Dependence of the measured pitch on the cylinder radius for coiled vesicles. The ratio of the radius to the pitch is 0.22 ± 0.09 , as obtained from the slope of the linear fit

used monovalent (NaCl, KCl) and divalent (CaCl₂, MgCl₂) salts. The positive ions screen the repulsive electrostatic interactions between SOPS head groups. Our results indicate that the yield of vesicles depends on the type of ion. Monovalent salts inhibit the formation of vesicles. On the other hand, divalent ions promote the formation of mainly spherical vesicles. These results are somewhat similar to those obtained by Akashi and coworkers [13] with a slightly different hydration method. Interestingly, no coiling was observed in the few cylindrical vesicles obtained in our experiments. It is not clear if this effect is only due to the low yield of cylindrical vesicles or to electrostatic effects related with the screening of the Coulomb interactions between PS head groups.

Note that other possible source of electrostatic effects is the pH of the solutions. In our case, we work in a slightly acidic media (pH = 6), thus effects due to protonation of the phospholipids should be negligible. In fact, the phosphatidylcholine head group has a strong zwitterionic character [3], i.e., it bears a positive electrical charge (associated with the nitrogen atom) as well as a negative electrical charge (phosphorous atom). On the basis of titrimetric assays, PC is known to preserve its zwitterionic characteristics over the entire pH range, $1 < \text{pH} < 12$ [14]. Thus, it is expected that a modification of pH, at least in this range, does not change the SOPC properties. On the other hand, SOPS is an anionic phospholipid [3]. Its head group has three ionizable groups (the diester phosphoric acid, the α -amino group and the carboxyl group), and it bears a net negative charge above a pH = 4.5 [14]. Below this value of pH, the carboxyl group protonates and SOPS is in the zwitterionic form (two opposite-sign electrical charges) [14]. Thus, if pH decreases below 4.5, SOPS loses its net negative charge and its properties change.

This behavior of the PC and PS head groups has been confirmed by potentiometric titration and surface potential measurements in mixed PC:PS vesicles [15]. We expect that in the case of the shapes of our SOPC:SOPS vesicles, no modifications would be observed if the pH is varied in the range above 4.5. However, due to protonation of the PS head group, one would expect modifications in the shape and properties of the SOPC:SOPS vesicles below a pH = 4.5. It would be an interesting point to investigate if coiling is possible for these pH values. We leave this issue for a future work.

Coiling of the SOPC:SOPS vesicles diluted with pure water depends on the composition of the sample because it is only observed for compositions between 90:10 and 70:30 [4]. However, it seems that the appearance of helicoidal vesicles is not only due to specific compositions but also to hydrodynamical stresses. In Fig. 6 we show the coiling of a SOPC:SOPS vesicle under a hydrodynamic perturbation. The composition of this vesicle is 80:20. The sequence was

obtained following a long cylindrical vesicle after solvent dilution. Right after sample preparation, the cylindrical vesicle was observed for a period of time of 30 min and only thermal fluctuations were observed (Fig. 6a). Afterwards, the sample was diluted adding a small quantity (10 μl) of solvent with a pipette. The effect was to coil both ends of the vesicle (Fig. 6b). The vesicle remained stable in this state for several minutes. Only thermal fluctuations were observed. Again we added the same volume of solvent and both ends of the vesicle continued to coil (Fig. 6c). The resulting vesicle was again stable for 30 min. This procedure was repeated until a final highly packed coiled aggregate was obtained (Fig. 6i). Note that the scale in Fig. 6 was changed in the last two pictures because of the small size of the final vesicle. This kind of highly packed aggregate was also observed in other samples with these phospholipid compositions. It seems to be the final stage of a coiling dynamics triggered by a hydrodynamical perturbation. Thus, coiling does not only depend on the composition of the membrane, but also on mechanical perturbations. This is a possible explanation of why the shapes of the population of vesicles obtained by hydration methods depend on the mechanical treatment of the samples. Note that the added solvent volume in each step of Fig. 6 reduces the phospholipid concentration of the sample. By performing this series of dilutions, at the final stage (Fig. 6i) we changed the total phospholipid concentration to about 20% of its original value. This new concentration is well above the typical cmc of phospholipids [5]. It is possible that preparing the vesicles with this concentration could lead to modifications in the aggregate characteristics. However, in the experiments depicted in Fig. 6 we did not perform all the hydration steps (drying, hydration, shaking). Instead, we just added the solvent to the already hydrated vesicles, without shaking the sample. The effect was to modify the preformed vesicle in the form observed in Fig. 6. We did not measure the characteristics of the other remaining vesicles, but just followed this cylindrical aggregate.

Discussion

As reported in reference [4], coiled vesicles have been observed in other systems [9–13, 16–19]. In some cases, coiling is induced by adding an additional component to cylindrical phospholipid vesicles. This component is either an ion [10] or a polymer [9, 16].

From a theoretical point of view, several mechanisms have been proposed in order to understand the existence of helicoidal vesicles.

Some of these approaches explain the coiling of the vesicles as a result of the interplay between favorable and

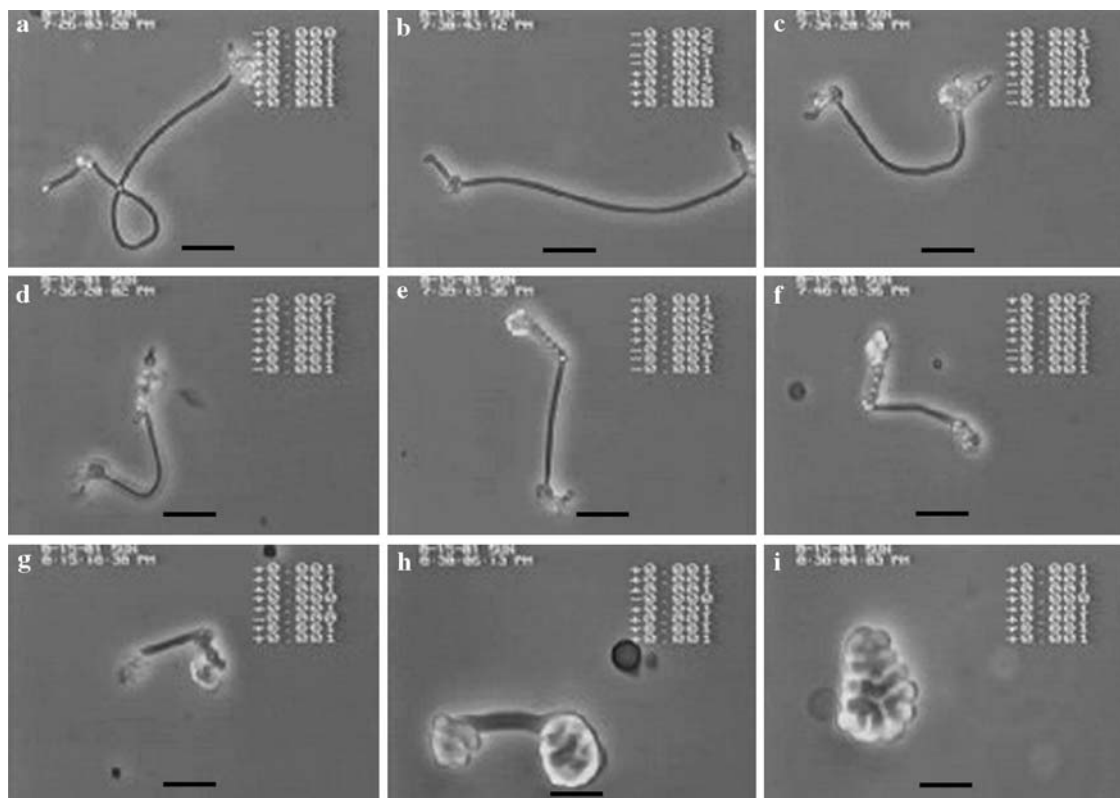


Fig. 6 Coiling dynamics of a SOPC:SOPS vesicle under a hydrodynamic perturbation (see text). The phospholipid composition of this vesicle is 80:20. **a** Unperturbed cylindrical vesicle undergoing thermal fluctuations. **b–i** Coiling of the vesicle observed after

hydrodynamic perturbation (flow of solvent) in each step. **i** Final highly-packed coiled vesicle. The bar represents 10 μm (**a–g**) and 5 μm in (**h**) and (**i**)

unfavorable forces. For instance, Lin et al. [10] have explained the Ca^{2+} -mediated induction of helical liposomes in mixtures of DMPC and cardiolipin by membrane–membrane binding forces; they argue that weak membrane–membrane binding energies can overcome curvature elastic energies and stabilize coiled vesicles. On the other hand, Mishima et al. [11] have reported coiling of cylindrical vesicles of egg-yolk lecithin. In this work, the proposed mechanism of coiling is an interplay between intermembrane attraction and the forces opposing helix formation which arise from the bending energy of the membranes. In the case of the SOPC:SOPS vesicles studied in this paper, membrane adhesion should be weak because the SOPS proportions are relatively small and adhesion forces should be similar to the case of pure SOPC [9]. In addition, the electrostatic repulsion of SOPS is unfavorable to adhesion. We thus rule out a mechanism related to a balance between favorable and unfavorable forces.

Another possible mechanism is the coupling between membrane composition and local membrane curvature. This is the driving force in the case of coiling induced by anchoring a hydrophobically modified polymer into cylindrical phospholipid vesicles [9, 16]. It has been proposed

that the added polymer diffuses and creates inhomogeneities that reduce the free energy of the system; this process locally induces a spontaneous curvature which drives the coiling of the cylinders [9, 16]. In our case, local inhomogeneities could appear after demixing of the two phospholipids composing the vesicle membranes. However, the DSC experiments show that our experiments were performed at a temperature well above the chain melting transition, regardless of the SOPC:SOPS proportion. Thus, phase transitions in the membrane can be ruled out as a driving force for coiling.

In our system, the exact mechanism of coiling is so far unclear. It is possible that the vesicles undergo a coiling transition due to some spontaneous curvature appearing at specific SOPC:SOPS compositions. This is a mechanism reported in the framework of a theoretical model by Santangelo and Pincus [19].

However, as shown in Fig. 6, coiling can also be induced by an appropriate flow of solvent. It is possible that the hydrodynamic perturbation produced by this flow creates asymmetric stresses or forces around the cylindrical vesicle so as to drag the cylinder to coil around itself. These forces could be of hydrodynamic origin, like those

explained by the Bernoulli equation of fluid dynamics [20]. One of the main effects predicted by this equation is a variation in pressure correlated with variations in the local velocity in an incompressible fluid. If the velocity of the fluid is higher in one point than in another, in the first point the fluid pressure is lower than in the second. This could give rise to two forces: a drag force, parallel to the free-stream velocity, and a lift force, perpendicular to the free-stream. The effect of the drag force is to push an object along the fluid flow. However, the lift force can lead to a bending of a flexible object. In the case of the vesicle of Fig. 6, it is possible that the solvent flow around the cylinder had an asymmetric velocity distribution. The side of the vesicle exposed to a low solvent velocity is subjected to a higher fluid pressure (as compared with the side exposed to a high solvent velocity). Thus, a lift force acts on the cylinder, pushing it from low-velocity to high-velocity regions. This effect, combined with appropriate shape or curvature fluctuations, could lead to the process depicted in Fig. 6. However, this is a point that needs more clarification, both theoretically as well as experimentally. Meanwhile, it is clear that in our case coiling is a process that depends on the way the system is prepared. This result has implications regarding the preparation of vesicles by hydration methods. Steps like stirring or shaking can induce flows that change the vesicle morphology as in the case of Fig. 6. In fact, these effects could explain some of the differences observed in the population of vesicles obtained by different hydration procedures.

Conclusions

We studied some properties of phospholipid vesicles prepared by hydration of mixtures of phosphatidylcholine (SOPC) and phosphatidylserine (SOPS) in different proportions. We investigated this system because in a previous work it has been shown that the shape of the vesicles depends on the SOPC:SOPS composition [4]. Using SAXS experiments we have confirmed that the vesicles are multilayered and that the periodicity distance inside a vesicle is or the order of $d \approx 60 \text{ \AA}$. On the other hand, DSC experiments have shown that the membranes are formed by a homogeneous mixture of the two phospholipids, with melting transitions well below room temperature. This result rules out effects related to phase transitions as a driving force for the coiling of cylindrical vesicles observed in this system. Finally, coiling was induced in a cylindrical vesicle by a hydrodynamic perturbation. This result shows that this process not only depends on the SOPC:SOPS composition, but also on mechanical forces applied to the phospholipid vesicles. This observation has implications for understanding the mechanisms behind the

differences observed in the shapes and properties of vesicles prepared by hydration methods.

Acknowledgments G.P.-Q. acknowledges a fellowship from Conacyt-Mexico. A.M. acknowledges financial support from Conacyt-Mexico (grants 32105E and 0074) and ANUIES-ECOS (MOOP03). H.A.-E. and G.P.-Q. thank Dennis Discher for allowing us to use his laboratory where initial experiments were carried out. We thank Raymond Ober and Ricardo López-Esparza for collaboration in the SAXS experiments.

References

- Yeagle PL (2005) The structure of biological membranes, 2nd edn. CRC Press, Boca Raton
- Svetina S, Žekš B (2002) Shape behavior of lipid vesicles as the basis of some cellular processes. *Anat Rec* 268:215–225
- Cevc G (ed) (1993) The phospholipid handbook, Marcel Dekker, NY
- Paredes G, Aranda H, Maldonado A (2006) Shapes of mixed phospholipid vesicles. *J Biol Phys* 32(2):177–181
- Israelachvili J (1992) Intermolecular and surface forces, 2nd edn. Academic Press, Orlando
- Huang JR, Swanson JE, Dibble ARG, Hinderliter AK, Feigenson GW (1993) Nonideal mixing of phosphatidylserine and phosphatidylcholine in the fluid lamellar phase. *Biophys J* 64:413–425
- Lygre H, Moe G, Skalevik R (2003) Interaction of Tricosan with eukaryotic membrane lipids. *H Eur J Oral Sci* 111:216–222
- Helfrich W (1973) Elastic properties of lipid bilayers: theory and possible experiments. *Z Naturforsch* 28C:693–703
- Tsafirir I, Guedeau-Boudeville MA, Kandel D, Stavans J (2001) Coiling instability of multilamellar membrane tubes with anchored polymers. *Phys Rev E* 63:031603
- Lin KC, Weiss RW, McConnell HM (1982) Induction of helical liposomes by Ca^{2+} mediated intermembrane binding. *Nature* 296:164–165
- Mishima K, Fukuda L, Suzuki K (1992) Double helix formation of phosphatidylcholine myelin figures. *Biochim Biophys Acta* 1108:115–118
- Nguyen TT, Gopal A, Lee KYC, Witten TA (2005) Surface charge relaxation and the pearling instability of charged surfactant tubes. *Phys Rev E* 72:051930
- Akashi KI, Miyata H, Itoh H, Kinoshita JK (1998) Formation of giant liposomes by divalent cations: critical role of electrostatic repulsion. *Biophys J* 74:2973–2982
- Hanahan DJ (1997) A guide to phospholipid chemistry. Oxford University Press, Oxford
- Tsui FC, Ojcius DM, Hubbel WL (1986) The intrinsic pKa values for phosphatidylserine and phosphatidylethanolamine in phosphatidylcholine host bilayers. *Biophys J* 49:459–468
- Frette V, Tsafirir I, Guedeau MA, Jullien L, Kandel D, Stavans J (1999) Coiling of cylindrical membrane stacks with anchored polymers. *Phys Rev Lett* 83:2465–2468
- Buchanan M, Egelhaaf SU, Cates ME (2000) Dynamics of interface instabilities in nonionic lamellar phases. *Langmuir* 16:3718–3726
- Huang JR, Zou LN, Witten TA (2005) Confined multilamellae prefer cylindrical morphology: a theory of myelin formation. *Eur Phys J E Soft Matter* 18:279–285
- Santangelo CD, Pincus P (2002) Coiling instabilities of multilamellar tubes. *Phys Rev E* 66:061501
- Shames IH (2003) Mechanics of fluids, 4th edn. Mc Graw-Hill, New York

Structures of the Ceramides from Porcine Palatal Stratum Corneum

Jennifer R. Hill · Philip W. Wertz

Received: 14 November 2008 / Accepted: 6 January 2009 / Published online: 29 January 2009
© The Author(s) 2009. This article is published with open access at Springerlink.com

Abstract Ceramides are the major type of lipid found in stratum corneum from the skin, gingiva and hard palate. The present study examined the ceramides of the stratum corneum from the hard palate. Six fractions of ceramides were isolated by preparative thin-layer chromatography. The least polar fraction contained an unusual acyl ceramide (EOS) consisting of long ω -hydroxy acids amide-linked to sphingosine with mostly saturated fatty acids ester-linked to the ω -hydroxyl group. The second and third fractions contained normal fatty acids amide-linked to sphingosine (NS) and phytosphingosine (NP), respectively. In each of these ceramides, the fatty acids consisted of a mixture of saturated and monoenoic species. The three most polar fractions all contain amide-linked α -hydroxy acids. The fourth fraction contained long α -hydroxy acids amide-linked to sphingosine (ASI), while the fifth fraction contained short α -hydroxy acids amide-linked to sphingosine (ASs). The most polar ceramide contained α -hydroxy acids amide-linked to phytosphingosine (AP). EOS, NS and NP differed from their epidermal counterparts in terms of the compositions of the normal fatty acids. ASI, ASs and AP from palatal stratum corneum were essentially identical to their epidermal counterparts. The differences between palatal and epidermal EOS, NS and NP contribute to the differences in permeability of palate compared to skin.

Keywords Lipid · Ceramide · Stratum corneum · Skin · Oral mucosa · Keratinization

Introduction

The epidermis covering the skin and the epithelium covering the hard palate are both keratinizing epithelia, and as such, they undergo terminal differentiation to produce a stratum corneum [1]. This consists of an array of flat, keratin-filled cells embedded in a lipid matrix. In both epidermal and oral stratum corneum, ceramides, cholesterol, and fatty acids are major lipid types [2], and the ceramides in both epidermis and hard palatal epithelium consist of the same set of six structural types as judged by thin-layer chromatographic comparison [3]. These lipids determine the permeability of the tissue. In either case, the six chromatographically separable ceramides (EOS, NS, NP, ASI, ASs, AP; the ceramide nomenclature is according to Motta et al. [4] with the addition of the suffixes l or s to indicate long-chain fatty acids or short-chain fatty acids, respectively.) make up about half of the total lipids. The proportions of these major lipids are similar in oral and epidermal stratum corneum, except that there is notably lower ceramide EOS in the oral tissue [3].

Unlike epidermal stratum corneum, palatal and gingival stratum corneum contains small but significant levels of phospholipids and glycolipids [2]. In the epidermis, these polar membrane lipids are completely catabolized in the late stages of the differentiation process leading to formation of the stratum corneum [5]. The oral stratum corneum also contains somewhat variable amounts of triglycerides which are not thought to contribute to barrier function and which may be contaminants [6].

J. R. Hill
University of Minnesota, Minneapolis, USA

P. W. Wertz (✉)
University of Iowa, N450 DSB, Iowa City, IA 52242, USA
e-mail: Philip-wertz@uiowa.edu

The phospholipids and glycolipids, with their relatively bulky polar head groups and unsaturated fatty acids, would be expected to cause disorder of chain-packing within membranes and thereby shift the balance from predominantly gel-phase membrane domains toward more permeable liquid crystalline domains [7, 8]. In accordance with this expectation, the permeability of oral stratum corneum is an order of magnitude greater than that of epidermal stratum corneum [2, 6].

The purpose of the present study was to determine the structures of the ceramides from porcine palatal stratum corneum and to compare them with the previously published structures of porcine epidermal ceramides [9]. The null hypothesis is that the oral ceramides will be identical in structure to the epidermal ceramides.

Materials and Methods

Stratum Corneum Lipids

Porcine hard palates were obtained at a local slaughter house. The epithelium was peeled off using forceps after 1 min of immersion in water heated to 65 °C [2]. The stratum corneum was isolated by digestion with 1% trypsin in phosphate buffered saline at 4 °C overnight, followed by extensive rinsing with distilled water [2]. The tissue was then frozen at –20 °C and lyophilized over night. During the freeze-drying process, the shelf temperature was kept at 0 °C, and the vacuum was below 13 Pa. In the morning the shelf temperature was raised to 23 °C for 30 min prior to releasing the vacuum.

Lipids were extracted from the dried stratum corneum using chloroform:methanol, 2:1, 1:1 and 1:2 for 2 h each at room temperature [10]. Solvent was removed by evaporation under a gentle stream of nitrogen in a 45 °C water bath.

Isolation of Individual Ceramides

Twenty × twenty centimeter glass plates coated with 0.25-mm-thick silica gel G (Adsorbosil-plus-1; Alltech Associates; Deerfield IL, USA) were washed with chloroform:methanol, 2:1, and activated in an oven at 110 °C. Stratum corneum lipids were dissolved in a small volume of chloroform:methanol, 2:1, and applied as a narrow streak 3 cm from the bottom edge of the plate. The chromatogram was then developed to the top with chloroform:methanol:acetic acid, 190:9:1, followed by hexane:ethyl ether:acetic acid, 70:30:1 [9]. After air drying, the plate was sprayed lightly with 0.01% 2',7'-dichlorofluorescein in ethanol. After drying again, the plate was viewed under ultraviolet light. Lipid bands

appeared as dark bands on a bright background. The lipid fractions of interest were marked using a pencil. The silica from each fraction of interest was scraped from the plate using a Teflon spatula and placed in a small glass column. Lipids were eluted from the silica gel with chloroform:methanol:water, 50:50:1. Solvent was evaporated under nitrogen at 45 °C.

Gas–Liquid Chromatography

Acyl ceramides (EOS) were isolated from both epidermal and palatal stratum corneum from the same pig. The EOS samples were treated with 10% boron trichloride in methanol at 50 °C for 60 min. The normal fatty acid methyl esters (FAME) were isolated by preparative thin-layer chromatography on silica gel with a mobile phase of toluene.

Each of the other ceramides from palatal stratum corneum was treated with 10% boron trichloride at 50 °C overnight to convert the amide-linked fatty acids into FAME, which were isolated by preparative thin-layer chromatography as described above.

The FAME were analyzed by gas–liquid chromatography using a Shimadzu GC-14A gas chromatograph equipped with a 30-m EC-Wax capillary column and a flame ionization detector. This was done isothermally with an oven temperature of 170 °C. The detector and injector temperatures were 250 °C. The standards used included one mixture containing methyl esters of linoleate (C18:2 ω 6), linolenate (C18:3 ω 3), arachidonate (C20:4 ω 6) and docosahexaenoate (C22:6 ω 3) and a second mixture containing straight-chained saturated FAME (C14:0, C16:0, C18:0, C20:0, C22:0 and C24:0). Fatty acids with chains longer than 24 carbons were identified using plots of \log_{10} (retention time) versus carbon number [11]. Such plots are linear for members of a homologous series.

Results

In epidermal stratum corneum the most abundant ester-linked fatty acids from ceramide EOS were linoleic acid (C18:2, 71.7%) and arachidic acid (C20:0, 14.3%). The remainder was mostly palmitic (C16:0) and stearic (C18:0) acids with only trace amounts of other components (Table 1). In contrast, the palatal ceramide EOS contained stearic acid (C18:0, 43.6%), palmitic acid (C16:0, 32.0%) as the most abundant species (Table 1). Linoleate was only 8.8% of the ester-linked fatty acid in palatal ceramide EOS. Longer saturated fatty acids (C20:0 and C22:0) were also present.

The compositions of the normal fatty acids from palatal ceramides EOS, NS and NP are given in Table 1. The

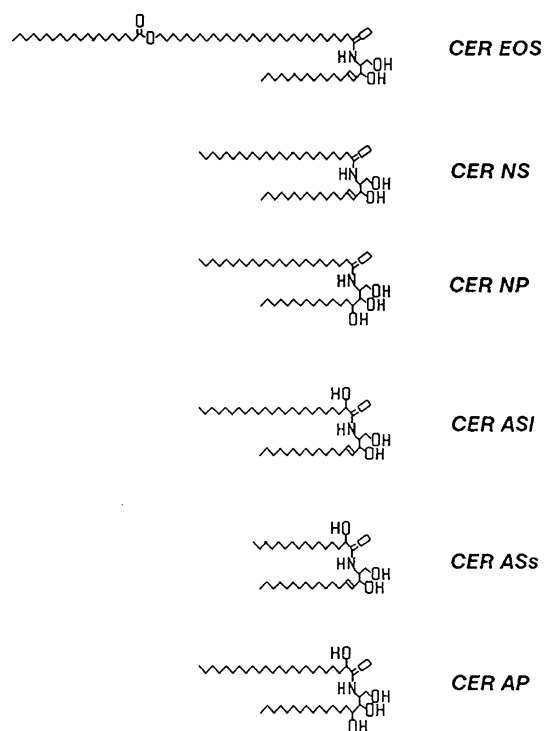
Table 1 Compositions (weight %) of normal fatty acids from epidermal ceramide EOS and palatal ceramides EOS, NS and NP

Fatty acid	Epidermal EOS	Palatal EOS	Palatal NS	Palatal NP
C16:0	6.4	32.0	5.1	9.1
C16:1			1.8	0.4
C17:0			0.7	0.4
C17:1			0.1	
C18:0	4.3	43.6	7.5	7.5
C18:1	2.1	5.5	2.8	1.7
C18:2 ω 6	71.7	8.8		
C19:0			0.7	0.4
C19:1			0.1	
C20:0	14.3	5.8	5.3	10.6
C20:1			5.2	0.6
C21:0			0.3	0.6
C21:1			0.4	
C22:0			1.9	4.2
C22:1			4.3	0.7
C23:0			0.6	0.7
C23:1			0.6	
C24:0			12.1	28.9
C24:1			1.7	4.0
C25:0			2.3	4.0
C25:1			0.7	
C26:0			11.5	14.6
C26:1			2.2	
C27:0			2.4	1.9
C27:1			0.3	
C28:0			17.6	7.7
C28:1			2.3	
C29:0			2.7	0.7
C29:1			0.3	
C30:0			5.3	1.4
C30:1			1.1	

amide-linked fatty acids from epidermal ceramides NS and NP were completely straight-chained saturated species, mainly C24:0, C26:0 and C28:0. The present findings for the ceramides NS and NP also contain C24:0, C26:0 and C28:0 as the most abundant species, but the presence of abundant monounsaturated species is in striking contrast to the findings with the epidermal ceramides. The compositions of the α -hydroxyacids from ceramides ASI, ASs and AP are listed in Table 2. In contrast with the findings with ceramides NS and NP, the α -hydroxyacids found in palatal ceramides ASI, ASs and AP are essentially identical to those found in their epidermal counterparts. Representative structures of the ceramides from porcine hard palatal stratum corneum are presented in Fig. 1. The long-chain bases were assigned on the basis of chromatographic comparisons with the well characterized epidermal ceramides [2, 3, 9].

Table 2 α -Hydroxy acids from palatal ceramides ASI, ASs and AP

Fatty acid	ASI	ASs	AP
C16:0		79.8	14.0
C17:0		2.0	1.2
C18:0		18.2	4.1
C19:0			0.2
C20:0			0.4
C21:0			0.4
C22:0			12.2
C23:0			1.2
C24:0	12.8		6.2
C25:0	3.6		2.5
C26:0	30.3		30.8
C27:0	7.9		4.4
C28:0	34.9		15.8
C29:0	4.6		1.7
C30:0	6.0		5.0

**Fig. 1** Representative structures of the ceramides from palatal stratum corneum

Discussion

Although the same structural types of ceramides are present in both oral and epidermal stratum corneum, the present results demonstrate numerous subtle differences in details of these structures. In epidermal ceramide EOS,

linoleate is the major ester-linked fatty acid [9]; however, in palatal stratum corneum straight-chained, saturated species prevail. Linoleate in ceramide EOS is essential for the barrier function of the skin [12]. Without a proper skin barrier, transepidermal water loss could lead to desiccation, thereby precluding life on dry land [13]. However, in the moist environment of the oral cavity there is no water gradient, and therefore, no need for a barrier to water loss.

As previously reported [9] for porcine epidermal ceramide NS, the major fatty acids in palatal ceramide NS are C24:0, C26:0 and C28:0; however, the presence of significant (23.9% of total) proportions of monounsaturated fatty acids is quite different. The amide-linked fatty acids from epidermal ceramide NS are entirely straight-chained saturated species. Also, palatal ceramide NP has C20:0, C22:0, C24:0, C26:0 and C28:0 as the most abundant amide-linked fatty acids as was the case with epidermal ceramide NP; however, there are again significant levels of monounsaturated fatty acids (7.4% of total) that are not found in epidermal ceramide NP.

Interestingly, the α -hydroxy-acid-containing ceramides (AS1, ASs and AP) are nearly identical to their epidermal counterparts. AS1 and ASs are presumed to be produced by hydroxylation of ceramide NS species with long or short fatty chains, respectively, and AP is presumed to be produced by vitamin C-dependent hydroxylation of NP [14]. Present results would be consistent with the suggestion that the α -hydroxylases that mediate these reactions act exclusively on substrates with saturated fatty acyl chains. The possibilities that fatty acids and/or dihydrosphingosine are hydroxylated prior to formation of the amide linkage cannot be ruled out.

As noted in the introduction, the presence of phosphoglycerides and glycosphingolipids in palatal stratum corneum would be expected to have a fluidizing effect on the intercellular membranes by virtue of having bulky polar head groups and some unsaturated acyl chains. The *cis* double bond in a monounsaturated fatty chain creates a kink in the chain thereby precluding a rod-like geometry and orderly chain-packing within membranes. The unsaturated fatty acids in palatal ceramides NS and NP would further contribute to membrane fluidization and, thereby, reduce barrier function.

One can only speculate about the effects of replacing most of the linoleate in ceramide EOS with saturated fatty acids. With epidermal stratum corneum lipids, it appears that ceramide EOS is required for the assembly of 13-nm trilamellar units [15, 16], and models have been proposed in which the linoleate chains from ceramide EOS are localized in the central lamella of these units [16, 17]. Perhaps the small proportion of linoleate in ceramide EOS is sufficient for formation of such functional units and

provision of a barrier function. The barrier requirements of oral mucosa are notably less than the requirements of skin. For one thing, the oral cavity is a wet environment, so there is no need for a water barrier. Perhaps, the EOS species with saturated fatty acids are capable of supporting an adequate barrier function for the oral cavity, and this allows for conservation of an essential nutrient—linoleic acid.

Aside from the roles of the ceramides in the permeability barrier of the stratum corneum, ceramides serve as substrates for ceramidases that liberate antimicrobial long-chain bases near the surface of the stratum corneum, thereby providing a microbial barrier [18].

Acknowledgments This work was supported in part by grants from the US National Institutes of Health (T32DE0 14678, T32DE0 07288 and R01 DE018032).

Open Access This article is distributed under the terms of the Creative Commons Attribution Noncommercial License which permits any noncommercial use, distribution, and reproduction in any medium, provided the original author(s) and source are credited.

References

1. Wertz PW, Squier CA (1996) Biochemical basis of the permeability barrier in skin and oral mucosa. In: Rathbone MJ (ed) Oral mucosal drug delivery. AAI, Wilmington, pp 1–26
2. Law S, Wertz PW, Swartzendruber DC, Squier CA (1995) Regional variation in content, composition and organization of porcine epithelial barrier lipids revealed by thin-layer chromatography and transmission electron microscopy. *Arch Oral Biol* 40:1085–1091
3. Wertz PW, Kremer M, Squier CA (1992) Comparison of lipids from epidermal and palatal stratum corneum. *J Invest Dermatol* 98:375–378
4. Motta SM, Monti M, Sesana S, Caputo R, Carelli S, Ghidoni R (1993) Ceramide composition of the psoriatic scale. *Biochim Biophys Acta* 1182:147–151
5. Yardley HJ, Summerly R (1981) Lipid composition and metabolism in normal and diseased epidermis. *Pharmacol Ther* 13:357–383
6. Squier CA, Cox P, Wertz PW (1991) Lipid content and water permeability of skin and oral mucosa. *J Invest Dermatol* 96:123–126
7. Forslind B (1994) A domain mosaic model of the skin barrier. *Acta Derm Venereol* 74:1–6
8. Wertz PW, van den Bergh BAI (1998) The physical, chemical and functional properties of lipids in the skin and other biological barriers. *Chem Phys Lipids* 91:85–96
9. Wertz PW, Downing DT (1983) Ceramides of pig epidermis: structure determination. *J Lipid Res* 24:759–765
10. Wertz PW, Downing DT (1983) Acylglucosylceramides of pig epidermis: structure determination. *J Lipid Res* 24:753–758
11. Downing DT, Krantz ZH, Murray KE (1960) Studies in waxes. *Aust J Chem* 13:80–94
12. Wertz PW (2000) Lipids and barrier function of the skin. *Acta Derm Venereol* 208:1–5
13. Attenborough D (1980) *Life on earth*. Little, Brown & Company, Boston

14. Ponec M, Weerheim A, Kempenaar J, Mulder A, Gooris GS, Bouwstra JA, Mommaas AM (1997) The formation of competent barrier lipids in reconstructed human epidermis requires the presence of vitamin C. *J Invest Dermatol* 109:348–355
15. Kuempel D, Swartzendruber DC, Squier CA, Wertz PW (1998) In vitro reconstitution of stratum corneum lipid lamellae. *Biochim Biophys Acta* 1372:135–140
16. Bouwstra JA, Dubbelaar FE, Gooris GS, Ponec M (2000) The lipid organization in the skin barrier. *Acta Derm Venereol Suppl* 208:23–30
17. Hill JR, Wertz PW (2003) Molecular models of the intercellular lipid lamellae from epidermal stratum corneum. *Biochim Biophys Acta* 1616:121–126
18. Drake DR, Brogden KA, Dawson DV, Wertz PW (2008) Antimicrobial lipids at the skin surface. *J Lipid Res* 49:4–11

Carbohydrate Restriction has a More Favorable Impact on the Metabolic Syndrome than a Low Fat Diet

Jeff S. Volek · Stephen D. Phinney · Cassandra E. Forsythe · Erin E. Quann · Richard J. Wood · Michael J. Puglisi · William J. Kraemer · Doug M. Bibus · Maria Luz Fernandez · Richard D. Feinman

Received: 6 October 2008 / Accepted: 20 November 2008 / Published online: 12 December 2008
© AOCs 2008

Abstract We recently proposed that the biological markers improved by carbohydrate restriction were precisely those that define the metabolic syndrome (MetS), and that the common thread was regulation of insulin as a control element. We specifically tested the idea with a 12-week study comparing two hypocaloric diets (~1,500 kcal): a carbohydrate-restricted diet (CRD) (%carbohydrate: fat:protein = 12:59:28) and a low-fat diet (LFD) (56:24:20) in 40 subjects with atherogenic dyslipidemia. Both interventions led to improvements in several metabolic markers, but subjects following the CRD had consistently reduced glucose (–12%) and insulin (–50%)

concentrations, insulin sensitivity (–55%), weight loss (–10%), decreased adiposity (–14%), and more favorable triacylglycerol (TAG) (–51%), HDL-C (13%) and total cholesterol/HDL-C ratio (–14%) responses. In addition to these markers for MetS, the CRD subjects showed more favorable responses to alternative indicators of cardiovascular risk: postprandial lipemia (–47%), the Apo B/Apo A-1 ratio (–16%), and LDL particle distribution. Despite a threefold higher intake of dietary saturated fat during the CRD, saturated fatty acids in TAG and cholesteryl ester were significantly decreased, as was palmitoleic acid (16:1n-7), an endogenous marker of lipogenesis, compared to subjects consuming the LFD. Serum retinol binding protein 4 has been linked to insulin-resistant states, and only the CRD decreased this marker (–20%). The findings provide support for unifying the disparate markers of MetS and for the proposed intimate connection with dietary carbohydrate. The results support the use of dietary carbohydrate restriction as an effective approach to improve features of MetS and cardiovascular risk.

Electronic supplementary material The online version of this article (doi:10.1007/s11745-008-3274-2) contains supplementary material, which is available to authorized users.

J. S. Volek (✉) · C. E. Forsythe · E. E. Quann · R. J. Wood · M. J. Puglisi · W. J. Kraemer
Department of Kinesiology, University of Connecticut,
2095 Hillside Road, Unit 1110, Storrs, CT 06269-1110, USA
e-mail: jeff.volek@uconn.edu

J. S. Volek
Department of Nutritional Science, University of Connecticut,
Storrs, CT, USA

S. D. Phinney · M. L. Fernandez
School of Medicine, University of California, Davis, Davis, CA,
USA

D. M. Bibus
Lipid Technologies, LLC, Austin, MN, USA

D. M. Bibus
University of Minnesota, Minneapolis, MN, USA

R. D. Feinman
Department of Biochemistry, SUNY Downstate Medical Center,
Brooklyn, NY, USA

Keywords Metabolic syndrome · HDL · LDL · Lipoprotein metabolism · Plasma lipids · Triglyceride metabolism · Dietary fat · Human

Abbreviations

Apo	Apolipoprotein
CA-IMT	Carotid artery intima-media thickness
CE	Cholesteryl ester
CRD	Carbohydrate-restricted diets
ChREBP	Carbohydrate response element binding protein
DSL	Diagnostics Systems Laboratory
HDL-C	HDL cholesterol

LDL-C	LDL cholesterol
LFD	Low-fat diets
MetS	Metabolic syndrome
NMR	Nuclear magnetic resonance
PAGE	Polyacrylamide gel electrophoresis
RBP4	Retinol binding protein 4
SCD-1	Stearoyl-coenzyme A desaturase 1
SFA	Saturated fatty acid
SREBP1c	Sterol response element binding protein
TAG	Triacylglycerols

Introduction

The codification of a set of physiologic markers as a metabolic syndrome (MetS) [1] 20 years ago is now recognized as a turning point in our understanding of metabolism as it plays out in the clinical states of obesity, diabetes and cardiovascular disease. The clustering of seemingly disparate markers—overweight, hyperglycemia, hyperinsulinemia, atherogenic dyslipidemia [high triacylglycerol (TAG) and low HDL-C]—can now be rationalized as the expression of a single physiologic state [2]. The underlying factor is generally considered to be insulin resistance and an increasing number of markers beyond the original definitions appear to be associated with the syndrome [3]. Notable among these is the predominance of small dense LDL-C, also called pattern B [4, 5]. Despite its theoretical importance, there is disagreement over whether diagnosing a patient's collective markers as a syndrome would lead to a different therapeutic strategy than treating the individual signs [6–10].

Whereas traditional approaches to MetS generally involve combination therapy [11, 12], we have suggested that a carbohydrate-restricted diet (CRD) provides a therapeutic intervention that will simultaneously target all of the traditional and emerging markers of MetS [13, 14]. The underlying mechanism is assumed to be readjustment of glycemic and insulin control. Thus, while insulin-sensitizing drugs, such as the thiazolidinediones, are associated with significant weight gain and edema and may be associated with some cardiovascular risk [15–17], improvement in insulin sensitivity with CRD is generally accompanied by weight loss [18–20]. Similarly, while there are several drugs that will raise HDL-C, none will affect the other markers of MetS and no treatment, pharmacologic or otherwise, is as effective as low-carbohydrate diets at lowering TAG [14, 21–24]. Low-fat diets may be effective for weight loss but tend to lower HDL-C and, in addition, generally *require* weight loss for beneficial effects whereas CRD do not [25, 26].

That a collection of markers is improved by a single type of intervention argues for the idea of a syndrome and the existence of a common (carbohydrate-sensitive) mechanism. From a practical standpoint, a physician treating any one marker by reducing carbohydrate has the potential to prevent the onset of others which may not be present at the moment.

We tested this hypothesis in a prospective study in which 40 overweight subjects with atherogenic dyslipidemia were randomly assigned either to a hypocaloric CRD (~1,500 kcal; %CHO:fat:protein = 12:59:28), or, as a control, to a diet restricted in fat (low fat diet, LFD: %CHO:fat:protein = 56:24:20). We previously reported the greater benefit of the CRD on weight loss and the relation between circulating fatty acid species and inflammatory markers [27]. Here we describe the broad panel of CVD risk markers that were differentially improved by these diets. Whereas the controls showed improvement in some of the physiologic markers studied, the CRD was generally (and in some cases dramatically) more effective. We also show, for the first time, that the CRD showed greater improvement in retinol binding protein 4 (RBP4), a novel mediator of insulin resistance [28–30].

Methods

Study Design and Participants

This study was a randomized, controlled, dietary intervention trial that compared a CRD to a LFD over a 12-week period in overweight subjects with atherogenic dyslipidemia. Participants were men and women aged 18–55 years with a BMI > 25 kg/m². Exclusion criteria were any metabolic and endocrine disorders, use of glucose-lowering, lipid-lowering or vasoactive prescriptions or supplements, consumption of a CRD at baseline, or weight loss greater than 5.0 kg in the past three months. Eligible subjects had a 12-h fasting blood sample taken and subjects with both moderately elevated TAG (150–500 mg/dL) and low HDL-C [<40 (men) or <50 (women) mg/dL] were randomly assigned to the CRD or LFD group after being matched by age and BMI. Twenty men and 20 women completed the study. All procedures were approved by the Institutional Review Board, and all subjects provided written informed consent.

Study Protocol

Prior to starting the diet treatment, subjects attended two baseline morning visits after a 12-h overnight fast and 24-h abstinence from alcohol and strenuous exercise. On Visit 1, body mass and body composition were assessed using

dual-energy X-ray absorptiometry (DXA), and a blood sample was obtained from an arm vein after the subjects rested quietly for 10 min in the supine position. Visit 2 involved a 6-h oral fat tolerance test to assess postprandial lipemic responses. The same tests were repeated after the 12-week dietary intervention period. In females, all blood samples were obtained during the early follicular phase to control for possible effects of menstrual phase on dependent variables. Habitual physical activity was maintained throughout the study intervention and was documented daily by all subjects. Dietary intake was assessed with detailed and weighed seven-day food records collected at baseline to assess habitual intake.

Dietary Intervention

Subjects received individual and personalized dietary counseling from registered dietitians prior to the dietary intervention. Detailed dietary booklets, specific to each dietary treatment, were provided that outlined dietary goals, lists of appropriate foods, recipes, sample meal plans, and food record log sheets. All subjects were given a multivitamin/mineral complex that provided micronutrients at levels <100% of the RDA and instructed to consume one pill every other day. No explicit instructions were provided regarding caloric intake for either diet to allow expression of any noncognitive aspects on food intake. Subjects received weekly follow-up counseling during which body mass was measured, compliance was assessed, and further dietetic education was provided. Seven-day weighed food records were kept during weeks 1, 6, and 12 of the intervention and were analyzed for energy and macro/micronutrient content (NUTRITIONIST PRO™, Version 1.3, First Databank Inc, The Hearst Corporation, San Bruno, CA, USA). The nutrient analysis program had no missing values for the nutrients reported, and the database was extensively updated with new foods and individualized recipes.

The main goal of the CRD was to restrict carbohydrate to a level that induced a low level of ketosis. Subjects monitored ketosis daily using urine reagent strips that produce a relative color change in the presence of one of the primary ketones, acetoacetic acid. In this diet there were no restrictions on the type of fat from saturated and unsaturated sources or cholesterol levels. Examples of foods consumed by the subjects included unlimited amounts of beef, poultry, fish, eggs, oils and heavy cream; moderate amounts of hard cheeses, low-carbohydrate vegetables and salad dressings; and small amounts of nuts, nut butters and seeds. Subjects restricted fruit and fruit juices, dairy products (with the exception of heavy cream and hard cheese), breads, grains, pasta, cereal, high-carbohydrate vegetables, and desserts. Subjects were

instructed to avoid all low-carbohydrate breads and cereal products, and were limited to a maximum of one sugar alcohol-containing, low-carbohydrate snack per day. The LFD was designed to provide <10% of total calories from saturated fat and <300 mg cholesterol. Foods encouraged included whole grains (breads, cereals, and pastas), fruit/fruit juices, vegetables, vegetable oils, low-fat dairy and lean meat products. Standard diabetic exchange lists were used to ensure a macronutrient balance of protein (~20% energy), fat (~25% energy), and carbohydrate (~55% of energy).

Body Mass and Composition

Body mass was measured in the morning after an overnight fast to the nearest 100 g on a calibrated digital scale. Whole body and regional body composition was assessed by DXA (Prodigy™, Lunar Corporation, Madison, WI, USA). Analyses were performed by the same blinded technician. Regional analysis of the abdomen was assessed by placing a box between L1 and L4 using commercial software (enCORE version 6.00.270). This abdominal region of interest has been shown to be a highly reliable and accurate determinant of abdominal obesity compared to multislice computed tomography [31]. Coefficients of variation for lean body mass, fat mass, and bone mineral content on repeat scans with repositioning on a group of men/women were 0.4, 1.4, and 0.6%, respectively.

Oral Fat Tolerance Test

An oral fat tolerance test was performed before and after each dietary treatment using standard procedures in our laboratory. A flexible catheter was inserted into a forearm vein and blood samples were obtained from a three-way stopcock. The catheter was kept patent with a constant saline drip. Prior to consumption of the test meal, subjects rested in a seated position for 10 min and a baseline blood sample was obtained. A high-fat meal (225 mL whipping cream, sugar-free instant pudding, 28.5 g macadamia nuts) was then consumed within a 15-min time frame, providing 908 kcal, 13% carbohydrate, 3% protein, and 84% fat. Postprandial blood samples were obtained immediately (0 h) and hourly for hours 1–6 following the meal. Subjects rested quietly in a seated position and consumed only water during the postprandial period.

Blood Analyses

Whole blood was collected into tubes without preservative or an anticoagulant and centrifuged at $1,500 \times g$ for 15 min and 4 °C, and promptly aliquoted into storage tubes. A portion of serum (~3 mL) was sent to a certified

medical laboratory (Quest Diagnostics, Wallingford, CT, USA) for determination of total cholesterol, HDL-C, TAG, and calculated LDL-C [32] concentrations using automated enzymatic procedures (Olympus America Inc., Melville, NY, USA). The remaining serum and plasma was stored frozen at -80°C and thawed only once before analysis. Glucose and insulin concentrations were analyzed in duplicate from serum using a YSI glucose/lactate analyzer (YSI 2300 STAT, Yellow Springs, OH, USA) and I^{125} radioimmunoassay [Diagnostic Systems Laboratory (DSL)-1600, Webster, TX, USA], respectively, and used to calculate an index of insulin resistance [33]. LDL particle size of was determined in serum using nongradient polyacrylamide gel electrophoresis (PAGE; Lipoprint LDL System, Quantimetrix Co., Redondo Beach, CA, USA), as previously described [34]. Lipoprotein (HDL, LDL, and VLDL) particle size and number was determined using H-nuclear magnetic resonance (NMR) on a 400 MHz NMR analyzer (Bruker BioSpin Corp, Billerica, MA, USA), as previously described [14]. Lipoprotein subclasses were grouped based on particle diameters: large VLDL (>60 nm), medium VLDL (35–60 nm), small VLDL (27–35 nm), IDL (23–27 nm), large LDL (21.2–23 nm), medium LDL (19.8–21.2 nm), small LDL (18–19.8 nm), large HDL (8.8–13 nm), medium HDL (8.2–8.8 nm), and small HDL (7.3–8.2 nm). Total ketone bodies were determined in duplicate from serum by a kinetic enzymatic, colorimetric method that measures both acetoacetate and 3-hydroxybutyrate (CV 3.6%); nonesterified fatty acids were analyzed in duplicate from serum with an ACS-ACOD method (Wako Chemicals USA, Richmond, VA, USA). Apo A-1 and Apo B were quantified in duplicate from serum using a turbidimetric immunoassay method (Wako Chemicals USA) with intra-assay CVs of 8.0 and 6.6%, respectively. Leptin was determined in duplicate using an ELISA with a sensitivity of 0.05 ng/mL (DSL, Webster, TX, USA). Serum RBP4 was measured by quantitative Western blotting using full-length recombinant RBP4 protein standards on each gel, as previously described [30]. For fatty acid analyses, serum total TAG and cholesteryl ester (CE) were separated on commercial silica gel G plates for determination of fatty acid methyl ester composition by capillary gas chromatography. A detailed description of the methods for fatty acid determination, as well as the complete fatty acid data focusing on the polyunsaturated fatty acid responses in relation to inflammatory markers, is published elsewhere [27]. Here we report only the TAG and CE saturated fatty acid (SFA) and 16:1n-7 data.

Statistical Analyses

The mean of two fasting blood draws performed at the same time of day on separate days to account for diurnal and

day-to-day variation in lipids was obtained. An ANOVA with one between-effect (CRD vs. LFD) and one within-effect (week 0 vs. week 12) was used to compare responses over time in both groups. Significant main or interaction effects were further analyzed using a Fishers LSD post hoc test. For postprandial biochemical variables, the area under the curve was calculated using the trapezoidal method. Relationships among selected variables were examined using Pearson's product-moment correlation coefficient. The alpha level for significance was set at 0.05.

Results

Dietary Intake

Average nutrient intake is provided in Table 1. Although not specifically counseled to reduce calories, there was a reduction in total caloric intake in both groups. Spontaneous reduction in calories on CRDs was first shown by LaRosa in 1980 [35], and there are several studies showing that, in practice, people tend to remove carbohydrate without replacement of either fat or protein (e.g., [36]). Interventions where weight loss is at least an implied goal may generally have this effect. The Women's Health Initiative was a large low-fat trial where weight was lost on a LFD in the first two years [37] although the effect did not persist. The diets, thus, did not differ in energy consumption averaged over the 12 weeks of the intervention. The nutrient composition, however, varied significantly between the CRD (1,504 kcal: %CHO:fat:protein = 12:59:28) and LFD (1,478 kcal: %CHO:fat:protein = 56:24:20). Subjects consuming the LFD were successful at reducing saturated fat to 7% of total energy, compared to 22% in subjects following the CRD. Because of the reduction in caloric intake, however, the increase in the absolute amount of saturated fat for the CRD group was not great, an average of 34 g/day in subjects' habitual diet compared to 36 g/day during the experiment. In the LFD group, the absolute amount of saturated fat fell from an average of 26–11.7 g/day. Dietary cholesterol was significantly higher and fiber significantly lower on the CRD compared to the LFD. The presence of urinary acetoacetic acid is a qualitative but sensitive indicator of carbohydrate restriction. During weeks 2–12 of the CRD intervention, subjects reported the presence of urinary ketones above trace on 85% of the days, indicating a high degree of compliance.

Dietary Carbohydrate Restriction Enhances Weight Loss and Reduces Adiposity Out of Proportion to the Caloric Deficit

Despite similar reductions in calories, weight loss in the CRD group was, on average, twofold greater than in the

Table 1 Average nutrient intake of men and women who consumed a carbohydrate-restricted (CRD) and low-fat diet (LFD)

	CRD (<i>n</i> = 20)		LFD (<i>n</i> = 20)		2 × 2 ANOVA	
	Week 0	Week 12	Week 0	Week 12	Time	T × G
Energy (kcal)	2351 ± 617	1504 ± 494	2082 ± 445	1478 ± 435	0.000	0.154
Protein (g)	95 ± 29	105 ± 34	82 ± 18	72 ± 21	0.756	0.009
Protein (%)	16 ± 3	28 ± 4	16 ± 3	20 ± 4	0.000	0.000
Carbohydrate (g)	270 ± 67	45 ± 19	267 ± 75	208 ± 70	0.000	0.000
Carbohydrate (%)	47 ± 8	12 ± 5	51 ± 10	56 ± 8	0.000	0.000
Total fat (g)	97 ± 35	100 ± 38	79 ± 30	40 ± 18	0.004	0.001
Total fat (%)	36 ± 7	59 ± 5	33 ± 10	24 ± 7	0.000	0.000
Saturated fat (g)	34 ± 14	37 ± 13	26 ± 11	12 ± 6	0.012	0.002
Monounsaturated fat (g)	19 ± 7	26 ± 11	18 ± 10	9 ± 5	0.830	0.000
Polyunsaturated fat (g)	12 ± 7	12 ± 8	11 ± 7	5 ± 3	0.064	0.019
18:1n-9 (g)	14 ± 5	21 ± 10	12 ± 7	7 ± 4	0.289	0.000
18:2n-6 (g)	7 ± 6	8 ± 5	6 ± 5	3 ± 2	0.215	0.042
18:3n-3 (mg)	989 ± 1199	879 ± 746	575 ± 398	325 ± 198	0.139	0.439
20:5n-3 (mg)	8 ± 10	46 ± 81	32 ± 50	32 ± 58	0.047	0.050
22:6n-3 (mg)	24 ± 24	117 ± 184	83 ± 116	82 ± 154	0.049	0.052
Alcohol (%)	1 ± 2	1 ± 1	0 ± 1	1 ± 2	0.232	0.056
Cholesterol (mg)	354 ± 120	605 ± 262	267 ± 111	144 ± 80	0.044	0.000
Dietary fiber (g)	13 ± 4	9 ± 5	16 ± 7	17 ± 10	0.083	0.021

Values are mean ± SD

low-fat control (10.1 kg vs 5.2 kg). This apparent decrease in caloric efficiency with carbohydrate restriction has been observed many times (reviews: [38, 39]), although the current report is one of the more dramatic demonstrations. There was substantial individual variation, but 9 of 20 subjects in the CRD group lost 10% of their starting weight, more than all of the subjects in the LFD group. Indeed, none of the subjects following the LFD lost as much weight as the average weight loss for the experimental group. The number of subjects who lost >5% of body weight was 19 of 20 subjects for the CRD compared to 12 of 20 for the LFD. Despite greater absolute fat intake and similar total caloric intake, whole body fat mass decreased significantly more in subjects following the CRD (5.7 kg) than in subjects following the LFD (3.7 kg) (Table 2). Fat mass in the abdominal region, associated with many features of the insulin resistance syndrome, was similarly decreased significantly more in subjects consuming the CRD than subjects following the LFD (−828 g vs −506 g).

Dietary Carbohydrate Restriction Improves Glycemic and Insulin Control

The CRD resulted in a significant average reduction of 12% in fasting glucose (Table 3). Responses in the control LFD were variable with little average change. Fasting insulin responses were also decreased to a greater extent in

subjects following the CRD than in subjects following the LFD (−49% vs −17%), as were postprandial insulin responses to a meal high in fat (−49% vs −6%). Similarly, the homeostasis model assessment (HOMA), a measure of insulin resistance, was reduced to a greater extent in subjects following the CRD than controls (−55% vs −18%). All subjects in this study were overweight and had elevated values for leptin at baseline, an indication of leptin resistance. These values were markedly reduced in subjects following the CRD (−42%) compared to a smaller decrease of 18% in control subjects following the LFD. The significantly greater decrease in leptin in subjects following the CRD persisted after normalization of values to body mass and fat mass.

Dietary Carbohydrate Restriction Enhances Mobilization and Utilization of Lipid Substrates and Inhibits Lipogenesis

The hormonal milieu associated with dietary carbohydrate restriction is proposed to create a unique metabolic state characterized by enhanced reliance on lipid sources and more efficient processing of dietary fat. Compared to baseline, fasting serum total ketones were not different after the LFD (103 ± 73–94 ± 65 μmol/L), but were elevated threefold after the CRD (77 ± 36–212 ± 91 μmol/L), signifying enhanced mobilization of fatty acids from adipose tissue (Table 4). In accord with enhanced lipolysis,

Table 2 Carbohydrate-restricted diet enhances weight loss and reduces adiposity

	CRD (<i>n</i> = 20)		LFD (<i>n</i> = 20)		2 × 2 ANOVA	
	Week 0	Week 12	Week 0	Week 12	Time	T × G
Age (year)	32.6 ± 11.3	–	36.9 ± 12.5	–		
Body mass (kg)	96.5 ± 13.7	86.4 ± 12.0	94.4 ± 15.2	89.2 ± 13.9	0.000	0.000
BMI (kg/m ²)	33.5 ± 5.2	30.0 ± 4.3	32.1 ± 4.1	30.3 ± 3.9	0.000	0.000
Fat mass (kg)	38.7 ± 7.7	33.1 ± 7.9	37.1 ± 10.0	33.4 ± 9.4	0.000	0.009
Lean body mass (kg)	54.4 ± 11.6	51.0 ± 10.9	55.1 ± 10.7	54.1 ± 9.9	0.000	0.009
Percent body fat (%)	40.6 ± 7.3	38.2 ± 8.5	39.0 ± 7.9	36.8 ± 7.9	0.000	0.642
Abdominal fat (g)	4152 ± 1261	3325 ± 1154	4059 ± 1165	3553 ± 1160	0.000	0.018

Values are mean ± SD

Table 3 Carbohydrate-restricted diet improves glycemic and insulin control and decreases leptin

	CRD (<i>n</i> = 20)		LFD (<i>n</i> = 20)		2 × 2 ANOVA	
	Week 0	Week 12	Week 0	Week 12	Time	T × G
Glucose (mg/dL)	101 ± 13	89 ± 8	96 ± 12	94 ± 9	0.000	0.006
Insulin (pmol/L)	107 ± 87	54 ± 57	70 ± 47	57 ± 57	0.000	0.017
Insulin AUC	1032 ± 901	529 ± 494	609 ± 306	573 ± 531	0.002	0.005
HOMA	2.9 ± 2.5	1.3 ± 1.4	1.7 ± 1.1	1.4 ± 1.4	0.000	0.009
Leptin (ng/mL)	59 ± 31	34 ± 27	50 ± 26	41 ± 26	0.000	0.004
Leptin (ng/mL)/BM	0.63 ± 0.35	0.41 ± 0.32	0.54 ± 0.29	0.46 ± 0.29	0.000	0.013
Leptin (ng/mL)/FM	1.47 ± 0.67	0.96 ± 0.66	1.24 ± 0.44	1.15 ± 0.61	0.000	0.004

Values are mean ± SD

HOMA, homeostatic model assessment; BM, body mass; FM, fat mass

Table 4 Carbohydrate-restricted diet enhances mobilization and utilization of lipid substrates and inhibits lipogenesis

	CRD (<i>n</i> = 20)		LFD (<i>n</i> = 20)		2 × 2 ANOVA	
	Week 0	Week 12	Week 0	Week 12	Time	T × G
Ketones (μmol/L)	77 ± 36	212 ± 91	103 ± 73	94 ± 65	0.000	0.000
Fatty acids (mEq/L)	0.23 ± 0.09	0.28 ± 0.14	0.30 ± 0.15	0.24 ± 0.12	0.780	0.025
Fatty acids AUC	1.20 ± 0.38	1.28 ± 0.34	1.30 ± 0.47	1.11 ± 0.38	0.360	0.033
Postprandial lipemia AUC	2005 ± 723	1062 ± 332	1890 ± 667	1606 ± 456	0.000	0.007
Total TAG SFA (%)	33.1 ± 5.0	29.2 ± 1.4	30.5 ± 4.0	29.0 ± 2.4	0.000	0.086
TAG 16:1n-7 (%)	4.5 ± 1.1	3.1 ± 0.7	4.5 ± 1.0	4.5 ± 1.1	0.000	0.000
Total CE SFA (%)	3.4 ± 1.5	12.1 ± 0.9	13.0 ± 1.3	12.7 ± 1.2	0.002	0.028
CE 16:1n-7 (%)	3.3 ± 0.9	1.8 ± 0.5	3.0 ± 1.0	3.0 ± 1.2	0.000	0.000

Values are mean ± SD

AUC, area under the curve; TAG, triacylglycerol; SFA, saturated fatty acids; CE, cholesteryl ester

fasting nonesterified fatty acids increased in subjects following the CRD and decreased in subjects following the LFD.

To better understand how carbohydrate restriction affects the processing of dietary fat, we measured clearance of an oral fat load providing 908 kcal and 85 g fat mainly from saturated fat. At baseline, we found that the fat

challenge induced a dramatic rise in TAG after 1 h that remained above fasting levels for the duration of the 6-h postprandial period. After 12 weeks on the CRD, the postprandial TAG pattern was dramatically decreased at all time points. The total postprandial TAG area under the curve (Fig. 1A) was significantly lower after the CRD than the LFD (−47 vs −15%). Although the CRD group

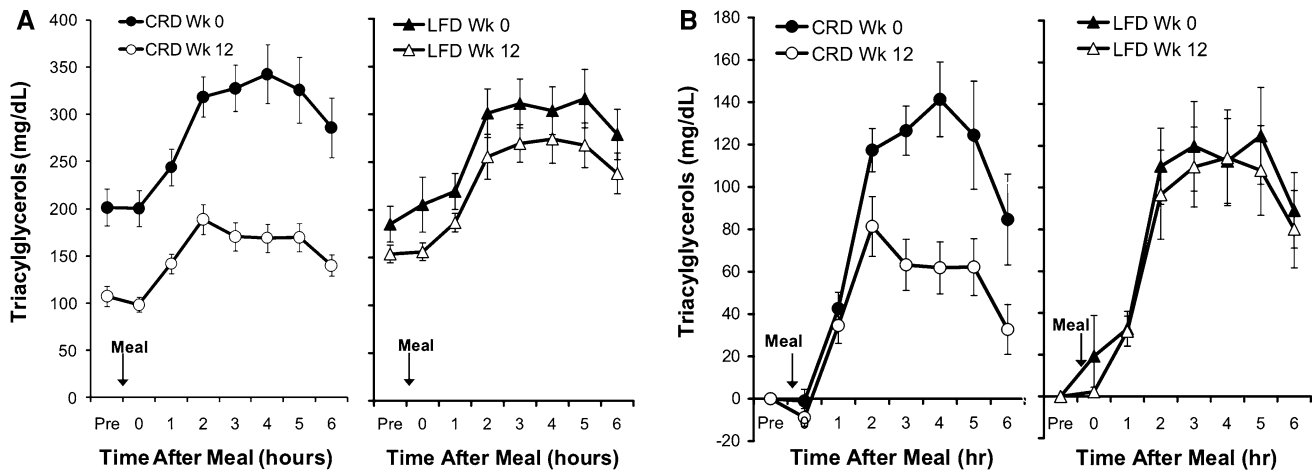


Fig. 1A–B Effect of diet on postprandial lipemic responses. Absolute (A) and integrated (B) TAG values in subjects who consumed a carbohydrate-restricted diet (CRD) or a low-fat diet (LFD) for

12 weeks. Mean total area under the curve (AUC) and integrated AUC were significantly different between the CRD and LFD ($P < 0.000$)

showed slightly lower fasting TAG levels, the area under the curve normalized to fasting TAG levels was significantly lower in subjects consuming the CRD (Fig. 1B).

Change in Fatty Acid Composition

To further explore the processing of dietary fat by carbohydrate restriction, we assessed fatty acid composition in serum lipid fractions (Table 5). The dietary intake of saturated fat was threefold higher on the CRD (36 g/day) compared to the LFD (12 g/day). Remarkably, the CRD showed consistently greater reductions in the relative proportions of most circulating SFAs in TAG and CE fractions (16), mainly attributed to greater reductions in myristic (14:0; 47% reduction) and palmitic (16:0; 10%) acids. With the exception of those with a low level at baseline, nearly all subjects consuming the CRD had a decrease in total saturates (17 of 20 subjects), whereas only half the subjects consuming the LFD had a decrease in saturates. Taking into account the change in absolute fasting TAG levels, the absolute concentration of total saturates in plasma TAG was reduced by 57% in response to the CRD, compared to 24% in response to the LFD. There was also a 31% decrease in palmitoleic acid (16:1n-7) in response to the CRD which, because of its low concentration in the diet, is a marker for de novo lipogenesis [40].

Dietary Carbohydrate Restriction Results in Consistently Greater Improvements in Atherogenic Dyslipidemia and Lipoprotein Markers

The CRD dramatically improved the features of atherogenic dyslipidemia compared to the LFD. Table 5 and Fig. 2 summarize the average and individual changes in

these parameters: the CRD shows more favorable responses in fasting TAG (−51 vs −19%), HDL-C (+13 vs −1%), and the TAG/HDL-C ratio (−54 vs −20%) ($P < 0.001$ in all cases). The dramatic decrease in TAG in response to carbohydrate reduction is one of the most reliable effects of any diet intervention [13, 41]. Whereas 12 of 20 subjects following the CRD showed a >10% increase in HDL-C, only 2 of 20 subjects following the LFD reached this point. Strikingly, the six subjects assigned to the CRD who already had the highest HDL at baseline further improved to a greater extent than any subject in LFD. An unexpected finding regarding HDL-C was a gender by diet effect, with women who started with higher baseline values exhibiting a more pronounced benefit on the CRD (17% women vs 8% men).

The CRD significantly improved other lipoprotein CVD risk factors. The total cholesterol/HDL-C ratio was reduced more in subjects during the CRD than during the LFD (−14 vs −4%). The Apo B/Apo A-1 ratio is considered the best indicator of risk for vascular disease [42] and was, similarly, improved in subjects following the CRD but was slightly worse on average for subjects of the LFD (−16 vs +8%). It should be pointed out, in addition, that the five subjects with the highest Apo B/Apo A-1 ratio in the CRD group improved (−29%), while the five subjects with the highest values in LFD got worse (4%).

Changes in LDL-C showed substantial variation in both the CRD and LFD groups. Although on average this marker was not reduced in subjects following the CRD, there were improvements in the vascular remodeling of particles, consistent with previous observations that the number of the small, dense, more atherogenic particles tend to increase as dietary carbohydrate is increased and dietary fat is reduced [4, 5, 26, 43]. We measured LDL subfractions

Table 5 Carbohydrate-restricted diet results in consistently greater improvements in atherogenic dyslipidemia and lipoprotein markers

	CRD (<i>n</i> = 20)		LFD (<i>n</i> = 20)		2 × 2 ANOVA	
	Week 0	Week 12	Week 0	Week 12	Time	T × G
Triacylglycerols (mg/dL)	211 ± 58	104 ± 44	187 ± 58	151 ± 38	0.000	0.000
HDL-C (mg/dL)	36 ± 7	40 ± 10	39 ± 6	38 ± 6	0.001	0.000
Triacylglycerols /HDL-C	6.2 ± 2.2	2.9 ± 1.8	5.0 ± 2.0	4.0 ± 1.1	0.000	0.000
Total cholesterol (mg/dL)	208 ± 26	197 ± 35	204 ± 32	195 ± 34	0.016	0.816
Total cholesterol/HDL-C	6.0 ± 1.2	5.1 ± 1.6	5.4 ± 1.1	5.2 ± 1.1	0.000	0.022
Apolipoprotein B (mg/dL)	109 ± 19	98 ± 21	104 ± 14	102 ± 19	0.012	0.067
Apolipoprotein A-1 (mg/dL)	107 ± 24	111 ± 23	124 ± 23	115 ± 28	0.545	0.075
Apo B/Apo A-1	1.1 ± 0.4	0.9 ± 0.3	0.9 ± 0.2	0.9 ± 0.3	0.128	0.001
LDL-C (mg/dL)	130 ± 22	135 ± 31	128 ± 31	126 ± 32	0.357	0.357
LDL mean size _{PAGE} (nm)	261 ± 7	269 ± 3	261 ± 4	261 ± 6	0.000	0.001
LDL peak size _{PAGE} (nm)	260.0 ± 9.9	270.6 ± 4.9	257.9 ± 8.6	259.9 ± 8.0	0.000	0.005
LDL-1 _{PAGE} (%)	9.7 ± 6.2	20.0 ± 6.5	9.7 ± 5.2	11.9 ± 6.2	0.000	0.000
LDL-2 _{PAGE} (%)	15.5 ± 4.9	13.7 ± 4.1	15.1 ± 3.8	16.6 ± 5.6	0.886	0.050
LDL-3+ _{PAGE} (%)	7.9 ± 4.8	1.7 ± 2.1	8.5 ± 5.3	7.1 ± 4.8	0.001	0.000
VLDL&CM total _{NMR} (nmol/L)	91 ± 27	79 ± 37	97 ± 30	92 ± 34	0.123	0.523
VLDL&CM large _{NMR} (nmol/L)	8 ± 4	1 ± 2	9 ± 7	5 ± 4	0.000	0.211
VLDL medium _{NMR} (nmol/L)	40 ± 18	24 ± 23	44 ± 24	38 ± 23	0.011	0.194
VLDL small _{NMR} (nmol/L)	43 ± 18	54 ± 19	45 ± 23	49 ± 20	0.038	0.398
LDL total _{NMR} (nmol/L)	1549 ± 322	1470 ± 439	1441 ± 359	1452 ± 367	0.493	0.373
IDL _{NMR} (nmol/L)	89 ± 39	62 ± 41	75 ± 45	65 ± 44	0.036	0.342
Large LDL _{NMR} (nmol/L)	227 ± 145	403 ± 152	313 ± 220	290 ± 153	0.022	0.004
Small LDL _{NMR} (nmol/L)	1234 ± 354	1005 ± 435	1053 ± 364	1097 ± 412	0.140	0.032
Medium small LDL _{NMR} (nmol/L)	247 ± 73	201 ± 85	207 ± 76	216 ± 83	0.170	0.046
Very small LDL _{NMR} (nmol/L)	986 ± 285	805 ± 353	846 ± 294	881 ± 330	0.141	0.033
HDL total _{NMR} (nmol/L)	27 ± 5	28 ± 6	29 ± 3	28 ± 3	0.799	0.431
HDL large _{NMR} (nmol/L)	2 ± 2	4 ± 2	3 ± 2	4 ± 2	0.001	0.100
HDL medium _{NMR} (nmol/L)	5 ± 4	2 ± 3	3 ± 3	4 ± 6	0.343	0.057
HDL small _{NMR} (nmol/L)	21 ± 5	22 ± 4	23 ± 4	20 ± 7	0.491	0.109
VLDL size _{NMR} (nm)	57.4 ± 8.8	43.3 ± 4.2	56.6 ± 10.4	48.7 ± 5.8	0.000	0.102
LDL size _{NMR} (nm)	20.1 ± 0.5	20.7 ± 0.5	20.4 ± 0.7	20.4 ± 0.7	0.009	0.010
HDL size _{NMR} (nm)	8.3 ± 0.2	8.6 ± 0.3	8.4 ± 0.3	8.5 ± 0.3	0.000	0.051

Values are mean ± SD

PAGE, polyacrylamide gel electrophoresis; NMR, nuclear magnetic resonance

using two methods based on high-resolution PAGE or on NMR. The results from PAGE confirmed previous observations, showing a significant ($P < 0.001$) LDL particle redistribution in subjects following the CRD as reflected by a shift from smaller (LDL-3) to larger (LDL-1) particles, whereas there was little change in the concentration or size of LDL particles on the LFD. NMR results showed a similar significant reduction in the quantity of small and very small LDL particles and a concomitant increase in the quantity of large LDL particles. Mean LDL size increased significantly in subjects following the CRD using both PAGE and NMR. In addition to increased LDL particle

size, there was a significant increase in NMR-determined HDL size in subjects following the CRD.

Weight Loss and Dyslipidemia

To understand the extent to which the measured parameters are related, we compared change in BMI to change in the TAG/HDL-C ratio. Figure 3 shows that there is a very poor correlation between these variables for either the CRD ($R^2 = 0.0529$ from linear regression) or the LFD ($R^2 = 0.0012$). Surprisingly, for the LFD group, 7 of the 11 subjects who had the largest change in BMI showed the smallest change in TAG/

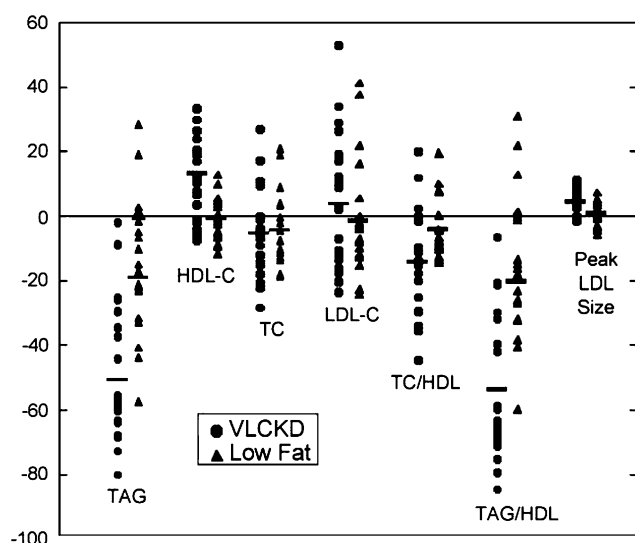


Fig. 2 Individual responses in lipid parameters after 12 weeks on indicated diets. Carbohydrate-restricted diet (CRD) is indicated by circles; low-fat diet (LFD) is indicated by triangles. Bars indicate mean values

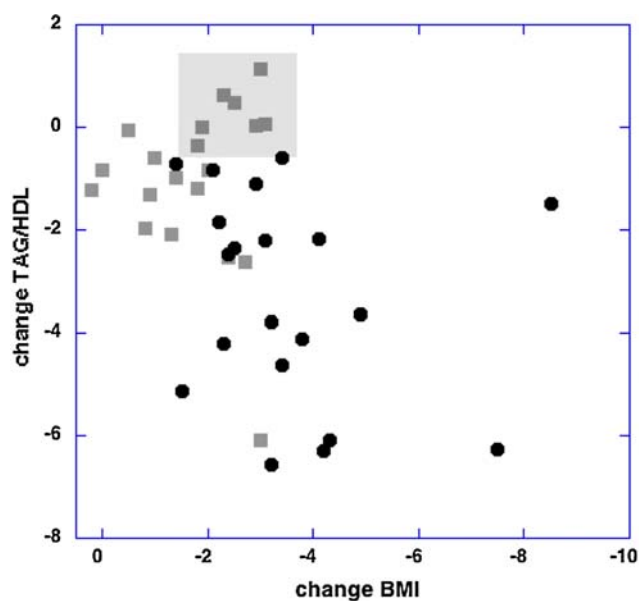


Fig. 3 Correlation of changes in BMI and changes in TAG/HDL ratio. Carbohydrate-restricted diet (CRD) is indicated by black circles; low-fat diet (LFD) is indicated by dark gray squares. The light gray square highlights 7 of the 11 subjects in the LFD with the largest change in BMI. Linear regression for VLCKD: $\Delta(\text{TAG}/\text{HDL}) = -0.24117 + 0.259 \times (\Delta\text{BMI})$, $R^2 = 0.0529$, for LFD: $\Delta(\text{TAG}/\text{HDL}) = -0.923 + 0.05325 \times (\Delta\text{BMI})$, $R^2 = 0.0012$

HDL. Similar poor correlations were found for other markers of weight loss and lipids (data not shown).

Dietary Carbohydrate Restriction Reduces RBP4

We further explored the response in serum RBP4, and the associations with dietary input and other markers of insulin

resistance. Changes in serum RBP4 levels were variable but showed a significantly greater reduction in subjects consuming the CRD (34.6 ± 11.7 – 27.6 ± 8.0 $\mu\text{g}/\text{mL}$) compared to LFD (37.1 ± 14.3 – 39.0 ± 18.6 $\mu\text{g}/\text{mL}$); only two of the subjects in the CRD group, but 8 of 20 controls showed an increase. Changes were significantly correlated to responses in several metabolic outcomes (“[Electronic supplementary material](#)”). The only dietary nutrient that correlated with the change in RBP4 was carbohydrate (g/day) during the CRD. The absolute and percent changes in RBP4 were associated with changes in measures of adiposity only in the LFD controls, not the CRD. On the other hand, RBP4 was correlated to improvement in glucose, fatty acids, insulin, HOMA, and leptin during the CRD but not the LFD. Changes in RBP4 were correlated with changes in LDL particle size on both diets and to total and LDL-C on the LFD. Changes in several serum fatty acid species were correlated with RBP4, but they differed for the CRD and LFD. The highest correlation was between changes in RBP4 and phospholipid 18:0 ($r = 0.77$). There were no correlations between changes in RBP4 and markers of inflammation as assessed by 20 separate inflammatory markers. These findings link the role of RBP4 in insulin resistance, with studies showing a tight connection between carbohydrate restriction and features of MetS.

Discussion

Several recent diet comparisons have been published showing that CRDs are at least as effective as LFDs on weight loss, lipid profile, and other health markers [18, 27, 44–46] (reviews: [14, 23, 47, 48]), the most recent being a two-year study from Shai et al. [49]. The current study is distinguished from these in that we specifically tested the idea that carbohydrate restriction targets the markers of MetS, particularly the atherogenic dyslipidemia. Our results support the hypothesis, and further show that CRDs improve a wide spectrum of lipid markers of CVD risk, including effects on LDL particle size. Two other novel findings were that a CRD resulted in a decrease in plasma SFAs despite higher dietary saturated intake, and resulted in a significant decrease in RBP4, a molecule of current interest because of its association with MetS. Finally, we show that weight loss in hypocaloric diets correlates poorly with changes in lipid profile.

Markers of CVD Risk

The atherogenic potential of LDL-C appears to reside in the small dense particles, whose concentration is independent of total LDL-C concentration [4, 5, 43]. Shoji et al., for

example, measured carotid artery intima-media thickness (CA-IMT) and showed that when results on LDL-C were broken into small dense and large buoyant fractions, only the small dense LDL showed a significant positive association with CA-IMT [50]. Small dense LDL are now considered a feature of MetS, but the dichotomy between LDL, still the most common marker for CVD risk, and atherogenic dyslipidemia is unresolved. The results presented here show a significant decrease in small LDL particles in subjects consuming the CRD, consistent with the tight connection between dietary carbohydrate and LDL size established in the literature [4, 5, 43].

The reductions in TAG associated with the CRD are particularly striking—an effect probably due to decreased de novo lipogenesis and VLDL-TAG secretion as well as increased VLDL-TAG clearance. Regardless of the mechanisms, elevated circulating TAG is an independent risk factor for CVD [24, 51], and elevations in the post-absorptive and postprandial period directly contribute to the dyslipidemic state characterized by low HDL-C and increased prevalence of small LDL-C. Considering the established importance of increasing HDL-C as a therapeutic target for both men and women [52], the effect on HDL-C is perhaps the most important result from this and other studies of CRDs. HDL-C is one of the major targets of health agencies and one for which existing drugs are not entirely satisfactory. Consistent with previous work [53, 54], we showed that a LFD has minimal effect on HDL-C, and that women experience a larger increase in response to carbohydrate restriction than men. We also assessed alternative lipid markers. Evidence has been presented that the ratio Apo B/Apo A-1 is the best predictor of CVD [42], and that, in the current study, the CRD was distinguished by the very dramatic reduction in this parameter. In summary, our results are consistent with previous work showing the benefit of CRD compared to LFD [13, 34, 41].

Dietary and Plasma Levels of SFA

Carbohydrate-restricted diets, although relatively high in SFA, show effects on plasma fatty acid that are very different from those seen in studies conducted in the presence of moderate to high dietary carbohydrate. A high-carbohydrate diet prolongs circulatory exposure to dietary (or endogenous) SFA, and conversely, dietary restriction of carbohydrate (via reduced secretion of insulin) allows for greater rates of lipid oxidation and management of the incoming lipid mix. High dietary fat is thus expected to be deleterious only if there is sufficient carbohydrate to provide the hormonal state in which the fat will be stored rather than oxidized. An expression of this effect is that the CRD with a greater proportion of fat and saturated fat led to a *reduction* in plasma SFA, particularly palmitic acid

(16:0), whose presence has been linked to higher levels of adiposity [55, 56]. The likely cause is greater fat oxidation and attenuation of hepatic de novo lipogenesis, as indicated by a parallel reduction in palmitoleic acid, the product of the stearoyl CoA desaturase-1 (SCD-1), and a minor constituent in dietary fat. That the reduced proportion of 16:1n-7 in serum lipids with the CRD is not due to downregulation of SCD-1 is indicated by the fact that both 16:0 and 16:1n-7 were reduced in the subjects consuming the CRD, whereas the proportion of 16:0 would be expected to rise if less were subject to desaturation. The results indicate a greater effect of the CRD on reduction of glucose disposal via lipogenesis.

Correlation of Weight Loss and Lipid Markers

The rationale for using carbohydrate restriction to treat MetS is that a (carbohydrate-sensitive) physiologic state is expressed in the various markers of the syndrome. It is not excluded that, beyond carbohydrate, per se, decreasing adipose mass contributes to the change in lipid markers since they are also affected by adipokines. It is difficult in general to distinguish between mechanisms in a hypocaloric experiment; however, the experiments presented here do not support the decreased adipose mass as the primary stimulus for inducing improvement in MetS in subjects consuming a CRD. Although the CRD was significantly better at effecting weight loss, all but two subjects consuming the LFD lost at least some weight; yet the performance of the latter group on some of the lipid markers was not good, even in a qualitative sense. In addition, as shown in Fig. 3, there is only a very weak correlation between weight loss and dyslipidemia in both groups, suggesting that, even in the LFD, the reduction in body mass may be one of several *parallel* consequences of some central physiologic change.

Experiments in the literature further support this idea. Normal-weight people [34, 57] and subjects with diabetes [58, 59] on low-carbohydrate diets constrained to maintain body mass show improvements in atherogenic dyslipidemia. Also, in comparative studies in which weight loss is similar between different diets, the carbohydrate-restricted group shows better response on other markers [60, 61]. Finally, experiments in which isocaloric changes in macronutrient composition are separated in time from weight loss point to the beneficial effects of carbohydrate reduction before caloric restriction [25, 26].

Mechanism of Improvement of Dyslipidemia by CRD

We recently summarized the mechanisms by which CRD are understood to improve dyslipidemia [14, 23]. In brief, high insulin represses lipolysis and increases de novo lipogenesis,

leading to increases in TAG. This, in turn, enhances overproduction of larger TAG-enriched VLDL particles and the formation of small LDL particles and reductions in HDL-C. These effects are also associated with decreased catabolism of Apo B-containing particles and increased catabolism of Apo A-1-containing HDL-C. Carbohydrate restriction ameliorates these processes. Lower glucose and insulin concentrations also reduce ChREBP and SREBP1c expression, which activate key lipogenic enzymes, thereby reducing hepatic lipogenesis and VLDL production. At the same time, carbohydrate restriction leads to decreases in malonyl-CoA concentration and dis-inhibition of the carnitine acyltransferase, allowing for enhanced mitochondrial shuttle and β -oxidation of fatty acids. Lower glucose (and lower fructose, which may be associated with high-carbohydrate diets) also limits glycerol-3-phosphate production for the re-esterification of free fatty acids.

RBP4

A novel finding was that RBP4 was reduced by the CRD (–20%) but not the LFD (5%). Several lines of evidence point to increased circulating levels of RBP4 in insulin-resistant states [29, 30]. Transgenic overexpression or injection of purified RBP4 results in impairment of insulin-stimulated signaling in muscle, indicating that RBP4 may directly contribute to insulin resistance. In humans, RBP4 is elevated in subjects with obesity and type 2 diabetes and is correlated with components of the MetS [29]. Energy restriction with LFDs resulting in weight loss has been shown to result in decreased serum RBP4 [62, 63], whereas short-term overfeeding apparently has no effect [64].

The Reality of Metabolic Syndrome

Despite the conceptual importance of MetS, several workers have raised the question of whether it is truly clinically useful. Most recently, a study by Sattar et al. [10] and an associated commentary by Kahn [65] concluded that “metabolic syndrome and its components are associated with type 2 diabetes but have weak or no association with vascular risk.” This surely overstates the case in that the vascular complications associated with hyperglycemia are the most deleterious outcomes of diabetes. In this sense, diabetes is a vascular disease. In the end, it is a question of whether identification of MetS would lead to a different treatment than the sum of the treatments of the different markers. The work presented here supports the idea that there is an across-the-board benefit to carbohydrate restriction. That the collection of markers—here emphasizing atherogenic dyslipidemia, response to fat challenge, reduction in RBP4, and the previously reported improvement in inflammatory markers—is improved by a single

type of intervention argues for their being viewed as a syndrome. The close connection between dietary carbohydrate and insulin metabolism provides the underlying biological basis, consistent with the generally agreed-on principle that “insulin resistance plays an important part in risk-factor clustering for the MetS [65].”

From a practical perspective, MetS is a collection of risk factors, and it is to be expected that the expression of each pathology would appear at a different time or in response to different environmental stimuli. It seems reasonable that the best bet will be to treat one marker with the methodology that has the potential to treat all. There is no guarantee that the signs in MetS for an individual patient might not be indications of isolated risk for one disease state, but, until we know how to distinguish these cases, carbohydrate restriction may be the “default” approach.

Limitations

This 12-week diet intervention in a group of 40 subjects could be viewed as short in duration and small in sample size in comparison to larger clinical trials. In contrast to large-scale dietary trials where dietary compliance and attrition are high, this study had a high level of experimental control, which allows direct comparison of the biological effects induced by diets varying in macronutrient composition, as opposed to studying the effects of *prescribing* a diet (as is the case in many diet trials where compliance is poor). Although the sample size of 20 subjects per group might be considered modest, statistical significance was achieved on most variables, again attributable to the high level of standardization and subject compliance. There is also little to suggest that the effects will not persist as long as there is compliance. In addition, longer studies generally support the relative superiority of CRDs [49, 60, 66]. The study of Foster et al. [60] in particular showed that improvements in CVD risk markers are stable beyond the point at which the diets become similar and weight loss differences become small. Finally, we did not perform a direct measure of insulin resistance, nor did we perform a glucose tolerance test to assess their metabolic status in respect to glucose metabolism.

Summary

The results presented here show that a diet restricted in carbohydrate can provide a more comprehensive improvement in the clinical risk factors associated with MetS than a LFD at reduced caloric intake. There are many options for treating obesity or the individual components of MetS, but carbohydrate restriction has the ability to target the range of markers with a single intervention. That this collection of

metabolic markers responds in concert to carbohydrate restriction provides support for considering them as a single syndrome, and treating any of the individual MetS markers with carbohydrate restriction holds the promise of potential benefits to the others. Low-carbohydrate diets therefore represent an alternative strategy for general health beyond weight regulation.

Acknowledgments We thank Timothy E. Graham and Barbara B. Kahn at the Division of Endocrinology, Diabetes, and Metabolism, Department of Medicine, Beth Israel Deaconess Medical Center and Harvard Medical School, Boston, MA for measuring serum RBP4 concentrations. This work was supported in part by funds from the Graduate School and the Health Disparity EXPORT Center at the University of Connecticut, USDA Hatch, the Dr. Robert C. Atkins Foundation, the Egg Nutrition Center, and the Research Foundation of the State University of New York.

References

- Reaven GM (1988) Role of insulin resistance in human disease. *Diabetes* 37:1595–1607
- Grundy SM, Cleeman JI, Daniels SR, Donato KA, Eckel RH, Franklin BA, Gordon DJ, Krauss RM, Savage PJ, Smith SC Jr et al (2006) Diagnosis and management of the metabolic syndrome: an American Heart Association/National Heart, Lung, and Blood Institute scientific statement. *Curr Opin Cardiol* 21:1–6
- Haffner S, Cassells HB (2003) Metabolic syndrome—a new risk factor of coronary heart disease? *Diabetes Obes Metab* 5:359–370
- Dreon DM, Fernstrom HA, Williams PT, Krauss RM (1999) A very low-fat diet is not associated with improved lipoprotein profiles in men with a predominance of large, low-density lipoproteins. *Am J Clin Nutr* 69:411–418
- Krauss RM (2005) Dietary and genetic probes of atherogenic dyslipidemia. *Arterioscler Thromb Vasc Biol* 25(11):2265–2272
- Kahn R, Buse J, Ferrannini E, Stern M (2005) The metabolic syndrome: time for a critical appraisal: joint statement from the American Diabetes Association and the European Association for the Study of Diabetes. *Diabetes Care* 28:2289–2304
- Lomangino K (2008) Metabolic syndrome diagnosis: clinical value called questionable. *Clin Nutr Insight* 34:7–8
- Reaven GM (2005) The metabolic syndrome: requiescat in pace. *Clin Chem* 51:931–938
- Sattar N (2006) The metabolic syndrome: should current criteria influence clinical practice? *Curr Opin Lipidol* 17:404–411
- Sattar N, McConnachie A, Shaper AG, Blauw GJ, Buckley BM, de Craen AJ, Ford I, Forouhi NG, Freeman DJ, Jukema JW et al (2008) Can metabolic syndrome usefully predict cardiovascular disease and diabetes? Outcome data from two prospective studies. *Lancet* 371:1927–1935
- Bloomgarden ZT (2005) 2nd International Symposium on Triglycerides and HDL: metabolic syndrome. *Diabetes Care* 28:2577–2584
- Boden G, Homko C, Mozzoli M, Zhang M, Kresge K, Cheung P (2007) Combined use of rosiglitazone and fenofibrate in patients with type 2 diabetes: prevention of fluid retention. *Diabetes* 56:248–255
- Volek JS, Feinman RD (2005) Carbohydrate restriction improves the features of metabolic syndrome. *Metabolic syndrome may be defined by the response to carbohydrate restriction. Nutr Metab (Lond)* 2:31
- Volek JS, Fernandez ML, Feinman RD, Phinney SD (2008) Dietary carbohydrate restriction induces a unique metabolic state positively affecting atherogenic dyslipidemia, fatty acid partitioning, and metabolic syndrome. *Prog Lipid Res* 47:307–318
- Bloomgarden ZT (2005) Thiazolidinediones. *Diabetes Care* 28(2):488–493
- Devchand PR (2008) Glitazones and the cardiovascular system. *Curr Opin Endocrinol Diabetes Obes* 15:188–192
- Richter B, Bandeira-Echtler E, Bergerhoff K, Clar C, Ebrahim SH (2007) Rosiglitazone for type 2 diabetes mellitus. *Cochrane Database Syst Rev* CD006063
- Nielsen JV, Joensson EA (2008) Low-carbohydrate diet in type 2 diabetes: stable improvement of bodyweight and glycemic control during 44 months follow-up. *Nutr Metab (Lond)* 5:14
- Boden G, Sargrad K, Homko C, Mozzoli M, Stein TP (2005) Effect of a low-carbohydrate diet on appetite, blood glucose levels, and insulin resistance in obese patients with type 2 diabetes. *Ann Intern Med* 142:403–411
- Yancy WS Jr, Foy M, Chalecki AM, Vernon MC, Westman EC (2005) A low-carbohydrate, ketogenic diet to treat type 2 diabetes. *Nutr Metab (Lond)* 2:34
- Ahrens E Jr (1986) Carbohydrates, plasma triglycerides, and coronary heart disease. *Nutr Rev* 44:60–64
- Hellerstein MK (2002) Carbohydrate-induced hypertriglyceridemia: modifying factors and implications for cardiovascular risk. *Curr Opin Lipidol* 13:33–40
- Karam J, Nessim F, McFarlane S, Feinman R (2008) Carbohydrate restriction and cardiovascular risk. *Curr Cardiovasc Risk Rep* 2:88–94
- Tirosh A, Rudich A, Shochat T, Tekes-Manova D, Israeli E, Henkin Y, Kochba I, Shai I (2007) Changes in triglyceride levels and risk for coronary heart disease in young men. *Ann Intern Med* 147:377–385
- Feinman RD, Volek JS (2006) Low carbohydrate diets improve atherogenic dyslipidemia even in the absence of weight loss. *Nutr Metab (Lond)* 3:24
- Krauss RM, Blanche PJ, Rawlings RS, Fernstrom HS, Williams PT (2006) Separate effects of reduced carbohydrate intake and weight loss on atherogenic dyslipidemia. *Am J Clin Nutr* 83:1025–1031
- Forsythe CE, Phinney SD, Fernandez ML, Quann EE, Wood RJ, Bibus DM, Kraemer WJ, Feinman RD, Volek JS (2008) Comparison of low fat and low carbohydrate diets on circulating fatty acid composition and markers of inflammation. *Lipids* 43:65–77
- Graham TE, Kahn BB (2007) Tissue-specific alterations of glucose transport and molecular mechanisms of intertissue communication in obesity and type 2 diabetes. *Horm Metab Res* 39:717–721
- Graham TE, Yang Q, Bluher M, Hammarstedt A, Ciaraldi TP, Henry RR, Wason CJ, Oberbach A, Jansson PA, Smith U et al (2006) Retinol-binding protein 4 and insulin resistance in lean, obese, and diabetic subjects. *N Engl J Med* 354:2552–2563
- Yang Q, Graham TE, Mody N, Preitner F, Peroni OD, Zabolotny JM, Kotani K, Quadro L, Kahn BB (2005) Serum retinol binding protein 4 contributes to insulin resistance in obesity and type 2 diabetes. *Nature* 436:356–362
- Glickman SG, Marn CS, Supiano MA, Dengel DR (2004) Validity and reliability of dual-energy X-ray absorptiometry for the assessment of abdominal adiposity. *J Appl Physiol* 97:509–514
- Friedewald WT, Levy RI, Fredrickson DS (1972) Estimation of the concentration of low-density lipoprotein cholesterol in plasma, without use of the preparative ultracentrifuge. *Clin Chem* 18:499–502

33. Matthews DR, Hosker JP, Rudenski AS, Naylor BA, Treacher DF, Turner RC (1985) Homeostasis model assessment: insulin resistance and beta-cell function from fasting plasma glucose and insulin concentrations in man. *Diabetologia* 28:412–419
34. Sharman MJ, Kraemer WJ, Love DM, Avery NG, Gomez AL, Scheett TP, Volek JS (2002) A ketogenic diet favorably affects serum biomarkers for cardiovascular disease in normal-weight men. *J Nutr* 132:1879–1885
35. Larosa JC, Fry AG, Muesing R, Rosing DR (1980) Effects of high-protein, low-carbohydrate dieting on plasma lipoproteins and body weight. *J Am Diet Assoc* 77:264–270
36. Volek JS, Sharman MJ, Gomez AL, DiPasquale C, Roti M, Pumerantz A, Kraemer WJ (2004) Comparison of a very low-carbohydrate and low-fat diet on fasting lipids, LDL subclasses, insulin resistance, and postprandial lipemic responses in overweight women. *J Am Coll Nutr* 23:177–184
37. Howard BV, Manson JE, Stefanick ML, Beresford SA, Frank G, Jones B, Rodabough RJ, Snetselaar L, Thomson C, Tinker L et al (2006) Low-fat dietary pattern and weight change over 7 years: the Women's Health Initiative Dietary Modification Trial. *JAMA* 295:39–49
38. Feinman RD, Fine EJ (2003) Thermodynamics and metabolic advantage of weight loss diets. *Metab Syndr Relat Disord* 1:209–219
39. Krieger JW, Sitren HS, Daniels MJ, Langkamp-Henken B (2006) Effects of variation in protein and carbohydrate intake on body mass and composition during energy restriction: a meta-regression 1. *Am J Clin Nutr* 83:260–274
40. Aarsland A, Wolfe RR (1998) Hepatic secretion of VLDL fatty acids during stimulated lipogenesis in men. *J Lipid Res* 39:1280–1286
41. Volek JS, Sharman MJ, Forsythe CE (2005) Modification of lipoproteins by very low-carbohydrate diets. *J Nutr* 135:1339–1342
42. Barter PJ, Ballantyne CM, Carmena R, Castro Cabezas M, Chapman MJ, Couture P, de Graaf J, Durrington PN, Faergeman O, Frohlich J et al (2006) Apo B versus cholesterol in estimating cardiovascular risk and in guiding therapy: report of the thirty-person/ten-country panel. *J Intern Med* 259:247–258
43. Dreon DM, Krauss RM (1997) Diet–gene interactions in human lipoprotein metabolism. *J Am Coll Nutr* 16:313–324
44. Gardner CD, Kiazand A, Alhassan S, Kim S, Stafford RS, Balise RR, Kraemer HC, King AC (2007) Comparison of the Atkins, Zone, Ornish, and LEARN diets for change in weight and related risk factors among overweight premenopausal women: the A TO Z weight loss study: a randomized trial. *JAMA* 297:969–977
45. Nuttall FQ, Schweim K, Hoover H, Gannon MC (2008) Effect of the LoBAG30 diet on blood glucose control in people with type 2 diabetes. *Br J Nutr* 99:511–519
46. Westman EC, Yancy WS Jr, Olsen MK, Dudley T, Guyton JR (2006) Effect of a low-carbohydrate, ketogenic diet program compared to a low-fat diet on fasting lipoprotein subclasses. *Int J Cardiol* 110:212–216
47. Feinman RD, Volek JS (2008) Carbohydrate restriction as the default treatment for type 2 diabetes and metabolic syndrome. *Scand Cardiovasc J* 42:256–263
48. Westman EC, Feinman RD, Mavropoulos JC, Vernon MC, Volek JS, Wortman JA, Yancy WS, Phinney SD (2007) Low-carbohydrate nutrition and metabolism. *Am J Clin Nutr* 86:276–284
49. Shai I, Schwarzfuchs D, Henkin Y, Shahar DR, Witkow S, Greenberg I, Golan R, Fraser D, Bolotin A, Vardi H et al (2008) Weight loss with a low-carbohydrate, Mediterranean, or low-fat diet. *N Engl J Med* 359:229–241
50. Shoji T, Hatsuda S, Tsuchikura S, Shinohara K, Kimoto E, Koyama H, Emoto M, Nishizawa Y (2008) Small dense low-density lipoprotein cholesterol concentration and carotid atherosclerosis. *Atherosclerosis* (in press)
51. Austin MA, Hokanson JE, Edwards KL (1998) Hypertriglyceridemia as a cardiovascular risk factor. *Am J Cardiol* 81:7B–12B
52. Toth PP (2005) High-density lipoprotein as a therapeutic target: clinical evidence and treatment strategies. *Am J Cardiol* 96(9A):50K–58K (discussion: 34K–35K)
53. Knopp RH, Paramsothy P, Retzlaff BM, Fish B, Walden C, Dowdy A, Tsunehara C, Aikawa K, Cheung MC (2005) Gender differences in lipoprotein metabolism and dietary response: basis in hormonal differences and implications for cardiovascular disease. *Curr Atheroscler Rep* 7:472–479
54. Fleming J, Sharman MJ, Avery NG, Love DM, Gomez AL, Scheett TP, Kraemer WJ, Volek JS (2003) Endurance capacity and high-intensity exercise performance responses to a high fat diet. *Int J Sport Nutr Exerc Metab* 13:466–478
55. Kunesova J, Zak A, Stunkard AJ (2002) Assessment of dietary and genetic factors influencing serum and adipose fatty acid composition in obese female identical twins. *Lipids* 37:27–32
56. Okada T, Furuhashi N, Kuromori Y, Miyashita M, Iwata F, Harada K (2005) Plasma palmitoleic acid content and obesity in children. *Am J Clin Nutr* 82:747–750
57. Volek JS, Sharman MJ, Gomez AL, Scheett TP, Kraemer WJ (2003) An isoenergetic very low carbohydrate diet improves serum HDL cholesterol and triacylglycerol concentrations, the total cholesterol to HDL cholesterol ratio and postprandial lipemic responses compared with a low fat diet in normal weight, normolipidemic women. *J Nutr* 133:2756–2761
58. Allick G, Bisschop PH, Ackermans MT, Endert E, Meijer AJ, Kuipers F, Sauerwein HP, Romijn JA (2004) A low-carbohydrate/high-fat diet improves glucoregulation in type 2 diabetes mellitus by reducing postabsorptive glycogenolysis. *J Clin Endocrinol Metab* 89:6193–6197
59. Gannon MC, Nuttall FQ (2006) Control of blood glucose in type 2 diabetes without weight loss by modification of diet composition. *Nutr Metab (Lond)* 3:16
60. Foster GD, Wyatt HR, Hill JO, McGuckin BG, Brill C, Mohammed BS, Szapary PO, Rader DJ, Edman JS, Klein S (2003) A randomized trial of a low-carbohydrate diet for obesity. *N Engl J Med* 348:2082–2090
61. Accurso A, Bernstein RK, Dahlqvist A, Draznin B, Feinman RD, Fine EJ, Glead A, Jacobs DB, Larson G, Lustig RH et al (2008) Dietary carbohydrate restriction in type 2 diabetes mellitus and metabolic syndrome: time for a critical appraisal. *Nutr Metab (Lond)* 5:9
62. Ng TW, Watts GF, Barrett PH, Rye KA, Chan DC (2007) Effect of weight loss on LDL and HDL kinetics in the metabolic syndrome: associations with changes in plasma retinol-binding protein-4 and adiponectin levels. *Diabetes Care* 30:2945–2950
63. Vitkova M, Klimcakova E, Kovacikova M, Valle C, Moro C, Polak J, Hanacek J, Capel F, Viguierie N, Richterova B et al (2007) Plasma levels and adipose tissue messenger ribonucleic acid expression of retinol-binding protein 4 are reduced during calorie restriction in obese subjects but are not related to diet-induced changes in insulin sensitivity. *J Clin Endocrinol Metab* 92:2330–2335
64. Shea J, Randell E, Vasdev S, Wang PP, Roebathan B, Sun G (2007) Serum retinol-binding protein 4 concentrations in response to short-term overfeeding in normal-weight, overweight, and obese men. *Am J Clin Nutr* 86(5):1310–1315
65. Kahn R (2008) Metabolic syndrome—what is the clinical usefulness? *Lancet* 371:1892–1893
66. Stern L, Iqbal N, Seshadri P, Chicano KL, Daily DA, McGrory J, Williams M, Gracely EJ, Samaha FF (2004) The effects of low-carbohydrate versus conventional weight loss diets in severely obese adults: one-year follow-up of a randomized trial. *Ann Intern Med* 140:778–785

Activation of T-Lymphocytes by LDL-Cholesterol

Borros Arneth

Received: 13 June 2008 / Accepted: 19 November 2008 / Published online: 17 December 2008
© AOCs 2008

Abstract Native LDL-cholesterol can be mechanically stressed by strong vortexing. According to one hypothesis, mechanical shear stress within the vessel can lead to an aggregation of LDL-cholesterol and subsequently to activation of CD4 and CD8 T-lymphocytes. The goal of this study was to determine the proportion of activated CD4 and CD8 T-lymphocytes that is induced by adding unstressed and mechanically stressed LDL-cholesterol to whole blood samples. Whole blood was taken from 12 healthy subjects. All probands fasted for at least 12 h before blood withdrawal. In each case, 1 ml of whole blood from each subject was incubated for 16 h at 32 °C (89.3 °F) with concanavalin A (A), without additive (B), with mechanically stressed LDL-cholesterol (C) or with native LDL-cholesterol (D). Subsequently, the samples were measured by four-color flow cytometry. CD3, CD4, CD8, and CD69 were measured as activity markers. CD69 was plotted against CD4 and CD8, and the proportions of activated CD4 and CD8 T-lymphocytes were determined. Native and vortexed LDL-cholesterol elicited significantly different types of T-cell activation. While native LDL activated CD4 T-cells to only a small extent, mechanically stressed (vortexed) LDL potently activated CD8 T-cells. Purely mechanically-induced changes in LDL-cholesterol may be one mechanism that contributes to the activation of CD8 cells and, as a consequence, the emergence of arteriosclerosis.

Keywords Arteriosclerosis · Activation · CD4 helper T cells · CD8 cytotoxic T cells · Cholesterol

Introduction

According to one theory [1], LDL-cholesterol under mechanical stress leads to a structural change in LDL-lipoprotein vesicles, and as a consequence, CD4 and CD8 T-lymphocytes become activated. The goal of this study was to determine the percentage of CD4 and CD8 T-lymphocytes that is activated after the addition of mechanically treated or untreated (unstressed) LDL-lipoprotein vesicles in human whole blood samples. Such methods may lead to a better understanding of pathophysiological processes in the human body since LDL-particles are also similarly mechanically stressed in systemic circulation. It is well known that patients who have high blood pressure and, in particular, patients who have a combination of high serum concentrations of LDL-cholesterol and high blood pressure, are at increased risk for arteriosclerosis [2, 3]. This association was first described in 1961 as a result of the Framingham study and has been confirmed in numerous subsequent studies [4, 5].

Experimental Procedure

Blood Withdrawal

From each of 12 healthy subjects, 9 ml whole blood was collected in the morning (Sarstedt S-monovettes[®], white 9 ml). Probands gave their informed consent and did not eat for at least 12 h before withdrawal. The study was approved by the relevant review board at the author's institution.

B. Arneth (✉)
Institute of Clinical Chemistry and Laboratory Medicine,
Johannes Gutenberg University, Building 505, 1.UG,
Room 202, Langenbeckstraße 1, 55131 Mainz, Germany
e-mail: arneth@zentrallabor.klinik.uni-mainz.de

Nadroparin (Fraxiparin[®], GSK, Glaxo Smith Kline, 16 IE/ml whole blood) was used as an anticoagulant and was added to the test tubes before blood withdrawal. Preliminary tests have shown that Nadroparin activates far fewer T-lymphocytes than Heparin. The whole blood was carefully mixed and aliquoted into nine tubes, each of which contained 1 ml.

Incubation

Isolated native LDL-cholesterol was mechanically stressed by vortexing for 15 min at maximal strength. Subsequently, the same quantities of mechanically stressed LDL and non-stressed (native) LDL were mixed with 1 ml-samples of fresh non-stressed human whole blood. The nine samples (tubes) per proband were then subjected to the following individual treatments: Tube No.1 (A), Concanavalin A as positive control (1 μ l, 1 μ g/ μ l, final concentration 1 μ g/ml); tube No.2 (B) remained untreated as negative control; tube No.3 (C) maximally vortexed LDL-cholesterol (10 μ l, 3 mg/ml), tube No.4 (D) native LDL-cholesterol (10 μ l, 3 mg/ml), tube No. 5 (E), a hemolyzing concentration of nadroparin (fraxiparin[®] 0.6 ml, 5700 IU anti-Xa), tube No. 6 (F), whole blood sample that was mechanically stressed (maximally vortexed for 15 min), tube No 7 (G), ascorbic acid in a lower concentration (20 μ l, 0.01 mg/ml), tube No 8 (H), ascorbic acid in a higher concentration (20 μ l, 0.05 mg/ml) and tube No 9 (I), a transfection reagent (Stratagene BioTrek protein delivery reagent, 1 cup per experiment).

Subsequently, the tubes were incubated for 16 h at 32 °C (89.6 °F). During this phase, the samples were carefully mixed every 2 h. Then, 50 μ l from each tube was stained with a dye that contained antibodies. Erythrocytes were lysed, and samples were evaluated by flow cytometry and the extent of CD4 and CD8 T-lymphocyte activation was examined.

The following conditions were fixed: Amount of LDL added, incubation time (16 h), incubation temperature (32 °C), and careful slight mixing of the samples every 2 h (Table 1).

LDL Preparation

The preparation of LDL was carried out according to Torzewski et al. [6]. Briefly, LDL particles were isolated from healthy subjects aged 18 to 65 years by preparative ultracentrifugation ($d = 1.019$ to 1.063 g/ml). Cholesterol concentrations refer to the total cholesterol concentration in the lipoprotein samples.

Plasma used for the isolation of LDL was obtained from healthy blood donors (blood bank). None of the donors had diabetes or hypertension, and none was taking any medication. No donors had any signs of ischemic heart disease.

Table 1 Human whole blood samples (1 ml each) from the same patient containing 16 I.U. Fraxiparin per ml whole blood were incubated for 16 h at 37 °C with these additives

Sample	Added
#1 A	Concanavalin A (positive control)
#2 B	Untreated control sample (negative control sample)
#3 C	15 min maximally vortexed LDL-cholesterol (10 μ l, 3 mg/ml)
#4 D	Native LDL-cholesterol (10 μ l, 3 mg/ml)
#5 E	A hemolyzing concentration of fraxiparin (0.6 ml, 5700 I.U. anti-Xa)
#6 F	A mechanically stressed whole-blood sample (maximally vortexed for 15 min)
#7 G	Ascorbic acid (20 μ l 0.01 mg/ml)
#8 H	Ascorbic acid (20 μ l 0.05 mg/ml)
#9 I	Transfection reagent (Biotrek, Stratagene)

Native LDL (nLDL, $d = 1.020$ to 1.062 g/ml) was isolated by a method based on preparative sequential ultracentrifugation using KBr gradients. The first gradient ultracentrifugation was accomplished using the density of the potassium bromide solution, $d = 1.019$ g/ml. Materials that have densities <1.019 g/ml migrate toward the surface, while those that have densities >1.019 g/ml are spun toward the bottom of the centrifuge container. One-third of the centrifuge container was filled at the bottom with a yellow sediment. The supernatant was discarded, and the sediment was further processed.

During the second centrifugation step using a potassium bromide solution of $d = 1.063$, a yellow supernatant was formed, filling approximately one-sixth (1/6) of the centrifuge container. This supernatant ($d < 1.063$ g/ml) represented the LDL fraction. Subsequently, LDL was purified by dialysis against Tris-NaCl buffer (5 mmol/l Tris and 150 mmol/l NaCl, pH 7.4). Cholesterol content, determined by an enzymatic test (Roche), was 300 mg/dl, triglyceride content was 73 mg/dl and protein content, analyzed by the Bradford method (Roth) was 2.1 mg/ml.

Therefore the cholesterol/triglyceride quotient was ~ 4.07 . The concentrations that are given refer to the total cholesterol concentration in the lipoprotein samples.

Mechanical Treatment of LDL

For each proband the LDL portion was first divided into two identical aliquots and placed in two reaction tubes. Then, one tube was vortexed, while the other tube remained untreated. Subsequently the contents of each reaction tube were transferred into the 1 ml whole blood samples, ensuring that the same amounts of cholesterol were added.

Under mechanical stress, the optical appearance of LDL-lipoprotein was changed. Native LDL-lipoprotein is a clear, slightly yellow solution, but its consistency changed when it was vortexed, turning cloudy. After strong vortexing (15 min at maximal strength), a white precipitate flocculated, resulting in a clear increase in turbidity caused by aggregated LDL particles.

Flow-Cytometric Investigation

To assess the phenotype of activated T-lymphocytes, four-color flow cytometry was used. In addition to CD4 and CD8, CD3 and CD69 also were measured.

In our assay, CD8 was labeled with fluorescein isothiocyanate (FITC), CD4 was labeled with allophycocyanin (APC), CD69 with phycoerythrin (PE), and CD3 with peridinin chlorophyll (PerCP). All reagents were purchased from Becton Dickinson Bioscience®. For flow cytometry, the FACS Calibur® Flow Cytometer was used (FACS Calibur, Becton Dickinson, New Jersey, US). First, in the CD3 versus side scatter plot, the T-lymphocytes were gated, and 30,000 lymphocytes were counted for each sample.

Next, the gated T-lymphocytes were measured on two different plots using Cell Quest Pro®-Software (Cell Quest Pro, Becton Dickinson, New Jersey, US): CD69 versus CD4, and CD69 versus CD8.

From these diagrams, the proportion of activated CD4 and CD8 T-cells was calculated using the following formula:

$$\begin{aligned} \% \text{ activated T-cells} &= q_4 \text{ or } q_8 \text{ respectively} \\ &= \text{UR}/(\text{UR} + \text{LR}) \times 100\%, \end{aligned} \quad (1)$$

where UR = number of events in the upper right quadrant and LR = number of events in the lower right quadrant.

To evaluate the effect of the additives, the differences in the proportion of activated CD4 and CD8 lymphocytes of treated samples and untreated samples (control samples) was calculated using the following formulas:

$$\Delta q_4 = (q_4 - q_{40}) \quad (2)$$

and

$$\Delta q_8 = (q_8 - q_{80}), \quad (3)$$

where q = proportion of activated T-cells, and q_{40} and q_{80} = proportion of activated T-cells in the untreated control sample of the same blood withdrawal from the same proband.

For each proband the same quantities of mechanically stressed LDL and unstressed (native) LDL were mixed with 1 ml fresh human whole blood. Afterwards, the amounts of activated CD4 and CD8 T-cells were examined by flow cytometry. Differences in activated T-cells were calculated for each proband.

Microscopy

All whole blood samples also were investigated by microscopy (Olympus CX21®, Olympus, Tokyo, Japan).

Statistical Analysis

For statistical analysis, paired Student t -tests were used (SPSS®, $P < 0.05$). The following experiments led to significant T-cell activations and/or inhibitions: addition of ascorbic acid in groups seven and eight led to significant CD8 activation compared to group two. Haemolysis in group five led to a significant CD8 activation and CD4 inhibition compared to group two. Comparison of groups three (addition of vortexed LDL) and four (addition of native LDL) revealed a significant difference in CD8 T-cell activation, which went from inhibition in the case of native LDL to activation in the case of vortexed LDL (Table 2).

Results

When native LDL was added to the whole blood sample, CD4 T-lymphocytes were clearly activated. In contrast, the addition of mechanically stressed LDL induced the activation of CD8 T-lymphocytes.

The same predominance of CD8 T-lymphocytes was seen after vortexing whole blood samples or after addition of a hemolytic quantity of nadroparin (fraxiparin®). Such a dominance of CD8 T-lymphocyte activation was seen under the following conditions:

Table 2 LDL, triglyceride, HDL and cholesterol values of the probands

Proband	LDL/ [mg/dl]	Triglyceride/ [mg/dl]	HDL/ [mg/dl]	Cholesterol/ [mg/dl]
#1	86	97	64	169
#2	110	115	42	175
#3	108	112	45	175
#4	125	130	48	199
#5	85	87	62	164
#6	95	113	41	158
#7	112	125	39	176
#8	117	135	42	186
#9	86	75	31	132
#10	97	112	69	188
#11	112	125	42	179
#12	114	135	41	182
Mean	104	113	47	174
Std	14	19	12	17

- Addition of mechanically stressed LDL–lipoprotein particles, sample no #3
- Mechanically stressed human whole blood, sample no #6
- Hemolytic human whole blood, sample no #5
- Ascorbic acid-treated human whole blood, samples no #7, #8
- Incubation with transfection reagent, sample #9,

The results of the incubation of human whole blood with native LDL-cholesterol (#4) compared to incubation with mechanically stressed LDL-cholesterol (#3) are shown in Figure 1 with respect to the activation of T-lymphocyte subpopulations (CD4, white bars and CD8, black bars). A significant difference emerged between blood that was incubated with native LDL and mechanically stressed LDL. The native LDL sample exhibited a CD4 increase, while the stressed LDL sample exhibited a CD8 increase. This CD8 activation was accompanied by a simultaneous inhibition of CD4+ activation.

Figure 1 additionally shows the results of samples 5 (hemolyzed by fraxiparin), 6 (hemolyzed by mechanical stress, strong vortexing), 7 (lower dose of vitamin C), 8 (higher dose of vitamin C) and 9 (transfection reagent). In all of these cases, an increase in CD8 activation developed.

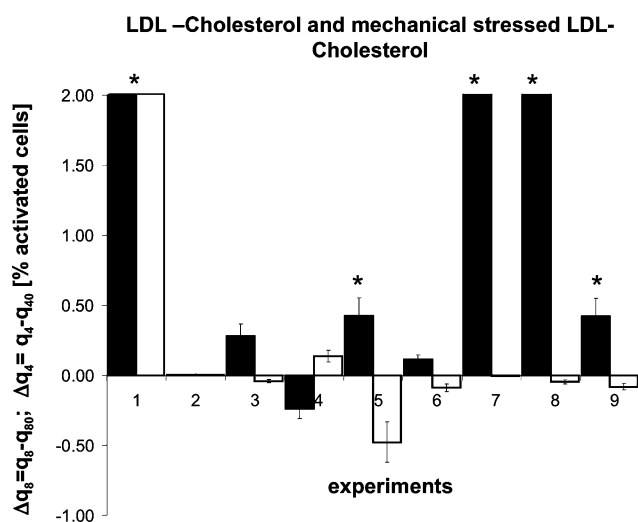


Fig. 1 Effect of native and mechanically stressed LDL-cholesterol on the activation of T-lymphocytes. On the ordinate, the portion of activated CD8 lymphocytes is given in comparison with the untreated control of the same proband (sample no 2). Increasing CD8 activity is given by the difference $q_8 - q_{80}$. This value (Δq_8) is shown by the black bars. Analogously, for CD4 activity, the $q_4 - q_{40}$ difference is relevant. This value (Δq_4) is represented by the white bars. Sample 1 was incubated with concanavalin A in each case and serves as a positive control. Sample 2 remained untreated in each case and serves as a negative control. Sample 3 was incubated in each case with mechanically stressed LDL-cholesterol, and Sample 4 was incubated with native LDL-cholesterol. Sample 5 was hemolyzed before incubation and Sample 6 was mechanically stressed (vortexed) before incubation. Samples 7 and 8 were treated with vitamin C. Sample 9 was treated with transfection reagent

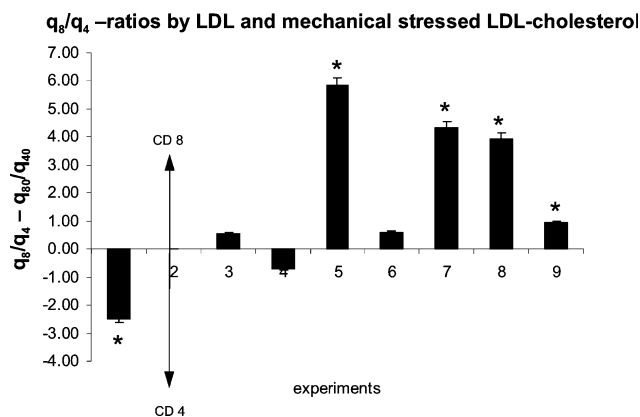


Fig. 2 Change of the q_8/q_4 quotients. These quotients are given in comparison with the untreated sample. This was performed because the CD8/CD4 quotients are clinically relevant, and because these quotients are frequently measured in patients. An increase of the q_8/q_4 quotient is indicative of an increase of CD8 activation or a reduction of CD4 activation. Accordingly, a reduction of this quotient is an indication of either CD4 increase or decrease of CD8 activation. A decrease of this quotient only appears after the addition of native LDL (sample 4). The remaining experiments, however, are accompanied by an increase of this quotient. Statistical significant difference to #2 ($*p < 0.05$)

Table 3 CD4 and CD8 cell counts of the probands

Proband	CD4%	CD4 count	CD8%	CD8 count	CD4/CD8
#1	45	942	32	670	1.41
#2	42	586	29	404	1.45
#3	40	692	31	536	1.29
#4	37	958	28	725	1.32
#5	31	636	24	492	1.29
#6	34	651	26	498	1.31
#7	38	647	28	477	1.36
#8	43	1264	32	940	1.34
#9	51	697	37	505	1.38
#10	48	1225	35	893	1.37
#11	41	933	32	728	1.28
#12	45	414	33	303	1.37

Increased CD8 activation also resulted after incubation with mechanically stressed LDL, similarly to incubation with a transfection reagent. Figure 2 shows the changes of the q_8/q_4 quotients compared with the untreated sample (q_{80}/q_{40}). This was calculated because the CD8/CD4 quotient is known to be clinically relevant, and because these values are measured frequently in patients (Table 3).

Discussion

In this study, only the influences of mechanically stressed LDL (vortexed LDL) were investigated. Other forms of

modified LDL, such as oxidised or enzymatically modified LDL, were not included.

Our results describe the occurrence of two different reaction mechanisms according to whether native or mechanically treated LDL-cholesterol was added to human whole blood. That CD4 activation developed after the addition of native LDL suggests an MHC II-mediated process. To activate CD4+ cells, antigen-presenting cells (APC) first must take up antigen and express it in the context of MHC II [7]. In our study, macrophages were also activated by both native LDL and by mechanically stressed LDL as seen by microscopy.

In contrast, mechanically stressed LDL appears to activate CD8 T-cells by an MHC I-mediated pathway. These mechanisms are expected to be important for the pathogenesis of arteriosclerosis and related diseases.

Logically, native LDL-cholesterol is recognized as an extracellular antigen and is treated accordingly. Subsequently, a CD4-dominated immunological reaction takes place. In contrast, mechanically stressed LDL-cholesterol leads to a CD8-dominated immunological reaction. Here, the vesicular structure of LDL-cholesterol particles is degraded by mechanical stress. Larger lipid aggregates are then formed that flocculate and generate turbidity [8–10]. On one hand, LDL-aggregation is described to be prevented by both HDL [10] and albumin [8]. On the other hand, aggregated LDL is thought to be taken up by macrophages more easily [9]. Therefore LDL dissolubility seems to be a sensitive equilibrium disturbed by HDL deficiency and/or mechanical stress leading to LDL-aggregation and subsequently to an activation of immune cells (macrophages and T-cells).

CD8-dominated immunological reactions also are observed after 16 h of incubation following the addition of a protein transfection reagent, such as the Peqlab® Bio-Porter® reagent (Peqlab, Erlangen Germany) or the Stratagene® Biotreck® protein transfection reagent (Stratagene, USA), to human whole blood samples. According to the manufacturers' data, these transfection reagents are lipid mixtures that transport proteins into human cells. It also is possible that mechanically stressed LDL particles function as de facto transfection reagents and develop the ability to transport serum proteins into human cells.

Within nearly all human cells, intracellular proteins (or as here mostly albumin, after transfection through stressed LDL) are digested by the proteasome and presented via MHC I receptors [7]. The newly formed MHC I-antigen complex is targeted to the cell surface, where it leads to an MHC I:CD8 T-cell interaction and subsequent activation of CD8 T-lymphocytes. The proposed reaction pathways described here may provide an explanation for our results. These pathways may be important in establishing a better understanding of pathophysiologically relevant processes,

caused by LDL that is exposed to mechanical stress as a result of systemic circulation.

From clinical studies, it is well known that patients who have high blood pressure, high serum cholesterol concentrations, and especially those who suffer from both conditions, are at increased risk for arteriosclerosis. Here, we proposed and investigated a pathway whereby mechanically induced structural changes in LDL-cholesterol particles effects a subsequent immunological reaction and inflammation that is caused by the transfection of endothelial cells. This model appears to be a plausible and possible mechanism.

Likewise, a CD8-dominated immunologic reaction also results when a blood sample incurs strong mechanical damage, such as that observed when whole blood samples were subjected to hemolytic damage by strong vortexing. To this end, blood samples incurred robust cellular damage in our experiments as a result of hemolytic activity.

Cellular damage is primarily characterized by a defect in the cell membrane. Due to the defective cellular membrane, the export and release of intracellular substances and proteins into the extracellular space, as well as the crossing of extracellular substances (such as albumin) into the cell are affected. In the latter case, the extracellular components then are recognized as foreign and lead to a CD8-dominated reaction. This reaction overshadows the activation of CD4 T-cells by macrophages, which is driven by the release of intracellular components as a result of pronounced damage. This predominance also may be favored due to the fact that phagocytic cells actively clear cellular remnants, curtailing the expected CD4 reaction after pronounced damage.

When high doses of vitamin C (ascorbic acid) are administered, a patient activation of CD8 T-cells was observed. It is unknown whether this activation results from a direct influence on the T-cells or from an indirect phenomenon. Thus, ascorbic acid can enter into the cell (ascorbic acid is able to cross the membrane [11, 12]) and form antigenic epitopes inside the cells by redox reactions (ascorbic acid reacts with peptides/proteins [13, 14]).

Taken together, our results suggest a molecular explanation for the pathogenesis of arteriosclerosis in patients who have high serum cholesterol and high blood pressure. Lastly, the benefit of high doses of vitamin C remains questionable.

The result of addition of vitamin C to whole blood was unexpected. We predicted a predominance of CD4 activation, however strong CD8 activation occurred.

Generally, ascorbic acid is regarded as beneficial, and vitamin C often is regarded as being protective against arteriosclerosis. Frequently, very high doses of vitamin C are recommended for this purpose. Furthermore, vitamin C may provide some protection from oxidation of

LDL-cholesterol. Additional studies will be needed to investigate this possibility.

Here, a possible protective effect of vitamin C as a result of direct activation of T-lymphocytes was examined. Vitamin C was incubated with whole blood using physiological concentrations that develop after intake of recommended amounts of vitamin C. Activation of very few T-lymphocytes would be expected, but in fact, a pronounced activation of CD8 T-lymphocytes was detected. The question then arises as to which mechanism causes this activation of CD8 T-cells by vitamin C. Although stimulation of immune cells by vitamin C might be viewed as a beneficial effect, it is noteworthy that this also can be part of an uncontrolled excessive immune reaction. In our study, however, only the influences of pure mechanical stress on LDL-cholesterol and on whole blood samples were examined. The effect of oxidative stress was not examined in this model. Therefore, a protective effect of vitamin C regarding oxidation cannot be supported nor excluded.

References

1. Arneth B (2003) Theory of mechanical immunology. *J Mech Med Biol* 3:285–297
2. Vinereanu D (2006) Risk factors for atherosclerotic disease: present and future. *Herz* 31(Suppl 3):5–24
3. von Eckardstein A (2005) Risk factors for atherosclerotic vascular disease. *Handb Exp Pharmacol* 170:71–105
4. Braunwald E (2005) Approach to the patient with cardiovascular disease. In: Kasper DL, Braunwald E et al (eds) *Harrison's principles of internal medicine*, 16th edn. McGraw Hill, New York, pp 1358–1367
5. Kannel WB, Castelli WP, Gordon T, McNamara PM (1971) Serum cholesterol, lipoproteins, and the risk of coronary heart disease. The Framingham study. *Ann Intern Med* 1:1–12
6. Torzewski M, Suriyaphol P, Paprotka K, Spath L, Ochsenhirt V, Schmitt A, Han SR, Husmann M, Gerl VB, Bhakdi S, Lackner KJ (2004) Enzymatic modification of low-density lipoprotein in the arterial wall: a new role for plasmin and matrix metalloproteinases in atherogenesis. *Arterioscler Thromb Vasc Biol* 11:2130–2136
7. Murphy KM, Travers P, Walport M (2008) *Janeway's immunobiology*. 7th edn. Garland Sciences, New York
8. Talbot RM, del Rio JD, Weinberg PD (2003) Effect of fluid mechanical stresses and plasma constituents on aggregation of LDL. *J Lipid Res* 44:837–845
9. Khoo JC, Miller E, McLoughlin P, Steinberg D (1988) Enhanced macrophage uptake of low density lipoprotein after self-aggregation. *Arteriosclerosis* 8:348–358
10. Khoo JC, Miller E, McLoughlin P, Steinberg D (1990) Prevention of low density lipoprotein aggregation by high density lipoprotein or apolipoprotein A-1. *J Lipid Res* 31:645–652
11. Hughes RE, Maton SC (1968) The passage of vitamin C across the erythrocyte membrane. *Br J Haematol* 14:247–253
12. Lohmann W (1983) Structure of ascorbic acid and its biological function. *Eur Biophys J* 10:205–210
13. Li S, Schoneich C, Wilson GS, Borchardt RT (1993) Chemical pathways of peptide degradation. Ascorbic acid promotes rather than inhibits the oxidation of methionine to methionine sulfoxide in small model peptides. *Pharm Res* 10:1572–1579
14. Haeffner F, Smith DG, Barnham KJ, Bush AI (2005) Model studies of cholesterol and ascorbate oxidation by copper complexes: relevance to Alzheimer's disease beta-amyloid metallochemistry. *J Inorg Biochem* 99:2403–2422

Reduction of Heat Shock Protein Antibody Levels by Statin Therapy

María C. Guisasola · Elena Dulín · Jesús Almendral · Pedro García-Barreno

Received: 1 July 2008 / Accepted: 30 October 2008 / Published online: 26 November 2008
© AOCS 2008

Abstract Atherosclerosis is a disease whose pathogenesis involves inflammatory and immunological mechanisms, including an autoimmune reaction against heat shock proteins (Hsps). The purpose of this study was to analyze whether the antiatherogenic effect of statin therapy was not limited to its lipid lowering effect, but also included anti-inflammatory and immunomodulatory effects, paying special attention to the measurement of circulating concentrations of anti-Hsp70 and anti-Hsp60 antibodies previously related to vascular disease. Two-hundred and seventy-five subjects aged 40–60 years, randomly selected in an epidemiological study on the incidence of vascular risk factors, were studied. Laboratory tests included a complete lipid profile after a 12-h fast and measurements of glucose, C-reactive-protein, anti-Hsp70 and anti-Hsp60 antibodies. Subjects with hypercholesterolemia had significantly higher concentrations of anti-Hsp70 antibodies as compared to subjects with normal cholesterol concentrations. Statin therapy was associated with 11.63 and 15.3% reductions in total and LDL-cholesterol ($P = 0.005$ and

0.017, respectively) as compared to untreated subjects, and with lower concentrations of circulating anti-Hsp70 ($P = 0.016$) antibodies. No differences were found in C-reactive-protein values. Since statin therapy not only reduces lipid profile, but also anti-Hsp70 and anti-Hsp60 antibody concentrations, without changing C-reactive-protein values, it is suggested that such an effect could not be accounted for by the anti-inflammatory properties of statins, but by their direct immunomodulatory properties through their effects on lymphocyte function.

Keywords Atherosclerosis · Inflammation · Immunology · Hyperlipidemia · Cholesterol · HMG-CoA reductase

Introduction

Cardiovascular disease is the leading cause of death in most western countries [1]. Experimental and epidemiological studies and genetic forms of hypercholesterolemia have shown the association between serum cholesterol, and particularly LDL cholesterol, and atherosclerosis [2]. Hypercholesterolemia causes focal endothelial activation in large and middle-sized arteries. LDL infiltration and retention in the arterial intima starts an inflammatory response in the arterial wall [3]. LDL cholesterol reduction using lipid lowering drugs is associated to significant decreases in cardiovascular morbidity and mortality both in primary and secondary prevention [4], and therefore represents the first pharmacological target for the adult treatment panel III (ATP III) [2]. The advent of statins at the end of the 1980s and the beginning of the 1990s revolutionized treatment of hypercholesterolemia, since they were safe drugs that were administered once daily and

M. C. Guisasola (✉) · P. García-Barreno
Unit of Experimental Medicine and Surgery,
Hospital General Universitario “Gregorio Marañón”,
Dr. Esquerdo 46, 28007 Madrid, Spain
e-mail: mguisasola@mce.hggm.es

E. Dulín
Department of Clinical Biochemistry,
Hospital General Universitario “Gregorio Marañón”,
Dr. Esquerdo 46, 28007 Madrid, Spain

J. Almendral
Department of Cardiology,
Hospital General Universitario “Gregorio Marañón”,
Dr. Esquerdo 46, 28007 Madrid, Spain

decreased LDL cholesterol levels by 25–35% [5]. Statins also decreased endothelial dysfunction, had direct anti-inflammatory effects, reducing content of inflammatory cells and their production of proinflammatory cytokines in the atherosclerotic plaque [6], and even exerted immunomodulatory effects, interfering with lymphocyte T function [7].

Both adaptive and innate immunity are also involved in the etiopathogenesis of atherogenesis [8]. Specific antigens starting immune response in atherosclerosis include oxidized LDL [9], heat shock proteins (Hsps) [10], and β 2-glycoprotein I [11].

Hsps have been involved in the pathogenesis of various diseases, and their role in atherosclerosis is among the most widely studied. Special attention has been paid to Hsp60 and Hsp70 [10]. Various studies have shown Hsp60 to be selectively located in atherosclerotic lesions rather than non-atherosclerotic areas of the arterial wall [12]. In advanced atherosclerotic lesions, Hsp70 are overexpressed in different cell types such as monocytes, macrophages, dendritic cells, and smooth muscle cells. Hsps have also been identified in soluble form in serum together with anti-Hsps antibodies, and various studies have shown a correlation between levels of these antibodies and severity of atherosclerosis. Anti-Hsp70 antibody concentrations are elevated in patients with established hypertension as compared to the normotensive control group [13] in patients with abdominal aortic aneurysm or peripheral vascular disease [14]. High titers of anti-Hsp60 antibodies have been found in patients with carotid atherosclerosis, coronary disease, or stroke [15].

The aim of this study was to explore whether statins not only achieved lower total and LDL cholesterol values in treated subjects as compared to an untreated population, but could also have anti-inflammatory and immunomodulatory effects in addition to their antiatherogenic effect, by measuring the circulating concentrations of anti-Hsp70 and anti-Hsp60 antibodies previously related to vascular disease.

Methods

Study Population and Design

This was an observational, cross-sectional, epidemiological study on the incidence of vascular risk factors. Inclusion criteria: randomly selected voluntary subjects of both sexes aged 40–60 years, employees (either active or not) of the Hospital General Universitario Gregorio Marañón in January 2004, who signed the informed consent. The study was approved by the Research Committee and the Clinical Research Ethics Committee of the center. All participants provided a clinical history and answered an epidemiological

survey including age, personal and family medical history, smoking (number of cigarettes per year and smoking duration; if former smokers, number of years elapsed since smoking cessation), alcohol intake (if yes, grams of alcohol daily), treatments, and occurrence or presence of disease of atherosclerotic etiology. Blood pressure (BP) was measured, and blood was taken for the appropriate laboratory measurements. Exclusion criteria included pregnancy or breast-feeding, any systemic infection in the past 3 months, current oncological disease or radiotherapy/chemotherapy, autoimmune disease (rheumatoid arthritis, systemic lupus erythematosus, sarcoidosis), endocrine disorders (except for diabetes), liver disease, renal failure, glomerulonephritis, congenital heart disorder, oncohematological disease, or allergic disorders.

Laboratory Tests

Venous blood was drawn after a 12-h fast and centrifuged, and serum samples were frozen at -70°C for subsequent testing. In order to assess causal and conditional vascular risk factors [4], total cholesterol, HDL cholesterol, LDL cholesterol, triglycerides, and glucose were quantified in a Hitachi Modular Analytic SVA autoanalyzer, Roche Diagnostics S.L., Barcelona, Spain. C-reactive protein (CRP) was quantified using a commercial ELISA (CRP-MTPL-EIA, DRG Instruments GMBH, Marburg, Germany) according to the manufacturer's instructions. Final absorbances were measured at 450 nm (Bio-Rad 3550 Microplate Reader, Bio-Rad Laboratories, Hercules, CA, USA). Values under $5\ \mu\text{g/mL}$ were considered normal. CRP concentrations in the samples were calculated by interpolation in the standard curve obtained (range $1.62\text{--}25\ \mu\text{g/mL}$). Homocysteine has been quantified by high performance liquid chromatography (HPLC); the established reference values (P_{95}) were $13\ \mu\text{mol/L}$ for men and $11\ \mu\text{mol/L}$ for women.

Definition of Vascular Risk Factors [2, 16]

Obesity

Obesity was defined as a body mass index (BMI kg/m^2) >30 , and overweight when the BMI was >25 .

Blood Pressure

The blood pressure (BP) of all participants was measured with an automated BP recording device after an individual had been sitting quietly for 5 min. Hypertension has been defined as a systolic blood pressure $\geq 140\ \text{mmHg}$ and/or a diastolic $\geq 90\ \text{mmHg}$ in at least two measurements taken separately.

Blood Lipids

Hypercholesterolemia was defined as a fasting total cholesterol level of ≥ 200 mg/dL, or LDL-cholesterol ≥ 130 mg/dL. By hypertriglyceridemia we understand a condition in which a fasting total triglyceride level is ≥ 150 mg/dL.

Blood Glucose

Diabetes has been defined as a fasting glycemia level ≥ 120 mg/dL, or post-prandial glucose of 130–160 mg/dL.

Measurement of Circulating Anti-Hsp70 and Anti-Hsp60 Antibodies

Titers of anti-Hsp70 and anti-Hsp60 antibodies in serum (diluted 1:1,000) were measured using two commercial

enzymimmunoassays [EKS-750, Anti-Human Hsp70 (IgG/IgM/IgA) ELISA Kit and EKS-650, Anti-Human Hsp60 (total) ELISA Kit, Stressgen Biotechnologies Corporation, Victoria, Canada] in a microplate coated with recombinant human Hsp70 or Hsp60, capturing anti-Hsp70 and anti-Hsp60 antibodies present in serum. The resulting absorbance was measured at 450 nm (Bio-Rad 3550 Microplate Reader, Bio-Rad Laboratories, Hercules, CA, USA). Anti-Hsp antibody concentrations in the samples, expressed as $\mu\text{g/mL}$, were obtained by interpolating in the standard curve the absorbances obtained in the samples.

Statistical Analysis

Results were analyzed using their means, medians, standard deviations, standard error of the mean (SEM), and ranges for quantitative variables, and using absolute frequencies and percentages for qualitative variables with a

Table 1 Characteristics of normocholesterolemic and hypercholesterolemic subjects

	Normocholesterolemic patients ($n = 116$)				Hypercholesterolemic patients ($n = 159$)				P^*
Anti-Hsp70 antibodies ($\mu\text{g/mL}$)	392.53 \pm 23.13				451.33 \pm 21.50				0.049
Patients under no treatment	404.27 \pm 24.34 ($n = 101$)				466.87 \pm 22.48 ($n = 140$)				0.041
Anti-Hsp60 antibodies ($\mu\text{g/mL}$)	57.99 \pm 5.84				49.94 \pm 3.48				NS
Age	47.66 \pm 0.75				49.36 \pm 0.48				NS
Sex									
Females	52				82				NS
Males	64				77				
Total cholesterol (mg/dL)	179.59 \pm 2.03				233.96 \pm 1.91				<0.001
LDL-cholesterol (mg/dL)	100.23 \pm 3.11				146.48 \pm 1.98				<0.001
HDL/LDL	0.63 \pm 0.02				0.047 \pm 0.01				<0.001
Blood glucose (mg/mL)	90.00 \pm 1.53				89.84 \pm 1.03				NS
Triglycerides (mg/mL)	107.11 \pm 5.77				115.98 \pm 5.47				NS
Homocysteinemia (mmol/L)	9.37 \pm 0.71				8.77 \pm 0.24				NS
CRP ($\mu\text{g/mL}$)	4.55 \pm 0.75				4.50 \pm 0.59				NS
Hypertension									
Yes	21				37				NS
No	95				122				
Smoking ^a									
Degree	0	1	2	3	0	1	2	3	NS
Number	89	17	10	0	109	35	17	1	
Alcohol intake ^b									
Degree	0	1	2	3	0	1	2	3	NS
Number	77	33	6	0	96	55	7	1	

Results given as mean \pm SEM

Hsp heat shock proteins, *CRP* C-reactive protein

* Referring to the effect of treatment on parameters analyzed in the Mann–Whitney test for two independent samples or an ANOVA test with Bonferroni correction

^a Smoking degree: 0: non-smoker; 1: 0–20 cigarettes/day; 2: 20–40 cigarettes/day; 3: >40 cigarettes/day

^b Alcohol intake degree: 0: none or less than 20 g of alcohol/day; 1: 20–40 g of alcohol/day; 2: 40–80 g of alcohol/day; 3: >80 g of alcohol/day

95% confidence interval. Variable means were compared using non-parametric tests. A Mann–Whitney's *U* test for two independent samples, a one-way ANOVA test with Bonferroni correction for three independent samples, or a Kruskal–Wallis test was used for quantitative variables. Qualitative variables were analyzed using a Spearman's correlation test. The statistical significance level selected was $P < 0.05$. SPSS 12.0 software for Windows was used for statistical analysis.

Results

A total of 275 subjects were included in the study, 134 females (age 48.95 ± 0.57 years) and 141 males (48.35 ± 0.62). Of these, 159 participants (57.8%) [82 females (51.57%) and 77 males (48.42%)] had total cholesterol levels higher than 200 mg/dL or LDL cholesterol levels higher than 130 mg/dL.

Hypercholesterolemic individuals had significantly higher titers of circulating anti-Hsp70 antibodies (451.32 ± 21.5 $\mu\text{g/mL}$) as compared to subjects with

normal cholesterol levels (392.53 ± 23.13 $\mu\text{g/mL}$) ($P < 0.05$, Mann–Whitney's test), with no differences between both groups in the incidence of other population (age, sex, and social level) or vascular risk factors (glucose, hypertension, triglyceridemia, homocysteinemia and CRP, smoking, alcohol intake and its extent). Both effects, hypercholesterolemia and titers of anti-Hsp70i antibodies, therefore appear to be directly related and not influenced by other potential factors acting on such antibodies (Table 1).

Thirty-four subjects (11 females and 23 males) were being treated with simvastatin 10 mg/day at the time of the study. This treatment was associated to a significant 11.63% lower total cholesterol levels ($P = 0.013$, Mann–Whitney's test) and a 11.07% LDL cholesterol levels as compared to subjects with no statin therapy ($P = 0.011$, Mann–Whitney's test). Patients treated with simvastatin also showed higher glucose, triglyceride, BP, and CRP values (Table 2), probably due to the presence of additional vascular risk factors [4]. In this latter case, when population was segmented based on the degree of vascular risk according to the Task Force [16] or considering the cases of established atherosclerosis, statin therapy caused no

Table 2 Differences between subjects with or without statin therapy at the time of study

	Patients with treatment ($n = 34$)				Patients without treatment ($n = 241$)				<i>P</i> *
Total cholesterol (mg/dL)	197.15 \pm 6.1				212.98 \pm 2.26				0.013
LDL cholesterol (mg/dL)	113.79 \pm 5.60				129.07 \pm 2.14				0.011
Anti-Hsp70 antibodies ($\mu\text{g/mL}$)	330.84 \pm 34.43				440.57 \pm 17.30				0.016
Anti-Hsp60 antibodies ($\mu\text{g/mL}$)	43.26 \pm 5.23				54.84 \pm 3.58				NS
Sex									
Females	11				123				0.042
Males	23				118				
Blood glucose (mg/mL)	98.82 \pm 3.74				88.65 \pm 0.89				0.002
Triglycerides (mg/mL)	133.44 \pm 10.842				109.26 \pm 4.27				0.005
Homocysteinemia (mmol/L)	9.44 \pm 0.74				8.93 \pm 0.36				NS
CRP ($\mu\text{g/mL}$)	7.42 \pm 1.68				4.12 \pm 0.47				0.04
Hypertension									
Yes	12				46				0.30
No	22				195				
Smoking ^a									
Degree	0	1	2	3	0	1	2	3	NS
Number	21	11	2	0	177	38	25	1	
Alcohol intake ^b									
Degree	0	1	2	3	0	1	2	3	NS
Number	21	11	2	0	152	77	11	1	

Results given as mean \pm SEM

Hsp heat shock proteins, CRP C-reactive protein

* Referring to the effect of treatment on parameters analyzed in the Mann–Whitney test for two independent samples or an ANOVA test with Bonferroni correction

^a Smoking degree: 0: non-smoker; 1: 0–20 cigarettes/day; 2: 20–40 cigarettes/day; 3: >40 cigarettes/day

^b Alcohol intake degree: 0: none or less than 20 g of alcohol/day; 1: 20–40 g of alcohol/day; 2: 40–80 g of alcohol/day; 3: >80 g of alcohol/day

Table 3 Differences in CRP between subjects with or without statin therapy by vascular risk (Task Force [16])

Group	Patients with treatment (n = 34)	Patients without treatment (n = 241)	P*
No VRF			0.918
N	5	141	
CRP (µg/mL)	2.83 ± 1.93	2.59 ± 0.44	
Moderate VRFs (10%)			0.722
N	12	80	
CRP (µg/mL)	5.34 ± 2.56	5.35 ± 0.93	
Established atherosclerosis			0.845
N	17	20	
CRP (µg/mL)	10.11 ± 2.64	10.26 ± 2.60	

Results given as mean ± SEM

CRP C-reactive protein, VRF vascular risk factors

* Referring to the effect of treatment on parameters analyzed in the Mann–Whitney test for two independent samples

significant changes in CRP concentrations (Table 3). However a significant trend to a lowering in the concentration of anti-Hsp70i antibodies in individuals with VRF or established atherosclerosis has been proven ($P = 0.024$, Kruskal–Wallis test). Patients with atherosclerosis show the lowest levels of circulating anti-Hsp70i antibodies [($P = 0.008$, Mann–Whitney test). Hsp70i is the inducible form of the HSP70 family and is also known as Hsp72, based on its molecular weight [17]. Therapy with statins reduces anti-Hsp70i antibodies concentrations significantly in patients with VRF and atherosclerosis in comparison to an identical group of patients without such therapy ($P = 0.043$, one-way ANOVA) (Table 4).

Treatment with simvastatin was very significantly associated with lower concentrations of circulating anti-Hsp70 antibodies ($P = 0.016$, Mann–Whitney's test). In order to rule out the potential effect of other population and vascular risk factors on the decrease in concentrations of circulating anti-Hsp70 antibodies seen in the statin-treated group, the potential association between such factors and anti-Hsp antibodies was tested in the study population.

Table 4 Differences in Anti-Hsp70 antibodies concentration (µg/mL) between subjects with or without statin therapy according to the degree of vascular risk (Task Force [16])

Group	Global	Patients with treatment	Patients without treatment	P*	P**
No VRF	458.72 ± 21.52 (n = 146)	510.65 ± 127.89 (n = 5)	456.87 ± 21.90 (n = 141)	0.024	0.043
Moderate VRFs (10–20%)	414.36 ± 27.99 (n = 92)	372.85 ± 44.77 (n = 12)	420.66 ± 31.54 (n = 80)		
Established atherosclerosis	349.93 ± 41.27 (n = 37)	265.95 ± 43.85 (n = 17)	421.31 ± 31.35 (n = 20)		

Results are given as means ± SEM

VRF vascular risk factors

* P refers to anti-HSP70i Abs level and their relevance in vascular disease (Kruskal–Wallis test)

** P refers to the effects of the treatment on Anti-Hsp70i Abs concentration in the different groups analyzed by the Anova-one-way test

Circulating concentrations of anti-Hsp70i antibodies in the overall population were not associated with factors such as age, sex, blood glucose, triglycerides, BP, homocysteinemia, or CRP (Table 5).

Discussion

Monocytes–macrophages and T lymphocytes are involved in atherosclerosis, a chronic inflammatory disease. Hsps are immunomodulatory molecules that act as potent autoantigens. Hsps recognition by T lymphocytes would trigger an autoimmune response potentially involved in the inflammatory etiopathogenesis of atherosclerosis [18]. The finding of a significant increase in anti-Hsp70 antibody concentrations in hypercholesterolemic patients as compared to normocholesterolemic subjects in age- and sex-matched populations, in the absence of a hypothetical etiopathogenetic role of other associated vascular risk factors, agrees with reports by other authors [19]. This could be explained by an enhanced immunoactivation status associated to atherosclerosis in this group. High cholesterol levels not only activate or damage endothelium per se but may modulate the function of T and B cells. Cholesterol has been shown to increase the antigen presentation function of monocytes, and oxidized LDL may activate dendritic cells and promote in vitro the proliferation of T lymphocytes mediated by dendritic cells [20].

Both the recommendations by the National Cholesterol Education Program [2] and those derived from the Second Joint Task Force of European societies [16] emphasize the need for controlling individual risk of coronary disease. Dyslipidemia is clearly a major risk factor for coronary disease, though it is often modulated by the presence of other additional risk factors. Both recommendations state that reduction of LDL cholesterol levels represents a recognized target, essential for reducing coronary risk. Drugs affecting lipoprotein metabolism include HMG-CoA reductase inhibitors (statins), fibrates, bile acid sequestrants (resins), and nicotinic acid and its derivatives. They have all been shown to decrease coronary disease progression in

Table 5 List of populational and biochemical parameters and anti-Hsp70 antibody levels in a randomly selected general population Anti-Hsp70 antibodies ($\mu\text{g/mL}$)

					<i>P</i> *
Sex					
Females (<i>n</i> = 134)	435.55 ± 22.07				NS
Males (<i>n</i> = 141)	418.88 ± 22.83				
Age					
40–44	375.65 ± 26.4				NS
45–49	465.62 ± 31.6				
50–54	432.04 ± 40.02				
55–60	448.56 ± 37.28				
Blood glucose (mg/mL)					
Normoglycemic	428.32 ± 16.83				NS
Hyperglycemic	411.86 ± 44.55				
Triglycerides (mg/mL)					
Normotriglyceridemia	432.46 ± 17.38				NS
Hypertriglyceridemia	394.94 ± 38.79				
Hypertension					
No	436.47 ± 18.93				NS
Yes	391.55 ± 25.16				
Homocysteinemia (mmol/L)					
Normal	419.56 ± 16.92				NS
Hyperhomocysteinemia	455.32 ± 42.09				
Smoking ^a					
Degree	0	1	2	3	NS
Number	198	48	27	1	
Anti-Hsp70 Abs ($\mu\text{g/mL}$)	435.96 ± 18.51	446.92 ± 35.41	518.41 ± 53.79	10,900	
Alcohol intake ^b					
Degree	0	1	2	3	NS
Number	173	88	13	1	
Anti-Hsp70 Abs ($\mu\text{g/mL}$)	420.82 ± 8.78	434.09 ± 31.76	458.65 ± 69.44	460.86	
CRP ($\mu\text{g/mL}$)					
Females (<i>n</i> = 134)	4.56 ± 0.72				NS ^c
Males (<i>n</i> = 141)	4.49 ± 0.60				
Anti-Hsp60 antibodies ($\mu\text{g/mL}$)					
Females (<i>n</i> = 134)	52.57 ± 4.47				NS ^c
Males (<i>n</i> = 141)	54.22 ± 4.61				

Results given as mean ± SEM

Hsp heat shock proteins, *CRP* C-reactive protein

* Referring to the effect of treatment on parameters analyzed in the Mann–Whitney test for two independent samples or an ANOVA test with Bonferroni correction

^a Smoking degree: 0: non-smoker; 1: 0–20 cigarettes/day; 2: 20–40 cigarettes/day; 3: >40 cigarettes/day

^b Alcohol intake degree: 0: none or less than 20 g of alcohol/day; 1: 20–40 g of alcohol/day; 2: 40–80 g of alcohol/day; 3: >80 g of alcohol/day

^c Spearman's correlation coefficient

angiographic studies. However, both the most convincing angiographic evidence and the best evaluation criteria in clinical trials have been obtained using statins [21]. These drugs are also the safest to date and the easiest to use. Thus, statins currently are the first-choice lipid lowering drugs [22].

The antiatherogenic effect of statins is not limited to their effects on the reduction of circulating total and LDL cholesterol levels. This study has shown that patients treated with simvastatin not only had significantly lower total and LDL cholesterol levels, but also showed significant lower anti-Hsp70 antibody concentrations and

relevant but not statistically significant lower anti-Hsp60 concentrations which agrees with reports from similar studies [23]. Since anti-Hsp antibodies are positively related to the risk of vascular disease and involved in the etiopathogenesis of atherosclerosis, their reduction may decrease the chronic inflammation characteristic of atherosclerosis and contribute to stabilization of the atherosclerotic plaque. The mechanism by which statin therapy is associated to a decrease in circulating anti-Hsp antibodies could be the pleiotropic effects of these drugs, including immunomodulation, that are independent from the decrease in cholesterol levels, as also shown in this study. Statins have also been shown to be able to inhibit binding of the lymphocyte function-associated antigen-1 (LFA-1) to the intercellular adhesion molecule-1 (ICAM-1), thereby preventing leukocyte adhesion and extravasation at inflammation sites, as well as antigen presentation, and lymphocyte T costimulation [24]. This would explain the significant lower circulating anti-Hsp70 antibodies detected in the group of treated subjects.

The immunosuppressant effect of statins is not only independent of their lipid lowering effect, but also of their documented anti-inflammatory properties, resulting from a decreased activation of the nuclear factor kappa B (NF- κ B) that induces expression of multiple proinflammatory molecules [25]. Since statin therapy reduced not only the lipid profile, but also circulating concentrations of anti-Hsp70 and anti-Hsp60 antibodies without changing—even in patients with established atherosclerotic disease—CRP concentrations, a systemic inflammation marker attributed by some authors to an active role not only in the onset of atherosclerosis, but also as a biomarker of its course and prognosis [26], it is suggested that such an effect cannot be completely explained by its anti-inflammatory effects, but by its direct immunomodulatory properties.

Acknowledgments The authors thank Mrs. Maria Jesús Sánchez for her invaluable help in sample processing. The study was supported by the FIS grant 13/0318 and Fundación Mutua Madrileña.

References

1. Grau M, Marrugat J (2008) Risk functions and the primary prevention of cardiovascular disease. *Rev Esp Cardiol* 61:404–416
2. Executive summary of the third report of the National Cholesterol Education Program (NCEP) (2001) Expert panel on detection, evaluation and treatment of high blood cholesterol in adults (adult treatment panel III). *JAMA* 285:2486–2497
3. Skalen K, Gustafsson M, Ryderg EK, Hultén LM, Wiklund O, Innerarity TL, Borén J (2002) Subendothelial retention of atherogenic lipoproteins in early atherosclerosis. *Nature* 417:750–754
4. Lahoz C, Mostaza JM (2007) La aterosclerosis como enfermedad sistémica. *Rev Esp Cardiol* 60:184–195
5. Jones PH (2001) Cholesterol: precursor to many lipid disorders. *Am J Manag Care* 7:S289–S298
6. Alvarez-Sala LA, Calderon M (2004) Colesterol, inflamación y aterosclerosis: efectos antiinflamatorios de las estatinas. *Rev Clin Esp* 204:18–29
7. Weitz-Schmidt G (2003) Lymphocyte function-associated antigen-1 blockade by statins: molecular basis and biological relevance. *Endothelium* 10:43–47
8. Jara LJ, Medina G, Vera-Lastra O, Amigo MC (2006) Accelerated atherosclerosis, immune response and autoimmune rheumatic diseases. *Autoimmun Rev* 5:195–201
9. Binder CJ, Hartvigsen K, Chang M-K, Miller M, Brode D, Palinski W et al (2004) IL-5 links adaptive and natural immunity specific for epitopes of oxidized LDL and protects from atherosclerosis. *J Clin Invest* 114:427–437
10. Mehta TA, Greenman J, Ettalaie C, Venkatasubramanian A, Chetter IC, McCollum PT (2005) Heat shock proteins in vascular disease. A review. *Eur J Vasc Endovasc Surg* 29:395–402
11. George J, Harats D, Gilburd B, Afek A, Shaish A, Kopolovic J et al (2000) Adoptive transfer of beta (2)-glycoprotein I-reactive lymphocytes enhances early atherosclerosis in LDL receptor-deficient mice. *Circulation* 102:1822–1827
12. Kol A, Sukhova GK, Lichtman AH, Libby P (1998) Chlamydial heat shock protein 60 localizes in human atheroma and regulates macrophage tumor necrosis factor- α and matrix metalloproteinase expression. *Circulation* 98:300–307
13. Pockley AG, De Faire U, Kiessling R, Lemne C, Thulin T, Frostegard J (2002) Circulating heat shock proteins and heat shock proteins antibodies in established hypertension. *J Hypertens* 20:1815–1820
14. Chan YC, Shukla N, Abdus-Samee M, Berwanger CS, Stanford J, Singh M M et al (1999) Anti-heat-shock protein 70 kDa antibodies in vascular patients. *Eur J Vasc Endovasc Surg* 18:381–385
15. Mandal K, Jahangiri M, Xu Q (2004) Autoimmunity to heat shock proteins in atherosclerosis. *Autoimmun Rev* 3:31–37
16. Task Force Report (1998) Prevention of coronary disease in clinical practice. Recommendations of the Second Joint Task Force of European, other societies on coronary prevention. *Eur Heart J* 19:1434–1503
17. Kampinga HH, Hageman J, Vos MJ, Kubota H, Tanguay RM, Brudford EA, et al (2008) Guideline for the nomenclature of the human heat shock proteins. *Cell Stress Chaperones*. doi: 10.1007/s12192-008-0068-7
18. Greaves DR, Channon KM (2002) Inflammation and immune responses in atherosclerosis. *Trends Immunol* 23:535–541
19. Ghayour-Mobarhan M, Lamb DJ, Lovell DP, Livingstone C, Wang T, Ferns GAA (2005) Plasma antibody titres to heat shock proteins-60, -65 and -70: their relationship to coronary risk factors in dyslipidaemic patients and healthy individuals. *Scand J Clin Lab Invest* 65:601–614
20. Lamb DJ, Tickner ML, Dreux AC, El-Sankary W, Hourani SMO, Eales-Reynolds LJ, Ferns GAA (2004) Impairment of vascular function following BCG immunisation is associated with immune responses to HSP-60 in the cholesterol-fed rabbit. *Atherosclerosis* 172:13–20
21. EUROASPIRE II Study Group (2001) Lifestyle and risk factor management and use of drug therapies in coronary patients from 15 countries: principal results from EUROASPIRE II Euro Heart Survey Programme. *Eur Heart J* 22:557–572
22. Gotto AM Jr, LaRosa JC (2005) The benefits of statin therapy—what questions remain? *Clin Cardiol* 28:499–503
23. Shin YO, Bae JS, Lee JB, Kim JK, Kim YJ, Kim C, Ahn JK et al (2006) Effect of cardiac rehabilitation and statin treatment on anti-Hsp antibody titers in patients with coronary artery disease after percutaneous coronary intervention. *Int Heart J* 47:671–682
24. Weitz-Schmidt G, Welzenbach K, Brinkmann V, Kamata T, Kallen J, Bruns C et al (2001) Statins selectively inhibit leukocyte

- function antigen-1 by binding to a novel regulatory integrin site. *Nat Med* 7:687–692
25. Ortego M, Bustos C, Hernández-Presa MA, Muñón J, Díaz C, Hernández G et al (1999) Atorvastatin reduces NF- κ B activation and chemokine expression in vascular smooth muscle cells and mononuclear cells. *Atherosclerosis* 147:253–261
26. Taubes G (2002) Cardiovascular disease. Does inflammation cut to the heart of the matter? *Science* 296:242–245

Fatty Acid Biomarkers of Symbionts and Unusual Inhibition of Tetracosapolyenoic Acid Biosynthesis in Corals (Octocorallia)

Andrey B. Imbs · Darya A. Demidkova ·
Tatyana N. Dautova · Nikolay A. Latyshev

Received: 2 September 2008 / Accepted: 31 October 2008 / Published online: 26 November 2008
© AOCS 2008

Abstract Seven zooxanthellae-free species of octocorals (the genera *Acanthogorgia*, *Acabaria*, *Chironephthya*, *Echinogorgia*, *Menella*, *Ellisella*, and *Bebryce*) and two zooxanthellate octocorals (the genera *Paralemnalia* and *Rumphella*) were examined to elucidate their fatty acid (FA) composition. Arachidonic (about 40% of the total FA) and palmitic acids were predominant in all the species studied. Seven furan FA (F-acids) (up to 9.7%) were identified in the azooxanthellate octocorals. The main F-acids were 14,17-epoxy-15-methyldocosa-14,16-dienoic and 14,17-epoxy-15,16-dimethyldocosa-14,16-dienoic acids. In all specimens of *Bebryce studeri*, C_{25–28} demospongiac FA (about 20%) were identified. These FA reflect the presence of a symbiotic sponge in *B. studeri* and can be used as the specific markers for other corals. A significant difference ($P < 0.01$) between azooxanthellate and zooxanthellate corals was found for odd-chain and methyl-branched saturated FA, 18:1n-7, and 7-Me-16:1n-10; that indicated the presence of an advanced bacterial community in azooxanthellate corals. The zooxanthellate species were distinguished by significant amounts of 18:3n-6, 18:4n-3, and 16:2n-7 acids, which are proposed as the markers of zooxanthellae in soft corals. Contrary to the normal level of 24:5n-6 (9.4%) and 22:4n-6 (0.6%), unexpected low concentrations of 24:5n-6 (0.4%) accompanied by a high content of 22:4n-6 (up to 11.9%) were detected in some specimens. The presence of an

unknown factor in octocorals, specific for n-6 PUFA, which inhibited elongation of 22:4n-6 to 24:4n-6, is conjectured.

Keywords Fatty acids · Octocorallia · Corals · Zooxanthellae · Symbionts · Tetracosapolyenoic acids · Furan acids · Demospongiac acids

Abbreviations

ECL	Equivalent chain length
F-acids	Furan fatty acids
FA	Fatty acids
FAME	Fatty acid methyl esters
GC	Gas chromatography
GC-MS	Gas chromatography–mass spectrometry
PUFA	Polyunsaturated fatty acids
TLC	Thin-layer chromatography
VLC	Very-long-chain

Introduction

Corals are polytrophic organisms, i.e. they simultaneously derive nutrients from various food sources, including the uptake of different classes of plankton and organic detritus [1–3]. In zooxanthellate coral species (zooxanthellae are endosymbiotic dinoflagellates of the *Symbiodinium* group), the phototrophic supply is delivered by symbiotic dinoflagellates living within gastrodermal host cells [4]. Filamentous algae colonize the skeletons in a variety of zooxanthellate and azooxanthellate scleractinian species [5]. A lot of bacteria associate with corals [6, 7]. All the food sources and the members of a whole coral colony mentioned above have different FA profiles and make their significant contributions to the total FA composition of corals. So, FA can serve as markers for a type of symbiotic

A. B. Imbs (✉) · D. A. Demidkova · T. N. Dautova ·
N. A. Latyshev
Laboratory of Comparative Biochemistry,
A. V. Zhirmunsky Institute of Marine Biology,
Far Eastern Branch of the Russian Academy of Sciences,
Palchevskogo str., 17, 690041 Vladivostok, Russia
e-mail: andreyimbs@hotmail.com

zooxanthellae [8]. The active transport of saturated and several unsaturated FA from zooxanthellae to the host is documented [9–13]. FA are most probably indicative of external food sources such as zoo- and phytoplankton [14]. The FA composition of corals is useful for the chemotaxonomic studies of reef-building and soft corals; and a clear division of coral specimens according to their family (sometimes, to their genus) has been consequently attained [15, 16].

A majority of investigations on the FA composition of corals have been performed on reef-building species. In general, octocorals exist in similar habitats as scleractinian corals but are able to tolerate a slightly wider range of conditions. For example, gorgonians survive in conditions where the temperature is between 19 °C and 36 °C (with a few exceptions). Studies of FA in soft corals have not so far been systematic, and data on the FA contents of total lipids of the corals, especially of gorgonian corals, are limited [17–24]. Only a few works describe the FA of symbiotic dinoflagellates of the reef-building corals [8, 11, 13, 25]. Data on the FA composition of zooxanthellae from soft corals have not been available until now. Nevertheless, it has been recently shown that the absence of an important lipid source, such as symbiotic dinoflagellates, leads to a significant difference in FA compositions between azooxanthellate and zooxanthellate soft corals [24].

Lipids of soft corals contain a large portion of unusual very-long-chain tetracosapolyenoic FA. Both 24:6n-3 and 24:5n-6 have been detected in the lipids of different octocorals [19, 20, 26]. It is noteworthy that the *Hexacorallia* species have no 24:6n-3 and 24:5n-6 acids; that is their main chemotaxonomic distinction from the *Octocorallia* species [19]. An investigation has recently been carried out on mammalian tissues and concluded that the tetracosahexaenoic FA are intermediates in the biosynthesis of C₂₂ Δ⁴ polyunsaturated fatty acids (PUFA) [27, 28]. Therefore, it is very likely that the *Octocorallia* species utilize a similar biosynthetic route, thus providing yet another interesting system for studying this type of biogenesis [29].

In our study, the FA composition of total lipids of nine octocoral species were examined to determine: (1) significant differences in the FA composition between zooxanthellate and azooxanthellate species; (2) the marker FA of organisms associated with corals; and (3) the distribution of tetracosapolyenoic FA and their biosynthetic intermediates.

Experimental Procedures

Nine soft coral species (Table 1) were collected by SCUBA in the South China Sea (Vietnam) in the Nha Trang Bay at depths of 2–4 m in November–December

2005, and one sample of *Bebryce studeri* was taken near Den Island (12°35'N, 109°18'E) at a 9-m depth in January 2005. The species identification was carried out under a light microscope (×200–400 magnification) using the arrangement of sclerites. The colonies were carefully cleaned of all noncoral debris. The samples collected were placed immediately into tanks under water at the collection site and transported to the laboratory within 0.5 h. Up to four different colonies of one species were used for a FA analysis.

The coral samples were crushed into 1–3 mm pieces, and total lipids were extracted by intensive homogenization in a chloroform/methanol (1:2, by vol.) mixture (30 ml for 10 g of coral weight). The homogenate obtained was filtered, and the residue was repeatedly extracted (6 h, 4 °C) in a chloroform/methanol (2:1, by vol.) mixture (2 × 30 ml). The extracts were then mixed and separated into layers by adding 35 ml of water and 30 ml of chloroform. The lower layer was evaporated, and the total lipids obtained were redissolved in chloroform and stored at –18 °C.

Fatty acid methyl esters (FAME) were obtained by a sequential treatment of the total lipids with 1% sodium methylate/methanol and 5% HCl/methanol according to Carreau and Dubacq [30] and purified by preparative silica gel thin-layer chromatography (TLC), using the precoated silica gel plates Sorbfil PTLC-AF-V (Sorbfil, Krasnodar, Russia) developed in benzene. *N*-acylpyrrolidide derivatives of FA were prepared according to Andersson [31] by direct treatment of the FAME with pyrrolidine/acetic acid (10:1, by vol.) in a capped vial (1 h, 100 °C) followed by ethereal extraction from the acidified solution and purification by preparative TLC developed in ethyl acetate.

A gas chromatography (GC) analysis of FAME was carried out on a Shimadzu GC-17A chromatograph (Shimadzu, Kyoto, Japan) with a flame ionization detector. A Supelco MDN-5S (Bellefonte, PA) capillary column (bonded and crosslinked (5% phenyl) methylpolysiloxane; 30 m × 0.25 mm i.d.) was used at 160 °C with a 2 °C/min ramp to 270 °C held for 30 min. The injector and detector temperatures were 270 °C. Helium was used as the carrier gas at a linear velocity of 30 cm/s (split ratio was 1:30). FAME were identified by a comparison with authentic standards (a mixture of PUFA methyl esters No. 3 from Menhaden oil was purchased from Supelco, Bellefonte, PA) and with the use of a table of equivalent chain-lengths (ECL) [32]. The structures of FA were confirmed by gas chromatography–mass spectrometry (GC–MS) of their methyl esters and *N*-acylpyrrolidide derivatives. GC–MS of FAME was performed with a Shimadzu GCMS-QP5050A instrument (Shimadzu, Kyoto, Japan). Ionization of samples was undertaken by electron impact at 70 eV. Helium was used as the carrier gas at a linear velocity of 30 cm/s (split ratio was 1:10). The Supelco MDN-5S was

Table 1 Fatty acid composition (% of total FAs) of total lipids of octocorals

Fatty acids	<i>Acabaria erithraea</i>	<i>Acanthogorgia isoxia</i>			<i>Chironephthya variabilis</i>			<i>Echinogorgia sp.</i>	<i>Ellisella plexauroides</i>			<i>Menella praelonga</i>			<i>Paralemmalia thyrsoides^a</i>		<i>Rumphella aggregata^a</i>	
14:0	0.8	1.7	1.6	1.4	2.0	1.8	1.5	2.9	1.5	1.0	1.5	1.2	0.6	1.3	4.5	3.5	2.0	1.2
i-15:0	–	–	–	–	–	0.1	–	–	–	–	–	–	–	–	–	–	–	–
ai-15:0*	–	0.1	0.1	0.1	0.1	0.1	0.1	0.2	–	0.1	0.1	–	–	0.1	–	–	–	–
15:0	0.4	0.7	0.8	0.9	0.8	0.5	0.9	0.9	0.6	0.4	0.5	0.5	0.2	0.8	0.2	0.5	0.3	0.1
16:2n-7	–	–	–	–	–	–	–	–	–	–	–	–	–	–	–	–	2.8	1.6
ai-16:0*	0.2	0.2	0.2	0.2	0.1	0.3	0.2	–	0.2	0.2	0.2	0.2	–	0.2	–	–	–	–
16:1n-9	0.5	0.4	0.5	0.1	0.2	0.3	1.6	1.0	2.1	0.2	0.4	0.3	–	0.1	–	1.5	0.2	0.2
16:1n-7	1.1	1.3	1.9	3.1	2.0	1.5	1.0	1.6	0.4	1.1	1.7	1.5	1.1	3.0	1.0	0.7	3.0	2.3
16:1n-5	0.5	0.2	–	0.8	0.3	0.3	0.2	–	–	0.3	0.3	0.3	–	0.6	0.1	–	–	0.2
16:0*	7.5	10.9	10.1	14.6	10.6	12.2	10.4	14.0	9.9	7.6	9.2	9.0	2.4	15.1	27.8	19.6	33.4	32.5
7-Me-16:1n-10	1.4	1.6	2.6	1.7	6.7	1.8	1.7	2.9	3.3	2.2	2.1	2.9	1.7	1.7	0.2	0.2	2.3	3.1
i-17:0*	0.1	0.3	0.6	0.7	0.7	0.5	0.5	0.5	1.0	0.7	0.5	0.8	–	0.8	0.2	–	–	–
2-Me-16:0	0.1	0.2	–	0.1	–	0.1	–	–	–	–	–	–	–	0.2	–	0.1	0.5	0.3
ai-17:0*	0.2	0.2	0.1	0.2	–	0.2	0.2	–	0.3	0.2	0.2	0.3	–	0.3	–	–	–	–
17:0*	0.6	0.9	0.7	1.8	0.7	0.8	1.0	0.9	1.2	1.5	1.3	1.1	–	2.0	0.3	0.3	0.1	0.1
18:3n-6	–	0.1	0.1	0.1	–	–	–	–	–	–	–	–	–	0.1	8.7	8.7	1.4	0.8
18:4n-3	0.4	0.1	0.1	0.3	–	0.1	–	–	0.1	0.2	0.1	0.1	0.5	0.2	1.8	3.9	3.0	1.3
br-18:0*	0.3	0.1	0.1	0.1	–	0.2	0.2	–	0.2	0.2	0.3	0.3	–	0.2	–	–	–	–
18:2n-9*	–	–	–	–	–	–	0.2	–	–	–	–	–	–	0.3	0.3	0.5	0.5	–
18:2n-7	–	–	–	–	–	–	–	–	–	–	–	–	–	–	–	–	2.6	1.9
18:2n-6	0.9	0.9	0.8	1.4	0.7	2.4	1.0	0.7	0.6	0.9	1.2	0.8	0.3	1.4	1.7	1.4	0.8	0.5
18:1n-9	2.4	3.9	2.2	3.7	2.4	6.7	3.0	3.1	2.4	2.5	3.1	2.0	0.5	3.9	3.6	3.1	3.5	4.2
18:1n-7*	1.9	1.1	1.5	3.8	1.8	1.8	1.3	2.2	1.8	2.5	3.3	1.2	0.5	4.1	0.2	0.1	0.4	0.3
18:0	6.5	6.3	4.5	7.7	5.3	5.7	6.4	5.3	5.1	8.8	8.3	6.1	0.9	8.9	12.4	8.6	8.2	11.0
ai-19:0*	0.1	–	–	–	–	0.1	–	–	–	0.1	–	0.1	–	0.1	–	–	–	–
Me-F18	2.7	–	–	–	0.5	–	–	–	0.5	0.1	–	0.3	1.0	–	–	–	–	–
19:0*	0.3	0.3	0.3	0.5	–	0.3	0.3	–	0.2	0.5	0.4	0.4	–	0.6	0.1	0.1	–	0.1
20:4n-6	37.2	43.7	48.2	24.4	34.9	40.2	46.2	47.6	42.3	37.3	38.3	40.6	57.0	21.5	22.4	28.7	13.8	12.5
20:5n-3	1.7	4.9	3.5	1.4	2.5	2.0	1.2	2.2	2.6	1.3	2.0	2.7	7.4	0.9	1.9	3.6	2.6	1.5
20:3n-6	0.4	0.4	–	1.4	–	0.3	0.3	0.2	0.2	0.5	0.3	–	–	1.4	0.4	0.5	1.6	1.1
20:4n-3	0.3	0.2	0.1	0.5	–	0.2	–	0.2	–	0.3	0.5	0.1	0.3	0.4	–	0.1	0.7	0.5
20:2n-6	0.4	–	–	0.5	–	0.1	–	–	–	0.2	0.2	–	–	0.6	–	–	–	0.1
20:1n-9	0.4	0.4	1.0	1.3	0.6	0.3	0.6	–	–	0.6	0.5	0.3	–	1.6	0.2	–	0.4	0.4
20:1n-7*	0.2	–	0.5	0.5	–	0.2	0.3	–	–	0.4	0.7	–	–	0.6	–	–	–	0.1
diMe-F18-3	–	–	–	–	0.7	–	–	–	0.8	–	–	0.4	–	–	–	–	–	–
20:0	0.3	0.3	0.6	0.7	0.3	0.3	0.4	–	0.3	0.6	0.3	0.4	–	0.8	0.9	0.7	5.3	8.1
Me-F20*	–	–	–	–	0.9	0.3	0.3	–	0.4	1.0	–	0.5	0.6	–	–	–	–	–
21:0	–	–	0.1	0.3	–	0.1	–	–	0.1	0.3	–	0.2	0.1	0.4	0.1	0.1	0.2	0.3
22:5n-6	5.7	0.4	0.2	2.8	0.5	0.8	0.8	0.2	0.3	1.2	1.2	0.4	0.4	3.0	–	–	0.1	0.1
22:6n-3	3.9	1.6	0.8	5.2	1.5	1.4	1.2	0.8	1.6	3.2	3.9	1.3	1.8	4.7	2.3	2.6	1.8	1.4
22:4n-6	0.6	0.5	0.4	10.6	0.4	0.3	1.4	0.4	0.4	14.7	11.8	0.5	0.7	10.6	0.1	0.2	0.7	0.6
22:5n-3	0.3	0.2	0.1	–	–	0.1	0.1	–	0.1	0.5	0.7	0.1	–	0.6	–	–	–	–
22:3n-6	–	–	–	0.5	–	–	–	–	–	–	–	–	–	0.5	–	–	0.1	0.1
diMe-F20*	–	–	–	–	0.8	0.2	0.2	–	0.5	0.6	0.2	0.5	0.6	–	–	–	–	–
diMe-F20-3	–	–	–	–	0.8	–	–	–	1.1	–	–	0.3	–	–	–	–	–	–
22:2n-6	–	0.2	–	–	–	–	–	–	–	–	–	–	0.3	0.2	–	–	0.3	0.5
22:1n-9	0.2	0.1	–	0.4	–	0.1	–	–	–	0.4	0.5	0.2	–	0.6	0.1	–	0.3	0.5

Table 1 continued

Fatty acids	<i>Acabaria erithraea</i>	<i>Acanthogorgia isoxia</i>	<i>Chironephthya variabilis</i>	<i>Echinogorgia</i> sp.	<i>Ellisella plexauroides</i>	<i>Menella praelonga</i>	<i>Paralemnalia thyrsoides</i> ^a	<i>Rumphella aggregata</i> ^a
22:1n-7	–	–	0.2	–	–	–	0.3	0.1
22:0	–	–	1.6	0.3	–	–	–	–
Me-F22*	0.1	–	–	1.7	0.2	0.2	–	–
24:5n-6	14.5	11.2	10.7	0.6	12.4	12.6	12.0	8.9
24:6n-3	2.3	3.0	2.4	1.8	1.6	1.2	1.1	2.6
diMe-F22	0.3	–	–	5.1	0.2	0.3	–	–
24:1n-9	–	–	–	0.2	–	–	–	–
24:1n-7	0.6	–	–	–	–	–	–	–
24:0	–	0.3	–	0.2	–	0.1	–	–

Me-F18 10,13-epoxy-11-methyloctadeca-10,12-dienoic acid, *Me-F20* 12,15-epoxy-13-methyleicosa-12,14-dienoic acid, *diMe-F20* 12,15-epoxy-13,14-dimethyleicosa-12,14-dienoic acid, *Me-F22* 14,17-epoxy-15-methyl docosa-14,16-dienoic acid, *diMe-F22* 14,17-epoxy-15,16-dimethyldocosa-14,16-dienoic acid, *diMe-F18-3* 12,15-epoxy-13,14-dimethyloctadeca-12,14-dienoic acid, *diMe-F20-3* 14,17-epoxy-15,16-dimethyleicosa-14,16-dienoic acid

* Indicate significant differences of FA contents between zooxanthellate and azooxanthellate species (*t* test $P < 0.05$)

^a Zooxanthellate species

used at 160 °C with a 2 °C/min ramp to 270 °C held for 20 min. The injector and detector temperatures being 270 °C and 240 °C, respectively. GC–MS of *N*-acylpyrrolidides was performed on the same instrument, the injector and detector temperatures being 300 °C and 270 °C, respectively, the column temperature was 210 °C with a 3 °C/min ramp to 300 °C that was held for 40 min.

To compare the differences between zooxanthellate and azooxanthellate species, Student's *t* test was performed using MS Excel 2002. Differences were considered statistically significant at $P < 0.05$.

Results

Tables 1 and 2 show the distribution of fatty acids (FA) in the total lipids of 22 soft coral specimens belonging to nine genera (*Acanthogorgia*, *Acabaria*, *Rumphella*, *Chironephthya*, *Echinogorgia*, *Menella*, *Paralemnalia*, *Ellisella*, and *Bebryce*). *Rumphella aggregata* and *Paralemnalia thyrsoides* contained zooxanthellae (endosymbiotic dinoflagellates), other genera were azooxanthellate [33]. Arachidonic (20:4n-6) and palmitic (16:0) acids were predominant in all species. Apart from *R. aggregata*, the content of 20:4n-6 amounted about 40% of total FA. Other principal FA were 14:0, 16:1n-7, 7-Me-16:1n-10, 18:0, 18:1, 20:5n-3, 22:5n-6, 22:6n-3, 24:5n-6, and 24:6n-3. For azooxanthellate species, the content of some ordinary even-chain acids, such as 18:2n-6, 18:4n-3, 20:1n-9, and 20:3n-6, did not exceed a value of 2%, but saturated odd-chain and methyl-branched FA were detected in a quite appreciable amount (up to 5.2% in the total). The average ratio between oleic and *cis*-vaccenic acids, 18:1n-9/18:1n-7 was 17.9 and

1.5 for zooxanthellate and azooxanthellate species, respectively. FA of (n-6) series were the predominant PUFA in the octocorals investigated, the (n-6)/(n-3) ratio ranged from 2.7 to 17.1 with the average value of 7.0. We did not detect a significant difference between zooxanthellate and azooxanthellate coral species in the (n-6)/(n-3) ratio.

Seven furan FA (F-acids) were detected in the most coral species investigated (Tables 1, 2, 3). Five of these F-acids were characterized by a furan ring, which carries in one α -position an unbranched FA chain with 9, 11 or 13 carbon atoms and in the other α -position a pentyl residue (Table 3). Either of the two β -positions of the furan ring were substituted by a methyl residue or, otherwise, only the β -position adjacent to the long aliphatic chain had a methyl group. The other two F-acids contained a furan ring with an unbranched FA chain with 11 or 13 carbon atoms in one α -position and a propyl group in the other α -position (Table 3). In this case, both β -positions of the furan ring were substituted by methyl group. Among all F-acids, the highest concentrations were registered for 14,17-epoxy-15-methyldocosa-14,16-dienoic acid (Me-F22) and 14,17-epoxy-15,16-dimethyldocosa-14,16-dienoic acid (diMe-F22) in *Menella praelonga* (2.0% of total FA) and *Chironephthya variabilis* (5.1%), respectively (Table 1).

The mass spectrum of Me-F22 acid methyl ester gave molecular ion peaks (M^+) at m/z 378 (Fig. 1). Allylic cleavage of alkyl carboxylic chain at the furan ring produced the base peak at m/z 165, whereas allylic cleavage of the alkyl chain yielded a fragment ion at m/z 321. The ring itself gave rise to a fragment ion at m/z 109 characteristic of trisubstituted furan acids [34–36]. The mass spectrum of diMe-F22 acid methyl ester is shown in Fig. 1.

Table 2 Fatty acid composition (% of total FAs, mean \pm SD, $n = 4$) of total lipids of *Bebryce studeri*

Fatty acids	Content
14:0	1.7 \pm 0.7
i-15:0	1.8 \pm 0.2
ai-15:0*	0.2 \pm 0.1
15:0	0.5 \pm 0.3
ai-16:0*	0.4 \pm 0.2
16:1n-9	0.3 \pm 0.1
16:1n-7	1.9 \pm 0.8
16:1n-5	0.3 \pm 0.1
16:0*	8.9 \pm 2.7
7-Me-16:1n-10	2.3 \pm 0.6
i-17:0*	1.3 \pm 0.7
ai-17:0*	0.6 \pm 0.2
17:0*	0.8 \pm 0.2
18:4n-3	0.3 \pm 0.3
br-18:0*	0.2 \pm 0.1
18:2n-6	0.7 \pm 0.1
18:1n-9	1.8 \pm 0.5
18:1n-7*	2.1 \pm 0.4
18:0	5.4 \pm 1.1
ai-19:0*	0.2 \pm 0.0
Me-F18	0.2 \pm 0.1
19:0*	0.5 \pm 0.1
20:4n-6	21.7 \pm 7.2
20:5n-3	2.0 \pm 0.9
20:3n-6	0.3 \pm 0.1
20:4n-3	0.1 \pm 0.1
20:1n-9	0.4 \pm 0.1
20:1n-7*	0.3 \pm 0.1
20:0	2.3 \pm 1.4
Me-F20*	0.5 \pm 0.3
21:0	0.5 \pm 0.2
22:5n-6	4.2 \pm 2.3
22:6n-3	3.5 \pm 1.8
22:4n-6	1.1 \pm 0.5
22:5n-3	0.5 \pm 0.3
diMe-F20*	0.2 \pm 0.1
22:1n-9	0.3 \pm 0.1
22:1n-7	0.2 \pm 0.0
22:0	0.9 \pm 0.5
Me-F22*	0.9 \pm 0.6
24:5n-6	7.2 \pm 2.5
24:6n-3	0.5 \pm 0.2
diMe-F22	0.9 \pm 0.9
24:1n-9	0.3 \pm 0.1
24:1n-7	0.6 \pm 0.4
24:0	0.6 \pm 0.4
25:2(5,9)	0.8 \pm 0.1

Table 2 continued

Fatty acids	Content
26:3(5,9,19)	0.8 \pm 0.5
26:2(5,9)	12.9 \pm 2.8
26:2	0.7 \pm 0.4
26:1	1.3 \pm 0.4
28:3(5,9,19)	2.7 \pm 0.9

Footnotes refer to Table 1

Analogously to Me-F22 acid methyl ester, the base peak at m/z 179 was produced by cleavage of the alkyl carboxylic chain, and a fragment ion at m/z 335 was yielded by cleavage of the butyl group. The tetrasubstituted furan ring itself gave rise to a fragment ion at m/z 123. The same fragmentation scheme was observed in mass spectra of other F-acid methyl esters (Table 3).

A number of very-long-chain saturated, mono-, and dioenoic FA (24:0, 24:1, 26:1, and 26:2) and demospongiac acids, such as 25:2(5,9), 26:2(5,9), 26:3(5,9,19), and 28:3(5,9,19), were identified in all specimens of *B. studeri* (Table 2).

The mass spectra of methyl esters of 24:0, 24:1, 26:1, and 26:2 gave molecular ion peaks (M^+) at m/z 382, m/z 380, m/z 408, and m/z 406, respectively, confirming the presence of a C_{24} or C_{26} chain and the corresponding number of double bonds in the original FA. Additionally, strong peaks at m/z 348 and m/z 376 ($[M-MeOH]^+$, characteristic of monoenoic FAME) were observed in mass spectra of 24:1 and 26:1. The mass spectra of the *N*-acylpyrrolidide derivatives of 24:1(n-9) and 24:1(n-7) gave molecular ion peaks at m/z 419 (M^+) and diagnostic fragments with the gap of 12 amu at m/z 280, 292 and m/z 308, 320, respectively [31].

The mass spectra of methyl esters of 25:2(5,9), 26:2(5,9), 26:3(5,9,19), and 28:3(5,9,19) acids gave molecular ion peaks (M^+) at m/z 392, m/z 406, m/z 404, and m/z 432, respectively. A combination of abundant ions at m/z 81, 109, and 141, which was observed in the mass spectra of these demospongiac acid methyl esters, indicated the presence of a 5,9-dienoic fragment in the fatty chain. The mass spectra of the *N*-acylpyrrolidide derivative of 25:2(5,9), 26:2(5,9), 26:3(5,9,19), and 28:3(5,9,19) acids gave molecular ion peaks (M^+) at m/z 431, m/z 445, m/z 443, and m/z 471, respectively. In these mass spectra, the gap of 12 amu between m/z 140 and 152, as well between m/z 194 and 206 confirmed the presence of double bonds in positions 5 and 9. The gap of 12 amu between m/z 332 and 344 was found in the mass spectra of the *N*-acylpyrrolidide derivative of trienoic demospongiac acids, indicating that double bond was localized at the 19th carbon atom of the original FA. Also, the spectra from 5,9-unsaturated FA

Table 3 Gas chromatography and mass spectra data (m/z , EI mode) for furan fatty acid methyl esters from octocorals

	Me-F18	diMe-F18-3	Me-F20	diMe-F20	diMe-F20-3	Me-F22	diMe-F22
n	7	9	9	9	11	11	11
m	3	1	3	3	1	3	3
GC retention time (min)	27.3	31.2	35.5	38.4	39.8	43.5	46.3
M^+	322	336	350	364	364	378	392
[M-MeOH + H] ⁺	291	305	319	333	333	347	361
[M-alkyl(C ₂ H ₅)] ⁺	–	307	–	–	335	–	–
[M-alkyl(C ₄ H ₉)] ⁺	265	–	293	307	–	321	335
[M-alkyl ester] ⁺ base peak	165	151	165	179	151	165	179
Furan fragment	109	123	109	123	123	109	123

FA names as in Table 1; n carbon atom numbers in alkyl chain; m carbon atom numbers in alkylester chain (refer to Fig. 1)

N-acylpyrrolidide derivatives exhibited an intensive peak at m/z 180 which was higher than a peak at m/z 126 [37].

One rather unusual 7-methyl-6-hexadecenoic acid was identified in all coral specimens with a relative abundance ranging from 0.2 to 6.7%. This acid was characterized by GC–MS as previously described [38]; an abundant ion at m/z 138 in the mass spectra of methyl ester is very characteristic for these compounds.

For each of the 56 C₁₄–C₂₄ FA from Tables 1 and 2, the average contents in four zooxanthellate specimens were compared to those in 18 azooxanthellate coral specimens. The statistically significant difference ($P < 0.05$) between the azooxanthellate and the zooxanthellate corals was indicated only for 14 FA, namely ai-15:0, ai-16:0, 17:0, i-17:0, ai-17:0, br-18:0, 18:1n-7, 18:2n-9, 19:0, ai-19:0, 20:1n-7, Me-F20, diMe-F20, and Me-F22. A comparison of the average contents of each FA between zooxanthellate *P. thyrsoides* and all azooxanthellate species indicated a statistically significant difference ($P < 0.01$) for 7-Me-16:1n-10, 18:3n-6, and 18:4n-3 (Fig. 2). Compared to all azooxanthellate species, the level of 7-Me-16:1n-10 in the zooxanthellate species *R. aggregata* did not differ significantly but, similar to *P. thyrsoides*, the average contents of 16:0, 18:3n-6, and 18:4n-3 were significantly higher (Fig. 2). Two (n-7) series FA, 16:2n-7 and 18:2n-7, were found in *R. aggregata* only, and contributed on the average 2.2 and 2.3% of total acids, respectively (Table 1).

The most gorgonians studied showed the presence of a high level of tetracosapolyenoic acid 24:5n-6 ($9.4 \pm 3.5\%$, in average \pm SD). However, an unexpected low concentration of 24:5n-6 (0.2–0.6% of total FA) was detected in the single specimens of *Acanthogorgia isoxia*, *M. praelonga*, and *Ellisella plexauroides* (Table 1). In all the cases, an extremely low amount of 24:5n-6 was accompanied by a substantial rise in the content of 22:4n-6 up to $11.9 \pm 1.9\%$ (in average \pm SD) from the value of $0.6 \pm 0.4\%$ calculated for the specimens with normal high level of 24:5n-6. At the same time, abrupt variations in the

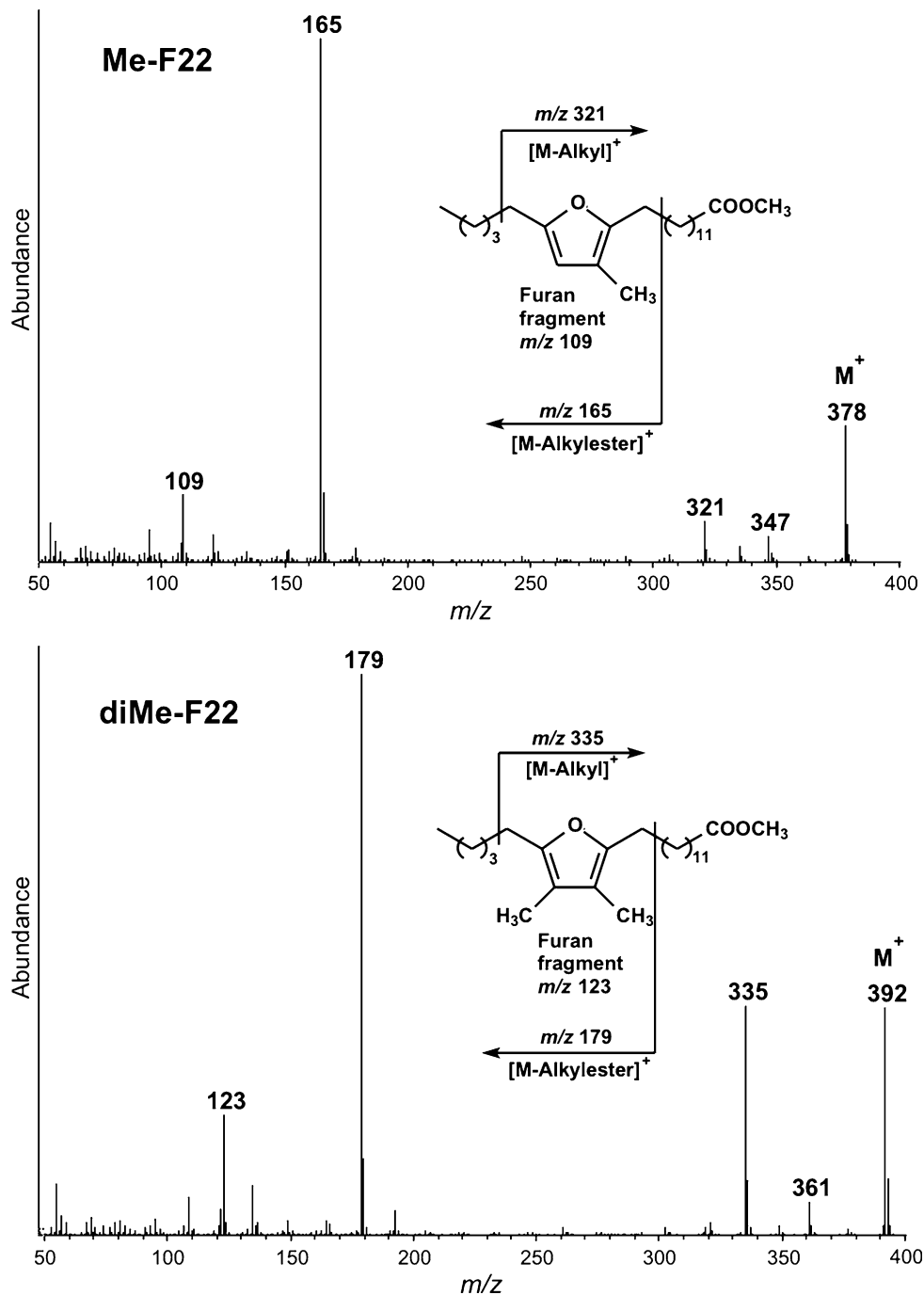
amounts of C_{22–24} (n-3) series FA, 22:5n-3, and 24:6n-3 were not found.

Discussion

The FA compositions of *Bebryce indica* and *R. aggregata* have been previously investigated by the use of a parked steel GC column [18, 39]. Incorrect determination of 18:4n-3 as 18:3n-3, 24:5n-6 as 24:5n-3, the loss of VLC FA, and other mistakes, made for *B. indica* and *R. aggregata*, were corrected in this study (Tables 1, 2). The FA compositions of octocorals of the genera *Acanthogorgia*, *Acabaria*, *Chironephthya*, *Echinogorgia*, *Menella*, *Paralemnalia*, and *Ellisella* were determined in the present study for the first time. In general, the qualitative FA profiles of total lipids of the nine coral genera investigated were similar enough and close to that of other gorgonians, such as *Mopsella aurantia* [18], *Paragorgia arborea* [19], *Euplexaura erecta*, *Subergorgia suberosa* [39], and *Leptogorgia piccola* [40] described earlier. The considerable proportion of arachidonic acid (about a half of the total FA), the high level of tetracosapolyenoic FA (24:5n-6 and 24:6n-3), and predomination of (n-6) polyunsaturated FA (n-6/n-3 > 1) should be considered as the distinguishing features of the gorgonian corals.

A lot of marine invertebrates, including corals, contain symbiotic bacteria and/or microalgae, and their FA make important contributions to the total FA composition of these organisms [41]. The FA composition and biosynthetic pathways of FA are essentially different in bacteria, photoautotrophic microalgae, and host animals [42]. The overwhelming majority of bacteria synthesize saturated and monounsaturated even- and odd-chain FA with 14–18 carbon atoms. Generally, only microalgae can synthesize C_{18–22} polyunsaturated fatty acids (PUFA) of the n-6 and n-3 series. The capability of marine invertebrates to produce C₁₈ PUFA is limited [43]. In a symbiont–host coral

Fig. 1 Electron impact mass spectra of methyl esters of 14,17-epoxy-15-methyldocos-14,16-dienoic acid (Me-F22) and 14,17-epoxy-15,16-dimethyldocos-14,16-dienoic acid (diMe-F22). Mass spectrometric conditions are described in the “Experimental Procedures”



community, different symbionts, such as endosymbiotic dinoflagellates (zooxanthellae), bacteria, filamentous algae or sponges which colonize the skeletons lay down their specific FA patterns that can be recognized in total coral lipids.

Numerous examinations of the interactions between corals and microbes have shown that there is a dynamic microbiota living on the surface and, possibly, within the tissue of corals [44, 45]. However, it is still unknown whether microbes play specific roles in coral biology or if

the observed associations are merely opportunistic interactions of the coral animal with water-column bacteria. The appreciable level of *cis*-vaccenic acid 18:1n-7 and the number of odd-chain and methyl-branched FA (Tables 1, 2) that are regarded as biomarkers of bacteria [46] were found in the FA of azooxanthellate coral species. The statistically significant difference ($P < 0.05$) between the azooxanthellate and the zooxanthellate corals was shown for the contents of these common bacterial FA. It indicated the presence of an advanced bacterial community in

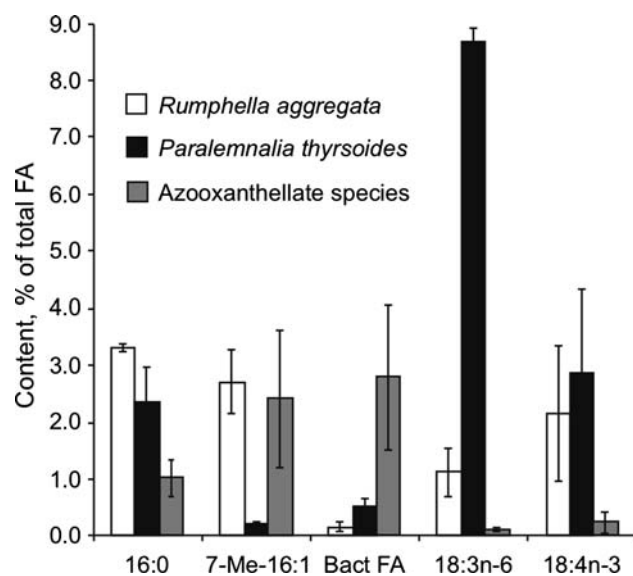


Fig. 2 Average contents of principal fatty acids (% of total FA) in *Rumphella aggregata*, *Paralemnalia thyrsoides* (zooxanthellate species), and azooxanthellate coral species (*Acabaria erithraea*, *Acanthogorgia isoxia*, *Chironephthya variabilis*, *Echinogorgia* sp., *Ellisella plexauroides*, *Menella praelonga*, *Bebrycce studeri*). BactFA was the sum of ai-15:0, ai-16:0, i-17:0, ai-17:0, 17:0, br-18:0, ai-19:0, and 19:0

azooxanthellate gorgonian species. A similar increase of the part of bacterial acids in total FA of azooxanthellate alcyonarians (the genus *Dendronephthya*) compared to the alcyonarians with zooxanthellae has been described earlier [24]. Also, this azooxanthellate alcyonarians are distinguished by the high level (up to 7.3% of total FA) of 7-methyl-6-hexadecenoic acid (7-Me-16:1n-10) presumably attributed to a bacterial origin. At the same time, the average concentration of this interesting component is $1.1 \pm 0.7\%$ (mean \pm SD) of total FA in 13 species of zooxanthellate alcyonarians [24]. In the azooxanthellate gorgonian specimens studied, the proportions of 7-Me-16:1n-10 ($2.4 \pm 1.2\%$ is the average \pm SD) were significantly higher than those in the zooxanthellate alcyonarians mentioned above ($P < 0.01$). This particular FA has been encountered before in several marine invertebrates, such as sponges, anemones, and gorgonians, it contributes on the average 2.9% of total acids of polar lipid fractions in the genus *Gorgonia* [20]. Nevertheless, the perceptible variations of the content of 7-Me-16:1n-10 and the occurrence of 2.7% of this acid in zooxanthellate *R. aggregata* (Table 1) did not allow us to fix unambiguously a direct correlation between the increase in the 7-Me-16:1n-10 content and the absence of zooxanthellae. Probably, 7-methyl-6-hexadecenoic acid does not characterize the whole bacterial community but can serve as a biomarker of some specific bacterial group associated with soft corals or consumed by the coral with food.

Another group of unusual acids, namely F-acids, which can be regarded as a useful biomarker, was identified in the gorgonians studied. These F-acids seem to be widely distributed in all living matter and are found in marine sponges, algae, invertebrates, crayfishes, crabs, and fishes [47]. It is recognized that plants and algae synthesize the carbon skeleton of F-acids from linoleic acid (18:2n-6). Then, the F-acids are elongated by acetate units to higher homologs. The occurrence and biosynthesis of F-acids in phototrophic bacteria has been reported by a few authors [34, 36]. All of these bacteria are common for many kinds of marine animals. It has been concluded that F-acids detected in the animals are derived from marine bacteria and/or algae [34]. Among corals, the presence of 3,4-dimethyl-5-pentylfuryl-proioic acid is reported for the soft corals *Sarcophyton glaucum* and *S. gemmatum* [48]. In the present study, a number of F-acids with 18–22 carbon atoms in the basic chain were for the first time identified in the six azooxanthellate gorgonian species (except for *A. isoxia*). All these compounds have been detected earlier among the predominant F-acids in the biological objects mentioned above [34, 36, 47].

Nevertheless, the F-acids were detected in all the specimens of the zooxanthellate corals studied. In the azooxanthellate species, the content of total F-acids varied between specimens appreciably namely from 0 to 9.7% of the total acids. Analogously to other marine animals, possible sources of F-acids in the octocorals may be microalgae consumed as a food or microorganisms associated with corals such as bacteria or microalgae. All the corals studied were collected at the same place and had similar food sources that, in general, resulted in a decrease in the differences in FA compositions between species. Taking this into account, we prefer the hypothesis of a temporary nonspecific association of azooxanthellate octocorals with phototrophic bacteria or/and some microalgae, which play a role of endosymbiotic dinoflagellates of the *Symbiodinium* group lacking there. In this case, the proportion of these associated microorganisms in the whole coral colony can be estimated by the content of F-acid markers.

At the beginning of our study, the unexpected occurrence of C_{25–28} Δ 5,9 unsaturated VLC FA (demospongiac acids) in *Bebrice* coral—the acids are very characteristic for sponges [49]—was perceived as an artifact. Nevertheless, the same demospongiac FA were found in all the three different colonies of *B. studeri* collected in the Nha Trang Bay and in one sample of the same species from the Den Island (Table 2). Demospongiac FA were never detected in other species studied. All *Bebrice* coral colonies were visually free of biofouling, but the presence of an endosymbiotic sponge has been described for the genus *Bebrice* by Fabricius and Alderslade [33]. Thus, the occurrence of

demospongiac acids in total FA unambiguously reflects the presence of a symbiotic sponge in the gorgonian coral *B. studeri*, and the acids can serve as a useful specific marker of symbiotic sponges for other coral species. It is known that FA constitute about 25 and 6% of tissue dry weight of corals and sponges, respectively. We found that the demospongiac acids amounted to $20.3 \pm 4.5\%$ (mean \pm SD) of the total FA of *B. studeri*. Thus, at a crude guess, the symbiotic sponge may contribute up to 50% of the total dry tissue of *B. studeri*.

According to different estimations, zooxanthellae may contribute from 5 to 30% of the total coral biomass [13]. The presence of this amount of zooxanthellae in a coral colony should appreciably influence the total FA composition, because the FA profile of photoautotrophic organisms significantly differs from that of the heterotrophic host animal. Another way of the influence on the FA composition of a whole colony consists in the transfer (and possible accumulation) of FA synthesized by zooxanthellae to the coral host [10, 12]. For reef-building corals, the transfer of saturated FA have been shown; the transfer of some PUFA have been supposed [9, 11, 13, 25], but the mechanism of this process is under discussion [50]. We described earlier for alcyonarians the significant excess of saturated FA in zooxanthellate species compared to species without zooxanthellae [24]. In the present investigation, the content of palmitic acid (16:0) was significantly higher ($P < 0.01$) in zooxanthellate corals (Table 1). If we suppose that zooxanthellae of octocorals, similar to those of Scleractinia, are a source of saturated FA for the host, the absence of this source may be the cause for the increased content of 16:0 discovered in zooxanthellate soft coral species.

The main PUFA of pure zooxanthellae isolated from reef-building corals are 18:3n-6, 18:4n-3, 18:5n-3, 20:4n-6, 20:5n-3, 22:4n-6, and 22:6n-3 [8, 25]. Data on FA composition of pure zooxanthellae from soft corals is not available, but zooxanthellae from reef-building and soft corals are attributed to the same *Symbiodinium* group of dinoflagellates. We suppose that PUFA profiles of the zooxanthellae from soft and reef-building corals are quite similar and some of these acids can be applied as zooxanthellae markers for soft corals. The use of C_{20–22} PUFA, such as 20:4n-6, 20:5n-3, 22:4n-6, and 22:6n-3, are limited, because high intraspecific variations of the content of these acids exceed interspecific differences [23, 24]. In the total FA of corals, octadecapentaenoic acid (18:5n-3) is absent or found only in trace amounts [15, 24]. At the same time, the comparison the average contents of 18:3n-6 and 18:4n-3 between the zooxanthellate *R. aggregata* and *P. thyrsoides* and the azooxanthellate species indicated the significant difference ($P < 0.01$) (Fig. 2). Therefore, 18:3n-6 and 18:4n-3 seem to be the

most suitable as the markers of zooxanthellae in soft corals.

The absence of 18:3n-6 and the low level of 18:4n-3 in azooxanthellate alcyonarians have been previously described [24]. Negligible amounts (less than 1% of total FA) of 18:3n-6 and 18:4n-3 are found in azooxanthellate reef-building corals *Tubastrea coccinea* and *T. micrantha* [51]. On the contrary, the level of these acids in hermatypic corals range from 2 to 15% of total FA [15, 51]. A comparison of the content of 18:3n-6 and 18:4n-3 in total FA of healthy and completely bleached colonies of the hermatypic coral *Pavona frondifera* has shown that the loss of zooxanthellae leads to decrease in the content from 12.2 to 1.8% [52]. Evidently, it is related to that 18:3n-6 and 18:4n-3 are the main FA of glycolipids, which play the key role in thylakoid membranes of zooxanthellae of reef-building corals [25, 53]. Thus, the presence of more than 2% of 18:3n-6 and 18:4n-3 in total FA can be regarded as the criterion of the presence of zooxanthellae in soft corals.

Genetic analyses based on ribosomal DNA have shown that zooxanthellate populations of scleractinian and soft corals are not homogeneous and contain different proportions of several *Symbiodinium* phylotypes [54, 55]. Variability of the FA profile in different species belonging to the same genus of the free-living dinoflagellates has been demonstrated by Mansour [56]. Also, the FA composition of zooxanthellae isolated from different species of reef-building corals, clams, and Foraminifera is found to vary according to the host [8, 25]. In the gorgonian coral *R. aggregata*, the level of 18:3n-6 was significantly low ($P < 0.01$) as compared to that in *P. thyrsoides* (Table 1; Fig. 2). The presence of a certain *Symbiodinium* phylotype with the specific FA composition may be the possible reason for this distinction. Two PUFA of the n-7 series (16:2n-7 and 18:2n-7) were detected in *R. aggregata* only (Table 1). The same 16:2n-7 acid is found in zooxanthellate alcyonarians (up to 11.9% of the total FA for *Sarcophyton* aff. *crassum*) [24]. Hence, 16:2n-7 acid is believed to originate mainly from a specific phylotype of zooxanthellae with the following elongation to 18:2n-7. The different FA markers may indicate different compositions of zooxanthellate populations in *P. thyrsoides* and *R. aggregata*. With its high level of 18:3n-6, the zooxanthellate population of *P. thyrsoides* was close to that of some hermatypic corals; and, because of the presence of 16:2n-7, the gorgonian coral *R. aggregata* is similar to the alcyonarians.

The Octocorallia species, irrespective of the presence of zooxanthellae, have 24:6n-3 and 24:5n-6 acids; that is their main chemotaxonomic distinction from the Hexacorallia species (stony corals) [20, 26]. Recently, newly revised pathways for the biosynthesis of n-3 and n-6 PUFA in animal cells have been proposed [27]. This report

concludes that 24:5n-6 is formed by elongation of 20:4n-6 to 22:4n-6 and then to 24:4n-6 followed by further desaturation (20:4n-6 → 22:4n-6 → 24:4n-6 → 24:5n-6); a similar formation of 24:6n-3 from 20:5n-3 have been proposed. C₂-degradation via β-oxidation of 24:5n-6 and 24:6n-3 acids is postulated as a pathway to 22:5n-6 and 22:6n-3 acids, respectively. It is very likely that gorgonians and other soft corals utilize a similar biosynthetic route, thus providing another interesting system for studying this type of biogenesis. It is noteworthy that C₂₄ PUFA are synthesized in the host cells of soft corals without a participation of zooxanthellae enzymes [24].

In the present investigation, several gorgonian specimens of *A. isoxia*, *E. plexauroides*, and *M. praelonga* were distinguished by extremely low quantities of 24:5n-6 acid (Table 1). The revised metabolic pathway for C₂₄ n-6 PUFA shows that three acids are chain-elongated, and two of these chain elongation reactions take place in the sequence 20:4n-6 → 22:4n-6 → 24:4n-6 [27]. The average content of 22:4n-6 acid was 20 times higher in the specimens with the deficiency of 24:5n-6 acid (Table 1); this showed an unusual inhibition of the second step of the chain-elongation reactions. Significant changes in the amount of analogical PUFA of n-3 series were not detected (Table 1). These results of our studies were consistent with the presence of both chain-length-specific condensing enzymes and different enzyme complexes for n-3 and n-6 series PUFA in gorgonians. The average content of 22:5n-6 acid in the abnormal specimens was also four times higher (Table 1) as a possible result of Δ⁴-desaturation of the excess of 22:4n-6 acid. The nature of a specific inhibitor of elongation of 22:4n-6 and 22:5n-6 acids is not clear and needs further investigation.

The comparative study of FA composition of the octocorals has allowed us to determine several lipid markers of microorganisms associated with the host coral; these markers will be useful for further investigation of the symbiotic community of soft corals. The octocorals were shown to be an interesting model system for studying the biosynthesis of C₂₂ Δ⁴ and C₂₄ Δ⁶ PUFA as well as a possible source of specific inhibitors for the regulation of biogenesis of the essential FA, e.g. docosahexaenoic acid.

Acknowledgment This work was supported by the grant 07-03-90001-Viet from the Russian Foundation for Basic Research.

References

- Sorokin YI (1993) Coral reef ecology. Springer, Berlin Heidelberg New York
- Ayukai T (1995) Retention of phytoplankton and planktonic microbes on coral reefs within the Great Barrier Reef, Australia. *Coral Reefs* 14:141–147
- Fabricius KE, Dommissie M (2000) Depletion of suspended particulate matter over coastal reef communities dominated by zooxanthellate soft corals. *Mar Ecol Prog Ser* 196:157–167
- Muscantine L, Weis V (1992) Productivity of zooxanthellae and biochemical cycles. In: Falkowski PG, Woodhead AD (eds) Primary productivity and biogeochemical cycles in the sea - Environmental Science Research, Plenum, New York, pp 257–271
- Schlichter D, Kampmann H, Conrady S (1997) Trophic potential and photoecology of endolithic algae living within coral skeletons. *Mar Ecol* 18:299–317
- Rohver F, Breitbart M, Jara J, Azam F, Knowlton N (2001) Diversity of bacteria associated with the Caribbean coral *Montastraea franksi*. *Coral Reefs* 20:85–91
- Beleneva IA, Dautova TI, Zhukova NV (2005) Characterization of communities of heterotrophic bacteria associated with healthy and diseased corals in Nha Trang Bay (Vietnam). *Russ J Microbiol* 74:579–587
- Zhukova NV, Titlyanov EA (2003) Fatty acid variations in symbiotic dinoflagellates from Okinawan corals. *Phytochemistry* 62:191–195
- Harland AD, Fixter LM, Davies PS, Anderson RA (1991) Distribution of lipids between the zooxanthellae and animal compartment in the symbiotic sea anemone *Anemonia viridis*—wax esters, triglycerides and fatty acids. *Mar Biol* 110:13–19
- Harland AD, Navarro JC, Davies PS, Fixter LM (1993) Lipids of some Caribbean and Red Sea corals—total lipid, wax esters, triglycerides and fatty acids. *Mar Biol* 117:113–117
- Al Moghrabi S, Allemant D, Couret JM, Jaubert J (1995) Fatty acids of the scleractinian coral *Galaxea fascicularis*—effect of light and feeding. *J Comp Physiol B* 165:183–192
- Ward S (1995) Two patterns of energy allocation for growth, reproduction and lipid storage in the scleractinian coral *Pocillopora damicornis*. *Coral Reefs* 17:87–90
- Papina M, Meziane T, van Woesik R (2003) Symbiotic zooxanthellae provide the host-coral *Montipora digitata* with polyunsaturated fatty acids. *Comp Biochem Physiol B* 135:533–537
- Widdig A, Schlichter D (2001) Phytoplankton: a significant trophic source for soft corals? *Helgol Mar Res* 55:198–211
- Imbs AB, Demidkova DA, Latypov YY, Pham QL (2007) Application of fatty acids for chemotaxonomy of reef-building corals. *Lipids* 42:1035–1046
- Luu VH, Doan LP, Pham QL, Imbs AB (2005) Fatty acids as chemotaxonomy of Vietnamese coral. *Vietnam J Sci Technol* 43:92–100
- Joseph JD (1979) Lipid composition of marine and estuarine invertebrates: Porifera and Cnidaria. *Prog Lipid Res* 18:1–30
- Lam CN, Nguen HK, Stekhov VB, Svetashev VI (1981) Phospholipids and fatty acids of soft corals. *Russ J Mar Biol* 6:44–47
- Vysotskii MV, Svetashev VI (1991) Identification, isolation and characterization of tetracosapolyenoic acids in lipids of marine coelenterates. *Biochim Biophys Acta* 1083:161–165
- Carballeira NM, Miranda C, Rodriguez AD (2002) Phospholipid fatty acid composition of *Gorgonia mariae* and *Gorgonia ventalina*. *Comp Biochem Physiol B* 131:83–87
- Yamashiro H, Oku H, Higa H, Chinen I, Sakai K (1999) Composition of lipids, fatty acids and sterols in Okinawan corals. *Comp Biochem Physiol B* 122:397–407
- Imbs AB, Demina OA, Demidkova DA (2006) Lipid class and fatty acid composition of the boreal soft coral *Gersemia rubiformis*. *Lipids* 41:721–725
- Imbs AB, Luu HV, Pham LQ (2007) Intra- and interspecific variability of fatty acid composition of the soft corals. *Russ J Mar Biol* 33:70–73

24. Imbs AB, Latyshev NA, Zhukova NV, Dautova TN (2007) Comparison of fatty acid compositions of azooxanthellate *Dendronephthya* and zooxanthellate soft coral species. *Comp Biochem Physiol B* 148:314–321
25. Bishop DG, Kenrick JR (1980) Fatty acid composition of symbiotic zooxanthellae in relation to their hosts. *Lipids* 15:799–804
26. Svetashev VI, Vysotsky MV (1998) Fatty acids of *Heliopora coerulea* and chemotaxonomic significance of tetracosapolyenoic acids in coelenterates. *Comp Biochem Physiol B* 119:73–75
27. Sprecher H (2000) Metabolism of highly unsaturated n-3 and n-6 fatty acids. *Biochem Biophys Acta* 1486:219–231
28. McKenzie JD, Black KD, Kelly MS, Newton LC, Handley LL, Scrimgeour CM, Raven JA, Henderson RJ (2000) Comparisons of fatty acid and stable isotope ratios in symbiotic and non-symbiotic brittlestars from Oban Bay, Scotland. *J Mar Biol Ass UK* 80:311–320
29. Berge J-P, Barnathan G (2005) Fatty acids from lipids of marine organisms: molecular biodiversity, roles as biomarkers, biologically active compounds, and economical aspects. *Mar Biotech I Adv Biochem Eng* 96:49–125
30. Carreau JP, Dubacq JP (1979) Adaptation of macro-scale method to the micro-scale for fatty acid methyl transesterification of biological lipid extracts. *J Chromatogr* 151:384–390
31. Andersson BA (1978) Mass spectrometry of fatty acid pyrrolidides. *Prog Chem Fats Other Lipids* 16:279–308
32. Christie WW (1988) Equivalent chain lengths of methyl ester derivatives of fatty acids on gas chromatography—a reappraisal. *J Chromatogr* 447:305–314
33. Fabricius C, Alderslade P (2001) Soft corals and sea fans: a comprehensive guide to the tropical shallow water genera of the Central-West Pacific, the Indian Ocean and the Red Sea. Australian Institute of Marine Science, Townsville
34. Shirasaka N, Nishi K, Shimizu S (1995) Occurrence of a furan fatty acid in marine bacteria. *Boichem Biophys Acta* 1258:225–227
35. Dembitsky VM, Rezanka T (1996) Furan fatty acids of some brackish invertebrates from the Caspian Sea. *Comp Biochem Physiol B* 114:317–320
36. Rontani J-F, Christodoulou S, Koblizek M (2005) GC–MS structural characterization of fatty acids from marine aerobic anoxygenic phototrophic bacteria. *Lipids* 40:97–108
37. Carballeira NM, Maldonado L (1986) Identification of 5, 9-hexadecadienoic acid in the marine sponge *Chondrilla nucula*. *Lipids* 21:470–471
38. Carballeira NM, Shalabi F (1994) Unusual lipids in the Caribbean sponges *Amphimedon viridis* and *Desmapsamma anchorata*. *J Nat Prod* 57:1152–1159
39. Imbs AB, Maliotin AN, Luu VH, Pham QL (2005) Study of fatty acid composition of 17 coral species of Vietnam. *Vietnam J Sci Tech* 43:84–91
40. Miralles J, Barnathan G, Galonnier R, Sall T, Samb A, Gaydou EM, Kornprobst JM (1995) New branched chain fatty acids from the Senegalese gorgonian *Leptogorgia piccola* (white and yellow morphs). *Lipids* 30:459–466
41. Volkman JK, Barrett SM, Blackburn SI, Mansour MP, Sikes EL, Gelin F (1998) Microalgal biomarkers: a review of recent research developments. *Org Geochem* 29:1163–1179
42. Pereira SL, Leonard AE, Mukerji P (2003) Recent advances in the study of fatty acid desaturases from animals and lower eukaryotes. *Prostaglandins Leukot Essent Fat Acids* 68:97–106
43. Dalsgaard J, John MS, Kattner G, Muller-Navarra D, Hagen W (2003) Fatty acid trophic markers in the pelagic marine environment. *Adv Mar Biol* 46:225–340
44. Sorokin YI (1973) Trophical role of bacteria in the ecosystem of the coral reef. *Nature* 242:415–417
45. Santavy DL (1995) The diversity of microorganisms associated with marine invertebrates and their roles in the maintenance of ecosystems. CAB International, Wallingford, pp 211–229
46. Kaneda T (1991) Iso-fatty and anteiso-fatty acids in bacteria—biosynthesis, function, and taxonomic significance. *Microbiol Rev* 55:288–302
47. Spiteller G (2005) Furan fatty acids: occurrence, synthesis, and reactions. Are furan fatty acids responsible for the cardioprotective effects of a fish diet? *Lipids* 40:755–771
48. Groweiss A, Kashman Y (1978) A new furanoid acid from the soft corals *Sarcophyton glaucum* and *S. gemmatum*. *Experientia* 34:299
49. Bergquist PR, Lawson MP, Lavis A, Cambie RC (1984) Fatty acid composition and the classification of the Porifera. *Biochem Syst Ecol* 12:63–84
50. Muscatine L, Gates RD, La Fontaine I (1994) Do symbiotic dinoflagellates secrete lipid droplets? *Limnol Oceanogr* 39:925–929
51. Latyshev NA, Naumenko NV, Svetashev VI, Latypov YY (1991) Fatty acids of reef-building corals. *Mar Ecol Prog Ser* 76:295–301
52. Bachok Z, Mfilinge P, Tsuchiya M (2006) Characterization of fatty acid composition in healthy and bleached corals from Okinawa, Japan. *Coral Reefs* 25:545–554
53. Tchernov D, Gorbunov MY, de Vargas C, Yadav SN, Milligan AJ, Haggblom M, Falkowski PG (2004) Membrane lipids of symbiotic algae are diagnostic of sensitivity to thermal bleaching in corals. *Proc Natl Acad Sci* 101:13531–13535
54. Fabricius KE, Mieog JC, Colin PL, Idip D, van Oppen MJH (2004) Identity and diversity of coral endosymbionts (zooxanthellae) from three Palauan reefs with contrasting bleaching, temperature and shading histories. *Mol Ecol* 13:2445–2458
55. van Oppen MJH, Mieog JC, Sanchez CA, Fabricius KE (2005) Diversity of algal endosymbionts (zooxanthellae) in octocorals: the roles of geography and host relationships. *Mol Ecol* 14:2403–2417
56. Mansour MP, Volkman JK, Jackson AE, Blackburn SI (1999) The fatty acid and sterol composition of five marine dinoflagellates. *J Phycol* 35:710–720

Macrobrachium borellii Hepatopancreas Contains a Mitochondrial Glycerol-3-Phosphate Acyltransferase Which Initiates Triacylglycerol Biosynthesis

M. Pellon-Maison · C. F. Garcia · E. R. Cattaneo ·
R. A. Coleman · M. R. Gonzalez-Baro

Received: 3 July 2008 / Accepted: 26 November 2008 / Published online: 8 January 2009
© AOCS 2008

Abstract Mammals express four isoforms of glycerol-3-phosphate acyltransferase (GPAT). The mitochondrial isoform GPAT1 may have been the acyltransferase that appeared first in evolution. The hepatopancreas of the crustacean *Macrobrachium borellii* has a high capacity for triacylglycerol (TAG) biosynthesis and storage. In order to understand the mechanism of glycerolipid biosynthesis in *M. borellii*, we investigated its hepatopancreas GPAT activity. In hepatopancreas mitochondria, we identified a GPAT activity with characteristics similar to those of mammalian GPAT1. The activity was resistant to inactivation by SH-reactive *N*-ethylmaleimide, it was activated by polymyxin-B, and its preferred substrate was palmitoyl-CoA. The reaction products were similar to those of mammalian GPAT1. A 70-kDa protein band immunoreacted with an anti-rat liver GPAT1 antibody. Surprisingly, we did not detect high GPAT specific activity in hepatopancreas microsomes. GPAT activity in microsomes was consistent with mitochondrial contamination, and its properties were similar to those of the mitochondrial activity. In microsomes, TAG synthesis was not dependent on the presence of glycerol-3 phosphate as a substrate, and the addition of monoacylglycerol as a substrate increased TAG synthesis 2-fold. We conclude that in *M. borellii* the de novo triacylglycerol biosynthetic pathway can be

completed in the mitochondria. In contrast, TAG synthesis in the ER may function via the monoacylglycerol pathway.

Keywords Triacylglycerol · Crustacean · Glycerolipid synthesis

Abbreviations

BSA	Bovine serum albumin
DGAT	Diacylglycerol acyltransferase
DTT	Dithiothreitol
EDTA	Ethylenediaminetetracetic acid
ER	Endoplasmic reticulum
GPAT	Glycerol-3-phosphate acyltransferase
NEM	<i>N</i> -ethylmaleimide
TAG	Triacylglycerols

Introduction

The most important organ for crustacean metabolism is the hepatopancreas, which is analogous to the vertebrate liver and insect fat body because it synthesizes and secretes digestive enzymes, absorbs digestive dietary products, stores mineral reserves and organic substances, metabolizes lipids and carbohydrates, and aids in distributing stored reserves during the intermoult cycle and xenobiotic metabolism [1]. The hepatopancreas of *Macrobrachium borellii*, a Decapod Crustacean, is active in triacylglycerol (TAG) biosynthesis. During the winter season the TAG content of hepatopancreas comprises more than 80% of the total lipid mass of the organ [2], and in vivo incubation of *M. borellii* with [¹⁴C]palmitic acid revealed that the hepatopancreas is the principal organ for TAG synthesis [3]. The hepatopancreas mobilizes TAG

M. Pellon-Maison · C. F. Garcia · E. R. Cattaneo ·
M. R. Gonzalez-Baro (✉)
Instituto de Investigaciones Bioquímicas de La Plata,
CCT La Plata, CONICET INIBIOLP, Fac. Cs. Médicas UNLP,
Calles 60 & 120, 1900 La Plata, Argentina
e-mail: mgbaro@atlas.med.unlp.edu.ar

R. A. Coleman
Department of Nutrition, University of North Carolina,
Chapel Hill, NC 27599, USA

when the animal is deprived of food or subjected to thermal stress [4, 5]. These facts suggest that, in addition to the hepatopancreas' digestive and biosynthetic roles, it functions to synthesize and store TAG, analogous to adipose tissue in vertebrates.

The first steps in the de novo biosynthesis of glycerolipids include the activation of fatty acids by acyl-CoA synthetases and their subsequent esterification by *sn*-glycerol-3-phosphate acyltransferases (GPAT, EC 2.3.1.15). Historically two types of GPAT have been characterized in mammals [6]: (1) a microsomal form, which comprises 90% of total GPAT activity in most organs, is sensitive to sulfhydryl reagents like *N*-ethylmaleimide (NEM), and lacks long-chain acyl-CoA substrate preference, and (2) a mitochondrial isoform that is resistant to NEM inactivation and prefers to use saturated acyl-CoA. The mitochondrial NEM-resistant isoform (GPAT1) was cloned twenty years ago from mouse and rat liver [7, 8]. More recently, a second mitochondrial NEM-sensitive isoform (GPAT2) [9] and two endoplasmic reticulum (ER) isoforms (GPAT3 and GPAT4) were cloned [10–12]. Although the specific roles of each isoform are not yet well understood, several studies [13, 14] strongly suggest that the mitochondrial NEM-resistant isoform (GPAT1) initiates the synthesis of TAG in rat liver under conditions of high carbohydrate feeding and caloric excess.

We previously reported that microsomes from *M. borellii* hepatopancreas have a significant acyl-CoA synthetase activity [15] and that the entire synthesis of TAG may occur in the ER of crustacean hepatopancreas [3]. Moreover, a mitochondrial type of acyl-CoA synthetase activity was described in this organ [16]. However, little is known about the acyltransferases that are present in invertebrates. Taking into account the preponderant role of *M. borellii* hepatopancreas in TAG synthesis, we hypothesized that glycerolipid biosynthesis compartmentalization in this crustacean would be similar to that of mammalian liver, so at least two GPAT isoforms would be present in both mitochondria and ER. Our aim was to characterize GPAT activity in these two cellular compartments in order to understand the mechanism of TAG synthesis in an organ intimately connected with versatile aspects of lipid metabolism.

Experimental Procedures

Animals

Adult specimens of *M. borellii* were collected in a freshwater stream near Rio de la Plata, Argentina. They were kept in the laboratory in glass aquaria containing

dechlorinated tap water at room temperature until they were used for experiments. All animal protocols were approved by the Committee for Care and Use of Laboratory Animals, School of Medicine, University of La Plata.

Isolation of Subcellular Fractions from Hepatopancreas of *M. borellii*

Approximately 60 animals were used in each isolation experiment. Specimens were kept on ice for 20 min and the hepatopancreas were quickly dissected and submerged in pre-cooled buffer H (10 mM Hepes-KOH, pH 7.4, 0.25 M sucrose, 1 mM EDTA, and 1 mM dithiothreitol (DTT)) with 0.002% v/v protease inhibitor cocktail (general use, Sigma). The total homogenate was prepared with 10 up-and-down strokes in a motor-driven Teflon-glass homogenizing vessel. Large debris and nuclei were removed by centrifuging twice at $600\times g$ at 4°C for 5 min, and the supernatant (post-nuclear homogenate) was centrifuged for 15 min at $10,000\times g$ at 4°C in a Sorvall refrigerated centrifuge. The resulting pellet was resuspended and recentrifuged twice with ice-cold buffer H to obtain the mitochondrial fraction. Additional purification of the mitochondrial fraction was performed by density-gradient centrifugation as previously described [17]. The combined supernatants were centrifuged for 1 h at $100,000\times g$ (Beckman LE-80K ultracentrifuge, rotor 70.1 Ti) to obtain microsomes. All steps were performed at 4°C and the fractions were aliquoted and frozen at -70°C . The total protein content of each fraction was determined with bovine serum albumin (BSA) as the standard [18].

GPAT Activity

GPAT activity was assayed in each fraction (100 μg of total protein) [19]. The incubation buffer contained 0.8 mM glycerol-3-phosphate (0.5 μCi [^{14}C]glycerol-3-phosphate, Amersham Biosciences), 75 mM Tris-HCl pH 7.4, 4 mM MgCl_2 , 2 mg/ml BSA, 8 mM NaF, 1 mM DTT, and the indicated concentrations of palmitoyl-CoA or oleoyl-CoA. The reaction was incubated at 30°C for 10 min and total radioactivity from the organic phase was quantified by liquid scintillation counting. In order to determine the effect of *N*-ethylmaleimide (NEM) or polymyxin B on GPAT activity, samples were pre-incubated for 30 min on ice in the presence of varying concentrations of NEM or polymyxin B. Products of the GPAT reaction were analyzed by thin-layer chromatography on silica-gel G plates. The solvent systems used to separate the products were hexane/ethyl ether/acetic acid (80:20:1.5; v/v) and chloroform/methanol/acetic acid/water (65:25:1:4; v/v) for neutral and polar lipids, respectively.

Marker Enzyme Activities

Arylesterase activity (ER marker) was measured as described previously [20], NADPH cytochrome c reductase (ER marker), and cytochrome c oxidase (inner mitochondrial membrane marker) were determined using cytochrome c oxidase and cytochrome c reductase (NADPH) assay kits (Sigma).

Immunoblotting

Fifty or one hundred microgram of total protein for each subcellular fraction were separated on an 8% SDS-PAGE, transferred to a polyvinylidene difluoride membrane (Bio-Rad), and probed with a 1/10,000 dilution of anti-GPAT1 antibody in phosphate buffer saline +0.05% Tween-20. Anti-GPAT1 antibody was obtained from rabbits immunized with recombinant rat liver GPAT1 expressed in insect cells and purified from inclusion bodies [21]. The membranes were then washed extensively and probed with horseradish peroxidase-conjugated goat anti-rabbit IgG (Pierce). For chemiluminescent detection, the membranes were incubated with Super Signal detection kit (Pierce).

Lipid Biosynthesis, Extraction and Separation

[¹⁴C]palmitate (3.5 nmol; 0.2 μCi) dissolved in 10 μl of propylene glycol was incubated with 300 μg of total microsomal or mitochondrial protein at 30°C for 60 min. The incubation mixture contained 75 mM Tris-HCl pH 7.4, 2 mM MgCl₂, 2 mg/ml BSA, 5 mM DTT, 5 mM ATP, and 0.2 mM CoASH (lithium salt) in a final volume of 0.35 ml. The reactions were carried out in either the presence or the absence of 20 mM glycerol-3-phosphate in the incubation mixture. 1-Monostearoyl-*rac*-glycerol dissolved in ethanol was added to the reaction in the absence of glycerol-3-phosphate at a final concentration of 100 μM. Lipids were extracted by the Folch procedure [22] and the radioactive lipid products were separated by thin-layer chromatography on silica-gel G plates using the same solvent systems described above. The radioactivity associated with each spot was quantified using a STORM 840 scanner (Amersham, Biosciences). Appropriate standards, run simultaneously, were visualized by exposure to iodine vapor.

Results

Characterization of the Cell Fractions Obtained from *M. borellii* Hepatopancreas

In this study we used total cellular homogenate, mitochondrial and microsomal subcellular fractions from

M. borellii hepatopancreas. To confirm the purity of these fractions, we tested them for marker enzymes that are widely used in mammals. The purity of the fractions was good (Table 1). Cytochrome c oxidase activity indicated some mitochondrial contamination of the microsomal fraction (near 20% of the total protein). Two different ER marker enzymes were tested: NADPH cytochrome c reductase and arylesterase activities. Both activities were present in the microsomal fraction but not in mitochondria. The mitochondrial fraction (10,000 g pellet) was further purified in a Percoll gradient. This technique is widely used to separate mitochondrial membranes from ER contaminants in lipid-biosynthetic organs like rat liver, and yields highly purified mitochondria and a separate band of ER-derived membranes [23, 24]. When *M. borellii* hepatopancreas mitochondria were purified by this method, no band corresponding to ER-derived membranes could be visualized (results not shown). These results are consistent with the absence of ER-markers in the 10,000 g mitochondrial pellet.

GPAT Activity was Primarily Recovered in the Mitochondrial Fraction

GPAT activity was assayed in hepatopancreas total homogenate, and in mitochondrial and microsomal fractions (Table 1, Fig. 1a). Because *M. borellii* GPAT is unstable after long freezing periods, all experiments were performed within two weeks of fractionation. GPAT activity was measured either in fresh and frozen-thawed samples, and no differences were observed in the specific activity values (results not shown). GPAT activity was highly enriched in the mitochondrial fraction (21-fold higher than homogenate) and 47% of total GPAT activity was recovered. In microsomes only 9% of the total GPAT activity was recovered and the enrichment was only 1.4-fold, similar to that of cytochrome c oxidase activity. These results suggest that all the GPAT activity present in microsomes was due to mitochondrial contamination.

The Main Product of GPAT Activity in Mitochondria was Phosphatidic Acid

Radioactive lipids were extracted from mitochondrial GPAT enzymatic assays and analyzed by thin-layer chromatography (Fig. 1b). The distribution of radioactivity associated with the glycerolipids synthesized from [¹⁴C]glycerol-3-phosphate was consistent with the products of the mammalian GPAT1 reaction [20]. In the mitochondrial fraction, the major product was phosphatidic acid (56%). The presence of diacylglycerols (11%) and TAG (32%) suggests that the enzymatic activities acyl-glycerol-3-phosphate acyltransferase (AGPAT), phosphatidic acid

Table 1 GPAT activity was enriched in the mitochondrial fraction of *M. borellii* hepatopancreas

	Cytochrome c oxidase			GPAT			Arylesterase			Cyt c Red		
	Specific activity (mU/mg)	Total activity (U)	Fold enrichment	Recovery (%)	Specific activity (pmol/mg min)	Total activity (pmol/min)	Fold enrichment	Recovery (%)	Specific activity ($\mu\text{mol/mg min}$)	Fold enrichment	Specific activity (mU/mg)	Fold enrichment
Total Homogenate	8.5 \pm 1.9	2.07	–	–	23 \pm 7	5,377	–	–	148 \pm 16	–	3.6 \pm 0.6	–
Mitochondria	181 \pm 14	1.43	21.3	69	322 \pm 38	2,524	14	47	–	–	–	–
Microsomes	11.9 \pm 1.0	0.44	1.4	21.2	34 \pm 7	515	1.5	9.6	519 \pm 32	3.5	10.9 \pm 0.7	3.0

GPAT specific activity was measured in total homogenate and in mitochondrial and microsomal fractions from *M. borellii* hepatopancreas. The purity of the fractions was monitored assaying the marker enzymes cytochrome c oxidase (mitochondria), NADPH cytochrome c reductase (Cyt c Red) and arylesterase (endoplasmic reticulum). Results are expressed as the means \pm SD of three independent experiments. Fold enrichment was calculated with respect to total homogenate

phosphohydrolase (PAPase), and diacylglycerol acyltransferase (DGAT) are also present in mitochondria. The amount of radioactivity obtained from GPAT assays in microsomes was not sufficient to analyze the reaction products.

Mitochondrial GPAT Preferred Saturated Fatty Acyl-CoA

The substrate specificity of GPAT was determined using palmitoyl-CoA and oleoyl-CoA as acyl-CoA donors. In the mitochondrial fraction, palmitoyl-CoA was the preferred substrate (Fig. 2a). The V_{max} value calculated with oleoyl-CoA as a substrate was 4-fold lower than the value obtained when the substrate was palmitoyl-CoA. Since higher concentrations of palmitoyl-CoA inhibited the GPAT activity, it was not feasible to determine a K_m value for this substrate. In contrast, oleoyl-CoA did not inhibit GPAT activity at a concentration as high as 120 μM and the apparent K_m value for this substrate, calculated by Lineweaver-Burk transformation, was 31.2 μM . The same experiments were performed using microsomes and identical substrate specificities were obtained, although the specific activities were 80% lower (Fig. 2b).

Mitochondrial GPAT Activity was NEM Resistant and Activated by Polymyxin B

Mitochondrial GPAT activity was resistant to inhibition by NEM at concentrations as high as 10 mM (Fig. 3). In contrast, preincubation of the mitochondrial fraction with the antibiotic polymyxin B markedly stimulated GPAT activity; at 0.5 mg/ml polymyxin B GPAT activity increased 2.7-fold (Fig. 3). The microsomal GPAT activity was also resistant to NEM-inactivation (results not shown).

Mitochondria from *M. borellii* Hepatopancreas Contained an Anti-GPAT1 Immunoreactive Protein

The polyclonal anti-GPAT1 antibody raised against rat liver GPAT1 recognized an immunoreactive protein with a molecular mass of 70 kDa in the mitochondrial fraction from hepatopancreas (Fig. 4). No immunoreactive protein was detected when 50 μg of total protein from microsomes were loaded on the gel, but a weak band was detected with 100 μg . Consistent with the low GPAT specific activity found in microsomes, this band might be the result of mitochondrial contamination. The presence of this immunoreactive band suggests that hepatopancreas mitochondria contain a protein homologous to GPAT1, consistent with NEM-resistant GPAT activity. The molecular weight of this protein was lower than that of rat liver GPAT1 (90 kDa). However, ER-GPAT 3 and 4 both have

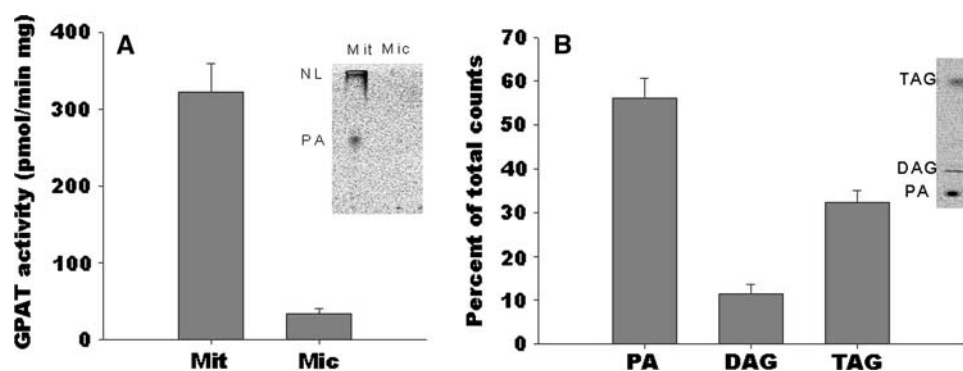


Fig. 1 **a** GPAT specific activity in mitochondrial (Mit) and microsomal (Mic) fractions from *M. borellii* hepatopancreas. Results are the means \pm S.E from three independent experiments. **b** Lipid classes distribution of [14 C]glycerol-3-phosphate esterified by mitochondria.

Results are representative of two independent experiments. The *inset* show the products of GPAT reaction resolved in TLC plates for polar (a) and neutral (b) lipids: PA phosphatidic acid; NL neutral lipids; DAG diacylglycerol; TAG triacylglycerol

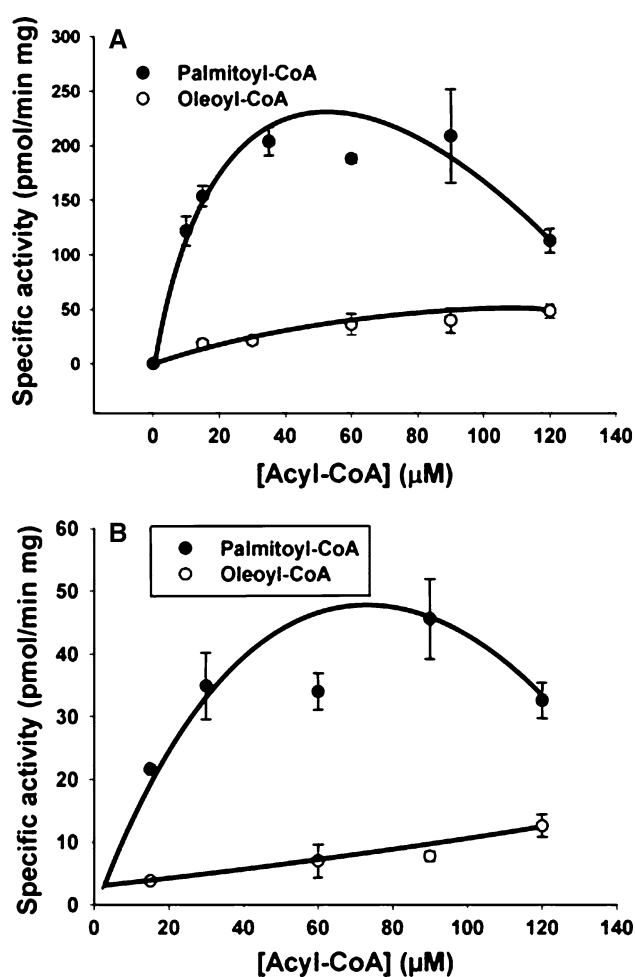


Fig. 2 Acyl-CoA substrate specificity of GPAT reaction in mitochondria (a) and microsomes (b). All assays contained 4 mM MgCl₂, 2 mg/ml BSA, 8 mM NaF, 1 mM DTT, 0.8 mM glycerol-3-phosphate (0.5 μ Ci [14 C]glycerol-3-phosphate per reaction) and the indicated concentrations of palmitoyl-CoA (filled circle) or oleoyl-CoA (open circle). Data points represent the means \pm SE of an experiment performed in duplicate and are representative of two independent experiments

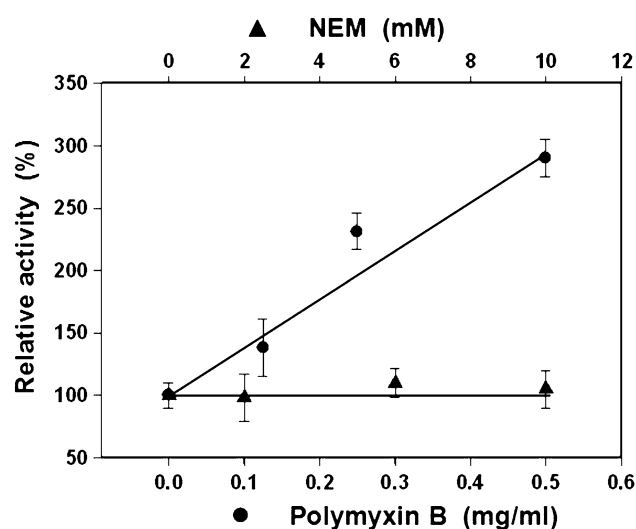


Fig. 3 Effect of NEM and polymyxin B on GPAT activity. Mitochondrial samples were pre-incubated for 30 minutes on ice in the presence of the indicated concentration of NEM (filled triangle) or polymyxin B (filled circle) in the incubation mixture. The results represent the means \pm SD from three independent experiments. The baseline specific activity was 322 \pm 38 pmol/min mg protein

molecular weights of approximately 40 kDa [10, 12], indicating that smaller GPAT proteins are also active.

Microsomes from *M. borellii* Hepatopancreas Esterified [14 C]Palmitate in the Absence of Glycerol-3-Phosphate

We had previously reported that microsomes from *M. borellii* hepatopancreas actively synthesized TAG [3]. To investigate the TAG synthesis pathway, experiments were performed under previously optimized experimental conditions in either the presence or absence of glycerol-3-phosphate and monoacylglycerol. When glycerol-3-phosphate (20 mM) was added to the reaction mixture, 54% of

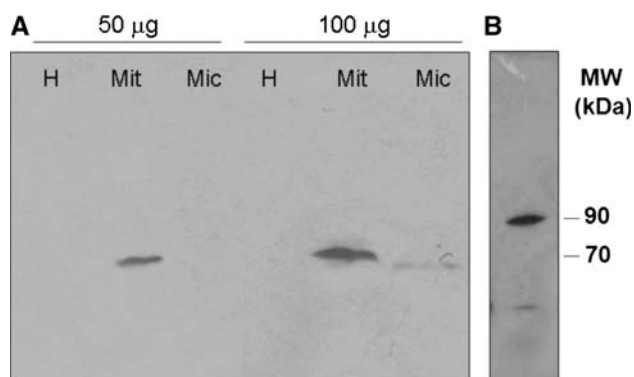


Fig. 4 Mitochondria from *M. borellii* contain an immunoreactive protein against GPAT1 antibody. **a** 50 µg or 100 µg of total protein from total homogenate (*H*), mitochondria (*Mit*), and microsomes (*Mic*) were loaded on SDS-PAGE 8%, transferred to PVDF membranes, probed with a polyclonal anti-rat liver GPAT1 antibody and visualized by ECL. The immunoreactive band molecular mass is 70 kDa. **b** 50 µg of rat-liver mitochondria were probed with the same antibody. The immunoreactive band molecular mass is 90 kDa

the [^{14}C]palmitate was esterified (104 pmol of esterified palmitate/min mg protein) (Table 2 and Fig. 5). Radioactivity was incorporated primarily into neutral glycerolipids (83.8%) and to a lesser extent into phospholipids (14%). The major neutral lipid product was TAG (about 65%). When glycerol-3-phosphate was omitted, 40% of the [^{14}C]palmitate was esterified, (78 pmol of esterified palmitate/min mg protein) and the distribution of the radioactivity among lipid classes was similar; under this condition adding 100 µM monostearoylglycerol increased TAG synthesis nearly 2-fold (Fig. 6).

In mitochondria, TAG synthesis required glycerol-3-phosphate as a substrate. [^{14}C]palmitate esterification into lipids was higher than in microsomes (74%, 144 pmol of esterified palmitate/min mg protein) (Table 2 and Fig. 5) and 70% of the radioactive palmitate was detected in the TAG fraction.

Discussion

In crustaceans, the hepatopancreas carries out essential functions of energy metabolism. We reported that the hepatopancreas of the fresh-water shrimp *M. borellii* is the major lipid-biosynthetic organ, and that the microsomal fraction synthesizes TAG [3]. Thus, we focused our studies on the enzyme that catalyzes the first and committed step in glycerolipid synthesis, GPAT, hypothesizing that, as in mammalian cells, more than one isoform might be present in different subcellular compartments to exert a specific metabolic function.

We measured GPAT activity following a method widely used in mammalian tissues [17]. Under these conditions,

Table 2 Microsomal and mitochondrial esterification of [^{14}C]palmitate

	Microsomes		Mitochondria
G3P addition	0	20 mM	20 mM
Specific activity (pmol/min mg) ^a	78 ± 4	104 ± 14	144.3 ± 10
Neutral lipids (%)	81.1 ± 7.3	83.8 ± 2.7	80.0 ± 8.2
Triacylglycerols (%)	56.6 ± 18.2	66.5 ± 11.3	70.7 ± 2
Phospholipids	18.4 ± 7.4	13.9 ± 4.2	17.8 ± 1.4

Esterification of [^{14}C]palmitate by microsomes and mitochondria from *M. borellii* hepatopancreas was measured either in the presence or absence of 20 mM glycerol-3-phosphate in the incubation mixture. Lipids were separated by TLC and the radioactivity quantified. Neutral glycerolipids include triacylglycerol, diacylglycerol, and monoacylglycerol. Triacylglycerol values are distinguished

^a Specific activity indicates the pmol of [^{14}C]palmitate esterified into lipids/min. mg protein

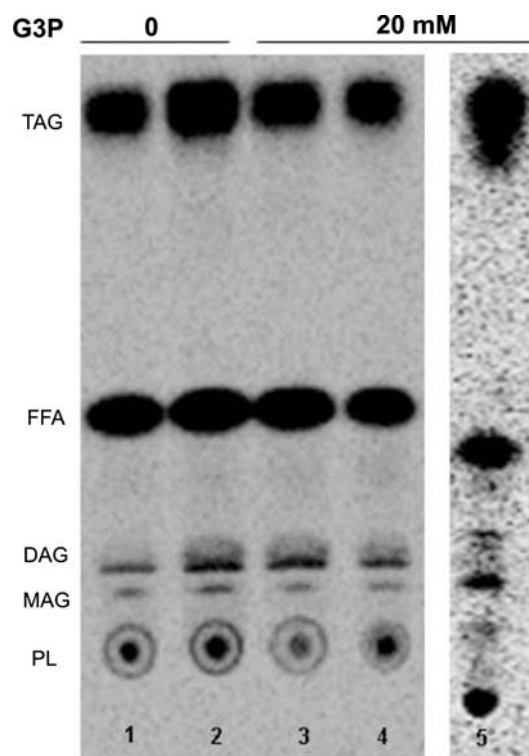


Fig. 5 Microsomal and mitochondrial glycerolipid biosynthesis from [^{14}C]palmitate. About 300 µg of hepatopancreas microsomal (lanes 1–4) or mitochondrial (lane 5) protein was incubated using [^{14}C]palmitate (0.2 µCi) as substrate either in the presence or in the absence of 20 mM glycerol-3-phosphate (G3P). Reaction products were analyzed by TLC and the radioactivity quantified by scanning proportional counting. TAG triacylglycerol, FFA free fatty acids, DAG diacylglycerol, MAG monoacylglycerol, PL phospholipids

GPAT activity can be detected in microsomes and mitochondria from rat liver. GPAT activities can be distinguished by their varying sensitivities to sulfhydryl reagents like

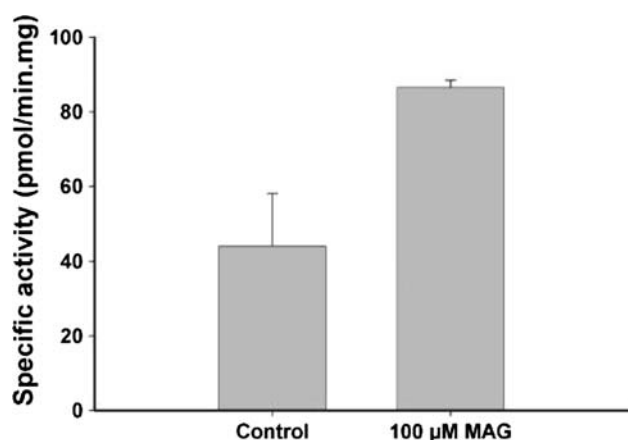


Fig. 6 Microsomal triacylglycerol biosynthesis is increased in the presence of monostearoylglycerol. About 300 μg of hepatopancreas microsomal protein was incubated using [14 C]palmitate (0.2 μCi) as substrate without any external source of glycerol (Control) and 100 μM monostearoylglycerol (MAG). Reaction products were analyzed by TLC and the radioactivity present in the TAG fraction quantified by scanning proportional counting. Specific activity values correspond to pmoles of synthesized triacylglycerol/min. mg of microsomal protein. Values represent the means \pm S.E of two independent experiments

NEM. In liver the NEM-sensitive activity comprises 50–60% of total GPAT activity whereas in most other organs it comprises about 90% of total GPAT activity [6]. In rat liver, the NEM-sensitive activity is attributed to microsomal GPAT3 and GPAT4 because expression of the mitochondrial NEM-sensitive isoform GPAT2 is very low [9].

Surprisingly, since microsomal fractions synthesize TAG [3], GPAT activity was recovered primarily in the mitochondrial fraction. Kinetic properties of the *M. borellii* mitochondrial activity were similar to those of rat and mouse GPAT1 [25]. The activity was NEM-resistant, it showed a preference for saturated-acyl-CoA substrates, and like mammalian GPAT1, it was activated by polymyxin B [26], an antibiotic that interferes with the glycerolipid packing in both bacteria and synthetic membranes. Activation of GPAT by polymyxin B was more striking in shrimp hepatopancreas than in rat liver mitochondria, suggesting that in the crustacean, membrane fluidity plays an important role in regulating GPAT activity. Finally, an anti-GPAT1 polyclonal antibody, raised against full-length recombinant rat GPAT1, recognized a single 70 kDa protein present in the mitochondrial fraction. These data suggest that GPAT1 from rat-liver mitochondria and the mitochondrial GPAT from *M. borellii* hepatopancreas may be homologous. Cloning and sequencing the *M. borellii* GPAT gene will be required to fully address this issue.

When hepatopancreas mitochondria were incubated with [14 C]glycerol-3-phosphate under the conditions optimized to measure GPAT activity, the major reaction product was phosphatidic acid, as observed in membranes

from rat liver that contain both GPAT and acyl-glycerol-3-phosphate acyltransferase. An additional 43% of the radiolabel was found in diacylglycerol and TAG. Under different conditions that were optimized for TAG synthesis, and which depended on the activities of several enzymes, the major reaction product was TAG (74%), indicating that mitochondria can perform the full pathway of de novo TAG synthesis.

Our results are consistent with the interpretation that the GPAT activity detected in microsomes is due to mitochondrial contamination. First, enrichment of GPAT activity in the microsomal fraction was equivalent to that of the mitochondrial marker enzyme cytochrome c oxidase. Second, the GPAT activity in microsomes had the same kinetic parameters and substrate preference as the mitochondrial activity. Finally, only a very faint band reactive to the anti-GPAT1 antibody was detected when 100 μg of microsomal protein was analyzed by western blot. Nevertheless, the possibility remains open that an independent microsomal GPAT isoform exists, that this activity has different kinetic parameters, and that the activity is not detectable under our experimental conditions.

The low GPAT activity in the microsomal fraction was unexpected because we had previously reported that the microsomal fraction incorporates [14 C]palmitate into TAG as the major product [3]. In that study, assays were performed in the presence of glycerol-3-phosphate, and we had assumed that TAG was synthesized de novo via the glycerol-3-phosphate pathway. In the present study, we showed that in the absence of glycerol-3-phosphate, microsomes retain 75% of their capacity to esterify [14 C]palmitate into glycerolipids. We attribute the difference in microsomal specific activity values for palmitate esterification in the presence and absence of high concentrations of glycerol-3-phosphate (104 and 78 pmol of esterified palmitic acid/min mg, respectively) to mitochondrial GPAT activity that is contaminating the microsomal fraction (about 20%).

Taking into account the absorptive function of the hepatopancreas and the TAG-lipase activity that has been reported in hepatopancreas cells from *M. borellii* [16] and other crustaceans [1], we considered the possibility that an alternative substrate, different from glycerol-3-phosphate, might account for the high rate of TAG synthesis observed in the microsomal fraction. Replacing glycerol-3-phosphate with 100 μM monoacylglycerol caused a 2-fold increase in TAG synthesis, suggesting that in microsomes, TAG synthesis occurs mainly via the monoacylglycerol pathway.

The initial step in glycerolipid synthesis in bacteria is catalyzed by a single gene product, *plsB* (GPAT) in Gram-negative bacteria and by *plsY* (acyl-ACP:phosphate transacylase) in Gram-positive bacteria. In contrast, both lower and higher eukaryotes express more than one GPAT

isoform and at least one of the isoforms is located in the ER. Information about TAG synthesis in invertebrates is scarce. Only a single report from more than three decades ago, described the incorporation of [^{14}C]glycerol-3-phosphate into the lipids of the insect *Ceratitis capitata* and demonstrated that TAG could be synthesized in mitochondria, although a higher rate of TAG synthesis was observed in microsomes [27].

We conclude here that de novo synthesis of TAG is initiated in mitochondria, whereas in microsomes TAG synthesis occurs by an alternate pathway, probably the monoacylglycerol pathway. Although the *M. borellii* GPAT gene has not yet been cloned, its properties suggest that it could be homologous to *PlsB* and to mitochondrial GPAT1, members of a highly conserved acyltransferase family.

Acknowledgments This work was supported by grants from the National Institutes of Health, NIH, (TW06034 and DK56598) and Consejo Nacional de Investigaciones Científicas y Técnicas, CONICET, (PIP6503). MPM and ERC are research fellows, and CFG and MRGB are members of the Carrera del Investigador Científico y Tecnológico, CONICET, Argentina.

References

1. Ceccaldi HJ (1989) Anatomy and physiology of digestive tract of Crustaceans Decapods reared in aquaculture. *Adv Trop Aquac* 9:243–259
2. Gonzalez-Baro MR, Pollero RJ (1988) Lipid characterization and distribution among tissues of the freshwater crustacean *Macrobrachium borellii* during an annual cycle. *Comp Biochem Physiol* 97B:711–715
3. Gonzalez-Baro MR, Pollero RJ (1993) Palmitic acid metabolism in the hepatopancreas of the freshwater shrimp *Macrobrachium borellii*. *Comp Biochem Physiol* 106B:71–75
4. Pollero RJ, Gonzalez-Baro MR, Irazu CE (1991) Lipid classes consumption related to fasting and thermal stress in the shrimp *Macrobrachium borellii*. *Comp Biochem Physiol* 99B:233–238
5. Sanchez-Paz A, Garcia-Careno F, Muhlia-Almazan A, Peregrino-Urriarte AB, Hernandez-Lopez J, Yepiz-Plascencia G (2006) Usage of energy reserves in crustaceans during starvation: status and future directions. *Insect Biochem Mol Biol* 36:241–249
6. Coleman RA, Lee DP (2004) Enzymes of triacylglycerol synthesis and their regulation. *Prog Lipid Res* 43:134–176
7. Bhat GB, Wang P, Kim JH, Black TM, Lewin TM, Fiedorek FT Jr, Coleman RA (1999) Rat sn-glycerol-3-phosphate acyltransferase: molecular cloning and characterization of the cDNA and expressed protein. *Biochim Biophys Acta* 1439:415–423
8. Paulauskis JD, Sul HS (1988) Cloning and expression of mouse fatty acid synthase and other specific mRNAs. Developmental and hormonal regulation in 3T3-L1 cells. *J Biol Chem* 263:7049–7054
9. Wang S, Lee DP, Gong N, Schwerbrock NM, Mashek DG, Gonzalez-Baro MR, Stapleton C, Li LO, Lewin TM, Coleman RA (2007) Cloning and functional characterization of a novel mitochondrial N-ethylmaleimide-sensitive glycerol-3-phosphate acyltransferase (GPAT2). *Arch Biochem Biophys* 465:347–358
10. Cao J, Li JL, Li D, Tobin JF, Gimeno RE (2006) Molecular identification of microsomal acyl-CoA:glycerol-3-phosphate acyltransferase, a key enzyme in de novo triacylglycerol synthesis. *Proc Natl Acad Sci U S A* 103:19695–19700
11. Chen YQ, Kuo MS, Li S, Bui HH, Peake DA, Sanders PE, Thibodeaux SJ, Chu S, Qian YW, Zhao Y, Bredt DS, Moller DE, Konrad RJ, Beigneux AP, Young SG, Cao G (2008) AGPAT6 is a novel microsomal glycerol-3-phosphate acyltransferase. *J Biol Chem* 283:10048–10057
12. Nagle CA, Vergnes L, Dejong H, Wang S, Lewin TM, Reue K, Coleman RA (2008) Identification of a novel sn-glycerol-3-phosphate acyltransferase isoform, GPAT4, as the enzyme deficient in *Agpat6*^{-/-} mice. *J Lipid Res* 49:823–831
13. Igal RA, Wang SL, Gonzalez-Baro MR, Coleman RA (2001) Mitochondrial glycerol phosphate acyltransferase directs the incorporation of exogenous fatty acids into triacylglycerol. *J Biol Chem* 276:42205–42212
14. Gonzalez-Baro MR, Lewin TM, Coleman RA (2007) Regulation of triglyceride metabolism. II. Function of mitochondrial GPAT1 in the regulation of triacylglycerol biosynthesis and insulin action. *Am J Physiol Gastrointest Liver Physiol* 292:G1195–G1199
15. Gonzalez-Baro MR, Irazu CE, Pollero RJ (1990) Palmitoyl-CoA ligase activity in the hepatopancreas and gill microsomes of the freshwater shrimp *Macrobrachium borellii*. *Comp Biochem Physiol* 97B:129–133
16. Lavarias S, Pollero RJ, Heras H (2006) Activation of lipid catabolism by the water-soluble fraction of petroleum in the crustacean *Macrobrachium borellii*. *Aquat Toxicol* 77:190–196
17. Pellon-Maison M, Montanaro MA, Coleman RA, Gonzalez-Baro MR (2007) Mitochondrial glycerol-3-P acyltransferase 1 is most active in outer mitochondrial membrane but not in mitochondrial associated vesicles (MAV). *Biochim Biophys Acta* 1771:830–838
18. Lowry OH, Rosebrough NJ, Farr AL, Randall RJ (1951) Protein measurement with the Folin phenol reagent. *J Biol Chem* 193:265–275
19. Pellon-Maison M, Coleman RA, Gonzalez-Baro MR (2006) The C-terminal region of mitochondrial glycerol-3-phosphate acyltransferase-1 interacts with the active site region and is required for activity. *Arch Biochem Biophys* 450:157–166
20. Shephard EH, Hubscher G (1969) Phosphatidate biosynthesis in mitochondrial subfractions of rat liver. *Biochem J* 113:429–440
21. Lewin TM, Kim JH, Granger DA, Vance JE, Coleman RA (2001) Acyl-CoA synthetase isoforms 1, 4, and 5 are present in different subcellular membranes in rat liver and can be inhibited independently. *J Biol Chem* 276:24674–24679
22. Folch J, Lees M, Sloane Stanley GH (1957) A simple method for the isolation and purification of total lipides from animal tissues. *J Biol Chem* 226:497–509
23. Hovius R, Lambrechts H, Nicolay K, de Kruijff B (1990) Improved methods to isolate and subfractionate rat liver mitochondria lipid composition of the inner and outer membrane. *Biochim Biophys Acta* 1021:217–226
24. Vance JE (1990) Phospholipid synthesis in a membrane fraction associated with mitochondria. *J Biol Chem* 265:7248–7256
25. Saggerson ED, Carpenter CA, Cheng CH, Sooranna SR (1980) Subcellular distribution and some properties of N-ethylmaleimide-sensitive and -insensitive forms of glycerol phosphate acyltransferase in rat adipocytes. *Biochem J* 190:183–189
26. Carroll MA, Morris PE, Grosjean CD, Anzalone T, Haldar D (1982) Further distinguishing properties of mitochondrial and microsomal glycerophosphate acyltransferase and the transmembrane location of the mitochondrial enzyme. *Arch Biochem Biophys* 214:17–25
27. Meier PJ, Spycher MA, Meyer UA (1981) Isolation and characterization of rough endoplasmic reticulum associated with mitochondria from normal rat liver. *Biochim Biophys Acta* 646:283–297

Influence of Commercial Dietary Oils on Lipid Composition and Testosterone Production in Interstitial Cells Isolated from Rat Testis

Graciela E. Hurtado de Catalfo ·
María J. T. de Alaniz · Carlos Alberto Marra

Received: 1 October 2008 / Accepted: 4 December 2008 / Published online: 8 January 2009
© AOCS 2008

Abstract The aim of this study was to examine the influence of dietary fat on lipid composition, as well as on the steroidogenic function of interstitial cells isolated from Wistar rats that had been fed semi-synthetic diets containing four different commercial oils (S soybean, O olive, C coconut, and G grape seed). Steroidogenic enzyme activities, lipid composition, and androgen production were measured in testicular interstitial cells. Lipid analysis included measurement of the contents of major lipid subclasses (neutral lipids, polar lipids, free and esterified cholesterol), as well as principal polar and neutral lipid fatty acyl compositions. Significant differences in lipid composition were observed among the groups, most of them reflecting the specific fatty acyl composition of the diet tested. Testosterone concentration was higher in O and C groups compared with S or G. In agreement with this observation, the activity of both key enzymes involved in testosterone biosynthesis (3β -HSD and 17β -HSD) was higher in O and C groups with significant differences between them ($O > C$). A significant negative correlation was found between cellular testosterone production and cellular cholesterol ester content. Additionally, testosterone concentration directly correlated with cholesterol levels. We conclude that dietary oils qualitatively and quantitatively modified the lipid composition of interstitial cells, producing either a direct or indirect regulatory effect on testicular steroidogenic function.

Keywords Lipid composition · Fatty acids · Testosterone production · Testicular interstitial cells · Dietary lipids

Abbreviations

C	Coconut
FC	Free cholesterol
CE	Esterified cholesterol
DBI	Double bond index
FA	Fatty acids
FAME	Fatty acid methyl esters
G	Grape seed
3β -HSD	3β -Hydroxysteroid dehydrogenase
17β -HSD	17β -Hydroxysteroid dehydrogenase
HPLC	High performance liquid chromatography
LH	Luteinizing hormone
MUFA	Monounsaturated FA
NL	Neutral lipids
O	Olive
PL	Polar lipids (phospholipids)
PUFA	Polyunsaturated FA
R _f	Relative chromatographic mobility
RIA	Radioimmunoassay
S	Soybean
SFA	Saturated FA
T	Testosterone
TL	Total lipids
TLC	Thin layer chromatography
TAG	Triacylglycerides

G. E. H. de Catalfo · M. J. T. de Alaniz · C. A. Marra (✉)
Instituto de Investigaciones Bioquímicas de La Plata
(INIBIOLP), CCT-La Plata-CONICET-UNLP,
Cátedra de Bioquímica, Facultad de Ciencias Médicas,
Universidad Nacional de La Plata, Calles 60 y 120 (1900),
La Plata, Argentina
e-mail: camarra@atlas.med.unlp.edu.ar

Introduction

It has long been known that changes in dietary fat [1–3] and/or cholesterol intake [4, 5] modify membrane

phospholipid composition in many tissues and cell types, thus influencing normal cell function. In the testis, it has been demonstrated that lipids strongly influence the histology and physiology of this tissue [6–8]. Different situations, such as essential fatty acid deficiency [9, 10] or alterations in fatty acid metabolism under diabetic conditions [10, 11], have been associated with testicular malfunction. Regarding androgen biosynthesis, it has been demonstrated that feeding rats with rapeseed oil rich in polyunsaturated fatty acids (PUFA) was associated with a high level of testosterone [12]. In contrast, decreased androgen concentration was measured in rats fed palm oil, which is rich in saturated fatty acids [12]. Total fat intake was also related to the level of sex steroid hormones. Some studies on men and rats have revealed that there was an increase in plasma androgen concentration after being fed a high-fat diet [13, 14]. In contrast, a reduction in total fat intake caused a decrease in plasma testosterone concentration [15]. Most studies on the relationship between dietary fat and testicular steroidogenesis have been carried out by analyzing the lipid composition of the whole testes. Additionally, we are unaware of any information concerning the possible relationship(s) between androgen production and a particular change in the lipid composition of interstitial cells. Therefore, the aim of this study was to evaluate the effect of diet supplementation, using four oils commercially available world wide, on lipid composition of interstitial cells and their impact on steroidogenic function.

Materials and Methods

Chemicals

Solvents (HPLC grade) were provided by Carlo Erba (Milano, Italy). Other chemicals were from Sigma Chem. Co. and Fluka Chemie AG (Buenos Aires, Argentina). Lipids used as standards were from the Serdary Research Lab (London, ON, Canada) or from Nu-Check-Prep (Elysian, MN). Collagenase was obtained from Worthington, Freehold, NJ. The commercially available oils that were added to the diets were from Molinos Río de La Plata SAIC and Platafarm SA (La Plata, Argentina).

Diets and Animal Treatment

Male Wistar rats weighing 180 ± 10 g with had been certified as specific-pathogen free (Laboratory Animal Care and Supply Facilities, Veterinary Medical School, UNLP) were used. Upon arrival, the rats were allowed to acclimatize for a week before starting the experiments. Rats were housed individually and maintained under controlled

conditions at a temperature of 25 ± 2 °C with a normal photoperiod of 12 h dark and 12 h light. They were fed with standard Purina chow (Cargill type “C”) from Ganave Co. (Santa Fe, Argentina) and water ad libitum throughout gestation and lactation. Clinical examinations together with body weight evaluation were performed every week during the experiment. Male pups (47 ± 4 g/animal) were divided into four groups of ten animals each, and fed specific diets ad libitum. Isocaloric diets (Table 1) were prepared in an identical manner, except for the lipid source, which was added as commercial oil (70 g/kg diet): soybean (S), olive (O), coconut (C), or grape seed (G). The fatty acyl composition of each diet is detailed in Table 2. Rats were fed according to the American Institute of Nutrition [16]. Animal maintenance and handling were conducted as recommended by NIH guidelines [17]. All procedures were approved by the local Laboratory Animal Committee, Facultad de Ciencias Médicas, UNLP, Argentina.

Experimental Design

Rats were sacrificed after being fed with the diets for 60 days. In order to avoid individual differences among animals, all rats were fasted for 24 h on day 59, giving access to the appropriate diet for 2 h, and killed by decapitation 12 h after the re-feeding period. Food intake,

Table 1 Composition of basal AIN-93 diet

Ingredients (g/kg)	
Casein, high protein	250.0
Sucrose	100.0
Corn starch	397.4
Cellulose	50.0
Commercial oil	70.0
Mineral mixture ^a	35.0
Sodium phosphate, monobasic	8.9
Potassium phosphate, monobasic	8.8
Calcium carbonate	12.5
Calcium phosphate–2H ₂ O	6.3
<i>tert</i> -Butylhydroquinone	0.014
Vitamin mixture ^b	10.0
Choline bitartrate	2.5
L-Cystine	3.0

^a Contained (g/kg mix.): NaCl 184, K₂SO₄ 136, C₆H₅O₇ (K)₃ 576, MgO 63, MnCO₃ 9.2, ferric citrate 17, ZnCO₃ 4.2, CuCO₃ 1, ammonium molybdate 0.03, Na₂SeO₃–5H₂O 0.03, CrK(SO₄)–12H₂O 1.0, KIO₄ 0.05, delipidated casein 8.09

^b Contained (g/kg mix): thiamine hydrochloride 0.5, riboflavin hydrochloride 0.5, niacin 0.5, pyridoxine 0.5, Ca-pantothenate 2.6, biotin 0.12, choline hydrochloride 50, folic acid 0.1, nicotinamide 1.26, *p*-aminobenzoic acid 0.5, inositol 50, Vitamin B12 0.006, Vitamin A 0.06, D-calciferol 0.01, α -tocopherol 1.5, menadione 2.5, ascorbate 6.0, L-methionine 2.0, delipidated casein 986.7

Table 2 Fatty acid composition of diets

Fatty acid	Diets			
	S	O	C	G
6:0			1.3 ± 0.1	
8:0			12.5 ± 0.3	
10:0			8.0 ± 0.2	
12:0			48.9 ± 1.1	
14:0		0.2 ± 0.0a	14.7 ± 0.3b	0.2 ± 0.0
15:0			0.1 ± 0.0	
16:0	11.5 ± 0.5a	15.5 ± 0.3a	6.9 ± 0.1b	7.5 ± 0.3b
16:1(n-7)	0.1 ± 0.0a	2.3 ± 0.1b	0.1 ± 0.0a	0.1 ± 0.0a
18:0	16.5 ± 0.4a	5.0 ± 0.1b	2.0 ± 0.1c	9.8 ± 0.2d
18:1(n-9)	9.7 ± 0.3a	68.5 ± 1.3b	4.0 ± 0.1c	16.8 ± 0.4d
18:1(n-7)		0.1 ± 0.0		0.1 ± 0.0
18:2(n-6)	55.1 ± 1.9a	8.2 ± 0.3b	1.3 ± 0.0c	65.1 ± 2.0d
18:3(n-6)	0.1 ± 0.0	0.1 ± 0.0		0.1 ± 0.0
18:3(n-3)	6.8 ± 0.1a	0.1 ± 0.0b		0.1 ± 0.0b
20:0			0.2 ± 0.0	
20:2(n-6)				0.1 ± 0.0
20:3(n-6)				0.1 ± 0.0
20:4(n-6)	0.1 ± 0.0			tr
20:5(n-3)	0.1 ± 0.0			
Analytical parameters				
ΣSFA	28.0 ± 0.7a	20.7 ± 0.3b	94.6 ± 0.9c	17.6 ± 0.7d
ΣMUFA	9.8 ± 0.2a	70.8 ± 0.9b	4.1 ± 0.1c	17.0 ± 0.9d
ΣPUFA	62.2 ± 1.8a	8.4 ± 0.2b	1.3 ± 0.0c	65.5 ± 1.8a
DBI	141.6 ± 3.3a	87.8 ± 1.4b	8.0 ± 0.2c	148.3 ± 4.4a
Σ(n-6)/ Σ(n-3)	7.9 ± 0.2a	83.0 ± 2.0b	∞c	654.0 ± 18d

Different letters on the same row indicate values significantly different ($P < 0.01$) as determined by one-way ANOVA and Tukey's post hoc test

Means below 0.1% are indicated as "tr"

Results are expressed as moles % (mean ± 1 SD; $n = 6$)

S soybean oil, O olive oil, C coconut oil, G grapeseed oil

c-GLC of the FAME was performed as indicated in "Materials and Methods"

Σ sum of: SFA saturated fatty acids, MUFA monounsaturated fatty acids, PUFA polyunsaturated fatty acids, DBI double bond index

water consumption, and body weight were individually registered during the feeding period. After sacrifice, testes were removed, weighed, and used for the isolation of interstitial cells.

Interstitial Cell Isolation

The technical procedure for interstitial cell isolation was described in detail in a previous report [18]. Briefly, cells were removed from the interstitial space of the testicular tissue by mechanical shaking with collagenase in a

metabolic incubator, at 34 °C, according to the method of Suescun et al. [19]. Cells were suspended in Krebs-Ringer bicarbonate glucose (KRBG 0.1%), albumin (0.1%), pH 7.4, examined for viability (85–90%) by exclusion of trypan blue [20], and counted in a hemocytometer to adjust cell concentration. Aliquots of cell suspensions were subjected to protein determination by the micromethod of Bradford [21]. Interstitial cell preparations consisted of Leydig cells (70%) and of spermatids, spermatocytes and small cytoplasmic fragments (21%). The homogeneity of cell preparations was assessed by means of observation of smears fixed in acetone and stained with hematoxylin-eosin.

Lipid Analysis of Diets and Interstitial Cells

The fatty acid compositions of the diets were routinely checked by gas-liquid chromatography after derivatization by methanolic boron trifluoride as described below for lipid cell isolation and analysis. Total cell lipids were extracted using the Folch procedure [22]. Neutral (NL) and phospholipids (PL) were isolated from the total lipid extract by silicic acid microchromatography [23]. Absolute content of the major lipid subclasses was obtained using commercial silicagel G-60 TLC plates (Merck, Darmstadt, Germany) as previously described [24]. The total amount of lipids in each fraction was determined by either inorganic phosphorous quantification [25] or gravimetrically [26]. Lipids separated by TLC were visualized and identified using the method of Nakamura and Handa [27]. R_f values were as reported previously [24]. Individual lipid components were quantified densitometrically [28]. Cholesterol content (FC) was enzymatically measured [29]. Triacylglyceride content (TAG) was assayed using a kit from the Wiener Lab (Rosario, Argentina). Total fatty acyl methyl esters (FAME) were prepared by transesterification with methanolic boron trifluoride [30] and analyzed by capillary gas-liquid chromatography (c-GLC) in a Hewlett Packard HP 6890, with a terminal computer integrator system. FAMES were identified by comparison of their relative retention times with authentic standards.

Steroidogenic Enzyme Activities

Sonicated interstitial cells were centrifuged (10,000g, 15 min, 1–2 °C). Aliquots of supernatants were employed to determine 3-β-hydroxysteroid-dehydrogenase (3-β-HSD) and 17-β-hydroxysteroid-dehydrogenase (17-β-HSD) enzyme activities using the method of Marugesan et al. [31].

Hormone Measurement

For the determination of testosterone levels in cells, interstitial cell suspensions were washed twice with cold

PBS and centrifuged (4,000g, 5 min). Pelleted cells were resuspended and homogenized by sonication (three 30-s bursts at 50% output in a Heat Systems Ultrasonic sonicator model W-220F from Plainview, NY) in 65 mM Tris–HCl buffer (pH 7.0) containing 10% sucrose and antiprotease inhibitor cocktail (from Sigma Chem. Co., Buenos Aires, Argentina) at the concentration recommended by the manufacturer. Cellular and plasma testosterone and plasma luteinizing hormone concentrations were determined by radioimmunoassay (RIA) using a commercial kit from Radim (Ponenzia, Italy).

Statistics

Statistical significance of data values was analyzed by one-way ANOVA followed by Tukey's test with the aid of Systat (Version 8.0 for Windows) from SPSS Science (Chicago, IL). Results were also plotted and analyzed using Sigma Scientific Graphing Software (Version 8.0) from Sigma Chem. Co. (St Louis, MO). Multivariable regression analysis was performed as described by Kleinbaum and Kupper [32].

Results

Fatty Acid Composition of Diets

Significant differences in fatty acyl composition were observed among diets (Table 2). Saturated fatty acids (SFA) represent approximately 95% of the total fatty acid (FA) content of Diet C and are mainly comprised of short or medium carbon chain fatty acids. Diet O was characterized by the highest content of monounsaturated fatty acids (MUFA), mainly oleic acid. Polyunsaturated fatty acid (PUFA) levels were high in both Diets S and G, with linoleic acid being the predominant FA. α -Linolenic acid was found in very low levels in all diets, except S (approximately 7%). As concerns the n-6/n-3 ratios, they were varied widely among diets. We observed that the relative proportion of n-6 versus n-3 fatty acyl chains decreased in the order C > G > O > S. In agreement with the fatty acyl composition of each diet, the corresponding double bond index (DBI) decreased in the order G = S > O > C.

Influence of Diets on Growth Parameters

The influence of diets on feeding parameters is listed in Table 3. Diets did not significantly influence water consumption (approximately 15 g/day). Initial body weights were similar in all groups. However, final body weights, rate of body weight gain, and food efficiency ratio were

significantly elevated in Group C when compared with the others. Both absolute and relative testicular weights were significantly higher in Group O when compared to the other groups.

Changes Induced by Diets on Major Lipid Subclasses

Table 4 shows the effects caused by the diets on the absolute amount of major lipid subclasses of interstitial cells. Rats fed on Diets C and O displayed major amounts of total lipids compared with Groups S and G. The highest concentrations of phospholipids (PL) were present in Group O and those of the neutral lipids (NL) in Group C. The NL/PL ratio was three times higher in Group C with respect to those ratios observed in the other experimental groups. Group C was enriched in triacylglycerides, as well as in free cholesterol (FC). Esterified cholesterol (CE) was present in relatively small amounts in all groups. When comparing the FC/CE ratios, we observed similar values in Groups C and O, which were approximately five times higher than those calculated for the other groups.

The influence of dietary lipids on the main phospholipid subclasses is shown in Table 5. Interstitial cells from rats fed on Diet O exhibited significantly higher concentrations of PC, PE, and PI than in the other groups. Other phospholipids such as phosphatidylserine, sphingomyelin, phosphatidic acid, and phosphatidylglycerol, were present in similar amounts in all groups.

Dietary Effect on Fatty Acyl Composition of Lipid Subclasses

The relative distribution of fatty acids in PC, PE, and TAG lipids of interstitial cells is shown in Tables 6, 7, 8, respectively. We observed significant differences among groups. One of the most important changes occurred in phosphatidylcholine (PC) (Table 6) from Group C, of which 73% was composed of SFA, mainly 16:0 and 18:0, with minor amounts of short and medium carbon chain fatty acids (14:0 and 15:0). This group also showed the lowest level of both MUFA and PUFA. Group O was characterized by the highest MUFA content, mainly oleic acid, as well as the lowest levels of SFA (16:0 and 18:0). PUFA levels were similar to those observed in Groups S and C. Cells isolated from grape seed-oil fed rats were characterized by the highest amount of PUFA (45%), mainly 18:2, 20:4, and 22:5 acids of the n-6 series, with relatively low levels of SFA and MUFA. Group S was characterized by its high content of SFA followed by PUFA, especially 20:4 and 22:5 acids from the n-6 series. DBI calculated from PC fatty acyl compositional data decreased in the order G > O > S > C. Despite the fact that PE fatty acyl composition (Table 7) differs from that

Table 3 Main feeding parameters associated to diets

Parameters	Diets			
	S	O	C	G
Initial body weight (g)	40.5 ± 0.3	41.1 ± 0.4	40.0 ± 0.2	42.3 ± 0.6
Final body weight (g)	162.6 ± 5.5a	160.1 ± 4.0a	188.9 ± 4.1b	159.7 ± 5.3a
Body weight gain (g)	122.1 ± 3.3a	119.0 ± 3.7a	148.9 ± 3.1b	117.4 ± 3.5a
Rate of body weight gain (g/day)	2.1 ± 0.1a	2.0 ± 0.1a	2.5 ± 0.1b	2.0 ± 0.1a
Food efficiency ratio ^a	8.5 ± 0.2a	7.9 ± 0.3a	9.5 ± 0.2b	8.5 ± 0.2a
Absolute testicular weight (g)	1.7 ± 0.1a	2.0 ± 0.1b	1.8 ± 0.2a	1.6 ± 0.1a
Relative testicular weight (mg/g) ^b	7.6 ± 0.4a	10.5 ± 0.3b	8.9 ± 0.5a	8.0 ± 0.4a

Different letters on the same row indicate values significantly different ($P < 0.01$) as determined by one-way ANOVA and Tukey's post hoc test. Values represent the mean ± 1 SD ($n = 10$).

S soybean oil, O olive oil, C coconut oil, G grapeseed oil

^a Food efficiency ratio = [body weight gain (g)/food intake (g)] × 10²

^b Relative testicular weight = testis weight (mg)/body mass (g)

Table 4 Effect of dietary lipids on the absolute amount of the major lipid subclasses of interstitial cells

Lipid subclass	Diets			
	S	O	C	G
Total Lipids ^a	86.5 ± 4.2a	107.6 ± 5.2b	128.1 ± 4.4c	80.0 ± 3.1a
Phospholipids (PL) ^b	55.5 ± 3.0a	72.3 ± 2.3b	44.1 ± 3.2c	59.3 ± 3.1a
Neutral lipids (NL) ^c	29.3 ± 1.5a	36.2 ± 3.1b	79.5 ± 2.3c	33.3 ± 2.1a
Triacylglycerides ^d	12.4 ± 0.6a	16.1 ± 1.4a	39.7 ± 1.1b	9.5 ± 0.3c
Free cholesterol (FC) ^e	17.8 ± 0.8a	23.8 ± 0.8b	31.1 ± 1.0c	15.3 ± 0.5a
Esterified cholesterol (CE) ^e	2.0 ± 0.1a	0.8 ± 0.1b	1.1 ± 0.1b	2.7 ± 0.2c
NL/PL	0.53 ± 0.02a	0.50 ± 0.03a	1.80 ± 0.08b	0.56 ± 0.02a
FC/CE	8.9 ± 0.2a	29.8 ± 0.5b	28.3 ± 0.7b	5.7 ± 0.2c

S soybean oil, O olive oil, C coconut oil, G grapeseed oil

Results represent the mean ± 1 SD, of four independent determinations assayed in triplicate

Different letters on the same row indicate values significantly different ($P < 0.01$) as determined by one-way ANOVA and Tukey's post hoc test

^a pg/mg protein

^b pmol inorganic phosphate/mg protein

^c pmol tripalmitin/mg protein

^d pmol linoleoyl-cholesterol/mg protein

of PC, the distribution pattern among different diets was similar. In summary, according to analytical parameters, SFA were the predominant fatty acids in Group C, MUFA were the most abundant acyl chains in Group O, and PUFA enriched the glycerolipids isolated from Groups S or G derived cells. Table 8 shows the fatty acyl composition of triacylglycerides (TAG) of interstitial cells. Group C exhibited the highest levels of SFA, as well as the lowest amount of MUFA. Group O was characterized by the highest levels of MUFA and the lowest levels of SFA. In Groups S and G, SFA amounts were quite similar. Group G exhibited the highest level of PUFA, similar to that of

Group O, followed by Groups S and C. However, the DBI in TAG decreased in the order O > G = S > C.

Dietary oils also influenced the fatty acyl composition of cholesterol esters (CE) (Table 9). In this case, the composition of the diet exerted a complex influence on the analytical profile, which did not reflect the relative abundance of the acyl chains in the oil. For example, the proportion of SFA was similar among groups and even less abundant (considering stearic acid level) in Group C, which was fed the most saturated oil. MUFA content was elevated in the olive-supplemented group, however, the other groups had similar proportions of oleic and palmitoleic acids. The

Table 5 Effect of dietary lipids on the main phospholipid subclasses from interstitial cells

Lipid subclass	S	O	C	G
Phosphatidylcholine ^a	25.3 ± 1.8a	34.4 ± 2.0b	21.0 ± 2.1c	29.7 ± 1.7a
Phosphatidylethanolamine ^a	18.6 ± 1.4a	23.5 ± 1.7b	11.1 ± 1.1c	18.0 ± 2.0a
Phosphatidylserine	5.5 ± 0.4	5.9 ± 0.2	5.5 ± 0.3	5.0 ± 0.2
Sphingomyelin	3.3 ± 0.2	4.0 ± 0.1	3.4 ± 0.2	3.1 ± 0.1
Phosphatidic acid	0.8 ± 0.1	0.7 ± 0.1	0.6 ± 0.0	0.9 ± 0.1
Lysophospholipids	1.7 ± 0.1a	2.2 ± 0.1b	1.5 ± 0.1a	2.2 ± 0.1a
Phosphatidylinositol	2.3 ± 0.2a	3.8 ± 0.2b	1.5 ± 0.2c	2.1 ± 0.2a
Phosphatidylglycerol	0.6 ± 0.0	0.7 ± 0.1	0.4 ± 0.0	0.5 ± 0.1

S soybean oil, O olive oil, C coconut oil, G grapeseed oil

Main phospholipid subclasses separated by HP-TLC as described in “Materials and Methods”

Values represented pmol of inorganic phosphate/mg cellular protein (mean ± 1 SD, *n* = 6)

Different letters on the same row indicate values significantly different (*P* < 0.01) as determined by one-way ANOVA and Tukey's post hoc test

^a These fractions include plasmanyl- and plasmeyl-species

Table 6 Effect of dietary lipids on the fatty acyl composition of phosphatidylcholine (PC) from interstitial cells

Fatty acids	S	O	C	G
14:0	tr a	tr a	3.1 ± 0.1b	0.1 ± 0.0a
15:0	tr a	tr a	0.2 ± 0.0b	tr a
16:0	44.4 ± 1.9a	29.9 ± 2.1b	64.1 ± 2.0c	33.3 ± 2.5b
16:1(n-7)	1.8 ± 0.2a	1.6 ± 0.1a	tr b	1.0 ± 0.2a
18:0	4.1 ± 0.1a	3.0 ± 0.1b	5.5 ± 0.1c	4.6 ± 0.0a
18:1(n-9)	18.0 ± 0.6a	37.5 ± 1.4b	2.0 ± 0.1c	15.1 ± 0.4a
18:2(n-6)	3.0 ± 0.1a	2.5 ± 0.1a	0.1 ± 0.0b	12.8 ± 2.2a
18:3(n-3)	0.2 ± 0.0a	tr b	tr b	0.1 ± 0.0c
20:3(n-6)	0.7 ± 0.1a	0.5 ± 0.1a	tr b	0.8 ± 0.1a
20:4(n-6)	11.5 ± 0.6a	10.0 ± 0.5a	4.3 ± 0.1b	15.5 ± 0.5c
22:4(n-6)	0.5 ± 0.0	0.1 ± 0.0b	tr c	1.0 ± 0.1d
22:5(n-6)	14.0 ± 1.0a	14.6 ± 0.7a	20.6 ± 0.6b	13.9 ± 0.4a
22:6(n-3)	0.6 ± 0.1a	0.3 ± 0.0b	0.1 ± 0.0c	0.7 ± 0.1a
Analytical parameters				
ΣSFA	48.5 ± 1.8a	32.9 ± 1.2b	72.9 ± 2.0c	38.0 ± 2.1b
ΣMUFA	19.8 ± 0.9a	39.1 ± 1.9b	2.0 ± 0.1c	16.1 ± 1.2a
ΣPUFA	30.5 ± 2.0a	28.0 ± 2.2a	25.1 ± 1.0a	44.8 ± 1.8b
DBI	139.5 ± 10.0a	160.8 ± 9.5b	121.0 ± 11.2c	186.3 ± 5.3d
Σ(n-6)/Σ(n-3)	37.1 ± 1.5a	92.3 ± 1.8b	251.0 ± 3.3c	55.0 ± 1.2d

S soybean oil, O olive oil, C coconut oil, G grapeseed oil

c-GLC of PC-FAME was performed as described in “Materials and Methods”

Values are expressed as mol% (mean ± 1 SD, *n* = 6)

Different letters on the same row indicate values significantly different (*P* < 0.01) as determined by one-way ANOVA and Tukey's post hoc test

Means below 0.1% are indicated as “tr”

Some minor components have been omitted; Σ sum of: SFA saturated fatty acids, MUFA monounsaturated fatty acids, PUFA polyunsaturated fatty acids, DBI double bond index

content of arachidonate (20:4n-6) was increased in Diet C, which was depleted in linoleic acid, while it was decreased in the other diets, especially those rich in MUFA (O). The content of 22:6n-3 fatty acid was approximately constant among groups and independent of the diet composition,

while the amount of 22:5n-6 was significantly different and not associated with the acyl composition of the dietary oil. For example, Group C had a 22:5n-6 level similar to that of Group G. The changes observed in the relative amounts of PUFA agreed with the DBI values calculated for each diet.

Table 7 Effect of dietary lipids on the fatty acyl composition of phosphatidylethanolamine (PE) from interstitial cells

Fatty acids	S	O	C	G
14:0	0.1 ± 0.0a	tr a	3.1 ± 0.1b	0.1 ± 0.0a
15:0	0.2 ± 0.0a	tr b	0.2 ± 0.0a	tr b
16:0	30.4 ± 2.1a	21.5 ± 2.2a	39.4 ± 2.3b	23.7 ± 2.2c
16:1(n-7)	0.8 ± 0.1a	1.1 ± 0.1a	tr b	0.9 ± 0.1a
18:0	9.8 ± 0.3a	7.0 ± 0.4a	18.3 ± 0.7b	7.6 ± 0.2a
18:1(n-9)	10.3 ± 0.4a	26.6 ± 0.5a	1.2 ± 0.1b	12.2 ± 0.5c
18:2(n-6)	2.5 ± 0.2a	3.0 ± 0.1a	0.1 ± 0.0b	6.2 ± 0.7c
18:3(n-3)	0.4 ± 0.0a	0.1 ± 0.0b	tr c	0.2 ± 0.0d
20:3(n-6)	1.0 ± 0.2a	0.6 ± 0.1b	0.1 ± 0.1c	0.9 ± 0.1a
20:4(n-6)	15.2 ± 0.5a	12.0 ± 0.4b	11.1 ± 0.2b	17.2 ± 2.3a
22:4(n-6)	1.1 ± 0.1a	0.7 ± 0.3b	0.1 ± 0.0c	1.5 ± 0.1a
22:5(n-6)	20.3 ± 1.8a	23.8 ± 1.1a	25.1 ± 1.2b	21.0 ± 0.5a
22:6(n-3)	3.2 ± 0.2a	2.1 ± 0.1b	1.0 ± 0.0c	2.7 ± 0.1d
Analytical parameters				
ΣSFA	40.5 ± 1.8a	28.5 ± 1.0b	57.7 ± 2.0c	31.4 ± 1.0b
ΣMUFA	11.1 ± 0.5a	27.7 ± 1.1b	1.2 ± 0.1c	13.1 ± 0.4a
ΣPUFA	43.7 ± 1.2a	42.3 ± 2.1a	37.5 ± 1.3b	49.7 ± 1.3c
DBI	214.8 ± 10.0a	221.4 ± 9.0a	178.7 ± 7.7b	238.0 ± 9.3c
Σ(n-6)/Σ(n-3)	11.1 ± 1.1a	18.2 ± 0.7b	36.5 ± 1.1b	13.0 ± 0.5c

S soybean oil, O olive oil, C coconut oil, G grapeseed oil

c-GLC of PC- FAME was performed as described in “Materials and Methods”

Values are expressed as mol% (mean ± 1 SD, $n = 6$)

Different letters on the same row indicate values significantly different ($P < 0.01$) as determined by one-way ANOVA and Tukey's post hoc test
Means below 0.1% are indicated as “tr”

Some minor components have been omitted; Σ sum of: SFA saturated fatty acids, MUFA monounsaturated fatty acids, PUFA polyunsaturated fatty acids, DBI double bond index

Influence of Dietary Lipids on Steroidogenic Function and Testosterone Production of Interstitial Cells

The activities of the two key enzymes for testosterone biosynthesis, 3- β -hydroxysteroid-dehydrogenase (3- β -HSD) and 17- β -hydroxysteroid-dehydrogenase (17- β -HSD), were significantly affected by the diets tested. Both enzyme activities were significantly decreased in interstitial cell homogenates from rats fed Diets S and G compared with the levels observed in Group O or C preparations (Fig. 1).

Testosterone concentrations in interstitial cell homogenates are shown in Fig. 2a. The highest androgen concentrations were found in cells from Groups O and C. The decrease in cellular testosterone concentration was in the order, O = C > S = G. Figure 2b shows the plasmatic levels of free testosterone and luteinizing hormone. The highest levels of testosterone were observed when the rat diet was supplemented with Oils O or C. In Groups S or G, plasma testosterone concentration was significantly lower. Luteinizing hormone followed the opposite trend (Fig. 2b)

with Groups S and G containing the highest levels and Groups O and C the lowest.

In Fig. 3 we have represented the linear correlation coefficient (r^2) between testosterone production and free or esterified cholesterol. Therefore, testosterone concentration directly correlated with free cholesterol (Fig. 3a). Additionally, a significantly negative correlation was found between cellular testosterone production and CE content (Fig. 3b).

Discussion

The control of testicular function is a complex process that requires the functional integrity of the seminiferous tubules and Leydig cells with a suitable multihormonal stimulation. The steroidogenic capacity of Leydig cells is essential for spermatogenesis. However, not only hormonal aspects are important in testis physiology; lipid composition is also crucial. Several factors have demonstrated that nutrition is an environmental factor of major importance [33]. Other

Table 8 Effect of dietary lipids on the fatty acyl composition of triacylglycerides (TAG) from interstitial cells

Fatty acids	S	O	C	G
12:0		tr a	0.5 ± 0.1b	
14:0	0.8 ± 0.1a	0.4 ± 0.0b	2.4 ± 0.2c	
15:0	0.1 ± 0.0a	tr b	0.1 ± 0.0	tr
16:0	28.8 ± 1.6a	22.9 ± 1.4b	44.8 ± 3.5c	25.3 ± 2.2b
16:1(n-7)	6.0 ± 0.2a	3.9 ± 0.1b	0.7 ± 0.1c	tr d
18:0	5.1 ± 0.2a	4.8 ± 0.2a	14.2 ± 0.6b	5.3 ± 0.1a
18:1(n-9)	19.7 ± 0.8a	24.7 ± 2.0b	8.0 ± 0.3c	21.1 ± 1.5a
18:1(n-7)	0.2 ± 0.0a	tr b	0.6 ± 0.1c	0.1 ± 0.0a
18:2(n-6)	10.0 ± 0.5a	11.1 ± 0.5b	5.1 ± 0.2c	21.0 ± 0.8d
18:3(n-6)	tr a	0.1 ± 0.0a	tr a	0.3 ± 0.0b
18:3(n-3)	0.2 ± 0.0a	tr b	tr b	tr b
20:2(n-6)	tr a	0.3 ± 0.0b	1.0 ± 0.1c	0.9 ± 0.1c
20:3(n-6)	0.3 ± 0.0a	2.5 ± 0.2b	0.1 ± 0.0a	1.3 ± 0.1c
20:4(n-6)	4.3 ± 0.1a	tr b	2.5 ± 0.1c	8.0 ± 0.2d
22:4(n-6)	3.1 ± 0.1a	2.8 ± 0.1a	0.2 ± 0.0b	4.5 ± 0.1c
22:5(n-6)	19.2 ± 1.1a	24.6 ± 0.9b	18.1 ± 1.9a	11.7 ± 0.4c
22:6(n-3)	1.1 ± 0.1a	1.0 ± 0.1a	0.4 ± 0.0b	0.2 ± 0.0c
Analytical parameters				
ΣSFA	34.8 ± 2.0a	28.1 ± 1.7b	62.0 ± 3.3c	30.6 ± 2.1b
ΣMUFA	25.9 ± 1.5a	28.6 ± 1.3b	9.3 ± 0.8c	21.2 ± 1.1d
ΣPUFA	38.2 ± 2.3a	42.4 ± 2.5b	27.4 ± 1.8c	47.9 ± 3.0b
DBI	178.7 ± 10.1a	199.4 ± 8.0b	125.5 ± 7.7c	184.8 ± 5.9a
Σ(n-6)/Σ(n-3)	28.5 ± 2.2a	42.4 ± 1.9b	68.5 ± 3.0c	239.5 ± 5.2d

S soybean oil, O olive oil, C coconut oil, G grapeseed oil

c-GLC of PC- FAME was performed as described in "Materials and Methods"

Values are expressed as mol% (mean ± 1 SD, n = 6)

Different letters on the same row indicate values significantly different ($P < 0.01$) as determined by one-way ANOVA and Tukey's post hoc test

Means below 0.1% are indicated as "tr"

Some minor components have been omitted; Σ sum of: SFA saturated fatty acids, MUFA monounsaturated fatty acids, PUFA polyunsaturated fatty acids, DBI double bond index

authors have demonstrated that dietary fats can modulate steroidogenic function of mammalian testis [12, 34]. However, little is known about the changes induced by dietary oils on lipid composition of interstitial cells and their eventual correlation with testosterone biosynthesis.

In this study, we demonstrated that commercial oils added to diets were able to affect lipid composition of interstitial cells, mainly Leydig cells, and that they markedly influenced their androgen biosynthesis capacity. The oils tested were selected by taking into account their massive consumption over the world and also because they were obtained from vegetable sources where cholesterol was absent. Differences among oils reflected their characteristics as a source of precursor FA, which, in turn, were then metabolized to MUFA and PUFA of the different fatty acid series.

Despite the fact that Oils S and G had the highest content of linoleic and/or linolenic acids they differed in the relative proportion of n-6 and n-3 fatty acid components. It was demonstrated that the ratio n-3/n-6 was important not only for cardiovascular disease prevention but also for a normal spermatogenesis [6]. However, the relationship between this analytical parameter and the androgenic capacity of interstitial cells is a matter that is still unsolved. We clearly demonstrated that oil-supplemented diets

strongly modified interstitial cell lipid composition. Especially important were the differences produced in the absolute amount of NL and PL, and in the ratios of FC/CE. Moreover, FA patterns of these major lipids strongly differed in their fatty acyl chains being SFA, MUFA and PUFA, concentrated in Groups C, O and S/G, respectively. Changes observed in the major lipid subclasses induced by the commercial oils were in accordance with those found for tissues other than testis [35].

The importance of the FA modifications observed in the main lipid subclasses is their capacity to influence the androgen metabolism. Testicular lipids have an active metabolism, and they arise from both dietary sources and from the processes of synthesis, elongation, desaturation, interconversion, esterification, and oxidation by the testicular tissue itself. Moreover, it is known that dietary fats can affect the testicular fatty acid composition in a similar way to that seen in hepatic tissue [7]. Also, certain dietary fats can modulate not only fatty acyl composition of testicular lipids, but also testosterone metabolism. It was demonstrated that diets rich in PUFAs depress Leydig cell function in rats [12]. In agreement with this report, our data demonstrated that diets supplemented with Oils S and G caused reductions in 3β - and 17β -HSD enzyme activities compared with Oils O and C. Decreased enzyme activities

Table 9 Effect of dietary lipids on the fatty acyl composition of cholesterol esters (CE) from interstitial cells

Fatty acids	S	O	C	G
14:0	2.3 ± 0.1a	1.9 ± 0.2a	4.5 ± 0.2b	1.0 ± 0.1c
15:0	1.0 ± 0.3	0.8 ± 0.2	0.7 ± 0.2	0.7 ± 0.1
16:0	17.6 ± 1.0a	18.4 ± 0.7a	19.2 ± 0.9a	13.3 ± 0.5b
16:1 (n-7)	0.3 ± 0.1a	1.5 ± 0.1b	0.4 ± 0.1a	0.3 ± 0.0a
18:0	23.0 ± 1.2a	25.4 ± 1.2b	19.9 ± 0.8c	21.8 ± 0.9a
18:1 (n-9)	15.3 ± 0.5a	20.0 ± 1.0b	13.0 ± 0.2c	14.4 ± 0.3c
18:2 (n-6)	1.1 ± 0.1a	1.2 ± 0.3a	0.8 ± 0.1a	3.8 ± 0.1b
18:3 (n-3)	0.3 ± 0.1a	tr b	tr b	tr b
20:3 (n-6)	1.5 ± 0.1a	1.3 ± 0.2a	1.0 ± 0.2a	3.1 ± 0.1b
20:4 (n-6)	8.6 ± 0.6a	5.1 ± 0.2b	12.3 ± 0.4c	11.7 ± 0.8c
22:2 (n-6)	1.6 ± 0.1a	1.8 ± 0.1a	0.8 ± 0.1b	1.3 ± 0.1a
22:3 (n-6)	0.1 ± 0.0a	tr a	0.1 ± 0.0a	0.2 ± 0.0b
22:4 (n-6)	0.9 ± 0.1a	0.1 ± 0.0b	0.5 ± 0.0c	0.7 ± 0.1a
22:5 (n-6)	13.8 ± 0.8a	9.5 ± 0.5b	16.7 ± 1.0c	16.2 ± 0.5c
22:5 (n-3)	0.2 ± 0.0a	0.2 ± 0.0a	tr b	0.1 ± 0.0b
22:6 (n-3)	12.0 ± 1.4	12.5 ± 0.8	10.1 ± 0.7	11.2 ± 1.0
Analytical parameters				
ΣSFA	43.9 ± 1.2a	46.5 ± 1.1a	44.3 ± 1.3a	36.8 ± 1.1a
ΣMUFA	15.6 ± 1.0a	21.5 ± 0.7b	13.4 ± 0.3c	14.7 ± 0.5a
ΣPUFA	40.1 ± 1.3a	31.7 ± 1.5b	42.3 ± 1.1a	48.3 ± 1.0c
DBI	205.8 ± 8.1a	175.7 ± 6.0b	185.2 ± 9.9c	233.1 ± 8.4d
Σ(n-6)/Σ(n-3)	2.2 ± 0.2a	1.5 ± 0.1b	3.1 ± 0.2c	3.3 ± 0.1c

S soybean oil, O olive oil, C coconut oil, G grapeseed oil

c-GLC of PC-FAME was performed as described in “Materials and Methods”

Values are expressed as mol% (mean ± 1 SD, $n = 6$)

Statistical analyses were performed as indicated in “Materials and Methods”

Different letters on the same row indicate values significantly different ($P < 0.01$) as determined by one-way ANOVA and Tukey’s post hoc test

Means below 0.1% are indicated as “tr”

Some minor components have been omitted; Σ sum of: SFA saturated fatty acids, MUFA monounsaturated fatty acids, PUFA polyunsaturated fatty acids, DBI double bond index

were in agreement with an inhibition in testosterone production by Leydig cells. This pattern of response was also reflected in peripheral plasma [34].

We also observed that Diets C and O had the best comparative performance in testosterone production despite their very different fatty acyl composition. The role of SFA and MUFA in steroidogenic function is a controversial issue. Oleic acid was provided predominantly by olive oil. This fatty acid has regulatory functions in many tissues [36–41] and it is accepted that its endogenous biosynthesis is insufficient for normal cell function. Thus, this acid must be obtained from dietary lipids [42]. However, previous reports have suggested that excessive oleic acid supplementation appears to inhibit testosterone synthesis by decreasing cholesteryl esterase activity [43]. This finding contradicts previous experimental evidence, indicating a stimulating effect of MUFA and an inhibitory effect exerted by n-3 PUFA [44]. Similar controversial

results were observed in the relative amount of saturated fatty acids [45]. Other researchers have also reported that FA could inhibit steroidogenesis at one of the steps preceding the conversion of cholesterol to pregnenolone [46]. Taking into account all these previous results, it is likely that both excessive PUFA and/or MUFA may be deleterious for testosterone production. However, our findings indicate that a diet enriched in MUFA (olive oil) may be important to keep androgenic synthesis within the normal values whereas PUFA diets appear to depress Leydig cell function. Such a conclusion denotes the importance of dietary lipids in Leydig cell function.

The availability of free cholesterol from cholesterol esters is influenced not only by the quantity and quality of FA but also by hormonal levels. In rat Leydig cells, the cholesterol side-chain cleaving enzyme is subjected to LH regulation in a complex way, which depends on both the time and the intensity of the gonadotrophic stimulus [47].

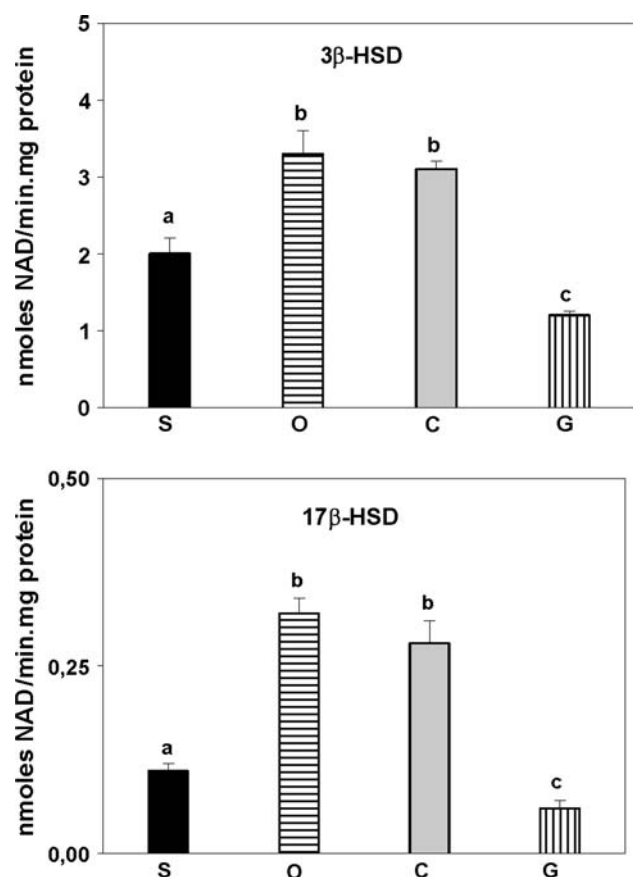


Fig. 1 Activities of the two key enzymes for testosterone biosynthesis: 3-beta-hydroxysteroid-dehydrogenase (3β -HSD) and 17-beta-hydroxysteroid dehydrogenase (17β -HSD) in interstitial cells from rats fed different diets (S soybean, O olive, C coconut, and G grape-seed oil-supplemented diet). Results presented as mean \pm 1 SD, $n = 10$. Different superscript letters indicate values significantly different ($P < 0.01$) as determined by one-way ANOVA and Tukey's post hoc test

As described in our paper, LH levels were elevated in Diets S and G compared to the other experimental groups. This stimulation may adversely affect the activity of the cholesteryl-side chain cleavage enzyme, and consequently, it may contribute to the inhibition of androgen production by decreasing the concentration of the precursor.

We also observed that the side chain of the esterified cholesterol is strongly influenced by the type of lipid present in the diet. This finding was in agreement with previous experimental evidence indicating that the composition of the cholesteryl esters in testis is more strongly affected than that of the other lipid subclasses [7].

The lipid changes we observed could also be involved in other mechanism(s) of action which depend on the physicochemical properties of interstitial cell membranes. It is well known that alterations in lipid proportions and/or fatty acyl chains acylated to complex lipids strongly influence several processes that occur in the cytoplasm and in the inner cell membranes, such as mitochondrial membranes

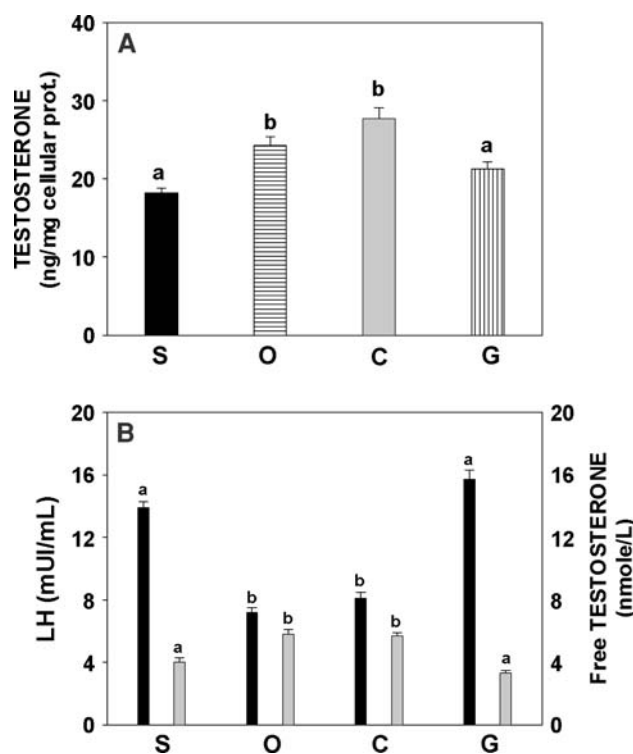


Fig. 2 Hormonal levels measured by RIA methodology for interstitial cells (a) or plasma (b) from rats fed different diets (S soybean, O olive, C coconut, and G grape-seed oil-supplemented diet). Values of free testosterone for interstitial cells were expressed as ng/mg cellular protein, and they were the mean \pm SD of ten independent determinations. Bars of b correspond to the concentration of LH (black mUI/mL) or free testosterone (gray nmole/L) in peripheral plasmas and they are the mean \pm SD of ten independent determinations. Statistical analyses were performed as indicated in "Materials and methods". In all cases different superscript letters indicate values significantly different ($P < 0.01$) as determined by one-way ANOVA and Tukey's post hoc test

[48–51]. Receptor-mediated signal transduction and even free cholesterol transport to the inner mitochondrial membrane are examples of processes that should be affected by lipid composition. It is well documented that the phospholipid content and the type of fatty acids acylated to phospholipids were both influenced by dietary manipulation and caused alterations on membrane-mediated gonadotropin action in testicular tissues [7].

Previous reports from other laboratories have described the stimulating effect of arachidonyl-CoA or free arachidonate on the activity of StAR protein and cholesterol transport into the mitochondria for androgen production [52]. Arachidonate involved in these regulatory processes would be obtained from the cholesteryl ester pool via the ACS4/Acot2 system [53] without the intervention of phospholipase A₂ [54]. The proportion of arachidonyl-side chains within the esterified cholesterol pool would probably regulate the proportion of free cholesterol available for testosterone biosynthesis. This speculation was not evident

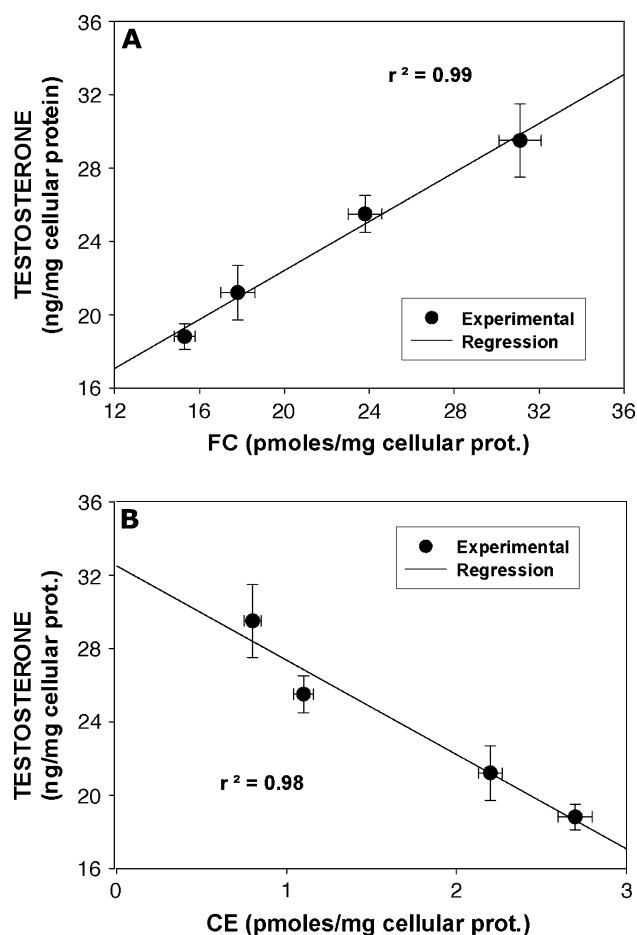


Fig. 3 Linear correlation coefficient (r^2) for regression plots between testosterone production by interstitial cells and (a) free cholesterol (FC) or (b) cholesterol ester (CE) levels. Data from Figure 1 and Table 4 were plotted and analyzed using the software described in “Materials and Methods”

from the compositional data. However, we demonstrated that the level of esterified cholesterol increased in the order $O > C > S > G$, while the level of the acylated cholesterol increased in the opposite way ($G > S > C > O$). Moreover, a positive linear correlation between androgen production and FC was evident, while this correlation became negative when CE was considered as the independent variable.

Data obtained from other laboratories also provide substantial support for the hypothesis that fat ingestion is sexually differentiated in humans. The regulatory stimuli controlling the consumption of fat arise from oral, gastric, intestinal, hepatic, and adipose sites [55]. However, environmental factors may modify this physiological behavior. In the past decades, a progressively significant worldwide decline in semen quality and androgenic performance was reported [56–59]. Within the environmental factors that determine this phenomenon, increasing pollutants for example [59–61], we think that lipid composition of the

diet should be considered as one of the most important. Future research in this area may contribute to the understanding of the mechanism(s) involved and also the prevention of the damage induced by an inadequate diet.

Acknowledgments The authors are grateful to Eva Illara de Bozzolo and Cristina Pallanza de Stringa for excellent technical assistance. This study was partially supported by grants from Consejo Nacional de Investigaciones Científicas y Técnicas (CONICET) and Universidad Nacional de La Plata (UNLP), Argentina.

References

- Clandinin MT, Field CJ, Hargreaves K, Morson L, Zsigmond E (1985) Role of diet fat in subcellular structure and function. *Can J Physiol Pharmacol* 63:546–556
- Stubbs CD, Smith AD (1984) The modification of mammalian membrane fluidity and function. *Biochim Biophys Acta* 779:89–137
- Levant B, Ozias MK, Carlson SE (2007) Diet (n-3) polyunsaturated fatty acid content and parity affect liver and erythrocyte phospholipid fatty acid composition in female rats. *J Nutr* 137:2425–2430
- Igal RA, INTde GómezDumm (1994) Changes in liver and adrenal gland polyunsaturated fatty acid biosynthesis in hypercholesterolemic rats. *Nutr Res* 14:241–254
- Igal RA, Hurtado de Catalfo G, de Gómez Dumm INT (1994) Polyunsaturated fatty acid biosynthesis in testis from rats fed a hypercholesterolemic diet. *J Nutr Biochem* 5:15–20
- Ayala S, Brenner RR, Gómez Dumm C (1977) Effect of polyunsaturated fatty acids of α -linolenic series on the development of rat testicles. *Lipids* 12:1017–1024
- Coniglio JG (1994) Testicular lipids. *Prog Lipid Res* 33:387–401
- Retterstol K, Haugen TB, Christophersen BO (2000) The pathway from arachidonic to docosapentaenoic acid (20:4n-6 to 22:5n-6) and from eicosapentaenoic to docosahexaenoic acid (20:5n-3 to 22:6n-3) studied in testicular cells from immature rats. *Biochim Biophys Acta* 1483:119–131
- Kirschman JC, Coniglio JC (1961) Polyunsaturated fatty acids in tissues of growing male and female rats. *Arch Biochem Biophys* 93:297–301
- Peluffo RO, Ayala S, Brenner RR (1970) Metabolism of fatty acids of the linoleic acid series in testicles of diabetic rats. *Am J Physiol* 218:669–673
- Hutson JC (1984) Altered biochemical responses by rat Sertoli cells and peritubular cells cultured under simulated diabetic conditions. *Diabetologia* 26:155–158
- Gromadzka-Ostrowska J, Przepiórka M, Romanowicz K (2002) Influence of dietary fatty acids composition, level of dietary fat and feeding period on some parameters of androgen metabolism in male rats. *Reprod Biol* 2:277–293
- Clinton SK, Mulloy AL, Li SP, Mangian HJ, Visek WJ (1997) Dietary fat and protein intake differ in modulation of prostate tumor growth, prolactin secretion and metabolism, and prostate gland prolactin binding capacity in rats. *J Nutr* 127:225–237
- Dorgan JF, Judd JT, Longcope Ch, Brown C, Schatzkin A, Clevidence BA, Campbell WS, Nair PP, Franz C, Kahle L, Taylor PR (1997) Effect of dietary fat and fiber on plasma and urine androgens and estrogens in men: a controlled feeding studies. *Am J Clin Nutr* 64:850–855
- Hamalainen EA, Adlercreutz H, Puska P, Pietinen P (1984) Diet and serum sex hormones in healthy men. *J Steroid Biochem* 20:459–464

16. Reeves PG, Nielsen FH, Fahley GC Jr (1993) AIN-93 Purified diets for laboratory rodents: final report of the American Institute of Nutrition ad hoc writing committee on the reformulation of the AIN-76A rodent diet. *J Nutr* 123:1939–1951
17. National Research Council, National Institute of Health. (1985) Guide for the care and use of laboratory animals. Bethesda, MD, Publication 85-23 (rev)
18. Hurtado de Catalfo GE, Mandon EC, Dumm IN (1992) Arachidonic acid biosynthesis in non-stimulated and adrenocorticotropic-stimulated sertoli and leydig cells. *Lipids* 27:593–598
19. Suescun MO, González SI, Chiauzzi VA, Calandra RS (1985) Effects of induced hypoprolactinemia on testicular function during gonadal maturation in the rat. *J Androl* 6:77–82
20. Jauregui HO, Hayner NT, Driscoll JL, Williams-Holland R, Lipsky MH, Galletti PM (1981) Trypan blue dye uptake and lactate dehydrogenase in adult rat hepatocytes freshly isolated cells, cell suspensions, and primary monolayer cultures. *In Vitro* 17:1100–1110
21. Bradford MM (1976) A rapid and sensitive method for the quantitation of microgram quantities of protein utilizing the principle of protein-dye binding. *Anal Biochem* 72:248–254
22. Folch J, Lees M, Sloane Stanley GH (1967) A simple method for the isolation and purification of total lipides from animal tissues. *J Biol Chem* 226:497–509
23. Hanahan DJ, Dittmer JC, Warashina E (1957) A column chromatographic separation of classes of phospholipids. *J Biol Chem* 228:685–700
24. Marra CA, de Alaniz MJT (1992) Incorporation and metabolic conversion of saturated and unsaturated fatty acids in SK-Hep1 human hepatoma cells in culture. *Mol Cell Biochem* 117:107–118
25. Chen PS, Toribara TY, Warner H (1956) Microdetermination of phosphorus. *Anal Chem* 33:1405–1406
26. Marra CA, de Alaniz MJT (1990) mineralocorticoids modify rat liver $\Delta 6$ desaturase activity and other parameters of lipid metabolism. *Biochem Int* 22:483–493
27. Nakamura K, Handa S (1984) Coomassie brilliant blue staining of lipids on thin-layer plates. *Anal Biochem* 142:406–410
28. Marra CA, de Alaniz MJT (2005) Neutral and polar lipid metabolism in liver microsomes of growing rats fed a calcium deficient diet. *Biochem Biophys Acta* 3:220–237
29. Allain CC, Poon LS, Chan CS, Richmond W, Fu PC (1974) Enzymatic determination of total serum cholesterol. *Clin Chem* 20:470–475
30. Morison WR, Smith LM (1964) Preparation of fatty acid methyl esters and dimethylacetals from lipids with boron fluoride-methanol. *J Lipid Res* 5:600–608
31. Marugesan P, Kanagaraj P, Yuvaraj S, Balasubramanian K, Aruldas MM, Arunakaran J (2005) The inhibitory effects of polychlorinated biphenyl Aroclor 1254 on Leydig cell LH receptors, steroidogenic enzymes and antioxidant enzymes in adult rats. *Reprod Toxicol* 201:117–126
32. Kleinbaum DG, Kupper LL (1997) Applied regression analysis and other multivariable methods, 3rd edn. Duxbury Press, Pacific Grove
33. Simopoulos AP (2002) The importance of the ratio omega-6/omega-3 essential fatty acids. *Biomed Pharmacother* 56:365–379
34. Mc Vey MJ, Cooke GM, Curran IH, Chan HM, Kubow S, Lok E, Mehta R (2008) Effects of dietary fats and proteins on rat testicular steroidogenic enzymes and serum testosterone levels. *Food Chem Toxicol* 46:259–269
35. Yaqoob P, Sherrington EJ, Jeffery NM, Sanderson P, Harvey DJ, Newsholme EA, Calder PC (1995) Comparison of the effects of a range of dietary lipids upon serum and tissue lipid composition in the rat. *Int J Biochem* 27:297–310
36. Velasco A, Tabernero A, Medina JM (2003) Role of oleic acid as neutrophic factor is supported in vivo by the expression of GAP-43 subsequent to the activation of SREBP-1 and the up-regulation of stearoyl-CoA desaturase during postnatal development of the brain. *Brain Res* 977:103–111
37. Rodriguez VM, Portillo MP, Picó C, Macarulla MT, Palou A (2002) Olive oil feeding up-regulates uncoupling protein genes in rat brown adipose tissue and skeletal muscle. *Am J Clin Nutr* 75:213–220
38. Picinato MC, Curi R, Machado UF, Carpinelli AR (1998) Soybean-and olive-enriched diets increase insulin secretion to glucose stimulus in isolated pancreatic rat islets. *Physiol Behav* 65:289–294
39. Viscardi RM, Strauss K, Hasday JD (1997) Oleic acid stimulates rapid translocation of choline phosphate cytidyltransferase in type II cells. *Biochim Biophys Acta* 1349:157–170
40. Lee HC, Dupont J (1991) Effects of dietary fatty acids on the activity of glucose transport in adipocytes. *J Nutr Biochem* 2:38–43
41. Giron MD, Mataix FJ, Faus MJ, Suárez MD (1989) Effect of long-term feeding olive and sunflower oils on fatty acid composition and desaturation activities of liver microsomes. *Biochem Int* 19:645–656
42. Bourre JE, Dumont OL, Clément ME, Durand GA (1997) Endogenous synthesis cannot compensate for absence of dietary oleic acid in rats. *J Nutr* 127:488–493
43. Meikle AW, Cardoso de Sousa JC, Hanzalova J, Murray DK (1996) Oleic acid inhibits cholesteryl esterase and cholesterol utilization for testosterone synthesis in mouse Leydig cells. *Metabolism* 45:293–299
44. Pham H, Ziboh VA (2002) 5 alpha-reductase-catalyzed conversion of testosterone to dihydrotestosterone is increased in prostatic adenocarcinoma cells: suppression by 15-lipoxygenase metabolites of gamma-linolenic and eicosapentaenoic acids. *J Steroid Biochem Mol Biol* 82:393–400
45. Raynaud JP, Cousse H, Martin PM (2002) Inhibition of type 1 and type 2 5 alpha-reductase activity by free fatty acids, active ingredients of Permixon. *J Steroid Biochem Mol Biol* 82:233–239
46. Meikle AW, Benson SJ, Liu XH, Boam WD, Stringham JD (1989) Non-esterified fatty acids modulate steroidogenesis in mouse Leydig cells. *Am J Physiol* 257:E937–E942
47. Brinkmann AO, Leemborg FG, Rommerts FF, van der Molen HJ (1984) Differences between the regulation of cholesterol side-chain cleavage in leydig cells from mice and rats. *J Steroid Biochem* 21:259–264
48. Valentine RC, Valentine DL (2004) Omega-3 fatty acids in cellular membranes: a unified concept. *Prog Lipid Res* 43:383–402
49. Stillwell W, Wassall SR (2003) Docosahexaenoic acid: membrane properties of a unique fatty acid. *Chem Phys Lipids* 126:1–27
50. Thewke D, Kramer M, Sinensky MS (2000) Transcriptional homeostatic control of membrane lipid composition. *Biochem Biophys Res Commun* 273:1–4
51. Hac-Wydro K, Wydro P (2007) The influence of fatty acid on model cholesterol/phospholipid membranes. *Chem Phys Lipids* 150:66–81
52. Wang XJ, Dyson MT, Mondillo C, Patrignani Z, Pignataro O, Stocco DM (2002) Interaction between arachidonic acid and cAMP signaling pathways enhances steroidogenesis and StAR gene expression in MA-10 Leydig tumor cells. *Mol Cell Endocrinol* 188:55–63
53. Maloberti P, Cornejo Maciel F, Castillo AF, Castilla R, Duarte A, Toledo MF, Meuli F, Mele P, Paz C, Podestá EJ (2007) Enzymes involved in arachidonic acid release in adrenal and leydig cells. *Mol Cell Endocrinol* 265:113–120
54. Cano F, Poderoso C, Cornejo Maciel F, Castilla R, Maloberti P, Castillo F, Neuman I, Paz C, Podestá EJ (2006) Protein tyrosine phosphatases regulate arachidonic acid release, StAR induction and steroidogenesis acting on a hormone-dependent arachidonic

- acid-preferring acyl-CoA synthetase. *J Steroid Biochem Mol Biol* 99:197–202
55. Geary N (2004) Is the control of fat ingestion sexually differentiated? *Physiol Behav* 83:659–771
56. Carlsen E, Giwercman A, Keiding N, Skakkebaek NE (1992) Evidence for decreasing quality of semen during past 50 years. *BMJ* 305:609–613
57. Auger J, Kunstmann JM, Czyglik F, Jouannet P (1995) Decline in semen quality among fertile men in Paris during the past 20 years. *N Engl J Med* 332:281–285
58. Ginsburg J, Okolo S, Prelevic G, Hardiman P (1994) Residence in London area and sperm density. *Lancet* 343:230
59. Saradha B, Mathur PP (2006) Effect of environmental contaminants on male reproduction. *Environ Toxicol Phar* 21:34–41
60. Cheek AO, McLachlan JA (1998) Environmental hormones and the male reproductive system. *J Androl* 19:5–10
61. Saradha B, Vaithinathan S, Mathur PP (2008) Single exposure to low dose of lindane causes transient decrease in testicular steroidogenesis in adult male wistar rats. *Toxicology* 244:190–197

Identification of Acylglycerols Containing Dihydroxy Fatty Acids in Castor Oil by Mass Spectrometry

Jiann-Tsyh Lin · Arthur Arcinas · Leslie A. Harden

Received: 15 September 2008 / Accepted: 5 November 2008 / Published online: 2 December 2008
© AOCS 2008

Abstract Ricinoleate, a monohydroxy fatty acid, in castor oil has many industrial uses. Dihydroxy fatty acids can also be used in industry. The C_{18} HPLC fractions of castor oil were analyzed by electrospray ionization mass spectrometry of lithium adducts to identify the acylglycerols containing dihydroxy fatty acids and the dihydroxy fatty acids. Four diacylglycerols identified were diOH18:1-diOH18:1, diOH18:2-OH18:1, diOH18:1-OH18:1 and diOH18:0-OH18:1. Eight triacylglycerols identified were diOH18:1-diOH18:1-diOH18:1, diOH18:1-diOH18:1-diOH18:0, diOH18:2-diOH18:1-OH18:1, diOH18:1-diOH18:1-OH18:1, diOH18:1-diOH18:0-OH18:1, diOH18:2-OH18:1-OH18:1, diOH18:1-OH18:1-OH18:1 and diOH18:0-OH18:1-OH18:1. The locations of fatty acids on the glycerol backbone were not determined. The structures of these three newly identified dihydroxy fatty acids were proposed as 11,12-dihydroxy-9-octadecenoic acid, 11,12-dihydroxy-9,13-octadecadienoic acid and 11,12-dihydroxyoctadecanoic acid. These individual acylglycerols were at the levels of about 0.5% or less in castor oil and can be isolated from castor oil or overproduced in a transgenic oil seed plant for future industrial uses.

Keywords Dihydroxy fatty acids · 11,12-Dihydroxy-9-octadecenoic acid · 11,12-Dihydroxy-9,13-octadecadienoic acid · 11,12-Dihydroxyoctadecanoic acid · Diacylglycerols · Triacylglycerols · Castor oil · Mass spectrometry · *Ricinus communis* L.

Introduction

Ricinoleate (OH18:1, Fig. 1a), a monohydroxy fatty acid, has many industrial uses such as the manufacture of aviation lubricant, plastic, paint and cosmetics. Ricinoleate occurs as acylglycerols (AG) in castor oil, and about 70% of castor oil is triricinolein (triricinoleoylglycerol) [1]. Castor oil is the only commercial source of ricinoleate. We have previously identified and quantified 14 molecular species of AG containing ricinoleate in castor oil using high-performance liquid chromatography (HPLC) and mass spectrometry (MS) methods [1–4]. We report here, the identification of 12 molecular species of AG containing dihydroxy fatty acids in castor oil. These dihydroxy fatty acids are proposed as 11,12-dihydroxy-9-octadecenoic acid (11,12-dihydroxyoleic acid, diOH18:1, Fig. 1b), 11,12-dihydroxy-9,13-octadecadienoic acid (diOH18:2, Fig. 1c), and 11,12-dihydroxyoctadecanoic acid (11,12-dihydroxystearic acid, diOH18:0, Fig. 1d). These fatty acids and the AG containing these fatty acids (Fig. 2) have not been previously reported. Dihydroxy fatty acids in higher plants also have not been previously reported. Oleic acid could convert to 7(*S*),10(*S*)-dihydroxy-8(*E*)-octadecenoic acid [5] and ricinoleic acid could convert to 10,12-dihydroxy-8(*E*)-octadecenoic acid [6] in a microbial culture. 8*R*-Hydroxyoctadecadienoic acid could convert to some dihydroxyoctadecadienoic acids in microbial cultures [7]. Dihydroxy fatty acids occur as eicosanoids in animals (acting as localized hormones) and cannot be used in industry as a source due to their low contents [8].

The presence of a hydroxyl group on fatty acid drastically changes the physical properties of the oil, e.g., viscosity, pour point, melting point, heat of fusion, solubility, crystal structure, and polymorphism [9]. Because of the physical and chemical changes from the normal fatty

J.-T. Lin (✉) · A. Arcinas · L. A. Harden
Western Regional Research Center,
Agricultural Research Service,
US Department of Agriculture,
800 Buchanan Street, Albany, CA 94710, USA
e-mail: jiann.lin@ars.usda.gov

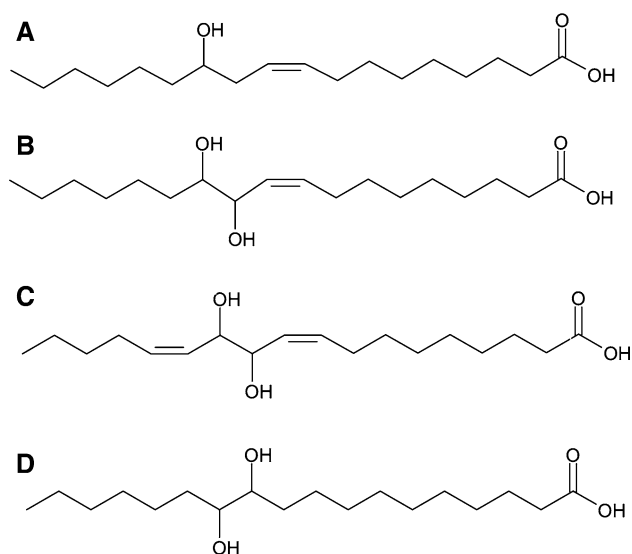


Fig. 1 The structure of ricinoleate and the proposed structures of dihydroxy fatty acids in castor oil. **a** Ricinoleate. **b** 11,12-Dihydroxy-9-octadecenoic acid. **c** 11,12-Dihydroxy-9,13-octadecadienoic acid. **d** 11,12-Dihydroxyoctadecanoic acid

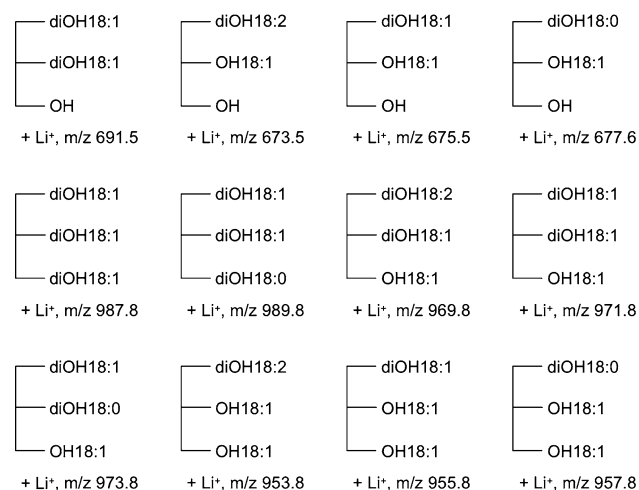


Fig. 2 The structures of 12 acylglycerols containing dihydroxy fatty acids in castor oil. The calculated m/z of the lithium adducts of acylglycerols are also shown. The stereospecific locations of the fatty acids were not determined

acids, many industrial uses of ricinoleate have been found. The physical and chemical properties of dihydroxy fatty acids and AG containing dihydroxy fatty acids are different from those of monohydroxy fatty acids and normal fatty acids. The dihydroxy fatty acids and AG containing dihydroxy fatty acids can be used in industry different from or similar to those of ricinoleate. These dihydroxy fatty acids have not been used in industry to date as there has been no practical source but, in the future it may be isolated from castor oil or produced by a transgenic oil seed plant.

Experimental Procedures

Materials

Castor oil, ricinoleate, 9,10-dihydroxyoctadecanoic acid, 12-hydroxyoctadecanoic acid and lithium acetate were obtained from Sigma (St Louis, MO, USA). HPLC and GC grade methanol and 2-propanol (Burdick & Jackson) for LC-MS were purchased from VWR International (West Chester, PA, USA). High-purity nitrogen for LC-MS was acquired from Praxair (Oakland, CA, USA). Research grade (99.999%) helium (Praxair) was used as a collision gas.

HPLC Fractionation of the Molecular Species of AG in Castor Oil

The fractionation of the molecular species of AG in castor oil was as previously reported [1]. Chromatographic fractionation was performed using a Waters HPLC (Waters Associate, Milford, MA, USA) and a C₁₈ analytical column (Gemini, 250 × 4.6 mm, 5 μm, C18, Phenomenex, Torrance, CA, USA). One mg of castor oil was chromatographed at 22 °C (room temperature) with a linear gradient from 100% methanol to 100% 2-propanol in 40 min, at a 1 mL/min flow rate, and detected at 205 nm. One-half minute fractions were collected and corresponding fractions were pooled from 15 HPLC runs. Fractions eluted before triricinolein (fraction #20, retention time 9.5–10.0 min) were used for MS studies. The final sample solutions were prepared for direct infusion into the mass spectrometer by combining approximately one-fourth of each fraction with 50 μL of a methanol solution of 100 mM lithium acetate and diluting it to a total volume of 200 μL. The same diluted sample solution was also used for high-resolution MS.

Electrospray Ionization Mass Spectrometry (ESI-MS)

An LCQ Advantage quadrupole ion-trap mass spectrometer with Xcalibur 1.3 software (ThermoFinnigan, San Jose, CA, USA) was utilized for MS analysis of the various molecular species of AG. The infusion at a 2.5 μL/min flow rate from a syringe pump produced stable singly charged lithiated parent ions which were subsequently fragmented for MS², MS³ and MS⁴ analysis. ESI source conditions were as follows: 50 arbitrary units (au) nitrogen sheath gas flow rate, 4.5 kV spray voltage, 250 °C ion-transfer capillary temperature, 1.5 m/z isolation width, 100–1,000 m/z mass range, 5 min acquisition time, 38 V capillary voltage and normalized collision energy ranging 35–39% for MS², MS³ and MS⁴ fragmentations, varying between molecular species of AG and fatty acids.

High-Resolution (HR) ESI-MS and MS/MS

Samples were analyzed by HR-ESI-MS using a hybrid quadrupole/time-of-flight (TOF) mass spectrometer (Q-STAR Pulsar I, MDS Sciex/ABI, Toronto, ON, Canada). The TOF mass analyzer was calibrated with two fragment ions generated by the collision-activated dissociation of the +2 charge state of glufibrogen (m/z 785.8). TOF resolution was typically 8,000–9,000 full width half maximum (fwhm). Eight microliter of the diluted sample solution (as described earlier) was loaded into an ESI spray capillary (NanoES, Proxeon Biosystems) using a 10 μ L gel pipette tip. The spray capillary was centrifuged briefly to displace air in the end of the closed spray capillary. The spray capillary was mounted onto the source head, and a backing pressure of 1–8 atm was applied from a 10 mL glass Luer-lock glass syringe. MS instrument parameters were as follows: 1,800 V spray voltage; 15 au of current gas; m/z 100–2,000 mass range; 1 s accumulation time; 3 min acquisition time; 50 au of declustering potential; 220 V focusing potential; 15 au second declustering potential; 11 μ s ion release delay; and 10 μ s ion release width. For MS/MS experiments, the collision gas setting was 5 au and the collision energy setting was 70 au. High-purity nitrogen, used for the curtain and a collision gas, was supplied from liquid nitrogen boil off from a large Dewar flask.

Results and Discussion

Castor oil was fractionated by reversed-phase C_{18} HPLC and the fractions that eluted before triricinolein (fraction #20, 0.5 min/fraction) were used for MS studies. The HPLC chromatogram of castor oil using this HPLC system was previously reported [1]. Fractions #9, 10, and 11 contained diacylglycerols according to the MS studies. Figure 3 is the MS^2 spectrum of diacylglycerol, dihydroxyoleoyl-ricinoleoyl-glycerol (diOH18:1-OH18:1), in fraction #9. The spectrum shows the fragment ions from the losses of dihydroxyoleate and ricinoleate as $[M + Li - diOH18:1]^+$ at m/z 361.2 and $[M + Li - OH18:1]^+$ at m/z 377.2. The two free fatty acids are also shown as $[diOH18:1 + Li]^+$ at m/z 321.2 and $[OH18:1 + Li]^+$ at m/z 305.3. Two other significant ions are $[M + Li - C_6H_{13}CHO]^+$ at m/z 561.4 and $[M + Li - C_5H_{11}CH=C=O]^+$ at m/z 563.4. The fragment ions from the loss of $C_6H_{13}CHO$ and $C_5H_{11}CH=C=O$ are also shown in Fig. 5. Similar to Fig. 3, Fig. 4 is the high-resolution MS^2 spectrum of dihydroxyoleoyl-ricinoleoyl-glycerol (diOH18:1-OH18:1) from HPLC fraction #9. The measured high-resolution masses, $[diOH18:1 + Li]^+$ at m/z 321.2601 and $[diOH18:1-OH18:1 + Li]^+$ at m/z 675.5319

matched well with the calculated masses of m/z 321.2617 and m/z 675.5387 individually.

Figure 5 is the MS^3 spectrum of dihydroxyoleate $[diOH18:1 + Li]^+$ at m/z 321.2. Three significant fragment ions are $[diOH18:1 + Li - H_2O]^+$ at m/z 303.2, $[diOH18:1 + Li - C_5H_{11}CH=C=O]^+$ at m/z 209.2 and $[diOH18:1 + Li - C_6H_{13}CHO]^+$ at m/z 207.1. The loss of $C_6H_{13}CHO$ (or shown earlier as $C_7H_{14}O$) has been previously reported [3, 4, 10] from the cleavage between C-11 and C-12 of the ricinoleoyl chain for TAG containing ricinoleate. The proposed fragmentation pathway of this ion at m/z 207.1 is shown as Fig. 6a. The fragmentation showed the cleavage was between C-11 and C-12 of diOH18:1 and the two hydroxyl groups were at both side of the cleavage. The fragment ion at m/z 207.1 had gained an extra hydrogen atom from the hydroxyl group at the C-12 position as shown in Fig. 6a. The location of this 12-hydroxyl group of diOH18:1 is the same as that of the 12-hydroxyl group of ricinoleate (Fig. 1a). The loss of ketene, $C_5H_{11}CH=C=O$, also has been previously reported [4, 11]. The proposed fragmentation pathway of the ion at m/z 209.2 is shown as Fig. 6b. The fragment ion at m/z 209.2 had gained three extra hydrogen atoms from the other side of the carbon-carbon cleavage between C-11 and C-12 of diOH18:1 as shown in Fig. 6b. Comparing between the MS spectra of diOH18:1 (Fig. 5) and ricinoleate (Fig. 7), the spectrum of ricinoleate $[OH18:1 + Li]^+$ at m/z 305.3 showed only the significant fragment ions of $[OH18:1 + Li - C_6H_{13}CHO]^+$ at m/z 191.1 and $[OH18:1 + Li - H_2O]^+$ at m/z 287.2, and the ion from the loss of ketene $[OH18:1 + Li - C_5H_{11}CH=C=O]^+$ at m/z 193 was not detected. Apparently the hydroxyl group at the C-11 position facilitated the fragment ion at m/z 209.2 (Fig. 5). The location of this hydroxyl group other than C-11 could not cause the cleavage between C-11 and C-12 as well as the fragmentation from the loss of ketene. We propose the structure of diOH18:1 as being 11,12-dihydroxy-9-octadecenoic acid (Fig. 1b) and the two hydroxyl groups are attached to adjacent carbon atoms at the C-11 and C-12 positions.

Figure 8 is the MS^4 spectrum of dihydroxyoctadecadienoic acid $[diOH18:2 + Li]^+$ at m/z 319.3. This was originated from the MS^2 of dihydroxyoctadecadienoyl-diricinoleoyl-glycerol $[M + Li]^+$ at m/z 953.6 from the HPLC fraction #15 of castor oil and then MS^3 of $[M + Li - OH18:1]^+$ at m/z 655.5. In the MS^2 spectrum, the relative abundance of $[diOH18:2 + Li]^+$ at m/z 319.3 was very low (2%) and we need to use the ion at m/z 319.3 in MS^3 spectrum (26%) for the MS^4 spectrum of $[diOH18:2 + Li]^+$ at m/z 319.3. Figure 8 shows three significant fragment ions, $[diOH18:2 + Li - H_2O]^+$ at m/z 301.2, $[diOH18:2 + Li - C_4H_6CH=C=C=O]^+$ at m/z 209.1 and $[diOH18:2 + Li - C_5H_{11}CH=CHOH]^+$ at m/z 205.2. The proposed fragmentation pathway to m/z 205.2 is shown as Fig. 6c. The proposed fragmentation pathway to

Fig. 3 Ion trap mass spectrum of ESI-MS² of dihydroxyoleyl-ricinoleoyl-glycerol $[M + Li]^+$ at m/z 675.5 in the HPLC fraction #9 of castor oil (collision energy 37%). diOH18:1 dihydroxyoleate, OH18:1 ricinoleate, C₅H₁₁CH=C=O ketene, C₆H₁₃CHO aldehyde

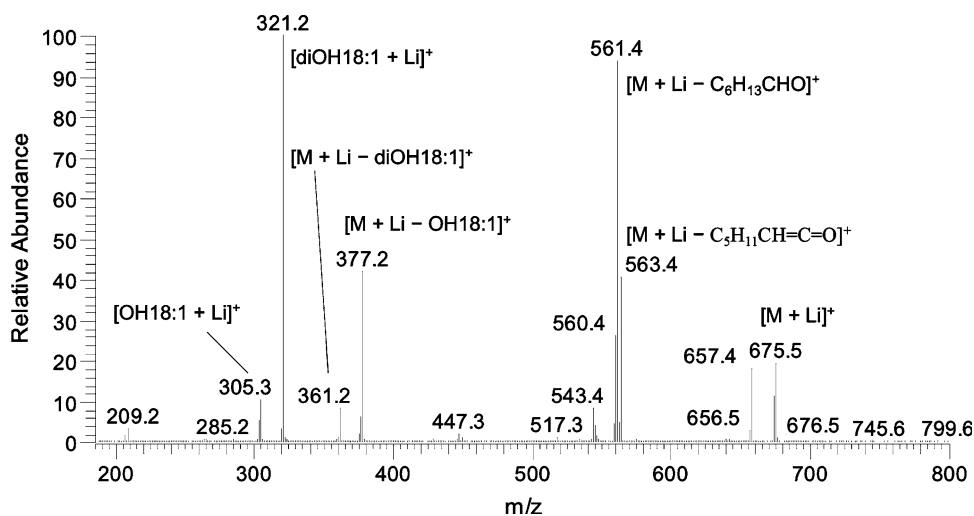


Fig. 4 Centroided high-resolution ESI-MS² mass spectrum of dihydroxyoleyl-ricinoleoyl-glycerol $[M + Li]^+$ at m/z 675.53 in the HPLC fraction #9 of castor oil. diOH18:1 dihydroxyoleate, OH18:1 ricinoleate, C₅H₁₁CH=C=O ketene

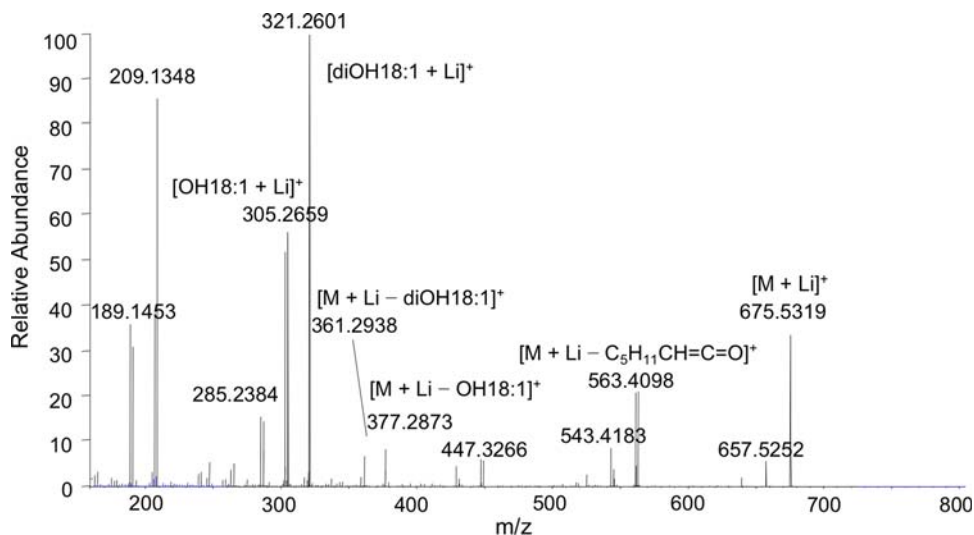
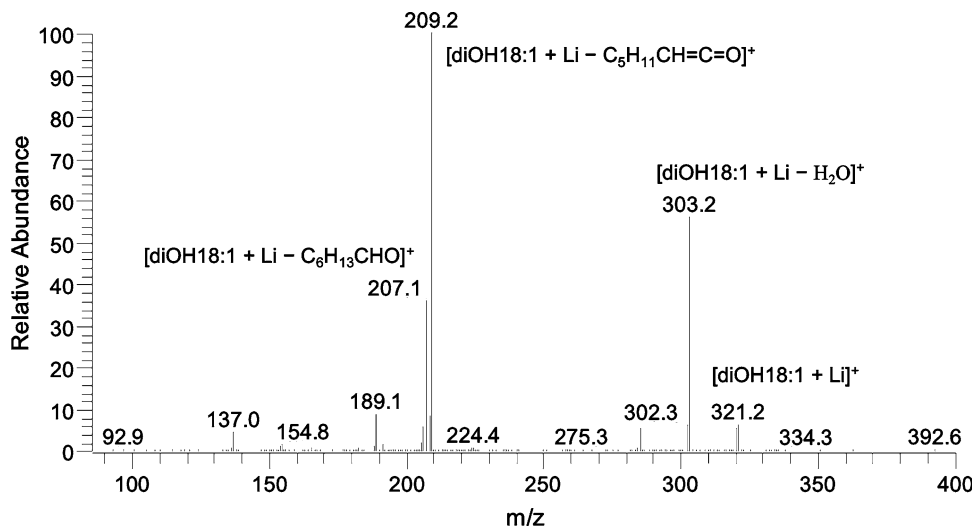


Fig. 5 Ion trap mass spectrum of ESI-MS³ of dihydroxyoleate $[diOH18:1 + Li]^+$ at m/z 321.2 (collision energy 36%). This was from $[diOH18:1 + Li]^+$ at m/z 321.2 shown in Fig. 3. For abbreviations, see Fig. 3. For proposed fragmentation pathways, see Fig. 6a and b



ion at m/z 209.1 is the same as that of Fig. 6b. We propose the structure of diOH18:2 as 11,12-dihydroxy-9,13-octadecadienoic acid (Fig. 1c).

Figure 9 is the MS⁴ spectrum of dihydroxyoctadecanoic acid $[diOH18:0 + Li]^+$ at m/z 323.3. This was originated from MS² of dihydroxyloctadecanoyl-diricinoleoyl-glycerol

Fig. 6 Proposed fragmentation pathways of dihydroxy fatty acids. **a** [diOH18:1 + Li – C₆H₁₃CHO]⁺ at *m/z* 207.1 shown in Fig. 5. **b** [diOH18:1 + Li – C₅H₁₁CH=C=O]⁺ at *m/z* 209.2 shown in Fig. 5. The cleavage of the bond between C-11 and C-12, the electron pair transfer *a*, was after the formation of the double bond at the C-10 position (*a*). The electron pair transfer *b* to the hydrogen atom at C-12 is after the migration of the hydrogen atom at C-13 to C-11 (*b*). **c** [diOH18:2 + Li – C₅H₁₁CH=CHO]⁺ at *m/z* 205.2 shown in Fig. 8

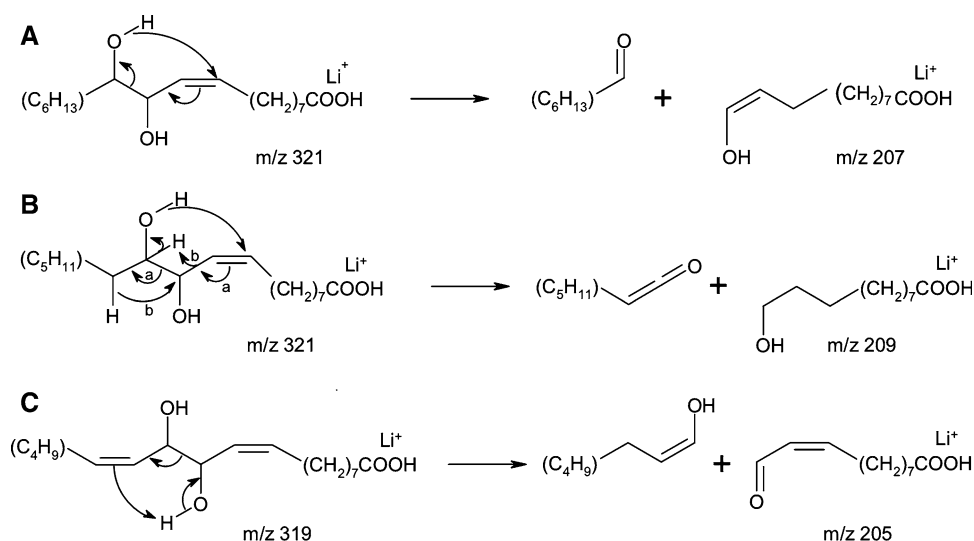
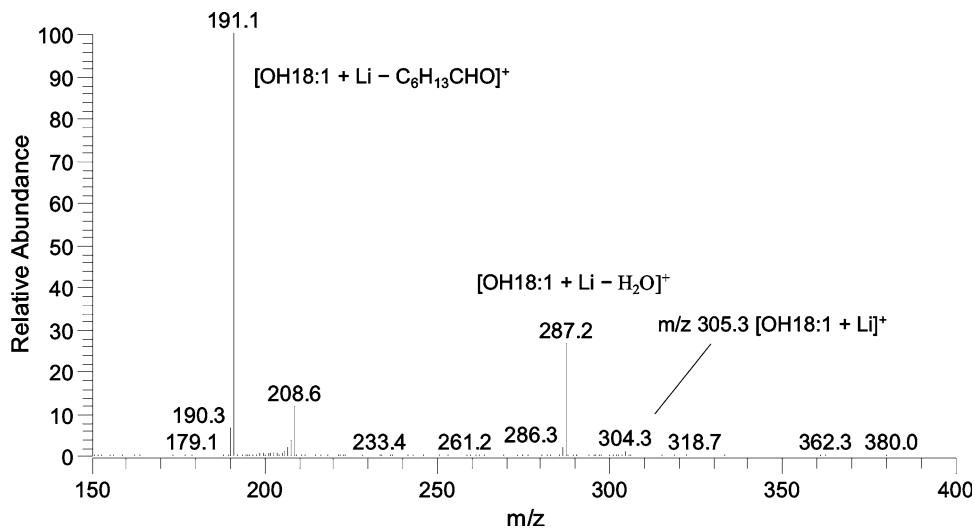


Fig. 7 Ion trap mass spectrum of ESI-MS² of ricinoleate standard (collision energy 36%)



[M + Li]⁺ at *m/z* 957.7 from the HPLC fraction #15 of castor oil and then MS³ of [M + Li – OH18:1]⁺ at *m/z* 659.5. Again in the MS² spectrum, the relative abundance of [diOH18:0 + Li]⁺ at *m/z* 323.3 was very low (2.5%) and we need to use the ion at *m/z* 323.3 in the MS³ spectrum (48%) for the MS⁴ spectrum of [diOH18:0 + Li]⁺ at *m/z* 323.3. Figure 9 shows only one significant fragment ion. The ion at *m/z* 305.2 was the dehydration of the precursor ion [diOH18:0 + Li – H₂O]⁺. The locations of the two hydroxyl groups of diOH18:0 were likely to be the same as those of the diOH18:1 and diOH18:2 (Fig. 1b, c). The standard 11,12-dihydroxyoctadecanoic acid is not commercially available. Instead we used the standard, 9,10-dihydroxyoctadecanoic acid, for MS² (spectrum not given here) to compare with Fig. 9 of diOH18:0 from castor oil. These two MS spectra were similar when the same collision energy 37% was used including the relative abundances of the precursor ions (about 23%). The MS spectrum of

standard 12-hydroxyoctadecanoic acid (not given here) at the same collision energy 37% also showed the only one significant fragment ion [OH18:0 + Li – H₂O]⁺ at *m/z* 289.2. However, the relative abundance of the precursor ion was only 1.5%. This suggested that the diOH18:0 in castor oil contained two hydroxyl groups attached to adjacent carbon atoms. The dehydration [diOH18:0 + Li – H₂O]⁺ with two hydroxyl groups attached to adjacent carbon atoms on the fatty acid chain required more collision energy than that of [OH18:0 + Li – H₂O]⁺ with monohydroxyl group on the chain. We propose here the structure of diOH18:0 as 11,12-dihydroxyoctadecanoic acid (Fig. 1d).

The three new dihydroxy fatty acids were confirmed, within 5 ppm of the calculated exact mass, by duplicate high-resolution accurate mass MS² measurements of their lithium adducts (Table 1). An example of an accurate mass MS² spectrum is shown in Fig. 4. The measured masses of the lithium adducts of diOH18:2 and diOH18:0 were from

Fig. 8 Ion trap mass spectrum of ESI-MS⁴ of dihydroxyoctadecadienoic acid [diOH18:2 + Li]⁺ at *m/z* 319.3 (collision energy 39%). This was from the MS² (collision energy 35%) of [diOH18:2-OH18:1-OH18:1 + Li]⁺ at *m/z* 953.6 from the HPLC fraction #15 of castor oil and then the MS³ (collision energy 38%) of [diOH18:2-OH18:1-OH18:1 + Li - OH18:1]⁺. For proposed fragmentation pathways, see Fig. 6b and c

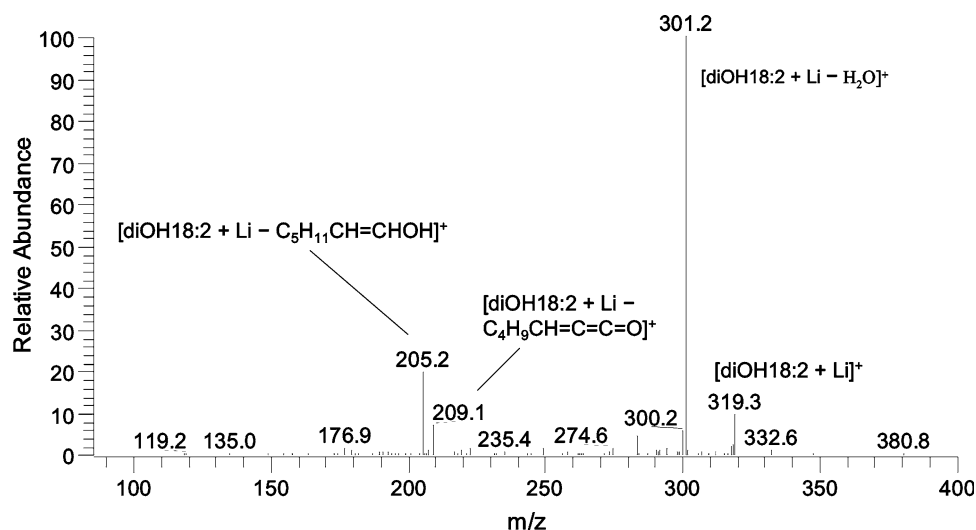
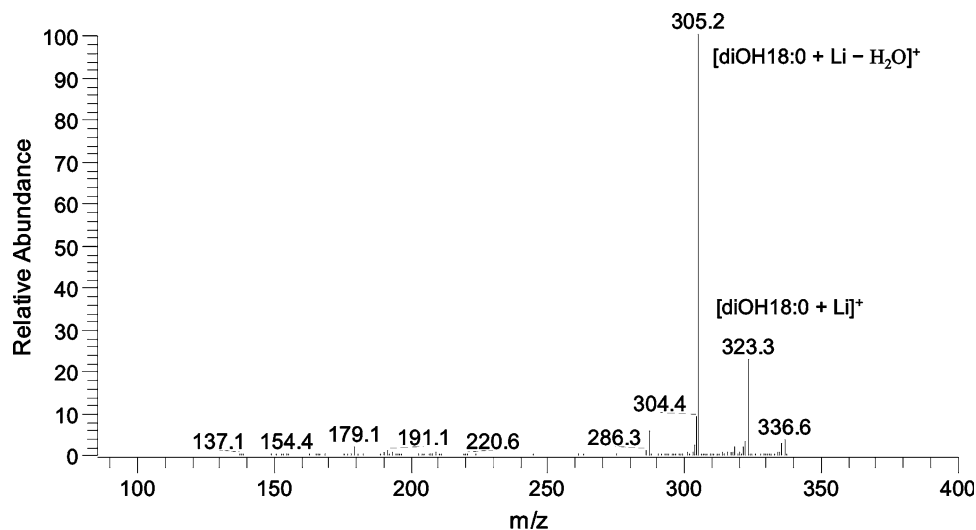


Fig. 9 Ion trap mass spectrum of ESI-MS⁴ of dihydroxyoctadecanoic acid [diOH18:0 + Li]⁺ at *m/z* 323.3 (collision energy 37%). This was originated from MS² (collision energy 36%) of [diOH18:0-OH18:1-OH18:1 + Li]⁺ at *m/z* 957.7 from the HPLC fraction #15 of castor oil and then MS³ (collision energy 39%) of [diOH18:0-OH18:1-OH18:1 + Li - OH18:1]⁺ at *m/z* 659.5



the high-resolution MS² spectra (not shown here) of [diOH18:2-OH18:1 + Li]⁺ at *m/z* 673.52 and [diOH18:0-OH18:1 + Li]⁺ at *m/z* 677.55 individually from the HPLC fraction #9. The errors were 5 ppm or less.

Figure 2 shows the four diacylglycerols and eight triacylglycerols containing dihydroxy fatty acids in castor oil identified by MS. The stereospecific locations of fatty acids on the glycerol backbones were not determined. The mass *m/z* of AG lithium adducts are also given in Fig. 2. Similar to Fig. 3, AG molecular species in Fig. 2 were identified by MS² of the individual AG lithium adducts. The MS² spectra (not shown here) showed the fragment ions from the loss of fatty acids, diOH18:2 *m/z* 312.2, diOH18:1 *m/z* 314.2, diOH18:0 *m/z* 316.2 and OH18:1 *m/z* 298.2. The MS³ (from diacylglycerols) and MS⁴ (from triacylglycerols) spectra (not shown here) of the dihydroxy fatty acids showed that these dihydroxy fatty acids were the same as those of the Figs. 5, 8 and 9.

Table 1 Calculated masses and duplicated measured masses by high-resolution MS² of lithium adducts of dihydroxy fatty acids [diOH-FA + Li]⁺ from the diacylglycerols in castor oil

diOH-FA	Calculated mass	Measured mass	Error in ppm
[diOH18:2 + Li] ⁺ ^a	319.2461	319.2446	5
[diOH18:2 + Li] ⁺ ^a	319.2461	319.2458	1
[diOH18:1 + Li] ⁺ ^b	321.2617	321.2601	5
[diOH18:1 + Li] ⁺ ^b	321.2617	321.2602	5
[diOH18:0 + Li] ⁺ ^c	323.2774	323.2760	4
[diOH18:0 + Li] ⁺ ^c	323.2774	323.2763	3

^a From the MS² of [diOH18:2-OH18:1 + Li]⁺ at *m/z* 673.52

^b From the MS² of [diOH18:1-OH18:1 + Li]⁺ at *m/z* 675.54

^c From the MS² of [diOH18:0-OH18:1 + Li]⁺ at *m/z* 677.55

In this HPLC fractionation, some AG detected by MS was eluted in many fractions (0.5 min/fraction). Individual AG in Fig. 2 were eluted in the fractions as: diOH18:1-

diOH18:1 (fractions #9–11), diOH18:2-OH18:1 (fractions #9, 10), diOH18:1-OH18:1 (fractions #8–12), diOH18:0-OH18:1 (fraction #9), diOH18:1-diOH18:1-diOH18:1 (fractions #11–14), diOH18:1-diOH18:1-diOH18:0 (fraction #13), diOH18:2-diOH18:1-OH18:1 (fraction #15), diOH18:1-diOH18:1-OH18:1 (fractions #12–18), diOH18:1-diOH18:0-OH18:1 (fractions #13–14), diOH18:2-OH18:1-OH18:1 (fraction #15), diOH18:1-OH18:1-OH18:1 (fractions #13–18), diOH18:0-OH18:1-OH18:1 (fractions #15–16). The HPLC resolutions of these AG containing dihydroxy fatty acids were not good and the accurate quantifications of these AG were difficult. However, according to the HPLC chromatogram of castor oil detected by evaporative light scattering detector using the same HPLC conditions published earlier [1]; the individual AG containing dihydroxy fatty acids were about 0.5% of castor oil or less. The total AG containing dihydroxy fatty acids was about 2.5% of castor oil. These AG were eluted before triricinolein. Among these 12 AG (Fig. 2), the contents of triacylglycerols diOH18:1-OH18:1-OH18:1, diOH18:0-OH18:1-OH18:1, diOH18:1-diOH18:1-OH18:1, diOH18:1-diOH18:0-OH18:1 and diacylglycerol diOH18:1-OH18:1 were higher than those of the other AG in castor oil.

We have reported the identification of 12 molecular species of acylglycerols containing dihydroxy fatty acids in castor oil. The structures of the three dihydroxy fatty acids were proposed as 11,12-dihydroxy-9-octadecenoic acid, 11,12-dihydroxy-9,13-octadecadienoic acid and 11,12-dihydroxyoctadecanoic acid.

References

- Lin JT, Turner C, Liao LP, McKeon TA (2003) Identification and quantification of the molecular species of acylglycerols in castor oil by HPLC using ELSD. *J Liq Chromatogr Relat Technol* 26:773–780
- Lin JT, Arcinas A, Harden LA, Fagerquist CK (2006) Identification of (12-ricinoleoylricinoleoyl) diricinoleoylglycerol and acylglycerol containing four acyl chains, in castor (*Ricinus communis* L.) oil by LC-ESI-MS. *J Agric Food Chem* 54:3498–3504
- Lin JT, Arcinas A (2007) Regiospecific analysis of diricinoleoylglycerols in castor (*Ricinus communis* L.) oil by electrospray ionization-mass spectrometry. *J Agric Food Chem* 55:2209–2216
- Lin JT, Arcinas A (2008) Regiospecific identification of 2-(12-Ricinoleoylricinoleoyl)-1,3-diricinoleoyl-*sn*-glycerol in castor (*Ricinus communis* L.) oil by ESI-MS4. *J Agric Food Chem* 56:3616–3622
- Hou CT, Bagby MO, Plattner RD, Koritala S (1991) A novel compound, 7,10-dihydroxy 8(*E*)-octadecenoic acid from oleic acid by bioconversion. *J Am Oil Chem Soc* 68:99–101
- Kim H, Kuo TM, Hou CT (2000) Production of 10,12-dihydroxy-8(*E*)-octadecenoic acid, an intermediate in the conversion of ricinoleic acid to 7,10,12-trihydroxy-8(*E*)-octadecenoic acid by *Pseudomonas aeruginosa* PR3. *J Ind Microbiol Biotechnol* 24:167–172
- Garscha U, Oliw EH (2008) Steric analysis of 8-hydroxy- and 10-hydroxyoctadecadienoic acids and dihydroxyoctadecadienoic acids formed from 8*R*-hydroxyoctadecadienoic acid by hydroperoxide isomerases. *Anal Biochem* 367:238–246
- Liu JW, Huang YS (2005) Separation and quantitation of polyunsaturated fatty acids and eicosanoids by HPLC. In: Lin JT, McKeon TA (eds) HPLC of acyl lipids, Chap 6. HNB Publishing, New York, pp 117–166
- Foubert I, Dewettinck K, Van de Walle D, Dijkstra AJ, Quinn PJ (2007) Physical properties: structural and physical characteristics. In: Gunstone FD, Harwood JL, Dijkstra AJ (eds) The lipid handbook, 3rd edn. CRC Press, Boca Raton, pp 535–590
- Byrdwell WC, Neff WE (1998) Analysis of hydroxyl-containing seed oils using atmospheric pressure chemical ionization mass spectrometry. *J Liq Chromatogr Relat Technol* 21:1485–1501
- Lin JT, Arcinas A (2008) Analysis of regiospecific triacylglycerols by electrospray ionization-mass spectrometry³ of lithiated adducts. *J Agric Food Chem* 56:4909–4915

Lipid and Phospholipid Profiling of Biological Samples Using MALDI Fourier Transform Mass Spectrometry

S. Mariccor A. B. Batoy · Sabine Borgmann · Karin Flick · Josephine Griffith · Jeffrey J. Jones · Viswanathan Saraswathi · Alyssa H. Hasty · Peter Kaiser · Charles L. Wilkins

Received: 11 September 2008 / Accepted: 17 October 2008 / Published online: 13 November 2008
© AOCs 2008

Abstract Here we describe a study of the feasibility of lipid and phospholipid (PL) profiling using matrix assisted laser desorption/ionization (MALDI) Fourier transform mass spectrometry (FTMS) for two different applications. In this work PL profiles of different mammalian tissues as well as those of whole cell organisms were examined. In particular, comparative analysis of lipid and PL profiles of tissues from mice fed different diets was done and, in another application, MALDI FTMS was used to analyze PL profiles of genetically modified *Saccharomyces cerevisiae*. Computational sorting of the observed ions was done in order to group the lipid and PL ions from complex MALDI spectra. The PL profiles of liver tissues from mice fed different diets showed a cross correlation coefficient of 0.2580, indicating significant dissimilarity, and revealed more than 30 significantly different peaks at the 99.9% confidence level. Histogram plots derived from the spectra of wild type and genetically modified yeast resulted in a

cross correlation coefficient 0.8941 showing greater similarity, but still revealing a number of significantly different peaks. Based on these results, it appears possible to use MALDI FTMS to identify PLs as potential biomarkers for metabolic processes in whole cells and tissues.

Keywords Matrix assisted laser desorption/ionization mass spectrometry (MALDI) · Fourier transform mass spectrometry (FTMS) · *Saccharomyces cerevisiae* · Yeast transcription factor Met4 · High fat diet

Introduction

Analysis of phospholipids (PLs) by matrix assisted laser desorption/ionization (MALDI) was first described by Harvey [1] over a decade ago. Around the same time, Marshall et al. reported initial experiments for MALDI Fourier transform mass spectrometry (FTMS) of a number of biological PLs [2]. Since then, MALDI FTMS also has been successfully used for analysis of di-acyl PL profiles of whole cell organisms [3, 4] and mammalian tissues [5]. Lipid compositions as main components [6] of cell membranes are vital for the physiological functionality of biological cells. Cellular signaling, metabolic processes, structural functions and regulatory roles are some of the processes where PLs are important [7, 8]. As demonstrated in 2006, MALDI FTMS allows rapid and precise monitoring of PL profiles of different types of mouse tissues (brain, heart and liver) [5].

This study aimed to apply the proposed approaches [3–5] to real biological problems in an optimized manner. Two different biological problems were selected, (1) monitoring the impact of high fat diets on PL profiles of *Mus musculus*

S. M. A. B. Batoy · J. Griffith · C. L. Wilkins (✉)
Department of Chemistry and Biochemistry,
University of Arkansas, Fayetteville, AR, USA
e-mail: cwilkins@uark.edu

S. Borgmann
Institute for Analytical Science (ISAS),
Bunsen-Kirchhoff-Strasse 11, 44139 Dortmund, Germany

J. J. Jones
Applied Proteomics Inc., Glendale, CA, USA

K. Flick · P. Kaiser
Department of Biological Chemistry, University of California,
Irvine, CA, USA

V. Saraswathi · A. H. Hasty
Department of Molecular Physiology and Biophysics,
Vanderbilt University, Nashville, TN, USA

(house mouse) and (2) evaluating the role of the yeast transcriptional regulator Met4 in PL homeostasis. Here the exceptional potential of MALDI high-resolution mass spectrometry ($>10^4$) for rapid, automated metabolite screens of complex biological samples is shown. This will allow researchers to achieve broader understanding of metabolic and signaling processes involving PLs.

Experimental Procedure

Reagents

The MALDI matrix used was 99% purity 2,5-dihydroxybenzoic acid (DHB) (Alfa Aesar, Shore Road, Heysham, Lancaster). Methanol was HPLC grade (EMC Chemical Inc., Gibbstown, NJ). Purified water was obtained from a Mill-Q gradient system (Millipore Corporation, Genay Cedex, France). The AIN-93G high fat diet was obtained from Dyets Inc., Bethlehem, PA. Trichloroacetic acid (TCA) was purchased from VWR, West Chester, PA.

Animal Care and Tissue Isolation

All animals were reared at Vanderbilt University. The protocols used in this study were performed and approved by the Institution for Animal Care and Use Committee of Vanderbilt University. Low density lipoprotein receptor LDLR $-/-$ mice on a C57BL/6J background were placed on high fat diets (39% calories from fat and 0.5% cholesterol) supplemented with 6% olive oil or 6% fish oil for 12 weeks. The fish oil in the mouse diet contained 140 mg eicosapentaenoic acid (EPA) and 95 mg docosahexaenoic acid (DHA) per gram of oil. The liver was removed, weighed and snap frozen before doing a MALDI FTMS analysis. Further experimental details are published elsewhere [9]. As matrix for homogenizing the frozen liver tissues, 1 M DHB in methanol/water (80:20, by volume) with 7.5% TCA was used.

Saccharomyces cerevisiae Growth Conditions

To analyze PL profiles of yeast, both wild type (wt) and mutant were grown in YEPD medium (1% yeast extract, 2% Bacto Peptone, 2% glucose, 0.04 g/L adenine sulfate, 0.04 g/L uracil) at 30 °C to mid-log phase ($OD_{600} = 1$). Yeast cells were harvested by filtration and washed in water. Washed cells were lysed in isopropanol with glass beads for 90 s at setting 4.5 in FastPrepTM FP120. Cell debris was separated by centrifugation (10 min 13,000 g). The supernatant was stored in dark tubes under nitrogen and analyzed within 2 days by MALDI FTMS. Yeast mutants lacking the *MET4* gene were generated by deleting

the entire open reading frame using a PCR-based strategy [10]. For MALDI FTMS a saturated solution of DHB in methanol/Mill-Q water (70:30 by volume) was used as matrix.

Instrumentation and Data Analysis

MALDI FTMS analysis was performed using the positive ion mode of a 9.4 Tesla FTMS (IonSpec/Varian, Lake Forest, CA) with an external ion source and a Nd-YAG laser operating at $\lambda = 355$ nm. PL assignments were accomplished via an optimized Windows version 3.8.28 of a lipid database and search program, utilizing a previously published assignment algorithm [4].

Results and Discussion

Following the methodology described above, reproducible MALDI FTMS spectra were observed. Figure 1 shows spectra of liver tissues from mice fed with different high fat diets. The spectra observed can be divided into three regions based on m/z values. PL fragment ions (PL-Hg) are found in the low mass region (550–700 m/z); PL ions such as those from phosphatidic acid (PA), phosphatidylethanolamine (PE), and phosphatidylcholine (PC) are found in the middle mass region (700–850 m/z); and the triacylglyceride ions (TAG) appear in the high mass region (850–1,000 m/z).

Triacylglycerides are of importance in this comparison because they are the major components of edible oils [11, 12]. In 2006 Lay et al. [11] observed that with the use of MALDI time-of-flight (TOF) mass spectrometry that edible oils can be identified through their TAG content. It is evident from the spectra shown in Fig. 1 that liver tissues from mice fed with the olive oil diet contain more TAG compared with liver tissues from mice fed with the fish oil diet. On the contrary, liver samples from fish oil fed mice have elevated PL contents compared with those from olive oil fed mice. The PLs and TAG content of the samples were binned together and a cross correlation calculation was done. The histogram correlation (Fig. 2) between the two samples is 0.2580 showing the expected low correlation. Based on these results, mice fed fish oil have lower TAG content than mice fed olive oil.

The results obtained in this study using MALDI FTMS are comparable to those obtained by Saraswathi et al. [9] using fatty acid methyl ester (FAME) analysis, wherein it was observed that the total TAG concentration in the liver for mice fed with the olive oil diet (74 mg/g tissue) is greater than that found in livers of fish oil fed mice (59 mg/g tissue). Although the biological importance of increased PLs in mice fed fish oil is not clear, our study demonstrates

Fig. 1 Representative spectra of liver tissues from mice fed high fat diets supplemented with 6% olive oil (*top*) and 6% fish oil (*bottom*). The spectra are divided into three regions **a** phospholipid fragments (PL-Hg) **b** PA phospholipids, PC, PE, etc., and **c** TAG triacylglycerides

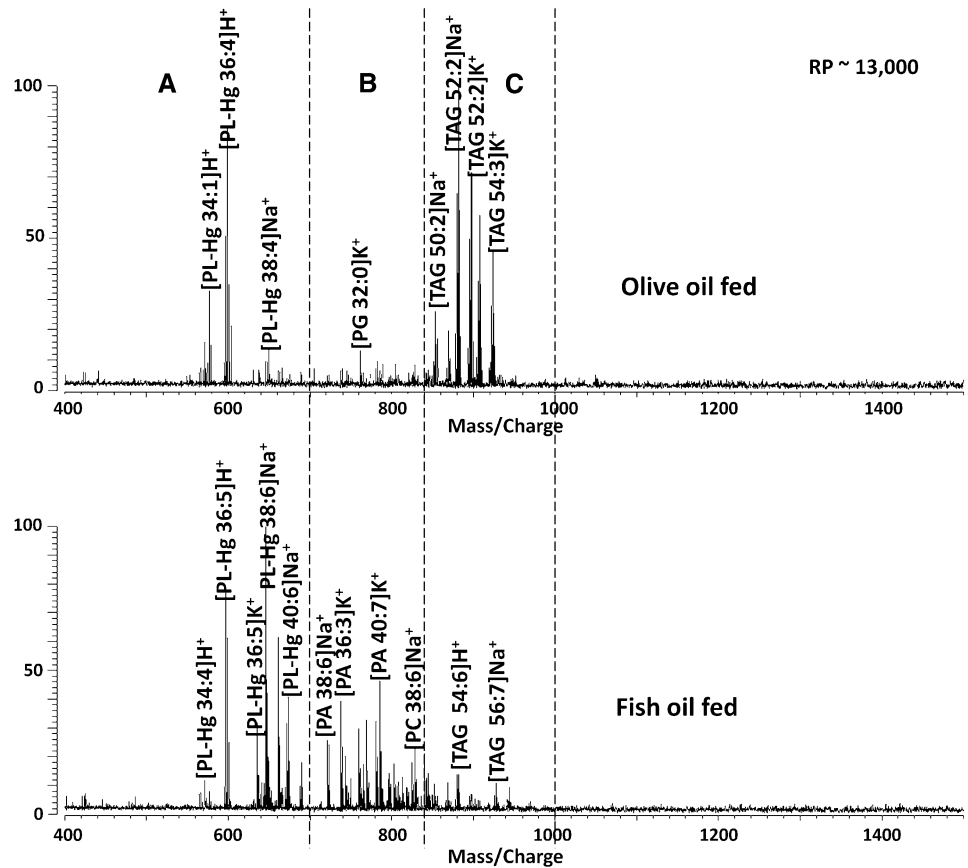
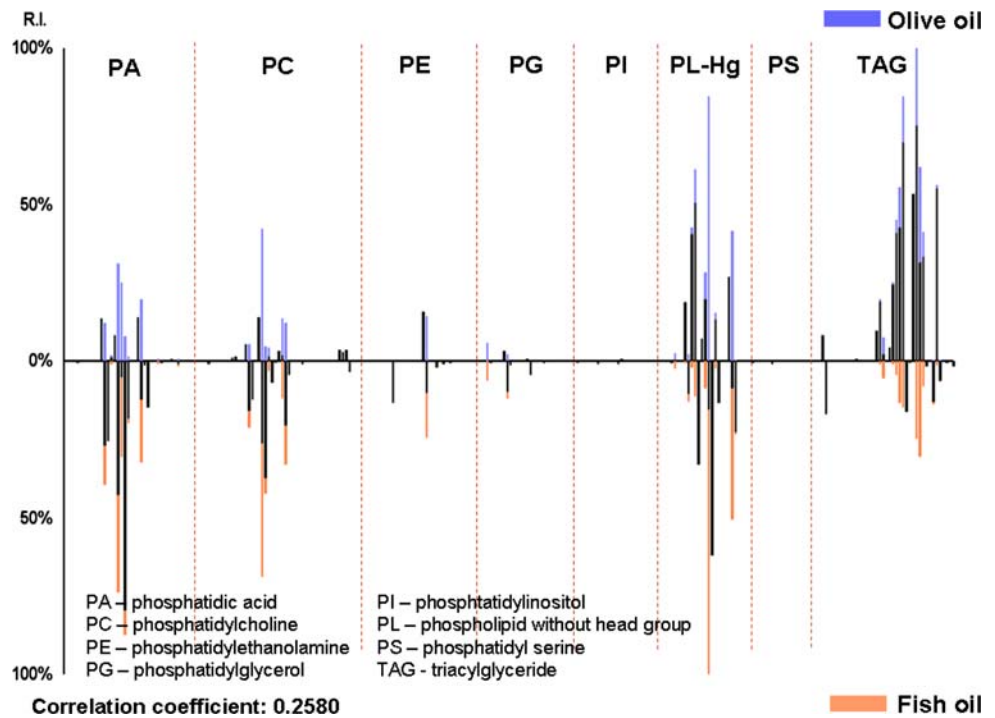


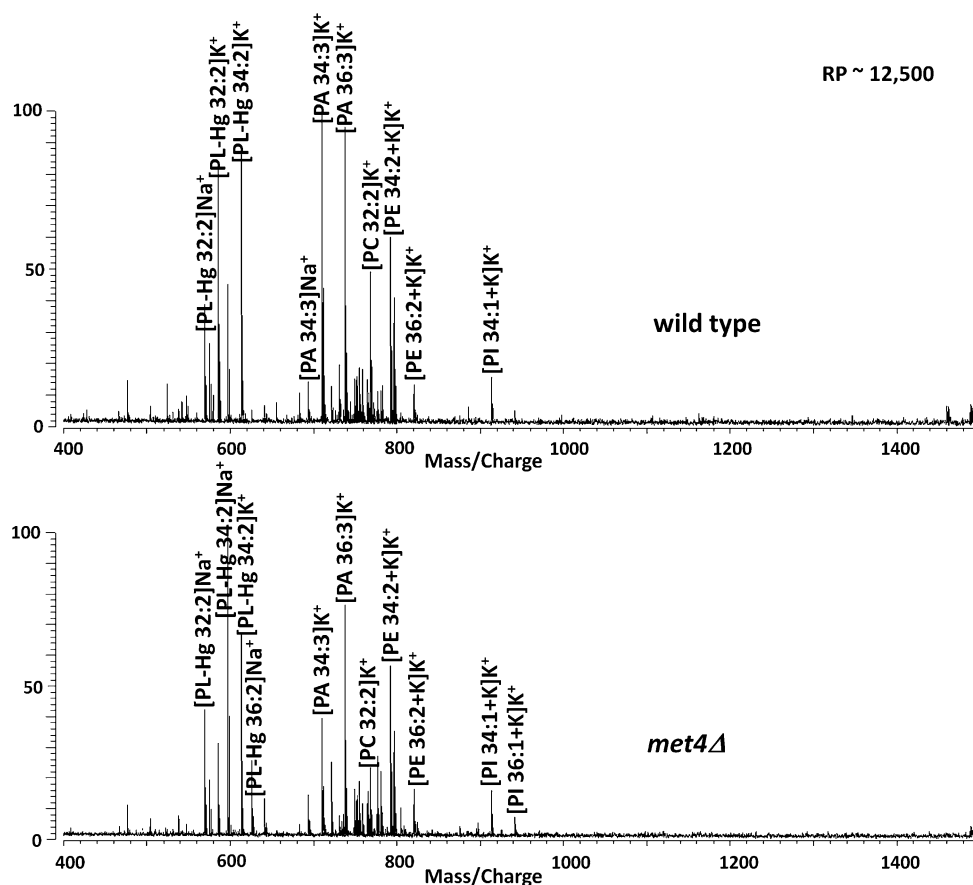
Fig. 2 Histogram plot of lipid and phospholipids found in liver tissues from mice fed a high fat diet supplemented with 6% olive oil (*top*) and fish oil (*bottom*)



that MALDI FTMS can be used to better characterize the PL species in biological samples. Several previous studies have analyzed the relationship between fish oil diets and

hypertriglyceridemia [13, 14] and all of their results reveal that dietary fish oil supplements reduce plasma TAG levels. The differences in their TAG content may be attributed to

Fig. 3 Representative MALDI FTMS spectra of wild type (wt) *S. cerevisiae* (top) and *met4Δ* mutant



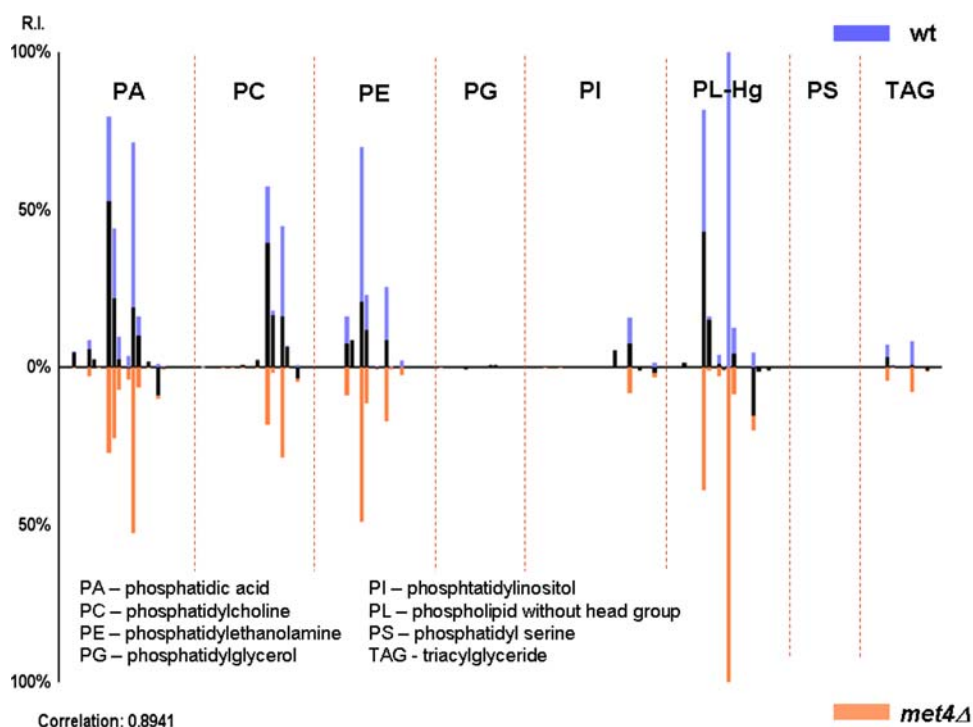
the fish oil's ability to reduce hepatic triacylglyceride synthesis [9, 15]. Hypertriglyceridemia and hepatic steatosis have been linked to their contribution to cardiovascular diseases and diabetes [16, 17].

We also applied our PL profiling strategy to analyze the role of the Met4 transcription factor in PL homeostasis. The activity of Met4 is tightly regulated by the ubiquitin ligase SCF^{Met30} [18]. Met30 the substrate specificity factor within this ubiquitin ligase has previously been linked to PL homeostasis based on genetic studies [18]. We were therefore interested in testing whether Met4 is involved in lipid homeostasis, given that its regulator was connected to lipid metabolism. Met4 is best known as a master regulator that coordinates the expression of genes involved in the synthesis of sulfur containing amino acids which include methionine, cysteine, and *S*-adenosylmethionine. Met4 can also induce a cell cycle arrest and thus links metabolic pathways with cell proliferation to protect cellular integrity when key metabolites are suboptimal [19, 20]. To investigate a potential role of Met4 in lipid metabolism we lysed wild type cells (wt) and *met4Δ* mutants, which lack the entire *MET4* gene and analyzed the lysates by MALDI FTMS. Representative spectra of the two strains are shown in Fig. 3. Although the most abundant ions are PL fragments, this does not necessary mean that these are the most

important ions. Based on the spectra, it is not evident which PLs differ, however when histogram plots (Fig. 4) derived from the spectra were cross-correlated, the correlation coefficient was 0.8941. Yeast lysates that lack the Met4 transcription factor (*met4Δ*) contain lower PL compared with lysates from wt samples based on the relative abundances of the binned PL peaks. This shows that inactivation of Met4 in yeast cells reduces the presence of PA, PC and PE. These results clearly link the transcriptional activator Met4 to lipid homeostasis in yeast. Since Met4 coordinates metabolic pathways with cell proliferation it is tempting to speculate that the Met4 pathway coordinates lipid homeostasis and cell cycle progression. Further studies will be required to dissect these functions and the role of other components in the Met4 system, but this analysis demonstrates that application of the MALDI FTMS strategy to a genetic model system is effective in linking gene function to lipid homeostasis.

To summarize, the use of MALDI FTMS has been demonstrated as a tool for PL profiling both in microorganisms with different genetic components as well as in mammalian tissues from mice fed different high fat diets. Our data have implications in understanding the cellular pathways involved in the biosynthesis and/or transport of PLs.

Fig. 4 Histogram plot of lipid and phospholipids found in wild type (top) and *met4Δ* mutant (bottom) *S. cerevisiae* lysates



Acknowledgments The authors are grateful for financial support from the Arkansas Biosciences Institute and NSF grants CHE-00-91868 and CHE-99-82045. P.K. acknowledges support from NIH-GM-66164. The authors appreciate discussions with R. M. O'Brien and support from the Arkansas Statewide Mass Spectrometry Facility.

References

- Harvey DJ (1995) Matrix-assisted laser desorption/ionization mass spectrometry of phospholipids. *J Mass Spectrom* 30:1333–1346
- Marto JA, White FM, Seldomddge S, Marshal AQ (1995) Structural characterization of phospholipids by matrix-assisted laser desorption/ionization Fourier transform ion cyclotron resonance mass spectrometry. *Anal Chem* 67:3979–3984
- Jones JJ, Stump MJ, Fleming RC, Lay JO, Wilkins CL (2004) Strategies and data analysis techniques for lipid and phospholipid chemistry elucidation by intact cell MALDI-FTMS. *J Am Soc Mass Spectrom* 15:1665–1674
- Jones JJ, Batoy SMAB, Wilkins CL (2005) A comprehensive and comparative analysis for MALDI FTMS lipid and phospholipid profiles from biological samples. *Comput Biol Chem* 29:294–302
- Jones JJ, Borgmann S, Wilkins CL, O'Brien RM (2006) Characterizing the phospholipid profiles in mammalian tissues by MALDI FTMS. *Anal Chem* 78:3062–3071
- Berg JM, Tymoczko JL, Stryer L (2006) *Biochemistry*. W.H. Freeman, New York
- Gurr MI, Harwood JL, Frayn KN (2002) *Lipid biochemistry—an introduction*. Blackwell, Oxford
- Ratledge C, Wilkinson SG (1988) An overview of microbial lipids. In: Ratledge C, Wilkinson SG (eds) *Microbial lipids*. Academic Press, London, pp 1–79
- Saraswathi V, Gao L, Morrow JD, Chait A, Niswender KD, Hasty AH (2007) Fish oil increases cholesterol storage in white adipose tissue with concomitant decreases in inflammation, hepatic steatosis, and atherosclerosis in mice. *J Nutr* 137:1776–1782
- Wach A, Brachat A, Pohlmann R, Philippsen P (1994) New heterologous modules for classical or PCR-based gene disruptions in *Saccharomyces cerevisiae*. *Yeast* 10:1793–1808
- Lay JO, Liyanage R, Durham B, Brooks J (2006) Rapid characterization of edible oils by direct matrix assisted laser desorption/ionization time-of-flight mass spectrometry analysis using triacylglycerols. *Rapid Commun Mass Spectrom* 20:952–958
- Gidden J, Liyanage R, Durham B, Lay JO (2007) Reducing fragmentation observed in the matrix-assisted laser desorption/ionization time-of-flight mass spectrometric analysis of triacylglycerols in vegetable oils. *Rapid Commun Mass Spectrom* 21:1951–1957
- Levy E, Thibault L, Turgeon J, Roy C, Gurbindo C, Lepage G, Godard M, Rivard G, Seidman E (1993) Beneficial effects of fish-oil supplements on lipids, lipoproteins, and lipoprotein lipase in patients with glycogen storage disease type I. *Am J Clin Nutr* 57:922–929
- Jonkers IJAM, Smelt AHM, Princen HMG, Kuipers F, Romijn JA, Boverhof R, Masclee AAM, Stellaard F (2006) Fish oil increases bile acid synthesis in male patients with hypertriglyceridemia. *J Nutr* 136:987–991
- Davidson MH (2006) Mechanisms for the hypotriglyceridemic effect of marine omega-3 fatty acids. *Am J Cardiol* 98:271–33i
- Citkowitz E (2005) Hypertriglyceridemia. In: Gambert SR, et al. (eds) *Hypertriglyceridemia*, eMedicine.com
- Coenen KR, Hasty AH (2002) Obesity potentiates development of fatty liver and insulin resistance, but not atherosclerosis, in high-fat diet-fed agouti LDLR-deficient mice. *Am J Physiol Endocrinol Metab* 293:E492–E499
- Schumacher MM, Choi JY, Voelker DR (2002) Phosphatidylserine transport to the mitochondria is regulated by ubiquitination. *J Biol Chem* 277:51033–51042
- Thomas D, Surdin-Kerjan Y (1997) Metabolism of sulfur amino acids in *Saccharomyces cerevisiae*. *Microbiol Mol Biol Rev* 61:503–532
- Kaiser P, Su N-Y, Yen JL, Ouni I, Flick K (2006) The yeast ubiquitin ligase SCF^{Met30}: connecting environment and intracellular conditions to cell division. *Cell Division* 1:16–23

Preparative Separation of *cis*- and *trans*-Isomers of Unsaturated Fatty Acid Methyl Esters Contained in Edible Oils by Reversed-Phase High-Performance Liquid Chromatography

Wakako Tsuzuki · Kaori Ushida

Received: 6 July 2008 / Accepted: 12 November 2008 / Published online: 16 December 2008
© AOCS 2008

Abstract In order to measure exactly the *trans*-fatty acids content in food materials, a preparative group separation of *cis*- and *trans*-isomers of unsaturated fatty acid methyl esters (FAMES) was achieved by an isocratic reversed-phase HPLC (RP-HPLC) method. The *trans*-isomers of 16:1, 18:1, 18:2, 18:3, 20:1 and 22:1 FAMES were readily separated from the corresponding *cis*-isomers by a COSMOSIL Cholester C18 column (4.6 mm I.D. × 250 mm, Nacalai Tesque) or a TSKgel ODS-100Z column (4.6 mm I.D. × 250 mm, TOSOH), using acetonitrile as the mobile phase. This method was applied for determining the *trans*-18:1 fatty acid content in partially hydrogenated rapeseed oil. The methyl esters of *cis*- and *trans*-18:1 isomers of the oil were collected as two separate fractions by the developed RP-HPLC method. Each fraction was analyzed by gas chromatography (GC) for both qualitative and quantitative information on its positional isomers. By a combination of RP-HPLC and GC methods, a nearly complete separation of *cis*- and *trans*-18:1 positional isomers was achieved and the *trans*-18:1 fatty acid content was able to be evaluated more precisely than is possible by the direct GC method. The reproducibility of *cis*- and *trans*-18:1 isomers fractionated by the RP-HPLC method was better than 98%. These results suggested that the preparative RP-HPLC method developed in this study could be a powerful tool for *trans*-fatty acid analysis in edible oils and food products as an alternative to silver-ion chromatography.

Keywords *trans*-Fatty acids · Configurational isomer · Reverse-phase HPLC

Introduction

The health risks of *trans*-fatty acids have been discussed for many years. It has been pointed out that excess consumption of *trans*-fatty acids increases the risk of coronary heart disease [1–3]. Therefore, some countries have issued regulations requiring manufacturers to label *trans*-fatty acid levels among the nutritional facts. These rules have prompted efforts to optimize the analysis of *trans*-fatty acid levels in food products. Such analysis is not so easy because of the wide range of positional monoene, diene and trine isomers. Generally, *trans*-fatty acid analysis is conducted by gas chromatography (GC) according to the official methods proposed by the academic societies [4, 5]. By the direct GC method, positional and geometrical isomers of monounsaturated fatty acid methyl esters (FAMES) can be resolved to some extent, but some of the *cis*-isomers overlap with the *trans*-isomers [6]. On the other hand, complete separation of *cis*- and *trans*-isomers of monounsaturated FAMES can be achieved by silver-ion chromatography (TLC or HPLC) and reversed-phase HPLC (RP-HPLC) prior to GC analysis. Among these methods, the silver-ion thin-layer chromatography (Ag-TLC) method is widely in use. But, Ag-TLC has some disadvantages; the most obvious being that it is a laborious process. The silver-ion HPLC method also has considerable potential for the separation of positional and configurational isomers of unsaturated fatty acids [7, 8]. Its difficulties include the low reproducibility and the contamination by a trace of silver salts into the fraction. Furthermore, small cartridge columns packed with a

W. Tsuzuki (✉) · K. Ushida
National Food Research Institute, Kannondai 2-1-12,
Tsukuba, Ibaraki 305-8642, Japan
e-mail: wakako@affrc.go.jp

bonded benzene sulfonate medium can be loaded with silver ions and used to achieve excellent separation of FAMES according not only to the geometrical configuration of the unsaturated bond but also to the degree of unsaturation [9].

As for the RP-HPLC method for preparative separation, Sevansson et al. first reported the geometric separation of long chain monounsaturated fatty acids by the RP-HPLC method [10]. Although RP-HPLC separation has been improved upon by various researchers [11–14], the method has not prevailed. In the previous RP-HPLC methods, plural HPLC columns and/or a gradient HPLC with polar organic solvents and water were needed for complete separation of *trans*- and *cis*-isomers of unsaturated FAMES. As a result, the volume of each fraction was considerably enlarged and its solvent contained water. These facts complicated the subsequent GC analysis.

The purpose of this study was to improve the RP-HPLC method for obtaining pure preparative fractions of *cis*- and *trans*-isomers of unsaturated FAMES. Recently, several RP-HPLC columns that can recognize the geometrical configuration of unsaturated double bonds in fatty acids have been developed. In this study, we selected two kinds of RP-HPLC columns in advance and examined the retention times of standard FAMES containing unsaturated *cis*- and *trans*-isomers using each column. After that, the method was applied to determine the exact *trans*-18:1 content of partially hydrogenated rapeseed oil.

Materials and Methods

Reagents

The chemical reagents were obtained from Wako Chem. Inc. (Osaka, Japan) and Sigma Chemicals Co. (St. Louis, MO, USA). Acetonitrile for the HPLC solvent was of analytical grade (Wako). Standard fatty acid methyl esters (FAMES) were purchased from SUPELCO (Bellefonte, PA, USA) and Funakoshi Co. Ltd. (Tokyo, Japan). Partially hydrogenated rapeseed oil was kindly donated by Tuki-shima Shokuhin Co. Ltd. (Tokyo, Japan). This oil was converted into corresponding FAMES using NaOH/methanol (0.5 mol/L) and BF₃/methanol (14%) according to the AOCS official method 2d-66.

HPLC Analysis

Separation of FAMES by the HPLC method was carried out on a solvent pump (JASCO 880-PU), a column oven (Shimadzu CTO-20AC), a UV spectrometer (Shimadzu SPD-20AV) and a chromatography manager (EZ Chrome, GL-Science, Tokyo, Japan). The injector was Rheodyne,

Model 7725-022. The columns selected for a preparative fractionation of FAMES were a COSMOSIL Cholesterol C18 column (4.6 mm I.D. × 250 mm, Nacalai Tesque, Kyoto, Japan) and a TSKgel ODS-100Z column (4.6 mm I.D. × 250 mm, TOSOH, Tokyo, Japan). The HPLC analysis was performed at 20 °C or 35 °C. Standard FAMES (about 5–10 µg, each) were chromatographed in 10 µL of acetonitrile to determine the retention time. The HPLC solvent system used for most FAMES was an isocratic one using 100% acetonitrile with a flow rate of 1 mL/min and initial pressure of 45 psi. For separation of *cis*- and *trans*-isomers of polyunsaturated FAMES, the isocratic solvent system was changed to 10% or 15% of water in acetonitrile, with a flow rate of 1 mL/min and initial pressure of 50–60 psi.

GC Analysis

The FAMES were analyzed by GC using a Shimadzu GC-2010 model, fitted with a split injector (250 °C) and a flame ionization detector (250 °C) coupled with a GC solution integrating system (Shimadzu). A CP-Sil 88 column (60 m × 0.25 mm I.D., 0.2 µm film thickness, SPELCO) was utilized and operated at 175 °C. For this column, nitrogen was used as a carrier at a velocity of 23.6 cm/s. Each FAME peak was identified and quantified with standard FAME mixtures of known composition. Most samples were run in triplicate.

Results and Discussions

The nature of the FAMES separation by RP-HPLC has been known for some time; i.e., that the retention time is prolonged depending on an increase in the total number of the carbon atoms of the fatty acids and is reduced by an increase in the total number of double bonds in this moiety [12–14]. Of the more than ten different kinds of RP-HPLC column examined in advance, the COSMOSIL Cholesterol C18 column (Cholesterol column) and TSK gel ODS-100Z column (100Z column) recognized best the configurational differences around unsaturated bonds of FAMES. The Cholesterol column possesses a cholesteryl group-bonded silica packing material. It offers strong stereo selectivity for hydrophobic compounds. On the other hand, the 100Z column contains a high-density monomeric C18 bonded phase for maximum retention and selectivity of small molecular weight compounds. Hence, the separation of various standard FAMES including the *cis*- and *trans*-isomers were investigated using the Cholesterol column and the 100Z columns. The retention times of FAMES eluted by the two kinds of column under various conditions are listed in Table 1. When 100% acetonitrile was used as the HPLC eluent and the column temperature was set at 20 °C,

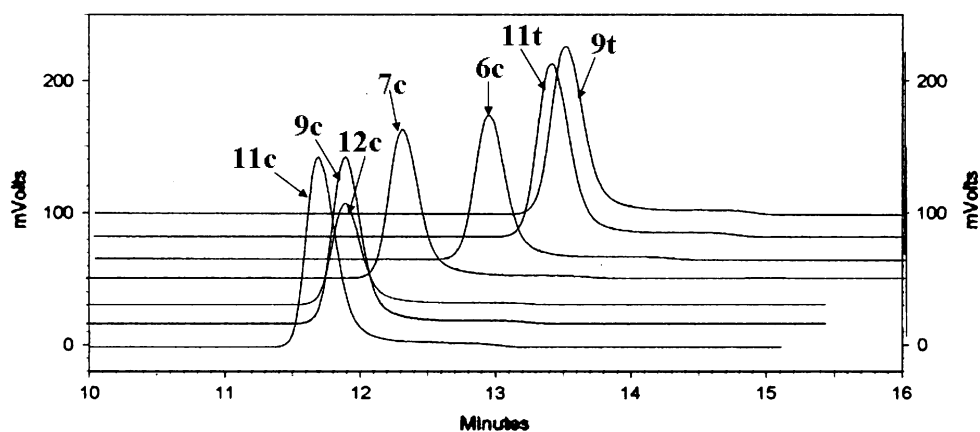
Table 1 Retention time (min) of standard fatty acid methyl esters (FAMES)

Column Solvent Temperature	Cholester				100Z	
	100% MeCN 20 °C	100% MeCN 35 °C	90% MeCN, 10% H ₂ O 35 °C	85% MeCN, 10% H ₂ O 35 °C	100% MeCN 20 °C	100% MeCN 35 °C
C8:0	3.83	3.74				
C10:0	4.68	4.37				
C12:0	6.27	5.45				
C14:0	9.28	7.31	11.35	17.80		
C16:0	14.78	10.39	24.79	38.88	18.10	14.22
C16:1,c9	7.75	6.35			12.32	9.68
C16:1,t9	8.69	6.92			13.02	10.11
C18:0	24.50	15.62	46.63	73.13	29.06	21.33
C18:1,c6	12.91				19.70	
C18:1,c7	12.32				19.33	
C18:1,c9	11.96	8.65	25.18	39.49	19.02	13.96
C18:1,c11	11.65		25.08	38.27	18.84	
C18:1,c12	11.91				18.82	
C18:1,t9	13.47	9.64	30.51	47.77	20.20	14.66
C18:1,t11	13.40				19.98	
C18:2,c9,c12	7.79	6.41	17.77	23.22	12.76	9.90
C18:2,c9,t12	8.69	6.82	19.80	26.10	13.41	10.35
C18:2,t9,c12	8.69	6.82	19.80	26.10	13.41	10.35
C18:2,t9,t12	8.69	6.82	20.44	27.04	13.74	10.56
C18:3,c9,c12,c15	6.04	5.32	12.37	16.02	9.07	7.51
C18:3,c6,c9,c12	6.04	5.32	12.16	15.79	9.07	7.51
C18:3 <i>trans</i> isomer	6.46	5.51	12.97	16.60	9.69	8.02
			13.29	17.18		
			13.39	18.01		
			14.59	18.56		
C20:0	40.66	23.35	94.96	121.21	47.14	32.66
C20:1,c11	17.52	12.21			29.92	20.73
C20:1,t11	18.01	12.93			31.84	21.81
C20:2	11.37	8.57			19.62	14.25
C20:3	8.02	6.47			13.38	10.43
C20:4	6.47	5.40			10.56	8.32
C20:5	5.05	4.70			7.34	6.12
C22:0	67.02	35.15			78.00	50.12
C22:1,c13	28.17	18.02			48.57	31.21
C22:1,t13	30.42	20.04			51.77	32.84
C22:6	5.35	4.98			8.22	6.68
C24:0	110.46	53.35				
C24:1,c15	46.99	27.50			80.99	48.35
C24:1,t15	49.65	29.93			86.49	50.87

elution patterns of saturated FAMES chromatographed by the Cholester column and by the 100Z column were similar to those obtained in previous RP-HPLC analysis [10, 11]. In the case of unsaturated FAMES, the retention times depended on the geometrical and positional configuration of the double bond, as shown in Table 1. In various 18:1

isomers of FAMES, *cis*-isomers were eluted slightly faster than the *trans*-isomers. For example, the retention times of *cis*-9 18:1 and *trans*-9 18:1 were 11.96 and 13.47 min, respectively, when the eluent was acetonitrile and the Cholester column was used at 20 °C (Fig. 1). Among the *cis*-18:1 isomers of FAMES, *cis*-11 18:1 was eluted the

Fig. 1 The reversed-phase HPLC separation of standard FAMES, *cis*-11 18:1, *cis*-9 18:1, *cis*-12 18:1, *cis*-7 18:1, *cis*-6 18:1, *trans*-11 18:1 and *trans*-9 18:1. Each standard (about 10 µg) in about 10 µL of 100% acetonitrile was chromatographed on one Cholesterol column at 20 °C. Eluent, 100% acetonitrile, flow rate = 1 mL/min



fastest, as shown in Fig. 1. The separation pattern of the geometrical isomers of 18:1 FAMES was in good accordance with that shown in previous reports using RP-HPLC methods [10, 11], although the chromatographic conditions of these previous works were more complicated than those of this study. Furthermore, not only 18:1 FAMES geometrical isomers but also of 16:1, 20:1, 22:1 and 24:1 FAMES were well separated using these RP-HPLC analysis conditions. It seemed to us that the RP-HPLC method just developed was very effective for a preparative isolation of *cis*- and *trans*-isomers of monounsaturated FAMES for further GC analysis.

In the case of 18:2 isomers, the *cis*-9/*cis*-12 18:2 FAME was separated from the other three isomers (*cis*-9/*trans*-12, *trans*-9/*cis*-12, *trans*-9/*trans*-12 18:2 FAMES), when they were chromatographed by Cholesterol column with an isocratic acetonitrile. By contrast, the 100Z column with acetonitrile resolved these four 18:2 geometrical isomers into three peaks. In addition to the *cis*-9/*cis*-12 18:2 FAME, the *trans*-9/*trans*-12 18:2 FAME was able to be isolated from the *cis*-9/*trans*-12 18:2 FAME and *trans*-9/*cis*-12 18:2 FAME, as shown in Table 1. When water was added to the HPLC eluent, the Cholesterol column could also resolve the geometrical differences of the four 18:2 isomers into three HPLC peaks (Table 1). Among the 18:3 isomers, *cis*-9/*cis*-12/*cis*-15 18:3 FAME was almost completely separated from the other seven *trans*-18:3 isomers by using acetonitrile/water (85/15, v/v) as an HPLC eluent. These results suggested that the RP-HPLC method examined in this study could also be applied to geometrical fractionation of polyunsaturated FAMES, especially for the effective separation of *trans*- from *cis*-isomers.

The RP-HPLC method was applied to the preparative separation of *trans*- and *cis*-18:1 isomers for estimating the exact content of *trans*-18:1 isomers in partially hydrogenated rapeseed oil. This oil was methylated and the FAMES were pre-fractionated by the RP-HPLC method. In the case of the Cholesterol column set at 20 °C using acetonitrile as

an eluent, the *trans*-18:1 isomer fraction of this oil was able to be successfully separated from the *cis*-18:1 isomer fraction, as shown in Fig. 2a. In the RP-HPLC analysis of the original oil, the head part of the first big peak around 11.7 min was composed of *cis*-11, 18:1 FAME (Fig. 2a upper), and that of the third peak around 13.5 min was of *trans*-11, 18:1 FAME, based on the elution time of each 18:1 isomer (Table 1 and Fig. 1). In the preparative separation by the RP-HPLC method, the peaks from 11.6 to 13.4 min were collected as a *cis*-fraction. For the *trans*-fraction, the peaks appeared from 13.4 to 15.4 min (Fig. 2a lower), in which the peak of 16:0 FAME was contained. In this *cis*-fraction, in addition to *cis*-11, 18:1 FAME, *cis*-6, *cis*-7, *cis*-8 and *cis*-12, 18:1 FAMES of the hydrogenated rapeseed oil should be present, at least from the results of each standard isomer analysis as shown in Fig. 1. Furthermore, no *trans*-18:1 isomers could be contained in this *cis*-fraction, because the *trans*-11, 18:1 FAME was eluted faster than any other *trans*-18:1 isomers under RP-HPLC conditions which were shown in Fig. 1 and in other previous studies [4, 12, 13]. The fractionated volume of the *cis*-fraction and that of the *trans* one were 1.8 mL and 2.0 mL, respectively, which were small enough to proceed with the subsequent GC analysis. The isomeric distribution of each fraction was examined by the GC method, after adding an internal standard (17:0 FAME). Gas chromatograms of the isomer distribution of 18:1 FAMES of the original partially hydrogenated rapeseed oil, of the *cis*-fraction and of the *trans*-fraction isolated by the RP-HPLC method are shown in Fig. 2b and c. Most peaks were assigned by the standard, commercially available FAMES, and by data from previous works [4, 12, 13]. The previous studies suggested that some *trans*-18:1 FAMES overlapped with the *cis* ones, as far example, *cis*-6,-7,-8 with *trans*-13,-14, 18:1 FAMES, *cis*-9 with *trans*-15, 18:1 FAME, and *cis*-14 with *trans*-16, 18:1 FAME [4, 12, 13]. In these experiments, the overlapping peaks were eluted in the retention time ranges from 16.3 to 16.6 min (*cis*-6,7,8 and

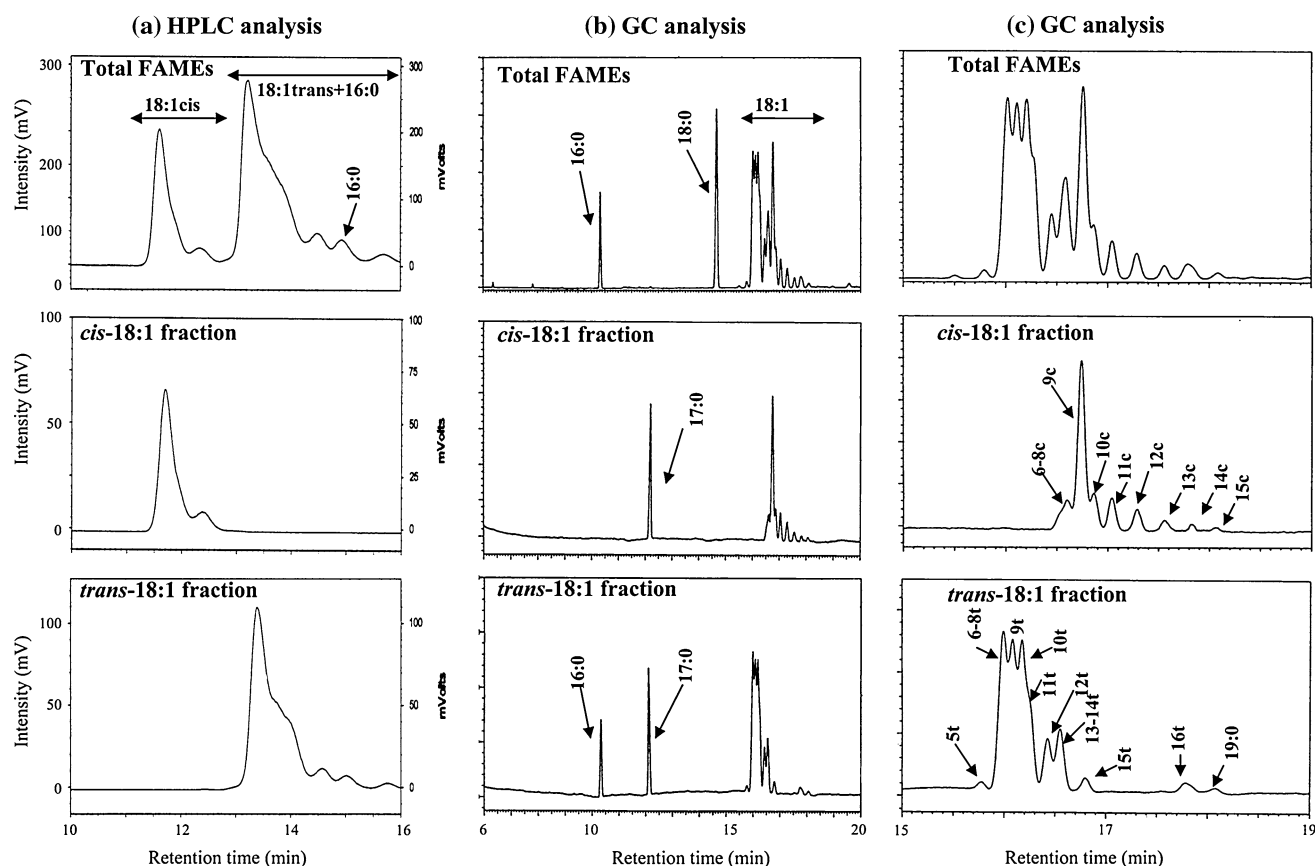


Fig. 2 **a** HPLC separation of total (original) 18:1 FAMES of hydrogenated rapeseed oil (upper). Methyl esterified hydrogenated rapeseed oil (about 0.1 mg) in about 10 μ L of 100% acetonitrile was chromatographed on one Cholesterol column at 20 $^{\circ}$ C. Eluent, 100% acetonitrile, flow rate = 1 mL/min. HPLC re-chromatogram of *cis*-18:1 fraction of **a** (middle). HPLC re-chromatogram of *trans*-18:1

fraction of **a** (lower). **b** GC separation of the total (original) 18:1 FAMES of hydrogenated rapeseed oil (upper), of the *cis*-18:1 fraction by the reversed HPLC method and 17:0 FAMES of internal standard (middle) and of *trans*-18:1 fraction by the reversed HPLC method and 17:0 of the internal standard (lower). **c** The same chromatograms as in **b**, with an expanded horizontal axis

trans-13,14), from 16.7 to 16.9 min (*cis*-9 and *trans*-15), and from 17.7 to 18.2 min (*cis*-14 and *trans*-16), respectively (Fig. 2c, upper and middle). In the case of unfractionated partially hydrogenated rapeseed oil, the peaks eluted in these regions were composed not only of *cis*-18:1 FAMES but also of *trans*-18:1 (Fig. 2b, c upper). The peaks of the *cis*-fraction eluted in these three regions must come from *cis*-18:1 isomers, but not *trans*-isomers, because the *cis*-fraction contained no *trans*-18:1 isomers as described for the RP-HPLC separation (Fig. 2c middle). For *trans*-fraction, the peaks eluted from 16.3 to 16.6 min and from 16.7 to 16.9 min were composed of *trans*-13,-14, 18:1 FAMES and *trans*-15, 18:1 FAMES, respectively, without contamination of *cis*-6,-7,-8, 18:1 FAMES and *cis*-9, 18:1 FAME. For the peaks from 17.7 to 18.2 min, the separation of *trans*-16, 18:1 FAME from *cis*-14, 18:1 FAME seemed to be incomplete. These results suggested that the developed RP-HPLC method was successful for a complete separation of *trans*-18:1 from *cis*-18:1 isomers.

When more than 3 mg of total FAMES from partially hydrogenated rapeseed oil was simultaneously injected into RP-HPLC for the pre-separation of *cis*- and *trans*-18:1 FAMES, the resultant contamination of *trans*-18:1 FAMES by *cis*-18:1 isomers was observed under our experimental conditions.

It is also worth noting that the preparative separation of *cis*- and *trans*-isomers by the RP-HPLC method developed in this study possessed high reproducibility. Indeed, two fractions, namely the *cis*-18:1 isomer fraction and the *trans*-18:1 isomer, which co-eluted with 16:0 FAME of partially hydrogenated rapeseed oils, were collected independently by the RP-HPLC method. The internal standard, 17:0 FAME, was added to these two fractions, before GC analysis. The absolute amount of total *cis*-18:1 isomers and total *trans*-18:1 isomers of the partially hydrogenated rapeseed oil was able to be determined easily by using both an internal standard (17:1 FAME) and 16:0 FAME co-eluted in the *trans*-18:1 fraction (Fig. 2b). The amounts of the two

Table 2 C18:1*cis*- and C18:1*trans*-fraction of hydrogenated rapeseed oil

	C18:1 <i>cis</i> -fraction (g/100 g)	C18:1 <i>trans</i> -fraction (g/100 g)	Total C18:1 (g/100 g)
Direct GC	20.2	13.1	33.3 (100.0)
HPLC/GC	22.1	10.6	32.7 (98.3)

Values in parentheses were the reproducibility (%)

The values were average of triplicated measurements

isomers were calculated from the results by the RP-HPLC method combined with GC analysis (HPLC/GC method) and which were compared with those obtained by the direct GC method. As shown in Table 2, the sum of *cis*-18:1 isomers and of *trans*-18:1 isomers by the HPLC/GC method was approximately the amount of the total 18:1 isomers estimated from the direct GC method. The yields of these two fractions were more than 98% of the original (Table 2), suggesting that a high reproducibility using the HPLC/GC method could be accomplished. In spite of the high reproducibility of the HPLC/GC method, the absolute amount of *trans*-18:1 isomers calculated by the HPLC/GC method (10.6 g/100 g) was about 20% less than that by the directed GC method (13.1 g/100 g), as shown in Table 2. Thus, the decrease must result from the complete elimination of *cis*-18:1 FAMES from the *trans*-fraction by the preparative RP-HPLC method. Thus, a more accurate measurement of *trans*-isomers of octadecenoic acid in partially hydrogenated rapeseed oil could be achieved by a prior preparative separation by the RP-HPLC method. It is suggested that the HPLC/GC method was essential for the accurate measurement of the total *trans*-18:1 content in food composed of partially hydrogenated edible oils.

In previous studies, *trans*-4, and *trans*-5, 18:1 isomers were not collected in the *trans*-18:1 fraction by the HPLC methods [12, 13]. On one hand, *trans*-5, 18:1 FAME was able to be fractionated by the RP-HPLC method developed in this study (Fig. 2c lower). On the other hand, the collection of *trans*-4 and *cis*-14, *cis*-15, 18:1 FAMES into the *trans*- and *cis*-fractions seemed to be incomplete even in this study. However, these isomers were a minor proportion in partially hydrogenated rapeseed oil (only a few percent of the total 18:1 isomers content).

Previously, the analysis of the isomeric distribution of *trans*-18:1 acid in milk fat was achieved by GC analysis with a pre-fractionation step by the RP-HPLC method [12, 13]. However, isomer distribution of *trans*-18:1 acid in partially hydrogenated edible oils has only been investigated by the silver-ion chromatographic method [15].

This study firstly demonstrated that the *trans*-18:1 isomer distribution (from *trans*-5 18:1 FAME to *trans*-16 18:1 FAME) contained in partially hydrogenated edible

oils could be analyzed by the RP-HPLC method. However, further investigation of preparative separation by RP-HPLC is needed to confirm the presence of minor *trans*-18:1 isomers, such as *trans*-4, and *trans*-16, 18:1 FAMES.

Because of the considerably higher reproducibility and simpler experimental procedure, the preparative separation of *trans*- and *cis*-isomers achieved by the RP-HPLC technique permits not only an accurate measurement of *trans*-18:1 acid content in food but also the analysis of the distribution of *trans*-18:1 isomers. Currently, silver-ion chromatography (Ag-TLC and Ag-HPLC methods) is widely used for complicated analysis of *trans*-fatty acids in foods. The RP-HPLC method developed in this study would be an attractive alternative to silver-ion chromatography for *trans*-isomer analysis.

In our laboratory, we are investigating the preparative separation of configurational isomers of other monounsaturated fatty acid (16:1, 20:1, 22:1 fatty acids) isomers contained in partially hydrogenated edible oils by the HPLC/GC method in order to identify their individual molecular conformations, which have not yet been identified. In future, the RP-HPLC method could be a powerful tool for the configurational separation of not only *trans*-isomers of monounsaturated FAMES but also those of polyunsaturated FAMES from corresponding *cis*-isomers.

Acknowledgments This work was supported (in part) by a grant-in-aid (Development of evaluation and management methods for supply of safe, reliable and functional food and farm produce) from the Ministry of Agriculture, Forestry and Fisheries of Japan.

References

1. Precht D, Molkentin J (1995) *trans* Fatty acids: implications for health, analytical methods, incidence in edible fats and intake. *Nahrung* 39:343–374
2. Vijver LPL, Kardinaal AFM, Couet C, Aro A, Kafatos A, Steingrimsdottir L (2000) Association between *trans* fatty acid intake and cardiovascular risk factors in Europe: the TRANS-FAIR study. *Eur J Clin Nutr* 54:126–135
3. Sacks FM, Katan M (2002) Randomized clinical trials on the effects of dietary fat and carbohydrate on plasma lipoproteins and cardiovascular disease. *Am J Med* 113(Suppl 9B):13S–24S
4. AOCS (2005) Determination of *cis*-, *trans*-saturated, monounsaturated and polyunsaturated fatty acids in vegetable or non-ruminant animal oils and fats by capillary GLC. Official Methods, Ce 1h-05
5. AOAC (2002) Fat (total, saturated unsaturated, and monounsaturated) in foods; hydrolytic extraction gas chromatographic method, 17th edn. Official Methods of Analysis (996.06). AOAC International, USA
6. Wolff RL, Bayard CC (1995) Improvement in the resolution of individual *trans*-18:1 isomers by capillary gas-liquid chromatography: use of a 100 m CP-Sil 88 column. *J Am Oil Chem Soc* 72:1197–1201
7. Molkentin J, Precht D (1995) Optimized analysis of *trans*-octadecenoic acids in edible fats. *Chromatographia* 41:267–272

8. Nikolova-Damyanova B, Herslof BG, Christie WW (1992) Silver ion high-performance liquid chromatography of derivatives of isomeric fatty acids. *J Chromatography* 609:133–140
9. Christie WW (1989) Silver ion chromatography using solid-phase extraction columns packed with a bonded-sulfonic acid phase. *J Lipid Res* 30:1471–1473
10. Svensson L, Sisifontes L, Nyborg G, Blomstrand R (1982) High performance liquid chromatography and glass capillary gas chromatography of geometric and positional isomers of long chain monounsaturated fatty acids. *Lipids* 17:50–59
11. Lin J-T, McKeon TA, Stafford AE (1995) Gradient reversed-phase high-performance liquid chromatography of saturated, unsaturated and oxygenated free fatty acids and their methyl esters. *J Chromatography A* 699:85–91
12. Juaneda P (2002) Utilisation of reversed-phase high-performance liquid chromatography as a alternative to silver-ion chromatography for the separation of *cis*- and *trans*-c18:1 fatty acid isomers. *J Chromatography A* 954:285–289
13. Destailats F, Golay P-A, Joffre F, Wispelaere M, Hug B, Giuffrida F, Fauconnot L, Dionisi F (2007) Comparison of available analytical methods to measure *trans*-octadecenoic acid isomeric profile and content by gas-liquid chromatography in milk fat. *J Chromatography A* 1145:222–228
14. Aveldano MI, VanRollins M, Horrocks LA (1983) Separation and quantitation of free fatty acids and fatty acid methyl esters by reverse phase high pressure liquid chromatography. *J Lipid Res* 24:83–93
15. Adlof RO, Copes LC, Emken EA (1995) Analysis of the monoenoic fatty acid distribution in hydrogenated vegetable oils by silver-ion high-performance liquid chromatography. *J Am Oil Chem Soc* 72:571–574

TLC and ^{31}P -NMR Analysis of Low Polarity Phospholipids

Mikhail Vyssotski · Andrew MacKenzie · Dawn Scott

Received: 15 July 2008 / Accepted: 12 November 2008 / Published online: 13 December 2008
© AOCS 2008

Abstract High-performance TLC and ^{31}P -NMR were assessed as methods of observing the presence of numerous low polarity phospholipids: bis-phosphatidic acid (BPA), semi-lyso bis-phosphatidic acid (SLBPA), *N*-acyl phosphatidylethanolamine (NAPE), *N*-(1,1-dimethyl-3-oxo-butyl)-phosphatidylethanolamine (diacetone adduct of PE, DOBPE), *N*-acetyl PE, phosphatidylmethanol (PM), phosphatidylethanol (PEt), phosphatidyl-*n*-propanol (PP), phosphatidyl-*n*-butanol (PB). Both techniques are non-discriminative and do not require the prior isolation of individual lipids. It appears that 2D TLC is superior to ^{31}P NMR in the analysis of low polarity phospholipids. All phosphatidylalcohols were well separated by 2D TLC. However, some compounds which can present difficulty in separation by 2D-TLC (e.g., SLBPA and NAPE; or DOBPE and *N*-acetyl PE) were easily distinguished using ^{31}P NMR so the methods are complimentary. A disadvantage of 2D TLC is that *R_f* values can vary with different brands and batches of TLC plates. The chemical shifts of ^{31}P NMR were less variable, and so a library of standards may not be necessary for peak identification. Another advantage of ^{31}P NMR is the ease of quantification of phospholipids. The applicability of the methods was tested on natural extracts of fish brain and cabbage stem.

Keywords ^{31}P -NMR · TLC · Phosphatidylmethanol · Phosphatidylethanol · *N*-acetone adduct · Phosphatidylpropanol · Phosphatidylbutanol · Bis-phosphatidic acid · Acyl phosphatidylglycerol · *N*-acyl phosphatidylethanolamine

Abbreviations

BPA	Bis-phosphatidic acid
DOBPE	<i>N</i> -(1,1-dimethyl-3-oxo-butyl)-phosphatidylethanolamine (diacetone adduct of PE)
EDTA	Ethylenediaminetetraacetic acid
CL	Cardiolipin
CPM	Ceramidophosphomethanol
GPB	Glycerophosphobutanol
GPE	Glycerophosphoethanolamine
GPEt	Glycerophosphoethanol
GPG	Glycerophosphoglycerol (diglycerophosphate)
GPM	Glycerophosphomethanol
GPP	Glycerophosphopropanol
LPC	Lyso PC
LPE	Lyso PE
LPM	Lyso PM
<i>N</i> -acetyl-GPE	<i>N</i> -acetyl glycerophosphoethanolamine
NAGPE	<i>N</i> -acyl glycerophosphoethanolamine
NAPE	<i>N</i> -acyl phosphatidylethanolamine
PA	Phosphatidic acid
PB	Phosphatidylbutanol
PC	Phosphatidylcholine
PE	Phosphatidylethanolamine
PEt	Phosphatidylethanol
PG	Phosphatidylglycerol
PI	Phosphatidylinositol
Pi	Inorganic phosphate
PM	Phosphatidylmethanol
PMG	Phosphonomethylglycine
PP	Phosphatidylpropanol
PS	Phosphatidylserine
SLBPA	Semi-lyso bis-phosphatidic acid (acyl phosphatidylglycerol)

M. Vyssotski (✉) · A. MacKenzie · D. Scott
Industrial Research Limited, Lower Hutt, New Zealand
e-mail: m.vyssotski@irl.cri.nz

SM	Sphingomyelin
SPE	Solid-phase extraction

Introduction

Beyond a widely known group of major phospholipids (phosphatidylethanolamine, phosphatidylcholine, phosphatidylinositol, phosphatidylserine, phosphatidylglycerol, cardiolipin, phosphatidic acid and sphingomyelin), a number of other phospholipid groups exist, including low polarity phospholipids, phosphonolipids, etc. While these other groups are generally represented by minor components, their importance in lipid metabolism and signalling may be high [1].

In this work we present and compare selected analytical techniques that allow identification of low polarity phospholipids, a group of phospholipids noted for their high mobility on silica gel TLC in solvent systems generally used in analysis of major phospholipids. Low polarity phospholipids are naturally existing or artefact lipids produced mostly by modification of polar moieties of phosphatidylcholine (PC), phosphatidylethanolamine (PE), or phosphatidylglycerol (PG) (Figs. 1–3).

Low polarity phospholipids include phosphatidylalcohols, mostly artefact lipids produced predominantly from PC when samples containing active phospholipase D (e.g., plant samples) are extracted with appropriate alcohols [2]. This process is usually accompanied by formation of phosphatidic acid (PA) due to the presence of water in extraction media (Fig. 1). Of all phosphatidylalcohols the most important seems to be phosphatidylethanol, currently considered as a biochemical marker of alcoholism [3], which was reported to form from phospholipids in mammalian cell membranes affected by ethanol [4]. Other phosphatidylalcohols (e.g., PM [5], PB [6], PP [7]) were found to be useful markers in phospholipase D activity assays due to the ease of their chromatographic separation from the bulk of phospholipids.

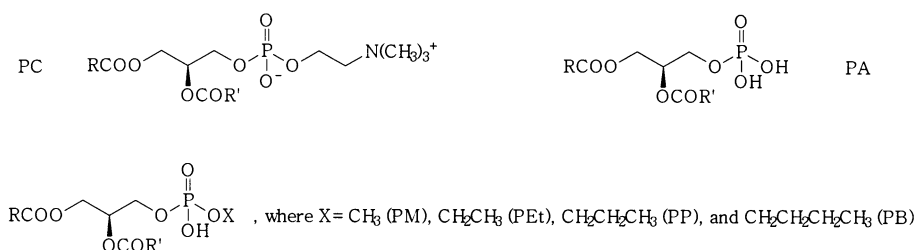


Fig. 1 Phosphatidylcholine (PC) and the products of its transphosphatidylation by phospholipase D: phosphatidic acid (PA) and phosphatidylalcohols—phosphatidylmethanol (PM), phosphatidylethanol (PEt), phosphatidylpropanol (PP) and phosphatidylbutanol (PB)

PE is able to form adducts with aldehydes and ketones. Acetone (more correctly—diacetone) adduct (DOBPE, Fig. 2) can be formed even from an acetone solution of PE stored in a fridge [8]. A recent study suggested that this lipid may also be formed in diabetic blood [9]. Still, the most important of the PE-derived low polarity phospholipids seems to be NAPE, the immediate precursor of endogenous bioactive *N*-acylethanolamines [10].

One of *N*-acylphosphatidylethanolamines, namely *N*-acetyl PE was allegedly found in the mammalian brain and placenta [11], but reliably confirmed only in zygomycete *Absidia corymbifera* [12].

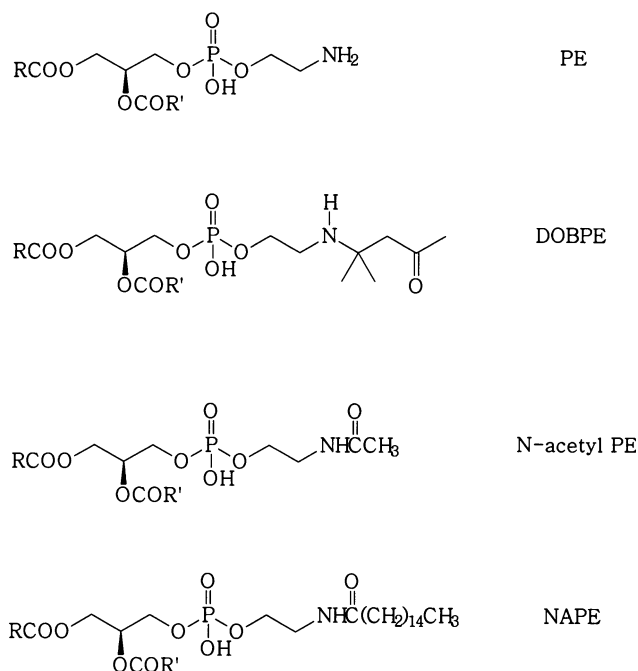
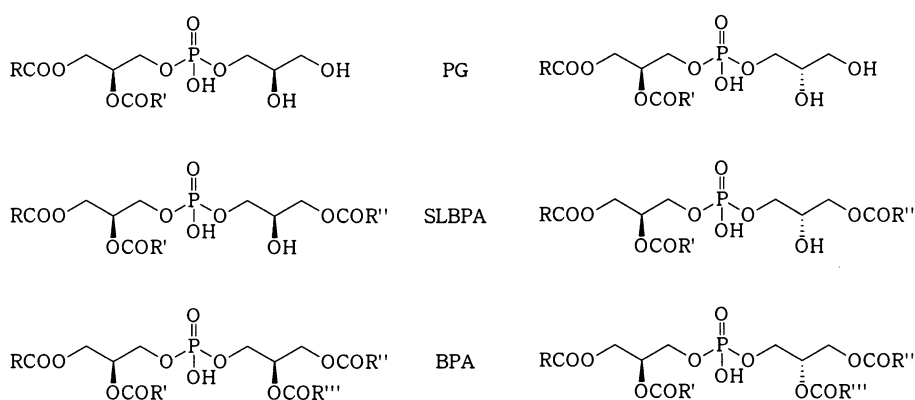


Fig. 2 Phosphatidylethanolamine (PE) and low polarity phospholipids, derived from PE: diacetone adduct, *N*-(1,1-dimethyl-3-oxobutyl)-derivative of phosphatidylethanolamine (DOBPE), *N*-acetyl PE, and *N*-palmitoyl PE (the major representative of *N*-acyl phosphatidylethanolamines, NAPE)

Fig. 3 Diastereomeric phosphatidylglycerols (PG), produced by transphosphatidylation of PC with glycerol, and low polarity phospholipids based on PG: semi-lyso bis-phosphatidic acid (SLBPA, also known as acyl phosphatidylglycerol), and bis-phosphatidic acid (BPA)



Two major low polarity phospholipids based on PG structure are BPA and SLBPA (Fig. 3). BPA was reported for marine bacteria [13], developing soybeans [14], fish brain [15], and degenerating cultured hamster fibroblasts [16]. BPA was also tentatively identified in some fish flesh [17]. SLBPA, also known as acyl phosphatidylglycerol, was found in a number of micro organisms, and also in plant and animal tissues [18].

The concern that some unnatural phospholipids, like PE adducts, may be produced during the course of industrial processing of food components, and as such may contribute to development of a pathology (e.g., diabetes) at epidemic or even pandemic scale was expressed recently [19]. However, it seems that low polarity phospholipids are not considered for quantitation by the majority of food quality control laboratories.

One of the reasons for that is the lack of analytical approaches to quantifying low polarity phospholipids. Attempts to identify low polarity lipids with chromatographic methods often resulted in misidentification. For example, low polarity phospholipids found in infarcted dog heart [20] and, later, in the brain of bony fish *Amia calva* [15] were identified as BPA. It took some time to find out that they were not BPA, but another low polarity phospholipid, NAPE [21], the structure already established for unusual dog heart phospholipid in another laboratory [22].

Similarly, controversial identifications were reported for other low polarity lipids. A phospholipid with high mobility on TLC found in developing soybean cotyledons was identified as NAPE [23], and as PM [24]. A phospholipid with chromatographic mobility higher than that of PE and containing nitrogen was found in beef brain lipids after prolonged contact with acetone. This lipid was identified as PE-acetone adduct [25] and as *N*-acetyl PE [11].

Application of MS and NMR-based techniques significantly improves reliability of low polarity phospholipids identification. For example, ^1H - ^{13}C 2D NMR experiments allowed distinguishing between SLBPA and NAPE in oats while HPLC-MS was useful in assessing their fatty acid composition [26]. A drawback of this approach is that a

combination of SPE and preparative TLC was required to isolate pure compounds for NMR.

It would be desirable to develop a non-discriminative technique that does not require isolation of individual lipids to distinguish between numerous low polarity phospholipids. In this publication we describe application of ^{31}P -NMR for analysis of low polarity phospholipids and compare the results with the data provided by high-performance TLC.

Materials and Methods

Egg yolk PE and PC were prepared according to Barsukov et al. [27].

Brain from three frozen and thawed red gurnards *Chelidonichthys kumu* was excised (total weight 839 mg) and extracted according to Bligh and Dyer [28]. The yield was 85 mg.

A methanolic solution of HCl (5%, 5 ml) was added to a portion of gurnard brain lipids for 5 min at 50 °C to remove vinyl ethers. Chloroform (0.5 ml) and water (0.5 ml) was added, and the mixture centrifuged. The lower layer was collected and solvent removed from the lipid under a stream of argon.

A cabbage (*Brassica oleracea* var. *capitata*) stem was extracted as follows:

1. 37.5 g of fresh stem was homogenised in the 100 ml Waring blender cup on high speed for two bursts of 30 s each, then extracted according to Bligh and Dyer method with 113 ml of chloroform-methanol (1:2, by v/v), followed by an extraction with 38 ml of chloroform, yielding 57.9 mg of lipids;
2. 37.6 g of fresh cabbage stem was boiled in water for 5 min, then extracted as above, yielding 89.4 mg lipids;
3. 34.7 g of fresh cabbage stem was homogenised in the 100 ml Waring blender cup on high speed for two bursts of 30 s each, then extracted as follows: 70 ml of

methanol was added, the mixture was homogenised again, and allowed to stay at room temperature for 20 min. After that, 35 ml of chloroform was added, the mixture was homogenised and filtered. The residue was extracted with 35 ml of chloroform. Combined extracts were rotary evaporated, yielding 72.8 mg lipids.

PG, PM, PEt, PP and PB were prepared by transphosphatidylation of corresponding alcohols (at 4% of media) and phosphatidylcholine by cabbage phospholipase D [2]. PG was produced by the same approach and purified by column chromatography on silica gel.

Bis-phosphatidic acid (BPA) and semi-lyso bis-phosphatidic acid (SLBPA) were prepared by acylation of PG by palmitoyl chloride using the method of Ellingson [29], modified by addition of few crystals of catalyst, 4-*N*, *N*-dimethylaminopyridine.

N-palmitoyl PE (NAPE) and *N*-acetyl PE were prepared by acylation of PE by palmitoyl chloride and acetyl chloride, correspondingly, using the method of Ellingson [29], modified as above.

N-(1,1-dimethyl-3-oxo-butyl)-derivative of phosphatidylethanolamine (acetone adduct of PE, DOBPE) was prepared by storing PE in acetone in a fridge for 2 weeks [8]. Other phospholipids were from Industrial Research Limited's collection of lipid standards.

Solvent systems for TLC were taken from Vaskovsky and Vysotskii [30]. To develop plates in the 1st direction the system used was chloroform–methanol–benzene–25% aqueous ammonia (60:15:10:1, by v/v/v/v). For 2nd direction the system acetone–benzene–glacial acetic acid–water (20:30:4:1, by v/v/v/v) was used. Development was performed in filter paper-lined tanks saturated with solvent systems for at least 1 h prior to development. Solvent systems in tanks were refreshed after each plate developed. TLC plates (10 × 10 cm glass-backed HPTLC-Plates Nano-Sil 20, Macherey-Nagel, Germany) were activated at 110 °C at least for 90 min and left to cool to room temperature in a vacuum desiccator prior to sample loading. Samples were loaded using 1- μ l capillary tubes (Billbatt Ltd, England). Between developments plates were ambient air-dried with a faint stream of argon applied.

Model mixtures of low polarity phospholipids were prepared as chloroform solutions with concentrations of individual components varying from 1 to 5 mg/ml.

Phospholipids were detected on TLC by phosphomolybdate spray prepared according to Vaskovsky et al. [31].

Complete removal of O-linked fatty acids from glycerolipids was achieved using monomethylamine [32]. Sample (10 mg) was weighed into a stoppered test tube and dispersed in ethanol (1.5 ml). Monomethylamine (40% solution in water, 4.5 ml) was added and the test tube

heated in a water bath at 55 °C for 1 h. Solvent was removed under a stream of argon on a heating block (60 °C). The residue was redispersed in ethanol (0.5 ml) and ethyl formate (100 μ l) added to neutralise any residual monomethylamine. The solvent was removed under argon and the sample dissolved in the NMR detergent as outlined below.

³¹P-NMR analysis was based on the method of Lehnhardt et al. [33]. A detergent solution was prepared containing: sodium cholate (10% w/w), EDTA (1% w/w) and phosphonomethylglycine (PMG) as an internal standard for quantification (0.3 g/L), pH was adjusted to 7.3 using sodium hydroxide. The detergent solution was an aqueous solution containing 20% D₂O for deuterium field-frequency lock capability. Sample (10 mg) was mixed with detergent solution (750 μ l) by vortexing, and then dispersed by ultrasonication at 60 °C for 10 min. The solution was then transferred to a 5-mm NMR tube for analysis.

Quantitative phosphorus NMR spectra using inverse gate proton decoupling for suppression of nuclear Overhauser effect were recorded on the two-channel Bruker Avance300 with the following instrument settings: spectrometer frequency for ³¹P 121.498 MHz, sweep width 6,067 Hz, 65,536 data points, 90 degree excitation pulse, 192 transients were normally taken, each with an 3.5 s delay time and free induction decay acquisition time of 5.4 s. Spectra were processed with a standard exponential weighting function with 0.2 Hz line broadening before Fourier transformation.

Chemical shifts were measured relative to the PMG internal standard, and also relative to SM [present naturally in samples which had been prepared from egg yolk lipids, or as an introduced standard (Avanti)].

Lecitase Ultra (5 μ l) was added to a NMR detergent containing fresh cabbage stem lipids followed by incubation at 40 °C for 20 min. The mixture was placed in boiling water for 10 min to deactivate the enzyme then reanalysed to confirm the peak positions of LPM regioisomers.

Results

Thin-Layer Chromatography

The use of the solvent systems developed for one-dimensional TLC separation of low polarity phospholipids [30] resulted in good separation for some lipids (Fig. 4).

Effect of chain length of polar heads of low polarity phospholipids on their TLC mobility was clearly observed: *N*-palmitoyl PE (NAPE) and *N*-acetyl PE were easily separated; PM, PEt and PP were also resolved from each other. Further increase in the substitute's chain length had

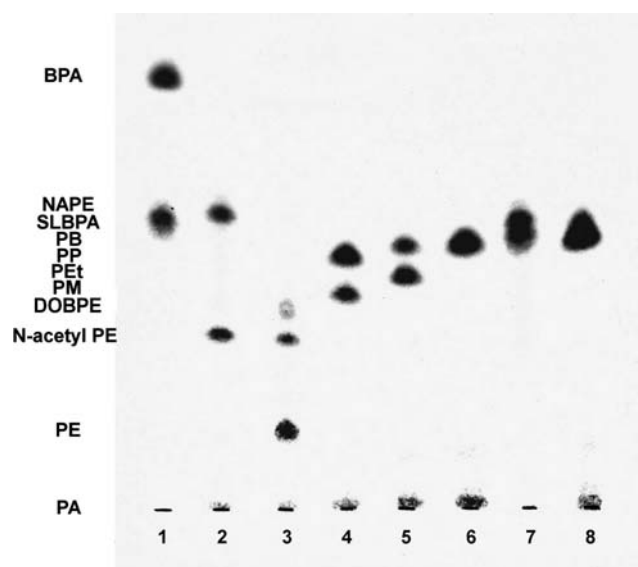


Fig. 4 TLC of low polarity phospholipids in solvent system chloroform-methanol-benzene-25% aqueous ammonia (60:15:10:1, by v/v/v), run twice. Detection—by phospholipid spray. Mixtures of phospholipids were applied as follows: *Lane 1* BPA + SLBPA; *Lane 2* NAPE + *N*-acetyl PE; *Lane 3* DOBPE + *N*-acetyl PE + PE; *Lane 4* PM + PP; *Lane 5* PEt + PB; *Lane 6* PB + SLBPA; *Lane 7* NAPE + SLBPA; *Lane 8* PP + SLBPA. Phosphatidylalcohols mixtures also small levels of PC and PA. DOPE exhibited a fainter spot than the other phospholipids which faded rapidly after visualisation

less pronounced effect: PB was clearly resolved from PP only at lower loadings.

SLBPA and PB were not resolved, while SLBPA and PP could be resolved only at low loadings. SLBPA and NAPE were poorly resolved even at low loadings under one-dimensional TLC.

Two-dimensional TLC produced significantly better separation of low polarity phospholipids (Fig. 5). All of the low polarity phospholipids were well resolved, including SLBPA and PB which could not be separated by one-dimensional TLC.

³¹P NMR

Results for the chemical shifts of the low polarity phospholipids relative to PMG and SM both as intact and deacylated lipids are presented in Table 1 with example spectra of mixtures of the nine less polar phospholipid classes in Figs. 6 and 7. Unlike with the TLC separation there is no clear trend in the chemical shifts based on the alcohol chain length of the phosphatidylalcohols. PM is well separated from the other phosphatidylalcohols, but PE, PP and PB are all within 0.03 ppm. The other low polarity phospholipids are well separated from each other.

Each of the low polarity phospholipids studied, except for BPA, produced a single signal. BPA produced two

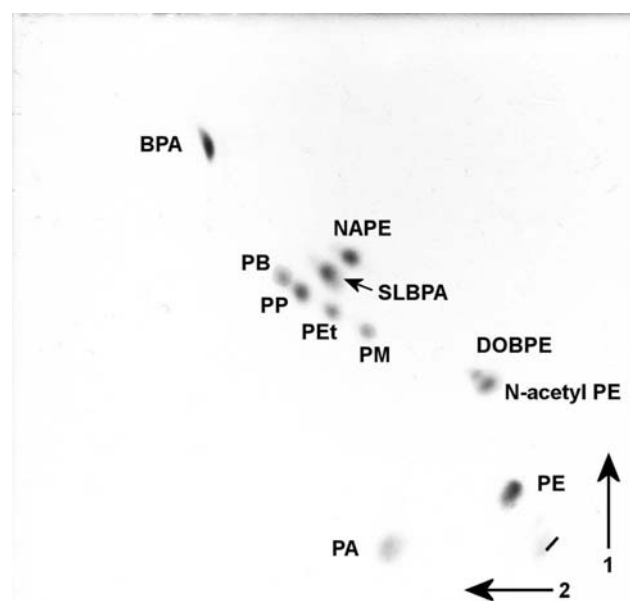


Fig. 5 Two-dimensional TLC of low polarity phospholipids in solvent systems. 1st direction: chloroform-methanol-benzene-25% aqueous ammonia (60:15:10:1, by v/v/v/v), run twice; 2nd direction: acetone-benzene-glacial acetic acid-water (20:30:4:1, by v/v/v/v). Detection—by phospholipid spray. A faint spot of PC was seen on the plate at the sample loading zone

signals, split by 0.09 ppm, which possibly reflects the existence of two diastereomeric forms. This view is supported by the finding that PG we used as starting material for BPA synthesis was produced from PC via transphosphatidylolation by cabbage phospholipase D. It was demonstrated that such PG is, in fact, a racemic mixture of 1-phosphatidyl-D-glycerol and 1-phosphatidyl-L-glycerol [2], and, therefore, BPA used in our experiments was a diastereomeric mixture of *sn*-3/*sn*-3' and *sn*-3/*sn*-1' isomers (Fig. 3). Differences in chemical shifts have been observed previously between the ³¹P NMR of mixtures containing L-PS compared to D-PS [34]. However, these differences were noted in phospholipid aggregates, whereas the Na cholate of the NMR detergent used in the current study is present to disrupt such aggregates and achieve sharper signals for individual phospholipids. Preparation of pure diastereomers of BPA is required to confirm that the peak splitting is due to diastereomeric differences, and for correct assignment of each peak. However, if this is the cause of the peak splitting then the ability to differentiate between the diastereomers is an advantage of ³¹P NMR over that of 2D TLC.

Unlike TLC where separation is based on polarity and thus the low polarity phospholipids by definition are well separated from other phospholipids, there is some overlap of the ³¹P-NMR chemical shifts of the low polarity phospholipids and some other phospholipids. The examples of

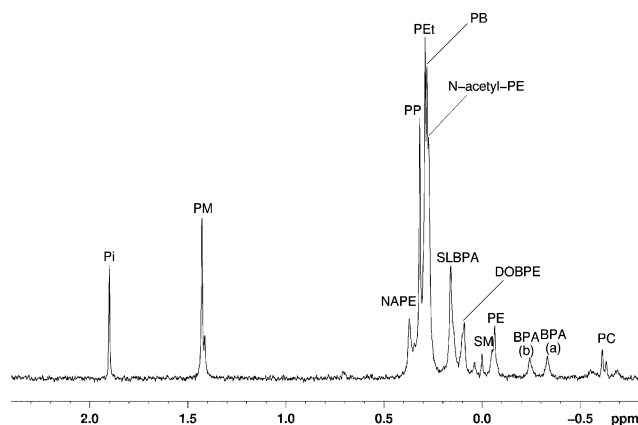
Table 1 ^{31}P -NMR chemical shifts for the low polarity phospholipids both intact and deacylated

Phospholipid	Chemical shift (ppm)	
	Relative to SM	Relative to PMG
Intact		
BPA(a) ^a	-0.33	-7.86
BPA(b) ^a	-0.24	-7.77
DOBPE	0.10	-7.43
SLBPA	0.16	-7.37
<i>N</i> -acetyl PE	0.27	-7.26
PB	0.28	-7.25
PEt	0.29	-7.24
PP	0.32	-7.22
NAPE	0.37	-7.16
PM	1.43	-6.10
Deacylated		
Deacylated DOBPE ^b	0.58	-6.95
<i>N</i> -acetyl GPE	0.87	-6.66
NAGPE	0.90	-6.63
GPEt	1.00	-6.53
GPG ^c	1.08	-6.45
GPB	1.10	-6.43
GPP	1.11	-6.43
GPM	2.12	-5.41

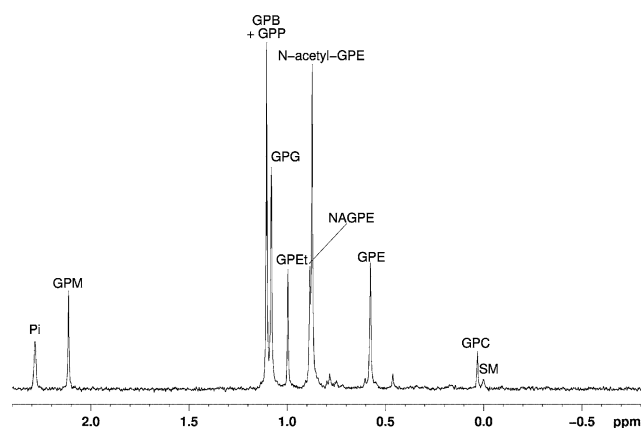
^a Unlike other phospholipids BPA gave two peaks (see text)

^b Identical to glycerophosphoethanolamine

^c Produced from deacylation of PG, BPA and SLBPA

**Fig. 6** ^{31}P -NMR spectrum of the intact mixture of nine less polar phospholipids in a sodium cholate/EDTA detergent system (pH 7.3). Test mixtures also contained PA and the internal standard PMG which were observed further downfield. Chemical shifts are shown relative to SM

this are: BPA(a) (-0.33 ppm relative to SM) and 1LPC (-0.34 ppm); BPA(b) (-0.24 ppm) and PS (-0.25 ppm); DOBPE (0.10 ppm) and dihydrosphingomyelin (0.09 ppm);

**Fig. 7** ^{31}P -NMR spectrum of the O-deacylated mixture of nine less polar phospholipids in a sodium cholate/EDTA detergent system (pH 7.6). Test mixtures also contained GPA and the internal standard PMG which were observed further downfield. Chemical shifts are shown relative to SM. The difference in chemical shift of Pi compared to the spectrum in Fig. 6 is due to a slightly higher pH

NAPE (0.37 ppm) and CL (0.36) and 2LPE (0.38 ppm) [35].

O-deacylation of the sample produced sharper peaks, which are better resolved both from other low polarity phospholipids and other phospholipids. GPB and GPP are not resolved, but all other O-deacylated low polarity phospholipids are separated from each other. However, deacylation converts BPA and SLBPA (as well as PG) to the single compound—glycerophosphoglycerol (GPG). Deacylation of DOBPE produced a single phosphorus-containing component, with chemical shift identical to that of glycerophosphoethanolamine, suggesting that acetone adduct is destroyed during deacylation.

To demonstrate the applicability of the described techniques to the real life samples analysis, a number of extracts were prepared. To illustrate a formation of an artefact phosphatidylmethanol during extraction of plant samples, a cabbage (*Brassica oleracea* var. *capitata*) stem was extracted as follows:

1. Fresh stem was extracted by a standard Bligh and Dyer method;
2. Boiled stem was extracted by a standard Bligh and Dyer method;
3. To demonstrate a danger of adding methanol first (as recommended sometimes, since methanol mixes better with tissues than chloroform), the methanol portion of Bligh and Dyer first extraction solvent was added first to the stem and allowed to stay for 20 min prior to addition of chloroform.

One-dimensional TLC demonstrated a formation of PM during extraction of fresh stem, especially when methanol was added prior to chloroform; no PM was formed during extraction of the boiled stem (Fig. 8).

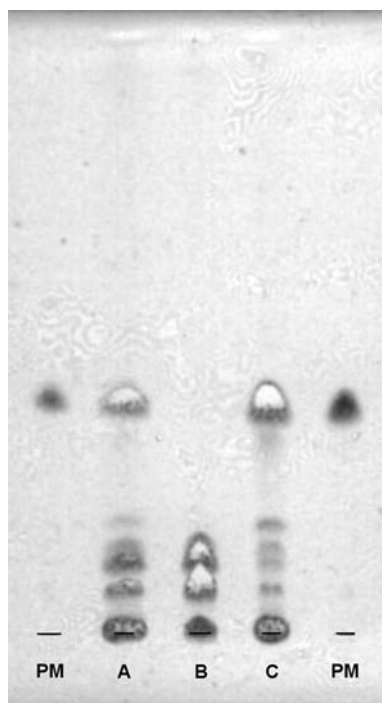


Fig. 8 TLC of cabbage stem extracts: *A*—fresh stem extract, *B*—boiled stem extract, *C*—fresh stem extract with methanol added first. *PM*—phosphatidylmethanol standard. Solvent system: chloroform-methanol-benzene-25% aqueous ammonia (60:15:10:1, by v/v/v/v), run twice. Detection—by phospholipid spray

Table 2 Phospholipid profiles (mol%) of Bligh and Dyer extracts from cabbage stem as measured by ^{31}P NMR (see text for details)

	Boiled cabbage	Fresh Standard	MeOH first
PC	45.7	10.7	1.8
PI	10.8	6.0	5.1
PS	2.1	1.4	0.5
2-LPC	2.5	1.1	
PE	29.9	12.0	0.9
CL	1.7	2.0	1.7
LPE ^a	0.5	1.1	
PG	3.5	2.0	0.4
PM	0.4	26.8	45.6
LPM ^a		0.8	1.4
CPM		4.2	5.6
PA	2.8	31.1	36.1

^a Sum of 1- and 2-lyso forms

^{31}P NMR measured high levels of PM in both extracts from fresh cabbage stem (Table 2). There was measurable PM (0.4 mol %) even in the extract from boiled cabbage indicating some residual phospholipase D activity. Peaks due to 1LPM and 2LPM (−5.79 and −5.63 ppm relative to PMG respectively) were confirmed by a partial phospholipase A1 hydrolysis of a fresh cabbage stem extract.

The presence of low polarity phospholipid in red gurnard (*Chelidonichthys kumu*) brain was demonstrated by two-dimensional TLC (Fig. 9, left pane), and the fact that it differs from SLBPA was demonstrated by spiking the sample with SLBPA standard (Fig. 9, right pane).

A comparison with the reference standard, SLBPA, and a known low polarity lipid two-dimensional TLC pattern (Fig. 5) suggests that the low polarity phospholipid from red gurnard brain is NAPE.

As discussed above, the ^{31}P -NMR peak position of NAPE is very close to that of 2LPE and CL. NAPE was not observed in the spectrum of intact gurnard brain lipids (Fig. 10). Analysis of deacylated red gurnard brain lipids did not result in a significant NAGPE peak, but a peak did appear at 0.77 ppm relative to SM. Acid treatment to destroy vinyl ethers, followed by deacylation resulted in the disappearance of this peak, and presence of a NAGPE peak. This indicates that most of the NAPE present in red gurnard brain is in the plasmalogen form.

Discussion

In our search for NAPE in bony and cartilaginous fish we found that it is difficult to distinguish SLBPA and NAPE even by high-performance TLC, and chemical transformations are required to attribute an unknown lipid to one of these without employing physico-chemical methods of structure elucidation [30]. Later we demonstrated that reliable separation of SLBPA and NAPE requires the use of homemade HPTLC-plates coated with silica sol-bound microfractionated silica gel KSK, and low humidity [36].

One-dimensional TLC is helpful in screening of significant number of samples for low polarity phospholipids, but it has shortcomings, like poor resolution of NAPE, SLBPA, PB and PP.

In contrast, 2D TLC, while requiring significantly longer procession times, allows the separation of all the above mentioned low polarity phospholipids.

TLC separation of low polarity phospholipids requires a careful selection of solvent systems. An inappropriate solvent system seemed to be used in the analysis of NAPE from kenaf seeds with *N*-linked acids being predominantly linoleic, palmitic and oleic [37], since it was reported to have the same chromatographic mobility as *N*-acetyl PE, while these are clearly separable as it was demonstrated in the current work.

Apart from NAPE, an unknown lipid identified as BPA was reported for developing soybeans and soybean suspension cultures [14]. The authors mentioned that chromatographic mobility of the latter lipid is lower than that of NAPE, which allows separation of these two lipids by preparative TLC. Considering the previous findings that

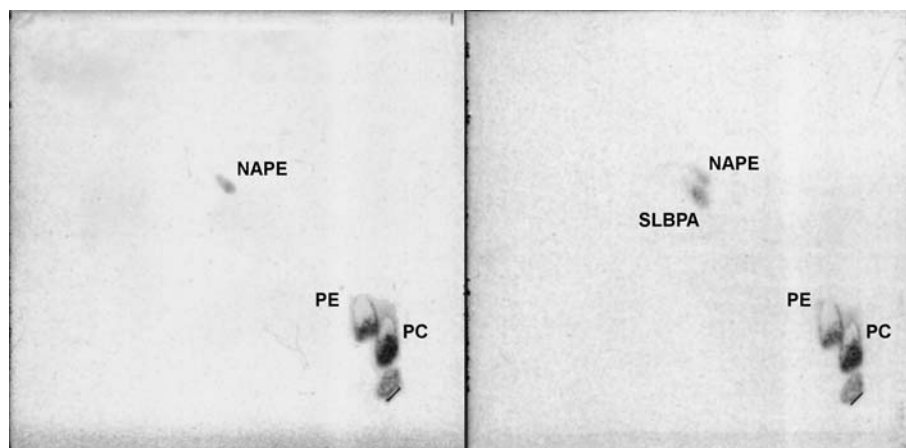
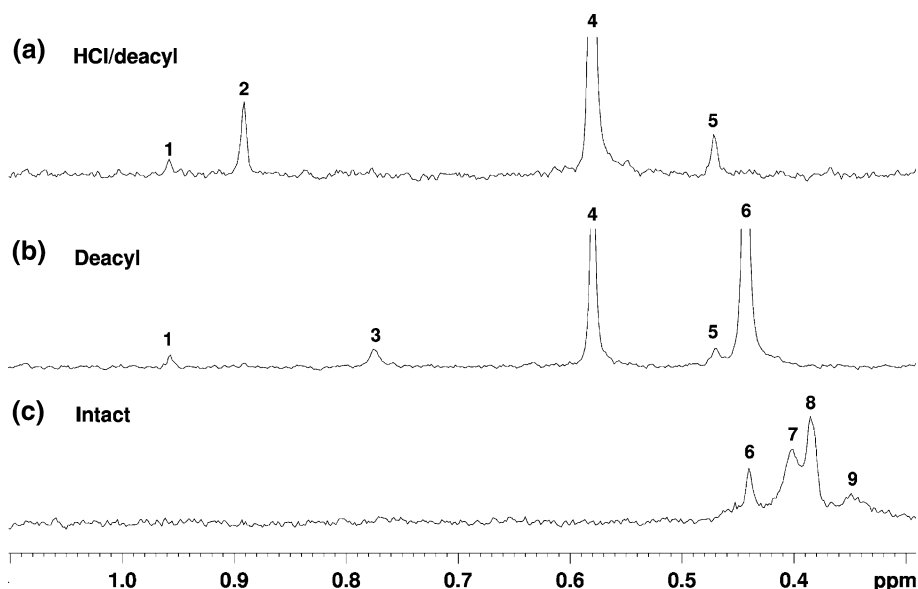


Fig. 9 Two-dimensional TLC of red gurnard brain phospholipids. *Left pane*—brain extract, *right pane*—brain extract spiked with SLBPA. Solvent systems: 1st direction—chloroform-methanol-benzene-25% aqueous ammonia (60:15:10:1, by v/v/v/v), run twice; 2nd direction—acetone-benzene-glacial acetic acid-water (20:30:4:1, by

v/v/v/v). Detection—by phospholipid spray. Note that while all spots were clearly visible on the TLC plate as blue spots on white background, the scanned images required enhancement to make the spots visible, thus resulting in darker background

Fig. 10 ^{31}P -NMR spectra of red gurnard brain lipid extract. **a** HCl treated to remove plasmalogens then deacylated, **b** Deacylated, **c** Intact. Peaks: 1 deacylated CL, 2 N-acyl GPE, 3 lyso NAPE-plasmalogen, 4 GPE, 5 1-alkyl GPE, 6 LPE plasmalogen, 7 NAPE-plasmalogen, 8 2-LPE, 9 CL



SLBPA (e.g., partially deacylated BPA, thus more polar than BPA) has a mobility on TLC similar or equal to that of NAPE [29], it seems rather unlikely for BPA to have lower mobility than that of NAPE in normal phase chromatography.

In summary, it appears that 2D TLC is superior to ^{31}P NMR in the analysis of low polarity phospholipids. However, some compounds which can present difficulty in separation by 2D-TLC (e.g., SLBPA and NAPE; or DO-BPE and *N*-acetyl PE) are easily distinguished using ^{31}P NMR so the methods are complimentary. A disadvantage of 2D TLC is that *R_f* values can vary with different brands and batches of TLC plates. It is therefore important in the 2D TLC analysis to have standards for confirmation of the

identity of spots in analysis of real samples. The chemical shifts of ^{31}P NMR are less variable, and such a library of standards may not be necessary for peak identification. Another advantage of ^{31}P NMR is the ease of quantification of phospholipids. The peak splitting observed in the ^{31}P NMR of BPA has been attributed to the presence of diastereomers. Unlike ^{31}P NMR, the 2D TLC method used in this study cannot distinguish between these diastereomers.

Acknowledgments This work was supported by the New Zealand Foundation for Research, Science and Technology grant C08X0709 “High value lipids”. The authors are grateful to Dr. O. Catchpole for reviewing the manuscript and to Dr. E. Nekrasov and Dr. H. Wong for help with NMR. M.V. is also grateful to Professor V. Vaskovsky for attracting his attention to low polarity phospholipids.

References

- Nicolaou A, Kokotos G (2004) Bioactive lipids. The Oily Press, Bridgewater
- Yang SF, Freer S, Benson AA (1967) Transphosphatidylation by phospholipase D. *J Biol Chem* 242:477–484
- Hannuksela ML, Liisanantti MK, Nissinen AET, Savolainen MJ (2007) Biochemical markers of alcoholism. *Clin Chem Lab Med* 45:953–961
- Alling C, Gustavsson L, Mansson JE, Benthin G, Anggard E (1984) Phosphatidylethanol formation in rat organs after ethanol treatment. *Biochim Biophys Acta* 793:122–199
- Vaskovsky VE, Khotimchenko SV (1983) Micro-chromatographic test of transphosphatidylic activity of phospholipase D in algae and other plants. *J Chromatogr* 261:324–328
- Randall RW, Bonser RW, Thompson NT, Garland LG (1990) A novel and sensitive assay for phospholipase D in intact cells. *FEBS* 264:87–90
- Mohn H, Chalifa V, Liscovitch M (1992) Substrate specificity of neutral phospholipase D from rat brain studied by selective labelling of endogenous synaptic membrane phospholipids in vitro. *J Biol Chem* 267:11131–11136
- Ando N, Ando S, Yamakawa T (1971) Structure and formation mechanism of *N*-acetone derivatives of phosphatidylethanolamine. *J Biochem* 70:341–348
- Kuksis A, Ravandi A, Schneider M (2005) Covalent binding of acetone to aminophospholipids in vitro and in vivo. *Ann N Y Acad Sci* 1043:417–439
- Schmid HHO, Schmid PC, Natarajan V (1990) *N*-Acylated glycerophospholipids and their derivatives. *Prog Lipid Res* 29:1–43
- Debuch H, Wendt G (1967) On a new group of colamine-containing glycerophosphatides from brain. *Hoppe-Seyler's Z Physiol Chem* 348:471–474
- Batracov SG, Konova IV, Sheichenko VI, Esipov SE, Galanina LA (2001) Two unusual glycerophospholipids from a filamentous fungus, *Absidia corymbifera*. *Biochim Biophys Acta* 1531:169–177
- McAllister DJ, De Siervo AJ (1975) Identification of bisphosphatidic acid and its plasmalogen analogues in the phospholipids of a marine bacterium. *J Bacteriol* 123:302–307
- Stearns EM, Morton WT (1977) Biosynthesis of fatty acids from acetate in soybean suspension cultures. *Lipids* 10:597–601
- Hack MH, Helmy FM (1975) Bis-phosphatidic acid plasmalogen in brain of *Amia calva* and its correlation with the infarct plasmalogen and cardiolipin (diphosphatidyl glycerol) series of phosphatides. *Comp Biochem Physiol C* 52(2):139–145
- Brotherus J, Renkonen O (1974) Isolation and characterization of bis-phosphatidic acid and its partially deacylated derivatives from cultured BHK-cells. *Chem Phys Lipids* 13:11–20
- Olley J (1956) The lipids of fish 7. Phosphate esters in the lipids of haddock and cod flesh. *Biochem J* 62:107–114
- Hsu F-F, Turk J, Shi Y, Groisman EA (2004) Characterization of acylphosphatidylglycerols from *Salmonella typhimurium* by tandem mass spectrometry with electrospray ionization. *J Am Soc Mass Spectrom* 15:1–11
- Elliott RB (2006) Diabetes—a man made disease. *Med Hypotheses* 67:388–391
- Hack MH, Ferrans VJ (1960) Nitrogen-free plasmalogen observed in infarcted myocardium of the dog. *Circulat Res* 8(4):738–741
- Hack MH, Helmy FM (1982) A reappraisal of the dog-heart infarct plasmalogen, its conception as a bis-phosphatidic acid and current recognition as an *N*-acylphosphatidylethanolamine. *Comp Biochem Physiol B* 73:873–879
- Epps DE, Natarajan V, Schmid PC, Schmid HHO (1980) Accumulation of *N*-acylethanolamine glycerophospholipids in infarcted myocardium. *Biochim Biophys Acta* 618:420–430
- Wilson RF, Rinne RW (1974) Phospholipids in the developing soybean seed. *Plant Physiol* 54:744–747
- Slack CR, Roughan PG, Balasingham N (1978) Labelling of glycerolipids in the cotyledons of developing oilseeds by [¹-¹⁴C] acetate and [²-³H] glycerol. *Biochem J* 170:421–433
- Helmy FM, Hack MH (1966) An ethanolamine plasmalogen artifact formed by acetone extraction of freeze-dried tissue. *Lipids* 1:279–281
- Holmback J, Karlsson AA, Arnoldsson KC (2001) Characterization of *N*-acylphosphatidylethanolamine and acylphosphatidylglycerol in oats. *Lipids* 36:153–165
- Barsukov LI, Batrakov SG, Bergelson LD, Dyatlovitskaya EV, Molotkovsky JG, Prokazova NV (1980) In: Bergelson LD (ed) Lipid biochemical preparations, Elsevier/North-Holland Biomedical Press, Amsterdam-New York-Oxford
- Bligh EG, Dyer WJ (1959) A rapid method of total lipid extraction and purification. *Can J Biochem Physiol* 37:911–917
- Ellingson JS (1980) Identification of (*N*-acyl)ethanolamine phosphoglycerides and acylphosphatidylglycerol as the phospholipids which disappear as *Dictyostelium discoideum* cells aggregate. *Biochemistry* 19:6176–6182
- Vaskovsky VE, Vysotskii MV (1985) *N*-acylphosphatidylethanolamine in fish brain. *Khim Prirodn Soedin* 1985:326–329 (in Russian)
- Vaskovsky VE, Kostetsky EY, Vasendin IM (1975) A universal reagent for phospholipid analysis. *J Chromatogr* 114:129–141
- Clarke NG, Dawson RM (1981) Alkaline O → *N*-transacylation. A new method for the quantitative deacylation of phospholipids. *Biochem J* 195:301–306
- Lehnhardt F-G, Röhn G, Ernestus R-I, Grüne M, Hoehn M (2001) ¹H- and ³¹P-NMR spectroscopy of primary and recurrent human brain tumors in vitro: malignancy-characteristic profiles of water soluble and lipophilic spectral components. *NMR Biomed* 14:307–317
- Epand RM, Stevenson C, Bruins R, Schram V, Glaser M (1998) The chirality of phosphatidylserine and the activation of protein kinase C. *Biochemistry* 37:12068–12073
- MacKenzie AD, Wong H, Braun RM (2005) Deacylation of phospholipids to improve resolution in the ³¹P NMR analysis of animal phospholipids. 26th World Congress and exhibition of the International Society of Fat Research (poster presentation), Prague, Czech Republic
- Vysotskii MV, Vaskovsky VE (1988) Micro-thin layer chromatography of low polarity phospholipids. Identification of *N*-acylphosphatidylethanolamine. VINITI deposited paper No.1036-B88, 16 pp. (in Russian)
- Tolibaev I, KhS Mukhamedova, Akramov ST (1976) *N*-acylated phospholipids and lysophospholipids of kenaf seeds. *Chem Nat Compd* 12:650–652

Sugar Cane Policosanols do not Reduce LDL Oxidation in Hypercholesterolemic Individuals

Amira N. Kassis · Stan Kubow · Peter J. H. Jones

Received: 12 December 2008 / Accepted: 4 March 2009 / Published online: 1 April 2009
© AOCS 2009

Abstract Sugar cane policosanols (SCP) have been shown to exert antioxidant properties in various studies conducted in Cuba. Independent studies have since reported no significant effect of SCP consumption on oxidized LDL levels. The objective of the present study was to confirm the effects of Cuban SCP on LDL oxidation using a high-precision capture ELISA procedure in hypercholesterolemic individuals. Twenty-one otherwise healthy hypercholesterolemic men and post-menopausal women participated in a randomized double blind crossover study where they received 10 mg/day of policosanol or a placebo incorporated in margarine as an evening snack for a period of 28 days. Subjects maintained their usual dietary and exercise habits throughout the duration of the study. Blood was collected on the first as well as the last 2 days of the trial. LDL oxidation was measured from plasma using a solid phase two-site enzyme immunoassay. A lack of effect of SCP was observed on LDL cholesterol levels, as well as no difference in LDL oxidation between the SCP treatment and placebo at the end of the intervention period. Subject body weights remained stable throughout the study and showed no significant correlation with LDL oxidation levels. Absolute levels of plasma LDL cholesterol were significantly ($P < 0.05$) correlated with plasma concentrations of oxidized LDL. The findings of the present study suggest that SCP do not significantly affect LDL oxidation.

Our results align with results of recent policosanol research questioning the efficacy of these natural extracts as cardio-protective agents.

Keywords Sugar cane policosanol · Low-density lipoprotein · Oxidation · Hypercholesterolemia · ELISA

Abbreviations

ANCOVA	Analysis of covariance
EDTA	Ethylenediaminetetraacetic acid
ELISA	Enzyme-linked immunosorbent assay
HDL	High-density lipoprotein
HMG CoA	3-Hydroxy-3-methyl-glutaryl-CoA
LDL	Low-density lipoprotein
MDA	Malonaldehyde
SCAP	Sugar cane policosanols
TBARS	Thiobarbituric acid reactive substances

Introduction

Atherosclerosis remains the leading cause of death not only in developed [17] but in developing countries as well [26, 27], making cardiovascular disease a substantial global health burden. Several processes have been implicated in early atherogenesis, with competing theories on the key triggering events including lipoprotein aggregation, macrophage chemotaxis, foam cell formation and lipoprotein oxidation [33]. Atherogenesis has been suggested as being triggered by the stimulation of intramural synthesis of molecules promoting lipoprotein retention and subsequent oxidation proposed to be the second most central process in the development of atherosclerosis [3, 33]. Sugar cane

A. N. Kassis · S. Kubow
School of Dietetics and Human Nutrition, McGill University,
Montreal, QC, Canada

P. J. H. Jones (✉)
Richardson Centre for Functional Foods and Nutraceuticals,
University of Manitoba, 196 Innovation Drive, Smart Park,
Winnipeg, MB R3T 6C5, Canada
e-mail: peter_jones@umanitoba.ca

policosanols (SCP), mixtures of long chain fatty alcohols, exert cardioprotective properties by reducing the susceptibility of LDL to oxidation as was shown in various studies by a research group based in Cuba [8, 19, 31]. Animal [20, 21, 24] and human [7, 23] studies have demonstrated reductions in lipid and LDL peroxidation as a result of SCP treatment, using markers of oxidative stress such as monitoring of conjugated dienes and measuring thiobarbituric acid reactive substances (TBARS). In animals [20, 21, 24] as well as humans [7, 23], SCP significantly prolonged the lag time, reduced the propagation of conjugated diene generation [7, 21, 23, 24] and decreased levels of TBARS [7, 20, 21, 23, 24]. TBARS and conjugated diene quantification are commonly used as an assessment method for lipid oxidation, however these methods have serious limitations such as lack of specificity and are often. Although independent research outside of Cuba examining the antioxidant power of SCP is limited, the outcomes of a recent study by Ng et al. failed to support previous positive findings, reporting no significant change of oxidation state in LDL from humans treated with a policosanol supplement [28]. While these negative findings have been supported by a growing body of evidence against the claimed cholesterol modulating properties of Cuban SCP [4, 9, 10, 14, 15, 25], no independent human trial had examined the antioxidant potential of this natural extract. Therefore, the objective of the present study was to evaluate the antioxidant effects of Cuban SCP in a compliance-controlled clinical feeding trial involving hypercholesterolemic individuals. It was hypothesized that there would be no significant difference in plasma oxidized LDL concentrations between subjects receiving SCP treatment versus placebo.

Materials and Methods

Subjects and Treatments

Potential participants were screened by phone interview, followed by blood biochemistry analyses to determine their lipid profile, as well as an examination conducted by the study physician. Subjects included in the clinical trial ($n = 21$) were healthy mildly hypercholesterolemic men and postmenopausal women living in the West Island of Montreal. Exclusion criteria included history of recent or chronic use of oral hypolipidemic therapy, chronic use of insulin, systemic antibodies, corticosteroids, androgens or phenytoin. Subjects were also excluded if they had experienced a myocardial infarction, coronary artery bypass or other major surgical procedures within the last 6 months, or reported recent onset of angina, congestive heart failure, inflammatory bowel disease, pancreatitis, or

hypothyroidism. Significant pre-existing diseases including cancer, chronic use of laxatives as well as smoking or consumption of more than two drinks per day were also considered to be part of the exclusion criteria. Before they were enrolled in the study, subjects were asked to sign a consent form outlining the details of the trial. The study protocol was approved by the Ethics committee of the medical faculty of McGill University. The SCP treatment administered to subjects during the trial was derived from Cuban SCP manufactured by Dalmer Laboratories (La Havana, Cuba) marketed under the brand Lipex, not to be confused with the simvastatin carrying the same name. SCP composition was 66.3% octacosanol, 13.0% triacontanol and 4.7% hexacosanol [18]. SCP pills were crushed into a powder and incorporated into margarine (Becel, Canada). Ten grams of the margarine containing 10 mg of SCP were spread on 60 g of bread and given daily to study participants as an evening snack. In the placebo margarine, the SCP powder was substituted by corn starch, the major excipient in the pill, which gave both margarines the same taste and texture. Subjects alternated between three types of bread snacks: zucchini bread, banana bread and tomato basil bread. The three snacks were adjusted to have similar macronutrient compositions. An average portion of 62 g contained on average 152 cal, 27.0 g of carbohydrates, 3.3 g of proteins, 3.7 g of fat and 1.0 g of fibre.

Protocol

The clinical trial was designed as a crossover whereby subjects consumed treatment and placebo margarines randomly over the course of two 28-day treatment phases. In order to eliminate the carryover effect of treatment, the two phases were separated by a 28-day washout period. During treatment and placebo phases, subjects were asked to maintain their habitual diets and exercise regimens and visit the research unit everyday to consume the evening snack under staff supervision at the Mary Emily Clinical Research Centre, in order to ensure absolute compliance. Alcohol was prohibited and caffeinated beverages were limited to one cup per day. We used 24 h recalls to ensure that subjects were following study guidelines. Body weights were recorded daily in order to monitor weight fluctuations throughout the study period. At the beginning and end of each feeding phase, blood draws were scheduled to check for health abnormalities at the onset of the trial and as a result of treatment. Subjects signed an informed consent form before entering the study.

LDL Oxidation Measurements

Subjects were scheduled for blood draws at the start and the end of each study phase. Blood was collected from

days 1 and 2 as baseline and 28 and 29 to determine endpoint oxidative states. Plasma was separated from red blood cells by centrifugation at 1,500 rpm for 20 min and was directly stored at -80°C until further analysis. Samples were maintained at -80°C prior to analysis and were analyzed within 2 years. Oxidized LDL was quantified using a solid phase two-site enzyme immunoassay (Oxidized LDL ELISA, Mercodia, Sweden) with murine monoclonal antibodies mAb-4E6. The plate wells used in this analysis were coated with the capture antibody. The test procedure was applied from the protocol accompanying the assay kit (Mercodia, Sweden). Briefly, plasma samples were thawed and diluted. Then, 25 μl of the sample was added to each coated well and incubated with assay buffer for 2 h at room temperature on a plate shaker. This first step insured that oxidized LDL in the sample bound to the solid phase antibodies. Wells were then thoroughly washed to eliminate other plasma components and peroxidase conjugated anti-human apolipoprotein B antibody was added to recognize the oxidized LDL attached to the solid phase. The labeled antibodies were detected upon the addition of 3,3', 5,5'-tetramethylbenzidine and absorbance at 450 nm was recorded. A standard curve was drawn for each run using four calibrators with different oxidized LDL concentrations as well as a low and a high concentration control. Plasma samples from the two phases belonging to each subject were run on one plate under the same laboratory conditions. Oxidized LDL concentrations of samples run on the same plate were calculated from the absorbance using the equation of a single standard curve.

Statistical Analysis

Effects of SCP on endpoint LDL oxidation were tested using a one way ANCOVA for crossover models including initial body weight and endpoint LDL cholesterol levels as covariates. Oxidized LDL values did not follow a normal distribution, therefore endpoint values were log transformed to achieve normality and differences in percent changes between groups were analyzed using the Wilcoxon Mann–Whitney non parametric test. Data were analyzed

using the SAS system for Windows version 8.0 (SAS Institute Inc.) and were reported as means \pm SEM. Statistical significance was set at $P < 0.05$.

Results

Twenty-two subjects were screened and accepted into the study. Twenty-one participants successfully completed the trial. Table 1 lists baseline characteristics of participants included in the trial. The policosanol treatment was odorless, colorless and tasteless; therefore subjects were not able to identify the SCP in their snacks. No adverse effects were noted during the study with the exception of four subjects reporting gastrointestinal discomfort and more frequent bowel movements. However, two of the subjects were allocated to the policosanol treatment, while the two others were allocated to the placebo intervention. Body weights remained stable throughout the study periods and blood biochemistry and hematology remained within normal ranges.

Plasma Lipid Levels

Plasma lipid levels were measured and results were published in a previous work [14]. Briefly, no significant differences were observed at endpoint between SCP treatment and placebo groups in plasma total, LDL, HDL and triglyceride levels. In addition, no significant effect of SCP was recorded on percent changes in lipid values.

Plasma Oxidized LDL Concentration

Concentrations of plasma oxidized LDL recorded at the end of the placebo and treatment phases are illustrated in Fig. 1. The effect of SCP on LDL oxidation was not significantly different from placebo ($P = 0.76$). When included in the model, initial body weight did not affect the concentration of oxidized LDL. A multiple regression of oxidized LDL on LDL, HDL cholesterol and triglyceride endpoint levels in the plasma demonstrated a significant effect of LDL cholesterol ($P = 0.03$) and approaching

Table 1 Baseline characteristics of subjects (means \pm SEM)

Variable	Males ($n = 12$)	Females ($n = 9$)	All ($n = 21$)
Age (years)	54.0 \pm 2.9 ^a	60.1 \pm 2.6 ^a	57.8 \pm 2.1
Weight (kg)	84.8 \pm 4.9 ^a	71.1 \pm 3.8 ^b	76.3 \pm 3.2
BMI (kg/m ²)	26.9 \pm 1.0 ^a	26.3 \pm 0.8 ^a	26.5 \pm 0.6
Total cholesterol	5.4 \pm 0.4 ^a	6.09 \pm 0.3 ^a	5.8 \pm 0.2
Low density lipoprotein	3.5 \pm 0.3 ^a	3.8 \pm 0.3 ^a	3.7 \pm 0.2
High density lipoprotein	1.2 \pm 0.1 ^a	1.6 \pm 0.1 ^b	1.4 \pm 0.09
Triglycerides	1.5 \pm 0.4 ^a	1.7 \pm 0.3 ^b	1.6 \pm 0.2

Values with different superscript letters are significantly different. Significance set at $P < 0.05$
Male/female ratio: 1.3
BMI body mass index

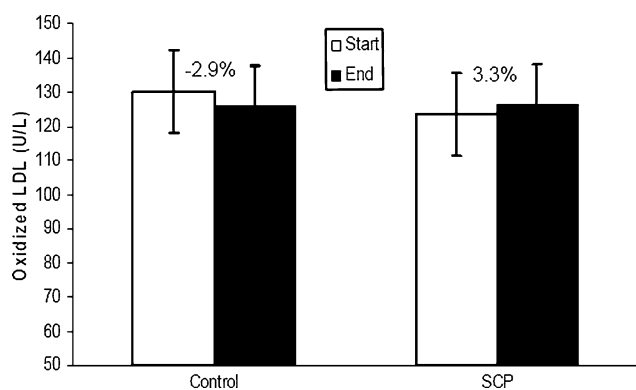


Fig. 1 Changes in oxidized LDL concentrations across treatment periods. Data reported as means \pm SEM. No significant difference recorded between control and SCP groups

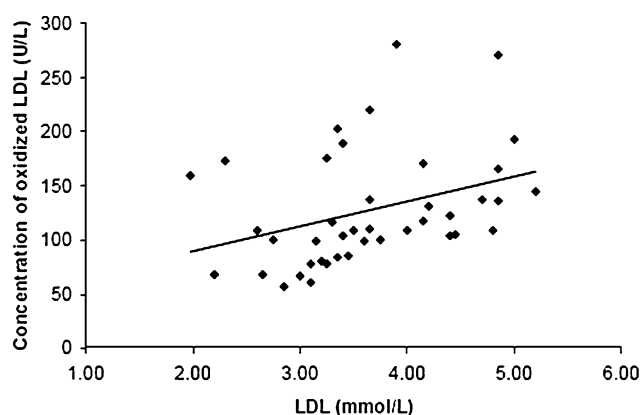


Fig. 2 Regression of oxidized LDL concentration and LDL cholesterol levels in plasma. Regression equation: $y = 23.24x + 42.53$; $r^2 = 0.0961$; $P = 0.02$

significance for triglycerides ($P = 0.06$) on LDL oxidation. Figure 2 illustrates a simple regression of oxidized LDL levels on LDL cholesterol concentrations in the study population as a whole. Results show a significant relationship between endpoint values ($r^2 = 0.13$; $P = 0.023$) and approached significance for percent change values ($r^2 = 0.091$; $P = 0.061$). When oxidized LDL concentrations were expressed relative to LDL levels in the plasma, no effect of treatment was recorded.

The effect of the treatment phase was significant suggesting that plasma collected during the first phase of the study had higher concentrations of oxidized LDL than those samples collected during the second phase. When the model was adjusted for storage time, the effect of treatment phase disappeared and the treatment remained non significant. Percent changes in LDL oxidation after placebo and SCP treatments are reported in Fig. 3 and showed no difference between the two study margarines in terms of their effect on LDL oxidation ($P = 0.61$).

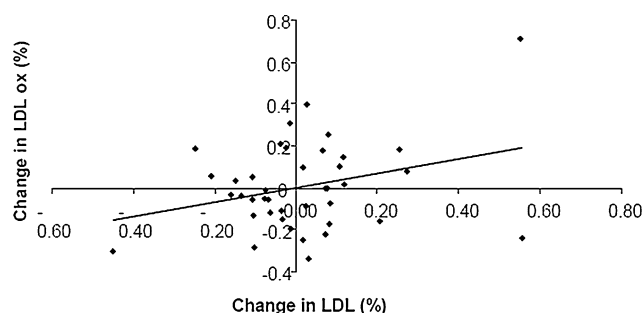


Fig. 3 Regression of change in oxidized LDL on change in LDL levels in plasma. Regression equation: $y = 0.34x + 0.012$; $r^2 = 0.09$; $P = 0.06$

Discussion

Results of the present randomized controlled study disagree with previous findings claiming efficacy of policosanols with respect to LDL oxidation reduction and agree with the independent in vitro study showing no antioxidant effect associated with SCP treatment [28]. Animal [1, 2, 20, 21, 24] and human [7, 23] trials previously demonstrated a clear-cut suppression of lipid peroxidation as a result of Cuban SCP treatment. In rabbits with exogenous hypercholesterolemia, SCP exerted a dose-dependant protective effect on atherosclerotic lesions, as 25 and 200 mg/kg of SCP resulted in less aortic fatty streaks with foam cells of macrophage origin [2]. Menendez et al. [21] conducted a dose response study in rats administering 0, 250 and 500 mg/kg/day to evaluate LDL oxidation induced by CuSO_4 . Continuous monitoring of conjugated dienes and TBARS showed a dose-dependent prolonged lag time, reduced propagation of conjugated diene generation and decreased levels of TBARS in LDL samples from rats on policosanol treatments. A similar experiment was conducted in healthy volunteers given 5 and 10 mg of SCP for a period of 8 weeks. SCP significantly decreased the rate of conjugated diene generation by 38% and lowered malondialdehyde (MDA) generation by 32% [23]. The antioxidant action of SCP was also compared to lovastatin, an HMG Co A reductase inhibitor, in a randomized double-blind study where both substances decreased conjugated diene and TBARS production, but only SCP increased the lag time of LDL peroxidation and total plasma antioxidant activity [7].

One limitation to the studies cited above was the methodology used to evaluate LDL-oxidation. Although TBARS is widely used for its simplicity, it is known to be affected by reaction conditions, namely the presence of EDTA [16]. In a comparative study conducted by Carru et al. [6], the authors reported that copper oxidation was not a suitable method for the clinical evaluation of LDL-oxidation because of the difficulty in standardizing the test and

the time needed to run it. More importantly, this procedure did not provide a reliable measurement of conjugated dienes. The method used in the present study was designed to quantify LDL oxidation using monoclonal antibodies directed at antigenic determinants of the oxidized apolipoprotein B molecule, making the test more specific than the assays used by the original research groups in terms of discriminating between the sources of oxidation. Since the conversion of native LDL to its oxidized form is a pivotal step in the process of atherogenesis, the choice of the test is crucial for the accurate determination of LDL oxidation. The LDL-ox ELISA method was also chosen in this study because its validity was shown not to be affected by storage time. Circulating oxidized LDL levels have been used as a coronary heart disease marker in previous studies in samples stored for up to 9 years [11, 12]. In addition, the LDL-ox ELISA was seen to be a reliable measure of LDL oxidation in a study examining different storage conditions, namely, freezing samples for up to 3 years [30]. Plasma samples from our subjects were stored at -80°C up to a maximum of 2 years; however, our results did show a significant effect of storage time on the concentration of oxidized LDL. Consequently, the data were adjusted for storage time as a covariate. Final results show that the difference between the treatment and placebo group remained non-significant.

The regression analysis and analysis of covariance performed on the present data revealed clear relationships between LDL levels as a predictor of oxidized LDL concentrations. Our results support previous research [11, 12] reporting this association. A multivariate analysis of the potential predictors of oxidized LDL concentrations showed that hypercholesterolemia is one of the strongest predictors of the LDL oxidation status [11]. These findings were later confirmed by a study investigating the relationship between oxidized LDL and other markers of atherosclerosis [12]. A significant powerful association was reported between circulating LDL levels and LDL oxidation [12]. Since LDL oxidation clearly varies with circulating LDL levels, the present data were also analyzed using standardized oxidized LDL concentrations relative to plasma LDL values for each subject. After normalization, the data continued to support the lack of antioxidant activity of SCP as shown by the absence of difference between the treatment and placebo groups.

The mechanisms of action by which SCP could potentially prevent *in vivo* LDL oxidation remain unclear, however, it was suggested that these alcohols possibly altered the lipid structure of LDL particles by affecting the ratio of unsaturated to saturated fatty acid content [23, 24]. Other fatty acids such as oleic acid have shown to reduce LDL oxidation by altering the fatty acid makeup of lipoproteins as well [5, 29]. Absorption rates of oleic acid

measured in the lymph reach 58% in rats [32]. In humans, fecal analysis of labeled oleic acid shows an absorption efficiency of 97.2% after a bolus administration [13]. If policosanol affects the lipid structure in a way similar to oleic acid as suggested by the original research group, it would be expected to have an absorption rate high enough to exert such an effect. Although the bioavailability of Cuban SCP has not been extensively researched, a study from Menendez et al. [22] demonstrated very low concentrations of octacosanol (30.1 ng/ml) and octacosanoic acid in plasma of hamsters after the administration of a 60 mg/kg SCP dose. These findings were later supported by Marinangeli et al. examining the content of the different alcohols in the plasma and tissues of hamsters on a SCP treatment [18]. The authors observed no trace of the alcohols in the plasma or tissues of the animals. Taken with the evidence originating from different independent laboratories showing no cholesterol-lowering effect on animals and humans [4, 9, 10, 15, 25], the authors' conclusion raises the possibility that SCP dose, absorption and uptake are not high enough to induce a systemic effect on lipoprotein metabolism and or oxidation status. Whether an action at the level of the intestinal wall is possible remains to be assessed.

In summary, the present investigation examined the claim that SCP play a preventive role in the development of atherosclerosis by reducing both circulating LDL concentrations and oxidation levels. The present data adds to the growing body of evidence raising doubts on the efficacy of SCP as a natural cholesterol-modulating antioxidant therapy.

Acknowledgments This study was supported by a research grant from the Advanced Foods and Materials Network—Networks of Centres of Excellence.

References

1. Arruzabala ML, Carbajal D, Mas R, Molina V, Valdes S, Laguna A (1994) Cholesterol-lowering effects of policosanol in rabbits. *Biol Res* 27:205–208
2. Arruzabala ML, Noa M, Menendez R, Mas R, Carbajal D, Valdes S, Molina V (2000) Protective effect of policosanol on atherosclerotic lesions in rabbits with exogenous hypercholesterolemia. *Braz J Med Biol Res* 33:835–840
3. Aviram M (1993) Modified forms of low density lipoprotein and atherosclerosis. *Atherosclerosis* 98:1–9
4. Berthold HK, Unverdorben S, Degenhardt R, Bulitta M, Gouni-Berthold I (2006) Effect of policosanol on lipid levels among patients with hypercholesterolemia or combined hyperlipidemia. A randomized controlled trial. *JAMA* 295:2263–2269
5. Bonanome A, Pagnan A, Biffanti S, Opportuno A, Sorgato F, Dorella M, Maiorino M, Ursini F (1992) Effect of dietary monounsaturated and polyunsaturated fatty acids on the susceptibility of plasma low density lipoproteins to oxidative modification. *Arterioscler Thromb* 12:529–533

6. Carru C, Zinellu A, Galistu F, Barca M, Pasciu V, Lumbau F, Sanna B, Tadolini B, Deiana L (2004) The evaluation of the oxidative state of native-LDL: three methods compared. *J Biochem Biophys Methods* 61:271–281
7. Castano G, Menendez R, Mas R, Amor A, Fernandez JL, Gonzalez RL, Lezcay M, Alvarez E (2002) Effects of policosanol and lovastatin on lipid profile and lipid peroxidation in patients with dyslipidemia associated with type 2 diabetes mellitus. *Int J Clin Pharmacol Res* 22:89–99
8. Chen JT, Wesley R, Shamburek RD, Pucino F, Csako G (2005) Meta-analysis of natural therapies for hyperlipidemia: plant sterols and stanols versus policosanol. *Pharmacotherapy* 25:171–183
9. Cubeddu LX, Cubeddu RJ, Heimowitz T, Restrepo B, Lamas GA, Weinberg GB (2006) Comparative lipid-lowering effects of policosanol and atorvastatin: a randomized, parallel, double-blind, placebo-controlled trial. *Am Heart J* 152:982. e1–5
10. Dulin MF, Hatcher LF, Sasser HC, Barringer TA (2006) Policosanol is ineffective in the treatment of hypercholesterolemia: a randomized controlled trial. *Am J Clin Nutr* 84:1543–1548
11. Holvoet P, Mertens A, Verhamme P, Bogaerts K, Beyens G, Verhaeghe R, Collen D, Muls E, Van de Werf F (2001) Circulating oxidized LDL is a useful marker for identifying patients with coronary artery disease. *Arterioscler Thromb Vasc Biol* 21:844–848
12. Hulthe J, Fagerberg B (2002) Circulating oxidized LDL is associated with subclinical atherosclerosis development and inflammatory cytokines (AIR Study). *Arterioscler Thromb Vasc Biol* 22:1162–1167
13. Jones PJ, Pencharz PB, Clandinin MT (1985) Absorption of ¹³C-labeled stearic, oleic, and linoleic acids in humans: application to breath tests. *J Lab Clin Med* 105:647–652
14. Kassis AN, Jones PJ (2006) Lack of cholesterol-lowering efficacy of Cuban sugar cane policosanols in hypercholesterolemic persons. *Am J Clin Nutr* 84:1003–1008
15. Kassis AN, Marinangeli CP, Jain D, Ebine N, Jones PJ (2007) Lack of effect of sugar cane policosanol on plasma cholesterol in golden Syrian hamsters. *Atherosclerosis* 194:153–158
16. Lapenna D, Ciofani G, Pierdomenico SD, Giamberardino MA, Cuccurullo F (2001) Reaction conditions affecting the relationship between thiobarbituric acid reactivity and lipid peroxides in human plasma. *Free Radic Biol Med* 31:331–335
17. Lefkowitz RJ, Willerson JT (2001) Prospects for cardiovascular research. *JAMA* 285:581–587
18. Marinangeli CP, Kassis AN, Jain D, Ebine N, Cunnane SC, Jones PJ (2007) Comparison of composition and absorption of sugar cane policosanols. *Br J Nutr* 97:381–388
19. Mas R, Castano G, Fernandez L, Illnait J, Fernandez J, Alvarez E (2001) Clinical use—effects of policosanol on lipid profile and cardiac events in older hypercholesterolaemic patients with coronary disease. *Clin Drug Investig* 21:485–499
20. Menendez R, Amor AM, Gonzalez RM, Jimenez S, Mas R (2000) Inhibition of rat microsomal lipid peroxidation by the oral administration of D002. *Braz J Med Biol Res* 33:85–90
21. Menendez R, Fraga V, Amor AM, Gonzalez RM, Mas R (1999) Oral administration of policosanol inhibits in vitro copper ion-induced rat lipoprotein peroxidation. *Physiol Behav* 67:1–7
22. Menendez R, Marrero D, Mas R, Fernandez I, Gonzalez L, Gonzalez RM (2005) In vitro and in vivo study of octacosanol metabolism. *Arch Med Res* 36:113–119
23. Menendez R, Mas R, Amor AM, Gonzalez RM, Fernandez JC, Rodeiro I, Zayas M, Jimenez S (2000) Effects of policosanol treatment on the susceptibility of low density lipoprotein (LDL) isolated from healthy volunteers to oxidative modification in vitro. *Br J Clin Pharmacol* 50:255–262
24. Menendez R, Mas R, Amor AM, Ledon N, Perez J, Gonzalez RM, Rodeiro I, Zayas M, Jimenez S (2002) Inhibition of rat lipoprotein lipid peroxidation by the oral administration of D003, a mixture of very long-chain saturated fatty acids. *Can J Physiol Pharmacol* 80:13–21
25. Murphy KJ, Saint DA, Howe PR (2008) Lack of effect of sugar cane and sunflower seed policosanols on plasma cholesterol in rabbits. *J Am Coll Nutr* 27:476–484
26. Murray CJ, Lopez AD (1997) Global mortality, disability, and the contribution of risk factors: global burden of disease study. *Lancet* 349:1436–1442
27. Murray CJ, Lopez AD (1997) Mortality by cause for eight regions of the world: global burden of disease study. *Lancet* 349:1269–1276
28. Ng CH, Leung KY, Huang Y, Chen ZY (2005) Policosanol has no antioxidant activity in human low-density lipoprotein but increases excretion of bile acids in hamsters. *J Agric Food Chem* 53:6289–6293
29. Parthasarathy S, Khoo JC, Miller E, Barnett J, Witztum JL, Steinberg D (1990) Low density lipoprotein rich in oleic acid is protected against oxidative modification: implications for dietary prevention of atherosclerosis. *Proc Natl Acad Sci U S A* 87:3894–3898
30. Perman J, Fagerlund C, Hulthe J (2004) Methodological aspects of measuring oxidized low density lipoproteins in human serum and plasma. *Scand J Clin Lab Invest* 64:753–755
31. Varady KA, Wang Y, Jones PJ (2003) Role of policosanols in the prevention and treatment of cardiovascular disease. *Nutr Rev* 61:376–383
32. Vistisen B, Mu H, Hoy CE (2006) The recovery of ¹³C-labeled oleic acid in rat lymph after administration of long chain triacylglycerols or specific structured triacylglycerols. *Eur J Nutr* 45:363–368
33. Williams KJ, Tabas I (1995) The response-to-retention hypothesis of early atherogenesis. *Arterioscler Thromb Vasc Biol* 15:551–561

The Carotid Artery Plaque Size and Echogenicity are Related to Different Cardiovascular Risk Factors in the Elderly

The Prospective Investigation of the Vasculature in Uppsala Seniors (PIVUS) study

Jessika Andersson · Johan Sundström · Lisa Kurland · Thomas Gustavsson · Johannes Hulthe · Anders Elmgren · Kersti Zilmer · Mihkel Zilmer · Lars Lind

Received: 6 March 2008 / Accepted: 29 December 2008 / Published online: 21 February 2009
© AOCs 2009

Abstract Carotid plaques can be characterised by ultrasound by size and echogenicity. Both size and echogenicity are predictors of cardiovascular events. The aim of this study was to examine whether traditional risk factors and markers of inflammation and oxidation were associated with plaque size and echogenicity. Computerised analysis of carotid plaque size and echogenicity (grey scale median, GSM) were performed by ultrasound in a population-based health survey in 1,016 subjects aged 70 years (PIVUS study). Information on cardiovascular risk factors was collected, together with markers of inflammation and oxidation. Increased Framingham risk score, systolic blood pressure, higher BMI and decreased HDL, lower glutathione levels were related to echolucent plaques. Previous or present smoking was common with significantly more pack-years related to the echorich plaques. Plaque size was associated with increased Framingham risk score, systolic

blood pressure, blood glucose levels, smoking, ApoB/A1 ratio, OxLDL, TNF alpha, HOMA insulin resistance, leucocyte count, decreased BCD-LDL and low levels of l-selectin. Low HDL, increased BMI and decreased glutathione levels were associated with the echolucency of carotid plaques, implying metabolic factors to play a role for plaque composition. Markers of inflammation were related to plaque size alone, implying inflammation to be predominantly associated with the amount of atherosclerosis. These results suggest that plaque size and echogenicity are influenced by different risk factors.

Keywords Atherosclerosis · Ultrasound · Plaque · Carotid artery · Risk factor · Lipids · Oxidation

Introduction

Plaque rupture is believed to be the precipitating event in the major clinical manifestations of atherosclerosis, e.g. myocardial and cerebral infarction. The vulnerable plaque is described as containing a large lipid-rich core, a thin fibrous cap and an increased number of inflammatory cells. The stable plaque, on the other hand, is characterised by a smaller amount of lipids, more collagen and calcium and less inflammatory cells. Apart from being able to quantify the size of the plaque, a useful imaging modality should also be able to analyse plaque composition.

The plaque can be characterised in two different dimensions, size and echogenicity by using externally applied ultrasound on the carotid arteries. Both size [1] and echogenicity [1–4] of carotid plaques have been shown to predict not only stroke, but also other clinical manifestations of atherosclerosis, such as acute coronary syndromes including myocardial infarction. Thus, both of these plaque

J. Andersson (✉) · J. Sundström · L. Kurland · L. Lind
Department of Medicine, Uppsala University Hospital, 751 85
Uppsala, Sweden
e-mail: jessika.andersson@medsci.uu.se;
jessika.andersson@akademiska.se

T. Gustavsson
Department of Signals and Systems,
Chalmers University of Technology,
Gothenburg, Sweden

J. Hulthe
Wallenberg Laboratory, Sahlgrenska University Hospital,
Gothenburg, Sweden

J. Hulthe · A. Elmgren
AstraZeneca R&D, Mölndal, Sweden

K. Zilmer · M. Zilmer
Department of Biochemistry, University of Tartu, Tartu, Estonia

dimensions are of interest for risk stratification. Analyses of carotid plaque specimens after endarterectomy indicates that the echogenicity reflects the different histopathological components, with echolucent plaques being associated with a high lipid and haemorrhage content [5].

While several studies have found that traditional risk factors, such as age, male gender, cigarette smoking, systolic blood pressure, high serum cholesterol, diabetes mellitus and low levels of HDL [6–10] are associated with carotid plaque size, determinants of plaque echogenicity are less well established. The presence of echolucent carotid plaques has been associated with low HDL levels [11], and with elevated levels of fasting and postprandial triglyceride rich lipoprotein [3]. Echolucent plaques in the femoral artery have also been found to be related to high levels of oxidised LDL and CRP [12]. Thus, lipid oxidation and inflammation may be important risk factors for plaque echogenicity.

Our hypothesis was that plaque size and echogenicity are associated with different risk factors. Earlier studies indicate that plaque echolucency is associated with lipid status [11]. Since both inflammation and oxidative stress have been advocated to play an important role in the development of atherosclerosis [13], several markers of inflammation and oxidative stress were investigated along with traditional risk factors. Treatment with statins are believed to induce regression of established atherosclerotic lesions, lower CRP levels [14], and possibly affect plaque composition [15]. Therefore, adjustment for statin treatment was made in all analyses.

Our aim was to investigate the relationship between carotid artery plaque size and echogenicity and cardiovascular risk factors, including markers of inflammation and oxidation in the PIVUS study, a population based cohort. We used the Prospective Investigation of the Vasculature in Uppsala Seniors (PIVUS) study, initiated in more than 1,000 subjects aged 70 living in the community of Uppsala, Sweden [16], to study the relationships.

Materials and Methods

For a detailed description of the basic characteristics of the PIVUS cohort see the previous publication by Stenborg et al. [17].

Subjects

The Prospective Investigation of the Vasculature in Uppsala Seniors (PIVUS) study is a population based cohort. All 70 year olds living in the community of Uppsala, Sweden were eligible. They received an invitation letter within 2 months of their 70th birthday. Of the total of

2,025 invited, 1,016 subjects participated giving a participation rate of 50, 1%. The study was approved by the ethics committee of the University of Uppsala and the participants gave informed consent. The present study was based on the 942 individuals in whom ultrasound pictures of high quality were obtained.

Basic Investigation

The participants answered a questionnaire disclosing their medical history, smoking habits and medication. All subjects were investigated in the morning after an over-night fast. Neither medication nor smoking was allowed after midnight preceding the investigations. Recordings of height, weight, abdominal and hip circumference were performed. Blood pressure was measured using a calibrated mercury sphygmomanometer in the non-cannulated arm after at least 30 min of rest in the supine position. The average of three recordings was used. Lipid variables and fasting blood glucose were measured by standard laboratory techniques. The Framingham risk score was calculated from these data [18].

Ultrasound System

The imaging was performed using an external B-mode ultrasound system (Acuson XP128 with a 10-MHz linear transducer, Acuson Mountain View, California, USA). All subjects were examined by the same ultrasonographer.

Ultrasound Procedure

The images were stored using the cine function during the electrocardiographic R-wave in the cardiac cycle. Frozen images of the arterial wall were saved and measurements subsequently performed on the stored digital images. Analyses were made using the AMS program package [19]. The common carotid artery, carotid bifurcation and internal carotid artery were examined bilaterally for the presence of plaques.

A local thickening of the intima-media by more than 50% compared with the surrounding IMT (but plaque area <10 mm²) was defined as stage 1 plaques. Plaque volume exceeding 10 mm² was defined as stage 2, and presence of an increased velocity distal to the plaque measured with Doppler, indicating >50% stenosis, as stage 3.

A region of interest (ROI) was manually positioned around the largest plaque. The grey scale median (GSM) was calculated from pixel analysis within in the range 0–256. The blood was used as the reference for black and the adventitia as the reference for white. Plaques were defined as echolucent if GSM value was lower than 70, and as echorich if GSM was higher than 70.

Also, the area of the ROI was calculated. This analysis was carried out by the same ultrasonographer blinded to the clinical data.

Measurements of GSM and plaque size were repeated in 25 random subjects yielding coefficients of variation (CV) of 8.3 and 11.2%, respectively.

Insulin Resistance

Serum insulin was measured with an enzymatic-immunological assay (Boehringer Mannheim). HOMA insulin resistance index was defined as fasting blood glucose time's serum insulin/22.5.

Markers of Inflammation

High sensitive CRP was measured in human serum by an ultra sensitive particle enhanced immunoturbidimetric assay (Orion Diagnostica, Espoo, Finland) on a Konelab 20 autoanalyser (Thermo Clinical LabSystems, Espoo, Finland). The inter assay CV was 3.2%.

Cytokines, chemokines and adhesion molecules were analysed on the Evidence[®] array biochip analyser (Randox Laboratories, Ltd., Crumlin, UK).

The functional sensitivity for the different inflammatory markers was as follows: interleukin 6 (IL-6): 0.3, interferon-gamma (InfG): 1.8, tumour necrosis factor alpha (TNF-alpha): 1.8, monocyte chemotactic protein 1 (MCP-1): 19.4, intercellular adhesion molecule 1 (ICAM-1): 18.6, vascular cell adhesion molecule 1 (VCAM-1): 3.1, endothelial selectin (e-selectin): 3.1, platelet-selectin (p-selectin): 11.2, lymphocyte selectin (l-selectin): 32.8, C reactive protein (CRP): 0.1, leukocyte count: 0.2.

Markers of Oxidative Stress

Baseline conjugated dienes of LDL (BCD-LDL) were measured by using a previously validated method (see Ref. [20] for details). The within assay CV for BCD-LDL was 4.4% and the between assay precision was 4.5%. Enzyme-linked immunoabsorbent assay (ELISA) kits (Merckodia, AB) were used to determine serum oxidised LDL, within-assay variation coefficient was 6.3% and between-assay CV was 4.7%. All glutathione indices, conjugated dienes (CD) and total antioxidant capacity (TAOC) values were measured and calculated as previously described [20]. Homocysteine was measured by using Enzyme Immunoassay method (Axis-Shield Diagnostics Ltd) with an intra-assay CV of 6.8%.

Statistics

IL-6, TNF alfa, InfG, e-selectin and homeostasis model assessment (HOMA) index were log-transformed in order

to achieve a normal distribution. ANOVA was used to evaluate differences between groups after adjustment for gender, with the Bonferroni post-hoc test using a pre-specified number of tests (abnormal groups versus the normal group). All analyses were adjusted for the influence of gender and statin use. Two-tailed significance values were given and $P < 0.05$ was regarded as significant. StatView (SAS Inc., NC, USA) was used for the statistical calculations.

Results

Approximately 6% of the cohort reported a history of myocardial infarction, 2% reported stroke and 9% reported diabetes mellitus. Almost half of the cohort reported some cardiovascular medication (45%), with antihypertensive medication being the most prevalent (31%).

Fifteen percent reported use of statins, while insulin and oral antiglycemic drugs were reported in 2 and 6% respectively (Table 1).

Evaluation of Non-Participants

As the participation rate in this cohort was only 50%, we carried out an evaluation of cardiovascular disorders and medications in 100 consecutive non-participants. The prevalence of cardiovascular drug intake, history of myocardial infarction, coronary revascularisation, antihypertensive

Table 1 Basic characteristics of the study sample (%)

Gender	Total <i>n</i> = 942	Men <i>n</i> = 469	Women <i>n</i> = 473
Hypertension ^a	678 (72%)	328 (70%)	350 (74%)
Statin use	141 (15%)	75 (16%)	66 (14%)
Heart failure	38 (4%)	19 (4%)	14 (3%)
Diabetes mellitus ^b	85 (9%)	52 (11%)	33 (7%)
Previous myocardial Infarction ^c	57 (6%)	84 (8%)	14 (3%)
Previous smoker	396 (42%)	230 (49%)	166 (35%)
Current smoker	94 (10%)	47 (10%)	52 (11%)
Use of Cardiovascular Medication	424 (45%)	211 (45%)	213 (45%)
Use of antihypertensive medication	292 (31%)	145 (31%)	147 (31%)
Previous stroke ^d	19 (2%)	14 (3%)	5 (1%)

^a Defined as systolic blood pressure >140 or diastolic >90, or use of antihypertensive medication

^b Defined as history of diabetes mellitus or fasting sugar level >6.1

^c Previous myocardial infarction which required hospitalisation

^d Previous stroke which required hospitalisation

medication, statin use and insulin treatment were similar to those in the investigated sample, while the prevalence of diabetes, congestive heart failure and stroke tended to be higher among the non-participants.

Prevalence of Carotid Artery Plaque

The prevalence of unilateral plaque, defined as at least 50% increase of the intima-media thickness, in the carotid arteries was 34%, while the prevalence of bilateral plaques was 27%. Plaques were in general slightly more prevalent in men ($n = 322$) than in women ($n = 293$).

Individuals with carotid artery plaques had significantly higher Framingham risk score ($P < 0.0001$), higher levels of systolic blood pressure ($P < 0.0001$), higher levels of fasting blood glucose ($P = 0.02$), LDL/HDL-ratio ($P = 0.04$), ApoB/A1-ratio ($P = 0.013$), LDL ($P = 0.02$) and also a higher average of pack-years of cigarette smoking ($P = 0.008$) after adjustment for gender and statin use. No significant differences were seen for HDL-cholesterol, serum triglyceride level, DBP or body mass index (Table 2).

Relationships Between Plaque Size, Traditional Risk Factors, Markers of Oxidative Stress and Inflammation

A similar picture emerged, as described above, when traditional risk factors were related to plaque size and not to plaque prevalence. Framingham risk score, SBP, blood glucose, ApoB/A1-ratio, HOMA resistance index and smoking were significantly related to plaque size after adjustment gender and statin use. However, these relationships were not all significant in the post-hoc analysis in the group with flow-restricting plaque since there were only 27 subjects in this group. No significant relationships

were seen between plaque size and LDL-cholesterol, HDL-cholesterol, LDL/HDL-ratio ($P = 0.07$), serum triglycerides, DBP, or body mass index (Table 3).

BCD LDL levels were significantly higher, among subjects with plaques. Conversely, the total antioxidant capacity (TAOC) was lower among these subjects as could be expected. There was a trend of decreased BCD levels with increased plaque size, however non-significant in the post hoc analysis. OxLDL levels showed a stepwise increase with increasing plaque size. No other markers of oxidative stress were significantly related to plaque size.

TNF alpha, l-selectin (inversely) and leukocyte count and all markers of inflammation, were significantly related to plaque size after adjustment for gender and statin use (Table 3).

Relationships Between Plaque Echogenicity and Traditional Risk Factors and Markers of Oxidative Stress and Inflammation

Echolucent plaques were correlated with an increased Framingham risk score, elevated systolic blood pressure and higher BMI after adjustment for gender and statin use, while the levels of HDL were lower. Previous or present smoking was common in both groups of echolucent and echorich plaques with significantly more pack-years related to the echorich plaques. None of the other traditionally risk factors were significantly related to plaque echogenicity (Table 4).

Levels of total glutathione (TGSH), reduced glutathione (GSH) and oxidised glutathione (GSSG) were significantly lower among the subjects with echolucent plaques when compared to individuals with echorich plaques. None of the other markers of inflammation and oxidative stress were significantly related (Table 4).

Table 2 Traditional risk factors in subjects with and without carotid artery plaques

	No plaque	Plaque	<i>P</i> -value
No.	327	594	
Framingham	10.4 ± 3.2	11.5 ± 3.4	<0.0001
SBP (mmHg)	146 ± 22	152 ± 23	<0.0001
LDL-cholesterol (mmol/l)	3.3 ± 0.9	3.4 ± 0.9	0.02
LDL/HDL-ratio	2.3 ± 0.8	2.4 ± 0.8	0.04
ApoB/A1-ratio	0.64 ± 0.2	0.67 ± 0.1	0.013
Fasting blood glucose (mmol/l)	5.1 ± 1.1	5.4 ± 1.7	0.02
Cigarette smoking (package years)	10 ± 15	13 ± 17	0.008

Differences between groups were calculated with ANOVA, adjusted for gender and statin use. Values presented as means ± SD

SBP systolic blood pressure, DBP diastolic blood pressure, LDL low density lipoprotein, ApoA1 apolipoprotein A1, ApoB apolipoprotein B

Discussion

The main result of this study was that different risk factors were related to the two different dimensions of carotid plaque, i.e. size and echogenicity. HDL-cholesterol, body mass index and glutathione were related to echogenicity; while markers of inflammation were related to plaque size and not to echogenicity.

Relationships Between Plaque Occurrence and Size and Cardiovascular Risk Factors

Plaque occurrence and size was associated with systolic blood pressure, fasting blood glucose, LDL, LDL/HDL-ratio, ApoB/A1-ratio and smoking in this population. These are established risk factors for carotid atherosclerosis.

Table 3 Relationships between plaque size and traditional risk factor and markers of inflammation and oxidation

	No plaque	Plaque <10 mm ²	Plaque >10 mm ²	Flow-obstructing plaque	P-value
No.	327	147	420	27	
Framingham risk score	10.4 ± 3.2	10.4 ± 3.2	11.8 ± 3.4***	12.7 ± 2.5**	<0.0001
SBP (mmHg)	145 ± 22	146 ± 23	153 ± 22***	157 ± 25*	<0.0001
Blood glucose (mmol/l)	5.2 ± 1.2	5.2 ± 1.1	5.5 ± 1.9*	5.6 ± 1.9	0.04
Cigarette smoking (pack years)	10.1 ± 15	12.7 ± 16	13 ± 17.5	20.5 ± 21*	0.0042
ApoB/ApoA1-ratio	0.64 ± 0.2	0.64 ± 0.2	0.67 ± 0.2*	0.70 ± 0.2	0.02
OxLDL (U/l)	129 ± 50	126 ± 45	137 ± 46	153 ± 56	0.002
TNFα (pg/ml)	1.4 (2.4–7.7)	1.4 (2.3–6.7)	1.4 (2.3–7.4)	1.7 (2.5–14.9)	0.03
I-Selectin (ng/l)	742 ± 145	707 ± 129	712 ± 141*	709 ± 149	0.038
BCD-LDL (μmol/l)	20.8 ± 7.2	23 ± 7.6*	21.5 ± 7.2	22.4 ± 7.8	0.011
TAOC (%)	38.1 ± 4	36.9 ± 4*	37.5 ± 4	38.2 ± 3	0.02
GSSG (μg/ml)	76 ± 38	83 ± 42	74 ± 33	68 ± 17	0.05
Leucocyte count	5.5 ± 1.3	5.5 ± 1.4	5.7 ± 1.5	6.5 ± 1.8*	0.005
HOMA resistance index (mmol/l* mU/l)	1.58 (0.90–3.44)	1.67 (0.8–4.1)	1.76 (0.87–4.4)	1.95 (1.1–9.2)	0.04

Data are given as means ± SD, or as median with 10–90th percentile in parenthesis. Differences between groups were calculated with ANOVA with adjustment for gender and statin use

* $P < 0.01$; ** $P < 0.001$; *** $P < 0.0001$ refer to post hoc analyses versus group with no plaque

SBP systolic blood pressure, DBP diastolic blood pressure, LDL low density lipoprotein, HDL high density lipoprotein, ApoA1 apolipoprotein A1, ApoB apolipoprotein B, BMI body mass index, OxLDL oxidised low density lipoprotein, BCD LDL baseline conjugated diens of low density lipoprotein, TAOC total antioxidant capacity, CD conjugated diens, TGSH total glutathione, GSH reduced glutathione, GSSG oxidised glutathione, IL-6 interleukin 6, TNF *alfa* tumour necrosis factor *alfa*, IntfG interferon gamma, VCAM-1 vascular cell adhesion molecule 1, ICAM-1 intercellular adhesion molecule, MCP-1 monocyte chemotactic protein 1, CRP C-reactive protein, HOMA index homeostasis model assessment index

Table 4 Relationships between echolucent and echorich plaques and traditional risk factors, markers of inflammation and oxidative stress

	Echolucent plaque <i>n</i> = 304	Echorich plaque <i>n</i> = 290	<i>P</i> value
Framingham risk score	11.8 ± 3.3	11.2 ± 3.4	0.04
SBP	153.4 ± 23.2	150.4 ± 22.7	0.005
HDL	1.44 ± 0.4	1.56 ± 0.5	0.047
Smoking, pack years	12.6 ± 17.4	15.7 ± 17.5	0.005
BMI	27.1 ± 4.0	26.5 ± 4.3	0.05
TGSH	887 ± 178	920 ± 222	0.03
GSH	816 ± 169	840 ± 212	0.0002
GSSG	71 ± 29	82 ± 40	0.0001

Data are given as mean value ± SD and *P*-value. Differences between groups were calculated with ANOVA with adjustment for gender and statin use. Echolucent plaques are defined as plaques with a GSM value of less than 70, and echorich plaques as plaques with a GSM value of more than 70

SBP systolic blood pressure, HDL high density lipoprotein, BMI body mass index, TGSH total glutathione, GSH reduced glutathione, GSSG oxidised glutathione

These findings being consistent with several earlier studies of asymptomatic carotid arteriosclerosis [7, 8, 21, 22].

In the present study, plaque size was also related to increased levels of TNF *alfa*, a high leukocyte count and

low levels of I-selectin. The relationship between with carotid atherosclerosis and inflammatory processes has previously been investigated. In the Rotterdam Study, increased fibrinogen was an independent predictor of carotid artery stenosis [7]. An elevated leukocyte count was associated with carotid arteriosclerosis in a study by Elkind and co-workers [23]. While high leukocyte count has been shown to predict future cardiovascular events [24, 25], less is known of the effects of I-selectin on atherosclerosis. However, in a small study, I-selectin levels were shown to be reduced in patients with ischemic heart disease compared to controls, and it was hypothesised that the chronic inflammatory process of atherosclerosis leads to downregulation of leukocyte expression of I-selectin, thus rendering lower circulating I-selectin levels. This hypothesis is supported by in vitro studies demonstrating that stimulation of leukocytes leads to a rapid downregulation of surface I-selectin expression [26].

The oxidative stress markers TAOC was reduced and BCD-LDL was increased in subjects with small plaques but not in those with larger plaques. This may be a pattern associated with the early stages of plaque growth, but it remains to be confirmed.

OxLDL levels have previously been associated with carotid artery atherosclerotic plaques [27], and we could confirm that carotid plaque size was linked to OxLDL in a stepwise fashion in the present study.

It should be emphasised that the vast majority of plaques observed in the present study are quite small and do not cause any obstruction of flow. Therefore, the present study should be regarded as a study of asymptomatic atherosclerosis. Other results could have been obtained if subjects with clinically important or symptomatic carotid stenosis had been investigated.

Relationships Between Plaque Echogenicity and Cardiovascular Risk Factors

The ANOVA analysis demonstrated that some of the risk factors related to plaque size were also related to the plaque echogenicity, while other risk factors were related to echogenicity alone. Body mass index, HDL and glutathione metabolism were factors mainly related to plaque echogenicity. Low levels of HDL-cholesterol have previously been shown to be associated with echolucent plaques, as well as with plaque progression [11]. In the present study, HDL was associated with the echogenicity but not size. HDL is known to be as a reverse cholesterol transporter and by the removal of cholesterol from the plaque and also other actions of HDL, such as anti-inflammatory actions, may influence the echogenicity of plaques.

Glutathione, an intracellular antioxidant widely distributed in human tissues, acts as a cofactor for glutathione peroxidase. This enzyme reduces H_2O_2 , a reactive oxidant species produced during the course of metabolism, to oxidised glutathione (GSSG) and water [28]. The GSSG level could be a result of a low glutathione peroxidase activity, indicating a reduced antioxidant activity in turn resulting in more echolucent plaques.

Another interesting finding was that BMI was associated with plaque echogenicity but not to plaque size. It has been shown that plaques that increase in GSM over time have a slow progress with respect to growth [29]. This finding could indicate that a good oxidative defence and a lean stature are characteristics that make a small plaque to increase in collagen and/or calcium content and in turn slowing down in plaque growth.

It has previously been reported that diabetics [30] and subjects with elevated inflammatory markers [31] have an increased prevalence of echolucent plaques. We could however not confirm these findings. Conversely, blood glucose levels and insulin resistance was related to plaque size, and none of the large number of inflammatory markers measured in this study were related to GSM in the plaque.

Limitation of the Study

The present sample is limited to Caucasians aged 70. Caution should therefore be made to draw conclusions to other ethnic and age groups.

The present study had a moderate participation rate. Therefore, we carried out an evaluation of cardiovascular disorders and medications in 100 consecutive subjects who refused to participate [13]. The prevalence of cardiovascular drug intake, history of myocardial infarction, coronary revascularisation, antihypertensive medication, statin use and insulin treatment were similar to those in the investigated sample, while the prevalence of diabetes, congestive heart failure and stroke tended to be higher among the non-participants.

A large number of variables were evaluated in order to obtain a broad view on risk factors for plaque size and echogenicity. This approach does however increase the risk of false positive findings. Thus, the results need to be repeated in other cohorts.

In conclusion, of the two carotid plaque dimensions, size and echogenicity, Framingham risk score, systolic blood pressure, fasting blood glucose, HOMA insulin resistance, cigarette smoking, ApoB/A, OxLDL, TNF alpha, low levels of I-selectin, decreased TAOC, increased leucocyte count were related to size, while HDL-cholesterol, glutathione and body mass index mainly were related to echogenicity. These results suggest that plaque size and echogenicity partly are influenced by different risk factors.

Acknowledgments The outstanding work at the endothelium laboratory performed by Nilla Fors, Jan Hall, Kerstin Marttala and Anna Stenborg in the collection and processing of the data is gratefully acknowledged. We also gratefully thank the staff at Analytical Biochemistry at AstraZeneca for performing the analyses of cytokines, chemokines, and adhesion molecules. The financial support from Uppsala University, Thureus foundation and AstraZeneca R&D is highly valued.

References

- Polak JF, Shemanski L, O'Leary DH, Lefkowitz D, Price TR, Savage PJ, Brant WE, Reid C (1998) Hypoechoic plaque at us of the carotid artery: an independent risk factor for incident stroke in adults aged 65 years or older. *Cardiovascular health study. Radiology* 208:649–654
- Honda O, Sugiyama S, Kugiyama K, Fukushima H, Nakamura S, Koide S, Kojima S, Hirai N, Kawano H, Soejima H, Sakamoto T, Yoshimura M, Ogawa H (2004) Echolucent carotid plaques predict future coronary events in patients with coronary artery disease. *J Am Coll Cardiol* 43:1177–1184
- Gronholdt ML, Nordestgaard BG, Schroeder TV, Vorstrup S, Sillesen H (2001) Ultrasonic echolucent carotid plaques predict future strokes. *Circulation* 104:68–73
- Seo Y, Watanabe S, Ishizu T, Moriyama N, Takeyasu N, Maeda H, Ishimitsu T, Aonuma K, Yamaguchi I (2006) Echolucent carotid plaques as a feature in patients with acute coronary syndrome. *Circ J* 70:1629–1634
- El-Barghouty NM, Levine T, Ladva S, Flanagan A, Nicolaidis A (1996) Histological verification of computerised carotid plaque characterisation. *Eur J Vasc Endovasc Surg* 11:414–416
- Prati P, Vanuzzo D, Casaroli M, Di Chiara A, De Biasi F, Feruglio GA, Touboul PJ (1992) Prevalence and determinants of

- carotid atherosclerosis in a general population. *Stroke* 23:1705–1711
7. Bots ML, Breslau PJ, Briet E, de Bruyn AM, van Vliet HH, van den Ouweland FA, de Jong PT, Hofman A, Grobbee DE (1992) Cardiovascular determinants of carotid artery disease. The Rotterdam elderly study. *Hypertension* 19:717–720
 8. Fabris F, Zanocchi M, Bo M, Fonte G, Poli L, Bergoglio I, Ferrario E, Pernigotti L (1994) Carotid plaque, aging, and risk factors. A study of 457 subjects. *Stroke* 25:1133–1140
 9. Bonithon-Kopp C, Scarabin PY, Taquet A, Touboul PJ, Malmejac A, Guize L (1991) Risk factors for early carotid atherosclerosis in middle-aged french women. *Arterioscler Thromb* 11:966–972
 10. Mathiesen EB, Joakimsen O, Bonna KH (2001) Prevalence of and risk factors associated with carotid artery stenosis: the Tromsø study. *Cerebrovasc Dis* 12:44–51
 11. Mathiesen EB, Bonna KH, Joakimsen O (2001) Low levels of high-density lipoprotein cholesterol are associated with echolucent carotid artery plaques: the Tromsø study. *Stroke* 32:1960–1965
 12. Sigurdardottir V, Fagerberg B, Wikstrand J, Schmidt C, Hulthe J (2007) Circulating oxidized low-density lipoprotein is associated with echolucent plaques in the femoral artery independently of hscrp in 61-year-old men. *Atherosclerosis* 190:187–193
 13. Lind L, Fors N, Hall J, Marttala K, Stenborg A (2005) A comparison of three different methods to evaluate endothelium-dependent vasodilation in the elderly: the prospective investigation of the vasculature in Uppsala seniors (pivus) study. *Arterioscler Thromb Vasc Biol* 25:2368–2375
 14. Ross R (1999) Atherosclerosis—an inflammatory disease. *N Engl J Med* 340:115–126
 15. Yu CM, Zhang Q, Lam L, Lin H, Kong SL, Chan W, Fung JW, Cheng KK, Chan IH, Lee SW, Sanderson JE, Lam CW (2007) Comparison of intensive and low-dose atorvastatin therapy in the reduction of carotid intimal-medial thickness in patients with coronary heart disease. *Heart* 93:933–939
 16. Watanabe K, Sugiyama S, Kugiyama K, Honda O, Fukushima H, Koga H, Horibata Y, Hirai T, Sakamoto T, Yoshimura M, Yamashita Y, Ogawa H (2005) Stabilization of carotid atheroma assessed by quantitative ultrasound analysis in nonhypercholesterolemic patients with coronary artery disease. *J Am Coll Cardiol* 46:2022–2030
 17. Lind L, Fors N, Hall J, Marttala K, Stenborg A (2006) A comparison of three different methods to determine arterial compliance in the elderly: the prospective investigation of the vasculature in Uppsala seniors (pivus) study. *J Hypertens* 24:1075–1082
 18. Wilson PW, D'Agostino RB, Levy D, Belanger AM, Silbershatz H, Kannel WB (1998) Prediction of coronary heart disease using risk factor categories. *Circulation* 97:1837–1847
 19. Liang Q, Wendelhag I, Wikstrand J, Gustavsson T (2000) A multiscale dynamic programming procedure for boundary detection in ultrasonic artery images. *IEEE Trans Med Imaging* 19:127–142
 20. Annuk M, Fellstrom B, Akerblom O, Zilmer K, Vihalemm T, Zilmer M (2001) Oxidative stress markers in pre-uremic patients. *Clin Nephrol* 56:308–314
 21. Mannami T, Konishi M, Baba S, Nishi N, Terao A (1997) Prevalence of asymptomatic carotid atherosclerotic lesions detected by high-resolution ultrasonography and its relation to cardiovascular risk factors in the general population of a Japanese city: the Suita study. *Stroke* 28:518–525
 22. O'Leary DH, Polak JF, Kronmal RA, Kittner SJ, Bond MG, Wolfson SK Jr, Bommer W, Price TR, Gardin JM, Savage PJ (1992) Distribution and correlates of sonographically detected carotid artery disease in the cardiovascular health study. The chs collaborative research group. *Stroke* 23:1752–1760
 23. Elkind MS, Cheng J, Boden-Albala B, Paik MC, Sacco RL (2001) Elevated white blood cell count and carotid plaque thickness: the northern manhattan stroke study. *Stroke* 32:842–849
 24. Imano H, Sato S, Kitamura A, Kiyama M, Ohira T, Shimamoto T, Iso H (2007) Leukocyte count is an independent predictor for risk of acute myocardial infarction in middle-aged Japanese men. *Atherosclerosis* 195:147–152
 25. Grau AJ, Boddy AW, Dukovic DA, Buggle F, Lichy C, Brandt T, Hacke W (2004) Leukocyte count as an independent predictor of recurrent ischemic events. *Stroke* 35:1147–1152
 26. Haught WH, Mansour M, Rothlein R, Kishimoto TK, Mainolfi EA, Hendricks JB, Hendricks C, Mehta JL (1996) Alterations in circulating intercellular adhesion molecule-1 and l-selectin: further evidence for chronic inflammation in ischemic heart disease. *Am Heart J* 132:1–8
 27. Wallenfeldt K, Fagerberg B, Wikstrand J, Hulthe J (2004) Oxidized low-density lipoprotein in plasma is a prognostic marker of subclinical atherosclerosis development in clinically healthy men. *J Int Med* 256:413–420
 28. Stocker R, Kearney JF Jr (2004) Role of oxidative modifications in atherosclerosis. *Physiol Rev* 84:1381–1478
 29. Johnsen SH, Mathiesen EB, Fosse E, Joakimsen O, Stensland-Bugge E, Njolstad I, Arnesen E (2005) Elevated high-density lipoprotein cholesterol levels are protective against plaque progression: a follow-up study of 1952 persons with carotid atherosclerosis the Tromsø study. *Circulation* 112:498–504
 30. Ostling G, Hedblad B, Berglund G, Goncalves I (2007) Increased echolucency of carotid plaques in patients with type 2 diabetes. *Stroke* 38:2074–2078
 31. Yamagami H, Kitagawa K, Nagai Y, Hougaku H, Sakaguchi M, Kuwabara K, Kondo K, Masuyama T, Matsumoto M, Hori M (2004) Higher levels of interleukin-6 are associated with lower echogenicity of carotid artery plaques. *Stroke* 35:677–681

Trans Fatty Acids and Fatty Acid Composition of Mature Breast Milk in Turkish Women and Their Association with Maternal Diet's

Gülhan Samur · Ali Topcu · Semra Turan

Received: 21 May 2008 / Accepted: 26 January 2009 / Published online: 12 March 2009
© AOCS 2009

Abstract The aim of this study was to determine the fatty acid composition and *trans* fatty acid and fatty acid contents of breast milk in Turkish women and to find the effect of breastfeeding mothers' diet on *trans* fatty acid and fatty acid composition. Mature milk samples obtained from 50 Turkish nursing women were analyzed. Total milk lipids extracts were transmethylated and analyzed by using gas liquid chromatography to determine fatty acids contents. A questionnaire was applied to observe eating habits and 3 days dietary records from mothers were obtained. Daily dietary intake of total energy and nutrients were estimated by using nutrient database. The mean total *trans* fatty acids contents was $2.13 \pm 1.03\%$. The major sources of *trans* fatty acids in mothers' diets were margarines-butter (37.0%), bakery products and confectionery (29.6%). Mothers who had high level of *trans* isomers in their milk consumed significantly higher amounts of these products. Saturated fatty acids, polyunsaturated fatty acids and monounsaturated fatty acids of human milk constituted $40.7 \pm 4.7\%$, $26.9 \pm 4.2\%$ and $30.8 \pm 0.6\%$ of the total fatty acids, respectively. The levels of fatty acids in human milk may reflect the current diet of the mother as well as

the diet consumed early in pregnancy. Margarines, bakery products and confectionery are a major source of *trans* fatty acids in maternal diet in Turkey.

Keywords Human milk · Diet · *Trans* fatty acids · Fatty acids

Introduction

Human milk has a 3–5% content of lipids which perform important functions in the breast-fed infants' nutrition. Lipids are the main source of calories in the human milk (approximately 50% of the total caloric value). Milk fatty acids (FAs) are either synthesized in the mammary gland or are derived from plasma FAs that originate from the diet, synthesis in nonmammary tissues, or lipid stores [1]. It is well established that the FA composition of the diet can alter milk FA composition [2]. *Trans* FAs are defined as those that contain at least one double bond in the *trans* configuration. They are formed during the chemical hydrogenation of vegetable oils to manufacture commercial fats or during the microbial biohydrogenation of FAs in the digestive tract of ruminant animals. Humans do not synthesize *trans* isomers of fatty acids therefore their presence in human milk is based on maternal diet. The consumption of *trans* FA-containing foods by lactating women results in the incorporation of *trans* FAs in their milk fat [3–5]. The content of *trans* fatty acids in human milk varies between countries, from 0.5% to 7.2% of total fatty acids [6, 7], because of variations in dietary exposure to *trans* isomers. In recent years, special attention has been given to the potential impairment of essential fatty acids metabolism to their long-chain metabolites by *trans* isomers in humans.

G. Samur (✉)
Department of Nutrition and Dietetics, Hacettepe University,
06100 Sımanpazarı, Ankara, Turkey
e-mail: gsamur@hacettepe.edu.tr

A. Topcu
Department of Food Engineering,
Hacettepe University, Ankara, Turkey

S. Turan
Department of Food Engineering,
Abant İzzet Baysal University, Bolu, Turkey

These long-chain polyunsaturates metabolites are physiologically important as essential membrane components and precursors for synthesis of prostaglandins and other eicosanoids during perinatal and postnatal development [8]. There have been several studies of the *trans* FA content of milk from women [9–21]. Many studies are available in the literature on the content of FAs in the milk of women from many countries, but little is known of the composition of FAs in the milk of Turkish women. Thus, this work was conducted to provide further information on the fatty acid composition of the milk of Turkish women living in Ankara, Turkey. The aim of this study was to determine the content of *trans* FAs and total FAs in mature human milk at 12–16th lactation weeks and to relate these results with the breastfeeding mothers' diet in Turkey.

Materials and Methods

This study involved 50 mothers who were exclusively breastfeeding their term (born at 37–41 weeks gestation) infants. Women having complication of pregnancy or other diseases and mothers of infants with any evidence of metabolic or physical abnormality were not included in the study. Infants who were given bottle feedings of formula or cow's milk were ineligible. Written informed consent was obtained from all participants. All mothers agreed to provide samples of breast milk at 12–16 weeks postpartum. No personal dietary instructions were given to any of the mothers and all women were consuming self-selected diets. Food and nutrient intake were estimated using 3 days dietary recall at 12–16 weeks of lactation. Each participant was informed and trained on how to carefully record all foods consumed, their quantity in grams or in household measures, and their brands. The 3 days food records were analyzed to determine the average daily intake of food products and total energy, protein, carbohydrates, fat and FAs for each individual by using a computer program including total nutrient contents of specific brand name food products and typical dishes in Turkey (BEBIS 11.3) [22]. Breastfeeding mothers' daily dietary intake of *trans* FAs was estimated on the basis of 3 days recall and *trans* fatty acid levels in food products were calculated by BEBIS and USDA nutrient database [22].

Samples (5–10 mL) of mature milk between 12–16th weeks of lactation were collected by manual expression from each mother into sterile polypropylene tubes, always after the first morning nourishing of the baby. Samples were immediately kept frozen in sterile plastic tubes and stored at -70°C until analysis. Analyses were performed within 3 months of collection.

Methods

Fatty Acid Analyses

Milk samples were defrosted at room temperature and tempered in a vortex mixer before analysis. Lipids were extracted using the method described by Bligh and Dyer [23] with some modifications. A 3-mL milk sample was mixed with 10 mL methanol, 5 mL chloroform and 1.30 mL of water (methanol:chloroform:water 2:1:0.8, v/v). The mixture was agitated for 30 min, followed by addition of 5 mL chloroform and 5 mL of 2% anhydrous sodium sulfate solution. The final mixture had a final proportion of 2:2:1.8 (methanol: chloroform:water). The mixture was agitated for 15 min and centrifuged at 2250g for 30 min. The lower phase was filtered through a filter paper containing about 2 g of anhydrous sodium sulfate. Chloroform (10 mL) was added to the remaining phase, and centrifuged under the same conditions. Extracts were pooled and solvent was evaporated under gentle nitrogen stream.

The preparation of the fatty acid methyl esters (FAMES) was conducted by the method described by Ledoux et al. [24]. One milliliter hexane solution (about 20 mg lipids) was transferred into a centrifuge tube and 0.5 mL internal standard (heptadecanoic acid methyl esters, 0.4 mg/mL (Sigma, ST Louis, MO) was added. The solvent was evaporated under nitrogen. Lipids were dissolved with 1 mL toluene, and esterified using 100 μL 2 N sodium methoxide (Merck, Darmstadt, Germany) for 20 min at room temperature. Then, 0.5 mL 14% boron trifluoride/methanol (Merck, Darmstadt, Germany) was added and allowed to react for 20 min at room temperature (ca. 20°C). FAMES were then extracted 2 times using 2 mL hexane in the presence of 5 mL sodium bicarbonate (Merck, Darmstadt, Germany). The FAMES were analyzed by gas liquid chromatography using a HP 5890 series II gas chromatograph (GC) (Hewlett Packard Company, Wilmington, DE) equipped with a flame ionization detector (FID) and an HP 7673A automatic injector (Agilent Technologies, Palo Alto, CA). Separations were performed on a DB 23 capillary column (60 m \times 0.25 mm i.d., 0.25 μm film thickness; J&W Scientific, Folsom, CA). The oven temperature was programmed from 140°C for 5 min, thereafter 3°C per minute up to 220°C , and maintained at this temperature for 20 min. Injector and detector temperatures were 250 and 260°C , respectively. Nitrogen was used as a carrier gas and the flow rate was 1 mL/min. The split ratio was 1/65. Peak identification was verified by comparison with reference standard mixes (37 component FAME mix, grain fatty acid methyl ester mix Supelco, Bellefonte, PA; linoleic acid methyl ester cis/trans isomers, linolenic acid methyl ester isomer mix standard, Sigma,

ST Louis, MO). Results were expressed as a percentage (% wt/wt) of all fatty acids detected with a chain length between 8 and 22 carbon atoms. Fatty acid analysis was performed in triplicate for single samples of each human milk samples and average values were reported.

Statistical Analysis

All data were analyzed by using Statistical Packages for Social Sciences (SPSS 13.0). Results were expressed as mean \pm SD. Correlations between the percentage by weight of each FA, total *trans* FAs, groups of similar FAs, and milk fat concentration were examined by using Pearson correlation coefficients. Analysis of variance was used to ascertain the relations between total *trans* and FA percentages. Relations were declared significant at $p < 0.05$.

Results

Physical Characteristics

The physical characteristics of lactating Turkish women are given in Table 1. The study was conducted in a moderate socio-economic status region in the city of Ankara in Turkey. Fifty lactating women meeting the criteria were selected, aged between 17–39 years old (mean \pm SD 26.16 ± 5.49 years). The mean body mass index (BMI) of the lactating women was 25.48 ± 4.61 kg/m². Age of marriage was 20.48 ± 3.89 years old. Age at first pregnancy was found to be low (21.44 ± 3.82 years). All of the subjects had only primary school education with an average attendance of 6.0 ± 1.9 years.

Fatty Acid Concentrations

The fatty acid distributions in Turkish mature breast milk are listed in the Table 2. The main fatty acids in the breast milk samples were oleic (18:1*c*; 27.3%), palmitic (16:0;

20.9%) and linoleic (18:2*n*-6; 24.3%) acids representing about 72.5% of the total FAs in the investigating stages (12–16th week) of lactation. The major FA groups and the total fat content (Table 3) were the saturated fatty acids (SFAs) (40.7%), of which 51.4% was palmitic acid, the monounsaturated fatty acids (MUFAs) (30.8%) of which 88.6% was oleic acid and the polyunsaturated fatty acids (PUFAs) (26.9%) of which 90.3% was linoleic acid. The mean total *trans* FA concentration was $2.13 \pm 1.03\%$ (min-max range 0.4–5.0%). As expected, *trans* isomeric octadecanoic acids (*trans*-18:1) made up the main *trans* isomer group in mature milk ($1.96 \pm 1.03\%$).

Trans fatty acids were found in all human milk samples but levels of *trans* isomers varied between mother. The mean value of *trans* isomers of octadecadienoic acid (18:2*t*) in mature milk was 0.15 ± 0.06 , whereas hexadecanoic acid (16:1*t*) *trans* isomers thereof were detected in very low concentrations and they were not present in all milk samples of mature milk at the investigated stage of lactation (Table 2).

On the basis of the wide variation in the total *trans* FA concentrations of these milk samples, the samples were grouped into 3 categories to evaluate the differences between the groups: high (samples containing $\geq 4\%$ total *trans* FAs; $n = 3$), medium (samples containing between 2–4% total *trans* FAs; $n = 20$), and low (samples containing $\leq 2\%$ total *trans* FAs; $n = 27$) *trans* FAs (Table 4). For simplicity, only data for major individual FAs and FA groups are shown. For stearic and linoleic acid concentrations, there were no significant differences between groups. Total SFA and PUFA concentrations were not significantly different between the groups; however MUFA concentrations were higher in the high *trans* FA group than in the low *trans* FA group ($p < 0.05$).

Maternal diet composition and major FAs profiles are listed in Table 5. Carbohydrates accounted for the 50.7%, protein for the 14.8% and lipids for the 34.5% of the total dietary energy intake. In the lipidic fraction, SFAs, MUFAs and PUFAs represent the 31.6%, 43.4% and 18.0% of the total dietary energy intake, respectively. The estimated daily intake of *trans* fatty acids was 2.16 ± 2.01 (min-max range 0.22–7.65) g/day in, representing 1.12 ± 1.09 (min-max range 0.06–4.75)% of the daily total energy intake and 3.16 ± 3.10 (min-max range 0.14–13.11)% of total fat (Table 5). The major sources of *trans* fatty acids in mothers' diets were margarines-butter (37.02%), bakery products such as cakes, cookies, pies, biscuits and muffins, confectionery, snack foods (29.62%) and breads (13.42%). Mothers who had high level of *trans* isomers in their milk consumed significantly higher amounts of these products (Table 6). However, the correlation between the human milk and maternal diet fatty acids was found statistically insignificant.

Table 1 Physical characteristics of the mothers ($n = 50$)

Physical characteristics	Mean \pm SD
Mother's age (y)	26.16 ± 5.49
Mother's height (cm)	1.56 ± 0.04
Weight (kg)	61.68 ± 10.91
Body mass index (kg/m ²)	25.48 ± 4.61
Age at first pregnancy (y)	21.44 ± 3.82
Age of marriage (y)	20.48 ± 3.89
Number of surviving children	1.66 ± 0.85
Number of pregnancies	1.86 ± 1.07

Table 2 Concentration of major fatty acids (FAs) in human milk samples

Fatty acids	% by wt of total FAs
Saturated fatty acids (SFAs)	
C 8:0	0.07 ± 0.05
C 10:0	1.02 ± 0.30
C 12:0	5.90 ± 1.71
C 14:0	6.46 ± 1.96
Total medium chain saturated fatty acids (MCSFAs)	13.45 ± 3.68
C 15:0	0.28 ± 0.09
C 16:0	20.90 ± 3.14
C 17:0	0.18 ± 0.13
C 18:0	5.66 ± 0.92
C 20:0	0.23 ± 0.10
C 22:0	TR
C 24:0	TR
Total long chain saturated fatty acids (LCSFAs)	27.25 ± 3.8
Total saturated fatty acids (SFAs)	40.7 ± 4.68
Monounsaturated fatty acids (MUFAs)	
C 14:1	0.14 ± 0.06
C 15:1	0.11 ± 0.10
C 16:1	1.51 ± 0.45
C 17:1	TR
C18:1 <i>trans</i>	1.96 ± 1.03
C18:1 <i>c9</i>	27.31 ± 2.86
C18:1 <i>c11</i>	1.22 ± 0.21
C 20:1	0.27 ± 0.05
C 22:1	TR
Total MUFAs	30.76 ± 0.59
Total <i>trans</i> fatty acids	2.13 ± 1.03
n-6 Polyunsaturated fatty acids (n-6 PUFAs)	
C 18:2 <i>trans</i>	0.15 ± 0.06
C18:2	24.31 ± 4.20
C18:3 <i>gamma</i>	0.18 ± 0.10
C 20:2	0.44 ± 0.09
C 20:3	0.44 ± 0.10
C 20:4	0.46 ± 0.16
C 22:2	TR
Total n-6 PUFAs	25.98 ± 0.79
Total long chain n-6 PUFAs (n-6 LCPUFAs)	1.34 ± 0.27
n-3 Polyunsaturated fatty acids (n-3 PUFAs)	
C18:3 <i>alpha</i>	0.59 ± 0.21
C18:4	0.23 ± 0.07
C20:5 (EPA)	TR
C22:6 (DHA)	0.15 ± 0.05
Total n-3 PUFAs	0.82 ± 0.14
Total long chain n-3 PUFAs (n-3 LCPUFAs)	0.15 ± 0.05

Table 2 continued

Fatty acids	% by wt of total FAs
Total PUFAs	26.89 ± 4.16

All values are means ± SD; *n* = 50

TR trace, EPA eicosapentaenoic acid, DHA docosahexaenoic acid

Table 3 Summary of selected fatty acids (FAs) and total fat of human milk

Fatty acids	% by wt of total FAs
Saturated fatty acids (SFAs)	40.70 ± 4.68
Monounsaturated fatty acids (MUFAs)	30.76 ± 0.59
Total <i>trans</i> fatty acids	2.13 ± 1.03
Total <i>trans</i> 18:1 isomers (18:1 <i>t</i>)	1.96 ± 1.03
Polyunsaturated fatty acids (PUFAs)	26.89 ± 4.16
n-6 PUFA	25.98 ± 0.79
n-3 PUFA	0.82 ± 0.14
PUFA/SFA	0.67 ± 0.17
PUFA/MUFA	0.89 ± 0.16
MUFA/SFA	0.75 ± 0.14
n-6/n-3	32.08 ± 8.46
Milk fat percentage	4.19 ± 1.95

All values are means ± SD; *n* = 50

Discussion

Fatty acids, an important component of milk, appear in milk as a result of dietary intake, mobilization from fat depots, and endogenous synthesis by the mammary gland [1]. FA composition of human milk responds rapidly and markedly to diet and is dependent on the amount and type of fat consumed, stage of lactation, and term or preterm milk and carbohydrate intakes, and also shows variance cross-culturally [2, 3]. The concentration of major FAs of Turkish lactating women milk (Table 2) with few exceptions were found differ from that of women consuming western diets in Europe and America. In this study, the SFA contents of mature milk (40.7% total FAs, Table 3) were very close to recent reviews on FA composition of human milk [7, 9, 18, 19]. Lactating women from Asian (Malay, India, Nepal) and Saudi Arabia showed higher SFA contents in milk lipid (51.7%, 50.5%, 65.8% and 56.2%, respectively) [9, 25, 26], whereas Chinese [9, 12], Canadian [7], Brazil [27], Western Iran [28] and European [29] lactating women showed similar values to those found in this study (38.5–44.9%). Percentages of medium-chain saturated FAs (C 8:0–C 14:0, MCSFAs) found in the milk of Turkish women (13.5%, Table 2) were within the range

Table 4 Comparison of composition of major fatty acids (FAs) and FA groups in human milk with different contents of *trans* FAs

Fatty acids	Total <i>trans</i> fatty acid content of human milk		
	0–2% (<i>n</i> = 27)	2–4% (<i>n</i> = 20)	≥4% (<i>n</i> = 3)
<i>% by wt of total FAs</i>			
16:0	21.06 ± 3.23	20.48 ± 3.14	22.20 ± 2.80
18:0	5.81 ± 0.98	5.37 ± 0.79	6.18 ± 0.63
18:1 <i>c</i>	27.17 ± 3.33	27.34 ± 2.35	28.27 ± 1.07
18:2 n-6	23.96 ± 4.67	25.24 ± 3.55	21.24 ± 2.06
18:3 n-3	0.58 ± 0.20	0.58 ± 0.23	0.62 ± 0.02
18:1 <i>t</i>	1.26 ± 0.49 ^a	2.51 ± 0.52 ^{ab}	4.58 ± 0.19 ^b
Total <i>trans</i> fatty acids	1.37 ± 0.51 ^a	2.68 ± 0.52 ^{ab}	4.76 ± 0.19 ^b
SFAs	40.20 ± 4.49	40.61 ± 5.10	40.37 ± 4.34
MUFAs	30.94 ± 3.74 ^b	29.55 ± 1.85 ^{ab}	31.64 ± 1.47 ^a
PUFAs	26.66 ± 4.67	27.70 ± 3.51	23.99 ± 1.99
Milk fat%	4.36 ± 2.11	4.19 ± 1.81	4.71 ± 0.96

All values are means ± SD. *c*, *cis* double bond; *t*, *trans* double bond; 18:1*t*, total *trans* 18:1 isomers; SFAs, total saturated FAs; MUFAs, total monounsaturated FAs; PUFAs, total polyunsaturated FAs. Means in the same row with different superscripts letters are significantly different, *p* < 0.05

of values found for other populations (range 12.7–42.5%) [25–31]. These FAs can either be synthesized *de novo* in mammary tissue or other maternal organs (primarily medium- and intermediate-chain fatty acids) or be derived from the mother's diet [18, 32–34]. The higher values of MCSFAs found in other studies were related to higher intakes of carbohydrates by the lactating women. Carbohydrate appears to favor the increased synthesis of MCSFAs by the mammary gland [33]. Van Beusekom et al. [34] found higher *de novo* FA synthesis in Dominican women, who had a diet richer in carbohydrates (70%) than in Belize women (55%). Similarly, Rocquelin et al. [31] and Kneebone et al. [9] observed human milk lipid in Congolese, Indian and Malay women populations, and they established the content of MCSFAs as to be 26.0% and 18.6% and 19.8% for those populations, respectively.

Bahrami et al. [28] reported that the milk of Iranian lactating women whose diet was mainly derived from low animal protein and high carbohydrates, showed MCSFAs contents of approximately 24%. The other study of Turkish lactating women who had a rich diet in carbohydrates (60–65%) [35] reported total SFA and MCSFA contents to be approximately 52.4%, and 28.4% respectively. In the present study, the content of MCSFAs was low (13.5%), probably depending on low carbohydrate intake (50.7%, Table 5).

Long-chain saturated fatty acids (LCSFAs, C15:0–24:0) contents were 27.3% (Table 2). These fatty acids are

Table 5 Daily energy and nutrient intakes of mothers (*n* = 50)

Nutrients	Mean ± SD
Energy (kcal)	1938.82 ± 555.30
Total protein (g)	70.94 ± 31.61
Percentage of energy (%)	14.84 ± 4.56
Animal protein (%)	49.64 ± 16.68
Plant protein (%)	50.36 ± 16.68
Total fat (g)	74.13 ± 26.49
Percentage of energy (%)	34.50 ± 7.57
Polyunsaturated fatty acids (PUFAs) (g)	13.86 ± 10.37
PUFA (% of fat)	18.05 ± 9.5
C18:2 n-6 (g)	10.68 ± 10.10
C18:3 n-3 (g)	1.19 ± 0.16
C18:2/C18:3	8.70 ± 6.86
C18:2 (% energy intake)	4.54 ± 3.26
C18:3 (% energy intake)	0.55 ± 0.18
Monounsaturated fatty acids (MUFAs) (g)	31.95 ± 12.54
MUFA (% of fat)	43.44 ± 8.66
Saturated fatty acids (SFA) (g)	23.30 ± 9.24
SFA (% of fat)	31.61 ± 6.25
PUFAs/SFAs	0.63 ± 0.48
MUFAs/SFAs	1.43 ± 0.43
Total <i>trans</i> fatty acids (TrFAs)(g)	2.16 ± 2.01
Percentage of total fat TrFAs (%)	3.16 ± 3.10
Percentage of energy TrFAs (%)	1.12 ± 1.09
Carbohydrate (g)	241.27 ± 85.88
Percentage of energy (%)	50.70 ± 8.39

derived especially from diet and their sources may be oils or fat used in food preparation, animal fat and proteins. Some reports have shown that LCSFA values of approximately 28–30% in the milk of lactating women whose diet was mainly derived from animal fat and proteins [1, 9, 33–36]. In this study, it has been found that the main source of LCSFAs was oils or fat used in food preparation (margarine, butter etc.) and animal protein for the lactating women (49.6% of total protein, Table 5).

In this study, MUFAs represented 30.8% of the total FAs in the milk lipid of the lactating women. The major fraction was formed by *cis* monoenoic FAs, for the most part represented by C18:1. Oleic acid, which is considered an important source of energy for the breast-fed infant, was the highest in human milk. Although monoenoic FAs are nonessential and can be synthesized by human, their dietary intake may have physiologic effects by influencing membrane fluidity and cholesterol metabolism [1, 10, 18]. Our mean 18:1*c* value (27.3%) is in the range of 25–38% reported for 18:1 in some recent studies [18–21, 27, 28, 37]. In relation to the lactating women's eating habits, the main source of these FAs was probably vegetable oils

Table 6 Major sources of the *trans* fatty acids in the diet of breastfeeding women in Turkey

	Grams per day		%
	18:1 <i>t</i>	T <i>t</i> FA	T <i>t</i> FA
Dairy products	0.10 ± 0.08	0.14 ± 0.11	6.48
Red meat	0.06 ± 0.02	0.14 ± 0.08	6.48
Poultry, chicken, broiler	0.10 ± 0.21	0.13 ± 0.09	6.01
Sausages, salami, giblets	0.05 ± 0.19	0.05 ± 0.01	2.31
Breads	0.23 ± 0.10	0.29 ± 0.13	13.42
Bakery products, confectionery, fried foods	0.41 ± 0.16	0.64 ± 0.16	29.62
Margarines	0.62 ± 0.27	0.64 ± 0.31	29.62
Butter	0.15 ± 0.04	0.16 ± 0.07	7.40
Total	1.77 ± 1.67	2.16 ± 2.01	100.00

All values are mean ± SD; *n* = 50

T*t*FA Total *trans* fatty acids

(soybean oil, olive oil) which contributed to their final content.

In the present study *trans* FAs accounted for 2.1% (min-max range 0.39–4.97). The major proportion of all of the *trans* isomers was contributed by 18:1*t* (1.96%), reflecting the composition of the maternal diet. The *trans* FA content in human milk depends mainly on the mother's recent dietary intake, most of which is derived from hydrogenated vegetable oils in margarines, shortenings, and processed foods [1, 3, 38].

The contribution of *trans* isomeric FAs to the FA composition of human milk in Turkey was found to be around 2% of the total FA content. This value is in good agreement with reports on mean percentage contributions of *trans* FAs to the FA composition of human milk in Europe [3, 10, 19, 20, 33, 39–41]. The mean values of *trans* FAs in mature milk reported for Poland (2.7%), Italy (Rome) (2.7%), Czech Republic (2.1%), France (2%) and Germany (2.4%) were all close to the value seen in our study. In contrast, considerably higher human milk *trans* FA values were reported for North America (Canada: 7.2%, USA: 7.0%) than for most European countries and the current study [42, 43]. The differences in total *trans* FAs in different countries may be partially attributed to differences in the diets consumed by the women in these various areas of the world. The consumption of foods that contain greater concentrations of *trans* FAs, such as processed foods made with partially hydrogenated vegetable oils and animal fat leads to greater intakes of total *trans* FAs, which are incorporated into milk fat [3, 38].

Our analysis of 3-day diet records estimated a mean *trans* FA intake of 2.16 g/day (min-max range 0.22–7.65 g/day), representing 1.12 (min-max range 0.06–4.75)% of energy intake and 3.16 (min-max range 0.14–13.11)% of total fat intake. The mean percentage of *trans* FAs in milk (2.13%) was similar to that calculated for the diet,

suggesting the estimated value of 2.16 g/day *trans* FAs is a reasonable estimation of the *trans* FA intake of the women in this study. The major sources of *trans* FAs in mothers' diets were margarines-butter (37.0%), bakery products (such as cakes, cookies, pies, and muffins), confectionery, snack foods, fried foods (29.62%) and breads (13.42%). Mothers who had a high level of *trans* isomers in their milk consumed significantly higher amounts of these products.

Numerous studies have shown that human milk FAs, particularly monounsaturated, n-6, n-3 and *trans* FAs, and their ratio change depending on maternal diet [19–21]. Concerns about dietary fat and health or lifestyle issues that alter maternal food choices may therefore influence the FA nutrition quality of breast-fed infants. It is particularly important to note that our results identified baked and prepared foods and breads as major sources of *trans* FAs providing <50% of the total *trans* FA intake. However, the relationship between intake dietary *trans* FAs and the *trans* FA level in mature breast milk was found to be statistically insignificant. Other factors may influence an increase in levels of *trans* FAs in milk. Besides dietary factors, maternal weight loss during lactation was also suggested as causing an increase of *trans* FAs in milk [3, 4, 13, 14, 38]. Numerous studies have shown that weight loss during lactation was an additional cause of the increase in *trans* FA concentrations in human milk [3, 4, 14]. In some studies, *trans* FAs have been shown to alter the incorporation of essential long-chain PUFAs into milk fat [7, 21, 38]. Larque et al. [38] showed that rats receiving dietary *trans* FAs had higher concentrations of linoleic acid in milk fat, but total long-chain PUFAs did not differ significantly. In contrast, other researchers [7, 21] found an inverse relation between essential all-*cis* n-6 and n-3 FAs and total *trans* FAs in human milk. However, in the current study, no correlation between total *trans* FAs or total 18:1*t* and linoleic, linolenic, total n-3, or total n-6 FAs in mature milk was detected (data not shown).

In this study, the total PUFA contents of mature milk were 26.9% (min-max range 16.1–38.9%) of total milk FAs (Table 2, 3). The levels of PUFA for the Turkish lactating women were higher than those found for the North American and European populations (10.0–16.6%) [18, 19, 28, 32, 44]. The essential fatty acid, linoleic (C18:2n-6), had a value of 24.3%. Linoleic acid contents in Turkish women milk lipid were higher (14.35–36.91%) than the range reported from different world locations (8.7–14.1%) [18, 19, 26–28, 32, 44, 45]. Dietary intake of 18:2 influences the content of this FA in milk [39]. Therefore, it seemed likely that the high percentage of 18:2 in the milk of Turkish women was a result of high dietary intakes of 18:2. Most of the women in our study group (95%) were consuming sunflower-based margarines and sunflower oil and also consumed olive oil.

The influence of maternal dietary fatty acids on the fatty acid composition of milk may be attributed to the great variation in the contents of linoleic (C18:2n-6), α -linolenic (C18:3n-3) acids. These changes are due to the consumption of polyunsaturated oils. For example, an increase in polyunsaturated oil consumption may lead to an increase in the content of PUFAs in the mother's milk [39]. Our results showed that there are relation between maternal PUFA intake and the content of PUFA in human milk. Mothers who had high level of n-6 PUFAs in their milk consumed significantly higher amounts of n-6 PUFA (Table 5). In this study, it was observed that the majority of the lactating women of Turkey used vegetable oils, especially sunflower oil as eating habit in their daily diets.

The essential FA, α -linolenic (C18:3n-3), presented a content of 0.59% (min-max range 0.26–1.29). It could be said that the α -linolenic acid level found in the milk of Turkish lactating women in this study was rather similar if range values reported for the world population (min-max range 0.10–1.4%) are considered [9, 19, 25, 26, 33]. The increased consumption of C18:2n-6 in Western societies would be capable of increasing the C18:2n-6/C18:3n-3 ratio in human milk. In USA the high level of C18:2n-6 in human milk also associated with an C18:3n-3 level often superior %1 of total FAs, so that the n-6/n-3 ratio generally never passes 16 [36]. In Turkey, it is quite different because C18:3n-3 only represents 0.59% of FAs in human milk. Thus, the C18:2n-6/C18:3n-3 ratio exceeds 20. A ratio superior to 20 in human milk has been recently observed by Scopesi et al. [44]. These observations suggest that different C18:3n-3 intakes are probably due to maternal dietary habits.

Total LCPUFAs showed a content of 1.49% in the milk lipids of Turkish lactating women (Table 2). In the present study, small proportions of n-6 LCPUFA (1.34%, min-max range 0.81–1.96%) were identified in the milk of the lactating women. The levels found for arachidonic acid (AA),

C20:4, (0.46%, min-max range 0.2–0.86%) were similar to those found in the milk lipids of women in France [36] (0.41–0.50%), Germany [18] (0.35%) and the USA [20] (0.47%). Koletzko [18] and Kneebone [9] demonstrated the lack of a correlation between linoleic (18:2n-6) and arachidonic acids (20:4n-6) in human milk and we did not find any correlation between both linoleic and α -linolenic acids and their respective LCPUFA metabolites either. Thus, the LCPUFA content of human milk appears not to be closely related to the maternal intake. This finding suggests inter-individual differences in the capacity of the desaturation/chain-elongation pathway and of the incorporation process of the LCPUFA metabolites into milk lipids. Among the n-3 LCPUFA, the main FA identified was docosahexaenoic acid (C22:6n-3) (0.15%, Table 2). The DHA (docosahexaenoic acid) was given with mean values of 0.45% for Western and 0.88% for Eastern women, and DHA value of 0.20–0.30% was accepted as a representative range [33, 39]. The amounts found in human milk corresponded to the amounts of DHA in foods, especially fish, in the diet of the lactating women [39]. In this study, DHA content was lower than the value recommended as representative. Because, Turkish lactating women do not habitually of consume fish frequently, the results found were probably due to the C18:3n-3 elongation–desaturation mechanisms.

In conclusion, this study showed that the milk of the women from Ankara, Turkey had a high content of linoleic acid and a low content of α -linolenic acid, confirming their frequent habit of consuming diets rich in polyunsaturated oils. Besides, low *trans* FAs contents were verified compared to populations from different localities. Thus, it is suggested that diet is an important factor that may influence and provide the differences observed in the compositions of FAs of populations from several regions worldwide. Although the negative effect of human milk *trans* FAs on breast-fed infants is not yet well documented, we suggest that infants ingest levels of *trans* FAs that reflect the current diets of breastfeeding mothers. In our study we identified margarines, butter, bakery products, and confectionery as the main sources of *trans* FAs in the maternal diet in Turkey and we conclude that breastfeeding mothers should avoid these products in their diet. However there is limited knowledge about *trans* FA levels in processed foods available in Turkey. Further studies are needed to improve the national nutrient database. In addition, more regional information is needed to fully describe the variation in the concentrations of *trans* FAs and FAs in human milk samples throughout the Turkey. The effect of *trans* FAs, PUFAs and LCPUFAs on human health is an important area of research. Identifying the concentrations of FAs in human milk fat will aid in identifying possible relations between *trans* FAs or FAs and infant growth or health.

References

- Jensen RG, Bitman J, Carlson SE, Couch SC, Hamosh M, Newburg DS (1995) Milk lipids A. Human milk lipids. In: Jensen RG (ed) Handbook of milk composition. Academic Press, San Diego, pp 495–575
- Neville MC, Picciano MF (1997) Regulation of milk lipid secretion and composition. *Annu Rev Nutr* 17:159–184
- Desci T (2003) Nutrition relevance of *trans* isomeric fatty acids in human milk. *Acta Paediatr* 92:1369–1371
- Chappell JE, Clandinin MT, Kearney-Volpe C (1985) *Trans* fatty acids in human milk lipids: influence of maternal diet and weight loss. *Am J Clin Nutr* 42:49–56
- Craig-Schmidt MC, Weete JD, Faircloth SA, Wickwire MA, Livant EJ (1984) The effect 390 of hydrogenated fat in the diet of nursing mothers on lipid composition and prostaglandin content of human milk. *Am J Clin Nutr* 39:778–786
- Craig-Schmidt MC (2006) Worldwide consumption of *trans* fatty acids. *Atheroscler Suppl* 7:1–4
- Chen Z-Y, Pelletier G, Hollywood R, Ratnayake WMN (1995) *Trans* fatty acid isomers in Canadian human milk. *Lipids* 30:15–21
- Decsi T, Burus I, Molnar S, Minda H, Veitl V (2001) Inverse association between *trans* isomeric and long-chain polyunsaturated fatty acids in cord blood lipids of full-term infants. *Am J Clin Nutr* 74:364–368
- Kneebone GM, Kneebone R, Gibson RA (1985) Fatty acid composition of breast milk from three racial groups from Penang, Malaysia. *Am J Clin Nutr* 41:765–769
- Precht D, Molkentin J (1999) C18:1, C18:2 and C18:3 *trans* and *cis* fatty acid isomers including conjugated *cis* 9, *trans* 11 linoleic acid (CLA) as well as total fat composition of German human milk lipids. *Nahrung* 43:233–244
- Koletzko B, Thiel I, Abiodun PO (1991) Fatty acid composition of mature human milk in Nigeria. *Z Ernahrungswiss* 30:289–297
- Chen ZY, Kwan KY, Tong KK, Ratnayake WM, Li HQ, Leung SS (1997) Breast milk fatty acid composition: a comparative study between Hong Kong and Chongqing Chinese. *Lipids* 32:1061–1067
- Dlouhy P, Tvrzická E, Stanková B, Buchčíková M, Pokorný R, Wiererová O, Bílková D, Rambousková J, Anđel M (2002) *Trans* fatty acids in subcutaneous fat of pregnant women and in human milk in the Czech Republic. *Ann NY Acad Sci* 967:544–547
- Aitchison JM, Dunkley WL, Canolty NL, Smith LM (1977) Influence of diet on *trans* fatty acids in human milk. *Am J Clin Nutr* 30:2006–2015
- Picciano MF, Perkins EG (1977) Identification of the *trans* isomers of octadecenoic acid in human milk. *Lipids* 12:407–408
- Clark RM, Ferris AM, Fey N, Hundrieser KE, Jensen RG (1980) The identity of the cholesteryl esters in human milk. *Lipids* 15:972–974
- Hundrieser KE, Clark RM, Brown PB (1983) Distribution of *trans* octadecenoic acid in the major glycerolipids of human milk. *J Pediatr Gastroenterol Nutr* 2:635–639
- Koletzko B, Mroczek M, Bremer HJ (1988) Fatty acid composition of mature human milk in Germany. *Am J Clin Nutr* 47:954–959
- Mojska H, Socha P, Socha J, Soplín'ska E, Jaroszewska-Balicka W, Szponar L (2003) *Trans* fatty acids in human milk in Poland and their association with breastfeeding mothers' diets. *Acta Paediatr* 98:1381–1387
- Mosley E, Wright L, McGuire MK, McGuire A (2005) *Trans* fatty acids in milk produced by women in the United States. *Am J Clin Nutr* 82:1292–1297
- Innis SM, King DJ (1999) *Trans* fatty acids in human milk are inversely associated with concentrations of essential all-*cis* n-6 and n-3 fatty acids and determine *trans*, but not n-6 and n-3, fatty acids in plasma lipids of breast-fed infants. *Am J Clin Nutr* 70:383–390
- BEBIS (2005) EbiSpro for Windows, Stuttgart, Germany; Turkish version BeBiS; Data Bases: Bundeslebensmittelschlüssel, 11.3 and other sources
- Bligh EG, Dyer JW (1959) A rapid method of total lipid extraction and purification. *Can J Biochem Physiol* 37:911–917
- Ledoux M, Chardigny J-M, Darbois M, Soustre Y, Sebedio J-L, Laloux L (2005) Fatty acid composition of French butters, with special emphasis on conjugated linoleic acid isomers. *J Food Comp Anal* 18:409–425
- Schmeits BL, Cook JA, Vanderjagt DJ, Magnussen MA, Bhatt SK, Bobik EG (1999) Fatty acid composition of the milk lipids of women in Nepal. *Nutr Res* 19:1339–1348
- Al-Othman AA, El-Fawaz HA, Hewdy FM, Abdullah NM (1996) Fatty acid composition of mature breast milk of Saudi lactating mothers. *Food Chem* 57:211–215
- Cunha J, Macedo da Costa TH, Ito MK (2005) Influences of maternal dietary intake and suckling on breast milk lipid and fatty acid composition in low-income women from Brasilia, Brazil. *Early Hum Dev* 81:303–311
- Bahrami G, Rahimi Z (2005) Fatty acid composition of human milk in Western Iran. *Eur J Clin Nutr* 59:494–497
- Koletzko B, Bremer HJ (1989) Fat content and fatty acid composition of infant formulas. *Acta Paediatr Scand* 78:513–521
- Knox E, Vanderjagt DJ, Shatima D, Huang YS, Chuang LT, Glew RH (2000) Nutritional status and intermediate chain-length fatty acids influence the conservation of essential fatty acids in the milk of northern Nigerian women. *Prostaglandins Leukot Essent Fatty Acids* 63:195–202
- Rocquelin G, Tapsoba S, Dop MC, Mbemba F, Traissac P, Martin-Prével Y (1998) Lipid content and essential fatty acid (EFA) composition of mature Congolese breast milk are influenced by mothers' nutritional status: impact on infants EFA supply. *Eur J Clin Nutr* 52:164–171
- De La Presa-Owens S, López-Sabater MC, Rivero-Urgell M (1996) Fatty acid composition of human milk in Spain. *J Pediatr Gastroenterol Nutr* 22:180–185
- Silva MHL, Silva MTC, Brandao SCC, Gomes JC, Peternelli LA, Franceschini SCC (2005) Fatty acid composition of mature breast milk in Brazilian women. *Food Chem* 93:297–303
- Van Beusekom CM, Martini IA, Rutgers HM, Boersma ER, Muskiet FAJ (1990) A carbohydrate-rich diet not only leads to incorporation of medium-chain fatty acids (6:0–14:0) in milk triglycerides but also in each milk-phospholipid subclass. *Am J Clin Nutr* 52:326–334
- Samur Eroglu G, Aksoy M, Kilic Z (1997) The effect of maternal dietary fatty acids intakes on the fatty acids composition of colostrum and mature milk as well as serum in Turkish Women. 16th International Congress of Nutrition, July 27–August 1, Montreal, Canada, p 85
- Guesnet P, Antonine JM, Lempdes A, Galent A, Durand G (1993) Polyunsaturated fatty acids composition of human milk in France: changes during the course of lactation and regional differences. *Eur J Clin Nutr* 47:700–710
- Vanderjagt DJ, Arndt CD, Okolo SN, Huang YS, Chuang LT, Glew RH (2000) Fatty acid composition of the milk lipids of Fulani women and the serum phospholipids of their exclusively breast fed infants. *Early Hum Dev* 60:73–87
- Larque E, Zamora S, Gil A (2001) Dietary *trans* fatty acids in early life: a review. *Early Hum Dev* 65 Suppl:31–41
- Jensen RG (1999) Lipids in human milk. *Lipids* 34:1243–1271
- Marhol P, Dlouhý P, Rambousková J, Pokorný R, Wiererová O, Hrnčířová D, Procházková B, Anđel M (2007) Higher content of C18:1 *trans* fatty acids in early human milk fat of Roma breast-feeding women. *Ann Nutr Metab* 51:461–467

41. Boatella J, Rafecas M, Codony R, Gibert A, Rivero M, Tormo R, Infante D, Sanchez-Valverde F (1993) *Trans* fatty acid content of human milk in Spain. *J Pediatr Gastroenterol Nutr* 16:432–434
42. Friesen R, Innis SM (2006) *Trans* fatty acids in human milk in Canada declined with the introduction of trans fat food labeling. *J Nutr* 136:2558–2561
43. Szabó E, Boehm G, Beermann C, Weyermann M, Brenner H, Rothenbacher D, Decsi T (2007) *Trans* octadecenoic acid and *trans* octadecadienoic acid are inversely related to long-chain polyunsaturates in human milk: results of a large birth cohort study. *Am J Clin Nutr* 85:1320–1326
44. Scopesi F, Ciangherotti S, Lantieri PB, Risso D, Bertini I, Compone F, Pedrotti A, Bonacci W, Serra G (2001) Maternal dietary PUFAs intake and human milk content relationships during the first month of lactation. *Clin Nutr* 20:393–397
45. Chardigny JM, Wolff RL, Mager E, Sebedio JL, Martine L, Juenada P (1995) *Trans* mono and polyunsaturated fatty acids in human milk. *Eur J Clin Nutr* 49:523–531

Plasma LCAT Activity and Lipid Subfraction Composition in Obese Beagles Undergoing Weight Loss

Rebecca Angell · Yuka Mitsuhashi ·
Karen Bigley · John E. Bauer

Received: 13 August 2008 / Accepted: 7 February 2009 / Published online: 3 March 2009
© AOCs 2009

Abstract The relationship between lecithin:cholesterol acyltransferase (LCAT) activity and weight loss in dogs was investigated. Four experimental weight-loss diets were fed to 12 obese female beagles for 56 days in a partial crossover design ($n = 6$). High- (HGI) or low- (LGI) glycemic index starch and diacylglycerol or triacylglycerol oils were combined to compose experimental diets with similar fatty acid profiles. Food intake and body weights were measured daily and weekly, respectively. Fasted blood samples were drawn at day 0, day 28, and day 56 to measure plasma LCAT activity and total (TC), unesterified (UC), and esterified (EC) cholesterol concentrations, and for fatty acid analysis of the phospholipid (PL) and EC fractions. The LGI groups lost more weight than the HGI groups due to starch digestibility differences. An HGI starch effect on TC and UC concentrations was observed but was unrelated to weight loss. LCAT activities increased over time but were not different after controlling for percentage weight loss. However, a positive linear correlation was found between LCAT and UC concentrations in all groups. Plasma PL fatty acid profiles reflected the diets fed, but increases in 16 and 18 carbon saturated and monounsaturated fatty acids in all groups appeared to be an effect of fatty acid mobilization from storage sites. Both plasma PL and EC fatty acid profiles were similar with both acylglycerol types and EC fatty acids reflected linoleic acid specificity with minimal diet or time effects.

Keywords Plasma esterified cholesterol composition · Plasma phospholipid composition · LCAT activity · Weight loss · Obese beagles

Abbreviations

DAG	Diacylglycerol
EC	Esterified cholesterol
FA	Fatty acid
FAMES	Fatty acid methyl esters
GC	Gas chromatography
HDL	High density lipoprotein
HGI	High-glycemic index
LCAT	Lecithin:cholesterol acyltransferase
LGI	Low-glycemic index
LPC	Lysophosphatidylcholine
MAG	Monoacylglycerol
MUFA	Monounsaturated fatty acid
PC	Phosphatidylcholine
PL	Phospholipid
PUFA	Polyunsaturated fatty acid
SFA	Saturated fatty acid
TAG	Triacylglycerol
TC	Total cholesterol
UC	Unesterified cholesterol

Introduction

Overweight and obesity are common problems among companion animals, affecting an estimated 25–40% of dogs and cats seen in private veterinary practice [1]. Significant health repercussions such as greater risk for earlier morbidity, shortened lifespan, insulin resistance, and osteoarthritis are associated with excess body weight in

R. Angell · Y. Mitsuhashi · K. Bigley · J. E. Bauer (✉)
Companion Animal Nutrition Lab, Department of Veterinary
Small Animal and Clinical Sciences,
College of Veterinary Medicine & Biomedical Sciences,
Texas A&M University, 4474 TAMU,
College Station, TX 77843-4474, USA
e-mail: jbauer@cvm.tamu.edu

dogs [2, 3]. Typically, this is addressed by decreasing calorie intake and increasing energy expenditure to promote weight loss [4]. Another approach proposed recently is the replacement of the typical form of fat found in the diet, triacylglycerol (TAG), with a form of fat normally found in very low quantities in the diet, diacylglycerol (DAG), especially 1,3-DAG [5].

Animal studies report suppression of diet-induced body weight and visceral fat gain in rats and obesity-prone mice fed diets containing 1,3-DAG versus TAG [5]. Human studies have demonstrated a decrease in visceral fat mass in normal weight, overweight, and obese subjects associated with 1,3-DAG versus TAG intake [5]. Because DAG and TAG oils have been observed to have similar digestibility, energy content per gram, and absorption, it has been hypothesized that the metabolic differences observed may be due to the structural differences between the two lipids [6, 7]. During digestion of TAG, the fatty acids at the sn-1 and sn-3 positions are hydrolyzed, resulting in 2-monoacylglycerols (2-MAG) and free fatty acids. After absorption into the intestinal mucosal cell, these components are re-esterified into TAG and packaged for circulation. In contrast, the digestion of 1,3-DAG produces free fatty acids (FA) and 1(3)-MAG, which exhibit less efficient re-esterification into TAG than 2-MAG in the intestinal mucosal cells [6, 8]. Alternatively, 1(3)-MAG may be entirely hydrolyzed to fatty acid and glycerol in the intestinal lumen prior to absorption but this process is not always complete [6]. The fate of the fatty acids that are not re-esterified in the intestinal mucosal cells after digestion of 1,3-DAG and absorption of its components is unclear. One possibility is that these fatty acids are oxidized within intestinal mucosal cells. Indeed, animal studies have demonstrated an increase in small intestinal β -oxidation in lean and obese mice fed diets high in DAG [9, 10].

One effect of obesity often observed in canines is increased plasma cholesterol [11]. This phenomenon has also been seen in cats, as well as a reduction in plasma cholesterol in conjunction with weight loss [12, 13]. This decrease in plasma cholesterol during weight loss could be explained by an increase in the activity of Lecithin:cholesterol acyltransferase (LCAT) in conjunction with efficient scavenging of the resultant esterified cholesterol (EC) as part of reverse cholesterol transport. LCAT facilitates reverse cholesterol transport by creating a concentration gradient of unesterified cholesterol (UC) between peripheral cells and high density lipoprotein (HDL) particles, onto which LCAT is reversibly anchored, resulting in cholesterol esterification [14–16]. Several studies have found strong positive correlations between plasma cholesterol concentrations and LCAT activities in both normal and obese subjects [17–19]. However, total

cholesterol concentrations do not appear to be determined by LCAT concentrations; instead the enzyme may be regulated as a response to changes in plasma cholesterol concentrations.

Current knowledge of canine LCAT activity is limited. No studies have reported the relationship between LCAT activity and weight loss in dogs, and few have reported the activity of canine LCAT in general. One study reported an increase in LCAT activity that was associated with an increase in plasma cholesterol concentrations in mixed-breed dogs fed a high-fat diet [16]. These data support the concept of a relationship between LCAT activity and cholesterol concentrations in dogs as has been found in other species. Through this dietary trial, relationships between LCAT activity and weight loss as well as plasma cholesterol concentrations were investigated. In addition, the effects of dietary DAG versus TAG on plasma PL and EC fatty acid compositions were studied. It was hypothesized that obese dogs undergoing weight loss would exhibit increased plasma LCAT activity and that the structural differences between DAG and TAG might influence plasma PL and EC fatty acid profiles.

Experimental Procedures

Animals and Diets

The protocol for this study was approved by the Texas A&M University Laboratory Animal Use Committee. Twelve adult intact female obese beagles, ages 2–6 years with body condition scores of 8–9 on a 9 point scale where five is ideal and nine is obese, were assigned equally to four diet groups. The dogs are part of an out-bred colony of beagles belonging to Texas A&M University. They were individually housed in approved sized kennels with 12 h light cycles and allowed free access to water and exercise during the study. All dogs were intentionally made obese by overfeeding a highly palatable mixed diet of commercial pet food, vegetable oil, and human grade cookies until stable obese body weights were attained. Complete details regarding the obesity induction and re-induction periods have been published [20]. Dogs were first fed an acclimation diet for 28 days and then one of the four experimental diets for 56 days, all at the estimated kcal required to maintain starting obese body weights. Initial levels of obesity were re-attained during a 17-week washout, weight re-gain period and a steady obese state was again achieved as evidenced by stable, yet high body weights. The acclimation and experimental diet periods were repeated in a partial crossover design. Food intake and body weights were measured daily and weekly, respectively.

Experimental diets incorporated gelatinized waxy corn starch (high glycemic index, HGI) or gelatinized high amylose corn starch (low glycemic index, LGI) paired with DAG or TAG oil having similar FA profiles (Table 1). The diets were designated HGI/DAG, HGI/TAG, LGI/DAG, and LGI/TAG. Starches and oils were provided by Kao Corporation (Tokyo, Japan). Chicken by-product meal (Tyson Foods, Inc., Oklahoma City, OK), starch, and a vitamin/mineral premix (Akey, Lewisburg, OH) constituted the dry diet mixture, which was combined with the specified oil and water to form gruel-based diets. Ingredients and FA profiles of the acclimation and experimental diets can be found in Tables 2 and 3, respectively. The acclimation diet consisted of a dry mixture of chicken by-product meal, HGI/LGI starch blend (50:50, by wt), and a vitamin/mineral premix combined with canola/vegetable oil blend (50:50, by vol) and water.

Blood Sample Collection and Analyses

Fasted blood samples (7 mL) were drawn into EDTA-tubes at day 0, day 28, and day 56 of experimental feeding. Plasma was harvested by low speed centrifugation and stored in aliquots at -20°C for subsequent analysis.

Plasma samples were analyzed in triplicate for TC, UC, and EC concentrations enzymatically according to the procedure described by Warnick [21]. Samples were also

assayed for LCAT activity in duplicate according to the procedure described by Gillett & Owens using radiolabeled tracer equilibrated with endogenous substrate [22]. Results were converted from percent UC esterified to nmol UC esterified/mL of plasma/h using individual plasma UC concentrations. LCAT activities were normalized between assays using control plasma samples from baseline which were determined with each assay.

Plasma lipids were extracted according to the method described by Folch et al. [23]. Lipid subfractions were separated by thin layer chromatography using hexane/ether/glacial acetic acid (80:20:1, by vol). The EC fraction was briefly visualized using I_2 vapor, outlined, and scraped into Teflon-lined screw capped tubes. Fatty acids in the PL and EC fraction were methylated by incubation with 4% H_2SO_4 in methanol for 1 h at 90°C . Fatty acid methyl esters (FAMES) were extracted into hexane and analyzed by gas chromatography (GC) using a Hewlett Packard 5890 Series II Gas Chromatograph (Hewlett Packard Co., Palo Alto, CA) with a flame ionization detector. The GC conditions were as follows: FAMEWAX fused silica capillary column (0.32 mm \times 30 m, 0.25 μm , Restek, Bellefonte, PA); initial velocity 28.3 cm/s and flow 1.25 mL/min of helium; initial oven temperature 160°C for 10 min, increased $1.0^{\circ}\text{C}/\text{min}$ until final temperature 220°C . Results were generated with Hewlett Packard ChemStation software package. Authentic FAMES standards (Nu-Check Prep, Inc., Elysian, MN) were used to identify individual FA peaks based on retention times.

Table 1 Fatty acid composition of DAG and TAG oils (relative %)

Fatty acid	DAG	TAG
14:0	TR	TR
16:0	2.76	4.94
16:1n-7	0.11	0.14
17:0	TR	TR
18:0	1.33	1.89
18:1	37.34	32.09
18:2n-6	47.60	50.31
18:3n-3	6.57	7.49
20:0	0.33	0.36
20:1	0.70	0.63
20:2n-6	TR	TR
20:3n-6	ND	ND
20:4n-6	ND	ND
22:0	0.29	0.26
22:1	TR	0.14
24:0/22:6n-3	0.10	TR
24:1n-9	0.10	0.10
Unidentified	2.53	1.34

Values are averages of two representative samples

ND not detected, TR trace ($<0.1\%$)

Data Analysis

Statistical analyses were performed using SPSS 15.0/16.0 for Windows. The Shapiro–Wilks test was used to determine normal distribution of data. Nearly all of the data were normally distributed. However, in a few cases, non-normally distributed data were analyzed using Kruskal–Wallis one-way ANOVA. Repeated measures ANOVA, was used to test all data for main effects of time, starch, and oil and for interactions. Where there was a significant interaction between factors, data within days was analyzed by a 2×2 factorial and least square means were compared among and within diet groups to determine significant effects. In addition, two-way ANCOVA using % body weight loss as a covariate was used followed by L-matrix analysis to test the data for main effects of starch and oil as well as starch \times oil interactions at each time point to control for differences in weight loss between the groups. For all data, a p -value <0.05 was considered significant and multiple comparisons were performed where appropriate using least squares differences and linear regression analyses.

Table 2 Ingredients and metabolizable energy of diets fed

Component (g/kg)	Diet				
	Acclimation period	LGI/DAG	LGI/TAG	HGI/DAG	HGI/TAG
Chicken byproduct meal	430	430	430	430	430
High amylose corn starch (LGI) ^a	215	430	430	–	–
Waxy corn starch (HGI) ^a	215	–	–	430	430
Vitamin/mineral pre-mix ^b	5	5	5	5	5
DAG oil	–	135	–	135	–
TAG oil	–	–	135	–	135
Canola/soybean oils (50/50, v/v)	135	–	–	–	–
Water	2,160	1,730	1,730	2,595	2,595
kcal/kg	4,228	4,228	4,228	4,228	4,228
Fat content (%)	19.7	19.7	19.7	19.7	19.7

^a High amylose corn starch contains 68% amylose; waxy corn starch contains 26% amylose

^bContains: copper 4,000 mg/kg; iodine 560 mg/kg; iron 2.4%; manganese 2,000 mg/kg; selenium 120 mg/kg; zinc 4.32%; vitamin A 218 mg/kg; vitamin D₃ 2.95 mg/kg; vitamin E 5455 mg/kg; vitamin B₁₂ 1.82 mg/kg; riboflavin 272.7 mg/kg; *d*-pantothenic acid 1,364 mg/kg; thiamine 75 mg/kg; niacin 3182 mg/kg; vitamin B₆ 90.9 mg/kg; folic acid 143.6 mg/kg; choline chloride 41.2 g/kg; choline 35.8 g/kg; *D*-biotin 4.5 mg/kg

Table 3 Fatty acid composition of diets fed (relative %)

Fatty acid	Diet				
	Acclimation period	LGI/DAG	LGI/TAG	HGI/DAG	HGI/TAG
14:0	0.30	0.23	0.19	0.25	0.38
14:1n-5	ND	ND	ND	TR	ND
16:0	13.77	11.55	12.54	10.30	16.40
16:1n-7	2.37	2.15	1.89	2.26	3.52
17:0	ND	TR	0.10	TR	0.12
17:1	ND	0.11	ND	0.11	ND
18:0	5.11	4.11	5.36	3.89	5.66
18:1n-7	3.17	3.89	3.56	2.89	3.31
18:1n-9	38.15	39.67	37.67	38.74	36.57
18:2n-6	28.31	30.10	29.86	32.91	27.08
18:3n-3	5.45	2.76	3.28	3.33	2.93
20:0	0.56	0.41	0.65	0.72	0.42
20:1n-9	0.62	0.93	0.94	0.65	0.58
20:2n-6	ND	ND	0.17	ND	ND
20:3n-3	ND	ND	ND	ND	ND
20:3n-6	ND	ND	ND	ND	ND
20:4n-6	0.41	0.37	0.28	0.43	0.37
20:5n-3	ND	ND	ND	ND	ND
22:0	ND	TR	0.60	0.39	0.41
22:1n-9	ND	ND	0.19	TR	0.13
22:4n-6	ND	TR	ND	TR	ND
22:5n-3	0.28	ND	ND	ND	ND
22:6n-3	0.41	0.36	0.78	0.42	0.68
24:0	0.33	ND	ND	ND	ND
24:1n-9	0.26	0.60	0.55	0.49	0.63
Unidentified	1.32	2.53	1.38	1.92	1.20

Values are averages of two representative samples. *ND* not detected, *TR* trace (<0.1%)

Results

Animals and Diets

The dogs consumed an average of only $68 \pm 4\%$ (mean \pm SEM) of the diets offered overall per day on a weight basis. Consequently, all dogs lost weight during the study with an average weight loss of $5.8 \pm 1.2\%$ (mean \pm SEM) by day 28 and $11.2 \pm 1.5\%$ (mean \pm SEM) by day 56 for all diet groups. However, dogs consuming the LGI-based diets lost significantly more weight as a percentage of starting weight than those eating the HGI-based diets (Table 4).

Plasma Cholesterol Concentrations

A time \times starch interaction was found for TC and UC concentrations using repeated measures ANOVA between day 0 and day 28 sample times. Further analysis revealed a starch effect for these cholesterol fractions at day 28 with HGI group values significantly higher than those of the LGI groups. Only a trend for this effect was observed at day 56 ($p < 0.066$) (Fig. 1). However, analysis of covariance using % body weight lost as a covariate eliminated any significant effects of starch during weight reduction of these dogs.

Plasma LCAT Activities

Repeated measures analysis revealed a main time effect but no diet effect or diet \times time interaction for LCAT activity (Fig 2). Plasma LCAT activity increased from day 0 to day 28 and remained elevated at day 56, though not as much as at day 28. Analysis of variance and covariance did not reveal any further significant differences among the diet groups or interactions. However, regression analysis revealed a significant positive linear correlation ($r = 0.638$, $p < 0.001$) between LCAT activities and UC concentrations but not with any other cholesterol fraction. These correlations were similarly positive whether the two starch diet groups were analyzed separately or together (HGI starch, $r = 0.622$,

Table 4 Body weights of dogs during the experimental period (kg)

Diet	Day 0	Day 28	Day 56
LGI/DAG	15.5 \pm 1.1	14.0 \pm 0.9 (9.7%) ^a	13.1 \pm 0.8 (15.5%) ^a
LGI/TAG	15.0 \pm 1.5	13.7 \pm 1.4 (8.7%) ^{a,b}	12.6 \pm 1.2 (16.0%) ^a
HGI/DAG	14.3 \pm 1.2	13.9 \pm 1.4 (2.8%) ^{b,c}	13.2 \pm 1.4 (7.7%) ^{a,b}
HGI/TAG	14.9 \pm 0.7	14.8 \pm 0.9 (0.7%) ^c	14.1 \pm 1.1 (5.4%) ^b

Values in parentheses indicate percentage of body weight lost compared to day 0

Letters not in common in a column are significantly different, $p < 0.05$

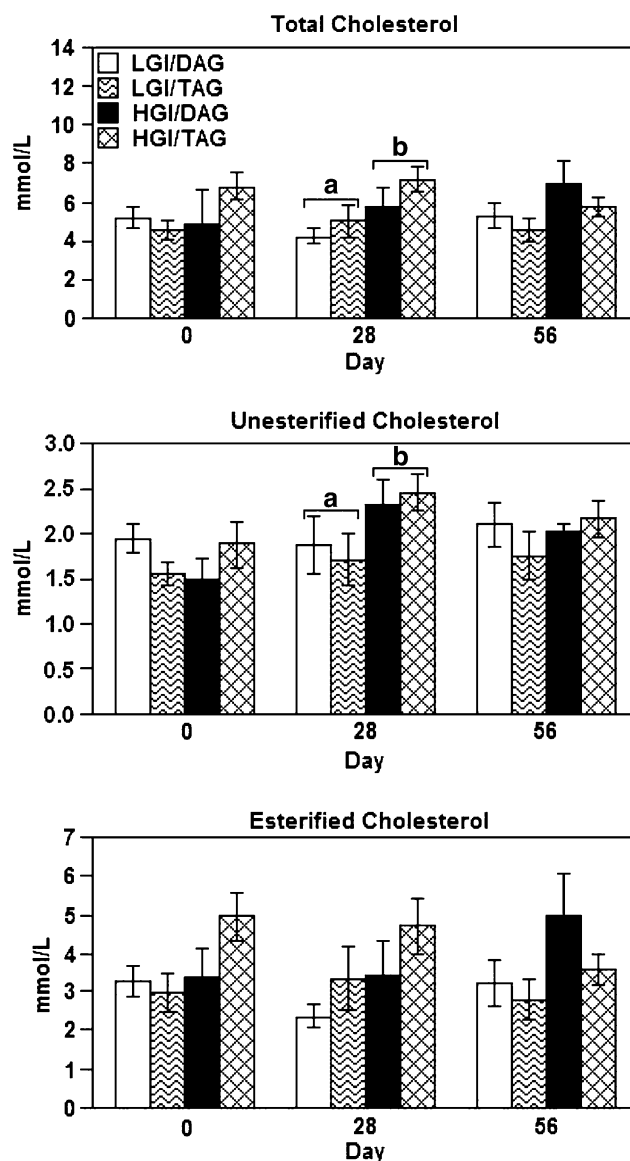


Fig. 1 Plasma total, unesterified, and esterified cholesterol concentrations of dogs fed diets differing in starch type (high-glycemic index [HGI] or low-glycemic index [LGI]) and oil type (diacylglycerol [DAG] or triacylglycerol [TAG]). Values are means \pm SEM; $n = 6$. Letters not in common indicate a significant difference between starch groups $p < 0.05$. When corrected for percent body weight loss, however, total cholesterol and unesterified cholesterol concentrations were not significantly different between starch groups

$p < 0.001$; LGI starch, $r = 0.658$, $p < 0.001$). Linear regression of LCAT activities with percent weight loss was only weakly positive with $r = 0.332$.

Plasma EC FA Composition

Few differences were observed between starch groups, oil groups, and diet (starch \times oil) groups in the plasma EC fatty acid profiles (Table 5).

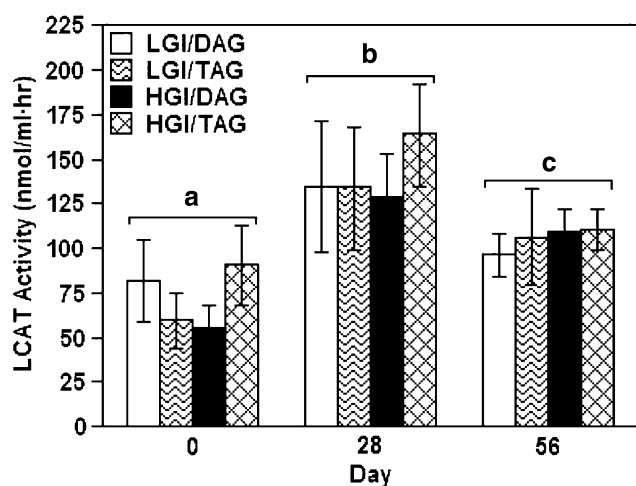


Fig. 2 Plasma LCAT activity of dogs fed diets differing in starch type (high-glycemic index [HGI] or low-glycemic index [LGI]) and oil type (diacylglycerol [DAG] or triacylglycerol [TAG]). Values are mean \pm SEM; $n = 6$. Letters not in common indicate a significant difference between days by repeated measures ANOVA, $p < 0.05$

When LGI starch was fed, plasma 16:1n-7 concentrations of dogs were statistically significantly higher when DAG was included compared to TAG at day 56. Within the two TAG groups, higher 16:1n-7 values were found at day 56 with HGI versus LGI starch. A similar pattern of statistically significant differences were seen with 18:1n-7. It should be noted, however, that these differences were of small magnitude (<1 relative % each) in all groups. Several main time effects were noted by repeated measures ANOVA over the course of the 56 days of feeding and weight loss which included modest increases in polyunsaturated fatty acids, primarily 18:2n-6. In addition, main starch effects were seen for 18:1n-9 (LGI groups higher than HGI groups) and 20:4n-6 (LGI groups lower than HGI groups) and a main oil effect for 18:3n-3 which decreased in DAG versus TAG groups but only at day 28.

Plasma PL FA Composition

Statistically significant differences over time were seen in nearly all plasma PL fatty acids using repeated measures ANOVA (Table 6). Saturates and monounsaturates (i.e., 14:0, 16:0, 16:1n-7, 18:0, and 18:1n7) were higher overall at day 28 versus day 0 but these decreased to baseline values at day 56. By contrast, polyunsaturates and longer chain monounsaturates were lower at day 28. These changes, while numerically modest, were nonetheless statistically significant. Main starch effects included higher concentrations of 22:5n-3, 24:0, and total n-3 fatty acids, but lower 16:0, in the HGI group versus the LGI group. Main oil effects seen overall were higher 18:1n-7 and lower 18:3n-3 in the DAG groups compared to TAG groups. Controlling for differences in % body weight lost

using ANCOVA revealed an oil \times starch interaction only for 16:1n-7. In addition, main oil effects for 18:1n-7 at day 56 (DAG $>$ TAG) and for 18:3n-3 at day 0 (TAG $>$ DAG) were observed as well as a main starch effect for 18:1n-9 at day 56 (LGI $>$ HGI).

Discussion

In this study, the dogs were offered an estimated number of calories required to maintain their baseline obese body weights. However, the gruel form of the experimental diets resulted in voluntary restriction of actual intake to a similar extent in all groups. Consequently, consistent weight loss occurred in all groups over the course of the study. However, the percentage of initial body weight lost in the LGI groups was greater than that in the HGI groups. The principal reason for this effect was significantly decreased starch digestibilities of the LGI diets compared to the HGI based diets resulting in lower calorie availability (data not shown).

The starch effect observed on both TC and UC concentrations at day 28 revealed higher values in animals fed the HGI starch diets during weight loss. This effect appeared independently of any effects of dietary fat feeding. However, after controlling for % body weight lost as a covariate, the statistically significant differences in TC and UC concentrations were no longer observed. While the reason for this starch effect is unknown, the possibility exists that the less digestible starch diets (i.e., LGI diets containing high amylose corn starch) may have prevented cholesterol elevations during the feeding period compared to the HGI diets resulting in statistically significant relative elevations in dogs fed the HGI diets at day 28. This effect did not appear to be due to percent of body weight lost but more likely due to differences in starch digestibilities. Indeed, studies in rats and hamsters have observed hypocholesterolemic effects of dietary high amylose corn starch, a low glycemic index starch [24–27]. One study found that this effect was mediated by an enlarged bile acid pool and increased fecal bile acid excretion along with decreased starch digestibilities [27]. Thus, when LGI diets were fed to dogs in the present study, the possibility exists that increased bile acid-starch binding and less bile acid hepatic recycling may have occurred. This phenomenon could then account for the statistically significant increase in plasma TC and UC that occurred at day 28 when the HGI diets were fed and may have been a result of decreased bile acid excretion.

Of additional interest is that the elevation of LCAT activities with time was positively correlated with plasma UC concentrations and appeared to coincide with a modest increase of UC in the HGI group at day 28. Correlations

Table 5 Plasma EC fatty acid composition (relative %, mean values)

FA	LGI/DAG			LGI/TAG			HGI/DAG			HGI/TAG			Overall SEM	Repeated Measures ANOVA ^a	Two-way ANCOVA
	D0	D28	D56	D0	D28	D56	D0	D28	D56	D0	D28	D56			
14:0	0.15	0.21	0.18	0.18	0.15	0.10	0.16	0.19	0.11	0.17	0.17	0.15	0.00	NS	NS
14:1n-5	TR	0.15	0.11	TR	0.12	TR	TR	0.12	TR	TR	0.10	ND	0.10	–	–
16:0	8.04	9.56	8.08	9.00	8.40	6.74	7.73	8.32	6.61	8.53	7.77	7.34	1.50	NS	NS
16:1n-7	1.05	1.40	1.17 ^b	1.23	1.19	0.82 ^{c,1}	1.21	1.09	0.84	1.17	0.97	1.00 ²	0.20	NS	0.008
17:0	0.19	0.11	0.11	0.14	TR	TR	0.14	0.22	0.21	0.35	0.34	TR	0.20	–	NS
18:0	5.06	3.05	2.70	4.84	3.06	3.11	3.25	3.74	2.36	5.12	4.66	2.38	1.10	0.044	NS
18:1n-7	4.08	4.26	3.76 ^b	4.14	3.91	3.03 ^{c,1}	3.81	3.84	3.33	3.86	3.41	3.64 ²	0.30	NS	0.008
18:1n-9	11.1	11.3	11.3	12.4	11.4	9.69	10.7	10.3	10.1	11.5	9.86	10.0	0.80	NS	0.016 ^d
18:2n-6	47.1	50.5	53.8	47.8	52.4	50.0	46.6	49.0	50.7	44.8	48.2	52.4	2.50	0.005	NS
18:3n-3	0.19	0.10	0.21	0.28	0.18	0.23	0.18	0.12	0.20	0.24	0.20	0.23	0.01	0.002 ^e	0.031 ^f
20:0	0.12	0.15	TR	0.21	0.33	0.13	0.25	TR	TR	0.24	TR	0.32	0.20	–	–
20:1n-9	ND	TR	TR	ND	ND	ND	TR	ND	ND	ND	ND	TR	–	–	–
20:2n-6	ND	ND	ND	ND	TR	ND	ND	TR	ND	ND	TR	TR	–	–	–
20:3n-3	ND	ND	TR	ND	ND	ND	TR	ND	ND	ND	ND	TR	–	–	–
20:3n-6	0.44	0.18	0.24	0.36	0.25	0.30	0.31	0.25	0.36	0.33	0.27	0.18	0.10	0.029	NS
20:4n-6	13.4	9.58	12.1	11.8	11.2	11.8	14.2	11.4	14.6	13.2	13.1	13.5	1.30	0.028	0.014 ^d
20:5n-3	TR	ND	ND	TR	TR	TR	TR	TR	TR	0.11	TR	TR	–	–	–
22:0	0.13	0.10	0.10	0.11	ND	0.19	TR	TR	TR	0.39	TR	TR	–	–	–
22:1n-9	ND	ND	ND	ND	ND	ND	ND	ND	ND	ND	ND	TR	–	–	–
22:4n-6	0.10	TR	TR	0.10	TR	TR	TR	TR	TR	TR	0.13	1.40	0.40	–	–
22:5n-3	0.33	0.20	0.12	0.27	0.12	0.12	0.25	0.13	0.13	0.34	0.27	0.12	0.10	0.030	NS
22:6n-3	ND	ND	ND	TR	ND	ND	TR	TR	ND	TR	ND	TR	–	–	–
24:0	ND	ND	ND	TR	ND	ND	TR	TR	ND	TR	ND	TR	–	–	–
24:1n-9	7.12	7.79	5.29	6.32	5.96	12.52	8.06	9.53	9.86	6.85	7.72	6.10	2.20	NS	NS
UI	1.25	1.25	0.65	0.69	1.12	0.98	2.47	1.53	0.42	2.60	2.65	0.84	0.70	–	–
SFA	13.7	13.2	11.2	14.5	12.0	10.3	11.6	12.6	9.31	14.8	13.0	10.4	0.53	NS	NS
MUFA	23.4	25.0	21.6	24.1	22.6	26.1	23.9	24.9	24.2	23.4	22.1	20.8	0.06	NS	NS
PUFA	61.7	60.6	66.5	60.7	64.2	62.6	61.9	61.0	66.0	59.2	62.3	68.0	0.80	0.044	NS
Total n-3	0.62	0.30	0.35	0.63	0.31	0.40	0.58	0.33	0.34	0.74	0.52	0.50	0.04	0.014	NS
Total n-6	61.1	60.3	66.1	60.0	63.9	62.2	61.3	60.7	65.7	58.4	61.8	67.5	0.80	0.037	NS

All groups $n = 6$, *ND* not detected, *NS* not significant, *Overall SEM* overall standard error of the mean, *TR* trace (<0.1%), *UI* unidentified

^a Main time effect at p -value shown

^{b,c} Letters not in common in a row at a time point indicate a significant difference within a starch group at p -value shown in Two-way ANCOVA

^d Main starch effect at day 28 at p -value shown

^e Also main oil effect at $p = 0.017$

^f Main oil effect at day 28 at p -value shown

^{1,2} Numbers not in common in a row at a time point indicate a significant difference within an oil group at p -value shown in Two-way ANCOVA

between LCAT and total cholesterol levels per se as well as over time have been previously reported in several studies [17–19]. Because UC serves as substrate for LCAT, enzyme induction may occur when its substrate concentrations are increased. After controlling for % body weight loss, no statistically significant effects were observed on LCAT activities. Thus, this enzyme activity did not change as a result of weight loss. Instead it was correlated with

plasma UC concentrations and may have been a response to relative elevations of this cholesterol fraction.

The acclimation and experimental diets used in this study were designed to have similar fatty acid profiles and any differences between them were likely due to normal variability in sampling and measurement. Consequently, fatty acid profiles of plasma EC and PL fractions demonstrated few statistically significant differences between

Table 6 Plasma PL fatty acid composition (relative %, mean values)

FA	LGI/DAG			LGI/TAG			HGI/DAG			HGI/TAG			Overall SEM	Repeated measures ANOVA		Two-way ANCOVA
	D0	D28	D56	D0	D28	D56	D0	D28	D56	D0	D28	D56		Time ^a	Oil/Starch	
14:0	TR	0.10	TR	TR	TR	TR	TR	0.10	TR	TR	TR	TR	0.00	0.001 ^a	NS	NS
14:1n-5	ND	ND	ND	ND	ND	ND	ND	ND	ND	ND	ND	TR	–	–	–	–
16:0	9.82	12.3	9.73	9.88	10.9	10.3	9.94	10.5	7.37	8.71	9.40	8.61	0.28	0.001 ^a	0.036 ^b	NS
16:1n-7	0.46	0.57	0.47	0.41	0.49	0.41	0.42	0.52	0.30	0.41	0.47	0.42	0.02	0.015 ^a	NS	0.040
17:0	0.48	0.45	0.42	0.44	0.39	0.38	0.41	0.30	0.34	0.44	0.40	0.40	0.01	0.003	NS	NS
18:0	33.5	35.0	30.6	30.7	31.9	29.9	32.4	34.2	30.9	31.5	32.4	32.1	0.37	0.024 ^a	NS	NS
18:1n-7	3.87	4.03	3.87	3.49	3.49	3.27	3.66	3.83	3.32	3.24	3.67	3.23	0.06	0.006 ^a	0.023 ^c	0.049 ^d
18:1n-9	5.60	5.85	7.04	6.39	6.22	6.66	5.60	5.69	5.89	5.80	7.47	5.92	0.16	0.044	NS	0.021 ^d
18:2n-6	15.8	15.9	17.1	18.3	17.6	18.6	16.3	15.6	16.5	16.1	15.8	15.7	0.31	NS	NS	NS
18:3n-3	0.20	0.14	0.18	0.24	0.17	0.20	0.18	0.14	0.19	0.23	0.18	0.23	0.01	0.002	0.035 ^c	0.022 ^e
20:0	0.44	0.39	0.36	0.34	0.28	0.32	0.37	0.30	0.31	0.33	0.39	0.39	0.02	NS	NS	NS
20:1n-9	0.21	0.15	0.26	0.22	0.16	0.19	0.16	0.13	0.20	0.22	0.19	0.23	0.01	0.001	NS	NS
20:2n-6	0.38	0.25	0.41	0.39	0.30	0.34	0.31	0.27	0.36	0.42	0.34	0.39	0.01	0.002	NS	NS
20:3n-3	TR	ND	TR	ND	ND	ND	TR	ND	ND	TR	TR	TR	–	–	–	–
20:3n-6	0.85	0.83	0.95	1.10	0.98	1.13	0.92	0.99	1.15	1.02	0.86	1.02	0.04	0.039	NS	NS
20:4n-6	21.1	18.2	21.4	21.0	21.1	21.0	22.1	21.3	24.7	23.4	21.9	22.9	0.43	NS	NS	NS
20:5n-3	0.20	0.11	0.20	0.24	0.17	0.20	0.17	0.16	0.21	0.22	0.17	0.24	0.01	0.000	NS	NS
22:0	0.58	0.49	0.57	0.54	0.43	0.54	0.49	0.32	0.55	0.52	0.45	0.57	0.02	0.008	NS	NS
22:1n-9	TR	TR	TR	TR	TR	TR	TR	TR	TR	TR	TR	TR	–	–	–	–
22:4n-6	0.91	0.73	1.04	0.98	0.97	1.04	0.95	0.84	1.21	1.06	0.96	1.16	0.04	0.015	NS	NS
22:5n-3	2.64	1.55	2.26	2.26	1.87	2.24	2.54	2.16	3.11	2.99	2.31	2.96	0.10	0.005	0.007 ^b	NS
22:6n-3	0.60	0.61	0.57	0.57	0.43	0.60	0.57	0.41	0.58	0.54	0.45	0.63	0.03	NS	NS	NS
24:0	0.33	0.23	0.38	0.31	0.26	0.29	0.33	0.28	0.43	0.46	0.35	0.44	0.02	0.007	0.041 ^b	NS
24:1n-9	1.40	1.28	1.49	1.58	1.29	1.68	1.32	1.16	1.65	1.61	1.34	1.84	0.06	0.001	NS	NS
UI	0.59	0.74	0.66	0.56	0.49	0.66	0.68	0.71	0.59	0.78	0.43	0.54				
SFA	45.2	49.0	42.1	42.3	44.3	41.8	44.1	46.0	40.0	42.0	43.4	42.6	0.52	0.011	NS	NS
MUFA	11.6	11.9	13.1	12.1	11.7	12.2	11.2	11.4	11.4	11.3	13.2	11.7	0.18	NS	NS	NS
PUFA	42.6	38.4	44.1	45.1	43.6	45.3	44.1	41.9	48.0	45.9	43.0	45.2	0.56	0.029	NS	NS
Total n-3	3.65	2.41	3.22	3.31	2.65	3.24	3.45	2.86	4.09	4.00	3.13	4.08	0.13	0.002	0.041 ^b	NS
Total n-6	39.0	36.0	40.9	41.8	40.9	42.1	40.6	39.0	43.9	41.9	39.8	41.1	0.51	NS	NS	NS

All groups $n = 6$, *ND* not detected, *NS* not significant, *Overall SEM* overall standard error of the mean, *TR* trace (<0.1%), *UI* unidentified

^a Main time effect overall at p -value shown (D0 vs. D28 and D28 vs. D56)

^b Main starch effect at p -value shown

^c Main oil effect at p -value shown

^d Main oil effect at day 56 at p -value shown

^e Main oil effect at day 0 at p -value shown

diets. As such, the isomeric differences between TAG and DAG oil did not translate into resultant differences in FA composition of the plasma PL or EC fractions. However, it is noteworthy that higher amounts of 16 and 18 carbon saturates and monounsaturates were seen in the PL and EC fractions over time during the feeding periods during weight loss, most notably at day 28. After controlling for percentage weight loss as a covariate at each time point in the analysis, only the amounts of 16:1n-7 remained statistically significant. Thus other factors besides weight loss

must have been responsible for this effect. One possibility is that it is due to differences in the fatty acid composition of diets fed. However, fatty acid compositions of the diets, including the acclimation diet, were similar to each other. Alternatively, these differences may be the result of calorie restriction and mobilization of these fatty acids types from storage depots. This possibility is consistent with the observation that adipose storage sites tend to be rich in 16 and 18 carbon saturates and monounsaturates in mammalian species [28]. Another possibility is that increased

de novo synthesis of these fatty acids may have occurred as a result of the dietary carbohydrate composition as has been reported by Forsythe et al. [29].

Finally, it should be noted that linoleic acid constituted the major fatty acid in plasma EC fractions in all diet groups, with concentrations much higher than those found in plasma PL. This finding is similar to an earlier report that canine LCAT exhibits substrate specificity for 18:2n6 [30]. Interestingly, this same phenomenon was also observed with 24:1. Concentrations of 24:1 detected in plasma EC were roughly five times those found in plasma PL on average, indicating that canine LCAT also shows specificity for this FA. A previous unpublished study in the authors' laboratory did not find substantial amounts of 24:1 in canine plasma EC; however, the experimental diets in that study did not contain detectable amounts of this fatty acid.

Summary

This investigation into diet and weight loss effects on LCAT activity and substrate specificity have contributed to the current knowledge of cholesterol metabolism in dogs. An increase in LCAT activity and positive correlation with plasma UC concentration was observed but did not appear to be associated with weight loss. Feeding diets containing HGI starch resulted in sustained plasma cholesterol concentrations during weight loss that became statistically significant when compared to LGI starch diets after 28 days of feeding. These effects also did not appear to be due to weight loss, per se, but possibly the result of decreased bile acid excretion with HGI starch and increased digestibility. Elevations of saturated and mono-unsaturated fatty acids occurred in all groups during weight loss most likely reflecting the composition of adipose storage sites in the animals. Finally, dietary oil type (TAG vs. DAG) did not affect the plasma EC or PL fatty acid compositions. This latter finding is likely due to the similar fatty acid composition of the experimental oils and indicates that positional isomers in oil do not affect resultant FA profiles.

Acknowledgments This research was supported by a grant from Kao Corporation, Tokyo, Japan, and by the Mark L. Morris Professorship in Clinical Nutrition, Texas A&M University. The authors wish to acknowledge the technical assistance of Daisuke Nagaoka and Dwayne Bandy during this study.

References

- McGreevy PD, Thomson PC, Pride C, Fawcett A, Grassi T, Jones B (2005) Prevalence of obesity in dogs examined by Australian veterinary practices and the risk factors involved. *Vet Rec* 156:695–707
- Kealy RD, Lawler DF, Ballam JM, Mantz SL, Biery DN, Greeley EH, Lust G, Segre M, Smith GK, Stowe HD (2002) Effects of diet restriction on life span and age-related changes in dogs. *J Am Vet Med Assoc* 220:1315–1320
- Rand JS, Fleeman LM, Farrow HA, Appleton DJ, Lederer R (2004) Canine and feline diabetes mellitus: nature or nurture? *J Nutr* 134:2072S–2080S
- Laflamme DP (2006) Understanding and managing obesity in dogs and cats. *Vet Clin North Am Sm Anim Pract* 36:1283–1295
- Rudkowska I, Roynette CE, Demonty I, Vanstone CA, Jew S, Jones PJH (2005) Diacylglycerol: efficacy and mechanism of action of an anti-obesity agent. *Obes Res* 13:1864–1876
- Kondo J, Hase T, Murase T, Tokimitsu I (2003) Digestion and assimilation features of dietary DAG in the rat small intestine. *Lipids* 38:25–30
- Taguchi H, Nagaro T, Watanabe H, Onizawa K, Matsuo N, Tokimitsu I, Itakura H (2001) Energy value and digestibility of dietary oil containing mainly 1,3-diacylglycerol are similar to those of triacylglycerol. *Lipids* 36:379–382
- Lehner R, Kuksis A, Itabashi Y (1993) Stereospecificity of monoacylglycerol and diacylglycerol acyltransferases from rat intestine as determined by chiral phase high-performance liquid chromatography. *Lipids* 28:29–34
- Murase T, Aoki M, Wakisaka T, Hase T, Tokimitsu I (2002) Anti-obesity effect of dietary diacylglycerol in C57BL/6J mice: dietary diacylglycerol stimulates intestinal lipid metabolism. *J Lipid Res* 43:1312–1319
- Murase T, Nagasawa A, Suzuki J, Wakisaka T, Hase T, Tokimitsu I (2002) Dietary α -linolenic acid-rich diacylglycerols reduce body weight gain accompanying the stimulation of intestinal β -oxidation and related gene expressions in C57BL/KsJ-db/db mice. *J Nutr* 132:3018–3022
- Jeusette IC, Lhoest ET, Istasse LP, Diez MO (2005) Influence of obesity on plasma lipid and lipoprotein concentrations in dogs. *Am J Vet Res* 66:81–86
- Hoening M, Wilkins C, Holson J, Ferguson D (2003) Effects of obesity on lipid profiles in neutered male and female cats. *Am J Vet Res* 64:299–303
- Szabo J, Ibrahim WH, Sunvold GD, Dickey KM, Rodgers JB, Toth IE, Boissonneault GA, Bruckner GG (2000) Influence of dietary protein and lipid on weight loss in obese ovariectomized cats. *Am J Vet Res* 61:559–565
- Jonas A (1998) Regulation of lecithin cholesterol acyltransferase activity. *Prog Lipid Res* 37:209–234
- Bauer JE (2004) Lipoprotein-mediated transport of dietary and synthesized lipids and lipid abnormalities of dogs and cats. *J Am Vet Med Assoc* 224:668–675
- McAlister KG, Bauer JE, Harte J, Rawlings JM, Markwell P (1996) Canine plasma lipoproteins and lecithin:cholesterol acyltransferase activities in dietary oil supplemented dogs. *Vet Clin Nutr* 3:50–56
- Albers JJ, Chen CH, Adolphson JL (1981) Lecithin:cholesterol acyltransferase (LCAT) mass; its relationship to LCAT activity and cholesterol esterification rate. *J Lipid Res* 22:1206–1213
- Sutherland WHF, Temple WA, Nye ER, Herbison PG (1979) Lecithin:cholesterol acyltransferase activity, plasma and lipoprotein lipids and obesity in men and women. *Atherosclerosis* 34:319–327
- Akanuma Y, Kuzuya T, Hayashi M, Ide T, Kuzuya N (1973) Positive correlation of serum lecithin:cholesterol acyltransferase activity with relative body weight. *Eur J Clin Invest* 3:136–141
- Nagaoka N, Mitsuhashi Y, Angell R, Bigley KE, Bauer JE (2008) Re-induction of obese body weight occurs more rapidly and at lower caloric intake in beagles. *J An Phys An Nutr* (in press)

21. Warnick GR (1986) Enzymatic methods for quantification of lipoprotein lipids. In: Albers JJ, Segrest JP (eds) *Methods in enzymology*, vol 129. Academic Press, New York
22. Gillett MPT, Owen JS (1992) Cholesterol esterifying enzymes—lecithin:cholesterol acyltransferase (LCAT) and acylcoenzyme A:cholesterol acyltransferase (ACAT). In: Converse CA, Skinner ER (eds) *Lipoprotein analysis: a practical approach*. Oxford University Press, New York
23. Folch J, Lees M, Sloane-Stanley GH (1957) A simple method for the isolation and purification of total lipids from animal tissues. *J Biol Chem* 226:497–506
24. Saquet E, Leprince C, Riottot M (1983) Effect of amylo maize starch on cholesterol and bile acid metabolisms in germfree (axenic) and conventional (holoxenic) rats. *Reprod Nutr Dev* 23:783–792
25. Kasaoka S, Morita T, Ikai M, Ohhhashi A, Kiriyaama S (1998) High amylose corn starch prevents increased serum lipids and body fat accretion in rats. *J Jpn Soc Nutr Food Sci* 51:345–353
26. Ranhotra GS, Gelroth JA, Leinen BS (1997) Hypolipidemic effect of resistant starch in hamsters is not dose dependent. *Nutr Res* 17:317–323
27. Kishida T, Nogami H, Ogawa H, Ebihara K (2002) The hypocholesterolemic effect of high amylose cornstarch in rats is mediated by an enlarged bile acid pool and increased fecal bile acid excretion, not by cecal fermented products. *J Nutr* 132:2519–2524
28. British Nutrition Foundation (1992) Functions of unsaturated fatty acids. In: *British Nutrition Task Force report*, Garton A (eds) *Unsaturated fatty acids, nutritional and physiological significance*. Chapman & Hall, London, pp 48–49
29. Forsythe CE, Phinney SD, Fernandez ML, Quan EE, Wood RJ, Bibus DM, Kraemer WJ, Feinman RD, Volek JS (2008) Comparison of low fat and low carbohydrate diets on circulating fatty acid composition and markers of inflammation. *Lipids* 43:65–77
30. Liu M, Bagdade JD, Subbaiah PV (1995) Specificity of lecithin:cholesterol acyltransferase and atherogenic risk: comparative studies on the plasma composition and in vitro synthesis of cholesteryl esters in 14 vertebrate species. *J Lipid Res* 36:1813–1824

Lysophosphatidylcholine Exhibits Selective Cytotoxicity, Accompanied by ROS Formation, in RAW 264.7 Macrophages

Cheon Ho Park · Mee Ree Kim · Jong-Min Han ·
Tae-Sook Jeong · Dai-Eun Sok

Received: 23 July 2008 / Accepted: 20 January 2009 / Published online: 28 February 2009
© AOCs 2009

Abstract Lysophosphatidylcholine (lysoPtdCho) is a component of oxidized low density lipoprotein, and is involved in the pathogenesis of atherosclerosis and inflammation. We studied the effects of lysoPtdCho on cytotoxicity, reactive oxygen species (ROS) production, activation of the extracellular signal-regulated kinase (ERK), mitogen-activated protein kinases and pro-inflammatory gene expression in RAW 264.7 murine macrophage cells. When cells were exposed to lysoPtdCho with various acyl chains in a culture medium containing 10% fetal bovine serum, only 1-linoleoyl (C18:2) lysoPtdCho showed a remarkable cytotoxicity, reaching the highest level at 24 h, and elicited ROS production, suggesting that oxidative stress might be implicated in the cytotoxicity of 1-linoleoyl (C18:2) lysoPtdCho. Presumably in support of this, antioxidants such as magnolol or trolox prevented 1-linoleoyl (C18:2) lysoPtdCho-induced cytotoxicity as well as ROS production, although only partially. Furthermore, the phosphorylation of ERK 1/2 and the expression of pro-inflammatory cytokines such as IL-1 β , CCL2 and CCL5 were augmented by 1-linoleoyl (C18:2) lysoPtdCho.

Meanwhile, there was no structural importance of the acyl chain for the cytotoxic action of lysoPtdCho during 10 min incubation in serum-free media. Taken together, it is suggested that in a serum-containing medium, 1-linoleoyl (C18:2) lysoPtdCho can cause a significant cytotoxicity through ROS production, probably accompanied by activation of ERK and induction of related inflammatory cytokines, in RAW 264.7 cells.

Keywords Delayed cytotoxicity · Lysophosphatidylcholine · Macrophage · Inflammation · NADPH oxidase · Atherosclerosis · Cytokines · Extracellular signal-regulated kinase · Antioxidants

Abbreviations

lysoPtdCho	Lysophosphatidylcholine
ROS	Reactive oxygen species
FBS	Fetal bovine serum
MTT	3-(4,5-Dimethylthiazole-2-yl)-2,5-diphenyltetrazolium bromide
ERK	Extracellular signal-regulated kinase
CCL	Chemotactic cytokines ligand

C. H. Park · D.-E. Sok (✉)
College of Pharmacy, Chungnam National University,
Gung-Dong 220, Yuseong-ku, Taejeon 305-764,
Republic of Korea
e-mail: daesok@cnu.ac.kr

M. R. Kim
Department of Food and Nutrition,
Chungnam National University, Gung-Dong 220,
Yuseong-ku, Taejeon 305-764, Republic of Korea

J.-M. Han · T.-S. Jeong
National Research Laboratory of Lipid Metabolism
and Atherosclerosis, KRIBB, Taejeon 305-333,
Republic of Korea

Introduction

Lysophosphatidylcholine (lysoPtdCho) is known to be generated from phosphatidylcholine by at least four enzymes, phospholipase A₂, lipoprotein-specific phospholipase A₂, lecithin/cholesterol acyltransferase or endothelial lipase [1, 2]. The cytoplasmic and secretory forms of PLA₂ are up-regulated in ischemia and inflammation, and a lipoprotein-associated PLA₂ is an independent risk factor for atherosclerotic complications [2]. Presumably in support of

this, lysoPtdCho accumulates in tissues during ischemia and in plasma of inflammatory arthritis [3]. In addition, a considerable increase in lysoPtdCho content during the routine storage of some blood cells has been reported [4]. However, a part of the lysoPtdCho in plasma may be bound by serum albumin or lipoproteins [5], albeit with a relatively lower affinity than alpha-1 acid glycoprotein, a major acute phase protein in plasma [6]. Alternatively, lysoPtdCho can be transferred directly to cell membranes from some specified lipids such as oxidized low density lipoprotein [7]. According to previous reports [8], lysoPtdCho elicits various pro-inflammatory and atherogenic phenomena. As a part of inflammatory actions of lysoPtdCho, previous studies reported that lysoPtdCho brought about the superoxide production in neutrophils [9]. In addition, lysoPtdCho caused superoxide generation by activating NADPH oxidase (NOX) in nonphagocytic cells, particularly in vascular endothelial cells [10]. Saturated lysoPtdCho such as 1-palmitoyl (C16:0) lysoPtdCho and 1-stearoyl (C18:0) lysoPtdCho were more potent in elevating the intracellular calcium ion level in neutrophils than 1-oleoyl (C18:1) lysoPtdCho [9]. In mechanistic analyses of lysoPtdCho effect, the increase of cytosolic Ca^{2+} and the reactive oxygen species (ROS) level was accompanied by stimulation of mitogen-activated protein kinase (MAPK) pathways [11]. A growing body of evidence suggests that ROS contribute to cell death, in part, through effects on various cellular signaling pathways including the MAPK pathways [12]. In addition, lysoPtdCho treatment elicits production of IL-1 β and MCP-1, proinflammatory cytokine, in human monocytes and rat aortic smooth muscle cells, respectively [13]. Further support for pro-inflammatory activity of lysoPtdCho is provided by the evidence of lysoPtdCho acting as a chemotactic factor for monocytes and T cells [14], and lysoPtdCho released by apoptotic cells has been proposed to constitute a phagocyte attraction signal [15]. However, most of the studies concerning the cellular effect of lysoPtdCho were performed in primary cell cultures using saturated lysoPtdCho or oleoylated lysoPtdCho [9, 16], and moreover, these studies were carried out in serum-free media, since serum components interfered with the action of lysoPtdCho. Therefore, it needs to be clarified further as to whether lysoPtdCho may exert any significant biological effect on cells in the medium containing serum. In the present study, we attempted to examine the effect of lysoPtdCho, saturated and unsaturated, on RAW 264.7 cells in either serum-free medium or serum-containing medium. Here, we report that 1-linoleoyl (C18:2) lysoPtdCho shows a selective cytotoxic effect on RAW 264.7 cells by causing ROS formation, accompanied by activation of extracellular signal-regulated kinase (ERK) and induction of inflammatory cytokines, in the medium containing serum.

Materials and Methods

Materials

1-Palmitoyl (C16:0) lysoPtdCho, 1-stearoyl (C18:0) lysoPtdCho, 1-myristoyl (C14:0) lysoPtdCho, 1-oleoyl (C18:1) lysoPtdCho, dilinoleoyl PtdCho and diarachidonoyl PtdCho were from Avanti Polar Lipids (Alabaster, AL, USA). Magnolol (purity >95%) was kindly provided by Dr K. Bae, College of Pharmacy, Chungnam National University. 2',7'-Dichlorofluorescein diacetate (DCFH₂-DA) was from Molecular Probe (Eugene, OR, USA), Dulbecco's modified Eagle's medium (DMEM), fetal bovine serum (FBS), penicillin, streptomycin and trypsin-EDTA were purchased from Gibco/BRL (Gaithersburg, MD, USA). Suramin, 3-(4,5-Dimethylthiazole-2-yl)-2,5-diphenyltetrazolium bromide (MTT), phosphor-specific antibodies against ERK were obtained from BD Biosciences (San Jose, CA, USA), and all other reagents were from Sigma-Aldrich (St Louis, MO, USA) unless specifically described. 1-Linoleoyl (C18:2) lysoPtdCho and 1-arachidonoyl (C20:4) lysoPtdCho were synthesized by PLA₂-catalyzed hydrolysis of corresponding phosphatidylcholine species as described previously [17].

Cell Culture

RAW 264.7 cells were cultured in DMEM-supplemented with, penicillin (100 U/mL) and streptomycin (100 μ g/mL), 10% (v/v) heat-inactivated FBS at 37 °C in a humidified atmosphere of 5% CO₂ as previously described [18], and used between passages 6–13 at ~80% confluence unless otherwise stated. Cells were plated at a density of 5×10^4 /well in 96-well plate, and incubated overnight to allow for adherence.

Determination of Cytotoxicity

Cell respiration, an indicator of cell viability, was determined by measuring the mitochondrial-dependent reduction of MTT to formazan [18]. Briefly, the cells (5×10^4 /well), plated in the media, were incubated for indicated times at 37 °C in a 5% CO₂ incubator. MTT solution was added to cells to a final concentration of 500 μ g/mL, and the incubation was continued for 4 h at 37 °C. Then, the medium was aspirated, and the formazan products were solubilized with dimethyl sulfoxide. The cell viability was determined by measuring the difference of absorbance at wavelength 570 nm vs. 690 nm. To see the cytotoxicity during 10 min incubation, the cells were incubated with lysoPtdCho for 10 min in a serum-free medium. Separately, for delayed cytotoxicity of

lysoPtdCho, the cells were incubated with lysoPtdCho for 24 h in DMEM containing 10% FBS.

Measurement of Intracellular ROS

Oxidative stress of the cells was determined by using the fluorescent probe DCFH₂-DA [19]; DCFH₂-DA, cell-permeable, is converted into the fluorescent 2,7-dichloro-fluorescein by oxidative substances in cells. Briefly, cells (5×10^4 /well) were pretreated with antioxidants of various concentrations for 2 h at 37 °C. Subsequently, lysoPtdCho was added to the cells, and the incubation was further extended according to the specified time. At the end of the incubation, the cells were treated with fluorescent probe DCFH₂-DA (10 μM) for 30 min. The degree of fluorescence, corresponding to intracellular ROS, was determined using a spectrofluorometer (Wallac 1420, Perkin-Elmer, Turku, Finland) at 485 nm excitation and 530 nm emission wavelengths.

Prevention Against Cytotoxicity or ROS Formation

Cells (5×10^4 /well) were pretreated with antioxidant or other drugs, and then lysoPtdCho was added to the cells. The incubation was continued for 10 min in a serum-free medium or for 24 h in the medium containing 10% FBS. Determination of cytotoxicity or ROS formation was performed as described above.

Western Blot Analysis

RAW 264.7 cells were stimulated with or without 10 μM lysoPtdCho or 0.1 μg/mL lipopolysaccharide for 10 min. Cytosolic extracts were prepared in lysis buffer consisting of 0.2% NP-40, 10 mM HEPES, 15 mM KCl, 2 mM MgCl₂, 1 mM dithiothreitol, 0.1 mM EDTA and 0.1 mM PMSF. Equal amounts of protein (20 μg/well) were separated by 10% SDS-polyacrylamide gel electrophoresis, and transferred to a nitrocellulose membrane (GE Healthcare UK Ltd, Buckinghamshire, UK). Each membrane was blocked overnight at 4 °C with a blocking solution (10 mM Tris-HCl, pH 7.4; 125 mM NaCl; 0.1% Tween 20; 5% skim milk) and then incubated with antibodies to ERK and phospho-ERK (Cell Signaling, Danvers, MA, USA) at room temperature for 3 h. The blots were washed three times with washing buffer (20 mM Tris, 160 mM NaCl and 0.1% Tween 20), followed by a 1-h incubation with appropriate horseradish peroxidase-conjugated secondary antibody. The peroxidase activity was detected using the Immobilon Western HRP detection reagent (Millipore, Billerica, MA, USA). This immunoblots analysis was performed three times independently.

Quantitative RT-PCR Analysis

RAW 264.7 cells were treated with or without 10 μM lysoPtdCho for 12 h. The cells were harvested and total RNA was extracted using an Easy-Blue™ kit (INtRON Biotechnology, Korea) according to the manufacturer's instructions. A sample (1 μg) of total RNA was used for the synthesis of the first strand cDNA using the Omniscript (Qiagen, Valencia, CA, USA) according to the manufacturer's instructions. PCR amplifications were quantified using the SYBRGreen™ PCR Master Mix (Applied Biosystems, Foster City, CA, USA) against the expression of genes involved in proinflammatory mediators such as IL-1β, CCL2 and CCL5. The primers were provided in Table 1. After obtaining real-time fluorescence measurements, cycle threshold values were determined. Standard curves in the linear range (i.e., the exponential amplification phase) were used to calculate the quantity of each mRNA. The final data are expressed as the ratio of indicated mRNA to GAPDH mRNA.

Statistical Analysis

All values are expressed as means ± SD. The statistical analysis was done on an SPSS (Chicago, IL, USA) program. One-way analysis of variance and Duncan's multiple range tests were used to examine the difference groups. A value of $P < 0.05$ was accepted as statistically significant, unless otherwise stated.

Results

Lysophosphatidylcholine has been believed to play an important role in atherosclerosis and inflammatory diseases by altering various functions in a number of cell-types [20]. Previously, it was reported that lysoPtdCho expressed cytotoxicity primarily by causing an increase of intracellular calcium ions and the formation of ROS through activation

Table 1 Sequences of the primers used in qRT-PCR analysis

mRNA	Gene number	Primers sequence (5'-3')
IL-1β	NM 008361	F 5'-ATGAGGACATGAGCACCTTC-3'
		R 5'-CATTGAGGTGGAGAGCTTTC-3'
CCL2	NM 011333	F 5'-TCACCTGCTGCTACTCATTTC-3'
		R 5'-TACAGAAGTGCTTGAGGTGG-3'
CCL5	NM 013653	F 5'-TCCCTGTCTATTGCTTGCTCTAG-3'
		R 5'-GAGCAGCTGAGATGCCCATTC-3'
GAPDH	NM 001001030	F 5'-CAGTGGCAAAGTGGAGATTG-3'
		R 5'-GTTGTCATGGATGACCTTGG-3'

of NOX in primary suspension cells in serum-free media [21]. Separately, a remarkable formation of ROS by unsaturated lysoPtdCho was observed in human neutrophils in the serum-free media [16]; the most dramatic effect was expressed by 1-oleoyl (C18:1) lysoPtdCho, followed by 1-linoleoyl (C18:2) lysoPtdCho. However, little is known about the cytotoxic effects of polyunsaturated lysoPtdCho on adherent cells in the presence of serum. First, in this study, we examined the cytotoxic effect of lysoPtdCho on RAW 264.7 cells, representative adherent cells, since lysoPtdCho was believed to play an important role in atherosclerosis by altering various functions in monocytes and macrophages [22]. For this purpose, RAW 264.7 cells were exposed to lysoPtdCho with various acyl chains, saturated or unsaturated, in the serum-free medium, and the viability was determined using MTT assays [18].

Effects of lysoPtdCho on Macrophage Viability During 10 min Incubation in a Serum-Free Medium

First, when RAW 264.7 cells were incubated with 1-palmitoyl (C16:0) lysoPtdCho for 10 min in serum-free media, it was observed that 1-palmitoyl (C16:0) lysoPtdCho decreased the viability in a concentration-dependent fashion (Fig. 1); the remaining viability was reduced to 21% of the control level after 10 min incubation with 1-palmitoyl (C16:0) lysoPtdCho (20 μ M). A similar cytotoxic effect was also exhibited by the other lysoPtdCho species such as 1-stearoyl (C18:0) lysoPtdCho (remaining viability 24.9%), 1-myristoyl (C14:0) lysoPtdCho (42.9%),

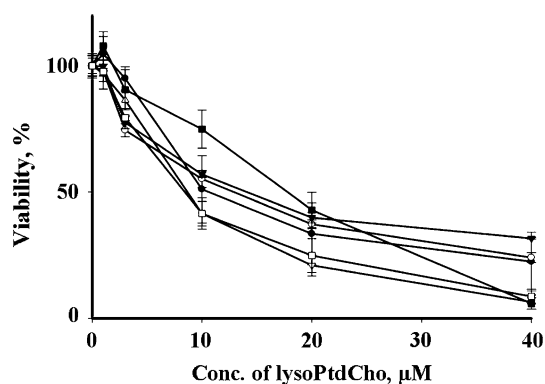


Fig. 1 Cytotoxicity of lysoPtdCho in RAW 264.7 cells during 10 min incubation in serum-free media. RAW 264.7 cells were incubated with various concentrations (0–40 μ M) of lysoPtdCho for 10 min in serum-free media. Cell viability was determined by MTT assay, and the viability was expressed as a percentage of viable cells among total cells. Data are shown as mean \pm SD of three parallel experiments. *Filled squares* indicate 1-myristoyl lysoPtdCho, *open inverted triangles* indicate 1-palmitoyl lysoPtdCho, *open squares* indicate 1-stearoyl lysoPtdCho, *filled circles* indicate 1-oleoyl lysoPtdCho, *open circles* indicate 1-linoleoyl lysoPtdCho, *filled inverted triangles* indicate 1-arachidonoyl lysoPtdCho

1-oleoyl (C18:1) lysoPtdCho (33.5%), 1-linoleoyl (C18:2) lysoPtdCho (37.3%) or 1-arachidonoyl (C20:4) lysoPtdCho (39.9%) after a 10-min incubation. In comparison (Table 2), the greatest cytotoxicity was expressed by 1-palmitoyl lysoPtdCho (IC_{50} , 9.0 μ M), followed by 1-stearoyl (C18:0) lysoPtdCho (IC_{50} , 9.9 μ M), 1-oleoyl (C18:1) lysoPtdCho (IC_{50} , 13.0 μ M), 1-linoleoyl (C18:2) lysoPtdCho (IC_{50} , 11.6 μ M), 1-arachidonoyl (C20:4) lysoPtdCho (IC_{50} , 13.7 μ M) and 1-myristoyl (C14:0) lysoPtdCho (IC_{50} , 17.5 μ M), indicating that the cytotoxic effect of lysoPtdCho may differ according to the type of acyl chain of the lysoPtdCho. The greater cytotoxicity of saturated lysoPtdCho such as 1-palmitoyl (C16:0) or 1-stearoyl (C18:0) lysoPtdCho may imply that lysoPtdCho acts as a detergent on the plasma membrane and thereby disturbs membrane stability. However, such a possibility is not supported by the additional finding that unsaturated lysoPtdCho, possessing relatively higher critical micelle concentration (CMC) values [23], also expresses a similar degree of cytotoxicity at the same concentration range. However, in media containing 10% FBS, no remarkable cytotoxicity (<5%) was exhibited by any of lysoPtdCho, suggesting that a component(s) of FBS prevented the cytotoxic action of lysoPtdCho.

Effects of lysoPtdCho on ROS Production in RAW 264.7 Cells During 10-min Incubation in a Serum-Free Medium

Reactive oxygen species have been suggested to be involved in the cytotoxic effect of lysoPtdCho [24], which has been reported to induce NAD(P)H oxidase, and increase the formation of superoxide anion radicals in nonphagocytic cells [25], particularly in vascular endothelial cells [20]. To determine whether the death of RAW 264.7 cells by lysoPtdCho is related to ROS production, we measured the ROS generation in RAW 264.7 cells using a fluorescent probe (DCFH₂-DA). As shown in Fig. 2, when

Table 2 IC_{50} value of lysoPtdCho-induced cytotoxicity in RAW 264.7 cells

LysoPtdCho-types	IC_{50} (μ M)
1-Myristoyl lysoPtdCho	17.5 \pm 0.57 ^a
1-Palmitoyl lysoPtdCho	9.0 \pm 0.45 ^e
1-Stearoyl lysoPtdCho	9.9 \pm 0.11 ^d
1-Oleoyl lysoPtdCho	13.0 \pm 0.52 ^b
1-Linoleoyl lysoPtdCho	11.6 \pm 0.18 ^c
1-Arachidonoyl lysoPtdCho	13.7 \pm 0.33 ^b

Cells were incubated with each lysoPtdCho in serum-free media for 10 min, as described in Fig. 1. Cell viability was determined by MTT assay. The values represent the means \pm SD of three independent experiments

each lysoPtdCho was incubated with RAW 264.7 cells in the serum-free medium for 10 min, 1-linoleoyl (C18:2) lysoPtdCho induced a considerable ROS production in RAW 264.7 cells in a concentration-dependent manner up to 20 μM , confirming the previous finding [16] that 1-linoleoyl (C18:2) lysoPtdCho-induced ROS formation in human neutrophils in serum-free media. In addition, a similar result was also observed with 1-arachidonoyl (C20:4) lysoPtdCho, although it caused a lower extent of ROS formation, compared to 1-linoleoyl (C18:2) lysoPtdCho. Meanwhile, other lysoPtdCho species including 1-oleoyl (C18:1) lysoPtdCho were not effective in inducing ROS formation. Thus, a considerable ROS generation was expressed only by lysoPtdCho with a 1-linoleoyl (C18:2) or a 1-arachidonoyl (C20:4) group, suggesting that ROS production might be related to the cytotoxicity of polyunsaturated lysoPtdCho in RAW 264.7 cells in the presence of serum. To confirm the above notion, the protective effect of antioxidant agents against 1-linoleoyl (C18:2) lysoPtdCho-induced ROS generation was evaluated. Figure 3 indicates that ROS generation by 1-linoleoyl (C18:2) lysoPtdCho was reduced by magnolol partially at 30 μM and fully at 100 μM . Nonetheless, the viability was not restored to the control level in the presence of magnolol even up to 100 μM . These results suggest that the formation of ROS may not be responsible for the cytotoxicity of unsaturated lysoPtdCho during a short incubation in serum-free medium. Thus, ROS appear to play a negligible role in lysoPtdCho-induced cytotoxicity during short time

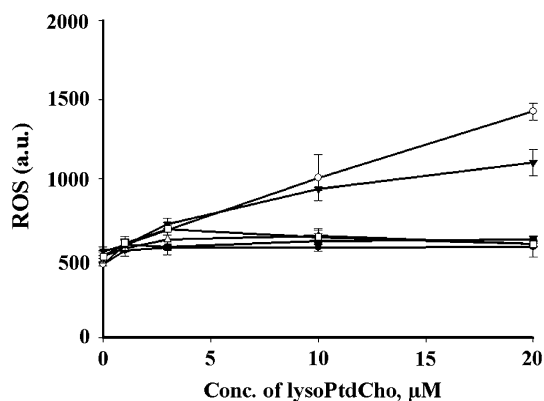


Fig. 2 Effect of lysoPtdCho on the formation of intracellular ROS. RAW 264.7 cells were incubated with various concentrations of lysoPtdCho (1, 3, 10 or 20 μM) for 10 min in serum-free media. Accumulation of intracellular ROS was monitored with DCFH₂-DA as described in the section “Materials and Methods”. Data are shown as means \pm SD of three parallel experiments. *Filled squares* indicate 1-myristoyl lysoPtdCho, *open inverted triangles* indicate 1-palmitoyl lysoPtdCho, *open squares* indicate 1-stearoyl lysoPtdCho, *filled circles* indicate 1-oleoyl lysoPtdCho, *open circles* indicate 1-linoleoyl lysoPtdCho, *filled inverted triangles* indicate 1-arachidonoyl lysoPtdCho

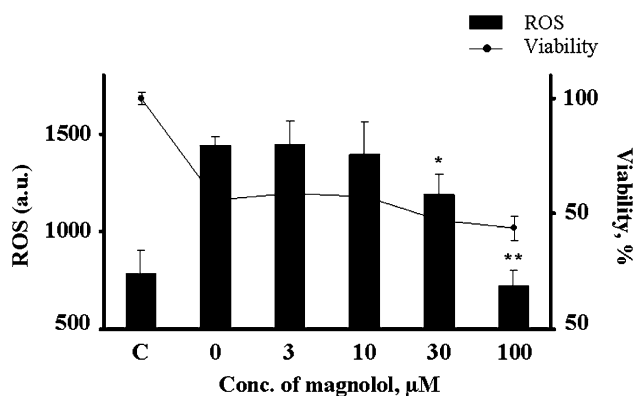


Fig. 3 Effect of antioxidants on lysoPtdCho-induced cytotoxicity and ROS production. RAW 264.7 cells were pretreated with magnolol (1–100 μM), and then incubated with 1-linoleoyl lysoPtdCho (20 μM) for 10 min in serum-free media. Data are shown as means \pm SD of three parallel experiments; * P < 0.05 vs. control, ** P < 0.01 vs. control. C without lysoPtdCho and magnolol

incubation in serum-free media. In the meantime, the inclusion of serum completely prevented the cytotoxicity of each lysoPtdCho as well as ROS formation by lysoPtdCho. These led us to examine whether the extended incubation of RAW 264.7 cells with lysoPtdCho may cause a remarkable cytotoxicity even in the presence of serum.

Effects of lysoPtdCho on Macrophage Viability During 24 h Incubation in a Medium Containing 10% FBS

In the subsequent experiment to see the delayed effect of lysoPtdCho, RAW 264.7 cells were incubated with each lysoPtdCho of various concentrations in media containing 10% FBS for 24 h, after which the viability of the remaining cells was analyzed by MTT assays [18]. First, when RAW 264.7 cells were incubated with lysoPtdCho of various concentrations for 24 h, a remarkable cytotoxic effect was demonstrated by 1-linoleoyl (C18:2) lysoPtdCho (Fig. 4); the viability decreased to 68.7% of control level after 24 h incubation with 1-linoleoyl (C18:2) lysoPtdCho (20 μM), and the increase of 1-linoleoyl (C18:2) lysoPtdCho concentration beyond 20 μM failed to further increase the cytotoxicity. Actually, the delayed cytotoxicity of 1-linoleoyl (C18:2) lysoPtdCho started to appear after 9 h incubation. In addition, 1-arachidonoyl (C20:4) lysoPtdCho also seemed to show a similar cytotoxic effect, although the maximal decrease of viability was limited to 9.8%. Meanwhile, the other lysoPtdCho species such as 1-oleoyl (C18:1) lysoPtdCho, 1-myristoyl (C14:0) lysoPtdCho, 1-palmitoyl (C16:0) lysoPtdCho or 1-stearoyl (C18:0) lysoPtdCho exerted no significant cytotoxic effect (<5%). Thus, it seems that the delayed cytotoxicity seems to be expressed selectively by 1-linoleoyl (C18:2) lysoPtdCho.

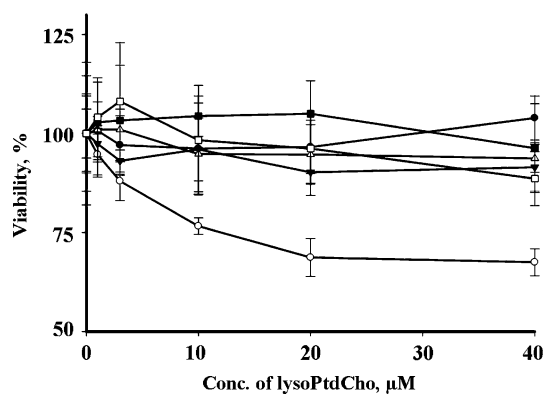


Fig. 4 Cytotoxicity of lysoPtdCho in RAW 264.7 cells during 24 h incubation in serum-containing media. Cells were incubated with each lysoPtdCho (0–40 μ M) for 24 h in media containing 10% FBS. Cell viability was determined by MTT assay, and the viability was expressed as a percentage of viable cells among total cells. Data are shown as mean \pm SD of three parallel experiments. *Filled squares* indicate 1-myristoyl lysoPtdCho, *open inverted triangles* indicate 1-palmitoyl lysoPtdCho, *open squares* indicate 1-stearoyl lysoPtdCho, *filled circles* indicate 1-oleoyl lysoPtdCho, *open circles* indicate 1-linoleoyl lysoPtdCho, *dark filled inverted triangles* indicate 1-arachidonoyl lysoPtdCho

Effect of lysoPtdCho on ROS Production During 24 h Incubation in a Medium Containing 10% FBS

To determine whether the delayed cell death of RAW 264.7 cells by 1-linoleoyl (C18:2) lysoPtdCho was related to ROS production, we measured ROS generation in RAW 264.7 cells exposed to 1-linoleoyl (C18:2) lysoPtdCho in a medium containing 10% FBS for 24 h. As shown in Fig. 5, 1-linoleoyl (C18:2) lysoPtdCho induced evidently a considerable ROS production in RAW 264.7 cells in a concentration-dependent manner (1–100 μ M), reaching its peak at 40 μ M. The effective concentrations (10–40 μ M) of 1-linoleoyl (C18:2) lysoPtdCho for ROS formation was close to those for its cytotoxicity in RAW 264.7 cells. Meanwhile, the other types of lysoPtdCho including 1-arachidonoyl (C20:4) lysoPtdCho failed to express a significant formation of ROS. These data suggest that the structural requirement of the acyl group for the cytotoxicity of lysoPtdCho in a serum-free medium is apparently different from that in a medium containing FBS.

Protection by Antioxidants Against Cytotoxicity of 1-Linoleoyl (C18:2) lysoPtdCho and ROS Formation

To further examine the mechanism by which 1-linoleoyl (C18:2) lysoPtdCho decreased the viability of RAW 264.7 cells during a 24-h incubation in the presence of FBS, the protective effect of antioxidant agents on the delayed cytotoxicity of 1-linoleoyl (C18:2) lysoPtdCho (20 μ M) was examined. As shown in Fig. 6a, magnolol (30 μ M)

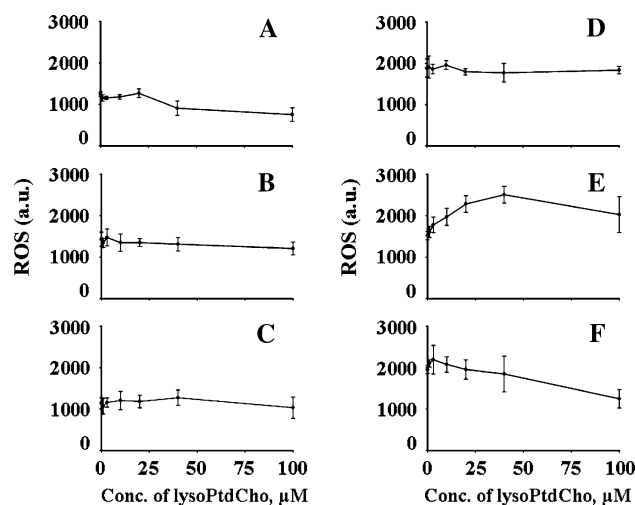


Fig. 5 Effect of lysoPtdCho on formation of intracellular ROS. RAW 264.7 cells were incubated with various concentrations of lysoPtdCho (1–100 μ M) for 24 h in media containing 10% FBS. Accumulation of intracellular ROS was monitored with DCFH₂-DA. Data are shown as means \pm SD of three parallel experiments. **a** 1-Myristoyl lysoPtdCho, **b** 1-palmitoyl lysoPtdCho, **c** 1-stearoyl lysoPtdCho, **d** 1-oleoyl lysoPtdCho, **e** 1-linoleoyl lysoPtdCho, **f** 1-arachidonoyl lysoPtdCho

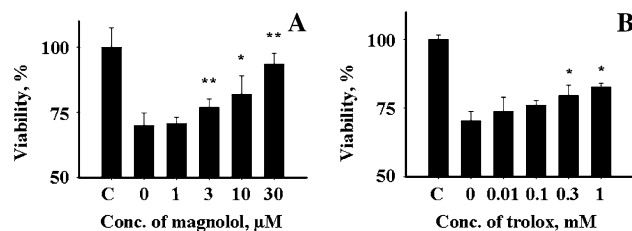


Fig. 6 Effect of antioxidants on lysoPtdCho-induced cell death. RAW 264.7 cells were pretreated with increasing magnolol concentrations (a) or increasing trolox concentrations (b), and then incubated with 1-linoleoyl lysoPtdCho (20 μ M) for 24 h in media containing 10% FBS. Cell viability was determined by MTT assay, and the viability was expressed as a percentage of viable cells among total cells. Data are shown as means \pm SD of three parallel experiments; * P < 0.05 vs. control, ** P < 0.01 vs. control. C without lysoPtdCho and magnolol

prevented the delayed cytotoxic action of 1-linoleoyl (C18:2) lysoPtdCho in a concentration-dependent manner; the viability, which decreased to 68.7% in the presence of 1-linoleoyl (C18:2) lysoPtdCho, was restored to 93.5% in the presence of magnolol with an EC₅₀ of 9.05 ± 1.79 μ M. Additionally, trolox, another antioxidant, augmented the viability to 82.8% with an EC₅₀ of 143 ± 21.1 μ M (Fig. 6b). In a separate experiment, the effect of antioxidant agents on the ROS formation in RAW 264.7 cells, exposed to 1-linoleoyl (C18:2) lysoPtdCho (20 μ M) for 24 h in a medium containing FBS, was examined. As shown in Fig. 7a, the inclusion of magnolol reduced the 1-linoleoyl (C18:2) lysoPtdCho-induced ROS formation in RAW 264.7 cells in a dose-dependent manner with an EC₅₀

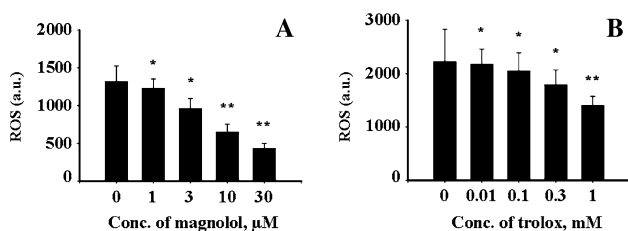


Fig. 7 Effect of antioxidants on lysoPtdCho-induced production of intracellular ROS. RAW 264.7 cells were pretreated with increasing concentrations of magnolol (a) or increasing concentrations of trolox (b), and then incubated with 20 μM 1-linoleoyl lysoPtdCho for 24 h in media containing 10% FBS. Data are shown as means \pm SD of three parallel experiments; * $P < 0.05$ vs. control, ** $P < 0.01$ vs. control

of $9.16 \pm 1.99 \mu\text{M}$. In addition (Fig. 7b), trolox also decreased the 1-linoleoyl (C18:2) lysoPtdCho-induced ROS formation in RAW 264.7 cells, although less effectively than magnolol. Thus, it is suggested that the delayed cytotoxicity of 1-linoleoyl (C18:2) lysoPtdCho in RAW 264.7 cells may be likely related to the increased ROS generation. Separately, suramin, a lysophosphatidic acid receptor antagonist, was tested for the prevention of 1-linoleoyl (C18:2) lysoPtdCho-induced cytotoxicity or ROS formation, since lysoPtdCho could be converted to lysophosphatidic acid during 24 h incubation. However, the lysophosphatidic acid receptor antagonist did not diminish the cytotoxicity of 1-linoleoyl (C18:2) lysoPtdCho or ROS formation in RAW 264.7 cells (data not shown), excluding the possibility that the cytotoxicity of 1-linoleoyl (C18:2) lysoPtdCho may be related to the action of lysophosphatidic acid, a degradation product of lysoPtdCho. Taken together, all the results suggest that oxidative stress may be implicated in the cytotoxicity of 1-linoleoyl (C18:2) lysoPtdCho in RAW 264.7 cells challenged with 1-linoleoyl (C18:2) lysoPtdCho.

Induction of Phosphorylation of ERK by 1-Linoleoyl (C18:2) lysoPtdCho

Since previous studies showed that the lysoPtdCho-induced activation of MAPKs pathways, dependent on ROS production, was observed in monocytes and endothelial cells [26], it was supposed that the production of ROS by 1-linoleoyl (C18:2) lysoPtdCho might be related to activation of MAPKs in macrophages. In this respect, RAW 264.7 cells were exposed to each lysoPtdCho, and the phosphorylation of ERK1/2 was evaluated. As demonstrated in Fig. 8, Western blot analysis clearly showed that 1-linoleoyl (C18:2) lysoPtdCho caused a significant increase in phosphorylation of ERK1/2 in a dose-dependent manner. However, the other lysoPtdCho such as 1-myristoyl (C14:0) lysoPtdCho, 1-palmitoyl (C16:0) lysoPtdCho

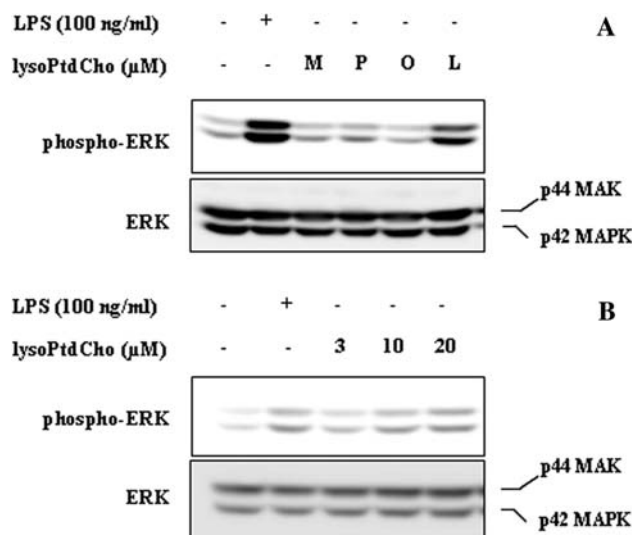


Fig. 8 Effects of lysoPtdCho on phosphorylation of ERK 1/2 in RAW 264.7 cells. Cells were treated with various lysoPtdCho (10 μM) or LPS (100 ng/mL) for 10 min. Harvested cells were lysed, and the extracted proteins were separated on 10% SDS-polyacrylamide gels and transferred to nitrocellulose membrane. Phosphorylation of ERK 1/2 was detected by Western blotting as described in the section “Materials and Methods”. The membrane was stripped and reprobed with ERK 1/2 antibody as an internal control (a). Separately, cells were treated with dose-dependent 1-linoleoyl lysoPtdCho or 100 ng/mL LPS, and were analyzed as described above (b). *M* 1-myristoyl lysoPtdCho, *P* 1-palmitoyl lysoPtdCho, *O* 1-oleoyl lysoPtdCho, *L* 1-linoleoyl lysoPtdCho

and 1-oleoyl (C18:1) lysoPtdCho even at 10 μM were not effective. These findings indicate that ERK1/2 phosphorylation may be related to 1-linoleoyl lysoPtdCho-induced ROS formation in RAW 264.7 cells.

LysoPtdCho Induces Proinflammatory Cytokine and Chemokine Gene Expression in RAW 264.7 Cells

In the next study to assess the lysoPtdCho-induced signal transduction pathway of cytokines responsible for inflammatory reactions, we examined the expression of cytokines in response to 1-linoleoyl (C18:2) lysoPtdCho or 1-palmitoyl (C16:0) lysoPtdCho. For this purpose, lysoPtdCho was incubated with murine macrophages to produce cytokines, and 12 h later, RNA was extracted from RAW 264.7 cells, and analyzed by graphical representations of the fold changes in cytokines. Figure 9 indicated that the production of IL-1 β and CCL2 was increased by about 20 times in the presence of 1-linoleoyl (C18:2) lysoPtdCho at 10 μM , and the gene expression of CCL5 was up-regulated by ≥ 10 -folds ($P < 0.05$), compared to control. Thus, a more dramatic induction was observed for CCL2 acting mainly in inflammatory reactions. Meanwhile, there was no significant difference of cytokines gene expression after the exposure to 1-palmitoyl (C16:0) lysoPtdCho. These results

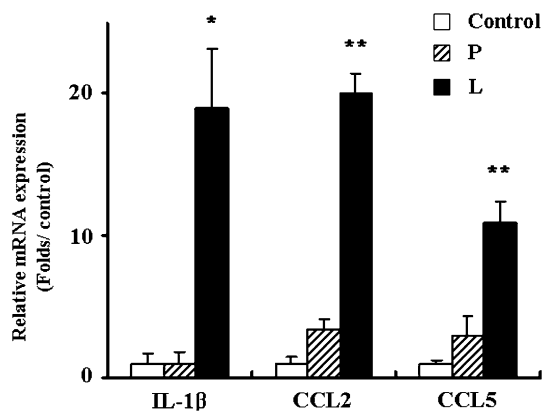


Fig. 9 Effect of lysoPtdCho on the expression of cytokines by RAW 264.7 cells. Cells were treated with 1-linoleoyl lysoPtdCho for 12 h. Expression levels of Interleukin-1 β (*IL-1 β*), CCL2 or CCL5, which were determined by a quantitative real time-polymerase chain reaction (qRT-PCR), were normalized to GAPDH, and plotted relative to those without 1-linoleoyl lysoPtdCho (control). All assays were performed in triplicate, and data are expressed as mean values \pm SD. * $P < 0.05$ vs. control, ** $P < 0.01$ vs. control. P 1-palmitoyl lysoPtdCho, L 1-linoleoyl lysoPtdCho

indicate that the cytotoxicity as well as ROS formation by 1-linoleoyl (C18:2) lysoPtdCho may implicate the upregulation of transcription of proinflammatory mediator genes in the RAW 264.7 cells.

Discussion

Lysophosphatidylcholine is believed to play an important role in patho-physiological conditions by altering various functions in a number of cell-types [27]. Earlier, the membrane effects of lysoPtdCho had been studied extensively in erythrocytes; lysoPtdCho, at concentrations above its CMC, disturbed membrane proteins, and disrupted plasma membrane integrity, leading to hemolysis [28]. Separately, lysoPtdCho, accumulating in the atherosclerotic arterial wall [29], has been suggested as playing a role in the progress of atherosclerosis, via receptor-mediated or independent actions, by causing vascular endothelial growth factor induction in macrophages, impairment of NO release, and upregulation of cell adhesion molecules, and acting as a monocyte chemoattractant [30]. In addition, the cytotoxicity of lysoPtdCho has been studied in vascular cells; for example, lysoPtdCho has been reported to induce apoptotic death in rat aorta smooth muscle cells at low concentrations (25–50 μ M), and induce necrosis at concentrations >100 μ M [31]. In human endothelial cells, lysoPtdCho at concentrations (25–300 μ M) has been shown to induce apoptosis, whereas primary necrosis has not been observed [22]. Our present data may provide an evidence for the cytotoxic effect of lysoPtdCho on RAW 264.7 cells. Thus, the effect of lysoPtdCho on cells may

depend on the lysoPtdCho concentration or the cell type as well as incubation conditions. Concerning the cytotoxicity of lysoPtdCho, lysoPtdCho as a detergent can be directly incorporated into the lipid matrix of cellular membranes and increase fluidity [28]. Further, lysoPtdCho at concentrations above its CMC values might induce micellar disruption, thus damaging membrane integrity. The present finding about the structure activity relationship for the cytotoxicity of saturated lysoPtdCho in RAW 264.7 cells in serum-free medium seemed to reflect the micellar property of lysoPtdCho [32] as had been observed with the cytotoxicity of lysoPtdCho in neutrophils [16]; the CMC value of saturated lysoPtdCho was inversely proportional to the size of acyl chain. However, this idea was not supported by another finding that 1-linoleoyl (C18:2) lysoPtdCho expressed a cytotoxicity below their CMC values (>20 μ M). Moreover, there was no significant difference of cytotoxicity between 1-oleoyl (C18:1) lysoPtdCho and 1-arachidonoyl (C20:4) lysoPtdCho, despite a great difference of their CMC values. Rather, it is supposed that the cytotoxic actions of lysoPtdCho may be explained by mechanisms different from detergent function [16]. One of them may involve the induction of oxidative stress, as had been previously observed in other types of cells [16, 31]. The formation of ROS through the activation of NOX had been observed with Jurkat T cells [33], fibroblast cell [32], human neutrophils [10] and endothelial cells [31] in the absence of serum, which prevented the cytotoxicity of lysoPtdCho [33]. However, in the present study, the cytotoxicity of lysoPtdCho during 10 min incubation in a serum-free medium was not addressed properly by ROS formation. Further, the cytotoxicity of lysoPtdCho was not prevented significantly by antioxidants. Meanwhile, the delayed cytotoxicity of 1-linoleoyl (C18:2) lysoPtdCho in medium containing 10% FBS was supposed to be related to ROS formation, since the delayed cytotoxicity was accompanied by ROS formation. A further support is from the finding that antioxidants such as magnolol and trolox diminished cytotoxicity as well as ROS formation in RAW 264.7 cells. It is worth noting that the delayed cytotoxicity in the presence of serum was expressed remarkably by 1-linoleoyl (C18:2) lysoPtdCho and slightly by 1-arachidonoyl (C20:4) lysoPtdCho, but not by saturated lysoPtdCho. Moreover, 1-oleoyl (C18:1) lysoPtdCho also failed to show a significant formation of ROS in RAW 264.7 cells in the presence of serum, despite a remarkable ROS formation by 1-oleoyl (C18:1) lysoPtdCho in human neutrophils in a serum-free medium [16]. Thus, it seems that the delayed cytotoxicity of lysoPtdCho may be peculiar to 1-linoleoyl (C18:2) lysoPtdCho in RAW 264.7 cells. Additionally, the delayed cytotoxicity of 1-linoleoyl (C18:2) lysoPtdCho might be cell-specific, since 1-linoleoyl (C18:2) lysoPtdCho did not show a delayed cytotoxic effect on RBL-2H3

cells. Taken together, the delayed cytotoxicity of 1-linoleoyl (C18:2) lysoPtdCho seems to depend on the types of cells or lysoPtdCho as well as the incubation conditions.

Although a previous study indicated that albumin and lipoprotein fractions of plasma contained higher amounts of saturated lysoPtdCho than unsaturated ones [31], this could not provide a relevant explanation of the selective cytotoxicity of 1-linoleoyl (C18:2) lysoPtdCho. Separately, alpha-1-acid glycoprotein was observed to show a strong binding affinity toward unsaturated lysoPtdCho [6]. However, such an action of alpha-1-acid glycoprotein may lead to the reduction in the cytotoxicity of 1-linoleoyl (C18:2) lysoPtdCho, although the possible delivery of lipids by alpha-1-acid glycoprotein to cell membrane may not be neglected. Rather, the delayed cytotoxicity of 1-linoleoyl (C18:2) lysoPtdCho is supposed to depend on free lysoPtdCho equilibrating with blood proteins- or lipoproteins-bound ones. Since the effective concentrations (10–20 μM) of 1-linoleoyl (C18:2) lysoPtdCho for delayed cytotoxicity was much below the reported CMC ($\sim 50 \mu\text{M}$) of lysoPtdCho in aqueous medium [34], it is more likely that the delayed cytotoxicity of 1-linoleoyl (C18:2) lysoPtdCho may be due to the specific interaction, rather than non-specific lipid interaction, between 1-linoleoyl (C18:2) lysoPtdCho and RAW 264.7 cells. The plasma concentration of lysoPtdCho ranges from 100 to 190 μM [35]; the most abundant lysoPtdCho species in fresh plasma samples was 1-palmitoyl (C16:0) lysoPtdCho, comprising $\sim 40\%$ of total lysoPtdCho, followed by 1-linoleoyl (C18:2) lysoPtdCho, corresponding to $\sim 20\%$ of total lysoPtdCho. Based on this, the plasma concentration of lysoPtdCho was estimated to be $\sim 40 \mu\text{M}$ for 1-palmitoyl (C16:0) lysoPtdCho and 20 μM for 1-linoleoyl (C18:2) lysoPtdCho. Since the concentrations (10–20 μM) of lysoPtdCho for delayed cytotoxicity of 1-linoleoyl (C18:2) lysoPtdCho were close to the physiological level, it is supposed that 1-linoleoyl (C18:2) lysoPtdCho may be one of plasma lysoPtdCho species implicated in the patho-physiological states. It is possible that lysophosphatidic acid, generated from the incubation of lysoPtdCho with RAW 264.7 cells, may be possibly responsible for the cytotoxicity. However, this is not supported by the observation that 1-linoleoyl (C18:2) lysophosphatidic acid was less cytotoxic than 1-palmitoyl (C16:0) lysophosphatidic acid in RAW 264.7 cells during 24 h incubation in medium containing FBS (data not shown). Separately, it is conceivable that the 1-(13-hydroperoxy) octadecadienoyl (C18:2) lysoPtdCho, generated from 24 h exposure of 1-linoleoyl (C18:2) lysoPtdCho to RAW 264.7 cells, may express the cytotoxicity. However, 1-(13-hydroperoxy) octadecadienoyl (C18:2) lysoPtdCho up to 10 μM failed to show any cytotoxic effect on RAW 264.7 cells (data not shown). All these observations suggest that the cytotoxic effect of

lysoPtdCho on RAW 264.7 cells differed according to the incubation conditions as well as types of cells or lysoPtdCho. Overall, saturated lysoPtdCho species were more cytotoxic than unsaturated lysoPtdCho species in the serum-free medium, but the reverse seemed to be true for the 24-h incubation in the medium containing FBS. Especially, 1-linoleoyl (C18:2) lysoPtdCho at physiological concentrations demonstrated a remarkable delayed cytotoxicity. Another important finding addressed by the present study is the involvement of the MAPK pathways in the selective cytotoxicity of 1-linoleoyl (C18:2) lysoPtdCho in RAW 264.7 cells. This may be consistent with previous findings that lysoPtdCho causes the activation of MAPK during apoptotic cell death in certain types of cells [36], and induces the activation of MAPK such as ERK 1/2 and JNK in endothelial cells [37]. However, most of these studies were done with 1-palmitoyl (C16:0) lysoPtdCho or 1-oleoyl (C18:1) lysoPtdCho, which failed to activate MAPK significantly in our present study. Although this discrepancy was not further examined in the present study, one possibility is that the selective interaction between 1-linoleoyl (C18:2) lysoPtdCho and RAW 264.7 cells may be responsible for the cytotoxicity of 1-linoleoyl (C18:2) lysoPtdCho as well as activation of MAPK. In support of this, there is a good correlation between the level of 1-linoleoyl (C18:2) lysoPtdCho-induced ERK activation and the cytotoxicity of 1-linoleoyl (C18:2) lysoPtdCho, accompanied by ROS formation. This idea may be somewhat relevant to a recent report that ERK can contribute to exerting apoptotic cell death during the cellular response to oxidative stress [38], although the role of the MAPK pathway in apoptosis is still controversial. Alternatively, it is conceivable that 1-linoleoyl (C18:2) lysoPtdCho-induced MAPK activation may be responsible for NOX-mediated ROS production according to a NOX–ROS–ERK-dependent pathway [27], since NOX-generated ROS may aid the phosphorylation of ERK and thereby contribute to upregulation in a downstream gene that is mediated by the ERK-dependent pathway. Additionally, we demonstrated that 1-linoleoyl (C18:2) lysoPtdCho markedly induces the expression of cytokine IL-1 β , and chemokines CCL2 (MCP-1) and CCL5 (RANTES) in RAW 264.7 cells while 1-palmitoyl (C16:0) lysoPtdCho failed to induce the expression. The mechanism for the increase in the production of cytokine by lysoPtdCho may be related to the activation of MAPK, as previously observed with inflammatory cells [36, 39]. In this regard, it is conceivable that the induction of CCL2 by 1-linoleoyl (C18:2) lysoPtdCho may contribute to the pro-inflammatory response in atherosclerosis. Taken together, present observations suggest that 1-linoleoyl (C18:2) lysoPtdCho may exert proinflammatory actions by selectively inducing ROS formation, activation of MAPK and gene expression of cytokines in

some specific cells. Further study employing *in vivo* methods may divulge the role of 1-linoleoyl (C18:2) lysophosphatidylcholine in pro-inflammatory conditions.

Acknowledgment This work was financially supported by a Korea Research Foundation Grant funded by the Korean Government (MOEHRD) (KRF-2007-531-C00067), Korea.

References

- Adibhatla Rao M, Hatcher JF (2006) Phospholipase A2, reactive oxygen species, and lipid peroxidation in cerebral ischemia. *Free Radic Biol Med* 40:376–387
- Zalewski A, Macphee CH (2005) Role of lipoprotein-associated phospholipase A2 in atherosclerosis: biology, epidemiology, and possible therapeutic target. *Arterioscler Thromb Vasc Biol* 25:923–931
- Daleau P (1999) Lysophosphatidylcholine, a metabolite which accumulates early in myocardium during ischemia, reduces gap junctional coupling in cardiac cells. *J Mol Cell Cardiol* 31:1391–1401
- Silliman CC, Clay KL, Thurman GW, Johnson CA, Ambruso DR (1994) Partial characterization of lipids that develop during the routine storage of blood and prime the neutrophil NADPH oxidase. *J Lab Clin Med* 124:684–694
- Thumser AE, Voysey JE, Wilton DC (1994) The binding of lysophospholipids to rat liver fatty acid-binding protein and albumin. *Biochem J* 301:801–806
- Ojala PJ, Hermansson M, Tolvanen M, Polvenen K, Hirvonen T, Impola U, Jauhainen M, Somerharju P, Parkkinen J (2006) Identification of alpha-1 acid glycoprotein as a lysophospholipid binding protein: a complementary role to albumin in the scavenging of lysophosphatidylcholine. *Biochemistry* 45:14021–14031
- Kugiyama K, Sakamoto T, Misumi I, Sugiyama S, Ohgushi M, Ogawa H, Horiguchi M, Yasue H (1993) Transferable lipids in oxidized low-density lipoprotein stimulate plasminogen activator inhibitor-1 and inhibit tissue-type plasminogen activator release from endothelial cells. *Circ Res* 73:335–343
- Huang F, Subbaiah PV, Holian O, Zhang J, Johnson A, Gertzberg N, Lum H (2005) Lysophosphatidylcholine increases endothelial permeability: role of PKC and RhoA cross talk. *Am J Physiol Lung Cell Mol Physiol* 289:L176–L185
- Silliman CC, Elzi DJ, Ambruso DR, Musters RJ, Hamiel C, Harbeck RJ, Bjornsen AJ, Wyman TH, Kelher M, England KM, McLaughlin-Malaxecheberria N, Barnett CC, Aiboshi J, Bannerjee A (2003) Lysophosphatidylcholines prime the NADPH oxidase and stimulate multiple neutrophil functions through changes in cytosolic calcium. *J Leukoc Biol* 73:511–524
- Nishioka H, Horiuchi H, Arai H, Kita T (1998) Lysophosphatidylcholine generates superoxide anions through activation of phosphatidylinositol 3-kinase in human neutrophils. *FEBS Lett* 441:63–66
- Guyton KZ, Liu Y, Gorospe M, Xu Q, Holbrook NJ (1996) Activation of mitogen-activated protein kinase by H₂O₂. Role in cell survival following oxidant injury. *J Biol Chem* 271:4138–4142
- Yamakawa T, Eguchi S, Yamakawa Y, Motley ED, Numaguchi K, Utsunomiya H, Inagami T (1998) Lysophosphatidylcholine stimulates MAP kinase activity in rat vascular smooth muscle cells. *Hypertension* 31:258–263
- Liu-Wu Y, Hurt-Camejo E, Wiklund O (1998) Lysophosphatidylcholine induces the production of IL-1beta by human monocytes. *Atherosclerosis* 137:351–357
- Quinn MT, Parthasarathy S, Steinberg D (1988) Lysophosphatidylcholine: a chemotactic factor for human monocytes and its potential role in atherogenesis. *Proc Natl Acad Sci USA* 85:2805–2809
- Lauber K, Bohn E, Krober SM, Xiao YJ, Blumenthal SG, Lindemann RK, Marini P, Wiedig C, Zobywalski A, Baksh S, Xu Y, Autenrieth IB, Schulze-Osthoff K, Belka C, Stuhler G, Wesselborg S (2003) Apoptotic cells induce migration of phagocytes via caspase-3-mediated release of a lipid attraction signal. *Cell* 113:717–730
- Ojala PJ, Hirvonen TE, Hermansson M, Somerharju P, Parkkinen J (2007) Acyl chain-dependent effect of lysophosphatidylcholine on human neutrophils. *J Leukoc Biol* 82:1501–1509
- Perez-Gilbert M, Veldink GA, Vliegthart JF (1998) Oxidation of linoleoyl phosphatidylcholine by lipoxigenase 1 from soybeans. *Arch Biochem Biophys* 354:18–23
- Mosmann T (1983) Rapid colorimetric assay for cellular growth and survival: application to proliferation and cytotoxicity assays. *J Immunol Methods* 65:55–63
- Oyama Y, Hayashi A, Ueha T, Meakawa K (1994) Characterization of 2',7'-dichlorofluorescein fluorescence in dissociated mammalian brain neurons: estimation on intracellular content of hydrogen peroxide. *Brain Res* 635:113–117
- Matsumoto T, Kobayashi T, Kamata K (2007) Role of lysophosphatidylcholine (LPC) in atherosclerosis. *Curr Med Chem* 14:3209–3220
- Takeshita S, Inoue N, Gao D, Rikitake Y, Kawashima S, Tawa R, Sakurai H, Yokoyama M (2000) Lysophosphatidylcholine enhances superoxide anions production via endothelial NADH/NADPH oxidase. *J Atheroscler Thromb* 7:238–246
- Kume N, Cybulsky MI, Gimborne MJ (1992) Lysophosphatidylcholine, a component of atherogenic lipoproteins, induces mononuclear leukocyte adhesion molecules in cultured human and rabbit arterial endothelial cells. *J Clin Invest* 90:1138–1144
- Croset M, Brossard N, Polette A, Lagarde M (2000) Characterization of plasma unsaturated lysophosphatidylcholine in human and rat. *Biochem J* 345:61–67
- Waring P (2005) Redox active calcium ion channels and cell death. *Arch Biochem Biophys* 434:33–42
- Watanabe N, Zmijewski JW, Takabe W, Umez-Goto M, Le Goffe C, Sekine A, Landar A, Watanabe A, Aoki J, Arai H, Kodama T, Murphy MP, Kalyanaraman R, Darley-Usmar VM, Noguchi N (2006) Activation of mitogen-activated protein kinases by lysophosphatidylcholine-induced mitochondrial reactive oxygen species generation in endothelial cells. *Am J Pathol* 168:1737–1748
- Komatsu D, Kato M, Nakayama J, Miyagawa S, Kamata T (2008) NADPH oxidase 1 plays a critical mediating role in oncogenic Ras-induced vascular endothelial growth factor expression. *Oncogene* 102:1–9
- Bergmann SR, Ferguson TB Jr, Sobel BE (1981) Effects of amphiphiles on erythrocytes, coronary arteries, and perfused hearts. *Am J Physiol* 240:H229–H237
- Bierbaum TJ, Bouma SR, Huestis WH (1979) A mechanism of erythrocyte lysis by lysophosphatidylcholine. *Biochim Biophys Acta* 555:102–110
- Portman OW, Alexander M (1969) Lysophosphatidylcholine concentrations and metabolism in aortic intima plus inner media: effect of nutritionally induced atherosclerosis. *J Lipid Res* 10:158–165
- Kugiyama M, Kern SA, Morrisett JD, Roberts R, Henry PD (1990) Impairment of endothelium-dependent arterial relaxation by lysolecithin in modified low-density lipoproteins. *Nature* 344:160–162
- Zhou L, Shi M, Guo Z, Brisbon W, Hoover R, Yang H (2006) Different cytotoxic injuries induced by lysophosphatidylcholine

- and 7-ketocholesterol in mouse endothelial cells. *Endothelium* 13:213–226
32. Li Z, Mintzer E, Bittman R (2004) The critical micelle concentrations of lysophosphatidic acid and sphingosylphosphorylcholine. *Chem Phys Lipids* 130:197–201
 33. Kim YL, Im YJ, Ha NC, Im DS (2007) Albumin inhibits cytotoxic activity of lysophosphatidylcholine by direct binding. *Prostaglandins Other Lipid Mediat* 83:130–138
 34. Weltzien HU, Arnold B, Reuther R (1977) Quantitative studies on lysolecithin-mediated hemolysis. Use of ether-deoxy lysolecithin analogs with varying aliphatic chain-lengths. *Biochim Biophys Acta* 466:411–421
 35. Okita M, Gaudette DC, Mills GB, Holub BJ (1997) Elevated levels and altered fatty acid composition of plasma lysophosphatidylcholine (lysoPC) in ovarian cancer patients. *Int J Cancer* 71:31–40
 36. Murugesan G, Sandhya Rani MR, Gerber CE, Mukhopadhyay C, Ransohoff RM, Chisolm GM, Kottke-Marchant K (2003) Lysophosphatidylcholine regulates human microvascular endothelial cell expression of chemokines. *J Mol Cell Cardiol* 35:1375–1384
 37. Ozaki H, Ishii K, Arai H, Kume N, Kita T (1999) Lysophosphatidylcholine activates mitogen-activated protein kinases by a tyrosine kinase-dependent pathway in bovine aortic endothelial cells. *Atherosclerosis* 143:261–266
 38. Feuerstein GZ, Young PR (2000) Apoptosis in cardiac disease: stress and mitogen-activated signaling pathways. *Cardiovasc Res* 45:560–569
 39. Jing Q, Xin S-M, Zhang W-B, Wang P, Qin Y-W, Pei G (2000) Lysophosphatidylcholine activates p38 and p42/44 mitogen-activated protein kinases in monocytic THP-1 cells, but only p38 activation is involved in its stimulated chemotaxis. *Circ Res* 87:52–59

Body Compositional Changes and Growth Alteration in Chicks from Hens Fed Conjugated Linoleic Acid

Vanessa A. Leone · Sharon P. Worzalla ·
Mark E. Cook

Received: 2 September 2008 / Accepted: 26 January 2009 / Published online: 18 February 2009
© AOCS 2009

Abstract Effects of feeding conjugated linoleic acid (CLA) to hens on progeny chick development and composition at hatch (NHC) and three weeks of age (TWC) were assessed. CLA (0 or 0.5%, composed of mixed isomers of *cis*-9,*trans*-11 or *trans*-10,*cis*-12-CLA) was fed to hens with either safflower (SO) or olive oil (OO) (3 or 3.5%) to assure successful hatch for 2 weeks prior to collection for incubation. Maternal CLA feeding had no effect on hatchability, but improved egg fertility ($p < 0.05$). Maternal feeding of CLA with SO increased 21 day-old progeny growth, while CLA with OO decreased growth (oil*CLA, $p < 0.05$). In 25 day-old chicks (TWC), but not NHC, maternal CLA decreased the proportion of total body water ($p < 0.05$) and increased body ash ($p < 0.05$). While monounsaturated fatty acids were decreased and saturated fatty acids increased in eggs and NHC from hens fed CLA, no differences in fatty acid composition were observed in chicks at 25 days of age from hens fed CLA. Maternal CLA feeding resulted in the presence of *c9,t11* and *t10,c12*-CLA in NHC, but only *c9,t11* in the TWC. In conclusion, hens fed CLA led to improved fertility and altered body composition at 3 weeks of age.

Keywords Conjugated linoleic acid (CLA) · Fatty acid modifications · Saturated fatty acids · Monounsaturated fatty acids · Desaturases · Dietary fat · Lipid absorption

Introduction

A considerable amount of research has been published on the effects of conjugated linoleic acid (CLA) on the body composition and fatty acid composition of growing animals, including mice [1–4], rats [5, 6], pigs [7–9], and chicks [10–12]. Maternal feeding of CLA has been shown to also affect the growth [13–15], body composition [15, 16], and fatty acid profile of tissues [13–16] in the progeny.

The progeny of rats [13, 15] and pigs [14] exposed to maternal CLA during gestation and lactation had increased rates of gain and improved feed efficiency in comparison to pups from control-fed dams. The body composition of growing male rats from dams fed 0.5% CLA appeared to be altered, in that gastrocnemius muscle was heavier and an increase of tail length was observed, indicative of increased lean mass and increased skeletal growth, respectively, in comparison to male pups from control-fed dams [15]. Bee [14] showed that 0.2% CLA incorporated into the diet of gestating sows did not alter birth or weaning weight, however, piglets reared by CLA-supplemented sows exhibited increased feed intake, increased daily gain, and higher final body weights than piglets reared on sows supplemented with 18:2(n-6). Consistently, in these mammalian species, the fatty acid composition of tissues obtained from the offspring was altered [13–15]. Bee [14] showed significantly increased levels of the predominant isomers of CLA fed to the mother (e.g., *cis*-9,*trans*-11 (*c9,t11*) and *trans*-10,*cis*-12 (*t10,c12*)) in the back fat of the progeny in comparison to progeny from control sows fed high levels of 18:2(n-6). Bee [14], Chin [13], and Poulos et al. [15] showed an increase in saturated fatty acids (SFA, e.g., 18:0) and a decrease in monounsaturated fatty acids (MUFA, e.g., 18:1(n-9)) [13–15] in progeny tissues, including back fat of pigs, as well as liver and inguinal fat

V. A. Leone · S. P. Worzalla · M. E. Cook (✉)
Department of Animal Sciences,
University of Wisconsin-Madison,
1675 Observatory Drive,
Madison, WI 53706, USA
e-mail: mcook@wisc.edu

V. A. Leone
e-mail: valeone@wisc.edu

pads of rats. Similar alteration in fatty acid data is also shown in tissues of newly hatched chicks from hens fed dietary CLA in comparison to tissues of offspring from control-fed hens [16].

The increased saturated fatty acids in eggs from laying hens fed 0.5% CLA in a basal diet with no added fat caused embryonic mortality [17–19]. Hatch of eggs obtained from CLA-fed hens could be “rescued” if the hen’s basal diet contained at least 3% oils exhibiting a fatty acid composition of either MUFA (e.g. olive oil or canola oil) or polyunsaturated fatty acids (PUFA, e.g. corn oil or soybean oil) [17, 19, 20]. Hence, the use of rescue oils allowed for the investigation of the effects of maternal CLA on avian progeny growth and composition. Using corn oil as a rescue oil, Cherian et al. [16] showed that newly hatched progeny from hens fed 0.5 or 1.0% CLA had decreased total carcass fat, while carcass weight, dry matter, and ash were not altered.

The purpose of this study was to extend the finding reported by Cherian et al. [16] in newly hatched chicks to the body composition and performance of chicks grown to three weeks of age that have hatched from hens fed mixed

isomers of CLA. To rescue hatchability in the presence of 0.5% maternal dietary CLA (containing equal parts *c9,t11* and *t10,c12*), oils rich in PUFA (safflower oil (SO), containing 80% 18:2(n-6)) or MUFA (olive oil (OO) containing 80% 18:1(n-9)) were used. The level of CLA selected was based on the lowest level reported by Cherian et al. [16] to reduce body fat in day old chicks without adversely affecting egg size, yolk weight, yolk lipid, or hatchability [18, 19, 21]. Hen egg production, egg fertility, fatty acid composition of yolk and subsequent offspring, as well as the body composition of newly hatched chicks (NHC) and three-week old chicks (TWC) was measured.

Experimental Procedure

Hens and Egg Management

Forty-eight individually housed single comb white leghorn (SCWL) hens were randomly assigned to 1 of 4 dietary treatments in a 2 × 2 factorial, where type of added fat and

Table 1 Composition of diets containing two types of added dietary fat with or without the presence of CLA

	SO	SO + CLA	OO	OO + CLA	Chick mash
Corn	60	60	60	60	63
Soybean meal (48% CP)	20.09	20.09	20.09	20.09	30.2
Corn gluten meal	3.29	3.29	3.29	3.29	–
Wheat middlings	2	2	2	2	–
Calcium carbonate ^a	8.46	8.46	8.46	8.46	1.48
Dicalcium phosphate	1.09	1.09	1.09	1.09	1.59
DL-methionine	0.07	0.07	0.07	0.07	0.18
Safflower oil	3.5	3	–	–	–
Olive oil	–	–	3.5	3	–
CLA ^b	–	0.5	–	0.5	–
Max-fat hog blend ^c	–	–	–	–	2.8
Salt	0.5	0.5	0.5	0.5	0.5
Vitamin premix ^d	1.0	1.0	1.0	1.0	0.25
Calculated linoleic acid content (%)	4.3	3.9	1.9	1.8	1.8

Diets were isonitrogenous and isocaloric, calculated to contain 15% CP and 2800 kcal/kg ME. Hen basal diet dry matter (ether extract) contained 4.02 g/100 g diet. Dietary inclusion g/100 g diet: SO, 3.5 g safflower oil/100 g; SO + CLA, 3 g safflower oil/100 g plus 0.5 g CLA/100 g; OO, 3.5 g olive oil/100 g; OO + CLA, 3 g olive oil/100 g plus 0.5 g CLA/100 g. Chick mash was fed to chicks post-hatch throughout the 3-week growing period

CP crude protein

^a Calcium carbonate was also given to SCWL as a free-choice top dress in the form of ground oyster shells

^b The source of commercial CLA contained 60% of CLA (BASF AG, Ludwigshafen, Germany). CLA accounts for *c9,t11* = 29.6%; *t10,c12* = 29.7% of the total free fatty acids. Other fatty acids include 5.5% 16:0, 4.6% 18:0, 23.4% 18:1(n-9), 1.4% 18:2(n-6)

^c Vegetable oil/animal fat mixture, supplied by Sanimax, MXO, Green Bay, WI

^d Hen diet supplied per kg of diet: vitamin A, 10,000 IU; vitamin D₃, 9790 IU; vitamin E, 121 IU; B-12, 20 µg; riboflavin, 4.4 mg; calcium pantothenate, 40 mg; niacin, 22 mg; choline, 840 mg; biotin, 30 µg; thiamin, 4 mg; zinc sulfate, 60 mg; manganese oxide, 60 mg. Chick mash diet supplied per kg of diet: vitamin A, 5500 IU; vitamin D₃, 634 IU; B-12, 10 µg; riboflavin, 6.6 mg; calcium pantothenate, 14 mg; niacin, 28 mg; choline chloride, 1268 mg; zinc sulfate, 27 mg; manganese oxide, 42 mg

presence of CLA were factors. Dietary treatments consisted of 3.5% safflower oil (SO) (80% 18:2(n-6)), 3.5% olive oil (OO) (80% oleic acid, 18:1(n-9)), 3% safflower oil + 0.5% CLA (SO + CLA), and 3% olive oil + 0.5% CLA (OO + CLA), where CLA consisted of CLA-60 (BASF AG, Ludwigshafen, Germany; equal parts 9*c*,11*t*; 10*t*,12*c*, see footnote, Table 1, for exact composition). Dietary composition is shown in Table 1, while dietary fatty acid composition is shown in Table 2. Hens were fed dietary treatments for 2 weeks and then artificially inseminated with 0.05 mL pooled, fresh New Hampshire rooster semen once per week. Hens remained on experimental treatments throughout the remainder of the experimental trial. Hens were exposed to a 16:8-h light/dark daily lighting schedule. All procedures involving animals were approved by the University of Wisconsin Animal Care and Use Committee. Eggs were collected and stored at 15 °C for a minimum of 24 h and incubated weekly at 37 °C and 85% relative humidity in a forced-air incubator. Eggs were candled weekly to detect fertility and embryonic mortality. Eggs that candled clear were broken out to detect infertility or very early embryonic mortality.

Table 2 Fatty acid composition of hen dietary treatments

Fatty acid	Dietary treatments ^a			
	SO	SO + CLA	OO	OO + CLA
	g/100 g fatty acid methyl esters			
14:0	0.3 ± 0.0	0.3 ± 0.0	0.2 ± 0.0	0.2 ± 0.0
16:0	12.0 ± 0.1	12.9 ± 0.2	15.1 ± 0.0	16.1 ± 0.3
16:1(n-7)	0.1 ± 0.0	0.1 ± 0.0	0.6 ± 0.0	0.7 ± 0.0
18:0	3.2 ± 0.0	4.1 ± 0.1	3.0 ± 0.0	3.8 ± 0.1
18:1(n-9)	19.8 ± 0.4	23.0 ± 0.5	51.4 ± 0.2	50.7 ± 0.9
18:2(n-6)	63.4 ± 0.6	52.3 ± 0.3	28.1 ± 0.2	22.4 ± 1.3
<i>cis</i> -9, <i>trans</i> -11 CLA	ND	3.3 ± 0.1	ND	2.4 ± 0.1
<i>trans</i> -10, <i>cis</i> -12 CLA	ND	3.2 ± 0.1	ND	2.3 ± 0.1
18:3(n-3)	1.3 ± 0.0	1.2 ± 0.0	1.4 ± 0.0	1.1 ± 0.0
20:4(n-6)	ND	ND	0.2 ± 0.0	0.1 ± 0.0
∑CLA	0.0 ± 0.0	6.5 ± 0.4	0.0 ± 0.0	4.7 ± 0.4
∑SFA	15.5 ± 0.2	17.3 ± 0.2	18.3 ± 0.1	20.1 ± 0.7
∑MUFA	19.9 ± 0.7	23.1 ± 0.9	52.0 ± 0.4	51.4 ± 1.7
∑PUFA	64.7 ± 1.0	60.0 ± 0.5	29.7 ± 2.3	28.3 ± 0.3

Values are means ± SD

∑ sum, CLA conjugated linoleic acid, SFA saturated fatty acid, MUFA monounsaturated fatty acid, PUFA polyunsaturated fatty acid, ND not detectable

^a Diets g/100 g diet: SO, 3.5 g safflower oil/100 g; SO + CLA, 3 g safflower oil/100 g plus 0.5 g CLA/100 g; OO, 3.5 g olive oil/100 g; OO + CLA, 3 g olive oil/100 g plus 0.5 g CLA/100 g

Growth and Feed Efficiency

To detect influences of maternal diet on growth and feed efficiency parameters, eggs from artificially inseminated hens fed the dietary treatments for 3 months were collected and incubated. Chicks that hatched were individually weighed and wing-banded. Chicks were then separated based on maternal dietary treatment and randomly assigned to 10 pens per maternal dietary treatment (5 chicks/pen). Individual chick weights and pen feed intake were measured weekly for 3 weeks and were used to determine growth rate and feed efficiency. Feed composition was the same across all chick treatment groups, as shown in Table 1.

Fatty Acid Composition

Relative fatty acid composition of diets, eggs, newly hatched chicks (NHC), and 25-day-old chicks (TWC) were determined. One 500 g sample of feed was taken from each hen dietary treatment and stored at −20 °C until analysis. Three eggs from each dietary treatment were randomly selected after hens were on diets for 14 days. Three NHC and 3 TWC from each maternal dietary treatment were euthanized via asphyxiation with CO₂ and frozen at −20 °C. Empty carcass weight (ECW) of TWC was determined post-euthanasia after flushing of the gastrointestinal tract with 0.8% NaCl solution. NHC and TWC were chopped and ground/pulverized with liquid nitrogen in a Waring blender. Freshly ground samples were thoroughly mixed and re-frozen at −20 °C. Three 1 g samples were taken from each feed sample, yolk, or chick slurry and fat was extracted using chloroform/methanol (2:1 v/v) according to the method of Folch et al. [22]. Briefly, fatty acid methyl esters (FAME) were prepared with 4 mL of HCl in 100 mL of methanol for 20 min at 60 °C. The composition of FAME in each sample was determined using gas chromatography (GC). GC was performed on an Agilent 6980N gas chromatograph (Agilent Technologies, Santa Clara, CA) fitted with a CP Sil 88 column (100 m × 0.25 mm i.d. × 0.2 μm film thickness; manufactured by Chromapack, Middleburg, The Netherlands, and available from Varian Inc., Mississauga, Canada). GC temperature settings were previously described by Kramer et al. [23]. FAME were determined by comparison of retention times with known standards (standards #463 and #UC-59M, Nu-Chek-Prep, Elysian, MN) and expressed as percentage of total FAME.

Body Composition

Total body composition was determined for NHC and TWC. Five NHC and five TWC were euthanized via asphyxiation with CO₂ from each of the maternal dietary treatment groups.

Table 3 Effect of maternal dietary conjugated linoleic acid (CLA) with two types of oil, safflower oil (SO) or olive oil (OO) on newly hatched chick body composition

	ECW (g)	% Water	% Protein	% Fat	% Ash
SO	37.0 ± 0.7	78.3 ± 0.6	14.2 ± 0.8	5.5 ± 0.4	2.0 ± 0.1
SO + CLA	37.4 ± 0.5	77.0 ± 0.4	15.4 ± 0.4	5.6 ± 0.3	2.0 ± 0.0
OO	37.8 ± 1.0	77.7 ± 0.4	15.0 ± 0.6	5.3 ± 0.4	1.9 ± 0.0
OO + CLA	38.2 ± 0.7	77.7 ± 0.3	14.6 ± 0.9	5.8 ± 0.2	2.0 ± 0.0
<i>p-Values</i>					
Oil type	0.31	0.45	0.97	0.95	0.05
CLA	0.61	0.44	0.52	0.36	0.51
Oil*CLA	1.0	0.92	0.22	0.61	0.81

Diets (g/100 g diet): SO, 3.5 g safflower oil/100 g; SO + CLA, 3 g safflower oil/100 g plus 0.5 g CLA/100 g; OO, 3.5 g olive oil/100 g; OO + CLA, 3 g olive oil/100 g plus 0.5 g CLA/100 g. Data are expressed as mean ± SE of 5 chicks per treatment group. No differences due to CLA, oil type, or oil type*CLA were found

ECW empty carcass weight (including the residual yolk)

Gut contents were removed via flushing with 0.8% NaCl solution from TWC post-euthanasia. Chick samples were then frozen at -20°C . NHC and TWC were chopped and ground/pulverized with liquid nitrogen in a Waring blender. Ground samples were then thoroughly mixed and weighed. Total ground NHC were placed in a freeze-drier for 60 h to determine total body water/dry matter content. Three 50 g samples of TWC were randomly selected from the ground slurry and placed in the freeze-drier for 60 h to determine total body water/dry matter content. Kjeldahl-N, lipid, and ash were determined in duplicate or triplicate on the freeze-dried ground samples (NHC) or sub-samples (TWC). Total body N was determined in samples digested with a sulfuric acid-hydrogen peroxide mixture [24] where ammonium levels were measured using a phenol-hypochlorite reaction [25]. Fat was extracted from freeze-dried sub-samples for both NHC and TWC using a soxhlet apparatus containing ethyl ether for 72 h and dried at 100°C for 24 h. Remaining fat-free dry material was then ashed at 750°C for 24 h and ash weight was determined.

Statistical Analysis

All data were analyzed by using two-way ANOVA as a 2×2 factorial with SAS (SAS Institute Inc., Cary, NC). Data were analyzed for main effects of added dietary oil, addition of CLA, as well as the oil*CLA interaction. Differences were considered significant at $p < 0.05$. Post-ANOVA analyses of mean treatment differences were determined using least squared differences.

Results and Discussion

Unlike previous reports involving mammalian species [1–9], where body composition was affected by maternal

CLA feeding, the body fat of the NHC and TWC progeny of CLA-fed SCWL hens was not reduced by maternally fed CLA (Tables 3 and 4, $p > 0.05$). In contrast to previous results, relative proportion of fat in TWC was increased (although not significantly, where the main effect of CLA was $p = 0.15$) and water was decreased (main effect of CLA was $p < 0.05$) as the result of maternally fed CLA regardless of additional fat source (no oil*CLA interaction, $p > 0.05$). The inability to show reduced total body fat in NHC from CLA-fed hens is in contrast to the finding of Cherian et al. [16]. In the work of Cherian et al. [16], newly hatched chicks from hens fed 0.5 or 1% CLA-75 (at the expense of 3% corn oil) had 16 and 26% less total carcass fat, respectively, than those obtained from control-fed hens. A significant reduction ($p < 0.05$) in hepatic total lipid and triacylglyceride content was also shown in their study, and it was suggested that the reduction was due to lack of mobilization of yolk lipid to the developing embryo. The inability to reproduce the significant body fat reductions ($p < 0.05$) in NHC due to maternal CLA feeding reported by Cherian et al. [16] in this study could be due to breed of hens. Cherian et al. [16] utilized heavier New Hampshire laying hens, whereas lighter SCWL hens were used in the present study. While similar levels of CLA were added to the maternal diets in both studies (0.5 g/100 g of feed), the New Hampshire females consume considerably more feed and were exposed to CLA-75, whereas SCWL hens [26] consume less and were exposed to CLA-60 hence, CLA exposure was likely higher in Cherian et al. [16].

The work reported here also extended the findings reported by Cherian et al. [16] in that the effects of maternal CLA on the composition of progeny grown to 25 days of age (TWC) was also investigated. A random sample of chicks ($n = 5$ or 6) from each treatment was selected from the larger population used to generate the gain data shown in Fig. 1, and body composition was

Table 4 Effect of maternal dietary conjugated linoleic acid (CLA) with two types of oil, safflower oil (SO) or olive oil (OO) on 25-day-old chick body composition

	ECW (g)	% Water	% Protein	% Fat	% Ash
<i>Treatment</i>					
SO	225.8 ± 10.1	71.1 ± 0.7 ^{ab}	20.4 ± 0.5	6.4 ± 0.5	2.2 ± 0.1 ^b
SO + CLA	215.0 ± 11.5	69.6 ± 0.8 ^{ab}	20.6 ± 1.2	7.3 ± 0.6	2.4 ± 0.1 ^{ab}
OO	225.8 ± 4.2	71.2 ± 1.1 ^a	21.3 ± 0.6	5.4 ± 0.6	2.2 ± 0.1 ^b
OO + CLA	210.8 ± 6.7	67.6 ± 1.1 ^b	22.1 ± 1.3	7.7 ± 0.7	2.7 ± 0.1 ^a
<i>p-Values</i>					
Oil type	0.77	0.87	0.16	0.40	0.10
CLA	0.17	0.03	0.69	0.15	0.009
Oil*CLA	0.82	0.12	0.69	0.17	0.42

Diets (g/100 g diet): SO, 3.5 g safflower oil/100 g; SO + CLA, 3 g safflower oil/100 g plus 0.5 g CLA/100 g; OO, 3.5 g olive oil/100 g; OO + CLA, 3 g olive oil/100 g plus 0.5 g CLA/100 g. Data are expressed as mean ± SE of 5 or 6 chicks per treatment group. Means with different letters within a column are significantly different ($p < 0.05$). Main effect of oil was not significant at $p < 0.05$ across all body composition measurements. Main effect of CLA on % water and % ash was significant at $p < 0.05$. Oil type*CLA interaction was not significant at $p < 0.05$ across all body composition measurements. Chicks were fed standard corn/soybean meal poultry chick mash ration from hatch until they were euthanized at 25 days of age. Chicks used in this analysis were a random sub-sample of chicks used to create data in Fig. 1. ECW (empty carcass weight) was greater than gain in Fig. 1 since the chicks were 4 days older and ECW also includes initial chick weight. ECW is not an accurate measurement of growth of the population due to random sub-sampling

ECW empty carcass weight

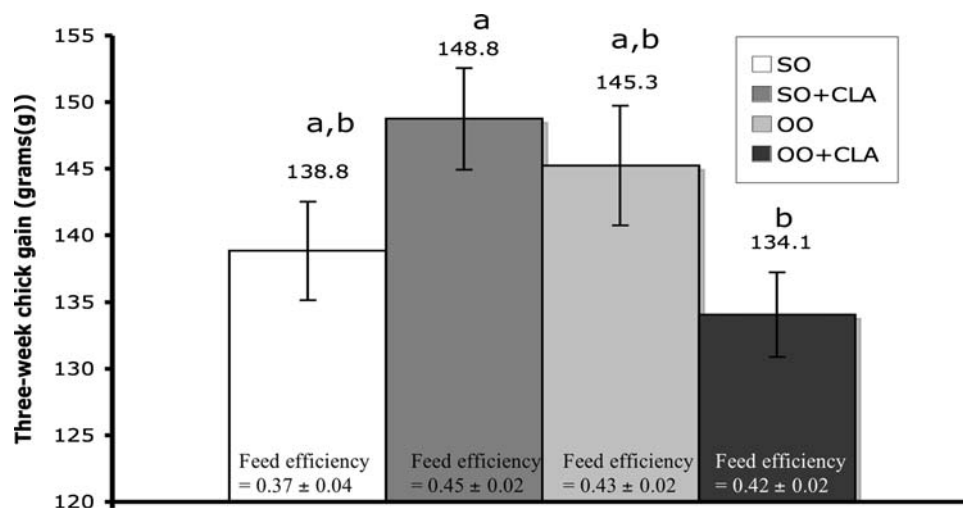


Fig. 1 Effect of maternal diets containing conjugated linoleic acid (CLA) with the presence of two types of oils, safflower oil (SO) or olive oil (OO) on 3-week progeny (chick) gain and feed efficiency. Diets: SO, 3.5 g safflower oil/100 g; SO + CLA, 3 g safflower oil/100 g plus 0.5 g CLA/100 g; OO, 3.5 g olive oil/100 g; OO + CLA, 3 g olive oil/100 g plus 0.5 g CLA/100 g. Feed efficiency = feed consumed per chick (g)/21 day gain per chick (g), where chicks consumed: SO = 375 g/chick; SO + CLA = 331 g/chick; OO = 338 g/chick; OO + CLA = 319 g/chick. Data are expressed as

means ± SE. Columns with different superscripts are significantly different, where $p < 0.05$, when analyzed as a 2×2 factorial, $n = 50$. Feed efficiency is shown at the bottom of each bar for each respective treatment. Main effect of oil type not significant, $p > 0.05$: growth, $p = 0.27$; feed efficiency, $p = 0.60$. Main effect of CLA not significant, $p > 0.05$: growth, $p = 0.80$; feed efficiency, $p = 0.29$. Oil type*CLA interaction significant, $p < 0.05$: growth, $p = 0.007$. Oil type*CLA interaction not significant, $p > 0.05$: feed efficiency, $p = 0.09$

analyzed as described in the experimental procedure. The mean treatment empty carcass weights (ECW, Table 4) of this small random sample were not significantly different between treatments and were not representative of the treatment differences shown in Fig. 1 in regards to gain. Even though ECW of randomly selected chicks did not

differ due to maternal treatment, an increase in % fat in TWC, due to maternal CLA feeding, was observed. This observation was unexpected based upon CLA's known effects on altering composition in mice, rats, and pigs [1–9]. However, the effect of CLA on body fat in the avian species has not been as consistent as in mammals. Javadi

et al. [10] reported a higher relative proportion of fat in broilers fed 1% CLA-80 for 21 days as compared to controls fed 1% Safflower oil. In contrast, Zhang et al. [11], using Beijingyou chickens showed that feeding 1–2% CLA-80 in place of maize oil for 126 days exhibited decreased intramuscular fat in breast and thigh as well as decreased abdominal fat. Similar results were shown by Szymczyk et al. [12] where abdominal fat was reduced in broiler chicks exposed to 0.5–1.5% dietary CLA-60 for 42 days in comparison to those fed corn oil. These conflicting results in regards to body fat could possibly be explained by the onset of CLA feeding during the growth phase of the chickens and/or length of CLA feeding. A significant CLA main effect on TWC body ash was unexpected (Table 4). Feeding CLA to growing mice has been shown to increase bone ash [2]. The mechanism by which dietary CLA increased bone mineral content was suggested to be related to CLA's inhibition of cyclooxygenase-2 and hence PGE₂ production in the bone tissue [27]. It is plausible that differences in carcass composition could have been partially affected by the random sampling method used in this experiment (e.g., treatment mean weight of sampled chicks were not reflective of the larger population used for determining gain).

Maternal feeding of CLA has been shown to improve the growth of the progeny in several mammalian model species [13–15]. In the study reported here, maternal feeding of CLA (main effect of CLA, $p > 0.05$) had no effect on progeny growth, feed intake, or feed efficiency to 3-weeks of age (3-week gain was 142 g vs. 141 g, consumption was 356 g/chick vs. 325 g/chick, and feed efficiency was 0.40 vs. 0.44 for maternal diets across oil type with 0 or 0.5% CLA, respectively, Fig. 1). Likewise, growth of progeny was not related to the maternal dietary oil used (3-week weight gain was 144 g vs. 140 g, consumption was 353 g/chick vs. 328 g/chick, and feed efficiency was 0.41 vs. 0.42 for maternal diets across CLA level with SO or OO, respectively). However, an oil type (SO or OO)*CLA interaction was observed ($p < 0.05$, Fig. 1) where feeding CLA increased growth when SO (7.2% increase) was fed, but decreased growth when OO (7.7% decrease) was fed in the maternal diet. Changes in gain were not likely due to differences in feed consumption since no difference in feed consumption and feed efficiency were observed ($p > 0.05$). One possible mechanism in which chick growth could have been reduced when the maternal diet contained OO + CLA was through a reduction of 18:2(n-6). Hargrave et al. [28] showed that the addition of CLA to diets marginal in 18:2(n-6) (coconut oil-based diet) resulted in a decrease in tissue 18:2(n-6), relative to those fed diets without CLA. However, the effect of these diets on growth rate was not reported. 18:2(n-6) has been shown to be an essential fatty acid

for avian growth and development [29]. Hopkins and Nesheim [30] showed that chicks from hens marginal in 18:2(n-6) (egg 18:2(n-6) content 3–4% total FAME) require increased 18:2(n-6) in the growing diets to achieve growth rates equal to chicks hatched from hens fed adequate levels of 18:2(n-6) (egg 18:2(n-6) content 12–16% total FAME). In the study reported here, the addition of CLA to the OO diet did not result in a further reduction of egg 18:2(n-6) (Table 5). Also, chick mash (Table 1) contained a calculated 18:2(n-6) content of 1.8% (Table 1). Hence the reduced growth due to the addition of CLA to the OO diet maternal diet did not appear to be 18:2(n-6)-dependent. It is possible that these differences are due to chance and additional studies may be necessary to validate the relevance of this significant interaction.

Maternal dietary treatments altered egg yolk and NHC tissue fatty acids in a similar manner (Tables 5 and 6), and in general were as expected based on the findings of others [16–21, 31]. Maternal diet effects on fatty acid profiles of egg yolk and NHC was unlikely due to changes in yolk weight and yolk lipid (not measured in this study) since 0.5% CLA has previously shown to have no effect on these parameters [18, 19, 21]. The maternal diets with SO (main effect of oil type) resulted in egg yolks and NHC with more 18:2(n-6) (and PUFA) and less 18:1(n-9) (and MUFA) as would be expected in comparison to egg yolks and NHC from mothers fed diets containing 3–3.5% OO, a fat source containing a high amount of 18:1(n-9) [20]. Feeding the hen SO resulted in a slightly higher 20:4(n-6) level in the egg yolk than eggs from hens fed OO ($p < 0.05$), but these differences were no longer evident in the NHC. The effects of oil type fed in maternal diets on fatty acid composition were no longer evident in TWC (Table 7).

In the egg yolk and NHC, maternal CLA feeding (main effect) decreased the MUFA and increased SFA. Effects of the *t10,c12* isomer on SCD-1 are well described [2, 32–34] and explain the reason for an increased relative abundance of SFA in the egg yolk and NHC. While egg yolk had reduced 20:4(n-6) due to CLA feeding, no differences in the NHC were evident. Maternal CLA feeding (main effect, $p < 0.05$) increased the relative abundance of egg yolk and NHC total CLA (*c9,t11* and *t10,c12*). The effects of maternal CLA feeding on fatty acid content of TWC was no longer evident, except that a small amount of *c9,t11* (0.1% total FAME) was still found in TWC. Disappearance of individual CLA isomers from tissues when dietary sources have been withdrawn has been previously reported in mice [35]. The *t10,c12* isomer appears to be metabolized more rapidly than the *c9,t11* isomer. The lack of fatty acid changes due to maternal feeding in the TWC seem to suggest that body compositional changes in the TWC (ash and water) due to maternal CLA feeding was likely the result of early (embryonic or at hatch) maternal effects on

Table 5 Effect of diets containing conjugated linoleic acid (CLA) with the presence of two types of oils, safflower oil (SO) or olive oil (OO) on egg yolk fatty acid profile

Fatty acids	Dietary treatments				Oil type	CLA	Oil*CLA
	SO g/100 g fatty acid	SO + CLA methyl esters	OO	OO + CLA			
14:0	0.8 ± 0.1 ^{ab}	0.9 ± 0.0 ^a	0.7 ± 0.0 ^b	0.8 ± 0.0 ^{ab}	0.08	0.02	0.61
16:0	31.3 ± 0.9 ^b	36.1 ± 0.3 ^a	30.2 ± 0.8 ^b	35.0 ± 0.6 ^a	0.14	0.0001	0.97
16:1(n-7)	1.5 ± 0.1 ^{ab}	1.1 ± 0.2 ^b	1.7 ± 0.1 ^a	1.1 ± 0.1 ^b	0.50	0.01	0.38
18:0	14.0 ± 0.6 ^b	18.2 ± 1.2 ^a	12.1 ± 0.3 ^b	17.1 ± 0.4 ^a	0.07	0.0002	0.69
18:1(n-9)	33.7 ± 1.0 ^b	24.1 ± 0.9 ^c	45.5 ± 0.8 ^a	34.0 ± 0.2 ^b	<0.0001	<0.0001	0.30
18:2(n-6)	16.9 ± 0.4 ^a	17.0 ± 0.5 ^a	8.0 ± 0.4 ^c	9.8 ± 0.2 ^b	<0.0001	0.04	0.05
<i>cis</i> -9, <i>trans</i> -11 CLA	ND	0.7 ± 0.0	ND	0.6 ± 0.1	0.40	<0.0001	0.41
<i>trans</i> -10, <i>cis</i> -12 CLA	ND	0.2 ± 0.0	ND	0.2 ± 0.0	0.50	<0.0001	0.40
18:3(n-3)	0.2 ± 0.0 ^a	0.2 ± 0.0 ^a	0.1 ± 0.0 ^b	0.2 ± 0.0 ^a	0.08	0.001	0.04
20:4(n-6)	1.7 ± 0.1 ^a	1.5 ± 0.0 ^b	1.5 ± 0.1 ^{ab}	1.2 ± 0.0 ^b	0.03	0.02	0.70
∑CLA	ND	0.9 ± 0.0	ND	0.8 ± 0.1	0.35	<0.0001	0.36
∑SFA	46.1 ± 0.7 ^c	55.2 ± 0.8 ^a	43.0 ± 0.6 ^d	52.9 ± 0.2 ^b	0.003	<0.0001	0.72
∑MUFA	35.2 ± 1.0 ^b	25.2 ± 1.0 ^c	47.2 ± 0.8 ^a	35.1 ± 0.3 ^b	<0.0001	<0.0001	0.09
∑PUFA	18.8 ± 0.5 ^a	19.6 ± 0.5 ^a	9.6 ± 0.4 ^c	12.0 ± 0.2 ^b	<0.0001	0.06	0.08

Values are means ± SE, *n* = 3. Means in a row with different superscript letters differ, *p* < 0.05. Diets (g/100 g diet): SO, 3.5 g safflower oil/100 g; SO + CLA, 3 g safflower oil/100 g plus 0.5 g CLA/100 g; OO, 3.5 g olive oil/100 g; OO + CLA, 3 g olive oil/100 g plus 0.5 g CLA/100 g. Data are expressed as mean ± SE of 3 eggs per treatment group collected on day 14 after the onset of feeding of experimental diets. Main effect of Oil type was significant at *p* < 0.05 for: 18:1(n-9), 18:2(n-6), 20:4(n-6), ∑SFA, ∑MUFA, ∑PUFA. Main effect of CLA was significant at *p* < 0.05 for: 14:0, 16:0, 16:1(n-7), 18:0, 18:1(n-9), 18:2(n-6), 18:3(n-3), 20:4(n-6), Other, *cis*-9,*trans*-11 CLA, *trans*-10,*cis*-12 CLA, ∑CLA, ∑SFA, ∑MUFA. Oil type*CLA was significant at *p* < 0.05 for: 18:3(n-3)

∑ sum, CLA conjugated linoleic acid, SFA saturated fatty acid, MUFA monounsaturated fatty acid, PUFA polyunsaturated fatty acid, ND not detectable

progeny development. Alternatively, the presence of *c*9,*t*11 in the chick at 3-weeks of age could be responsible for the compositional changes seen in TWC.

The addition of CLA plus 3% rescue oil (SO or OO) to the laying hen diet did not effect egg production or hatchability (% hatch of fertile eggs, Fig. 2). Aydin et al. [20] showed that when CLA is added to a laying diet with no added fat, eggs completely fail to hatch within 6 days following the addition of dietary CLA. Aydin [17] also showed that the addition of 3% vegetable oil to the breeding hen diet in the presence of 0.5% CLA would prevent CLA-induced embryonic mortality. Hence the findings in this experiment are consistent with previous work. While egg production and hatchability were not altered as a result of feeding SCWL hens CLA, the addition of CLA to SO or OO in the laying hen diet led to an increase in fertility (main effect of CLA, *p* < 0.05) of approximately 5 and 10%, respectively, when compared to their respective control-fed hens. To the authors' knowledge, this is the first report of CLA's beneficial effects on fertility in the avian species. Bauman et al. [36] reported that incorporation of mixed isomers of *c*9,*t*11 and *t*10,*c*12 CLA into dairy cattle rations either prior to calving or at the onset of calving improves reproductive

performance in the cow. In a study where cows were fed less than 20 g/day of each CLA isomer, the interval between calving and first ovulation was shortened and maintenance of pregnancy was improved. These findings may be due to an improvement in energy balance post-calving, although the exact mechanism behind the improvement has not been elucidated. A possible reason that improved fertility was not observed by Aydin [17] may have been the use of both candling and egg breakout for the assessment of fertility in the current study. Aydin's [17] fertility assessment was by candling only at day 7 of incubation. Interestingly, previous reports have shown that a high amount of 18:2(n-6) in the laying hen's diet can negatively effect fertility and thereby cause a significant decrease in the reproductive success of the avian species [37–39]. In this study, there was not a decrease in fertility when the hens were fed 3% oil high in 18:2(n-6) compared to 3% oil high in 18:1(n-9) (main effect of oil type was not significant, *p* > 0.05). Since CLA tended to increase fertility regardless of the fat type used, the increase in fertility appeared to be independent of a direct effect of CLA on 18:2(n-6).

Noble and Cocchi [40] showed that the presence of 18:1(n-9) is necessary for the transport of yolk lipids to the

Table 6 Effect of diets containing conjugated linoleic acid (CLA) with the presence of two types of oil, safflower oil (SO) or olive oil (OO), on whole, newly hatched chick fatty acid profile

Fatty acid	Dietary treatments				Oil type	CLA	Oil*CLA
	SO g/100 g fatty acid	SO + CLA methyl esters	OO	OO + CLA			
16:0	25.0 ± 0.2	26.8 ± 1.5	24.7 ± 0.2	27.0 ± 1.3	0.34	0.25	0.73
16:1(n-7)	0.9 ± 0.1 ^{ab}	0.7 ± 0.0 ^b	1.0 ± 0.1 ^a	0.7 ± 0.0 ^b	0.33	0.003	0.36
18:0	12.4 ± 0.5 ^b	16.5 ± 1.4 ^a	12.5 ± 0.4 ^b	14.7 ± 0.7 ^{ab}	0.30	0.01	0.54
18:1(n-9)	29.3 ± 0.9 ^b	24.7 ± 1.7 ^c	39.7 ± 2.0 ^a	34.0 ± 0.2 ^{ab}	0.0004	0.01	0.85
18:2(n-6)	26.5 ± 0.5 ^a	24.5 ± 1.9 ^a	14.8 ± 1.1 ^b	17.0 ± 0.8 ^b	<0.0001	0.85	0.08
<i>cis</i> -9, <i>trans</i> -11 CLA	ND	0.5 ± 0.1	ND	0.5 ± 0.0	0.60	<0.0001	0.60
<i>trans</i> -10, <i>cis</i> -12 CLA	ND	0.1 ± 0.0	ND	0.1 ± 0.0	0.20	0.002	0.20
18:3(n-3)	0.2 ± 0.0 ^{ab}	0.2 ± 0.0 ^a	0.2 ± 0.0 ^b	0.2 ± 0.0 ^a	0.24	0.06	0.33
20:4(n-6)	4.9 ± 0.3	5.3 ± 0.4	5.9 ± 0.4	5.1 ± 0.1	0.38	0.53	0.32
22:6(n-3)	0.8 ± 0.0 ^b	0.7 ± 0.1 ^b	1.2 ± 0.1 ^a	0.8 ± 0.1 ^b	0.01	0.04	0.29
∑CLA	ND	0.6 ± 0.1	ND	0.6 ± 0.0	0.34	<0.0001	0.34
∑SFA	37.4 ± 0.5 ^{ab}	43.3 ± 2.9 ^a	37.2 ± 0.4 ^b	41.7 ± 1.8 ^{ab}	0.44	0.03	0.87
∑MUFA	30.2 ± 0.9 ^b	25.4 ± 1.7 ^c	40.7 ± 2.1 ^a	34.7 ± 0.2 ^{ab}	0.0005	0.01	0.89
∑PUFA	32.4 ± 0.6 ^a	30.7 ± 2.0 ^a	22.1 ± 0.7 ^b	23.1 ± 0.7 ^b	<0.0001	0.63	0.13

Values are means ± SE, *n* = 3. Means in a row with different superscript letters differ, *p* < 0.05. Diets: SO, 3.5 g safflower oil/100 g; SO + CLA, 3 g safflower oil/100 g plus 0.5 g CLA/100 g; OO, 3.5 g olive oil/100 g; OO + CLA, 3 g olive oil/100 g plus 0.5 g CLA/100 g. Data are expressed as mean ± SE of 3 chicks per treatment group. Main effect of Oil type significant at *p* < 0.05 for: 18:1(n-9), 18:2(n-6), ∑MUFA, ∑PUFA. Main effect of CLA significant at *p* < 0.05 for: 16:1(n-7), 18:0, 18:1(n-9), 18:3(n-3), *cis*-9,*trans*-11 CLA, *trans*-10,*cis*-12 CLA, 22:6(n-3), ∑CLA, ∑SFA, ∑MUFA. Oil type*CLA was not significant at *p* < 0.05 across all fatty acid measurements

∑ sum, CLA conjugated linoleic acid, SFA saturated fatty acid, MUFA monounsaturated fatty acid, PUFA polyunsaturated fatty acid, ND not detectable

developing embryo. Nobel [41] suggested that the egg levels of 18:1(n-9) may be important for the reproductive success of avian species. Since both CLA (*t*10,*c*12 isomer) and 18:2(n-6) are inhibitors of SCD-1 [32–34, 42] the addition of both CLA and 18:2(n-6) as the predominate fatty acids in the diet of some of the hens used in this study (SO + CLA) should provide a means of testing the importance of 18:1(n-9) for embryonic chick development. Eggs from hens fed SO + CLA had approximately half the 18:1(n-9) content of eggs from hens fed OO. While the hatchability of the eggs from hens fed SO + CLA (72%) appeared reduced relative to those fed OO (82%), significant differences were not detected in this study. Using purified 18:2(n-6) or 18:1(n-9) fatty acids, Aydin [17] also showed that reducing the relative proportion of egg 18:1(n-9) from 38.3 to 16.6% by feeding 18:2(n-6) + CLA did not have an adverse effect on hatchability. Hence, the value of 18:1(n-9) in the egg for the developing embryo appeared adequate within the limits shown in this study (see Table 5).

The content of individual isomers of CLA in the diet of the hens showed a higher CLA concentration in the diet containing SO as compared to OO (Table 2). The differences observed cannot be explained within the context of artifacts described by Park et al. [43]. Methods used for

analyzing CLA in the diet attempted to minimize the formation of artifacts [43]. Yurawecz et al. [44] pointed out that the most appropriate method of hydrolysis and esterification can be largely matrix dependent. When the OO-based diet was analyzed using the HCl/MeOH acid-catalyzed methylation procedure [43], the content of the two CLA isomers were as predicted from calculation. The same procedure on the SO-based diets overestimated the isomer content. This overestimate of CLA when analyzing the SO-based diet is clearly an analytical artifact since the relative content of CLA and each of its isomers in the egg and day-old chick was similar between samples collected from hens fed the SO + CLA and the OO + CLA diets (Tables 5 and 6).

In conclusion, unlike results obtained in mammals, maternal feeding of CLA to SCWL did not result in improved progeny growth or feed conversion. Maternal feeding of CLA does alter progeny body composition (increased ash and decreased water) up to 25 days after hatch. Changes in body composition may be directly dependent on the fatty acid composition supplied maternally during embryogenesis or the early post hatch developmental stage; however, the effects were not evident until later in life. The increased fertility resulting from maternal CLA feeding, regardless of dietary rescue oil

Table 7 Effect of diets containing conjugated linoleic acid (CLA) with the presence of two types of oils, safflower oil (SO) or olive oil (OO), on whole, three-week-old chick fatty acid profile

Fatty acid	Dietary treatments				Oil type	CLA	Oil*CLA
	SO	SO + CLA	OO	OO + CLA			
	g/100 g fatty acid methyl esters						
					<i>p</i> -Values		
16:0	27.0 ± 0.8	27.8 ± 0.8	26.6 ± 0.2	27.7 ± 0.3	0.37	0.07	0.43
16:1(n-7)	5.5 ± 0.6	5.7 ± 0.8	5.4 ± 0.3	5.8 ± 0.4	0.87	0.55	0.83
18:0	11.2 ± 0.4	10.7 ± 0.9	12.2 ± 0.8	10.9 ± 0.4	0.60	0.35	0.75
18:1(n-9)	38.8 ± 1.1	39.3 ± 0.8	40.1 ± 1.0	40.2 ± 0.9	0.62	0.42	0.71
18:2(n-6)	15.3 ± 1.1	14.5 ± 0.7	13.4 ± 0.3	13.3 ± 0.2	0.04	0.77	0.48
<i>cis</i> -9, <i>trans</i> -11 CLA	ND	0.1 ± 0.0 ^a	ND	0.1 ± 0.0 ^a	0.45	0.01	0.49
<i>trans</i> -10, <i>cis</i> -12 CLA	ND	ND	ND	ND	NA*	NA	NA
18:3(n-3)	0.7 ± 0.1	0.7 ± 0.0	0.6 ± 0.0	0.7 ± 0.0	0.36	0.30	0.37
20:4(n-6)	1.5 ± 0.2	1.2 ± 0.3	1.6 ± 0.1	1.3 ± 0.3	0.87	0.38	0.89
∑CLA	ND	0.1 ± 0.0 ^a	ND	0.1 ± 0.0 ^a	0.45	0.01	0.49
∑SFA	38.2 ± 0.6	38.5 ± 0.1	38.8 ± 0.7	38.6 ± 0.4	0.72	0.30	0.62
∑MUFA	44.3 ± 1.2	45.0 ± 1.5	45.5 ± 1.2	46.0 ± 1.0	0.75	0.38	0.71
∑PUFA	17.5 ± 1.1	16.4 ± 1.0	15.6 ± 0.2	15.3 ± 0.5	0.07	0.65	0.49

Values are means ± SE, $n = 3$. Means in a row with different superscript letters differ, $p < 0.05$. Diets: SO, 3.5 g safflower oil/100 g; SO + CLA, 3 g safflower oil/100 g plus 0.5 g CLA/100 g; OO, 3.5 g olive oil/100 g; OO + CLA, 3 g olive oil/100 g plus 0.5 g CLA/100 g. Data are expressed as mean ± SE of 3 chicks per treatment group. Main effect of oil type was not significant at $p < 0.05$ across all fatty acid measurements. Main effect of CLA significant at $p < 0.05$ for: *cis*-9,*trans*-11 CLA, ∑CLA. Oil type*CLA interaction was not significant at $p < 0.05$ across all fatty acid measurements

∑ sum, CLA conjugated linoleic acid, SFA saturated fatty acid, MUFA monounsaturated fatty acid, PUFA polyunsaturated fatty acid, NA not applicable, ND not detectable

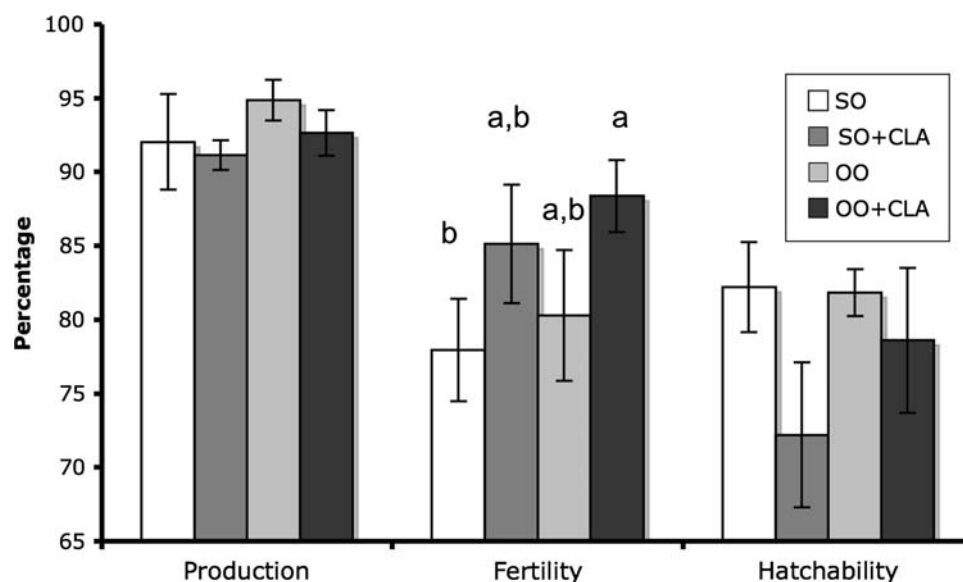


Fig. 2 Effect of diets containing conjugated linoleic acid (CLA) with the presence of two types of oils, safflower oil (SO) or olive oil (OO) on egg production, fertility, and hatchability. Diets (g/100 g diet): SO, 3.5 g safflower oil/100 g; SO + CLA, 3 g safflower oil/100 g plus 0.5 g CLA/100 g; OO, 3.5 g olive oil/100 g; OO + CLA, 3 g olive oil/100 g plus 0.5 g CLA/100 g. Parameters measured were hen egg day production, fertility (# fertile eggs/# of eggs produced), and hatchability (# eggs hatched/# of fertile eggs), where fertile eggs were determined via candling and egg breakout, $n = 12$ hens/trt. Data are

expressed as means ± SE. Columns with different superscripts are significantly different, where $p < 0.05$, when analyzed as a 2×2 factorial. Main effects of oil type: production, $p = 0.30$; fertility, $p = 0.42$; hatchability, $p = 0.46$. Main effects of CLA: production, $p = 0.45$; fertility, $p = 0.04$; hatchability, $p = 0.10$. Oil type*CLA interaction: production, $p = 0.74$; fertility, $p = 0.90$; hatchability, $p = 0.39$. Main effects of oil type and CLA, as well as oil type*CLA interaction were not significant for production or hatchability, however, fertility main effect of CLA was significant, $p < 0.05$

used, was unexpected and could prove of value for improving reproduction of avian species.

Acknowledgments The authors express their gratitude to S&R Farms (Whitewater, WI) for providing laying hens and to the staff at the University of Wisconsin-Madison Poultry Research Lab (Dawn Irish, George Bradley, and Angel Gutierrez) for support of research. The authors would like to thank Shane Huebner for his assistance in fatty acid analysis, Debra Schneider for her assistance in body composition analysis, and David Trott for assistance in certain aspects of this project. Research was supported through royalties received from the Wisconsin Alumni Research Foundation (WARF), as one of the authors (MEC) is an inventor on CLA patents assigned to WARF.

References

- Park Y, Albright KJ, Liu W, Storkson JM, Cook ME, Pariza MW (1997) Effect of conjugated linoleic acid on body composition in mice. *Lipids* 32:852–858
- Park Y, Storkson JM, Albright KJ, Liu W, Pariza MW (1999) Evidence that the *trans*-10, *cis*-12 isomer of conjugated linoleic acid induces body composition changes in mice. *Lipids* 34:235–241
- Hayman A, MacGibbon A, Pack RJ, Rutherford K, Green JH (2002) High intake, but not low intake, of CLA impairs weight gain in growing mice. *Lipids* 37:689–692
- Terpstra AH, Javadi M, Beynen AC, Kocsis S, Lankhorst AE, Lemmens AG, Mohede IC (2003) Dietary conjugated linoleic acids as free fatty acids and triacylglycerols similarly affect body composition and energy balance in mice. *J Nutr* 133:3181–3186
- Choi N, Kwon D, Yun SH, Jung MY, Shin HK (2004) Selectively hydrogenated soybean oil with conjugated linoleic acid modifies body composition and plasma lipids in rats. *J Nutr Biochem* 15:411–417
- Yamasaki M, Ikeda A, Oji M, Tanaka Y, Hirao A, Kasai M, Iwata T, Tachibana H, Yamada K (2003) Modulation of body fat and serum leptin levels by dietary conjugated linoleic acid in Sprague-Dawley rats fed various fat-level diets. *Nutrition* 19:30–35
- Ostrawska E, Muralitharan M, Cross RF, Bauman DE, Dunshea FR (1999) Dietary conjugated linoleic acids increase lean tissue and decrease fat deposition in growing pigs. *J Nutr* 129:2037–2042
- Thiel-Cooper RL, Parrish FC Jr, Sparks JC, Wiegand BR, Ewan RC (2001) Conjugated linoleic acid changes swine performance and carcass composition. *J Anim Sci* 79:1821–1828
- Corl BA, Mathews-Oliver SA, Lin X, Oliver WT, Ma Y, Harrell RJ, Odle J (2008) Conjugated linoleic acid reduces body fat accretion and lipogenic gene expression in neonatal pigs fed low- or high-fat formulas. *J Nutr* 138:449–454
- Javadi M, Geelen MJ, Everts H, Hovenier R, Javadi S, Kappert H, Beynen AC (2007) Effect of dietary conjugated linoleic acid on body composition and energy balance in broiler chickens. *Br J Nutr* 98:1152–1158
- Zhang GM, Wen J, Chen JL, Zhao GP, Zheng MQ, Li WJ (2007) Effect of conjugated linoleic acid on growth performances, carcass composition, plasma lipoprotein lipase activity and meat traits of chicken. *Br Poult Sci* 48:217–223
- Szymczyk B, Pisulewski P, Szczurek W, Hanczakowski P (2001) Effects of conjugated linoleic acid on growth performance, feed conversion efficiency, and subsequent carcass quality in broiler chickens. *Br J Nutr* 85:465–473
- Chin SF, Storkson JM, Albright KJ, Cook ME, Pariza MW (1994) Conjugated linoleic acid is a growth factor for rats as shown by enhanced weight gain and improved feed efficiency. *J Nutr* 124:2344–2349
- Bee G (2000) Dietary conjugated linoleic acid consumption during pregnancy and lactation influences growth and tissue composition in weaned pigs. *J Nutr* 130:2981–2989
- Poulos SP, Sisk M, Hausman DB, Azain MJ, Hausman GJ (2001) Pre- and postnatal dietary conjugated linoleic acid alters adipose development, body weight gain and body composition in Sprague-Dawley rats. *J Nutr* 131:2722–2731
- Cherian G, Ai W, Goeger MP (2005) Maternal dietary conjugated linoleic acid alters hepatic triacylglycerol and tissue fatty acids in hatched chicks. *Lipids* 40:131–136
- Aydin R (2000) The effects of dietary CLA on avian lipid metabolism. Dissertation, University of Wisconsin-Madison
- Aydin R, Cook ME (2004) The effect of dietary conjugated linoleic acid on egg yolk fatty acids and hatchability in Japanese quail. *Poult Sci* 83:2016–2022
- Muma E, Palander M, Nasi M, Pfeiffer A-M, Keller T, Grinnari JM (2006) Modulation of conjugated linoleic acid-induced loss of chicken egg hatchability by dietary soybean oil. *Poult Sci* 85:712–720
- Aydin R, Pariza MW, Cook ME (2001) Olive oil prevents the adverse effects of dietary conjugated linoleic acid on chick hatchability and egg quality. *J Nutr* 131:800–806
- Cherian G, Holsonbake TB, Goeger MP, Bidfell R (2002) Dietary CLA alters yolk and tissue FA composition and hepatic histopathology of laying hens. *Lipids* 37:751–757
- Folche J, Lees M, Sloane-Stanley GH (1957) A simple method for the isolation and purification of total lipids from animal tissues. *J Biol Chem* 226:497–507
- Kramer JK, Blackadar CB, Zhou J (2002) Evaluation of two GC columns (60-m SUPELCOWAX 10 and 100-m CP Sil 88) for analysis of milkfat with emphasis on CLA, 18:1, 18:2, and 18:3 isomers, and short- and long-chain FA. *Lipids* 37:823–835
- Brotz PG, Schaefer DM (1984) Nitrogen, calcium, and phosphorous determination from a single digestion of feed or feces. *J Anim Sci* 59:S408
- Broderick GA, Kang JH (1980) Automated simultaneous determination of ammonia and total amino acids in ruminal fluid and in vitro media. *J Dairy Sci* 63:64–75
- National Research Council (NRC) (1994) Nutrient requirements of poultry. National Academy Press, Washington, DC
- Watkins BA, Seifert MF (2000) Conjugated linoleic acid and bone biology. *J Am Coll Nutr* 19:S478–S486
- Hargrave KM, Meyer BJ, Li C, Azain MJ, Baile CA, Miner JL (2004) Influence of dietary conjugated linoleic acid and fat source on body fat and apoptosis in mice. *Obes Res* 12:1435–1444
- Bieri JG, Briggs GM, Fox MR, Ortiz LO, Pollard CJ (1956) Essential fatty acids in the chick. 1. Development of fat deficiency. *Proc Soc Exp Biol Med* 93:237–240
- Hopkins DT, Nesheim MC (1967) The linoleic acid requirement of chicks. *J Poult Sci* 46:872–880
- Latour MA, Devitt AA, Meunier RA, Stewart JJ, Watkins BA (2000) Effects of conjugated linoleic acid. 1. Fatty acid modification of yolks and neonatal fatty acid metabolism. *Poult Sci* 79:817–821
- Choi Y, Kim Y, Han Y, Park Y, Pariza MW, Ntambi JM (2000) The *trans*-10, *cis*-12 isomer of conjugated linoleic acid down-regulates Stearoyl-CoA desaturase 1 gene expression in 3T3-L1 adipocytes. *J Nutr* 130:1920–1924
- Park Y, Storkson JM, Ntambi JM, Cook ME, Sih CJ, Pariza MW (2000) Inhibition of hepatic Stearoyl-CoA desaturase activity by *trans*-10, *cis*-12 conjugated linoleic acid and its derivatives. *Biochim Biophys Acta* 1486:285–292
- Choi YJ, Park Y, Pariza MW, Ntambi JM (2001) Regulation of Stearoyl-CoA desaturase activity by the *trans*-10, *cis*-12 isomer

- of conjugated linoleic acid in HepG2 cells. *Biochem Biophys Res Commun* 284:689–693
35. Park Y, Albright KJ, Storkson JM, Liu W, Cook ME, Pariza MW (1999) Changes in body composition in mice during feeding and withdrawal of conjugated linoleic acid. *Lipids* 34:243–248
 36. Bauman DE, Castaneda-Gutierrez E, Butler WR, de Veth M, Pfeiffer A (2007) Method of enhancing reproductive function of mammals by feeding of conjugated linoleic acids. US Patent Application 2007/0191483 A1
 37. Halle I (1999) The effect of palm oil and safflower oil in the feed of parent fattening hens on fertility, hatchability and growth of progeny. *Arch Tierernahr* 52:371–390
 38. Latour MA, Peebles ED, Doyle SM, Pansky T, Smith TW, Boyle CR (1998) Broiler breeder age and dietary fat influence the yolk fatty acid profiles of fresh eggs and newly hatched chicks. *Poult Sci* 77:47–53
 39. Vilchez C, Touchburn SP, Chavez ER, Chan CW (1991) Effect of feeding palmitic, oleic, and linoleic acids to Japanese quail hens (*Coturnix coturnix japonica*). 1. Reproductive performance and tissue fatty acids. *Poult Sci* 70:2484–2493
 40. Noble RC, Cocchi M (1990) Lipid metabolism and the neonatal chicken. *Prog Lipid Res* 29:107–140
 41. Nobel RC (1987) Lipid metabolism in the chick embryo: some recent ideas. *J Exp Zool* 1:S65–S73
 42. Sessler AM, Kaur N, Palta JP, Ntambi JM (1996) Regulation of Stearoyl-CoA desaturase mRNA stability by polyunsaturated fatty acids in 3T3-L1 adipocytes. *J Biol Chem* 271:29854–29858
 43. Park Y, Albright KJ, Cai ZY, Pariza MW (2001) Comparison of methylation procedures for conjugated linoleic acid and artifact formation by commercial (trimethylsilyl) diazomethane. *J Agric Food Chem* 49:1158–1164
 44. Yurawecz MP, Kramer JKG, Ku Y (1999) Methylation procedures for conjugated linoleic acid. In: Yurawecz MP, Mossoba MM, Kramer JKG, Pariza MW, Nelson GJ (eds) *Advances in conjugated linoleic acid research*, vol 1. AOCS Press, Champaign, pp 64–82

Conjugated Linoleic Acid Decreases MCF-7 Human Breast Cancer Cell Growth and Insulin-Like Growth Factor-1 Receptor Levels

Danielle L. Amarù · Catherine J. Field

Received: 13 July 2008 / Accepted: 26 January 2009 / Published online: 6 March 2009
© AOCS 2009

Abstract In vitro work suggests that conjugated linoleic acid (CLA) isomers (c9,t11 and t10,c12) are cytotoxic to human breast cancer cells, however the mechanism remains unknown. Using human MCF-7 breast cancer cells, we examined the effects of c9,t11 and t10,c12 CLA compared to oleic acid (OA), linoleic acid (LA), or untreated cells on cell membrane phospholipid composition, cell survival, and the insulin-like growth factor-I (IGF-I) and the downstream insulin receptor substrate-1 (IRS-1). Both CLA isomers were incorporated into membrane phospholipids ($p < 0.05$). Compared to untreated cells, c9,t11 or t10,c12 CLA significantly reduced the metabolic activity of IGF-I stimulated MCF-7 cells, increased lactate dehydrogenase (LDH) release, and decreased cellular concentrations of the IGF-I receptor (IGF-IR) and insulin receptor substrate-1 ($p < 0.05$). Incubation with t10,c12 CLA also reduced the levels of phosphorylated IGF-1R. The effects on all of these measures were greater ($p < 0.05$) for t10,c12 CLA compared to c9,t11 CLA. There were few differences between LA-treated and c9,t11 CLA-treated cells, whereas cellular metabolic activity, LDH release, and IGF-IR concentrations differed between t10,c12 CLA-treated and LA-treated cells ($p < 0.05$). OA stimulated growth compared to the untreated condition ($p < 0.05$). In summary, this study demonstrated that the t10,c12 CLA isomer inhibits growth of MCF-7 cells and suggested that this may be mediated through incorporation into cellular phospholipids and

interference with the function of IGF-I and related signaling proteins.

Keywords c9,t11 CLA · t10,c12 CLA · Breast cancer · Conjugated linoleic acid · Insulin-like growth factor-I · IGF-I receptor · Insulin receptor substrate-1 · Mammary · MCF-7 · Tumour

Abbreviations

AA	Arachidonic acid
BSA	Bovine serum albumin
c9, t11 CLA	<i>Cis</i> -9, <i>trans</i> -11 CLA
CLA	Conjugated linoleic acid
DHA	Docosahexaenoic acid
DMEM	Dulbecco's modified Eagle medium
FBS	Fetal bovine serum
IGF-I	Insulin-like growth factor I
IGF-IR	Insulin-like growth factor-I receptor
IRS-1	Insulin receptor substrate-1
LA	Linoleic acid
LDH	Lactate dehydrogenase
MUFA	Monounsaturated fatty acids
OA	Oleic Acid
PUFA	Polyunsaturated fatty acid
SFA	Saturated fatty acids
t10,c12 CLA	<i>trans</i> -10, <i>cis</i> -12 CLA

Introduction

The role of dietary fat in the prevention or treatment of breast cancer remains controversial. The relationship between total fat intake and breast cancer risk or treatment outcome is not clear, potentially due to opposing effects of

D. L. Amarù · C. J. Field (✉)
Alberta Institute for Human Nutrition,
Department of Agricultural, Food and Nutritional Science,
University of Alberta, 4-126A HRIF East,
Edmonton, AB T6G 2P5, Canada
e-mail: Catherine.Field@ualberta.ca

the different dietary fats on tumour growth. Recently, there has been considerable interest in the potential anti-carcinogenic properties of conjugated linoleic acid (CLA). CLA consists of a group of positional and geometric (*cis-trans*) stereoisomers of linoleic acid (LA) that are commercially synthesised from plant oils [1] or formed during the biohydrogenation of LA by ruminant animals [2]. The *cis-9,trans-11* (c9,t11) CLA isomer is the most prevalent form found in ruminant-derived foods (e.g. milk and meat) [2]. The *trans-10,cis-12* (t10,c12) CLA isomer is present only in trace amounts in animal foods but is found in an approximate 50:50 ratio with c9,t11 CLA in many commercial CLA preparations [2]. The cytotoxicity (growth inhibition and induction of cell death) of CLA isomers in various animal and cell culture models of mammary cancer is well established [3]. The c9,t11 and t10,c12 CLA isomers have been shown in animal models to inhibit mammary tumour initiation, promotion and progression [4] and to reduce growth of human breast cancer cell lines in vitro [4–6]. Most of the animal research has used mixtures of CLA isomers, however in vitro work suggests that both major isomers (c9,t11 and t10,c12) have cytotoxic effects against cancer cells [7–10].

The mechanism by which the c9,t11 and/or t10,c12 CLA isomers inhibit mammary tumour growth is not clear. The plasma membrane is important in mediating cell growth and death [11], and alterations in membrane phospholipid composition by other dietary fats have been demonstrated to alter tumour cell function by changing membrane-mediated events and receptor functions [12]. The possible disruptive effect of the unique conjugated double bond structure of CLA on membrane function has not been studied in human breast cancer cells and may offer a possible mechanism for the anti-cancer effects of CLA. In vitro, CLA is incorporated into MDA-MB-231 breast cancer cell membrane phospholipids [8]. However, to our knowledge no studies have examined the effect of CLA incorporation into membrane phospholipids on the signal transduction of membrane bound proteins such as growth factor receptors.

Insulin-like growth factor I (IGF-I) is a mitogenic peptide that is believed to play a role in breast cancer development. In vitro, IGF-I stimulates growth and inhibits apoptosis of breast cells [13]. In humans, high circulating levels of IGF-I are associated with an increased risk of premenopausal breast cancer [14, 15]. During puberty, the formation of terminal end buds (the primary sites where breast cancer develops) is dependent on IGF-I signaling [16, 17]. CLA fed to rodents during puberty reduced the development of mammary tumours by altering mammary gland development, specifically by reducing the number of terminal end buds [18]. In vitro, Kim et al. [19] reported that CLA reduced HT-29 colon cancer cell responsiveness

to IGF-I signaling. These studies provide indirect evidence that CLA might influence IGF-I mediated effects.

The IGF-I receptor (IGF-IR) is located in the outer membrane of the cell. Upon binding of IGF-I, the IGF-IR is phosphorylated and initiates various signalling cascades, resulting in an increase in cellular proliferation and an inhibition of apoptosis [13]. The insulin receptor substrate-1 (IRS-1) is an essential component of IGF- type 1 receptor (IGF-IR) signaling, and links the receptor to key downstream signaling cascades [20]. Decreasing the amount of IRS-1 has been recently demonstrated to decrease the growth of MCF-7 cells [21]. The effect of CLA on IGF-I and related molecules has not been examined in breast cancer cell lines. The purpose of this study was to first establish whether the c9,t11 and t10,c12 CLA isomers inhibit IGF-I-induced proliferation of MCF-7 human breast cancer cells, which exhibit upregulated IGF-IR levels and IGF signaling [22]. Second, we sought to determine the effects of incubating c9,t11 and t10,c12 CLA on membrane phospholipid composition, the content of the total and phosphorylated IGF-1 receptor and the content of the insulin receptor substrate-1 (IRS-1), an important signaling protein in these breast cancer cells.

Experimental Procedure

Cell Culture

MCF-7 estrogen receptor-positive breast cancer cells were obtained from the American Type Culture Centre (Cedarlane Laboratories Ltd, Burlington, ON, Canada). The cells were cultured in 1:1 Dulbecco's Modified Eagle Medium: Nutrient Mix F-12 (DMEM:F12) with 15 mM HEPES and 365 mg/L of L-glutamine containing 5% v/v fetal bovine serum (FBS) and 1% v/v antibiotic/antimycotic (Invitrogen/Gibco Corporation, Burlington, ON, Canada). Cells were maintained at 37 °C in a humidified atmosphere in 5% v/v CO₂. The medium was changed every 2 days and cells were routinely passaged at 80–90% confluence.

Fatty Acids

Linoleic acid (LA; C18:2n-6), oleic acid (OA; C18:1n-9), and CLA isomers (C18:2-c9,t11 and C18:2-t10,c12) were purchased from Matreya (Pleasant Gap, PA). Stock solutions of fatty acids were prepared in ethanol or hexane at a concentration of 10 mg/mL and stored at –80 °C under N₂(g) until needed. Fatty acids were complexed to bovine serum albumin (BSA) depleted of essential fatty acids (Sigma-Aldrich Canada Ltd., Oakville, ON, Canada) at a 4:1 ratio as previously described [23]. Briefly, a 12-mg aliquot of the fatty acid stock was dried under nitrogen, and

then incubated with 1 mL KOH (0.1 M) for 10 min at 50 °C in a shaking water bath. Nine millilitres of sterile-filtered 7.5% v/v BSA in doubly distilled water was added. Solutions were vortexed, kept at room temperature for 3 h, incubated at 4 °C overnight, and then stored in sterile microcentrifuge tubes (Medicorp Inc., Montreal, PC, Canada) at –30 °C until used.

Determination of Growth Inhibition of IGF-I-Stimulated MCF-7 Cells

Growth experiments were performed in which the experimental fatty acids were added in isolation (at 128 or 256 μ M) or in combination with LA (128 μ M fatty acid + 128 μ M LA). An untreated condition was also included, in which no exogenous fatty acids were added to the medium. Cells were plated in 96-well flat-bottomed tissue culture plates (Thermo Fisher Scientific, Edmonton, AB, Canada) at a density of 3,000 cells/well in 200 μ L of 5% v/v FBS supplemented DMEM:F12 medium. After culture for 48 h, the medium was replaced with serum-free, phenol red-free DMEM:F12 (Invitrogen/Gibco) containing 0.5 mg/mL BSA (Sigma). After 24 h, cells were incubated for 24 or 48 h in serum-free medium containing 50 nM IGF-I (human recombinant expressed in *E. coli*; Sigma) plus one of the fatty acid treatments described above. Following incubation, viable cell counts were performed on a hemacytometer (Fisher Scientific, Edmonton, AB, Canada) by trypan blue and the WST-1 cell proliferation assay (Roche, Indianapolis, IN) was used to assess proliferation. Fresh serum-free medium was added (100 μ L/well) with 10 μ L/well of WST-1 cell proliferation reagent, and plates were incubated in a humidified atmosphere at 37 °C for 2 h. The assay principle is based upon the reduction of the tetrazolium salt WST-1 to formazan by cellular dehydrogenases. The plates were premixed for 60 s and the generation of the dark yellow coloured formazan is measured on a microplate spectrophotometer (Spectramax Plus, Molecular Devices, Sunnyvale, CA) was read at an absorbance of 440 nm. For all subsequent assays, the experimental fatty acids were provided in combination with LA (128 μ M).

Lactate Dehydrogenase Release during IGF-I Stimulation

MCF-7 cells were seeded and grown in 96-well flat-bottomed plates as above. After 24 h of fatty acid treatment, the medium was removed and centrifuged at 250 \times g. The supernatant was collected and analysed immediately or frozen at –30 °C until analysis. Lactate dehydrogenase (LDH) release was measured using the CytoTox 96 Nonradioactive Cytotoxicity Assay Kit (Thermo Fisher

Scientific, Edmonton, AB, Canada) according to the manufacturer's instructions. To determine maximum LDH release, some cells were lysed with 200 μ L of 1.5% v/v Triton X-100 (Thermo Fisher Scientific, Edmonton, AB, Canada) for 60 min at 37 °C, and the supernatant collected for analysis.

Membrane Phospholipid Fatty Acid Composition

Lipids were extracted from whole cell pellets after 24 h of treatment with IGF-I and fatty acids using a modified Folch procedure [24] as previously described [25]. Total phospholipids were isolated on silica gel thin layer chromatography plates (Thermo Fisher Scientific, Edmonton, AB, Canada) using an 80:20:1 v/v/v ratio of solvents (petroleum ether/diethyl ether/glacial acetic acid). The phospholipid band was identified using 8-anilino-1-naphthalene-sulfonic acid under long wave ultraviolet light. Fatty acid methyl esters were prepared by the addition of sodium methoxide and benzene [26] with heating at 50 °C for 10 min. Samples were then dissolved in hexane and the fatty acids were separated by automated gas liquid chromatography using hydrogen gas on a 100 m CP-Sil 88 fused capillary column (Varian Inc., Mississauga, ON, Canada) as previously described [27].

Western Blot Analysis for Total IGF-IR, IRS-1 and Phosphorylated IGF-IR

Whole cell protein lysates were prepared from IGF-I-stimulated and fatty acid-treated cells as previously described [28]. Protein content was determined by bicinchoninic acid protein assay (Sigma). Equal amounts of protein (40 μ g) from each treatment were separated by SDS-PAGE as previously described [28]. Precision Plus ProteinTM All Blue (BioRad Laboratories (Canada) Ltd., Mississauga, ON, Canada) molecular weight standards were used to monitor protein separation. Membranes were blocked for 1 h at room temperature in Tris-buffered saline plus Tween-20 (TBST: 0.01 M Tris-HCl pH 6.8, 0.15 M NaCl, 0.1% v/v Tween-20) and 5% w/v powdered milk. After rinsing with TBST, membranes were incubated overnight at 4 °C with either IGF-IR β C-20 primary antibody (Santa Cruz Biotechnology, Santa Cruz, CA) diluted 1:10,000 in TBST containing 1% w/v powdered milk, or IRS-1 (59G8) primary antibody (Cell Signaling Technology, Cedarlane Laboratories Ltd., Hornby, ON, Canada) diluted 1:1,000 in TBST containing 5% w/v BSA. For the phosphorylated-IGF-IR (2B9) (Santa Cruz Biotechnology, CA), the primary antibody was diluted 1:100 in TBST supplemented with 0.5% BSA and 0.5% milk. A 50 μ g aliquot of T-47D Cell Lysate (Santa Cruz Biotechnology, CA) was used as a positive control for the p-IGF-IR.

A 1:10,000 dilution of the secondary antibody, horseradish peroxidase-conjugated donkey anti-rabbit IgG (Jackson ImmunoResearch Labs, Cedarlane Laboratories), or goat anti-mouse IgG (Invitrogen, Burlington, ON, Canada) in TBST with 1% w/v powdered milk was incubated with the membranes for 1 h at room temperature. Membranes were developed using enhanced chemiluminescence (ECL Plus™) western blotting detection reagents (Amersham Biosciences, GE Healthcare, Baie d'Urfe, Quebec, Canada) and read on a Typhoon™ Trio+ variable mode imager (Amersham Biosciences). The intensity of target bands was quantified using ImageQuant™ TL software (Amersham Biosciences). Beta actin (Sigma, Oakville, ON, Canada) was used as an internal loading control as we found that it was not altered by treatments.

Statistical Analysis

Statistical analyses were conducted using SAS, version 9 (SAS Institute, Cary, NC) to compare the effects of fatty acid treatment on MCF-7 breast cancer growth and death. A one-way analysis of variance was used, blocking for passage number. When a significant effect of treatment ($p < 0.05$) was found, least squared means was used for post hoc analysis. Data are presented as means \pm SEM.

Results

CLA Isomers are Incorporated into MCF-7 Cell Membrane Phospholipids

The c9,t11 and t10,c12 CLA isomers were significantly incorporated into membrane phospholipids but t10,c12 CLA incorporation occurred to a greater extent than c9,t11 CLA incorporation (32% vs. 22% of total fatty acids, respectively; Table 1). The higher incorporation of t10,c12 CLA occurred at the expense of total saturated fatty acids (SFA), which made up a significantly lower proportion of total fatty acids than among c9,t11 CLA-treated cells. The relative content of total n-6 and n-3 fatty acids and the proportion of arachidonic acid (AA, C20:4n-6) did not differ between the two CLA treatment groups (Table 1).

Incubation with LA or OA significantly increased the incorporation of these fatty acids into membrane phospholipids (Table 1). Compared to the OA treatment group (which had the greatest cell growth), phospholipids from all other treatment groups had significantly less C18:1n-9. Compared to LA-treated cells, phospholipids from all other treatment groups had significantly less LA and C20:2n-6. There were significantly more SFA in the phospholipids of

LA-treated cells compared to those incubated with t10,c12 CLA (Table 1). Untreated cells had significantly less total n-6 PUFA, especially LA, compared to all fatty acid treatments; however the content of AA was higher than all other treatment groups. The untreated group had a greater proportion of SFA compared to OA- and t10,c12 CLA-treated cells, and a greater proportion of monounsaturated fatty acids (MUFA) compared to LA-, c9,t11 CLA- and t10,c12 CLA-treated cells (Table 1).

CLA Isomers Inhibit the Growth of MCF-7 Breast Cancer Cells Stimulated by IGF-I

MCF-7 cells were grown in IGF-I-containing serum-free medium for 48 h with or without 128 or 256 μ M of the experimental fatty acids. At both fatty acid concentrations, cells incubated with t10,c12 CLA had a significantly lower rate of proliferation ($p < 0.05$), as defined by their metabolic activity, compared to cells incubated with LA, c9,t11 CLA or no fatty acids (Fig. 1). When cells were incubated with the various experimental fatty acids in combination with 128 μ M LA, all fatty acid treatments stimulated metabolic activity ($p < 0.05$) after 24 h compared to untreated cells (Fig. 2). However, at 24 h there were significantly fewer viable cells in the wells from the t10,c12 CLA treated cells. After 48 h of treatment, both CLA isomers significantly inhibited growth compared to OA-treated, LA-treated or untreated cells ($p < 0.01$, Fig. 2); OA increased growth compared to all other fatty acid treatments ($p < 0.01$, Fig. 2). After 48 h, the t10,c12 CLA treatment reduced growth to a greater extent ($p < 0.01$) than the c9,t11 CLA treatment (Fig. 2).

t10,c12 CLA Increases Cell Death in IGF-1-Stimulated MCF-7 Cells

LDH release was measured to estimate cell death/necrosis. After 24 h, the t10,c12 CLA isomer in combination with LA resulted in a significantly higher LDH release ($p < 0.01$) compared to all other fatty acid treatments (Fig. 3). LDH release by the untreated or OA-treated cells was significantly less than the other fatty acid treatment groups ($p < 0.01$, Fig. 3).

t10,c12 CLA Reduces Total Cellular Total and Phosphorylated IGF-IR Levels in MCF-7 Cells

Treatment with the t10,c12 CLA isomer reduced total cellular IGF-IR protein levels in MCF-7 cells compared to all other treatment groups (Fig. 4). Both LA and c9,t11 CLA significantly reduced IGF-IR protein compared to OA-treated and untreated cells, but not compared to each

Table 1 Fatty acid composition of whole cell phospholipids

Fatty acid	Fatty acid treatment ¹					Significance (<i>p</i> -values)
	Untreated	LA	c9,t11 CLA	t10,c12 CLA	OA	
	% of total fatty acids					
14:0	3.5 ± 1.0 ^a	0.8 ± 0.2 ^b	1.1 ± 0.2 ^b	1.1 ± 0.2 ^b	1.1 ± 0.1 ^b	<0.05
14:1	2.8 ± 1.6 ^a	1.2 ± 0.7 ^{ab}	0.0 ± 0.0 ^b	0.0 ± 0.0 ^b	0.0 ± 0.0 ^b	<0.05
16:0	14 ± 1.0	10.2 ± 0.4	14.9 ± 6.8	7.4 ± 0.4	8.3 ± 0.7	NS
16:1(n-9)	11.7 ± 2.3 ^a	1.4 ± 0.4 ^b	2.1 ± 0.3 ^b	1.7 ± 0.5 ^b	1.5 ± 0.4 ^b	<0.01
8:0	14.0 ± 3.0 ^b	17.6 ± 3.3 ^a	11.0 ± 1.5 ^b	11.3 ± 2.0 ^b	13.0 ± 2.8 ^b	<0.01
18:1(n-9)	26.1 ± 0.4 ^b	12.1 ± 1.5 ^c	13.5 ± 4.2 ^c	10.0 ± 1.0 ^c	38.3 ± 3.3 ^a	<0.01
18:1(n-11)	5.6 ± 0.7 ^a	1.6 ± 0.2 ^b	1.6 ± 0.3 ^b	1.3 ± 0.2 ^b	1.2 ± 0.2 ^b	<0.01
18:2(n-6)	8.5 ± 3.5 ^c	47.8 ± 4.1 ^a	25.8 ± 6.2 ^b	27.9 ± 1.8 ^b	29.1 ± 2.7 ^b	<0.01
c9,t11 CLA	ND	ND	22.0 ± 5.4	ND	ND	<0.01
t10,c12 CLA	ND	ND	0.1 ± 0.5	32.0 ± 4.0	ND	<0.01
18:3(n-3)	0.4 ± 0.1 ^b	0.7 ± 0.3 ^{ab}	0.3 ± 0.1 ^b	0.5 ± 0.2 ^b	1.0 ± 0.2 ^a	<0.01
20:1(n-9)	0.01 ± 0.0 ^b	0.1 ± 0.1 ^b	1.3 ± 0.5 ^a	1.3 ± 0.3 ^a	0.1 ± 0.1 ^b	<0.01
20:2(n-6)	0.1 ± 0.0 ^b	2.8 ± 0.5 ^a	1.2 ± 0.5 ^b	0.4 ± 0.1 ^b	1.0 ± 0.1 ^b	<0.01
20:3(n-6)	0.6 ± 0.1 ^a	0.1 ± 0.1 ^c	0.2 ± 0.1 ^{bc}	0.2 ± 0.0 ^{bc}	0.3 ± 0.0 ^b	<0.01
20:4(n-6)	4.3 ± 0.6 ^a	1.2 ± 0.2 ^b	1.2 ± 0.3 ^b	1.3 ± 0.2 ^b	1.4 ± 0.3 ^b	<0.01
22:6(n-3)	1.1 ± 0.2 ^a	0.7 ± 0.3 ^b	0.3 ± 0.0 ^c	0.5 ± 0.2 ^c	0.6 ± 0.2 ^{bc}	<0.01
∑ SFA	33 ± 2 ^a	29.1 ± 3.4 ^{ab}	28.8 ± 7.8 ^{ab}	20.3 ± 2.6 ^c	23.6 ± 3.1 ^{bc}	<0.01
∑ MUFA	48.9 ± 4.4 ^a	16.9 ± 0.7 ^b	19.6 ± 4.0 ^b	15.5 ± 1.2 ^b	42.1 ± 3.7 ^a	<0.01
∑ PUFA ²	16.8 ± 2.9 ^c	51.3 ± 2.4 ^{ab}	48.9 ± 10.9 ^{bc}	60.4 ± 2.4 ^a	32.6 ± 1.3 ^{bc}	<0.05
∑ n-6 PUFA	13.9 ± 2.8 ^c	52.4 ± 3.9 ^a	28.7 ± 6.7 ^b	30.1 ± 1.6 ^b	32.5 ± 2.0 ^b	<0.01
∑ n-3 PUFA	4.1 ± 1.9 ^a	1.6 ± 0.5 ^{ab}	0.9 ± 0.1 ^b	1.4 ± 0.5 ^b	1.8 ± 0.4 ^{ab}	<0.05

MCF-7 breast cancer cells were exposed to fatty acids for 24 h in serum-free conditions. Values are percentages of total fatty acids and are expressed as means ± SEM, determined from 3 to 4 experiments. Values within a row that do not share a common superscript letter are significantly different ($p < 0.05$). LA Linoleic acid; OA oleic acid; CLA conjugated linoleic acid; NS not significant; ND not detectable; SFA saturated fatty acids; MUFA monounsaturated fatty acids; PUFA polyunsaturated fatty acids. Fatty acids not shown: C17:0, C20:0, C22:0, C16:1(t9), C18:1(t11), C22:2(6), C22:4(6), C22:5(6), C20:5(3), C22:5(3)

¹ The fatty acid treatment used were, untreated (no additional fatty acids added), LA (256 μM LA), c9,t11 CLA (128 μM LA + 128 μM c9t11 CLA), t10,c12 CLA (128 μM LA + 128 μM t10,c12 CLA), OA (128 μM LA + 128 μM OA)

² Both CLA isomers contain two double bonds, therefore they are included in the total PUFA calculation

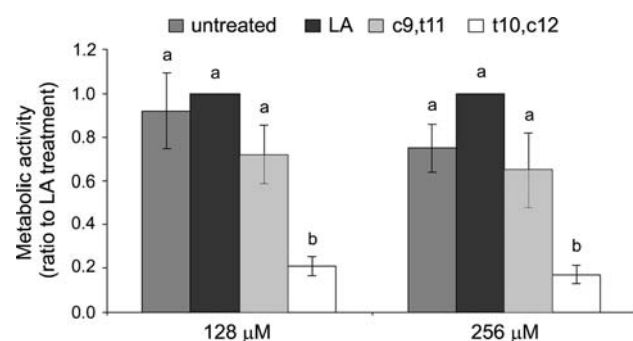


Fig. 1 Metabolic activity (mitochondrial enzyme activity) of IGF-I-stimulated MCF-7 breast cancer cells treated with 128 μM (mean absorbance was 1.66 ± 0.26) or 256 μM (mean absorbance was 1.50 ± 0.16) fatty acids for 48 h. Values are expressed as a ratio to the LA treatment, and represent the means ± SEM of three experiments. The untreated condition contained no additional fatty acids. Within each concentration, bars that do not share a common letter are significantly different ($p < 0.05$)

other (Fig. 4). The levels of phosphorylated IGF-1 were lower in MCF-7 cells incubated with t10,c12 CLA compared to LA. Band intensity ($n = 2$ /treatment), expressed, relative to LA, was for untreated cells ($1.56 ± 0.41$), c9,t11 CLA ($1.0 ± 0.01$), t10,c12 CLA ($0.52 ± 0.27$) and OA ($1.52 ± 0.68$).

CLA Reduces Total Cellular IRS-1 Levels Compared to Untreated and OA-Treated MCF-7 Cells

Treatment with c9,t11 CLA or t10,c12 CLA reduced total cellular IRS-1 protein levels in MCF-7 cells compared to untreated and OA-treated cells (Fig. 5). Although IRS-1 protein levels were affected by treatments in a pattern similar to that seen for IGF-IR, the CLA-induced reductions in IRS-1 protein levels were not statistically different from LA-treated cells (Fig. 5).

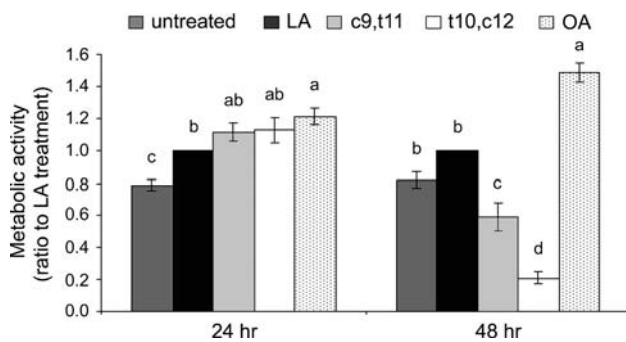


Fig. 2 Metabolic activity (mitochondrial enzyme activity) of IGF-1-stimulated MCF-7 breast cancer cells treated with various fatty acids in combination with LA for 24 or 48 h. Values are expressed as a ratio to the 256 μ M LA treatment (mean absorbance was 0.256 ± 0.037) and represent the means \pm SEM of 3–4 experiments. Each of the fatty acid treatments contained 128 μ M LA + 128 μ M of the experimental fatty acid. The untreated condition contained no additional fatty acids. Within each time point, bars that do not share a common letter are significantly different ($p < 0.05$). Cell counts ($\times 10^6$ /mL) were performed ($n = 5$ /group) at 24 h; untreated 19.2 ± 1.1^a , LA 17.5 ± 1.5^a , OA 17.4 ± 1.5^a , c9,t11 CLA 15.6 ± 1.7^a , t10,c12 CLA 9.6 ± 1.0^b

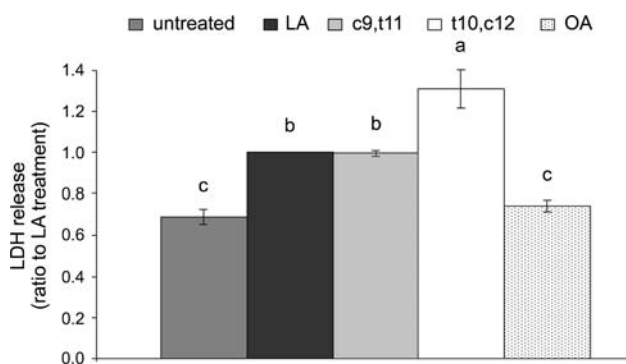


Fig. 3 LDH release from IGF-1-stimulated MCF-7 breast cancer cells treated with various fatty acids in combination with LA for 24 h. Values are expressed as a ratio to the 256 μ M LA treatment (mean % LDH released into media was 38 ± 6), and represent the means \pm SEM of 3–4 experiments. Each of the fatty acid treatments contained 128 μ M LA + 128 μ M of the experimental fatty acid. The untreated condition contained no additional fatty acids. Bars that do not share a common letter are significantly different ($p < 0.05$)

Discussion

The two most common dietary CLA isomers, c9,t11 and t10,c12, have been reported to reduce the incidence and size of mammary tumours in rodent models when fed together or individually [4, 29]. Consistent with the animal models, the anti-carcinogenic activity of these two isomers has been demonstrated in human breast cell lines [7–10]. While both isomers are reported to have anti-cancer activity, their respective level of growth inhibition and the mechanism by which they mediate their cytotoxic activity against tumour cells has not been established. In the current

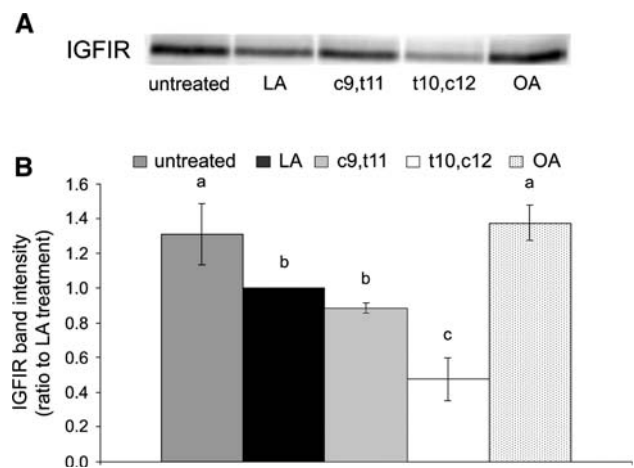


Fig. 4 Total IGF-IR protein levels in IGF-I-stimulated MCF-7 breast cancer cells after treatment with various fatty acids in combination with LA for 24 h. **a** Western blot analysis of total IGF-IR protein and β -actin levels among fatty-acid treated cells. The blot shown is representative of three independent experiments. **b** IGF-IR band intensity. Each of the fatty acid treatments contained 128 μ M LA + 128 μ M of the experimental fatty acid. The untreated condition contained no additional fatty acids. Bars that do not share a common letter are significantly different ($p < 0.05$)

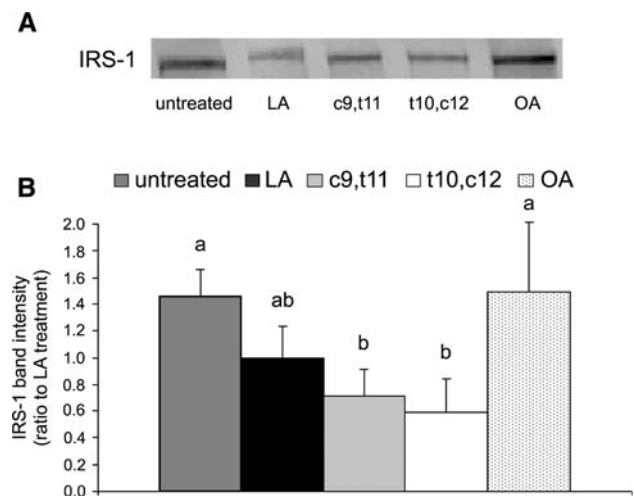


Fig. 5 Total IRS-1 protein levels in IGF-I-stimulated MCF-7 breast cancer cells after treatment with various fatty acids in combination with LA for 24 h. **a** Western blot analysis of total IRS-1 protein and β -actin levels among fatty-acid treated cells. The blot shown is representative of 4 independent experiments. **b** IRS-1 band intensity. Each of the fatty acid treatments contained 128 μ M LA + 128 μ M of the experimental fatty acid. The untreated condition contained no additional fatty acids. Bars that do not share a common letter are significantly different ($p < 0.05$)

study, the t10,c12 CLA isomer decreased metabolic activity after 48 h compared to all other treatment groups. These results are consistent with the literature [6, 9, 30] and demonstrate that on a gram per gram basis, t10,c12 CLA has a greater growth inhibitory effect (metabolic activity and cell number) on estrogen receptor positive MCF-7

cells. Previous work on CLA and cancer cells lines have performed experiments using the cell maintenance media that contains a very low concentration of fatty acids (only that from the serum), as the ‘control’ treatment [6, 7, 9, 10, 19, 31]. Serum provides only a very low (at 5% v/v would result in a concentration of 3 μ M LA; [8]) amount of essential fatty acids. CLA isomers have been reported to interfere with n-6 essential fatty acid metabolism when LA is in limited supply [32] but not when there is a sufficient level in the diet [33]. In most in vivo situations, LA is usually not in limited supply, thus we added LA to the media of all our experimental treatments to prevent concluding that the in vitro growth inhibition effects of CLA isomers on MCF-7 cells was due to effects on the availability of LA. Through a series of preliminary experiments we determined that the addition of 125 μ M LA to the media enabled us to maintain the concentration of LA in the membrane PL (higher than the untreated condition) and the concentration of C20:4(6) similar to the LA treatment (Table 1). Our work extends earlier growth studies by confirming that growth inhibition by the t10,c12 CLA isomer is maintained in the presence of LA and that the growth inhibitory effects of c9,t11 CLA appear when LA is present in the media.

The effect of CLA isomers on increasing LDH release (estimate of cell death) is consistent with the reduced metabolic activity measured in the WST-1 assay. Interestingly, incubation with t10,c12 CLA did not significantly decrease the metabolic activity of MCF-7 cells after 24 h, but it did increase our measure of cytotoxicity (LDH release) compared to the other treatments at 24 h. This might be a result of the ways that these two assays are measured. LDH release assesses the amount of LDH released into the media while the Wst-1 viability assay looks at the remaining live cells and assesses mitochondrial reductase activity. Our results suggest that at 24 h, a significant number of t10,c12 CLA-treated cells had died but the remaining cells had a similar mitochondrial activity to the other groups. We did not measure apoptosis in the current study; however, incubation of MCF-7 cells with mixtures of CLA isomers has been demonstrated to increase apoptosis by increasing pro-apoptotic and decreasing anti-apoptotic genes and proteins [34–36]. However, a recent study suggested that CLA isomers can inhibit the growth of MCF-7 cells without increasing apoptosis [37].

The orientation of fatty acid double bonds (e.g. *cis*, *trans*), or the length of a fatty acid chain, impacts the positioning and spacing of neighbouring fatty acids in the plasma membrane [38]. Changes to the fatty acid composition of the plasma membrane and subsequently the physical structure have been shown to alter lipid-protein interactions, and ultimately the function of the membrane

[38, 39]. Due to its conjugated *cis* and *trans* double bonds, the mechanism by which t10,c12 CLA inhibits MCF-7 breast cancer cell growth may be related to its incorporation into and subsequent disruption of cellular membrane functions. Both CLA isomers, c9,t11 and t10,c12, are structurally similar in that they contain two conjugated double bonds, one in the *cis* formation and the other in the *trans* position. Using synthetic model membranes, Yin et al. showed that incorporation of c9,t11 CLA perturbed membrane structure at the location of the conjugated double bonds and increased oxygen permeability, as compared to LA, MUFA and SFA [40]. Although this study used only the c9,t11 CLA isomer, the results are likely relevant to t10,c12 CLA. As t10,c12 CLA was incorporated into the cell membrane to a greater extent than c9,t11 CLA (33% vs. 22%, respectively) in the present study, this suggests that the membrane might be more disrupted by t10,c12 CLA treatment. In support of this, recently, it was demonstrated that the physical properties of these two isomers are quite different [41]. The greater incorporation of t10,c12 CLA was at the expense of SFA as compared to the LA- and c9,t11 CLA-treated groups. However it is unlikely that the change in SFA concentration in the membrane accounts entirely for the differences in growth as the concentration of SFA in the t10,c12 CLA treated group was not different from that of the OA treated group. Our results suggest that the high incorporation of the t10,c12 CLA isomer might be responsible for the difference in biological function, rather than the displacement of a specific saturated or unsaturated fatty acid. Future studies are planned to determine if the alteration in phospholipid composition, altered the positional distribution (sn-1 and sn-2) of fatty acids in membrane phospholipids.

Previously, OA has been shown to stimulate the proliferation of MCF-7 cells as compared to untreated cells [42]. Interestingly, the mixture of OA and LA in the presence of IGF-I led to a 1.5 fold increase in metabolic activity as compared to either LA-treated or untreated cells and resulted in the lowest level of LDH release at 24 h. To our knowledge there are no published studies that have examined the supplementation of LA and OA together on the viability of breast cancer cells. OA-treated and untreated cells had a higher relative content of MUFA than the other three treatments. The greater proportion of MUFA in the OA treated group was due to the high incorporation of OA, whereas for the untreated group 16:1n-9, 18:1n-9, and 18:1n-11 were all higher than the CLA- or LA-treated groups. The increased MUFA in the OA group occurred without a proportional replacement of any one specific fatty acid or fatty acid group. Our data suggests that a higher MUFA content (particularly 18:1) in phospholipids is associated with better survival/growth of MCF-7 cells. In support of this conclusion, incubation with

OA was reported to promote cell survival in MDA-MB-231, MDA-MB-468 and T47D breast cancer cells under serum-free conditions [42, 43] compared to LA, AA, docosahexaenoic acid (DHA) and palmitate [44].

Changes in the fatty acid composition of membrane phospholipids can alter the functional activity of cell membranes, including the activity of membrane associated receptors [45, 46]. Addition of long chain polyunsaturated fatty acids (DHA but not AA) was reported to increase the number of insulin receptors in retinoblastoma cells, although this same study did not find a change in the binding ability of IGF-I receptors, nor did they study the addition of LA or trans fatty acids [47]. The observed changes in total IGF-IR, phosphorylated IGF-IR and IRS-1 protein levels observed among the different treatments are consistent with the growth inhibition and LDH results. The untreated and OA-treated groups demonstrated the least amount of LDH release/cell death, higher metabolic activity, and had the greatest amount of total and phosphorylated IGF-IR and total IRS-1. In contrast, the t10,c12 CLA-treated group had the greatest cell death, lowest metabolic activity and the lowest amounts of total and phosphorylated IGF-IR and IRS-1. The amount of phosphorylated IRS-1 was not measured in the current study; however, it was recently demonstrated that the amount of IRS-1 in the cell was important for cell proliferation as reducing the translation of IRS-1 suppressed the growth of MCF-7 cells [21].

Consistent with our results, in HT-29 colon cancer cells, Kim et al. [19] demonstrated that a mixture of CLA decreased the amount of total IGF-1R and inhibited the IGF-1 induced phosphorylation of the IGF-1R in cells. Their work demonstrated that this decrease was associated with a reduced recruitment of the P85 PI3K to the receptor and the phosphorylation of Akt and extracellular signal-regulated kinase (ERK)-phosphorylation [19]. Our results confirm this observation in human breast cancer cells and unlike the previous work studied the effects of the two major CLA isomers. Additionally our findings demonstrated the effect of CLA isomers on the amount of IRS-1, which is upstream from Akt and Erk signalling.

As changes to the total protein levels of these signaling molecules are most likely due to changes at the genetic or transcription level, in the current study it is not possible to directly link the changes in total IGF-IR and IRS-1 protein levels to specific lipid changes in membrane phospholipids. However, the dramatic incorporation of t10,c12 CLA into cell phospholipids indicates a probable disruption of the function of these and/or other membrane associated proteins. Future studies are warranted to examine the activity levels of these molecules, and their downstream signaling mediators (e.g. phosphatidylinositol 3-kinase, extracellular

signal-related kinase). In addition, further studies are needed to examine the effects of CLA isomers on lipid “rafts” (microdomains of saturated lipids that cluster together in the plasma membrane) [48]. Our group has shown that incubation of estrogen-receptor negative MDA-MB-231 breast cancer cells with n-3 PUFA alters the fatty acid composition of lipid rafts, resulting in a reduction of raft-associated epidermal growth factor receptors (EGFR) and an increase in whole cell tyrosine phosphorylated EGFR, which was consistent with an increase in apoptosis [12]. As IGF-IR [49] and IRS-1 [50] have been reported to be located in lipid rafts, the disruption of the lipid composition of these microdomains due to CLA is a future area of investigation to pursue.

The CLA concentration (128 μ M) used in the current study is within the range used in previous studies to demonstrate an effect on cell growth on human breast cancer cell lines [6, 30, 34, 36, 51, 52]. Although the growth inhibition is similar to what is observed in animal feeding studies [5, 53–56], the physiological relevance of the amount of CLA incorporated into membranes remains to be determined. In summary, the results of this study demonstrate that the t10,c12 isomer of CLA inhibits the growth of MCF-7 cells and suggest that this may be mediated through incorporation into cellular phospholipids and interference with the function of IGF-I and related signaling proteins. Further investigation is required to definitively link this interference with modifications to the membrane of breast cancer cells.

Acknowledgments The authors would like to acknowledge the help of Patricia Biondo in putting together this manuscript and the technical assistance of Marnie Newell, Paige Sorochan and Susan Goruk. D. Amariù was the recipient of a post-graduate studentship from the Natural Sciences and Engineering Research Council of Canada. Funding for this study came from the CLA network through a grant from the Alberta Agriculture Research Funding Consortium.

References

1. Sebedio JL, Gnaedig S, Chardigny JM (1999) Recent advances in conjugated linoleic acid research. *Curr Opin Clin Nutr Metab Care* 2:499–506
2. Dhiman TR, Nam SH, Ure AL (2005) Factors affecting conjugated linoleic acid content in milk and meat. *Crit Rev Food Sci Nutr* 45:463–482
3. Kelley NS, Hubbard NE, Erickson KL (2007) Conjugated linoleic acid isomers and cancer. *J Nutr* 137:2599–2607
4. Ip C, Dong Y, Ip MM, Banni S, Carta G, Angioni E, Murru E, Spada S, Melis MP, Saebo A (2002) Conjugated linoleic acid isomers and mammary cancer prevention. *Nutr Cancer* 43:52–58
5. Ip MM, Masso-Welch PA, Ip C (2003) Prevention of mammary cancer with conjugated linoleic acid: role of the stroma and the epithelium. *J Mammary Gland Biol Neoplasia* 8:103–118
6. Wang LS, Huang YW, Sugimoto Y, Liu S, Chang HL, Ye W, Shu S, Lin YC (2005) Effects of human breast stromal cells on conjugated linoleic acid (CLA) modulated vascular endothelial

- growth factor-A (VEGF-A) expression in MCF-7 cells. *Anticancer Res* 25:4061–4068
7. Park Y, Allen KG, Shultz TD (2000) Modulation of MCF-7 breast cancer cell signal transduction by linoleic acid and conjugated linoleic acid in culture. *Anticancer Res* 20:669–676
 8. Ma DW, Field CJ, Clandinin MT (2002) An enriched mixture of *trans*-10, *cis*-12-CLA inhibits linoleic acid metabolism and PGE2 synthesis in MDA-MB-231 cells. *Nutr Cancer* 44:203–212
 9. Kemp MQ, Jeffy BD, Romagnolo DF (2003) Conjugated linoleic acid inhibits cell proliferation through a p53-dependent mechanism: effects on the expression of G1-restriction points in breast and colon cancer cells. *J Nutr* 133:3670–3677
 10. Chujo H, Yamasaki M, Nou S, Koyanagi N, Tachibana H, Yamada K (2003) Effect of conjugated linoleic acid isomers on growth factor-induced proliferation of human breast cancer cells. *Cancer Lett* 202:81–87
 11. Grunicke HH (1991) The cell membrane as a target for cancer chemotherapy. *Eur J Cancer* 27:281–284
 12. Schley PD, Brindley DN, Field CJ (2007) (n-3) PUFA alter raft lipid composition and decrease epidermal growth factor receptor levels in lipid rafts of human breast cancer cells. *J Nutr* 137:548–553
 13. Pollak MN (2004) Insulin-like growth factors and neoplasia. *Novartis Found Symp* 262:84–98
 14. Schernhammer ES, Holly JM, Pollak MN, Hankinson SE (2005) Circulating levels of insulin-like growth factors, their binding proteins, and breast cancer risk. *Cancer Epidemiol Biomarkers Prev* 14:699–704
 15. Renehan AG, Zwahlen M, Minder C, O'dwyer ST, Shalet SM, Egger M (2004) Insulin-like growth factor (IGF)-I, IGF binding protein-3, and cancer risk: systematic review and meta-regression analysis. *Lancet* 363:1346–1353
 16. Kleinberg DL, Feldman M, Ruan W (2000) IGF-I: an essential factor in terminal end bud formation and ductal morphogenesis. *J Mammary Gland Biol Neoplasia* 5:7–17
 17. Sternlicht MD (2006) Key stages in mammary gland development: the cues that regulate ductal branching morphogenesis. *Breast Cancer Res* 8:201
 18. Ip C, Singh M, Thompson HJ, Scimeca JA (1994) Conjugated linoleic acid suppresses mammary carcinogenesis and proliferative activity of the mammary gland in the rat. *Cancer Res* 54:1212–1215
 19. Kim EJ, Kang IJ, Cho HJ, Kim WK, Ha YL, Park JH (2003) Conjugated linoleic acid downregulates insulin-like growth factor-I receptor levels in HT-29 human colon cancer cells. *J Nutr* 133:2675–2681
 20. Kaburagi Y, Yamauchi T, Yamamoto-Honda R, Ueki K, Tobe K, Akanuma Y, Yazaki Y, Kadowaki T (1999) The mechanism of insulin-induced signal transduction mediated by the insulin receptor substrate family. *Endocr J* 46(Suppl):S25–S34
 21. Zhang J, Du YY, Lin YF, Chen YT, Yang L, Wang HJ, Ma D (2008) The cell growth suppressor, mir-126, targets IRS-1. *Biochem Biophys Res Commun* 377:136–140
 22. Peyrat JP, Bonnetterre J, Dusanter-Fourt I, Leroy-Martin B, Djiane J, Demaille A (1989) Characterization of insulin-like growth factor 1 receptors (IGF1-R) in human breast cancer cell lines. *Bull Cancer* 76:311–319
 23. Keating AF, Kennelly JJ, Zhao FQ (2006) Characterization and regulation of the bovine stearoyl-CoA desaturase gene promoter. *Biochem Biophys Res Commun* 344:233–240
 24. Folch J, Lees M, Sloane Stanley GH (1957) A simple method for the isolation and purification of total lipides from animal tissues. *J Biol Chem* 226:497–509
 25. Field CJ, Ryan EA, Thomson AB, Clandinin MT (1988) Dietary fat and the diabetic state alter insulin binding and the fatty acyl composition of the adipocyte plasma membrane. *Biochem J* 253:417–424
 26. Kramer JK, Fellner V, Dugan ME, Sauer FD, Mossoba MM, Yurawecz MP (1997) Evaluating acid and base catalysts in the methylation of milk and rumen fatty acids with special emphasis on conjugated dienes and total trans fatty acids. *Lipids* 32:1219–1228
 27. Cruz-Hernandez C, Kramer JK, Kennelly JJ, Glimm DR, Sorensen BM, Okine EK, Goonewardene LA, Weselake RJ (2007) Evaluating the conjugated linoleic acid and trans 18:1 isomers in milk fat of dairy cows fed increasing amounts of sunflower oil and a constant level of fish oil. *J Dairy Sci* 90:3786–3801
 28. Schley PD, Jijon HB, Robinson LE, Field CJ (2005) Mechanisms of omega-3 fatty acid-induced growth inhibition in MDA-MB-231 human breast cancer cells. *Breast Cancer Res Treat* 92:187–195
 29. Ip C, Chin SF, Scimeca JA, Pariza MW (1991) Mammary cancer prevention by conjugated dienoic derivative of linoleic acid. *Cancer Res* 51:6118–6124
 30. Tanmahasamut P, Liu J, Hendry LB, Sidell N (2004) Conjugated linoleic acid blocks estrogen signaling in human breast cancer cells. *J Nutr* 134:674–680
 31. Cho HJ, Kim WK, Jung JI, Kim EJ, Lim SS, Kwon DY, Park JH (2005) *Trans*-10, *cis*-12, not *cis*-9, *trans*-11, conjugated linoleic acid decreases ErbB3 expression in HT-29 human colon cancer cells. *World J Gastroenterol* 11:5142–5150
 32. Banni S, Angioni E, Casu V, Melis MP, Carta G, Corongiu FP, Thompson H, Ip C (1999) Decrease in linoleic acid metabolites as a potential mechanism in cancer risk reduction by conjugated linoleic acid. *Carcinogenesis* 20:1019–1024
 33. Turpeinen AM, Barlund S, Freese R, Lawrence P, Brenna JT (2006) Effects of conjugated linoleic acid on linoleic and linolenic acid metabolism in man. *Br J Nutr* 95:727–733
 34. Majumder B, Wahle KW, Moir S, Schofield A, Choe SN, Farquharson A, Grant I, Heys SD (2002) Conjugated linoleic acids (CLAs) regulate the expression of key apoptotic genes in human breast cancer cells. *FASEB J* 16:1447–1449
 35. Seo JH, Moon HS, Kim IY, Guo DD, Lee HG, Choi YJ, Cho CS (2008) PEGylated conjugated linoleic acid stimulation of apoptosis via a p53-mediated signaling pathway in MCF-7 breast cancer cells. *Eur J Pharm Biopharm* 70:621–626
 36. Guo DD, Moon HS, Arote R, Seo JH, Quan JS, Choi YJ, Cho CS (2007) Enhanced anticancer effect of conjugated linoleic acid by conjugation with pluronic F127 on MCF-7 breast cancer cells. *Cancer Lett* 254(2):244–254
 37. Miglietta A, Bozzo F, Gabriel L, Bocca C, Canuto RA (2006) Extracellular signal-regulated kinase 1/2 and protein phosphatase 2A are involved in the antiproliferative activity of conjugated linoleic acid in MCF-7 cells. *Br J Nutr* 96:22–27
 38. Stubbs CD, Smith AD (1984) The modification of mammalian membrane polyunsaturated fatty acid composition in relation to membrane fluidity and function. *Biochim Biophys Acta* 779:89–137
 39. Grimble RF, Tappia PS (1995) Modulatory influence of unsaturated fatty acids on the biology of tumour necrosis factor-alpha. *Biochem Soc Trans* 23:282–287
 40. Yin JJ, Mossoba MM, Kramer JK, Yurawecz MP, Eulitz K, Morehouse KM, Ku Y (1999) Effects of conjugated linoleic acid on oxygen diffusion-concentration product and depletion in membranes by using electron spin resonance spin-label oximetry. *Lipids* 34:1017–1023
 41. Uehara H, Suganuma T, Negishi S, Uda Y, Furukawa Y, Ueno S, Sato KJ (2008) Physical properties of two isomers of conjugated linoleic acid. *Am Oil Chem Soc* 85:29–36

42. Hardy S, Langelier Y, Prentki M (2000) Oleate activates phosphatidylinositol 3-kinase and promotes proliferation and reduces apoptosis of MDA-MB-231 breast cancer cells, whereas palmitate has opposite effects. *Cancer Res* 60:6353–6358
43. Przybytkowski E, Joly E, Nolan CJ, Hardy S, Francoeur AM, Langelier Y, Prentki M (2007) Upregulation of cellular triacylglycerol—free fatty acid cycling by oleate is associated with long-term serum-free survival of human breast cancer cells. *Biochem Cell Biol* 85:301–310
44. Hardy S, El-Assaad W, Przybytkowski E, Joly E, Prentki M, Langelier Y (2003) Saturated fatty acid-induced apoptosis in MDA-MB-231 breast cancer cells. A role for cardiolipin. *J Biol Chem* 278:31861–31870
45. Hulbert AJ, Turner N, Storlien LH, Else PL (2005) Dietary fats and membrane function: implications for metabolism and disease. *Biol Rev Camb Philos Soc* 80:155–169
46. Spector AA, Burns CP (1987) Biological and therapeutic potential of membrane lipid modification in tumors. *Cancer Res* 47:4529–4537
47. Yorek M, Leeney E, Dunlap J, Ginsberg B (1989) Effect of fatty acid composition on insulin and IGF-I binding in retinoblastoma cells. *Invest Ophthalmol Vis Sci* 30:2087–2092
48. Brown DA, London E (1998) Functions of lipid rafts in biological membranes. *Annu Rev Cell Dev Biol* 14:111–136
49. Huo H, Guo X, Hong S, Jiang M, Liu X, Liao K (2003) Lipid rafts/caveolae are essential for insulin-like growth factor-1 receptor signaling during 3T3-L1 preadipocyte differentiation induction. *J Biol Chem* 278:11561–11569
50. Remacle-Bonnet M, Garrouste F, Baillat G, Andre F, Marvaldi J, Pommier G (2005) Membrane rafts segregate pro- from anti-apoptotic insulin-like growth factor-I receptor signaling in colon carcinoma cells stimulated by members of the tumor necrosis factor superfamily. *Am J Pathol* 167:761–773
51. desBordes C, Lea MA (1995) Effects of C18 fatty acid isomers on DNA synthesis in hepatoma and breast cancer cells. *Anticancer Res* 15:2017–2021
52. Choi Y, Park Y, Storkson JM, Pariza MW, Ntambi JM (2002) Inhibition of stearoyl-CoA desaturase activity by the cis-9, trans-11 isomer and the trans-10, cis-12 isomer of conjugated linoleic acid in MDA-MB-231 and MCF-7 human breast cancer cells. *Biochem Biophys Res Commun* 294:785–790
53. Visonneau S, Cesano A, Tepper SA, Scimeca JA, Santoli D, Kritchevsky D (1997) Conjugated linoleic acid suppresses the growth of human breast adenocarcinoma cells in SCID mice. *Anticancer Res* 17:969–973
54. Hubbard NE, Lim D, Erickson KL (2003) Effect of separate conjugated linoleic acid isomers on murine mammary tumorigenesis. *Cancer Lett* 190:13–19
55. Corl BA, Barbano DM, Bauman DE, Ip C (2003) cis-9, trans-11 CLA derived endogenously from trans-11 18:1 reduces cancer risk in rats. *J Nutr* 133:2893–2900
56. Lock AL, Corl BA, Barbano DM, Bauman DE, Ip C (2004) The anticarcinogenic effect of trans-11 18:1 is dependent on its conversion to cis-9, trans-11 CLA by delta9-desaturase in rats. *J Nutr* 134:2698–2704

Plasma Lipid Transfer Enzymes in Non-Diabetic Lean and Obese Men and Women

Faidon Magkos · B. S. Mohammed ·
Bettina Mittendorfer

Received: 8 December 2008 / Accepted: 13 January 2009 / Published online: 6 February 2009
© AOCS 2009

Abstract There are considerable differences in the plasma lipid profile between lean and obese individuals and between men and women. Little, however, is known regarding the effects of obesity and sex on the plasma concentration of enzymes involved in intravascular lipid remodeling. Therefore, we measured the immunoreactive protein mass of lipoprotein lipase (LPL), hepatic lipase (HL), cholesterol-ester transfer protein (CETP) and lecithin-cholesterol acyl transferase (LCAT) in fasting plasma samples from 40 lean and 40 obese non-diabetic men and premenopausal women. Women, compared with men, had ~5% lower plasma LCAT ($p < 0.041$), ~35% greater LPL ($p = 0.001$) and ~10% greater CETP ($p = 0.085$) concentrations. Obese, compared with lean individuals of both sexes, had ~30% greater plasma LCAT ($p < 0.001$), ~20% greater CETP ($p < 0.001$) and ~20% greater LPL ($p = 0.071$) concentrations. Plasma HL concentration was not different in lean men and women. Obesity was associated with increased (by ~50%) plasma HL concentration in men ($p = 0.018$) but not in women; consequently, plasma HL concentration was lower in obese women than

obese men ($p = 0.009$). In addition, there were direct correlations between plasma lipid transfer enzyme concentrations and lipoprotein particle concentrations and sizes. There are considerable differences in basal plasma lipid transfer enzyme concentrations between lean and obese subjects and between men and women, which may be partly responsible for respective differences in the plasma lipid profile.

Keywords Adiposity · Sex differences · Lipid transport · Lipid profile · Lipoprotein subclasses

Abbreviations

VLDL	Very low-density lipoprotein
LDL	Low-density lipoprotein
HDL	High-density lipoprotein
LPL	Lipoprotein lipase
HL	Hepatic lipase
CETP	Cholesterol-ester transfer protein
LCAT	Lecithin-cholesterol acyl transferase
CVD	Cardiovascular disease

F. Magkos · B. S. Mohammed · B. Mittendorfer
Center for Human Nutrition,
Washington University School of Medicine,
St. Louis, MO, USA

F. Magkos
Department of Nutrition and Dietetics,
Harokopio University, Athens, Greece

B. Mittendorfer (✉)
Division of Geriatrics & Nutritional Science,
Washington University School of Medicine,
660 South Euclid Avenue, Campus Box 8031,
St. Louis, MO 63110, USA
e-mail: mittendb@wustl.edu; mittendb@dom.wustl.edu

Introduction

Obese subjects and men are at greater risk for cardiovascular disease (CVD) than lean subjects and women, probably because obese individuals and men have a more pro-atherogenic plasma lipid profile than lean subjects and women, respectively [1]. Several mechanisms, including hepatic and intestinal secretion of very low-density lipoproteins (VLDL), high-density lipoproteins (HDL), and possibly also low-density lipoproteins (LDL), intravascular delipidation and remodeling, and final catabolism and

removal from the circulation, act in concert to maintain a more or less pro-atherogenic lipid profile [2]. Intravascular remodeling of lipoproteins involves the exchange of core and surface lipids and apolipoproteins, mediated largely by the action of plasma lipid transfer enzymes, i.e., lipoprotein lipase (LPL), hepatic lipase (HL), cholesterol-ester transfer protein (CETP), and lecithin-cholesterol acyl transferase (LCAT) [3]. Although differences between lean and obese subjects and between men and women in the plasma lipid and lipoprotein profile are well established [1, 4], we know little regarding the effects of obesity and sex on the plasma concentration (i.e., the protein mass) of enzymes involved in intravascular lipid remodeling [5, 6]. A better understanding of the regulation of plasma lipid transfer enzyme concentrations may be clinically important because the immunoreactive protein mass of these enzymes has recently been shown to be related to CVD risk [7–12]. The relationship between plasma lipid transfer enzyme concentrations and CVD risk could simply be a reflection of their enzymatic actions and consequent changes in plasma lipid profile but likely goes beyond that because their function is not only limited to their catalytic activity, e.g., LPL [13] and HL [14] serve as bridges/ligands that facilitate lipoprotein uptake by various cell types. The purpose of our study therefore was to examine potential differences in basal plasma lipid transfer enzyme concentrations between lean and obese men and women. We studied non-diabetic, healthy, normoglycemic and normotriglyceridemic subjects with normal oral glucose tolerance to avoid potential confounding due to obesity-related metabolic complications [15, 16].

Experimental Procedure

Subjects

Eighty subjects between the ages of 18 and 50 years participated in the study: 40 (18 men; 22 premenopausal women) were lean with a body mass index (BMI) between 18.5 and 25 kg/m² and 40 (13 men; 27 premenopausal women) were obese with a BMI between 30 and 45 kg/m². Lean and obese subjects and men and women were matched on age. All subjects were considered to be in good health after completing a medical evaluation, which included a history and physical examination and standard blood tests. Subjects were included in the study if they were free of hypertension (blood pressure <140/90 mmHg) and were normoglycemic (plasma glucose concentration <5.5 mmol/L) and normotriglyceridemic (plasma triglyceride concentration <1.69 mmol/L); in addition, all obese subjects had normal oral glucose tolerance (plasma glucose concentration 2 h after a 75 g oral glucose challenge

<7.77 mmol/L). None of the subjects satisfied the criteria for metabolic syndrome, and none were smoking or taking medications known to affect glucose or lipid metabolism. Total body fat was determined by using dual-energy X-ray absorptiometry (Delphi-W densitometer, Hologic, Waltham, MA), and total abdominal, intra-abdominal, and subcutaneous abdominal fat areas were determined by magnetic resonance imaging on a 1.5T scanner (Siemens, Iselin, NJ), as previously described [17]. Written informed consent was obtained from all subjects before their participation in the study, which was approved by the Human Studies Committee and the General Clinical Research Center (GCRC) Advisory Committee at Washington University School of Medicine in St. Louis, MO.

Sample Collection and Analyses

Subjects were instructed to adhere to their regular diet and to refrain from physical activity for a minimum of 3 days before they were admitted to the GCRC where they consumed a standardized meal at ~1930 h, and then fasted (except for water) and rested in bed until fasting venous blood (total volume ~20 mL) was collected in chilled tubes containing sodium EDTA between 0700 and 0800 h the next day. Plasma was separated by centrifugation (3,000 rpm for 15 min at 4 °C) and stored at –80 °C until analyses were performed.

The concentrations of LPL, LCAT and CETP in plasma were determined with commercially available ELISA kits (Daiichi Pure Chemicals, Tokyo, Japan) [18] and plasma HL concentration was determined by using a sandwich ELISA method with monoclonal antibodies generated against human HL [19]; the assays used for LPL and HL do not cross-react with each other or with pancreatic lipase.

Plasma glucose concentration was determined by using an automated glucose analyzer (YSI 2300 STAT plus, Yellow Spring Instrument Co., Yellow Springs, OH). Total plasma triglyceride, VLDL-triglyceride and HDL-cholesterol concentrations, and plasma concentrations of VLDL, LDL, and HDL particles and average lipoprotein particle sizes (diameter in nm) were determined (LipoScience, Raleigh, NC) by using an AVANCE INCA NMR Chemical Analyzer equipped with a Bruker BioSpin UltraShield super-conducting magnet (Bruker BioSpin, Billerica, MA), as previously described [4].

Statistical Analysis

All data sets were normally distributed and are presented as means ± standard error (SEM). Two-way analysis of variance was used to evaluate the significance of differences between lean and obese subjects and men and women. In a secondary analysis, we compared the LPL, LCAT, and

CETP data obtained from a subgroup of 15 men and 15 women who were matched on percent body fat to evaluate the effect of sex independently of differences in body composition between men and women, by using the Student's *t*-test for independent samples. Plasma HL concentration measurements were excluded from this secondary analysis because we detected a significant interaction between sex and obesity on plasma HL concentration. Associations between variables of interest were assessed with Pearson's linear correlation analysis. A *p*-value < 0.05 was considered statistically significant.

Results

Plasma LCAT concentration was ~5% lower and plasma LPL concentration was ~35% higher in women than in men; women also tended to have higher plasma CETP concentration than men (Table 1). Obese subjects had 20–30% higher plasma LCAT and CETP concentrations than lean subjects, irrespective of sex; they also tended to have higher plasma LPL concentration than lean subjects (Table 1).

Plasma HL concentration was not different in lean men and women. Obesity was associated with ~50% higher plasma HL concentration in men but not in women; consequently, obese women had ~30% lower plasma HL concentration than obese men (Table 1).

There were no differences in plasma LPL and CETP concentrations between men and women who were matched on percent body fat (Table 2). However, women had ~20% lower plasma LCAT concentration than men, even when matched on percent body fat (Table 2).

Total body fat (% body weight) correlated positively with plasma LCAT ($r = 0.296$, $p = 0.008$), LPL ($r = 0.473$, $p < 0.001$), and CETP ($r = 0.351$, $p = 0.002$) concentrations, but not with HL concentration ($r = 0.104$, $p = 0.362$). Total abdominal fat (in cm²) was positively associated with plasma LCAT ($r = 0.451$, $p < 0.001$) and LPL ($r = 0.329$, $p = 0.013$) concentrations, but not with plasma CETP ($r = 0.181$, $p = 0.175$) and HL ($r = 0.201$, $p = 0.131$) concentrations. Intra-abdominal fat (% total abdominal fat) was not significantly associated with plasma lipid transfer enzyme concentrations (all *p*-values > 0.05).

Plasma LCAT concentration was inversely correlated with average HDL particle size. Plasma HL concentration correlated directly with average VLDL particle size and negatively with average LDL particle size (Table 3). There was no relationship between plasma LPL concentration and average VLDL, LDL, or HDL particle sizes. In addition, plasma LCAT concentration was directly correlated with VLDL (all), LDL (total and small), and HDL (total and small and medium) particle concentrations (Table 3). Plasma CETP concentration was directly correlated with the concentrations (total and small) of VLDL, LDL, and HDL in plasma (Table 3). Plasma HL concentration was

Table 1 Plasma lipid transfer enzyme concentrations in lean and obese men and women

	Lean (<i>n</i> = 40)		Obese (<i>n</i> = 40)		Two-way ANOVA <i>p</i> -values		
	Men	Women	Men	Women	Obesity	Sex	Interaction
<i>n</i>	18	22	13	27			
Body mass index (kg/m ²)	22.6 ± 0.4	22.4 ± 0.3	34.5 ± 1.2	35.1 ± 0.7	<0.001	0.793	0.547
Body fat (% body weight)	14.1 ± 1.3	28.2 ± 0.8	33.9 ± 2.2	48.2 ± 1.1	<0.001	<0.001	0.929
Abdominal fat (cm ²)	133 ± 28	166 ± 18	625 ± 66	561 ± 36	<0.001	0.692	0.221
Intra-abdominal fat (% total)	39 ± 6	23 ± 3	46 ± 3	25 ± 2	0.291	<0.001	0.478
Plasma glucose (mmol/L)	4.98 ± 0.09	4.86 ± 0.04	5.25 ± 0.09	4.95 ± 0.06	0.012	0.003	0.202
Plasma triglyceride (mmol/L)	0.80 ± 0.04	0.67 ± 0.04	1.21 ± 0.06	1.14 ± 0.06	<0.001	0.072	0.596
VLDL-triglyceride (mmol/L)	0.54 ± 0.03	0.40 ± 0.03	0.89 ± 0.06	0.78 ± 0.05	<0.001	0.012	0.730
HDL-cholesterol (mmol/L)	0.91 ± 0.05	1.16 ± 0.05	0.79 ± 0.05	0.90 ± 0.04	<0.001	0.001	0.198
LCAT (μg/mL)	548 ± 20	513 ± 20	730 ± 39	654 ± 26	<0.001	0.041	0.446
CETP (μg/mL)	170 ± 7	175 ± 6	192 ± 8	215 ± 8	<0.001	0.085	0.248
LPL (ng/mL)	31 ± 2	40 ± 3	35 ± 3	48 ± 3	0.071	0.001	0.436
HL (ng/mL)	6.6 ± 0.8	6.8 ± 0.9	10.0 ± 1.1*,**	6.8 ± 0.6	–	–	0.048

Values are means ± SEM

* Significantly different from corresponding value in lean men ($p = 0.018$)

** Significantly different from corresponding value in obese women ($p = 0.009$)

VLDL very-low density lipoprotein; HDL high-density lipoprotein; LCAT lecithin-cholesterol acyl transferase; LPL lipoprotein lipase; CETP cholesterol-ester transfer protein; HL hepatic lipase

Table 2 Plasma lipid transfer enzyme concentrations in men and women matched on percent body fat

	Men	Women	<i>p</i> -value
<i>n</i>	15	15	
Body fat (% body weight)	32.5 ± 2.1	33.0 ± 2.3	0.874
Intra-abdominal fat (% total)	44 ± 3	28 ± 5	0.024
Plasma glucose (mmol/L)	5.17 ± 0.09	5.05 ± 0.07	0.359
Plasma triglyceride (mmol/L)	1.15 ± 0.07	0.85 ± 0.10	0.016
VLDL-triglyceride (mmol/L)	0.84 ± 0.06	0.54 ± 0.08	0.005
HDL-cholesterol (mmol/L)	0.78 ± 0.04	1.05 ± 0.07	0.002
LCAT (μg/mL)	694 ± 42	570 ± 40	0.040
CETP (μg/mL)	186 ± 8	186 ± 9	0.993
LPL (ng/mL)	34 ± 3	36 ± 3	0.660

Values are means ± SEM

VLDL very-low density lipoprotein; HDL high-density lipoprotein; LCAT lecithin-cholesterol acyl transferase; LPL lipoprotein lipase; CETP cholesterol-ester transfer protein

directly correlated with the plasma concentration of small LDL and small HDL particles and inversely related to the concentration of large HDL particles. No robust relationships were found between plasma LPL concentration and lipoprotein concentrations (Table 3).

Discussion

We measured the immunoreactive protein mass of plasma lipid transfer enzymes in non-diabetic lean and obese men and women with normal oral glucose tolerance and plasma triglyceride concentrations, and found considerable

differences in plasma LPL, CETP, LCAT, and HL concentrations between sexes and between lean and obese subjects.

A few previous studies evaluated the effect of obesity on plasma CETP concentration without considering potential sex differences [5], and measured plasma LPL concentration in men and women without considering the potential role of obesity [6]. Furthermore, both of these studies included subjects with hypertriglyceridemia and of unknown glucose tolerance status, which might have confounded the results [15, 16]. We found that obese individuals have higher plasma LPL, CETP, and LCAT concentrations than lean individuals and obese men (but not obese women) also have higher plasma HL concentration than lean men. LPL is the central enzyme in plasma triglyceride hydrolysis, however, LPL also functions as a molecular bridge to enhance lipoprotein uptake into cells via pathways that are independent of its catalytic activity [13]. The absence of robust relationships between the immunoreactive protein mass of LPL and plasma lipoprotein concentrations suggests that the relationship between plasma LPL concentration and CVD risk [7, 12] may be related to recently discovered non-catalytic functions of the enzyme, such as tissue binding of VLDL [13] and native and oxidized LDL [20], and the facilitation of monocyte adhesion [21]. CETP primarily carries triglyceride from VLDL in exchange for cholesterol esters from other lipoproteins, especially HDL but also LDL [22, 23]. Depletion of core triglyceride makes the VLDL particle smaller and denser, whereas triglyceride enrichment of LDL [24] and HDL [25] eventually leads to the generation of small and dense LDL and small HDL particles. Consistent with

Table 3 Relationships between plasma lipid transfer enzyme concentrations and lipoprotein profile

	LCAT	LPL	CETP	HL
Total VLDL particle concentration	0.414*	0.128	0.299*	0.003
Large VLDL particles	0.315*	0.114	0.143	0.162
Medium VLDL particles	0.457*	−0.067	0.074	−0.099
Small VLDL particles	0.287*	0.203	0.370*	0.047
Average VLDL particle size	0.167	0.044	−0.001	0.237*
VLDL-triglyceride concentration	0.445*	0.137	0.183	0.109
Total LDL particle concentration	0.333*	0.232*	0.459*	0.184
Large LDL particles	0.031	0.099	0.169	−0.124
Small LDL particles	0.327*	0.198	0.401*	0.235*
Average LDL particle size	−0.157	−0.125	−0.198	−0.227*
Total HDL particle concentration	0.595*	−0.034	0.287*	0.021
Large HDL particles	−0.114	−0.182	−0.070	−0.269*
Medium HDL particles	0.245*	0.232*	0.105	−0.206
Small HDL particles	0.477*	−0.045	0.249*	0.338*
Average HDL particle size	−0.389*	−0.053	−0.193	−0.189
HDL-cholesterol concentration	0.062	−0.104	0.030	−0.185

Pearson's simple correlation coefficients are shown;

* *p* < 0.05

LCAT lecithin-cholesterol acyl transferase; LPL lipoprotein lipase; CETP cholesterol-ester transfer protein; HL hepatic lipase; VLDL very-low density lipoprotein; LDL low-density lipoprotein; HDL high-density lipoprotein

this metabolic cascade, we observed positive associations between plasma CETP mass and small VLDL, LDL, and HDL particles.

Differences between men and women in plasma LPL and CETP concentrations (women greater than men) seem to manifest secondary to typical male and female phenotypes (i.e., greater body fat in women than men). This is consistent with the observation that CETP and LPL mRNA is highly expressed in mammalian adipose tissue [26], as well as with the positive relationships found between percent body fat and CETP and LPL concentrations in plasma. On the other hand, sex differences in plasma LCAT and HL concentrations are independent of differences in total body fat accumulation between men and women, and might be considered true sexual dimorphism rather than a secondary phenomenon.

Plasma LCAT concentration was ~30% greater in obese than lean subjects and slightly (~5%) but significantly lower in women than men. Since women have more body fat than men, the difference in plasma LCAT concentration is unlikely to be due to differences in body composition between men and women. Indeed, in our subset of men and women who were matched on percent body fat, plasma LCAT concentration was ~20% lower in women than in men. LCAT is a lipoprotein-associated enzyme responsible for esterifying free cholesterol to cholesterol esters, primarily on the surface of HDL; hydrophobic cholesterol esters then move to the core of HDL thereby maintaining a free-cholesterol gradient from cells to HDL, which is essential for reverse cholesterol transport [9]. Thus, our results are in agreement with the lower HDL-cholesterol concentration and smaller HDL particle size in obese compared with lean subjects and in men compared with women [1, 4], because LCAT in plasma is mainly associated with HDL particles and large, cholesterol-rich HDL particles (in lean subjects and women) contain little or no LCAT [27]. Corroborating these observations, we found that plasma LCAT concentration correlated positively with small HDL particles and negatively with average HDL size.

In agreement with an earlier study that measured post-heparin plasma HL activity [5], we found that obesity was associated with increased plasma HL concentration in men but not in women. Although HL in non-heparinized plasma is catalytically mostly inactive [28], the difference in HL protein mass may be important for our understanding of the regulation of lipid metabolism because HL has multiple roles in lipoprotein metabolism and cellular lipid uptake. It hydrolyzes triglycerides and phospholipids present in circulating plasma lipoproteins, including intermediate-density lipoproteins and lipoprotein remnants, LDL, and HDL, resulting in the generation of smaller LDL and HDL particles [14, 29], consistent with the observed

relationships between plasma HL concentration and small LDL and HDL particles and average particle sizes. Besides its function as lipase, HL serves as a ligand that facilitates lipoprotein uptake by various cell types [14].

In summary, there are considerable differences in the plasma lipid transfer enzyme concentrations between lean and obese subjects and between men and women, which may be partly responsible for respective differences in the plasma lipid profile and CVD risk.

Acknowledgments This publication was made possible by Grant Number UL1 RR024992 from the National Center for Research Resources (NCRR), a component of the National Institutes of Health (NIH), and NIH Roadmap for Medical Research, by National Institutes of Health grants AR 49869, HD 057796, DK 56341 (Clinical Nutrition Research Unit), RR 00036 (General Clinical Research Center), and grants from the American Heart Association (0365436Z and 0510015Z). We wish to thank Megan Steward for help in subject recruitment and the study subjects for their participation.

References

1. National Cholesterol Education Program (2002) Third report of the national cholesterol education program (NCEP) expert panel on detection, evaluation, and treatment of high blood cholesterol in adults (adult treatment panel III) final report. *Circulation* 106:3143–3421
2. Betteridge DJ, Illingworth DR, Shepherd J (1999) Lipoproteins in health and disease. Arnold Publishers, London
3. Havel RJ, Goldstein JL, Brown MS (1980) Lipoproteins and lipid transport. In: Bondy PK, Rosenberg LE (eds) *Metabolic control and disease*, 8th edn. W. B. Saunders Company, Philadelphia, PA, pp 393–494
4. Magkos F, Mohammed BS, Mittendorfer B (2008) Effect of obesity on the plasma lipoprotein subclass profile in normoglycemic and normolipidemic men and women. *Int J Obes (Lond)* 32:1655–1664
5. Arai T, Yamashita S, Hirano K, Sakai N, Kotani K, Fujioka S, Nozaki S, Keno Y, Yamane M, Shinohara E et al (1994) Increased plasma cholesteryl ester transfer protein in obese subjects. A possible mechanism for the reduction of serum HDL cholesterol levels in obesity. *Arterioscler Thromb* 14:1129–1136
6. Watanabe H, Miyashita Y, Murano T, Hiroh Y, Itoh Y, Shirai K (1999) Preheparin serum lipoprotein lipase mass level: the effects of age, gender, and types of hyperlipidemias. *Atherosclerosis* 145:45–50
7. Rip J, Nierman MC, Wareham NJ, Luben R, Bingham SA, Day NE, van Miert JN, Hutten BA, Kastelein JJ, Kuivenhoven JA, Khaw KT, Boekholdt SM (2006) Serum lipoprotein lipase concentration and risk for future coronary artery disease: the EPIC-Norfolk prospective population study. *Arterioscler Thromb Vasc Biol* 26:637–642
8. Cuchel M, Rader DJ (2007) Is the cholesteryl ester transfer protein proatherogenic or antiatherogenic in humans? *J Am Coll Cardiol* 50:1956–1958
9. Movva R, Rader DJ (2008) Laboratory assessment of HDL heterogeneity and function. *Clin Chem* 54:788–800
10. Boekholdt SM, Kuivenhoven JA, Wareham NJ, Peters RJ, Jukema JW, Luben R, Bingham SA, Day NE, Kastelein JJ, Khaw KT (2004) Plasma levels of cholesteryl ester transfer protein and the risk of future coronary artery disease in apparently healthy men and women: the prospective EPIC (European Prospective

- Investigation into Cancer and nutrition)-Norfolk population study. *Circulation* 110:1418–1423
11. Borggreve SE, Hillege HL, Dallinga-Thie GM, de Jong PE, Wolffenbuttel BH, Grobbee DE, van Tol A, Dullaart RP (2007) High plasma cholesteryl ester transfer protein levels may favour reduced incidence of cardiovascular events in men with low triglycerides. *Eur Heart J* 28:1012–1018
 12. Hitsumoto T, Ohsawa H, Uchi T, Noike H, Kanai M, Yoshinuma M, Miyashita Y, Watanabe H, Shirai K (2000) Preheparin serum lipoprotein lipase mass is negatively related to coronary atherosclerosis. *Atherosclerosis* 153:391–396
 13. Merkel M, Kako Y, Radner H, Cho IS, Ramasamy R, Brunzell JD, Goldberg IJ, Breslow JL (1998) Catalytically inactive lipoprotein lipase expression in muscle of transgenic mice increases very low density lipoprotein uptake: direct evidence that lipoprotein lipase bridging occurs in vivo. *Proc Natl Acad Sci U S A* 95:13841–13846
 14. Santamarina-Fojo S, Gonzalez-Navarro H, Freeman L, Wagner E, Nong Z (2004) Hepatic lipase, lipoprotein metabolism, and atherogenesis. *Arterioscler Thromb Vasc Biol* 24:1750–1754
 15. Hanyu O, Miida T, Obayashi K, Ikarashi T, Soda S, Kaneko S, Hirayama S, Suzuki K, Nakamura Y, Yamatani K, Aizawa Y (2004) Lipoprotein lipase (LPL) mass in preheparin serum reflects insulin sensitivity. *Atherosclerosis* 174:385–390
 16. Sandhofer A, Kaser S, Ritsch A, Laimer M, Engl J, Paulweber B, Patsch JR, Ebenbichler CF (2006) Cholesteryl ester transfer protein in metabolic syndrome. *Obesity (Silver Spring)* 14:812–818
 17. Magkos F, Patterson BW, Mohammed BS, Klein S, Mittendorfer B (2007) Women produce fewer but triglyceride-rich very low density lipoproteins than men. *J Clin Endocrinol Metab* 92:1311–1318
 18. Magkos F, Wright DC, Patterson BW, Mohammed BS, Mittendorfer B (2006) Lipid metabolism response to a single, prolonged bout of endurance exercise in healthy young men. *Am J Physiol Endocrinol Metab* 290:E355–362
 19. Bensadoun A (1996) Sandwich immunoassay for measurement of human hepatic lipase. *Methods Enzymol* 263:333–338
 20. Olin KL, Potter-Perigo S, Barrett PH, Wight TN, Chait A (1999) Lipoprotein lipase enhances the binding of native and oxidized low density lipoproteins to versican and biglycan synthesized by cultured arterial smooth muscle cells. *J Biol Chem* 274:34629–34636
 21. Obunike JC, Paka S, Pillarisetti S, Goldberg IJ (1997) Lipoprotein lipase can function as a monocyte adhesion protein. *Arterioscler Thromb Vasc Biol* 17:1414–1420
 22. Morton RE, Zilversmit DB (1983) Inter-relationship of lipids transferred by the lipid-transfer protein isolated from human lipoprotein-deficient plasma. *J Biol Chem* 258:11751–11757
 23. Yen FT, Deckelbaum RJ, Mann CJ, Marcel YL, Milne RW, Tall AR (1989) Inhibition of cholesteryl ester transfer protein activity by monoclonal antibody. Effects on cholesteryl ester formation and neutral lipid mass transfer in human plasma. *J Clin Invest* 83:2018–2024
 24. Berneis KK, Krauss RM (2002) Metabolic origins and clinical significance of LDL heterogeneity. *J Lipid Res* 43:1363–1379
 25. Lamarche B, Rashid S, Lewis GF (1999) HDL metabolism in hypertriglyceridemic states: an overview. *Clin Chim Acta* 286:145–161
 26. Jiang XC, Moulin P, Quinet E, Goldberg IJ, Yacoub LK, Agellon LB, Compton D, Schnitzer-Polokoff R, Tall AR (1991) Mammalian adipose tissue and muscle are major sources of lipid transfer protein mRNA. *J Biol Chem* 266:4631–4639
 27. Borggreve SE, De Vries R, Dullaart RP (2003) Alterations in high-density lipoprotein metabolism and reverse cholesterol transport in insulin resistance and type 2 diabetes mellitus: role of lipolytic enzymes, lecithin:cholesterol acyltransferase and lipid transfer proteins. *Eur J Clin Invest* 33:1051–1069
 28. Nishimura M, Ohkaru Y, Ishii H, Sunahara N, Takagi A, Ikeda Y (2000) Development and evaluation of a direct sandwich-enzyme-linked immunosorbent assay for the quantification of human hepatic triglyceride lipase mass in human plasma. *J Immunol Methods* 235:41–51
 29. Zambon A, Bertocco S, Vitturi N, Polentarutti V, Vianello D, Crepaldi G (2003) Relevance of hepatic lipase to the metabolism of triacylglycerol-rich lipoproteins. *Biochem Soc Trans* 31:1070–1074

Dietary n-3 and n-6 PUFA Enhance DHA Incorporation in Retinal Phospholipids Without Affecting PGE₁ and PGE₂ Levels

Coralie Schnebelen · Stéphane Grégoire · Bruno Pasquis ·
Corinne Joffre · Catherine P. Creuzot-Garcher ·
Alain M. Bron · Lionel Bretillon · Niyazi Acar

Received: 18 November 2008 / Accepted: 3 February 2009 / Published online: 26 February 2009
© AOCs 2009

Abstract The purpose of this study was to determine whether dietary n-3 and n-6 PUFA may affect retinal PUFA composition and PGE₁ and PGE₂ production. Male Wistar rats were fed for 3 months with diets containing: (1) 10% eicosapentaenoic acid (EPA) and 7% docosahexaenoic acid (DHA), or (2) 10% γ -linolenic acid (GLA), or (3) 10% EPA, 7% DHA and 10% GLA, or (4) a balanced diet deprived of EPA, DHA, and GLA. The fatty acid composition of retinal phospholipids was determined by gas chromatography. Prostaglandin production was measured by enzyme immunoassay. When compared to rats fed the control diet, the retinal levels of DHA were increased in rats fed both diets enriched with n-3 PUFA (EPA + DHA and EPA + DHA + GLA diets) and decreased in those supplemented with n-6 PUFA only (GLA diet). The diet enriched with both n-6 and n-3 PUFA resulted in the greatest increase in retinal DHA. The levels of PGE₁ and PGE₂ were significantly increased in retinal homogenates of rats fed with the GLA-rich diet when compared with those of animals fed the control diet.

These higher PGE₁ and PGE₂ levels were not observed in animals fed with EPA + DHA + GLA. In summary, GLA added to EPA + DHA resulted in the highest retinal DHA content but without increasing retinal PGE₂ as seen in animals supplemented with GLA only.

Keywords Dietary polyunsaturated fatty acids · Retina · Prostaglandin · Rat

Abbreviations

ALA	α -Linolenic acid
ARA	Arachidonic acid
dGLA	Dihomo γ -linolenic acid
DHA	Docosahexaenoic acid
DPA	Docosapentaenoic acid
EPA	Eicosapentaenoic acid
GLA	γ -Linolenic acid
LA	Linoleic acid
LC-PUFA	Long chain polyunsaturated fatty acids
PG	Prostaglandins

C. Schnebelen · S. Grégoire · B. Pasquis · C. Joffre ·
L. Bretillon · N. Acar
Eye and Nutrition Research Group, INRA,
UMR1129 FLAVIC, 21000 Dijon, France

C. P. Creuzot-Garcher · A. M. Bron
University of Burgundy, UMR1129 FLAVIC,
21000 Dijon, France

C. P. Creuzot-Garcher · A. M. Bron
Department of Ophthalmology,
University Hospital, 21000 Dijon, France

N. Acar (✉)
Eye and Nutrition Research Group, INRA,
UMR1129 FLAVIC, 17 rue Sully,
BP 86510, 21065 Dijon Cedex, France
e-mail: acar@dijon.inra.fr

Introduction

Long chain n-6 and n-3 polyunsaturated fatty acids (LC-PUFA) are essential components of cell structures and key factors influencing various cellular functions such as neurotransmission or inflammation [1]. Even if very few studies have documented the responses of tissue composition to increased dietary n-6 and n-3 PUFA, it has been shown that supplementing with n-3 PUFA in the absence of n-6 PUFA increases docosahexaenoic acid (DHA, 22:6n-3) but reduces tissue arachidonic acid (ARA, 20:4n-6) [2–4]. Thus it is generally agreed that LC-PUFA from both

families should be provided simultaneously. A recent work carried out on piglets confirmed these observations except for the brain and the retina where ARA accumulation was unresponsive to dietary ARA [5]. Previously, we reported that a dietary supplementation with eicosapentaenoic acid (EPA, 20:5n-3), DHA and γ -linolenic acid (GLA, 18:3n-6) is efficient in increasing the retinal levels of EPA, DHA and dihomo- γ -linolenic acid (dGLA, 20:3n-6) but not those of ARA after a 3-month supplementation in the rat [6].

Since some PUFA are metabolic precursors of eicosanoids, modifications in fatty acid composition of membrane phospholipids can have consequences on the production of these molecules [7]. Eicosanoids are composed of prostaglandins (PG), thromboxanes and leukotrienes that are involved in inflammatory processes. PG are the major eicosanoids that are synthesized from PUFA during inflammatory processes via the cyclooxygenase (COX) pathway. Series 2 PG (including PGE₂) are the most abundant eicosanoids derived from ARA [8, 9] and have pro-inflammatory properties [10]. Series 1 and 3 PG (including PGE₁ and PGE₃) are derived from dGLA [11] and EPA [12, 13], respectively. PGE₁ and PGE₃ are known to be less pro-inflammatory than PG from series 2 [14]. Because PUFA from n-6 and n-3 families compete for the same enzymes responsible for their conversion into either LC-PUFA (desaturases and elongases) or PG (COX), the dietary composition in n-6 and n-3 PUFA may affect the production and tissue accretion of PG. Considering the differences between PG in terms of induction of inflammation, a decrease in the ARA level counterbalanced by an increase in dGLA and EPA levels in cell membranes may reduce the cellular inflammatory potential by modifying the nature of the PG produced. Moreover, it is well known that EPA limits its own biosynthesis through the inhibition of $\Delta 5$ -desaturase, the enzyme that also converts dGLA into ARA [6, 15, 16]. As a consequence, EPA may limit the biosynthesis of ARA from dGLA and favor the production of PGE₁ at the expense of PGE₂. Therefore, EPA allows both the biosynthesis of PGE₃ and the limitation of PGE₂ production. Since GLA, a dietary metabolic precursor of dGLA, is able to increase PGE₁ [17], a diet combining EPA and GLA may decrease the inflammatory potential of the tissues in which they are incorporated.

Given that dietary PUFA such as EPA and GLA may affect the composition of retinal membranes in the rat [6], the aim of the present study was to investigate whether these modifications affect PGE₁ and PGE₂ levels in the retina.

Experimental Procedure

All experiments on the animals were conducted in accordance with the Association for Research in Vision and

Ophthalmology (ARVO) as well as the French regulations (personal agreement number 21CAE104 for C.S. and animal quarters agreement number A21 231010EA).

Animals and Diets

Animals were housed in animal quarters under controlled temperature (22 ± 1 °C) and light conditions (12-h light, 12-h dark cycle). Male Wistar rats (8 weeks of age, Centre d'élevage Janvier, Le Genest Saint Isle, France) were fed for 3 months with diets (Table 1) containing either: (1) 10% EPA and 7% DHA, (2) 10% GLA, (3) 10% EPA, 7% DHA and 10% GLA, or (4) no EPA, DHA and GLA, as previously described [6]. The fat components of the diets were prepared by using sunflower oil and canola oil in order to supply linoleic acid (LA, 18:2n-6) and α -linolenic acid (ALA, 18:3n-3), respectively. High oleic sunflower oil and palm oil were added to balance the levels of oleic acid and palmitic acid, respectively, whereas borage and tuna oils were specifically used to ensure GLA and EPA+DHA supplies, respectively. The detailed composition of dietary lipids is presented in Table 2. These dietary PUFA concentrations were chosen since they have been shown to significantly modify the retinal fatty acid composition in rats after 3 months of diet [6]. At the end of the feeding period, animals were euthanized and the retinas were carefully excised from the ocular globe, quickly frozen in liquid nitrogen and stored at -80 °C until further analyses.

Table 1 Composition of diets

Ingredient	Amount (g/kg diet)
Casein	180
Cornstarch	460
Sucrose	230
Cellulose	20
Fat ^a	50
Mineral mix ^b	50
Vitamin mix ^c	10

^a Represented by oil mixes prepared with variable amounts of sunflower oil, canola oil, high oleic sunflower oil, palm oil, borage oil, and tuna oil

^b Composition (g/kg diet): sucrose, 5.535; CaCO₃, 12; K₂HPO₄, 10.75; CaHPO₄, 10.75; MgSO₄ · 7H₂O, 5; NaCl, 3; MgO, 2; FeSO₄ · 7H₂O, 0.4; ZnSO₄ · 7H₂O, 0.35; MnSO₄ · H₂O, 0.1; CuSO₄ · 5H₂O, 0.05; Na₂SiO₇ · 3H₂O, 0.025; AlK(SO₄)₂ · 12H₂O, 0.01; K₂CrO₄, 0.0075; NaF, 0.005; NiSO₄ · 6H₂O, 0.005; H₂BO₃, 0.005; CoSO₄ · 7H₂O, 0.00025; KIO₃, 0.002; (NH₄)₆Mo₇O₂₄ · 4H₂O, 0.001; LiCl, 0.00075; Na₂SeO₃, 0.00075; NH₄VO₃, 0.0005

^c Composition (g/kg diet): sucrose, 5.4945; retinyl acetate, 0.01; cholecalciferol, 0.0025; DL- α -tocopheryl acetate, 0.2; phylloquinone, 0.001; thiamin HCl, 0.01; riboflavin, 0.01; nicotinic acid, 0.05; calcium pantothenate, 0.025; pyridoxine HCl, 0.01; biotin, 0.01; folic acid, 0.002; cyanobalamin, 0.025; choline HCl, 2; DL-methionin, 2; *p*-aminobenzoic acid, 0.05; inositol, 0.1

Table 2 Fatty acid composition of dietary lipids

Fatty acids	Control	EPA+DHA	GLA	EPA+DHA+GLA
Total saturated fatty acids	25.8	30.5	21.1	31.5
Total monounsaturated fatty acids	60.4	34.2	43.6	19.4
C18:2n-6 (LA)	11.7	15.2	24.0	20.0
Trans C18:2	0.4	nd	0.2	nd
C18:3n-6 (GLA)	nd	nd	10.2	9.9
C20:4n-6 (ARA)	nd	nd	nd	0.6
Total n-6 fatty acids	12.1	15.2	34.4	30.5
C18:3n-3 (ALA)	1.7	0.9	0.9	0.9
C20:5n-3 (EPA)	nd	10.9	nd	10.0
C22:5n-3	nd	1.1	nd	1.1
C22:6n-3 (DHA)	nd	7.2	nd	6.6
Total n-3 fatty acids	1.7	20.1	0.9	18.6
Total n-6+n-3 fatty acids	13.8	35.3	35.3	49.1
n-6/n-3 ratio	7.1	0.7	38.2	1.7

Values are expressed as a percentage of total fatty acids; nd: not detected (under the limit for the detection by gas chromatography, <0.05%)

Lipid Assay

Total lipids were extracted from retinas according to the Folch procedure [18] ($n = 6$ in each group). Total phospholipids were separated from neutral lipids using silica cartridges according to Juaneda and Rocquelin's method [19]. The phospholipid fraction was transesterified using boron trifluoride in methanol according to Morrison and Smith [20]. Fatty acid methyl esters (FAMES) were analyzed by gas chromatography on a Hewlett Packard Model 5890 gas chromatograph (Palo Alto, CA, USA) using a CPSIL-88 column (100 m \times 0.25 mm i.d. film thickness 0.20 μ m; Varian, Les Ulis, France) equipped with a flame ionization detector. Hydrogen was used as a carrier gas (inlet pressure, 210 kPa). The oven temperature was held at 60 °C for 5 min, increased to 165 °C at 15 °C/min and held for 1 min, and then to 225 °C at 2 °C/min and finally held at 225 °C for 17 min. The injector and the detector were maintained at 250 and 280 °C, respectively. FAMES were identified by comparison with commercial and synthetic standards. The data were processed using the EZChrom Elite software (Agilent Technologies, Massy, France).

Measurement of Prostaglandin Levels in the Retina

Retinas were immersed in 500 μ L of cell lysis reagent (CellLytic™ M, Sigma-Aldrich, Saint Quentin Fallavier, France) containing 10% of a protease inhibitor cocktail

(Sigma-Aldrich). After mechanical crushing and sonication for 30 min, samples were incubated overnight at 4 °C. Samples were then centrifuged for 10 min, at 1,000g, 4 °C. The supernatants were collected and stored at –80 °C until PG assay using an enzyme immunoassay kit (Assay Designs, Euromedex, Souffelweyersheim, France) according to the manufacturer's instructions. A cross-reactivity of 70% with PGE₁ was announced by the manufacturer for PGE₂ immunoassay. Since the neuronal tissue levels of PGE₂ are about 10-fold higher than those of PGE₁, we expected this cross-reactivity to have a minor influence on PGE₂ quantification [21–23]. Concerning PGE₁ immunoassay, the cross-reactivity with PGE₂ was of 6.5% only. PGE₁ and PGE₂ levels in the homogenates were expressed in picograms per milligram of total protein quantified using the Bradford method [24] ($n = 6$ in each group). We did not observe any difference in total protein content of retinal homogenates between the different diet groups.

Statistical Analyses

Data were expressed as means \pm standard deviation (SD). The Student–Newman–Keuls test was used to compare the data from the different groups using SAS software (SAS Institute, Cary, NC, USA). *p*-Values less than 0.05 were considered as significant.

Results and Discussion

Confirming our previous results [6], feeding the animals with GLA only significantly increased the retinal levels of ARA and docosapentaenoic acid n-6 (DPAn-6, 22:5n-6) compared to control animals (Table 3). The amount of total n-6 PUFA was increased from 12.1% in controls to 20.2% in the GLA group. Conversely, the amount of total n-3 PUFA was decreased from 31.7% in controls to 29.5% of total fatty acids in the GLA group, certainly as a result of the competition between n-6 and n-3 PUFA families for enzymes responsible for their conversion. The n-6/n-3 ratio was thus significantly enhanced in the GLA group (0.68) when compared to controls (0.38). These modifications in retinal lipid composition had repercussions on the PG levels, as shown by the significant increases in the retinal amounts of PGE₁ and PGE₂ when compared to retinas from controls (Fig. 1).

Animals fed with the EPA+DHA diet showed contrasting retinal fatty acid compositions when compared to those fed with GLA (Table 3). We observed a significant increase in the retinal levels of EPA and DHA compared to the control group, whereas the n-6 end-chain products were significantly decreased (ARA and DPAn-6). In the retina of animals from the EPA+DHA group, the level of PGE₁ was

Table 3 Retinal phospholipid fatty acid composition of rats fed 3 months with diets enriched with n-3 and n-6 long-chain polyunsaturated fatty acids

Fatty acids	Control <i>n</i> = 6	EPA+DHA <i>n</i> = 8	GLA <i>n</i> = 7	EPA+DHA+GLA <i>n</i> = 6
C16:0	15.5 ± 0.3 ^a	14.1 ± 0.9 ^b	10.2 ± 1.5 ^c	9.7 ± 1.2 ^c
C18:0	25.9 ± 1.3	25.1 ± 0.6	26.5 ± 0.9	25.8 ± 0.9
Total saturated fatty acids	41.9 ± 1.7 ^a	39.6 ± 1.0 ^b	37.1 ± 0.8 ^c	35.8 ± 0.9 ^c
C16:1n-7	0.25 ± 0.05 ^{a,b}	0.29 ± 0.07 ^a	0.14 ± 0.06 ^c	0.17 ± 0.11 ^{b,c}
C18:1n-9	7.7 ± 0.7 ^a	8.5 ± 1.0 ^b	6.7 ± 0.3 ^c	6.8 ± 0.3 ^c
C18:1n-7	2.4 ± 0.1 ^a	2.3 ± 0.3 ^a	2.2 ± 0.1 ^{a,b}	2.0 ± 0.1 ^b
Total monounsaturated fatty acids	10.8 ± 0.8 ^a	11.6 ± 1.1 ^a	9.5 ± 0.4 ^b	9.4 ± 0.4 ^b
C18:2n-6	0.46 ± 0.15 ^a	0.67 ± 0.15 ^b	0.51 ± 0.13 ^{a,b}	0.54 ± 0.17 ^{a,b}
C18:3n-6 (GLA)	nd	nd	nd	nd
C20:2n-6	nd	nd	nd	nd
C20:3n-6 (dGLA)	0.12 ± 0.01 ^a	0.18 ± 0.02 ^b	0.21 ± 0.04 ^b	0.33 ± 0.07 ^c
C20:4n-6 (ARA)	8.9 ± 0.4 ^a	7.7 ± 0.5 ^b	10.3 ± 0.3 ^c	9.5 ± 0.3 ^d
C22:4n-6	1.4 ± 0.1 ^a	0.9 ± 0.1 ^b	2.3 ± 0.1 ^c	1.4 ± 0.1 ^a
C22:5n-6 (DPA)	1.1 ± 0.2 ^a	0.08 ± 0.01 ^b	6.7 ± 0.8 ^c	0.16 ± 0.04 ^b
Total n-6 fatty acids	12.1 ± 0.5 ^a	9.7 ± 0.7 ^b	20.2 ± 0.6 ^c	12.2 ± 0.4 ^a
C18:3n-3	nd	nd	nd	nd
C20:5n-3 (EPA)	<0.1 ^a	0.52 ± 0.1 ^b	nd ^a	0.23 ± 0.03 ^c
C22:5n-3	0.33 ± 0.02 ^a	1.0 ± 0.1 ^b	0.30 ± 0.03 ^a	0.90 ± 0.07 ^c
C22:6n-3 (DHA)	31.3 ± 1.5 ^a	33.8 ± 2.4 ^b	29.2 ± 1.4 ^c	37.8 ± 1.2 ^d
Total n-3 fatty acids	31.7 ± 1.6 ^a	35.4 ± 2.3 ^b	29.5 ± 1.4 ^c	38.9 ± 1.2 ^d
Total n-6+n-3 fatty acids	43.7 ± 1.7 ^a	45.0 ± 1.6 ^a	49.6 ± 1.1 ^b	51.0 ± 1.1 ^b
n-6/n-3 ratio	0.38 ± 0.04 ^a	0.28 ± 0.02 ^b	0.68 ± 0.05 ^c	0.31 ± 0.02 ^b

Values are expressed as means ± SD in percentage of total fatty acids (*n* = 6–8). Values with different superscript letters (a, b, c, d) are significantly different (*p* < 0.05). nd: not detected (under the limit for the detection by gas chromatography, <0.05%)

similar to that of control animals despite a significant increase in the dGLA level, although moderate (from 0.12 to 0.18% of total fatty acids in control and EPA+DHA groups, respectively; *p* < 0.05) (Fig. 1). This slight but significant increase in dGLA can be explained by the retro-inhibition of $\Delta 5$ -desaturase by EPA [15], thus limiting the conversion of dGLA to ARA. However, the decrease observed in retinal n-6 end-chain products and particularly in ARA did not result in any significant change in the retinal PGE₂ level, suggesting that the level of PGE₂ is not limited to substrate availability (Fig. 1). Nevertheless, and considering the significant increase in the EPA level (from <0.1 to 0.52% of total fatty acids in control and EPA+DHA groups, respectively; *p* < 0.05), we would expect an increase in the level of PGE₃ [13]. Unfortunately, the methodology we used did not allow us to analyse that eicosanoid, which can only be quantified by high-performance liquid chromatography coupled with electrospray ionization tandem mass spectrometry (LC/MS/MS) [25].

Feeding the animals with EPA and DHA together with GLA resulted in retinal levels of ARA, and DPA n-6 that were higher than those of control animals and lower than

those of animals fed with GLA only (Table 3). These results are not in accordance with previous reports showing that the levels of cerebral and retinal ARA are unchanged after DHA and ARA supplementations on newborn piglets [5, 26, 27]. The specific incorporation rates of LC-PUFA during neonatal development and the fact that our supplements are not based on ARA itself but on GLA and EPA may have contributed to these differential responses of the retina to dietary LC-PUFA. Within fatty acids from the n-3 family, we observed a strong increase in retinal DHA, whose levels were above those measured in the EPA+DHA group (35.4 vs. 38.9% of total fatty acids in EPA+DHA and EPA+DHA+GLA groups, respectively; *p* < 0.05). This observation was confirmed by the amounts of total n-3 PUFA and total n-6+n-3 PUFA, whose values were higher than those observed in the EPA+DHA and GLA groups. Within retinal n-3 PUFA, the levels of EPA were reduced by more than 55% in animals fed both n-6 and n-3 PUFA when compared to those supplemented with n-3 PUFA only whereas the levels of C22:5n-3 were reduced by 10% only. Indeed, the strong increase in retinal DHA of animals supplemented with both n-6 and n-3

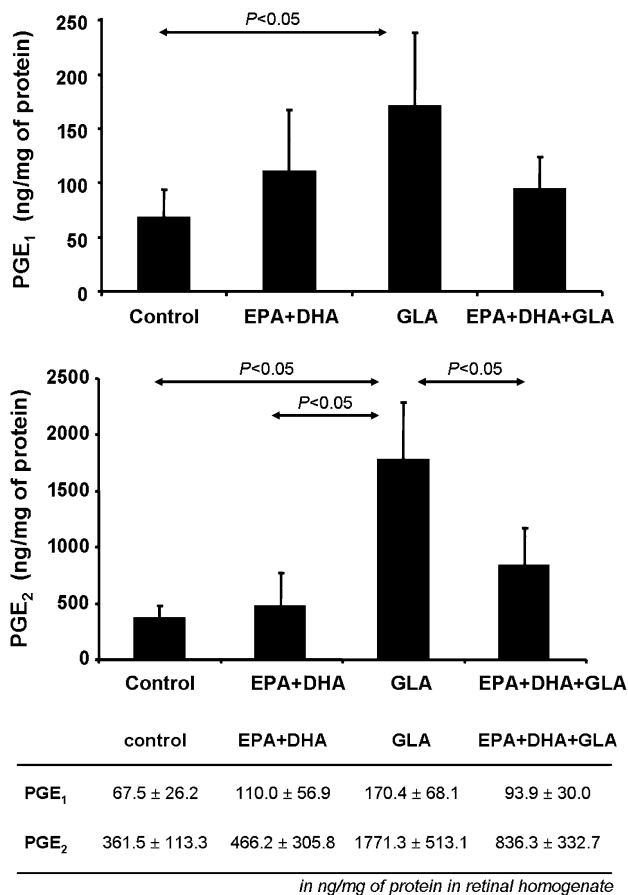


Fig. 1 PGE₁ and PGE₂ content of retinal homogenates of rats fed 3 months with diets enriched with n-3 and n-6 long-chain polyunsaturated fatty acids ($n = 6$ in each group). Results are expressed as means \pm SD in ng per mg of total protein in retinal lysate

PUFA may be at least partly due to the contribution of EPA to form DHA. However, the reasons why dietary GLA may potentially influence the conversion of n-3 PUFA remain unknown. The repercussions of these modifications on the retinal PGE₂ level matched expectations, since the measured values followed the ARA values by being comparable to those from control animals (Fig. 1). However, and unexpectedly, the level of PGE₁ in the EPA+DHA+GLA group was also unmodified when compared to control animals (Fig. 1), despite significantly higher amounts of dGLA (0.33 vs. 0.12% of total fatty acids in EPA+DHA+GLA and control groups, respectively; $p < 0.05$). This result suggests either that the increase of dGLA was not sufficient to significantly modify the retinal level of PGE₁ or that the level of PGE₁ is not limited to substrate availability. Nevertheless, this lack of repercussion on the PGE₁ level can be explained by the low concentrations of dGLA in the retinas, particularly when compared to the other PUFA such as ARA.

In conclusion, although the data we provide do not show a clear relationship between dietary PUFA and retinal

inflammatory potential through retinal PGE₁ and PGE₂ levels, we show that a concomitant supply of targeted PUFA from both n-6 and n-3 families, namely GLA, EPA and DHA (i) can enhance the retinal levels of DHA above those observed with n-3 PUFA supplementation only, (ii) without modifying the basal levels of retinal PGE₁ and PGE₂.

Acknowledgments A Ph.D. fellowship to Coralie Schnebelen was supported by a grant from Chauvin, Bausch & Lomb Laboratories (France) and the Regional Council of Burgundy (France). The authors gratefully acknowledge Linda Northrup (PhD, ELS, English Solutions, Voiron, France) for the English language editing of the manuscript.

References

- SanGiovanni JP, Chew EY (2005) The role of omega-3 long-chain polyunsaturated fatty acids in health and disease of the retina. *Prog Retin Eye Res* 24:87–138
- Carlson SE, Cooke RJ, Werkman SH, Tolley EA (1992) First year growth of preterm infants fed standard compared to marine oil n-3 supplemented formula. *Lipids* 27:901–907
- Carlson SE, Werkman SH, Peebles JM, Cooke RJ, Tolley EA (1993) Arachidonic acid status correlates with first year growth in preterm infants. *Proc Natl Acad Sci USA* 90:1073–1077
- Koletzko B, Agostoni C, Carlson SE, Clandinin T, Hornstra G, Neuringer M, Uauy R, Yamashiro Y, Willatts P (2001) Long chain polyunsaturated fatty acids (LC-PUFA) and perinatal development. *Acta Paediatr* 90:460–464
- Huang MC, Brenna JT, Chao AC, Tschanz C, Diersen-Schade DA, Hung HC (2007) Differential tissue dose responses of (n-3) and (n-6) PUFA in neonatal piglets fed docosahexaenoate and arachidonoate. *J Nutr* 137:2049–2055
- Snebelen C, Viau S, Gregoire S, Joffre C, Creuzot-Garcher C, Bron A, Bretillon L, Acar N (2009) Nutrition for the eye: different susceptibility of the retina and the lacrimal gland to dietary omega-6 and omega-3 polyunsaturated fatty acid incorporation. *Ophthalmic Res* 884 (in press)
- Calder PC (2002) Dietary modification of inflammation with lipids. *Proc Nutr Soc* 61:345–358
- Kelley DS, Taylor PC, Nelson GJ, Mackey BE (1998) Arachidonic acid supplementation enhances synthesis of eicosanoids without suppressing immune functions in young healthy men. *Lipids* 33:125–130
- Peterson LD, Jeffery NM, Thies F, Sanderson P, Newsholme EA, Calder PC (1998) Eicosapentaenoic and docosahexaenoic acids alter rat spleen leukocyte fatty acid composition and prostaglandin E2 production but have different effects on lymphocyte functions and cell-mediated immunity. *Lipids* 33:171–180
- Calder PC (2006) n-3 polyunsaturated fatty acids, inflammation, and inflammatory diseases. *Am J Clin Nutr* 83:1505S–1519S
- Levin G, Duffin KL, Obukowicz MG, Hummert SL, Fujiwara H, Needleman P, Raz A (2002) Differential metabolism of dihomogamma-linolenic acid and arachidonic acid by cyclo-oxygenase-1 and cyclo-oxygenase-2: implications for cellular synthesis of prostaglandin E1 and prostaglandin E2. *Biochem J* 365:489–496
- Santoli D, Zurier RB (1989) Prostaglandin E precursor fatty acids inhibit human IL-2 production by a prostaglandin E-independent mechanism. *J Immunol* 143:1303–1309
- Yang P, Chan D, Felix E, Cartwright C, Menter DG, Madden T, Klein RD, Fischer SM, Newman RA (2004) Formation and

- antiproliferative effect of prostaglandin E(3) from eicosapentaenoic acid in human lung cancer cells. *J Lipid Res* 45:1030–1039
14. Bagga D, Wang L, Farias-Eisner R, Glaspy JA, Reddy ST (2003) Differential effects of prostaglandin derived from omega-6 and omega-3 polyunsaturated fatty acids on COX-2 expression and IL-6 secretion. *Proc Natl Acad Sci USA* 100:1751–1756
 15. Barham JB, Edens MB, Fonteh AN, Johnson MM, Easter L, Chilton FH (2000) Addition of eicosapentaenoic acid to gamma-linolenic acid-supplemented diets prevents serum arachidonic acid accumulation in humans. *J Nutr* 130:1925–1931
 16. Miles EA, Banerjee T, Calder PC (2004) The influence of different combinations of gamma-linolenic, stearidonic and eicosapentaenoic acids on the fatty acid composition of blood lipids and mononuclear cells in human volunteers. *Prostaglandins Leukot Essent Fatty Acids* 70:529–538
 17. Fan YY, Ramos KS, Chapkin RS (1997) Dietary gamma-linolenic acid enhances mouse macrophage-derived prostaglandin E1 which inhibits vascular smooth muscle cell proliferation. *J Nutr* 127:1765–1771
 18. Folch J, Lees M, Sloane Stanley GH (1957) A simple method for the isolation and purification of total lipids from animal tissues. *J Biol Chem* 226:497–509
 19. Juaneda P, Rocquelin G (1985) Rapid and convenient separation of phospholipids and non phosphorus lipids from rat heart using silica cartridges. *Lipids* 20:40–41
 20. Morrison WR, Smith LM (1964) Preparation of fatty acid methyl esters and dimethylacetals from lipids with boron fluoride-methanol. *J Lipid Res* 5:600–608
 21. Bell JG, Tocher DR, MacDonald FM, Sargent JR (1995) Diets rich in eicosapentaenoic acid and gamma-linolenic acid affect phospholipid fatty acid composition and production of prostaglandins E1, E2 and E3 in turbot (*Scophthalmus maximus*), a species deficient in delta 5 fatty acid desaturase. *Prostaglandins Leukot Essent Fatty Acids* 53:279–286
 22. Bell JG, Tocher DR, Sargent JR (1994) Effect of supplementation with 20:3(n-6), 20:4(n-6) and 20:5(n-3) on the production of prostaglandins E and F of the 1-, 2- and 3-series in turbot (*Scophthalmus maximus*) brain astroglial cells in primary culture. *Biochim Biophys Acta* 1211:335–342
 23. Galli C, Petroni A (1990) Eicosanoids and the central nervous system. *Ups J Med Sci Suppl* 48:133–144
 24. Bradford MM (1976) A rapid and sensitive method for the quantitation of microgram quantities of protein utilizing the principle of protein-dye binding. *Anal Biochem* 72:248–254
 25. Yang P, Felix E, Madden T, Fischer SM, Newman RA (2002) Quantitative high-performance liquid chromatography/electrospray ionization tandem mass spectrometric analysis of 2- and 3-series prostaglandins in cultured tumor cells. *Anal Biochem* 308:168–177
 26. Alessandri JM, Goustard B, Guesnet P, Durand G (1998) Docosahexaenoic acid concentrations in retinal phospholipids of piglets fed an infant formula enriched with long-chain polyunsaturated fatty acids: effects of egg phospholipids and fish oils with different ratios of eicosapentaenoic acid to docosahexaenoic acid. *Am J Clin Nutr* 67:377–385
 27. Craig-Schmidt MC, Stieh KE, Lien EL (1996) Retinal fatty acids of piglets fed docosahexaenoic and arachidonic acids from microbial sources. *Lipids* 31:53–59

Abies koreana Essential Oil Inhibits Drug-Resistant Skin Pathogen Growth and LPS-Induced Inflammatory Effects of Murine Macrophage

Weon-Jong Yoon · Sang-Suk Kim · Tae-Heon Oh ·
Nam Ho Lee · Chang-Gu Hyun

Received: 12 November 2008 / Accepted: 16 March 2009 / Published online: 7 April 2009
© AOCS 2009

Abstract Since acne vulgaris is the combined result of a bacterial infection and the inflammatory response to that infection, we examined whether *Abies koreana* essential oil (AKE) possessed anti-inflammatory and antibacterial activities against skin pathogens. In this study, AKE showed excellent antibacterial activities against drug-susceptible and -resistant *Propionibacterium acnes* and *Staphylococcus epidermidis*, which are acne-causing bacteria. In addition, AKE reduced the LPS-induced secretion of tumor necrosis factor- α (TNF- α), interleukin-1 β (IL-1 β), IL-6, NO and PGE₂ in RAW 264.7 cells, indicating that it has anti-inflammatory effects. Therefore, we suggest that AKE may be an attractive candidate for promoting skin health.

Keywords *Abies koreana* · Acne vulgaris · Essential oil · Inflammation · Skin pathogen

Introduction

Propionibacterium acnes is a skin-colonizing, gram-positive bacterium associated with sebum-excreting pilosebaceous follicles. *P. acnes* is involved in the development of inflamed lesions during the course of acne, in which an induced inflammatory response is presumably directed

against propionibacterial antigens [1]. In contrast, *Staphylococcus epidermidis*, an aerobic organism, is usually involved in superficial infections within the sebaceous unit [2].

Mild to moderate inflammatory acne sometimes responds well to topical treatment with anti-bacterial agents, usually erythromycin or clindamycin and less often tetracycline [3, 4]. Over the past 2½ decades, the incidence of resistance to erythromycin, clindamycin and/or tetracycline has increased among propionibacterial populations associated with inflammatory acne; this resistance presents a worldwide problem for the treatment of this condition [3, 5]. The development of antibiotic resistance is multifactorial, involving the specific nature of the relationship of bacteria to antibiotics, how the anti-bacterial is used, host characteristics and environmental factors. To overcome the problem of antibiotic resistance, essential oils have been extensively studied as alternative treatments for disease [2, 6]. Therapeutic agents for acne are also employed to inhibit inflammation. However, these remedies have been known to induce side effects. Benzoyl peroxide and retinoid cause xerosis cutis and skin irritation if they are used excessively [7], and several reports also suggest that prolonged use of antibiotics can lead to organ damage and immunohypersensitivity [8–10]. In addition, triclosan is converted into an environmental hormone when exposed to light, inducing severe environmental pollution [10]. Therefore, many researchers have sought to develop therapeutic agents for acne that have high antibacterial and anti-inflammatory activities with no side effects [11–16].

As part of our ongoing alternative medicine programs, we have directed our attention toward the identification of essential oils that combine a relatively narrow spectrum of activity against erythromycin- and clindamycin-resistant strains with good anti-inflammatory activity for potential

W.-J. Yoon · C.-G. Hyun (✉)
Research Group for Cosmetic Materials, Jeju Biodiversity
Research Institute (JBRI), Jeju High-Tech Development Institute
(HiDI), Jeju 697-943, Korea
e-mail: cghyun@jejuhidi.or.kr

S.-S. Kim · T.-H. Oh · N. H. Lee
Department of Chemistry, Cheju National University,
Jeju 690-756, Korea

topical applications in patients with mild to moderate inflammatory acne. Here we report on the anti-bacterial and anti-inflammatory activities of *Abies koreana* essential oil (AKE) against drug-resistant *P. acnes* and *S. epidermidis*.

Experimental Procedures

An ethnobotanical survey was conducted on Jeju Island, South Korea, in October 2007. Voucher specimens were deposited at the herbarium of Jeju Biodiversity Research Institute (Jeju, Korea). The AKE was extracted by hydro-distillation as described by Baik et al. [17]. Briefly, approximately 1 kg of fresh *A. koreana* leaves was immersed in 3.5 l of distilled water in a 5-l three-neck flask. The sample was steam distilled for 12 h at atmospheric pressure. Gas chromatographic analyses were performed on a Hewlett-Packard 5890 gas chromatograph equipped with a polar Supelcowax column (30 m × 0.25 mm × 0.25 μm), an apolar DB-1HT column (30 m × 0.25 mm) and a split-splitless injection port (split mode). The temperature was set at 40°C for 5 min, ramped to 210°C at 10°C/min and held at 250°C for 28 min. Compounds were identified by their retention indices on both columns and by GC-MS using a Hewlett-Packard MSD 5972 mass spectrometer at 70 eV coupled to an HP 5890GC equipped with a DB-1HT column (30 m × 0.32 mm × 0.1 μm).

Nitric oxide production was assayed in the culture medium of cells stimulated with LPS (1 μg/ml) for 24 h in the presence of AKE. Cytotoxicity was determined using the LDH method. Supernatants were collected and PGE₂ concentration in the supernatants was determined by ELISA. iNOS and COX-2 mRNA expression and protein levels were determined by RT-PCR and immunoblotting, respectively. The primers used in this study were: β-actin (forward primer 5'-GTGGGCCCGCCCTAGGCACCAG-3' and reverse primer 5'-GGAGGAAGAGGATGCGGCA GT-3'), iNOS (forward primer 5'-CCCTCCGAAGTT TCTGGCAGCAGC-3' and reverse primer 5'-GGCTGTCA GAGCCTCGTGGCTTTGG-3'), COX-2 (forward primer 5'-CACTACATCCTGACCCACTT-3' and reverse primer 5'-ATGCTCCTGCTTGAGTATGT-3'). PCR products were electrophoresed in 1.5% agarose gels and stained with ethidium bromide. The β-actin, iNOS and COX-2 primers produced the expected amplified products of 603, 496 and 696 bp, respectively. The Student's *t*-test and one-way ANOVA were used to determine statistically significant differences between the values for the various experimental and control groups. Data are expressed as means ± standard errors (SEM) and the results are taken from at least three independent experiments performed in triplicate.

Values are the mean ± SEM of triplicate experiments. **P* < 0.05; ***P* < 0.01

Results and Discussion

Abies koreana is a shrub or broadly pyramidal evergreen tree endemic to the high mountains in southern Korea, including Mt. Halla. Recent reports demonstrated that *A. koreana* has several medicinal functions, including anti-tumor [18, 19] and memory-enhancing effects [20]. In addition, Jeong et al. [21] elucidated 68 chemical components and demonstrated the anti-microbial activity of AKE. However, anti-inflammatory effects or anti-bacterial activities against drug-resistant skin pathogens by AKE have not been described. In our study, *A. koreana* leaves were subjected to steam distillation. Nineteen compounds were identified in *A. koreana* leaves by GC/MS, representing more than 85.05% of the volatile compounds (Table 1). Bornyl acetate (30.35%) and limonene (18.95%) were the major components. Other chemical components included α-pinene (8.10%), camphene (7.39%), α-elemene (3.51%), alloaromadendrene (2.45%), γ-selinene (2.21%) and borneol (1.96%). In contrast, the main compounds identified by Jeong were borneol (27.9%), α-pinene

Table 1 Chemical composition of the essential oils from *A. Koreana*

RT	RI	Components	Peak area
4.885	908.0	Tricyclene	0.78
5.348	919.2	α-Pinene	8.10
5.723	928.2	Camphene	7.39
6.714	952.2	β-Pinene	1.06
7.783	978.0	β-Myrcene	0.87
8.405	993.1	δ-Carene	0.87
9.546	1015.0	Limonene	18.95
14.608	1103.4	Limonene oxide	0.51
16.459	1132.5	Borneol	1.96
20.304	1193.0	2-Norbornanol	1.28
24.524	1259.4	Bornyl acetate	30.35
31.448	1371.0	Isolongifolene	0.74
35.987	1440.9	γ-Selinene	2.21
36.296	1445.4	δ-Selinene	1.12
37.453	1462.6	Alloaromadendrene	2.45
37.998	1470.6	7-epi-α-Selinene	0.62
38.747	1481.7	1-β-Bisabolene	0.89
41.865	1535.3	Caryophyllene oxide	1.39
45.368	1601.5	α-Elemene	3.51

The GC/MS retention indices were calculated using a homologous series of *n*-alkanes C₆–C₃₁. Components were characterized based on library and literature searches and only those components showing matches exceeding 90% were selected. *RI* retention index, *RT* retention time

(23.2%), β -pinene (5.8%), terpinene-4-ol (3.8%), bornyl acetate (3.4%) and α -terpineol (3.1%). This difference in the main components may be due to the provenance of plant, harvest time or development stage, extraction technique, or the use of fresh or dried plant material. These are all factors that influence the chemical composition and biological activity.

The *in vitro* anti-bacterial activity of AKE against *P. acnes* and *S. epidermidis* was assessed by the presence or absence of inhibition zones and by MIC values. The MIC was recorded as the lowest concentration (highest dilution) of essential oils that inhibited visible growth (no turbidity). The MIC of AKE was determined using a two-fold serial dilution method. As shown in Table 2, AKE exhibited excellent anti-bacterial activity against drug-susceptible and -resistant *P. acnes* and *S. epidermidis*. We also determined the MIC of the major components of AKE (bornyl acetate, camphene, limonene, and α -pinene) and commercial essential oils (tea tree, lavender, and peppermint oils). In this experiment, the antibacterial activities of AKE were similar to those of the major components of AKE and the commercial essential oils. The MIC of AKE was far superior to those of the other compounds and oils against clindamycin-resistant *P. acne* SKA4.

In many studies, anti-inflammatory compounds have been investigated for their potential inhibitory effects *in vitro* using lipopolysaccharide (LPS)-stimulated RAW264.7 macrophages. Bacterial LPS is one of the best-characterized stimuli used to induce upregulation of pro-inflammatory proteins such as cyclooxygenase-2 (COX-2) and inducible nitric oxide synthase (iNOS). Inducible COX-2 is responsible for the high prostaglandin levels observed in many inflammatory pathologies. Similarly, iNOS produces large amounts of nitric oxide (NO) and is thought to play a central role in inflammatory disease. Numerous studies have

reported that NO and prostaglandin E₂ (PGE₂) participate in inflammatory and nociceptive events.

Since acne vulgaris is the combined result of a bacterial infection and the inflammatory response to that infection, we next examined whether AKE possessed anti-inflammatory activity. To investigate the effect of AKE on NO production, we measured the accumulation of nitrite, a stable oxidized product of NO, in culture media [22, 23] of RAW 264.7 cells stimulated with LPS for 24 h in the presence or absence of AKE. Nitrite levels in LPS-stimulated cells increased significantly compared to that in control cells. As shown in Fig. 1a, AKE (12.5, 25 and 50 μ g/ml) markedly and dose-dependently inhibited LPS-induced NO production by RAW 264.7 cells. COX-2 is induced by cytokines and other activators, such as LPS, in a variety of inflammatory cells, including macrophages, resulting in the release of large amounts of PGE₂ at inflammatory sites. Therefore, we examined the effects of AKE on PGE₂ production in LPS-stimulated RAW 264.7 macrophages. When macrophages were stimulated with LPS (1 μ g/ml) for 24 h, the levels of PGE₂ increased in the culture medium. As shown in Fig. 1b, AKE (12.5, 25 and 50 μ g/ml) suppressed LPS-induced PGE₂ production in a dose-dependent manner. As expected, the reference compounds, NS-398 (COX-2 inhibitor) and 2-amino-4-methyl pyridine (iNOS inhibitor) potently inhibited PGE₂ and NO production at 20 μ M, respectively.

Western blot and RT-PCR analyses were performed to determine if the inhibitory effects of AKE on pro-inflammatory mediators (NO and PGE₂) were related to the modulation of iNOS and COX-2 expressions. In unstimulated RAW 264.7 cells, iNOS and COX-2 protein and mRNA were not detected. But, LPS upregulated their protein levels, and pre-treatment with AKE inhibited this upregulation. To determine if the inhibition of

Table 2 MIC values of AKE, its components, and commercial essential oils

Drug-resistant patterns of skin pathogens (MIC; μ g/ml)	Strains	MIC values (μ l/mL)							
		AKE	Tea tree Oil	Lavender oil	Peppermint oil	Bornyl acetate	Camphene	Limonene	α -pinene
Susceptible	<i>S. epidermidis</i> SK4	0.625	0.125	1.000	0.125	<0.300	0.500	0.500	0.500
Erythromycin (>32), Clindamycin (>16), Chloramphenicol (64)	<i>S. epidermidis</i> SK 9	0.312	1.000	0.125	0.500	0.300	>4.000	>4.000	1.000
Tetracycline (>32)	<i>S. epidermidis</i> SK19	5.000	1.000	1.000	0.500	>10.00	10.00	10.00	4.000
Susceptible	<i>P. acnes</i> ATCC 3314	0.312	0.250	0.250	0.250	5.000	<0.156	<0.625	0.500
Clindamycin (64)	<i>P. acnes</i> SKA 4	0.312	2.500	1.250	0.625	20.00	>20.00	>20.00	10.00
Clindamycin (64)	<i>P. acnes</i> SKA 7	0.625	0.250	0.250	0.060	20.00	<0.156	<0.625	0.125

Skin pathogens were grown at 37°C for 24 h or 48 h (for *Propionibacterium* sp.) in each media. Culture suspensions were adjusted by comparing against 0.5 McFarland standard. For determination of MIC, the microdilution broth susceptibility assay was used

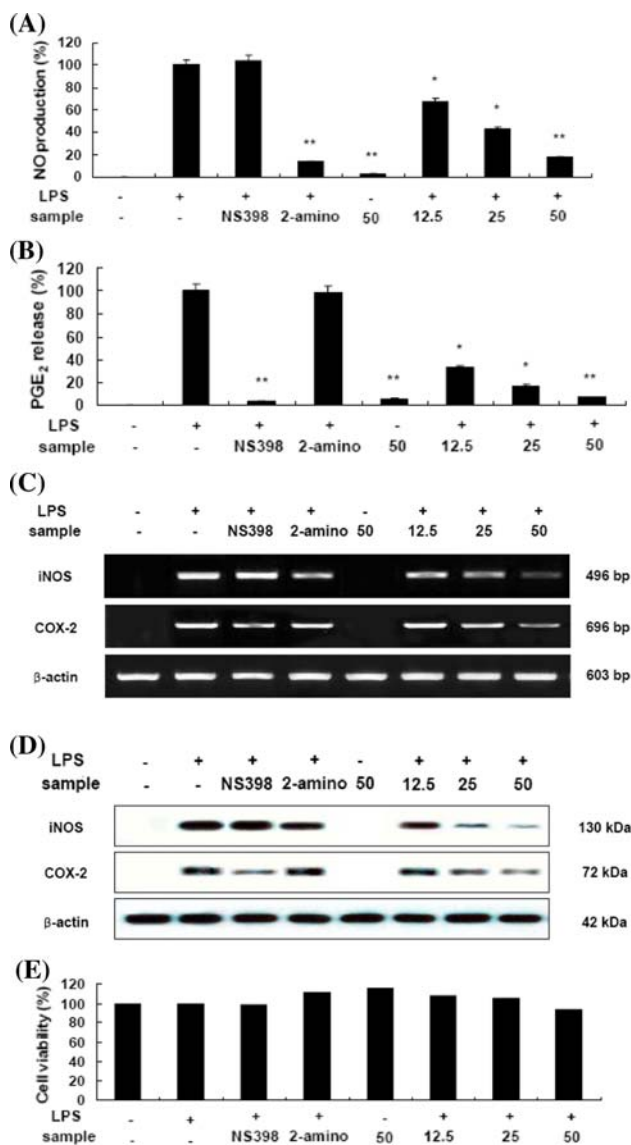


Fig. 1 Inhibitory effects of AKE on iNOS and COX-2 expressions in macrophage RAW264.7 cells. Nitric oxide production was assayed in the culture medium of cells stimulated with LPS (1 μ g/ml) for 24 h in the presence of AKE (a). Supernatants were collected and PGE₂ concentration in the supernatants was determined by ELISA (b). iNOS and COX-2 mRNA expression (c) and protein levels (d) were determined by RT-PCR and immunoblotting, respectively. Cytotoxicity was determined using the LDH method (e). As positive controls, we used 2-amino-4-methyl pyridine (20 μ M) and NS398 (20 μ M), which inhibit NO and PGE₂ production, respectively. Values are the mean \pm SEM of triplicate experiments. * P < 0.05; ** P < 0.01

LPS-stimulated NO and PGE₂ production by AKE was mediated by iNOS and COX-2 gene regulation, RT-PCR analyses were performed. As shown in Fig. 1c, AKE reduced the expressions of iNOS and COX-2 mRNA in a dose-dependent manner. By comparison, AKE did not affect β -actin expression, a housekeeping gene. As shown in Fig. 1d, AKE also dose-dependently reduced the expressions

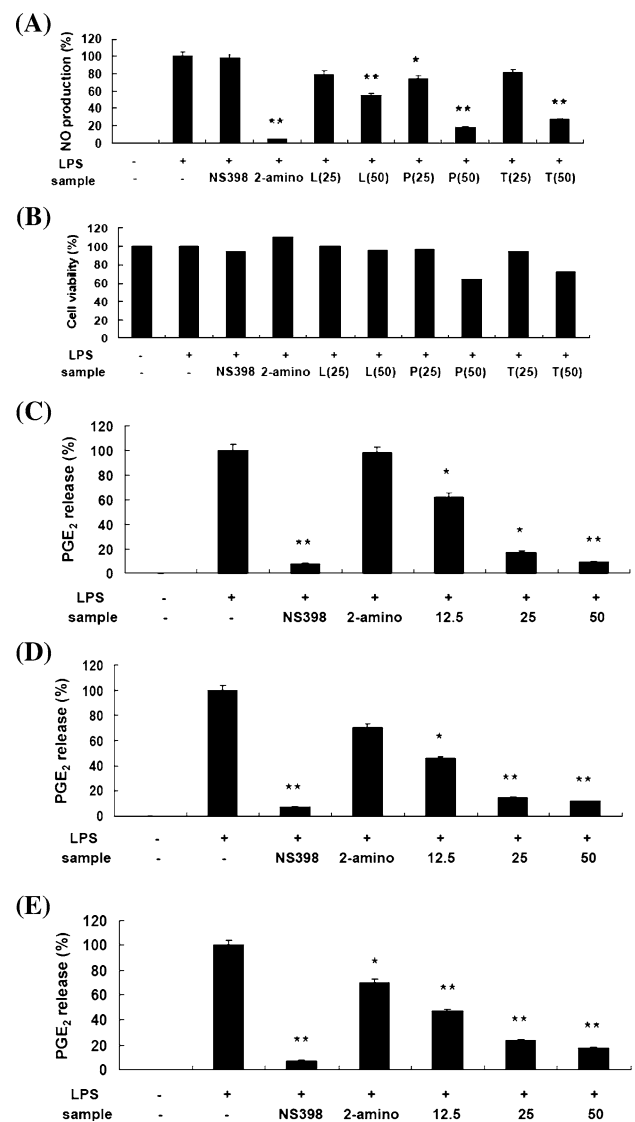


Fig. 2 Inhibitory effects of oil extract of lavender (L), peppermint (P), and tea tree (T) oils on nitric oxide and PGE₂ production in RAW 264.7 cells. Nitric oxide production was assayed in the culture medium of cells stimulated with LPS (1 μ g/ml) for 24 h in the presence of commercial oils (12.5, 25 and 50 μ g/ml), NS-398 (20 μ M) and 2-amino-4-methyl pyridine (20 μ M). Cytotoxicity was determined using the LDH method (b). (c), lavender oil; (d), peppermint oil; (e), tea tree oils. Values are the mean \pm SEM of triplicate experiments. * P < 0.05; ** P < 0.01

of iNOS and COX-2 protein. In general, these results indicate that the inhibitory effects of AKE on LPS-induced NO and PGE₂ production resulted from iNOS and COX-2 suppression. Furthermore, based on the RT-PCR analyses, the mRNA levels of iNOS and COX-2 correlated with their protein levels. The numbers of viable activated macrophages, as determined by LDH assays, were not altered by AKE, indicating that the inhibition of NO synthesis by AKE was not simply due to cytotoxic effects (Fig. 1e). Therefore, the inhibitory effect of AKE on iNOS and COX-2

gene expressions appears to be one of the mechanisms for the anti-inflammatory action of AKE.

We also investigated the *in vitro* anti-inflammatory effects of tea tree, lavender, and peppermint oils as commercially available essential oils in this study. As shown in Fig. 2, we found that low concentrations of commercial oils also inhibited the production of NO and PGE₂ within LPS-stimulated murine macrophages. The inhibitory effect of AKE on NO and PGE₂ production is greater than those of commercial oils in this study. Peppermint and tea tree oil exhibited cytotoxicities at 50 µg/ml. Also, many of the major components of AKE, including bornyl acetate, camphene, limonene, and α-pinene, had no inhibitory effect on NO and PGE₂ production and caused severe cytotoxicities above 25 µg/ml. Only limonene had an inhibitory effect on PGE₂ production (data not shown).

IL-1β, IL-6 and TNF-α are produced primarily by activated monocytes or macrophages. Because AKE potently inhibited pro-inflammatory mediators, we investigated its effects on LPS-induced IL-1β, IL-6 and TNF-α release by enzyme immunoassay (EIA). After 18-h pre-incubation, mRNA expression of pro-inflammatory cytokines was determined from a 24-h culture stimulated with LPS (1 µg/ml) in the presence of AKE. After 24-h incubation with both LPS and AKE, TNF-α, IL-1β and IL-6 production were remarkably inhibited in RAW264.7 cells.

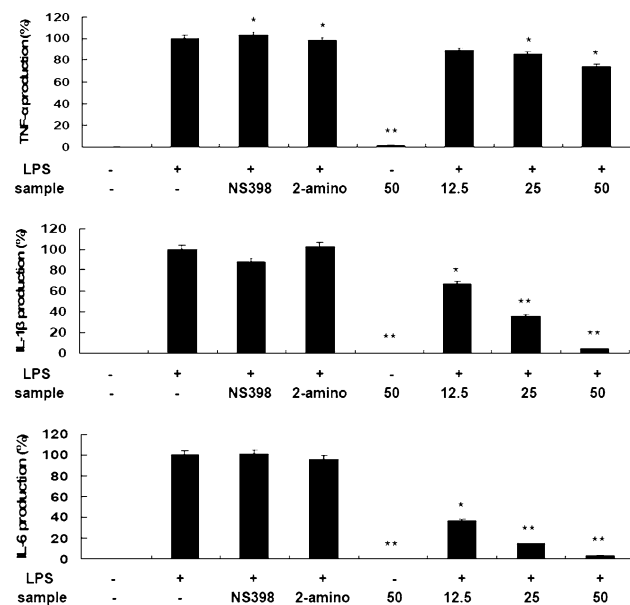


Fig. 3 Inhibitory effects of AKE on TNF-α, IL-1β and IL-6 production by RAW 264.7 cells. Cells (1.5×10^5 cells/ml) were stimulated with LPS (1 µg/ml) for 24 h in the presence of AKE (12.5, 25, and 50 µg/ml). Supernatants were collected, and the pro-inflammatory cytokine concentrations in the supernatants were determined by ELISA. Values are the mean \pm SEM of triplicate experiments. * $P < 0.05$; ** $P < 0.01$

However, NS-398 and 2-amino-4-methyl pyridine had no effect on inflammatory cytokine production (Fig. 3).

In conclusion, we demonstrated that AKE has good anti-bacterial and anti-inflammatory effects. Therefore, we suggest that AKE should be explored further as a potential therapeutic agent to promote skin health.

Acknowledgments This research was supported by the Regional Technology Innovation Program (RTI04-02-07), which is managed by the Ministry of Knowledge and Economy, Korea.

References

- Dreier J, Amantea E, Kellenberger L, Page MG (2007) Activity of the novel macrolide BAL19403 against ribosomes from erythromycin-resistant *Propionibacterium acnes*. *Antimicrob Agents Chemother* 51:4361–4365
- Chomnawang MT, Surassmo S, Nukoolkarn VS, Gritsanapan W (2005) Antimicrobial effects of Thai medicinal plants against acne-inducing bacteria. *J Ethnopharmacol* 101:330–333
- Heller S, Kellenberger L, Shapiro S (2007) Antipropionibacterial activity of BAL19403, a novel macrolide antibiotic. *Antimicrob Agents Chemother* 51:1956–1961
- Ross JI, Snelling AM, Carnegie E, Coates P, Cunliffe WJ, Bettoli V, Tosti G, Katsambas A, Galvan Pérez Del Pulgar JI, Rollman O, Török L, Eady EA, Cove JH (2003) Antibiotic-resistant acne: lessons from Europe. *Br J Dermatol* 148:467–478
- Eady EA, Gloor M, Leyden JJ (2003) *Propionibacterium acnes* resistance: a world-wide problem. *Dermatology* 206:54–56
- Swanson JK (2003) Antibiotic resistance of *Propionibacterium acnes* in acne vulgaris. *Dermatol Nurs* 15:359–362
- Zesch A (1988) Adverse reactions of externally applied drugs and inert substances. *Derm Beruf Umwelt* 36:128–133
- Eady EA (1998) Bacterial resistance in acne. *Dermatology* 196:59–66
- Wawruch M, Bozekova L, Krcmery S, Kriska M (2002) Risks of antibiotic treatment. *Bratisl Lek Listy* 103:270–275
- Park J, Lee J, Jung E, Park Y, Kim K, Park B, Jung K, Park E, Kim J, Park D (2004) *In vitro* antibacterial and anti-inflammatory effects of honokiol and magnolol against *Propionibacterium sp.* *Eur J Pharmacol* 496:189–195
- Jain A, Basal E (2003) Inhibition of *Propionibacterium acnes*-induced mediators of inflammation by Indian herbs. *Phytomedicine* 10:34–38
- Lim YH, Kim IH, Seo JJ (2007) *In vitro* activity of kaempferol isolated from the *Impatiens balsamina* alone and in combination with erythromycin or clindamycin against *Propionibacterium acnes*. *J Microbiol* 45:473–477
- Joo SS, Jang SK, Kim SG, Choi JS, Hwang KW, Lee DI (2008) Anti-acne activity of *Selaginella involvens* extract and its non-antibiotic antimicrobial potential on *Propionibacterium acnes*. *Phytother Res* 22:335–339
- Kim SS, Kim JY, Lee NH, Hyun CG (2008) Antibacterial and anti-inflammatory effects of Jeju medicinal plants against acne-inducing bacteria. *J Gen Appl Microbiol* 54:101–106
- Leyden J (2008) New developments in topical antimicrobial therapy for acne. *J Drugs Dermatol* 7:s8–11
- Marcinkiewicz J, Wojas-Pelc A, Walczewska M, Lipko-Godlewska S, Jachowicz R, Maciejewska A, Bialecka A, Kasproicz A (2008) Topical taurine bromamine, a new candidate in the treatment of moderate inflammatory acne vulgaris: a pilot study. *Eur J Dermatol* 18:433–439

17. Baik JS, Kim SS, Lee JA, Oh TH, Kim JY, Lee NH, Hyun CG (2008) Chemical composition and biological activities of essential oils extracted from Korean endemic citrus species. *J Microbiol Biotechnol* 18:74–79
18. Kim HJ, Choi EH, Lee IS (2004) Two lanostane triterpenoids from *Abies koreana*. *Phytochemistry* 65:2545–2549
19. Kim HJ, Le QK, Lee MH, Kim TS, Lee HK, Kim YH, Bae K, Lee IS (2001) A cytotoxic secocycloartenoid from *Abies koreana*. *Arch Pharm Res* 24:527–531
20. Kim K, Bu Y, Jeong S, Lim J, Kwon Y, Cha DS, Kim J, Jeon S, Eun J, Jeon H (2006) Memory-enhancing effect of a supercritical carbon dioxide fluid extract of the needles of *Abies koreana* on scopolamine-induced amnesia in mice. *Biosci Biotechnol Biochem* 70:1821–1826
21. Jeong SI, Lim JP, Jeon H (2007) Chemical composition and antibacterial activities of the essential oil from *Abies koreana*. *Phytother Res* 21:1246–1250
22. Kim JY, Oh TH, Kim BJ, Kim SS, Lee NH, Hyun CG (2008) Chemical composition and anti-inflammatory effects of essential oil from *Farfugium japonicum* flower. *J Oleo Sci* 57:623–628
23. Yoon WJ, Ham YM, Kim KN, Park SY, Lee NH, Hyun CG, Lee WJ (2009) Anti-inflammatory activity of brown alga *Dictyota dichotoma* in murine macrophage RAW 264.7 cells. *J Med Plant Res* 3:1–8

Cholesterol Synthesis Inhibitor U18666A and the Role of Sterol Metabolism and Trafficking in Numerous Pathophysiological Processes

Richard J. Cenedella

Received: 6 October 2008 / Accepted: 16 December 2008 / Published online: 14 May 2009
© AOCs 2009

Abstract The multiple actions of U18666A have enabled major discoveries in lipid research and contributed to understanding the pathophysiology of multiple diseases. This review describes these advances and the utility of U18666A as a tool in lipid research. Harry Rudney's recognition that U18666A inhibited oxidosqualene cyclase led him to discover a pathway for formation of polar sterols that he proved to be important regulators of 3-hydroxy-3-methyl-glutaryl coenzyme A reductase. Laura Liscum's recognition that U18666A inhibited the egress of cholesterol from late endosomes and lysosomes led to greatly improved perspective on the major pathways of intracellular cholesterol trafficking. The inhibition of cholesterol trafficking by U18666A mimicked the loss of functional Niemann–Pick type C protein responsible for NPC disease and thus provided a model for this disorder. U18666A subsequently became a tool for assessing the importance of molecular trafficking through the lysosomal pathway in other conditions such as atherosclerosis, Alzheimer's disease, and prion infections. U18666A also provided animal models for two important disorders: petite mal (absence) epilepsy and cataracts. This was the first chronic model of absence epilepsy. U18666A is also being used to address the role of oxidative stress in apoptosis. How can one molecule have so many effects? Perhaps because of its structure as an amphipathic cationic amine it can interact and inhibit diverse proteins. Restricting the availability of cholesterol for membrane formation through inhibition of cholesterol synthesis and intracellular trafficking could also be a mechanism for broadly affecting many processes.

Another possibility is that through intercalation into membrane U18666A can alter membrane order and therefore the function of resident proteins. The similarity of the effects of natural and enantiomeric U18666A on cells and the capacity of intercalated U18666A to increase membrane order are arguments in favor of this possibility.

Keywords U18666A · Cholesterol · Polar sterols · Lysosome · Epilepsy · Cataracts · Niemann–Pick type C disease · Intracellular trafficking · Apoptosis · Enantiomer

Abbreviations

ACAT	Acyl cholesterol acyl transferase
APP	β -Amyloid precursor protein
AY-9944	<i>trans</i> 1, 4-bis(2-Chlorobenzylaminoethyl)cyclohexane
CHO	Chinese hamster ovary
DHCR24	7-Dehydrocholesterol reductase 24
DRM	Detergent-resistant membranes
EEG	Electroencephalogram
ER	Endoplasmic reticulum
GABA	Gamma aminobutyric acid
HMGCoA	3-Hydroxy-3-methyl-glutaryl coenzyme A
LDL	Low density lipoproteins
Mer 29 (triparanol)	(1-[<i>p</i> -(β -Diethylaminoethoxy)-phenyl]-1-(<i>p</i> -tolyl)-2-(<i>p</i> -chlorophenyl) ethanol
MVB	Multivesicular bodies
NPC	Niemann–Pick type C disease
PM	Plasma membrane
OSC	2, 3-Oxidosqualene cyclase
SDO	Squalene 2, 3:22,23-dioxide

R. J. Cenedella (✉)
Department of Biochemistry, A.T. Still University of Health Sciences, 800 West Jefferson Street, Kirksville, MO 63501, USA
e-mail: rcenedella@atsu.edu

SO	Squalene oxide
U18666A	3- β -[2-(Diethylamino)ethoxy]androst-5-en-17-one

Introduction

The amphipathic steroid 3- β -[2-(diethylamino)ethoxy]androst-5-en-17-one, identified as U18666A by the Upjohn Company (Fig. 1), is a versatile chemical tool used in addressing questions on control of cholesterol biosynthesis, intracellular trafficking of cholesterol, trafficking of other molecules through endosomal and lysosomal compartments; and in understanding the pathophysiology of several diseases including epilepsy, cataracts, Niemann–Pick type C disease, atherosclerosis, Alzheimer’s disease, prion infections, and others.

After some historical perspective, the review will address the multiple actions of U18666A on sterol synthesis and its central role in discovery of the oxysterol synthesis pathway. The epilepsy and cataract disease models induced by the drug will be discussed, with less attention to cataracts because this model was previously reviewed [1]. The utility of U18666A in understanding intracellular trafficking of cholesterol and the mechanism of Nieman–Pick type C disease deserves special attention. Finally, the roles of oxidative stress and apoptosis in the actions of U18666A will be considered. I apologize in advance for failure to cite every article that used U18666A.

U18666A and Sterol Synthesis

Cavallini and Massarani [2] described the synthesis of 3- β -[2-(diethylamino)ethoxy]androst-5-en-17-one along with

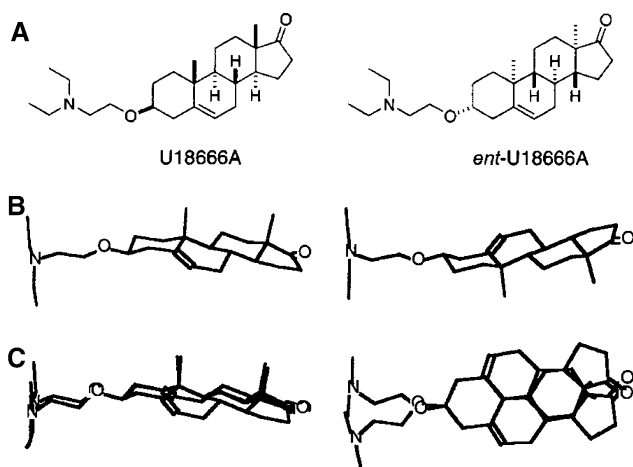


Fig. 1 **a** Two-dimensional structures of the nonprotonated amine forms of U18666A. **b** Three-dimensional models of the two enantiomers. **c** An edge and top view of the superimposed enantiomers. (Reprinted with permission: Cenedella et al. [21])

the synthesis of other di-alkyl-amino-ethyl esters in 1951. The compounds were said to be strong coronary vasodilators, a claim not substantiated in the literature. The next mention of the compound, now named U18666A, was in 1963 when Upjohn Company made it available to Phillips and Avigan [3] to study its capacity to inhibit cholesterol biosynthesis. How Upjohn acquired rights to the compound is unclear. The late 1950s and early 1960s marked the start of a search for hypocholesterolemic drugs that culminated in the introduction of the statins in the mid-1980s. Several 3-dialkylaminoethoxy compounds were tested in the early 1960s for hypocholesterolemic activity. Most, including U18666A, caused the substitution of desmosterol for cholesterol [4–6]. One, {1-[*p*-(β -diethylaminoethoxy)-phenyl]-1-(*p*-tolyl)-2-(*p*-chlorophenyl)ethanol}, known as Mer 29 or triparanol, was introduced into humans and then promptly withdrawn from clinical use because of drug-related cataract formation [7, 8]. We reported in 1979 that U18666A was cataractogenic in rats and that it inhibited desmosterol reductase [9]. We found that it also inhibited sterol synthesis at a site prior to formation of squalene [10], but much higher drug levels were required to inhibit at the early site compared with reduction of desmosterol.

A controversy between Harry Rudney and Joseph Volpe over the consequences of U18666A inhibition of sterol synthesis on ubiquinone formation led Rudney to discover a pathway for formation of polar sterols and a regulatory role for polar sterols in cholesterol biosynthesis. Volpe and Obert [11] reported that ubiquinone synthesis was markedly increased in cultured C-6 glial cells exposed to 200 ng/mL of U18666A (about 0.5×10^{-6} M). A block at squalene synthase could divert isoprenes formed from mevalonate to ubiquinone. However, Rudney’s group [12], using cultured rat intestinal epithelial cells, clearly proved a year later that it was not ubiquinone that increased but rather squalene 2,3:22,23-dioxide (SDO). Squalene oxide (SO), the substrate for the inhibited 2,3-oxidosqualene cyclase (OSC), was diverted to SDO. Upon removal of U18666A from the media, SDO was converted to polar sterols. Both SO and SDO are substrates for the cyclase. In their following paper, Panini et al. [13] observed that 3-hydroxy-3-methyl-glutaryl coenzyme A (HMGCoA) reductase activity was decreased by addition of low concentrations of U18666A to the culture media, but activity increased when higher drug levels were added. They concluded that SDO formed at low drug levels underwent cyclization and conversion to polar sterols that inhibited HMGCoA reductase. As the concentration of U18666A was increased, cyclization of SDO was inhibited and formation of polar sterols ceased. These two seminal studies [12, 13], made possible because of the actions of U18666A, led the Rudney group to identify the oxysterols formed in the SDO pathway and their roles in regulating HMGCoA reductase [14, 15].

U18666A has continued to serve as a useful tool in studies of sterol synthesis in both plants and animals. In addition to inhibiting OSC and desmosterol reductase, it also has been shown to be an inhibitor of sterol- Δ^8 - Δ^7 isomerase, called sigma receptor or emopamil-binding protein [16, 17]. Thus, U18666A inhibits at least three membrane-bound enzymes in sterol synthesis. The inhibition of all three (OSC [18], sterol Δ^8 - Δ^7 isomerase [17], and Δ^{24} reductase or desmosterol reductase [19]) is reported as noncompetitive [18, 19]. The mechanism of inhibition, at least of OCS could involve mimicking a carbocationic intermediate due to the drug's cationic amine [18]; however, the kinetics of OCS inhibition by U18666A could be complex. Lenhart et al. [20] suggested that the OSC inhibitors could be “kinetically captured in the sequestering cavity, feigning a noncompetitive case.” We suggested that physical effects of U18666A on membrane order might also contribute to inhibiting multiple enzymes that catalyze different types of reactions. U18666A and its enantiomer equally inhibited sterol synthesis by cultured cells and induced apoptosis [21], and when added to model membranes, U18666A increased membrane structural order [22].

U18666A and Epilepsy

Our awareness of U18666A came from studies of changes in brain cholesterol and cholesterol ester levels associated with implantation of a small piece of cobalt wire in the cerebral cortex of rat [23]. The implanted rats developed epilepsy, and the affected cerebral cortex displayed a marked reduction in the concentration of unesterified cholesterol and a great increase in cholesterol ester [24]. George Bierkamper (then my student) posed the question in our journal club (1974), “Could drug-induced changes in brain sterols produce epilepsy?” Jim Culberson from the Anatomy Department of West Virginia University (Morgantown, West Virginia, USA) brought our attention to a then-recently published paper by Jurgelski et al. [25] that described induction of chronic epilepsy in opossums treated with U18666A (it was one of a number of cholesterol synthesis inhibitors tested). Based on their work, we succeeded in developing chronic epilepsy in rats with U18666A, but, unlike the opossum, the rat developed “absence” or petit mal epilepsy [26]. This epilepsy is defined by electroencephalogram seizure pattern without major motor involvement. As with the opossum, brain total sterols were essentially unchanged, but desmosterol replaced much of the cholesterol. However, Jurgelski et al. concluded that desmosterol is not the cause of the seizure state because another inhibitor of desmosterol reductase (Mer 29) increased brain desmosterol without causing

epilepsy. Even though the physical properties of cholesterol and desmosterol differed [27], we agreed with Jurgelski et al. that desmosterol was not the answer. Desmosterol can account for 80% of the total sterol in the ocular lens of U18666A-treated rats and yet the lens can remain clear [28], and replacement of cholesterol by desmosterol causes no structural or functional changes in the retina [29, 30]. Furthermore, desmosterol can support the normal growth of cultured cells [31, 32]. The epilepsy may be better related to desmosterol-independent changes in control of neural GABA_A receptor responses [33]. Perhaps of special significance to epilepsy, Sparrow et al. [34] reported that U18666A blocked voltage-regulated calcium channels in cultured neuroblastoma cells secondary to inhibiting potassium-evoked release of norepinephrine. The effect was attributed to U18666A's well-established inhibition of cholesterol synthesis and intracellular transport in cultured cells. As mentioned earlier, the effects of U18666A on membrane-related activities might also be due, at least partially, to drug-induced changes in membrane structure.

In 1990 Smith and Bierkamper [35] described how treatment of the neonatal rat with AY-9944 [*trans* 1,4-bis(2-chlorobenzylaminoethyl)cyclohexane] at 2 days of age followed by seven subsequent injections at 6-day intervals produced permanent petit mal (absence-like) epilepsy. AY-9944 was reported by Krami et al. in 1964 to be a potent inhibitor of 7-dehydrocholesterol reductase [36]. The mechanism of the AY-9944 seizure model appeared to involve GABA-ergic receptor stimulation, which was assumed to be secondary to replacement of 60–70% of the brain cholesterol with 7-dehydrocholesterol [35]. Perhaps because of the simplicity of treatment, the AY-9944 model has largely replaced U18666A in the study of epilepsy and has become a standard tool [37–50]. Studies continue to focus on the roles of GABA receptors in the mechanism of AY-9944-generated epilepsy and the importance of brain sterol changes. An unresolved question is why epileptiform activity persists after discontinuation of drug treatment and the subsequent normalization of brain sterols (disappearance of 7-dehydrocholesterol). Permanent damage to a localized region of the brain during the treatment phase might account for the continued seizures [39]. More recently, Serbanescu et al. [41] measured changes in brain sterols and development of absence seizures in rats treated with U18666A, AY-9944, or lovastatin. Both U18666A and AY-9944 increased 7-dehydrocholesterol (surprising for U18666A since others see elevation of desmosterol); and AY-9944, but not U18666A, decreased brain total sterol. Both AY-9944 and U18666A produced seizure activity as anticipated, but surprisingly lovastatin increased the abnormal brain electrical activity without any major effect on brain sterols. The authors

speculated that very localized changes in brain sterols might account for these findings or that the epilepsy is unrelated to sterols per se and might involve decreased synthesis of neurosteroids [41].

U18666A and Cataracts

Soon after beginning studies of epilepsy in U18666A-treated rats, we noticed development of cataracts in some animals. Increasing the dose caused cataracts in all animals. Several factors led us to begin studies into the mechanism of cataract induction by U18666A and other inhibitors of cholesterol biosynthesis. The National Eye Institute was interested in new animal models of cataracts, drug companies were becoming aware that appearance of cataracts in toxicology assessment could be a limiting factor in the development of hypocholesterolemic drugs, and recognition was developing that inherited diseases involving enzymes of the sterol synthesis pathway uniformly displayed increased risk of cataracts as a feature of the condition [reviewed in 51]. The working hypothesis was that altering the sterol content and composition of the lens fiber cell plasma membrane (PM) was the basis of lens opacification caused by treatment with hypocholesterolemic drugs or by genetic defect. Essentially all of the lens' total lipids are present in this unusual membrane, unusual because it contains the highest molar ratio of cholesterol to phospholipid in any known membrane, as high as 4 to 1 [1]. Treatment of rats with U18666A caused a decrease in this ratio, which led to altered membrane structure [1, 52], binding of crystalline proteins to the membrane, and presumed formation of light-scattering aggregates. New findings made since this mechanism was proposed [1] suggest that perturbation of lens membrane structure due to intercalation of U18666A could contribute to lens opacification. By using small-angle X-ray diffraction approaches, lens membrane structure was found to be more complex than anticipated, possessing "highly ordered, immiscible cholesterol domains" [53, 54]. The effects of U18666A on the order of membranes constructed from lens lipids were evaluated by both X-ray diffraction analysis and measurement of changes in the anisotropy of probes incorporated into these membranes [22]. Both approaches indicated that the presence of U18666A increased membrane order, which alone might contribute to increased light scatter. Analysis of the X-ray scatter data showed that U18666A intercalated into the hydrocarbon core of the membrane, resulting in a broad condensing effect. U18666A also induced apoptosis *in vitro* and *in vivo* in lens epithelial cells [22]. The possibility that physical properties of U18666A contribute to its assault on the lens is supported by finding that the natural and enantiomeric

forms of the drug equally inhibit sterol synthesis and induce apoptosis in lens epithelial cells [21]. The possible involvement of apoptosis in accounting for the multiple actions of U18666A is addressed later.

Role of U18666A in Understanding Trafficking of Cellular Cholesterol

U18666A's seminal role in understanding intracellular trafficking of cholesterol started with the key observation by Panini et al. that U18666A could completely block low density lipoprotein (LDL) suppression of HMGCoA reductase without affecting degradation of LDL [13]. The observation was unexplained since it is well established that LDL taken up by cells is degraded by lysosomes, that esterified cholesterol is converted to unesterified cholesterol, and that the free cholesterol is then released from lysosomes and acts to inhibit HMGCoA reductase activity in the endoplasmic reticulum [55]. Liscum and Faust [56] solved the paradox by demonstrating that U18666A inhibited the release of cholesterol from lysosomes. This discovery established the foundation for research into pathways of intracellular trafficking of cholesterol and led the Liscum laboratory and others to demonstrate that there is brisk transport of free cholesterol from lysosome to the PM and to the endoplasmic reticulum (ER) where it is re-esterified by acyl cholesterol acyl transferase (ACAT) and then stored as inert cholesterol ester. In the presence of U18666A, cultured cells accumulate free cholesterol in lysosomes, and LDL added to the media can neither support cell growth, suppress HMGCoA reductase, nor promote cholesterol re-esterification [56]. These observations were confirmed [57, 58] and extended to generate a broader view of the effects of U18666A on cellular cholesterol transport and, thereby, a clearer view of cholesterol transport pathways.

U18666A was shown to decrease movement of cholesterol from the lysosome to the ER, from the lysosome to the PM, and from the PM to the ER [59, 60]. It was without effect on the movement of LDL cholesterol to lysosomes. The transport of cholesterol from lysosomes to the ER was especially sensitive to inhibition by U18666 [61] and suggested that a distinct pathway utilizing vesicles was involved [60]. This selective sensitivity was more recently confirmed by Feng and Tabas [62]. They reported that concentrations of U18666A that blocked cholesterol trafficking to the ER by 90% decreased movement to the PM by only 10%.

Lange and coworkers proposed an alternative model for cholesterol exchange between cellular compartments based on their observations of U18666A effects on cholesterol trafficking [63–65]. They found little evidence for the

direct movement of cholesterol from lysosomes to ER, but rather movement from lysosomes to PM and from PM to ER [63]. U18666A was suggested to block cholesterol movement from PM to ER rather than from lysosomes to PM [63, 64]. The massive accumulation of cholesterol in lysosomes in U18666A-treated cells was attributed to accumulation of a special class of lysosomes, ones containing abundant lipid arranged as lamellar bodies from which egress of cholesterol is very slow [64].

The Liscum group affirmed their conclusion that U18666A and similar cationic-hydrophobic amines block efflux of cholesterol from the lysosome to the PM [60]. They suggested that Lange et al. [63] failed to see a U18666A-induced decrease in PM cholesterol because the cholesterol oxidase used reached an intracellular pool of cholesterol. Cholesterol oxidase is intended to attack cholesterol in only the outer leaflet of the PM. On the basis of the work of Liscum et al. described above and that of others [66–69], one can say that U18666A broadly inhibits intracellular trafficking of cholesterol and principally inhibits the movement of cholesterol out of lysosomes. What mechanism is responsible for this action?

Although the mechanism(s) by which U18666A inhibits cellular cholesterol trafficking (lysosome to ER and PM, and PM to ER) are unclear, several observations lead to a working hypothesis. U18666A inhibition of cholesterol trafficking appears independent of protein synthesis, integrity of the cytoskeleton, energy availability, pH of the lysosome, or *P*-glycoprotein function [57, 59]. Rather, U18666A's effects on cholesterol trafficking could involve direct interference with the Niemann–Pick type C protein (more on this below) or interference with this protein secondary to altering membrane lipid organization. Underwood et al. [61] reported that U18666A bound with high specificity to intact Chinese hamster ovary (CHO) cell membrane and suggested that this binding can alter the organization of membrane lipids. Other amphipathic cationic amines (imipramine, stearylamine, and sphinganine) could antagonize the binding and also interfere with cholesterol trafficking [61, 67], but they were orders of magnitude less potent than U18666A [61, 67]. Thus, physical properties of U18666A could contribute to its effects on intracellular cholesterol transport and perhaps to the many other actions of the drug. U18666A incorporation into model membranes increased structural order, which resulted in a broad condensing effect on membrane lipids. The equal capacity of natural and enantiomeric U18666A to inhibit cholesterol synthesis and induce apoptosis suggested that the drug might alter cell function because of physical characteristics of the molecule rather than through stereospecific interaction with proteins [21].

Role of U18666A in Understanding Niemann–Pick Type C Disease

U18666A has been used as a tool to probe the roles of cholesterol trafficking in numerous diseases and states. These include Niemann–Pick type C disease, atherosclerosis, Alzheimer's disease, prion infections, AIDS, Wilson's disease, and others.

Niemann–Pick type C disease is an autosomal recessive condition caused by a loss of function mutation in the protein product of the NPC1 gene. NPC is a hydrophobic–polytopic transmembrane protein that promotes lipid sorting and vesicular trafficking of both LDL-derived and endocytotic cholesterol [70–72]. The protein appears to reside in a novel set of vesicles or organelles that associate with lysosomes and functions to shuttle endocytotic cholesterol to the PM and ER [73–75]. Free or unesterified cholesterol accumulates in peripheral tissues, and glycosphingolipids accumulate in brain of patients lacking functional NPC protein [70, 76]. Although NPC protein may primarily affect intracellular trafficking of glycosphingolipids in brain, it may have a role in the transport of endogenously made cholesterol from neuronal cell body to distal axon where it is used for membrane synthesis. Axonal growth is impaired in primary cultures of neurons from mice with mutation in the NPC1 gene [77]. Autophagic cell death can result from blocking egress of cholesterol from endosomes/lysosomes due to NPC disease [78]. Autophagy is a process of cellular self-digestion that normally functions to aid survival during periods of starvation or deficiency in essential molecules [79]. The inaccessibility of the cell to the cholesterol trapped in lysosomes can be viewed as a nutritional deficiency.

U18666A has been a widely used chemical tool to model Niemann–Pick type C disease [70, 77, 78, 80–84]. The transport and subcellular distribution of NPC protein is altered when egress of cholesterol from lysosomes is blocked by U18666A [74, 80], and U18666A may produce its effects through direct interaction with the NPC protein [70]. A link between the NPC protein and U18666A is reinforced by seeing marked increases in NPC1 mRNA and protein levels when U18666A is added to normal steroidogenic cells [81]. Furthermore, Sugimoto et al. [83] demonstrated that U18666A's effect on lipid accumulation by NPC-deficient CHO cells is at least partially dependent on the presence of intact NPC protein. When transfected with mutated-nonfunctional NPC, cultured cells accumulate cholesterol and gangliosides, and treatment with U18666A causes no further increase. But “knock in” of the NPC protein restores U18666A's capacity to block lipid trafficking and raises cellular lipid content [83].

In summary, the presence of resident NPC protein in vesicles and organelles is necessary for the intracellular movement of lipids from lysosomes and late endosomes to various membrane compartments. The lysosomal lipids that accumulate in Niemann–Pick type C disease reflect defects in the intracellular trafficking of lipids (from both endocytotic and extracellular sources) due to a nonfunctional NPC protein. The capacity of U18666A to mimic Niemann–Pick disease appears at least partially due to blocking the NPC protein. The block may involve direct interaction of U18666A with the protein or changes in NPC protein function secondary to altering the membrane domain in which the protein resides. As described earlier, U18666A can alter the structure of model membranes [22], and it binds to intact cells with high affinity [61]. Since U18666A readily enters cells and associates with intracellular membrane [85], it may also alter intracellular membranes and the function of their resident proteins.

Role of U18666A in Understanding the Pathophysiology of Other Diseases

Atherosclerosis (Macrophage, High Density Lipoproteins)

Cholesterol ester-laden macrophages are foam cells, which accumulate in early atherosclerotic disease. Free cholesterol generated from esterified cholesterol through the action of cholesterol ester hydrolase is toxic to the foam cells and can lead to their death and necrosis [86–88]. U18666A has been used to explore the consequences of free cholesterol accumulation to the macrophage [86–88]. U18666A protects macrophages from free cholesterol, although U18666A-treated cells accumulate free cholesterol [88]. Location provides the answer to this paradox. The protection comes from trapping free cholesterol in the lysosome, which decreases the cholesterol concentration in the remainder of the cell. U18666A has also been used as a tool to reveal that the ABCA1 transporter protein can function intracellularly to withdraw endocytotic lipids from late endosomes and lysosomes and combine them with apoprotein A1 to form nascent high density lipoproteins that are then secreted from the cell [89].

Alzheimer's Disease

Interest in Alzheimer's disease and U18666A came from observations that endocytotic trafficking might play roles in the processing of β -amyloid precursor protein (APP) and secretion of the pathogenic amyloid β proteins. A 99 kDa fragment of the amyloid precursor protein carboxy terminal

was cleaved by secretases to generate peptides of 40 and 42 kDa, $A\beta_{40}$ and $A\beta_{42}$, respectively [90]. Blockage of lipid trafficking by treatment of cultured cells with U18666A induced increases of both free cholesterol and $A\beta_{42}$ amyloid in late endosomes [91]. The $A\beta_{42}$ amyloid was released from the endosome upon removal of the drug, but $A\beta$ amyloids were released as aggregates [91]. Furthermore, treatment of cultured neuronal cells with U18666A influenced the processing of amyloid proteins, reducing β -cleavage of full-length APP but increasing γ -secretase activity on the APP C-terminal resulting in increased production of both $A\beta$ fragments [92]. These changes were attributed to altered intracellular cholesterol trafficking. Kametaka et al. [93] also used U18666A to reveal that the APP-cleaving enzyme moves through a late endosomal compartment of HeLa cells. In the presence of U18666A, the protein appeared in multivesicular bodies (MVB) derived from late endosomes. These studies collectively demonstrated that many of the hallmark proteins associated with Alzheimer's disease require transit through late endosomal–lysosomal pathways for activation and function.

Can a common mechanism explain the cellular models of Niemann–Pick and Alzheimer's diseases induced by U18666A? U18666A has three known, broad actions that may account for its varied effect on cells: It inhibits cholesterol biosynthesis at multiple sites [10, 12, 13, 16–19], it interferes with intracellular trafficking of cholesterol [56–69], and it can intercalate into membranes and alter their order [22]. Addition of as little as 0.1 μ M U18666A to cultured cells can markedly inhibit sterol synthesis [21] and esterification of LDL-derived cholesterol [60, 61]. However, the inhibition of esterification appears independent of reducing cholesterol synthesis since U18666A continues to block esterification of cholesterol in cells treated with mevinolin, an inhibitor of HMGCoA reductase [56]. Blockage of cholesterol movement through the endosome may arise from direct interaction of U18666A with the NPC protein [70, 81, 83]. Although direct interference with the NPC protein may contribute to reduced transit of various molecules through the endosomal compartment, such as $A\beta_{42}$ -amyloid, a more generalized action of U18666A may also account for its diverse effects. When added to membrane preparations, it increases the anisotropic values of probes and has a broad condensing effect on membrane order as determined by Fourier transform analysis of X-ray scatter data; [22]. Thus, increased order of membrane domains may account for reduced transit of many molecules through endosomal compartments that are dependent on NPC or other regulatory proteins as a result of restricting the mobility of these proteins.

Prion Diseases

Once again, U18666A's capacity to alter cellular cholesterol trafficking led to its use to examine mechanisms and treatment of disease. The nonpathogenic (normal) prion protein PrP^c is anchored to neural membranes by attachment to glycosylphosphatidylinositol located in detergent-resistant membrane (DRM) domains. The pathogenic prion protein PrP^{Sc}, responsible for Creutzfeldt-Jakob disease in humans and bovine spongiform encephalopathy in cattle, replicates by inducing misfolding of the normal host protein. Because U18666A can cause redistribution of membrane cholesterol through interfering with cholesterol trafficking and biosynthesis, it was tested for antiprion activity [94]. U18666A added to infected neuroblastoma cells caused a major redistribution of cholesterol from the PM to intracellular sites and displayed very strong antiprion activity, that is, an EC₅₀ of 100 nM. U18666A caused total displacement of the infectious prion from DRM domains. The capacity of U18666A to halt progression of pathogenic prions in cultured neural cells was confirmed by Hagiwara et al. [95], EC₅₀ of 10 nM. But treatment of prion-infected mice with U18666A did not affect survival. The lack of effect was not surprising since there were no changes in the composition of brain sterols following treatment of 6-week-old mice. The absence of an effect was probably due to the age of mice at onset of treatment. We observed that almost all rats developed cataracts if treatment with U18666A started at one day of age, but few developed cataracts if treatment was delayed until 14 days of age [96].

Wilson Disease

Wilson disease is a genetic disorder characterized by the accumulation of copper in body tissues due to deficiency of ATP7B, which is a copper-transporting ATPase responsible for regulating copper secretion into plasma (with ceruloplasmin) and copper excretion into bile. ATP7B colocalized with NPC1 in late endosomes of Huh7 cells [97]. Addition of U18666A caused formation of late endosome-lysosome hybrid organelles.

HIV and Other Uses

GAG protein of HIV-1 is localized primarily to the host's PM in T-cells. In macrophages, however, GAG accumulates in MVB when treated with U18666A, indicating that trafficking of GAG through MVB is required for HIV particle production [98]. U18666A has also been used to probe the role of cycling through endosomal-lysosomal compartments in the activation and functions of annexins [99], small GTPase Rab7 [100], and the mannose 6-phosphate receptor [101, 102].

U18666A-Induced Apoptosis Could Contribute to Its Multiple Actions

Beginning in 2004, reports clearly established that U18666A can induce apoptosis in lens epithelial cells [22], melanoma cells [103], and cultured murine cortical neurons [104–109]. The apoptosis in all three models can be triggered by oxidative stress. Lipid peroxidation increases in lenses of U18666A-treated rats [110]. Apoptosis in the melanoma cells was attributed to U18666A inhibition of the product of the 7-dehydrocholesterol reductase 24 gene, also known as seladin-1 [103]. The gene product is desmosterol reductase. Seladin-1 stands for SElective Alzheimer Disease indicator 1 because it can protect neurons from the toxicity caused by β -amyloid peptide and is anti-apoptotic. The apoptosis induced by U18666A is dependent on oxidative stress and may occur through an action on the antioxidant pathway [103].

Cheung and coworkers investigated U18666A-induced apoptosis in cultured murine cortical neurons as it relates to Niemann–Pick type C disease and Alzheimer's disease [104–109]. Activation of caspases accompanied U18666A-induced apoptosis [104, 105]. Disruption of mitochondrial function and caspase activation was attributed to U18666A impairment of intracellular cholesterol transport [106]. Abundant cholesterol was seen to accumulate in the cultured neurons [104]. The group conducted an interesting experiment to examine the contribution of de novo cholesterol synthesis to the U18666A-induced cytotoxicity. Pravastatin, an HMGCoA reductase inhibitor, essentially blocked cell death from U18666A when added to the culture [104]. Since the concentration of U18666A was more than adequate to block cholesterol synthesis completely (0.5 μ g/mL) [10, 12], the protective effect of pravastatin was likely independent of decreasing cholesterol production. Since the flow of carbon through the sterol pathway would be blocked at squalene, the protective effect of pravastatin suggested that something in the sterol pathway between mevalonic acid and squalene was cytotoxic and could contribute to the apoptosis induced by U18666A.

As seen with U18666A in cultured melanoma cells [103], oxidative stress accompanied induction of apoptosis in the cortical neuronal cells. Here, U18666A increased reactive oxygen species and increased neuronal levels of A β 40 and A β 42 amyloid proteins [107]. The connection between damaging oxidation, accumulation of A β amyloid, and U18666A induction of apoptosis in the cultured neuronal was recently confirmed by Koh et al. [107]. The link between U18666A and apoptotic cell death was shown to be complex, involving decreased available energy, disruption of mitochondria, and increased production of reactive oxygen species with accompanying oxidation of cellular molecules such as lipids, proteins, and nucleic

acids. All of the following events could arise from the multiple actions of U18666A: inhibition of sterol synthesis, disruption of cellular cholesterol trafficking, and alteration of membrane order or fluidity. The combined actions of inhibited cholesterol synthesis and inhibited access to LDL cholesterol may induce autophagy, which could lead to apoptosis secondary to degradation of cytoplasmic organelles [111].

Summary/Conclusions

How can one drug have so many different effects and induce such widely different diseases in animals? U18666A inhibits three membrane-bound enzymes in sterol synthesis that catalyze very different reactions (a ring-forming cyclase, an isomerase, and a reductase); it blocks the egress of cholesterol and other molecules from lysosomes; it blocks the movement of cholesterol from the PM to the ER; it induces apoptosis *in vivo* and in cultured cells; when given to young rats it can cause permanent petite mal epilepsy and cataracts; and when added to cultured cells it can cause massive accumulation of unesterified cholesterol and thereby mimic the fatal human Niemann–Pick type C disease. Its structure as an amphipathic-cationic amine may be the basis of the diversity. Similar compounds can duplicate U18666A effects but generally at much higher concentrations. The finding that the natural and enantiomeric forms of U18666A equally inhibit sterol synthesis and induce apoptosis also argues for actions based on physical properties of the molecule. When incorporated into membranes, U18666A has an ordering or condensing effect. Whereas these observations do not exclude U18666A acting through binding to specific proteins, as for example the NPC1 protein, they do support the possibility that U1866A (and perhaps similar compounds) produces its actions by altering the physical properties of membranes and the function of the membrane's resident proteins.

Acknowledgments This work was supported by USPHS NIH grant EY02568-29. The author remembers Harry Rudney for his encouragement and George Bierkamper for his great ideas and friendship.

References

- Cenedella RJ (1996) Cholesterol and cataracts. *Surv Ophthalmol* 40:320–337
- Cavallini G, Massarani E (1951) Contributo Alle Relazioni Fra Costituzioni Chimica Ed Attivita Biologica. *Sci.e tee (pavia)* 6:291–299
- Phillips WA, Avigan J (1963) Inhibition of cholesterol biosynthesis in the rat by 3 β (2-diethylamino-ethoxy) androst-5-en-17-one, hydrochloride (28003). *Proc Soc Exp Bld Med* 112:233–236
- Avigan J, Steinberg D, Vroman HE, Thompson MJ, Mosestigg E (1960) I. The identification of desmosterol in serum and tissues

- of animals and man treated with MER-29. *J Biol Chem* 235:3123–3126
- Gordon S, Cantrall EW, Cekeleniak WP, Albers HJ, Littell R, Bernstein S (1961) The hypocholesterolemic effect of 3 β -(β -dimethylaminoethoxy)-androst-5-en-17-one and its mechanism of action. *Biochem Biophys Res Comm* 6:359–363
- Cantrall EW, Littell R, Stolar SM, Cakleniak WP, Albers HJ, Gordon S, Bernstein S (1963) Steroids and lipid metabolism. I The hypocholesterolemic effect of 3-(β -dialkylaminoethoxy)-substituted steroids. *Steroids* 1:173–178
- Kirby TJ, Achor RWP, Perry HO, Winkelmann RK (1962) Cataract formation after triparanol therapy. *Arch Ophthalmol* 68:486–489
- Laughlin RC, Carey TF (1962) Cataracts in patients treated with triparanol. *JAMA* 181:339–340
- Cenedella RJ, Bierkamper GG (1979) Mechanism of cataract production by 3- β -(2-diethylaminoethoxy) androst-5-en-17-one hydrochloride, U18666A: an inhibitor of cholesterol biosynthesis. *Exp Eye Res* 28:673–688
- Cenedella RJ (1980) Concentration-dependent effects of AY-9944 and U18666A on sterol synthesis in brain. *Biochem Pharm* 29:2751–2754
- Volpe JJ, Obert KA (1982) Interrelationships of ubiquinone and sterol syntheses in cultured cells of neural origin. *J Neurochem* 38:931–938
- Sexton RC, Panini SR, Azran F, Rudney H (1983) Effects of 3 β -[2-diethylaminoethoxy]androst-5-en-17-one on the synthesis of cholesterol and ubiquinone in rat intestinal epithelial cell cultures. *Am Chem Soc* 22:5687–5691
- Panini SR, Sexton RC, Rudney H (1984) Regulation of 3-hydroxy-3-methylglutaryl coenzyme A reductase by oxysterol by-products of cholesterol biosynthesis. *J Biol Chem* 259:7767–7771
- Gupta A, Sexton RC, Rudney H (1986) Modulation of regulatory oxysterol formation and low density lipoprotein suppression of 3-hydroxy-3-methylglutaryl coenzyme A (HMG-CoA) reductase activity by ketoconazole. *J Biol Chem* 261:8348–8356
- Panini SR, Sexton PR, Gupta AK, Parish EJ, Chitrakorn S, Rudney H (1986) Regulation of 3-hydroxy-3-methylglutaryl coenzyme A reductase activity and cholesterol biosynthesis by oxysterols. *J Lipid Res* 27:1190–1204
- Bae SH, Seong J, Paik YK (2001) Cholesterol biosynthesis from lanosterol: molecular cloning, chromosomal localization, functional expression and liver-specific gene regulation of rat sterol Δ^8 -isomerase, a cholesterologenic enzyme with multiple functions. *Biochem J* 353:689–699
- Moebius FF, Reiter RJ, Bermoser K, Glossmann H, Cho SY, Paik YK (1998) Pharmacological analysis of sterol Δ^8 - Δ^7 isomerase proteins with [3 H] ifenprodil. *Mol Pharm* 1998:591–598
- Duriatti A, Bouvier-Nave P, Benveniste P, Schuber F, Delprino L, Balliano G, Cattel L (1985) *In vitro* inhibition of animal and higher plants 2, 3-oxidosqualene-sterol cyclases by 2-aza-2, 3-dihydrosqualene and derivatives, and by other ammonium-containing molecules. *Biochem Pharm* 34:2765–2775
- Bae SH, Paik YK (1997) Cholesterol biosynthesis from lanosterol: development of a novel assay method and characterization of rat liver microsomal lanosterol Δ^{24} -reductase. *Biochem J* 326:609–616
- Lenhart A, Reinert DJ, Dehmlow H, Morand OH, Schulz GE (2003) Binding structures and potencies of oxidosqualene cyclase inhibitors with the homologous Squalene-Hopene cyclase. *J Med Chem* 46:2083–2092
- Cenedella RJ, Sexton PS, Krishnan K, Covey DF (2005) Comparison of effects of U18666A and enantiomeric on sterol synthesis and induction of apoptosis. *Lipids* 40:635–640
- Cenedella RJ, Jacob R, Borchman D, Tang D, Neely AR, Samadi A, Mason RP, Sexton P (2004) Direct perturbation of

- lens membrane structure may contribute to cataracts caused by U18666A, an oxidosqualene cyclase inhibitor. *J Lipid Res* 45:1232–1241
23. Colassanti BK, Hartman ER, Craig CR (1974) Electrocorticogram and behavioral correlates during the development of chronic experimental epilepsy. *Epilepsia* 15:361–373
 24. Bierkamper GG, Cenedella RJ (1978) Cerebral cortical cholesterol changes in cobalt-induced epilepsy. *Epilepsy* 19:155–167
 25. Jurgelski W Jr, Hudson PM, Vogel FS (1973) Induction of a chronic somatosensory epilepsy in the opossum (*Didelphis virginiana* Kerr) with an inhibitor of cholesterol biosynthesis. *Brain Res* 64:466–471
 26. Bierkamper GG, Cenedella RJ (1978) Induction of chronic epileptiform activity in the rat by an inhibitor of cholesterol synthesis, U18666A. *Brain Res* 150:343–351
 27. Vainio S, Jansen M, Koivusalo M, Rog T, Karttunen M, Vattulainen I, Ikonen E (2006) Significance of sterol structural specificity desmosterol cannot replace cholesterol in lipid rafts. *J Biol Chem* 281:348–355
 28. Cenedella RJ (1985) Regional distribution of lipids and phospholipase A₂ activity in normal and cataractous rat lens. *Curr Eye Res* 4:113–119
 29. Fliesler SJ, Richards MJ, Miller CY, Peachey NS, Cenedella RJ (2000) Retinal structure and function in an animal model that replicates the biochemical hallmarks of desmosterolosis. *Neurochem Res* 25:685–694
 30. Fliesler SJ, Richards MJ, Miller CY, Cenedella RJ (2000) Cholesterol synthesis in the vertebrate retina: effects of U18666A on rat retinal structure, photoreceptor membrane assembly and sterol metabolism and composition. *Lipids* 35:289–296
 31. Rujanavech C, Silbert DF (1986) LM cell growth and membrane lipid adaptation to sterol structure. *J Biol Chem* 261:7196–7203
 32. Xu F, Rychnovsky SD, Belani JD, Hobbs HH, Cohen JC, Rawson RB (2005) Dual roles for cholesterol in mammalian cells. *Proc Natl Acad Sci USA* 102:14551–14556
 33. Wu J, Ellsworth K, Ellsworth M, Schroeder KM, Smith K, Fisher RS (2004) Abnormal benzodiazepine and zinc modulation of GABA_A receptors in an acquired absence epilepsy model. *Brain Res* 1013:230–240
 34. Sparrow SM, Carter JM, Ridgway ND, Cook HW, Byers DM (1999) U18666A inhibits intracellular cholesterol transport and neurotransmitter release in human neuroblastoma cells. *Neurochem Res* 24:69–77
 35. Smith KA, Bierkamper GG (1990) Paradoxical role of GABA in a chronic model of Petit Mal (absence)-like epilepsy in the Rat. *Eur J Pharm* 176:45–55
 36. Krami M, Bagli JF, Dvornik KD (1964) Inhibition of conversion of 7-dehydrocholesterol to cholesterol nu AY-9944. *Biochim Biophys Acta* 15:455–457
 37. Smith KA, Fisher RS (1996) The selective GABAB antagonist CGP-35348 blocks spike-wave bursts in the cholesterol synthesis rat absence epilepsy model. *Brain Res* 729:147–150
 38. Cortez MA, McKlerie C, Snead OC III (2001) A model of atypical absence seizures. *Neurology* 56:341–349
 39. Cortez MA, Cunnane SC, Snead OC III (2002) Brain sterols in the AY-9944 rat model of atypical absence seizures. *Epilepsia* 43:3–8
 40. Persad V, Cortez MA, Snead OC III (2002) A chronic model of atypical absence seizures: studies of developmental and gender sensitivity. *Epilepsy Res* 48:111–119
 41. Serbanescu I, Ryan MA, Shukla R, Cortez MA, Snead OC III, Cunnane SC (2004) Lovastatin exacerbates atypical absence seizures with only minimal effects on brain sterols. *J Lipid Res* 45:2038–2043
 42. Persad V, Ting Wong CG, Cortez MA, Wang YT, Snead OC III (2004) Hormonal regulation of atypical absence seizures. *Ann Neurol* 55:353–361
 43. Chan KF, Jia Z, Murphy PA, Burnham WM, Cortez MA, Snead OC III (2004) Learning and memory impairment in rats with chronic atypical absence seizures. *Exp Neurol* 190:328–336
 44. Serbanescu I, Cortez MA, McKlerie C, Snead OC III (2004) Refractory atypical absence seizures in rat: a two hit model. *Epilepsy Res* 62:53–63
 45. Li H, Kraus A, Wu J, Huguenard JR, Fisher RS (2006) Selective changes in thalamic and cortical GABAA receptor subunits in a model of acquired absence epilepsy in the rat. *Neuropharmacology* 51:121–128
 46. Stewart LS, Bercovici E, Shukla R, Serbanescu I, Persad V, Mistry N, Cortez MA, Snead OC III (2006) Daily rhythms of seizure activity and behavior in a model of atypical absence epilepsy. *Epilepsy Behav* 9:564–572
 47. Chan KF, Burnham WM, Jia Z, Cortez MA, Snead OC III (2006) GABAB receptor antagonism abolishes the learning in rats with chronic atypical absence seizures. *Eur J Pharmacol* 541:64–72
 48. Bercovici E, Cortez MA, Wang X, Snead OC III (2006) Serotonin depletion attenuates AY-9944-mediated atypical absence seizures. *Epilepsia* 47:240–246
 49. Bercovici E, Cortez MA, Snead OC III (2007) 5-HT₂ modulation of AY-9944 induced atypical absence seizures. *Neurosci Lett* 418:13–17
 50. Li H, Huguenard JR, Fisher RS (2007) Gender and age difference in expression of GABAA receptor subunits in rat somatosensory thalamus and cortex in an absence epilepsy model. *Neurobiol Dis* 25:623–630
 51. Cenedella RJ, Kuszak JR, Al-Ghoul KJ, Qin S, Sexton PS (2003) Discordant expression of the sterol pathway in lens underlies simvastatin-induced cataracts in Chbb: Thom Rats. *J Lipid Res* 44:198–211
 52. Kuszak JR, Khan AR, Cenedella RJ (1988) An ultrastructural analysis of plasma membrane in the U18666A cataract. *Ophthalmol Vis Sci* 29:261–267
 53. Jacob RF, Cenedella RJ, Mason RP (1999) Direct evidence for immiscible cholesterol domains in human ocular lens fiber cell plasma membranes. *J Biol Chem* 274:31613–31618
 54. Jacob RF, Cenedella RJ, Mason RP (2001) Evidence for distinct cholesterol domains in fiber cell membranes from cataractous human lenses. *J Biol Chem* 276:13573–13578
 55. Brown MS, Goldstein JL (1986) A receptor-mediated pathway for cholesterol homeostasis. *Science* 232:34–47
 56. Liscum L, Faust JR (1989) The intracellular transport of low density lipoprotein-derived cholesterol is inhibited in Chinese hamster ovary cells cultures with 3-β-[2-(Diethylamino)ethoxy]androst-5-en-17-one*. *J Biol Chem* 264:11796–11806
 57. Liscum L (1990) Pharmacological inhibition of the intracellular transport of low-density lipoprotein-derived cholesterol in Chinese hamster ovary cells. *Biochim Biophys Acta* 1045:40–48
 58. Liscum L, Collins GJ (1991) Characterization of Chinese hamster ovary cells that are resistant to 3-β-[2-(diethylamino)ethoxy]androst-5-en-17-one inhibition of low density lipoprotein-derived cholesterol metabolism. *J Biol Chem* 266:16599–16606
 59. Liscum L, Dahl NK (1992) Intracellular cholesterol transport. *J Lipid Res* 33:1239–1254
 60. Underwood KW, Jacobs NL, Howley A, Liscum L (1997) Evidence for a cholesterol transport pathway from lysosomes to endoplasmic reticulum that is independent of the plasma membrane. *J Biol Chem* 273:4266–4274

61. Underwood KW, Andermariam B, McWilliams GL, Liscum L (1996) Quantitative analysis of hydrophobic amine inhibition of intracellular cholesterol transport. *J Lipid Res* 37:1556–1568
62. Feng B, Tabas I (2002) ABCA1-mediated cholesterol efflux is defective in free cholesterol-loaded macrophages. *J Biol Chem* 277:43271–43280
63. Lange Y, Ye J, Chin J (1997) The fate of cholesterol exiting lysosomes. *J Biol Chem* 272:17018–17022
64. Lange Y, Ye J, Steck TL (1998) Circulation of cholesterol between lysosomes and the plasma membrane. *J Biol Chem* 273:18915–18922
65. Lange Y, Ye J, Rigney M, Steck TL (1999) Regulation of endoplasmic reticulum cholesterol by plasma membrane cholesterol. *J Lipid Res* 40:2264–2270
66. Butler JD, Blanchette-Mackie J, Goldin E, O'Neill RR, Carstea G, Roff CF, Patterson MC, Patel S, Comly ME, Cooney A, Vanier MT, Brady RO, Pentchev PG (1992) Progesterone blocks cholesterol translocation from lysosomes. *J Biol Chem* 267:23797–23805
67. Roff CF, Goldin E, Comly ME, Cooney A, Brown A, Vanier MT, Miller SPF, Brady RO, Pentchev PG (1991) Type C Niemann–Pick disease: use of hydrophobic amines to study defective cholesterol transport. *Dev Neurosci* 13:315–319
68. Sparrow SM, Carter JM, Ridgway ND, Cook HW, Byers DM (1999) U18666A inhibits intracellular cholesterol transport and neurotransmitter release in human neuroblastoma cells. *Neurochem Res* 24:69–77
69. Issandou M, Guillard R, Boullay AB, Linhart V, Lopez-Perez E (2004) Up-regulation of low-density lipoprotein receptor in human hepatocytes is induced by sequestration of free cholesterol in the endosomal/lysosomal compartment. *Biochem Pharmacol* 67:2281–2289
70. Liscum L, Klansek JJ (1998) Niemann–Pick disease type C. *Curr Opin Lipidol* 9:131–135
71. Lange Y, Ye J, Rigney M, Steck T (2000) Cholesterol movement in Niemann–Pick type C cells and in cells treated with amphiphiles. *J Biol Chem* 275:17468–17475
72. Blanchette-Mackie EJ (2000) Intracellular cholesterol trafficking: role of the NPC1 protein. *Biochim Biophys Acta* 1486:171–183
73. Neufeld EB, Wastney M, Patel S, Suresh S, Cooney AM, Dwyer NK, Roff CF, Ohno K, Morris JA, Carstea ED, Incardona JP, Strauss JF III, Vanier MT, Patterson MC, Brady RO, Pentchev PG, Blanchette-Mackie EJ (1999) The Niemann–Pick C1 protein resides in a vesicular compartment linked to retrograde transport of multiple lysosomal cargo. *J Biol Chem* 274:9627–9635
74. Ko DC, Gordon MD, Jin JY, Scott MP (2001) Dynamic movements of organelles containing Niemann–Pick C1 protein: NPC1 involvement in late endocytic events. *Am Soc Cell Biol* 12:601–614
75. Cruz JC, Sugii S, Yu C, Chang TY (2000) Role of Niemann–Pick type C1 protein in intracellular trafficking of low density lipoprotein-derived cholesterol. *J Biol Chem* 275:4013–4021
76. Vanier MT (1999) Lipid changes in Niemann–Pick disease type C brain: personal experience and review of the literature. *Neurochem Res* 24:481–489
77. Karten B, Vance DE, Campenot RB, Vance JE (2003) Trafficking of cholesterol from cell bodies to distal axons in Niemann–Pick C1-deficient Neurons. *J Biol Chem* 278:4168–4175
78. Pacheco CD, Kunkel R, Lieberman AP (2007) Autophagy in Niemann–Pick C disease is dependent upon Beclin-1 and responsive to lipid trafficking defects. *Hum Mol Gene* 16:1495–1503
79. Munafo DB, Colombo MI (2001) A novel assay to study autophagy: regulation of autophagosome vacuole size by amino acid deprivation. *J Cell Sci* 114:3619–3629
80. Higgins ME, Davies JP, Chen FW, Ioannou YA (1999) Niemann–Pick C1 is a late endosome-resident protein that transiently associates with lysosomes and the trans-Golgi network. *Mol Genet Metab* 68:1–13
81. Watari H, Blanchette-Mackie EJ, Dwyer NK, Sun G, Glick JM, Patel S, Neufeld EB, Pentchev PG, Strauss JF III (2000) NPC1-containing compartment of human granulosa-lutein cells: a role in the intracellular trafficking of cholesterol supporting steroidogenesis. *Exp Cell Res* 25:56–66
82. Lange Y, Ye J, Rigney M, Steck TL (2002) Dynamics of lysosomal cholesterol in Niemann–Pick type C and normal human fibroblasts. *J Lipid Res* 43:198–204
83. Sugimoto Y, Ninomiya H, Ohsaki Y, Higaki K, Davies JP, Ioannou YA, Ohno K (2001) Accumulation of cholera toxin and GM1 ganglioside in the early endosome of Niemann–Pick C1-deficient cells. *Proc Natl Acad Sci USA* 98:12391–12396
84. Mohammadi A, Perry RJ, Storey MK, Cook HW, Byers DM (2001) Golgi and phosphorylation of oxysterol binding protein in Niemann–Pick C and U18666A-treated cells. *J Lipid Res* 42:1062–1071
85. Cenedella RJ, Sarkar CP, Towns L (1981) Studies on the mechanism of the epileptiform activity induced by U18666A. II. Concentration, half-life and distribution of radiolabeled U18666A in the brain. *Epilepsia* 23:257–268
86. Tangirala RK, Mahlberg FH, Glick JM, Jerome WG, Rothblat GH (1993) Lysosomal accumulation of unesterified cholesterol in model macrophage foam cells. *J Biol Chem* 268:9653–9660
87. Delton-Vandenbroucke I, Bouvier J, Makino A, Besson N, Pageaux JF, Lagarde M, Kobayashi T (2007) Anti-bis (monoacylglycerol)phosphate antibody accumulates acetylated LDL-derived cholesterol in cultured macrophages. *J Lipid Res* 48:543–552
88. Kellner-Weibel G, Jerome WG, Small DM, Warner GJ, Stoltenberg JK, Kearney MA, Corjay MH, Phillips MC, Rothblat GH (1997) Effects on intracellular free cholesterol accumulation on macrophage viability a model for foam cell death. *Arterioscler Thromb Vasc Biol* 18:423–431
89. Neufeld EB, Stonik JA, Demosky SJ Jr, Knapper CL, Combs CA, Cooney A, Comly M, Dwyer N, Blanchette-Mackie J, Remaley AT, Santamarina-Fojo S, Brewer HB Jr (2004) The ABCA1 transporter modulates late endocytic trafficking. *J Biol Chem* 279:15571–15578
90. Jin LW, Maezawa I, Vincent I, Bird T (2004) Intracellular accumulation of amyloidogenic fragments of amyloid- β precursor protein in neurons with Niemann–Pick type C defects is associated with endosomal abnormalities. *J Pathol* 164:975–985
91. Yamazaki T, Chang TY, Haass C, Thara Y (2001) Accumulation and aggregation of amyloid β -Protein in late endosomes of Niemann–Pick Type C Cells. *J Biol Chem* 276:4454–4460
92. Runz H, Rietdorf J, Tomic I, de Bernard M, Beyreither K, Pepperkok R, Hartmann T (2002) Inhibition of intracellular cholesterol transport alters presenilin localization and amyloid precursor protein processing in neuronal cells. *J Neurosci* 22:1679–1689
93. Kametaka S, Shibata M, Moroe K, Kanamori S, Ohsawa Y, Waguri S, Sims PJ, Emoto K, Umeda M, Uchiyama Y (2003) Identification of phospholipid scramblase 1 as a novel interacting molecule with β -secretase (B β Site amyloid precursor protein (APP) cleaving enzyme (BACE)). *J Biol Chem* 278:15239–15245
94. Klingenstein R, Lober S, Kujala P, Godsava S, Leliveld SR, Gmeiner P, Peters P, Korth C (2006) Tricyclic antidepressants, quinacrine and a novel, synthetic chimera thereof clear prions by

- destabilizing detergent-resistant membrane compartments. *J Neuro Chem* 98:748–759
95. Hagiwara K, Nakamura Y, Nishijima M, Yamakawa Y (2007) Prevention of prion propagation by dehydrocholesterol reductase inhibitors in cultured cells and a therapeutic trial in mice. *Biol Pharm Bull* 30:835–838
96. Cenedella RJ (1983) Source of cholesterol for the ocular lens, studied with U18666A: a cataract-producing inhibitor of lipid metabolism. *Exp Eye Res* 37:33–43
97. Harada M, Kawaguchi T, Kumemure H, Terada K, Ninomiya H, Taniguchi E, Hanada S, Baba S, Maeyama M, Koga H, Ueno T, Furuta K, Suganuma T, Sugiyama T, Sata M (2005) The Wilson disease protein ATP7B resides in the late endosomes with Rab 7 and the Niemann–Pick C1 Protein. *J Pathol* 166:499–510
98. Lindwasser OW, Resh MD (2004) Human immunodeficiency virus type 1 gag contains a dileucine-like motif that regulates association with multivesicular bodies. *J Virol* 78:6013–6023
99. de Diego I, Schwartz F, Siegfried H, Dauterstedt P, Heeren J, Beisiegel U, Enrich C, Grewal T (2002) Cholesterol modulates the membrane binding and intracellular distribution of annexin 6. *J Biol Chem* 277:32187–32194
100. LeBrand C, Corti M, Goodson H, Cosson P, Cavalli V, Mayran N, Faure J, Gruenberg J (2002) Late endosome motility depends in lipids via the small GTPase Rab 7. *EMBO J* 21:1289–1300
101. Umeda A, Fujita H, Kuronita T, Hirosako K, Himeno M, Tanaka Y (2003) Distribution and trafficking of MPR300 is normal in cells with cholesterol accumulated in late endocytic compartments: evidence for early endosome-to-TGN trafficking of MPR300. *J Lipid Res* 44:1821–1832
102. Tomiyama Y, Waguri S, Kanamori S, Kametaka S, Wakasugi M, Shibata M, Ebisu S, Uchiyama Y (2004) Early-phase redistribution of the cation-independent mannose 6-phosphate receptor by U18666A treatment in HeLa cells. *Cell Tissue Res* 317:253–264
103. Stasi DD, Vallacchi V, Campi V, Ranzani T, Daniotti M, Chiodini E, Fiorentini S, Greeve I, Prinetti A, Rivoltini L, Pierotti MA, Rodolfo M (2005) DHCR24 gene expression is upregulated in melanoma metastases and associated to resistance to oxidative stress-induced apoptosis. *Int J Cancer* 115:224–230
104. Cheung NS, Koh CHV, Bay BH, Qi RZ, Choy MS, Li QT, Wong KP, Whiteman M (2004) Chronic exposure to U18666A induces apoptosis in cultured murine cortical neurons. *Biochem Biophys Res Commun* 315:408–417
105. Koh CHV, Qi RZ, Qu D, Melendez A, Manikandan J, Bay BH, Duan W, Cheung NS (2006) U18666A-mediated apoptosis in cultured murine cortical neurons: role of caspases, calpains and kinases. *Sci Dir* 18:1572–1583
106. Huang Z, Hou Q, Cheung NS, Li QT (2006) Neuronal cell death caused by inhibition of intracellular cholesterol trafficking is caspase dependent and associated with activation of the mitochondrial apoptosis pathway. *J Neurochem* 97:280–291
107. Koh CH, Whiteman M, Li QX, Halliwell B, Jenner AM, Wong BS, Laughton KM, Wenk M, Masters CL, Beart PM, Bernard O, Cheung NS (2006) Chronic exposure to U18666A is associated with oxidative stress in cultured murine cortical neurons. *J Neurobiochem* 98:1278–1289
108. Koh CHV, Cheung NS (2006) Cellular mechanism of U18666A-mediated apoptosis in cultured murine cortical neurons: bridging Niemann–Pick disease type C and Alzheimer’s disease. *Sci Dir* 18:1844–1853
109. Koh CH, Peng ZF, Ou K, Melendez A, Manikandan J, Qi RZ, Cheung NS (2007) Neuronal apoptosis mediated by inhibition of intracellular cholesterol transport: microarray and proteomics analyses in cultured murine cortical neurons. *Cell Physiol* 211:63–87
110. Yadav S, Rawal UM (1992) Cholesterol and lipid peroxidation in 3 beta-(2-diethylaminoethoxy)-androst-5-en-17-one HCl (U18666A) induced cataractogenesis in rats. *Indian J Exp Biol* 30:147–148
111. Bursch W, Ellinger A (2005) Autophagy—a basic mechanism and a potential role for neurodegeneration. *Folia Neuropathol* 43:297–310

Inhibition of Fatty Acid Synthase by Orlistat Accelerates Gastric Tumor Cell Apoptosis in Culture and Increases Survival Rates in Gastric Tumor Bearing Mice In Vivo

Shawn Dowling · James Cox · Richard J. Cenedella

Received: 24 October 2008 / Accepted: 16 March 2009 / Published online: 21 April 2009
© AOCS 2009

Abstract Orlistat, an anti-obesity drug, is a potent inhibitor of fatty acid synthase (FAS) and tumor cell viability. It can also induce apoptotic cancer cell death. We examined the effects of Orlistat on cultured NUGC-3 gastric cancer cells. We identified that inhibition of FAS via Orlistat exposure results in rapid cellular damage preceded by a direct but short-lived autophagic response. The Orlistat induced damage can be reversed through the addition of lipid containing media in a process that normally leads to cell death. By limiting exogenous lipid availability and inhibiting FAS using Orlistat, we demonstrated both a greater sensitivity and amplified cancer cell death by activation of apoptosis. We have identified “windows of opportunity” at which time apoptosis can be aborted and cells can be reversed from the death pathway. However, when challenged beyond the window of recovery, cell death becomes all but certain as the ability to be rescued decreases considerably. In vivo examination of Orlistat’s ability to inhibit gastrointestinal cancer was examined using heterozygous male C57BL/6J APC-Min mice, which spontaneously develop a fatal gastrointestinal cancer. Mice were fed either a high fat (11%) or low fat (1.2%) diet containing no Orlistat or 0.5 mg Orlistat/g of chow. Orlistat treated mice fed the high fat, but not low fat diet, survived 7–10% longer than the untreated controls.

Keywords Thin layer chromatography · Analytical Techniques · Lipid biochemistry · General Area · Lipases · Lipoproteins · Metabolism ·

Cancer · Physiology · Fatty acids · Specific Lipids · Sterols

Introduction

Fatty acid synthase (FAS) functions to form palmitic acid from acetyl and malonyl coenzymeA. It is highly expressed in many tumors that are dependent on de novo synthesis to supply the fatty acid needed for growth and proliferation [1–5]. The capacity of FAS inhibitors to kill cancer cells suggests a new approach to treatment of human cancers [6]. Orlistat is one of these FAS inhibitors.

Orlistat, an over-the-counter anti-obesity drug, decreases absorption of dietary fat by inhibiting gastric and pancreatic lipases through covalent modification of the enzymes [7]. It is also a potent inhibitor of FAS [8]. Using an activity-based proteomics screen for serine hydrolases, Kridel et al. [8] discovered that Orlistat irreversibly inhibits the thioesterase activity of FAS. The capacity of Orlistat to inhibit the proliferation of prostatic cancer cells cultured in serum free media appeared to be due to restricting the availability of fatty acids for growth, since the addition of palmitic acid to the media reversed the inhibition [8]. A decrease in DNA synthesis, arrest of cell progression through the G1/S boundary, and apoptotic cell death are all consequences of inhibiting FAS in cultured cancer cells with Orlistat [6, 9].

The effects of Orlistat on proliferation and viability of tumor cells have typically been examined after 24–72 h [8, 10] and even after 4–5 days [10] of continuous exposure to the drug. This approach assumes that the Orlistat has a linear-accumulative effect on tumor cells. Possible immediate or very rapid effects of Orlistat on tumor cells have not been reported. We searched for such effects and

S. Dowling · J. Cox · R. J. Cenedella (✉)
Biochemistry, A.T. Still University of the Health Sciences,
Kirksville, USA
e-mail: rcenedella@atsu.edu

observed that as little as one-half hour exposure of NUGC-3 cells to 100–500 μM Orlistat induced transient autophagy. In addition, we observed that 4 h exposure followed by removal of the drug reduced viability when examined at hour 48. The presence of Orlistat for the first 8 h of culture resulted in near total loss of viability when measured 40 h later. Acute-irreversible damage appeared to occur at the interface between 4 and 8 contact hours with Orlistat. We probed the mechanism of reduced viability by examining NUGC-3 cells for the emergence of autophagy and apoptosis following short-term exposure to the drug. Rapid onset of apoptosis was attributed to nutritional stress, in which altering the availability of nutrients places a stress on the cell to acquire alternative sources of nutrients to meet the cells biogenesis needs. In this case, nutritional stress was caused by the deprivation of fatty acids since the apoptosis could be arrested by addition of whole serum to the culture media.

Although Kridel et al. [8] demonstrated that intraperitoneally injected Orlistat suppressed the growth of implanted tumor cells, use of Orlistat to treat systemic tumors is limited by the fact that it is essentially unabsorbed following oral dosage [11]. However, since orally administered Orlistat would directly contact the gastrointestinal mucosa, the drug might be of value in treating gastrointestinal tumors exposed to the intestinal lumen. We tested this possibility by examining the effect of orally given Orlistat on the survival of C57BL/6J APC-Min mice (Min). The Min mice provide an excellent *in vivo* model for human gastrointestinal cancer, since the adenomas that develop in these animals result from inactivation of the same tumor suppressor gene associated with most human colon cancers [12]. The tumors develop due to a mutation in the murine AP gene, a homolog of the human APC gene (JAX MICE literature, The Jackson Laboratory). However, Min mice develop a heavy tumor load in the small rather than large intestines which results in death at several months of age [13–15].

Materials and Methods

Cell Culture and Reagents

All reagents were from Sigma Chemical Co. (St. Louis, MO) unless otherwise noted. NUGC-3 gastric cancer cells (human stomach) were obtained from the Health Science Research Resource Bank (Osaka, Japan). Bovine lens epithelial cells (local source) were used as a normal cell control. Cells were seeded at 30,000–40,000 per well in 96 well dishes and grown at 37°C and 5% carbon dioxide in RPMI-1640 media containing 10% fetal calf serum (FCS) plus 0.25% antibiotic/antimycotic containing mix. This is

called whole media (WM). Experiments were started 1–2 days later with cell layers 70–90% confluent. Orlistat from 5 to 120 mg Zenical™ capsules (obtained from a local pharmacy) was extracted by homogenization in 3–5 ml aliquots of 1:1 (v/v) chloroform:methanol and transferred to a weighed test tube. After evaporation of the solvent under nitrogen and further drying overnight under vacuum, the recovered Orlistat was dissolved in ethanol at 50 mg/ml. Aliquots were added to WM or serum deficient media (DM) containing 0.1% FCS to yield 500 μM . Serial dilutions provided media containing 200, 100, 50, and 25 μM Orlistat. The capacity of Orlistat to decrease cell viability was also examined in non-cancerous (normal) bovine lens epithelial cells. Culture conditions were as we described before [16].

Cell Viability

Cell layers in groups of 5 or 6 wells were incubated for 4–48 h at 37°C with 200 μl of WM or DM containing 0–500 μM Orlistat. Cell viability was assessed by the MTT (thiazolyl blue tetrazolium bromide) assay essentially as described by Carmichael et al. [17]. Test media was replaced with 200 μl of WM, 25 μl of MTT solution (5 mg/ml water) was added, and the samples incubated for 4 h at 37°C. The MTT solution was replaced with 100 μl of DMSO and the optical density at 570 nm measured 1 h later. Absorbance for each group was expressed as the mean \pm SEM. Statistical significance of differences ($P \leq 0.05$) was assessed by one-way ANOVA.

Measurement of Fatty Acid and Synthesis

Near confluent layers of NUGC-3 cells were washed twice in serum free media, after which 200 μl of plain RPMI-1640 media was added followed by 1 μl of ^{14}C -acetate (55 mCi/mmol, ARC Inc, St. Louis, MO). Serum free media was used to avoid dilution of the labeled acetate with competing sources of unlabeled acetate. Following 4-hour incubation in the absence or presence of varying concentrations of Orlistat, cell layers were washed twice with PBS. The cell layer in each well was dissolved in 200 μl of 1 N NaOH in 50% ethanol containing 100 μg of triolein and 100 μg of cholesterol added as carrier. Each well was washed with 4 additional 200 μl -aliquots of the 1 N NaOH and pooled into screw capped test tubes with the first 200 μl . Samples were saponified for 2 h at 100°C, diluted with 1 ml of water, acidified and the non-saponifiable plus saponifiable lipids extracted with 2–4 ml aliquots of hexane. The hexane extracts were washed with an equal volume of water to remove any water-soluble radiolabel. The hexane extracts were evaporated and the lipids separated by thin layer chromatography in silica gel

using a solvent of hexane:diethyl ether:glacial acetic acid (73:25:2; v/v/v). The sterol (cholesterol) band and the fatty acid band were recognized by exposure to iodine vapor and marked. After loss of the iodine by sublimation, the cholesterol and fatty acid bands were recovered and the radiolabel measured by scintillation counting.

We accounted for variation in incorporation from well to well in any given group by expressing the level of fatty acid synthesis as a ratio of incorporation of ^{14}C into fatty acid to cholesterol. Cholesterol controls were run to determine Orlistat's effect on total sterol synthesis. Significant differences were not seen in the disintegrations per minute (dpm) of ^{14}C -acetate incorporated into cholesterol between control and Orlistat treated cell layers. Decreases in the fatty acid:cholesterol ratio reflects inhibition of fatty acid synthesis, since Orlistat has no known effects on cholesterol biosynthesis.

Western Blotting: Changes in the Relative Mass of Fatty Acid Synthase (FAS)

NUGC-3 cells were grown in RPMI-1640 on 35 mm plastic dishes to assure adequate protein. Cell layers exposed or unexposed to Orlistat under varying condition were washed twice with PBS and dissolved in 0.50 ml of lysis buffer [18]. Samples were assayed for protein (aliquots containing 50 μg protein were separated on 8% PAGE gels 94% stacking gel), transferred to membranes which were then probed with 0.8 $\mu\text{g}/\text{ml}$ rabbit-polyclonal, antihuman FAS-antiserum (Santa Cruz Biotechnology) and HRP-conjugated goat-antirabbit IgG secondary antibody (1/60,000 dilution). Immunoreactive protein was detected by enhanced chemiluminescences and relative concentrations estimated by densitometric scanning of the exposed X-ray film as done before [18].

Detection of Autophagy and Apoptosis

Autophagic vacuoles were labeled with monodansylcadaverine (MDC) using a modified protocol as described by Biederbick et al. [19]. Briefly, cells were grown on coverslips, incubated at 37°C in WM, and DM \pm 500 μM Orlistat for varying time intervals. Media was removed; cells were washed once with PBS, and replaced with PBS supplemented with 0.1 mM MDC. Cells were allowed to incubate for 10 min at 37°C. Following incubation, cells were washed three times with PBS, fixed using 4% paraformaldehyde, and mounted using Fluoromount. Cells were examined using a NIKON Eclipse 80i upright fluorescent microscope equipped with a V2-A filter system (excitation 340 nm, barrier 514 nm). Images were captured using a NIKON DS-Qi1 digital camera and were processed using Image J.

Autophagic vacuole formation was measured using methods described by Munafo and Colombo [20]. Briefly, cells were grown in 60 mm dishes and treated using varying concentrations of WM and DM \pm Orlistat. To identify autophagy activity and duration, MDC incorporation was measured after 0.5, 1, 2, 4, 6, 8, and 10-hour Orlistat exposure. After varying times the media was removed and PBS was added with the addition of 0.1 mM of MDC and incubated at 37°C for 10 min. Following incubation the cells were washed three times with PBS and collected in 10 mM Tris-HCl, pH 8 with 0.1% Triton X-100. Intracellular MDC incorporation was measured using a BioTek FLx 800 Microplate Fluorescent Reader equipped with an excitation filter of 365/20 nm and an emissions filter of 528/20 nm. The number of cells per well were normalized by the addition of ethidium bromide to a final concentration of 0.1 μM to each well followed by the measuring of DNA fluorescence (excitation filter 528/20 nm and emission filter of 590/20 nm). The MDC measured was expressed as the percent of autophagic activity relative to whole media control.

The mechanism of cell death (apoptosis) was determined through the use of fluorochrome inhibitor of caspases (FLICA) (Immunochemistry Technologies, LCC). Activated caspase is an enzyme found active only in cells undergoing apoptosis. FLICA irreversibly binds to caspases (caspase-1, -3, -4, -5, -6, -7, -8, -9) allowing apoptosis to be measured [21, 22]. Caspase activity was visually examined using the suggested manufactures protocol for labeling caspases with FLICA. Briefly, cells were grown on coverslips and treated with various concentrations of Orlistat substituted in DM. Cells were then treated with FLICA solution in a 1:30 ratio (10 μl FLICA:290 μl media) and incubated for 1 h. Next, media was removed and replaced with fresh media (300 μl) containing 1.5 μl of 200 $\mu\text{g}/\text{ml}$ stock Hoechst stain solution (Immunochemistry). After 5 min cells were rinsed with wash buffer (Immunochemistry) and examined immediately using a NIKON Eclipse 80i upright fluorescent microscope equipped with a V2-A filter system (excitation 340 nm, barrier 514 nm). Images were captured using a NIKON DS-Qi1 digital camera and were processed using Image J.

Animals and Treatments

Heterozygous male C57BL/6J APC-Min (multiple intestinal neoplasia) mice were purchased from The Jackson Laboratory (Bar Harbor, ME). Heterozygous mice were used for these studies because homozygous mice die in utero. Mice in groups of 4–8 were fed either a high fat (11% fat) or low fat (1.2%) diet containing no Orlistat or Orlistat at 0.5 mg/g chow. Mice were started on the diets at either 50–60 days (Experiments 1 and 3) or 33–34 days

(Experiment 2) of age. Age at death varied from 104–229 days of age. Mice were housed in the Animal Care Facility at KCOM/ATSU and maintained according to the “Guide of the Care and Use of Laboratory Animals” from the National Research Council.

Recovery of Orlistat and Preparation of Test Diets

The contents of 4–6 Zenical capsules, each containing 120 mg of Orlistat, were pooled and extracted three times with 5 ml of 1:1 chloroform–methanol (v/v) using a Polytron-type homogenizer. The solvent from the pooled extracts recovered after centrifugation was evaporated under nitrogen. The residue was dried overnight to constant weight under high vacuum, and dissolved in ethanol to give a stock solution of 50 mg/ml. Mice in two studies were fed ground Purina Mouse Diet 5015 that contained 11% fat plus 0 (control) or 0.5 mg Orlistat/g chow. In a third study, mice were fed a customized powdered diet (AIN-93M, Purina Mills TESTDIET, Richmond, IN) containing 0.2% fat, from saturated and monounsaturated fatty acids, to which we added 1% linoleic acid to guard against essential fatty acid deficiency. Orlistat was added at 0 (control) or 0.5 mg/g (test) to this very low fat diet.

HPLC Analysis of Orlistat

The HPLC method of Souri et al. [11] was used to confirm the concentration of Orlistat in chow and to estimate the distribution of Orlistat in the mouse gut following oral dosage. Samples of mouse chow (11% fat) with Orlistat and sections of mouse gut removed at 4 h after oral dosage were extracted with 1:1 chloroform–methanol, and the recovered lipids were fractionated by thin layer chromatography on Silica Gel G plates using a solvent of hexane: diethyl ether:glacial acetic acid (73:25:2). Orlistat, visualized by exposure to iodine vapor, migrated with an R_f of between 0.1 and 0.2. After sublimation of the iodine, the TLC zone containing Orlistat was recovered and extracted twice with 3 ml aliquots of methanol. The residue remaining after evaporation of the methanol was dissolved in several hundred microliters of acetonitrile:0.1% orthophosphoric acid in water (90:10), centrifuged and aliquots injected onto a Waters C18 reverse phase column (10 μ m, 3.9 \times 300 mm, 125 A μ Bondapak) eluted at 1 ml/min with the 90:10 acetonitrile-acidic water and absorbance monitored at 205 nm. Ten micrograms of Orlistat standard (injected in 100 μ l) eluted at about 6 min.

Survival Statistical Analyses

To determine the effects of Orlistat on mouse survival, the end point analyzed was the difference in day of death

between untreated (control) and Orlistat treated animals (test). The Kaplan–Meier procedure [18] was used to estimate the probability of surviving a given time. Since all untreated animals die prematurely (4–7 months) compared to wild type mice (1.5–2 years), even slight prolongation of life due to treatment can be recognized. Using a statistical computer program (GraphPad Prism version 5.0 for Windows, GraphPad Software, San Diego, CA, USA) survival curves were generated by the Kaplan–Meier procedure [23] and analyzed by the Log-Rank (Mantel–Cox) and the Gehan–Wilcoxon Tests. The Log-Rank test is more powerful and gives equal weight to all time points.

Results

Potential use of Orlistat as an anticancer drug would likely be restricted to treatment of gastrointestinal tumors since it is essentially unabsorbed following oral dosage [2]. Therefore, we chose to examine the effects of Orlistat on a human derived gastric cancer cell line, NUGC-3 [24]. Viability of cells cultured for 48 h in serum deficient media, DM (0.10% serum), was decreased by more than 70% when continuously exposed to 25 μ M Orlistat (Fig. 1). Near complete inhibition was seen at 100 μ M. The dose response curve was markedly shifted to the right by including 10% serum in the media, called whole media (WM).

Although cell viability assays are typically performed following 48 h or more of continuous exposure to an inhibitor, we considered the possibility that the decreased viability observed at 48 h was due in part or total to cell injury induced soon after adding Orlistat rather than to a

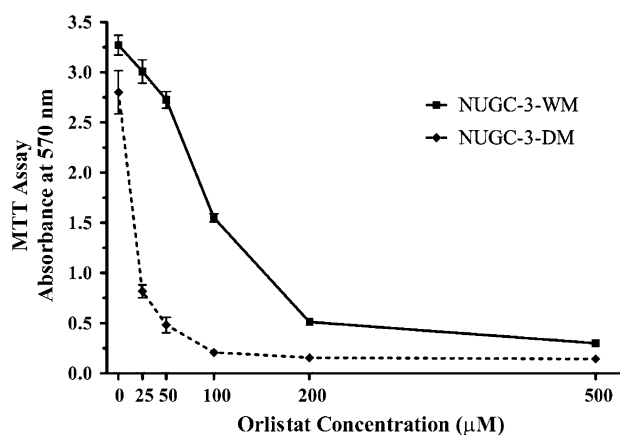


Fig. 1 Effect of Orlistat on the viability of NUGC-3 gastric tumor cells. Cells were cultured for 48 h in RPMI-1640 media containing 10% fetal calf serum (whole media, WM) or 0.10% serum (deficient media, DM) and varying concentrations of Orlistat. Cell viability was assessed by the MTT assay. Each point is the mean \pm SEM of 6 cell wells

sustained accumulation of injury. Cells were incubated for 4, 8 or 12 h in DM containing 0 (control), 100 or 500 μM Orlistat, and then incubated to hour 48 in drug free media. Cell viability was significantly reduced from only 4-hour exposure to 500 μM Orlistat and an 8-hour exposure to 100 μM Orlistat (Fig. 2a). Four-hour exposure to 500 μM Orlistat decreased viability by about 65%, while 8-hour exposure to 100 μM decreased viability by about 40%. These brief exposure periods accounted for about two-thirds and one-half of the total decrease seen for cells cultured the entire 48 h in DM with 500 and 100 μM Orlistat, respectively. Addition of WM rather than DM to the NUGC-3 cell layers after 4 h exposure to 500 μM Orlistat and after 8 h exposure to 100 μM Orlistat totally rescued the cells; that is, there was no decrease in viability compared to cells cultured in the absence of Orlistat measured at 48 h (Fig. 2b). However, there were limits to the capacity of WM to rescue Orlistat exposed cell. For example, 12 h of exposure to 500 μM Orlistat in DM committed the cells to detachment and disintegration.

Orlistat toxicity likely begins with inhibition of fatty acid synthesis. Incubation of NUGC-3 cells with 200 μM Orlistat for 4 h decreased incorporation of ^{14}C -acetate into total fatty acids by about 75% (Fig. 3a). We expressed effects on fatty acid synthesis as a decrease in the ratio of incorporation of ^{14}C -acetate into fatty acid to total sterol. Since Orlistat had no effect on sterol synthesis, this

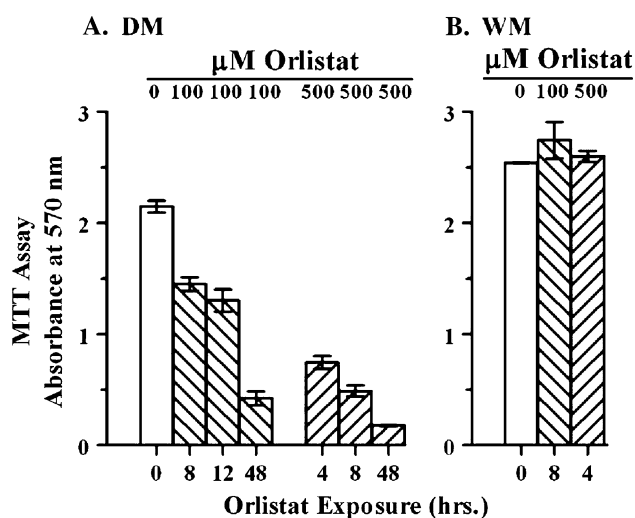


Fig. 2 Early effects of Orlistat on cell viability. **a** NUGC-3 cell layers were incubated in serum deficient media containing 0, 100 or 500 μM Orlistat. After 4, 8 or 12 h of incubation the media was replaced with Orlistat free DM and the incubation continued to hour 48 at which time cell viability was measured. Controls were cultured for 48 h in Orlistat free DM. The “48” hour groups were cells incubated with either 100 or 500 μM Orlistat-DM. **b** Controls are cells cultured for 48 h in Orlistat free WM. Cells were incubated for 4 h in DM containing 500 μM Orlistat or 8 h with 100 μM Orlistat and then switched to Orlistat free WM and the culture continued to hour 48 at which time viability was measured

expression should account for potential differences in cell numbers from well to well. Not only does Orlistat inhibit fatty acid synthesis, but also once exposed to this drug the inhibition seems permanent. Fatty acid synthesis continued to be inhibited after Orlistat was removed from the media. NUGC-3 cells were incubated for 4 h in media containing 200 μM Orlistat, the cell layers were washed and then incubated an additional 4 h in Orlistat free media containing ^{14}C -acetate. Synthesis was still inhibited by 80% (Fig. 3b). This finding supports the idea that Orlistat binds irreversibly to the thioesterase domain of FAS [8]. Up regulation of FAS expression might be a means to circumvent the near total inhibition of fatty acid synthesis; however, FAS protein levels (assessed by Western blotting) were not increased following exposure of Orlistat (data not shown). Thus, once exposed to Orlistat fatty acid synthesis appears permanently inhibited. This would make the cells dependent upon uptake of lipids from the media as the only source of fatty acids to sustain membrane turnover and cell proliferation.

As shown (Fig. 2), there was a narrow window of opportunity to rescue NUGC-3 cell from permanent injury and death when cultured in DM containing Orlistat. The response of the cells to this nutritional stress, no source of fatty acids, was extremely rapid induction of autophagy (Fig. 4). The autophagic response was Orlistat dose dependent, peaked at one-half hour of incubation and returned to baseline by 2 h. Thus, it seems unlikely that autophagy accounts for the irreversible injury and consequent cell

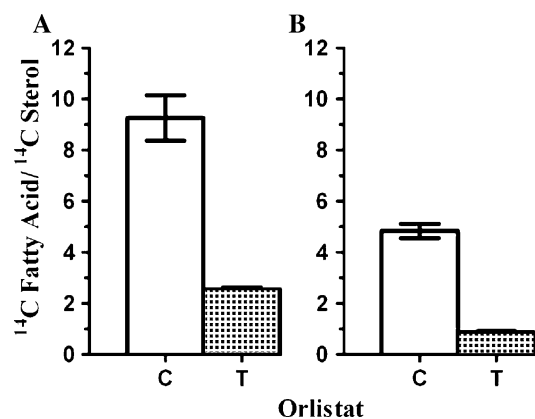
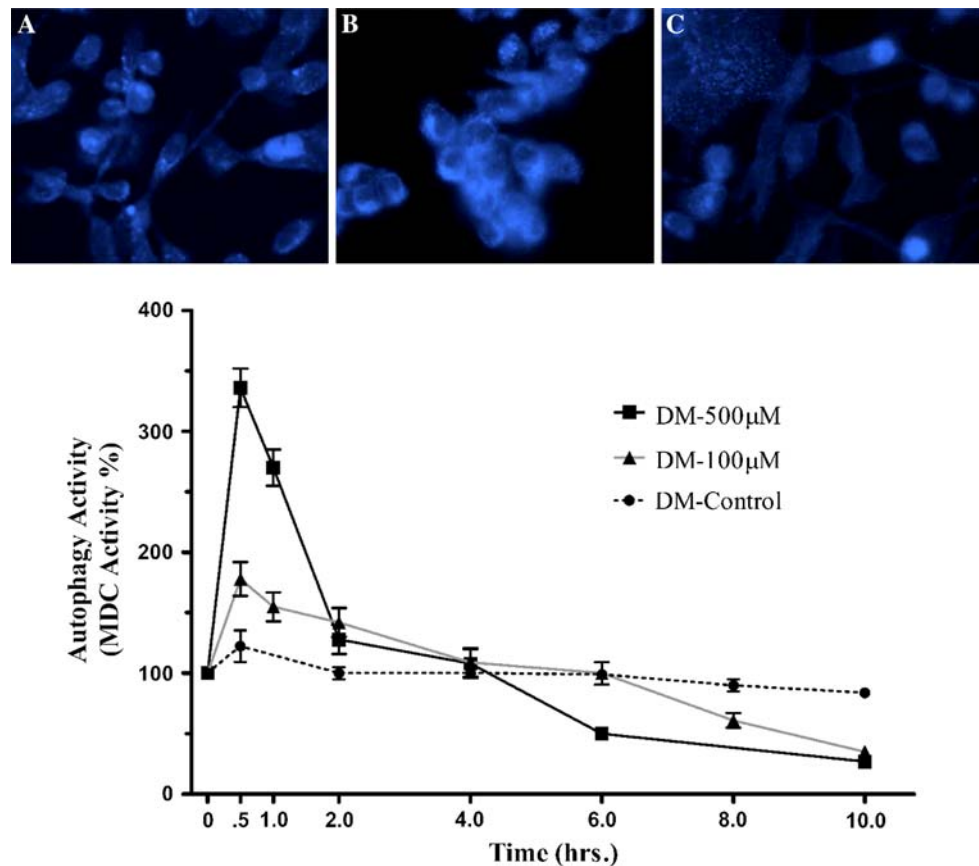


Fig. 3 Irreversible inhibition of fatty acid synthesis by Orlistat in NUGC-3 tumor cells. **a** Subconfluent cell layers in 96 well dishes were incubated for 4 h in serum free RPMI-1640 media containing 1 μCi of ^{14}C -acetate and 0 (Control C) or 200 μM Orlistat (Treated T). Total fatty acids and sterols recovered after saponification were separated by TLC, fractions isolated, the ^{14}C -content measured and results expressed as the ratio of incorporation into fatty acids to sterols. Each value is the mean \pm SEM of 5 cell layers. **b** Cell layers were incubated for 4 h with 0 or 200 μM Orlistat in the absence of ^{14}C -acetate; the media was then replaced with Orlistat free media containing the ^{14}C -acetate and incubated for a second 4-hour interval. Values are the mean \pm SEM of five cell layers

Fig. 4 Rapid induction and disappearance of the autophagic response to Orlistat. Fluorescence microscopy showing autophagic vesicles in NUGC-3 cells unexposed to Orlistat (a), exposed to 500 μ M Orlistat for 30 min (b) or 6 h (c). The graph shows the time course of autophagic response to varying concentrations of Orlistat. Values are the mean \pm SEM of 3 cell layers. Differences in cell numbers between wells normalized using ethidium bromide [21]



death seen with longer-term exposure. Rather, cell death could be due to induction of apoptosis. The onset and progression of apoptosis paralleled the loss of cell viability. Apoptosis was seen after 8 h exposure to 100 μ M Orlistat in DM (Fig. 5e), but not at 4 h (Fig. 5c). Loss of cell viability occurred after 8 but not 4 h exposure to 100 μ M (Fig. 2 a). At the higher drug concentration (500 μ M), apoptosis was evident after 4 h of incubation (Fig. 5d) and markedly increased by the 8 h of drug exposure (Fig. 5f). The progression of apoptosis over the 4–8 h interval was largely halted by exchanging the Orlistat-DM media for drug-free WM at hour four (Fig. 5g). This parallels the time-interval boundaries for rescue of NUGC-3 cell viability from exposure to 500 μ M Orlistat (Fig. 2).

Applying the information garnered from in vitro experiments, the potential of Orlistat to inhibit in vivo gastrointestinal cancer was evaluated by examining the effect of orally administered Orlistat on the survival of APC-Min mice that spontaneously develop a fatal gastrointestinal cancer. Mice were fed a high fat (11%) or low fat (1.2%) diet containing 0 or 500 mg Orlistat/kg chow. Each mouse weighed approximately 25 g and consumed an average of 3 g of chow per day, resulting in delivery of about 60 mg of Orlistat/kg body weight. The fecal fat content of Orlistat treated mice increased 4-to-6-fold

compared to untreated control mice when the animals were fed chow containing 11% fat (Table 1). In animals fed chow containing 1.2% fat, fecal fat increased about 2.5-fold in Orlistat treated mice versus untreated controls (Table 1). The increased fecal fat obviously reflects the inhibition of gastric lipases by the drug.

Orally administered Orlistat moves quickly through the GI tract. Four hours after giving a single oral 50 mg/kg dose of Orlistat (in aqueous emulsion) by gavage, the drug was detected almost exclusively in the large intestines (Fig. 6). Similar results were seen in a replicate experiment. This observation is consistent with GI transit times in the mouse being 4–6 h [25].

Considering the browsing feeding pattern of mice, the gut should receive multiple exposures to Orlistat during the day. The 500 mg of Orlistat/kg of chow corresponds to about 1 mM (MW = 497.5), a concentration in great excess of that needed to inhibit the viability of cultured, human-derived, NUGC-3 gastrointestinal cancer cells (Fig. 1). Fifty μ M Orlistat in serum deficient media (0.1% serum) and 200 μ M Orlistat in whole media (10% serum) both inhibited cell viability by about 80% (Fig. 1). Similar results were seen in replicate experiments.

Three experiments were conducted to evaluate the effect of orally administered Orlistat on survival times of the

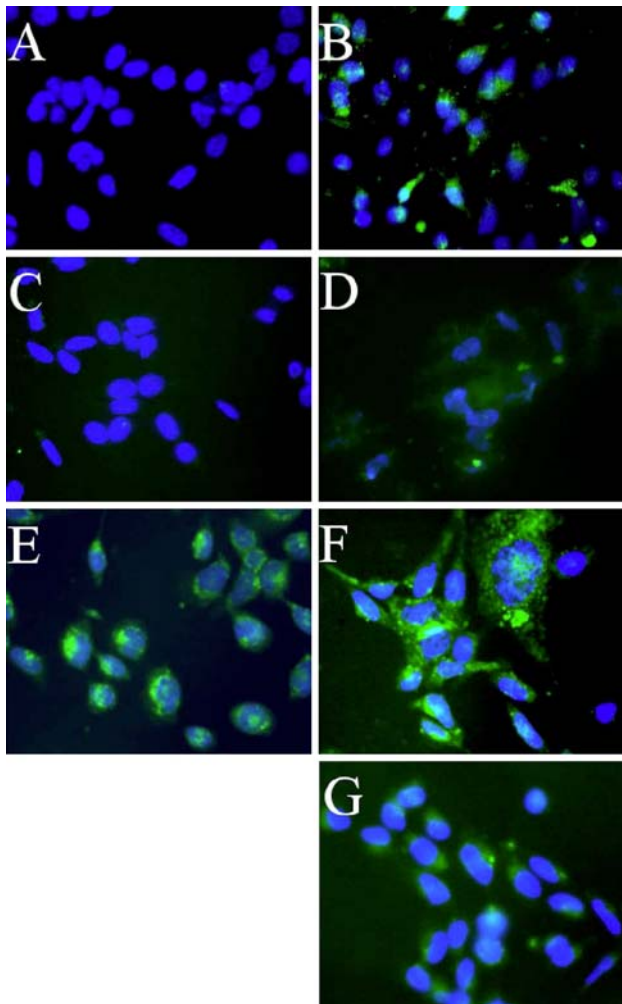


Fig. 5 Antagonism of Orlistat induced apoptosis. Images show overlap fluorescence of apoptotic caspase stained (*green*) and nucleic acid stained (*blue*) cells. All cell layers, except **b** and **g**, were incubated in DM. **a** Control. **b** Staurosporine, 500 nM in WM for 3 h. **c** Orlistat, 100 μ M for 4 h. **d** Orlistat, 500 μ M for 4 h. **e** Orlistat, 100 μ M for 8 h. **f** Orlistat, 500 μ M for 8 h. **g** Cell layers were incubated for 4 h with 500 μ M Orlistat, the media was replaced with Orlistat free WM and the incubation continued an additional 4 h. These results are representative of triplicate experiments (color figure online)

APC-min mice (Fig. 7). Median survival times were increased 7–10% (25.5 and 9 days, experiments 1 and 2, respectively) in Orlistat fed mice (Fig. 7 top and middle panels). The difference was statistically significant by the log-rank test ($P = 0.047$) and the Wilcoxon test ($P = 0.0318$) in experiment 1 and was not significant in experiment 2 (Table 2). Experiment 3, using a low fat (1.2%) diet produced no significant results (Table 2), however, control mice fed the low fat diet produced a greater median survival time than their treated counterparts (Table 1).

Table 1 Effect of Orlistat on fecal fat content and median survival times

Experiment	Group	Fecal fat content ^a (mg fat/g dry feces)	Starting age (days)	Median survival (days)
1 High fat	Control	45.3	50–60	147
	Treated	197.8		172.5
2 High fat	Control	63.7	33–40	122
	Treated	388.8		131
3 Low fat	Control	22.4	58	194.5
	Treated	52		136

^a Controls were fed diets with either 11% high fat (Experiment 1 and 2) or 1.2% low fat (Experiment 3). Treated mice received the same diet but containing 0.5 mg Orlistat/g chow. Feces was collected from the cages of the various groups

Discussion

As stated above, cancer cells can place a great demand on FAS to supply the fatty acids required for membrane turnover and cell proliferation. NUGC-3 cells cultured in serum deficient media (0.1% serum) grew as well as when cultured in media containing 10% serum, indicating that lipogenesis can sustain growth. In contrast to cancer cells, viability of a normal cell line (bovine lens epithelial) decreased by about 50% when cultured in serum deficient media, indicating a major reliance on extracellular lipids (Fig. 8). Also, the normal bovine lens epithelial cells were virtually resistant to the growth inhibition mediated by high concentrations of Orlistat in WM, indicating little reliance on fatty acid synthesis (Fig. 8). The general toxicity of Orlistat is also addressed by this data. Since the viability of lens epithelial cells cultured in WM containing no Orlistat and high levels of Orlistat (200 and 500 μ M) were similar, Orlistat has no apparent toxicity to these cultured cells independent of its effect on FAS. This would appear to also include toxicity due to inhibition of triacylglycerol lipases, the basis of its use as an anti-obesity drug [7].

Perhaps the major findings of this work are the speed with which Orlistat can insult the cultured cancer cells and the capacity of whole media to rescue the cells from this insult, at least up to a point. The rapid untoward effects are attributed to near total restriction of fatty acids due to inhibition of synthesis coupled with the absence of media lipids. Because membrane phospholipids are highly dynamic and can turnover with half-lives in the minutes [26], a block in the availability of fatty acids could rapidly compromise membrane integrity. In view of this rapid turnover and because the restriction of fatty acids constitutes nutritional stress, it is not surprising that autophagy was activated within minutes of adding Orlistat. However, it was surprising that the autophagic response was over

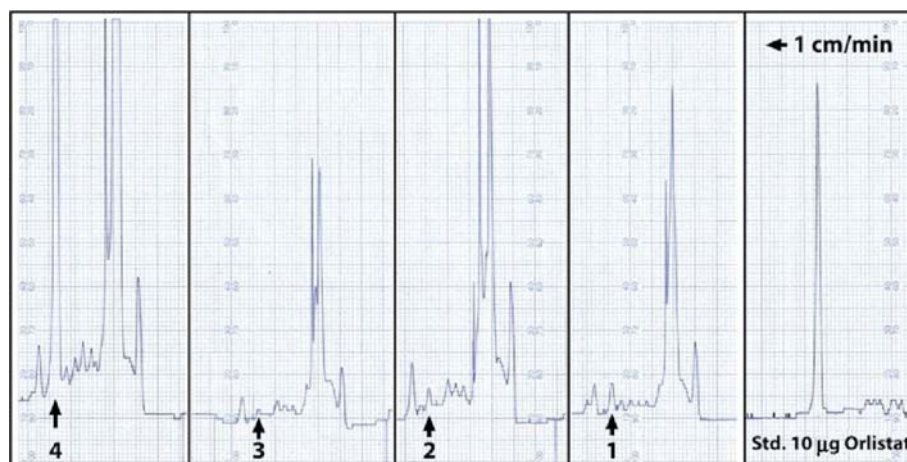


Fig. 6 Distribution of Orlistat in the gastrointestinal tract estimated by HPLC analysis. Relative concentration of Orlistat in the GI tract at 4 h after a mouse was given (by gavage) 50 mg/kg of Orlistat in aqueous emulsion. Nearly all of the drug was found in the large

intestine and colon. Similar results were seen in a replicate experiment. The Orlistat standard (10 µg injected in 100 µl) eluted at about 6 min. Zones: 1 Stomach, 2 Upper small intestine, 3 Lower small intestines, 4 Large intestines and colon

within 2 h. This could reflect that there is a limited pool of cellular substrates for the autophagic response. The extent to which the autophagy damaged the cells is unclear, but it is clear that apoptosis was activated by 4–8 h of culture, depending on the concentration of Orlistat. Early signs of apoptosis, cellular blebbing, were observed in as little as 4 h following treatment with 500 µM Orlistat substituted DM and 12 h exposure to 100 µM Orlistat substituted DM. The apoptosis is linked to the nutritional deficiency since adding a source of fatty acids to the media suppressed its progression and reversed the signs of cellular blebbing. Apparently the cells can recover, re-attain normal viability, from initiated apoptosis. However, there is clearly a threshold of apoptosis inducing cell injury beyond which the cells cannot recover.

Knowles and coworkers [9] describe in a paper that the apoptosis induced in mammary and prostate cell tumor lines by Orlistat was dependent on inhibition of FAS but independent of fatty acid availability. This paradox is explained by a pleiotropic consequence of inhibiting FAS that involves up-regulation of a stress responsive gene, DDIT4, which inhibits the mTOR pathway. Our findings with the NUGC-3 gastric tumor cells are more consistent with apoptosis arising from nutritional stress due to decreased availability of fatty acids. Addition of lipid-containing media to NUGC-3 cells exposed to Orlistat for 4 h halted progression of apoptosis over the next 4 h. Even though Orlistat was removed from the media in the second incubation, FAS continued to be inhibited (Fig. 2b). Thus, in the face of continued inhibition of FAS, whole media alone (lipids) halted apoptosis. The differences between our findings and those of Knowles et al. [9] could be related to differences in the duration of incubation with Orlistat. Eight hours exposure of NUGC-3 cells to 100 µM Orlistat

clearly induced apoptosis (Fig. 5e). Perhaps a higher level of stress develops with 24 and 48 h of continuous exposure that activated the DDIT4 initiated apoptosis. Although we used higher concentrations of Orlistat, their observations at 50 µM and ours at 100 µM should be similar. Our use of a gastric cell line may also have contributed to differences between our findings. As stated above, if Orlistat is to have a role in treating cancer it would be most likely for gastrointestinal tumors that could come in direct contact with the orally administered drug.

The greater sensitivity to inhibition of NUGC-3 cells in serum deficient media was likely due to the low lipid content of this media, since viability was greater in WM. This observation is consistent with FAS being Orlistat's target in cancer cells and Orlistat being more toxic to the cancer cells when they are wholly dependent on FAS to supply the fatty acids needed for phospholipid synthesis and, therefore, membrane formation.

Because increased cell death was seen in cultured cancer cells treated with Orlistat in DM, we applied this information to one of our in vivo experiments. Orlistat was fed in a very low fat diet in experiment 3. Animals were 58 days of age at the start. Previous work in our laboratory had showed that when added to a lipid emulsion, Orlistat partitioned into the lipid phase (data not shown). Given this result, we reasoned that Orlistat might similarly partition into the increased intestinal fat content generated by inhibition of lipases, and therefore, be less available to the tumors. Therefore, Orlistat was administered in a very low fat diet in the third experiment with the goal of enhancing drug exposure to gastrointestinal tumors. No statistically significant differences were seen between control and Orlistat treated groups (Fig. 7 bottom panel, Table 2). Although no significant difference was observed, the

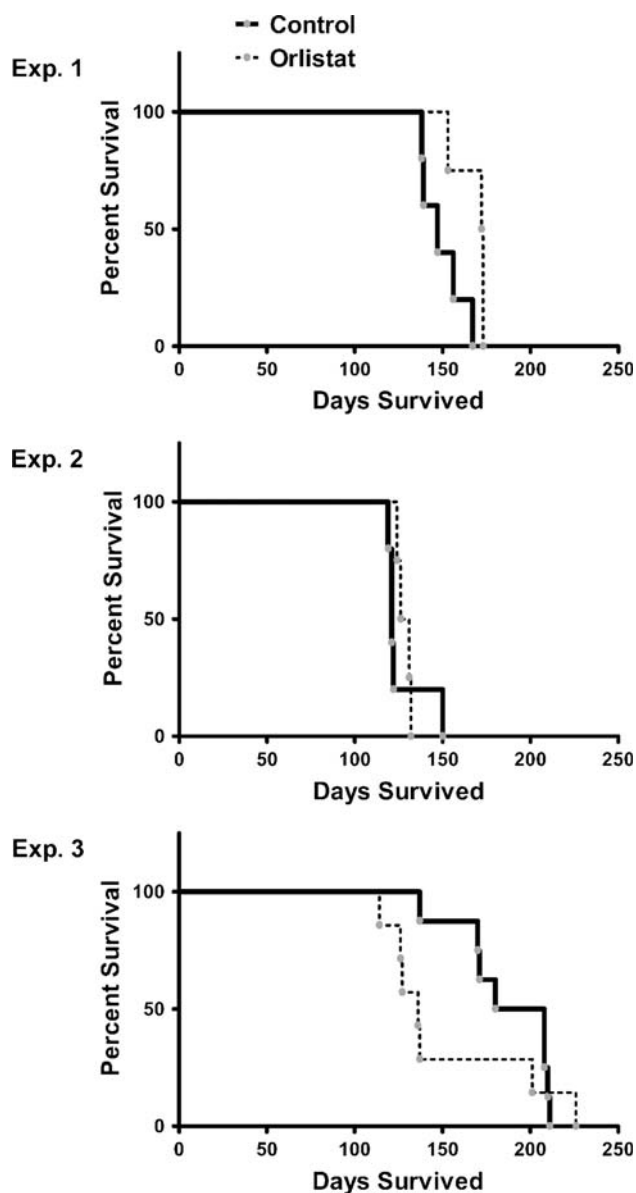


Fig. 7 Survival curves of control and Orlistat treated APC-min/+ mice. In experiments 1 and 2 mice were fed an 11% fat diet containing no Orlistat or 0.5 mg Orlistat/g chow. In experiment 3 mice were fed a 1.2% fat diet with and without 0.5 mg Orlistat/g chow

Table 2 Statistical analyses of experiments

	Experiment 1	Experiment 2	Experiment 3
Log-Rank (Mantel–Cox) Test			
Chi Square	4.609	0.3990	0.8191
P Value	0.0318	0.5276	0.3654
Gehan–Breslow–Wilcoxon Test			
Chi Square	3.938	2.201	3.530
P Value	0.0472	0.1379	0.0602

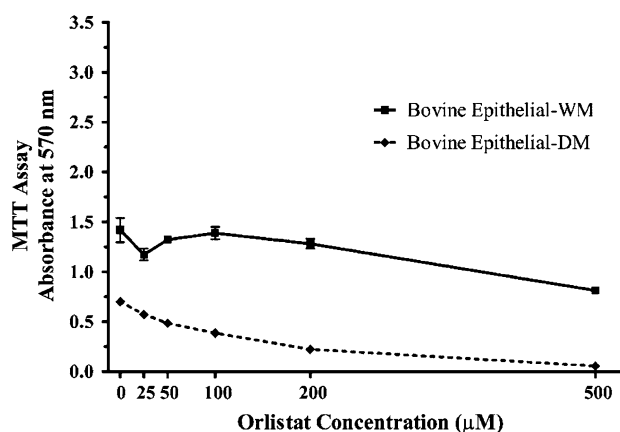


Fig. 8 Effect of Orlistat on the viability of bovine lens epithelial cells. Cells in 96 well plates were cultured for 48 h with varying concentrations of Orlistat added in either serum deficient DMEM (0.1% calf serum), DM, or DMEM containing 10% serum, WM. Cell viability was measured at hour 48 by the MTT assay. Values are mean \pm SEM of 4 wells

median survival time for untreated mice fed the low fat diet exceeded that of the Orlistat treated group. This data suggest that limiting exogenous sources of fatty acids via diet restrictions may offer potential in treating gastrointestinal cancers. However, a significant difference was seen when Orlistat was supplemented into the high fat diet. This data suggest that when supplemented into a high fat diet, Orlistat produced more beneficial results than supplemented into an already fat limited diet.

In conclusion, Orlistat appeared to slightly prolong the survival of mice with a fatal-genetic gastrointestinal cancer. There was no evidence that Orlistat accelerated death in these tumor-bearing animals. If the findings are applicable to humans, they support the idea that Orlistat inhibits this type of cancer. Long-term survival studies in rats and other mice strains are needed to further evaluate the potential of Orlistat to inhibit GI cancer.

Acknowledgments This work was funded by grants from the A.T. Still University of Health Sciences.

References

- Kuhajda FP (2006) Fatty acid synthase and cancer: new application of an old pathway. *Cancer Res* 66:5977–5980
- Kuhajda FP (2000) Fatty-acid synthase and human cancer: new perspectives on its role in tumor biology. *Nutrition* 16:202–208
- Milgraum LZ, Witters LA, Pasternack GR, Kuhajda FP (1997) Enzymes of the fatty acid synthesis pathway are highly expressed in in situ breast carcinoma. *Clin Cancer Res* 3:2115–2120
- Pizer ES, Pflug BR, Bova GS, Han WF, Udan MS, Nelson JB (2001) Increased fatty acid synthase as a therapeutic target in androgen-independent prostate cancer progression. *Prostate* 47:102–110

5. Rossi S, Graner E, Febbo P, Weinstein L, Bhattacharya N, Onody T, Bubley G, Balk S, Loda M (2003) Fatty acid synthase expression defines distinct molecular signatures in prostate cancer. *Mol Cancer Res* 1:707–715
6. Pizer ES, Chrest FJ, DiGiuseppe JA, Han WF (1998) Pharmacological inhibitors of mammalian fatty acid synthase suppress DNA replication and induce apoptosis in tumor cell lines. *Cancer Res* 58:4611–4615
7. (2006) PDR guide to drug interactions, side effects, and indications. Thomson PDR, Montvale, NJ
8. Kridel SJ, Axelrod F, Rozenkrantz N, Smith JW (2004) Orlistat is a novel inhibitor of fatty acid synthase with antitumor activity. *Cancer Res* 64:2070–2075
9. Knowles LM, Axelrod F, Browne CD, Smith JW (2004) A fatty acid synthase blockade induces tumor cell-cycle arrest by down-regulating Skp2. *J Biol Chem* 279:30540–30545
10. Menendez JA, Vellon L, Lupu R (2005) Orlistat: from anti-obesity drug to anticancer agent in Her-2/neu (erbB-2)-over-expressing gastrointestinal tumors? *Exp Biol Med* (Maywood) 230:151–154
11. Souri E, Jalalizadeh H, Kebriaee-Zadeh A, Zadehvakili B (2007) HPLC analysis of orlistat and its application to drug quality control studies. *Chem Pharm Bull (Tokyo)* 55:251–254
12. Jacoby RF, Seibert K, Cole CE, Kelloff G, Lubet RA (2000) The cyclooxygenase-2 inhibitor celecoxib is a potent preventive and therapeutic agent in the min mouse model of adenomatous polyposis. *Cancer Res* 60:5040–5044
13. Chiu CH, McEntee MF, Whelan J (1997) Sulindac causes rapid regression of preexisting tumors in Min/+mice independent of prostaglandin biosynthesis. *Cancer Res* 57:4267–4273
14. Moser AR, Dove WF, Roth KA, Gordon JI (1992) The Min (multiple intestinal neoplasia) mutation: its effect on gut epithelial cell differentiation and interaction with a modifier system. *J Cell Biol* 116:1517–1526
15. Taketo MM (2006) Mouse models of gastrointestinal tumors. *Cancer Sci* 97:355–361
16. Hitchener WR, Cenedella RJ (1985) Absolute rates of sterol synthesis estimated from [³H]water for bovine lens epithelial cells in culture. *J Lipid Res* 26:1455–1463
17. Carmichael J, DeGraff WG, Gazdar AF, Minna JD, Mitchell JB (1987) Evaluation of a tetrazolium-based semiautomated colorimetric assay: assessment of chemosensitivity testing. *Cancer Res* 47:936–942
18. Sexton PS, Neely AR, Cenedella RJ (2004) Distribution of caveolin-1 in bovine lens and redistribution in cultured bovine lens epithelial cells upon confluence. *Exp Eye Res* 78:75–82
19. Biederbick A, Kern HF, Elsasser HP (1995) Monodansylcadaverine (MDC) is a specific in vivo marker for autophagic vacuoles. *Eur J Cell Biol* 66:3–14
20. Munafo DB, Colombo MI (2001) A novel assay to study autophagy: regulation of autophagosome vacuole size by amino acid deprivation. *J Cell Sci* 114:3619–3629
21. Darzynkiewicz Z, Bedner E, Smolewski P, Lee BW, Johnson GL (2002) Detection of caspases activation in situ by fluorochrome-labeled inhibitors of caspases (FLICA). *Methods Mol Biol* 203:289–299
22. Grabarek J, Amstad P, Darzynkiewicz Z (2002) Use of fluorescently labeled caspase inhibitors as affinity labels to detect activated caspases. *Hum Cell* 15:1–12
23. Daniel WW (2005) Biostatistics: a foundation for analysis in the health sciences. Wiley, Hoboken, NJ
24. Akiyama S, Amo H, Watanabe T, Matsuyama M, Sakamoto J, Imaizumi M, Ichihashi H, Kondo T, Takagi H (1988) Characteristics of three human gastric cancer cell lines, NU-GC-2, NU-GC-3 and NU-GC-4. *Jpn J Surg* 18:438–446
25. Garcia SB, Barros LT, Turatti A, Martinello F, Modiano P, Ribeiro-Silva A, Vespucio MV, Uyemura SA (2006) The anti-obesity agent Orlistat is associated to increase in colonic preneoplastic markers in rats treated with a chemical carcinogen. *Cancer Lett* 240:221–224
26. Hao M, Maxfield FR (2000) Characterization of rapid membrane internalization and recycling. *J Biol Chem* 275:15279–15286

Over-expression of the Anti-apoptotic Protein Bcl-2 Affects Membrane Lipid Composition in HL-60 Cells

Catherine Cantrel · Alain Zachowski ·
Blandine Geny

Received: 1 October 2008 / Accepted: 12 February 2009 / Published online: 12 March 2009
© AOCs 2009

Abstract We studied modifications induced at the membrane lipid level by over-expression of the anti-apoptotic protein Bcl-2. When total cell phospholipids were analyzed, the transformation led to a moderate decrease in poly-unsaturated fatty acids, compensated by an increase in mono-unsaturated species. At the mitochondrial membrane level, the changes were more important and occurred in saturated and dimethyl acetal fatty acids, which became more abundant, while unsaturated fatty acid content diminished. This indicates a decline in oxidation-sensitive fatty acids (unsaturated species) together with a gain in oxidation-insensitive saturated fatty acids and in plasmalogen (as detected by dimethyl acetal fatty acids) considered as oxygen species scavengers. These changes, combined with the protective role of Bcl-2 against oxidation due to its effect on the redox potential, should protect cells from apoptosis starting in mitochondria.

Keywords Bcl-2 · Fatty acid species · Phospholipids · Mitochondrion · Plasmalogens · Cardiolipin

Abbreviations

ADP	Adenosine 5'-diphosphate
ANT-1	Adenine nucleotide translocase-1
ATP	Adenosine 5'-triphosphate
BSA	Bovine serum albumin
C:16	16 Carbon-long fatty acids
C:18	18 Carbon-long fatty acids
DMA	Dimethylacetal
EDTA	Ethylenediaminetetraacetate
FA	Fatty acid
GLC	Gas liquid chromatography
HRP	Horse radish peroxidase
MUFA	Mono-unsaturated fatty acid
NADPH	β -Nicotinamide adenine dinucleotide phosphate, reduced
PBS	Phosphate buffered saline
PtdCho	Phosphatidylcholine
PtdEtn	Phosphatidylethanolamine
PtdIns	Phosphatidylinositol
PtdSer	Phosphatidylserine
PKC	Protein kinase C
PUFA	Poly-unsaturated fatty acid
SFA	Saturated fatty acid
TLC	Thin layer chromatography
TMRM	Tetramethylrhodamine methyl ester

Electronic supplementary material The online version of this article (doi:10.1007/s11745-009-3292-8) contains supplementary material, which is available to authorized users.

C. Cantrel · A. Zachowski
Physiologie Cellulaire et Moléculaire des Plantes,
UPMC Univ Paris 06, UR 5, 75005 Paris, France

B. Geny
Département de Microbiologie, Institut Pasteur,
Unité des Bactéries Anaérobies et Toxines,
25 rue du Docteur Roux, 75015 Paris, France

A. Zachowski (✉)
Physiologie Cellulaire et Moléculaire des Plantes,
UR 5, Université Pierre et Marie Curie, 3 rue Galilée,
94200 Ivry-sur-Seine, France
e-mail: alain.zachowski@upmc.fr

Introduction

The lipid composition of membranes directly affects their physical properties that are, among other roles, important

for the cell structure. It is well established that the fatty acid composition of phospholipids plays a role in membrane packing and lipid-protein interaction in the bilayer [1–5]. Thus, membrane curvature, cell deformation, vesicle formation and membrane fusion are dependent on the lipid composition of each membrane compartment [6–8]. Moreover, several lipids and lipid metabolites are involved in signaling pathways in response to various stimuli [9]. Modification in fatty acid and phospholipid composition can affect membrane association of extrinsic proteins, including some involved in signal transduction [10, 11]. Thus, both structural and signaling properties of lipids are involved in control of cell functions, such as proliferation, endocytosis, exocytosis, polarity, migration, or cell death by apoptosis [12–15].

The oncogene bcl-2 was first identified on the basis of its involvement in B cell malignancies where chromosomal translocation t(14;18) activates bcl-2 in many human B-cell lymphomas [16]. This protein is present in several membrane compartments, in particular in the outer membrane of mitochondria [17–20] and possesses an ion channel activity [21]. Its role as a blocker of apoptotic cell death is to maintain the integrity of the mitochondrial barrier by preventing its nonspecific permeabilization [22, 23]. However, Bcl-2 would maintain the exchange of small molecules including ATP, ADP, NADPH, and thus, normal mitochondrial functions (see reviews [24, 25]). Most of Bcl-2 effects were confirmed by gene transfer experiments in various cell types. Bcl-2 over-expression blocks cell death generated in a wide variety of cells by various agents, including growth factor withdrawal, cytotoxic lymphokines, virus infection, DNA damage, anticancer drug and radiation. However, it has no protective effect on programmed cell death induced by other stimuli [26].

So far, only a few studies have dealt with the effect of Bcl-2 expression on lipids (e.g. [27]) although the role of lipids in maintaining membrane integrity is essential. However, it is well established that apoptosis is accompanied by exposure of phosphatidylserine at the cell surface as assessed by annexin V binding to plasma membrane, a modification used for apoptosis measurement [28].

In the present study, we investigated whether a change in Bcl-2 expression could have an effect on membrane phospholipid distribution or on fatty acid species associated with phospholipids in HL-60 cells.

Materials and Methods

Materials

RPMI-1640, antibiotics and glutamine were purchased from Gibco BRL. Fetal bovine serum was from Dutcher.

All inorganic solvents were obtained from VWR and were of analytical grade.

Silica gel 60A plates (20 × 20 cm) for thin layer chromatography (TLC) were obtained from Merck and the fused-silica capillary column (50 m × 0.32 mm) used for GLC came from SGE.

Mouse monoclonal antibodies recognizing a human 65-kDa mitochondrial protein (mAB 1273), Bcl-2 (clone 7) and porin (clone 31HL) were purchased from Chemicon, BD Transduction laboratories and Calbiochem, respectively; rabbit polyclonal antibodies against adenine nucleotide translocase-1 (ANT-1) were from Oncogene Research products. HRP conjugated secondary antibodies to mouse and rabbit IgG were purchased from Cellular Signaling and anti-mouse IgG conjugated with fluorescein was from Cappel. Antibodies were used at the dilution indicated by the manufacturer. Tetramethylrhodamine methyl ester (TMRM) was obtained from Molecular Probes Europe BV.

Methods

Cell Culture and Cell Treatments with Agents

A stable clone of HL-60 cells transfected with the empty vector (neo) and a HL-60 clone over-expressing Bcl-2 were obtained from Dr. M. Allouche (Toulouse, France) and cultured in the presence of G418 (0.5 mg/ml) as reported [29]. Both clones were cultured in suspension in RPMI-1640 medium containing 10% fetal bovine serum, 2% L-glutamine, 1% penicillin-streptomycin and 1% G418 to maintain the gene selection at 37 °C in a humidified incubator containing 5% CO₂.

Purification of Mitochondria

Mitochondria from the two clones of HL-60 cells (see above) were purified according to Susin et al. [30]. Briefly, two to three liters of cells at confluency ($2\text{--}3 \times 10^9$ cells) were centrifuged, washed three times with ice-cold PBS and resuspended in cold homogenization buffer made of 300 mM saccharose, 5 mM Tris(hydroxymethyl)methyl-2-aminomethanesulfonic acid (TES), 0.2 mM EDTA, pH7.2, and containing a cocktail of protease inhibitors (complete mini tablets (Roche)). All the subsequent steps were performed at 4 °C. Cells were homogenized in a Potter homogenizer and the homogenate was centrifuged for 10 min at 800 g to remove nuclei. The supernatant was centrifuged for 10 min at 9,000g. After centrifugation, the pellet was recovered and resuspended in 1 ml of the homogenization buffer, put on the top of a discontinuous Percoll-saccharose gradient made of equal volumes of 60%, 30%, and 15% Percoll solutions, and centrifuged for

10 min at 9,000g. Mitochondria at the lower interface (between 60 and 30% Percoll) were recovered with a syringe, diluted 10 times in a buffer made of 10 mM MOPS-KOH, 10 mM KCl, 1 mM EDTA, pH 7.3, and centrifuged. The pellet of purified mitochondria was resuspended in 0.7 ml and lipids were then extracted as described below after removal of an aliquot kept for protein analysis.

Protein Analysis by SDS-PAGE and Immunoblotting

The amount of three mitochondrial proteins, namely Bcl-2, ANT-1 and porin, was measured in purified mitochondria from neo and Bcl-2 over-expressing HL-60 cells. Equal amounts of mitochondrial proteins purified from the two clones were loaded on a polyacrylamide gel (PAGE) and analyzed by SDS-PAGE. Samples separated by SDS-PAGE were transferred to nitrocellulose membrane (Hybond™ C-extra, Amersham) and blocked in phosphate-buffered saline containing 0.1% Tween 20 (PBST) and 5% BSA and incubated with primary antibodies diluted in PBST for 1 h at room temperature then washed 5 times for 10 min and incubated for 1 h at room temperature with species-matched HRP-conjugated secondary antibody diluted in PBST. After membrane washing in PBST, the specific signal was detected by enhanced chemiluminescence (ECL kit; Pierce). Quantitation of immunoblots was performed using a densitometer (Fuji-system) and expressed as mean \pm SD of three experiments.

Flow Cytometry Analysis

Flow cytometry was used to analyze cell size and to measure mitochondrial membrane potential in living cells using tetramethylrhodamine methyl ester (TMRM), as described in [31].

Analysis of Mitochondrial Density and Morphology by Immunofluorescence

Cells were fixed at room temperature with 3% paraformaldehyde (PFA) for 20 min and incubated in a solution of NH_4Cl (50 mM) containing 10 mM CaCl_2 and 10 mM MgCl_2 for 10 min. After several washes with PBS, cells were permeabilized with Triton X-100 (0.5% final) for 5 min. The primary antibody, diluted in PBS containing 0.5% BSA, was then incubated for 1 h with cells and after several washes, the fluorescent-labeled secondary antibody was incubated for 30 min with cells at the required dilution. After cell washing, samples were mounted in Mowiol and observed with a confocal laser scanning microscope (BioRad MRC-100) attached to a diaphot 300 microscope (Nikon). Using the Metamorph analysis program, the number of mitochondrial structures, their size and intensity

of fluorescence were measured on 7 cell pictures acquired using the same parameters.

Lipid Extraction, Preparation of Total Phospholipid Extract, Separation of Phospholipid Classes and Fatty Acid Analysis by Gas Chromatography

Cells (1.20×10^8) were initially washed three times in PBS containing 0.1 mM EDTA, and resuspended in the same medium at a density of 40×10^6 cells/ml. Lipids were then extracted according to Folch et al. [32] and separated on silica gels plates by 2-D thin layer chromatography (TLC) developed by chloroform/methanol/ammonia 28% (65/25/5 v/v/v) (first dimension), and chloroform/methanol/acetone/acetic acid/water, (50/10/20/10/4, v/v/v/v/v) (second dimension) [33]. The spots of lipid were visualized by iodine vapor (supplemental Fig. 1) and phospholipid spots were scraped off. As the PtdSer and PtdIns spots were very frequently overlapping, these two phospholipids were treated as a whole. Phospholipids were then transmethylated by methanol/sulfuric acid (97.5/2.5) at 70 °C for 60 min [34]. FA methyl esters were then analyzed by fused-silica capillary column (50 m \times 0.32 mm) coated with carbowax 20 M on GLC (Model 3300; Varian). Quantitative analysis of fatty acid methyl esters was carried out using methylheptadecanoate (C17) as an internal standard introduced before transmethylation reaction. Capillary GLC allows a good separation of DMAs and FA isomers, particularly of long chain polyunsaturated FAs. A similar protocol was used to analyze lipids from purified mitochondria.

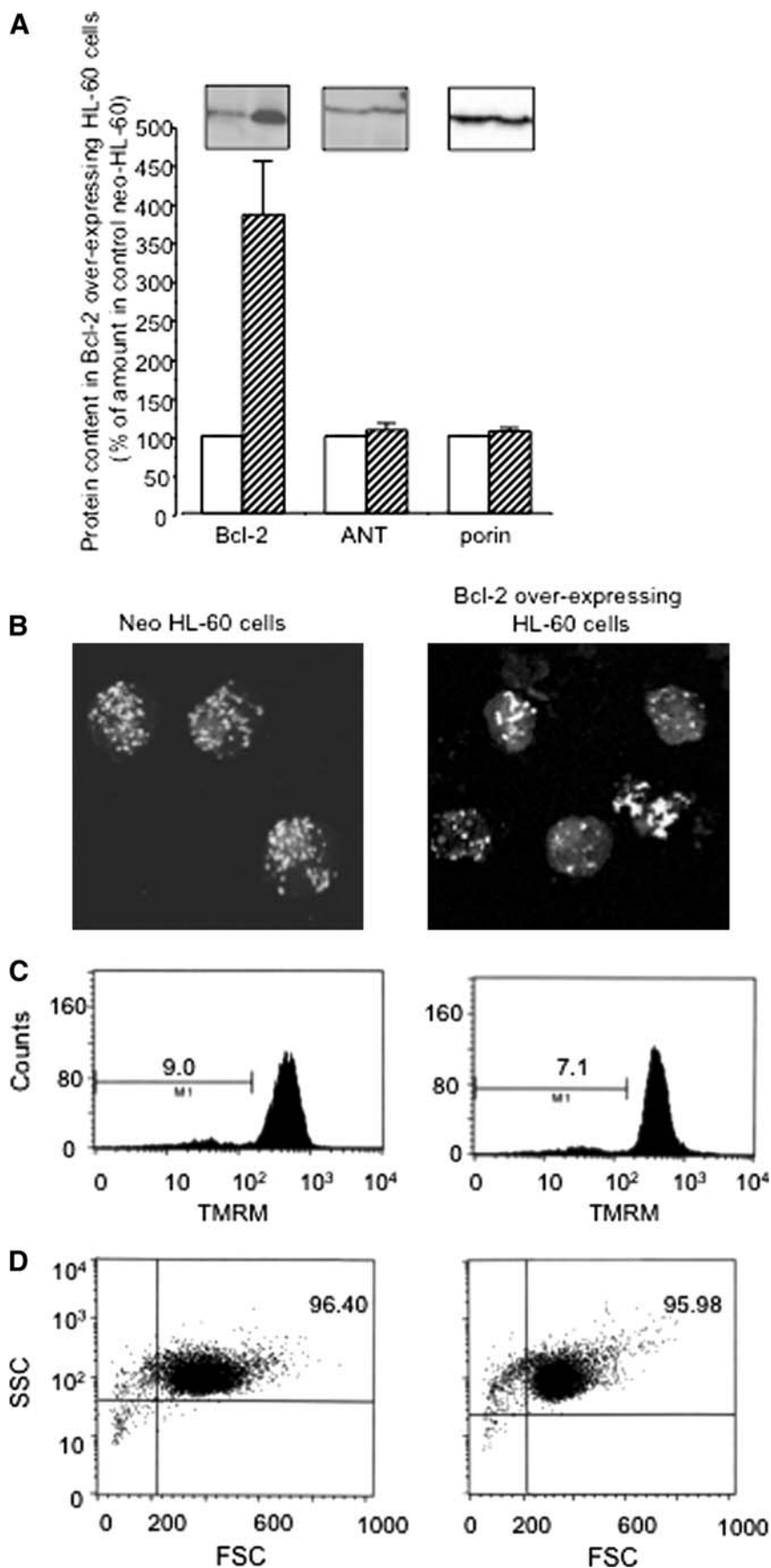
Statistical Analysis

The values are expressed as weight per cent of the total FAs \pm SD. Statistical differences between Neo HL-60 cells and Bcl-2 over-expressing HL-60 cells were calculated by the Student *t* test applied to unpaired samples, **P* < 0.05.

Results

The effect of Bcl-2 over-expression in an established HL-60 clone was initially checked by studying a few characteristics of mitochondria. Firstly, the amount of this anti-apoptotic mitochondrial protein as well as that of two other mitochondrial proteins, ANT-1 (located in the internal membrane) and porin (also called voltage-dependent anion channel and located in the external membrane), were measured in Bcl-2 over-expressing HL-60 cells and compared to those present in neo HL-60 cells. As reported in Fig. 1a, the Bcl-2 over-expressing HL-60 cells contained

Fig. 1 Modifications at mitochondrion level and of cell size induced by Bcl-2 over-expression. Mitochondria from HL-60 cells over-expressing or not Bcl-2 were analyzed for different parameters. **a** Bcl-2, ANT-1 and porin levels were measured in purified mitochondria from neo (*empty bars*) and from Bcl-2 over-expressing HL-60 cells (*stripped bars*). **b** Neo and Bcl-2 over-expressing HL-60 cells were examined by confocal immunofluorescence microscopy after fixation with PFA followed by staining with a mouse monoclonal antibody to mitochondria (mAB 1273) and revealed with a secondary antibody labeled with FITC. **c** Mitochondrial membrane potential ($\Delta\Psi_m$) was measured with tetramethylrhodamine methyl ester (TMRM) as described in [31]. **d** Cell size was measured by forward scatter (FSC)



4 times more Bcl-2 than neo-HL-60 cells. In contrast, no modification in the amount of ANT or porin was observed between both clones indicating that over-expression of Bcl-2 did not induce major changes in the amounts of other well known proteins of the mitochondrion. Cell content in mitochondria and morphology of these organelles were then studied in both clones, using an antibody (mAB1273) against a 65-kDa mitochondrial protein. As observed in Fig. 1b, the number of mitochondria in Bcl-2 over-expressing cells was lower than in neo cells, 45 ± 24 and 69 ± 28 , respectively. Mitochondria were bigger in Bcl-2 over-expressing cells than in neo-HL-60 cells (36.2 ± 18.9 and 15.8 ± 6.2 surface units, respectively). Moreover, intensity of fluorescence of these organelles was increased in Bcl-2 over-expressing cells (9462 ± 5825 arbitrary units) compared to that in Neo cells (2315 ± 442). All data on mitochondria analysis in neo and Bcl-2 over-expressing cells are expressed as means \pm SD (number of cells studied = 7). All these observations on mitochondria suggest that a high level of Bcl-2 might modify mitochondrial membranes. Whether Bcl-2 over-expression could have an impact on mitochondrial membrane potential was then explored. As shown in Fig. 1c, over-expression of the anti-apoptotic Bcl-2 protein does not modify the cell mitochondrial membrane potential ($\Delta\Psi_m$) as only 9% and 7% of control and Bcl-2 over-expressing cells, respectively, exhibited a low $\Delta\Psi_m$. As observed by flow cytometry analysis, cells over-expressing Bcl-2 were slightly smaller than neo HL-60 cells (Fig. 1d). In the HL-60 cell-line used to establish both Bcl-2 and neo clones, cells of different sizes were present, thus, the difference in cell size observed between the two clones could be due to their clonal origin. Bcl-2 is well established to play a role in cell survival (for a review, see [35]) and its over-expression together with that of c-myc has been shown to initiate proliferation [36]. Therefore, cell growth was measured in the two clones. As shown in Fig. 2, no obvious difference was observed in the growth curves between neo-HL-60 cells and Bcl-2 over-expressing cells cultured in the same conditions. Through these characteristics, concerning cell growth, mitochondrion protein expression (except, as expected, that of Bcl-2) and mitochondrial morphology and function, no gross differences could be detected between the two clones.

Lipids are known to play an important role in membrane stability and in various signaling pathways. Membrane content in proteins often modifies lipid composition. Thus, we analyzed the fatty acid composition of total phospholipid content in neo and Bcl-2 over-expressing HL-60 cells. Phospholipids present in membranes were separated by two-dimensional thin layer chromatography and the respective percentage of each phospholipid was estimated. Then, fatty acid composition of each major phospholipid

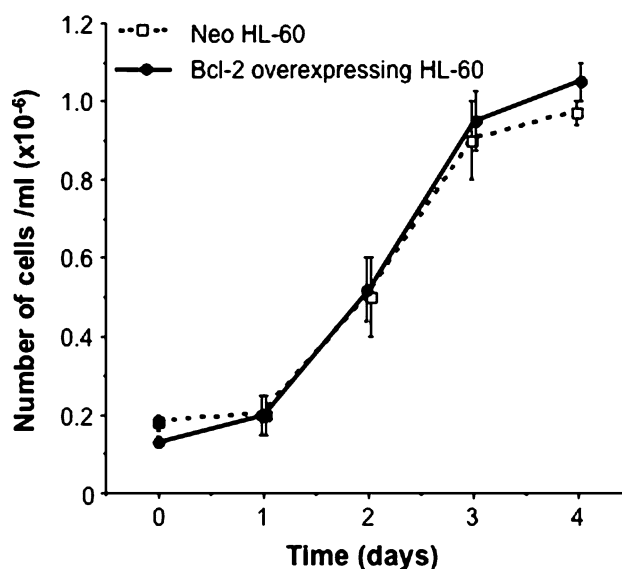


Fig. 2 Cell growth curves of neo and Bcl-2 over-expressing HL-60 cells. On day 0, cells were diluted in RPMI 1640 medium supplemented with 10% FCS and the number of cells/ml was counted in 3 different samples. Cells were then counted every day before being diluted on day 4. Data represent the means \pm SD of three different experiments

class was analyzed. To determine whether specific changes would occur at the level of mitochondrial membranes, we purified these organelles from the two clones and subsequently the same FA composition analysis of total lipids and specific phospholipid classes were performed.

As reported in Table 1, no drastic change in the whole cell content of fatty acids was observed between HL-60 cells transfected with the empty vector or with the vector containing the bcl-2 gene. However, mono-unsaturated fatty acid (MUFA) content appeared to be slightly higher in cells over-expressing Bcl-2 than in neo cells, at the expense of polyunsaturated fatty acids (PUFAs). Amongst the polyunsaturated fatty acids detected, arachidonate, which is the most abundant, appeared to be the most affected representing 8% of total fatty acids in neo HL-60 cells and only about 3% in cells over-expressing Bcl-2. The change in the MUFA vs. PUFA ratio that occurred in the Bcl2 overexpressor is consistent with what was reported in a human keratinocyte cell line [27]. However, in this latter case, the amount of saturated fatty acids (SFAs) also decreased, so that the unsaturation index of the surexpressor cell was slightly increased (from 129.6 to 138.5). In our cell system, the amount of SFAs did not change in the total cell extract, and the decrease in PUFAs led to a decrease of the unsaturation index (from 118.3 to 93.8).

In purified mitochondria, the most significant changes in total lipid composition due to Bcl-2 over-expression were an increase in the percentage of saturated fatty acids, in particular that of 16:0, and a decrease mostly in PUFAs. In

Table 1 Fatty acid species in phospholipids from HL-60 cells transfected with empty vector (neo cells) and with bcl-2 gene (Bcl-2 over-expressing cells), and from their mitochondria

Fatty acid species	Lipids from total cell extracts		Lipids from purified mitochondria	
	Neo cells (<i>n</i> = 4) Mean ± SD	Bcl-2 over-expressing cells (<i>n</i> = 4) Mean ± SD	Neo cells (<i>n</i> = 3) Mean ± SD	Bcl-2 over-expressing cells (<i>n</i> = 3) Mean ± SD
14:0	2.55 ± 0.67	4.34 ± 0.44*	2.12 ± 0.54	3.35 ± 1.04
14:1	0.13 ± 0.01	0.18 ± 0.06	0.11 ± 0.02	0.51 ± 0.05*
16 DMA	2.79 ± 1.36	2.82 ± 0.80	1.25 ± 0.12	1.76 ± 0.15
16:0	23.50 ± 1.14	21.53 ± 0.70	16.68 ± 1.85	22.14 ± 2.25
16:1(n-9 + n-7)	6.98 ± 0.99	11.89 ± 1.59*	12.86 ± 1.04	10.27 ± 0.90
18 DMA	0.38 ± 0.66	0.47 ± 0.82	0.59 ± 0.04	2.83 ± 1.03
18:0	12.92 ± 1.10	13.10 ± 1.45	14.40 ± 1.52	16.77 ± 1.63
18:1(n-9 + n-7)	30.21 ± 4.71	33.19 ± 3.36	33.84 ± 2.85	30.61 ± 2.15
18:2n-6	1.53 ± 1.06	0.91 ± 0.69	4.75 ± 1.04	2.95 ± 0.90
18:3	0.09 ± 0.08	ND	0.70 ± 0.40	2.05 ± 0.16*
20:0	0.14 ± 0.24	0.09 ± 0.15	0.20 ± 0.01	ND
20:1n-9	0.40 ± 0.14	0.63 ± 0.54	0.82 ± 0.25	0.27 ± 0.20
20:3 (n-9 + n-6)	2.56 ± 1.57	2.26 ± 0.73	ND	ND
20:4n-6	8.01 ± 3.19	3.29 ± 0.97	6.22 ± 1.04	2.95 ± 0.95
20:5n-3	0.99 ± 0.86	0.82 ± 0.20	0.95 ± 0.35	0.44 ± 0.23
22:4n-6	0.19 ± 0.16	0.29 ± 0.31	ND	ND
24:1n-9	1.48 ± 0.16	0.25 ± 0.22*	2.10 ± 0.55	2.21 ± 0.84
22:6n-3	3.69 ± 1.14	2.09 ± 0.94	0.15 ± 0.16	ND
24:0	ND	0.16 ± 0.15	0.19 ± 0.20	ND
22:5n-3	1.63 ± 0.83	1.62 ± 0.35	2.67 ± 0.25	2.56 ± 0.30
Fatty acid composition				
Saturated fatty acids (%)	39.11	39.22	33.59	42.26
Mono-unsaturated fatty acids (%)	39.20	46.14	49.00	43.87
Poly-unsaturated fatty acids (%)	18.60	11.28	15.44	8.39
DMA fatty acids (%)	3.17	3.29	1.84	5.59

Lipids were extracted from whole cells and purified mitochondria preparations of HL-60 cells transfected either with the empty vector (neo cells) or with the bcl-2 gene (Bcl-2 over-expressing cells). Fatty acid composition of lipids were analyzed by capillary GLC as described in Materials and Methods. The values are expressed as weight per cent of the total FAs ± SD

* Significantly different from control cells with $P < 0.05$

Table 2 Phospholipid species in lipids extracted from HL-60 cells transfected with empty vector (neo cells) and with bcl-2 gene (Bcl-2 over-expressing cells) and from their mitochondria

Phospholipid species	Lipids from total cell extracts		Lipids from purified mitochondria	
	Neo HL-60 cells (<i>n</i> = 4) Mean ± SD	Bcl-2 over-expressing HL-60 cells (<i>n</i> = 4) Mean ± SD	Neo HL-60 cells (<i>n</i> = 3) Mean ± SD	Bcl-2 over-expressing HL-60 cells (<i>n</i> = 3) Mean ± SD
Phosphatidylcholine (%)	53.49 ± 2.66	63.69 ± 5.47	48.33 ± 2.15	44.29 ± 2.52
Phosphatidylethanolamine (%)	24.31 ± 2.11	20.67 ± 2.31	20.12 ± 0.55	21.93 ± 1.62
Phosphatidylinositol (%)	14.32 ± 1.78	12.03 ± 2.98	5.87 ± 0.15	9.98 ± 1.75*
Cardiolipin (%) (Diphosphatidylglycerol)	7.77 ± 1.00	3.81 ± 0.97*	26.61 ± 0.56	23.79 ± 5.38

After lipid extraction from whole cell and purified mitochondria preparations of HL-60 cells transfected either with the empty vector (neo cells) or with bcl-2 gene (Bcl-2 over-expressing cells), phospholipids were separated on silica gel plates by 2-D thin layer chromatography as described in the Methods section. The amount of each phospholipid is expressed as a percentage of the total phospholipids ± SD

* Significantly different from control cells with $P < 0.05$

Table 3 Fatty acid species in phosphatidylcholine (PtdCho) from HL-60 cells transfected with empty vector (neo cells) and with bcl-2 gene (Bcl-2 over-expressing cells), and from their mitochondria

Fatty acid species	PtdCho from total cell extracts		PtdCho from purified mitochondria	
	Neo cells (<i>n</i> = 3) Mean ± SD	Bcl-2 over-expressing cells (<i>n</i> = 3) Mean ± SD	Neo cells (<i>n</i> = 3) Mean ± SD	Bcl-2 over-expressing cells (<i>n</i> = 3) Mean ± SD
14:0	4.90 ± 0.61	7.17 ± 0.98	3.14 ± 0.19	5.48 ± 0.74
14:1	0.21 ± 0.21	0.91 ± 0.72	0.23 ± 0.20	0.24 ± 0.10
16 DMA	0.85 ± 0.75	0.88 ± 0.61	0.82 ± 0.16	1.36 ± 0.03*
16:0	32.45 ± 4.60	27.81 ± 1.24	24.72 ± 0.27	28.48 ± 2.20
16:1(n-9 + n-7)	10.29 ± 1.05	17.47 ± 0.95*	14.11 ± 0.29	17.90 ± 2.54
18 DMA	0.12 ± 0.19	0.06 ± 0.13	0.33 ± 0.03	1.51 ± 0.23*
18:0	5.83 ± 2.24	7.47 ± 0.77	8.14 ± 0.35	8.56 ± 0.48
18:1(n-9 + n-7)	36.54 ± 3.98	33.34 ± 2.58	37.88 ± 0.05	29.79 ± 2.99*
18:2n-6	1.84 ± 0.53	1.00 ± 0.46	3.65 ± 0.02	2.21 ± 0.72
18:3	ND	0.12 ± 0.12	0.27 ± 0.02	ND
20:0	0.06 ± 0.08	0.16 ± 0.03	0.20 ± 0.01	ND
20:1n-9	1.19 ± 0.94	0.83 ± 0.18	0.95 ± 0.03	1.79 ± 0.32*
20:3 (n-9 + n-6)	0.78 ± 0.76	0.59 ± 0.38	ND	ND
20:4n-6	2.64 ± 0.72	0.42 ± 0.30*	3.27 ± 0.06	0.22 ± 0.23
20:5n-3	0.72 ± 0.50	0.28 ± 0.48	0.47 ± 0.03	ND
22:4n-6	ND	ND	0.04 ± 0.05	ND
24:1n-9	ND	0.15 ± 0.14	0.12 ± 0.02	2.42 ± 1.66
22:6n-3	1.98 ± 1.94	0.63 ± 0.51	0.15 ± 0.02	ND
24:0	ND	0.20 ± 0.19	1.30 ± 0.09	ND
22:5n-3	0.15 ± 0.35	0.11 ± 0.14	ND	ND
Fatty acid composition				
Saturated fatty acids (%)	43.24	42.81	37.52	42.52
Mono-unsaturated fatty acids (%)	48.23	52.70	53.29	52.14
Poly-unsaturated fatty acids (%)	8.11	3.35	7.90	2.43
DMA fatty acids (%)	0.97	0.94	1.15	2.87

After separation of phospholipids by TLC followed by their transmethylation as described in the Methods section, Fatty acid composition of phosphatidylcholine was analyzed by capillary GLC. The values are expressed as weight per cent of the total FAs ± SD

* Significantly different from control cells with $P < 0.05$

addition, DMA fatty acids, derived from plasmalogens by methanolysis, were increased by a factor 3 in Bcl-2 over-expressing mitochondria, whereas they were not modified in total lipid cell extracts.

As shown in Table 2, in lipid cellular extracts, Bcl-2 over-expression induced an increase in the percentage of PtdCho to the detriment of the other classes. Moreover, it is normal that the percentage of cardiolipin, a specific lipid of mitochondria, was limited in these extracts. In contrast, it represents about a quarter of the total lipid content in purified mitochondria from neo and Bcl-2 over-expressing cells (Table 2).

To investigate whether changes observed in the fatty acid composition of Bcl-2 over-expressing cells concern all phospholipids, fatty acid compositions of the three major phospholipid spots separated by TLC from total cell extracts were analyzed. These major spots contained

phosphatidylcholine (PtdCho), phosphatidylethanolamine (PtdEtn), and phosphatidylserine (PtdSer) plus phosphatidylinositol (PtdIns).

The tendency to an increase in the percentage of MUFAs at the expense of PUFAs found in total phospholipids of cells over-expressing Bcl-2 compared to those of neo HL-60 cells was also observed in each individual glycerophospholipid (see Tables 3, 4, 5). It was more marked in PtdEtn than in the other phospholipids. In addition, in PtdEtn, over-expression of Bcl-2 induced a substantial decrease in total SFAs, which concerned only stearic acid (18:0) (Table 4). In PtdCho, PtdSer and PtdIns, DMA FAs, reflecting plasmalogen content, represented less than 1%. In PtdEtn this content reached 10% in control cells, and subsequently increased to more than 15% upon Bcl-2 over-expression.

Analysis of the impact of Bcl-2 over-expression on FA composition of PtdCho, PtdEtn, PtdIns and cardiolipin

Table 4 Fatty acid species in phosphatidylethanolamine (PtdEtn) from HL-60 cells transfected with empty (neo cells) and with bcl-2 gene (Bcl-2 over-expressing cells), and from their mitochondria

Fatty acid species	PtdEtn from total cell extracts		PtdEtn from purified mitochondria	
	Neo (<i>n</i> = 3) Mean ± SD	Bcl-2 over-expressing cells (<i>n</i> = 3) Mean ± SD	Neo (<i>n</i> = 3) Mean ± SD	Bcl-2 over-expressing cells (<i>n</i> = 3) Mean ± SD
14:0	0.70 ± 0.61	1.04 ± 0.28	1.50 ± 0.10	1.50 ± 0.06
14:1	0.48 ± 0.53	0.80 ± 1.12	0.04 ± 0.04	0.72 ± 0.39
16 DMA	9.57 ± 4.39	10.87 ± 1.01	1.48 ± 0.57	2.66 ± 0.04*
16:0	6.82 ± 1.59	6.35 ± 1.01	14.79 ± 3.55	21.50 ± 2.04*
16:1(n-9 + n-7)	3.91 ± 0.87	8.02 ± 1.85	10.20 ± 0.32	9.81 ± 0.60
18 DMA	2.03 ± 2.52	4.60 ± 3.04	0.71 ± 0.11	2.85 ± 0.02*
18:0	20.49 ± 2.20	14.37 ± 1.98	26.72 ± 0.86	21.60 ± 2.90
18:1(n-9 + n-7)	26.77 ± 2.82	31.97 ± 5.20	34.55 ± 0.11	30.90 ± 3.92
18:2n-6	3.06 ± 2.30	2.86 ± 1.73	3.78 ± 0.21	3.85 ± 0.92
18:3	ND	ND	0.33 ± 0.34	ND
20:0	ND	0.19 ± 0.29	0.07 ± 0.08	ND
20:1n-9	0.32 ± 0.66	0.26 ± 0.51	0.58 ± 0.17	2.69 ± 0.11*
20:3 (n-9 + n-6)	4.88 ± 2.65	3.11 ± 2.00	ND	ND
20:4n-6	13.43 ± 3.89	10.77 ± 1.90	3.99 ± 2.34	0.50 ± 0.50
20:5n-3	2.49 ± 0.08	2.25 ± 1.39	0.55 ± 0.60	ND
22:4n-6	ND	ND	ND	ND
24:1n-9	0.22 ± 0.47	ND	0.17 ± 0.18	1.45 ± 0.16*
22:6n-3	0.33 ± 0.62	ND	ND	ND
24:0	ND	ND	ND	ND
22:5n-3	4.46 ± 2.92	2.50 ± 2.45	0.42 ± 0.50	ND
Fatty acid composition				
Saturated fatty acids (%)	28.01	21.95	43.08	44.60
Mono-unsaturated fatty acids (%)	31.70	41.05	45.54	45.57
Poly-unsaturated fatty acids (%)	28.65	21.49	8.74	4.35
DMA fatty acids (%)	11.60	15.47	2.19	5.51

After separation of phospholipids by TLC followed by their transmethylation as described in the Methods section, Fatty acid composition of phosphatidylethanolamine was analyzed by capillary GLC. The values are expressed as weight per cent of the total FAs ± SD

* Significantly different from control cells with $P < 0.05$

from purified mitochondria showed that in the three first phospholipids, over-expression of Bcl-2 induced a marked decrease in PUFA percentage by a factor 3, 2 and 1.5 in PtdCho, PtdEtn and PtdIns, respectively. Moreover, DMA fatty acids representing in neo cell mitochondrial phospholipids around 1, 2 and 4%, respectively, of total FAs, were increased to about 3, 5 and 12% in those from Bcl-2 over-expressing HL-60 cells (see Tables 3, 4, 5). As to cardiolipin, specifically located in mitochondria, more drastic changes were observed upon Bcl-2 over-expression. SFAs were doubled in Bcl-2 over-expressing cells whereas PUFAs were halved. Moreover, DMA fatty acids were also doubled compared to those present in neo cells (Table 6). These major changes in cardiolipin FA composition are likely to be related to the increased expression of Bcl-2 in these organelles and to be involved in the protection against apoptosis from mitochondrial origin.

Discussion

In the present work we have shown that in the human promyelocytic cell line, HL-60, over-expression of the major anti-apoptotic protein Bcl-2 leads to changes in membrane lipids that could take a part in their observed resistance to apoptosis. Although PUFAs represented only a small percentage of all FAs, their content decreased upon Bcl-2 over-expression in total cell lipids and in individual phospholipid classes. Taken together with the increase in MUFAs observed in cellular lipid extracts and in individual phospholipid classes, PUFA decrease might suggest a lower sensitivity of Bcl-2 over-expressing cells to oxidation, a phenomenon that contributes to cell apoptosis.

Looking at changes in mitochondrion composition induced by over-expression of Bcl-2 protein, they all indicate that this organelle would be less prone to injuries

Table 5 Fatty acid species in phosphatidylserine (PtdSer) plus phosphatidylinositol (PtdIns) from HL-60 cells transfected with empty vector (neo cells) and with bcl-2 gene (Bcl-2 over-expressing cells), and in phosphatidylinositol (PtdIns) from their mitochondria

Fatty acid species	PtdSer + PtdIns from total cell extracts		PtdIns from purified mitochondria	
	Neo (<i>n</i> = 3) Mean ± SD	Bcl-2 over-expressing cells (<i>n</i> = 3) Mean ± SD	Neo (<i>n</i> = 3) Mean ± SD	Bcl-2 over-expressing cells (<i>n</i> = 3) Mean ± SD
14:0	0.26 ± 0.17	0.39 ± 0.08	0.92 ± 0.18	0.84 ± 0.21
14:1	0.16 ± 0.18	0.12 ± 0.24	0.61 ± 0.05	0.98 ± 0.14
16 DMA	0.14 ± 0.17	0.28 ± 0.19	1.80 ± 0.13	4.75 ± 0.44*
16:0	6.49 ± 1.93	7.40 ± 1.01	13.65 ± 0.38	14.69 ± 0.66
16:1(n-9 + n-7)	2.88 ± 0.56	3.87 ± 0.87	1.99 ± 0.05	1.71 ± 0.19
18 DMA	ND	0.08 ± 0.16	1.99 ± 0.06	7.15 ± 0.71*
18:0	49.51 ± 3.76	46.31 ± 3.03	36.40 ± 0.11	35.05 ± 6.61
18:1(n-9 + n-7)	29.17 ± 2.27	31.65 ± 2.79	26.22 ± 1.32	19.30 ± 6.64*
18:2n-6	0.72 ± 0.10	0.82 ± 0.37	3.77 ± 0.25	7.80 ± 0.80*
18:3	0.12 ± 0.14	0.21 ± 0.30	0.38 ± 0.02	1.68 ± 0.33*
20:0	0.27 ± 0.22	0.51 ± 0.10	0.46 ± 0.46	ND
20:1n-9	0.36 ± 0.45	0.46 ± 0.15	1.63 ± 1.08	1.23 ± 0.3
20:3 (n-9 + n-6)	1.71 ± 0.23	1.33 ± 0.70	ND	ND
20:4n-6	4.75 ± 1.11	1.22 ± 0.33*	7.06 ± 0.96	ND
20:5n-3	1.25 ± 0.58	1.01 ± 0.62	0.95 ± 0.12	ND
22:4n-6	ND	ND	ND	ND
24:1n-9	ND	0.71 ± 0.84	0.56 ± 0.60	4.20 ± 0.5*
22:6n-3	2.18 ± 1.62	2.88 ± 0.69	0.22 ± 0.23	ND
24:0	ND	ND	0.67 ± 0.06	ND
22:5n-3	ND	0.72 ± 0.81	0.58 ± 0.57	ND
Fatty acid composition				
Saturated fatty acids (%)	56.53	54.61	52.10	50.58
Mono-unsaturated fatty acids (%)	32.57	36.81	31.01	27.42
Poly-unsaturated fatty acids (%)	10.73	8.19	12.96	9.48
DMA fatty acids (%)	0.14	0.36	3.79	11.90

After separation of phospholipids by TLC followed by their transmethylation as described in the Methods section, Fatty acid composition of phosphatidylserine plus phosphatidylinositol from whole cell preparation and from phosphatidylinositol from mitochondria preparations was analyzed by capillary GLC. The values are expressed as weight per cent of the total FAs ± SD

* Significantly different from control cells with $P < 0.05$

leading to apoptosis. As expected, the Bcl-2 content is greatly increased, and this protein is known to have anti-apoptotic properties when apoptosis is induced by agents that activate caspase via the intrinsic pathway initiated by mitochondrial outer membrane and release of cytochrome *c* [37]. In addition, over-expression of Bcl-2 regulates amplification of caspase activation by cytochrome *c*. In addition, over-expression of Bcl-2 has been shown to shift the cellular redox potential to a more reduced state (see reviews [38, 39]) not favoring oxidation of cell components. Using the same two clones, we have previously reported that apoptosis by disruption of mitochondrial homeostasis induced by the lethal toxin from *Clostridium sordellii* did not occur in Bcl-2 over-expressing cells [40].

The changes in mitochondrial lipid composition noted in Bcl-2 over-expressing cells are indicating that the

membranes are significantly less unsaturated. There was a net decrease in PUFA content (ca. 2 times) together with a smaller reduction in MUFA content. These decreases were compensated by an increase (ca. 10%) in SFAs and in DMA-FAs. All together, these changes led to a drop of ca. 20% in the unsaturation index of the mitochondrial membrane (from 105.2 to 82.7). However, this rearrangement in fatty acid composition has to be further analyzed to show the tendency of the membrane to be more resistant to (per)oxidation. Indeed, susceptibility to peroxidation of fatty acids is complex, with number of unsaturations, chain length and n-3 and n-6 series being important [41]. Combining all these parameters, it is possible to calculate a peroxidation index, which is a measure of the membrane susceptibility to peroxidation [41]. This index was lower by ca. 30% (66.4 vs. 47.8) in mitochondrial membranes

Table 6 Fatty acid species of cardiolipin (DPG) in purified mitochondria from HL-60 cells transfected with empty vector (Neo) and with *bcl-2* gene

Fatty acid species	Neo (<i>n</i> = 3) Mean ± SD	Bcl-2 over-expressing cells (<i>n</i> = 3) Mean ± SD
14:0	0.75 ± 0.47	2.39 ± 0.90
14:1	0.07 ± 0.04	0.51 ± 0.13*
16 DMA	1.42 ± 0.55	2.66 ± 0.94
16:0	3.05 ± 0.15	9.42 ± 2.95
16:1(n-9 + n-7)	21.51 ± 4.01	20.07 ± 2.42
18 DMA	0.80 ± 0.11	3.05 ± 0.91
18:0	6.39 ± 4.80	9.60 ± 5.64
18:1(n-9 + n-7)	40.70 ± 5.63	35.65 ± 1.89
18:2n-6	12.00 ± 1.70	5.39 ± 2.16*
18:3	ND	ND
20:0	0.95 ± 0.61	ND
20:1n-9	0.57 ± 0.13	2.41 ± 0.51*
20:3 (n-9 + n-6)	ND	ND
20:4n-6	6.72 ± 3.28	3.82 ± 3.83
20:5n-3	0.88 ± 0.62	0.75 ± 0.75
22:4n-6	ND	ND
24:1n-9	0.6 ± 0.34	1.50 ± 0.38
22:6n-3	ND	ND
24:0	ND	0.70 ± 0.70
22:5n-3	3.34 ± 2.50	2.26 ± 2.27
Fatty acid composition		
Saturated fatty acids (%)	11.14	22.11
Monounsaturated fatty acids (%)	63.45	60.14
Poly-unsaturated fatty acids (%)	22.94	12.22
DMA fatty acids (%)	2.22	5.71

After separation of phospholipids by TLC followed by their trans-methylation as described in the Methods section, Fatty acid composition of cardiolipin from mitochondria preparations was analyzed by capillary GLC. The values are expressed as weight per cent of the total FAs ± SD

* Significantly different from control cells with $P < 0.05$

purified from Bcl-2 over-expressors, confirming that the bilayer should be less prone to oxidative damages.

DMA-FAs originate from plasmalogens, a class of lipids which are known to act as scavengers, protecting other lipids from oxidative reactions [42, 43]. The increase (2.5–3 times) in plasmalogen species was found in all the lipid classes of mitochondrial membranes.

Changes in unsaturation of fatty acyl chains concerned all the mitochondrial phospholipids, especially cardiolipin. Indeed, its content in SFAs doubled while the amount of PUFAs was diminished by 50%. Thus, cardiolipin should become more resistant to (per)oxidation (peroxidation index decreasing by 33%), disfavoring cytochrome *c* release leading to apoptosis [44].

Although the amount of cardiolipin was not affected by Bcl-2 over-expression, the fatty acid composition changes could modify interactions with apoptotic or anti-apoptotic proteins, either in the inner membrane or at the contact sites where this lipid is enriched [45].

In conclusion, the present work shows that over-expression of Bcl-2 protects from apoptosis starting in mitochondria not only through the specific properties of the protein, but also by changes in membrane fatty acids.

Acknowledgments B. Geny is a senior scientist from the Institut National de la Santé et de la Recherche Médicale (INSERM, France). A. Zachowski is a senior scientist and C. Cantrel is a research engineer of the Centre National de la Recherche Scientifique (CNRS, France). This work was supported by the Association de la Recherche sur le Cancer (ARC; grant number 9452 M), the Centre National de la Recherche Scientifique (CNRS, France) and the Université Pierre et Marie Curie (UPMC, France).

References

- Harder T (2003) Formation of functional cell membrane domains: the interplay of lipid- and protein-mediated interactions. *Philos Trans R Soc Lond B Biol Sci* 358:863–868
- Lee AG (2003) Lipid-protein interactions in biological membranes: a structural perspective. *Biochim Biophys Acta* 1612:1–40
- Nyholm TK, Ozdirekcan S, Killian JA (2007) How protein transmembrane segments sense the lipid environment. *Biochemistry* 46:1457–1465
- Schmitz G, Grandi M (2008) Update on lipid membrane microdomains. *Curr Opin Clin Nutr Metab Care* 11:106–112
- Sui SF (2000) Membrane-induced conformational change of proteins. *Adv Colloid Interface Sci* 85:257–267
- Huttner WB, Zimmerberg J (2001) Implication of lipid microdomains for membrane curvature, budding and fission. *Curr Opin Cell Biol* 13:478–484
- van der Sluijs HP, van Meer G (2001) How proteins move lipids and lipid move proteins. *Nat Rev* 2:504–513
- Farsad K, De Camilli P (2003) Mechanisms of membrane deformation. *Curr Opin Cell Biol* 15:372–381
- Pitson SM (2008) Lipids as central mediators of cellular signaling. *IUBMB Life* 58:449–450
- Powner DJ, Wakelam MJO (2002) The regulation of phospholipase D by inositol phospholipids and small GTPases. *FEBS Lett* 531:62–64
- Escriba PV, Wedegaertner PB, Goni FM, Vögler O (2007) Lipid-protein interactions in GPCR-associated signaling. *Biochim Biophys Acta* 1768:836–852
- Mukherjee S, Maxfield FR (2000) Role of membrane organization and membrane domains in endocytic lipid trafficking. *Traffic* 1:203–211
- Emoto K, Umeda M (2001) Membrane lipid control of cytokinesis. *Cell Struct Funct* 26:659–665
- Gomez-Munoz A (2006) Ceramide 1-phosphate/ceramide, a switch between life and death. *Biochim Biophys Acta* 1758:2049–2056
- Deigner HP, Hermetter A (2008) Oxidized phospholipids: emerging lipid mediators in pathophysiology. *Curr Opin Lipidol* 19:289–294
- Kusenda J (1998) Bcl-2 family proteins and leukemia. *Neoplasma* 45:117–122

17. Hockenbery D, Nunez G, Milliman C, Schreiber RD, Korsmeyer SJ (1990) Bcl-2 is an inner mitochondrial membrane protein that blocks programmed cell death. *Nature* 348:334–336
18. Monaghan P, Robertson D, Amost TAS, Dyer MJS, Mason DY, Greaves MF (1992) Ultrastructural localization of Bcl-2 protein. *J Histochem Cytochem* 40:1819–1825
19. Krajewski S, Tanaka S, Takayama S, Schibler MJ, Fenton W, Reed JC (1993) Investigation of the subcellular distribution of the bcl-2 oncoprotein: residence in the nuclear envelope, endoplasmic reticulum and outer mitochondrial membranes. *Cancer Res* 53:4701–4714
20. de Jong D, Prins FA, Mason DY, Reed JC, van Ommen GB, Kluin PM (1994) Subcellular localization of the bcl-2 protein in malignant and normal lymphoid cells. *Cancer Res* 54:256–260
21. Schendel SL, Xie Z, Oblatt-Montal M, Matsuyama S, Montal M, Reed JC (1997) Channel formation by antiapoptotic protein Bcl-2. *Proc Natl Acad Sci USA* 94:5113–5118
22. Yang J, Liu X, Bhalla K, Kim CN, Ibrado AM, Cai J, Peng Y-I, Jones DP, Wang X (1997) Prevention of apoptosis by Bcl-2: release of cytochrome *c* from mitochondria blocked. *Science* 275:1129–1132
23. Kluck RM, Bossy-Wetzell E, Green DR, Newmeyer DD (1997) The release of cytochrome *c* from mitochondria: a primary site for Bcl-2 regulation of apoptosis. *Science* 275:1132–1136
24. Schendel SL, Montal M, Reed JC (1998) Bcl-2 family proteins as ion-channels. *Cell Death Diff* 5:372–380
25. Harris MH, Thompson CB (2000) The role of the Bcl-2 family in the regulation of outer mitochondrial membrane permeability. *Cell Death Diff* 7:1182–1191
26. Reed JC (1994) Bcl-2 and the regulation of programmed cell death. *J Cell Biol* 124:1–6
27. Virgili F, Santini MP, Canali R, Polakowska RR, Haake A, Perozzi G (1998) Bcl-2 overexpression in the HaCaT cell line is associated with a different membrane fatty acid composition and sensitivity to oxidative stress. *Free Rad Biol Med* 24:93–101
28. Martin SJ, Reutelingsperger CPM, McGahon AJ, Rader JA, van Schie RCAA, LaFace DM, Green DR (1995) Early redistribution of plasma membrane phosphatidylserine is a general feature of apoptosis regardless of the initiating stimulus: inhibition by overexpression of Bcl-2 and Abl. *J Exp Med* 182:1545–1556
29. Allouche M, Bettaib A, Vindis C, Rousse A, Grignon C, Laurent G (1997) Influence of Bcl-2 overexpression on the ceramide pathway in daunorubicin-induced apoptosis of leukemic cells. *Oncogene* 14:1837–1846
30. Susin SA, Larochette N, Geurkens M, Kroemer G (2000) Purification of mitochondria for apoptosis assays. *Meth Enzymol* 322:205–213
31. De Giorgi F, Lartigue L, Bauer MKA, Schubert A, Grimm S, Hanson GT, Remington SJ, Youle RJ, Ichas F (2002) The permeability transition pore signals apoptosis by directing Bax translocation and multimerization. *FASEB J* 16:607–609
32. Folch G, Lees M, Sloane-Stanley GH (1957) A simple method for isolation and purification of total lipids from animal tissues. *J Biol Chem* 226:497–509
33. Rouser G, Fleischer S, Yamamoto A (1970) Two dimensional thin layer chromatographic separation of polar lipids and determination of phospholipids by phosphorus analysis of spots. *Lipids* 5:494–496
34. Metcalfe LD, Schmitz AA, Palka JR (1966) Rapid preparation of fatty acid esters from lipids for gas chromatographic analysis. *Anal Chem* 38:514–515
35. Bonnefoy-Berard N, Auouacheria A, Vershelde C, Quemerer L, Marcais A, Marvel J (2004) Control of proliferation by Bcl-2 family members. *Biochim Biophys Acta* 1644:159–168
36. Ifandi V, Al-Rubeai M (2005) Regulation of cell proliferation and apoptosis of CHO-K1 cells by the co-expression of c-myc and Bcl-2. *Biotechnol Prog* 21:671–677
37. Cosulich SC, Savory PJ, Clarke PR (1999) Bcl-2 regulates amplification of caspase activation by cytochrome *c*. *Curr Biol* 9:147–150
38. Elleby L, Elleby H, Park M, Sunghi M, Holleran AL, Murphy AN, Fiskum G, Kane DJ, Testa MP, Kayalar C, Bresden DE (1996) Shift of the cellular oxidation-reduction potential in neural cells expressing Bcl-2. *J Neurochem* 67:1259–1267
39. Voehringer DW, Meyn RE (2000) Redox aspects of Bcl-2 function. *Antioxid Redox Signal* 2:537–550
40. Petit PX, Bréard J, Montalescot V, Ben El Hadj N, Levade T, Popoff M, Geny B (2003) Lethal toxin from *Clostridium sordellii* induces apoptotic cell death by disruption of the mitochondrial homeostasis in HL-60 cells. *Cell Microbiol* 5:761–771
41. Hulbert AJ, Pamplona R, Buffenstein R, Buttemer WA (2007) Life and death: metabolic rate, membrane composition and life span of animals. *Physiol Rev* 87:1175–1213
42. Nagan N, Zoeller RA (2001) Plasmalogens: biosynthesis and functions. *Prog Lipid Res* 40:199–229
43. Brites P, Waterham HR, Wanders RJA (2004) Functions and biosynthesis of plasmalogens in health and disease. *Biochim Biophys Acta* 1636:219–231
44. Gonzalez F, Gottlieb E (2007) Cardiolipin: setting the beat of apoptosis. *Apoptosis* 12:877–885
45. Daum G, Vance JE (1997) Import of lipids into mitochondria. *Prog Lipid Res* 36:103–130

StAR Overexpression Decreases Serum and Tissue Lipids in Apolipoprotein E-deficient Mice

Yanxia Ning · Leyuan Xu · Shunlin Ren ·
William M. Pandak · Sifeng Chen · Lianhua Yin

Received: 23 January 2009 / Accepted: 24 March 2009 / Published online: 17 April 2009
© AOCs 2009

Abstract Cholesterol metabolism as initiated by mitochondrial sterol 27-hydroxylase (CYP27A1) is a ubiquitous pathway capable of synthesizing multiple key regulatory oxysterols involved in lipid homeostasis. Previously we have shown that the regulation of its activities within hepatocytes is highly controlled by the rate of mitochondrial cholesterol delivery. In the present study, we hypothesized that increasing expression of the mitochondrial cholesterol delivery protein, steroidogenic acute regulatory protein (StAR), is able to lower lipid accumulation in liver, aortic wall, as well as in serum in a well-documented animal model, apolipoprotein E-deficient (apoE^{-/-}) mice. ApoE^{-/-} mice, characterized by increased serum, liver, and endothelial cholesterol and triglyceride levels by 3 months of age, were infected with recombinant cytomegalovirus (CMV)-StAR adenovirus to increase StAR protein expression. Six days following infection, serum total cholesterol and triglycerides had decreased 19 and 30% ($P < 0.01$), respectively, with a compensatory 40% ($P < 0.01$) increase in serum HDL-cholesterol in increased StAR expressing mice as compared to controls (no or control virus). Histologic and biochemical analysis of the liver demonstrated not only a dramatic decrease in cholesterol ($\downarrow 25\%$; $P < 0.01$), but an even more marked decrease in triglyceride ($\downarrow 56\%$; $P < 0.01$)

content. En bloc Sudan IV staining of the aorta revealed a $>80\%$ ($P < 0.01$) decrease in neutral lipid staining. This study demonstrates for the first time a possible therapeutic role of the CYP27A1-initiated pathway in the treatment of dyslipidemias.

Keywords Lipids · Cholesterol · Lipoproteins · Steroidogenic acute regulatory protein

Abbreviations

ALP	Alkaline phosphatase
ALT	Alanine aminotransferase
apoE ^{-/-}	Apolipoprotein E-deficient
AST	Aspartate aminotransferase
BAS	Bile acid synthesis
CMV	Cytomegalovirus
CTX	Cerebrotendinous xanthomatosis
CYP7A1	Cholesterol 7 alpha-hydroxylase
CYP27A1	Sterol 27-hydroxylase
EGFP	Enhanced Green fluorescent protein
HDL	High density lipoprotein
HDL-CHO	HDL cholesterol
IDL	Intermediate-density lipoproteins
LDL	Low density lipoprotein
NS	Normal saline
O.C.T	Optimum cutting temperature compound
PC-TP	Phosphatidylcholine transfer protein
PPAR γ	Proliferation peroxysome activator receptor gamma
StAR	Steroidogenic acute regulatory protein
START	StAR-related lipid transfer domain
T-CHO	Total cholesterol
TG	Triglyceride
VLDL	Very low-density lipoproteins

Y. Ning · L. Xu · S. Chen (✉) · L. Yin (✉)
Department of Physiology and Pathophysiology, Shanghai
Medical College, Fudan University, PO Box 224, 138 Yixueyuan
Road, 200032 Shanghai, People's Republic China
e-mail: chen1216@fudan.edu.cn

L. Yin
e-mail: lhyin@shmu.edu.cn

S. Ren · W. M. Pandak
Department of Medicine, Veterans Affairs Medical Center
and Virginia Commonwealth University, Richmond, VA, USA

Introduction

Dyslipidemias, as characterized by abnormal serum lipoprotein profiles, are a risk factor for atherosclerosis [1]. Although current strategies have led to significant advances in their treatment, there is great interest in exploring new therapeutic strategies to treat and prevent what remains a leading cause of morbidity and mortality throughout the world.

Steroidogenic acute regulatory protein (StAR/StarD1), an intracellular cholesterol transport protein, was first identified in steroidogenic tissues. This protein is a member of a family that contains a StAR homologue domain that has been found capable of binding and transporting sterols within cells. This family includes the phosphatidylcholine transfer protein (PC-TP/StarD2) [2], MLN64 (StarD3) [3, 4], and the newly discovered StarD4, StarD5, and StarD6 [5–8]. All of these proteins have a similar structural lipid-binding domain referred to as the StAR-related lipid transfer (START) domain. StAR, first detected in the adrenal, was shown to facilitate cholesterol delivery to the inner mitochondrial cholesterol side-chain cleavage system in the initiation of steroidogenesis [9, 10]. StAR was initially considered to be confined to steroidogenic tissues such as adrenal gland, ovary, and testicle [7, 11]. However, StAR has since been found in other tissues/cells inclusive of the liver, brain, endothelium, and macrophages [12–15].

In the liver, StAR has been shown to facilitate cholesterol delivery to the inner membrane of the mitochondria where cholesterol can be oxidized by sterol 27-hydroxylase (CYP27A1) to an important regulatory oxysterol, 27-hydroxycholesterol, before ultimately being metabolized to bile acids [16]. Most recently, we have shown that in addition to its metabolism of cholesterol to 27-hydroxycholesterol and subsequently to bile acids, CYP27A1 is also capable of metabolizing cholesterol to 25-hydroxycholesterol with subsequent conversion to its sulfated form [17]. Like 27-hydroxycholesterol, both 25-hydroxycholesterol and sulfated 25-hydroxycholesterol are regulators of intracellular lipid metabolism [17–19]. Both 27- and 25-hydroxycholesterol are known to down-regulate cholesterol synthesis while stimulating cell cholesterol secretion [18, 19]. Sulfated 25-hydroxycholesterol has recently been shown to decrease fatty acid synthase as well as activate a nuclear receptor responsible for fatty acid mobilization/secretion [20].

It is possible that increased metabolism of cholesterol as initiated through the CYP27A1 could result in a coordinated lipids lowering response. Increasing StAR expression would be expected to not only increase cholesterol catabolism to bile acids as we have previously shown, but produce key regulatory oxysterols of intracellular lipid homeostasis [12, 16, 21]. In support of this supposition, our recent *in vitro* findings in THP-1 macrophages showed that up-regulation

of StAR induced a coordinated mobilization and reduction of cell cholesterol [14]. Therefore, it seems reasonable to hypothesize that the StAR/CYP27A1-initiated metabolism of cholesterol is not only a pathway of cholesterol catabolism, but an important intracellular pathway capable of directing intracellular lipid homeostasis.

Apolipoprotein-E mediates the clearance of serum lipids such as cholesterol and triglyceride [22]. Apolipoprotein E-deficient (apoE^{-/-}) mice develop hypercholesterolemia as a result of an accumulation of chylomicron remnants, very low-density lipoproteins (VLDL), and intermediate-density lipoproteins (IDL) [23]. Mice homozygous for the inactivated apoE gene spontaneously develop hypercholesterolemia and aortic lipid accumulation [24, 25]. The lipid lesions which develop in the aortas of mice fed a standard rodent chow diet are similar to the early lipid accumulations found in humans [23, 26, 27]. In addition, apoE^{-/-} mice are also known to develop significant hepatic lipid (i.e. cholesterol/triglyceride) accumulation. Therefore, apoE^{-/-} mice provide not only a practical model for the study of early developmental atherosclerosis [28], but an excellent model for the outlined study.

The described trial was simply designed as “an *in-vivo* proof of concept” that increasing CYP27A1-initiated cholesterol metabolism as facilitated by the mitochondria-directed cholesterol transport protein, StAR, could represent a novel approach to reduce serum and tissue cholesterol and triglyceride levels. As shown, increased StAR expression led to a coordinated response in serum triglycerides and HDL cholesterol. Furthermore, hepatic cholesterol was significantly reduced. Of equal importance, neutral lipid levels in the serum, liver, and aorta were also dramatically reduced in this classic animal model of dyslipidemia.

Experimental Procedure

Materials

TRIzol reagent and SuperScript TMIII First-Strand Synthesis System for RT-PCR were purchased from Invitrogen (Carlsbad, CA). Taq DNA Polymerase, dNTP mix and PageRuler Prestained Protein Ladder were purchased from Fermentas MBI (San Diego, CA). Primary antibody against StAR and GAPDH were purchased from Abcam Ltd (Cambridge Science Park, Cambridge, UK) and Kangcheng Bio-Tech (Shanghai, China), respectively. Second antibody against rabbit and mouse IgG were obtained from Kirkegaard & Perry Laboratories (Guildford, UK). SuperSignal West Pico Chemiluminescent Substrate was obtained from Pierce Biotechnology, Inc (Rockford, IL). All other reagents were from Sigma-Aldrich Chemical Co. (St. Louis, MO) unless otherwise indicated.

Experimental Animals

C57BL/6 J mice and homozygous apoE^{-/-} mice (same inherited background as the C57BL/6 J mice) were purchased from the Department of Laboratory Animal Science, Peking University Health Science Center (Beijing, China). The animals were allowed to acclimatize for 1 week while being maintained at a room temperature of 22 ± 2°C on a 12 h light/dark cycle with free access to standard rodent chow food and water (Standard sustain feed, from Institute of Laboratory Animal Science, Shanghai, China). Housing facilities and all experimental protocols were approved by the Animals Care and Use Committee of Fudan University Shanghai Medical College which adopts the guidelines for the care and use of laboratory animals published by the US National Institutes of Health (NIH Publication No. 85–23, revised 1996).

Ninety-six C57BL/6 J and apoE^{-/-} mice of both sexes at 1, 3 and 5 months old were used to determine serum level of lipids. An additional 27 6-month-old male apoE^{-/-} mice were used to investigate the effect of StAR overexpression on serum, liver, and aortic lipid levels. Prior to and post infusion, the animals dietary intake was not significantly different from either control group. Before sacrificing, the mice were fasted for 12 h. The mice were then anesthetized (60 mg pentobarbital/kg body weight, intravenously) and euthanized. Blood was collected from the retro-orbital plexus and aliquots of plasma were stored at –70°C until determination of serum parameters as described below. The liver was excised, weighed, snap frozen in liquid nitrogen, and stored at –70°C until further analysis. The aorta and liver were harvested for gross and histological examination.

Preparation of Recombinant Adenoviruses

The recombinant adenoviruses encoding StAR were prepared as previously described [29]. The virus was then amplified by infecting confluent monolayers of human embryonic kidney 293 cells as previously described [30]. Aliquots of the amplified virus were stored at –70°C until used. The control adenoviruses expressing the enhanced green fluorescence protein were purchased from the Vector Gene Technology Company Ltd (Beijing, China). The infection and particle titers of the viruses were determined using plaque and optical density assays, respectively.

Intravenous Infusion of Adenovirus

For the adenovirus infections, the 27 6-month-old apoE^{-/-} mice fed a standard rodent chow diet were equally and randomly divided into three groups. Eighteen of mice were tail vein injected with 1 × 10¹¹ virus particles of

Ad~CMV~StAR or Ad~CMV~EGFP. In nine non-transduced (control) mice the virus was replaced with the same volume of normal saline (NS). Six days after infection, the animals were briefly anesthetized and euthanized after fasting for 12 h. Blood was collected for determination of serum alanine aminotransferase (ALT), aspartate aminotransferase (AST), alkaline phosphatase (ALP) and lipid levels. Organs were harvested for histology and biochemical analysis. The histological specimens were fixed in 10% formalin. Additional tissue (liver) was quickly frozen in liquid nitrogen and stored at –70°C for further analysis.

Determination of Blood Parameters

The levels of triglyceride (TG), total cholesterol (T-CHO), and HDL cholesterol (HDL-CHO) in serum were measured by enzymatic methods [31] according to the manufacturer's instructions using the detection kit purchased from Rongsheng Biotechnology Company Ltd (Shanghai, China). Serum ALT, AST, and ALP activities were determined by the clinical laboratory at the Longhua Hospital (Shanghai, China).

Histology

After adenoviruses infection, the StAR protein expression in heart, coronary artery and liver were detected by immunohistochemistry by ABC methods as previously described by the authors [13]. A portion of liver was harvested and embedded in optimum cutting temperature compound (O.C.T compound, Sakura Finetek, Inc., Torrance, CA), mixed with sucrose (20%), and stored at –80°C. Ten-micrometer cryosections were made lengthwise through the liver lobe. All cryosections were fixed for 1 min in formaldehyde solution, stained for 10 min with Oil Red O (stains lipids red), and counterstained for 1 min with hematoxylin. En face lipid accumulation was determined by removing the aortas from the aortic arch to the ileal bifurcation. The aortas were fixed in 10% neutral buffered formalin. To increase the reliability of lipid quantification, only the aortic segment from left subclavian artery to ileal bifurcation was used for the measurement. The aortas were cut longitudinally, splayed, and pinned in a dish filled with Sudan IV stain for 10 min, destained in 80% ethanol for 5 min, and then photographed. Quantitation of neutral lipid staining was performed by measuring stained area using ImageM software (Department of Physiology and Pathophysiology, Shanghai Medical College, Fudan University, China). The accumulated stained area in a given aorta was calculated as a percentage of the total surface area of the aorta.

Liver Lipid Measurement

Lipids were extracted from liver according to a published method [32]. Triglyceride and cholesterol were measured using the same method described previously for blood lipid analysis [31].

Determination StAR Protein Levels in Tissues

Total proteins of heart, lung, liver, spleen, and adrenal gland from the infected mice were isolated using $1 \times$ SDS-PAGE sample buffer (50 mM Tris-Cl buffer, pH 6.8, 2% (w/v) SDS, 2% mercaptoethanol, 10% (v/v) glycerol, and 0.1% (w/v) bromophenol blue). Protein was quantitated using the bicinchoninic acid assay purchased from Pierce (Rockford, IL). Fifty micrograms of total protein were separately on 10% SDS-PAGE gels. Western blot analysis of StAR was performed as previously described by the authors [13].

Statistics

Data were reported as mean \pm standard deviation (SD) and subjected to ANOVA analysis. *F* test and the *Student-Neuman-Keuls post* test analyses were performed on these data to analyze the variances and significances between groups. Statistical significance was defined as $P < 0.05$.

Results

Plasma Lipid Levels Increased in ApoE^{-/-} Mice

The absence of apoE^{-/-} in humans and animal models is associated with increases in serum, liver, and aortic lipid

levels. To simply confirm the apoE^{-/-} mouse model available as representative and as a viable model for examining the effects of increased StAR expression on serum, aortic, and liver lipids, serum lipids were determined at 1, 3, and 5 months of age and compared to C57BL/J6 mice. On a standard rodent chow diet (4.4% fat; 0.06% cholesterol), apoE^{-/-} mice had a significantly higher T-CHO and a significantly lower HDL-CHO at all time periods versus age-matched C57BL/6 J mice (Table 1). Serum triglycerides were not significantly different. Of note is that a significant steady decrease in HDL-CHO was observed from month 1 to 5 in apoE^{-/-} mice. The results indicated that the apoE^{-/-} mice available for study to be a representative and would serve as a viable apoE^{-/-} model. Certain assumptions were made, i.e. that there would be significant liver and aortic lipid accumulation.

Recombinant StAR Gene was Successfully Expressed in ApoE^{-/-} Mice

To determine if StAR protein was being overexpressed following mouse infection with Ad~CMV~StAR, 6 days following infection selected organs were screened for StAR protein expression by immunohistochemistry and Western blotting. After infection, StAR expression was higher in the mice infused with adenovirus encoding CMV-StAR than the other two groups in heart, coronary artery and liver tissue. The increases of StAR in the heart and coronary arteries were marginal (Fig. 1a). StAR protein was detected in the adrenal gland, spleen, liver, and lung of controls (NS: normal saline, Ad~CMV~EGFP), with large amounts of StAR found in the spleen and adrenal gland. Following Ad~CMV~StAR infection, StAR protein was found in all

Table 1 Increased plasma lipid levels in apoE^{-/-} mice

Mice	Total cholesterol		Triglyceride		HDL-cholesterol	
	Female	Male	Female	Male	Female	Male
Wild type						
1 M	1.98 \pm 0.14	2.32 \pm 0.25	1.96 \pm 0.83	1.60 \pm 0.54	1.29 \pm 0.02	1.73 \pm 0.05
3 M	2.08 \pm 0.14	2.22 \pm 0.21	1.18 \pm 0.59	1.26 \pm 0.19	1.52 \pm 0.17	1.74 \pm 0.21
5 M	1.76 \pm 0.34	2.31 \pm 0.11	0.94 \pm 0.41	0.97 \pm 0.95	1.15 \pm 0.16	1.97 \pm 0.43
ApoE ^{-/-}						
1 M	7.55 \pm 3.42*	7.53 \pm 3.26*	0.84 \pm 0.53*	1.31 \pm 0.52	0.63 \pm 0.33*	0.95 \pm 0.20*
3 M	9.58 \pm 1.53*	7.81 \pm 3.88*	1.08 \pm 0.64	1.50 \pm 0.46	0.56 \pm 0.15*	0.78 \pm 0.41*
5 M	9.98 \pm 0.97*	8.96 \pm 0.67*	1.02 \pm 0.25*	1.54 \pm 1.29	0.36 \pm 0.15*	0.53 \pm 0.31*

Values are mmol/L

ApoE^{-/-} apolipoprotein E-deficient

Values are presented as means \pm SD; $n = 6$

Statistical analyses were performed by one-way ANOVA within each age group

* $P < 0.01$ versus wild type C57BL/6 J mice at the same age

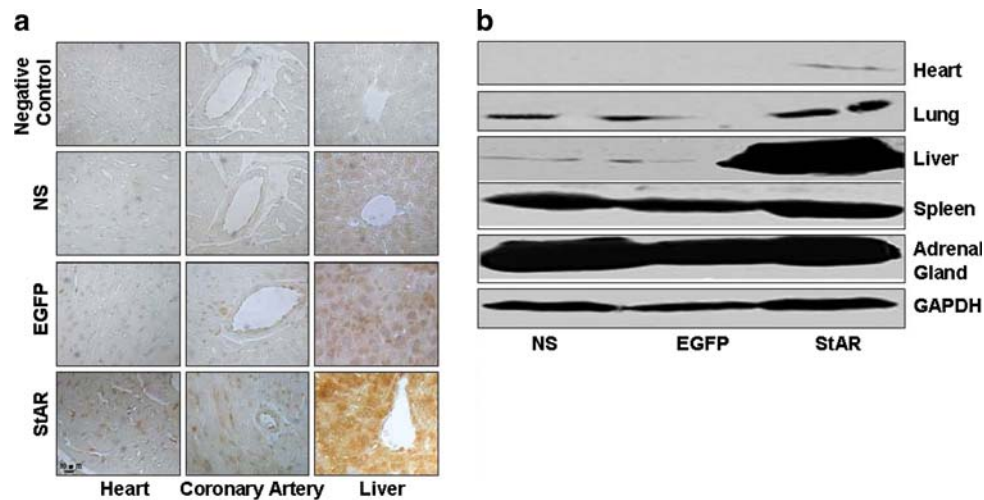


Fig. 1 Successful gene transduction of StAR in apoE^{-/-} mice fed with normal diet. The StAR expression in paraffin imbedded slices of heart, coronary artery and liver were detected by immunohistochemistry as shown in **a**. Western blot of StAR protein levels in different

major organs after StAR overexpression as shown in **b**. NS apoE^{-/-} mice injected with normal saline, EGFP apoE^{-/-} mice injected with control adenovirus encoding CMV-EGFP, StAR apoE^{-/-} mice injected with adenovirus encoding CMV-StAR. Bar 10 μ m

tested tissues with the largest increases found in the liver, a known reservoir for infecting adenovirus (Fig. 1b).

Liver Transaminases

Serum ALT, AST, and ALP activity levels in mice were measured to determine if there was liver injury following adenovirus infection. No significant differences were observed among the three groups of NS, Ad ~ CMV ~ StAR and Ad ~ CMV ~ EGFP (data not shown).

Transduction of Ad ~ CMV ~ StAR Decreases Lipid Accumulation in the Serum and Liver of ApoE^{-/-} Mice

Sera six days following infection with Ad ~ CMV ~ StAR, the serum T-CHO and TG were 19 and 30% ($P < 0.01$) lower in apoE^{-/-} mice receiving Ad ~ CMV ~ StAR than in those receiving NS or Ad ~ CMV ~ EGFP, respectively. In contrast, there was a dramatic reversal in the HDL-CHO levels with HDL-CHO in their plasma about 40% higher ($P < 0.01$) than controls (Table 2).

Liver tissues Liver sections stained with Oil Red O to evaluate the hepatic accumulation of lipids showed that the lipid levels were significantly less in the livers of Ad ~ CMV ~ StAR mice as compared to NS and Ad ~ CMV ~ EGFP mice (Fig. 2a). To confirm these results, lipids were extracted from the liver tissues and measured using commercial colorimetric kits for both cholesterol and triglycerides (Rongsheng Biotechnology Company Ltd, Shanghai, China). The hepatic cholesterol and triglyceride concentrations in the Ad ~ CMV ~ StAR mice decreased 25 and 56% ($P < 0.01$) as compared to NS and

Table 2 The level of plasma lipids in apoE^{-/-} mice after StAR overexpression

	NS	Ad ~ CMV ~ EGFP	Ad ~ CMV ~ StAR
T-CHO	13.53 \pm 1.17	13.76 \pm 1.21	11.01 \pm 0.62 ^{***}
TG	1.25 \pm 0.30	1.12 \pm 0.08	0.82 \pm 0.14 ^{**}
HDL-CHO	0.73 \pm 0.08	0.67 \pm 0.13	1.00 \pm 0.19 ^{***}

Values are mmol/L

Values are presented as means \pm SD

NS apoE^{-/-} mice injected with normal saline, Ad ~ CMV ~ EGFP apoE^{-/-} mice injected with control adenovirus encoding CMV-EGFP, Ad ~ CMV ~ StAR apoE^{-/-} mice injected with adenovirus encoding CMV-StAR

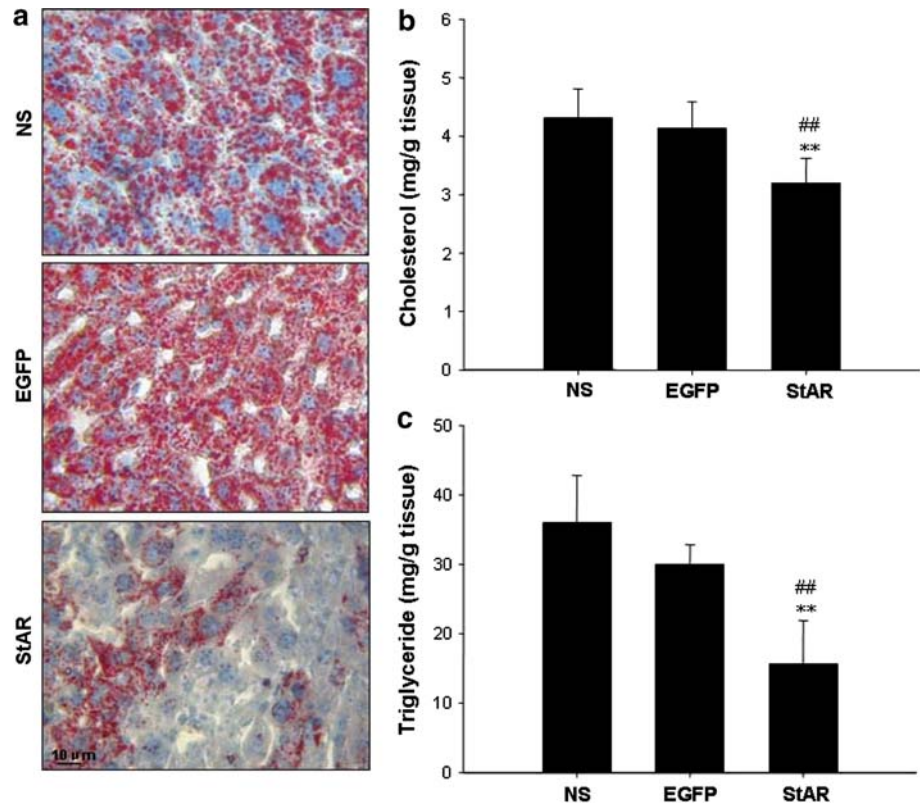
** $P < 0.01$ versus NS group, *** $P < 0.01$ versus Ad ~ CMV ~ EGFP group, # $P < 0.05$ versus Ad ~ CMV ~ EGFP group

Ad ~ CMV ~ EGFP mice, respectively (Fig. 2b, c). There were no significant differences in hepatic cholesterol and triglyceride levels between the NS and Ad ~ CMV ~ EGFP groups (Fig. 2b, c).

Transduction of StAR Reduces Aortic Neutral Lipid Accumulation in ApoE^{-/-} Mice

A previous study has shown that apoE^{-/-} mice will develop visible aortic lipid accumulation at 20 weeks on a normal mouse diet [23]. We found the microscopic presence of aortic lipid accumulation by the 3rd month with accumulation grossly visible by the 5th month in apoE^{-/-} mice fed a similar diet. Six days following Ad ~ CMV ~ StAR transduction, examination en face of aortas from

Fig. 2 Transduction of Ad~CMV~StAR decreases lipid accumulation in the liver of apoE^{-/-} mice fed with normal diet. **a** Oil Red O-stained liver sections (*bar* 10 μ m) of apoE^{-/-} mice. **b** Total hepatic cholesterol. **c** Hepatic triglyceride. Data are mean \pm SD. ***P* < 0.01 versus NS mice. ##*P* < 0.01 versus Ad~CMV~EGFP mice. NS apoE^{-/-} mice injected with normal saline (*n* = 11). EGFP apoE^{-/-} mice injected with control adenovirus encoding CMV-EGFP (*n* = 9). StAR apoE^{-/-} mice injected with adenovirus encoding CMV-StAR (*n* = 9)



Ad~CMV~StAR injected mice using ImageM software revealed significantly less neutral lipid than in NS or Ad~CMV~EGFP mice (Fig. 3a). The amount of lipid accumulation in aortas between NS and Ad~CMV~EGFP mice was found to not be different (Fig. 3a). The accumulated area of lipid stained lesions had decreased from $21.03 \pm 2.66\%$ and $19.42 \pm 2.39\%$ in NS and Ad~CMV~EGFP mice, respectively, to $3.74 \pm 1.57\%$ (Fig. 3b).

Discussion

Hyperlipidemia is an important risk factor for atherosclerosis. The treatment response to current medications is frequently inadequate. Therefore, there remains great interest in developing new therapeutic strategies. Based upon recent observations, it was hypothesized that facilitating mitochondria-directed cholesterol transport could elicit in an in vivo model a sequence of metabolic events resulting in both serum and tissue cholesterol lowering. The current study was designed to explore this hypothesis by increasing expression of StAR, a mitochondrial directed cholesterol transport protein, in a well-described animal model of dyslipidemia.

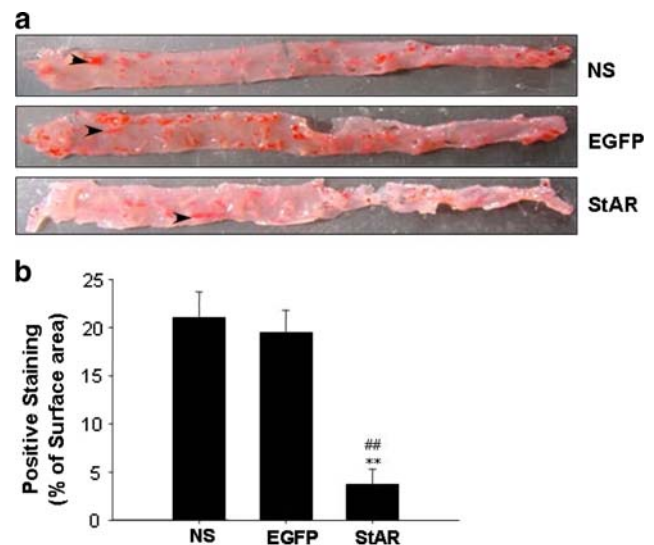


Fig. 3 Effect of transduction of StAR on aortic lipid accumulation in apoE^{-/-} mice. **a** En face staining of Sudan IV-stained aortas of mice fed with normal diet. Arrows indicate neutral lipid stained plaques. **b** Quantification of neutral lipid staining presented as percentage of total en face aorta surface area of mice fed with normal diet (see “Experimental Procedure”). ***P* < 0.01 versus NS. ##*P* < 0.01 versus Ad~CMV~EGFP. NS, EGFP and StAR represent apoE^{-/-} mice injected with normal saline, control adenovirus encoding CMV-EGFP, and adenovirus encoding CMV-StAR, respectively

Cholesterol metabolism as initiated via mitochondrial CYP27A1 is subsequently metabolized to key regulatory oxysterols of cholesterol homeostasis; and within the liver, continued catabolism to bile acids. For proper function, inner mitochondrial cholesterol levels must be tightly controlled, and it has been suggested that the key function of CYP27A1 is to initiate the metabolism of cholesterol to a metabolite that can be more easily mobilized out of the mitochondria. As CYP27A1 has been detected in all examined peripheral tissues as well as the liver, others have suggested that the conversion of cholesterol to 27-hydroxycholesterol as important under conditions of cholesterol excess. Under these conditions it has been proposed that the 27-hydroxylation can facilitate a process of reverse cholesterol transport of cholesterol from peripheral tissues to the liver with 27-hydroxycholesterol's subsequent elimination as bile acids [16, 33–36]. In support of this hypothesis, CTX (Cerebrotendinous xanthomatosis), characterized by the inability of cells to 27-hydroxylate sterols, is associated in humans with early dementia, premature atherosclerosis, and cataracts due to abnormal tissue sterol accumulation [37, 38]. As a function of these observations, CYP27A1 was overexpressed in transgenic mice, but interpreted as having little appreciable effect on lipid metabolism [39]. We also found that following overexpression of CYP27A1 in hepatocyte cultures only a modest increase in the rates of bile acid synthesis was observed as compared to the 8 to 10-fold increase consistently seen following CYP7A1 overexpression [40]. This suggested that inner mitochondrial substrate availability could be the rate-determining step in the CYP27A1-initiated pathway.

As described, StAR has been shown to not only facilitate cholesterol delivery to the inner mitochondrial cholesterol side-chain cleavage system in the initiation of steroidogenesis, but that increasing its expression would markedly increase steroidogenesis [9, 10]. Applying this concept to hepatocytes, we demonstrated that increased StAR expression markedly increased the rates of bile acid synthesis (BAS) in both in vitro and in vivo models [16, 21]. Our inability to up-regulate bile acid synthesis in CYP27A1^{-/-} mouse hepatocytes demonstrated that StAR's effects were mediated through the CYP27A1-initiated pathway [17].

Recently, Ren et al. demonstrated for the first time that CYP27A1 also metabolizes cholesterol to 25-hydroxycholesterol. 25-hydroxycholesterol, in a manner like 27-hydroxycholesterol, can down-regulate cholesterol synthesis, stimulate cholesterol secretion and stimulate fatty acid synthesis [17, 18]. Sulfated 25-hydroxycholesterol, a newly uncovered and subsequent metabolite of 25-hydroxycholesterol, like its precursor, also down-regulates cholesterol synthesis [17–19]. However, in direct contrast to 25-hydroxycholesterol and 27-hydroxycholesterol,

sulfated 25-hydroxycholesterol down-regulates fatty acid synthetase [19]. Furthermore, it is capable of activating PPAR γ , a nuclear receptor known to play a role in the redistribution of body fat as well as increase tissue insulin responsiveness [41, 42]. All three oxysterols are increased following increased StAR expression as evidenced by their increased cytosolic and nuclear levels [16, 18, 21, 30]. Furthermore, in addition to their intestinal lipid solubilization properties, bile acids, an end product of cholesterol/27-hydroxycholesterol metabolism, are also known regulators of key steps of lipid homeostasis [43–45].

Based on these observations, we hypothesized that increased cholesterol metabolism as initiated by the CYP27A1 pathway and stimulated by increased StAR expression would result, not only in increased cholesterol elimination as bile acids, but elicit a homeostatic response as a function of increased levels of at least three known regulatory oxysterols. More specifically, these oxysterols, working in a coordinate fashion, should lead to decreased cholesterol synthesis and increased cholesterol export; responses that would be expected to decrease serum and tissue cholesterol levels. Although not originally considered, a metabolic response in fatty acid metabolism should have been entertained given how tightly cholesterol and fatty acid metabolism are interwoven.

The apoE^{-/-} mouse was chosen as the animal model to explore this hypothesis as it is a well studied model of atherogenesis that on a rodent chow diet will develop serum and tissue dyslipidemia as it ages. The model was first confirmed with serum lipid analysis. As predicted, based upon prior in-vivo studies in rats and mice, 6 month old mice tolerated the level of increased StAR expression for 6 days without any detectable adverse effects or dietary differences from controls. Increased StAR expression led to a dramatic normalization of both serum and tissue cholesterol levels in apoE^{-/-} mice. Serum and tissue triglyceride levels demonstrated an even greater response. These responses demonstrate for the first time a possible therapeutic role for the CYP27A1-initiated pathway in the treatment of dyslipidemias.

Acknowledgments This work was supported by the National Natural Science Foundation of China (30871021) of the People's Republic of China (Yin, L), and the United States National Institutes of Health R01HL078898 (Ren, S).

References

1. Ansell BJ (2008) Hyperlipidaemia and cardiovascular disease. *Curr Opin Lipidol* 19:433–434
2. Cohen DE, Green RM, Wu MK, Beier DR (1999) Cloning, tissue-specific expression, gene structure and chromosomal localization of human phosphatidylcholine transfer protein. *Biochim Biophys Acta* 1447:265–270

3. Alpy F, Stoeckel ME, Dierich A, Escola JM, Wendling C, Chenard MP, Vanier MT, Gruenberg J, Tomasetto C, Rio MC (2001) The steroidogenic acute regulatory protein homolog MLN64, a late endosomal cholesterol-binding protein. *J Biol Chem* 276:4261–4269
4. Watari H, Arakane F, Moog-Lutz C, Kallen CB, Tomasetto C, Gerton GL, Rio MC, Baker ME, Strauss JFIII (1997) MLN64 contains a domain with homology to the steroidogenic acute regulatory protein (StAR) that stimulates steroidogenesis. *Proc Natl Acad Sci USA* 94:8462–8467
5. Romanowski MJ, Soccio RE, Breslow JL, Burley SK (2002) Crystal structure of the *Mus musculus* cholesterol-regulated START protein 4 (StarD4) containing a StAR-related lipid transfer domain. *Proc Natl Acad Sci USA* 99:6949–6954
6. Tsujishita Y, Hurley JH (2000) Structure and lipid transport mechanism of a StAR-related domain. *Nat Struct Biol* 7:408–414
7. Maxfield FR, Wustner D (2002) Intracellular cholesterol transport. *J Clin Invest* 110:891–898
8. Soccio RE, Adams RM, Maxwell KN, Breslow JL (2005) Differential gene regulation of StarD4 and StarD5 cholesterol transfer proteins. Activation of StarD4 by sterol regulatory element-binding protein-2 and StarD5 by endoplasmic reticulum stress. *J Biol Chem* 280:19410–19418
9. Christenson LK, Strauss JFIII (2000) Steroidogenic acute regulatory protein (StAR) and the intramitochondrial translocation of cholesterol. *Biochim Biophys Acta* 1529:175–187
10. Stocco DM (2000) Intramitochondrial cholesterol transfer. *Biochim Biophys Acta* 1486:184–197
11. Jefcoate C (2002) High-flux mitochondrial cholesterol trafficking, a specialized function of the adrenal cortex. *J Clin Invest* 110:881–890
12. Hall EA, Ren S, Hylemon PB, Rodriguez-Agudo D, Redford K, Marques D, Kang D, Gil G, Pandak WM (2005) Detection of the steroidogenic acute regulatory protein, StAR, in human liver cells. *Biochim Biophys Acta* 1733:111–119
13. Ning Y, Chen S, Li X, Ma Y, Zhao F, Yin L (2006) Cholesterol, LDL, and 25-hydroxycholesterol regulate expression of the steroidogenic acute regulatory protein in microvascular endothelial cell line (bEnd.3). *Biochem Biophys Res Commun* 342:1249–1256
14. Ning Y, Bai Q, Lu H, Li X, Pandak WM, Zhao F, Chen S, Ren S, Yin L (2008) Overexpression of mitochondrial cholesterol delivery protein, StAR, decreases intracellular lipids and inflammatory factors secretion in macrophages. *Atherosclerosis*. doi:10.1016/j.atherosclerosis.2008.09.006
15. Ma Y, Ren S, Pandak WM, Li X, Ning Y, Lu C, Zhao F, Yin L (2007) The effects of inflammatory cytokines on steroidogenic acute regulatory protein expression in macrophages. *Inflamm Res* 56:495–501
16. Pandak WM, Ren S, Marques D, Hall E, Redford K, Mallonee D, Bohdan P, Heuman D, Gil G, Hylemon P (2002) Transport of cholesterol into mitochondria is rate-limiting for bile acid synthesis via the alternative pathway in primary rat hepatocytes. *J Biol Chem* 277:48158–48164
17. Li X, Pandak WM, Erickson SK, Ma Y, Yin L, Hylemon P, Ren S (2007) Biosynthesis of the regulatory oxysterol, 5-cholesten-3 β , 25-diol 3-sulfate, in hepatocytes. *J Lipid Res* 48:2587–2596
18. Ren S, Hylemon P, Zhang ZP, Rodriguez-Agudo D, Marques D, Li X, Zhou H, Gil G, Pandak WM (2006) Identification of a novel sulfonated oxysterol, 5-cholesten-3 β , 25-diol 3-sulfonate, in hepatocyte nuclei and mitochondria. *J Lipid Res* 47:1081–1090
19. Ren S, Li X, Rodriguez-Agudo D, Gil G, Hylemon P, Pandak WM (2007) Sulfated oxysterol, 25HC3S, is a potent regulator of lipid metabolism in human hepatocytes. *Biochem Biophys Res Commun* 360:802–808
20. Ma Y, Xu L, Rodriguez-Agudo D, Li X, Heuman DM, Hylemon PB, Pandak WM, Ren S (2008) 25-Hydroxycholesterol-3-sulfate regulates macrophage lipid metabolism via the LXR/SREBP-1 signaling pathway. *Am J Physiol Endocrinol Metab* 295:E1369–E1379
21. Ren S, Hylemon PB, Marques D, Gurley E, Bodhan P, Hall E, Redford K, Gil G, Pandak WM (2004) Overexpression of cholesterol transporter StAR increases in vivo rates of bile acid synthesis in the rat and mouse. *Hepatology* 40:910–917
22. Harris JD, Schepelmann S, Athanasopoulos T, Graham IR, Stannard AK, Mohri Z, Hill V, Hassall DG, Owen JS, Dickson G (2002) Inhibition of atherosclerosis in apolipoprotein-E-deficient mice following muscle transduction with adeno-associated virus vectors encoding human apolipoprotein-E. *Gene Ther* 9:21–29
23. Plump AS, Smith JD, Hayek T, Alto-Setälä K, Walsh A, Verstuyft JG, Rubin EM, Breslow JL (1992) Severe hypercholesterolemia and atherosclerosis in apolipoprotein E-deficient mice created by homologous recombination in ES cells. *Cell* 71:343–353
24. Nakashima Y, Plump AS, Raines EW, Breslow JL, Ross R (1994) ApoE-deficient mice develop lesions of all phases of atherosclerosis throughout the arterial tree. *Arterioscler Thromb* 14:133–140
25. d'Uscio LV, Baker TA, Mantilla CB, Smith L, Weiler D, Sieck GC, Katusic ZS (2001) Mechanism of endothelial dysfunction in apolipoprotein E-deficient mice. *Arterioscler Thromb Vasc Biol* 21:1017–1022
26. Tamminen M, Mottino G, Qiao JH, Breslow JL, Frank JS (1999) Ultrastructure of early lipid accumulation in ApoE-deficient mice. *Arterioscler Thromb Vasc Biol* 19:847–853
27. Cyrus T, Witztum JL, Rader DJ, Tangirala R, Fazio S, Linton MF, Funk CD (1999) Disruption of the 12/15-lipoxygenase gene diminishes atherosclerosis in apo E-deficient mice. *J Clin Invest* 103:1597–1604
28. Zhang SH, Reddick RL, Piedrahita JA, Maeda N (1992) Spontaneous hypercholesterolemia and arterial lesions in mice lacking apolipoprotein E. *Science* 258:468–471
29. Pandak WM, Bohdan P, Franklund C, Mallonee DH, Eggertsen G, Bjorkhem I, Gil G, Vlahcevic ZR, Hylemon PB (2001) Expression of sterol 12 α -hydroxylase alters bile acid pool composition in primary rat hepatocytes and in vivo. *Gastroenterology* 120:1801–1809
30. Ren S, Hylemon P, Marques D, Hall E, Redford K, Gil G, Pandak WM (2004) Effect of increasing the expression of cholesterol transporters (StAR, MLN64, and SCP-2) on bile acid synthesis. *J Lipid Res* 45:2123–2131
31. Belcher JD, Egan JO, Bridgman G, Baker R, Flack JM (1991) A micro-enzymatic method to measure cholesterol and triglyceride in lipoprotein subfractions separated by density gradient ultracentrifugation from 200 microliters of plasma or serum. *J Lipid Res* 32:359–370
32. Carlson SE, Goldfarb S (1977) A sensitive enzymatic method for determination of free and esterified tissue cholesterol. *Clin Chim Acta* 79:575–582
33. Babiker A, Diczfalusy U (1998) Transport of side-chain oxidized oxysterols in the human circulation. *Biochim Biophys Acta* 1392:333–339
34. Babiker A, Andersson O, Lund E, Xiu RJ, Deeb S, Reshef A, Leitersdorf E, Diczfalusy U, Bjorkhem I (1997) Elimination of cholesterol in macrophages and endothelial cells by the sterol 27-hydroxylase mechanism. Comparison with high density lipoprotein-mediated reverse cholesterol transport. *J Biol Chem* 272:26253–26261
35. Lund E, Andersson O, Zhang J, Babiker A, Ahlborg G, Diczfalusy U, Einarsson K, Sjövall J, Bjorkhem I (1996) Importance of a novel oxidative mechanism for elimination of intracellular cholesterol in humans. *Arterioscler Thromb Vasc Biol* 16:208–212
36. Westman J, Kallin B, Bjorkhem I, Nilsson J, Diczfalusy U (1998) Sterol 27-hydroxylase- and apoAII/phospholipid-mediated efflux

- of cholesterol from cholesterol-laden macrophages: evidence for an inverse relation between the two mechanisms. *Arterioscler Thromb Vasc Biol* 18:554–561
37. Cali JJ, Hsieh CL, Francke U, Russell DW (1991) Mutations in the bile acid biosynthetic enzyme sterol 27-hydroxylase underlie cerebrotendinous xanthomatosis. *J Biol Chem* 266:7779–7783
38. Oftebro H, Bjorkhem I, Skrede S, Schreiner A, Pederson JI (1980) Cerebrotendinous xanthomatosis: a defect in mitochondrial 26-hydroxylation required for normal biosynthesis of cholic acid. *J Clin Invest* 65:1418–1430
39. Meir K, Kitsberg D, Alkalay I, Szafer F, Rosen H, Shpitzen S, Avi LB, Staels B, Fievet C, Meiner V, Bjorkhem I, Leitersdorf E (2002) Human sterol 27-hydroxylase (CYP27) overexpressor transgenic mouse model. Evidence against 27-hydroxycholesterol as a critical regulator of cholesterol homeostasis. *J Biol Chem* 277:34036–34041
40. Hall E, Hylemon P, Vlahcevic Z, Mallonee D, Valerie K, Avadhani N, Pandak W (2001) Overexpression of CYP27 in hepatic and extrahepatic cells: role in the regulation of cholesterol homeostasis. *Am J Physiol Gastrointest Liver Physiol* 281:G293–G301
41. Bouhrel MA, Staels B, Chinetti-Gbaguidi G (2008) Peroxisome proliferator-activated receptors—from active regulators of macrophage biology to pharmacological targets in the treatment of cardiovascular disease. *J Intern Med* 263:28–42
42. Chinetti G, Lestavel S, Bocher V, Remaley AT, Neve B, Torra IP, Teissier E, Minnich A, Jaye M, Duverger N, Brewer HB, Fruchart JC, Clavey V, Staels B (2001) PPAR-alpha and PPAR-gamma activators induce cholesterol removal from human macrophage foam cells through stimulation of the ABCA1 pathway. *Nat Med* 7:53–58
43. Javitt NB (2002) 25R, 26-Hydroxycholesterol revisited: synthesis, metabolism, and biologic roles. *J Lipid Res* 43:665–670
44. Lefebvre P, Cariou B, Lien F, Kuipers F, Staels B (2009) Role of bile acids and bile acid receptors in metabolic regulation. *Physiol Rev* 89:147–191
45. Li T, Chen W, Chiang JY (2007) PXR induces CYP27A1 and regulates cholesterol metabolism in the intestine. *J Lipid Res* 48:373–384

Common Variants of *ABCB4* and *ABCB11* and Plasma Lipid Levels: A Study in Sib Pairs with Gallstones, and Controls

Monica Acalovschi · Simona Tirziu ·
Erica Chiorean · Marcin Krawczyk ·
Frank Grünhage · Frank Lammert

Received: 12 January 2009 / Accepted: 1 April 2009 / Published online: 30 April 2009
© AOCs 2009

Abstract Most epidemiological surveys have confirmed the association of low HDL-cholesterol and high triglyceride levels with cholesterol gallstones. Our objective was to analyze the relationship between plasma lipid levels and common polymorphisms of *ABCB11* (encoding the bile salt export pump, BSEP) and *ABCB4* (encoding the phospholipid transporter into bile, MDR3) genes. Plasma lipids were measured in 108 index patients of sib pairs with gallstones and in 260 controls. Using PCR-based assays with 5'-nuclease and fluorescence detection (TaqMan), the *ABCB11* coding SNP p.A444V and four haplotype-tagging SNPs covering the *ABCB4* gene (c.504C > T, c.711T > A, p.R652G, *rs31653* in intron 26) were genotyped. Plasma lipids were compared in carriers of the common versus rare allele of these polymorphisms using Student's *t* test and Pearson's correlation. BMI and triglyceride levels were higher and HDL-cholesterol levels were lower in affected siblings than in controls. Among cases, triglyceride and cholesterol levels were higher in carriers of the common versus rare (hetero/homozygous carriers) allele of the SNPs p.A444V of *ABCB11* and C.504C > T of *ABCB4*. HDL-

cholesterol was lower in carriers of the common allele of *rs31653*. In controls, significant differences of cholesterol and HDL-cholesterol levels were found in carriers of *ABCB4* polymorphisms. Our results do not support the hypothesis of a link between *ABCB4* and *ABCB11* polymorphisms, lithogenic dyslipidemia, and gallstone risk.

Keywords Serum triglycerides · HDL cholesterol · Gallstones · Candidate genes · Polymorphisms · *ABCB4* · *ABCB11*

Introduction

The prevalence of cholesterol gallstone disease is rising in industrialized countries in Europe and North America [1–6]. Given the higher incidence at advanced ages, the longer life expectancy of the population, and the high costs of cholecystectomy, gallstones are a significant burden for these societies. Sustained efforts are presently directed to elucidate the genetic susceptibility factors of this common disease, with the objective of identifying high-risk groups and preventing gallstone formation.

Although supersaturation of bile with cholesterol is a prerequisite of lithogenesis, and cholesterol and bile acids in bile are the only ways of eliminating cholesterol from the body, even the largest series did not find an association between serum cholesterol level and gallstones. However, most case-control studies have confirmed the association of low serum HDL-cholesterol levels and hypertriglyceridemia with cholesterol gallstones [7, 8].

In a previous study we found that some common polymorphisms in the *ABCG5/ABCG8* genes, which encode the hepatic cholesterol transporter into bile, were significantly associated with high triglyceride and low HDL-cholesterol

M. Acalovschi · S. Tirziu · E. Chiorean
3rd Medical Clinic, University Iuliu Hatieganu,
Cluj-Napoca, Romania

M. Krawczyk · F. Grünhage · F. Lammert
2nd Medical Clinic, Saarland University Hospital,
Homburg, Germany

M. Acalovschi (✉)
3rd Medical Clinic, University of Medicine and Pharmacy,
Str. Croitorilor No.19-23, 400162 Cluj-Napoca, Romania
e-mail: monacal@umfcluj.ro

levels in siblings with gallstones, in contrast to gallstone carriers without positive family history [9].

Cholesterol gallstone formation is not only because of elevated biliary cholesterol concentrations, but also related to the bile acid and phospholipid contents of bile.

Serum lipid profiles in patients with rare mutations causing familial intrahepatic cholestasis are scarce, but point to increased triglyceride levels and the appearance of triglyceride-rich LDL particles in the setting of normal total cholesterol and low HDL levels [10–12], which are reminiscent of alterations reported for gallstone patients. Therefore, we have now evaluated levels of plasma lipids in siblings with gallstones in relation to common polymorphisms in the *ABCB4* and *ABCB11* genes encoding the hepatobiliary phospholipid and bile acid transporters, respectively. *ABCB11* (the gene encoding BSEP, the bile salt export pump) and *ABCB4* (the gene encoding MDR3, the phospholipid transporter across the canalicular membrane of the hepatocyte) have been designated as candidate genes for gallstone formation in mice, but studies in humans regarding the association of common variants of these genes with gallstone disease are sparse.

Materials and Methods

Subjects

All subjects were recruited prospectively at the Department of Gastroenterology, University of Cluj-Napoca, between November 2002 and April 2007.

The inclusion criteria for patients were: previous cholecystectomy for gallbladder stones or actual gallbladder stones (abdominal ultrasound) plus a family history of gallstone disease (at least one sibling with gallstones). Age, sex, and body mass index (BMI) were recorded on inclusion in the study. From 229 siblings with gallstones, belonging to 108 sib pairs, the index patients (i.e. the first ones recruited from each pair) were analyzed—94 females and 14 males with a mean age of 54.6 ± 11.2 years.

The inclusion criteria for the controls were: absence of gallstones or cholecystectomy, no relation to cases, and negative personal or family history of gallstone disease. Controls were comparable with cases with respect to ethnicity, geographical residence, hospitalization, and time of recruitment. Two hundred and sixty controls matched for gender and age were recruited (228 females and 32 males, mean age 52.9 ± 10.9 years).

Informed consent was obtained from each subject included in the study. The study protocol was approved by the Ethical Committee of the University of Medicine and Pharmacy at Cluj-Napoca.

Clinical Chemistry

Plasma levels of cholesterol, HDL-cholesterol, and triglycerides were assessed, after an overnight 12-h fast, by use of standard enzymatic colorimetric methods (Konelab 30 equipment, Finland).

Genotype Analysis

Genomic DNA was isolated using the QIAamo DNA extraction procedure (Qiagen). Employing PCR-based assays with 5'-nuclease and fluorescence detection (Taq-Man), the following SNPs were genotyped: the *ABCB11* coding SNP p.A444V (*rs2287622*), which is known to affect transporter expression (*rsXX*), and four haplotype-tagging SNPs covering the *ABCB4* gene (c.504C > T – *rs1202283*; c.711T > A – *rs2109505*; p.R652G – *rs8187799*; *rs31653* in intron 26), which were identified in our previous study [13].

Statistical Analysis

Results are expressed as mean \pm standard deviation (SD). Siblings with gallstone disease were divided into:

1. homozygotes for the common allele, and
2. heterozygotes or homozygotes for the minor allele.

Allele and genotype frequencies between cases and controls were compared by use of the χ^2 test and Armitage's trend test, respectively. Plasma lipid values were analyzed in cases and controls, and in carriers of the common allele versus carriers of the rare allele of the studied polymorphisms by using Student's *t* test for independent variables. Statistical significance was defined as a probability of $P < 0.05$. The correlation between lipid levels and BMI was calculated using Pearson's correlation coefficient.

Power Calculation

Power calculations were performed using the P&S power and sample size program that is available online (<http://biostat.mc.vanderbilt.edu>). The study population was designed to detect a 2.5-fold increase of relative risk with a power of 85% based on a frequency of the risk allele of ≥ 0.1 (significance level 0.05).

Results

We analyzed 108 index patients with gallstones belonging to 108 distinct families. Most (96; 88.8%) pedigrees

consisted of two affected siblings; eleven pedigrees contained three affected siblings, and one pedigree was composed of four affected siblings.

BMI and plasma lipid levels were significantly different in the index patients of the sib pairs than in controls. Triglyceride levels were higher, whereas total and HDL-cholesterol levels were lower in siblings with gallstones (Table 1).

Allele and genotype frequencies for index patients and controls are given in Table 2. Of note, all minor allele frequencies are >5%, indicating that the polymorphisms are common in our population. Allele and genotype frequencies did not differ between cases and controls (all $P > 0.05$).

Significant differences were found for the following plasma lipid levels in the index patients of the sib pairs with gallstones (Table 3): higher triglyceride levels in carriers of the common versus rare alleles of the *ABCB11* SNP *rs2287622*, higher triglyceride and cholesterol levels in carriers of the common allele of the *ABCB4* polymorphism *rs1202283*; and lower HDL-cholesterol in carriers of the common allele of the *ABCB4* SNP *rs31653*.

Among the index patients, we found a correlation between plasma triglyceride levels and BMI for carriers of the rare allele of SNP *rs1202283* ($r = 0.266$, $P < 0.05$), and for carriers of the common alleles of *rs2109505* ($r = 0.219$, $P < 0.05$) and *rs8187799* ($r = 0.227$, $P = 0.02$), all of which are located in the *ABCB4* gene. No correlations of triglyceride levels with age or with other polymorphisms of the two genes studied were detected in these patients.

In controls, the following plasma lipid changes were significant (Table 4): higher cholesterol levels in carriers of the common versus rare alleles of SNPs *rs2109505* and *rs8187799*, and lower HDL-cholesterol for carriers of the rare versus common allele of *rs31653*. No changes of the triglyceride levels were found between carriers of the common and rare alleles of these polymorphisms.

When we compared the index patients with the controls, we found significant differences for triglyceride levels,

Table 1 Characteristics and plasma lipid levels (mean \pm SD) in the study groups

	Siblings with gallstones (108)	Controls (260)	<i>P</i>
Gender (females/males)	94/14	228/32	NS
Age (years)	54.66 \pm 11.21	52.95 \pm 10.98	NS
BMI (kg/m ²)	28.86 \pm 5.22	25.93 \pm 5.62	<0.001
Triglycerides (mg/dl)	172.6 \pm 95.51	136.59 \pm 83.28	<0.001
Cholesterol (mg/dl)	214.16 \pm 48.71	228.4 \pm 49.11	<0.02
HDL-cholesterol (mg/dl)	49.55 \pm 15.32	55.64 \pm 13.95	<0.001

Table 2 Allele and genotype frequencies in index patients and controls

SNP	Allele/genotype	Allele/genotype frequency	
		Index patients	Controls
<i>ABCB11</i>			
<i>rs2287622</i>	C	0.54	0.58
	T	0.46	0.42
	CC	0.26	0.32
	CT	0.56	0.53
	TT	0.19	0.15
<i>ABCB4</i>			
<i>rs1202283</i>	C	0.62	0.57
	T	0.38	0.43
	CC	0.33	0.27
	CT	0.47	0.48
	TT	0.19	0.25
<i>rs2109505</i>	T	0.83	0.85
	A	0.17	0.15
	TT	0.69	0.71
	TA	0.30	0.27
	AA	0.01	0.2
<i>rs8187799</i>	A	0.89	0.87
	G	0.11	0.13
	AA	0.81	0.75
	AG	0.18	0.25
	GG	0.02	0.01
<i>rs31653</i>	G	0.92	0.92
	A	0.08	0.08
	GG	0.83	0.86
	GA	0.17	0.14
	AA	0.0	0.0

which were higher in siblings than in controls for carriers of the common alleles of almost all the polymorphisms studied. Cholesterol levels were higher in controls for carriers of the common alleles of the polymorphisms *rs2109505* and *rs8187799*, and HDL-cholesterol levels were lower in siblings versus controls for carriers of the rare alleles of SNPs *rs2287622* and *rs1202283* and of the common allele of SNP *rs31653*. These differences were in accordance with those between the mean values of triglyceride and HDL-cholesterol levels in affected siblings and controls (Table 1).

Discussion

Cholesterol gallstone disease is a complex disease, characterized by a genetic (polygenic) predisposition to develop gallstones associated with an important environmental effect. Many of the environmental (modifiable) risk

Table 3 Age, BMI, and plasma lipid levels of 108 index patients of sibling pairs with gallstones in relation to the common and rare (homozygous and heterozygous carriers) alleles of the *ABCB4* and *ABCB11* polymorphisms

	Allele	No. patients	Age (years)	BMI (kg/m ²)	Triglycerides (mg/dl)	Cholesterol (mg/dl)	HDL cholesterol (mg/dl)
<i>ABCB11</i> p.A444 V <i>rs2287622</i>	Common	28	55.14 ± 12.45	27.82 ± 4.54	198.03 ± 118.71*	228.96 ± 56.5	52.13 ± 17.74
	Rare	80	54.28 ± 10.8	29.36 ± 5.39	162.53 ± 85.86	207.78 ± 44.44	48.61 ± 14.8
<i>ABCB4</i> c.504C > T <i>rs1202283</i>	Common	34	56.26 ± 10.14	29.86 ± 5.85	204.67 ± 122.54*	230.55 ± 48.56 [§]	51.17 ± 15.86
	Rare	74	54.0 ± 11.53	28.94 ± 5.36	159.02 ± 77.04	204.42 ± 46.44	48.36 ± 15.02
<i>ABCB4</i> c.711T > A <i>rs2109505</i>	Common	75	53.77 ± 10.24	29.06 ± 5.56	173.77 ± 97.35	213.36 ± 49.01	49.23 ± 14.56
	Rare	33	56.9 ± 13.22	28.7 ± 4.37	170.87 ± 92.49	214.21 ± 48.78	49.5 ± 16.75
<i>ABCB4</i> p.R652G <i>rs8187799</i>	Common	83	54.36 ± 11.97	29.45 ± 5.27	181.31 ± 102.99	213.55 ± 48.34	49.39 ± 14.52
	Rare	21	55.95 ± 7.61	28.86 ± 5.7	159.61 ± 64.21	209.38 ± 54.05	46.31 ± 16.16
<i>ABCB4</i> <i>rs31653</i>	Common	89	54.5 ± 11.03	29.12 ± 5.4	172.95 ± 96.19	210.61 ± 48.64	48.77 ± 15.75*
	Rare	19	55.0 ± 12.18	27.66 ± 4.2	170.94 ± 94.85	230.78 ± 46.74	54.53 ± 13.07

Values given in bold are significantly different from controls—carriers of the same allele (Table 4)

* Significantly different than in carriers of the rare allele

Table 4 Age, BMI, and plasma lipid levels of 260 controls in relation to the common and rare (homozygous and heterozygous carriers) alleles of the *ABCB4* and *ABCB11* polymorphisms

	Allele	No. controls	Age (years)	BMI (kg/m ²)	Triglycerides (mg/dl)	Cholesterol (mg/dl)	HDL cholesterol (mg/dl)
<i>ABCB11</i> p.A444 V <i>rs2287622</i>	Common	79	53.99 ± 10.55	26.28 ± 4.11	128.11 ± 59.43	228.4 ± 37.15	57.11 ± 15.11
	Rare*	181	52.76 ± 11.18	25.78 ± 5.04	140.33 ± 91.75	229.21 ± 53.62	55.01 ± 13.41
<i>ABCB4</i> c.504C > T <i>rs1202283</i>	Common	69	52.41 ± 10.25	26.26 ± 5.54	152.52 ± 108.06	231.01 ± 53.21	55.06 ± 13.26
	Rare	191	53.15 ± 11.25	25.81 ± 4.46	130.92 ± 71.95	227.47 ± 47.69	55.84 ± 14.12
<i>ABCB4</i> c.711T > A <i>rs2109505</i>	Common	185	52.46 ± 9.87	26.32 ± 4.92	142.27 ± 92.03	233.89 ± 50.93*	56.34 ± 14.48
	Rare	75	54.17 ± 13.32	24.98 ± 4.26	122.15 ± 53.0	214.45 ± 41.29	53.85 ± 12.42
<i>ABCB4</i> p.R652G <i>rs8187799</i>	Common	192	52.37 ± 10.96	26.21 ± 4.62	142.06 ± 90.91	234.19 ± 51.2*	51.47 ± 14.22
	Rare	68	54.58 ± 10.95	25.13 ± 5.13	121.25 ± 54.36	212.14 ± 39.65	56.09 ± 13.30
<i>ABCB4</i> <i>rs31653</i>	Common	219	52.93 ± 10.70	25.43 ± 4.77	133.73 ± 84.53	228.92 ± 50.42	56.32 ± 14.21*
	Rare	38	52.79 ± 12.63	26.10 ± 4.81	148.08 ± 67.14	223.0 ± 40.30	51.61 ± 11.66

* Significantly different from carriers of the rare allele

factors—obesity, rapid weight loss, hypertriglyceridemia, high calorie diet, highly absorbable sugars, low fibre diet—have been identified in epidemiological studies and measures targeting them have been included in the preventive strategy for gallstone formation. The current challenge is to identify the genetic factors determining susceptibility to lithogenesis, and research is very intense both in experimental models and in humans. More than 20 cholesterol

gallstone susceptibility genes (*Lith*) have been identified in mice by quantitative trait locus (QTL) mapping.

In humans, in most cases, no Mendelian inherited trait could be demonstrated for gallstone disease. With the exception of cholesterol gallstone disease associated with low biliary phospholipid levels because of rare mutations in the *ABCB4* gene [14–16] and of gallstone disease induced by single mutations in the cholesterol 7-alpha

hydroxylase gene (*CYP7A1*) [17] or the gene encoding the CCK receptor A [18], no variants have been linked to cholesterol gallstones. Additional analyses regarding common variants of *ABCB4* [19], *ABCB11* [19, 20], and *CCKAR* [21] did not confirm their association with cholesterol gallstone disease in the populations studied.

A translational study that confirmed an association of a mouse *Lith* locus (*Lith9* on chromosome 17) as a susceptibility factor for cholelithiasis in humans, or a human *LITH* gene, was recently reported [22]. The polymorphism *rs11887534* (p.D19H) of the *ABCG8* gene, which encodes the hepatobiliary cholesterol hemitransporter, is the first identified susceptibility factor for gallstones in humans [22, 23]. Our previous study of plasma lipid levels in siblings with gallstones, carriers of common polymorphisms of *ABCG5/ABCG8*, identified significant associations of SNP *rs11887534* with plasma cholesterol and triglyceride levels [9].

There have been no previous studies evaluating the plasma lipid profile in carriers of the common polymorphisms of the genes encoding the membrane transporters of the other two major lipids into bile, phospholipids and bile acids. We evaluated plasma lipid levels in patients with gallstones and a positive family history (at least one sibling with gallstones) and in controls with a negative family history in order to find evidence of a possible relationship with common polymorphisms of the *ABCB4* (*MDR3*) and *ABCB11* (*BSEP*) genes.

The *ABCB4* gene encodes the hepatic canalicular transporter for the major phospholipid phosphatidylcholine, which acts as a phospholipid floppase [24]. *ABCB4* mutations result in a wide spectrum of phenotypes, ranging from progressive familial intrahepatic cholestasis (PFIC type 3) to intrahepatic cholestasis of pregnancy or intrahepatic and gallbladder microlithiasis (low phospholipid associated cholelithiasis, LPAC syndrome) [14, 15, 25]. The *Mdr2*^{-/-} mouse model supports the concept that this gene is a monogenic risk factor for cholesterol gallstones [26]. Some variants of *ABCB4* have been identified and studied in women with intrahepatic cholestasis of pregnancy [13, 27]. Although rare *ABCB4* variants contribute to gallstone formation in LPAC, studies investigating the relationship between gallstone susceptibility and common *ABCB4* polymorphisms in German patients failed to find an association [19].

The bile salt export pump (BSEP) encoded by the *ABCB11* gene is also a member of the ABC transporter family. BSEP is the major hepatocanalicular efflux system for the excretion of conjugated bile salts. Inhibition of BSEP by some drugs might lead to drug-induced cholestasis. Defects in the gene coding for BSEP can cause hereditary disorders such as progressive familial intrahepatic cholestasis (PFIC type 2), whereas some missense

mutations have been found to cause benign recurrent intrahepatic cholestasis (BRIC type 2) [28]. *Abcb11* (*Bsep*) co-localizes with the *Lith1* locus in mice, and congenic mouse strains carrying susceptible *Lith1* alleles develop cholesterol gallstones when fed a lithogenic diet [29]. Nevertheless, further studies failed to find different levels of the BSEP protein in gallstone-susceptible versus resistant strains of mice [30]. In humans, a study performed in the POPGEN cohort in Northern Germany [20] showed that the common gallstone trait is not allelic to PFIC type 2 at the *ABCB11* locus. Recent studies have confirmed that the common *ABCB11* coding SNP *rs2287622* (p.A444V), which is known to affect transporter expression [31, 32], is not associated with an increased risk of gallstones [19].

In this study we evaluated sibling pairs in whom the *ABCG8* variant *rs11887534* has been found to confer genetic susceptibility to gallstone disease [22]. The relationship of plasma lipid values to common variants of the genes controlling two other hepatobiliary lipid transporters (*ABCB4* and *ABCB11*) were compared between siblings with gallstones and controls without gallstones. Although plasma lipid levels were significantly different among these groups for carriers of common alleles of some polymorphisms (Table 3), these differences were similar to those found between the mean values of plasma lipids in patients and controls (Table 1). We did not find any association between plasma lipid levels and the common variants of *ABCB11* and *ABCB4* in gallstone-affected siblings as compared with stone-free controls.

Our results do not support the hypothesis of a link between *ABCB4* and *ABCB11* common variants and gallstone risk and confirm previous studies suggesting that common polymorphisms of these genes are not related to gallstone susceptibility.

Acknowledgment Supported by grants from the Romanian National Council of Scientific Research in Universities (CNCSIS 1263/2005 to M.A.), the German Research Council (Deutsche Forschungsgemeinschaft DFG LA 997/3-1 to F.L.), and the University of Bonn, Germany (BONFOR O-107.0083 to F.G.).

References

1. Acalovschi M, Dumitrascu DL, Caluser I, Ban A (1987) Comparative prevalence of gallstone disease at 100-year interval in a large Romanian town. A necroptic study. *Dig Dis Sci* 32:354–357
2. Bates T, Harrison M, Lowe D, Lawson C, Padley N (1992) Longitudinal study of gallstone prevalence at necropsy. *Gut* 33:103–107
3. Acalovschi M, Pascu M, Iobagiu S, Petrescu M, Olinici CD (1995) Increasing gallstone prevalence and cholecystectomy rate in a large Romanian town. *Dig Dis Sci* 40:2582–2586
4. Lammert F, Sauerbruch T (2005) Mechanisms of disease: the genetic epidemiology of gallbladder stones. *Nat Clin Pract Gastroenterol Hepatol* 2:423–433

5. Everhart JE, Khare M, Hill M, Maurer KR (1999) Prevalence and ethnic differences in gallbladder disease in the United States. *Gastroenterology* 117:632–639
6. Portincasa P, Moschetta A, Palasciano G (2006) Cholesterol gallstone disease. *Lancet* 368:230–239
7. Ahlberg J (1979) Serum lipid levels and hyperlipoproteinaemia in gallstone patients. *Acta Chir Scand* 145:373–377
8. Petitti D, Friedman GD, Klatsky AL (1981) Association of a history of gallbladder disease with a reduced concentration of high-density-lipoprotein cholesterol. *N Engl J Med* 304:1396–1398
9. Acalovschi M, Ciocan A, Mosteanu O, Tarziu S, Chiorean E, Keppeler H, Schirin-Sokhan R, Lammert F (2006) Are plasma lipid levels related to ABCG5/ABCG8 polymorphisms? A preliminary study in siblings with gallstones. *Eur J Int Med* 17:490–494
10. Nagasaka H, Yorifuji T, Egawa H, Yanai H, Fujisawa T, Kosugiyama K, Matsui A, Hasegawa M, Okada T, Takayanagi M, Chiba H, Kobayashi K (2005) Evaluation of risk for atherosclerosis in Alagille syndrome and progressive familial intrahepatic cholestasis: two congenital cholestatic diseases with different lipoprotein metabolisms. *J Pediatr* 146:329–335
11. Nagasaka H, Chiba H, Hui SP, Takikawa H, Miida T, Takayanagi M, Yorifuji T, Hasegawa M, Ota A, Hirano K, Kikuchi H, Tsukahara H, Kobayashi K (2007) Depletion of high-density lipoprotein and appearance of triglyceride-rich low-density lipoprotein in a Japanese patient with FIC1 deficiency manifesting benign recurrent intrahepatic cholestasis. *J Pediatr Gastroenterol Nutr* 45:96–105
12. Davit-Spraul A, Gonzales E, Baussan C, Jacquemin E (2009) Progressive familial intrahepatic cholestasis. *Orphanet J Rare Dis* 4. doi:10.1186/1750-1172-4-1
13. Wasmoth HE, Glantz A, Keppeler H, Simon E, Bartz C, Rath W, Mattsson LA, Marschall HU, Lammert F (2007) Intrahepatic cholestasis of pregnancy: the severe form is associated with common variants of the hepatobiliary phospholipid transporter ABCB4 gene. *Gut* 56:265–270
14. Rosmorduc O, Hermelin B, Boelle PY, Parc R, Taboury J, Poupon R (2003) ABCB4 gene mutation-associated cholelithiasis in adults. *Gastroenterology* 125:452–459
15. Jacquemin E (2001) Role of multidrug resistance 3 deficiency in pediatric and adult liver disease: one gene for three diseases. *Semin Liver Dis* 21:551–562
16. Shoda J, Oda K, Suzuki H, Sugiyama Y, Ito K, Cohen DE (2001) Etiologic significance of defects in cholesterol, phospholipid and bile acid metabolism in the liver of patients with intrahepatic calculi. *Hepatology* 33:1194–1205
17. Pullinger CR, Eng C, Salen G, Shefer S, Erickson SK, Verhagen A, Rivera CR, Mulvihill SJ, Malloy MJ, Kane JP (2002) Human cholesterol 7 α -hydroxylase (CYP7A1) deficiency has a hypercholesterolemic phenotype. *J Clin Invest* 110:109–117
18. Miller LJ, Holicky EL, Ulrich CD, Wieben ED (1995) Abnormal processing of the human cholecystokinin receptor gene in association with gallstones and obesity. *Gastroenterology* 109:1375–1380
19. Krawczyk M, Wolska M, Grünhage F, Sauerbruch T, Acalovschi M, Lammert F (2008) Common ABCB4 and ABCB11 transporter gene variants are not associated with susceptibility to gallstone formation in the general population. *Z Gastroenterol* 46:150 (abstr.)
20. Schafmayer C, Tepel J, Franke A, Buch S, Lieb S, Seeger M, Lammert F, Kremer B, Fölsch UR, Fändrich F, Schreiber S, Hampe J (2006) Investigation of the Lith1 candidate genes ABCB11 and LXRA in human gallstone disease. *Hepatology* 44:650–657
21. Miyasaka K, Takata Y, Funakoshi A (2002) Association of cholecystokinin A receptor polymorphism with cholelithiasis and the molecular mechanisms of this polymorphism. *J Gastroenterol* 37:102–106
22. Grunhage F, Acalovschi M, Tirziu S, Walier M, Wienker TF, Ciocan A, Mosteanu O, Sauerbruch T, Lammert F (2007) Increased gallstone risk in humans conferred by common variant of hepatic atp-binding cassette transporter for cholesterol. *Hepatology* 46:793–801
23. Buch S, Schafmayer C, Völzke H, Becker C, Franke A, von Eller-Eberstein H, Kluck C, Bässmann I, Brosch M, Lammert F, Miquel JF, Nervi F, Wittig M, Roskopf D, Timm B, Höll C, Seeger M, ElSharawy A, Lu T, Egberts J, Fändrich F, Fölsch UR, Krawczak M, Schreiber S, Nürnberg P, Tepel J, Hampe J (2007) A genome-wide association scan identifies the hepatic cholesterol transporter ABCG8 as a susceptibility factor for human gallstone disease. *Nat Genet* 39:995–999
24. Oude Elferink RPJ, Ottenhoff R, van Wijland M, Frijters CMG, van Nieuwkerk C, Groen AK (1996) Uncoupling of biliary phospholipid and cholesterol secretion in mice with reduced expression of mdr2 P-glycoprotein. *J Lipid Res* 37:1065–1075
25. Rosmorduc O, Hermelin R, Poupon R (2001) MDR3 gene defect in adults with symptomatic intrahepatic and gallbladder cholesterol cholelithiasis. *Gastroenterology* 120:1459–1467
26. Lammert F, Wang DQ, Hillebrandt S, Geier A, Fickert P, Trauner M, Matern S, Paigen B, Carey MC (2004) Spontaneous cholelithiasis and hepatolithiasis in Mdr2^{-/-} mice: a model for low-phospholipid-associated cholelithiasis. *Hepatology* 39:117–128
27. Mullenbach R, Linton KJ, Wiltshire S, Weerasekera N, Chambers J, Elias E, Higgins CF, Johnston DG, McCarthy MI, Williamson C (2003) ABCB4 gene sequence variation in women with intrahepatic cholestasis of pregnancy. *J Med Genet* 40:e70
28. Van Mil SWC, Van der Woerd WL, Van der Brugge G, van der Brugge G, Sturm E, Jansen PL, Bull LN, van den Berg IE, Berger R, Houwen RH, Klomp LW (2004) Benign recurrent intrahepatic cholestasis type 2 is caused by mutations in ABCB11. *Gastroenterology* 127:379–384
29. Lammert F, Carey MC, Paigen B (2001) Chromosomal organization of candidate genes involved in cholesterol gallstone formation: a murine gallstone map. *Gastroenterology* 120:221–238
30. Muller O, Challa C, Scheibner J, Stange EF, Fuchs M (2002) Expression of liver plasma membrane transporters in gallstone-susceptible and gallstone-resistant mice. *Biochem J* 361:673–679
31. Lang C, Meier Y, Stieger B, Beuers U, Lang T, Kerb R, Kullak-Ublick GA, Meier PJ, Pauli-Magnus C (2007) Mutations and polymorphisms in the bile salt export pump and the multidrug resistance protein 3 associated with drug-induced liver injury. *Pharmacogenet Genomics* 17:47–60
32. Meier Y, Pauli-Magnus C, Zanger UM, Klein K, Schaeffeler E, Nussler AK, Nussler N, Eichelbaum M, Meier PJ, Stieger B (2006) Interindividual variability of canalicular ATP-binding-cassette (ABC)-transporter expression in human liver. *Hepatology* 44:62–74

Bile Acids Conjugation in Human Bile Is Not Random: New Insights from ^1H -NMR Spectroscopy at 800 MHz

G. A. Nagana Gowda · Narasimhamurthy Shanaiah ·
Amanda Cooper · Mary Maluccio · Daniel Raftery

Received: 6 December 2008 / Accepted: 16 March 2009 / Published online: 17 April 2009
© AOCs 2009

Abstract Bile acids constitute a group of structurally closely related molecules and represent the most abundant constituents of human bile. Investigations of bile acids have garnered increased interest owing to their recently discovered additional biological functions including their role as signaling molecules that govern glucose, fat and energy metabolism. Recent NMR methodological developments have enabled single-step analysis of several highly abundant and common glycine- and taurine- conjugated bile acids, such as glycocholic acid, glycodeoxycholic acid, glycochenodeoxycholic acid, taurocholic acid, taurodeoxycholic acid, and taurochenodeoxycholic acid. Investigation of these conjugated bile acids in human bile employing high field (800 MHz) ^1H -NMR spectroscopy reveals that the ratios between two glycine-conjugated bile acids and their taurine counterparts correlate positively ($R^2 = 0.83\text{--}0.97$; $p = 0.001 \times 10^{-2}\text{--}0.006 \times 10^{-7}$) as do the ratios between a glycine-conjugated bile acid and its taurine counterpart ($R^2 = 0.92\text{--}0.95$; $p = 0.004 \times 10^{-3}\text{--}0.002 \times 10^{-10}$). Using such correlations, concentration of individual bile acids in each sample could be predicted in good agreement with the experimentally determined values. These insights into the pattern of bile acid conjugation in human bile between

glycine and taurine promise useful clues to the mechanism of bile acids' biosynthesis, conjugation and enterohepatic circulation, and may improve our understanding of the role of individual conjugated bile acids in health and disease.

Keywords Human gallbladder bile · Conjugation pattern · Glycine-conjugated bile acids · Taurine-conjugated bile acids · ^1H -NMR · Single-step analysis · Metabolite profiling

List of abbreviations

GCA	Glycocholic acid
GDCA	Glycodeoxycholic acid
GCDCA	Glycochenodeoxycholic acid
TCA	Taurocholic acid
TDCA	Taurodeoxycholic acid
TCDCa	Taurochenodeoxycholic acid
NMR	Nuclear magnetic resonance

Introduction

Bile acids constitute a group of structurally closely related molecules. Their steroid-like moieties consist of mono-, di-, or tri-hydroxy groups. Tri- and di-hydroxy bile acids, such as cholic acid and chenodeoxycholic acid, respectively, are known as primary bile acids because they are biosynthesized from cholesterol in hepatocytes. The others are known as secondary bile acids. Secondary bile acids are thought to be the products of gut bacterial deconjugation during enterohepatic circulation. In human bile, both primary and secondary bile acids are normally conjugated to glycine or taurine. Conjugated bile acids are the major components of human bile, with their total concentration exceeding that of any other metabolite in bile.

Electronic supplementary material The online version of this article (doi:10.1007/s11745-009-3296-4) contains supplementary material, which is available to authorized users.

G. A. Nagana Gowda (✉) · N. Shanaiah · D. Raftery
Department of Chemistry, Purdue University, West Lafayette,
IN 47907, USA
e-mail: ngowda@purdue.edu

A. Cooper · M. Maluccio (✉)
Department of Surgery, Indiana University School of Medicine,
Indianapolis, IN 46202, USA
e-mail: mmalucci@iupui.edu

Bile acids have long been known to play an important, but less appreciated, biological role in lipid absorption and cholesterol catabolism. Recently, they have also been recognized as signaling molecules with systemic endocrine functions [1]. In addition, it is shown that increased bile acid levels facilitate liver regeneration and decreased levels inhibit re-growth [2]. The role of bile acids in maintaining energy homeostasis has been recently highlighted [3]. Strong evidence for a previously unknown mechanism by which conjugated bile acids facilitate their antimicrobial effects in the small intestine was recently presented [4]. Bile acids are also shown to have close links with human diseases including hepatocellular carcinoma and cholangiocarcinoma [5–8]. Key differences in bile acid metabolism observed in diabetes based on investigations of human subjects, suggest yet another important role of bile acid metabolism [9, 10].

The link between bile acids and a multitude of deleterious effects in humans has increased the interest in better understanding of the bile acid physiology [11, 12]. Although, mass spectrometry based methods are highly useful for analyzing bile acids, establishing the relationship between glycine- and taurine-conjugation has not been possible so far [13–16]. This may be due to the tedious and often not so reproducible separation procedures associated with such analysis methods. In contrast, NMR spectroscopy is highly reproducible and quantitative. Hence, it is an attractive technique for analyzing a large number of bile acids in a single-step, particularly when the concentration is not a limiting factor. Recently, from a series of comprehensive NMR studies of human bile and authentic bile acids, we reported simple NMR methodologies for detecting and quantifying major bile metabolites including a number of conjugated bile acids in human bile [17–20]. Subsequently, using these methods we have shown significant differences in the concentrations of bile metabolites between liver disease patients and controls [21]. Such developments would be useful for discovering biomarkers in light of the emerging area of ‘metabolomics’, which is based on single-step analysis of multiple metabolites in biological systems [22–27]. In the present study, we hypothesized that understanding of the conjugation pattern of bile acids is important to explore its pathophysiological significance in human health and disease. Accordingly, continuing our studies of human bile, we have investigated bile acids conjugation pattern using NMR spectroscopy at high magnetic fields (800 MHz). The investigations reveal that glycine- and taurine-conjugation of bile acids in human bile is not random, but follows a highly correlative pattern. Such findings open new avenues for exploring physiology of bile acids in health and understanding the possible links between conjugation pattern and liver diseases.

Materials and Methods

Chemicals

Deuterium oxide (D_2O), and sodium salt of trimethylsilylpropionic acid- d_4 (TSP) were purchased from Sigma-Aldrich (Milwaukee, WI, USA).

Human Gallbladder Bile

Gallbladder bile was obtained from 44 patients (22 male; 22 female; mean age 50.7 years). These included both liver disease ($n = 27$) and non-liver disease patients ($n = 17$). Liver disease included both malignant, hepatocellular carcinoma ($n = 10$) and cholangiocarcinoma ($n = 7$), and non-malignant ($n = 9$) disease patients. Non-malignant liver disease included patients with alcoholic cirrhosis ($n = 3$); cirrhosis due to hepatitis C infection ($n = 3$); non-alcoholic steatohepatitis cirrhosis ($n = 1$); choledochal cyst ($n = 1$) and primary sclerosing cholangitis ($n = 1$).

Bile Collection and Storage

Gallbladder bile was taken at the beginning of the case, prior to any devascularization of the gallbladder. A purse string suture was placed in the fundus of the gallbladder. Through an 18-gauge needle, 10 mL of bile was removed and placed immediately into a red top tube treated with 0.1% sodium azide. The suture was tied down to eliminate any bile leakage and the gallbladder taken off the liver. Bile specimen was then divided into 1-mL aliquots and stored at $-80^\circ C$ until analysis. An Institutional Review Board protocol, approved at both Indiana University School of Medicine and Purdue University, was in place for the collection, storage, and analysis of human bile for research purposes.

NMR Experiments

All 1H -NMR experiments were performed on a Bruker Biospin Avance 800 MHz NMR spectrometer using a 5-mm CHN inverse probehead equipped with automatic tune and match, and shielded triple axis (x, y, z) gradients.

Bile solutions were prepared for NMR analysis by diluting 100 μL of bile to 600 μL using doubly distilled water. A reusable co-axial capillary tube containing TSP in D_2O was inserted into the NMR tube before recording 1H -NMR spectra. While D_2O served as a field-frequency locking solvent, TSP served as chemical shift as well as a quantitative reference. Recently, from the comprehensive analysis of bile 1H -NMR spectra, we have shown that the characteristic amide signals constituting three

glycine-conjugated bile acids, glycocholic acid (GCA), glycodeoxycholic acid (GDCA), glycochenodeoxycholic acid (GCDCA), and their taurine counterparts, taurocholic acid (TCA), taurodeoxycholic acid (TDCA) and taurochenodeoxycholic acid (TCDCA), invariably appear in the region 7.8–8.1 ppm [20]. We have also shown that these bile acids signals are better distinguished when the coupling between amide protons and the attached methylene protons is removed by decoupling. Hence, one dimensional $^1\text{H-NMR}$ spectra were obtained using a one pulse sequence with (and without) homonuclear decoupling of the methylene protons. Simultaneous decoupling of the amide protons of all the conjugated bile acids was achieved by setting the decoupling frequency at 3.65 ppm, in between the chemical shifts of methylene protons of conjugated taurine (3.56 ppm) and conjugated glycine (3.75 ppm).

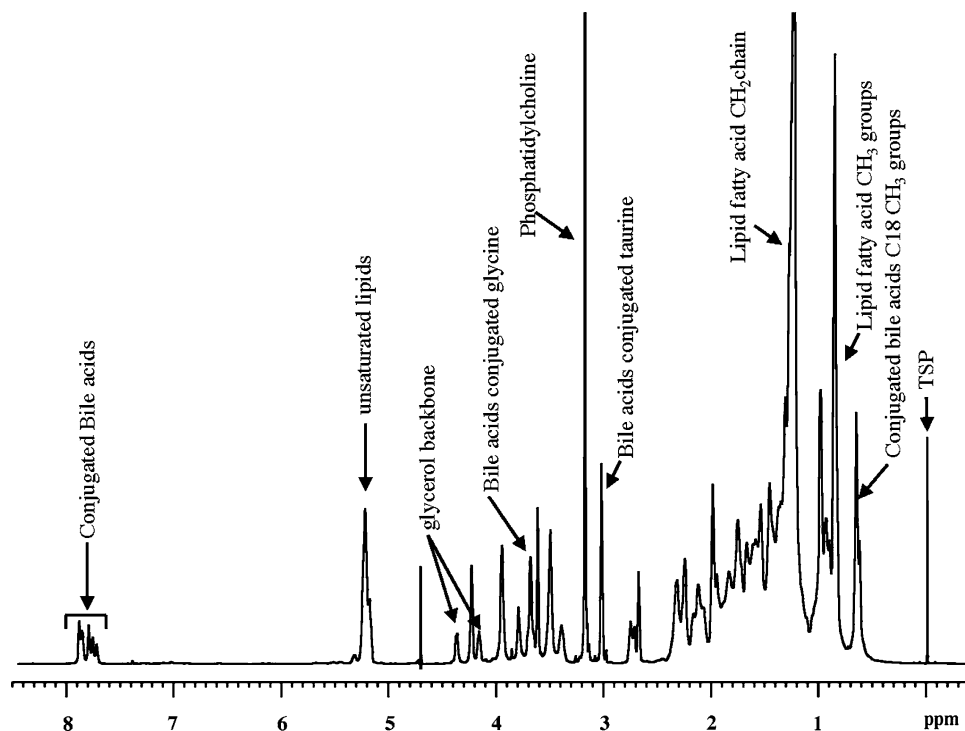
It is shown from the experiments performed at different pH that the amide signals of individual conjugated bile acids represent more quantitatively over the pH range 6 ± 0.5 [18, 20]. Hence, the pH of each bile solution was adjusted to this range by the addition of 1–2 μL of 1 N hydrochloric acid. Typical parameters used were: spectral width: 12,000 Hz; time domain data points: 32 K; flip angle: 45° ; acquisition time: 1.4 s; relaxation delay: 3 s; number of transients: 64; spectrum size: 32 K points. This resulted in an acquisition time of 4.6 min for each NMR experiment. Water signal suppression was achieved by presaturation during the relaxation delay while

homonuclear decoupling was performed during the data acquisition. The recycle delay was chosen based on the optimization studies performed earlier using delays varying from 1 to 10 s [20]. Thus, we rule out any change in intensity of the amide signals either due to relaxation or NOE buildup during decoupling of the adjacent methylene protons.

Quantitative Estimation of Individual Conjugated Bile Acids

Peak areas for the characteristic bile acids' amide signals (between 7.8 and 8.1 ppm; see Figs. 1, 2) and the TSP reference were obtained by integration. The total bile acid concentration in each bile sample was first determined using these integrals and the concentration of the reference compound after taking into account the number of protons contributed from the bile acids as well as the reference compound. Subsequently, the relative area under each conjugated bile acid signal was determined by signal deconvolution using Bruker xwinnmr software. For the deconvolution of the spectra, Lorentzian line shape was used. The concentration of individual bile acids was then determined using the relative integrals of individual bile acids and the amount of total bile acids as determined above. Decoupled spectra were used for the analysis of bile acids.

Fig. 1 Typical $^1\text{H-NMR}$ spectrum at 800 MHz of human gallbladder bile (100 μL bile diluted to 600 μL)



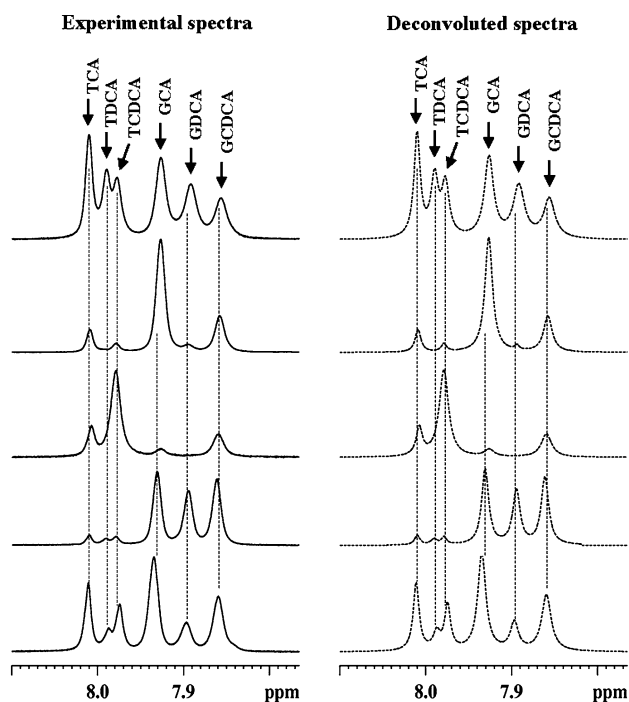


Fig. 2 *Left* Portions of the 800 MHz ^1H -NMR spectra of gallbladder bile from five different patients (four from non-liver disease controls and one from hepatitis C patient). The spectra were obtained by decoupling methylene protons of glycine-/taurine-conjugated bile acids. *Right* The corresponding deconvoluted spectra obtained for estimating the integrals. *GCA* glycocholic acid; *GCDCA* glycochenodeoxycholic acid; *GDCA* glycodeoxycholic acid; *TCA* taurocholic acid; *TCDC*A: taurochenocholic acid and *TDCA* taurodeoxycholic acid

Assessment of Bile Acids Conjugation

Glycine- and taurine-conjugation in human bile samples was assessed by comparing the bile acids individually and in the following combinations. (1) The ratio between glycine- and the corresponding taurine-conjugated bile acid in different bile samples was assessed by comparison. (2) The ratio between two glycine-conjugated bile acids was compared with the ratio between the corresponding taurine-conjugated counterparts. (3) The ratio between a glycine-conjugated bile acid and its taurine-conjugated counterpart was compared with the ratio between another glycine-conjugated bile acid and its taurine-conjugated counterpart. Linear regression analysis was performed for the ratios obtained in the latter two steps (steps 2 and 3) to estimate the inter-relationship between the ratios of the bile acids.

Finally, concentration of each conjugated bile acid was predicted using experimentally determined values of the other three bile acids. This prediction was based on the results of the regression analysis as described below which indicate that the ratio between two glycine-conjugated bile acids linearly correlates with the ratio between the

corresponding taurine-conjugated bile acids or, alternatively, the ratio between a glycine-conjugated bile acid and its taurine-conjugated counterpart linearly correlates with the ratio between another glycine-conjugated bile acid and its taurine-conjugated counterpart. The predicted bile acids concentrations were then compared with the experimentally determined values from the NMR spectra for the six conjugated bile acids, individually.

Statistical Analysis

All linear regression analyses were made using Microsoft Excel and R statistical package (version 2.8.1). The Excel software was first used to calculate the ratios of various combinations of the glycine- and taurine-conjugated bile acids (*TCA/TCDC*A, *GCA/GCDCA*, *TCA/TDC*A, *GCA/GDCA*, *TDCA/TCDC*A, *GDCA/GCDCA*, *GCA/TCA*, *GCDCA/TCDC*A, *GCA/TCA*, *GDCA/TDC*A, *GCDCA/TCDC*A versus *GDCA/TDC*A) for each patient using the concentration of individual bile acids obtained from ^1H -NMR spectra. The plots of the ratio of *TCA/TCDC*A versus *GCA/GCDCA*, *TCA/TDC*A versus *GCA/GDCA*, *TDCA/TCDC*A versus *GDCA/GCDCA*, *GCA/TCA* versus *GCDCA/TCDC*A, *GCA/TCA* versus *GDCA/TDC*A and *GCDCA/TCDC*A versus *GDCA/TDC*A were then made to assess the correlation of the ratios. Subsequently, using the Excel software, the linear regression analysis was made and, the equations for the line-fitting and the correlation coefficient (R^2) were determined. Further, the statistical significance of the correlations was determined using the R program using Pearson product moment correlation analysis.

Results

This investigation aims at understanding the conjugation pattern of glycine- and taurine-conjugated bile acids in humans. Considering the fact that the glycine and taurine conjugation depends on a number of factors and the amount of bile acids varies widely between the two types even across the non-liver disease patients (as shown later), it will not be possible to trace possible relationship between the two types of bile acids in humans from a glycine- and a taurine-conjugated bile acids. It thus necessitated comparison of the ratios of a pair of glycine- conjugated bile acids with the corresponding pair of taurine-conjugated bile acids. Hence, all the bile samples that showed less than a pair of glycine and the corresponding taurine-conjugated bile acids were omitted from the analysis (see for example, supplementary Fig. S1). In addition, four bile samples in which individual bile acids could not be quantified

Table 1 Patient profile and the number of bile acids observed by NMR

Disease type	Number of patients	Number of patients in which all six conjugated bile acids were detected ^a	Number of patients in which only four conjugated bile acids were detected ^b
Hepatocellular carcinoma	6	2	4
Cholangio-carcinoma	3	1	2
Hepatitis C	2	0	2
Alcoholic cirrhosis	1	0	1
Non-alcoholic steatohepatitis cirrhosis	1	0	1
Non-liver disease	11	7	4

^a Six bile acids detected were GCA, GCDCA, GDCA, TCA, TCDCA, and TDCA

^b Secondary bile acids, GDCA, and TDCA, were not detected in these patients

accurately due to excessive line broadening were also omitted to avoid possible error in the measurement of the signal integrals adversely influencing the outcome of the study (see for example, supplementary Fig. S2). Of the 44 bile samples, 24 met the minimum requirement which were used for evaluating the bile acids conjugation pattern. Table 1 shows the patient profile and the number of conjugated bile acids detected in each category of patients considered in this study.

Figure 1 shows a typical one-dimensional ¹H-NMR spectrum of intact human gallbladder bile obtained at 800 MHz. Owing to the amphipathic nature of major bile metabolites such as phospholipids, cholesterol and bile acids which exist in aggregated form, the spectral lines appear somewhat broad as seen in the figure. All major metabolites which contribute to the bulk of the complex NMR spectra of bile have recently been individually identified by exhaustive NMR studies at different magnetic fields [20]. Six of the metabolites were bile acids conjugated to glycine or taurine (GCA, GCDCA, GDCA, TCA, TCDCA, and TDCA). In the present study, all the six conjugated bile acids were observed in 14 of 24 bile samples, while only four (GCA, GCDCA, TCA, and TCDCA) were observed in the remaining 10 (Table 1). It may be noted that, in the entire set of 24 bile samples, all the glycine- conjugated bile acids were the counterparts of the taurine-conjugated bile acids or vice versa.

Not surprisingly, the concentration of the individual bile acids varied significantly across the sample set as shown in Figs. 2 and 3. Even the ratios between the total glycine- and taurine-conjugated bile acids (Fig. 4a) or between a glycine-conjugated bile acid and its taurine counterpart varied significantly (Fig. 4b–d). Interestingly, however, the ratios between two glycine-conjugated bile acids and between their taurine counterparts linearly correlated (Fig. 5) and the significance of the correlations was very high for all the ratios. The correlation coefficients and p values were, $R^2 = 0.83$ and $p = 0.006 \times 10^{-7}$ for the correlation of ratio of GCA and GCDCA with the ratio of TCA and TCDCA (Fig. 5a); 0.97 and 0.004×10^{-4} for the correlation of the ratio of GCA and GDCA with the ratio of

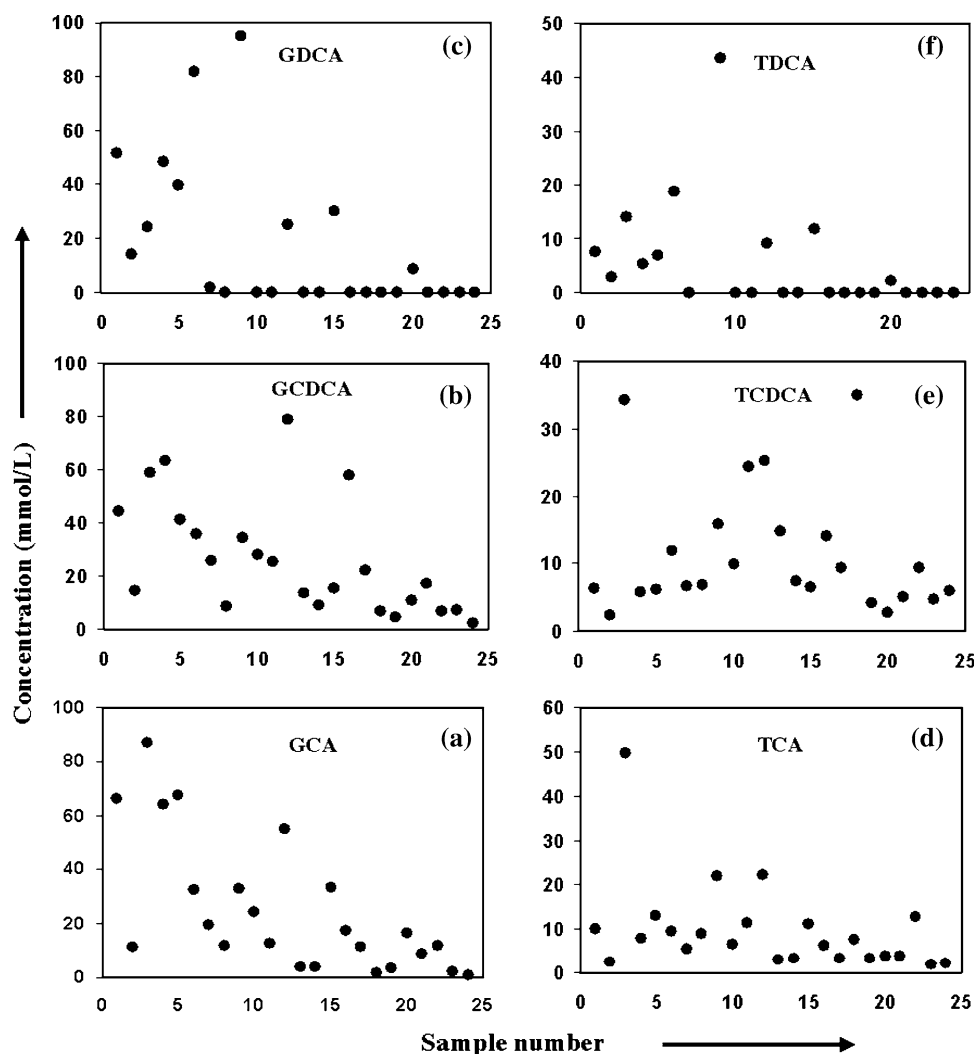
TCA and TDCA (Fig. 5b) and 0.92 and 0.001×10^{-2} for the correlation of the ratio of GDCA and GCDCA with the ratio of TDCA and TCDCA (Fig. 5c). Similarly the ratios between glycine-conjugated bile acid and its taurine counterpart, and those between another glycine-conjugated bile acid and its taurine counterpart were also highly linearly correlated: $R^2 = 0.92$ and $p = 0.002 \times 10^{-10}$ for the correlation of the ratio of GCA and TCA with that of GCDCA and TCDCA (Fig. 5d); 0.95 and 0.003×10^{-3} for the correlation of the ratio of GCA and TCA with that of GDCA and TDCA (Fig. 5e) and 0.94 and 0.004×10^{-3} for the correlation of the ratio of GCDCA and TCDCA with that of GDCA and TDCA (Fig. 5f). The regression equations of the correlations show a slope of close to one for the ratios of bile acids as shown in Fig. 5.

The concentration of individual bile acids in each bile sample was predicted using such correlations and experimentally determined values of the other three bile acids as follows. The concentration of GCA was predicted using the experimental values of TCA, GCDCA, and TCDCA; the concentration of GDCA using GCA, TCA, and TDCA; the concentration of GCDCA using GCA, TCA, and TCDCA; the concentration of TCA using GCA, GCDCA, and TCDCA; the concentration of TDCA using GCA, TCA, and GDCA and the concentration of TCDCA using GCA, TCA, and GCDCA. The correlations between the experimental and predicted values for the six conjugated bile acid are shown in the supplementary Fig. S3; as excepted from the results shown in Fig. 5, the experimental and predicted values for all the bile acids were highly correlated (supplementary Fig. S3).

Discussion

This study takes advantage of recent methodological advancements in NMR which enabled identification of major bile metabolites in intact human bile [19, 20]. Employing these methodologies and using ¹H-NMR spectroscopy at 800 MHz, we have studied human bile to investigate glycine and taurine conjugation patterns of bile acids.

Fig. 3 Concentration of individual bile acids (in mmol/L) for different bile samples. Abbreviations are as described before in Fig. 2 caption



Generally, in human bile, six conjugated bile acids can be detected using a simple one-dimensional NMR experiment (Fig. 1). These constitute two primary bile acids, cholic acid and chenodeoxycholic acid, and a secondary bile acid, deoxycholic acid, each of which is conjugated to glycine, resulting in GCA, GCDCA, and GDCA, or taurine, resulting in TCA, TCDCA, and TDCA. Depending upon the status of the liver, concentration of these bile acids vary in individual patients so much that, in the present study, bile acids in 16 patients were either undetectable or fewer than four. Since our aim was to investigate the conjugation pattern by comparing and correlating the ratios between two glycine-conjugated bile acids and their taurine counterparts or the ratios between glycine-conjugated bile acid and its taurine counterpart, we considered only those bile samples which showed at least a pair of glycine-conjugated bile acids and their taurine counterparts.

Significant variation in each of these bile acids concentration across the sample set (Figs. 2, 3) may be attributed to a number of factors such as altered

biosynthesis, cholestatic liver disease, bile acid malabsorption or disturbed enterohepatic circulation arising from the heterogeneity of the patients used in this study. Interestingly, from the systematic comparison of the variation in glycine- and taurine-conjugated bile acids concentrations within a bile sample as well as across a set of bile samples, a fundamental relationship between glycine- and taurine-conjugated bile acids levels in human bile could be established (Figs. 2, 5). Despite many factors that can affect individual bile acid concentration and the heterogeneity of the human subjects involved, who varied from non-liver disease patients to patients with liver diseases including hepatocellular carcinoma and cholangiocarcinoma, the ratios between glycine-conjugated bile acids and between taurine-conjugated bile acids did not vary randomly. This is particularly true for the six conjugated bile acids, GCA, GCDCA, GDCA, TCA, TCDCA, and TDCA commonly detected by NMR in a single step. The slope of nearly one for the line-fitting obtained from linear regression analysis and a very low *p* value clearly shows the

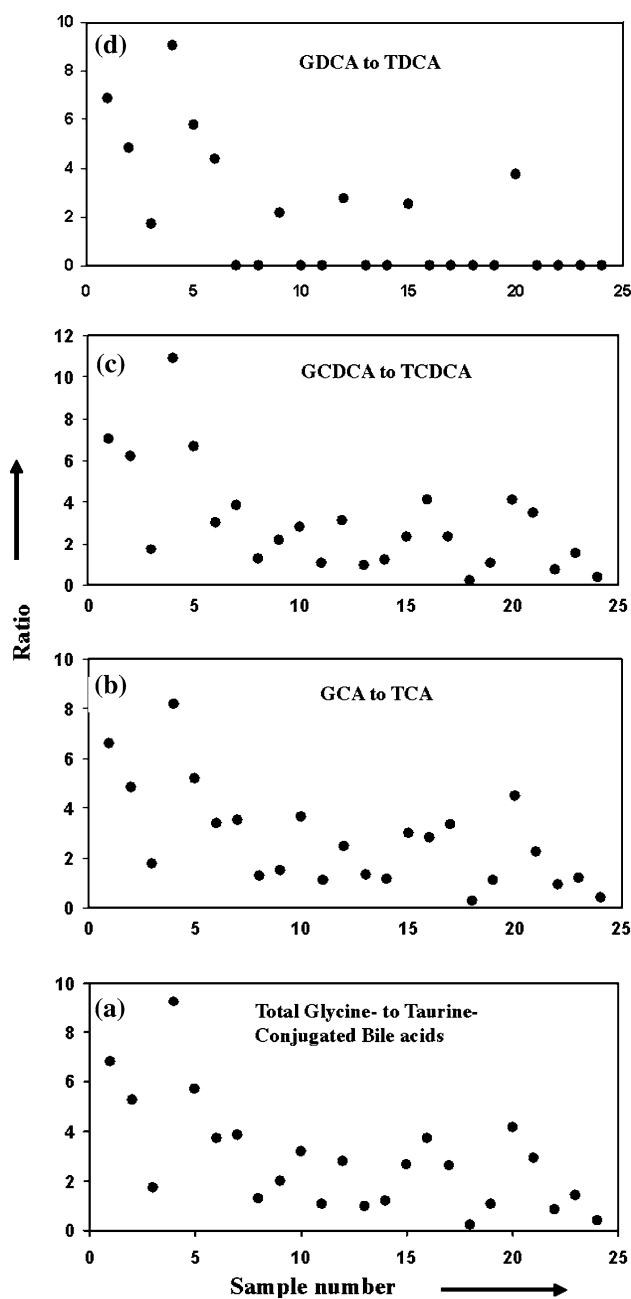


Fig. 4 Ratios of a glycine- to taurine-conjugated bile acids and b–d glycine to the corresponding taurine-conjugated bile acid. Abbreviations are as described before in Fig. 2 caption

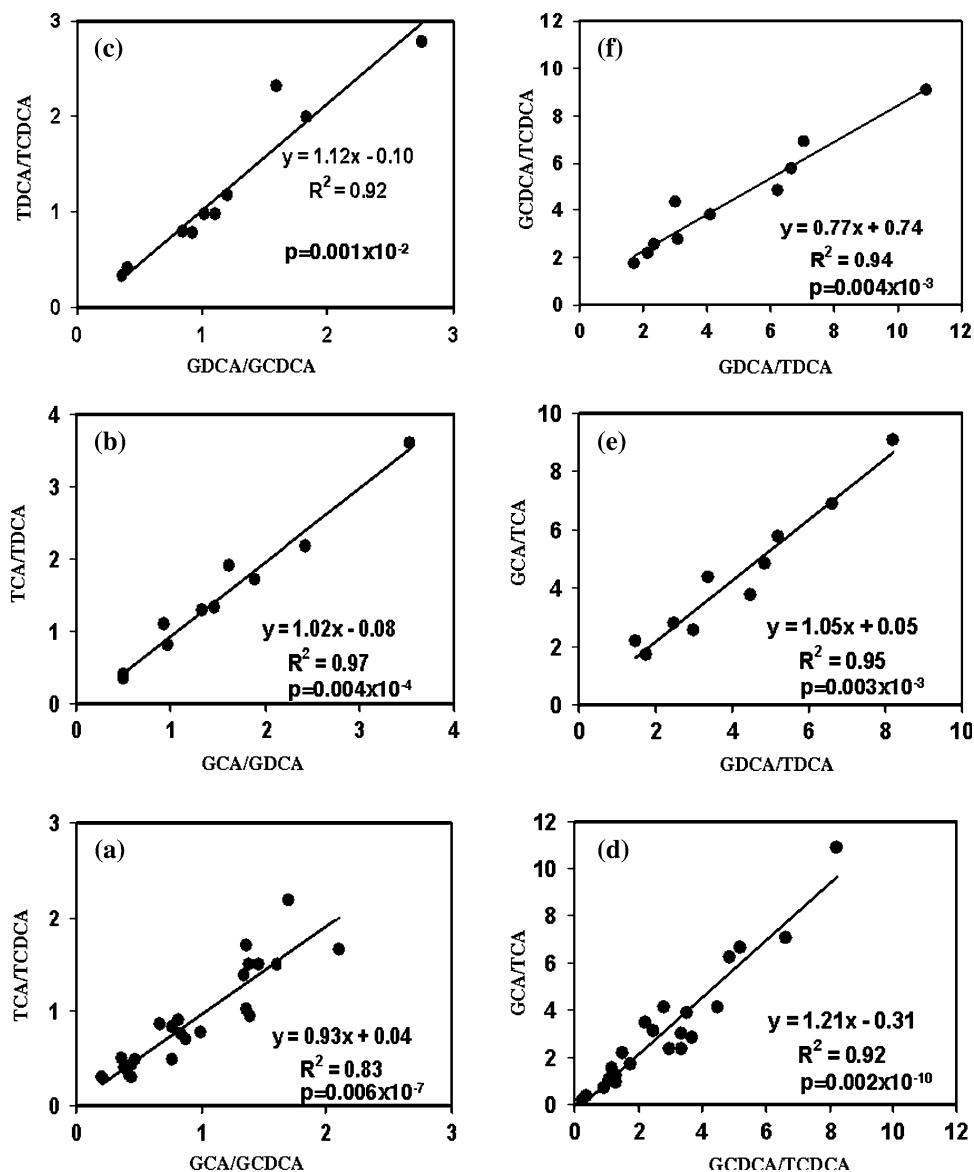
linearity of correlation of bile acids ratios. An earlier investigation of bile using high pressure liquid chromatography reported somewhat constant proportion of the three glycine-conjugated bile acids in healthy humans (GCA, GCDCA, and GDCA) [28]. These results are in accordance with the relationship between glycine- and taurine-conjugated bile acids observed in the present study. Further, these results indicate that it is even possible to predict the concentration of a bile acid utilizing the

relationship of co-variation of the bile acids ratios (supplementary Fig. S3). Considering the fact that numerous factors affect individual bile acid's concentration and that it is not yet known whether damage to bile acids during enterohepatic circulation is corrected in the hepatocytes, either partially or completely [29], the findings of the present study that the individual bile acids do not vary randomly may provide clues to the mechanism of the regulatory make up of bile acids in the hepatocytes.

Interest in better understanding bile acids metabolism and their role in a variety of diseases has increased since the recent discovery of a nuclear receptor for bile acids, which regulates bile acids synthesis and controls glucose, fat and energy metabolism. A very recent study on bile acids kinetics showed significantly higher cholic acid synthesis in type 2 diabetes patients [9]. Although bile acids have common structural features, the number and the position of the hydroxyl groups, and the nature of conjugation is anticipated to make each of the bile acids exhibit widely differing biological functions. For example, taurodeoxycholic acid, but not glycodeoxycholic acid, has inhibitory potential against apoptosis [30], and chenodeoxycholic acid levels in blood exceeding 15 $\mu\text{mol/L}$ are indicative of end stage liver disease [31]. Hence, understanding the metabolism and physiology of individual bile acid conjugation becomes an important aspect of the study of bile acids. Most of the literature about bile acids to date deals with bile acids as a whole, such as the primary bile acids, cholic acid and chenodeoxycholic acid, and the secondary acids, deoxycholic acid and lithocholic acid. Specific roles for the individual taurine- or glycine-conjugated bile acids have not been extensively explored.

Present investigation was based on the six conjugated bile acids, GCA, GCDCA, GDCA, TCA, TCDCA, and TDCA that are commonly found in human bile at high concentrations. Conjugates of ursodeoxycholic acid and lithocholic acid that are also thought to be present commonly in bile were not detected by NMR in this study, probably, owing to their low concentrations. It is also quite likely that such undetected low concentration conjugated bile acids overlap with the signals of the abundant bile acids. In our earlier investigation, we have shown that all the bile acids' signals are resolved even at low magnetic fields (400 MHz) except the two, TCDCA and TDCA, and at 800 MHz, all the signals get resolved [20]. Now that the relationship between glycine- and taurine-conjugated bile acids is established, it would be possible to predict the concentrations of TCDCA and TDCA, even if they overlap, provided the integrals of the other four are known as described in the supplementary Fig. S3. Thus, the analysis of individual bile acids can be performed even using instruments with lower magnetic fields (for example 400 MHz) as long as the correlation of the ratios is valid.

Fig. 5 Plots showing the linear correlation of the ratios **a–c** between a pair of glycine-conjugated bile acids and between the corresponding taurine-conjugated bile acids; and **d–f** between a glycine-conjugated bile acid and its taurine counterpart and between another glycine-conjugated bile acid and its taurine counterpart. Abbreviations are as described before in Fig. 2 caption



Conclusions

Bile acids have been intensively studied over the last several decades; however, investigations with an emphasis on bile acids conjugation are sparse. With a multitude of new roles for bile acids in several diseases coming to light, the need to investigate and understand the specific role of each member of the bile acid family has gained significance. Utilizing the latest methodological developments in bile acids analysis, we have made a detailed correlative analysis of individual glycine- and taurine-conjugated bile acids, which normally occur abundantly in human bile. We show here that glycine- and taurine-conjugated bile acids do not vary randomly but follow a definite correlative relationship, despite significantly altered levels of individual bile acids across the sample set. Although, this

investigation involves a small sample set and only six conjugated bile acids, the correlations between the two classes of conjugated bile acids are highly consistent and striking. Further studies using a greater number of bile samples targeting additional number of bile acids that are undetected in the present study are needed to substantiate the findings and to further our understanding of the physiology of bile acids' conjugation. Further, it will be interesting and useful to understand the pathophysiological circumstances which contribute to the deviation of such a correlation, although present study on a small sample set has not detected any difference between liver diseases and non-liver disease controls.

Acknowledgments This work was supported by the Walther Cancer Institute Multi-Institution Cancer Research Seed Project, the Purdue Oncological and Cancer Centers, and a collaborative research grant

between Purdue University/Discovery Park and the Indiana University School of Medicine.

References

- Houten SM, Watanabe M, Auwerx J (2006) Endocrine functions of bile acids. *EMBO J* 25(7):1419–1425
- Huang W, Ma K, Zhang J, Qatanani M, Cuvillier J, Liu J, Dong B, Huang X, Moore DD (2006) Nuclear receptor-dependent bile acid signaling is required for normal liver regeneration. *Science* 312(5771):233–236
- Watanabe M, Houten SM, Matakai C, Christoffolete MA, Kim BW, Sato H, Messaddeq N, Harney JW, Ezaki O, Kodama T, Schoonjans K, Bianco AC, Auwerx J (2006) Bile acids induce energy expenditure by promoting intracellular thyroid hormone activation. *Nature* 439(7075):484–489
- Inagaki T, Moschetta A, Lee YK, Peng L, Zhao G, Downes M, Yu RT, Shelton JM, Richardson JA, Repa JJ, Mangelsdorf DJ, Kliewer SA (2006) Regulation of antibacterial defense in the small intestine by the nuclear bile acid receptor. *Proc Natl Acad Sci USA* 103:3920–3925
- Hofmann AF (1999) The continuing importance of bile acids in liver and intestinal disease. *Arch Intern Med* 159(22):2647–2658
- Jansen PL (2007) Endogenous bile acids as carcinogens. *J Hepatol* 47(3):434–435
- Kim I, Morimura K, Shah Y, Yang Q, Ward JM, Gonzalez FJ (2007) Spontaneous hepatocarcinogenesis in farnesoid X receptor-null mice. *Carcinogenesis* 28:940–946
- Yang F, Huang X, Yi T, Yen Y, Moore DD, Huang W (2007) Spontaneous development of liver tumors in the absence of the bile acid receptor farnesoid X receptor. *Cancer Res* 67:863–867
- Brufau G, Kuipers F, Prado K, Abbey S, Jones M, Schwartz S, Stellaard F, Murphy E (2008) California altered bile salt metabolism in type 2 diabetes mellitus, 68th scientific sessions of the American Diabetes Association, San Francisco, June 6–10, abstract No. 1553-P
- Meinders AE, Van Berge Henegouwen GP, Willekens FL, Schwerzel AL, Ruben A, Huybregts AW (1981) Biliary lipid and bile acid composition in insulin-dependent diabetes mellitus. Arguments for increased intestinal bacterial bile acid degradation. *Dig Dis Sci* 26(5):402–408
- Scotti E, Gilardi F, Godio C, Gers E, Krneta J, Mitro N, De Fabiani E, Caruso D, Crestani M (2007) Bile acids and their signaling pathways: eclectic regulators of diverse cellular functions. *Cell Mol Life Sci* 64:2477–2491
- Zimber A, Gispach C (2008) Bile acids and derivatives, their nuclear receptors FXR, PXR and ligands: role in health and disease and their therapeutic potential. *Anticancer Agents Med Chem* 8(5):540–563
- Burkard I, von Eckardstein A, Rentsch KM (2005) Differentiated quantification of human bile acids in serum by high-performance liquid chromatography-tandem mass spectrometry *J Chrom B Anal. Technol Biomed Life Sci* 826(1–2):147–159
- Ding M, Ye L, Wang M, Shan Y (2007) Simultaneous determination of free and conjugated bile acids in serum by high performance liquid chromatography–tandem mass spectrometry. *Chin J Anal Chem* 35(10):1506–1508
- Kandrac J, Kevresan S, Gu JK, Mikov M, Fawcett JP, Kuhajda K (2006) Isolation and determination of bile acids. *Eur J Drug Metab Pharm* 31(3):157–177
- Wang Y, Griffiths WJ (2007) Modern methods of bile acid analysis by mass spectrometry: a view into the metabolome. *Cur Anal Chem* 3(2):103–126
- Ijare OB, Somashekar BS, Jadegoud Y, Nagana Gowda GA (2005) ^1H and ^{13}C NMR characterization and stereochemical assignments of bile acids in aqueous media. *Lipids* 40:1031–1041
- Ijare OB, Somashekar BS, Nagana Gowda GA, Sharma A, Kapoor VK, Khetrpal CL (2005) Quantification of glycine and taurine conjugated bile acids in human bile using ^1H NMR spectroscopy. *Magn Reson Med* 53(6):1441–1446
- Nagana Gowda GA, Somashekar BS, Ijare OB, Sharma A, Kapoor VK, Khetrpal CL (2006) One step analysis of major bile metabolites in human bile using ^1H -NMR spectroscopy. *Lipids* 41:577–589
- Nagana Gowda GA, Ijare OB, Somashekar BS, Sharma A, Kapoor VK, Khetrpal CL (2006) Single step analysis of individual conjugated bile acids in human bile using ^1H -NMR Spectroscopy. *Lipids* 41:591–603
- Nagana Gowda GA, Shanaiah N, Cooper A, Maluccio M, Raftery D (2009) Visualization of bile homeostasis using ^1H -NMR spectroscopy as a route for assessing liver cancer. *Lipids* 44:27–35
- Bollard ME, Stanley EG, Lindon JC, Nicholson JK, Holmes E (2005) NMR-based metabolomic approaches for evaluating physiological influences on biofluid composition. *NMR Biomed* 18(3):143–162
- Chen H, Pan Z, Talaty N, Raftery D, Cooks RG (2006) Combining desorption electrospray ionization mass spectrometry and nuclear magnetic resonance for differential metabolomics without sample preparation. *Rapid Commun Mass Spectrom* 20:1577–1584
- Lindon JC, Holmes E, Nicholson JK (2004) Metabonomics and its role in drug development and disease diagnosis. *Expert Rev Mol Diagn* 4(2):189–199
- Nagana Gowda GA, Zhang S, Gu H, Asiago V, Shanaiah N, Raftery D (2008) Metabolomics-based methods for early disease diagnostics *Expert Rev. Mol Diagn* 8(5):617–633
- Pan Z, Raftery D (2007) Comparing and combining NMR spectroscopy and mass spectrometry in metabolomics. *Anal Bioanal Chem* 387(2):525–527
- Shanaiah N, Desilva A, Nagana Gowda GA, Raftery MA, Hainline BE, Raftery D (2007) Metabolite class selection of amino acids in body fluids using chemical derivatization and their enhanced ^{13}C NMR. *Proc Natl Acad Sci USA* 104(28):11540–11544
- Rossi SS, Converse JL, Hofmann AF (1987) High pressure liquid chromatographic analysis of conjugated bile acids in human bile: simultaneous resolution of sulfated and unsulfated lithocholyl amides and the common conjugated bile acids. *J Lipid Res* 28(5):589–595
- Hofmann AF, Hagey LR (2008) Bile acids: chemistry, pathochemistry, biology, pathobiology, and therapeutics. *Cell Mol Life Sci* 65(16):2461–2483
- Hirano F, Haneda M, Makino I (2006) Chenodeoxycholic acid and taurochenodeoxycholic acid induce anti-apoptotic cIAP-1 expression in human hepatocytes *Source. J Gastro Hepatol* 21(12):1807–1813
- Azer SA, Coverdale SA, Byth K, Farrell GC, Stacey NH (1996) Sequential changes in serum levels of individual bile acids in patients with chronic cholestatic liver disease. *J Gastroenterol Hepatol* 11(3):208–215

Plasma Lipid Levels of Rats Fed a Diet Containing Pork Fat as a Source of Lipids after Splenic Surgery

Ana Paula Gonçalves Dinis · Ruy Garcia Marques · Fernanda Correia Simões ·
Cristina Fajardo Diestel · Carlos Eduardo Rodrigues Caetano ·
Dióscuro José Ferreira Secchin · José Firmino Nogueira Neto ·
Margareth Crisóstomo Portela

Received: 5 November 2008 / Accepted: 9 April 2009 / Published online: 5 May 2009
© AOCS 2009

Abstract Experimental studies have suggested an important role of the spleen in lipid metabolism, although with controversial results. Our purpose was to analyze the effect of a nutritionally balanced (NB) diet and a diet containing pork fat (PF) as source of lipids on the lipid profile of rats submitted to splenic surgery. Sixty adult male Wistar rats were divided into six groups of 10 animals each: 1 sham-operated, NB diet; 2 sham-operated, PF diet; 3 total splenectomy (TS), NB diet; 4 TS, PF diet; 5 TS followed by splenic autotransplantation (SA), NB diet; and 6 SA, PF diet. Blood samples were collected at the beginning (D0) and after 12 weeks of the experiment (D + 12) for plasma lipid determination. Morphologic regeneration of splenic tissues was observed, with no differences between groups 5 and 6. When D + 12 plasma lipid levels were compared to D0 levels there were no differences in groups 1, 3, and 5, while in groups 2, 4, and 6 total cholesterol (TC), low density lipoprotein (LDL), very low density lipoprotein (VLDL), and triacylglycerols (TAG) increased, and high density lipoprotein (HDL) decreased. At D + 12, groups 2, 4, and 6 had lower HDL than group 3. In conclusion, regardless of the surgical procedure applied to the spleen, an NB diet maintained

plasma lipid levels while a diet with PF as source of lipids changed the animals' lipid profile.

Keywords Splenectomy · Spleen · Autotransplants · Cholesterol · Dietary fats · Experimental surgery · Rats

Abbreviations

AIN-93	American Institute of Nutrition (1993)
D0	Beginning of the experiment
D + 12	12 Weeks after the beginning of the experiment
HDL	High density lipoprotein
LDL	Low density lipoprotein
NB	Nutritionally balanced
PF	Pork fat
SA	Splenic autotransplantation
TC	Total cholesterol
TAG	Triacylglycerols
TS	Total splenectomy
VLDL	Very low density lipoprotein

Introduction

It is well known that the spleen plays an important role in immunological processes and hemorheological homeostasis [1]. Since an increased risk of severe infection has been recognized to occur after splenectomy, even after many years, spleen-saving techniques, including autotransplantation of spleen fragments, have been performed when possible [2]. It has been demonstrated that splenic autotransplantation at an appropriate site successfully preserves splenic tissue after total splenectomy. Splenic autotransplants acquire the macro- and microscopic architecture of a

A. P. G. Dinis · R. G. Marques (✉) · F. C. Simões ·
C. F. Diestel · C. E. R. Caetano · D. J. F. Secchin ·
J. F. N. Neto · M. C. Portela
Laboratory of Experimental Surgery, Postgraduate Program
in Physiopathology and Surgical Sciences, Rio de Janeiro State
University, Rio de Janeiro, Brazil
e-mail: Rmarques@uerj.br

R. G. Marques
Rua Clóvis Salgado 255/204, Recreio, Rio de Janeiro,
RJ 22795-230, Brazil

normal spleen and are capable of restoring immune function [3–5].

A possible role of the spleen in plasma lipid level regulation was first suggested by Robinette and Fraumeni Jr (1977) who showed a high incidence of ischemic heart disease in splenectomized World War II veterans [6]. Both clinical and experimental studies have documented the spleen's influence on lipid metabolism in two different situations, i.e., hyperesplenism and asplenia [7–10].

Previous studies on patients with myeloproliferative disorders associated with splenomegaly have shown decreased plasma cholesterol levels, which normalize after total splenectomy [11–13]. Conversely, an increase in plasma cholesterol and triglyceride levels has been demonstrated in animals after total splenectomy [12, 14, 15]. Other studies have also suggested that the presence of splenic tissue, even in small amounts, can prevent such metabolic disorders [10, 16, 17].

Hypercholesterolemia is a cause of concern in our society since it constitutes one of the major risk factors for the development of cardiovascular diseases such as atherosclerosis and its complications, remaining the leading cause of death and disability in the world [18, 19]. Diet is the first line of therapy for the management of plasma lipid levels in the prevention and treatment of cardiovascular disease, with particular emphasis on fatty acid quality, much more than total fat content proper [20, 21]. Controlled feeding studies have consistently found that a reduction in the consumption of dietary saturated fatty acids decreases plasma total cholesterol and LDL levels, reducing the morbidity and mortality due to cardiovascular disease [22, 23].

Based on the possible correlation between the spleen and lipid metabolism and on the lack of studies considering the effect of different sources of fat on lipid profile after surgical procedures affecting the spleen, the purpose of the present study was to assess the impact of a nutritionally balanced diet and a diet containing pork fat as the source of lipids on plasma lipid levels of rats submitted to total splenectomy alone or in combination with splenic autotransplantation.

Experimental Procedure

Animals

Sixty adult male Wistar rats weighing 240–270 g were housed in individual cages under conditions of controlled temperature and humidity and on a 12-h light/12-h dark photoperiod. The animals were randomly divided into six groups of 10 animals each: group 1 – Control – sham-operated, fed a nutritionally balanced (NB) diet; group

2 – Control – sham-operated, fed a diet containing pork fat (PF) as a source of lipid; group 3 – total splenectomy (TS), fed the NB diet; group 4 – TS, fed the PF diet; group 5 – splenic autotransplantation (SA), fed the NB diet; and group 6 – SA, fed the PF diet.

After animals were submitted to different surgical procedures at the beginning of the experiment, they were fed two types of diet, according to the groups, and were monitored daily over a period of 12 weeks. Then, animals were killed with an anesthetic overdose at the end of the experiment. The study was approved by the Ethics Committee on Animal Research of the Biology Institute Roberto Alcantara Gomes, Rio de Janeiro State University Brazil. All procedures rigorously followed current regulations on animal experimentation [24, 25].

Surgical Procedures

After a 12-h fast, the surgical procedures were carried out under conditions of asepsis and antisepsis and under general anesthesia with a combination of ketamine hydrochloride (50 mg/kg) (Ketamina Agener®, Agener União, Saúde Animal) and xylazine (5 mg/kg) (Calmiun®, Agener União, Saúde Animal) administered intraperitoneally. The day of the operation was considered to be the first day of the experiment (D0).

A supraumbilical midline laparotomy was performed. In the sham-operated groups (1 and 2), the animals were submitted to mobilization of the spleen to the wound surface followed by replacement to its original position in the abdomen. In groups 3 and 4, total splenectomy was performed, and in groups 5 and 6, the removed spleen was weighed and cut transversely into five slices, each about 2 mm thick. The splenic sections were implanted into the greater omentum using continuous 4-0 polyglycolic acid (Dexon II®, Brasmédica S/A, São Paulo, SP, Brazil) sutures. Slices were introduced alternately between the omentum and splenic tissue to allow interposition of omental tissue between them. Laparorrhaphy was carried out on two planes (peritoneal-aponeurotic plane and skin) using continuous 3-0 polyglycolic acid (Dexon II®, Brasmédica S/A, São Paulo, SP, Brazil) sutures.

Blood Analysis

Blood samples were first collected from the animals immediately before the surgical procedure by cardiac puncture under anesthesia and then 12 weeks later at the end of the experiment. The following biochemical parameters were analyzed: total cholesterol (TC), low-density lipoprotein (LDL), very low-density lipoprotein (VLDL), high-density lipoprotein (HDL), and triacylglycerols (TAG). Plasma concentrations of TC, HDL, and TAG were

measured by the enzymatic colorimetric method after centrifugation using an automatic analyzer A15 (BioSystems®). LDL and VLDL levels were determined by the Friedewald formula, as follows:

$$\text{VLDL(mg/dL)} = \text{TAG}/5$$

$$\text{LDL(mg/dL)} = \text{TC} - \text{VLDL} - \text{HDL}$$

Animal Feeding

The animals received commercial rat chow (Focus 1722 Roedores, Agrocere®) and had unrestricted access to water until reaching the ideal weight for the experiment. Starting during the immediate postoperative period, all animals received a manipulated rat chow based on the recommendations of the American Institute of Nutrition Rodents Diets (AIN-1993) [26]. Groups 1, 3, and 5 were fed a nutritionally balanced diet with soybean oil as the source of fat, as recommended by AIN-93M. Groups 2, 4, and 6 were fed a diet containing the same amount of fat, but with pork fat as the main source, which contains a high percentage of saturated fatty acids compared to soybean oil. The composition of the two diets is presented in Table 1. In these groups, 18% of the total fat was soybean oil in order to guarantee essential fatty acid content [27]. Animal's intake of chow as well as body weight were controlled weekly, always at the same time of day.

Statistical Analysis

Descriptive analysis was applied to calculate the mean and standard deviation for the following variables: chow intake, weight gain, percentage of splenic mass regeneration, and TAG, TC, HDL, LDL, and VLDL levels. The Wilcoxon test was applied to compare preoperative and postoperative plasma lipid levels. The Kruskal–Wallis test and Dunn's post-test were used to compare plasma lipid levels between groups at the beginning and at the end of the experiment, as well as data regarding body weight variation and chow

Table 1 Composition of the nutritionally balanced (NB) and pork fat (PF) diets used during the experiment (g/100 g)

Composition	NB diet (g)	PF diet
Carbohydrates	62.10	62.10 g
Protein	14	14 g
Fat	4	4 g
Saturated fat	0.67	1.56 g
Monounsaturated fat	0.97	1.65 g
Polyunsaturated fat	2.37	0.79 g
Trans fat	0	0 g
Cholesterol	0	2.36 mg
Fiber	5	5 g

intake. The Student *t*-test for independent samples was applied to compare splenic mass between groups 5 and 6. The level of significance was set at $P \leq 0.05$ in all analyses. Statistical analysis was performed with the Graph Pad Prism 4® software for Windows version 4.0 (2003) and the SAS Statistical Software Package® for Windows 2007.

Morphologic Study

Removed splenic implants were placed in a solution containing 10% buffered formalin. The tissue was processed with increasing concentrations of alcohol and xylol, cut into 4-mm-thick slices and embedded in paraffin. Slides prepared from these slices were stained with hematoxylin and eosin and analyzed by light microscopy.

Results

During the immediate postoperative period the animals recovered rapidly from the surgical procedure. No complications resulting from anesthesia or surgery were observed. Only one animal (group 4) died during the 6th week of the experiment. Examination of the abdominal and thoracic cavity of the dead rat did not reveal the possible cause of death.

Regeneration of the splenic implants was observed in all animals of groups 5 and 6, with no difference in percent regeneration between them ($P = 0.7716$). Microscopic examination revealed a normal morphological appearance in all animals submitted to total splenectomy combined with splenic autotransplantation, with the presence of red and white pulps, besides lymphoid follicles (Fig. 1).

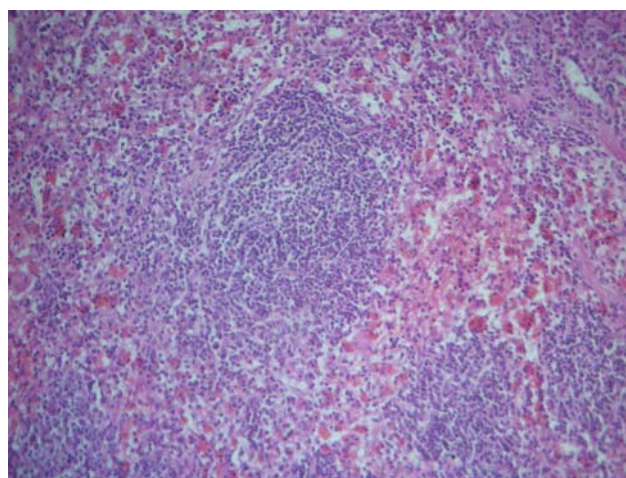


Fig. 1 Microscopic morphology of a regenerated splenic autotransplant showing the presence of white pulp containing lymphoid follicles and of red pulp with pigments of hemosiderin phagocytized by macrophages ($\times 40$)

Table 2 Comparison of TC, HDL, LDL, VLDL, and TAG levels at weeks 0 and 12 of the experiment in each group of animals—*P* values

Variable	Group 1	Group 2	Group 3	Group 4	Group 5	Group 6
TC	0.8457	0.0273*	0.1934	0.0234*	0.1289	0.0039*
HDL	0.6406	0.0039*	0.2031	0.0234*	0.9219	0.0039*
LDL	0.4316	0.0391*	0.8457	0.0234*	0.3750	0.0039*
VLDL	0.2969	0.0020*	0.0840	0.0156*	1.0	0.0039*
TAG	0.4961	0.0020*	0.0645	0.0039*	0.1309	0.0039*

TC total cholesterol, HDL high density lipoprotein, LDL low density lipoprotein, VLDL very low density lipoprotein, TAG triacylglycerols

* Statistically significant

No difference was observed in body weight gain ($P = 0.8542$) or in chow intake ($P = 0.1846$) between the various animal groups during the 12 weeks of the experiment. All groups had similar plasma lipid levels at the beginning of the experiment. When plasma lipids were compared at weeks 0 and 12, no significant difference in levels of TC, LDL, HDL, VLDL, and TAG was observed in groups 1, 3, and 5, while in groups 2, 4, and 6 there was an increase in TC, LDL, VLDL, and TAG levels, and a decrease in HDL levels (Table 2; Fig. 2).

When all animal groups were compared at the end of the experiment, only the HDL levels of groups 2, 4, and 6 were lower than those of group 3 (Fig. 2). Additionally, when groups 1 versus 3 versus 5 and 2 versus 4 versus 6 were compared in order to identify the separate effect of the surgical procedures on the spleen, no difference was observed.

Discussion

For many years, total splenectomy has been usually performed due to trauma, some diseases, and for diagnostic purposes, since there was insufficient knowledge about its consequences [2, 15]. Once the importance of the spleen in host defense was recognized, the immunological consequences of total splenectomy were given more attention and the development of new conservative spleen procedures was recommended, in an attempt to avoid the complications of asplenism [28, 29]. Subtotal and partial splenectomies have been recommended in many situations. Nevertheless, when total splenectomy is unavoidable, splenic autotransplantation seems to be the only alternative [30, 31].

A variety of studies have confirmed morphological regeneration of autotransplanted splenic tissue [32–35]. However, splenic regeneration does not necessarily mean recovery of organ function. Several authors have shown that splenic autotransplantation is a simple, effective procedure [30, 36] and that, when performed at appropriate sites, it successfully maintains some spleen functions after total splenectomy, as demonstrated by indirect laboratory methods and scintigraphic techniques [4, 37]. Due to their blood supply and venous drainage into the portal vein, as is the case for the spleen in situ, splenic implants in the greater omentum seem to develop and function better than at other sites [38, 39]. Although the regeneration sequence begins hours after autotransplantation, the time needed for the occurrence of morphological and functional

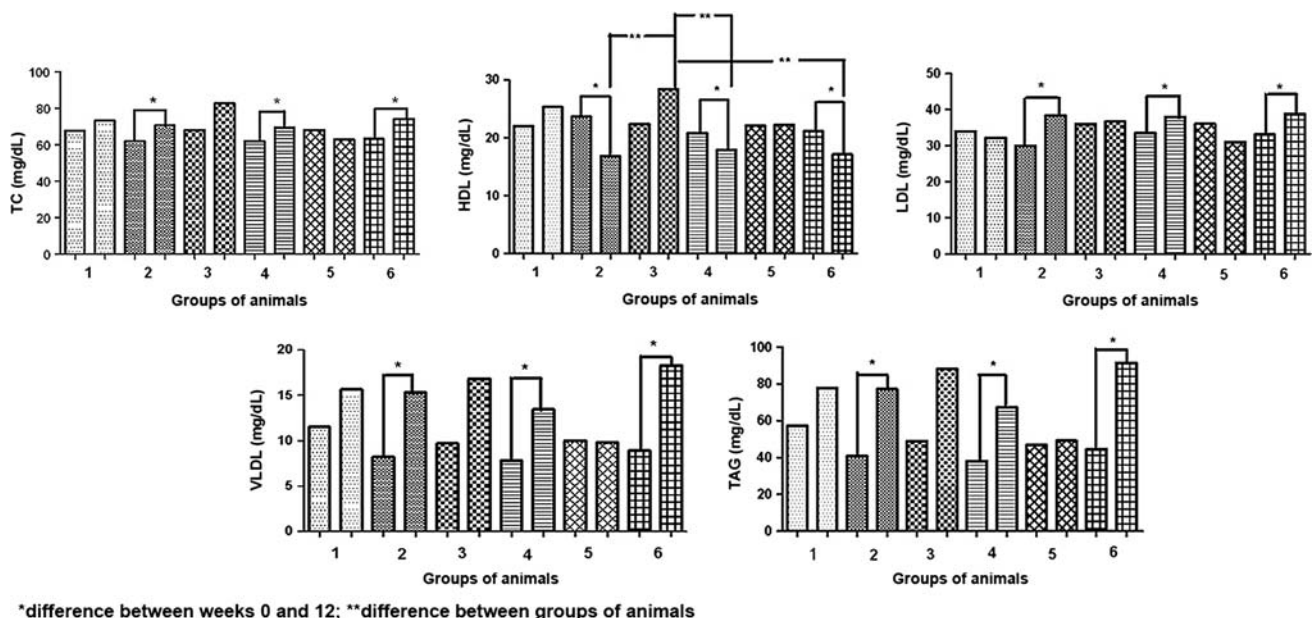


Fig. 2 Comparison over time of the experiment (*Wilcoxon test*) and between groups of animals at the end of the experiment (*Kruskal–Wallis test*) of TC, HDL, LDL, VLDL, and TAG levels at weeks 0

(left column in each group) and 12 (right column in each group) in all groups of animals

regeneration has been reported to range from 8 to 12 weeks [40, 41].

In the present study, rats were submitted to total splenectomy for the induction of an asplenic condition in order to identify a possible role of the spleen in plasma lipid levels 12 weeks after the beginning of the experiment. Splenic autotransplantation following total splenectomy was performed to determine if such a simple procedure would protect the animals from these changes. Additionally, rats were fed two diets with different sources of lipids in order to identify the effect of such diets on the lipid profile of the animals after these surgical procedures.

The participation of the spleen in lipid metabolism has been investigated in clinical and experimental studies [42–44]. Studies performed in rats have demonstrated increased levels of cholesterol after TS, although with controversial results. Animals fed standard chow have been reported to show an increase in TAG and a decrease in HDL levels after TS compared with sham-operated animals [14], in contrast to the results from other studies showing an increase in TC and LDL and a decrease in HDL levels after the same procedure, with no alterations in TAG or VLDL levels [10], or elevation of all of these parameters [17].

Some theories have been proposed to explain the possible role of the spleen in plasma lipid levels. Increased macrophage activity in myeloproliferative disorders would lead to hypocholesterolemia through an increase in LDL catabolism [45–48]. Schmidt et al. [49] compared the spleen to a lipid reservoir that accumulates a great part of the fat in states of hypersplenism. Another explanation for the participation of the spleen in lipid metabolism would be the production of anti-oxidized LDL antibody, with spleen-associated immune activity protecting against the development of atherosclerosis [50].

Most of the studies that showed a correlation between the spleen and plasma lipid level regulation did not consider chow intake or weight gain during the experiment. In the present study, all animal groups showed similar weight gain and chow intake. There is evidence that excess body adiposity can lead to a worsening of cardiovascular risk factors, including dyslipidemia [51, 52], making the control of such variables extremely relevant in order to guarantee a correct interpretation of the results, avoiding, for example, an erroneous attribution of lipid profile alteration to a surgical procedure on the spleen.

Some authors have increased fat content in rat chow during the post-splenectomy period in order to induce hyperlipidemia and emphasize possible alterations in the lipid profile by adding cholesterol to the commercial chow [9, 17, 43]. Others have shown that increasing dietary

cholesterol results in higher plasma cholesterol concentrations [53, 54], with the addition of cholesterol itself being expected to alter plasma lipid levels. However, most studies have also demonstrated that dietary cholesterol is a less potent regulator of plasma cholesterol concentrations than dietary fatty acids [18, 55].

Recent evidence suggests that a consistent reduction in the risk of cardiovascular disease due to changes in the plasma lipoprotein profile can be achieved through changes in fat source consumption, such as replacing *trans* and saturated fat with mono- and polyunsaturated fatty acids [56–58]. In the present study, we changed the fat source instead of increasing fat content in an attempt to identify the impact of fat quality on lipid profile, using pork fat due to its high saturated fatty acid content.

In contrast to other experimental studies [12, 14–16], we did not observe any changes in plasma lipid levels after any surgical procedure on the spleen when rats were fed a nutritionally balanced diet. Thus, surgical trauma and total splenectomy alone or in combination with splenic autotransplantation did not influence the lipid profile of the animals. Rezende et al. [44] also showed similar plasma levels of cholesterol and its fractions in groups of mice fed a similar diet and submitted to the same surgical procedures. Comparable results were obtained by Caligiuri et al. [59], who did not detect changes in cholesterol levels in splenectomized mice, although atherosclerosis had drastically worsened after the surgical procedure.

When animals were fed a chow containing pork fat as a source of lipids, a worsening of all parameters was observed. Again, these changes occurred in all animals regardless of the surgical procedure on the spleen. Our findings confirm the results obtained in other studies that showed an increase in TC and LDL levels with the use of a high saturated fat diet [60–62]. Alterations in HDL, VLDL, and TAG levels may be due to changes in the fat content or fatty acid profile with the chow used during the postoperative period compared to the commercial chow used during the preoperative period.

Despite the possible role of the spleen in myeloproliferative diseases and in protective immunity against atherosclerosis, we did not find any effect of the spleen on plasma lipid levels. It was the quality of the fat, rich in saturated fatty acids, that significantly worsened the lipid profile of rats in contrast to a nutritionally balanced diet. This result suggests that the spleen, in the absence of diseases, does not seem to have an important role in the regulation of plasma lipid levels. Further studies dealing with other animal models and different contents and sources of fat in the diet are necessary to better elucidate the correlation between the spleen and the lipid profile.

Acknowledgments The authors wish to thank Albanita Viana de Oliveira (Discipline of Pathologic Anatomy of Sciences Medical School, Rio de Janeiro State University) for her support with morphological tissue analysis. This work was partially supported by a grant from *Fundação Carlos Chagas Filho de Amparo à Pesquisa do Estado do Rio de Janeiro* (FAPERJ), Brazil.

References

- Miko I, Nemeth N, Sipka S, Brath E, Peto K, Gulyas A, Furka I, Zhong R (2006) Hemorheological follow up after splenectomy and spleen autotransplantation in mice. *Microsurgery* 26:38–42
- Timens W, Leemans R (1992) Splenic autotransplantation and the immune system. *Ann Surg* 215:256–260
- Marques RG, Petroianu A, Coelho JM (2003) Bacterial phagocytosis by macrophage of autogenous splenic implant. *Braz J Biol* 63:491–495
- Patel JM, Williams JS, Shmigel B, Hinshaw JR (1981) Preservation of splenic function by autotransplantation of traumatized spleen in man. *Surgery* 90:683–688
- Petroianu A, Vidigal FM, Costa VC, De Oliveira SC (2000) Splenic autotransplantation in Gaucher's disease. *Dig Surg* 17:181–183
- Robinette CD, Fraumeni JF Jr (1977) Splenectomy and subsequent mortality in veterans of the 1939–1945 war. *Lancet* 16:127–129
- Wysocki A, Drozd W, Dolecki M (1999) Spleen and lipids metabolism—is there any correlation? *Med Sci Monit* 5:524–527
- Gilbert HS, Ginsberg H (1983) Hypocholesterolemia as a manifestation of disease activity in chronic myelocytic leukemia. *Cancer* 51:1428–1433
- Paulo ICAL, Paulo DNS, Kalil M, Guerra AJ, Guerzet EA, Silva AL (2007) Effects of two types of diet on plasma lipids in rats submitted to splenic surgery. *Rev Assoc Med Bras* 53:171–177
- Petroianu A, Veloso DFM, Costa GR, Alberti LR (2006) Effects of spleen surgeries on lipidogram of rats. *Rev Assoc Med Bras* 52:56–59
- Sugihara T, Miyashima K, Yawata Y (1984) Disappearance of microspherocytes in peripheral circulation and normalization of decreased lipids in plasma and in red cells of patients with hereditary spherocytosis after splenectomy. *Am J Hematol* 17:129–139
- Aviram M, Brook JG, Tatarsky I, Levy Y, Carter A (1986) Increased low-density lipoprotein levels after splenectomy: a role for the spleen in cholesterol metabolism in myeloproliferative disorders. *Am J Med Sci* 291:25–28
- Gilbert HS, Ginsberg H, Fagerstrom R, Brown WV (1981) Characterization of hypocholesterolemia in myeloproliferative disease. Relation to disease manifestations and activity. *Am J Med* 71:595–602
- Fatouros M, Bourantas K, Bairaktari E, Elisaf M, Tsolas O, Cassioumis D (1995) Role of the spleen in lipid metabolism. *Br J Surg* 82:1675–1677
- Paulo DNS, Paulo ICAL, Kalil M, Vargas PM, Silva AL, Baptista JFA, Guerra AJ (2006) Subtotal splenectomy preserving the lower pole in rats: technical, morphological, and functional aspects. *Acta Cir Bras* 21:321–327
- Paulo DNS, Silva AL (2001) The plasma lipids after total and partial splenectomy in dogs. *Rev Col Bras Cir* 28:264–270
- Paulo ICAL, Paulo DNS, Silva AL, Foletto RM, Colnago GL, Vargas PM (2005) Plasma lipid levels in rats after total splenectomy, simultaneous ligation of the splenic vessels and subtotal splenectomy with inferior pole preservation. *Rev Col Bras Cir* 32:229–236
- Schaefer EJ (2002) Lipoproteins, nutrition, and heart disease. *Am J Clin Nutr* 75:191–202
- McCullough ML, Feskanich D, Stampfer MJ, Giovannucci EL, Rimm EB, Hu FB, Spiegelman D, Hunter DJ, Colditz GA, Willett WC (2002) Diet quality and major chronic disease risk in men and women: moving toward improved dietary guidance. *Am J Clin Nutr* 76:1261–1271
- Lichtenstein AH, Appel LJ, Brands M, Carnethon M, Daniels S, Franch HA, Franklin B, Kris-Etherton P, Harris WS, Howard B, Karanja N, Lefevre M, Rudel L, Sacks F, Van Horn L, Winston M, Wylie-Rosett J (2006) Diet and lifestyle recommendations revision 2006: a scientific statement from the American Heart Association Nutrition Committee. *Circulation* 114:82–96
- Yu-Poth S, Zhao G, Etherton T, Naglak M, Jonnalagadda S, Kris-Etherton PM (1999) Effects of the National Cholesterol Education Program's Step I and Step II dietary intervention programs on cardiovascular disease risk factors: a meta-analysis. *Am J Clin Nutr* 69:632–646
- Stone NJ, Nicolosi RJ, Kris-Etherton PM, Ernst ND, Krauss RM, Winston M (1996) Summary of the scientific conference on the efficacy of hypocholesterolemic dietary interventions. *Circulation* 94:3388–3391
- Kris-Etherton PM, Yu S (1997) Individual fatty acid effects on plasma lipids and lipoproteins: human studies. *Am J Clin Nutr* 65:1628S–1644S
- Petroianu A (1996) Ethical aspects on the research in animals. *Acta Cir Bras* 11:157–164
- Marques RG, Morales MM, Petroianu A (2009) Brazilian law for scientific use of animals. *Acta Cir Bras* 24:69–74
- Reeves PG (1997) Components of the AIN-93 Diets as improvements in the AIN-76A diet. *J Nutr* 127:838S–841S
- Soriguer F, Moreno F, Rojo-Martinez G, Garcia-Fuentes E, Tinahones F, Gomez-Zumaquero JM, Cuesta-Muñoz AL, Cardona F, Morcillo S (2003) Monounsaturated n-9 fatty acids and adipocyte lipolysis in rats. *Br J Nutr* 90:1015–1022
- Barbuscia M, Praticò C, Pergolizzi FP, Lizio R, Ilaqua A, Minniti C, Sofia L, Gorgone S (2007) Closed trauma of the spleen. Indications to surgical treatment. *G Chir* 28:217–221
- Malago R, Reis NS, Araújo MR, Andreollo NA (2008) Late histological aspects of spleen autologous transplantation in rats. *Acta Cir Bras* 23:274–281
- Marques RG, Petroianu A, De Oliveira MB, Bernardo-Filho M, Boasquevisque EM, Portela MC (2002) Bacterial clearance after total splenectomy and splenic autotransplantation in rats. *Appl Radiat Isot* 57:767–771
- Marques RG, Petroianu A, Coelho JM, Portela MC (2002) Regeneration of splenic autotransplants. *Ann Hematol* 81:622–626
- Pabst R, Kamran D (1986) Autotransplantation of splenic tissue. *J Pediatr Surg* 21:120–124
- Pabst R (1999) Regeneration of autotransplanted splenic fragments: basic immunological and clinical relevance. *Clin Exp Immunol* 117:423–424
- Tavassoli M, Ratzan RJ, Crosby WH (1973) Studies on regeneration of heterotopic splenic autotransplants. *Blood* 41:701–709
- Liaunigg A, Kastberger C, Leitner W, Kurz ME, Bergmann ES, Seifriedsberger M, Weinlich D, Pimpl W, Thalhammer J (1992) Regeneration of autotransplanted splenic tissue at different implantation sites. *Cell Tissue Res* 269:1–11
- Karagülle E, Hoşçoşkun Z, Kutlu AK, Kaya M, Baydar S (2007) The effectiveness of splenic autotransplantation: an experimental study. *Ulus Travma Acil Cerrahi Derg* 13:13–19
- Hathaway JM, Harley RA, Self S, Schiffman G, Virella G (1995) Immunological function in post-traumatic splenosis. *Clin Immunol Immunopathol* 74:143–150

38. Patel J, Williams JS, Naim JO, Hinshaw JR (1982) Protection against pneumococcal sepsis in splenectomized rats by implantation of splenic tissue into an omental pouch. *Surgery* 91:638–641
39. Inuma H, Okinaga K, Sato S, Tomioka M, Matsumoto K (1992) Optimal site and amount of splenic tissue for autotransplantation. *J Surg Res* 53:109–116
40. Sipka S Jr, Brath E, Toth FF, Aleksza M, Kulcsar A, Fabian A, Barath S, Balogh P, Sipka S, Furka I, Miko I (2006) Cellular and serological changes in the peripheral blood of splenectomized and spleen autotransplanted mice. *Transpl Immunol* 16:99–104
41. Willführ KU, Westermann J, Pabst R (1990) Absolute numbers of lymphocyte subsets migrating through the compartments of the normal and transplanted rat spleen. *Eur J Immunol* 20:903–911
42. Simões FC, Marques RG, Diestel CF, Caetano CER, Dinis APG, Horst NL, Neto JFN, Portela MC (2007) Lipid profile among rats submitted to total splenectomy isolated or combined with splenic autotransplant. *Acta Cir Bras* 22:46–51
43. Asai K, Kuzuya M, Naito M, Funaki C, Kuzuya F (1988) Effects of splenectomy on serum lipids and experimental atherosclerosis. *Angiology* 39:497–504
44. Rezende AB, Nunes SI, Farias RE, Vieira FR, Petroianu A, Teixeira HC (2007) Influence of the spleen, asplenism, and autologous splenic implants on lipid metabolism in mice. *Rev Col Bras Cir* 34:177–182
45. Goldstein JL, Brown MS (1977) The low-density lipoprotein pathway and its relation to atherosclerosis. *Annu Rev Biochem* 46:897–930
46. Le NA, Gibson JC, Rubinstein A, Grabowski GA, Ginsberg HN (1988) Abnormalities in lipoprotein metabolism in Gaucher type 1 disease. *Metabolism* 37:240–245
47. Ho YK, Smith RG, Brown MS, Goldstein JL (1978) Low-density lipoprotein (LDL) receptor activity in human acute myelogenous leukemia cells. *Blood* 52:1099–1114
48. Vitols S, Angelin B, Ericsson S, Gahrton G, Juliusson G, Masquelier M, Paul C, Peterson C, Rudling M, Söderberg-Reid K (1990) Uptake of low density lipoproteins by human leukemic cells in vivo: relation to plasma lipoprotein levels and possible relevance for selective chemotherapy. *Proc Natl Acad Sci USA* 87:1598–1602
49. Schmidt HH, Wagner S, Manns M (1997) The spleen as a storage pool in lipid metabolism [letter]. *Am J Gastroenterol* 92:1072
50. Witztum JL (2002) Splenic immunity and atherosclerosis: a glimpse into a novel paradigm? *J Clin Invest* 109:721–724
51. Ezquerra EA, Vázquez JMC, Barrero AA (2008) Obesity, metabolic Syndrome, and diabetes: cardiovascular implications and therapy. *Rev Esp Cardiol* 61:752–764
52. Kannel WB, D'Agostino RB, Cobb JL (1996) Effect of weight on cardiovascular disease. *Am J Clin Nutr* 63(4):19S–122S
53. Hopkins PN (1992) Effects of dietary cholesterol on serum cholesterol: a meta-analysis and review. *Am J Clin Nutr* 55:1060–1070
54. Brown SA, Morrisett J, Patsch JR, Reeves R, Gotto AM Jr, Patsch W (1991) Influence of short term dietary cholesterol and fat on human plasma Lp[a] and LDL levels. *J Lipid Res* 32:1281–1289
55. Lichtenstein AH, Ausman LM, Carrasco W, Jenner JL, Ordovas JM, Schaefer EJ (1994) Hypercholesterolemic effect of dietary cholesterol in diets enriched in polyunsaturated and saturated fat. Dietary cholesterol, fat saturation, and plasma lipids. *Arterioscler Thromb* 14:168–175
56. Hu FB, Stampfer MJ, Manson JE, Rimm E, Colditz GA, Rosner BA, Hennekens CH, Willett WC (1997) Dietary fat intake and the risk of coronary heart disease in women. *N Engl J Med* 337:1491–1499
57. Yu-Poth S, Etherton TD, Reddy CC, Pearson TA, Reed R, Zhao G, Jonnalagadda S, Wan Y, Kris-Etherton PM (2000) Lowering dietary saturated fat and total fat reduces the oxidative susceptibility of LDL in healthy men and women. *J Nutr* 130:2228–2237
58. Willett WC (2000) Will high-carbohydrate/low-fat diets reduce the risk of coronary heart disease? *Proc Soc Exp Biol Med* 225:187–190
59. Caligiuri G, Nicoletti AP, Poirier B, Hansson GK (2002) Protective immunity against atherosclerosis carried by B cells of hypercholesterolemic mice. *J Clin Invest* 109:745–753
60. Hooper L, Summerbell CD, Higgins JP, Thompson RL, Clements G, Capps N, Davey S, Riemersma RA, Ebrahim S (2001) Reduced or modified dietary fat for preventing cardiovascular disease. *Cochrane Database Syst Rev* 3:CD002137
61. Cobb MM, Teitlebaum H (1994) Determinants of plasma cholesterol responsiveness to the diet. *Br J Nutr* 71:271–282
62. Mensink RP, Zock PL, Katan MB, Hornstra G (1992) Effect of dietary *cis* and *trans* fatty acids on serum lipoprotein[a] levels in humans. *J Lipid Res* 33:1493–1501

Cloning and Characterization of the $\Delta 6$ Polyunsaturated Fatty Acid Elongase from the Green Microalga *Parietochloris incisa*

Umidjon Iskandarov · Inna Khozin-Goldberg ·
Rivka Ofir · Zvi Cohen

Received: 18 December 2008 / Accepted: 4 March 2009 / Published online: 7 May 2009
© AOCS 2009

Abstract The very-long-chain polyunsaturated fatty acid (VLC-PUFA), arachidonic acid (ARA, 20:4 ω -6) is a component of neuron tissues such as brain and retina cells and a primary substrate for the biosynthesis of biologically active eicosanoids. The green freshwater microalga *Parietochloris incisa* (Trebouxiophyceae) has been shown to accumulate an extraordinary high content of ARA-rich triacylglycerols. It was thus interesting to characterize the genes involved in lipid biosynthesis in this alga. We report here the identification of a cDNA encoding for a *P. incisa* PUFA elongase (*PiELO1*) and demonstrate that the expression of *PiELO1* in yeast *Saccharomyces cerevisiae* confers its elongase activity on C18 $\Delta 6$ PUFA. Phylogenetic analysis indicated that *PiELO1* is highly similar to functionally characterized $\Delta 6$ PUFA elongase genes from other green algae and lower plants. Quantitative real-time PCR expression studies showed that *PiELO1* is upregulated under nitrogen starvation, the condition triggering and enhancing storage oil and ARA accumulation in *P. incisa*.

Keywords Arachidonic acid · Fatty acid elongation · Nitrogen starvation · *Parietochloris incisa* · Subtractive hybridization · VLC-PUFA

Abbreviations

ARA	Arachidonic acid
DGLA	Dihomo- γ -linolenic acid
DHA	Docosahexaenoic acid
GLA	γ -Linolenic acid
EPA	Eicosapentaenoic acid
STA	Stearidonic acid
VLC-PUFA	Very-long-chain polyunsaturated fatty acid

Introduction

The very-long-chain polyunsaturated fatty acid (VLC-PUFA), arachidonic acid (ARA, 20:4 ω -6), is a component of neuron tissues such as brain and retina cells and an important component of the human diet. ARA is a primary substrate for the biosynthesis of eicosanoids, including the 2-group prostaglandins, 4-group leukotrienes, thromboxanes, and lipoxins that serve as biological effectors involved in inflammatory and immune responses and cell signaling [1, 2]. Being an important and dominant VLC-PUFA in human breast milk, ARA needs to be externally supplied for normal development of preterm babies if they are not breast-fed [1, 3]. Because of its beneficial properties there is a growing interest in the production of ARA for baby formulae. At present, the major commercial source of ARA is the filamentous fungus *Mortierella alpina* [4].

Microalgae are one of the richest sources of VLC-PUFAs [5–8]. Furthermore, algae can be used as sources of genes for implementation of VLC-PUFA biosynthesis in genetically engineered oil crops [9, 10]. Genetic information on enzymes involved in the biosynthesis of VLC-PUFA in some algae led to in-vivo applications of VLC-PUFA production in seed oil [11]. The gene pool

U. Iskandarov · I. Khozin-Goldberg (✉) · Z. Cohen
The Microalgal Biotechnology Laboratory,
The Jacob Blaustein Institutes for Desert Research,
Ben-Gurion University of the Negev, Sede Boker Campus,
84990 Midreshet Ben-Gurion, Israel
e-mail: khozin@bgu.ac.il

R. Ofir
Dead Sea and Arava Science Center, Ben-Gurion University
of the Negev, Beer Sheva, Israel

of the green freshwater microalga *Parietochloris incisa* (Trebouxiophyceae) is of special interest because it is the only microalga known to be able to accumulate extraordinary high amounts of ARA-rich triacylglycerols (TAG) [7, 8]. When *P. incisa* is cultivated under nitrogen starvation, the condition triggering storage oil accumulation, ARA constitutes about 60% of total fatty acids (TFA) and over 95% of cellular ARA is deposited in TAG in cytoplasmic lipid bodies [12].

The biosynthesis of VLC-PUFAs in algae follows various pathways, initiating from oleic acid exported from the chloroplast and employing polar extraplasmic lipids. In the $\omega 6$ and $\omega 3$ pathways, linoleic acid (LA; 18:2 ω -6) and α -linolenic acid (ALA; 18:3 ω -3) are successively converted by $\Delta 6$ desaturase, $\Delta 6$ elongase, and $\Delta 5$ desaturase to ARA and eicosapentaenoic acid (EPA, 20:5 ω -3), respectively [6]. For example, in *P. incisa* and in the red microalga *Porphyridium cruentum*, ARA biosynthesis proceeds via the $\omega 6$ pathway [13, 14]. Unusual elongations and desaturations leading to the biosynthesis of VLC-PUFA have been reported in the marine haptophyte *Isochrysis galbana* [15] and the fresh-water euglenophyte *Euglena gracilis* [16, 17]. In the alternative route, elongation of 18:2 ω -6 and 18:3 ω -3 by a C18- $\Delta 9$ -specific fatty acid elongase to the respective C20 intermediates precedes sequential $\Delta 8$ and $\Delta 5$ desaturations to ARA and EPA, respectively. It is assumed that in *E. gracilis* EPA produced by the $\omega 3$ - $\Delta 8$ pathway is further $\Delta 4$ desaturated and finally elongated to docosahexaenoic acid (DHA, 22:6 ω -3) [17].

Fatty acid elongation is a multi-step process involving four sequential enzymatic reactions: rate limiting condensation (of malonyl-CoA and acyl-CoA), reduction, dehydration and enoyl reduction [18]. Only the expression of the condensing enzyme component is required to reconstitute elongase activity in the heterologous host; there is no requirement for the co-expression of any other component of the elongase complex. Multiple microsomal elongation systems with different specificities to the acyl chain length exist in various organisms. Recent studies have identified and characterized PUFA-specific elongases, responsible for the elongation of PUFA in the nematode *Caenorhabditis elegans*, mammals, fish, algae, lower plants, and fungi [19–25]. The elongation of 18:3 ω -6 to 20:3 ω -6, the immediate precursor of ARA, was shown to be the rate-limiting step in ARA biosynthesis in *M. alpina* [26, 27]. Functional expression of the PUFA elongase condensation component in yeast revealed enzymes of various specificities for C18 and C20 acyl substrates. Thus, two types of PUFA elongases engaged in DHA biosynthesis have been cloned from the green microalga *Ostreococcus tauri* and the diatom *Thalassiosira pseudonana*: OtELO1 and TpELO1 are $\Delta 6$ C18-PUFA-specific and involved in the elongation of 18:3 ω -6 and 18:4 ω -3,

whereas OtELO2 and TpELO2 are $\Delta 5$ C20-PUFA elongases involved in the elongation of 20:5 ω -3 [28]. Bifunctional PUFA elongases able to elongate both $\Delta 6$ and $\Delta 5$ PUFA, and elongases of wide substrate specificity utilizing both C20 and C22 PUFA substrates, have been isolated from aquatic animals [28, 29].

In this paper we report the identification of a cDNA encoding for a *P. incisa* elongase (PiELO1) and that the expression of PiELO1 in yeast cells conferred its $\Delta 6$ PUFA elongase activity. Quantitative real-time PCR expression studies showed that *PiELO1* is up-regulated during nitrogen starvation and that the level of expression is correlated with the production of ARA precursors.

Experimental Procedures

Growth Conditions

Axenic cultures of *P. incisa* were cultivated on BG-11 nutrient medium [30] in 250-ml Erlenmeyer glass flasks in an incubator shaker under an air/CO₂ atmosphere (99:1, v/v) and controlled temperature (25°C) and illumination (115 $\mu\text{mol quanta m}^{-2} \text{s}^{-1}$) at a speed of 170 rpm [13]. For nitrogen starvation experiments, cells of daily-diluted cultures were collected by centrifugation, washed thrice in sterile double-distilled water, and resuspended in nitrogen-free BG-11 medium. Cultures were further grown under the same conditions for 14 days. To prepare nitrogen-free medium, NaNO₃ was omitted from the BG-11 medium and ferric ammonium citrate was substituted with ferric citrate.

RNA Isolation

Cells for RNA isolation were harvested from 40 ml log-phase culture (Time 0) grown in complete BG11 and cultured on nitrogen-free medium for 3, 7, and 14 days. The cultures were filtered through a glass-fiber paper filter (GF-52, Schleicher & Schuell, Germany), and cells were collected by scraping and immediately flash-frozen in liquid nitrogen and stored at -80°C for further use. Total RNA was isolated either using the RNeasy Plant Mini kit (Qiagen, Hilden, Germany) or by the procedure described by Bekesiova et al. [31], with minor modifications. Three independent RNA isolations were conducted for each growth period. For real-time PCR studies, the total RNA samples were further treated with RNAase-free DNAase (Epicentre, Madison, WI, USA).

Construction of Subtracted cDNA Library

The subtracted complementary DNA (cDNA) library was prepared from cDNAs enriched for differentially expressed

sequences obtained from *P. incisa* cultures in the log phase (driver) and after three days of nitrogen starvation (tester) [32], using a PCR-Select cDNA Subtraction Kit (Clontech, Mountain View, CA, USA). First, a double-stranded cDNA was synthesized from total RNA isolated from cells during log phase and N-starvation and digested with *RsaI*. Subtraction was then done in both directions. To enrich for “log phase” cDNAs, the cDNA sequences of N-starved cells were subtracted from those of log phase cells; conversely, to enrich for cDNAs of N-starved cells, log phase cDNA sequences were subtracted from those of N-starved cells. Two portions of the tester cDNA were ligated to adaptor primers. After two cycles of hybridization with excess of driver over tester, the ends of the enriched tester cDNA population were filled in by DNA polymerase and selectively amplified by PCR. Following a subsequent PCR with nested primers, the two differentially expressed cDNA populations were cloned into a pGEM-T vector (Promega, Madison, WI, USA) to produce clones of the subtracted libraries. Plasmids were sequenced by an ABI automated sequencer. Among the 56 differentially expressed sequence tags (ESTs) clones, one was found to be highly similar to PUFA elongases.

Generation of 5' and 3' End Fragments of the Putative *P. incisa* PUFA Elongase

To generate the full-length cDNA of the putative PUFA elongase, 3' and 5' rapid amplification of the cDNA ends (RACE) was performed using a BD smart RACE cDNA Amplification Kit (BD Biosciences Clontech, Foster City, CA, USA) according to the manufacturer's manual. To amplify the 5' end, the reverse gene-specific primers (GSP) 5'-CCCGGCTGCTGCCATGCTTCTGTG (EL5R1) and the nested 5'-TGGGGTAGGGAGAGTAGGCCCAAGT (EL5RN) were designed using Primer3 online software (<http://frodo.wi.mit.edu>). Based on the nucleotide sequence of the 5'-end fragment obtained, two forward GSPs, 5'-GCCTACATGTCCTCTGCCGCTGCTA (EL3R1) and the nested 5'-GCGGGACATGGGAGGGCTCATCTATA CC (EL3R2) were constructed to amplify the 3' end of the target gene. RACE PCR reactions were conducted using 5' and 3'-RACE-Ready cDNAs made from 1 µg total RNA of N-starved cells with 50× BD Advantage 2 polymerase mix (Clontech Laboratories, Mountain View, CA, USA). The PCR products of the expected size were excised, purified from the gel (NucleoSpin Extract II purification kit; Macherey-Nagel, Duren, Germany) and ligated into a pGEM T-Easy vector (Promega). The full-length cDNA corresponding to the *P. incisa* putative PUFA elongase (designated *PiELO1*) was assembled from the 5' and 3' RACE fragments and its ORF was further subcloned into a pYES2 vector (Invitrogen, Carlsbad, CA, USA).

Expression and Functional Characterization of *PiELO1* cDNA in the Yeast *Saccharomyces cerevisiae*

The ORF encoding for *PiELO1* was amplified using *PfuUltra* II fusion HS DNA polymerase (Stratagene, La Jolla, CA, USA) with the forward primer 5'-AGGAATT CAAAATGGCATTGACGGCGGCCT (PUFAEL5RES1) containing a restriction site (underlined) and a yeast translation consensus followed by ATG (bold) and the reverse primer 5'-CATTCTAGATTACTGCAGCTTTTGCTTGG CTGC (PUFAEL3RES2) containing a restriction site (underlined) and a stop codon (bold). The amplified sequence was then restricted with *EcoRI* and *XbaI* (NEB, Ipswich, MA, USA). The expected bands were gel-purified with NucleoSpin Extract II purification kit (Macherey-Nagel) and ligated into a *EcoRI-XbaI* cut pYES2 vector, yielding pY*PiELO1*. *Saccharomyces cerevisiae* strain W303 was transformed with pY*PiELO1* by the PEG/lithium acetate method [33]. The yeast cells harboring the empty pYES2 vector were used as control. Transformants were selected by uracil prototrophy on yeast synthetic medium (YSM) lacking uracil (Invitrogen). For functional expression, a minimal selection medium containing 2% (w/v) raffinose was inoculated with the pY*PiELO1* transformants and grown at 27°C for 24 h in a water bath shaker. Five milliliters of sterile YSM, containing 1% (w/v) Tergitol-40 and 250 µM of the appropriate fatty acid, was inoculated with raffinose-grown cultures to obtain an OD of 0.2 at 600 nm. Expression was induced by adding galactose to a final concentration of 2% (w/v) and cultures were further grown at 27°C for 48 h. Cells were harvested by centrifugation, washed twice with 0.1% NaHCO₃, freeze-dried, and used for fatty acid analysis.

Fatty Acid Analysis

Fatty acid methyl esters (FAMES) were obtained by transmethylation of the freeze-dried yeast or *P. incisa* cells with dry methanol containing 2% (v/v) H₂SO₄ and heating at 80°C for 1.5 h while stirring under an argon atmosphere. Gas chromatographic analysis of FAMES was performed on a Thermo Ultra gas chromatograph (Thermo Scientific, Italy) equipped with PTV injector, FID, and a fused silica capillary column (30 m × 0.32 mm; ZB WAXplus, Phenomenex). FAMES were identified by co-chromatography with authentic standards (Sigma Chemical, St Louis, MO, USA) and FAME of fish oil (Larodan Fine Chemicals, Sweden). Each sample was analyzed in duplicate.

Real-Time Quantitative RT-PCR

Template cDNA for real-time quantitative PCR (RTQPCR) was synthesized using 1 µg total RNA in a total volume

using the PrimerQuest tool (<http://test.idtdna.com/Scitools/Applications/Primerquest/>). Conditions were set for a primer length of 19–26 bp, primer melting temperature of $60.0 \pm 1.0^\circ\text{C}$, and an amplicon length of 90–150. Primer pairs were validated using seven serial 50-fold dilutions of cDNA samples, and standard curves were plotted to test for linearity of the response. The primer pairs and primer concentrations with reaction efficiencies of $100 \pm 10\%$ were chosen for quantitative RT-PCR analysis of relative gene expression. The nucleotide sequences and characteristics of primers used for quantitative RT-PCR analysis are presented in Table 1.

Gene Expression Profiling

Gene expression profiling was done by real-time quantitative PCR using duplicate reactions for each sample of three independent RNA isolations with a gene-specific primer pair using Absolute Blue QPCR SYBR Green ROX Mix (ABgene) in a real-time PCR 7500 system (Applied Biosystems). The amplification procedure was 50°C for 2 min, 95°C for 15 min, 40 cycles of 95°C for 15 s, and 60°C for 1 min. A dissociation curve was obtained for each pair of primers to confirm that a single, specific product was produced in each reaction.

Calculation of Gene Transcript Levels

The mean changes in gene expression, as multiples of the original values, were calculated according to the $2^{-\Delta\Delta\text{Ct}}$ method [34] using the average of threshold cycle (Ct) values from triplicate cDNA-primer samples. The ΔCt followed by the $\Delta\Delta\text{Ct}$ was calculated from the average Ct values of the target and the endogenous genes. The transcript abundance of the *PiELO1* gene was normalized to the endogenous control 18S SSU rRNA gene. The change in gene expression was calculated using $2^{-\Delta\Delta\text{Ct}}$ to find the expression level of the target gene which was normalized to the endogenous gene, relative to the expression of the target gene at time 0.

Results

Identification and Characterization of PiELO1

The BLASTX analysis (<http://www.ncbi.nlm.nih.gov/blast>) of clones obtained through subtractive hybridization revealed a clone of 141 bp whose putative amino acid sequence was highly homologous to the C-terminal region of PUFA elongases. Using GSP primers, the 870-bp 5'-end fragment was amplified and the sequence information was used to obtain the 3' end fragment from the 3' RACE

Ready cDNA. Alignment of the 800 bp 3'-end sequence with that of the 5'-end fragment provided an overlapping nucleotide sequence and included the partial 141 bp sequence, thus confirming the amplification of both ends of the expected gene. The assembled complete 867 bp cDNA sequence, designated *PiELO1*, was preceded and followed by 22 and 150 bp nucleotides at 5' and 3' UTR, respectively. *PiELO1* contained an ORF for 289 predicted amino acid residues consistent with functionally characterized PUFA elongase ORFs from fungi, lower plants, and algae (Fig. 1). The deduced amino acid sequence of the *PiELO1* was 50% identical to functionally characterized $\Delta 6$ PUFA elongases from *O. tauri* and *M. polymorpha*, while sharing 48 and 44% identity with *P. patens* $\Delta 6$ elongase and *M. polymorpha* $\Delta 5$ elongase, respectively. PiELO1 was also similar, yet with a lower score, to $\Delta 6$ elongases of fungal origin. It shared 40 and 36% identity with the $\Delta 6$ PUFA elongases of *Thraustochytrium* sp. and *M. alpina* (not included in the alignment), respectively. PiELO1 was 98% similar to a putative protein of the green microalga *Myrmecea incisa* (accession number ACF60496) which was not functionally characterized.

The predicted amino acid sequence of the PiELO1 contained four conserved motifs that are characteristic of PUFA elongases (Fig. 1, highlighted). The hydropathy plot of the PiELO1-deduced amino acid sequences was obtained using the algorithm available in the DAS transmembrane prediction server (<http://www.sbc.su.se/~miklos/DAS>) [35].

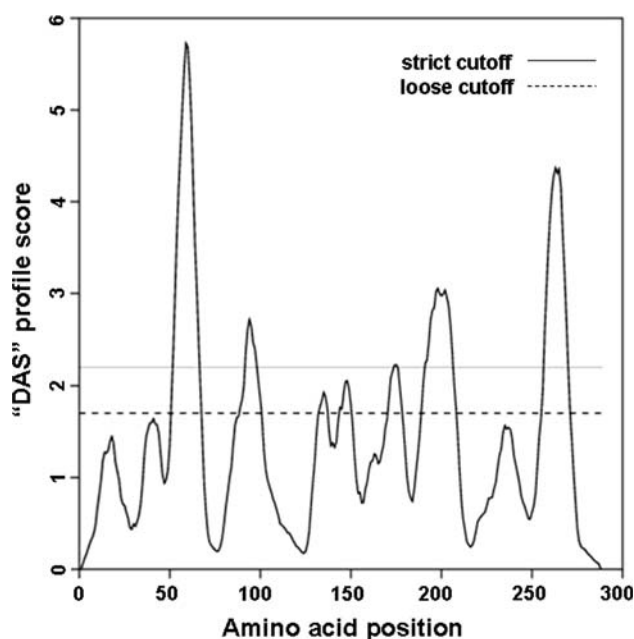


Fig. 2 Hydropathy plot of the amino acid sequence of PiELO1. The lower dashed line and the upper line represent the loose transmembrane region cutoff and the strict transmembrane region cutoff, respectively

The two strictly hydrophobic transmembrane domains were found about 50 amino acids downstream and upstream from the N and C termini, respectively, while the two less hydrophobic domains were located about 100 amino acids downstream and upstream from the N and C termini, respectively (Fig. 2).

Phylogenetic Analysis

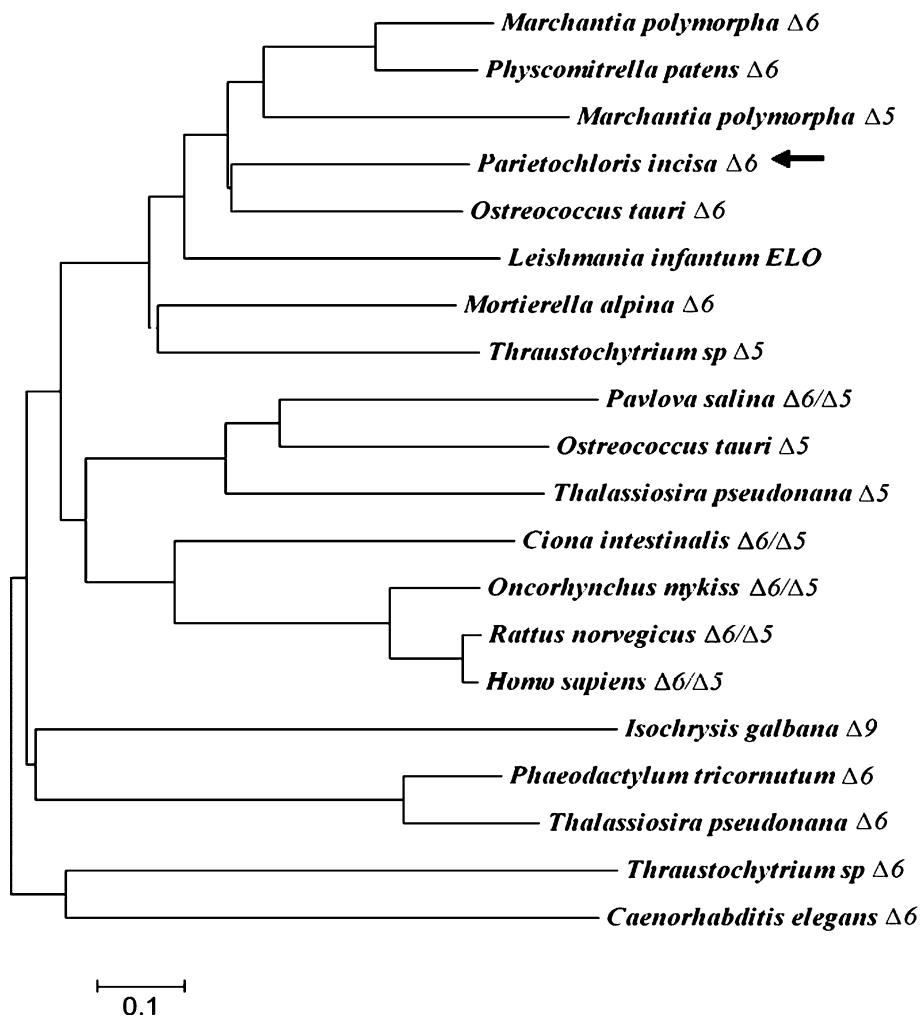
An unrooted phylogenetic tree of PiELO1 and several functionally characterized PUFA elongases was constructed to identify their functional and phylogenetic relationships by the neighbor-joining program in MEGA4 [36]. From Fig. 3 one can see that PiELO1 falls into a group of PUFA elongases of lower eukaryotes. Although the group contains mostly PUFA elongases with $\Delta 6$ activity, some $\Delta 5$ elongases, e.g., those of *M. polymorpha* and *Thraustochytrium* sp., are more related to $\Delta 6$ elongases of lower eukaryotes than to $\Delta 5$ elongases of higher eukaryotes. PiELO1 makes a closely related subgroup with OtELO1, MpELO1, MpELO2, and PpELO1, the OtELO1 being the closest one.

Functional Expression of PiELO1 in *S. cerevisiae*

To characterize the enzymatic activity of PiELO1, the pYES2 plasmid containing the *PiELO1* ORF downstream of the *GAL1* promoter was transformed into *S. cerevisiae*. PiELO1 was expressed in the presence of the $\Delta 6$ PUFA elongase substrates, 18:3 ω -6 (γ -linolenic acid, GLA) and 18:4 ω -3 (stearidonic acid, STA). GC analysis of the FAMES of transformed yeast cells showed that PiELO1 elongated both GLA and STA, converting them into di-homo- γ -linoleic acid (DGLA, 20:3 ω -6) and eicosatetraenoic acid (20:4 ω -3), respectively (Fig. 4; Table 2). The yeast cells harboring the empty vector alone did not demonstrate any elongation activity on the added substrates, confirming that the *PiELO1* encoded enzyme has a $\Delta 6$ PUFA elongase activity. Feeding the *PiELO1* transformants with the $\omega 6$ fatty acids LA and ARA did not result in their elongation (not shown).

Real-time quantitative PCR was performed to quantitate the alterations in expression levels of the $\Delta 6$ *PiELO1* in *P. incisa* cells under nitrogen starvation. The change in the

Fig. 3 Unrooted phylogram of PiELO1 and some other functionally characterized PUFA elongases. The alignment was generated by the CLUSTAL W program and the unrooted phylogram was constructed by the neighbor-joining method using MEGA4 software [36]. GeneBank accession numbers for the PUFA elongases are: ACK99719 ($\Delta 6$, *P. incisa*), AAV67797 ($\Delta 6$, *O. tauri*), AAV67798 ($\Delta 5$, *O. tauri*), AAT85662 ($\Delta 6$, *M. polymorpha*), BAE71129 ($\Delta 5$, *M. polymorpha*), AAL84174 ($\Delta 6$, *P. patens*), CAJ30819 ($\Delta 6$, *Thraustochytrium* sp.), CAM55873 ($\Delta 5$, *Thraustochytrium* sp.), AAF70417 ($\Delta 6$, *M. alpina*), XP_001467802 (*L. infantum*), AAV67803 ($\Delta 6/\Delta 5$, *O. mykiss*), NP_001029014 ($\Delta 6/\Delta 5$, *C. intestinalis*), NP_068586 ($\Delta 6/\Delta 5$, *H. sapiens*), AAY15135 ($\Delta 5$, *P. salina*), CAM55851 ($\Delta 6$, *P. tricornutum*), AAL37626 ($\Delta 9$, *I. galbana*), AAV67799 ($\Delta 6$, *T. pseudonana*), AAV67800 ($\Delta 5$, *T. pseudonana*), CAA92958 ($\Delta 6$, *C. elegans*), and NP_599209 ($\Delta 6/\Delta 5$, *R. norvegicus*)



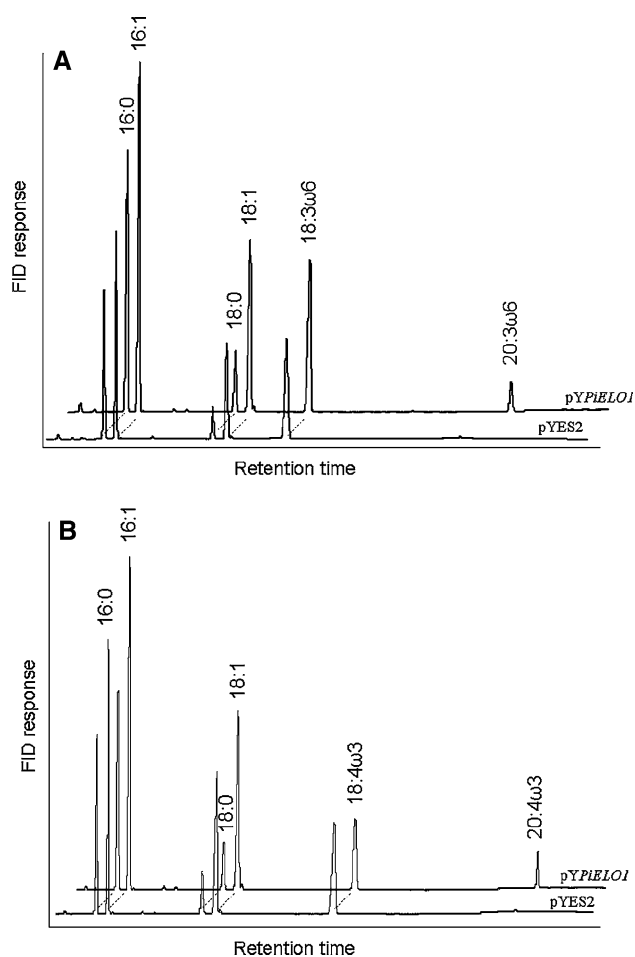


Fig. 4 GC of FAMES of recombinant yeast harboring pYES2 (control) and pYPIELO1 fed with 18:3 ω -6 (a) and 18:4 ω -3 (b)

Table 2 Fatty acid composition of *Saccharomyces cerevisiae* (W303) transformed with the pYES2 vector or the pYPIELO1 construct

Fatty acid (% of total)	Control (pYES2)		pYPIELO1	
	+18:3 ω -6	+18:4 ω -3	+18:3 ω -6	+18:4 ω -3
16:0	20.1	21.6	22.1	20.3
16:1	26.0	28.9	26.8	31.2
18:0	6.0	6.9	7.3	6.5
18:1	18.0	22.7	19.4	25.2
18:3 ω -6	29.9	–	20.4	–
18:4 ω -3	–	19.9	–	12.6
20:3 ω -6	–	–	4.0	–
20:4 ω -3	–	–	–	4.1
Percent elongated			16.4	24.6

The experiments were performed in two biological replicates, each analyzed in duplicate

expression level of the target gene in *P. incisa* cells grown for 3, 7, and 14 days on N-free medium was calculated relative to the expression level of the target gene in the log

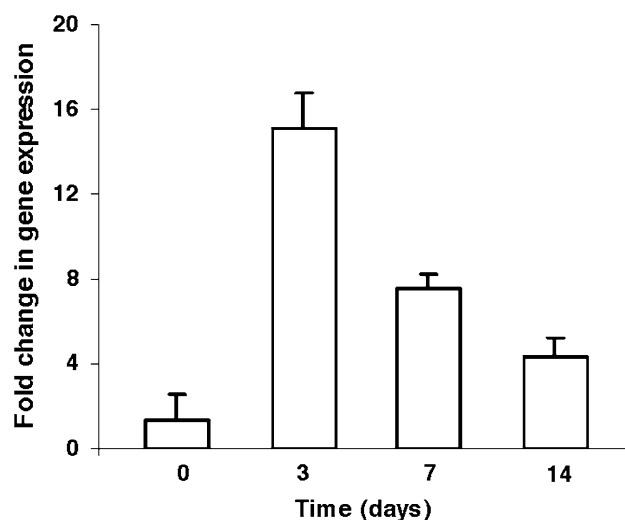


Fig. 5 Quantitative real-time PCR analysis of the *PiELO1* gene expression in the log phase (time 0) and nitrogen starved (3, 7 and 14 days) cells of *P. incisa*. The transcript abundance of the gene was normalized to that of 18S SSU rRNA gene

phase (time 0). The results showed that during nitrogen starvation the mRNA of the *PiELO1* gene was induced to its highest level at day 3 (14-fold increase over time 0), decreasing thereafter to a level still higher than that of day 0 (Fig. 5). After 7 and 14 days, the expression level of the *PiELO1* gene was still 7.5 and 4.3-fold higher, respectively. The level of expression of the *PiELO1* gene correlated with the increase in the share of ARA and the C20/ (C16 + C18) elongation ratio (Table 3). The share of the elongation product, DGLA, increased sharply at day 3 (50% increase over time 0) and decreased thereafter.

Discussion

Recent successes in the production of VLC-PUFA by genetically modified oil plants has elicited further investigations concerning the characterization, role, and regulation of the genes and enzymes involved in VLC-PUFA biosynthesis. We isolated from *P. incisa* a cDNA (*PiELO1*) of an elongase encoding for a deduced protein, structurally similar to Δ 6 PUFA elongase gene products from microalgae, lower plants, and fungi (Fig. 1). The deduced amino acid sequence of the *PiELO1* ORF was about 50% identical with that of Δ 6 elongases from the liverwort *M. polymorpha* (AAT85662), the green marine microalga *O. tauri* (AAV67797), and the moss *P. patens* (AAL84174). In similarity to recently cloned PUFA elongases, the predicted protein is highly hydrophobic and has two strongly hydrophobic transmembrane regions, the first located about 50 amino acids downstream of the N-terminus and the second in the vicinity of the C-terminus. We identified in the *PiELO1* sequence a

Table 3 Major fatty acid composition of *P. incisa* cells grown under N-starvation

Time (days)	Fatty acid composition (% of total fatty acids)												TFA (% DW)
	16:0	16:2	16:3	18:0	18:1	18:2	18:3 ω -6	18:3 ω -3	20:3 ω -6	20:4 ω -6	20:5 ω -3	Elo. ratio ^a	
0	19.1	4.1	2.9	3.1	9.1	20.1	1.2	6.0	0.5	23.0	0.7	0.34	6.4
3	12.7	1.5	1.9	3.8	15.2	13.5	1.6	2.0	0.9	39.7	0.6	0.74	11.0
7	10.7	0.6	1.1	3.5	14.9	10.0	1.1	0.9	1.0	50.0	0.5	1.10	21.2
14	9.0	0.3	0.8	3.1	13.4	8.8	0.9	0.6	0.9	56.9	0.6	1.44	28.9

^a Elongation ratio, C20/(C18 + C16)

C-terminal lysine-rich motif, important for the endoplasmic reticulum targeting [37], and four conserved motifs FYxSKxxEFxDT, QxxxLHVYHHxxI, NSxxHVxMYxYY, and TxxQxxQF, including a conserved histidine-rich box, suggested to be functionally important for PUFA elongation [28] (Fig. 1). These conserved motifs were not found in other classes of plant microsomal elongases, β ketoacyl CoA synthases, and fatty acid elongases (FAE) involved in extraplasmidial elongation of saturated and monounsaturated fatty acids. A variant histidine box, containing three amino acid replacements, in C18- Δ 9-PUFA-specific elongase from *I. galbana* (IgASE1), was shown to be essential for optimal enzymatic activity rather than for substrate specificity [38].

Similarly to GLELO of *M. alpina*, PiELO1 prefers the Δ 6 C18 PUFA substrates, GLA and STA [25]. Only these Δ 6 fatty acids were, when exogenously added, elongated to the respective products by *S. cerevisiae* cells transformed with *PiELO1* (Fig. 4). Transformation of a higher plant so as to render it to produce Δ 6 PUFA requires that the elongase used will have a high selectivity for Δ 6 PUFA, thereby reducing the appearance of side products in the transformed plant [11, 39, 40]. Bifunctional invertebrate PUFA elongases with both Δ 6 and Δ 5 activities (OmELO, XiELO, and CiELO) are less desirable in plant transformations [20, 28].

Phylogenetic analysis showed (Fig. 3) that the PUFA elongases are not strictly divided according to their substrate specificity. The Δ 6 elongases of algal (OtELO1, TpELO1, PiELO1) and moss (PpELO1) origin are functionally restricted to the elongation of Δ 6-C18-PUFAs, however, these elongases are placed in separate groups on the phylogenetic tree (Fig. 3) [28]. PiELO1 is closely related to OtELO1 isolated from a chloropyte and a lower plant rather than to a ELO1 gene isolated from a diatom, although both are specific for the elongation of Δ 6-C18-PUFAs (Fig. 3). PiELO1 is highly similar to, and is placed in the same group with, both Δ 6 and Δ 5 elongases of the liverwort *M. polymorpha*. Kajikawa et al. [41] suggested that MpELO2, a Δ 5 elongase, is likely to have originated through gene duplication of the *MpELO1* gene. In contrast, Δ 5 and Δ 6 PUFA elongases of *Thraustochytrium* sp. are located in distinct branches. The Δ 5 PUFA elongases of a marine chloropyte, a diatom and a haptophyte, OtELO2,

TpELO2 and the *P. salina* ELO1 [42], respectively, are more likely to share a common branch with the mammalian and animal Δ 5 PUFA elongases, OmELO [28] and HELO1 [20], while they are also similar to bifunctional PUFA elongases such as CiELO1/2 [28].

Quantitative real time PCR studies revealed that the expression level of the *PiELO1* gene was up-regulated during the time course of N-starvation (Fig. 5). Nitrogen starvation led to a continuous increase in the share of ARA and the C20/(C16 + C18) elongation ratio (Table 3). However, a major transcriptional activation of *PiELO1* which occurred on day 3 (14-fold increase in transcript level) coincided with the steep rise in ARA accumulation and elongation ratio (Table 3). The increase in *PiELO1* transcription level followed by enhanced biosynthesis of ARA may be interpreted as an increase in the PiELO1 enzyme level and/or enzymatic activity. The importance of the transcriptional activation of PiELO1 is supported by the fact that PUFA elongase gene was the only ARA biosynthesis-related gene that was obtained from the subtractive library. Possibly, the elongation of GLA by PiELO1 could be rate-limiting in ARA biosynthesis as it is in *M. alpina*. However, the significance of the coordinated transcription and action of desaturases, elongases, and enzymes of TAG assembly in biosynthesis of ARA-rich TAG in *P. incisa* is yet to be elucidated. Abbadì et al. [11] suggested that in transgenic plants modified with VLC-PUFA biosynthesis genes, substrate availability rather than enzymatic activity is rate-limiting in the Δ 6 elongation of PUFA. Moreover, the selective acyl channeling to TAG in engineered plant seeds is of major importance in regulating the final TAG acyl quality [11, 39].

In conclusion, PiELO1 is a Δ 6 PUFA elongase, specifically elongating GLA and STA to 20:3 ω -6 and 20:4 ω -3, respectively. The *PiELO1* gene is up-regulated under oleogenic conditions. This gene is a likely candidate for genetic transformations of oil seed plants that will enable the production of VLC-PUFAs in the transgenic plants. The up-regulation of the *PiELO1* gene under nitrogen starvation conditions must have significant physiological importance for adaptation of *P. incisa* cells to nitrogen deficiency.

Accession Numbers GenBank accession numbers for PiELO1 and 18S SSU rRNA of *P. incisa* are ACK99719 and FJ548971, respectively.

Acknowledgments This work was supported by a grant from the Israeli ministry of science, culture and sport.

References

- Funk CD (2001) Prostaglandins and leukotrienes: advances in eicosanoid biology. *Science* 294:1871–1875
- Hansen J, Schade D, Harris C, Merkel K, Adamkin D, Hall R, Lim M, Moya F, Stevens D, Twist P (1997) Docosahexaenoic acid plus arachidonic acid enhance preterm infant growth. *Prostaglandins Leukot Essent Fatty Acids* 57:196
- Crawford MA, Golfetto I, Ghebremeskel K, Min Y, Moodley T, Poston L, Phylactos A, Cunnane S, Schmidt W (2003) The potential role for arachidonic and docosahexaenoic acids in protection against some central nervous system injuries in preterm infants. *Lipids* 38:303–315
- Gill I, Valivety R (1997) Polyunsaturated fatty acids, part 1: occurrence, biological activities and applications. *Trends Biotechnol* 15:401–409
- Arao T, Sakaki T, Yamada M (1994) Biosynthesis of polyunsaturated lipids in the diatom, *Phaeodactylum tricorutum*. *Phytochemistry* 36:629–635
- Cohen Z, Norman HA, Heimer YM (1995) Microalgae as a source of ω 3 fatty acids. In: Simopoulos AP (ed) *Plants in human nutrition*, vol. 77. World Rev Nutr Diet. Karger, Basel, pp 1–31
- Bigogno C, Khozin-Goldberg I, Boussiba S, Vonshak A, Cohen Z (2002) Lipid and fatty acid composition of the green oleaginous alga *Parietochloris incisa*, the richest plant source of arachidonic acid. *Phytochemistry* 60:497–503
- Cohen Z, Khozin-Goldberg I (2005) Searching for PUFA-rich microalgae. In: Cohen Z, Ratledge C (eds) *Single cell oils*. J Am Oil Chem Soc, Champaign, pp 53–72
- Qi B, Fraser T, Mugford S, Dobson G, Sayanova O, Butler J, Napier JA, Stobart AK, Lazarus CM (2004) Production of very long chain polyunsaturated omega-3 and omega-6 fatty acids in plants. *Nat Biotechnol* 22:739–745
- Robert SS, Singh SP, Zhou X, Petrie JR, Blackburn SI, Mansour PM, Nichols PD, Liu Q, Green AG (2005) Metabolic engineering of *Arabidopsis* to produce nutritionally important DHA in seed oil. *Funct Plant Biol* 32:473–479
- Abbadi A, Domergue F, Bauer J, Napier JA, Welti R, Zähringer U, Cirpus P, Heinz E (2004) Biosynthesis of very-long-chain polyunsaturated fatty acids in transgenic oilseeds: constraints on their accumulation. *Plant Cell* 16:2734–2748
- Khozin-Goldberg I, Bigogno C, Shrestha P, Cohen Z (2002) Nitrogen starvation induces the accumulation of arachidonic acid in the freshwater green alga *Parietochloris incisa* (Trebouxio-phyceae). *J Phycol* 38:991–994
- Bigogno C, Khozin-Goldberg I, Adlerstein D, Cohen Z (2002) Biosynthesis of arachidonic acid in the oleaginous microalga *Parietochloris incisa* (Chlorophyceae): radiolabeling studies. *Lipids* 37:209–216
- Khozin-Goldberg I, Adlerstein D, Bigogno C, Heimer YM, Cohen Z (1997) Elucidation of the biosynthesis of eicosapentaenoic acid in the microalga *Porphyridium cruentum*. *Plant Physiol* 114:223–230
- Qi B, Beaudoin F, Fraser T, Stobart AK, Napier JA, Lazarus CM (2002) Identification of a cDNA encoding a novel C18- Δ 9 polyunsaturated fatty acid-specific elongating activity from the docosahexaenoic acid (DHA)-producing microalga, *Isochrysis galbana*. *FEBS Lett* 510:159–165
- Nichols BW, Appleby RS (1969) The distribution of arachidonic acid in algae. *Phytochemistry* 8:1907–1915
- Meyer A, Cirpus P, Ott C, Schlecker R, Zähringer U, Heinz E (2003) Biosynthesis of Docosahexaenoic acid in *Euglena gracilis*: biochemical and molecular evidence for the involvement of a Δ 4-fatty acyl group desaturase. *Biochemistry* 42:9779–9788
- Lassner MW, Lardizaba K, Metz JG (1996) A jojoba [β]-Ketoacyl-CoA synthase cDNA complements the canola fatty acid elongation mutation in transgenic plants. *Plant Cell* 8:281–292
- Beaudoin F, Michaelson LV, Hey SJ, Lewis MJ, Shewry PR, Sayanova O, Napier JA (2000) Heterologous reconstitution in yeast of the polyunsaturated fatty acid biosynthetic pathway. *Proc Natl Acad Sci USA* 97:6421–6426
- Leonard AE, Bobik EG, Dorado J, Kroeger PE, Chuang LT, Thurmond JM, Parker-Barnes JM, Das T, Huang YS, Mukerji P (2000) Cloning of a human cDNA encoding a novel enzyme involved in the elongation of long-chain polyunsaturated fatty acids. *Biochem J* 3:765–770
- Agaba MK, Tocher DR, Zheng X, Dickson CA, Dick JR, Teale AJ (2005) Cloning and functional characterization of polyunsaturated fatty acid elongases of marine and freshwater teleost fish. *Comp Biochem Physiol* 42:342–352
- Domergue F, Lerchl J, Zähringer U, Heinz E (2002) Cloning and functional characterization of *Phaeodactylum tricorutum* front-end desaturases involved in eicosapentaenoic acid biosynthesis. *Eur J Biochem* 269:4105–4113
- Kaewsuwan S, Cahoon EB, Perroud PF, Wiwat C, Panvisavas N, Quatrano RS, Cove DJ, Bunyapraphatsara N (2006) Identification and functional characterization of the moss *Physcomitrella patens* Δ 5-desaturase gene involved in arachidonic and eicosapentaenoic acid biosynthesis. *J Biol Chem* 281:21988–21997
- Kajikawa M, Yamato KT, Kohzu Y, Nojiri M, Sakuradani E, Shimizu S, Saka Y, Fukuzawa H, Ohyama K (2004) Isolation and characterization of Δ 6-desaturase, an ELO-like enzyme and Δ 5-desaturase from the liverwort *Marchantia polymorpha* and production of arachidonic and eicosapentaenoic acids in the methylotrophic yeast *Pichia pastoris*. *Plant Mol Biol* 54:335–352
- Parker-Barnes JM, Das T, Bobik E, Leonard AE, Thurmond JM, Chuang LT, Huang YS, Mukerji P (2000) Identification and characterization of an enzyme involved in the elongation of n-6 and n-3 polyunsaturated fatty acids. *Proc Natl Acad Sci USA* 97:8284–8289
- Wynn JP, Ratledge C (2000) Evidence that the rate-limiting step for the biosynthesis of arachidonic acid in *Mortierella alpina* is at the level of the 18:3 to 20:3 elongase. *Microbiology* 146:2325–2331
- Takeno S, Sakuradani E, Murata S, Inohara-Ochiai M, Kawashima H, Ashikari T, Shimizu S (2005) Molecular evidence that the rate-limiting step for the biosynthesis of arachidonic acid in *Mortierella alpina* is at the level of an elongase. *Lipids* 40:25–30
- Meyer A, Kirsch H, Domergue F, Abbadi A, Sperling P, Bauer J, Cirpus P, Zank TK, Moreau H, Roscoe TJ, Zähringer U, Heinz E (2004) Novel fatty acid elongases and their use for the reconstitution of docosahexaenoic acid biosynthesis. *J Lipid Res* 45:1899–1909
- Agaba M, Tocher DR, Dickson CA, Dick JR, Teale AJ (2004) Zebra fish cDNA encoding multifunctional fatty acid elongase involved in production of eicosapentaenoic (20:5n-3) and docosahexaenoic (22:6n-3) acids. *Mar Biotechnol* 6:251–261
- Stanier RY, Kunisawa R, Mandel M, Cohen-Bazire G (1971) Purification and properties of unicellular blue-green algae (order Chroococcales). *Bacteriol Rev* 35:171–205
- Bekesiova I, Nap JP, Mlynarova L (1999) Isolation of high quality DNA and RNA from leaves of the carnivorous plant *Drosera rotundifolia*. *Plant Mol Biol Rep* 17:269–277

32. Diatchenko L, Lau YF, Campbell AP, Chenchik A, Moqadam F, Huang B, Lukyanov S, Lukyanov K, Gurskaya N, Sverdlov ED, Siebert PD (1996) Suppression subtractive hybridization: a method for generating differentially regulated or tissue-specific cDNA probes and libraries. *Proc Natl Acad Sci USA* 93:6025–6030
33. Ausubel FM, Brent R, Kingston RE, Moore DD, Seidman JG, Smith JA, Struhl K, Albright LM, Cohen DM, Varki A (1995) *Current protocols in molecular biology*. Wiley, New York
34. Livak KJ, Schmittgen TD (2001) Analysis of relative gene expression data using real-time quantitative pcr and the $2^{-\Delta\Delta Ct}$ method. *Methods* 25:402–408
35. Cserző M, Wallin E, Simon I, Heijne G, Elofsson A (1997) Prediction of transmembrane alpha-helices in prokaryotic membrane proteins: the dense alignment surface method. *Protein Eng* 10:673–676
36. Tamura K, Dudley J, Nei M, Kumar S (2007) MEGA4: molecular evolutionary genetics analysis (MEGA) software version 4.0. *Mol Biol Evol* 24:1596–1599
37. Jackson MR, Nilsson T, Peterson PA (1990) Identification of a consensus motif for retention of transmembrane proteins in the endoplasmic reticulum. *EMBO J* 9:3153–3162
38. Qi B, Fraser T, Bleakley CL, Shaw EM, Stobart AK, Lazarus CM (2003) The variant ‘his-box’ of the C18- $\Delta 9$ -PUFA-specific elongase IgASE1 from *Isochrysis galbana* is essential for optimum enzyme activity. *FEBS Lett* 547:137–139
39. Wu G, Truksa M, Datla N, Vrinten P, Bauer J, Zank T, Cirpus P, Heinz E, Qiu X (2005) Stepwise engineering to produce high yields of very long-chain polyunsaturated fatty acids in plants. *Nat Biotech* 23:1013–1017
40. Zank TK, Zähringer U, Beckmann PG, Boland W, Holtort H, Reski J, Lerchl J, Heinz E (2002) Cloning and functional characterization of an enzyme involved in the elongation of a $\Delta 6$ -polyunsaturated fatty acids from the moss *Physcomitrella patens*. *Plant J* 31:255–268
41. Kajikawa M, Yamato K, Sakai Y, Fukuzawa H, Ohyama K, Kohchi T (2006) Isolation and functional characterization of fatty acid $\Delta 5$ -elongase gene from the liverwort *Marchantia polymorpha* L. *FEBS Lett* 580:149–154
42. Pereira SL, Leonard AE, Huang YS, Chuang LT, Mukerji P (2004) Identification of two novel microalgal enzymes involved in the conversion of the omega 3-fatty acid, eicosapentaenoic acid, into docosahexaenoic acid. *Biochem J* 384:357–366

Cloning and Molecular Characterization of the Acyl-CoA: Diacylglycerol Acyltransferase 1 (DGAT1) Gene from *Echium*

A. Mañas-Fernández · M. Vilches-Ferrón ·
J. A. Garrido-Cárdenas · E.-H. Belarbi ·
D. L. Alonso · F. García-Maroto

Received: 12 February 2009 / Accepted: 8 April 2009 / Published online: 2 May 2009
© AOCs 2009

Abstract Boraginaceae species, such as those from the genus *Echium*, contain high levels of the Δ^6 -desaturated γ -linolenic (18:3n-6) and octadecatetraenoic (18:4n-3) acids. These are unusual fatty acids among the plant kingdom that are gaining interest due to their benefits to human health. The potential utility of acyltransferases aimed at an increase in oil yield and fatty acid profiling has been reported. In this work, a gene encoding an acyl-CoA:diacylglycerol acyltransferase (DGAT, EC 2.3.1.20) was cloned from *Echium pitardii*. Genomic and cDNA sequences obtained revealed a gene structure composed of 16 exons, yielding a protein (EpDGAT) of 473 amino acids with high similarity to DGAT1 enzymes of plants. Protein features such as a predicted structure with a highly hydrophilic N-terminus followed by 10 transmembrane domains, as well as the presence of diverse specific signatures, also indicate that EpDGAT belongs to the DGAT1 family. indeed. DGAT activity of the protein encoded by *EpDGAT* was confirmed by heterologous expression of the full-length cDNA in a yeast mutant (H1246) defective in the synthesis of triacylglycerols. Fatty acid composition of the triacylglycerols synthesized by EpDGAT in H1246

yeast cultures supplemented with polyunsaturated fatty acids suggest a substrate preference for the trienoic fatty acids α -linolenic acid (18:3n-3) and γ -linolenic acid over the dienoic linoleic acid (18:2n-6). Site-directed mutagenesis has revealed the presence of a critical residue (P¹⁷⁸ in EpDGAT) within a reported thiolase signature for binding of acyl-enzyme intermediates that might be involved in the active site of the enzyme. Transcript analysis for *EpDGAT* shows an ubiquitous expression of the gene which is increased in leaves during senescence.

Keywords *Echium pitardii* · Boraginaceae · Diacylglycerol acyltransferase · Triacylglycerol · Seed oil

Abbreviations

ALA	Alpha-linolenic acid
cDNA	Complementary DNA
CTAB	Cetyl trimethylammonium bromide
DAG	Diacylglycerol
DGAT	Acyl-CoA:diacylglycerol acyltransferase
DIG	Digoxigenin
FFA	Free fatty acids
GC	Gas chromatography
GLA	Gamma-linolenic acid
IPCR	Inverse PCR
LNA	Linoleic acid
NL	Neutral lipids
PCR	Polymerase chain reaction
PL	Polar lipids
PUFA	Polyunsaturated fatty acid
RT-PCR	Reverse transcriptase PCR
SDS	Sodium dodecylsulfate
SE	Steryl esters

Electronic supplementary material The online version of this article (doi:10.1007/s11745-009-3303-9) contains supplementary material, which is available to authorized users.

A. Mañas-Fernández · M. Vilches-Ferrón ·
J. A. Garrido-Cárdenas · D. L. Alonso · F. García-Maroto (✉)
Laboratorio Genética III, Edificio CITE-II B, Universidad
de Almería, 04120 Almería, Spain
e-mail: fgmaroto@ual.es

E.-H. Belarbi
Departamento Ingeniería Química, Universidad de Almería,
04120 Almería, Spain

ST	Sterols
TAG	Triacylglycerol
TL	Total lipids
TLC	Thin layer chromatography

Introduction

Plant oils have become important renewable resources as biofuel and for human consumption [1–3]. Nowadays there is a growing demand, mainly due to an increase in the biodiesel market specially in Europe [1]. Consequently, any improvement in seed oil production is of interest, and great efforts are being made with this aim within the biotechnology field.

Plant oil is mostly composed of triacylglycerol (TAG), the main storage lipid. TAG is usually synthesized by sequential incorporation of acyl groups through the glycerol-3-phosphate (G3P) pathway, also known as the Kennedy pathway [4–6]. Briefly, G3P is first acylated by the action of the acyl-CoA:glycerol-3-phosphate acyltransferase (GPAT; EC 2.3.1.15), followed by a second acylation step catalyzed by the acyl-CoA:lysophosphatidate acyltransferase (LPAT; also called acyl-CoA:acyl-glycerol-3-phosphate acyltransferase, AGPAT; EC 2.3.1.51). The phosphatidic acid obtained is then dephosphorylated by a phosphatidate phosphatase (PAP; EC 3.1.3.4) to generate diacylglycerol (DAG) which is finally used as substrate for the acyl-CoA:diacylglycerol acyltransferase (DGAT; EC 3.2.1.20) to produce TAG [5, 6]. GPAT and LPAT are acyltransferases common to TAG and membrane-lipid biosynthesis while DGAT catalyze the only step which is committed to TAG biosynthesis [4, 5, 7].

Two alternative pathways for the synthesis of TAG have also been described involving the phospholipid:diacylglycerol acyltransferase (PDAT) and DAG:DAG transacylase (DGTA) enzymes, respectively [5, 8]. It has been suggested that PDAT has a role in directing unusual fatty acids (such as ricinoleic acid) to TAG, thus avoiding their incorporation into polar lipids and possible disturbances of membrane functions [9, 10]. The presence of PDAT in plants lacking such unusual fatty acids indicates that it may play a different role in lipid biosynthesis, though this function remains still unknown [11, 12]. Nevertheless, current evidence strongly suggests that PDAT is not a major determinant of TAG production in seed plants [9, 12–14]. With regard to DGTA, involvement in remodeling of TAG was proposed [15] although it does not seem to affect the net biosynthesis [8, 13].

There is growing evidence supporting a major contribution of DGAT to TAG synthesis in seed plants [14, 16]. The *AS11 Arabidopsis* mutant, bearing reduced DGAT

activity, showed a 75% reduction in seed lipids [17]. Conversely, DGAT over-expression determines a net increase in seed oil content in *Arabidopsis* [18]. Additional evidence is also available from studies of soybean [19], oil-seed rape [20], olive [21] and maize [3]. In agreement with this, it is considered that DGAT catalyzes a rate limiting step within the TAG biosynthesis pathway [5, 18, 20, 22, 23]. Consequently, DGAT is also regarded as being a key enzyme, from a biotechnological point of view, in order to increase oil content in oleaginous species [7, 23–27].

Another area of active research is the biosynthesis of oils containing particular fatty acid profiles. In this regard, the importance of acyltransferases for the production of ‘designer oils’ in genetically engineered plants has been emphasized [14, 24]. Though initial studies on DGAT activity had suggested a wide substrate utilization by this enzyme [24], later works indicated that the DGAT specificity is species-dependent. While DGAT from plant species like saffron or peanut showed wide acyl utilization [28], in others such as spinach, maize [28], castor bean [29], *Arabidopsis* [17], *Garcinia indica* [30], *Vernonia galamensis* and *Stokesia laevis* [31], this enzyme exhibited some acyl preference. This behavior opens the possibility of using appropriate *DGAT* genes to engineer TAG fatty acid profiles.

The first eukaryotic *DGAT* gene was cloned from the mouse, based on similarity to the acyl-CoA:cholesterol acyltransferase (ACAT) enzyme [32]. A similar gene was later cloned from *Arabidopsis* [33–35] and other plants species [36–41], all of them encoding proteins related to ACAT. A different family of enzymes with DGAT activity was uncovered after cloning of the *DGAT* gene from *Mortierella rammaniana* [42], and finding of similar genes in different plant species [13, 41]. Members of this group share homology with a broader family of genes that transfer acyl groups from coenzyme A to neutral lipids including monoacylglycerol, diacylglycerol, and fatty alcohol species [43]. Thus, two evolutionary unrelated DGAT families are present in plants, encoding membrane bound proteins, that have been named as DGAT1 (ACAT-related) and DGAT2 [23]. Recently, a new *DGAT* gene was reported encoding a soluble cytosolic enzyme [44]. This protein is closely related to bacterial bifunctional DGAT/wax ester synthetase, thus representing a third unrelated group named as DGAT3 [14].

Experimental evidence indicates that DGAT1 and DGAT2 are the major isoenzymes acting in the biosynthesis of TAG [14], while the contribution of DGAT3 seems to be just marginal [44]. The importance of DGAT1 for the synthesis of TAG in the seed has been well documented in *Arabidopsis thaliana* [12, 17, 18, 34, 35, 45, 46] and more recently in maize [3]. On the other hand, DGAT2 has proven to be essential in determining both TAG profile

and TAG content in *Vernicia fordii* [41]. Paradoxically, in that work, DGAT2 was shown to be less active in vitro than DGAT1, and yeast transformed with *DGAT1* were more efficient in producing TAG than that transformed with *DGAT2* [41]. Similar studies performed in castor bean (*Ricinus communis*) suggested that DGAT2 was the main enzyme for TAG synthesis in seeds [13] and metabolic engineering of *Arabidopsis* with both castor bean fatty acid hydroxylase 12 and DGAT2 resulted in a significant increase in ricinoleic acid in the seed oil [47]. However, another study on *R. communis* has shown a DGAT1 activity pattern matching in time to that of TAG accumulation [48]. Moreover, an extensive search for DGAT2 was unsuccessful in *Tropaeolum majus* suggesting that DGAT1 may be the sole DGAT in this plant species [7], and *Arabidopsis* DGAT2 showed no detectable activity in yeast complementation assays [41]. Therefore, the question about the relative contribution to TAG synthesis by DGAT1 versus DGAT2 is far from being answered [14, 23]. In this regard, it has been suggested that both DGAT isoenzymes may play distinct roles in different tissues and plant species [41, 48].

In this work, we report on the cloning of the *DGAT1* gene from *Echium pitardii* A. Chev. ex D. Bramwell (Boraginaceae). Boraginaceae species such as those from genus *Echium* are characterized by the accumulation of high levels of the Δ^6 -desaturated fatty acids, γ -linolenic (18:3n-6, GLA) and octadecatetraenoic (18:4n-3) acids, that are unusual among the plant kingdom. More specifically, Macaronesian species of *Echium* such as *E. pitardii* are considered among the richest sources of GLA found in nature, reaching 28% of total fatty acids in the seeds of *E. gentianoides* [49]. *E. pitardii* was chosen for our work since its herbaceous habit makes it appropriate for the study in the laboratory [50]. The highest content of GLA (19% for *E. pitardii*) is found in the seed, but it is also accumulated, although at a lower level, in other organs of the plant such as the leaves, roots and stem [50].

Molecular characterization of the *Echium DGAT* was performed in our study that included confirmation of the DGAT activity by heterologous expression in a yeast system.

Experimental Procedure

Biological Material

Seeds of *E. pitardii* A. Chev. ex D. Bramwell (= *E. lancerolettense* Lems et Holz) were collected from plants located in their natural habitat at Lanzarote (Canary Islands). Seedlings (6–8 leaves stage) were grown at 25°C, under the controlled conditions of growth cabinets with a 16 h

light/8 h dark photoperiod and 70% relative humidity. Leaf material from seedlings was used as a DNA source, while the different tissues of *E. pitardii* utilized for RNA extraction and Northern blot analysis were sampled from mature plants cultivated in a greenhouse.

The wild type yeast strain INVSc1 (purchased from Invitrogen), and the H1246 mutant strain (*Mat α yor245c::KanMX4 lro1::TRP1 are1::HIS3 are2::LEU2 ADE2 ura3*) [51], kindly provided by Dr. Stymne (Swedish University of Agricultural Sciences, Uppsala) were used to assay DGAT activities by heterologous expression.

Cloning of the DGAT1 Gene of *E. pitardii*

Cloning of the *EpDGAT* gene was achieved by RT-PCR amplification of a partial cDNA sequence, followed by bi-directional walking through inverse PCR (IPCR) on genomic DNA. Briefly, a cDNA was synthesized from 5 μ g of total RNA obtained from developing flowers of *E. pitardii* (RNeasy Plant Mini Kit, QIAGEN) by employing the kit “SuperScript First-Strand Synthesis System for RT-PCR” (Invitrogen), and following the manufacturer’s instructions. RT-PCR amplification on the cDNA was done using the degenerated oligonucleotide primers DAG1-Up (5'-ATTATCGARAAYYTIATGAAR TAYGG-3') and DAG2-Down (5'-GCRTTCCACCART CYTTRTARAAAYTC-3') designed against the DGAT conserved motifs IENLMKYG and EFYKDWNA, respectively. The reaction was performed using a proof-reading polymerase (AccuTaq, Sigma) and a program consisting of a denaturation step of 2 min at 94°C, followed by 40 cycles of 15 s at 94°C, 30 s at 45°C and 75 s at 72°C, ending with a 5 min step at 72°C. The resulting fragment (about 800 bp, spanning the central coding region) was cloned in the vector pGEM-T-Easy[®] (Promega), and several clones were sequenced that resulted in their being all identical. Starting with this partial sequence, a total of five successive IPCR rounds were carried out following the method reported in [52] with minor modifications [53]. DNA clones were sequenced on both strands using a Perkin-Elmer ABI-310 DNA automated sequencer, and the BigDye[®] Terminator v3.1 chemistry. About 7.5 Kb of genomic sequence were assembled which included the whole coding sequence and about 700 bp of the 5'-region upstream the ATG. A whole cDNA was obtained by RT-PCR as described before on mRNA from developing fruits, using the flanking primers DAG2-Up (5'-CATAGGTTACCATGGCAATATGGGAGTCGCCGG A-3') and DAG2-Down (5'-CATACTCGAGTCAGTTTGCATTAACCTTTTCTATTCAAGAC-3') which contained suitable restriction sites for cloning in the pYES2 vector and a single nucleotide change involving the second codon, ACA (Thr) \rightarrow GCA (Ala), to conform the Kozak

consensus and maximize expression in yeast. The cDNA and genomic sequences were deposited in the GenBank under the accession numbers FJ226588 and FJ226589, respectively.

Cladistic Analysis

Alignment of DGAT protein sequences was achieved using the program Clustal X v.1.7 [54] using the default settings, and further refined by visual inspection. The alignment output was used to generate a cladogram based on the minimum evolution method [55], as implemented in the MEGA package v3.1 [56]. The Poisson model was used together with the pairwise deletion of gaps option, and confidence of the tree branches was checked by bootstrap generated from 1,000 replicates. Rooting of the tree was accomplished by using the plant cytosolic DGAT3 sequences as outgroup. For sequences selected in Fig. 1, the alignment was visualized using the Boxshade v. 3.21 software.

Southern and Northern Blot Analysis

Genomic DNA was isolated from *Echium* seedlings by a CTAB-based extraction procedure [57]. DNA (about 5 µg) was restricted with the appropriate restriction enzymes, separated on a 0.8% agarose gel, and transferred by capillarity onto Hybond[®] N⁺ nylon membranes (Amersham). Filters were UV-crosslinked, pre-hybridized at 42°C for 5 h in the 50% formamide/high SDS buffer recommended by the DIG manufacturer (Boehringer-Mannheim), and hybridized at the same temperature and same buffer solution (stringent conditions), containing the digoxigenin-labeled *DGAT* specific probe. High stringency washes were performed twice at 65°C during 15 min in buffer containing 0.1× SSC, 0.1% SDS, and the luminogenic substrate CSPD[®] was used for the detection, following the instructions provided with the DIG detection kit. Images were obtained by exposure of Biomax[®] ML films (Kodak) for 10–25 min and final developing by standard procedures. The *DGAT* probe was obtained by random primed labeling from a cDNA fragment spanning 512 bp of the 5'-coding sequence.

Total RNA was extracted from different tissues of *Echium* plants, using the Concert[™] Plant RNA Reagent (Invitrogen) following the protocol provided by the manufacturer. About 10 µg per lane of total RNA was loaded onto an agarose/formaldehyde gel, electrophoretically separated, and transferred to Hybond[®]-N⁺ membranes. Filters were hybridized at 50°C (stringent conditions) as described for Southern analysis, and using the same *DGAT* specific probe. Stringent washes, accomplished at 68°C, and detection of the DIG-labelled probe were as indicated before.

Heterologous Expression of *EpDGAT* in Yeast

The whole *EpDGAT* coding sequence was transcriptionally fused to the *GALI* inducible promoter of the pYES2[®] expression vector (Stratagene), and the resulting plasmid used to transform *Saccharomyces cerevisiae* (INVSc1 or H1246 strains) according to the LiAcO method [58]. Cultures were grown at 28°C in standard minimal medium supplemented with the auxotrophic requirement of the strain plus 1% (w/v) raffinose, and expression was further induced on a 0.4 OD₆₀₀ culture by the addition of galactose 2% (w/v). Incubation under inductive conditions was prolonged for 48 h at the same temperature. Supplementation of cultures with LNA, ALA and GLA in some experiments was carried out with 0.5 mM of each, in the presence of 0.1% Tween-40 in the induction medium. Yeast cells were collected by centrifugation, further washed with 1.3% NaCl, and the resulting biomass subjected to lyophilization and pulverization in a mortar. The material was stored at –25°C until processed for lipid analysis.

Lipid Analysis

Fatty acid composition of the different materials (lipid extract, lipid fractions, etc.) was analyzed by GC of methyl esters, as previously described [59] and using heptadecanoic acid as the internal standard.

Total lipids were extracted from 200 mg of yeast lyophilized biomass as described elsewhere [60]. Particular care was taken with the procedure to minimize the action of endogenous lipases and subsequent liberation of free fatty acids. The lipid extract was dried in a rotary evaporator under an argon stream and then resolubilized in 2 ml of CHCl₃. The lipid extract was fractionated by column chromatography (CC) on a silica gel cartridge (Sep-Pack Classic, Waters) accordingly to [60] with some modifications. Briefly, after cartridge equilibration with CHCl₃, the lipid extract was adsorbed into the silica gel cartridge and lipid fractions were sequentially eluted with 30 ml of CHCl₃ (neutral lipids, NL) and then 30 ml of MeOH (polar lipids, PL). Lipid fractions were dried in a rotary evaporator as described above and resuspended in 2 ml CHCl₃.

Neutral lipid classes were separated by one-dimensional TLC using silica gel plates (Macherey Nagel). Plates were activated in an oven at 120°C for 2 h before use. Solvents employed were: petrol–Et₂O–HOAc (80:20:1) [61]. NL classes were visualized by iodine vapor, marked with a pencil and immediately scrapped-off and analyzed individually by GC as previously described. NL classes were identified by co-chromatography with authentic standards. The areas corresponding to NL classes were always scrapped-off and processed even when they were not

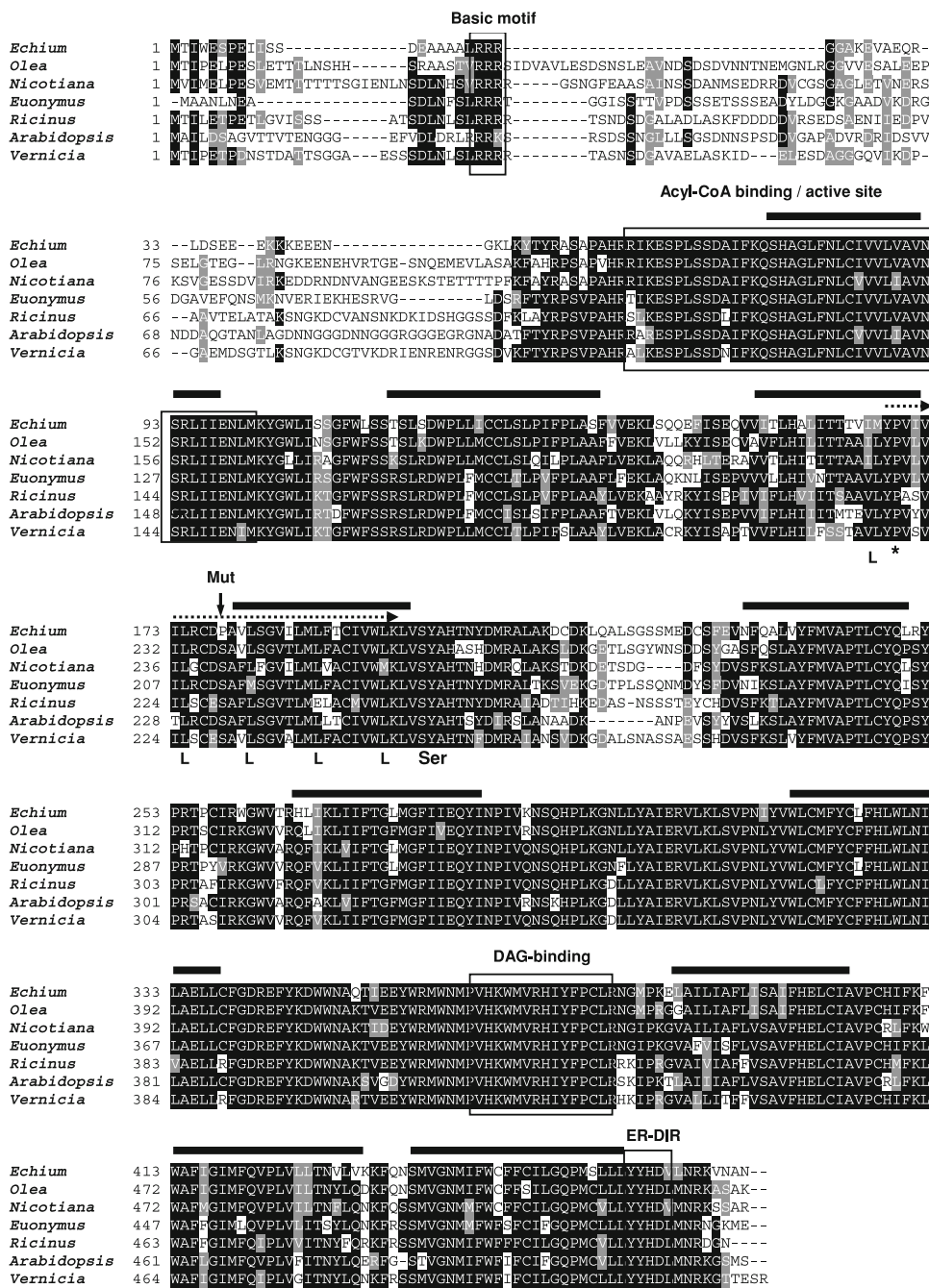


Fig. 1 Sequence comparison of EpDGAT with related DGAT1 enzymes from higher plants. The amino acid sequence of EpDGAT (GenBank accession no. FJ226588) was aligned, using the software ClustalX v1.7 together with those of characterized DGAT1 type I DGAT from *Olea europaea* (acc. no. AAS01606), *Nicotiana tabacum* (acc. no. AAF19345), *Euonymus alatus* (acc. no. AAV31083), *Ricinus communis* (acc. no. AAR11479), *Arabidopsis thaliana* (acc. no. AAF19262), and *Vernicia fordii* (acc. no. ABC94471). The Boxshade program is used to highlight the homology between protein sequences. Shading is applied when there is agreement for a fraction of sequences above 0.5. Amino acids identical to EpDGAT are enclosed in *black boxes* while similar residues are in *grey*. Gaps

introduced for maximum alignment are represented by *dashes*. Transmembrane domains inferred from the TMpred software [62] are marked by *horizontal solid bars*. Conserved motifs or putative signatures (see text for details) are boxed, such as the N-terminal basic motif, the Acyl-CoA binding signature, and DAG-binding and putative ER retrieval motifs (ER-DIR). The region containing a conserved leucine repeat (L) coinciding with a thiolase acyl-enzyme intermediate binding signature is also marked (*pointed arrow*) besides previously described critical Pro and Ser residues which are marked by *asterisks*. Position of the Pro residue in EpDGAT which was analyzed in this work by site-directed mutagenesis is indicated by an *arrow*

endoplasmic reticulum (ER) membrane. Little conservation is found for the amino terminal domain, which is unusually short in the *Echium* protein, except for the characteristic basic repeat [36] consisting of three arginine residues in EpDGAT. Also relevant is the presence of the reported acyl-CoA binding signature R⁶¹–G⁷⁹ [18, 37] close to residues (R⁹⁴–N⁹⁹) that have been involved in the active site, as well as a DAG/phorbol ester binding motif [18, 35]. A previously reported leucine zipper motif [23, 36] is also found overlapping with a putative thiolase acyl-enzyme intermediate binding motif reported for the *Arabidopsis* and *Tropaeolum* DGAT1 [7, 35]. This sequence contains an invariant proline residue (P¹⁶⁹ in EpDGAT, Fig. 1) that has been shown critical for DGAT1 activity [7]. Within the same domain it is also remarkable the presence of a proline residue at position 178 of EpDGAT instead of the extremely conserved serine present in other DGAT1 (Figs. 1, 7a). The relevance of the Pro replacement in EpDGAT was assessed in this work by site directed mutagenesis (see results below). A C-terminal YYHDV motif conforming the putative ER retrieval motif is also present in the *Echium* DGAT similarly to other DGAT1 proteins of plants [13].

Gene Structure and Genomic Organization of EpDGAT

A comparison between the genomic and cDNA sequences allows the identification of 15 introns interrupting the coding region (Fig. 3a, GenBank accession no. FJ226589). The same structure is also shared by *DGAT1* genes of dicot plant species such as *Arabidopsis* [35], *N. tabacum* [36], and *V. fordii* [41]. An exception to this rule are the DGAT genes of the legumes *Lotus* and *Glycine*, with only 14 introns, a difference that is likely due to combination of the last two exons [40]. When sequences around the inferred splicing sites are analyzed (Table 1 in Supplementary data) the usual GT pair in all donor splice sites is found, although a non-consensus acceptor splice sequence is observed in the third intron of the *EpDGAT* gene whose sequence (GG) differ from the common AG. This particular deviation has also been observed in other organisms and has been illustrated in the case of *A. thaliana* (http://www.tigr.org/tdb/e2k1/ath1/Arabidopsis_nonconsensus_splice_sites.shtml).

Genomic organization of the *EpDGAT* gene was investigated by Southern-blot on genomic DNA restricted with different enzymes under highly stringency conditions (Fig. 3b). The pattern obtained is in agreement to that

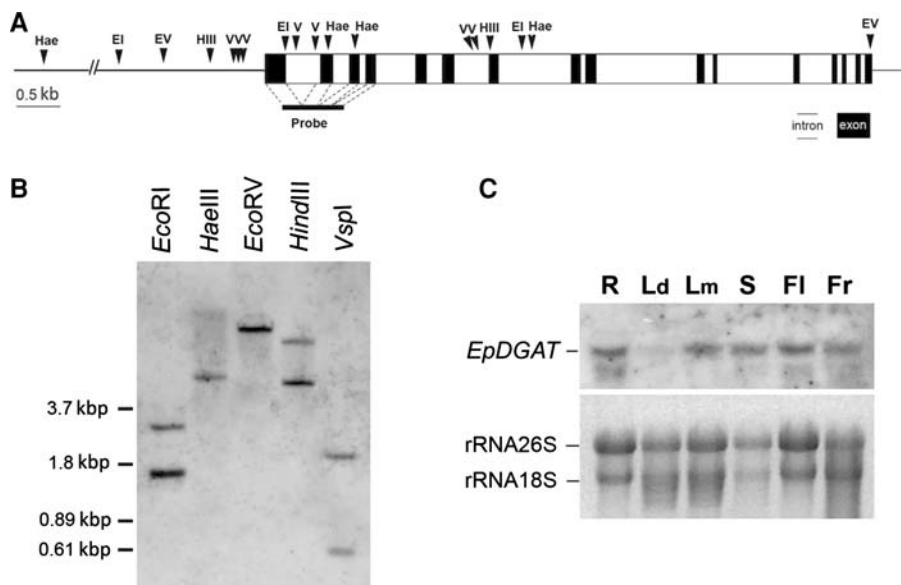


Fig. 3 **a** Genomic structure of *EpDGAT* together with a restriction map showing relevant endonuclease sites (Hae, *Hae*III; E1, *Eco*RI; EV, *Eco*RV; HIII, *Hind*III; V, *Vsp*I) for Southern analysis. Position of the cDNA probe used for hybridization experiments is represented correlating with exons covered in the genomic DNA. **b** Analysis of the genomic organization of *EpDGAT* by Southern blot. Genomic DNA of *E. pitardii* was restricted with the different enzymes indicated above each lane and analyzed as indicated in “[Experimental Procedure](#)”, using a digoxigenine labeled cDNA as a probe (see *upper panel*). Marker sizes (Kbp) are indicated. **c** Expression analysis of

EpDGAT by Northern blot in different tissues of *E. pitardii*. Equivalent amounts of total RNA (10 μ g) from roots (*R*) developing (*Ld*) or mature (*Lm*) leaves, floral stem (*S*) developing flowers (*Fl*) and developing fruits (*Fr*), collected from adult plants, were subjected to electrophoresis in an agarose/formaldehyde gel, run for 1 h at 110 V, blotted and hybridized with the *EpDGAT*-specific probe (see above) under highly stringency conditions, as indicated in “[Experimental Procedure](#)”. The ethidium bromide staining of the gel is also shown as a loading control

expected from the known genomic sequence and the cDNA probe used in the analysis (Fig. 3a, b). This also indicates that the *DGAT1* gene is represented by a single copy in the *Echium* genome. This is also suggested by the finding of identical sequences for the different cDNA clones obtained in the initial RT amplification using primers against highly conserved motifs (see “[Experimental Procedure](#)”).

Expression Analysis of *EpDGAT*

The transcript level of *EpDGAT* was determined by Northern blot on total RNA. An ubiquitous expression is observed among the different organs of the plant (Fig. 3c). This generalized expression pattern is also found for *DGAT1* genes of other plants such as *Arabidopsis*, *Brassica* and soybean [33, 35, 40, 45, 63], where expression is not restricted to typical oil-accumulating organs like seeds. As in the case of *Echium*, relatively high transcript levels are also present in flowers, stem, roots, and leaves, which may indicate a more generalized function in the plant. Low expression levels, though comparable to those of developing seeds, are found in the leaves of *Ricinus* [13] and tung tree [41], where a second DGAT enzyme (DGAT2) is also present with a location predominantly in the seed. However, a seed-specific pattern of *DGAT1* has been reported in the case of *Tropaeolum* [7]. It seems likely that differences may exist in the contribution of the DGAT isozymes and metabolic pathways to the synthesis of TAG in the diverse organs, among the plant species considered.

Interestingly, the mRNA level was remarkably higher in the old leaves of *Echium* than in young developing leaves. Up-regulation of the *DGAT1* gene during senescence has been also reported in *Arabidopsis* and soybean [40, 63], and a role in sequestering fatty acids mobilized from plastid galactolipids into TAG has been proposed [63]. Related to this, is the presence of two ethylene responsive motifs (ERE) in the 5'-regulatory region of *EpDGAT* located at -350 and -380 as a part of a wider direct repeat CACCTATATTTCAA (see GenBank accession no. FJ226589). Two direct ERE motifs are also found in the promoter of the *Arabidopsis DGAT1* gene that have been related with seed maturation [45]. However, a possible involvement of the ERE motifs in the regulation of *DGAT1* during the leaf senescence remains unknown, but it is also likely given the involvement of ethylene in the senescence of vegetative tissues [64, 65].

The Protein Encoded by *EpDGAT* Shows TAG Biosynthetic Activity

To assess DGAT activity of the *EpDGAT* product, a complementation assay was carried out using the H1246 strain of *S. cerevisiae* [51]. This is a *dgal1 lro1 are1 are2*

quadruple mutant that is defective in the *DAG1* and *LRO1* genes which are responsible for the TAG synthesis in the yeast, besides two other genes, *ARE1* and *ARE2*, with overlapping acyl-CoA:sterol acyltransferase (ASAT) activities, thus rendering the yeast unable to synthesize both triacylglycerol (TAG) and steryl ester (SE) [51]. Yeast transformation was performed with a pYES2 expression plasmid containing the *EpDGAT* gene, or the empty vector as a control. The lipid content (as total fatty acids, TFA) from galactose induced cultures was determined from the lipid extract and the lipid extract was fractionated into polar lipids (PL) and neutral lipids (NL) as indicated in “[Experimental Procedure](#)”. As shown in Fig. 4a, nearly a fourfold increase (from 11 to 40 mg/g) in the NL fraction is obtained relative to the control, when the yeast mutant is transformed with *EpDGAT*, while a reduction in the PL was found. Expressed as percentages, this results in an increment of the NL from 22 to 66% and a parallel decrease of the PL from 78 to 34%. Similarly, expression of *EpDGAT* in a wild type yeast strain (INVSc1) also results in a clear increase of the NL fraction (Fig. 4a). The higher PL content in the H1246 mutant as compared to the same cells transformed with *EpDGAT* or with the wild type strain may be attributed to the higher availability of the DAG, an intermediary that is also employed for the synthesis of major phospholipids in yeast [66].

The NL fraction was further analyzed by resolving the lipid classes by TLC, and each saponifiable NL class was quantitated by GC (see “[Experimental Procedure](#)”). As expected for the mutant strain H1246 [51] neither SE nor TAG was detected in the NL fraction of the pYES2 control, where the predominant NL classes were free fatty acids (FFA) (73%) and DAG (27%) (Fig. 4b). Conversely, TLC plates of NL reveal the appearance of a prominent band corresponding to TAG in the yeast transformed with *EpDGAT* that is lacking in the pYES2 control (Fig. 4b). Most of NL of yeast expressing *EpDGAT* correspond to TAG (91%), with FFA in much lower amount (9%), and undetectable levels of DAG and SE. These results indicate that *EpDGAT* encodes a protein with TAG biosynthetic activity, what together with sequence identity suggests that it is a DGAT1 enzyme.

Analysis of the Acyl-CoA Preference of *EpDGAT*

Echium pitardii accumulates substantial amounts of GLA, an ‘unusual’ PUFA in higher plants. Since it has been reported that DGAT enzymes from plant species with ‘unusual’ fatty acids (e.g. ricinoleic, vernolic, eleostearic acids) exhibit preference for substrates containing its ‘unusual’ fatty acid, it may be hypothesized that *EpDGAT* could exhibit preference for some PUFAs. In this regard, we devised an “in vivo” experiment in yeast to get some hint

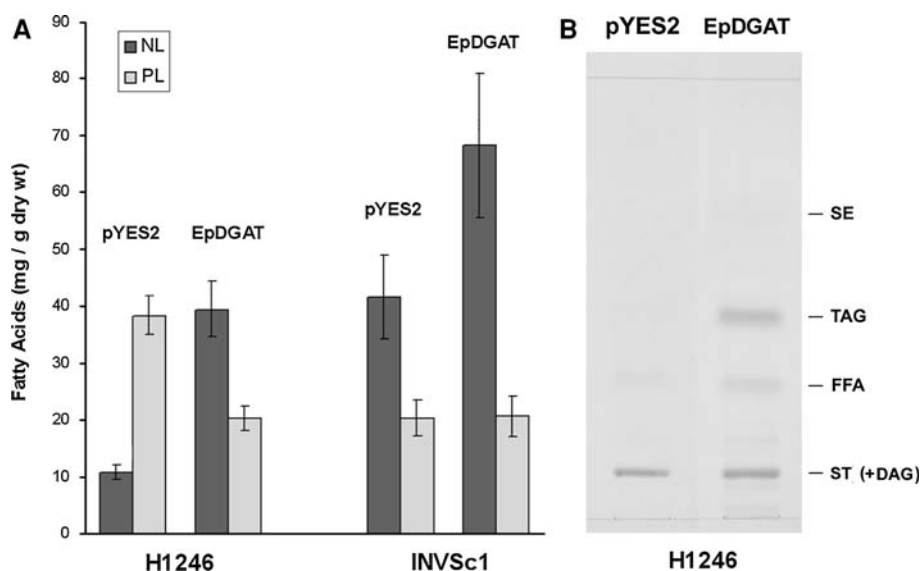


Fig. 4 Synthesis of TAG directed by heterologous expression of *EpDGAT* in yeast cells. **a** Fatty acids content of the NL (black bars) and PL (grey bars) fractions from the defective H1246 or wild type INVSc1 yeast strains transformed with the empty expression vector (pYES2) or the same plasmid containing the *Echium* DGAT gene (*EpDGAT*). Lipids were extracted from the induced yeast cells and processed as indicated in the “Experimental Procedure” to obtain the NL and PL fractions. Fatty acids of acyl-lipids in these fractions were quantitated by GC analysis of methyl esters, as described in the “Experimental Procedure”, and expressed relative to the dry wt

biomass. Mean values ($n = 3$) are represented together with their SE. **b** Lipid analysis by TLC of the NL fraction obtained from H1246 cells transformed with the empty vector (pYES2) or with the plasmid containing *EpDGAT*. Lipids were visualized by iodine staining. Predominant acyl-lipid classes in the NL fractions are indicated: triacylglycerol (TAG), steryl esters (SE), free fatty acids (FFA) and diacylglycerols (DAG). In our chromatography system DAG overlap with sterols (ST), and estimation of the DAG amount is therefore not possible from direct visualization of the band intensity

on the possible acyl-CoA preference of *EpDGAT*. We compared the fatty acid profiles of the H1246 yeast mutant transformed with the *EpDGAT* gene with that containing the empty vector. Since the yeast does not synthesize PUFAs we supplemented the culture with equimolar amounts of LNA, GLA, and ALA together. As will be shown, these exogenous fatty acids are efficiently incorporated to the different cellular lipids. Similarly to the previous experiment, the lipid extract from the induced cultures was fractionated into PL and NL. As represented in Fig. 5a, the amount of PL fraction did not change significantly while a considerable increase was observed for the NL which increased from 14 mg/g in the pYES2 control to 129 mg/g in the yeast expressing *EpDGAT*. Overall these results are similar to those obtained in the experiment without added PUFAs, though a greater increase of the NL suggests a limitation of the FA supply for the synthesis of TAG in the non supplemented yeast, at least under our experimental conditions. Lipid class composition in the NL fraction reveals that, as expected, TAG are the main component (76%) when the yeast are transformed with *EpDGAT* (Fig. 5b). When fatty acid composition of the NL was determined (Fig. 5c) differences were observed among them, with a lower proportion of C16 fatty acids (16:0 and 16:1n-7) in *EpDGAT* expressing cells, relative to the control, while 18:0 is increased and 18:1n-9 remains

unchanged. With regard to the three PUFAs, exogenously provided, the trienoic acids, GLA and ALA, increased while LNA decreased in *EpDGAT* transformed yeast relative to the control (Fig. 5c). These differences were statistically significant as shown by ANOVA and non-parametric tests.

When PUFA contributions to the different lipids are compared (Fig. 6) several observations are remarkable. The three PUFAs are efficiently incorporated into the different lipids if we compare them to the endogenous fatty acids of the yeast. Nevertheless, GLA is incorporated in all lipids to a lower extent than LNA and ALA (Fig. 6), even though they are supplied to cultures in equimolar amounts. This indicates that, in the yeast, GLA is discriminated against by some of the yeast enzymes (acyl-CoA synthetases and/or acyltransferases) involved up to the synthesis of DAG. Thus, a LNA:GLA:ALA ratio of 1:0.25:0.93 in the total lipid extract (TL), and 1:0.36:1 in the NL fraction are obtained for the pYES2 control (Fig. 6a). However, when cells are transformed with *EpDGAT*, a remarkable change in the ratio of PUFAs is observed both in TL (1:0.57:1.56) and NL (1:0.69:1.86), so that LNA contribution is reduced relative to GLA and ALA, thus indicating that these two PUFAs are being favored in their incorporation to the TAG by the *Echium* DGAT (Fig. 6a) as compared to the rest of acyl-lipids. This suggestion is also supported by comparison of the PUFA composition of lipid

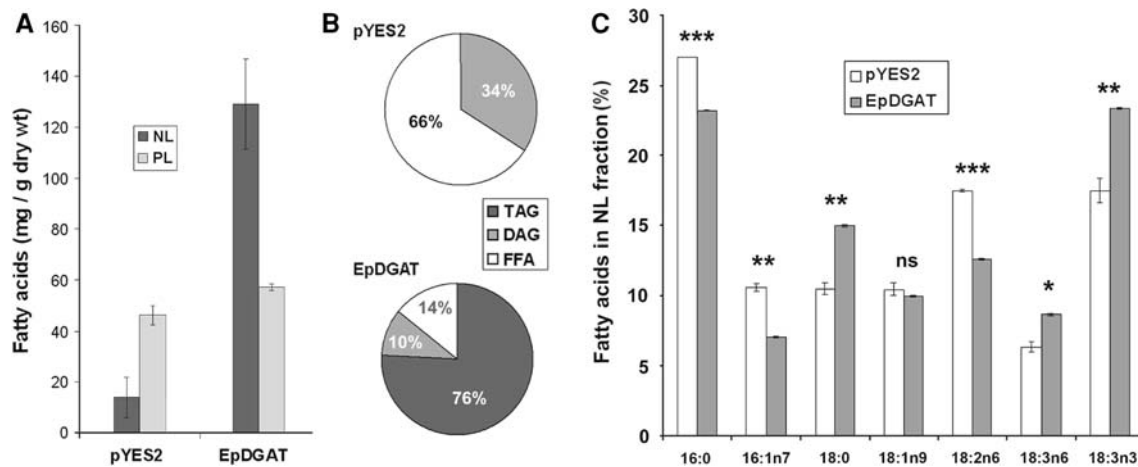
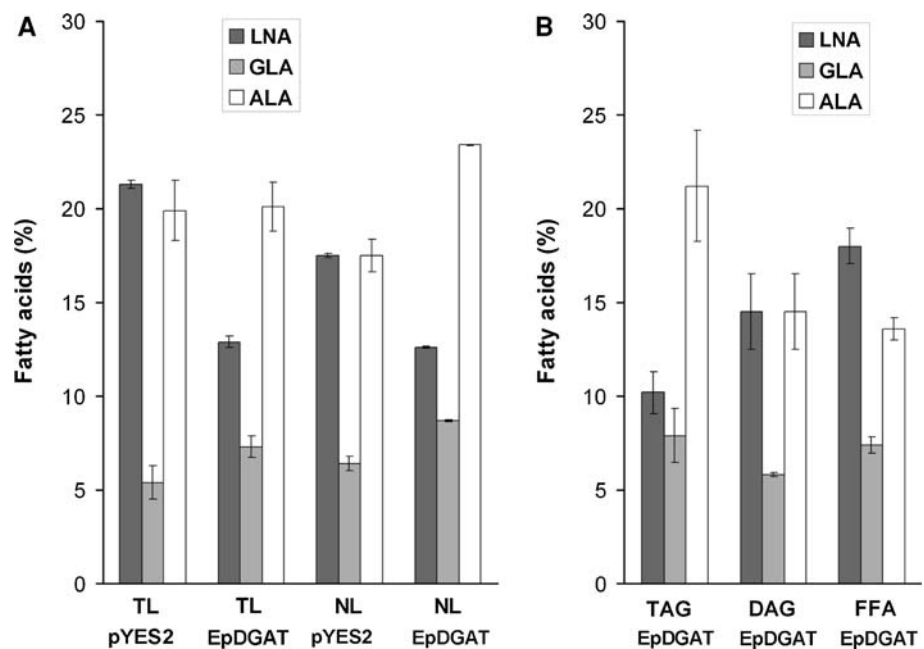


Fig. 5 Lipid synthesis directed by *EpDGAT* in H1246 yeast supplemented with PUFAs. **a** Fatty acids content of the NL (black bars) and PL (grey bars) fractions from the defective H1246 yeast strain transformed with the empty expression vector (pYES2) or the same plasmid containing the *Echium* DGAT gene (*EpDGAT*), and cultivated in the presence of equimolar amounts of LNA, ALA and GLA. Lipids were analyzed as in Fig. 4a. **b** Contributions of individual fatty acids in the NL fractions of H1246 yeast cells

transformed with pYES2 alone or the plasmid containing *EpDGAT* from cultures supplemented with PUFAs (see above). Values are expressed as percentage over total fatty acids in the NL fraction. Mean values ($n = 3$) are represented together with their SE. Significance of the differences was checked by ANOVA and non-parametric tests (*ns* non significant; $*P < 0.05$; $**P < 0.01$; $***P < 0.001$)

Fig. 6 PUFAs composition in different lipid fractions of H1246 yeast cells transformed with the empty vector (pYES2) or the vector containing *EpDGAT* (see experiment in Fig. 5). LNA, GLA and ALA contributions are represented for the total lipids in the biomass (TL in panel a), the NL (in panel a), and individual NL classes (TAG, DAG and FFA in panel b). Values correspond to percentages on the total FAs in each fraction. Acyl-lipid composition of the NL fraction is represented as a percentage for each lipid class (panel c). Mean values ($n = 3$) are represented besides their SE

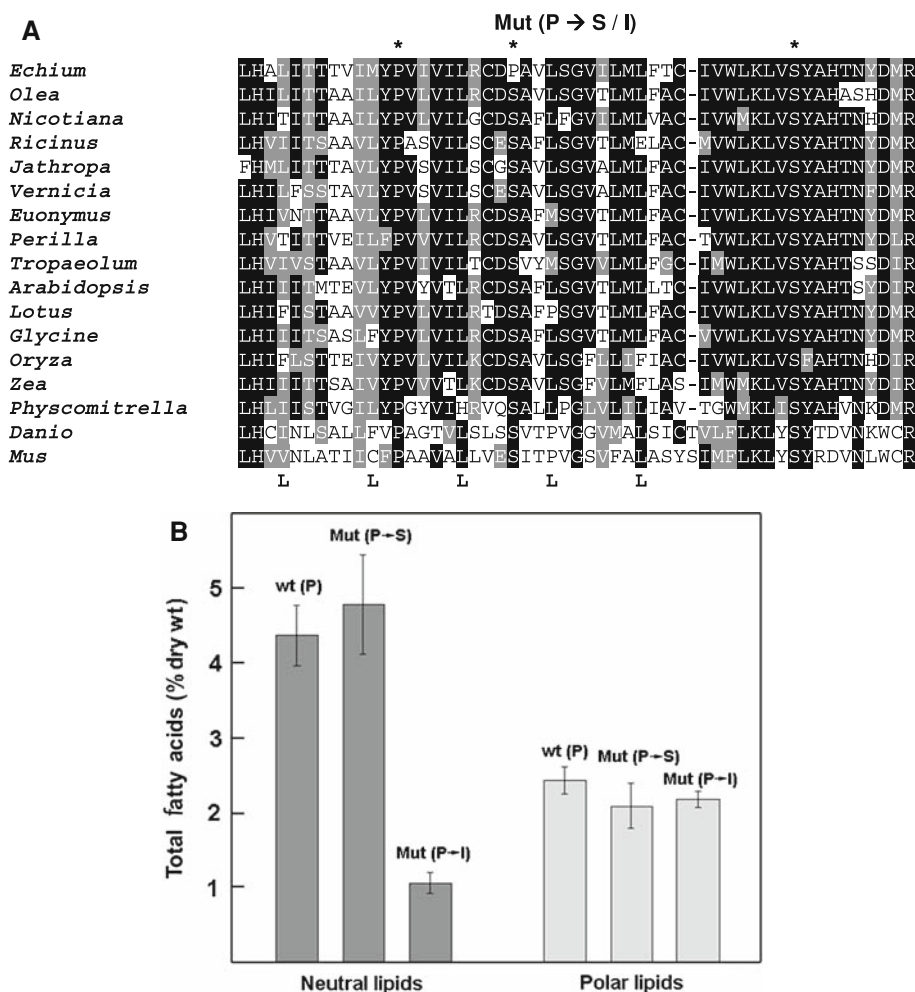


classes in the NL fraction of *EpDGAT* transformed yeast (Fig. 6b). A PUFA ratio of 1:0.77:2.08 was obtained for TAG while, in DAG and FFA, the ratios were 1:0.40:1 and 1:0.41:0.76, respectively, fairly similar to that of the NL fraction in control cells. In other words, GLA and ALA increased from DAG to TAG while LNA decreased (Fig. 6b). These differences in PUFA percentages between DAG and TAG were statistically significant ($P < 0.05$) by ANOVA and non-parametric tests. Since in the H1246 cells the synthesis of TAG comes exclusively from the

acylation of DAG via *EpDGAT* it seems likely that ALA and GLA are being preferentially selected against LNA in their incorporation to DAG by *EpDGAT*, thus increasing the proportion of the trienoic acids in TAG relative to that in the DAG substrate.

A number of reports on DGAT activity using microsomes from different species have indicated a preference for substrates containing particular acyl groups [23]. This is exemplified in plants like *Cuphea* and *Ricinus*, producing unusual and potentially toxic fatty acids such as lauric and

Fig. 7 Site-directed mutagenesis of EpDAGAT. **a** Protein alignment of the leucine repeat region showing the P¹⁶⁹ residue in EpDAGAT which was replaced either by Ser (P→S) or Ile (P→I). Positions of other critical amino acids in the same region, revealed in previous studies, are marked by asterisks. **b** Fatty acids content of the NL (grey bars) and PL (white bars) fractions from the defective H1246 yeast strain transformed with the wild type *EpDGAT* gene (wt) and the two replacement mutants (P→S and P→L). Lipids were extracted from the induced yeast cells and processed as indicated in the “Experimental Procedure” to obtain the NL and PL fractions. Fatty acids of acyl-lipids in these fractions were quantitated by GC analysis of methyl esters and expressed as a percentage over the dry wt biomass. The experiment was performed three times using independent cultures, and the mean value is shown besides their SE



ricinoleic acids, respectively [29]. In these cases it was proposed that fast conversion of DAG to TAG would act as a way to prevent incorporation of harmful fatty acids to membrane phospholipids [29]. Channeling of particular fatty acids into TAG has also been described in cocoa, for stearic acid [67], and rape, for erucic acid [68].

However, studies on substrate preference dealing with particular DGAT isoenzymes (DGAT1, DGAT2) are still scarce, and even a clear picture of their particular roles and distribution within the plant is lacking at the moment. It has been shown that DGAT1 of some plants like *Ricinus* [38] and *Tropaeolum* [7] favor the incorporation of their respective unusual ricinoleic and erucic fatty acids into TAG. However, in other species like *Vernonia* [69] and *Vernicia* [41], the DGAT1 enzyme does not show preference for vernolic and eleostearic acids, respectively, contrary to the results obtained with seed microsomes. In these cases the DGAT2 isoenzyme was proposed to be responsible for channeling of the unusual fatty acids. It seems therefore that substrate preference and isoenzyme contribution to the synthesis of TAG may be different in each plant.

There is little information available for Boraginaceae species. The analysis carried out with *Borago* seed microsomes indicated a strong selectivity of the DGAT activity by GLA-CoA [70]. Even though interpretation of our results must be cautious, data obtained for *Echium* DGAT do not show a strong preferential utilization of GLA-CoA. It is possible, as described above for other species, that additional activities (e.g. DGAT2) are involved in determining the fatty acid profile of TAG in Boraginaceae species. It should be also noticed that, contrary to *Borago*, the seeds of *Echium* accumulate high amounts of ALA [49], which is consistent with the observed preference of the *Echium* DGAT1 enzyme for this fatty acid.

Site Directed Mutagenesis of the Pro178 Residue of EpDAGAT

As previously stated, a proline residue is present at position 178 of EpDAGAT, a place where a serine is invariably found for DGAT1 proteins of plants and animals (Fig. 7a). We have performed SDM on this residue in

order to assess its importance for DGAT activity. In particular, the P¹⁷⁸ was replaced either by serine (P → S), the common residue, or by isoleucine (P → I), and DGAT activity was recorded by yeast complementation of the defective H1246 strain, as described before. As shown in Fig. 7b, the P → S replacement does not have an appreciable effect on the synthesis of TAG, estimated by the NL content, which is predominantly composed by TAG, as it was shown previously. On the contrary, changing of the P¹⁷⁸ to Ile produces a drastic reduction of the NL content thus showing the critical role of this residue for DGAT1 activity. As expected, none of the replacements had an appreciable effect on the PL content (Fig. 7).

Different studies have underlined the importance of this region for DGAT1 activity. Thus, two critical positions have been identified (Fig. 7a), a serine residue (Ser¹⁹⁹ in EpDGAT) which is essential for ACAT activity [71], and an extremely conserved proline (Pro¹⁶⁹ in EpDGAT) present in diverse acyltransferases [72]. This Pro was demonstrated to act as a catalytic site in GPAT enzymes [72], and a recent work also proved its importance for DGAT1 activity [7]. As stated before the P¹⁷⁸ is located between these two amino acids as a part of a sequence that contains a thiolase signature (PCDO0092) for binding of acyl-enzyme intermediates [7, 35]. The loss of activity produced by the P→I replacement suggests the possible involvement of this residue as a part of the DGAT1 active site. On the other hand, it was noticed that DGAT1 proteins of plants contain a regularly spaced leucine repeat overlapping the thiolase signature (Fig. 7a) which has been proposed to act as a leucine zipper in protein to protein interactions [37]. However, specialized leucine zipper prediction tools such as TRESPASSER [73] or 2ZIP [74] fail to recognize this structure, and it should also be noticed that the Leu repeat is absent from animal enzymes. The notion that this motif may not represent a leucine zipper is in agreement with our results since the presence in the EpDGAT of the Pro residue, a typical helix breaker, does not seem to affect enzyme activity which is similar to that of the Ser containing mutant.

The cloning and molecular characterization of the gene encoding the DGAT1 enzyme of *Echium* was achieved. Functional assay by heterologous expression in yeast show that the encoded protein promotes the synthesis of TAG, and increases the oil amount. We also report evidence that *Echium* DGAT1 catalyzes a preferential incorporation of ALA over LNA, and that it does not discriminate the GLA negatively. This is interesting regarding the possible utility of this gene to modify the fatty acid profile of transgenic plants in order to increase the contribution of trienoic fatty acids in oils, including the ‘unusual’ GLA.

Acknowledgments This work was supported by grants from the Ministerio de Ciencia y Tecnología (MCYT, AGL2005-01498/AGR) and Junta de Andalucía (P05-189-AGR). J.A. Garrido-Cárdenas and A. Mañas-Fernández were recipients of postgraduate fellowships from the MCYT and Junta de Andalucía, respectively. We are also grateful to J. Pérez-Parra and J.C. Gázquez for providing greenhouse facilities and technical assistance in plant culture at the “Estación Experimental Las Palmerillas (CAJAMAR)”. Dr. Stymne (Swedish University of Agricultural Sciences, Uppsala) kindly provided the mutant strain of *S. cerevisiae* H1246, and is gratefully acknowledged.

References

- Dyer JM, Stymne S, Green AG, Carlsson AS (2008) High-value oils from plants. *Plant J* 54:640–655
- Durrett TP, Benning C, Ohlrogge J (2008) Plant triacylglycerols as feedstocks for the production of biofuels. *Plant J* 54:593–607
- Zheng P, Allen WB, Roesler K, Williams ME et al (2008) A phenylalanine in DGAT is a key determinant of oil content and composition in maize. *Nat Genet* 40:367–372
- Dircks L, Sul HS (1999) Acyltransferases of de novo glycerophospholipid biosynthesis. *Prog Lipid Res* 38:461–479
- Lehner R, Kuksis A (1996) Biosynthesis of triacylglycerols. *Prog Lipid Res* 35:169–201
- Coleman RA, Lee DP (2004) Enzymes of triacylglycerol synthesis and their regulation. *Prog Lipid Res* 43:134–176
- Xu J, Francis T, Mietkiewska E, Giblin EM et al (2008) Cloning and characterization of an acyl-CoA-dependent diacylglycerol acyltransferase 1 (DGAT1) gene from *Tropaeolum majus*, and a study of the functional motifs of the DGAT protein using site-directed mutagenesis to modify enzyme activity and oil content. *Plant Biotechnol J* 6:799–818
- Stobart AK, Mancha M, Lenman M, Dahlqvist A, Stymne S (1997) Triacylglycerols are synthesized and utilized by transacylation reactions in microsomal preparations of developing safflower (*Carthamus tinctorius* L.) seeds. *Planta* 203:58–66
- Dahlqvist A, Stahl U, Lenman M, Banas A et al (2000) Phospholipid:diacylglycerol acyltransferase: an enzyme that catalyzes the acyl-CoA-independent formation of triacylglycerol in yeast and plants. *Proc Natl Acad Sci USA* 97:6487–6492
- Millar AA, Smith MA, Kunst L (2000) All fatty acids are not equal: discrimination in plant membrane lipids. *Trends Plant Sci* 5:95–101
- Banas A, Carlsson AS, Huang B, Lenman M et al (2005) Cellular sterol ester synthesis in plants is performed by an enzyme (phospholipid:sterol acyltransferase) different from the yeast and mammalian acyl-CoA:sterol acyltransferases. *J Biol Chem* 280:34626–34634
- Mhaske V, Beldjilali K, Ohlrogge J, Pollard M (2005) Isolation and characterization of an *Arabidopsis thaliana* knockout line for phospholipid: diacylglycerol transacylase gene (At5g13640). *Plant Physiol Biochem* 43:413–417
- Kroon JT, Wei W, Simon WJ, Slabas AR (2006) Identification and functional expression of a type 2 acyl-CoA:diacylglycerol acyltransferase (DGAT2) in developing castor bean seeds which has high homology to the major triglyceride biosynthetic enzyme of fungi and animals. *Phytochemistry* 67:2541–2549
- Cahoon EB, Shockey JM, Dietrich CR, Gidda SK et al (2007) Engineering oilseeds for sustainable production of industrial and nutritional feedstocks: solving bottlenecks in fatty acid flux. *Curr Opin Plant Biol* 10:236–244

15. Mancha M, Osorio J, Garces R, Ruso J et al (1994) New sunflower mutants with altered seed fatty acid composition. *Prog Lipid Res* 33:147–154
16. Bao X, Ohlrogge J (1999) Supply of fatty acid is one limiting factor in the accumulation of triacylglycerol in developing embryos. *Plant Physiol* 120:1057–1062
17. Katavic V, Reed DW, Taylor DC, Giblin EM et al (1995) Alteration of seed fatty acid composition by an ethyl methane sulfonate-induced mutation in *Arabidopsis thaliana* affecting diacylglycerol acyltransferase activity. *Plant Physiol* 108:399–409
18. Jako C, Kumar A, Wei Y, Zou J et al (2001) Seed-specific over-expression of an *Arabidopsis* cDNA encoding a diacylglycerol acyltransferase enhances seed oil content and seed weight. *Plant Physiol* 126:861–874
19. Settlage SB, Kwanyuen P, Wilson RF (1998) Relation between diacylglycerol acyltransferase activity and oil concentration in soybean. *J Am Oil Chem Soc* 75:775–781
20. Perry HJ, Bligny R, Gout E, Harwood JL (1999) Changes in Kennedy pathway intermediates associated with increased triacylglycerol synthesis in oil-seed rape. *Phytochemistry* 52:799–804
21. Giannoulia K, Haralampidis K, Poghosyan Z, Murphy DJ, Hatzopoulos P (2000) Differential expression of diacylglycerol acyltransferase (DGAT) genes in olive tissues. *Biochem Soc Trans* 28:695–697
22. Triki S, Ben Hamida J, Mazliak P (2000) Diacylglycerol acyltransferase in maturing sunflower seeds. *Biochem Soc Trans* 28:689–692
23. Lung SC, Weselake RJ (2006) Diacylglycerol acyltransferase: a key mediator of plant triacylglycerol synthesis. *Lipids* 41:1073–1088
24. Frentzen M (1998) Acyltransferases from basic science to modified seed oils. *Fett-Lipid* 100:161–166
25. Thelen JJ, Ohlrogge JB (2002) Metabolic engineering of fatty acid biosynthesis in plants. *Metab Eng* 4:12–21
26. Dyer JM, Mullen RT (2005) Development and potential of genetically engineered oilseeds. *Seed Sci Res* 15:255–267
27. Lardizabal KD, Effertz R, Levering CK, Mai JT et al (2008) Expression of *Umbelopsis ramanniana* DGAT2A in seed increases oil in soybean. *Plant Physiol* 148:89–96
28. Ichihara K, Takahashi T, Fujii S (1988) Diacylglycerol acyltransferase in maturing safflower seeds: its influences on the fatty acid composition of triacylglycerol and on the rate of triacylglycerol synthesis. *Biochim Biophys Acta* 958:125–129
29. Vogel G, Browne J (1996) Cholinephosphotransferase and diacylglycerol acyltransferase (substrate specificities at a key branch point in seed lipid metabolism). *Plant Physiol* 110:923–931
30. Daniel J, Abraham L, Balaji K, Rajasekharan R (2003) Biosynthesis of stearate-rich triacylglycerol in developing embryos and microsomal membranes from immature seeds of *Garcinia indica* Choisy. *Curr Sci* 85:363–370
31. Yu K, McCracken CT Jr, Li R, Hildebrand DF (2006) Diacylglycerol acyltransferases from *Vernonia* and *Stokesia* prefer substrates with vernolic acid. *Lipids* 41:557–566
32. Cases S, Smith SJ, Zheng YW, Myers HM et al (1998) Identification of a gene encoding an acyl CoA:diacylglycerol acyltransferase, a key enzyme in triacylglycerol synthesis. *Proc Natl Acad Sci USA* 95:13018–13023
33. Hobbs DH, Lu C, Hills MJ (1999) Cloning of a cDNA encoding diacylglycerol acyltransferase from *Arabidopsis thaliana* and its functional expression. *FEBS Lett* 452:145–149
34. Routaboul JM, Benning C, Bechtold N, Caboche M, Lepiniec L (1999) The TAG1 locus of *Arabidopsis* encodes for a diacylglycerol acyltransferase. *Plant Physiol Biochem* 37:831–840
35. Zou J, Wei Y, Jako C, Kumar A et al (1999) The *Arabidopsis thaliana* TAG1 mutant has a mutation in a diacylglycerol acyltransferase gene. *Plant J* 19:645–653
36. Bouvier-Nave P, Benveniste P, Oelkers P, Sturley SL, Schaller H (2000) Expression in yeast and tobacco of plant cDNAs encoding acyl CoA:diacylglycerol acyltransferase. *Eur J Biochem* 267:85–96
37. Nykiforuk CL, Furukawa-Stoffer TL, Huff PW, Sarna M et al (2002) Characterization of cDNAs encoding diacylglycerol acyltransferase from cultures of *Brassica napus* and sucrose-mediated induction of enzyme biosynthesis. *Biochim Biophys Acta* 1580:95–109
38. He X, Turner C, Chen GQ, Lin JT, McKeon TA (2004) Cloning and characterization of a cDNA encoding diacylglycerol acyltransferase from castor bean. *Lipids* 39:311–318
39. Milcamps A, Tumaney AW, Paddock T, Pan DA et al (2005) Isolation of a gene encoding a 1, 2-diacylglycerol-sn-acetyl-CoA acetyltransferase from developing seeds of *Euonymus alatus*. *J Biol Chem* 280:5370–5377
40. Wang HW, Zhang JS, Gai JY, Chen SY (2006) Cloning and comparative analysis of the gene encoding diacylglycerol acyltransferase from wild type and cultivated soybean. *Theor Appl Genet* 112:1086–1097
41. Shockey JM, Gidda SK, Chapital DC, Kuan JC et al (2006) Tung tree DGAT1 and DGAT2 have nonredundant functions in triacylglycerol biosynthesis and are localized to different subdomains of the endoplasmic reticulum. *Plant Cell* 18:2294–2313
42. Lardizabal KD, Mai JT, Wagner NW, Wyrick A et al (2001) DGAT2 is a new diacylglycerol acyltransferase gene family: purification, cloning, and expression in insect cells of two polypeptides from *Mortierella ramanniana* with diacylglycerol acyltransferase activity. *J Biol Chem* 276:38862–38869
43. Turkish AR, Henneberry AL, Cromley D, Padamsee M et al (2005) Identification of two novel human acyl-CoA wax alcohol acyltransferases: members of the diacylglycerol acyltransferase 2 (DGAT2) gene superfamily. *J Biol Chem* 280:14755–14764
44. Saha S, Enugutti B, Rajakumari S, Rajasekharan R (2006) Cytosolic triacylglycerol biosynthetic pathway in oilseeds. Molecular cloning and expression of peanut cytosolic diacylglycerol acyltransferase. *Plant Physiol* 141:1533–1543
45. Lu CL, de Noyer SB, Hobbs DH, Kang J et al (2003) Expression pattern of diacylglycerol acyltransferase-1, an enzyme involved in triacylglycerol biosynthesis, in *Arabidopsis thaliana*. *Plant Mol Biol* 52:31–41
46. Zhang FY, Yang MF, Xu YN (2005) Silencing of DGAT1 in tobacco causes a reduction in seed oil content. *Plant Sci* 169:689–694
47. Bursal J, Shockey J, Lu C, Dyer J et al (2008) Metabolic engineering of hydroxy fatty acid production in plants: RcDGAT2 drives dramatic increases in ricinoleate levels in seed oil. *Plant Biotechnol J* 6:819–831
48. Chen GQ, Turner C, He X, Nguyen T et al (2007) Expression profiles of genes involved in fatty acid and triacylglycerol synthesis in castor bean (*Ricinus communis* L.). *Lipids* 42:263–274
49. Guil-Guerrero JL, Gomez-Mercado F, Rodriguez-Garcia I, Campra-Madrid P, Garcia-Maroto F (2001) Occurrence and characterization of oils rich in gamma-linolenic acid (III): the taxonomical value of the fatty acids in *Echium* (Boraginaceae). *Phytochemistry* 58:117–120
50. Garcia-Maroto F, Garrido-Cardenas JA, Rodriguez-Ruiz J, Vilches-Ferron M et al (2002) Cloning and molecular characterization of the Delta 6-desaturase from two *Echium* plant species: production of GLA by heterologous expression in yeast and tobacco. *Lipids* 37:417–426
51. Sandager L, Gustavsson MH, Stahl U, Dahlqvist A et al (2002) Storage lipid synthesis is non-essential in yeast. *J Biol Chem* 277:6478–6482
52. Ochman H, Ajioka JW, Garza D, Hartl DL (1990) Inverse polymerase chain reaction. *Biotechnology* 8:759–760

53. Garcia-Maroto F, Garrido-Cardenas JA, Michaelson LV, Napier JA, Alonso DL (2007) Cloning and molecular characterisation of a Delta(8)-sphingolipid-desaturase from *Nicotiana tabacum* closely related to Delta(6)-acyl-desaturases. *Plant Mol Biol* 64:241–250
54. Thompson JD, Gibson TJ, Plewniak F, Jeanmougin F, Higgins DG (1997) The CLUSTAL_X windows interface: flexible strategies for multiple sequence alignment aided by quality analysis tools. *Nucleic Acids Res* 25:4876–4882
55. Rzhetsky A, Nei M (1992) Statistical properties of the ordinary least-squares, generalized least-squares, and minimum-evolution methods of phylogenetic inference. *J Mol Evol* 35:367–375
56. Kumar S, Tamura K, Jakobsen IB, Nei M (2001) MEGA2: molecular evolutionary genetics analysis software. *Bioinformatics* 17:1244–1245
57. Taylor B, Powel A (1982) Isolation of plant DNA and RNA. *Focus* 4:4–6
58. Elble R (1992) A simple and efficient procedure for transformation of yeasts. *BioTechniques* 13:18–20
59. Rodriguez-Ruiz J, Belarbi EH, Sanchez JLG, Alonso DL (1998) Rapid simultaneous lipid extraction and transesterification for fatty acid analyses. *Biotechnol Tech* 12:689–691
60. Alonso DL, Belarbi EL, Rodriguez-Ruiz J, Segura CI, Gimenez A (1998) Acyl lipids of three microalgae. *Phytochemistry* 47:1473–1481
61. Kates M (1988) *Techniques of lipidology: isolation, analysis, and identification of lipids*. Elsevier, Amsterdam
62. Hofmann K, Stoffel W (1993) TMbase—a database of membrane spanning proteins segments. *Biol Chem Hoppe-Seyler* 374:166
63. Kaup MT, Froese CD, Thompson JE (2002) A role for diacylglycerol acyltransferase during leaf senescence. *Plant Physiol* 129:1616–1626
64. Oh SA, Park JH, Lee GI, Paek KH et al (1997) Identification of three genetic loci controlling leaf senescence in *Arabidopsis thaliana*. *Plant J* 12:527–535
65. John I, Drake R, Farrell A, Cooper W et al (1995) Delayed leaf senescence in ethylene-deficient ACC-oxidase antisense tomato plants: molecular and physiological analysis. *Plant J* 7:483–490
66. Athenstaedt K, Daum G (1999) Phosphatidic acid, a key intermediate in lipid metabolism. *Eur J Biochem* 266:1–16
67. Griffiths G, Harwood JL (1991) The regulation of triacylglycerol biosynthesis in cocoa (*Theobroma cacao*) L. *Planta* 184:279–284
68. Cao YZ, Huang AH (1987) Acyl coenzyme A preference of diacylglycerol acyltransferase from the maturing seeds of *Cuphea*, maize, rapeseed, and canola. *Plant Physiol* 84:762–765
69. Yu K, Li R, Hatanaka T, Hildebrand D (2008) Cloning and functional analysis of two type 1 diacylglycerol acyltransferases from *Vernonia galamensis*. *Phytochemistry* 69:1119–1127
70. Griffiths G, Stobart AK, Stymne S (1988) Delta 6- and delta 12-desaturase activities and phosphatidic acid formation in microsomal preparations from the developing cotyledons of common borage (*Borago officinalis*). *Biochem J* 252:641–647
71. Cao G, Goldstein JL, Brown MS (1996) Complementation of mutation in acyl-CoA:cholesterol acyltransferase (ACAT) fails to restore sterol regulation in ACAT-defective sterol-resistant hamster cells. *J Biol Chem* 271:14642–14648
72. Lewin TM, Wang P, Coleman RA (1999) Analysis of amino acid motifs diagnostic for the sn-glycerol-3-phosphate acyltransferase reaction. *Biochemistry* 38:5764–5771
73. Hirst JD, Vieth M, Skolnick J, Brooks CL 3rd (1996) Predicting leucine zipper structures from sequence. *Protein Eng* 9:657–662
74. Bornberg-Bauer E, Rivals E, Vingron M (1998) Computational approaches to identify leucine zippers. *Nucleic Acids Res* 26:2740–2746

A Simplified Method to Distinguish Farmed (*Salmo salar*) from Wild Salmon: Fatty Acid Ratios Versus Astaxanthin Chiral Isomers

Peter Andrew Megdal · Neal A. Craft ·
Garry J. Handelman

Received: 18 June 2008 / Accepted: 23 February 2009 / Published online: 19 May 2009
© The Author(s) 2009. This article is published with open access at Springerlink.com

Abstract Mislabeling of farmed and wild salmon sold in markets has been reported. Since the fatty acid content of fish may influence human health and thus consumer behavior, a simplified method to identify wild and farmed salmon is necessary. Several studies have demonstrated differences in lipid profiles between farmed and wild salmon but no data exists validating these differences with government-approved methods to accurately identify the origin of these fish. Current methods are both expensive and complicated, using highly specialized equipment not commonly available. Therefore, we developed a testing protocol using gas chromatography (GC), to determine the origin of salmon using fatty acid profiles. We also compared the GC method with the currently approved FDA (United States Food and Drug Administration) technique that uses analysis of carotenoid optical isomers and found 100% agreement. Statistical validation ($n = 30$) was obtained showing elevated 18:2n-6 ($z = 4.56$; $P = 0.0001$) and decreased 20:1n-9 ($z = 1.79$; $P = 0.07$) in farmed samples. The method is suitable for wide adaptation because fatty acid methyl ester analysis is a well-established procedure in labs that conduct analysis of lipid composition and food constituents. GC analysis for determining the origin of North American salmon compared favorably with the astaxanthin isomer technique used by the FDA and showed that the fatty acid 18:2n-6 was the key indicator associated with the origin of these salmon.

Keywords Farmed salmon · Gas chromatography · Cultivated salmon · Wild salmon · Astaxanthin · HPLC

Abbreviations

GC Gas chromatography
EPA Eicosapentaenoic acid
DHA Docosahexaenoic acid
HPLC High performance liquid chromatography

Introduction

Farmed Atlantic salmon (*Salmo salar*) production currently provides approximately 50% of world-wide salmon consumption [1]. This popularity is due, in part, to the year-round availability of fresh farmed salmon and the low-cost which can be half that of wild salmon [2]. A direct result of these lower prices is greater availability of a high omega three fish product to the public. Additionally, as the catch of wild salmon becomes more variable, farmed salmon may provide a more stable supply. However, some concern exists over ecological damage from salmon cultivation. Extensive salmon farming may result in negative effects including dwindling fisheries of the small pelagic fish used as feed, interruption of salmon breeding patterns, dilution of the wild salmon gene pool by escaped farmed salmon, and transmission of infections from farmed to wild populations [3–7]. Farmed salmon have been reported to contain on average much higher levels of polychlorinated biphenyls (PCBs) and other nonpolar contaminants than their wild counterparts even after correction for the higher fat content of the farmed salmon [8, 9]. It may be possible to solve these problems;

P. A. Megdal (✉) · G. J. Handelman
University of Massachusetts Lowell,
Lowell, MA, USA
e-mail: pmegdal@efasciencesinc.com

N. A. Craft
Craft Technologies, Wilson, NC, USA

some farmed salmon, such as those from Chile, have very favorable contamination profiles which may rival wild salmon such as Chinook [10–12]. Mozaffarian and Rimm make the valid point that some common foods also may have similar concentrations of PCBs to farmed salmon and although eating such fish may have certain risks, they believe the health benefits exceed the dangers [2].

Contaminated fishmeal and depletion of pelagic fish used in fishmeal may be motivating commercial fish farmers to develop alternate feeding strategies. The nutritional requirements of farmed salmon can be met in part by the substitution of plant derived oils and protein such as rapeseed, corn, palm, or soybean [13–16]. Some studies indicate that resultant feeds containing up to 100% terrestrial plant oils are well tolerated, support normal growth rates, and provide filets with acceptable flavor [14, 15, 17].

Deep cold water fish such as salmon have low delta-6 desaturase enzyme activity and therefore have a limited ability to convert linoleic acid (18:2n-6, LNA) to arachidonic acid (20:4n-6, ARA), and linolenic acid (18:3n-3, ALA) to eicosapentaenoic acid (20:5n-3, EPA) and docosahexaenoic acid (22:6n-3, DHA) [15, 17, 18]. Consequently, farmed deep cold water fish must be fed a “finishing diet” containing increased amounts of fish oils for the last few weeks before slaughter. This diet maintains the most beneficial fatty acid balance, including the higher levels of EPA and DHA that are fundamental to the health benefits of fatty fish consumption [13, 14, 19].

To maintain the characteristic reddish-orange color of their flesh, salmon must consume the carotenoids astaxanthin and canthaxanthin. Farmed salmon are fed fishmeal supplemented with various isomers of these carotenoids; wild salmon assimilate carotenoids by consuming krill. It is interesting to note that the color differences between wild and farmed salmon are often indistinguishable by visual inspection and thus advanced analytical techniques are required for authentication [14, 19–23].

Interest in farmed and wild salmon by both consumers and scientists has led to increased pressure to determine accurately the origin of different fish provided to the marketplace. In 1998, the United States Food and Drug Administration (FDA) developed an accurate method to authenticate the origin of salmon by measuring unique isomer ratios of astaxanthin [20]. The origin of the salmon in our study was verified by the FDA method that uses high performance liquid chromatography (HPLC) analysis of astaxanthin isomers. The HPLC method requires specialized equipment such as specific chiral columns or derivatization with chiral reagents. Our objective was to establish a facile gas chromatography (GC) fatty acid analysis technique for distinguishing wild and farmed salmon that

could be readily implemented with the resources of a typical biochemistry laboratory.

Materials and Methods

Thirty salmon filet samples were provided to our laboratory by Craft Technologies in Wilson, NC, USA. These samples had been collected during the interval between 2004 and 2006 at various fish markets in the Northeastern and central United States. All samples were stored frozen at -80°C and transported on dry ice.

Craft Technologies tested all samples for carotenoid profiles using the FDA method which includes a combination of normal-phase and chiral HPLC as described in references [20, 24]. Astaxanthin was extracted from the fish samples by homogenization with acetone. After centrifugation to remove protein debris, the extract was injected on a Chromegabond diol column (ES Industries), 15×0.46 cm, $5 \mu\text{m}$ particle size, with 96% hexane/4% isopropanol mobile phase, at 1.5 mL/min flow rate. Detection was at 450 nm. The astaxanthin fraction was collected, the solvent was evaporated, and the sample re-dissolved in 85% hexane/15% acetone for the next HPLC step. The isolated astaxanthin fraction was re-analyzed for enantiomer composition with two chiral columns in series: Chiralcel C18 250×4.6 mm (Diacel Chemical Industries, Ltd), $5 \mu\text{m}$ particle size. The mobile phase was 85% hexane/15% acetone, at 0.8 mL/min flow rate, and detection was at 450 nm [20].

Preparation of Fatty Acid Methyl Esters

One gram of each salmon filet was minced with single-edged razor blades and homogenized in 10 mL of 0.15 M NaCl, using a handheld glass Potter–Elvehem homogenizer. For extraction of lipids, 1 mL of the tissue homogenate was vortexed with 2 mL of chloroform/methanol (2:1) and 0.1% BHT as antioxidant. After centrifugation, the lower organic layer was collected and evaporated in an 8-mL vial under nitrogen.

The methylation reagent was generated by mixing 1 mL of acetyl chloride with 30 mL of MeOH, and was used within 5 days of preparation. One milliliter of this reagent was added to the residue from extraction, along with 200 μL of hexane in a tightly sealed 10-mL Teflon-capped glass vial, and the sample was heated at 100°C for 1 h to convert fatty acids to methyl esters. After addition of 1 mL of 0.15 M sodium bicarbonate and 2 mL of hexane, the sample was vortexed, centrifuged, and the upper hexane layer was transferred to a second 10-mL glass vial, evaporated under a nitrogen stream, and dissolved in 200 μL chloroform for GC analysis.

GC Analysis and Peak Identification

Samples were analyzed on an HP 5890 GC (Avondale, PA, USA), equipped with a flame-ionization detector. The column was a DB-23, 30M × 0.25 mm i.d. with film thickness of 0.25 μM (J & W Scientific, Folsom, CA, USA). The stationary phase was a (50% phenyl)-methylpolysiloxane. Helium was used as the carrier gas at 30 psi column pressure. One microlitre of sample was injected using an HP-6331 auto-injector, with a 1:15 split ratio. Initial column temperature was 160 °C, with a 1 °C/min gradient to 200 °C, and an additional 5 min at 200 °C. The injector and detector were set at 240 °C.

Calibration was done with fatty acid methyl ester standards from Nu-Chek Prep (Elysian, MN, USA). Chromatograms were collected and integrated with Lab-Calc software (Galactic Industries, Salem, NH, USA), on an IBM-PC. The total peak areas of the following fatty acids were determined: 14:0 myristic acid, 16:0 palmitic acid, 18:0 stearic acid, 18:1n-9 oleic acid, 18:1n-7 vaccenic acid, 18:2n-6 linoleic acid, 20:1n-9 eicosenoic acid, 20:4n-6 arachidonic acid, 20:5n-3 eicosapentaenoic acid, and 22:6n-3 docosahexaenoic acid. Each peak of interest was reported as weight percent of the sum of these major fatty acid components.

Research Design and Selection of Criterion Value

Our research design required two sample groups. The initial batch had five wild and five farmed salmon samples with known identities as determined by carotenoid chiral isomer ratios. This first batch was used to establish a criterion value for categorizing salmon as either wild or farmed. The second batch contained 20 samples whose categorization (wild or farmed) was not disclosed to the team analyzing the fatty acid composition.

After reviewing several fatty acids that might be used for discrimination within the sample of ten salmon with known classifications, we determined that LNA was the best indicator, as there was no overlap of LNA concentrations within the distribution of the pre-identified wild and farmed salmon. We then calculated the criterion value by choosing the lowest LNA (9.96%) value for the known farmed samples and the highest value (2.19%) from the known wild samples, and then taking the midpoint between those two values (6.1%).

We then tested the criterion value of 6.1% LNA on the remaining 20 unknown samples. The “unknown” samples were sent by Craft Technologies without any indication as to their carotenoid ratios or their classification as wild or farmed. Craft Technologies had previously categorized these 20 samples using the FDA-approved carotenoid chiral isomer ratios test.

Using the proposed 6.1% LNA criterion value, the 20 unknown samples were classified as farmed (LNA over 6.1%) or wild (LNA below 6.1%). The classifications for each of these 20 samples were then unblinded by Craft Technologies. The match between the criterion value classification and the carotenoid chiral isomer ratios classification was 100%.

Fatty Acid Statistics

Significant differences between farmed and wild salmon sample fatty acid ratios were noted by comparison of chromatographic peak areas. These results were recorded as percent of total weight of fatty acids. Difference of proportions tests were calculated on each fatty acid to determine statistical significance between farmed and wild salmon samples. This test produces *z* scores which are subsequently converted to *P* values, see Table 1 [25, 26].

Table 1 Fatty acid retention times, mean percent weight, standard deviation (SD) and *P* values

Fatty acid	Retention Time (min)	Mean peak area (%) Wild salmon	SD	Mean peak area (%) Farmed salmon	SD	<i>P</i> value
14:0	4	4.40	1.58	4.68	1.02	0.85
16:0	6.7	21.59	4.36	18.36	1.75	0.64
18:00	11.1	6.04	1.70	5.17	0.50	0.64
18:1n-9	11.7	25.68	8.31	29.10	8.47	0.73
18:1n-7	11.9	7.23	6.03	4.16	0.25	0.11
18:2n-6	13	2.10	0.61	12.73	2.59	0.0001
20:1n-9	18.5	4.75	3.21	2.65	0.94	0.07
20:4n-6	22.1	0.80	0.24	0.98	0.18	0.12
20:5n-3	24.8	11.84	4.01	9.97	3.41	0.62
22:6n-3	35.6	15.57	5.67	12.20	4.08	0.49
Total sat (%)	–	32.0	4.1	28.2	2.8	–
Mono (%)	–	37.7	8.6	35.9	8.4	–
n-6 (%)	–	2.9	0.5	13.7	2.5	–
n-3 (%)	–	27.4	7.7	22.2	7.2	–

All *P* values were determined by differences of fatty acids between all farmed and wild salmon tested *n* = 30 (note 18:2n-6 has a very high *P* value)

These calculations were carried out using Microsoft Excel version 2000.

Results

The fatty acid results for the initial sample of ten salmon that were analyzed are shown in Table 2. These salmon had all been pre-identified by chiral carotenoid analysis.

The highest LNA for wild salmon in this sample was 2.19%, and the lowest LNA for farmed salmon was 9.96%.

Representative carotenoid analyses are shown in Fig. 1. Wild salmon ingest predominantly a mixture of an astaxanthin from copepods and krill, which contain mostly the 3*R*,3'*R* and 3*S*,3'*S* astaxanthin isomers, and very little of the 3*R*,3'*S* isomer. Salmon fed yeast astaxanthin in their diet show primarily the 3*S*,3'*S* isomer, and salmon fed synthetic astaxanthin show an abundance of the central “meso” peak on the HPLC analysis, the 3*R*,3'*S* isomer.

Table 1 summarizes the fatty acid retention times and percent of total for each of the fatty acids reported in this analysis. This table was assembled after all the salmon samples had been classified as wild or farmed, using the criterion value of 6.1% LNA obtained from the initial set of identified salmon. There was complete agreement between assignment using LNA content and assignment using carotenoid analysis. These results are provided graphically in the histogram in Fig. 2, which emphasizes that LNA was the major peak that differs between wild and farmed.

Representative fatty acid profiles by GC of wild and farmed salmon are shown in Fig. 3. The elevated 18:2*n*-6 peak is highly distinctive and easily identifiable on the trace of the cultivated sample. Farmed samples may have

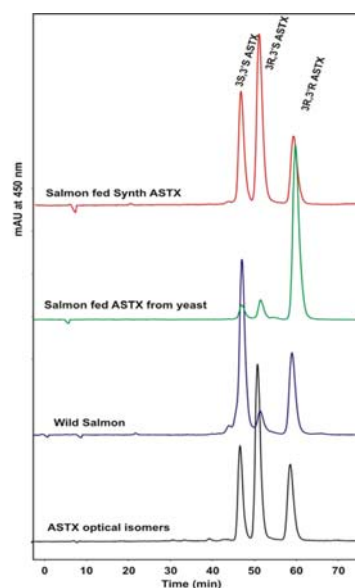
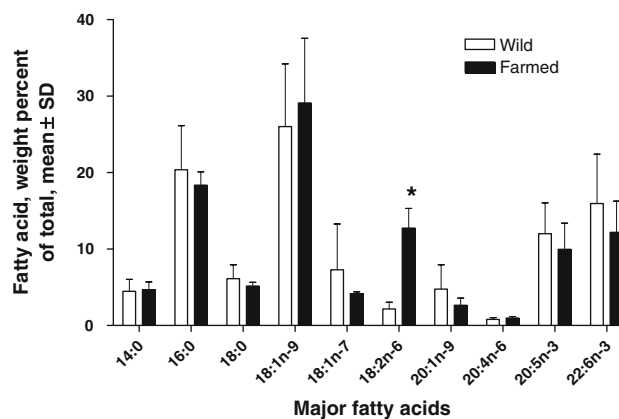


Fig. 1 HPLC comparison of astaxanthin isomers found in wild and farmed salmon. Wild salmon have very little 3*R*,3'*S* while farmed salmon have either very high levels of synthetic 3*R*,3'*S* or 3*R*,3'*R* from yeast



* Z score, 4.56, $p = 0.0001$, wild vs farmed

Fig. 2 Histogram comparing ratios of fatty acid content as percent of total major fatty acids. All fatty acids shown are not different statistically except for 18:2*n*-6

lower 20:1*n*-9, but this fatty acid was not statistically significant ($P = 0.07$). The other fatty acid components are generally comparable between wild and cultivated salmon and are not statistically different. Also, there was a non-significant trend toward decreasing percent of several major fatty acids in cultivated salmon reflecting the presence of increased 18:2*n*-6 (see Table 1; Fig. 2). The 22:1*n*-11 peak (sometimes called cetoleic acid), which elutes at 26.8 min in Fig. 3, is more abundant in many of the wild samples than in the farmed samples, but exhibits a high variance between samples. The peak is present at low abundance in all the farmed samples (1–2%) and in some

Table 2 Derivation of criterion value for determining wild from farmed salmon

Identifier	Wild or farmed	Percent (w) 18:2 <i>n</i> -6
1	W	2.19 ^a
2	W	1.90
3	W	1.73
4	W	1.54
5	W	1.95
6	F	11.60
7	F	11.57
8	F	9.96 ^b
9	F	13.72
10	F	13.89

Criterion value = average 18:2*n*-6 (highest wild and lowest farmed value of controls) = 6.1

Original identification based on astaxanthin levels

^a Highest wild value

^b Lowest farmed value

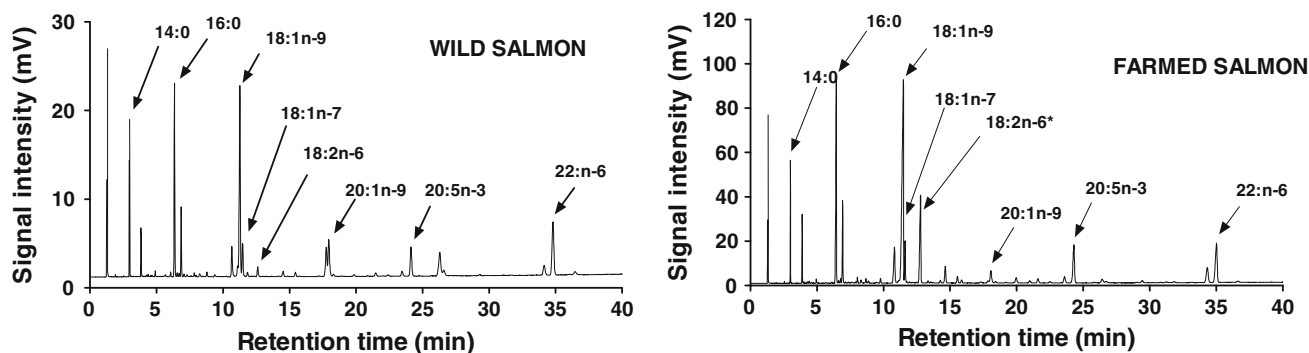


Fig. 3 Two representative gas chromatograms of farmed and wild salmon with major fatty acids and the prominent 18:2n-6 peak for the farmed salmon

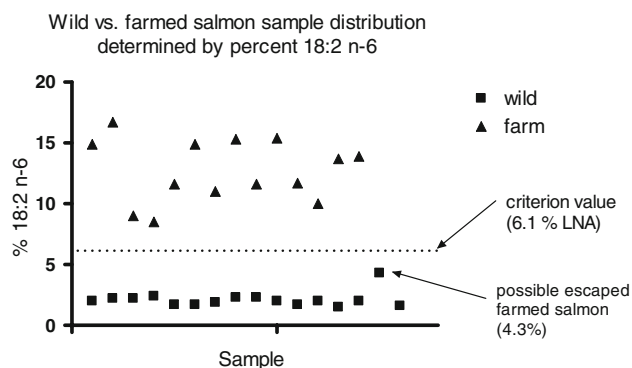


Fig. 4 The criterion value of 6.1 separates farmed from wild salmon samples by the percentage of 18:2n-6. Note that one sample of the wild salmon appears very close to the criterion value. See text for explanation

wild samples. This may reflect the fact that some of the wild-caught fish consumed copepods or other foods rich in 22:1n-11. Although of potential interest, this fatty acid cannot be reliably used for classifying the origin of the fish. Thomas et al. [27] also observed a much greater variance for 22:1n-11 in wild salmon than the other fatty acids reported in their study.

The percentage of LNA was plotted separately for all samples in Fig. 4; one sample, classified as wild by the LNA criterion, had a somewhat higher LNA content (4.3%) than the other 14 wild samples. This sample had an unusual carotenoid profile as well, intermediate between what is typically seen for wild and farmed salmon. Based on both the LNA content and carotenoid profile, we hypothesize that this sample is a farmed salmon that escaped and consumed a natural diet in the wild for an extended period.

Discussion

Wild and farmed salmon are similar in appearance and therefore it may be difficult for consumers to distinguish

between them by visual inspection. For this reason, the FDA developed the accurate, but complicated, HPLC method using chiral isomers of astaxanthin to identify farmed salmon. In our study, we analyzed fatty acid profiles in salmon samples that had been pre-identified using the FDA HPLC method.

Trends in the feeding practices for cultivated salmon could decrease the reliability of carotenoid analysis for determination of fish origins since wild krill and *Haematococcus* microalgae are being employed as part of the fish rations, and the astaxanthin isomer ratio in these fish could resemble that of wild salmon (see Fig. 1 for typical astaxanthin profiles) [23, 28]. By contrast, fatty acid analysis should continue to be a reliable method for classification. For example, Bell et al. [16] reported that when salmon flesh fatty acid content is plotted against their dietary intake of fatty acid for 20:5n-3 and 22:1, $r = 1.0$, while other fatty acids such as 18:2n-6 and 18:1n-9 result in the slightly lower flesh values of $r = 0.97$ and 0.98 , respectively. Current trends in fish feed development may lead to increased levels of 18:2n-6 in farmed fish, emphasizing the utility of fatty acid analysis in identifying farmed and wild salmon [15, 16, 19, 22, 29, 30].

Due primarily to price pressures, mislabeling of the origins of commercially sold salmon has been previously reported [27, 31]. Without quick, accurate, inexpensive, and commonly available testing procedures to authenticate wild and farmed salmon, mislabeling could become increasingly problematic. It therefore may be useful that readily available procedures such as fatty acid analysis by GC be applied to this question, and it should be possible to accomplish this analysis using the facilities in many nutrition and food science laboratories.

Our identification of farmed and wild salmon samples using fatty acid analysis demonstrated 100% agreement with the carotenoid isomer identification technique established by the FDA. The higher percent of 18:2n-6 in the farmed salmon flesh is an excellent marker for distinguishing

farmed and wild salmon, based on current feeding practices. Statistically, the percent of 18:2n-6 had a value of $P = 0.0001$ when the differences between all farmed and all wild ($n = 30$) samples were compared, indicating a high level of certainty that the amount of this fatty acid is dissimilar between the two groups of salmon. The only other fatty acid that approached statistical significance was the 20:1n-9, but it failed to reach 95% significance ($P = 0.07$). We chose not to employ it as a marker for identification.

As noted earlier, the fatty acids that salmon consume are assimilated into their flesh in proportion to dietary content (less any amount used for energy derived through beta-oxidation) [19]. Cultivated fish are currently being fed meal formulations with increasing ratios of plant-based oils [15, 16, 19, 22]. This change may reduce persistent organic contaminants, decrease the cost of fish feed, and ultimately increase the sustainability of aquaculture as a whole by preserving threatened pelagic fisheries [14, 16]. The practice of switching from fish oils to terrestrial plant oils leads directly to the increased 18:2n-6 content reported here, since 18:2n-6 is a major constituent of corn, rapeseed, and soybean oils that are typically used as components of the diet of farmed salmon. North American suppliers of salmon feed may use largely soybean oil and corn oil, consistent with the elevated n-6 fatty acid content of salmon feed in North America [32]. Salmon feed employed in Europe may have a different fatty acid profile, and the 18:2n-6 fatty acid content of farmed salmon from Scotland can be lower for some fish than farmed salmon from North America [8, 32].

Several studies that address the content of highly unsaturated fatty acids such as EPA and DHA have found that the relative percentages of these fatty acids were similar between farmed and wild salmon, but the total content of these fatty acids was higher in farmed fish because of the higher total lipid content [8, 22, 30, 33–35]. The percentage of EPA and DHA was not statistically different between wild and farmed salmon in the samples reported here, but we did demonstrate a consistently higher percentage of 18:2n-6 as seen in Table 1 and Fig. 2. In several previous studies, 18:2n-6 was also found to be significantly higher in farmed than in wild fish [27, 29, 30, 34]. However, our group was the first to apply a prospective blinded study design to test the hypothesis that 18:2n-6 could be an accurate marker for determining wild or farmed origin as compared with the current FDA-approved method. In one recent study, Thomas et al. [27] found 18:2n-6 to be the most reliable fatty acid for classification, but their validation procedure also used complex and expensive isotope ratio mass spectrometers. We feel that the mass spec method, which uses several different isotopic mass spectrometers equipped with either chemical analyzers or pyrolysis ovens [27], may be prohibitively

complex and expensive. Our data suggests that with this limited sample of fish obtained from North America, 18:2n-6 may be as accurate as using carotenoid chiral isomers, and therefore could be used as the sole identifier of farmed and wild salmon instead of the FDA-approved method. Additionally, the instrumentation for the HPLC analysis would require a capital investment of \$30,000, compared to \$10,000 for a standard GC. The labor required is also very different. A technician can complete 40 samples per week using fatty acid analysis, as opposed to ten samples per week for the FDA-approved astaxanthin chiral isomer identification test.

With any testing method for salmon, there may be samples that seem ambiguous. In our study, there was one wild sample with 18:2n-6 content of 4.3%, which approached the criterion value of 6.1% (see Fig. 4). The carotenoid profile of this fish was somewhat ambiguous as well. Farmed salmon sometimes escape from their pens and become feral salmon that are caught as wild. One study estimated that the number of escaped farmed salmon could be up to 40% of the total salmon caught as wild in the North Atlantic near the Faroe Islands, a center of fish farming [36]. The number was far lower for catches in the Pacific which averaged below 1%, although in some years higher numbers of escaped farmed salmon caught as wild in the Pacific have been reported [37]. It therefore is reasonable to expect that we could find at least one sample of wild caught salmon that could be a feral Atlantic salmon that escaped, was subsequently caught, and was identified with an intermediate fatty acid profile. Since it takes months for fatty acid and carotenoid profiles to change significantly, escapees may have a fatty acid profile with a ratio between that of typical wild and farmed salmon (see Fig. 4). For example, fish caught near the Faroe Islands might be more difficult to identify by either carotenoid or fatty acid profiles since this area is a center for salmon farming with a high escape rate. Therefore, to ensure consistency and accuracy with our method, continuous monitoring of the fatty acid composition of both cultivated and wild salmon should be considered. If a major change in LNA composition was detected for a given salmon population, the criterion value could be adjusted accordingly. This would eliminate error due to changes in either fishmeal fatty acid content or seasonal variation in wild salmon's diet. If greater assurances were needed, more sophisticated and time-consuming techniques, such as fish scale identification or multiprobe and multielement isotopic analyses [27, 38], could be employed.

One possible limitation of this study is that we reported each fatty acid as a percentage by weight, instead of the quantitative method using an internal standard to determine the absolute amount of each fatty acid per gram tissue. This study was focused on establishing a rapid, simple and

convenient procedure to distinguish farmed from wild salmon, thus the use of the percentage by weight of each fatty acid satisfies these requirements. Some investigators may want to quantify the amount of EPA and DHA in a sample to help identify fish that provide more of these fatty acids in the diet.

To our knowledge, this is the first published study to compare the FDA developed chiral isomer astaxanthin analysis method to the fatty acid analysis by the GC method of identifying farmed and wild salmon. The procedures reported herein are accurate, facile, and may be readily adapted in facilities with capillary GC. For this reason, fatty acid profiles could be of general value for discriminating wild and farmed salmon, with the potential to be applied to other seafood.

Acknowledgments Lori Megdal is acknowledged for her help on the statistical analysis and manuscript preparation, Edward Dratz for his help with editing this manuscript, and Eugene Rogers for his help with the analysis and identification of fatty acids and GC preparation.

Open Access This article is distributed under the terms of the Creative Commons Attribution Noncommercial License which permits any noncommercial use, distribution, and reproduction in any medium, provided the original author(s) and source are credited.

References

- Murphy WL, Andersen JM, Ebelin RM (2002) Assessment of geology as it pertains to modeling uplift in jointed rock: a basis for inclusion of uncertainty in flow models. <http://libweb.wes.army.mil/uhtbin/hyperion/TR-02-2.pdf>
- Mozaffarian D, Rimm EB (2006) Fish intake, contaminants, and human health: evaluating the risks and the benefits. *JAMA* 296(15):1885–1899
- Naylor RL, Goldburg RJ, Primavera JH, Kautsky N, Beveridge MC, Clay J, Folke C, Lubchenco J, Mooney H, Troell M (2000) Effect of aquaculture on world fish supplies. *Nature* 405(6790):1017–1024
- Pauly D, Watson R, Alder J (2005) Global trends in world fisheries: impacts on marine ecosystems and food security. *Philos Trans R Soc Lond B Biol Sci* 360(1453):5–12
- Fleming IA, Hindar K, Mjølnerod IB, Jonsson B, Balstad T, Lamberg A (2000) Lifetime success and interactions of farm salmon invading a native population. *Proc Biol Sci* 267(1452):1517–1523
- McGinnity P, Prodohl P, Ferguson A, Hynes R, Maoileidigh NO, Baker N, Cotter D, O’Hea B, Cooke D, Rogan G, Taggart J, Cross T (2003) Fitness reduction and potential extinction of wild populations of Atlantic salmon, *Salmo salar*, as a result of interactions with escaped farm salmon. *Proc Biol Sci* 270(1532):2443–2450
- Norford BS (1999) Introduction to papers on the Cambrian-Ordovician boundary. *Geol Mag* 125(4):323
- Hamilton MC, Hites RA, Schwager SJ, Foran JA, Knuth BA, Carpenter DO (2005) Lipid composition and contaminants in farmed and wild salmon. *Environ Sci Technol* 39(22):8622–8629
- Hayward D, Wong J, Krynitsky AJ (2007) Polybrominated diphenyl ethers and polychlorinated biphenyls in commercially wild caught and farm-raised fish fillets in the United States. *Environ Res* 103(1):46–54
- Hites RA, Foran JA, Carpenter DO, Hamilton MC, Knuth BA, Schwager SJ (2004) Global assessment of organic contaminants in farmed salmon. *Science* 303(5655):226–229
- Dewailly E, Ayotte P, Lucas M, Blanchet C (2007) Risk and benefits from consuming salmon and trout: a Canadian perspective. *Food Chem Toxicol* 45(8):1343–1348
- Huang X, Hites RA, Foran JA, Hamilton C, Knuth BA, Schwager SJ, Carpenter DO (2006) Consumption advisories for salmon based on risk of cancer and noncancer health effects. *Environ Res* 101(2):263–274
- Seierstad SL, Seljeflot I, Johansen O, Hansen R, Haugen M, Rosenlund G, Froyland L, Arnesen H (2005) Dietary intake of differently fed salmon; the influence on markers of human atherosclerosis. *Eur J Clin Invest* 35(1):52–59
- Torstensen BE, Bell JG, Rosenlund G, Henderson RJ, Graff IE, Tocher DR, Lie O, Sargent JR (2005) Tailoring of Atlantic salmon (*Salmo salar* L.) flesh lipid composition and sensory quality by replacing fish oil with a vegetable oil blend. *J Agric Food Chem* 53(26):10166–10178
- Bell JG, McEvoy J, Tocher DR, McGhee F, Campbell PJ, Sargent JR (2001) Replacement of fish oil with rapeseed oil in diets of Atlantic salmon (*Salmo salar*) affects tissue lipid compositions and hepatocyte fatty acid metabolism. *J Nutr* 131(5):1535–1543
- Bell JG, Henderson RJ, Tocher DR, McGhee F, Dick JR, Porter A, Smullen RP, Sargent JR (2002) Substituting fish oil with crude palm oil in the diet of Atlantic salmon (*Salmo salar*) affects muscle fatty acid composition and hepatic fatty acid metabolism. *J Nutr* 132(2):222–230
- Miller MR, Nichols PD, Carter CG (2007) Replacement of dietary fish oil for Atlantic salmon parr (*Salmo salar* L.) with a stearidonic acid containing oil has no effect on omega-3 long-chain polyunsaturated fatty acid concentrations. *Comp Biochem Physiol B Biochem Mol Biol* 146(2):197–206
- Zheng X, Torstensen BE, Tocher DR, Dick JR, Henderson RJ, Bell JG (2005) Environmental and dietary influences on highly unsaturated fatty acid biosynthesis and expression of fatty acyl desaturase and elongase genes in liver of Atlantic salmon (*Salmo salar*). *Biochim Biophys Acta* 1734(1):13–24
- Bell JG, Henderson RJ, Tocher DR, Sargent JR (2004) Replacement of dietary fish oil with increasing levels of linseed oil: modification of flesh fatty acid compositions in Atlantic salmon (*Salmo salar*) using a fish oil finishing diet. *Lipids* 39(3):223–232
- Turujman SA, Wamer WG, Wei RR, Albert RH (1997) Rapid liquid chromatographic method to distinguish wild salmon from aquacultured salmon fed synthetic astaxanthin. *J AOAC Int* 80(3):622–632
- Moretti VM, Mentasti T, Bellagamba F, Luzzana U, Caprino F, Turchini GM, Giani I, Valfre F (2006) Determination of astaxanthin stereoisomers and colour attributes in flesh of rainbow trout (*Oncorhynchus mykiss*) as a tool to distinguish the dietary pigmentation source. *Food Addit Contam* 23(11):1056–1063
- Bell JG, McEvoy J, Webster JL, McGhee F, Millar RM, Sargent JR (1998) Flesh lipid and carotenoid composition of Scottish farmed Atlantic Salmon (*Salmo salar*). *J Agric Food Chem* 46(1):119–127
- Lorenz RT, Cysewski GR (2000) Commercial potential for Haematococcus microalgae as a natural source of astaxanthin. *Trends Biotechnol* 18(4):160–167
- Abu-Lafi S, Turujman SA (1997) A chiral HPLC method for the simultaneous separation of configurational isomers of the predominant cis/trans forms of astaxanthin. *Enantiomer* 2(1):17–25
- Blalock HM (1979) *Social statistics*, 2nd edn. McGraw Hill, New York

26. <http://www.graphpad.com/quickcalcs/Pvalue2.cfm>
27. Thomas DSG, Shaw PA (1999) Late Cenozoic drainage evolution in the Zambezi basin—geomorphological evidence from the Kalahari rim. *J Afr Earth Sci Middle East* 8(2):40–42
28. Suountama J, Kiessling A, Melle W, Waagbo R, Olesn RE (2007) Protein from Northern krill (*Thysanoessa inermis*), Antarctic krill (*Euphausia superba*) and the Arctic amphipod (*Themisto libellula*) can partially replace fish meal in diets to Atlantic salmon (*Salmo salar*) without affecting product quality. *Aquac Nutr* 13:50–58
29. Sargent JR, Tacon AG (1999) Development of farmed fish: a nutritionally necessary alternative to meat. *Proc Nutr Soc* 58(2):377–383
30. Blanchet C, Lucas M, Julien P, Morin R, Gingras S, Dewailly E (2005) Fatty acid composition of wild and farmed Atlantic salmon (*Salmo salar*) and rainbow trout (*Oncorhynchus mykiss*). *Lipids* 40(5):529–531
31. Burros M (2005) Stores say wild salmon, but tests say farm bred. *New York Times*
32. Olsen Y, Skjervold H (1995) Variation in content of 3 fatty acids in farmed Atlantic salmon, with special emphasis on effects of non-dietary factors. *Aquac Int* 3:22–35
33. Cahu C, Salen P, de Lorgeril M (2004) Farmed and wild-fish in the prevention of cardiovascular diseases: assessing possible differences in lipid nutritional values. *Nutr Metab Cardiovasc Dis* 14(1):34–41
34. Nettleton J (2000) Fatty acids in cultivated and wild-fish. In: *Proceedings of the International Institute of Fisheries Economics and Trade Oregon State University, Corvallis*. <http://www.orst.edu/Dept/IIFET/html/i2ktoc.pdf>
35. van Vliet T, Katan MB (1990) Lower ratio of n-3 to n-6 fatty acids in cultured than in wild-fish. *Am J Clin Nutr* 51(1):1–2
36. Hansen LP, Jacobsen JA, Lund RA (1999) The incidence of escaped farmed Atlantic salmon, *Salmo salar* L. in the Faroese fishery and estimates of catches of wild salmon. *ICES J Mar Sci* 56:200–206
37. Thomson AJ, Mckinnell S (1996) Recent events concerning Atlantic salmon escapees in the Pacific. *J Mar Sci* 54:1221–1225
38. Hansen P, Jacobsen JA, Lund RA (1993) High numbers of farmed Atlantic salmon, *Salmo salar*, observed in oceanic waters north of the Faroe Islands. *Aquac Fisheries Management* 24:777–781

Low and High Fat Diets Inconsistently Induce Obesity in C57BL/6J Mice and Obesity Compromises n-3 Fatty Acid Status

Diana L. Tallman · Amy D. Noto · Carla G. Taylor

Received: 18 August 2008 / Accepted: 26 September 2008 / Published online: 3 June 2009
© AOCS 2009

Sir,

C57BL/6J mice are the background strain for multiple models of obesity and diabetes that have genes homologous to those identified in human obesity [1, 2]. C57BL/6J mice are also models of gene-environment induced obesity because they are more susceptible to an environment permissive to obesity and several publications show that high fat (HF) feeding (~40–70% of kcal) induces obesity, insulin resistance, hyperglycemia and leptin resistance [3–9]. We have used this model of high fat feeding to examine interactions of obesity and zinc status but showed neither level of dietary fat nor zinc had an effect on body weight, body mass index, glycemia, insulinemia or leptinemia in C57BL/6J mice [10]. This led to an opportunity to examine whether the inconsistency in development of diet induced obesity (DIO) is related to dietary fat level, or the metabolic derangements associated with greater weight gain. Thus, mice from the original data set [10] were stratified into low body weight (LBW) and high body weight (HBW) groups to determine relationships with metabolic parameters associated with obesity including variations in adipose tissue fatty acid composition and zinc status.

The LBW and HBW groups comprised mice fed both low fat (LF) and HF diets, and similar numbers of zinc deficient, control and supplemented mice (Fig. 1). The HBW group displayed greater fasting serum glucose and leptin concentrations (9.8 ± 0.5 vs. 8.2 ± 0.6 mmol/L and 42.6 ± 5.9 vs. 20.3 ± 4.4 ng/ml, respectively; $P < 0.05$) compared to the LBW mice. Fasting serum insulin,

homeostasis model assessment (HOMA) and zinc were not different between LBW and HBW mice (data not shown). Notably, mice fed a LF diet based on the AIN-93G diet (7 g soybean oil/100 g diet; 16% of calories as fat), were susceptible to obesity, contrary to what others have reported [11–13]. Furthermore, approximately half the mice fed the HF diet were resistant to obesity. The HF diet in our experiment contained a combination of lard and soybean oil (20.9 and 8.8 g/100 g diet, respectively; 55% of calories as fat) to ensure adequate intake of essential fatty acids and this resulted in a HF diet with slightly lower saturated fatty acid content and higher polyunsaturated fatty acid content from linoleic acid compared to protocols in which the high fat diet contains less soybean oil [6, 11]. There are other reports that show HF feeding does not consistently produce obesity in C57BL/6J mice [4, 8].

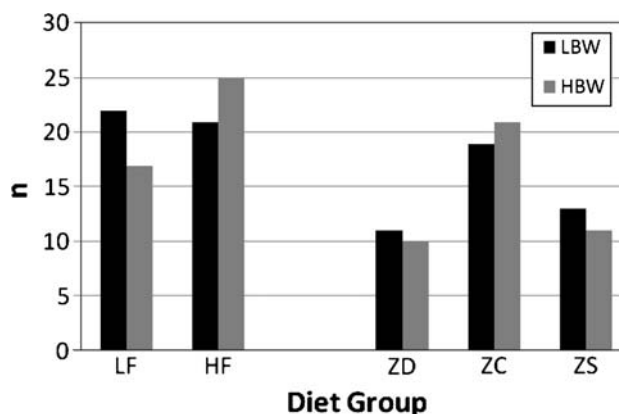


Fig. 1 Distribution of low and high body weight C57BL/6J mice by dietary treatment. *LF* low fat, *HF* high fat, *ZD* zinc deficient, *ZC* zinc control, *ZS* zinc supplemented; *LBW* low body weight, *HBW* high body weight. The distribution of LBW and HBW mice by level of dietary fat or zinc were not different by Chi-square analysis

D. L. Tallman · A. D. Noto · C. G. Taylor (✉)
Department of Human Nutritional Sciences, University
of Manitoba, H507 Duff Roblin Building, Winnipeg,
Manitoba R3T 2N2, Canada
e-mail: ctaylor@cc.umanitoba.ca

Burcelin et al. [8], fed C57BL/6J mice a HF diet [72% kcal from corn oil and lard (proportions not specified)] for 9 months and found that only about 50% of the mice became obese with diabetes. Koza et al. [4] reported a fourfold difference in fat mass among C57BL/6J mice fed a HF diet (33.4 g hydrogenated coconut oil and 2.5 g soybean oil/100 g diet; 58% kcal from fat) and found important gene variations in mice that were high gainers compared to those that were low gainers, thus showing the importance of gene–diet interactions. Given that the level of fat used in the current study was comparable to what others have reported induces DIO [3–9, 11–13] and the findings of Koza et al. [4], these observations support a strong genetic predisposition to obesity in the affected mice. There are now over 30 candidate genes on 6 chromosomes linked to adiposity in mice. Some of the target pathways include CCAAT/enhancer binding protein

(C/EBP)- α , sterol regulatory element binding protein (SREBP)-1, peroxisome proliferator activated protein (PPAR)- γ and secreted frizzled-related sequence protein (SFRP)-5/Wnt signalling [2, 4, 14–16], to which the fatty acid environment of adipose tissue may be important [17].

Our results also demonstrate that adipose PL fatty acid composition was affected by diet and obesity (Table 1), whereas adipose TAG fatty acid composition generally resembled the dietary fatty acid content. The HBW mice had more C16:0 (15.3 ± 0.4 vs. $14.3 \pm 0.4\%$), C18:3n-3 (0.35 ± 0.07 vs. $0.24 \pm 0.04\%$) and C22:5n-3 (0.52 ± 0.02 vs. $0.46 \pm 0.02\%$), less C22:6n-3 (3.94 ± 0.22 vs. $4.49 \pm 0.25\%$), and a greater n-6:n-3 ratio (5.88 ± 0.24 vs. 5.15 ± 0.23) in adipose PL compared to LBW mice. There was an interaction of diet fat and body weight such that the HBW-LF mice had more C18:3n-3 and less C20:5n-3 in adipose PL than the LBW-LF mice, suggesting reduced

Table 1 Fatty acid profiles (% and ratios) of epididymal adipose tissue phospholipids for low and high body weight C57BL/6J mice by low or high fat diet^a

Fatty acid ^{b,c}	LBW mice		HBW mice		<i>F</i> values ^d		
	Low fat diet	High fat diet	Low fat diet	High fat diet	Diet fat	Body weight	Diet fat \times body weight
Percentages							
C16:0	15.7 ± 0.4	12.9 ± 0.2	16.7 ± 0.2^e	13.8 ± 0.4	<0.0001	0.0037	NS
C18:0	17.8 ± 0.7	22.2 ± 0.3	18.0 ± 0.4	21.2 ± 0.5	NS	NS	NS
C18:1n-9	8.9 ± 0.4	12.7 ± 0.4	9.8 ± 0.4	13.1 ± 0.5	0.0002	NS	NS
C18:2n-6	18.0 ± 0.7	16.5 ± 0.9	18.4 ± 0.4	17.3 ± 0.5	0.0482	NS	NS
C18:3n-3	0.25 ± 0.07	0.23 ± 0.06	0.59 ± 0.06^e	0.11 ± 0.02	0.0001	0.0514	0.0004
C20:0	1.2 ± 0.1	1.1 ± 0.1	1.2 ± 0.1	1.0 ± 0.1	0.0363	NS	NS
C20:4n-6	10.2 ± 0.6	11.8 ± 1.1	10.2 ± 0.4	12.1 ± 0.5	0.0147	NS	NS
C20:5n-3	0.43 ± 0.05	0.20 ± 0.04	0.21 ± 0.04^e	0.28 ± 0.06	NS	NS	0.0056
C22:0	2.3 ± 0.2	2.1 ± 0.2	2.3 ± 0.1	1.6 ± 0.1^f	0.0046	NS	NS
C22:5n-3	0.48 ± 0.03	0.43 ± 0.03	0.52 ± 0.03	0.52 ± 0.02	NS	0.0319	NS
C22:6n-3	5.0 ± 0.2	4.0 ± 0.4	4.6 ± 0.2	3.2 ± 0.2^f	0.0001	0.0474	NS
Totals							
mg FA/g	0.9 ± 0.1	1.3 ± 0.1	0.9 ± 0.1	1.1 ± 0.1	0.0081	NS	NS
Total SFA	39.1 ± 0.8	40.3 ± 0.5	40.5 ± 0.3	39.2 ± 0.5	NS	NS	0.0384
Total MUFA	16.0 ± 0.4	18.1 ± 0.5	16.1 ± 0.5	19.2 ± 0.5	<0.0001	NS	NS
Total PUFA	36.7 ± 0.8	35.4 ± 0.8	37.1 ± 0.5	35.7 ± 0.8	NS	NS	NS
Total n-6	29.7 ± 0.7	29.9 ± 0.5	30.7 ± 0.4	30.7 ± 0.9	NS	NS	NS
Total n-3	6.7 ± 0.2	5.3 ± 0.4	5.8 ± 0.2^e	4.8 ± 0.2	NS	NS	NS
Ratios							
PUFA/SFA	1.0 ± 0.1	0.9 ± 0.1	0.9 ± 0.1	0.9 ± 0.1	NS	NS	NS
n-6/n-3	4.4 ± 0.2	5.9 ± 0.3	5.3 ± 0.1^e	6.5 ± 0.4	<0.0001	0.0104	NS

^a Mice were divided by median body weight: low body weight mice ≤ 39.6 g, high body weight mice ≥ 39.6 g

^b Values are means \pm SEM, $n = 8$ /group

^c SFA saturated fat, MUFA monounsaturated fat, PUFA polyunsaturated fat. Fatty acids are expressed as % composition (g/100 g fatty acids) except for total milligrams of fatty acid per gram (mg FA/g) and the ratios

^d *F* values determined by ANOVA

^e LBW-LF different from HBW-LF

^f LBW-HF different from HBW-HF

conversion of ALA to EPA in the HBW-LF mice (Table 1). These findings may be due to differences in delta 6 and delta 5 desaturation, β -oxidation or incorporation into membrane PL [18, 19], but this study is limited by the fact that these factors were not examined. Interestingly, both desaturase enzymes are regulated by SREBP-1 and PPAR α in mice [20], targeted genes in the pathology of obesity. Furthermore, people with diabetes have defects of delta 6 and delta 5 desaturases [21].

Insulin stimulates delta 6 desaturase and zinc is one cofactor, thus, it is also of interest that we have shown a reduced zinc concentration in adipose, pancreatic and liver tissue (Fig. 2a) in conjunction with a lower n-3 fatty acid status in adipose tissue PL in the HBW mice, independent of dietary fat (Table 1). However, when total zinc content was calculated in the same tissues, the effect was lost (Fig. 2b), implying that it was due to a dilution effect of excess fat and/or larger fat cells. Other studies investigating zinc status in obese or diabetic states have reported reduced tissue zinc concentrations but have not considered the effect on total tissue zinc content. For example, lower zinc concentrations were found in carcasses of obese mice,

pancreatic tissue of diabetic and obese mice, and hair or serum of obese people [22–26]. Recently it has been reported that zinc finger proteins (e.g. zinc finger protein 36) from omental fat are inversely related to insulin and insulin resistance in women [27] and zinc finger transcription factors (e.g. SLUG) are important for adipocyte differentiation in humans [28]. Thus, further investigation into mechanisms between zinc, obesity and lipid metabolism appear warranted.

In summary, these results suggest that body fat accumulation in C57BL/6J is not dependent entirely on a HF diet, and can in fact occur on a LF diet. Additionally, obesity in this model resulted in an unfavourable adipose PL n-3 fatty acid status which may be a result of, or further complicate obesity and diabetes.

Acknowledgments We would like to acknowledge Marily Latta and Thi Ly, Department of Human Nutritional Sciences for technical assistance, and the staff of the animal holding facility at the University of Manitoba.

References

- Zuberi A, Chagnon YC, Weisnagel SJ et al (2006) The human obesity gene map: the 2005 update. *Obesity* 14:529–644
- Wuschke S, Dahm S, Schmidt C, Joost HG, Al-Hasani H (2007) A meta-analysis of quantitative trait loci associated with body weight and adiposity in mice. *Int J Obes (Lond)* 31:829–841
- Nishikawa S, Yasoshima A, Doi K, Nakayama H, Uetsuka K (2007) Involvement of sex, strain and age factors in high fat diet-induced obesity in C57BL/6J and BALB/cA mice. *Exp Anim* 56:263–272
- Koza RA, Nikonova L, Hogan J, Rim JS, Mendoza T, Faulk C, Skaf J, Kozak LP (2006) Changes in gene expression foreshadow diet-induced obesity in genetically identical mice. *PLoS Genet* 2:e81
- Ruzickova J, Rossmeisl M, Prazak T et al (2004) Omega-3 PUFA of marine origin limit diet-induced obesity in mice by reducing cellularity of adipose tissue. *Lipids* 39:1177–1185
- Williams TD, Chambers JB, Roberts LM, Henderson RP, Overton JM (2003) Diet-induced obesity and cardiovascular regulation in C57BL/6J mice. *Clin Exp Pharmacol Physiol* 30:769–778
- Ahren B, Pacini G (2002) Insufficient islet compensation to insulin resistance vs. reduced glucose effectiveness in glucose-intolerant mice. *Am J Physiol Endocrinol Metab* 283:E738–E744
- Burcelin R, Crivelli V, Dacosta A, Roy-Tirelli A, Thorens B (2002) Heterogeneous metabolic adaptation of C57BL/6J mice to high-fat diet. *Am J Physiol Endocrinol Metab* 282:E834–E842
- Weigle DS, Kuijper JL (1996) Obesity genes and the regulation of body fat content. *Bioessays* 18:867–874
- Tallman DL, Taylor CG (2003) Effects of dietary fat and zinc on adiposity, serum leptin and adipose fatty acid composition in C57BL/6J mice. *J Nutr Biochem* 14:17–23
- Jiang T, Wang Z, Proctor G, Moskowitz S, Liebman SE, Rogers T, Lucia MS, Li J, Levi M (2005) Diet-induced obesity in C57BL/6J mice causes increased renal lipid accumulation and glomerulosclerosis via a sterol regulatory element-binding protein-1c-dependent pathway. *J Biol Chem* 280:32317–32325
- Kim S, Sohn I, Lee YS, Lee YS (2005) Hepatic gene expression profiles are altered by genistein supplementation in mice with diet-induced obesity. *J Nutr* 135:33–41

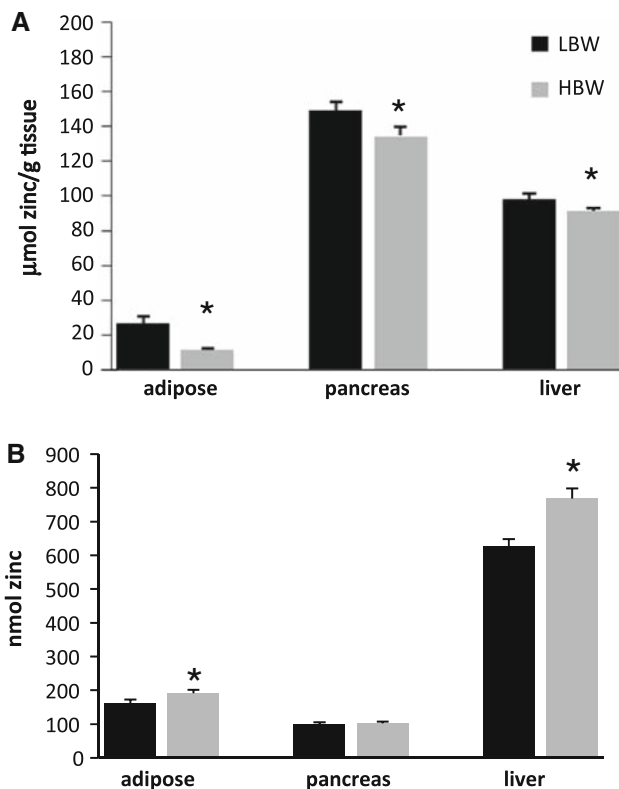


Fig. 2 Adipose, pancreas and liver zinc concentrations (a) and contents (b) of low and high body weight C57BL/6J mice. Values are mean \pm SEM for adipose: $n = 28$ (LBW) or 31 (HBW); pancreas $n = 31$ (LBW) or 29 (HBW); liver $n = 33$ (LBW) or 30 (HBW); *LBW different from HBW mice ($P < 0.05$). Zinc concentrations based on dry weight of tissue. Zinc contents calculated from zinc concentration/wet weight of tissue \times organ wet weight

13. Lin S, Thomas TC, Storlien LH, Huang XF (2000) Development of high fat diet-induced obesity and leptin resistance in C57Bl/6J mice. *Int J Obes Relat Metab Disord* 24:639–646
14. Fisler JS, Warden CH, Pace MJ, Lusk AJ (1993) BSB: a new mouse model of multigenic obesity. *Obes Res* 1:271–280
15. York B, Truett AA, Monteiro MP, Barry SJ, Warden CH, Naggert JK, Maddatu TP, West DB (1999) Gene–environment interaction: a significant diet-dependent obesity locus demonstrated in a congenic segment on mouse chromosome 7. *Mamm Genome* 10:457–462
16. Chiu S, Kim K, Haus KA, Espinal GM, Millon LV, Warden CH (2007) Identification of positional candidate genes for body weight and adiposity in subcongenic mice. *Physiol Genomics* 31:75–85
17. Takada R, Satomi Y, Kurata T, Ueno N, Norioka S, Kondoh H, Takao T, Takada S (2006) Monounsaturated fatty acid modification of Wnt protein: its role in Wnt secretion. *Dev Cell* 11:791–801
18. Sprecher H, Luthria DL, Mohammed BS, Baykousheva SP (1995) Reevaluation of the pathways for the biosynthesis of polyunsaturated fatty acids. *J Lipid Res* 36:2471–2477
19. Marzo I, Alava MA, Pineiro A, Naval J (1996) Biosynthesis of docosahexaenoic acid in human cells: evidence that two different delta 6-desaturase activities may exist. *Biochim Biophys Acta* 1301:263–272
20. Matsuzaka T, Shimano H, Yahagi N, Amemiya-Kudo M, Yoshikawa T, Hastly AH, Hamura Y, Osuga J, Okazaki H, Iizuka Y, Takahashi A, Sone H, Gotoda T, Ishibashi S, Yamada N (2002) Dual regulation of mouse Delta(5)- and Delta(6)-desaturase gene expression by SREBP-1 and PPARalpha. *J Lipid Res* 43:107–114
21. Das UN (2007) A defect in the activity of Delta6 and Delta5 desaturases may be a factor in the initiation and progression of atherosclerosis. *Prostaglandins Leukot Essent Fatty Acids* 76:251–268
22. Simon SF, Taylor CG (2000) Dietary zinc supplementation attenuates hyperglycemia in db/db mice. *Exp Biol Med* 226:43–51
23. Kennedy ML, Failla ML, Smith JC (1987) Influence of genetic obesity on tissue concentrations of zinc, copper, manganese and iron in mice. *J Nutr* 116:1432–1441
24. Chen MD, Lin PY, Cheng V, Lin W-H (1996) Zinc supplementation aggravates body fat accumulation in genetically obese mice and dietary-obese mice. *Biol Trace Elem Res* 52:125–132
25. Chen M-D, Liou S-J, Lin P-Y, Yang VC, Alexander PS, Lin W-H (1998) Effects of zinc supplementation on the plasma glucose level and insulin activity in genetically obese (ob/ob) mice. *Biol Trace Elem Res* 61:303–311
26. Di Martino G, Matera MG, De Martino B, Vacca C, Di Martino S, Rossi F (1993) Relationship between zinc and obesity. *J Med* 24:177–183
27. Bouchard L, Vohl MC, Deshaies Y, Rheaume C, Daris M, Tchernof A (2007) Visceral adipose tissue zinc finger protein 36 mRNA levels are correlated with insulin, insulin resistance index, and adiponectinemia in women. *Eur J Endocrinol* 157:451–457
28. Perez-Mancera PA, Bermejo-Rodriguez C, Gonzalez-Herrero I, Herranz M, Flores T, Jimenez R, Sanchez-Garcia I (2007) Adipose tissue mass is modulated by SLUG (SNAI2). *Hum Mol Genet* 16:2972–2986

Modification of Palm Oil for Anti-Inflammatory Nutraceutical Properties

Zaida Zainal · Andrea J. Longman · Samantha Hurst ·
Katrina Duggan · Clare E. Hughes · Bruce Caterson ·
John L. Harwood

Received: 9 January 2009 / Accepted: 3 April 2009 / Published online: 16 May 2009
© AOCS 2009

Abstract Palm oil is one of the most important edible oils in the world. Its composition (rich in palmitate and oleate) make it suitable for general food uses but its utility could be increased if its fatty acid quality could be varied. In this study, we have modified a palm olein fraction by transesterification with the n-3 polyunsaturated fatty acids, α -linolenate or eicosapentaenoic acid (EPA). Evaluation of the potential nutritional efficacy of the oils was made using chondrocyte culture systems which can be used to mimic many of the degenerative and inflammatory pathways involved in arthritis. On stimulation of such cultures with interleukin-1 α , they showed increased expression of cyclooxygenase-2, the inflammatory cytokines tumour necrosis factor- α (TNF- α), IL-1 α and IL-1 β and the proteinase ADAMTS-4. This increased expression was not affected by challenge of the cultures with palm olein alone but showed concentration-dependent reduction by the modified oil in a manner similar to EPA. These results show clearly that it is possible to modify palm oil conveniently to produce a nutraceutical with effective anti-inflammatory properties.

Keywords Interesterification · Palm oil · n-3 PUFA · Eicosapentaenoic acid (EPA) · Chondrocyte cultures · Arthritis

A. J. Longman · S. Hurst · K. Duggan ·
C. E. Hughes · B. Caterson · J. L. Harwood (✉)
School of Biosciences, Cardiff University,
Cardiff CF10 3AX, UK
e-mail: Harwood@Cardiff.ac.uk

Present Address:

Z. Zainal
Malaysian Palm Oil Board, Persiaran Institutusi,
43000 Kajang, Selangor, Malaysia

Abbreviations

ADAMTS-4	A disintegrin and metalloproteinase with thrombospondin motifs (aggrecanase-1)
COX-2	Cyclooxygenase-2
DHA	All <i>cis</i> -4, 7, 10, 13, 16, 19-docosahexaenoic acid
EPA	All <i>cis</i> -5, 8, 11, 14, 17-eicosapentaenoic acid
FCS	Fetal calf serum
GAPDH	Glyceraldehyde 3-phosphate dehydrogenase
TAG	Triacylglycerol
TNF- α	Tumour necrosis factor- α
VLCPUFA	Very long chain (>18C) polyunsaturated fatty acid

Introduction

The oil palm is one of the major commodity species grown in the world [1] and is, currently, the main crop grown for oil [2]. The oil palm produces two products. Palm kernel oil (which is enriched in laurate) is used by the soap, detergent and cosmetic industries as well as having specialised edible uses [1]. Palm oil, on the other hand, contains mainly palmitate (43–46%) and oleate (36–41%), and is used generally in the food industry.

Palm oil is a major source of sustainable and renewable raw material for the world's food, oleochemical and biofuel industries [3]. In that connection, there has been increasing interest in diversifying the use of palm oil. This could be done if its composition could be varied. However, genetic manipulation is more problematic for palm trees than for annual, dicotyledonous crops (such as soybean or canola) and limited progress has been made [4]. Alternative

strategies include the identification of suitable individual varieties (e.g. *Elaeis oleifera*) or by modification or fractionation of the crude palm oil.

There has been much recent interest in the beneficial properties of dietary omega n-3 PUFA [5]. There is strong evidence that such compounds can be of benefit for good health, particularly with regard to cardiovascular disease, brain development and function, arthritis and various other chronic inflammatory diseases [6]. Recently, there has been progress in elucidating the mechanisms by which n-3 PUFA exert this effect at the molecular level [7–9] where they reduce the metabolism of n-6 fatty acids to pro-inflammatory mediators, produce competing non- or anti-inflammatory metabolites as well as reduce the expression of pro-inflammatory cytokines and enzymes [6].

The first evidence for an important role of dietary n-3 fatty acids on inflammation was derived from epidemiological observations of the low incidence of autoimmune and inflammatory disorders in Inuits [see 10]. In addition, the first study showing positive effects with n-3 PUFA dietary supplementation was published in 1985 [11] although it has to be noted that a report in the London Medical Journal in 1783 extols the virtues of cod liver oil for the treatment of ‘rheumatism’ amongst other disorders [12]. Discussions of the potential anti-inflammatory properties of n-3 fatty acids relevant to arteriosclerosis, asthma and arthritis will be found in [13–22].

n-3 PUFA are produced by algae and plants and accumulate, via the food chain, in fish oils. The latter have traditionally been the main dietary source of very long chains (VLCs), such as eicosapentaenoic (EPA, all *cis*-5, 8, 11, 14, 17-eicosapentaenoic) or docosahexaenoic (DHA; all *cis*-4, 7, 10, 13, 16, 19-docosahexaenoic) acids [5]. With the decline in fish stocks in many parts of the world, there have been attempts to genetically manipulate plants to produce VLCs [23, 24] and also to use some of the waste products of the fishing industry better [25].

In this paper, we describe the lipase-mediated modification of palm oil using n-3 fatty acids and the utilisation of an in vitro model system which can be used to mimic some of the pathological pathways occurring in arthritis [26, 27]. Challenge of the chondrocyte cultures with mixtures of fatty acids allowed us to demonstrate that the n-3 PUFA EPA was able to reduce expression of inflammatory mediators and enzymes including proteinases important in the aetiology of arthritis. Although palm oil itself had no effect, the modified material (containing EPA) reduced the inflammatory factors that lead to cartilage matrix degradation in arthritis. These data show that it is possible to produce a value-added product from palm oil which would be beneficial to the health status of consumers.

Experimental Procedures

Materials

Collagenase TypeII, prepared from *Clostridium histolyticum* was obtained from Worthington Biochem. Corp. (NJ 08701, USA), pronase (*Streptomyces griseus*) from Boehringer (Bracknell, Berks RG12 8YS, UK) and DMEM and fetal calf serum from Gibco-BRL (now Invitrogen) (Paisley PA4 9RF, UK). Refined palm olein was obtained from the Malaysian Palm Oil Board (43000 Kajang, Selangor, Malaysia). Fatty acid standards were from Nu-Chek Prep. (Elysian, MN 56028, USA) and recombinant human interleukin-1 α was from Totam Biological (Peterborough PE1 5TX, UK). Other chemicals were of the best available grades and were from Sigma–Aldrich Co. (Gillingham, Dorset SP8 4XT, UK) or from Boehringer–Mannheim (now Roche Diagnostics Ltd., Burgess Hill, RH15 9RY, UK).

Isolation and Culture of Bovine Chondrocytes

Bovine metacarpo- and metatarsophalangeal joints (7-day-old calves) were obtained from the local abattoir. Cartilage was removed from the joint surfaces under sterile conditions and digested in 0.1% (w/v) pronase in DMEM containing 5% (w/v) fetal calf serum (FCS) for 3 h at 37 °C with roller agitation. It was further digested with 0.04% (w/v) collagenase in DMEM with 5% FCS for 24 h at 37 °C with roller agitation. After 24 h, cells were separated from debris by filtration through a 40 μ m Nitex filter (BD Bioscience, Bedford MA, 01730, USA) before cell numbers were estimated by microscopy. Cells were resuspended at 6×10^6 cells/ml in DMEM. Monolayer cultures were established in 60-mm dishes by plating 1 ml of the above medium/dish (to give a final density of approximately 20×10^5 cells/cm²). Experimental medium (4 ml/dish, DMEM containing 50 μ g/ml gentamicin) was then added to the cultures which were maintained at 37 °C under 5% (v/v) CO₂ for 6 h by which time monolayers had established.

Fatty acids to be added were made up in a complex with defatted bovine serum albumin. For the palm olein and modified palm olein preparations, these were hydrolysed first and then unesterified fatty acids purified by TLC. 300 μ g fatty acid/ml medium (20 mM HEPES, 140 mM NaCl, 4.5 mM KCl, 1 mM MgCl₂, 2.5 mM CaCl₂, 11 mM glucose, 3.5 mg BSA, pH 7.4) was incubated overnight (16 h) at 37 °C under nitrogen. After incubation, the mixture was filtered through a Sartorius (0.2 μ m pore size) Minisart filter unit (Sartorius Ltd., Epsom KT19 9QQ, UK) to sterilise the solution and ensure that any unbound, excess, fatty acids were removed. GC analysis was

performed to quantify the fatty acid–BSA complex and was found necessary, as samples could vary significantly in concentration after sterile filtration. Samples were diluted appropriately to give the final concentrations of fatty acids needed for experiments. Controls had medium alone added to the cultures. All cultures were maintained for 8 h in the absence or presence of fatty acids to allow for uptake into cells and incorporation into membrane lipids. Control experiments showed that uptake of fatty acids over 8 h was proportional to the amount added [28].

After 8 h incubation, the cultures were carefully washed three times with DMEM without FCS and incubated further for 4 days in DMEM with or without 10 ng/ml IL-1 α .

Determination of Lactate and Glycosaminoglycan in the Culture Medium

Lactate production was used as a measure of the metabolic activity of viable chondrocytes under the different experimental conditions. The concentration of lactate in the culture medium was measured with a lactate assay kit (Sigma–Aldrich) used according to the manufacturer’s instructions. Proteoglycan content in the culture medium was measured as sulphated glycosaminoglycan using a 1,9-dimethylmethylene blue (DMMB) assay [29] with chondroitin sulphate C as standard.

Transesterification

Lipozyme 1M60 in an immobilised form was purchased from Novo Nordisk A/S (Bagsvaerd 2880, Denmark). Other dried-powder lipases (*Pseudomonas* sp. Lip LS, *Rhizopus delemar* Lip D, *Rhizopus oryzae* Lip F, *Candida lipolytica* LipAk, *Rhizopus niveus* Lip N, *Penicillium roqueforti* Lip R) were a kind gift from Amano Enzyme Inc. (Nagoya 460-8630, Japan). The lipases were used at 10% (g/g) with the substrate mixture (except when the effect of enzyme amount was tested) at 55 °C. 10 ml hexane/g substrate was used and transesterification carried out in capped glass vials for up to 24 h with reciprocal shaking in a water bath at 100 r.p.m. All experiments were carried out in triplicate. For the experiment where the re-use of the enzyme preparation was tested, the Lipozyme 1M60 was filtered from the reaction mixture with glass wool, washed twice with hexane and dried under vacuum before re-use.

Analysis of Lipids

Samples were taken from the esterification mixture and extracted by the method of Garbus et al. [30]. The extracted lipids were separated by TLC on pre-coated silica gel 60 plates (Merck, 64293 Darmstadt, Germany) using

petroleum ether/diethylether/acetic acid (80:20:1, by vol.) as solvent. Lipid bands were detected by spraying plates with 0.2% 8-anilino-4-naphthalene sulphonic acid and exposing to UV light. Lipid standards (Sigma–Aldrich) were used to identify the TAG, monoacylglycerol, diacylglycerol, non-esterified fatty acid and fatty acid methyl ester bands. Bands were scraped off and lipids methylated with 2.5% H₂SO₄ in dry methanol/toluene (2:1, v/v) for 2 h at 70 °C.

Fatty acid methyl esters were separated on a glass column (1.5 m \times 4 mm) packed with 10% SP-2330 on 100/120 Supelcoport (Supelco, Sigma–Aldrich) using a Perkin–Elmer Autosystem X2 gas chromatogram. FAMES were identified using standard mixtures (Nu-Chek) and quantification performed using Perkin–Elmer internal software and a pentadecanoate internal standard.

RT-PCR Reactions and Semi-Quantification of Message Levels

RNA was extracted from chondrocyte cultures using Tri-reagent and isolated using RNeasy minicolumns and reagents (Qiagen Ltd., Crawley RH10 9NQ, UK). Reverse transcription-polymerase chain reactions (RT-PCR) were performed using a RNA PCR core kit (Applied Biosystems, Warrington WA3 7QH, UK). Primers and the annealing temperatures used are listed in Table 1. Hot-start was used for the IL-1 α and TNF- α and cold-start for the others. Thirty-four cycles were used. The fidelity of the primers was confirmed by isolation of the reaction product on agarose gels (below) and sequencing.

Following PCR, the reaction products were size fractionated on 2% (w/v) agarose gels containing ethidium bromide. Bands were visualised under UV light, photographed and stored as image files for further analysis. Individual gels ($n = 3$) were scanned using Kodak Digital IB Image Analysis apparatus to provide densitometric values for each of the PCR products of interest. Densitometric values of PCR products to the genes of interest were normalised to the densitometric values obtained for GAPDH (used as a constitutive gene) from the same cDNA samples.

Results

Interesterification Conditions for Palm Olein and Methyl Linolenate

In order to find efficient conditions for the incorporation of n-3 fatty acids into palm olein, we began investigative studies by screening a number of lipases (see “[Experimental Procedures](#)”). Two lipases (from *Penicillium*

Table 1 Primers used for RT-PCR

Target template	PCR primer sequences (5'-3')	Product size for bovine product (bp)	Annealing temperature (°C)
GAPDH	5'-TGG ATCGTGGAAGGGCTCAT 5'-ATGGGAGTTGCTGTTGAAGTC	370	50.0
IL-1 α	5'-AAGGAGAATGTGGTGATGGTG 5'-CAGAAGAAGAGGAGGTTGGTC	470	53.2
IL-1 β	5'-GCTCTCCACCTCCTCTCACAG 5'-TACATTCTTCCCTTCCCTTCT	454	54.5
TNF- α	5'-CTCAAGCCTCAAGTAACAAGC 5'-GCAATGATCCCAAAGTAGACC	454	57.6
COX-2	5'-GCTCTTCCCTGTGCCTGAT 5'-CATGGTTCTTCCCTTAGTGA	229	52.3
ADAMTS-4	5'-TGGATCCTGAGGAGCCCTG 5'-TGGCGGTCAGCATCATAGTC	151	55.5

All products were verified by isolation on agarose gels and sequencing

roqueforti and *Rhizopus niveus*) showed low activity while three enzyme preparations (*Rhizopus miehei* Lipozyme 1M60, *Pseudomonas* sp. LipPS, *Rhizopus delemar* LipD) showed good activity (data not shown). Under standard conditions, all of the above three enzymes showed essentially complete equilibrium of palm olein with added methyl α -linolenate by the end of the reaction time with Lipozyme 1M60 giving a slightly higher percentage α -linolenate (48%) in the final triacylglycerol fraction. Because Lipozyme 1M60 was also an immobilized enzyme preparation, this was chosen for further use.

Varying the amount of Lipozyme 1M60 (with substrate) showed that a rapid equilibrium in lipid class composition (Fig. 1a) and also incorporation of α -linolenate into triacylglycerol (TAG) were reached with about 10 g enzyme prep./100 g substrates (Fig. 1b). Higher concentrations of enzyme did not increase the yield of TAG (Fig. 1a) nor its content of linolenate significantly (Fig. 1b) but led to elevated levels of free (un-esterified) fatty acids in the products (Fig. 1a), perhaps because of a residual amount of water in the immobilized enzyme preparation.

Examination of the reaction course showed that incorporation of α -linolenate into TAG was nearly complete after 30 min with only a small increase over the next 150 min (Fig. 1d). There was little change in the lipid class distribution over the first 2 h of incubation, apart from an initial release of unesterified fatty acids (Fig. 1c). The effect of temperature on the reaction in the range 40–80 °C was also examined. There was rather little change in the product composition over the range but the percentage of linolenate in the TAG fraction increased in the range 40–55 °C after which it plateaued (data not shown). The temperature of 55 °C was chosen for further incubations.

In order to modify a crude oil with a chosen fatty acid by interesterification, there is a trade-off between the cost

of the fatty acid and efficiency of its transfer into the TAG fraction. Examination of the effect of substrate ratio on lipid class distribution showed that, as expected, the final products reflected well the starting substrate ratio (Fig. 2a). Moreover, although there was a small increase in the percentage linolenate in the final TAG fraction on increasing the ratio of methyl linolenate: palm olein above 1:1 (Fig. 2b), the latter substrate ratio was efficient and a compromise with the potential cost of n-3 PUFA.

Although the initial experiments had been carried out using hexane as solvent, other solvents were checked for their efficiency. Twelve different solvents were tested (“[Experimental Procedures](#)”) and the more efficient ones in terms of TAG yield are shown in Table 2. Three other solvents gave yields of TAG which were comparable with that using hexane. These were acetone, petroleum ether and pentane. However, when the fatty acid composition of the final TAG product was analysed, then it was clear that little interesterification had taken place with acetone (Table 2). Since neither of the other two hydrocarbons showed any advantage to using hexane, the latter was used as the standard solvent throughout the research.

One possible advantage to using an immobilized enzyme preparation (certainly in commercial applications) would be that it has potential re-usability. Therefore, the enzyme activity of Lipozyme 1M60 was examined over a series of consecutive incubations (Table 3). Although the quality of the TAG product did not change noticeably, there was a steady decline in the amount of TAG yielded. This was mirrored by the increase of partial glycerides and unesterified fatty acids as the immobilised enzyme was re-used. However, although the yield of TAG declined, it was still present at high levels after three re-uses of the lipase preparation (Table 3).

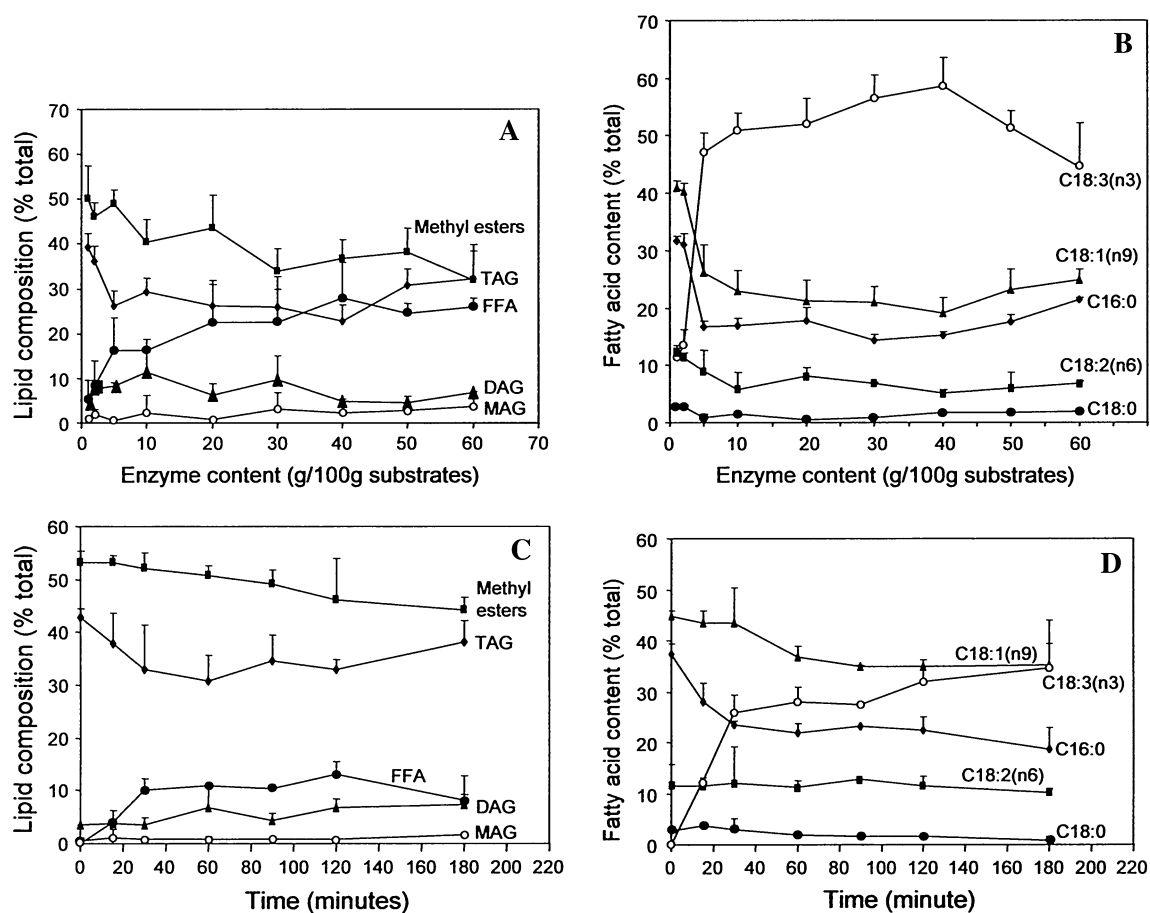


Fig. 1 Effect of enzyme concentration and incubation time on the reaction products following interesterification of palm olein with methyl linolenate. The figures show means \pm SD ($n = 3$) for lipid class distribution (a) and fatty acid composition of the TAG fraction (b) versus enzyme concentration, lipid class distribution (c) and fatty acid composition of the TAG fraction (d) versus incubation time.

Incubations were with Lipozyme 1M60 under conditions described in “Experimental Procedures” (except for changes in enzyme concentration or incubation time). TAG triacylglycerol, DAG diacylglycerol, MAG monoacylglycerol, FFA free (non-esterified) fatty acid, 16:0 palmitate, 18:0 stearate, 18:1 oleate, 18:2 linoleate, 18:3 α -linoleate

Interesterification with Eicosapentaenoate

Although α -linolenate is generally the major n-3 PUFA in human diets, it is not converted efficiently to the 20C precursor, EPA, for eicosanoid production [20]. Accordingly, most dietary advice suggests using eicosapentaenoate such as is found in oily fish or certain algae [1]. Since one of the major purposes of this work was to test the anti-inflammatory activity of modified palm oil, the interesterification reaction with EPA was also examined.

Lipozyme 1M60 proved to also interesterify efficiently with methyl EPA as the co-substrate. Incorporation of EPA into the TAG fraction of palm olein (Fig. 3b) was slower than that of linolenate (Fig. 1) but had still achieved values of 35% (total acids) by 3 h. The distribution of lipid classes in the products (Fig. 3a) was also similar to that found for transesterification with linolenate (Fig. 1). Other parameters for optimal enzyme activity were similar for the two

fatty acid substrates [28] and these standard incubation conditions were also used with EPA.

A large-scale preparation of palm olein TAG, containing EPA was made. The purified TAG fraction had a content of about 25% EPA (Table 4) and this preparation was used for the anti-inflammatory experiments.

In Vitro Model for Cytokine-Induced Cartilage Matrix Degradation in Arthritis

Monolayer cultures of bovine chondrocytes in the presence and absence of inflammatory cytokines are a useful test system with which to study inflammation in relation to osteoarthritis [26]. The chondrocytes can be easily stimulated by the inflammatory cytokine interleukin-1 α which increases transcription and activity of inflammatory mediators, prostaglandins, cytokines and cartilage matrix-degrading proteinases.

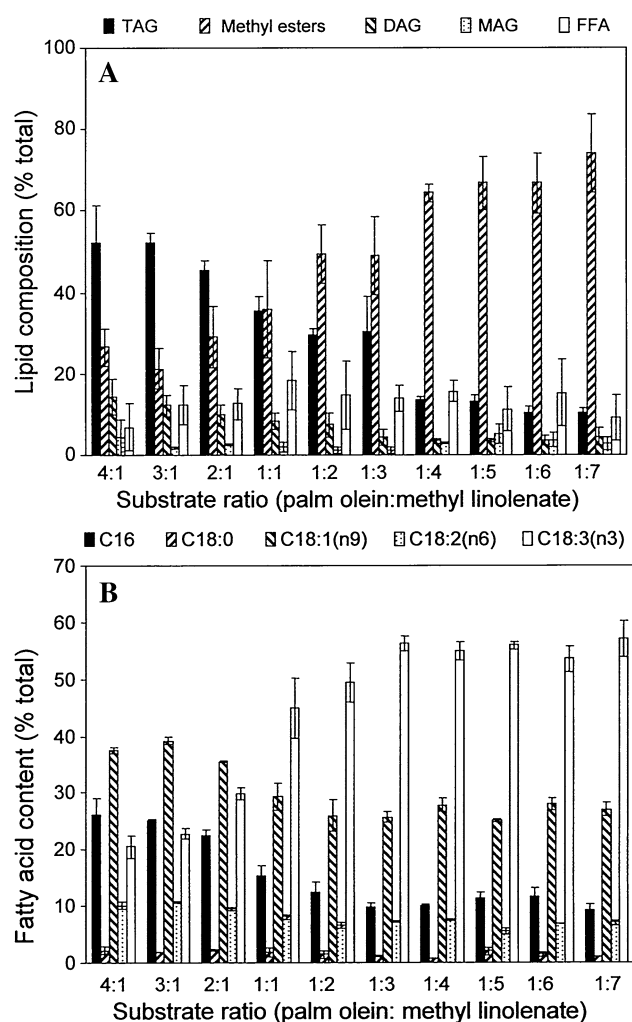


Fig. 2 Effect of substrate ratio on the reaction products and incorporation of linolenate into triacylglycerol. Lipid classes (a) were separated by TLC following incubation under standard conditions apart from changes in the ratio of substrates (palm olein, methyl α -linolenate). The fatty acid composition of the isolated TAG fraction is shown in (b). Means \pm SD ($n = 3$) shown. TAG triacylglycerol, DAG diacylglycerol, MAG monoacylglycerol, FFA free (non-esterified) fatty acid, 16:0 palmitate, 18:0 stearate, 18:1 oleate, 18:2 linoleate, 18:3 α -linoleate

In order to monitor cell viability and metabolism the cultures were examined by light microscopy and lactate production measured. The latter test can be used routinely to examine the metabolic state of the cells in such culture systems. Typical results are displayed in Fig. 4a. Lactate production was increased in all cultures by the addition of interleukin-1 α and this rise was not altered by previous incubation of the cultures with any of the fatty acid preparations up to 30 μ g/ml. The three fatty acid preparations (from palm olein, modified palm olein or EPA itself) did not have any effect on lactate production when they alone were added to control cultures. This showed that overall cell viability and metabolism was not affected by addition of the fatty acid preparation.

Table 2 Effect of solvent on the products of interesterification

	H	A	PE	B	T	P
Lipid class products (%)						
TAG	34 \pm 3	37 \pm 5	34 \pm 3	28 \pm 10	21 \pm 2	34 \pm 3
DAG	8 \pm 2	7 \pm 2	14 \pm 6	13 \pm 1	11 \pm 1	12 \pm 6
MAG	2 \pm 3	2 \pm 1	3 \pm 2	7 \pm 2	2 \pm 2	2 \pm 2
FFA	19 \pm 4	27 \pm 2	20 \pm 6	10 \pm 3	22 \pm 3	15 \pm 3
Methyl esters	37 \pm 2	27 \pm 3	29 \pm 6	42 \pm 4	44 \pm 5	37 \pm 3
TAG fatty acids (%)						
16:0	18 \pm 4	32 \pm 12	17 \pm 1	29 \pm 4	14 \pm 2	15 \pm 3
18:0	2 \pm tr	3 \pm 1	2 \pm 1	5 \pm 3	2 \pm tr	2 \pm 1
18:1	25 \pm 4	45 \pm 9	26 \pm 3	48 \pm 3	31 \pm 1	25 \pm 3
18:2	7 \pm 1	11 \pm 2	8 \pm 1	9 \pm 3	9 \pm tr	7 \pm 2
18:3	48 \pm 10	8 \pm 3	47 \pm 3	9 \pm 4	44 \pm 2	51 \pm 3

Results show means \pm SD ($n = 3$). Incubations were carried out under standard conditions for 24 h with different solvents substituting for hexane

H hexane, A acetone, PE petroleum ether (60–80° fraction), B butanol, T toluene, P pentane, TAG triacylglycerol, DAG diacylglycerol, MAG monoacylglycerol, FFA free (non-esterified) fatty acid, 16:0 palmitate, 18:0 stearate, 18:1 oleate, 18:2 linoleate, 18:3 α -linoleate, trace less than 0.5%

Table 3 Effect of enzyme re-use on product quality

Enzyme use	Lipid class distribution (% total)				
	TAG	DAG	MAG	ME	FFA
1	45 \pm 4	4 \pm 4	Trace	45 \pm 3	6 \pm 1
2	36 \pm 6	10 \pm 8	1 \pm 1	44 \pm 4	9 \pm 4
3	32 \pm 4	8 \pm 2	2 \pm tr	43 \pm 4	15 \pm 4
Fatty acid composition of TAG (% total acids)					
	16:0	18:0	18:1	18:2	18:3
1	15 \pm 10	2 \pm 1	40 \pm 6	8 \pm 3	35 \pm 8
2	20 \pm 2	3 \pm 1	35 \pm 2	9 \pm tr	32 \pm 4
3	15 \pm 1	2 \pm tr	35 \pm 2	9 \pm 1	39 \pm 3

Results show means \pm SD ($n = 3$). Incubations were carried out under standard conditions for 24 h

TAG triacylglycerol, DAG diacylglycerol, MAG monoacylglycerol, ME methyl esters, FFA free (non-esterified) fatty acid, 16:0 palmitate, 18:0 stearate, 18:1 oleate, 18:2 linoleate, 18:3 α -linoleate, trace less than 0.5%

Modified Palm Olein Reduces mRNA Levels for 'Inflammatory' Proteins

RT-PCR was used to examine whether the modified palm olein was able to show any anti-inflammatory properties when tested for its ability to reduce the expression of enzymes or proteins known to be involved in cartilage

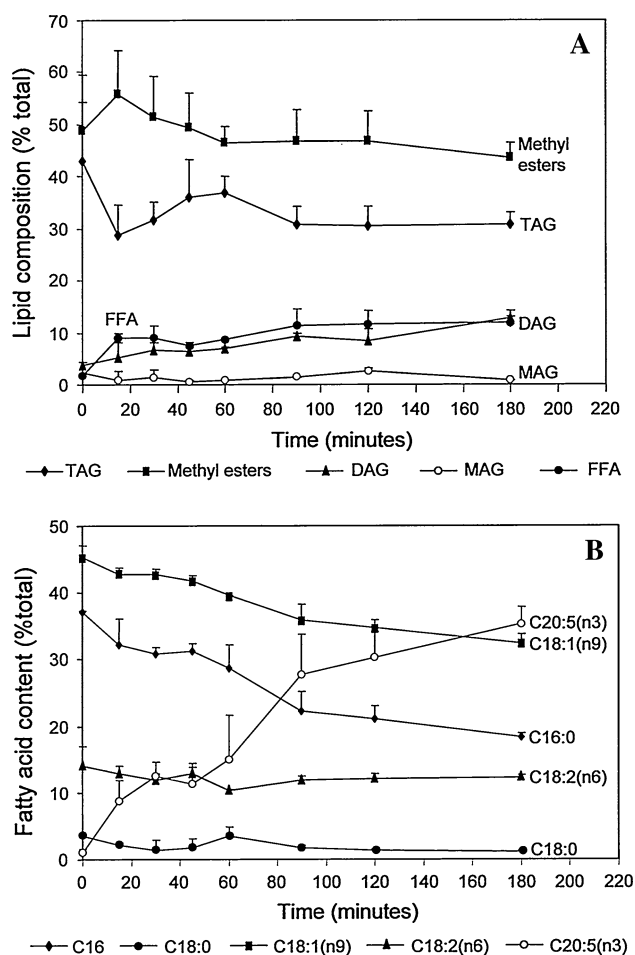


Fig. 3 Time-course for the incorporation of eicosapentaenoic acid into palm olein triacylglycerol by the action of Lipozyme IM60. EPA n-3 eicosapentaenoic acid. **a** Shows the reaction product distribution with incubation time and **b** Shows the change in TAG composition with time. Standard incubation conditions were used (“[Experimental Procedures](#)”) and means + SD ($n = 3$) are shown

matrix degradation during the pathogenesis of degenerative joint diseases; e.g. osteoarthritis.

We tested the action of the three fatty acid mixtures on the mRNA levels for cyclooxygenase-2 (COX-2, the inducible cyclooxygenase activity present in inflamed joints) and ADAMTS-4 (a disintegrin and metalloproteinase with

thrombospondin motifs, aggrecanase-1), which is one of the primary candidate enzymes believed to be responsible for aggrecan degradation in cartilage pathology (Fig. 5).

COX-2 mRNA levels were barely detectable in control cells, as expected for samples obtained from young, (healthy) joint tissue (Fig. 5a). However, COX-2 expression was clearly stimulated by the pro-inflammatory cytokine interleukin-1 α (IL-1 α). Pre-incubation of cultures with palm olein had no effect on the IL-1 α induced levels. In contrast, the modified palm olein was able to reduce COX-2 mRNA levels progressively with increasing concentrations of fatty acids. By 20 or 30 μ g/ml of the modified palm olein, the mRNA band for COX-2 was barely detectable. As expected, EPA was somewhat more effective with very low levels of the mRNA at 10 μ g/ml.

ADAMTS-4 expression was increased markedly by IL-1 α treatment and there was no obvious reduction in this by palm olein. However, again, both modified palm olein and EPA itself were able to reduce mRNA expression levels for ADAMTS-4 so that there was none detectable with modified palm olein at 30 μ g/ml and none at 20 μ g EPA/ml (Fig. 5b).

The expression of mRNA for a number of inflammatory cytokines was also monitored. Results for three of these (IL-1 α , IL-1 β and TNF- α) are shown in Fig. 6. Endogenous expression of IL-1 α by the cells was undetectable until they were stimulated by exogenous cytokine (Fig. 6a). The induced level of mRNA was unaffected by palm olein but reduced to undetectable levels by 20–30 μ g modified palm olein/ml or by 10–30 μ g EPA/ml. Similarly, IL-1 β mRNA was also induced by exogenous IL-1 α and this induction was reversed to very low levels by 30 μ g modified palm olein/ml or 20–30 μ g EPA/ml (Fig. 6b).

When tumour necrosis factor- α (TNF- α) was examined, exogenous IL-1 α induced detectable mRNA levels which were again unaffected by pre-incubation with palm olein. However, the modified palm olein was clearly able to reduce mRNA levels so that they were barely detectable at 30 μ g/ml. EPA reduced the TNF- α mRNA to very low levels at 10 μ g/ml (Fig. 6c).

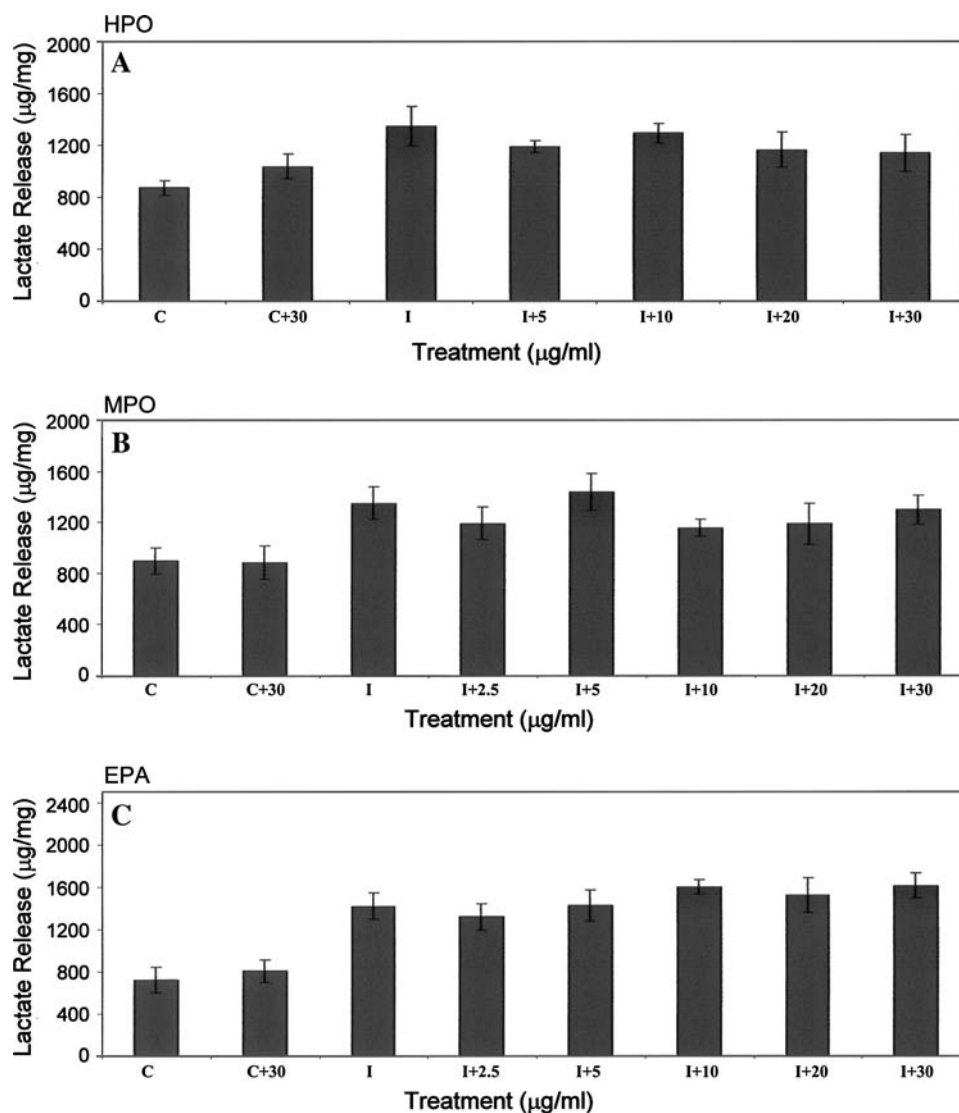
Table 4 Fatty acid composition of the palm olein triacylglycerols used for anti-inflammatory testing in chondrocyte culture systems

	Fatty acid composition (% total)						
	14:0	16:0	18:0	18:1	18:2	18:3	20:5
Palm olein	1.1 \pm 0.4	36.8 \pm 1.2	3.2 \pm 0.2	44.6 \pm 0.2	13.7 \pm 0.9	0.6 \pm 0.3	n.d.
Modified palm olein	0.3 \pm 0.1	27.9 \pm 1.6	2.9 \pm 0.8	35.0 \pm 2.6	8.6 \pm 4.4	0.2 \pm 0.1	25.2 \pm 7.4

Data as means \pm SD ($n = 3$). TAG fractions were purified by T.L.C and analysed further by G.L.C. (see “[Experimental Procedures](#)”)

n.d. not detected, 14:0 myristate, 16:0 palmitate, 18:0 stearate, 18:1 oleate, 18:2 linoleate, 18:3 α -linoleate, trace less than 0.5%, 20:5 n-3 eicosapentaenoate

Fig. 4 Test for monolayer chondrocyte viability and metabolism. Lactate release into the culture medium during the incubation is shown. Means \pm SD ($n = 3$) are displayed. The culture medium was supplemented with fatty acids ($\mu\text{g/ml}$) for 8 h before washing and continuing the incubation for 4 days in the presence (I) or absence (C) of interleukin-1 α . EPA eicosapentaenoate, MPO modified palm olein, HPO hydrolysed palm olein



Discussion

Palm oil is the world's most abundant edible oil and huge quantities are exported from Indonesia and Malaysia [1]. However, there is a perceived need to diversify the fatty acyl quality of the oil [4]. One area would be to modify palm oil for added nutritional value and, with the increasing interest in n-3 s, this is one aspect where an obvious market exists. By incorporating n-3 fatty acids into palm oil by interesterification, one can produce a product which also has the good anti-oxidant properties of palm oil (e.g. with high β -carotene and vitamin E contents [31–33]).

We have shown that it is possible to modify palm olein by the incorporation of up to 50% of its fatty acids with either of the n-3 fatty acids, α -linolenate or EPA. A lipase from *Rhizomucor miehei* (Lipozyme 1M60) was the most effective of the seven lipases tested which also agreed with

recent reported data [34]. Lipozyme 1M60 is *sn*-1,3-specific so that, in theory, the *sn*-2 position of palm olein should not be involved in acyl exchange. However, it is well known that some acyl groups at the *sn*-2 position are always exchanged [1] and, indeed, the fatty acid compositions of modified palm olein (Table 4) would bear out this conclusion since the *sn*-2 position of palm oil is enriched in unsaturated acids (especially linoleate) [1]. Nevertheless, enrichment of the modified oil with n-3 fatty acids at the *sn*-1 and *sn*-3 positions might have a nutritional advantage since pancreatic lipase also shows specificity for the primary acyl esters [35].

Among many regioselective lipases tested for their ability to incorporate fatty acids into triacylglycerols, the best consistent results have been obtained with lipases from *Rhizomucor miehei* (such as Lipozyme 1M60), *Rhizopus delamar* and *Candida antarctica* [36, 37]. Lipozyme 1M60

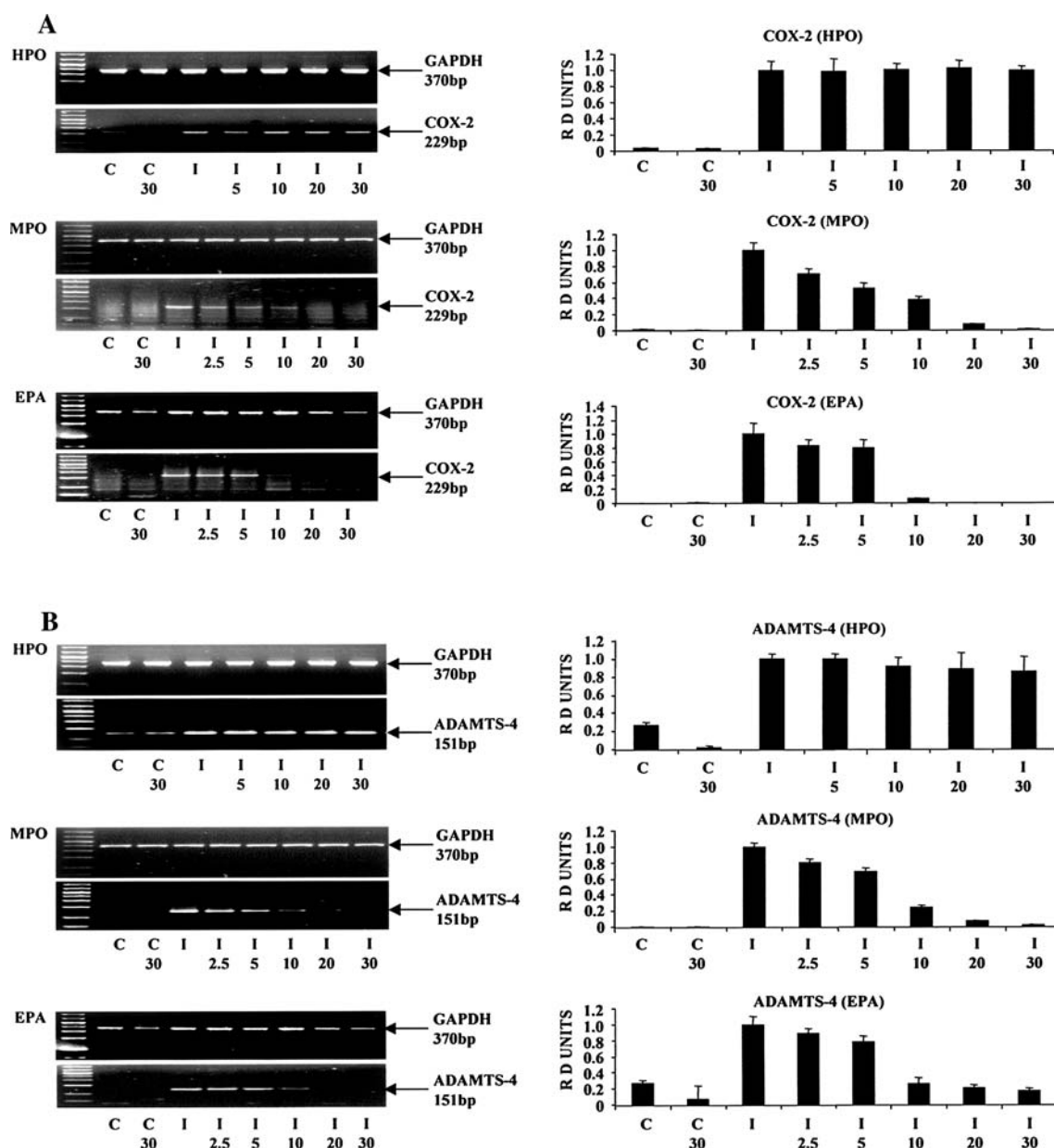


Fig. 5 Changes in mRNA levels for cyclooxygenase-2 (a) and ADAMTS-4 (b) in bovine monolayer cultures following exposure to interleukin-1 α and lipid preparations. The activity of EPA (eicosapentaenoic acid) and modified palm olein (MPO) are compared with those of hydrolysed palm olein (HPO). The culture medium was supplemented with fatty acids ($\mu\text{g}/\text{ml}$) for 8 h before washing and continuing the incubation for 4 days in the presence (I) or absence (C) of interleukin-1 α . For incubation details see “[Experimental](#)

[Procedures](#)”. Representative gel scans are shown and the histograms show semi-quantitative, relative, mRNA levels (means \pm SD) for three separate experiments [RD (arbitrary relative density) Units] corrected for gel loading by GAPDH mRNA levels. Control incubations (no cytokine) are indicated with C. Incubations in the presence of 10 ng/ml IL-1 α are labelled I. The amount of fatty acid added is shown in $\mu\text{g}/\text{ml}$

has been used extensively for the incorporation of n-3 fatty acids into edible oils [38–40] due to its high activity and temperature stability [41].

The reaction characteristics for interesterification were typical of other lipase-catalysed procedures [42–44]. The lipase used was stable to high temperatures, worked well with equal proportions of the substrates and preferred non-

polar solvents. Akoh and Huang [45] also showed that Lipozyme 1M60 gave good yields with hexane as solvent but poor incorporation with acetone (see Table 1). Other immobilised lipases have also been reported to prefer non-polar solvents [46]. While small amounts of water are needed for interesterification, it is known that it is necessary to carefully control quantities for efficient reactions

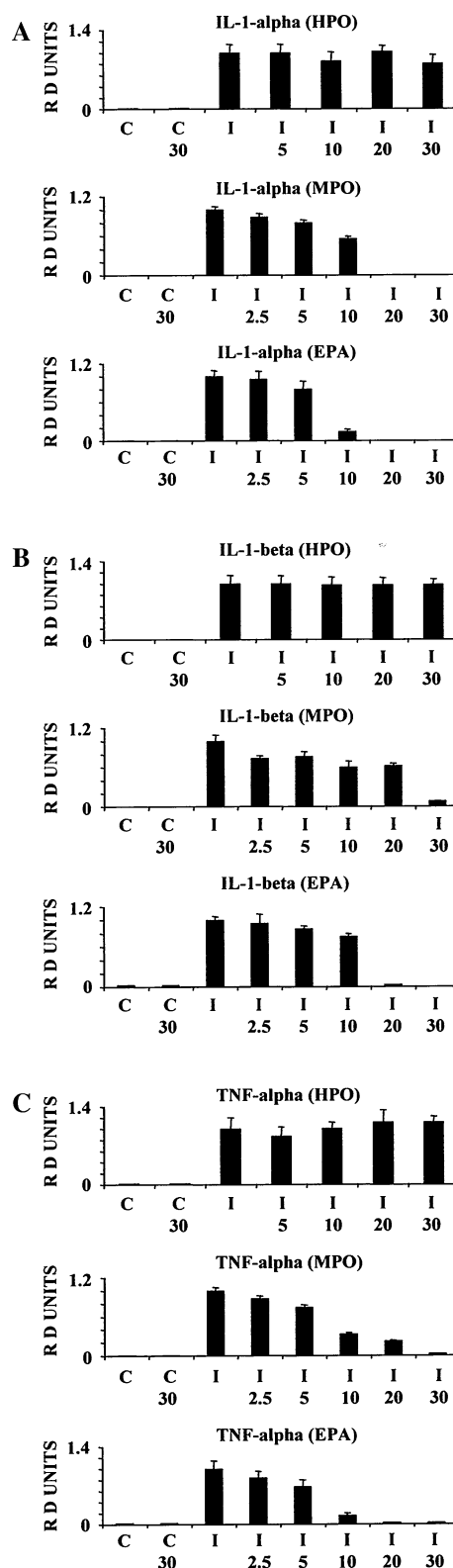
Fig. 6 Changes in mRNA levels for interleukin-1 α (a), interleukin-1 β (b) or TNF- α (c) in bovine monolayer cultures following exposure to interleukin-1 α and lipid preparations. The culture medium was supplemented with fatty acids ($\mu\text{g/ml}$) for 8 h before washing and continuing the incubation for 4 days in the presence (I) or absence (C) of interleukin-1 α . Incubation details are given in “Experimental Procedures”. Histograms show semi-quantitative, relative, mRNA levels (means \pm SD) for three separate experiments corrected for gel loading by GAPDH mRNA levels. EPA eicosapentaenoate, MPO modified palm olein, HPO hydrolysed palm olein

[47]. Indeed, the appreciable amounts of non-esterified fatty acids and partial glycerides which were found in some of our reactions can be attributed to the presence of water in the incubations. This water content would be increased successively during re-use of the immobilised enzyme [48] and the results of this were clearly seen in Table 3 where the yield of TAG decreased and that of the hydrolysis products increased with re-use.

Under the reaction conditions utilised, we were able to incorporate up to 52% α -linolenate and 45% EPA into the TAG fraction. In similar experiments for the modification of palm oil, Fajardo et al. [40] also used Lipozyme 1M60 but, despite using a higher ratio of n-3 PUFA to TAG, only obtained average incorporations of 21% EPA (and 16% docosahexaenoate) in their studies. Others have used different immobilised lipase preparations to incorporate n-3 PUFA into vegetable oils. Huang and Akoh [36] found a *Mucor miehei* (1,3-specific) lipase to be more efficient than that from *Candida antarctica* (non-specific) for the incorporation of EPA or DHA into soybean oil. However, when ethyl esters of EPA or DHA were used then the lipase from *C. antarctica* was more efficient.

The chondrocyte cell culture system used to test for anti-inflammatory properties of exogenous lipids has been well utilised as a model system to follow aspects of cartilage matrix degradation in degenerative joint disease; e.g. osteoarthritis. In these cultures, challenge with interleukin-1 α has been shown to up-regulate inflammatory mediators and cartilage-degrading proteinases [26]. While palm olein had virtually no effect on the IL-1 induced increases in mRNA levels for COX-2, ADAMTS-4, IL-1 α or IL-1 β or TNF- α , EPA was able to reduce these significantly when cultures were subsequently challenged with IL-1 α to induce an inflammatory response. This may be due to a direct effect of the n-3 PUFA on gene expression [49, 50] or indirectly through a change in the balance of eicosanoids [51] or other lipid mediators, such as E-series resolvins [52]. The anti-inflammatory properties of n-3 PUFA have been well-studied through feeding experiments and include their effects on cytokine release [e.g. 16].

The modified palm olein (containing about 25% EPA) was also able to reduce inflammatory responses in the chondrocyte culture system, as measured by lower levels of mRNA for ‘inflammatory’ proteins. These data indicate



that the nutritional properties of palm oil should be significantly enhanced by the incorporation of EPA into the TAG fraction. It would seem better to use EPA rather than

α -linolenate for this purpose because EPA has been shown to be more biologically potent than linolenate [19]. This would also agree with deductions from feeding studies [20] and with the fact that EPA can be converted directly to eicosanoids [21]. The effects of EPA on COX-2 (but not COX-1) [28] mRNA are also timely in that specific COX-2 inhibitors, which showed much promise for the treatment of chronic inflammatory diseases, have had to be withdrawn recently from pharmaceutical use [53].

Our results therefore reinforce information from epidemiological and clinical surveys that have shown significant benefits for the use of dietary n-3 fatty acids for the treatment of inflammation and pain in human arthritic disease [54, 55]. They also show that palm oil may be modified conveniently to produce a nutraceutical with effective anti-inflammatory properties.

Acknowledgments The authors acknowledge grant support from the Biotechnology and Biological Sciences Research Council (D16961) and a studentship provided by the Malaysian Palm Oil Board, for which we are grateful.

References

- Gunstone FD, Harwood JL, Dijkstra AJ (eds) (2007) The lipid handbook, 3rd edn. Taylor and Francis, Boca Raton
- Gunstone FD (2006) Fats and oils forecast. *Inform* 17:667–669
- Basiron Y (2007) Palm oil production through sustainable plantations. *Eur J Lipid Sci Technol* 109:289–295
- Murphy DJ (2007) Future prospects for oil palm in the 21st century: biological and related challenges. *Eur J Lipid Sci Technol* 104:296–306
- Lands WEM (2005) Fish, omega-3 and human health, 2nd edn. AOCS Press, Champaign
- Harwood JL, Caterson B (2006) Dietary omega-3 polyunsaturated fatty acids and inflammation. *Lipid Technol* 18:7–10
- Calder PC, Knapp HR (eds) (2004) Lipids as determinants of cell function and human health. Proceedings of the 6th Congress of ISSFAL. *Lipids* 39:1045–1247
- Bordoni A, Astolfi A, Morandi L, Pession A, Danesi F et al (2007) n-3 s modulate global gene expression profile in cultured rat cardiomyocytes. Implications in cardiac hypertrophy and heart failure. *FEBS Lett* 581:923–929
- Massaro M, Habib A, Lubrano L, Del Turco S, Lazzarini G et al (2006) The omega-3 fatty acid docosahexaenoate attenuates cyclooxygenase-2 induction through both NADP(H) oxidase and PKC ϵ inhibition. *Proc Natl Acad Sci USA* 103:15184–15189
- Connor WE (2000) Importance of n-3 fatty acids in health and disease. *Am J Clin Nutr* 71:171–175
- Kremer JM (2000) n-3 Fatty acid supplements in rheumatoid arthritis. *Am J Clin Nutr* 71:349–351
- Percival T (1783) Observations on the medicinal uses of oleum jecoris aselli, or cod liver oil, in the chronic rheumatism and other painful disorders. *Lond Med J* 3:393–401
- Panash P (1983) Diet therapy for rheumatoid arthritis. *Arthritis Rheum* 26:462–471
- Simopoulos AP (1991) Omega-3 fatty acids in health and disease and in growth and development. *Am J Clin Nutr* 54:438–463
- Okuyama H, Kohayashi T, Watanabe S (1997) Dietary fatty acids—the n6/n3 balance and chronic elderly diseases. *Prog Lipid Res* 35:409–457
- Calder PC (1998) Immunoregulatory and antiinflammatory effects of n-3 polyunsaturated fatty acids. *Braz J Med Biol Res* 31:467–490
- Simopoulos AP (1999) Essential fatty acids in health and chronic disease. *Am J Clin Nutr* 70:560–569
- Calder PC (2001) n-3 Polyunsaturated fatty acids, inflammation and immunity: pouring oil on troubled waters or another fishy tale? *Nutr Res* 21:309–341
- Simopoulos AP (2001) Omega-3 fatty acids in inflammation and autoimmune diseases. *J Am Coll Nutr* 21:495–505
- Cunnane SC (2003) Problems with essential fatty acids: time for a new paradigm? *Prog Lipid Res* 42:544–568
- Calder PC (2004) n-3 Fatty acids and cardiovascular disease: evidence explained and mechanisms explored. *Clin Sci* 107:1–11
- Calder PC (2005) Polyunsaturated fatty acids and inflammation. *Biochem Soc Trans* 33:409–457
- Wu G, Truksa M, Datla N, Vrinten P, Bauer J et al (2005) Stepwise engineering to produce high yields of very long-chain polyunsaturated fatty acids in plants. *Nat Biotechnol* 23:1013–1017
- Qi B, Frazer T, Mugford S, Dobson G, Sayanova O et al (2004) Production of very long chain polyunsaturated omega-3 and omega-6 fatty acids in plants. *Nat Biotechnol* 22:739–745
- Aidos I, van der Padt A, Luten JB, Boom RM (2002) Seasonal changes in crude and lipid composition of herring fillets, byproducts and respective produced oils. *J Agric Food Chem* 50:4589–4599
- Caterson B, Flannery CR, Hughes CE, Little CB (2000) Mechanisms involved in cartilage proteoglycan metabolism. *Matrix Biol* 19:333–344
- Little CB, Hughes CE, Curtis CL, Janus M, Bohne R et al (2002) Matrix metalloproteinases are involved in C-terminal and interglobular domain processing of cartilage aggrecan in late stage cartilage degradation. *Matrix Biol* 21:271–288
- Zainal Z (2005) How can palm oil be modified to give improved dietary benefits? Ph.D. thesis. Cardiff University, UK
- Farndale RW, Buttle DJ, Barrett AJ (1986) Improved quantification and discrimination of sulphated glycosaminoglycans by use of dimethylmethylene blue. *Biochim Biophys Acta* 883:173–177
- Garbus J, De Luca HF, Loomans ME, Strong FM (1963) The rapid incorporation of phosphate into mitochondrial lipids. *J Biol Chem* 238:59–63
- Choo MY (1994) Palm oil carotenoids. *Food Nutr Bull* 15:1–13
- Chandrasekharan NCT (2002) The palm oil debate—health considerations. Malaysian Medical Association. www.mma.org.my/info/1_palm_88.htm
- Mayamol PN, Balachandran C, Samuel T, Sundaresan A, Arumughan C (2007) Process technology for the production of micronutrient rich red palm olein. *J Am Oil Chem Soc* 84:587–596
- Hamam F, Shakidi F (2007) Enzymatic incorporation of selected long-chain fatty acids into triolein. *J Am Oil Chem Soc* 84:533–541
- Jensen RG (1971) Lipolytic enzymes. *Prog Chem Fats Other Lipids* 11:347–394
- Huang KH, Akoh CC (1994) Lipase-catalysed incorporation of n-3 polyunsaturated fatty acids into vegetable oils. *J Am Oil Chem Soc* 71:1277–1280
- Soumanou MM, Bornscheuer UT, Schmid RD (1998) Two-step enzymatic reaction for the synthesis of pure structured triacylglycerides. *J Am Oil Chem Soc* 75:703–710
- Senanoyake SPI, Shahidi F (2002) Structured lipids via lipase-catalysed incorporation of eicosapentaenoic into borage and evening primrose oils. *J Agric Food Chem* 50:477–483
- Xu X, Skands ARC, Hoy C-E, Mu H, Balchen S et al (1998) Production of specific-structured lipids by enzymatic interesterification: elucidation of acyl migration by response surface design. *J Am Oil Chem Soc* 75:1179–1186

40. Fajardo AR, Akoh CC, Lai OM (2002) Lipase-catalysed incorporation of n-3 PUFA into palm oil. *J Am Oil Chem Soc* 80:1197–1200
41. Bornscheuer UT, Adamczak M, Soumanou MM (2003) Lipase-catalysed synthesis of modified lipids. In: Gunstone FD (ed) *Lipids for functional foods and nutraceuticals*. Oily Press, Bridgwater, pp 149–182
42. Beisson F, Tiss A, Riviere C, Verger R (2000) Methods for lipase detection and assay: a critical review. *Eur J Lipid Sci Technol* 1:133–153
43. Hayes DG (2004) Enzyme-catalyzed modification of oilseed materials to produce eco-friendly products. *J Am Oil Chem Soc* 81:1077–1103
44. Schmid U, Bornscheuer UT, Soumanou MM, McNeill GP, Schmid RD (1998) Optimization of the reaction conditions in the lipase-catalyzed synthesis of structured triglycerides. *J Am Oil Chem Soc* 75:1527–1531
45. Akoh CC, Huang KH (1995) Enzymatic synthesis of structured lipids: transesterification of triolein and caprylic acid. *J Food Lipids* 2:219–230
46. Guncheva M, Zhiryakova D, Radchenkova N, Kabourova M (2008) Acidolysis of tripalmitin with oleic acid catalyzed by a newly isolated thermostable lipase. *J Am Oil Chem Soc* 85:129–132
47. Rozendaal A, Macrae AR (1997) Interesterification of oils and fats. In: Gunstone FD, Padley FB (eds) *Lipid technologies and applications*. Marcel Dekker, New York, pp 223–264
48. Diks RMM (2000) Lipase stability in oil. *Lipid Technol* 14:10–14
49. Clarke SD (2001) Polyunsaturated fatty acid regulation of gene transcription: a molecular mechanism to improve the metabolic syndrome. *J Nutr* 131:1129–1132
50. Jump DB (2002) The biochemistry of n-3 polyunsaturated fatty acids. *J Biol Chem* 277:8753–8758
51. Gurr MI, Harwood JL, Frayn KN (2002) *Lipid biochemistry*, 5th edn. Blackwell, Oxford
52. Serhan CN, Gotlinger K, Hong S, Arita M (2004) Resolvins, docosatrienes and neuroprotectins, novel omega-3-derived mediated mediators and their aspirin-triggered endogenous epimers: an overview of their protective roles in catabasis. *Prostaglandins Other Lipid Mediat* 73:155–172
53. Drazen JM (2005) A lesson in unexpected problems. *New Engl J Med* 352:1131–1132
54. Cleland LG, James MJ (2001) Fish oil and rheumatoid arthritis: anti-inflammatory and collateral health benefits. *J Rheumatol* 27:2305–2307
55. Calder PC, Zurier RB (2001) Polyunsaturated fatty acids and rheumatoid arthritis. *Curr Opin Clin Nutr Metab Care* 4:115–121

Effects of Dietary Coconut Oil on the Biochemical and Anthropometric Profiles of Women Presenting Abdominal Obesity

Monica L. Assunção · Haroldo S. Ferreira ·
Aldenir F. dos Santos · Cyro R. Cabral Jr ·
Telma M. M. T. Florêncio

Received: 12 September 2008 / Accepted: 22 April 2009 / Published online: 13 May 2009
© AOCS 2009

Abstract The effects of dietary supplementation with coconut oil on the biochemical and anthropometric profiles of women presenting waist circumferences (WC) >88 cm (abdominal obesity) were investigated. The randomised, double-blind, clinical trial involved 40 women aged 20–40 years. Groups received daily dietary supplements comprising 30 mL of either soy bean oil (group S; $n = 20$) or coconut oil (group C; $n = 20$) over a 12-week period, during which all subjects were instructed to follow a balanced hypocaloric diet and to walk for 50 min per day. Data were collected 1 week before (T1) and 1 week after (T2) dietary intervention. Energy intake and amount of carbohydrate ingested by both groups diminished over the trial, whereas the consumption of protein and fibre increased and lipid ingestion remained unchanged. At T1 there were no differences in biochemical or anthropometric characteristics between the groups, whereas at T2 group C presented a higher level of HDL (48.7 ± 2.4 vs. 45.00 ± 5.6 ; $P = 0.01$) and a lower LDL:HDL ratio (2.41 ± 0.8 vs. 3.1 ± 0.8 ; $P = 0.04$). Reductions in BMI

were observed in both groups at T2 ($P < 0.05$), but only group C exhibited a reduction in WC ($P = 0.005$). Group S presented an increase ($P < 0.05$) in total cholesterol, LDL and LDL:HDL ratio, whilst HDL diminished ($P = 0.03$). Such alterations were not observed in group C. It appears that dietetic supplementation with coconut oil does not cause dyslipidemia and seems to promote a reduction in abdominal obesity.

Keywords Medium chain fatty acids · Lauric acid · Dyslipidemia

Abbreviations

BMI	Body mass index
BMR	Basal metabolic rate
CVD	Cardiovascular disease
LCFA	Long chain fatty acids
MCFA	Medium chain fatty acid
SFA	Saturated fatty acid
TC	Total cholesterol
TEV	Total energy value
UFA	Unsaturated fatty acid
US-CRP	Ultra-sensitive C reactive protein
WC	Waist circumference

This article based in part on the Master's Dissertation of M.L. Assunção, presented to the Faculdade de Nutrição, Universidade Federal de Alagoas, Maceió, AL, Brazil, in 2007. A summary of the paper was presented at the IX Congresso Nacional da Sociedade Brasileira de Alimentação e Nutrição, São Paulo, SP, Brazil, 2007.

M. L. Assunção · H. S. Ferreira (✉) · C. R. Cabral Jr ·
T. M. M. T. Florêncio
Faculdade de Nutrição, Universidade Federal de Alagoas,
Maceió, AL 57072-970, Brazil
e-mail: haroldo.ufal@gmail.com

A. F. dos Santos
Faculdade de Ciências Biológicas e da Saúde, Fundação Jayme
de Altavila, Maceió, AL 57051-160, Brazil

Introduction

In many countries obesity has reached epidemic levels, representing a serious public health problem and a matter of considerable concern for government and health services. In Brazil, the prevalence of obesity has risen from 5.7 to 10.8% of the adult population within the last 30 years, and currently 40.5% of adults are considered to

be overweight. Although dramatic increases in average body weight have affected the entire socioeconomic strata, they have been proportionally greater amongst poor women [1, 2].

Obesity results from a positive energy balance that leads to the accumulation of body fat at various anatomical sites. If fat accumulation occurs predominantly in the abdominal region the condition is known as visceral obesity, a factor that is strongly associated with increased risk of cardiovascular diseases (CVDs) [3]. The type of fat provided by the diet influences the incidence of obesity and also plays a significant role in the aetiology of various metabolic disorders including dyslipidemia [4]. Although many theories concerning the types of fatty acids that are beneficial or deleterious to health are contentious, it is generally considered that saturated fatty acids (SFAs) are hypercholesterolemic whereas unsaturated fatty acids (UFAs) are hypocholesterolemic [5].

Oil from coconuts (*Cocos nucifera* L.) contains a high proportion of medium chain fatty acids (MCFAs), principally the SFA lauric acid (12:0), in proportions that range from 45 to 50% [6]. A possible association between dietary intake of coconut oil and the incidence of CVDs was suggested four decades ago following studies carried out by the food industry involving hydrogenation of the oil and modification of some of the UFAs present, particularly oleic and linoleic acids. On the basis that the harmful effects of coconut oil observed in experimental animals resulted from the hydrogenation of UFAs, health professionals began to recommend the replacement of coconut oil by UFA-rich soy bean (*Glycine max* L.) oil [7]. However, studies involving African and South Pacific populations, whose diets contain large proportions of coconut oil (80% of daily lipid intake), have revealed that there is no association between the ingestion of coconut oil and the occurrence of obesity and/or dyslipidemia [8–10]. Additionally, coconut oil is frequently used in the treatment of obesity by virtue of its high content of MCFAs [11], since such lipids are easily oxidised and are not normally stored in the adipose tissue, thus diminishing the basal metabolic rate (BMR). However, the use of coconut oil in the diet remains controversial owing to the possible detrimental effects of SFAs and their association with dyslipidemia and CVDs [4, 12, 13].

Obesity is a particularly serious problem in the State of Alagoas, which is located in the north-east of Brazil and is a major producer of coconut oil. Considering the lack of evidence concerning the physiological effects of intake of coconut oil, the aim of the present study was to investigate the effects of dietary supplementation with coconut oil on the biochemical and anthropometric profiles of a population of women of low socioeconomic status living in Alagoas and suffering from abdominal obesity.

Materials and Methods

Study Design and Subjects

The project of work was submitted to and approved by the Ethical Committee in Research of the Faculdade de Ciências Biológicas e da Saúde, Fundação Educacional Jayme de Altavila, Maceió, AL, Brazil. Written informed consent was obtained from all participants prior to the commencement of the study.

The study took the form of a randomised, double-blind, clinical trial involving 40 women selected from those attending an outpatients unit located in Marechal Deodoro, AL, Brazil. The selection criteria were: (1) age between 20 and 40-years-old, (2) low socioeconomic status (per capita family income <USD\$1/day), and (3) presenting abdominal obesity as defined by waist circumference (WC) >88 cm [14]. Pregnant women were excluded from the selection, as were subjects presenting arterial hypertension, chronic degenerative diseases, endocrinopathies or body mass index (BMI) >35 kg/m². The exclusion of women >40-years-old and with a BMI >35 kg/m² was intended to reduce the probability of including individuals with unknown or undiagnosed morbidities in the sample population, as well as women with menopausal hormone alterations and those presenting a degree of obesity unresponsive to dietetic treatment.

The study population was randomly divided in two groups of 20, paired according to BMI, one of which (group S) received soy bean oil as dietary supplement, while the second (group C) received coconut oil. Individual dietary counselling for all participants was provided by a nutritionist throughout the entire experimental period of 12 weeks. Subjects were instructed to follow a diet that was balanced in respect of macronutrients with increased consumption of fruits and vegetables and reduced consumption of simple carbohydrates and animal fat. Participants were also advised to drink adequate amounts of water and to reduce or eliminate alcohol consumption and smoking. Under the supervision of a fitness trainer, all of the participants took part on 4 days every week in a physical activity program comprising elongation followed by 50 min walking. Both, the physical trainer and the nutritionist were not aware of the distribution of the individuals between the study groups.

The dietary intervention consisted in the daily ingestion of either 30 mL of soy bean oil (group S) or 30 mL of coconut oil (group C) distributed through the three main meals. Participants were instructed that the daily oil supplement should be used in the preparation of food as normal, but that the nutritional recommendations provided must be followed. Each subject received a supply of oil (sufficient for the experimental period) contained in a

numbered flask, together with a standardised measuring spoon. In order to ensure that neither the participant nor the researchers had knowledge of the dietary supplement applied, the oil flasks were filled and numbered according to a supplement key prepared by an investigator, who was not involved in the collection of data, and the flasks were distributed to the participants by another researcher who had no knowledge of the contents of the supplement key. Data relating to the variables of interest were collected 1 week before the start of dietary intervention (T1) and again 1 week after the 12th week of intervention (T2). The supplement key was not revealed to the participants or to the research team until all data had been collected and analysed.

Origin and Composition of Oil Supplements

Filtered coconut oil, obtained by pressing coconut pulp that had been dehydrated at 60 °C, was provided by a local manufacturer (Sococo Indústria Alimentícia, Maceió, AL, Brazil). Soy bean oil (Bunge Alimentos, Pernambuco, Brazil) was purchased from a local supermarket. The compositions of the oil supplements (Table 1) were determined by an accredited laboratory (SFDK Laboratório de Análise de Produtos Ltda, São Paulo, SP, Brazil). The two types of oil were of a similar colour but differed slightly with respect to odour and flavour. In order to conceal the differences, the oils were bottled in 600 mL amber flasks and could not be readily distinguished except by direct comparison.

Socioeconomic Evaluation

Socioeconomic information was obtained from each participant by application of a specific questionnaire relating to the type of accommodation occupied, number of rooms,

sanitary facilities, schooling, occupation and family income, number of family members, alcohol intake and smoking habits, and physical activities.

Anthropometric Evaluation

The body mass of each subject wearing light clothes was determined using Filizola SA (São Paulo, SP, Brazil) Personal PL 180 portable digital scales with a maximum capacity of 180 kg and a precision of 100 g. Heights of subjects (with bare feet) were measured using a WCS (Curitiba, PR, Brazil) stadiometer connected to a non-extendable 220-cm measuring tape (1 mm precision). WC was measured (with subjects standing upright and immediately after exhalation) at the mid point between the last rib and the anterior superior iliac spine using a non-extendable measuring tape of 200 cm. BMI was calculated by dividing body mass (kg) by the square of the height (m). Values were categorised in accordance with the cut-off points recommended by the World Health Organisation guidelines [14] for BMI [<18.5 , 18.5–24.9 (or <25.0), 25.0–29.9 (or <30.0) and >30.0 ; kg/m²] and WC ($</>88$ cm) or were considered as continuous variables.

Dietary Evaluation

In order to evaluate compliance with expected dietary intake, the effects of lipid supplementation, and possible confusing effects between the different groups, a 24 h dietary recall was applied to subjects for a 3 day period (1 day of which was during a weekend) immediately before and 12 weeks after dietary intervention. Images depicting different quantities of food were used to assist participants in assessing the amounts of food consumed [15]. Data were collected by the researcher in charge of nutritional supervision and were processed using Nutwin software (Departamento de Informática em Saúde, Universidade Federal de São Paulo, SP, Brazil). BMR values were calculated according to the procedure of the Food and Agriculture Organisation [16] taking into consideration differences between the age groups as follows: BMR (18–30 years) = $(14.7 \times \text{weight}) + 496$ BMR (30–60 years) = $(8.7 \times \text{weight}) + 829$.

Biochemical Evaluation

Blood samples were collected 1 week before the start of dietary intervention (T1) and 1 week after the 12th week of intervention (T2). In each case blood was taken in the morning following a 12 h overnight fast. Glucose, triglycerides, total cholesterol (TC) and LDL/HDL fractions were determined in triplicate for each sample using standard laboratory kits (Boehringer Mannheim, Germany).

Table 1 Main fatty acids present in soy bean and coconut oils

Fatty acid	Composition (%)	
	Soy bean ^a oil	Coconut ^b oil
Lauric acid (12:0)	0	49.0
Myristic acid (14:0)	0.1	17.5
Palmitic acid (16:0)	10.3	9.0
Stearic acid (18:0)	3.8	3.0
Oleic acid (18:1 ω -9)	22.8	5.0
Linoleic acid (18:2 ω -6)	51.0	1.8
Total	100.0	100.0

Source: SFDK Laboratório de Análise de Produtos Ltda., São Paulo, SP, Brazil

^a *Glycine max* L.

^b *Cocos nucifera* L.

The quotients TC/HDL and LDL/HDL were calculated on the basis of the plasma lipoprotein values. The levels of fibrinogen, ultra-sensitive C reactive protein (US-CRP) and insulin were determined by thermo-precipitation, nephelometry and chemiluminescence, respectively. The secretory function of pancreatic beta cells and insulin resistance were calculated using the homeostatic model assessments (HOMA- $\beta\%$ and HOMA-S, respectively) according to the equations proposed by Mathews et al. [17].

$$\text{HOMA-}\beta\% = \frac{20 \times \text{insulin}(\mu\text{U/mL})}{\text{glucose}(\text{mmol/L}) - 3.5}$$

$$\text{HOMA-S} = \frac{\text{insulin}(\mu\text{U/mL}) \times \text{glucose}}{22.5}$$

Statistical Analysis

The experiment was carried out according to a totally randomised design and took the form of a 2×2 factorial scheme (factor A—type of oil tested on the two groups; factor B—two assay periods during the 12 weeks of dietary intervention). There were four treatments: (1) soy bean oil at zero time, (2) soy bean oil after 12 weeks, (3) coconut oil at zero time; and (4) coconut oil after 12 weeks. The interaction between factors A and B was analysed statistically.

In order to reduce the magnitude of the error variance, analysis of covariance (ANCOVA), was performed considering or not the significant differences between the two groups in relation to the supposed covariate age. In this context, H_0 implies that all β_I are equal to β , whilst H_1 requires at least one β_I is not equal to β for the same factor means. The equation applied was $y_{ij} = \mu + \tau_i + \beta_I x_{ij} + e_{ij}$. The χ^2 test was used to determine if there were significant differences between the two groups of women with respect to frequency of alcohol consumption or smoking habit. The normality of the distribution and the homoskedasticity of the residual variances were analysed using Shapiro–Wilk and Levene tests, respectively, for all studied variables. These tests were also used to determine if body mass, BMI, US-CRP, triglycerides, insulin, HOMA- $\beta\%$ and HOMA-S obeyed the parametric assumptions. The values relating to these variables were then subjected to logarithmic transformation, i.e. $y_i = \log(X_i)$. The percentage values of protein components were arcsine transformed, i.e. $y_i = \arcsin X_i$. After the application of the Snedecor test (F test), multiple comparisons between treatments were carried out using the post hoc Bonferroni test ($P < 0.05$) with correction factor. Both tests were applied to all dependent variables.

The level of significance was established at 5% for all statistical tests. However, when the probability of the experimental error was >5 and $<10\%$ (i.e. $0.05 > P < 0.1$), the difference was taken to indicate the probability of a biological significance.

Results

Most participants (60%) lived in brick houses comprising three rooms on average but lacking sewage facilities. Most women were illiterate (68.2%) and their sole occupation was to act as housewife (90%). Each family unit consisted on average of 5 members with a per capita income of R\$ 1.86/day (equivalent to US\$ 0.82/day in January 2006). Approximately a quarter of the women (22.5%; 4 in group S and 5 in group C) smoked regularly, and more than half of the participants (52.5%; 11 in group S and 10 in group C) ingested alcohol occasionally. There were no significant differences ($P \geq 0.05$) between the two groups with respect to the variables alcohol and smoking habits (χ^2 alcoholism = 0.10 and χ^2 smoking = 0.143; $df = 1$ for both variables; P values = 0.759 and 0.705, respectively), indicating that these covariables exerted no significant antagonism or synergism on the outcomes.

The median height of the studied population was found to be 1.55 m, corresponding to an estimated ideal weight of 51.63 kg and an ideal daily energy intake of 1,975.6 kcal. The daily energy consumption of the population was determined to be 1,893 kcal on average at the start of the trial, and this corresponded to 95.8% of the ideal requirement estimated on the basis of assessed height.

The results at T1 showed that the diet of the participants was poor in lipids [19% of total energy value (TEV)] and proteins (0.77 g/kg of body mass per day), and this was associated with an elevated ingestion of carbohydrates (69% of TEV). Tubers, flour and bread derived from traditional carbohydrate-rich plants were consumed with abundance. The frequency of ingestion of foods with cardio-protective properties, such as fruit and vegetables, was practically zero, while the intake of fibre was around 10 g a day.

The relative contribution of macronutrients to the daily energy intake varied little between T1 and T2 for the S and C groups. The TEV supplied by carbohydrates was reduced from 69 to 61.8% during this period, whilst the TEV supplied by lipids remained almost unaltered (changing from 19 to 20.8%) despite supplementation of the diet with 30 mL/day of oil (equivalent to 270 kcal). Regarding proteins, at T1 the participants ingested a hypoproteic diet whereas at T2 the diet was considered normoproteic (0.99 g/kg of weight a day). The mean TEV was reduced from 1,893 (T1) to 1,732 kcal/day (T2) as a result of the hypocaloric diet presented to the subjects and supervised by researchers during the 12 week dietary intervention.

The results of the 24 h dietary recall performed at T1 and T2 are presented in Table 2. The energy intake and the amounts of carbohydrates, lipids, proteins and fibre were similar in both S and C groups. Within the groups, however, some differences of similar magnitude could be

Table 2 Dietetic profiles of women presenting abdominal obesity determined before and after dietary supplementation with soy bean (group S) and coconut (group C) oils during a 12-week period

Variables	24 h Dietary recall	Study population		P value ^b
		Group S (n = 20) ^a	Group C (n = 20) ^a	
Energy (kcal)	First evaluation (T1)	1,887.3 ± 163.9	1,894.0 ± 190.6	0.916
	Second evaluation (T2)	1,700.1 ± 154.7	1,696.9 ± 176.5	0.958
	Δ% ^c	-9.9**	-10.4**	
Protein (g)	First evaluation (T1)	54.2 ± 7.6	58.8 ± 7.2	0.084
	Second evaluation (T2)	62.4 ± 6.3	61.7 ± 7.2	0.769
	Δ% ^c	15.0***	4.9*	
Carbohydrates (g)	First evaluation (T1)	327.2 ± 33.6	325.2 ± 36.0	0.874
	Second evaluation (T2)	272.2 ± 28.6	272.9 ± 33.8	0.946
	Δ% ^c	-16.8***	-16.1***	
Lipids (g)	First evaluation (T1)	40.2 ± 1.6	39.8 ± 2.7	0.607
	Second evaluation (T2)	40.2 ± 2.3	39.8 ± 2.1	0.653
	Δ% ^c	0.2 ns	0.1 ns	
Fibres (g)	First evaluation (T1)	10.03 ± 1.0	9.97 ± 1.1	0.872
	Second evaluation (T2)	14.98 ± 1.6	15.02 ± 1.8	0.944
	Δ% ^c	49.4***	50.7***	

ns Not significant

* $P < 0.05$; ** $P < 0.01$; *** $P < 0.001$

^a Mean values ± standard deviations

^b According to Bonferroni test

^c $\Delta\% = [(T2 - T1)/T1] \times 100$

observed. For example, there was a reduction of 10% in total energy intake and 16% in the ingestion of carbohydrates. In contrast, there was an increase (of approximately 50%) in the ingestion of proteins and fibres. The ingestion of lipids, however, remained unaltered.

The biochemical and anthropometrical data collected at T1 and T2 are presented in Table 3. ANCOVA analysis showed that there were no significant differences ($P \geq 0.05$) between groups S and C concerning the covariate age as determined by the H_o value. The Snedecor test (F test) showed a significant difference ($P < 0.05$) between the two groups concerning the type of oil (factor A) and assessment time (factor B). However, there was no significant interaction between factors A and B ($P \geq 0.05$) for any of the variables in this study (Table 3).

At the end of the trial period, reductions in body mass and BMI were observed in both groups ($P < 0.05$), but only group C presented a significant reduction ($P = 0.005$) in WC. The levels of total cholesterol, LDL and LDL:HDL ratio were significantly ($P < 0.05$) increased in group S, whilst the level of HDL was significantly ($P = 0.03$) diminished. Such alterations in the lipid profile did not occur in group C. In contrast, this group presented a tendency towards increased HDL although the alteration was not statistically significant ($P = 0.09$). At T1 the HDL level of group S tended ($P = 0.08$) to be higher than that of

group C, whilst at T2 the situation was reversed and the HDL level of group C was significantly higher, as shown by a P value of 0.03 consequently, at T2 the LDL:HDL ratio of group C was significantly ($P = 0.04$) lower than that of group S. According to the LDL:HDL ratios determined in the present study, the S and C groups cannot be considered to be at risk with respect to CVDs since the values were below 3.5.

The glucose levels of the S and C groups at T1 and T2 were similar. There was no change in the release of insulin in group S, whereas in group C the increase in hormone release observed, although not statistically significant ($P = 0.09$), was sufficient to increase the HOMA-S value of group C to a level significantly higher ($P = 0.03$) than that of group S. There were no significant differences between the S and C groups with respect to the remaining parameters (i.e. height, age, levels of triglycerides, US-CRP, fibrinogen, glucose and HOMA-β%) at both evaluations.

Discussion

The two groups of women presenting abdominal obesity endured similar socioeconomic conditions and lifestyles. The reductions in body mass and BMI of both S and C

Table 3 Metabolic and anthropometric profiles of women presenting abdominal obesity determined before and after dietary supplementation with soy bean (group S) and coconut (group C) oils during a 12-week period

Variables	Desirable values	Group S (<i>n</i> = 20)				Group C (<i>n</i> = 20)			
		First evaluation (T1) ¹	Second evaluation (T2) ¹	Δ (T2 – T1)	<i>P</i>	First evaluation (T1) ¹	Second evaluation (T2) ¹	Δ (T2 – T1)	<i>P</i>
Height (m)	–	1.56 ± 0.07	–	–	–	1.54 ± 0.05	–	–	–
Age (years)	–	28.5 ± 6.7	–	–	–	31.0 ± 6.4	–	–	–
Body mass (kg)	–	76.0 ± 9.0	75.0 ± 9.1	–1.0*	0.02	73.2 ± 9.0	72.1 ± 9.1	–1.1*	0.002
BMI (kg/m ²)	18.5–24.9	31.1 ± 3.2	30.7 ± 3.3	–0.4*	0.02	31.0 ± 3.6	30.5 ± 3.6	–0.5*	0.003
Waist circumference (cm)	<88	96.4 ± 5.1	97.0 ± 6.5	0.6	0.39	98.8 ± 6.7	97.4 ± 7.0	–1.4*	0.005
Total cholesterol (mg/dL)	<200	189.5 ± 22.2	209.3 ± 28.5	19.8*	0.001	192.5 ± 41.2	198.1 ± 39.0	5.6	0.69
HDL (mg/dL)	40–60	51.5 ± 10.0 ^C	45.00 ± 5.6 ^A	–6.5*	0.04	45.5 ± 7.1 ^c	48.7 ± 2.4 ^a	3.2 [‡]	0.11
LDL (mg/dL)	<100	108.6 ± 15.9	134.1 ± 28.7	25.5*	0.01	112.6 ± 37.8	116.5 ± 36.8	3.9	0.69
Triglycerides (mg/dL)	<150	147.2 ± 75.2	148.2 ± 64.8	1.0	0.93	172.8 ± 88.1	179.7 ± 93.7	6.9	0.65
LDL:HDL [18]	≤2.9	2.2 ± 0.5	3.1 ± 0.8 ^B	0.9*	0.002	2.49 ± 0.8	2.41 ± 0.8 ^b	–0.1	0.73
US-CRP (mg/L)	<1	4.9 ± 4.0	4.2 ± 3.2	–0.7	0.52	5.7 ± 4.9	3.7 ± 1.7	–2.0	0.11
Fibrinogen (mg/dL)	200–400	241.5 ± 41.5	243.6 ± 43.9	2.1	0.91	254.0 ± 42.2	243.8 ± 41.9	–10.2	0.85
Glucose (mg/dL)	70–100	81.8 ± 9.0	78.5 ± 9.9	–3.3	0.36	83.5 ± 7.8	82.8 ± 5.4	–0.7	0.81
Insulin (μU/mL)	<29.1	8.9 ± 3.3	7.6 ± 2.1	–1.3	0.27	9.0 ± 4.5	9.8 ± 4.1	0.8 [‡]	0.09
HOMA-S% [19]	1.66 ± 0.81	1.83 ± 0.82	1.48 ± 0.45 ^D	–0.4	0.20	1.8 ± 0.9	2.0 ± 0.9 ^d	0.2	0.11
HOMA β% [19]	> 100%	35.3 ± 13.0	31.8 ± 9.8	–3.5	0.44	36.1 ± 20.1	39.4 ± 18.0	3.3	0.20

US-CRP Ultra-sensitive C reactive protein

* Difference statistically significant ($P < 0.05$) and [‡]difference biologically significant ($P \geq 0.05$ to <0.1) according to Bonferroni test

¹ Mean values ± standard deviations

^{A/a,B/b} Difference statistically significant ($P < 0.05$) according to Bonferroni test

^{C/c,D/d} Difference biologically significant ($P \geq 0.05$ to <0.1) according to Bonferroni test

groups observed at T2 may be attributed to the negative energy balance resulting from healthier habits (i.e. a more balanced diet and additional physical activity) arising from the counselling administered during dietary intervention. The reduction in abdominal fat in individuals of group C can be explained by their consumption of MCFA-rich coconut oil, since these components are not readily incorporated into the triglycerides of adipose tissue [20]. Moreover, unlike triglycerides containing long chain fatty acids (LCFAs), those comprising MCFAs are more susceptible to oxidation even under resting conditions. This difference may be explained by the fact that LCFAs are dependent on carnitine for mitochondrial transport, whilst MCFAs are transported through the inner mitochondrial membrane independent of the carnitine acyl transferase system [21].

Studies on the effects of a diet rich in MCFAs (equivalent to 45% of TEV) compared with a diet rich in LCFAs administered over a 21-day period showed that plasma TC, LDL and triglyceride levels increased by 11, 12 and 22%, respectively, as a result of the ingestion of MCFAs, while HDL levels remained unchanged [22]. However, a diet

providing an intake of MCFAs in excess of 30 g/day would be nutritionally unbalanced and likely to produce undesirable collateral effects, which might explain the results observed [23]. In the present study, the hypocaloric diet adopted by the individuals of group C was supplemented with MCFA-rich coconut oil (as the main source of lipids), but no undesirable alterations were observed in the lipid profile of the participants after 12 weeks. In contrast, some researchers [24] have observed that subjects supplied with an amount of lauric acid significantly greater than that used in the present study, exhibited hypercholesterolemia. These results may be explained, however, by the unbalanced relation between saturated, monounsaturated and polyunsaturated fatty acids in the diet applied.

The majority of studies that have focussed on the hypercholesterolemic effect of MCFAs have employed hyperlipidic diets from which essential mono and polyunsaturated fatty acids, such as linoleic (18:1) and arachidonic (20:4) acids, were absent. Arachidonic acid is an important modulator of anti-inflammatory responses and is a precursor of the eicosanoids (leukotrienes, prostaglandins, thromboxanes and lipoxins), which present diverse biochemical

and physiological roles [25]. Such diets would, therefore, have been unbalanced and could have given rise to numerous metabolic disorders.

The reduction in HDL levels within group S observed in the present study may be explained by the high content of linoleic acid (51%) present in the soy bean oil, which may have undergone conformational changes during cooking. The process of heating transforms *cis*-linoleic and *cis*-linolenic acids into their respective *trans* isomers leading to alterations in lipid metabolism and to the under-expression of LDL receptors and, consequently, to an increase in blood LDL [26]. Whilst no evidence was obtained in the present study to confirm the formation of *trans* UFAs, the ingestion of soy bean oil by subjects of group S definitely induced an increase in the concentration of serum LDL after 12 weeks. There is a consensus amongst researchers concerning the deleterious effects on the levels of LDL of *trans* UFAs in comparison with SFAs. For example, Roos and co-workers [27] carried out a comparative study of a diet rich in lauric acid and a diet rich in *trans* UFAs derived from soy bean oil and observed that individuals supplied with the former presented a healthier lipid profile. In the present study, it is clear from the 24 h dietary recall that the participants used the oil provided for frying foods and as a supplement to the diet. However, the time spent in cooking, the temperature used in the processes, and the possible formation of *trans* isomers were not directly investigated. Undoubtedly, the influence of such variables warrants consideration and such a study would contribute to the knowledge already gathered. Nevertheless, it is important to emphasise that prior to nutritional intervention, several participants reported that they used the same cooking oil twice or three times as an economy measure. Although such practice was strongly discouraged during the study and the amount of oil supplied was ample for the needs of the participants and their families, full compliance was out of the control of the research team.

Much research has focussed on attempts at elucidating the real effects of SFAs on the lipid profile and the possible association with CVDs [28–30] but the results achieved are controversial since the amounts of oil employed, together with their fatty acid compositions, varied in the different studies. Further factors that could also explain the diverse results deriving from the various investigations include the duration of the dietary intervention, the ingestion of dietary cholesterol, and the level of antioxidants ingested. In the present study, the daily ingestion of 30 g of coconut oil during a 12-week period did not alter the lipid metabolism of the women of group C, including those who had exhibited some degree of hypertriglyceridaemia at T1. This result may be explained by the rapid oxidation of MCFAs, particularly lauric acid, as well as by their low incorporation into VLDLs. MCFAs are poor substrates for Δ^6 and Δ^9

fatty acid desaturases and, unlike palmitic acid (16:0), cannot undergo elongation. The hypercholesterolemic activity of palmitic acid is a consequence of such elongation reactions and the subsequent formation of LCFAs [31]. The presence of antioxidant polyphenols in the coconut oil could also have contributed to the results obtained in the present study. It is of interest to note that reduced levels of LDL, VLDL and total cholesterol, together with increased levels of HDL, have been reported in experimental animals that had been fed with coconut oil [32].

Regarding the carbohydrate profile, it has been postulated that the secretion of insulin varies according to the type of fatty acids supplied in the diet [33]. UFAs, such as linoleic and linolenic acids, potentiate insulin secretion in response to the basal concentration of glucose, whereas SFAs diminish the response of the islets of Langerhans to glucose concentration [34]. In the present study, individuals of group C exhibited a tendency towards increased insulin secretion following 12 weeks on a diet rich in lauric acid, a finding that is in agreement with a previous report that supplementation of lauric acid in experimental animals stimulated the secretion of insulin [35].

It is important to emphasise that the HOMA-S values representing insulin resistance were higher than normal in both groups and at both evaluations, a condition probably associated with abdominal obesity that was common to all participants of the study. The levels of USCRP, an inflammatory marker and an independent predictor of CVD risk [35], were also above the normal limit (<1 mg/L) in both groups and at both evaluations. The levels of fibrinogen were, however, normal at both T1 and T2. This protein is an important component of platelet aggregation and is an indicator of acute conditions. When the levels are normal, fibrinogen performs a cardio-protective function even in the presence of high levels of cholesterol [36].

It is important to stress that the background diet of participants in the present study was richer in carbohydrates (about 70%) than that of most Western populations (around 50–55%). Stable isotope experiments have shown that individuals submitted to carbohydrate-rich diets exhibit higher rates of de novo lipogenesis [37, 38] and decreased VLDL clearance and fat oxidation [39] compared with those ingesting diets poor in carbohydrates and rich in fat. Considering that the subjects of this study did not increase fat intake significantly, and that the carbohydrate intake diminished by more than 15%, it is possible that metabolic adaptations were induced by their normal diet pattern that could have influenced the results obtained. For this reason, the effects of coconut oil reported here cannot be extrapolated to other populations. Additionally, the 24-h dietary recall presented various limitations that must be considered in the evaluation of food consumption. Among such limitations are recall bias and the fact that a

single dietary recall does not characterise the habitual feeding habits of an individual owing to high intra-personal variability [40]. In order to minimise reporting bias a photo album containing images of different portions of food was employed, and to reduce intra-personal variability three different 24 h dietary recalls were conducted including one at the weekend when variations in the usual consumption pattern are most likely to occur.

In conclusion, the ingestion of coconut oil did not produce undesirable alterations in the lipid profile of women presenting abdominal obesity, although dietary supplementation with this oil did give rise to a reduction in WC, which is considered to confer some protection against CVDs. On the other hand, the ingestion of coconut oil appeared to have induced an increase in peripheral insulin resistance. The results presented here indicate that SFAs cannot be characterised as the sole aetiological cause of obesity, dyslipidemia and risk factor for CVDs, but that the overall composition of the diet, particularly the fatty acid, cholesterol and antioxidant fractions, as well as the lifestyle of the individuals, must be taken into consideration. Within this context, it would be important to evaluate the effects of coconut oil over a prolonged period, and to investigate the composition and effects of the polyphenolic fraction of the oil.

References

- Instituto Brasileiro de Geografia e Estatística (accessed June 2008). Pesquisa de orçamentos familiares: 2002–2003. Análise da disponibilidade domiciliar de alimentos e do estado nutricional no Brasil. IBGE; Rio de Janeiro, 2004. <http://www.ibge.gov.br/home/estatistica/populacao/condicaoodevida/pof/2002analise/pof2002analise.pdf>
- Peixoto MRG, Benicio MHA, Jardim PCBV (2007) The relationship between body mass index and lifestyle in a Brazilian adult population: a cross-sectional survey. *Cad Saude Publica* 23:2694–2740
- Klein S, Allison DB, Heymsfield SB, Kelley DE, Leibel RL, Nonas C, Kahn R (2007) Waist circumference and cardiometabolic risk: a consensus statement from shaping America's health: Association for weight management and obesity prevention; NAASO, The Obesity Society; the American Society for Nutrition; and the American Diabetes Association. *Diabetes Care* 30:1647–1652
- Schaefer EJ (2002) Lipoproteins, nutrition, and heart disease. *Am J Clin Nutr* 75:191–212
- Costa AG, Bressan J, Sabarense CM (2006) Trans fatty acids: foods and effects on health. *Arch Latinoam Nutr* 56:12–21
- Li DF, Thaler RC, Nelssen JL, Harmon DL, Allee GL, Weeden TL (1990) Effect of fat sources and combinations on starter pig performance, nutrient digestibility and intestinal morphology. *J Anim Sci* 68:3694–3704
- Enig MG (1999) Coconut: in support of good health in the 21st century. http://www.coconutoil.com/coconut_oil_21st_century.htm. Accessed July 2007
- Lipoeto NI, Agus Z, Oenzil F, Wahlqvist M, Wattanapenpaiboon N (2004) Dietary intake and the risk of coronary heart disease among the coconut-consuming Minangkabau in West Sumatra, Indonesia. *Asia Pac J Clin Nutr* 13:377–384
- Prior IA, Davidson F, Salmond CE, Czochanska Z (1981) Cholesterol, coconuts, and diet on Polynesian atolls: a natural experiment: the Pukapuka and Tokelau Island studies. *Am J Clin Nutr* 34:1552–1561
- Amarasiri WA, Dissanayake AS (2006) Coconut fats. *Ceylon Med J* 51:47–51
- Calbom C, Calbom J (2005) The coconut diet. Grand Central Publishing, New York
- Lima FEL, Menezes TN, Tavares MP, Szarfarc SC, Fisberg RM (2000) Ácidos graxos e doenças cardiovasculares: uma revisão. *Rev Nutr* 13:73–80
- Puska P (2002) Nutrition and global prevention on non-communicable diseases. *Asia Pacific J Clin Nutr* 11:S755–S758
- World Health Organisation (1998) Obesity: preventing and managing the global epidemic. Report of a WHO consultation on obesity. WHO, Geneva
- Zabotto CB, Viana RPT, Gil MF. Registro fotográfico para inqueritos dietéticos: utensílios e porções (1996) Photographic record to dietetic inquiries: appliances and portions, UFG Goiânia
- FAO/WHO/UNU (1985) Energy and protein requirements. WHO—technical report series # 724. WHO, Geneva
- Mathews DR, Hosker JP, Rudenski AS, Naylor BA, Treacher DF, Turner RC (1985) Homeostasis model assessment: insulin resistance and B-cell function from fasting plasma glucose and insulin concentrations in man. *Diabetologia* 28:412–419
- Castelli WP (2006) Cholesterol and lipids in the risk of coronary artery disease—the Framingham heart study. *Can J Cardiol* 4:5A–10A
- Geloneze B, Repetto EM, Geloneze SR, Tambascia MA, Ermetice MN (2006) The threshold value for insulin resistance (HOMA-IR) in an admixed population: IR in the Brazilian metabolic syndrome study. *Diabetes Res Clin Pract* 72:219–220
- Colleone VV (2002) Aplicações clínicas dos ácidos graxos de cadeia média. In: Curi R, Pompéia C, Miyasaka CK, Procópio J (eds) Entendendo a Gordura: os Ácidos Graxos. Manole, Barueri
- Gomes RV, Aoki MS (2003) A suplementação de triglicérides de cadeia média promove efeito ergogênico sobre o desempenho no exercício de endurance? *Rev Bras Med Esporte* 9:162–168
- Tholstrup T, Ehnholm C, Jauhiainen M (2004) Effects of medium-chain fatty acids and oleic acid on blood lipids, lipoproteins, glucose, insulin, and lipid transfer protein activities. *Am J Clin Nutr* 79:564–569
- Ferreira AMD, Barbosa PEB, Ceddia RB (2003) A influência da suplementação de triglicérides de cadeia média no desempenho em exercícios de ultra-resistência. *Rev Bras Med Esporte* 9:413–419
- Sundram K, Ismail A, Hayes KC, Jeyamalar R, Pathmanathan R (1997) Trans (elaidic) fatty acids adversely affect the lipoprotein profile relative to specific saturated fatty acids in humans. *J Nutr* 127:514–520
- Honstra G (2000) Essential fatty acids in mothers and their neonates. *Am J Clin Nutr* 71:1262S–1269S
- Ascherio A, Willett WC (1997) Health effects of trans fatty acids. *Am J Clin Nutr* 66:1006S–1010S
- de Roos NM, Schouten EG, Katan MB (2001) Consumption of a solid fat rich in lauric acid results in a more favorable serum lipid profile in healthy men and women than consumption of a solid fat rich in *trans*-fatty acids. *J Nutr* 131:242–245
- Kumar PD (1997) The role of coconut and coconut oil in coronary heart disease in Kerala, South India. *Trop Doct* 27:215–217
- Oliveros LB, Videla AM, Gimenez MS (2004) Effect of dietary fat saturation on lipid metabolism, arachidonic acid turnover and peritoneal macrophage oxidative stress in mice. *Braz J Med Biol Res* 37:311–320

30. Grundy SM, Denke MA (1990) Dietary influences on serum lipids and lipoproteins. *J Lipid Res* 31:1149–1172
31. Verlengia R, Lima TM (2002) Síntese de ácidos graxos. In: Curi R, Pompéia C, Miyasaka CK, Procopio J (eds) *Entendendo a Gordura: os Ácidos Graxos*. Manole, Barueri
32. Nevin KG, Rajamohan T (2006) Virgin coconut oil supplemented diet increases the antioxidant status in rats. *Food Chem* 99:260–266
33. Haber EP, Carpinelli AR, Carvalho CRO, Cury R (2001) Secreção de insulina: efeito autócrino da insulina e modulação por ácidos graxos. *Arq Bras Endocrinol Metab* 45:219–227
34. Garfinkel M, Lee S, Opara EC, Akwari OE (1992) Insulinotropic potency of lauric acid: a metabolic rationale for medium chain fatty acids (MCF) in TNP formulation. *J Surg Res* 52:328–333
35. Sepulveda JL, Metha JL (2005) C-Reactive protein and cardiovascular disease: a critical appraisal. *Curr Opin Cardiol* 20:407–416
36. Frankel S, Elwood P, Sweetnam P, Yarnell J, Smith GD (1996) Birth weight, body-mass index in middle age, and incident coronary heart disease. *Lancet* 348:1478–1480
37. Hudgins LC, Hellerstein M, Seidman C, Neese R, Diakun J, Hirsch J (1996) Human fatty acid synthesis is stimulated by a eucaloric low fat, high carbohydrate diet. *J Clin Invest* 97:2081–2091
38. Mittendorfer B, Sidossis LS (2001) Mechanism for the increase in plasma triacylglycerol concentrations after consumption of short-term, high-carbohydrate diets. *Am J Clin Nutr* 73:892–899
39. Parks EJ, Krauss RM, Christiansen MP, Neese RA, Hellerstein MK (1999) Effects of a low-fat, high-carbohydrate diet on VLDL-triglyceride assembly, production, and clearance. *J Clin Invest* 104:1087–1096
40. Fisberg RM, Slater B, Marchioni DML, Martini LA (2005) *Inquéritos alimentares: métodos e bases científicas (nutritional surveys: methodology and scientific bases)*. Manole, Barueri

Effect of ALA-Enriched Food Supply on Cardiovascular Risk Factors in Males

Isabelle Sioen · Mirjam Hacquebard · Gaëlle Hick ·
Veronique Maindix · Yvan Larondelle ·
Yvon A. Carpentier · Stefaan De Henauw

Received: 11 December 2008 / Accepted: 22 April 2009 / Published online: 19 May 2009
© AOCS 2009

Abstract The outcome of a total dietary approach using a wide range of n-3 polyunsaturated fatty acids (PUFA) enriched food items on cardiovascular diseases called for further investigation. The study objective was to assess the effect of an ALA-enriched food supply on cardiovascular risk factors in healthy males. A dietary intervention (single-blind field trial with pre- and post-measurements) was performed with 59 healthy males in a Belgian prison. Over a period of 12 weeks they were supplied with an n-3 enriched diet (containing 6.5 g n-3 PUFA/day compared to 4 g n-3 PUFA/day in the standard diet) that was substituted for their regular diet, increasing mainly the α -linolenic acid intake

(from 2.8 to around 5 g/day). The results indicated no impact on subjects waist circumference, weight and BMI or systolic blood pressure. In contrast, the diastolic blood pressure significantly decreased during the intervention period (from 74.6 ± 8.2 to 71.7 ± 10.1 mmHg; $P < 0.02$). Moreover, the HDL-cholesterol level increased in non-smoking participants (from 0.97 ± 0.25 to 1.06 ± 0.23 mmol/l; $P < 0.03$). In summary, the study demonstrated that enrichment of commonly eaten food items with n-3 fatty acids provides the opportunity to increase the n-3 fatty acid intake and to decrease the n-6/n-3 ratio which results in a decreasing diastolic blood pressure and an increase of HDL-cholesterol (in non-smokers).

I. Sioen (✉) · S. De Henauw
Department of Public Health, Faculty of Medicine and Health
Science, Ghent University, UZ-2 Blok A, De Pintelaan 185,
9000 Ghent, Belgium
e-mail: Isabelle.Sioen@UGent.be

I. Sioen
Department of Food Safety and Food Quality,
Faculty of Bioscience Engineering, Ghent University,
Ghent, Belgium

M. Hacquebard · Y. A. Carpentier
L. Deloyers Laboratory for Experimental Surgery,
Erasmus Hospital, Université Libre de Bruxelles,
Brussels, Belgium

G. Hick
Groupement d'Intérêt Economique 'Equilibrium Industrial
Partnership', Brussels, Belgium

V. Maindix
Dietetic Department, Institut Paul Lambin, Brussels, Belgium

Y. Larondelle
Biochimie Cellulaire, Nutritionnelle et Toxicologique,
Institut des Sciences de la Vie, Université catholique de Louvain,
Louvain-la-Neuve, Belgium

Keywords Dietary intake · Omega-3 ·
Cardiovascular risk factors · Blood pressure · Cholesterol ·
A-linolenic acid

Abbreviations

AA	Arachidonic acid
ALA	Alpha-linolenic acid
Apo A1	Apolipoprotein A1
Apo B	Apolipoprotein B
CHD	Coronary heart disease
CRP	C-reactive protein
CVD	Cardiovascular diseases
DHA	Docosahexaenoic acid
DPA	Docosapentaenoic acid
EPA	Eicosapentaenoic acid
γ GT	Gamma glutamic transpeptidase
GOT	Glutamic oxaloacetic transaminase
GPT	Glutamic pyruvate transaminase
HDL-C	HDL-cholesterol
LA	Linoleic acid

LC	Long-chain
LDL-C	LDL-cholesterol
PUFA	Polyunsaturated fatty acids
SFA	Saturated fatty acids
TC	Total cholesterol
TG	Triglycerides

Introduction

Cardiovascular diseases (CVD) are among the leading causes of disability and premature death in Western populations [1]. High LDL-cholesterol (LDL-C), low HDL-cholesterol (HDL-C) plasma levels and hypertension are among the major cardiovascular risk factors [2]. Nutrition can influence the development of CVD by modifying one or more of these risk factors. Within the diet, fat, particularly the type of fat rather than the amount consumed, seems to be the most important macronutrient in relation to CVDs. There is a growing body of evidence demonstrating that the regular consumption of n-3 PUFA is associated with significant health benefits in the prevention of CVD [3]. In the meantime, there are considerable indications that the current intake of n-3 PUFA via the Western diet is too low [4–8]. A possible solution to increase the n-3 PUFA intake is to increase the fatty fish consumption, the most important natural source of long-chain (LC) n-3 PUFA. However, Western societies consume little fish and many barriers exist to increase this current pattern [9]. Moreover, limited availability of fish stocks is an issue that has to be considered in the future [10]. An alternative strategy for enhancing n-3 PUFA intake may be to provide a wide range of commercial food products and ingredients fortified with n-3 PUFA, which can be incorporated in an existing diet. Many of these food items are currently available. Most of them have an increased content of α -linolenic acid (ALA; C18:3n-3), precursor of LC n-3 PUFA [11]. The Lyon as well as the Indo-Mediterranean Diet Heart Studies showed that a Mediterranean diet rich in ALA prevented the recurrence of cardiovascular events [12, 13]. Nevertheless, there is considerable evidence that LC n-3 PUFA have much greater efficacy in the prevention of CVD [14, 15]. Still, the efficacy of such n-3 PUFA enriched food items for the prevention and control of CVD remains a matter of debate.

The main objective of this study was to investigate the effect of an ALA enrichment in the diet of healthy male human volunteers on different cardiovascular risk factors. A group of volunteer prisoners were supplied with an n-3 enriched diet for 12 weeks. By using ALA-enriched food items, this total dietary approach—simulating a real-life situation—differed from previous supplementation studies

which used ALA-enriched capsules or single fortified products [16–19]. The study questioned whether this approach can be a useful nutritional strategy to prevent CVD.

Materials and Methods

The design of this dietary intervention study was a single-blind field trial with pre- and post-measurements in a group of healthy men. Each individual served as his own control.

Study Population

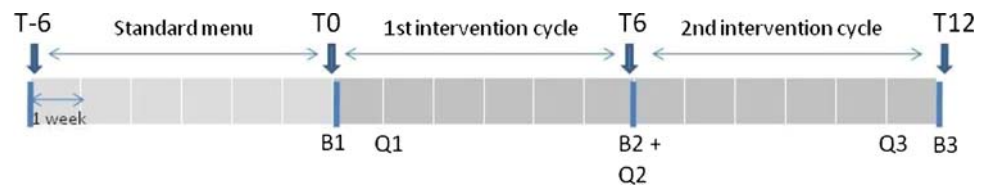
The study took place in a highly protected penitentiary institution (Andenne, Belgium) for male persons sentenced to long imprisonment (>5 years), with a capacity of 400 prisoners. Volunteers were recruited among 396 men present in the prison at the start of the study. The exclusion criteria were: specific diseases or organ dysfunction, special diet (vegetarian, diabetic, ...), alcohol abuse or use of drugs for CVD treatment or specific types of medication (e.g. medication decreasing the blood pressure). On the basis of these exclusion criteria, 102 men were eligible for participation. All eligible participants received a letter explaining the study's goal, timing and practical aspects. A short movie presentation was also made available in which the details of the dietary intervention study were explained by the organizing and scientific committee. Finally, an informative meeting was organised to answer prisoners' questions. After receiving complete information, 70 volunteers (68.8% of the eligible prisoners) registered to participate in the study and signed a written informed consent. During the study, 11 dropped out, resulting in a final group of 59 participants. Apart from one death (because of brain haemorrhage caused by aneurysm rupture), reasons for the volunteers' drop out were essentially being set at liberty or transfer to another prison. The organizing committee covered television subscription costs during the 5 months of the study as compensation for participation from the beginning until the end of the study.

The study protocol and the process for obtaining informed consent were approved by the Ethical Committee of the Erasmus hospital, Brussels.

Dietary Intervention

The standard catering system in the prison of Andenne follows repeating menu cycles consisting of 6 weeks. This study lasted three cycles in the year 2007 (from January to June) of which the first cycle did not include an n-3 intervention (Fig. 1). During the first cycle (standard menu), nothing was changed in the supplied food of the

Fig. 1 Graphical presentation of the time line of the dietary intervention study and the moments of blood sampling (*B*) and completion of the dietary questionnaires (*Q*)



participants except for the bread and the fact that all pre-packed foods were now packed in a neutral package. The refined bread provided by standard catering was changed in the first study cycle to wholemeal bread since the n-3 fortified bread used during dietary intervention (second and third cycle) was not available in a refined version. During the n-3 intervention cycles several standard supplied food items were replaced by n-3 fortified versions in the participants' menus, i.e. bread, margarine, meat and meat products (beef, pork, chicken), dairy products, cheese and eggs. The replacement was done for food items of breakfast, lunch and dinner. The quantity of n-3 fortified foods per day was determined by dietitians in order to reach an optimal ratio of linoleic acid (LA; C18:2n-6) and ALA, i.e. a ratio of less than 4 to 1 [20]. The n-3 fortified foods were provided by Belgian industrial companies of the ESV/GIE EQUILIBRIUM Industrial Partnership. The fatty acid composition of some food items used in the intervention is given in Table 1. For most of the food items of animal origin, the increased n-3 PUFA content resulted from feeding the animals with ALA-enriched feed. Apart from the higher n-3 content, all these foods were equal to the standard supplied versions for all other nutritional parameters, organoleptic characteristics, taste, etc. Moreover, during the whole study period (the cycle before the intervention and the two intervention cycles), the food items were prepacked in neutral package and identification could only be done by specific serial numbers, so that the participants could not notice the changes in their diet at T0. To determine the actual changes in the fatty acid content of the food provided during the three different menu cycles, chemical analyses of the supplied food were performed during the 18 study weeks. For this, two duplicate samples were collected each day from standard meal portions of all meals throughout the day. Samples were immediately frozen by the prison personnel and stored at -25°C for chemical analyses. The samples were thawed at 55°C and the edible part of the meal was isolated and weighed. All the food samples of a same day were mixed together in a R8 mixer (Robocoupe, Monceau-en-Bourgogne, France). For each sample, the total fat content was gravimetrically determined according to the general Weibuhl method, as described in the reference method ISO 1443. Furthermore, fat components were extracted according to the method of Folch et al. [21] adapted by Christie [22] to determine the fatty acid pattern by gas chromatography [23].

Dietary Questionnaire

On three different occasions during the study (Fig. 1), the participants had to complete questionnaires to evaluate their dietary habits. The questionnaires were specifically developed for the study purpose. A first questionnaire was used to evaluate the participants' dietary habits before the intervention, whereas the second and the third questionnaires were used to evaluate their behaviour during the two intervention cycles. Examples of questions used are given in Table 2. Two individual scores were calculated expressing the participants' compliance based on their answers. A first score (diet_score) was calculated as an indicator of the overall compliance to the provided menu. A second score called (fish_score) was determined to provide an indication on whether the participant consumed the fish present in the menu. A mean score for the three different study cycles was calculated per participant. Based on their individual score participants were divided in tertiles. These scores were not an endpoint as such but were used further as confounders in the statistical analyses.

Clinical Measurements

All participants underwent three medical visits which took place during the initial week of the first (T0) and second (T6) intervention cycle and during the first week after the intervention (T12). During these visits the medical staff of the prison measured waist circumference, weight and height. Further, two consecutive measurements of systolic and diastolic blood pressure were performed from the same arm, with subjects in a sitting position, after 15 min rest from the time the cuff had been placed on the arm. An extra blood pressure measurement was done 2.5 months after the end of the intervention in those participants who were still present in the institution, i.e. 48 out of the 59 participants who completed the whole study. At each medical visit, fasting blood samples were collected and immediately handled to analyse fatty acid profile in platelet phospholipids, plasma lipids, plasma apolipoproteins B (apo B) and A1 (apo A1), glucose, C-reactive protein (CRP; indicator of inflammation) and hepatic function tests. Platelet-rich plasma was separated from blood samples by low speed centrifugation at 228g for 10 min in a J2.21 centrifuge (Beckman Instruments, Fullerton, CA, USA). Platelets were then isolated from plasma by centrifugation at 1430g

Table 1 The fatty acid composition of some n-3 PUFA enriched food items used in both intervention cycles (NA: not available, no value given by the industry providing these foods)

Food item	Total fat g/100 g	SFA g/100 g	MUFA g/100 g	PUFA g/100 g	C18:2 n-6 mg/100 g	C20:4 n-6 mg/100 g	C18:3 n-3 mg/100 g	C20:5 n-3 mg/100 g	C22:5 n-3 mg/100 g	C22:6 n-3 mg/100 g
Cooked ham	4	1.2	1.7	1	651	44	184	12	20	4
Smoked ham	2.2	0.8	1	0.3	200	21	59	6	10	1
Pâté	15	5.8	6.2	2.8	1852	157	594	11	48	12
Smoked bacon	22.9	7.2	8.8	4.1	2472	39	1173	19	55	6
Roasted pork	6	1.8	2.2	1.2	775	72	265	22	32	5
Minced pork	18	6	7.2	3.4	2110	56	914	19	56	12
Beef	1.78	0.8	0.8	0.2	102	30	26	10	17	1
Chicken	11.36	3.5	4.12	3.8	2380	57	1200	13	0	16
Non-skimmed milk	3.5	2.3	1.04	0.2	108	NA	42	NA	NA	NA
Butter	82	53	24.5	3.6	2520	NA	976	NA	NA	NA
Cheese	27	18	8.06	1.2	832	NA	321	NA	NA	NA
Eggs	7.95	2.2	3.21	2.4	1415	95	708	17	29	136
Bread (six cereals)	6.5	0.9	2.37	3.2	1920	10	876	NA	NA	NA
Smoked mackerel ^a	30.1	6.3	12.87	8.9	479	2	452	1959	364	3297

^a This food item is naturally rich in n-3 PUFA and is regularly put on the menu in the prison (not only during the intervention)

for 20 min. Fatty acid pattern was determined in platelet phospholipids by gas chromatography after separation of lipid components by thin layer chromatography [24]. Plasma total cholesterol (TC) and triglycerides (TG) were measured using enzymatic kits (Roche Diagnostics GmbH, Mannheim, Germany). HDL-cholesterol (HDL-C) was determined as the cholesterol remaining in plasma supernatant after precipitation of apolipoprotein B-containing lipoproteins with phosphotungstic acid manganese chloride [25, 26]. LDL-cholesterol (LDL-C) was calculated by the Friedewald formula [27]. Apo B and A1 were measured in plasma by ELISA using rabbit polyclonal antibodies for apo B and A1, respectively [28]. Plasma CRP level was determined by using high sensitive CRP immuno-turbidimetric method [29]. Finally, plasma glucose levels as well as common hepatic function tests consisting in the determination of glutamic oxaloacetic transaminase (GOT), glutamic pyruvate transaminase (GPT) and gamma glutamic transpeptidase (γ GT) were determined by standard clinical testing methods.

Statistics

The results of the measurements at the different time points (T0, T6 and T12) were compared on an individual level using a general linear model (GLM) for repeated measurements. The following parameters were taken into account as potential confounders: smoking behaviour, age, diet_score, and fish_score. When an interaction was found with one of these confounders, the GLM for repeated measurements was stratified by this confounder. For all

Table 2 Examples of questions used in the dietary questionnaires (the moments on which the questionnaires were completed are indicated in Fig. 1)

Examples of questions used in the dietary questionnaires
1. During the last 6 weeks, how frequently did you consume breakfast/lunch/diner?
2. During the last 6 weeks, did you use the margarine/bread/... [asked separately]
that was distributed?
2.1. If yes, what was your average bread consumption:
(a) I ate all the bread
(b) I left some bread (if yes, how many slices)
(c) I ate all the bread and I even ate extra self-bought bread
3. How frequently did you eat fish (or eggs or meat [asked separately]):
(a) Every time when it was on the menu
(b) From time to time
(c) Never

analyses, a significant effect of the intervention was assumed for a P value ≤ 0.05 . The statistical analyses were performed using SPSS software version 12.0.

Results

Dietary Intervention

As shown in Table 3, the mean contents of total fat, saturated fatty acids (SFA) and monounsaturated fatty acids (MUFA) in the supplied food were lower during the

Table 3 The mean content of fat and different fatty acids (g/day) of the supplied foods for the three menu cycles (mean value for a period of 6 weeks) calculated on the basis of two duplicates of all meals (breakfast, lunch and dinner) provided to the prisoners per day

		Standard menu	Intervention cycle 1	Intervention cycle 2
g/day	Total fat	109.92	107.26	104.30
	Saturated fatty acids (SFA)	45.01	42.34	38.84
	Mono-unsaturated fatty acids (MUFA)	39.78	36.90	37.79
	Poly-unsaturated fatty acids (PUFA)	23.28	25.62	25.95
	n-6 PUFA	19.33	19.18	19.69
	C18:2n-6 (LA)	18.07	17.86	17.82
	C20:4n-6 (AA)	0.18	0.17	0.17
	n-3 PUFA	4.03	6.48	6.50
	C18:3n-3 (ALA)	2.83	4.85	5.01
	C20:5n-3 (EPA)	0.30	0.40	0.38
	C22:5n-3 (DPA)	0.09	0.14	0.13
	C22:6n-3 (DHA)	0.50	0.66	0.61
	LA/ALA	6.24	3.59	3.82
	n-6/n-3	5.75	3.39	3.26

n-3 dietary intervention compared to the standard menu. In contrast, the mean content of PUFA in the supplied food increased. The mean n-3 PUFA content increased from 4.0 to 6.5 g/day; this was mostly accounted for by an increased supply of ALA (~5.0 vs. 2.8 g/day in the standard menu). Still, the LC n-3 PUFA content was also slightly increased (see Table 3). In contrast, the n-6 PUFA content (with LA and arachidonic acid (AA; C20:4n-6) as most important fatty acids) did not differ between the standard diet and the intervention diet (19.3 vs. 19.7 g/day). As a result, the LA/ALA and n-6/n-3 ratios decreased, respectively from 6.2 to 3.8 and from 5.8 to 3.3 during the intervention.

Subjects Baseline Characteristics

The 59 male volunteers who completed the study were aged from 22 to 65 years (a mean age of 41.5 ± 9.8 years). Of the 59 participants, 41 were smokers and 18 non-smokers. Anthropometrical and clinical characteristics of the participants at baseline can be found in Table 4.

Compliance to the Diet

On the basis of the dietary questionnaires and the calculated diet_scores, the participants were divided into tertiles: 19 were defined as having a poor compliance to the provided menu, 20 of them a moderate compliance and the other 20 participants a good compliance (on a relative scale). With respect to the calculated fish_score and the division in tertiles, 14 of the 59 participants did not consume regularly the provided fish, 24 consumed it from time to time, and 21 consumed most of the provided fish.

Effect of Dietary Intervention on Anthropometrical and Clinical Measurements

n-3 Dietary intervention had no significant effect on subjects anthropometrical characteristics (Table 4). Also no significant effect of the intervention was found on the systolic blood pressure. In contrast, n-3 dietary intervention was associated with a significant decrease of diastolic blood pressure from 74.6 ± 8.2 (T0) and 74.4 ± 9.3 mmHg (T6) to 71.7 ± 8.8 mmHg (T12) ($P < 0.02$). The diastolic blood pressure measured at 2.5 months after the end of the dietary intervention showed a return to initial values (74.7 ± 10.1 mmHg).

No significant effect of the intervention was found on TG, TC, LDL-C, Apo B, Apo A1, glucose, CRP and hepatic function tests (GOT, GPT, γ -GT) (Table 4). In contrast, the dietary intervention led to a significant increase of HDL-C, from 0.97 ± 0.25 on T0 to 1.06 ± 0.23 mmol/l on T12 in the group of non-smoking participants ($P < 0.03$).

Fatty Acid Composition in Platelet Phospholipids

The dietary intervention decreased the relative content of saturated, palmitic acid (C16:0) and arachidic acid (C20:0) in platelet phospholipids (Table 4). This was accompanied by an increase in the relative content of LA. For several other fatty acids, statistical analyses indicated a significant effect from one of the confounders. In particular, an effect of fish_score was found for C18:0, C20:4n-6 (AA), C20:5n-3 (EPA), and C22:6n-3 (DHA) (Table 5). Volunteers who consumed the fish provided by the diet most of the time showed a decrease in the relative content of AA, together with an increase of EPA and DHA; this led to decreased AA/EPA or AA/LC n-3 ratios.

Table 4 Anthropometrical and clinical characteristics and fatty acid composition of platelet phospholipids (molar % of total fatty acids) and at T0, T6 and T12 (mean \pm standard deviation) for the 59 participants

	Baseline (T0)	T6	T12
Waist circumference (cm)	95.4 \pm 12.4 ^a	95.0 \pm 12.0 ^a	96.6 \pm 12.7 ^a
Weight (kg)	87.7 \pm 15.7 ^a	88.2 \pm 15.8 ^a	87.3 \pm 16.2 ^a
BMI (kg/m ²)	28.3 \pm 4.9 ^a	28.3 \pm 4.9 ^a	28.4 \pm 4.9 ^a
Systolic blood pressure (mmHg)	115 \pm 14 ^a	119 \pm 13 ^a	119 \pm 14 ^a
Diastolic blood pressure (mmHg)	74.6 \pm 8.2 ^a	74.4 \pm 9.3 ^a	71.7 \pm 8.8 ^b
Total cholesterol (mmol/l)	4.80 \pm 1.03 ^a	4.57 \pm 0.98 ^a	4.76 \pm 1.06 ^a
LDL-cholesterol (mmol/l)	3.30 \pm 0.92 ^a	3.05 \pm 0.92 ^a	3.25 \pm 0.98 ^a
HDL-cholesterol (HDL-C) (mmol/l)	0.90 \pm 0.22 ^a	0.87 \pm 0.19 ^a	0.92 \pm 0.23 ^a
HDL-C (smokers; <i>n</i> = 41) (mmol/l)	0.87 \pm 0.21 ^a	0.83 \pm 0.19 ^a	0.86 \pm 0.21 ^a
HDL-C (non-smokers; <i>n</i> = 18) (mmol/l)	0.97 \pm 0.25 ^a	0.96 \pm 0.19 ^a	1.06 \pm 0.23 ^b
Apolipoprotein B (mg/dl)	115.6 \pm 32.2 ^a	112.0 \pm 33.1 ^a	113.6 \pm 34.1 ^a
Apolipoprotein A1 (mg/dl)	160.0 \pm 28.4 ^a	158.4 \pm 28.0 ^a	153.3 \pm 27.4 ^a
Glucose (mmol/l)	4.5 \pm 0.9 ^a	4.3 \pm 0.9 ^a	4.6 \pm 1.0 ^a
Triglycerides (mmol/dl)	1.3 \pm 0.6 ^a	1.4 \pm 1.0 ^a	1.3 \pm 0.8 ^a
GOT (UI/l)	24.6 \pm 7.8 ^a	28.4 \pm 11.3 ^a	26.1 \pm 10.2 ^a
GPT (UI/l)	31.4 \pm 21.7 ^a	37.3 \pm 29.0 ^a	32.8 \pm 25.6 ^a
γ GT (UI/l)	27.6 \pm 15.9 ^a	29.2 \pm 17.5	29.1 \pm 19.8 ^a
CRP (ng/dl)	0.28 \pm 0.33 ^a	0.31 \pm 0.34 ^a	0.42 \pm 1.25 ^a
C16:0	19.96 \pm 1.00 ^a	19.90 \pm 1.16 ^a	19.63 \pm 0.97 ^b
C18:0 ^A	16.85 \pm 0.52	16.74 \pm 0.72	16.96 \pm 0.57
C20:0	1.26 \pm 0.12 ^a	1.16 \pm 0.23 ^b	1.14 \pm 0.20 ^b
C22:0	2.50 \pm 0.18 ^a	2.51 \pm 0.20 ^a	2.53 \pm 0.20 ^a
C24:0	1.31 \pm 0.19 ^a	1.35 \pm 0.17 ^a	1.35 \pm 0.25 ^a
C18:1n-9	13.86 \pm 0.67 ^a	14.06 \pm 0.8 ^b	13.97 \pm 0.76 ^{ab}
C20:1n-9	0.62 \pm 0.16 ^a	0.66 \pm 0.18 ^a	0.63 \pm 0.16 ^a
C18:2n-6 (LA)	6.28 \pm 0.84 ^a	6.46 \pm 0.73 ^b	6.57 \pm 0.71 ^b
C20:4n-6 (AA) ^A	29.09 \pm 1.07	28.59 \pm 1.54	28.87 \pm 1.20
C22:4n-6	1.72 \pm 0.27 ^a	1.63 \pm 0.36 ^b	1.67 \pm 0.31 ^b
C20:5n-3 (EPA) ^A	0.50 \pm 0.21	0.67 \pm 0.41	0.54 \pm 0.21
C22:5n-3 (DPA)	2.12 \pm 0.29 ^a	2.35 \pm 0.34 ^b	2.31 \pm 0.36 ^b
C22:6n-3 (DHA) ^A	2.62 \pm 0.72	2.8 \pm 0.87	2.69 \pm 0.72
EPA + DHA ^A	3.12 \pm 0.86	3.48 \pm 1.20	3.22 \pm 0.86
EPA + DPA + DHA ^A	5.25 \pm 0.92	5.83 \pm 1.23	5.53 \pm 0.92
AA/EPA ^A	66.65 \pm 25.37	53.73 \pm 21.48	62.51 \pm 23.92
AA/EPA + DPA + DHA ^A	5.73 \pm 1.14	5.14 \pm 1.15	5.38 \pm 1.04

The detection limit for fatty acid analysis was 3.59 μ mol/l which corresponded to 0.1–0.6 mol% depending on the amount of fatty acid present in platelet phospholipid samples

GOT glutamic oxaloacetic transaminase, *GPT* glutamic pyruvate transaminase, γ *GT* gamma glutamic transpeptidase

Values within a row with different superscript letters indicate significant differences at $P = 0.05$ (general linear model for repeated measures)

^A For these fatty acids, fish_score was a confounder with a significant effect. Detailed results can be found in Table 5

Discussion

This study evaluated the effect of replacing various commonly eaten food items by dietary products naturally fortified with ALA for a period of 12 weeks on several cardiovascular risk markers in a group of middle-aged men. By using a wide range of ALA-enriched food items this

total dietary approach differed from previous supplementation studies which used ALA-enriched capsules or single fortified dietary products [16]. A systematic review of these previous supplementation studies found, however, that ALA supplementation did not appear to affect most cardiovascular risk markers, which is in contrast with the results of the study presented in this paper. Possibly, the

Table 5 Fatty acid composition of platelet phospholipids (mol% of total fatty acids) at T0, T6 and T12 (mean \pm standard deviation) per group with a different fish_score (FS1: did not regularly consume the provided fish; FS2: consumed the provided fish from time to time; FS3: consumed the provided fish most of the time)

		T0	T6	T12
C18:0	FS1 (<i>n</i> = 14)	17.04 \pm 0.62 ^a	17.00 \pm 0.76 ^a	17.03 \pm 0.65 ^a
C18:0	FS2 (<i>n</i> = 24)	16.84 \pm 0.43 ^a	16.89 \pm 0.61 ^a	17.12 \pm 0.46 ^b
C18:0	FS3 (<i>n</i> = 21)	16.74 \pm 0.53 ^a	16.42 \pm 0.73 ^b	16.74 \pm 0.59 ^a
AA	FS1 (<i>n</i> = 14)	29.11 \pm 1.23 ^a	28.87 \pm 1.60 ^a	29.01 \pm 1.34 ^a
AA	FS2 (<i>n</i> = 24)	29.30 \pm 0.99 ^a	29.15 \pm 1.09 ^a	29.23 \pm 1.11 ^a
AA	FS3 (<i>n</i> = 21)	28.85 \pm 1.04 ^a	27.77 \pm 1.64 ^b	28.38 \pm 1.09 ^c
EPA	FS1 (<i>n</i> = 14)	0.37 \pm 0.15 ^a	0.47 \pm 0.15 ^b	0.38 \pm 0.10 ^a
EPA	FS2 (<i>n</i> = 24)	0.48 \pm 0.22 ^a	0.55 \pm 0.23 ^a	0.50 \pm 0.18 ^a
EPA	FS3 (<i>n</i> = 21)	0.59 \pm 0.19 ^a	0.94 \pm 0.54 ^b	0.69 \pm 0.21 ^a
DHA	FS1 (<i>n</i> = 14)	2.17 \pm 0.60 ^a	2.14 \pm 0.56 ^a	2.16 \pm 0.63 ^a
DHA	FS2 (<i>n</i> = 24)	2.58 \pm 0.75 ^a	2.59 \pm 0.69 ^a	2.56 \pm 0.62 ^a
DHA	FS3 (<i>n</i> = 21)	2.96 \pm 0.60 ^a	3.46 \pm 0.79 ^b	3.15 \pm 0.61 ^a
EPA + DHA	FS1 (<i>n</i> = 14)	2.54 \pm 0.64 ^a	2.61 \pm 0.59 ^a	2.54 \pm 0.58 ^a
EPA + DHA	FS2 (<i>n</i> = 24)	3.06 \pm 0.89 ^a	3.15 \pm 0.87 ^a	3.06 \pm 0.72 ^a
EPA + DHA	FS3 (<i>n</i> = 21)	3.55 \pm 0.73 ^a	4.39 \pm 1.22 ^b	3.84 \pm 0.77 ^c
EPA + DPA + DHA	FS1 (<i>n</i> = 14)	4.85 \pm 0.72 ^a	5.22 \pm 0.66 ^b	5.05 \pm 0.69 ^{ab}
EPA + DPA + DHA	FS2 (<i>n</i> = 24)	5.13 \pm 1.03 ^a	5.43 \pm 1.02 ^b	5.30 \pm 0.82 ^{ab}
EPA + DPA + DHA	FS3 (<i>n</i> = 21)	5.61 \pm 0.79 ^a	6.68 \pm 1.28 ^b	6.10 \pm 0.88 ^c
AA/EPA	FS1 (<i>n</i> = 14)	77.84 \pm 19.97 ^a	67.04 \pm 17.82 ^b	82.76 \pm 24.01 ^a
AA/EPA	FS2 (<i>n</i> = 24)	72.06 \pm 29.00 ^a	59.94 \pm 19.35 ^a	65.30 \pm 19.25 ^{ab}
AA/EPA	FS3 (<i>n</i> = 21)	54.33 \pm 18.91 ^a	38.69 \pm 17.09 ^b	46.93 \pm 17.84 ^{ab}
AA/LCn-3	FS1 (<i>n</i> = 14)	6.15 \pm 1.05 ^a	5.63 \pm 0.91 ^b	5.84 \pm 0.99 ^{ab}
AA/LCn-3	FS2 (<i>n</i> = 24)	5.93 \pm 1.24 ^a	5.56 \pm 1.04 ^b	5.65 \pm 0.93 ^b
AA/LCn-3	FS3 (<i>n</i> = 21)	5.26 \pm 0.94 ^a	4.34 \pm 1.00 ^b	4.78 \pm 0.93 ^c

Values within a row with different superscript letters indicate significant differences at $P = 0.05$ (general linear model for repeated measures)

overall dietary approach used in this study and resulting not only in an increase of ALA and LC n-3 PUFA but also in a reduction of total fat, SFA and MUFA, can explain this difference.

The dietary intervention provided the participants with a more balanced diet regarding the fatty acid composition by substantially increasing ($\sim +50\%$) the supply of n-3 fatty acids, essentially ALA, and slightly decreasing the supply of saturated fatty acids. Nevertheless, it must be mentioned that the LC n-3 PUFA content of the standard menu was already high. The explanation is that fatty fish (a.o. mackerel, fatty acid composition of mackerel shown in Table 1) was regularly put on the menu in the prison. The increase in n-3 PUFA supply during the intervention led to a LA/ALA ratio of 4/1 and an n-6/n-3 ratio of 3/1; this allowed the diet to meet current dietary guidelines [20]. LA/ALA and n-6/n-3 ratios averaged 6/1 in the standard menu which was relatively low compared to data from national PUFA dietary consumption reports. Indeed, a study based on food consumption data of Belgian women collected in 2002 found a mean LA/ALA and n-6/n-3 ratio

averaging both 8-7/1 [5]. However, regarding this n-6/n-3 ratio, it recently came up that this is not the ideal dietary measure to use in the context of cardiovascular health, but that the absolute amounts of LA and ALA are of relevance to the efficiency of conversion of ALA to EPA and DHA [30]. Therefore, the fact that the absolute amount of LA in the supplied menu decreased while the absolute amount of ALA increased (Table 4) possibly had a beneficial effect on the ALA conversion to EPA and DHA.

Changes in the fatty acid composition of platelets appeared to be largely influenced by the fish consumption habits of the volunteers. Indeed, the relative content of LC n-3 PUFA increased in platelet phospholipids from participants regularly consuming the fish that was provided. This is in accordance with a previous study reporting increases in LC n-3 PUFA in platelet phospholipids [31].

Volunteers included in the study were slightly overweight but presented normal systolic and diastolic blood pressure. Dietary manipulation did not modify weight and BMI nor did it affect systolic blood pressure. Still, a significant decrease of 3 mmHg in diastolic blood pressure

was found after 12 weeks of n-3 enriched diet on a population level. The diastolic blood pressure returned to basal values when volunteers received their standard diet again. These results are in line with a recent international cross-sectional epidemiologic study (INTERMAP study) which concluded that dietary n-3 PUFA intake (ALA and LC) is inversely related to blood pressure in hyper- and normotensive persons [32]. However, in the INTERMAP study, a reduction of the systolic and diastolic blood pressure was found, whereas in our study no significant effect on the systolic blood pressure was found. No clear explanation for this difference could be found. Further, Paschos et al. [33] recently showed that supplementation with flaxseed oil, rich in ALA, lowers blood pressure in middle-aged men [33]. Since the blood pressure level is directly related to coronary heart disease (CHD) mortality [34], the decrease in diastolic blood pressure observed in the present study may be associated with a significant reduction in CHD risk and have important public health implications. Indeed, a decrease of 5 mmHg of diastolic blood pressure appears to be associated with a 20% lower risk of CHD and a 30% decrease of stroke [35].

Volunteers of the study manifested a dyslipidaemic profile with high LDL-C and low HDL-C plasma levels while the mean values for fasting plasma TC and TG levels were within normal ranges. Dietary manipulation had no effect on TC, LDL-C and TG levels; this is in accordance with previous short and long-term ALA supplementation studies [36–38]. In contrast, HDL-C levels which were low at the start of the study increased by more than 2 mg/dl during the intervention period in non-smoker participants. Such an increase in HDL-C may represent another important health benefit in relation to CHD. Indeed, every 1 mg/dl increase in HDL-C appears to decrease cardiovascular risk by 2–3% [39]. An increase in HDL-C was not found for the smoking participants, which can be explained by the fact that smoking decreases HDL-C [40].

For both effects, a reduced diastolic blood pressure and an increased HDL-C in non-smokers, the statistical analyses indicated no significant confounding effect of fish_score, indicating that the consumption of fish is not the crucial explanation behind both effects. Moreover, the diastolic blood pressure lowering effect and the HDL-C raising effect was only seen after the second intervention cycle, and not after the first intervention cycle. This can be explained by the fact that clinical benefits of dietary supplementation with n-3 PUFA are not immediate. The time course to alter clinical events may occur within weeks or months to years depending on the clinical effect studied as well as the type of n-3 PUFA used for supplementation. As reviewed by Mozaffarian et al. [41], the beneficial effect of fish or fish oil intake on blood pressure lowering occurs only within months of intake.

A limitation of this study is the control of the food consumption. The compliance to the provided diet was evaluated on the basis of questionnaires which do not reflect the precise amount of food ingested. Furthermore, volunteers also had access to food that they bought themselves in the canteen of the prison. On the basis of the data on purchasing behaviour which were listed up by the administration of the prison at any time, it could however be concluded that there was no difference in purchasing behaviour of food items during the intervention period compared to the standard period (details not shown).

In summary, providing ALA through a variety of fortified foods enables to considerably increase the n-6/n-3 ratio in the diet without changing the subject's dietary habits. Such an increased n-3 supply in a group of middle-aged men has beneficial effects on at least two CHD risk factors by lowering their diastolic blood pressure and increasing HDL-C in non-smokers.

Acknowledgments First of all, we wish to thank all the participants of the study as well as the director and all the staff members of the penitentiary institute, in particular the medical staff and the kitchen staff for their enthusiastic and fruitful collaboration. The dietician Thierry Denies is acknowledged for the excellent help in the organisation of the fieldwork and Professor Jean-Marie Pycke is acknowledged for the analyses of the food samples. We would like to express our appreciation to Patricia D'Hont, Valérie Delforge, Arleta Chwalik and Annie Dufour for their excellent technical assistance. All companies of the ESV/GIE EQUILIBRIUM Industrial Partnership are thanked for sponsoring this study by providing the n-3 fortified foods. Els Clays is thanked for statistical advice. The work was partly financed by the Walloon region of Belgium through the competitiveness cluster 'WALGRALIM'.

References

1. World Health Organization (2003) Diet, nutrition and the prevention of chronic diseases. WHO Technical report series, 916. Geneva, WHO
2. Mann J (2004) Cardiovascular disease. In: Gibney MJ, Margetts B, Kearney J, Arab L (eds) Public health nutrition. Blackwell, Oxford, pp 317–329
3. Deckelbaum RJ, Akabas SR (2006) n-3 Fatty acids and cardiovascular disease: navigating toward recommendations. *Am J Clin Nutr* 84(1):1–2
4. Loosemore ED, Judge MP, Lammi-Keefe CJ (2004) Dietary intake of essential and long-chain polyunsaturated fatty acids in pregnancy. *Lipids* 39(5):421–424
5. Sioen IA, Pynaert I, Matthys C, De Backer G, Van Camp J, De Henauw S (2006) Dietary intakes and food sources of fatty acids for Belgian women, focused on n-6 and n-3 polyunsaturated fatty acids. *Lipids* 41(5):415–422
6. Astorg P, Arnault N, Czernichow S, Noisette N, Galan P, Hercberg S (2004) Dietary intakes and food sources of n-6 and n-3 PUFA in French adult men and women. *Lipids* 39(6):527–535
7. Howe P, Meyer B, Record S, Baghurst K (2006) Dietary intake of long-chain [omega]-3 polyunsaturated fatty acids: contribution of meat sources. *Nutrition* 22(1):47–53

8. Meyer BJ, Mann NJ, Lewis JL, Milligan GC, Sinclair AJ, Howe PRC (2003) Dietary intakes and food sources of omega-6 and omega-3 polyunsaturated fatty acids. *Lipids* 38(4):391–398
9. Verbeke W, Sioen I, Pieniak Z, Van Camp J, De Henauw S (2005) Consumer perception versus scientific evidence about health benefits and safety risks from fish consumption. *Public Health Nutr* 8(4):422–429
10. FAO (2006) The state of world fisheries and aquaculture. 1-148. 2007. Rome, FAO communication division
11. Din JN, Newby DE, Flapan AD (2004) Science, medicine, and the future omega 3 fatty acids and cardiovascular disease: fishing for a natural treatment. *BMJ* 328(7430):30–35
12. de Lorgeril M, Salen P (2006) The Mediterranean diet in secondary prevention of coronary heart disease. *Clin Invest Med* 29(3):154–158
13. Singh RB, Dubnov G, Niaz MA, Ghosh S, Singh R, Rastogi SS, Manor O, Pella D, Berry EM (2002) Effect of an Indo-Mediterranean diet on progression of coronary artery disease in high risk patients (Indo-Mediterranean diet heart study): a randomised single-blind trial. *Lancet* 360(9344):1455–1461
14. Burdge GC, Calder PC (2005) Conversion of alpha-linolenic acid to longer-chain polyunsaturated fatty acids in human adults. *Reprod Nutr Dev* 45(5):581–597
15. Wang C, Harris WS, Chung M, Lichtenstein AH, Balk EM, Kupelnick B, Jordan HS, Lau J (2006) n-3 Fatty acids from fish or fish-oil supplements, but not {alpha}-linolenic acid, benefit cardiovascular disease outcomes in primary- and secondary-prevention studies: a systematic review. *Am J Clin Nutr* 84(1):5–17
16. Wendland E, Farmer A, Glasziou P, Neil A (2006) Effect of alpha linolenic acid on cardiovascular risk markers: a systematic review. *Heart* 92(2):166–169
17. Finnegan YE, Minihane AM, Leigh-Firbank EC, Kew S, Meijer GW, Muggli R, Calder PC, Williams CM (2003) Plant- and marine-derived n-3 polyunsaturated fatty acids have differential effects on fasting and postprandial blood lipid concentrations and on the susceptibility of LDL to oxidative modification in moderately hyperlipidemic subjects. *Am J Clin Nutr* 77(4):783–795
18. Bemelmans WJ, Broer J, Feskens EJ, Smit AJ, Muskiet FA, Lefrandt JD, Bom VJ, May JF, Meyboom-de Jong B (2002) Effect of an increased intake of {alpha}-linolenic acid and group nutritional education on cardiovascular risk factors: the Mediterranean alpha-linolenic enriched Groningen dietary intervention (MARGARIN) study. *Am J Clin Nutr* 75(2):221–227
19. Balk EM, Lichtenstein AH, Chung M, Kupelnick B, Chew P, Lau J (2006) Effects of omega-3 fatty acids on serum markers of cardiovascular disease risk: a systematic review. *Atherosclerosis* 189(1):19–30
20. de Lorgeril M, Salen P (2004) Alpha-linolenic acid and coronary heart disease. *Nutr Metab Cardiovasc Dis* 14(3):162–169
21. Folch J, Lee M, Sloane-Stanley GH (1957) A simple method for the isolation and purification of total lipids from animal tissues. *J Biol Chem* 226:497–509
22. Christie WW (2008) Gas chromatography and lipids, a practical guide, 2nd edn. The Oily press Ltd, ed. Dundee
23. Dieffenbacher A, Pocklington WD (2008) Standard methods for the analysis of oils, fats and derivatives, first supplement to the 7th edn. IUPAC, ed. Blackwell, Oxford
24. Dahlan W, Richelle M, Kulapongse S, Rossle C, Deckelbaum RJ, Carpentier YA (1992) Effects of essential fatty-acid contents of lipid emulsions on erythrocyte polyunsaturated fatty-acid composition in patients on long-term parenteral-nutrition. *Clin Nutr* 11(5):262–268
25. Burstein M, Scholnick HR, Morfin R (1970) Rapid method for the isolation of lipoproteins from human serum by precipitation with polyanions. *J Lipid Res* 11(6):583–595
26. Lopes-Virella MF, Stone P, Ellis S, Colwell JA (1977) Cholesterol determination in high-density lipoproteins separated by three different methods. *Clin Chem* 23(5):882–884
27. Friedewald W, Frederick D, Levy RI (1972) Estimation of concentration of low-density lipoprotein cholesterol in plasma, without use of preparative ultracentrifuge. *Clin Chem* 18(6):499
28. Dubois DY, Cantraine F, Malmendier CL (1987) Comparison of different sandwich enzyme immunoassays for the quantitation of human apolipoprotein-A-I and apolipoprotein-A-II. *J Immunol Methods* 96(1):115–120
29. Cotton F, Thiry P, Hsain AB, Boeynaems JM (2001) Analyzer transfer of a broad range high-sensitivity C-reactive protein immunoassay. *Clin Lab* 47(7–8):405–409
30. Griffin BA (2008) How relevant is the ratio of dietary n-6 to n-3 polyunsaturated fatty acids to cardiovascular disease risk? Evidence from the OPTILIP study. *Curr Opin Lipidol* 19(1):57–62
31. Metcalf RG, James MJ, Mantzioris E, Cleland LG (2003) A practical approach to increasing intakes of n-3 polyunsaturated fatty acids: use of novel foods enriched with n-3 fats. *Eur J Clin Nutr* 57(12):1605–1612
32. Ueshima H, Stamler J, Elliott P, Chan Q, Brown IJ, Carnethon MR, Daviglus ML, He K, Moag-Stahlberg A, Rodriguez BL, Steffen LM, Van Horn L, Yarnell J, Zhou B, for the INTERMAP Research Group (2007) Food omega-3 fatty acid intake of individuals (total, linolenic acid, long-chain) and their blood pressure: INTERMAP study. *Hypertension* 50(2):313–319
33. Paschos GK, Magkos F, Panagiotakos DB, Votteas V, Zampelas A (2007) Dietary supplementation with flaxseed oil lowers blood pressure in dyslipidaemic patients. *Eur J Clin Nutr* 61(10):1201–1206
34. Van den Hoogen PCW, Feskens EJM, Nagelkerke NJD, Menotti A, Nissinen A, Kromhout D (2000) The relation between blood pressure and mortality due to coronary heart disease among men in different parts of the world. *N Engl J Med* 342(1):1–8
35. Law M, Wald N, Morris J (2003) Lowering blood pressure to prevent myocardial infarction and stroke: a new preventive strategy. *Health Technol Assess* 7(31):1–94
36. Liou YA, King DJ, Zibrik D, Innis SM (2007) Decreasing linoleic acid with constant {alpha}-linolenic acid in dietary fats increases (n-3) eicosapentaenoic acid in plasma phospholipids in healthy men. *J Nutr* 137(4):945–952
37. Harper CR, Edwards MC, Jacobson TA (2006) Flaxseed oil supplementation does not affect plasma lipoprotein concentration or particle size in human subjects. *J Nutr* 136(11):2844–2848
38. Pang D, Iman-Farinelli MA, Wong T, Barnes R, Kingham KM (1998) Replacement of linoleic acid with alpha-linolenic acid does not alter blood lipids in normolipidaemic men. *Br J Nutr* 80(2):163–167
39. Gordon DJ, Probstfield JL, Garrison RJ, Neaton JD, Castelli WP, Knoke JD, Jacobs DR Jr, Bangdiwala S, Tyroler HA (1989) High-density lipoprotein cholesterol and cardiovascular disease. Four prospective American studies. *Circulation* 79(1):8–15
40. Hata Y, Nakajima K (2000) Life-style and serum lipids and lipoproteins. *J Atheroscler Thromb* 7(4):177–197
41. Mozaffarian D, Rimm EB (2006) Fish intake, contaminants, and human health: evaluating the risks and the benefits. *JAMA* 296(15):1885–1899

Effect of *trans*8, *cis*10+*cis*9, *trans*11 Conjugated Linoleic Acid Mixture on Lipid Metabolism in 3T3-L1 Cells

Shama V. Joseph · Jessica R. Miller ·
Roger S. McLeod · H el ene Jacques

Received: 23 September 2008 / Accepted: 15 April 2009 / Published online: 22 May 2009
  AOCs 2009

Abstract Evidence suggests that minor isomers of conjugated linoleic acid (CLA), such as *trans*8, *cis*10 CLA, can elicit unique biological effects of their own. In order to determine the effect of a mixture of *t*8, *c*10+*c*9, *t*11 CLA isomers on selected aspects of lipid metabolism, 3T3-L1 preadipocytes were differentiated for 8 days in the presence of 100 μ M linoleic acid (LA); *t*8, *c*10+*c*9, *t*11 CLA; *t*10, *c*12+*c*9, *t*11 CLA or purified *c*9, *t*11 CLA. Whereas supplementation with *c*9, *t*11 and *t*10, *c*12+*c*9, *t*11 CLA resulted in cellular triglyceride (TG) concentrations of 3.4 ± 0.26 and 1.3 ± 0.11 μ g TG/ μ g protein, respectively ($P < 0.05$), TG accumulation following treatment with CLA mixture *t*8, *c*10+*c*9, *t*11 was significantly intermediate (2.5 ± 0.22 μ g TG/ μ g protein, $P < 0.05$) between the two other CLA treatments. However, these effects were not attributable to an alteration of the Δ^9 desaturation index. Adiponectin content of adipocytes treated with *t*8, *c*10+*c*9, *t*11 mixture was similar to the individual isomer *c*9, *t*11 CLA, and both the *t*8, *c*10+*c*9, *t*11 and *c*9, *t*11 CLA groups were greater ($P < 0.05$) than in the *t*10, *c*12+*c*9, *t*11 CLA group. Overall, these results suggest that *t*8, *c*10+*c*9, *t*11 CLA mixture affects TG accumulation in 3T3-L1 cells differently from the *c*9, *t*11 and *t*10, *c*12 isomers.

Furthermore, the reductions in TG accumulation occur without adversely affecting the adiponectin content of these cells.

Keywords Conjugated linoleic acid · Isomers · Triglycerides · Adiponectin · 3T3-L1 cells

Abbreviations

BSA	Bovine serum albumin
CLA	Conjugated linoleic acid
DMEM	Dulbecco's Modified Eagle's Medium
FAME	Fatty acid methyl ester
FFA	Free fatty acid
GC-FID	Gas chromatograph(y)-flame ionisation detector
LA	Linoleic acid
MUFA	Monounsaturated fatty acid
NL	Neutral lipid
SCD	Stearoyl CoA desaturase
TG	Triglyceride
TLC	Thin layer chromatography

Introduction

Conjugated linoleic acid (CLA), a group of positional and geometric isomers of linoleic acid with conjugated double bonds, has been demonstrated to impact aspects of health and disease as varied as cancer, cardiovascular disease, diabetes, immune function and bone health [1]. The specific ability of CLA to affect body fat metabolism and consequently reduce fat mass accumulation in animals, including mice [2] and pigs [3], has led to a flurry of research activity into its potential use as an anti-obesity agent. The *cis*9, *trans*11 CLA (*c*9, *t*11 CLA), also known as

S. V. Joseph · H. Jacques (✉)
Department of Food Science and Nutrition,
Institute of Nutraceuticals and Functional Foods,
Laval University, 2425 Agriculture St.,
Paul-Comtois Building, Quebec, QC G1V 0A6, Canada
e-mail: helene.jacques@fsaa.ulaval.ca

J. R. Miller · R. S. McLeod
Department of Biochemistry and Molecular Biology,
Dalhousie University, 5850 College Street, Room 9C Sir Charles
Tupper Medical Building, Halifax, NS B3H 1X5, Canada

'ruminic acid' is the predominant isomer occurring in nature and the most widely studied. It has recently become clear that many of the biological effects are attributable to the *trans*10, *cis*12 CLA (*t*10, *c*12 CLA), which is a minor isomer and occurs naturally only in small amounts. However, it can be obtained in the same proportion as the *c*9, *t*11 isomer from dietary CLA supplements [4]. It is thought to act through inhibition of TG accumulation via decreased activity of lipoprotein lipase and stearoyl CoA desaturase, decreasing preadipocyte differentiation, and by increasing fat oxidation and perhaps lipolysis [5]. Of importance, however, is the fact that results are varied and somewhat equivocal according to the model used, the dosage and the duration of supplementation. In addition, the presence of small amounts of various lesser-known isomers in the mixture may also play a role.

It is well known that the synthesis of monounsaturated fatty acids (MUFA), the preferred fatty acid (FA) for incorporation into triglyceride (TG), membrane phospholipids and cholesteryl esters, is catalysed by the central lipogenic enzyme, stearoyl CoA desaturase (SCD1). Palmitoleate (16:1) and oleate (18:1) are the major MUFA synthesised by this enzyme from palmitate (16:0) and stearate (18:0), respectively. Perturbations in the ratio of MUFA to saturated FA have been shown to influence several disease states such as obesity, dyslipidemia and insulin resistance [6]. There is evidence to indicate that inhibition of SCD1 activity can improve glucose signalling and prevent obesity in SCD null mice [7], although the mechanism for this effect is unknown. In a recent study [8], targeted SCD1 inhibition in mice fed a high-fat diet improved hepatic insulin signalling, suggesting that SCD1 activity is implicated in the development of insulin resistance. It is already known that SCD1 activity can be modulated by CLA in animals [9, 10] and cell lines, and that the *t*10, *c*12 CLA isomer decreases the activity of this enzyme in 3T3-L1 preadipocytes [11] and HepG2 cells [12] with a decrease in the synthesis of MUFA.

Adiponectin is an adipocyte specific cytokine that is involved in carbohydrate and lipid metabolism. Circulating levels of this hormone are found to be depressed in obesity. Moreover, low plasma levels of the hormone have been associated with low HDL, high TG levels and small, dense LDL particles, which are risk factors for the development of heart disease. Furthermore, adiponectin is required for normal insulin action. It is thought that lowered adiponectin could contribute towards development of insulin resistance and Type 2 diabetes [13].

Results from very early studies report essentially the combined effects of crude CLA mixtures containing different amounts of various isomers. It is now becoming increasingly clear that the range of individual isomers that comprise CLA are likely to exert unique biological effects

of their own. It is important to have knowledge of such isomers that exert either beneficial effects or might be detrimental to health so that they might be excluded from, or included in the manufacture of dietary supplements. One isomer that has received very little attention to date is the *trans*8, *cis*10 CLA (*t*8, *c*10 CLA), which is present as a minor component of dietary CLA supplements [14]. This isomer, which can be formed as a by-product during the commercial production of CLA, used to be present as an 'impurity' in the CLA mixtures that were used in studies conducted in the 1990s [15]. Methodologies have since been developed to avoid the generation of the *t*8, *c*10 isomer in order to produce CLA supplements of a higher quality. Therefore, knowledge of the specific biological effects of this isomer might be useful in better interpreting the results of those earlier studies on CLA. More recently, however, this isomer has been produced in substantial amounts as part of an equimolar mixture of *t*8, *c*10 and *c*9, *t*11 CLA when high CLA containing butterfat was heated under specific conditions [16]. The results of this study suggest that this isomer can be produced during cooking of milk and other dairy products containing the *c*9, *t*11 isomer and can thus be potentially obtained from the diet. In addition, CLA supplements for animals such as cows and pigs sometimes contain the *t*8, *c*10 isomer [14, 17], which might be incorporated into the food derived from these animals, providing yet another potential dietary source of this isomer. In light of these findings, a study was recently conducted in which hamsters fed a purified diet supplemented with an equal mixture of *t*8, *c*10 and *c*9, *t*11 at 2% (w/w) showed increased plasma VLDL TG and cholesterol concomitantly with an increase in plasma glucose, compared with an equal mixture of *t*10, *c*12+*c*9, *t*11 CLA [18].

The objectives of this study were, therefore, to further investigate the physiological effects of *t*8, *c*10+*c*9, *t*11 CLA mixture in relation to TG metabolism in the adipocyte. For this purpose, we compared a mixture of *t*8, *c*10+*c*9, *t*11 CLA, which was the only source of *t*8, *c*10 CLA available on the market, with a pure *c*9, *t*11 CLA isomer, a mixture of *t*10, *c*12+*c*9, *t*11 CLA, and linoleic acid (LA). The well-characterised mouse preadipocyte cell line, 3T3-L1, was selected as a suitable model for conducting this research.

Based on previous data [18, 19], we hypothesised that the *t*8, *c*10+*c*9, *t*11 mixture of CLA would increase TG accumulation through effects on stearoyl CoA desaturase, as estimated by the desaturation index, compared with the pure *c*9, *t*11 CLA and *t*10, *c*12+*c*9, *t*11 CLA mixture. We also expected to see a decrease in adiponectin content following the *t*8, *c*10+*c*9, *t*11 treatment compared with the pure *c*9, *t*11 CLA and *t*10, *c*12+*c*9, *t*11 CLA mixture. LA has been used as a reference.

Materials and Methods

Chemicals

A mixture of *t*8, *c*10+*c*9, *t*11 CLA, in free fatty acid (FFA) form, was obtained from Natural Lipids (Hovdebygda, Norway) and contained approximately 40% each of the two isomers. Pure *c*9, *t*11 and *t*10, *c*12 CLA were purchased from Matreya LLC (PA, USA). The fatty acids used in all studies were complexed to 10% BSA. The *t*10, *c*12+*c*9, *t*11 CLA used in the experiments was a 50:50 mixture of the two purified isomers. Bovine serum albumin (BSA) and LA treated cells were used as controls. The fatty acid composition of the experimental fatty acids is presented in Table 1. LA as sodium linoleate, BSA, dexamethasone (DEX), isobutyl methylxanthine (IBMX), trimethylsilyl (TMS) and sodium methoxide were obtained from Sigma-Aldrich, Inc. (Oakville, ON, Canada). BSA standard for the protein assay was purchased from Pierce Biotechnology Inc. (Rockford, IL, USA). Dulbecco's Modified Eagle's Medium (DMEM), trypsin-EDTA and fetal bovine serum (FBS) were obtained from Invitrogen (Burlington, ON, Canada). Di-ethyl ether for thin layer chromatography (TLC) was obtained from EMD Chemicals Inc. (Hawthorne, NY, USA).

Cell Culture

3T3-L1 mouse preadipocytes (#CL-173) were purchased from the American Type Culture Collection (VA, USA) and were routinely maintained in a growth medium of Dulbecco's Modified Eagle's Medium (DMEM) supplemented with 10% fetal bovine serum at 37 °C in a humidified atmosphere of 5% CO₂. Medium was changed

Table 1 Fatty acid composition of the experimental fatty acids (relative area %)

Fatty acid	<i>trans</i> 8, <i>cis</i> 10+ <i>cis</i> 9, <i>trans</i> 11 CLA	<i>cis</i> 9, <i>trans</i> 11 CLA	<i>trans</i> 10, <i>cis</i> 12 CLA	LA
16:0	<0.1			
18:0	<0.1			
<i>cis</i> 9 18:1	3.7			
<i>cis</i> 9, <i>cis</i> 12 18:2	<0.1			99
<i>cis</i> 9, <i>trans</i> 11 18:2	~40	>98		
<i>trans</i> 8, <i>cis</i> 10 18:2	~40			
<i>trans</i> 10, <i>cis</i> 12 18:2	1.9		>98	
Other conjugated 18:2	~13.1			

Obtained from certificates of analysis provided by manufacturers (Matreya LLC for *cis*9, *trans*11 and *trans*10, *cis*12 CLA and LA, and Natural Lipids for *trans*8, *cis*10+*cis*9, *trans*11 CLA)

LA linoleic acid, CLA conjugated linoleic acid

every 2 days and cell monolayers were passaged at regular intervals until use in experiments.

For studies on TG accumulation and adiponectin expression, cells that were 50–60% confluent were seeded into 12-well cell culture cluster plates (Corning, NY, USA). For the fatty acid profile studies, cells were seeded into 60-mm cell culture plates (BD Falcon, Mississauga, ON, Canada). Cell layers in all culture dishes were allowed to grow to confluence.

Adipocyte Differentiation and Fatty Acid Treatments

Two days after 3T3-L1 cells had reached confluence, the differentiation process was induced by replacing growth medium with induction medium comprising DMEM, 10% FBS, 250 nM DEX, 0.5 μM IBMX and 5 μg/mL insulin (this was day 'zero' of the experiment). After 48 h, the induction medium bathing the differentiating cells was replaced by DMEM containing 10% FBS, 5 μg/mL insulin and either 100 μM BSA, LA, *c*9, *t*11 CLA, *c*9, *t*11+*t*10, *c*12 CLA mixture, or *t*8, *c*10+*c*9, *t*11 CLA. Media were changed on alternate days with addition of fresh BSA or fatty acids to each medium change. On day 10 of the experiment, cells were washed and harvested in 1 mL isotonic sucrose buffer containing 29 mM sucrose, 73 μM tris-HCl (pH 8) and 24 μM EDTA, and stored at –20 °C until the lipid extraction process. A further step was included for cells that were harvested for TG, protein and adiponectin measurements: cell layers were centrifuged to remove sucrose buffer, resuspended in 100 μL phosphate buffered saline, sonicated for 10 s at 20% output and stored at –20 °C.

Estimation of TG Content

TG content of 3T3-L1 cells was measured with a commercially available colorimetric kit from Diagnostic Chemicals Limited (Charlottetown, PEI, Canada) using glycerol as standard. Briefly, triglycerides are hydrolysed to glycerol and fatty acids. The glycerol moiety is phosphorylated and oxidised leading to the formation of hydrogen peroxide ultimately resulting in reactions leading to the formation of quinoneimine dye, which can be measured spectrophotometrically at 490 nm on a Microplate Reader (model 3550; Bio-Rad, Ramsey, MN, USA). The amount of dye formed is directly proportional to the amount of triglyceride. TG contents of samples were normalised to total cell protein and expressed as μg TG/μg protein.

Estimation of Protein Content

The DC Bio-Rad Protein micro-assay kit (Bio-Rad Laboratories, CA, USA) was used to estimate the protein

content of 3T3-L1 cells with BSA as the standard. This procedure is based on the principle of the Lowry assay [20] involving detergent solubilisation of the samples and colorimetric analysis on a Microplate Reader at 655 nm (model 3550; Bio-Rad, Ramsey, MN, USA).

Estimation of Adiponectin Content

The adiponectin content of 3T3-L1 cells was determined by western blotting analysis using mouse anti-mouse adiponectin antibody (Chemicon International Inc., Temecula, CA, USA) and goat anti-mouse secondary antibody (Bio-Rad Laboratories, CA, USA). Protein in 2 μ l whole cell homogenate was resolved, under reducing conditions, on a 10% SDS–polyacrylamide gel. The separated bands were transferred onto a nitrocellulose membrane (Bio-Rad Laboratories, CA, USA), blocked, and probed with the primary antibody followed by incubation with the horseradish peroxidase conjugated secondary antibody. The membrane was then revealed with BM Chemiluminescence Blotting Substrate solution (POD) (Roche Diagnostics, Laval, QC, Canada) and the signals recorded by autoradiography. Data were analysed using Scion Imaging Software (Scion Corporation, Frederick, MD, USA).

Extraction of Total Lipids from 3T3-L1 Cells

Total lipids were extracted from 3T3-L1 cells according to a modification of the method of Hara and Radin [21] using 40:1 ratio of isopropanol:hexane (v/v). Cell lipids thus obtained were separated into FFA and neutral lipid (NL) fractions. Thin layer chromatography (TLC) was used to further separate the NL fraction into its constituent lipid classes, including triglycerides.

Thin Layer Chromatography for Separation of Neutral Lipids

The NL fraction retained in hexane from the initial lipid extraction process was dried down under nitrogen, dissolved in 50 μ l of chloroform, and spotted on a silica TLC plate (250 μ m coating thickness, Sigma–Aldrich) that had been baked at 50°C for at least an hour and scored to accommodate multiple samples. A 0.02 g/mL standard of phosphatidylcholine/triolein/cholesterol oleate was also spotted on the plate. A double development method was used to separate the neutral lipids. The phospholipids were first separated by placing the plates in a glass chamber equilibrated with chloroform:methanol:acetic acid:water (70:30:12:1), and this was followed by separation of the triglyceride and cholesteryl ester fractions with hexane:diethyl ether:acetic acid (70:30:1). The plates were

dried in air, developed with iodine vapor and bands identified by comparison with the standard.

Preparation of Fatty Acid Methyl Esters (FAME)

FAME of FFA lipid fraction were prepared by incubation with 10% trimethylsilyl–diazomethane in hexane for 30 min at room temperature by the method of Hashimoto et al. [22]. Cellular triglycerides were trans-esterified to their methyl esters by heating for 20 min at 50°C in the presence of methanolic sodium methoxide [23].

Determination of Fatty Acid Composition by GC-FID Analysis

Analysis of all FAME, except those derived from cells treated with *t8*, *c10+c9*, *t11* CLA mixture, were performed on an Hewlett-Packard 6890 Capillary FID gas chromatograph equipped with a 60 m column (0.25 mm inside diameter) coated with 50% cyanopropyl polysiloxane (0.25 μ m film thickness; J&W DB-23; Folsom, CA, USA), and temperature programmed as isothermal at 153°C for 2 min, ramp at 1.7°C/min and hold at 174°C for 0.2 min, ramp at 2.5°C/min and hold at 220°C for 3 min. Methyl heptadecanoic acid (C17:0) was used as the internal standard. Data were analysed using HP ChemStation software (Hewlett-Packard, Agilent Technologies, Mississauga, ON, Canada).

The *t8*, *c10+c9*, *t11* CLA FAME were analysed separately on a 6890 Series II gas chromatograph (Hewlett-Packard) using the temperature and pressure program described previously by Destailats et al. [16]. This step was requisite as the two isomers co-elute when subjected to GC analysis under the conditions described above. Peaks were identified by comparing with commercially available mixture of FAME (GLC 15A), as well as pure *c9*, *t11* and *t10*, *c12* CLA methyl esters obtained from Nu-Check Prep (Elysian, MN, USA). The response factor for C17:0 was used to quantify the identified fatty acids.

Statistical analysis

Data were analysed using SPSS[®] (Statistical Package for Social Sciences; SPSS Inc., IL, USA), SAS[®] (Statistical Analysis Software; SAS Institute Inc., NC, USA) and GraphPad Prism software (GraphPad software Inc., San Diego, CA, USA). Means of the treatment groups were compared using one-way ANOVA with Tukey's post hoc test to detect significant differences between means at $P < 0.05$. Pearson's correlation coefficient was used to calculate relationship between cellular TG concentration and adiponectin content.

Results

Effect of Fatty Acid Treatments on TG Accumulation

The effect of fatty acid supplementation on TG accumulation in differentiating 3T3-L1 cells is presented in Fig. 1. The TG content in cells treated with *c9*, *t11* CLA was significantly higher ($3.4 \pm 0.26 \mu\text{g TG}/\mu\text{g protein}$, $P < 0.05$) than the two other CLA treatments, LA and BSA (no fatty acid). In direct contrast, *t10*, *c12+c9*, *t11* CLA mixture significantly inhibited TG accumulation in 3T3-L1 cells compared with all other treatment groups ($1.3 \pm 0.11 \mu\text{g TG}/\mu\text{g protein}$, $P < 0.05$). Cells that had been supplemented with *t8*, *c10+c9*, *t11* CLA mixture accumulated TG ($2.5 \pm 0.22 \mu\text{g TG}/\mu\text{g protein}$) to an extent that was intermediate between the pure *c9*, *t11* and the *t10*, *c12+c9*, *t11* CLA mixture ($P < 0.05$). This effect, however, was similar to that of both LA and BSA control.

Effect of Fatty Acid Treatments on Δ^9 desaturation index

Data on the Δ^9 desaturation index of the cellular TG fraction are presented in Table 2. This index is the ratio of monounsaturated to saturated fatty acid of palmitic acid (palmitoleic acid/palmitic acid; 16:1/16:0) and stearic acid (oleic acid/stearic acid; 18:1/18:0), and is used as an indicator of the activity of the lipogenic enzyme, stearoyl CoA desaturase. Supplementation of differentiating 3T3-L1 cells with *t10*, *c12+c9*, *t11* CLA mixture resulted in a significant decrease ($P < 0.05$) in the Δ^9 desaturation index, suggesting a decrease in the enzyme's activity when compared with BSA, LA, *c9*, *t11* CLA, or the *t8*, *c10+c9*, *t11* CLA mixture. No statistically significant differences were observed between the LA, *c9*, *t11* CLA, or the *t8*, *c10+c9*, *t11* CLA mixture groups.

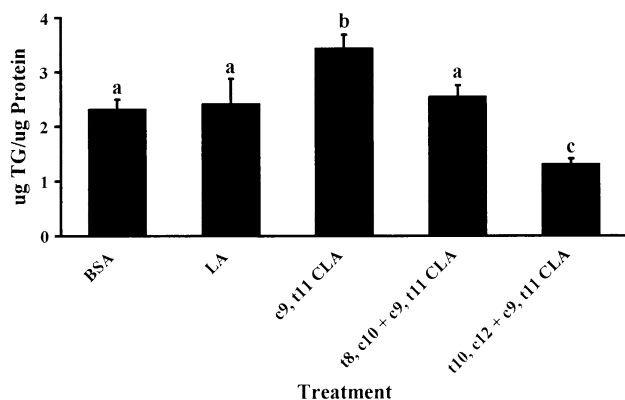


Fig. 1 Effect of 100 μM BSA, LA, *c9*, *t11* CLA, *t8*, *c10+c9*, *t11* CLA or *t10*, *c12+c9*, *t11* CLA on TG accumulation in 3T3-L1 mouse (pre)adipocytes. Data are means \pm SD ($n = 3$). Means for a variable without a common letter differ at $P < 0.05$

Table 2 Effect of fatty acid treatment on Δ^9 desaturation index

Treatment	16:1/16:0	18:1/18:0
BSA	0.79 ± 0.16	5.00 ± 0.76
LA	0.52 ± 0.15	$2.89 \pm 0.52^\dagger$
<i>cis9</i> , <i>trans11</i> CLA	0.60 ± 0.20	3.92 ± 0.21
<i>trans8</i> , <i>cis10+cis9</i> , <i>trans11</i> CLA	0.53 ± 0.14	3.47 ± 0.98
<i>trans10</i> , <i>cis12+cis9</i> , <i>trans11</i> CLA	$0.07 \pm 0.06^*$	$0.25 \pm 0.05^*$

Desaturation indices in TG fraction of 3T3-L1 cells treated with fatty acids. Values are means \pm SD ($n = 3$)

BSA bovine serum albumin, LA linoleic acid, CLA conjugated linoleic acid, 16:1 palmitoleic acid, 16:0 palmitic acid, 18:1 oleic acid, 18:0 stearic acid

* Significantly different from all other treatment groups at $P < 0.05$

† Significantly different from BSA at $P < 0.05$

Effect of Fatty Acid Treatments on Adiponectin Content

The results on the adiponectin content of 3T3-L1 cells in response to fatty acid supplementation are presented in Fig. 2. Among the five treatments, *t10*, *c12+c9*, *t11* CLA mixture had the most profound effect on adiponectin content of the differentiating cells by more than 30% compared to the other fatty acids ($P < 0.05$). Cells treated with this CLA mixture had the same level of adiponectin as cells treated without fatty acid. No significant differences in adiponectin were observed between cells treated with LA, pure *c9*, *t11* CLA or the *t8*, *c10+c9*, *t11* CLA mixture.

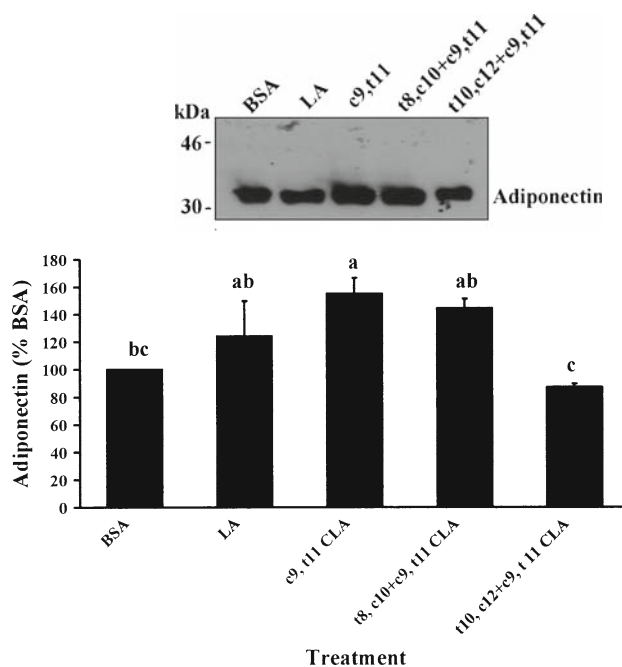


Fig. 2 Adiponectin content of 3T3-L1 mouse (pre)adipocytes treated with 100 μM BSA or fatty acids. Data are means \pm SD ($n = 3$). Means for a variable without a common letter differ at $P < 0.05$

Correlation Between TG Accumulation and Adiponectin Content

Correlation analysis revealed that there was a positive association between cellular TG concentration and adiponectin content in 3T3-L1 cells treated with BSA or different fatty acids ($n = 15$, $r = 0.72$, $P = 0.002$).

Discussion

The present study provided evidence that the *t8*, *c10+c9*, *t11* CLA mixture behaves in a manner that is unique compared to the other CLA isomers used in this study with regards to selected aspects of lipid metabolism in 3T3-L1 cells. The differences included TG accumulation, desaturation index, and cellular content of the cytokine adiponectin. 3T3-L1 preadipocytes are considered the gold standard for studying adipogenesis at the cellular level, and have been used in a number of studies to determine the effects of CLA on various aspects of lipid metabolism. 3T3-L1 is a non-transformed cell line derived from disaggregated mouse embryo cells that were selected for their ability to accumulate triglyceride droplets. These cells have undergone commitment, and when appropriately stimulated develop into fully functional adipocytes exhibiting the same metabolic features as adipocytes derived from adipose tissue [24]. In culture, these cells are responsive to the same differentiation-inducing agents as adipose tissue in vivo, and thereby represent appropriate models of preadipocyte differentiation [25]. A novel aspect of our research was the observation that *t8*, *c10+c9*, *t11* CLA mixture did not promote lipid filling of 3T3-L1 preadipocytes. In fact, this study shows that *t8*, *c10+c9*, *t11* CLA mixture partially counteracted the lipid filling of *c9*, *t11* CLA isomer, but did not reproduce the anti-adipogenic action of *t10*, *c12+c9*, *t11* CLA mixture.

The results on TG accumulation from the present study are in agreement with previously published data using similar experimental conditions from our lab [26], and others [27] comparing 41 μM *c9*, *t11* pure isomer with 100 μM *t10*, *c12+c9*, *t11* CLA mixture. It has been reported that the *c9*, *t11* CLA by itself elevates TG accumulation by increasing PPAR- γ dependent gene expression [28, 29]. In our previous study [26], TG levels in cells treated with *t10*, *c12* CLA alone, or with the *t10*, *c12+c9*, *t11* CLA mixture, were reduced similarly compared with the *c9*, *t11* pure isomer, suggesting that *t10*, *c12* was the CLA isomer exerting a dominant effect in the mixed isomer preparation. In support of this, in the present study, *c9*, *t11* isomer alone increased TG levels by 41% compared with LA, whereas the presence of *t10*, *c12* CLA in the *t10*, *c12+c9*, *t11* CLA mixture not only abolished the *c9*, *t11*

effect but additionally decreased TG levels by 46% compared with LA. On the other hand, the *t10*, *c12* isomer can suppress TG accumulation in 3T3-L1 cells at concentrations even as low as 25 μM [30], but usually within the range of 50–100 μM . The lower limit concentration of 50 μM (50% of the total concentration of the *t10*, *c12+c9*, *t11* CLA mixture) was used in the present study. Interestingly, a lower concentration range (3–30 μM) of this isomer was sufficient to produce similar results in human preadipocytes [31].

The exact mechanism by which *t10*, *c12* isomer reduces TG content is still unclear. The *t10*, *c12* CLA might act in adipocytes through such mechanisms as decreased de novo FA synthesis [29] and increased FA oxidation. In addition, the *t10*, *c12* CLA may also inhibit differentiation of preadipocytes by down regulating PPAR- γ expression and its downstream targets involved in fatty acid metabolism. This results in the formation of a fibroblast-like cell that demonstrates certain characteristics of a mature adipocyte such as leptin expression, but has a diminished ability to store TG [32]. It has been suggested by Choi et al. [11] that the *t10*, *c12* isomer of CLA may influence adiposity by inhibiting SCD activity, thereby reducing the monounsaturated to saturated fatty acid ratio, termed the ‘desaturation index’, as observed in the present study. According to Ntambi and Miyazaki [33] a decrease in the activity of SCD1 leads to decreased FA esterification, and thereby to reduced synthesis and accumulation of TG.

Reduced TG content of 3T3-L1 cells treated with the *t8*, *c10+c9*, *t11* CLA mixture compared with the *c9*, *t11* CLA isomer was, however, not due to a reduction in the desaturation index, such as was observed with the *t10*, *c12+c9*, *t11* CLA mixture. Indeed, in the present study, the palmitoleic/palmitic and oleic/stearic acid ratios elicited by the *t8*, *c10+c9*, *t11* CLA mixture were similar to those observed with LA and the *c9*, *t11* CLA, but greater than that observed with the *t10*, *c12+c9*, *t11* CLA mixture. In this respect, Choi et al. [11] suggest that a decrease in SCD1 activity might only be partly responsible for reduction in TG content. Therefore, the moderate but significant decrease in TG accumulation that was seen with the *t8*, *c10+c9*, *t11* mixture compared with the *c9*, *t11* CLA isomer alone suggests a mechanism other than direct inhibition of SCD1. It is possible that the presence of 40% *t8*, *c10* isomer in the *t8*, *c10+c9*, *t11* CLA mixture could have partially inhibited the PPAR- γ dependent gene expression stimulated by *c9*, *t11* CLA with a consequent reduction in TG accumulation.

Decreases in cellular and circulating adiponectin concentrations are usually seen as being unfavourable, and are associated with the development of obesity, insulin resistance, Type 2 diabetes and heart disease [34]. A decrease in adiponectin production is seen in obesity, where larger adipocytes with larger amounts of TG do not produce as much

hormone as their smaller counterparts [13]. On the other hand, low adiponectin concentrations could also indicate inadequate function of adipocytes. Therefore, the cellular level of adiponectin, which is a hormone secreted exclusively by adipocytes, may be considered a useful marker of differentiation and proper functioning of these cells. In the present study, there was a positive association between cellular TG concentration and adiponectin content in 3T3-L1 cells treated with BSA or different fatty acids ($n = 15$, $r = 0.72$, $P = 0.002$), suggesting that in the present context, adiponectin levels and TG accumulation together in the adipocyte may be seen as indicators of adequate functioning of 3T3-L1 cells. With supplementation of the *t8, c10+c9, t11* CLA mixture, there was no significant decrease in the cellular adiponectin content of 3T3-L1 cells and was similar to values for the pure *c9, t11* CLA and LA treatment groups, indicating adequate preadipocyte differentiation.

In marked contrast, this hormone was significantly lower in cells treated with the *t10, c12+c9, t11* CLA mixture than in those treated with LA or the other CLA isomers. There was a concomitant decrease in TG content of cells treated with the *t10, c12+c9, t11* CLA mixture, suggesting that the *t10, c12+c9, t11* CLA treatment could not sustain proper cell differentiation. Although this is in direct contrast to epidemiological data which indicates that reduced adiposity is associated with higher circulating adiponectin levels [35], it is in keeping with recent studies in mice where supplementation with the *t10, c12* isomer resulted in decreased concentrations of circulating adiponectin [36, 37] concomitant with a reduction in adipose tissue [36].

To the best of our knowledge, this is the first study to investigate the effects of a CLA mixture containing the *t8, c10* CLA isomer on lipid metabolism in the murine 3T3-L1 cell line. We have previously studied the effects of *c9, t11+t8, c10* CLA mixture compared to those of *c9, t11+t10, c12* CLA mixture and LA on lipoprotein profile, hepatic lipids, body composition and digestibility of dietary fat in hamsters [18]. We showed that whereas the *c9, t11+t8, c10* CLA mixture deteriorated VLDL TG and cholesterol, as well as glycemia compared with LA treatment [18], the *c9, t11* and *t10, c12* CLA isomers given separately had no effect on VLDL TG and cholesterol [19], thus indicating that the *c9, t11+t8, c10* effect on VLDL TG and glycemia could not be attributed to the *c9, t11* CLA isomer alone. This suggests a high possibility that the *t8, c10* CLA, although found at 35% concentration in this mixture, might be the physiologically active CLA isomer, being aware that other isomers could have also played a role [18].

In the present study, the *t8, c10+c9, t11* CLA induced similar TG accumulation as LA, and decreased TG accumulation in 3T3-L1 cells when compared with the *c9, t11* pure CLA isomer. Since the *t8, c10* CLA was supplemented as part of a mixture, it is difficult to attribute the

observed effects to this isomer alone. We cannot rule out the presence of other minor isomers (~15%) that could have affected the TG response in the preadipocytes, neither exclude the possibility that the TG response could also be a result of the lower concentration (40%) of *c9, t11* CLA in the mixture compared to the 98% purity of this isomer in the individual *c9, t11* CLA treatment. On the other hand, Brown et al. [27] have demonstrated that 3T3-L1 cells treated with half the concentration (41 μ M) of *c9, t11* CLA isomer had significantly higher TG content than 3T3-L1 cells treated with LA (100 and 44 μ M), *c9, t11+t10, c12* CLA mixture (100 μ M) and *t10, c12* CLA (44 μ M). Taken together, these data and the results of the present study suggest that the *c9, t11* CLA supplemented at either 100 μ M or half the concentration (~50 μ M) could both promote higher lipid accumulation than LA, the *t8, c10+c9, t11* and the *c9, t11+t10, c12* CLA mixtures in 3T3-L1 preadipocytes. Nevertheless, a limitation of the present study was the use of *t8, c10* CLA as a mixture with *c9, t11* CLA, rather than as the *t8, c10* single isomer. This prevents us from making clear distinctions between the effects of the two isomers. Therefore, all the results observed for this treatment group should be considered a combined effect of the isomers present in the *t8, c10+c9, t11* CLA mixture. However, because the *t8, c10* isomer was present at a proportion of ~40% in the mixture used, there is also a possibility that the suppressive effect on TG accumulation might be more pronounced with the *t8, c10* isomer administered in its pure form. Specific biological effects of the *t8, c10* isomer will be thus determined when the pure form of this isomer becomes available.

In conclusion, our CLA isomer mixture of interest, *t8, c10+c9, t11* CLA, can beneficially decrease TG accumulation as compared to the individual *c9, t11* CLA, without adversely affecting adiponectin content in 3T3-L1 cells, and in turn adipocyte differentiation, as did the *t10, c12+c9, t11* CLA mixture. Further studies on the *t8, c10* pure CLA isomer are needed to investigate metabolic effects in animals, and ultimately humans, in order to evaluate its potential usefulness in safe weight loss formulations of CLA.

Acknowledgment This study was conducted with the support of the Advanced Foods and Materials Network, as part of the Networks of Centres of Excellence, Canada.

References

1. Belury MA (2002) Dietary conjugated linoleic acid in health: physiological effects and mechanisms of action. *Annu Rev Nutr* 22:505–531
2. Park Y, Albright KJ, Liu W, Storkson JM, Cook ME, Pariza MW (1997) Effect of conjugated linoleic acid on body composition in mice. *Lipids* 32:853–858

3. Ostrowska E, Muralitharan M, Cross RF, Bauman DE, Dunshea FR (1999) Dietary conjugated linoleic acids increase lean tissue and decrease fat deposition in growing pigs. *J Nutr* 29:2037–2042
4. Wahle KW, Heys SD, Rotondo D (2004) Conjugated linoleic acids: are they beneficial or detrimental to health? *Prog Lipid Res* 43:553–587
5. Pariza MW (2004) Perspective on the safety and effectiveness of conjugated linoleic acid. *Am J Clin Nutr* 79:1132S–1136S
6. Flowers MT, Miyazaki M, Liu X, Ntambi M (2006) Probing the role of stearoyl-CoA desaturase-1 in hepatic insulin resistance. *J Clin Invest* 116:1478–1481
7. Ntambi JM, Miyazaki M, Stoehr JP, Lan H, Kendzierski CM, Yandell BS, Song Y, Cohen P, Friedman JM, Attie AD (2002) Loss of stearoyl-CoA desaturase-1 function protects mice against adiposity. *Proc Natl Acad Sci USA* 99:11482–11486
8. Gutierrez-Juarez R, Pocai A, Mulas C, Ono H, Bhanot S, Monia BP, Rossetti L (2006) Critical role of stearoyl-CoA desaturase-1 (SCD1) in the onset of diet-induced hepatic insulin resistance. *J Clin Invest* 116:1686–1695
9. Park Y, Storkson JM, Ntambi JM, Cook ME, Sih CJ, Pariza MW (2000) Inhibition of hepatic stearoyl-CoA desaturase activity by *trans*-10, *cis*-12 conjugated linoleic acid and its derivatives. *Biochim Biophys Acta* 1486:285–292
10. Wendel AA, Belury MA (2006) Effects of conjugated linoleic acid and troglitazone on lipid accumulation and composition in lean and Zucker diabetic fatty (*fa/fa*) rats. *Lipids* 41:241–247
11. Choi Y, Kim YC, Han YB, Park Y, Pariza MW, Ntambi JM (2000) The *trans*-10, *cis*-12 isomer of conjugated linoleic acid downregulates stearoyl-CoA desaturase 1 gene expression in 3T3-L1 adipocytes. *J Nutr* 130:1920–1924
12. Choi Y, Park Y, Pariza MW, Ntambi JM (2001) Regulation of stearoyl-CoA desaturase activity by the *trans*-10, *cis*-12 isomer of conjugated linoleic acid in HepG2 cells. *Biochem Biophys Res Commun* 284:689–693
13. Havel PJ (2004) Update on adipocyte hormones: regulation of energy balance and carbohydrate/lipid metabolism. *Diabetes* 53:S143–S151
14. Perfield JW, Saebo A, Bauman DE (2004) Use of conjugated linoleic acid (CLA) enrichments to examine the effects of *trans*-8, *cis*-10 CLA, and *cis*-11, *trans*-13 CLA on milk-fat synthesis. *J Dairy Sci* 87:1196–1202
15. Reany MJT, Liu Y, Westcott ND (1999) Advances in conjugated linoleic acid research, vol 1. AOCS Press, Champaign
16. Destailats F, Japiot C, Chouinard PY, Arul J, Angers P (2005) Short communication: rearrangement of rumenic acid in ruminant fats: a marker of thermal treatment. *J Dairy Sci* 88:1631–1635
17. Ostrowska E, Cross RF, Muralitharan M, Bauman DE, Dunshea FR (2003) Dietary conjugated linoleic acid differentially alters fatty acid composition and increases conjugated linoleic acid content in porcine adipose tissue. *Br J Nutr* 90:915–928
18. Bissonauth V, Chouinard PY, Marin J, Leblanc N, Richard D, Jacques H (2008) Altered lipid response in hamsters fed *cis*-9, *trans*-11+*trans*-8, *cis*-10 conjugated linoleic acid mixture. *Lipids* 43:251–258
19. Bissonauth V, Chouinard Y, Marin J, Leblanc N, Richard D, Jacques H (2006) The effects of τ 10, τ 12 CLA isomer compared with ϵ 9, τ 11 CLA isomer on lipid metabolism and body composition in hamsters. *J Nutr Biochem* 17:597–603
20. Lowry OH, Rosebrough NJ, Farr AL, Randall RJ (1951) Protein measurement with the Folin phenol reagent. *J Biol Chem* 193:265–275
21. Hara A, Radin NS (1978) Lipid extraction of tissues with a low-toxicity solvent. *Anal Biochem* 90:420–426
22. Hashimoto N, Aoyama T, Shiori T (1981) New methods and reagents in organic synthesis: a simple efficient preparation of methyl esters with trimethylsilyldiazomethane (TMSCHN₂) and its application to gas chromatographic analysis of fatty acids. *Chem Pharm Bull* 29:1475–1478
23. Yurawecz MP, Kramer JK, Ku Y (1999) Methylation procedures for conjugated linoleic acid. AOCS Press, Champaign
24. MacDougald O, Lane M (1995) Transcriptional regulation of gene expression during adipocyte differentiation. *Annu Rev Biochem* 64:345–373
25. Evans M, Lin X, Odle J, McIntosh M (2002) *Trans*-10, *cis*-12 conjugated linoleic acid increases fatty acid oxidation in 3T3-L1 preadipocytes. *J Nutr* 132:450–455
26. Miller JR, Siripurkpong P, Hawes J, Majdalawieh A, Ro HS, McLeod RS (2008) The *trans*-10, *cis*-12 isomer of conjugated linoleic acid decreases adiponectin assembly by PPAR γ -dependent and PPAR γ -independent mechanisms. *J Lipid Res* 49:550–562
27. Brown M, Evans M, McIntosh M (2001) Linoleic acid partially restores the triglyceride content of conjugated linoleic acid-treated cultures of 3T3-L1 preadipocytes. *J Nutr Biochem* 12:381–387
28. Evans M, Park Y, Pariza M, Curtis L, Kuebler B, McIntosh M (2001) *Trans*-10, *cis*-12 conjugated linoleic acid reduces triglyceride content while differentially affecting peroxisome proliferator activated receptor γ 2 and α 2 expression in 3T3-L1 preadipocytes. *Lipids* 36:1223–1232
29. Brown JM, Halvorsen YD, Lea-Currie YR, Geigerman C, McIntosh M (2001) *Trans*-10, *cis*-12, but not *cis*-9, *trans*-11, conjugated linoleic acid attenuates lipogenesis in primary cultures of stromal vascular cells from human adipose tissue. *J Nutr* 131:2316–2321
30. Granlund L, Larsen LN, Nebb HI, Pedersen JI (2005) Effects of structural changes of fatty acids on lipid accumulation in adipocytes and primary hepatocytes. *Biochim Biophys Acta* 1687:23–30
31. Brown JM, McIntosh MK (2003) Conjugated linoleic acid in humans: regulation of adiposity and insulin sensitivity. *J Nutr* 133:3041–3046
32. Brown JM, Boysen MS, Jensen SS, Morrison RF, Storkson J, Lea-Currie R, Pariza M, Mandrup S, McIntosh MK (2003) Isomer-specific regulation of metabolism and PPAR γ signaling by CLA in human preadipocytes. *J Lipid Res* 44:1287–1300
33. Ntambi JM, Miyazaki M (2003) Recent insights into stearoyl-CoA desaturase-1. *Curr Opin Lipidol* 14:255–261
34. Pischon T, Rimm EB (2006) Adiponectin: a promising marker for cardiovascular disease. *Clin Chem* 52:797–799
35. Fu Y, Luo N, Klein RL, Garvey WT (2005) Adiponectin promotes adipocyte differentiation, insulin sensitivity, and lipid accumulation. *J Lipid Res* 46:1369–1379
36. Poirier H, Shapiro JS, Kim RJ, Lazar MA (2006) Nutritional supplementation with *trans*-10, *cis*-12-conjugated linoleic acid induces inflammation of white adipose tissue. *Diabetes* 55:1634–1641
37. Cooper M, Miller JR, Mitchell PL, Currie DL, McLeod RS (2008) Conjugated linoleic acid isomers have no effect on atherosclerosis and adverse effects on lipoprotein and liver lipid metabolism in apoE(-/-) mice fed a high-cholesterol diet. *Atherosclerosis* 200:294–302

Characterization of Both Polyunsaturated Fatty Acid Biosynthetic Pathways in *Schizochytrium* sp.

J. Casey Lippmeier · Kristine S. Crawford ·
Carole B. Owen · Angie A. Rivas ·
James G. Metz · Kirk E. Apt

Received: 4 March 2009 / Accepted: 1 May 2009 / Published online: 3 June 2009
© AOCS 2009

Abstract *Schizochytrium* produces long chain polyunsaturated fatty acids (PUFAs) via a PUFA synthase. Targeted mutagenesis of one gene of this synthase was conducted to confirm PUFA synthase function and determine its metabolic necessity. The resulting mutants were auxotrophic and required supplementation with PUFAs. In vivo labeling experiments with radioactive fatty acids demonstrated the presence of several elongase and desaturase activities associated with the standard pathway of PUFA synthesis. However, this system was missing a critical $\Delta 12$ desaturase activity and was therefore not capable of synthesizing PUFAs from the 16- or 18-carbon saturated fatty acid products of the fatty acid synthase. Because *Schizochytrium* uses a PUFA synthase system for the production of PUFAs, the existence of a partial desaturase-elongase system (if not a simple vestige) is suggested to be either a scavenging mechanism for intermediate fatty acids prematurely released by the PUFA synthase or for PUFAs found in the organism's native environment.

Keywords Fatty acid metabolism · Metabolism · Polyunsaturated fatty acids (PUFA) · Specific lipids · Radiotracer · Analytical techniques · Marine lipid biochemistry · General area · Molecular biology · Miscellaneous

Abbreviations

DHA Docosahexaenoic acid
DPA Docosapentaenoic acid

Introduction

Schizochytrium sp. is one of several heterotrophic eukaryotic organisms used to make commercial amounts of long chain polyunsaturated fatty acids (PUFAs) by fermentation. *Schizochytrium* is a member of the Stramenopiles, a kingdom consisting of photosynthetic diatoms, brown algae and other algae commonly referred to as chromophytes [1]. Within this kingdom, the phylum Labyrinthulomycota contains two orders, the Labyrinthulales and the Thraustochytriales; the genus *Schizochytrium* is a member of the latter. *Schizochytrium* makes two PUFAs: docosahexaenoic acid (DHA) and docosapentaenoic acid (DPA) n-6. These fatty acids occur in a 3:1 ratio among total cellular lipids of this microalgae and are found in most known Thraustochytrids (although in different ratios) [2]. DHA and DPA n-6 can comprise >60% of the total lipid-associated fatty acids of cultured *Schizochytrium*, which in turn can be as much as 43% of the dry cell weight [2, 3].

Three genes, designated *PFA1*, 2 and 3 (and formerly *ORF A*, *B* and *C*) have been implicated in *Schizochytrium* PUFA biosynthesis [4, 5] based on sequence similarity to the products of the PUFA synthase gene clusters from the marine bacteria *Shewanella* [6] and *Moritella* [7] and on their functional expression in bacteria [8]. The mechanism behind double-bond insertion in PUFA synthase systems, proposed by Metz et al. [4, 5] is thought to be similar to the FAS-mediated biosynthesis of monounsaturated fatty acids in *E. coli*, which employs dual dehydratase and 2,3-isomerase activities of the FabA enzyme. The mechanics of

J. C. Lippmeier (✉) · K. S. Crawford ·
C. B. Owen · A. A. Rivas · K. E. Apt
Martek Biosciences Corporation, 6480 Dobbin Rd,
Columbia, MD 21045-5825, USA
e-mail: clippmeier@martek.com

J. G. Metz
Martek Biosciences Corporation, Boulder, CO 80301, USA

double-bond formation by the *Schizochytrium* PUFA synthase are thought to differ from the synthesis of *E. coli* monounsaturates in the need for an additional novel 2,2-isomerase activity [4].

Desaturase genes involved in the standard pathway of PUFA biosynthesis have also been identified in *Schizochytrium* [4], putting the relative contribution of the PUFA synthase for PUFA accumulation in this organism into question. Additionally, genes encoding enzymes for the standard pathway have been found in other thraustochytrids. *Thraustochytrium aureum*, a close relative of *Schizochytrium*, harbors several enzymes of the standard pathway of PUFA biosynthesis, including the first-discovered $\Delta 4$ desaturase [9]. To reconcile the apparent presence of two biosynthetic pathways for PUFA production in *Schizochytrium* [10], two different approaches were utilized. A transformation system for *Schizochytrium* was previously developed and data indicated that it was capable of vector-mediated homologous recombination [11]. This vector-directed homologous recombination method was used to disrupt the *PFAI* PUFA synthase gene in *Schizochytrium*. Second, the standard pathway elongase and desaturase activities were characterized by supplementation with radiolabeled precursors. This study presents direct functional evidence that the PUFA synthase is the sole system responsible for de novo biosynthesis of PUFAs in *Schizochytrium* and that those PUFAs are essential nutrients for this organism. The data also illustrate that while several fatty acid desaturase and elongase activities are present in *Schizochytrium*, that pathway for PUFA synthesis is incomplete.

Materials and Methods

Host Strains, Transformations, and Culture Conditions

All vectors and constructs were propagated in *E. coli* UltraMax DH5- α FT chemically competent cells (Invitrogen, Carlsbad, CA) for plasmid purification using Qiagen kits appropriate for a given scale of culture (Qiagen, Valencia, CA).

Schizochytrium sp. was isolated from a single colony of an ATCC stock culture (ATCC# 20888). *Schizochytrium* cultures were typically grown in 50 mL of “PB26-M2B” media consisting of 10 g L⁻¹ glucose, 0.8 g L⁻¹ (NH₄)₂SO₄, 5 g L⁻¹ Na₂SO₄, 2 g L⁻¹ MgSO₄·7H₂O, 0.5 g L⁻¹ KH₂PO₄, 0.5 g L⁻¹ KCl, 0.1 g L⁻¹ CaCl₂·2H₂O, 0.1 M MES (pH 6.0) 0.1% PB26 metals and 0.1% PB26 Vitamins (v/v). PB26 vitamins consisted of 50 mg mL⁻¹ vitamin B12, 100 μ g mL⁻¹ thiamine, and 100 μ g mL⁻¹ Ca-Pantothenate. PB26 metals were adjusted to pH 4.5 and consisted of 3 g L⁻¹ FeSO₄·7H₂O, 1 g L⁻¹ MnCl₂·4H₂O,

800 mg mL⁻¹ ZnSO₄·7H₂O, 20 mg mL⁻¹ CoCl₂·6H₂O, 10 mg mL⁻¹ Na₂MoO₄·2H₂O, 600 mg mL⁻¹ CuSO₄·5H₂O, and 800 mg mL⁻¹ NiSO₄·6H₂O. PB26 stock solutions were filter sterilized separately and added to the broth after autoclaving. Glucose, KH₂PO₄, and CaCl₂·2H₂O were each autoclaved separately from the remainder of the broth ingredients before mixing to prevent salt precipitation and carbohydrate caramelizing. All media ingredients were purchased from Sigma, St. Louis, MO. Cultures of *Schizochytrium* sp. were grown to log-scale and transformed with a biolistic particle bombardier (BioRad, Hercules, CA) with the gene disruption construct described below. The biolistic transformation procedure was essentially the same as described previously [12]. Primary transformants were selected on solid PB26-M2B media containing 20 g L⁻¹ agar (VWR, West Chester, PA), 50 μ g mL⁻¹ zeocin, and 0.5 mM DHA, DPA n-6 or myristic acid (NuChekPrep, Elysian, MN) complexed with 10–30 g L⁻¹ randomly methylated β -cyclodextrins (Cyclodextrin Technologies Development, Inc., High Springs, FL). All primary transformants were manually transferred to grid-plates containing or lacking polyunsaturated free fatty acid supplements. Putative auxotrophs were confirmed by a second round of inoculation on these plates. Transformants were further characterized after growth in liquid PB26-M2B with 15 g L⁻¹ β -cyclodextrins and 0.5 mM PUFA as indicated in the text. Equilibrium-radiolabeled cultures were typically grown in 10 mL of liquid “790” media; 1 g yeast extract, 1 g peptone, 5 g glucose (VWR), all per liter of Instant Ocean™ artificial seawater (Aquarium Systems, Mentor, OH) and 0.1 μ Ci mL⁻¹ of a 1-[¹⁴C]-labeled fatty acid (American Radiolabeled Chemicals, St. Louis, MO) as indicated in the text. Equilibrium-labeled cultures were grown under agitation (120 rpm) for at least 2 days at 27 °C.

Vector Construction

Materials used for cloning procedures including restriction enzymes, alkaline phosphatase, and T7 DNA polymerase were purchased from New England Biolabs (Beverly, MA) and used according to the manufacturer’s instructions. Restriction fragment and amplicon purification was done with either PCR clean-up kits or Qiaex gel extraction kits from Qiagen. Agarose gels were made with 1% SeaKem Agarose or 1% low-melt Agarose (Cambrex BioScience Rockland, Inc., Rockland, ME). DNA ligations were performed with the Rapid DNA Ligation Kit (Roche Diagnostics Corporation, Indianapolis, IN) and 2 μ L of each ligation were used to transform DH5- α competent cells (Invitrogen). Transformed bacterial colonies were grown in 5 mL mini-cultures of Luria broth (LB), 100 μ g mL⁻¹ ampicillin [13]. Plasmids were extracted from mini-cultures

with miniprep kits (Qiagen). All constructs were verified by DNA sequencing (Lark Technologies, Houston, TX). All reagents and kits described were used according to the manufacturer's instructions unless otherwise noted.

Construction of a vector harboring *Schizochytrium* PFAI (pBSK:A) and a vector capable of conferring resistance to zeocin when used to transform *Schizochytrium* (pTUB-ZEO11-2) have been described elsewhere [11]. Briefly, the vector contains the *ble* gene of *Streptoalloteichus hindustanus* [14] to confer resistance to zeocin. The endogenous *Schizochytrium* promoter for α -tubulin was used to drive expression of this selectable marker. A terminator from the SV40 virus coat protein locus (genbank accession M24873) follows the *ble* coding region. These three elements: promoter, *ble* coding region, and terminator, are collectively referred to hereafter as a "zeocin resistance cassette". Vector pBSK:A, which harbored only the coding region of PFAI in the vector background pBLUESCRIPT SK, was digested and linearized with *Sma*I. The zeocin resistance cassette was liberated from pTUBZEO11-2 by digestion with *Pst*I. The fragment was treated with T7 DNA polymerase to create blunt ends before ligation to the linear pBSK:A. *E. coli* cells were transformed directly with this ligation mix. Resulting transformants were mini-cultured from colonies and plasmids were purified and digested to screen for insertion of the zeocin cassette. One clone was selected for having a zeocin cassette encoded on the plus strand, relative to PFAI transcription. This plasmid, pBSK- Δ ORFA-zeoR#2, was prepared in large scale for use in *Schizochytrium* transformation.

Gas and High Pressure Liquid Chromatography

Fatty acid methyl esters (FAMES) were extracted and derived from freeze-dried biomass according to the method described elsewhere [15]. Injections of FAMES in 1 μ L volumes were separated on a GC fitted with a flame-ionizing detector and a FAMEWAX 30-meter column (0.25 mm i.d., 0.25 μ m) [16]. Eluted FAMES were identified and quantified by comparison to authentic standards.

HPLC separations of FAMES were performed using an adaptation of a common reverse phase protocol [17]. FAMES were resuspended in 50–200 μ L of acetonitrile after evaporating \sim 2 mL of hexane from the FAME reaction. FAME injections of 5–20 μ L were separated by HPLC with a Metachem 3 Taxsil, 250 \times 4.6 mm column (Varian, Palo Alto, CA) into which a gradient of acetonitrile was applied in water; 60% from 0 to 35 min, 60–70% from 35 to 40 min, 70% from 40 to 60 min, 70–60% from 60 to 61 min, and lastly held at 70% for an additional 9 min. Eluted radioactive FAMES were mixed in-line with Scintiverse LC (Fisher, Hampton, NH) liquid scintillant (1:2, v:v) for detection of beta-particle emissions. Fatty

acids were qualified and quantified by comparison to authentic reference standards.

Nucleic Acid Isolation

Wet pellets from 1 L of overnight *Schizochytrium* wild-type and mutant cultures were washed with sterile water, weighed, and lysed with Extraction Buffer (20 mM Tris-HCl pH 8.0, 50 mM NaCl, 10 mM EDTA, 0.5% SDS) (1 mL Extraction Buffer per 100 mg wet cell pellet) and 100 μ g mL⁻¹ proteinase K for \sim 45 min at 50 °C. After this, 100 μ g mL⁻¹ of DNase-free RNase A was added and the lysate incubated at 37 °C for an additional 15 min. DNA was then extracted from the lysate twice with an equal volume of phenol:chloroform:isoamyl alcohol (24:24:1) by gentle shaking for 30 min at room temperature. The aqueous phase of the extract was further extracted twice with an equal volume of chloroform:isoamyl alcohol (24:1). Genomic DNA (gDNA) was precipitated from the remaining aqueous fraction by addition of 0.1 v of 3 M sodium acetate and 2 v of 100% ethanol. DNA was gently wound out of the solution with a glass rod, washed with 70% ethanol, dried and resuspended in Tris-buffered water (pH 8.0).

For RNA preparation, flash-frozen pellets from 1 L of log-phase wild-type and auxotrophic mutant cultures of *Schizochytrium* were pulverized in liquid nitrogen-cooled mortars that had been oven-baked overnight at 350 °F. Total RNA was extracted from the resulting frozen powder in 30 mL of buffer containing 0.1 M Tris-HCl (pH 7.5), 1.5 M NaCl, 50 mM EDTA (pH 8.0), 20 g L⁻¹ cetyl trimethyl ammonium bromide (CTAB), and fresh dithiothreitol (DTT, 8 mg mL⁻¹). The slurry was centrifuged at 5,000 \times g for 20 min before mixing the supernatant with an equal volume of phenol:chloroform:isoamyl alcohol (25:24:1) (Biotechnology Grade, Midwest Scientific, St. Louis, MO). Phases were separated by centrifugation at 10,000 \times g for 30 min and the aqueous phase was re-extracted with phenol:chloroform:isoamyl alcohol. The aqueous phase was then mixed with an equal volume of isopropanol and allowed to chill at 4 °C overnight. The resulting precipitate was pelleted at 5,000 \times g for 20 min, washed with 80% ethanol, dried briefly, and resuspended in RNase-free water before treatment with RNase-free DNase (New England Biolabs, Beverly, MA) at 37 °C for 2 h. RNA was again extracted and precipitated as above.

Southern and Northern Blotting

100 μ g of gDNA was digested overnight at 37 °C with *Nco*I. Digested DNA was fractionated on 1% agarose gels (10 μ g per lane) and transferred to Nytran-Supercharge membranes (Whatman, Middlesex, UK) while RNA was

fractionated (10 µg per lane) using 2.2 M formaldehyde agarose gels [13] and transferred to Nytran-N membranes (Whatman) using the manufacturer's protocol for neutral transfers or RNA transfers as appropriate.

All probes were synthesized using dCT[³²P] (ICN, Costa Mesa, CA) and the Prime-a-Gene labeling system (Promega, Madison, WI) according to the manufacturer's instructions. A *PFA1*-specific probe template was created by digestion of *PFA1* (in pBSK:A) with *Nco*I and *Bsr*GI and gel purification of the resulting 1,146 bp band. RNA millenium markers (Ambion, Austin, TX) were electrophoresed and blotted with total RNA samples, while the Quanti-Ladder markers (Origene, Rockville, MD) were electrophoresed and blotted with DNA samples. Both marker-ladders were detected with probes made from *Hind*III digested, lambda phage DNA (Origene).

Southern and northern blots were probed in UltraHyb hybridization buffer according to the manufacturer's protocol (Ambion). After drying, blots were wrapped in cellophane and imaged on a BioRad Personal Molecular Imager FX (BioRad).

Results

Disruption Vector Construction

A vector construct for the disruption of *PFA1* of the *Schizochytrium* PUFA synthase was made to test the feasibility of PUFA synthase inactivation. The construct contained the coding region of *PFA1* (but not its corresponding promoter or terminator) and an additional insert of ~1,100 bp which conferred resistance to the antibiotic zeocin (Fig. 1). In some systems, long homologous flanking sequences have been reported to correlate with higher recombination efficiencies [18, 19]. Therefore, to improve the potential for recombination in this system, the construct was designed such that 1,500–7,500 bp of target gene sequence flanked either side of the zeocin cassette.

Generation of *Schizochytrium* Disruption Mutants

Cells bombarded with vector-coated tungsten particles were allowed to recover overnight before being transferred to solid media containing zeocin and myristic, docosapentaenoic (n-6), and docosahexaenoic acids complexed with cyclodextrins for further growth. One bombardment with supercoiled vector typically yielded 10–100 primary transformants. Each primary transformant was then re-plated to screen for auxotrophy by observing its ability to grow on solid media containing zeocin and cyclodextrins, but no free fatty acids. Between 10 and 40% of the

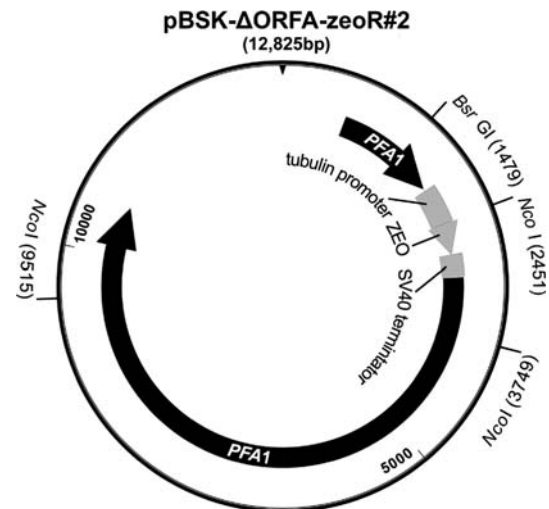


Fig. 1 Cartoon depicting the position of the zeocin disruption cassette in the *PFA1* coding region in a vector construct intended to mediate disruption of *PFA1* of the *Schizochytrium* PUFA synthase. The *PFA1* sequence is translated in the direction shown by an open arrow. The encoded resistance marker, “ZEO” protein (*sh ble*) is translated in the same direction as *PFA1*. The tubulin promoter, the SV40 terminator and the coding region of the zeocin resistance gene are indicated. Numbers given in parentheses or along the vector ruler are in base pairs, numbered from the first base pair of the bacterial backbone vector, pBLUESCRIPT SK

primary transformants failed to grow indicating that these clones were fatty acid auxotrophs.

Phenotyping of the Disruption Mutants of *Schizochytrium*

Verified auxotrophic mutants were further characterized by observing growth on solid media supplemented with a number of fatty acids (Table 1). The phenotypes of all verified auxotrophic mutants were similar. None were able to grow without supplemented PUFAs less complex than linolenic acid. Polyunsaturated fatty acids of 20 and 22 carbons in length were found to permit better growth of the mutant than linolenic acid. One *PFA1*-disrupted (*ZEO::PFA1*) mutant clone (A14) was grown in liquid cultures supplemented with several free fatty acids. The cultures were harvested for FAME derivation and analysis by GC (Table 2). These data show that the PUFAs which permitted growth of the mutants were converted to several more complex PUFAs; however, complete conversion to DHA and DPA n-6 did not appear necessary for survival.

Genotyping of the Gene Disruption of *Schizochytrium* Auxotrophs

To verify that the observed auxotrophies were caused by a targeted gene disruption event, nucleic acids of a

Table 1 Observed growth of *Schizochytrium* wild-type and an auxotrophic, PUFA synthase-disrupted “knockout” on solid PB26-M2B media supplemented with the indicated free fatty acids

Supplemented FFA	<i>PFA1</i> knockout	Wild-type
22:6n-3	++	++
20:5n-3	++	++
20:4n-6	++	++
18:3n-3	+	++
18:3n-6	+	++
18:2n-6	–	++
18:1n-9	–	++
16:1n-9	–	++
16:0	–	++
14:0	–	++
None	–	++

Inocula were grown to saturation at 27 °C in liquid PB26-M2B media supplemented with DHA. Plates were inoculated with 100 µL of this culture and incubated for 3 days at 27 °C

++ Growth indistinguishable from wild-type

+ Impaired growth

– No observed growth

Schizochytrium mutant were compared to those of wild-type by Southern and northern blotting. Total gDNA was purified from a wild-type culture and from a putative *PFA1* disruption mutant clone (A20), which was identical in phenotype to all other PUFA auxotrophs. These gDNA preparations were digested with *NcoI* and separated on agarose gels for blotting. Blots were probed with fragments which specifically hybridized to coding regions of *PFA1*. Maps of wild-type *PFA1* and the integrated *PFA1* disruption cassette are shown in panels (a) and (b), respectively of Fig. 2. Probe annealing locations and predicted sizes of detectable *NcoI* fragments are also featured in these panels. The observed migrations of labeled fragments in the *PFA1*-probed Southern agreed relatively well with a predicted

single crossover event resulting in the genomic structure proposed in Fig. 2b.

Total RNA was also purified from a wild-type culture and from disruption mutant clone A20. These RNA samples were separated on agarose gels for northern blotting. Blots were probed with the same fragments used for Southern blotting. As shown in Fig. 3, transcripts of the *PFA1* disruption mutant A20 are clearly fragmented into weak bands of ~2,700 bases and ~1,800 bases, while the size of the band observed in the wild-type sample lane agrees with the expected size of a wild-type *PFA1* transcript (8,730 bases for the open reading frame, plus 5' and 3' UTR sequence lengths).

Characterization of the Standard Pathway in Wild-type *Schizochytrium*

To determine which standard pathway enzymes are active in *Schizochytrium*, liquid cultures of wild-type cells were equilibrium-labeled with [1-¹⁴C]-free fatty acids and patterns of conversion were observed (Table 3). Radiolabeled compounds were added during culture inoculation. After ~2 days growth, the culture was harvested and lipids were extracted and derivitized for radio-HPLC analysis as detailed in the previous section.

For improved sensitivity, an HPLC apparatus fitted with an in-line liquid scintillant β-RAM detector was used for separating and identifying radiolabeled FAMES. As is common with HPLC separations, some FAMES co-migrated precluding distinct quantification [17]. Specifically, 18:3 n-3, 20:4 n-3 and 22:5 n-3 all co-migrated. Separately, 18:3 n-6 and 22:6 n-3 co-migrated as a single peak as did 16:0 and 18:1 n-9 in yet another single peak. Despite the co-migrations, the data shown in Table 3 indicate that wild-type *Schizochytrium* possesses many but not all of the activities associated with a standard PUFA biosynthesis pathway. Total percent FAMES are listed in the column corresponding to the structurally simplest member of a

Table 2 FAMES derived from total lipids of wild-type and *PFA1*-disrupted *Schizochytrium* cultures grown for 48 h at 27 °C in PB26-M2B liquid media supplemented with 0.5 mM of the indicated free fatty acids

Fatty acid added to medium	Percentage FAME recovered in:											
	14:0	16:0	16:1	18:0	18:1	18:3n-6	20:3n-6	20:4n-6	20:5n-3	22:5n-3	22:5n-6	22:6n-3
None*	9.7	33.8	7.5	0.9	6.5	–	0.2	0.5	0.7	–	11.1	27.4
18:3n-6	1.1	16.5	3.2	1.0	21.3	11.6	32.5	1.8	–	–	1.2	–
20:4n-6	8.3	43.0	11.0	1.8	16.0	0.1	0.8	6.8	0.2	0.3	0.4	–
20:5n-3	8.5	43.5	17.6	1.9	13.6	–	–	0.1	3.2	8.3	–	0.2
22:5n-6	10.6	44.0	8.0	1.7	10.1	0.1	0.3	1.0	–	–	22.0	0.2
22:6n-3	5.8	37.7	11.2	1.7	14.4	–	–	0.1	1.6	0.4	–	24.5

*wild-type culture, all other cultures were Δ*PFA1* mutant clone A14. All values are expressed as a FAME area percent of total FAME peaks

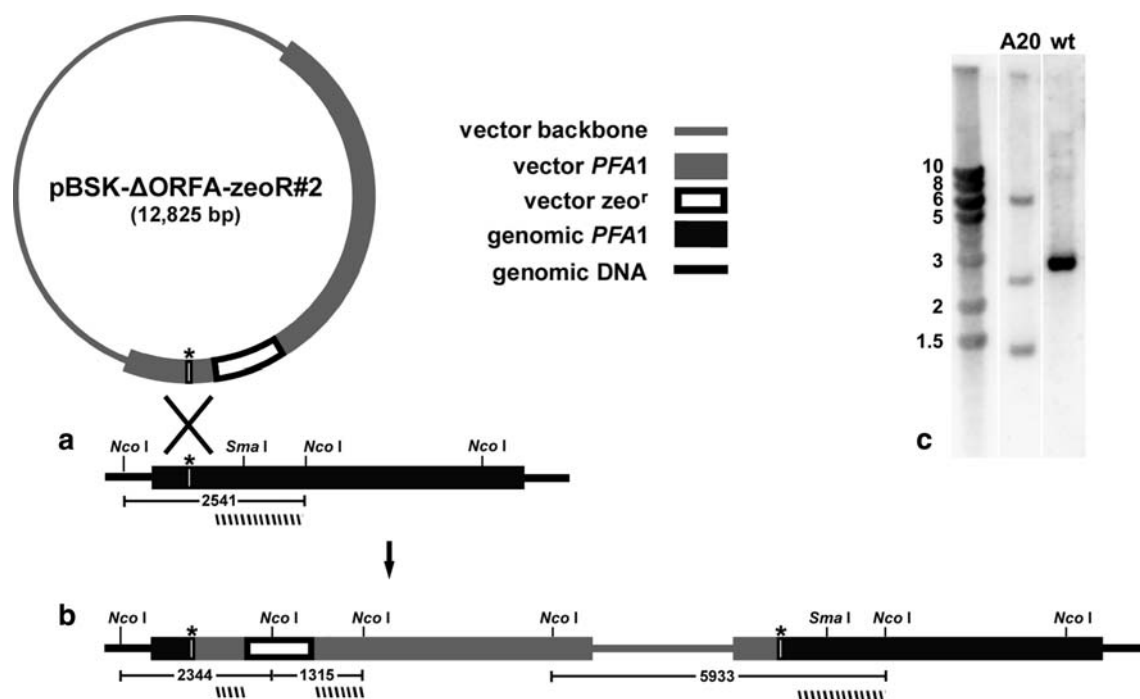


Fig. 2 *Schizochytrium* PUFA synthase *PFA1* disruption. **a** and **b** show maps of expected arrangement of *PFA1* gDNA resulting from a single crossover event in auxotrophic mutants transformed with pBSK- Δ ORFA-zeoR#2. The maps illustrate the locations of *PFA1*-specific probe annealing regions (*hatched bars*) and detectable *Nco*I restriction fragments, labeled according to their predicted size in base pairs, 2,541, 2,344, 1,315, and 5,933 (*stroked goalposts*). The proposed recombination site between the vector, within the *PFA1* coding region and upstream of the ZEO expression cassette is also shown (*asterisk*). Vector-backbone sequences are indicated by *grey lines* and genomic DNA sequences (other than *PFA1*) are indicated by *black lines*. The vector-encoded Zeocin resistance cassette, vector-encoded *PFA1*, and genome-encoded *PFA1* are shown as *open black*

boxes, *grey bars*, and *black bars*, respectively. All genes are transcribed left to right in linear sequence representations and counter-clockwise in circular representations. The *Sma* I site was used for cloning the zeocin resistance cassette and thus only appears in the wild-type *PFA1* reading frame. The Southern blot of *Nco*I-digested gDNA samples from wild-type “wt” and disruption mutant clone A20 (**c**) was labeled with an *PFA1*-specific probe created from a restriction fragment of wild-type *PFA1* (see Sect. “Materials and Methods”). The lane at left in **c**, containing molecular weight markers, was probed separately with a lambda virus-specific probe preparation and the bands are labeled according to their size in kilobase pairs

co-migrating group. Retro-conversion and β -oxidation of fatty acids was not observed, however, some fatty acids were converted to minor extractable products which did not co-migrate with any of the used standards.

Discussion

This study provides evidence for the essential role of the PUFA synthase in DHA and DPA biosynthesis in *Schizochytrium*. In addition to the *PFA1* disruption mutants described, disruption mutants of *PFA2* and *3* were also created and analyzed with similar results (data not shown). These mutants resulted from recombination events where components of the PUFA synthase were disrupted with a dominant selectable marker for zeocin resistance. All auxotrophic mutants generated had identical phenotypes and required supplementation with PUFAs for growth, indicating that each PUFA synthase component is

necessary for PUFA synthesis. This work confirms that of Metz et al. [4] and Hauvermale et al. [8] supporting the role of the PUFA synthase genes, *PFA1*, *2*, and *3* of *Schizochytrium* in PUFA biosynthesis and additionally demonstrates that this PUFA synthase is a critical enzyme component required for primary metabolism in *Schizochytrium*. This work also reveals a secondary and partially functional fatty acid desaturase and elongase-mediated PUFA pathway.

Wild-type *Schizochytrium* does not accumulate any significant amounts of PUFA other than DHA and DPA. However, knock-out mutants of the PUFA synthase components were able to grow when supplemented with PUFAs, some of which were only minimally converted to DHA or DPA, demonstrating a nutritional flexibility for complementation by fatty acids less complex than DHA and DPA. However, auxotrophs fed 20- and 22-carbon PUFAs grew significantly better than those fed 18-carbon PUFAs, indicating that PUFA auxotrophs preferred

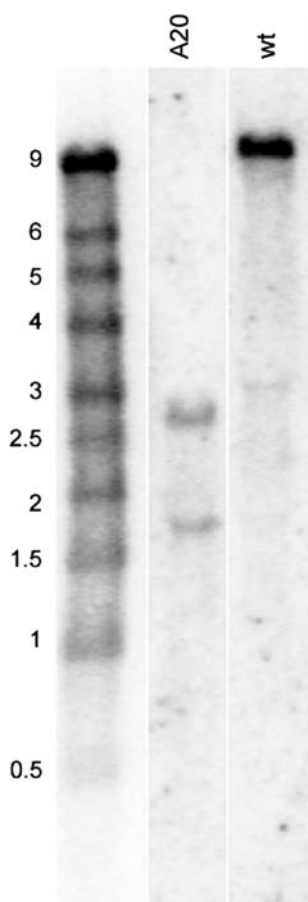


Fig. 3 Northern blot of total RNA samples extracted from wild-type “wt” *Schizochytrium* and disruption mutant clone A20. Blots were labeled with the same *PFAI*-specific probe illustrated in Fig. 2. The lane at left was labeled separately with a lambda virus-specific probe preparation and the bands are annotated according to their size in kilobases

supplementation with longer chain PUFAs (Table 1). Additional studies will be needed to specifically address whether the requirement for PUFAs is limited to 22-carbon PUFAs or if unconverted 18- or 20-carbon PUFAs are adequate for minimal complementation of PUFA synthase mutants.

A requirement for monounsaturated fatty acids has been well documented among diverse organisms [20–22]. The absolute requirement for certain PUFAs (as observed here for *Schizochytrium*) might be considered unusual though, because other PUFA-producing organisms, such as the fungus *Mortierella alpina* and the cyanobacterium *Synechocystis* PCC6803, remain viable after suffering mutations that interrupt certain parts of PUFA biosynthesis (depending upon growth conditions) [22, 23]. Unlike the *Schizochytrium* system, however, both *M. alpina* and *Synechocystis* employ a standard pathway for PUFA synthesis, therefore any given mutation in a desaturase resulted in the accumulation of other structurally analogous PUFAs

which might have complemented the loss of the most complex PUFA made by the wild-type strain.

The nature of the genetic defect in these auxotrophic mutants of *Schizochytrium* was analyzed by Southern and northern blotting (Figs. 2, 3, respectively). The described disruption construct was designed to integrate at the loci encoding the PUFA synthase component, *PFAI*. The data are consistent with a single crossover event in the *PFAI* disruption mutant A20. Homologous recombination via a single crossover event should yield two copies of the targeted gene separated by the backbone of the vector encoding an ampicillin resistance gene and bacterial origin of replication (Fig. 2). Since the *PFAI* disruption construct only contained the coding regions of *PFAI* (and no *PFAI* promoter), the second, introduced copy of *PFAI* should not have appeared as an expressible gene, as long as the crossover occurred upstream of the zeocin selection cassette. The resulting *PFAI* locus would have a 5′ copy of *PFAI* containing the zeocin cassette and a second, uninterrupted 3′ copy of *PFAI*. The largest band of the Southern blot of A20 agrees well with the predicted size of the vector-backbone containing fragment found between the 3′-most *NcoI* site in the upstream, interrupted copy of *PFAI* and the first *NcoI* site found in the coding region of the downstream, uninterrupted, promoter-less copy of *PFAI*. The remaining bands also agree well with their predicted sizes. Northern blots (Fig. 3) demonstrate that the *PFAI* transcript was affected in the auxotrophic mutant. As shown, the *PFAI* transcript in the mutant appears as two fragments detectable by the probe used. These fragments, ~2,700 bases and ~1,800 bases in size, obviously do not sum to the wild-type transcript size (>9,000 bases). The size of the larger band agrees with the size expected for a transcript initiated by the *PFAI* promoter and stopped at the zeo cassette terminator. The smaller band may also have been formed by initiation from the *PFAI* promoter, but with premature termination or transcript fragmentation occurring at some point within the sequence of the zeocin cassette promoter.

Although our method of generating “knockout” mutants worked well for the current study, one might expect double cross-over recombination events to occur more frequently if linear vector had been used, as is the case in many other systems. Transformation efficiencies with linear vectors are being improved and should yield more facile recombinations in future studies.

A secondary desaturase/elongase PUFA pathway (a “standard” pathway) was detected in *Schizochytrium*, however, the enzymes of this pathway were unable to rescue cultures from the lethality of PUFA synthase disruption. The apparent absence of a $\Delta 12$ desaturation activity for 18:1 n-9 seems the most likely cause of this inability to self-complement disruptions of the PUFA

Table 3 Radiolabeled FAMES derived from total lipids of wild-type *Schizochytrium* cultures grown at 27 °C in 10 mL 790 liquid media supplemented with 1 μCi of the indicated 1-[¹⁴C] labeled free fatty acids

¹⁴ C-Fatty acid added	Wild-type <i>Schizochytrium</i> culture FAME percentage of label recovered in:																	
	16:0	18:0	18:1 n-6	18:2 n-3	18:3 n-6	18:3 n-3	18:4 n-6	20:2 n-6	20:3 n-6	20:3 n-9	20:4 n-3	20:4 n-6	20:5 n-3	22:4 n-6	22:5 n-3	22:5 n-6	22:6	?
16:0	97 ^φ	–	Φ	–	–	–	–	–	–	–	–	–	–	–	–	–	–	3
18:0		92	–	–	–	–	–	–	–	–	–	–	–	–	–	–	–	7.9
18:1 n-9			92.3	–	–	–	–	–	–	–	–	–	–	–	–	–	–	7.7
18:2 n-6				69.5	13.4*	4.2 [#]	–	–	–	–	*	–	–	–	*	–	#	12.9
18:3 n-3					47.8*	–	1.9	–	–	–	*	–	43.1	–	*	–	–	1
18:3 n-6						49.1 [#]	–	–	5.4	–	6.5*	7.4	31.4	–	*	–	#	–
18:4 n-3							26.6	–	–	–	7.5*	–	59.1	–	*	–	4.8	–
20:2 n-6								93.2	–	–	–	–	–	–	–	–	–	6.8
20:3 n-6									31.3	–	1.3*	19.1	43.6	–	*	–	3.2	–
20:3 n-9										76.9	–	–	2.1	–	–	2.5	15.1	3.5
20:4 n-3											30.9*	–	61	–	*	–	5.6	–
20:4 n-6												39.4	46	–	–	3.2	8.6	–
20:5 n-3													74.9	–	8.2	–	16	–
22:4 n6														31.0	42.1	17.2	19.8	–
22:5 n-3															26.2	–	73.8	–
22:5 n-6																74.3	25.7	–

All values are expressed as percent of total recovered activity per FAME. Three distinct groups of FAME standards appeared as a single co-migrating peak during HPLC separation, precluding quantification of these FAMES individually:

* FAMES of 18:3 n-3, 20:4 n-3 and 22:5 n-3 co-migrated

FAMES of 18:3 n-6 and 22:6 n-3 co-migrated

φ FAMES of 16:0 and 18:1 co-migrated

? Includes percent activities of minor peaks which did not elute with any of the authentic standards used

synthase. This lesion in the standard pathway may not be limited entirely to the absence of the Δ12 desaturase activity. Even though the conversion of radiolabeled 18:2 to 18:3 was observed, 18:2 (and 20:2 n-6, data not shown) were unable to support growth of the PUFA synthase mutants, suggesting that the kinetics of these conversions are severely limited. Downstream of 18:2, most biosynthetic steps expected for the standard pathway could be identified or inferred (Fig. 4). Specifically, an omega-3 desaturase activity for the conversion of ARA to EPA was seen, as were several elongase activities. Additionally, Δ6 and Δ9 elongase activities for the conversion of both isomers of 18:3 to their 20 carbon products, and a Δ5 elongase activity for the conversion of EPA to 22:5 n-3, were observed.

It may be worth noting that conversion of 18:0 to 18:1 n-9 was not detected in the radiolabeling experiment (Table 3) despite the fact that the wild-type strain clearly accumulates an isomer of 18:1 (Table 2). The reason for this is unclear although it may be that the cultures responded differently to the different culture volumes and media compositions used in each set of experiments. The most

significant difference in media compositions being the masses of substrates used in the two experiments (0.5 mM unlabeled FFA vs. ~2 μM labeled FFA). This may also explain the fact that very little conversion of ARA or DPA n-6 was seen in cultures fed unlabeled substrate (Table 2), whereas these fats were converted more when fed as radiolabeled substrates (Table 3). Some of these differences might also be explained by potential alterations in the regulation of standard pathway enzymes in response to PUFA synthase disruption, when compared to wild-type cultures. It should additionally be noted that *Schizochytrium* has previously been shown to produce 18:1 n-7 and 16:1 n-7 along with 18:1 n-9 [24]. The n-7 isomer of 18:1 was not used as a substrate in this study because radiolabeled standard was not available and because no precedence exists for the conversion of n-7 fatty acids to n-3 or n-6 products. Double-bond positions of FAME products corresponding to 18:1 were not specified in Tables 2 or 3 because neither of the FAME separation techniques used in this study would have easily resolved the different mono-unsaturated fatty acid isomers. The primary products of the *Schizochytrium* FAS [8] are 14:0 and 16:0. Stearic acid is

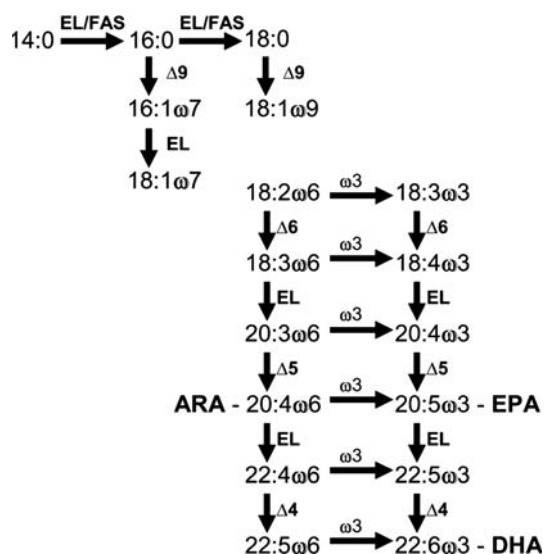


Fig. 4 A summary of elongation and desaturation activities corresponding to wild-type and auxotrophic mutant cultures of *Schizochytrium*. The most apparent “missing” activity corresponds to a Δ 12 desaturase although other activities immediately adjacent to the Δ 12 desaturase in the above pathway may be so inefficient as to be essentially non-functional. EL elongase, EL/FAS elongase or fatty acid synthase, ω 3 omega-3 desaturase activity, Δ 9 delta-9 desaturase activity, Δ 6 delta-6 desaturase activity, Δ 5 delta-5 desaturase activity, Δ 4 delta-4 desaturase activity. The saturated and monounsaturated fatty acid conversions shown are hypothetical and were not demonstrated by radiolabeling in this investigation. Their inclusion in the pathway above is based on the observed accumulation of each unlabeled saturated and monounsaturated fatty acid in *Schizochytrium* cultures described here and in other studies referenced in the text. Accumulation of stearic acid and monounsaturates in *Schizochytrium* appears to be dependent on culture conditions different from those used for radiolabeling experiments here

either a minor product of the FAS or a minor elongation product of 16:0 in wild-type cells. Disruption of the PUFA synthase appears to promote greater accumulation of 18:1 (Table 2), presumably formed either via elongation of 16:1 n-7 to 18:1 n-7 or desaturation of 18:0 to the n-7 or n-9 isomer of 18:1. If the predominant isomer produced by *Schizochytrium* PUFA synthase knockouts is 18:1 n-7, then the absence of a mechanism to form substantial quantities of 18:1 n-9 may represent yet another lesion in the standard pathway of this organism.

Lastly, *Schizochytrium* appears to harbor a Δ 4 desaturase activity as evidenced by the accumulation of DHA in cultures fed 22:5 n-3. This desaturase is likely to be very similar to its counterpart in *Thraustochytrium* [9]. In contrast to our results, Meyer et al. [25] reported that *Schizochytrium* was not able to convert significant amounts of DPA n-3 to DHA during 24 h incubation with label. All of the *Schizochytrium* fatty acid labeling data presented in this work was obtained using 2 day incubations, simply because preliminary experiments had established that

equilibrium was not yet attained after just 24 h. The *Schizochytrium* Δ 4 desaturase activity and others were only revealed when these longer incubation times were used.

As noted earlier, Thraustochytrid PUFA synthases [5, 26], like that of *Schizochytrium*, are most similar to PUFA synthases of proteobacterial systems. However, the Δ 4 desaturase isolated from *Thraustochytrium* (Genbank accession AAM09688) is, by BLASTP analysis, most similar to other “front-end” desaturases of other eukaryotes such as the Δ 4 desaturase of *Euglena* (of the alveolates), the Δ 5 desaturases of the liverwort, *Marchantia* (of the viridiplantae), and the fungi, *Mortierella* (Genbank accessions AAQ19605, AAT85663, and AAR28035, respectively). Isolation of additional standard PUFA synthesis pathway genes from other members of the order Labyrinthulida coupled with detailed phylogenetic studies may reveal that the desaturases and elongases were likely the only components of a PUFA pathway present in ancestors of *Thraustochytrium* and *Schizochytrium*, and that the PUFA synthase was a later, horizontally transferred acquisition from a bacterium to the *Schizochytrium* progenitor (and perhaps other ancestral eukaryotes). Precedence for such bacteria-to-eukaryote horizontal gene transfers exists beyond the common examples associated with the acquisition of plastids and mitochondria (especially among protists) [27]. Hypothetically, once the PUFA synthase stabilized in this ancestor, selective pressure to retain the standard pathway components could have been diminished to a secondary role in scavenging for environmental PUFAs or prematurely released PUFA synthase intermediates (possibly 18:5 n-3 for example, which could be converted to 20:5 n-3 (EPA) via a single β -ketoacyl synthase-mediated condensation, according to the scheme of Metz et al. [4]). Under such conditions, one would predict that the standard pathway enzymes involved in conversion of PUFAs with the least structural analogy to the native PUFAs, DHA and DPA would be under the least selective pressure and would thus decay faster. An environment rich in sources of 18-carbon PUFAs (perhaps from decaying vegetation) may relax the selective pressure on the early parts of the standard pathway in these organisms even further. Analysis of other members of Labyrinthulida (or even other eukaryotes) may reveal standard pathways in greater or lesser stages of decay depending upon specific environmental needs and the strength of an endogenous PUFA synthase system.

Acknowledgments We would like to acknowledge Jerry Kuner, Brad Rosenzweig, Craig Weaver, and Dan Doherty for helpful discussions and for supplying vectors without which this work would not have been possible. We would also like to acknowledge Paul Roessler’s development of the *Schizochytrium* transformation system and his observations of homologous recombination with it. Colin Ratledge is thanked for review of portions of the manuscript.

References

1. Cavalier-Smith T, Allsopp MTEP, Chao EE (1994) *Thraustochytrids* are chromists, not fungi: 18 s rRNA signatures of heterokonta. *Philos Trans R Soc Lond B Biol Sci* 346:387–397
2. Barclay WR (2002) Fermentation process for producing long chain omega-3 fatty acids with euryhaline microorganisms. US Patent 6,451,567
3. Cohen Z, Ratledge C (2005) *Single Cell Oils*. AOCS Publishing, Champaign, 36–52, 208–210
4. Metz JG, Roessler P, Facciotti D, Levering C, Dittrich F, Lassner M, Valentine R, Lardizabal K, Domergue F, Yamada A, Yazawa K, Knauf V, Browse J (2001) Production of polyunsaturated fatty acids by polyketide synthases in both prokaryotes and eukaryotes. *Science* 293:290–293
5. Metz JG, Lassner M, Facciotti D (2000) Production of polyunsaturated fatty acids by expression of polyketide-like synthesis genes in plants. US Patent 6,140,486
6. Yazawa K (1996) Production of eicosapentaenoic acid from marine bacteria. *Lipids* 31(Suppl):S297–300
7. Morita N, Tanaka M, Okuyama H (2000) Biosynthesis of fatty acids in the docosahexaenoic acid-producing bacterium *Moritella marina* strain MP-1. *Biochem Soc Trans* 28:943–945
8. Hauvermale A, Kuner J, Rosenzweig B, Guerra D, Diltz S, Metz JG (2006) Fatty acid production in *Schizochytrium* sp.: involvement of a polyunsaturated fatty acid synthase and a type I fatty acid synthase. *Lipids* 41:739–747
9. Qiu X, Hong H, Mackenzie SL (2001) Identification of a $\Delta 4$ fatty acid desaturase from *Thraustochytrium* sp. involved in the biosynthesis of docosahexanoic acid by heterologous expression in *Saccharomyces cerevisiae* and *Brassica juncea*. *J Biol Chem* 276:31561–31566
10. Qiu X (2003) Biosynthesis of docosahexanoic acid (DHA, 22:6-4, 7, 10, 13, 16, 19): two distinct pathways. *Prostaglandins Leukot Essent Fatty Acids* 68:181–186
11. Roessler PG, Matthews TD, Ramseier TM, Metz JG (2006) Product and process for transformation of Thraustochytriales microorganisms. US Patent 7,001,772
12. Apt KE, Kroth-Pancic PG, Grossman AR (1996) Stable nuclear transformation of the diatom *Phaeodactylum tricorutum*. *Mol Gen Genet* 252:572–579
13. Sambrook J, Russell DW (2001) *Molecular cloning: a laboratory manual*, 3rd edn. Cold Spring Harbor Laboratory Press, New York
14. Gatignol A, Durand H, Tiraby G (1988) Bleomycin resistance conferred by a drug-binding protein. *FEBS Lett* 230:171–175
15. Morrison WR, Smith LM (1964) Preparation of fatty acid methyl esters and dimethylacetals from lipids with boron fluoride-methanol. *J Lipid Res* 5:600–608
16. Arterburn LM, Boswell KD, Henwood SM, Kyle DJ (2000) A developmental safety study in rats using DHA- and ARA-rich single-cell oils. *Food Chem Toxicol* 38:763–771
17. Ozcimder M, Hammers WE (1980) Fractionation of fish oil fatty acid methyl esters by means of argentation and reversed-phase high-performance liquid chromatography, and its utility in total fatty acid analysis. *J Chromatogr* 187:307–317
18. Deng C, Capecchi MR (1992) Reexamination of gene targeting frequency as a function of the extent of homology between the targeting vector and the target locus. *Mol Cell Biol* 12:3365–3371
19. Negritto MT, Wu X, Kuo T, Chu S, Bailis AM (1997) Influence of DNA sequence identity on efficiency of targeted gene replacement. *Mol Cell Biol* 17:278–286
20. Stuke JE, McDonough VM, Martin CE (1989) Isolation and characterization of OLE1, a gene affecting fatty acid desaturation from *Saccharomyces cerevisiae*. *J Biol Chem* 264:16537–16544
21. Campbell JW, Cronan JE Jr (2001) *Escherichia coli* FadR positively regulates transcription of the *fabB* fatty acid biosynthetic gene. *J Bacteriol* 183:5982–5990
22. Certik M, Sakuradani E, Shimizu S (1998) Desaturase-defective fungal mutants: useful tools for the regulation and overproduction of polyunsaturated fatty acids. *Trends Biotechnol* 16:500–505
23. Wada H, Murata N (1989) *Synechocystis* PCC6803 mutants defective in desaturation of fatty acids. *Plant Cell Physiol* 30:971–978
24. Michaud AL, Guan-Yeu D, Abril R, Brenna JT (2002) Double bond localization in minor homoallylic fatty acid methyl esters using acetonitrile chemical ionization tandem mass spectrometry. *Anal Biochem* 307:348–360
25. Meyer A, Cirpus P, Ott C, Schlecker R, Zähringer U, Heinz E (2003) Biosynthesis of docosahexanoic acid in *Euglena gracilis*: biochemical and molecular evidence for the involvement of a $\Delta 4$ -fatty acyl group desaturase. *Biochemistry* 42:9779–9788
26. Metz JG, Flatt JH, Kuner JM, Barclay WR (2007) Pufa polyketide synthase systems and uses thereof. US Patent 7,256,022
27. Gogarten JP (2003) Gene transfer: gene swapping craze reaches eukaryotes. *Curr Biol* 13:R53–R54

Effect of Bilayer Phospholipid Composition and Curvature on Ligand Transfer by the α -Tocopherol Transfer Protein

Wen Xiao Zhang · Grant Frahm · Samantha Morley ·
Danny Manor · Jeffrey Atkinson

Received: 15 July 2008 / Accepted: 28 April 2009 / Published online: 21 May 2009
© AOCS 2009

Abstract We report here our preliminary investigations on the mechanism of α -TTP-mediated ligand transfer as assessed using fluorescence resonance energy transfer (FRET) assays. These assays monitor the movement of the model α -tocopherol fluorescent derivative ((*R*)-2,5,7,8-tetramethyl-chroman-2-[9-(7-nitro-benzo[1,2,5]oxadiazol-4-yl amino)-nonyl]-chroman-6-ol; NBD-Toc) from protein to acceptor vesicles containing the fluorescence quencher TRITC-PE. We have found that α -TTP utilizes a collisional mechanism of ligand transfer requiring direct protein–membrane contact, that rates of ligand transfer are greater to more highly curved lipid vesicles, and that such rates are insensitive to the presence of anionic phospholipids in the acceptor membrane. These results point to hydrophobic features of α -TTP dominating the binding energy between protein and membrane.

Keywords α -Tocopherol · α -Tocopherol transfer protein · Lipid transfer protein · Membrane curvature · Unilamellar vesicles · LUV · SUV · FRET

Abbreviations

AVED Ataxia with vitamin E deficiency

Electronic supplementary material The online version of this article (doi:10.1007/s11745-009-3310-x) contains supplementary material, which is available to authorized users.

W. X. Zhang · G. Frahm · J. Atkinson (✉)
Department of Chemistry, Centre for Biotechnology,
Brock University, 500 Glenridge Ave, St. Catharines,
ON L2S 3A1, Canada
e-mail: jatkin@brocku.ca

S. Morley · D. Manor
Department of Nutrition, School of Medicine, Case Western
Reserve University, Cleveland, OH 44106-4954, USA

DOPA	Dioleoylphosphatidic acid
DOPC	Dioleoylphosphatidylcholine
EDTA	Ethylenediaminetetraacetic acid
FABP	Fatty acid binding protein
FRET	Fluorescence resonance energy transfer
HDL	High density lipoprotein
LBPA	Lysobisphosphatidic acid
LDL	Low density lipoprotein
LUV	Large unilamellar vesicle
MVB	Multivesicular body
NBD-Toc	(<i>R</i>)-2,5,7,8-tetramethyl-chroman-2-[9-(7-nitro-benzo[1,2,5]oxadiazol-4-yl amino)-nonyl]-chroman-6-ol
PC	Phosphatidylcholine
PE	Phosphatidylethanolamine
PI	Phosphatidylinositol
PIPs	Phosphoinositide phosphates
PMSF	Phenylmethanesulfonyl fluoride
PS	Phosphatidylserine
POPC	1-Palmitoyl-2-oleoyl phosphatidylcholine
PUFA	Polyunsaturated fatty acid
SUV	Small unilamellar vesicle
TRITC-PE	<i>N</i> -(6-tetramethylrhodaminethio-carbamoyl)-1,2-dihexadecanoyl- <i>sn</i> -glycero-3-phospho-ethanol-amine, triethylammonium salt
VLDL	Very low density lipoprotein

Introduction

The human α -tocopherol transfer protein (α -TTP) is a soluble 32 kDa-protein chiefly expressed in the liver that is understood to be responsible for the selective retention of α -tocopherol from dietary sources over other forms of

vitamin E [1]. This role is exemplified by mutant forms of the protein that are known to cause neurological deficits in persons having “ataxia with vitamin E deficiency” (AVED) [2–6]. It is further underscored by mice in which the *tppA* gene has been deleted, that exhibit very low levels of plasma and tissue α -tocopherol [7–10] and present AVED-like neuropathological symptoms [11]. Despite these demonstrations of α -TTP centrality to tocopherol bioavailability and distribution, little is known about the molecular mechanism of α -tocopherol transport in hepatocytes, nor the means by which α -TTP assists in the re-secretion of α -tocopherol into the plasma where it is carried to extrahepatic tissues by plasma lipoproteins. For instance, while it is well documented that the majority of plasma tocopherol is carried by LDL and HDL, treatment of cultured hepatocytes with brefeldin A, which inhibits lipoprotein construction and secretion outside the cell, did not inhibit tocopherol secretion [12]. Similarly, mice in which the expression of liver microsomal triglyceride transfer protein (MTTP) is disrupted and thus do not secrete VLDL remain tissue-sufficient in tocopherol [13].

Lipid transfer proteins enable cells to transport hydrophobic compounds (e.g., fatty acids, phospholipids, sterols, retinoids, and α -tocopherol) across aqueous media inside cells. The means by which this is accomplished has been most thoroughly described for the fatty acid binding proteins (FABPs) that, in all cases except for the liver FABP [14, 15], bind directly to membrane surfaces where they extract or deliver their preferred ligand(s). In order to accomplish this task, FABPs take advantage of electrostatic forces between a collection of basic residues on an α -helical portal region and negatively charged membrane phospholipids [16].

In previous work using cultured hepatocyte cells it was shown [17, 18] that expressed α -TTP co-locates with a fluorescent form of α -tocopherol ((*R*)-2,5,7,8-tetramethylchroman-2-[9-(7-nitro-benzo[1, 2, 5]oxadiazol-4-yl amino)-nonyl]-chroman-6-ol; NBD-Toc) [19] in the late endosomal compartment. The localization of α -TTP to endosomes raises the possibility that the protein may prefer to associate with membranes of specific phospholipid composition, or defined curvature. We report here our investigations on the mechanism of α -TTP-mediated ligand transfer assessed using fluorescence resonance energy transfer (FRET) assays that monitor the movement of NBD-Toc from protein to acceptor vesicles. We have found that α -TTP utilizes a collisional mechanism of ligand transfer requiring direct protein–membrane contact, that rates of ligand transfer are greater for more highly curved lipid vesicles, and that such rates are insensitive to the presence of anionic phospholipids in the acceptor membrane.

Materials and Methods

Materials

Glutathione agarose and DNase I were purchased from Invitrogen (Burlington, ON, Canada). N-(6-tetramethylrhodaminethio-carbamoyl)-1,2-dihexadecanoyl-*sn*-glycero-3-phosphoethanol-amine, triethylammonium salt (TRITC-DHPE) was from Molecular Probes (Invitrogen, Oregon, USA). Thrombin was obtained from GE Healthcare (Piscataway, NJ, USA). RNase A and Triton X-100 were from Sigma (St. Louis, MI, USA). Polycarbonate membranes for lipid extrusion were purchased from Avestin, Inc (Ottawa, ON, Canada). The following phospholipids were obtained from Avanti Polar Lipids (Alabaster, AL, USA): Liver bovine L- α -phosphatidylcholine (liver PC), soy L- α -phosphatidylcholine (soy PC), porcine brain L- α -phosphatidylserine (PS), bovine liver phosphatidylinositol (PI), 1,2-dioleoyl-*sn*-glycerol-3-phosphocholine (DOPC), oleoyl lysobisphosphatidic acid (LBPA), and 1,2-dioleoyl-*sn*-glycerol-3-phosphate (DOPA). NBD-Toc was previously synthesized in our lab [19]. All other reagents were from BioShop Canada Inc. (Burlington, ON, Canada).

Protein Expression and Purification

Human α -TTP flanked by NotI and SalI restriction sites was subcloned into pGEX-4T-3 vector. This construct was transformed into *E. coli* BL21 (DE3) for protein expression [20]. *E. coli* cultures were grown in baffled flasks at 37 °C until OD 600 nm was between 0.4 and 0.6. The bacterial culture was cooled to room temperature before being induced with 400 μ M IPTG. To improve the production of soluble α -TTP, the culture was grown at room temperature for 18 h. The cells were harvested and stored at –80 °C until use.

After being frozen and thawed three times, the *E. coli* pellet was re-suspended in buffer A (150 mM Tris pH 8.0, 150 mM NaCl, 1 mM EDTA, 10% glycerol, 0.1 mM DTT and 0.1 mM PMSF). Lysozyme (4 mg/ml) was added to the cell suspension and followed by 30 min incubation on ice. Nucleic acids were digested with the addition of 10 mM MgCl₂, DNase I (1,000 units/ml lysate) and RNase (50 μ g/ml), followed by an additional 30 min incubation on ice. The cells were then homogenized and centrifuged at 40,000g for 30 min at 4 °C. The supernatant was applied to a glutathione affinity column, and nonspecific binding proteins were removed by 15 column volumes wash each of buffer B (Buffer A plus 0.5% Triton X and 10 mM MgCl₂) and buffer C (50 mM Tris, pH 8, 150 mM NaCl, 10 mM MgCl₂ and 0.1 mM DTT), respectively. On-column thrombin cleavage of GST-TTP was completed after 2 h of incubation at RT with 50 units of thrombin in PBS

per 1 ml of resin. The α -TTP was eluted in buffer C and a final concentration of 0.5 mM PMSF was added to prevent further thrombin-induced degradation. GST bound on the column was eluted with PBS containing 20 mM glutathione, and the column was regenerated with 3 M NaCl in PBS. Each purified sample was subjected to SDS-PAGE analysis. The Bradford assay was used to determine protein concentration. Purified protein was stored at 4 °C and used within a few days after the purification. In general, α -TTP ligand transfer activity remained intact within 5 days of purification.

Lipid Vesicle Preparation

Acceptor lipid vesicles for ligand transfer assays contained 97 mol% PC and 3 mol% quencher TRITC-PE, unless otherwise specified. For anionic lipid vesicles, 15 mol% of indicated anionic phospholipid was incorporated in vesicle preparations. Chloroform was evaporated from lipid mixtures under a stream of N₂ and residual solvent removed by continued evaporation under 0.5 mmHg. Lipid mixtures were rehydrated in SET buffer (250 mM Sucrose, 100 mM KCl, 50 mM Tris, 1 mM EDTA, pH 7.4). The lipid suspensions were vortexed and incubated for 30 min at room temperature before liposome preparation. Large unilamellar vesicles (LUV) were prepared with a Liposfast mini-extruder (Avestin, Inc.). Briefly, lipid suspensions were extruded through a polycarbonate membrane (100-nm membrane for standard LUV preparation) for 15 passages to produce uniform size LUV. Small unilamellar vesicles (SUV) were prepared, following the procedure described by Schroeder and Thompson [21] with minor modifications. Briefly, lipid suspensions were sonicated using a titanium microprobe and a W-375 cell disruptor (Heat Systems-Ultrasonic, Inc.). Lipid samples were sonicated on ice for 45 min with output setting level of 2.5 and 35% duty cycle. The resulting liposomes were centrifuged at 110,000g for 2 h at 4 °C to remove large vesicles and titanium particles. To compare the difference between probe and bath sonicated SUV, SUV were also prepared by sonication for 45 min with a Branson bath sonicator Model 2510 (Branson, USA). SUV produced from both methods appeared to behave similarly toward α -TTP mediated tocopherol transfer. Ideally, a phosphorous assay should be performed to determine the phospholipid concentration after each vesicle preparation. However, due to the presence of a high sucrose content in the SET buffer, lipid samples turned black during acidic digestion at 190 °C, and thus such assays could not be used regularly to assess phospholipid concentration. To confirm that there is no loss of phospholipids due to extrusion and sonication procedures, the phosphorous assay was performed initially with SET buffer without sucrose, and the result suggested that

the lipid concentration remains the same before and after the preparation. For the experiments that compared the vesicles of different size, the same rehydrated lipid mixture (multilamellar vesicles) was used to generate SUVs or LUVs of the same stock concentration. An estimation of vesicle concentration can be determined based on the emission spectrum of quencher TRITC-PE at approximately 575 nm. Lipid samples were prepared freshly for each experiment.

We measured the size of all lipid vesicles using a single angle (90°) quasi-elastic light scattering (QELS) instrument (Bookhaven Instruments Corporation) with a Melles Griot HeNe Laser (35 mW, 632.8 nm) and BI-APD 8590 digital auto-correlator. A cumulative statistical method was used to calculate particle size distributions. We found that all vesicles have nominal diameters larger than expected from the pore size of the filters when the extrusion method is used. We also note that the sucrose-containing buffer elicited a significant background signal that led to an overestimation of the size of small vesicles. Increased vesicle size has been seen previously with vesicles made in sucrose-containing buffers [22]. In general, the size variation is larger than expected for smaller vesicles than for bigger ones.

The average diameters of vesicles (nm) and their polydispersity index (in parentheses) were, by probe sonication; 106 nm (0.283), bath sonication; 134 nm (0.262); and by extrusion through polycarbonate filters of nominal pore size 30 nm (91 nm, 0.122), 50 nm (107 nm, 0.119), 100 nm (158 nm, 0.116), and 200 nm (219, 0.103). When vesicles of expected size 100 nm were prepared in Tris buffer rather than SET, the average size was 114 nm (0.085) emphasizing the overestimation of vesicle size that occurs in SET buffer.

We also separately determined the size of the smallest vesicles we prepared by sonication and extrusion on a DyanPro™ NanoStar (Wyatt Technology). In this case probe sonication gave vesicles of an average size of 67 nm (polydispersity 0.326) and extruded vesicles using 30 nm filters, 55 nm (0.034).

Partition Coefficient of NBD-Toc Between α -TTP and PC Lipid Vesicles

Kinetic analyses of FRET-based ligand transfer assays are only useful if the transfer is essentially unidirectional. In this work we have monitored the decrease in fluorescence intensity as NBD-Toc bound to α -TTP (where the signal is high) is transferred to PC vesicles containing the quencher TRITC-PE (where the signal is low). In order to be assured of unidirectional transfer, the partition coefficient (K_p) of NBD-Toc between α -TTP and vesicles must be known. Once K_p is known, appropriate concentrations of donor

protein-ligand complex and acceptor vesicles can be chosen. The K_p of NBD-Toc was measured following literature procedures for fluorescent fatty acid transfer from albumins and FABPs to lipid vesicles [15, 23]. Briefly, several solutions were prepared containing a 9:1 ratio of α -TTP:NBD-Toc (final protein and ligand concentrations were 1 μ M α -TTP:0.1 μ M NBD-Toc in SET, pH 7.4) that assured the absence of appreciable amounts of free NBD-Toc. (The K_d of NBD-Toc for α -TTP was determined to be between 8.5 [24] and 56 nM [19] depending on the assay conditions and whether the α -TTP used was a GST or His-tagged fusion. Natural α -tocopherol has a K_d of 25 nM using a tritiated-tocopherol binding assay [25]). These high affinities of the protein for the ligand suggest that the α -TTP concentrations for both kinetic and partitioning experiments are sufficient to bind all available NBD-Toc. The samples were incubated for 15 min with gentle rotation. To each of these solutions were added amounts of LUVs or SUVs containing TRITC-PE (measured as μ M total phospholipid) so that the final lipid concentration ranged from 50 to 400 μ M. The resulting mixture was incubated for 15 min to allow NBD-Toc to equilibrate between α -TTP and acceptor SUVs or LUVs, the fluorescence spectrum of NBD-Toc from 475 to 600 nm was recorded, and the changes in the fluorescence at 520 nm were applied to the following equation [23, 26] to calculate partition coefficients:

$$1/\Delta F = 1/K_p(1/\Delta F_{\max})(\text{mol } \alpha\text{-TTP/mol PC}) + 1/\Delta F_{\max} \quad (1)$$

where ΔF is the difference between the initial fluorescence of NBD-Toc bound to α -TTP and the fluorescence at a given protein/PC ratio, and ΔF_{\max} is the maximum fluorescence change [15]. A plot of $1/\Delta F$ versus $(1/\Delta F_{\max})(\text{mol } \alpha\text{-TTP/mol PC})$ gave a straight line whose slope was equal to $1/K_p$.

Transfer of NBD-Toc to Lipid Vesicles Investigated by FRET

The rate of NBD-Toc transfer from α -TTP to lipid vesicles was investigated utilizing a FRET assay. Experiments were performed using a Photon Technologies, Inc. QuantaMaster-QM-2001-4 fluorometer (Photon Technologies International, Inc.) equipped with SPF-17 stopped-flow device which were used to determine the kinetics of NBD-Toc transfer to quencher TRITC-PE containing acceptor vesicles. The emission spectrum of NBD-Toc overlaps with the excitation spectrum of TRITC-PE, thus, upon mixing of donor (α -TTP bound NBD-Toc) and acceptor (TRITC-PE containing vesicles), the fluorescence intensity decreases with time. The excitation and emission wavelengths used were 466 and 526 nm, respectively. Standard transfer

experiments were performed by incubating 0.45 μ M NBD-Toc with 4 μ M α -TTP for 15 min prior to mixing with 200 μ M acceptor vesicles using the SPF-17 stopped-flow device. The final concentrations after mixing were 0.225 μ M NBD-Toc, 2 μ M α -TTP and 100 μ M vesicles. The ratio of α -TTP to NBD-Toc was kept at 9:1 to ensure that there was no free ligand and that the fluorescence signal was solely attributed to protein-bound NBD-Toc. A 50-fold excess of acceptor vesicle was used based on the partition coefficient of NBD-Toc between α -TTP and vesicles. All experiments were performed at 20 °C. The fluorescence quench was monitored over time and normalized to the starting fluorescent intensity of NBD-Toc bound to α -TTP as 100%. To study the intervesicular transfer of NBD-Toc, 1 mol% of NBD-Toc was incorporated into PC SUV or LUV, and the transfer of NBD-Toc from these vesicles to PC LUV or SUV were monitored. In our assay condition, after subtraction of the signal due to slight ligand photobleaching, the rate of NBD-Toc transfer was best fitted with a single exponential decay Eq. 2 provided by Prism software (version 5, GraphPad Software, Inc., El Camino Real, San Diego, CA, USA).

$$y = (y_0 - y_{\text{inf}}) * \exp(-k * x) + y_{\text{inf}} \quad (2)$$

where y_0 is the initial fluorescence when NBD-Toc bound to α -TTP, k is the rate constant, x is the half time, and y_{inf} is the remaining fluorescence signal after NBD-Toc has been transferred to the acceptor vesicle, which in our case is approximately 55% of the original fluorescence signal.

Results

A representative determination of the partition coefficient of NBD-Toc between α -TTP and vesicles of different size is shown in Fig. 1. The slopes of the lines for both LUVs and SUVs over this lipid concentration range are very similar and shallow. The average values of the determined partition coefficient, K_p , of NBD-Toc between α -TTP and bovine liver phosphatidylcholine unilamellar vesicles were determined to be 0.064 ± 0.026 ($n = 4$) for LUVs and 0.098 ± 0.035 ($n = 3$) for SUVs. These values are not significantly different from each other. As the units of K_p are (mol lipid-bound NBD-Toc/mol phospholipid)/(mol protein-bound NBD-Toc/mol protein) the magnitude of K_p shows that NBD-Toc binds to α -TTP with ~ 10 – 15 times greater affinity than to lipid. Thus, for our transfer assay conditions to reflect unidirectional movement from protein to vesicle, an excess of phospholipids must be provided. Our assays use a 50-fold molar excess of phospholipids over α -TTP and represent a convenient concentration that assures unidirectional transfer, is not wasteful of phospholipids, and maintains the rate of transfer within the

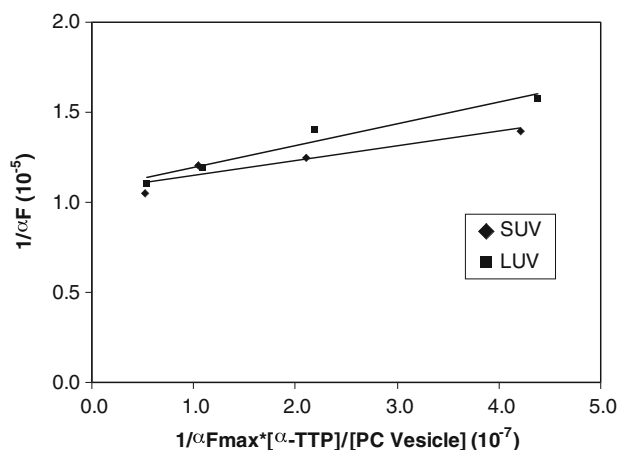


Fig. 1 Partitioning of NBD-Toc between α -TTP and SUVs or LUVs. Titration of NBD-Toc (0.225 μ M) bound to α -TTP (2 μ M) with PC SUVs (filled diamonds) or LUVs (filled squares) at a concentration of 50, 100, 200 and 400 μ M. The change in fluorescence intensity between NBD-Toc bound to α -TTP and vesicles at each lipid concentration is expressed as ΔF . The partition coefficients determined for this particular experiment are 0.122 and 0.082 for SUVs and LUVs, respectively

kinetic window of our stopped-flow device (mixing dead time \sim 20 ms). At equilibrium, the assays show a \sim 50% loss of the original fluorescence from protein-bound NBD-Toc.

However, it was observed that spontaneous intervesicular ligand transfer in the absence of α -TTP occurred at a higher rate for donor SUVs than donor LUVs (Fig. 2). Note that the fastest observed rate was for movement of NBD-Toc from donor SUV to acceptor SUV; when the donor vesicles were LUVs the rates were lowered by about 50%. This may represent a combination of the enhanced water-solubility of NBD-Toc (calculated $\log P = 7.34$) compared to natural α -tocopherol ($\log P = 9.60$), and the ease of ligand movement from the differing lipid packing of SUVs and LUVs. Our previous work with NBD-tocopherol in hepatocytes [17, 18] showed that this ligand partitions to membranes and that residence time in mainly endosomal membranes is dependent on the inducible expression of TTP that clears the fluorescence signal from the cell. This behavior completely mimics similar secretion assays done using 14 C- α -tocopherol. Furthermore, we recently reported on the effect of tocopherols on aspects of membrane curvature using differential scanning calorimetry (DSC) [27]. All of the tocopherols and tocotrienols lowered both the gel to liquid crystalline transition temperature (T_M) and the liquid crystalline to inverted hexagonal transition (T_H) of dielaidoyl phosphatidylethanolamine. We have repeated such measurements with NBD- α -tocopherol and found them to be more similar to natural α -tocopherol than any other tocopherol. In the above-cited work, the numbers for α -tocopherol were: ΔT_M ($^{\circ}$ C/mol fraction) = -41 ± 4 and ΔT_H

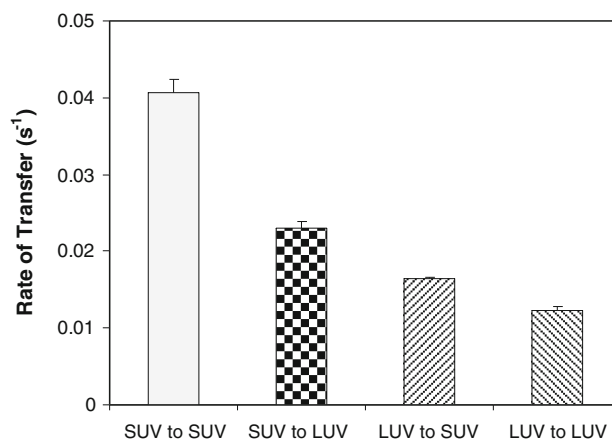


Fig. 2 Intervesicular transfer of NBD-Toc from donor vesicles to acceptor vesicles. 1 μ M NBD-Toc incorporated in 100 μ M donor PC SUVs or LUVs was transferred to 100 μ M acceptor bovine liver PC SUVs or LUVs containing 3% TRITC-PE. Data shown represent an average of six determinations \pm the standard deviation

($^{\circ}$ C/mol fraction) = -300 ± 35 . The values for NBD- α -tocopherol were $\Delta T_M = -33 \pm 4$ and $\Delta T_H = -262 \pm 17$, suggesting that NBD-tocopherol has the same effect on the physical attributes of a membrane as does α -tocopherol.

To test whether α -TTP uses a collisional mechanism of transfer where membrane binding is required [16], the concentration of acceptor phospholipids was increased while keeping the protein:ligand concentration constant. If protein-membrane collision is required then the rate of transfer should increase with increasing concentration of phospholipid. As shown in Fig. 3, the rate of transfer of NBD-Toc from α -TTP is quite insensitive to LUV concentration. However, the rates did increase about 50% (0.011 ± 0.0017 – 0.017 ± 0.005 s^{-1}) when the LUV concentration was increased from 50 to 750 μ M. When SUVs were the ligand acceptor the enhancement of transfer was much more dramatic as the lipid amount was raised, increasing \sim 4.5-fold from 25 to 625 μ M phospholipids. Indeed, we have noted a 4-nm red-shift of the intrinsic tryptophan fluorescence of α -TTP when bound to PC SUVs [28] suggesting that α -TTP binding to these vesicles is accompanied by a significant environmental change around tryptophan residues.

Supporting evidence for a collisional versus diffusional mechanism can be obtained if the rate of transfer is not affected by an increase in ionic strength of the medium. High ionic strength slows the rate of transfer if the ligand must first leave the protein and diffuse to a nearby membrane. Hydrophobic compounds such as α -tocopherol and NBD-Toc, which already have very low aqueous solubility, would be even less likely to exist free in buffer due to the increased solvent polarity of the high salt buffer. This has been demonstrated for the liver FABP [15]. Figure 4 shows

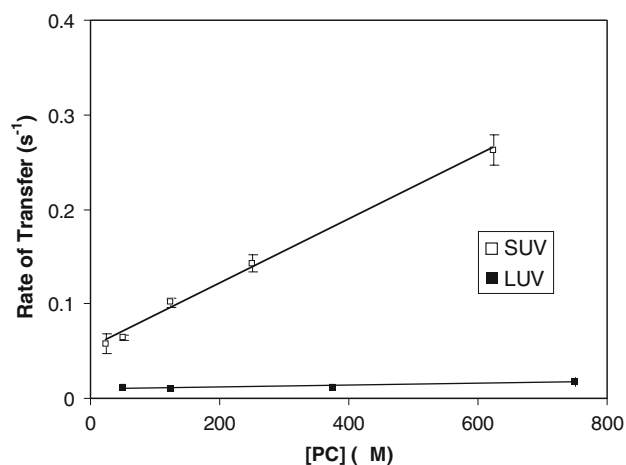


Fig. 3 Effect of lipid concentration on the rate of NBD-Toc transfer from α -TTP to PC SUVs and LUVs. Transfer of $0.125 \mu\text{M}$ NBD-Toc from $1.25 \mu\text{M}$ α -TTP to SUVs (open squares) or LUVs (filled squares) at the indicated concentration was monitored at room temperature. Results are the average of three curves \pm the standard deviation

that there is no transfer rate reduction for movement of NBD-Toc from α -TTP to SUVs (100% PC or 15 mol% PS in PC) up to 1.0 M salt.

We hypothesized that α -TTP would show enhanced rates of ligand transfer to membranes that contained anionic lipids, since this has been noted for other lipid transfer proteins such as the FABPs [26, 29–32], and cellular retinol binding protein I [33]. However, when SUVs were prepared containing 15% of anionic phospholipids such as bovine liver PI, DOPS, LBPA, or DOPA, rates of NBD-

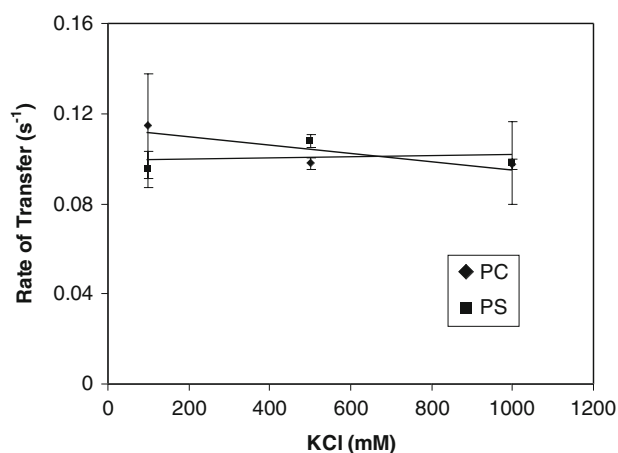


Fig. 4 Effect of ionic strength on the rate of NBD-Toc transfer to PC or PS SUVs. $0.225 \mu\text{M}$ NBD-Toc transferred from $2 \mu\text{M}$ α -TTP to $100 \mu\text{M}$ PC SUVs (filled circles) or PC SUVs containing 15% PS (filled squares) in the presence of an increasing concentration of KCl. Data shown represents an average \pm the standard deviation, $n = 12$ for PC at 100 mM KCl, $n = 3$ for other conditions tested. The data shown are compiled from separate experiments with different protein and lipid preparations

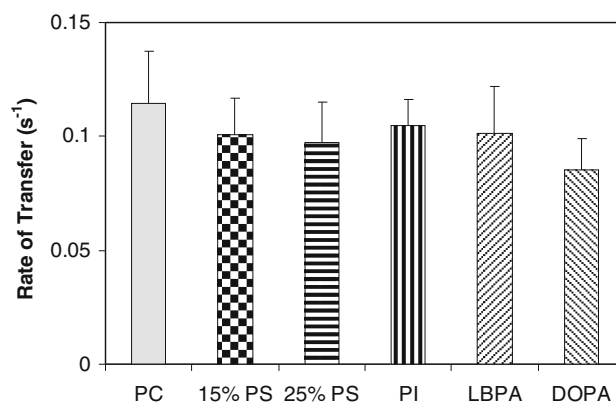


Fig. 5 NBD-Toc transfer from α -TTP to anionic SUVs. Transfer of $0.225 \mu\text{M}$ NBD-Toc from $2 \mu\text{M}$ α -TTP to $100 \mu\text{M}$ bovine liver PC SUVs containing 15 mol% of PS, PI, LBPA and DOPA or 25 mol% of PS. Results are the average \pm the standard deviation, $n = 3$ for PI, PS, LBPA and DOPA and $n = 12$ for PC only controls. No statistical differences were observed between PC vesicles and those of variant lipid composition, as assessed by unpaired t tests

Toc transfer by α -TTP showed only minor rate variations (Fig. 5). An increase in the concentration of PS from 15 to 25% did not significantly increase the observed rate. Transfer rates from TTP to LUV were 4–10 times slower than for SUVs (data not shown). Inclusion of 15% cholesterol in bovine liver PC vesicles (both SUV and LUV) had no effect on the rate of transfer when compared to vesicles without cholesterol. The greater rate of transfer to SUV over LUV was, however, maintained (data not shown).

To explore further the effect of membrane surface curvature, vesicles of differing size were prepared by liposome extrusion through specific pore size filters and by sonication. The rates of NBD-Toc transfer to PC vesicles of 50-, 100-, or 200-nm diameters were similar ($k = \sim 0.017 \pm 0.0009 \text{ s}^{-1}$, Fig. 6). Sonicated vesicles, using either an immersion probe or bath sonicator, are generally accepted to yield SUVs of about $\sim 25 \text{ nm}$ in diameter [34, 35] and consistently showed 5–7 fold faster rates of ligand transfer than larger vesicles. For the probe-sonicated vesicles the rate was $0.114 \pm 0.023 \text{ s}^{-1}$ and for bath sonicated was $0.098 \pm 0.005 \text{ s}^{-1}$.

To assess the influence of lipid packing on the transfer process, the rate of NBD-Toc transfer to acceptor phospholipid vesicles of differing degrees of unsaturation is shown in Fig. 7. Three different sources of phosphatidylcholine were tested: soy PC (that has a saturated to unsaturated lipid ratio (S/U) of 0.30 and is composed predominantly 18:2 acyl chains; synthetic dioleoylphosphatidylcholine (DOPC); and bovine liver PC (which has a S/U ratio of 0.91). (Product data from Avanti Polar Lipids, Alabaster, AL). The rates of α -TTP mediated ligand transfer were faster to SUV than LUV acceptors, and soy

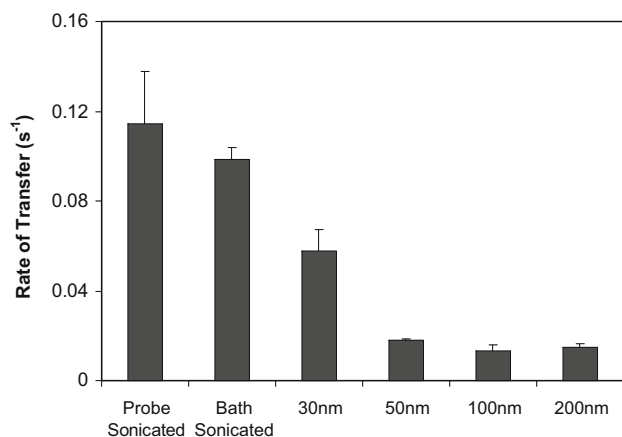


Fig. 6 Effect of vesicle size on the rate of NBD-Toc transfer from α -TTP. PC vesicles were prepared by probe sonication, bath sonication or extrusion. The transfer of NBD-Toc (0.225 μ M) from 2 μ M α -TTP to 100 μ M vesicles of various sizes was monitored. Data shown represents the average \pm the standard deviation $n = 12$ for the probe-sonicated PC SUV, $n = 18$ for 100 nm PC LUV, $n = 3$ for other conditions tested. Vesicles sizes represent the nominal pore size of the filters used for extrusion. For full details on the vesicles size distribution see “Materials and Methods”

PC lipids that contain a larger fraction of unsaturated acyl chains supported a transfer rate twice as fast as either DOPC or bovine liver PC.

Discussion

The α -tocopherol transfer protein is one important mechanism for the selective retention of α -tocopherol over other forms of vitamin E found in the diet. The selectivity of α -tocopherol binding to α -TTP [25, 36], coupled with

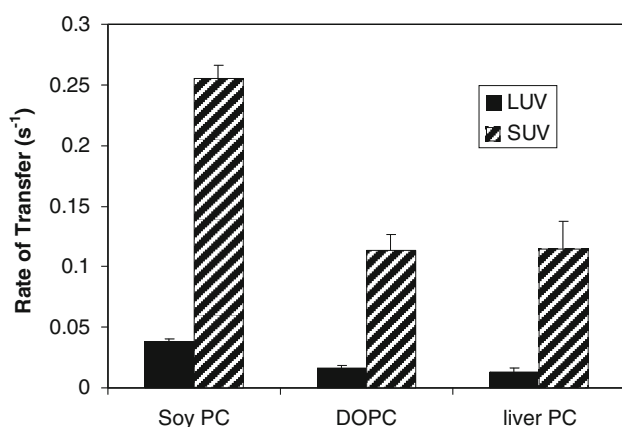


Fig. 7 Effect of lipid saturation on α -TTP mediated NBD-Toc transfer. Transfer of 0.225 μ M NBD-Toc from 2 μ M α -TTP to 100 μ M PC LUVs (closed bar) and SUVs (hatched bar) of soy PC, DOPC or liver PC was monitored. Data shown represents an average \pm the standard deviation, $n = 3$ for soy PC and DOPC, $n = 12$ for PC SUVs and $n = 18$ for PC LUVs

enhanced oxidative metabolism of non- α -tocols [37, 38], explains how plasma levels of α -tocopherol exceed those of γ -tocopherol for North Americans despite the dietary surplus of γ -tocopherol [39]. Once bound to α -TTP, α -tocopherol is secreted from hepatocytes by an as yet unknown mechanism, and carried in plasma by lipoproteins [1, 40, 41].

α -TTP is a soluble protein that is assumed to bind peripherally to membranes given its localization to late endosomes [18] and its ability to bind phospholipid vesicles in vitro [28]. The membrane-binding characteristics of peripheral membrane proteins are known to combine both electrostatic interactions and hydrophobic forces [42]. Proteins that depend chiefly on the presence of anionic phospholipids such as PS for favorable membrane binding include lipopolysaccharide binding protein (LBP) [43, 44], and bactericidal/permeability-increasing protein (BPI) [45, 46]. BPI (a family member along with PLTP and LBP) has a group of basic residues on its amino terminus that are responsible for recognition of acidic sites on bacterial endotoxin. The fatty acid binding proteins (FABPs) also have a cluster of basic residues on the loop capping the binding cavity that are key to their recognition of anionic membranes [16, 26, 29]. Figure 5 shows that when anionic lipids were incorporated at 15 mol% (and 25% PS) there was no effect on the rate of ligand transfer to SUV or LUVs. It remains possible that more significant differences might be apparent at much higher anionic lipid concentration, but we chose to use 15 mol% of these lipids since PI, PA, and LBPA rarely if ever occur in concentrations higher than this.

Other proteins have been shown to rely more on hydrophobic surface penetration into the lipid bilayer. The human phospholipid transfer protein (PLTP) uses a hydrophobic patch in the N-terminal tip of the protein for membrane binding. Mutations of these residues showed reduced binding [47]. Other contributions of hydrophobic residues for membrane binding have been noted for bee venom secreted PLA₂ [48] and human group \times secreted PLA₂ [49, 50].

A protein that uses predominantly hydrophobic interactions for membrane binding would presumably have difficulty arriving at any specific cellular bilayer membrane since all bilayers contain a hydrophobic core. Many proteins are directed to membranes that contain specific lipids such as the phosphatidylinositol phosphates (PIPs) through protein motifs such as the FYVE and PX domains that specifically recognize these anionic lipids [51–54]. Indeed, it has been recently noted that α -TTP may also have some specificity for membranes containing PIPs even though α -TTP does not contain a FYVE or PX domain [55].

Bilayer curvature is also a variable in membrane recognition and binding by proteins. Biological membranes

are in constant flux, undergoing fusion, exo- and endocytosis processes, all of which generate areas of high curvature and/or curvature stress [56–58]. The size of the organelle thus does not necessarily reflect local membrane curvature or curvature stress since such forces can occur in local portions of larger membranes [59].

α -TTP is known to localize to late endosomes [17, 60], structures that have complex membrane dynamics and topology [61–63]. Late endosomes occur in dense tubular, multi-lamellar, and multi-vesicular subclasses [64] and are reported to be 200–750 nm in diameter [64–66]. The endosome-specific phospholipid LBPA (lysobisphosphatidic acid, also known as bis(monoacylglycerol)phosphate, BMP) [67, 68] appears key to multivesicular body (MVB) structure and function. The interior vesicles of the MVB (called “exosomes” as they are destined for exocytosis) are “pinched” from the MVB limiting membrane at sites rich in LBPA and lysolipids that, at low pH, stabilize this highly curved membrane substructure [69]. The exosomes, however, are not enriched in LBPA [70]. α -TTP has been shown to co-localize with LBPA in rat McARH7777 cells transfected with α -TTP [71]. Our results suggest that this is not due to a specific attraction of α -TTP for LBPA, but rather the effect of LBPA on the properties of the endosomal membrane and the pH-dependent formation of the highly curved MVB [72–74]. The failure of LBPA to enhance α -TTP transfer of NBD-Toc in our assays may be due to lack of an internal acidic pH as in MVBs or, more likely, that SUVs—whether they contain LBPA or not—already have sufficient membrane curvature to enhance *in vitro* α -TTP binding and thus ligand transfer. Therefore, the co-localization of α -TTP with LBPA [71] may be a secondary effect (high curvature) rather than due to a direct interaction of α -TTP with LBPA. Contrarily, the Niemann-Pick-type C2 protein that also occurs in endosomes has recently been shown to exhibit enhanced cholesterol transfer in the presence of SUVs containing 25% anionic lipids such as PI and PS, but is most pronounced in the presence of LBPA [75].

The sensitivity of membrane binding proteins to bilayer curvature is common. For example, an increased rate of ligand transfer from protein to SUVs over LUVs has been observed previously for FABPs [30, 76, 77]. The binding of sterol carrier protein 2 [78], and the glycolipid transfer protein (GLTP) [79] have also been shown to favor more highly curved membranes. The lipid-packing sensor of Arf GTPase activating protein 1 (arfGAP1) known as ALPS2, also preferentially binds to the more highly curved surface of SUVs [80, 81].

Wootan and Storch [82] observed faster rates of fluorescent fatty acid transfer from adipocyte and heart fatty acid bind protein (A- and H-FABP) to SUVs. They noted that this may be due to the greater number of SUVs versus

LUVs prepared from an equal amount of lipid, and suggested that this could be the prime reason for the approximately ten-fold greater rate for transfer to SUVs than LUVs. We observed approximately the same increased rate of transfer to extruded 30 nm vesicles (~5-fold) and sonicated vesicles (~11-fold) as did Wootan and Storch. These authors also noted, however, that tighter packing of the phospholipid acyl chains in LUV due to their more flat lamellar structure may also have decreased rates of ligand transfer to LUVs. Our preparation of vesicles of different size used equal molar amounts of phospholipids. If we assume that vesicles are of uniform size and unilamellar, that the membrane thickness is ~5 nm, and that the area per phospholipid (here assumed to be DOPC) is 67.4 nm² [83], then the total available surface area for protein lipid interaction can be calculated (See Supplementary Material). The area available on the outer leaflet of vesicles increases by only 1.5 times when vesicle size is reduced from 200 to 20 nm when an equal amount of phospholipid is used for all samples. If the rate of ligand transfer was determined solely by the available surface area, we should have seen no more than an ~1.5 fold increase in transfer rate as vesicle size was varied from the larger 200 nm LUVs to smaller SUVs. However, we repeatedly saw transfer rate increases of ~11-fold on moving from extruded LUVs, to SUVs prepared by either extrusion or sonication, substantiating that TTP prefers to bind to SUV membranes of higher curvature.

It is worth noting that the spontaneous rates of NBD-tocopherol transfer between vesicles shown in Fig. 2 clearly shows that LUVs are both poorer donors and acceptors of NBD-tocopherol. Coupling this with our previous observation that TTP binds much better to SUVs than LUVs [28], suggests that in fact, the transfer of NBD-tocopherol to SUVs is faster due to the ease of both protein and ligand insertion into the membrane.

The collisional insertion of a ligand into a membrane by a protein can, in theory, be broken into two discrete steps: (1) binding of the protein-ligand complex to the acceptor membrane, and (2) insertion of the ligand into the bulk of the membrane. Our results do not rule out the possibility that ligand insertion occurs at different rates when the membrane structure is perturbed. However, the spontaneous rate of ligand movement from LUV donors to SUV or LUV acceptors suggests that NBD-Toc (as a model of α -tocopherol) inserts equally well into both membrane types. The presence of anionic lipids could enhance protein binding through electrostatic interactions between the protein and the phospholipid head group, or it might make ligand insertion easier if the anionic phospholipids have changed the packing density of the membrane. The present work cannot rule out packing density changes in the acceptor membrane, but the fact that each anionic

phospholipid supported near equal transfer rates whether they are present in SUVs or LUVs suggests that packing is not an important variable in rates of NBD-Toc transfer by α -TTP.

The only phospholipid composition that changed the rate of NBD-Toc transfer to vesicles by α -TTP were soy PC lipids. The higher degree of unsaturation in these plant lipid samples may provide a more receptive membrane environment for tocopherol as it is well-known that tocopherols prefer to partition into those phospholipid phases that are rich in polyunsaturated lipids [27].

In this report we have used only the wild type α -TTP to explore the variables that affect the rates of ligand movement from protein to membrane. The lack of effect of anionic phospholipids suggests that membrane recognition may rely more on hydrophobic forces, something that has been well interpreted by several comprehensive surveys [84–88]. We have now begun studies with mutant forms of α -TTP that perturb the putative hydrophobic face of the protein that is offered to membranes. We will soon report their ability to bind membranes and effect ligand transfer.

The α -TTP is selective for more highly curved membranes as observed by its fast transfer of NBD-Toc to small unilamellar vesicles of ~ 25 nm diameter versus vesicles of diameter larger than ~ 50 nm, but does not show any preference for anionic lipids when binding membranes. This preference for highly curved membranes may be linked to the localization of α -TTP to the late endosomes whose membranes are quite dynamic, and form small internal vesicles with the aid of the endosome-specific phospholipid LBPA. The degree of phospholipid unsaturation may also be a controlling feature for delivery of tocopherol to membranes since the plant-derived soy PC supported faster ligand transfer than did pure DOPC or bovine liver PC, both of which have a lower unsaturation content.

Acknowledgment We thank Richard and Raquel Epanand (Biochemistry, McMaster University) for the DSC measurements with NBD- α -tocopherol; Doug Keller and Yuguang Cui (Chemical Engineering, McMaster University) and Sigrid Kuebler (Wyatt Technology Corporation) for measurement of vesicle sizes. This work was supported by a grant from the Natural Sciences and Engineering Research Council of Canada to J.A. and, in part, by award DK067494 to D.M.

References

- Manor D, Morley S (2007) The alpha-tocopherol transfer protein. *Vitam Horm* 76:45–65
- Federico A (2004) Ataxia with isolated vitamin E deficiency: a treatable neurologic disorder resembling Friedreich's ataxia. *Neurol Sci* 25:119–121
- Hoshino M, Masuda N, Ito Y, Murata M, Goto J, Sakurai M, Kanazawa I (1999) Ataxia with isolated vitamin E deficiency: a Japanese family carrying a novel mutation in the alpha-tocopherol transfer protein gene. *Ann Neurol* 45:809–812
- Cavalier L, Ouahchi K, Kayden HJ, Di Donato S, Reutenauer L, Mandel JL, Koenig M (1998) Ataxia with isolated vitamin E deficiency: heterogeneity of mutations and phenotypic variability in a large number of families. *Am J Hum Genet* 62:301–310
- Ouahchi K, Arita M, Kayden H, Hentati F, Ben Hamida M, Sokol R, Arai H, Inoue K, Mandel J, Koenig M (1995) Ataxia with isolated vitamin E deficiency is caused by mutations in the alpha-tocopherol transfer protein. *Nat Genet* 9:141–145
- Hentati A, Deng H, Hung W, Nayer M, Ahmed M, He X, Tim R, Stumpf D, Siddique T (1996) Human alpha-tocopherol transfer protein: gene structure and mutations in familial vitamin E deficiency. *Ann Neurol* 39:295–300
- Nishida Y, Yokota T, Takahashi T, Uchihara T, Jishage KI, Mizusawa H (2006) Deletion of vitamin E enhances phenotype of Alzheimer disease model mouse. *Biochem Biophys Res Commun* 350:530–536
- Leonard SW, Terasawa Y, Farese RV, Traber MG (2002) Incorporation of deuterated RRR- or all-rac-alpha-tocopherol in plasma and tissues of alpha-tocopherol transfer protein-null mice. *Am J Clin Nutr* 75:555–560
- Jishage K, Arita M, Igarashi K, Iwata T, Watanabe M, Ogawa M, Ueda O, Kamada N, Inoue K, Arai H, Suzuki H (2001) alpha-tocopherol transfer protein is important for the normal development of placental labyrinthine trophoblasts in mice. *J Biol Chem* 276:1669–1672
- Terasawa Y, Ladha Z, Leonard SW, Morrow JD, Newland D, Sanan D, Packer L, Traber MG, Farese RV (2000) Increased atherosclerosis in hyperlipidemic mice deficient in alpha-tocopherol transfer protein and vitamin E. *Proc Natl Acad Sci USA* 97:13830–13834
- Yokota T, Igarashi K, Uchihara T, Jishage K, Tomita H, Inaba A, Li Y, Arita M, Suzuki H, Mizusawa H, Arai H (2001) Delayed-onset ataxia in mice lacking alpha-tocopherol transfer protein: Model for neuronal degeneration caused by chronic oxidative stress. *Proc Natl Acad Sci USA* 98:15185–15190
- Arita M, Nomura K, Arai H, Inoue K (1997) α -Tocopherol transfer protein stimulates the secretion of α -tocopherol from a cultured liver cell line through a brefeldin A-insensitive pathway. *Proc Natl Acad Sci USA* 94:12437–12441
- Minehira-Castelli K, Leonard SW, Walker QM, Traber MG, Young SG (2006) Absence of VLDL secretion does not affect alpha-tocopherol content in peripheral tissues. *J Lipid Res* 47:1733–1738
- Corsico B, Liou HL, Storch J (2004) The alpha-helical domain of liver fatty acid binding protein is responsible for the diffusion-mediated transfer of fatty acids to phospholipid membranes. *Biochemistry* 43:3600–3607
- Thumser AE, Storch J (2000) Liver and intestinal fatty acid-binding proteins obtain fatty acids from phospholipid membranes by different mechanisms. *J Lipid Res* 41:647–656
- Storch J, Thumser AE (2000) The fatty acid transport function of fatty acid-binding proteins. *Biochim Biophys Acta* 1486:28–44
- Qian J, Atkinson J, Manor D (2006) Biochemical consequences of heritable mutations in the alpha-tocopherol transfer protein. *Biochemistry* 45:8236–8242
- Qian J, Morley S, Wilson K, Nava P, Atkinson J, Manor D (2005) Intracellular trafficking of vitamin E in hepatocytes: the role of tocopherol transfer protein. *J Lipid Res* 46:2072–2082
- Nava P, Cecchini M, Chirico S, Gordon H, Morley S, Manor D, Atkinson J (2006) Preparation of fluorescent tocopherols for use in protein binding and localization with the alpha-tocopherol transfer protein. *Bioorg Med Chem* 14:3721–3736

20. Morley S, Panagabko C, Shineman D, Mani B, Stocker A, Atkinson J, Manor D (2004) Molecular determinants of heritable vitamin E deficiency. *Biochemistry* 43:4143–4149
21. Schroeder F, Barenholz Y, Gratton E, Thompson TE (1987) A fluorescence study of dehydroergosterol in phosphatidylcholine bilayer vesicles. *Biochemistry* 26:2441–2448
22. Konigsberg PJ, Debrick JE, Pawlowski TJ, Staerz UD (1999) Liposome encapsulated aurothiomalate reduces collagen-induced arthritis in DBA/1 J mice. *Biochim Biophys Acta* 1421:149–162
23. Massey JB, Bick DH, Pownall HJ (1997) Spontaneous transfer of monoacyl amphiphiles between lipid and protein surfaces. *Biophys J* 72:1732–1743
24. Morley S, Cross V, Cecchini M, Nava P, Atkinson J, Manor D (2006) Utility of a fluorescent vitamin E analogue as a probe for tocopherol transfer protein activity. *Biochemistry* 45:1075–1081
25. Panagabko C, Morley S, Hernandez M, Cassolato P, Gordon H, Parsons R, Manor D, Atkinson J (2003) Ligand specificity in the CRAL-TRIO protein family. *Biochemistry* 42:6467–6474
26. Falomir-Lockhart LJ, Laborde L, Kahn PC, Storch J, Corsico B (2006) Protein–membrane interaction and fatty acid transfer from intestinal fatty acid-binding protein to membranes. Support for a multistep process. *J Biol Chem* 281:13979–13989
27. Atkinson J, Epand RF, Epand RM (2008) Tocopherols and tocotrienols in membranes: a critical review. *Free Radic Biol Med* 44:739–764
28. Morley S, Cecchini M, Zhang W, Virgulti A, Noy N, Atkinson J, Manor D (2008) Mechanisms of ligand transfer by the hepatic tocopherol transfer protein. *J Biol Chem* 283:17797–17804
29. Liou HL, Storch J (2001) Role of surface lysine residues of adipocyte fatty acid-binding protein in fatty acid transfer to phospholipid vesicles. *Biochemistry* 40:6475–6485
30. Smith ER, Storch J (1999) The adipocyte fatty acid-binding protein binds to membranes by electrostatic interactions. *J Biol Chem* 274:35325–35330
31. Herr FM, Aronson J, Storch J (1996) Role of portal region lysine residues in electrostatic interactions between heart fatty acid binding protein and phospholipid membranes. *Biochemistry* 35:1296–1303
32. Herr FM, Matarese V, Bernlohr DA, Storch J (1995) Surface lysine residues modulate the collisional transfer of fatty acid from adipocyte fatty acid binding protein to membranes. *Biochemistry* 34:11840–11845
33. Herr FM, Li E, Weinberg RB, Cook VR, Storch J (1999) Differential mechanisms of retinoid transfer from cellular retinoid binding proteins types I and II to phospholipid membranes. *J Biol Chem* 274:9556–9563
34. Huang C (1969) Studies on phosphatidylcholine vesicles. Formation and physical characteristics. *Biochemistry* 8:344–352
35. Szoka F Jr, Papahadjopoulos D (1980) Comparative properties and methods of preparation of lipid vesicles (liposomes). *Annu Rev Biophys Bioeng* 9:467–508
36. Hosomi A, Arita M, Sato Y, Kiyose C, Ueda T, Igarashi O, Arai H, Inoue K (1997) Affinity for alpha tocopherol transfer protein as a determinant of the biological activities of vitamin E analogs. *FEBS Lett* 409:105–108
37. Parker RS, Sontag TJ, Swanson JE, McCormick CC (2004) Discovery, characterization, and significance of the cytochrome p450 omega-hydroxylase pathway of vitamin E catabolism. In: Kelly F, Meydani M, Packer L (eds) *Vitamin E and Health*. NYAS, New York, pp 13–21
38. Sontag TJ, Parker RS (2007) Influence of major structural features of tocopherols and tocotrienols on their omega-oxidation by tocopherol-omega-hydroxylase. *J Lipid Res* 48:1090–1098
39. Wagner KH, Kamal-Eldin A, Elmadfa I (2004) Gamma-tocopherol—an underestimated vitamin? *Ann Nutr Metab* 48:169–188
40. Traber MG (2007) Vitamin E bioavailability. In: Preedy VR, Watson RR (eds) *The encyclopedia of vitamin E*. CABI International, Wallingford
41. Traber MG, Burton GW, Hamilton RL (2004) Vitamin E trafficking. In: Kelly F, Meydani M, Packer L (eds) *Vitamin E and health*. NYAS, New York, pp 1–12
42. Mulgrew-Nesbitt A, Diraviyam K, Wang J, Singh S, Murray P, Li Z, Rogers L, Mirkovic N, Murray D (2006) The role of electrostatics in protein–membrane interactions. *Biochim Biophys Acta* 1761:812–826
43. Schumann RR, Latz E (2000) Lipopolysaccharide-binding protein. *Chem Immunol* 74:42–60
44. Lamping N, Hoess A, Yu B, Park TC, Kirschning CJ, Pfeil D, Reuter D, Wright SD, Herrmann F, Schumann RR (1996) Effects of site-directed mutagenesis of basic residues (Arg 94, Lys 95, Lys 99) of lipopolysaccharide (LPS)-binding protein on binding and transfer of LPS and subsequent immune cell activation. *J Immunol* 157:4648–4656
45. Schultz H, Weiss JP (2007) The bactericidal/permeability-increasing protein (BPI) in infection and inflammatory disease. *Clin Chim Acta* 384:12–23
46. Gazzano-Santoro H, Parent JB, Conlon PJ, Kasler HG, Tsai CM, Lill-Elghanian DA, Hollingsworth RI (1995) Characterization of the structural elements in lipid A required for binding of a recombinant fragment of bactericidal/permeability-increasing protein rBPI23. *Infect Immun* 63:2201–2205
47. Desrumaux C, Labeur C, Verhee A, Tavernier J, Vandekerckhove J, Rosseneu M, Peelman F (2001) A hydrophobic cluster at the surface of the human plasma phospholipid transfer protein is critical for activity on high density lipoproteins. *J Biol Chem* 276:5908–5915
48. Bollinger JG, Diraviyam K, Ghomashchi F, Murray D, Gelb MH (2004) Interfacial binding of bee venom secreted phospholipase A2 to membranes occurs predominantly by a nonelectrostatic mechanism. *Biochemistry* 43:13293–13304
49. Pan YH, Yu BZ, Singer AG, Ghomashchi F, Lambeau G, Gelb MH, Jain MK, Bahnson BJ (2002) Crystal structure of human group \times secreted phospholipase A2. Electrostatically neutral interfacial surface targets zwitterionic membranes. *J Biol Chem* 277:29086–29093
50. Winget JM, Pan YH, Bahnson BJ (2006) The interfacial binding surface of phospholipase A2s. *Biochim Biophys Acta* 1761:1260–1269
51. Kutateladze TG (2007) Mechanistic similarities in docking of the FYVE and PX domains to phosphatidylinositol 3-phosphate containing membranes. *Prog Lipid Res* 46:315–327
52. Kutateladze TG, Capelluto DG, Ferguson CG, Cheever ML, Kutateladze AG, Prestwich GD, Overduin M (2004) Multivalent mechanism of membrane insertion by the FYVE domain. *J Biol Chem* 279:3050–3057
53. De Matteis MA, D'Angelo G (2007) The role of the phosphoinositides at the Golgi complex. *Biochem Soc Symp* 74:107–116
54. De Matteis MA, Godi A (2004) PI-lotting membrane traffic. *Nat Cell Biol* 6:487–492
55. Arai H (2006) Molecular mechanisms of α -tocopherol transfer protein (α -TTP)-dependent α -tocopherol transfer in hepatocytes. *FASEB J* 20:LB44
56. Kozlovsky Y, Chernomordik LV, Kozlov MM (2002) Lipid intermediates in membrane fusion: formation, structure, and decay of hemifusion diaphragm. *Biophys J* 83:2634–2651
57. Kozlovsky Y, Kozlov MM (2003) Membrane fission: model for intermediate structures. *Biophys J* 85:85–96
58. Burger KN (2000) Greasing membrane fusion and fission machineries. *Traffic* 1:605–613
59. Morris R, Cox H, Mombelli E, Quinn PJ (2004) Rafts, little caves and large potholes: how lipid structure interacts with membrane

- proteins to create functionally diverse membrane environments. *Subcell Biochem* 37:35–118
60. Qian JH, Morley S, Wilson K, Nava P, Atkinson J, Manor D (2005) Intracellular trafficking of vitamin E in hepatocytes: the role of tocopherol transfer protein. *J Lipid Res* 46:2072–2082
 61. Gruenberg J (2001) The endocytic pathway: a mosaic of domains. *Nat Rev Mol Cell Biol* 2:721–730
 62. Gruenberg J (2003) Lipids in endocytic membrane transport and sorting. *Curr Opin Cell Biol* 15:382–388
 63. Gruenberg J, Stenmark H (2004) The biogenesis of multivesicular endosomes. *Nat Rev Mol Cell Biol* 5:317–323
 64. Ganley IG, Carroll K, Bittova L, Pfeffer S (2004) Rab9 GTPase regulates late endosome size and requires effector interaction for its stability. *Mol Biol Cell* 15:5420–5430
 65. Mullock BM, Hinton RH, Peppard JV, Slot JW, Luzio JP (1987) The preparative isolation of endosome fractions: a review. *Cell Biochem Funct* 5:235–243
 66. Genisset C, Puhar A, Calore F, de Bernard M, Dell'Antone P, Montecucco C (2007) The concerted action of the *Helicobacter pylori* cytotoxin VacA and of the v-ATPase proton pump induces swelling of isolated endosomes. *Cell Microbiol* 9:1481–1490
 67. Kobayashi T, Beuchat MH, Lindsay M, Frias S, Palmiter RD, Sakuraba H, Parton RG, Gruenberg J (1999) Late endosomal membranes rich in lysobisphosphatidic acid regulate cholesterol transport. *Nat Cell Biol* 1:113–118
 68. Kobayashi T, Stang E, Fang KS, de Moerloose P, Parton RG, Gruenberg J (1998) A lipid associated with the antiphospholipid syndrome regulates endosome structure and function. *Nature* 392:193–197
 69. Subra C, Laulagnier K, Perret B, Record M (2007) Exosome lipidomics unravels lipid sorting at the level of multivesicular bodies. *Biochimie* 89:205–212
 70. Laulagnier K, Grand D, Dujardin A, Hamdi S, Vincent-Schneider H, Lankar D, Salles JP, Bonnerot C, Perret B, Record M (2004) PLD2 is enriched on exosomes and its activity is correlated to the release of exosomes. *FEBS Lett* 572:11–14
 71. Horiguchi M, Arita M, Kaempf-Rotzoll DE, Tsujimoto M, Inoue K, Arai H (2003) pH-dependent translocation of alpha-tocopherol transfer protein (alpha-TTP) between hepatic cytosol and late endosomes. *Genes to Cells* 8:789–800
 72. Matsuo H, Chevallier J, Mayran N, Le Blanc I, Ferguson C, Faure J, Blanc NS, Matile S, Dubochet J, Sadoul R, Parton RG, Vilbois F, Gruenberg J (2004) Role of LBPA and Alix in multivesicular liposome formation and endosome organization. *Science* 303:531–534
 73. van der Goot FG, Gruenberg J (2006) Intra-endosomal membrane traffic. *Trends Cell Biol* 16:514–521
 74. Hayakawa T, Makino A, Murate M, Sugimoto I, Hashimoto Y, Takahashi H, Ito K, Fujisawa T, Matsuo H, Kobayashi T (2007) pH-dependent formation of membranous cytoplasmic body-like structure of ganglioside G(M1)/bis(monoacylglycero)phosphate mixed membranes. *Biophys J* 92:L13–L16
 75. Cheruku SR, Xu Z, Dutia R, Lobel P, Storch J (2006) Mechanism of cholesterol transfer from the Niemann-Pick type C2 protein to model membranes supports a role in lysosomal cholesterol transport. *J Biol Chem* 281:31594–31604
 76. Kleinfeld AM, Storch J (1993) Transfer of long-chain fluorescent fatty acids between small and large unilamellar vesicles. *Biochemistry* 32:2053–2061
 77. Davies JK, Thumser AE, Wilton DC (1999) Binding of recombinant rat liver fatty acid-binding protein to small anionic phospholipid vesicles results in ligand release: a model for interfacial binding and fatty acid targeting. *Biochemistry* 38:16932–16940
 78. Huang H, Ball JM, Billheimer JT, Schroeder F (1999) Interaction of the N-terminus of sterol carrier protein 2 with membranes: role of membrane curvature. *Biochem J* 344(Pt 2):593–603
 79. Rao CS, Lin X, Pike HM, Molotkovsky JG, Brown RE (2004) Glycolipid transfer protein mediated transfer of glycosphingolipids between membranes: a model for action based on kinetic and thermodynamic analyses. *Biochemistry* 43:13805–13815
 80. Mesmin B, Drin G, Levi S, Rawet M, Cassel D, Bigay J, Antony B (2007) Two lipid-packing sensor motifs contribute to the sensitivity of ArfGAP1 to membrane curvature. *Biochemistry* 46:1779–1790
 81. Bigay J, Casella JF, Drin G, Mesmin B, Antony B (2005) ArfGAP1 responds to membrane curvature through the folding of a lipid packing sensor motif. *Embo J* 24:2244–2253
 82. Wootan MG, Storch J (1994) Regulation of fluorescent fatty acid transfer from adipocyte and heart fatty acid binding proteins by acceptor membrane lipid composition and structure. *J Biol Chem* 269:10517–10523
 83. Kucerka N, Nagle JF, Sachs JN, Feller SE, Pencer J, Jackson A, Katsaras J (2008) Lipid bilayer structure determined by the simultaneous analysis of neutron and X-ray scattering data. *Biophys J* 95:2356–2367
 84. Lomize AL, Pogozheva ID, Lomize MA, Mosberg HI (2007) The role of hydrophobic interactions in positioning of peripheral proteins in membranes. *BMC Struct Biol* 7:44
 85. Lomize AL, Pogozheva ID, Lomize MA, Mosberg HI (2006) Positioning of proteins in membranes: a computational approach. *Protein Sci* 15:1318–1333
 86. Lomize MA, Lomize AL, Pogozheva ID, Mosberg HI (2006) OPM: orientations of proteins in membranes database. *Bioinformatics* 22:623–625
 87. Bhardwaj N, Stahelin RV, Langlois RE, Cho W, Lu H (2006) Structural bioinformatics prediction of membrane-binding proteins. *J Mol Biol* 359:486–495
 88. Bhardwaj N, Stahelin RV, Zhao G, Cho W, Lu H (2007) MeTaDoR: a comprehensive resource for membrane targeting domains and their host proteins. *Bioinformatics* 23:3110–3112

Dietary Lipid Level Induced Antioxidant Response in Manchurian Trout, *Brachymystax lenok* (Pallas) Larvae

Hui Zhang · Zhenbo Mu · LiangMei Xu · Gefeng Xu ·
Min Liu · Anshan Shan

Received: 5 December 2008 / Accepted: 21 April 2009 / Published online: 6 June 2009
© AOCs 2009

Abstract This study was designed to determine the nutritional lipid requirement of Manchurian trout and to investigate the effects of lipid concentrations on the antioxidant status in larvae with experimental diets with different lipid levels. Oxidative stress differences between different organs and tissues were also assessed. Manchurian trout larvae were fed for 35 days and, during that period, growth and survival, the activity of superoxide dismutase (SOD), catalase (CAT), glutathione peroxidase (GPX) and content of malondialdehyde (MDA) in viscera, muscle, gill and brain of four diets, lipid levels from 15 to 30%, and control treatment were measured. Growth rates were similar, but survival was low, between high and low dietary lipid levels. SOD activity was stimulated in viscera, muscle and brain in high lipid diets, but reduced in gills with increased lipid content. SOD was kept lower in the control group. GPX activity was inhibited in viscera and stimulated in gill, muscle and brain. CAT activities were enhanced by all treatments and showed the lowest values in the control. Lipid peroxidation of the diet was promoted in all organs, excluding the gill which showed no regular pattern. MDA content increased with increased dietary lipid levels in viscera, muscle and brain. Our results indicate that the most appropriate lipid requirement is probably 20–25% and a higher dietary level of lipids might induce oxidative stress in Manchurian trout larvae. The brain and

gill were probably the most sensitive organs to oxidative damage.

Keywords *Brachymystax lenok* · Lipid · Antioxidant enzyme · Stress · Larvae

Abbreviations

DLL	Dietary lipid level
SOD	Superoxide dismutase
CAT	Catalase
GPX	Glutathione peroxidase
MDA	Malondialdehyde
DHA	Docosahexaenoic acid
EPA	Eicosapentaenoic acid

Introduction

Reactive oxygen species (ROS) are free radicals and/or oxygen derivatives produced during normal cellular functions [1]. The biological handicap associated with oxidative stress could be estimated by a physicochemical condition in which an increase in the steady-state levels of oxidative species e.g. H_2O_2 , $HO\cdot$, O^{-2} , R^- and $ROO\cdot$ occurs [2]. At low concentrations, the ROS may be beneficial or even indispensable in processes such as defenses against microorganisms, contributing to phagocytic bactericidal activity. Cellular defense systems involving antioxidant enzymes; such as superoxide dismutase (SOD), glutathione peroxidase (GPX), catalase (CAT), and non-enzymatic scavengers—glutathione, vitamin A, and E—protect the organism against such oxyradical damages as DNA strand breaks, protein oxidation and the induction of lipid peroxidation [3]. An increase in the activated form of molecular oxygen

H. Zhang · L. Xu · M. Liu · A. Shan (✉)
College of Animal Science and technology, Northeast
Agricultural University, 59 Mucai road, Xiangfang district,
Harbin, Heilongjiang, People's Republic of China
e-mail: zhanghuisystem@yahoo.com.cn

Z. Mu · G. Xu
Heilongjiang Fishery Institute, Harbin, Heilongjiang,
People's Republic of China

species due to overproduction and/or to inability to destroy them may lead to damage to the DNA structure and thus, cause mutations, chromosomal aberrations and carcinogenesis [4]. To counter the increase in superoxide radical levels, cells will increase activities of SOD and CAT. Free radicals may also stimulate cell growth by damaging specific genes that control the growth rate and differentiation during the promotion phase. In heavily polluted waters, an elevated activity of CAT and SOD among bivalves has been reported [5]. In the liver of the common carp, GPX activity is reduced under hypoxia and re-oxygenation, while CAT, SOD and Glutathione-S-transferase (GST) enzymes are unaffected [6].

In contrast, high doses and/or inadequate removal of ROS result in oxidative stress that may cause severe metabolic malfunctions and finally impair the health status of animal. Under a normal physiological state, the harmful effects of ROS are effectively neutralized by an antioxidant defense system which is an important mechanism to maintain the balance of ROS. As in higher vertebrates, fish also possess two major antioxidant defenses—the non-enzymatic system (vitamins and other molecules such as glutathione, etc.) and enzymatic system (SOD, CAT, GPX)—to protect the cells from damage by ROS. Most of the studies involving alteration of antioxidant defenses in aquatic animals have focused on stress induced by salinity changes, temperature fluctuations, hypoxia, aging, pollution of pesticide and heavy metal, etc. [7–11]. Only few have examined the influence of varying nutritional status on antioxidant enzymes in fish [12–14].

Little attention has been paid to evidence with regard to the influence of dietary lipids on the stress response [15, 16]; despite the facts that the production of prostaglandins is affected by dietary lipids and that prostaglandins may also play a role in stress hormone release [17, 18]. Dietary fatty acids can also influence the susceptibility of tissue lipids to peroxidative damage. Increasing dietary n-3 polyunsaturated fatty acids (PUFA) can elevate the unsaturation index of lipids in fish tissues and make them more prone to free radical attack [19]. High levels of dietary lipid and carbohydrate increase the growth and condition factor of an organism. However, high dietary fat also increases cholesterol concentration in blood plasma that, in turn, could influence the activity of the heart and other organs to weaken the physiological state and immune system [20, 21]. Nutrients misused, such as by high lipid intake, have been demonstrated to be harmful to animal health [22, 23]. Although high lipid diets had been fed to different species [24–27] and found to stimulate relevant metabolic enzymes [28, 29], the effect of antioxidant status in fish, especially in larvae is still unknown.

Being an endangered species in China, the population of Manchurian trout has declined in recent years [30, 31] and

has received increased attention through a program of artificial propagation for the purpose of restocking to a sustainable level since the 1990s. Few nutritional studies have been undertaken on this species.

This study attempted to establish a correlation between lipid nutrition and antioxidant stress of different organs in trout larvae, collating the data on physiological indicators and oxidative markers and evaluating possible effects on physiological status.

Materials and Methods

Fish and Diets

Brachymystax lenok (Pallas) larvae were propagated and maintained in an indoor water flow-through system at the BoHai experimental station of Heilongjiang Fishery Institute. Water temperature was regulated at $13 \pm 2^\circ\text{C}$ and the fish were fed a trial diet six times per day. At first, the larvae diet consisted exclusively of daphnia for 10 days. Then the larvae were divided into one control and four experimental groups (four tanks per group). The four groups were fed for 35 days with four formulated diets with an equal protein level (48%) with increasing fat levels (15, 20, 25, 30%) and decreasing carbohydrate levels (20–0%). The diets were designated as L15, L20, L25, and L30 (Table 1). The control groups were fed with daphnia and worm (*Branchiura sowerbyi* Beddard). In the added lipid, the soy lecithin/cod liver oil ratio was maintained at 0.8.

Diet formulation took into account the estimated requirements of salmonidae larvae in phospholipids and in the main highly unsaturated fatty acids, eicosapentaenoic acid (EPA) and docosahexaenoic acid (DHA) (Table 2). Thiobarbituric acid reactive substances (TBARs) values were measured and diets should be under 0.3 mmol/kg as a standard. The size of the microparticulate diets was 125–200 μm during the first 5 days, then 200–400 μm . Fish were fed six times per day (6:00, 9:00, 12:00, 15:00, 18:00, 21:00) with excess. Food ingestion was monitored by observing the larvae digestive tract under a binocular microscope, as the dietary microparticles are visible in transparent tracts. Five hundred juvenile larvae were acclimated with diets for 3 days in each column. The prepared diets were kept in refrigerator until use.

Sample Collection

To monitor growth, ten larvae per tank each ($n = 4$ tanks for each dietary group) were taken in 10 days intervals. For this, water volume was lowered and ten larvae were collected at one time using an appropriate net at random. Before sampling, the larvae were starved for 24 h to

Table 1 Composition of the experimental diets

Ingredients ^a	L15	L20	L25	L30
Constant ingredients				
Fish meal ^a	660	660	660	660
Soy lecithin	40	40	40	40
Vitamin mixture ^b	80	80	80	80
Mineral mixture ^c	40	40	40	40
Betaine	10	10	10	10
CMC	4	4	4	4
Variable ingredients				
Fish oil ^a	30	30	30	30
Soybean oil ^a	10	66	118	136
Precooked starch	126	60	26	0
Protein (N × 6.25)	484	484	484	484
Carbohydrate	170	135	97	66
Lipid	156	201	256	305
Ash	135	136	133	125
Energy ^d (kJ/kg)	16.07	16.82	19.16	19.58

^a Dietary ingredients were commercially obtained. Fish meal and fish oil from Denmark. The soy lecithin and soybean oil from Jiusan Co. (China). The potato precooked starch was from the Haerbin pharmaceutical group

^b Per kilogram of vitamin mixture: thiamine-HCl, 3.2; riboflavin, 7.2; niacinamide, 25.6; biotin, 0.08; Ca-pantothenate, 14.4; pyridoxine-HCl, 2.4; folic acid, 0.96; menadione, 0.8; vitamin B12, 2.67; inositol, 125; ascorbic acid, 60.0; para-amino benzoic acid, 20; vitamin D2, 0.4; BHA, 0.75; celite, 735.8

^c Per kilogram of mineral mixture: CaCO₃, 21; CaHPO₄·2H₂O, 735; K₂HPO₄, 81; K₂SO₄, 68; NaCl, 30.6; Na₂HPO₄·6H₂O, 21.4; MnO, 25.0; FeC₆H₅O₇·3H₂O, 5.58; MnCO₃, 4.18; CuCO₂, 0.34; ZnCO₃, 0.81; KI, 0.01; NaF, 0.02; CoCl₂, 0.2; citric acid, 6.88

^d Calculated as total carbohydrate × 16.7 kJ/kg; fat × 37.7 kJ/kg; protein × 16.7 kJ/kg

Table 2 Composition of lipid fraction in the experimental diets

	L15	L20	L25	L30
g/kg dry diet				
Neutral lipids	118	145	180	210
Phospholipids	15	21	25	35
DHA + EPA	17	22	26	30

DHA and EPA: eicosapentaenoic and docosahexaenoic

evacuate feces. These ten larvae were thus representative of the tank population. At the end of the experiment, larval survival rates were determined by counting individuals.

At days 0, 10, 20 and 30, 20 larvae were collected for enzymatic studies from each tank before morning food distribution; larvae were immediately stored at -80°C pending dissection and assays. Dissection under the microscope was conducted on a glass maintained at 0°C .

Individuals were cut into four parts: head, gill, viscera and trunk muscle, in order to limit the assay of enzymes to specific segments. This dissection of viscera produced a mixture of organs in each segment which containing liver, heart, intestine and pancreas.

All the segments were individually weighed and placed immediately in liquid nitrogen and stored at -80°C .

Tissues were homogenized into ten volumes (v/wt) in 0.25 M pH 7.4 sucrose buffer using a glass homogenizer for 1 min at 10,000 rpm/min and then centrifuged at 1,000g for 30 min in a Beckman centrifuge at 4°C , and the supernatant was used for biochemical analyses.

Enzyme Assay

SOD (EC 1.15.1.1) activity was determined immediately after centrifugation of the homogenates by measuring the inhibition of the auto-oxidation of pyrogallol using a modification of a published method [32]. Samples were assayed in a solution of 10 mL 50 mM phosphate buffer, pH 8.2, and 0.25 mL 20 mM pyrogallol (dissolved in 10 mM HCl). The rate of pyrogallol auto-oxidation was measured with a Shanghai UV-220 spectrophotometer at 325 nm. One unit of enzyme activity was defined as the amount of enzyme exhibiting 50% inhibition of the auto-oxidation rate of 0.1 mM pyrogallol in 1 mL solution at 25°C .

The assay of CAT (EC 1.11.1.6) followed that described by Abei [33] and involved monitoring the decrease in absorbance at 240 nm due to decomposition of 10 mM H₂O₂ (omitted for control) ($\epsilon = 0.0394 \text{ mmol L}^{-1} \text{ cm}^{-1}$). The reaction took place in 50 mM imidazole (pH 7.1 at 4°C).

GPX (EC 1.11.1.9) activity was measured following the method of Flohé and Günzler [34]. A freshly prepared glutathione reductase solution (2.4 U mL^{-1} in 0.1 M potassium phosphate buffer, pH 7.0) was added to a 50 mM potassium phosphate buffer (pH 7.0), 0.5 mM EDTA, 1 mM sodium azide, 0.15 mM NADPH and 0.15 mM H₂O₂. After the addition of 1 mM GSH (reduced glutathione), the NADPH consumption rate was monitored at 340 nm.

Protein was determined by the Bradford method [35] using bovine serum albumin as a standard.

Lipid Peroxidation

The MDA concentration, an index of lipid peroxidation, was measured following the method described by Esterbauer and Cheeseman [36] on homogenized tissues. The homogenized tissue (0.5 mL), previously treated with 25 μL of butylhydroxytoluene 1% v/v in glacial acetic, was mixed with 0.2 mL of sodium lauryl sulphate (8%), 1 mL

of acetic acid (20% v/v) and 1 mL of 0.8% thiobarbituric acid. This mixture was then heated at 95°C for 30 min. The resulting chromogen was extracted with 3 mL of *n*-butyl alcohol and, after centrifugation (1,500g for 10 min). The absorbance of the organic phase was determined at 532 nm. 1,1,3,3 tetramethoxypropane was used as a standard. Values were presented as $\mu\text{mol MDA/g tissue}$.

Statistical Analysis

For the comparison of various enzyme activities and lipid peroxidation products, one way ANOVA and LSD (used as a post hoc test) were performed by SPSS 10.1 (SPSS, Chicago). Differences were considered significant at $p = 0.05$ for all analyses. Values in the text are given as means \pm SD (standard deviation).

Results

Growth and Survival

Survival rate of L15, L20, L25, L30 and the control were as follows: 70, 75, 82, 64 and 80%. Final larval weights are shown in Fig. 1. Fish fed with control diet grew fast and steady. At day 10, fish fed with artificial diets exhibited lower weights than that with the control diet, but at 30th day, similar weights were obtained. Only L25 was heavier than that of control. Final survival rates changed greatly, 82% of L25 was the highest and similar as that of the control. The survival rate of L30 was the lowest at only 64%. Larval growth is similar with each other at different time interval, except at 10 day sampling, when the control group is better than those of other treatments, but there is no statistics difference. Due to acclimation to diets, larvae show less weight in the experiment groups than the control. Body weights (BW) of L30 at 20 and 30 day were similar as the control, but heavier than that of other three groups.

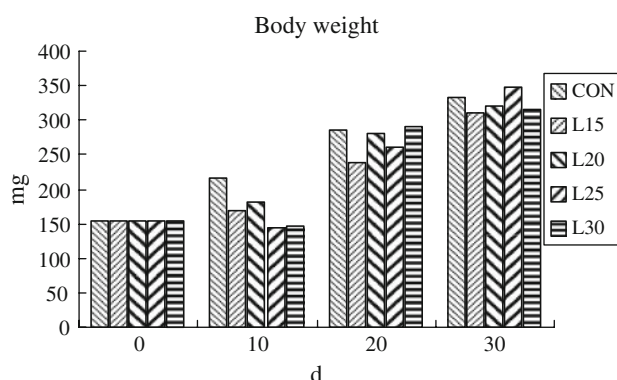


Fig. 1 Body weights at different time intervals

At 30 day, BW of L25 was the highest, but there were no significant difference with the others.

Antioxidant Enzyme

SOD

SOD activities of viscera and brain were maintained at 200–420 U/mg protein (Table 3; Fig. 2). The values in muscles were the lowest compared to other tissues. The highest activity was found in the gill.

In muscle, activities continued to increase steadily and the highest value achieved with L30. SOD activities were still low and steady in the control. But those larvae fed formulated diets showed an increase with time and L30 had the highest value. In the gill, the lowest activities were in the control, but there was no difference among those on different diets. The activities in brain remained steady among diets and showed a significant difference from that of the control.

CAT

The highest values were obtained in viscera compared with other tissues, but there was no consistency among organs (Table 3; Fig. 3).

In viscera, CAT activities of L30 exhibited higher value than other group, and declined with time, similar in this regard with L20 and L25 at the final experiment. The control group and L15 showed low activities from the beginning to the end (Fig. 3a).

CAT activities of muscle were the lowest among all tissues tested. L30 showed higher values compared with other treatments and increased with time. The highest value was determined at the end of experiment. The control groups were the lowest and showed significant differences to the others ($p < 0.05$) (Fig. 3b).

In gill and brain tissues, CAT activities of the control were lower compared to other treatments and showed significant differences ($p < 0.05$) except for the brain. Highest activities in gills were detected in L25 and showed significantly difference ($p < 0.05$) from the others. CAT in gill remained almost constant during the experiment and was higher than the other groups. CAT in gill of the control remained steady and that of L30 showed a decline. In brain, L30 showed the highest CAT values during the trial and appeared significantly different from the others (Fig. 3d).

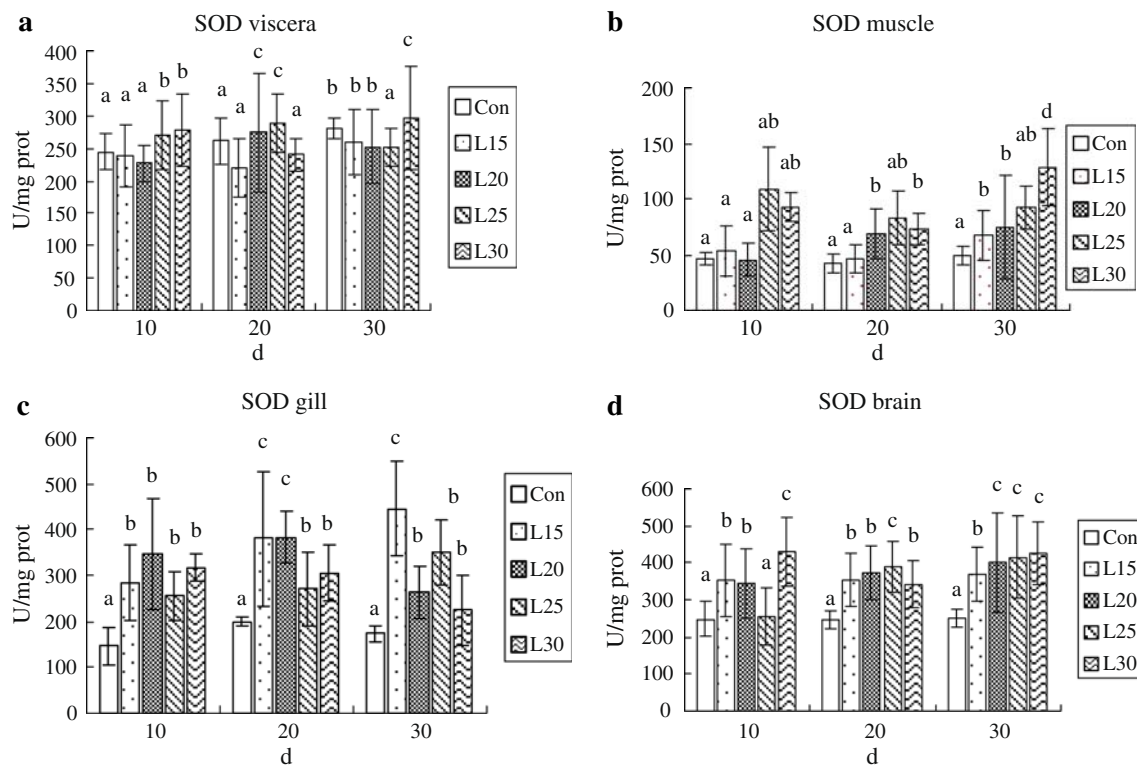
GPX

Activities of GPX in viscera showed higher values, compared with other tissues (Table 3; Fig. 4). GPX were significantly different among treatments and were lowered in

Table 3 SOD, CAT, GPX and MDA content in different tissues of the control group of *Lenok* larvae

	Viscera time interval (days)				Muscle time interval (days)			
	0	10	20	30	0	10	20	30
SOD (U/mg pro)	228.1 ± 13.9	244.5 ± 27.2	261.5 ± 35.1	280.1 ± 15.9	52.9 ± 11.4	47.0 ± 5.7	42.2 ± 7.9	49.8 ± 8.2
CAT (U/mg pro)	8.0 ± 0.9	4.8 ± 0.6	7.3 ± 1.3	6.9 ± 0.5	1.3 ± 0.6	0.9 ± 0.4	0.6 ± 0.1	1.0 ± 0.2
GPX (U/mg pro)	334.3 ± 87.8	465.1 ± 48.1	520.3 ± 59.5	532.1 ± 63.9	40.4 ± 14.3	50.3 ± 4.4	38.6 ± 14.5	44.0 ± 5.4
MDA (nmol/mg pro)	0.55 ± 0.17	0.60 ± 0.10	0.62 ± 0.06	0.56 ± 0.05	0.22 ± 0.04	0.17 ± 0.02	0.23 ± 0.03	0.20 ± 0.02

	Gill time interval (days)				Brain time interval (days)			
	0	10	20	30	0	10	20	30
SOD (U/mg pro)	187.6 ± 33.5	147.0 ± 41.0	199.6 ± 10.4	174.6 ± 17.4	233.6 ± 17.7	248.2 ± 46.7	246.2 ± 23.7	249.4 ± 24.3
CAT (U/mg pro)	1.4 ± 0.9	2.3 ± 1.1	1.7 ± 0.4	1.4 ± 0.3	6.4 ± 1.6	5.1 ± 1.2	7.3 ± 1.3	6.9 ± 0.5
GPX (U/mg pro)	70.1 ± 21.1	84.9 ± 16.0	47.3 ± 13.5	57.1 ± 17.2	73.2 ± 37.5	46.3 ± 8.3	35.4 ± 16.7	34.9 ± 13.8
MDA (nmol/mg pro)	0.36 ± 0.07	0.37 ± 0.05	0.35 ± 0.07	0.36 ± 0.07	0.44 ± 0.08	0.37 ± 0.08	0.43 ± 0.13	0.34 ± 0.04

**Fig. 2** SOD activities of different tissues **a** viscera, **b** muscle, **c** gill, **d** brain

artificial diets. GPX in viscera of the L30 group was the highest and increased with dietary lipid levels, except the control.

In muscle, activities of moderate lipid diets showed higher than that of control and L30. Activities of L15 kept very steady from the start and was different to the others. The GPX of L30 declined and became the lowest at the end.

The values of gills were lower compared with those of the brain. There was no obvious tendency for treatment in gills except low activity of L15 in 10 days. GPX of L25 and L30 stayed at a higher level during the experiment in the gills. The GPX of the brain showed significant differences and decreased in the control. Activities of L30 remains at a high level and increased to the highest at 30 days. In the end, similar values were achieved except for

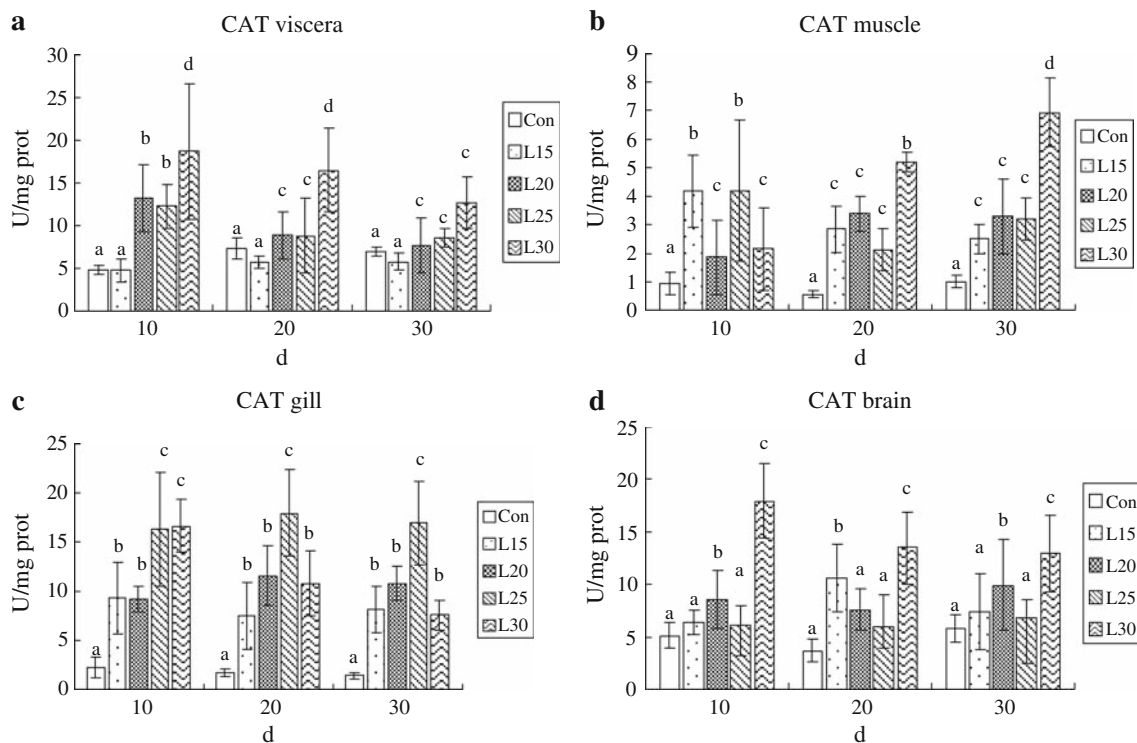


Fig. 3 CAT activities of different tissues **a** viscera, **b** muscle, **c** gill, **d** brain

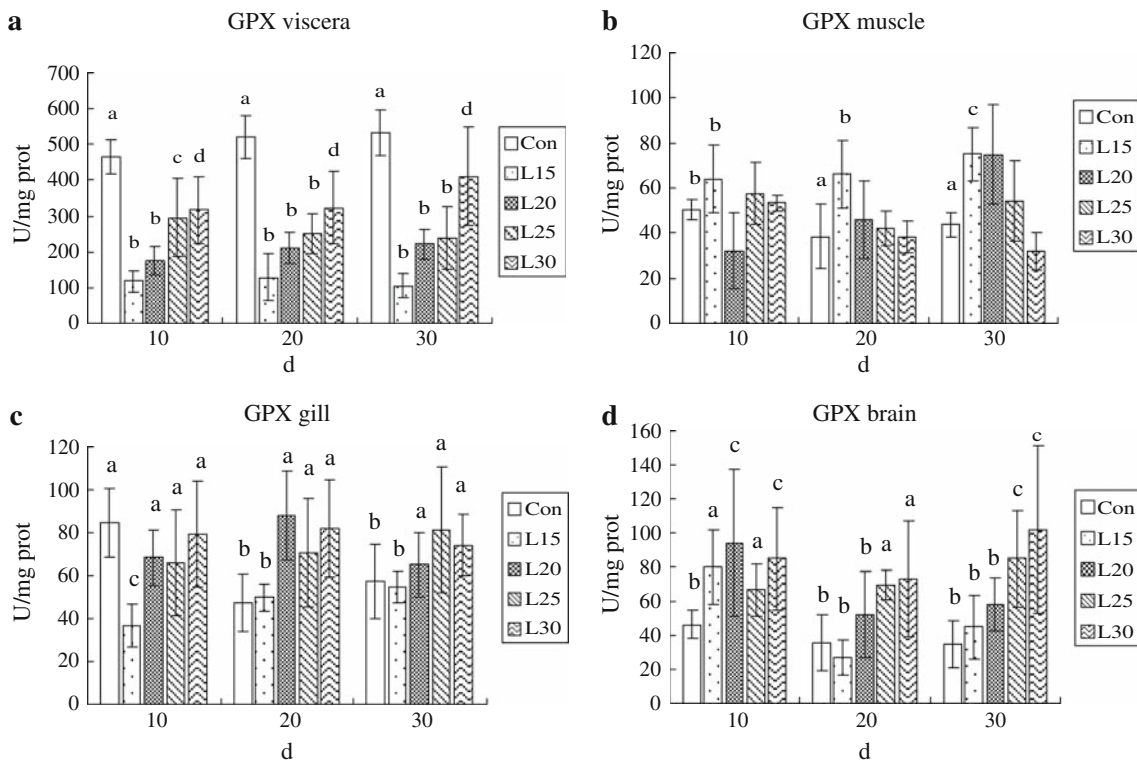


Fig. 4 GPX activities of different tissues **a** viscera, **b** muscle, **c** gill, **d** brain

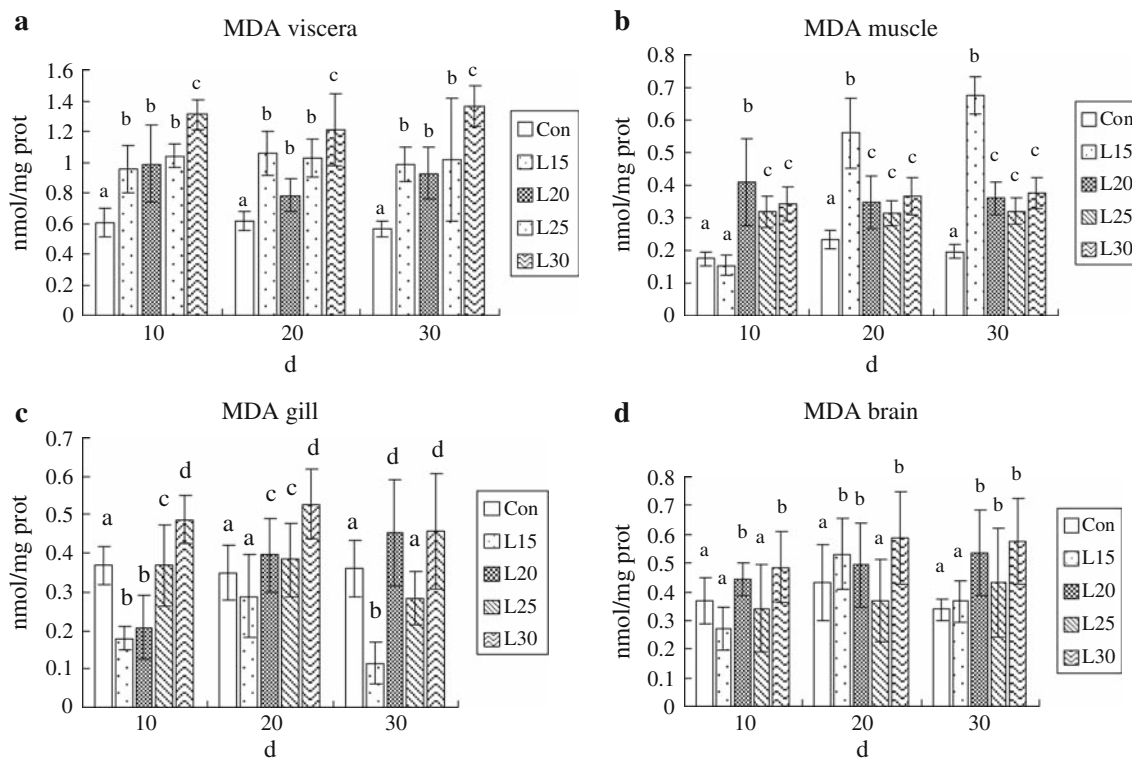


Fig. 5 MDA concentration of different tissues **a** viscera, **b** muscle, **c** gill, **d** brain

L25 and L30 and significant differences were found among treatments.

Lipid Peroxidation

MDA

The highest MDA contents were detected with an increase in dietary lipid level and time in viscera (Fig. 5a). Larvae with live food showed low values in tissues.

Compared with other treatments, the highest MDA content of viscera was found in L30 and showed a statistical difference ($p < 0.05$) to the others. The value of the control remained steady, under 0.8 nmol/mg protein, and significantly lower than experimental diets. The content of treatments from 0.8 to 1.2 $\mu\text{mol/mg}$ protein displayed no difference among treatments except for L30.

Values of artificial diets showed inclined pattern in muscle, but that of the control kept steady and maintained at low level. High values were found in low lipid diets, L15 and L20. Values of L15 increased sharply and were significant different with others. Content of L20 to L30 showed no difference and remained at a medium level.

There were significant differences among treatments and no tendency was found except for L30 in gill. From the start, the highest MDA content of L30 was observed and

higher than 0.4 nmol/mg protein, but no differences were found. Lower values obtained from L15 and significantly lower comparing with others.

MDA content in brain increased with time except that of the control. Results of L30 kept steady and significantly higher ($p < 0.05$). Values of the control remained constant. With increasing dietary lipid levels, high MDA production took place in the brain and maintained steady in L30.

Discussion

This study was to investigate relation between the dietary lipid requirements and the antioxidant status of fish larvae. The use of a compound diet as the only source is common in cold water fish, such as rainbow trout, and usually used to domesticate larvae. But there was no information on nutrition in Manchurian trout larvae, especially with regards to lipids. Indeed, larvae were carefully fed live prey, *Artemia* and crumbled worm at the developmental stage in previous feeding practices. A compound diet formulated to meet the specific nutritional requirements of fish larvae could replace live prey in larvae feeding and would lower the juvenile production costs and mortality in hatcheries. The lack of a compound diet available for the early larval stages explains the poor knowledge of larval nutritional requirements.

Lipids are very important for egg and larval development [24, 37, 38]. Research on lipid nutrition mainly focuses on the requirement of the total quantity and fatty acids, few studies have been conducted on physiological response of organs to dietary lipid levels, especially on antioxidant stress caused by poor diets in larvae [13, 14]. In sea bass (*Dicentrarchus labrax*) larvae, high DLL levels enhance digestive tract maturation and improve larval development [24].

In the experiment, the four diets were able to sustain some growth and survival in trout larvae. Final weight of L15 was the lowest. With dietary lipid concentration increasing from 15 to 30%, high growth gain was achieved. A maximal twofold increase was observed in the weight of fish larvae from day 10 to 30. With regard to the final body weight of experimental larvae, the highest weight of L25 showed that lipid contents can increase the growth rate and a high survival rate was achieved. It could be assumed that such a growth rate requires high energy diets, but DLL had a profoundly positive effect on Atlantic salmon growth and feed conversion, and gave fillets with nearly two times the fat content found in fish fed a low lipid diet [39].

In the same way, the increasing DLL positively affected the larval survival rate. The best survival rate in this study, 82% in the L25 group, was similar to that of the control, 80%. Survival rate increased with dietary lipid content and the lowest was 64% in L30, the highest lipid content group. Survival of control is 80% and only with L25 over 80%. These results indicated that the optimal lipid concentration in the diet for larvae might be 25%, higher than the 10–20%, generally adopted in other cold water species larvae diets (Fig. 6).

According to Panserat et al. [28] and Zambonino Infante and Cahu [24], high DLL could act on digestive physiology and to improve metabolism of nutrients. Our results indicated that appropriate DLL could alter growth and survival in trout larvae. Diet with 25% lipid might be appropriate to achieve better culture regime.

SOD is the first enzyme to respond to oxygen radicals [40] and is the one that offers the greatest response to oxidative stress [41]. Any situation that increases oxygen

consumption by the mitochondria proportionally increases the generation of O_2^- [42]. Experimental tests in animals demonstrate a correlation between SOD and tolerance to oxygen toxicity [43].

It is known that vertebrate liver exhibits a high metabolism and oxygen consumption, and it probably best represents the status of antioxidant defense in organisms, and therefore, it is frequently referred to in the literature [44]. Thus, the profile of SOD activities in tissues found in Manchurian trout larvae agreed with the literature in reference to the other fish [44–47].

In our study, the results were similar to rainbow trout [47] and SOD activity in muscle was the lowest compare with other tissues and indicated that fewer free radicals might take place. In muscle, lowest activities were found, which means lipid level cause less oxidative stress and whether lipid was accumulated is uncertain. In viscera, SOD showed significant difference and the control increased steady, but in L25 and L30, high values nearly always remained high and constant from the start to the end. The higher activities revealed that DLL played the key role in production of free radicals. Addition of fish oil in rat diet had been proved to alter the antioxidant status [48] and that might be helpful in explaining the results, which means that not only lipid level but fatty acids could alter fish antioxidant status, especially SOD.

The gills appear to be susceptible to oxidation, partly because of their defensive phagocytic activity [49] and partly for presenting fewer antioxidant resources in comparison with other tissues, such as liver [50]. In our results, SOD of artificial diets in gills showed higher values than that of the control. The high value indicated DLL might influence susceptibility in gills and induce responses to ROS to protect organ from damage.

Activities of SOD in brain showed different patterns unlike the organs mentioned above. Enzyme activities of larvae fed artificial diets were higher than that of the control. Rueda-Jasso et al. [51] found that juvenile Senegalese sole fed a high lipid diet had a different oxidation susceptibility. SOD activities increased with lipid level. Other experiments showed lipid levels and fatty acids influenced the species physiological status [22, 27, 52]. From our results, high SOD activities in the brain might be responses to free radicals derived from oxidation of lipids, but whether ROS could be removed completely is uncertain. Different fish with a different response to redox homeostasis might be helpful in explaining the harmful effects in larval development [53]. The response of SOD in the brain might indicate that neural system development could be influenced in Manchurian trout larvae in our experiment.

CAT is an enzyme present in nearly all animal and plant cells [54]. CAT combines rapidly with hydrogen peroxide to catalyze H_2O_2 , breakdown into oxygen and water. In

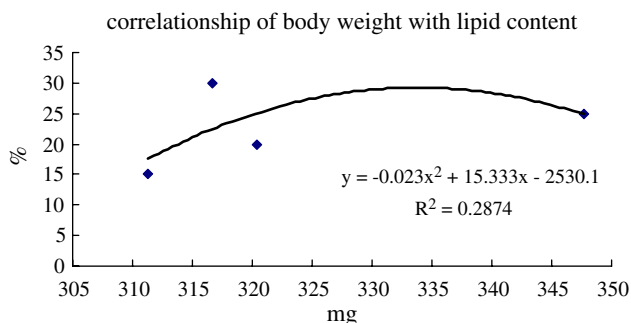


Fig. 6 Correlation between dietary lipid level and body weight

many cases, the enzyme is localized in subcellular organelles such as peroxisomes of the liver or in much smaller aggregates such as the microperoxisomes found in a variety of other cells. Chance et al. [54] documented that the physiological variation of CAT concentrations in different organs and tissues lead to different steady-state levels of hydrogen peroxide concentration for the same rate of hydrogen peroxide generation. Furthermore, CAT is uniquely fitted to provide a homeostasis for hydrogen peroxide concentrations in the cells [54].

CAT had been studied in many fish species with different situation [12, 55–57]. Tort et al. [55] reported that CAT activity in the livers of treated fish was not significantly different from the activity in control fish livers when hydrogen peroxide as a chemotherapeutant to treat walleye. However, CAT levels in the gills were significantly higher in the treated fish when compared to the control fish, indicating an induction of CAT activity in the gills of the fish treated with low concentration of hydrogen peroxide. Ozone and hyperoxic conditions increased SOD activity on red blood cell after exposure and CAT was only increase 10 min after exposure, suggesting other mechanisms rather than enzyme induction [56].

The increase of CAT in different tissues was obvious in L25 and L30 in our experiment. As in viscera and muscle, significant difference ($p < 0.05$) was found that might indicate antiperoxidative protection took place due to diets. As absorption and deposition of dietary lipid occurred mainly in viscera and muscle, high values were determined in L30 that might be indicator of oxidative reaction. Especially in brain, CAT of L30 maintained at high level indicated that brain was also a key organ influenced from start by DLL. Interestingly, among all groups, the control showed lower activity compared to the others. In *Solea senegalensis* larvae, Fernandez-Diaz et al. [16] found that larvae fed with both inert diets showed similar biomarker activities, but these activities were different ($p < 0.05$) from larvae fed with Artemia. SOD, CAT activities increased in inert diets and GPX showed a higher level in larvae fed with Artemia, but MDA did not markedly and was parallel with GPX. Varghese and Oommen [29] carried out a study that indicated that dietary lipids depress hepatic lipogenic activity in a teleost (*Anabas testudineus* Bloch) as well as lipid peroxidation products by maintaining high levels of antioxidant enzymes. All these demonstrated that dietary lipids in larvae might affected antioxidant enzymes and induced responses to artificial diet. In our experiment, DLL really induced an antioxidant response, especially in high lipid diets.

GPX catalyzes the reduction of H_2O_2 derived from oxidative metabolism as well as peroxides from oxidation of lipids and is considered the most effective enzyme against lipid peroxidation [41]. Its activity is considered

complementary to CAT activity, being especially suited for hydroperoxide detoxification at low substrate concentrations [43]. In our experiment, the determinations in viscera showed the highest levels, with similar values in other tissues (Fig. 3).

The increase of GPX activity observed in viscera is similar to the results reported by Li et al. [58], who studied the responses of the antioxidant systems in the hepatocytes of common carp (*Cyprinus carpio* L.) to microcystin-LR. Interestingly, THE GPX of the control in viscera remained at a high level during the experiment and that might be influenced by live prey's free radicals. An increasing tendency was found in muscle, especially significantly different was L30 with others. The increase in GPX activity probably reflects an adaptation to the oxidative conditions to which the fish had been exposed [59]. However, GPX activity increased in gills and brain after the longer exposure time, corroborating the ROS increase in this organ; this may be explained because gills and brain are less efficient than muscle and viscera at neutralizing the impact of peroxidative damage [50]. The fermented vegetable products (FVP)-fed fish showed a higher GPX activity of liver than the control fish which also demonstrated the influence of food on the tissues [57].

Estimation of lipid peroxidation in particular has been found to have high predictive importance as revealed by a credible number of research papers describing its use as a biomarker to great effect [60]. MDA is the main oxidation product of peroxidized PUFA and an increased MDA level is an important indicator of lipid peroxidation.

Similar to the Olsen et al. [61] and Rueda-Jasso et al. [51] results, MDA content in viscera and muscle increased with dietary lipid. The value of the controls was maintained at a low level and almost kept steady from start to finish in all groups, which might indicate that lipid from live prey could be assimilated well. Compared to the control fish, MDA in the viscera of fish fed supplemented diets achieved significant differences ($p < 0.05$).

In respiratory organs, a lower MDA concentration was determined than with other organs, which might be related to the excretion of the oxidative product and environmental stress [47, 49, 62, 63].

Studies on the addition of antioxidants to diets had been widely undertaken in animals [64, 65] and these may be beneficial to health. Our results showed that MDA in viscera and brain increased with dietary lipid levels and accumulated in the two organs with time. More peroxidative products produced meant that the protective mechanism could be operated to offset damaging effects caused by MDA.

However, it should be pointed out that more MDA is produced in the brain with higher dietary lipid level. In cold-temperature adaptive fish, high oxygen solubility and

a lipid diet might induce production of free radicals and stimulate the antioxidant defense mechanism [66]. The aging process might be related to DNA damage by oxidative stress in animals [67]. The accumulation of MDA in the brain with increased dietary lipid levels indicates that more oxidative stress might be induced and probably damage to the normal physiological function.

Lipids are an important energy store for larval metabolism [9, 11–13, 15, 26, 29] and play a role in digestive maturation [24, 25, 28]. In cultured fish, high dietary lipids may be utilized well and be beneficial to larval development and enhance survival [15, 16, 24–26, 28]. In our experimental diet, DLL increased and carbohydrate decreased. As a consequence, antioxidant enzyme activity showed variation in organs. With increased energy content in diets, high survival and growth were achieved, and the antioxidant status changed. As an energy resource, the lipid level might be more important than protein content in experimental treatments comparing with the control group (more than 80% protein in live organism, but a low lipid level, under 14%). For young animals, a high metabolism rate is a common phenomenon and more energy is needed to fuel development [42, 65], but fish species exhibited antioxidant differences to nutrients [16, 51] and few studies have focused in this area.

In recent studies, *Solea senegalensis* larvae fed on live and microencapsulated diets, these activities were different ($p < 0.05$) from larvae fed with *Artemia* [16]. That is, CAT and Hsp70 (stress protein) levels were lower in larvae fed with live prey and GPX and lipid peroxidation levels were lower in larvae fed with the inert food. Among the factors responsible for increased antioxidant defenses were the initiation of metamorphosis and the use of inert food. However, *Solea senegalensis* larvae in non-protein energy levels [51], lipid peroxidation was founded in fish with high lipid content diets and CAT, SOD activities were influenced by the type of dietary starch in the diet. These data suggest that lipid and carbohydrate energy sources affect the oxidative status of Senegalese sole. However, our results showed that decreased carbohydrate levels and increased lipid levels have been effective in regulating the antioxidant status in Manchurian larvae and improving growth.

In this study we have demonstrated that dietary lipid supplementation altered the antioxidant status in Manchurian trout larvae. Indices of oxidative stress directly measured in any organs indicated that the high DLL induced significant long-term oxidative stress due to antioxidant enzymes stimulated and peroxidative products increased, especially in brain and viscera, which were a key function in neuron regulation and the adsorption location. Our results demonstrated that trout larvae are susceptible to dietary components and these require appropriate lipid

contents. Moreover, if the high DLL did initially result in oxidative stress, then some organs adapted by increasing antioxidant defenses mechanism as demonstrated in this study. This may have been responsible for the protective effects against exogenous free radicals that are produced by absorbing and disposing them. Diet containing 20–25% lipid might meet larvae requirements and the antioxidant response would be moderate. The effects of fatty acids containing polyunsaturated bonds needs to be investigated in the future.

Acknowledgment The research was funded by Heilongjiang science and technology project, GC05B510, and national science supporting plan, 2006BAD03B08. The editorial help from Dr. Maynard Chen is appreciated.

References

- Mate's JM (2000) Effects of antioxidant enzymes in the molecular control of reactive oxygen species toxicology. *Toxicology* 153:83–104
- Ansaldo M, Luquet CM, Evelson PA, Polo JM, Llesuy S (2000) Antioxidant levels from different Antarctic fish caught around South Georgia Island and Shag rocks. *Polar Biol* 23:160–165
- Winzer K, Becker W, Van Noorden CJF, Köhler A (2000) Short-time induction of oxidative stress in hepatocytes of the European flounder (*Platichthys flesus*). *Mar Environ Res* 50:495–501
- Akyol Ö, Arslanoglu R, Durak I (1995) Activities of free radical and DNA turn-over enzymes in cancerous and non-cancerous human brain tissues. *Redox Report* 1:255–259
- Porte C, Sol M, Albaigs J, Livingstone DR (1991) Responses of mixed-function oxygenase and antioxidant enzyme system of *Mytilus* sp. to organic pollution. *J Comp Biochem Physiol* 100C:183–186
- Lushchak VI, Bagnyukova TV, Lushchak OV, Storey JM, Storey KB (2005) Hypoxia and recovery perturb free radical processes and antioxidant potential in common carp (*Cyprinus carpio*) tissues. *J Int Biochem Cell Biol* 37:1319–1330
- Guerriero G, Di Finizio A, Ciarcia C (2002) Stress-induced changes of plasma antioxidants in aquacultured sea bass, *Dicentrarchus labrax*. *J Comp Biochem Physiol* 132:205–211
- Viarengo A, Canesi L, Martinez PG, Peters LD, Livingstone DR (1995) Pro-oxidant processes and antioxidant defence systems in the tissues of the Atlantic scallop (*Adamussium colbecki*) compared with the Mediterranean scallop (*Pecten jacobaeus*). *J Comp Biochem Physiol* 111B:119–126
- Lushchak V, Lushchak LP, Mota AA, Hermes-Lima M (2001) Oxidative stress and antioxidant defenses in goldfish, *Carassius auratus* during anoxia and reoxygenation. *Am J Physiol Regul Integr Comp Physiol* 280:100–107
- Welker TL, Congleton JL (2004) Oxidative stress in juvenile chinook salmon, *Oncorhynchus tshawytscha* (Walbaum). *Aquac Res* 35:881–887
- Götz ME, Malz CR, Dirr A, Blum D, Gsell W, Schmidt S, Burger R, Pohli S S, Riederer P (2005) Brain aging phenomena in migrating sockeye salmon, *Oncorhynchus nerka nerka*. *J Neural Transm* 112:1177–1199
- Mourente G, Diaz-Salvago E, Tocher DR, Bell JG (2000) Effects of dietary polyunsaturated fatty acid/vitamin E (PUFA/tocopherol) ratio on antioxidant defense mechanisms of juvenile gilt-head sea bream (*Sparus aurata* L., *Osteichthyes*, Sparidae). *J Fish Physiol Biochem* 23:337–351

13. Tocher DR, Mourente G, Van Der Eecken A, Evjemo JO, Diaz E, Wille M, Bell JG, Olsen Y (2003) Comparative study of antioxidant defense mechanisms in marine fish fed variable levels of oxidised oil and vitamin E. *Aquac Int* 11:195–216
14. Puangkaew J, Kiron V, Satoh S, Watanabe T (2005) Antioxidant defense of rainbow trout (*Oncorhynchus mykiss*) in relation to dietary n-3 highly unsaturated fatty acids and vitamin E contents. *J Comp Biochem Physiol* 140C:187–196
15. Welker TL, Congleton JL (2003) Relationship between dietary lipid source, oxidative stress, and the physiological response to stress in sub-yearling chinook salmon (*Oncorhynchus tshawytscha*). *J Fish Physiol Biochem* 29:225–235
16. Fernandez-Diaz C, Kopecka I, Canavate JP, Sarasquete C, Sole M (2006) Variations on development and stress defences in *Solea senegalensis* larvae fed on live and microencapsulated diets. *Aquaculture* 251:573–584
17. Gupta OP, Lahlou B, Botella J, Porthé-Nibelle J (1985) In vivo and in vitro studies on the release of cortisol from interrenal tissue in trout I. Effects of ACTH and prostaglandins. *J Exp Biol* 43:201–212
18. Wales NAM (1988) Hormone studies in *Myxine glutinosa*: effects of the eicosanoids arachidonic acid, prostaglandin E₁, E₂, A₂, F_{2α}, thromboxane B₂ and of indomethacin on plasma cortisol, blood pressure, urine flow and electrolyte balance. *J Comp Physiol* 158B:621–626
19. Stéphan G, Guillaume J, Lamour F (1995) Lipid peroxidation in turbot (*Scophthalmus maximus*) tissue: effect of dietary vitamin E and dietary n-6 or n-3 polyunsaturated fatty acids. *Aquaculture* 130:251–268
20. Lie O (2001) Flesh quality—the role of nutrition. *Aquac Res* 32(Suppl 1):341–348
21. Torstensen BE, Lie O, Hamre K (2001) A factorial experimental design for investigation of effects of dietary lipid content and pro- and antioxidants on lipid composition in Atlantic salmon (*Salmo salar*) tissues and lipoproteins. *Aquac Nutr* 7:265–276
22. Basso MM, Eynard AR, Valentich MA (2006) Dietary lipids modulate fatty acid composition, gamma glutamyltranspeptidase and lipid peroxidation levels of the epididymis tissue in mice. *Anim Reprod Sci* 92:364–372
23. Bhattacharya A, Sun DX, Rahman M, Fernandes G (2007) Different ratios of eicosapentaenoic and docosahexaenoic omega-3 fatty acids in commercial fish oils differentially alter pro-inflammatory cytokines in peritoneal macrophages from C57BL/6 female mice. *J Nutr Biochem* 18:23–30
24. Zambonino Infante JL, Cahu CL (1999) High dietary lipid levels enhance digestive tract maturation and improve *Dicentrarchus labrax* larval development. *J Nutr* 129:1195–1200
25. Geurden I, Bergot P, Schwarz L, Sorgeloos P (1998) Relationship between dietary phospholipid classes and neutral lipid absorption in newly-weaned turbot, *Scophthalmus maximus*. *Fish Physiol Biochem* 19:217–228
26. Bell JG, McEvoy J, Tocher DR, McGhee F, Campbell PJ, Sargent JR (2001) Replacement of fish oil with rapeseed oil in diets of Atlantic salmon (*Salmo salar*) affects tissue lipid compositions and hepatocyte fatty acid metabolism. *J Nutr* 131:1535–1543
27. Bhattacharya A, Sun DX, Rahman M, Fernandes G (2007) Different ratios of eicosapentaenoic and docosahexaenoic omega-3 fatty acids in commercial fish oils differentially alter pro-inflammatory cytokines in peritoneal macrophages from C57BL/6 female mice. *J Nutr Biochem* 18:23–30
28. Panserat S, Perrin A, Kaushik S (2002) High dietary lipids induce liver glucose-6-phosphatase expression in rainbow trout (*Oncorhynchus mykiss*). *J Nutr* 132:137–141
29. Varghese S, Oommen OV (2000) Long-term feeding of dietary oils alters lipid metabolism, lipid peroxidation, and antioxidant enzyme activities in a teleost (*Anabas testudineus* Bloch). *Lipids* 35:757–762
30. Dong CZ (1999) Aquatic organism resources and their utilization in Heilongjiang river system. *J Chin Fis* 12:22–27
31. Zhao YH, Zhang CG, Threatened fishes of the world: *Brachymystax lenok tsinlingensis* Li, 1966 (Salmonidae). *Environ Biol Fish* doi:10.1007/s10641-008-9337-7
32. Marklund S, Marklund G (1974) Involvement of the superoxide anion radical in the autooxidation of pyrogallol and a convenient assay for superoxide dismutase. *J Eur Biochem* 47:469–474
33. Abei H (1984) Catalase in vitro. *Methods Enzymol* 105:121–126
34. Flohé L, Günzler WA (1984) Assay of glutathione peroxidase. *Methods Enzymol* 105:115–121
35. Bradford MM (1976) A rapid sensitive method for the quantification of microgram quantities of protein utilizing the principle of protein-dye binding. *J Anal Biochem* 72:248–254
36. Esterbauer H, Cheeseman KH (1990) Determination of aldehydic lipid peroxidation products: malonaldehyde and 4-hydroxynon-etal. *Methods Enzymol* 186:407–421
37. Desvillettes C, Bourdier G, Breton JC (1997) Changes in lipid class and fatty acid composition during development in pike (*Esox lucius* L) eggs and larvae. *Fish Physiol Biochem* 16:381–393
38. Arnil C, Emata H, Ogata Y, Esteban SG, Hirofumi F (2003) Advanced broodstock diets for the mangrove red snapper and a potential importance of arachidonic acid in eggs and fry. *Fish Physiol Biochem* 28:489–491
39. Hamre K, Christiansen R, Waagb R, Maage A, Torstensen BE, Lygren B, Lie Ø, Wathne E, Albrektsen S (2004) Antioxidant vitamins, minerals and lipid levels in diets for Atlantic salmon (*Salmo salar* L.): effects on growth performance and fillet quality. *Aquacult Nutr* 10:113–123
40. McCord JM, Fridovich J (1969) Superoxide dismutase: an enzymatic function for erythrocyte (hemocuprein). *J Biol Chem* 244:6049–6055
41. Winston GW, Di Giulio RT (1991) Prooxidant and antioxidant mechanisms in aquatic organisms. *Aquac Toxicol* 19:137–161
42. Camougrand N, Rigoulet M (2001) Aging and oxidative stress: studies of some genes involved both in aging and in response to oxidative stress. *Respir Physiol* 15:393–401
43. Pérez-Campo R, López-Torres M, Rojas C, Cadenas S, Barja G (1993) A comparative study of free radicals in vertebrates—I Antioxidant enzymes. *J Comp Biochem Physiol* 105B:745–749
44. Wilhelm-Filho DW, Boveris A (1993) Antioxidant defenses in marine fish—II Elasmobranchs. *J Comp Biochem Physiol* 106C:415–418
45. Wdziedzicak J, Zalesna G, Wujec E, Peres G (1982) Comparative studies on superoxide dismutase, catalase and peroxidase levels in erythrocytes and livers of different freshwater and marine fish species. *J Comp Biochem Physiol* 73B:361–365
46. Avci A, Kaçmaz M, Durak I (2005) Peroxidation in muscle and liver tissues from fish in a contaminated river due to a petroleum refinery industry. *Ecotoxicol Environ Saf* 60:101–105
47. Trenzado C, Hidalgo MC, García-Gallego M, Morales AE, Furné M, Domezain A, Domezain J, Sanz A (2006) Antioxidant enzymes and lipid peroxidation in sturgeon *Acipenser naccarii* and trout *Oncorhynchus mykiss*. A comparative study. *Aquaculture* 254:758–767
48. Jahangiri A, Wayne RL, Karen LK, Edwards JMM (2006) Dietary fish oil alters cardiomyocyte Ca²⁺ dynamics and antioxidant status. *Free Radic Biol Med* 40:1592–1602
49. Parihar MS, Dubey AK (1995) Lipid peroxidation and ascorbic acid status in respiratory organs of male and female freshwater catfish, *Heteropneustes fossilis* exposed to temperature increase. *J Comp Biochem Physiol* 112C:309–313
50. Fatima M, Ahmad Y, Sayeed Y, Athar M, Raisuddin S (2000) Pollutant-induced over-activation of phagocytes is concomitantly

- associated with peroxidative damage in fish tissues. *Aquac Toxicol* 49:243–250
51. Rueda-Jasso R, Conceicao LEC, Dias J, Gomesc E, Reese JF, Soaresb F, Dinisb MT, Sorgeloos P (2004) Effect of dietary non-protein energy levels on condition and oxidative status of Senegalese sole (*Solea senegalensis*) juveniles. *Aquaculture* 231:417–433
 52. Devereux G, Seaton A (2005) Diet as a risk factor for atopy and asthma. *J Clin Immunol* 115(6):1110–1117
 53. Bermejo-Nogales A, Saera-Vila A, Calduch-Giner JA, Navarro JC, Sitjà-Bobadilla A, Pérez-Sánchez J (2007) Differential metabolic and gene expression profile of juvenile common dentex (*Dentex dentex* L.) and gilthead sea bream (*Sparus aurata* L.) in relation to redox homeostasis. *Aquaculture* 267:213–224
 54. Chance B, Sies H, Boveris A (1979) Hydroperoxide metabolism in mammalian organs. *Physiol Rev* 59:527–605
 55. Tort MJ, Hurley D, Fernandez-Cobas C, Wooster GA, Bowser PR (2005) Effects of hydrogen peroxide treatments on catalase and glutathione activity in walleye *Sander vitreus*. *J World Aqua Soc* 36(4):578–586
 56. Ritola O, Peters LD, Livingstone DR, Lindstorm-Seppa P (2002) Effects of in vitro exposure to ozone and/or hyperoxia on superoxide dismutase, catalase, glutathione and lipid peroxidation in the red blood cells and plasma of rainbow trout, *Oncorhynchus mykiss* (Walbaum). *Aqua Res* 33:165–175
 57. Ashida T, Takei Y, Takagaki M, Matsuura Y, Okimasu E (2006) The dietary effects of a fermented vegetable product on glutathione peroxidase activity and lipid peroxidation of Japanese flounder (*Paralichthys olivaceus*). *Fish Sci* 72:179–184
 58. Li XY, Liu YD, Song LR, Liu JT (2003) Responses of antioxidant systems in the hepatocytes of common carp (*Cyprinus carpio* L.) to the toxicity of microcystin-LR. *Toxicol* 42:85–89
 59. Lenartova V, Holovska K, Pedrajas JR, Martinez-Lara E, Peinado J, Lopez-Barea J, Rosival I, Kosuth P (1997) Antioxidant and detoxifying fish enzymes as biomarkers of river pollution. *Biomarkers* 2:247–252
 60. Krumschnabel G, Lackner R (1993) Stress responses in rainbow trout *Oncorhynchus mykiss* alevins. *J Comp Biochem Physiol* 104A:777–784
 61. Olsen RE, Løvaas E, Lie Ø (1999) The influence of temperature, dietary polyunsaturated fatty acids, α -tocopherol and spermine on fatty acid composition and indices of oxidative stress in juvenile Arctic char *Salvelinus alpinus* (L.). *J Fish Physiol Biochem* 20:13–29
 62. Otto DME, Moon TW (1996) Endogenous antioxidant systems of two teleost fish, the rainbow trout and the black bullhead, and the effect of age. *J Fish Physiol Biochem* 15:349–358
 63. Angel DL, Fielder U, Eden N, Kress N, Adelung D, Herut B (1999) Catalase activity in macro- and microorganisms as an indicator of biotic stress in coastal waters of the Eastern Mediterranean sea. *Helgol Mar Res* 53:209–218
 64. Bell MV, Batty RS, Dick JR, Fretwell K, Navarro JC, Sargent JR (1995) Dietary deficiency of docosahexaenoic acid impairs vision at low light intensities in juvenile herring (*Clupea harengus* L.). *Lipids* 30:443–449
 65. Hemre G-I, Sandnes K (1999) Effect of dietary lipid level on muscle composition in Atlantic salmon, *Salmo salar*. *Aquac Nutr* 5:9–16
 66. Doris A, Puntarulo S (2004) Formation of reactive species and induction of antioxidant defence systems in polar and temperate marine invertebrates and fish. *Comp Biochem Physiol A* 138:405–415
 67. Barja G (2004) Aging in vertebrates, and the effect of caloric restriction: a mitochondrial free radical production—DNA damage mechanism? *J Biol Rev* 79:235–251

New 17-Methyl-13-Octadecenoic and 3,16-Docosadienoic Acids from the Sponge *Polymastia penicillus*

Claire Denis · Gaëtane Wielgosz-Collin · Anne Bretéché ·
Nicolas Ruiz · Vony Rabesaotra · Nicole Boury-Esnault ·
Jean-Michel Kornprobst · Gilles Barnathan

Received: 12 September 2008 / Accepted: 8 February 2009 / Published online: 6 March 2009
© AOCs 2009

Abstract The phospholipid fatty acid composition of the North-East Atlantic sponge *Polymastia penicillus* (South Brittany, France) was investigated. Sixty fatty acids (FA) were identified as methyl esters (FAME) and *N*-acyl pyrrolidides (NAP) by gas chromatography–mass spectrometry (GC/MS), including eight $\Delta 5,9$ unsaturated FA and three long-chain 2-hydroxylated FA. The major phospholipid FA were palmitic (14.3% of the total FA mixture), vaccenic (12.7%), 15(*Z*)-docosenoic (13.4%) and 5(*Z*),9(*Z*)-hexacosadienoic (13.3%) acids. In addition to the *iso*- and *anteiso*-branched saturated FA, several unusual short-chain branched saturated FA were identified. In addition to the known $\Delta 5,9$ FA, and interestingly regarding their identification by GC–MS as *N*-acyl pyrrolidides, was the co-occurrence of unusual FA possessing a $\Delta 3$, $\Delta 4$ and $\Delta 5$ double bond such as *iso*-4-pentadecenoic, *iso*-5-heptadecenoic, *anteiso*-5-heptadecenoic and two new compounds, not hitherto found in nature, namely 17-methyl-13-octadecenoic (0.8%) and 3,16-docosadienoic (1.1%) acids.

Keywords 3,16-Docosadienoic acid · Fatty acids · Phospholipids · *Polymastia* · Sponge ·

17-Methyl-13-octadecenoic · *N*-Acyl pyrrolidides · Non-methylene-interrupted fatty acids

Abbreviations

amu	Atomic mass unit
FA	Fatty acid(s)
FAME	Fatty acid methyl ester(s)
GC/MS	Gas chromatography–mass spectrometry
MS	Mass spectrum (spectra)
NAP	<i>N</i> -Acyl pyrrolidide(s)
NMI	Non-methylene-interrupted
TLC	Thin layer chromatography

Introduction

Marine sponges are primitive invertebrates with a remarkable ability to adapt to environmental changes. Thus, they have given rise to intensive investigations into the basic lipid components of their cell membranes since the pioneer studies [1, 2]. The phospholipid fatty acid composition is important for the functions of the cell membranes [3, 4]. In addition, sponge phospholipid classes have also been examined [3–5]. Moreover, sponges have proved to be a rich source of many unusual sterols and fatty acids (FA). Common polyunsaturated FA from the n-6 and n-3 series, such as eicosapentanoic acid EPA and docosahexaenoic acid DHA, are quite rare in sponge phospholipids, that instead usually contain very long-chain (C_{22} – C_{34}) non-methylene-interrupted (NMI) FA including the particular unsaturation pattern $\Delta 5,9$ [3, 4, 6–11].

Sponges from the genus *Polymastia* are known to contain secondary metabolites with biological activity but there have been, in comparison, few investigations of

C. Denis · G. Wielgosz-Collin · A. Bretéché · N. Ruiz ·
V. Rabesaotra · J.-M. Kornprobst · G. Barnathan (✉)
Groupe MMS (Mer, Molécules, Santé) EA 2160, Equipe Lipides
Marins, Faculté de Pharmacie, Pôle Mer et Littoral,
Université de Nantes, 2 rue de La Houssinière, BP 92208,
44322 Nantes Cedex 03, France
e-mail: Gilles.Barnathan@univ-nantes.fr

N. Boury-Esnault
UMR 6540 DIMAR, Centre d'Océanologie de Marseille, Station
Marine d'Endoume, CNRS-Université de la Méditerranée,
rue Batterie des Lions, 13007 Marseille, France

their primary metabolites such as FA and sterols to date. Thus, organic extracts of *Polymastia janeirensis* demonstrated in vitro cytotoxicity against HT29 colorectal tumor cell lines [12]. *Polymastia croceus* has been farmed in order to produce quantities of bioactive compounds of medicinal interest [13, 14]. *Polymastia penicillus* is usually found in the North Atlantic in shallow waters and to depths of 600 m [15, 16]. The phospholipids of *P. gleneni*, collected around the Glenan Islands (South Brittany, France) were shown to contain a unique series of saturated 2-acetoxy long chain FA ranging from C₂₂ to C₃₀ chains [17].

As part of our ongoing investigations of sponge lipids [11, 18, 19], we present here the phospholipid FA composition of *P. penicillus* and the identification of several new and unusual Δ 3, Δ 4, Δ 5 and Δ 13 unsaturated FA.

Materials and Methods

Sponge Material

Samples of *Polymastia penicillus* were collected by hand (scuba) at a depth of 17 m, in the Etel River, Gulf of Morbihan, Brittany, France, in June 2005. Sponge identification was determined according to the recent classification [20, 21], and voucher specimens were deposited in the Marine Station of Endoume, Marseille, France. Like all Polymastiidae, this sponge is encrusting, hemispherical and cushion shaped, always with numerous papillae, but is characterized by the absence of a collagenous layer and by the absence of spicules in internal laminae, and spicules are tylostyles [15, 16].

Extraction, Isolation and Analysis of Phospholipids

The collected specimens were immediately transported to the laboratory for immediate lipid extraction. The sponges were washed in seawater, carefully cleaned, cut in small pieces and steeped twice in dichloromethane/methanol (1:1, v/v) for 24 h at room temperature. The combined extracts yielded the crude total lipids. Total lipid content (wt.%) was determined as the ratio total lipids versus sum of sponge dried residue plus total lipids. Total lipids were rapidly subjected to lipid class separation. Phospholipids were separated from other lipids by column chromatography on silica gel (70–230 mesh) successively eluted with dichloromethane (neutral lipids), acetone (glycolipids) and methanol (phospholipids) [10, 11]. The phospholipid classes were investigated by thin-layer chromatography on silica gel 60F₂₅₄ plates (0.2 mm thickness, SDS Carlo Erba, Val de Reuil, France) and dichloromethane/methanol

(70:30, v/v) was the eluent with phospholipid standards purchased from Sigma (Saint-Quentin Fallavier, France).

Preparation of Fatty Acid Methyl Esters and *N*-Acyl Pyrrolidides

Fatty acid methyl esters (FAME) were obtained by phospholipid transmethylation (40 min under reflux with 5% methanolic hydrogen chloride). *N*-Acyl pyrrolidide derivatives (NAP) were prepared by direct treatment of the FAME with pyrrolidine/acetic acid (10:1, v/v) for 2 h under reflux and purified by TLC on 0.5 mm silica gel layers using hexane/diethyl ether (1:2, v/v) [10, 22–26].

Fourier Transform Infrared Spectroscopy

Infrared spectra were recorded by means of a Bruker Vector-22 Fourier transform infrared spectrometer (Bruker Spectrospin, Karlsruhe, Germany) on liquid films between NaCl plates. Spectra were collected over the wavenumber range 4,000 to 600 cm⁻¹.

Gas Chromatography–Mass Spectrometry Analyses

Gas chromatography–mass spectrometry (GC/MS) coupling experiments were performed on a Hewlett-Packard HP-5890 chromatograph linked to a HP-5989-A mass spectrometer (70 eV) equipped with a HP-9000-345 integrator, and using a 30 m × 0.32 mm i.d. fused silica capillary column coated with HP-1 (0.25 μm phase thickness). The carrier gas was helium. The temperatures of injector and source were held at 240 °C, and the temperature of the GC–MS interface was held at 290 °C.

The column temperature was programmed for FAME and NAP from 180 to 310 °C at 3 °C/min. Equivalent chain length (ECL) were determined for FAME and for NAP in some cases since the observed ECL values have proved to be very similar for both derivatives except for highly branched FA [25].

Mass spectral data for the novel fatty acid structures are presented below.

17-Methyl-13-octadecenoic acid methyl ester MS *m/z* (rel. int.) [M⁺] 310 (6.5), 279 (13.7), 227 (2.3), 211 (8.7), 194 (17.4), 185 (6.5), 171 (19.5), 152 (2.5), 139 (28.3), 125 (21.7), 111 (13.0), 97 (32.6), 95 (21.2), 87 (8.7), 83 (50.0), 81 (20.6), 74 (16.3), 69 (100), 55 (76.1), 43 (23.7), 41 (30.4).

17-Methyl-13-octadecenoic acid pyrrolidide MS *m/z* (rel. int.) [M⁺] 349 (16.1), 334 (4.5), 320 (1), 306 (5.4), 292 (4.5), 278 (3.4), 264 (4.5), 252 (2.7), 238 (2.7), 224 (4.5), 210 (3.6), 196 (3.4), 182 (3.6), 168 (4.5), 154 (1.8), 140

(3.6), 126 (23.8), 113 (100), 98 (11.6), 85 (4.5), 71 (9.8), 55 (9.8).

3,16-Docosadienoic acid methyl ester MS *m/z* (rel. int.) [M⁺] 350 (4.8), 337 (1.0), 319 (14.8), 304 (3.7), 290 (3.7), 276 (12.1), 261 (5.1), 247 (5.5), 191 (3.7), 171 (2.8), 163 (7.4), 150 (14.8), 135 (20.4), 123 (20.4), 115 (19.7), 109 (31.5), 95 (53.7), 87 (11.1), 81 (63.0), 71 (40.7), 69 (46.3), 67 (48.4), 55 (100), 43 (37.0), 41 (64.8).

3,16-Docosadienoic acid pyrrolidide MS *m/z* (rel. int.) [M⁺] 389 (32.2), 374 (2.5), 360 (4.1), 346 (4.2), 332 (11), 318 (19.5), 304 (7.6), 292 (5.1), 278 (3.4), 264 (7), 250 (6.8), 236 (6.8), 222 (10.2), 208 (11.9), 194 (8.5), 180 (4.2), 166 (8.5), 152 (61.9), 139 (13.6), 126 (30.5), 124 (9.3), 113 (100), 98 (30.5), 81 (8.5), 72 (30.5), 55 (8.5).

Results and Discussion

Total lipids accounted for 5.3% of the dried sponge residues after extraction. Total phospholipids of *P. penicillus* accounted for 29.6% of the total lipids. As determined by thin layer chromatography, the most abundant phospholipids were phosphatidylserine, phosphatidylcholine and phosphatidylinositol, while phosphatidylethanolamine occurred at a significant level and phosphatidylglycerol was present at a lower amount. Acid methanolysis provided a complex phospholipid FA mixture. Sixty fatty acids (FA) were identified by gas chromatography–mass spectrometry (GC/MS) of their methyl esters (FAME) and *N*-acyl pyrrolidides (NAP) as shown in Table 1.

Many of the FA reported in Table 1 were identified by comparing their equivalent chain lengths (ECL) and their mass spectra (MS) with those of known standards. Unsaturated FA, mainly monoenes and dienes, accounted for almost 61% of the FA mixture. The Fourier transform infrared spectrum of the whole phospholipid FAME showed absorption at 3,004 cm⁻¹ (=C–H stretching), strong peaks at 2,923 and 2,852 cm⁻¹ (C–H stretching), 1,743 cm⁻¹ (C=O stretching, ester), significant peaks at 1,465 cm⁻¹ (CH₂ scissors deformation) and 720 cm⁻¹ (CH₂ rocking/C=C *cis*), and displayed no absorption in the region 940–980 cm⁻¹ (C=C–H out-of-plane), indicating the absence of (*E*)-unsaturation [27]. Thus, double bonds in major unsaturated phospholipid FA from *P. penicillus*, such as those at more than 1% have the (*Z*) configuration. It should be noted that the Δ^{5,9} FA have been generally reported to have the (*Z*) configuration [3, 4].

Five long-chain dimethylacetal derivatives occurred as minor compounds in the phospholipid FA mixture. All their MS displayed the fragmentation ion *m/z* 75 ([CH₃O)₂–CH]⁺ as the base peak, and a appreciable [M–MeO]⁺ ion [26, 28]. Unfortunately, complete identification

Table 1 Phospholipid fatty acids identified from the sponge *Poly-mastia penicillus*

Fatty acid (symbol)	ECL ¹ (HP-1)	Abundance (wt%)
Saturated fatty acids (SFA)		
Dodecanoic (12:0)	12.00	0.6
Tetradecanoic (14:0)	14.00	1.3
10-Methyltetradecanoic (br-15:0)	14.58	2.7
13-Methyltetradecanoic (<i>i</i> -15:0)	14.60	0.4
Pentadecanoic (15:0)	15.00	0.3
12-Methylpentadecanoic (br-16:0)	15.52	2.1
14-Methylpentadecanoic (<i>i</i> -16:0)	15.62	0.6
Hexadecanoic (16:0)	16.00	4.3
15-Methylhexadecanoic (<i>i</i> -17:0)	16.60	1.2
14-Methylhexadecanoic (<i>ai</i> -17:0)	16.71	1.8
Heptadecanoic (17:0)	17.00	0.2
Octadecanoic (18:0)	18.00	2.6
15-Methylnonadecanoic (br-20:0)	19.60	0.6
18-Methylnonadecanoic (<i>i</i> -20:0)	19.66	0.5
17-Methylnonadecanoic (<i>ai</i> -20:0)	19.72	0.3
Eicosanoic (20:0)	20.00	1.0
19-Methyleicosanoic (<i>i</i> -21:0)	20.63	0.6
Tricosanoic (23:0)	23.00	0.5
Hexacosanoic (26:0)	26.00	0.6
Total SFA: 32.2%		
2-Hydroxy fatty acids (HFA)		
2-Hydroxytetracosanoic (2-OH-24:0)	25.23	3.4
2-Hydroxypentacosanoic (2-OH-25:0)	26.22	0.8
2-Hydroxyhexacosanoic (2-OH-26:0)	27.14	2.8
Total HFA: 7.0%		
Monounsaturated fatty acids (MFA)		
13-Methyl-4-tetradecenoic (<i>i</i> -15:1)	14.28	0.4
(<i>Z</i>)-9-Hexadecenoic (16:1)	15.65	1.6
15-Methyl-5-hexadecenoic (<i>i</i> -17:1)	16.28	0.7
14-Methyl-5-hexadecenoic (<i>ai</i> -17:1)	16.40	0.4
(<i>Z</i>)-9-Heptadecenoic (17:1)	16.81	1.0
5-Octadecenoic (18:1)	17.49	0.6
(<i>Z</i>)-11-Octadecenoic (18:1)	17.82	12.7
17-Methyl-13-octadecenoic (<i>i</i> -19:1) ²	18.21	0.8
9-Nonadecenoic (19:1)	18.70	0.8
12-Nonadecenoic (19:1)	18.82	0.6
11-Eicosenoic (20:1)	19.76	0.5
13-Eicosenoic (20:1)	19.82	0.4
x ₁ -Heneicosenoic (21:1)	20.80	0.6
x ₂ -Heneicosenoic (21:1)	20.84	0.4
(<i>Z</i>)-15-Docosenoic (22:1)	21.87	13.4
16-Tetracosenoic (23:1)	22.82	0.3
(<i>Z</i>)-15-Tetracosenoic (24:1)	23.62	1.7
(<i>Z</i>)-17-Tetracosenoic (24:1)	23.81	1.5
19-Tetracosenoic (24:1)	23.88	0.7
(<i>Z</i>)-17-Hexacosenoic (26:1)	25.61	2.3

Table 1 continued

Fatty acid (symbol)	ECL ¹ (HP-1)	Abundance (wt%)
Total MFA: 41.4%		
Diunsaturated fatty acids (DFA)		
(5Z,9Z)-5,9-Octadecadienoic (18:2)	17.40	1.4
(9Z,12Z)-9,12-Octadecadienoic (18:2)	17.62	0.8
(5Z,9Z)-5,9-Eicosadienoic (20:2)	19.39	0.3
11,15-Eicosadienoic (20:2)	19.60	0.4
3,16-Docosadienoic (22:2) ²	21.55	1.1
(5Z,9Z)-5,9-Tetracosadienoic (24:2)	23.44	0.9
(5Z,9Z)-5,9-Pentacosadienoic (25:2)	24.50	0.7
(5Z,9Z)-5,9-Hexacosadienoic (26:2)	25.52	13.3
Total DFA: 18.9%		

Identified minor (<0.2%) fatty acids: *i*-14:0 (13.64), 10-Me-16:0 (16.52), 13-Me-16:0 (16.56), 14-Me-17:0 (17.55), Phytanic (17.74), 15-20:1 (19.88), 23:0 (23.00), 5,9,*x*-25:3 (24.20), br-5,9-25:2 (24.22), 5,9-27:2 (26.48)

¹ FAME

² Not previously found in nature

of these derivatives failed due to their very small amounts and that they were co-eluted with other compounds. It is known that they are obtained from particular phospholipids named plasmalogens (1-*O*-alk-1'-enyl-2-acyl-glycerophospholipids) of great biological interest, and were found in some sponges [29, 30]. Dimethylacetals are produced from fatty aldehydes, which are liberated from plasmalogen vinyl ether bonds on methanolic acid hydrolysis.

Saturated Fatty Acids

Twenty-five saturated FA of Table 1 were identified accounting for more than 32% of the total FA, including fourteen monobranched ones from C₁₄ to C₂₁ (almost 11%).

The highly branched phytanic acid present as trace was readily identified as methyl ester with an ECL value of 17.74 and diagnostic fragmentation ions including the molecular ion at *m/z* 326 and a base peak at *m/z* 101 (C-3 methyl branching), as previously described [25, 26]. It was the sole isoprenoid FA identified in the present mixture.

As usually, *iso*- and *anteiso*-branched FA were identified as FAME and NAP from their ECL values and their MS typical of saturated FA (*m/z* 74 base peak, McLafferty, *m/z* 87). The MS of their NAP displayed the corresponding molecular ion and a diminished peak for the ions [M-CH₃-CH₂]⁺ and [M-CH₃-2CH₂]⁺, respectively [10, 18, 19, 22, 24].

In addition to the *iso*- and *anteiso*-branched FA, seven various monomethyl-branched FA occurred in phospholipids of *P. penicillus*. Six of them with short-chains were

detected as FAME from their ECL values of 14.58, 15.52, 16.52, 16.56, 17.55 and 19.60, respectively, and from their MS that exhibited molecular ions at *m/z* 256, 270, 284 (two compounds) and 326, respectively. Thus, we dealt with branched pentadecanoic, hexadecanoic, heptadecanoic, eicosanoic acid structures. The MS of the 15:0 pyrrolidide showed a very low fragmentation ion at *m/z* 224 (C₁₀ fragment) and enhanced peaks at *m/z* 210 and 238 indicating a methyl branch at C-10 [10, 22, 24]. Thus, the unusual 10-methyltetradecanoic acid was identified. Another branched 17:0 acid was identified as FAME and as NAP. As FAME its MS showed the molecular ion at *m/z* 284 and an expected ion at *m/z* 227 of very low intensity, while the ions at *m/z* 213 and 241 were highly enhanced (methyl branch at C-13) [24, 29]. The branched 17:0 acid was then identified (FAME) as 13-methylhexadecanoic acid and this structure was confirmed by the MS of the NAP which showed a molecular ion at *m/z* 323. The expected ion *m/z* 266 was lacking, while the ions at *m/z* 252 and *m/z* 280 were highly enhanced (methyl branching at C-13). Mass spectra of NAP of 13-methyl- and 15-methyl-branched saturated FA were shown in a recent report [29]. The quite unusual 12-methylpentadecanoic, 14-methylheptadecanoic and 15-methylnonadecanoic acids were characterized as methyl esters since their MS showed the molecular ions at *m/z* 270, 298 and 326 (16:0, 18:0 and 20:0 structures) [24, 29]. Among these FA, the branched 20:0 acid (FAME) was identified as 15-methylnonadecanoic acid since the expected ion at *m/z* 255 was lacking, while the ions at *m/z* 241 and 269 were present (methyl branch at C-14) [22, 29].

Iso- and *anteiso* FA are typical for the occurrence of bacteria and the other monomethyl-branched short-chain FA probably have the same origin [31–34], although one of the most frequent bacterial phospholipids, namely phosphatidylglycerol, accounted here for a relatively low percentage [3, 4]. Branched-chain FA (*iso* and *anteiso*) are characteristic for gram-positive bacteria [34]. The 13-methylhexadecanoic acid was described in previous reports [22, 29]. Branched saturated FA (C₁₅–C₁₉) have been used as biomarkers for bacteria including anaerobic bacteria and the sulfate-reducing bacteria [33–37]. The 10-methyl-14:0, 10-methyl-15:0 and 10-methyl-16:0 acids were found in bacteria [33–35], and it was assumed that methyl branching on the tenth carbon atom in the acyl chain seems specific for actinomycetes [33, 38]. The 10-methylhexadecanoic acid was observed in a *Cinachyrella* sponge [10] and in a pioneering report on the sponge *Aplysina fistularis* [4]. The occurrence of bacteria in sponges has already been evidenced and studied in several reports [39, 40].

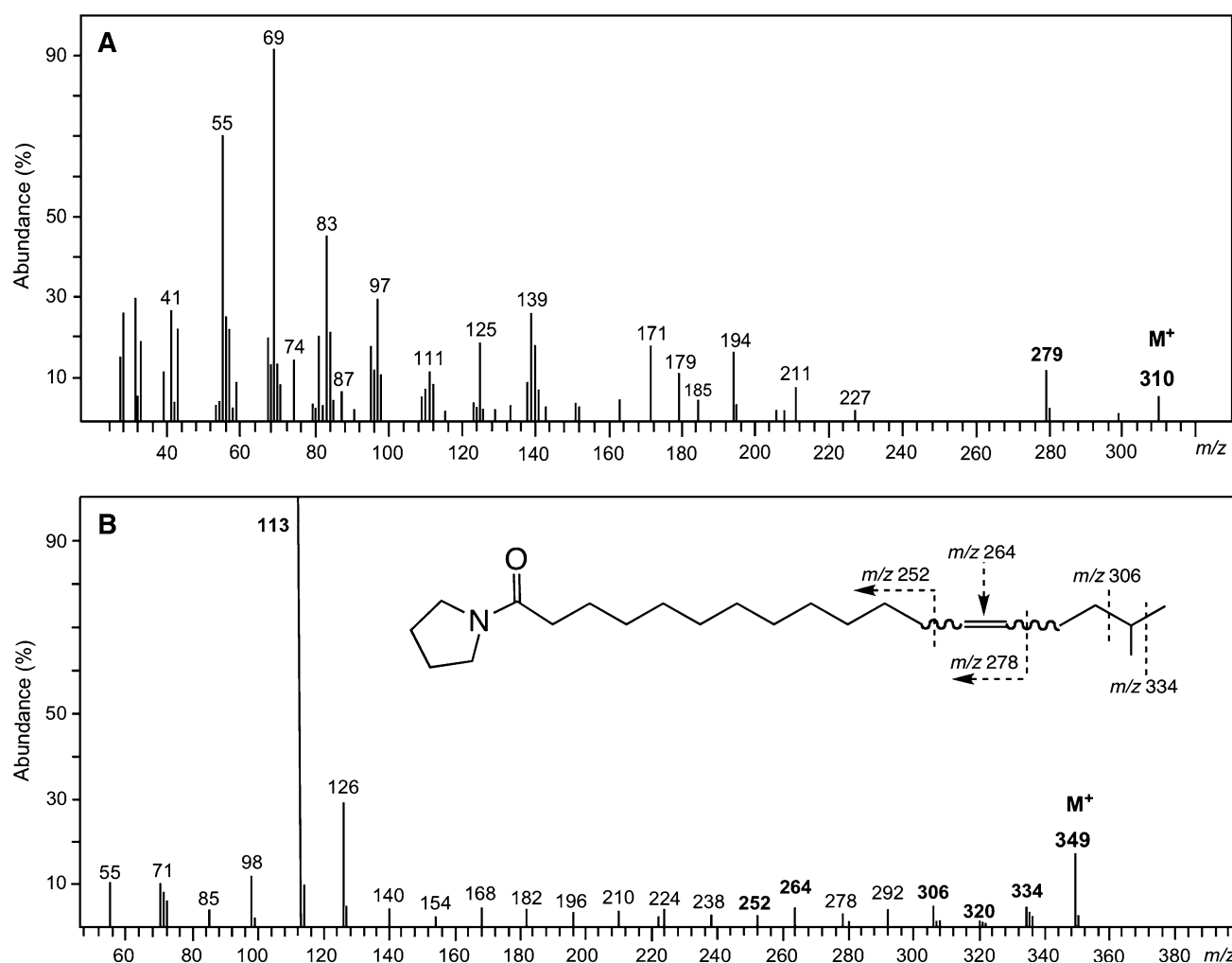


Fig. 1 Mass spectra of methyl ester (a) and pyrrolidide derivative (b) of 17-methyl-13 octadecenoic acid from *Polymastia penicillus*

2-Hydroxylated Fatty Acids

Three 2-hydroxylated FA (7.0% of FA mixture; C₂₄, C₂₅ and C₂₆) were readily identified by GC/MS as FAME since their MS displayed diagnostic fragmentation ions at *m/z* 90 (McLafferty) and 103, and the corresponding molecular ions at *m/z* 398, 412 and 426, respectively. Diagnostic ions of 2-hydroxy acids have been described in previous reports such as those on series of 2-hydroxylated FA found in two sponges of the family Suberitidae [29] and in two Caribbean sponges [31]. The M⁺ and *m/z* 90 and 103 ions were accompanied by the corresponding related ions [M–MeOH]⁺ at *m/z* 366, *m/z* 380 and *m/z* 394, respectively, and [M–COOMe]⁺ at *m/z* 339, *m/z* 353 and *m/z* 367, respectively. Mass spectra of NAP derivatives showed the corresponding molecular ions and the major ions at *m/z* 129 (McLafferty, base peak), *m/z* 113, *m/z* 100 and *m/z* 98, thus confirming the hydroxylated structures.

Monounsaturated Fatty Acids

Twenty-one monounsaturated FA listed in Table 1 were identified, accounting for more than 41% of the total FA, including four *iso*- and *anteiso*-branched FA. Three unusual short-chain monoenoic acids were readily identified in phospholipids of *P. penicillus*.

A short-chain acid was readily identified as a branched pentadecenoic acid (0.4%; ECL 14.28) since its NAP displayed a molecular ion at *m/z* 293 (15:1), and major fragment ions at *m/z* 126 and *m/z* 152, a peak at *m/z* 138 of low intensity, a very intense peak at *m/z* 166 (almost 70% of the base peak *m/z* 113; Δ4), and lacking the expected *m/z* 264, the ions at *m/z* 250 and *m/z* 278 being enhanced. Thus, we identified the *iso*-4-pentadecenoic acid, which was early observed in phospholipids from *Suberites massa* [29]. In addition, some examples of MS of NAP of Δ4 FA are shown in Christie's homepage "www.lipidlibrary.co.uk"

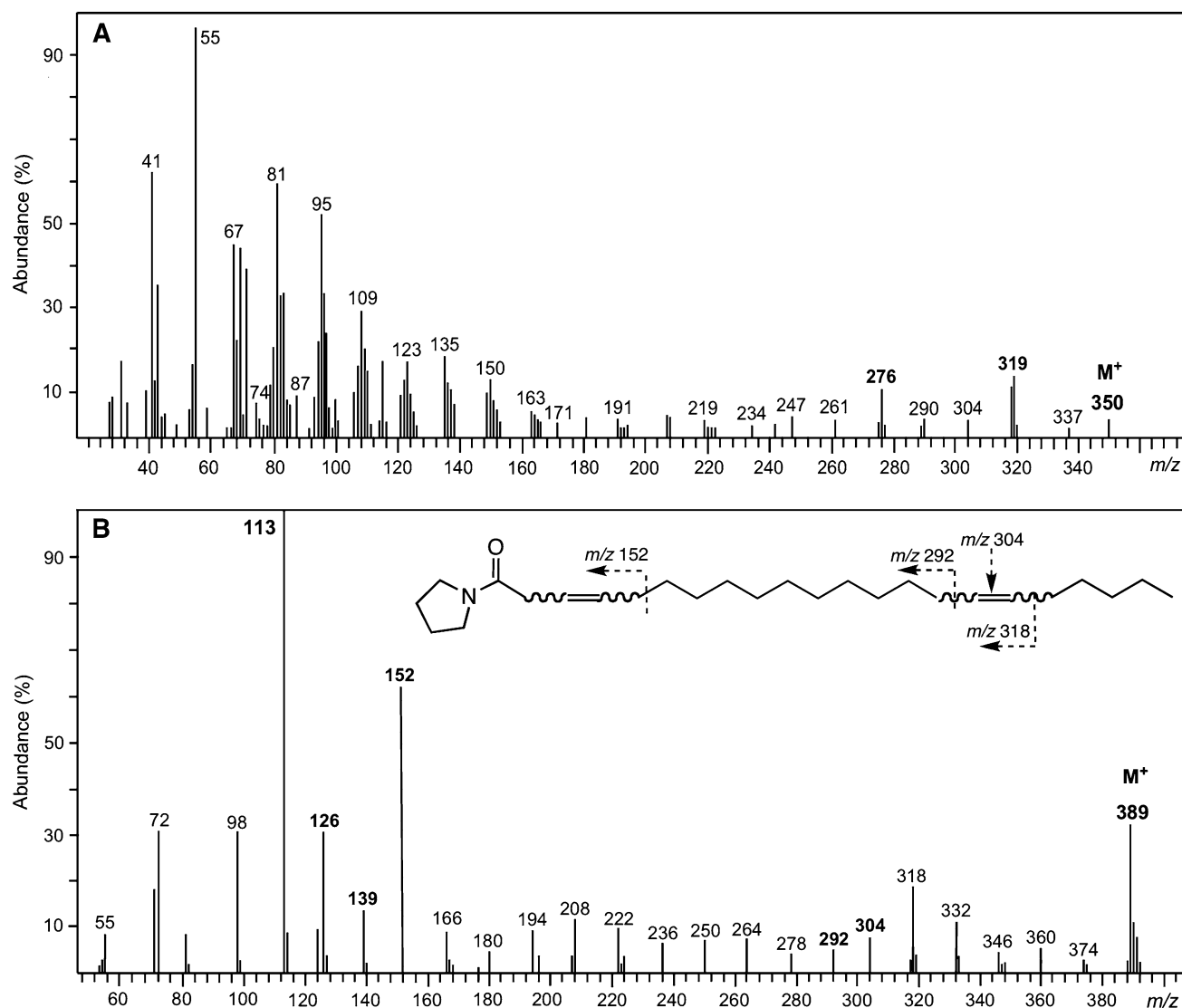


Fig. 2 Mass spectra of methyl ester (a) and pyrrolidide derivative (b) of 3,16-docosadienoic acid from *Polymastia penicillus*

[23, 24, 26]. Another $\Delta 4$ monounsaturated FA occurred in the freshwater sponge *Baicalospongia bacilifera*, namely *iso*-4-octadecenoic acid [41]. The latter sponge also contained $\Delta 5$ FA as shown with the use of the iodolactonization method [41].

Two closely related FA were identified as monounsaturated and monomethyl-branched FA since their MS showed a molecular ion (as FAME) at m/z 282, and that their ECL values were 16.28 and 16.40. Mass spectra of their NAP showed the expected molecular ion at m/z 321 and a gap of 12 amu between an appreciable m/z 140 and 152, while the ion at m/z 166 was enhanced, indicative of $\Delta 5$ unsaturation. The first br-17:1 acid was identified as 15-methylhexadecenoic (*iso*-17:1) acid because of the low relative intensity of the fragment ion at m/z 294 (C_{15}), while the ions at m/z 278 (C_{14}) and 306 (C_{16} ; M- CH_3) were enhanced. The second br-17:1 acid was identified as

14-methylhexadecenoic (*anteiso*-17:1) acid due to the low relative intensity of the fragment ion at m/z 278 (C_{14}), while the ions at m/z 264 (C_{13}) and 292 (C_{15}) were enhanced. Thus, we characterized two not-so-common FA, namely 15-methyl-5-hexadecenoic and 14-methyl-5-hexadecenoic acids. These *iso* and *anteiso* monounsaturated $\Delta 4$ or $\Delta 5$ FA probably originated from associated bacteria. Present at low growth temperatures in bacteria from the genera *Bacillus*, *Brevibacter* and *Streptomyces*, the *iso*- $\Delta 5$ -hexadecenoic, *anteiso*- $\Delta 5$ -pentadecenoic and *anteiso*- $\Delta 5$ -heptadecenoic acids were identified as methyl esters [42].

Another branched monoenoic FA was detected by GC-MS as FAME and characterized as NAP (Fig. 1).

This acid (FAME) showed a molecular ion at m/z 310, and a (M- CH_3O)⁺ at m/z 279, corresponding to a 19:1 acid structure, and an ECL value of 18.21, implying methyl branching (Fig. 1a). The usual peaks for FA methyl esters

at m/z 74 and m/z 87 were present as minor fragment ions. Other abundant fragments were not relevant for the characterization of structure. The molecular ion peak of the corresponding NAP was present at m/z 349 confirming the 19:1 structure (Fig. 1b). The gap of 12 amu between homologous fragment ions at m/z 252 (C_{12}) and m/z 264 (C_{13}) indicated $\Delta 13$ unsaturation. A diminished peak at m/z 320 (C_{17}) flanked by an elevated peak at m/z 306 (C_{16}), and an appreciable peak at m/z 334 (C_{18}), indicated a methyl branch at C-17. Thus, we identified the new 17-methyl-13-octadecenoic acid, which to our knowledge, has not been reported from any natural source.

Diunsaturated Fatty Acids

Ten dienoic FA were identified accounting for about 19% and including the 9,12-octadecadienoic acid (0.8%), a series of eight FA possessing the 5,9-unsaturation pattern common in sponges, and two other interesting NMI FA.

The FA with the 5(*Z*),9(*Z*)-unsaturation, ranged from C_{18} to C_{27} , were readily characterized by GC–MS. Mass spectra of all their methyl esters displayed the corresponding molecular ion and the ion at m/z 81 (base peak), while spectra of their NAP displayed a significant ion at m/z 180 arising from the activated double allylic cleavage. Mass spectra of both derivatives showed corresponding molecular ions. They had been already found in sponges [4, 6–11, 18, 19, 26, 29, 31, 32]. It is now well known that lipids of most sponge species contain various $\Delta 5$ olefinic FA mainly including $\Delta 5,9$ FA. Interestingly, $\Delta 5,9$ FA displayed antiprotozoal activity, antitumor activity, and topoisomerase I inhibitory activity [43, 44]. Only one triunsaturated FA occurred as a minor component in the FA mixture and was identified as 5,9,*x*-pentacosatrienoic acid since its methyl ester (ECL of 24.20) showed the molecular ion at m/z 390 and the base peak at m/z 81.

A first additional NMI FA (0.3%) had an ECL value of 19.60 as methyl ester and a molecular ion at m/z 322 indicative of a 20:2 acid structure. The MS of the NAP showed a molecular ion at m/z 361 (20:2 acid structure). The two double bonds were located by the 12 amu differences between the peaks at m/z 224 (C_{10}) and m/z 236 (C_{11}), indicating of $\Delta 11$ unsaturation, and between the peaks at m/z 278 (C_{14}) and m/z 290 (C_{15}), indicating $\Delta 15$ unsaturation. Thus, we dealt with the rare 11,15-eicosadienoic acid, which was firstly reported from the sponge *Amphimedon complanata* [45] and observed in *Stylissa carteri* [19]. This FA has been considered as a biosynthetic intermediate of the unusual dienoic FA 17,21-hexacosadienoic and 19,23-octacosadienoic acids [10].

The second interesting dienoic NMI FA (1.1%) as a methyl ester had an ECL value of 21.55 and a molecular ion at m/z 350, and elevated ions at m/z 319 ($[M-74]^+$) and

m/z 276 ($[M-31]^+$), indicative of a 22:2 acid structure (Fig. 2a).

The usual peaks for FA methyl esters at m/z 74 and m/z 87 were present as minor fragment ions. The relatively abundant ions at m/z 304 (C_{16}), m/z 290 (C_{15}), and m/z 276 (C_{14}) confirmed a 22:2 FA structure. The MS of the NAP showed a molecular ion at m/z 389 (22:2 structure) (Fig. 2b). A first double bond was readily located by the 12 amu gap between the peaks at m/z 292 (C_{15}) and m/z 304 (C_{16}), indicating of $\Delta 16$ unsaturation. The second double bond was located with the sequence of m/z 113 (base peak), m/z 126, m/z 139, m/z 152 (the second-most prominent ion at more than 60% of the relative intensity) and m/z 166, indicating a $\Delta 3$ unsaturation according to Andersson [23, 24]. It should be noted that the ion at m/z 152 was the second-most prominent ion in the MS of the NAP of the novel 3(*Z*),9(*Z*),12(*Z*)-octadecatrienoic acid that also exhibited the two appreciable m/z 126 and m/z 139 [26, 46]. Also available on the Christie's homepage, MS of the NAP of the 3(*E*),9(*Z*)-octadecadienoic acid allows another useful comparison [26]. Indeed, the m/z 152 ion is also the second-most prominent ion but there is a prominent ion at m/z 124 suggesting a probable isomerization to 2,9-18:2 during the derivatization step. Thus, MS of the NAP of 2,6-18:2 shows intense ions at m/z 124 without the m/z 126, and at m/z 139 (base peak) [26]. In addition, MS of 2-16:1 and 2-18:1 show similar features with a major ion at m/z 152, a prominent ion at m/z 124 and a minor ion at m/z 126 [26].

In the MS of the 22:2 (NAP), from *P. penicillus*, the ion at m/z 126 is intense in accordance with a $\Delta 3$ double bond. Nevertheless, the presence of the ion at m/z 124 with a lower intensity than the ion at m/z 126 in the SM depicted in Fig. 2 suggested a possible partial isomerization $\Delta 3$ to $\Delta 2$ [26]. Thus, we identified the new 3,16-docosadienoic acid, which to our knowledge, has not been reported from any natural source.

In summary, phospholipids from the sponge *P. penicillus* contained a lot of monomethyl-branched monoenoic FA, several $\Delta 5,9$ FA, and two novel FA, namely 17-methyl-13-octadecenoic and 3,16-docosadienoic.

Acknowledgments We express our thanks to scientists from the MMS research group (EA 2160, University of Nantes), Prof. Jean-François Biard and Dr. Karina E. Petit, for their help in collecting specimens of *P. penicillus*, and Mr. Denis Loquet for his help for additional GC/MS measurements. Mrs. Maryvonne Luçon, Faculty of Sciences and Techniques of Nantes, Department of Chemistry, is greatly acknowledged for FTIR measurements.

References

1. Litchfield C, Morales RW (1976) Are Demospongiae membranes unique among living organisms? In: Harrison FW, Cowden RR

- (eds) Aspects of sponge biology. Academic Press, New York, pp 183–200
2. Litchfield C, Greenberg AJ, Noto G, Morales RW (1976) Unusually high levels of C₂₄–C₃₀ fatty acids in sponges of the class Demospongiae. *Lipids* 11:567–570
 3. Djerassi C, Lam WK (1991) Sponge phospholipids. *Acc Chem Res* 24:69–75
 4. Walkup RD, Jamieson GC, Ratcliff MR, Djerassi C (1981) Phospholipid studies of marine organisms: 2. Phospholipid-bound fatty acids and free sterols of the sponge *Aplysina fistularis* (Pallas) *forma fulva* (= *Verongia thiona*). Isolation and structure elucidation of unprecedented branched fatty acids. *Lipids* 16:631–646
 5. Genin E, Wielgosz-Collin G, Njinkoué JM, Kornprobst JM, Vacelet J, Barnathan G (2008) New trends of phospholipid class composition in marine sponges. *Comp Biochem Physiol B* 150:427–431
 6. Carballeira NM, Reyes ED (1990) Identification of the new 23-methyl-5, 9-pentacosadienoic acid in the sponge *Cribochalina vasculum*. *Lipids* 25:69–71
 7. Carballeira NM, Reyes ED, Shalabi F (1993) Identification of novel iso/anteiso nonacosadienoic acids from the phospholipids of the sponges *Chondrosia remiformis* and *Myrmekioderma styx*. *J Nat Prod* 56:1850–1855
 8. Barnathan G, Mirallès J, Gaydou EM, Boury-Esnault N, Kornprobst JM (1992) New phospholipid fatty acids from the marine sponge *Cinachyrella alloclada* Ulicza. *Lipids* 27:779–784
 9. Barnathan G, Doumenq P, Njinkoué JM, Debitus C, Levi C, Kornprobst JM (1994) Sponge fatty acids-3. Occurrence of complete series of n-7 monoenoic and iso-5,9 dienoic long-chain phospholipid fatty acids in the marine sponge *Cinachyrella* aff. *schulzei*. *Lipids* 29:297–303
 10. Barnathan G, Kornprobst JM, Doumenq P, Mirallès J (1996) Sponge new unsaturated long-chain fatty acids in the phospholipids from the Axinellida sponges *Trikenrion loeve* and *Pseudaxinella* cf. *lunaecharta*. *Lipids* 31:193–200
 11. Barnathan G, Genin E, Velosaotsy NE, Kornprobst JM, Al-Lihaibi S, Al-Sofyani A, Nongonierma R (2003) Phospholipid fatty acids and sterols of two *Cinachyrella* sponges from the Saudi Arabian Red Sea: comparison with *Cinachyrella* species from other origins. *Comp Biochem Physiol B* 135:297–308
 12. Monks NR, Lerner C, Henriques AT, Farias FM, Schapoval EES, Suyenaga ES, da Rocha AB, Schwartzmann G, Mothes B (2002) Anticancer, antichemotactic and antimicrobial activities of marine sponges collected off the coast of Santa Catarina, southern Brazil. *J Exper Mar Biol Ecol* 281:1–12
 13. Duckworth AR, Battershill CN (2003) Developing farming structures for production of biologically active sponge metabolites. *Aquaculture* 217:139–156
 14. Duckworth AR, Battershill CN, Schiel DR (2004) Effects of depth and water flow on growth, survival and bioactivity of two temperate sponges cultured in different seasons. *Aquaculture* 242:237–250
 15. Boury-Esnault N (1987) The *Polymastia* species (Demosponges, Hadromerida) of the Atlantic area. In: Vacelet J, Boury-Esnault N (eds) *Taxonomy of Porifera NATO*, vol G13. ASI Series Springer, Berlin, pp 29–66
 16. Plotkin A, Boury-Esnault N (2004) Alleged cosmopolitanism in sponges: the example of a common Arctic *Polymastia* (Porifera, Demospongiae, Hadromerida). *Zoosystema* 28:13–20
 17. Ayanoglu E, Kurtz K, Kornprobst JM, Djerassi C (1985) New natural 2-acetoxy fatty acids using chemical ionization and electron impact mass spectrometry. *Lipids* 20:141–144
 18. Barnathan G, Kornprobst JM (2000) Fatty acids from marine organisms: recent research developments. In: Baudimant G, Guezennec J, Roy P, Samain JF (eds) *Marine Lipids*. IFREMER Press, Brest, pp 35–43
 19. Velosaotsy NE, Genin E, Nongonierma R, Al-Lihaibi S, Kornprobst JM, Vacelet J, Barnathan G (2004) Phospholipid distribution and phospholipid fatty acids in four Saudi Red Sea sponges. *Boll Mus Ist Biol Univ Genova* 68:639–645
 20. Hooper JNA, van Soest RWM (2002) *Systema Porifera*. A guide to the classification of sponges, vol. 2. Kluwer/Plenum, New York, 1708 pp
 21. Boury-Esnault N (2002) Family Polymastiidae Gray, 1867. In: Hooper JNA, van Soest RWM (eds) *Systema Porifera*. A guide to the classification of sponges. Kluwer/Plenum, New York, pp 201–219
 22. Andersson BÅ, Holman RT (1975) Mass spectrometric localization of methyl branching in fatty acids using acylpyrrolidines. *Lipids* 10:716–718
 23. Andersson BÅ, Holman RT (1974) Pyrrolidides for mass spectrometric determination of the position of the double bond in monounsaturated fatty acids. *Lipids* 9:185–190
 24. Andersson B (1978) Mass spectrometry of fatty acid pyrrolidides. *Progr Chem Fats Lipids* 16:279–308
 25. Mirallès J, Barnathan G, Galonnier R, Sall T, Samb A, Gaydou EM, Kornprobst JM (1995) New branched-chain fatty acids from the Senegalese Gorgonian *Leptogorgia piccola* (white and yellow morphs). *Lipids* 30:459–466
 26. Christie WW The lipid library. www.lipidlibrary.co.uk, section updated 07.05.08
 27. Albuquerque MLS, Guedes I, Alcantara P Jr, Moreira SC (2003) Infrared absorption spectra of Burity (*Mauritia flexuosa* L.) oil. *Vibr Spectrosc* 33:127–131
 28. Christiansen K, Mahadevan V, Viswanathan CV, Holman RT (1969) Mass spectrometry of long-chain aldehydes, dimethyl acetals and alk-1-enyl ethers. *Lipids* 4:421–427
 29. Barnathan G, Kornprobst JM, Doumenq P, Mirallès J, Boury-Esnault N (1993) Sponge fatty acids. 5. Characterization of complete series of 2-hydroxy long-chain fatty acids in phospholipids of two Senegalese marine sponges from the family Suberitidae: *Pseudosuberites* sp. and *Suberites massa*. *J Nat Prod* 56:2104–2113
 30. Nagan N, Zoeller RA (2001) Plasmalogens: biosynthesis and functions. *Prog Lipid Res* 40:199–229
 31. Carballeira NM, Shalabi F, Negron V (1989) 2-Hydroxy fatty acids from marine sponges 2. The phospholipid fatty acids of the Caribbean sponges *Verongula gigantea* and *Aplysina archeri*. *Lipids* 24:229–232
 32. Nechev J, Christie WW, Robain R, de Diego F, Popov S (2004) Chemical composition of the sponge *Hymeniacion sanguinea* from the Canary Islands. *Comp Biochem Physiol A* 137:365–374
 33. Ratledge C, Wilkinson G (1988) *Microbial lipids*. Academic Press, London, 963 pp
 34. Kaneda T (1991) Iso- and anteiso-fatty acids in bacteria; biosynthesis, function, and taxonomic significance. *Microbiol Rev* 55:288–302
 35. Cronan JE (2003) Bacterial membrane lipids: where do we stand? *Annu Rev Microbiol* 57:203–224
 36. Haack SK, Garchow H, Odelson DA, Forney LJ, Klug MJ (1994) Accuracy, reproducibility, and interpretation of fatty acid methyl ester profiles of model bacterial communities. *Appl Environ Microbiol* 60:2483–2493
 37. Cravo-Laureau C, Hirschler-Réa A, Matheron R, Grossi V (2004) Growth and cellular fatty-acid composition of a sulphate-reducing bacterium, *Desulfatibacillum aliphaticivorans* strain CV2803T, grown on n-alkenes. *C R Biologies* 327:687–694
 38. Saddler GS, O'Donnel AG, Goodfellow M, Minnikin DE (1987) SIMCA pattern recognition on the analysis of streptomycete fatty acids. *J Gen Microbiol* 133:1137–1147

39. Vacelet J (1975) Etude en microscopie électronique de l'association entre bactéries et Spongiaires du genre *Verongia* (Dictyoceratida). *J Microsc Biol Cell* 3:271–288
40. Gillan FT, Stoilov IL, Thompson JE, Hogg RW, Wilkinson CR, Djerassi C (1988) Fatty acids as biological markers for bacterial symbionts in sponges. *Lipids* 23:1139–1145
41. Imbs AB, Latyshev NA (1998) New $\Delta 5$ and $\Delta 4$ unsaturated medium- and long-chain fatty acids in the freshwater sponge *Baicalospongia bacilifera*. *Chem Phys Lipids* 92:117–125
42. Suutari M, Laasko S (1993) Signature GLC-MS ions in identification of $\Delta 5$ - and $\Delta 9$ -unsaturated *iso*- and *anteiso*-branched fatty acids. *J Microbiol Methods* 17:39–48
43. Bergé JP, Barnathan G (2005) Recent advances in fatty acids from lipids of marine organisms: molecular biodiversity, roles as biomarkers, biologically-active compounds and economical aspects. In: Le Gal Y, Ulber R (eds) *Marine Biotechnology*. *Adv Biochem Eng Biotechnol* 96:49–125
44. Carballeira NM (2008) New advances in fatty acids as antimalarial, antimycobacterial and antifungal agents. *Prog Lipid Res* 47:50–61
45. Carballeira NM, Restituyo J (1991) Identification of the new 11, 15-icosadienoic acid and related acids in the sponge *Amphimedon complanata*. *J Nat Prod* 54:315–317
46. Tsevegsuren N, Fujimoto K, Christie WW, Endo Y (2003) Occurrence of a novel *cis, cis, cis*-octadeca-3, 9, 12-trienoic (*Z,Z,Z*-octadeca-3,9,12-trienoic) acid in *Chrysanthemum (Tanacetum) zawadskii* Herb. (Compositae) seed oil. *Lipids* 38:573–578

Differences in Sterol Composition between Male and Female Gonads of Dominant Limpet Species

Hideki Kawashima · Masao Ohnishi ·
Satoshi Ogawa

Received: 14 February 2009 / Accepted: 25 April 2009 / Published online: 19 May 2009
© AOCS 2009

Abstract The present study demonstrated here for the first time that there are statistically significant differences in sterol composition between male and female gonads of the dominant limpets *Cellana grata* and *Cellana toreuma*, which are intertidal gastropods. Among 11 different sterols identified in this study, unusually high levels (11.2–19.8% of total sterols) of the Δ^8 -sterols 5 α -cholest-8-en-3 β -ol (zymostenol) and 5 α -cholesta-8,24-dien-3 β -ol (zymosterol), which have never been reported in aquatic invertebrate gonads, were present in only the male gonads.

Keywords *Cellana grata* · *Cellana toreuma* · Limpet gonad(s) · Zymostenol · Zymosterol

Abbreviations

GC–MS Gas chromatography–mass spectrometry
GC Gas chromatography
MS Mass spectrum
TMS Trimethylsilyl ether

H. Kawashima (✉)
Bioscience Laboratory, Miyako College,
Iwate Prefectural University, Miyako 027-0039, Japan
e-mail: ajoe@iwate-pu.ac.jp

M. Ohnishi
Department of Agriculture and Life Science,
Obihiro University of Agriculture and Veterinary Medicine,
Obihiro 080-8555, Japan

S. Ogawa
Department of Chemical Engineering, Faculty of Engineering,
Iwate University, Morioka 020-8551, Japan

Introduction

Our previous studies of male and female gonads of the dominant limpet species of intertidal gastropods are characterized by significant differences in their proportions of 16:0, 20:4n-6, and 20:5n-3 fatty acids and their composition of unusual nonmethylene-interrupted fatty acids, which differ widely in chain length and unsaturation [1, 2]. Furthermore, the female limpet gonads of *Cellana grata* had a wide range of unusual fatty acid isomers, including di-, tri-, tetra-, and pentaenoic fatty acids with a 5,9-double bond system in the triacylglycerols as one of the most usually abundant lipid classes [3, 4]. The previously observed sex-based differences in limpet gonad fatty acids stimulated us to characterize the sterols of these and other organs in limpets, although sterol composition has been reported from only whole bodies of the limpets *Lepetodrilus* spp. and *Patella vulgata* [5, 6]. Therefore, we characterized the occurrence and distribution of sterols in two representative dominant limpet species, *C. grata* and *C. toreuma*, which are widely distributed in northern Japan, using capillary GC and GC–MS, and further determined whether a sexual difference exists in the limpet gonads.

Experimental Procedures

Reagents

Most chemicals, cholesterol, desmosterol, and lathosterol were purchased from Sigma-Aldrich (St. Louis, MO, USA). Brassicasterol, 24-methylcholesterol, and sitosterol were kindly provided by Mr. K. Omata (Tama Biochemical Co. Ltd., Tokyo, Japan). Cholestanol, 24-methylenecholesterol,

and isofucosterol were prepared from the marine bivalve *Megangulus zyoensis* [7].

Sampling

The dominant limpets of the genus *Cellana*, *C. grata* and *C. toreuma*, were collected on intertidal rocky shores between June and August 2007. Specimens of *C. toreuma* ranging from 37.7 ± 0.6 ($n = 54$) mm in shell length and *C. grata* ranging from 39.2 ± 5.2 ($n = 54$) mm were collected from the coastal waters of Otsuchi and Funakoshi Bays, Iwate Prefecture, northern Japan.

Extraction of Lipids from Limpets

After collection, all limpets were immediately dissected in the laboratory. The gonads were distinguished as female or male by microscopic examination. The muscle, viscera, and gonads of males and females of each dominant limpet ($n = 54$) were dissected and separated. Each of group of muscles, viscera, or gonads (each of three pooled samples) was suspended in chloroform–methanol (2:1, v/v) and then homogenized for 1 min at 11,000 rpm by using an IKA Ultra Turrax[®] T25 Basic homogenizer (IKA Japan KK, Nara, Japan). Lipids were extracted by the method of Bligh and Dyer [8]. The different lipid classes were analyzed by thin-layer chromatography on silica gel 60 G plates (Merck, Darmstadt, Germany) as described previously [4, 9].

Preparation of Trimethylsilyl (TMS) Derivatives

Each sample of total lipids (2–5 mg) was saponified with 1.5 mL of 1.6 M KOH in 73% ethanol (v/v) at 90 °C for 1 h. After addition of 0.5 mL distilled water, the nonsaponifiables were extracted twice with 1.5 mL diethyl ether. The organic solvents were combined, dried over anhydrous sodium sulfate, filtered, and evaporated to dryness under a gentle stream of nitrogen at room temperature. The residue was converted to TMS derivatives of sterols by treatment with 0.3 mL of Sylon BFT, *N,O-bis* (trimethylsilyl) trifluoroacetamide containing 1% trimethylchlorosilane (v/v) (Supelco Inc., Bellefonte, PA, USA) at 80 °C for 1 h. The reaction mixture was evaporated under a gentle stream of nitrogen at 40 °C, and the derivatives were redissolved in 0.1 mL of *n*-hexane.

GC and GC–MS Analyses

The TMS derivatives of sterols were analyzed by GC using a Shimadzu GC-1700 chromatograph (Shimadzu Seisakusho Co., Kyoto, Japan) equipped with a flame ionization detector and an SACTM-5 capillary column (30 m × 0.25 mm i.d., 0.25 μm film thickness; Supelco Inc.). The injector and

detector temperatures were maintained at 290 °C, while the column temperature was isothermal at 270 °C for 30 min. The carrier gas was helium at a flow rate of 1.0 mL/min, and the injection split ratio was 1:36. GC–MS analyses of the TMS derivatives of sterols were performed in an electron impact mode at 70 eV with a scanning range 50–550 *m/z* using a Shimadzu GC-MS-QP2010 mass spectrometer (Shimadzu Seisakusho Co.) equipped with the same column used for in GC analysis. The column and injection temperatures were isothermal at 270 °C for 30 min, and the injection split ratio was 1:25. The carrier gas was helium at a flow rate of 1.0 mL/min, and pressure programming was used in a constant flow mode. Sterols were identified by comparison of their relative retention times, MS analysis of their free forms and TMS derivatives, published mass spectral data [10–12], and the Wiley Mass Spectral Library database (7th edition). All chromatographic analyses were performed within 48 h of sample preparation.

Statistical Analysis

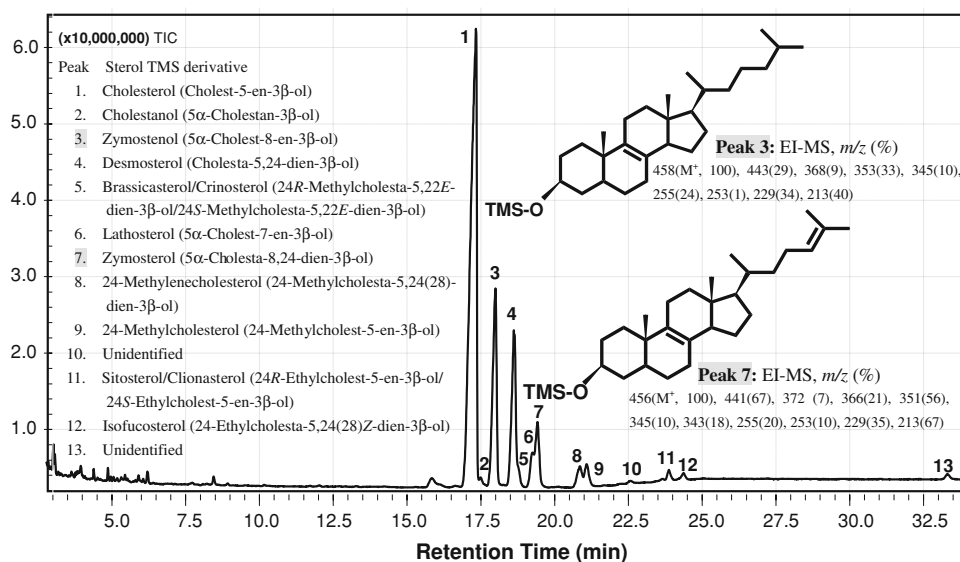
The procedures were repeated three times for three different sets of pooled male or female muscle, viscera, and gonads. Data are expressed as means ± SD. Statistical comparisons between sterols of male and female limpets were made using Student's *t*-test. A value of $P < 0.05$ was considered significant.

Results and Discussion

Of 11 different sterols identified in this study, the two Δ^8 -sterols 5α -cholest-8-en- 3β -ol (zymostenol) and 5α -cholesta-8,24-dien- 3β -ol (zymosterol), which have never been reported in aquatic invertebrate gonads, were found to be the major sterol components (Fig. 1). The prominent and characteristic molecular ions were *m/z* 458 for zymostenol ($[M]^+$) and *m/z* 456 for zymosterol ($[M]^+$), but neither of these sterols gave the cleavage of the fragment ion *m/z* 129 due to the presence of a Δ^5 double bond in the B-ring structure of seven sterols (Δ^5 -sterols) identified in this study [7]. Although the mass spectra of lathosterol and zymostenol are rather similar, the intensity of the fragment ion *m/z* 255 ($[M-TMSOH\text{-side chain}]^+$) of lathosterol was about three times as much as that of zymostenol, and their relative retention times to cholesterol were markedly different (Fig. 1). These results are in accord with published studies [10, 11].

Although no statistically significant difference in sterol composition was found between male and female muscles or male and female viscera in either of the dominant limpets *C. grata* and *C. toreuma*, there were statistically significant

Fig. 1 Total ion current chromatogram of the TMS derivatives of sterols in male limpet gonads of *C. grata*. The chromatogram was obtained on an SACTM-5 capillary column (30 m × 0.25 mm i.d., 0.25 μm film thickness) at 270 °C



differences between the levels of cholesterol and total Δ^5 -sterols in the male and female gonads of these limpets. In addition, there was also a statistically significant difference between the level of desmosterol in the male and female gonads in *C. toreuma*. In this study cholesterol was consistently the most abundant sterol in muscle, viscera, and gonad tissues, followed by desmosterol. However, high levels of zymostenol and zymosterol were present in only the male gonads of *C. grata* and *C. toreuma*, respectively, as shown in Table 1. The major sterols in the male limpet gonads of *C. grata* were cholesterol, desmosterol, and zymostenol, which were present at levels of 56.8, 15.3, and 15.0%, respectively, of total sterols. In contrast, the concentration of zymosterol as a major sterol, accounting for 9.0% of total sterols, in the male gonads of *C. toreuma* was nearly twice as high as that in *C. grata*, while that of zymostenol in the male gonads of *C. grata* was about eight times higher than in *C. toreuma*. The total sterol composition of whole bodies of *Patella vulgata* and *Lepetodrilus* spp. has been reported to contain the cholesterol levels of 79 and 90%, respectively. Although lathosterol was not found in *P. vulgata*, fucosterol and desmosterol accounted for 11 and 9%, respectively, of total sterols [5, 6]. In contrast, both desmosterol and lathosterol in *Lepetodrilus* spp. were less than 3% of total sterols, and fucosterol was not detected. In this study, a variety of unusual sterol components, including zymosterol and lathosterol, together with large amounts of cholesterol, desmosterol, and zymostenol, and other minor sterols, were found in the male gonads of *C. grata*, as compared with those of *C. toreuma*.

Interestingly, among the previously identified biologically active Δ^8 -sterols, zymosterol has also been reported to activate meiosis, which induced the maturation of rat oocytes and improved the formation of two-cell-preembryos in an in vitro maturation and fertilization mouse model [12–14],

although it has mainly been recognized as an important intermediate in ergosterol synthesis in both yeasts and fungi [15–18] and in cholesterol synthesis in mammalian cells [11, 19, 20]. However, the physiological function of zymostenol remains unclear. Cultures of human breast cancer cells, such as MCF-7 and MDA-MB-231, in the presence of tamoxifen, a selective estrogen-receptor modulator widely used for breast cancer treatment, or *N*-pyrrolidino-2-[4-(benzyl)-phenoxy]-ethanamine, a selective antiestrogen binding-site ligand that inhibits the growth of tumor cell lines in vitro and in vivo, produced massive accumulations of zymostenol as the most abundant sterol, together with minor amounts of zymosterol, desmosterol, and several other sterols [19]. This result suggests that the 3β -hydroxysterol- Δ^8 - Δ^7 -isomerase and 3β -hydroxysterol- Δ^7 -reductase involved in cholesterol biosynthesis were inhibited by these drugs [19]. In contrast, high levels of zymostenol (18% of total sterols) have been reported in cultures of a soil bacterium *Nannocystis exedens* Na e1 without any enzyme inhibitor [21], but both the major sterol components zymostenol and/or zymosterol and other sterols are most commonly present in *Nannocystis* strains that produce sterols [22].

Less is known about the biosynthesis of sterols by limpets than by marine bivalves [23–26]. The limpet *P. vulgata* is able to biosynthesize cholesterol *de novo* as well as produce cholesterol from phytosterols by a C-24 dealkylation process [6]. The results suggest that limpet gonads may be able to biosynthesize not only cholesterol but also the cholesterol precursors zymostenol and zymosterol detected in this study. Both the precursors may be biosynthesized by male limpet gonads rather than originating in their diets because these sterols were not detected in either muscle or viscera tissues of limpets. Although Δ^8 -sterols are converted into Δ^7 -sterols by 3β -hydroxysterol- Δ^8 - Δ^7 -isomerase, which is an essential enzyme on the sterol biosynthesis pathway in eukaryotes [16,

Table 1 Sterol compositions (% of total sterols) of different tissues of dominant limpets *C. grata* and *C. toreuma*

Sterol ^a	Muscle						Viscera						Gonads										
	<i>C. grata</i>			<i>C. toreuma</i>			<i>C. grata</i>			<i>C. toreuma</i>			<i>C. grata</i>			<i>C. toreuma</i>							
	Male	Female	tr	Male	Female	tr	Male	Female	tr	Male	Female	tr	Male	Female	tr	Male	Female	tr					
Cholesterol	84.1 ± 2.6 ^b	83.5 ± 2.6	85.8 ± 2.6	85.3 ± 0.1	56.0 ± 2.3	54.0 ± 3.2	71.1 ± 5.0	72.0 ± 1.5	56.8 ± 1.2	75.3 ± 1.7*	61.2 ± 3.2	86.6 ± 1.7*	0.5 ± 0.4	0.7 ± 0.7	0.3 ± 0.2	tr ^c	0.3 ± 0.2	0.5 ± 0.5	0.6 ± 0.5	0.8 ± 0.1	1.0 ± 0.3	2.2 ± 1.1	0.3 ± 0.4
Cholestanol	0.5 ± 0.4	0.7 ± 0.7	0.3 ± 0.2	tr ^c	0.7 ± 0.7	0.4 ± 0.6	0.6 ± 0.5	0.6 ± 0.5	0.8 ± 0.1	1.0 ± 0.3	tr	0.3 ± 0.4	0.3 ± 0.4	0.7 ± 0.7	0.4 ± 0.6	0.4 ± 0.6	0.6 ± 0.5	0.6 ± 0.5	0.8 ± 0.1	1.0 ± 0.3	2.2 ± 1.1	0.3 ± 0.4	
Zymosterol	– ^d	–	–	–	–	–	–	–	–	–	–	–	–	–	–	–	–	–	–	–	–	–	–
Desmosterol	11.1 ± 2.0	11.5 ± 1.6	9.4 ± 1.2	9.4 ± 1.0	36.3 ± 2.8	36.3 ± 2.8	21.2 ± 3.1	22.5 ± 1.1	15.3 ± 1.9	20.3 ± 2.9	23.7 ± 2.6	6.4 ± 1.1*	0.6 ± 0.6	0.8 ± 0.8	0.7 ± 0.6	0.7 ± 0.8	0.5 ± 0.7	0.3 ± 0.4	tr	0.5 ± 0.9	–	–	0.5 ± 0.5
Brassicasterol/Crinosterol	–	–	–	–	–	–	–	–	–	–	–	–	–	–	–	–	–	–	–	–	–	–	–
Lathosterol	–	–	–	–	–	–	–	–	–	–	–	–	–	–	–	–	–	–	–	–	–	–	–
Zymosterol	–	–	–	–	–	–	–	–	–	–	–	–	–	–	–	–	–	–	–	–	–	–	–
24-Methylenecholesterol	1.0 ± 0.5	1.1 ± 0.8	2.3 ± 0.2	2.5 ± 0.8	1.9 ± 1.2	0.8 ± 0.3	3.6 ± 0.6	2.8 ± 0.5	1.0 ± 0.4	1.1 ± 0.3	2.6 ± 0.4	3.0 ± 0.7	1.5 ± 1.3	1.2 ± 1.1	tr	2.0 ± 1.8	2.1 ± 0.5	–	1.2 ± 0.9	1.1 ± 0.9	tr	–	–
24-Methylcholesterol	0.6 ± 0.3	0.5 ± 0.1	tr	tr	1.3 ± 0.3	1.1 ± 0.2	1.0 ± 0.7	0.4 ± 0.7	0.6 ± 0.3	0.5 ± 0.2	0.2 ± 0.2	0.3 ± 0.3	0.6 ± 0.3	0.5 ± 0.1	tr	1.3 ± 0.3	1.1 ± 0.2	1.0 ± 0.7	0.6 ± 0.3	0.5 ± 0.2	0.2 ± 0.2	0.3 ± 0.3	
Sitosterol/Clionasterol	tr	tr	0.4 ± 0.3	0.4 ± 0.4	0.5 ± 0.5	0.2 ± 0.3	1.4 ± 0.5	0.8 ± 0.7	0.3 ± 0.1	0.4 ± 0.1	0.5 ± 0.5	0.7 ± 0.7	0.6 ± 0.6	1.5 ± 0.2	1.3 ± 0.6	1.3 ± 0.6	0.7 ± 1.1	0.4 ± 0.4	1.3 ± 0.8	0.6 ± 0.2	0.7 ± 0.3	1.4 ± 0.8	
Isofucosterol	0.6 ± 0.6	1.5 ± 0.2	1.1 ± 0.7	1.5 ± 0.2	1.3 ± 0.6	1.3 ± 0.6	0.7 ± 1.1	0.4 ± 0.4	1.3 ± 0.8	0.6 ± 0.2	0.7 ± 0.3	0.7 ± 0.7	0.6 ± 0.6	1.5 ± 0.2	1.3 ± 0.6	1.3 ± 0.6	0.7 ± 1.1	0.4 ± 0.4	1.3 ± 0.8	0.6 ± 0.2	0.7 ± 0.3	1.4 ± 0.8	
Unidentified	98.9 ± 0.9	98.7 ± 0.9	98.9 ± 0.4	98.5 ± 0.2	98.0 ± 0.3	98.7 ± 0.5	98.7 ± 0.7	99.1 ± 0.8	75.1 ± 1.7	98.6 ± 0.5*	86.2 ± 0.1	98.2 ± 0.6*	–	–	–	–	–	–	–	–	–	–	–
Total Δ ⁵ -sterols	–	–	–	–	–	–	–	–	–	–	–	–	–	–	–	–	–	–	–	–	–	–	–
Total Δ ⁷ -sterols	–	–	–	–	–	–	–	–	–	–	–	–	–	–	–	–	–	–	–	–	–	–	–
Total Δ ⁸ -sterols	–	–	–	–	–	–	–	–	–	–	–	–	–	–	–	–	–	–	–	–	–	–	–

^a For abbreviations see Fig. 1^b Values are presented as means ± SD of three independent assays^c tr, <0.1%; ^d–, not detectedAn asterisk in the same row indicates a significant difference of $P < 0.05$ compared to male gonads

19, 27–31], and previous studies have provided evidence that this enzyme regulates the overall rate of cholesterol biosynthesis [31], the biosynthesis of both zymostenol and zymosterol by limpets is not well understood. Therefore, experimentation with inhibitors of 3β -hydroxysterol- Δ^8 - Δ^7 -isomerase and elucidation of the regulatory mechanism of related enzymes responsible for the accumulation of Δ^8 -sterols in limpets are necessary. The findings of this study may have important implications for clarification of the physiological roles and functions of unusual cholesterol precursors occurring in marine mollusk gonads rather than yeasts, fungi, and mammalian cells.

Acknowledgments This study was done as a cooperative research program (No. 104) with the International Coastal Research Center, Ocean Research Institute, The University of Tokyo.

References

- Kawashima H, Ohnishi M, Uchiyama H (2002) Sexual differences in gonad fatty acid compositions in dominant limpets species from the Sanriku coast in northern Japan. *J Oleo Sci* 51:503–508
- Kawashima H (2005) Unusual minor nonmethylene-interrupted di-, tri-, and tetraenoic fatty acids in limpet gonads. *Lipids* 40:627–630
- Kawashima H, Ohnishi M (2006) Occurrence of novel nonmethylene-interrupted C_{24} polyenoic fatty acids in female gonad lipids of the limpet *Cellana grata*. *Biosci Biotechnol Biochem* 70:2575–2578
- Kawashima H, Ohnishi M, Ogawa S, Matsui K (2008) Unusual fatty acid isomers of triacylglycerols and polar lipids in female limpet gonads of *Cellana grata*. *Lipids* 43:559–567
- Phleger CF, Nelson MM, Groce AK, Cary SC, Coyne KJ, Nichols PD (2005) Lipid composition of deep-sea hydrothermal vent tubeworm *Riftia pachyptila*, crabs *Munidopsis subsquamosa* and *Bythograea therydron*, mussels *Bathymodiolus* sp. and limpets *Lepetodrilus* spp. *Comp Biochem Physiol* 141B:196–210
- Collignon-Thiennot F, Allais JP, Barbier M (1973) Existence de deux voies de biosynthèse du cholestérol chez un mollusque : la Patelle *Patella vulgata* L. (Gastéropodes, Prosobranches, Archéogastéropodes). *Biochimie* 55:579–582 Summary in English
- Kawashima H, Ohnishi M, Negishi Y, Amano M, Kinoshita M (2007) Sterol composition in muscle and viscera of the marine bivalve *Megangulus zyanoensis* from coastal waters of Hokkaido, northern Japan. *J Oleo Sci* 56:231–235
- Bligh EG, Dyer WJ (1959) A rapid method of total lipid extraction and purification. *Can J Biochem Physiol* 37:911–917
- Kawashima H, Ohnishi M (2003) Fatty acid composition of various tissue lipids in the marine bivalves, *Megangulus venulosus* and *Megangulus zyanoensis*, from coastal waters of Hokkaido, northern Japan. *J Oleo Sci* 52:309–315
- Gerst N, Ruan B, Pang J, Wilson WK, Schroepfer Jr GJ (1997) An updated look at the analysis of unsaturated C_{27} sterols by gas chromatography and mass spectrometry. *J Lipid Res* 38:1685–1701
- Wolthers BG, Walrecht HT, van der Molen JC, Nagel GT, Van Doormaal JJ, Wijnandts PN (1991) Use of determinations of 7-lathosterol (5α -cholest-7-en- 3β -ol) and other cholesterol precursors in serum in the study and treatment of disturbances of sterol metabolism, particularly cerebrotendinous xanthomatosis. *J Lipid Res* 32:603–612
- Byskov AG, Andersen CY, Leonardsen L, Baltzen M (1999) Meiosis activating sterols (MAS) and fertility in mammals and man. *J Exp Zool (Mol Dev Evol)* 285:237–242
- Byskov AG, Andersen CY, Leonardsen L (2002) Role of meiosis activating sterols, MAS, in induced oocyte maturation. *Mol Cell Endocrinol* 187:189–196
- Steffensen KR, Robertson K, Gustafsson J-Å, Andersen CY (2006) Reduced fertility and inability of oocytes to resume meiosis in mice deficient of the *Lxr* genes. *Mol Cell Endocrinol* 256:9–16
- Ariga N, Hatanaka H, Nagai J, Katsuki H (1978) Accumulation of zymosterol in yeast grown in the presence of ethionine. *J Biochem* 83:1109–1116
- Yabusaki Y, Nishino T, Ariga N, Katsuki H (1979) Studies on Δ^8 - Δ^7 -isomerization and methyl transfer of sterols in ergosterol biosynthesis of yeast. *J Biochem* 85:1531–1537
- Berg LR, Patterson GW (1986) Phylogenetic implications of sterol biosynthesis in the oomycetes. *Exp Mycol* 10:175–183
- Steel CC, Baloch RI, Mercer EI, Baldwin BC (1989) The intracellular location and physiological effects of abnormal sterols in fungi grown in the presence of morpholine and functionally related fungicides. *Pestic Biochem Physiol* 33:101–111
- Kedjouar B, de Médina P, Oulad-Abdelghani M, Payré B, Silvente-Poirot S, Favre G, Faye JC, Poirot M (2004) Molecular characterization of the microsomal tamoxifen binding site. *J Biol Chem* 279:34048–34061
- Holleran AL, Lindenthal B, Aldaghlis TA, Kelleher JK (1998) Effect of tamoxifen on cholesterol synthesis in HepG2 cells and cultured rat hepatocytes. *Metabolism* 47:1504–1513
- Kohl W, Gloe A, Reichenbach H (1983) Steroids from the Myxobacterium *Nannocystis exedens*. *J Gen Microbiol* 129:1629–1635
- Bode HB, Zeggel B, Silakowski B, Wenzel SC, Reichenbach H, Müller R (2003) Steroid biosynthesis in prokaryotes: identification of myxobacterial steroids and cloning of the first bacterial 2, 3(S)-oxidosqualene cyclase from the myxobacterium *Stigmatella aurantiaca*. *Mol Microbiol* 47:471–481
- Voogt PA (1975) Investigations of the capacity of synthesizing 3β -sterols in mollusca—XIII. Biosynthesis and composition of sterols in some bivalves (Anisomyaria). *Comp Biochem Physiol* 50B:499–504
- Voogt PA (1975) Investigations of the capacity of synthesizing 3β -sterols in mollusca—XIV. Biosynthesis and composition of sterols in some bivalves (Eulamellibranchia). *Comp Biochem Physiol* 50B:505–510
- Holden MJ, Patterson GW (1991) Absence of sterol biosynthesis in oyster tissue culture. *Lipids* 26:81–82
- Teshima S, Kanazawa A (1974) Biosynthesis of sterols in abalone, *Haliotis gurneri*, and mussel, *Mytilus edulis*. *Comp Biochem Physiol* 47B:555–561
- Gaylor JL, Delwhiche CV, Swindell AC (1966) Enzymatic isomerization ($\Delta^8 \rightarrow \Delta^7$) of intermediates of sterol biosynthesis. *Steroids* 8:353–363
- Schroepfer Jr GJ (1961) Conversion of zymosterol- C^{14} and zymostenol- H^3 to cholesterol by rat liver homogenates and intact rats. *J Biol Chem* 236:1668–1673
- Yamaga N, Gaylor JL (1978) Characterization of the microsomal steroid-8-ene isomerase of cholesterol biosynthesis. *J Lipid Res* 19:375–382
- Paik Y-K, Billheimer JT, Magolda RL, Gaylor JL (1986) Microsomal enzymes of cholesterol biosynthesis from lanosterol. Solubilization and purification of steroid 8-isomerase. *J Biol Chem* 261:6470–6477
- Kang M-K, Kim C-K, Johng T-N, Paik Y-K (1995) Cholesterol biosynthesis from lanosterol: Regulation and purification of rat hepatic sterol 8-isomerase. *J Biochem* 117:819–823

Effect of ALA-Enriched Food Supply on Cardiovascular Risk Factors in Males

Isabelle Sioen · Mirjam Hacquebard · Gaëlle Hick ·
Veronique Maindiaux · Yvan Larondelle ·
Yvon A. Carpentier · Stefaan De Henauw

Published online: 24 June 2009
© AOCS 2009

Erratum to: *Lipids* DOI 10.1007/s11745-009-3307-5

The first sentence of the last paragraph of the manuscript contains a mistake.

“In summary, providing ALA through a variety of fortified foods enables to considerably increase the n-6/n-3

ratio in the diet without changing the subject’s dietary habits.”

must be replaced by

“In summary, providing ALA through a variety of fortified foods enables to considerably decrease the n-6/n-3 ratio in the diet without changing the subject’s dietary habits”.

The online version of the original article can be found under doi:[10.1007/s11745-009-3307-5](https://doi.org/10.1007/s11745-009-3307-5).

I. Sioen (✉) · S. De Henauw
Department of Public Health, Faculty of Medicine and Health
Science, Ghent University, UZ-2 Blok A, De Pintelaan 185,
9000 Ghent, Belgium
e-mail: Isabelle.Sioen@UGent.be

I. Sioen
Department of Food Safety and Food Quality,
Faculty of Bioscience Engineering, Ghent University,
Ghent, Belgium

M. Hacquebard · Y. A. Carpentier
L. Deloyers Laboratory for Experimental Surgery,
Erasmus Hospital, Université Libre de Bruxelles,
Brussels, Belgium

G. Hick
Groupement d’Intérêt Economique
‘Equilibrium Industrial Partnership’, Brussels, Belgium

V. Maindiaux
Dietetic Department, Institut Paul Lambin, Brussels, Belgium

Y. Larondelle
Biochimie Cellulaire, Nutritionnelle et Toxicologique,
Institut des Sciences de la Vie, Université catholique de Louvain,
Louvain-la-Neuve, Belgium

Docosahexaenoic Acid Activates Some SREBP-2 Targets Independent of Cholesterol and ER Stress in SW620 Colon Cancer Cells

Gro Leite Størvold · Karianne Giller Fleten · Cathrine Gøberg Olsen · Turid Follestad · Hans Einar Krokan · Svanhild Arentz Schønberg

Received: 6 May 2009 / Accepted: 15 June 2009 / Published online: 7 July 2009
© AOCs 2009

Abstract The SREBP-2 transcription factor is mainly activated by low cellular cholesterol levels. However, other factors may also cause SREBP-2 activation. We have previously demonstrated activation of SREBP-2 by the polyunsaturated fatty acid docosahexaenoic acid (DHA) in SW620 colon cancer cells. Despite activation of SREBP-2, only a few target genes were induced and cholesterol biosynthesis was reduced. In the present study, gene expression analysis at early time points verified the previously observed SREBP-2 target gene expression pattern. Activation of SREBP-2 using siRNAs targeting Niemann Pick C1 protein (NPC1) led to increased expression of all SREBP target genes examined, indicating that activation of some SREBP-2 target genes is inhibited during DHA-treatment. Cholesterol supplementation during DHA treatment did not abolish SREBP-2 activation. We also demonstrate that activation of SREBP-2 is independent of ER stress and eIF2 α phosphorylation, which we have previously observed in DHA-treated cells. Thapsigargin-induced ER stress repressed expression of SREBP-2 target

genes, but with a different pattern than observed in DHA-treated cells. Moreover, oleic acid (OA) treatment, which does not induce ER stress in SW620 cells, led to activation of SREBP-2 and induced a target gene expression pattern similar to that of DHA-treated cells. These results indicate that DHA and OA may activate SREBP-2 and inhibit activation of SREBP-2 target genes through a mechanism independent of cholesterol level and ER stress.

Keywords SREBP-2 · Cholesterol biosynthesis · ER stress · Transcriptional regulation · eIF2 α

Abbreviations

ATF6	Activating transcription factor 6
DHA	Docosahexaenoic acid
DnaJA4	DnaJ (Hsp 40) homolog-subfamily A-member 4
ER	Endoplasmic reticulum
eIF2 α	Eukaryote translation initiation factor 2 alpha
FA	Fatty acid
FDFT	Farnesyl diphosphate farnesyltransferase
HMGCR	3-Hydroxy-3-methylglutaryl-coenzyme A reductase
IDI	Isopentenyl-diphosphate delta isomerase
Insig	Insulin induced gene
LDLR	Low density lipoprotein receptor
NPC1	Niemann Pick C1
OA	Oleic acid
PUFA	Polyunsaturated fatty acid
SCAP	SREBP cleavage activating protein
siRNA	Small interfering RNA
SRE	Sterol regulatory element
SREBP	SRE binding protein
mSREBP	Mature SREBP

G. L. Størvold · K. G. Fleten · C. G. Olsen ·

S. A. Schønberg (✉)

Department of Laboratory Medicine, Children's and Women's Health, Norwegian University of Science and Technology (NTNU), Erling Skjalgssons gate 1, 7489 Trondheim, Norway
e-mail: svanhild.schonberg@ntnu.no

T. Follestad

Department of Mathematical Sciences, Norwegian University of Science and Technology (NTNU), Erling Skjalgssons gate 1, 7489 Trondheim, Norway

H. E. Krokan

Department of Cancer Research and Molecular Medicine, Norwegian University of Science and Technology (NTNU), Erling Skjalgssons gate 1, 7489 Trondheim, Norway

SQS	Squalene synthetase
Tg	Thapsigargin
UFA	Unsaturated fatty acid

Introduction

The sterol regulatory element binding proteins (SREBPs) are transcription factors regulating fatty acid (FA) and cholesterol synthesis. Three family members have been identified to date; SREBP-1a, SREBP-1c and SREBP-2. SREBP-1a and SREBP-1c are transcribed from the same gene using alternate promoters, while SREBP-2 is transcribed from a separate gene [1]. The SREBP-2 and SREBP-1c isoforms are expressed in liver and most other tissues, while in cultured cells SREBP-2 and SREBP-1a are the most dominant isoforms [2]. SREBP-1c mainly regulates genes involved in FA biosynthesis, while SREBP-2 activates genes involved in cholesterol biosynthesis [3]. SREBP-1a, which has a longer transcription activating domain than the SREBP-1c isoform, is able to induce expression of genes involved in both FA and cholesterol biosynthesis [1, 4].

The SREBP transcription factors are synthesized as inactive precursor proteins localized in the endoplasmic reticulum (ER) membrane [5]. The SREBP precursor protein forms a complex with another ER-localized protein, the SREBP cleavage activating protein (SCAP), which contains a cholesterol sensing domain [6]. Binding of cholesterol when ER cholesterol levels are high induces a conformational change in SCAP. This enables binding of the SCAP-SREBP complex to another ER resident protein; insulin-induced gene 1 (Insig1), which retains the SCAP-SREBP complex in the ER [7, 8]. When cells are depleted of sterols, SCAP dissociates from Insig-1, and the SCAP-SREBP complex is translocated to the Golgi where the SREBP precursor is cleaved by two proteases; site-1 protease (S1P) and site-2 protease (S2P) [5]. This releases the N-terminal fraction of the protein, termed mature SREBP (mSREBP), which contains the transcription factor domain. The active transcription factor is translocated to the nucleus where it induces expression of target genes, including the SREBP transcription factors themselves [3, 5]. SREBP target genes contain a sterol regulatory element (SRE) sequence or modified forms of this sequence in their promoters, while SREBP-1c target genes mainly contain E-boxes or E-box like sequences [9, 10]. The SREBP transcription factors have weak transcriptional domains, and require co-factors like NF-Y or Sp1 to activate target genes [9, 11].

In addition to cholesterol, unsaturated fatty acids (UFAs) have been shown to regulate mSREBP levels. A unified mechanism explaining the regulation of SREBP by UFAs has not yet been established. It has been demonstrated that UFAs may inhibit the proteolytic processing of the precursor protein [12–15], reduce SREBP-1 mRNA stability [16], as well as transcription [12, 17–19]. Studies performed on hepatic tissue *in vivo* or in hepatic cell lines have demonstrated that polyunsaturated FAs (PUFAs), but not the monounsaturated FA oleic acid (OA), reduce the levels of mSREBP-1 [15, 16, 19] or both SREBP-1 and -2 [20]. Other studies have demonstrated that OA as well as PUFAs, reduce the levels of both SREBP-1 and -2 [13, 14]. In a study using the non-hepatic 293T fibroblast-like cell line, both OA and arachidonic acid (AA) reduced SREBP-1 levels, while no alterations in SREBP-2 levels were found [12]. A similar response was seen when the CaCo-2 colon adenocarcinoma cell line was treated with PUFAs, while OA had no effect [18].

Regulation of the SREBP transcription factors independent of cholesterol and FA levels has also been reported. Several studies have demonstrated activation of the SREBP transcription factors by cellular stress like hypotonic shock [21], ER stress [21–23] or apoptosis [24].

ER stress is induced by disturbances in ER homeostasis and leads to initiation of the unfolded protein response (UPR). The response is mediated by three ER-localized transmembrane proteins; activating transcription factor 6 (ATF6), inositol-requiring enzyme 1 (IRE1) and the eukaryote translation initiation factor 2 alpha (eIF2 α) kinase 3 (EIF2AK3/PERK). Activated PERK phosphorylates eIF2 α [25], thereby inducing a global inhibition of translation resulting in reduced protein synthesis and depletion of short lived proteins like cyclin D1 [26].

We have previously demonstrated that treatment of SW620 human colon cancer cells with the PUFA docosahexaenoic acid (DHA; 22:6n-3) leads to reduced levels of SREBP-1 [27], while the SREBP-2 transcription factor is activated [28]. Despite increased levels of the activated transcription factor, only a few SREBP-2 target genes were up-regulated at mRNA level, and synthesis of cholesterol from acetate was reduced in DHA-treated cells [28]. In addition, DHA treatment induced accumulation of cholesteryl esters in SW620 cells without a corresponding increase in total cholesterol [27, 28]. These data made us hypothesize that free cholesterol was redistributed from the ER membrane to cholesterol esters, inducing local cholesterol depletion in the ER and activation of SREBP-2. DHA treatment also induced ER stress in SW620 cells [28], and it was hypothesized that depletion of cholesterol in the ER could lead to the observed ER stress and growth inhibition observed in DHA-treated SW620 cells.

In the present study we demonstrate that activation of SREBP-2 by DHA is not caused by cholesterol depletion or ER stress induction. Treatment of SW620 cells with OA, which does not induce cholesteryl ester accumulation [27] or eIF2 α phosphorylation [28], also lead to activation of SREBP-2, indicating that UFAs may have a common mechanism for SREBP-2 activation. Further, we observe that in DHA- and OA- treated cells, despite activated SREBP-2, expression of only a few target genes is increased. In cells where SREBP-2 is activated by cholesterol depletion all target genes examined are induced, indicating that activation of some SREBP-2 target genes is inhibited during DHA and OA treatment.

Experimental Procedures

Cell Culture

The human colon adenocarcinoma cell line SW620 was obtained from ATCC (Rockville, MD). Cells were cultured in Leibowitz's L-15 medium (Cambrex, BioWhittaker, Walkersville, MD) supplemented with L-glutamine (2 mM), FBS (10%) and gentamicin (45 mg/l) (complete growth medium) and maintained in a humidified atmosphere of 5% CO₂: 95% air at 37 °C.

Fatty Acid, Cholesterol and Thapsigargin Treatment

Stock solutions of DHA and OA in ethanol (Cayman Chemical, Ann Arbor, MI) were stored at –20 °C and diluted in complete growth medium before experiments (final concentration of ethanol <0.01% v/v). Cholesterol and Tg (both Sigma, St. Louis, MO) were dissolved in ethanol. Stock solutions were kept at –20 °C and diluted in complete growth medium before experiments. Complete growth medium with an equal volume of ethanol as for the treatment media was used as the control media in the experiments. For all treatments cells were plated at a density of 3.5×10^6 cells /175 cm² flask and allowed to attach over night, further FA, cholesterol or Tg was added and cells were treated for the indicated time periods. For DHA and cholesterol treatments, cells were also plated in triplicates in 6-well trays treated in parallel with the 175 cm² flasks to assay cell growth. Cells were harvested by trypsination and counted using a Coulter Counter (Beckman Coulter, Fullerton, CA).

Immunoblot Analysis

Preparation of total protein extracts was performed as described previously [27]. An equal amount of protein was separated on 10% precast denaturing NuPAGE gels

(Invitrogen, Carlsbad, CA) and transferred to PVDF membranes (Millipore, Billerica, MA). Membranes were blocked in PBS supplied with 5% nonfat dry milk and 0.1% Tween[®]-20 (BioRad, Hercules, CA) and further incubated over night at 4 °C with the indicated primary antibodies. The following primary antibodies were used to probe the membranes; LDLR (Progen, Germany), FDFT1/SQS (Abgent, San Diego, CA), Insig-1 (Santa Cruz, Santa Cruz, CA), SREBP-2 (BD Biosciences, San Jose, CA), IDI1 and β -actin (both AbCam, UK). Membranes were further incubated with HRP-conjugated secondary antibodies (DAKO, Carpinteria, CA) and detected by chemiluminescence using Super Signal West Femto Maximum Sensitivity Substrate (Pierce, Rockford, IL) and visualized by Kodak Image Station 4000R (Eastman Kodak Company, Rochester, NY). Quantification was performed using Kodak Molecular Imaging Software (version 4.0.1).

siRNA Transfection

siRNAs targeting Niemann Pick C1 protein (NPC1) (NCBI accession number NM_000271) and eukaryote translation initiation factor 2 alpha (eIF2 α) (NCBI accession number NM_004094) were purchased from Dharmacon (Lafayette, CO) (NPC1si#2, eIF2 α si#14) and Ambion (Austin, TX) (NPC1si#7). A non-targeting siRNA (Dharmacon, Lafayette, CO) was used as a control. siRNAs were dissolved in 1 \times siRNA buffer (Dharmacon, Lafayette, CO) and stock solutions were aliquoted and stored at –80 °C. For siRNA transfection experiments, 8.17×10^6 cells were plated in 175 cm² flasks in complete growth media without gentamicin. Cells were transfected 24 h after plating using siRNA (50 nM) and Dharmafect 1 transfection reagent (Dharmacon). The media was changed 24 h after transfection, and the cells were allowed to recover for 6 h before they were sub-cultured at a density of 3.5×10^6 cells/175 cm² flask for further growth or DHA treatment. Cells were harvested by scraping in ice cold PBS, and total cell extracts were prepared as described above.

RNA Isolation

For RNA isolation 3.5×10^6 cells were seeded in 175 cm² flasks and allowed to attach over night. The following morning, the growth medium was replaced with media supplemented with DHA (70 μ M) or an equal volume of ethanol (control). After 6 h, cells were harvested by scraping in ice cold PBS and stored at –80 °C. Total RNA was isolated using the High Pure RNA Isolation Kit (Roche, Mannheim, Germany) according to the instruction manual. RNase inhibitor rRNasin (40U/ μ l, 1 μ l) (Promega, Madison, WI) was added and RNA was up-concentrated on a speed vac and resuspended in RNase free distilled H₂O.

RNA concentration and quality were determined using the NanoDrop1000 (NanoDrop Technologies, Wilmington, Delaware) and agarose gel electrophoresis.

Gene Expression Profiling

A 5- μ g amount of total RNA was used for cDNA- and cRNA synthesis according to the eukaryote expression manual (Affymetrix, Santa Clara, CA). cRNA was hybridized to the Human Genome U133 Plus 2.0 Arrays (Affymetrix). Washing and staining were performed using the Fluidics Station 450 and the arrays were scanned using an Affymetrix GeneChip Scanner 3000 with autoloader (Affymetrix, USA). Expression profiling was performed in triplicate at all time points using RNA from independent biological replicates, except for the 1 h time point when only two control experiments were used. All experiments were submitted to ArrayExpress with accession number E-MEXP-2010. The statistical analysis was performed based on summary expression measures of the probe sets of the GeneChips, using the raw data (CEL) files and a linear statistical model for background-corrected, quantile normalized and log-transformed PM values, performed by the robust multiarray average (RMA) method [29, 30]. Data from all time points (0.5, 1, 3, and 6 h) were used in the statistical analysis.

For each transcript, a linear regression model including parameters representing treatment and time effects and treatment-time interactions was fitted to the RMA expression measures. Based on the estimated effects, tests for significant differential expression due to DHA treatment and time were performed using moderated *t* tests, in which gene-specific variance estimates are replaced by variance estimates found by borrowing strength from data on the remaining genes [31]. To account for multiple testing, adjusted *P* values controlling the false discovery rate (FDR) were calculated [32]. Differentially expressed genes were selected based on a threshold of 0.05 on the adjusted *P*-values.

The statistical analysis was performed in *R* (<http://www.r-project.org>), using the packages Limma and affy from Bioconductor [33]. Differentially expressed genes were annotated using the NetAffx Analysis Centre (<http://www.Affymetrix.com>) and NMC Annotation Tool/eGOn V2.0 (<http://www.GeneTools.no>).

Results

Expression of mSREBP-2 Target Genes at mRNA and Protein Level in DHA-Treated SW620 Cells

We have previously found that only some SREBP-2 target genes are up-regulated in SW620 cells after 12–48 h of

DHA treatment despite activation of SREBP-2 [28]. In the present study, gene expression analysis was performed on SW620 cells treated with DHA for short time periods using arrays covering the whole human genome. No SREBP-2 target genes were found differentially expressed at mRNA level after 0.5, 1 and 3 h treatment with DHA. However, after 6 h of DHA treatment up-regulation of some, but not all, SREBP-2 target genes was observed (Table 1), in agreement with our previous findings [28]. In addition, two SREBP-2 target genes that were not present on the Focus arrays previously used were found up-regulated at mRNA level; farnesyl-diphosphate farnesyltransferase 1 (FDFT1), encoding for squalene synthetase (SQS), an enzyme in the cholesterol biosynthetic pathway, and DnaJ (Hsp40) homolog, subfamily A, member 4 (DnaJA4), recently demonstrated to be a SREBP-2 target gene (Table 1) [34].

Several of the SREBP-2 target genes were also analyzed at protein level by Western blot. Increased protein levels of low density lipoprotein receptor (LDLR), SQS/FDFT1 and DnaJA4 were observed after 12 h of DHA treatment, and remained elevated up to 48 h of treatment (Fig. 1a). The level of the SREBP target gene isopentenyl-diphosphate delta isomerase 1 (IDI1), also an enzyme in the cholesterol biosynthetic pathway, was not changed by DHA treatment neither at mRNA nor protein level (Table 1, Fig. 1a).

Treatment of SW620 cells with OA, resulted in a similar protein expression pattern as for DHA-treated cells. Protein levels of mSREBP-2 and SQS were increased after 24 h of OA treatment, while IDI1 was unchanged (Fig. 1b).

Activation of SREBP-2 by NPC1 Knockdown Induces Expression of all Target Genes Examined in SW620 Cells

Activated SREBP-2 has been demonstrated to generally induce expression of all target genes [35–37]. In order to investigate whether activation of SREBP-2 by NPC1 knockdown would induce expression of target genes not activated during DHA treatment, SW620 cells were transfected with siRNAs targeting NPC1. The NPC1 protein is involved in intracellular cholesterol transport of LDLR-derived cholesterol from the lysosomes to the interior of the cell, and inhibition of NPC1 function leads to cholesterol depletion in the ER [38]. Significantly reduced NPC1 protein levels were observed in cells transfected with NPC1 siRNA, as well as increased levels of mSREBP-2 (Fig. 2a). Further, induction of both SQS and IDI1 was observed (Fig. 2a), in contrast to DHA-treated cells where only SQS was induced. These results demonstrate that SW620 cells are able to increase expression all target genes examined after activation of SREBP-2 by cholesterol depletion induced by NPC1 knockdown.

Table 1 Significant differentially expressed transcripts of SREBP target genes in SW620 cells treated with DHA (70 μ M) for 6 h

Gene symbol	Affymetrix ID	Refseq NCBI ID	Description	SW620 fold change 6 h
Chaperones/protein folding				
DnaJA4	1554333_at	NM_18602.3	DnaJ (Hsp40) homolog, subfamily A, member 4	2.39
	1554334_a_at			2.18
	225061_at			2.45
Cholesterol biosynthesis, uptake, metabolism and transport				
LDLR	202068_s_at	NM_000527	Low density lipoprotein receptor	2.28
	202067_s_at			1.55
NPC1	202679_at	NM_000271	Niemann-Pick disease, type C1	1.58
SC4MOL	209146_at	NM_001017369	Sterol-C4-methyl oxidase-like	2.2
		NM_006745		
FDFT1	243658_at	NM_004462	Farnesyl-diphosphate farnesyltransferase 1	2.89
	241954_at			2.08
	238666_at			1.93
HMGCS1	221750_at	NM_002130	3-hydroxy-3-methylglutaryl-coenzyme A synthase 1 (soluble)	1.5
		NM_001098272		
VLDLR	209822_s_at	NM_001018056	Very low density lipoprotein receptor	3.23
		NM_003383		
IDI1	204615_x_at	NM_004508	Isopentenyl-diphosphate delta isomerase 1	NC
	208881_x_at			
	233014_at			
	242065_x_at			

*NC no change

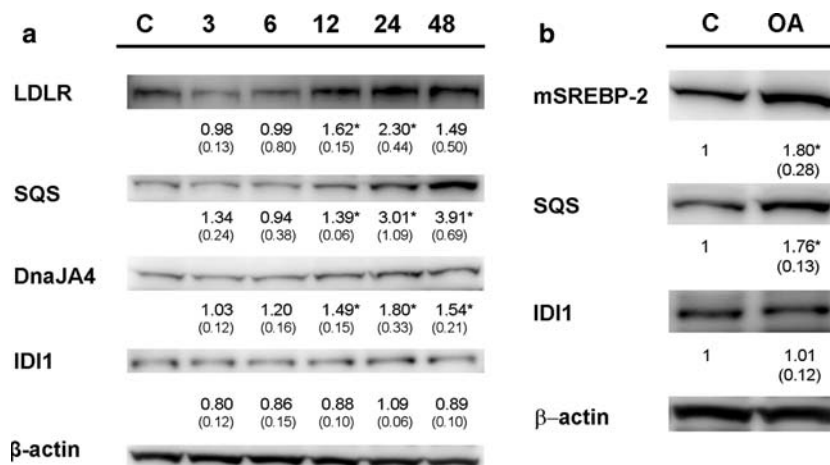


Fig. 1 Analysis of protein levels of mSREBP-2 and selected SREBP target genes after DHA and OA treatment. **a** Western blot analysis of mSREBP-2 target gene protein levels in total protein extracts from SW620 cells treated with DHA (70 μ M) for the indicated time periods (h). Controls were harvested at all time points, only 24 h control (C) is shown. **b** Western blot analysis of mSREBP-2 and SREBP target gene protein levels in total protein extracts from SW620 cells treated with OA (70 μ M) for 24 h. β -actin was used as a control for equal protein loading. The blots were quantified and protein band intensities

normalized relative to β -actin. For results in Fig. 1a, the β -actin adjusted band intensities from the DHA and control membranes were further normalized relative to the 24 h control band, present at all membranes, to adjust for differences in signal intensities between the membranes. The numbers under the blots represent mean fold change (with standard deviation(SD)) of DHA- or OA- treated samples relative to control at indicated time points for three independent experiments. *Significantly different from control (Student's *t* test, $P < 0.05$)

Cholesterol Supplementation During DHA Treatment Does Not Inhibit Activation of SREBP-2 or Relieve DHA-Induced Cell Cycle Arrest

We have previously observed increased cholesterol esterification in addition to reduced de novo cholesterol synthesis in SW620 cells treated with DHA [27, 28]. This may lead to depletion of cholesterol in the ER, which could lead to the observed activation of SREBP-2 [28] and possibly cause growth inhibition [39]. To further investigate this, we incubated SW620 cells with cholesterol alone or in combination with DHA. Cholesterol treatment alone reduced the level of mSREBP-2 compared to control, indicating uptake of sterols in ER and inhibition the proteolytic activation of the SREBP-2 transcription factor (Fig. 2b). When cells were treated with DHA in the presence of cholesterol, a significant increase in mSREBP-2 levels relative to control was observed (1.45 ± 0.16 relative to control with cholesterol only, $P < 0.05$), demonstrating activation of SREBP-2 by DHA in the presence of excess cholesterol. Further, the cell cycle arrest observed in SW620 cells after DHA treatment [27] was not rescued by co-incubation with cholesterol. Cholesterol treatment alone did not affect cell growth (results not shown). The data indicates that activation of mSREBP-2 and the growth arrest observed in SW620 cells after DHA treatment are not caused by depletion of cholesterol.

DHA Regulates mSREBP-2 and Target Genes Independent of ER Stress and eIF2 α Function

We have previously observed induction of ER stress and phosphorylation of eIF2 α in SW620 cells during DHA treatment [28]. Previous reports have demonstrated that ER stress activates SREBP-2 [22, 23], but may inhibit SREBP-2 target gene expression [40]. To investigate whether ER stress related mechanisms are causing the activation of mSREBP-2 and repression of target genes in our system, we used three different approaches; (1) induction of ER stress by thapsigargin (Tg), (2) measuring the level of the negative regulatory protein Insig-1 and (3) siRNAs targeting eIF2 α .

Thapsigargin Treatment Regulates mSREBP-2 and Target Genes

Tg induces ER stress by perturbing ER calcium homeostasis. Activation of SREBP-2 was observed when SW620 cells were treated with Tg for 6 h (Fig. 3a), but the level of mSREBP-2 was higher than in cells treated with DHA for the same time period [28]. The level of mSREBP-2 declined after 24 h of Tg treatment, but was still significantly higher than control (Fig. 3a). These results demonstrate that ER stress may lead to activation of SREBP-2 in SW620 cells, but that the response differs from the

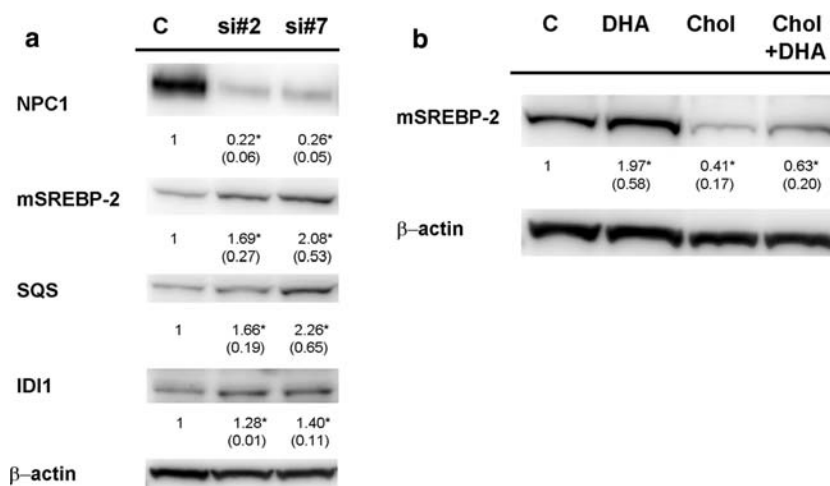


Fig. 2 Analysis of protein levels of mSREBP-2 and selected SREBP target genes after induction of cholesterol depletion or cholesterol supplementation. **a** Western blot analysis of protein levels of NPC1, mSREBP-2 and mSREBP-2 targets in total protein extracts from SW620 cells transfected with NPC1 siRNAs. Cells were transfected with two siRNAs targeting independent sequences in the NPC1 transcript (NPCsi#2 and NPCsi#7), while control cells were transfected with a non-targeting siRNA. Cells were harvested for analysis 72 h after transfection. The blots were quantified and protein band intensities normalized relative to β -actin loading control. The numbers under the blots represent mean fold change (with SD) of

NPC1 siRNA transfected samples relative to control at indicated time points ($n = 3$). **b** Western blot analysis of mSREBP-2 levels in total protein extracts from SW620 cells after DHA treatment and cholesterol supplementation. Cells were incubated for 24 h in control media (C), DHA (70 μ M), 30 μ g/ml cholesterol (Chol), or both cholesterol (30 μ g/ml) and DHA (70 μ M); (Chol + DHA). The blots were quantified and intensities normalized relative to β -actin loading control. The numbers under the blots represent mean fold change (and SD) relative to control for three independent experiments. *Significantly different from control (Student's t test, $P < 0.05$)

response observed after DHA treatment, where the level of mSREBP-2 remained elevated up to 48 h of treatment [28]. The same response was also observed when using a tenfold lower concentration of Tg, indicating that the difference in response is not caused by high concentrations of Tg with a corresponding stronger ER stress response. The protein levels of selected SREBP-2 target genes were assayed after Tg-treatment of SW620. Unexpectedly, SQS and DnaJA4, both induced by DHA treatment, were down-regulated in Tg-treated cells (Fig. 3a). Furthermore, expression of IDI1, which was unchanged in DHA treated cells, was increased relative to control after 24 h of Tg-treatment (Fig. 3a).

mSREBP-2 Activation is not Caused by Depletion of the Regulatory Protein Insig-1

It has been suggested that activation of mSREBP-2 upon cellular stress may be caused by depletion of the negative regulatory protein Insig-1 due to eIF2 α phosphorylation and inhibition of protein translation [21]. However, the level of Insig-1 was not altered upon Tg nor DHA treatment in SW620 cells (Fig. 3a, b) demonstrating that SREBP-2 is not activated by Insig-1 depletion in these settings.

Inhibition of Protein Translation Using siRNAs Targeting eIF2 α

To investigate whether inhibition of protein translation would lead to activation of SREBP-2 through a mechanism other than reduced level of Insig-1, siRNAs targeting eIF2 α were used to deplete the protein from the cells. Transfection with siRNA significantly reduced the level of eIF2 α , and a significant reduction in cyclin D1 level was also observed, indicating inhibition of protein translation (Fig. 3c). Knockdown of eIF2 α did not result in increased levels of mSREBP-2, indicating that inhibition of protein translation does not lead to mSREBP-2 activation in SW620 cells. Instead decreased levels mSREBP-2 was observed (Fig. 3c). When eIF2 α siRNA transfected cells were treated with DHA for 24 h, increased level of mSREBP-2 relative to cells not treated with DHA was observed (Fig. 3d). These results indicate that activation of mSREBP-2 by DHA is independent of ER stress and eIF2 α function.

Discussion

Activation of the SREBP-2 transcription factor and induction of cholesterol biosynthesis are mainly regulated by cellular cholesterol levels [1]. However, cellular stress and ER stress have also been reported to activate SREBP-2,

independent of cholesterol levels [21, 22]. We have previously demonstrated that DHA treatment leads to activation of the SREBP-2 transcription factor in the human colon cancer cell line SW620, but that the activated transcription factor only induces expression of some SREBP target genes [28]. In the present study we demonstrate that activation of SREBP-2 by DHA occurs independent of cholesterol levels and ER stress induction, and that activation of some SREBP-2 target genes is inhibited during DHA treatment.

In our previous study, activation of the SREBP-2 transcription factor was observed as early as after 3 h of DHA treatment [28], and in the present study we demonstrate by gene expression analysis that increased mRNA levels of SREBP target genes can be observed after 6 h of DHA treatment. The gene expression analysis also verified the previously observed expression pattern in DHA-treated SW620 cells where activation of only a few SREBP-2 target genes was observed despite the activated transcription factor. In SW620 cells treated with OA, we observe a similar effect as for DHA on mSREBP-2 and target gene protein levels.

Previous studies have demonstrated that when SREBP-2 is activated by cholesterol depletion or by over-expression of the active transcription factor, expression of all known target genes is generally induced [35–37]. In line with this we demonstrate that SREBP-2 activated by knockdown of NPC1 is able to induce all target genes examined, unlike the response observed in DHA-treated cells. These results demonstrate that during DHA treatment activated SREBP-2 is not able to increase expression of all target genes.

Previously we have demonstrated increased protein levels of 3-hydroxy-3-methylglutaryl-coenzyme A reductase (HMGCR) and NPC1 in SW620 cells treated with DHA [28], and in the present study we demonstrate increased protein levels of LDLR. Together with the observed activation of mSREBP-2 [28], these results suggest an increased demand for intracellular cholesterol. However, our data demonstrate that activation of SREBP-2 is not inhibited by cholesterol supplementation to the cell culture media during DHA treatment. It has been suggested that cholesterol dissolved in ethanol added to cell culture media will not be efficiently absorbed by cells [41], and that observed effects could be caused by oxysterol impurities that are more easily absorbed. Thus, reduced levels of mSREBP-2 observed after cholesterol supplementation to SW620 cells could be caused by oxysterols present in the cholesterol. However, oxysterols are not able to substitute for the cellular functions of cholesterol [5, 41]. Also, others have demonstrated by using the same approach, that cholesterol supplementation may restore growth in cholesterol depleted cells [39, 42]. These results strongly indicate that SREBP-2 activation in DHA-treated cells is not caused by

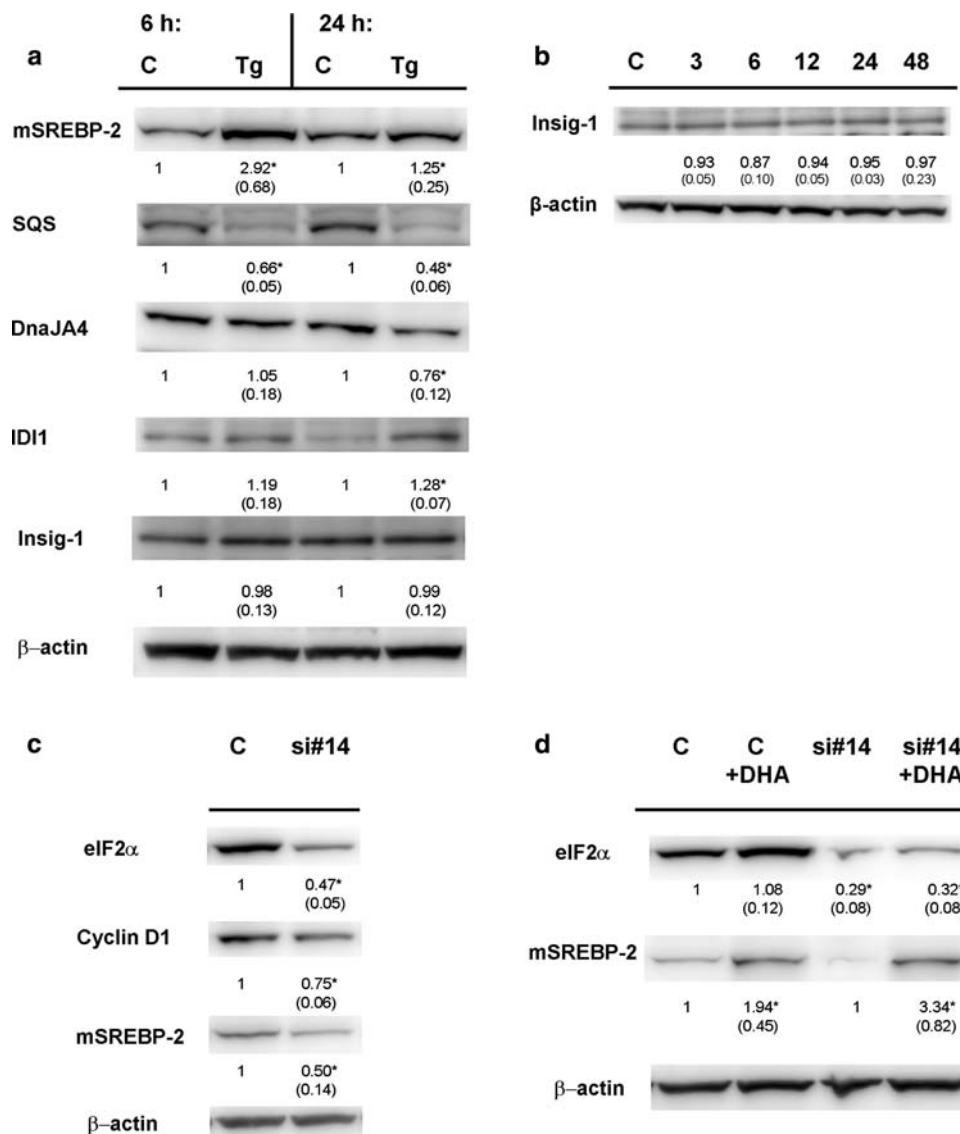


Fig. 3 Regulation of protein levels of mSREBP-2 and SREBP target genes by ER stress and eIF2 α knockdown. **a** Western blot analysis of the protein levels of mSREBP-2 and mSREBP-2 target genes in total protein extracts from SW620 cells treated with 0.2 μ M thapsigargin (Tg) for the indicated time periods (h). The blots were quantified and protein band intensities normalized relative to β -actin loading control. The numbers under the blots represent mean fold change (with SD) of Tg-treated samples relative to control at indicated time points for three independent experiments. **b** Western blot analysis of Insig-1 protein levels in total protein extracts from SW620 cells treated with DHA (70 μ M) for the indicated time periods (h). Controls were harvested at all time points; only 24 h control (C) is shown. The blots were quantified and protein band intensities normalized relative to β -actin. The β -actin adjusted band intensities from the DHA and control membranes were further normalized relative to the 24 h control band, present at all membranes, to adjust for differences in signal intensities

cholesterol depletion, despite the accumulation of cholesteryl esters and reduced cholesterol biosynthesis observed previously [27, 28]. Furthermore, OA treatment of SW620 cells does not induce cholesteryl ester

between the membranes. The numbers under the blots represent mean fold change (with SD) of DHA treated samples relative to control at indicated time points for three independent experiments. **c** Western blot analysis of the protein levels of eIF2 α , cyclin D1 and mSREBP-2 in total protein extracts from SW620 cells transfected with a siRNA targeting eIF2 α . Cells were harvested for analysis 48 h after transfection. **d** Western blot analysis of the protein levels of eIF2 α and mSREBP-2 in total protein extracts from SW620 cells transfected with a siRNA targeting eIF2 α and further treated with DHA for 24 h. For all eIF2 α experiments control cells were transfected with a non-targeting siRNA. The blots were quantified and protein band intensities normalized relative to β -actin loading control. The numbers under the blots represent mean fold change (with SD) of siRNA transfected cells relative to the corresponding control at indicated time points for three independent experiments. *Significantly different from control (Student's *t* test, $P < 0.05$)

accumulation [27], but we observe activation of SREBP-2 (this work). The data demonstrates that both DHA and OA may activate SREBP-2 independent of cellular cholesterol levels, possibly through a mechanism common for UFAs.

We further demonstrate that activation of SREBP-2 by DHA treatment is most likely not caused by ER stress or inhibition of protein translation, and that it is independent of Insig-1 protein levels and eIF2 α function. In SW620 cells treated with OA we observe activation of SREBP-2, but not induction of ER stress and eIF2 α phosphorylation [28]. These data further support a common mechanism for UFAs for activation of SREBP-2 independent of both cholesterol levels and ER stress.

Activation of SREBP-2 by induction of apoptosis has also been reported [24], but we have previously not detected induction of apoptosis or activation of caspases in DHA-treated SW620 cells [27, 28].

Inhibition of transcription of SREBP-2 target genes has previously been associated with ER stress-induced activation and cleavage of ATF6 [40]. Tg treatment activates both ATF6 [40] and mSREBP-2, as demonstrated in our study. The reduced protein levels of SQS and DnaJA4 observed after Tg treatment are most likely caused by ATF6 interaction with SREBP-2 transcription, since reduced levels of SQS after ATF6 activation have been demonstrated previously [40]. Unexpectedly, proteins that were repressed in Tg-treated cells were the same proteins found induced upon SREBP-2 activation in DHA treated cells. ATF6 activation was not assayed in this work, but it could be speculated that the ER stress response or activation of ATF6 in DHA-treated cells may be weaker than in Tg-treated cells, or that all the branches of the ER stress response are not equally activated upon DHA treatment [35]. In OA-treated cells, where no ER stress has been observed, the SREBP targets SQS and IDI1 display the same response as observed in DHA-treated cells. Together the data indicates that lack of activation of some SREBP-2 target genes during DHA or OA treatment is not caused by activation of ER stress and ATF6.

Regulation of the SREBP transcription factors by UFAs have been shown in several studies [12, 13, 17], but our study is the first to demonstrate increased levels of mSREBP-2 after UFA treatment. Why UFA treatment would cause activation of SREBP-2 in the SW620 colon cancer cell line is not known and remains to be investigated in our system. However, activation of SREBP-2 by DHA does not result in activation of all target genes and increased cholesterol biosynthesis. Instead, activation of some SREBP-2 target genes in DHA- and OA-treated cells seems to be inhibited, and a significant reduction in de novo cholesterol biosynthesis has previously been observed after DHA treatment [28].

Protein modification of the SREBP-2 transcription factor by phosphorylation, acetylation, sumoylation or ubiquitination may affect the binding affinity or activation of target promoters [43–45]. UFAs could also possibly affect co-factors or regulate repressors that are involved in

SREBP-2 target gene transcription [46, 47]. The SREBP-1a transcription factor has also been demonstrated to be involved in the regulation of genes involved in cholesterol biosynthesis [10, 36, 37]. We have previously observed reduced levels of mSREBP-1 in DHA-treated SW620 cells [27]. SREBP-1 levels were not altered in NPC1 siRNA transfected cells, where expression of all SREBP target genes examined were induced (results not shown). Whether the observed SREBP-2 target gene expression pattern induced by DHA and OA could be caused by reduced SREBP-1 levels, or if it is caused by other factors, remains to be investigated.

The liver is the main site for cholesterol biosynthesis in the body, but extra-hepatic tissue also synthesizes a significant amount of cholesterol (reviewed in [48]). In addition cancer cells and tumors display increased rates of cholesterol biosynthesis [49]. In spite of this, most studies investigating the effect of dietary fatty acids on cholesterol metabolism have been performed in fibroblasts or hepatic cell lines or tissues [14–16, 19, 20, 50]; only a few studies have addressed regulation of SREBPs or cholesterol biosynthesis in other tissues and cell types [18, 51]. The results from our study have revealed that UFAs may affect cholesterol homeostasis and reduce cholesterol biosynthesis in a colon cancer-derived cell line by interfering with induction of SREBP-2 transcription. This is in line with previous observations where UFA treatment reduced transcriptional levels of cholesterologenic enzymes or reduced cholesterol biosynthesis in both hepatic tissue and cells, as well as glioma cells [19, 20, 50, 51]. Altered levels of cholesterol biosynthesis in the liver may contribute to altered plasma cholesterol levels [48], and it has been suggested that the reduction in cholesterologenesis induced by UFAs may be a mechanism explaining the plasma cholesterol-lowering effect that has been observed in some studies after UFA treatment [20, 50]. In addition reduced levels of cholesterol biosynthesis in cancer cells may contribute to reduced cancer cell growth [52, 53]. However, further studies are needed to confirm our observations and investigate possible implications in other cancer cell lines.

Together the data presented in this report demonstrate that DHA and OA activate SREBP-2 independent of cholesterol levels and ER stress, possibly through a mechanism common for UFAs. Further, we show that activation of SREBP-2 by these FAs only increases expression of some SREBP target genes. The mechanisms by which DHA and OA increase the level of mSREBP-2, but inhibit induction of some SREBP target genes in SW620 human colon cancer cells remain to be investigated.

Acknowledgments Technical assistance from Caroline Hild Hakvaag Pettersen, Mari Sæther and Jens Erik Slagsvold is highly

appreciated. The project was financed by The Faculty of Medicine, NTNU, The Cancer Research Fund, Trondheim University Hospital and The Research Council of Norway through grants from the Functional Genomics Program (FUGE). Microarray experiments were performed at the microarray core facility at the Norwegian Microarray Consortium (NMC), Trondheim, which is supported by FUGE.

References

- Brown MS, Goldstein JL (1997) The SREBP pathway: regulation of cholesterol metabolism by proteolysis of a membrane-bound transcription factor. *Cell* 89:331–340
- Shimomura I, Shimano H, Horton JD, Goldstein JL, Brown MS (1997) Differential expression of exons 1a and 1c in mRNAs for sterol regulatory element binding protein-1 in human and mouse organs and cultured cells. *J Clin Invest* 99:838–845
- Horton JD, Goldstein JL, Brown MS (2002) SREBPs: activators of the complete program of cholesterol and fatty acid synthesis in the liver. *J Clin Invest* 109:1125–1131
- Pai JT, Guryev O, Brown MS, Goldstein JL (1998) Differential stimulation of cholesterol and unsaturated fatty acid biosynthesis in cells expressing individual nuclear sterol regulatory element-binding proteins. *J Biol Chem* 273:26138–26148
- Brown MS, Goldstein JL (1999) A proteolytic pathway that controls the cholesterol content of membranes, cells, and blood. *Proc Natl Acad Sci USA* 96:11041–11048
- Hua X, Nohturfft A, Goldstein JL, Brown MS (1996) Sterol resistance in CHO cells traced to point mutation in SREBP cleavage-activating protein. *Cell* 87:415–426
- Goldstein JL, Bose-Boyd RA, Brown MS (2006) Protein sensors for membrane sterols. *Cell* 124:35–46
- Sun LP, Li L, Goldstein JL, Brown MS (2005) Insig required for sterol-mediated inhibition of Scap/SREBP binding to COPII proteins in vitro. *J Biol Chem* 280:26483–26490
- Shimano H (2001) Sterol regulatory element-binding proteins (SREBPs): transcriptional regulators of lipid synthetic genes. *Prog Lipid Res* 40:439–452
- Amemiya-Kudo M, Shimano H, Hasty AH, Yahagi N, Yoshikawa T, Matsuzaka T, Okazaki H, Tamura Y, Iizuka Y, Ohashi K, Osuga J, Harada K, Gotoda T, Sato R, Kimura S, Ishibashi S, Yamada N (2002) Transcriptional activities of nuclear SREBP-1a, -1c, and -2 to different target promoters of lipogenic and cholesterologenic genes. *J Lipid Res* 43:1220–1235
- Bengochea-Alonso MT, Ericsson J (2007) SREBP in signal transduction: cholesterol metabolism and beyond. *Curr Opin Cell Biol* 19:215–222
- Hannah VC, Ou J, Luong A, Goldstein JL, Brown MS (2001) Unsaturated fatty acids down-regulate srebp isoforms 1a and 1c by two mechanisms in HEK-293 cells. *J Biol Chem* 276:4365–4372
- Thewke DP, Panini SR, Sinensky M (1998) Oleate potentiates oxysterol inhibition of transcription from sterol regulatory element-1-regulated promoters and maturation of sterol regulatory element-binding proteins. *J Biol Chem* 273:21402–21407
- Worgall TS, Sturley SL, Seo T, Osborne TF, Deckelbaum RJ (1998) Polyunsaturated fatty acids decrease expression of promoters with sterol regulatory elements by decreasing levels of mature sterol regulatory element-binding protein. *J Biol Chem* 273:25537–25540
- Yahagi N, Shimano H, Hasty AH, Amemiya-Kudo M, Okazaki H, Tamura Y, Iizuka Y, Shionoiri F, Ohashi K, Osuga J, Harada K, Gotoda T, Nagai R, Ishibashi S, Yamada N (1999) A crucial role of sterol regulatory element-binding protein-1 in the regulation of lipogenic gene expression by polyunsaturated fatty acids. *J Biol Chem* 274:35840–35844
- Xu J, Nakamura MT, Cho HP, Clarke SD (1999) Sterol regulatory element binding protein-1 expression is suppressed by dietary polyunsaturated fatty acids. A mechanism for the coordinate suppression of lipogenic genes by polyunsaturated fats. *J Biol Chem* 274:23577–23583
- Ou J, Tu H, Shan B, Luk A, Bose-Boyd RA, Bashmakov Y, Goldstein JL, Brown MS (2001) Unsaturated fatty acids inhibit transcription of the sterol regulatory element-binding protein-1c (SREBP-1c) gene by antagonizing ligand-dependent activation of the LXR. *Proc Natl Acad Sci USA* 98:6027–6032
- Field FJ, Born E, Murthy S, Mathur SN (2002) Polyunsaturated fatty acids decrease the expression of sterol regulatory element-binding protein-1 in CaCo-2 cells: effect on fatty acid synthesis and triacylglycerol transport. *Biochem J* 368:855–864
- Kim HJ, Takahashi M, Ezaki O (1999) Fish oil feeding decreases mature sterol regulatory element-binding protein 1 (SREBP-1) by down-regulation of SREBP-1c mRNA in mouse liver. A possible mechanism for down-regulation of lipogenic enzyme mRNAs. *J Biol Chem* 274:25892–25898
- Le Jossic-Corcus C, Gonthier C, Zaghini I, Logette E, Shechter I, Bournot P (2005) Hepatic farnesyl diphosphate synthase expression is suppressed by polyunsaturated fatty acids. *Biochem J* 385:787–794
- Lee JN, Ye J (2004) Proteolytic activation of sterol regulatory element-binding protein induced by cellular stress through depletion of Insig-1. *J Biol Chem* 279:45257–45265
- Colgan SM, Tang D, Werstuck GH, Austin RC (2007) Endoplasmic reticulum stress causes the activation of sterol regulatory element binding protein-2. *Int J Biochem Cell Biol* 39:1843–1851
- Werstuck GH, Lentz SR, Dayal S, Hossain GS, Sood SK, Shi YY, Zhou J, Maeda N, Krisans SK, Malinow MR, Austin RC (2001) Homocysteine-induced endoplasmic reticulum stress causes dysregulation of the cholesterol and triglyceride biosynthetic pathways. *J Clin Invest* 107:1263–1273
- Wang X, Zelenski NG, Yang J, Sakai J, Brown MS, Goldstein JL (1996) Cleavage of sterol regulatory element binding proteins (SREBPs) by CPP32 during apoptosis. *EMBO J* 15:1012–1020
- Schroder M, Kaufman RJ (2005) ER stress and the unfolded protein response. *Mutat Res* 569:29–63
- Brewer JW, Hendershot LM, Sherr CJ, Diehl JA (1999) Mammalian unfolded protein response inhibits cyclin D1 translation and cell-cycle progression. *Proc Natl Acad Sci USA* 96:8505–8510
- Schonberg SA, Lundemo AG, Fladvad T, Holmgren K, Bremseth H, Nilsen A, Gederaas O, Tvedt KE, Egeberg KW, Krokan HE (2006) Closely related colon cancer cell lines display different sensitivity to polyunsaturated fatty acids, accumulate different lipid classes and downregulate sterol regulatory element-binding protein 1. *FEBS J* 273:2749–2765
- Jakobsen CH, Størvold GL, Bremseth H, Føllestad T, Sand K, Mack M, Olsen KS, Lundemo AG, Iversen JG, Krokan HE, Schonberg SM (2008) DHA induces ER stress and growth arrest in human colon cancer cells—associations with cholesterol and calcium homeostasis. *J Lipid Res* 49:2089–2100
- Irizarry RA, Bolstad BM, Collin F, Cope LM, Hobbs B, Speed TP (2003) Summaries of Affymetrix GeneChip probe level data. *Nucleic Acids Res* 31:e15
- Bolstad BM, Irizarry RA, Astrand M, Speed TP (2003) A comparison of normalization methods for high density oligonucleotide array data based on variance and bias. *Bioinformatics* 19:185–193
- Smyth GK (2004) Linear models and empirical bayes methods for assessing differential expression in microarray experiments. *Stat Appl Genet Mol Biol* 3: Article 3
- Benjamini Y, Hochberg Y (1995) Controlling the false discovery rate - practical and powerful approach to multiple testing. *J Royal Statistical Soc* 57:289–300

33. Gentleman RC, Carey VJ, Bates DM, Bolstad B, Dettling M, Dudoit S, Ellis B, Gautier L, Ge Y, Gentry J, Hornik K, Hothorn T, Huber W, Iacus S, Irizarry R, Leisch F, Li C, Maechler M, Rossini AJ, Sawitzki G, Smith C, Smyth G, Tierney L, Yang JY, Zhang J (2004) Bioconductor: open software development for computational biology and bioinformatics. *Genome Biol* 5:R80
34. Robichon C, Varret M, Le L, X, Lasnier F, Hajduch E, Ferre P, Dugail I (2006) DnaJA4 is a SREBP-regulated chaperone involved in the cholesterol biosynthesis pathway. *Biochim Biophys Acta* 1761:1107–1113
35. Harding HP, Zhang Y, Khersonsky S, Marciniak S, Scheuner D, Kaufman RJ, Javitt N, Chang YT, Ron D (2005) Bioactive small molecules reveal antagonism between the integrated stress response and sterol-regulated gene expression. *Cell Metab* 2:361–371
36. Horton JD, Shah NA, Warrington JA, Anderson NN, Park SW, Brown MS, Goldstein JL (2003) Combined analysis of oligonucleotide microarray data from transgenic and knockout mice identifies direct SREBP target genes. *Proc Natl Acad Sci USA* 100:12027–12032
37. Sakakura Y, Shimano H, Sone H, Takahashi A, Inoue N, Toyoshima H, Suzuki S, Yamada N (2001) Sterol regulatory element-binding proteins induce an entire pathway of cholesterol synthesis. *Biochem Biophys Res Commun* 286:176–183
38. Liscum L, Ruggiero RM, Faust JR (1989) The intracellular transport of low density lipoprotein-derived cholesterol is defective in Niemann-Pick type C fibroblasts. *J Cell Biol* 108:1625–1636
39. Martinez-Botas J, Suarez Y, Ferruelo AJ, Gomez-Coronado D, Lasuncion MA (1999) Cholesterol starvation decreases p34(cdc2) kinase activity and arrests the cell cycle at G2. *FASEB J* 13:1359–1370
40. Zeng L, Lu M, Mori K, Luo S, Lee AS, Zhu Y, Shyy JY (2004) ATF6 modulates SREBP2-mediated lipogenesis. *EMBO J* 23:950–958
41. Gill S, Chow R, Brown AJ (2008) Sterol regulators of cholesterol homeostasis and beyond: the oxysterol hypothesis revisited and revised. *Prog Lipid Res* 47:391–404
42. Metherall JE, Waugh K, Li H (1996) Progesterone inhibits cholesterol biosynthesis in cultured cells. Accumulation of cholesterol precursors. *J Biol Chem* 271:2627–2633
43. Sundqvist A, Bengoechea-Alonso MT, Ye X, Lukiyanchuk V, Jin J, Harper JW, Ericsson J (2005) Control of lipid metabolism by phosphorylation-dependent degradation of the SREBP family of transcription factors by SCF(Fbw7). *Cell Metab* 1:379–391
44. Raghov R, Yellaturu C, Deng X, Park EA, Elam MB (2008) SREBPs: the crossroads of physiological and pathological lipid homeostasis. *Trends Endocrinol Metab* 19:65–73
45. Giandomenico V, Simonsson M, Gronroos E, Ericsson J (2003) Coactivator-dependent acetylation stabilizes members of the SREBP family of transcription factors. *Mol Cell Biol* 23:2587–2599
46. Teran-Garcia M, Rufo C, Nakamura MT, Osborne TF, Clarke SD (2002) NF-Y involvement in the polyunsaturated fat inhibition of fatty acid synthase gene transcription. *Biochem Biophys Res Commun* 290:1295–1299
47. Wang Y, Rogers PM, Su C, Varga G, Stayrook KR, Burris TP (2008) Regulation of cholesterologenesis by the oxysterol receptor, LXRalpha. *J Biol Chem* 283:26332–26339
48. Dietschy JM, Turley SD, Spady DK (1993) Role of liver in the maintenance of cholesterol and low density lipoprotein homeostasis in different animal species, including humans. *J Lipid Res* 34:1637–1659
49. Rao KN (1995) The significance of the cholesterol biosynthetic pathway in cell growth and carcinogenesis (review). *Anticancer Res* 15:309–314
50. Sugiyama E, Ishikawa Y, Li Y, Kagai T, Nobayashi M, Tanaka N, Kamijo Y, Yokoyama S, Hara A, Aoyama T (2008) Eicosapentaenoic acid lowers plasma and liver cholesterol levels in the presence of peroxisome proliferators-activated receptor alpha. *Life Sci* 83:19–28
51. Natali F, Siculella L, Salvati S, Gnoni GV (2007) Oleic acid is a potent inhibitor of fatty acid and cholesterol synthesis in C6 glioma cells. *J Lipid Res* 48:1966–1975
52. Brusselmans K, Timmermans L, Van de ST, Van Veldhoven PP, Guan G, Shechter I, Claessens F, Verhoeven G, Swinnen JV (2007) Squalene synthase, a determinant of Raft-associated cholesterol and modulator of cancer cell proliferation. *J Biol Chem* 282:18777–18785
53. Kaneko R, Tsuji N, Asanuma K, Tanabe H, Kobayashi D, Watanabe N (2007) Survivin down-regulation plays a crucial role in 3-hydroxy-3-methylglutaryl coenzyme A reductase inhibitor-induced apoptosis in cancer. *J Biol Chem* 282:19273–19281

Artificial Rearing of Infant Mice Leads to n-3 Fatty Acid Deficiency in Cardiac, Neural and Peripheral Tissues

Nahed Hussein · Irina Fedorova · Toru Moriguchi ·
Kei Hamazaki · Hee-Yong Kim · Junji Hoshiba ·
Norman Salem Jr.

Received: 7 October 2008 / Accepted: 3 June 2009 / Published online: 9 July 2009
© US Government 2009

Abstract The ability to control the fatty acid content of the diet during early development is a crucial requirement for a one-generation model of docosahexaenoic acid (DHA; 22:6n3) deficiency. A hand feeding method using artificial rearing (AR) together with sterile, artificial milk was employed for feeding mice from postnatal day 2–15. The pups were fed an n-3 fatty acid adequate (3% α -linolenic acid (LNA; 18:3n3) + 1% 22:6n3) or a deficient diet (0.06% 18:3n3) with linoleic acid (LA; 18:2n6) as the only dietary source of essential fatty acids by AR along with a dam-reared control group (3.1% 18:3n3). The results indicate that restriction of n-3 fatty acid intake during postnatal development leads to markedly lower levels of brain, retinal, liver, plasma and heart 22:6n3 at 20 weeks of age with

replacement by docosapentaenoic acid (DPAn6; 22:5n6), arachidonic acid (ARA; 20:4n6) and docosatetraenoic acid (DTA; 22:4n6). A detailed analysis of phospholipid classes of heart tissue indicated that phosphatidylethanolamine, phosphatidylcholine and cardiolipin were the major repositories of 22:6n3, reaching 40, 29 and 15%, respectively. A novel heart cardiolipin species containing four 22:6n3 moieties is described. This is the first report of the application of artificially rearing to mouse pup nutrition; this technique will facilitate dietary studies of knockout animals as well as the study of essential fatty acid (EFA) functions in the cardiovascular, neural and other organ systems.

Keywords Artificial rearing · Artificial mouse milk · Docosahexaenoic acid · Docosapentaenoic acid · Brain · Heart · Retina · Liver · Plasma · Phospholipid class

N. Hussein
Faculty of Specific Education, Ain Shams University,
Cairo, Egypt

I. Fedorova · T. Moriguchi · N. Salem Jr.
Laboratory of Membrane Biochemistry and Biophysics,
National Institute on Alcohol Abuse and Alcoholism,
National Institutes of Health, 5625 Fishers Lane, Room 3N-07,
Bethesda, MD 20892-9410, USA

K. Hamazaki · H.-Y. Kim
Laboratory of Molecular Signaling,
National Institute on Alcohol Abuse and Alcoholism,
National Institutes of Health, 5625 Fishers Lane, Room 3N-07,
Bethesda, MD 20892-9410, USA

J. Hoshiba
Department of Animal Resources, Advanced Science Research
Center, Okayama University, Okayama, Japan

N. Salem Jr. (✉)
Martek Biosciences Corp., 6480 Dobbin Road, Columbia,
MD 21045, USA
e-mail: nsalem@martek.com

Abbreviations

AR Artificial rearing
n-3 Adq n-3 Fatty acid adequate group
n-3 Def n-3 Fatty acid deficient group

Introduction

Nutritional studies during the early postnatal period are difficult to conduct since mammals are dependent upon maternal breast milk for nourishment and the breast milk composition cannot be controlled since it differs from the maternal diet. The artificial rearing (AR) method permits precise control of dietary essential fatty acids when used in combination with artificial milk and allows for a rapid induction of neural 22:6n3 deficiency in the newborn rat

[1–3]. Hoshiba has introduced a new type of nursing bottle for use in AR employing hand feeding that supports excellent pup survival [4] and recently it has been adapted for essential fatty acid research [3, 5]. This work has employed rats; however, mice are the most widely used animal in molecular biological work where genetic mutants are readily available. Thus, a practical method of artificially rearing mouse pups is desirable for neonatal nutrition.

Experimental animal, human and cell culture studies have reported anti-arrhythmic actions of omega 3 fatty acids [6]. Ku et al. [7] showed that the recovery of cardiac function after cold storage was impaired in hyperlipidemic rats fed a high-fat diet, but was restored in the presence of omega-3 fatty acids. The administration of a lipid preparation (medium chain-triacylglycerols (MCT): fish oil (FO) or MCT: triolein (OO)) improved cardiac function during aerobic reperfusion post-ischemia. In addition to the previous effect; the bolus injection of MCT:FO opposed the deleterious effect of long-term n-3 fatty acid deficiency and, in this respect, was superior to MCT:OO [8]. In a recent study by Porto et al. [9] the alteration of cardiac function in n-3 deficient rats and its improvement after injection of MCT:FO emulsion coincides with parallel changes in heart lipid fatty acid content and pattern.

In humans, Mori et al. [10] have also shown that compared with a placebo, heart rate was significantly reduced by 22:6n3 and increased by eicosapentaenoic acid (EPA; 20:5n3). The beat-to-beat variability correlated directly with the 22:6n3 content of platelet membranes in survivors of myocardial infarction [11]. The recent GISSI-Prevention study of 11,324 patients showed a marked decrease in the risk of sudden cardiac death as well as a reduction in all-cause mortality in the group taking omega-3 fatty acid ethyl esters, despite the use of other secondary prevention drugs, including beta-blockers and lipid-lowering therapy [12].

The fatty acid composition of myocardial membrane phospholipids is sensitive to the type of fatty acids consumed in the diet. Indeed, the myocardium and the myocardial membrane phospholipids are rich in n-3 PUFA after feeding fish oils [13–15]. Kramer [16] observed no effect of dietary lipids on the proportions of the major phospholipids of rat heart after feeding various plant oil supplements. These observations thus indicate that dietary lipid induced changes in the fatty acid composition of cardiac phospholipids are due primarily to changes in the fatty acid content of the lipids, rather than to altering lipid class profiles. Garg et al. [17] demonstrated for the first time that short-term supplementation with fish oil concentrate results in significant incorporation of long chain n-3 PUFA with a concomitant depletion of the eicosanoid substrate 20:4n6 in the human atrium.

In the present study, an AR system was employed to produce mice with lower levels of brain 22:6n3 in the first generation by feeding diets with only 18:2n6 as a source of essential fatty acids; a second group of mice were fed an identical diet to which 18:3n3 and 22:6n3 were substituted for a portion of the oleate (18:1n9). The fatty acid content of neural and peripheral tissues is presented.

Materials and Methods

Animals and Study Design

Time-pregnant, female ICR mice of 2-day gestational age were obtained from Harlan (Indianapolis, IN) and immediately placed on a diet (maternal diet) containing 3.1% 18:3n3 as the source of n-3 fatty acids (Table 1). They were maintained in our animal facility under conventional conditions with controlled temperature (23 ± 1 °C) and illumination (12 h; 06.00–18.00 h) and water was provided ad libitum. At postnatal day (PND) 2, one male pup was selected from various litters, born within a 48 h time window and randomly allocated into one of two experimental groups with the constraint that the groups had an equal mean body weight. A third male group served as another reference group and was allowed to suckle from dams fed on the maternal diet (dam-reared group; $n = 16$) containing 3.1 wt % 18:3n3. The two experimental groups were artificially fed one of the two artificial milks: n-3 fatty acid deficient (n-3 Def; $n = 14$) milk (18:2n6 only added as EFA) or an identical milk except that 3.1 wt % 18:3n3 and 1 wt % 22:6n3 were added (n-3 Adq; $n = 14$) in place of some of the monounsaturated fat (Table 2). All experimental procedures were approved by the Animal Care and Use Committee of the National Institute on Alcohol Abuse and Alcoholism, National Institute of Health.

Artificial Rearing System

The AR procedure used was a hand-feeding technique with a newly developed nursing bottle as described by Hoshiba [4] and recently adapted for essential fatty acid research [3, 5]. The AR system consisted of a custom made nursing bottle, container, cage, digital microprocessor incubator (Quincy Lab, Inc., Chicago, IL) with a thermo-hygrometer (Sper Scientific Ltd., Scottsdale, AZ).

Artificial Milk

The artificial milk formula was modified from the method of Yajima et al. [18, 19]. Table 2 shows the ingredients used as well as their commercial sources. Casein, whey

Table 1 Nutrient and fatty acid composition of pelleted diets given to dams and pups at weaning

Ingredient	Amount (g/100 g)		
	Maternal	n-3 Def	n-3 Adq
Casein, vitamin free ^a	20		
Carbohydrate	60		
Corn starch	15		
Sucrose	10		
Dextrose	19.9		
Maltose-dextrin	15		
Cellulose	5		
Mineral and salt mix ^b	3.5		
Vitamin mix ^c	1		
L-Cystine	0.3		
Choline bitartrate	0.25		
TBHQ ^d	0.002		
Fat			
Hydrogenated coconut oil	7.75	8.1	7.45
Safflower oil	1.77	1.9	1.77
Flaxseed oil	0.48	–	0.48
DHASCO ^e	–	–	0.3
Fatty acid composition (wt %)			
∑ Saturated	74.6	80.9	71.1
∑ Monounsaturated	5.1	3.5	6.0
18:2n6	15.3	13.4	16.0
18:3n3	3.1	0.09	2.9
22:6n3	–	–	1.6
n-6/n-3	5.8	143	3.5

^a Dyets Inc. catalogue #400625 for maternal diet and ALACID casein (NZMP North America Inc) for n-3 Def and n-3 Adq diet

^b Dyets Inc. catalogue #210025

^c Dyets Inc. catalogue #310025

^d TBHQ is tert-butyl hydroquinone

^e Martek Biosciences Corporation. DHASCO refers to a mixture of oil extracted from the unicellular algae *Cryptocodinium cohnii* and high oleic sunflower oil, the resulting mixed oil contains 44% of product weight as 22:6n3

protein hydrolysate and whey protein were used as protein sources and lactose was used as the carbohydrate. The protein sources were carefully chosen so as not to introduce significant levels of n-3 fatty acids, as this is often the major source of introduction of these components into n-3 fatty acid deficient diets [25]. For complete dissolution, all ingredients were mixed in the order described by Kanno et al. [20] so as to minimize precipitation. The milk was then homogenized two times under high pressure (120 kg/cm²) using a homogenizer with a two-stage valve (Model #HP50–250 FES International, Pomona, CA) that had been cleaned by rinsing with 0.1 M NaOH and then neutralized with sterilized water. The homogenized milk was tyndalized twice at 63 °C for 30 min, 6 h apart. The complete

Table 2 Nutrient composition of the artificial milk for mouse pups

Ingredient	Amount (weight/100 mL milk)	
	n-3 Def	n-3 Adq
Protein (g)		
Whey protein (Alacen, WPI) ^a	3.64	3.64
Whey protein Hydrolysate ^g	4.00	4.00
Casein (Alacid, acid casein) ^a	3.46	3.46
Carbohydrate (g)		
alpha-Lactose ^b	2.6	2.6
Fat (g)		
MCT oil ^d	2.08	2.08
Coconut oil (hydrogenated) ^e	4.32	4.32
18:1n9 ethyl ester ^f	7.2	6.6
18:2n6 ethyl ester ^f	2.4	2.4
18:3n3 ethyl ester ^f	—	0.48
22:6n3 ethyl ester ^f	—	0.16
Cholesterol ^b	0.04	0.04
Vitamins (g)		
Vitamin mix ^c	0.50	0.50
Vitamin C ^b	0.02	0.02
Tricholine citrate ^b	0.37	0.37
Minerals (mg)		
NaOH ^b	102.5	102.5
KOH ^b	170	170
GlyCaPO ₄ ^b	800	800
MgCl ₂ 6H ₂ O ^b	183	183
CaCl ₂ 2H ₂ O ^b	210	210
Ca ₃ -4H ₂ O-citrate ^b	250	250
Na ₂ HPO ₄ ^b	114	114
KH ₂ PO ₄ ^b	51	51
FeSO ₄ ^b	3.0	3.0
ZnSO ₄ ^b	6.0	6.0
CuSO ₄ ^b	1.6	1.6
MnSO ₄ ^b	0.075	0.075
NaF ^b	0.15	0.15
KI ^b	0.18	0.18
K ₂ SO ₄ ^b	163.1	163.1
Na ₂ SeO ₄ ^b	0.036	0.036
(NH ₄) ₂ MoO ₄ ^b	0.028	0.028
Na ₂ O ₃ Si 9H ₂ O ^b	5.075	5.075
CrK(SO ₄) ₂ 12H ₂ O ^b	0.963	0.963
LiCl ^b	0.061	0.061
H ₃ BO ₃ ^b	0.285	0.285
NiCO ₃ ^b	0.111	0.111
NH ₄ VO ₃ ^b	0.023	0.023
Others (g)		
Carnitine ^b	0.004	0.004
Picolinate ^b	0.002	0.002
Ethanolamine ^b	0.004	0.004
Taurine ^b	0.015	0.015

Table 2 continued

Ingredient	Amount (weight/100 mL milk)	
	n-3 Def	n-3 Adq
Serine ^b	0.03	0.03
Cystine ^b	0.3	0.3
Tryptophan ^b	0.03	0.03
Methionine ^b	0.005	0.005
Actual fatty acid composition of artificial mouse milk (wt %) ^h		
∑ Saturated	30.62	32.62
∑ Monounsaturated	49.09	45.79
18:2n6	16.72	16.9
18:3n3	0.06	3.14
22:6n3	–	0.93
n-6/n-3	207.6	4.2

Component sources were as follows: ^a NZMP (North America) Inc, Santa Rosa, CA; ^b Sigma-Aldrich Corp. St. Louis, MO; ^c Harlan, Madison, WI; ^d Novartis Medical Nutrition, Fremont, MI; ^e Dyets, Bethlehem, PA; ^f Nu-Chek Prep. Inc. Elysian, MN; ^g Chicago Sweeteners, Chicago, IL

^h This fatty acid profile was analyzed by transmethylation of each artificial milk and GC analysis. Only trace quantities of the long-chain polyunsaturated fatty acids 20:4n6, 20:5n3, 22:5n3 were detected (i.e., <0.01%). Other minor peaks were not included

milk was poured into 50 mL sterilized polypropylene bottles (Falcon, San Jose, CA) and stored at -40°C . The milks contained 16 wt % lipids composed of saturated fat (medium chain triglycerides and hydrogenated coconut oil) and the ethyl ester form of purified unsaturated fatty acids (Nu-Chek Prep, Inc., Elysian, MN). The n-3 fatty acid deficient milk (n-3 Def) contained 16.7% of 18:2n6 and 0.06% of 18:3n3 and the n-3 fatty acid adequate (n-3 Adq) milk contained 16.9% of 18:2n6 and 3.1% 18:3n3 and 0.93% of 22:6n3 upon actual analysis (Table 2). The addition of the 18:3n3 and 22:6n3 to the n-3 Adq diet was substituted for an equal quantity of ethyl 18:1n9; this introduced only a 4% difference in 18:1n9 content between the two diets. Saturated, monounsaturated, and 18:2n6 were balanced leaving only the level of 18:3n3 and 22:6n3 as a dietary variable. Insulin-Like Growth Factor-I (IGF-I), (Fitzgerald Industries International, Concord, MA) was added to the milk as studies suggest that milk-borne IGF-I is important in modulation of somatic and gastrointestinal tract growth in the neonatal rat [21]. The IGF-I was added to the artificial mouse milk in the following manner: the IGF-I (10 μg in 0.5 mL of 0.1 M acetic acid) was added to Pyrex screw cap culture tubes (13 \times 100 mm, Corning). Tube contents were lyophilized and stored at -20°C until use. Each morning, 0.2 mL of Tris buffer (50 mM, pH 7.4) was added to each

tube and subjected to gentle mixing, then transferred into sterile polypropylene bottles with 20 mL of artificial milk to achieve a final IGF-I concentration of 500 ng IGF-I/mL of artificial milk.

Pelleted Diets

The three pelleted diets used were based on the AIN-93 [22] formulation with several modifications to obtain the extremely low n-3 fatty acid level required in this study (Table 1). The diets were obtained commercially and used a cold pelleting process to preserve unsaturated fats (Dyets, Bethlehem, PA). Pups were weaned to pelleted diets with a fat composition similar to that fed during the AR period; the dam-reared group was weaned onto the same diet as their dams and they were maintained on these diets until they were killed. All three diets contained 10 wt % fat and had a similar content of 18:2n6. The fatty acid data in Tables 1 and 2 represent actual gas chromatographic (GC) analyses of the entire diet (rather than theoretical values or analysis of just the lipid mixtures).

Lipid Extraction

The mice were killed by decapitation at 20 weeks of age, tissue samples including brain, liver, heart, plasma and retina were collected and stored at -80°C . The total lipid extracts of tissues were prepared according to the method of Folch et al. [23]. Aliquots of the lipid extracts were transmethylated with 14% BF_3 -methanol (Alltech Associates, Deerfield, IL) at 100°C for 60 min by a modification of the method of Morrison and Smith [24] with hexane addition [25]. The total lipids in the artificial milk and pelleted diets were transmethylated by the method of Lepage and Roy [26] as this is more accurate when shorter chain fatty acids (e.g. 8–12C) occur at appreciable levels. The fatty acid methyl esters were analyzed by a fast gas chromatographic method as previously described [27]. Data were expressed as a percentage of total fatty acid weight (% by wt) or referenced to an internal standard and expressed as an absolute concentration ($\mu\text{g}/\text{mg}$ tissue wet weight).

High Performance Liquid Chromatography (HPLC) Separations of Heart Lipid Classes

HPLC Procedures

Normal-phase HPLC was performed using a HP1100 consisting of a quaternary pump, online degasser, auto-sampler and variable wavelength detector (Agilent Technologies, Wilmington, DE). The column was an Advantage

silica 5 μm (60 \AA) 250 \times 4.6 mm purchased from Thomson Instrument Company (Clear Brook, VA). A guard column of 4.0 \times 10 mm packed with silica was used in conjunction with the analytical column.

An aliquot of 0.3–0.6 mg of the heart tissue lipid extract was dissolved in 20 μL chloroform and injected into the HPLC system. Phospholipid separations were achieved with a solvent system consisting of hexane:2-propanol:25 mM potassium acetate (pH 7.0):ethanol:glacial acetic acid (250:607:62: 100:0.6) (by volume) (Buffer A) and hexane:2-propanol:25 mM potassium acetate (pH 7.0):acetonitrile:glacial acetic acid (442:490:62:25:0.6) (by volume) (Buffer B) at 50 $^{\circ}\text{C}$ using a modification of the method of Lesnefsky et al. [28]. The first 65 min of the elution scheme was designed to separate various lipid classes, starting with Buffer A for 15 min for elution of neutral lipids (which included triacylglycerol, cholesterol, and cholesterol esters) and subsequently phosphatidylethanolamine followed by a linear gradient from A to B for elution of phosphatidylinositol and cardiolipin. The flow rate was increased from 1.0 to 1.25 mL/min at 26 min and then held constant until the end of the elution scheme for elution of phosphatidylserine and phosphatidylcholine. A 30 min period with Buffer A at the end of each run was used to reequilibrate the column prior to the next injection with a flow rate of 1 mL/min. Chromatographic peaks were identified using ultraviolet absorbance at 208 nm. Individual phospholipid peaks were identified by comparison of retention time to commercial standards. Phospholipid fractions were collected and stored at -80°C until later analysis for fatty acid content.

HPLC Materials

HPLC-grade hexane, water and potassium acetate were obtained from EMD Chemicals Inc. (Gibbstown, NJ), 2-propanol, acetonitrile and glacial acetic acid were obtained from J. T. Baker Inc. (Phillipsburg, NJ), ethanol was obtained from Pharmco products Inc. (Brookfield, CT). Phospholipid standards were obtained from Avanti Polar lipids (Alabaster, AL).

Transesterification and Gas Chromatography

The lipid fractions prepared by HPLC were transesterified as follows: 1 mL of hexane and 1 mL of 14% BF_3 -methanol was added and the mixture was incubated at 100 $^{\circ}\text{C}$ for 1 h. The fatty acid methyl esters were extracted with hexane and analyzed by gas chromatography as described above. A pulsed splitless mode was used for GC analysis of methyl esters from phosphatidylinositol, phosphatidylserine and cardiolipin due to the low concentration of these fractions. GC methodology was as previously described

[27] with the exception that ramp pressure was initially 55.5 psi with a 0.63 min hold; thereafter pressure was ramped at a rate of 50 psi/min to 14.50 psi, with a 60 min hold. The run time for a single sample was 74 min, with a sample injection-to injection time of 76 min.

Phospholipid Molecular Species Analysis of Cardiolipin

For phospholipid molecular species analysis, heart lipids were extracted in the presence of deuterium-labeled phospholipid standards and analyzed using reversed-phase high-performance liquid chromatography/electrospray ionization–mass spectrometry (HPLC/ESI–MS) with a C18 column (Prodigy, 150 \times 2.0 mm, 5 μm ; Phenomenex, Torrance, CA) as described previously [29]. The separation was accomplished using a linear solvent gradient (water:0.5% ammonium hydroxide in methanol:hexane), changing from 12:88:0 to 0:88:12 in 17 min after holding the initial solvent composition for 3 min at a flow rate of 0.4 mL/min [30]. An Agilent 1100 LC/MSD instrument (Palo Alto, CA) was used to detect the separated phospholipid molecular species. For electrospray ionization, the drying gas temperature was 350 $^{\circ}\text{C}$; the drying gas flow rate and nebulizing gas pressure were 11 L/min and 45 psi, respectively. The capillary and fragmentor voltages were set at 4,500 and 300 V, respectively. Identification of individual phospholipid molecular species was based on the monoglyceride, diglyceride and protonated molecular ion peaks [31].

Statistical Analysis

All data were expressed as the mean \pm SEM. Mouse growth was tested using repeated measures ANOVA (Statsoft, Tulsa, OK). Tissue fatty acid comparisons at 20 weeks of age were performed using a one-way ANOVA. The analysis was followed by Tukey HSD post hoc test for determination of statistical significance among the three dietary groups.

Results

Body and Organ Weights of Dam-Reared and Artificially Reared Mice

The AR pups had a significantly lower body weight than that of dam-reared pups from PND 2 to PND 21; Fig. 1 illustrates changes in body weight in the three groups. There was no significant difference in body weight at PND 21 and the mean body weights were 10.68 \pm 0.33 g for the n-3 Def, 10.73 \pm 0.19 g for the n-3 Adq, and 12.12 \pm 0.27 g for the dam-reared groups. After PND 21, the AR pups gained

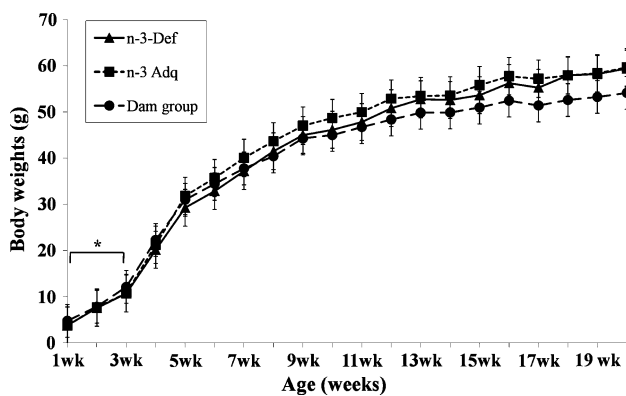


Fig. 1 Growth curves of artificially reared and dam-reared mouse pups from PND2 through week 20. The body weight is presented as the mean \pm SEM, with an $n = 14$ or 16. Asterisk indicates $P < 0.001$ for Dam's group versus the artificially reared groups from PND2–PND21

weight rapidly so as to catch up and surpass the dam-reared pups. At 20 weeks of age, the mean body weights were 59.4 ± 1.5 g for the n-3 Def, 59.4 ± 1.0 g for the n-3 Adq, and 54.1 ± 1.4 g for the dam-reared groups. At 20 weeks of age there were no differences detected by one-way ANOVA in excised tissue weights between the AR and dam-reared groups except for the brain (the organ weights were for the brain (dam-reared group, 0.50 ± 0.01 g; n-3 Adq, 0.47 ± 0.01 g; n-3 Def, 0.460 ± 0.004 g), liver (dam-reared group, 2.66 ± 0.18 g; n-3 Adq, 3.13 ± 0.19 g; n-3 Def, 2.98 ± 0.24 g), heart (dam-reared group, 0.22 ± 0.01 g; n-3 Adq, 0.20 ± 0.01 g; n-3 Def, 0.21 ± 0.01 g), and retina (dam-reared group, 5.18 ± 0.42 mg; n-3 Adq, 5.64 ± 0.38 mg; n-3 Def, 5.43 ± 0.51 mg).

Fatty Acid Composition of Tissues

The 22:6n3 was significantly lower in the n-3 Def group as compared with the dam-reared and n-3 Adq groups in all tissues. In the n-3 Adq group, the 22:6n3 was similar to the dam-reared animals in all tissues, except liver. The decreased content of 22:6n3 for the n-3 Def group was largely replaced by a marked elevation in the percentage of 22:5n6 ($P < 0.0001$).

The 20:4n6 and 22:4n6 were also increased in the n-3 Def group compared with levels in the dam-reared and n-3 Adq groups except in heart tissue where there was no significant difference among the three dietary groups in the percentage of 22:4n6.

The brain, retina, and heart tissues had significantly lower docosapentaenoic acid (DPAn3; 22:5n3) in the n-3 Def group compared with the dam-reared and n-3 Adq groups whereas the plasma had significantly higher 22:5n3 in n-3 Def group compared with the dam-reared and n-3

Adq groups; the 22:5n3 was significantly different among the three dietary groups in the liver.

In the liver and retina, there were statistically significant differences in the ratio of 22:5n6/22:6n3 and n-6/n-3 between the dam-reared and n-3 Adq groups versus the n-3 Def group ($P < 0.0001$ for 22:5n6/22:6n3, $P < 0.0001$ for the n-6/n-3); for the liver, plasma and heart, there were significant differences in the ratio of 22:5n6/22:6n3 and n-6/n-3 in the n-3 Def group compared with those of the dam-reared and n-3 Adq groups ($P < 0.0001$ for 22:5n6/22:6n3, $P < 0.0001$ for n-6/n-3).

In brain, retina, heart and plasma the n-3 Def group showed a significantly higher percentage of total n-6 and a lower percentage of total n-3 compared with the n-3 Adq and the dam-reared group. In liver, the n-3 Def group showed a significantly lower percentage of total n-3 compared with those of the dam-reared, and n-3 Adq groups; there was no significant differences in total n-6 PUFA among the three dietary groups.

It must be noted that significant differences in weight percent do not necessary imply significant differences in absolute weight due to differences in some cases of absolute total fatty acid content. It should be noted in this regard that the absolute concentration of liver total fatty acid was significantly greater in the two controlled diets relative to the dam-reared control (Table 5) and this may suggest steatosis. This may be due to the very high content of saturated fatty acids (about 71–81%) in the two controlled diets due to the restriction in the use of vegetable oils in the basal fat that contained omega-3 fatty acids. Although the maternal diet also had a similarly high content of saturated fatty acids, the maternal milk composition could not be controlled in this regard. Since the two experimental diets (n-3 Adq and n-3 Def) had a similar liver total fatty acid content, the differences noted above in the weight percent data also correspond to differences in absolute concentrations.

When the results are presented on a relative percentage basis, the percentage of each fatty acid is influenced by changes in the other fatty acids. On the other hand, if the fatty acid results were reported as absolute concentrations, changes in fatty acids would be independent of each other. Detailed fatty acid compositions, including total fatty acid concentrations of each dietary group for each tissue, are included in Tables 3, 4, 5, 6, and 7.

Heart Lipid Classes

Since heart total lipid exhibited an extremely high 22:6n3 level when dietary 22:6n3 was supplied, a percentage much higher than that observed in any other tissue, it was of interest to further delineate the lipid pools within which the 22:6n3 resided. A non-uniform distribution of the major phospholipid classes in cardiac muscle has been reported

Table 3 Brain fatty acid composition of the two artificially reared groups and a dam-reared reference group at 20 week of age (wt % of total fatty acids)

	Dietary group		
	Dam-reared (n = 16)	n-3 Adq (n = 14)	n-3 Def (n = 14)
Fatty acids			
12:0	0.021 ± 0.002 ^a	0.028 ± 0.002 ^b	0.020 ± 0.002 ^a
14:0	0.94 ± 0.03 ^a	0.91 ± 0.03 ^a	0.78 ± 0.03 ^b
16:0 DMA	0.04 ± 0.01 ^a	ND ^a	0.52 ± 0.08 ^b
16:0	19.67 ± 0.14	20.19 ± 0.27	19.89 ± 0.22
18:0 DMA	ND	ND	0.22 ± 0.07
18:0	18.17 ± 0.14 ^a	18.99 ± 0.33 ^b	18.49 ± 0.11 ^{ab}
20:0	0.39 ± 0.01	0.35 ± 0.02	0.36 ± 0.02
22:0	0.51 ± 0.02 ^a	0.46 ± 0.02 ^a	0.62 ± 0.03 ^b
24:0	1.08 ± 0.07	0.99 ± 0.11	0.90 ± 0.05
Total saturates	40.83 ± 0.20	41.94 ± 0.56	41.81 ± 0.25
16:1n7	0.95 ± 0.06	0.88 ± 0.07	0.86 ± 0.05
18:1 DMA	ND	ND	0.13 ± 0.03
18:1n9	15.38 ± 0.16 ^a	14.17 ± 0.33 ^b	13.70 ± 0.15 ^b
18:1n7	3.71 ± 0.04 ^a	3.42 ± 0.07 ^b	3.82 ± 0.04 ^a
20:1n9	2.19 ± 0.08 ^a	1.81 ± 0.12 ^b	1.81 ± 0.09 ^b
22:1n9	0.28 ± 0.01 ^a	0.22 ± 0.01 ^b	0.23 ± 0.02 ^b
24:1n9	3.29 ± 0.11	2.91 ± 0.22	2.82 ± 0.11
Total monounsaturates	25.80 ± 0.39 ^a	23.41 ± 0.74 ^b	23.37 ± 0.40 ^b
18:2n6	0.53 ± 0.01 ^a	0.50 ± 0.02 ^a	0.37 ± 0.02 ^b
18:3n6	ND	ND	ND
20:2n6	0.131 ± 0.004 ^a	0.13 ± 0.01 ^a	0.10 ± 0.01 ^b
20:3n6	0.55 ± 0.01 ^a	0.54 ± 0.01 ^a	0.25 ± 0.01 ^b
20:4n6	7.06 ± 0.12 ^a	7.85 ± 0.16 ^b	9.01 ± 0.14 ^c
22:2n6	ND	ND	ND
22:4n6	2.19 ± 0.05 ^a	2.43 ± 0.04 ^b	3.68 ± 0.04 ^c
22:5n6	0.19 ± 0.01 ^a	0.25 ± 0.01 ^a	6.45 ± 0.19 ^b
Total n-6 PUFA	10.65 ± 0.14 ^a	11.70 ± 0.17 ^b	19.86 ± 0.26 ^c
18:3n3	0.060 ± 0.003 ^a	0.061 ± 0.004 ^a	0.041 ± 0.003 ^b
20:5n3	0.090 ± 0.004 ^a	0.08 ± 0.01 ^b	ND ^c
22:5n3	0.26 ± 0.01 ^a	0.23 ± 0.01 ^a	0.10 ± 0.02 ^b
22:6n3	14.57 ± 0.32 ^a	15.70 ± 0.35 ^b	7.74 ± 0.20 ^c
Total n-3 PUFA	14.97 ± 0.32 ^a	16.07 ± 0.36 ^b	7.88 ± 0.20 ^c
16:1n7/16:0	0.05 ± 0.003	0.04 ± 0.004	0.04 ± 0.003
18:1n9/18:0	0.85 ± 0.01 ^b	0.75 ± 0.03 ^a	0.74 ± 0.01 ^a
20:4n6/20:3n6	12.94 ± 0.40 ^b	14.70 ± 0.35 ^b	36.17 ± 1.30 ^a
20:4n6/20:5n3	81.12 ± 4.24	109.54 ± 6.52	ND
20:4n6/22:6n3	0.49 ± 0.01 ^b	0.50 ± 0.01 ^b	1.17 ± 0.03 ^a
20:5n3/22:6n3	0.01 ± 0.0003	0.005 ± 0.0004	ND
22:5n6/22:6n3	0.013 ± 0.001 ^a	0.016 ± 0.001 ^a	0.84 ± 0.03 ^b
22:5n6+22:6n3	14.75 ± 0.31 ^a	15.95 ± 0.35 ^b	14.19 ± 0.26 ^a
n-6/n-3	0.71 ± 0.01 ^a	0.73 ± 0.01 ^a	2.54 ± 0.07 ^b
n-6+n-3	25.62 ± 0.42 ^a	27.76 ± 0.50 ^b	27.74 ± 0.36 ^b
Total fatty acids (µg/mg wet brain)	41.26 ± 0.46 ^a	39.16 ± 0.49 ^b	40.99 ± 0.44 ^a

Each parameter is presented as the mean (±SEM). Means with different alphabetical superscripts (a, b, c) indicate significant differences across diets by Tukey's HSD at $P < 0.05$

ND not detected (i.e., <0.01%), DMA dimethyl acetal

[32]. Both the distribution of the major heart phospholipid classes, as well as their fatty acid composition was determined, in order to more clearly define the extent of the diet-

induced changes. Significant changes in the distribution of phosphatidylcholine ($P < 0.01$), phosphatidylethanolamine ($P < 0.05$), neutral lipid ($P < 0.05$), cardiolipin

Table 4 Retina fatty acid composition of the two artificially reared groups and a dam-reared reference group at 20 week of age (wt % of total fatty acids)

	Dietary group		
	Dam-reared (<i>n</i> = 16)	n-3 Adq (<i>n</i> = 14)	n-3 Def (<i>n</i> = 14)
Fatty acids			
10:0	0.13 ± 0.02 ^a	0.26 ± 0.06 ^{ab}	0.36 ± 0.03 ^b
12:0	0.052 ± 0.005 ^a	0.10 ± 0.01 ^b	0.09 ± 0.01 ^{ab}
14:0	1.14 ± 0.06 ^a	1.30 ± 0.07 ^a	0.46 ± 0.02 ^b
16:0	19.78 ± 0.35 ^a	20.72 ± 0.50 ^a	18.44 ± 0.15 ^b
18:0	17.11 ± 0.37	17.08 ± 0.40	18.01 ± 0.28
20:0	0.23 ± 0.01 ^{ab}	0.25 ± 0.01 ^a	0.21 ± 0.01 ^b
22:0	0.16 ± 0.01 ^a	0.19 ± 0.02 ^a	0.12 ± 0.01 ^b
24:0	0.13 ± 0.01 ^a	0.14 ± 0.02 ^a	0.23 ± 0.01 ^b
Total saturates	38.72 ± 0.62 ^{ab}	40.05 ± 0.63 ^a	37.92 ± 0.21 ^b
12:1	0.25 ± 0.09	0.18 ± 0.06	0.18 ± 0.05
14:1	0.27 ± 0.06	0.65 ± 0.20	0.67 ± 0.08
16:1n7	0.69 ± 0.06 ^{ab}	0.89 ± 0.10 ^a	0.55 ± 0.06 ^b
18:1n7	1.54 ± 0.06 ^a	1.71 ± 0.06 ^a	1.97 ± 0.05 ^b
18:1n9	10.51 ± 0.59	11.39 ± 0.57	9.76 ± 0.38
20:1n9	0.64 ± 0.06 ^a	0.50 ± 0.06 ^{ab}	0.36 ± 0.03 ^b
22:1n9	0.03 ± 0.01	0.04 ± 0.01	0.027 ± 0.002
24:1n9	0.20 ± 0.02	0.27 ± 0.04	0.21 ± 0.02
Total monounsaturates	14.14 ± 0.66	15.64 ± 0.75	13.73 ± 0.47
18:2n6	0.69 ± 0.03 ^a	0.84 ± 0.07 ^b	0.45 ± 0.02 ^c
18:3n6	0.022 ± 0.001 ^a	0.07 ± 0.03 ^b	0.048 ± 0.003 ^{ab}
20:2n6	0.10 ± 0.01	0.16 ± 0.05	0.13 ± 0.01
20:3n6	0.38 ± 0.01 ^a	0.37 ± 0.02 ^a	0.26 ± 0.02 ^b
20:4n6	7.17 ± 0.21 ^a	7.93 ± 0.21 ^b	9.86 ± 0.15 ^c
22:2n6	0.025 ± 0.003 ^a	0.04 ± 0.01 ^{ab}	0.05 ± 0.01 ^b
22:4n6	0.84 ± 0.04 ^a	0.96 ± 0.03 ^a	2.44 ± 0.10 ^b
22:5n6	0.11 ± 0.01 ^a	0.13 ± 0.01 ^a	5.72 ± 0.66 ^b
Total n-6 PUFA	9.33 ± 0.24 ^a	10.50 ± 0.21 ^a	18.96 ± 0.79 ^b
18:3n3	0.018 ± 0.003 ^a	0.033 ± 0.004 ^b	0.046 ± 0.004 ^c
20:3n3	0.025 ± 0.003	0.028 ± 0.004	0.03 ± 0.01
20:5n3	0.47 ± 0.03 ^a	0.39 ± 0.03 ^b	0.017 ± 0.002 ^c
22:5n3	0.67 ± 0.02 ^a	0.63 ± 0.03 ^a	0.27 ± 0.02 ^b
22:6n3	18.91 ± 1.41 ^a	18.31 ± 1.58 ^a	12.95 ± 0.78 ^b
Total n-3 PUFA	20.09 ± 1.39 ^a	19.38 ± 1.57 ^a	13.32 ± 0.78 ^b
16:1n7/16:0	0.03 ± 0.003	0.04 ± 0.005	0.03 ± 0.003
18:1n9/18:0	0.62 ± 0.04 ^{ab}	0.67 ± 0.04 ^a	0.55 ± 0.03 ^b
20:4n6/20:3n6	19.23 ± 0.79 ^a	21.84 ± 1.05 ^a	40.49 ± 3.48 ^b
20:4n6/20:5n3	15.99 ± 1.04 ^a	21.55 ± 1.32 ^a	661.14 ± 64.04 ^b
20:4n6/22:6n3	0.41 ± 0.03 ^a	0.48 ± 0.04 ^a	0.81 ± 0.06 ^b
20:5n3/22:6n3	0.03 ± 0.003 ^a	0.02 ± 0.003 ^a	0.001 ± 0.0002 ^b
22:5n6/22:6n3	0.007 ± 0.001 ^a	0.008 ± 0.001 ^a	0.43 ± 0.03 ^b
22:5n6+22:6n3	19.02 ± 1.41	18.44 ± 1.58	18.66 ± 1.39
n-6/n-3	0.46 ± 0.03 ^a	0.54 ± 0.05 ^a	1.42 ± 0.05 ^b
n-6+n-3	29.42 ± 1.42	29.89 ± 1.54	32.28 ± 1.50
Total fatty acids (µg/mg wet retina)	23.72 ± 2.13 ^b	19.63 ± 1.76 ^b	36.78 ± 4.02 ^a

* Each parameter is presented as the mean (± SEM). Means with different alphabetical superscripts (a, b, c) indicate significant differences across diets by Tukey's HSD at *P* < 0.05

Table 5 Liver fatty acid composition of the two artificially reared groups and a dam-reared reference group at 20 week of age (wt % of total fatty acids)

	Dietary group		
	Dam-reared (n = 16)	n-3 Adq (n = 14)	n-3 Def (n = 14)
Fatty acids			
10:0	0.014 ± 0.002	0.013 ± 0.01	0.011 ± 0.001
12:0	0.32 ± 0.03	0.25 ± 0.01	0.31 ± 0.02
14:0	1.38 ± 0.05 ^{ab}	1.24 ± 0.05 ^a	1.56 ± 0.10 ^b
16:0	24.56 ± 0.35	24.13 ± 0.51	23.98 ± 0.54
18:0	5.90 ± 0.30 ^a	4.24 ± 0.43 ^b	4.47 ± 0.57 ^{ab}
20:0	0.41 ± 0.03 ^a	0.26 ± 0.03 ^b	0.22 ± 0.02 ^b
22:0	0.29 ± 0.02 ^a	0.16 ± 0.03 ^b	0.13 ± 0.02 ^b
24:0	0.033 ± 0.004 ^a	0.05 ± 0.02 ^{ab}	0.09 ± 0.02 ^b
Total saturates	32.91 ± 0.38 ^a	30.35 ± 0.52 ^b	30.77 ± 0.43 ^b
12:1	0.010 ± 0.002	0.011 ± 0.01	0.009 ± 0.001
14:1	0.09 ± 0.01	0.08 ± 0.01	0.14 ± 0.01
16:1n7	4.10 ± 0.16 ^a	4.58 ± 0.35 ^a	4.68 ± 0.30 ^b
18:1n7	4.66 ± 0.27 ^a	5.38 ± 0.24 ^a	7.35 ± 0.33 ^b
18:1n9	26.69 ± 1.68 ^a	35.92 ± 1.55 ^a	34.35 ± 2.14 ^b
20:1n9	0.85 ± 0.04 ^a	0.99 ± 0.04 ^b	0.99 ± 0.03 ^b
22:1n9	0.100 ± 0.005	0.09 ± 0.01	0.08 ± 0.01
24:1n9	0.20 ± 0.01	0.14 ± 0.02	0.15 ± 0.04
Total monounsaturates	36.70 ± 1.96 ^a	47.21 ± 1.88 ^b	47.74 ± 2.25 ^b
18:2n6	10.89 ± 0.80 ^a	8.53 ± 0.83 ^{ab}	7.57 ± 0.79 ^b
18:3n6	0.11 ± 0.01	0.08 ± 0.01	0.10 ± 0.01
20:2n6	0.21 ± 0.01	0.17 ± 0.02	0.16 ± 0.03
20:3n6	1.05 ± 0.05 ^a	0.75 ± 0.07 ^b	0.73 ± 0.11 ^b
20:4n6	3.21 ± 0.21 ^a	2.50 ± 0.35 ^a	5.33 ± 0.88 ^b
22:2n6	0.021 ± 0.003 ^a	0.02 ± 0.01 ^a	0.051 ± 0.004 ^b
22:4n6	0.09 ± 0.01 ^a	0.09 ± 0.01 ^a	0.20 ± 0.04 ^b
22:5n6	0.048 ± 0.004 ^a	0.05 ± 0.01 ^a	1.32 ± 0.24 ^b
Total n-6 PUFA	15.63 ± 0.96	12.19 ± 1.11	15.46 ± 1.95
18:3n3	0.60 ± 0.06 ^a	0.53 ± 0.07 ^a	0.054 ± 0.004 ^b
20:3n3	0.060 ± 0.004 ^a	0.05 ± 0.01 ^{ab}	0.038 ± 0.004 ^a
20:5n3	0.68 ± 0.05 ^a	0.35 ± 0.04 ^b	0.025 ± 0.002 ^c
22:5n3	0.42 ± 0.05 ^a	0.26 ± 0.03 ^b	0.017 ± 0.004 ^c
22:6n3	7.70 ± 0.66 ^a	4.32 ± 0.50 ^b	0.38 ± 0.06 ^c
Total n-3 PUFA	9.46 ± 0.79 ^a	5.50 ± 0.60 ^b	0.51 ± 0.07 ^c
16:1n7/16:0	0.17 ± 0.01	0.19 ± 0.01	0.20 ± 0.01
18:1n9/18:0	4.94 ± 0.58 ^b	9.77 ± 1.07 ^a	8.95 ± 0.93 ^a
20:4n6/20:3n6	3.06 ± 0.11 ^a	3.26 ± 0.22 ^a	7.29 ± 0.43 ^b
20:4n6/20:5n3	5.03 ± 0.43 ^a	8.05 ± 1.21 ^a	217.77 ± 28.19 ^b
20:4n6/22:6n3	0.44 ± 0.03 ^a	0.59 ± 0.04 ^a	14.05 ± 0.28 ^b
20:5n3/22:6n3	0.09 ± 0.004	0.08 ± 0.01	0.08 ± 0.01
22:5n6/22:6n3	0.007 ± 0.001 ^a	0.011 ± 0.001 ^a	3.39 ± 0.18 ^b
22:5n6+22:6n3	7.75 ± 0.67 ^a	4.37 ± 0.51 ^b	1.70 ± 0.30 ^c
n-6/n-3	1.65 ± 0.07 ^a	2.22 ± 0.08 ^a	30.17 ± 0.91 ^b
n-6+n-3	25.09 ± 1.73 ^a	17.69 ± 1.70 ^b	15.98 ± 2.02 ^b
Total fatty acids (µg/mg wet liver)	49.69 ± 3.07 ^b	86.06 ± 9.85 ^a	78.72 ± 7.26 ^a

Each parameter is presented as the mean (±SEM). Means with different alphabetical superscripts (a, b, c) indicate significant differences across diets by Tukey's HSD at $P < 0.05$

Table 6 Plasma fatty acid composition of the two artificially reared groups and a dam-reared reference group at 20 week of age (wt % of total fatty acids)

	Dietary group		
	Dam-reared (<i>n</i> = 16)	n-3 Adq (<i>n</i> = 14)	n-3 Def (<i>n</i> = 14)
Fatty acids			
10:0	0.21 ± 0.02 ^a	0.11 ± 0.02 ^b	0.08 ± 0.01 ^b
12:0	3.69 ± 0.32 ^a	2.06 ± 0.33 ^b	1.07 ± 0.16 ^b
14:0	2.73 ± 0.19 ^a	1.64 ± 0.18 ^b	1.06 ± 0.11 ^b
16:0	18.27 ± 0.20 ^a	17.95 ± 0.21 ^a	14.77 ± 0.44 ^b
18:0	9.22 ± 0.16	9.05 ± 0.20	8.82 ± 0.31
20:0	0.37 ± 0.02 ^a	0.25 ± 0.02 ^b	0.19 ± 0.01 ^b
22:0	0.37 ± 0.02 ^{ab}	0.30 ± 0.01 ^a	0.48 ± 0.06 ^b
24:0	0.16 ± 0.01 ^a	0.14 ± 0.01 ^a	0.29 ± 0.03 ^b
Total saturates	35.01 ± 0.55 ^a	31.50 ± 0.68 ^b	26.75 ± 0.75 ^c
12:1	0.03 ± 0.01	0.022 ± 0.001	0.032 ± 0.004
14:1	0.06 ± 0.01 ^a	0.036 ± 0.004 ^b	0.049 ± 0.005 ^{ab}
16:1n7	2.84 ± 0.12	2.64 ± 0.18	2.42 ± 0.12
18:1n7	2.63 ± 0.20 ^a	2.85 ± 0.21 ^a	3.71 ± 0.19 ^b
18:1n9	14.65 ± 0.77 ^{ab}	16.30 ± 0.75 ^a	13.03 ± 0.41 ^b
20:1n9	0.61 ± 0.02 ^a	0.53 ± 0.03 ^{ab}	0.49 ± 0.03 ^b
22:1n9	0.12 ± 0.01 ^a	0.10 ± 0.01 ^a	0.39 ± 0.09 ^b
24:1n9	0.32 ± 0.01 ^a	0.41 ± 0.03 ^a	0.82 ± 0.07 ^b
Total monounsaturates	21.26 ± 0.96	22.89 ± 0.95	20.94 ± 0.52
18:2n6	22.54 ± 0.73 ^a	20.36 ± 0.76 ^a	16.53 ± 0.89 ^b
18:3n6	0.34 ± 0.01 ^a	0.27 ± 0.02 ^a	0.14 ± 0.03 ^b
20:2n6	0.21 ± 0.01 ^{ab}	0.25 ± 0.01 ^a	0.15 ± 0.03 ^b
20:3n6	1.58 ± 0.08 ^a	2.06 ± 0.13 ^b	1.96 ± 0.09 ^b
20:4n6	5.40 ± 0.38 ^a	8.89 ± 0.88 ^b	17.70 ± 0.83 ^c
22:2n6	0.04 ± 0.01 ^a	0.028 ± 0.002 ^a	0.39 ± 0.10 ^b
22:4n6	0.08 ± 0.01 ^a	0.10 ± 0.01 ^a	0.59 ± 0.07 ^b
22:5n6	0.058 ± 0.004 ^a	0.09 ± 0.01 ^a	2.19 ± 0.12 ^b
Total n-6 PUFA	30.25 ± 0.58 ^a	32.05 ± 0.80 ^a	39.65 ± 0.68 ^b
18:3n3	0.75 ± 0.05 ^a	0.49 ± 0.05 ^b	0.025 ± 0.002 ^c
20:3n3	0.05 ± 0.01	0.042 ± 0.003	0.17 ± 0.09
20:5n3	1.02 ± 0.04 ^a	0.94 ± 0.07 ^a	0.21 ± 0.06 ^b
22:5n3	0.34 ± 0.02 ^a	0.28 ± 0.02 ^a	0.63 ± 0.13 ^b
22:6n3	6.54 ± 0.14 ^a	6.91 ± 0.19 ^a	0.90 ± 0.07 ^b
Total n-3 PUFA	8.71 ± 0.16 ^a	8.67 ± 0.21 ^a	1.94 ± 0.28 ^b
16:1n7/16:0	0.16 ± 0.01	0.15 ± 0.01	0.16 ± 0.01
18:1n9/18:0	1.61 ± 0.10	1.83 ± 0.11	1.50 ± 0.06
20:4n6/20:3n6	3.42 ± 0.16 ^a	4.38 ± 0.38 ^a	9.19 ± 0.51 ^b
20:4n6/20:5n3	5.41 ± 0.46 ^a	10.52 ± 1.51 ^a	207.79 ± 42.69 ^b
20:4n6/22:6n3	0.83 ± 0.06 ^a	1.28 ± 0.12 ^a	21.17 ± 1.80 ^b
20:5n3/22:6n3	0.16 ± 0.01	0.14 ± 0.01	0.24 ± 0.06
22:5n6/22:6n3	0.009 ± 0.001 ^a	0.013 ± 0.002 ^a	2.43 ± 0.29 ^b
22:5n6+22:6n3	6.60 ± 0.14 ^a	7.00 ± 0.20 ^a	3.09 ± 0.15 ^b
n-6/n-3	3.47 ± 0.05 ^a	3.70 ± 0.11 ^a	20.42 ± 5.12 ^b
n-6+n-3	38.96 ± 0.71 ^a	40.72 ± 0.89 ^{ab}	41.59 ± 0.55 ^b
Total fatty acids (µg/ml plasma)	5.48 ± 0.29 ^a	5.50 ± 0.33 ^a	4.28 ± 0.32 ^b

Each parameter is presented as the mean (±SEM). Means with different alphabetical superscripts (a, b, c) indicate significant differences across diets by Tukey's HSD at *P* < 0.05

Table 7 Heart fatty acid composition of the two artificially reared groups and a dam-reared reference group at 20 week of age (wt % of total fatty acids)

	Dietary group		
	Dam-reared (<i>n</i> = 16)	n-3 Adq (<i>n</i> = 14)	n-3 Def (<i>n</i> = 14)
Fatty acids			
10:0	0.019 ± 0.001	0.019 ± 0.002	0.022 ± 0.002
12:0	0.61 ± 0.04	0.59 ± 0.07	0.61 ± 0.06
14:0	1.72 ± 0.05	1.83 ± 0.06	1.70 ± 0.05
16:0	12.99 ± 0.13 ^a	13.48 ± 0.23 ^a	11.57 ± 0.14 ^b
18:0	17.31 ± 0.21 ^a	16.16 ± 0.37 ^b	16.68 ± 0.24 ^{a,b}
20:0	0.35 ± 0.01 ^a	0.30 ± 0.01 ^b	0.29 ± 0.01 ^b
22:0	0.26 ± 0.01	0.26 ± 0.01	0.24 ± 0.01
24:0	0.06 ± 0.02 ^a	0.02 ± 0.01 ^a	0.163 ± 0.004 ^b
Total saturates	33.33 ± 0.28 ^a	32.65 ± 0.22 ^a	31.28 ± 0.25 ^b
12:1	0.020 ± 0.002 ^a	0.018 ± 0.001 ^a	0.029 ± 0.002 ^b
14:1	0.66 ± 0.01 ^a	0.73 ± 0.02 ^b	0.67 ± 0.01 ^a
16:1n7	0.98 ± 0.10	1.13 ± 0.15	1.31 ± 0.11
18:1n7	2.08 ± 0.09 ^a	2.57 ± 0.09 ^b	2.63 ± 0.14 ^b
18:1n9	6.99 ± 0.29 ^a	9.04 ± 1.01 ^{ab}	10.35 ± 0.45 ^b
20:1n9	0.28 ± 0.01 ^{ab}	0.24 ± 0.02 ^a	0.33 ± 0.02 ^b
22:1n9	0.046 ± 0.002	0.045 ± 0.002	0.05 ± 0.01
24:1n9	0.06 ± 0.01 ^a	0.10 ± 0.04 ^a	0.19 ± 0.01 ^b
Total monounsaturates	11.12 ± 0.40 ^a	13.88 ± 1.12 ^b	15.56 ± 0.50 ^b
18:2n6	10.87 ± 0.64 ^a	9.15 ± 0.47 ^a	14.56 ± 0.55 ^b
18:3n6	0.25 ± 0.01	0.22 ± 0.01	0.23 ± 0.01
20:2n6	0.16 ± 0.01	0.15 ± 0.01	0.15 ± 0.01
20:3n6	0.93 ± 0.04 ^a	0.99 ± 0.03 ^a	1.13 ± 0.04 ^b
20:4n6	3.73 ± 0.12 ^a	4.35 ± 0.19 ^a	11.63 ± 0.27 ^b
22:2n6	0.017 ± 0.001 ^a	0.021 ± 0.001 ^a	0.14 ± 0.03 ^b
22:4n6	0.12 ± 0.01	0.18 ± 0.01	0.51 ± 0.21
22:5n6	0.15 ± 0.01 ^a	0.22 ± 0.03 ^a	14.28 ± 0.71 ^b
Total n-6 PUFA	16.23 ± 0.57 ^a	15.28 ± 0.47 ^a	42.63 ± 0.58 ^b
18:3n3	0.24 ± 0.01 ^a	0.20 ± 0.02 ^a	0.021 ± 0.001 ^b
20:3n3	0.027 ± 0.001 ^a	0.024 ± 0.001 ^a	0.06 ± 0.01 ^b
20:5n3	0.126 ± 0.004 ^a	0.09 ± 0.01 ^b	0.024 ± 0.003 ^c
22:5n3	0.93 ± 0.03 ^a	0.94 ± 0.04 ^a	0.31 ± 0.02 ^b
22:6n3	32.48 ± 0.59 ^a	31.05 ± 0.89 ^a	2.78 ± 0.10 ^b
Total n-3 PUFA	33.80 ± 0.59 ^a	32.31 ± 0.90 ^a	3.19 ± 0.11 ^b
16:1n7/16:0	0.08 ± 0.01 ^a	0.08 ± 0.01 ^a	0.11 ± 0.01 ^b
18:1n9/18:0	0.41 ± 0.02 ^b	0.58 ± 0.09 ^a	0.63 ± 0.03 ^a
20:4n6/20:3n6	4.11 ± 0.22 ^a	4.48 ± 0.28 ^a	10.43 ± 0.32 ^b
20:4n6/20:5n3	29.96 ± 1.48 ^a	49.56 ± 4.47 ^a	550.68 ± 45.88 ^b
20:4n6/22:6n3	0.12 ± 0.004 ^a	0.14 ± 0.01 ^a	4.25 ± 0.19 ^b
20:5n3/22:6n3	0.004 ± 0.0002 ^a	0.003 ± 0.0002 ^a	0.009 ± 0.001 ^b
22:5n6/22:6n3	0.0045 ± 0.0004 ^a	0.007 ± 0.001 ^a	5.13 ± 0.35 ^b
22:5n6+22:6n3	32.62 ± 0.59 ^a	31.27 ± 0.89 ^a	17.07 ± 0.72 ^b
n-6/n-3	0.48 ± 0.02 ^a	0.48 ± 0.02 ^a	13.60 ± 0.56 ^b
n-6+n-3	50.03 ± 0.46 ^a	47.58 ± 1.02 ^b	45.82 ± 0.56 ^b
Total fatty acids (µg/mg wet heart)	23.53 ± 0.31	24.33 ± 0.71	23.94 ± 0.59

Each parameter is presented as the mean (±SEM). Different alphabetical superscripts (a, b, c) indicate significant differences across diets by Tukey's HSD at *P* < 0.05

Table 8 Lipid class distribution in mouse heart of two artificially reared groups and a dam-reared reference group at 20 week of age

Phospholipids class	Diets		
	Dam-reared (<i>n</i> = 8)	n-3 Adq (<i>n</i> = 7)	n-3 Def (<i>n</i> = 8)
Phosphatidylcholine	43.0 ± 1.0 ^b	43.4 ± 0.9 ^b	39.0 ± 0.9 ^a
Phosphatidylethanolamine	21.8 ± 0.6 ^{ab}	19.9 ± 0.9 ^a	22.8 ± 0.6 ^b
Neutral lipids	20.8 ± 0.6 ^{ab}	19.5 ± 0.8 ^a	22.3 ± 0.6 ^b
Cardiolipin	5.8 ± 0.3 ^b	7.8 ± 0.5 ^a	5.9 ± 0.3 ^b
Phosphatidylserine	1.1 ± 0.2	1.6 ± 0.3	1.9 ± 0.2
Phosphatidylinositol	0.6 ± 0.1 ^a	1.4 ± 0.4 ^{ab}	2.0 ± 0.2 ^b

Values given are mean ± SEM for peak areas of HPLC chromatogram. Different alphabetical superscripts (a, b) indicate significant differences across diets by Tukey's HSD at $P < 0.05$. Neutral lipids included triacylglycerol, cholesterol, and cholesteryl esters

($P < 0.001$) and phosphatidylinositol ($P < 0.01$) were observed between the dietary groups (Table 8). The amount of the remaining material was below the level required for accurate determination of other lipid classes with the method employed.

When examining the fatty acid composition across the phospholipid classes under investigation, we find that, in general, there was no effect of the diet upon the distribution of the major saturated fatty acids (palmitic acid, 16:0; stearic acid, 18:0). 22:6n3 was concentrated in the phosphatidylethanolamine, phosphatidylcholine and cardiolipin fractions reaching 40, 29 and 15%, respectively, of total fatty acids in diets containing preformed 22:6n3. Again 22:5n6 replaced 22:6n3 in the n-3 Def case, and also 20:4n6 was very significantly elevated in all phospholipid classes relative to the n-3 Adq and dam-reared groups. While cardiac cardiolipin makes up only about 6–8% of the total phospholipid of cardiac muscle membranes, it contains a very high proportion of 18:2n6 compared with other phospholipid classes (See Tables 9 and 10).

In further investigation of the reservoirs for 22:6n3, a molecular species analysis of cardiolipins was performed. It was observed, for the first time, that the heart cardiolipin in the 22:6n3-supplemented group contained molecular species with four 22:6n3 moieties. HPLC/EIS-MS analysis of heart phospholipids indicated that cardiolipin in the n-3 Adq dietary group contained abundant 22:6 species, including 22:6,22:6/22:6,22:6, 22:6,22:6/18:2,22:6, 18:2, 22:6/18:2,22:6, 18:2,22:6/18:2,18:2, 18:2,22:6/18:2,18:1, 18:2,18:1/18:1,22:6, and 18:1,18:1/18:2,22:6 species. These assignments were based on the diglyceride ions detected at m/z 600, 648, 602, 650 and 696, representing 18:2,18:2 (di-linoleoyl), 18:2,22:6 (linoleoyl, docosahexaenoyl), 18:1,18:2 (oleoyl, linoleoyl), 18:1,22:6 (oleoyl, docosahexaenoyl) and 22:6,22:6 (di-docosahexaenoyl) species, respectively. Considering that cardiolipin contains

four fatty acyl chains, two diglyceride fragment peaks overlapping in the ion chromatogram indicated the presence of these cardiolipin molecular species, although positional information cannot be obtained using this approach. In contrast, in the n-3 Def diet group, 18:2,18:2/18:2,18:2 is the predominant molecular species in cardiolipin, with the 22:5-containing species 18:2,18:2/18:2,22:5 and 18:2,18:2/16:0,22:5 species as rather minor species. No 22:5,22:5 ion at m/z 700 was detected in the cardiolipin. These data suggested that 22:6n3 may be the preferred fatty acid incorporated into cardiolipin in comparison to 22:5n6.

Discussion

The AR technique has provided nutritionists with a powerful research tool. The main advantage of the AR technique is that it allows precise control of the amount and composition of milk-substitute that each pup receives. Historically, the species most studied using the AR technique is the rat. In addition to the obvious cost advantages of feeding and housing a smaller animal, the rat has emerged as a species of choice for these studies because of its well-defined nutritional requirements and long history of use in metabolic studies. The relatively large number of pups in a rodent litter also enables control and experimental animals to be chosen from the same litters. Finally, the small size of the rat makes its rearing apparatus easy to design and assemble. This work established that the Hoshiba [4] artificial rearing system could be applied to the mouse for studies of essential fatty acid nutrition throughout the neonatal period.

The body weight of the mice in the present study has the same pattern as reported previously [5, 33]; that is the AR groups showed lower weight gain than the dam-reared group until the time of weaning. No significant differences were detected between the growths of the two experimental diet groups. It should be noted that body weights were not reported beyond the weaning period in the above mentioned studies, hence comparison is not possible. From the later observation, it appears that the AR procedures may have induced some difference in ad libitum feeding behavior.

In our study, the mortality of pups was 12% in the artificially reared groups. Three pups in the n-3 Def group and one pup in the n-3 Adq group died after aspirating milk into the lungs. Different sizes of nipples were used that better fit the mouth of the pups as they aged so as to avoid bloating that can occur due to air aspiration through the gap between the incisors and nipple as we noted that this can lead to pup mortality.

Although the AR technique has several advantages, some limitations do exist, although future refinements will

Table 9 The fatty acid composition of phosphatidylethanolamine, phosphatidylcholine and neutral lipids in mouse heart of two artificially reared groups and a dam-reared reference group at 20 week of age (wt % of total fatty acids)

Fatty acids	Phosphatidylethanolamine			Phosphatidylcholine			Neutral lipids		
	Dam-reared (n = 8)	n-3 Adq (n = 7)	n-3 Def (n = 8)	Dam-reared (n = 8)	n-3 Adq (n = 7)	n-3 Def (n = 8)	Dam-reared (n = 8)	n-3 Adq (n = 7)	n-3 Def (n = 8)
Non-essential									
12:0	0.05 ± 0.01	0.05 ± 0.01	0.031 ± 0.002	0.34 ± 0.22	0.08 ± 0.01	0.08 ± 0.01	5.02 ± 0.82	4.18 ± 0.34	4.78 ± 0.49
14:0	0.30 ± 0.13	0.41 ± 0.17	0.44 ± 0.14	0.60 ± 0.13 ^b	0.42 ± 0.05 ^{ab}	0.29 ± 0.04 ^a	5.79 ± 0.38	4.99 ± 0.30	5.19 ± 0.39
16:0	6.26 ± 0.28 ^b	6.58 ± 0.42 ^b	4.73 ± 0.17 ^a	24.67 ± 3.99	21.65 ± 1.37	17.66 ± 0.34	18.84 ± 0.65	18.67 ± 0.75	17.09 ± 0.91
18:0	26.79 ± 0.47	25.29 ± 0.60	26.34 ± 0.45	27.52 ± 5.02	21.96 ± 0.57	22.24 ± 0.43	5.98 ± 0.48	4.68 ± 0.48	4.68 ± 0.50
20:0	0.28 ± 0.07	0.13 ± 0.02	0.13 ± 0.02	0.12 ± 0.02	0.11 ± 0.01	0.13 ± 0.03	0.55 ± 0.06 ^b	0.36 ± 0.05 ^{ab}	0.33 ± 0.06 ^a
16:1	0.32 ± 0.02	0.28 ± 0.01	0.30 ± 0.04	0.51 ± 0.08	0.40 ± 0.07	0.48 ± 0.05	5.75 ± 0.75	6.13 ± 1.11	7.07 ± 1.16
18:1n9	3.53 ± 0.15 ^a	4.37 ± 0.13 ^b	4.94 ± 0.21 ^b	7.28 ± 1.40 ^b	6.01 ± 0.16 ^b	11.12 ± 0.55 ^a	23.25 ± 1.15 ^a	28.73 ± 0.69 ^b	29.05 ± 1.06 ^b
18:1n7	0.74 ± 0.06 ^a	1.07 ± 0.09 ^b	1.40 ± 0.10 ^c	2.30 ± 0.44	2.37 ± 0.15	3.20 ± 0.12	2.51 ± 0.21 ^b	3.39 ± 0.33 ^{ab}	3.59 ± 0.34 ^a
20:1n9	0.21 ± 0.02 ^b	0.17 ± 0.02 ^b	0.31 ± 0.04 ^a	0.24 ± 0.08	0.16 ± 0.01	0.22 ± 0.05	1.23 ± 0.12 ^{ab}	0.84 ± 0.06 ^b	1.36 ± 0.16 ^a
n-6 PUFA									
18:2n6	2.01 ± 0.10 ^a	1.31 ± 0.08 ^b	2.51 ± 0.15 ^c	6.92 ± 0.75 ^b	4.39 ± 0.36 ^a	7.78 ± 0.57 ^b	16.41 ± 0.91 ^b	13.76 ± 0.53 ^a	11.46 ± 0.29 ^a
20:2n6	0.07 ± 0.02 ^b	0.046 ± 0.004 ^b	0.16 ± 0.04 ^a	0.12 ± 0.02	0.14 ± 0.04	0.15 ± 0.04	0.24 ± 0.03	0.36 ± 0.16	0.56 ± 0.18
20:3n6	0.20 ± 0.01 ^b	0.23 ± 0.01 ^b	0.33 ± 0.01 ^a	0.57 ± 0.13 ^b	0.50 ± 0.02 ^b	1.01 ± 0.05 ^a	0.46 ± 0.05	0.51 ± 0.09	0.60 ± 0.11
20:4n6	3.59 ± 0.22 ^b	4.23 ± 0.23 ^b	13.29 ± 0.65 ^a	2.61 ± 0.48 ^b	3.10 ± 0.38 ^b	11.81 ± 0.38 ^a	1.22 ± 0.12 ^b	1.50 ± 0.27 ^b	3.03 ± 0.40 ^a
22:4n6	0.12 ± 0.02 ^b	0.21 ± 0.02 ^b	2.34 ± 0.12 ^a	0.28 ± 0.12 ^b	0.15 ± 0.05 ^b	1.88 ± 0.09 ^a	0.11 ± 0.02 ^b	0.18 ± 0.03 ^b	0.64 ± 0.13 ^a
22:5n6	0.47 ± 0.08 ^b	0.54 ± 0.09 ^b	23.17 ± 1.17 ^a	0.72 ± 0.21 ^b	0.50 ± 0.12 ^b	12.16 ± 0.85 ^a	0.21 ± 0.08 ^b	0.22 ± 0.07 ^b	1.25 ± 0.22 ^a
n-3 PUFA									
18:3n3	0.34 ± 0.06	0.20 ± 0.03	0.21 ± 0.05	0.077 ± 0.004 ^a	0.05 ± 0.01 ^b	0.015 ± 0.005 ^c	1.02 ± 0.06 ^a	0.84 ± 0.03 ^b	0.11 ± 0.02 ^c
20:5n3	0.14 ± 0.01 ^a	0.09 ± 0.01 ^b	0.014 ± 0.003 ^c	0.08 ± 0.01	0.05 ± 0.01	0.05 ± 0.01	0.16 ± 0.01 ^b	0.12 ± 0.02 ^b	0.020 ± 0.005 ^a
22:5n3	0.82 ± 0.05 ^b	0.91 ± 0.06 ^b	0.405 ± 0.025 ^a	1.15 ± 0.23 ^b	1.06 ± 0.06 ^b	0.30 ± 0.04 ^a	0.57 ± 0.06 ^b	0.59 ± 0.12 ^b	0.044 ± 0.004 ^a
22:6n3	40.64 ± 0.74 ^b	39.59 ± 1.05 ^b	4.56 ± 0.19 ^a	27.92 ± 0.72 ^b	29.21 ± 0.65 ^b	1.93 ± 0.08 ^a	3.72 ± 0.45 ^b	3.48 ± 0.55 ^b	0.31 ± 0.12 ^a
22:5n6/22:6n3	0.012 ± 0.002 ^b	0.014 ± 0.003 ^b	5.17 ± 0.39 ^a	0.021 ± 0.004 ^b	0.018 ± 0.005 ^b	6.26 ± 0.31 ^a	0.05 ± 0.02 ^b	0.06 ± 0.02 ^b	5.55 ± 0.96 ^a
22:5n6+22:6n3	41.11 ± 0.68 ^b	40.13 ± 0.97 ^b	27.73 ± 1.11 ^a	33.94 ± 5.50 ^b	29.71 ± 0.57 ^b	14.09 ± 0.91 ^a	3.93 ± 0.50 ^b	3.66 ± 0.57 ^b	1.56 ± 0.32 ^a
n-6+n-3	48.39 ± 0.78	47.34 ± 0.89	47.00 ± 0.50	45.65 ± 7.08	39.10 ± 0.82	37.02 ± 0.84	24.12 ± 1.42 ^b	21.53 ± 1.55 ^{ab}	18.07 ± 1.01 ^a
Total fatty acids (ug/mg)	0.39 ± 0.04	0.48 ± 0.07	0.39 ± 0.06	0.27 ± 0.03	0.32 ± 0.06	0.31 ± 0.03	0.45 ± 0.06	0.52 ± 0.11	0.44 ± 0.07

Each parameter is presented as the mean (±SEM). Different alphabetical superscripts (a, b, c) indicate significant differences across diets by Tukey's HSD at $P < 0.05$. Neutral lipids included triacylglycerol, cholesterol, and cholesteryl esters

Table 10 The fatty acid composition of phosphatidylserine, phosphatidylinositol and cardiolipin in mouse heart of two artificially reared groups and a dam-reared reference group at 20 week of age (wt % of total fatty acids)

Fatty acids	Phosphatidylserine			Phosphatidylinositol			Cardiolipin		
	Dam-reared (n = 8)	n-3 Adq (n = 7)	n-3 Def (n = 8)	Dam-reared (n = 8)	n-3 Adq (n = 7)	n-3 Def (n = 8)	Dam-reared (n = 8)	n-3 Adq (n = 7)	n-3 Def (n = 8)
Non-essential									
16:0	20.34 ± 2.18	17.38 ± 1.75	15.04 ± 1.18	25.10 ± 1.97	21.75 ± 1.21	19.97 ± 1.31	2.97 ± 0.41	2.95 ± 0.41	2.50 ± 0.45
18:0	41.18 ± 1.92	42.17 ± 1.46	39.99 ± 1.80	38.34 ± 1.49 ^{ab}	39.62 ± 0.85 ^b	32.75 ± 2.37 ^a	3.47 ± 0.64	3.21 ± 0.65	3.82 ± 0.75
16:1	3.11 ± 0.19	2.88 ± 0.34	2.64 ± 0.17	3.59 ± 0.36	3.28 ± 0.50	2.55 ± 0.20	2.17 ± 0.13	2.03 ± 0.22	2.11 ± 0.12
18:1n9	4.72 ± 0.40	5.89 ± 0.43	5.13 ± 0.37	4.96 ± 0.42	6.02 ± 0.52	6.17 ± 0.38	9.81 ± 0.74 ^b	14.84 ± 0.70 ^a	8.59 ± 0.87 ^b
18:1n7	0.81 ± 0.17	1.27 ± 0.19	1.11 ± 0.16	0.74 ± 0.09 ^b	1.16 ± 0.13 ^{ab}	1.57 ± 0.15 ^a	4.56 ± 0.37 ^b	8.22 ± 0.57 ^a	3.57 ± 0.26 ^b
n-6 PUFA									
18:2n6	5.34 ± 0.87 ^b	4.48 ± 0.79 ^b	12.14 ± 2.23 ^a	2.53 ± 0.37 ^b	2.71 ± 0.23 ^b	9.47 ± 2.81 ^a	54.55 ± 2.20 ^a	40.79 ± 1.77 ^b	63.40 ± 3.11 ^c
20:3n6	0.69 ± 0.08	0.95 ± 0.11	0.89 ± 0.07	0.34 ± 0.04 ^b	0.44 ± 0.09 ^{ab}	0.91 ± 0.22 ^a	2.64 ± 0.23 ^b	3.46 ± 0.17 ^a	2.92 ± 0.23 ^{ab}
20:4n6	1.82 ± 0.45 ^b	1.76 ± 0.17 ^b	3.38 ± 0.28 ^a	1.81 ± 0.22 ^b	2.40 ± 0.35 ^b	5.12 ± 0.65 ^a	0.71 ± 0.06 ^b	0.95 ± 0.05 ^b	1.46 ± 0.11 ^a
22:4n6	0.28 ± 0.03 ^b	0.32 ± 0.05 ^b	0.87 ± 0.15 ^a	0.33 ± 0.07	0.30 ± 0.07	0.55 ± 0.09	0.03 ± 0.01 ^b	0.02 ± 0.005 ^b	0.35 ± 0.09 ^a
22:5n6	1.28 ± 0.16 ^b	1.32 ± 0.21 ^b	7.08 ± 0.98 ^a	1.55 ± 0.13 ^b	1.50 ± 0.29 ^b	7.07 ± 0.77 ^a	0.39 ± 0.09 ^b	0.41 ± 0.08 ^b	3.13 ± 0.36 ^a
n-3 PUFA									
22:5n3	0.29 ± 0.03 ^b	0.30 ± 0.04 ^b	0.009 ± 0.002 ^a	ND	ND	ND	0.15 ± 0.02 ^a	0.23 ± 0.02 ^b	0.08 ± 0.01 ^a
22:6n3	5.85 ± 0.80 ^b	7.60 ± 1.05 ^b	0.99 ± 0.12 ^a	4.95 ± 0.83 ^b	6.82 ± 1.32 ^b	0.85 ± 0.11 ^a	9.79 ± 0.87 ^a	14.57 ± 0.88 ^b	0.37 ± 0.04 ^c
22:5n6/22:6n3	0.27 ± 0.08 ^b	0.22 ± 0.07 ^b	7.48 ± 1.18 ^a	0.38 ± 0.06 ^b	0.31 ± 0.11 ^b	8.64 ± 0.55 ^a	0.04 ± 0.01 ^b	0.03 ± 0.01 ^b	8.46 ± 0.66 ^a
22:5n6+22:6n3	7.13 ± 0.75	8.92 ± 1.00	8.07 ± 1.05	6.50 ± 0.79	8.32 ± 1.17	7.92 ± 0.88	10.18 ± 0.86 ^a	14.98 ± 0.83 ^b	3.50 ± 0.39 ^c
n-6+n-3	15.55 ± 1.07 ^b	16.73 ± 1.55 ^b	25.36 ± 2.77 ^a	11.51 ± 1.06 ^b	14.18 ± 1.69 ^b	23.97 ± 3.34 ^a	68.26 ± 1.70 ^{ab}	60.44 ± 2.07 ^b	71.70 ± 2.38 ^a
Total fatty acids (ng/mg)	7.55 ± 0.32	7.87 ± 1.25	7.95 ± 1.47	7.02 ± 0.85	9.22 ± 2.49	9.40 ± 1.17	63.80 ± 10.98	96.83 ± 33.53	78.66 ± 18.17

Each parameter is presented as the mean (±SEM). Different alphabetical superscripts (a, b, c) indicate significant differences across diets by Tukey's HSD at $P < 0.05$. ND not detected (i.e., <0.01%)

likely overcome these. One such limitation is that it eliminates many of the maternal interactions experienced by naturally reared pups. Lack of these interactions may have profound effects on brain and behavioral development. Also, the presence or absence of some unknown factor(s) in the milk-substitute formula that are present in mother's milk may promote normal organ development, especially of the intestine [21, 34].

Other studies have used a mouse model for feeding a diet deficient in n-3 fatty acids including three [35]; two [36, 37]; and one generation models [38]. Because of the increasing availability of tools for genetic manipulation [39, 40], the mouse has become the most popular animal model; development of this technique will provide a means to perform studies involving nutritional manipulation of essential fatty acids in neonatal mice in conjunction with genetically derived enzymatic modifications of interest including desaturase knock out [41], fat1 [39] and SCD-1 [42] deficiency. In addition, it should be clear that any nutrient whose content can be controlled in the artificial milk can provide an independent variable for an AR experiment and so there should be many applications of this method for nutritional studies.

It was important initially to establish whether this "one generation" model can generate large enough losses in the nervous system as well as other organ levels of 22:6n3 so that functional changes can be observed. It must first be considered what the extent of brain/retinal DHA losses are necessary for behavioral/physiological parameters to be significantly altered. Lim et al. [43] have shown that adult rats with a 70% loss in brain 22:6n3 performed more poorly in spatial tasks. Weisinger et al. [44] showed that there was a loss in retinal sensitivity and b-wave implicit times in rats after three generations of n-3 deficiency. However, these rats had only a 55% loss of retinal 22:6n3, and showed no differences in α -wave amplitudes or in most of the phototransduction parameters measured. Moriguchi and Salem [45] have demonstrated, in a 22:6n3 repletion paradigm, that spatial task performance is altered when the brain level of 22:6n3 declines by 40% or more. Thus, a one generation model of n-3 fatty acid deficiency that better mimics the human situation but that still produces a substantial decline in brain and retinal 22:6n3 of 40–50% or more would be very valuable for the development of this field.

This method was shown to be an efficient means for inducing brain and peripheral organ n-3 fatty acid deficiency as the pups fed the n-3 Def formula exhibited a loss of 51% of their brain 22:6n3 by 20 weeks of age, replacing it primarily with 22:5n6. These changes were consistent with the proposal by Salem et al. [46] that reciprocal replacement of 22:6n3 with 22:5n6 should be extended to include other n-6 fatty acids like 20:4n6 and 22:4n6 since

for the case of the retina and brain, only when both 22:5n6 and 22:4n6 were summed together with 22:6n3 was reciprocal replacement of 22:6n3 complete at all time points when comparing n-3 fatty acid adequate and deficient diets. The liver, heart, plasma, and the retinal percentages of 22:6n3 were 91, 90, 86 and 29% lower, respectively, in the pups fed the n-3 Def milk formula relative to those fed the same formula to which 3.1% of 18:3n3 and 0.93% of 22:6n3 had been added. As expected then, the peripheral organ losses in 22:6n3 and other n-3 fatty acids was much more drastic than those observed in the nervous system. Thus, the present feeding method results in nutritional deficiencies comparable to those observed in multiple generational models and should prove useful for studies of 22:6n3 function in the nervous system as well as peripheral organs.

It must be noted here that the percentage of 22:6n3 in the n-3 Adq group in the heart reached 31%, a level much greater than that of the brain or retina, prompting us to investigate in which lipid classes the 22:6n3 was concentrated. Our data indicate that phosphatidylethanolamine and phosphatidylcholine were the major repositories of 22:6n3 in the mouse heart, with 22:6n3 contents of 40 and 29%, respectively. In a review by Wessels and Sedmera [47]; the authors concluded that, apart from the obvious differences in size, the mouse and human heart are anatomically remarkably similar throughout development. They also concluded that employing the mouse as a model system for the human heart is useful. This extremely high level of heart 22:6n3 in a diet containing 22:6n3 has not been previously noted, to our knowledge. It is also noteworthy that the level of 22:6n3 provided in our diet was less than 1 wt % of fatty acids, a level obtained in many modern diets. Perhaps the critical factor leading to a remarkably high 22:6n3 content in mouse heart is the feeding from the very beginning of life where fatty acid compositions are more malleable.

When comparing the level of 22:6n3 in the mouse heart versus that of the rat, the 22:6n3 content of the rat heart is much lower than the mouse heart reaching 10% for a diet containing only 18:3n3 (3.1% of 18:3n3 and no 22:6n3) and 15% for a diet containing 2.6% of 18:3n3 plus 1.3% of 22:6n3 (unpublished data). This then prompts the question of what this apparent species difference may be due to. The underlying differences in metabolism leading to this very significant response to dietary 22:6n3 between these species is unclear but it is noted that the murine heart has an elevated heart rate of 500–700 beats/min, whereas the rat has a heart rate of 300–400 beats/min [48]. It has previously been reported that 22:6n3 is concentrated in tissues, such as the hummingbird flight muscles, that have extremely high metabolic activity [49].

Observational, clinical, and experimental studies have demonstrated that long-chain n-3 PUFA supplementation reduces the risk of heart disease in humans including cardiac arrhythmias [50, 51]. In n-3 depleted rats, it was observed that within 2 h after intravenous bolus injection with medium chain-triacylglycerols: fish oil, the emulsion modifies several cationic events likely to be involved in contractile functions of aortic ring preparations [52]. A positive association between levels of circulating n-3 fatty acids derived from normal dietary variation and endothelial function was shown in young adults who smoked or had higher levels of fasting insulin, glucose or triglycerides. Given the central position of the endothelium in early atherogenesis, a protective influence of 22:6n3 may, in part, explain the epidemiological association between increased fish intake and reduced cardiovascular mortality and morbidity [53].

In a recent study by Garg et al. [17]; the authors demonstrated that short-term supplementation with a fish oil concentrate results in increased levels of 20:5n3 and 22:6n3, whereas the levels of the eicosanoid substrate, 20:4n6 decreased in the human atrium. However, more 22:6n3 than 20:5n3 is incorporated in the atrium total lipids (22:6n3/20:5n3 ratio of 2.54) and phospholipids (22:6n3/20:5n3 ratio of 2.78) despite the fish oil supplement supplying a higher amount of 20:5n3 than 22:6n3. The author also concluded that the enrichment of the phospholipid fraction with long-chain n-3 PUFA suggests that these fatty acids were readily available for release as non-esterified acids should an arrhythmic event occur. The accumulation of 20:5n3 and 22:6n3 was also observed during fish oil supplementation in myocardial fatty acids in humans [54] and that was at the expense of 20:4n6; 22:6n3 accumulated in atrial phospholipids more rapidly than did 20:5n3, even though 22:6n3 and 20:5n3 were present in equal proportions in the fish oil supplement used. The rapid accumulation of 22:6n3 was also reported in rat cardiac phospholipids without a similar increase in heart 20:5n3 content [13], and it was also confirmed in this mouse study; suggesting a specific mechanism for the uptake and/or retention of 22:6n3. The content of 20:5n3 in mouse cardiac muscle phospholipids was very low. This was apparent in both the total phospholipids (Table 7) and in all the major phospholipid classes examined in detail (Table 9). In the present study, consistent with these reports, the 20:5n3 content was very low in all tissues studied when dietary sources of 18:3n3 and 22:6n3 were provided.

In mammals, cardiolipin may contain up to 85 wt % of fatty acids as 18:2n6. However, this composition is known to be malleable as when the influence of maternal dietary fatty acids on the acyl composition of offspring cardiolipin was examined, feeding fish oil resulted in replacement of a substantial portion of 18:2n6 with 22:6n3 in 42-day-old

mice concomitant with a reduction in 18:2n6 from 62% (safflower oil fed) to 12% [55]. In the present study, the 18:2n6 content of the cardiolipin was 63% in the n-3 Def group and 41% in the n-3 Adq group. Watkins et al. [56] reported that cardiolipin did not accumulate more 22:6n3 than other phospholipid classes, and the mass of cardiolipin per g of heart did not change in response to a crocodile oil diet (containing 3% 22:6n3 and 1% 20:5n3) fed to weanling, 21-day-old mice until the 112th day of age. Heart phospholipids were enriched with the metabolic products of 18:3n3 in mice fed soybean oil suggesting that either 18:3n3 was converted to 22:6n3 within the heart itself or that the heart preferentially accumulated fatty acids from a plasma lipid pool enriched in 22:6n3. A novel observation in the present study was that in mice fed preformed 22:6n3, heart cardiolipin contained species with three and four 22:6n3 moieties. The occurrence of these rather extraordinary species has never been previously observed, to our knowledge. Together with phosphatidylcholine and phosphatidylethanolamine, the cardiolipin forms a repository for a high degree of 22:6n3 accretion in the mouse heart. This study lays the groundwork for studies of the unique biophysical role of tetra-22:6n3-cardiolipin species.

In conclusion, this study demonstrates the rather remarkable extent to which tissue fatty acid composition of internal organs, particularly the heart, but also nervous system tissues can be modified when the dietary fatty acid intake is controlled from the first days of life. The AR method employed here should be a boon to the study of EFA function, especially when combined with suitable genetically modified lines of mice. For example, desaturase knockout mice can be reared with or without particular essential fatty acids so that the relationship to physiological functions can be understood. It was notable that the mouse appeared to be a very responsive species in its organ fatty acid composition with respect to a diet containing preformed 22:6n3. Mouse heart phospholipids incorporated a very high level of 22:6n3 and a species of cardiolipin containing four 22:6n3 molecules were described for the first time.

References

1. Moriguchi T, Lim SY, Greiner R, Lefkowitz W, Loewke J, Hoshiba J, Salem N Jr (2004) Effects of an n-3-deficient diet on brain, retina, and liver fatty acyl composition in artificially reared rats. *J Lipid Res* 45:1437–1445
2. Ward G, Woods J, Reyzer M, Salem N Jr (1996) Artificial rearing of infant rats on milk formula deficient in n-3 essential fatty acids: a rapid method for the production of experimental n-3 deficiency. *Lipids* 31:71–77

3. Lim SY, Hoshiba J, Moriguchi T, Salem N Jr (2005) N-3 fatty acid deficiency induced by a modified artificial rearing method leads to poorer performance in spatial learning tasks. *Pediatr Res* 58:741–748
4. Hoshiba J (2004) Method for hand-feeding mouse pups with nursing bottles. *Contemp Top Lab Anim Sci* 43:50–53
5. Lim SY, Hoshiba J, Salem N Jr (2005) An extraordinary degree of structural specificity is required in neural phospholipids for optimal brain function: n-6 docosapentaenoic acid substitution for docosahexaenoic acid leads to a loss in spatial task performance. *J Neurochem* 95:848–857
6. Leaf A, Kang JX (1996) Prevention of cardiac sudden death by N-3 fatty acids: a review of the evidence. *J Intern Med* 240:5–12
7. Ku K, Oku H, Kaneda T, Onoe M, Zhang Z (1999) Beneficial effects of omega-3 fatty acid treatment on the recovery of cardiac function after cold storage of hyperlipidemic rats. *Metabolism* 48:1203–1209
8. Peltier S, Malaisse WJ, Portois L, Demaison L, Novel-Chate V, Chardigny JM, Sebedio JL, Carpentier YA, Leverve XM (2006) Acute in vivo administration of a fish oil-containing emulsion improves post-ischemic cardiac function in n-3-depleted rats. *Int J Mol Med* 18:741–749
9. Portois L, Peltier S, Sener A, Malaisse WJ, Carpentier YA (2008) Perturbation of phospholipid and triacylglycerol fatty acid positional location in the heart of rats depleted of n-3 long-chain polyunsaturates. *Nutr Res* 28:51–57
10. Mori TA, Bao DQ, Burke V, Puddey IB, Beilin LJ (1999) Docosahexaenoic acid but not eicosapentaenoic acid lowers ambulatory blood pressure and heart rate in humans. *Hypertension* 34:253–260
11. Christensen JH, Korup E, Aaroe J, Toft E, Moller J, Rasmussen K, Dyerberg J, Schmidt EB (1997) Fish consumption, n-3 fatty acids in cell membranes, and heart rate variability in survivors of myocardial infarction with left ventricular dysfunction. *Am J Cardiol* 79:1670–1673
12. Marchioli R, Barzi F, Bomba E, Chieffo C, Di Gregorio D, Di Mascio R, Franzosi MG, Geraci E, Levantesi G, Maggioni AP, Mantini L, Marfisi RM, Mastrogiuseppe G, Mininni N, Nicolosi GL, Santini M, Schweiger C, Tavazzi L, Tognoni G, Tucci C, Valagussa F (2002) Early protection against sudden death by n-3 polyunsaturated fatty acids after myocardial infarction: time-course analysis of the results of the Gruppo Italiano per lo Studio della Sopravvivenza nell'Infarto Miocardico (GISSI)-Prevenzione. *Circulation* 105:1897–1903
13. Charnock JS, Abeywardena MY, McLennan PL (1986) Comparative changes in the fatty-acid composition of rat cardiac phospholipids after long-term feeding of sunflower seed oil- or tuna fish oil-supplemented diets. *Ann Nutr Metab* 30:393–406
14. McLennan PL (2001) Myocardial membrane fatty acids and the antiarrhythmic actions of dietary fish oil in animal models. *Lipids* 36(Suppl):S111–S114
15. Nair SS, Leitch J, Falconer J, Garg ML (1999) Cardiac (n-3) non-esterified fatty acids are selectively increased in fish oil-fed pigs following myocardial ischemia. *J Nutr* 129:1518–1523
16. Kramer JK (1980) Comparative studies on composition of cardiac phospholipids in rats fed different vegetable oils. *Lipids* 15:651–660
17. Garg ML, Leitch J, Blake RJ, Garg R (2006) Long-chain n-3 polyunsaturated fatty acid incorporation into human atrium following fish oil supplementation. *Lipids* 41:1127–1132
18. Yajima M, Kanno T, Yajima T (2006) A chemically derived milk substitute that is compatible with mouse milk for artificial rearing of mouse pups. *Exp Anim* 55:391–397
19. Yajima M, Hoshiba J, Terahara M, Yajima T (2007) Reduced thymic size and numbers of splenic CD4+ and CD8+ cells in artificially reared mouse pups. *Biosci Biotechnol Biochem* 71:2420–2427
20. Kanno T, Koyanagi N, Katoku Y, Yonekubo A, Yajima T, Kuwata T, Kitagawa H, Harada E (1997) Simplified preparation of a refined milk formula comparable to rat's milk: influence of the formula on development of the gut and brain in artificially reared rat pups. *J Pediatr Gastroenterol Nutr* 24:242–252
21. Philipps AF, Anderson GG, Dvorak B, Williams CS, Lake M, Lebouton AV, Koldovsky O (1997) Growth of artificially fed infant rats: effect of supplementation with insulin-like growth factor I. *Am J Physiol* 272:R1532–R1539
22. Reeves PG, Nielsen FH, Fahey GC Jr (1993) AIN-93 purified diets for laboratory rodents: final report of the American Institute of Nutrition ad hoc writing committee on the reformulation of the AIN-76A rodent diet. *J Nutr* 123:1939–1951
23. Folch J, Lees M, Sloane Stanley G (1957) A simple method for the isolation and purification of total lipids from animal tissues. *J Biol Chem* 226:497–509
24. Morrison W, Smith L (1964) Preparation of fatty acid methyl esters and dimethylacetals from lipids with boron fluoride-methanol. *J Lipid Res* 5:600–608
25. Salem N Jr, Reyzer M, Karanian J (1996) Losses of arachidonic acid in rat liver after alcohol inhalation. *Lipids* 31(Suppl):S153–S156
26. Lepage G, Roy CC (1986) Direct transesterification of all classes of lipids in a one-step reaction. *J Lipid Res* 27:114–120
27. Masood A, Stark KD, Salem N Jr (2005) A simplified and efficient method for the analysis of fatty acid methyl esters suitable for large clinical studies. *J Lipid Res* 46:2299–2305
28. Lesnfsky EJ, Stoll MS, Minkler PE, Hoppel CL (2000) Separation and quantitation of phospholipids and lysophospholipids by high-performance liquid chromatography. *Anal Biochem* 285:246–254
29. Wen Z, Kim HY (2004) Alterations in hippocampal phospholipid profile by prenatal exposure to ethanol. *J Neurochem* 89:1368–1377
30. Ma YC, Kim HY (1995) Development of the on-line high-performance liquid chromatography/thermospray mass spectrometry method for the analysis of phospholipid molecular species in rat brain. *Anal Biochem* 226:293–301
31. Kim HY, Wang TC, Ma YC (1994) Liquid chromatography/mass spectrometry of phospholipids using electrospray ionization. *Anal Chem* 66:3977–3982
32. Charnock JS, Abeywardena MY, Tan D, McLennan PL (1991) Omega-3 and omega-6 PUFA's have different effects on the phospholipid fatty acid composition of rat myocardial muscle when added to a saturated fatty acid dietary supplement. *Nutr Res* 11:1013–1024
33. Lefkowitz W, Lim SY, Lin Y, Salem N Jr (2005) Where does the developing brain obtain its docosahexaenoic acid? Relative contributions of dietary alpha-linolenic acid, docosahexaenoic acid, and body stores in the developing rat. *Pediatr Res* 57:157–165
34. Motouri M, Matsuyama H, Yamamura J, Tanaka M, Aoe S, Iwanaga T, Kawakami H (2003) Milk sphingomyelin accelerates enzymatic and morphological maturation of the intestine in artificially reared rats. *J Pediatr Gastroenterol Nutr* 36:241–247
35. Wainwright PE, Huang YS, Coscina DV, Levesque S, McCutcheon D (1994) Brain and behavioral effects of dietary n-3 deficiency in mice: a three generational study. *Dev Psychobiol* 27:467–487
36. Carrie I, Clement M, de Javel D, Frances H, Bourre JM (2000) Specific phospholipid fatty acid composition of brain regions in mice. Effects of n-3 polyunsaturated fatty acid deficiency and phospholipid supplementation. *J Lipid Res* 41:465–472

37. Wainwright PE, Huang YS, Bulman-Fleming B, Levesque S, McCutcheon D (1994) The effects of dietary fatty acid composition combined with environmental enrichment on brain and behavior in mice. *Behav Brain Res* 60:125–136
38. Fedorova I, Hussein N, Di Martino C, Moriguchi T, Hoshiba J, Majchrzak S, Salem N Jr (2007) An n-3 fatty acid deficient diet affects mouse spatial learning in the Barnes circular maze. *Prostaglandins Leukot Essent Fatty Acids* 77:269–277
39. Kang JX (2007) Fat-1 transgenic mice: a new model for omega-3 research. *Prostaglandins, Leukot Essent Fatty Acids* 77:263–267
40. Flowers MT, Ntambi JM (2008) Role of stearoyl-coenzyme A desaturase in regulating lipid metabolism. *Curr Opin Lipidol* 19:248–256
41. Stoffel W, Holz B, Jenke B, Binczek E, Gunter RH, Kiss C, Karakesisoglou I, Thevis M, Weber AA, Arnhold S, Addicks K (2008) Delta 6-desaturase (FADS2) deficiency unveils the role of omega 3- and omega 6-polyunsaturated fatty acids. *EMBO J* 27:2281–2292
42. Flowers JB, Rabaglia ME, Schueler KL, Flowers MT, Lan H, Keller MP, Ntambi JM, Attie AD (2007) Loss of stearoyl-CoA desaturase-1 improves insulin sensitivity in lean mice but worsens diabetes in leptin-deficient obese mice. *Diabetes* 56:1228–1239
43. Lim SY, Moriguchi T, Lefkowitz B, Loewke J, Majchrzak S, Hoshiba J, Salem N Jr (2003) Artificial feeding of an n-3 essential fatty acid-deficient diet leads to a loss of brain function in the first generation. In: Huang YS, Lin SJ, Huang PC (eds) *Essential fatty acids and eicosanoids*. AOCs Press, Champaign
44. Weisinger HS, Armitage JA, Jeffrey BG, Mitchell DC, Moriguchi T, Sinclair AJ, Weisinger RS, Salem N Jr (2002) Retinal sensitivity loss in third-generation n-3 PUFA-deficient rats. *Lipids* 37:759–765
45. Moriguchi T, Salem N Jr (2003) Recovery of brain docosahexaenoate leads to recovery of spatial task performance. *J Neurochem* 87:297–309
46. Salem N Jr, Loewke J, Catalan JN, Majchrzak S, Moriguchi T (2005) Incomplete replacement of docosahexaenoic acid by n-6 docosapentaenoic acid in the rat retina after an n-3 fatty acid deficient diet. *Exp Eye Res* 81:655–663
47. Wessels A, Sedmera D (2003) Developmental anatomy of the heart: a tale of mice and man. *Physiol Genomics* 15:165–176
48. Banerjee I, Fuseler JW, Price RL, Borg TK, Baudino TA (2007) Determination of cell types and numbers during cardiac development in the neonatal and adult rat and mouse. *Am J Physiol Heart Circ Physiol* 293:H1883–H1891
49. Infante JP, Kirwan RC, Brenna JT (2001) High levels of docosahexaenoic acid (22:6n-3)-containing phospholipids in high-frequency contraction muscles of hummingbirds and rattlesnakes. *Comp Biochem Physiol B Biochem Mol Biol* 130:291–298
50. Mozaffarian D, Ascherio A, Hu FB, Stampfer MJ, Willett WC, Siscovick DS, Rimm EB (2005) Interplay between different polyunsaturated fatty acids and risk of coronary heart disease in men. *Circulation* 111:157–164
51. Siscovick DS, Lemaitre RN, Mozaffarian D (2003) The fish story: a diet-heart hypothesis with clinical implications: n-3 polyunsaturated fatty acids, myocardial vulnerability, and sudden death. *Circulation* 107:2632–2634
52. Courtois P, Louchami K, Portois L, Chardigny JM, Sener A, Carpentier YS, Malaisse WJ (2005) Effects of a medium-chain triglyceride:fish oil emulsion administered intravenously to omega 3 fatty acid-depleted rats on cationic fluxes in aortic rings. *Int J Mol Med* 16:1089–1093
53. Leeson CP, Mann A, Kattenhorn M, Deanfield JE, Lucas A, Muller DP (2002) Relationship between circulating n-3 fatty acid concentrations and endothelial function in early adulthood. *Eur Heart J* 23:216–222
54. Metcalf RG, James MJ, Gibson RA, Edwards JR, Stubberfield J, Stuklis R, Roberts-Thomson K, Young GD, Cleland LG (2007) Effects of fish-oil supplementation on myocardial fatty acids in humans. *Am J Clin Nutr* 85:1222–1228
55. Berger A, Gershwin ME, German JB (1992) Effects of various dietary fats on cardiolipin acyl composition during ontogeny of mice. *Lipids* 27:605–612
56. Watkins SM, Lin TY, Davis RM, Ching JR, DePeters EJ, Halpern GM, Walzem RL, German JB (2001) Unique phospholipid metabolism in mouse heart in response to dietary docosahexaenoic or alpha-linolenic acids. *Lipids* 36:247–254

Involvement of Lipids in Dimethoate-Induced Inhibition of Testosterone Biosynthesis in Rat Interstitial Cells

Mariana Astiz · Graciela E. Hurtado de Catalfo ·
María J. T. de Alaniz · Carlos Alberto Marra

Received: 25 November 2008 / Accepted: 13 May 2009 / Published online: 5 July 2009
© AOCs 2009

Abstract The mechanism involved in the inhibition of testosterone (Te) biosynthesis after a sub-chronic exposure to low doses of dimethoate (D) was studied in rat interstitial cells (IC). Expression of COX-2 in IC isolated from D-treated rats increased by 44% over C data, while transcription of StAR decreased by approx. 50% and the expression of this protein was diminished by approximately 40%. PGE₂ and PGF_{2α} were increased by 61 and 78%, respectively. Te concentration decreased by 49% in IC homogenates. Concomitantly, plasma concentration of LH and FSH both increased. Arachidonic acid (ARA) and C₂₂ fatty acyl chains in phospholipids from IC mitochondrial fraction decreased by approx. 30% after D treatment. Protein carbonyls, lipoperoxides and nitrite content increased while α-tocopherol and the antioxidant capacity of the soluble cellular fraction decreased significantly. Stimulation with h-CG 10 nM overnight failed to overcome the inhibition caused by D on both Te biosynthesis and 3β- and 17β-hydroxysteroid dehydrogenases. Decreased Te biosynthesis may be attributed to (1) inhibition of StAR protein activity due to the stimulation of COX-2 and the overproduction of PGF_{2α}, (2) decreased stimulatory effect of ARA on StAR with a subsequent reduction in the availability of CHO for the androgenic pathway, and/or (3) indirect inhibition of steroidogenic enzymes by a lower transcriptional rate caused by elevated

PGF_{2α}. Rofecoxib administration prevents the deleterious effect(s) exerted by D.

Keywords Arachidonic acid · COX-2 · Dimethoate · Oxidative stress · Prostaglandins · Rat interstitial cells · StAR · h-CG · Rofecoxib · TROLOX

Abbreviations

C	Control group
CM	Cytoplasmic membrane
D	Dimethoate
FSH	Follicle-stimulating hormone
LH	Luteinizing hormone
LPO	Lipid peroxidation
MDA	Malonedialdehyde
N	Nucleus
OS	Oxidative stress
RNS	Reactive nitrogen species
PS	Protein synthesis
R	Rofecoxib
ROS	Reactive oxygenated species
StAR	Steroidogenic acute regulatory protein
T	TROLOX®
TBARS	Thiobarbituric acid-reactive substances
Te	Testosterone

M. Astiz · G. E. Hurtado de Catalfo · M.
J. T. de Alaniz · C. A. Marra (✉)
Instituto de Investigaciones Bioquímicas de La Plata
(INIBIOLP), CCT La Plata, CONICET-UNLP, Cátedra de
Bioquímica y Biología Molecular, Facultad de Ciencias
Médicas, Universidad Nacional de La Plata, Calles 60 y 120,
1900 La Plata, Argentina
e-mail: camarra@atlas.med.unlp.edu.ar;
contactocarlos@hotmail.com

Introduction

The growing amount of experimental evidence documenting endocrine dysfunction in male wildlife has led to the hypothesis that environmental contaminants adversely affect testosterone production and caused deleterious

effects on the male reproductive system [1]. In an interesting work, Carlsen et al. [2] reported that a significant worldwide decline in semen quality has occurred over the past 50 years. Retrospective studies performed in sperm banks from Paris [3] and London [4] have supported this conclusion. The hypothesis of environmental pollution as a causative factor is casually related to higher declines in sperm quality observed in developed countries characterized by important agrotechnical activities [5, 6]. Other authors reported that environmental chemicals can mimic estrogen action and also disrupt androgen signaling pathways [6]. Moreover, alterations were also observed not only in reproductive performance, but also in the incidence of cryptorchidism and testicular cancer [7]. Many contaminants demonstrated antiandrogenic activity both in whole animals and in receptor binding-in vitro assays [1]. Important evidence for this mechanism of action was obtained with the herbicide Linuron. This chemical agent binds to the androgen receptor with an affinity similar to that of flutamide, which is a potent antiandrogenic drug. As a result, feedback control to the pituitary is interrupted and serum LH and estrogen concentrations increase significantly. The ultimate outcome of Linuron exposure is Leydig cell cancer due to over-stimulation of steroidogenesis [8]. Several pesticides and their metabolites have similar effects [6, 9]. Currently, the levels of environmental exposure to these substances and their derivatives are completely unknown. Thus, predictions about alterations in male reproductive function or fertility cannot be made [6, 10]. This fact has generated considerable public and scientific concern about the relationship existing between environmental contaminants and alterations to the male reproductive system [11].

Some of the most used agrochemicals have been shown to disturb pro-oxidant/anti-oxidant balance in testicular cells and consequently decrease the androgen production [6]. Free radical generation in response to toxicants [12] plays different and complex roles in the Leydig cell physiology [6]. For example, high levels of corticosterone produced during oxidative stress may bring about, in part, the decline in testosterone biosynthesis since this steroid is able to induce Leydig cell apoptosis [13]. In addition, testosterone production is profoundly affected by the prostaglandin $F_{2\alpha}$ ($PGF_{2\alpha}$) level. The inducible enzyme cyclooxygenase-2 (COX-2) is responsible for the biosynthesis of $PGF_{2\alpha}$ from its precursor arachidonic acid (ARA). $PGF_{2\alpha}$ not only inhibits progesterone production but also activates its own biosynthetic pathway by induction of COX-2 via protein kinase C in an autoamplification cascade [14]. In this scenario it is possible to assume that pesticides induce oxidative stress (OS) and disturb the conversion of ARA into $PGF_{2\alpha}$ via COX-2. In addition, other laboratories have demonstrated that COX-2 and

$PGF_{2\alpha}$ are both inhibitors of Leydig cell steroidogenesis [14, 15].

In Leydig cells, cholesterol is converted to testosterone through various steps catalyzed by different enzymes [16]. The delivery of free cholesterol to the inner mitochondrial membrane is the true rate-limiting step of steroidogenesis and it is mediated mainly by the steroidogenic acute-regulatory protein (StAR) [16, 17]. The biological activity of this protein depends on many factors such as ARA, PGF levels, COX-2 activity, and free radical production in a complex interrelationship not fully understood yet [14, 15, 18–20]. StAR is also sensitive to various pesticides as demonstrated by Walsh et al. [21].

Some organophosphorus compounds are known to impair fertility, suppress libido, cause testicular degeneration, and a deterioration in semen quality [22]. Dimethoate (D; 2-dimethoxyphosphonylthio-*N*-methylacetamine) is an organophosphorus pesticide extensively used as a systemic insecticide and acaricide which proved to be neurotoxic [22] and to disturb StAR gene expression [21]. Toxicity of D on testicular Leydig cell function is still unexplored. Therefore, in the present study we aimed to investigate the action of a sub-chronic exposure of Wistar rats to low doses of D on Leydig cell steroidogenesis, free radical production, and StAR and COX-2 expression. The testis is the major site for testosterone production. It plays a crucial role in the development of secondary sexual characteristics and initiation, as well as regulation of spermatogenesis. Thus, reduction in testosterone production due to exposure to environmental toxicants (such as D) has the potential to adversely affect normal sexual development in humans.

Experimental Procedure

Chemicals

All chemicals used were of reagent grade and obtained from Sigma Chem. Co. (CA, USA, or Buenos Aires, Argentina) or Merck Laboratories (Darmstadt, Germany). Organic solvents were from Carlo Erba (Milano, Italy). α -Tocopheryl-diacetate (TROLOX[®], 98% pure) and rofecoxib (99% pure) were from Saporitti S.A., Buenos Aires, Argentina. Other chemicals employed were purchased from local commercial sources and they were of analytical grade. Dimethoate (2-dimethoxyphosphonylthio-*N*-methylacetamine) was obtained as a gift from INTA (Castelar, Argentina). Hormone measurements [luteinizing (LH), follicle-stimulating (FSH), total and free testosterone] were performed using commercial kits (KP7CT, KP6CT, KS24CT, and KS33CTN, respectively) from Radim (Radim SpA, Pomezia, Italy).

Animals and Treatments

Male Wistar rats weighing 190 ± 20 g with specific-pathogen free-certified status were used. Upon arrival, the rats were allowed to acclimatize for a week before starting the experiment. Rats were maintained under controlled conditions of temperature (25 ± 2 °C), and a normal photoperiod of 12 h dark and 12 h light. They were fed with standard Purina chow from Ganave S.A. (Santa Fe, Argentina) and water ad libitum. Clinical examination together with body weight evaluation was performed every week during the experiment. Animals were randomly divided into two groups of six rats each, assigned as control rats (C) injected i.p. with polyethylene-glycol 400 (PEG-400), or D-treated rats injected with 15 mg D/kg body weight dissolved in PEG-400. All animals were injected three times a week for 5 weeks. The dose used was in accordance with previous reports [23–26]. This model was chosen for simulation of a sub-chronic exposition to low doses of pesticide incorporated from the living environment [27]. Other experiment was designed to study the effect of the antioxidant α -tocopheryl diacetate (TROLOX[®]) and the COX inhibitor rofecoxib administered alone or in combination with dimethoate. In this experimental protocol TROLOX[®] (T) and rofecoxib (R) were dissolved in PBS with PEG-400 and administered i.p. to groups of 4 rats each at a doses of 12.5 and 5.0 mg/kg body weight, respectively. Two groups of rats received TROLOX[®] (CT) or rofecoxib (CR), other two groups were simultaneously injected with D and T (DT) or D and R (DR). Finally, other groups of animals were injected with the vehicle alone (C), dimethoate alone (D), or a combination of the three drugs (DTR). Animal maintenance and handling were in accordance with the NIH guide for the care and use of laboratory animals [28]. All procedures were approved by the local Laboratory Animal Bioethics Committee, Facultad de Ciencias Médicas, UNLP, Argentina.

Sample Collection

At the end of the treatment, the animals were decapitated. Blood was collected using heparin (10 UI/mL) as anticoagulant in graduated ice-cold polypropylene tubes. Plasma samples were immediately prepared by centrifugation ($4,000 \times g$, 10 min) and then stored at -80 °C until analyzed. Testes were rapidly excised, washed, weighed, and homogenized in ice-cold phosphate buffer 100 mM with 6 mM of EDTA pH 7.40 (3 ml of buffer to 1 g of tissue). Homogenates were stored at -80 °C until assayed.

Analytical Methods

Various biomarkers of oxidative stress and cell damage were measured in plasma and testicular interstitial cells.

Lipid peroxidation was assayed as authentic lipoperoxides (ROOHs) by the FOX assay [29]. ROOHs were expressed as nmol malondialdehyde (MDA)/mg protein. The sum of nitrates and nitrites ($[\text{NO}_x]$) was measured as the main end-metabolite products of nitric oxide (NO) and peroxy nitrite anion (ONOO^-) by the method of Miranda et al. [30]. Results were expressed as nmol of nitrites/mg protein. Protein carbonyls (nmol/mg of protein) were measured using the method of Reznick and Packer [31] as a biomarker of oxidative damage to proteins. We also measured parameters of the antioxidant defense system. The FRAP (ferric reducing ability of plasma) assay was determined by the method of Benzie and Strain [32] and the results were expressed as μM of equivalent TROLOX[®] or α -tocopheryl acetate. Vitamin E (α -tocopherol) was measured after extraction by the method of Buttriss and Diplock [33] using the HPLC technique of Bagnati et al. [34] which can detect and quantify both α - and γ -tocopherols. Total glutathione (GSH) was measured by the method of Anderson and Meister [35] and expressed as $\mu\text{mol}/\text{mg}$ of protein. Protein contents were determined according to the method of Bradford [36].

Cell Culture and Treatment

Technical procedure for Leydig cell isolation was described in detail in a previous report [37]. Briefly, Leydig cells were removed from the interstitial space of testicular tissue by mechanical shaking with collagenase (Sigma Chem. Co., type IV) in a metabolic incubator, at 34 °C, according to Suescon et al. [38]. Cells were suspended in Krebs Ringer bicarbonate glucose (KRBG) solution (pH 7.4), examined for viability (90%) by trypan blue exclusion [39], and counted in a hemocytometer to adjust cell concentration. Aliquots of cell suspensions were subjected to protein determination by the micromethod of Bradford [36]. Preparations of interstitial cells comprised a high percentage of Leydig cells. The homogeneity of cell preparations was assessed by means of the observation of smears fixed in acetone and stained with H&E. Interstitial cell preparations consisted of Leydig cells (79%) and 21% of spermatids, spermatocytes and small cytoplasmic fragments.

Functional Assay

The functional response of cultured interstitial cells was assayed by stimulation with chorionic gonadotrophin (h-CG, Ovusyn[®] from Syntex S.A., Buenos Aires, Argentina) 10 nM for 12 h. Cells were detached from the surface culture using mechanical harvesting, transferred to graduated polypropylene ice-cold tubes, and pelleted at $600 \times g$ for 10 min. The pellet was washed twice with sonication buffer (65 mM Tris-HCl, pH 7.0, containing 10% sucrose)

and resuspended in the same medium. Cellular homogenates were prepared by sonication (three 30-s bursts at medium power in a Heat Systems Ultrasonic sonicator model W-220F from Plainview, NY). Crude extracts were centrifuged at $2,000\times g$ for 15 min and the supernatants were used for hormone measurements.

Immunoblotting

Cells were homogenized by sonication as described above in Tris/HCl/sucrose buffer with a 1% antiprotease cocktail (Sigma Chem. Co, Bs. As., Argentina), and 2% SDS. After heating the samples (20 μ g) at 95 °C for 3 min with 10% mercaptoethanol, aliquots were supplemented with 10% glycerol and 0.01% bromophenol blue and loaded on 12% SDS-PAGE mini-slabs (Mini protean II, Bio-Rad, Hercules, CA). Proteins were electrophoretically transferred overnight to PVDF membranes (Bio-Rad, Hercules, CA) using a transfer buffer containing 25 mM Tris, 190 mM glycine and 20% methanol. COX-2 protein levels were analyzed using a polyclonal antibody (Santa Cruz Biotechnology Inc., CA) while StAR protein was detected with a rabbit polyclonal antibody generated against amino acids 88–98 of the 30 kDa StAR protein prepared according to Clark et al. [17]. Blots were re-analyzed for α -tubulin as the reference protein to control both loading and transfer processes. A polyclonal anti- α -tubulin antibody from Oncogene (San Diego, CA) was used. Immunocomplexes were revealed with peroxidase-labeled secondary antibodies from Amersham Pharmacia Biotech AB (Uppsala, Sweden). Semi-quantitation of Western blots was performed using the GeneGenius gel documentation system and GeneTools software from Syngene (Cambridge, UK). Results were normalized to α -tubulin signal and expressed as “fold change” relative to the control (basal assay) which was assigned a value of 1.

Northern Blot Analysis

To determine StAR mRNA expression, Leydig cells were collected by centrifugation at 2 °C ($3,000\times g$ for 10 min) and washed twice with PBS. Total RNA purification was performed with TRIzol reagent following the manufacturer's instructions (Gibco-BRL, Grand Island, NY). Quantification and purities were checked by determination of the absorbance ratio at 260/280 nm. Electrophoretic separation was performed in an agarose/formaldehyde gel with a linear gradient from 1 to 5%. Hybond-P membranes (Amersham, GE Healthcare Ltd., Buckinghamshire, UK) were used for blotting the slabs. Membranes were stripped with a buffer containing 15 mM NaCl, 15 mM Na citrate and 1% SDS (pH 7) for 40 min at 52 °C. StAR mRNA on the membrane was probed with biotin-labeled mouse StAR

cDNA and detected using the North2South Chemiluminescent Nucleic Acid Hybridization and Detection Kit from Pierce (Pierce Biotechnology Inc. Rockford, IL) following the manufacturer's instructions.

PGF_{2 α} and PGE₂ Assays

For assessment of PGF_{2 α} and PGE₂ contents in the incubation media of interstitial cells, samples were centrifuged at $15,000\times g$ for 20 min at 2 °C. Supernatants were filtered through Millipore 0.2 μ m filters and concentrated by lyophilization in a Telstar Lyobeta freeze drying unit (Madrid, Spain). The residues were dissolved with HCl 2 N adjusting the pH to 3.5. These solutions were injected into a 200-mg C₁₈ reverse phase Sep-columns (Peninsula Lab, Belmont, CA) and then eluted with ethyl acetate. The eluted fractions were evaporated to dryness under a nitrogen stream and reconstituted in buffers for enzyme-immuno assay (EIA) determinations. Prostaglandins were determined using commercially available kits Prostaglandin F_{2 α} EIA Kit and Prostaglandin E₂ Express EIA Kit from Cayman, Migliore Laclaustra S.R.L. (Buenos Aires, Argentina) with a minimum detection of 4 and 30 pg/mL, respectively. Intra- and inter-assay coefficients of variation were in the range of 8–12% for both kits.

Lipid Analysis

Total lipids were extracted by the method of Folch et al. [40]. The phospholipid fraction was separated from the Folch extracts by the micro-column chromatography method described elsewhere [41] and quantified as phosphorus content [42] after mineralization of an aliquot from the silicic acid partition. GLC of the FAME (fatty acid methyl esters) was performed as indicated in one of our previous papers [43] except that in this case we used a capillary column mounted on a Hewlett Packard HP 6890 Series GC System Plus (Avondale, PA) equipped with a terminal computer integrator and data station. The FAMES were identified by comparison of their relative retention times with authentic standards and mass distribution was calculated electronically by quantification of the peak areas. Eicosamonoenoic acid (20:1) was used as the internal standard. Cholesterol content was enzymatically measured according to Allain et al. [44] using a commercial kit from Wiener Lab. (Rosario, Argentina).

Steroidogenic Enzyme Activities

Appropriate aliquots of supernatants were employed to determine 3- β -hydroxysteroid-dehydrogenase (3 β HSD) and 17- β -hydroxysteroid-dehydrogenase (17 β HSD) [EC 1.1.1.51] enzyme activities following the method of

Marugesan et al. [45]. Sonicated interstitial cells were centrifuged (10,000 × g, 15 min, 1–2 °C). Supernatants were mixed with charcoal in order to remove the endogenous steroids and the samples were again centrifuged (10,000 × g 15 min, 2 °C). The reaction conditions were defined in preliminary experiments, in which the enzyme activities were tested by varying the incubation times and concentrations of substrates, protein, and cofactors. Assays were performed under initial velocity conditions in a reaction mixture (250 µL final volume) containing 10 µM of the steroid substrate (Δ^4 -androstenedione or pregnenolone for 17 β HSD and 3 β HSD, respectively), 1 mM NADPH (17 β HSD) or 0.2 mM NAD⁺ (3 β HSD), and 0.1 M phosphate buffer (pH 7.4). Mixtures were incubated under air in a spectrophotometric cell holder thermostated at 37 °C. The reactions were started by the addition of the supernatant aliquots and OD changes of the nicotinamide cofactor(s) were measured. The incubation mixture deprived of substrate(s) was used as control.

Statistical Analysis

Results were analyzed by one way analysis of variance (ANOVA) followed by the Tukey multiple comparison test. Data were expressed as means \pm standard deviation (SD) of six independent determinations. They were considered different with respect to control data at the level of significance of * $P < 0.05$ or ** $P < 0.01$. In some of the Figures or Tables where multiple comparisons can be done we used different superscript letters to indicate statistical significances among results. Correlation and regression analyses and data plotting were automatically performed with the aid of Systat (version 12.0 for Windows) from SPSS Science (Chicago, IL) or Sigma Scientific Graphing Software (version 8.0) from Sigma Chem. Co. (St. Louis, MO).

Results

Influence of Treatments on Growth Parameters

The influence of the treatments on feeding parameters is shown in Table 1. Dimethoate treatment did not influence significantly the water consumption (approximately 15 mL/day), the final body weights, the rate of body weight gain, or the food efficiency ratio. Similar conclusions were obtained for the other treatments assayed (R, T or combined administrations; data not shown). We did not find absolute and relative testicular weight changes. Pesticide exposure—alone or in combination with the other drugs—did not affect the animal behavior. Also, no visible signs of toxicity and/or cholinergic effects were observed during the entire experimental period.

Table 1 Main feeding parameters associated with experimental treatments

Parameters	Treatments	
	C	D
Initial body weight (g)	181.0 \pm 3.7	174.0 \pm 7.3
Final body weight (g)	307.5 \pm 13.7	288.8 \pm 20.9
Body weight gain (g)	126.5 \pm 3.4	114.8 \pm 5.5
Rate of body weight gain (g/day)	3.6 \pm 0.1	3.3 \pm 0.2
Food efficiency ratio ^a	9.5 \pm 0.2	8.7 \pm 0.3
Absolute testicular weight (g)	2.8 \pm 0.1	2.9 \pm 0.1
Relative testicular weight (mg/g) ^b	9.1 \pm 0.3	10.0 \pm 0.4

Values represent the means \pm SD ($n = 8$)

C control rats, D dimethoate-treated rats

^a Food efficiency ratio = [body weight gain (g)/food intake (g)] $\times 10^2$

^b Relative testicular weight = testis weight (mg)/body mass (g)

Testosterone Biosynthesis

Plasmas from dimethoate (D)-treated rats contained less free and bound testosterone compared to control animals (Table 2). In samples from dosed rats, a decrease of approximately 20% was observed in both parameters whereas the ratio free/bound testosterone was not modified. We observed a more significant decrease in testosterone levels (approximately 50%) when sonicated interstitial cells were analyzed. Plasma estradiol concentration was decreased in D-treated rats by approximately 30%, while LH and FSH were increased by 58 and 76%, respectively (Table 2).

Table 2 Hormone levels in plasma and interstitial cellular homogenates from control (C) or dimethoate-treated (D) rats

Determinations	C	D
Plasma		
Free testosterone (nM)	4.7 \pm 0.2	3.9 \pm 0.1**
Bound testosterone (nM)	22.2 \pm 1.5	17.1 \pm 3.0**
Free/bound testosterone $\times 10^3$	212 \pm 15	228 \pm 12
Estradiol (pg/mL)	15.1 \pm 0.6	11.0 \pm 0.4**
LH (mU/mL)	7.7 \pm 0.2	12.2 \pm 0.6**
FSH (mU/mL)	8.1 \pm 0.4	14.3 \pm 0.8**
Cellular homogenates		
Total testosterone (pmol/mg protein)	27.9 \pm 1.3	14.2 \pm 0.9**

Hormone levels were analyzed using RIA kits commercially available from Radim as indicated in the Experimental procedures. Data were expressed as the means \pm standard error of six independent determinations assayed in triplicate

Results significantly different to those of the corresponding control value are indicated with asterisks ($P < 0.01$)

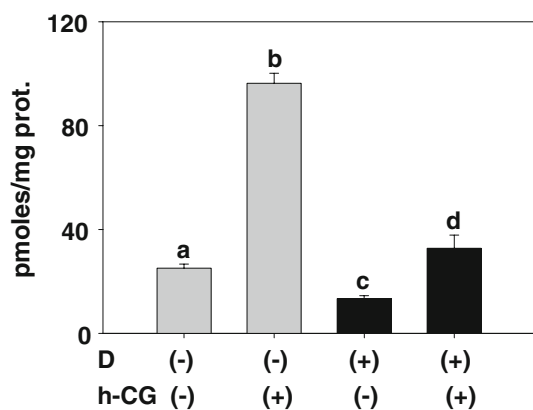


Fig. 1 Testosterone production of interstitial cells isolated from control (*gray bars*) or dimethoate (D)-treated (*black bars*) rats incubated in the presence or not of h-CG 10 nM for 12 h. Results were the means \pm SD of six independent determinations performed by RIA as indicated in the “[Experimental procedure](#)”. Different superscript letters correspond to statistically significant differences at $P < 0.01$

Interstitial cell cultures from C or D rats exhibited a very different behavior after 12-h stimulation with 10 nM human chorionic gonadotrophin (h-CG) (Fig. 1). Cells isolated from C rats released four times the basal testosterone production after overnight stimulation. In contrast, the cells isolated from D-treated rats exhibited significantly decreased basal levels and they only doubled the concentration of testosterone after the functional test with h-CG. Thus, we observed a 50% reduction in androgen production in h-CG-stimulated cells from D rats (Fig. 1).

Direct measurement of the two key androgenic enzyme activities which regulate testosterone biosynthesis were performed in supernatants from interstitial cell sonicates after a h-CG stimulation assay (Fig. 2). Both enzymes activities, 3β - and 17β -hydroxysteroid dehydrogenases (3β HSD and 17β HSD, respectively) (Fig. 2A, B), were significantly lower (40–50%) after dimethoate treatment. Neither of the two enzymes exhibited a significant change after h-CG stimulation independent of the previous treatment of the animals and cells (Fig. 2).

Oxidative Stress Biomarkers

A condition of oxidative stress (OS) was clearly established in D-treated rats. This condition was characterized by a general failure of the antioxidant defense enzymes, a lower level of α -tocopherol and increased concentrations of oxidative damage biomarkers in plasma (data not shown). In interstitial cells of D-treated rats, a significantly higher level of ROOHs which are reliable biomarkers of lipid oxidative damage (Fig. 3A). Levels of protein carbonyls

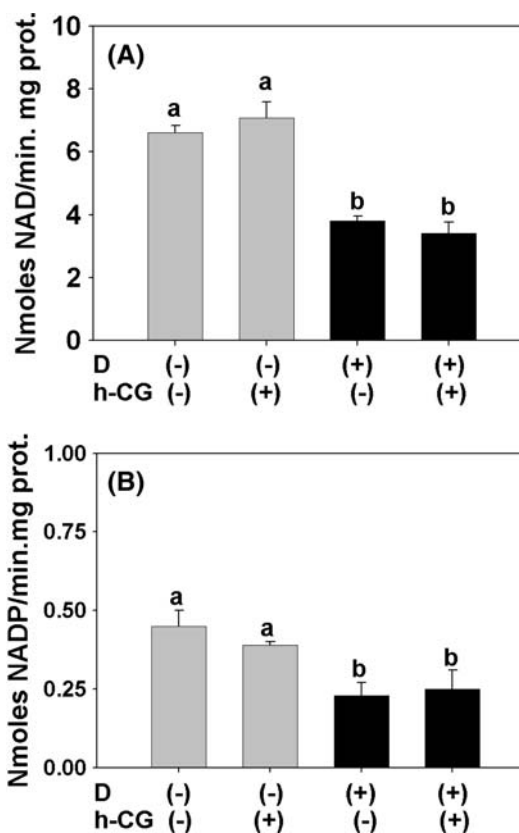


Fig. 2 Steroidogenic enzyme activities in interstitial cells prepared from control (*gray bars*) or dimethoate (D)-treated (*black bars*) rats previously incubated or not with h-CG 10 nM for 12 h. Enzyme activities (A 3β HSD, B 17β HSD) were expressed as nmol of NAD or NADP/min mg protein and correspond to the means of six independent assays performed in duplicates \pm SD. See “[Experimental procedure](#)” for details. Different superscript letters correspond to statistically significant differences at $P < 0.01$

and $[\text{NO}_x]$ (nitrates + nitrites), which reflects the oxidative damage to proteins and the stimulation of NOS activity, respectively, were both increased by the administration of the pesticide (Fig. 3A). After dimethoate treatment, the total glutathione concentration increased (Fig. 3A) while α -tocopherol decreased (Fig. 3B). The FRAP assay was performed in sonicated interstitial cells from C and D rats as a biomarker of the total antioxidant ability. In cells from D-treated rats, FRAP was lower by approximately 30% compared with control animals (Fig. 3C).

StAR and COX-2 Expression

The level of StAR mRNAs was estimated by Northern blotting. A representative result is shown in Fig. 4A. Lanes 1 and 2 correspond to control interstitial cells while lanes 3 and 4 to cells isolated from D-treated rats. Chorionic gonadotrophin was added to the cultures analyzed in lanes 2 and 4. The same scheme was followed when the

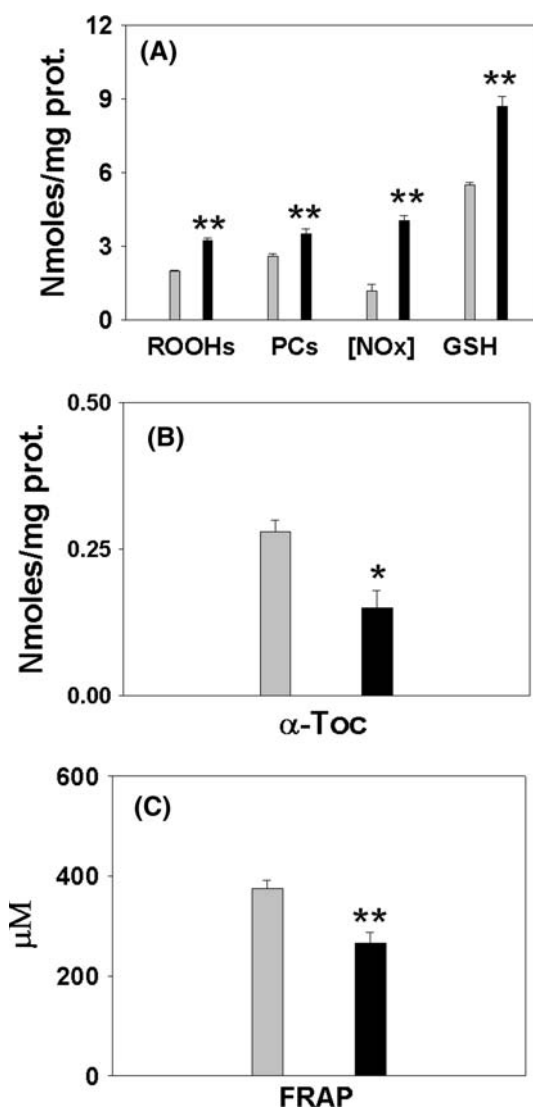


Fig. 3 Oxidative stress biomarkers measured in interstitial cells from control (gray bars) or dimethoate-treated (black bars) rats. **A** Data for authentic lipoperoxides (ROOHs), protein carbonyls (PCs), nitrates + nitrites ([NO_x]), and glutathione (GSH) levels. **B** α-tocopherol concentration (α-Toc), **C** the assay of the total antioxidant capacity (FRAP). Each value was expressed as the mean of six independent determinations ±SD. Asterisks indicate significant difference with respect to control value **P* < 0.05 and ***P* < 0.01

expression of StAR or COX-2 proteins were tested by Western blotting (Fig. 4B). Relative quantification of the signals appeared in Fig. 5A and B. The h-CG stimulation provoked a significant increment of StAR at both transcriptional (Fig. 5A) and translational (Fig. 5B) levels. These increments were completely abolished by dimethoate treatment. Moreover, the pesticide evoked a reduction in the expression of StAR mRNAs, and also in its translation products (StAR protein). In contrast, dimethoate increased the biosynthesis of COX-2 protein at levels

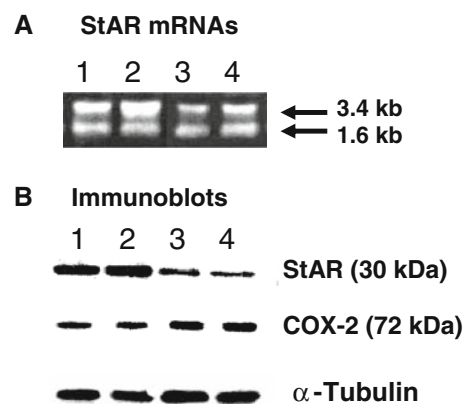


Fig. 4 Expression of mRNA StAR (**A**) and protein level for StAR and COX-2 (**B**) in interstitial cells. Lanes were: 1 control cells, 2 control stimulated with hCG 10 nM for 12 h, 3 D-treated cells, 4 D-treated cells stimulated with h-CG. Results are representative of six different incubations run in duplicate. See details in the “Experimental procedure” part

which were very similar to those observed in both h-CG stimulated and non-stimulated cells (Fig. 5C).

Arachidonate Metabolism and Cholesterol Level

The analysis of interstitial cell phospholipids demonstrated that the content of total inorganic phosphate per mg protein was unaffected by dimethoate treatment (data not shown). However, the pesticide significantly modified the fatty acyl composition of membrane phospholipids (Fig. 6). Saturated palmitic and stearic acids were increased while arachidonic, docosapenta-, and docosahexaenoic acids were diminished. Similar alterations were observed in neutral lipids (data not shown).

The total lipid extract from the mitochondrial fraction was also analyzed by the absolute content of cholesterol and arachidonic acid (Table 3) using a coupled enzymatic procedure with cholesterol oxidase and quantitative capillary gas-liquid chromatography, respectively. Clear correlations between the androgen production and the content of these lipids were observed (Fig. 7). Testosterone concentrations in whole cells were linearly and positively correlated with cholesterol content ($r^2 = 0.92$) and arachidonate levels ($r^2 = 0.98$) in mitochondrial fractions from interstitial cells.

Cyclooxygenase-related metabolites of arachidonate were also studied in interstitial cells under basal or h-CG-stimulated conditions using EIA methods (Fig. 8). Prostaglandins F_{2α}, and its precursor (PGE₂), were both significantly higher in rats treated with dimethoate. Stimulation with h-CG provoked in both types of cellular cultures (control or D-treated) a slight—but not significant—change in the concentration of the prostaglandins analyzed compared with the corresponding reference culture (Fig. 8).

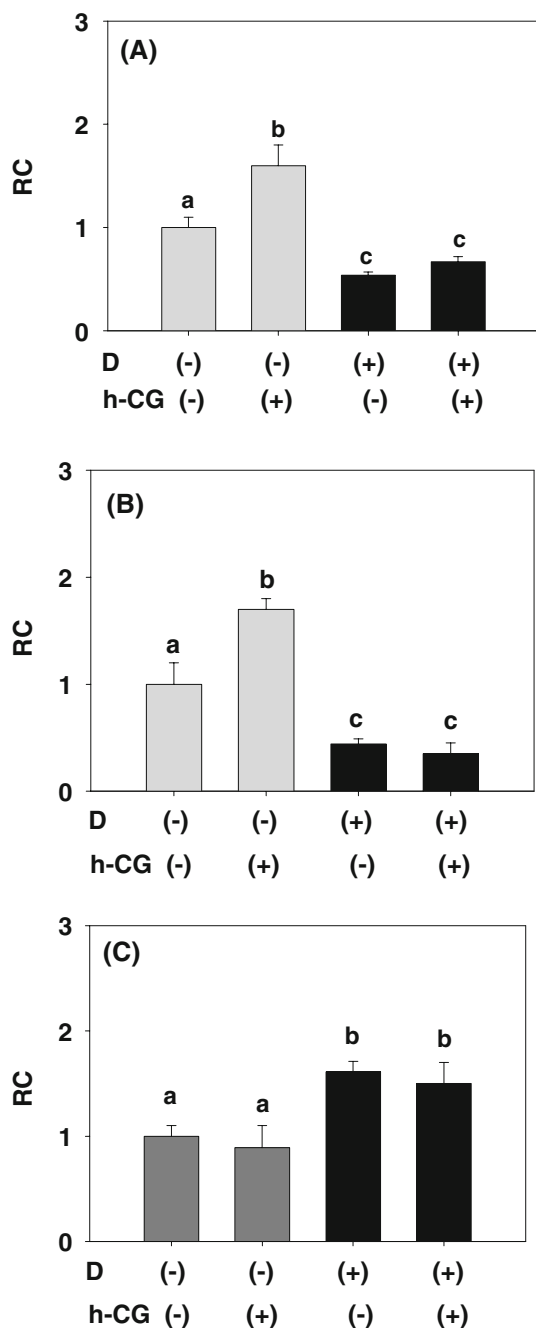


Fig. 5 Relative changes (RC) of the expression of StAR mRNA (A), StAR protein (B) or COX-2 protein (C), quantified by densitometry using the GeneGenius gel documentation system and GeneTools software from Syngene (Cambridge, UK). Results were normalized to α -tubulin signal and expressed as “fold change” relative to the control (basal assay) which was assigned a value of 1. Mean \pm SD. Different superscript letters correspond to statistically significant differences at $P < 0.01$

Antioxidant and COX-Inhibitor Effects

The effects of the antioxidant TROLOX[®] or the COX inhibitor rofecoxib on various experimental parameters

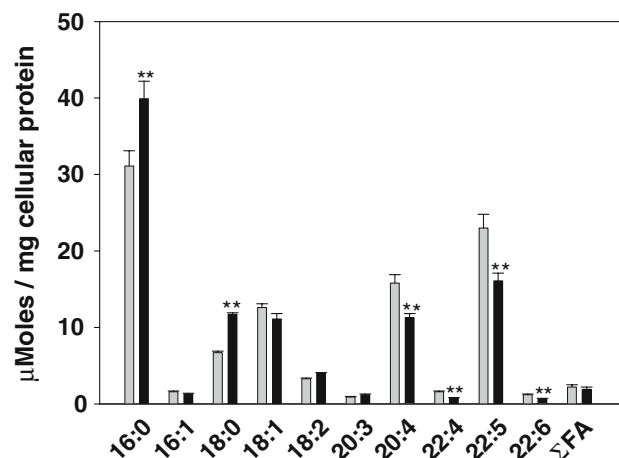


Fig. 6 Fatty acid composition of total phospholipids isolated from the mitochondrial fraction of interstitial cells prepared from control (gray bars) or dimethoate-treated (black bars) rats. Fatty acids were derivatized to methyl esters (FAMES) and analyzed by capillary gas-liquid chromatography under the conditions described in the “Experimental procedures”. FAMES were identified with authentic standards, quantified using eicosamonoenoic acid as internal standard and expressed as μ mol of fatty acid per mg cellular protein (mean of six independent analyses \pm SD). Double asterisks indicate significant difference with respect to control value at $P < 0.01$. Σ FA corresponds to the sum of other C₂₂ and C₂₄ fatty acids not identified in the chromatogram

measured on dimethoate-treated rats appear in Tables 4 (absolute values) and 5 (relative changes). Drugs were administered alone or in combination at dosages that effectively inhibited lipid peroxidation and COX-2 activity. TROLOX[®] produced a strong decrease in the formation of D-induced ROOHs. However, the hormonal alterations evoked by dimethoate administration (essentially decreased testosterone biosynthesis and raised levels of the main gonadotrophin) were not normalized by simultaneous treatment with D and T. The levels of ARA were not affected by the treatment with the antioxidant alone. In addition, the decreased level of ARA observed after D administration was not restored when the pesticide was associated with T. Injection of R raised the level of ARA and at the same time significantly decreased the biosynthesis of PGF_{2 α} . Interestingly, testosterone concentration in both plasma and cellular homogenates was slightly (but significantly) higher while LH was lower under R treatment. Simultaneous administration of D and R normalized hormonal disturbances induced by D; notwithstanding the production of ROOHs still persistent and markedly elevated (Table 4). The ARA and PGF_{2 α} D-induced changes were completely reverted by the opposite and proportional effects displayed by R (Table 5). When the three drugs were administered in combination (DTR) all the parameters of those of control rats were indistinguishable. From these

Table 3 Cholesterol and arachidonic acid levels of total lipids from the mitochondrial fraction isolated from interstitial cells from control or dimethoate-treated rats

Cells	Control		Dimethoate	
Treatment	None	+h-CG	None	+h-CG
Lipids				
Cholesterol (ng/ μ g protein)	27.1 \pm 5.0 ^a	63.6 \pm 15.0 ^b	20.4 \pm 5.2 ^c	16.2 \pm 5.6 ^c
Arachidonic acid (μ mol/mg protein)	36.2 \pm 6.6 ^a	57.3 \pm 3.2 ^b	25.5 \pm 5.0 ^c	31.2 \pm 4.3 ^c

Total lipids were extracted from the mitochondrial fraction of the interstitial cells prepared from control or dimethoate-treated rats after incubation with or without h-CG 10 nM for 12 h. Total lipid fractions were fractionated into neutral and polar lipids using silicic acid partition, and then analyzed for cholesterol and arachidonic acid levels using enzymatic and chromatographic methods as described in “[Experimental procedure](#)”. Results were expressed as the means of six independent determinations \pm 1 SD of the mean. Different superscript letters correspond to statistically significant differences at $P < 0.01$

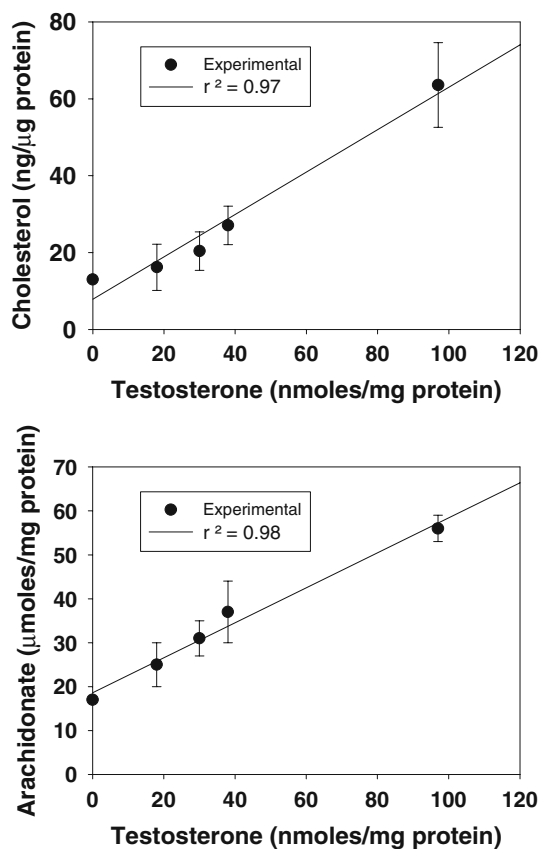


Fig. 7 Linear regressions and linear correlation coefficients (r^2) for the relationship between cholesterol content of the mitochondrial fraction of interstitial cells and testosterone production (*upper panel*), or arachidonic acid level of the mitochondrial fraction of interstitial cells and testosterone production (*lower panel*). Data were obtained from basal or h-CG-stimulated cells from control or dimethoate-treated rats, and they were expressed as the means \pm SD of six independent measurements. Plots and r^2 were automatically generated by means of the statistical software described in the “[Experimental procedure](#)”

results, the main conclusion obtained is that there is an inverse proportionality between the changes induced by each drug assayed (D, T or R) that results in neutralization

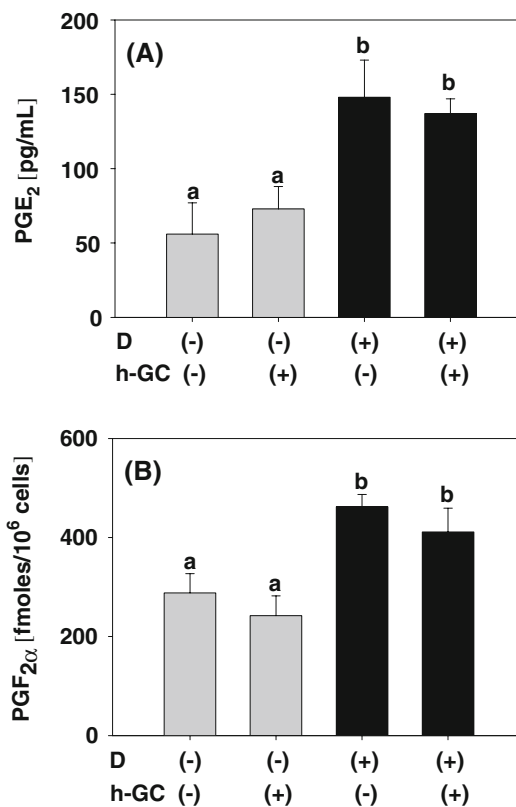


Fig. 8 Prostaglandins (PG) production from interstitial cell suspension prepared from control (*gray bars*) or dimethoate (D)-treated (*black bars*) rats incubated in presence or absence of h-CG 10 nM for 12 h. PGE₂ (A) or PGF_{2 α} (B) were analyzed by EIA as described in the “[Experimental procedure](#)” section. Each datum is the mean \pm SD of six independent assays. Different *superscript letters* correspond to statistically significant differences at $P < 0.01$

of the effects when they are combined. For example, the decrease in testosterone or the increased biosynthesis of PGF_{2 α} produced by D were almost exactly compensated by simultaneous treatment with R. Also, it is evident that the generation of ROOHs does not parallel the changes of ARA concentrations suggesting that other fatty acids (in addition to ARA) are involved in the generation of free radicals.

Table 4 Main experimental parameters determined after dimethoate (D), TROLOX[®] (T), or rofecoxib (R) treatments to rats

Analytical parameters	Experimental groups						
	C	CT	CR	D	DT	DR	DTR
ARA ($\mu\text{mol}/\text{mg}$ cell protein)	15.5 \pm 0.7 ^a	16.2 \pm 0.8 ^a	19.4 \pm 0.9 ^b	9.8 \pm 0.1 ^c	10.1 \pm 0.5 ^c	15.3 \pm 0.6 ^a	14.9 \pm 0.8 ^a
PG F _{2α} (fmol/10 ⁶ cells)	294.7 \pm 11.9 ^a	319.3 \pm 6.5 ^b	95.3 \pm 8.5 ^c	454.4 \pm 9.1 ^d	486.5 \pm 12.3 ^c	301.9 \pm 15.8 ^a	301.0 \pm 9.6 ^a
ROOHs (nmol/mg protein)	3.1 \pm 0.2 ^a	2.9 \pm 0.3 ^a	3.4 \pm 0.3 ^a	5.3 \pm 0.1 ^b	3.6 \pm 0.1 ^c	6.1 \pm 0.8 ^b	3.7 \pm 0.1 ^a
Hormones							
Plasma testosterone (nM)	5.0 \pm 0.2 ^a	4.9 \pm 0.1 ^a	5.9 \pm 0.2 ^a	3.8 \pm 0.1 ^b	4.0 \pm 0.1 ^b	4.8 \pm 0.1 ^a	5.1 \pm 0.2 ^a
Cellular testosterone (pmol/mg protein)	26.6 \pm 1.1 ^a	27.2 \pm 0.8 ^a	32.1 \pm 0.9 ^a	12.5 \pm 1.0 ^b	14.3 \pm 0.8 ^a	24.5 \pm 0.8 ^a	27.1 \pm 1.2 ^a
Plasma LH (mU/mL)	6.9 \pm 0.2 ^a	7.0 \pm 0.1 ^a	5.8 \pm 0.2 ^a	15.1 \pm 0.7 ^b	13.5 \pm 0.5 ^b	7.3 \pm 0.1 ^a	6.8 \pm 0.2 ^a

Data are expressed as the means \pm SD (four independent determinations assayed in duplicate). C, control group (injected with vehicle alone). CT, CR and D were treated with TROLOX[®], rofecoxib or dimethoate, respectively. DT, DR, and DTR received combined administration of the drugs. Determinations were performed as described in the “[Experimental procedure](#).” Statistical comparisons (ANOVA plus Tukey’s test) among experimental groups within a same row were indicated with different superscript letters

Discussion

The increasing use for organophosphorus insecticides has introduced a serious and novel hazard for humans and livestock animals [22]. Dimethoate is one of the most used agrochemicals around the world. Experimental evidence indicates that it impairs fertility, suppresses libido, causes testicular degeneration, and deteriorates semen quality [22]. Despite its residual action, this drug is extensively used in horticulture as a systemic insecticide and acaricide for treating gardens, vineyards, and field crops, and it is also applied externally for the control of fly larvae in cattle [22]. Previous studies from other laboratories demonstrated its adverse effects on semen performance [22] which were attributed to the presence of the dimethyl group in the moiety [46]. In our experiments, the testes were macroscopically examined to find visible evidence of toxic effect(s). We observed considerable changes in appearance, volume, and consistence of both testes of treated rats that suggest tissue edema. However, we did not observe significant changes in absolute and/or relative weights such as those reported by Farag et al. [47]. This probably could be due to differences in animal species, time/route of treatment, and the dose of dimethoate administered. Since the wet weights were conserved, this finding may indicate loss of testicular-specific structural tissue. This was strongly supported by the aspects of the testes previously decapsulated, and it is in agreement with findings of Sayim et al. [48, 49] that revealed a dimethoate-dose depended histopathological features of rat testes. Alterations reported were characterized by moderate to severe seminiferous tubule degeneration as sloughing, atrophy, germ cell degeneration, and partial arrest of spermatogenesis [48, 49].

Dimethoate was also involved in hormonal unbalance. Thomas et al. [50] suggested that this pesticide could block

the uptake of steroid hormones at the interstitial cell receptor level. However, other research has previously proposed that dimethoate exerts a direct cytotoxic action not associated with alterations in LH, FSH, or other hormonal regulators implicated in androgen biosynthesis [51, 52]. The present work demonstrate that low doses of dimethoate administered i.p. chronically are able to produce significant alterations in the levels of circulating gonadotrophin hormones which raise in response to a decrease testosterone production. The LH and FSH increases may have important consequences in the differentiation status of Leydig cells. In fact, previous studies demonstrated that this chronic stimulation is closely related to increased cancer degeneration [8]. The estradiol level, which reflects testosterone metabolism, is also significantly reduced after dimethoate treatment. Our results agree with an early investigation by Afifi et al. [22] who reported a decrease testosterone level of rats dosed orally with dimethoate for 2 months. We are unaware of any other studies that have examined in more detail the hormonal profile after dimethoate intoxication.

Oxidative stress is a well-known consequence of intoxication with environmental contaminants. This condition was repeatedly observed under metal overload [14, 53–56] or after intoxication with agrochemicals [20, 57, 58]. Some of the detrimental effects produced by pesticides in the male reproductive system were explained as a consequence of the exacerbated free radical production caused by these drugs [59]. It was proposed that most pesticides may act as pseudosubstrates for the generation of free radicals, which in turn, can damage P450 enzymes [6]. However, this suggestion is not accepted for all researchers since antioxidant supplementation failed to restore testosterone biosynthesis after intoxication by, for example, octylphenols [57]. Our results indicate that cultures of interstitial cells isolated from D-treated rats have a clear

oxidative stress condition hallmarked by a general loss of the antioxidant capacity and elevation of biomarkers of OS damage. Interestingly, we observed an increased amount of the water-soluble antioxidant glutathione that could be ascribed to a compensatory mechanism of scavenging against the increased production of free radicals induced by dimethoate. This explanation is in agreement with previous experimental evidence indicating that γ -glutamyl-cysteinyl synthetase—which controls the biosynthesis of glutathione—is induced by a prolonged oxidative stress condition [60, 61]. At the same time, the decreased level of α -tocopherol could be the consequence of its increased rate of consumption within the lipophilic compartment of the interstitial cells. The loss of the lipid-soluble antioxidant capacity correlates well with the observed increase in the ROOHs production and the lower FRAP values. These findings led us to the idea that the testosterone level may be restored by antioxidant treatment. However, in agreement with the results reported by Muroño et al. [57] (for the octylphenol inhibitory effect on testosterone biosynthesis) we did not find any positive effect caused by concomitant administration of D and T (Tables 4, 5).

From this scenario, a first explanation for the decreased testosterone production could be proposed. Biosynthesis of this androgen in Leydig cells depends on the activities of two key enzymes (3β HSD and 17β HSD) which were inhibited in our experimental system in a clear correlation with the observed decrease in both the production of testosterone by Leydig cells and the plasma testosterone level. During the last years, free radical production has been linked to its possible role in reducing steroidogenesis [62–65]. In addition, studies from Murugesan et al. [20, 45, 66] and Kostic et al. [67] suggested that androgenic dehydrogenases could be significantly inhibited by free radical overproduction. Thus, we think that—as judged by the normalization of ROOHs—OS induced by dimethoate treatment can be reverted by T administration; however, this fact may not contribute at least crucially to the loss of the androgenic capacity via 3β - and 17β -dehydrogenase inhibition. These results support the assumption that D does not act as a pseudosubstrate that binds to the steroid-binding site of P450 enzymes (P450_{scc} and P450_{c17}) disrupting hydroxylation and leading to electron leakage and free radical production [57]. Also, it is unlikely that OS condition affects significantly the availability of NADPH that is required for the normal hydroxylation of steroids during P450 pathway for testosterone biosynthesis.

Another question concerning OS and steroidogenic activity can be discussed. It is well known that lipids can be destroyed by free radical attack. In particular, lipid peroxidation is now considered to be the main mechanism by which oxygen- or nitrogen-derived radicals can cause damage leading to impaired normal cellular function in

testis [68]. Mammalian spermatozoa, being rich in polyunsaturated fatty acids (PUFAs) are more susceptible to oxidative damage resulting in sperm deterioration [6, 49]. Similar consequences can be assumed for Leydig cells which are also very rich in PUFAs [69]. Induction of OS by pesticides has been a focus of research over the last decade as a possible mechanism for infertility [6, 70]. We observe that after intoxication with dimethoate a significant loss of PUFAs occurred in interstitial cells, specially arachidonic, docosapenta- and hexaenoic fatty acids (Fig. 6). C₂₂ PUFAs are involved in spermatogenesis [71] while arachidonic acid (ARA) is directly linked to the androgenic activity of Leydig cells [16, 19]. Thus, it is possible that chronic OS may be an important mechanism for the arachidonate-dependent loss of steroidogenic ability since this fatty acid is essential for the biological activity of the steroidogenic acute regulatory protein (StAR) [72]. ARA level in Leydig cells is controlled by a hormone-regulated mechanism which involves an acyl-CoA synthetase (ACS4) and a mitochondrial acyl-CoA thioesterase (Acot2). Recent findings have demonstrated that, in steroidogenic cells, ARA release does not operate through the activation of the phospholipase A₂ pathway [73]. Experimental evidence supports the idea that ARA is released from the cholesteryl-ester pool and immediately converted into arachidonoyl-CoA by ACS4 [19]. This thioester binds to the acyl-CoA binding protein (DBI), which in turn, binds to the translocator protein (TSPO) located in the outer mitochondrial membrane. This would possibly facilitate a direct transference of arachidonoyl-CoA into the mitochondria [72]. In addition, ARA is transformed into lipoxygenated products which induce the transcription of StAR gene [72]. Thus, the conversion of cholesterol to testosterone is limited by the transport of cholesterol from the outer to the inner mitochondrial membrane. This event is controlled by StAR activity [21] and also by the ARA level [73, 74]. We have demonstrated that both ARA and cholesterol concentration are decreased in cells isolated from dimethoate-treated rats. Reduction of ARA, which in turn leads to the reduction of mitochondrial cholesterol content, could be produced by oxidative destruction of PUFAs due to D-induced OS, by an increased utilization via the COX-2 pathway, or both. Previous studies with rat mitochondrial fractions subjected to peroxidative conditions support the assumption that PUFA content can be effectively depleted by overproduction of free radicals [75]. In addition, recent studies from our laboratory indicated that plasmalogen subfraction is particularly enriched in ARA and very sensible to oxidative damage [76]. In addition, another pathway for ARA metabolism which is very active in interstitial cells, is the cyclooxygenase route that converts the precursor ARA into prostaglandins G₂, H₂, E₂, D₂ and F_{2 α} [77]. Cyclooxygenase isoenzymes types

Table 5 Statistical comparisons and percent changes among experimental parameters determined after dimethoate (D), TROLOX® (T), or rofecoxib (R) treatments to rats

Parameters	Groups					
	CT	CR	D	DT	DR	DTR
ARA	4.5 ± 0.1 n.s.	25.2 ± 1.2*	-36.7 ± 1.6**	-34.8 ± 1.1**	-1.3 ± 0.1 n.s.	-3.9 ± 0.2 n.s.
PGF _{2α}	8.3 ± 0.2 n.s.	-67.7 ± 2.1**	54.2 ± 1.5**	65.1 ± 2.4**	2.4 ± 0.2 n.s.	2.1 ± 0.3 n.s.
ROOHs	-6.5 ± 0.2 n.s.	9.7 ± 0.3 n.s.	70.9 ± 1.9**	16.1 ± 0.5*	96.7 ± 2.1**	19.4 ± 0.4*
Te (plasma)	-2.0 ± 0.1 n.s.	18.0 ± 0.4*	-24.0 ± 0.6**	-20.0 ± 0.5*	-4.0 ± 0.1 n.s.	2.0 ± 0.1 n.s.
Te (cells)	2.2 ± 0.1 n.s.	17.1 ± 0.3*	-53.0 ± 2.1**	-46.2 ± 1.1**	-7.9 ± 0.3 n.s.	1.9 ± 0.1 n.s.
LH (plasma)	1.4 ± 0.1 n.s.	-15.9 ± 0.5*	118.8 ± 4.6**	95.6 ± 3.1**	5.8 ± 0.2 n.s.	-1.4 ± 0.1 n.s.

Data were obtained from Table 4 and assayed by ANOVA plus Tukey's test. Percentage changes (expressed as means ± SD) for a determined treatment were calculated as $[X - C] \times 100/C$, being X and C the tested and control paired data, respectively, within each group under comparison

ARA arachidonic acid, PGF_{2α} prostaglandin F_{2α}, ROOHs authentic hydroperoxides, Te testosterone

Statistical significances were indicated by asterisks (* $P < 0.05$ and ** $P < 0.01$), or with "n.s." (non-significant difference respect to the corresponding control group)

I (COX-1) and II (COX-2) are key enzymes that function coordinately and are controlled differentially by regulating the amount of ARA and lipid peroxides [78]. Previous studies from other laboratories suggested that COX-1 and COX-2 may not be important for male reproductive performance, at least in mice [77]. However, this early general view is being challenged by recent findings. COX-2 is overexpressed in human testis from men with impaired spermatogenesis, infertility, or degenerative disorders [79, 80]. Moreover, PGF_{2α} has been reported to significantly decrease StAR expression in porcine, rat, and human tissues [81–84]. In addition, Frungieri et al. [74] demonstrated that PGF_{2α} inhibition of h-CG-induced testosterone production in Leydig cells is accompanied by the down-regulation of both StAR and 17βHSD. Moreover, we observed elevated levels of trophic hormones in peripheral blood which failed to restore the androgenic capacity. This was in agreement with a previously demonstrated blockage of PGF_{2α} of the LH- or FSH-stimulatory pathway [85]. In vitro studies using MA-10 mouse Leydig cells further proved that inhibition of COX-2 activity significantly increased StAR protein expression and steroid production [86]. Our results strongly suggest that COX-2 is implicated in the inhibition of testosterone biosynthesis by dimethoate. We observed a significant increase in the level of COX-2 protein in cells isolated from dosed animals which correlated with the higher concentrations of both PGE₂ and PGF_{2α}. Concomitantly, StAR protein is diminished at both the gene expression and protein levels. These results also agree with those of Arakane et al. [87] who reported an inhibition of StAR gene expression by PGF_{2α}. Concerning the role of COX-2 in testosterone production, we demonstrated that simultaneous administration of rofecoxib and dimethoate normalizes the hormonal levels to control values although the COX inhibitor was not able to modify the

ROOHs production (Tables 4, 5). From these results, we assume that the main target of dimethoate effect on steroidogenic route is COX-2 activity that leads to the overproduction of PGE₂ and F_{2α} and subsequent inhibition of the StAR regulatory mechanism.

The status of androgenesis is usually tested (in vivo or in vitro) by the commonly accepted method of h-CG stimulation followed by the measurement of the testosterone production [12]. Interestingly, in our experimental system, the functional assay of stimulation with physiological concentration of h-CG does not normalize the changes induced by dimethoate, suggesting that the pesticide could act independently of gonadotrophin receptor-mediated events. This fact should be considered as another mechanism by which dimethoate can depress the pathway for androgen production. It remains to be explored whether this inhibitory response was initially triggered by overproduction of free radicals, and to what extent the overall effect can be attributed to the other(s) (synergistic) mechanism(s) involved. For example, previous studies by Diemer et al. [85] demonstrated that free radicals per se are able to inhibit StAR activity. However, results from Tables 4 and 5 suggest that OS may not have a crucial role in blocking StAR signal cascade directly or indirectly via gonadotrophin receptors. Whenever this crosstalk may (or not) occur, it seems quite possible that the ARA level was not (at least not entirely) depleted as a consequence of the oxidative stress condition since administration of D or R decrease and increase, respectively, the level of the acid in a clear correspondence with the COX-2 activity changes (Tables 4, 5). Thus, the increased production of PGE₂ and PGF_{2α} should be produced—as observed in our experiments—through an important stimulation of the COX-2 activity which is inversely associated to the concentration of its substrate (ARA). As a consequence, StAR activity

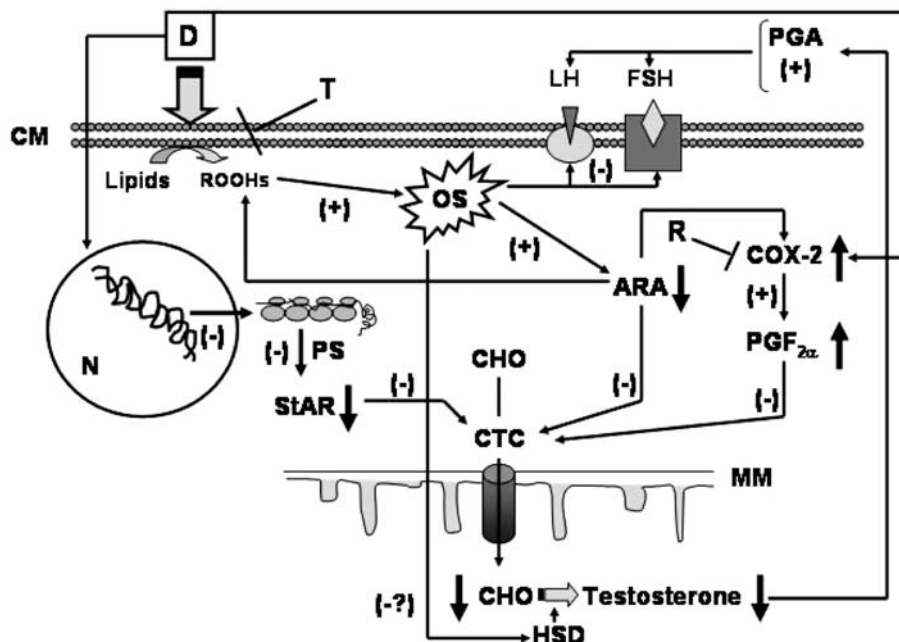


Fig. 9 Effects of chronic dimethoate intoxication on the steroidogenic status in rat testis. Dimethoate (*D*) evokes a general failure in the antioxidant system and exacerbates the production of lipoperoxides (*ROOHs*) which leads to an oxidative stress condition (*OS*). This effect is effectively blocked by administration of TROLOX® (*T*). The arachidonic acid (*ARA*) level decreases by conversion into peroxides principally due to exacerbated COX-2 activity rather than the destruction by free radicals. This condition diminishes the efficiency of the cholesterol transport complex (*CTC*) located at the mitochondrial membrane (*MM*). *ARA* is converted by the induced cyclooxygenase-2 (*COX-2*) into prostaglandin F_{2x} (*PGF_{2x}*) that inhibits the activity of the *CTC*. Rofecoxib (*R*) blocks the activity

of COX-2 and prevents the deleterious effect(s) of dimethoate (*D*). Administration of *D* also reduces the expression of the gene which encodes the steroid acute regulatory protein (*StAR*) and its translation into active protein. The decreased production of *StAR* further inhibits the input of cholesterol (*CHO*) by the mitochondria. All these effects act in concert to decrease the availability of *CHO* and its conversion into testosterone. Additional effects should be exerted on the activities of the 3 β - and 17 β -hydroxysteroid dehydrogenases (*HSD*), and on the signal transduction of LH and FSH which are increased by the pituitary–gonadal axis (*PGA*) in response to the decreased production of testosterone. *CM* cytoplasmic membrane, *N* nucleus, *PS* protein synthesis

would be inhibited indirectly by either a decreased availability of *ARA* or an increased concentration of PGF_{2x} . As reported previously, steroidogenesis is sensitive to small changes in *StAR* protein expression [21]. This question is important since *StAR* plays a key role in steroid production by gonads as well as in the steroidogenesis of adrenal glands. As a result, a disruption in *StAR* protein expression may impair more than just fertility. The biosynthesis of mineralo- and glucocorticoids may affect carbohydrate metabolism, immune system, and water balance. Such a general disturb may underline many of the toxic effects of environmental pollutants [21, 88].

As a conclusion, we propose that dimethoate inhibits testosterone biosynthesis by multiple mechanisms of action (Fig. 9). Chronic intoxication, even at the low doses used in our experiments, provokes an oxidative stress which in turn raises the level of lipoperoxides and the activity of COX-2. As a consequence, a decreased rate of the *StAR*-stimulated cholesterol transport into the mitochondria was observed. Dimethoate treatment also blocks the activities

of the hydroxysteroid dehydrogenases and impairs the LH- or FSH-dependent signal for stimulation of androgen biosynthesis by a mechanism(s) that do not depend crucially on the *ROOHs* level. At the same time, increased COX-2 protein decreases *StAR* transcription and translation. The subsequent elevation of PGF_{2x} further inhibits *StAR* protein action decreasing both the availability of cholesterol and the rate of testosterone biosynthesis probably by inhibition of the 17 β HSD mRNA transcription. The final biological effect suggests that the androgenesis status could provide a highly sensitive test for estimating the damage exerted by residual agrochemicals in chronically exposed populations. These conclusions should stimulate further research concerning the androgen functionality and the hormone level of men involuntarily exposed to dimethoate or others organophosphorus compounds. This fact also raised concern about the generality of the toxic action(s) of this kind of drugs on both the reproductive functions and the other metabolic pathways controlled by steroid hormones.

Acknowledgments This study was supported by a grant from Consejo Nacional de Investigaciones Científicas y Técnicas (CONICET), Argentina. We would like to thank Mrs. Agustina Zardis de Cobefias, Eva Illara de Bozzolo, and Norma Cristalli for their excellent technical assistance.

References

- Cheek AO, McLachlan JA (1998) Environmental hormones and the male reproductive system. *J Androl* 19:5–10
- Carlsen E, Giwercman A, Keiding N, Skakkeback NE (1992) Evidence for decreasing quality of semen during past 50 years. *Biochem Med J* 305:609–613
- Auger J, Kunstmann JM, Czyglik F, Jouannet P (1995) Decline in semen quality among fertile men in Paris during the past 20 years. *New Engl J Med* 332:281–285
- Ginsburg J, Okolo S, Prelevic G, Hardiman P (1994) Residence in the London area and sperm density. *Lancet* 343:230
- Swan SH, Elkin EP, Fenster L (1997) Have sperm densities declined? A reanalysis of global trend data. *Environ Health Perspect* 105:1228–1232
- Saradha B, Mathur PP (2006) Effect of environmental contaminants on male reproduction. *Environ Toxicol Pharmacol* 21:34–41
- Swan SH, Kruse RL, Liu F, Barr DB, Drobnis EZ, Redmon JB, Wang C, Brazil C, Overstreet JW (2003) Semen quality in relation to biomarkers of pesticide exposure. *Environ Health Perspect* 111:1478–1484
- Cook JC, Mullin LS, Frame SR, Biegel LB (1993) Investigation of a mechanism for leydig cell tumorigenesis by linuron in Rats. *Toxicol Appl Pharmacol* 119:195–204
- Fry DM (1995) Reproductive effects in birds exposed to pesticides and industrial chemicals. *Environ Health Perspect* 103:165–171
- Wong C, Kelce WR, Sar M, Wilson EM (1995) Androgen receptor antagonist versus agonist activities of the fungicide vinclozolin relative to hydroxyflutamide. *J Biol Chem* 270:19998–20003
- Irvine DS (2000) Male reproductive health: cause for concern? *Andrologia* 32:195–208
- Andric NL, Andric SA, Zoric SN, Kostic TS, Stojilkovic SS, Kovacevic RZ (2003) Parallelism and dissociation in the actions of an aroclor 1260-based transformer fluid on testicular androgenesis and antioxidant enzymes. *Toxicology* 194:65–75
- Wang GM, Ge RS, Latif SA, Morris DJ, Hardy MP (2002) Expression of 11 β -hydroxylase in rat Leydig cells. *Endocrinology* 143:621–626
- Gunnarsson D, Svensson M, Selstam G, Nordberg G (2004) Pronounced induction of testicular PGF_{2 α} and suppression of testosterone by cadmium-prevention by zinc. *Toxicology* 200:49–58
- Wang X, Dyson MT, Jo Y, Stocco DM (2003) Inhibition of cyclooxygenase-2 activity enhances steroidogenesis and steroidogenic acute regulatory gene expression in MA-10 mouse Leydig cells. *Endocrinology* 144:3368–3375
- Payne AH, Hales DB (2004) Overview of steroidogenic enzymes in the pathway from cholesterol to active steroid hormones. *Endocr Rev* 25:947–970
- Clark BJ, Wells J, King SR, Stocco DM (1994) The purification, cloning, and expression of a novel luteinizing hormone-induced mitochondrial protein in MA-10 mouse Leydig tumor cells. Characterization of the steroidogenic acute regulatory protein (StAR). *J Biol Chem* 269:28314–28322
- Chen H, Liu J, Luo L, Baig MU, Kim JM, Zirkin BR (2005) Vitamin E, aging and Leydig cell steroidogenesis. *Exp Gerontol* 40:728–736
- Cano F, Poderoso C, Cornejo Maciel F, Castilla R, Maloberti P, Castillo F, Neuman I, Paz C, Podestá EJ (2006) Protein tyrosine phosphatases regulate arachidonic acid release, StAR induction and steroidogenesis acting on a hormone-dependent arachidonic acid-preferring acyl-CoA synthetase. *J Steroid Biochem Mol Biol* 99:197–202
- Murugesan P, Baladaneshi M, Balasubramanian K, Arunakaran J (2007) Effects of polychlorinated biphenyl (Aroclor 1254) on steroidogenesis and antioxidant system in cultured adult rat Leydig cells. *J Endocrinol* 192:325–338
- Walsh LP, McCormick C, Martin C, Stocco DM (2000) Roundup inhibits steroidogenesis by disrupting steroidogenic acute regulatory (StAR) protein expression. *Environ Health Perspect* 108:769–776
- Affi NA, Ramadan A, Ae-Aziz MI, Saki EE (1991) Influence of dimethoate on testicular and epididymal organs, testosterone plasma level and their tissue residues in rats. *Dtsch Tierärztl Wschr* 98:419–423
- Bagchi D, Bagchi M, Hassoun EA, Stohs SJ (1995) In vitro and in vivo generation of reactive oxygen species, DNA damage and lactate dehydrogenase leakage by selected pesticides. *Toxicology* 104:129–140
- Bolognesi C, Morasso G (2000) Genotoxicity of pesticides: potential risk for consumers. *Trends Food Sci Tech* 11:182–187
- John S, Kale M, Rathore N, Bhatnagar D (2001) Protective effect of vitamin E in dimethoate and malathion induced oxidative stress in rat erythrocytes. *J Nutr Biochem* 12:500–504
- Sivapiriya V, Jayanthisakthisekaran Venkatraman S (2006) Effects of dimethoate (O, O-dimethyl S-methyl carbamoyl methyl phosphorodithioate) and ethanol in antioxidant status of liver and kidney of experimental mice. *Pest Biochem Physiol* 85:115–121
- Cory-Slechta DA (2005) Studying toxicants as single chemicals: does this strategy adequately identify neurotoxic risk? *Neurotoxicol* 26:491–510
- National Research Council (1985) Guide for the care and use of laboratory animals. Publication no. 85–23 (rev). National Institute of Health, Bethesda
- Nourooz-Zadeh J, Tajaddini-Sarmandi J, McCarthy S, Betteridge DJ, Wolff SP (1995) Elevated levels of authentic plasma hydroperoxides in NIDDM. *Diabetes* 44:1054–1058
- Miranda KM, Espey MG, Wink DA (2001) A rapid, simple spectrophotometric method for simultaneous detection of nitrate and nitrite. *Nitric Oxide* 5:62–71
- Reznick AZ, Packer L (1994) Oxidative damage to proteins: spectrophotometric method for carbonyl assay. *Methods Enzymol* 233:357–363
- Benzie IF, Strain JJ (1996) The ferric reducing ability of plasma (FRAP) as a measure of “antioxidant power”: the FRAP assay. *Anal Biochem* 239:70–76
- Buttriss JL, Diplock AT (1984) High-performance liquid chromatography methods for vitamin E in tissues. *Methods Enzymol* 105:131–138
- Bagnati M, Bordone R, Perugini C, Cau C, Albano E, Bellomo G (1998) Cu(I) availability paradoxically antagonizes antioxidant consumption and lipid peroxidation during the initiation phase of copper-induced LDL oxidation. *Biochem Biophys Res Commun* 253:235–240
- Anderson ME, Meister A (1984) Enzymic assay of GSSG plus GSH. *Methods Enzymol* 105:448–450
- Bradford MM (1976) A rapid and sensitive method for the quantification of microgram quantities of protein utilizing the principle of protein–dye binding. *Anal Biochem* 72:248–254

37. Hurtado de Catalfo GE, Mandon EC, de Gómez Dumm IN (1992) Arachidonic acid biosynthesis in non-stimulated and adrenocorticotropic-stimulated sertoli and Leydig cells. *Lipids* 27:593–598
38. Suescun MO, González SI, Chiauuzzi VA, Calandra RS (1985) Effects of induced hypoprolactinemia on testicular function during gonadal maturation in the rat. *J Androl* 6:77–82
39. Jauregui HO, Hayner NT, Driscoll JL, Williams-Holland R, Lipsky MH, Galletti PM (1981) Trypan blue dye uptake and lactate dehydrogenase in adult rat hepatocytes-freshly isolated cells, cell suspensions, and primary monolayer cultures. *In Vitro* 17:1100–1110
40. Folch J, Lees M, Sloane GH (1957) A simple method for the isolation and purification of total lipids from animal tissues. *J Biol Chem* 226:497–509
41. Hanahan DJ, Dittner JC, Warashina E (1957) A column chromatographic separation of classes of phospholipids. *J Biol Chem* 228:685–690
42. Chen PS, Toribara TY, Warner H (1956) Microdetermination of phosphorus. *Anal Chem* 33:1405–1406
43. Marra CA, de Alaniz MJT (1989) Influence of testosterone administration on the biosynthesis of unsaturated fatty acids in male and female rats. *Lipids* 24:1014–1019
44. Allain CC, Poon LS, Chan CS, Richmond W, Fu PC (1974) Enzymatic determination of total serum cholesterol. *Clin Chem* 20:470–475
45. Murugesan P, Kanagaraj P, Yuvaraj S, Balasubramanian K, Aruldas MM, Arunakaran J (2005) The inhibitory effects of polychlorinated biphenyl Aroclor 1254 on Leydig cell LH receptors, steroidogenic enzymes and antioxidant enzymes in adult rats. *Reprod Toxicol* 20:117–126
46. Jackson H, Jones AR (1968) Antifertility action and metabolism of trimethyl-phosphate in rodents. *Nature* 220:591–592
47. Farag AT, El-Aswad AF, Shaaban NA (2007) Assessment of reproductive toxicity of orally administered technical dimethoate in male mice. *Reprod Toxicol* 23:232–238
48. Sayim F (2007) Histopathological effects of dimethoate on testes of rats. *Bull Environ Contam Toxicol* 78:479–484
49. Sayim F (2007) Dimethoate-induced biochemical and histopathological changes in the liver of rats. *Exp Toxicol Pathol* 59:237–243
50. Thomas JA, Donovan MD, Schein LG (1978) Biochemical bases for insecticide-induced changes in the male reproductive system. *Toxicol Appl Pharmacol* 45:291–295
51. Krause W (1977) Influence of DDT, DDVP, and malathion on FSH, LH and testosterone serum levels, and testosterone concentration in testes. *Bull Environ Contam Toxicol* 18:231–242
52. Krause W, Homola S (1974) Alterations of the seminiferous epithelium and the Leydig cells of the mouse testis after application of dichlorvos. *Bull Environ Contam Toxicol* 11:429–433
53. Lucesoli F, Fraga CG (1999) Oxidative stress in testes of rats subjected to chronic iron intoxication and α -tocopherol supplementation. *Toxicology* 132:179–186
54. Lucesoli F, Caligiuri M, Roberti MF, Perazzo JC, Fraga CG (1999) Dose-dependent increase of oxidative damage in the testes of rats subjected to acute iron overload. *Arch Biochem Biophys* 372:37–43
55. Guo CH, Huang CJ, Chen ST, Wang Hsu GS (2001) Serum and testicular testosterone and nitric oxide products in aluminium-treated mice. *Environ Toxicol Pharmacol* 10:53–60
56. Guo CH, Lin CY, Yeh MS, Hsu GSW (2005) Aluminium-induced suppression of testosterone through nitric oxide production in male mice. *Environ Toxicol Pharmacol* 19:33–40
57. Muroño EP, Derk RC, de León JH (2000) Octylphenol inhibits testosterone biosynthesis by cultured precursor and immature Leydig cells from rat testes. *Reprod Toxicol* 14:275–288
58. Muroño EP, Derk RC, de León JH (2001) Differential effects of octylphenol, 17 β -estradiol, endosulfan, or bisphenol A on the steroidogenic competence of cultured adult rat Leydig cells. *Reprod Toxicol* 15:551–560
59. Taylor CT (2001) Antioxidants and reactive oxygen species in human fertility. *Environ Toxicol Pharmacol* 10:189–198
60. Dringen R (2000) Metabolism and function of glutathione in brain. *Prog Neurobiol* 62:649–671
61. Dringen R (2005) Oxidative and antioxidative potential of brain microglial cells. *Antioxid Redox Signal* 7:1223–1233
62. Latchoumycandane C, Chitra KC, Mathur PP (2002) The effect of 2, 3, 7, 8-tetrachlorodibenzo-*p*-dioxin on mitochondrial and microsomal fractions of rat testis. *Toxicology* 171:127–135
63. Latchoumycandane C, Mathur PP (2002) Effect of methoxychlor on the antioxidant system in mitochondrial and microsome-rich fractions of rat testis. *Toxicology* 176:67–75
64. Chitra KC, Latchoumycandane C, Mathur PP (2003) Induction of Oxidative Stress by Bisphenol A in the Epididymal Sperm of Rats. *Toxicology* 185:119–127
65. Chitra KC, Mathur PP (2004) Vitamin E prevents nonylphenol-induced oxidative stress in testis of Rats. *Ind J Exp Biol* 42:220–223
66. Murugesan P, Senthilkumar J, Balasubramanian K, Aruldas MM, Arunakaran J (2005) Impact of polychlorinated biphenyl Aroclor 1254 on testicular antioxidant system in adult rats. *Hum Exp Toxicol* 24:61–66
67. Kostic TS, Andric SA, Maric D, Kovacevic RZ (2000) Inhibitory effects of stress-activated nitric oxide on antioxidant enzymes and testicular steroidogenesis. *J Steroid Biochem Mol Biol* 75:299–306
68. Cao L, Leers-Sucheta S, Azhar S (2004) Aging alters the functional expression of enzymatic and non-enzymatic anti-oxidant defence systems in testicular rat Leydig cells. *J Steroid Biochem Mol Biol* 88:61–67
69. Coniglio JG (1994) Testicular lipids. *Prog Lipid Res* 33:387–401
70. Abdollabi M, Shadnia S, Nikfar S, Rezale A (2004) Pesticides and oxidative stress: a review. *Med Sci Monit* 10:RA141–RA147
71. Ayala S, Brenner RR, Dumm CG (1977) Effect of polyunsaturated fatty acids of the α -linolenic series on the development of rat testicles. *Lipids* 12:1017–1024
72. Maloberti P, Maciel FC, Castillo AF, Castilla R, Duarte A, Toledo MF, Meuli F, Mele P, Paz C, Podestá EJ (2007) Enzymes involved in arachidonic acid release in adrenal and Leydig cells. *Mol Cell Endocrinol* 265(266):113–120
73. Wang XJ, Dyson MT, Mondillo C, Patrignani Z, Pignataro O, Stocco DM (2002) Interaction between arachidonic acid and cAMP signalling pathways enhances steroidogenesis and StAR gene expression in MA-10 Leydig tumor cells. *Mol Cell Endocrinol* 188:55–63
74. Catalá A (2007) The ability of melatonin to counteract lipid peroxidation in biological membranes. *Curr Mol Med* 7:638–649
75. Frungieri MB, González-Calvar SI, Parborell F, Albrecht M, Mayerhofer A, Calandra RS (2006) Cyclooxygenase-2 and Prostaglandin F₂ α in Syrian Hamster Leydig cells: inhibitory role on luteinizing hormone/human chorionic-stimulated testosterone production. *Endocrinology* 147:4476–4485
76. Hurtado de Catalfo GE, de Alaniz MJT, Marra CA (2008) Dietary lipids modify redox homeostasis and steroidogenic status in rat testis. *Nutrition* 24:717–726
77. Smith WL, DeWitt DL, Garavito RM (2000) Cyclooxygenases: structural, cellular, and molecular biology. *Annu Rev Biochem* 69:145–182
78. Frungieri MB, Weidinger S, Meineke V, Köhn FM, Mayerhofer A (2002) Proliferative action of mast-cell tryptase is mediated by PAR2, COX-2, prostaglandins, and PPAR γ : possible relevance to human fibrotic disorders. *Proc Natl Acad USA* 99:15072–15077

79. Hase T, Yoshimura R, Matsuyama M, Kawahito Y, Wada S, Tsuchida K, Sano H, Nakatani T (2003) Cyclooxygenase-1 and -2 in human testicular tumours. *Eur J Cancer* 39:2043–2049
80. Chung PH, Sandhoff TW, McLean MP (1998) Hormone and prostaglandin F₂ alpha regulation of messenger ribonucleic acid encoding steroidogenic acute regulatory protein in human corpora lutea. *Endocrine* 8:153–160
81. Fiedler EP, Plouffe LJr, Hales DB, Hales KH, Khan I (1999) Prostaglandin F(2Alpha) induces a rapid decline in progesterone production and steroidogenic acute regulatory protein expression in isolated rat corpus luteum without altering messenger ribonucleic acid expression. *Biol Reprod* 61:643–650
82. Diaz FJ, Wiltbank MC (2005) Acquisition of luteolytic capacity involves differential regulation by prostaglandin F₂Alpha of genes involved in progesterone biosynthesis in the porcine corpus luteum. *Domest Anim Endocrinol* 28:172–189
83. Shea-Eaton W, Sandhoff TW, Lopez D, Hales DB, McLean MP (2002) Transcriptional repression of the rat steroidogenic acute regulatory (StAR) protein gene by the AP-1 family member c-Fos. *Mol Cell Endocrinol* 188:161–170
84. Fuchs AR, Chantabratsri U (1981) Prostaglandin F_{2α} regulation of LH-stimulated testosterone production in rat testis. *Biol Reprod* 25:492–501
85. Wang X, Dyson MT, Jo Y, Stocco DM (2008) Inhibition of cyclooxygenase-2 activity enhances steroidogenesis and steroidogenic acute regulatory gene expression in MA-10 mouse Leydig cells. *Endocrinology* 149:851–857
86. Arakane F, Kallen CB, Watari H, Foster JA, Sepuri NB, Pain D, Stayrook SE, Lewis M, Gerton GL, Strauss JF 3rd (1998) The mechanism of action of steroidogenic acute regulatory protein (StAR). StAR acts on the outside of mitochondria to stimulate steroidogenesis. *J Biol Chem* 273:16339–16345
87. Diemer T, Allen JA, Hales KH, Hales DB (2003) Reactive oxygen disrupts mitochondria in MA-10 tumor Leydig cells and inhibits steroidogenic acute regulatory (StAR) protein and steroidogenesis. *Endocrinology* 144:2882–2891
88. Reinhart AJ, Williams SC, Stocco DM (1999) Transcriptional regulation of the StAR gene. *Mol Cell Endocrinol* 151:161–169

Association of ER-Alpha Gene Polymorphism with Metabolic Phenotypes in Chinese Hans

Yan Chen · Xiao-yan Jiang · Li Xu ·
Xia Li · Fei-fei Cao · Lei Li ·
Ming Lu · Li Jin · Xiao-feng Wang

Received: 7 April 2009 / Accepted: 16 June 2009 / Published online: 4 July 2009
© AOCs 2009

Abstract Recently, two polymorphisms (rs1884052 and rs3778099) of estrogen receptor α (ER-alpha) gene were identified as being associated with primary quantitative bone mineral density (BMD) in a genome-wide association (GWA) study in Framingham cohorts. In this study we aimed at investigating the association of rs1884052 and rs3778099, and another polymorphism (rs2234693) located at intron 1 of the ER-alpha gene with BMD, body mass index (BMI), glucose, triglyceride, and total cholesterol

(CHO) levels in Chinese Hans. We recruited 425 consecutive adult volunteers who had a physical examination in the Jinan Maternity and Child Care Hospital. We did not observe significant association of rs1884052 and rs3778099 with BMD, BMI, glucose, triglyceride, and total cholesterol (CHO) levels. For rs2234693, increased levels of BMD for hip, spine or whole-body regions were consistently observed in TT/TC genotype carriers than in CC genotype carriers, although the board line significance diminished after adjusting for age and gender. However, significant association of rs2234693 with glucose and CHO levels were observed in our sample. Subjects with TC/CC genotypes were associated with an increased level of glucose ($p = 0.013$) and CHO ($p = 0.032$) levels than subjects with TT genotypes. In conclusion, we did not confirm the association of rs1884052 and rs3778099 with BMD originally discovered in a GWA study; however, we made novel discoveries that rs2234693 was associated with glucose and CHO levels in Chinese Hans.

Y. Chen and X. Jiang have contributed equally.

Y. Chen · L. Xu · X. Li
Department of Gynecologic Endocrine, Jinan Maternity
and Child Care Hospital, 250001 Jinan,
People's Republic of China

X. Jiang
Department of Pharmacology, Tongji University School
of Medicine, 1239, Si-Ping Road, 200092 Shanghai,
People's Republic of China

F. Cao · M. Lu
Clinical Epidemiology Units,
Qilu Hospital of Shandong University,
250000 Jinan, People's Republic of China

L. Li · L. Jin · X. Wang (✉)
State Key Laboratory of Genetic Engineering
and MOE Key Laboratory of Contemporary Anthropology,
School of Life Sciences and Institutes of Biomedical Sciences,
Fudan University, 220 Handan Road, 200433 Shanghai,
People's Republic of China
e-mail: xiaofengautomatic@gmail.com

L. Jin · X. Wang
CMC Institute of Health Sciences,
225300 Taizhou, Jiangsu, People's Republic of China

Keywords Bone mineral density · Bone mineral content · Polymorphism · Estrogen receptor · Glucose · Cholesterol

Abbreviations

ANOVA	Analysis of variance
ANCOVA	Analysis of covariance
BMD	Bone mineral density
BMI	Body mass index
CHO	Total cholesterol
ER-alpha	Estrogen receptor α
GWA	Genome-wide association
LD	Linkage disequilibrium
SD	Standard deviation
SNP	Single nucleotide polymorphism

Introduction

Bone mineral density (BMD), the major determinant and predictor of osteoporotic fracture risk [1], is a quantitative trait determined by multiple environmental, genetic, and metabolic factors. Despite years of hard research identifying major genetic variants, determining BMD in the general population remains elusive. The genes linked to BMD in one population have often been replicated inconsistently in other populations.

Recently, Kiel et al. [2] conducted a genome-wide association (GWA) study to examine genetic associations with ten primary BMD quantitative traits using the Affymetrix 100 K single nucleotide polymorphism (SNP) Gene Chip marker set in the Framingham cohort. Several genes (e.g., methylenetetrahydrofolate reductase, low-density lipoprotein receptor-related protein 5, vitamin D receptor, ER- α) were associated with BMD in this study. Among them, rs3778099 and rs1884052 in the ER- α gene were identified to be associated with femoral BMD and neck width, respectively.

The ER- α gene encodes an estrogen receptor, a ligand-activated transcription factor composed of several domains important for hormone binding, DNA binding, and activation of transcription. ER- α is expressed widely in human reproductive or non-reproductive tissues, including bone [3], cerebrovascular endothelial system [4], skeletal muscle [5], central nervous system [6], involved in several pathological processes in these tissues. ER- α knockout mice also exhibit insulin resistance, impaired glucose tolerance, and obesity, which support pleiotropic effects on metabolic phenotypes of ER- α [7].

In the present study, we aimed at investigating the association of rs1884052 and rs3778099, and another important polymorphism (rs2234693) located in intron 1 of the ER- α gene with BMD and metabolic phenotypes in Chinese Hans. China is composed of 56 ethnic groups. Among them the Han nationality accounts for about 92% (1.1367 billion) of the overall population, and the other 55 minority nationalities make up the remaining 8% [8].

Methods

Subjects

The study was performed at Jinan Maternity and Child Care Hospital from January to December of 2006. A total of 425 consecutive adult volunteers who had a physical examination (203 male and 222 female), aged 18–74 years (average 48.9 ± 12.5), were recruited. All the participants were of the same ancestry of the Jinan population. To

improve the representation of Jinan Han subjects, we recruited subjects from a variety of sources by advertisement (the relatives and friends of hospital workers, the relative and friends of the inpatients and outpatients at Jinan Maternity and Child Care Hospital, members of the social gathering, and blood donors). Participants were excluded if they reported to have chronic disease or were taking medication. Whole body scans were performed using a dual energy X-ray absorptiometry (DXA) scanner (Lunar Prodigy densitometer; Wisconsin, MA, USA), using the pencil beam mode to determine areal BMD (g/cm^2) of the total body, spine and hip. Body weight and height were measured to calculate BMI (the body weight in kilograms divided by the square of height in meters). The blood specimens were drawn after overnight fasting and subjected to centrifugation immediately and analyzed within 8 h for glucose, triglyceride, and CHO. Serum glucose, triglyceride, and CHO concentrations were measured using enzyme methods and commercial kits (Centronic, GmbH, Germany) on Advia 1650 Autoanalyzer (Bayer Diagnostics Leverkusen, Germany). Written informed consent was obtained from all subjects in this study. The Human Ethics Committee of Jinan Maternity and Child Care Hospital approved the research.

Genotyping

Blood was taken into EDTA-containing receptacles and DNA samples were prepared from blood, using a method described by Boom et al. [9]. Sample DNA (10 ng) was amplified by PCR following the recommendations of the manufacturer. Fluorescence was detected by using an ABI 7900HT and the alleles were scored by using Sequence Detection Software (ABI). The assay identifications of the Taqman probes of rs2234693, rs31884052 and rs3778099 were C_3163590_10, C_11918426_10 and C_2823740_10, respectively. Laboratory personnel were blinded to clinical status. In addition to quality control samples included in each batch by the laboratory, blinded quality control samples were included to monitor the reproducibility of the genotyping assays. The concordance of duplicate samples was >99%.

Statistical Analysis

Values are expressed as the means \pm standard deviation (SD). All rs2234693, rs1884052 and rs3778099 were divided into two genotype groups (TT vs. TC/CC; CC vs. CG/GG; TT vs. TC/CC). The differences between genotype groups were tested by using analysis of variance (ANOVA) and analysis of covariance (ANCOVA) including gender and age as covariates. For haplotype construction, genotype data were used to estimate

inter-marker Linkage Disequilibrium (LD) by measuring pair-wise D' and r^2 and defining LD blocks. Haplotype block structure was determined using Haploview version 3.32 [10].

Results

The genotype successful rates of rs2234693, rs1884052, and rs3778099 were 99.3, 99.6, and 98.4%, respectively. The frequencies of TT, TC, and CC genotypes and C allele of rs2234693 were 0.38, 0.46, 0.16, and 0.39, respectively. The frequencies of CC, CG, and GG genotypes and G allele of rs1884052 were 0.42, 0.46, 0.12, and 0.35, respectively. The frequencies of TT, TC, and CC genotypes and C allele of rs3778099 were 0.41, 0.45, 0.14, and 0.36, respectively. LD analysis revealed that the pair-wise LDs of the rs1884052, rs3778099, and rs2234693 were weak (r^2 ranged from 0 to 0.04) (data not shown).

Although the hip BMD, spine BMD, and total BMD were decreased in the CG/GG genotype carriers than in CC genotype carriers for rs1884052 and TC/CC genotype carriers than in TT genotype carriers for rs3778099, non-significant association were observed. Lack of association was also observed for BMI, glucose, triglyceride, and CHO with respect to rs1884052 and rs3778099 (Table 1).

For rs2234693, increased levels of hip BMD, spine BMD, and total BMD were consistently observed in TT/TC genotype carriers in comparison with CC genotype carriers, although the board line significance of spine ($p = 0.034$) and total BMD ($p = 0.040$) diminished after adjusting for age and gender. However, we observed a significantly higher level of glucose ($p = 0.013$) and CHO ($p = 0.032$) in TC/CC genotype carriers than in TT genotype carriers. The significant association of rs2234693 with glucose and CHO remained after adjusting for covariate age and gender ($p = 0.029$, and $p = 0.045$, respectively) (Table 2).

Discussion

In the present study, we did not find the association between rs1884052 and rs3778099 and BMD originally discovered in a GWA study conducted on Caucasians [2]. Nevertheless, we observed a significant association of rs2234693 with spine BMD, total BMD, glucose, and CHO levels in Chinese Hans. SNP rs2234693 is located in intron 1 of the ER-alpha gene. The functional significance of rs2234693 is still unknown. However, rs2234693 is located within a potential transcription factor binding site, in which subjects carrying CC genotype results in a relatively high level of ER-alpha transcription as compared with CT carriers [11]. Alternatively, rs2234693 is in strong LD with

Table 1 Clinical characteristics of subjects according to rs1884052 and rs3778099 genotypes in Hans

Variables	rs1884052		rs3778099	
	CC ($n = 178$)	CG/GG ($n = 245$)	TT ($n = 171$)	TC/CC ($n = 247$)
Hip BMD (g/cm^2)	1.14 \pm 0.15	1.13 \pm 0.15	1.14 \pm 0.15	1.12 \pm 0.14
Spine BMD (g/cm^2)	1.11 \pm 0.14	1.09 \pm 0.15	1.10 \pm 0.15	1.09 \pm 0.14
Total BMD (g/cm^2)	1.17 \pm 0.11	1.15 \pm 0.12	1.16 \pm 0.11	1.15 \pm 0.11
BMI (kg/m^2)	26.43 \pm 4.23	26.38 \pm 4.49	26.50 \pm 4.09	26.24 \pm 4.59
Triglyceride (mmol/L)	1.49 \pm 1.06	1.66 \pm 1.49	1.72 \pm 1.42	1.46 \pm 1.24
CHO (mmol/L)	4.77 \pm 0.77	4.76 \pm 0.84	4.72 \pm 0.79	4.78 \pm 0.87
Glucose (mmol/L)	6.01 \pm 1.51	5.77 \pm 1.38	5.90 \pm 1.62	5.84 \pm 1.31

Table 2 Clinical characteristics of subjects according to rs2234693 genotypes in Hans

Variables	TT ($n = 159$)	TC/CC ($n = 263$)	p	Adjusted p
Hip BMD (g/cm^2)	1.12 \pm 0.16	1.15 \pm 0.14	0.056	0.159
Spine BMD (g/cm^2)	1.08 \pm 0.14	1.10 \pm 0.15	0.034	0.078
Total BMD (g/cm^2)	1.14 \pm 0.11	1.17 \pm 0.11	0.040	0.133
BMI (kg/m^2)	26.07 \pm 4.21	26.53 \pm 4.48	0.289	0.370
Triglyceride (mmol/L)	1.51 \pm 1.42	1.64 \pm 1.26	0.331	0.478
CHO (mmol/L)	4.65 \pm 0.92	4.84 \pm 0.78	0.032	0.045
Glucose (mmol/L)	5.64 \pm 0.91	6.01 \pm 1.67	0.013	0.029

Adjusted p : adjusted for age and gender

another TA repeat polymorphism in the promoter region of the ER-alpha gene in Caucasians [12].

Although the functional significance of rs2234693 remains to be elucidated, the relationship of this polymorphism with bone phenotypes was studied extensively. In women of four races/ethnicities who were premenopausal or in early perimenopause, Greendale et al. [13] observed that African American and Japanese women with the rs2234693 CC genotype had higher LS-BMDs than did their peers with the TT genotype ($p = 0.009$ and $p = 0.04$, respectively). In postmenopausal Japanese women, Kitamura et al. [14] discovered that the effect of lean tissue mass on femoral neck BMD was significantly larger for those with the TC/CC genotype than for those with the TT genotype for the rs2234693 polymorphism. In a cohort of 11-year-old European Caucasian girls, Tobias et al. [15] observed that differences in spinal area-adjusted bone mineral content in late puberty were two times greater in girls who were homozygous for the C alleles of rs2234693 ($p = 0.001$). However, In a meta-analysis of individual-level data involving standardized genotyping of 18,917 individuals in eight European centers, Ioannidis et al. [16] did not find a statistically significant effect of rs2234693 on BMD in adjusted or unadjusted analyses. Based on the above conflicting results and our observation on BMD in Chinese Hans, the role of rs2234693 polymorphism with regard to BMD needs further exploration.

There are also studies addressing the role of rs2234693 to cardiovascular or metabolic phenotypes. In a population-based offspring cohort of the Framingham Heart Study and in a meta-analysis including more than 7,000 whites in five cohorts from four countries, Individuals with CC genotype of rs2234693 were found to have a substantial increase in the risk of myocardial infarction [17, 18]. In an estrogen replacement and atherosclerosis trial with respect to 10 ER-alpha polymorphisms, Herrington et al. [19] discovered that the 18.9% of the women who had the rs2234693 CC genotype had an increased HDL cholesterol level with hormone-replacement therapy that was more than twice the increase observed in the other women. Interestingly, rs2234693 had been associated with lower waist circumference [20] and lower small LDL concentration [21, 22] in White Americans in the Framingham cohort, while this allele was associated with reduced insulin sensitivity index in multigenerational African-Americans and Hispanic Americans [23]. The C allele of rs2234693 was also associated with increased glucose and CHO concentration in our Chinese Hans. As far as we know, we are the first to report the association of rs2234693 with CHO concentration. However, in a recent study conducted in Framingham cohorts, Klos et al. [24] observed the association between other intron 1 genetic variants rs9322331 and rs9340799 and apoC-II, and TG concentrations in 15-year-olds

and younger. The relationship between rs2234693 and rs9322331 and rs9340799 needs further exploration.

The rs1884052 is located in intron 4 of the ER-alpha gene and 128 kb away from rs2234693. The rs1884052 is located in intron 7 of the ER-alpha gene and 255 kb away from rs2234693. The pair-wise LD constructed by rs2234693, rs1884052, and rs3778099 is weak in our Han population (D' ranged from 0 to 0.21, r^2 range from 0 to 0.04). Thus, rs2234693, rs1884052, and rs3778099 may represent different haplotype blocks in the Han population, and the effects of rs2234693 on BMD, glucose and CHO levels are independent of rs1884052 or rs3778099 in our samples.

In this study, we did not replicate the association of rs1884052, and rs3778099 with BMD originally discovered in a GWA study, which needs cautious explanation. To increase the representative of the Jinan Han general population, we examined a sample of adults of different ages. For females, we also included subjects before and after menopause. However, the sample size of the present study is relatively small which may decrease the statistical power to detect the genotype phenotype association, especially when the age spread of the subjects is broad. The negative results of rs1884052 and rs3778099 may be due to lack of statistical power owing to insufficient sample size. The differences in genetic background may be another explanation. As could be seen from the data released from the International Hapmap Project (http://www.hapmap.org/cgi-perl/gbrowse/hapmap26_B36/), the frequency of G allele of rs1884052 varies between Caucasians (10%), Chinese (31%), Japanese (35%), and Africans (2%). The frequency of C allele of rs3778099 are also varies between Caucasians (7%), Chinese (33%), Japanese (32%), and Africans (19%).

In summary, we did not confirm the association of rs1884052 and rs3778099 with the BMD originally discovered in a GWA study; however, we made novel discoveries that rs2234693 was associated with metabolic phenotypes in Chinese Hans. Due to the relative small sample size of our study and the novel observation that rs2234693 is linked to CHO levels in Chinese, the role of these polymorphisms on metabolic phenotypes needs further exploration in other large sample studies.

Acknowledgments This work was supported by a grant from the Major Program of National Natural Science Foundation (30890034), a grant from the Health Bureau of Jinan city in Shandong (2007058), and a grant from Outstanding Youth Science Foundation of Tongji University (2007KJ065).

References

1. Kanis JA, Melton LJ, Christiansen C, Johnston CC, Khaltaev N (1994) The diagnosis of osteoporosis. *J Bone Miner Res* 9:1137–1141

2. Kiel DP, Demissie S, Dupuis J, Lunetta KL, Murabito JM, Karasik D (2007) Genome-wide association with BMD and geometry in the Framingham Heart Study. *BMC Med Genet* 8(Suppl 1):S14
3. Bord S, Horner A, Beavan S, Compston J (2001) Estrogen receptors alpha and beta are differentially expressed in developing human bone. *J Clin Endocrinol Metab* 86:2309–2314
4. Stirone C, Duckles SP, Krause DN (2003) Multiple forms of estrogen receptor alpha in cerebral blood vessels: regulation by estrogen. *Am J Physiol Endocrinol Metab* 284:E184–E192
5. Capozza F, Combs TP, Cohen AW, Cho YR, Park SY, Schubert W, Williams TM, Brasaemle DL, Jelicks LA, Scherer PE, Kim JK, Lisanti MP (2005) Caveolin-3 knockout mice show increased adiposity and whole body insulin resistance, with ligand-induced insulin receptor instability in skeletal muscle. *Am J Physiol Cell Physiol* 88:C1317–C1331
6. Osterlund MK, Grandien K, Keller E, Hurd YL (2000) The human brain has distinct regional expression patterns of estrogen receptor alpha mRNA isoforms derived from alternative promoters. *J Neurochem* 75:1390–1397
7. Heine PA, Taylor JA, Iwamoto GA, Lubahn DB, Cooke PS (2000) Increased adipose tissue in male and female estrogen receptor-alpha knockout mice. *Proc Natl Acad Sci USA* 97:12729–12734
8. <http://www.paulnoll.com/China/Minorities/China-Nationalities.html>
9. Boom R, Sol CJ, Salimans MM, Jansen CL, Wertheim-van Dillen PM, van der Noordaa J (1990) Rapid and simple method for purification of nucleic acids. *J Clin Microbiol* 28:495–503
10. Barrett JC, Fry B, Maller J, Daly MJ (2005) Haploview: analysis and visualization of LD and haplotype maps. *Bioinformatics* 21:263–265
11. Herrington DM, Howard TD, Brosnihan KB, McDonnell DP, Li X, Hawkins GA, Reboussin DM, Xu J, Zheng SL, Meyers DA, Bleecker ER (2002) Common estrogen receptor polymorphism augments effects of hormone replacement therapy on E-selectin but not C-reactive protein. *Circulation* 105:1879–1882
12. Becherini L, Gennari L, Masi L, Mansani R, Massart F, Morelli A, Falchetti A, Gonnelli S, Fiorelli G, Tanini A, Brandi ML (2000) Evidence of a linkage disequilibrium between polymorphisms in the human estrogen receptor alpha gene and their relationship to BMD variation in postmenopausal Italian women. *Hum Mol Genet* 9:2043–2050
13. Greendale GA, Chu J, Ferrell R, Randolph JF Jr, Johnston JM, Sowers MR (2006) The association of bone mineral density with estrogen receptor gene polymorphisms. *Am J Med* 119:S79–S86
14. Kitamura I, Ando F, Koda M, Okura T, Shimokata H (2007) Effects of the interaction between lean tissue mass and estrogen receptor alpha gene polymorphism on bone mineral density in middle-aged and elderly Japanese. *Bone* 40:1623–1629
15. Tobias JH, Steer CD, Vilarino-Güell C, Brown MA (2007) Estrogen receptor alpha regulates area-adjusted bone mineral content in late pubertal girls. *J Clin Endocrinol Metab* 92:641–647
16. Ioannidis JP, Ralston SH, Bennett ST, Brandi ML, Grinberg D, Karassa FB, Langdahl B, van Meurs JB, Mosekilde L, Scollen S, Albagha OM, Bustamante M, Carey AH, Dunning AM, Enjuanes A, van Leeuwen JP, Mavilia C, Masi L, McGuigan FE, Nogues X, Pols HA, Reid DM, Schuit SC, Sherlock RE, Uitterlinden AG, GENOMOS Study (2004) Differential genetic effects of ESR1 gene polymorphisms on osteoporosis outcomes. *JAMA* 292:2105–2114
17. Shearman AM, Cupples LA, Demissie S, Peter I, Schmid CH, Karas RH, Mendelsohn ME, Housman DE, Levy D (2003) Association between estrogen receptor alpha gene variation and cardiovascular disease. *JAMA* 290:2263–2270
18. Shearman AM, Cooper JA, Kotwinski PJ, Miller GJ, Humphries SE, Ardlie KG, Jordan B, Irenze K, Lunetta KL, Schuit SC, Uitterlinden AG, Pols HA, Demissie S, Cupples LA, Mendelsohn ME, Levy D, Housman DE (2006) Estrogen receptor alpha gene variation is associated with risk of myocardial infarction in more than seven thousand men from five cohorts. *Circ Res* 98:590–592
19. Herrington DM, Howard TD, Hawkins GA, Reboussin DM, Xu J, Zheng SL, Brosnihan KB, Meyers DA, Bleecker ER (2002) Estrogen-receptor polymorphisms and effects of estrogen replacement on high-density lipoprotein cholesterol in women with coronary disease. *N Engl J Med* 346:967–974
20. Fox CS, Heard-Costa NL, Wilson PW, Levy D, D'Agostino RB Sr, Atwood LD (2004) Genome-wide linkage to chromosome 6 for waist circumference in the Framingham Heart Study. *Diabetes* 53:1399–1402
21. Shearman AM, Demissie S, Cupples LA, Peter I, Schmid CH, Ordovas JM, Mendelsohn ME, Housman DE (2005) Tobacco smoking, estrogen receptor alpha gene variation and small low density lipoprotein level. *Hum Mol Genet* 14:2405–2413
22. Demissie S, Cupples LA, Shearman AM, Gruenthal KM, Peter I, Schmid CH, Karas RH, Housman DE, Mendelsohn ME, Ordovas JM (2006) Estrogen receptor alpha variants are associated with lipoprotein size distribution and particle levels in women: the Framingham Heart Study. *Atherosclerosis* 185:210–218
23. Gallagher CJ, Langefeld CD, Gordon CJ, Campbell JK, Mychaleckyj JC, Bryer-Ash M, Rich SS, Bowden DW, Sale MM (2007) Association of the estrogen receptor-alpha gene with the metabolic syndrome and its component traits in African-American families: the insulin resistance atherosclerosis family study. *Diabetes* 56:2135–2141
24. Klos KL, Boerwinkle E, Ferrell RE, Turner ST, Morrison AC (2008) ESR1 polymorphism is associated with plasma lipid and apolipoprotein levels in Caucasians of the Rochester family heart study. *J Lipid Res* 49:1701–1706

Characterization of Mutant Serine Palmitoyltransferase 1 in LY-B Cells

Amin A. Momin · Hyejung Park · Jeremy C. Allegood ·
Martina Leipelt · Samuel L. Kelly ·
Alfred H. Merrill Jr. · Kentaro Hanada

Received: 26 January 2009 / Accepted: 26 May 2009 / Published online: 18 June 2009
© AOCS 2009

Abstract CHO-LY-B cells have been useful in studies of sphingolipid metabolism and function because they lack serine palmitoyltransferase (SPT) activity. Cloning and sequencing of the SPT1 transcript of LY-B cells identified the mutation as a guanine to adenine change at nucleotide 738, causing a G246R transformation. Western blots revealed low expression of the mutant SPT1 peptide, but activity was not detectable by mass spectrometric analysis of [¹³C]-palmitate incorporation into sphinganine, sphingosine, 1-deoxysphinganine, or 1-desoxymethylsphinganine. Treatment of LY-B cells with chemical chaperones (DMSO or glycerol) increased the amounts of mutant SPT1 as well as SPT2, but SPT activity was not restored. This study has established that G246R mutation in hamster SPT1 results in the loss of SPT activity.

Keywords Sphingolipid · Sphingoid base · Serine palmitoyltransferase · Mutant enzyme

Abbreviations

1-deoxy-Sa	1-Deoxysphinganine and 1-desoxymethylsphinganine
1-desoxymethyl-Sa	1-Desoxymethylsphinganine
BSA	Bovine serum albumin
CHO	Chinese hamster ovary
Cer	Ceramide
DMSO	Dimethyl sulfoxide
FBS	Fetal bovine serum
FB ₁	Fumonisin B ₁
GAPDH	Glyceraldehyde 3-phosphate dehydrogenase
HA	Human influenza hemagglutinin
HexCer	Hexosylceramide
HSN1	Hereditary sensory neuropathy type 1
LCB	Long-chain base
LCB1	Long-chain base subunit 1
LCB2	Long-chain base subunit 2
LC ESI-MS/MS	Liquid chromatography electrospray ionization mass spectrometry
LY-B	Chinese hamster ovary cells strain with defective SPT
LY-B/cLCB1	LY-B cells stably transfection with LCB1 cDNA
PBS	Phosphate buffer saline
PDB	Protein data bank
Sa	Sphinganine
SaP	Sphinganine 1-phosphate
SM	Sphingomyelin
So	Sphingosine
SoP	Sphingosine 1-phosphate

A. A. Momin · H. Park · M. Leipelt · S. L. Kelly ·
A. H. Merrill Jr. (✉)

School of Biology, The Petit Institute for Bioengineering and Bioscience, Georgia Institute of Technology, Atlanta, GA 30332, USA
e-mail: al.merrill@biology.gatech.edu

J. C. Allegood · A. H. Merrill Jr.
School of Chemistry and Biochemistry, The Petit Institute for Bioengineering and Bioscience, Georgia Institute of Technology, Atlanta, GA 30332, USA

K. Hanada
Department of Biochemistry and Cell Biology, National Institute of Infectious Diseases, 1-23-1, Toyama, Shinjuku-ku, Tokyo 162-8640, Japan

Present Address:

J. C. Allegood
Department of Biochemistry, Virginia Commonwealth University, Richmond, VA 23298, USA

SPT	Serine palmitoyltransferase
SPT1	Serine palmitoyltransferase subunit 1
SPT2	Serine palmitoyltransferase subunit 2
SPTLC1	Serine palmitoyltransferase long-chain base subunit 1
SPTLC2	Serine palmitoyltransferase long-chain base subunit 2
TBST	Tris buffered saline Tween-20

Introduction

Sphingolipids are a structurally diverse and important family of compounds [1] characterized by having a sphingoid base backbone [2]. Sphingoid base biosynthesis is initiated by serine palmitoyltransferase (SPT; EC2.3.1.50) [3], an activity that is essential for cells in culture unless the medium is supplemented with sphingolipids [4]. SPT is comprised of two [3], and possibly more [5, 6], subunits and homozygous deletion of two subunits (Sptlc1 and Sptlc2, also known as LCB1/LCB2 or SPT1/SPT2) in mice is embryonic lethal [7]. Mutations in *SPTLC1* are responsible for human hereditary sensory neuropathy type 1 (HSN1) [8, 9].

LY-B cells lack SPT activity due to mutation of *Sptlc1* [4], and have been useful tools for studies of de novo sphingolipid biosynthesis and the functions of sphingolipids [4]. This report describes the point mutation that results in the loss of SPT activity in LY-B cells, and notes that small amounts of SPT1 polypeptide can be detected by Western blotting, especially when the cells are treated with ‘chemical chaperones’ [10] such as DMSO and glycerol, but without restoration of activity.

Experimental Procedures

Materials

Chinese hamster ovary (CHO) derived lines LY-B and LY-B/cLCB1 (which are stably transfected with the Chinese hamster LCB1 cDNA to restore SPT activity) were available from previous studies [4]. Ham’s F12 medium was from Gibco (Carlsbad, CA) and fetal bovine serum was obtained from Hyclone (Logan, UT). The sources for the antibodies were BD Biosciences (San Jose, CA) for the anti-LCB1 monoclonal antibody, Cayman (Ann Arbor, MI) for the anti-SPT2 monoclonal antibody, Sigma (St. Louis, MO) for the anti-beta actin and anti-HA antibodies, Ambion (Austin, TX) for the anti-GAPDH antibody, and David Uhlinger (Johnson & Johnson Pharmaceutical Research & Development, Raritan, NJ) for another anti-

SPT1 antibody [11]. The enhanced chemifluorescence (ECF) Western blotting kit was purchased from GE healthcare (Piscataway, NJ). Mass spectrometry internal standards were obtained from Avanti Polar Lipids (Alabaster, AL) and [U-¹³C]-palmitic acid was purchased from Cambridge Isotope (Andover, MA). Fumonisin B₁ (FB₁) was obtained from Biomol (Plymouth Meeting, PA). All other reagents and solvents were of high quality.

Cell Culture and Treatments

LY-B and LY-B/cLCB1 cells were cultured in Ham’s F12 medium containing 10% fetal bovine serum, penicillin G (100 U/ml) and streptomycin sulfate (100 µg/ml) in 5% CO₂ at 37 °C. During stable isotope labeling studies, the media was supplemented with 0.1 mM [U-¹³C]-palmitic acid complexed with equimolar fatty acid free BSA (Calbiochem, Gibbstown, NJ). After 12 or 24 h, depending on the experiment, the incorporation of the stable isotope into sphingolipids was measured by liquid chromatography, electrospray ionization tandem mass spectrometry (LC ESI-MS/MS) as previously described [12] except as noted below.

To analyze whether LY-B and LY-B/cLCB1 cells produce both ‘typical’ (i.e., sphinganine and sphingosine) and ‘atypical’ sphingoid bases (1-deoxysphinganine and 1-desoxymethylsphinganine) [13, 14], 25-µM FB₁ was added to the medium 1 h before addition of 0.1 mM [U-¹³C]-palmitic acid–BSA complex to cause the sphingoid bases to accumulate [13].

For chemical chaperone treatment, the LY-B cells were grown to ~50% confluence and changed to media supplemented with different concentrations of DMSO (up to 3%) or glycerol (up to 1 M) for 24 h. To determine how this affected SPT amount, the SPT1 and SPT2 peptides were visualized by Western blotting as described below. GAPDH was used as the protein loading control because DMSO and glycerol influence actin expression [15–17]. To determine how SPT activity was affected, the cells were incubated for 12 h in the same medium supplemented with 0.1 mM [U-¹³C]-palmitic acid–BSA complex then analyzed by LC ESI-MS/MS.

Cloning and Sequencing of SPT1 from LY-B cells

Total RNA was extracted from LY-B cells by the Absolutely RNA Miniprep Kit (Qiagen, Valencia, CA) and reverse transcribed to cDNA using the cDNA Synthesis System Kit (TaKaRa, Mountain View, CA). PCR was performed to amplify the SPT1 transcript using primers (5′-atggcgatggcggcgaggca and 3′-ctacagcagcagcctgggca), which represent the start and stop codon for hamster SPT1 open reading frame. The amplified PCR transcript was

ligated into pUC18 cloning vector and restriction digested with EcoRI to determine the clones with the correct inserts. 15 selected clones were sequenced (Nevada Genomics Center, Reno, NV) and compared to wildtype CHO SPT1 mRNA by multiple sequence alignment using T-coffee [18].

Western Blotting

Cells were rinsed with PBS then scraped from the dishes using PBS containing complete mini protease inhibitor cocktail (Roche Diagnostics, Indianapolis, IN), lysed by brief sonication, incubated for 30 min at 25 °C with Benzonase Nuclease (Novagen, Madison, WI), then boiled briefly in Tris-HEPES-SDS (100 mM Tris, 100 mM HEPES, pH 8.0, 3 mM SDS) before loading onto a 12% SDS-PAGE (Pierce, Rockford, IL) minigel (40 µg of protein/well) and electrophoresed. The separated proteins were transferred onto a nitrocellulose membrane (Whatman, Florham park, NJ) and blocked with 5% milk-TBST (Tris buffered saline Tween-20) (20 mM Tris-HCl, pH 7.6, 137 mM NaCl, 0.1% Tween-20) solution. The membrane was incubated with primary antibodies (anti-LCB1, diluted 1:2,000; Anti-SPT1, diluted 1:3,000; anti-SPT2, diluted 1:1,000) overnight at 4 °C and washed with TBST solution before being probed with a secondary anti-fluorescein antibody (ECF kit) for 1 h. The protein bands were visualized by incubating the membrane with the ECF substrate for 30 min and imaged using FLA-3000 imager (Fujifilm, Stamford, CT). Pixel density was measured using Multi Gauge (Fujifilm) image analysis software. Statistical significance was defined at a *P* value of 0.05 using the Kruskal–Wallis rank sum test in R v2.61 (www.r-project.org).

LC ESI-MS/MS Analysis of Sphingolipids

The sphingolipids were analyzed in positive ionization mode by LC ESI-MS/MS [12] using ABI 3000 triple quadrupole and ABI 4000 quadrupole-linear ion trap mass spectrometers (Applied Biosystems, Foster city, CA). Since the major fragmentation products of ceramides (Cer) and ceramide monohexosides (HexCer) (e.g., ions with *m/z* 264.4 for sphingosine and *m/z* 266.4 for sphinganine) retain the carbon atoms originally derived from palmitoyl-CoA, the sphingolipids made de novo via incorporation of [^{13}C]-palmitate into the sphingoid base backbones were determined by adding 16 mass units to the precursor-product pairs for species labeled in only the sphingoid base backbone, and by adding 32 mass units to the precursor ion and 16 to the product for compounds labeled in both the fatty acid and the sphingoid base. Since these product ions are of very low abundance from sphingomyelins (SM) [12],

the incorporation of [^{13}C]-palmitate into the sphingoid base backbones of SM was determined by treatment of an aliquot of the lipid extract with the phospholipase D from *Streptomyces chromofuscus* (Sigma) to produce ceramide 1-phosphates [19, 20], which do provide definitive information about [^{13}C] labeling of the sphingoid base backbone [12, 21]. This treatment was conducted by incubating dried lipid extracts with 50 units of the enzyme suspended in 0.1 ml of 100 mM Tris-HCl, pH 8.0, and 3 mM decylglucopyranoside (Sigma), at 37 °C for 30 min. The reaction was dried by speedvac and analyzed by LC ESI-MS/MS.

Analysis of the biosynthesis of sphinganine (So), sphingosine (Sa), 1-deoxysphinganine (1-deoxy-Sa), and 1-desoxymethylsphinganine (1-desoxymethyl-Sa) [14, 22] from cells incubated [^{13}C]-palmitate and 25-µM FB₁ was conducted by LC ESI-MS/MS in positive ionization mode using multiple reaction monitoring with Q1 and Q3 set to pass the following precursor and product ions: 316.5/298.3 ([^{13}C]-So), 318.5/300.3 ([^{13}C]-Sa), 302.4/284.4 ([^{13}C]-1-deoxy-Sa), and 288.3/270.3 ([^{13}C]-1-desoxymethyl-Sa). The LC conditions were the same as described previously [13, 22], i.e., using a reverse phase LC column (Supelco 2.1 × 50 mm Discovery C18 column, Sigma, St. Louis, MO) and a binary solvent system at a flow rate of 0.6 mL/min; the binary system began with equilibration of the column with 60% mobile phase A (CH₃OH/H₂O/HCOOH, 58/41/1, v/v/v, with 5 mM ammonium formate) and 40% mobile phase B (CH₃OH/HCOOH, 99/1, v/v, with 5 mM ammonium formate), sample injection and elution for 1.3 min in the same mobile phase, followed by a linear gradient over 2.8 min to 100% B (then a column wash with 100% B for 0.5 min followed by re-equilibration with the original A/B mixture before the next run).

Homology Modelling of Mutant SPT1

Homology modelling was performed by comparing SPT with two POAS enzymes [23], with one being the SPT from *Sphingomonas paucimobilis* (PDB ID: 2JG2) [24]. The crystal structures of PDB ID: 2JG2 and 1FC4 were selected as templates because they were identified to have 30% sequence identity with hamster SPT1 by a blast search of the PDB database. The sequences of the templates and mutant SPT1 protein were aligned using T-coffee [18], refined manually into a PIR format alignment file that was used to generate the homology model with Modeller v6.1 [25], which provides a consensus structure of the target protein without a bias towards a single template [26, 27], and visualized by VMD v1.8.6 [28]. The 2JG2 template has 55% identity with hamster SPT1 for the amino acid residues located within a 5-Å radius of the mutated amino acid residue, R246, of SPT1 from LY-B cells.

Results and Discussion

Analysis of the Gene Sequence for Mutant SPT1 in LY-B Cells

Sequencing of the mutated SPT1 from LY-B cells revealed a guanine to adenine mutation at nucleotide residue 738, which would result in the substitution of Arg for Gly246, which is conserved across numerous species (*C. griseus*, *M. musculus*, *H. sapiens* and *S. cerevisiae*), as shown in Fig. 1a. To investigate the impact of G246R substitution on SPT1, a homology model was prepared and residues within 5 Å of G246R were compared to 2JG2 template by multiple sequence alignment, which revealed 55% sequence homology. The analysis revealed the presence of non-polar residues such as Val, Leu and Phe within 3–5 Å distance from the point mutation, while polar residues Glu and Ser were conserved between SPT1 and 2JG2, which may play a role in protein folding. The steric hindrance resulting from G246R substitution in a conserved region of SPT1 may destabilize the protein structure.

Analysis of Mutant SPT1 Polypeptide in LY-B Cells

Previous studies have not detected an SPT1 peptide in LY-B cells by Western blotting [4], however, a very faint

A	LY-B	237	VTRRFIVVERLYMNTGT	253
	<i>C.griseus</i>	237	VTRRFIVVEGLYMNTGT	253
	<i>H.sapiens</i>	237	VTRRFIVVEGLYMNTGT	253
	<i>M.musculus</i>	237	VTRRFIVVEGLYMNTGT	253
	<i>S.cerevisiae</i>	283	IPRKFIVTEGIFHNSGD	299

*

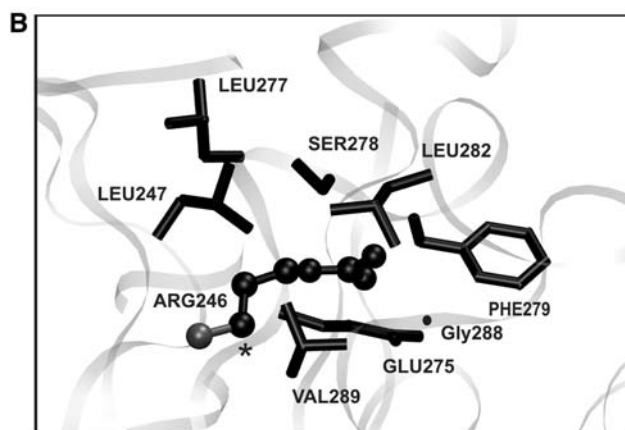


Fig. 1 Sequence comparison and homology model of the SPT1 mutant protein of LY-B cells. **a** Protein sequences of SPT1 were compared from LY-B cells, CHO, human, mouse and *S. cerevisiae* using T-coffee. The point mutation G246R in LY-B cells is indicated by an asterisk. **b** This homology model for mutant SPT1 from LY-B cells was prepared using Modeller v6.1. The illustrated figure shows the G246R mutation (indicated in a ball-and-stick representation) to be located in a pocket of hydrophobic residues (Phe279, Leu282, Val289, Leu247) was visualized by VMD

band is discernable when larger amounts of protein (40 µg) are examined using two antibodies (anti-LCB1 and anti-SPT1) (Fig. 2a, b) but not using an antibody to another polypeptide epitope not found in the cells (HA) (Fig. 2c). Also shown is the immunoblotting of SPT1 in LY-B/cLCB1 cells, which have been stably transfected with the wild-type SPT1 gene (Fig. 2a, b).

Analysis of Mutant SPT Activities in LY-B Cells

To ascertain whether this small amount of mutant SPT1 afforded detectable de novo sphingolipid biosynthesis, cells were incubated with [¹³C]-palmitic acid and analyzed for incorporation of [¹³C] into the sphingoid base backbone (with free sphingoid bases in Fig. 3a and complex sphingolipids in Fig. 3b–d); LY-B/cLCB1 cells were used as a positive control because they have SPT activities comparable to wild-type CHO cells [4]. When all of the subspecies are summed, the amounts of backbone [¹³C]-labeled sphingolipids in the LY-B/cLCB1 cells at 6 h were 62 ± 0.3 pmol Cer/mg protein, 54 ± 0.8 pmol

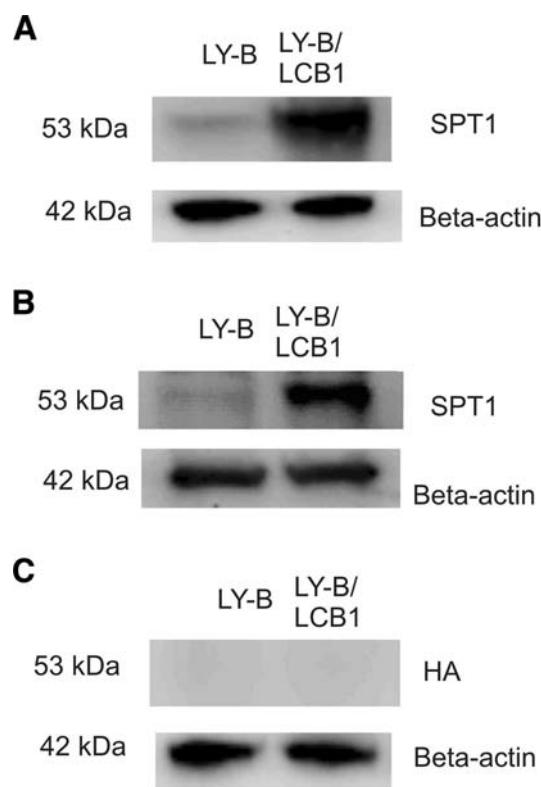


Fig. 2 Western blots of SPT1 in LY-B and LY-B/cLCB1 cells. Whole cell lysates of LY-B and LY-B/cLCB1 cells were prepared and equal amounts (40 µg) of protein were separated by an SDS-PAGE gel. Replicate membranes were probed with **a** a commercial LCB1 antibody; **b** an independent anti-SPT1 polyclonal antibody, and **c** an anti-HA antibody as a negative control. The detection of β-actin with an anti-β-actin antibody was used as a protein loading control

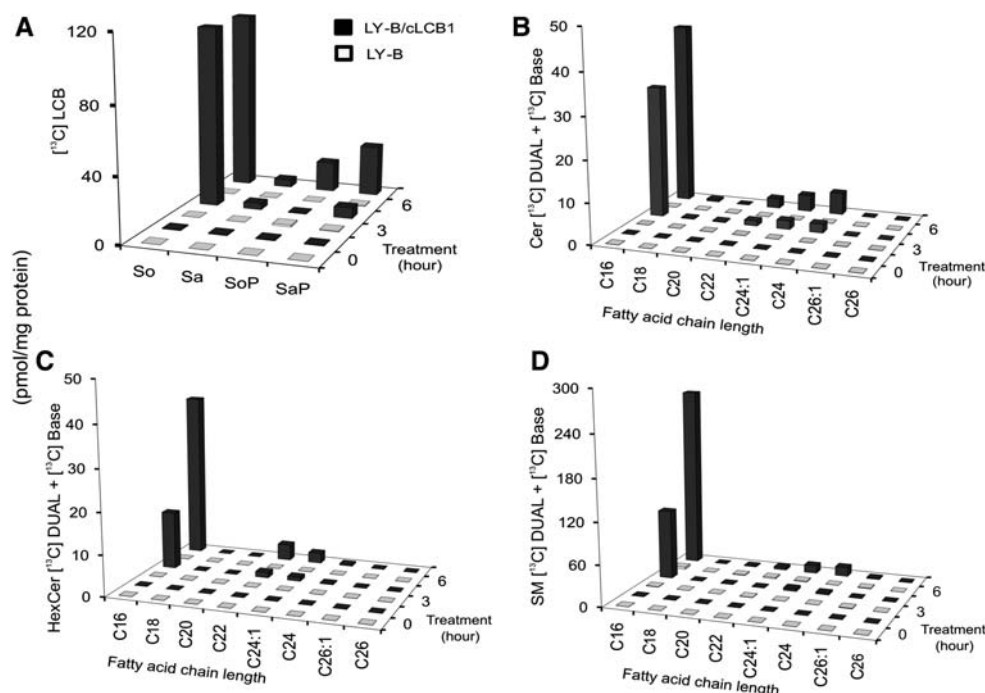


Fig. 3 Comparison of de novo sphingolipid biosynthesis in LY-B and LY-B/cLCB1 cells. LY-B and LY-B/cLCB1 cells were incubated with 0.1 mM [^{13}C]-palmitic acid for 0, 3 and 6 h and the sphingolipids labeled in the sphingoid base alone (BASE) plus the sphingoid base and fatty acid (DUAL) were measured by LC ESI-MS/MS. The *black bars* represent the sphingolipids in LY-B/cLCB1 cells while the *white bars* indicate the LY-B cells. **a** [^{13}C]-labeled long-

chain bases (LCB) sphingosine *So*, sphinganine *Sa*, sphingosine 1-phosphate *SoP*, and sphinganine 1-phosphate *SaP*. **(b–d)** provide the sum of the label in the BASE and DUAL subspecies of ceramide *Cer*, monohexosylceramides *HexCer*, and sphingomyelins *SM*, based on variation in the chain length of the amide-linked fatty acid (shown by chain length:number of double bonds)

HexCer/mg protein and 300 ± 14 pmol SM/mg protein, for a total of ~ 416 pmol/mg protein; for LY-B cells, the amounts were below the limits of detection for *Cer* and *HexCer* (~ 0.1 pmol/mg protein) and very low for *SM* (5.5 ± 16 pmol SM/mg protein) which, based on the high noise in the signal (reflected in the high SD), might be due to other compounds with similar ionization characteristics. Thus, even counting the possibility that this represents *SM*, the maximum amount of labeled backbone sphingolipids in the LY-B cells would only $\sim 1\%$ that in LY-B/cLCB1 cells. This is in agreement with a previous study [4] which has shown that SPT activity in the microsomal fraction of LY-B cells was less than 5% of that in CHO-K1 cells.

As has been shown before [4], although LY-B cells are defective in sphingolipid biosynthesis de novo, they contain appreciable amounts of sphingolipids if grown in medium that contains sphingolipids (e.g., from serum). In these studies, the pmol of unlabeled sphingolipids/mg protein for LY-B versus LY-B/cLCB1 cells (measured by LC ESI-MS/MS) were, respectively: 140 ± 18 versus $1,073 \pm 17$ for *Cer*; 122 ± 7 versus 447 ± 87 for *HexCer*; and $3,474 \pm 452$ versus $5,143 \pm 167$ for *SM* (data not shown).

As another way to assess sphingoid base biosynthesis, the cells were incubated with FB_1 to allow accumulation of the [^{13}C]-labeled sphingoid bases which are otherwise rapidly N-acylated to complex sphingolipids, and thus less easily tracked. These results are shown in Fig. 4 as the relative ion yields for the precursor/product pairs as they elute from the reverse phase column. Production of [^{13}C]-*So* (Fig. 4a), [^{13}C]-*Sa* (Fig. 4c), [^{13}C]-1-deoxy-*Sa* (Fig. 4b) and [^{13}C]-1-deoxy-methyl-*Sa* (Fig. 4d) were readily detected with the LY-B/cLCB1 cells, but the signal was not above background for the LY-B cells, which further confirms the conclusion from Fig. 3 that the LY-B cells do not synthesize detectable amounts of sphingoid bases de novo. The appearance of [^{13}C]-sphingosine in LY-B/cLCB1 cells was somewhat surprising because desaturation of sphinganine is thought to occur only after N-acylation [29], but it is possible that this concentration of FB_1 did not completely block [^{13}C]-*Cer* biosynthesis and this [^{13}C]-sphingosine arose from turnover.

Partial Stabilization of Mutant SPT in LY-B Cells

Some misfolded proteins can be stabilized by so-called chemical chaperones such as DMSO and glycerol [30–32].

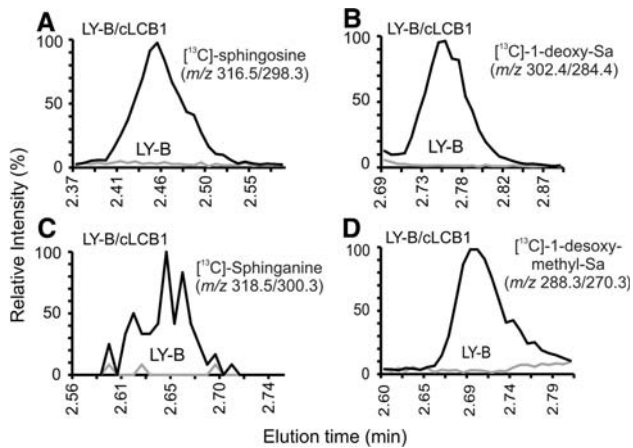


Fig. 4 Relative amounts of typical and atypical [^{13}C]-labeled sphingoid bases produced by LY-B and LY-B/cLCB1 cells upon co-treatment with FB_1 . Shown are the relative ion intensities of the shown precursor/product pairs in the LC ESI-MS/MS eluates. The LC retention times for these species matched that of standards for these compounds (not shown). The samples for these analyses were obtained by incubating LY-B and LY-B/cLCB1 cells with 0.1 mM [^{13}C]-palmitic acid and 25 μM FB_1 for 24 h; the *grey line* indicates LY-B cells and the *black line* represents LY-B/cLCB1 cells

When LY-B cells were treated for 24 h with DMSO or glycerol at concentrations where they have previously been effective [30, 32], there were noticeable increases in both SPT1 and SPT2 by Western blotting (Fig. 5, upper), with

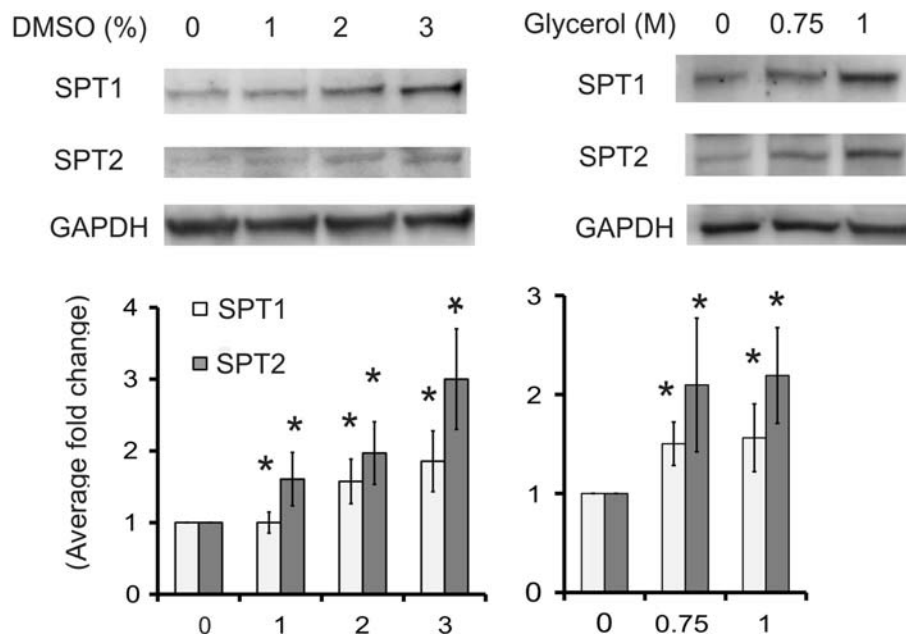


Fig. 5 Elevation of the amounts of SPT1 and SPT2 in LY-B cells treated with chemical chaperones. LY-B cells were treated with DMSO (*left panels*) or glycerol (*right panels*) at the shown concentrations for 24 h then analyzed by Western blotting (*upper panels*), with GAPDH as the loading control. The lower panels are the relative differences in protein amounts as estimated from the pixel

the average increases in five experiments being between two and threefold (Fig. 5, lower). Lower concentrations had no effect, and higher were toxic (data not shown). In case these treatments also resulted in restoration of SPT activity, the incorporation of [^{13}C]-palmitate into sphingolipids was measured after LY-B cells had been treated with either 3% DMSO or 1 M glycerol for 24 h (the [^{13}C]-palmitate was added to the same medium and the cells were incubated for 12 h before extraction for sphingolipid analysis by LC ESI-MS/MS). As noted earlier, the ion yields for the [^{13}C]-labeled species were very low, but by manually averaging the ion counts in the samples versus the background, we would estimate that the amounts of newly made sphingolipids (i.e., [^{13}C]-labeled in the sphingoid base backbone) were 2.0 ± 0.5 pmol/mg protein for the LY-B cells in medium alone, 1.6 ± 0.2 pmol/mg protein for the LY-cells incubated with 3% DMSO and 2.3 ± 1.2 pmol/mg protein for LY-B cells in 1 M glycerol. Therefore, there was no evidence that the small amounts of SPT1 detected upon treatment of the cells with these chemical chaperones restored SPT activity.

Concluding Comments

The finding that the sequence of the SPT1 transcript from LY-B cells has a G246R substitution is not surprising because these cells were produced using ethyl methanesulfonate [4], a mutagen that causes the random replacement of

densities of the bands from five independent Western blots (*bottom panels*), with the standard error indicated by the *bars*. Ratios that were significantly different from the control (no treatment, 0) at $P \leq 0.05$, as determined by the Kruskal–Wallis rank sum test, are indicated by an *asterisk*

guanine(s) with adenine. Furthermore, the very low amounts of detectable mutant SPT1 polypeptide is consistent with the translated protein being unstable, which would be predicted upon localization of a positively charged Arg in a hydrophobic region of the enzyme, as suggested by the homology model [33]. It was worthwhile, nonetheless, to test for possible SPT activity given the recent discovery that SPT is able to produce not only sphinganine (and downstream sphingosine) but also the atypical sphingoid bases, 1-deoxysphinganine (from alanine) and 1-desoxymethylsphinganine (from glycine) [13, 22]; furthermore, it has been suggested that these are elevated in the mutated SPTLC1 found in human sensory neuropathy type 1 (HSN1) [14]. However, the LY-B cells produced no detectable sphingoid bases of any of these types.

Therefore, for most studies, the presence of small amounts of mutant SPT1 polypeptide is not likely to interfere with the investigation. Its presence should be kept in mind, nonetheless, during investigations where the residual protein might become stabilized and complicate interpretation of studies of protein–protein interactions or other phenomena.

Acknowledgments This work was supported by NIH grant GM076217, and a MEXT grant of Japan.

References

- Merrill AH Jr, Wang MD, Park M, Sullards MC (2007) (Glyco)sphingolipidology: an amazing challenge and opportunity for systems biology. *Trends Biochem Sci* 32:457–468
- Pruett ST, Bushnev A, Hagedorn K, Adiga M, Haynes CA, Sullards MC, Liotta DC, Merrill AH Jr (2008) Biodiversity of sphingoid bases (“sphingosines”) and related amino alcohols. *J Lipid Res* 49:1621–1639
- Hanada K (2003) Serine palmitoyltransferase, a key enzyme of sphingolipid metabolism. *Biochim Biophys Acta* 1632:16–30
- Hanada K, Hara T, Fukasawa M, Yamaji A, Umeda M, Nishijima M (1998) Mammalian cell mutants resistant to a sphingomyelin-directed cytolysin. Genetic and biochemical evidence for complex formation of the LCB1 protein with the LCB2 protein for serine palmitoyltransferase. *J Biol Chem* 273:33787–33794
- Gable K, Slife H, Bacikova D, Monaghan E, Dunn TM (2000) Tsc3p is an 80-amino acid protein associated with serine palmitoyltransferase and required for optimal enzyme activity. *J Biol Chem* 275:7597–7603
- Hornemann T, Richard S, Rutti MF, Wei Y, von Eckardstein A (2006) Cloning and initial characterization of a new subunit for mammalian serine-palmitoyltransferase. *J Biol Chem* 281:37275–37281
- Hojjati MR, Li Z, Jiang XC (2005) Serine palmitoyl-CoA transferase (SPT) deficiency and sphingolipid levels in mice. *Biochim Biophys Acta* 1737:44–51
- Bejaoui K, Wu C, Scheffler MD, Haan G, Ashby P, Wu L, de Jong P, Brown RH Jr (2001) SPTLC1 is mutated in hereditary sensory neuropathy, type 1. *Nat Genet* 27:261–262
- Dawkins JL, Hulme DJ, Brahmabhatt SB, Auer-Grumbach M, Nicholson GA (2001) Mutations in SPTLC1, encoding serine palmitoyltransferase, long chain base subunit-1, cause hereditary sensory neuropathy type I. *Nat Genet* 27:309–312
- Tatzelt J, Zuo J, Voellmy R, Scott M, Hartl U, Prusiner SB, Welch WJ (1995) Scrapie prions selectively modify the stress response in neuroblastoma cells. *Proc Natl Acad Sci USA* 92:2944–2948
- Batheja AD, Uhlinger DJ, Carton JM, Ho G, D’Andrea MR (2003) Characterization of serine palmitoyltransferase in normal human tissues. *J Histochem Cytochem* 51:687–696
- Merrill AH Jr, Sullards MC, Allegood JC, Kelly S, Wang E (2005) Sphingolipidomics: high-throughput, structure-specific, and quantitative analysis of sphingolipids by liquid chromatography tandem mass spectrometry. *Methods* 36:207–224
- Zitomer NC et al (2009) Ceramide synthase inhibition by fumonisin B1 causes accumulation of 1-deoxysphinganine: a novel category of bioactive 1-deoxysphingoid bases and 1-deoxydihydroceramides biosynthesized by mammalian cell lines and animals. *J Biol Chem* 284:4786–4795
- Hornemann T, Penno A, von Eckardstein A (2008) The accumulation of two atypical sphingolipids cause hereditary sensory neuropathy type 1 (HSAN1). *Chem Phys Lipids* 154:62
- Iwatani M, Ikegami K, Kremenska Y, Hattori N, Tanaka S, Yagi S, Shiota K (2006) Dimethyl sulfoxide has an impact on epigenetic profile in mouse embryonic body. *Stem Cells* 24:2549–2556
- Hegner B, Weber M, Dragan D, Schulze-Lohoff E (2005) Differential regulation of smooth muscle markers in human bone marrow-derived mesenchymal stem cells. *J Hypertens* 23:1191–1202
- Wiebe JP, Kowalik A, Gallardi RL, Egeler O, Clubb BH (2000) Glycerol disrupts tight junction-associated actin microfilaments, occludin, and microtubules in Sertoli cells. *J Androl* 21:625–635
- Notredame C, Higgins DG, Heringa J (2000) T-Coffee: a novel method for fast and accurate multiple sequence alignment. *J Mol Biol* 302:205–217
- Malmqvist T, Mollby R (1981) Enzymatic hydrolysis by bacterial phospholipases C and D of immobilized radioactive sphingomyelin and phosphatidylcholine. *Acta Pathol Microbiol Scand [B]* 89:363–367
- Brogden KA, Engen RL, Songer JG, Gallagher J (1990) Changes in ovine erythrocyte morphology due to sphingomyelin degradation by *Corynebacterium pseudotuberculosis* phospholipase D. *Microb Pathog* 8:157–162
- Shaner RL, Allegood JC, Park H, Wang E, Kelly S, Haynes CA, Sullards MC, Merrill AH Jr (2009) Quantitative analysis of sphingolipids for lipidomics using triple quadrupole and quadrupole linear ion trap mass spectrometers. *J Lipid Res* (in press)
- Zitomer NC, Mitchell T, Voss KA, Bondy GS, Pruett ST, Garnier-Amblard EC, Liebeskind LS, Park H, Wang E, Sullards MC, Merrill AH Jr, Riley RT (2009) Ceramide synthase inhibition by fumonisin B1 causes accumulation of 1-deoxysphinganine: a novel category of bioactive 1-deoxysphingoid bases and 1-deoxydihydroceramides biosynthesized by mammalian cell lines and animals. *J Biol Chem* 284:4786–4795
- Gable K, Han G, Monaghan E, Bacikova D, Natarajan M, Williams R, Dunn TM (2002) Mutations in the yeast LCB1 and LCB2 genes, including those corresponding to the hereditary sensory neuropathy type I mutations, dominantly inactivate serine palmitoyltransferase. *J Biol Chem* 277:10194–10200
- Yard BA et al (2007) The structure of serine palmitoyltransferase: gateway to sphingolipid biosynthesis. *J Mol Biol* 370:870–886
- Marti-Renom MA, Stuart AC, Fiser A, Sanchez R, Melo F, Sali A (2000) Comparative protein structure modeling of genes and genomes. *Annu Rev Biophys Biomol Struct* 29:291–325
- Venclovas C, Margelevicius M (2005) Comparative modeling in CASP6 using consensus approach to template selection, sequence-structure alignment, and structure assessment. *Proteins* 61(Suppl 7):99–105
- Zhang Y, Skolnick J (2005) The protein structure prediction problem could be solved using the current PDB library. *Proc Natl Acad Sci USA* 102:1029–1034

28. Humphrey W, Dalke A, Schulten K (1996) VMD: visual molecular dynamics. *J Mol Graph* 14(33–8):27–28
29. Rother J, van Echten G, Schwarzmann G, Sandhoff K (1992) Biosynthesis of sphingolipids: dihydroceramide and not sphinganine is desaturated by cultured cells. *Biochem Biophys Res Commun* 189:14–20
30. Burrows JA, Willis LK, Perlmutter DH (2000) Chemical chaperones mediate increased secretion of mutant alpha 1-antitrypsin (alpha 1-AT) Z: a potential pharmacological strategy for prevention of liver injury and emphysema in alpha 1-AT deficiency. *Proc Natl Acad Sci USA* 97:1796–1801
31. Kubota K et al (2006) Suppressive effects of 4-phenylbutyrate on the aggregation of Pael receptors and endoplasmic reticulum stress. *J Neurochem* 97:1259–1268
32. Ohashi T, Uchida K, Uchida S, Sasaki S, Nihei H (2003) Intracellular mislocalization of mutant podocin and correction by chemical chaperones. *Histochem Cell Biol* 119:257–264
33. Myers JK, Pace CN (1996) Hydrogen bonding stabilizes globular proteins. *Biophys J* 71:2033–2039

The HMG-CoA Reductase Gene and Lipid and Lipoprotein Levels: the Multi-Ethnic Study of Atherosclerosis

Yi-Chun Chen · Yii-Der I. Chen · Xiaohui Li ·
Wendy Post · David Herrington · Joseph F. Polak ·
Jerome I. Rotter · Kent D. Taylor

Received: 12 January 2009 / Accepted: 18 May 2009 / Published online: 25 June 2009
© US Government 2009

Abstract HMG-CoA reductase (HMGCR) is an enzyme involved in cholesterol synthesis. To investigate the contribution of the *HMGCR* gene to lipids and lipoprotein subfractions in different ethnicities, we performed an association study in the Multi-Ethnic Study of Atherosclerosis (MESA). In total, 2,444 MESA subjects [597 African-Americans (AA), 627 Chinese-Americans (CHA), 612 European-Americans (EA), and 608 Hispanic-Americans

(HA)] without statin use were included. Participants had measurements of blood pressure, anthropometry, and fasting blood samples. Subjects were genotyped for 10 single nucleotide polymorphisms (SNPs). After excluding SNPs with minor allele frequency <5%, a single block was constructed. The most frequent haplotype was H1 (41–56%) in all ethnic groups except AA (H2a, 44.9%). Lower triglyceride level was associated with the H2a haplotype in AA and H2 in HA. In HA, H4 carriers had higher levels of triglyceride and small low-density lipoprotein (s-LDL), and lower high-density lipoprotein cholesterol (HDL-c), while carriers with H7 or H8 had associations with these traits in the opposite direction. No significant association was discovered in both CHA and EA. The total variation for triglyceride that could be explained by H2 alone was 2.6% in HA and 1.4% in AA. In conclusion, *HMGCR* gene variation is associated with multiple lipid/lipoprotein traits, especially with triglyceride, s-LDL, and HDL-c. The impact of the genetic variance is modest and differs greatly among ethnicities.

Y.-C. Chen · Y.-D. I. Chen · X. Li · J. I. Rotter · K. D. Taylor
Medical Genetics Institute, Cedars-Sinai Medical Center,
Los Angeles, CA, USA

Y.-C. Chen
Department of Neurology, Chang Gung Memorial Hospital
and College of Medicine, Chang-Gung University,
Taipei, Taiwan

W. Post
Division of Cardiology, Department of Medicine, Bloomberg
School of Public Health, Johns Hopkins University,
Baltimore, MD, USA

W. Post
Department of Epidemiology, Bloomberg School of Public
Health, Johns Hopkins University, Baltimore, MD, USA

D. Herrington
Department of Internal Medicine/Cardiology,
Wake Forest University Health Sciences,
Winston-Salem, NC, USA

J. F. Polak
Department of Radiology, Tufts-New England Medical Center,
Boston, MA, USA

Y.-C. Chen (✉)
Department of Neurology, Chang Gung Memorial Hospital,
Linkou Medical Center, 333, Kueishan, Taoyuan, Taiwan
e-mail: asd108@adm.cgmh.org.tw

Keywords Hydroxymethylglutaryl CoA reductases ·
Association study · Cholesterol · Triglyceride ·
Low-density lipoprotein size

Abbreviations

HMGCR	HMG-CoA reductase
<i>HMGCR</i>	HMG-CoA reductase gene
TG	Triglyceride
HDL-c	High-density lipoprotein cholesterol
LDL-c	Low-density lipoprotein cholesterol
s-LDL	Small low-density lipoprotein
VLDL	Very low-density lipoprotein
CVD	Cardiovascular diseases

BMI	Body mass index
TC	Total cholesterol
AA	African-Americans
CHA	Chinese-Americans
EA	European-Americans
HA	Hispanic-Americans
SNPs	Single nucleotide polymorphisms
BP	Blood pressure
DM	Diabetes mellitus
LD	Linkage disequilibrium
MAF	Minor allele frequency
HWE	Hardy-Weinberg equilibrium
GLM	General linear model
GWAS	Genome-wide association study

Introduction

Elevated triglyceride (TG), low levels of high-density lipoprotein cholesterol (HDL-c), and elevated small, dense low-density lipoprotein particles (s-LDL) have been established as important risk factors for cardiovascular diseases (CVD) [1]. Several studies have revealed ethnic differences in the variation in lipid/lipoprotein traits [2, 3]. Compared to other ethnic groups, despite a higher prevalence of hyperglycemia, hypertension, and obesity, the prevalence of hypertriglyceridemia and low HDL-c is lower in blacks [2–4]. In contrast, Asians had higher TG and lower HDL-c than whites despite the lower body mass index (BMI) [5]. The interethnic disparity in lipid/lipoprotein profile could not be solely explained by the differences in environmental or nutritional factors [2].

Genetic effects on lipid/lipoprotein phenotypes have been shown in numerous studies. Atherogenic lipoprotein phenotype was demonstrated to segregate in Caucasian families [6], and heritability of LDL particles was estimated to range from 0.34 to 0.60 in Caucasian and Hispanic families [7–10]. Linkage studies have reported several chromosome loci with lipid/lipoprotein traits in multiple ethnicities [11–15]. Two independent groups [11, 15] have reported a promising locus on 5q13–14, which suggests as a potential candidate gene the HMG-CoA reductase gene (*HMGCR*). This locus was linked to TG and total cholesterol (TC) levels in Turkish/Mediterranean families [15] and to LDL peak particle diameter and TG levels in Québec families [11].

HMGCR is the rate-limiting enzyme in cholesterol biosynthesis and is the target of statin therapy [16]. Pharmacokinetic studies have identified interethnic differences in statin responses [17, 18]. Previous studies [19, 20] have shown that the *HMGCR* gene contributed to the differences in response to statins. A major role of *HMGCR* alternative

splicing in influencing lipid response to statin therapy [21] and LDL-c variation [22] has been shown in the previous reports. Although the *HMGCR* gene was associated with the baseline LDL-c, it has not been clarified to what extent the *HMGCR* gene contributes to lipids and lipoprotein subfractions in multiple ethnic groups. To investigate the contribution of the *HMGCR* gene to the lipid/lipoprotein traits in different ethnicities, we utilized the Multi-Ethnic Study of Atherosclerosis study (MESA) to test the association between the *HMGCR* gene and a comprehensive profile of lipid and lipoprotein subfractions in African-Americans (AA), Chinese-Americans (CHA), European-Americans (EA), and Hispanic-Americans (HA). We used a tagged-single-nucleotide-polymorphisms (SNPs) approach to assess gene variation comprehensively.

Methods

Subjects

MESA is a prospective cohort study designed to study the progression of subclinical cardiovascular disease, consisting of 6,814 subjects who were free of clinical cardiovascular disease at entry. The participants were recruited from six communities (Baltimore, Chicago, Forsyth County, Los Angeles County, northern Manhattan, and St. Paul). The sampling procedures have been described in detail [23] and are available at <http://www.mesa-nhlbi.org>. A subcohort of 2,880 MESA subjects (720 in each ethnic group with matched age and gender) were randomly selected from subjects who gave informed consent for genetic studies. After excluding subjects with statin use, we included 2,444 subjects in the current study (597 AA, 627 CHA, 612 EA, and 608 HA).

Phenotyping

All data were collected at the first MESA examination (2000–2002), when participants had measurements taken of blood pressure (BP), anthropometry, and fasting blood samples. Three resting BP readings were recorded, and hypertension was defined as a mean systolic BP \geq 140 or diastolic BP \geq 90 mmHg, or use of antihypertensive medication. Diabetes mellitus (DM) was defined as a fasting glucose $>$ 6.88 mmol/L or use of antidiabetic medication.

Using CDC-standardized methods, lipid levels were measured on samples obtained after an overnight fast. LDL-c was calculated in plasma specimens having a TG value $<$ 400 mg/dL by the Friedewald equation. Measurements for lipoprotein particles have been previously described [24].

Genotyping

Genomic DNA was extracted from peripheral leukocytes isolated from packed cells of anticoagulated blood by use of a commercially available DNA isolation kit (Puregene; Gentra Systems, Minneapolis, MN). The DNA was quantified by determination of absorbance at 260 nm followed by PicoGreen analysis (Molecular Probes, Eugene, OR).

Because of linkage disequilibrium (LD) in the human genome, genotyping of chosen SNPs will provide sufficient information to assess the remainder of the common SNPs and to construct each of the common haplotypes in a specific region [25]. Using International HapMap data on NCBI Build 35 assembly for whites, Asian, and Yoruban populations, we selected 10 SNPs to tag major haplotypes with Haploview v4 [26]. Selection of single nucleotide polymorphisms (tagSNPs) in candidate gene loci was according to the following criteria: (1) location within the proximal and distal 10-kb regions 5' and 3' to the given candidate gene (NCBI Build 35); (2) compatibility with the Illumina GoldenGate technology [27, 28] as determined by the Assay Design Tool (TechSupport, Illumina, San Diego, CA, USA); (3) minor allele frequency (MAF) >0.05 or a tag (r^2 value >0.8) for another SNP with MAF >0.05 as determined by applying the multilocus or “aggressive” “Tagger” option of Haploview v3 [26, 29] using International HapMap project data for CEPH and Yoruban populations (release 19) (International HapMap Consortium 2003). All ten SNPs were used for haplotyping, except for the SNP rs5908, since its MAF was <0.05 in all MESA ethnic groups, and thus would provide little information in an association study.

The 10 SNPs were rs3761738 (G/A, mRNA untranslated region, UTR), rs3761739 (G/A, UTR), rs4704209 (A/G, intron), rs10038095 (A/T, intron), rs2303152 (G/A, intron), rs3846662 (G/A, intron), rs5908 (reference allele A/G, I637V), rs17238540 (A/C, intron), rs3846663 (G/A, intron), and rs5909 (G/A, UTR). As is well-known, G/A is the most common change in the human genome due to a methylation of the C on the opposite strand followed by deamination to a T. Although the MAF of the SNP rs5908 in CEPH shown in the International HapMap was 0.034, which is borderline lower than 0.05, it was still considered to be genotyped in this study because of its function as a nonsynonymous polymorphism (reference allele A, I637V).

Genotyping was performed by Illumina genotyping services (GoldenGate assay, Illumina, San Diego, CA). All 10 SNPs were successfully typed with a genotype calling rate of 100%. Each SNP was in Hardy-Weinberg equilibrium (HWE, significance level of 0.005) in each ethnic group. We utilized the SNPs with minor allele frequency (MAF) ≥ 0.05 to evaluate LD in each ethnic group and in the combined group with Haploview v4 [26]. Because the MAF of rs5908 was <0.05 in all ethnic groups, it was not included

in haplotype construction. In each ethnic group, there was a single block structure composed of a portion of the remaining nine SNPs. Because the MAF was different for each SNP between ethnicities, different ethnic groups had different portions of the nine SNPs for the same haplotype (see “Appendix”). For example, the H2 haplotype was separated into H2a and H2b in AA based on the variation of rs17238540, in which the MAF was 0.08 in AA but <0.05 in the others. Haplotypes were reconstructed based on the LD results in each ethnic group by PHASE 2.0 [30]. Haplotypes with frequency <1% were excluded and were numbered in the order of their frequency in the combined sample.

Statistical Analysis

Interethnic differences in the demographic/phenotypic characteristics and haplotype distribution were performed by ANOVA or the Pearson's χ^2 test where appropriate. We used haplotypes to examine the possible associations because it is expected that haplotype analyses will provide greater power than single SNPs since certain untyped SNPs may be in LD with a combination of typed SNPs [31]. Association tests for individual SNPs were only applied to those that differentiate the haplotypes with significant association results. We use a general linear model (GLM) to estimate association in each ethnic group. Covariates included age, gender, BMI, and DM. Dominant models for SNP analyses were used because the majority of the SNPs had minor allele homozygotes <10. Parameter estimates were derived from the same models. Permutation testing of 10,000 replicates was performed for empirical estimates to account for the multiple testing. To identify the interaction between significant haplotypes and ethnic groups, the multiplicative term of significant haplotypes and ethnic groups was examined by the GLM. R^2 was calculated to estimate the proportion of explained variation of the outcome variable as a function of independence in the GLM.

Under the sample of 600 independent individuals and a priori TC data in MESA, we tested the ability to detect an association between a SNP and TC. At the 0.005 significance level, for detectable effect size >0.4, we had sufficient power (>0.80) to identify the association under a dominant model with disease allele frequency >0.10.

Results

The prevalence of DM and hypertension, and the quantitative traits of BMI, waist circumference, and lipid/lipoprotein levels, significantly differed among ethnicities (Table 1), but age and gender did not. The prevalence of hypertension was higher in AA (52%) than the others (35–40%). BMI and waist circumference were higher in AA and HA, and lower in

Table 1 Mean values with standard deviations or percentage distributions of clinical, lipid, and lipoprotein variables in each MESA ethnic group

	AA (<i>n</i> = 597)	CHA (<i>n</i> = 627)	EA (<i>n</i> = 612)	HA (<i>n</i> = 608)	All (<i>n</i> = 2444)
Age (years)	60.9 ± 10.0	61.4 ± 10.3	60.9 ± 10.6	60.5 ± 10.2	60.9 ± 10.3
Male gender (%)	45.7	49.8	45.6	45.9	46.8
Diabetes mellitus (DM)* (%)	43.0	44.2	28.2	46.9	40.5
Hypertension* (%)	52.4	34.9	35.8	39.8	40.6
BMI (kg/m ²)*	30.0 ± 5.7	23.9 ± 3.3	27.6 ± 5.3	29.6 ± 5.1	27.7 ± 5.5
Waist circumference (cm)*	100.6 ± 14.3	86.8 ± 9.9	97.2 ± 15.3	100.3 ± 13.0	96.1 ± 14.4
Total cholesterol (mg/dL)*	192 ± 37	195 ± 31	199 ± 34	201 ± 37	196 ± 35
LDL-c (mg/dL)†	117 ± 33	118 ± 28	120 ± 31	122 ± 31	119 ± 31
l-LDL (nmol/L)*	421 ± 204	345 ± 190	434 ± 203	372 ± 215	392 ± 206
s-LDL (nmol/L)*	837 ± 459	947 ± 441	855 ± 422	1024 ± 472	916 ± 455
Triglyceride (mg/dL)*	104 ± 60	141 ± 82	130 ± 82	158 ± 88	133 ± 81
l-VLDL (nmol/L)*	2.3 ± 3.7	3.5 ± 5.5	4.1 ± 5.3	6.0 ± 7.1	4.0 ± 5.7
m-VLDL (nmol/L)*	24 ± 22	45 ± 29	31 ± 23	37 ± 26	34 ± 26
s-VLDL (nmol/L)*	36 ± 20	40 ± 19	40 ± 21	43 ± 19	40 ± 20
HDL-c (mg/dL)*	53 ± 15	49 ± 12	53 ± 16	47 ± 12	50 ± 14
l-HDL (μmol/L)*	7.6 ± 4.0	6.9 ± 3.6	7.1 ± 4.2	6.0 ± 3.5	6.9 ± 3.9
m-HDL (μmol/L)*	3.4 ± 3.7	3.2 ± 3.5	5.7 ± 4.8	5.3 ± 4.2	4.4 ± 4.2
s-HDL (μmol/L)*	20 ± 5	21 ± 5	19 ± 5	19 ± 4	20 ± 5
TG/HDL-c ratio*	2.3 ± 1.9	3.3 ± 2.6	2.9 ± 2.7	3.8 ± 2.8	3.1 ± 2.5

The frequency of DM and hypertension and the traits of BMI, waist circumference, lipid, and lipoprotein were all significantly different among race/ethnic groups (* $P < 0.0001$, † $P = 0.035$)

AA African-Americans, CHA Chinese-Americans, EA European-Americans, HA Hispanic-Americans, l-HDL large HDL, m-HDL medium HDL, s-HDL small HDL, l-LDL large LDL, s-LDL small LDL, l-VLDL large VLDL/chylomicron, m-VLDL medium VLDL, s-VLDL small VLDL

To convert mg/dL to mmol/L, multiply LDL-C, HDL-c, and total cholesterol values by 0.02586 and triglycerides by 0.011

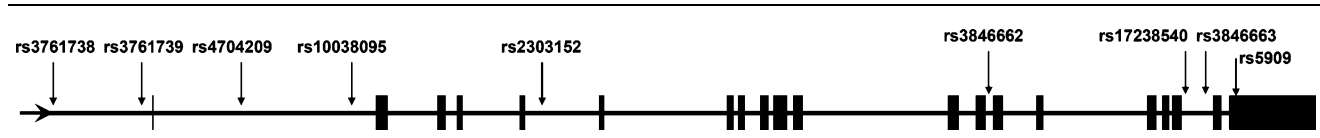
CHA. Compared to the other groups, AA had a more protective lipid/lipoprotein phenotype.

Haplotype structure and frequencies of the *HMGCR* gene in each ethnic group are shown in Table 2 and the Appendix. The frequency of each haplotype differed significantly among ethnic groups (χ^2 test, $P < 0.0001$). The H1 haplotype was the most frequent haplotype in every ethnic group except AA, in which 44.9% had H2a.

There was no significant association between any of the lipid traits and the *HMGCR* gene in both EA and CHA. However, lower TG was associated with H2a in AA ($P = 0.005$) and H2 in HA ($P = 0.021$) (Table 3). TG/HDL-c ratio was also lower in the H2a carriers in AA ($P = 0.023$). In HA, the H4 haplotype was associated with the lipid/lipoprotein traits, specifically, higher TG ($P = 0.012$), TG/HDL-c ratio ($P = 0.003$), s-LDL ($P = 0.016$), l-VLDL ($P = 0.012$), and m-VLDL ($P = 0.002$), and lower HDL-c ($P = 0.004$) and l-HDL ($P = 0.0004$) (Fig. 1). In contrast, H8 was associated with these traits in the opposite direction, including lower TG ($P = 0.002$), TG/HDL-c ratio ($P = 0.0005$), s-LDL ($P = 0.009$), l-VLDL ($P = 0.021$), and s-VLDL ($P = 0.039$), and higher HDL-c ($P = 0.002$)

and l-HDL ($P = 0.002$). In HA, the H7 haplotype was also associated with lower TG ($P = 0.013$), lower TG/HDL-c ratio ($P = 0.032$), and lower s-VLDL ($P = 0.017$), but to a lesser magnitude compared with H8. In addition, H7 was associated with lower TC ($P = 0.026$) and m-VLDL ($P = 0.012$), but not significantly associated with the subclasses of LDL and HDL. LDL-c was not associated with any of the examined haplotypes in any ethnic group. In HA, when combining the subjects carrying H7 or H8, carriers had lower TC ($P = 0.04$), lower TG ($P < 0.0001$), higher HDL-c ($P = 0.01$), lower l-VLDL ($P = 0.003$), and higher l-HDL ($P = 0.001$) than noncarriers (Fig. 1), and had lower TC ($P = 0.03$), TG ($P < 0.0001$), s-LDL ($P = 0.02$), and l-VLDL ($P = 0.0004$), and higher HDL-c ($P = 0.003$) and l-HDL ($P = 0.0003$) levels than the H4 carriers.

Examination of the interaction effect of H2 and the ethnicity of AA and HA on TG levels was performed to determine if the higher frequency of H2 in AA could explain their lower TG levels. The H2 haplotype was associated with lower TG in both AA and HA. However, compared to HA, both H2 carriers and noncarriers in AA had lower TG levels (Fig. 2). The differences in TG level

Table 2 Haplotype frequencies of the *HMGCR* gene in each MESA ethnic group


Haplotype	Ethnic groups	Ethnic groups				
		Combined, <i>n</i> (%)	AA, <i>n</i> (%)	CHA, <i>n</i> (%)	EA, <i>n</i> (%)	HA, <i>n</i> (%)
H1	GGAAGAAGG	2,024 (41.4)	157 (13.2)	610 (48.7)	681 (55.9)	576 (47.5)
H2a	GGAAGGAGG	869 (17.8)	536 (44.9)	–	67 (5.5)	174 (14.3)
H2b	GGAAGGCGG		96 (8.0)			
H3	GGATGGAAG	652 (13.3)	*	281 (22.4)	160 (13.1)	123 (10.1)
H4	GAGTGGAAG	420 (8.6)	*	231 (18.4)	*	88 (7.3)
H5	GGATAGAAG	386 (7.9)	63 (5.3)	96 (7.7)	130 (10.7)	97 (8.0)
H6	AAATGGAAA	315 (6.4)	*	*	125 (10.3)	125 (10.3)
H7	GGATGGAGG	128 (2.6)	106 (8.9)	–	–	16 (1.3)
H8	GAATGGAAG	86 (1.8)	*	*	*	15 (1.2)
			236 (19.8) ^a	35 (2.8) ^a	55 (4.5) ^a	

Haplotypes were constructed in the above SNP order. Detailed haplotype structure is provided in the [Appendix](#)

AA African-Americans, CHA Chinese-Americans, EA European-Americans, HA Hispanic-Americans

– Very rare (<1% frequency) haplotype

*Haplotypes that were not differentiated because of certain rare SNPs (MAF < 0.05)

^a Sum of haplotypes marked by *

between H2 carriers and noncarriers were similar in AA and HA ($P = 0.70$). The interethnic difference in TG thus could not be solely explained by the H2 effect only. The total variation for TG that could be explained by H2 alone was 2.6% in HA and 1.4% in AA when controlling for covariates.

Associations were examined for the SNPs that differentiated significant haplotypes, including rs3846662 (separating H2a and H1), rs17238540 (H2a and H2b), and rs10038095 (H2a and H7) in AA, and rs3846662 (H2 and H1), rs3846663 (H7 and H3), rs3761739 (H8 and H3), and rs4704209 (H4 and H8) in HA. All three selected SNPs in AA and rs3846662 and rs3761739 in HA showed no contribution toward the associations of the relevant haplotypes (data not shown). In contrast, the minor allele of rs3846663 was associated with higher TG ($P = 0.001$), higher TG/HDL-c ratio ($P = 0.006$), and higher m-VLDL ($P = 0.002$) in HA, which was consistent with the association and the direction of H7. The association with rs4704209 was entirely equivalent to that with the H4 haplotype in HA.

Discussion

To our knowledge, this is the first report regarding the interethnic differences in the distribution of *HMGCR*

haplotypes and the differential associations of *HMGCR* gene with lipid/lipoprotein levels. The significant associations occurred mainly in HA. In HA, the H4 haplotype was associated with higher TG, s-LDL, and VLDL and lower HDL-c; and the haplotypes H2, H7, and H8 were associated with lower TG, s-LDL, and VLDL and higher HDL-c. The H2 haplotype was associated with lower TG and lower VLDL in AA as well. The absence of H2 in CHA and the lack of distinct, separable H4 and H8 haplotypes in AA and EA could well have accounted for ethnic differences in the associations. In HA, SNP analyses suggested that the association of H7 and H4 could be attributed to rs3846663 and rs4704209, respectively (or any SNP in complete LD with the two SNPs). This study supports that AA have less proportion of hypertriglyceridemia and low HDL-c than the other ethnic groups. Although AA had a remarkably high frequency (44.9%) of H2a, this study revealed that the *HMGCR* H2a haplotype had only a modest effect on TG level and did not have a significant effect on the interethnic differences in TG levels. In summary, the *HMGCR* gene variation is associated with multiple lipid/lipoprotein traits. The impact of the genetic variance is modest and differs greatly among ethnicities.

The first published MESA genetic study [32] utilized a MESA sample ($n = 969$, white = 448, Chinese = 97, AA = 205, HA:219) from the overall baseline MESA cohort who were randomly selected from the 5,030 MESA

Table 3 Differences (95% confident intervals) in lipid traits as a function of the presence or absence of *HMGC*R haplotypes in African-Americans (AA) and Hispanic-Americans (HA) in MESA

	TC (mg/dl)	TG (mg/dl)	TG/HDL-c	LDL		VLDL (nmol/L)		HDL				
				LDL-c (mg/dl)	s-LDL (nmol/L)	l-VLDL	m-VLDL	s-VLDL	HDL-c (mg/dl)	l-HDL (nmol/L)		
AA												
H2a	-3.1 (-9, 3)	-10.7† (-18, -3)	-0.2‡ (-0.4, -0.03)	-1.1 (-7, 5)	1.0 (-74, 76)	-0.2 (-0.5, 0.1)	-3.9‡ (-7, -0.6)	-5.2† (-9, -2)	0.4 (-2, 3)	0.6 (-0.4, 0.9)		
H2b	4.8 (-3, 13)	1.6 (-8, 12)	0.01 (-0.2, 0.3)	4.0 (-3, 11)	56.6 (-39, 152)	0.1 (-0.3, 0.5)	0.8 (-3, 5)	-1.8 (-6, 3)	0.7 (-2, 4)	0.1 (-0.7, 0.9)		
HA												
H2	-0.9 (-7, 6)	-14.8‡ (-26, -2)	-0.3 (-0.6, 0.1)	3.1 (-3, 9)	15.5 (-69, 100)	-0.6 (-1.3, 0.1)	-2.9 (-7, 1.5)	0.5 (-3, 4)	-0.5 (-2, 1.4)	0.09 (-0.5, 0.7)		
H4	3.2 (-5, 12)	21.7‡ (4.6, 41)	0.7† (0.2, 1.3)	0.1 (-7, 8)	127.2‡ (24, 231)	1.3‡ (0.3, 2.6)	9.2† (3.6, 14.8)	2.7 (-2, 7)	-3.3† (-5.3, -1)	-1.1* (-1.8, -0.5)		
H7	-19.3‡ (-34, -3)	-37.3‡ (-60, -9)	-0.9‡ (-1.5, -0.1)	-13.5 (-29, 2)	17.2 (-208, 242)	-1.6 (-2.7, 0.1)	-13.3‡ (-24, -3)	-11.9‡ (-21, -2)	1.5 (-3, 7)	1.0 (-0.6, 2.6)		
H8	-5.3 (-22, 13)	-46.3† (-67, -19)	-1.4* (-1.8, -0.7)	-5.3 (-21, 11)	-310.7† (-542, -80)	-1.9‡ (-2.9, -0.4)	-11.0 (-22, -0.6)	-10.5‡ (-20, -0.6)	8.6† (3, 15)	2.7† (1.0, 4.5)		
HA												
3846662	2.1 (-4, 8)	2.7 (-9, 15)	0.06 (-0.3, 0.4)	0.4 (-5, 6)	11.9 (-67, 90)	0.2 (-0.5, 1.0)	0.5 (-3.6, 4.5)	0.6 (-3, 4)	-0.2 (-2, 1.6)	0.09 (-0.4, 0.6)		
3846663	4.8 (-1, 11)	18.2† (7, 30)	0.4† (0.1, 0.8)	0.8 (-4, 6)	45.1 (-28, 118)	0.8‡ (0.2, 1.6)	5.9† (2.2, 9.7)	1.9 (-1, 5)	-0.4 (-2, 1.2)	-0.3 (-0.8, 0.2)		
3761739	6.7‡ (0.7, 13)	13.3‡ (1.4, 26)	0.3 (-0.01, 0.7)	3.0 (-2, 8)	45.5 (-30, 122)	0.5 (-0.2, 1.3)	6.5† (2.5, 10.5)	2.4 (-0.9, 6)	-0.5 (-2, 1.3)	-0.2 (-0.8, 0.3)		
4704209	3.2 (-5, 12)	21.7‡ (4.6, 41)	0.7† (0.2, 1.3)	0.1 (-7, 8)	127.2‡ (24, 231)	1.3‡ (0.3, 2.6)	9.2† (3.6, 14.8)	2.7 (-2, 7)	-3.3† (-5.3, -1)	-1.1* (-1.8, -0.5)		

Parameter estimates (95% CI) derived from GLM models that included age, sex, BMI, and diabetes as independent variables show the difference in each trait in carriers (haplotype or genotype consisting at least one minor allele) compared to noncarriers. Definition for minor allele is based on the allele frequency of each SNP in all cohort subjects

* $P < 0.001$, † $P < 0.01$, ‡ $P < 0.05$

The *negative signs* mean the level of each trait in carriers is lower to that in noncarriers

To convert mg/dL to mmol/L, multiply LDL-C, HDL-C, and total cholesterol values by 0.02586 and triglycerides by 0.011

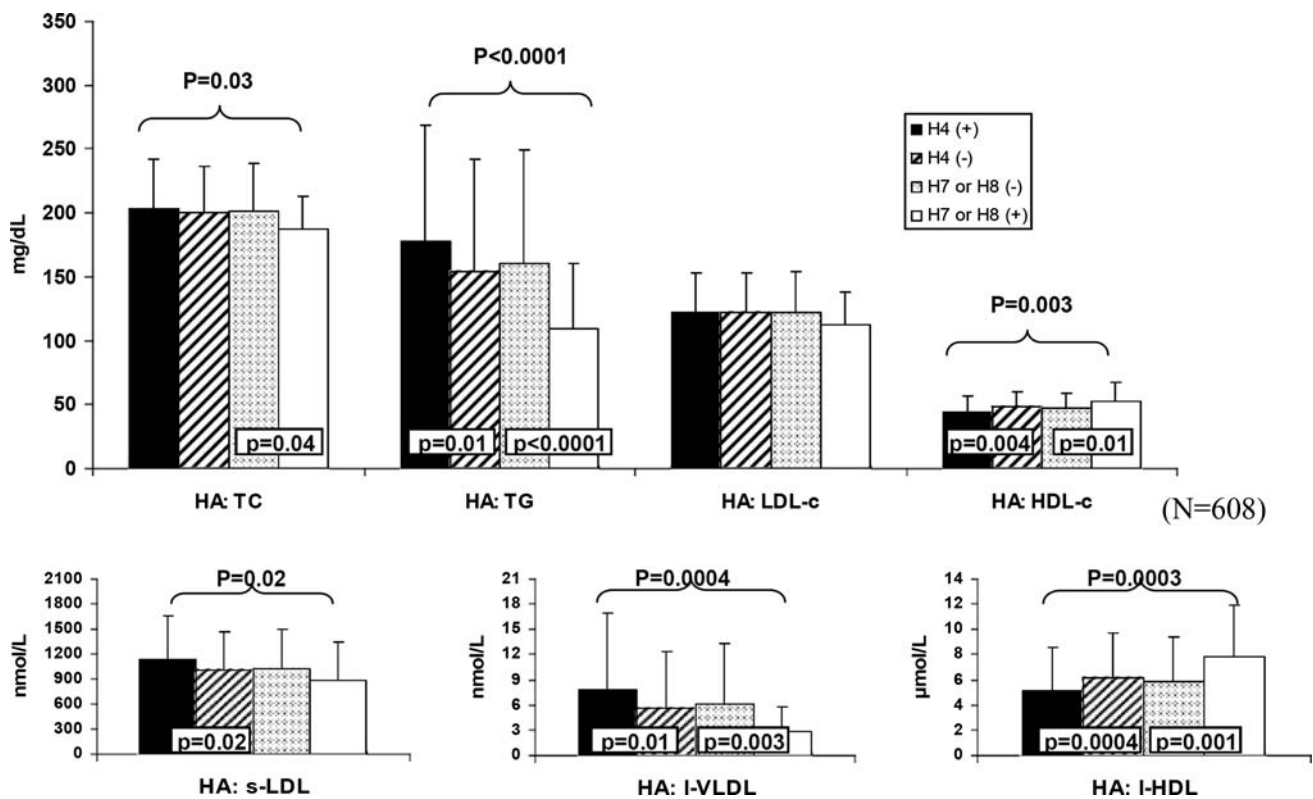


Fig. 1 Comparisons of lipid/lipoprotein levels between the carriers and noncarriers of the *HMGR* H4 and the combination of H7 and/or H8 in Hispanic-Americans. Data are presented as mean of the levels. Subjects carrying the H4 haplotype [H4 (+)] have significantly higher TG, lower HDL-c, higher s-LDL, higher l-VLDL, and lower l-HDL than noncarriers. In contrast, H7 or H8 carriers [H7/H8 (+)] have

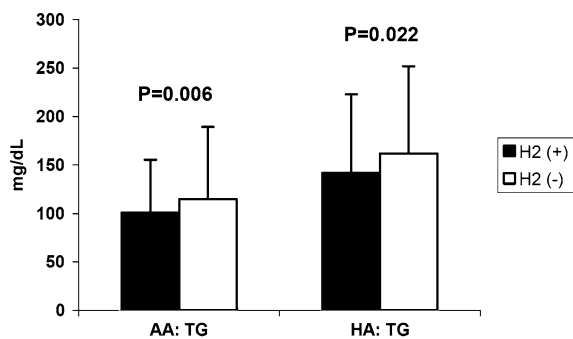
lower total cholesterol (TC) and TG, higher HDL-c, lower l-VLDL, and higher l-HDL than noncarriers. H4 carriers have higher TC, TG, s-LDL, and l-VLDL, and lower HDL-c and l-HDL levels than H7/H8 carriers. To convert mg/dL to mmol/L, multiply LDL-c, HDL-c, and total cholesterol values by 0.02586 and TG by 0.011

participants enrolled prior to February 2002, before the completion of the overall recruitment. That study found ethnic differences in the association between *ABCA1* gene SNPs and HDL-c as well as subclinical atherosclerosis. The multi-ethnic composition of the MESA cohort is both a strength (analyses in multiple ethnicities) and a potential limitation (relatively small sample sizes) [32].

The limitations of the present study included moderate sample sizes of each population group, which could limit the capacity to reveal valid genetic information for the complex phenotype of lipoprotein levels. Independent confirmation or further replication is needed to verify these associations. The other potential limitation of this study was that the LDL-c level was calculated by the Friedewald equation instead of direct tests; therefore, LDL-c of subjects with TG value greater than 400 mg/dL was not included in the genetic analysis. However, there were only 1.4% (34 subjects) with elevated TG who were excluded from analyses. This study did not show any association between *HMGR* gene and lipid traits in EA and CHA. It is possible that lipids were associated with

other SNPs and haplotypes in the *HMGR* gene that have more potent associations with lipid/lipoprotein traits. In addition, the MESA subjects included only subjects free from known cardiovascular diseases at baseline, and this study has excluded subjects who took statins; both of the above selection criteria may lead to somewhat different results. The strengths of this study included the multiple samples of different ethnicities, extensive LD mapping and haplotyping of the locus, comparisons of haplotype frequency and genetic associations across ethnic groups, and the consistent associations between lower triglyceride level and the *HMGR* haplotype 2 in two ethnic groups, AA and HA.

The *HMGR* gene map locus is at 5q13.3–q14. Previous studies showed linkage evidence of this locus with several lipid/lipoprotein traits, mainly in whites [11, 15]. In AA, CHA, or HA, there were no promising data supporting this linkage [12–14]. In contrast to the linkage reports, the associations between *HMGR* gene and the lipid/lipoprotein traits in our study were most striking in HA and AA, but not in EA. In EA, the absence of association between



	β coefficient	P-value
H2 haplotype	-0.13	0.005
Ethnicity	0.35	<0.0001
Interaction of H2 and ethnicity	0.02	0.70

Fig. 2 Triglyceride levels in H2 carriers and noncarriers in African-Americans (AA) and Hispanic-Americans (HA). The H2 haplotype had lower TG level in both AA and HA. Both H2 carriers and noncarriers in HA had higher TG levels (142 ± 81 and 162 ± 90 mg/dL, respectively) than AA (101 ± 55 and 115 ± 75 mg/dL, respectively). The difference in TG level between H2 carriers and noncarriers was similar in AA and HA (14 and 20 mg/dL, respectively), without interaction between the H2 haplotype and ethnicity ($P = 0.70$)

the *HMGR* gene and lipid/lipoprotein traits was consistent with findings in previous studies [19, 20]. The Pravastatin Inflammation/CRP Evaluation (PRINCE) study and the Cholesterol and Pharmacogenetics (CAP) study have demonstrated that the *HMGR* gene contributed to the differences in response to statins [19, 20]. The PRINCE study did not find an association between the *HMGR* gene and the baseline LDL-c level in the studied population, which consisted mainly of whites (88.7%). The CAP study showed an association of their Hap2 (haplotype 2) and/or Hap7 (haplotype 7) with lower baseline LDL-c level in blacks, but not in whites. The CAP Hap2 and Hap7 are analogous to our H2a and H2b in AA, respectively; the combination of Hap2 and Hap7 is analogous to our H2 in the other ethnic groups. The study herein supports the association of H2 with lower TG in both AA and HA. In addition, the percentage of the designated Hap2 in the CAP study was higher in AA (32%) than EA (2%), which was similar to our results (H2a, 44.9% in AA; H2, 5.5% in EA). In AA, we observed the association of the H2 haplotype with lower TG instead of LDL-c level shown in the previous study [20]. In HA, this is the first association data that showed significant associations between *HMGR* haplotypes with multiple lipid/lipoprotein traits, especially with TG, s-LDL, and HDL-c. In CHA, we did not observe any association, although an association between the 8302A/C variation of the *HMGR* gene and lipids was

reported in one Chinese study [33]. It should be noted that the absence of H2 in CHA and the lack of the distinct, separable H4 and H8 haplotypes in AA and EA could well have accounted for the ethnic differences in the associations. Because the associations of the *HMGR* gene with lipid/lipoprotein traits were mainly in AA and HA, and the haplotype distribution was remarkably different among ethnicities, future studies of statin therapy will need to include adequate representation from several ethnic groups, such as AA and HA.

Recently, a genome-wide association study (GWAS) [34] using variance-weighted meta-analysis from up to four GWAS revealed an association between SNP rs12654264 of *HMGR* and LDL-c level in the European population ($P = 1 \times 10^{-20}$). A simultaneous GWAS [35] using similar study cohorts did not report this association (threshold $P = 5 \times 10^{-7}$). Based on the CEU data in HapMap, SNP rs12654264 is in LD with rs3846662 ($r^2 = 0.84$) and rs3846663 ($r^2 = 0.97$); however, in our white group, neither SNP exhibited any significant association with lipid levels in EA ($P > 0.05$). The SNP rs12654264 is in complete LD with rs3846662 and rs3846663 in HapMap's CHB and JPT data. In our CHA group, neither of the two SNPs was associated with lipid traits. The SNP rs12654264 is not in LD with any of our tagSNPs in the AA group, and the two SNPs rs3846662 and rs3846663 showed no association with lipid traits in AA. The only association discovered in our study between lipids and the two SNPs was rs3846663 with TG levels and l-VLDL and m-VLDL in HA. We had no LD information between rs3846663 and rs12654264 in our Hispanic groups. The inconsistency among the two GWAS and our reports might be caused by the different sample size and study/analysis methods. Independent study into this inconsistency is necessary. Further studies addressing the function related to the SNP and the intermediate phenotypes such as mevalonate and HMG-CoA reductase would increase the functional biochemical evidence for the association.

It is somewhat surprising that the *HMGR* gene was associated with TG and HDL-c because *HMGR* does not play a direct role in TG synthesis and hydrolysis. The association may be indirectly caused by the requirement of hepatic cholesterol for VLDL assembly [36], regulation of LDL receptor number, and the conversion of s-LDL from large TG-rich VLDL particles [36]. Several studies have also shown the effect of statins on lowering TG and increasing HDL-c [16]. The *HMGR* gene is thus a potential contributor, at least to some extent, to the differences in statin response of TG and HDL-c.

In summary, *HMGR* gene variations were associated with multiple lipid/lipoprotein traits in African-Americans and Hispanic-Americans. The impact of the *HMGR* gene

on lipid/lipoprotein levels appears modest and differs greatly among ethnicities.

Acknowledgments This research was supported by contracts N01-HC-95159 through N01-HC-95169 (MESA), RO1HL071205 (MESA family), and HL069757 (PARC) from the NHLBI. We thank the other investigators, the staff, and the participants of the MESA study for their

valuable contributions. A full list of participating MESA investigators and institutions can be found at <http://www.mesa-nhlbi.org>.

Appendix

See Table 4.

Table 4 Haplotype structure and frequencies of the *HMGR* gene in each MESA ethnic group

Haplotype: <i>n</i> (%)	SNP MAF (%) in all								
	rs3761738 (G/A, UTR) (6.5)	rs3761739 (G/A, UTR) (16.9)	rs4704209 (A/G, intron) (8.6)	rs10038095 (A/T, intron) (41.0)	rs2303152 (G/A, intron) (8.2)	rs3846662 (G/A, intron) (40.9)	rs17238540 (A/C, intron) (3.6)	rs3846663 (G/A, intron) (38.4)	rs5909 (G/A, UTR) A (6.5)
AA									
H1: 157 (13.2)	*	*	*	A	G	A	A	G	*
H2a: 536 (44.9)	*	*	*	A	G	G	A	G	*
H2b: 96 (8.0)	*	*	*	A	G	G	C	G	*
H3, 4, 6, 8: 236 (19.8)	*	*	*	T	G	G	A	A	*
H5: 63 (5.3)	*	*	*	T	A	G	A	A	*
H7: 106 (8.9)	*	*	*	T	G	G	A	G	*
CHA									
H1: 610 (48.7)	*	G	A	A	G	A	*	G	*
H3: 281 (22.4)	*	G	A	T	G	G	*	A	*
H4: 231 (18.4)	*	A	G	T	G	G	*	A	*
H5: 96 (7.7)	*	G	A	T	A	G	*	A	*
H6, 8: 35 (2.8)	*	A	A	T	G	G	*	A	*
H2, H7: 0 (0)	–	–	–	–	–	–	–	–	–
EA									
H1: 681 (55.9)	G	G	*	A	G	A	*	G	G
H2: 67 (5.5)	G	G	*	A	G	G	*	G	G
H3: 160 (13.1)	G	G	*	T	G	G	*	A	G
H5: 130 (10.7)	G	G	*	T	A	G	*	A	G
H6: 125 (10.3)	A	A	*	T	G	G	*	A	A
H4, 8: 55 (4.5)	G	A	*	T	G	G	*	A	G
H7: 0 (0)	–	–	–	–	–	–	–	–	–
HA									
H1: 576 (47.5)	G	G	A	A	G	A	*	G	G
H2: 174 (14.3)	G	G	A	A	G	G	*	G	G
H3: 123 (10.1)	G	G	A	T	G	G	*	A	G
H4: 88 (7.3)	G	A	G	T	G	G	*	A	G
H5: 97 (8.0)	G	G	A	T	A	G	*	A	G
H6: 125 (10.3)	A	A	A	T	G	G	*	A	A
H7: 16 (1.3)	G	G	A	T	G	G	*	G	G
H8: 15 (1.2)	G	A	A	T	G	G	*	A	G
ALL									
H1: 2024 (41.4)	G	G	A	A	G	A	*	G	G
H2: 869 (17.8)	G	G	A	A	G	G	*	G	G
H3: 652 (13.3)	G	G	A	T	G	G	*	A	G
H4: 420 (8.6)	G	A	G	T	G	G	*	A	G
H5: 386 (7.9)	G	G	A	T	A	G	*	A	G
H6: 315 (6.4)	A	A	A	T	G	G	*	A	A

Table 4 continued

Haplotype: <i>n</i> (%)	SNP MAF (%) in all								
	rs3761738 (G/A, UTR) (6.5)	rs3761739 (G/A, UTR) (16.9)	rs4704209 (A/G, intron) (8.6)	rs10038095 (A/T, intron) (41.0)	rs2303152 (G/A, intron) (8.2)	rs3846662 (G/A, intron) (40.9)	rs17238540 (A/C, intron) (3.6)	rs3846663 (G/A, intron) (38.4)	rs5909 (G/A, UTR) (6.5)
H7: 128 (2.6)	G	G	A	T	G	G	*	G	G
H8: 86 (1.8)	G	A	A	T	G	G	*	A	G

Haplotypes were constructed in the above SNP order. Haplotype frequency (%) shows the percentage for each haplotype in each race/ethnic group. The distribution of haplotypes was significantly different among the ethnic groups (χ^2 test, $P < 0.0001$)

– Absent or very rare (<1% frequency) haplotype

*SNPs with minor allele frequency (MAF) <5% were not included in haplotype construction

References

- Lewington S, Whitlock G, Clarke R, Sherliker P, Emberson J, Halsey J, Qizilbash N, Peto R, Collins R (2007) Blood cholesterol and vascular mortality by age, sex, and blood pressure: a meta-analysis of individual data from 61 prospective studies with 55,000 vascular deaths. *Lancet* 370:1829–1839
- Johnson JL, Slentz CA, Duscha BD, Samsa GP, McCartney JS, Houmar JA, Kraus WE (2004) Gender and racial differences in lipoprotein subclass distributions: the STRRIDE study. *Atherosclerosis* 176:371–377
- Ford ES, Giles WH, Dietz WH (2002) Prevalence of the metabolic syndrome among US adults: findings from the third National Health and Nutrition Examination Survey. *JAMA* 287:356–359
- Freedman DS, Strogatz DS, Eaker E, Joesoef MR, DeStefano F (1990) Differences between black and white men in correlates of high density lipoprotein cholesterol. *Am J Epidemiol* 132:656–669
- Anand SS, Yusuf S, Vuksan V, Devanesen S, Teo KK, Montague PA, Kelemen L, Yi C, Lonn E, Gerstein H, Hegele RA, McQueen M (2000) Differences in risk factors, atherosclerosis, and cardiovascular disease between ethnic groups in Canada: the Study of Health Assessment and Risk in Ethnic groups (SHARE). *Lancet* 356:279–284
- Austin MA, King MC, Vranizan KM, Krauss RM (1990) Atherogenic lipoprotein phenotype a proposed genetic marker for coronary heart disease risk. *Circulation* 82:495–506
- Edwards KL, Mahaney MC, Motulsky AG, Austin MA (1999) Pleiotropic genetic effects on LDL size, plasma triglyceride, and HDL cholesterol in families. *Arterioscler Thromb Vasc Biol* 19:2456–2464
- Rainwater DL, Martin LJ, Comuzzie AG (2001) Genetic control of coordinated changes in HDL and LDL size phenotypes. *Arterioscler Thromb Vasc Biol* 21:1829–1833
- Barzilai N, Atzmon G, Schechter C, Schaefer EJ, Cupples AL, Lipton R, Cheng S, Shuldiner AR (2003) Unique lipoprotein phenotype and genotype associated with exceptional longevity. *JAMA* 290:2030–2040
- Bosse Y, Vohl MC, Despres JP, Lamarche B, Rice T, Rao DC, Bouchard C, Perusse L (2003) Heritability of LDL peak particle diameter in the Quebec Family Study. *Genet Epidemiol* 25:375–381
- Bosse Y, Chagnon YC, Despres JP, Rice T, Rao DC, Bouchard C, Perusse L, Vohl MC (2004) Genome-wide linkage scan reveals multiple susceptibility loci influencing lipid and lipoprotein levels in the Quebec Family Study. *J Lipid Res* 45:419–426
- Hsiao CF, Chiu YF, Chiang FT, Ho LT, Lee WJ, Hung YJ, Chen YD, Donlon TA, Jorgenson E, Curb D, Risch N, Hsiung CA (2006) Genome-wide linkage analysis of lipids in nondiabetic Chinese and Japanese from the SAPPPIRe family study. *Am J Hypertens* 19:1270–1277
- Duggirala R, Blangero J, Almasy L, Dyer TD, Williams KL, Leach RJ, O'Connell P, Stern MP (2000) A major susceptibility locus influencing plasma triglyceride concentrations is located on chromosome 15q in Mexican Americans. *Am J Hum Genet* 66:1237–1245
- Kullo IJ, Ding K, Boerwinkle E, Turner ST, de AM (2006) Quantitative trait loci influencing low density lipoprotein particle size in African Americans. *J Lipid Res* 47:1457–1462
- Yu Y, Wyszynski DF, Waterworth DM, Wilton SD, Barter PJ, Kesaniemi YA, Mahley RW, McPherson R, Waeber G, Bersot TP, Ma Q, Sharma SS, Montgomery DS, Middleton LT, Sundseth SS, Mooser V, Grundy SM, Farrer LA (2005) Multiple QTLs influencing triglyceride and HDL and total cholesterol levels identified in families with atherogenic dyslipidemia. *J Lipid Res* 46:2202–2213
- Vaughan CJ, Gotto AM Jr (2004) Update on statins: 2003. *Circulation* 110:886–892
- Lee E, Ryan S, Birmingham B, Zalikowski J, March R, Ambrose H, Moore R, Lee C, Chen Y, Schneck D (2005) Rosuvastatin pharmacokinetics and pharmacogenetics in white and Asian subjects residing in the same environment. *Clin Pharmacol Ther* 78:330–341
- Simon JA, Lin F, Hulley SB, Blanche PJ, Waters D, Shiboski S, Rotter JI, Nickerson DA, Yang H, Saad M, Krauss RM (2006) Phenotypic predictors of response to simvastatin therapy among African-Americans and Caucasians: the Cholesterol and Pharmacogenetics (CAP) Study. *Am J Cardiol* 97:843–850
- Chasman DI, Posada D, Subrahmanyam L, Cook NR, Stanton VP Jr, Ridker PM (2004) Pharmacogenetic study of statin therapy and cholesterol reduction. *JAMA* 291:2821–2827
- Krauss RM, Mangravite LM, Smith JD, Medina MW, Wang D, Guo X, Rieder MJ, Simon JA, Hulley SB, Waters D, Saad M, Williams PT, Taylor KD, Yang H, Nickerson DA, Rotter JI (2008) Variation in the 3-hydroxy-3-methylglutaryl coenzyme A reductase gene is associated with racial differences in low-density lipoprotein cholesterol response to simvastatin treatment. *Circulation* 117:1537–1544
- Medina MW, Gao F, Ruan W, Rotter JI, Krauss RM (2008) Alternative splicing of 3-hydroxy-3-methylglutaryl coenzyme A reductase is associated with plasma low-density lipoprotein cholesterol response to simvastatin. *Circulation* 118:355–362
- Burkhardt R, Kenny EE, Lowe JK, Birkeland A, Josowitz R, Noel M, Salit J, Maller JB, Pe'er I, Daly MJ, Altschuler D, Stoffel M, Friedman JM, Breslow JL (2008) Common SNPs in HMGCR in Micronesians and whites associated with LDL-cholesterol levels

- affect alternative splicing of exon13. *Arterioscler Thromb Vasc Biol* 28:2078–2084
23. Bild DE, Bluemke DA, Burke GL, Detrano R, ez Roux AV, Folsom AR, Greenland P, Jacob DR Jr, Kronmal R, Liu K, Nelson JC, O'Leary D, Saad MF, Shea S, Szklo M, Tracy RP (2002) Multi-ethnic study of atherosclerosis: objectives and design. *Am J Epidemiol* 156:871–881
 24. Mora S, Szklo M, Otvos JD, Greenland P, Psaty BM, Goff DC Jr, O'Leary DH, Saad MF, Tsai MY, Sharrett AR (2007) LDL particle subclasses, LDL particle size, and carotid atherosclerosis in the Multi-Ethnic Study of Atherosclerosis (MESA). *Atherosclerosis* 192:211–217
 25. Carlson CS, Eberle MA, Rieder MJ, Yi Q, Kruglyak L, Nickerson DA (2004) Selecting a maximally informative set of single-nucleotide polymorphisms for association analyses using linkage disequilibrium. *Am J Hum Genet* 74:106–120
 26. Barrett JC, Fry B, Maller J, Daly MJ (2005) Haploview: analysis and visualization of LD and haplotype maps. *Bioinformatics* 21:263–265
 27. Fan JB, Gunderson KL, Bibikova M, Yeakley JM, Chen J, Wickham GE, Lebruska LL, Laurent M, Shen R, Barker D (2006) Illumina universal bead arrays. *Methods Enzymol* 410:57–73
 28. Gunderson KL, Kruglyak S, Graige MS, Garcia F, Kermani BG, Zhao C, Che D, Dickinson T, Wickham E, Bierle J, Doucet D, Milewski M, Yang R, Siegmund C, Haas J, Zhou L, Oliphant A, Fan JB, Barnard S, Chee MS (2004) Decoding randomly ordered DNA arrays. *Genome Res* 14:870–877
 29. de Bakker P (2004) Tagger. <http://www.broad.mit.edu/mpg/tagger>
 30. Stephens M, Smith NJ, Donnelly P (2001) A new statistical method for haplotype reconstruction from population data. *Am J Hum Genet* 68:978–989
 31. Crawford DC, Nickerson DA (2005) Definition and clinical importance of haplotypes. *Annu Rev Med* 56:303–320
 32. Benton JL, Ding J, Tsai MY, Shea S, Rotter JJ, Burke GL, Post W (2007) Associations between two common polymorphisms in the ABCA1 gene and subclinical atherosclerosis: Multi-Ethnic Study of Atherosclerosis (MESA). *Atherosclerosis* 193:352–360
 33. Tong Y, Zhang S, Li H, Su Z, Kong X, Liu H, Xiao C, Sun Y, Shi JJ (2004) 8302A/C and (TTA)_n polymorphisms in the HMG-CoA reductase gene may be associated with some plasma lipid metabolic phenotypes in patients with coronary heart disease. *Lipids* 39:239–241
 34. Kathiresan S, Melander O, Guiducci C, Surti A, Burtt NP, Rieder MJ, Cooper GM, Roos C, Voight BF, Havulinna AS, Wahlstrand B, Hedner T, Corella D, Tai ES, Ordovas JM, Berglund G, Vartiainen E, Jousilahti P, Hedblad B, Taskinen MR, Newton-Cheh C, Salomaa V, Peltonen L, Groop L, Altshuler DM, Orho-Melander M (2008) Six new loci associated with blood low-density lipoprotein cholesterol, high-density lipoprotein cholesterol or triglycerides in humans. *Nat Genet* 40:189–197
 35. Willer CJ, Sanna S, Jackson AU, Scuteri A, Bonnycastle LL, Clarke R, Heath SC, Timpson NJ, Najjar SS, Stringham HM, Strait J, Duren WL, Maschio A, Busonero F, Mulas A, Albai G, Swift AJ, Morken MA, Narisu N, Bennett D, Parish S, Shen H, Galan P, Meneton P, Hercberg S, Zelenika D, Chen WM, Li Y, Scott LJ, Scheet PA, Sundvall J, Watanabe RM, Nagaraja R, Ebrahim S, Lawlor DA, Ben-Shlomo Y, vey-Smith G, Shuldiner AR, Collins R, Bergman RN, Uda M, Tuomilehto J, Cao A, Collins FS, Lakatta E, Lathrop GM, Boehnke M, Schlessinger D, Mohlke KL, Abecasis GR (2008) Newly identified loci that influence lipid concentrations and risk of coronary artery disease. *Nat Genet* 40:161–169
 36. Packard CJ, Shepherd J (1997) Lipoprotein heterogeneity and apolipoprotein B metabolism. *Arterioscler Thromb Vasc Biol* 17:3542–3556

Metabolites from an Endophytic Fungus *Sphaceloma* sp. LN-15 Isolated from the Leaves of *Melia azedarach*

An-Ling Zhang · Li-Ying He · Jin-Ming Gao ·
Xu Xu · Shi-Qing Li · Ming-Sheng Bai ·
Jian-Chun Qin

Received: 3 March 2009 / Accepted: 4 May 2009 / Published online: 20 June 2009
© AOCs 2009

Abstract Two new natural compounds, a symmetrical disulfide dimer didodecyl 3,3''-dithiodipropionate (**1**) and a pregnane steroid 5,16-pregnadien-3 β -ol-20-one acetate (**2**), were isolated together with two known compounds, ergosta-4,6,8(14),22-tetraen-3-one (**3**) and ergosterol peroxide (**4**), from the ethyl acetate soluble extract of fermentation broth of an endophytic fungus, *Sphaceloma* sp. LN-15 isolated from the leaves of *Melia azedarach* L. and grown in pure culture. Their structures were determined on the basis of spectroscopic methods including 1D and 2D nuclear magnetic resonance spectroscopy (NMR) experiments and by mass spectrometric measurements (MS). These fungal metabolites were isolated for the first time from the genus *Sphaceloma*. The structure of **1** was also confirmed by chemical synthesis.

Keywords *Melia azedarach* L. · Endophytic fungus · *Sphaceloma* sp. · Disulfide dimer · Didodecyl 3,3''-dithiodipropionate · 5,16-Pregnadien-3 β -ol-20-one acetate · Fungal metabolites

Abbreviations

CC	Column chromatography
COSY	Correlation spectroscopy
DCC	<i>N,N'</i> -Dicyclohexylcarbodiimide
DEPT	Distortionless enhancement by polarization transfer
DMAP	<i>N,N</i> -Dimethylpyridin-4-amine
EI-MS	Electron impact-mass spectrometry
EC ₅₀	Effective concentration for 50% growth inhibition
ESI-MS	Electrospray ionization-mass spectrometry
FAB-MS	Fast atom bombardment-mass spectrometry
HMBC	Heteronuclear multiple bond correlation
HMQC	Heteronuclear multiple quantum correlation
HR	High resolution
MS	Mass spectrometric measurements
NMR	Nuclear magnetic resonance spectroscopy
PDA	Potato dextrose agar
TLC	Thin layer chromatography

Introduction

Endophytes are microorganisms that live in the intercellular spaces of the tissues of host plants without causing any discernible manifestation of disease [1, 2]. All higher plants seem to be hosts to one or more endophytic microbes. Of all the world's plants, however, only a few grass species were thoroughly studied for their endophytes [2]. As a result, the opportunity to find new and interesting endophytes among a variety of plants is enormous. Recent comprehensive studies have indicated that 51% of the biologically active substances isolated from endophytic fungi were previously unknown [3]. Most of these compounds have shown various interesting bioactivities such as

A.-L. Zhang · J.-M. Gao (✉) · X. Xu · M.-S. Bai · J.-C. Qin
Research Centre for Natural Medicinal Chemistry,
College of Science, Northwest A&F University,
712100 Yangling, Shaanxi, China
e-mail: jinminggao@nwsuaf.edu.cn

L.-Y. He
College of Life Sciences, Northwest A&F University,
712100 Yangling, Shaanxi, China

S.-Q. Li
State Key Laboratory of Soil Erosion and Dryland Farming
on the Loess Plateau, Institute of Soil and Water Conservation,
Chinese Academy of Science, 712100 Yangling, Shaanxi, China

cytotoxic and antitumor, antimicrobial, phytotoxic and antileishmanial (active against *Leishmania aethiopica*, a parasitic trypanosome protozoa that is the causative agent of leishmaniasis) activities [3–5]. Hence, compared with only 38% of novel substances from soil microflora, endophytes have recently been recognized as prolific sources of structurally novel and biologically active secondary metabolites to be chemically explored [3–5].

Melia azedarach Linn (Meliaceae), also known as Chinaberry or Persian lilac tree, is a deciduous tree that is native to northwestern India and has long been recognized for its insecticidal properties [6]. This plant produces a class of low molecular weight metabolites, modified oxygenated triterpenoids, known as limonoids [7, 8]. However, little is known about secondary metabolites of endophytes harbored inside the healthy tissues of *M. azedarach* [9–12].

In the course of our ongoing study of biologically active metabolites from plant endophytes [13–15], we investigated the chemical constituents produced by an endophytic fungus *Sphaceloma* sp. found inside *M. azedarach* and isolated four compounds, including two new natural products, a fatty alcoholic disulfide dimer didodecyl 3,3''-dithiodipropionate (**1**) and a pregnane steroid 5,16-pregnadien-3 β -ol-20-one acetate (**2**), together with two known ergosterol derivatives ergosta-4,6,8(14),22-tetraen-3-one (**3**) and 5 α ,8 α -epidioxy-(22*E*,24*R*)-ergosta-6,22-dien-3 β -ol (**4**). In this paper, we describe the isolation and structural characterization of these two new natural products.

Materials and Methods

General Experimental Procedure

Melting points were obtained on an XRC-1 apparatus and uncorrected. Optical rotations were measured on a Perkin Elmer Model 341 polarimeter. NMR spectra were recorded on a Bruker DRX-500 instrument with TMS as an internal standard. Mass spectra were recorded on a VG Auto Spec-3000 spectrometer (Micromass, UK) and Thermo Finnigan LCQ Advantage. IR spectra were obtained in KBr pellets with a Bio-Rad FTS-135 infrared spectrophotometer. Column chromatography (CC) was performed over silica gel (200–300 mesh, Qingdao Marine Chemical Ltd., Qingdao, China) and Sephadex LH-20 (Pharmacia, Uppsala, Sweden). Silica gel 60 F₂₅₄ TLC plates (Qingdao Marine Chemical Ltd., Qingdao, China) and RP-18 F₂₅₄ TLC plates (Merck, Darmstadt, Germany) were used for analysis. Fractions were monitored by thin layer chromatography (TLC), and spots were visualized by spraying with 10% H₂SO₄ in ethanol, followed by heating. All other chemicals used in this study were of analytical grade.

Fungal Material

The endophytic fungal strain was isolated from the fresh leaves of the tree *M. azedarach* L. growing in the campus of Northwest A&F University, Yangling, Shaanxi province, China. The isolate was identified as *Sphaceloma* sp. LN-15 by morphological analysis and was deposited at the Research Centre for Natural Medicinal Chemistry, Northwest A&F University.

Cultivation

The fungal strain was cultured on the slants of potato dextrose agar (PDA) at 28 °C for 6 days. Then three pieces (size 8 mm², each) of mycelium were transferred to PDA liquid media. A suspension (1 ml) of the strain was inoculated aseptically to 500-ml Erlenmeyer flasks each containing 180 ml of PDA culture medium comprising potato (20%) and glucose (2%). The flask cultures were incubated at 28 °C for 7 days on a rotary shaker at 120 rpm.

Extraction and Isolation

The strain cultures (20 l) were filtered to collect mycelia. The filtrate was concentrated in vacuo at 45 °C, and then successively extracted four times with an equal volume of AcOEt to give a crude extract. The extract was fractionated by silica gel CC using petroleum ether–acetone gradient elution to provide seven fractions (Fr.1–Fr.7). Fr.3 (1.12 g) was subsequently fractionated by Silica gel CC using petroleum ether–AcOEt gradient elution to obtain Fr.3.1–3. Fr.3.2 was subsequently purified by Sephadex LH-20 column chromatography using acetone as solvents to yield compound **3** (10 mg). Fr.4 was chromatographed by RP-18 silica gel (40–75 μ m, 72 g) column using MeOH–H₂O (60:40–100:0) gradient elution to provide fr.4.1–4. Fr.4.3 eluted with MeOH–H₂O (90:10) was purified by Sephadex LH-20 using acetone to give compound **4** (8 mg). Fr.4.4 eluted with MeOH–H₂O (100:0) was subjected to CC over Silica gel using petroleum ether–AcOEt (95:5 and 85:15) to give Fr.4.4.1 and Fr.4.4.2; Fr.4.4.2 was separated by Sephadex LH-20 CC using MeOH, followed by Silica gel CC using petroleum ether–acetone (95:5 and 90:10) to afford compound **1** (4 mg). Fr.4.1 was separated by Sephadex LH-20 CC using MeOH, followed by Silica gel CC using petroleum ether–acetone (95:5, 90:10), and petroleum ether–AcOEt (87:13) to give compound **2** (6 mg).

Didodecyl 3,3''-dithiodipropionate (**1**)

White needles (acetone), m.p. 39–40 °C; IR (KBr) ν : 2,955, 2,920, 2,850, 1,741, 1,463, 1,376, 1,264, 1,188,

1,125, 1,099, 803, 728, 568, 479 cm^{-1} ; ^{13}C -NMR (125 MHz, CDCl_3): $\delta = 170.4$ (s, C-1), 28.5 (t, C-2), 48.8 (t, C-3), 65.8 (t, C-1'), 27.0 (t, C-2'), 25.8 (t, C-3'), 29.4 (t, C-4'), 29.7 (t, C-5'), 29.6 (t, C-6'), 29.5 (t, C-7'), 29.6 (t, C-8'), 29.2 (t, C-9'), 31.9 (t, C-10'), 22.7 (t, C-11'), 14.1 (q, C-12'); ^1H -NMR (500 MHz, CDCl_3): $\delta = 4.13$ (2H, t, $J = 6.8$ Hz, H-1'), 3.35 (2H, t, $J = 7.5$ Hz, H-3), 2.89 (2H, t, $J = 7.5$ Hz, H-2), 1.58–1.66 (6H, m, H-3'–H-9'), 1.27–1.42 (14H, m, H-10' and 11'), 0.89 (3H, t, $J = 8.2$ Hz, H-12'); ESI-MS (positive mode): $m/z = 569$ [$\text{M} + \text{Na}$] $^+$ (2.5), 570 [$\text{M} + \text{Na} + \text{H}$] $^+$ (1.0), 585 [$\text{M} + \text{K}$] $^+$ (1.0); FAB-MS (positive mode): $m/z = 547$ [$\text{M} + \text{H}$] $^+$ (100), 361 [$\text{M}-\text{C}_{12}\text{H}_{25}\text{O}$] $^+$ (6.0), 169 [$\text{M}-\text{C}_{18}\text{H}_{33}\text{O}_4\text{S}_2$] $^+$ (1.5), 211 [$\text{M}-\text{C}_{17}\text{H}_{33}\text{O}_2\text{S}_2-2\text{H}$] $^+$ (6.0); EI-MS (70 eV): m/z (relative intensities) = 361 [$\text{M}-\text{C}_{12}\text{H}_{25}\text{O}$] $^+$ (1.5), 241 [$\text{M}-\text{C}_{15}\text{H}_{29}\text{O}_2\text{S}_2$] $^+$ (8.0), 213 [$\text{M}-\text{C}_{17}\text{H}_{33}\text{O}_2\text{S}_2$] $^+$ (4.5), 211 [$\text{M}-\text{C}_{17}\text{H}_{33}\text{O}_2\text{S}_2-2\text{H}$] $^+$ (36.0), 193 [$\text{C}_6\text{H}_9\text{O}_3\text{S}_2$] $^+$ (100), 169 [$\text{M}-\text{C}_{18}\text{H}_{33}\text{O}_4\text{S}_2$] $^+$ (4.5), 121(65); high resolution ESI-MS (positive mode): $m/z = 569.3681$ (calc. 569.3674 for $\text{C}_{30}\text{H}_{58}\text{O}_4\text{S}_2\text{Na}$); HR-EI-MS (70 eV): m/z 193.0024 (calc. 193.0032 for $\text{C}_6\text{H}_9\text{O}_3\text{S}_2$).

5,16-Pregnadien-3 β -ol-20-one acetate
(=16-dehydropregnenolone acetate, **2**)

White needles (acetone), m.p. 169–174 °C (170–173 °C) (Ying et al. [18]); $[\alpha]_{\text{D}}^{20} = -118^\circ$ ($c = 0.5$, CHCl_3). IR (KBr) ν : 2,942, 2,905, 2,865, 1,728 (C = O), 1,659 (C = O), 1,583 (C = C = O), 1,439, 1,367, 1,234, 1,035, 976, 654 cm^{-1} . ^1H -NMR (500 MHz, CDCl_3): $\delta = 6.72$ (1H, dd, $J = 2.3, 3.90$ Hz, H-16), 5.40 (1H, brd, H-6), 4.57–4.64 (1H, m, H-3 α), 2.34–2.29 (2H, m, H-4), 2.28 (3H, s, H-21), 2.05 (3H, s, $-\text{OCOCH}_3$), 1.89–1.86 (2H, m, H-15), 1.69–1.60 (2H, m, H-7), 1.59–1.26 (4H, m, H-1 and H-2), 1.06 (3H, s, H-19), 0.92 (3H, s, H-18). ^{13}C -NMR (125 MHz, CDCl_3): $\delta = 36.7$ (t, C-1), 27.7 (t, C-2), 73.8 (d, C-3), 38.1 (t, C-4), 140.2 (s, C-5), 122.0 (d, C-6), 31.5 (t, C-7), 30.1 (d, C-8), 56.3 (d, C-9), 36.8 (s, C-10), 20.6 (t, C-11), 34.5 (t, C-12), 46.0 (s, C-13), 50.3 (d, C-14), 32.2 (t, C-15), 144.4 (d, C-16), 155.3 (s, C-17), 15.7 (q, C-18), 19.2 (q, C-19), 197.0 (s, C-20), 27.1 (q, C-21), 170.5 (s, $-\text{OCOCH}_3$), 21.4 (q, $-\text{OCOCH}_3$). ESI-MS (positive mode) m/z : 357 [$\text{M} + \text{H}$] $^+$ (2.5), 379 [$\text{M} + \text{Na}$] $^+$ (5.5), 395 [$\text{M} + \text{K}$] $^+$ (1.5); HR-ESI-MS (positive mode): $m/z = 357.2432$ (calc. 357.2430 for $\text{C}_{23}\text{H}_{33}\text{O}_3$).

Ergosta-4,6,8(14),22-tetraen-3-one (**3**)

Yellow crystals, m.p. 112–114 °C; IR (KBr) ν : 2,982, 1,675 (C = O), 1,590 (C = C), 1,270, 1,223, 965 cm^{-1} ; EI-MS (70 eV) m/z (relative intensities): 392 (M^+ , 19.5), 377 (1.5) 349 (1.5), 268 (42), 253 (6), 240 (3.5), 214 (7.5),

173 (7), 129 (6). ^1H and ^{13}C NMR: identical with those of an authentic specimen.

5 $\alpha,8\alpha$ -Epidioxy-(22E,24R)-ergosta-6,22-dien-3 β -ol (**4**)

Colorless crystals, m.p. 182–184 °C (*n*-hexane); $[\alpha]_{\text{D}}^{23} = -34^\circ$ ($c = 0.6$, CHCl_3); IR (KBr) ν : 3,525, 3,309, 2,957, 2,873, 1,653, 1,459, 1,377, 1,046, 1,029, 985, 970, 858 cm^{-1} ; EI-MS (70 eV) m/z (relative intensities): 428 (M^+ , 5), 410 (4), 396 (100), 363 (35), 271 (7), 251 (14), 152 (30), 107 (22), 81 (43), 69 (63). ^1H - and ^{13}C -NMR: identical with those of an authentic specimen.

Synthesis of Compound **1**

Method A. DCC (412.7 mg, 2 mmol) and DMAP (24.4 mg, 0.2 mmol) were added to a stirred solution of 3,3'-dithiodipropionic acid (210.3 mg, 1 mmol) and dodecanol (410 mg, 2.2 mmol) in dichloromethane (10 ml) at room temperature. The reaction was monitored by TLC. After about 6 h, the reaction mixture was then quenched by addition of several drops of acetic acid. After filtration, the mixture was washed with saturated aqueous sodium hydrogen carbonate, saturated NaCl solution and dried (MgSO_4) and the solvents evaporated. CC (SiO_2 , petroleum ether/acetone, 97:3) gave the crude product, which was crystallized from acetone–methanol to afford **1** (398.6 mg, 73%) as white plate-like crystals.

Method B. A catalytic amount of con. H_2SO_4 was added to a mixture of 3,3'-di-thiodipropionic acid (210.3 mg, 1.0 mmol) and dodecanol (2,490 mg, 13.36 mmol) at 60 °C under stirring. The reaction mixture was then heated to 120 °C under stirring. The reaction was monitored by TLC. After 5 h, the reaction mixture was then cooled to room temperature, and dichloromethane (5 ml) was added. The organic layer was washed with saturated aqueous sodium carbonate, saturated aqueous NaCl solution and dried (MgSO_4) and concentrated at reduced pressure. CC (SiO_2 , petroleum ether/acetone, 100:2) gave **1** (382 mg, 70%) as white plate-like crystals. Its NMR spectroscopic data were identical with those reported for the natural product (see “[Extraction and Isolation](#)”).

Antimicrobial Assays

In vitro antifungal activity was tested against the pathogenic fungi, *Alternaria solani*, *Fusarium oxysporium*, *Sclerotinia sclerotiorum*, *Exserohilum turcicum* and *Colletotrichum loeosporioides*, by the mycelial growth inhibitory rate method. These fungi were grown on PDA medium in Petri plates. All samples were dissolved in methanol.

The tested fungi (4 mm diameter) were inoculated at the centre of agar medium discs incorporating test samples. Three replicate plates for each fungus were incubated at 26 (± 2) °C for all test fungi. Control plates containing medium mixed with methanol (1 ml) were included. After incubation for 72–96 h, the mycelial growth of fungi (mm) in both treated (*T*) and control (*C*) Petri dishes were measured in three different directions (decussation method) until the fungal growth in the control dishes was almost complete. The growth inhibition rate (*I*) was calculated using the following formula $I (\%) = [(C - T)/C - 4] \times 100$.

Results and Discussion

The fungal strain was cultivated on PDA plates for 6 days at 28 °C. The extract of the culture was partitioned between AcOEt and water. The AcOEt extract was subjected to silica gel, RP-18 gel, and Sephadex LH-20 column chromatographic purification steps to yield four products **1–4** (Fig. 1), including a new fatty alcohol disulfur dimer **1** and a new pregnane steroid **2**.

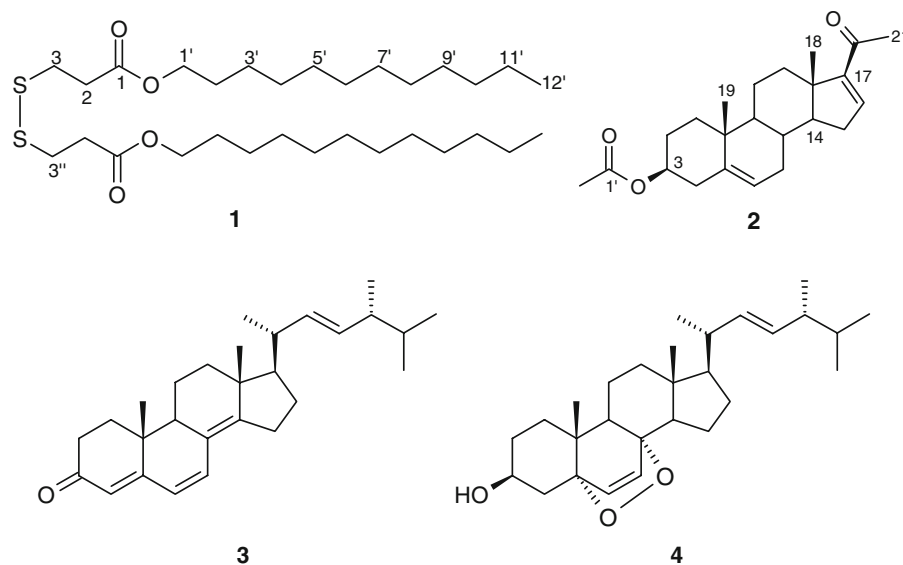
In order to determine if any of the four isolated compounds in this study were derived from the medium as control, the AcOEt extract of the sterile medium treated equally but without inoculation of the microorganism was examined by LC-MS. This showed that all the isolates were produced by the endophytic fungus.

Compound **1** was obtained as a white needle-shaped crystal from acetone (m.p. 39–40 °C). It showed quasi-molecular ion peaks at m/z 569 $[M + Na]^+$, 570 $[M + Na + H]^+$, and 585 $[M + K]^+$, as well as at m/z 547 $[M + H]^+$ in the positive ESI-MS and in the positive

FAB-MS spectra, respectively, suggesting its relative molecular weight of 546. Its molecular formula was determined to be $C_{30}H_{58}O_4S_2$ by the positive high resolution ESI-MS (calc. for $[M + Na]^+$: 569.3674; found: 569.3681) and NMR data, indicating 2° of unsaturation. The IR spectrum of compound **1** suggested the presence of alkane ($2,920\text{ cm}^{-1}$, C–H stretch), ester carbonyl ($1,741\text{ cm}^{-1}$), methylene ($1,463\text{ cm}^{-1}$, $-\text{CH}_2$ bend), methyl ($1,376\text{ cm}^{-1}$, $-\text{CH}_3$ bend), ester ($1,264$, $1,188$, $1,125$, $1,099\text{ cm}^{-1}$, C–O), and di-sulfur (568 , 479 cm^{-1} , S–S) groups. The ^{13}C NMR (DEPT) and HMQC spectra further established the presence of 15 carbon signals, which were recognized as one methyl group [δ_{C} 14.1(*q*)], 13 methylenes [δ_{C} 22.7–65.8 (*t*)] including one oxygen-linked methylene [δ_{C} 65.8 (*t*)], one sulfur-linked methylene [δ_{C} 48.8(*t*)], and a carbonyl carbon [δ_{C} 170.4]. The ^1H NMR spectrum of **1** also supported the presence of one methyl [δ_{H} 0.89, (3H, t, $J = 8.2$ Hz)], 13 methylenes including three signals [δ_{H} 4.13 (2H, t, $J = 6.8$ Hz), 3.35 (2H, t, $J = 7.5$ Hz), 2.89 (2H, t, $J = 7.5$ Hz)] and ten ones [δ_{H} 1.58–1.66 (overlap) and 1.27–1.42 (overlap)]. These data indicate that this compound belongs to long chain fatty alcohol esters.

All these signals formed the partial structure moiety $-\text{S}(\text{CH}_2)_2\text{COO}(\text{CH}_2)_{11}\text{CH}_3-$. Taking the molecular formula and molecular weight into account, therefore, compound **1** should be a complete symmetric structure linked by a disulfur bond, which could match the molecular formula and mass of this molecule. Moreover, the proposed structure gained further reinforcement from its EI mass spectrum, which displayed prominent ion peaks at m/z 379, 361, 211, 193 (base peak), and 169, as shown in Fig. 2. Among them, this ion peak at m/z 193, consistent with the molecular composition of $C_6H_9O_3S_2$ (calc. for $[M + H]^+$:

Fig. 1 Chemical structures of four compounds isolated from *Sphaceloma* sp. Didodecyl 3,3''-dithiodipropionate (**1**). 5,16-Pregnadien-3 β -ol-20-one acetate (**2**). Ergosta-4,6,8(14),22-tetraen-3-one (**3**). Ergosterol peroxide (**4**)



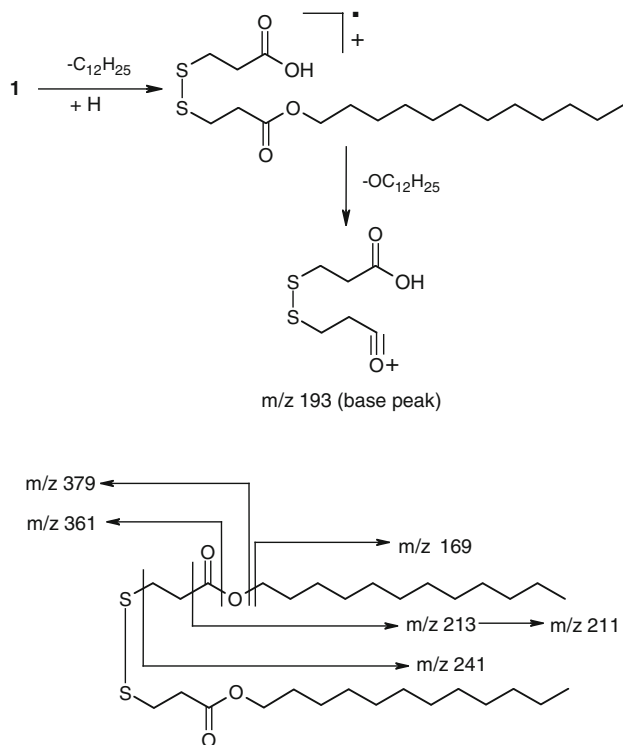


Fig. 2 Proposed EI-MS fragmentation pathways of didodecyl 3,3''-dithiodipropionate (**1**). $[\text{HOOCCH}_2\text{CH}_2\text{SSCH}_2\text{CH}_2\text{CO}]^+$ at m/z 193 (base peak)

193.0032; found: 193.0024) was substantiated by high resolution EI-MS analysis. Further evidence to support the structure of **1** was obtained from ^1H - ^{13}C -long-range couplings observed in the HMBC and COSY spectra (Fig. 3). The HMBC and COSY spectra of compound **1** displayed the key correlations of H-3 (δ 3.35) with C-1 (δ 170.4) and C-2 (δ 27.0), and correlations of H-2 (δ 2.89) with C-1 (δ 170.4) and C-3 (δ 48.7); similarly, H-1' (δ 4.13) showed correlation to C-1 (δ 170.4), C-2' (δ 28.5) and C-3' (δ 29.6). Accordingly, the comprehensive analysis of MS, 1D and 2D NMR data led to the elucidation of compound **1** as didodecyl 3,3''-dithiodipropionate, which was synthesized [16] as sulfur-based antioxidant.

To the best of our knowledge, the structure of compound **1** has not previously been reported to occur naturally. Also, dithiopropionic acid, the “de-alcoholated” version of this natural product also has not been reported to occur naturally. Perhaps in *Sphaceloma* sp. dithiopropionic acid is biosynthesized by joining two cysteine molecules via an S-S bond, and both cysteines are also deaminated. Although it is reasonable to speculate that this fungus may also contain some of the mono-dodecyl form of the disulfide dimer, it was not detected in this study.

Compound **2** was obtained as an optically active white needle. Its molecular formula was deduced as $\text{C}_{23}\text{H}_{32}\text{O}_3$ by

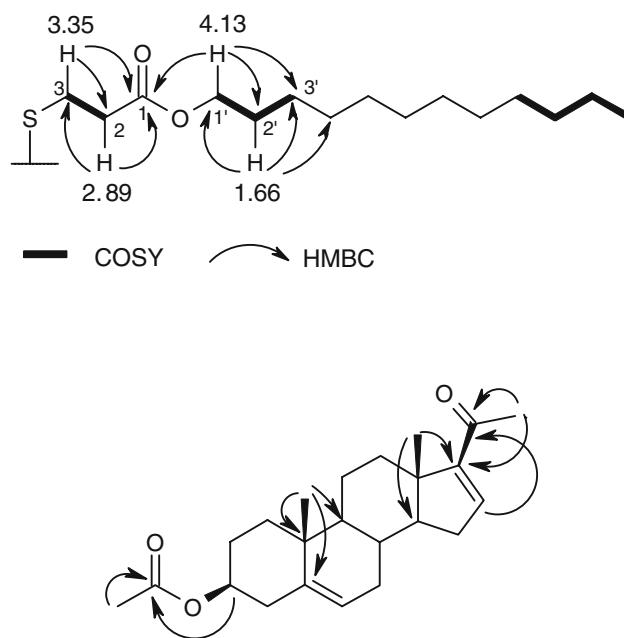


Fig. 3 Selected H-H COSY and HMBC correlations of didodecyl 3,3''-dithiodipropionate (**1**) and 5,16-pregnadien-3 β -ol-20-one acetate (**2**)

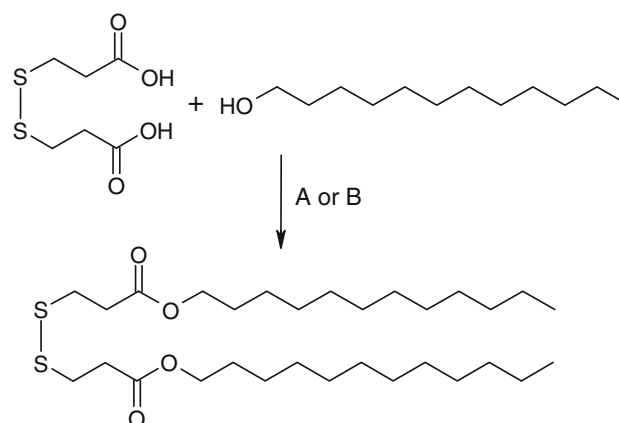
the positive HR-ESI-MS at m/z 357.2432 $[\text{M} + \text{H}]^+$ (calc. 357.2430) and NMR data possessing 8 degrees of unsaturation. Its IR spectrum suggested the presence of an ester carbonyl ($1,728\text{ cm}^{-1}$) and a conjugated carbonyl ($1,659\text{ cm}^{-1}$) group. The ^{13}C -NMR spectrum of compound **2** showed resonances for 23 carbon atoms, and the DEPT spectrum indicated the presence of four methyl groups containing two tertiary ones, seven methylenes, six methines and six quaternary carbon atoms including two carbonyls [δ = 197.0 (C-20) and 170.5 (C-1')]. The ^1H - and ^{13}C -NMR spectra showed signals for two trisubstituted double bonds at δ = 6.72 (1H, dd, J = 2.3, 3.9 Hz, H-16), and 5.40 (1H, brd, H-6), and at δ = 140.2 (s, C-5) and 122.0 (d, C-6), and 144.4 (d, C-16) and 155.3 (s, C-17). The appearance of resonances for six sp^2 carbons including two carbonyl carbons in the ^{13}C -NMR spectrum indicated that 4 $^\circ$ of unsaturation were attributed to the presence of four double bonds and that the remaining degrees could be satisfied by the assignment of four rings in the molecule. In the ^1H -NMR spectrum, the multiplet at δ = 4.57–4.64 had a complexity normally seen for a 3 α -carbinol proton [17]. The ^1H -/ ^{13}C -NMR spectrum of **2** indicated resonances of two tertiary methyl groups [$\delta_{\text{H/C}}$ = 0.92 (3H, s)/15.7, 1.06 (3H, s)/19.2], which were assigned as 18- CH_3 and 19- CH_3 , respectively. These observations suggested that compound **2** has a steroidal skeleton. As a result of the HMBC correlations (Fig. 3) of H-3 and C-1' (δ 170.5), H-16 and C-20, and H₃-21 and C-17, one acetoxy and acetyl groups were clearly located at C-3 and C-17, respectively. In

addition, in comparison with NMR spectroscopic data of the synthetic known compound, 5,16-pregnadien-3 β -ol-20-one acetate, reported in the literature [18], compound **2** was thus assigned as 5,16-pregnadien-3 β -ol-20-one acetate, namely, 16-dehydropregnenolone acetate, belonging to a type of pregnane steroids. This compound, which is a well-known key intermediate in the synthesis of steroidal hormones in pharmaceutical industry, has been synthesized from a readily available natural product diosgenin via a sequence of fission of rings E and F in acetic anhydride–acetic acid and oxidative degradation [18].

In addition, two known compounds **3** and **4** were identified as ergosta-4,6,8(14),22-tetraen-3-one and 5 α ,8 α -epidioxy-(22*E*,24*R*)-ergosta-6,22-dien-3 β -ol, respectively, by comparison of their spectroscopic data with those in the literature [17]. They were isolated for the first time from this endophytic fungus, *Sphaceloma* sp.

The co-occurrence of two ergosterol-derived compounds **3** and **4**, typical and common metabolites of fungi, confirms that the pregnane steroid isolated from the culture broth is in fact of fungal origin. Biogenetically, the transformation of $\Delta^{5,7}$ -ergosterol compounds to the pregnane derivative **2** may be involved in the ergosterol side-chain cleavage, including sequential hydroxylation, and scission of the C-20–C-22 dihydroxylated bond in the presence of a family of oxidase enzymes like cytochrome P-450. This bioconversion is similar to that of cholesterol to pregnane steroids [19]. More recently, some new naturally occurring pregnane steroidal analogues, such as 3 β ,4 α -dihydroxy-5 α -pregnan-17(20)-(Z)-en-16-one and its *E*-isomer 3 β ,4 α -dihydroxy-5 α -pregnan-17(20)-(E)-en-16-one, were recorded in the genus *Melia* [20], but so far there is no evidence of this group of pregnane metabolites in *M. azedarach*. In the present study, the first discovery of compound **2** present in this endophytic fungus *Sphaceloma* sp. seems to further account for the established relationship between analogous secondary metabolites produced by the host and the endophytic fungus [3, 4]. Due to gene recombination during evolution, endophytic microorganisms have often developed biochemical abilities to produce compounds either similar or identical to those produced by their host plants [4]. On the other hand, it has been reported that the pregnane steroids are distributed not only in marine organisms such as corals, sponges, and gorgonians [19, 21–23], but also in terrestrial plants [24]; however, they are rare in fungi.

To verify the proposed structure of the disulfide compound **1** and to obtain further compounds for biological testing, we employed two synthetic methods to prepare compound **1**. The synthesis of the disulfide dimer **1** is based on the esterification reaction of a carboxylic acid with fatty alcohol. Dithiodicarboxylic acid was subjected to esterification reaction with dodecanol under the condition of H₂SO₄ or *N,N'*-dicyclohexylcarbodiimide (DCC) in the



Scheme 1 Reagents and conditions: method **a** DCC, DMAP, CH₂Cl₂, room temperature, 6 h (73%); method **b** H₂SO₄, 60–120 °C, 5 h (70%)

Table 1 Inhibitory effects of compounds **1–2** against some phytopathogenic fungi (EC₅₀ μ g ml⁻¹)

Compound	<i>E. t</i>	<i>C. l</i>	<i>S. s</i>	<i>A. s</i>	<i>F. o</i>
1	NA	210.5	NA	230.5	221.6
2	NA	200.8	NA	230.7	NA
Amphotericin B	NA	210.6	NA	NA	200.4

E. t *Exserohilum turcicum*, *C. l* *Colletotrichum loeosporioides*, *S. s* *Sclerotinia sclerotiorum*, *A. s* *Alternaria solani*, *F. o* *Fusarium oxysporium*, NA not active

presence of *N,N*-dimethylpyridin-4-amine (DMAP) in dichloromethane (Scheme 1) [25]. The residue was purified by silica gel CC to afford propanoate **1** in good yield. Its physicochemical, MS, and NMR data were in full agreement with those of the natural product.

The *in vitro* antifungal activities of the individual isolated metabolites **1–4** were examined using the reference agar dilution method using amphotericin B as a positive control. The inhibitory activities (the effective concentration for 50% growth inhibition, EC₅₀ values) were summarized in Table 1.

The results indicated that only compounds **1** and **2** displayed weak activities against several plant pathogenic fungi. Compound **1** showed growth inhibition against *Colletotrichum loeosporioides*, *Alternaria solani*, and *Fusarium oxysporium*. Compound **2** inhibited growth of *Colletotrichum loeosporioides* and *Alternaria solani*.

Two new natural fungal products **1–2** were isolated from an endophytic fungus, *Sphaceloma* sp. isolated from *M. azedarach* and their structures were confirmed by spectral data and chemical synthesis. To the best of our knowledge, this is the first report of these two metabolites from natural sources. Moreover, a naturally occurring symmetrical disulfide dimer lipid **1** containing a dithiodipropionic acid structure is rare in natural environment.

A limited number of symmetrical disulfide compounds have been previously isolated from marine sources [26, 27], a basidiomycete mushroom of the *Cortinarius* genus [28], and plants of the *Allium* genus [29, 30]. Interestingly, the isolation and structural elucidation of three co-metabolites, a pregnane derivative 5,16-pregnadien-3 β -ol-20-one acetate (**2**) and two ergosterol congeners appear to lend support for a shared steroidal nucleus produced via a biosynthetic pathway.

Acknowledgments We would like to acknowledge the National Natural Science Foundation of China (30670221 and 30770237), as well as the Program for Changjiang Scholars and Innovative Research Team in University (IRT0749) and from the Program for New Century Excellent Talents in University (NCET-05-0852).

References

1. Strobel GA, Long DM (1998) Endophytic microbes embody pharmaceutical potential. *ASM News* 64:263
2. Strobel GA (2002) Rainforest endophytes and bioactive products. *Crit Rev Biotechnol* 22:315–333
3. Strobel GA, Daisy B, Castillo U, Harper J (2004) Natural products from endophytic microorganisms. *J Nat Prod* 67:257–268
4. Tan RX, Zou WX (2001) Endophytes: a rich source of functional metabolites. *Nat Prod Rep* 18:448–459
5. Stierle A, Strobel G, Stierle D (1993) Taxol and taxane production by *Taxomyces andreanae*, an endophytic fungus of pacific yew. *Science* 260:214–216
6. Yang JA, Ma YH, Su YQ, Ye GS (2004) Review and prospect of research and development in Chinaberry Tree. *J Northwest For Univ* 19:115–118
7. Champagne DE, Koul O, Isman MB, Scudder GGE, Towers GHN (1992) Biological activity of limonoids from the rutales. *Phytochemistry* 31:377–394
8. Zhou H, Hamazaki A, Fontana JD, Takahashi H, Wandscheer CB, Fukuyama Y (2005) Cytotoxic limonoids from Brazilian *Melia azedarach*. *Chem Pharm Bull* 53:1362–1365
9. Wang Q, Fu Y-H, Gao J-M, Wang Y-Q, Li X-M, Zhang A-L (2007) Preliminary isolation and screen of endophytic fungi from *Melia azedarach* L. *Acta Agric Boreali Occidentalis Sin* 16:224–227
10. Pastre R, Marinho AMR, Rodrigues-Filho E, Souzam AQL, Pereira JO (2007) Diversity of polyketides produced by *Penicillium* species isolated from *Melia azedarach* and *Murraya paniculata*. *Quim Nova* 30:1867–1871
11. Campos FR, Barison A, Daolio C, Ferreira AG, Rodrigues-Filho E (2005) Complete ¹H and ¹³C NMR assignments of aurasperone A and fonsecinone A, two bis-naphthopyrones produced by *Aspergillus aculeatus*. *Magn Reson Chem* 43:962–965
12. Geris dos Santos RM, Rodrigues-Filho E (2003) Structures of meroterpenes produced by *Penicillium* sp., an endophytic fungus found associated with *Melia azedarach*. *J Braz Chem Soc* 14:722–727
13. Qin J-C, Zhang Y-M, Gao J-M, Bai M-S, Yang S-X, Laatsch H, Zhang A-L (2009) Bioactive metabolites produced by *Chaetomium globosum*, an endophytic fungus isolated from *Ginkgo biloba*. *Bioorg Med Chem Lett* 19:1572–1574
14. Qiao L-R, Yuan L, Gao J-M, Zhao P-J, Kang Q-J, Shen Y-M (2007) Tricycloalternarene derivatives produced by an endophyte *Alternaria alternata* isolated from *Maytenus hookeri*. *J Basic Microbiol* 47:340–343
15. Wei G-H, Yang X-Y, Zhang J-W, Gao J-M, Ma Y-Q, Fu Y-Y, Wang P (2007) Rhizobialide, a new stearylactone produced by rhizobial *Mesorhizobium* sp. CCNWX022, an endophyte from *Glycyrrhiza uralensis*. *Chem Biodivers* 4:893–898
16. Kohout JV (1967) Fats and their stabilization in feed mixtures by antioxidants. *Agrochimica (Bratislava)* 7:154–156
17. Gao JM, Hu L, Liu JK (2001) A novel sterol from Chinese truffles *Tuber indicum*. *Steroids* 66:771–775
18. Ying MH, Lin YL, Tan JJ, Jiang SH, Zhu DY (2003) Separation and structure elucidation of minute impurities in pregnadienolone acetate. *Chin J Pharm* 34:347–349
19. Dorta E, Díaz-Marrero AR, Cueto M, D’Croz L, Maté JL, San-Martín A, Darias J (2004) Unusual chlorinated pregnanes from the eastern Pacific octocoral *Carijoca multiflora*. *Tetrahedron Lett* 45:915–918
20. Da Silva MF, das GF, Agostinho SMM, de Paula JR, Neto JO, Castro-Gamboa I, Filho ER, Fernandes JB, Vieira PC (1999) Chemistry of *Toona ciliata* and *Cedrela odorata* graft (Meliaceae): chemosystematic and ecological significance. *Pure Appl Chem* 71:1083–1087
21. Ciavatta ML, Gresa MPL, Manzo E, Gavagnin M, Wahidulla S, Cimino G (2004) New C₂₁ Δ^{20} pregnanes, inhibitors of mitochondrial respiratory chain, from Indopacific octocoral *Carijoca* sp. *Tetrahedron Lett* 45:7745–7748
22. Blunt JW, Copp BR, Munro MHG, Northcote PT, Prinsep MR (2004) Marine natural products. *Nat Prod Rep* 21:1–49
23. Ortega MJ, Zubia E, Rodríguez S, Carballo JL, Salvá J (2002) Muricenones A and B: new degraded pregnanes from a gorgonian of the genus *Muricea*. *Eur J Org Chem* 19:3250–3253
24. Deepak D, Khare A, Khare MP (1989) Plant pregnanes. *Phytochemistry* 12:3255–3263
25. Felder D, Gutiérrez Nava M, del Pilar Carreon M, Eckert J-F, Luccisano M, Schall C, Masson P, Gallani J-L, Heinrich B, Guillon D, Nierengarten J-F (2002) Synthesis of amphiphilic fullerene derivatives and their incorporation in 1 Langmuir and Langmuir-blodgett films. *Helv Chim Acta* 85:288–319
26. Nogle LM, Gerwick WH (2002) Somocystinamide A, a novel cytotoxic disulfide dimer from a Fijian marine cyanobacterial mixed assemblage. *Org Lett* 4:1095–1098
27. Suyama TL, Gerwick WH (2008) Stereospecific total synthesis of somocystinamide A. *Org Lett* 10:4449–4452
28. Nicholas GM, Blunt JW, Munro MHG (2001) Cortamidine oxide, a novel disulfide metabolite from the New Zealand basidiomycete (mushroom) *Cortinarius* Species. *J Nat Prod* 64:341–344
29. Cavallito CJ, Bailey JH (1944) Allicin, the antibacterial principle of *Allium sativum*. I. isolation, physical properties and antibacterial action. *J Am Chem Soc* 66:1950–1951
30. Cavallito CJ, Bailey JH, Buck JS (1945) The antibacterial principle of *Allium sativum*. III. Its precursor and essential oil of garlic. *J Am Chem Soc* 67:1032–1033

Overexpression of a FAD3 Desaturase Increases Synthesis of a Polymethylene-Interrupted Dienoic Fatty Acid in Seeds of *Arabidopsis thaliana* L.

Debbie Puttick · Melanie Dauk · Sharla Lozinsky · Mark A. Smith

Received: 7 April 2009 / Accepted: 15 May 2009 / Published online: 23 June 2009
© Her Majesty the Queen in Right of Canada 2009

Abstract A cDNA encoding the *Arabidopsis* extraplastidic linoleate desaturase (FAD3) was overexpressed in the seeds of wild-type *Arabidopsis* and in a mutant line that accumulates high levels of oleic acid. In the transformed wild-type plants, linolenic acid (18:3 Δ 9,12,15) increased from 19% to nearly 40% of total seed fatty acids, with a corresponding decrease in linoleate content (18:2 Δ 9,12). In the high oleate mutant, a large increase in the level of a fatty acid identified by gas-chromatography/mass-spectrometry as mangiferic acid (18:2 Δ 9,15) was observed. The results demonstrate that the polymethylene-interrupted dienoic fatty acid, mangiferic acid, can be produced in seed oil through the overexpression of a fatty acid n-3 desaturase.

Keywords Linoleate desaturase · Mangiferic acid · Polymethylene-interrupted dienoic fatty acid · *Arabidopsis* · Seed oil

Abbreviations

FAMES Fatty acid methyl esters
PMIFA Polymethylene-interrupted fatty acid
PUFA Polyunsaturated fatty acid
VLCFA Very long chain fatty acid

Introduction

The predominant dienoic fatty acid of higher plants is linoleic acid (octadeca-9-*cis*,12-*cis*-dienoic acid, 18:2 Δ 9,12).¹ The methylene-interrupted (MI) *cis*-double-bond configuration of this fatty acid is characteristic of most plant polyunsaturated fatty acids. Polymethylene-interrupted fatty acids (PMIFA), where double bonds are separated by more than one methylene group, are uncommon but can be abundant within individual plant families. Seed oils of many conifer species, for example, are rich in Δ 5-polyunsaturated fatty acids and contain dienoic PMIFAs such as taxoleic acid (octadeca-5-*cis*,9-*cis*-dienoic acid, 18:2 Δ 5,9) and the very long chain fatty acid (VLCFA) eicosa-5-*cis*,11-*cis*-dienoic acid, 20:2 Δ 5,11. These species also produce a variety of polyunsaturated fatty acids containing double bonds in both MI and PMI configurations [1]. Fatty acids with Δ 5 unsaturation are also the major components of meadowfoam oil, obtained from the seeds of *Limnanthes alba* [2]. This oil contains an unusual VLC-PMIFA, docosa-5-*cis*,13-*cis*-dienoic acid (22:2 Δ 5,13), that accounts for up to 16% of total seed fatty acids [3, 4].

Biochemical studies have indicated that in *Limnanthes* species, 22:2 Δ 5,13 is synthesized by the action of a Δ 5 desaturase on the VLC-monounsaturated fatty acid erucic acid (22:1 Δ 13) [5]. The PMIFA therefore results from the activity of a desaturase that inserts a double bond at a

D. Puttick · M. Dauk · S. Lozinsky · M. A. Smith (✉)
Plant Biotechnology Institute, National Research Council
Canada, 110 Gymnasium Place, Saskatoon, SK S7N 0W9,
Canada
e-mail: mark.smith@nrc-cnrc.gc.ca

¹ Fatty acid nomenclature: X:Y Δ z, where X is chain length, Y is number of double bonds, and Δ z is double-bond position relative to the carboxyl end of the molecule. In fatty acids designated using n-x or ω x nomenclature, the position of the double bond is described relative to the methyl end of the molecule.

specific position in the fatty acid on the carboxyl side of an existing double bond. This activity is referred to as “front-end desaturation” and is distinct from the “methyl-end” desaturation catalyzed by the majority of plant desaturases [6]. It is likely that $\Delta 5$ desaturation of monounsaturated fatty acids in conifers also results in the formation of PMIFAs.

In addition to PMIFAs containing $\Delta 5$ unsaturation, a novel 18-carbon PMIFA, sometimes referred to as mangiferic acid, has been reported from the pulp of ripe mango fruit (*Mangifera indica* L.) grown in the Philippines [7], in the seed oil of *Arabidopsis* lines deficient in linoleate desaturase activities [8, 9], and in some high oleic lines of soybean [10]. In these reports, the fatty acid was suggested to be a result of low-level activity of an $\omega 3$ -desaturase, such as the plastidial or extraplastidial linoleate desaturases, acting on oleic acid (18:1 $\Delta 9$). The *ox* designation refers to a fatty acid desaturase that catalyzes double-bond formation at a specific position relative to the methyl end of a fatty acid [6]. Ectopic expression of a plant extraplastidial desaturase and an $\omega 3$ -desaturase from the nematode *Caenorhabditis elegans* in the yeast *Saccharomyces cerevisiae* confirmed the low-level activity of these enzymes on oleic acid and resulted in production of small amounts of 18:2 $\Delta 9,15$ [9, 11].

Polyunsaturated fatty acids (PUFAs) with double bonds that are not in methylene-interrupted positions are likely to have better oxidative stability and different physical properties compared to their MI isomers. Very little attention has been paid to these fatty acids as possible raw materials for industrial uses. To attempt to determine whether production of 18:2 $\Delta 9,15$ in a seed oil was possible by metabolic engineering, we overexpressed a gene encoding a linoleate desaturase in the seeds of *Arabidopsis*. Transformed plants accumulated this novel dienoid fatty acid in their seed oil to levels of up to 8% of total seed fatty acids.

Materials and Methods

Construction of the Plant Transformation Vector

A full-length cDNA encoding the *Arabidopsis* extraplastidial linoleate desaturase (Clone U11701, *FAD3*, At2g29980) was obtained from the Arabidopsis Biological Resource Center, DNA Stock Center (Ohio State University; www.arabidopsis.org). An expression cassette comprising the seed-specific *Lesquerella* hydroxylase promoter [12], the *FAD3* cDNA, and an *Arabidopsis* oleosin terminator (kindly provided by Prof. M. Moloney, SemBioSys, Calgary, Canada) was assembled in the binary vector pBar1 [13] to create the vector pDP5.

Arabidopsis Lines and Plant Transformation

Wild-type (Columbia ecotype) and *fad2/fae1* mutant *Arabidopsis* plants [14] were transformed with the binary vector pDP5 using the floral dip method [15]. For screening, T₁ seeds were sown onto moist potting soil, vernalized at 4°C for 72 h then transferred to a growth chamber at 23°C with constant light (fluorescent bulbs giving an intensity of 100 $\mu\text{E m}^{-2} \text{s}^{-1}$ at pot level), and allowed to grow until the first true leaves were clearly visible. Plants were sprayed three times at 2-day intervals with a solution containing 0.1 mL/L Silwet (Lehle Seeds, Round Rock, TX, USA) and 80 mg/L glufosinate ammonium (WipeOut herbicide, CIL Nu-Gro IP, Brantford, ON). Surviving plants were grown to maturity, and seeds (T₂ generation) were harvested from individual plants.

Gas Chromatography of Fatty Acid Methyl Esters

For determination of total seed fatty acid composition, three samples, each of approximately 100 seeds, collected from each individual *Arabidopsis* plant to be analyzed were placed in separate Pyrex screw-cap tubes with 2 mL 1 M HCl in methanol (Supelco) and 300 μL of hexane. The tubes were tightly capped and heated at 80°C for 2 h. After cooling, 2 mL of 0.9% NaCl was added, and fatty acid methyl esters (FAMES) were recovered by collecting the hexane phase. Gas chromatography of FAMES was conducted using an Agilent 6890N GC fitted with a DB-23 capillary column (0.25 mm \times 30 m, 0.25 μm thickness; J & W, Folsom, CA, USA) as described previously [16].

Identification of Fatty Acids by Mass Spectrometry

For identification of fatty acids by mass spectrometry, diethylamide derivatives were prepared, based on the method of [17]. Free fatty acids were generated from total seed lipids by grinding approximately 200 seeds in methanol and directly saponifying with 8.5% methanolic KOH. Fatty acids were dissolved in 400 μL of chloroform, 50 μL of pyridine was added, followed by the dropwise addition of 150 μL of acetyl chloride with continuous shaking. The mixture was diluted with 600 μL of chloroform, and 500 μL of diethylamine was added dropwise with continuous shaking. Excess reagent was removed by extracting twice with 1 mL of water, and the solvent phase was dried under a stream of nitrogen gas. The sample was dissolved in 200 μL of chloroform and 2 μL was directly injected (40:1 split ratio) onto a 30 m DB-23 capillary column in an Agilent 7890A GC equipped with a 5975C mass selective detector (ionizing energy of 70 eV). After an initial hold for 1 min at 160°C, the temperature was ramped at a rate of 4°C/min until reaching 240°C, and then held for 10 min.

Results

To demonstrate the activity of the FAD3 desaturase encoded by vector pDPP5, we transformed wild-type *Arabidopsis* plants with this vector. Transformed plants exhibited increased levels of linolenic acid (18:3 Δ 9,12,15) and reduced amounts of 18:2 Δ 9,12 in their seed oil (Fig. 1b), corresponding to the expected linoleate desaturase activity of the enzyme. Total C18-PUFA (18:2 + 18:3) levels, and the levels of other seed fatty acids were largely unchanged (Table 1). The vector was also used to transform a mutant line of *Arabidopsis* deficient in the activities of the extraplastidic oleate desaturase (FAD2) and seed-specific β -ketoacyl-CoA synthetase (FAE1) [14]. The seeds

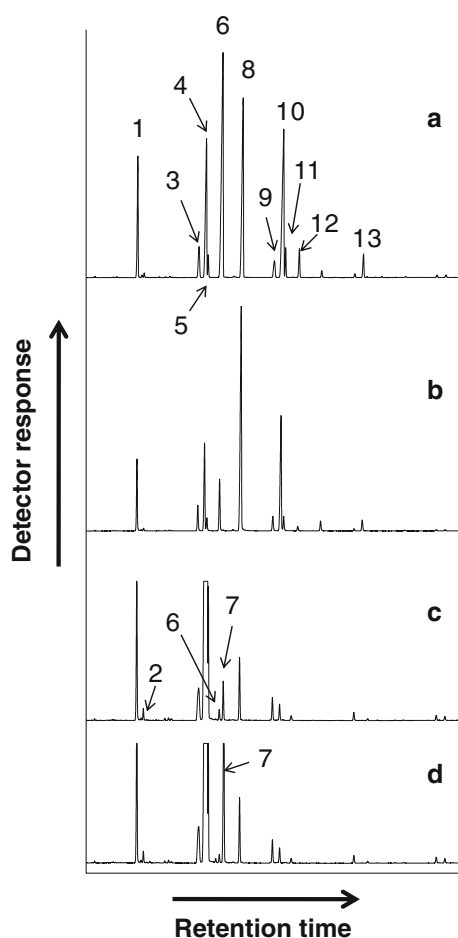


Fig. 1a–d Gas chromatogram traces of FAMES prepared from total seed lipids of *Arabidopsis*. **a** Wild-type. **b** Wild-type expressing the *Arabidopsis* FAD3 desaturase. **c** *Arabidopsis fad2/fae1* mutant. **d** *Arabidopsis fad2/fae1* mutant expressing the *Arabidopsis* FAD3 desaturase. Fatty acids: 1 palmitic acid (16:0); 2 palmitoleic acid (16:1 Δ 9); 3 stearic acid (18:0); 4 oleic acid (18:1 Δ 9); 5 *cis*-vaccenic acid (18:1 Δ 11); 6 linoleic acid (18:2 Δ 9,12); 7 mangiferic acid (18:2 Δ 9,15); 8 linolenic acid (18:3 Δ 9,12,15); 9 eicosanoic acid (20:0); 10 11-eicosenoic acid (20:1 Δ 11); 11 13-eicosenoic acid (20:1 Δ 13); 12 11,14-eicosadienoic acid (20:1 Δ 11, 14); 13 erucic acid (22:1 Δ 13)

of these plants contain over 82% oleic acid and less than 3% linolenic acid (Table 1, Fig. 1c). They also contain two 18-carbon dienoic fatty acids, linoleic acid (18:2 Δ 9,12) and mangiferic acid (18:2 Δ 9,15), at an average of 0.4 and 1.4%, respectively. Preliminary identification of 18:2 Δ 9,15 was based on the work of [9] who observed its presence in the seed lipids of a *fad2* mutant line of *Arabidopsis*. *Fad2/fae1* mutant lines expressing the FAD3 transgene showed increased levels of 18:2 Δ 9,15 and a reduction in 18:1 Δ 9. They also showed lower levels of 18:2 Δ 9,12 and an increase in 18:3 Δ 9,12,15 (Table 1, Fig. 1d). The highest level of PMIFA (18:2 Δ 9,15) observed in the transformed plants was 8.2% of total seed fatty acids. Total C18-PUFA (total 18:2 + 18:3) increased to 11.0% from an average of 4.1%, and a slight increase in total saturated fatty acid content was observed.

To confirm the identity of the putative PMIFA, GC/MS analysis was conducted using a diethylamide derivative of the fatty acid. The mass spectrum (Fig. 2) displayed a molecular ion at $m/z = 335$, suggesting a C18 dienoic fatty acid. Diagnostic ions differing by 12 amu at $m/z = 198$ and 210 and $m/z = 280$ and 292 locate the double bonds at the Δ 9 and Δ 15 (ω 9 and ω 3) positions, respectively. The 14-amu spacing of fragment ions at $m/z = 224$, 238, 252, and 266 demonstrates that there are no double bonds between the Δ 9 and Δ 15 positions. The abundant ion at $m/z = 115$ is suggested to be the McLafferty rearrangement ion, characteristic of fatty acid diethylamide derivatives [17]. An identical mass spectrum was obtained from the diethylamide derivative of the fatty acid identified as 18:2 Δ 9,15 in the seed oil of the untransformed *fad2/fae1* lines. Double-bond configuration (*cis/trans*) was not determined.

Discussion

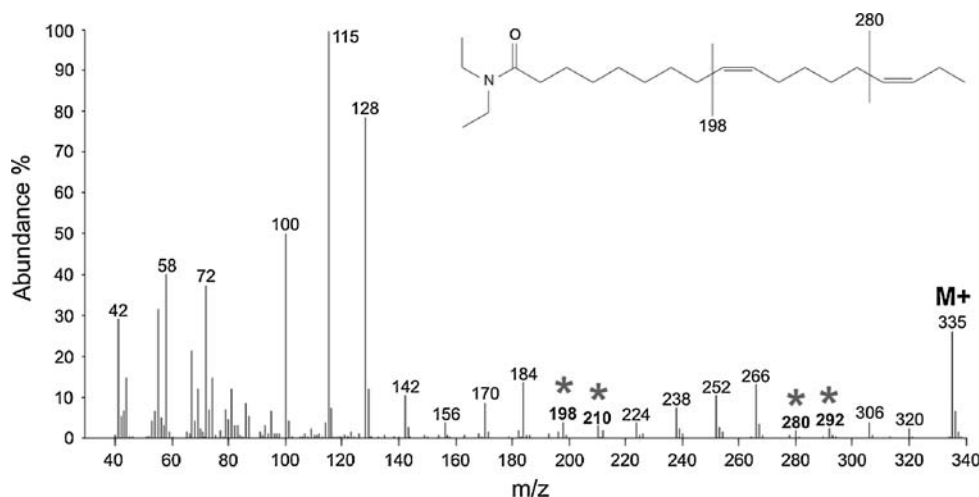
Previous studies have observed the presence of an unusual dienoic acid in the seed oil of *Arabidopsis* linoleate desaturase-deficient lines. The fatty acid was identified by GC/MS as 18:2 Δ 9,15 and was suggested to result from the ω 3 desaturation of oleic acid [8, 9]. In soybean, low levels of mangiferic acid observed in certain *fad2-1* (oleate desaturase) mutant lines were not seen when plants were crossed with a line containing a suppressed FAD3 gene [10]. We have shown that overexpression of the *Arabidopsis* FAD3 extraplastidic linoleate desaturase in lines containing high 18:1 content results in a substantial increase in the amount of 18:2 Δ 9,15 accumulating in the seed oil. Plant FAD3 desaturases are considered to have ω 3 (methyl-end) rather than Δ 15 (carboxyl-end) regioselectivity. Preferred substrates have ω 6 double bonds, but low-level activity is observed on ω 9 unsaturated fatty acids [9].

Table 1 Seed fatty acid composition of control *Arabidopsis* lines and lines transformed with a cDNA encoding the *Arabidopsis* FAD3 desaturase

Major fatty acid	<i>Arabidopsis</i> seed fatty acid composition (%)			
	WT	WT + <i>FAD3</i>	<i>fad2/fae1</i>	<i>fad2/fae1</i> + <i>FAD3</i>
16:0	7.6 ± <0.1	8.5 ± 0.2	5.6 ± <0.1	6.3 ± <0.1
16:1Δ9	0.3 ± <0.1	0.3 ± <0.1	0.3 ± <0.1	0.4 ± <0.1
18:0	3.2 ± <0.1	3.4 ± 0.1	2.6 ± 0.1	3.0 ± 0.1
18:1Δ9	13.2 ± 0.2	12.4 ± 0.2	82.8 ± 0.2	74.6 ± 0.3
18:1Δ11	1.3 ± 0.1	1.7 ± 0.1	3.0 ± 0.1	2.8 ± 0.2
18:2Δ9,12	27.5 ± >0.1	7.6 ± 0.4	0.4 ± <0.1	0.3 ± <0.1
18:2Δ9,15	ND	ND	1.3 ± <0.1	8.2 ± 0.1
18:3Δ9,12,15	19.4 ± 0.1	39.6 ± 0.1	2.4 ± 0.1	2.5 ± <0.1
20:0	2.0 ± <0.1	2.1 ± 0.2	0.9 ± <0.1	0.9 ± <0.1
20:1Δ11	19.2 ± 0.1	18.9 ± 0.5	0.6 ± <0.1	0.6 ± <0.1
20:1Δ13	1.8 ± 0.1	1.9 ± 0.1		
22:1	1.8 ± <0.1	1.6 ± 0.1		
Total saturate	12.8	14.0	9.1	10.3
Total C18 PUFA	46.8	47.1	4.1	11.0

Results given ± standard deviation

WT Wild-type, ND not detected

Fig. 2 Mass spectrum of diethylamide derivative of 18:2Δ9,15

Overexpression of *FAD3* in seeds that have high levels of oleic acid (ω 9 unsaturation) and low levels of linoleic acid (ω 9 + ω 6 unsaturation) leads to the accumulation of the PMIFA 18:2Δ9,15. A corresponding decrease in 18:1Δ9 content was observed suggesting that the PMIFA results from ω 3 desaturation of oleic acid. To demonstrate the activity of the *Arabidopsis* FAD3 desaturase used in this work, we used the same construct to overexpress *FAD3* in wild-type *Arabidopsis*. Transformed plants synthesized increased amounts of linolenic acid with a corresponding decrease in the substrate fatty acid linoleic acid. Overall levels of PUFAs in these plants were largely unchanged, indicating that the limiting activity in C18 PUFA biosynthesis is likely to be the formation of linoleic acid.

A seed oil rich in dienoic PMIFAs would have novel chemical properties compared to existing oils in which dienoic acids have a MI configuration. Such fatty acids may serve as valuable chemical feed stocks. Recent advances in the development of catalysts for olefin metathesis chemistry, for example, could allow the production of novel hydrocarbon monomers such as α -olefins, α - ω -dienes, and short- to medium-chain ω -unsaturated methyl esters [18]. Metathetical cleavage using ethene (ethenolysis) of fatty acids from meadowfoam oil has been considered as a process for the production of 5-hexenoic acid for polymer biosynthesis [19]. A second product from this oil was 1,9-decadiene resulting from cleavage of 22:2Δ5,13. Ethenolysis of mangiferic methyl ester would

yield methyl-9-decenoate, 1,7-octadiene, and 1-butene. All of these compounds have potential industrial uses. The C18 PMIFA reported in this work results from the activity of an ω 3 desaturase on a suboptimal substrate. PMIFA levels of over 8% of seed fatty acids were however achieved in *Arabidopsis*. Molecular engineering of an ω 3 desaturase to improve its ability to utilize oleic acid offers intriguing possibilities for the generation of new plant oils suitable for use as industrial feed stocks.

During the course of this work, we determined the fatty acid profile of the pulp from ripe mangoes (*Mangifera indica* L., cultivar unknown) purchased from a local supermarket. Palmitic acid (30%) was the major fatty acid, 18:2 Δ 9,12 (25%) and 18:3 Δ 9,12,15 (19%) were also abundant, but no mangiferic acid was detected. The fatty acid profile was different from that reported previously for ripe fruit obtained from the Philippines [7] in which 18:2 Δ 9,12 was only present at levels close to 1% of total pulp fatty acids. It is likely that the material we analyzed is not from the same variety of mango, however, the very low levels of ω 6 unsaturation observed in the previous study may indicate that those fruit differ in oleate desaturase activity, resulting in low levels of 18:2 Δ 9,12. Endogenous ω 3 desaturase activity with 18:1 Δ 9, rather than 18:2 Δ 9,12, as substrate may account for the mangiferic acid previously observed in the fruit pulp.

Acknowledgments The authors would like to thank Dr. Alison Ferrie and Dr. Patrick Covello for critical review of the manuscript and Dr. Sue Abrams for advice on mass spectroscopy. NRC-PBI publication number 50144.

References

1. Wolff RL, Deluc LG, Marpeau AM (1996) Conifer seeds: oil content and fatty acid composition. *J Am Oil Chem Soc* 73:765–771
2. Miller RW, Daxenbichler ME, Earle FR, Gentry HS (1964) Search for new industrial oils VIII. The genus *Limnanthes*. *J Am Oil Chem Soc* 41:167–169
3. Nikolova-Damyanova B, Christie WW, Herslof B (1990) The structure of the triacylglycerols of meadowfoam oil. *J Am Oil Chem Soc* 67:503–507
4. Knapp SJ, Crane JM (1995) Fatty acid diversity of section inflexae *Limnanthes* (meadowfoam). *Ind Crop Prod* 4:219–227
5. Pollard MR, Stumpf PK (1980) Biosynthesis of C20 and C22 fatty acids by developing seeds of *Limnanthes alba*; chain elongation and Δ 5 desaturation. *Plant Physiol* 66:649–655
6. Sperling P, Ternes P, Zank TK, Heinz E (2003) The evolution of desaturases. *Prostaglandins Leukot Essent Fatty Acids* 68:73–79
7. Shibahara A, Yamamoto K, Shinkai K, Nakayama T, Kajimoto G (1993) *Cis*-9, *cis*-15-octadecadienoic acid: a novel fatty acid found in higher plants. *Biochim Biophys Acta* 1170:245–252
8. Browse J, Kunst L, Anderson S, Hugly S, Somerville C (1988) A mutant of *Arabidopsis* deficient in the chloroplast 16:1/18:1 desaturase. *Plant Physiol* 90:522–529
9. Reed DW, Schafer UA, Covello PS (2000) Characterization of the *Brassica napus* extraplasmidial linoleate desaturase by expression in *Saccharomyces cerevisiae*. *Plant Physiol* 122:715–720
10. Kinney AJ (1996) Development of genetically engineered soybean oils for food applications. *J Food Lipids* 3:273–292
11. Meesapyodsuk D, Reed DW, Savile CK, Buist PH, Ambrose SJ, Covello PS (2000) Characterization of the regiochemistry and cryptoregiochemistry of a *Caenorhabditis elegans* fatty acid desaturase (*FAT-1*) expressed in *Saccharomyces cerevisiae*. *Biochemistry* 39:11948–11954
12. Broun P, Boddupalli S, Somerville C (1998) A bifunctional oleate 12-hydroxylase: desaturase from *Lesquerella fendleri*. *Plant J* 13:201–210
13. Holt BF, Boyes DC, Ellerstrom M, Seifers N, Wiig A, Kauffman S, Grant MR, Dangl JL (2002) An evolutionarily conserved mediator of plant disease resistance gene function is required for normal *Arabidopsis* development. *Dev Cell* 2:807–817
14. Smith MA, Moon H, Chowrira G, Kunst L (2003) Heterologous expression of a fatty acid hydroxylase gene in developing seeds of *Arabidopsis thaliana*. *Planta* 217:507–516
15. Clough SJ, Bent AF (1998) Floral dip: a simplified method for *Agrobacterium*-mediated transformation of *Arabidopsis thaliana*. *Plant J* 16:735–743
16. Kunst L, Taylor DC, Underhill EW (1992) Fatty acid elongation in developing seeds of *Arabidopsis thaliana*. *Plant Physiol Biochem* 30:425–434
17. Nilsson R, Liljenberg C (1991) The determination of double bond positions in polyunsaturated fatty acids—gas chromatography/mass spectrometry of the diethylamide derivative. *Phytochem Anal* 2:253–259
18. Mol JC (2002) Application of olefin metathesis in oleochemistry: an example of green chemistry. *Green Chem* 4:5–13
19. Warwel S, Bruse F, Demes C, Kunz M (2004) Polymers and polymer building blocks from meadowfoam oil. *Ind Crop Prod* 20:301–309

An Isomeric Mixture of Novel Cerebrosides Isolated from *Impatiens pritzellii* Reduces Lipopolysaccharide-Induced Release of IL-18 from Human Peripheral Blood Mononuclear Cells

Xuefeng Zhou · Lan Tang · Yonghong Liu

Received: 13 April 2009 / Accepted: 9 June 2009 / Published online: 17 July 2009
© AOCs 2009

Abstract An isomeric mixture of two cerebrosides, soya-cerebrosides I and II, was isolated from an ethno drug, the rhizomes of *Impatiens pritzellii* Hook. f. var. *hupehensis* Hook. f., and their structures were identified by spectroscopic (NMR, MS) analysis. In order to determine the immunomodulatory activities of soya-cerebrosides I and II, the effects of the mixture of cerebrosides (MC) on cytotoxicity of human peripheral blood mononuclear cells (PBMC) and the inhibitory activities to lipopolysaccharide (LPS)-induced interleukin (IL)-18 in PBMC were studied. The MC at concentrations of 10 and 1 μ M, without toxicity to PBMC in 24 h, showed obvious inhibitory activity on IL-18 secretion. Because of this effect of modulating the cellular immune response, soya-cerebrosides I and II were considered to be the active substances of this ethno drug.

Keywords Soya-cerebrosides · Mixture of cerebrosides · Interleukin-18 · Cytotoxicity · Peripheral blood mononuclear cells

Abbreviations

AZP Azothioprine
COSY Correlation spectroscopy

ELISA	Enzyme-linked immunosorbent assay
FA	Fatty acid
HMBC	Heteronuclear multiple-bond correlation
HR-FABMS	High resolution fast atom bombardment mass spectra
IL	Interleukin
LCB	Long-chain base
LPS	Lipopolysaccharide
MC	Mixture of cerebrosides
MTT	3-(4,5-Dimethylthiazol-2-yl)-2,5-diphenyl tetrazolium bromide
PBMC	Peripheral blood mononuclear cells
RA	Rheumatoid arthritis

Introduction

The rhizomes of *Impatiens pritzellii* Hook. f. var. *hupehensis* Hook. f. (*I. pritzellii*) are used as an ethno drug for the treatment of rheumatoid arthritis in the northwest district of Hubei province and the Wan county of Chongqing, China [1]. In our previous study, the chemical constituents [2–4] and their immunomodulatory effect in the treatment of rheumatoid arthritis (RA) in mice were investigated [5].

Interleukin (IL)-18, which was formerly called as “IFN- γ -inducing factor”, is a novel cytokine with pleiotropic activities that is critical to the development of Th1 responses [6]. It can induce many other cytokines or components, which play important roles in RA, including IFN- γ , TNF- α , IL-1, GM-CSF, NO and PGE2 [7]. It has been reported that IL-18 is a potential therapeutic target in RA [8]. IL-18 could be secreted from monocytes or macrophages activated by lipopolysaccharide (LPS) [9].

X. Zhou · Y. Liu
Key Laboratory of Marine Bio-resources Sustainable Utilization,
South China Sea Institute of Oceanology,
Chinese Academy of Sciences,
510301 Guangzhou, China
e-mail: zhou-xuefeng@hotmail.com

L. Tang (✉)
School of Pharmaceutical Sciences,
Southern Medical University,
510515 Guangzhou, China
e-mail: tanglan_tongji@hotmail.com

Cerebrosides, a family of glycosphingolipids, are important components of a wide variety of tissues and organs in biological systems. Some cerebrosides have been proven to serve as structural support and texture determinants of cell membranes, and act as mediators of biological events such as activation, cell agglutination, intracellular communication and cell development. The biological activities of cerebrosides are very wide, for example, immunomodulatory, antitumor/cytotoxic, COX-2 and histidine decarboxylase inhibitory, anti-HIV-1, and so on [10].

Soya-cerebrosides I and II were isolated from the rhizomes of *I. pritzellii* and their chemotaxonomic significance were discussed in our previous study [3]. But their biological activities were not studied except their ionophoretic activity for Ca^{2+} ion [11, 12], and the antihepatotoxicity of soya-cerebroside II [13]. In order to discuss the immunomodulatory activities of soya-cerebrosides I and II, the isomeric mixture of these two cerebrosides was prepared and studied for the effect to lipopolysaccharide (LPS)-induced IL-18 in human peripheral blood mononuclear cells (PBMC).

Materials and Methods

General Experimental Procedure

$^1\text{H-NMR}$ and $^{13}\text{C-NMR}$ data were recorded on a Bruker AM-400 spectrometer. FABMS and HR-FABMS were conducted using a VG Auto Spec-3000 instrument. Optical rotation was determined on a Perkin–Elmer digital polarimeter. GC was carried out on a GC-14C gas chromatograph (Shimadzu, Japan) with a DB-17 fused silica capillary column (30 m \times 0.25 mm \times 0.25 μm) (J & W Scientific); FID detection; N_2 ; 230 $^\circ\text{C}$ for injector and detector; 150 $^\circ\text{C}$ for 1 min and then raised to 230 $^\circ\text{C}$ at the rate of 5 $^\circ\text{C}/\text{min}$. Silica gel (100–200, 200–300 mesh, Qingdao Marine Chemical Group Co., Qingdao, China) and Sephadex LH-20 (Amersham Pharmacia Biotech AB, Uppsala, Sweden) were used for column chromatography.

Plant Material

The rhizomes of *Impatiens pritzellii* Hook. f. var. *hupehensis* Hook. f. (Balsaminaceae) were collected in Enshi, Hubei province, China, and identified by Prof. Dingrong Wan (Hubei Province Institute for Drug Control, China). A voucher specimen (P 20020713) was deposited at the Faculty of Pharmaceutical Sciences, Tongji Medical College of Huazhong University of Science and Technology, Wuhan, China.

Extraction and Isolation

The extraction and isolation were briefly described previously [8], but this time compound **1** (soya-cerebroside I, 8 mg) and the mixture of cerebrosides (MC, soya-cerebrosides I and II, 36 mg) were isolated.

Preparation of Monocytes

Human PBMC were obtained from three healthy male volunteers after informed consent. Twenty milliliters of peripheral blood was withdrawn from the vein of the forearm. PBMC were isolated from the buffy coat of human peripheral blood by centrifugation on Nycoprep 1.077 (AXIS-SHIELD, Oslo, Norway) and then washed three times in RPMI 1640 medium (Nissui Co. Ltd., Tokyo, Japan). PBMC were suspended at a final concentration of 1×10^6 cells/mL in RPMI 1640 medium supplemented with 10% (v/v) heat-inactivated fetal calf serum.

Cytotoxicity Assay

The cytotoxicity of MC on PBMC was determined by 3-(4,5-dimethylthiazol-2-yl)-2,5-diphenyl tetrazolium bromide (MTT) assay.

Briefly, PBMC (1×10^6 cells/mL) were incubated with MC (1, 10, and 50 μM , with 1% DMSO) in 96-well plates to determine the cytotoxicity or proliferation effect of MC to PBMC. Meanwhile, PBMC were incubated together with MC and LPS (1 $\mu\text{g}/\text{mL}$, Sigma, MO, USA) to determine the effect of MC to LPS induced proliferation of PBMC [14]. PBMC incubated with 1% DMSO were used as control. All of these were prepared in three 96-well plates for different incubation periods (12, 24 and 48 h). After incubating in 37 $^\circ\text{C}$, 5% CO_2 and 90% humidity incubator for corresponding period (either 12, 24 or 48 h), 20 μL of MTT (Sigma, MO, USA) at 5 mg/mL was added into each well in the 96-well plate and incubated for 4 h at 37 $^\circ\text{C}$, 5% CO_2 and 90% humidity in an incubator. The solution was removed and 100 μL DMSO was added to dissolve the MTT formazan crystals. The plates were mixed on a microshaker for 10 min and then read the OD value on a microplate reader (Stat Fax-2100, USA) at 570 nm. Each concentration and control was assayed in triplicate three times. The cytotoxicity and cell survival were evaluated by the following formula:

$$\text{Cytotoxicity (\%)} = (\text{OD}_{\text{control}} - \text{OD}_{\text{sample}}) / \text{OD}_{\text{control}} \times 100\%$$

$$\text{Cell survival (\%)} = (\text{OD}_{\text{sample}} / \text{OD}_{\text{control}}) \times 100\%$$

Cytokine Assays

PBMC (1×10^6 cells/mL) were co-incubated with MC (1, 10, and 50 μ M, with 1% DMSO) and LPS (1 μ g/mL) at 37 $^{\circ}$ C, 5% CO₂ and 90% humidity in an incubator. PBMC incubated with LPS (1 μ g/mL) and 1% DMSO was used as model group and azothioprine (AZP, 1 and 10 μ M, Jiufu Drug Co., Shanghai, China) as positive control. After 24 h of culture, the cell suspensions were transferred into Eppendorf tubes and centrifuged. The cell-free supernatant fractions were assayed for IL-18 protein. IL-18 levels were measured using commercially available enzyme-linked immunosorbent assay (ELISA) kits (Human IL-18 INSTANT ELISA, BMS, Vienna, Austria) after standardization of the protein concentrations, and the detection limit was 10 pg/mL. The IL-18 level in untreated PBMC was also measured.

Statistical Analysis

Data are presented as means \pm SD. The results were statistically analyzed by one-way analysis of variance (ANOVA), followed by Dunnett's *t* test. *P* values < 0.05 were considered significant.

Results and Discussion

Compound **1** (soya-cerebroside I, 8 mg) and the mixture of cerebroside (MC, soya-cerebroside I and II, 36 mg) were isolated from the rhizomes of *I. pritzellii*. Compound **1** was obtained as white powder and had the molecular formula C₄₀H₇₅NO₉ as deduced from negative-ion HR-FABMS (*m/z* 712.5480 [M–H][–], calcd 712.5442) and ¹³C-NMR data. The signals of two long and branchless carbon chains, an amide group and a sugar moiety in ¹H and ¹³C-NMR spectrum suggested compound **1** was a cerebroside. Acid hydrolysis of **1** yielded D-glucose, as determined by TLC (EtOAc–MeOH–H₂O–HOAc, 6:1:1:1, *R_f* = 0.32), GC analyses (*R_t* = 23.37, D-glucose derivative) [15] and optical rotation (positive polarity), together with authentic sugar samples. The locations of hydroxyl groups and double bonds were determined by HMBC and ¹H–¹H COSY experiments. The configurations of two double bonds were determined to be *E* from the ¹³C-NMR chemical shift of the methylene carbon adjacent to the olefinic carbon as described in the literature [16]. The length of two long carbon chains, long-chain base (LCB) and fatty acid (FA), were determined by negative-ion FABMS: *m/z* 712 ([M–1][–]), 550 ([M–C₆H₁₀O₅–H][–]), 296 (LCB, [C₁₈H₃₄NO₂][–]) and 254 (FA, [C₁₆H₃₁O₂–H][–]). The ¹H and ¹³C-NMR spectrum and optical rotation of **1** ([α]_D²⁰ + 9.5 $^{\circ}$, *c* 0.1, MeOH) suggested that **1** has the same

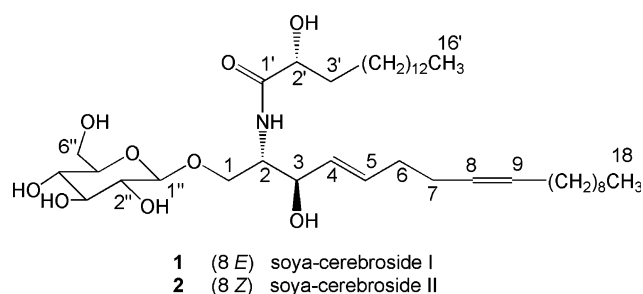


Fig. 1 Chemical structures of soya-cerebroside I and II

absolute configuration as that of AS-1-4 (2*S*, 3*R*, 2'*R*) in the literature [16]. So, compound **1** was identified as 1-*O*- β -D-glucosyl-(2*S*, 3*R*, 4*E*, 8*E*, 2'*R*)-*N*-(2'-hydroxypalmitoyl)-2-amino-4,8-octadecadiene-1,3-diol (soya-cerebroside I) (Fig. 1).

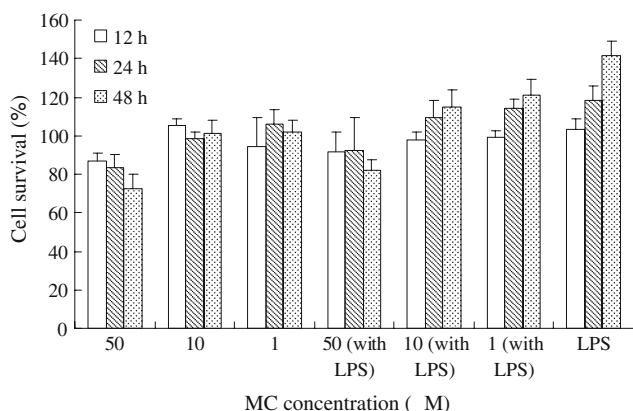
The MC was obtained as white powder and the negative-ion FABMS showed the same molecular ion peak as compound **1** (*m/z* 712 [M–1][–]). The ¹H and ¹³C-NMR spectrum were similar with those of compound **1**, except the redundant signals of two olefinic carbons (δ 129.5, 130.7) and two methylene carbons (δ 27.4, 27.6). These redundant signals suggested there was another isomeric compound besides **1**. The *Z* configuration of double bond at C-8,9 was fit those four redundant carbon signals perfectly [16]. So, the other component in the mixture was determined as 1-*O*- β -D-glucosyl-(2*S*, 3*R*, 4*E*, 8*Z*, 2'*R*)-*N*-(2'-hydroxypalmitoyl)-2-amino-4,8-octadecadiene-1,3-diol (soya-cerebroside II). The ¹³C-NMR data of compound **1** and MC were showed in Table 1. MC was identified as isomeric mixture of soya-cerebroside I and II by comparing those NMR data in the literature [16].

The MTT assay was used to determine the cytotoxicity of MC on PBMC before evaluating the interleukin inhibitory activities (Fig. 2). MC showed obvious cytotoxicity to PBMC, at a concentration of 50 μ M, with survival of 86.67 ± 4.04 , 83.33 ± 6.66 , $72.67 \pm 7.57\%$ in 12, 24, 48 h, respectively. While MC at the concentration of 10 and 1 μ M showed no cytotoxicity. The proliferation effect of LPS (1 μ g/mL) to PBMC increased when the culture time was extended to 24 and 48 h, with a survival rate of 118.33 ± 7.57 and $141.33 \pm 7.64\%$, respectively. We found that MC had obvious inhibitory effect to LPS induced proliferation of PBMC at concentration of 50 μ M, which might be due to its cytotoxicity. At lower concentration (10 and 1 μ M), MC showed inhibitory effects to LPS-induced proliferation of PBMC when the co-culture time was extended to 48 h, and this revealed MC could effect the survival of PBMC activated by LPS when co-culture long enough.

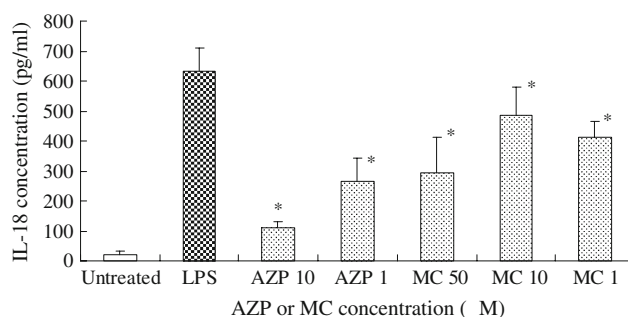
The levels of IL-18 in PBMC co-cultured with MC and LPS were determined by ELISA kits (Fig. 3), and the

Table 1 ^{13}C -NMR data of compound **1** and MC (400 MHz, in Pry-d_5)

Position	Pure compound	MC	
	1	1	2
1	70.1	70.2	
2	54.7	54.6	
3	72.3	72.4	
4	132.1	132.1	
5	132.0	132.1	
6	32.8	32.8	
7	32.1	32.2	27.4
8	130.0	130.0	129.5
9	131.1	131.1	130.7
10	32.9	32.9	27.6
11–16	29.5–30.0	29.5–30.0	
17	22.9	23.0	
18	14.3	14.3	
1'	175.6	175.7	
2'	72.5	72.5	
3'	35.7	35.7	
4'–14'	29.5–30.0	29.5–30.0	
15'	22.9	23.0	
16'	14.3	14.3	
1''	105.7	105.7	
2''	75.1	75.1	
3''	78.5	78.5	
4''	71.6	71.6	
5''	78.6	78.6	
6''	62.7	62.7	

**Fig. 2** Effect of MC in different concentrations on cell survival of PBMC at 12, 24 and 48 h. The concentration of LPS is $1 \mu\text{g/mL}$. 1% DMSO was used in every group and each concentration was assayed in triplicate three times. The results are presented as means \pm SD

culture time was 24 h. The significant effect of MC, at the concentration of $50 \mu\text{M}$, to inhibit the production of IL-18 in vitro might be partly due to its cytotoxicity to PBMC.

**Fig. 3** Effects of MC on LPS-induced IL-18 level in PBMC at 24 h. AZP: azothioprine. The concentration of LPS is $1 \mu\text{g/mL}$. 1% DMSO was used in every group including model and untreated groups. IL-18 levels were measured by ELISA kits. The results were presented as means \pm SD ($n = 8$). One-way ANOVA revealed significant effects between model and treatment groups ($P < 0.001$). * $P < 0.05$ compared with model (Dunnett's t test)

However, MC at concentrations of 10 and $1 \mu\text{M}$, which showed no toxicity to PBMC in 24 h, were found inhibitory to IL-18 secretion. This result suggested MC might potentially modulate the cellular immune response in monocytes [17]. Moreover, the inhibitory activity of MC at concentration of $1 \mu\text{M}$ was somewhat higher than that for $10 \mu\text{M}$. Intracellular IL-18 represents a storage pool, which may be initially depleted by MC before their reduction in the excretion into the supernatant [18]. MC with the concentration of $1 \mu\text{M}$ could cause a marked decrease in extracellular levels of IL-18, as well as in intracellular. However, at the concentration of $10 \mu\text{M}$, MC might inhibit the intracellular IL-18 extremely, which was not seen by measuring cytokine level in cellular supernatants by ELISA technique. The toxicity of MC with $10 \mu\text{M}$, which were not observed by MTT measurement, affected the function of transportation of cytokines through the cell membrane. These results suggest that higher concentrations of MC result in a direct toxic or breaking the cellular function of PMBC compared with an immunosuppressive effect at lower concentration ($1 \mu\text{M}$). In addition, there is more than one mechanism of inhibitory of the IL-18 production of MC, as well as more than one pathway of the cytokine secretion [19]. The level of IL-18 and its effects on Th1/Th2 balance in immune cells were considered to be dependent on the coexisting cytokine and the state of activation of subsets [20]. So, the mechanisms of effects on the IL-18 secretion of MC might be much complicated and further study should be continued.

The IL-18 inhibitory activities of MC and its cytotoxicity on PBMC suggested MC could potentially modulate the cellular immune response. Because of the pleiotropic activities of IL-18 in the development of Th1 responses [6, 7], MC could be considered to modulate the cytokines levels in monocytes.

Our previously study revealed methanol extract of the rhizomes of *I. pritzellii* could modulate the cytokines levels, including down-regulation of the levels of IL-18, in serum of mice with RA model [5]. Soya-cerebrosides I and II, whose immunomodulatory effect was investigated in current study, were indicated to be the active substances in *I. pritzellii*.

Acknowledgments This research was supported by the National Natural Science Foundation of China (No. 30371733).

References

- Wan DR, Li AJ, Feng HL (1989) Pharmacognostic studies of *Impatiens pritzellii* var. *hupehensis*. *Zhong Yao Cai* 12:18–20
- Zhou XF, Zhao XY, Tang L, Ruan HL, Zhang YH, Pi HF, Xiao WL, Sun HD, Wu JZ (2007) Three new triterpenoid saponins from the rhizomes of *Impatiens pritzellii* var. *hupehensis*. *J Asian Nat Prod Res* 9:379–385
- Zhou XF, Tang L, Zhang YH, Pi HF, Ruan HL, Wu JZ (2007) Nitrogenous compounds from *Impatiens pritzellii* var. *hupehensis* (Balsaminaceae). *Biochem Syst Ecol* 35:308–310
- Zhao XY, Zhou XF, Ruan HL, Zhang YH, Pi HF, Sun HD, Wu JZ (2005) Chemical constituents of *Impatiens pritzellii*. *Chin J Nat Med* 3:354–356
- Zhou X, Zhao X, Tang L, Zhang Y, Ruan H, Pi H, Qiu J, Wu J (2007) Immunomodulatory activity of the rhizomes of *Impatiens pritzellii* var. *hupehensis* on collagen-induced arthritis mice. *J Ethnopharmacol* 109:505–509
- Wei XQ, Leung BP, Arthur H, McInnes IB, Liew FY (2001) Reduced incidence and severity of collagen-induced arthritis in mice lacking IL-18. *J Immunol* 166:517–521
- Gracie JA, Forsey RJ, Chan WL, Gilmour A, Leung BP, Greer MR, Kennedy K, Carrer R, Wei XQ, Xu D, Field M, Foulis A, Liew FY, McInnes IB (1999) A proinflammatory role for IL-18 in rheumatoid arthritis. *J Clin Invest* 104:1393–1401
- Bessis N, Boissier MC (2001) Novel pro-inflammatory interleukins: potential therapeutic targets in rheumatoid arthritis. *Joint Bone Spine* 68:477–481
- Stoll S, Jonuleit H, Schmitt E, Muller G, Yamauchi H, Kurimoto M, Knop J, Enk AH (1998) Production of functional IL-18 by different subtypes of murine and human dendritic cells (DC): DC-derived IL-18 enhances IL-12-dependent Th1 development. *Eur J Immunol* 28:3231–3239
- Tan RX, Chen JH (2003) The cerebroside. *Nat Prod Rep* 20:509–534
- Shibuya H, Kawashima K, Sakagami M, Kawanishi H, Shimomura M, Ohashi K, Kitagawa I (1990) Sphingolipids and glycerolipids. I. Chemical structures and ionophoretic activities of soya-cerebrosides I and II from soybean. *Chem Pharm Bull* 38:2933–2938
- Kurosu M, Katayama S, Shibuya H, Kitagawa I (2007) A study of the calcium complex of a glucosylceramide, soya-cerebroside II. *Chem Pharm Bull* 55:1758–1761
- Kim SY, Choi YH, Huh H, Kim J, Kim YC, Lee HS (1997) New antihepatotoxic cerebroside from *Lycium chinense* Fruits. *J Nat Prod* 60:274–276
- Takahashi HK, Iwagaki H, Mori S, Yoshino T, Tanaka N, Nishibori M (2004) Histamine inhibits lipopolysaccharide-induced interleukin (IL)-18 production in human monocytes. *Clin Immunol* 112:30–34
- Fang W, Ruan J, Wang Z, Zhao Z, Zou J, Zhou D, Cai Y (2006) Acetylated flavanone glycosides from the rhizomes of *Cyclosorus acuminatus*. *J Nat Prod* 69:1641–1644
- Inagaki M, Harada Y, Yamada K, Isobe R, Higuchi R, Matsuura H, Itakura Y (1998) Isolation and structure determination of cerebroside from Garlic, the bulbs of *Allium sativum* L. *Chem Pharm Bull* 46:1153–1156
- Swamy SMK, Tan BKH (2000) Cytotoxic and immunopotentiating effects of ethanolic extract of *Nigella sativa* L. seeds. *J Ethnopharmacol* 70:1–7
- Yuengsrigul A, Chin TW, Nussbaum E (1999) Immunosuppressive and cytotoxic effects of furosemide on human peripheral blood mononuclear cells. *Ann Allergy Asthma Immunol* 83: 559–566
- Stow JL, Ching Low P, Offenhäuser C, Sangermani D (2009) Cytokine secretion in macrophages and other cells: Pathways and mediators. *Immunobiology*. doi:10.1016/j.imbio.2008.11.005
- Takahashi HK, Yoshida A, Iwagaki H, Yoshino T, Itoh H, Morichika T, Yokoyama M, Akagi T, Tanaka N, Mori S, Nishibori M (2002) Histamine regulation of interleukin-18-initiating cytokine cascade is associated with down-regulation of intercellular adhesion molecule-1 expression in human peripheral blood mononuclear cells. *J Pharmacol Exp Ther* 300:227–235

Development of a High-Density Assay for Long-Chain Fatty Acyl-CoA Elongases

Hidefumi Kitazawa · Yasuhisa Miyamoto ·
Ken Shimamura · Akira Nagumo · Shigeru Tokita

Received: 17 February 2009 / Accepted: 10 June 2009 / Published online: 4 July 2009
© AOCs 2009

Abstract We established a convenient assay method for measuring elongation of very long chain fatty acids (ELOVLs) using a Unifilter-96 GF/C plate. The Unifilter GF/C plate preferentially interacts with hydrophobic end products of ELOVLs (i.e., long chain fatty acid), with minimal malonyl-CoA (C2 unit donor for fatty acid elongation) interaction. This new method results in the quick separation and detection of [¹⁴C] incorporated end products (e.g., [¹⁴C] palmitoyl-CoA) from reaction mixtures containing excessive amounts of [¹⁴C] malonyl-CoA. In the Unifilter-96 GF/C plate assay, recombinantly expressed human ELOVLs (i.e., ELOVL1,-2,-3,-5 and -6) displayed appreciable assay windows (>2-fold vs. mock-transfected control), enabling us to conduct comprehensive substrate profiling of ELOVLs. The substrate concentration profile of ELOVL6 in the Unifilter-96 GF/C plate assay is consistent with that obtained from the conventional liquid extraction method, thus, supporting the reliability of the Unifilter-96 GF/C plate assay. We then examined the substrate specificities of ELOVLs in a comprehensive fashion. As previously reported, ELOVL1,-3 and -6 preferably elongated the saturated fatty acyl-CoAs while

ELOVL2 and ELOVL5 preferentially elongated the polyunsaturated fatty acyl-CoAs. This further confirms the Unifilter-96 GF/C plate assay reliability. Taken together, our newly developed assay provides a convenient and comprehensive assay platform for ELOVLs, allowing investigators to conduct high density screening and characterization of ELOVLs chemical tools.

Keywords ELOVL · Elongase · Long chain fatty acyl-CoA · Malonyl-CoA · Long chain fatty acid · Obesity · Diabetes · Metabolic disorder

Abbreviations

BSA	Bovine serum albumin
CoA	Coenzyme A
EDTA	Ethylenediaminetetraacetic acid
ELOVL	Elongase of long chain fatty acyl-CoA
LCFA	Long chain fatty acid
NADPH	Reduced nicotinamide adenine dinucleotide phosphate
SDS	Sodium lauryl sulfate
TBS	Tris-buffered saline

H. Kitazawa and Y. Miyamoto were contributed equally to this work.

Electronic supplementary material The online version of this article (doi:10.1007/s11745-009-3320-8) contains supplementary material, which is available to authorized users.

H. Kitazawa · Y. Miyamoto · K. Shimamura · A. Nagumo · S. Tokita (✉)
Department of Metabolic Disorder Research,
Tsukuba Research Institute, BANYU Pharmaceutical Co., Ltd.,
Okubo 3, Tsukuba, Ibaraki 300-2611, Japan
e-mail: shigeru.tokita@po.rd.taisho.co.jp

Y. Miyamoto
e-mail: myashsa@mx6.nisiq.net

Introduction

Obesity, a complex condition associated with an increased risk of type 2 diabetes, hypertension, and cardiovascular diseases, is becoming a global epidemic. Accumulating evidence indicates that alternations in intracellular lipid metabolism play a prominent role in the pathology of obesity and diabetes [1]. An increase in fat storage in the nonadipose tissues such as the liver, leads to tissue

dysfunction, i.e., insulin resistance. Although it is unclear how increased intracellular lipid content exacerbates tissue and whole body insulin sensitivity, it has been suggested that increased levels of long chain fatty acyl-CoA antagonize the metabolic actions of insulin. Interestingly, recent reports have suggested that alternations of the specific fatty acid component (i.e., palmitoleate) have a significant impact on the insulin sensitivity of the liver and whole body [2, 3].

De novo lipogenesis plays a major role in maintaining energy storage and membrane fluidity. Fatty acid synthase (FAS), a cytosolic and multifunctional enzyme, is responsible for de novo synthesis of acyl-CoAs with fatty acid chains of C2 up to C16 (palmitoyl-CoA), while the elongation of very long chain fatty acids (ELOVL) family enzymes, microsome resident enzymes, are responsible for the elongation of fatty acids with longer chain fatty acids [4]. It is reported that fatty acid elongation in microsomal fractions occurs through four sequential steps: (1) condensation by ELOVL (elongase of long chain fatty acyl-CoA), (2) reduction by β -ketoacyl-CoA reductase, (3) dehydrogenase by β -hydroxyacyl-CoA dehydrogenase, and (4) reduction by trans-2,3-enoyl-CoA reductase [5, 6]. Given NADPH-dependent activity of β -ketoacyl-CoA reductase, the condensation activities of ELOVLs can be monitored in the absence of NADPH [7, 8].

In mammals, seven ELOVL enzymes (ELOVL1-7) have been identified [7, 9–13]. Accumulating evidence suggests that each ELOVL exhibits different fatty acid substrate preferences. In addition to the diverse substrate preference, it has been reported that ELOVLs are expressed in distinct tissues and their expressions were differently regulated. This suggests ELOVLs have distinct physiological roles [13–15]. Recent progress in this area revealed the potential physiological and pathological roles of ELOVLs. It was reported that overexpression of ELOVL2, but not ELOVL3, enhanced triglyceride synthesis and lipid accumulation in preadipocytes cells [16], suggesting ELOVL2 plays an important role in adipose tissues. ELOVL3 has been identified as a long chain fatty acid elongase that is highly expressed in brown adipocytes and skin. ELOVL3 is upregulated by cold-exposure in vivo. In addition, ELOVL3-deficient mice displayed a distinct skin phenotype including impaired barrier function, suggesting ELOVL3 plays a critical role in the regulation of thermogenesis and body temperature [17].

ELOVL6 has gained much attention in the field of metabolic disorders; Matsuzaka and his colleagues reported ELOVL6-deficient mice displayed improved insulin sensitivity and glucose homeostasis as compared with the wild-type mice when fed a high-fat diet. Therefore, ELOVL6 might serve as a therapeutic target for metabolic disorders [2].

In this study, we describe a convenient high density assay method (96-well format) for ELOVLs, which provides a comprehensive analysis of substrate specificities of ELOVLs.

Materials and Methods

Reagents

[2-¹⁴C] malonyl-CoA (1.92 GBq/mmol) was purchased from GE Healthcare Bioscience (Tokyo, Japan). [1-¹⁴C] palmitic acid, [1-¹⁴C] stearic acid, Unifilter-96 GF/C plate and MICROSCINT 0 were all purchased from PerkinElmer Japan (Kanagawa, Japan). [1-¹⁴C] behenic acid (C22:0), [1-¹⁴C] Δ -7,10,13,16-docosatetraenoic acid (C22:4), [1-¹⁴C] arachidic acid (C20:0) and [1-¹⁴C] Δ -11-eicosenoic acid (C20:1) were from Muromachi-Yakuhin (Tokyo, Japan). Other reagents were purchased from Sigma-Aldrich Japan (Tokyo, Japan).

Cloning of Human ELOVLs from Human Liver cDNA and Expression Vector Construction

The full-length human ELOVLs cDNAs were amplified by polymerase chain reaction (PCR) using gene specific primers from human liver cDNA (Clontech, Mountain View, CA) as the template. The primer sequence for cloning each elongase (Supplemental Table 1) was designed based on sequences obtained from GenBank and 5'-primers and 3'-primers introduced the *NotI* and *XbaI* sites in the 5'-end, respectively. The PCR products were subcloned into pEF1/V5-His vector (Invitrogen, Carlsbad, CA), which express C-terminal tag encoding V5-epitope and polyhistidine. The integrity of all PCR products and ligation was confirmed by DNA sequencing.

Cell Culture and Transfection

COS-7 cells (African green monkey kidney fibroblast cells) were grown in Dulbecco's modified Eagle's medium (DMEM; Invitrogen) containing 10% fetal bovine serum, supplemented with 100 units/ml penicillin and 100 μ g/ml streptomycin. For transfection, COS-7 cells were plated at a density of 5×10^7 cells/500 cm² square dish in DMEM. After overnight culture, cells were transfected with 240 μ g pEF1/V5-His plasmids harboring each ELOVL open reading frame (ORF) using 600 μ l Lipofectamine2000 reagent (Invitrogen), according to the manufacturer's instructions. After 48 h transfection, cells were washed three times with cold PBS and harvested in 10 ml of cold PBS. The cells were collected by centrifugation and stored at -80°C until use.

Preparation of Microsome Fractions Overexpressing Recombinant Human ELOVLs

The cell pellets were suspended in the homogenization buffer (10 mM Tris-HCl, pH 7.4, 1 mM EDTA, 0.25 M sucrose) containing protease inhibitor cocktail (Roche, Basel, Switzerland) and homogenized with POLYTRON homogenizer (Kinematica, Lucerne, Switzerland). Cell homogenates were centrifuged at 1,000g for 10 min at 4°C and the supernatant was centrifuged at 10,000g for 10 min at 4°C. The resulting supernatant was further centrifuged at 100,000g for 1 h at 4°C. The pellet was resuspended in buffer (50 mM Tris-HCl, pH 7.4, 1 mM EDTA, 20% glycerol) with protease inhibitor cocktail, and centrifuged again at 100,000g for 1 h at 4°C. The pellet was resuspended in buffer and used as microsomal protein. Concentration of the microsomal protein was determined by BCA protein assay kit (Pierce, Rockford, IL) and stored at -80°C until use.

Immunoblot Analysis

The expressions of V5 epitope-tagged human ELOVLs in microsomes from transfected COS-7 cells were examined by Immunoblot analysis using anti-V5-epitope antibody. In brief, cytosolic and microsomal protein (20 µg) were electrophoresed on a 10% SDS-polyacrylamide gel and transferred to PVDF membrane (Immobilon-P, Millipore) using the standard procedure. The membrane was blocked for 1 h at room temperature in TBS, 0.05% Tween-20 (TTBS) containing 1% dried non-fat milk, and then incubated with a 1:1,000 dilution of the horseradish peroxidase-conjugated anti-V5 monoclonal antibody conjugated (Anti-V5-HRP, Invitrogen) in TTBS for 1 h at room temperature. After 3 washes with TTBS, antibody-protein complexes were visualized using an ECL Plus kit (GE Healthcare Bioscience).

Binding of Malonyl-CoA and Long Chain Fatty Acids to the GF/C Filter

Radiolabelled C22:0, C22:4, C20:0, C20:1, C18:1 and malonyl-CoA (60 µM) were dissolved in the assay buffer containing 100 mM potassium phosphate buffer (pH 6.5), 200 µM BSA (fatty acid free), 500 µM NADPH, 1 µM rotenone and were applied to the Unifilter-96 GF/C plate. After three times washing with distilled water, the residual radioactivity values on the GF/C filter were measured by TopCount. The radioactivity values of fatty acids and malonyl-CoA on non-washed wells were also measured and defined as total radioactivity values. Remaining % of the respective fatty acids and malonyl-CoA are determined as follows;

$$\text{Remaining (\%)} = \left[\frac{\text{residual radioactivity after washing}}{\text{total radioactivity (non-wash)}} \right] \times 100$$

To compare the relative remaining (%) of fatty acids over malonyl-CoA, the remaining (%) of respective fatty acid was standardized by the remaining (%) of malonyl-CoA to yield the ratios of the respective fatty acids to Malonyl-CoA as follows:

$$\text{Remaining ratio} = \left[\frac{\text{remaining (\%)} \text{ of fatty acid}}{\text{remaining (\%)} \text{ of malonyl-CoA}} \right]$$

Fatty Acyl-CoA Elongation Assay

Reaction Step

Fatty acyl CoA elongation using the microsome fractions was performed by the method previously described [7] with slight modifications. Briefly, 30 µl reaction mixtures (100 mM potassium phosphate buffer (pH 6.5), 200 µM BSA (fatty acid free), 500 µM NADPH, 1 µM rotenone, 20 µM malonyl-CoA, 833 kBq/ml [2-¹⁴C] malonyl-CoA and 40 µM long chain fatty acyl-CoA) were used as the substrate mixture, and then the elongation reaction was initiated with the addition of 20 µl microsomal protein. The reaction step was performed on a 96 well plate with gentle shaking.

Separation Step

After 1 h incubation at 37°C, 50 µl of 5 M HCl was added to hydrolyze acyl-CoAs. The reaction mixtures were then filtered through the Unifilter-96, GF/C plate (Perkin Elmer) using FilterMate cell harvester (Perkin Elmer). The 96-well GF/C filter plate was subsequently washed with distilled water to remove the excess amount of [2-¹⁴C] malonyl-CoA. After drying the plate, 25 µl MICROSCINT 0 was added to each well and the residual radioactivity was measured by TopCount (Perkin Elmer). In order to compare the performance of our assay method with that of the conventional one, the separation step was conducted according to the previously described conventional method [7]. Briefly, after hydrolysis, the resulting mixtures were transferred into the glass tubes and extracted with 1 mL of n-hexane (3 times). The hexane layers were collected to a scintillation vial and dried up under nitrogen stream. The resulting materials were mixed with 3 mL of Clear-sol II (Nacalai tesque, Kyoto, Japan) and their radioactivity were measured by the liquid scintillation analyzer TRICARB 2300 (PerkinElmer).

Results

Expression of ELOVLs in Microsome Fraction of the Transfected COS-7 Cells

COS-7 cells were transfected transiently with a cDNA encoding V5 epitope-tagged human ELOVLs. Cytosolic fractions and microsome fractions from the transfected cells were prepared and subjected to western blot analyses with anti-V5 antibody (Fig. 1). We observed the specific bands showing the expected molecular weight (ca. 30 kDa) for each ELOVLs in microsome fractions but not in cytosolic fractions. This confirmed successful expression of recombinant ELOVLs in the microsomal fractions.

Different Binding Properties of Malonyl-CoA and Long Chain Fatty Acids to GF/C Filter

ELOVLs are rate-limiting enzymes for elongation of long chain fatty acid (LCFA) and catalyze the condensation between LCFA-CoA and malonyl-CoA, a C2 unit for elongation. Therefore, elongase activities are monitored by measuring the incorporation of [¹⁴C] into the reaction products (i.e., LCFA-CoAs) from [¹⁴C] malonyl-CoA after removing excessive [¹⁴C] malonyl-CoA from the reaction mixture. In the conventional assay, separation of radiolabelled hydrophobic products from reaction mixtures is achieved by organic solvent extraction or solid phase chromatography. We assumed that the GF/C filter could separate radiolabelled LCFAs from the reaction mixture by preferentially absorbing LCFAs while interacting to a lesser extent with malonyl-CoA, a more hydrophilic substance. Considering its potential application to the ELOVL

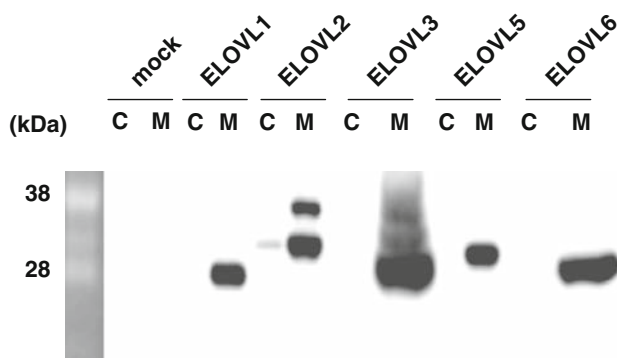


Fig. 1 Expression of V5-tagged human ELOVLs in microsomal fractions of transfected COS-7 cells. COS-7 cells were transiently transfected with the V5-tagged human ELOVLs cDNA expression vectors or the vector alone (mock). After 48 h transfection, the cells were harvested and the cytosolic and microsomal fractions were isolated according to the standard procedure. Twenty micrograms of cytosolic (C) and microsomal (M) protein were subjected to SDS-PAGE and immunoblot analysis

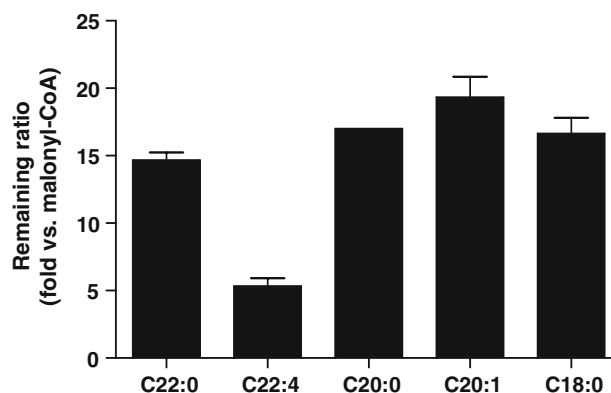


Fig. 2 Binding profiles of malonyl-CoA and long chain fatty acids to the GF/C filter. Radiolabelled fatty acids and malonyl-CoA (60 μM) were dissolved in assay buffer and applied to the Unifilter-96 GF/C plate. After washing, the residual radioactivity values on the GF/C filter were measured by TopCount. The horizontal axis indicates the fold of the residual radioactivity of respective fatty acids compared to that of malonyl-CoA. Data are expressed as means ± SD

assay, we evaluated the binding profiles of malonyl-CoA and the expected ELOVL end-products such as C22:0-, C22:4-, C20:0-, C20:1- and C18:0-fatty acids (for ELOVL1, -2, -3, -5 and -6, respectively) as described in the [Materials and Methods](#). LCFAs were retained on the GF/C filter by 5- to 20-fold as compared with malonyl-CoA following the washing step (Fig. 2).

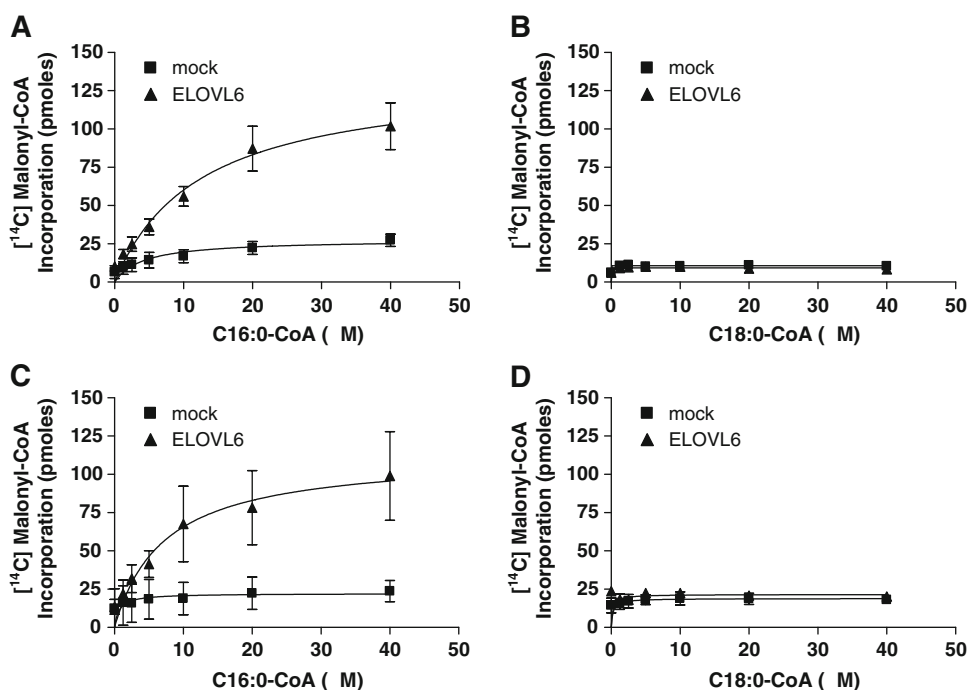
Assay Validation

In order to validate our new assay method, we examined the substrate specificity of ELOVL6 reported to elongate myristoyl-CoA (C14:0-CoA) and palmitoyl-CoA (C16:0-CoA), but not stearoyl-CoA (C18:0-CoA) [7]. As expected, we observed that human ELOVL6-transfected microsome fractions preferentially elongated myristoyl-CoA and palmitoyl-CoA with greater efficacy (4-fold) as compared with mock-transfected microsome fractions (Figs. 3a, 5e). In contrast, we could not see any differences in the elongation activities between the ELOVL6- and mock-transfected microsome fractions when stearoyl-CoA and other acyl-CoAs with longer, unsaturated fatty acids were used as substrates (Figs. 3b, 5e). Taken together, these results support the substrate specificity of ELOVL6 that was determined by the conventional assay method (Figs. 3c, 3d); thus demonstrating the reliability of the GF/C filter plate assay.

Application to Other Elongases

Since our newly developed assay method has been validated for ELOVL6, we have applied it to the other representative fatty acid elongases: ELOVL1, -2, -3 and -5. The

Fig. 3 Substrate concentration profiles for human ELOVL6 activity in microsomes from transfected COS-7 cells. Microsome fractions were prepared from COS-7 cells transfected with human ELOVL6 or mock vectors. The elongation activities against C16:0-CoA (**a, c**) or C18:0-CoA (**b, d**) were examined using the filtration assay method (**a, b**) and conventional assay method (**c, d**) as described in the [Materials and Methods](#). The elongation activities were represented by malonyl-CoA incorporation (pmol). Data are expressed as means \pm SEM from three independent experiments



microsome fractions overexpressing human recombinant ELOVL1, -2, -3 and -5 were prepared and used to test the elongase assays using the GF/C filter plates (Figs. 1, 4, 5). For the substrate concentration profile studies, representative substrates were used for each ELOVL: C20:0-CoA for ELOVL1, C20:4-CoA for ELOVL2, C18:0-CoA for ELOVL3 and C18:1-CoA for ELOVL5. As shown in Fig. 4, the ELOVL-transfected microsome fractions displayed dose-dependent activities that were 2.4-fold, 2.4-fold, 3.2-fold, and 3.2-fold higher than that of the mock transfected microsomes, respectively. These results suggest that under the current conditions, each ELOVL retains its own elongase activity and the GF/C filter assay plate assay is applicable to the measurement of these representative ELOVLs.

Comparison of the Substrate Preferences of Human ELOVLs

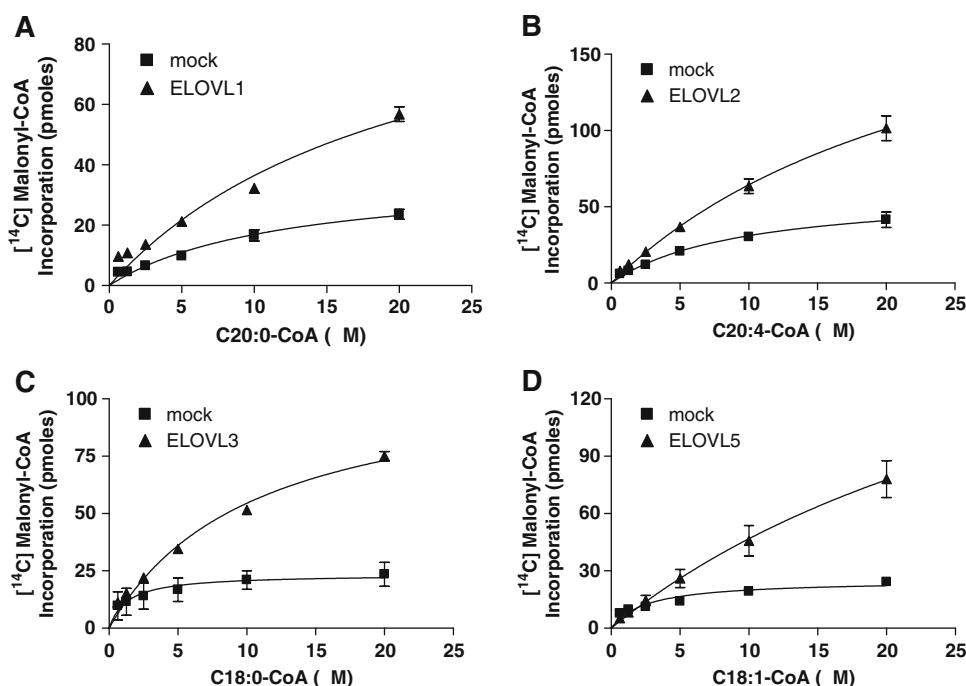
Up till now, seven ELOVLs (i.e., ELOVL1-7) have been genetically identified in mammals and characterized by several investigators using recombinantly expressed enzymes. To date, there have been no other studies using identical platforms for the expression and assay methods for ELOVLs. Since we observed significantly increased elongase activities of each recombinant ELOVL using the respective substrate (vs. mock-transfected controls), we have examined the substrate specificity of ELOVLs using a series of saturated and unsaturated fatty acyl-CoAs as substrates (Fig. 5a–e). ELOVL1, -3 and -6 preferably elongated the saturated fatty acyl-CoA (ELOVL1; C18:0,

C20:0 and C22:0, ELOVL3; C14:0, C16:0, C18:0 and C20:0, ELOVL6; C14:0, and C16:0), while ELOVL2 and -5 preferably elongated the mono- and poly unsaturated fatty acyl-CoA (ELOVL2; C20:4, ELOVL5; C16:1, C18:1, C18:2, and C20:4). These results are in good agreement with previous reports except that ELOVL5 also elongated the saturated acyl-CoAs (i.e., C14:0 and C16:0) in addition to the unsaturated acyl-CoAs.

Discussion

We have described our newly developed assay system for the measurement of long chain fatty acid elongases (i.e., ELOVLs) and its application in ELOVL primary characterization. This assay method is based on the findings that [14 C] malonyl-CoA (hydrophilic substance) and elongated long chain fatty acids (hydrophobic substance) are separated by the GF/C filter (Fig. 2). In conventional fatty acid elongase assays, the separation steps of radioactive products from reaction mixtures by organic solvent extraction or solid phase chromatography are required [7, 18] (Fig. 6). Although these methods are reliable and widely utilized, they are too labor intensive; meaning they are not suitable for screening a chemical library and head-to-head characterization or comparison of elongase activities. Regarding several cytosolic lipogenic enzymes such as FAS and farnesyl pyrophosphate synthase (FPPS), Glickman et al. reported that the FlashPlate assay provides investigators with robust assay windows, where the hydrophobic products preferably associate with a lipid-coated surface

Fig. 4 Substrate concentration profiles for human ELOVL1, -2, -3, and -5 activities in microsomes from transfected COS-7 cells. Microsome fractions were prepared from COS-7 cells transfected with human ELOVL1, -2, -3, -5 or mock vectors. The elongation activities of ELOVL1, -2, -3, or -5 were determined using C20:0-CoA (a), C20:4-CoA (b), 18:0-CoA (c) or C18:1-CoA (d) as the substrate and [14 C] malonyl-CoA as a C2 unit donor. The elongation activities were represented malonyl-CoA incorporation (pmol). Data are expressed as means \pm SEM from four or five independent experiments



[19, 20]. In the case of membrane enzymes such as ELOVLs, the enzyme fraction (i.e., microsome) provides a significant amount of lipid to the reaction mixture, which in turn interferes with the association of a hydrophobic end product and a lipid-coated surface. This gives rise to high background noise and increasing non-specific interactions of radioactive mixtures with the lipid-coated surface (data not shown).

Assay Development and Validation

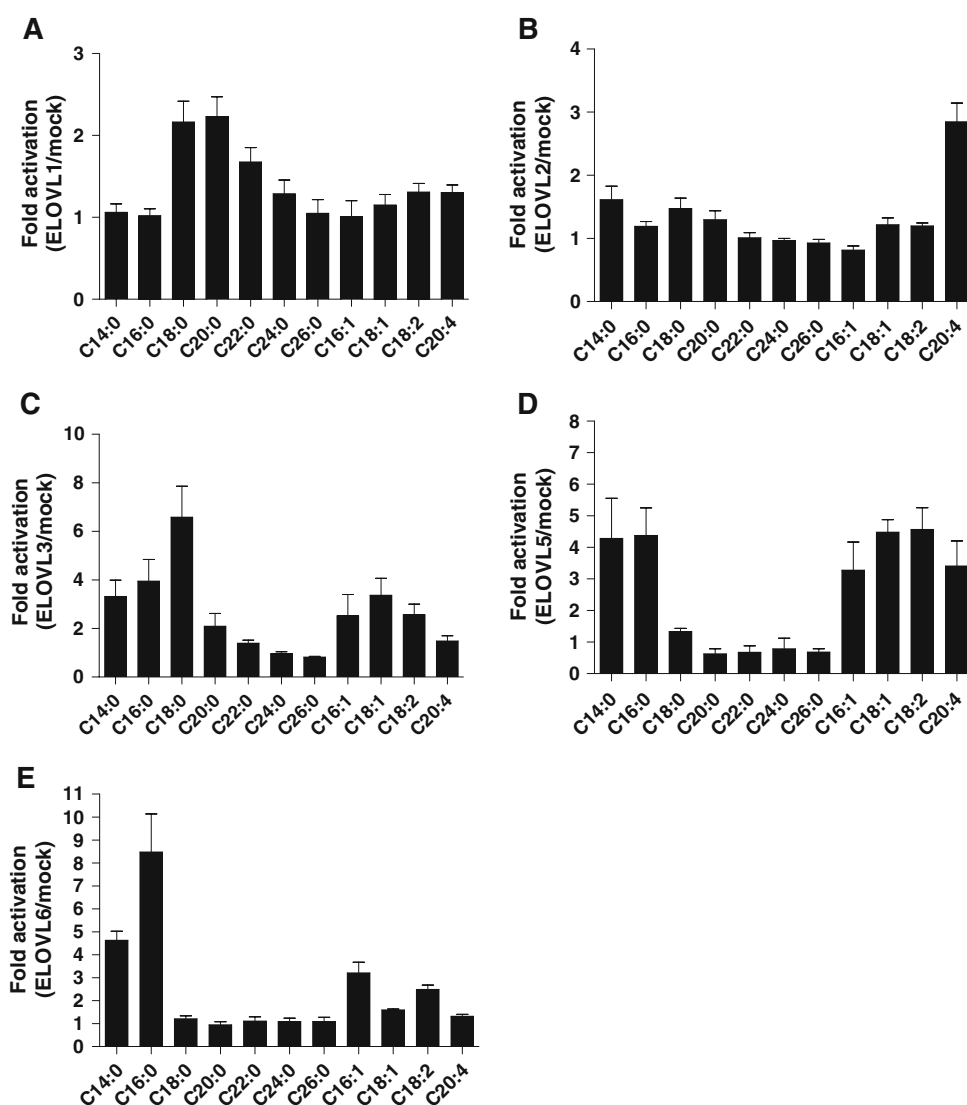
In our elongation assay, [14 C] malonyl-CoA was incorporated into long chain fatty acids and the excess amount of [14 C] malonyl-CoA was efficiently removed from the reaction mixtures by washing the GF/C filter. This resulted in the establishment of a quick and convenient ELOVL assay method in a 96-well format (Fig. 6). As expected from their hydrophobic properties associated with long chain fatty acid components (cLogP of C22:0, C22:4, C20:0, C20:1 and C18:0; >7.9 vs. cLogP of malonyl-CoA; -4.3 , cLogP was calculated by ACD software), long chain fatty acids corresponding to the representative end-products of each ELOVL enzyme remain on the GF/C filter with greater efficacy than malonyl-CoA after washing (Fig. 2). Among the long chain fatty acids tested, although C22:4, the end product of ELOVL2 (i.e., elongation of C20:4), displayed relatively low remaining efficacy, its remaining efficacy was still 5 times larger than that of malonyl-CoA. This enabled us to conduct the primary characterization of ELOVL2 (Figs. 4b, 5b). Although further research is necessary, the relatively low remaining

property of C22:4 (5-fold) may be associated with its higher desaturation degree as compared with the corresponding saturated fatty acid (vs. C22:0; 15-fold).

In order to validate our newly developed assay methods, we first examined the substrate profile of ELOVL6 because the substrate specificity of ELOVL6 has been well characterized with conventional assays [7]. Regarding the enzyme materials, immunoblot analysis has confirmed that recombinant ELOVL6 is successfully expressed in the microsome fractions without altering its intrinsic compartment location (Fig. 1). Furthermore, recombinant ELOVL6 displayed selective elongation activities against myristoyl-CoA (C14:0-CoA) and palmitoyl-CoA (C16:0-CoA), recapitulating the reported substrate profiles of ELOVL6. Taken together, this suggests C-terminally tagged recombinant ELOVL proteins and the GF/C-filter method are reliable for measuring ELOVL activities. In support of this, we similarly observed that the microsomes from ELOVL-transfected cells, but not mock-transfected cells, displayed dose-dependent increases in elongation activities against the acyl-CoA substrates, respectively, with appreciable assay windows (Fig. 4).

Because there had been no report that compares the substrate specificities of human ELOVLs using the same format, we further examined and compared the detailed substrate profiles of the representative ELOVLs; ELOVL1, -2, -3, -5 and -6. Consistent with previous reports [4, 7, 12, 21, 22], ELOVL1, -3, and -6 preferentially elongated the saturated acyl-CoAs while ELOVL2 and ELOVL5 elongated the unsaturated acyl-CoAs (Fig. 5). With regard to

Fig. 5 Comparison of the substrate specificity of human ELOVL enzymes. The substrate specificities of human ELOVL enzymes were assessed using a series of saturated (C14:0, C16:0, C18:0, C20:0, C22:0, C24:0 and C26:0), monounsaturated (C16:1 and C18:1), and polyunsaturated (C18:2 and C20:4) fatty acyl-CoAs. Data were expressed as fold activities of ELOVLs-transfected microsomes (a ELOVL1, b ELOVL2, c ELOVL3, d ELOVL5, e ELOVL6) compared to that of mock transfected microsomes. Data are expressed as means \pm SEM from three independent experiments for each ELOVL enzyme

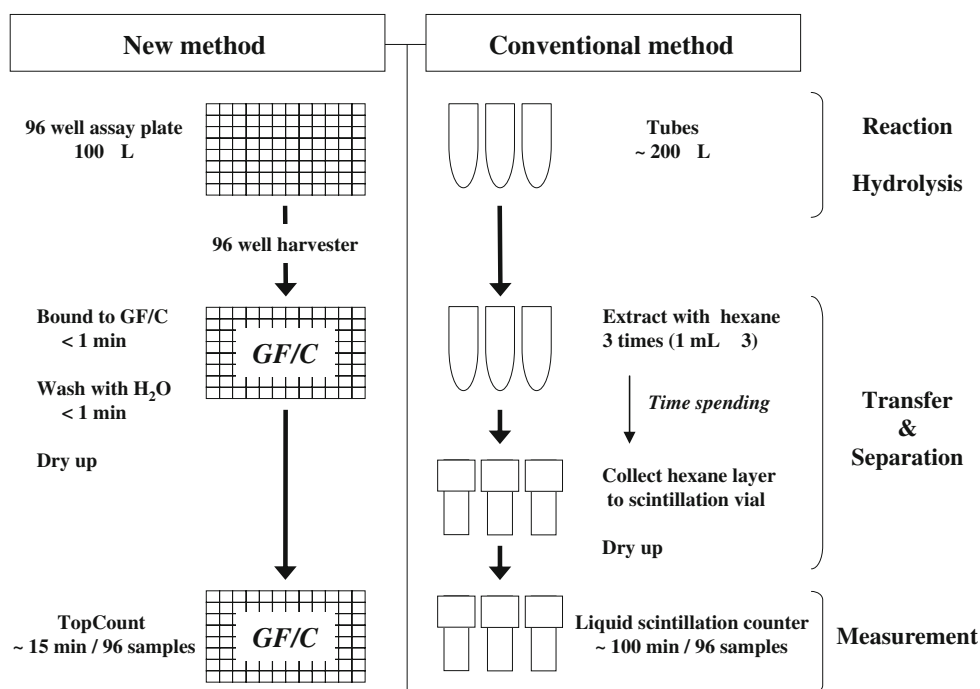


ELOVL3, there has been no study reporting the substrate specificity in a direct manner by using recombinantly expressed ELOVL3 so far. Under our assay conditions, ELOVL3 preferentially elongates C18:0 with relatively moderate-to-low elongation activities on other saturated fatty acids such as C14:0, C16:0 and C20:0. Although previous reports have not assessed ELOVL3 activity toward C14:0, we observed similar substrate specificity of ELOVL3 in the conventional assay (supplemental Fig. 2b), suggesting that ELOVL3 also elongates C14:0. Considering the highest sequence homology between ELOVL3 and ELOVL6 (46%) among the ELOVL family enzymes, it is not surprising that ELOVL3 and ELOVL6 show the overlapped substrate specificity for saturated fatty acids such as C14:0 and C16:0.

Under our assay conditions, ELOVL5 elongates the saturated acyl-CoAs such as myristoyl-CoA (C14:0-CoA)

and palmitoyl-CoA (C16:0-CoA); a 4-fold increase in elongation activities in the ELOVL5 transfected microsome versus the mock-transfected microsome (Fig. 5d). We observed the elongation activities of ELOVL5 for these acyl-CoAs under the conventional assay method, suggesting that the discrepancy between the current and previous reports is not due to the assay methods (data not shown). At present, we cannot exclude the possibility that the C-terminal tag may affect the substrate profile of ELOVL5. Further studies using recombinant ELOVL5 with no-tag will help us to understand the potential limits of using the modified recombinant enzymes for detailed profiling of ELOVLs. If this is the case, development of specific antibodies against native sequences of each ELOVL proteins might facilitate the confirmation of unmodified ELOVL expression and support our assay method when using unmodified enzymes.

Fig. 6 Scheme of elongation assay procedure (new vs. conventional method)



Drug Discovery

The lack of convenient ELOVL assay protocols keeps researchers from discovering new ELOVL drugs despite increasing interest. In order to establish an assay protocol that is amenable to high-throughput screening, we improved upon the 3 assay steps of the conventional assay by introducing 96-well-based devices (Fig. 6). (1) *Transfer step*: The 96-well harvester (FilterMate cell harvester: PerkinElmer) simplifies the transfer step as compared to the conventional method that requires time-consuming transfer of reaction mixtures to glass tubes. (2) *Separation step*: The use of the Unifilter-96 GF/C plate considerably reduced the experimental time needed for the separation procedure; now only 2–3 min are required to treat 96 samples (one plate). (3) *Measurement step*: We use the TopCount (PerkinElmer) to measure elongation activity. TopCount is capable of measuring 96 samples (one plate) within 15 min whereas the conventional method requires ~100 min when counting 96 samples.

Here we combined each step of the conventional assay using the Unifilter-96 GF/C filter plate, establishing a high-throughput assay that allows investigators to conduct (1) screening of a chemical library and further characterization of hit compounds and (2) a detailed characterization of ELOVL enzymes using the same format with reduced work load.

As demonstrated in this study, the respective ELOVLs have distinct substrate specificity. Furthermore, ELOVLs have different expression patterns in human tissues (Supplemental Fig. 1), suggesting ELOVLs have distinct

physiological roles. Recent studies using transgenic approaches strongly suggest that altered expressions of ELOVLs might be associated with diseases such as metabolic disorders and dyslipidemia [2, 23, 24]. We believe our 96-well format assay will help further ELOVL research, not only in industry but also in academic institutions. In turn, our new method will advance drug research.

References

- McGarry JD (2002) Banting lecture 2001: dysregulation of fatty acid metabolism in the etiology of type 2 diabetes. *Diabetes* 51:7–18
- Matsuzaka T, Shimano H, Yahagi N, Kato T, Atsumi A, Yamamoto T, Inoue N, Ishikawa M, Okada S, Ishigaki N, Iwasaki H, Iwasaki Y, Karasawa T, Kumadaki S, Matsui T, Sekiya M, Ohashi K, Hasty AH, Nakagawa Y, Takahashi A, Suzuki H, Yatoh S, Sone H, Toyoshima H, Osuga J, Yamada N (2007) Crucial role of a long chain fatty acid elongase, Elov16, in obesity-induced insulin resistance. *Nat Med* 13:1193–1202
- Cao H, Gerhold K, Mayers JR, Wiest MM, Watkins SM, Hotamisligil GS (2008) Identification of a lipokine, a lipid hormone linking adipose tissue to systemic metabolism. *Cell* 134:933–944
- Jacobsson A, Westerberg R, Jacobsson A (2006) Fatty acid elongases in mammals: their regulation and roles in metabolism. *Prog Lipid Res* 45:237–249
- Bernert JT Jr, Sprecher H (1977) An analysis of partial reactions in the overall chain elongation of saturated and unsaturated fatty acids by rat liver microsomes. *J Biol Chem* 252:6736–6744
- Nugteren DH (1965) The enzymic chain elongation of fatty acids by rat-liver microsomes. *Biochim Biophys Acta* 106:280–290

7. Moon YA, Shah NA, Mohapatra S, Warrington JA, Horton JD (2001) Identification of a mammalian long chain fatty acyl elongase regulated by sterol regulatory element-binding proteins. *J Biol Chem* 276:45358–45366
8. Moon YA, Horton JD (2003) Identification of two mammalian reductases involved in the two-carbon fatty acyl elongation cascade. *J Biol Chem* 278:7335–7343
9. Tvrdik P, Asadi A, Kozak LP, Nedergaard J, Cannon B, Jacobsson A (1997) Cig30, a mouse member of a novel membrane protein gene family, is involved in the recruitment of brown adipose tissue. *J Biol Chem* 272:31738–31746
10. Tvrdik P, Westerberg R, Silve S, Asadi A, Jakobsson A, Cannon B, Loison G, Jacobsson A (2000) Role of a new mammalian gene family in the biosynthesis of very long chain fatty acids and sphingolipids. *J Cell Biol* 149:707–717
11. Zhang K, Kniazeva M, Han M, Li W, Yu Z, Yang Z, Li Y, Metzker ML, Allikmets R, Zack DJ, Kakuk LE, Lagali PS, Wong PW, MacDonald IM, Sieving PA, Figueroa DJ, Austin CP, Gould RJ, Ayyagari R, Petrukhin K (2001) A 5-bp deletion in ELOVL4 is associated with two related forms of autosomal dominant macular dystrophy. *Nat Genet* 27:89–93
12. Leonard AE, Bobik EG, Dorado J, Kroeger PE, Chuang LT, Thurmond JM, Parker-Barnes JM, Das T, Huang YS, Mukerji P (2000) Cloning of a human cDNA encoding a novel enzyme involved in the elongation of long chain polyunsaturated fatty acids. *Biochem J* 350:765–770
13. Matsuzaka T, Shimano H, Yahagi N, Yoshikawa T, Amemiya-Kudo M, Hasty AH, Okazaki H, Tamura Y, Iizuka Y, Ohashi K, Osuga J, Takahashi A, Yato S, Sone H, Ishibashi S, Yamada N (2002) Cloning and characterization of a mammalian fatty acyl-CoA elongase as a lipogenic enzyme regulated by SREBPs. *J Lipid Res* 43:911–920
14. Wang Y, Botolin D, Xu J, Christian B, Mitchell E, Jayaprakasam B, Nair MG, Peters JM, Busik JV, Olson LK, Jump DB (2006) Regulation of hepatic fatty acid elongase and desaturase expression in diabetes and obesity. *J Lipid Res* 47:2028–2041
15. Brolinson A, Fourcade S, Jakobsson A, Pujol A, Jacobsson A (2008) Steroid hormones control circadian Elov13 expression in mouse liver. *Endocrinology* 149:3158–3166
16. Kobayashi T, Zdravec D, Jacobsson A (2007) ELOVL2 over-expression enhances triacylglycerol synthesis in 3T3–L1 and F442A cells. *FEBS Lett* 581:3157–3163
17. Westerberg R, Tvrdik P, Uden AB, Mansson JE, Norlen L, Jakobsson A, Holleran WH, Elias PM, Asadi A, Flodby P, Toftgard R, Capecchi MR, Jacobsson A (2004) Role for ELOVL3 and fatty acid chain length in development of hair and skin function. *J Biol Chem* 279:5621–5629
18. Nagi MN, Cook L, Suneja SK, Peluso PS, Laguna JC, Osei P, Cinti DL (1989) Evidence for two separate beta-ketoacyl CoA reductase components of the hepatic microsomal fatty acid chain elongation system in the rat. *Biochem Biophys Res Commun* 165:1428–1434
19. Glickman JF, Schmid A (2007) Farnesyl pyrophosphate synthase: real-time kinetics and inhibition by nitrogen-containing bisphosphonates in a scintillation assay. *Assay Drug Dev Technol* 5:205–214
20. Weiss DR, Glickman JF (2003) Characterization of fatty acid synthase activity using scintillation proximity. *Assay Drug Dev Technol* 1:161–166
21. Leonard AE, Kelder B, Bobik EG, Chuang LT, Lewis CJ, Kopchick JJ, Mukerji P, Huang YS (2002) Identification and expression of mammalian long chain PUFA elongation enzymes. *Lipids* 37:733–740
22. Westerberg R, Mansson JE, Golozoubova V, Shabalina IG, Backlund EC, Tvrdik P, Retterstøl K, Capecchi MR, Jacobsson A (2006) ELOVL3 is an important component for early onset of lipid recruitment in brown adipose tissue. *J Biol Chem* 281:4958–4968
23. Moon YA, Hammer RE, Horton JD (2009) Deletion of ELOVL5 leads to fatty liver through activation of SREBP-1c in mice. *J Lipid Res* 50:412–423
24. Wang Y, Torres-Gonzalez M, Tripathy S, Botolin D, Christian B, Jump DB (2008) Elevated hepatic fatty acid elongase-5 activity affects multiple pathways controlling hepatic lipid and carbohydrate composition. *J Lipid Res* 49:1538–1552

Michael T. Arts, Michael T. Brett, Martin J. Kainz (eds): Lipids in aquatic ecosystems

Springer 2009

Néstor M. Carballeira

Received: 28 July 2009 / Accepted: 28 July 2009 / Published online: 3 September 2009
© AOCS 2009

Lipids in aquatic ecosystems is a much needed and timely volume that encompasses how lipids progress in the food chain across freshwater and marine ecosystems. The book tries to cover the role of lipids from lower to higher trophic levels. In 14 chapters the editors have succeeded in gathering a nice compilation of very important and instructive chapters, by experts in the field, which should appeal to a broad audience of researchers and educators in the lipid ecological area. Each chapter starts with a well-drafted introduction to the topic, and finishes with a conclusion that opens the door for future research in the field.

Chapter one begins with a relatively short overview of the lipid composition of algae but the emphasis of the chapter is on how environmental factors such as temperature, salinity, pH, and nutrient effects affect algal glycerolipid biochemistry.

Chapter two describes the formation and transfer of fatty acids in aquatic microbial food webs with a special emphasis on the role of heterotrophic protists (unicellular eukaryotes). This chapter presents a precise summary of the biosynthetic pathways of polyunsaturated fatty acids (PUFA) in heterotrophic protists and tells us that many of the biosynthetic pathways found in protists can be understood based on their phylogenetic histories. We leave the chapter with the awareness that future research in this area is much needed and important.

Chapter three focuses on the ecological significance of sterols in aquatic food webs. After a relatively short introduction to sterols we get a quick and simplified scheme of the sterol biosynthetic capabilities of the

different taxa. The exploitation of sterols from aquatic microorganisms for nutritional purposes is highlighted and we are left with the idea that sterol limitation might be one important factor that could have a negative impact on aquatic food webs.

In Chapter four, probably my favorite in this book, fatty acids and oxylipins that can act as semiochemicals are reviewed and their potential to modify intra and extracellular aquatic processes is discussed. One plus of this chapter is that it nicely describes the mechanistic pathways resulting in the production of polyunsaturated aldehydes (PUA) and hydrocarbons, compounds that can be detrimental to plankton interactions with a multitude of mechanisms and consequences.

Chapter five successfully presents how lipids and xenobiotic chemicals (contaminants) interact and move in aquatic food webs. This is a very important chapter since lipids are ecotoxicologically important for determining the extent to which lipophilic organic contaminants are bioaccumulated in aquatic organisms. Chapter five should have great appeal to environmental chemists.

Chapter six describes how taxonomic affiliation, temperature, and diet influence the fatty acid composition of freshwater and marine zooplankton based on the fact that ocean and freshwater lakes have markedly different fatty acid compositions. The chapter ends with a series of unanswered questions in the field that should certainly spark much needed research in this area. Chapter six is certainly a good source of research ideas for aquatic ecologists.

Chapter seven defines specific optima between omega-3 and omega-6 fatty acids in freshwater fish, zooplankton and zoobenthos. This chapter is an excellent reference on n-3/n-6 ratios in marine biota (several reference tables with n-3/n-6 ratios are presented at the end of the chapter) and

N. M. Carballeira (✉)
Department of Chemistry, University of Puerto Rico,
Rio Piedras, PR, USA
e-mail: nmcarballeira@uprrp.edu

presents a good discussion on the physiological and ecological importance of these PUFA. When reading the chapter the reader can easily identify knowledge gaps in the field. We are told that there are large effects on these n-3/n-6 ratios when comparing wild vs. cultured fish and that diet has a strong influence on the PUFA composition.

Chapter eight gives an estimate of the transfer of omega-3 highly unsaturated fatty acids (HUFA) from aquatic to terrestrial ecosystems based on the available literature. We learn that the main flux of aquatic HUFA to terrestrial ecosystems originates from inland waters and estuaries rather than from the ocean. Algae are a main source of HUFA for many terrestrial animals but the role of birds and humans is also discussed.

Chapter nine is a good concise account of the biochemistry and molecular biology involved in the various pathways of polyunsaturated fatty acids and their inter-conversions in aquatic ecosystems. A well-referenced summary of the present knowledge of the biosynthesis of fatty acids in fish is presented and potential future directions of research are discussed. We are left with the message that fish will remain a major source of n-3 HUFA for humans, but fish will be cultivated using diets containing transgenic seed oils.

Chapter 10 is a short chapter dealing with the influence of lipids on membrane fluidity and immune response. The role that specific fatty acids play in maintaining the health and conditions of teleost cell membranes in terms of temperature adaptation is discussed. The author succeeds in conveying the message that biochemical methods are complimentary measures to assess the condition and underlying health of fish.

In Chapter 11, the emphasis now moves to global warming. The role of lipids in marine copepods is reviewed as the case study. The copepod lipid profiles have evolved in response to the specific habitats and temperature regimes

occupied by the various species. The copepods accumulate large resources of energy-rich lipids (as wax esters) and they play a key role in the transfer of energy through the food web. The lipid levels of zooplankton in polar regions can comprise more than half of the total carbon source and changes in temperature may have effects on these lipid profiles that may not be straightforward or predictable but it will have a decisive effect on future life in the oceans.

Chapter 12 emphasizes the need for a more quantitative method for using fatty acid trophic markers to explain food web dynamics. The author recognizes that fatty acids can be used as powerful trophic tracers of carbon flow and predator–prey interactions. The use of the statistical tool quantitative fatty acid signature analysis (QFASA) is discussed in detail and seems to be the way to go in the future. Therefore, chapter 12 is very important for those who want to move further in this field.

Chapter 13 questions what the essential fatty acids in aquatic food webs really are. The author states that it is time to reexamine whether the two fatty acids EPA and DHA are enough to describe adequately the essential fatty acid states in aquatic food webs. The last chapter in the book, Chapter 14, examines the position of humans in the global food web and calls for an urgent need to protect the aquatic food web → human connection.

The editors of *Lipids in Aquatic Ecosystems* correctly and clearly identify that this book should appeal to plankton ecologists, nutritionists, aquaculturists, toxicologists, environmental chemists and environmental managers. I would add that it should also appeal to lipid educators since the volume contains valuable material and information that could be incorporated in several sections of a course in lipid chemistry. Overall, this is a well-drafted and easy to read volume that should be in the shelves of most lipid chemists' libraries.

Marine Two-Headed Sphingolipid-Like Compound Rhizochalin Inhibits EGF-Induced Transformation of JB6 P⁺ Cl41 Cells

Sergey N. Fedorov · Tatyana N. Makarieva ·
Alla G. Guzii · Larisa K. Shubina · Jong Y. Kwak ·
Valentin A. Stonik

Received: 6 February 2009 / Accepted: 15 June 2009 / Published online: 5 July 2009
© AOCS 2009

Abstract Rhizochalin [(2*R*,3*R*,26*R*,27*R*)-2,27-diamino-3-hydroxy-26-[(2*R*,3*R*,4*S*,6*R*)-3,4,5-trihydroxy-6-(hydroxymethyl)tetrahydro-2*H*-pyran-2-yl]oxy]octacosan-11-one], an antimicrobial and cytotoxic marine two-headed sphingolipid-like natural product, isolated from the sponge *Rhizochalina incrustata*, and some related compounds were studied as anticarcinogenic and proapoptotic agents. The corresponding effects were tested on the mouse skin epidermal JB6 P⁺ Cl 41 cell line, its stable transfectants, THP-1, HeLa, and SNU-C4 human tumor cells using a variety of assessments, including cell viability (MTS), flow cytometry, anchorage-independent soft agar, and luciferase assays. At 5–10 μM concentrations, rhizochalin was effective as an inhibitor of the malignant transformation of JB6 P⁺ Cl 41 cells or colony formation of human tumor cells, which exerted its action, at least in part, through the induction of p53-dependent apoptosis. Structure–activity relationship study showed aglycon of rhizochalin to be the most active while peracetylated aglycon was the least active among the compounds studied.

Keywords Marine two-headed sphingolipid-like compound · Anticarcinogenic properties · Tumor cells · p53-dependent apoptosis

Abbreviations

MTS	5-(3-Carboxymethoxyphenyl)-2-(4,5-dimethylthiazolyl)-3-(4-sulfophenyl) tetrazolium, inner salt
JB6 P ⁺ Cl 41, THP-1, HeLa, SNU-C4	Cell lines
EGF	Epidermal growth factor
FBS	Fetal bovine serum
IAC ₅₀	Induction of apoptosis C ₅₀
IC ₅₀	Inhibition concentration
INCC ₅₀	Inhibition of the number of the colonies C ₅₀
MEM,RPMI,BME	Medium for cell growth
SAR	Structure–activity relationship
p53	Tumor suppressor protein
AP-1	Activator protein 1
TPA	12- <i>O</i> -Tetradecanoylphorbol-13-acetate
MAPK	Mitogen-activated protein kinase

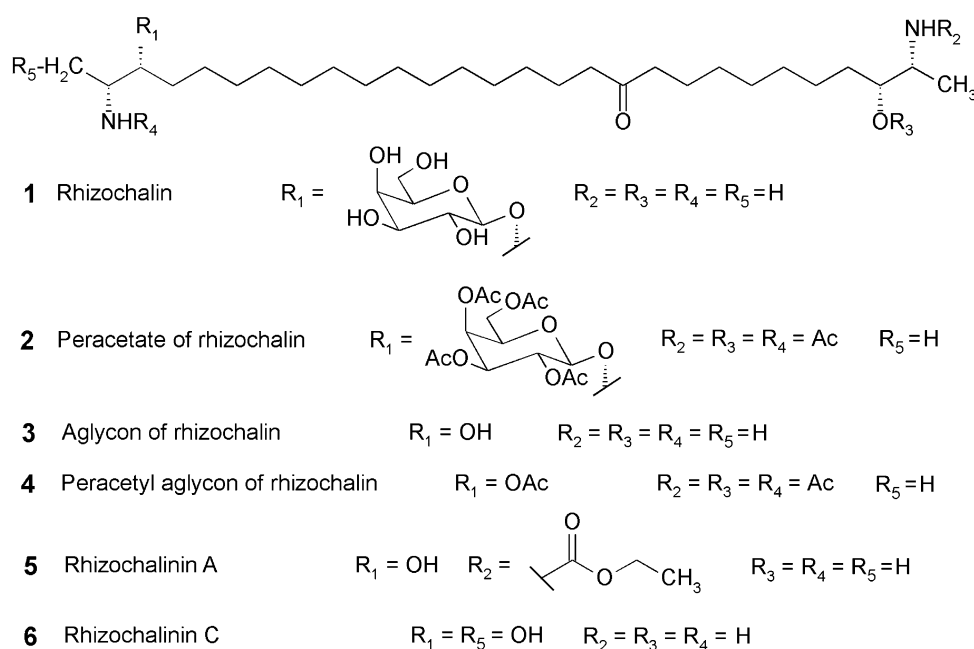
Introduction

Since the isolation in 1989 of an unusual two-headed sphingolipid-like metabolite rhizochalin (**1**, Fig. 1) [1], a series of related natural products have been reported [2–10]. Two-headed sphingolipid-like compounds differ from classical sphingolipids in the presence of polar groups in α,ω -positions. These polar groups resemble a polar end of sphingoid bases, but contain often a terminal methyl group instead of hydroxymethyl group. Thus, these natural products represent a unique group of bipolar lipids.

S. N. Fedorov (✉) · T. N. Makarieva · A. G. Guzii ·
L. K. Shubina · V. A. Stonik
Pacific Institute of Bioorganic Chemistry,
Vladivostok 690022, Russian Federation
e-mail: fedorov@piboc.dvo.ru

J. Y. Kwak
Medical Research Center for Cancer Molecular Therapy,
Dong-A University, Busan 602-714, Republic of Korea

Fig. 1 Structures of rhizochalin and its analogs and derivatives



Rhizochalin and analogs were reported to possess antibacterial, antifungal, and cytotoxic activities [2–10]. Beside preliminary data on blocking phytosphingolipid biosynthesis by the related metabolite oceanalin A [6], no information exists regarding the molecular mechanism that determines the physiological activities of rhizochalin and its analogs. In the present study we investigated the cancer-preventive and anticancer cytotoxic activities of rhizochalin (**1**) and its analogs (**5**, **6**) and derivatives (**2–4**).

Cancer chemopreventive agents are usually natural products or their synthetic analogs that inhibit either the transformation of normal cells to premalignant cells or the progression of premalignant cells to malignant cells [11–13]. Therefore, an effective chemopreventive agent should step in the process of carcinogenesis to eliminate premalignant cells before they become malignant [14–16]. Some chemopreventive agents (e.g. retinoids and antiestrogens) promote cytostatic effects in transformed cells by modulating cell proliferation or differentiation [11, 14, 16]. These agents should be long-term administered to healthy individuals who have an increased cancer risk. In this case long-term toxicity and the possibility of developing resistance to chemopreventive agents could limit the application of the substances [14]. An alternative chemopreventive approach calls for the use of agents that quickly eliminate premalignant cells by inducing them to undergo apoptosis. An increasing number of chemopreventive agents have been shown to stimulate apoptosis in premalignant and malignant cells in vitro and in vivo [17–22]. By using this approach, chronic exposure to a chemopreventive agent would not be necessary, thereby limiting the risk of long-term toxicity or the development of chemoresistance [14–16].

Herein, we report results of the study on rhizochalin and related compounds capability to inhibit the EGF-induced malignant transformation of JB6 P⁺ Cl41 and colony formation of several human cancer cell lines in anchorage-independent assay experiments. Some detailed data regarding the molecular mechanism of **1–6** action are also given. The JB6 cell system of clonal genetic variants, including promotion-sensitive (P⁺), promotion-resistant (P⁻), or malignantly transformed, enables the search of chemopreventive compounds and helps to study their cancer-preventive properties at the molecular level. The JB6 P⁺, P⁻, and transformed variants are a series of cell lines representing earlier-to-late stages of preneoplastic-to-neoplastic progression [23–27]. JB6 P⁺ cells transform when stimulated with EGF or TPA resulting in the formation of colonies in soft agar. The transformation involves the activation of the AP-1 nuclear factor which regulates the transcription of various genes related to inflammation, proliferation and metastasis [24, 28]. Cancer cells, in contradistinction from JB6 P⁺ Cl41 cells, do not need EGF or any other carcinogen for activation. The process of carcinogenesis initiated, promoted and perpetuated malignant phenotype in these cells. The colony formation of cancer cells in soft agar is a result of their phenotype expression [29, 30]. The investigation of rhizochalin and its analogs as anticancer agents requires the study of their activity against various human cancer cell lines. Anticancer activity of one and the same compound often differs significantly from one cancer cell line to another. We studied the anticancer activity of the substances using human THP-1 (acute monocytic leukemia), HeLa (cervical carcinoma), and SNU-C4 (colorectal

cancer) cell lines from the NCI panel. These cell lines are widely used in many laboratories all over the world, so the activities of rhizochalin and its analogs can be easily compared with those of a number of other anticancer agents.

Experimental Procedure

General Procedures

Cell colonies in the anchorage-independent transformation assay were scored using the LEICA DM IRB inverted research microscope (Leica Mikroskopie und Systeme GmbH, Germany) and Image-Pro Plus software, version 3.0 for Windows (Media Cybernetics, Silver Spring, MD, USA). The MTS reduction assay to determine cell viability was carried out using the μ Quant microplate reader (Bio-Tek Instruments, Inc, USA). The onset of apoptosis was analyzed by flow cytometry using the Becton-Dickinson FACSCalibur (BD Biosciences, San Jose, CA, USA). Data analysis was performed using CellQuest software (Becton-Dickinson, CA, USA). The luminescence assay for p53 nuclear factor-dependent transcriptional activity was measured using the Luminoscan Ascent Type 392 microplate reader (Labsystems, Helsinki, Finland).

Rhizochalin or Its Analogs and Derivatives

Rhizochalin and its analogs and derivatives were extracted, purified and prepared as described previously [1, 7–9] and were pure in accordance with NMR, MS, TLC, and HPLC data. Briefly, the fresh collection of the sponges *R. incrustata* was immediately lyophilized and kept at $-20\text{ }^{\circ}\text{C}$. The lyophilized material was extracted with EtOH (200 ml \times 3). The combined EtOH extract was concentrated under vacuum and dissolved in EtOH/H₂O (9:1, by vol). This solution was partitioned three times with equal volumes of *n*-hexane. The aqueous EtOH layer was evaporated in vacuo at $50\text{ }^{\circ}\text{C}$ to give a brown oil, which was purified from salts using reversed phase column chromatography. The rhizochalin-containing fraction (ninhydrine positive) was eluted with 50% EtOH and separated on a Si gel column [CHCl₃/EtOH/H₂O (3:2:0.2, by vol)] to give a rhizochalin-containing mixture. Preparative HPLC of the mixture using a C₁₈ reversed phase column [MeOH/H₂O/TFA (80:20:0.1, by vol)] gave rhizochalin or its analogs. Aglycons of rhizochalin or analogs were obtained after hydrolysis of the initial glycosides using 2 N HCl. Acetate of rhizochalin or peracetylated aglycon of rhizochalin were obtained after acetylation of rhizochalin or aglycon of rhizochalin in the mixture of pyridine/Ac₂O (1:1, by vol), rt for 12 h.

Reagents

Minimum essential medium (MEM), and RPMI medium were purchased from Gibco Invitrogen Corporation (Carlsbad, CA, USA). Fetal bovine serum (FBS) was from Gemini Bio-Products (Calabasas, CA, USA); penicillin/streptomycin and gentamycin were from Bio-Whittaker (Walkersville, MD, USA); and L-glutamine was from Mediatech, Inc. (Herndon, VA, USA). Epidermal growth factor (EGF) was obtained from Collaborative Research (Bedford, MA, USA). The luciferase assay substrate and Cell Titer 96 Aqueous One Solution Reagent [5-(3-carboxymethoxyphenyl)-2-(4,5-dimethylthiazolyl)-3-(4-sulfophenyl) tetrazolium, inner salt (MTS)] kit for the cell viability assay were from Promega (Madison, WI, USA). The Annexin V-FITC Apoptosis Detection kit was from Medical & Biological Laboratories (Watertown, MA, USA).

Cell Culture

The JB6 P⁺ Cl41 mouse epidermal cell line and its stable transfectants JB6 Cl41 DN-JNK1 mass1, JB6 Cl41 DN-p38 G7, JB6 Cl41 DN-ERK2 B3 mass1, JB6 Cl41-Lucp53 (PG-13) cells were cultured in monolayers at $37\text{ }^{\circ}\text{C}$ and 5% CO₂ in MEM containing 5% FBS, 2 mM L-glutamine, 100 U/ml penicillin and 100 $\mu\text{g/ml}$ streptomycin [23]. The human cancer cell lines THP-1, HeLa, and SNU-C4 were obtained from the American Type Culture Collection (Rockville, MD, USA) and were cultured at $37\text{ }^{\circ}\text{C}$ and 5% CO₂ in RPMI containing 10% FBS, 2 mM L-glutamine, 100 U/ml penicillin and 100 $\mu\text{g/ml}$ streptomycin. Information regarding the genetic background of these cell lines is available online.

Anchorage-independent Transformation or Phenotype Expression Assay

The cancer-preventive effect of rhizochalin or its analogs were evaluated using an anchorage-independent neoplastic transformation or phenotype expression assay. For evaluation of the anticancer effects of the substances in human cancer cell lines using a phenotype expression assay, no additional stimulus was required. EGF (10 ng/ml) was used for stimulating neoplastic transformation of JB6 P⁺ Cl 41 cells. The assay was carried out in six-well tissue culture plates. Human HeLa, THP-1, SNU-C4, or mouse JB6 P⁺ Cl 41 cells (8×10^3 per ml) were treated with various concentrations of the substances in 1 ml of 0.33% basal medium Eagle (BME) agar containing 10% FBS over 3 ml of 0.5% BME agar containing 10% FBS and various concentration of the substances. The cultures were maintained in a $37\text{ }^{\circ}\text{C}$, 5% CO₂ incubator for 1 week. Then cell colonies were scored.

Cell Viability Assay

The effect of the compounds on cell viability was evaluated using MTS reduction into its formazan product [31]. The cells were cultured for 12 h in 96-well plates (6,000 cells/well) in the corresponding medium (100 μ l/well) containing 10% FBS (5% for JB6 Cl 41 cells). The medium was then replaced with 10% FBS-medium (5% for JB6 Cl 41 cells) containing the indicated concentrations of the compounds, and the cells were incubated for 22 h. Then 20 μ l amount of MTS reagent was added into each well, and MTS reduction was measured 2 h later spectrophotometrically at 492 and 690 nm as background.

Apoptosis Assay

The onset of early and late apoptosis was analyzed by flow cytometry using Annexin V-FITC and propidium iodide (PI) double staining. THP-1 cells, 1×10^6 /10 cm dish, in 10% FBS-RPMI were treated with various concentrations of rhizochalin or its derivatives for 24 h. After incubation, cells were washed with PBS by centrifugation at 1,000 rpm (170 rcf) for 5 min, and processed for detection of apoptosis using Annexin V-FITC and PI staining according to the manufacturer's protocol. In brief, 1×10^5 to 5×10^5 cells were resuspended in 500 μ l of $1 \times$ binding buffer (Annexin V-FITC Apoptosis Detection Kit, Medical & Biological Laboratories). Then, 5 μ l of Annexin V-FITC and 5 μ l of PI were added, and the cells were incubated at room temperature for 15 min in the dark and were analyzed by flow cytometry.

Assay for p53-dependent Transcriptional Activity

The ability of rhizochalin or its aglycon to influence p53-dependent transcriptional activity in the mouse JB6 Cl 41 cell line was evaluated using the luciferase method. JB6 Cl41-Lucp53 (PG-13) cells (6×10^3) suspended in 100 μ l 5% FBS-MEM were added into each well of a 96-well plate. Plates were incubated for 12 h and then treated with various concentrations of the substances in 100 μ l of 10% FBS-MEM. After incubation with the substances for 24 h, the cells were extracted for 1 h at room temperature with 100 μ l/well of lysis buffer [0.1 M potassium phosphate buffer at pH 7.8, 1% Triton X-100, 1 mM dithiothreitol (DTT), 2 mM EDTA]. Then 30 μ l of lysate from each well was transferred in a plate used for luminescent analysis, and luciferase activity was measured using 100 μ l/well of the luciferase assay buffer [0.47 mM D-luciferin, 20 mM Tricin, 1.07 mM magnesium carbonate hydroxide pentahydrate ($\text{MgCO}_3)_4 \times \text{Mg(OH)}_2 \times 5\text{H}_2\text{O}$, 2.67 mM $\text{MgSO}_4 \times 7\text{H}_2\text{O}$, 33.3 mM DTT, 0.53 mM ATP, 0.27 mM CoA, and 0.1 mM EDTA (pH 7.8)].

Statistics

The statistical computer program Statistica 6.0 for Windows (StatSoft, Inc., Tulsa, OK, USA, 2001) was used for analysis of the data obtained. The value of the $n = 6$ (six samples of two independent experiments). Nonparametric Mann–Whitney U test was used to compare two independent groups of data. Method of regressions was used to compute IC_{50} , IAC_{50} or INCC_{50} in corresponding experiments.

Results

Cancer-preventive Properties

To assess whether rhizochalin or its derivatives can prevent tumor promoter-induced neoplastic transformation of mouse epidermal JB6 P⁺ Cl41 cells or inhibit phenotype expression of human cancer cell lines, we used the well-accepted anchorage-independent assay in soft agar and EGF (10 ng/ml) as a promoter of JB6 P⁺ Cl41 cells colony formation [24, 25, 32, 33].

Our experiments showed that rhizochalin (**1**) at 5–12 μ M concentrations, in a dose-dependent manner inhibited EGF-induced malignant transformation of JB6 P⁺ Cl41 cells (Fig. 2a–c). Specifically, a 50% inhibition of EGF-induced JB6 P⁺ Cl41 cells colony formation (INCC_{50}) by rhizochalin was achieved at a concentration of 8.6 μ M (Fig. 2a). Similar effects were observed for suppression of phenotype expression of several human tumor cell lines in a soft agar. For example, the INCC_{50} for phenotype expression of HeLa (cancer of cervix) cells (Fig. 2b) or THP-1 (monocytic leukemia) cells (Fig. 2c), were 12.6 and 5.4 μ M, respectively. Aglycon of rhizochalin (**3**) was significantly more active as inhibitor of SNU-C4 cells colony formation with $\text{INCC}_{50} = 1.7 \mu\text{M}$ (Fig. 2d).

Cytotoxic Activity and SAR Study

The MTS method [31] was applied to examine the cytotoxicity of rhizochalin or its analogs and derivatives against JB6 P⁺ Cl41, HeLa, or THP-1 cell lines. The results (Table 1) showed that the cytotoxic effect of the compounds (**1–6**) depends on their chemical structure. Thus, aglycon of rhizochalin (**3**) together with rhizochalinin A (**5**) and rhizochalinin C (**6**) were the most cytotoxic, while peracetylated aglycon of rhizochalin (**4**) was the least active among the compounds studied. Furthermore, peracetate of rhizochalin (**2**) was two times less active against THP-1 cells than rhizochalin (**1**). SAR study among the compounds **1–6** using MTS method (Table 1) indicated

Fig. 2 Rhizochalin inhibited EGF-induced malignant transformation of JB6 P⁺ Cl41 cells (a) or phenotype expression of human cancer HeLa (b) or THP-1 (c) cells. Aglycon of rhizochalin suppressed phenotype expression of human cancer SNU-C4 cells (d). Each bar represents the mean \pm SD from six samples of two independent experiments. * $p < 0.05$

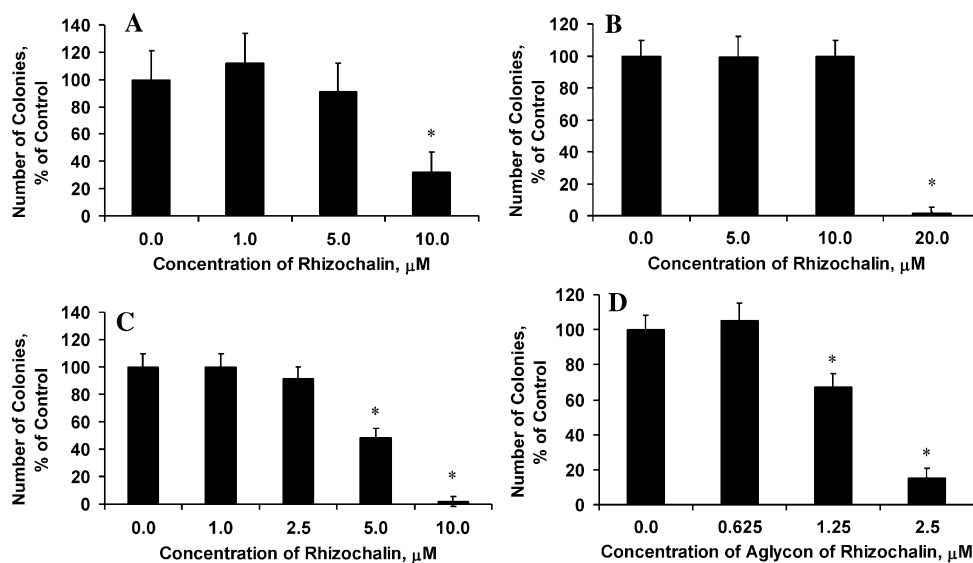


Table 1 Cytotoxic activity (IC₅₀, μ M) of the compounds (1–6)

Compound	JB6 P ⁺ Cl 41	HeLa	THP-1
Rhizochalin (1)	8.8	22.1	13.6
Peracetate of rhizochalin (2)	n/s	n/s	26.8
Aglycon of rhizochalin (3)	2.8	8.5	3.2
Peracetylated aglycon of rhizochalin (4)	>30	>30	63.3
Rhizochalinin A (5)	n/s	n/s	7.5
Rhizochalinin C (6)	n/s	n/s	6.7

n/s: Cytotoxicity was not studied

that unsubstituted hydroxyl groups at both α - and ω -ends of the molecule are important for the anticancer action of rhizochalin or its analogs and derivatives. Then, the results of the cell viability experiments were compared with the results of the soft agar experiments. As shown, rhizochalin (1) demonstrated cancer-preventive properties at non-cytotoxic concentrations against HeLa or THP-1 cells. In the case of JB6 P⁺ Cl 41 cells the active concentrations were about the same in both soft agar and cell viability experiments.

The dominant-negative mutant (DNM) JB6 Cl 41 cells and the MTS method were used to elucidate the effect of rhizochalin on the main MAPK signaling pathways in JB6 Cl 41 cells. The results (Fig. 3) demonstrated cytotoxic effect of rhizochalin to be different in respect to various DNM JB6 Cl 41 cells. Specifically, rhizochalin was significantly more active against JB6 Cl 41 DN-ERK2 or JB6 Cl 41 DN-JNK1 cells than against JB6 Cl 41 DN-p38 or non-transfected JB6 P⁺ Cl 41 cells (Fig. 3). Furthermore, JB6 Cl 41 DN-p38 and JB6 P⁺ Cl 41 cells showed the even sensitivity to the action of rhizochalin (Fig. 3). These

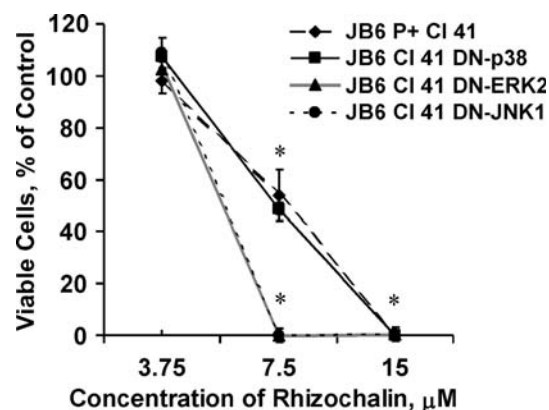


Fig. 3 Cytotoxic activity of rhizochalin against various JB6 Cl41 DNM cells. Each datapoint represents the mean \pm SD from six samples of two independent experiments. * $p < 0.05$

findings indicated that probably no one of the main MAPK kinases mediate the cytotoxic effect of rhizochalin.

Rhizochalin Induces Apoptosis in Human Leukemia Cells

Induction of apoptosis by rhizochalin was evaluated by flow cytometry using Annexin V-FITC and propidium iodide double staining. Rhizochalin was found to induce a dose-dependent apoptosis of human leukemia THP-1 cells with IAC₅₀ (induction of apoptosis C₅₀) 6.5 μ M (Fig. 4).

Rhizochalin Induces Basal p53 Transcriptional Activation in JB6 Cl41 Cells

The effect of the compounds 1 or 3 on p53 transcriptional activation was investigated in JB6 Cl41 p53 cells stably expressing a luciferase reporter gene controlled by a p53

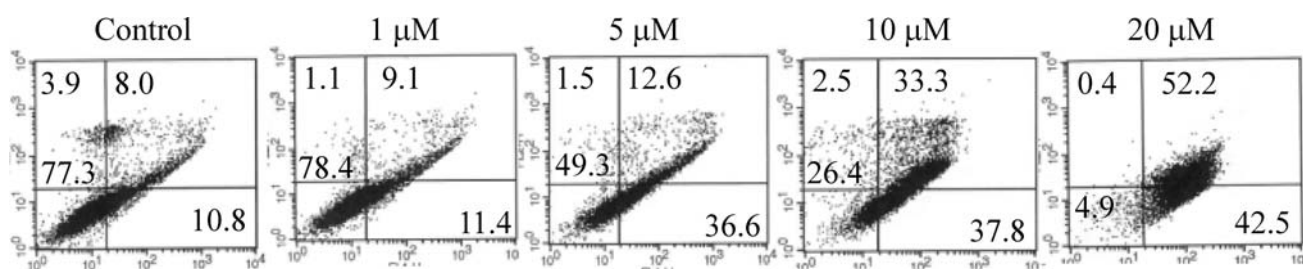


Fig. 4 The induction of apoptosis by rhizochalin in human leukemia THP-1 cells as analyzed by flow cytometry. Representative experiment is shown

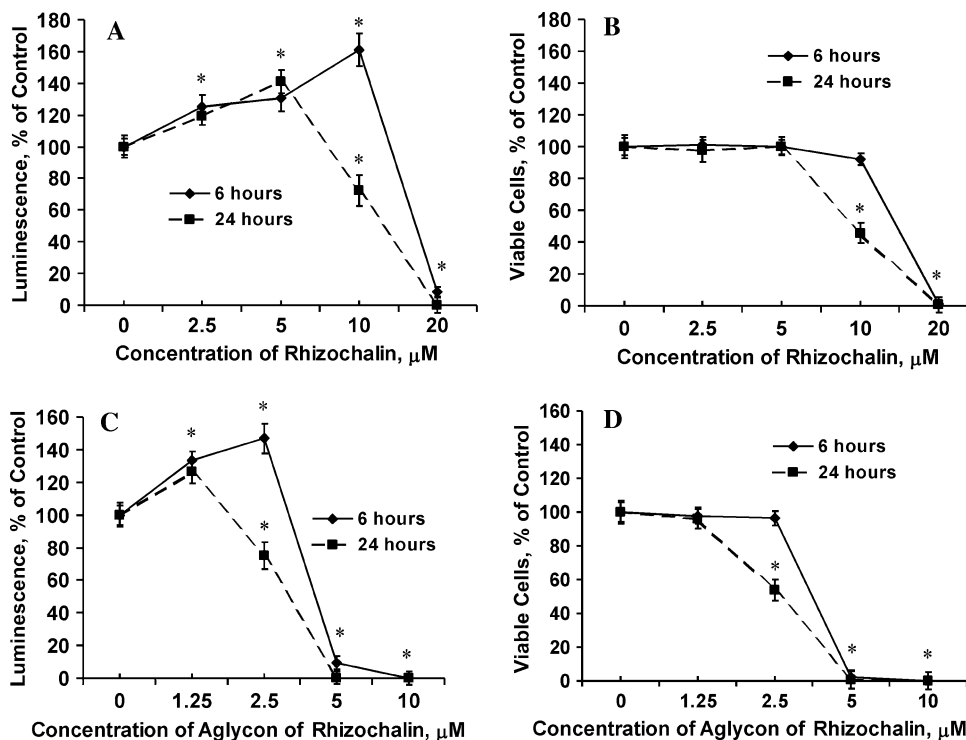
DNA binding sequence (Fig. 5a, c). Beside p53-dependent transcriptional activity, the effect of **1** or **3** on JB6 Cl41 p53 cells viability (Fig 5b, d) was also evaluated. Rhizochalin (Fig. 5a) or aglycon of rhizochalin (Fig. 5c) at active concentrations of 5–10 or 1.25–2.5 μM (Fig. 5b or d), respectively, and in a dose-dependent manner induced basal p53-dependent transcriptional activity in JB6 Cl 41 cells. It was demonstrated that about 100% of cells were still alive after 6 h of the treatment with the active concentrations of **1** or **3** (Fig. 5b, d). At these conditions, the p53-dependent transcriptional activity was induced 1.3–1.6 times more, when compared with untreated control cells (Fig. 5a, c). Only about 50% of cells were alive (Fig. 5b, d) after 24 h of the treatment with 10 μM of **1** or 2.5 μM of **3**. Nevertheless, luminescence was about 80% in comparison with that of untreated control cells (Fig. 5a, c) indicating thus the 1.6 times increase of p53-dependent transcriptional

activity in JB6 Cl 41 p53 cells treated with the active concentrations of rhizochalin (**1**) or aglycon of rhizochalin (**3**). These findings suggest that rhizochalin exerts its anticancer properties at least in part through the induction of p53-dependent pathway.

Discussion

The fact that most cancers are not of hereditary origin and that lifestyle factors, such as dietary habits, smoking, alcohol consumption, and infections have a profound influence on their development [34] provides major opportunities for cancer prevention. Natural products, including those of marine origin that show cancer-preventive and anticancer properties, attract more and more attention as probable candidates to be used in cancer-

Fig. 5 Rhizochalin (a) or aglycon of rhizochalin (c) induces basal p53-dependent transcriptional activity in JB6 Cl 41 p53 cells. The effect of rhizochalin (b) or aglycon of rhizochalin (d) on the cell viability of JB6 Cl 41 p53 cells evaluated after 6 or 24 h of incubation with the compounds. Each bar represents the mean \pm SD from six samples of two independent experiments. * $p < 0.05$



preventive or chemotherapeutic anticancer strategies [35–42]. The cancer-preventive effects of the most common natural chemopreventive compounds, such as resveratrol, caffeine, epigallocatechin-3-gallate were established using promotion-sensitive JB6 P⁺ Cl41 cells. All these compounds prevent EGF- or TPA-induced transformation of JB6 P⁺ Cl41 cells [43–45]. Our results also showed that rhizochalin (**1**) and its derivative, aglycon of rhizochalin (**3**), in a dose-dependent manner inhibited EGF-induced malignant transformation of JB6 P⁺ Cl41 cells and colony formation of human tumor HeLa or THP-1 cells in soft agar (Fig. 2). Rhizochalin and analogs also demonstrated the cytotoxic activity against various human cancer cells (Table 1). SAR study revealed that this activity depends on the chemical structure of the compounds **1–6** and that free hydroxyl groups at both α - and ω -ends of the molecule are important for the anticancer action of rhizochalin or its analogs and derivatives.

Three different MAPK signaling pathways have been identified in mammalian cells: ERKs, JNKs, and p38 kinase. In general, JNKs and p38 kinase are primarily activated by environmental stresses, whereas ERKs respond mainly to mitogenic and proliferative stimuli [46]. Many of the changes which drive the process of carcinogenesis in a cell occur in MAPK signaling pathways that regulate proliferation and apoptosis [47]. The chemopreventive compounds can modulate signaling by affecting MAP kinase activity. For example, antimutagenic effect of epigallocatechin-3-gallate depends on the ERKs pathway [48], flavonoid baicalein induces cancer cells death by the induction of p38 kinase activity [49], while novel flavonoid protoapigenone induces apoptosis in human prostate cancer cells through activation of JNKs and p38 kinase [50]. To determine effects of rhizochalin on the main MAP kinases in cells, the cytotoxic activity of rhizochalin in respect to dominant-negative ERK2, p38, or JNK1 JB6 Cl 41 cells was evaluated (Fig. 3). The results suggest that probably no one of three main MAPK signaling pathways, p38, ERKs or JNKs, mediate the effect of rhizochalin or its analogs. Moreover, JNKs and/or ERKs signaling pathways may counteract against cytotoxic action of the compounds **1–6**.

Apoptosis is a general mechanism for removal of unwanted cells from organisms playing a protective role against carcinogenesis [51]. Evidence from both in vivo and in vitro experiments shows that apoptosis is involved in successful cancer treatment using many drugs and other chemical substances [52]. A number of factors and signaling pathways in a cell can lead to apoptosis and one of the most important pathways extends through activation of the p53 tumor suppressor protein. The tumor suppressor protein p53 normally exists in cells as a short-lived protein and functions to negatively regulate cell growth following damage by inducing cell cycle arrest and apoptosis [53–55]. A plethora

of evidence exists that p53 is involved in the chemopreventive effects of many natural compounds. For example resveratrol, epigallocatechin-3-gallate, caffeine, and many other cancer-preventive substances suppress normal cell transformation or induce antiproliferative effects with subsequent apoptosis in cancer cells through a p53-dependent pathway [43, 45, 56–67]. To explore a possible mechanism of the cancer-preventive action of rhizochalin and analogs, we studied pro-apoptotic properties of rhizochalin and the effect of the compounds **1** or **3** on p53 transcriptional activation in JB6 Cl41 p53 cells stably expressing a luciferase reporter gene controlled by a p53 DNA binding sequence. As it was shown, rhizochalin also exerts its cancer-preventive properties at least in part through the induction of p53-dependent apoptosis (Figs. 4, 5).

In conclusion, our results indicate that rhizochalin (**1**) and some analogs (**2–6**) represent a new group of marine secondary metabolites having cancer-preventive and anticancer properties. These compounds induce also the apoptosis of human cancer cells and increase the p53-dependent transcriptional activity. Both cancer-preventive and cytotoxic effects of rhizochalin and its analogs may be explained, at least in part, by the induction of p53-dependent apoptosis. It was also found that aglycon of rhizochalin (**3**), rhizochalinin A (**5**), or rhizochalinin C (**6**) are the most active compounds while peracetate of rhizochalin aglycon (**4**) is the least active among the compounds studied. We conclude that free hydroxyl groups at the both α - and ω -ends of the molecule are important for the anticancer properties of rhizochalin and related compounds. Therefore, further search for cancer-preventive and anticancer two-headed sphingolipids and their synthetic analogs might be prospective to find new pharmaceutical leads and/or useful tools for the study on molecular mechanisms of anticancer action of different compounds.

Acknowledgments This work was supported by the Grant 2813.2008.4 for Support of the Leading Russian Science Schools, Program of Presidium of RAS “Molecular and Cell Biology”, Grant RFFI 09-04-00015-a, and FEB RAS Grants 09-III-A-05-139 and 09-III-A-05-146. The Korean co-authors are grateful for financial support from the KOSEF through the Medical Research Center for Cancer Molecular Therapy at Dong-A University. The authors are grateful to Prof. Zigang Dong (Hormel Institute of Minnesota University, USA) who kindly donated the JB6 cell lines, which were used in the present study.

References

1. Makarieva TN, Denisenko VA, Stonik VA, Milgrom YM, Rashkes YV (1989) Rhizochalin, a novel secondary metabolite of mixed biosynthesis from the sponge *Rhizochalina incrustata*. *Tetrahedron Lett* 30:6581–6584
2. Kong F, Faulkner DJ (1993) Leucettamols A and B, two antimicrobial lipids from the calcareous sponge *Leucetta micro-raphis*. *J Org Chem* 58:970–971

3. Willis RH, De Vries DJ (1997) BRS1, a C30 bis-amino, bis-hydroxy polyunsaturated lipid from an Australian calcareous sponge that inhibits protein kinase C. *Toxicon* 35:1125–1129
4. Nicholas GM, Hong TW, Molinski TF, Lerch ML, Cancilla MT, Lebrilla CB (1999) Oceanapiside, an antifungal bis- α , ω -amino alcohol glycoside from the marine sponge *Oceanapia phillipensis*. *J Nat Prod* 62:1678–1681
5. Zhou BN, Mattern MP, Johnson RK, Kingston DG (2001) Structure and stereochemistry of a novel bioactive sphingolipid from a *Calyx* sp. *Tetrahedron* 57:9549–9554
6. Makarieva TN, Denisenko VA, Dmitrenok PS, Guzii AG, Santalova EA, Stonik VA, MacMillan JB, Molinski TF (2005) Oceanalin A, a hybrid α , ω -bifunctionalized sphingoid tetrahydroisoquinoline β -glycoside from the marine sponge *Oceanapia* sp. *Org Lett* 7:2897–2900
7. Makarieva TN, Guzii AG, Denisenko VA, Dmitrenok PS, Santalova EA, Pokanevich EV, Molinski TF, Stonik VA (2005) Rhizochalin A, a novel two-headed sphingolipid from the sponge *Rhizochalina incrustata*. *J Nat Prod* 68:255–257
8. Makarieva TN, Dmitrenok PS, Zakharenko AM, Denisenko VA, Guzii AG, Li R, Skepper CK, Molinski TF, Stonik VA (2007) Rhizochalins C and D from the sponge *Rhizochalina incrustata*. A rare three-sphingolipid and a facile method for determination of the carbonyl position in α , ω -bifunctionalized ketosphingolipids. *J Nat Prod* 70:1991–1998
9. Makarieva TN, Zakharenko AM, Denisenko VA, Dmitrenok PS, Guzii AG, Shubina LK, Kapustina II, Fedorov SN (2007) Rhizochalinin A, a new antileukemic two-headed sphingolipid from the sponge *Rhizochalina incrustata*. *Chem Nat Comp* 43:468–469
10. Makarieva TN, Guzii AG, Denisenko VA, Dmitrenok PS, Stonik VA (2008) New two-headed sphingolipid-like compounds from the marine sponge *Oceanapia* sp. *Rus Chem Bull* 57:669–673
11. Hong WK, Sporn MB (1997) Recent advances in chemoprevention of cancer. *Science* 278:1073–1077
12. Sporn MB (1976) Approaches to prevention of epithelial cancer during the preneoplastic period. *Cancer Res* 36:2699–2702
13. Umar A, Viner JL, Hawk ET (2001) The future of colon cancer prevention. *Ann NY Acad Sci* 952:88–108
14. Wattenberg LW (1995) What are the critical attributes for cancer chemopreventive agents? *Ann NY Acad Sci* 768:73–81
15. Smith TJ, Hong J-Y, Wang Z-Y, Yang CS (1995) How can carcinogenesis be inhibited? *Ann NY Acad Sci* 768:82–90
16. Kelloff GJ, Crowell JA, Steele VE, Lubet RA, Boone CW, Malone WA et al (1999) Progress in cancer chemoprevention. *Ann NY Acad Sci* 889:1–13
17. Gupta S, Hastak K, Ahmad N, Lewin JS, Mukhtar H (2001) Inhibition of prostate carcinogenesis in TRAMP mice by oral infusion of green tea polyphenols. *Proc Natl Acad Sci USA* 98:10350–10355
18. Lu Y-P, Lou Y-R, Li XH, Xie J-G, Brash D, Huang M-T et al (2000) Stimulatory effect of oral administration of green tea or caffeine on ultraviolet light-induced increases in epidermal wild-type p53, p21 (WAF1/CIP1), and apoptotic sunburn cells in SKH-1 mice. *Cancer Res* 60:4785–4791
19. Lu Y-P, Lou Y-R, Li XH, Xie J-G, Yen P, Huang M-T, Conney AH (1997) Inhibitory effect of black tea on the growth of established skin tumors in mice: effects on tumor size, apoptosis, mitosis and bromodeoxyuridine incorporation into DNA. *Carcinogenesis* 18:2163–2169
20. Samaha HS, Kelloff GJ, Steele V, Rao CV, Reddy BS (1997) Modulation of apoptosis by sulindac, curcumin, phenylethyl-3-methylcaffeate and 6-phenylhexyl isothiocyanate apoptotic index as a biomarker in colon cancer chemoprevention and promotion. *Cancer Res* 57:1301–1305
21. Yang K, Lamprecht SA, Liu Y, Shinozaki H, Fan K, Leung D et al (2000) Chemoprevention studies on the flavonoids quercetin and rutin in normal and azoxymethane-treated mouse colon. *Carcinogenesis* 21:1655–1660
22. Tanaka T, Kohno H, Sakata K, Yamada Y, Hirose Y, Sugie S et al (2002) Modifying effects of dietary capsaicin and rotenone on 4-nitroquinoline-1-oxide-induced rat tongue carcinogenesis. *Carcinogenesis* 23:1361–1367
23. Huang C, Ma WY, Young MR, Colburn N, Dong Z (1998) Shortage of mitogen-activated protein kinase is responsible for resistance to AP-1 transactivation and transformation in mouse JB6 cells. *Proc Natl Acad Sci USA* 95:156–161
24. Dong Z, Birrer MJ, Watts RG, Matrisian LM, Colburn NH (1994) Blocking of tumor promoter-induced AP-1 activity inhibits induced transformation in JB6 mouse epidermal cells. *Proc Natl Acad Sci USA* 91:609–613
25. Dong Z, Watts SG, Sun Y, Colburn NH (1995) Progressive elevation of AP-1 activity during preneoplastic-to-neoplastic progression as modeled in mouse JB6 cell variants. *Int J Oncol* 7:359–364
26. Bernstein LR, Colburn NH (1989) AP1/jun function is differentially induced in promotion-sensitive and resistant JB6 cells. *Science* 244:566–569
27. Dong Z et al (2002) Harvesting cells under anchorage-independent cell transformation conditions for biochemical analyses. *Sci STKE* PL7
28. Huang C, Ma W-Y, Dawson MI, Rincon M, Flavell RA, Dong Z (1997) Blocking activator protein-1 activity, but not activating retinoic acid response element, is required for the antitumor promotion effect of retinoic acid. *Proc Natl Acad Sci USA* 94:5826–5830
29. Johannsen W (1911) The genotype conception of heredity. *Am Nat* 45:129–159
30. Churchill FB (1974) William Johannsen and the genotype concept. *J Hist Biol* 7:5–30
31. Baltrop JA, Owen TC, Cory AH, Cory JG (1991) 5-(3-Carboxymethoxyphenyl)-2-(4, 5-dimethylthiazolyl)-3-(4-sulfophenyl) tetrazolium, inner salt (MTS) and related analogs of 3-(4, 5-dimethylthiazolyl)-2, 5-diphenyltetrazolium bromide (MTT) reducing to purple water-soluble formazans as cell-viability indicators. *Bioorg Med Chem Lett* 1:611–614
32. Colburn NH, Former BF, Nelson KA, Yuspa SH (1979) Tumour promoter induces anchorage independence irreversibly. *Nature* 281:589–591
33. Strickland J, Sun Y, Dong Z, Colburn NH (1997) Grafting assay distinguishes promotion sensitive from promotion resistant JB6 cells. *Carcinogenesis* 18:1135–1138
34. Irigaray P, Newby JA, Clapp R, Hardell L, Howard V, Montagnier L, Epstein S, Belpomme D (2007) Lifestyle-related factors and environmental agents causing cancer: an overview. *Biomed Pharmacother* 61:640–658
35. Haefner B (2003) Drugs from the deep: marine natural products as drug candidates. *DDT* 8:536–544
36. Altman K-H, Gertsch J (2007) Anticancer drugs from nature—natural products as a unique source of new microtubule-stabilizing agents. *Nat Prod Rep* 24:327–357
37. Delmas D, Lancon A, Colin D, Jannin B, Latruffe N (2006) Resveratrol as a chemopreventive agent. *Curr Drug Targets* 7:423–442
38. Lu YP, Low YR, Xie JG, Peng QY, Liao I, Yang CS, Huang MT (2002) Topical applications of caffeine or (-)-epigallocatechin gallate (EGCG) inhibit carcinogenesis and selectively increase apoptosis in UVB-induced skin tumor in mice. *Proc Natl Acad Sci USA* 99:12455–12460
39. Rogozin EA, Lee KW, Kang NJ, Yu H, Nomura M, Miyamoto KI, Conney AH, Bode AM, Dong Z (2008) Inhibitory effects of caffeine analogues on neoplastic transformation: structure–activity relationship. *Carcinogenesis* 29:1228–1234

40. Fedorov SN, Radchenko OS, Shubina LK, Balaneva NN, Bode AM, Stonik VA, Dong Z (2006) Evaluation of cancer-preventive activity and structure-activity relationships of 3-demethylubiquinone Q2, isolated from the ascidian *Aplidium glabrum*, and its synthetic analogs. *Pharm Res* 23:70–81
41. Fedorov SN, Shubina LK, Bode AM, Stonik VA, Dong Z (2007) Dactylone inhibits epidermal growth factor-induced transformation and phenotype expression of human cancer cells and induces G₁-S arrest and apoptosis. *Cancer Res* 67:5914–5920
42. Fedorov SN, Shubina LK, Kicha AA, Ivanchina NV, Kwak JY, Jin JO, Bode AM, Dong Z, Stonik VA (2008) Proapoptotic and anticarcinogenic activities of leviusculoside G from the starfish *Henricia leviuscula* and probable mechanism. *Nat Prod Commun* 3:1575–1580
43. Huang C, Ma WY, Goranson A, Dong Z (1999) Resveratrol suppresses cell transformation and induces apoptosis through a p53-dependent pathway. *Carcinogenesis* 20:237–242
44. Nomura M, Ichimatsu D, Moritani S, Koyama I, Dong Z, Yokogawa K, Miyamoto K (2005) Inhibition of epidermal growth factor-induced cell transformation and Akt activation by caffeine. *Mol Carcinog* 44:67–76
45. Qin J, Chen He-Ge, Yan Q, Deng M, Jinping Liu, Doerge S, Ma W, Dong Z, Li DW (2008) Protein Phosphatase-2A is a target of epigallocatechin-3-gallate and modulates p53-Bak apoptotic pathway. *Cancer Res* 68:4150–4162
46. Kyriakis JM, Avruch J (2001) Mammalian mitogen-activated protein kinase signal transduction pathways activated by stress and inflammation. *Physiol Rev* 81:807–869
47. Manson MM, Holloway KA, Howells LM, Hudson EA, Plummer SM, Squires MS, Prigent SA (2000) Modulation of signal-transduction pathways by chemopreventive agents. *Biochem Soc Trans* 28:7–12
48. Hung P-F, Wu B-T, Chen H-C, Chen Y-H, Chen C-L, Wu M-H, Liu H-C, Lee M-J, Kao Y-H (2005) Antimitogenic effect of green tea (-)-epigallocatechin gallate on 3T3-L1 preadipocytes depends on the ERK and Cdk2 pathways. *Am J Physiol Cell Physiol* 288:1095–1108
49. Chao J-I, Su W-C, Liu H-F (2007) Baicalein induces cancer death and proliferation retardation by the inhibition of cdc₂ kinase and survivin associated with opposite role of p38 mitogen-activated protein kinase and AKT. *Mol Cancer Ther* 6:3039–3048
50. Chang H-L, Wu Y-C, Su J-H, Yeh Y-T, Yuan S-SF (2008) Protoapigenone, a novel flavonoid induces apoptosis in human prostate cancer cells through activation of p38 mitogen activated protein kinase and c-Jun NH₂-terminal kinase 1/2. *J Pharmacol Exp Ther* 325:841–849
51. Bursch W, Oberhammer F, Schulte-Hermann R (1992) Cell death by apoptosis and its protective role against disease. *Trends Pharmacol Sci* 13:245–251
52. Hickman JA (1992) Apoptosis induced by anticancer drugs. *Cancer Metastasis Rev* 11:121–139
53. Levine AJ (1997) p53, the cellular gatekeeper for growth and division. *Cell* 88:323–331
54. Prives C, Hall PA (1999) The p53 pathway. *J Pathol* 187:112–126
55. Vousden KH (2000) p53: death star. *Cell* 103:691–694
56. He Z, Ma W-Y, Hashimoto T, Bode AM, Yang CS, Dong Z (2003) Induction of apoptosis by caffeine is mediated by the p53, Bax, and caspase 3 pathways. *Cancer Res* 63:4396–4401
57. Song G, Mao YB, Cai QF, Yao LM, Ouyang GL, Bao SD (2005) Curcumin induces human HT-29 colon adenocarcinoma cell apoptosis by activating p53 and regulating apoptosis-related protein expression. *Braz J Med Biol Res* 38:1791–1798
58. Tanigawa S, Fujii M, Hou D-X (2008) Stabilization of p53 is involved in quercetin-induced cell cycle arrest and apoptosis in HepG2 cells. *Biosci Biotechnol Biochem* 72:797–804
59. Katiyar SK, Roy AM, Baliga MS (2005) Silymarin induces apoptosis primarily through a p53-dependent pathway involving Bcl-2/Bax, cytochrome c release, and caspase activation. *Mol Cancer Ther* 4:207–216
60. Dhanalakshmi S, Agarwal C, Singh RP, Agarwal R (2005) Silibinin up-regulates DNA-protein kinase-dependent p53 activation to enhance UVB-induced apoptosis in mouse epithelial JB6 Cells. *JBC* 280:20375–20383
61. Ito K, Nakazato T, Yamato K, Miyakawa Y, Yamada T, Hozumi N, Segawa K, Ikeda Y, Kizaki M (2004) Induction of apoptosis in leukemic cells by homovanillic acid derivative, capsaicin, through oxidative stress: implication of phosphorylation of p53 at Ser-15 residue by reactive oxygen species. *Cancer Res* 64:1071–1078
62. Corbiere C, Liagre B, Terro F, Beneytout J-L (2004) Induction of antiproliferative effect by diosgenin through activation of p53, release of apoptosis-inducing factor (AIF) and modulation of caspase-3 activity in different human cancer cells. *Cell Res* 14:188–196
63. Hsu JC, Dev A, Wing A, Brew C, Bjeldanes LF, Firestone GL (2006) Indole-3-carbinol mediated cell cycle arrest of LNCaP human prostate cancer cells required the induced production of activated p53 tumor suppressor protein. *Biochem Pharmacol* 72:1714–1723
64. Fimognari C, Nusse M, Berti F, Iori R, Cantelli-Forti G, Hrelia P (2002) Cyclin D₃ and p53 mediate sulforafane-induced cell cycle delay and apoptosis in non-transformed human T-lymphocytes. *Cell Mol Life Sci* 59:2004–2012
65. Gali-Muhtasib H, Diab-Assaf M, Boltze C, Al-Hmaria J, Hartig R, Roessner A, Schneider-Stock R (2004) Thymoquinone extracted from black seed triggers apoptotic cell death in human colorectal cancer cells via a p53-dependent mechanism. *Int J Oncol* 25:857–866
66. Huang C, Ma WY, Li J, Hecht SS, Dong Z (1998) Essential role of p53 in phenethyl isothiocyanate-induced apoptosis. *Cancer Res* 58:4102–4106
67. Fedorov SN, Bode AM, Stonik VA, Gorshkova IA, Schmid PC, Radchenko OS, Berdyshev EV, Dong Z (2004) Marine alkaloid polycarpine and its synthetic derivative dimethylpolycarpine induce apoptosis in JB6 cells through p53- and caspase 3-dependent pathways. *Pharm Res* 21:2307–2319

Tocotrienols Suppress Proinflammatory Markers and Cyclooxygenase-2 Expression in RAW264.7 Macrophages

Mun-Li Yam · Sitti Rahma Abdul Hafid ·
Hwee-Ming Cheng · Kalanithi Nesaretnam

Received: 14 May 2009 / Accepted: 23 June 2009 / Published online: 5 August 2009
© AOCs 2009

Abstract Tocotrienols are powerful chain breaking anti-oxidant. Moreover, they are now known to exhibit various non-antioxidant properties such as anti-cancer, neuroprotective and hypocholesterolemic functions. This study was undertaken to investigate the anti-inflammatory effects of tocotrienol-rich fraction (TRF) and individual tocotrienol isoforms namely δ -, γ -, and α -tocotrienol on lipopolysaccharide-stimulated RAW264.7 macrophages. The widely studied vitamin E form, α -tocopherol, was used as comparison. Stimulation of RAW264.7 with lipopolysaccharide induced the release of various inflammatory markers. 10 $\mu\text{g/ml}$ of TRF and all tocotrienol isoforms significantly inhibited the production of interleukin-6 and nitric oxide. However, only α -tocotrienol demonstrated a significant effect in lowering tumor necrosis factor- α production. Besides, TRF and all tocotrienol isoforms except γ -tocotrienol reduced prostaglandin E_2 release. It was accompanied by the down-regulation of cyclooxygenase-2 gene expression by all vitamin E forms except α -tocopherol. Collectively, the data suggested that tocotrienols are better anti-inflammatory agents than α -tocopherol and the most effective form is δ -tocotrienol.

Keywords Tocotrienols · α -Tocopherol · Inflammation · RAW264.7 · Cyclooxygenase-2 · Vitamin E

Abbreviations

COX-1	Cyclooxygenase-1
COX-2	Cyclooxygenase-2
IL-6	Interleukin-6
LPS	Lipopolysaccharide
NO	Nitric oxide
PGE_2	Prostaglandin E_2
TNF- α	Tumor necrosis factor
TRF	Tocotrienol-rich fraction
αT	Alpha-tocopherol
αT_3	Alpha-tocotrienol
γT_3	Gamma-tocotrienol
δT_3	Delta-tocotrienol

Introduction

Inflammation is a complex response that protects the body from various harmful agents such as microbes and toxins [1]. Nevertheless, it is a known fact that unregulated inflammation is associated with many chronic diseases, contributing to the increase in worldwide morbidity and mortality rates. The relationship between cancer and inflammation was hypothesized in 1863 by Rudolf Virchow that cancer originates from sites of chronic inflammation where the inflammatory event serves as the cofactor in carcinogenesis [2]. The imbalance in inflammatory mediators during chronic inflammation causes damage to the cartilage and bone, leading to the debilitating rheumatoid arthritis [3]. Besides that, inflammation has also

This study was supported by Malaysian Palm Oil Board (MPOB).

M.-L. Yam · S. R. Abdul Hafid · K. Nesaretnam (✉)
Malaysian Palm Oil Board, 6 Persiaran Institusi,
Bandar Baru Bangi, 43000 Kajang,
Selangor, Malaysia
e-mail: sarnesar@mpob.gov.my

M.-L. Yam · H.-M. Cheng
Department of Physiology, Faculty of Medicine,
University of Malaya, 50603 Kuala Lumpur,
Malaysia

been found to participate in all phases of the atherosclerotic process, from the initial atherogenesis through lesions progression and finally, the subsequent thrombotic complications [4]. In other words, inflammation plays a great role in the underlying mechanisms of almost all pathological states and diseases.

Nonsteroidal anti-inflammatory drugs (NSAIDs) are among the most widely prescribed drugs in inflammation therapy. Alleviation of pain and arrestment of the tissue-damaging process serve as the therapeutic strategies in patients with inflammation [5]. However, the short-coming of these drugs is their association with a wide range of adverse effects on the gastrointestinal tract, hematological, and renal functions [5, 6]. A study by Tomisato and colleagues shows that NSAIDs have the possibility of inducing gastric lesions through direct cytotoxic effects on the gastric mucosa [7]. Moreover, it has been put forward that a causal association exists between bowel perforation or hemorrhage and NSAIDs ingestion [8]. Hence, any alternatives to address the shortcomings of NSAIDs would be hailed.

Palm vitamin E comprising 30% tocopherols and 70% tocotrienols has been extensively studied for its nutritional properties and health benefits [9]. Both tocopherols and tocotrienols have different biological properties and are further separated into four isoforms, α -, β -, δ - and γ -, respectively. It is widely known that vitamin E possesses potent antioxidant properties as well as other beneficial values. It confers protection against peroxynitrite-induced lipid oxidation in vivo and prevents cholesterol-induced atherosclerotic lesions in rabbits [10, 11]. Besides, tocotrienols are shown to inhibit the growth of a human breast cancer cell line, ZR-75-1 [12]. Reactive oxygen metabolites are involved in the mediation of tissue injuries as well as amplifying the existing inflammatory response [13]. Therefore, it is possible that the use of antioxidants may have direct or indirect effects on inflammation. Moreover, some vitamin E forms have been shown to possess anti-inflammatory effects in vivo and in vitro [14, 15].

Materials and Methods

Chemicals and Reagents

Tocotrienol-rich fraction (TRF) was obtained from Golden Hope Plantations (Selangor, Malaysia). α -Tocopherol (α T) was purchased from Aldrich Chemical Company Inc. (Milwaukee, USA) whereas δ -, γ -, and α -tocotrienol (T_3) were acquired from Eisai Food & Chemical Co. Ltd. (Tokyo, Japan). All media and reagents for tissue culture were purchased from GIBCO BRL (Paisley, Scotland). A 3-(4,5-dimethylthiazol-2-yl)-2,5-diphenyl tetrasodium

bromide (MTT) kit for cell viability assay was purchased from Chemicon (Temecula, CA, USA). Lipopolysaccharide (LPS) from a *Escherichia coli* source was obtained from Sigma (St Louis, Missouri, USA). ELISA kit for tumor necrosis factor (TNF)- α and interleukin (IL)-6 was from eBioscience (San Diego, CA, USA) and the Amersham Prostaglandin E₂ Biotrak Enzyme immunoassay (EIA) System was from GE Healthcare Ltd. (Buckinghamshire, UK). Griess reagent for the determination of nitrite was purchased from Molecular Probes (Eugene, Oregon, USA). Meanwhile, TRI reagent was from the Molecular Research Center, Inc (Cincinnati, OH, USA) and reagents for polymerase chain reaction (PCR) applications were all from Invitrogen Life Technologies (Carlsbad, CA, USA). Protein assay dye reagent concentrate for the Bradford assay was from Bio-Rad (Hercules, CA, USA).

Cell Culture

RAW264.7 macrophages were purchased from American Type Culture Collection (ATCC) (Manassas, Virginia, USA) and grown in high-glucose Dulbecco's modified Eagle's medium (DMEM) supplemented with 10% fetal bovine serum (FBS), 1% penicillin-streptomycin and 1% L-glutamine in a humidified atmosphere of 5% CO₂ at 37 °C. For treatment, cells were cultured in RPMI medium without phenol red, supplemented with 5% FBS, 1% penicillin-streptomycin and 1% L-glutamine. 1×10^5 cells/well were plated in 96-well plates and incubated overnight. The next day, treatments and stimulant were given accordingly and the cells were incubated for 24 h. Cell supernatant was collected for the measurement of cytokines (IL-6 and TNF- α), nitric oxide (NO) and prostaglandin E₂ (PGE₂).

Cell Viability Assay

RAW264.7 macrophages were cultured and left overnight in 96-well plates at a density of 1×10^5 cells/well. The next day, treatment with different concentrations of TRF, α T, and tocotrienol isoforms (δ -, γ -, and αT_3) in the presence of 10 ng/ml LPS were given. The cells were incubated for 24 h. MTT solution was added into the wells containing fresh RPMI medium and the cultures were returned to the incubator. Four hours later, the blue formazan crystals that had formed were dissolved in isopropanol-HCl and the optical density was measured at 570 nm using a microplate reader.

Cytokine Assays

1×10^5 cells/well of RAW264.7 macrophages were incubated overnight in 96-well plates. Next, 10 ng/ml of

LPS was added for stimulation, together with 10 µg/ml of vitamin E supplementation and the cells were incubated for 24 h. The levels of IL-6 and TNF- α in culture supernatants were determined using commercially available ELISA kits (eBioscience). Assays were carried out according to the manufacturer's instructions. Plates were read at 540 nm using a microplate reader.

Griess Assay

Determination of NO production was performed using a Griess reagent kit (Molecular Probes) which measures the levels of nitrite formed from the spontaneous oxidation of NO. Briefly, 1×10^5 cells/well of RAW264.7 were cultured overnight in DMEM in 96-well plates, and then subjected to their respective treatments for another 24 h in the presence of 10 ng/ml of LPS. To measure nitrite, supernatants were incubated for 30 min with an equal volume of *N*-(1-naphthyl)ethylenediamine dihydrochloride and sulfanilic acid against a nitrite standard. Absorbance was measured using a microplate reader at 548 nm.

Prostaglandin E₂ Enzyme Immunoassay

Measurement of PGE₂ in the cell culture supernatant of treated RAW264.7 was carried out using the Amersham Prostaglandin E₂ Biotrak Enzyme immunoassay (EIA) System according to the manufacturer's instructions. Optical density was read at 450 nm using a microplate reader.

RNA Extraction and Reverse Transcriptase-PCR

RAW264.7 macrophages were maintained in DMEM in culture flasks. Upon confluency, treatments were given in the presence of 10 ng/ml LPS and incubated for 24 h in 5% CO₂. Total RNA was extracted using TRI reagent (Molecular Research Center, Inc.) according to manufacturer's instructions. Next, the RNA was reverse transcribed into cDNA using reverse transcriptase and the resultant cDNA was subjected to PCR using gene-specific primers. The primers for β -actin was designed using Primer 3 software whereas the sequences for *COX-1* and *COX-2* have previously been reported [16, 17]. All the primers were purchased from Invitrogen (Carlsbad, CA, USA). The sequences and the product sizes are as follows: β -actin (forward: 5'-GTG GGGCGCCCCAGGCACCA-3', reverse: 5'-CTCCTTAAT GTCACGCACGATTTTC-3') 540 bps, *COX-1* (forward: 5'-CTTTGCACAACACTTCACCCACC-3', reverse: 5'-AG CAACCCAAACACCTCCTGG-3') 285 bps, and *COX-2* (forward: 5'-GCATTCTTTGCCAGCACTT-3', reverse: 5'-AGACCAGGCACCAGACCAAAGA-3') 299 bps. The amplified products were resolved on a 1.5% agarose gel

containing ethidium bromide and visualized using an imager. The bands were quantified using ImageJ software and results were expressed as the relative fold change after normalization against β -actin [18].

Real-Time RT-PCR

Total RNA was subjected to DNase treatment. Gene expression of *COX-2* was examined using SuperScript III Platinum SYBR Green kit (Invitrogen) which employs the ABI PRISM 7000 Sequence Detection System (Applied Biosystems, CA, USA). β -Actin was used as the endogenous control. Primers for β -actin and *COX-2* were purchased from Invitrogen (Carlsbad, CA, USA) and Bioneer (Korea), respectively. The primer sequences are: β -actin (forward: 5'-AGAAGGATTCCTATGTGGGGG-3', reverse: 5'-CAT GTCGTCCCAGTTGGTGAC-3') and *COX-2* (forward: 5'-CATACTCAAGCAGGAGCATCC-3', reverse: 5'-ACC GCTCAGGTGTTGCACGTAGTC-3'). The reactions were assayed as triplicates and performed in a final volume of 50 µl. Melting curve analysis was also done. The mRNA levels for *COX-2* were normalized against β -actin and expressed as fold change relative to control. The quantification was done using the delta-delta C_t method.

Western Blot

Total proteins were extracted from treated-RAW264.7 for Western blot analysis. Briefly, cells were trypsinized, washed with ice-cold PBS and resuspended in lysis buffer (10 mM Tris-HCl pH 7.4, 1.92 mM MgCl₂, 1 mM EDTA pH 8.0, 50 mM NaCl, 6 mM β -mercaptoethanol and 2% Triton X-100) containing 1% protease inhibitor cocktail (Calbiochem, San Diego, CA, USA) and incubated for 5 min on ice. Afterwards, the cells were passed through a 21G needle syringe twice, and sonicated for 5 min. The lysates were then centrifuged at 1,000g for 10 min and the supernatants were collected. Determination of protein concentration was done using the Bradford method. A 30-µg amount of the protein lysates were resolved on 10% SDS-PAGE gels and electroblotted onto nitrocellulose membranes using a semi-dry transfer system (Bio-Rad, CA, USA). The membranes were then incubated overnight at 4 °C with 5% blocking agent (Amersham, UK) in wash buffer (0.1% (v/v) Tween 20 in PBS). After the blocking step, membranes were probed with rabbit polyclonal COX-2 antibody (Santa Cruz, USA) for 1 h at room temperature. Subsequently, the membranes were incubated for another hour at room temperature with anti-rabbit secondary antibody (Amersham, UK). Detection was performed using an ECL detection kit from Amersham (UK), according to the manufacturer's instructions. Following that, the membranes

were stripped off from the probed antibodies, blocked, and re-incubated with mouse monoclonal actin (Sigma, USA) followed by horseradish peroxidase-labeled anti-mouse secondary antibody (Santa Cruz, USA). Bands on autoradiography films were quantified using ImageJ software and normalized against actin [18].

Statistical Analysis

All results were expressed as means \pm SD and analyzed using one way ANOVA. Dunnett's multiple comparisons test was applied to determine the significant differences between treatment groups. Results were accepted to be significant at $P < 0.05$.

Results

Effects of TRF, α T, and Individual Tocotrienol Isoforms (δ -, γ -, and α T₃) on the Viability of LPS-Stimulated RAW264.7

An MTT assay was performed to determine the viability of RAW264.7 following treatment with different vitamin E forms. Figure 1 shows the percent cell viability of LPS-stimulated RAW264.7 after 24 h incubation with different concentrations of TRF, α T and tocotrienol isoforms. It demonstrated that 10 ng/ml of LPS, the concentration used for RAW264.7 stimulation throughout the study, did not

cause any change in RAW264.7 viability. No cytotoxicity was observed in all treatment groups for up to 15 μ g/ml except for δ - and γ T₃. A significant decrease in the percentage cell viability was observed in these two groups at 15 μ g/ml.

TRF, α T and Tocotrienol Isoforms (δ -, γ -, and α T₃) Have Different Effects on Proinflammatory Cytokines (IL-6 and TNF- α)

IL-6 and TNF- α are two important proinflammatory cytokines that are released in various inflammatory conditions. The presence of 10 ng/ml of LPS stimulated the release of these cytokines in RAW264.7 (Fig. 2a, b). TRF and all tocotrienol isoforms (δ -, γ -, and α T₃) at 10 μ g/ml significantly reduced the release of IL-6 in LPS-stimulated RAW264.7 when compared to the untreated LPS-stimulated group (Fig. 2a). On the other hand, α T has no effect on this context. Of all the treatments, δ T₃ showed the best inhibitory effect, being able to reduce the production of IL-6 by more than 50%, followed by γ T₃, α T₃ and TRF. In contrast, co-treatment of vitamin E forms and LPS has different effects on the production of TNF- α in RAW264.7 (Fig. 2b). TNF- α levels were increased in TRF, α T and δ T₃-treated groups, remained unaltered in a γ T₃-treated group, but underwent a significant decrease in α T₃-treated RAW264.7. This decrease was equivalent to a 12% inhibition when compared to an untreated LPS-stimulated group. The significant increase in TNF- α production was

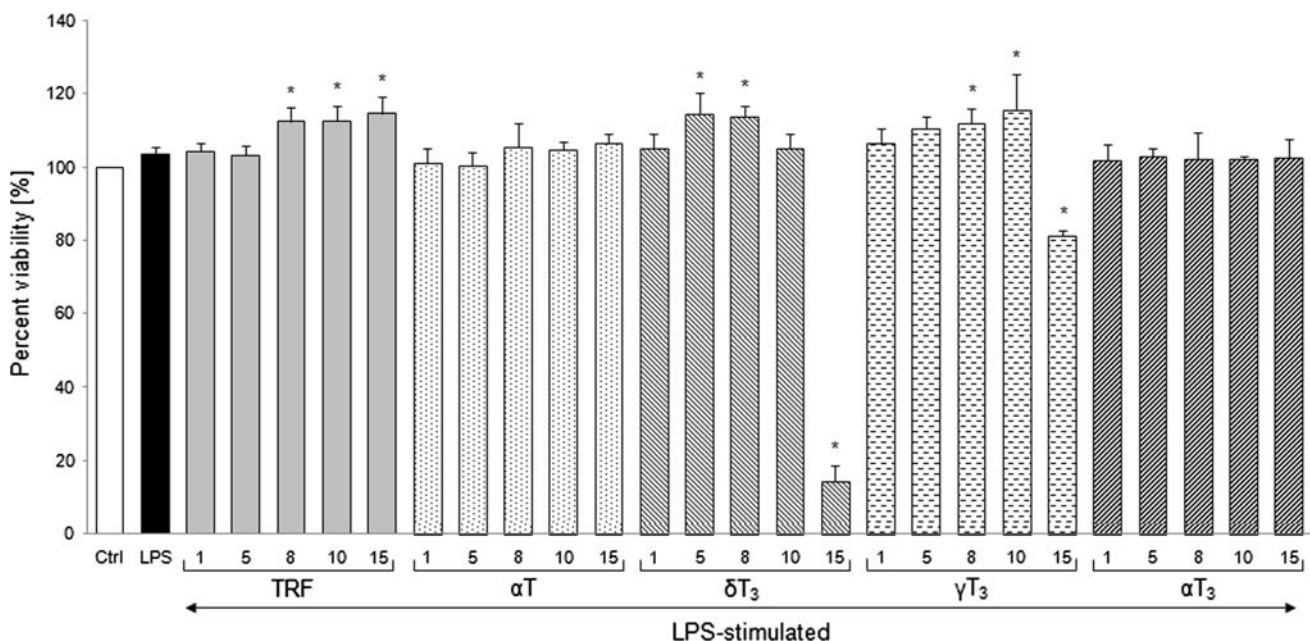
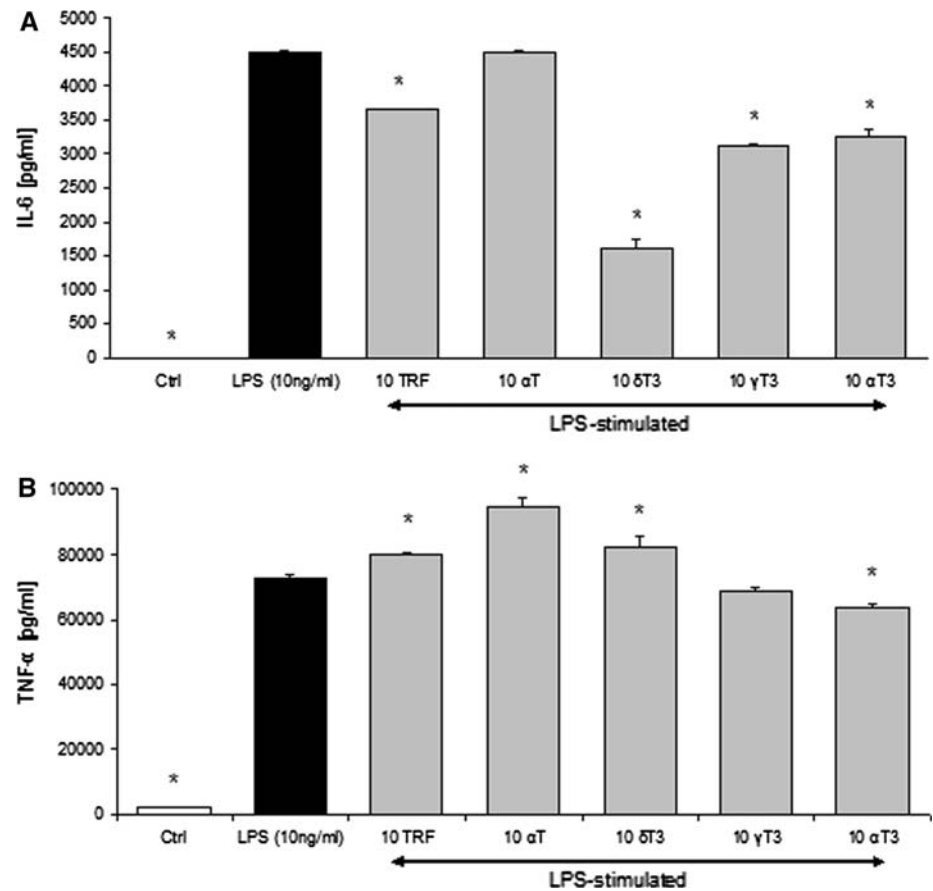


Fig. 1 Percentage cell viability of LPS-stimulated RAW264.7 following 24 h incubation with TRF, α T, and tocotrienol isoforms (δ -, γ -, and α T₃) as assessed using the MTT assay. Data are expressed as means \pm SD of triplicate wells. * $P < 0.05$ compared with control group

Fig. 2 The changes in (a) IL-6 and (b) TNF- α levels in LPS-stimulated RAW264.7 after 24 h treatment with various vitamin E forms. Supernatants were collected and assayed by ELISA. Data are presented as means \pm SD. * P < 0.05 compared with LPS group



highest in an α T-treated group, followed by δ T₃- and TRF-treated groups. Data suggested a possible proinflammatory effect of these vitamin E forms in LPS-stimulated RAW264.7.

All Vitamin E Forms Inhibited the Production of NO in LPS-Stimulated RAW264.7

The addition of 10 ng/ml LPS to RAW264.7 macrophages stimulated the production of NO from a baseline 0.2 μ M in the control to 37 μ M in the LPS group (Fig. 3). Treatment with 10 μ g/ml of all vitamin E forms showed a positive effect in inhibiting NO production. The best effect was observed in the δ T₃-treated group in which the level of NO was limited to 26 μ M which corresponds to a 31% inhibition when compared to the LPS-stimulated group. It was followed by γ T₃ which showed a 19% inhibition at 30 μ M, compared to the LPS group. Compared to δ - and γ T₃, other treatments also showed significant inhibitory effects in NO production although not as strongly. The levels of NO were detected at 33, 34, and 35 μ M in α T₃, TRF, and α T-treated groups, respectively. It is significant that α T treatment demonstrated the least inhibitory effect of only 5% when compared to the other vitamin E forms.

Tocotrienols Inhibited the Production of PGE₂ in LPS-Stimulated RAW264.7

Following LPS stimulation, the level of PGE₂ in the culture supernatant increased to approximately 1,000 pg/ml (Fig. 4). Treatment of LPS-stimulated RAW264.7 with TRF and tocotrienols, except γ T₃, significantly inhibited the level of PGE₂ when compared with the LPS group. The greatest inhibition was exerted by δ T₃, which showed approximately 55% reduction, followed by TRF and α T₃. No change in the level of PGE₂ was seen in the γ T₃-treated group. It was interesting that the PGE₂ level was significantly elevated in the α T-treated group when compared to the LPS group.

Effects of TRF, α T and Tocotrienol Isoforms (δ -, γ -, and α T₃) on COX-1 and COX-2 Gene Expression in LPS-Stimulated RAW264.7

COX-1 and COX-2 are two isoforms of the COX enzyme which regulate the synthesis of various prostanoids via the arachidonic acid pathway [19]. COX-1, being the constitutive isoform is important in the regulation of homeostasis whereas COX-2 is the inducible isoform that plays

Fig. 3 The production of NO in LPS-stimulated RAW264.7 following treatment with different vitamin E forms. Griess assay that measures nitrite formation was used as an indirect method to determine the levels of NO accumulation in culture supernatants. The data are expressed as means \pm SD of triplicate wells. * $P < 0.05$ compared with LPS group

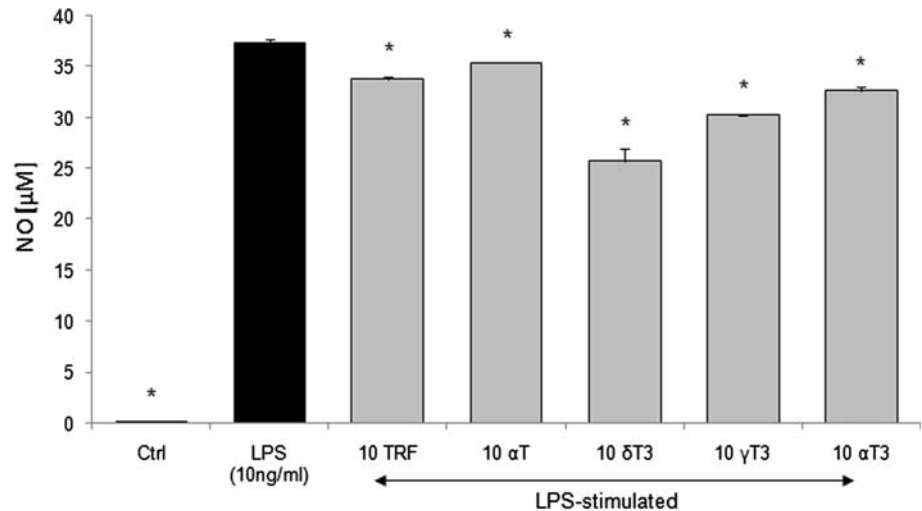
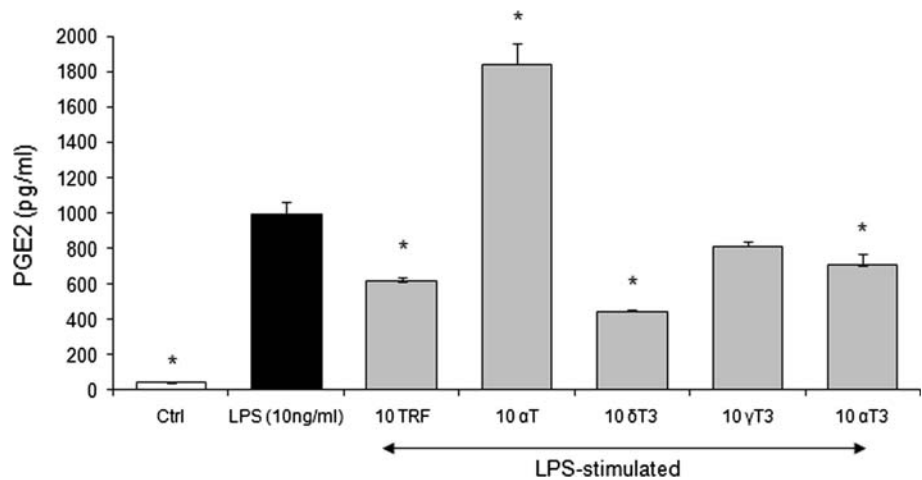


Fig. 4 The changes in PGE₂ release following treatment of LPS-stimulated RAW264.7 with different vitamin E forms. The PGE₂ levels in cell supernatants were measured using an enzyme immunoassay kit. The data are expressed as means \pm SD of triplicate wells. * $P < 0.05$ compared with LPS group



important roles in the pathophysiological aspects of inflammation (20). The expression of COX-2 can be initiated by a variety of stimuli and LPS is known to be a potent inducer for these enzymes [21, 22]. In order to elucidate the effects of different vitamin E forms on *COX-1* and *COX-2* gene expressions in LPS-stimulated RAW264.7, RT-PCR was performed using gene-specific primers. Data showed that gene expression of *COX-1* remained unaltered in all groups (Fig. 5b). This observation agrees with the fact that COX-1 remains a constitutive isoform of COX and being expressed equally in all samples. Meanwhile, 10 ng/ml of LPS up-regulated the expression of *COX-2* to a significant 6.4-fold relative to the control. Among the treated groups, δ T₃ showed the best inhibition in *COX-2* expression. δ T₃, at 10 μ g/ml down-regulated the expression of *COX-2* for 1.5-fold when compared with the LPS group but the change was not statistically significant.

TRF and Individual Tocotrienol Isoforms, but Not α T Down-Regulated the Expression of *COX-2* as Determined Using Semi-Quantitative Real-Time PCR

To ascertain the *COX-2* expression results obtained using the conventional RT-PCR method, semi-quantitative Real-Time PCR was applied. Real-Time PCR is a more sensitive method for direct detection of PCR product during the exponential phase of the reaction [23]. Data obtained showed a 145-fold increase in *COX-2* expression when compared to control (Fig. 6). Supplementation of LPS-stimulated RAW264.7 with all the vitamin E forms at 10 μ g/ml effectively reduced the expression of *COX-2*. However, the down-regulation was only statistically significant for TRF and other tocotrienol isoforms, but not α T. The most apparent change was seen in the δ T₃-treated group where the expression of *COX-2* was reduced 29-fold

Fig. 5 Gene expressions of *COX-1* and *COX-2* in LPS-stimulated RAW264.7. Total RNA was extracted from the treated macrophages and RT-PCR was carried out to study the gene expressions of *COX-1* and *COX-2*. (a) PCR bands as visualized from ethidium bromide-stained agarose gel. The images are representatives of three independent experiments. (b) Gene expressions are expressed as relative fold change following normalization against β -actin. Data are shown as means \pm SD of three replicates. * $P < 0.05$ compared with LPS group

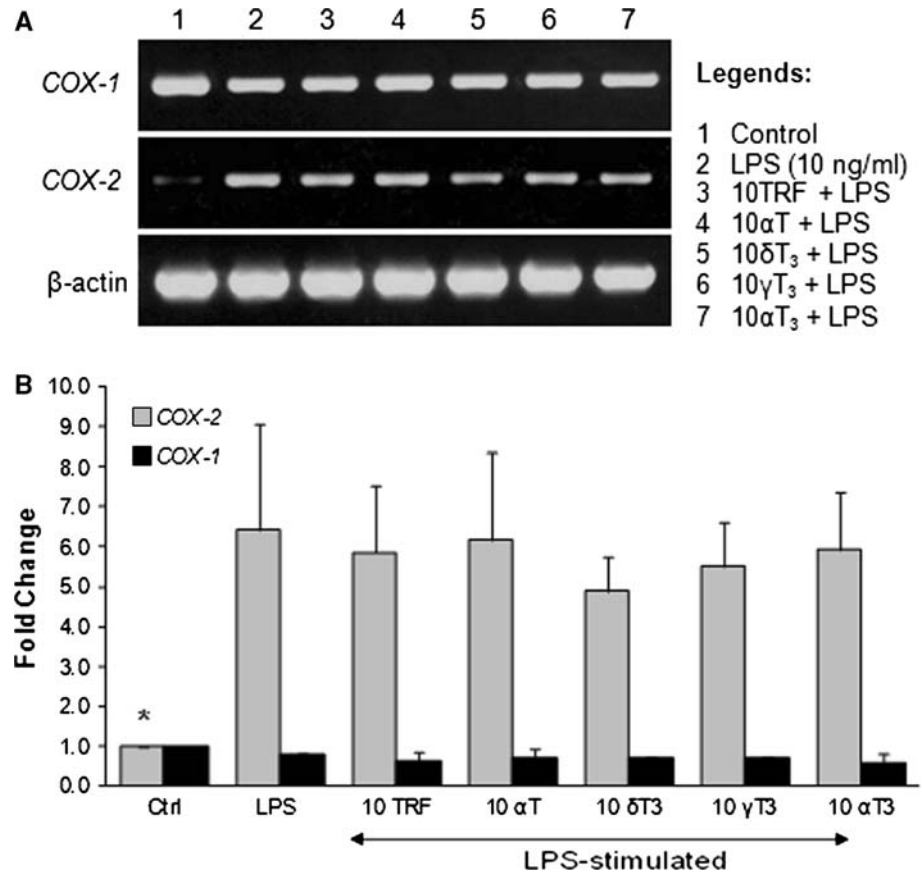
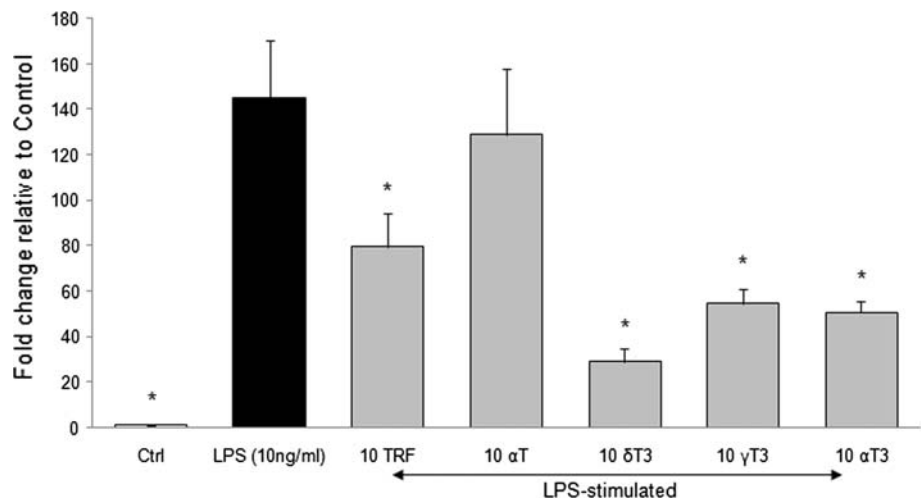


Fig. 6 Relative *COX-2* mRNA expression in LPS-stimulated RAW264.7 after 24 h treatment with TRF, α T and tocotrienol isoforms (δ -, γ -, and α T₃) as determined by Real-Time PCR. Total RNA extracted using the TRIzol method was DNase-treated and subjected to Real-Time PCR to determine the expression of *COX-2*. Data represent expressional fold change relative to control after normalization against β -actin. Data are expressed as means \pm SD of triplicate wells. * $P < 0.05$ compared with LPS group

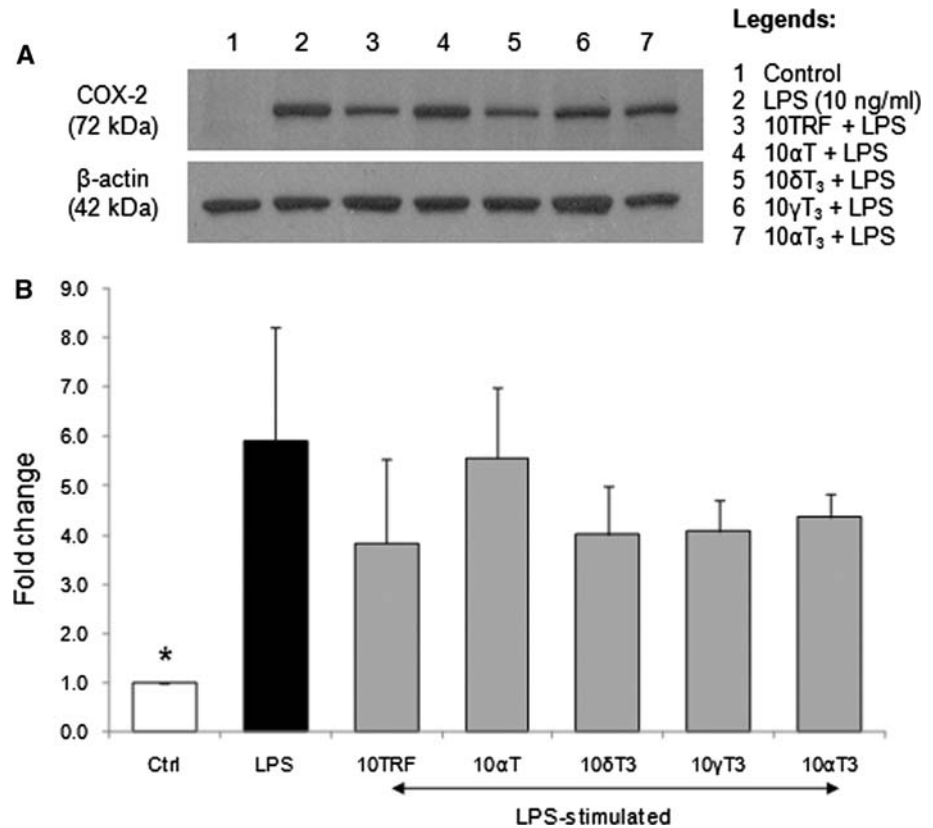


relative to the control, which was equivalent to a 116-fold difference from the LPS group. It was followed by α T₃, γ T₃, TRF and α T with *COX-2* expression levels at 51-, 55-, 79- and 129-fold relative to the control, respectively. In terms of differences from the LPS group, it corresponded to 94-, 90-, 66-, and 16-fold, respectively. Using this more sensitive approach to determine the expression of the *COX-2* gene, it showed that the most effective *COX-2* inhibitor was δ T₃ while α T has no effect.

Effects of TRF, α T and Tocotrienol Isoforms (δ -, γ -, and α T₃) on *COX-2* Protein Expression

Next, the effects of vitamin E forms on protein expression of *COX-2* were evaluated using Western blot analysis. Stimulation of RAW264.7 with 10 ng/ml of LPS significantly up-regulated the expression of *COX-2* protein to 5.9-fold relative to control (Fig. 7b). TRF, at the concentration tested showed the best effect in down-regulating the

Fig. 7 Protein expression of COX-2 in LPS-stimulated RAW264.7. Cell lysates from treated macrophages were obtained and analyzed for COX-2 protein expression by Western blot. (a) COX-2 and β -actin bands on autoradiography films following Western blotting. Images are representatives of three separate experiments. (b) Following densitometry analysis, data are expressed as the number of times the change is relative to the control group after normalization against β -actin. * $P < 0.05$ compared with the LPS group



expression of COX-2 protein. In the TRF group, COX-2 protein expression level was 3.8-fold relative to the control and this corresponded to a 2.1-fold difference from the LPS group. However, this down-regulation shown by TRF was not statistically significant. Other treated groups (δ -, γ -, and α T₃) also demonstrated a slight decrease in the number of times different compared to the LPS group but again, the changes were not significant. No obvious effect was seen in the α T-treated group.

Discussion

Recent studies have shown that tocotrienols possess powerful neuroprotective, anti-cancer, as well as hypocholesterolemic properties that are not seen in tocopherols [24]. The objective of the study was to investigate the anti-inflammatory effects of TRF and individual tocotrienol isoforms (δ -, γ -, and α T₃), using α T as comparison. RAW264.7, a transformed murine macrophages cell line was used as the in vitro model for the study. The cells were incubated for 24 h with 10 μ g/ml of one of the vitamin E forms together with 10 ng/ml of LPS as stimulation. The concentration of vitamin E form used, 10 μ g/ml, was selected based on the cell viability assay as the highest non-toxic concentration for all tested vitamin E forms. The levels of IL-6 in the culture supernatant were found to be

reduced in all treated groups except α T. The decrease was not due to the cytotoxic effects of the treatments because as shown by the MTT assay, cells were still viable at 10 μ g/ml for each treatment. On the contrary, treatment with vitamin E forms not only failed to reduce TNF- α levels, its production was increased in α T, δ T₃ and TRF-treated groups. When compared with the LPS group, only α T₃ was able to inhibit TNF- α significantly whereas its production was unaffected by γ T₃. NO, as estimated using Griess assay for the measurement of nitrite, was significantly reduced by all the vitamin E forms when compared with the LPS group. All the treatments, with the exception of α T and γ T₃ also inhibited the release of PGE₂. In addition, gene expression of COX-2 was found to be down-regulated in all treated group except α T. Of all the treatments, δ T₃ exhibited the best effect, followed by α T₃, γ T₃, and finally, TRF. No significant effect was observed in all the treated groups on the expression of COX-2 protein.

IL-6 and TNF- α are among the main cytokines produced by activated macrophages which are involved in both acute and chronic inflammation [25]. Many studies have used these two cytokines as important markers of inflammation [26, 27]. The up-regulation of IL-6 and TNF- α is seen in many disorders such as rheumatoid arthritis, multiple myeloma and chronic obstructive pulmonary disease [28–30]. Our findings on IL-6 release showed that all treatments except α T were able to reduce the production of

this cytokine significantly. This result contradicts a previous finding which showed a significant decrease in IL-6 level when 20 μ M of α T was supplemented [27]. The same report also demonstrated a reduction in TNF- α production at the same concentration of α T. This is in opposition to what we obtained where all the vitamin E forms except α T₃ failed to demonstrate a significant reduction in TNF- α production. The discrepancies in the results may be probably due to the use of different approaches in the experimental protocols as the effects caused by a particular mediator depend on the nature of the toxicant, target and quantities of the mediator produced [31].

NO is an important mediator that is involved in the regulation of homeostatic conditions and immune responses. Synthesis of NO requires the amino acid L-arginine as substrate and the process is catalyzed by a group of enzymes termed the nitric oxide synthases (NOS) [32, 33]. NOS co-exist in three isoforms, each with its own biological functions. The constitutive form of NOS, the cNOS, is important in maintaining homeostasis and it is further divided into the neuronal NOS (nNOS or type 1 NOS) and endothelial NOS (eNOS or type 3 NOS). The third isoform, the inducible NOS (iNOS or type 2 NOS) is the form that is involved in a wide range of pathophysiological events. Our findings showed that all vitamin E forms at 10 μ g/ml significantly reduced the generation of NO as assayed using Griess reagent that measures nitrite, the breakdown product of NO. This may be attributed to the antioxidant properties of vitamin E. NO is an effector molecule of innate immunity that forms the pro-oxidant and toxic peroxynitrite (ONOO⁻) in the presence of superoxide (O₂⁻) [34]. In addition, the data also agree with those reported by Berharka and colleagues stating that supplementation of vitamin E reduces the production of inducible NO in peritoneal macrophages derived from aged mice [35]. Study of *iNOS* gene expression was also carried out but none of the treatments showed a significant effect (results not shown). This suggested that vitamin E forms can only inhibit iNOS activity as demonstrated by the reduction in NO synthesis, and not at the gene level.

Being one of the most studied prostaglandins, PGE₂ is produced by fibroblasts, macrophages, and some types of malignant cells and its over-production is implicated in various pathophysiological and diseased states [36, 37]. Similar to NOS, the COX enzymes can be divided into the constitutive and inducible isoforms. COX-1, being the constitutive isoform plays important roles in the regulation of various physiological functions such as gastric cytoprotection, and the maintenance of kidney and platelet functions [20, 38]. On the other hand, COX-2 is the inducible isoform of COX, being expressed by immune cells and engages in the pathological aspects of inflammation [38]. The present study revealed that treatment of

LPS-stimulated RAW264.7 with TRF, δ -, and α T₃ suppressed the release of PGE₂ into the culture supernatant. On the other hand, study of gene expression demonstrated that treatment with 10 μ g/ml of TRF and tocotrienol isoforms (δ -, γ -, and α T₃) down-regulated the expression of COX-2. These levels of COX-2 expression were in accordance with the amount of PGE₂ measured in the cell supernatants. The expression level of COX-1, the constitutive isoform which is responsible for various housekeeping roles, remained unaffected in all groups. This shows that the changes of PGE₂, as shown in Fig. 4, have nothing to do with COX-1 activity. The down-regulation of the COX-2 gene suggested that vitamin E forms show an effect at the gene transcriptional level, subsequently affecting the levels of PGE₂ released. Although some marginal down-regulation was observed in the present study, treatment with all vitamin E forms seemed to have no significant effect on the protein translational level. Previous findings have shown that PGE₂ inhibition is accompanied by the down-regulation of the COX-2 gene and protein expression [39]. However, other findings also demonstrated that it does not necessarily follow in that manner as COX-2 enzymatic activity could be altered without any effects being shown at the transcription and translation levels [40, 41]. This suggests that each tocotrienol forms could modulate PGE₂ production through different mechanisms.

Tocotrienols, the vitamin E form which has previously been neglected, are now starting to gain attention due to their newly found properties. Besides their novel antioxidant functions, researchers have shown great interest in the non-antioxidant properties of this vitamin E form [42]. On top of that, studies are beginning to strengthen the notion that tocotrienols are superior to tocopherols in many aspects. TRF and individual tocotrienols, in particular δ - and γ T₃, are potent anti-proliferative agents, being able to induce apoptosis and cell cycle arrest in PC-3, a human prostate cancer cell line [43]. α T and α T₃ show no effect in that context. Besides, α T₃ is shown to provide the best neuroprotective effects in rat striatal cultures while α T failed to do so [44]. In the inflammation context, palm TRF has been shown to suppress the transcription of proinflammatory cytokines, and blocking the expression of COX-2 and iNOS in THP-1, a human monocytic cell line [45]. γ T₃ was found to inhibit the production of PGE₂ in human lung epithelial A549 cells activated by interleukin-1 β while no effect was seen in α T [46]. Meanwhile, another study has demonstrated that γ T₃, but not tocopherol, is a potent inhibitor of nuclear factor- κ B (NF- κ B) activation that leads to the down-regulation of various gene products including COX-2, as well as potentiating apoptosis [47]. NF- κ B is a principal transcription factor that modulates the expression of various cytokines, growth factors and

proinflammatory enzymes [48]. The activation of NF- κ B pathway is involved in the pathogenesis of many diseases such as those related to inflammation, enhanced cellular proliferation, infections and genetic diseases [49]. The expression of many proinflammatory genes including *COX-2* and *iNOS* is regulated by the activation of NF- κ B [50]. Therefore it is plausible that the inhibitory effects of vitamin E forms on *COX-2* expression in this study were due to the blockade of the NF- κ B pathway. Suppression of the NF- κ B pathway will eventually lead to a lower expression of proinflammatory enzymes and/or cytokines.

In conclusion, the results of this study showed that TRF and tocotrienol isoforms (δ -, γ -, and α T₃) possess anti-inflammatory properties with each displaying different levels of potency. It should be remembered that different effects might be observed if other cell types or different stimulation and incubation methods were used. Nevertheless, in this model of LPS-stimulated RAW264.7 macrophages, δ T₃ was demonstrated to be the most effective anti-inflammatory agent among all the vitamin E forms tested, being able to suppress the production of IL-6, NO, PGE₂, and at the same time inhibiting the expression *COX-2*. α T showed the least effect in alleviating an inflammatory response. It was suggested that individual isoforms of tocotrienol might have distinct and different effects, depending on the cell-type and on which parameters are being studied.

References

- Mitchell RN, Cotran RS (2003) Acute and chronic inflammation. In: Cotran RS, Kumar V, Robbins SL (eds) Robbins basic pathology, 7th edn. Saunders, Philadelphia, pp 33–59
- Balkwill F, Mantovani A (2001) Inflammation and cancer: back to Virchow? *Lancet* 357:539–545
- Choy EHS, Panayi GS (1997) Cytokine pathways and joint inflammation in rheumatoid arthritis. *N Engl J Med* 344(12):907–916
- Libby P, Ridker PM, Maseri A (2002) Inflammation and atherosclerosis. *Circulation* 105:1135–1143
- Furst DE, Munster T (2001) Nonsteroidal anti-inflammatory drugs, disease-modifying antirheumatic drugs, nonopioid analgesics, & drugs used in gout. In: Katzung BG (ed) Basic & clinical pharmacology, 8th edn. New York, McGraw Hill, pp 596–623
- Peura DA (2002) Gastrointestinal safety and tolerability of non-selective nonsteroidal anti-inflammatory agent and cyclooxygenase-2-selective inhibitors. *Cleve Clin J Med* 69:SI31–SI39
- Tomisato W, Tsutsumi S, Hoshino T, Hwang HJ, Mio M, Tsuchiya T, Mizushima T (2004) Role of direct cytotoxicity effects of NSAIDs in the induction of gastric lesions. *Biochem Pharmacol* 67:575–585
- Langman MJS, Morgan L, Worrall A (1985) Use of anti-inflammatory drugs by patients admitted with small or large bowel perforations and haemorrhage. *Br Med J* 290:347–349
- Sundram K, Sambanthamurthi R, Tan YA (2003) Palm fruit chemistry and nutrition. *Asia Pac J Clin Nutr* 12(3):355–362
- Christen S, Woodall AA, Shigenaga MK, Southwell-Keely PT, Duncan MW, Ames BN (1997) γ -Tocopherol traps mutagenic electrophiles such as NO_x and complements α -tocopherol: physiological implications. *Proc Natl Acad Sci USA* 94:3217–3222
- Ozer NK, Azzi A (2000) Effect of vitamin E on the development of atherosclerosis. *Toxicology* 148(2–3):179–185
- Nesaretnam K, Dorasamy S, Darbre PD (2000) Tocotrienols inhibit growth of ZR-75-1 breast cancer cells. *Int J Food Sci Nutr* 51(Suppl):S95–S103
- Conner EM, Grisham MB (1996) Inflammation, free radicals and antioxidants. *Nutrition* 12(4):274–277
- Jiang Q, Ames BN (2003) γ -Tocopherol, but not α -tocopherol, decreases proinflammatory eicosanoids and inflammation damage in rats. *FASEB J* 17:816–822
- Jiang Q, Elson-Schwab I, Courtemanche C, Ames BN (2000) γ -Tocopherol and its major metabolite, in contrast to α -tocopherol, inhibit cyclooxygenase activity in macrophages and epithelial cells. *Proc Natl Acad Sci USA* 97(21):11494–11499
- Rozen S, Skaletsky HJ (2000) Primer3 on the WWW for general users and for biologist programmers. In: Krawetz S, Misener S (eds) Bioinformatics methods and protocols: methods in molecular biology. Humana Press, New Jersey, pp 365–386
- Lazarus M, Munday CJ, Eguchi N, Matsumoto S, Killian GJ, Kubata BK, Urade Y (2002) Immunohistochemical localization of microsomal PGE synthase-1 and cyclooxygenase in male mouse reproductive organs. *Endocrinology* 143(6):2410–2419
- Rasaband WS (1997–2007) Image J, U. S. National Institutes of Health, Bethesda, MD, USA. <http://rsb.info.nih.gov/ij/>
- Méric J-B, Rottey S, Olaussen K, Soria JC, Khayat D, Rixe O, Spano J-P (2006) Cyclooxygenase-2 as a target for anticancer drug development. *Crit Rev Oncol Hematol* 59:51–64
- Hinz B, Brune K (2002) Cyclooxygenase-2—10 years later. *J Pharmacol Exp Ther* 300:367–375
- Leiro J, Álvarez E, Arranz JA, Laguna R, Uriarte E, Orallo F (2004) Effects of *cis*-resveratrol on inflammatory murine macrophages: antioxidant activity and down-regulation of inflammatory genes. *J Leukoc Biol* 75:1156–1165
- Salvemini D, Misko TP, Masferrer JL, Seibert K, Currie MG, Needleman P (1993) Nitric oxide activates cyclooxygenase enzymes. *Proc Natl Acad Sci USA* 90:7240–7244
- Giulietti A, Overbergh L, Valckx D, Decallonne B, Bouillon R, Mathieu C (2001) An overview of real-time quantitative PCR: applications to quantify cytokine gene expression. *Methods* 25:386–401
- Sen CK, Khanna S, Roy S (2006) Tocotrienols: vitamin E beyond tocopherols. *Life Sci* 78:2088–2098
- Feghali CA, Wright TM (1997) Cytokines in acute and chronic inflammation. *Front Biosci* 2:d12–d26
- Won J-H, Im H-T, Kim Y-H, Yun K-J, Park H-J, Choi J-W, Lee K-T (2006) Anti-inflammatory effect of buddlejasaponin IV through the inhibition of iNOS and COX-2 expression in RAW264.7 macrophages via the NF- κ B inactivation. *Br J Pharmacol* 148:216–225
- Jung W-J, Sung M-K (2004) Effects of major dietary antioxidants on inflammatory markers of RAW264.7 macrophages. *BioFactors* 21:113–117
- Houssiao FA (1995) Cytokines in rheumatoid arthritis. *Clin Rheumatol* 14(Suppl):10–13
- Nachbaur DM, Herold M, Maneschg A, Huber H (1991) Serum levels of interleukin-6 in multiple myeloma and other haematological disorders: correlation with disease activity and other prognostic parameters. *Ann Hematol* 62:54–58
- Chung KF (2001) Cytokines in chronic obstructive disease. *Eur Respir J* 18:50S–59S

31. Laskin DL, Laskin JD (2001) Role of macrophages and inflammatory mediators in chemically induced toxicity. *Toxicology* 160:111–118
32. Moncada S, Higgs A (1993) The L-arginine-nitric oxide pathway. *N Engl J Med* 329:2002–2012
33. Singh S, Evans TW (1997) Nitric oxide, the biological mediator of the decade: fact or fiction? *Eur Respir J* 10:699–707
34. Beckman JS, Koppenol WH (1996) Nitric oxide, superoxide, and peroxynitrite: the good, the bad, and the ugly. *Am J Physiol Cell Physiol* 271:C1424–C1437
35. Beharka AA, Han SN, Adolfsson O, Wu D, Smith D, Lipman R, Cao G, Meydani M, Meydani S (2002) Long-term dietary antioxidant supplementation reduces production of selected inflammatory mediators by murine macrophages. *Nutr Res* 20(2):281–296
36. Harris SG, Padilla J, Koumas L, Ray D, Phipps RP (2002) Prostaglandins as modulators of immunity. *Trends Immunol* 23:144–150
37. Herschman HR (1996) Prostaglandin synthase 2. *Biochim Biophys Acta* 1299:125–140
38. Botting RM (2006) Cyclooxygenase: past, present and future. A tribute to John R. Vane (1927–2004). *J Therm Biol* 31:208–219
39. Abate A, Yang G, Dennery PA, Oberle S, Schröder H (2000) Synergistic inhibition of cyclooxygenase-2 expression by vitamin E and aspirin. *Free Radic Biol Med* 29:1135–1142
40. Jin DZ, Yin LL, Ji XQ, Zhu XZ (2006) Cryptotanshinone inhibits cyclooxygenase-2 enzyme activity but not its expression. *Eur J Pharmacol* 549:166–172
41. Barrios-Rodiles M, Keller K, Belley A, Chadee K (1996) Non-steroidal anti-inflammatory drugs inhibit cyclooxygenase-2 enzyme activity but not mRNA expression in human macrophages. *Biochem Biophys Res Commun* 225:896–900
42. Nesaretnam K, Wong WY, Wahid MB (2007) Tocotrienols and cancer: beyond antioxidant activity. *Eur J Lipid Sci Technol* 109:445–452
43. Nesaretnam K, Teoh HK, Selvaduray KR, Bruno RS, Ho E (2008) Modulation of cell growth and apoptosis response in human prostate cancer cells supplemented with tocotrienols. *Eur J Lipid Sci Technol* 110:23–31
44. Osakada F, Hashino A, Kume T, Katsuki H, Kaneko S, Akaike A (2004) α -Tocotrienol provides the most neuroprotection among vitamin E analogs on cultured striatal neurons. *Neuropharmacology* 47:904–915
45. Wu SJ, Liu PL, Ng LT (2008) Tocotrienol-rich fraction of palm oil exhibits anti-inflammatory property by suppressing the expression of inflammatory mediators in human monocytic cells. *Mol Nutr Food Res* 52(8):921–929
46. Jiang Q, Yin X, Lill MA, Danielson ML, Freiser H, Huang J (2008) Long-chain carboxychromanols, metabolites of vitamin E, are potent inhibitors of cyclooxygenases. *Proc Natl Acad Sci USA* 105(51):20464–20469
47. Ahn KS, Sethi G, Krishnan K, Aggarwal BB (2007) γ -Tocotrienol inhibits nuclear factor- κ B pathway through inhibition of receptor-interacting protein and TAK1 leading to suppression of antiapoptotic gene products and potentiation of apoptosis. *J Biol Chem* 282(1):809–820
48. Chen F, Castranova V, Shi XL, Demers LM (1999) New insights into the role of nuclear factor- κ B, a ubiquitous transcription factor in the initiation of diseases. *Clin Chem* 45(1):7–17
49. Kumar A, Takada Y, Boriek AM, Aggarwal BB (2004) Nuclear factor- κ B: its role in health and disease. *J Mol Med* 82:434–448
50. Aggarwal BB (2001) Nuclear factor- κ B: the enemy within. *Cancer Cell* 6:203–208

Phospholipid, Oleic Acid Micelles and Dietary Olive Oil Influence the Lutein Absorption and Activity of Antioxidant Enzymes in Rats

R. Lakshminarayana · M. Raju ·
M. N. Keshava Prakash · V. Baskaran

Received: 26 April 2009 / Accepted: 30 June 2009 / Published online: 14 August 2009
© AOCs 2009

Abstract This study reports on the results of repeated gavages and dietary feeding of lutein dispersed either in phospholipids or fatty acid micelles or vegetable oils and the effects on lutein bioavailability and antioxidant enzymes in rats. For the gavage study, rats ($n = 5/\text{group}$) were intubated with lutein solubilized either in oleic acid (OLA, 18:1n-9) or linoleic acid (LNA, 18:2n-6) or phosphatidylcholine (PC) or lysophosphatidylcholine (LPC) or no phospholipid (NoPL) micelles for 10 days. For the dietary study, rats ($n = 5/\text{group}$) were fed a diet containing fenugreek leaf (lutein source), either with olive (OO) or sunflower (SFO) or groundnut (GNO, control) oil or L- α -lecithin (PL) for 4 weeks. The gavage study showed that the plasma, liver and eye lutein levels in OLA and LPC groups were higher by 23.9, 20.8 and 25.5% and 16.1, 28.5 and 14.0% than LNA and PC groups, respectively. The dietary study showed the plasma (35.0 and 43.5%) and eye (18.5 and 37.0%) lutein levels in OO were higher than SFO and GNO groups. The plasma and eye lutein levels in the PL group were higher by 20 and 31.3% than in the control. It is evident that OO and PL modulate lutein absorption, which in turn modulates antioxidant enzymes and fatty acids in plasma and tissues compared to SFO. Hence,

selection of the fat source may be vital to enhancing the lutein bioavailability.

Keywords Antioxidant enzymes · Bioavailability · Fatty acids · Lutein · Phospholipids

Abbreviations

GNO	Groundnut oil
LNA	Linoleic acid
LPC	Lysophosphatidylcholine
MDA	Malonaldehyde
OLA	Oleic acid
OO	Olive oil
PC	Phosphatidylcholine
PL	L- α -Lecithin
SFO	Sunflower oil
SOD	Superoxide dismutase

Introduction

Dietary ingestion is the only source of lutein, as humans cannot synthesize it. Consumption of lutein-rich food is associated with a lower risk of cataracts and age-related macular degeneration (AMD) [1]. Lutein is ingested along with other food matrices, reported to interfere with lutein absorption [2]. Herden et al. [3] reported that intestinal absorption of carotenoids depends on the concentration and origin of the dietary fat consumed. Dietary fat is reported to improve the absorption of β -carotene [4], by influencing the release of bile and the formation of mixed micelles in the intestine [5]. Plasma lutein response was improved after a meal with sufficient fat, but reduced when fat is absent or too

R. Lakshminarayana · M. Raju · V. Baskaran (✉)
Department of Biochemistry and Nutrition, Central Food
Technological Research Institute, CSIR, Mysore 570020, India
e-mail: basrev@yahoo.co.in

M. N. Keshava Prakash
Department of Fruit and Vegetable Technology, Central Food
Technological Research Institute, CSIR, Mysore 570020, India

Present Address:

R. Lakshminarayana
Department of Biotechnology, Jnana Bharathi Campus,
Bangalore University, Bangalore 560056, India

low [6]. Baskaran et al. [7] and others [8, 9] reported that a single oral dose of specific phospholipids in mixed micelles influenced the intestinal uptake of β -carotene and lutein in mice, rats and human intestinal Caco-2 cells, respectively.

There are studies which investigated the effects of vegetable fat on carotenoids bioavailability in animal and human subjects. Hu et al. [10] studied the effect of dietary sunflower oil and beef tallow on the level of β -carotene in plasma triacylglyceride-rich lipoproteins in women. Clark et al. [11] observed that lycopene and astaxanthin absorption in rats was greater with an orally administered emulsion with olive oil compared to corn oil. Despite the importance of dietary lipids as carriers for lutein, little is known with relation to their influence on lutein bioavailability in vivo. Hence, it is appropriate to study the role of dietary fat on lutein bioavailability. Earlier, we reported that a single oral dose of phospholipid micelles and olive oil significantly enhanced the plasma lutein level in rat and mice models [7, 12, 13]. This study appraises the effect of repeated gavages and dietary feeding of lutein with phospholipids, fatty acids and vegetable oils on its bioavailability, fatty acid profile and activity of certain antioxidant enzymes in rats. Although gerbils and monkeys are considered as being superior models for xanthophyll absorption studies, a rat model was chosen in this study because the results obtained can be considered valid and comparable with other animal models. Earlier, we had established by LC-MS that lutein and zeaxanthin are present in the rats' eye [13].

Materials and Methods

Chemicals and Materials

Lutein (99%), DL- α -tocopherol, monooleoylglycerol, sodium taurocholate, linoleic acid, oleic acid (~99%), phosphatidylcholine (99%) and lysophosphatidylcholine (99%) were purchased from Sigma-Aldrich (St. Louis, MO, USA). All other chemicals and solvents were of analytical reagent grade, unless otherwise mentioned, and were obtained from Sisco Research Laboratories (Mumbai, India). Food grade casein, cellulose, sucrose, methionine, vitamins, minerals, choline chloride and L- α -lecithin (L- α -phosphatidylcholine from soybean) were purchased from Himedia Laboratories Pvt. Ltd. (Mumbai, India). Refined olive, sunflower, and groundnut oils were obtained from a local super market.

Animals

Animal experiments were conducted after due approval from the Institutional Animal Ethics Committee. Male

albino rats [OUTB-, Wistar, IND-cft (2c)] weighing 42 ± 2 g were housed in individual steel cages at room temperature ($28 \pm 2^\circ\text{C}$) with a 12-h dark/light cycle in the institute's animal house facility.

Gavage Studies

Mixed micelles in phosphate buffered saline (pH, 7.0) containing monooleoylglycerol (2.5 mM), sodium taurocholate (12 mM), lutein (200 μM) either with 3 mM PC or LPC or no phospholipids (NoPL) or with 7.5 mM OLA or LNA was prepared separately [11]. Rats were divided into six groups ($n = 5/\text{group}$) and housed individually in metabolic cages for 7 days. Rats were fed orally a daily dose (0.2 ml/day) of micellar lutein containing NoPL (control) or PC or LPC or OLA or LNA for 10 days. Feed (Amrut feeds, Sangli, India) and water was made available ad lib throughout the experimental run. Feed samples were processed for lutein analysis before feeding to ascertain its level.

Urine was collected in amber bottles contained 0.5 ml of toluene (to prevent bacterial growth) and 0.2 ml of 2 mM α -tocopherol and faecal matter was collected separately from the individual rats for 6 days from days 2 to 8 and used for lutein analysis. At the termination of the experiment, the rats were anesthetized with diethyl ether, sacrificed; blood, liver and eyes were sampled and processed for lutein analysis.

Dietary Studies

The rats ($n = 5/\text{group}$) were fed an isocaloric diet [14] containing powdered fenugreek leaf (0.421%) as the source of lutein (2.69 mg/kg diet), 10% either olive oil (oleic acid source, OO group) or sunflower oil (linoleic acid source, SFO group) or groundnut oil (control, GNO group) or 10% soy lecithin (phospholipids source, PL group), casein (20%), DL-methionine (0.3%), sucrose (59.57%), cellulose (5%), vitamin mix (1%), mineral mix (3.5%) and choline bitartrate (0.2%), respectively, for 4 weeks. Rats had free access to food and water and the daily food intake and weekly gain-in-body weight were monitored. At the termination of experiment, rats were anesthetized with diethyl ether, sacrificed; blood, liver and eyes were sampled and processed for lutein analysis. Samples were handled on ice under dim yellow light to minimize isomerization and oxidation of lutein by light irradiation.

HPLC Analysis of Lutein

Lutein levels in the extracts of plasma, liver, eyes, urine, feces, fenugreek leaf powder and diet were analyzed by HPLC [12, 13]. In brief, lutein was separated under

isocratic condition at a flow rate of 1 mL/min on SGE C-18 (ODS) column, 25 cm × 4.6 mm id, 5 nm, 120A0 (SGE Co., India) using acetonitrile: methanol: dichloromethane (60:20:20, v/v/v) containing 0.1% ammonium acetate, as a mobile phase at 450 nm with UV–visible detector (Shimadzu, Japan). Peak identities, λ_{\max} and levels of lutein and zeaxanthin were confirmed and quantified by their retention time, characteristic spectra and peak area of reference standards, recorded with a Shimadzu model LC-10Avp series equipped with SPD-10AVP detector. In the case of eye samples, lutein and zeaxanthin levels are presented together as lutein + zeaxanthin, due to their unsatisfactory resolution.

Assay for Antioxidant Enzymes and Lipid Peroxides

Liver and eyes were homogenized separately in phosphate buffer (10%, pH 7.0), centrifuged at 600g for 15 min at 4 °C and the supernatant was used for enzyme assays. Superoxide dismutase (SOD, EC 1.15.1.1) activity was measured by the inhibition of cytochrome-C reduction mediated via superoxide anions generated by xanthine-xanthine oxidase and measured using spectrophotometer (Shimadzu-Japan, 1601) at 550 nm [15]. One unit of superoxide dismutase was defined as the amount-required to inhibit the reduction of cytochrome-C by 50%. Glutathione peroxidase (GSH-Px, EC 1.11.1.9) activity was measured by initiating reaction with *tert*-butyl hydroperoxide (100 μ l) and recorded decrease in absorbance at 340 nm for 5 min [16]. The activity is expressed as nmol of NADPH oxidized/min/mg protein (\sum 340–6.22 $\text{mM}^{-1}\text{cm}^{-1}$). The glutathione level was measured by monitoring the rate of 5-thio-2-nitrobenzoic acid formation at 412 nm [17]. Protein content and lipid peroxides (nmol MDA/mg protein) in plasma and tissue were estimated as per Lowry et al. [18] and a thiobarbituric acid reactive substances assay [19].

Analysis of Lipid Profile

Total lipids [20], triacylglycerides [21], cholesterol [22] and phospholipids [23] were analyzed from plasma and tissues by adopting standard procedures. Fatty acids were analyzed as methyl esters prepared using boron trifluoride in methanol [24] and analyzed by gas chromatography (Shimadzu 14B, fitted with FID) using a fused silica capillary column 25 cm × 0.25 mm (Parma bond FFAP-DF-0.25: Machery-Nagel GmbH co. Duren, Germany). The gas chromatography operating conditions were: initial column (160 °C), injector (210 °C) and detector temperature (250 °C) and the column temperature were programmed to rise at 6 °C/min to the final temperature of 240 °C. Nitrogen gas was used as the carrier. Fatty acids

were identified with their respective standards (Nu Chek Prep, Elysian, MN, USA).

Statistical Analysis

Data were tested for homogeneity of variances by the Bartlett test. When homogenous variances were confirmed, the data were tested by ANOVA and significant differences between the groups were evaluated by Tukey's test. Differences in means were considered significant at $P < 0.05$.

Results

Gavage Studies

Influence of Phospholipids on Lutein Bioavailability

The plasma lutein levels for the PC and LPC groups were higher by 19.2 and 32.3% than NoPL group, while the value for the LPC group was 16.1% higher than the PC group. The liver lutein levels in PC and LPC groups were 30 and 50% higher than the NoPL group, whereas in the LPC group it was 28.5% higher than the PC group. Similarly, lutein concentration in the eyes of PC and LPC groups were higher by 25.8 and 36.2% compared with the NoPL group, but it was 14.0% higher in the LPC than in the PC group (Table 1). Lutein excreted through the urine of the PC group was higher by 30.1 and 50.9% than the NoPL and LPC groups. However, lutein levels in feces of the PC group were higher by 8.3 and 38.8% than the NoPL and LPC groups (Table 1). The plasma TG response (mg/dl) on feeding PC was higher (257.3 ± 27.4) than LPC (183.6 ± 43.2) and NoPL (250.3 ± 25.2) groups.

Influence of fatty Acids on Lutein Bioavailability

The plasma, liver and eyes lutein response in the OLA group was higher by 23.9, 20.8 and 25.5% than in the LNA group (Table 1). The level of lutein excreted in urine was higher in the OLA group (25.2%) and its level in feces was slightly higher in the LNA group (Table 1). Likewise, a higher (44.8%) TG level was recorded in the plasma of the OLA in comparison to the LNA group.

Dietary Studies

The experimental diet had lutein (2.69 μ g/g diet) as the major carotenoid. No difference was noticed in mean food intake and gain-in-body weight among groups. Diet was analyzed for their fatty acid composition prior to use (Table 2). OLA (74.3%) and LNA (64.9%) are major fatty acids in olive oil and sunflower oil, whereas, lecithin

Table 1 Lutein level in plasma, liver, eyes, urine and feces of rats after 10 days of gavaging of lutein solubilized in either phospholipids or fatty acid micelles

Dietary factor	Group	Plasma (pmol/ml)	Liver (pmol/g)	Eyes* (pmol/g)	Urine (pmol/ml/day/rat)	Feces (nmol/g/day/rat)
Phospholipids	NoPL or OLA	4.6 ± 0.8 ^a	9.1 ± 1.8 ^a	49.7 ± 9.2 ^a	11.1 ± 3.5 ^a	1.2 ± 0.2 ^a
	PC	5.7 ± 0.3 ^a	13.0 ± 1.9 ^b	66.1 ± 11.8 ^a	15.9 ± 5.9 ^a	1.8 ± 0.4 ^a
	LPC	6.8 ± 2.0 ^a	18.2 ± 2.7 ^c	76.9 ± 18.3 ^a	7.8 ± 3.1 ^b	1.1 ± 0.5 ^a
Fatty acids	OLA	4.6 ± 0.8 ^a	9.1 ± 1.8 ^a	49.7 ± 9.2 ^a	11.1 ± 3.5 ^a	1.2 ± 0.2 ^a
	LNA	3.5 ± 0.2 ^b	7.2 ± 2.5 ^a	37.0 ± 11.8 ^a	8.3 ± 1.5 ^{a,b}	1.3 ± 0.2 ^a

Values are means ± SEM of five rats. Values not sharing a common superscript within a column are statistically significant at $P < 0.05$

* Since lutein and zeaxanthin did not resolve clearly in plasma, tissues and excreted products, results are presented as lutein + zeaxanthin

Table 2 Fatty acid profile of experimental diets containing powdered fenugreek leaves as the lutein source either with vegetable oils or L- α -lecithin

Fatty acids (%)	GNO	OO	SFO	PL
14:0	ND	ND	ND	2.1 ± 0.3
16:0	1.3 ± 0.1 ^a	4.5 ± 0.3 ^b	0.3 ± 0.0 ^c	16.1 ± 0.2 ^d
16:1	0.3 ± 0 ^a	ND	0.8 ± 0.3 ^a	5.5 ± 0.5 ^b
18:0	15.0 ± 2.1 ^a	5.0 ± 1.2 ^b	0.3 ± 0.0 ^c	8.7 ± 0.3 ^d
18:1	52.9 ± 5.6 ^a	74.3 ± 7.8 ^b	14.6 ± 2.0 ^c	38.2 ± 2.0 ^d
18:2 (n-6)	19.5 ± 1.3 ^a	1.2 ± 0.1 ^b	64.9 ± 4.7 ^c	19.5 ± 3.2 ^{a,d}
18:3 (n-3)	6.0 ± 2.1 ^a	7.2 ± 0.7 ^a	11.6 ± 1.3 ^b	5.9 ± 0.2 ^a
20:0	1.0 ± 0.3 ^a	2.1 ± 0.2 ^b	5.9 ± 0.8 ^c	3.7 ± 0.4 ^d
20:4 (n-6)	0.4 ± 0.1 ^a	2.6 ± 0.2 ^b	0.2 ± 0.0 ^b	ND
20:5 (n-3)	ND	0.7 ± 0.0	0.3 ± 0.0	ND
22:0	3.4 ± 1.0 ^a	1.4 ± 0.0 ^b	0.7 ± 0.2 ^c	0.3 ± 0.0 ^d
22:6 (n-3)	ND	1.0 ± 0.1	0.3 ± 0.0	ND

Values are means ± SEM of three samples. Values not sharing a common superscript within a row are statistically significant at $P < 0.05$

ND not detected

contained OLA as the major fatty acid (38.2%), followed by LNA (19.5%). Vegetable oils used in this study were chosen based on their fatty acid composition so as to compare with the results of specific fatty acids employed in the gavage studies.

Influence of Vegetable Oils and Lecithin on Lutein Bioavailability

At 0 day (baseline values), the plasma (nmol/l), liver and eyes (pmol/g) lutein levels were 4.7 ± 0.4 , 94.5 ± 17.4 and 32.7 ± 3.2 , respectively, and their levels were elevated after 4 weeks feeding of lutein dispersed in vegetable oils. The OO and SFO groups recorded higher plasma (43.5 and 13.1%) and eyes (37 and 22.7%) lutein levels than the GNO group. In comparison, the value for the OO group was 35 and 18.5% higher than the SFO group (Table 3). In contrast, no difference was noticed in the liver lutein levels

Table 3 Lutein levels in rats at 0 day and after 4 weeks feeding of a diet containing powdered fenugreek leaves as the lutein source either with vegetable oils or L- α -lecithin

Groups	Plasma (nmol/l)	Liver (pmol/g)	Eyes (pmol/g)*
Base line values	7.0 ± 0.4	94.5 ± 17.4	32.7 ± 3.2
GNO	28.5 ± 6.2 ^a	145.9 ± 18.5 ^a	88.4 ± 7.5 ^a
OO	50.5 ± 3.0 ^b	161.0 ± 4.0 ^a	140.5 ± 9.3 ^b
SFO	32.8 ± 4.5 ^{a,c}	177.5 ± 11.4 ^b	114.4 ± 13.5 ^c
PL	35.6 ± 2.4 ^c	183.3 ± 10.2 ^b	128.8 ± 12.8 ^b

Values are means ± SEM of five rats. Values not sharing a common superscript within a column are statistically significant at $P < 0.05$

* Lutein and zeaxanthin are expressed together due to their low resolution in eyes

among the groups. The plasma TG level was higher by 26.0 and 22.4% in the OO and SFO groups compared with the GNO group. The plasma, liver and eye lutein level in the PL group was higher by 19.9, 20.4 and 31.3% compared to the GNO group (Table 3).

Antioxidant Enzymes

The activity of SOD in plasma was higher by 17.4% (SFO group) and lower by 38% (OO group) compared with the GNO group, wherein its activity in the OO group was lower by 40% compared to the SFO group. In contrast, no significant difference was noticed in the liver of the SFO group compared with the GNO and OO groups. Similarly, no difference was noticed in SOD activity in eyes between SFO and OO groups and plasma, liver and eye of the PL group compared to the GNO group (Table 4).

The activity of GSH-Px in plasma of the SFO group increased slightly and it was lower (32%) in the OO than in the GNO group in comparison, the OO group displayed 30.6% lower activity than the SFO group. Activity of GSH-Px was higher by 15.4 and 37.4% in liver and eyes of the SFO group and it was non-significantly lower in the OO group than in the GNO group. Data further reveal that the activity of enzyme in liver and eyes of the OO group was

Table 4 Activity of antioxidant enzymes, glutathione and MDA levels in plasma, liver and eyes of rats fed on a diet containing powdered fenugreek leaves as lutein source either with vegetables oils or L- α -lecithin

Parameters	Plasma				Liver*				Eyes*			
	GNO	OO	SFO	PL	GNO	OO	SFO	PL	GNO	OO	SFO	PL
Superoxide dismutase (U/min/mg protein)	2.9 ± 0.2 ^a	2.1 ± 0.2 ^a	3.5 ± 0.2 ^a	3.2 ± 0.7 ^a	4.9 ± 0.7 ^a	4.5 ± 0.6 ^a	5.4 ± 0.8 ^a	5.2 ± 1.0 ^a	5.1 ± 0.4 ^a	5.5 ± 0.4 ^a	5.4 ± 0.8 ^a	5.2 ± 1.0 ^a
Glutathione peroxidase (μ mol/min/mg protein)	21.3 ± 1.2 ^a	16.1 ± 2.9 ^b	23.2 ± 5.5 ^c	27.1 ± 1.9 ^a	31.8 ± 1.2 ^a	26.7 ± 4.2 ^b	37.6 ± 3.5 ^c	33.2 ± 2.2 ^a	38.3 ± 1.2 ^a	36.1 ± 4.2 ^a	57.7 ± 8.1 ^b	43.2 ± 2.2 ^a
Glutathione (μ mol/ml)	22.8 ± 4.3 ^a	28.5 ± 6.3 ^a	31.1 ± 7.6 ^a	26.4 ± 3.6 ^{a,b}	52.0 ± 2.3 ^a	68.8 ± 5.2 ^b	62.8 ± 5.7 ^b	57.9 ± 3.1 ^b	62.0 ± 6.4 ^a	78.3 ± 7.1 ^b	82.4 ± 9.6 ^b	64.4 ± 6.2 ^a
MDA (nmol/mg protein)	9.2 ± 2.0 ^a	10.1 ± 1.4 ^a	15.1 ± 1.2 ^b	13.1 ± 2.8 ^b	15.3 ± 3.2 ^b	18.1 ± 2.1 ^a	25.1 ± 1.8 ^b	29.1 ± 3.2 ^b	42.3 ± 4.2 ^a	46.1 ± 2.3 ^a	55.1 ± 1.7 ^b	47.1 ± 2.2 ^a

Values are means \pm SEM of five samples. Values not sharing a common superscript within a row are statistically significant at $P < 0.05$

* Per ml of 10% tissue homogenate

lower by 28.9 and 37.4% than in the SFO group. The activity of GSH-Px in the PL group was higher in plasma (21.4%), while no difference was noticed in liver and eyes compared with the GNO group (Table 4).

Plasma glutathione levels in the SFO and OO groups increased by 26.6 and 20% over the GNO group. In case of liver and eyes, the levels of glutathione was 17.1, 24.7 and 24.4, 5.0% higher in SFO and OO groups than in the GNO group, wherein its level was slightly lower in the OO group than in the SFO group. Glutathione level in plasma, liver and eyes of the PL group were non-significantly higher than the control group (Table 4).

Lipid Peroxides

Elevated levels (39.1 and 9%) of MDA were recorded in the plasma of the SFO and OO groups compared to the GNO group, wherein it was lower by 33% in the OO group in comparison to the SFO group. Similarly, the MDA level in the liver of the SFO group was higher (40 and 15.4%) and in eyes not much difference was observed compared to the OO and GNO groups. The plasma, liver and eyes MDA level in the PL group was higher by 29, 47.2 and 10.1% compared to the GNO group (Table 4).

Plasma and Tissues Lipid Profile

In the OO group, the plasma TG level was higher by 21.1 and 35.9% and cholesterol level was lower by 29.1 and 55.0% than in the SFO and GNO groups, respectively. No significant difference was found in plasma phospholipids levels among groups (Table 5). OLA and LNA levels (%) in plasma, liver and eye of 0 weeks (base line value) were recorded as 16.3 ± 2.7 and 23.9 ± 0.5 , 18.4 ± 2.1 , 19.2 ± 1.1 and 16.3 ± 4.5 and 18.8 ± 2.3 , respectively. The plasma fatty acid profile of the OO, SFO and GNO groups show that the OLA and LNA levels were 54 and 21.5% in the OO and SFO groups. However, the proportion of OLA and LNA levels in the GNO group were 42.6 and 17.9%, respectively (Table 6).

The triacylglyceride level in the liver of the OO group was 22.5 and 12.7% higher than those of the SFO and GNO groups, while cholesterol and phospholipids levels were not altered significantly (Table 5). Feeding OO and SFO resulted in elevated levels of OLA (28.4%) and LNA (29.6%) in the liver. There was non-significant alteration in the lipid profile studied in the eyes of the OO and SFO groups compared with the GNO group while, fatty acid profile show that the OLA is a major fatty acid in the OO (36.1%) and SFO (21.4%) groups (Table 5). The plasma, liver and eyes lipid profile of the PL group was not significantly changed compared with the control group, whereas the fatty acid profile showed higher OLA

Table 5 Lipid profile of plasma, liver and eyes of rats after four weeks feeding a diet containing powdered fenugreek leaves along with vegetable oils or L- α -lecithin

Parameter	Plasma (mg/dl)				Liver (mg/g)				Eyes (mg/g)			
	GNO	OO	SFO	PL	GNO	OO	SFO	PL	GNO	OO	SFO	PL
Triglycerides	139.0 ± 10.4 ^a	189.0 ± 11.2 ^b	149.2 ± 15.1 ^a	125.6 ± 12.2 ^a	120.0 ± 10.4 ^a	137.6 ± 7.0 ^b	106.6 ± 8.5 ^c	128.9 ± 12.5 ^{ab}	102.5 ± 13.8 ^a	93.8 ± 12.5 ^a	110.6 ± 9.0 ^a	120.3 ± 3.3 ^b
Phospholipids	138.7 ± 9.2 ^a	161.6 ± 15.0 ^a	152.8 ± 12.2 ^a	188.3 ± 21.5 ^b	160.6 ± 15.7 ^a	180.0 ± 8.0 ^a	159.6 ± 7.9 ^{ab}	220.0 ± 10.3 ^c	66.8 ± 4.7 ^a	67.0 ± 9.3 ^a	62.3 ± 4.3 ^a	86.4 ± 2.8 ^b
Cholesterol	219.2 ± 19.9 ^a	155.2 ± 20.8 ^b	140.7 ± 16.7 ^b	235.4 ± 23.8 ^{ab}	231.7 ± 21.8 ^a	212.5 ± 15.5 ^a	194.0 ± 15.8 ^b	235.4 ± 43.5 ^a	112.0 ± 13.6 ^b	131.3 ± 4.4 ^b	118.6 ± 18.6 ^{ab}	142.5 ± 3.6 ^c

Values are means ± SEM of five samples. Values not sharing a common superscript within a row are statistically significant at $P < 0.05$

Table 6 Fatty acid profile in plasma, liver and eyes of rats after 4 weeks of feeding experimental diets

FA (%)	Plasma				Liver				Eyes			
	GNO	OO	SFO	PL	GNO	OO	SFO	PL	GNO	OO	SFO	PL
14:0	ND	ND	ND	3.4 ± 0.2	ND	ND	ND	1.2 ± 0.2	ND	ND	ND	ND
16:0	21.4 ± 2.2 ^a	19.2 ± 5.2 ^a	23.9 ± 3.7 ^b	18.4 ± 2.5 ^a	28.4 ± 1.4 ^a	22.5 ± 1.4 ^b	20.3 ± 2.8 ^b	23.4 ± 2.1 ^b	33.2 ± 2.9 ^a	35.4 ± 3.1 ^a	28.2 ± 2.4 ^b	30.0 ± 5.1 ^{a,b}
16:1	4.7 ± 1.1 ^a	4.3 ± 1.6 ^a	3.9 ± 1.1 ^a	10.2 ± 0.5 ^b	5.2 ± 1.1 ^a	8.3 ± 1.9 ^b	7.0 ± 1.8 ^b	12.2 ± 0.5 ^c	5.8 ± 0.2 ^a	4.2 ± 0.8 ^b	7.1 ± 0.7 ^c	6.3 ± 1.2 ^c
18:0	8.1 ± 1.8 ^a	9.8 ± 3.8 ^a	8.4 ± 1.8 ^a	8.7 ± 1.3 ^a	7.4 ± 1.8 ^a	7.1 ± 2.7 ^a	7.8 ± 1.1 ^a	10.2 ± 1.3 ^b	23.4 ± 3.8 ^a	12.7 ± 1.0 ^b	13.7 ± 4.2 ^b	14.1 ± 1.0 ^{b,c}
18:1	42.6 ± 2.1 ^a	54.1 ± 3.8 ^b	21.5 ± 1.4 ^c	36.2 ± 5.0 ^d	17.8 ± 2.5 ^a	28.4 ± 7.6 ^b	29.6 ± 3.5 ^b	31.3 ± 4.0 ^b	26.3 ± 2.7 ^a	36.1 ± 8.2 ^b	21.4 ± 2.5 ^c	35.3 ± 4.0 ^d
18:2(n-6)	17.9 ± 0.6 ^a	8.8 ± 2.0 ^b	32.7 ± 1.5 ^c	14.5 ± 0.9 ^d	18.3 ± 4.2 ^a	17.3 ± 3.2 ^a	23.3 ± 2.8 ^b	14.1 ± 0.8 ^c	4.6 ± 0.9 ^a	6.5 ± 0.5 ^b	14.2 ± 2.9 ^c	7.5 ± 1.0 ^a
18:3(n-3)	ND	ND	ND	ND	12.6 ± 2.0 ^a	10.2 ± 2.7 ^a	5.2 ± 1.0 ^b	2.3 ± 0.4 ^c	2.4 ± 0.4 ^a	ND	3.8 ± 0.2 ^b	2.1 ± 0.6 ^a
20:0	ND	ND	ND	6.5 ± 0.8	ND	ND	ND	4.4 ± 0.3	ND	ND	ND	1.4 ± 0.1 ^d
20:4(n-6)	4.6 ± 0.7 ^a	3.8 ± 0.4 ^a	8.7 ± 0.9 ^b	ND	9.6 ± 1.6	5.7 ± 0.8 ^a	ND	ND	2.2 ± 0.3 ^a	2.7 ± 0.5 ^a	3.2 ± 0.2 ^a	ND
20:5(n-3)	ND	ND	ND	ND	ND	ND	6.1 ± 0.0 ^a	ND	1.7 ± 0.4 ^a	0.6 ± 0.2 ^b	2.1 ± 0.9 ^a	ND
22:0	ND	ND	ND	1.34 ± 0.0	ND	ND	ND	0.85 ± 0.0	ND	ND	ND	0.8 ± 0.0
22:6(n-3)	ND	ND	ND	ND	ND	ND	ND	ND	ND	1.6 ± 0.2 ^a	6.2 ± 0.4 ^b	2.3 ± 0.1 ^c

Values are means ± SEM of five samples. Values not sharing a common superscript within a row are statistically significant at $P < 0.05$

FA fatty acid; ND not detected

accumulation in plasma (36.2%), liver (31.3%) and in eyes (28.3%) (Table 6).

Feeding vegetable oils resulted in altered plasma, liver and eyes fatty acid composition (Table 6). Rats fed on SFO and OO diets had 25 and 45% lower level of LNA in the plasma compared to those fed on a GNO diet. Plasma of the SFO group had 15% of total fatty acid as LNA, whereas, LNA was not detected in the GNO group. OLA and LNA were present only in rats fed on the OO diet and they were 1.3 and 1.4% of total fatty acids. Rats fed with the SFO diet contained LNA to the extent of 2.9% of total fatty acids in liver. The basal level of LNA and OLA in the GNO group was 9.6% of total fatty acids and it increased to 12.7 and 14.4%, respectively, in the SFO and OO groups. The eyes of rats fed with the SFO diet contained 4.9% of LNA of total fatty acids, whereas, it was not detected in other dietary groups.

Discussion

The plasma response of lutein was considered as a measure of intestinal absorption. This study indicates that repeated gavages of lutein solubilized in LPC micelles resulted in an enhanced plasma lutein level compared to PC micelles in rats. This is inconsistent with our earlier single dose studies [7, 9], reported that PC inhibited β -carotene and lutein absorption in rodents and Caco-2 cells, indicating that incomplete hydrolysis of PC in the intestine may affect the rate of solubilization and transfer of lutein from mixed micelles to the enterocytes [12]. Evidence has been reported [25] showing that the presence of intact PC in mixed micelles slows the transfer of cholesterol and α -tocopherol from the micellar matrix. This could be a reason for a higher level of lutein excreted in the feces of rats fed with PC compared to LPC micelles. In contrast, the present study shows that the plasma, liver and eyes lutein levels of the PC group were higher compared with the NoPL group. Repeated intake of PC may stimulate the phospholipases [9], which hydrolyses PC to LPC in the intestine resulting in an increased lutein absorption suggesting that the hydrolysis of phospholipids in the intestinal tract is vital, although PC plays a significant role in the solubilization of carotenoids in lipid emulsions [26]. PC with two long-chain acyl moieties is more hydrophobic than LPC, which has one acyl moiety and a free hydroxyl group, may slow the intestinal uptake of PC more than LPC [25]. Thus, PC can strongly retain the hydrophobic lutein in the mixed micelles thereby suppressing its intestinal uptake [9]. These properties of phospholipids could make it possible to modify the lutein bioavailability.

The dietary study revealed that the plasma lutein level was higher in the OO group than in the SFO group. The

differences in plasma triglycerides and the fatty acids profile indicate that the ingested dietary lipid readily altered the plasma TG. Hollander and Ruble [27] reported that oleic acid in micellar perfusate enhanced the β -carotene absorption more than linoleic acid indicating that the rate of transport depends upon the hydrophobicity of the fatty acids. A more elevated lutein level in the eyes of the OLA group than in the LNA group suggests that, OLA not only influences the intestinal accessibility but also sways the transport of newly absorbed lutein to target tissue. An elevated level of plasma TG further supports the above hypothesis, it being a carrier molecule for lutein. A lower level of plasma lutein after 10 days of intubation and its higher level in eyes further suggests the basis for clearance of absorbed lutein as being via TG (Table 1).

The lipid sources used in this study differ in TG and fatty acid composition (Table 4). OO is rich in oleic acid whereas, SFO is rich in linoleic acid. Borel et al. [28] and Odeberg et al. [29] reported that incorporation of β -carotene and astaxanthin into chylomicrons in human subjects was lower with emulsions containing medium-chain than long-chain triglycerides and suggested that medium-chain triglycerides are mainly transported by portal blood and do not favor the lymphatic transport of lipoproteins. In fact, the higher levels of plasma TG recorded in this study after repeated gavages and dietary feeding support the above mechanism.

Although, specific fatty acids or vegetable lipids play a vital role in lutein bioavailability, they are found to be involved in the regulation of oxidative mechanism. The present results demonstrate that OLA-rich OO is found to protect tissue from lipid peroxidation more than LNA-rich SFO [30]. The effect of a feeding diet with olive oil on tissue lipid composition and the activity of SOD and GSH-PX were comparatively lower than SFO while slightly higher than in the control rats. This could be the reason for lower MDA levels in the OO group. Changes in the liver fatty acid composition may be due to unsaturated lipids in SFO; in turn they may enhance the efficiency of the SOD and GSH-Px [31, 32]. Since lutein is an antioxidant, it may be involved in the protective action against oxidative reactions [1]. This has been supported by the fact that retinal cells treated with lutein had decreased oxidative stress-induced lipid peroxidation and apoptosis [32]. The present data suggest that high levels of dietary unsaturated fat as a carrier for lutein may be avoided if oxidative stress is a critical issue in nutrition-related degenerative diseases like AMD.

In conclusion, the choice of carrier lipid and its fatty acid profile is critical to achieving an enhanced bioavailability of dietary lutein. The relative bioavailability of lutein could be improved either by single, repeated and dietary feeding of lutein either with OLA micelles or

dispersed in olive oil which, in turn, may help in modulating the activity of antioxidant molecules.

Acknowledgment The authors thank the Director and Head, Department of Biochemistry and Nutrition, CFTRI for their encouragement. R. Lakshminarayana and M. Raju acknowledge the CSIR, New Delhi, India for the granting of Senior Research Fellowships.

References

- Krinsky NI (2002) Possible biologic mechanisms for a protective role of xanthophylls. *J Nutr* 132:540S–542S
- Handelman GJ, Nightingale ZD, Liechtenstein AH, Schaefer EJ, Blumberg JB (1999) Lutein and zeaxanthin concentration in plasma after dietary supplementation with egg yolk. *Am J Clin Nutr* 70:247–251
- Herden E, Diaz V, Svanberg U (2002) Estimation of carotenoids accessibility from carrots determined by an in vitro digestion method. *Eur J Clin Nutr* 56:425–430
- Dimitrov NV, Meyer C, Ulrey DE, Chenoweth W, Michelakis A, Malone W, Boone C, Fink G (1988) Bioavailability of β -carotene in humans. *Am J Clin Nutr* 48:298–304
- Roodenberg AJC, Leenen R, Van het hof KH, Weststrate JA, Tijburg LBM (2000) Amount of fat in the diet affects bioavailability of lutein esters but not of β -carotene, and vitamin-E in humans. *Am J Clin Nutr* 71:1187–1193
- Van het Hof KH, West CE, Weststrate JA, Hautvast JGA (2000) Dietary factors that affect the bioavailability of carotenoids. *J Nutr* 130:503–506
- Baskaran V, Sugawara T, Nagao A (2003) Phospholipids affect the intestinal absorption of carotenoids in mice. *Lipids* 38:705–711
- Raju M, Lakshminarayana R, Krishnakantha TP, Baskaran V (2005) Influence of phospholipids on β -carotene absorption and conversion into vitamin A in rats. *J Nutr Sci Vitaminol* 51:216–222
- Sugawara T, Kushiro M, Zhang H, Nara E, Ono H, Nagao A (2001) Lysophosphatidylcholine enhances carotenoid uptake from mixed micelles by Caco-2 human intestinal cells. *J Nutr* 131:2921–2927
- Hu X, Jandacek RJ, White WS (2000) Intestinal absorption of β -carotene ingested with a meal rich in sunflower oil or beef tallow: postprandial appearance in triacylglycerol-rich lipoproteins in women. *Am J Clin Nutr* 71:1170–1180
- Clark RM, Yao L, She L, Furr HC (2000) A comparison of lycopene and astaxanthin absorption from corn oil and olive oil emulsions. *Lipids* 37:803–806
- Lakshminarayana R, Raju M, Krishnakantha TP, Baskaran V (2006) Enhanced bioavailability of lutein by lyso-phosphatidylcholine in mixed micelles. *Mol Cell Biochem* 281:103–110
- Lakshminarayana R, Raju M, Krishnakantha TP, Baskaran V (2007) Lutein and zeaxanthin in leafy greens and their bioavailability: olive oil influences the absorption of dietary lutein and its accumulation in adult rats. *J Agric Food Chem* 55:6395–6400
- Report (1977) of the American Institute of Nutrition Ad. Hoc committee on standards for nutritional studies. *J Nutr* 170:1340–1348
- Flohe L, Otting F (1984) Superoxide dismutase assays. *Methods Enzymol* 105:93–104
- Flohe L, Gunzler W (1984) Assays of glutathione peroxidase. *Methods Enzymol* 105:114–121
- Owens CWI, Belcher RV (1965) A colorimetric micro-method for the determination of glutathione. *Biochem J* 94:705–711
- Lowry OH, Rosebrough NJ, Farr AL, Randall RJ (1951) Protein estimation with Folin phenol reagent. *J Biol Chem* 193:265–275
- Ohkawa H, Ohishi N, Yagi H (1979) Assay for lipid peroxides in animal tissues by thiobarbituric acid reaction. *Anal Biochem* 95:351–358
- Folch J, Lee M, Sloane SGH (1957) A simple method for isolation and purification of total lipids from animal tissue. *J Biol Chem* 226:497–509
- Fletcher MJ (1968) A colorimetric method for estimating serum triacylglycerol. *Clin Chem Acta* 22:303–307
- Searcy RL, Bergquist LM (1960) A new color reaction for the quantification of serum cholesterol. *Clin Chem Acta* 5:192–196
- Stewart JCM (1980) Colorimetric estimation of phospholipids with ammonium ferrothiocyanate. *Anal Biochem* 104:10–14
- Morrison MR, Smith M (1963) Preparation of fatty acids methyl esters and dimethyl acetyls from lipids with boron fluoride methanol. *J Lipid Res* 5:600–608
- Homan R, Hamlehle KL (1998) Phospholipase A₂ relieves phosphatidylcholine inhibition of micellar cholesterol absorption and transport by human intestinal cell line Caco-2. *J Lipid Res* 39:1197–1209
- Borel P, Grolier P, Armand M, Partier A, Lafont H, Lairon D, Azais-Braesco V (1996) Carotenoids in biological emulsions: solubility, surface-to-core distribution and release from lipid droplets. *J Lipid Res* 37:250–261
- Hollander D, Ruble PE (1978) β -Carotene intestinal absorption: bile, fatty acids, pH and flow rate effects on transport. *Am J Physiol* 235:E686–E691
- Borel P, Tyssandier V, Mekki N, Grolier P, Rochette Y, Alexandre-Gouabau MC, Azais-Braesco V (1998) Chylomicron β -carotene and retinyl palmitate responses are dramatically diminished when men ingest β -carotene with medium-chain rather than long-chain triglycerides. *J Nutr* 128:1361–1367
- Odeberg JM, Lingnell A, Pettersson A, Hoglund P (2003) Oral bioavailability of the antioxidant astaxanthin in humans is enhanced by incorporation of lipid based formulations. *Eur J Pharm Sci* 19:299–304
- Mataix J, Quiles JL, Huertas JR, Battino M, Manas M (1998) Tissue specific interactions of exercise, dietary fatty acids and vitamin-E in lipid peroxidation. *Free Radic Biol Med* 24:511–521
- Ruiz-Gutierrez V, Perez-Espinosa A, Vazquez CM, Santa-Maria C (1999) Effect of dietary fats (fish, olive and high-oleic acid sunflower oils) on lipid composition and antioxidant enzymes in rat liver. *Br J Nutr* 82:233–241
- Cai J, Nelson KC, Wu M, Steinberg P Jr, Jones DP (2000) Oxidative damage and protection of the retinal pigment epithelium. *Prog Ret Eye Res* 19:205–221

Radical Scavenging Activity of Lipophilized Products from Transesterification of Flaxseed Oil with Cinnamic Acid or Ferulic Acid

Wee-Sim Choo · Edward John Birch · Ian Stewart

Received: 10 June 2009 / Accepted: 7 August 2009 / Published online: 29 August 2009
© AOCS 2009

Abstract Lipase-catalyzed transesterification of flaxseed oil with cinnamic acid (CA) or ferulic acid (FA) using an immobilized lipase from *Candida antarctica* (E.C. 3.1.1.3) was conducted to evaluate whether the lipophilized products provided enhanced antioxidant activity in the oil. Lipase-catalyzed transesterification of flaxseed oil with CA or FA produced a variety of lipophilized products (identified using ESI-MS-MS) such as monocinnamoyl/feruloyl-diacylglycerol, dicinnamoyl-monoacylglycerol and monocinnamoyl-monoacylglycerol. The free radical scavenging activity of the lipophilized products of lipase-catalyzed transesterification of flaxseed oil with CA or FA toward 2,2-diphenyl-1-picrylhydrazyl radical (DPPH·) were both examined in ethanol and ethyl acetate. The polarity of the solvents proved important in determining the radical scavenging activity of the substrates. Unesterified FA showed the highest free radical scavenging activity among all substrates tested while CA had negligible activity. The esterification of CA or FA with flaxseed oil resulted in significant increase and decrease in the radical scavenging activity compared with the native phenolic acid,

respectively. Based on the ratio of a substrate to DPPH· concentration, lipophilized FA was a much more efficient free radical scavenger compared to lipophilized CA and was able to provide enhanced antioxidant activity in the flaxseed oil. Lipophilized cinnamic acid did not provide enhanced radical scavenging activity in the flaxseed oil as the presence of natural hydrophilic antioxidants in the oil had much greater radical scavenging activity.

Keywords Lipase-catalyzed transesterification · Cinnamic acid · Ferulic acid · Free radical scavenging activity · Antioxidant

Abbreviations

CA	Cinnamic acid
DPPH·	2,2-Diphenyl-1-picrylhydrazyl radical
ESI-MS	Electrospray ionization-mass spectroscopy
ESI-MS-MS	Electrospray ionization-mass spectroscopy-mass spectroscopy
FA	Ferulic acid
HPLC	High performance liquid chromatography

Presented at the 100th AOCS Annual Meeting and Expo, Orlando, Florida, USA, 3–6 May 2009.

W.-S. Choo
School of Science, Monash University Sunway Campus, Jalan
Lagou Selatan, 46150 Bandar Sunway, Selangor, Malaysia

E. J. Birch (✉)
Department of Food Science, University of Otago,
P.O. Box 56, Dunedin 9054, New Zealand
e-mail: john.birch@otago.ac.nz

I. Stewart
Department of Chemistry, University of Otago,
P.O. Box 56, Dunedin 9054, New Zealand

Introduction

Flaxseed oil is rich in alpha linolenic acid (ALA), an essential n-3 fatty acid. The oil usually contains greater than 50% of ALA [1]. The high content of ALA in flaxseed oil, however, renders the oil susceptible to oxidation. Flaxseed oil is not recommended to be used for frying, pan-heating or preparation of food when heat is involved [2]. Today, flaxseed oil is usually cold-pressed from the seed and is increasingly sold as a health food.

There is growing interest in modifying fats and oils to form structured lipids with specific properties for nutritional and pharmaceutical applications [3, 4]. Modification of natural lipids can be achieved by enzymatic means. Long et al. [5] investigated the effect of enzymatic transesterification of palm stearin and palm olein with flaxseed oil on the melting behaviour of palm stearin and palm olein with the objective of expanding the application of the oils. Phenolic acids are natural antioxidants that occur ubiquitously in fruits, vegetables, spices and aromatic herbs [6]. Phenolic acids are hydrophilic in character, which may reduce their antioxidant effectiveness in stabilizing fats and oils. Lipophilization of phenolic acids, which involves the esterification of the phenolic acid with a lipophilic moiety resulting in new molecules with modified hydrophilic/lipophilic balance is a way to utilize their antioxidative properties [7–9]. The lipophilized phenolic acids should maintain its original functional properties such as antioxidant, antimicrobial and UV filtering ability [10, 11].

The esterification of phenolic acids with non-triacylglycerol structures such as alcohol have been previously investigated [12–15]. Literature pertaining to studies involving direct esterifying of phenolic acids on oils has been mainly limited to studies conducted by two groups of researchers. Compton and Laszlo [16], Laszlo et al. [17], Laszlo and Compton [18], and Compton et al. [19] focused mainly on using lipase-catalyzed reactions of vegetable oils such as soybean oil to synthesize structured lipids with properties suitable for use as possible sunscreen reagents. These structured lipids were examined for their ultraviolet-absorbing efficacy but not their free radical scavenging activity. Sabally et al. [20, 21] and Karboune et al. [22] investigated lipase-catalyzed reactions using fish liver oil or flaxseed oil with phenolic acids to synthesize nutraceutical phenolic lipids.

The objectives of this research were to characterize the lipophilized products from lipase-catalyzed transesterification of flaxseed oil with cinnamic acid or ferulic acid, to evaluate the antioxidant activity of the lipophilized products and to investigate whether the lipophilized products provided enhanced antioxidant activity in the flaxseed oil.

Experimental Procedure

Materials

An organic, unrefined, cold-pressed flaxseed oil (abbreviated as OSELO) was obtained from Oil Seed Extractions Ltd, Ashburton, New Zealand. The triacylglycerol profile of OSELO was as follows: trilinolenoylglycerol,

dilinolenoyl-linoleoylglycerol, dilinolenoyl-oleoylglycerol, dilinolenoyl-stearoylglycerol, dioleoyl-linolenoylglycerol, dioleoyl-linoleoylglycerol and trioleoylglycerol. The percentage of free fatty acids was determined as $0.30 \pm 0.05\%$. Peroxide value and *p*-anisidine value were 0.91 ± 0.12 milliequivalent peroxide/kg sample and 0.70 ± 0.05 , respectively. Commercially available immobilized lipase B from *Candida antarctica* [E.C. 3.1.1.3; Novozym 435, with an activity of 10,000 propyl laurate units per solid gram (PLU)], was a gift from Novozymes (Bagsværd, Denmark). CA, FA and DPPH \cdot were purchased from Sigma Chemicals Co. (St. Louis, MO, USA). All the chemicals and solvents used were of analytical or HPLC grade.

Enzymatic Transesterification

The enzymatic transesterification of OSELO with CA or FA was carried out according to a modified method of Karboune et al. [23]. OSELO (1,000 mg) was dissolved in 10 mL of *n*-hexane in a 50-mL Erlenmeyer flask. CA (170 mg) or FA (56 mg) was added to the reaction mixture followed by Novozym 435 (234 mg for CA system; 211 mg for FA system). The mol ratio of OSELO:CA and OSELO:FA was 1:1 and 4:1, respectively. The flask was incubated under nitrogen at 50 °C, with continuous shaking, in an orbital shaker at 120 rpm (Model SS70, Chiltern Scientific, Auckland, New Zealand) for 2 weeks. The enzymatic reaction was stopped by termination of contact with immobilized lipase by filtration using Whatman glass microfibre filter paper C. The removal of unreacted CA/FA by aqueous solvent washing of reaction components and hydrolysis of lipophilized products for quantification were carried out according to the method of Choo and Birch [24]. Briefly, the reaction components in *n*-hexane were washed with four volumes of acetone:methanol:water (7:7:6). Each volume was 6 mL. This was followed by drying the recovered hexane fraction under nitrogen at room temperature. Lipophilized products free from unreacted CA or FA (2.0–7.0 mg) were weighed into a glass tube (15.0 cm \times 1.3 cm with Teflon-lined screw cap). One mL of 4 N methanolic NaOH was added and the hydrolysis was carried out under nitrogen at 50 °C for 3 h, followed by acidification with concentrated HCl. Acidity was checked using litmus paper. This solution was then evaporated to dryness. The dried sample was dissolved in 2 mL isopropanol:hexane (4:1) prior to HPLC analysis. The conversion of CA or FA was calculated as w/w ratio of CA or FA released from the hydrolysis of lipophilized products to its initial amount. Quantification was based on an external standard method where a calibration curve [25, 50, 75, 100, 125 and 150 μ g CA or FA dissolved in 1 mL of isopropanol:hexane (4:1)] was prepared.

HPLC Analysis of Reaction Components

The enzymatic reaction components were monitored by HPLC analysis, according to the method of Sabally et al. [25]. The separation of reaction components was performed on a C-18 Phenosphere-Next column (250 × 4.6 mm, 5 μm; Phenomenex, Torrance, CA, USA) using a Varian 9010 solvent delivery system (Varian Associates, Inc., Walnut Creek, CA, USA), a SPD-M10AV diode array detector (Shimadzu, Kyoto, Japan) and an analyzing software, Shimadzu Class-M10A. Detection of reaction components was achieved at 215 and 280 nm (CA system) and 215 and 290 nm (FA system). These wavelengths, 280 and 290 nm, were selected from the absorption spectrum of CA and FA, respectively. Elution of a 20-μL injected sample was carried out with a gradient system using an acetonitrile/methanol mixture (7:5, vol/vol) as solvent A and isopropanol as solvent B; the elution was initiated by a flow of 100% solvent A for 10 min, followed by a 20-min linear gradient to 100% solvent B, which was maintained for an additional 5 min. The flow rate was 1 mL/min. Typically, a 10-min equilibration period was used between samples, requiring about 45 min/sample.

Electrospray ionization-mass spectroscopy (ESI-MS) and electrospray ionization-mass spectroscopy-mass spectroscopy (ESI-MS-MS) were used for the analysis of reaction components.

The reaction components were recovered by HPLC and analyzed using an ESI-MS system, Bruker microTOFQ (Bruker Daltronics, Bremen, Germany). Samples were introduced using direct infusion into the ESI source in a positive mode with a collision energy of 10 eV. Capillary voltage of −4.5 kV and a dry gas of 99% N₂ at 180 °C were employed. Sampling was averaged for 3 min over a *m/z* range of 100–1,000 amu. The mass was calibrated using an external calibrant of sodium formate clusters. Spectra were processed using Compass software version 1.3 (Bruker Daltronics, Bremen, Germany). Selected ions that were tentatively identified were chosen to undergo further analysis by ESI-MS-MS with collision energy between 20 and 40 eV. High resolution MS data (to five decimal points) was obtained but all the MS data was presented to the nearest mass unit for simplicity.

Determination of Radical Scavenging Activity

The free radical scavenging activity of compounds was measured using a modified DPPH· radical method of Silva et al. [6]. The concentration of sample and DPPH· solution was modified to suit the rate of reactivities of the samples analyzed here. All assays were carried out in triplicate. For the evaluation of free radical scavenging activity of the CA/FA system, five samples were tested (Fig. 1). OSELO

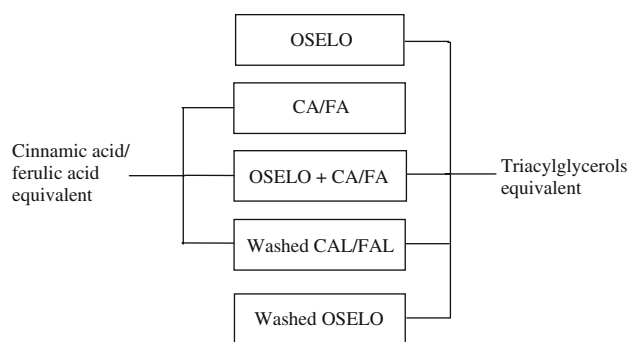


Fig. 1 Samples for evaluation of free radical scavenging activity of the CA/FA system. Lipophilized product including unreacted OSELO from lipase-catalyzed transesterification of OSELO and CA/FA was abbreviated as CAL/FAL. As CAL/FAL underwent aqueous solvent washing to remove unreacted CA/FA, it was labelled as ‘washed CAL/FAL’. Washed OSELO underwent the same aqueous solvent washing. The mixture of OSELO and CA/FA without transesterification was abbreviated as OSELO + CA/FA

concentration was set at 25.0 mM. The amount of CA/FA tested was equivalent to the amount of CA/FA esterified to the acylglycerols of OSELO in CAL/FAL. Taking into consideration the unreacted triacylglycerols (calculated using percentage of conversion) in the CAL/FAL fraction, the amount of CAL/FAL was estimated and set at 25.0 mM. The sample for analysis was mixed with 2×10^{-4} M DPPH· solution in ethanol or ethyl acetate. The ratio of a substrate to DPPH· concentration was $1:8 \times 10^{-3}$. The reduction of DPPH· radical was monitored spectrophotometrically at 517 nm over a period of 30 min against a blank assay. The percentage of the remaining radical was calculated as the absorbance of the sample at 517 nm, divided by that of the DPPH· control at the same time, multiplied by 100.

Results and Discussion

Figure 2 shows a chromatogram of reaction components of the lipase-catalyzed transesterification of OSELO and CA after removal of the enzyme followed by aqueous solvent washing. Unreacted CA was removed from the reaction components by aqueous solvent washing for the quantification of the amount of CA that has been converted to lipophilized products. The average percentage conversion of CA in this lipase-catalyzed transesterification of OSELO and CA was 44.6%. Lipophilized product and CA were detected at both $\lambda = 215$ and 280 nm. Unreacted OSELO triacylglycerols were detected at $\lambda = 215$ nm as trilinolenoylglycerol (25.133 min), dilinolenoyl-linoleoylglycerol (26.150 min), dilinolenoyl-oleoylglycerol (27.254 min), dilinolenoyl-stearoylglycerol (28.252 min), dioleoyl-linolenoylglycerol (29.181 min) and dioleoyl-linoleoylglycerol

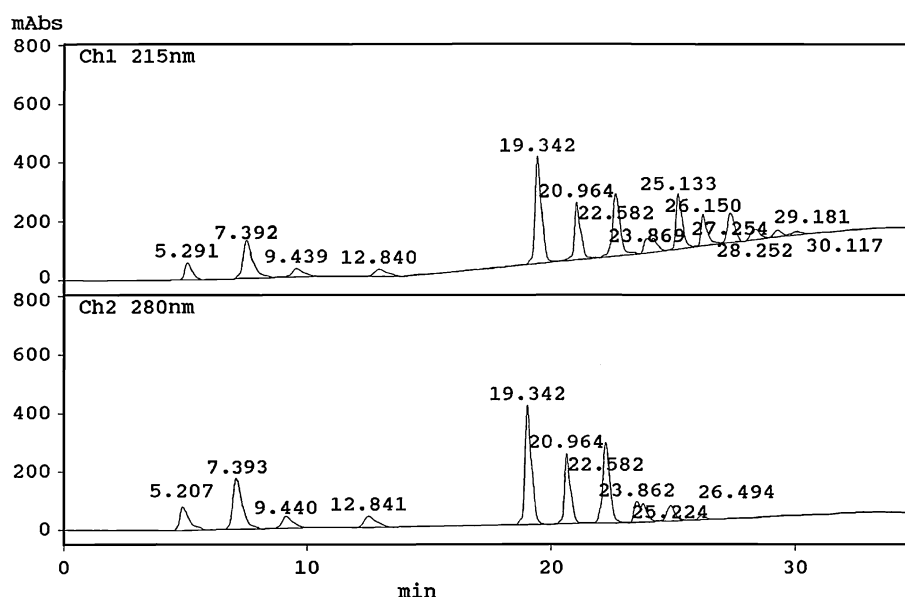


Fig. 2 HPLC chromatogram at 215 nm and 280 nm of reaction components of the lipase-catalyzed transesterification of OSELO and CA after removal of the enzyme followed by aqueous solvent washing. Peaks were identified as follows: monocinnamoyl-linolenoylglycerol (5.207); dicinnamoyl-linolenoyl-glycerol (7.393); dicinnamoyl-linoleoylglycerol (9.440); dicinnamoyl-oleoylglycerol (12.841); monocinnamoyl-dilinolenoylglycerol (19.342); monocinnamoyl-oleoyl-

linolenoylglycerol (20.964); monocinnamoyl-linoleoyl-linolenoylglycerol (22.582); monocinnamoyl-oleoyl-linoleoylglycerol (23.862); trilinolenoylglycerol (25.133); dilinolenoyl-linoleoylglycerol (26.150); dilinolenoyl-oleoylglycerol (27.254); dilinolenoyl-stearoylglycerol (28.252); dioleoyl-linolenoylglycerol (29.181); dioleoyl-linoleoylglycerol (30.117)

(30.117 min), respectively. The first peak at 5.207 min at 280 nm in Fig. 2 was found to be monocinnamoyl-linolenoylglycerol, with two positions on the glycerol having acyl groups (one CA and one linolenic acid) and one position having a hydroxyl (–OH) group (Table 1). Peaks at 7.393, 9.440 and 12.841 min at 280 nm in Fig. 2 were found to be dicinnamoyl-monoacylglycerols whereas peaks at 19.342, 20.964, 22.582 and 23.862 min were found to be monocinnamoyl-diacylglycerols. The identification of lipophilized products for peaks 25.224 and 26.494 min at 280 nm in Fig. 2 was not successful. This was most likely due to the unreacted OSELO triacylglycerols co-eluting at the same retention times, detected at 215 nm. As shown in Fig. 2, the lipophilized products peaks at 25.224 and 26.494 min at 280 nm were minor peaks as compared to the larger respective peaks at 25.133 and 26.150 min at 215 nm.

Figure 3 shows a chromatogram of the reaction components of the lipase-catalyzed transesterification of OSELO and FA after removal of the enzyme followed by aqueous solvent washing. Unreacted FA was removed from the reaction components by aqueous solvent washing for the quantification of the amount of FA that has been converted to lipophilized products. The average percentage conversion of FA in this lipase-catalyzed transesterification of OSELO and FA was 23.7%. Lipophilized products and FA are detected at both $\lambda = 215$ nm and 290 nm.

Unreacted OSELO triacylglycerols were detected at $\lambda = 215$ nm. The four lipophilized product peaks at 15.933, 18.084, 19.987 and 21.383 min at 290 nm in Fig. 3 were found to be monoferuloyl-diacylglycerols (Table 2). Diferuloyl-monoacylglycerol was not detected in this study although Compton et al. [26] reported the presence of diferuloyl-monoacylglycerol in their study of lipase-catalyzed transesterification of soybean oil with ethyl ferulate. This is most likely due to the use of different transesterification conditions and substrates in this study. Unreacted OSELO triacylglycerols (peak 25.064, 26.082, 27.182, 28.113, 29.103, 30.027 and 30.912 min at 215 nm in Fig. 3) were trilinolenoylglycerol, dilinolenoyl-linoleoylglycerol, dilinolenoyl-oleoylglycerol, dilinolenoyl-stearoylglycerol, dioleoyl-linolenoylglycerol, dioleoyl-linoleoylglycerol and trioleoylglycerol, respectively.

The free radical scavenging activity of the lipophilized products of lipase-catalyzed transesterification of OSELO with CA or FA toward DPPH \cdot were examined both in ethanol and ethyl acetate. To examine the comparative free radical scavenging activity of the lipophilized products (CAL and FAL), four control samples were examined (Figs. 4, 5). CA showed very limited free radical scavenging activity in ethanol and ethyl acetate. This is in agreement with the free radical scavenging activity of CA found by Karboune et al. [23] and Choo and Birch [24]. Although Sabally et al. [20] and Karboune et al. [22]

Table 1 Summary of ESI-MS data of lipophilized products of the lipase-catalyzed transesterification of OSELO with CA

Lipophilized products	HPLC (280 nm; Fig. 2) retention time (min)	Molecular weight	ESI-MS	ESI-MS-MS fragmentation
Monocinnamoyl-linolenoylglycerol	5.207	482	505 (M + 23) ⁺	357 [-CA] 227 [-C18:3]
Dicinnamoyl-linolenoylglycerol	7.393	612	635 (M + 23) ⁺	487 [-CA] 357 [-C18:3]
Dicinnamoyl-linoleoylglycerol	9.440	614	637 (M + 23) ⁺	489 [-CA] 357 [-C18:2]
Dicinnamoyl-oleoylglycerol	12.841	616	639 (M + 23) ⁺	491 [-CA] 357 [-C18:1]
Monocinnamoyl-dilinolenoylglycerol	19.342	742	765 (M + 23) ⁺	617 [-CA] 487 [-C18:3]
Monocinnamoyl-oleoyl-linolenoylglycerol	20.964	746	747 (M + 1) ⁺	599 [-CA] 469 [-C18:3] 465 [-C18:1]
Monocinnamoyl-linoleoyl-linolenoylglycerol	22.582	744	745 (M + 1) ⁺	597 [-CA] 467 [-C18:3] 465 [-C18:2]
Monocinnamoyl-oleoyl-linoleoylglycerol	23.862	748	771 (M + 23) ⁺	623 [-CA] 491 [-C18:2] 489 [-C18:1]

(M + 23)⁺ represents the sodiated molecular ion and (M + 1)⁺ represents the protonated molecular ion

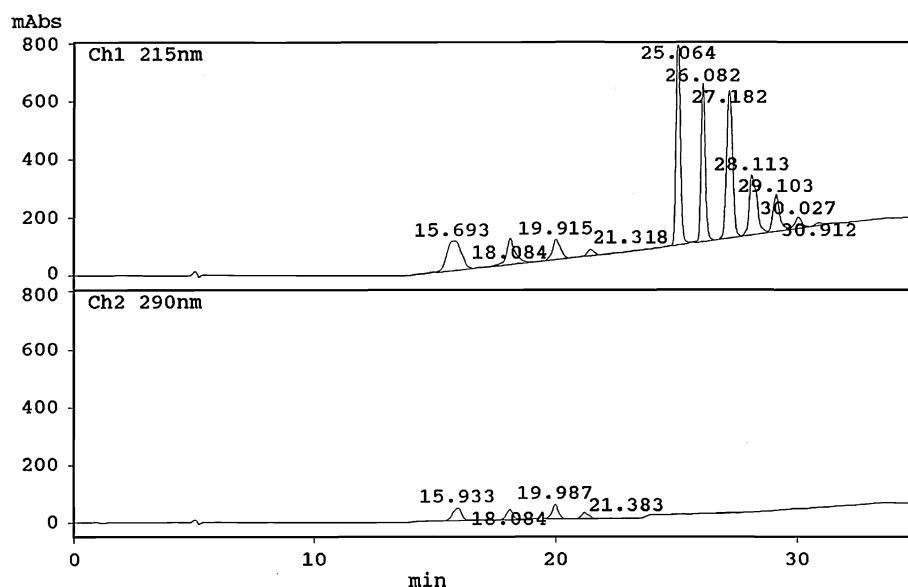


Fig. 3 HPLC chromatogram at 215 and 290 nm of reaction components of the lipase-catalyzed transesterification of OSELO and FA after removal of enzyme followed by aqueous solvent washing. Peaks were identified as follows: monoferuloyl-dilinolenoylglycerol (15.933); monoferuloyl-linoleoyl-linolenoylglycerol

(18.084); monoferuloyl-dioleoylglycerol (19.987); monoferuloyl-oleoyl-linoleoylglycerol (21.383); trilinolenoylglycerol (25.064); dilinolenoyl-linoleoylglycerol (26.082); dilinolenoyl-oleoylglycerol (27.182); dilinolenoyl-stearoylglycerol (28.113); dioleoyl-linolenoylglycerol (29.103); dioleoyl-linoleoylglycerol (30.027); trioleoylglycerol (30.912)

investigated the enzymatic transesterification of flaxseed oil with selected phenolic acids, the free radical scavenging activity of flaxseed oil was not determined. The free radical

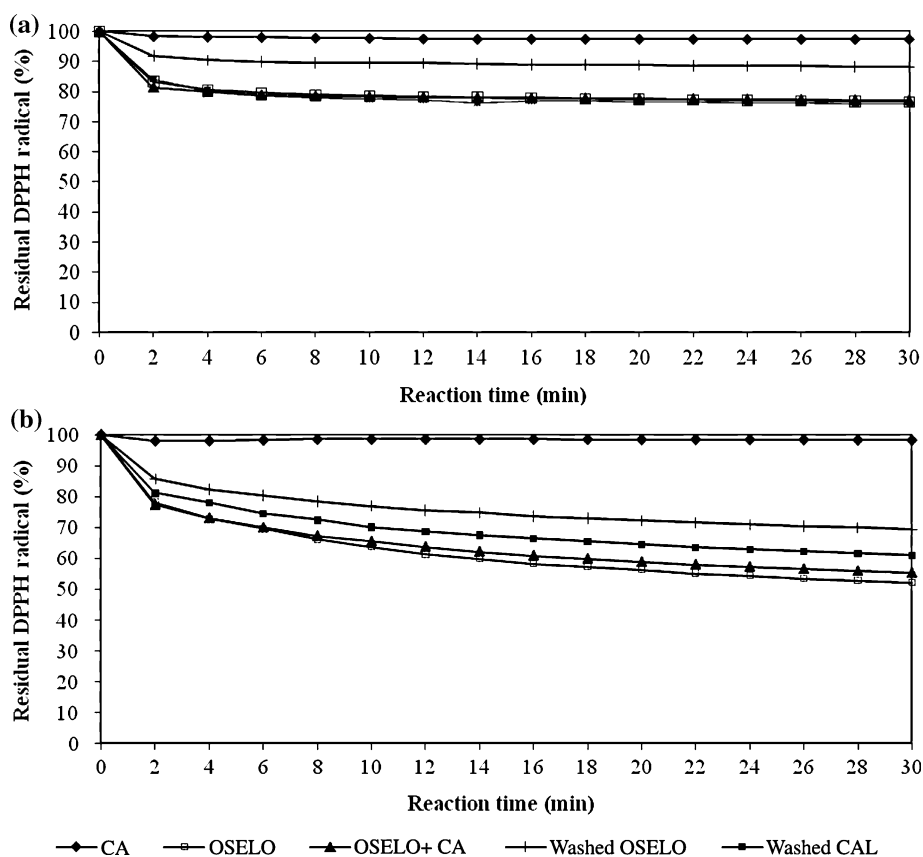
scavenging of OSELO in ethanol and ethyl acetate was 23.5 and 47.8%, respectively (Fig. 4). This activity was due to the presence of naturally occurring antioxidants such

Table 2 Summary of ESI-MS data of lipophilized products of the lipase-catalyzed transesterification of OSELO with FA

Lipophilized products	HPLC (290 nm; Fig. 3) retention time (min)	Molecular weight	ESI-MS (M + 23) ⁺	ESI-MS-MS fragmentation
Monoferuloyl-dilinolenoylglycerol	15.933	788	811	617 [-FA] 533 [-C18:3]
Monoferuloyl-linoleoyl-linolenoylglycerol	18.084	790	813	619 [-FA] 535 [-C18:3] 533 [-C18:2]
Monoferuloyl-dioleoylglycerol	19.987	796	819	625 [-FA] 537 [-C18:1]
Monoferuloyl-oleoyl-linoleoylglycerol	21.383	794	817	623 [-FA] 537 [-C18:2] 535 [-C18:1]

(M + 23)⁺ represents the sodiated molecular ion

Fig. 4 Time course for DPPH· radical scavenging activity of CA system tested in ethanol (a) and ethyl acetate (b). All standard deviations values were below 3.6%. The lipophilized product including unreacted OSELO and CA from the lipase-catalyzed transesterification of OSELO and CA was abbreviated as CAL. Washed CAL and washed OSELO refer to the aqueous solvent washing that CAL and OSELO underwent. The mixture of OSELO and CA without transesterification was abbreviated as OSELO + CA

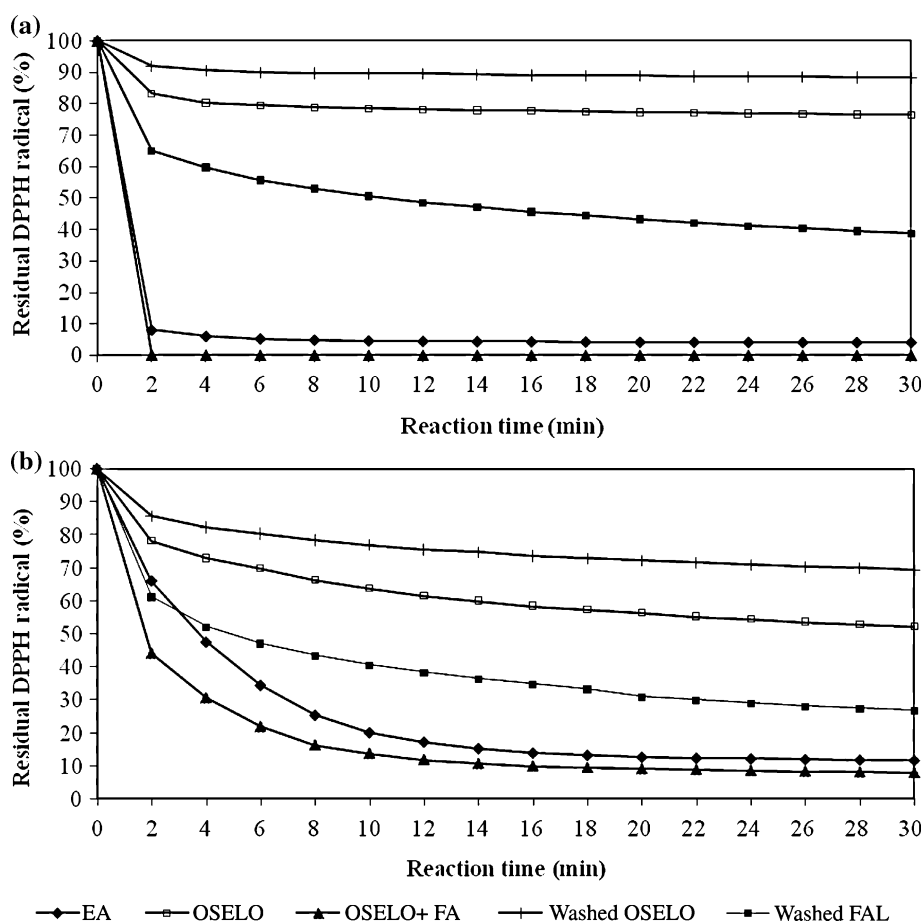


as phenolic acids and tocopherols in OSELO. OSELO showed higher free radical scavenging activity in ethyl acetate than that in ethanol and this indicates that the polarity of the solvent and solubility of substrate may have affected the free radical scavenging activity. When CA was added to OSELO and mixed without transesterification, no significant change in free radical scavenging activity was found for this mixture (OSELO + CA) as compared with

OSELO (Fig. 4). This result reaffirmed that CA has limited free radical scavenging activity at the level tested.

As CAL underwent aqueous solvent washing to remove unreacted CA, a control OSELO was subjected to the same aqueous solvent washing. The aqueous solvent washing removed not only unreacted CA from CAL, it also removed hydrophilic antioxidants present in the oil. This resulted in a loss of free radical scavenging activity in washed OSELO as

Fig. 5 Time course for DPPH· radical scavenging activity of FA system tested in ethanol (a) and ethyl acetate (b). All standard deviation values were below 3.4%. Lipophilized product including unreacted OSELO and FA from lipase-catalyzed transesterification of OSELO and FA was abbreviated as FAL. As FAL underwent aqueous solvent washing to remove unreacted FA, it was labelled as 'washed FAL'. Washed OSELO underwent the same aqueous solvent washing. The mixture of OSELO and FA without transesterification was abbreviated as OSELO + FA



compared with unwashed OSELO (Fig. 4). However, lipophilic tocopherols were not removed by the aqueous solvent washing and contributed to the free radical scavenging of washed OSELO in ethanol (11.8%) and ethyl acetate (30.6%). There was no significant difference in the free radical scavenging activity of OSELO, OSELO + CA and washed CAL tested in ethanol (Fig. 4a). However, a difference was observed among the three samples tested in ethyl acetate (Fig. 4b). The free radical scavenging of OSELO tested in ethyl acetate was 8.9% units higher than that of washed CAL whereas the free radical scavenging activity of washed CAL was 8.3% units higher than that of washed OSELO. These results indicate the esterification of the carboxyl group of CA resulted in a slight increase of its free radical scavenging activity. Alkyl substituents in the carboxylic ethylene side chain of lipophilized CA may have donated electrons inductively to the benzene ring and increased the rate of hydrogen atom transfer reactions and hence an increase in the free radical scavenging activity [24]. However, the radical scavenging activity of natural antioxidants in unwashed OSELO was much greater. The increase in the free radical scavenging activity of CAL was in agreement with the findings of Karboune et al. [23]

and Choo and Birch [24]. For CAL to provide higher enhancement of free radical scavenging activity in OSELO, a higher level of lipophilized CA may be needed, however the conversion to lipophilized CA was already high.

Figure 5 shows the time courses for DPPH· scavenging of the FA system tested in ethanol and ethyl acetate, respectively. The free radical scavenging activity of FA tested in ethanol and ethyl acetate was 96.0 and 88.3%, respectively. The higher free radical scavenging activity obtained for FA in ethanol than that in ethyl acetate was in agreement with the study of Choo and Birch [24]. When FA was added to OSELO and mixed without transesterification, the free radical scavenging activity obtained for this mixture (OSELO + FA) was higher than that of OSELO (Fig. 5). The OSELO activity was due to the contribution of free radical scavenging activity of naturally occurring antioxidants in OSELO. These results were in agreement with that of Warner and Laszlo [27] who reported that ferulic acid acted as an antioxidant when added to soybean oil used for frying potato chips and those of Nag [28], Bera et al. [29, 30] and Jaswir et al. [31, 32] who used natural antioxidants such as capsicum extract, ajowan extract, oleoresin rosemary extract and sage extract

to improve the oxidative stability of flaxseed oil. Like washed CAL, FAL underwent aqueous solvent washing to remove unreacted FA. The free radical scavenging activity of washed FAL tested in ethanol and ethyl acetate was 61.3 and 73.2%, respectively. The higher free radical scavenging activity obtained for washed FAL in ethyl acetate than that in ethanol again indicates that the polarity of the solvent and solubility of substrate may have affected the free radical scavenging activity of washed FAL. The free radical scavenging of washed FAL tested in ethanol and ethyl acetate was 34.7 and 15.1% units lower than those of FA, respectively. The decrease in free radical scavenging activity after esterification of the carboxyl group of FA was in agreement with the findings of Safari et al. [33] and Choo and Birch [24]. The electron-donating alkyl group in the carboxylic ethylene side chain of lipophilized FA may have decreased the reactivity of the phenolic hydroxyl group toward electron transfer reactions and hence a decrease in the free radical scavenging activity [24]. The free radical scavenging of washed FAL tested in ethanol and ethyl acetate was 37.8 and 25.6% units higher than those of OSELO, respectively, and much higher than those of washed OSELO. These results indicate that FAL provided enhanced antioxidant activity in the flaxseed oil.

Conclusions

FAL was a much more efficient free radical scavenger compared to CAL and was able to provide enhanced antioxidant activity in OSELO. The level of CAL required to achieve a noticeable change in antioxidant activity of OSELO would be extreme due to the presence of natural antioxidants in OSELO. Nevertheless, CAL may be useful for unsaturated oils with a small amount of natural antioxidants in them. CAL and FAL demonstrated higher free radical scavenging activities in ethyl acetate than those in ethanol. FA demonstrated a higher free radical scavenging activity in ethanol than that in ethyl acetate. These results strongly suggest that the most suitable polarity medium with respect to the hydrophilicity or lipophilicity of a substrate should be sought in evaluating the free radical scavenging activity of the substrate as it controls the ability of the substrate to reach the true site of free radical attack.

References

- Daun JK, Barthet VJ, Chornick TL, Duguid S (2003) Structure composition and variety development of flaxseed. Flaxseed in human nutrition. AOCS Press, Champaign
- Choo WS, Birch EJ, Dufour JP (2007) Physicochemical and quality characteristics of cold-pressed flaxseed oils during pan-heating. *J Am Oil Chem Soc* 84:735–740
- Willis WM, Lenck RW, Marangoni AG (1998) Lipid modification strategies in the production of nutritionally functional fats and oils. *Crit Rev Food Sci Nutr* 38:639–674
- Compton DL, Laszlo JA, Berhow MA (2000) Lipase-catalyzed synthesis of ferulate esters. *J Am Oil Chem Soc* 77:513–519
- Long K, Zubir I, Hussin AB, Idris N, Ghazali HM, Lai OM (2003) Effect of enzymatic transesterification with flaxseed oil on the high-melting glycerides of palm stearin and palm olein. *J Am Oil Chem Soc* 80:133–137
- Silva FAM, Borges F, Ferreira MA (2001) Effects of phenolic propyl esters on the oxidative stability of refined sunflower oil. *J Agric Food Chem* 49:3936–3941
- Buisman GJH, van Helteren CTW, Kramer GFH, Veldsink JW, Derksen JTP, Cuperus FP (1998) Enzymatic esterifications of functionalized phenols for the synthesis of lipophilic antioxidants. *Biotechnol Lett* 20:131–136
- Stamatis H, Sereti V, Kolisis FN (1999) Studies on the enzymatic synthesis of lipophilic derivatives of natural antioxidants. *J Am Oil Chem Soc* 76:1505–1510
- Figuroa-Espinoza MC, Villeneuve P (2005) Phenolic acids enzymatic lipophilization. *J Agric Food Chem* 53:2779–2787
- Ha TJ, Nihei KI, Kubo I (2004) Lipoxygenase inhibitory activity of octyl gallate. *J Agric Food Chem* 52:3177–3181
- Nihei K, Nihei A, Kubo I (2004) Molecular design of multi-functional food additives: antioxidative antifungal agents. *J Agric Food Chem* 52:5011–5020
- Priya K, Chadha A (2003) Synthesis of hydrocinnamic esters by *Pseudomonas cepacia* lipase. *Enzyme Microb Technol* 32:485–490
- Lue BM, Karboune S, Yeboah FK, Kermasha S (2005) Lipase-catalyzed esterification of cinnamic acid and oleyl alcohol in organic solvent media. *J Chem Tech Biotechnol* 80:462–468
- Weitkamp P, Vosmann K, Weber N (2006) Highly efficient preparation of lipophilic hydroxycinnamates by solvent-free lipase-catalyzed transesterification. *J Agric Food Chem* 54:7062–7068
- de Pinedo AT, Penalver P, Perez-Victoria Rondon D, Morales JC (2007) Synthesis of new phenolic fatty acid esters and their evaluation as lipophilic antioxidants in an oil matrix. *Food Chem* 105:657–665
- Compton DL, Laszlo JA (2002) Sunscreens from vegetable oil and plant phenols. US Patent 6,346,236
- Laszlo JA, Compton DL, Eller FJ, Taylor SL, Isbell TA (2003) Packed-bed bioreactor synthesis of feruloylated monoacyl- and diacylglycerols: clean production of a “green” sunscreen. *Green Chem* 5:382–386
- Laszlo JA, Compton DL (2006) Enzymatic glycerolysis and transesterification of vegetable oil for enhanced production of feruloylated glycerols. *J Am Oil Chem Soc* 83:765–770
- Compton DL, Kenar JA, Laszlo JA, Felker FC (2007) Starch-encapsulated, soy-based, ultraviolet-absorbing composites with feruloylated monoacyl- and diacylglycerol lipids. *Ind Crops Prod* 25:17–23
- Sabally K, Karboune S, St-Louis R, Kermasha S (2006) Lipase-catalyzed transesterification of dihydrocaffeic acid with flaxseed oil for the synthesis of phenolic lipids. *J Biotechnol* 127:167–176
- Sabally K, Karboune S, St-Louis R, Kermasha S (2007) Lipase-catalyzed synthesis of phenolic lipids from fish liver oil and dihydrocaffeic acid. *Biocatal Biotransform* 25:211–218
- Karboune S, St-Louis R, Kermasha S (2008) Enzymatic synthesis of structured phenolic lipids by acidolysis of flaxseed oil with selected phenolic acids. *J Mol Catal B Enzym* 52–53:96–105

23. Karboune S, Safari M, Lue BM, Yeboah FK, Kermasha S (2005) Lipase-catalyzed biosynthesis of cinnamoylated lipids in a selected organic solvent medium. *J Biotechnol* 119:281–290
24. Choo WS, Birch EJ (2009) Radical scavenging activity of lipophilized products from lipase-catalyzed transesterification of triolein with cinnamic and ferulic acids. *Lipids* 44:145–152
25. Sabally K, Karboune S, St-Louis R, Kermasha S (2006) Lipase-catalyzed transesterification of trilinolein or trilinolenin with selected phenolic acids. *J Am Oil Chem Soc* 83:101–107
26. Compton DL, Laszlo JA, Berhow MA (2006) Identification and quantification of feruloylated mono-, di-, and triacylglycerols from vegetable oils. *J Am Oil Chem Soc* 83:753–758
27. Warner K, Laszlo JA (2005) Addition of ferulic acid, ethyl ferulate, and feruloylated monoacyl- and diacylglycerols to salad oils and frying oils. *J Am Oil Chem Soc* 82:647–652
28. Nag A (2000) Stabilization of flaxseed oil with capsicum antioxidant. *J Am Oil Chem Soc* 77:799–800
29. Bera D, Lahiri D, Nag A (2004) Novel natural antioxidant for stabilization of edible oil: the ajowan (*Carum copticum*) extract case. *J Am Oil Chem Soc* 81:169–172
30. Bera D, Lahiri D, Nag A (2006) Studies on a natural antioxidant for stabilization of edible oil and comparison with synthetic antioxidants. *J Food Eng* 74:542–545
31. Jaswir I, Kitts DD, Man YBC, Hassan TH (2004) Synergistic effect of rosemary, sage and citric acid on fatty acid retention of heated flaxseed oil. *J Oleo Sci* 53:581–591
32. Jaswir I, Kitts DD, Man YBC, Hassan TH (2005) Physico-chemical stability of flaxseed oil with natural antioxidant mixtures during heating. *J Oleo Sci* 54:71–79
33. Safari M, Karboune S, St-Louis R, Kermasha S (2006) Enzymatic synthesis of structured phenolic lipids by incorporation of selected phenolic acids into triolein. *Biocatal Biotransform* 24:272–279

The Hypolipidemic Effect of an Ethyl Ester of Algal-Docosahexaenoic Acid in Rats Fed a High-Fructose Diet

Alan S. Ryan · Eileen Bailey-Hall · Edward B. Nelson · Norman Salem Jr

Received: 15 April 2009 / Accepted: 20 July 2009 / Published online: 5 August 2009
© AOCS 2009

Abstract Preclinical and clinical studies demonstrate that the omega-3 fatty acids docosahexaenoic acid (DHA) and eicosapentaenoic acid (EPA) as a triacylglycerol (TAG) or an ethyl ester are protective against cardiovascular disease. Both have significant TAG-lowering effects. We developed a concentrated ethyl ester of DHA (MATK-90, 900 mg/g) using microalgae as its source. This study evaluated the effects that different doses of MATK-90 had on lipid levels and clinical parameters in male Wistar rats fed a high-fructose diet used to induce hypertriglyceridemia ($\text{TAG} \geq 300 \text{ mg/dL}$). Effects of MATK-90 were compared to those produced by a pharmaceutical product (Lovaza, formerly Omacor, P-OM3; 465 mg EPA + 375 mg DHA), a TAG oil used in food (DHASCO, algal-DHA, 40% DHA by weight), and a control (corn oil). Doses of MATK-90 (0.6, 1.3, 2.5, 5.0 $\text{g kg}^{-1} \text{ day}^{-1}$), algal-DHA (2 g DHA $\text{kg}^{-1} \text{ day}^{-1}$), and P-OM3 (5.0 $\text{g kg}^{-1} \text{ day}^{-1}$) were administered by oral gavage for 28 days. A significant dose-related decrease was observed in TAG and cholesterol levels in all but the lowest dose of MATK-90 treatment group vs. control. The high-dose group of MATK-90 and the P-OM3 group produced similar reductions in TAG levels.

Keywords Docosahexaenoic acid · Omega-3 fatty acids · Triacylglycerol lowering · Cholesterol · Clinical chemistry

Abbreviations

Apo E-KO Apolipoprotein E-knockout mice
CHOL Cholesterol

DHA	Docosahexaenoic acid
EPA	Eicosapentaenoic acid
GRAS	Generally recognized as safe
HDL-C	High-density lipoprotein cholesterol
HTG	Hypertriglyceridemia
LC-PUFAs	Long-chain polyunsaturated fatty acids
LDL-C	Low-density lipoprotein cholesterol
LSMEAN	Least square means
P-OM3	Lovaza TM , formerly Omacor [®]
RANCOVA	Repeated measure analysis of covariance
TAG	Triacylglycerol

Introduction

The omega-3 long-chain polyunsaturated fatty acids (LC-PUFAs), particularly docosahexaenoic acid (DHA) and eicosapentaenoic acid (EPA), are known to have many cardiovascular benefits in animals and humans. Both DHA and EPA not only lower triacylglycerol (TAG) levels but may also reduce the risk of sudden death [1, 2], decrease the risk of arrhythmia and atherosclerosis [3–5], increase plaque stabilization [6], and reduce blood pressure and heart rate in both normotensive and mildly hypertensive individuals [7–9]. The TAG-lowering effects of DHA and EPA appear to be due to the combination of decreased hepatic TAG secretion and enhanced clearance of TAG from the plasma [10] that can occur in the fasting state or post-prandially [11, 12].

Several animal studies have considered the effects of DHA and EPA on plasma lipid levels and metabolism, but the findings have been inconsistent [13, 14]. In Wistar rats fed a standard diet, a cholesterol (CHOL) diet (2% CHOL),

A. S. Ryan (✉) · E. Bailey-Hall · E. B. Nelson · N. Salem Jr
Martek Biosciences Corporation, 6480 Dobbin Road,
Columbia, MD 21045, USA
e-mail: alryan@martek.com

or a pelleted chow diet with highly purified DHA (92% pure) at different doses (0.5, 1, 1.5 g kg⁻¹ day⁻¹), there was no significant decrease in hepatic and plasma concentration of TAG after 10 days of treatment [13]. However, a TAG-lowering effect was reported after 1 day in Wistar rats fed a standard diet after receiving 1.5 g kg⁻¹ day⁻¹ of EPA [14].

Highly purified ethyl esters of EPA (93%) and DHA (91%) were added at a 3% level to a hypercholesterolemic diet (52.5% sucrose, 5% lard, 0.5% CHOL, and 25% sodium cholate) and administered to male Sprague–Dawley rats [15]. In addition to the hypercholesterolemic diet, four experimental diets were considered (5% olive oil, 2% olive oil + 3% ethyl-linoleate, 2% olive oil + 3% EPA, and 2% olive oil + 3% DHA). The animals were fed the experimental diets for up to 20 days. Serum total CHOL level was significantly lower in the rats fed the diet that included DHA, whereas serum TAG level was significantly lower only in the rats fed the diet that included EPA.

The mechanisms and degree of suppression of postprandial hypertriglyceridemia (HTG) resulting from a fish oil diet rich in DHA (6.7 g/100 g EPA, 20.5 g/100 g DHA) were considered in a study of Sprague–Dawley rats [12]. TAG levels were significantly lower in animals fed the DHA-rich fish oil diet than in those fed safflower oil for 3 weeks. The authors reported that the TAG-lowering was due to the suppression of hepatic fatty acid and TAG synthesis [12].

To investigate the effect that fish oil had on serum lipid levels and atherosclerotic lesions in apolipoprotein E-knockout (Apo E-KO) mice, 1% dietary fish oil was added to a mouse chow containing 9% (w/w) fat and 0.2% (w/w) CHOL for 14 days [16]. Apo E-KO mice develop spontaneous atherosclerosis and high plasma TAG and CHOL levels. Aortic atherosclerosis was assessed by histological and morphological techniques. Although levels of DHA and EPA increased significantly in plasma free fatty acids and plasma TAG, phospholipid, and cholesteryl ester fractions, there were significant increases in plasma TAG levels, and the development of atherosclerotic plaque was not prevented. The authors suggested that the lack of the effect of fish oil on TAG levels may be related to the role that Apo E has on metabolism of fatty acids and TAG-rich lipoprotein particles [16]. Apo E is needed for clearance of TAG-rich particles and therefore the lack of Apo E was probably responsible for the absence of the TAG-lowering effect typically reported for fish oil.

Studies in animals have shown that insulin resistance can be improved with diets containing LC-PUFAs [17, 18]. Results from human studies have been less conclusive [19, 20]. In a study of insulin-resistant mice fed a lipid modified diet with DHA and/or DHA blends, TAG levels significantly decreased by ~40%, but insulin sensitivity and

fasting plasma glucose were not altered [21]. In a study that compared a diet with EPA to one containing safflower oil, EPA-fed diabetic-prone rats had lower TAG and CHOL levels and improved insulin resistance [22].

The effects of dietary fish oil (17.6 g of DHA and 7.7 g of EPA per 100 g of fatty acid, respectively) on lipid peroxidation and serum TAG levels were considered in a study of psychologically stressed female BALB/c mice [23]. The animals were initially group-housed (four mice/cage) and fed a diet containing fish oil, soybean oil, or olive oil for 3 weeks. The animals were then housed under the same conditions or individually housed to generate psychological stress for 2 weeks. In the fish-oil-fed mice, a significant reduction in serum TAG levels was observed versus the soybean-oil- or olive-oil-fed mice. The reduction was more profound in the isolation stress group. The authors suggested that dietary intake of LC-PUFAs could exert more beneficial effects against the onset of cardiovascular disease under conditions of isolation stress [23]. The isolation stress group had increased levels of LC-PUFAs in the liver and serum when compared with the group-housed animals. This increase may account for the more profound reduction in the serum TAG levels in the fish-oil-fed mice subjected to isolation stress compared with their group-housed counterparts.

Cardiovascular benefits of LC-PUFAs also have been observed in large animals. Thirteen thoroughbred or standard bred horses were assigned to diets with fish oil or corn oil for 63 days [24]. The fish-oil diet contained 10.8% EPA and 8% DHA. The oils were added to timothy hay and a mixed-grain concentrate at rates necessary to maintain body weight (324 mg/kg of body weight). Compared with horses receiving corn oil, those receiving fish oil had significantly lower TAG levels after 63 days. Serum CHOL, platelet number, prothrombin and partial prothrombin time, red blood cell number, and lymphocyte percentage did not change with either diet.

In humans, DHA and EPA are obtained primarily from marine mammals and fatty fish that have consumed microalgae containing these LC-PUFAs. However, the consumption of DHA and EPA from fatty fish is relatively low, particularly in Westerners, and normal dietary intake is unlikely to provide a significant TAG-lowering effect in individuals with relatively high TAG levels. Consequently, DHA and EPA can be provided through a pharmaceutical product. Lovaza (formerly Omacor, P-OM3) was approved by the U.S. Federal Drug Administration to reduce elevated TAG levels in adult patients with very high (≥ 500 mg/dL) TAG levels. Each gram capsule of P-OM3 contains 900 mg of ethyl esters of omega-3 fatty acids including EPA (approximately 465 mg) and DHA (approximately 375 mg). The U.S. recommended daily dose of P-OM3 is 4 g per day.

As discussed above, most studies in humans and animals have considered experimental diets that contain mixtures of EPA and DHA. However, there is growing evidence that DHA alone provides cardioprotective benefits similar to those seen with products containing both EPA and DHA [25]. A microalgal source of DHA, which contains only trace amounts of EPA and other omega-3 fatty acids, is available for food use and for dietary supplements. The DHA is derived from the microalga *Cryptocodinium cohnii* in a controlled fermentation process to produce a TAG oil (DHASCO, algal-DHA, Martek Biosciences, Columbia, MD, USA). Algal-DHA oil naturally contains approximately 40–50% DHA by weight. Algal-DHA is generally recognized as safe (GRAS) for use in food products and dietary supplements. A highly concentrated ethyl ester of DHA derived from algal-DHA (~900 mg/g DHA) was manufactured for clinical evaluation (MATK-90, Martek Biosciences).

To date, it is not known whether a highly concentrated ethyl ester of DHA from algae devoid of EPA affects plasma lipids in a similar fashion as algal-DHA triacylglycerol oil or the combination of DHA and EPA ethyl esters from fish oil. However, highly purified ethyl esters of DHA and EPA from fish oil each decrease TAG levels in humans [26]. These ethyl esters from fish oil are not 100% pure; each may contain up to 5–10% of the corresponding LC-PUFA [26]. In the present study, we evaluated the effects that different doses of MATK-90 had on plasma lipid levels, fatty acid levels, and clinical parameters in male Wistar rats fed a hyperlipidemic (high fructose) diet. The effects of MATK-90 were compared with those produced by P-OM3, algal-DHA, and a control (corn oil modified with vitamin E).

Materials and Methods

Animals and Experimental Design

Male Wistar rats, 41–44 days of age, were provided by Charles River Laboratories, Montreal, Quebec, Canada, and were maintained in their testing facility in Shrewsbury, MA. The study was conducted according to Good Laboratory Practices standards. The animals were examined for signs of disease or injury upon receipt, and 84 males were assigned to the study. On the day of receipt, animals (including spare animals) weighed 168–236 g. The animals were individually housed in clear polycarbonate cages with contact bedding, as recommended by the National Research Council [27]. Environmental controls maintained temperatures at 18–26 °C (64–79°F) with a relative humidity of 30–70%. A 12-h light/12-h dark cycle was maintained (lights on at approximately 0300 h and lights

off at approximately 1500 h). At least 10 air changes per hour were maintained in the animal room.

Charles River Laboratories is accredited by the Association for the Assessment and Accreditation of Laboratory Animal Care, International, and registered with the United States Department of Agriculture to conduct research in laboratory animals. The study was conducted in conformity with the Public Health Service Policy on Humane Care and Use of Laboratory Animals and was approved by the Institutional Animal Care and Use Committee at the facility.

All animals were fed a high-fructose diet (Research Diet D07121202, Research Diets, New Brunswick, NJ, USA) (Table 1) ad libitum for approximately 5 weeks before the initial dose administration (designated here as week -5). The high-fructose diet was used to induce HTG. Animals with a pretreatment TAG level of <299 mg/dL were excluded from the study. Thirty-three animals were excluded based on the TAG-level study entry criterion.

Table 1 Composition of basal diet^a

Component	Percentage
Fructose	57.5%
Casein	18.9
Corn starch	8.5
Cellulose	4.7
Mineral mix	4.7
Lard	4.2
Vitamin mix	1.0
Choline bitartrate	0.3
L-cystine	0.2
Fatty acid composition (% of total fatty acid)	
14:0	1.6
16:0	22.2
16:1	1.9
18:0	12.1
18:1	39.7
18:2	18.4
18:3 n-3	1.1
20:0	0.2
20:1	0.7
20:2	0.7
20:4 n-6	0.4
20:5 n-3	ND ^a
24:0	ND
22:5 n-3	ND
22:6 n-3	ND
22:6 n-3	ND
Others	1.0

ND Not detected

^a Research Diet D07121202

Table 2 Fatty acid composition of MATK-90, algal-DHA, P-OM3, and corn oil (control)

Fatty acid	Fatty acid composition (% of total fatty acid)			
	MATK-90	Algal-DHA	P-OM3	Corn oil
10:0	ND ^a	1.1	ND	ND
12:0	ND	5.4	ND	ND
14:0	ND	15.6	ND	ND
16:0	0.3	13.9	ND	10.2
16:1	0.1	2.1	ND	ND
18:0	ND	0.7	ND	1.9
18:1 n-9	2.8	18.3	ND	28.7
18:2 n-6	ND	0.9	ND	57.1
18:3 n-3	ND	ND	2.8	0.9
20:0	ND	ND	ND	0.4
20:4 n-6	ND	ND	1.9	ND
20:5 n-3	ND	0.2	48.3	ND
24:0	ND	ND	ND	0.3
22:4 n-6	ND	ND	2.0	ND
22:5 n-3	1.1	ND	3.0	ND
22:6 n-3	93.6	41.1	38.3	ND
28:8 n-3	1.3	ND	ND	ND
Others	0.8	0.7	3.7	0.5

ND Not detected

Animals enrolled into the study were fed the high-fructose diet continuously throughout the study except during times of fasting.

Test materials for the treatment groups are described in Table 2. Doses were prepared by diluting the MATK-90, P-OM3, and algal-DHA with corn oil stripped of tocopherol (item #401101, Dyets, Bethlehem, PA). α -Tocopherol (0.4%) was added to MATK-90, algal-DHA, and control oil to match the level found in P-OM3. Eighty-four animals were assigned to one of seven treatment groups, and each group contained 12 animals. The experimental design is provided in Table 3. Animals were 10–11 weeks of age at

the time of dosing. Doses were administered once daily via oral gavage, within 3 h of the onset of the dark cycle, for 28 consecutive days. The animals were dosed at a volume of 10 mL/kg.

The first day of dosing was day 1. The doses were given at approximately the same time each day and were based upon the most recently collected body weight. Doses were rounded to the nearest 0.1 mL.

Clinical Observations

Clinical observations were performed at least once daily starting before the initiation of the high-fructose diet and continuing until the completion of the study. Body weights were measured before the initiation of the high-fructose diet and at least three times per week during the pretreatment time period. After group assignment, body weights were measured before the initial dose administration (day -1); on day 1, 3, 5, 8, 10, 12, 15, 17, 19, 22, 24, and 26; and before necropsy on day 29.

Food consumption was quantitatively measured before the initiation of the high-fructose diet (pretreatment) and at least three times per week before the treatment administration. After group assignment and treatment, food consumption was measured on day 1, 3, 5, 8, 10, 12, 14, 15, 17, 19, 22, 24, 26, and 28.

Biochemical Analyses

Blood samples to determine TAG entry levels were collected 1 and 3 weeks prior to dosing. Serum samples were also collected before the high-fructose diet initiation (week -5), before initial dose on day -1, and on day 14 and 28 to determine levels of glucose, urea nitrogen, creatinine, total protein, albumin, calculated globulin and albumin/globulin ratio, calcium, phosphorus, electrolytes, total CHOL, total albumin, TAG, alanine aminotransferase, aspartate aminotransferase, alkaline phosphatase, and gamma glutamyltransferase. Levels

Table 3 Experimental design

Group number	Number of animals	Test material	Dose level (g kg ⁻¹ day ⁻¹)	Dose volume (mL/kg)	Dose DHA (g/kg) ^a	Dose EPA (g/kg) ^a
1	12	Vehicle (corn oil)	0.0	10.0	0.00	0.00
2	12	Algal-DHA	5.0	10.0	2.18	0.00
3	12	P-OM3 ^b	5.0	10.0	1.99	2.53
4	12	MATK-90	0.6	10.0	0.54	0.00
5	12	MATK-90	1.3	10.0	1.26	0.00
6	12	MATK-90	2.5	10.0	2.34	0.00
7	12	MATK-90	5.0	10.0	4.38	0.00

^a Based on actual analysis of DHA and EPA. Assumes the specific gravity conversion factor of 0.9

^b Each gram of P-OM3 contains 465 mg EPA and 375 g DHA

of high-density lipoprotein cholesterol (HDL-C) and low-density lipoprotein cholesterol (LDL-C) were measured before the initial treatment on day -1 and on day 28.

Whole blood samples collected into serum separator tubes were centrifuged. Serum chemistry parameters were determined at Charles River Laboratories using the Olympus AU640 chemistry immune analyzer (Center Valley, PA, USA). Blood samples for fatty acid analysis (DHA and EPA) were collected on day 14 and 29 before necropsy. Plasma total lipid fatty acids were analyzed as described previously [28]. The fatty acid profiles were expressed as area percent of fatty acids.

Fasting (specified as a minimum of 6 h, not to exceed 8 h) was conducted before all blood collections, including the terminal blood collection. Water was provided *ad libitum* during times of fasting.

Statistical Analysis

Statistical analysis was performed on body weights, food consumption, and serum chemistry parameters. Each analysis endpoint was analyzed with a repeated measure analysis of covariance (RANCOVA). Factors in the model included treatment, duration of treatment, and the treatment \times duration interaction. The baseline measurement was included as a covariate. Least square means (LSMEAN) and their standard deviations were produced. Initially, the control and the MATK-90 dose groups were included in the statistical analysis. The monotonic dose–response relationship was evaluated for the control and four MATK-90 groups using sequential linear trend tests based on ordinal spacing of dose levels [29]. The trend tests were conducted at the 0.05 significance level for each post-dose day as well as across the pooled post-dose days.

To evaluate responses that occurred in a non-dose-related fashion, non-monotonic dose responses were evaluated whenever no significant linear trends were detected, but when either treatment or the treatment \times duration interaction was significant at the 0.01 level. Within the framework of the RANCOVA, pairwise comparisons were made for each individual MATK-90 group with the control group through linear contrasts. The comparisons were conducted at the 0.01 significance level for each post-dose day as well as across the pooled post-dose days.

Pairwise comparisons were made using Dunnett's test at the 0.05 significance level to compare the MATK-90 dose groups to P-OM3. The pairwise comparisons were conducted for each post-dose day as well as across the pooled post-dose days.

To compare algal-DHA to P-OM3 and to the control, if either the treatment or treatment \times duration interaction was significant, Duncan's multiple range test was used to make all possible pairwise comparisons of the three groups for each

post-dose day as well as across the pooled post-dose days. Both the Dunnett's test and Duncan's multiple range test were adjusted for multiple comparisons. All statistical analyses were conducted with SAS software (Cary, NC, USA).

Results

Clinical Observations, Body Weights, and Food Consumption

Treatment-related mortality was not observed during the study. No unusual clinical signs were observed. One accidental death was observed for an animal in the P-OM3 group; this animal died immediately after the day 14 blood collection. A comprehensive necropsy revealed that the death was related to the blood collection procedure.

Before the initiation of the high-fructose diet, mean body weights in each group were comparable, ranging from 249 ± 6.2 to 262 ± 11.4 g; during week -1, mean body weights in each group ranged from 405 ± 19.8 to 431 ± 23.6 g. Over time, body weight trends were similar among the control, algal-DHA, MATK-90, and P-OM3 treatment groups.

Throughout the approximately 5-week high-fructose diet prestudy feeding period, all groups demonstrated a similar food intake pattern. Upon initiation of treatment, all groups exhibited an immediate 1.4- to 1.8-fold decrease in food intake, relative to baseline, that remained until the completion of study. After the initiation of treatment, over time, food intakes were similar between groups. The decrease in food consumption was attributed to the higher caloric density of the test diets.

Triacylglycerols and Other Serum Chemistry Parameters

Before the initiation of the high-fructose diet (approximately week -5), serum chemistry values were comparable among groups and within expected ranges for the Wistar rat. During the high-fructose diet prestudy feeding period, TAG levels were evaluated for progressive increases over time to gauge the induction of HTG. Mean TAG levels increased 3.4- to 4.8-fold relative to the baseline diet levels after approximately 4 weeks of the high-fructose diet (approximately week -1), demonstrating successful induction of HTG. Before the initiation of treatments (day -1), baseline serum chemistry values were comparable among groups, and serum chemistry values were within expected ranges for the Wistar rat, with the exception of the TAG levels. Changes in CHOL and HDL-C were also observed as anticipated with diet induction. The pretreatment (day -1) mean values for TAG, CHOL, and HDL-C

levels were 476 ± 179.3 , 127 ± 22.3 , and 43 ± 6.9 mg/dL, respectively.

Overall Trends in TAG Levels vs. Control

MATK-90 treatment at 0.6, 1.3, 2.5, or 5.0 g kg⁻¹ day⁻¹ resulted in an overall significant ($p < 0.05$) trend for reduced TAG levels during the dosing phase, relative to the control group. On day 14, mean (LSMEAN) TAG levels in the 0.6, 1.3, 2.5, and 5.0 g kg⁻¹ day⁻¹ MATK-90 treatment groups were significantly ($p < 0.05$) decreased and were 65, 67, 47, and 43% of the control group (Fig. 1). Mean (LSMEAN) TAG values for the 1.3, 2.5, and 5.0 g kg⁻¹ day⁻¹ MATK-90 treatment groups on day 28 were 60, 60, and 47% of the control group ($p < 0.05$), respectively. On day 28, the mean (LSMEAN) TAG value for the 0.6 g kg⁻¹ day⁻¹ MATK-90 treatment group was not significantly different from that of the control group.

Mean (LSMEAN) TAG levels in both the algal-DHA- and P-OM3-treated animals were significantly ($p < 0.05$) lower overall compared to the control-treated animals. On day 14, mean (LSMEAN) values were 47 and 48% of the control in the P-OM3- and algal-DHA-treated animals, respectively ($p < 0.05$). On day 28, mean (LSMEAN) TAG levels in the P-OM3-treated but not the algal-DHA-treated animals were significantly lower (35%, $p < 0.05$) than that in the control group.

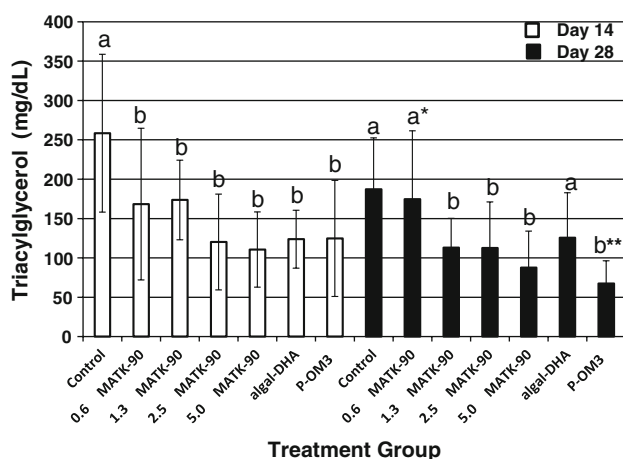


Fig. 1 Mean (LSMEAN) TAG levels in Wistar rats at day 14 and 28 after treatment with MATK-90, algal-DHA, or P-OM3. Different letters indicate significant differences ($p < 0.05$) between treatment groups vs. the control. On day 28, asterisks indicate significant differences ($p < 0.05$) between 0.6 g kg⁻¹ day⁻¹ of MATK-90 vs. P-OM3. On day 14, mean TAG levels in the 0.6, 1.3, 2.5, and 5.0 g kg⁻¹ day⁻¹ MATK-90 treatment groups were significantly ($p < 0.05$) decreased vs. the control. On day 28, the mean TAG level in the 0.6 g kg⁻¹ day⁻¹ MATK-90-treated animals was 2.7 times greater ($p < 0.05$) than that of the P-OM3 group. The high-dose group of MATK-90 and the P-OM3 group produced similar reductions in TAG levels at day 14 and 28

TAG Levels of MATK-90 and Algal-DHA vs. P-OM3

There were no significant differences in the mean (LSMEAN) TAG levels between the 1.3, 2.5, and 5.0 g kg⁻¹ day⁻¹ MATK-90 and P-OM3-treated animals at day 14 and day 28. However, on day 28, the mean (LSMEAN) TAG level in the 0.6 g kg⁻¹ day⁻¹ MATK-90-treated animals was 2.7 times greater ($p < 0.05$) than that of the P-OM3 group. There were no differences overall in TAG levels between the DHASCO-treated and P-OM3-treated animals.

Overall Trends in CHOL Levels vs. control

There was an overall significant trend ($p < 0.05$) toward reduced CHOL levels, relative to the control, in all of the MATK-90 dose groups. Significantly reduced mean (LSMEAN) CHOL levels were observed on day 28, relative to the control, in the 1.3 (62%), 2.5 (71%), and 5.0 (61%) g kg⁻¹ day⁻¹ MATK-90-treated animals (Fig. 2). There was a statistically significant ($p < 0.05$) overall trend for reduced mean (LSMEAN) CHOL levels, relative to the control, in the P-OM3-treated animals but not the algal-DHA-treated animals. However, there was no statistically significant difference in mean (LSMEAN) CHOL levels between the P-OM3-treated and the control-treated animals on days 14 and 28.

CHOL levels of MATK-90 and algal-DHA vs. P-OM3

Mean (LSMEAN) CHOL levels were similar at day 14 and 28 in the MATK-90-, algal-DHA, and P-OM3-treated animals.

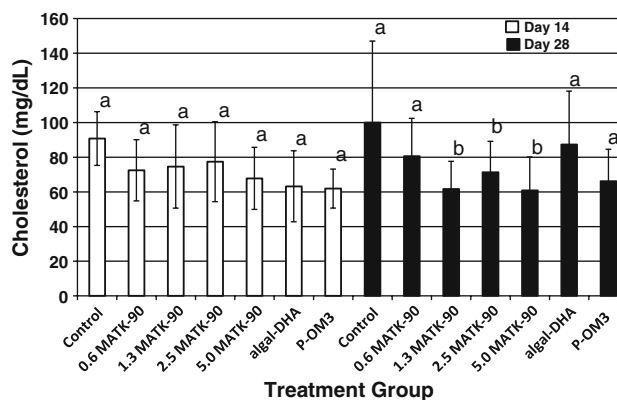


Fig. 2 Mean (LSMEAN) CHOL levels in Wistar rats at day 14 and 28 after treatment with MATK-90, algal-DHA, or P-OM3. Different letters indicate significant differences ($p < 0.05$) between treatment groups vs. the control. Significantly reduced mean CHOL levels were observed on day 28, relative to the control in the 1.3, 2.5, and 5.0 g kg⁻¹ day⁻¹ MATK-90-treated animals

Overall Trends in HDL Levels vs. Control

There were no significant trends for HDL-C levels relative to the control in any of the MATK-90, algal-DHA, or P-OM3 treatment groups. On day 28, the mean HDL-C level in the control-treated animals was 68% (44.7 ± 8.6 vs. 30.5 ± 3.1 mg/dL) of the day -1 baseline level. Similar decreased mean (LSMEAN) values (53–65%) on day 28 in HDL-C, relative to baseline, occurred in the algal-DHA-treatment group (41.9 ± 8.4 vs. 25.0 ± 5.6 mg/dL), the MATK-90 treatment groups (0.6 g kg⁻¹ day⁻¹: 42.5 ± 6.1 vs. 27.8 ± 3.6 mg/dL; 1.3 g kg⁻¹ day⁻¹: 42.8 ± 7.4 vs. 25.0 ± 3.6 mg/dL; 2.5 g kg⁻¹ day⁻¹: 44.0 ± 8.4 vs. 26.1 ± 4.2 mg/dL; 5.0 g kg⁻¹ day⁻¹: 42.0 ± 5.0 vs. 23.5 ± 6.2 mg/dL) and the P-OM3-treated animals (42.0 ± 4.5 vs. 22.1 ± 3.5 mg/dL).

LDL-C Levels

A large percentage of LDL-C samples were below the lower limit of detection (< 7 mg/dL) at approximately week -5, day -1, and day 28 (20, 59, and 66%, respectively). These values were not included in the statistical analyses, and the data for LDL-C are not presented here.

Other Serum Chemistry Values

After the initiation of the high-fructose diet (approximately week -5), except for the serum lipid values considered above, the other chemistry values were comparable among groups and within expected ranges for the Wistar rat.

Fatty Acid Analysis

The administration of MATK-90 (0.6–5.0 g kg⁻¹ day⁻¹), algal-DHA (2.0 g DHA kg⁻¹ day⁻¹), or P-OM3 (5 g kg⁻¹ day⁻¹) resulted in a statistically significant ($p < 0.05$) increase in DHA levels in plasma (day 29) compared with baseline (day -1) values (Fig. 3). On day 14 and 29, in the MATK-90 groups, there was a dose-dependent response in DHA levels. Also observed was a significant ($p < 0.05$) increase in EPA levels, with the greatest increase in animals that were administered P-OM3 (5 g kg⁻¹ day⁻¹), which contained ~55% EPA. Algal-DHA and MATK-90 contained only traces of EPA, yet animals treated with the algal-DHA or MATK-90 exhibited significant increases in EPA levels (Fig. 4). This increase in EPA level was thus attributed to the retroconversion of DHA to EPA. The increases in EPA with MATK-90 treatment were dose-related, and retroconversion of DHA to EPA demonstrated that saturation was not achieved at the highest dose of 5.0 g kg⁻¹ day⁻¹ in this animal model.

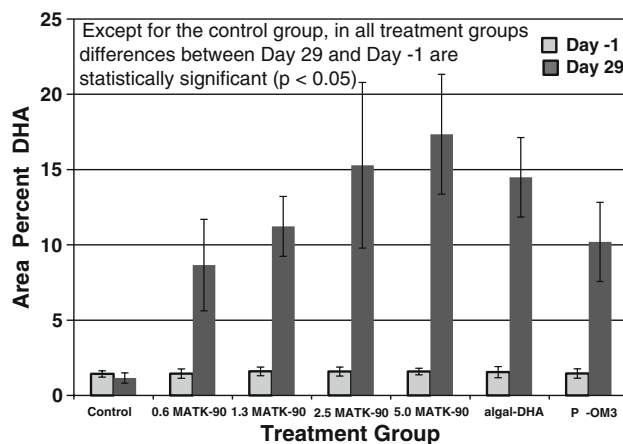


Fig. 3 Mean DHA fatty acid area percent levels in Wistar rats prior to treatment (day -1) and after treatment (day 29) with MATK-90, algal-DHA, or P-OM3. Administration of MATK-90 (0.6–5.0 g kg⁻¹ day⁻¹), algal-DHA (2.0 g DHA kg⁻¹ day⁻¹), or P-OM3 (5 g kg⁻¹ day⁻¹) resulted in a statistically significant ($p < 0.05$) increase in DHA levels in plasma compared with baseline (day -1) values

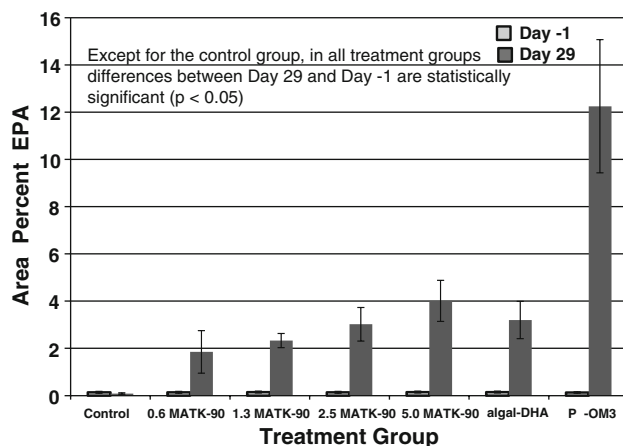


Fig. 4 Mean EPA fatty acid area percent levels in Wistar rats prior to treatment (day -1) and after treatment (day 29) with MATK-90, algal-DHA, or P-OM3. There was a significant ($p < 0.05$) increase in EPA levels vs. baseline (day -1), with the greatest increase in animals that were administered P-OM3 (5 g kg⁻¹ day⁻¹), which contained ~55% EPA. Algal-DHA and MATK-90 contained less than 1% EPA, yet animals treated with algal-DHA or MATK-90 exhibited significant increases in EPA levels vs. baseline. This increase in EPA level was attributed to the retroconversion of DHA to EPA

Discussion

This study was designed to evaluate the potential TAG-lowering effects of a highly purified ethyl ester of algal-DHA (MATK-90) in male Wistar rats fed a high-fructose diet to induce HTG. Different doses of MATK-90 were administered (0.6–5.0 g kg⁻¹ day⁻¹) for 28 days and the results were compared to those observed in animals fed a high dose of a commercially available algal-DHA triacylglycerol oil (DHASCO; 2 g DHA/kg per day), a

prescription formulation of omega-3-fatty acid ethyl esters of DHA and EPA (Lovaza;P-OM3, 5 g kg⁻¹ day⁻¹), and a placebo (corn oil). Results indicated that MATK-90 at 1.3, 2.5, or 5.0 g kg⁻¹ day⁻¹ was effective at reducing TAG levels relative to the control group at day 14 and 28. There were no significant differences in the mean TAG levels between the 1.3, 2.5, and 5.0 g kg⁻¹ day⁻¹ MATK-90-treated and the P-OM3-treated animals at day 14 and day 28.

There may be concern that the degree of TAG-lowering observed with DHA might not have resulted had a high-fat diet been used rather than the high-fructose diet used in the present study. A high-fructose diet may allow for a better evaluation of the inhibitory effect of DHA on hepatic conversion of fructose to fatty acid and then esterification to TAG. However, in a recent study of mice fed high-fat diets (18% fat wt/wt) with different fatty acid compositions (soy vs. a high-DHA fish oil) for 4 months, the fish-oil diet significantly reduced plasma TAG concentration by ~50% both in fasting and postprandial states [30]. Further, in humans who consume a typical “western” diet, which may be high in fat, moderate amounts of DHA (1–2 g/day) have been shown to lower TAG levels significantly in subjects with both normal and elevated TAG levels [25].

In humans, LC-PUFAs typically do not affect total CHOL levels, although significant reduction in the level of total CHOL has been observed in subjects who have received both LC-PUFAs and statins [31, 32]. As demonstrated here with Wistar rats, MATK-90 at 1.3 g kg⁻¹ day⁻¹ or greater, but not P-OM3, was effective in markedly reducing total plasma CHOL. It is unclear why MATK-90 reduced total CHOL in this animal model.

LC-PUFAs modestly increase HDL-C levels in humans [25, 33]. However, in the present study, there were no significant trends for HDL-C levels, relative to the control, in any of the treatment groups considered. In all groups, levels of HDL-C declined relative to baseline and the changes were of similar magnitude. This finding suggests that the decline in HDL-C levels may be specific to the animal model considered.

DHA was clearly bioavailable based on the dose-dependent increase in the level of DHA in plasma. Administration of DHA also led to a dose-dependent increase in EPA. The increase in EPA was probably related to retroconversion of DHA to EPA [34]. These results corroborate earlier findings from a 28-day Sprague–Dawley rat study with algal-DHA [35]. The retroconversion of DHA to EPA is also observed in other tissues such as heart and liver [36]. In humans receiving 280 mg of DHA, a retroconversion rate of ~1.4% has been reported [34], but rates as high as 12% have also been noted in subjects who received 1.62 g DHA [37, 38].

No safety issues were identified with MATK-90 even at the relatively high concentrations administered in this study. In the present study, the dose of DHA per kilogram of body weight was up to 100-fold higher than the DHA doses found to lower TAG levels in humans (i.e., 1–2 g/day). As in many preclinical studies, doses of investigational product administered to animals are typically much higher than those given to humans. Higher doses are needed to account for increased metabolic rates in small animals; they may also shed light on any issues with toxicity. The safety of DHA, as contained in algal-DHA, has been evaluated in several animal studies [36, 39–44]. These studies included tests for genetic, acute, subchronic, and developmental toxicity. Many of these studies considered pregnant, lactating, and/or neonatal animals. Results demonstrated that algal-DHA is not a genetic, reproductive, or developmental toxicant, and the effects of acute toxicity are negligible. Rat subchronic toxicology studies documented doses of algal-DHA of up to 500 and 1,250 mg kg⁻¹ day⁻¹. Higher doses than would normally be consumed in a diet or as a supplement or drug have been considered in studies of healthy human volunteers (up to 6 g DHA or 15 g algal-DHA oil per day) [45]; no adverse events were reported. Algal-DHA is used in capsule form as a dietary supplement or as oil in infant formulas and food products throughout the world. The findings from the present study suggest that MATK-90, the concentrated ethyl ester form of DHA, is well tolerated in this animal model. Further research is needed to demonstrate efficacy and safety of MATK-90 in humans.

From studies in healthy volunteers, and those with dyslipidemia, it is clear that DHA and EPA lower blood TAG levels. Many factors related to the development of atherosclerosis and its complications are positively influenced by DHA and EPA [46]. These factors include TAG levels, platelet aggregation, hemostatic parameters, blood pressure, and endothelial aggregation. In 16 clinical studies in humans [25], it was unexpectedly shown that supplementation of 1–2 g/day of algal-DHA alone as a TAG oil is associated with a marked reduction in serum TAG levels (up to 26%) in normal individuals and in those with HTG or combined hyperlipidemia. Algal-DHA devoid of EPA was also associated with increased HDL-C levels, increased LDL-C particle size, and a modest reduction in blood pressure and heart rate in many subjects. This study demonstrated that the benefits of TAG reduction accomplished using combined ethyl esters of DHA and EPA from fish oil may also be attainable with an ethyl ester of algal-DHA alone.

Acknowledgments The authors are grateful to Dr. Joan F. Flanagan from at Charles River Laboratories who provided thoughtful discussions relating to this study.

References

- Albert CM, Hennekens CH, O'Donnell CJ, Ajani UA, Carey VJ, Willett WC, Ruskin JN, Manson JE (1998) Fish consumption and risk of sudden death. *JAMA* 279:23–28
- GISSI-Prevenzione Investigators (1999) Dietary supplementation with n-3 polyunsaturated fatty acids and vitamin E after myocardial infarction: results of the GISSI-Prevenzione trial. *Lancet* 354:447–455
- Chung MK (2008) Omega-3 fatty acid supplementation for the prevention of arrhythmias. *Curr Treat Options Cardiovasc Med* 10:398–407
- Calo L, Bianconi L, Colivicchi LF, Lamberti F, Loricchio ML, de Ruvo E, Meo A, Pandozi C, Staibano M, Santini M (2005) N-3 fatty acids for the prevention of atrial fibrillation after coronary artery bypass surgery: a randomized controlled trial. *J Am Coll Cardiol* 45:1723–1728
- Kris-Etherton PM, Harris WS, Appel LJ, for the Nutrition Committee (2002) Fish consumption, fish oil, omega-3 fatty acids, and cardiovascular disease. *Circulation* 106:2747–2757
- Thies F, Garry J, Yaqoob P, Rerkasem K, Williams J, Shearman CP, Gallagher PJ, Calder PC, Grimble RF (2003) Association of n-3 polyunsaturated fatty acids with stability of atherosclerotic plaque: a randomized controlled trial. *Lancet* 361:477–485
- Bonna KH, Thelle DS (1991) Association between blood pressure and serum lipids in a population: the Tromso Study. *Circulation* 83:1305–1314
- Mori TA, Bao DQ, Burke V, Puddey IB, Beilen LJ (1999) Docosahexaenoic acid but not eicosapentaenoic acid lowers ambulatory blood pressure and heart rate in humans. *Hypertension* 34:253–260
- Mozaffarian D, Geelen A, Brouwer IA, Geleijnse JM, Zock PL, Katan MB (2005) Effect of fish oil on heart rate in humans: a meta-analysis of randomized controlled trials. *Circulation* 112:1945–1952
- Harris WS, Miller M, Tighe AP, Davidson MH, Schaefer EJ (2008) Omega-3 fatty acids and coronary heart disease risk: clinical and mechanistic perspectives. *Atherosclerosis* 197:12–24
- Agren JJ, Hanninen O, Julkunen A, Fogelholm L, Vidgren H, Schwab U, Pynnonen O, Uustipa M (1996) Fish diet, fish oil and docosahexaenoic acid rich oil lower fasting and postprandial plasma lipid levels. *Eur J Clin Nutr* 50:765–771
- Ikeda I, Kumamaru J, Nakatani N, Sakono M, Murota I, Imaizumi K (2001) Reduced hepatic triglyceride secretion in rats fed docosahexaenoic acid-rich fish oil suppresses postprandial hypertriglyceridemia. *J Nutr* 131:1159–1164
- Willumsen N, Hexeberg S, Skorve J, Lundquist M, Berge RK (1993) Docosahexaenoic acid shows no triglyceride-lowering effects but increases the peroxisomal fatty acid oxidation in liver of rats. *J Lipid Res* 34:13–22
- Willumsen N, Skorve J, Hexeberg S, Rustan AC, Berge RK (1993) The hypotriglyceridemic effect of eicosapentaenoic acid in rats is reflected in increased mitochondrial fatty acid oxidation followed by diminished lipogenesis. *Lipids* 28:683–690
- Kobayashi Y, Kuroda K, Jinnouchi H, Nishide E, Innami S (1984) Differential effects of dietary eicosapentaenoic acid and docosahexaenoic fatty acids on lowering triglyceride and cholesterol levels in the serum of rats on hypercholesterolemic diet. *J Nutr Sci Vitaminol* 30:357–372
- Xu Z, Riediger N, Innis S, Moghadasian MH (2007) Fish oil significantly alters fatty acid profiles in various lipid fractions but not atherogenesis in apo E-KO mice. *Eur J Nutr* 46:103–110
- Storbien LH, Jenkins AB, Chisholm DJ, Pascoe WS, Khouri S, Kraegen EW (1991) Influence of dietary fat composition on development of insulin resistance in rats: relationship to muscle triglyceride and omega-3 fatty acids in muscle phospholipid. *Diabetes* 40:280–289
- Behme M (1996) Dietary fish oil enhances insulin sensitivity in miniature pigs. *J Nutr* 126:1549–1553
- Nettleton JA, Katz R (2005) N-3 long-chain polyunsaturated fatty acids in type 2 diabetes: a review. *J Am Diet Assoc* 105:428–440
- Farmer A, Montori V, Dinneen S, Clar C (2001) Fish oil in people with type 2 diabetes mellitus. *Cochrane Database Syst Rev* 3:CD003205
- Mustad VA, DeMichele S, Huang Y-S, Mika A, Lubbers N, Berthiaume N, Polakowski J, Zinker B (2006) Differential effects of n-3 polyunsaturated fatty acids on metabolic control and vascular reactivity in the type 2 diabetic *ob/ob* mouse. *Metab Clin Exp* 55:1365–1374
- Minami A, Ishimura N, Sakamoto S, Takishita E, Mawatari K, Okada K, Nakaya Y (2002) Effect of eicosapentaenoic acid ethyl ester v. oleic acid-rich safflower oil on insulin resistance in type 2 diabetic model rats with hypertriglyceridemia. *Br J Nutr* 87:157–162
- Oarada M, Tsuzuki T, Gono T, Igarashi M, Kamei K, Nikawa T, Hirasaka K, Ogawa T, Miyazawa T, Nakagawa K, Kurita N (2008) Effects of dietary fish oil on lipid peroxidation and serum triacylglycerol levels in psychologically stressed mice. *Nutrition* 24:67–75
- O'Connor CL, Lawrence LM, Hayes SH (2007) Dietary fish oil supplementation affects serum fatty acid concentrations in horses. *J Animal Sci* 85:2183–2189
- Ryan AS, Keske MA, Hoffman JP, Nelson EB (2009) Clinical overview of algal-docosahexaenoic acid: effects on triglyceride levels and other cardiovascular risk factors. *Am J Ther* 16:183–192
- Grimsgaard S, Bonna KH, Hansen J-B, Nordoy A (1997) Highly purified eicosapentaenoic acid and docosahexaenoic acid in humans have similar triacylglycerol-lowering effects but divergent effects on serum fatty acids. *Am J Clin Nutr* 66:649–659
- National Research Council (1996) Guide for the care and use of laboratory animals. National Academy Press, Washington DC
- Arterburn LM, Oken HA, Hoffman JP, Bailey-Hall E, Chung G, Rom D, Hamersley J, McCarthy D (2007) Bioequivalence of docosahexaenoic acid from different algal oils in capsules and in a DHA-fortified food. *Lipids* 42:1011–1024
- Tukey JW, Ciminera JL, Heyse JF (1985) Testing the statistical certainty of a response to increasing doses of a drug. *Biometrics* 41:295–301
- Qi K, Fan C, Jiang J, Zhu H, Haiyan Z, Jiao H, Meng Q, Deckerbaum RJ (2008) Omega-3 fatty acid containing diets decrease plasma triglyceride concentrations in mice by reducing endogenous triglyceride synthesis and enhancing the blood clearance of triglyceride-rich particles. *Clin Nutr* 27:424–430
- Keller DD, Jurgilas S, Perry B, Blum J, Farino B, Reynolds J, Keilson L (2007) Docosahexaenoic acid (DHA) lowers triglyceride levels and improves low density lipoprotein particle size in a statin-treated cardiac risk population. *J Clin Lipidol* 1:151(A)
- Davidson M, Stein E, Bays H, Maki K, Doyle R, Shalwitz R, Ballantyne C, Ginsberg H, on behalf of the COMBination of prescription Omega-3 with Simvastatin (COMBOS) investigators (2007) Efficacy and tolerability of adding prescription omega-3 fatty acids 4 g/d to simvastatin 40 mg/d in hypertriglyceridemic patients: an 8-week, randomized, double-blind, placebo-controlled study. *Clin Ther* 29:1354–1367
- Mori TA, Woodman R (2006) The independent effects of eicosapentaenoic acid and docosahexaenoic acid on cardiovascular risk factors in humans. *Curr Opin Nutr Metab Care* 9:95–104
- Brossard N, Croset M, Pachiaudi C, Riou JP, Tayot JL, Lagarde M (1996) Retroconversion and metabolism of [¹³C]22:6n-3 triacylglycerols. *Am J Clin Nutr* 64:577–586

35. Boswell K, Koskelo E-K, Carl L, Glaza S, Hensen DJ, Williams KD, Kyle DJ (1996) Preclinical evaluation of single-cell oils that are highly enriched with arachidonic acid and docosahexaenoic acid. *Food Chem Toxicol* 34:585–593
36. Arterburn LM, Boswell KD, Koskelo E-K, Kassner SL, Kelly C, Kyle DJ (2000) A combined subchronic (90-day) toxicity and neurotoxicity study of a single-cell source of docosahexaenoic acid triglyceride (DHASCO[®] oil). *Food Chem Toxicol* 38:35–39
37. Conquer JA, Holub BJ (1996) Supplementation with an algae source of docosahexaenoic acid increases (n-3) fatty acid status and alters selected risk factors for heart disease in vegetarian subjects. *J Nutr* 126:3032–3039
38. Conquer JA, Holub BJ (1997) Dietary docosahexaenoic acid as a source of eicosapentaenoic acid in vegetarians and omnivores. *Lipids* 32:341–345
39. Wilbert GJ, Burns RA, Diersen-Schade DA, Kelley CM (1997) Evaluation of single cell sources of docosahexaenoic acid and arachidonic acid: a 4-week oral safety study. *Food Chem Toxicol* 35:967–974
40. Arterburn LM, Boswell KD, Lawlor T, Cifone MA, Murli H, Kyle DJ (2000) In vitro genotoxicity of ARASCO[®] and DHASCO[®] oil. *Food Chem Toxicol* 38:971–976
41. Arterburn LM, Boswell KD, Henwood SM, Kyle DJ (2000) A developmental safety study in rats using DHA- and ARA-rich single-cell oils. *Food Chem Toxicol* 38:3761–3771
42. Weiler HA (2000) Dietary supplementation of arachidonic acid is associated with higher whole body weight and bone mineral density in growing pigs. *Pediatr Res* 47:692–697
43. Mathews SA, Oliver WT, Phillips OT, Odle J, Diersen-Schade DA, Harrell RJ (2002) Comparison of triglycerides and phospholipids as supplemental sources of dietary long-chain polyunsaturated fatty acids in piglets. *J Nutr* 132:3081–3089
44. Huang M-C, Chao A, Kirwan R, Tschanz C, Peralta JM, Diersen-Schade DA, Cha S, Brenna JT (2002) Negligible changes in piglet serum clinical indicators or organ weights due to dietary single-cell long-chain polyunsaturated oils. *Food Chem Toxicol* 40:453–460
45. Nelson GJ, Schmidt PS, Bartolini GL, Kelley DS, Kyle DJ (1997) The effect of dietary docosahexaenoic acid on platelet function, platelet fatty acid composition, and blood coagulation. *Lipids* 32:1129–1136
46. Von Schacky C (2006) A review of omega-3 ethyl esters for cardiovascular prevention and treatment of increased blood triglyceride levels. *Vasc Health Risk Manag* 2:251–262

Comparison of Seal Oil to Tuna Oil on Plasma Lipid Levels and Blood Pressure in Hypertriglyceridaemic Subjects

Barbara J. Meyer · A. E. Lane · N. J. Mann

Received: 15 April 2009 / Accepted: 20 July 2009 / Published online: 29 August 2009
© AOCS 2009

Abstract As meat is a rich source of the omega-3 fatty acid docosapentaenoic acid (DPA) and Australians consume six times more meat than fish, investigation of the potential health benefit of DPA is warranted. The aims were to compare the effects of seal oil supplementation with fish oil, on measures of plasma lipids and blood pressure in hypertriglyceridaemic subjects. Forty-eight volunteers were recruited from the Wollongong community and were randomly allocated to one of three groups either receiving 1 g/day of long-chain omega-3 polyunsaturated fatty acids (LC n-3 PUFA) using one of three oils: seal oil capsules (340 mg eicosapentaenoic acid (EPA), 230 mg DPA, 450 mg DHA), fish oil capsules (210 mg EPA, 30 mg DPA, 810 mg DHA) or placebo capsules (containing sunola oil) for 6 weeks. Plasma triglycerides remained unchanged in the placebo group, whilst reductions of 7 and 14% ($P < 0.05$) were seen in the fish oil and seal oil groups respectively. Systolic blood pressure improved by 8 and 5 mmHg with

seal oil and fish oil respectively ($P < 0.05$). The mean arterial pressure was significantly lower after seal oil supplementation ($P < 0.005$) compared with the placebo group. These results indicate that seal oil is as effective as fish oil in lowering plasma triglycerides and blood pressure.

Keywords Docosapentaenoic acid · Omega-3 polyunsaturated fatty acids · Cardiovascular disease · Blood pressure · Dyslipidaemia

Abbreviations

ANOVA	Analysis of variance
ARA	Arachidonic acid
BMI	Body mass index
CVD	Cardiovascular disease
DBP	Diastolic blood pressure
DHA	Docosahexaenoic acid
DPA	Docosapentaenoic acid
EDTA	Ethylenediamine tetra-acetic acid
EPA	Eicosapentaenoic acid
FSANZ	Food standards Australia and New Zealand
HDL	High density lipoprotein
IMT	Intimal-medial thickness
LC n-3 PUFA	Long-chain omega-3 polyunsaturated fatty acids
LDL	Low density lipoprotein
MAP	Mean arterial pressure
NHMRC	National Health and Medical Research Council
NRV	Nutrient reference values
SBP	Systolic blood pressure
UoW	University of Wollongong

B. J. Meyer (✉) · A. E. Lane
School of Health Sciences, Metabolic Research Centre,
Smart Foods Centre, University of Wollongong,
Wollongong, NSW 2522, Australia
e-mail: bmeyer@uow.edu.au

Present Address:

A. E. Lane
Free Radical Group, Heart Research Institute,
7 Eliza St, Newtown, NSW 2042, Australia

N. J. Mann
School of Applied Sciences, RMIT University,
Melbourne, VIC 3000, Australia

Introduction

Cardiovascular disease (CVD) is the greatest single cause of mortality in Australia, accounting for 34 and 39% of male and female deaths, respectively [1]. Numerous clinical trials have shown that highly unsaturated long-chain omega-3 polyunsaturated fatty acids (LC n-3 PUFA) such as eicosapentaenoic acid (EPA; 20:5n-3) and docosahexaenoic acid (DHA; 22:6n-3) benefit cardiovascular disease outcomes in primary and secondary prevention [2]. Risk factors for CVD include hypertension and dyslipidaemia, with increased plasma triglycerides emerging as an independent risk factor [3]. EPA and DHA are effective in lowering plasma triglyceride levels [4]. Yet there is almost no data available regarding the potential health benefits of the only other common highly unsaturated LC n-3 PUFA, docosapentaenoic acid (DPA; 22:5n-3).

Epidemiological evidence indicates that intakes of all three of the LC n-3 PUFA (EPA, DHA, DPA) are significantly and inversely related to carotid intimal-medial thickness (IMT) [5]. The quartiles of gram EPA intakes (0.00–0.15; 0.16–0.29; 0.30–0.41; 0.42+); of gram DHA intakes (0.01–0.27; 0.28–0.45; 0.46–0.63; 0.64+) and of gram DPA intakes (0.02–0.04; 0.05–0.07; 0.08–0.10; 0.11+) all correlated negatively with IMT, which suggests that the cardiovascular benefits attributed to LC n-3 PUFA are not just attributable to EPA and DHA, but also to DPA [5]. Furthermore, the Kuopio Ischaemic Heart Disease Risk Factor Study showed that the men with the highest quintile of serum DHA plus DPA (>3.58% of total fatty acids) had a 44% reduced risk of acute coronary events compared with men in the lowest quintile (<2.38% of total fatty acids), and there were no associations with EPA levels [6]. The significance was due to DHA plus DPA, not just DHA alone. Hence there is scientific evidence that DPA has cardiovascular health benefits but this evidence is limited.

DPA can be found in relative abundance in most red meat. Australian grass fed beef contains 32 mg EPA, 49 mg DPA and 6 mg DHA per 100 g lean beef, as opposed to grain fed beef which contains much lower values (16 mg EPA, 37 mg DPA and 5 mg DHA per 100 g) [7]. This is consistent with beef from USA with range fed beef containing 0.62% EPA, 0.71% DPA and 0.09% DHA as percent of total fatty acids compared with only 0.13% EPA, 0.26% DPA and 0.04% DHA in feed-lot (grain fed) beef [8]. Hence meat contains more DPA and EPA, whereas fish/seafood contains more DHA and much less DPA.

Actual DPA intakes have been reported as 90 mg/day for men and 52 mg/day for women in Australia [9] which is comparable to that of France (75 mg/day for men and 56 mg/day for women, [10]) and Japan (90 mg/day for both men and women in Japan [5]), but both France and Japan consume more fish/seafood than Australians and

hence their EPA and DHA intakes are higher than Australian intakes [5, 9, 10]. As Australians consume more meat than fish/seafood, in the Australian diet, meat contributes up to 42.7% of LC n-3 PUFA intake which is similar to the new estimate of fish and seafood of 48% [9, 11]. This would indicate that DPA intakes are threefold higher than previously thought [9, 11]. Importantly, DPA intakes contribute up to 30% towards the intakes of LC n-3 PUFA in the Australian adult diet [9]. Given this level of DPA in the Australian diet, it is pertinent to understand its potential health benefit.

However for research studies on DPA, no purified or enriched form is commercially available. The richest commercial source of DPA is seal oil. There have been limited trials assessing the effect of seal oil supplementation on cardiovascular disease risk factors. One study showed a significant reduction in plasma triglycerides after seal oil supplementation for 6 weeks in healthy people [12], whilst another similar study showed no significant lowering of plasma triglycerides [13]. However these studies were conducted in people with normal plasma triglyceride levels. Therefore the aim of this study was to assess the ability of seal oil supplementation to lower plasma triglyceride levels and blood pressure in people with hypertriglyceridaemia in comparison to fish oil containing similar levels of EPA and DHA in a placebo controlled double blind intervention trial.

Experimental Procedures

Notification of Clinical Trial and Ethics Approval

The study on the cardiovascular effects of DPA was registered with the Australian Clinical Trial Register, number ACTRNO. 12605000641695 and notification forwarded to the Therapeutics Goods Administration. Ethics approval was granted by the University of Wollongong (UoW) Human Research Ethics Committee and informed consent was obtained from all study participants prior to the commencement of the clinical trial.

Recruitment and Study Population

Hypertriglyceridaemic subjects were recruited via newspaper advertisements, email to UoW community, social clubs and on local ABC radio. The UoW media release unit also generated interest from the media. Fifty-six volunteers were recruited and eligible for the study (i.e. plasma triglycerides >1.5 mmol/l) and 48 completed the study. Reasons for dropping out of the study included suffering from diarrhoea, forgetting to come to their 6-week appointment, losing their job and not being contactable for

their 6-week appointment or no discernable reasons. People already taking fish oil supplements were excluded from the study.

Seal Oil, Fish Oil and Placebo Capsule Supplementation

The capsules were 500 mg in weight and their composition is shown in Tables 1A and 1B. All three groups were provided with two separate bottles of capsules and they were asked to take 10 capsules per day; four capsules before breakfast and six capsules before dinner, such that all three groups were taking the same number of capsules per day. The target LC n-3 PUFA intake of the Seal Oil (BGI Atlantic Marine Product Inc, Canada) and Fish Oil (NuMega Ingredients Ltd, Sydney) groups was 1 g/day. Therefore the Seal Oil group took 10 Seal Oil capsules per day (which provided 340 mg EPA, 230 mg DPA, 450 mg DHA per day); the Fish Oil group took four placebo capsules and six Fish Oil capsules per day (which provided 210 mg EPA, 30 mg DPA, 810 mg DHA per day). The third group took 10 placebo capsules per day (Sunola oil, NuMega Ingredients Ltd, Sydney, which provided no LC n-3 PUFA but did provide approximately 4 g monounsaturated oil per day). The placebo group intake of monounsaturated oil in quantity is trivial compared to the dietary intake of monounsaturated fat. Furthermore as the seal oil capsules contained squalene (12.5 mg/500 mg capsule), the fish oil and placebo groups took one squalene capsule (875 mg) per week for 6 weeks equivalent to 125 mg/day, an identical intake to the seal oil group. Seal oil provided a 7.6-fold increase in the amount of DPA; a 1.6-fold increase in the amount of EPA and a 1.8-fold decrease in the amount of DHA compared to fish oil (Table 1B).

Seal oil also contains 0.3 mg/100 g vitamin A and 4.5 mg/100 g alpha-tocopherol [14]. Tuna oil contains less than 10 International Units of vitamin A and 0.21% of mixed natural tocopherols (NuMega Ingredients Ltd, Sydney).

Table 1A Individual capsule composition by principal fatty acid (mg per 500 mg capsule)

Fatty acid	Sunola oil capsules (mg/500 mg)	Fish oil capsules (mg/500 mg)	Seal oil capsules (mg/500 mg)
C18:1n-9	425	61	142
C20:5n-3	0	35	34
C22:5n-3	0	5	23
C22:6n-3	0	135	45

Study Design

A randomised, parallel, placebo-controlled, double-blind study was conducted in 56 hypertriglyceridaemic subjects, 48 of whom completed the study. They were randomly allocated to one of three groups and all three groups took ten 500-mg capsules per day for a 6 week intervention trial. Blood pressure and fasting blood samples were taken at baseline and at 6-week post intervention. Blood samples were assessed for erythrocyte fatty acids and plasma lipids (triglycerides, total cholesterol, LDL-cholesterol and HDL-cholesterol).

Erythrocyte Fatty Acids

Fasting blood samples were collected in tubes containing ethylenediamine tetra-acetic acid (EDTA) and placed on ice. The erythrocytes were separated from the plasma by centrifugation (10 min, 2,000×g, 4 °C). Erythrocyte and plasma samples were stored at −80 °C until analysed.

Erythrocyte membranes were isolated from 400 µl of packed erythrocytes and prepared for fatty acid analysis. The erythrocytes were lysed in 10 ml TRIS buffer (10 mM TRIS buffer, 2 mM EDTA, pH 7.2) and the membranes were pelleted after ultracentrifugation (200,000×g, 4 °C, 30 min). The erythrocyte membrane pellets were resuspended in 200 µl water and 150 µl was transferred into glass tubes for direct transesterification as described by Lepage and Roy [15]. Briefly, 2 ml of methanol:toluene (4:1) was added to each sample. While vortexing, 200 µl of acetyl chloride was added dropwise to each sample using a positive displacement pipette. Samples were then heated for 60 min at 100 °C in a heating block. After the tubes had been cooled in cold water, 3 ml of potassium chloride (10%) and 100 µl of toluene were added to each tube before centrifugation for 10 min (2,000×g, 4 °C). The fatty acid methyl esters, contained in the upper toluene phase, were removed and placed in GC vials. The fatty acid methyl esters were analysed by flame-ionisation gas chromatography (model GC-17A, Shimadzu) using a 30 m × 0.25 mm internal diameter capillary column (Varian). Individual fatty acids were identified upon comparison with known fatty acid standards (NuChek, Sigma, Australia, mix C10–C24 plus added DPA).

Plasma Lipids

HDL was isolated from plasma by precipitation of the apoB containing lipoproteins using dextran sulphate and magnesium chloride according to Warnick et al. [16]. All lipid analyses (plasma triglyceride, total cholesterol, HDL-cholesterol) were carried out using enzymatic colorimetric assays using the Konelab autoanalyser. LDL-cholesterol was calculated using the Friedewald calculation [17].

Table 1B Amount of principal fatty acids supplemented per group per day (mg per day)

Fatty acid	Sunola oil group (placebo) (mg per day)	Fish oil group (mg per day)	Seal oil group (mg per day)
C18:1n-9	4,250	1,944	1,420
C20:5n-3	0	210	340
C22:5n-3	0	30	230
C22:6n-3	0	810	450
Total LC n-3 PUFA	0	1,050	1,020

The placebo group consumed 10 placebo capsules per day; the fish oil group consumed six fish oil capsules per day plus four placebo capsules per day; the seal oil group consumed 10 seal oil capsules per day

Blood Pressure

Systolic blood pressure (SBP), diastolic blood pressure (DBP) and mean arterial pressure (MAP) were measured using the Omron blood pressure instrument (Medisave Australasia). These measurements were taken in triplicate at baseline (duplicate days) and after 6 weeks intervention (duplicate days). An average of the six baseline readings were obtained for each study participant and similarly after 6 weeks intervention.

Statistical Analysis

Statistical analysis was carried out using a JMP statistical analysis package (SAS Institute Inc Windows NT v5.1) and where variables were not normally distributed (plasma triglycerides), log transformation was used prior to analysis. One-way ANOVA was used to assess the change in plasma triglycerides and blood pressure between the three groups. One-way ANOVA was also used to assess the change in erythrocyte EPA and DHA levels and the change in plasma triglycerides per group. Pearson correlation analyses were conducted using Microsoft Excel. Statistical significance was set at $\alpha = 0.05$ for all analyses.

Results

Study Participant Characteristics and Baseline Blood Pressure and Plasma Lipids

The study participant baseline characteristics and baseline blood pressure and plasma lipids are shown in Table 2. There were no significant differences in age, sex, weight, body mass index (BMI) and blood pressure lowering medication used, between the three groups at baseline. On average, the study population was overweight, and ranging from middle age to elderly. All subjects were hypertriglyceridaemic, but with relatively normal plasma

cholesterol levels. Systolic blood pressures were greater than 140 mmHg in 23% of the study population whilst diastolic blood pressures were greater than 90 mmHg in 10% of the study population. The study volunteers did not change their body weight throughout the intervention (results not shown) (Table 2).

Erythrocyte Fatty Acids

The main erythrocyte LC PUFA measured at baseline (0 weeks) and after 6 weeks of intervention (week 6) in all three groups are shown in Table 3. The placebo group showed no changes over the 6 weeks period. In comparison to its own baseline value (0 weeks), fish oil supplementation resulted in decreases in arachidonic acid (ARA, 20:4n-6 ($P < 0.01$), adrenic acid (22:4n-6, $P < 0.05$) and DPA (22:5n-3, $P < 0.05$) and an increase in DHA (22:6n-3, $P < 0.01$). In comparison to its own baseline value (0 weeks), seal oil supplementation significantly decreased levels of ARA ($P < 0.05$) and adrenic acid ($P < 0.05$) and significantly increased the mean levels of EPA ($P < 0.001$), DPA ($P < 0.001$) and DHA ($P < 0.0005$) (Table 3, Fig. 1).

Figure 1 shows the comparison of the percentage changes in erythrocyte fatty acids in the three groups after 6 weeks supplementation. In comparison to the change in the placebo group (0–6 weeks), there were no significant difference in ARA, EPA and DPA in the fish oil group (0–6 weeks), but there were significant decreases in adrenic acid ($P < 0.05$) and increases in DHA ($P < 0.0005$). In comparison to the change in the placebo group (0–6 weeks), there was no significant difference in ARA in the seal oil group (0–6 weeks), but there were significant decreases in adrenic acid ($P < 0.05$) and significant increases in EPA ($P < 0.001$), DPA ($P < 0.001$) and DHA ($P < 0.0001$).

Plasma Lipids

The change in plasma lipids (mmol/l) from baseline (0 weeks) to 6 weeks for all three groups are shown in Fig. 2. Plasma triglycerides remained unchanged in the placebo group (2.31 vs. 2.36 mmol/l), but were reduced by 7% in the fish oil group (2.24 vs. 2.09 mmol/l, $P > 0.05$) and 14% in the seal oil group (2.54 vs. 2.19 mmol/l) ($P < 0.05$) and these changes were significantly different to the changes in the placebo group. No differences were seen in the total cholesterol, LDL-cholesterol or HDL-cholesterol between any of the groups (Fig. 2).

Blood Pressure

The changes in blood pressure results are shown in Fig. 3. Systolic blood pressure (SBP) decreased significantly in both the fish oil (-5.3 mmHg, $P < 0.05$) and the seal oil

Table 2 Study participant characteristics, plasma lipids and blood pressure at baseline ($n = 48$)

	Placebo ($n = 17$)	Fish oil ($n = 15$)	Seal oil ($n = 16$)
Male/female (n)	9/8	6/9	9/7
Age (years)	57 ± 7 ^a (42–70)	59 ± 7 (49–73)	54 ± 7 (45–69)
Weight (kg)	86 ± 12 (63–114)	79 ± 18 (53–108)	79 ± 11 (62–107)
Body mass index (kg/m ²)	29 ± 3 (25–37)	28 ± 5 (19–36)	27 ± 3 (22–34)
Plasma triglycerides (mmol/l)	2.31 ± 0.73 (1.69–3.61)	2.24 ± 0.18 (1.57–3.67)	2.54 ± 0.27 (1.57–5.26)
Total cholesterol (mmol/l)	5.14 ± 0.22 (3.61–6.52)	5.31 ± 0.18 (3.68–6.82)	5.60 ± 0.25 (4.13–6.67)
LDL-cholesterol ^b (mmol/l)	3.06 ± 0.18 (1.93–4.23)	3.38 ± 0.18 (2.34–4.40)	3.63 ± 0.22 (2.41–4.83)
HDL-cholesterol (mmol/l)	1.12 ± 0.07 (0.75–1.91)	1.12 ± 0.10 (0.63–1.90)	1.03 ± 0.05 (0.65–1.34)
Systolic blood pressure (mmHg)	126 ± 13 (99–151)	131 ± 14 (100–147)	137 ± 21 (119–189)
Diastolic blood pressure (mmHg)	73 ± 9 (60–85)	74 ± 11 (57–93)	79 ± 9 (70–92)
Mean arterial pressure (mmHg)	93 ± 10 (73–107)	95 ± 10 (77–106)	102 ± 14 (88–129)
Blood pressure medication (M/F)	2/1	2/2	0/2

n is number of participants as males and females

^a Values are mean ± SD (range)

^b LDL-C was calculated using the Friedewald calculation [17]

Table 3 Red Blood Cell Fatty Acids (expressed as % of total fatty acids)

	20:4n-6	22:4n-6	20:5n-3	22:5n-3	22:6n-3
Placebo ($n = 17$)					
0 weeks	12.8 ± 0.3 ^a	2.3 ± 0.1	1.1 ± 0.1	2.5 ± 0.1	5.0 ± 0.2
6 weeks	12.5 ± 0.3	2.3 ± 0.1	1.1 ± 0.1	2.4 ± 0.2	5.0 ± 0.2
Fish oil ($n = 13$)					
0 weeks	12.6 ± 0.2	2.5 ± 0.2	1.1 ± 0.2	2.6 ± 0.1	5.2 ± 0.3
6 weeks	12.1 ± 0.2**	2.1 ± 0.1*	1.3 ± 0.1	2.4 ± 0.1*	6.4 ± 0.3***
Seal oil ($n = 16$)					
0 weeks	12.6 ± 0.2	2.2 ± 0.1	1.0 ± 0.1	2.5 ± 0.1	4.8 ± 0.2
6 weeks	12.0 ± 0.2*	2.0 ± 0.2*	1.8 ± 0.1****	2.7 ± 0.1****	5.8 ± 0.1***

* $P < 0.05$, ** $P < 0.01$, *** $P < 0.005$, **** $P < 0.0001$, differences between 0 and 6 weeks

^a Values are means ± SEM

groups (−7.7 mmHg, $P < 0.01$) in comparison to the placebo group (6 mmHg). The mean arterial pressure (MAP) was significantly reduced (−8.3 mmHg, $P < 0.01$) in the seal oil group and tended towards a reduction (−3.5 mmHg, n.s.) in the fish oil versus the placebo group (3.9 mmHg). There were no statistical differences in diastolic blood pressure (DBP) in the three groups (Fig. 3).

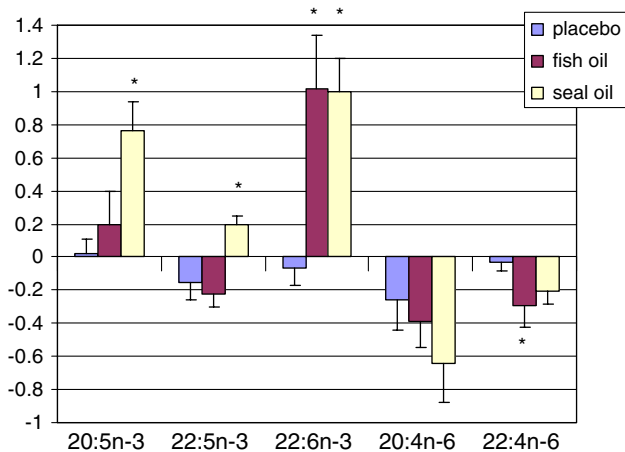
Correlations between the Change in Erythrocyte EPA and DHA Levels and the Change in Plasma Triglycerides and Blood Pressure

The change in erythrocyte EPA + DHA levels correlated with the change in plasma triglycerides in the seal oil group, $r = 0.52$ ($P < 0.05$) but there were no correlations in the fish oil or placebo oil groups with the change in plasma triglycerides (Table 4).

There were several significant correlations (see Table 4) between the change in erythrocyte EPA and DHA levels and the change in SBP, DBP and MAP in the fish oil groups with correlation coefficients ranging from 0.56 to 0.76 ($P < 0.05$). As expected there were no correlations with erythrocyte LC n-3 PUFA and blood pressure in the placebo group (Table 4).

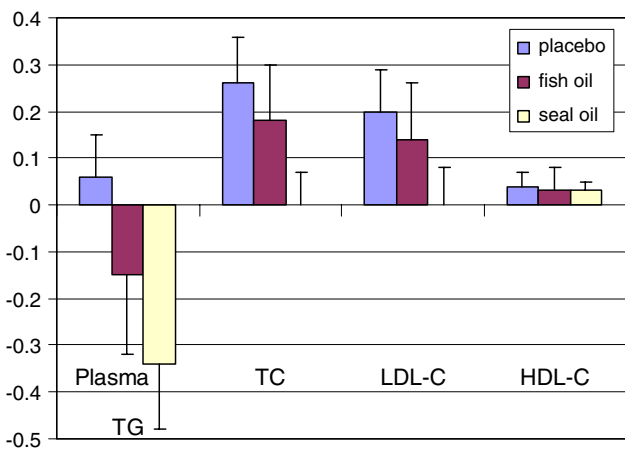
Discussion

The supplementation of 1 g of LC n-3 PUFA per day supplied by fish oil capsules for 6 weeks resulted in a significant increase in erythrocyte DHA levels, which is in agreement with previous studies using similar doses of fish oil and similar duration of intervention [18, 19]. However, the supplementation of 1 g of LC n-3 PUFA per day



* significantly different from the change in the placebo group ($p < 0.05$)

Fig. 1 The percent change in erythrocyte fatty acids (6 weeks minus baseline) from the three groups from left to right: placebo, fish oil and seal oil group. The fatty acid abbreviations: *20:5n-3* is eicosapentaenoic acid, *22:5n-3* is docosapentaenoic acid, *22:6n-3* is docosahexaenoic acid, *20:4n-6* is arachidonic acid and *22:4n-6* is adrenic acid. *Significantly different from the change in the placebo group ($P < 0.05$)

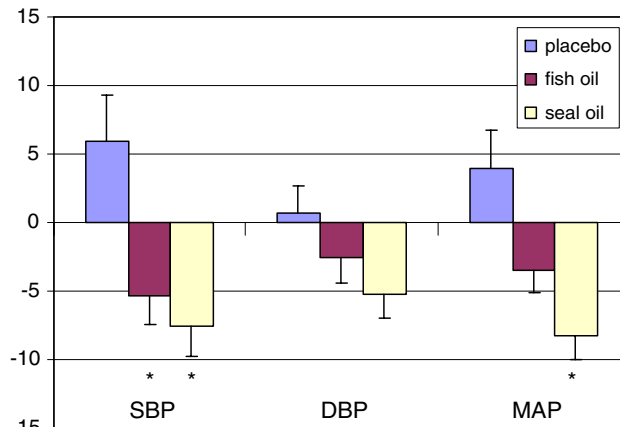


* significantly different from the change in the placebo group ($p < 0.05$)

Fig. 2 The change in plasma lipids (mmol/l) in the three groups from left to right: placebo, fish oil and seal oil group. Plasma lipid abbreviations: *TG* triglycerides, *TC* total cholesterol, *LDL-C* low density lipoprotein cholesterol and *HDL-C* high density lipoprotein cholesterol. *Significantly different from the change in the placebo group ($P < 0.05$)

supplied by seal oil capsules for 6 weeks differed to that of fish oil, in that DPA and EPA in addition to DHA were significantly increased, which is in agreement with a previous study using the same 1 g dose of seal oil for 6 weeks [12].

It has been shown previously that intakes of EPA and DHA correlate significantly with erythrocyte EPA and DHA levels respectively [20]. However, there was no correlation between DPA intakes and erythrocyte DPA



* significantly different from the change in the placebo group ($p < 0.05$)

Fig. 3 The change in blood pressure (mmHg) in the three groups from left to right: placebo, fish oil and seal oil group. Blood pressure abbreviations; *SBP* systolic blood pressure, *DBP* diastolic blood pressure and *MAP* mean arterial pressure. *Significantly different from the change in the placebo group ($P < 0.05$)

levels (correlation coefficient $r = 0.05$, $P = 0.71$), despite quite reasonable correlations between dietary intakes and erythrocyte levels of EPA, DHA and total LC n-3 PUFA [20]. Since that publication, another study assessed the validity of a PUFA questionnaire by comparison to 3 day weighed food record and erythrocyte fatty acids using the methods of triads [21]. In that triangulation of DPA intakes from PUFA questionnaire versus DPA intake from 3 day weighed food record versus DPA in erythrocytes (or plasma)—a validity co-efficient could not be determined as the estimate was >1 for erythrocytes and negative for plasma. This lack of correlation between dietary intake of DPA and circulating levels of DPA has been shown by another group [22] who assessed a different questionnaire. Using the methods of triads they found a similar negative validity co-efficient when assessing plasma DPA to their questionnaire and weighed food records [22]. Hence whilst there is a direct correlation between EPA and DHA intakes and EPA and DHA erythrocyte levels respectively, this does not hold true for DPA as there is no direct correlation between DPA intake and erythrocyte or plasma levels of DPA.

Therefore to interpret the DPA results in this study it is probably better to look at DPA intakes rather than erythrocyte levels of DPA. In this study the fish oil group consumed 210 mg/day EPA, 30 mg/day DPA and 810 mg/day DHA, whilst the seal oil group consumed 340 mg/day EPA, 230 mg/day DPA and 450 mg/day DHA. The difference between the fish oil and seal oil groups is the seal oil group consumed 130 mg/day more EPA; 200 mg/day more DPA and 360 mg/day less DHA than the fish oil group. This difference corresponds to a 1.6-fold increase in

EPA; a 7.6-fold increase in DPA and a 1.8-fold decrease in DHA, where the magnitude of dietary change is greatest in DPA.

This study showed a trend towards a 7% reduction plasma triglyceride levels with 1 g LC n-3 PUFA per day fish oil supplementation, which is less than a recently published study that assessed a dose response with DHA rich fish oil supplementation which showed 6% (n.s.), 20 and 25% reductions with approx 0.7, 1.3 and 2 g of fish oil supplementation per day for 6 weeks [19]. The seal oil 1 g LC n-3 PUFA per day supplementation for 6 weeks resulted in 14% reduction in plasma triglyceride which was also less than 21% reduction previously reported [12], however another seal oil study showed no significant lowering of plasma triglycerides [13]. Both Bonefeld-Jorgensen et al. [12] and Conquer et al. [13] were conducted in healthy people with normal plasma triglyceride levels which could explain the lack of effect in the latter study. The Bonefeld-Jorgensen et al. study [12] was not a placebo-controlled study and the reductions in plasma triglyceride seen could have been due to other factors.

In terms of the mechanism in plasma triglyceride lowering effect, a decrease in hepatic VLDL output has been attributed to increased hepatic fatty acid oxidation and a decreased rate of lipogenesis [23, 24]. EPA and DHA have been shown to be ligands for nuclear receptors such as PPAR-alpha [23–25] and sterol regulatory element binding proteins [23, 26], which modulate the expression of key genes in these metabolic processes. Now DPA may also be involved in these processes. Certainly in a well controlled rat study (where seal oil and fish oil supplemented rat groups had constant PUFA/MUFA/SAFA levels and the control rat group had linoleic acid as their sole PUFA in the diet), the seal oil was more effective than fish oil in lowering serum triglyceride levels [27]. In this rat model the activities of fatty acid synthase, glucose-6-phosphate dehydrogenase and hepatic lipase were all lower in the seal oil group compared to the control group, whereas only the activity of hepatic lipase was lower in the fish oil group compared to the control group. However, the activities of peroxisomal beta-oxidation and lipoprotein lipase in adipose tissue were significantly higher in the fish oil group compared to the controls [27]. Hence the hypotriglyceridaemic effect of the seal oil was attributed to suppression in fatty acid synthesis. As the main difference between seal oil and fish oil is the eightfold increased level of DPA in seal oil, the authors surmised that this higher DPA content could be the primary agent responsible for triglyceride lowering.

Moreover, a study comparing the effects of EPA rich oil versus DHA rich oil on circulating plasma triglyceride levels in humans found that the DHA rich oil was more effective than EPA rich oil and remained significant when

compared to the olive-oil placebo group, whereas the EPA rich oil did not [28]. Interestingly, the authors pointed out that the DHA rich oil contained a sixfold greater amount of DPA than the EPA rich oil, but the hypotriglyceridaemic effect of DPA was unknown and that it warranted further study [28].

In the present study, both fish oil and seal oil supplementation resulted in improvements in blood pressure. The reduction in blood pressure as a result of fish oil supplementation is well documented with several meta-analyses showing benefits as described in the review by Mori [29]. However, most of these trials required doses of 3–4 g per day to achieve the blood pressure lowering benefits. This study showed significant reductions in SBP (fish oil and seal oil groups) and MAP (seal oil group) but no significant reductions in DBP (all groups) using a 1-g dose of LC n-3 PUFA per day for 6 weeks. There was an increase in SBP in the placebo group, however, upon re-analysis with estimating zero change in SBP in the placebo group, the changes in SBP in the seal oil and fish oil groups remained significantly lower compared to placebo.

However the increase in erythrocyte EPA + DHA after fish oil but not seal oil supplementation correlated with the change in blood pressure. EPA correlated with SBP whilst DHA correlated with DBP (Table 4). Mori et al. [30] showed that purified DHA capsules lowered 24-h ambulatory blood pressure in mild hyperlipidaemic subjects, whilst purified EPA capsules had no effect. Even though similar study populations were assessed, it is not clear why the differential effect of EPA on SBP and DHA on DBP is seen in this current study. However, other studies have shown limited effect of EPA and DHA on blood pressure in normotensive people [31] and in study populations taking multiple medications [29].

Even though there was no correlation between the changes in erythrocyte EPA + DHA levels and the change in blood pressure in the seal oil treated group, in this study, seal oil resulted in a significant 8 mmHg reduction in SBP. Usually high doses of EPA + DHA of 3–4 g per day are needed to reduce blood pressure as shown by meta-analyses [32, 33]. It is conceivable that the significant reduction in SBP in the current study could be due to (1) the study population having an average blood pressure of 130/75 mmHg of which 23% had SBP greater than 140 mmHg and 10% had DBP greater than 90 mmHg and (2) less than 20% of the study population were taking medication to lower their blood pressure, thereby allowing the omega-3 PUFA to be effective. A study by Vericel et al. [34] showed that supplementation for 42 days with 150 mg DHA and 30 mg EPA per day in an elderly un-medicated population resulted in 14 mmHg reduction in SBP, which is consistent with the current study showing the effect of low dose omega-3 PUFA and reduction in SBP.

Table 4 Correlations between the changes in erythrocyte LC n-3 PUFA and changes in plasma triglyceride and changes in blood pressure

	<i>r</i>		
	Placebo (<i>n</i> = 17)	Fish oil (<i>n</i> = 15)	Seal oil (<i>n</i> = 16)
Change in TG (6-0)			
Change in EPA	0.094	0.028	0.283
Change in DPA	-0.106	0.131	-0.210
Change in DHA	-0.127	0.077	0.381
Change in EPA + DHA	-0.024	0.067	0.520*
Change in EPA + DPA + DHA	-0.099	0.089	0.442
Change in SBP (6-0)			
Change in EPA	0.055	0.634*	-0.165
Change in DPA	-0.270	0.065	0.023
Change in DHA	-0.156	0.451	-0.181
Change in EPA + DHA	-0.080	0.556*	-0.282
Change in EPA + DPA + DHA	-0.290	0.558*	-0.264
Change in DBP (6-0)			
Change in EPA	-0.201	0.330	-0.190
Change in DPA	0.286	-0.444	0.222
Change in DHA	-0.398	0.756*	0.428
Change in EPA + DHA	-0.421	0.714*	0.299
Change in EPA + DPA + DHA	-0.148	0.651*	0.330
Change in MAP (6-0)			
Change in EPA	-0.090	0.446	-0.282
Change in DPA	-0.056	-0.010	0.255
Change in DHA	-0.203	0.608*	0.103
Change in EPA + DHA	-0.206	0.628*	-0.078
Change in EPA + DPA + DHA	-0.232	0.647*	-0.023

**P* < 0.05

The mechanisms of action of LC n-3 PUFA on blood lowering effects have been described by Mori et al. [29]. The mechanisms include (1) the LC n-3 PUFA having vasodilatory effects by increasing the release of nitric oxide; (2) modifying the release of ADP, vasoactive prostanoids (such as thromboxane A₂ and prostacyclin I₂) (3) and the LC n-3 PUFA incorporation into plasma and cellular membranes, altering the physicochemical structure of the membrane and leading to changes in fluidity, permeability and function of the membrane and membrane-bound proteins [29].

Given the health benefits of seal oil containing DPA, what are some DPA rich containing foods? Australian red meat is a relatively rich source of DPA [9, 11] and Australians consume six times more meat (158 g per day [35], 164 g per day [36]) than fish/seafood (26 g per day [35], 28 g per day [36]). Abalone is another DPA rich food [37] but the consumption is also much lower than meat. The National Health and Medical Research Council (NHMRC)

in Australia has released Nutrient Reference Values (NRV) for LC n-3 PUFA intakes which includes EPA, DPA and DHA [38]. However, DPA is not included in the LC n-3 PUFA nutrient claim in the current Food Standards Australia and New Zealand (FSANZ) Code [39]. The exclusion of DPA precludes many cuts of meat qualifying for this LC n-3 PUFA nutrient claim. Hence these standards favour fish and seafood as well as fortified foods containing LC n-3 PUFA over those with intrinsic DPA content [40]. The rationale for the exclusion of DPA is a lack of scientific evidence. Hence more research is warranted to ascertain the potential health benefits of DPA. Therefore larger trials with more pure forms of DPA are warranted.

In conclusion, 1 g/day of LC n-3 PUFA from seal oil is just as effective as 1 g/day of LC n-3 PUFA from fish oil in reducing plasma triglyceride levels and SBP in hypertriglyceridaemic subjects; however, studies using (as yet unavailable) purified DPA are warranted.

Acknowledgments The authors would like to acknowledge the time and effort of all the study participants as well as funding from the Meat & Livestock Australia.

References

1. National Heart Foundation (2007) The burden of cardiovascular disease in Australia for the Year 2003 July 2007. Available at http://www.heartfoundation.org.au/Heart_Information/Statistics.htm. Accessed 12 February 2009
2. Wang C, Harris WS, Chung M, Lichtenstein AH, Balk EM, Kupelnick B, Jordan HS, Lau J (2006) N-3 fatty acids from fish or fish-oil supplements, but not alpha-linolenic acid, benefit cardiovascular disease outcomes in primary- and secondary-prevention studies: a systematic review. *Am J Clin Nutr* 84(1):5–17
3. Malloy MJ, Kane JP (2001) A risk factor for atherosclerosis: triglyceride-rich lipoproteins. *Adv Internal Med* 47:111–136
4. Weber P, Raederstorff D (2000) Triglyceride-lowering effect of omega-3 LC-polyunsaturated fatty acids—a review. *Nutr Metab Cardiovasc Dis* 10:28–37
5. Hino A, Adachi H, Toyomasu K, Yoshida N, Enomoto M, Hiratsuka A, Hirai Y, Satoh A, Imaizumi T (2004) Very long chain N-3 fatty acids intake and carotid atherosclerosis: an epidemiological study evaluated by ultrasonography. *Atherosclerosis* 176:145–149
6. Rissanen T, Voutilainen S, Nyyssonen K, Lakka TA, Salonen JT (2000) Fish-oil derived fatty acids, docosahexaenoic acid and docosapentaenoic acid and the risk of acute coronary events: the Kuopio ischaemic heart disease risk factor study. *Circulation* 102:2677–2679
7. Ponnampalam EN, Mann NJ, Sinclair AJ (2006) Effect of feeding systems of omega-3 fatty acids, conjugated linoleic acid and trans fatty acids in Australian beef cuts: potential impact on human health. *Asia Pac J Clin Nutr* 15(1):21–29
8. Rule DC, Broughton KS, Shellito SM, Maiorano G (2002) Comparison of muscle fatty acid profiles and cholesterol concentration of bison, beef cattle, elk and chicken. *J Anim Sci* 85(1):1202–1211
9. Howe PRC, Meyer BJ, Record S, Baghurst K (2006) Dietary intake of long chain omega-3 polyunsaturated fatty acids: contribution of meat sources. *Nutrition* 22(1):47–53

10. Astorg P, Arnault N, Czernichow S, Noisette N, Galan P, Hercberg S (2004) Dietary intake and food sources of n-6 and n-3 PUFA in French adult men and women. *Lipids* 34(6):527–535
11. Meyer BJ, Mann NJ, Lewis JL, Milligan GC, Sinclair AJ, Howe PRC (2003) Dietary intakes and food sources of omega-6 and omega-3 polyunsaturated fatty acids. *Lipids* 38:391–398
12. Bonefeld-Jorgensen EC, Moller SM, Hansen JC (2001) Modulation of atherosclerotic risk factors by seal oil: a preliminary assessment. *Int J Circumpolar Health* 60:25–33
13. Conquer JA, Cheryk LA, Chan E, Gentry PA, Holub BJ (1999) Effect of supplementation with dietary seal oil on selected cardiovascular risk factors and hemostatic variables in healthy male subjects. *Thrombosis Res* 96:239–250
14. Brunborg LA, Madland TM, Lind RA, Arslan G, Berstad A, Froyland L (2008) Effects of short-term oral administration of dietary marine oils in patients with inflammatory bowel disease and joint pain: a pilot study comparing seal oil and cod liver oil. *Clin Nutr* 27:614–622
15. Lepage G, Roy CC (1986) Direct transesterification of all classes of lipids in a one-step reaction. *J Lipid Res* 27:114–120
16. Warnick GR, Albers JJ (1978) A comprehensive evaluation of the heparin/manganese precipitation procedure for estimating HDL cholesterol. *J Lipid Res* 9:65–76
17. Friedewald WT, Levy RI, Fredrickson DS (1972) Estimation of the concentration of LDL cholesterol in plasma without the use of the preparative ultracentrifuge. *Clin Chem* 18:499–502
18. Brown AJ, Pang E, Roberts DC (1991) Persistent changes in the fatty acid composition of erythrocyte membranes after moderate intake of N-3 polyunsaturated fatty acids: study design implications. *Am J Clin Nutr* 54:668–673
19. Milte CM, Coates AM, Buckley JD, Hill AM, Howe PRC (2008) Dose-dependent effects of docosahexaenoic acid-rich fish oil on erythrocyte docosahexaenoic acid and blood lipid levels. *Br J Nutr* 99:1083–1088
20. Sullivan BL, Williams PG, Meyer BJ (2006) Biomarker validation of a long-chain omega-3 polyunsaturated fatty acid food frequency questionnaire. *Lipids* 41:845–850
21. Swierk M, Williams PG, Jennifer Wilcox J, Russell KG, Meyer BJ (2009) Validation of an Australian electronic food frequency questionnaire to measure polyunsaturated fatty acid intake (submitted)
22. McNaughton SA, Hughes MC, Marks GC (2007) Validation of a FFQ to estimate the intake of PUFA using plasma phospholipid fatty acids and weighed food records. *Br J Nutr* 97:561–568
23. Jump DB, Clark SD (1999) Regulation of gene expression by dietary fat. *Annu Rev Nutr* 19:63–90
24. Price PT, Nelson CM, Clarke SD (2000) Omega-3 polyunsaturated fatty acid and regulation of gene expression. *Curr Opin Lipidol* 11:3–7
25. Clark SD (2000) Polyunsaturated fatty acid regulation of gene transcription: a mechanism to improve energy balance and insulin resistance. *Br J Nutr* 83:S59–S66
26. Xu J, Nakamura MT, Cho HP, Clarke SD (1999) Sterol regulation element binding protein-1 expression is suppressed by dietary polyunsaturated fatty acids. *J Biol Chem* 274:840–848
27. Yoshida H, Mawatari M, Ikeda I, Imaizumi K, Seto A, Tsuji H (1999) Effect of dietary seal and fish oils on triacylglycerol metabolism in rats. *J Nutr Sci Vitaminol (Tokyo)* 45(4):411–421
28. Buckley R, Shewring B, Turner R, Yaqoob P, Minihane AM (2004) Circulating triacylglycerol and apo E in response to EPA and docosahexaenoic acid supplementation in adult human subjects. *Br J Nutr* 92:477–483
29. Mori TA (2006) Omega-3 fatty acids and hypertension in humans. *Clin Exp Pharmacol Physiol* 33:842–846
30. Mori TA, Bao DQ, Burke V, Puddey IB, Beilin LJ (1999) Docosahexaenoic acid but not eicosapentaenoic acid lowers ambulatory blood pressure and heart rate in humans. *Hypertension* 34:253–260
31. Grimsgaard S, Bonna KH, Hansen JB, Muhre ESP (1998) Effects of highly purified eicosapentaenoic acid and docosahexaenoic acid on hemo-dynamics in humans. *Am J Clin Nutr* 68:52–59
32. Geleijnse JM, Giltay EJ, Grobbee DE, Donders ART, Kok FJ (2002) Blood pressure response to fish oil supplementation: meta-regression analysis of randomized trials. *J Hypertension* 20:1493–1499
33. Morris MC, Sacks F, Rosner B (1993) Does fish oil lower blood pressure? A meta-analysis of controlled studies. *Circulation* 88:523–533
34. Vericel E, Calzada C, Chapuy P, Lagarde M (1999) The influence of low intake of N-3 fatty acids on platelets in elderly people. *Atherosclerosis* 147:187–192
35. McLennan W, Podger A (1997) National nutrition survey, selected highlights, Australia. Australian Government Publishing Service, Canberra. ISBN 0 642 25793 0
36. Ollis TE, Meyer BJ, Howe PRC (1999) Australian food sources and intakes of omega-6 and omega-3 polyunsaturated fatty acids. *Ann Nutr Metab* 43:346–355
37. Nichols PD, Virtue P, Mooney BD, Elliot NG, Yearsley GK (1998) Seafood, the Good Food. The oil content and composition of Australian commercial fishes, shellfishes and crustaceans. FRDC Project 95/122. Guide Prepared for the Fisheries Research and Development Corporation CSIRO Marine Research Hobart. ISBN 0 643 06177 0
38. National Health and Medical Research Council (2006) Nutrient reference values for Australia and New Zealand. Commonwealth of Australia. Canberra. <http://www.nhmrc.gov.au/publications/synopses/n35syn.htm>
39. Food Standards Australia New Zealand (2002) Proposal P234—criteria and conditions for making nutrition content and related claims. pp 62–63. http://www.foodstandards.gov.au/_srcfiles/P234_DAR.pdf
40. Howe P, Buckley J, Meyer B (2007) Long-chain omega-3 fatty acids in red meat. *Nutr Dietet* 64(Suppl):S135–S139

Organ-Specific Distributions of Lysophosphatidylcholine and Triacylglycerol in Mouse Embryo

Takahiro Hayasaka · Naoko Goto-Inoue ·
Nobuhiro Zaima · Yoshishige Kimura ·
Mitsutoshi Setou

Received: 17 June 2009 / Accepted: 21 July 2009 / Published online: 15 August 2009
© AOCs 2009

Abstract Imaging mass spectrometry (IMS) has been developed as a method for determining and visualizing the distribution of proteins and lipids across sections of dissected tissue. Although lipids play an important role in mammal development, their detailed distributions have not been analyzed by conventional methods. In this study, we tried to determine and visualize lysophosphatidylcholine (LysoPtdCho) and triacylglycerol (TAG) in a mouse embryo by matrix-assisted laser desorption/ionization (MALDI) hybrid quadrupole time-of-flight (TOF) mass spectrometer. Many peaks were detected from a raster scan of the whole embryonic sections. The peaks at m/z 496.33, 524.36, 879.72, 881.74, and 921.74 were identified by MS/MS analyses as [LysoPtdCho (16:0) + H]⁺, [LysoPtdCho (18:0) + H]⁺, [TAG (16:0/18:2/18:1) + Na]⁺, [TAG (16:0/18:1/18:1) + Na]⁺, and [TAG (16:0/20:3/18:1) + K]⁺, respectively. The ion images constructed from the peaks revealed that LysoPtdCho were distributed throughout the body and TAGs were distributed around the brown adipose tissue and in the liver at embryo day 17.5. Thus, IMS system based on MALDI hybrid quadrupole TOF MS revealed the distribution of LysoPtdCho and, more importantly, the organ-specific distribution of TAGs

in the embryonic stages of mammals for the first time. We can conclude that this technique enables us to analyze the roles of various lipids during embryogenesis and gives insight for lipid research.

Keywords Lysophosphatidylcholine · Triacylglycerol · Phosphatidylcholine · Mouse · Embryo · Imaging mass spectrometry · Matrix-assisted laser desorption/ionization · Time of flight

Abbreviations

ARA	Arachidonic acid
Da	Dalton
DHA	Docosahexaenoic acid
DHB	2,5-Dihydroxybenzoic acid
H&E	Hematoxylin and eosin
IMS	Imaging mass spectrometry
ITO	Indium-tin-oxide
LPA	Lysophosphatidic acid
LysoPtdCho	Lysophosphatidylcholine
LPLD	Lysophospholipase D
MALDI	Matrix-assisted laser desorption/ionization
MW	Molecular weight
NL	Neutral loss
OCT	Optimal cutting temperature
PtdCho	Phosphatidylcholine
PL	Phospholipid
PLA2	Phospholipase A2
PUFA	Polyunsaturated fatty acid
SM	Sphingomyelin
TAG	Triacylglycerol
TFA	Trifluoroacetic acid
TOF	Time of flight
TRPV	Transient receptor potential vanilloid

T. Hayasaka · N. Goto-Inoue · N. Zaima · Y. Kimura ·
M. Setou (✉)
Department of Molecular Anatomy,
Molecular Imaging Frontier Research Center,
Hamamatsu University School of Medicine,
1-20-1 Handayama, Higashi-ku, Hamamatsu,
Shizuoka 431-3192, Japan
e-mail: setou@hama-med.ac.jp

Introduction

The techniques of metabolomics [1], proteomics [2, 3], and transcriptomics [4, 5] have been used for detailed analyses of metabolites, proteins, and RNAs. In these techniques, distributional information for the biomolecules of interest is lost due to the homogenization during sample preparation. In methods used to visualize the distribution of proteins in a living organism, antibodies [6, 7] and various fluorescent proteins [8, 9] are used to label target proteins. However, the antibodies and fluorescent proteins are not usually able to identify detailed structural differences, such as the posttranslational changes in protein and fatty acid composition in lipids [10]. Recently, imaging mass spectrometry (IMS) has been used to directly reveal the distribution of these biomolecules, such as phospholipids (PLs) [11–13], proteins [11, 14], and glycolipids [15, 16]. In IMS, a tissue section sprayed with matrix solution is directly raster-scanned by matrix-assisted laser desorption/ionization (MALDI) [17, 18]. The biomolecules in the section are ionized by MALDI and separated by time of flight (TOF) [19, 20]. The distribution of a biomolecule is two-dimensionally visualized as the relative signal intensities among the measurement points on the tissue section [11]. In this way, a great number of signals can be analyzed using a single IMS measurement.

In parallel with other groups [13, 21–27], our research group has contributed to the development of IMS [11, 28]. A large number of signals can now be detected from a tissue section because the detection sensitivity has been improved by the introduction of pretreatment techniques [14, 29–32] and new approaches for the processing and analysis of IMS data have been developed [33, 34]. The improved IMS has been applied to the imaging of various samples, such as the organs of various animals [11, 12, 14, 30–33, 35], human pathological samples [36–38], the brains of knock-out mice [39], and drug-treated animals [40]. Moreover, a MALDI-TOF-based IMS system has enabled us to perform structural analyses of PLs and peptides in tissue sections by MS/MS analysis [11, 12]. When the biomolecules are well-known lipid species, MS/MS analysis can easily figure out its detailed structure, including the difference of fatty acids, using other MALDI-TOF instruments, such as the QSTAR XL system used in the present study. With this technique, the distributions of phosphatidylcholine (PtdCho), lysophosphatidylcholine (LysoPtdCho), and triacylglycerol (TAG) are now able to be visualized by IMS.

Polyunsaturated fatty acids (PUFA), in particular arachidonic acid (ARA; 20:4) and docosahexaenoic acid (DHA; 22:6), are important structural components of membrane PLs and are required for normal development. Responding to nutritional intake, mammal development

has mainly been analyzed for lipids and/or the fatty acid composition in the liver [41], heart [41], endothelium [42], kidney [42], adipose [43], red blood cell [44], brain [41], plasma [41], and retina [45]. The important roles of PUFA in neural development have been reported not only in mammals but also in other invertebrate model animals. In *C. elegans*, for example, a subset of PUFA is implicated for the chemosensory and nociceptive behavior through transient receptor potential vanilloid (TRPV) channel signaling [46]. These results indicated that the synthesis and/or intake of nutritional sources rich in PUFA contributed to normal development and prevented several diseases associated with PUFA deficiency. However, distributional information was completely lost due to the homogenization during sample preparation in the previous analyses.

When PtdCho is hydrolyzed by phospholipase A2 (PLA2), it is changed to LysoPtdCho. LysoPtdCho is a signal mediator. LysoPtdCho possesses a charged head-group like PLs with only a single fatty acid as a consequence of the hydrolytic cleavage of one of the two fatty acids of PtdCho [47]. As an intermediate in the metabolism of PtdCho, LysoPtdCho is present in a variety of mammalian tissues and accumulates rapidly in diseases such as cardiac ischemia and diabetic cardiomyopathy [48]. However, the distribution of LysoPtdCho has not been well characterized by IMS. The characterization of accumulated LysoPtdCho would be of great significance for the analysis of diseases. TAGs are important long-term fuel-storage molecules that contain three fatty acid substituents esterified to a glycerol backbone. These three substituents may consist of one type, or may consist of two or three distinct types, each of which can have varying chain lengths, degrees of unsaturation, and locations of double bonds. Although TAGs have long been viewed as passive storage molecules, recent evidence suggests that TAGs are present at certain levels within cells, and that accumulation of excessive levels of TAGs impairs cellular functions [49]. With respect to IMS, TAGs have very recently been detected and visualized using TOF secondary-ion mass spectrometry [21]. This method allowed the detection of precise m/z values from a tissue section, and TAGs were identified by the m/z values and the result that fatty acid and TAGs were colocalized in the ion images. However, there are many kinds of lipids in the mass range of m/z 700–1,000. Moreover, the distribution of TAG was constructed from multiple peaks [21]. We believed that MS/MS analysis is preferable for discriminating the different kinds of lipids.

In this study, we identified and visualized PtdCho, LysoPtdCho, and TAGs in a mouse embryo with a MALDI hybrid quadrupole TOF-based IMS system. Embryogenesis is an important process for most organisms to generate the body plan specific for every species. During this dynamic

event, cells are dividing, migrating, and differentiating to form the mature tissue structures. The mechanism of development has been studied genetically and biochemically through the regulation of proteins thus far. On the other hand, the nature of other components, such as sugars and lipids, is not well known. Considering the dynamic change of morphology and migration of embryonic cells, lipids—important signaling mediators as well as the main component of plasma membrane—are expected to change their distribution and composition according to the stage of development. Many regulatory genes during development are known to be reactivated in abnormal involved tissues in adult, which means that analysis of embryogenesis can reveal not only the mechanism of development but also the nature of human diseases. To study the roles of lipids during embryogenesis, we prepared mouse embryos, which are most commonly used for developmental analysis. Sagittal sections of a mouse embryo at embryonic age of 17.5 days (E17.5) were analyzed by IMS. Based on the MS/MS analyses, we were able to perform IMS-based identification of LysoPtdCho, PtdCho, and TAG. Moreover, our IMS analyses also demonstrated the distributions of these lipids in the mouse embryos. This is the first finding of the specific distribution of LysoPtdCho, PtdCho, and TAG in mouse embryos.

Experimental Procedure

Reagents

Trifluoroacetic acid (TFA) and methanol were purchased from Kanto Chemical Company (Tokyo, Japan). 2,5-Dihydroxybenzoic acid (DHB) matrix was purchased from Bruker Daltonics (Bremen, Germany). Human angiotensin II and human bradykinin fragment 1–7 were purchased from Sigma Aldrich (St. Louis, MO). Ultrapure water was purchased from Kanto Chemical Company and used for the preparation of all buffers and solvents. All the chemicals used in this study were of the highest purity available.

Sample Preparation

The care and use of laboratory animals were in accordance with the Animal Experiment Regulations at Hamamatsu University School of Medicine, which follow the Guidelines for the Proper Conduct of Animal Experiments by the Science Council of Japan. Pregnant ICR mice were purchased from SLC (Shizuoka, Japan). The mice were euthanized and the embryos were isolated immediately. The embryonic age was 17.5 days. After washing twice with 0.1 M phosphate buffer, the embryos were frozen on dry-ice powder and stored at -80°C . Before sectioning, the

embryos were left for 30 min at -20°C . Frozen whole-body sagittal sections of the mouse embryo were sliced to a thickness of 8 μm using a cryostat (CM 1950; Leica Microsystems, Wetzlar, Germany). Sections were thaw-mounted onto an indium-tin-oxide (ITO)-coated glass slide (Bruker Daltonics) and dried at room temperature. The glass slide was cut to the proper size by a thin-layer chromatography (TLC) plate cutter (OM laboratory, Kanagawa, Japan) before thaw-mounting. The sections were placed in a polycarbonate tube and stored at -80°C until their analysis. An optimal cutting temperature (OCT) compound (Sakura Finetek, Torrance, CA) was used only to fix each mouse embryo body onto the support stand of the cryostat, and was not used for embedding the embryo body, because the residual polymer on the sections might have degraded the mass spectra. The sections were thawed in their tubes at room temperature for 20 min. A thin matrix layer was applied to the surface by a 0.2-mm nozzle caliber airbrush (Procon Boy FWA Platinum; Mr. Hobby, Tokyo, Japan). Spraying with 500 μL DHB matrix solution (50 mg/mL DHB in 70% methanol/0.1% TFA) was performed and each section was allowed to dry at room temperature. During spraying, the distance between the nozzle and the tissue surface was kept at 15 cm. After drying, the ITO-coated glass slide was adhered to an MS target plate with double-sided conductive adhesive tape to facilitate electrical conduction.

IMS System

A MALDI hybrid quadrupole TOF-type mass spectrometer (QSTAR XL; Applied Biosystems/MDS Sciex, Foster City, CA) equipped with an orthogonal MALDI source was used to acquire MALDI-MS and MALDI-MS/MS spectra. All analyses were performed in positive-ion and reflector modes after external calibration with human angiotensin II ($[\text{M} + \text{H}]^+$, m/z 1,046.54) and human bradykinin fragment 1–7 ($[\text{M} + \text{H}]^+$, m/z 757.40 Da). The laser shot was run at 100 Hz. The MS method was optimized on biological molecules on the tissue surface coated with DHB matrix to maximize the sensitivity of the tissue analysis. MALDI-MS spectra were obtained from an Nd:YAG laser per image spot with a 1 s accumulation time. The instrument is equipped with an oMALDI Server application. oMALDI Server version 4 includes a graphical user interface that allows the user to specify the area to be imaged and the step size between laser shots (lateral resolution). The oMALDI Server then directs the acquisition software (Analyst QS version 1.1) to acquire data, treating each laser spot as one sample in a batch run. Analyst QS allows the user to specify the instrument acquisition method to be used, the time to be accumulated in a spectrum, and the mass ranges of interest to monitor. As the profiles are being

acquired, the sample stage is moved from spot to spot, creating a raster of desorbed areas over the tissue surface. A spectrum is acquired at each spot, and the intensity of each signal from all of the mass ranges specified is stored in “wiff” format file. In the present study, when the “wiff” format file was converted to an “analyze” format file using the function of oMALDI Server version 5.1, the interval value of m/z was set to 0.2. The ion density maps were constructed by BioMap software (Novartis, Basel, Switzerland) and highlighted the signal intensities obtained from each area of interest within the tissue. The images from mouse whole-body sections were acquired from a raster scan with a step size of 200 μm . After raster-scanning, the section was soaked in 100% methanol for 30 s to wash off the DHB matrix and then stained with hematoxylin and eosin (H&E) for anatomical visualization. The optical images were taken with a microscope (LMD6000; Leica Microsystems) to adjust the ion images constructed by BioMap.

MS/MS analysis

In the MS/MS analysis, collisional activation of selected ions was carried out using the relative collision energy from 20 to 35 V with argon as the collision gas. The selectivity of precursor ions was increased by selecting a high mass selection mode. In the product-ion spectrum, when the fragment peaks were identical to the specific neutral loss (NL) of trimethylamine $[(\text{CH}_3)_3\text{N}]$ and/or the cyclophosphane ring $[(\text{CH}_2)_2\text{PO}_4\text{H}]$ and to specific ions of the headgroup $[(\text{CH}_3)_3\text{N}(\text{CH}_2)_2\text{PO}_4\text{H}]$ from LysoPtdCho and PtdCho and of each fatty acid from TAG, the m/z value of the precursor ion was transferred to the Lipid Search (http://lipidsearch.jp/manual_search/) and the Metabolite MS Search (<http://www.hmdb.ca/labm/jsp/mlims/MSDbParent.jsp>). These websites provide information on the carbons and unsaturated bonds included in LysoPtdCho, PtdCho, and TAG. In this study, to reveal the detailed composition of fatty acids, the NL of fatty acids from LysoPtdCho, PtdCho, and TAG was detected by MS/MS analysis.

Results

Mass Spectra Obtained from Mouse E17.5 Sections

After raster-scanning, the sections were stained with H&E (Fig. 1a). Eight organs were selected from the whole body and the name of each was indicated on the optical image (Fig. 1a). The spectra recorded for each of the organs are presented in the panels of Fig. 1 as follows: b, brain; c, brown adipose tissue; d, lung; e, liver; f, hypoglossitis; g,

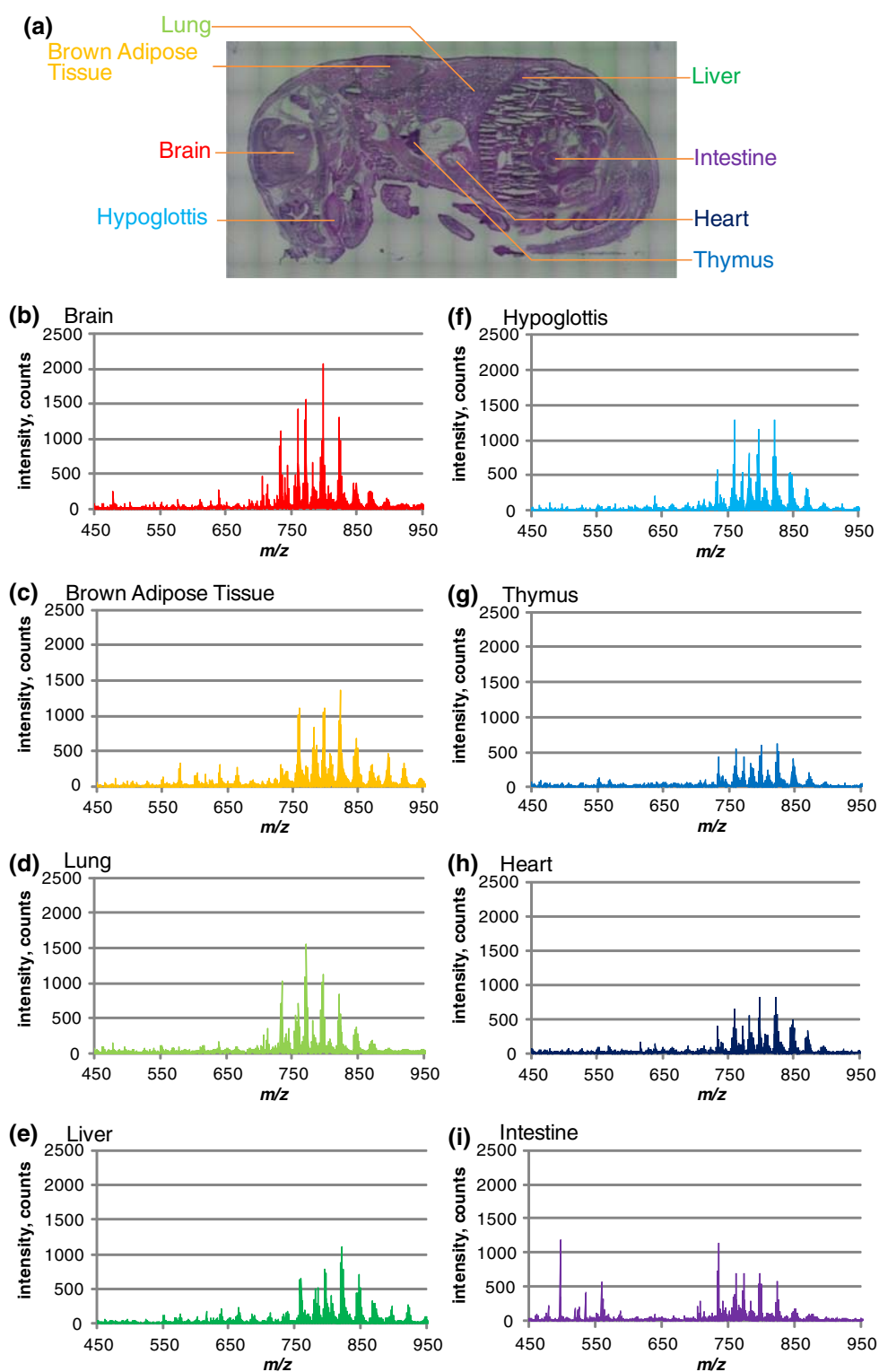
thymus; h, heart; i, intestine. The mass spectra were obtained from representative points in each organ using BioMap software, and displayed in the mass range of m/z 450–950. The intensity counts were highest in the spectrum of the brain (Fig. 1b). The spectrum in the intestine was different from the other spectra (Fig. 1i). The peaks detected from the intestine had higher intensities at m/z 490–570. In each organ, the top ten peaks with higher intensity were selected. The peaks were identified by MS/MS analysis to be revealed as major lipids. The representative molecular species are presented in Table 1. Although four peaks, m/z 558.25, 786.58, 794.46, and 846.48, could not be identified, we speculated that they were $[\text{LysoPtdCho (18:2) + K}]^+$, $[\text{PtdCho (18:1/18:1) + H}]^+$, $[\text{PtdCho (16:0/18:3) + K}]^+$, and $[\text{PtdCho (18:1/20:4) + K}]^+$, respectively, based on previous reports. In the results, almost all biomolecules were PtdCho and had at least one unsaturated fatty acid. There was only one PtdCho composed of two saturated fatty acids, i.e., PtdCho (16:0/16:0).

Distribution of LysoPtdCho and PtdCho

The product-ion spectra were obtained by MS/MS analysis (Fig. 2a, b). In the product-ion spectrum of m/z 496.33 (Fig. 2a), fragment peaks at m/z 184.08 and 313.28 were detected. In the MS/MS analyses for PtdCho and sphingomyelin (SM), a NL of 183 Da from a precursor peak was detected. The NL corresponds to the headgroup $(\text{CH}_3)_3\text{N}(\text{CH}_2)_2\text{PO}_4\text{H}$ of PtdCho and SM. So, the fragment peaks at m/z 184.08 and 313.28 correspond to $[(\text{CH}_3)_3\text{N}(\text{CH}_2)_2\text{PO}_4\text{H} + \text{H}]^+$ and an NL of 183 Da from a precursor peak, respectively. The product-ion spectrum even indicated peaks at m/z 104.11 and 125.00. These peaks correspond to $[(\text{CH}_3)_3\text{N}(\text{CH}_2)_2\text{O} + \text{H}]^+$ and $[(\text{CH}_2)_2\text{PO}_4\text{H} + \text{H}]^+$ from the headgroup, respectively. The m/z value of 496.33 is too small for PtdCho and SM because they are detected as the m/z value at the range of m/z 600–900. In addition, the ions of SM are detected as the odd number by the nitrogen rule. Therefore, the biomolecule may be LysoPtdCho. Moreover, the m/z value of 496.33 was retrieved from Lipid Search and we identified the biomolecule as $[\text{LysoPtdCho (16:0) + H}]^+$ from the results of the retrieval. In the same way, the peak at m/z 524.36 was identified as $[\text{LysoPtdCho (18:0) + H}]^+$. Although the NL of 183 Da does not appear in the MS/MS analysis of LysoPtdCho using electrospray-ionization MS, the spectrum in the MS/MS analysis of $[\text{LysoPtdCho (18:0) + H}]^+$ also showed the peak corresponding to the NL. Therefore the discrepancy was deemed to be due to the kind of ionization.

In the MS/MS analysis for m/z 782.59 (Fig. 2b), fragment peaks at m/z 599.52 and 723.51 were detected. PtdCho adducted with a cation often has these two fragment peaks

Fig. 1 Mass spectra obtained from mouse E17.5 sections. The analyzed section was stained with H&E: **a** the spectra recorded for each of the organs are presented in the panels as follows: **b** brain, **c** brown adipose tissue, **d** lung e liver, **f** hypoglottis, **g** thymus, **h** heart, and **i** intestine. The mass spectra were obtained from representative *points* in each organ using BioMap software, and displayed in the mass range of m/z 450–950



corresponding to NLs of 59 Da [trimethylamine, $(\text{CH}_3)_3\text{N}$] and 183 Da [headgroup, $(\text{CH}_3)_3\text{N}(\text{CH}_2)_2\text{PO}_4\text{H}$] from a precursor peak [50]. Because the two peaks from m/z 782.59

were also consistent with the NLs, the biomolecule is a PtdCho with a cation. The kind of cation adducted to a biomolecule is usually considered to be a sodium ion or a

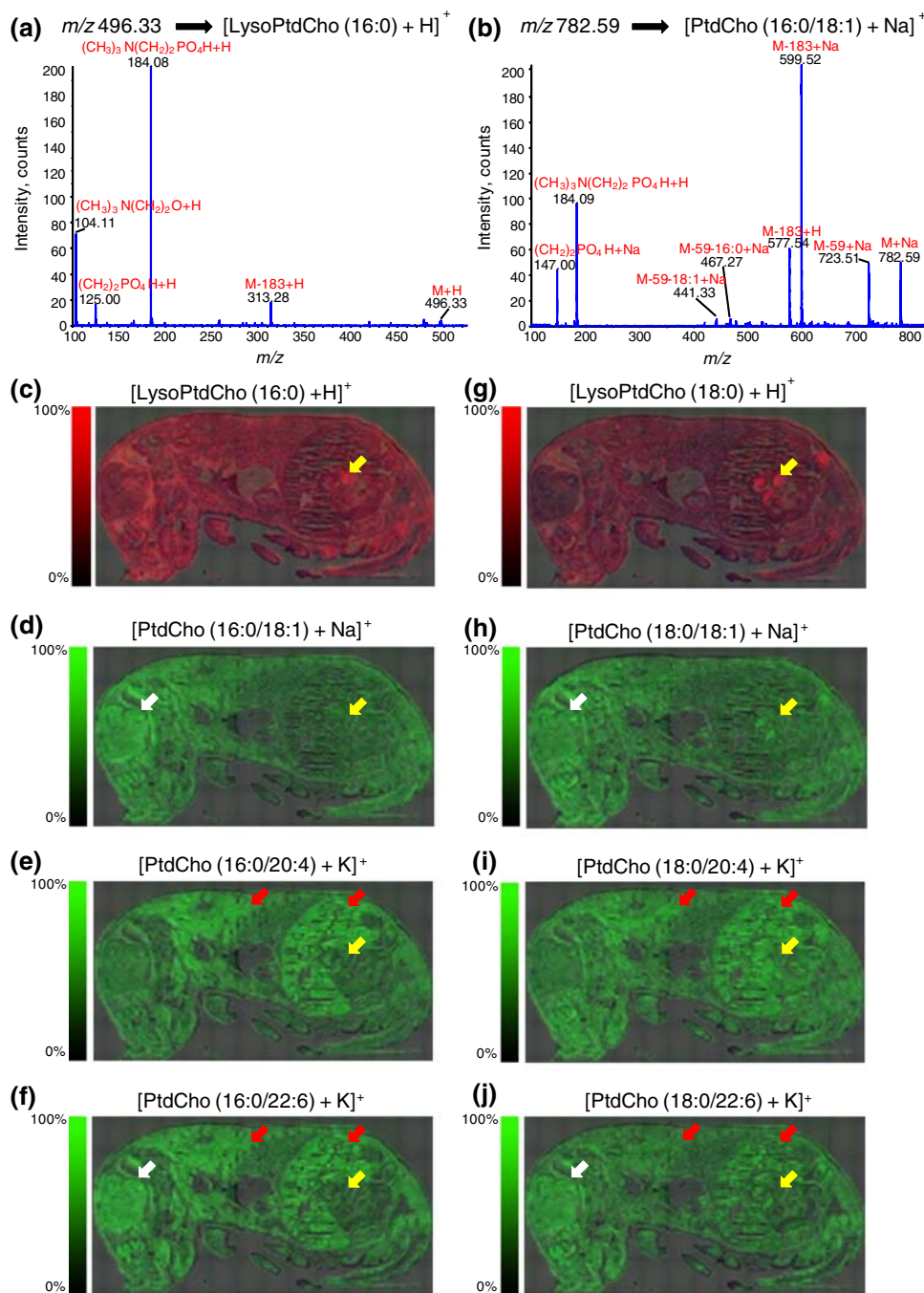
Table 1 The representative molecular species for the top ten peaks in each organ

Organ	Molecular species	Observed	Calculated	Error	Organ	Molecular species	Observed	Calculated	Error
Brain	PtdCho(16:0/18:1) + K	798.51	798.54	0.03	Hypoglossitis	PtdCho(16:0/18:1) + H	760.56	760.59	0.03
	PtdCho(16:0/16:0) + K	772.50	772.53	0.03		PtdCho(18:1/18:2) + K	822.49	822.54	0.05
	PtdCho(16:0/18:1) + H	760.56	760.59	0.03		PtdCho(16:0/18:1) + K	798.51	798.54	0.03
	PtdCho(18:1/18:2) + K	822.49	822.54	0.05		PtdCho(16:0/18:1) + Na	782.54	782.57	0.03
	PtdCho(16:0/16:1) + K	770.49	770.51	0.02		PtdCho(16:0/18:2) + K	796.49	796.53	0.04
	PtdCho(16:0/16:0) + H	734.55	734.57	0.02		PtdCho(16:0/20:4) + K	820.48	820.53	0.02
	PtdCho(16:0/18:2) + K	796.49	796.53	0.04		PtdCho(16:0/20:2) + K	824.50	824.46	0.04
	PtdCho(16:0/20:2) + K	824.50	824.46	0.04		PtdCho(16:0/18:2) + H	758.55	758.57	0.02
	PtdCho(16:0/16:1) + H	732.53	732.55	0.02		PtdCho(16:0/16:0) + H	734.55	734.57	0.02
	PtdCho(16:0/18:3) + K	794.46	794.51	0.05		PtdCho(16:0/16:0) + K	772.50	772.53	0.03
Brown adipose tissue	PtdCho(18:1/18:2) + K	822.49	822.54	0.05	Thymus	PtdCho(18:1/18:2) + K	822.49	822.54	0.05
	PtdCho(16:0/18:1) + H	760.56	760.59	0.03		PtdCho(16:0/18:1) + K	798.51	798.54	0.03
	PtdCho(16:0/18:1) + K	798.51	798.54	0.03		PtdCho(16:0/18:1) + H	760.56	760.59	0.03
	PtdCho(16:0/18:2) + K	796.49	796.53	0.04		PtdCho(16:0/20:2) + K	824.50	824.46	0.04
	PtdCho(16:0/18:2) + H	758.55	758.57	0.02		PtdCho(16:0/18:2) + K	796.49	796.53	0.04
	PtdCho(16:0/20:4) + K	820.48	820.53	0.05		PtdCho(16:0/16:0) + K	772.50	772.53	0.03
	PtdCho(16:0/20:2) + K	824.50	820.46	0.04		PtdCho(16:0/16:0) + H	734.55	734.57	0.02
	PtdCho(16:0/18:1) + Na	782.54	782.57	0.03		PtdCho(18:0/20:4) + K	848.51	848.57	0.06
	PtdCho(18:0/20:4) + K	848.51	848.57	0.06		PtdCho(16:0/20:4) + K	820.48	820.53	0.05
	PtdCho(18:1/18:1) + H	786.58	786.60	0.02		PtdCho(16:0/18:1) + Na	782.54	782.57	0.02
Lung	PtdCho(16:0/16:0) + K	772.50	772.53	0.03	Heart	PtdCho(18:1/18:2) + K	822.49	822.54	0.05
	PtdCho(16:0/18:1) + K	798.51	798.54	0.03		PtdCho(16:0/18:1) + K	798.51	798.54	0.03
	PtdCho(16:0/16:1) + K	770.49	770.51	0.02		PtdCho(16:0/18:1) + H	760.56	760.59	0.03
	PtdCho(16:0/16:0) + H	734.55	734.57	0.02		PtdCho(16:0/20:2) + K	824.50	824.46	0.04
	PtdCho(16:0/18:2) + K	796.49	796.53	0.04		PtdCho(16:0/18:1) + Na	782.54	782.57	0.03
	PtdCho(18:1/18:2) + K	822.49	822.54	0.05		PtdCho(16:0/20:4) + K	820.48	820.53	0.05
	PtdCho(16:0/18:1) + H	760.56	760.59	0.03		PtdCho(16:0/18:2) + K	796.49	796.53	0.04
	PtdCho(16:0/16:1) + H	732.53	732.55	0.02		PtdCho(18:0/20:4) + K	848.51	848.57	0.06
	PtdCho(16:0/18:3) + K	794.46	794.51	0.05		PtdCho(18:1/20:4) + K	846.49	846.54	0.05
	PtdCho(16:0/20:2) + K	824.50	820.46	0.04		PtdCho(16:0/16:0) + H	734.55	734.57	0.02
Liver	PtdCho(18:1/18:2) + K	822.49	822.54	0.05	Intestine	LysoPtdCho(16:0) + H	496.33	496.34	0.01
	PtdCho(16:0/20:4) + K	820.48	820.53	0.05		PtdCho(16:0/16:0) + H	734.55	734.57	0.02
	PtdCho(16:0/20:2) + K	824.50	820.46	0.04		PtdCho(16:0/16:1) + H	732.53	732.55	0.02
	PtdCho(16:0/18:2) + K	796.49	796.53	0.04		PtdCho(16:0/18:2) + K	796.49	796.53	0.04
	PtdCho(16:0/18:1) + K	798.51	798.54	0.03		PtdCho(16:0/16:0) + K	772.50	772.53	0.03
	PtdCho(18:0/20:4) + K	848.51	848.57	0.06		PtdCho(16:0/18:1) + H	760.56	760.59	0.03
	PtdCho(16:0/18:1) + H	760.56	760.59	0.03		PtdCho(18:1/18:2) + K	822.49	822.54	0.05
	PtdCho(16:0/18:2) + H	758.55	758.57	0.02		LysoPtdCho(18:2) + K	558.25	558.29	0.04
	PtdCho(18:1/18:1) + H	786.58	786.60	0.02		PtdCho(16:0/18:1) + K	798.51	798.54	0.03
	PtdCho(16:0/18:1) + Na	782.54	782.57	0.03		PtdCho(16:0/18:3) + K	794.46	794.51	0.05

potassium ion from the biological tissue. The product-ion spectrum of m/z 782.59 indicated peaks at m/z 577.54. The value of 577.54 is 21.98 away from 599.52. In the MS/MS analysis for PtdCho with a cation, such a characteristic fragment peak is often detected [12, 50]. The fragment peak is produced when a cation replaces a proton. In this case, the value of 21.98 Da was consistent with the replacement of a

sodium ion [molecular weight (MW) 23 Da] with a proton (MW 1 Da). This consideration is supported by the fact that the peak at m/z 147.00 corresponded to $[(\text{CH}_2)_2\text{PO}_4\text{H} + \text{Na}]^+$. The results of the retrieval from Lipid Search also indicated that the biomolecule is PtdCho (1-acyl 32:1). Moreover, there are two minor peaks, m/z 441.33 and 467.27, in the product-ion spectrum. We considered that

Fig. 2 Distributions of LysoPtdCho and PtdCho. The structural analyses of two peaks as respective biomolecules were performed. The product-ion spectra from **a** m/z 496.33 and **b** m/z 782.59 as precursor ions were obtained by MS/MS analyses on a mouse embryonic section. Their biomolecules were identified by the production and the neutral loss as follows: **a** [LysoPtdCho (16:0) + H]⁺ and **b** [PtdCho (16:0/18:1) + Na]⁺. In the same way, six more biomolecules were identified. The ion images constructed from the peaks showed the distribution of biomolecules as a relative difference in signals detected in the mouse embryo: **c** [LysoPtdCho (16:0) + H]⁺, **d** [PtdCho (16:0/18:1) + Na]⁺, **e** [PtdCho (16:0/20:4) + K]⁺, **f** [PtdCho (16:0/22:6) + K]⁺, **g** [LysoPtdCho (18:0) + H]⁺, **h** [PtdCho (18:0/18:1) + Na]⁺, **i** [PtdCho (18:0/20:4) + K]⁺, and **j** [PtdCho (18:0/22:6) + K]⁺. The ion images were merged with the optical image of a section stained with H&E



these peaks were consistent with NLs of (59 + 282 Da) and (59 + 256 Da) from the precursor peak. The values of 282 and 256 Da corresponded to fatty acids 18:1 and 16:0. There are many lipids in the range of m/z 700–850. Our IMS system, which directly detects the ions on the biological tissue, cannot separate the peak completely and the productions are not sufficiently abundant. However, we could identify each lipid as a major biomolecule by MS/MS analysis. In general, saturated fatty acids are esterified at the *sn*-1 position while unsaturated fatty acids are esterified at

the *sn*-2 position [51, 52]. We determined *sn*-1 and *sn*-2 positions based on previous works. Therefore, in this experiment, we identified the biomolecule of m/z 782.59 as [PtdCho (16:0/18:1) + Na]⁺. In the same way, the peaks at m/z 810.4, 820.48, 844.48, 848.51, and 872.50 were identified as [PtdCho (18:0/18:1) + Na]⁺, [PtdCho (16:0/20:4) + K]⁺, [PtdCho (16:0/22:6) + K]⁺, [PtdCho (18:0/20:4) + K]⁺, and [PtdCho (18:0/22:6) + K]⁺.

We constructed the ion image from the peaks identified as above on the embryonic section using the BioMap

software (Fig. 2c–j). The ion images showed the relative difference of signals detected on the mouse embryonic section. The ion images of LysoPtdCho (16:0) and LysoPtdCho (18:0) showed that both biomolecules were distributed throughout the body, and were especially prominent in the intestines (yellow arrows in Fig. 2c, g). The ion images of PtdCho (16:0/18:1) (Fig. 2d), PtdCho (16:0/20:4) (Fig. 2e), and PtdCho (16:0/22:6) (Fig. 2f), which have the same fatty acid of 16:0 at *sn*-1, indicated a specific disappearance in the intestine (yellow arrows in Fig. 2d–f). In the same way, the specific distribution of LysoPtdCho (18:0) (Fig. 2g) was also compared with the distributions of PtdCho (18:0/18:1) (Fig. 2h), PtdCho (18:0/20:4) (Fig. 2i), and PtdCho (18:0/22:6) (Fig. 2j). All four molecules had similar distributions in the intestines (yellow arrows in Fig. 2g–j).

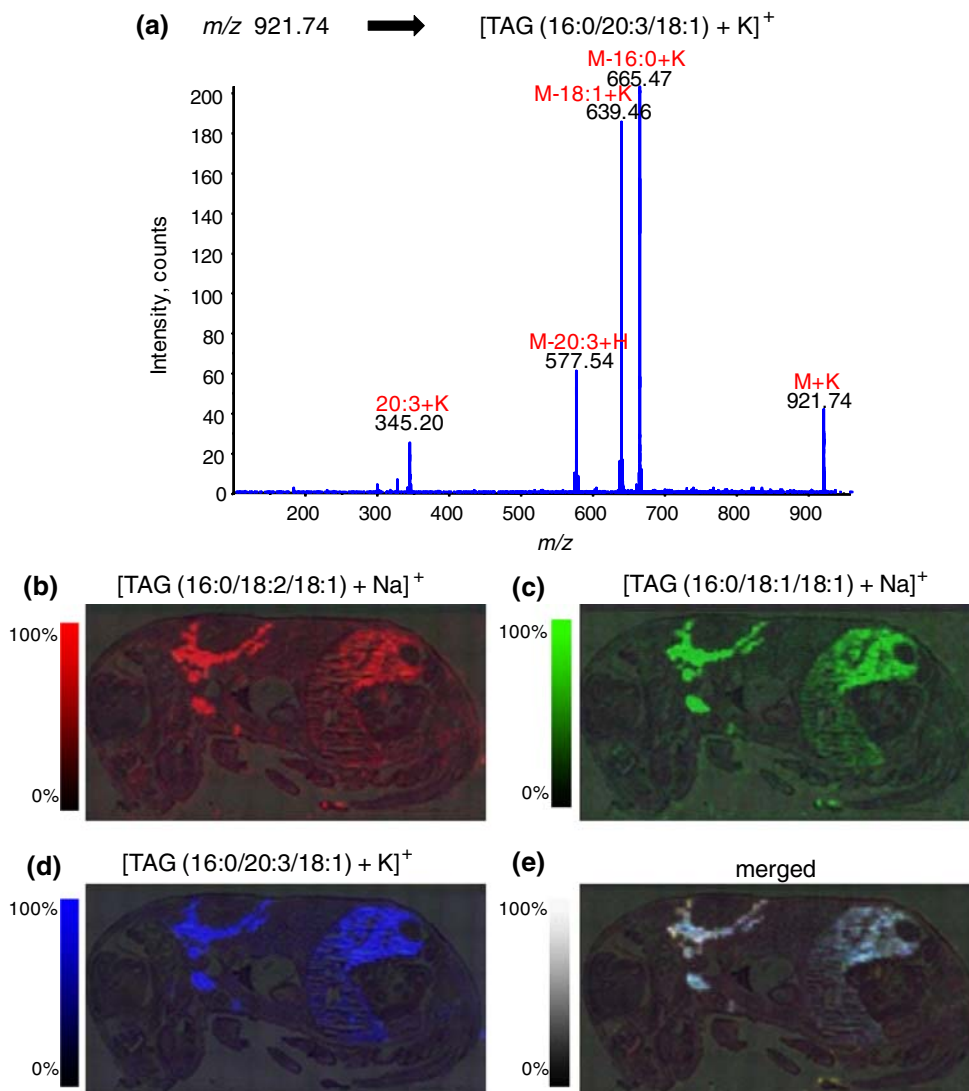
There was heterogeneity of the distribution among PtdCho. PtdCho (16:0/18:1) and PtdCho (16:0/22:6) were

strongly distributed in the brain (white arrows in Fig. 2d, f). PtdCho (16:0/20:4) and PtdCho (16:0/22:6) were distributed around brown adipose tissue and in the liver (red arrows in Fig. 2e, f). Similarly, PtdCho with the same fatty acid at *sn*-2, such as PtdCho (16:0/18:1) and PtdCho (18:0/18:1), showed the same distribution (white arrows in Fig. 2d, h).

Distribution of TAG

The product-ion spectrum of m/z 921.74 was markedly different from the other spectra that were identified as LysoPtdCho and PtdCho (Fig. 3a). The major peaks were m/z 639.46 and 665.47, which corresponded to NLs of 282 Da (18:1) and 256 Da (16:0) from a precursor ion. These NLs have been reported [53] and are characteristic of the MS/MS analysis for TAG. Moreover, there are two abundant peaks, m/z 345.20 and 577.54, in the product-ion

Fig. 3 Distribution of TAG. The structural analysis of one peak was performed. The product-ion spectrum from **a** m/z 921.74 as a precursor ion was obtained by MS/MS analysis on a mouse embryonic section. The biomolecules were identified by neutral loss as TAG (16:0/20:3/18:1). In the same way, two more biomolecules were identified. The ion images constructed from the peaks showed the distribution of biomolecules on the mouse embryo: **b** [TAG (16:0/18:2/18:1) + Na]⁺, **c** [TAG (16:0/18:1/18:1) + Na]⁺, and **d** [TAG (16:0/20:3/18:1) + K]⁺. The ion images were merged with the optical image of a section stained with H&E. The three merged TAG images demonstrate the same distribution



spectrum. We considered that these peaks were consistent with the ion of $[20:3 + K]^+$ and NL of 344.20 Da from the precursor ion. The product-ion reflecting neutral loss of the *sn*-2 fatty acid substituent was less abundant than the corresponding ions reflecting such losses of either *sn*-1 or the *sn*-3 fatty acid substituent [54]. Therefore, we identified this biomolecule as $[TAG (16:0/20:3/18:1) + K]^+$. In the same way, the peaks at *m/z* 879.72 and 881.74 were identified as $[TAG (16:0/18:2/18:1) + Na]^+$ and $[TAG (16:0/18:1/18:1) + Na]^+$. Three ion images of TAG demonstrated the same distribution, which is illustrated by the merged image (Fig. 3b–e).

Discussion

In this study, we aimed to identify and visualize biomolecules in the mouse embryo. E17.5 embryo was chosen because the embryonic organs are highly similar to those of adult mice at this age. Since different organs should be compared in the same slide, we can visualize all the tissues at the same time. Late stage of embryo is suitable for this purpose. We are also able to obtain detailed information about the identity and distribution of embryonic metabolites, which can be compared with those of adults. The ion image constructed from the peaks is often merged with the optical image to reveal the detailed distribution of biomolecules in IMS. This method was also used in the present study: all sections analyzed by IMS were stained, and the optical images were merged with the ion images (Figs. 2c–j, 3b–e).

Whole-body sections were prepared from a mouse E17.5, and raster-scanned by a QSTAR XL system. The spectra recorded for each of the organs are presented in the panels of Fig. 1b–i. The intensity counts in the mass spectra obtained from representative points in each organ indicated the abundance of PLs in the brain (Fig. 1b). Therefore, the intensity counts which we detected in the brain are reasonable. However, the characteristic spectrum was detected in intestine (Fig. 1i). The peaks had higher intensities at the range of low molecules. The results of MS/MS analyses indicated that some of the low molecule was LysoPtdCho (Fig. 2a and Table 1). Moreover, the ion images of LysoPtdCho (16:0) and LysoPtdCho (18:0) showed that both biomolecules were especially prominent in the intestines (yellow arrows in Fig. 2c, g). It is known that PLs are hydrolyzed to lyso-PLs with any phospholipase. The detected peaks suggest that the enzyme exists and acts in the intestine. LysoPtdCho is produced by the hydrolysis of PtdCho with an enzyme such as PLA2 and is changed to lysophosphatidic acid (LPA) by an enzyme such as lysophospholipase D (LPLD) [55]. These results

imply two different aspects. One is that most PLA2 acted on PtdCho at this location because PLA2, especially pancreatic PLA2, is prominent in the intestines. However, the ion images of PtdCho did not show the specific disappearance in the intestine (Fig. 2d–f). Therefore, we thought that the increase of LysoPtdCho in the intestine was not dependent on the nonspecific action of pancreatic PLA2. Another is that LPLD activity was lower in the intestines and LysoPtdCho accumulated before changing to LPA. Anyway, IMS enabled us to screen the distribution of LysoPtdCho as well as PtdCho.

The distribution among PtdCho indicated heterogeneity (Fig. 2d–f, h–j). These results suggest that the fatty acids at *sn*-2 play specific roles in the normal development and function of each organ. Both fatty acids of 20:4 (ARA) and 22:6 (DHA) were minor species in this study. However, these fatty acids are important structural components of membrane PLs and are required for normal development. Deficiencies in these fatty acids result in abnormal development and several diseases [41, 44, 56]. For example, the amount and composition of fatty acids are controlled precisely; complete loss of fatty acid synthesis results in early embryonic lethality [57]. Therefore, we thought that the detection of these fatty acids by IMS analysis would be more useful for many researchers.

In a previous report, TAG was identified by its exact *m/z* value, without MS/MS analysis [21]. In addition, Murphy et al. [58] visualized the peak at *m/z* 879.7 on the mouse kidney section and identified the peak as $[TG (16:0/20:4/18:1) + H]^+$ in their previous report [59], which revealed product-ions at *m/z* 623.5, 597.5, and 575.5 from the extraction of RAW 264.7 cells using electrospray mass spectrometry. However, since there are numerous lipids in the mass range of *m/z* 700–1,000 and the main composition of fatty acids is different for a biological sample, it is preferable that MS/MS analysis be performed for the same kind of sample. Thus, we proved that the identification can be performed fairly accurately by detecting the NLs of fatty acids in the product-ion spectrum for TAG on the whole-body mouse embryonic sections, which produce specific signals (Fig. 3a).

We demonstrated the merged image from three ion images of TAG (Fig. 3b–d). This merged image showed a distinctly different distribution from the LysoPtdCho and PtdCho images (Fig. 3d). It is clear from the image merged with the optical image stained with H&E that the distribution was localized around brown adipose tissue and in the liver. Intriguingly, the signals hardly existed in other areas. Moreover, the image merged from the distribution of three TAG highlighted the complete correspondence of their distributions (Fig. 3e). This fascinating localization pattern probably reflects functional difference of each TAG

during embryogenesis, which was not established by conventional methods.

Thus, we identified and visualized the lipid species in a mouse embryo with a MALDI hybrid quadrupole TOF-based IMS system. The IMS system detected a number of peaks in the analysis of the whole embryonic sections, and the spectra were different in each organ. Eleven specific peaks were analyzed with MS/MS analyses. The biomolecules were identified as LysoPtdCho (16:0), LysoPtdCho (18:0), PtdCho (16:0/18:1), PtdCho (16:0/20:4), PtdCho (16:0/22:6), PtdCho (18:0/18:1), PtdCho (18:0/20:4), PtdCho (18:0/22:6), TAG (16:0/18:1/18:1), TAG (16:0/18:2/18:1), and TAG (16:0/20:3/18:1). In addition, the ion images constructed from the peaks of the biomolecules showed their distribution in the whole body. Interestingly, the distributions of the three PtdCho were different from one another, which is dependent on the fatty acid at *sn*-2. In contrast, the distributions of TAG were the same, with a predominance around the brown adipose tissue and in the liver. TAG might accumulate in such organs to maintain body temperature or to supply TAG for other organs. This is the first successful visualization of LysoPtdCho and TAG localization in the embryonic stage of a mammal using an IMS system based on MALDI hybrid quadrupole TOF. In the future, this method will help to combine developmental biology and lipid research.

Acknowledgments We are grateful to Masako Suzuki (Hamamatsu University School of Medicine) for technical support with the operation of the QSTAR XL system. This work was supported by a Grant-in-Aid for SENTAN from the Japan Science and Technology Agency (to M.S.) and a Grant-in-Aid for Young Scientists B (to T.H.).

References

- Kiep L, Burkhardt J, Seifert K (2008) Drug metabolism studies with the incubated hen's egg. Identification of 2,3,5-trihydroxybenzoic acid as a metabolite of gentisic acid. *Arzneimittelforschung* 58:469–474
- Ikegami K, Heier RL, Taruishi M, Takagi H, Mukai M, Shimma S, Taira S, Hatanaka K, Morone N, Yao I, Campbell PK, Yuasa S, Janke C, Macgregor GR, Setou M (2007) Loss of alpha-tubulin polyglutamylation in ROSA22 mice is associated with abnormal targeting of KIF1A and modulated synaptic function. *Proc Natl Acad Sci USA* 104:3213–3218
- Yao I, Takagi H, Ageta H, Kahyo T, Sato S, Hatanaka K, Fukuda Y, Chiba T, Morone N, Yuasa S, Inokuchi K, Ohtsuka T, Macgregor GR, Tanaka K, Setou M (2007) Scrapper-dependent ubiquitination of active zone protein RIM1 regulates synaptic vesicle release. *Cell* 130:943–957
- Matsumoto M, Setou M, Inokuchi K (2007) Transcriptome analysis reveals the population of dendritic RNAs and their redistribution by neural activity. *Neurosci Res* 57:411–423
- Gobert GN, Jones MK (2008) Discovering new schistosome drug targets: the role of transcriptomics. *Curr Drug Targets* 9:922–930
- Setou M, Nakagawa T, Seog DH, Hirokawa N (2000) Kinesin superfamily motor protein KIF17 and mLin-10 in NMDA receptor-containing vesicle transport. *Science* 288:1796–1802
- Ahnfelt-Ronne J, Jorgensen MC, Hald J, Madsen OD, Serup P, Hecksher-Sorensen J (2007) An improved method for three-dimensional reconstruction of protein expression patterns in intact mouse and chicken embryos and organs. *J Histochem Cytochem* 55:925–930
- Setou M, Seog DH, Tanaka Y, Kanai Y, Takei Y, Kawagishi M, Hirokawa N (2002) Glutamate-receptor-interacting protein GRIP1 directly steers kinesin to dendrites. *Nature* 417:83–87
- Popova E, Rentsch B, Bader M, Krivokharchenko A (2008) Generation and characterization of a GFP transgenic rat line for embryological research. *Transgenic Res* 17:955–963
- Kitamura Y, Okazaki T, Nagatsuka Y, Hirabayashi Y, Kato S, Hayashi K (2007) Immunohistochemical distribution of phosphatidylglucoside using anti-phosphatidylglucoside monoclonal antibody (DIM21). *Biochem Biophys Res Commun* 362:252–255
- Shimma S, Sugiura Y, Hayasaka T, Zaima N, Matsumoto M, Setou M (2008) Mass imaging and identification of biomolecules with MALDI-QIT-TOF-based system. *Anal Chem* 80:878–885
- Hayasaka T, Goto-Inoue N, Sugiura Y, Zaima N, Nakanishi H, Ohishi K, Nakanishi S, Naito T, Taguchi R, Setou M (2008) Matrix-assisted laser desorption/ionization quadrupole ion trap time-of-flight (MALDI-QIT-TOF)-based imaging mass spectrometry reveals a layered distribution of phospholipid molecular species in the mouse retina. *Rapid Commun Mass Spectrom* 22:3415–3426
- Woods AS, Jackson SN (2006) Brain tissue lipidomics: direct probing using matrix-assisted laser desorption/ionization mass spectrometry. *AAPS J* 8:E391–395
- Groseclose MR, Andersson M, Hardesty WM, Caprioli RM (2007) Identification of proteins directly from tissue: in situ tryptic digestions coupled with imaging mass spectrometry. *J Mass Spectrom* 42:254–262
- Goto-Inoue N, Hayasaka T, Sugiura Y, Taki T, Li YT, Matsumoto M, Setou M (2008) High-sensitivity analysis of glycosphingolipids by matrix-assisted laser desorption/ionization quadrupole ion trap time-of-flight imaging mass spectrometry on transfer membranes. *J Chromatogr B Analyt Technol Biomed Life Sci* 870:74–83
- Sugiura Y, Shimma S, Konishi Y, Yamada MK, Setou M (2008) Imaging mass spectrometry technology and application on ganglioside study; visualization of age-dependent accumulation of C20-ganglioside molecular species in the mouse hippocampus. *PLoS One* 3:e3232
- Tanaka K, Waki H, Ido Y, Akita S, Yoshida Y, Yoshida T, Matsuo T (1988) Protein and polymer analyses up to *m/z* 100,000 by laser ionization time-of-flight mass spectrometry. *Rapid Commun Mass Spectrom* 2:151–153
- Karas M, Hillenkamp F (1988) Laser desorption ionization of proteins with molecular masses exceeding 10,000 daltons. *Anal Chem* 60:2299–2301
- Hillenkamp F, Karas M, Beavis RC, Chait BT (1991) Matrix-assisted laser desorption/ionization mass spectrometry of biopolymers. *Anal Chem* 63:1193A–1203A
- Kaufmann R, Spengler B, Lutzenkirchen F (1993) Mass spectrometric sequencing of linear peptides by product-ion analysis in a reflectron time-of-flight mass spectrometer using matrix-assisted laser desorption ionization. *Rapid Commun Mass Spectrom* 7:902–910
- Touboul D, Brunelle A, Halgand F, De La Porte S, Laprevote O (2005) Lipid imaging by gold cluster time-of-flight secondary ion mass spectrometry: application to Duchenne muscular dystrophy. *J Lipid Res* 46:1388–1395

22. Northen TR, Yanes O, Northen MT, Marrinucci D, Uritboonthai W, Apon J, Golledge SL, Nordstrom A, Siuzdak G (2007) Clathrate nanostructures for mass spectrometry. *Nature* 449:1033–1036
23. Chaurand P, Latham JC, Lane KB, Mobley JA, Polosukhin VV, Wirth PS, Nanney LB, Caprioli RM (2008) Imaging mass spectrometry of intact proteins from alcohol-preserved tissue specimens: bypassing formalin fixation. *J Proteome Res* 7:3543–3555
24. Seeley EH, Oppenheimer SR, Mi D, Chaurand P, Caprioli RM (2008) Enhancement of protein sensitivity for MALDI imaging mass spectrometry after chemical treatment of tissue sections. *J Am Soc Mass Spectrom* 19:1069–1077
25. Broersen A, van Liere R, Altelaar AF, Heeren RM, McDonnell LA (2008) Automated, feature-based image alignment for high-resolution imaging mass spectrometry of large biological samples. *J Am Soc Mass Spectrom* 19:823–832
26. Baluya DL, Garrett TJ, Yost RA (2007) Automated MALDI matrix deposition method with inkjet printing for imaging mass spectrometry. *Anal Chem* 79:6862–6867
27. Wiseman JM, Ifa DR, Zhu Y, Kissinger CB, Manicke NE, Kissinger PT, Cooks RG (2008) Special feature: desorption electrospray ionization mass spectrometry: imaging drugs and metabolites in tissues. *Proc Natl Acad Sci USA* 105:18120–18125
28. Burnum KE, Tranguch S, Mi D, Daikoku T, Dey SK, Caprioli RM (2008) Imaging mass spectrometry reveals unique protein profiles during embryo implantation. *Endocrinology* 149:3274–3278
29. Shimma S, Furuta M, Ichimura K, Yoshida Y, Setou M (2006) A novel approach to in situ proteome analysis using a chemical inkjet printing technology and MALDI-QIT-TOF tandem mass spectrometer. *Surf Int Anal* 38:1712–1714
30. Sugiura Y, Shimma S, Setou M (2006) Thin sectioning improves the peak intensity and signal-to-noise ratio in direct tissue mass spectrometry. *J Mass Spectrom Soc Jpn* 54:45–48
31. Sugiura Y, Shimma S, Setou M (2006) Two-step matrix application technique to improve ionization efficiency for matrix-assisted laser desorption/ionization in imaging mass spectrometry. *Anal Chem* 78:8227–8235
32. Taira S, Sugiura Y, Moritake S, Shimma S, Ichiyangi Y, Setou M (2008) Nanoparticle-assisted laser desorption/ionization based mass imaging with cellular resolution. *Anal Chem* 80:4761–4766
33. Hosokawa N, Sugiura Y, Setou M (2008) Spectrum normalization method with external standard in mass spectrometric imaging (MSI). *J Mass Spectrom Soc Jpn* 56:77–81
34. Norris JL, Cornett DS, Mobley JA, Andersson M, Seeley EH, Chaurand P, Caprioli RM (2007) Processing MALDI mass spectra to improve mass spectral direct tissue analysis. *Int J Mass Spectrom* 260:212–221
35. Setou M, Hayasaka T, Shimma S, Sugiura Y, Matsumoto M (2008) Protein denaturation improves enzymatic digestion efficiency for direct tissue analysis using mass spectrometry. *Surf Int Anal* 255:1555–1559
36. Shimma S, Sugiura Y, Hayasaka T, Hoshikawa Y, Noda T, Setou M (2007) MALDI-based imaging mass spectrometry revealed abnormal distribution of phospholipids in colon cancer liver metastasis. *J Chromatogr B Analyt Technol Biomed Life Sci* 855:98–103
37. Shimma S, Setou M (2007) Mass microscopy to reveal distinct localization of heme B (m/z 616) in colon cancer liver metastasis. *J Mass Spectrom Soc Jpn* 55:145–148
38. Chaurand P, Cornett DS, Caprioli RM (2006) Molecular imaging of thin mammalian tissue sections by mass spectrometry. *Curr Opin Biotechnol* 17:431–436
39. Yao I, Sugiura Y, Matsumoto M, Setou M (2008) In situ proteomics with imaging mass spectrometry and principal component analyses in the Scrapper-Knockout mouse brain. *Proteomics* 8:3692–3701
40. Khatib-Shahidi S, Andersson M, Herman JL, Gillespie TA, Caprioli RM (2006) Direct molecular analysis of whole-body animal tissue sections by imaging MALDI mass spectrometry. *Anal Chem* 78:6448–6456
41. Novak EM, Dyer RA, Innis SM (2008) High dietary omega-6 fatty acids contribute to reduced docosahexaenoic acid in the developing brain and inhibit secondary neurite growth. *Brain Res* 1237:136–145
42. Rousseau D, Helies-Toussaint C, Raederstorff D, Moreau D, Grynberg A (2001) Dietary n-3 polyunsaturated fatty acids affect the development of renovascular hypertension in rats. *Mol Cell Biochem* 225:109–119
43. Farkas K, Ratchford IA, Noble RC, Speake BK (1996) Changes in the size and docosahexaenoic acid content of adipocytes during chick embryo development. *Lipids* 31:313–321
44. Innis SM, Friesen RW (2008) Essential n-3 fatty acids in pregnant women and early visual acuity maturation in term infants. *Am J Clin Nutr* 87:548–557
45. Alessandri JM, Goussard B, Guesnet P, Durand G (1998) Docosahexaenoic acid concentrations in retinal phospholipids of piglets fed an infant formula enriched with long-chain polyunsaturated fatty acids: effects of egg phospholipids and fish oils with different ratios of eicosapentaenoic acid to docosahexaenoic acid. *Am J Clin Nutr* 67:377–385
46. Kahn-Kirby AH, Dantzer JL, Apicella AJ, Schafer WR, Browne J, Bargmann CI, Watts JL (2004) Specific polyunsaturated fatty acids drive TRPV-dependent sensory signaling in vivo. *Cell* 119:889–900
47. Choy PC, Tran K, Hatch GM, Kroeger EA (1997) Phospholipid metabolism in the mammalian heart. *Prog Lipid Res* 36:85–101
48. Kinnaird AA, Choy PC, Man RY (1988) Lysophosphatidylcholine accumulation in the ischemic canine heart. *Lipids* 23:32–35
49. Hirano K, Ikeda Y, Zaima N, Sakata Y, Matsumiya G (2008) Triglyceride deposit cardiomyovascularopathy. *N Engl J Med* 359:2396–2398
50. Hsu FF, Turk J (2003) Electrospray ionization/tandem quadrupole mass spectrometric studies on phosphatidylcholines: the fragmentation processes. *J Am Soc Mass Spectrom* 14:352–363
51. Amate L, Ramirez M, Gil A (1999) Positional analysis of triglycerides and phospholipids rich in long-chain polyunsaturated fatty acids. *Lipids* 34:865–871
52. Yang LY, Kuksis A, Myher JJ, Steiner G (1995) Origin of triacylglycerol moiety of plasma very low density lipoproteins in the rat: structural studies. *J Lipid Res* 36:125–136
53. Al-Saad KA, Zabrouskov V, Siems WF, Knowles NR, Hannan RM, Hill HH Jr (2003) Matrix-assisted laser desorption/ionization time-of-flight mass spectrometry of lipids: ionization and prompt fragmentation patterns. *Rapid Commun Mass Spectrom* 17:87–96
54. Hsu FF, Turk J (1999) Structural characterization of triacylglycerols as lithiated adducts by electrospray ionization mass spectrometry using low-energy collisionally activated dissociation on a triple stage quadrupole instrument. *J Am Soc Mass Spectrom* 10:587–599
55. Allenmark S, Sjobahl E, Sjobahl R, Tagesson C (1980) Purification of an enzyme with lysophospholipase activity from rat intestinal mucosa by hydrophobic chromatography. *Prep Biochem* 10:463–471
56. Burdge GC, Slater-Jefferies JL, Grant RA, Chung WS, West AL, Lillycrop KA, Hanson MA, Calder PC (2008) Sex, but not maternal protein or folic acid intake, determines the fatty acid composition of hepatic phospholipids, but not of triacylglycerol, in adult rats. *Prostaglandins Leukot Essent Fatty Acids* 78:73–79

57. Chirala SS, Chang H, Matzuk M, Abu-Elheiga L, Mao J, Mahon K, Finegold M, Wakil SJ (2003) Fatty acid synthesis is essential in embryonic development: fatty acid synthase null mutants and most of the heterozygotes die in utero. *Proc Natl Acad Sci USA* 100:6358–6363
58. Murphy RC, Hankin JA, Barkley RM (2008) Imaging of lipid species by MALDI mass spectrometry. *J Lipid Res*
59. McAnoy AM, Wu CC, Murphy RC (2005) Direct qualitative analysis of triacylglycerols by electrospray mass spectrometry using a linear ion trap. *J Am Soc Mass Spectrom* 16:1498–1509

Four New Fatty Acid Esters from the Feces of *Trogopterus xanthipes*

Nian-Yun Yang · Wei-Wei Tao · Jin-Ao Duan ·
Jian-Ming Guo · Ling-Ling Cao

Received: 29 May 2009 / Accepted: 13 July 2009 / Published online: 1 August 2009
© AOCS 2009

Abstract Four new fatty acid esters have been isolated from Feces *Trogopterus*. Their structures were determined by spectroscopic and chemical methods to be bis(7-hydroxyheptyl) icosanedioate (**1**), bis(7-hydroxyheptyl) heptadecanedioate (**2**), bis(7-hydroxyheptyl) decanedioate (**3**), and bis(7-hydroxyheptyl) octanedioate (**4**). In the anticoagulative assay, compounds **3** and **4** had significant antithrombin activity.

Keywords Feces *Trogopterus* · Fatty acid ester · Antithrombin activity

Abbreviations

COSY	Correlation spectroscopy
ESI	Electrospray ionization
FAME	Fatty acid methyl ester
HMBC	Heteronuclear multiple bond correlation
HMQC	Heteronuclear multiple quantum correlation
HR	High resolution
IR	Infrared
MS	Mass spectrometry
NMR	Nuclear magnetic resonance
Tris	Trishydroxymethylaminomethane
TT	Thrombin time

Introduction

Feces *Trogopterus*, called “Wulingzhi”, are the dry excrement of *Trogopterus xanthipes* Milne-Edwards (Petauristidae).

Feces *Trogopterus* promote blood circulation and remove stasis, and in traditional Chinese medicine are often used for treatment of amenorrhea, dysmenorrhea, menses pain, and retained lochia due to stasis. The literature reports that the chemical constituents of Feces *Trogopterus* are mainly terpenoids, phenolic acids, and sterols, and these have the pharmacological activity of anticoagulation, enhancing immunity, and anti-inflammation [1]. Different solvent extracts of Feces *Trogopterus* were screened in our current study, which showed that the ethyl acetate extract was the important active part. The ethyl acetate extract was, therefore, investigated chemically and contained four new fatty acid esters. Fatty alcohols, fatty acids, and their esters are important lipid compounds reported to have many biological and pharmacological functions, including inhibiting cholesterol synthesis, increasing low-density lipoprotein processing, and anti-thrombosis and anti-platelet aggregation activity [2–4]. In this study we deal with the isolation and structure elucidation of four new fatty acid esters, bis(7-hydroxyheptyl) icosanedioate (**1**), bis(7-hydroxyheptyl) heptadecanedioate (**2**), bis(7-hydroxyheptyl) decanedioate (**3**), and bis(7-hydroxyheptyl) octanedioate (**4**), and a new natural product, bis(7-hydroxyheptyl) hexanedioate (**5**) (Fig. 1), and report some of their anticoagulative activity. Their structures were elucidated by means of chemical and extensive spectroscopic analysis.

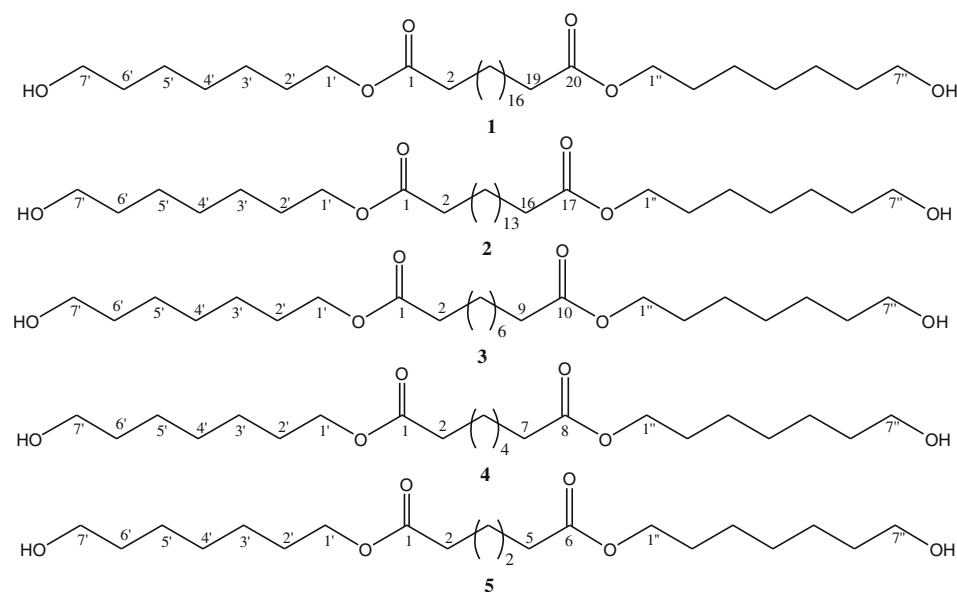
Materials and Methods

General Experimental Procedures

Melting points were determined with a WRS-IB melting point apparatus (Shanghai Precision and Scientific Instrument, Shanghai, P.R. China) and are uncorrected. Optical

N.-Y. Yang · W.-W. Tao · J.-A. Duan (✉) · J.-M. Guo ·
L.-L. Cao
Jiangsu Key Laboratory for TCM Formulae Research,
Nanjing University of Traditional Chinese Medicine,
Nanjing 210046, People's Republic of China
e-mail: duanja@163.com

Fig. 1 Chemical structures of compounds **1–5**



rotation was measured on a Perkin–Elmer 341 polarimeter. IR spectra were taken on a Nicolet IR-100 FT-IR spectrometer in KBr discs. NMR spectra were measured on a Bruker AV-500 MHz (500 MHz for ^1H NMR and 125 MHz for ^{13}C NMR), using TMS as internal standard; chemical shifts were recorded as δ values. ESI-MS and HR-ESI-MS spectra were obtained on a Micromass Q/TOF mass spectrometer. Anticoagulative assay was performed on an LG-PABER-I coagulation-analysis instrument. The blood sample was treated on an Anke TDL-40B centrifuge.

Materials and Chemicals

Feces Trogopterus were collected in June 2008 from Hebei province of China, and identified as the dry feces of *T. xanthipes* by Associate Professor Nianyun Yang of Nanjing University of Traditional Chinese Medicine. A voucher specimen (GS-20080610) was kept in the Herbarium of Nanjing University of Traditional Chinese Medicine.

Silica gel for column chromatography (CC) (200–300 mesh) and TLC plates (10–40 μm) were the products of Qingdao Marine Chemical (Qingdao, P.R. China). All solvents used were of analytical grade (Nanjing Chemical Plant, Nanjing, P.R. China). Thrombin was purchased from Xisen Sanhe (Leling, P.R. China). Trishydroxymethylaminomethane (Tris) was the product of Shanghai Jingxi Chemical Industry (Shanghai, P.R. China). Sodium citrate was purchased from Shanghai Lingfeng Chemical Reagent (Shanghai, P.R. China). Heparin sodium (biotech grade, 150 U mg^{-1}) was purchased from Amresco (Solon, USA). A rabbit (3.8 kg) was supplied by Shanghai Sikelai Experimental Animal (Shanghai, P.R. China).

Extraction and Isolation

Air-dried and powdered Feces Trogopterus (3 kg) were extracted with 60% $\text{C}_2\text{H}_5\text{OH}$ (2 \times 50 L) for 2 h under reflux, and the combined extracts were concentrated under reduced pressure. The resulting extract (370 g) was suspended in H_2O and extracted successively with ethyl acetate and *n*-butanol to give the respective extracts after solvent removal. The combined ethyl acetate extracts were evaporated under reduced pressure to leave a residue (277 g) which was chromatographed on silica gel (2 kg) eluting with a CHCl_3 – CH_3OH stepwise gradient (100:0 \rightarrow 5:1); five fractions were collected. Fraction 1 (10 g) was separated on silica gel (CH_2Cl_2) to yield compounds **1** (50 mg) and **2** (55 mg). Fraction 2 (15 g) was separated on silica gel (CH_2Cl_2 – CH_3OH 20:1) to yield compounds **3** (300 mg), **4** (550 mg), and **5** (500 mg).

Bis(7-hydroxyheptyl) icosanedioate (1)

white powder, m.p. 130–132°C, IR (KBr) λ_{max} 3209, 2911, 1626, 1534, 1470, 1,270, 1,060, 1,018, 720 cm^{-1} ; ^1H NMR (CD_3OD , 500 MHz) δ 4.06 (4H, t, $J = 6.5$ Hz, H-1', 1''), 3.53 (4H, t, $J = 6.7$ Hz, H-7', 7''), 2.30 (4H, t, $J = 7.4$ Hz, H-2, 19), 1.62 (12H, m, H-3, 18, 2', 2'', 6', 6''), 1.28–1.30 (40H, br s, H-3'–5', 3''–5'', 4–17); ^{13}C NMR (CD_3OD , 125 MHz) δ 177.6 (C-1, 20), 66.0 (C-1', 1''), 63.6 (C-7', 7''), 35.7 (C-2, 19), 34.2 (C-6', 6''), 30.9–31.2 (C-4–17, 4', 4''), 30.8 (C-2', 2''), 27.4 (C-3', 3'', 5', 5''), 26.5 (C-3, 18); ESI-MS: m/z 571 $[\text{M}+\text{H}]^+$, 593 $[\text{M}+\text{Na}]^+$; HR-ESI-MS: m/z 593.4775 $[\text{M}+\text{Na}]^+$ ($\text{C}_{34}\text{H}_{66}\text{O}_6\text{Na}$, calc. 593.4757).

Bis(7-hydroxyheptyl) heptadecanedioate (2)

white powder, m.p. 127–128°C, IR (KBr) λ_{\max} 3210, 2909, 1624, 1535, 1471 1270, 1060, 1015, 722 cm^{-1} ; ^1H NMR (CD_3OD , 500 MHz) δ 4.07 (4H, t, $J = 6.6$ Hz, H-1', 1''), 3.53 (4H, t, $J = 6.7$ Hz, H-7', 7''), 2.29 (4H, t, $J = 7.4$ Hz, H-2, 16), 1.62 (12H, m, H-3, 15, 2', 2'', 6', 6''), 1.28–1.30 (34H, br s, H-3'-5', 3''-5'', 4–14); ^{13}C NMR (CD_3OD , 125 MHz) δ 177.7 (C-1, 17), 66.0 (C-1', 1''), 63.6 (C-7', 7''), 35.8 (C-2, 16), 34.2 (C-6', 6''), 30.9–31.2 (C-4–14, 4', 4''), 30.7 (C-2', 2''), 27.4 (C-3', 3'', 5', 5''), 26.5 (C-3, 15); ESI-MS: m/z 529 $[\text{M}+\text{H}]^+$, 551 $[\text{M}+\text{Na}]^+$; HR-ESI-MS: m/z 551.4305 $[\text{M}+\text{Na}]^+$ ($\text{C}_{31}\text{H}_{60}\text{O}_6\text{Na}$, calc. 551.4288).

Bis(7-hydroxyheptyl) decanedioate (3)

white powder, m.p. 118–120°C, IR (KBr) λ_{\max} 3211, 2905, 1626, 1535, 1473 1271, 1062, 1015, 721 cm^{-1} ; ^1H NMR (CD_3OD , 500 MHz) δ 4.06 (4H, t, $J = 6.6$ Hz, H-1', 1''), 3.53 (4H, t, $J = 6.7$ Hz, H-7', 7''), 2.29 (4H, t, $J = 7.4$ Hz, H-2, 9), 1.60 (12H, m, H-3, 8, 2', 2'', 6', 6''), 1.27–1.29 (20H, br s, H-3'-5', 3''-5'', 4–7); ^{13}C NMR (CD_3OD , 125 MHz) δ 176.2 (C-1, 10), 66.0 (C-1', 1''), 63.6 (C-7', 7''), 35.7 (C-2, 9), 34.2 (C-6', 6''), 30.9–31.2 (C-4–7, 4', 4''), 30.7 (C-2', 2''), 27.4 (C-3', 3'', 5', 5''), 26.6 (C-3, 8); ESI-MS: m/z 431 $[\text{M}+\text{H}]^+$, 453 $[\text{M}+\text{Na}]^+$; HR-ESI-MS: m/z 453.3203 $[\text{M}+\text{Na}]^+$ ($\text{C}_{24}\text{H}_{46}\text{O}_6\text{Na}$, calc. 453.3192).

Bis(7-hydroxyheptyl) octanedioate (4)

white powder, m.p. 103–104°C, IR (KBr) λ_{\max} 3210, 2906, 1624, 1533, 1469 1268, 1060, 1012, 722 cm^{-1} ; ^1H NMR (CD_3OD , 500 MHz) δ 4.06 (4H, t, $J = 6.6$ Hz, H-1', 1''), 3.55 (4H, t, $J = 6.7$ Hz, H-7', 7''), 2.28 (4H, t, $J = 7.4$ Hz, H-2, 7), 1.60 (12H, m, H-3, 6, 2', 2'', 6', 6''), 1.27–1.29 (16H, br s, H-3'-5', 3''-5'', 4, 5); ^{13}C NMR (CD_3OD , 125 MHz) δ 177.9 (C-1, 8), 66.0 (C-1', 1''), 63.7 (C-7', 7''), 35.7 (C-2, 9), 34.2 (C-6', 6''), 30.9–31.2 (C-4, 5, 4', 4''), 30.7 (C-2', 2''), 27.4 (C-3', 3'', 5', 5''), 26.6 (C-3, 6); ESI-MS: m/z 403 $[\text{M}+\text{H}]^+$, 425 $[\text{M}+\text{Na}]^+$; HR-ESI-MS: m/z 425.2890 $[\text{M}+\text{Na}]^+$ ($\text{C}_{22}\text{H}_{42}\text{O}_6\text{Na}$, calc. 425.2879).

Bis(7-hydroxyheptyl) hexanedioate (5)

white powder, m.p. 100–102°C, IR (KBr) λ_{\max} 32109, 2903, 1624, 1535, 1470 1269, 1061, 1011, 722 cm^{-1} ; ^1H NMR (CD_3OD , 500 MHz) δ 4.06 (4H, t, $J = 6.6$ Hz, H-1', 1''), 3.55 (4H, t, $J = 6.7$ Hz, H-7', 7''), 2.28 (4H, t, $J = 7.4$ Hz, H-2, 5), 1.60 (12H, m, H-3, 4, 2', 2'', 6', 6''), 1.27–1.29 (12H, br s, H-3'-5', 3''-5''); ^{13}C NMR (CD_3OD , 125 MHz) δ 177.9 (C-1, 6), 66.0 (C-1', 1''), 63.6 (C-7', 7''), 35.7 (C-2, 9), 34.2 (C-6', 6''), 31.0 (C-4', 4''), 30.7 (C-2', 2''), 27.4 (C-3', 3'', 5', 5''), 26.6 (C-3, 4); ESI-MS: m/z 375

$[\text{M}+\text{H}]^+$, 397 $[\text{M}+\text{Na}]^+$; HR-ESI-MS: m/z 397.2576 $[\text{M}+\text{Na}]^+$ ($\text{C}_{20}\text{H}_{38}\text{O}_6\text{Na}$, calc. 397.2566).

Methanolysis of 1–5

Compounds 1–5 (ca. 1 mg) were heated with 10% HCl in MeOH (1 mL each) at 80°C for 14 h. The reaction mixtures were then extracted with *n*-hexane. The upper and lower layers were analyzed by ESI-MS to identify the chemical structures of the reaction products.

Anticoagulative Assay

The anticoagulative activity of the different solvent extracts and pure compounds 1–5 was evaluated by use of the thrombin time (TT) method. All samples were dissolved in ethanol. A sample of blood was taken from the rabbit common carotid artery and mixed with anticoagulant (3.8% sodium citrate) in the proportion 9:1. The mixture was centrifuged at 2,500 rev min^{-1} for 15 min to collect the plasma. The plasma (50 μL) was placed in a plastic cup for 3 min at 37°C, and 100 μL thrombin solution (15 U mL^{-1}) diluted with 0.1 mol mL^{-1} pH 7.4 Tris-HCl buffer was also placed in the plastic cup, with 10 μL sample solution. The coagulation analysis instrument was then started and the thrombin clotting time was recorded. The same experiment was done for the positive control drug heparin sodium and the blank solvent ethanol. Each analyte was tested several times, and an average value was calculated. TT prolongation rate and lgTT prolongation rate were calculated to assess the anticoagulative activity of the samples.

Results and Discussion

The anticoagulative ethyl acetate extract of *Feces Troglodytes* was separated by CC on silica gel to give two fractions and further purified by silica gel to yield compounds 1–5. Their structures were elucidated as follows.

Compound 1 was isolated as a white powder. The molecular formula of 1 was established as $\text{C}_{34}\text{H}_{66}\text{O}_6$ by HRESI-MS (m/z 593.4775 $[\text{M} + \text{Na}]^+$). The positive ESI-MS showed quasi molecular ion peaks at m/z 571 $[\text{M} + \text{H}]^+$ and 593 $[\text{M} + \text{Na}]^+$. The ^1H and ^{13}C NMR spectra were typical of a fatty acid ester, but the ^1H and ^{13}C NMR spectra did not reveal any methyl signals, which suggested that 1 is a symmetric dibasic acid diester [5]. The proton signals at δ 4.06 (4H, t, $J = 6.5$ Hz) and 3.53 (4H, t, $J = 6.7$ Hz) and the carbon signals at δ 66.0 and 63.6 indicated that 1 is a terminal diol ester. When 1 was methanolized with methanolic HCl, a fatty acid methyl ester (FAME) was obtained together with a fatty alcohol. On the

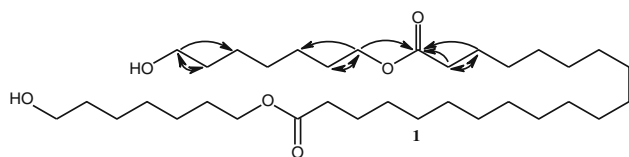


Fig. 2 Key ^1H - ^1H COSY and HMBC correlations of compound **1**

basis of ESI-MS analysis, the FAME was characterized as dimethyl icosanedioate from a quasi molecular ion peak at m/z 371 $[\text{M} + \text{H}]^+$, and the fatty alcohol was identified as 1,7-heptanediol from a quasi molecular ion peak at m/z 133 $[\text{M} + \text{H}]^+$. Assignments of all protons and carbons in **1** were also made on the basis of ^1H - ^1H COSY, HMQC, and HMBC spectra (Fig. 2). Thus, the structure of compound **1** was determined as bis(7-hydroxyheptyl) icosanedioate.

Compound **2** was isolated as a white powder. The molecular formula of **2** was established as $\text{C}_{31}\text{H}_{60}\text{O}_6$ by HRESI-MS (m/z 551.4305 $[\text{M} + \text{Na}]^+$). The positive ESI-MS showed quasi molecular ion peaks at m/z 529 $[\text{M} + \text{H}]^+$ and 551 $[\text{M} + \text{Na}]^+$. The ^1H and ^{13}C NMR spectra were very similar to that of **1**. The quasi molecular ion peak at m/z 529 $[\text{M} + \text{H}]^+$ indicated a deficiency of 42 Da in comparison with that of **1**, which suggested lack of three CH_2 units in **2**. When **2** was methanolized with methanolic HCl, a fatty acid methyl ester (FAME) was obtained together with a fatty alcohol. On the basis of ESI-MS analysis, the FAME was characterized as dimethyl heptadecanedioate from a quasi molecular ion peak at m/z 329 $[\text{M} + \text{H}]^+$, and the fatty alcohol was identified as 1,7-heptanediol from a quasi molecular ion peak at m/z 133 $[\text{M} + \text{H}]^+$. Thus, the structure of compound **2** was determined as bis(7-hydroxyheptyl) heptadecanedioate.

Compound **3** was isolated as a white powder. The molecular formula of **3** was established as $\text{C}_{24}\text{H}_{46}\text{O}_6$ by HRESI-MS (m/z 453.3203 $[\text{M} + \text{Na}]^+$). The positive ESI-MS showed quasi molecular ion peaks at m/z 431 $[\text{M} + \text{H}]^+$ and 453 $[\text{M} + \text{Na}]^+$. The ^1H and ^{13}C NMR spectra were very similar to that of **1**. The quasi molecular ion peak at m/z 431 $[\text{M} + \text{H}]^+$ indicated a deficiency of 140 Da in comparison with that of **1** which suggested lack of ten CH_2 units in **3**. When **3** was methanolized with methanolic HCl, a fatty acid methyl ester (FAME) was obtained together with a fatty alcohol. On the basis of ESI-MS analysis, the FAME was characterized as dimethyl decanedioate from a quasi molecular ion peak at m/z 231 $[\text{M} + \text{H}]^+$, and the fatty alcohol was identified as 1,7-heptanediol from a quasi molecular ion peak at m/z 133 $[\text{M} + \text{H}]^+$. Thus, the structure of compound **3** was determined as bis(7-hydroxyheptyl) decanedioate.

Compound **4** was isolated as a white powder. The molecular formula of **4** was established as $\text{C}_{22}\text{H}_{42}\text{O}_6$ by HRESI-MS (m/z 425.2890 $[\text{M} + \text{Na}]^+$). The positive

ESI-MS showed quasi molecular ion peaks at m/z 403 $[\text{M} + \text{H}]^+$ and 425 $[\text{M} + \text{Na}]^+$. The ^1H and ^{13}C NMR spectra were very similar to that of **1**. The quasi molecular ion peak at m/z 403 $[\text{M} + \text{H}]^+$ indicated a deficiency of 168 Da in comparison with that of **1** which suggested lack of twelve CH_2 units in **4**. When **4** was methanolized with methanolic HCl, a fatty acid methyl ester (FAME) was obtained together with a fatty alcohol. On the basis of ESI-MS analysis, the FAME was characterized as dimethyl octanedioate from a quasi molecular ion peak at m/z 203 $[\text{M} + \text{H}]^+$, and the fatty alcohol was identified as 1,7-heptanediol from a quasi molecular ion peak at m/z 133 $[\text{M} + \text{H}]^+$. Thus, the structure of compound **4** was determined as bis(7-hydroxyheptyl) octanedioate.

Compound **5** was isolated as a white powder. The molecular formula of **5** was established as $\text{C}_{20}\text{H}_{38}\text{O}_6$ by HRESI-MS (m/z 397.2576 $[\text{M} + \text{Na}]^+$). The positive ESI-MS showed quasi molecular ion peaks at m/z 375 $[\text{M} + \text{H}]^+$ and 397 $[\text{M} + \text{Na}]^+$. The ^1H and ^{13}C NMR spectra were very similar to that of **1**. The quasi molecular ion peak at m/z 375 $[\text{M} + \text{H}]^+$ indicated a deficiency of 196 Da in comparison with that of **1** which suggested lack of fourteen CH_2 units in **5**. When **5** was methanolized with methanolic HCl, a fatty acid methyl ester (FAME) was obtained together with a fatty alcohol. On the basis of ESI-MS analysis, the FAME was characterized as dimethyl hexanedioate from a quasi molecular ion peak at m/z 175 $[\text{M} + \text{H}]^+$, and the fatty alcohol was identified as 1,7-heptanediol from a quasi molecular ion peak at m/z 133 $[\text{M} + \text{H}]^+$. Thus, the structure of compound **5** was determined as bis(7-hydroxyheptyl) hexanedioate, which has been reported in the literature [6].

The in-vitro anticoagulative activity of the different solvent extracts and of compounds **1**–**5** was tested using the thrombin time method assay with heparin sodium as a positive control. As can be appreciated from the results summarized in Table 1, compounds **3** and **4** significantly prolonged thrombin time with a good dose–effect relationship.

The thrombin time is a coagulation assay which is usually performed in order to detect for the therapeutic level of the anticoagulant heparin, and it is one of the most procedurally simple methods for screening potential thrombin inhibitors [7]. A bioassay called the optimized thrombin time was successfully developed in our laboratory for determining the anti-thrombin activity of a series of Chinese blood-activating medicines and some active components [8]. The isolated fatty acid esters **1**–**5** from *Feces Troglodytes* might be metabolic products of *T. xanthipes*. The coagulative assay results suggested that these fatty acid esters are the important anticoagulative constituents of *Feces Troglodytes*. The antithrombin

Table 1 Antithrombin activity of the different solvent extracts and compounds 1–5 ($\bar{x} \pm s$, $n = 6-8$)

Sample	Dosage (mg mL ⁻¹)	TT prolongation rate (%)	lgTT prolongation rate (%)
60% Ethanol extract	10.00	23.62 ± 1.34	1.37 ± 0.03
Ethyl acetate extract	10.00	39.32 ± 1.89	1.59 ± 0.01
<i>n</i> -Butanol extract	10.00	–	–
Compound 1	1.00	17.52 ± 0.91	1.24 ± 0.02
Compound 2	1.00	22.34 ± 0.89	1.34 ± 0.01
Compound 3	1.00	1184.49 ± 109.68	3.07 ± 0.04
	0.50	204.22 ± 10.01	2.31 ± 0.02
	0.25	70.30 ± 4.31	1.85 ± 0.02
	0.10	59.13 ± 2.94	1.77 ± 0.01
	0.05	44.62 ± 3.10	1.65 ± 0.03
Compound 4	1.00	321.56 ± 14.63	2.51 ± 0.02
	0.50	55.20 ± 5.35	1.74 ± 0.04
	0.25	24.35 ± 1.52	1.39 ± 0.02
	0.10	12.41 ± 0.78	1.09 ± 0.03
	0.05	7.13 ± 0.57	0.85 ± 0.03
Compound 5	1.00	41.37 ± 2.97	1.62 ± 0.04
Heparin sodium	0.05	73.25 ± 3.14	1.86 ± 0.02

– stands for no effect

activity of the compounds is related to the carbon chain length of the fatty acid.

Acknowledgments This work was financially supported by the 2006 Great Basic Science Research Project of Jiangsu College and University (no. 06KJA36022). We also thank Drs Er-Xin Shang and Shu-Lan Su for other helpful assistance.

References

- Tang XG, Huang WQ (2008) A summary of pharmacology and clinical application of *Feces Trogopteris*. *J Emerg Tradit Chin Med* 17:101–102
- Berthold HK, Unverdothen S, Degenhardt R, Bulitta M (2006) Effect of policosanol on lipid levels among patients with hypercholesterolemia or combined hyperlipidemia. *JAMA* 295:2262–2269
- Peter RC, Howe PMC, Michael JJ (1999) Equal antithrombotic and triglyceride-lowering effectiveness of eicosapentaenoic acid-rich and docosahexaenoic acid-rich fish oil supplements. *Lipids* 34:307–308
- Tremoli E, Maderna P, Marangoni F, Colli S, Eligini S, Catalano I, Angeli MT, Pazzucconi F, Gianfranceschi G, Davi G (1995) Prolonged inhibition of platelet aggregation after n-3 fatty acid ethyl ester ingestion by healthy volunteers. *Am J Clin Nutr* 61:607–613
- Liang S, Chen HS, Wang HP, Jin L, Qiao LM, Lu J (2007) Study on chemical constituents of *Tabernaemontana divaricata* (II). *Acad J Sec Mil Med Univ* 28:425–426
- Dimian AF, Jones FN (1988) Liquid crystalline oligoester diols as thermoset coatings binders. *ACS Symp Ser* 367:324–334
- Michele MF, Ronda C, George MR (2003) Comparison of five thrombin time reagents. *Clin Chem* 49:169–172
- Liu L, Ma HY, Duan JA, Tang YP, Su SL, Guo JM (2009) The development of a bioassay called thrombin time and application of the bioassay in study on Siwu decoction and its serial decoctions. *Chin J Exp Tradit Med Formulae* 15:68–71

Nitro-fatty Acids Occur in Human Plasma in the Picomolar Range: a Targeted Nitro-lipidomics GC–MS/MS Study

Dimitrios Tsikas · Alexander A. Zoerner ·
Anja Mitschke · Frank-Mathias Gutzki

Received: 21 April 2009 / Accepted: 2 July 2009 / Published online: 22 August 2009
© AOCS 2009

Abstract First studies on the occurrence of nitrated fatty acids in plasma of healthy subjects revealed basal concentrations of 600 nM for free/nonesterified nitro-oleic acid (NO₂-OA) as measured by liquid chromatography tandem mass spectrometry (LC–MS/MS). We recently showed by a gas chromatography tandem mass spectrometry (GC–MS/MS) method the physiological occurrence of two isomers, i.e., 9-NO₂-OA and 10-NO₂-OA, at mean basal plasma concentrations of 880 and 940 pM, respectively. In consideration of this large discrepancy we modified our originally reported method by replacing solid-phase extraction (SPE) by solvent extraction with ethyl acetate and by omitting the high-performance liquid chromatography (HPLC) step for a more direct detection and with the potential for lipidomics studies. Intra-assay imprecision and accuracy of the modified method in human plasma were 1–34% and 91–221%, respectively, for added NO₂-OA concentrations in the range 0–3,000 pM. This method provided basal plasma concentrations of 306 ± 44 pM for 9-NO₂-OA and 316 ± 33 pM for 10-NO₂-OA in 15 healthy subjects. Nitro-arachidonic acid and nitro-linolenic acid were not detectable in the plasma samples. In summary, our studies show 9-NO₂-OA and 10-NO₂-OA as endogenous nitrated fatty acids in human plasma in the pM range; HPLC is recommendable as a sample clean-up step for reliable quantification of nitro-oleic acids by GC–MS/MS.

Keywords Fatty acids · GC–MS/MS · HPLC · Interferences · LC–MS/MS · Lipidomics · Nitration · Quantification · Stable isotopes · Validation

Abbreviations

CID	Collision-induced dissociation
GC–MS/MS	Gas chromatography tandem mass spectrometry
HAc	Acetic acid
LC–MS/MS	Liquid chromatography tandem mass spectrometry
MeCN	Acetonitrile
MeOH	Methanol
<i>m/z</i>	Mass-to-charge
NO ₂ -OA	Nitro-oleic acid
PFB	Pentafluorobenzyl
PFB-Br	Pentafluorobenzyl bromide
QC	Quality control
S/N	Signal-to-noise
SPE	Solid-phase extraction
SRM	Selected reaction monitoring
TSQ	Triple-stage quadrupole

Introduction

Nitrated fatty acids are a newly discovered class of biologically active nitro-compounds [1–12]. For the first time, the nonesterified nitro-oleic acid (NO₂-OA) has been found by LC–MS/MS in human plasma, at a basal concentration of about 600 nM [5]. Recently, our group has reported on the development, validation, and application of a highly specific GC–MS/MS method for the quantification

D. Tsikas (✉) · A. A. Zoerner · A. Mitschke · F.-M. Gutzki
Institute of Clinical Pharmacology, Hannover Medical School,
Carl-Neuberg-Strasse 1, 30625 Hannover, Germany
e-mail: tsikas.dimitros@mh-hannover.de

of NO₂-OA in human plasma [13]. In order to avoid potential interferences we incorporated in this GC–MS/MS method a HPLC step for separation and isolation of NO₂-OA. In freshly obtained plasma from 15 healthy subjects we identified by GC–MS/MS two isomers of nitro-oleic acid, namely 9-NO₂-OA and 10-NO₂-OA, and determined their concentration to be on the threshold of the pM-to-nM range [13]. The 9-NO₂-OA and 10-NO₂-OA concentrations measured by us are about three orders of magnitude lower than those firstly reported by Freeman and co-workers by using the LC–MS/MS methodology [5]. The large discrepancy between the findings of our and other groups is difficult to reconcile because the analytical performance of the LC–MS/MS method in terms of accuracy, precision, and specificity has not been reported [5]. A recent study [14], in which nitro-oleic acid could not be found in mouse plasma, argues against the originally reported concentration of nitro-oleic acid and supports our findings that 9-NO₂-OA and 10-NO₂-OA occur in human plasma in the pM-to-nM range [13].

In consideration of this contradiction, we have performed additional work to verify our originally reported data on 9-NO₂-OA and 10-NO₂-OA. For this, we have made two modifications, i.e., we performed solvent extraction instead of SPE and omitted the HPLC step (Fig. 1). These modifications were aimed at simplifying and making the method more direct, with the potential for lipidomics studies. The modified method reported here revealed plasma 9-NO₂-OA and 10-NO₂-OA concentrations of 300 pM, which support our previous findings [13]. On the basis of the new analytical facts, this article discusses the importance of nitro-fatty acids with regard to their physiological and pathological roles.

Experimental Procedures

Materials

2,3,4,5,6-Pentafluorobenzyl bromide (PFB-Br) was obtained from Sigma–Aldrich (Steinheim, Germany). *cis*-9-Nitro-9-octadecenoic acid (9-NO₂-OA) and *cis*-10-nitro-9-octadecenoic acid (10-NO₂-OA) were obtained from Cayman Chemical (Ann Arbor, MI, USA) and were stored at –20°C. The preparation, isolation, characterization, and standardization of the ¹⁵N-labeled 9-NO₂-OA (9-¹⁵NO₂-OA) and 10-NO₂-OA (10-¹⁵NO₂-OA), which were used as internal standards in the present study, have been described in detail elsewhere [13]. Toluene was purchased from Baker (Deventer, The Netherlands). Acetonitrile, ethyl acetate, and *N*-ethyl-diisopropylamine were from Merck (Darmstadt, Germany).

Solvent Extraction of Free 9- and 10-Nitro-oleic Acid from Human Plasma

For the present work we used plasma samples that were generated and analyzed for nitro-oleic acid using GC–MS/MS and HPLC (Fig. 1, procedure A) in a previous work of our group [13]. Healthy adults had volunteered to donate blood and had given written consent to the use of their blood samples for analytical examination in the frame of scientific experiments only. Blood had been drawn from antecubital veins of healthy volunteers using 9-mL syringes containing ethylenediamine tetraacetic acid (EDTA), put immediately on ice, and centrifuged (4,240 × *g*, 4°C, 5 min). Plasma samples had been proportioned into 1-mL fractions and stored at –80°C until further analysis.

Only once-thawed plasma samples were placed in an ice bath and spiked with a mixture of 9-¹⁵NO₂-OA and 10-¹⁵NO₂-OA as specified in the respective studies, mixed by vortexing, and allowed to condition for 30 min in the ice bath (Fig. 1). Then, plasma samples were acidified to pH 5 by using 20 vol% acetic acid (HAc). Substances were extracted by solvent extraction with ethyl acetate (750 μL) by vortex-mixing for 2 min (Fig. 1, procedure B). After centrifugation (4,240 × *g*, 4°C, 5 min) the upper ethyl acetate phase (600 μL) was decanted and dried over anhydrous Na₂SO₄, and the solvent was evaporated under a stream of nitrogen. The residue was reconstituted in molsieve-dried acetonitrile (MeCN, 100 μL) and methanol (MeOH, 10 μL), and fatty acid pentafluorobenzyl (PFB) esters were prepared using PFB-Br (30 vol% in MeCN) as the derivatization agent and *N*-ethyl-diisopropylamine as the catalyst [13]. After incubation for 60 min at 30°C, solvents and reagents were evaporated to dryness under nitrogen and the residue was reconstituted in toluene (50 μL) from which 1-μL aliquots were injected into the GC–MS/MS instrument in the splitless mode by means of the autosampler.

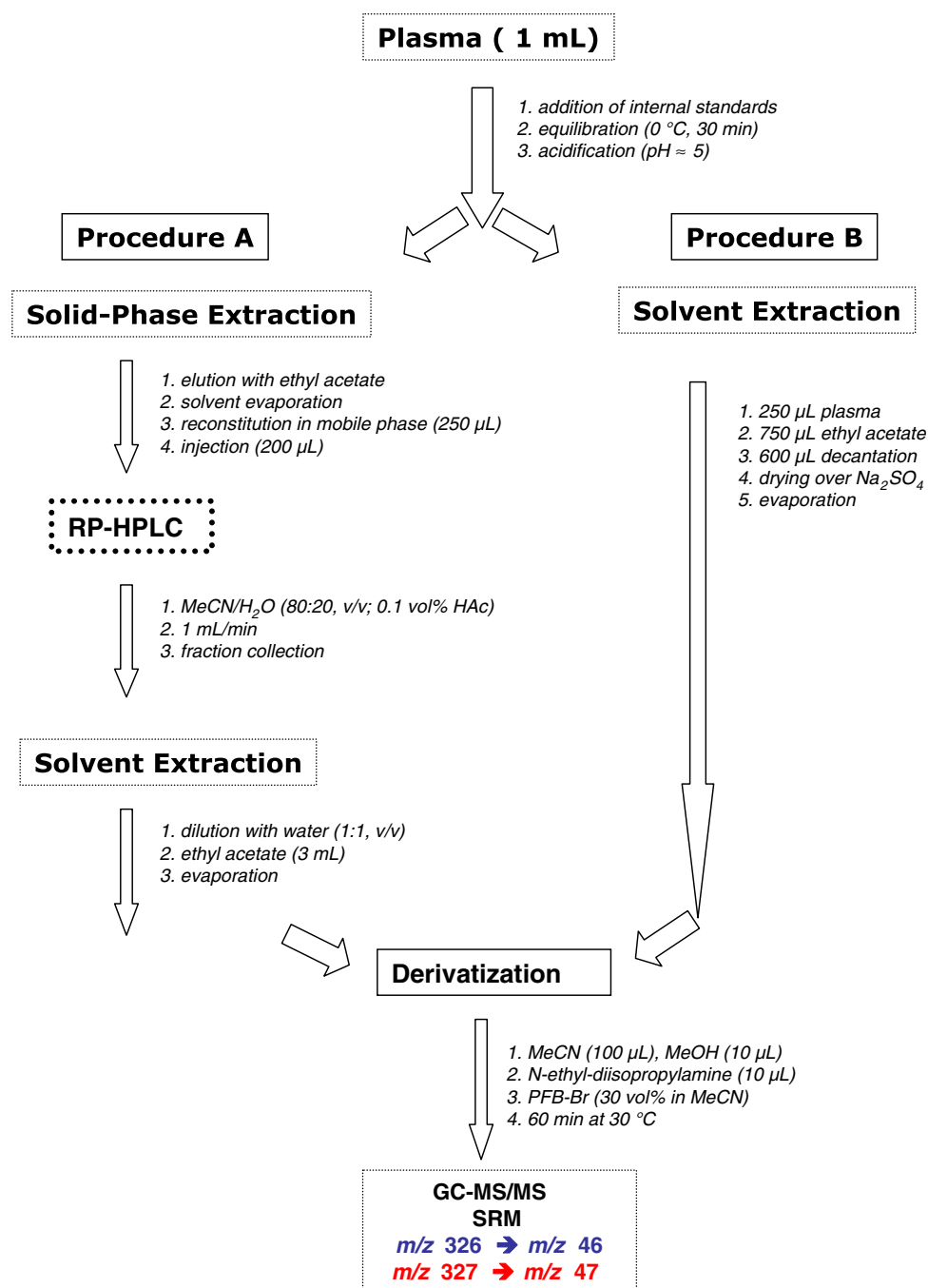
HPLC Conditions

HPLC with ultraviolet (UV) absorbance detection at 263 nm was carried out on a Summit apparatus from Dionex (Idstein, Germany) as described elsewhere [13]. A Nucleodur C18 Gravity column (250 mm × 4.6 mm i.d., 5 μm particle size) from Macherey-Nagel (Düren, Germany) was used. The mobile phase was 80 vol% MeCN and 0.1 vol% acetic acid and was pumped at a flow rate of 1 mL/min.

GC–MS/MS Conditions

The GC–MS/MS conditions used in the present study were essentially the same as described elsewhere [13]. Analyses were carried out on a triple-stage quadrupole (TSQ)

Fig. 1 Schematic of the GC–MS/MS method for the quantification of free 9- and 10-nitro-oleic acid (9-NO₂-OA and 10-NO₂-OA) in human plasma. In procedure A (*left panel*), SPE and HPLC are used [13]. Procedure B was used in the present work to measure nitro-oleic acid in human plasma. *HAc* acetic acid



ThermoQuest TSQ 7000 mass spectrometer (Finnigan MAT, San Jose, CA, USA) directly interfaced with a Trace 2000 series gas chromatograph equipped with an autosampler AS 2000 and a BEST programmable temperature vaporizer (PTV) injector (CE Instruments, Austin, TX, USA). A 15-m-long fused-silica DB-5ht capillary column (0.25 mm i.d., 0.25-μm film thickness) from Agilent (Santa Clara, CA, USA) was used. The following oven temperature program was used with helium as the carrier gas at constant flow rate of 1 mL/min: 1 min at 90°C, then increased to 225°C and 320°C at a rate of 15°C/min and

30°C/min, respectively. Interface and ion source were kept at 280°C and 180°C, respectively.

In quantitative analyses, sample injection was performed by PTV starting at an injector temperature of 70°C, which was increased to 280°C at 10°C/s. Electron energy and electron current were set to 200 eV and 300 μA, respectively. Methane (530 Pa) and argon (0.13 Pa collision pressure) were used as reagent and collision gas, respectively. The collision energy was 15 eV. Quantification was performed by selected reaction monitoring (SRM) of the product ions *m/z* 46 ([¹⁴NO₂]⁻) and *m/z* 47

($[^{15}\text{NO}_2]^-$) produced by collision-induced dissociation (CID) of the parent ions $[\text{M}-\text{PFB}]^-$ at m/z 326 and m/z 327 for endogenous nitro-oleic acids and the internal standards, respectively. The dwell time was 100 ms for each mass transition.

Results

Intra-assay Precision and Accuracy of the Method

Intra-assay imprecision (relative standard deviation, RSD, %) and accuracy (recovery, %) were determined by analyzing in duplicate 9-NO₂-OA and 10-NO₂-OA in human plasma before and after their addition at 300, 900, and 3,000 pM each. The results from the intra-assay validation are summarized in Table 1. Figure 2 shows chromatograms from the GC–MS/MS analysis (procedure B) of the plasma sample before and after addition of 300 pM of 9-NO₂-OA or 10-NO₂-OA. The respective basal concentrations of 9-NO₂-OA and 10-NO₂-OA in the plasma used to validate the method was determined to be 102 and 205 pM.

Basal Plasma Concentrations of 9-NO₂-OA and 10-NO₂-OA in Healthy Humans

The results from the quantitative analysis of 9-NO₂-OA and 10-NO₂-OA in plasma samples of 15 healthy subjects by GC–MS/MS without preceding HPLC separation, i.e., by using procedure B, are summarized in Table 2. The results previously obtained by analyzing the same plasma samples by using procedure A that includes HPLC separation [13] (Fig. 1) are also presented in Table 2 for comparison. The samples in the present study were worked up and analyzed within a single run. The quality of these analyses was evaluated by co-processing four 250- μL aliquots of a pooled plasma which served as a quality control (QC). In both the 15 study plasma samples and the

QC plasma sample analyzed by the present method we identified the two isomers of nitro-oleic acid, i.e., 9-NO₂-OA and 10-NO₂-OA. The concentration of 9-NO₂-OA and 10-NO₂-OA in the QC plasma sample was determined to be 288 ± 11 and 334 ± 40 pM with an intra-assay precision (RSD) of about 4% and 12%, respectively, indicating satisfactory analytical precision.

Representative chromatograms from the GC–MS/MS analysis of 9-NO₂-OA and 10-NO₂-OA in two aliquots of the same plasma sample worked up by the two procedures (Fig. 1) are shown in Fig. 3. These GC–MS/MS chromatograms clearly show how effective the HPLC step is from the analytical point of view. HPLC analysis of the ethyl acetate eluate from the SPE step of procedure A: (1) separates potentially interfering substances co-extracted from plasma, (2) improves the gas chromatography of the PFB ester derivatives of the isomeric 9-NO₂-OA and 10-NO₂-OA, and (3) enhances the sensitivity of the method by improving the signal-to-noise (S/N) ratio as compared with the rather rough and not further purified extract from solvent extraction of the plasma sample in procedure B. To quantitate this effect we used the S/N ratios observed for the internal standards 9-¹⁵NO₂-OA and 10-¹⁵NO₂-OA. Without the HPLC step the mean S/N ratio was determined to be 667:1 (RSD, 8.7%) for 9-¹⁵NO₂-OA and 949:1 (RSD, 15%) for 10-¹⁵NO₂-OA. With the use of the HPLC step the mean S/N ratio was determined to be 25,400:1 (RSD, 57%) for 9-¹⁵NO₂-OA and 28,000:1 (RSD, 58%) for 10-¹⁵NO₂-OA. Considering the spike of 40 pmol of 9-¹⁵NO₂-OA or 10-¹⁵NO₂-OA in procedure A with HPLC (1 mL plasma) and 6.25 pmol of 9-¹⁵NO₂-OA or 10-¹⁵NO₂-OA in procedure B without HPLC (0.25 mL plasma) (Fig. 1), it is calculated that the internal standards were analyzed with about five to six times more sensitivity when the HPLC step was implemented. Presumably, this factor also applies to the endogenous 9-NO₂-OA and 10-NO₂-OA (Fig. 3).

Incorporation of the HPLC step into the method always provided symmetric GC peaks of very similar peak areas

Table 1 Intra-assay imprecision (RSD, %) and accuracy (recovery, %) of the GC–MS/MS method for 9-NO₂-OA and 10-NO₂-OA in human plasma without the use of HPLC

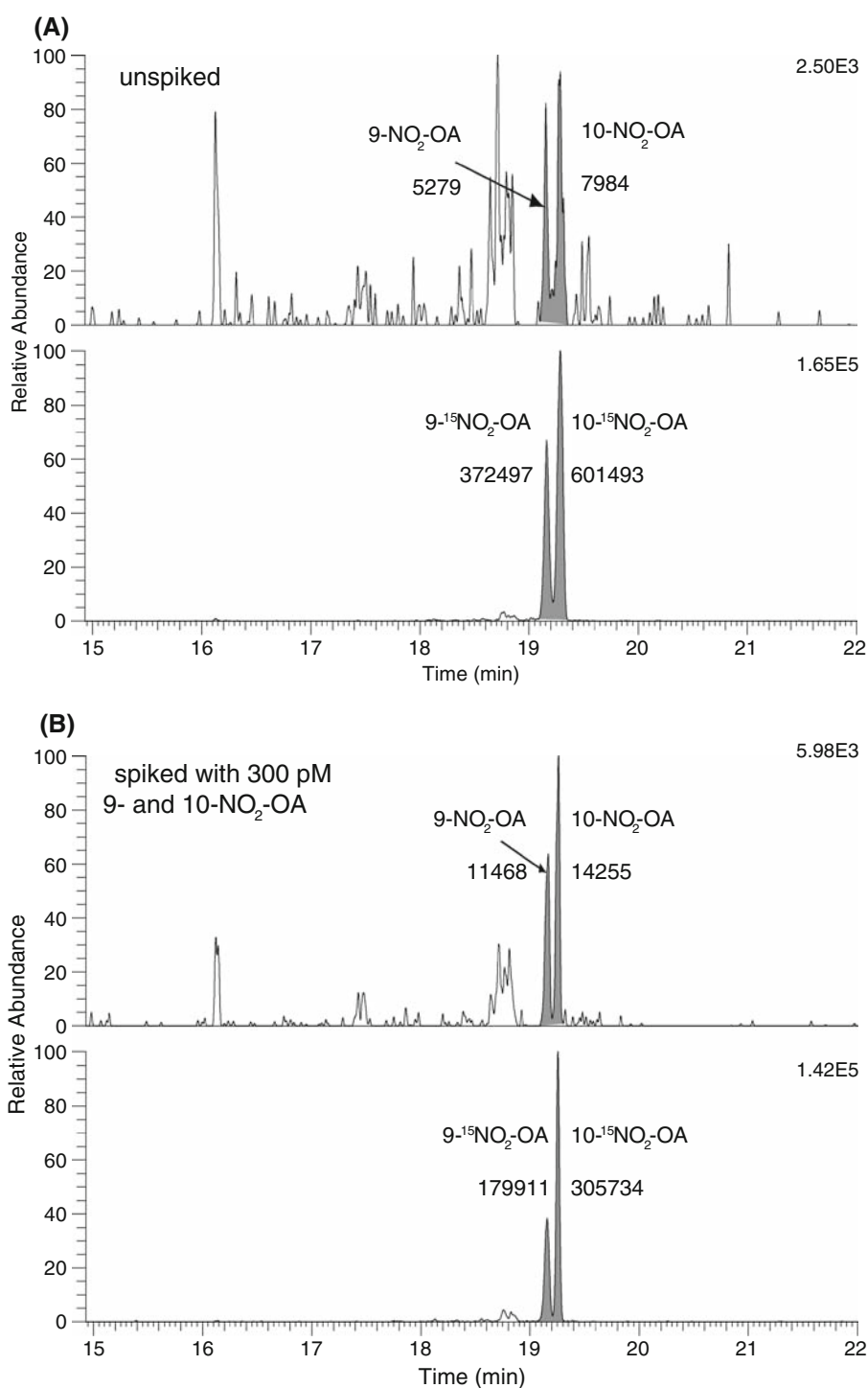
Added (pM)	Measured (pM) ^a		Imprecision (%)		Recovery (%) ^b	
	9-NO ₂ -OA	10-NO ₂ -OA	9-NO ₂ -OA	10-NO ₂ -OA	9-NO ₂ -OA	10-NO ₂ -OA
0	102 ± 27	205 ± 69	26	34	N.A.	N.A.
300	427 ± 36	868 ± 41	8.4	4.7	108	221
900	920 ± 50	1316 ± 14	5.4	1.1	91	123
3000	3204 ± 117	3695 ± 262	3.7	7.1	103	116

N.A. not applicable

^a The internal standards 9-¹⁵NO₂-OA and 10-¹⁵NO₂-OA were used at final concentrations of 6,400 and 19,500 pM, respectively. Data are presented as mean ± standard deviation from duplicate analyses

^b Recovery was calculated by using the formula: recovery = [(measured concentration – basal concentration)/added concentration] × 100

Fig. 2 Partial chromatograms from simultaneous quantitative GC–MS/MS analysis of 9-NO₂-OA and 10-NO₂-OA in a plasma sample from a healthy volunteer using procedure B (no use of HPLC) before (a) and after (b) addition of 300 pM of 9-NO₂-OA or 10-NO₂-OA. ¹⁵N-Labeled 9- and 10-nitro-oleic acid were used as the internal standards at final added plasma concentrations of 6.37 and 19.5 nM, respectively. SRM of *m/z* 46 and *m/z* 47 produced by CID of the parent ions at *m/z* 326 for unlabeled 9-NO₂-OA and 10-NO₂-OA (*upper traces*) and *m/z* 327 for the internal standards (*lower traces*). Endogenous 9-NO₂-OA and 10-NO₂-OA and internal standards were analyzed as their PFB derivatives. The numbers beside the peaks provide the peak areas. The longer retention times of these derivatives in this figure as compared with those shown in Fig. 3 and reported in the *text* are due to the use of a new GC column. See also Fig. 1 and Table 1



and peak heights for both isomers (Fig. 3b). By contrast, omission of the HPLC step resulted in chromatographically considerably differing GC peaks, with the 9-NO₂-OA peak being always wider than that of 10-NO₂-OA (Fig. 3a). However, our analyses show that the internal standards 9-¹⁵NO₂-OA and 10-¹⁵NO₂-OA behave obviously identically to their endogenous analogs from the chromatography point of view, so that quantification of 9-NO₂-OA and

10-NO₂-OA extracted from plasma by ethyl acetate is possible with reasonable precision and accuracy nevertheless (see also Table 1). Thus, within the whole study group, 9-NO₂-OA and 10-NO₂-OA basal plasma concentrations were fairly close and of the order of 0.3 nM and their molar ratio was close to unity (Table 2). This order of magnitude is about 1,000 times lower than that reported initially by others for free, i.e., nonesterified, NO₂-OA [5].

Table 2 Nitro-oleic concentrations in plasma of 15 healthy subjects measured by GC–MS/MS with and without use of HPLC

No.	Procedure A (with HPLC) ^a		Ratio ^b	Procedure B (without HPLC)		Ratio ^b
	9-NO ₂ -OA (nM)	10-NO ₂ -OA (nM)		9-NO ₂ -OA (nM)	10-NO ₂ -OA (nM)	
1	1.66	1.55	1.07	0.285	0.363	0.785
2	0.91	1.03	0.88	0.240	0.296	0.811
3	1.03	1.06	0.97	0.300	0.324	0.926
4	0.84	0.82	1.02	0.338	0.301	1.123
5	0.66	1.07	1.07	0.258	0.332	0.777
6	0.60	0.67	0.88	0.296	0.262	1.130
7	1.41	1.38	1.02	0.378	0.257	1.471
8	0.71	0.80	0.89	0.262	0.325	0.806
9	0.88	1.04	0.85	0.316	0.344	0.919
10	0.68	0.62	1.10	0.328	0.360	0.911
11	0.81	0.79	1.02	0.247	0.351	0.704
12	0.69	0.81	0.86	0.281	0.279	1.007
13	0.86	0.94	0.92	0.346	0.309	1.120
14	0.77	0.84	0.91	0.352	0.305	1.154
15	0.67	0.74	0.91	0.366	0.328	1.116
	0.88 ± 0.29	0.94 ± 0.26	0.96 ± 0.08	0.306 ± 0.044	0.316 ± 0.033	0.98 ± 0.2

^a Data from using procedure A are taken from a previous study of our group [13]. The concentration of the internal standards 9-¹⁵NO₂-OA and 10-¹⁵NO₂-OA was 50 nM in procedure A and 25 nM in procedure B

^b Molar ratio of 9-NO₂-OA to 10-NO₂-OA

Interestingly, the concentrations determined by the present method (procedure B, without HPLC) are consistently three times lower than those measured by procedure A utilizing the HPLC step (Table 2) [13]. Also, it is worth mentioning that the molar ratio of 9-NO₂-OA and 10-NO₂-OA varied considerably more in the procedure without HPLC as compared with that using the HPLC clean-up step, i.e., by 20.4% versus 8.3% (RSD). Another interesting and unexpected finding of the present study is that there was no correlation between 9-NO₂-OA and 10-NO₂-OA when they were quantitated without preceding HPLC separation, in contrast to the procedure that uses the HPLC clean-up step (Fig. 4) [13].

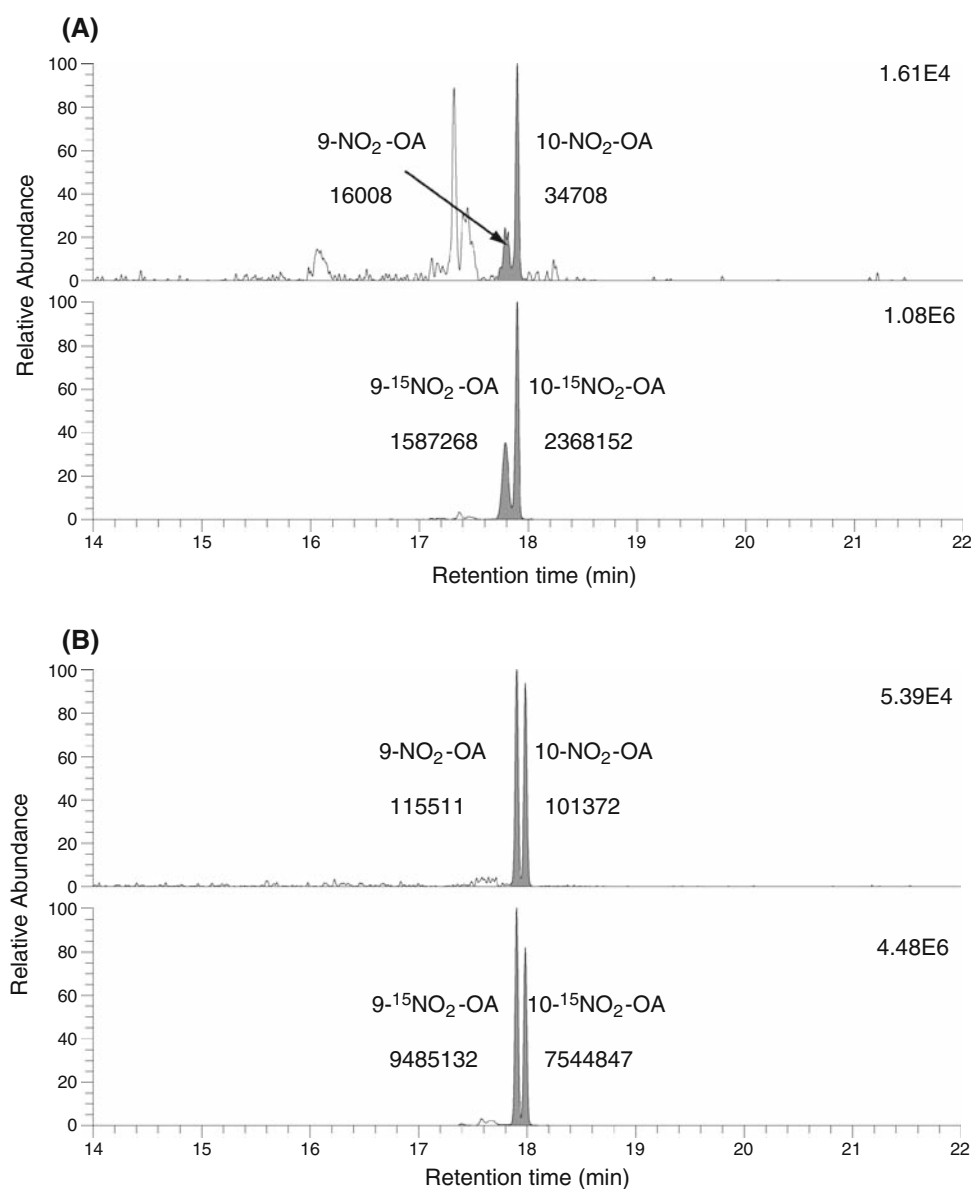
Nitro-lipidomics of Human Plasma

Leaving out the HPLC step after the extraction of plasma with water-immiscible organic solvents such as ethyl acetate as used in the present study allows performance of lipidomics studies on nitrated fatty acids in plasma. On the reasonable assumption that the PFB esters of the expected nitrated fatty acids undergo ionization to the parent ions [M–PFB][–] and that their CID fragmentation in GC–MS/MS occurs analogously to 9-NO₂-OA and 10-NO₂-OA and produces the common characteristic product ion nitrite at *m/z* 46 ([¹⁴NO₂][–]), we searched for the appearance of endogenous nitro metabolites of various unsaturated fatty acids in human plasma samples by SRM of the calculated mass are summarized in Table 3.

Figure 5 shows representative GC–MS/MS chromatograms from the nitro-lipidomics analysis of the PFB esters of nitro-fatty acids extracted by solvent extraction with

ethyl acetate from a plasma sample of a healthy subject. As expected, both endogenous nitro-oleic acid isomers and their externally added synthetic ¹⁵N-labeled analogs were identified on the basis of their retention time at 17.78 min for 9-NO₂-OA/9-¹⁵NO₂-OA and at 17.87 min for 10-NO₂-OA/10-¹⁵NO₂-OA. The tracing for nitro-arachidonic acid is very poor in peaks at relevant retention times and suggests that no nitro-arachidonic acid is endogenously present in the plasma sample analyzed. However, because the limits of detection (LOD) and limits of quantitation (LOQ) of the present method have not been determined for nitro-arachidonic acids, the physiological occurrence of nitro-arachidonic acids at concentrations below about 100 pM in human plasma cannot be excluded. This may also apply to nitro-linolenic acid and nitro-palmitoleic acid, the PFB esters of which are expected to elute in front of the nitro-oleic acid derivatives (Table 3). With regard to nitro-linoleic acid we obtained two groups of peaks, of which only the earlier-eluting group at about 16.5 min and 16.7 min deserves consideration, because the PFB esters of nitro-linoleic acids are expected to elute in front of the PFB esters of nitro-oleic acids. These findings are supportive of the physiological occurrence of nitro-linoleic acid in plasma of healthy humans at concentrations presumably not higher than those of the nitro-oleic acids. Nitro-linoleic acid concentrations of the order of 300 pM would be greatly contradictory to previous reports on the physiological occurrence of nitro-linoleic acid in human plasma at about 80 nM for the free form and 550 nM for the esterified form [2]. However, unequivocal identification and quantification of nitro-linoleic acids and other nitro-fatty

Fig. 3 Partial chromatograms from simultaneous quantitative GC–MS/MS analysis of 9-NO₂-OA and 10-NO₂-OA in the same plasma sample from a healthy volunteer. **(a)** Procedure B (no use of HPLC) was applied as described in the present work. **(b)** Procedure A (use of HPLC) was applied as described elsewhere [13]. ¹⁵N-labeled 9- and 10-nitro-oleic acid were used as the internal standards (50 nM each in procedure A, and 25 nM each in procedure B). SRM of *m/z* 46 and *m/z* 47 produced by CID of the parent ions at *m/z* 326 for unlabeled 9- and 10-nitro-oleic acid (*upper traces*) and *m/z* 327 for ¹⁵N-labeled 9- and 10-nitro-oleic acid (*lower traces*). 9-NO₂-OA and 10-NO₂-OA and internal standards were analyzed as their PFB derivatives. The numbers beside the peaks provide the peak areas. See also Figs. 1 and 2



acids in human plasma require use of well-characterized stable-isotope-labeled internal standards and preceding separation by HPLC, as described by us for the nitro-oleic acid isomers [13].

Discussion

First publications on nitro-fatty acids reported physiological occurrence of nitro-oleic acid in human plasma at concentrations of the order of 600 nM [5]. Based on our experience on quantitative analysis of nitrated biomolecules and fatty acids, a plasma concentration of 600 nM for nitro-oleic acid in healthy humans appeared to us as very high. Our first goal was, therefore, to develop a GC–MS/MS method for the unequivocal identification and accurate

quantification of nitro-oleic acid in human plasma. This goal was achieved by incorporating a HPLC step for the isolation of two expectable nitro-oleic acid isomers, i.e., 9-NO₂-OA and 10-NO₂-OA. After adequate validation we applied the method to determine their concentration in plasma of 15 healthy subjects in the basal state. This method, i.e., procedure A in Fig. 1, revealed mean plasma concentrations of 880 pM for 9-NO₂-OA and 940 pM for 10-NO₂-OA, which are almost three orders of magnitude lower than that initially reported by others [5]. In consideration of this discrepancy we performed additional studies to verify our initial findings and to examine whether the HPLC step might have led to loss of nitro-oleic acid despite the use of synthetic ¹⁵N-labeled analogs as internal standards. Expectedly, this quite “rough” method, i.e., procedure B in Fig. 1, provided analyses at considerably lower

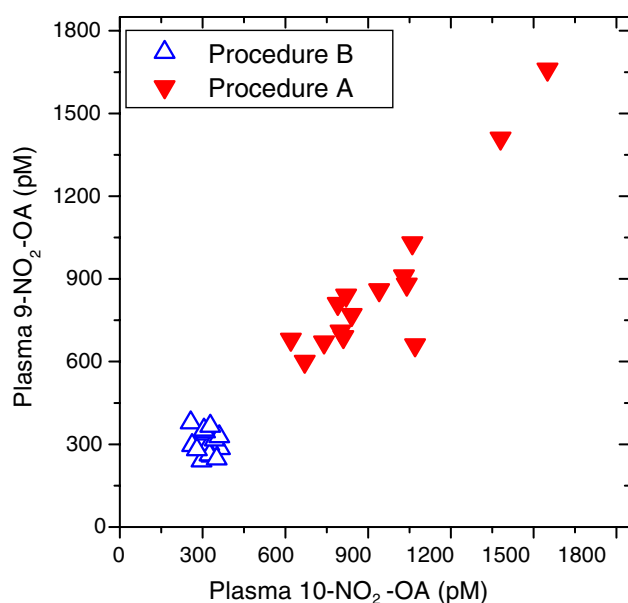


Fig. 4 Relationship between 9-NO₂-OA and 10-NO₂-OA in plasma of 15 healthy volunteers as measured by GC–MS/MS using two different procedures. This figure was constructed with data generated in the present work (i.e., procedure B, without use of HPLC) and with those previously reported by our group (i.e., procedure A, with use of HPLC) [13]

S/N values and poorer chromatography (Figs. 2, 3) due to co-extracted “background,” but allowed quantification with satisfactory precision and accuracy, as reported in the present work. These analyses provided even lower concentrations than the method using HPLC separation [13], presumably as a result of suboptimum gas chromatography. On the other hand, an advantage of leaving out the HPLC step in the GC–MS/MS method for nitro-fatty acids is that the sample obtained is suitable for rather qualitative lipidomics studies. Technological advancements in mass chromatography and improvements in chromatographic techniques in the area of lipidomics research and biomarker discovery have been recently reviewed [15].

Figures 2, 3, and 5 and Table 1 clearly indicate that renunciation of the HPLC step in nitro-fatty acid

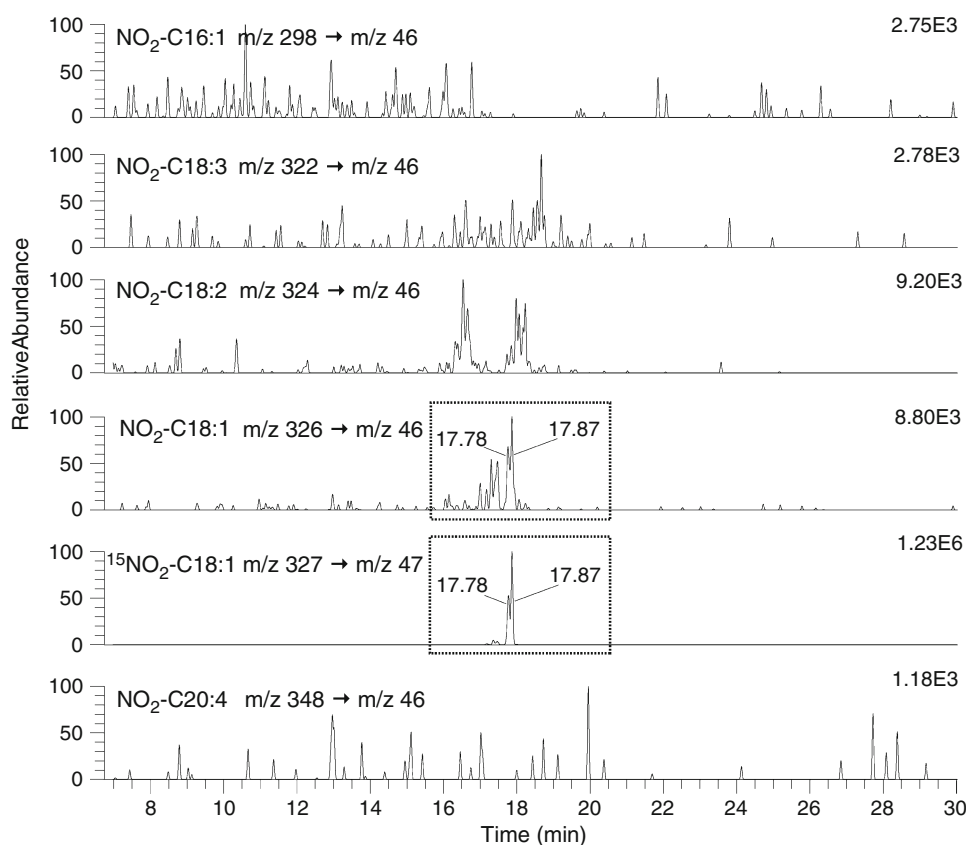
quantification by GC–MS/MS is not recommended due to deterioration of the analytical performance, notably in terms of loss of accuracy, precision, and sensitivity. This especially applies to 10-NO₂-OA, which can be measured by GC–MS/MS using procedure B with acceptable accuracy in human plasma only if present at the very high concentration of 3,000 pM, which is about 15 times higher than its putative basal concentration (Table 1). In addition, use of “rough” yellow-colored ethyl acetate extracts for “shotgun” GC–MS/MS would inevitably require much more frequent need for maintenance of the whole GC–MS/MS apparatus, unlike the “pure” colorless HPLC fractions provided by procedure A.

Because the ethyl acetate extract of human plasma in procedure A contains many more compounds than the ethyl acetate extract of the HPLC fraction in procedure B, it is likely that some of the co-extracted compounds aggravate the gas chromatography of the PFB ester derivatives of 9-NO₂-OA and 10-NO₂-OA, as can be seen in Figs. 3–5. The presence of a much higher number of analytes in the ethyl acetate fraction in procedure B enhances the baseline, so that the S/N ratio decreases and consequently the LOD and LOQ values of the method increase. In LC–MS/MS, ion suppression and ion enhancement effects are very well recognized and investigated, and methods have been developed for their identification, quantification, and exclusion or minimization [16, 17]. Theoretically, such effects may also have occurred in our GC–MS/MS method for nitro-oleic acid using procedure B, but to a much lesser degree using procedure A (with HPLC). Use of stable-isotope-labeled analogs may attenuate such effects. However, because we used the internal standards 9-¹⁵N-NO₂-OA and 10-¹⁵N-NO₂-OA in high molar excess over their endogenous counterparts (about 80-fold), it may be that their high concentration was suboptimal, unlike in procedure A in which the molar excess was about 60-fold [13]. In addition, during gas chromatography, *trans*-nitration may occur [18]. Together with the use of high molar excess of the internal standards over the endogenous nitro-oleic acids and with the presence of numerous other compounds in the ethyl

Table 3 Calculated mass-spectrometry-related data for pentafluorobenzyl (PFB) esters of putative vinylic nitro-fatty acids from major unsaturated fatty acids

Parent fatty acid	Molecular mass	Putative nitro-fatty acid	Molecular mass	[M–PFB] [–]	Mass transition (<i>m/z</i> → <i>m/z</i>)	Relative retention time
Palmitoleic acid	254.4	Nitro-palmitoleic acid	299.4	298.4	298.4 → 46.0	<1.0
Linoleic acid	280.5	Nitro-linoleic acid	325.5	324.5	324.5 → 46.0	<1.0
Linolenic acid	278.4	Nitro-linolenic acid	323.4	322.4	322.4 → 46.0	<1.0
Oleic acid	282.5	Nitro-oleic acid	327.5	326.5	326.5 → 46.0	1.0
Oleic acid	282.5	[¹⁵ N]-Nitro-oleic acid	328.5	327.5	327.5 → 47.0	≈ 1.0
Arachidonic acid	304.5	Nitro-arachidonic acid	349.5	348.5	348.5 → 46.0	>1.0

Fig. 5 Representative partial chromatograms from targeted nitro-lipidomics GC–MS/MS analysis of a plasma sample from a healthy subject. 9-NO₂-OA and 10-NO₂-OA, their internal standards added to plasma (at 25 nM each), and other putative nitro-fatty acids were analyzed using procedure B (Fig. 1). The mass transitions monitored are summarized in Table 3. A dwell time of 100 ms was used for each mass transition



acetate extract of procedure B, these unfavorable circumstances may have resulted in lower 9-NO₂-OA and 10-NO₂-OA concentrations in plasma as compared with procedure A involving the HPLC step. In consideration of the potential importance of matrix effects and ion suppression/enhancement in GC-based methods, these phenomena deserve thorough investigation.

Our previous study [13] and the present work suggest that presumably nitro-oleic acid is the most abundant nitrated unsaturated fatty acid in human plasma. It occurs as two isomers with basal plasma concentrations in the pM range. With regard to other nitrated fatty acids our present study only allows a rough estimation of their concentration in human plasma. Thus, nitro-linoleic acid seems to occur physiologically at concentrations in the lower pM range. On the other hand, nitro-linolenic acid and nitro-arachidonic acid, i.e., the nitro-derivatives of higher unsaturated fatty acids, are to be expected at much lower concentrations in plasma of healthy humans. Validated GC–MS/MS methods and use of stable-isotope-labeled analogs of these nitro-fatty acids are required for accurate determination of their basal concentrations in human plasma.

Endogenous nitrated fatty acids, first and foremost nitro-oleic acid, have been proposed as a new class of cell-signaling molecules, storage and transport forms of NO bioactivity within the vasculature, and anti-inflammatory

mediators [2–7, 10]. Presumably, the basis for these proposals has been the finding by LC–MS/MS that the sum of nitro-fatty acids and their esterified forms occur at concentrations of the order of almost 1,000 nM in human blood [2, 5]. These reports have initiated much scientific work in the field of NO research. However, the findings of our group (present study and [13]) and the results reported in a recent paper [14] challenge the originally reported concentrations of nitro-fatty acids [2, 5].

As discussed by us recently [13], the reasons for this discrepancy and for the inability of Freeman's group to confirm originally reported concentrations for nitro-oleic acid and other nitro-fatty acids are unknown at present. The analytical performance of the LC–MS/MS method originally used for quantitative analyses has not been described adequately [5]. Thus, from the quantitative perspective the reliability of the LC–MS/MS method used in previous studies cannot be properly evaluated. Theoretically, differences may also be due to the different species investigated, i.e., mouse [5] versus human (present study and [13]). However, given the fair comparability between mouse and human with regard to fatty acid [19] composition and quantity in blood and urine, as well as to the nitric oxide (NO) pathway [20], it is unlikely that species differences may account for a three-order-of-magnitude discrepancy. Indeed, pointing out the discrepancies between

initial and recent reports, Rudolph et al. discussed in their recent paper that “We and others have detected nitro-oleate in rodents and humans in other instances, as well as metabolites reported herein” [14]. Unlike other nitrosated and nitrated biomolecules such as *S*-nitrosothiols [21] and 3-nitrotyrosine [22, 23], artifactual formation of nitro-fatty acids is unlikely [13]. We can therefore only hypothesize that mainly analytical factors, such as lack of specificity of the LC–MS/MS method used, have resulted in severe artefacts. The large discrepancy and the inadequate description of the analytical performance of the LC–MS/MS method used in previous studies [2, 5] underscore the pressing need for validation of analytical methods and reporting of their analytical performance in detail prior to their use in quantitative analyses. The discrepancy seen in reported nitro-fatty acid plasma concentrations emphasizes the observation that the L-arginine/NO area of research is highly susceptible to analytical difficulties [24].

Freeman and co-workers have recently provided the following two explanations for their failure to detect nitro-oleic acid unlike in their previous studies [14, 25]: (1) “The initial report of ~500 nM nitro-oleate in human plasma (1) is now viewed to be higher than current measurements, with the original value complicated by non-covalent complexes of nitrite and oleate.”; and (2) “These previous estimates of free and esterified *cis*-nitroalkenes derivatives are now viewed to be overestimated in concentration due to electrophilic adduction of biological nucleophiles [100] and the co-elution of an isobaric molecule that is not covalently nitrated.¹”. These explanations are not clear and not likely from the chemical and analytical point of view, in our opinion, and deserve clarification.

Very recently, Schopfer et al. reported that nitro-oleic acid forms protein adducts, with endogenous protein-adducted nitro-oleic acid being, however, not detectable in plasma of untreated mice as measured by LC–MS/MS [25]. This finding argues against the assumption that “electrophilic adduction of biological nucleophiles” might have interfered [26]. Furthermore, this finding suggests that the fraction of non-protein-adducted nitro-oleic acid should be considered rather minor due to the rather inert vinyl functionality of nitro-oleic acid against nucleophiles such as sulfhydryl groups. For example, the cyclopentenone ring of prostaglandins such as 15-deoxy-prostaglandin J₂ (15-d-PGJ₂) is highly reactive towards nucleophiles, so that the non-protein-adducted and nonconjugated forms are practically not detectable in human plasma and urine (≤ 150 pM) as measured by us using GC–MS/MS (unpublished results). As stated above for nonadducted nitro-fatty acids, it may also be concluded for adducts of nitro-fatty acids that analytical methods need to be validated and proven prior to their use in quantitative analyses of such adducts which require additional analytical steps.

So far, there are no *in vivo* studies to indicate any involvement of endogenous nitro-fatty acids such as nitro-oleic acid in physiology and pathology based on the use of reportedly really reliable analytical quantitative methods. In consideration of the likely analytical inadequacy one may also question results generated by the same LC–MS/MS method [14, 26], which is now assumed to be not free of artefacts. Also, biological effects seen in association with nitro-fatty acids, such as anti-inflammatory actions and NO signaling, originate from the use of synthetic nitro-fatty acids at extraordinarily high concentrations [26] compared with their basal plasma concentrations. In this context, it is worth mentioning that nitro-arachidonic acid had to be used at concentrations of 1,000–5,000 nM in order to achieve any appreciable biological response [10, 27]. Presumably, and on a rather conservative basis, the concentration of nitro-arachidonic acid used *in vitro* is 10,000–50,000 times higher than the concentration of endogenous nitro-arachidonic acids in tissue. This may equally apply to nitro-oleic acid and nitro-linoleic acid [28–30]. Such concentrations are most likely beyond any pathophysiological relevance. With regard to a potential pharmacological relevance of nitro-fatty acids several factors need to be considered, including their rather very low potency, for instance regarding NO-dependent vasorelaxation, their rapid and extensive metabolism [14], and presumably their very high protein binding. In synergy, these factors may make mandatory the administration of very high doses with the potential risk of severe adverse effects.

To conclude, in view of the possibly lacking occurrence of nitro-arachidonic acid and nitro-linolenic acid and of the most likely pM concentrations of the simply unsaturated nitro-oleic acid in human blood, the physiology, pathology, and pharmacological potential of nitro-fatty acids demand thorough revision and consideration of the new analytical facts (present study and [13, 14]). Reliable, thoroughly validated, and adequately reported analytical methods are required and are the key to achieving reliable scientific results and to progress.

References

1. Balazy M, Iesaki T, Park JL, Jiang H, Kaminski PM, Wolin MS (2001) Vicinal nitrohydroxyeicosatrienoic acids: vasodilator lipids formed by reaction of nitrogen dioxide with arachidonic acid. *J Pharmacol Exp Ther* 299:611–619
2. Baker PRS, Schopfer FJ, Sweeney S, Freeman BA (2004) Red cell membrane and plasma linoleic acid nitration products: synthesis, clinical identification, and quantitation. *Proc Natl Acad Sci USA* 101:11577–11582
3. Kalyanaraman B (2004) Nitrated lipids: a class of cell-signaling molecules. *Proc Natl Acad Sci USA* 101:11527–11528

4. Schopfer FJ, Baker PRS, Giles G, Chumley P, Batthyany C, Crawford J, Patel RP, Hogg N, Branchaud BP, Lancaster JR Jr, Freeman BA (2005) Fatty acid transduction of nitric oxide signalling. *J Biol Chem* 280:19289–19927
5. Baker PRS, Lin Y, Schopfer FJ, Woodcock SR, Groeger AL, Bathany C, Sweeney S, Long MH, Iles KE, Baker LMS, Branchaud BP, Chen YE, Freeman BA (2005) Fatty acid transduction of nitric oxide signalling. *J Biol Chem* 280:42464–42475
6. Lima ES, Bovini MG, Augusto O, Barbero HV, Souza HP, Abballa DSP (2005) Nitrated lipids decompose to nitric oxide and lipids radicals and cause vasorelaxation. *Free Radic Biol Med* 39:532–539
7. Cui T, Schopfer FJ, Zhang J, Chen K, Ichikawa T, Baker PRS, Bathany C, Chacko BK, Feng X, Patel RP, Agarwal A, Freeman BA (2005) Nitrated fatty acids: endogenous anti-inflammatory signalling mediators. *J Biol Chem* 281:35686–35698
8. Woodcock SR, Marwitz AJV, Bruno P, Branchoud BP (2006) Synthesis of nitrolipids. All four possible diastereomers of nitrooleic acids: (*E*)- and (*Z*)-, 9- and 10-nitro-octadec-9-enoic acids. *Org Lett* 8:3931–3934
9. Jain K, Siddam A, Marathi A, Roy U, Falck JR, Balazy M (2008) The mechanism of oleic acid nitration by $\cdot\text{NO}_2$. *Free Radic Biol Med* 45:269–283
10. Trostchansky A, Rubbo H (2008) Nitrated fatty acids: mechanism of formation, chemical characterization, and biological properties. *Free Radic Biol Med* 44:1887–1896
11. Rubbo H, Radi R (2008) Protein and lipid nitration: role in redox signaling and injury. *Biochim Biophys Acta* 1780:1318–1324
12. Freeman BA, Baker PRS, Schopfer FJ, Woodcock SR, Napoletano A, d'Ischia M (2008) Nitro-fatty acid formation and signaling. *J Biol Chem* 283:15515–15519
13. Tsikas D, Zoerner A, Mitschke A, Homsy Y, Gutzki FM, Jordan J (2009) Specific GC–MS/MS stable-isotope dilution methodology for free 9- and 10-nitro-oleic acid in human plasma challenges previous LC–MS/MS reports. *J Chromatogr B* 877:2895–2908
14. Rudolph V, Schopfer FJ, Khoo NKH, Rudolph TK, Cole MP, Woodcock S, Bonacci G, Groeger AL, Golin-Bisello F, Chen CS, Baker PRS, Freeman BA (2009) Nitro-fatty acid metabolome: saturation, desaturation, β -oxidation, and protein adduction. *J Biol Chem* 284:1461–1473
15. Hu C, van der Heijden R, Wang M, van der Greef J, Hankemeier T, Xu G (2009) Analytical strategies in lipidomics and applications in disease biomarker discovery. *J Chromatogr B* 877:2836–2846
16. Annesley TM (2003) Ion suppression in mass spectrometry. *Clin Chem* 49:1041–1044
17. Matuszewski BK (2006) Standard line slopes as a measure of a relative matrix effect in quantitative HPLC–MS bioanalysis. *J Chromatogr B* 820:293–300
18. Tsikas D, Dehnert S, Urban K, Surdacki A, Meyer HH (2009) GC–MS analysis of *S*-nitrosothiols after conversion to *S*-nitroso-*N*-acetylcysteine ethyl ester and in-injector nitrosation of ethyl acetate. *J Chromatogr B*. doi:10.1016/j.jchromb.2009.06.032
19. Christeff N, Homo-Delarche F, Thobie N, Durant S, Dardenne M, Nunez EA (1994) Free fatty acid profiles in the non-obese diabetic (NOD) mouse: basal serum levels and effects of endocrine manipulation. *Prostaglandins Leukot Essent Fatty Acids* 51:125–131
20. Jobgen WS, Jobgen SC, Li H, Meininger CJ, Wu G (2007) Analysis of nitrite and nitrate in biological samples using high-performance liquid chromatography. *J Chromatogr B* 851:71–82
21. Giustarini D, Milzani A, Dalle-Donne I, Rossi R (2007) Detection of *S*-nitrosothiols in biological fluids: a comparison among the most widely applied methodologies. *J Chromatogr B* 851:124–139
22. Tsikas D, Caidahl K (2005) Recent methodological advances in the mass spectrometric analysis of free and protein-associated 3-nitrotyrosine in human plasma. *J Chromatogr B* 814:1–9
23. Ryberg H, Caidahl K (2007) Chromatographic and mass spectrometric methods for quantitative determination of 3-nitrosotyrosine in biological samples and their application to human samples. *J Chromatogr B* 851:160–171
24. Tsikas D (2008) A critical review and discussion of analytical methods in the *L*-arginine/nitric oxide (NO) area of basic and clinical research. *Anal Biochem* 379:139–163
25. Schopfer FJ, Batthyany C, Baker PRS, Bonacci G, Cole MP, Rudolph V, Groeger A, Rudolph TK, Nadochiy S, Brookes PS, Freeman BA (2009) Detection and quantification of protein adduction by electrophilic fatty acids: mitochondrial generation of fatty acid nitroalkene derivatives. *Free Radic Biol Med* 46:1250–1259
26. Baker PRS, Schopfer FJ, O'Donnell VB, Freeman BA (2009) Convergence of nitric oxide and lipid signaling: anti-inflammatory nitro-fatty acids. *Free Radic Biol Med* 46:989–1003
27. Trostchansky A, Souza JM, Ferreira A, Ferrari M, Blancko F, Trujillo M, Castro D, Cerecetto H, Baker RP, O'Donnell VB, Rubbo H (2007) Synthesis, isomer characterization, and anti-inflammatory properties of nitroarachidonate. *Biochemistry* 46:4645–4653
28. Chen L, Bosworth CA, Pico T, Collawn JF, Varga K, Gao Z, Clancy JP, Fortenberry JA, Lancaster JR Jr, Matalon S (2008) DETANO and nitrated lipids increase chloride secretion across lung airway cells. *Am J Respir Cell Mol Biol* 39:150–162
29. Iles KE, Wright MM, Cole MP, Welty NE, Ware LB, Matthay MA, Schopfer FJ, Baker PRS, Agarwal A, Freeman BA (2009) Fatty acids transduction of nitric acid signalling: nitrooleic acid mediates protective effects through regulation of the ERK pathway. *Free Radic Biol Med* 46:866–875
30. Taylor-Clark TE, Ghatta S, Bettner W, Udem BJ (2009) Nitrooleic acid, an endogenous product of nitrative stress, activates nociceptive sensory nerves via the direct activation of TRPA1. *Mol Pharmacol* 75:820–829

Liquid Chromatography–High-Resolution Mass Spectrometry for Quantitative Analysis of Gangliosides

Bertram Fong · Carmen Norris · Edwin Lowe · Paul McJarrow

Received: 20 April 2009 / Accepted: 22 June 2009 / Published online: 26 July 2009
© AOCs 2009

Abstract Gangliosides are a large family of glycosphingolipids that are abundant in the brain, and have been shown to affect neuronal plasticity during development, adulthood, and aging. We developed a fast, efficient, and sensitive liquid chromatography–mass spectrometry method to quantify eight different classes of gangliosides (GM₁, GM₂, GM₃, GD₃, GD_{1a}, GD_{1b}, GT_{1b}, GQ_{1b}) in the brains of 2-day-old and 80-day-old Wistar rats. The gangliosides were extracted from rat brain using a modified Svennerholm and Fredman method. After ganglioside class separation using a hydrophilic high performance liquid chromatography (HPLC) column, the resolving power of the LTQ-OrbitrapTM mass spectrometer was used to extract and sum the major species of each ganglioside class, generating fully resolved extracted ion current peaks for both standards and samples. The flexibility and the specificity of this method are such that it can be applied to the analysis of other ganglioside species/classes not discussed in this paper, provided appropriate standards are available. The method had good repeatability (coefficient of variation 4.8–12.3%) and mean recoveries in the range 92–107%.

Keywords Electrospray ionisation–mass spectrometry · Glycosphingolipids · LTQ-OrbitrapTM · Ganglioside quantification

Abbreviations

CV	Coefficient of variation
LBSA	Lipid-bound sialic acid
LOD	Limit of detection
LOQ	Limit of quantification
NANA	<i>N</i> -acetylneuraminic acid
NGNA	<i>N</i> -glycolylneuraminic acid

Introduction

Gangliosides, a large family of complex lipids that are abundant in the brain, have been shown to affect neuronal plasticity during development, adulthood, and aging and are considered to be possible therapeutics [1–3]. Gangliosides in human milk and infant milk formula are considered to be bioactive components in human infant nutrition and have an important role during early infancy, modifying the intestinal microflora and promoting the development of intestinal immunity in the neonate [4].

Thin layer chromatography (TLC) coupled with densitometry detection [5, 6] and high performance liquid chromatography (HPLC) [7–12] methods have traditionally been used to measure ganglioside levels in tissues.

More recently, liquid chromatography–mass spectrometry (LC–MS) methods have been used for the quantification of selected gangliosides. LC–MS offers improved sensitivity and selectivity over the more traditional TLC and HPLC methods for ganglioside detection. For example, Sorensen [13] used an LC–electrospray tandem MS method (LC–MS/MS) for the quantification of two ganglioside classes (GM₃ and GD₃) in bovine milk and in infant formulae using a standard addition technique. Gu et al. [14]

B. Fong (✉) · C. Norris · E. Lowe · P. McJarrow
Fonterra Research Centre, Dairy Farm Road,
Private Bag 11029, Palmerston North 4412,
New Zealand
e-mail: bertram.fong@fonterra.com

used an LC–MS/MS method for the quantification of a single species of both GM₁ and GM₂ in cerebrospinal fluid, using isotope dilution techniques. Sommer et al. [15] also used an LC–MS method to measure four gangliosides (GM₃, GM_{1a}, GD_{1a}, and GT_{1b}) in human lipoprotein lipids. Quantification was based on the signal area of single ion chromatograms at the appropriate retention time.

In this study, we used the resolving power of an LTQ–OrbitrapTM mass spectrometer to extract and sum the major ganglioside species [16, 17] present within eight classes of ganglioside (GM₁, GM₂, GM₃, GD₃, GD_{1a}, GD_{1b}, GT_{1b}, and GQ_{1b}) in order to quantitatively determine the amount of these ganglioside classes present in rat brain samples. The advantage of this LC–MS method is its ability to measure eight individual ganglioside classes simultaneously and to give detail on the relative proportions of the molecular species present within each ganglioside class.

The described method was used to compare the ganglioside composition in the brains of 2-day-old and 80-day-old rats. Although a large number of gangliosides are present in rat brain, many are minor. The eight classes were chosen for analysis by LC–MS, based on the reported abundance [18] and the availability of commercial standards.

Experimental Procedure

Standards and Chemicals

Ganglioside standards were obtained from Matreya, LLC (Pleasant Gap, PA). All solvents used were of LC grade (Merck, Darmstadt, Germany), except for chloroform which was analytical grade (ethanol stabilized).

Sample Preparation

Rat brains were obtained from 2-day-old and 80-day-old Wistar rats. The brain lipids were extracted using a modified Svennerholm and Fredman extraction protocol [19]. This method was used to remove the phospholipids present in the tissue, as we found that the presence of high levels of phospholipids in the extract suppresses ionization of the gangliosides.

Briefly, the left hemisphere of rat brain was homogenized in 3 ml of water for 1–2 min in an ice bath using an ultrasonicator probe. A portion of the rat brain homogenate (0.5 ml) was weighed into a 10-ml Kimax tube. Water (0.5 ml) was added to the homogenate, followed by methanol (2.7 ml) and chloroform (1.35 ml) at room temperature. The mixture was allowed to rock gently for 30 min on a rocker before centrifugation at 2,000g for 30 min. The supernatant was transferred to a 15-ml Kimax

tube and the pellet was re-extracted using water (0.5 ml) and chloroform/methanol (1:2, 2 ml). After mixing and centrifugation (30 min at 2,000g), the supernatants were pooled and the pellet was discarded. Solvent partition of the supernatant was achieved by the addition of water (1.3 ml) and gentle inversion three to four times, followed by centrifugation (2,000g for 30 min). The upper phase was transferred to a 10-ml volumetric flask. KCl (0.01 M, 0.5 ml) was added to the remaining lower phase and any interfacial fluff (minimal) and was centrifuged (2,000g, 20 min). The upper phase was pooled into the 10-ml volumetric flask without disturbing any interfacial fluff, and the flask was made up to the mark with methanol (50%). The upper phase was used for ganglioside analysis.

Standard Preparation

Ganglioside stock standards [GM₁ (bovine brain), GM₂ (human brain), GM₃ (bovine buttermilk), GD_{1a} (bovine brain), GD_{1b} (bovine brain), GD₃ (bovine buttermilk), GT_{1b} (bovine brain), and GQ_{1b} (bovine brain)] were obtained from Matreya, LLC (Pleasant Gap, PA) and were prepared at 1 mg/ml or 0.5 mg/ml in methanol (50%). An intermediate mixed standard solution was prepared from each stock solution into a 5-ml volumetric flask, and was serially diluted further in methanol (50%) to give a seven-point calibration curve (Fig. 1). All solutions were stored at –80 °C.

High Performance Liquid Chromatography

The HPLC analysis was performed on an Agilent 1100 series HPLC system (Santa Clara, CA) consisting of a quaternary pump, binary pump, degasser, column heater (60 °C), and refrigerated auto-sampler (5 °C). Samples or standards (10 µl) were initially loaded (0.5 ml/min; 50%

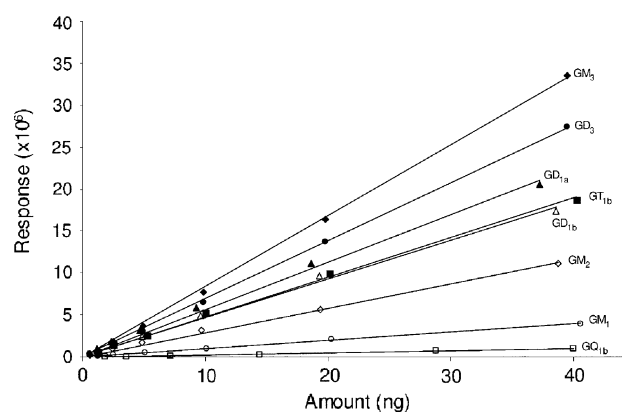


Fig. 1 Ganglioside calibration curve. The correlation coefficient r for every ganglioside is >0.9 . Amount (ng) refers to the ng of each ganglioside loaded onto the HPLC column

Table 1 HPLC mobile phase solvent gradient for separation of the gangliosides

Time (min)	Trap valve position	A (%)	B (%)	C (%)
0	Waste	95	5	0
2		95	5	0
4		95	5	0
8	Detector			
15		10	90	0
16		0	0	100
18		0	0	100
19	Waste	95	5	0
25		95	5	0

Solvent A consisted of acetonitrile (100%), solvent B consisted of 50:50 acetonitrile/50 mM ammonium acetate buffer, pH 5.6, and solvent C consisted of 50:50 methanol/water. The flow rate was 0.5 ml/min

methanol) on to a wide pore, reversed-phase trap (C18, 4 mm × 2.0 mm, 5 μm, Phenomenex, CA) for pre-concentration/desalting. After 8 min, the trap was switched in-line with an APS-2 hypersil hydrophilic column (150 mm × 2.1 mm, 3 μm, Thermo Electron Corporation, Waltham, MA) coupled to an APS-2 guard column (10 mm × 2.1 mm inner diameter). The gangliosides were separated with an acetonitrile/ammonium acetate buffer gradient as described in Table 1.

Mass Spectrometry

The eluate from the HPLC system was introduced into an LTQ-OrbitrapTM mass spectrometer (Thermo Electron Corporation, Waltham, MA) using an ESI probe inlet. Ions were generated and focused using an ESI voltage of −3,750 V, a sheath gas flow of 30 L/min, an auxiliary gas flow of 10 L/min, and a capillary temperature of 300 °C. MS data acquisition was carried out with the LTQ-OrbitrapTM mass spectrometer scanning in negative ion mode over 700–1,650 *m/z*, with a resolution of 30,000 @ 400 *m/z*. The system was calibrated with ganglioside standards obtained from Matreya, LLC (Pleasant Gap, PA) as described above. The HPLC run was diverted to waste for the first 9 min and after 18 min. The total run time was 25 min.

The resolving power of the LTQ-OrbitrapTM mass spectrometer was used to filter post analysis for known masses of ganglioside species present within each class of ganglioside measured. Three factors were considered when compiling our extract mass lists for filtering post analysis.

Sphingosine group and fatty acid side chains

The exact ganglioside masses extracted (including three carbon 13 isotopes) were based on sphingosine d18:1 and

d20:1, and dihydrosphingosine d18:0 with fatty acid side chains C16:0, C18:0, C18:1, C20:0, C21:0, C22:0, C23:0, and C24:0. These ganglioside species represent the major proportion of the ganglioside species present in rat brain [17, 20].

Sugar moiety

Only gangliosides containing *N*-acetylneuraminic acid (NANA), and not *N*-glycolylneuraminic acid (NGNA), were included in the mass list calculations, as these species make up the majority of gangliosides observed in rat brain [18].

Charge state

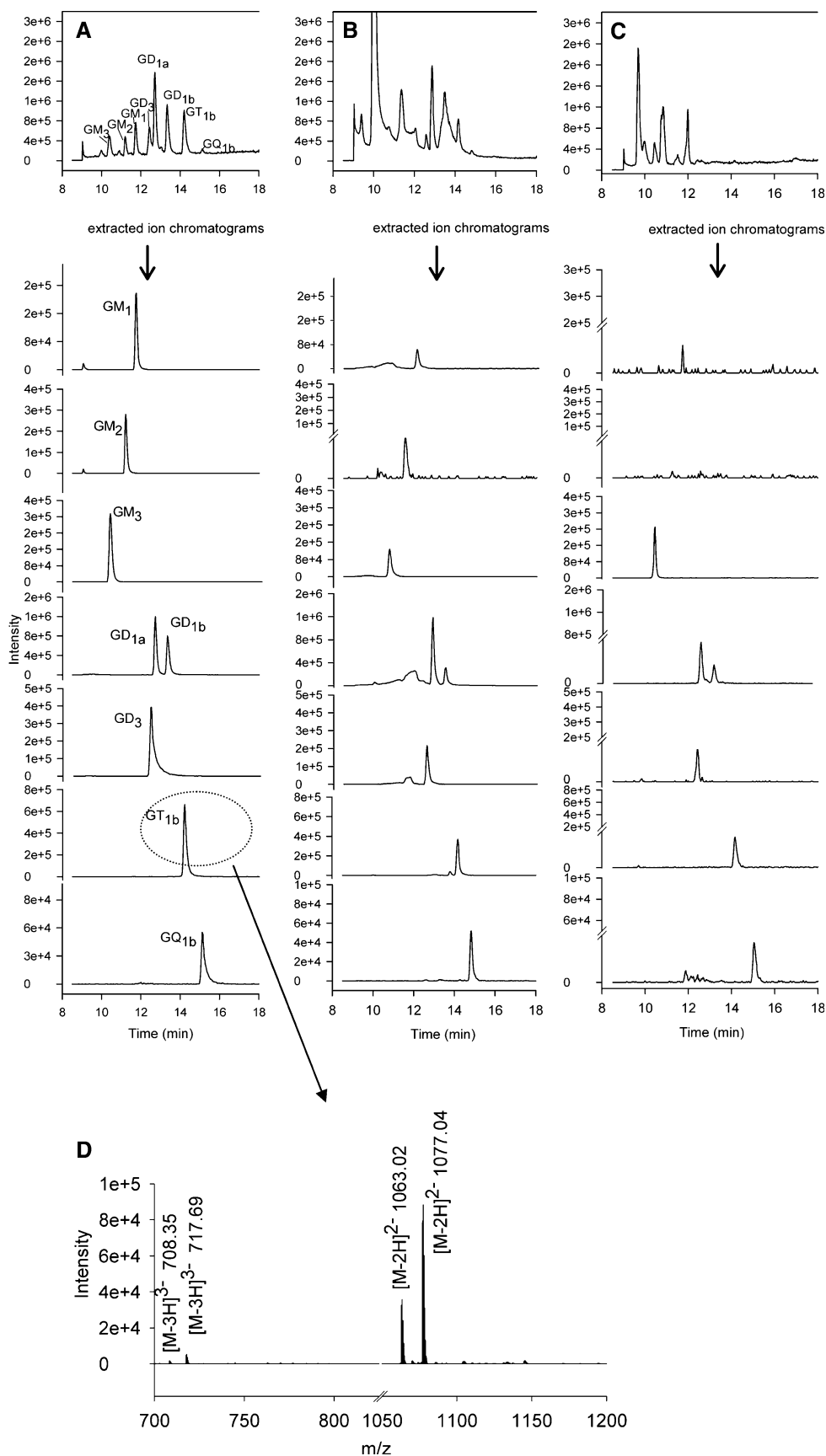
The number of NANA residues present on a ganglioside molecule determines the number of possible charge states that may be observed in the (electrospray) mass spectra of that ganglioside. Where more than one charge state existed for a given class of ganglioside, the charge state(s) observed in the greatest intensity were those used for compiling our mass lists. Figure 2d shows an extracted ion spectrum of calibration standard GT_{1b} displaying prominent species (most likely dC18:1/C18:0 and dC20:1/C18:0) in their −2 and −3 charge states [16]. The charge state(s) selected for each ganglioside class were as follows: (GM₁ [M−H][−], GM₂ [M−H][−], GM₃ [M−H][−], GD_{1a} [M−2H]^{2−}, GD_{1b} [M−2H]^{2−}, GD₃ [M−2H]^{2−}, GT_{1b} [M−2H]^{2−}, [M−3H]^{3−}, and GQ_{1b} [M−2H]^{2−}, [M−3H]^{3−}).

The excellent specificity of the method allowed us to use it confidently to quantify gangliosides in rat serum samples (extracted using the modified Svennerholm and Fredman extraction protocol where the serum samples were treated the same as homogenised brains), which have proportionally much lower levels of gangliosides than brain extracts (Fig. 2). The flexibility of this technique may also allow for quantification of other ganglioside species (e.g., NGNA-containing or *O*-acetylated gangliosides) or classes such as GM₄ that are present in tissue or serum samples and that are not discussed in this paper, provided that appropriate standards are available. Qualitative comparison using theoretical molecular masses could also be undertaken when standards are not available.

Accuracy and Repeatability

The accuracy and the repeatability of the method were evaluated by performing recovery studies, the between-day precision, and the within-day precision using an 80-day-old rat brain.

Fig. 2 Total ion current of the calibration mix (20 ng, **a**), rat brain extract (**b**), and rat serum (**c**) followed by the extracted ion chromatograms of each ganglioside class analyzed. The extracted ion spectrum of calibration standard GT_{1b} (**d**) shows the two dominant species present in the mix (most likely dC18:1/C18:0 ([M–2H]^{–2} 1063.02, [M–3H]^{–3} 708.35) and dC20:1/C18:0 ([M–2H]^{–2} 1077.04, [M–3H]^{–3} 717.69). The quantification of each class of ganglioside was carried out using the peak areas obtained from each extracted ion chromatogram



Results and Discussion

HPLC–MS

Figure 2 shows a separation of the gangliosides in a standard mixture, and in sample (rat brain and serum). We used a hydrophilic HPLC column because of its ability to separate gangliosides largely by sugar moiety or class, as opposed to reversed-phase columns which separate gangliosides largely by carbon number, leading to multiple peaks for each class of ganglioside [21]. It was important to condition the column before use to stabilize the retention time, particularly for GT_{1b} and GQ_{1b}. Conditioning was achieved by repeated injection of the standards and samples overnight. Adequate blanks were run prior to analysis to avoid any carryover issues.

Calibration Curve

The HPLC–MS method used an external standard to quantify the relative amounts of gangliosides present in rat brain. A typical calibration curve obtained by the method is given in Fig. 1. The linear calibration range used routinely in this study was up to 40 ng on-column but could be extended to twice that magnitude. The variation in response between different ganglioside classes observed in Fig. 1 may in part be explained by the size of the glycan portion of the ganglioside and the position of NANA on the ganglioside molecule, bound to the internal or terminal galactose. The possibility of NANA loss from the gangliosides due to front end collision induced dissociation (CID) causing this reduction in response was investigated. No fragments arising from the loss of NANA were observed in the spectra.

The current method was used to compare samples derived from the same sample matrix, i.e., 2-day-old and 80-day-old rat brains, and results were not corrected for any variation in ionization efficiencies of species within a given ganglioside class that may exist. Consequently the results may not be absolute. Variation in ionization efficiency has been corrected by the use of internal standards for the quantification of other classes of lipids, e.g., phospholipids [22–24]. The need for this correction for ganglioside analysis is currently being investigated in our laboratory.

Accuracy and Precision

Matrix Effects

The brain extracts were serially diluted and compared with their respective standard curves. Only GQ_{1b} showed any matrix effects; at high concentration, suppression of the

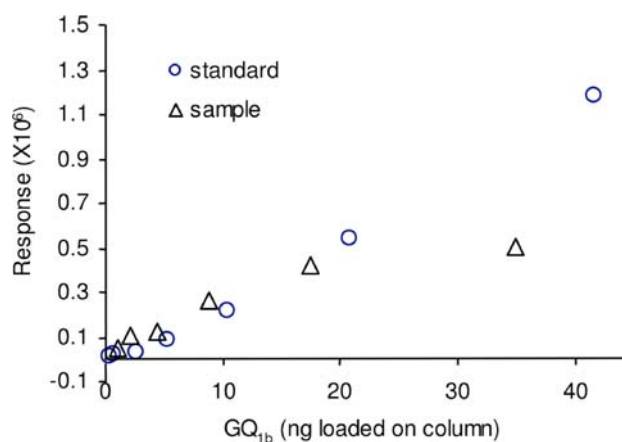


Fig. 3 Response of gangliosides in standards and sample (*control*) solutions. All gangliosides, except GQ_{1b}, showed the same response over the measured concentration range

response was observed at above approximately 20 ng loaded. Dilution of the extract to below 20 ng/10 μ l loaded was required to eliminate this matrix effect (Fig. 3). It is unclear what components in the matrix were affecting the GQ_{1b} response.

Spiked Recovery

Recovery experiments were conducted using homogenized rat brains spiked with a mixed ganglioside standard. The spiking solutions were measured into 10 ml Kimax tubes and were evaporated to near dryness under a stream of nitrogen at 25 °C. Homogenized brain (1 ml) or water (1 ml) was added and extraction proceeded as outlined previously. Given the nature of the method, solvent/solvent extraction, the recoveries (Table 2) were extremely good, ranging from 84 to 110%. Higher than 100% recovery can be explained by the coefficients of variance of the method measuring the endogenous gangliosides.

Method Repeatability

The repeatability of the method was calculated using the pooled standard deviation determined from 48 samples analyzed in duplicate across the control, low treatment, and

Table 2 Recovery (%) of gangliosides after spiking into a water blank and into rat brain homogenate

	GM ₁	GM ₂	GM ₃	GD ₃	GD _{1a}	GD _{1b}	GT _{1b}	GQ _{1b}
Water	95	95	102	90	93	89	No data	No data
	92	96	84	94	103	104		
Rat brain	94	94	96	103	96	92	101	94
	102	93	104	110	97	97		
	111	101	92		98	102		

Table 3 Repeatability percentage coefficient of variation (CV) for gangliosides, determined from the pooled standard deviation of 48 duplicate analyses of rat brain across the control, low treatment, and high treatment groups

Ganglioside	Mean ($\mu\text{g/g}$)	CV (%)
GM ₃	47.2	8.8
GM ₂	13.9	12.3
GM ₁	383.1	7.2
GD ₃	21.9	4.8
GD _{1a}	531.1	5.7
GD _{1b}	324.1	5.0
GT _{1b}	615.9	5.1
GQ _{1b}	814.9	6.0

high treatment groups. The coefficients of variation ranged from 4.8 to 12.3% (Table 3).

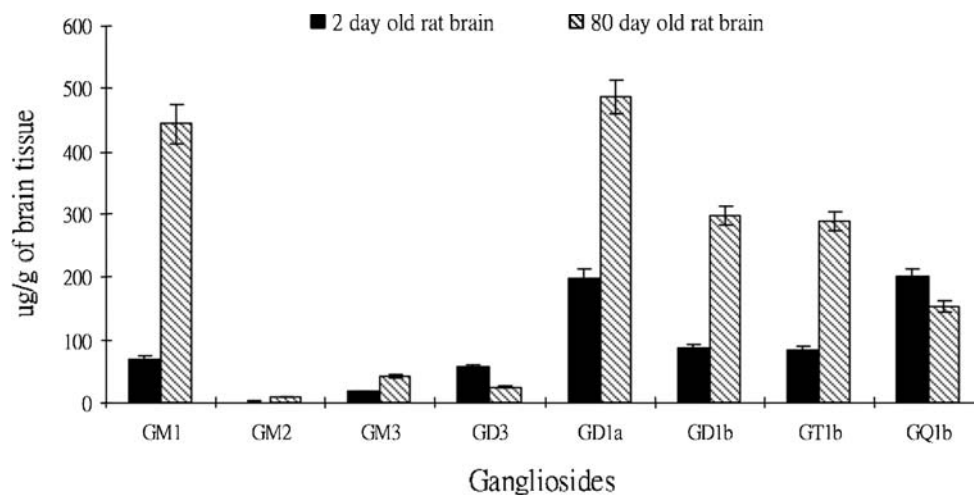
Limit of Detection (LOD) and Limit of Quantification (LOQ)

The LOD was estimated by loading decreasing amounts of ganglioside standard on to the HPLC–MS system until the peak was three times the noise level. The LOQ was estimated as three times the LOD. The LODs were determined to be 0.34, 0.08, 0.16, 0.09, 0.08, 0.16, 0.17, 0.84 and LOQs 1.00, 0.25, 0.50, 0.30, 0.25, 0.50, 0.50, 2.50 ng on column for GM₁, GM₂, GM₃, GD_{1a}, GD_{1b}, GD₃, GT_{1b} and GQ_{1b}, respectively. Sensitivity could be further improved by using a hydrophilic column with a smaller column diameter as they become available.

Gangliosides in the Brains of 2-Day-Old and 80-Day-Old Rats

The distributions of the individual ganglioside classes in 2-day-old and 80-day-old rat brains are shown in Fig. 4

Fig. 4 Ganglioside distribution in 2-day-old ($n = 22$) and 80-day-old ($n = 11$) rat brain



(as μg ganglioside/g brain (wet weight)) and Table 4 (as percentage of total ganglioside). Figure 4 shows an increase in the amount of ganglioside as the rat brain developed, consistent with results reported by Vanier et al. [25]. The substantial decrease in GQ_{1b} and the substantial increase in GT_{1b}, as a percentage of total ganglioside shown in Table 4, are consistent with trends outlined by Rosner et al. [26] as the rat brain ages, but disagree with those reported by Yu et al. [18], where the GQ_{1b} percentage of lipid-bound sialic acid (LBSA) remained the same and the GT_{1b} (percentage of LBSA) decreased with age. The gangliosides GM₁, GM₃ and GD_{1a} increase in concentration between the two ages (Fig. 4) as the concentration of total gangliosides increases. The significant rise in the percentage of GM₁ between the day 2 and day 80 tissues (Table 4) is consistent with both Rosner et al. [28] and Yu et al. [27] but GD_{1a} and GM₃ do not increase as a percentage of LBSA which is consistent with Yu et al. [18], but not Rosner et al. [26].

We compared our 2-day-old and 80-day-old rat brain ganglioside results (percentage ganglioside) with similar results (newborn and adult rat brain) reported by Yu et al. [27] (Table 4). Whereas the 80-day-old and adult rat brain analyses compared very well for all the measured ganglioside classes (Table 4), the 2-day-old and newborn rat brain analyses compared well for all ganglioside classes except GQ_{1b}, GD₃, and GT_{1b}. The difference in age between the newborn and the 2-day-old rat brain samples may go some way to explaining the discrepancies observed between the two sets of data, as, just after birth, the rat brain is developing rapidly [25]. The influence of the different methods of analysis, the strain of rat and the number of individuals sampled in this study and that of Yu et al. [27] may also help to explain the discrepancies between the results. Certainly, Rosner et al. [26] indicated a small increase in the relative concentration of GD₃ just after birth and there is also an increasing percentage of GT₁/GD_{1b}

Table 4 Ganglioside distribution in newborn and adult rats

	Molecular weight ^a	Lipid-bound sialic acid (%) Newborn ^b	Ganglioside (%)		Lipid-bound sialic acid (%) Adult ^b	Ganglioside (%)	
			Newborn ^c	2-day-old ^d		Adult ^c	80-day-old ^d
GM ₁	1,546.87	5.4	10	10	12.9	22	25
GM ₂	1,383.82	1	2	0	0.4	1	0
GM ₃	1,180.74	1.5	2	2	1.7	2	2
GD ₃	1,472.84	3.3	3	8	0.6	0	1
GD _{1a}	1,836.97	29	31	28	27.8	28	28
GD _{1b}	1,836.97	11	12	12	15.8	16	17
GT _{1b}	2,128.06	34.4	29	12	25.4	20	17
GQ _{1b}	2,419.16	11	8	28	11.5	8	9
GT _{1a}	2,128.06	Not detected	0	Not measured	Not detected	0	Not measured
GD ₂	1,674.92	3.4	3	Not measured	3.8	3	Not measured
Total sialic acid		286.9			768		

Comparison of results obtained from this study with those reported in the literature

^a The molecular weight of the most dominant ganglioside class species (dC18:1/C18:0) was used to convert lipid-bound sialic acid to ganglioside equivalent

^b Lipid-bound sialic acid data obtained from Yu et al. [27]

^c Lipid-bound sialic acid results from Yu et al. [27] converted to percentage ganglioside equivalent to allow direct comparison with our data

^d Total ganglioside levels were estimated by summing the amounts of the eight ganglioside classes measured in this study

around this time. The small number of studies that have investigated the ganglioside levels at this rapidly changing developmental stage of the rat brain makes it difficult to compare in detail this method and others with our 2-day-old rat brain analysis. With respect to the analysis of young adult rat brains (day 80) for gangliosides the results obtained using this study's methodology are consistent with those previously published [25, 27, 28] for adult rat brain ganglioside levels and individual ganglioside species distribution using this study's methodology are consistent with those previously published.

In conclusion, an LC–MS method for the simultaneous measurement of gangliosides in rat brain was developed. The flexibility of this method is such that it can be applied to the analysis of ganglioside classes not presented in this paper. This method could also be extended to measure the ganglioside (GM₁, GM₂, GM₃, GD₃, GD_{1a}, GD_{1b}, GT_{1b}, GQ_{1b}) content in other tissues or serum.

Acknowledgments The authors would like to thank Kathleen Schoeman for technical support, Charles Yang and Alastair MacGibbon for LC–MS discussions, Claire Woodhall for editing this manuscript, and Mark Vickers (Liggins Institute, Auckland University) for providing the rat brains.

References

- Hungund BL, Ross DC, Gokhale VS (1994) Ganglioside gm1 reduces fetal alcohol effects in rat pups exposed to ethanol in utero. *Alcohol Clin Exp Res* 18:1248–1251
- Laev H, Karpiak SE, Gokhale VS, Hungund BL (1995) In utero ethanol exposure retards growth and alters morphology of cortical cultures: gm1 reverses effects. *Alcohol Clin Exp Res* 19:1226–1233
- Saito M, Mao RF, Wang R, Vadasz C, Saito M (2007) Effects of gangliosides on ethanol-induced neurodegeneration in the developing mouse brain. *Alcohol Clin Exp Res* 31:665–674
- Wang B, McVeagh P, Petocz P, Brand-Miller J (2003) Brain ganglioside and glycoprotein sialic acid in breast-fed compared with formula-fed infants. *Am J Clin Nutr* 78:1024–1029
- Ando S, Chang NC, Yu RK (1978) High-performance thin-layer chromatography and densitometric determination of brain ganglioside compositions of several species. *Anal Biochem* 89:437–450
- Kasperzyk JL, El-Abbadi MM, Hauser EC, d'Azzo A, Platt FM, Seyfried TN (2004) *N*-butyldeoxygalactonojirimycin reduces neonatal brain ganglioside content in a mouse model of GM1 gangliosidosis. *J Neurochem* 89:645–653
- Nakabayashi H, Iwamori M, Nagai Y (1984) Analysis and quantitation of gangliosides as para-bromophenacyl derivatives by high-performance liquid-chromatography. *J Biochem* 96:977–984
- Ullman MD, McCluer RH (1985) Quantitative-analysis of brain gangliosides by high-performance liquid-chromatography of their perbenzoyl derivatives. *J Lipid Res* 26:501–506
- Miyazaki K, Okamura N, Kishimoto Y, Lee YC (1986) Determination of gangliosides as 2,4-dinitrophenylhydrazides by high-performance liquid-chromatography. *Biochem J* 235:755–761
- Traylor TD, Koontz DA, Hogan EL (1983) High-performance liquid-chromatographic resolution of para-nitrobenzylxyamine derivatives of brain gangliosides. *J Chromatogr* 272:9–20
- Wagener R, Kobbe B, Stoffel W (1996) Quantification of gangliosides by microbore high performance liquid chromatography. *J Lipid Res* 37:1823–1829
- Gazzotti G, Sonnino S, Ghidoni R (1985) Normal-phase high-performance liquid chromatographic separation of non-derivatized ganglioside mixtures. *J Chromatogr* 348:371–378

13. Sorensen LK (2006) A liquid chromatography/tandem mass spectrometric approach for the determination of gangliosides GD3 and GM3 in bovine milk and infant formulae. *Rapid Commun Mass Spectrom* 20:3625–3633
14. Gu JH, Tiffit CJ, Soldin SJ (2008) Simultaneous quantification of G(M1) and G(M2) gangliosides by isotope dilution tandem mass spectrometry. *Clin Biochem* 41:413–417
15. Sommer U, Herscovitz H, Welty FK, Costello CE (2006) LC–MS-based method for the qualitative and quantitative analysis of complex lipid mixtures. *J Lipid Res* 47:804–814
16. Avrova NF, Zabelins Sa (1971) Fatty acids and long chain bases of vertebrate brain gangliosides. *J Neurochem* 18:675
17. Rosenber A, Stern N (1966) Changes in sphingosine and fatty acid components of gangliosides in developing rat and human brain. *J Lipid Res* 7:122
18. Yu RK, Ledeen RW (1970) Gas–liquid chromatographic assay of lipid-bound sialic acids: measurement of gangliosides in brain of several species. *J Lipid Res* 11:506–516
19. Svennerholm L, Fredman P (1980) A procedure for the quantitative isolation of brain gangliosides. *Biochim Biophys Acta* 617:97–109
20. Valsecchi M, Palestini P, Chigorno V, Sonnino S (1996) Age-related changes of the ganglioside long-chain base composition in rat cerebellum. *Neurochem Int* 28:183–187
21. Ikeda K, Shimizu T, Taguchi R (2008) Targeted analysis of ganglioside and sulfatide molecular species by LC/ESI–MS/MS with theoretically expanded multiple reaction monitoring. *J Lipid Res* 49:2678–2689
22. Koivusalo M, Haimi P, Heikinheimo L, Kostianen R, Somerharju P (2001) Quantitative determination of phospholipid compositions by ESI–MS: effects of acyl chain length, unsaturation, and lipid concentration on instrument response. *J Lipid Res* 42:663–672
23. Brugger B, Erben G, Sandhoff R, Wieland FT, Lehmann WD (1997) Quantitative analysis of biological membrane lipids at the low picomole level by nano-electrospray ionization tandem mass spectrometry. *Proc Natl Acad Sci U S A* 94:2339–2344
24. Ahn EJ, Kim H, Chung BC, Moon MH (2007) Quantitative analysis of phosphatidylcholine in rat liver tissue by nanoflow liquid chromatography/tandem mass spectrometry. *J Sep Sci* 30:2598–2604
25. Vanier MT, Holm M, Ohman R, Svennerh L (1971) Developmental profiles of gangliosides in human and rat brain. *J Neurochem* 18:581–592
26. Rosner H, Alaqtum M, Rahmann H (1992) Gangliosides and neuronal differentiation. *Neurochem Int* 20:339–351
27. Yu RK, Macala LJ, Taki T, Weinfeld HM, Yu FS (1988) Developmental-changes in ganglioside composition and synthesis in embryonic rat-brain. *J Neurochem* 50:1825–1829
28. Rosner H (2003) Developmental expression and possible roles of gangliosides in brain development. *Prog Mol Subcell Biol* 32:49–73

New Bioactive Oxylipins Formed by Non-Enzymatic Free-Radical-Catalyzed Pathways: the Phytoprostanes

Thierry Durand · Valérie Bultel-Poncé ·
Alexandre Guy · Susanne Berger ·
Martin J. Mueller · Jean-Marie Galano

Received: 24 July 2009 / Accepted: 11 September 2009 / Published online: 30 September 2009
© AOCs 2009

Abstract In animals and plants, fatty acids with at least three double bonds can be oxidized to prostaglandin-like compounds via enzymatic and non-enzymatic pathways. The most common fatty acid precursor in mammals is arachidonic acid (C20:4) (AA) which can be converted through the cyclooxygenase pathway to a series of prostaglandins (PG). Non-enzymatic cyclization of arachidonate yields a series of isoprostanes (IsoP) which comprises all PG (minor compounds) as well as PG isomers that cannot be formed enzymatically. In contrast, in plants, α -linolenic acid (C18:3) (ALA) is the most common substrate for the allene oxide synthase pathway leading to the jasmonate (JA) family of lipid mediators. Non-enzymatic oxidation of linolenate leads to a series of C18-IsoPs termed dinor IsoP or phytoprostanes (PP). PP structurally resemble JA but cannot be formed enzymatically. We will give an overview of the biological activity of the different classes of PP and also discuss their analytical applications and the strategies developed so far for the total synthesis of PP, depending on the synthetic approaches according to the targets and which key steps serve to access the natural products.

Keywords Phytoprostanes · Oxidative stress · Total synthesis · Biological properties

Abbreviations

AA	Arachidonic acid
Ac	Acetyl
ALA	α -Linolenic acid
<i>Bet</i> -APE	<i>Betula alba</i> L. aqueous pollen extracts
BINAL-H	Lithium (1,1'-binaphthyl-2,2'-dioxy) aluminum dihydride
Bz	Benzoyl
BzCl	Benzoylchloride
CAL-B	<i>Candida antarctica</i> lipase B
CH ₂ N ₂	Diazomethane
Co ₂ (CO) ₆	Hexacarbonyldicobalt complex
COII	Coronatine-insensitive1 (COII)
CuSO ₄	Copper sulfate
DABCO	Diazabicyclo[2.2.2]octane
DBU	1,8-Diazabicyclo[5.4.0]undec-7-ene
DCE	1,2-Dichloroethane
DCM	Dichloromethane
DMF	Dimethylformamide
DMP	Dess-Martin Periodinane
DMSO	Dimethylsulfoxide
dPPJ ₁	Deoxy-J ₁ -Phytoprostane
GC	Gas chromatography
GC-MS	Gas chromatography-mass spectrometry
HEK cell	Human embryonic kidney cell
HPLC	High performance liquid Chromatography

T. Durand (✉) · V. Bultel-Poncé · A. Guy · J.-M. Galano
Institut des Biomolécules Max Mousseron, IBMM,
UMR 5247, CNRS, Université Montpellier I,
Université Montpellier II,
Faculté de Pharmacie, 15. Av. Ch. Flahault,
34093 Montpellier Cedex 05, France
e-mail: Thierry.Durand@univ-montp1.fr

S. Berger · M. J. Mueller
Julius-von-Sachs-Institute for Biosciences,
Pharmaceutical Biology, University of Wuerzburg,
Julius-von-Sachs-Platz 2, 97082 Wuerzburg, Germany

HPLC–ESI–MS/MS	High performance liquid chromatography–Electrospray tandem mass spectrometry	TES	Triethylsilyl
HWE	Horner–Wadsworth–Emmons	TFA	Trifluoroacetic acid
IL	Interleukin	TGA	Transcription factors
IsoP	Isoprostane	THF	Tetrahydrofuran
JA	Jasmonic acid	THP	Tetrahydropyran-2-yl
JA-Ile	Isoleucine–jasmonic acid conjugate	Ts	Tosyl
KHMDS	Potassium hexamethyldisilazide	TsCl	Tosyl chloride
KOH	Potassium hydroxide	UV	Ultra-violet
LAH (LiAlH ₄)	Lithium aluminum hydride		
LC	Liquid chromatography		
LiHMDS	Lithium hexamethyldisilazide		
MAPK	Mitogen-activated protein kinases		
MeAlCl ₂	Methyl aluminum dichloride		
mRNA	Messenger ribonucleic acid		
MS	Mass spectrometry		
NaH	Sodium hydride		
NaHMDS	Sodium hexamethyldisilazide		
NaOH	Sodium hydroxide		
NEt ₃	Triethylamine		
NeuroP	Neuroprostane		
NF-κB	Nuclear factor-kappa B		
NICI	Negative ion capture chemical ionization		
NMO	<i>N</i> -Methylmorpholine <i>N</i> -oxide		
[¹⁸ O ₃]PPE1	Oxygen-18-labeled phytoprostane E1		
OPDA	12-Oxophytodienoic acid		
PAL	Phenylalanine ammonia lyase		
Pd(OAc) ₂	Palladium II acetate		
PG	Prostaglandin		
PP	Phytoprostane		
PPA ₁	Phytoprostane A ₁		
PPAR	Peroxisome proliferator-activated receptor		
PPB ₁	Phytoprostane B ₁		
PPD ₁	Phytoprostane D ₁		
PPE ₁	Phytoprostane E ₁		
PPF ₁	Phytoprostane F ₁		
PPG ₁	Phytoprostane G ₁		
PPh ₃	Triphenylphosphine		
PPJ ₁	Phytoprostane J ₁		
PUFA	Polyunsaturated fatty acid		
Pyr.	Pyridine		
ROS	Reactive oxygen species		
r. t.	Room temperature		
SPE	Solid phase extraction		
TBDPS	<i>Tert</i> -butyldiphenylsilyl		
TBS	<i>Tert</i> -butyldimethylsilyl		
TEA	Triethylamine		

Introduction

In animals and plants, fatty acids with at least three double bonds can be oxidized to prostaglandin-like compounds via enzymatic and non-enzymatic pathways [1]. The most common fatty acid precursor in mammals is arachidonic acid (C20:4) (AA) which can be converted through the cyclooxygenase pathway to a series of prostaglandins (PG). Non-enzymatic cyclization of arachidonate yields a series of isoprostanes (IsoP) which comprises all PG (minor compounds) as well as PG isomers that cannot be formed enzymatically. In contrast in plants, α -linolenic acid (C18:3) (ALA) is the most common substrate for the allene oxide synthase pathway leading to the jasmonate (JA) family of lipid mediators. Non-enzymatic oxidation of linolenate leads to a series of C18-IsoPs termed dinor IsoP or phytoprostanes (PP). PP structurally resemble JA but cannot be formed enzymatically.

PG and JA are short lived, local mediators that have important functions in animal and plant development, respectively. In both kingdoms, these mediators are essential for reproduction. Moreover, PG and JA can be rapidly formed by *de novo* synthesis in response to a variety of biotic (microorganisms) and abiotic (UV-light, wounding) stresses. In the acute stress response, PG and JA induce a massive defense response on a cellular level by reprogramming cellular metabolism through binding to extracellular receptors (PG) and through binding to intracellular receptors (JA, cyclopentenone prostanoids). As discussed below, IsoP and PP display some but not all biological activities of PG and JA. It is generally assumed that chemically synthesized isoprostanooids are accidentally formed by autoxidation and may incidentally bind to receptors involved in PG/JA signaling.

From an evolutionary point of view, PG and JA pathways evolved rather late and separately in the animal and plant kingdom. Although PG and JA can be found in some lower organisms, they are only common and display essential functions in mammals and higher land plants. In contrast, non-enzymatic formation of isoprostanooids takes place *in vivo* in all aerobic organisms that use polyunsaturated fatty

acids as membrane modules. Hence, isoprostanooids are an evolutionary ancient class of compounds which occur in most organisms.

Biosynthesis and Nomenclature of Phytoprostanes

IsoP have been well established as markers of oxidative stress in animals [2]. In plants, PG and IsoP cannot be formed, since higher plants generally lack the enzymatic capacity to form arachidonic acid.

α -Linolenic acid (C18:3 ω 3) is beside linoleic acid (C18:2 ω 6), the predominant polyunsaturated fatty acid in plant membranes [3]. α -Linolenate can be released from membrane lipids and metabolized via an enzymatic pathway to prostaglandin-like compounds of the JA family. The best studied jasmonates are 12-oxo-phytodienoic acid (OPDA), JA and its isoleucine conjugate (JA-Ile) [4]. However, the autoxidation of fatty acids that have more than two double bonds yields a series of oxylipins for which no enzymatic biosynthetic pathways have yet evolved in plants. Since α -linolenic acid is a major unsaturated fatty acid in plants and only a trace fatty acid in animals, these compounds have been termed phytoprostanes.

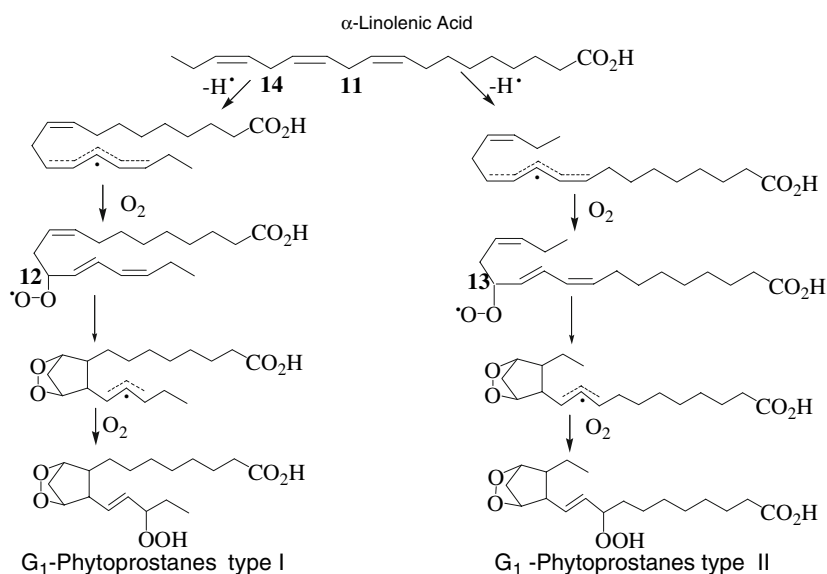
The free radical-initiated peroxidation of ALA and its esters generates mixtures of primary hydroperoxides and cyclic peroxides. Two regioisomeric series are formed from the oxidation of linolenate depending on the site of initial hydrogen abstraction and subsequent oxygen insertion (Fig. 1). Hydrogen atom abstraction at C-14 generates type I PP whereas hydrogen abstraction at C-11 yields type II PP, according to the nomenclature by Rokach et al. [5].

Each series is composed of 16 isomers and 32 PPG₁ can be formed in total. These PPG₁ are major products of linolenate peroxy radicals and are thought to be formed in situ in membrane lipids, similar to the corresponding IsoPs in animals. Unstable PPG₁ spontaneously rearrange and/or are reduced to D₁-, E₁- and F₁- ring compounds (Fig. 2). Finally, D₁- and E₁-PP may further dehydrate and isomerize to J₁-, deoxy-J₁, A₁ and B₁- PP.

Analytical Applications of Phytoprostanes

First evidence for the formation of PP in plants was discovered by Parchmann and Mueller in 1998 [6]. Highly sensitive and specific analysis methods were needed to overcome the daunting task of the sheer numbers of primary and secondary metabolites present in plant materials. Initially, gas chromatography-mass spectrometry (GC-MS) and HPLC coupled to a fluorescent detector were the instruments of choice for analysis quantification. However as detailed below, GC-MS methods require extensive and laborious sample preparation and derivatization procedures. More recently, HPLC-ESI-MS/MS has become the method of choice for the analysis of all classes of PP since this analytical method can be applied to simple methanol extracts of plant materials without further purification or derivatization. In any case, internal standard are required for accurate analysis. The best internal standards are oxygen-18 labeled PP which could be obtained by two methods. In the first procedure [¹⁸O₃]PPE₁ and [¹⁸O₃]PPF₁ standards were obtained by autoxidation of linolenate in oxygen-18 atmosphere. While PPB₁ was synthesized from [¹⁸O₃]PPE₁ by base-catalyzed dehydration [6, 7]. The

Fig. 1 Non-enzymatic phytoprostane biosynthesis from α -linolenic acid



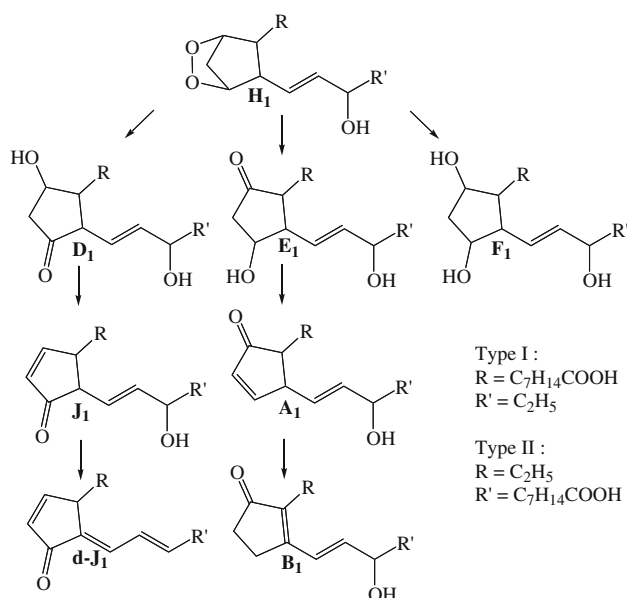


Fig. 2 The Phytoprostane pathway in plants

second method, that can be generally applied to oxylipins, is the lipase- or base-catalyzed exchange of the two oxygen atoms in the carboxyl group by oxygen-18 using H₂¹⁸O [8].

Within the PPE₁ series, comprised of 32 possible isomers, quantification was achieved by chromatographic separation (HPLC or solid phase extraction, SPE) of PPE₁ from PPB₁. Next, the pre-purified crude mixture of PPE₁ was converted to PPB₁ (comprising only two regioisomers) by brief exposure to KOH followed by another SPE purification step. PPB₁ were subsequently derivatized into pentafluorobenzyl ester and trimethylsilyl ether derivatives. GC–MS analysis in the negative chemical ionization mode against [¹⁸O]₁PPB₁ internal standard permitted quantification of the two regioisomers of PPB₁ representing the endogenous PPE₁ regioisomers (type I and type II). Both regioisomers can be well chromatographically separated and quantified [6].

PPF₁ quantification required another method to separate the large amount of acyclic triols (derived from both enzymatic and non-enzymatic oxidation of linolenate in plants) to cyclic triols of the PPF₁ type. Although acyclic and cyclic compounds have similar chromatographic and mass spectrometric properties and the same molecular weight, they differ by their number of double bonds. However after hydrogenation, PPF₁ could be differentiated from the acyclic compounds by their molecular weight. Thereafter, another step of SPE purification was necessary followed by derivatization of the hydrogenated PPF₁ to their corresponding pentafluorobenzyl ester and trimethylsilyl ether derivatives. PPF₁ isomers could only be partially resolved on the GC column and were quantified by GC–NICI–MS [9].

Table 1 Prostaglandin-like oxylipins in tomato leaves

Cyclopentane phytoprostanes (ng/g DW)	
PPD ₁ -I (459 ± 130)	PPD ₁ -II (698 ± 161)
PPE ₁ -I (35 ± 8)	PPE ₁ -II (35 ± 12)
PPF ₁ -I (75 ± 25)	PPF ₁ -II (75 ± 25)
Cyclopentenone phytoprostanes (ng/g DW)	
PPA ₁ -I (3.3 ± 2.0)	PPA ₁ -II (1.2 ± 2.0)
PPB ₁ -I (1.2 ± 1.1)	PPB ₁ -II (0.75 ± 1.5)
dPPJ ₁ -I (293 ± 20)	dPPJ ₁ -II (1668 ± 202)
Jasmonates (ng/g DW)	
12-Oxo-phytodienoic acid (212 ± 51)	Jasmonic acid (20 ± 5)

Levels of non-enzymatically formed Phytoprostanes and enzymatically biosynthesized jasmonates in tomato leaves (*Lycopersicon esculentum* cv. moneymaker) were quantitated by GC–MS or HPLC/fluorescence detection. Data are means ± SD of leaves collected from three different plants

PPD₁ and deoxy-J₁-phytoprostane (dPPJ₁) were analyzed using a novel method based on the unique capability of dPPJ₁ to bind covalently to thiol groups. After separation of PPD₁ and dPPJ₁ by SPE, dPPJ₁ were covalently linked to 7-mercapto-4-methyl-coumarin and analyzed by HPLC coupled with a fluorescence detector. All regioisomers eluted in one peak and 15-deoxy-Δ^{12,14}-PGJ₂ was used as the internal standard. PPD₁ were converted to dPPD₁ by acid dehydration and analyzed as above using PGD₂ as internal standard (transformed into PGJ₂ by acid treatment) [10].

The analysis of cyclopentenone PPA₁ and B₁ had to be accomplished by the combination of two different analyses. After extraction of PPA₁/PPB₁ by SPE and derivatization (see PPE₁), GC–NICI–MS analysis revealed that PPA₁ had isomerized into PPB₁. Quantification of the sum was performed using [¹⁸O]PPB₁ as an internal standard (added prior to work-up). Furthermore, methoxime derivatization of the carbonyl group to prevent isomerization of PPA₁ into PPB₁ into the GC injector revealed the endogenous ratio of PPA₁ to PPB₁. From both analyses, levels of PPA₁ and PPB₁ could be calculated indirectly [11].

Non-enzymatic peroxidation of ALA produces a large spectrum of PP in plant tissues. In plant species studied to date (more than 20 from taxonomically different plant species) all types of free PP and dPPJ₁ have been found to occur ubiquitously at greater levels than their mammalian congeners, the IsoP [6, 7, 10, 12]. The relative abundance of all the aforementioned PP classes has been established in tomato leaves (*Lycopersicon esculentum* cv. moneymaker) (see Table 1) [11].

PPE₁ and PPF₁ are for instance at least 2 to 3 orders of magnitude higher in plants tissues than IsoP in mammalian tissues. Furthermore, PPD₁ and dPPJ₁ are the most abundant PP in most plant species [10]. Free PPA₁ and PPB₁ are

also found in vivo to the contrary of their mammalian congeners which are apparently below the limit of detection at basal levels [13–15]. Moreover, glutathione conjugates of PPA₁ dramatically accumulate after pathogen infection in *Arabidopsis thaliana*.

High levels of isoprostanoids in plants could be the cause of enhanced formation (arachidonates are more reactive toward autoxidation but are prone to further polyoxygenation) or slower metabolism of PP in plants. However, oxygenic photosynthesis in chloroplasts has been shown to be a major source of reactive oxygen species, especially singlet oxygen. In green plant tissues, lipid peroxidation is predominately dependent on singlet oxygen and leads to the accumulation of fatty acid hydroperoxides esterified in chloroplast galactolipids. It is assumed that the pool of lipid peroxidation products is prone to further free radical-catalyzed peroxidation of chloroplast membranes, hence leading to the accumulation of PP. In contrast, levels of lipid peroxidation products in plant roots (that do not form singlet oxygen) are about 10-fold lower than in leaves and comparable to levels found in mammalian tissues. Hence, singlet oxygen formed during photosynthesis in the plant specific chloroplast organelle may accelerate free radical driven lipid peroxidation [16].

Investigation of PP in human diet showed that levels increase when plants are dried and stored after harvest. Indeed, up to a 250-fold of free and esterified PPF₁ (in the range of 3,000–20,000 and 10,000–55,000 ng/g of dry weight, respectively) were found in fresh plant parts [9]. An impressive high amount of free PPF₁ (more than 32,000 ng/g) was also found in fresh birch pollen [9], and *Betula alba* L. (*Bet*-APE) pollen were found to contain E₁, F₁, A₁, and B₁ PP, of which PPE₁ levels were eightfold more abundant than the others [17].

A recent investigation showed that PPF₁, PPE₁, PPA₁, and PPB₁ are found in vegetable oils and parenteral nutrition (intralipid) in remarkably high levels (0.09–99 mg/L) [18]. It was demonstrated that PPF₁ were absorbed after oral consumption, and found to circulate in plasma in an unknown conjugated form. They were excreted in free form in urine. Because cyclopentenone-PP display potent anti-inflammatory and apoptosis-inducing activities similar to PGA₁, deoxy-PGJ₂, A₂-IsoP, and J₂-IsoP, this study indicates that PP may contribute to the beneficial effects of the Mediterranean diet. In addition, a study by Barden et al. show that after 4 weeks supplementation with flaxseed oil, plasma phospholipid ALA was significantly increased and PPF₁ were elevated in plasma and urine, in men [19].

Similar to IsoP in mammals, PP have been shown to represent a reliable marker of oxidative stress in vivo [9, 12].

Levels of free PPF₁ transiently increased by more than 15- and 30-fold, respectively, after treatment of *Eschscholzia californica* cell cultures with butyl hydroperoxide

(10 mM) or copper ions (500 μM) with maximum levels of 1.7 and 2.7 μg/g of dry weight, respectively. Wounding which causes an increase in endogenous reactive oxygen species generated a 4- to 5-fold increase in both free and esterified PPF₁, showing that PPF₁ is clearly inducible by oxidative stress in plants [7]. A recent study showed that levels of free and esterified PPF₁ increased after pathogen treatment. The fact that the increase in esterified compounds occurred earlier than in free compounds suggests that non-enzymatic lipid oxidation occurs predominantly in membranes from which oxidized lipids can be released [20].

Other PP are also produced during oxidative stress, and indeed butyl hydroperoxide treatment of tobacco cell cultures resulted in an accumulation of E₁-, A₁- and B₁-PP [12]. Furthermore, necrotrophic plant fungi like *Botrytis cinerea* induced an oxidative burst in infected tomato leaves and triggered a three- to four-fold increase of E₁-, A₁- and B₁-PP, reflecting generation of ROS by the necrotrophic plant fungus. It was interesting to notice that the PP pathway can be triggered independently of the JA pathway (hydroperoxide treatment) or simultaneously (*Botrytis cinerea*) depending on the environmental conditions [12].

Biological Activity of Phytoprostanes

PP have been reported to possess a broad spectrum of biological activities in different plant species. The best studied compounds are the cyclopentenone-PP of the A and B classes. In several studies it was shown that exogenous application of these classes of PP regulates gene expression in *Arabidopsis thaliana* and tomato [12, 15, 21]. A whole genome transcriptome analysis of *A. thaliana* treated with 75 μM PPA₁ for 4 h revealed that the expression of 157 genes was up-regulated by a factor of three or more while the expression of 211 genes was repressed [15]. 28% of the up-regulated genes were related to detoxification, stress responses and secondary metabolism. In agreement with gene regulation, the levels of secondary metabolites increase upon PP treatment. This accumulation in response to PPB₁ was shown for different classes of phytoalexins in different plant species: the indole-alkaloid camalexin in *A. thaliana*, the coumarin scopoletin in tobacco, the isobavachalcone in *Crotalaria cobalticola* and the alkaloid sanguinarine in *Eschscholzia californica* [21].

Detoxification genes which were up-regulated by PPA₁ and PPB₁ comprised genes involved in the xenobiotic response in animals such as phase I enzymes (CytP450 enzymes, aldehyde dehydrogenases, OPDA-reductases), phase II conjugating enzymes (glutathione-S-transferases and glycosyltransferases) and putative phase III xenobiotica transporters (ABC transporters) [21]. Enhanced

activities of these enzymes might be useful in the deactivation of xenobiotics as well as endogenous compounds such as peroxidized lipids [22]. Also, the increased expression of stress-related genes encoding heat shock proteins and heat shock factors indicate the activation of mechanisms which might help to improve cellular metabolism under stress conditions. Recently, Dueckershoff et al. [23] reported the impact of PPA₁ on the proteome of *A. thaliana* showing that the PPA₁-regulated proteins were localized in chloroplast and mitochondria—locations where internal oxidative stress is generated.

These results suggest that cyclopentenone PP may be archetypal mediators of oxidative stress: they trigger the first adaptive responses thus limiting the consequences of oxidative stress by inducing several plant-protection mechanisms [19, 24].

In agreement with this hypothesis, it has been shown that PPB₁ may induce cell protection genes which enables plant cells to survive subsequent, otherwise lethal stress [21]. Pretreatment of a tobacco cell culture with PPB₁ decreased cell death caused by a severe oxidative stress generated by CuSO₄ [21].

PP also display inhibitory effects on gene regulation and on the physiological level. In *A. thaliana*, PPA₁ down-regulate the expression of genes related to cell division and growth. In accordance with gene regulation, treatment with PPA₁ resulted in inhibition of root growth and of cell cycle progression. With respect to inhibition of root growth, it has been found that the cyclopentenones OPDA and PPA₁ mediate their activities through the COI1 complex, an established receptor for the JA-isoleucine conjugate (JA-Ile). Most biological activities of PPA₁ and OPDA, however, are independent of the JA-COI1-signaling pathway and are mediated through TGA transcription factors [15]. It is assumed that cyclopentenone prostanoids exert their biological activities by covalently binding to free thiol groups of target proteins such as transcription factors and redox-regulated enzymes. While several target proteins such as NF- κ B and PPAR γ have been identified in animals, little is known about the primary cyclopentenone target proteins in plants [25].

For most biological activity studies, mixtures of various PP isomers have been used. Only in a few studies, the effect of different regioisomers was investigated with interesting results. In tomato cell culture (*Lycopersicon esculentum*), exogenous application of PPA₁-I/II, deoxy-PPJ-I/II and PPB₁-II activated significantly the mitogen-activated protein kinases (MAPK) whereas PPB₁-I did not [12, 26]. In the same system, PPB₁-I/II but not PPA₁ led to an increase in the mRNA levels of *Lin6* (encoding an extracellular invertase) after 3 h. PPB₁-I/II also induced the expression of *PAL* (phenylalanine ammonia lyase) in tomato cell suspension cultures in 30 to 60 min. PPA₁ did

not up-regulate the expression of *PAL* in tomato cells but induced strongly expression of the orthologous gene in tobacco [12]. In addition, the regulation of gene expression by PPB₁ in an *A. thaliana* cell suspension culture was dependent on the regioisomer: the spectrum of induced genes was similar but the response to PPB₁-I was stronger than to PPB₁-II. In contrast, the induction of phytoalexins in three different models (tobacco, *C. cobalticola*, *E. californica* cell culture) was stronger with PPB₁-II in comparison to PPB₁-I. The allylic alcohol configuration, the free acid or the esterified form did not affect phytoalexin formation [21]. These results clearly demonstrate the importance of investigating the response to specific, defined stereoisomers. The comparison of different stereoisomers is necessary to learn more about the mechanisms involved in mediating the effects of PP.

PP also display several biological activities in animal models. PPE₁ inhibit in vitro dendritic cell interleukin-12 (IL-12) production and increase Th2 cell polarization [17, 27]. In contrast, in vivo, PPE₁ and PPF₁ inhibit partially the Th1 and Th2 cytokine production [28].

Finally, Mueller and coworkers reported that the cyclopentenones PPA₁ and dPPJ₁, displayed an anti-inflammatory activity at the same concentration (10–50 μ M) similar to PGA₁ and dPGJ₂ in human embryonic kidney (HEK) cells and RAW264.7 murine macrophages by down-regulating NF- κ N and inhibiting nitric oxide synthesis, respectively. Moreover, the authors reported that PPA₁-I induced apoptosis in leukemia Jurkat T cell, at the same concentration as PGA₁ (10–40 μ M) but at a higher degree (60 vs. 33% apoptosis). dPPJ₁-I, dPPJ₁-II showed the same activity at a concentration range of 20–40 μ M, whereas PPA₁-II, PPB₁-I and -II were completely inactive [18]. This indicates that biological activities exerted in animals also depend on the stereochemistry of the compound.

Synthetic Approaches to Phytoprostanes and Analogs

Many efforts towards the total synthesis of IsoPs and analogs, metabolites derived from peroxidation of arachidonic acid and other polyunsaturated fatty acids (PUFA) have been made in the last 15 years [29, 30]. Since the discovery of IsoP [31], neuroprostanes (NeuroP) [32, 33] and more recently, the PP [7] there has been a growing interest in the total synthesis of such molecules in order to supply sufficient amounts for their identification, quantification as well as their biological properties.

Without the synthetic strategies developed so far, the field of IsoP and PP would not have advanced to its current status. However, as can be seen in the following section, only selected members of some PP families have been

synthesized. One of the greatest needs is the development of novel synthetic approaches that are more efficient with respect to number of steps and time to execute them. Approaches to synthetic PP and analogs have been reported by several groups during the last 5 years. Nevertheless, much remains to be learned concerning the functions of these new bioactive lipids. We will concentrate our review on the outline of the general strategies and the involved key steps to assemble the respective intermediates.

Most of the published total syntheses use one of three basic synthetic strategies of the PP skeletons.

1. The side chains were introduced at the same time or subsequently to suitably functionalized cyclopentane rings. This strategy is very flexible for the synthesis of more than one member of different regioisomeric series of PP. Since the configuration of cyclopentane stereocenters directs the incoming side chains strongly, a potential limitation is the accessibility of diastereomeric structures.
2. Precursors containing the fully assembled PP chain with the desired functionality were assembled first. The key step was a cyclization reaction to afford the natural products. Potential limiting factors of this strategy are a considerable synthetic effort to prepare the cyclization precursors and a low flexibility to apply the methodology to a largest range of substrates.
3. An approach via a two component coupling process, where at first one of the side chains is disconnected. The cyclopentane ring with the other side chain in place is available by a number of cyclization reactions. Here, the methodology can be rather easily developed, divergent stereochemical control opportunities exist, albeit precursor's synthesis may be somewhat more difficult than the other strategies pointed above.

Synthesis of Phytoprostanes by Attachment of the Side Chains to a Suitably Functionalized Cyclopentane Ring

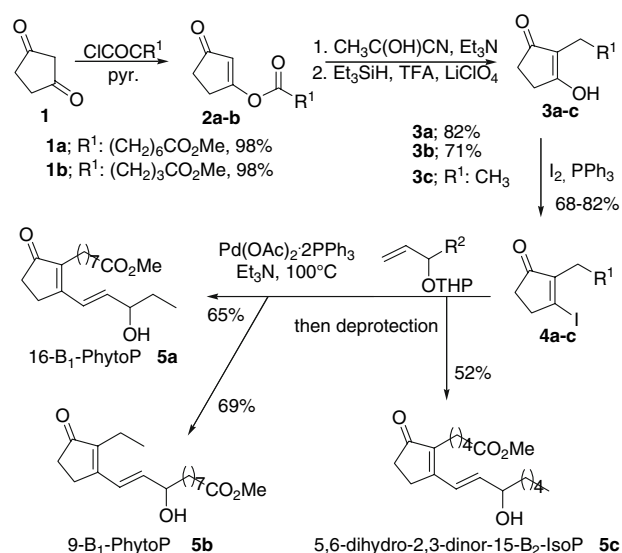
Synthesis from Functionalized Cyclopentenones

In 2007, Boland and coworkers developed a very short and general strategy for the synthesis of B₁-PP, dinor-IsoP and several analogs (Scheme 1) [34]. Their approach is based on five key operations to introduce the two side chains. Starting from 1,3-cyclopentanedione **1**, a three-step procedure consisting of *O*-acylation with acyl chlorides to **2**, subsequent 1,3-*O,C*-acyl shift with acetone cyanohydrin/*N*Et₃ and reduction of the exocyclic keto function by triethylsilane yielded the desired C-alkylated 3-hydroxyenones **3a–c** with the first lateral chain in place. Reaction with the iodine-triphenylphosphine complex gave access to 2-alkyl-3-iodocyclopentenones **4a–c**, which served as

precursors for the introduction of the second side chains by Heck-type cross-coupling reactions employing a 2:1 mixture of PPh₃ and Pd(OAc)₂ as the catalyst in the presence of Et₃N. THP-protected 1-alken-3-ols proved to be the coupling substrates of choice. THP-deprotection completed the total synthesis of 16-PPB₁ **5a**, of 9-PPB₁ **5b** and of 5,6-dihydro-2,3-dinor-15-B₂-IsoP **5c** in good overall yield. The flexibility of this approach was also demonstrated by the synthesis of acetylenic and *O*-alkylated PP analogs (not shown).

Cyclization Reactions Followed by Attachment of the Remaining Side Chain

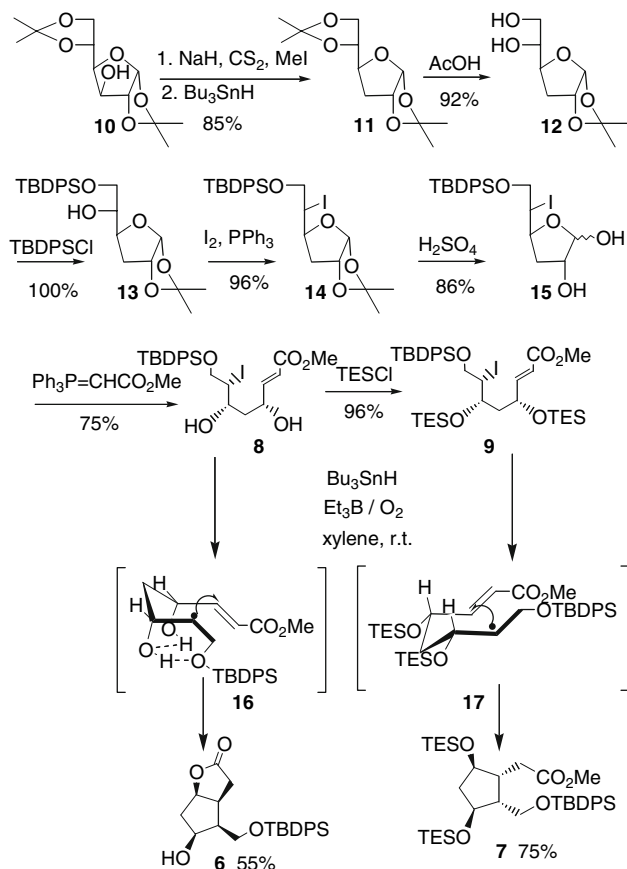
Radical Cyclizations Since radical cyclizations are well-suited to approach cyclopentane rings with *cis*-oriented substituents [35], they are attractive to synthesize IsoP intermediates. At the beginning of the 1990s, the Durand/Rossi group along with Rokach's team reported the synthesis of key intermediate **6**, a diastereomer of Corey's formyl-lactone, via an acyclic thionocarbonate [36]. Durand and Rossi developed subsequently radical carbocyclizations of functionalized iodo precursors **8** and **9** (Scheme 2) [37], which replace the thionocarbonate precursors initially proposed advantageously. The synthesis of **6** started with commercially available 1,2,5,6-di-*o*-isopropylidene- α -D-glucufuranose **10**, which was transformed to the corresponding 3-deoxy-sugar **11** in 85% yield using the Barton-McCombie procedure. A selective deprotection of the isopropylidene group at 5,6-position to diol **12** was accomplished in the presence of 70% aqueous acetic acid in good yield. Protection of the primary alcohol using 1.1 equiv. of *tert*-butyldiphenylsilyl chloride in



Scheme 1 Total synthesis of PPB₁ according to Boland et al. [34]

DMF and imidazole led to the pure mono silyl ether **13**. Introduction of iodine at C5 to **14** was accomplished in 96% yield by using I₂, Ph₃P and imidazole in xylene in a procedure developed earlier by our group [37].

Hydrolysis of the isopropylidene group at 1,2-position was achieved in the presence of 10% aqueous sulfuric acid in THF-dioxane (3:1) to afford the diol **15** in 86% yield. The next step was a Wittig reaction with methyl triphenylphosphoranylidene acetate affording the cyclization precursor **8** in 75% yield. Protection of the two hydroxy groups in **8** with triethylsilyl chloride in pyridine gave **9** in 96% yield. The crucial radical 5-*exo* cyclizations were conducted in the presence of tributyltin hydride initiated by triethylborane/oxygen under ambient conditions. The factors controlling the cyclization diastereoselectivity of these polyhydroxylated hex-5-enyl radicals were carefully examined and shown to be strongly dependent on the protecting group pattern of the two secondary hydroxy groups in **8** and **9** [38]. Compound **8** with free hydroxy groups cyclizes preferentially via hydrogen-bonded transition state **16** to all-*cis*-**6**. The bis(TES) derivative **9**, in contrast, cyclizes via a Beckwith-Houk transition state **17** to *syn-anti-syn*-**7**. All reactions shown for D-glucose were also performed with



Scheme 2 Synthesis of cyclopentane key intermediates according to Durand, Rossi and co-workers [37]

L-glucose to make all stereoisomers of the *syn-anti-syn* and all-*cis* cyclopentane families accessible.

Compounds **6** and **7** were converted to a large set of enantiomerically pure IsoP, NeuroP, and PP by the following standard methods: (a) sequential appendage of the side chains by Wittig and/or HWE reactions; (b) protection/deprotection reactions; (c) regioselective oxidation; and (d) enantioselective reduction.

This is illustrated by the first total synthesis of PPF₁ type II methyl ester **18**, which was achieved in 2004 starting from *syn-anti-syn* cyclopentane **7** (Scheme 3) [39]. After the reduction of the methyl ester **7** and activation of the hydroxy group with toluenesulfonyl chloride, followed by reduction, once again, by LAH the methyl group of the α chain is obtained in 83% yield.

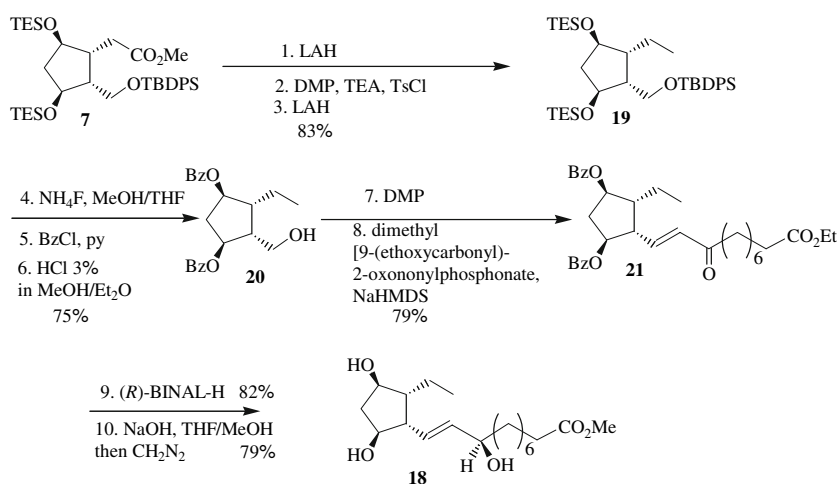
Introduction of the ω chain in *syn-anti-syn* derivative **19** was achieved by a HWE reaction with dimethyl [9-(ethoxycarbonyl)-2-oxononylphosphonate/NaHMDS and afforded the enone β -**21**. Diastereoselective reduction of the C9 keto group in **21** with the chiral reducing agent [40] (*R*)-BINAL-H gave the desired pure 9(*R*) derivative in 82% yield. Finally, deprotection of the benzoyl groups, in presence of 1 N NaOH, followed by excess of CH₂N₂, afforded the desired *ent*-PPF₁ type II methyl ester **18** in ten steps and 38% yield from the cyclopentane **7**.

Using this radical pathway, starting from D- and L-glucose, all diastereomers of PPF₁ summarized in Scheme 4 were synthesized [41].

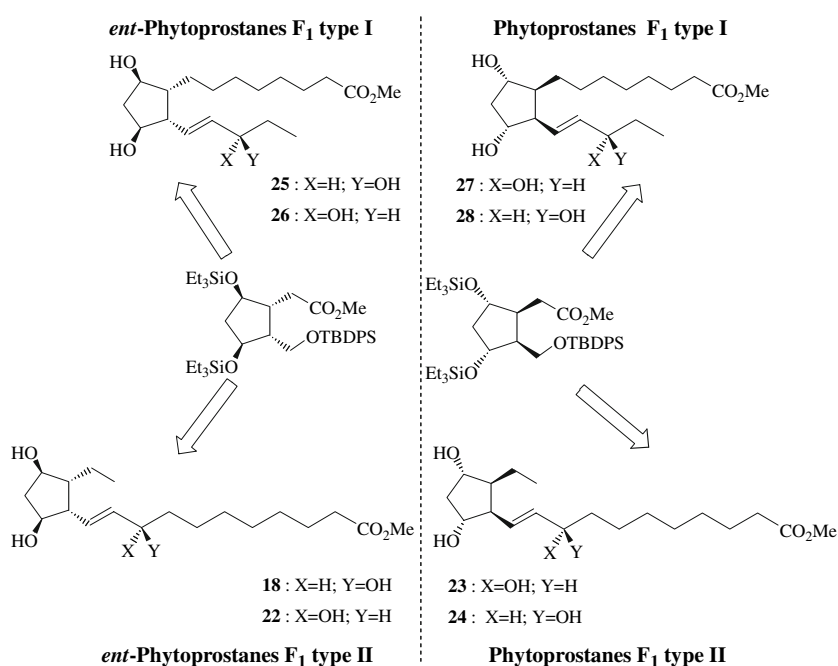
Transition Metal-Catalyzed Cyclization Reactions Leading to Phytoprostanes The Evans group reported an interesting Pauson-Khand strategy for the synthesis of J-type IsoP or PP (Scheme 5) [42, 43]. The reaction between Co₂(CO)₆-complexed trimethylsilylacetylene **29** and norbornadiene **30** led to racemic key intermediate **31**. The yield of this cyclization step was optimized by using thermal microwave heating. The following key step represents an adaption of the well-known three-component coupling for PG synthesis consisting of copper(I)-catalyzed conjugate addition of 7-silyloxyheptylmagnesium bromide to **31** followed by an aldol addition of *trans*-oct-2-enal. The construction of the cross-conjugated dienone unit **32** was achieved by subsequent Peterson olefination under acidic conditions and gave an initial 1:3 13*E*/13*Z*-diene mixture.

After removal of the silicon protecting group and separation, the individual diene isomers (12*Z*)-**32** and (12*E*)-**32** were isolated in 25 and 28% yield, respectively. The authors named this procedure conjugate addition-Peterson olefination reaction. Conversion of the primary alcohol **22** into the methyl ester **33** was achieved using a three-step protocol. Alcohol (12*E*)-**32** was oxidized with Dess-Martin periodinane and subsequently sodium chlorite to the

Scheme 3 Total synthesis of PPF₁ type II according to Durand, Rossi and co-workers [41]



Scheme 4 Four diastereoisomers of PPF₁ synthesized by Durand/Rossi group [41]

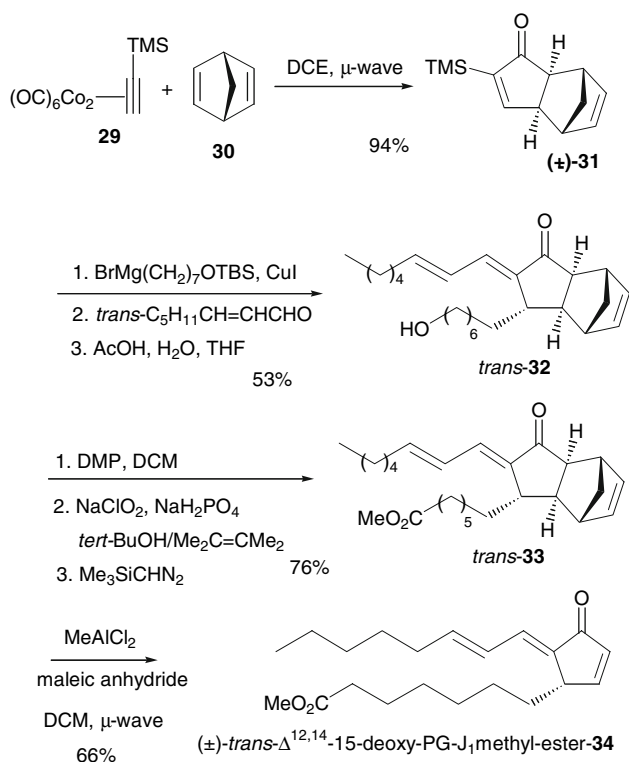


corresponding carboxylic acid, which was esterified with (trimethylsilyl)diazomethane in good yield. The total synthesis was completed by retro-Diels–Alder reaction of the cyclopentadienyl-protected methyl ester **33** with MeAlCl₂ and maleic anhydride under microwave conditions to give 52% of (\pm)-*trans*- $\Delta^{12,14}$ -15-deoxy-PGJ₁ methyl ester **34** and 14% of its *cis*-isomer (not shown).

In 2005, Evans' group associated with Riera's group published the synthesis of optically pure 13,14-dehydro-12-oxophytodienoic acids **37** and **38** (dPPJ₁) using an asymmetric version of their earlier approach (Scheme 6) [26]. This was achieved by ligand exchange of **29** with bidentate chiral ligand **35** in the presence of 1,4-diazabicyclo[2.2.2]octane (DABCO) in toluene to give the two diastereomeric cobalt complexes **36a** and **36b** in good yield, which were separated by crystallization and/or

chromatography. The Pauson–Khand reaction of **36a** with norbornadiene **30** in the presence of *N*-methylmorpholine *N*-oxide (NMO) in dichloromethane furnished (+)-**31** in excellent yield and enantiomeric excess.

Using similar conditions as in the synthesis of racemic compound **34** (cf. Scheme 5), the synthesis of (+)-*trans*,-*trans*-dPPJ₁ type I **37** as a single isomer was accomplished from (+)-**31** in a six-step sequence including 1,4-conjugate addition using 7-(silyloxy)heptylmagnesium bromide, a Peterson olefination with *trans*-pent-2-enal and finally the removal of the cyclopentadienyl-protecting group with MeAlCl₂ and maleic anhydride under microwave irradiation conditions. A similar sequence with lithium diethyl cuprate and the appropriate functionalized α,β -unsaturated aldehyde provided (+)-*trans*,*trans*-dPPJ₁ type II **38** in good yield (Scheme 6).



Scheme 5 Total synthesis of J-type IsoP and PP according to Evans and co-workers [42, 43]

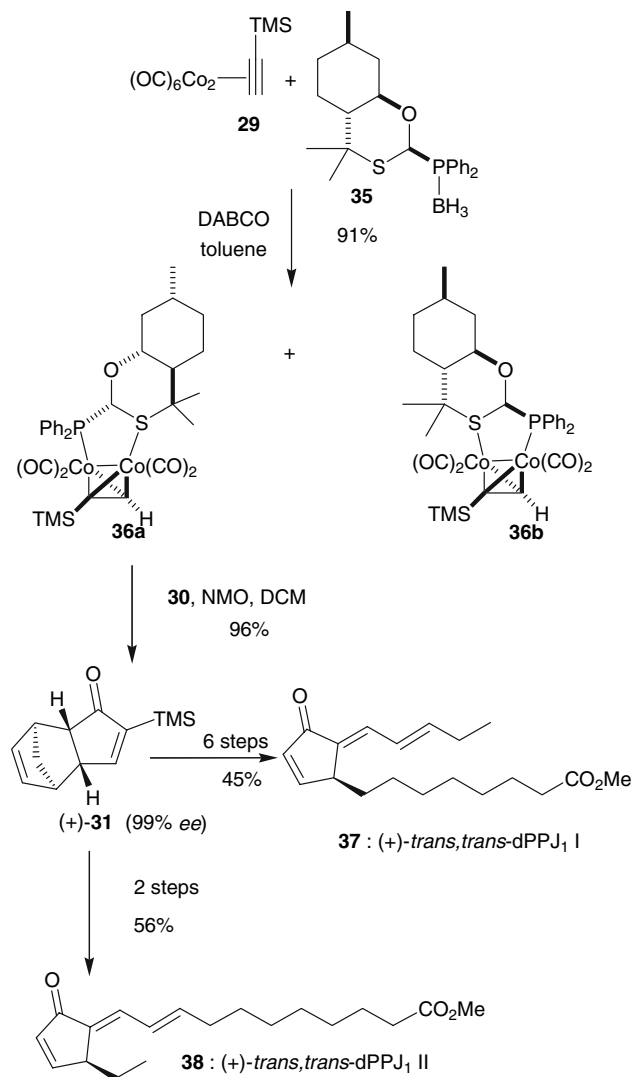
In 2009, Riera and coworkers developed a new approach using an intermolecular Pauson–Khand reaction of internal alkynes (Scheme 7) for the synthesis of PGB₂ and PPB1 [44].

The synthesis required internal alkynes **39**, easily prepared from propargylic alcohol and the corresponding bromo acid. The alkynes were treated with octacarbonyl dicobalt to give the related cobalt complexes. The Pauson–Khand reaction was performed at room temperature in a pressure reactor under ethylene, NMO and powered 4-Å molecular sieves with good yield. After a quantitative silyl group removal using HF.Pyr. , the Pauson–Khand adduct **41** was converted into an aldehyde **42** under Swern conditions in an excellent yield.

The first attempt of Riera's group to introduce the ω chain by a Wittig reaction on the aldehyde **42** afforded a mixture of stereoisomers in low yield. Finally, they succeeded in their approach by using a Julia olefination to introduce the chiral ω chain.

Mikolajczyk et al. reported the synthesis of a key intermediate (Scheme 8), the 3-(phosphorylmethyl)cyclopent-2-enone **46** which turned out to be an excellent building block in the synthesis of naturally cyclopentenone derivatives [45].

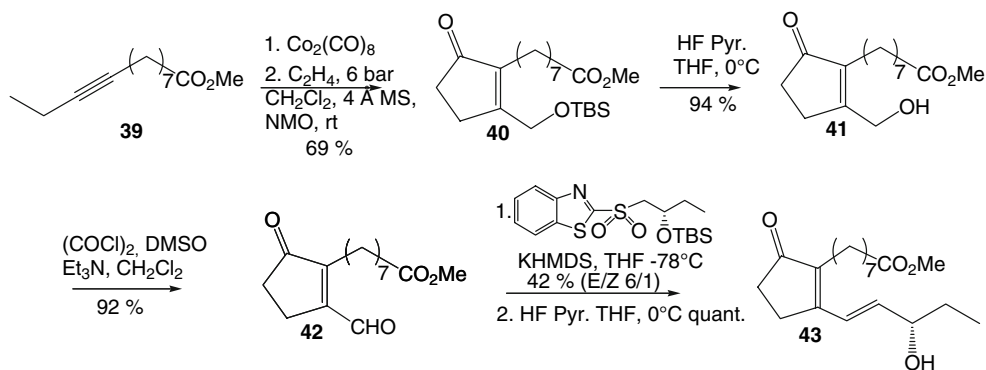
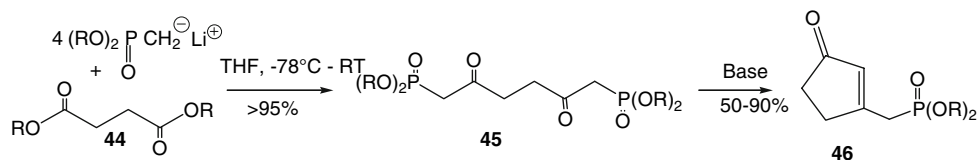
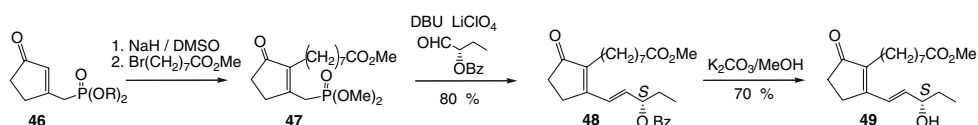
The cyclopentenone **46** was obtained in the reaction between the α -phosphonate carbanions and dicarboxylic



Scheme 6 Synthesis of optically pure dPPJ₁ type II according to Riera, Evans and co-workers [26]

acid esters **44** to afford the bis- β -ketophosphonates **45**. Under basic conditions, this latter yielded through an intramolecular HWE reaction the desired cyclopentenones **46**.

Recently, by a controlled combination of the alkylation and Horner reaction of the anion generated from **46** the authors were able to reach the PPB₁ type I (Scheme 9). The anion of **46** generated from NaH in DMSO reacts with the 8-bromooctanoate to afford the corresponding C2-alkylated derivative **47**. Then, the Horner reaction of **47** with the enantiopure (–)-*S*- α -benzyloxybutanal yielded the olefination product **48** which after saponification of the methyl ester afforded the enantiopure PPB₁ **49** in a 25% overall yield [46]. Starting from (+)-*R*- α -benzyloxybutanal, the authors reported the synthesis of the enantiomer of PPB₁ type I.

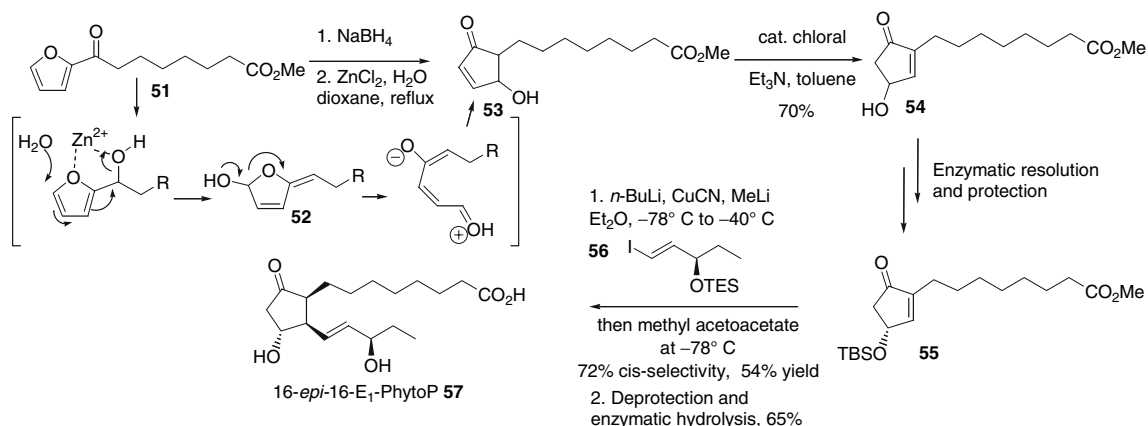
Scheme 7 Synthesis of PPB₁ type I according to Riera et al. [44]**Scheme 8** Synthesis of 3-(phosphorylmethyl)cyclopent-2-enone according to Mikolajczyk [45]**Scheme 9** Synthesis of PPB₁ type I according to Mikolajczyk [46]

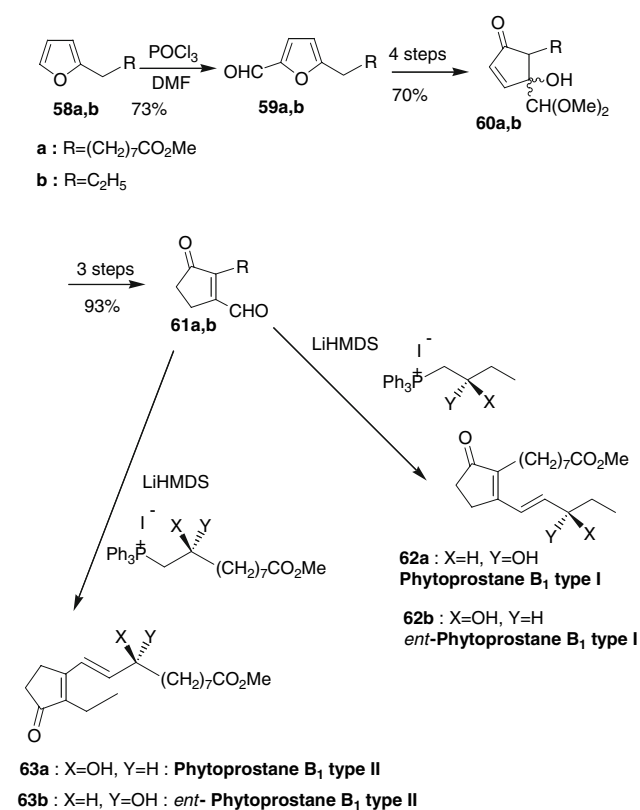
Phytosteranes Syntheses Based on Furan Ring Transformations

Spur and coworkers developed very efficient syntheses of the PPE₁ via a two components coupling process typically used for the synthesis of PG and analogs [47–49]. By simply modifying “work-up” conditions using chelating proton sources, a switch from PG *trans*-dialkyl stereochemistry to PP *cis*-dialkyl stereochemistry was accomplished. The synthesis of chiral cyclopentenone component **55** started with a Friedel–Crafts acylation of furan and the mixed anhydride of azelaic acid monoester to give furyl ester **51** (Scheme 10) [50]. NaBH₄ reduction followed by

rearrangement with ZnCl₂ in dioxane/water at reflux afforded 4-hydroxycyclopentenone **53**, probably via ring opening of intermediate **52** and subsequent intramolecular aldol addition. Treatment of **53** with chloral yielded the more stable 4-hydroxycyclopentenone **54** in 70% overall yield.

Enzymatic resolution and TBS protection gave **55**, which was subjected to conjugate addition with a chiral component, obtained by lithium-iodine exchange of the corresponding vinyl iodide **56**. The resulting 2,3-dialkylcyclopentanone enolate intermediate was then added to a cool solution of methyl acetoacetate to provide a *cis*-2,3-dialkylcyclopentanone with 72% selectivity. Finally,

**Scheme 10** Synthesis of PPE₁ according to Spur et al. [50]

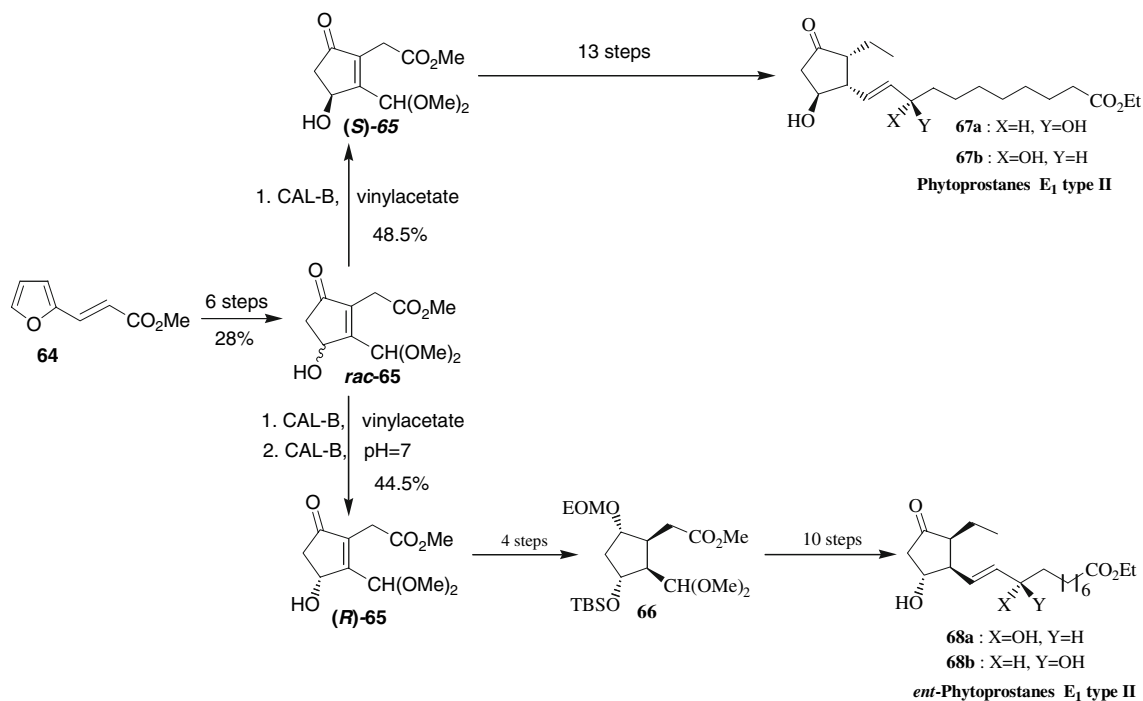


Scheme 11 Synthesis of PPB₁ according to Durand et al. [54]

deprotection and ester hydrolysis gave 16-*epi*-16-E₁-PP **57**. *ent*-16-E₁-PP was also synthesized starting from the enantiomer of **55** [51, 52].

Since 2004, Durand's group became interested in developing new and flexible routes to B-, D-, E-IsoP and -PP starting from two common intermediates reported by Freimanis, namely the 4-hydroxy-2-cyclopentenone precursors **60a,b** (Scheme 11) [53]. The synthesis started with a Vilsmeier formylation reaction at 5-position of the furans **58a,b**. A selective rearrangement of **59a,b** yielded the 4-hydroxy-2-cyclopentenones **60a,b** after four steps. The two 4-hydroxycyclopent-2-enone acetals **60a,b** were transformed to 3-oxocyclopentenecarbaldehydes **61a,b** in three steps and served as precursors for the synthesis of both enantiomers of PPB₁ type I methyl ester **62** as well as of PPB₁ type II methyl ester **63** by Wittig reactions using chiral β-hydroxy phosphonium salts [54].

In another synthetic venture (Scheme 12), methyl *trans*-3-(2-furyl)acrylate **64** was transformed in six steps to racemic 4-hydroxycyclopentenone **65** using the above procedure. An efficient enzymatic resolution for this compound to the two enantiomerically pure hydroxycyclopentenones (*R*)-**65** and (*S*)-**65** using CAL-B was developed [55]. Following a similar strategy, but applying **64** as a starting material and different coupling partners, other PP, such as all diastereomers of PPE₁ type II (**67** and **68**) were obtained [56].



Scheme 12 Synthesis of PPE₁ type II according to Durand et al. [55, 56]

Conclusion

During the last 10 years the chemistry, analysis, biology, and application of PP has undergone significant developments.

PP are generated by free radical-catalyzed oxidation of esterified linolenate in membranes in situ, from which they may be released preformed by lipases similar to IsoP in mammals. PPF₁ have been shown to occur predominantly esterified in plant lipids, presumably in plastidic galactolipids.

Pure synthetic PP are necessary as analytical standard for the unequivocal structure determination, the quantification and the exact elucidation of their potential biological properties. Without the synthetic strategies developed so far, the field of PP would not have advanced to its current status.

In parallel to these synthetic and analytical achievements, recent studies indicate that several PP display similar biological activities as OPDA which are mediated to a large part through TGA-transcription factors. In addition, PP also share biological activities with JA which are in part mediated through the COI1 signaling pathway such as induction of phytoalexin biosynthesis in plants and root growth inhibition. Cyclopentenone PP rapidly activate mitogen activated protein kinase (MAPK) and trigger activation of genes involved in stress responses and detoxification, hence, resembling the mammalian xenobiotic response. The Pollen-derived PPE₁ modulate DC function via PPAR γ -gamma dependent pathways that lead to inhibition of NF- κ B activation and result in reduced DC IL-12 production and consecutive T(H)2 polarization. Work is in progress to elucidate the signal transduction mechanisms of phytoprostanes in humans and animals in more detail.

A recent investigation showed that PPF₁, PPE₁, PPA₁, and PPB₁ are found in vegetable oils and parenteral nutrition (Intralipid) in remarkably high levels (0.09–99 mg/L). In addition, a study by Bardeen et al. show that after 4 weeks supplementation with flaxseed oil, plasma phospholipid ALA was significantly increased and PPF₁ were elevated in plasma and urine (data not shown). Since PP are contained in the human diet the profile of their pharmacological activities in humans and animals needs also to be explored.

Acknowledgment We are deeply grateful to Pr. Jean-Yves Lallemand and the ICSN for their generous financial support and a part of this work was supported by the University Montpellier I grant (BQR-2008).

References

- Nugteren D, Vonkeman H, van Dorp D (1967) Non-enzymatic conversion of all-*cis* 8, 11, 14-eicosatrienoic acid into prostaglandin E₁. *Recl Trav Chim Pays Bas* 86:1237–1245
- Roberts LJ II, Morrow JD (2000) Measurement of F(2)-isoprostanes as an index of oxidative stress in vivo. *Free Radic Biol Med* 28:505–513
- Conconi A, Miquel M, Browse JA, Ryan CA (1996) Intracellular levels of free linolenic and linoleic acids increase in tomato leaves in response to wounding. *Plant Physiol* 111:797–803
- Mueller MJ (1997) Enzymes involved in jasmonic acid biosynthesis. *Physiol Plant* 100:653–663
- Rokach J, Khanapure SP, Hwang SW, Adiyaman M, Lawson JA, FitzGerald GA (1997) Nomenclature of isoprostanes: a proposal. *Prostaglandins* 54:853–873
- Parchmann S, Mueller MJ (1998) Evidence for the formation of dinor isoprostanes E₁ from alpha-linolenic acid in plants. *J Biol Chem* 273:32650–32655
- Imbusch R, Mueller MJ (2000) Formation of isoprostane F(2)-like compounds (phytoprostanes F(1)) from alpha-linolenic acid in plants. *Free Radic Biol Med* 28:720–726
- Mueller MJ, Mene-Saffrane L, Grun C, Karg K, Farmer EE (2006) Oxylipin analysis methods. *Plant J* 45:472–489
- Imbusch R, Mueller MJ (2000) Analysis of oxidative stress and wound-inducible dinor isoprostanes F(1) (phytoprostanes F(1)) in plants. *Plant Physiol* 124:1293–1304
- Krischke M, Loeffler C, Mueller MJ (2003) Biosynthesis of 14, 15-dehydro-12-oxo-phytodienoic acid and related cyclopentenones via the phytoprostane D(1) pathway. *Phytochemistry* 62:351–358
- Thoma I, Krischke M, Loeffler C, Mueller MJ (2004) The isoprostanoic pathway in plants. *Chem Phys Lipids* 128:135–148
- Thoma I, Loeffler C, Sinha AK, Gupta M, Krischke M, Steffan B, Roitsch T, Mueller MJ (2003) Cyclopentenone isoprostanes induced by reactive oxygen species trigger defense gene activation and phytoalexin accumulation in plants. *Plant J* 34:363–375
- Morrow JD, Minton TA, Mukundan CR, Campbell MD, Zackert WE, Daniel VC, Badr KF, Blair IA, Roberts LJ 2nd (1994) Free radical-induced generation of isoprostanes in vivo. Evidence for the formation of D-ring and E-ring isoprostanes. *J Biol Chem* 269:4317–4326
- Chen Y, Morrow JD, Roberts LJ 2nd (1999) Formation of reactive cyclopentenone compounds in vivo as products of the isoprostane pathway. *J Biol Chem* 274:10863–10868
- Mueller S, Hilbert B, Dueckershoff K, Roitsch T, Krischke M, Mueller MJ, Berger S (2008) General detoxification and stress responses are mediated by oxidized lipids through TGA transcription factors in *Arabidopsis*. *Plant Cell* 20:768–785
- Triantaphylides C, Krischke M, Hoerberichts FA, Ksas B, Gresser G, Havaux M, Van Breusegem F, Mueller MJ (2008) Singlet oxygen is the major reactive oxygen species involved in photo-oxidative damage to plants. *Plant Physiol* 148:960–968
- Traidl-Hoffmann C, Mariani V, Hochrein H, Karg K, Wagner H, Ring J, Mueller MJ, Jakob T, Behrendt H (2005) Pollen-associated phytoprostanes inhibit dendritic cell interleukin-12 production and augment T helper type 2 cell polarization. *J Exp Med* 201:627–636
- Karg K, Dirsch VM, Vollmar AM, Cracowski JL, Laporte F, Mueller MJ (2007) Biologically active oxidized lipids (phytoprostanes) in the plant diet and parenteral lipid nutrition. *Free Radic Res* 41:25–37
- Barden A, Croft K, Durand T, Guy A, Mueller M-J, Mori TJ (2009) F1-phytoprostanes following ALA supplementation in men: a randomised controlled trial. *J Nutr* 10:1890–1895
- Grun C, Berger S, Matthes D, Mueller MJ (2007) Early accumulation of non-enzymatically synthesised oxylipins in *Arabidopsis thaliana* after infection with *Pseudomonas syringae*. *Funct Plant Biology* 34:65–71
- Loeffler C, Berger S, Guy A, Durand T, Bringmann G, Dreyer M, von Rad U, Durner J, Mueller MJ (2005) B1-phytoprostanes

- trigger plant defense and detoxification responses. *Plant Physiol* 137:328–340
22. Martinez-Lara E, Leaver M, George S (2002) Evidence from heterologous expression of glutathione *S*-transferases A and A1 of the plaice (*Pleuronectes platessa*) that their endogenous role is in detoxification of lipid peroxidation products. *Mar Environ Res* 54:263–266
 23. Dueckershoff K, Mueller S, Mueller MJ, Reinders J (2008) Impact of cyclopentenone-oxylipins on the proteome of *Arabidopsis thaliana*. *Biochim Biophys Acta* 1784:1975–1985
 24. Mueller MJ (2004) Archetype signals in plants: the phytoprostanes. *Curr Opin Plant Biol* 7:441–448
 25. Mueller M-J, Berger S (2009) Reactive electrophilic oxylipins: Pattern recognition and signaling. *Phytochemistry*. <http://dx.doi.org/10.1016/j.phytochem.2009.05.018>
 26. Iqbal M, Evans P, Lledo A, Verdaguer X, Pericas MA, Riera A, Loeffler C, Sinha AK, Mueller MJ (2005) Total synthesis and biological activity of 13, 14-dehydro-12-oxo-phytodienoic acids (deoxy-J1-phytoprostanes). *Chem Bio Chem* 6:276–280
 27. Mariani V, Gilles S, Jakob T, Thiel M, Mueller MJ, Ring J, Behrendt H, Traidl-Hoffmann C (2007) Immunomodulatory mediators from pollen enhance the migratory capacity of dendritic cells and license them for Th2 attraction. *J Immunol* 178:7623–7631
 28. Gutermuth J, Bewersdorff M, Traidl-Hoffmann C, Ring J, Mueller MJ, Behrendt H, Jakob T (2007) Immunomodulatory effects of aqueous birch pollen extracts and phytoprostanes on primary immune responses in vivo. *J Allergy Clin Immunol* 120:293–299
 29. Roberts LJ II, Durand T (2004) Preface. *Chem Phys Lipids* 128:1–194
 30. Jahn U, Galano JM, Durand T (2008) Beyond prostaglandins—chemistry and biology of cyclic oxygenated metabolites formed by free-radical pathways from polyunsaturated fatty acids. *Angew Chem Int Ed Engl* 47:5894–5955
 31. Morrow JD, Hill KE, Burk RF, Nammour TM, Badr KF, Roberts LJ 2nd (1990) A series of prostaglandin F2-like compounds are produced in vivo in humans by a non-cyclooxygenase, free radical-catalyzed mechanism. *Proc Natl Acad Sci USA* 87:9383–9387
 32. Nourooz-Zadeh J, Liu EH, Anggard E, Halliwell B (1998) F4-isoprostanes: a novel class of prostanoids formed during peroxidation of docosahexaenoic acid (DHA). *Biochem Biophys Res Commun* 242:338–344
 33. Roberts LJ II, Montine TJ, Markesbery WR, Tapper AR, Hardy P, Chemtob S, Dettbarn WD, Morrow JD (1998) Formation of isoprostane-like compounds (neuroprostanes) in vivo from docosahexaenoic acid. *J Biol Chem* 273:13605–13612
 34. Schmidt A, Boland W (2007) General strategy for the synthesis of b(1) phytoprostanes, dinor isoprostanes, and analogs. *J Org Chem* 72:1699–1706
 35. Beckwith AJJ, Schiesser CH (1985) Regio- and stereoselectivity of alkenyl radical ring closure: a theoretical study. *Tetrahedron* 41:3925–3941
 36. Rondot B, Durand T, Girard JP, Rossi JC, Schio L, Khanapure SP, Rokach J (1993) A free radical route to syn lactones and other prostanoid intermediates in isoprostaglandin synthesis. *Tetrahedron Lett* 34:8245–8248
 37. Rondot B, Durand T, Rossi J-C, Rollin P (1994) Synthesis of 3,5-dideoxy-5-iodo-1,2-O-isopropylidene-beta-L-lyxo-hexofuranose derivatives. *Carbohydr Res* 261:149–156
 38. Krause N, Ebert S, Haubrich A (1997) Diastereoselective protonation of chiral enolates with chelating proton donors under reagent control: scope, mechanism, and applications. *Liebigs Ann*:2409–2418
 39. Roland A, Durand T, Rondot B, Vidal J-P, Rossi J-C (1996) A practical asymmetric synthesis of ent-12-epi-PGF-2 alpha methyl ester. *Bull Soc Chim Fr* 133:1149–1154
 40. Noyori R, Tomino I, Yamada M, Nishizawa M (1984) Asymmetric synthesis via axially dissymmetric molecules. 7. Synthetic applications of the enantioselective reduction by binaphthol-modified lithium aluminum hydride reagents. *J Am Chem Soc* 106:6717–6725
 41. El Fangour S, Guy A, Despres V, Vidal J-P, Rossi J-C, Durand T (2004) Total synthesis of the eight diastereomers of the *syn-anti-syn* phytoprostanes F1 types I and II. *J Org Chem* 69:2498–2503
 42. Iqbal M, Evans P (2003) Conjugate addition-Peterson olefination reactions: expedient routes to cross conjugated dienones. *Tetrahedron Lett* 44:5741–5745
 43. Iqbal M, Li Y, Evans P (2004) Synthesis of D12, 14–15-deoxy-PG-J1 methyl ester and epi-D12–15-deoxy-PG-J1. *Tetrahedron* 60:2531–2538
 44. Vasquez-Romero A, Cardenas L, Blasi E, Verdaguer X, Riera A (2009) Synthesis of prostaglandin and phytoprostanes B1 via regioselective intramolecular Pauson–Khand reactions. *Org Lett* 11:3104–3107
 45. Mikolajczyk M, Midura WH, Mohamed Ewas AM, Perlikowska W, Mikina M, Jankowiak A (2008) Horner olefination reaction in organic sulfur chemistry and synthesis of natural and bioactive products. *Phosphorus Sulfur Silicon Relat Elem* 183:313–325
 46. Perlikowska W, Mikolajczyk M (2009) A short synthesis of enantiomeric phytoprostanes B1 Type I. *Synthesis* 16:2715–2718
 47. Sih CJ, Price P, Sood R, Salomon RG, Peruzzotti G, Casey M (1972) Total synthesis of prostaglandins. II. Prostaglandin E1. *J Am Chem Soc* 94:3643–3644
 48. Alvarez FS, Wren D, Prince A (1972) Prostaglandins. IX. Synthesis of (+)-prostaglandin E1, (+)-11-deoxyprostaglandins E1, F1.alpha., and F1.beta., and (+)-9-oxo-13-*cis*-prostenic acid by conjugate addition of vinylcopper reagents. *J Am Chem Soc* 94:7823–7827
 49. Kluge AF, Untch KG, Fried JH (1972) Prostaglandins. X. Synthesis of prostaglandin models and prostaglandins by conjugate addition of a functionalized organocopper reagent. *J Am Chem Soc* 94:7827–7832
 50. Rodriguez AR, Spur BW (2003) First total synthesis of the E type I phytoprostanes. *Tetrahedron Lett* 44:7411–7415
 51. Rodriguez AR, Spur BW (2002) Total synthesis of E1 and E2 isoprostanes by diastereoselective protonation. *Tetrahedron Lett* 43:9249–9253
 52. Rodriguez AR, Spur BW (2002) Total synthesis of isoprostanes via the two-component coupling process. *Tetrahedron Lett* 43:4575–4579
 53. Loza E, Lola D, Freimanis J, Turovskii I, Gavars M, Liepina A (1985) 2,5-Disubstituted furans in the synthesis of 2-cyclopentenone derivatives. *Latvijas PSR Zinatnu Akademijas Vestis, Kimijas Serija* 4:465–472
 54. El Fangour S, Guy A, Vidal J-P, Rossi J-C, Durand T (2005) A flexible synthesis of the phytoprostanes B1 type I and II. *J Org Chem* 70:989–997
 55. Pinot E, Guy A, Guyon A-L, Rossi J-C, Durand T (2005) Enzymatic kinetic resolution of a functionalized 4-hydroxycyclopentenone: synthesis of the key intermediates in the total synthesis of isoprostanes. *Tetrahedron Asymmetry* 16:1893–1895
 56. Pinot E, Guy A, Fournial A, Balas L, Rossi J-C, Durand T (2008) Total synthesis of the four enantiomerically pure diastereoisomers of the phytoprostanes E1 Type II and of the 15-E2t-Isoprostanes. *J Org Chem* 73:3063–3069

Contrasting Effects of n-3 and n-6 Fatty Acids on Cyclooxygenase-2 in Model Systems for Arthritis

Samantha Hurst · Sarah G. Rees ·
Peter F. Randerson · Bruce Caterson ·
John L. Harwood

Received: 8 June 2009 / Accepted: 24 August 2009 / Published online: 26 September 2009
© AOCS 2009

Abstract Cyclooxygenase-2 (COX-2) is intimately involved in symptoms of arthritis while dietary n-3 polyunsaturated fatty acids (PUFA) are thought to be beneficial. In these experiments, using both bovine and human in vitro systems that mimic features of arthritis, we show that the n-3 PUFA eicosapentaenoic acid (EPA) is able to reduce mRNA and protein levels of COX-2. Activity, as assessed through prostaglandin E₂ formation, was also reduced in a dose-dependent manner. These effects of EPA contrasted noticeably with the n-6 PUFA, arachidonic acid. The data provide direct evidence for a molecular mechanism by which dietary n-3 PUFA, such as EPA, can reduce inflammation and, hence, associated symptoms in arthritis.

Keywords Cyclooxygenase-2 (COX-2) expression · COX-2 activity · Arthritis · n-3 Polyunsaturated fatty acids

Abbreviations

ARA	Arachidonic acid
BCIP	5-bromo-4-chlorindolyl phosphate
COX	Cyclooxygenase
DHA	All <i>cis</i> - Δ 4, 7, 10, 13, 16, 19-docosahexaenoic acid
DMEM	Dulbecco's modified Eagle's medium
EPA	All <i>cis</i> - Δ 5, 8, 11, 14, 17-eicosapentaenoic acid
FCS	Foetal calf serum

FGF	Fibroblast growth factor
GAPDH	Glyceraldehyde-3-phosphate dehydrogenase
IL-1	Interleukin-1
NBT	Nitroblue tetrazolium
NSAIDs	Non-steroidal anti-inflammatory drugs
OA	Osteoarthritis
PDGF	Platelet-derived growth factor
PG	Prostaglandin
PUFA	Polyunsaturated fatty acid
RA	Rheumatoid arthritis
TNF- α	Tumour necrosis factor- α
TSA	TRIZMA saline azide

Introduction

There are two classes of essential polyunsaturated fatty acids (PUFA), the n-3 compounds such as α -linolenic acid and the n-6 series such as linoleic acid. Both types of PUFA are needed in a healthy diet [1] but there has been a continuous debate about the amounts and the ratio of n-3/n-6 PUFA which are required [2]. Although the plant-derived PUFA, linoleate and α -linolenate, are the main dietary components it is their 20C metabolites, arachidonate (ARA) and eicosapentaenoate (EPA), respectively, which are the direct precursors of the biologically-active eicosanoids. Moreover, the n-3 PUFA, EPA and docosahexaenoate (DHA), can also give rise to newly-discovered mediators such as resolvins and neuroprotectins [3]. One complication when considering dietary requirements for n-3 and n-6 PUFA is the relatively poor conversion of the 18C precursors into the respective 20C (or 22C) PUFA [4]. For that reason, acids such as EPA or DHA, as present in oily fish,

S. Hurst · P. F. Randerson · B. Caterson · J. L. Harwood (✉)
Cardiff School of Biosciences, Cardiff University,
Museum Avenue, Cardiff CF10 3AX, UK
e-mail: Harwood@Cardiff.ac.uk

S. G. Rees
School of Medicine, Swansea University, Singleton Park,
Swansea SA2 8PP, UK

are often considered important for a healthy diet [5] and are regarded in some circumstances as conditionally-essential [6].

It is accepted generally that dietary n-3 PUFA can have a beneficial effect on the etiology and progression of chronic inflammatory complaints [7], such as cardiovascular disease [8], Alzheimer's disease [9] or arthritis [10]. This is in contrast to the n-6 PUFA which are usually regarded as pro-inflammatory [11] and the predominance of such acids in the Western diet has led to calls for an urgent adjustment of the ratio of dietary n-3/n-6 PUFA in order to help with the prevention and management of chronic diseases [2].

The molecular mechanism(s) by which n-3 PUFA can exert their beneficial effects is uncertain but may include actions on membranes (and membrane rafts) [12], competition with n-6 PUFA in metabolism [13, 14], the production of anti- or less-inflammatory metabolites [3, 11] and effects on gene expression [15].

Arthritis, particularly osteo- and rheumatoid arthritis, is a major problem world-wide with an estimated 30% of the W. Europe or US populations having symptoms and up to 10% experiencing disability [16]. A beneficial effect for fish oil was first noted in 1783 [17] and, in the last twenty years there have been many clinical studies (e.g. [18–20]) showing clear clinical benefits for n-3 PUFA which mainly relate to reduction of the inflammatory response associated with arthritic conditions [10, 11, 21]. Overproduction of pro-inflammatory and immunoregulatory cytokines is associated with chronic inflammatory diseases [22] and both TNF- α and IL-1 have been implicated as mediators of arthritic joint pathology [4, 10]. The production of such cytokines may be modulated by eicosanoids [22] or n-3 PUFA may influence their expression via the NF- κ B pathway [15].

A key enzyme in mediating the effects of n-3 and n-6 PUFA is cyclooxygenase (COX) [23]. Indeed, non-steroidal anti-inflammatory drugs (NSAIDs), which inhibit cyclooxygenase, are widely prescribed to alleviate symptoms of arthritis (e.g. [24]) and can show chondroprotective effects in vitro [25]. There are two main isoforms of COX; COX-1 and COX-2. These enzymes are the products of different genes although their protein products are highly homologous [26]. COX-1 is present in most cell types and is usually expressed constitutively. In contrast, COX-2 expression is typically transient and is often induced by inflammatory factors such as endotoxin or cytokines. Not only is COX-2 expression under control by multiple factors but the degradation of its protein is rapid due, in particular, to a unique 27 amino acid sequence near its C-terminus. Thus, while COX-1 degradation is slow or undetectable, the $T_{1/2}$ for COX-2 protein degradation varies from 2 to 7 h [26].

n-3 PUFA have been implicated in the reduction of COX-2 expression in a number of tissues [27–29] particularly in relation to malignant cells [30–33]. Moreover, a short report suggested beneficial effects of α -linolenic acid on inflammation and prostaglandin E_2 production in horse joint tissue [34]. Because of the persuasive evidence for a central role for COX-2 activity in the pathogenesis of arthritis, we decided to examine the effect of PUFA on expression and activity of COX-2 using in vitro tissue culture model systems that mimic cartilage matrix degradation in degenerative joint diseases. The results show that, while the n-6 PUFA arachidonate had no beneficial effect in lowering the IL-1 induced levels of COX-2, the n-3 PUFA EPA reduced mRNA and protein levels down to control values. Activity, as measured by PGE $_2$ production, was also reduced in a dose-dependent manner by EPA. These data provide evidence for a molecular mechanism underlying the beneficial effect of dietary n-3 PUFA in arthritis patients.

Experimental Procedures

Materials

Collagenase Type II, isolated from *Clostridium histolyticum* was from Worthington, pronase (*Streptomyces griseus*) from Boehringer and Dulbecco's modified Eagle's medium (DMEM) and foetal calf serum (FCS) from Gibco-BRL (now Invitrogen). Fatty acid standards were from Nu-Chek Prep. or Sigma-Aldrich and recombinant human interleukin-1 α (IL-1 α) or IL-1 β from Totam Biologics. Other chemicals were of the best available grades and were from Sigma-Aldrich or Boehringer-Mannheim (now Roche Diagnostics).

Isolation and Culture of Bovine Chondrocytes

Bovine metacarpo- or metatarsophalangeal joints from 7 day-old calves were obtained from the local abattoir. Human tissue was obtained from patients undergoing total knee replacement surgery for osteoarthritis (Llandough Hospital, S. Wales, UK). All procedures had Local Ethical Committee Approval. Cartilage tissue slices were obtained in sterile conditions and placed in DMEM before subjecting them to pronase and collagenase digestion to isolate the chondrocytes [35]. Monolayer cultures were established in 60 mm culture dishes by plating 1 ml/dish of a suspension of 6×10^6 chondrocytes/ml of DMEM. In the case of human chondrocytes these had to be passaged several times to obtain enough cells for analysis. Cultures were maintained overnight in the absence or presence of 1–10 μ g/ml (for bovine cultures) or 10–30 μ g/ml (for human cultures)

of the n-3 polyunsaturated fatty acid (PUFA), eicosapentaenoic acid (all *cis* Δ5, 8, 11, 14, 17–20:5, EPA) or the n-6 PUFA arachidonic acid (all *cis* Δ5, 8, 11, 14–20:4, ARA). Previous experiments had established that these were appropriate concentrations to observe changes in gene expression in these two tissues (see e.g. [36]). Prior to addition to the cultures, all PUFA were incubated for 16 h at 37 °C in Tyrode-HEPES buffer (20 mM HEPES, 140 mM NaCl, 4.5 mM KCl, 1 mM MgCl₂, 2.5 mM CaCl₂, 11 mM glucose, pH 7.4) containing 3.5 mg/ml fatty acid-free bovine albumin. Following incubation with the PUFA, the culture medium was removed, the cells washed in fresh DMEM and new media (without PUFA) added with supplementation with or without 10 ng/ml IL-1 α or IL-1 β for bovine or human cultures, respectively. The cells were further incubated at 37 °C for 4 days before harvesting.

Explant Cultures

Cartilage explants were obtained from both bovine metacarpal- and metatarsophalangeal joints (7 day-old calves) and from human patients undergoing total knee replacement surgery for OA as described above. The explant cultures were established by taking diced cartilage (20–70 mg wet weight) and maintaining them in 1 ml of DMEM containing 10% FCS (plus 50 μ g/ml gentamicin, 0.5% antibiotic/antimycotic solution 100 \times for the human cultures) for 72 h at 37 °C, with aeration using 5% CO₂/95% air. Following pre-culture, the explants were washed (3 \times 10 min) in serum-free DMEM and maintained for 24 h in individual wells of 24-well plates with 1 ml of serum-free DMEM with or without 1–10 μ g/ml (for bovine cultures) or 10–30 μ g/ml (for human cultures) n-3 or n-6 PUFA. After this culture period, the medium was removed and explants washed and fresh medium (no PUFA) added with or without 10 ng/ml IL-1 α (for bovine tissue) or IL-1 β (for human tissue) and cultured for a further 4 days before harvesting.

RNA Extraction and PCR Analysis

Total RNA was extracted from intact cartilage explants. Explants were snap-frozen in liquid nitrogen and then

subjected to pulverisation with a Braun Mikro-Dismembrator for 1 min at 2000 rpm. Tri-reagent (Sigma-Aldrich) was added to the powdered cartilage (1 ml for samples up to 100 mg) prior to RNA isolation using the Qiagen RNeasy miniprep kit. To 1 ml of Tri-Reagent, 0.2 ml of CHCl₃ was added and the mixture left at room temperature for 15 min. Following centrifugation at 13200 rpm for 15 min, the upper phase was transferred to a sterile 1.5-ml tube containing 375 μ l of 70% ethanol and mixed by inverting. The mixture was applied to a spin column and RNA was isolated following the manufacturer's protocol (Qiagen).

Reverse transcription-polymerase chain reactions (RT-PCR) were performed using an RNA PCR kit (Perkin-Elmer) as described previously [37] using oligonucleotide primers specific to cyclooxygenase cDNA sequences (see Table 1). Following an initial denaturation step of 1 min at 95 °C, amplification consisted of 30–45 cycles of 1 min at 95 °C, 45 s at the individual annealing temperature of the primers (Table 1), 30 s at 72 °C, followed by a final extension step of 5 min at 72 °C. The PCR products were visualised on 3% agarose gels (containing 0.5 μ g/ml ethidium bromide) under UV light.

The Wizard PCR Preps DNA Purification System (Promega) was used to purify the PCR products following the manufacturer's guidelines. The PCR products were sequenced to check the template specificity of each primer by using an Applied Biosystems AB1310 Genetic Analyser. This was followed by alignment of nucleotide sequences using the MacDNASIS sequence analyser software package (Hitachi).

Individual gels were scanned using a Kodak Digital IB Image Analysis apparatus to provide densitometric values for the PCR products. These densitometric values were normalised to those for GAPDH (used as a constitutive gene) from the same cDNA samples.

SDS-PAGE and Western blot Analysis of Cyclooxygenase Protein

Monolayer cultures were washed twice with cold phosphate-buffered saline (PBS) and, using a rubber cell

Table 1 Oligonucleotide primers used in RT-PCR

	Target	PCR Primer sequence (5'-3')	Annealing Temp (°C)	Product size (bp)
Sequences, annealing temperatures and product sizes are shown. The products were verified by isolation on agarose gels and sequencing	GAPDH	5'-TGGCATCGTGGAAGGGCTCAT 5'-ATGGGAGGTGCTGTTGAAGTC	50	370
	Bovine COX-2	5'-GCTCTTCCTCCTGTGCTGAT 5'-CATGGTTCTTTCCCTTAGTGA	52.3	229
	Human COX-2	5'-GGCTGTCCCTTTACTTCATTC 5'-ACATCTTTACTTTCGTCCTTA	48.2	438

scraper, the chondrocytes were scraped from their plates into 1 ml of cold lysis buffer (40 mM Tris, 1 mM EDTA, 250 mM sucrose, 5 mM DTT, 0.2 M Na_3VO_4 , 0.5 mM phenylmethylsulphonyl fluoride (PMSF), 10 $\mu\text{g}/\text{ml}$ leupeptin, 1 $\mu\text{g}/\text{ml}$ anitpain, 1 $\mu\text{g}/\text{ml}$ pepstatin A), placed into tubes and kept on ice. The suspension was subjected to homogenisation by 30 passages through a narrow gauge needle and syringe. The homogenate was centrifuged at 13,000 rpm for 10 min and the supernatant kept as the protein source [38]. Samples were then dialysed and lyophilised.

The lyophilised sample was initially prepared by diluting with 2 \times Sample Buffer (0.125 M Tris HCl, pH 6.8, 4% SDS, 20% glycerol, 0.01% bromophenol blue) and Milli-Q water. The samples were reduced by adding β -mercaptoethanol at 10% of the final loading volume and the mixture heated for 10 min at 70 °C prior to gel loading. The samples were separated on 10% polyacrylamide gels (poured using acrylagel and bisacrylagel from National Diagnostics) in SDS. After electrophoresis, the fractionated proteins were transferred electrophoretically to nitrocellulose membranes (Schleicher and Schuell), blocked with 5% BSA (w/v) in TRIZMA saline azide (TSA) (50 mM TRIZMA, 200 mM NaCl, 0.02% (w/v) NaN_3 , pH 7.4 with HCl (1 h) and immuno-blotted with a polyclonal primary antibody specific to the 72 kDa COX-2 protein (Santa Cruz Biotechnology). Anti-COX-2 was used at 1:1000 dilution, overnight. The primary antibody was poured off and a secondary antibody, alkaline-phosphatase conjugated anti-goat (Sigma-Aldrich), was added at a concentration of 1:10,000 for 1 h. All antibodies were diluted with 1% BSA/TSA. The membrane was subjected to three 10 min washes in TSA and developed in alkaline phosphatase substrate; 10 ml of buffer (100 mM Tris, 100 mM NaCl, 5 mM MgCl_2 , pH 9.55) with 66 μl of nitroblue tetrazolium (NBT) (50 mg/ml in 70% dimethylformamide and 33 μl of 5-bromo-4-chloro-1-indolyl phosphate (BCIP; Promega) for 10–15 min until the optimum colour had developed.

Quantification of Prostaglandin E_2 (PGE_2)

The PGE_2 immunoassay kit from R & D Systems is a competitive enzyme immunoassay designed to measure PGE_2 concentrations in cell culture supernatants and other biological samples. This kit shows some cross-reactivity with a few eicosanoids (mainly PGE_3 and PGE_1) but no interference at mid-range PGE_2 concentrations, such as found in present study (Manufacturer's brochure). Explant culture medium was harvested and either frozen at -20 °C or assayed immediately. The assay was carried out following the manufacturer's protocol and absorbance was read at 405 nm prior to statistical analysis using Statview 4.02 package for Macintosh (Abacus Concepts Inc.).

Results

Metabolic Activity of Explant Cultures

Previous experiments with model in vitro culture systems for arthritis [38] demonstrated that fatty acids could be added as a complex with BSA, which is the natural way in which they are supplied in vivo. Such complexes have been shown to allow transport of fatty acids through the cartilage matrix at measurable rates [39].

Explant cultures of tissue from joints have been shown, when cultured appropriately, to mimic many of the features of matrix degradation found in arthritic tissues [40]. Lactate production by explants from both bovine and human joints was unaffected by the addition of IL-1, by the n-3 PUFA, EPA or the n-6 PUFA, ARA (Fig. 1a, b). These results show that general metabolism, as measured by lactate production, was not affected by any of the additions performed.

In contrast, degradation of matrix components was monitored by glycosaminoglycan (GAG) release and this was increased significantly by IL-1 α challenge in bovine explants (Fig. 1c). In control cultures, the level of GAG release was low as expected for healthy tissue. However, the level of GAG release, which was raised by IL-1 α addition, was reduced successively by increasing amounts of EPA but not by ARA (Fig. 1c). For the explants of human joint tissues, the control samples showed high levels of GAG release which fitted well with the fact that these samples were obtained from patients with advanced osteoarthritis. The amount of GAG release in these tissues was only slightly increased by IL-1 β challenge and the addition of fatty acids had no significant effect (Fig. 1d).

Effect of PUFA on COX-2 Expression

We now used these in vitro explant cultures to examine cyclooxygenase expression and activity. In control bovine tissues which had not been pre-treated with PUFA or stimulated with IL-1 α , low levels of COX-2 mRNA were found (Fig. 2a). Expression was stimulated by exposure to the inflammatory cytokine IL-1 α and this was abrogated by previous incubation of the explants with the n-3 PUFA EPA but not by the n-6 PUFA ARA (Fig. 2a).

In contrast, for the human explant cultures, COX-2 expression was significant in controls (Fig. 2b). This was indicative of the pathological state of the osteoarthritic cartilage which had been obtained from patients awaiting knee-replacement surgery. Nevertheless, expression levels of COX-2 were increased further by exposure to IL-1 β . Furthermore, COX-2 mRNA levels were reduced significantly by pre-incubation with EPA but not by

Fig. 1 Lactate production and glycosaminoglycan (GAG) release in healthy bovine (a, c) or osteoarthritic human (b, d) cartilage explant cultures. Cultures were supplemented with 1–30 μg (as shown) fatty acid/ml medium for 24 h followed by culture in the presence or absence of 10 ng/ml IL-1 for 4 days. Data show means \pm SDs ($n = 3-4$) each carried out in triplicate. * Data significantly (t test, $P < 0.05$) different from control; + Significantly different from IL-1 treated explants. The upper histograms (a, b) show lactate levels and the lower histograms (c, d) are for GAG release. Open bars without IL-1 challenge and the shaded bars for incubations in the presence of IL-1

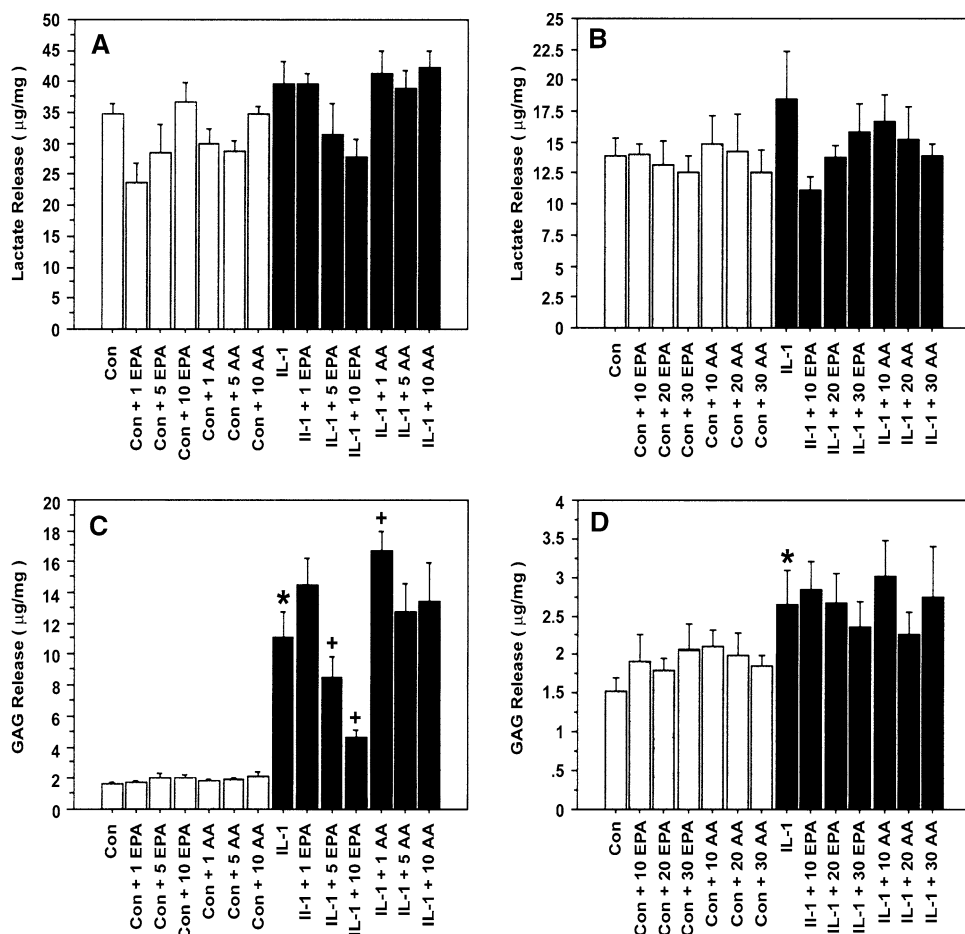
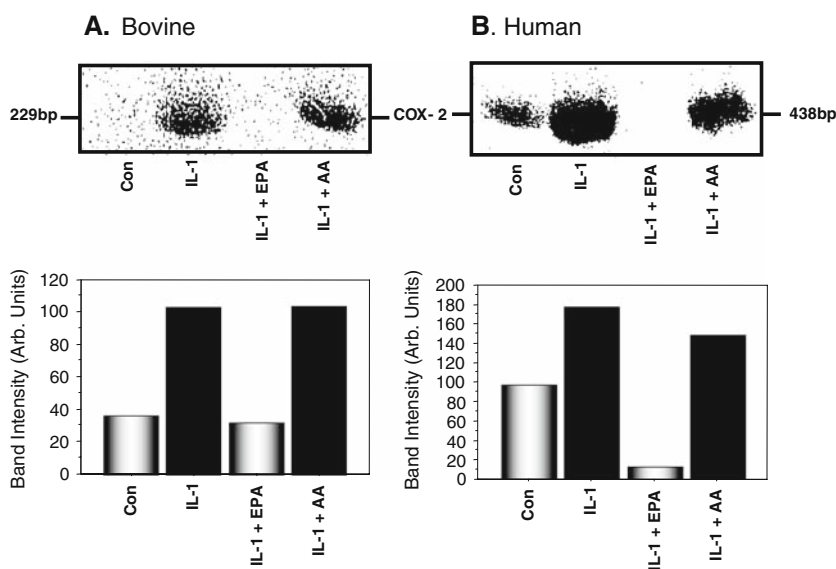


Fig. 2 mRNA levels for cyclooxygenase-2 (COX-2) in bovine (a) and human (b) cartilage explant cultures. Cultures were supplemented with 10 $\mu\text{g}/\text{ml}$ (bovine) or 30 $\mu\text{g}/\text{ml}$ (human) EPA or ARA for 24 h followed by culture in the presence or absence of 10 ng/ml IL-1 α (bovine cultures) or IL-1 β (human cultures) for 4 days. RT-PCR was carried out using specific primers (Table 1) and the Figure shows gel images in the upper portion and quantification using the NIH Image and Statview 4.02 software packages in the lower part. Representative experiments are depicted



pre-incubation with ARA (Fig. 2b). Thus, in both human and bovine cartilage explants, COX-2 mRNA was increased by the inflammatory cytokine IL-1 and this increase was strongly inhibited by the n-3 PUFA, EPA but not by the n-6 PUFA, ARA.

EPA and ARA have Opposite Effects on COX-2 Protein Levels

Because changes in gene expression are not necessarily paralleled by similar alterations in protein levels (and

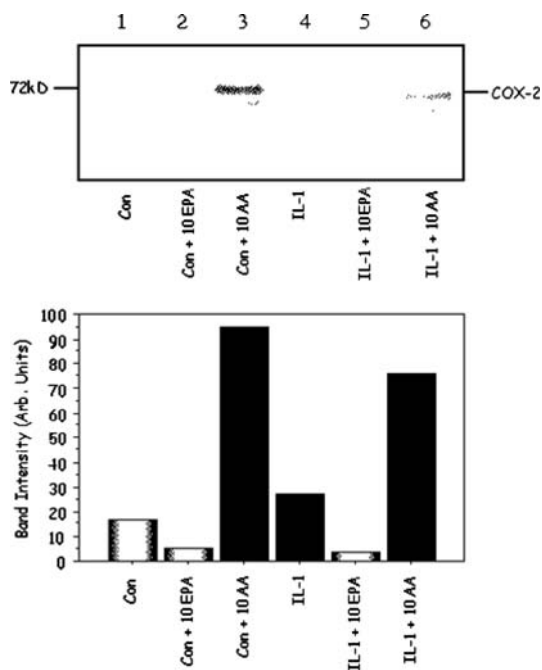


Fig. 3 Western blot analysis to show the effects of 10 $\mu\text{g/ml}$ EPA or ARA on COX-2 protein levels in bovine chondrocyte cultures. Cultures were pre-incubated with fatty acids and treated with IL-1 α as described in Fig. 2

activity), we examined the effect of PUFA on COX-2 protein in IL-1 challenged bovine tissues (Fig. 3). As expected for tissue preparations from young, healthy animals, little COX-2 protein was detected in controls. Pre-incubation with EPA caused a small (non-significant) reduction in protein levels whereas ARA increased COX-2 protein more than 5-fold (Fig. 3). Incubation with IL-1 α caused a moderate increase in COX-2 protein and this was clearly abrogated by pre-incubation with EPA. In contrast, pre-incubation with ARA resulted in elevated COX-2 protein levels (Fig. 3). Similar experiments using chondrocyte preparations from the human osteoarthritic tissue were attempted several times but could not be achieved because of the small numbers of viable cells available.

Cyclooxygenase-2 Activity

Having shown beneficial effects of EPA on COX-2 expression (at both mRNA and protein levels), we quantified prostaglandin E₂ (PGE₂) as a measure of COX-2 activity. This eicosanoid is also thought to be particularly relevant to the etiology of arthritis (see [10]).

In Fig. 4, the effect of pre-incubation with different concentrations of EPA is shown. For control bovine explants there were very low concentrations of PGE₂ detected—as expected given the low levels of COX-2 expression (Fig. 2) in such preparations. Pre-incubation

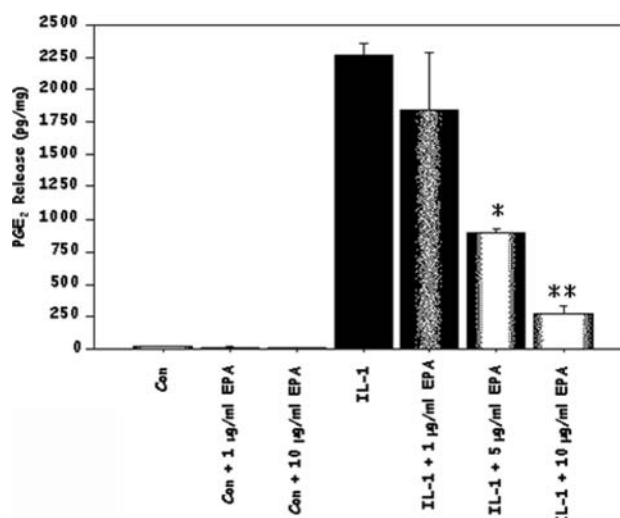


Fig. 4 Prostaglandin E₂ (PGE₂) production in bovine explant cultures is stimulated by IL-1 α and reduced dose-dependently by EPA. Cultures were supplemented with or without 1–10 $\mu\text{g/ml}$ EPA for 24 h and then challenged with 10 $\mu\text{g/ml}$ IL-1 α for 4 days. Means (pg PGE₂/mg fresh wt. of tissue) \pm SD ($n = 4$) shown. ***/** Significantly different (t test, $P < 0.05/P < 0.01$) from IL-1-treated alone

with EPA did not change the amount of PGE₂ released. Exposure to IL-1 α caused a large elevation in PGE₂ levels and these were progressively reduced by pre-incubation of the tissue with increased amounts of EPA (Fig. 4).

For human explant cultures, significant PGE₂ release was found in controls, due to the pathological state of the original tissue. This varied between 4 and 31 pg/mg fresh wt. tissue for preparations from different patients. In order to allow comparisons, results (Fig. 5) are expressed as a percentage of the level of PGE₂ which was induced by incubation with IL-1 β . On average this caused about a five-fold increase in the PGE₂ detected relative to control. However, pre-incubation with EPA was able to reduce PGE₂ back to control levels whereas pre-incubation with ARA had no effect on the IL-1 β -induced PGE₂ concentrations (Fig. 5).

Discussion

In arthritis it is well accepted that inflammatory changes are critical to the development and exacerbation of the disease. IL-1 and TNF- α are the main cytokines involved [10] and here we have used IL-1 to induce molecular changes in model systems that mimic cartilage degradation in arthritis. IL-1, which is raised in arthritic tissue [33], also increases expression of COX-2 in a variety of cell types such as cardiac [41] or venous epithelial cells [28] and our experiments (Figs. 2, 3) are consistent with these findings. While dietary n-6 PUFA increase inflammatory cytokines,

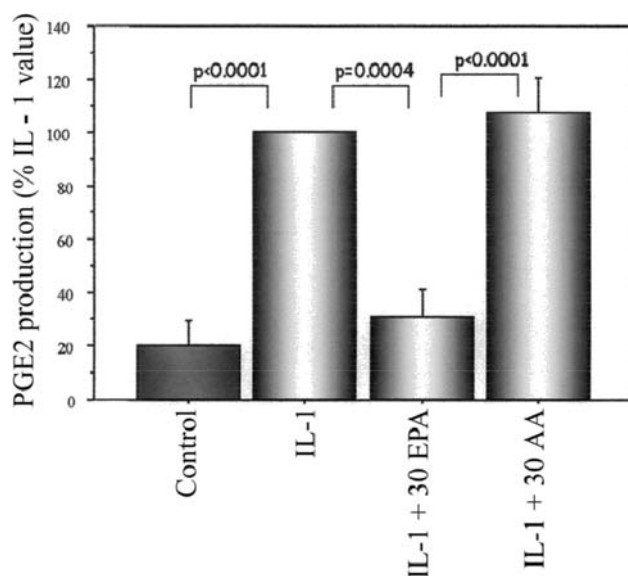


Fig. 5 Prostaglandin E₂ (PGE₂) production in human osteoarthritic joint explant cultures is reduced by EPA but not by ARA. Treatments as in Fig. 2. The data are expressed as % of the +IL-1 β value which had a mean of 400 pg/mg fresh wt. of tissue for the 8 patients. Means \pm SD ($n = 8$) shown. Significant differences (t test) shown

such as IL-1 and TNF- α , as well as COX enzymatic products [2], dietary n-3 PUFA reduce inflammatory gene expression [42, 43] including that of COX-2 [15]. Some of the effects of the n-3 PUFA may be via resolvins [44] in addition to the classic eicosanoids [23]. In addition, the n-3 and n-6 PUFA have antagonistic effects on TNF receptors [45].

Here we show that the n-3 PUFA, EPA, is able to reduce COX-2 expression, protein levels and activity in both bovine and human tissue cultures, which act as models for cartilage degradation in arthritis. These effects suggest a functional manifestation of the benefit of dietary n-3 PUFA. These data parallel other experiments showing that n-3 PUFA reduce COX-2 expression and/or activity in several other systems [28, 46], especially neoplastic tissues [29, 31–33]. Furthermore, in chondrocyte cultures (as used in this work) we showed that EPA was the most effective n-3 PUFA [36].

The molecular basis for the dietary benefits of n-3 PUFA is not yet resolved and it is probably multifactorial [23]. Such dietary components may affect the expression of COX-2 via Toll-like receptors [47] and inflammatory signalling pathways such as NF κ B [48]. Indeed, the latter has been proposed as a potential therapeutic target for arthritis [49]. Here we have been able to show that the reduction of PGE₂, which is a therapeutic goal for the use of COX-2 inhibitors in arthritis treatment [24], is dose-dependent on the n-3 PUFA, EPA, and that this, in turn, is due to a reduction in both COX-2 gene and protein expression.

Whether the alterations in gene expression are mediated through NF κ B, such as has been proposed from work related to cardiovascular disease using venous epithelial cells [28], requires further experiments. Nevertheless, our data indicate interesting parallels between the two chronic inflammatory conditions, cardiovascular disease and arthritis [7], both of which benefit from dietary n-3 PUFA.

Acknowledgments This investigation was supported financially by the Arthritis Research Campaign and the Biotechnology and Biological Sciences Research Council (Grant D16961) for which we are grateful.

References

1. Gunstone FD, Harwood JL, Dijkstra AJ (eds) (2006) The lipid handbook, 3rd edn. Taylor and Francis, Boca Raton
2. Simopoulos AP (2006) Evolutionary aspects of diet, the omega-6/omega-3 ratio and genetic variation: nutritional implications for chronic diseases. *Biomed Pharmacother* 60:502–507
3. Serhan CN, Makato A, Hong S, Gotlinger K (2004) Resolvins, docosatrienes and neuroprotectins, novel omega-3-derived mediators and their endogenous aspirin-triggered epimers. *Lipids* 39:1125–1132
4. MacLean CH, Mojica WA, Morton SC, Pencharz J, Hasenfeld R et al (2004) Effects of omega-3 fatty acids on lipids and glycemic control in Type II diabetes and the metabolic syndrome and on inflammatory bowel disease, rheumatoid arthritis, renal disease, systemic lupus erythematosus and osteoporosis. Summary, Evidence Report/Technology Assessment no. 89. AHRQ Publication no. 04-E012-1. Rockville
5. Lands WEM (2005) Fish, omega-3 and human health, 2nd edn. American Oil Chemists Society, Champaign
6. Cunnane SC (2003) Problems with essential fatty acids: time for a new paradigm? *Prog Lipid Res* 42:544–568
7. Harwood JL, Caterson B (2006) Dietary omega-3 polyunsaturated fatty acids and inflammation. *Lipid Technol* 18:7–10
8. von Schacky C, Harris WS (2007) Cardiovascular benefit of omega-3 fatty acids. *Cardiovasc Res* 73:310–315
9. Morris MC, Evans DA, Bienias JC, Tangney CC, Bennett DA et al (2003) Consumption of fish and n-3 fatty acids and risk of incident Alzheimer's disease. *Arch Neurol* 60:940–946
10. Rayman M, Callaghan A (2006) Nutrition and arthritis. Blackwell, Oxford
11. Calder PC, Zurier RB (2001) Polyunsaturated fatty acids and rheumatoid arthritis. *Cur Opin Clin Nutr Metab Care* 4:115–121
12. Vigh L, Escriba PV, Sonnleiter A, Piotto S, Maresca B et al (2005) The significance of lipid composition for membrane activity: new concepts and ways of assessing function. *Prog Lipid Res* 44:303–344
13. Calder PC (2006) n-3 Polyunsaturated fatty acids, inflammation and inflammatory diseases. *Am J Clin Nutr* 83:1505S–1519S
14. Harris WS (2007) Omega-3 fatty acids and cardiovascular disease: a case for omega-3 index as a new risk factor. *Pharmacol Res* 55:217–223
15. Deckelbaum RJ, Worgall TS, Seo T (2006) n-3 Fatty acids and gene expression. *Am J Clin Nutr* 83:1520S–1525S
16. West SG (2002) Rheumatology secrets, 2nd edn. Hanley and Belfus, Philadelphia
17. Percival T (1783) Observations on the medicinal uses of the Oleum Jecoris Aselli, or cod liver oil in the chronic rheumatism and other painful disorders. *London Med J* 3:393–401

18. Kremer JM (2000) n-3 Fatty acid supplements in rheumatoid arthritis. *Am J Clin Nutr* 71:349S–351S
19. Cleland LG, James MJ (2000) Fish oil and rheumatoid arthritis: anti-inflammatory and collateral health benefits. *J Rheumatol* 27:2305–2307
20. Sundrarjun T, Komindr S, Archararit N, Dahlan W, Puchaiwatananon O et al (2004) Effects of n-3 fatty acids on serum interleukin-6, tumour necrosis factor- α and soluble tumour necrosis factor receptor p55 in active rheumatoid arthritis. *J Int Med Res* 32:443–454
21. James MJ, Proudman SM, Cleland LG (2003) Dietary n-3 fats as adjunctive therapy in a prototypic inflammatory disease: issues and obstacles for use in rheumatoid arthritis. *Prostaglandins Leukotr Essential Fatty Acids* 68:399–405
22. Calder PC (1997) n-3 Polyunsaturated fatty acids and cytokine production in health and disease. *Ann Nutr Metab* 41:203–234
23. Smith WL (2007) Nutritionally essential fatty acids and biologically-indispensable cyclooxygenases. *Trends Biochem Sci* 33:27–37
24. Silverstein FE, Faich G, Goldstein JL, Simon LS, Pincus T et al (2000) Gastrointestinal toxicity with celecoxib vs non-steroidal anti-inflammatory drugs for osteoarthritis and rheumatoid arthritis: the CLASS study; a randomised controlled trial. Celecoxib long-term arthritis safety study. *JAMA* 284:1247–1255
25. de Boer TN, Huisman AM, Polak AA, Niehoff AG, van Rinsum RC et al (2009) The chondroprotective effect of selective COX-2 inhibition in osteoarthritis: ex vivo evaluation of human cartilage tissue after in vivo treatment. *Osteoarthr Cartilage* 17:482–488
26. Kang Y-J, Mbye UR, DeLong CJ, Wada M, Smith WL (2007) Regulation of intracellular cyclooxygenase levels by gene transcription and protein degradation. *Prog Lipid Res* 46:108–125
27. Bagga D, Wag L, Farias-Eisner R, Glaspy JA, Reddy ST (2003) Differential aspects of prostaglandins derived from n-6 and n-3 polyunsaturated fatty acids on COX-2 expression and IL-6 secretion. *Proc Natl Acad Sci USA* 100:1751–1756
28. Massaro M, Habib A, Lubrano L, Del Turco S, Lazzzerini G et al (2006) The omega-3 fatty acid docosahexaenoate attenuates endothelial cyclooxygenase-2 induction through both NADP(H) oxidase and PKC ϵ inhibition. *Proc Natl Acad Sci USA* 103:15184–15189
29. Badawi AF, El-Soheby A, Stephen LL, Ghoshal AK, Archer MC (1998) The effect of dietary n-3 and n-6 polyunsaturated fatty acids on the expression of cyclooxygenase 1 and 2 and levels of p21^{ras} in rat mammary glands. *Carcinogenesis* 19:905–910
30. Calviello G, Resci F, Serini S, Piccioni E, Toesca A et al (2007) Docosahexaenoic acid induces proteasome-dependent degradation of β -catenin, down-regulation of survivin and apoptosis in human colorectal cancer cells not expressing COX-2. *Carcinogenesis* 28:1202–1209
31. Llor X, Pons E, Roca A, Alvarez M, Mane J et al (2003) The effects of fish oil, olive oil, oleic acid and linoleic acid on colorectal neoplastic processes. *Clin Nutr* 22:71–79
32. Denkins Y, Kempf D, Ferniz M, Nileshwar S, Marchetti D (2005) Role of n-3 polyunsaturated fatty acids on cyclooxygenase-2 metabolism in brain-metastatic melanoma. *J Lipid Res* 46:1278–1284
33. Vecchini A, Ceccarelli V, Susta F, Caligiana P, Orvietani P et al (2004) Dietary alpha-linolenic acid reduces COX-2 expression and induces apoptosis of hepatoma cells. *J Lipid Res* 45:308–316
34. Munsterman AS, Bertone AL, Zachos TA, Weisbrode SE (2005) Effects of the omega-3 fatty acid, α -linolenic acid, on lipopolysaccharide-challenged synovial explants from horses. *Am J Vet Res* 66:1503–1508
35. Hughes CE, Little CB, Buttner FH, Bartnik E, Caterson B (1998) Differential expression of aggrecanase and matrix metalloproteinase activity in chondrocytes isolated from bovine and porcine articular cartilage. *J Biol Chem* 273:30576–30582
36. Zainal Z, Longman AJ, Hurst S, Duggan K, Caterson B et al (2009) Relative efficacies of omega-3 polyunsaturated fatty acids in reducing expression of key proteins in a model system for studying osteoarthritis. *Osteoarthr Cartilage* 17:882–891
37. Rees SG, Flannery CR, Little CB, Hughes CE, Caterson B, Dent C (2000) Catabolism of aggrecan, decorin and biglycan in tendon. *Biochem J* 350:181–188
38. Thomas B, Thirion S, Humbert L, Tan L, Goldring MB et al (2002) Differentiation regulates interleukin-1 β -induced cyclooxygenase-2 in human articular chondrocytes: role of p38 mitogen-activated protein kinase. *Biochem J* 362:367–373
39. Arkill KP, Winlove CP (2006) Fatty acid transport in articular cartilage. *Arch Biochem Biophys* 456:71–78
40. Caterson B, Flannery CR, Hughes CE, Little CB (2000) Mechanisms involved in cartilage proteoglycan metabolism. *Matrix Biol* 19:333–344
41. Barbieri SS, Weksler BB (2007) Tobacco smoke cooperates with interleukin-1 β to alter β -catenin trafficking in vascular endothelium resulting in increased permeability and induction of cyclooxygenase-2 expression in vitro and in vivo. *FASEB J* 21:1831–1843
42. Bordoni A, Astolfi A, Morandi L, Pession A, Danesi F et al (2007) N-3 PUFAs modulate global gene expression profile in cultured rat cardiomyocytes. Implications for cardiac hypertrophy and heart failure. *FEBS Lett* 581:923–929
43. Sierra S, Lara-Villoslada F, Comalada M, Olivares M, Xaus J (2006) Dietary fish oil n-3 fatty acids increase regulatory cytokine production and exert anti-inflammatory effects in two murine models of inflammation. *Lipids* 41:1115–1125
44. Connor KP, SanGiovanni JP, Lofqvist C, Aderman CM, Chen J et al (2007) Increased dietary intake of ω -3-polyunsaturated fatty acids reduces pathological retinal angiogenesis. *Nat Med* 13:868–873
45. Moghaddami N, Irvine J, Gao X, Grover PK, Costabile M et al (2007) Novel action of n-3 polyunsaturated fatty acids. *Arth Rheum* 56:799–808
46. Bryan D-L, Forsyth KD, Hart PH, Gibson RA (2006) Polyunsaturated fatty acids regulate cytokine and prostaglandin E $_2$ production by respiratory cells in response to mast cell mediators. *Lipids* 41:1101–1107
47. Lee JY, Plakidas A, Lee WH, Heikkinen A, Chanmugam P et al (2003) Differential modulations of toll-like receptors by fatty acids: preferential inhibition by n-3 polyunsaturated fatty acids. *J Lipid Res* 44:479–486
48. Denys A, Hichami A, Khan NA (2005) n-3 PUFAs modulate T-cell activation via protein kinase C- α and - ϵ and the NF κ B signalling pathway. *J Lipid Res* 46:752–758
49. Roman-Blas JA, Jimenez SA (2006) NF κ B as a potential therapeutic target in osteoarthritis and rheumatoid arthritis. *Osteoarthr Cartilage* 14:839–848

Ezetimibe Inhibits Expression of Acid Sphingomyelinase in Liver and Intestine

Yajun Cheng · Fuli Liu · Jun Wu · Yao Zhang · Åke Nilsson · Rui-Dong Duan

Received: 24 March 2009 / Accepted: 3 September 2009 / Published online: 24 September 2009
© AOCs 2009

Abstract Ezetimibe inhibits cholesterol absorption in the intestine. Sphingomyelin has strong interactions with cholesterol. We investigated the effects of ezetimibe on Sphingomyelinase (SMase) expression in intestine and liver. After feeding rats with ezetimibe (5 mg/kg per day) for 14 days, acid SMase activities in the liver and in the proximal part of small intestine were reduced by 34 and 25%, respectively. Alkaline SMase (alk-SMase) was increased in the proximal part of the small intestine. Administration of lower doses of ezetimibe reduced acid SMase only in the liver by 14% ($P < 0.05$). In cell culture studies, ezetimibe decreased acid SMase activity in Hep G2 and Caco-2 cells dose-dependently. The reductions were more rapid for Hep G2 cells than for Caco-2 cells. Western blot showed that acid SMase protein was decreased in both Hep G2 and Caco-2 cells by 100 μ M ezetimibe. The SM content was increased in Hep G2 cells but not Caco-2 cells, and total cholesterol content was increased in both cell lines 24 h after stimulation with 100 μ M ezetimibe. Mevastatin, the inhibitor of cholesterol synthesis, induced a mild increase in acid SMase activity in Hep G2 cells but not Caco-2 cells. Following the reduction of acid SMase, ezetimibe at high dose slightly increased alk-SMase activity. In conclusion, the study demonstrates an inhibitory effect of ezetimibe on acid SMase activity and expression in both liver and intestine.

Keywords Acid sphingomyelinase · Ezetimibe · Sphingomyelin · Cholesterol · Rat · Hep G2 cells · Caco-2 cells · Intestine · Liver

Abbreviations

Alk-SMase	Alkaline sphingomyelinase
NPC1	Niemann–Pick C1
NPC1L1	Niemann–Pick C1 like 1 protein
SM	Sphingomyelin
SMase	Sphingomyelinase

Introduction

Ezetimibe is an effective drug that inhibits the absorption of biliary and dietary cholesterol from the small intestine. In the intestinal tract, ezetimibe is glucuronidated, transported to the liver, and in turn secreted in the intestine in response to diet [1]. The glucuronide form is more potent than ezetimibe itself. Studies using Niemann–Pick C1 like 1 (NPC1L1) protein deficient mice indicated that NPC1L1 is the target of ezetimibe [2, 3]. NPC1L1 is a membrane protein that shares 42% identity with Niemann–Pick C1 (NPC1) protein [4]. NPC1L1 is expressed in the intestine and also several other organs including liver, and plays important roles in mediating cholesterol absorption and uptake. Besides the effect on absorption of cholesterol in the intestine, ezetimibe has also been shown to affect the metabolism of lipoproteins, such as to increase HDL levels, and enhance clearance of LDL via upregulation of LDL receptors [1]. In addition, ezetimibe may have other effects such as to improve insulin resistance in obese mice, improve the liver function in non-alcohol fatty liver disease

Y. Cheng · F. Liu · J. Wu · Y. Zhang · Å. Nilsson · R.-D. Duan (✉)
Gastroenterology and Nutrition Lab, BMC, B11,
Institution of Clinical Sciences,
Lund University, 221 84 Lund, Sweden
e-mail: Rui-dong.duan@med.lu.se

[5], and reduce the formation of gallstones [6]. The mechanisms underlying these effects are largely unknown.

Sphingomyelin (SM) is a type of sphingolipid, which interacts strongly with cholesterol to form a stable complex. Previous studies have shown that hydrolysis of membrane SM by sphingomyelinase (SMase) affects cholesterol metabolism. Treating the fibroblasts with exogenous SMase increases the mass cholesterol ester in the cells associated with an increase in ACAT [7] and HMG-CoA reductase activities [8], whereas in the cells isolated from Niemann–Pick diseases, the trafficking of cholesterol into the cells is impaired [9]. SM levels in the intestine may also affect cholesterol absorption. Chan et al. [10] showed that treating Caco-2 cells with exogenous SMase reduces the uptake of cholesterol. We previously showed that when animals were fed cholesterol together with SM, the cholesterol absorption decreased with increasing the amount of SM in the diet [11]. In the intestinal tract, the levels of SM are mainly regulated by two types of SMases: acid SMase and alkaline SMase (alk-SMase) [12, 13]. Acid SMase activity is relatively high in the proximal part of the intestine and liver. The main function of acid SMase is to degrade the internalized SM associated with endocytosis. Genetic lack of acid SMase causes Niemann–Pick disease, which is characterized by an accumulation of both SM and cholesterol in lysosomes [14]. Alk-SMase is distributed mainly in the middle part of the intestine and is the main enzyme for hydrolyzing dietary SM and also affects the membrane bound SM of the mucosal cells.

The present study investigated whether ezetimibe changes activity and expression of SMases in the intestine and liver both *in vivo* and *in vitro*. Our results disclosed an inhibitory effect of ezetimibe on acid SMase expression.

Materials and Methods

Materials

Female Sprague–Dawley rats weighing about 225 g were obtained from Mollegaard, Denmark and kept under normal housing conditions with free access to drinking water. The Hep G2 and Caco-2 cells were obtained from American Tissue Culture Collection. SM was purified from bovine milk and labeled with [^{14}C -CH $_3$] choline ([^{14}C -SM]). Antibody against acid SMase was purchased from Santa Cruz and antiserum against alk-SMase was generated as described earlier [15]. The cell culture media and other chemical agents used were purchased from Sigma Co. (Stockholm, Sweden). Ezetimibe tablets (10 mg/tablet) and purified ezetimibe were obtained from Schering–Plough Research Institute (Kenilworth, NJ, USA). ^{14}C -cholesterol

(0.1 mCi/ml) was purchased from American Radiolabeled Chemicals (Malmö, Sweden).

Preparation of Ezetimibe for Animal Study

Two types of animal studies were performed. In type 1, the tablets of ezetimibe (10 mg/tablet) were ground, dissolved in distilled water, and then given to the animals by gavage according to Deushi [5]. In the second type of experiment, dietary chows containing ezetimibe were prepared based on the method of Lillienau et al. [16]. Briefly, standard chow R34 (Lactamin AB, Sweden) was soaked in 100 ml 99.5% ethanol containing 9 mg ezetimibe. After saturation, the reduction of the solution volume was measured and the amount of ezetimibe incorporated into the pellets was calculated. The pellets were air-dried at room temperature overnight. Using this procedure, a chow containing 0.001% (w/w) ezetimibe was obtained. The diet was stored at 4 °C, and given to the animals daily.

Animal Study

In the type 1 study, six rats were given ezetimibe by gavage once a day at a dose of 5 mg/kg in a volume of 1 ml for 14 days. Those in the control group ($n = 6$) were given distilled water only. In the type 2 study, six rats were provided with 25 g pellets containing ezetimibe per day for 14 days, and another six rats in the control group were given 25 g normal pellets. The remaining food was weighed everyday and the food intake was recorded. After feeding, all the animals were anesthetized with an intramuscular injection of ketamine (60 mg/kg body weight) and xylazine (8 mg/kg body weight), and killed by puncture of the aorta. The liver and whole gastrointestinal tract were removed. A part of the liver was homogenized in 0.15 M NaCl containing 6 mM taurodeoxycholate and 1 mM benzamidine. The homogenate was centrifuged at 12,000g for 10 min and the supernatant was saved for biochemical analysis. The small intestine was cut into three segments in equal length, representing the proximal, middle and distal parts of the organ. The intestinal content was washed out with ice cold 0.15 M NaCl, and the intestinal mucosa was scraped and homogenized as previously described [17]. After centrifugation, the supernatant was saved for biochemical analysis. The colon was used as a single segment and one piece of feces was collected. The research was conducted in conformity with PHS policy and was approved by the animal ethical committee of Lund University, Sweden.

Cell Culture Study

Hep G2 cells and Caco-2 cells were cultured in RPMI-1640 medium and DMEM medium, respectively, containing

4.5 g/l glucose, 2 mM glutamine, 100 IU/ml penicillin, 10 µg/ml streptomycin, and 10% heat inactivated FBS. Pure ezetimibe was dissolved in DMSO as a stock. After culturing with ezetimibe at different concentrations, the cells were scraped, lysed, sonicated and centrifuged as described previously [15]. The supernatant was used for biochemical analysis. For a time-course study, the cells were incubated with ezetimibe (50 µM) for 8, 16, 24 and 48 h. The cells in control groups were incubated with the vehicle DMSO only. At each time point, the cells in both control and experimental groups were lysed and the activities of acid and alkaline SMase were determined. The changes of the activities were expressed as percentage of the values in control group at each time point.

Assay Cholesterol Absorption and Cholesterol Content in the Cells

The efficiency of ezetimibe used was checked by examining its effect on cholesterol absorption in Caco-2 cells according to Chen et al. [10]. The cells were cultured with micelles contained ^{14}C -cholesterol (50 µCi) for 4 h in the presence of different concentrations of ezetimibe. After treatment, the cells were washed, scraped and lysed in 0.2 M NaOH, and the absorbed ^{14}C -cholesterol was determined by liquid scintillation. For measuring the total cholesterol content in the cells, both Hep G2 and Caco-2 cells were treated with ezetimibe at different concentrations for 24 h. The total cholesterol in the cells was extracted by sonication of the cells in 0.5 ml of isopropyl alcohol according to Heider and Boyett [18]. After centrifugation at 8,000g for 10 min, the cholesterol in the supernatant was measured fluorometrically using a cholesterol assay kit purchased from Cayman (Ann Arbor, USA). The final concentration of isopropyl in the assay system is 1.7 µl in 1 ml assay buffer for both control and ezetimibe-treated samples. The cell pellet was dissolved in 0.2 M NaOH and the protein content was determined. The total cholesterol levels were expressed against the protein levels.

Sphingomyelinase Assay

The activities of different types of SMase activity were analyzed with different buffers as described [19]. The assay buffers used were 50 mM Tris–maleate buffer pH 5.0 containing 0.15 M NaCl and 0.12% Triton 100× for acid SMase, 50 mM Tris–HCl buffer pH 7.5 containing 4 mM Mg^{2+} and 0.12% Triton 100× for neutral SMase, and 50 mM Tris–HCl pH 9.0, containing 2 mM EDTA, 0.15 M NaCl, and 6 mM taurocholate for alk-SMase. Each sample in 10 µl was mixed with 90 µl of the corresponding buffer containing 80 pmol [^{14}C]-SM (~8,000 dpm) and

incubated at 37 °C for 30 min. The reaction was terminated by adding 0.4 ml of chloroform/methanol (2/1, v/v) followed by centrifugation at 10,000g for 5 s. An aliquot of the upper phase was taken and the production of ^{14}C -phosphocholine was determined by liquid scintillation. The preparation of the fecal samples for SMase assay was described previously [20].

Western Blot

Seventy micrograms of proteins in cell lysate were subjected to 7.5% SDS-PAGE for acid SMase or to 10% SDS PAGE for alk-SMase. The resolved proteins in the gel were transferred to a nitrocellulose membrane electrophoretically overnight. The membranes were either incubated with anti acid SMase (1:5,000) or anti alk-SMase antibody (1:2,500), and then with the second antibody (1:50,000) conjugated with horseradish peroxidase. The specific acid SMase and alk-SMase bands were identified by enhanced chemiluminescence advance reagent. The membranes were then stripped and re-probed with anti-actin antibody as a loading control. The details of the methods have been described elsewhere [15]. The densities of the bands were quantified by use of the software Scion Image (www.scioncorp.com).

Changes of SM in Cells after Ezetimibe Treatment

The changes of SM in the cells were determined as described [15]. In brief, the cells were first incubated with [^3H]-choline chloride (0.5 µCi/ml) for 48 h to label the endogenous SM. After that, the excess ^3H -choline chloride was removed and the cells were then treated with ezetimibe for 24 h in the absence of ^3H -choline chloride. The cell-free extract was prepared as described above and the protein concentration in the lysate was determined. The total lipids in the lysate were extracted according to Bligh and Dyer [21] and applied to the 60F Silica Gel plate (0.25 mM) for TLC. The plates were developed with chloroform/methanol/ammonium hydroxide (65/25/4 v/v/v) and stained with iodine vapor. The bands of SM were scraped according to the authentic standards and the radioactivity in the various bands was counted by liquid scintillation. The levels of SM were adjusted to the protein concentrations of the cell lysate.

Direct Effects of Ezetimibe on SMase Activity

To investigate whether ezetimibe has a direct effect on acid SMase activity, 30 µl of cell-free extract from Hep G2 or Caco-2 cells was incubated with ezetimibe at 0, 50 and 100 µM at 37 °C for 1 h or with DMSO as a control. The enzyme activities were then determined. The changes of

enzyme activity were expressed as percentage of control. For investigating the direct effect of ezetimibe on alk-SMase, purified alk-SMase (15 nmol/h per ml) was incubated with ezetimibe in a way similar to that above.

Other Biochemical Determinations

The acid and alkaline phosphatase activities were analyzed as described previously [20] using *p*-nitrophenylphosphate as a substrate. Proteins were determined with a kit from Bio-Rad using bovine albumin as a standard.

Results

Ezetimibe Administration Reduced Acid SMase Activities in Rat Accompanied by a Slight Increase in Alk-SMase Activities

After feeding rats with ezetimibe in either high or low doses, there were no great differences in body weight and food intake between the control and the treated animals (data not shown). When SMase activities were determined, the acid SMase activity in the liver of the rats fed high dose of ezetimibe was significantly decreased by 34% (Fig. 1, upper panel). Neutral SMase activity was not changed and alk-SMase activity was not detectable in rat liver. Feeding animals with the low dose of ezetimibe also decreased hepatic acid SMase activity, but to a lesser extent (lower panel). When the activities in the intestine were examined, a significant reduction of acid SMase activity by 25% (Fig. 2a) and an increase in alk-SMase by 52% (Fig. 2b) were identified by high dose, but not low dose of ezetimibe (Fig. 2c, d). The changes were observed only in the proximal part of the small intestine. There was also no change of SMase in either colonic mucosa or stool of the rats in both high and low dose experiments (data not shown).

Changes of Acid and Alk-SMase Activity in Hep G2 and Caco-2 Cells after Ezetimibe Treatment

For further characterizing the effects of ezetimibe on SMases found in vivo, we examined the effects of ezetimibe on SMases in Hep G2 liver cells and Caco-2 intestinal cells. Before starting such experiments, the efficiency of ezetimibe was checked by measuring its inhibitory effects on cholesterol absorption in Caco-2 cells. We found that ezetimibe ranging from 12.5 to 100 μ M dose-dependently inhibited cholesterol absorption (data not shown). In these concentrations, we found that ezetimibe inhibited acid SMase activities in both cell lines (Fig. 3 upper panel). The effects occurred at concentrations higher than 25 μ M. The Caco-2 cells appeared less sensitive than

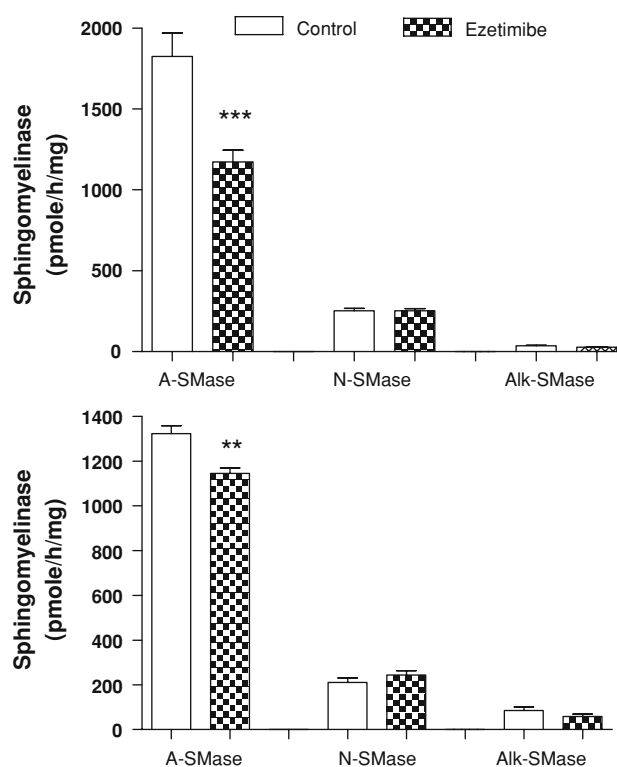


Fig. 1 Changes of SMase activity in rat liver after ezetimibe administration. In the *upper panel*, rats were fed ezetimibe by gavage at a dose of 5 mg/kg for 14 days. In the *lower panel*, the animals had free access to chow pellets containing 0.001% ezetimibe for 14 days. The activities of three types of SMase in the liver were determined. Results are mean \pm SE, $n = 6$. ** $P < 0.01$, *** $P < 0.001$ compared with control

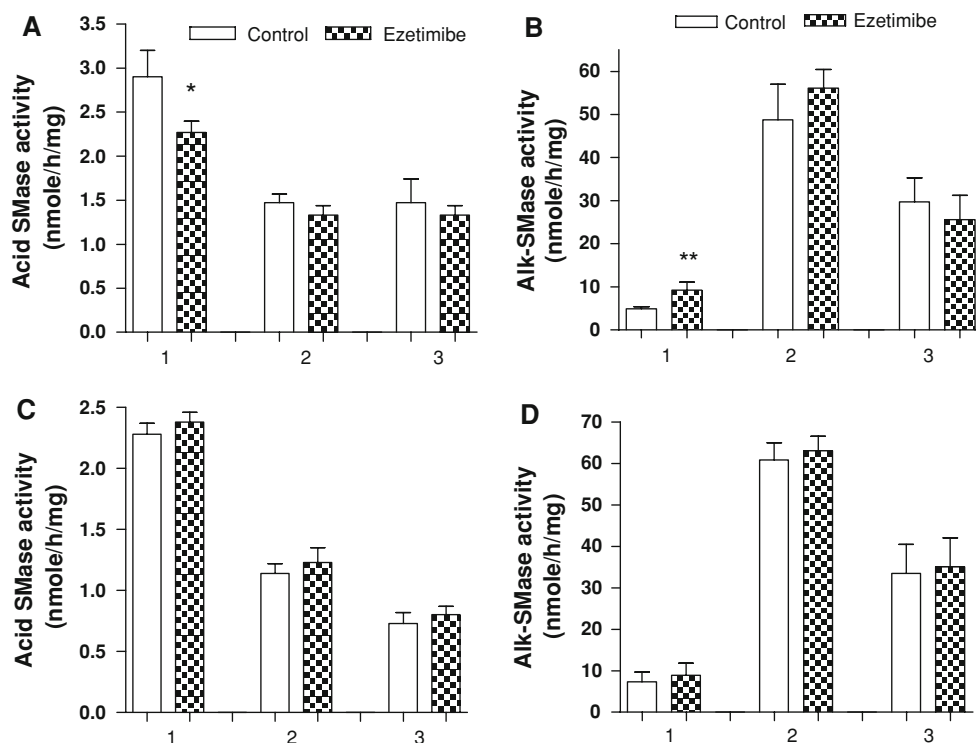
that of Hep G2 cells. As for alk-SMase (lower panel), the basal activity was higher in Caco-2 cells than in Hep G2 cells. Ezetimibe appeared increasing alk-SMase activity, but a statistically significant increase was demonstrated only after stimulation with ezetimibe at 100 μ M.

The time courses for the changes of SMases were shown in Fig. 4. The ezetimibe-induced reduction of acid SMase was more rapid in Hep G2 cells than in Caco-2 cells, with the maximal reduction occurred earlier in Hep G2 cells than in Caco-2 cells. For the changes of alk-SMase, a significant increase was demonstrated 48 h after incubation in both cell lines.

Mevastatin Mildly Increased Acid SMase Activity in Hep G2 Cells

When we identified the changes of SMase in the cells after ezetimibe treatment, we also examined whether mevastatin, the inhibitor of cholesterol biosynthesis had a similar effect on SMases activity. We treated the cells with mevastatin at the same concentrations as ezetimibe for 24 h.

Fig. 2 Changes of SMase activity in rat intestine after ezetimibe administration. Rats were either fed ezetimibe at a dose of 5 mg/kg by gavage or had free access to chow pellets containing 0.001% ezetimibe for 14 days. The small intestine was removed and cut into three parts, representing proximal, middle and distal small intestine. The acid and alkaline SMase activities in the mucosa were determined. **a** Acid SMase, high dose of ezetimibe, **b** alk-SMase, high dose of ezetimibe, **c** acid SMase, lower dose of ezetimibe, and **d** alk-SMase, low dose of ezetimibe. Results are mean \pm SE $n = 6$. * $P < 0.05$, ** $P < 0.01$ compared with control



A mild increase of acid SMase activity in Hep G2 cells was identified (Table 1).

Western Blots Showed a Reduced Expression of Acid SMase by Ezetimibe in Hep G2 and Caco-2 Cells

To examine whether the changed SMase activities were associated with changes of the enzyme proteins, Western blots were performed. A representative result is shown in panel a and b in Fig. 5. Ezetimibe decreased the expression of acid SMase in both Hep G2 and Caco-2 cells. However, the effects were obvious in the cells treated with 100 μ M of ezetimibe. Density determination of six samples in three separate experiments found that ezetimibe decreased acid SMase mass by 57.2 ± 10.3 ($P < 0.001$) and $74.4 \pm 5\%$ ($P < 0.0001$) in Hep G2 and Caco-2 cells, respectively. As to alk-SMase, ezetimibe at 100 μ M showed 43 and 23% increases in the protein in Caco-2 and Hep G2 cells, respectively.

Changes of SM and Cholesterol Levels in Hep G2 and Caco-2 Cells by Ezetimibe

Whether the changed acid and alkaline SMase expression affects the SM levels in the cells is shown in Fig. 6. We found that incubating the cells with 50 μ M ezetimibe for 24 h did not induce significant changes of SM content in

both Hep G2 and Caco-2 cells, whereas incubating the cells with 100 μ M ezetimibe increased the SM content in Hep G2 cells, but not in Caco-2 cells. Incubating the Caco-2 cells even for 48 h with ezetimibe did not induce an accumulation of SM levels (data not shown). Ezetimibe up to 50 μ M had no effects on total cholesterol levels in both Hep G2 and Caco-2 cells. However, 100 μ M ezetimibe increased total cholesterol levels in both cell lines, the effect being greater in Hep G2 cells than in Caco-2 cells (Table 2).

Other Effects of Ezetimibe

In order to assess the specificity of the changes of SMases found in this study, we determined acid and alkaline phosphatase activities in the cells treated with ezetimibe. Ezetimibe up to 50 μ M had no effects on acid phosphatase activity in both Hep G2 and Caco-2 cells. At the highest concentration (100 μ M) ezetimibe only decreased acid phosphatase activity by 20%. No change of alkaline phosphatase activity was identified by ezetimibe.

We also examined whether ezetimibe can directly affect the acid and alkaline SMase activities. Pre-treating the cell lysate with ezetimibe up to 100 μ M in test tubes at 37 $^{\circ}$ C for 1 h did not change the acid and alkaline SMase activity (data not shown). Incubating the purified alk-SMase with ezetimibe also did not affect the enzyme activity.

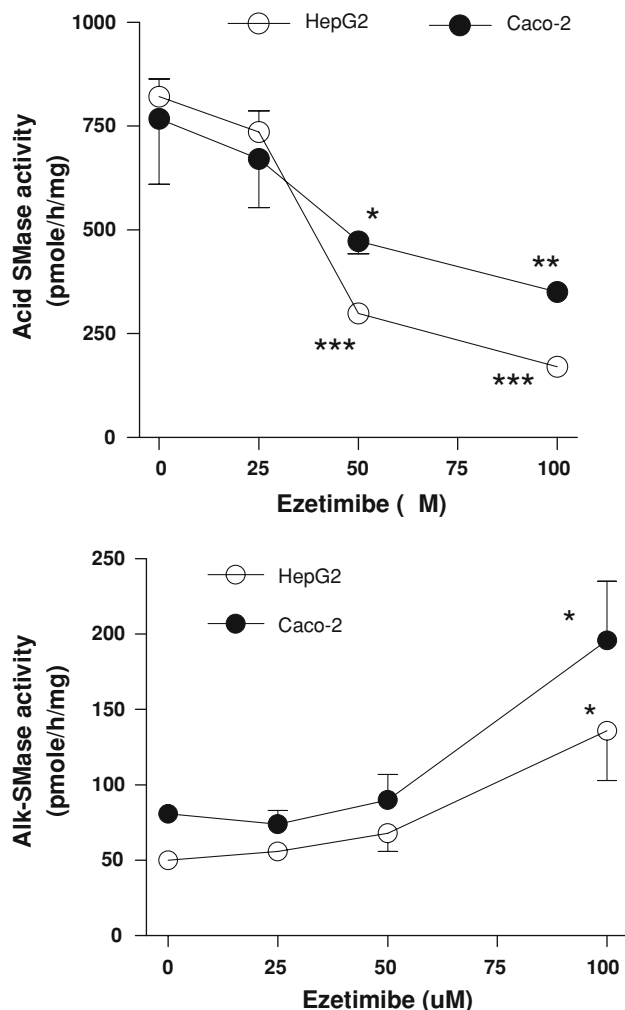


Fig. 3 Changes of acid SMase (*upper panel*) and alk-SMase (*lower panel*) in Hep G2 and Caco-2 cells. The cells were treated with ezetimibe for 24 h and the activities of acid and alkaline SMases were determined. Results are mean \pm SE in triple cell culture flasks in two separate experiments (six samples). * $P < 0.05$, ** $P < 0.01$, and *** $P < 0.001$ compared with the 0 concentration

Discussion

Ezetimibe is a well known inhibitor of cholesterol absorption and is used in the treatment of patients with hypercholesterolemia. The effects are believed to be mediated by interference of a specific intestinal sterol transporter NPC1L1, which is located on the apical membrane of absorptive mucosal cells [2]. The present study discovered a novel effect of ezetimibe, i.e., to inhibit acid SMase expression both in the intestinal tract and liver, and both in animal studies and human cell cultures. The effects showed a dose-dependent pattern, and the effective concentration was higher than 25 μ M in culture studies after 24 h incubation. Although the effective concentration in vitro was higher than that measured in the peripheral blood of human beings [22], the portal concentration reaching the

liver and the luminal concentration in the small intestine could be much higher. Particularly, our in-vivo study showed that a low dose of ezetimibe (chows containing 0.001% ezetimibe w/w) did decrease acid SMase in the liver of the rat, indicating that a clinical relevance should be considered. The effect is likely to be specific, as ezetimibe had no similar effect on acid phosphatase, another lysosomal enzyme.

Comparing the reduction of acid SMase activity with the levels of enzyme protein on Western blot, we found that the reduction of activity occurred earlier than the reduction of the enzyme protein. When 50 μ M ezetimibe decreased acid SMase activity by about 50%, no similar reduction of acid SMase protein could be found in Western blot examination. This discrepancy may not be explained by a direct inhibition of ezetimibe on the enzyme, as pre-incubation of cell lysate with ezetimibe in vitro did not change acid SMase activity. The hypothesis is that ezetimibe at lower doses can affect post-translational regulation of acid SMase and at high doses, the translation or transcription of the acid SMase gene. It has been demonstrated that post-translational modification which involves glycosylation, phosphorylation, and proteolytic processing, as recently reviewed [23], is an important step for maturation of acid SMase and therefore its activity. Further study may be required to examine whether ezetimibe could affect any process of the maturation of acid SMase.

Of interest is that liver appears more sensitive than the intestine in response to ezetimibe. Feeding high doses of ezetimibe to rats decreased acid SMase activity to a greater extent in the liver than in the small intestine, and feeding low doses of ezetimibe only reduced acid SMase in the liver, not in the small intestine. Time course experiments also showed that the reduction of acid SMase in Hep G2 cells occurred more rapidly than in Caco-2 cells. The reason for such differences is not known. The effect of ezetimibe on cholesterol absorption is thought to be mediated by an inhibition of NPC1L1. Whether the inhibitory effect on acid SMase is also mediated by NPC1L1 inhibition is unknown. Our result, that reduction of acid SMase occurs only in the proximal part of small intestine, may indicate an involvement of NPC1L1, as NPC1L1 is highly expressed in this part of the small intestine [2]. However, regarding the different sensitivities between liver and intestine, there is no evidence indicating that the level of NPC1L1 is higher in liver than in the small intestine in rats [24]. The involvement of other mechanisms secondary or independent of the effects on NPC1L1 cannot be excluded. In fact, such a hypothesis was indicated previously by several studies [25].

Acid SMase has been considered to play important roles in the lysosomal degradation of SM that is internalized by endocytosis. Niemann–Pick disease, a genetic disease due

Fig. 4 Time course of the changes of acid and alkaline SMases induced by ezetimibe in Hep G2 (left) and Caco-2 (right) cells. The cells were treated with or without ezetimibe (EZ) (50 μ M) for different times. After treatment, the cells were lysed and the enzyme activities were determined in comparison with the control group in each time points. The activities in the control group were taken as 100%. Results were means \pm SE from duplicate culture flasks in three separate experiments (six samples)

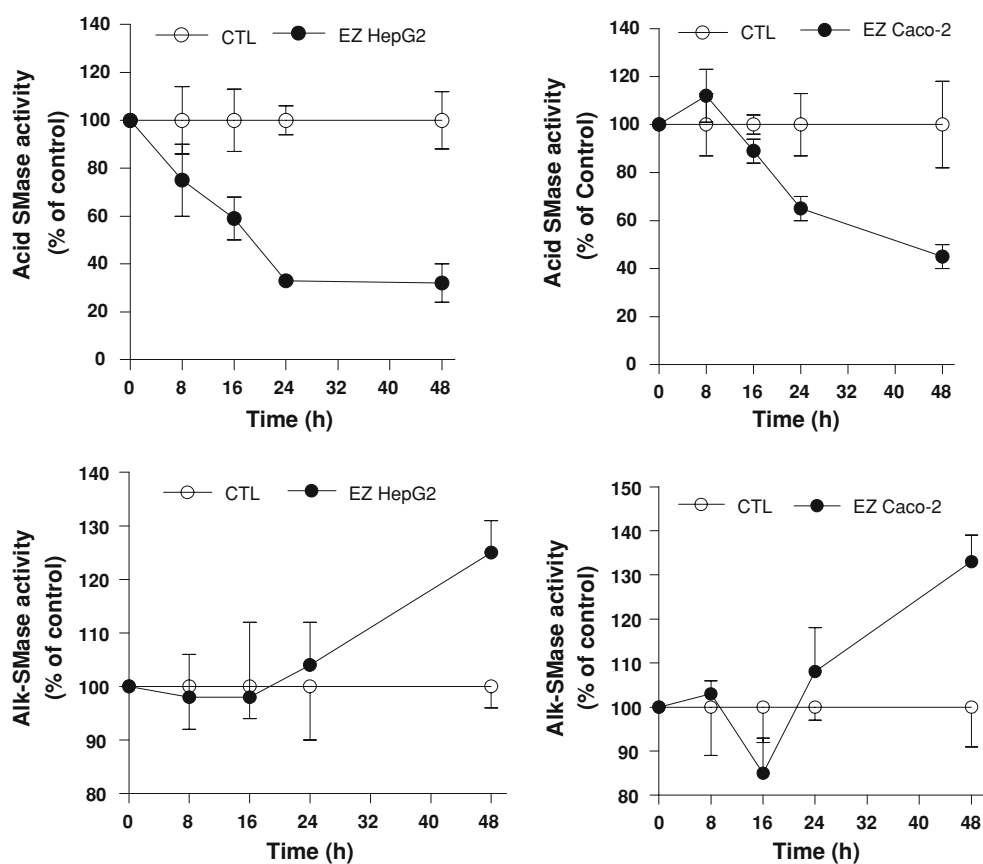


Table 1 Effects of mevastatin on SMase activity (pmol/mg per h) in Hep G2 and Caco-2 cells

	0	25	50	100 (μ M)
Hep G2				
Acid SMase	619 \pm 21	677 \pm 78	710 \pm 32*	740 \pm 65
Alk-SMase	60.8 \pm 6.8	61.0 \pm 2.2	70.5 \pm 5.7	74.6 \pm 5.8
Caco-2				
Acid SMase	788 \pm 79	773 \pm 65	751 \pm 30	807 \pm 43
Alk-SMase	66.1 \pm 7.5	74.7 \pm 15.1	94.2 \pm 18.5	88.6 \pm 14.4

The cells were treated with mevastatin at different concentrations for 24 h. The cell-free extracts were prepared and the activities of SMases were determined and expressed as pmol/mg per h. Results are means \pm SE in triple samples in two separate experiments (six samples). * $P < 0.05$ compared with 0 concentration

to deficiency of acid SMase, causes a mass accumulation of SM and cholesterol in the lysosomes [14]. Under the conditions studied in this paper, we found increases of total SM and cholesterol in Hep G2 cells and increased cholesterol in Caco-2 cells by ezetimibe at 100 μ M. High levels of cholesterol in the cells have been shown to inhibit acid SMase expression in NPC1 mutant cells [26]. Whether the increase in cholesterol found in this study is responsible for reduced acid SMase expression is tempting to

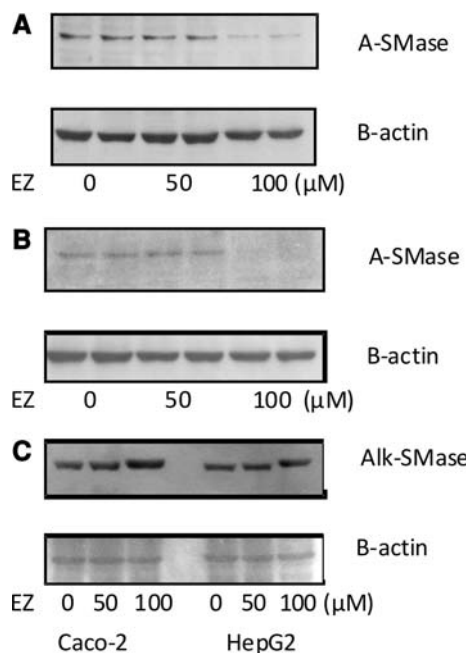


Fig. 5 Western blot for acid and alkaline SMase in the cells. The cells were treated with ezetimibe (EZ) for 24 h. The cell lysate was prepared and subjected to SDS-PAGE and Western blots. **a** For acid SMase in Hep G2 cells. **b** For acid SMase in Caco-2 cells. **c** For alk-SMase in Caco-2 and Hep G2 cells. The loading control was checked by reaction of the membrane with anti β -actin antibody

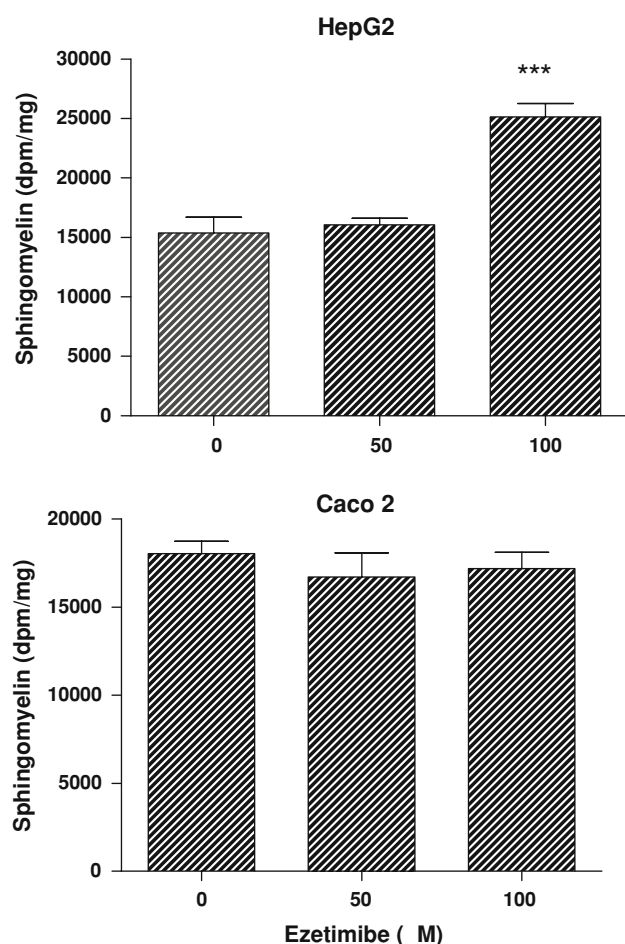


Fig. 6 The changes of SM content in Hep G2 cells and Caco-2 cells after treatment of ezetimibe. The endogenous SM was labeled with ^3H -choline chloride for 48 h before stimulation with ezetimibe for 24 h. The lipids in the cell lysate were extracted and separated by TLC. The radioactivity in the SM band was counted by liquid scintillation counting. Results were obtained from triple cell culture flasks in two separate experiments (six samples). *** $P < 0.005$ as compared with the 0 concentration of ezetimibe

speculate. Our results that mevastatin increased acid SMase activity support the hypothesis. How ezetimibe increases the cholesterol content in the cells was not examined in detail in the present work. Previous studies showed that, in NPC1L1 deficient mice, the expression of HMG-CoA synthase was significantly increased in both liver and

intestine [3], and treating the LDL receptor deficiency mice with ezetimibe resulted in a significant increase of hepatic cholesterol [27]. On the other hand, the increase in cholesterol found in this study may also be a consequence secondary to the changed SM and acid SMase activity, since high SM levels may increase the biosynthesis of cholesterol [28]. Further kinetic characterizations of the changes of SM, cholesterol, and the enzymes involved are required to address such questions.

The present study also identified an increase of alk-SMase activity in the intestinal tract by ezetimibe. Alk-SMase is the major enzyme in the intestinal tract that hydrolyzes dietary SM to form ceramide, which in turn to be degraded by ceramidase to sphingosine [29]. Previous studies have shown that alk-SMase may have anticancer and antiinflammatory effects in the gut through its ability to generate ceramide and to inactivate platelet activating factor [13]. Alk-SMase may also inhibit cholesterol uptake, because hydrolysis of membrane SM has been shown to reduce cholesterol uptake [10, 13]. However, the increase of alk-SMase induced by ezetimibe is relatively mild and occurred only in the proximal part of small intestine where alk-SMase is not high. The importance of such changes in cholesterol absorption may be questionable.

Finally it should be emphasized that our finding that ezetimibe significantly reduced acid SMase activity has clinical relevance. Acid SMase not only functions as a lysosomal enzyme, but also has signaling effects. In response to stress and pathogen stimuli, acid SMase can be relocated to the outer leaflet of the plasma membrane to hydrolyze SM and generate ceramide, a key molecule in favor of apoptosis [30]. Acid SMase activity is relatively high in the liver and has been shown to be an important enzyme for hepatic functions and liver diseases [31], such as in apoptosis induced by $\text{TNF-}\alpha$ [32] and CD95 [33]. Deficiency of acid SMase in hepatic cells may increase the risk of inflammation and proliferation, due to the resistance to apoptosis. Although ezetimibe is considered as a safe drug, case reports recently showed that it may induce liver swelling, hepatitis, and abnormal changes in liver enzymes [34–37]. How the reduction of acid SMase by ezetimibe may be involved in these phenomena is unknown. On the other hand, high levels of acid SMase in some organs

Table 2 Changes of total cholesterol (nmol/mg protein) after ezetimibe treatment in Hep G2 and Caco-2 cells

Ezetimibe	0	25	50	100 (μM)
Hep G2	140.7 \pm 11.2	135.7 \pm 13.2	137.5 \pm 14.1	313.5 \pm 58.3**
Caco-2	113.0 \pm 5.6	129.0 \pm 9.4	118.5 \pm 4.3	130.3 \pm 4.9*

The cells were cultured with ezetimibe for 24 h and then suspended in 0.5 ml isopropanol followed by sonication for 10 s. After centrifugation, the cholesterol in the supernatant was determined fluorometrically using a kit purchased from Cayman Chemical Company. The cell pellets were dissolved in 0.5 ml 0.2 M NaOH and the protein concentration was determined. The levels of cholesterol are expressed as nmol/mg cell proteins. Results are means \pm SE in triple samples in two separate experiments (six samples). * $P < 0.05$, ** $P < 0.01$ compared with 0 concentration

particularly the endothelial cells in blood vessels may have important implications in the pathogenesis of atherosclerosis, heart failure, insulin resistance and obesity, as recently reviewed [23]. It was recently shown that acid SMase could promote lipoprotein retention within early atheromata and thus accelerate the lesion progress [38]. Whether ezetimibe, by inhibiting the expression of acid SMase in endothelial cells and thus reducing the risk of cardiovascular disease would be of interest to explore. Improvement of insulin resistance after intravenous administration of ezetimibe has already been reported [5]. Our results raise questions for further investigations.

Acknowledgments The work was supported by grants from Albert Pålsson Foundation, Swedish Cancer Foundation, Swedish Research Council, and the Research Foundation of Lund University Hospital. Merck Sharp & Dohme (Sweden) AB is thanked for providing ezetimibe and financial support for this study.

References

- Bays HE, Neff D, Tomassini JE, Tershakovec AM (2008) Ezetimibe: cholesterol lowering and beyond. *Expert Rev Cardiovasc Ther* 6:447–470
- Altmann SW, Davis H R Jr, Zhu LJ, Yao X, Hoos LM, Tetzloff G, Iyer SP, Maguire M, Golovko A, Zeng M, Wang L, Murgolo N, Graziano MP (2004) Niemann–Pick C1 like 1 protein is critical for intestinal cholesterol absorption. *Science* 303:1201–1204
- Davis H R Jr, Zhu LJ, Hoos LM, Tetzloff G, Maguire M, Liu J, Yao X, Iyer SP, Lam MH, Lund EG, Detmers PA, Graziano MP, Altmann SW (2004) Niemann–Pick C1 like 1 (NPC1L1) is the intestinal phytosterol and cholesterol transporter and a key modulator of whole-body cholesterol homeostasis. *J Biol Chem* 279:33586–33592
- Davies JP, Levy B, Ioannou YA (2000) Evidence for a Niemann–Pick C (NPC) gene family: identification and characterization of NPC1L1. *Genomics* 65:137–145
- Deushi M, Nomura M, Kawakami A, Haraguchi M, Ito M, Okazaki M, Ishii H, Yoshida M (2007) Ezetimibe improves liver steatosis and insulin resistance in obese rat model of metabolic syndrome. *FEBS Lett* 581:5664–5670
- Zuniga S, Molina H, Azocar L, Amigo L, Nervi F, Pimentel F, Jarufe N, Arrese M, Lammert F, Miquel JF (2008) Ezetimibe prevents cholesterol gallstone formation in mice. *Liver Int* 28:935–947
- Slotte JP, Bierman EL (1988) Depletion of plasma-membrane sphingomyelin rapidly alters the distribution of cholesterol between plasma membranes and intracellular cholesterol pools in cultured fibroblasts. *Biochem J* 250:653–658
- Gupta AK, Rudney H (1991) Plasma membrane sphingomyelin and the regulation of HMG-CoA reductase activity and cholesterol biosynthesis in cell cultures. *J Lipid Res* 32:125–136
- Byers DM, Morgan MW, Cook HW, Palmer FB, Spence MW (1992) Niemann–Pick type II fibroblasts exhibit impaired cholesterol esterification in response to sphingomyelin hydrolysis. *Biochim Biophys Acta* 1138:20–26
- Chen H, Born E, Mathur SN, Johlin F C Jr, Field FJ (1992) Sphingomyelin content of intestinal cell membranes regulates cholesterol absorption. Evidence for pancreatic and intestinal cell sphingomyelinase activity. *Biochem J* 286:771–777
- Nyberg L, Duan RD, Nilsson A (2000) A mutual inhibitory effect on absorption of sphingomyelin and cholesterol. *J Nutr Biochem* 11:244–249
- Nilsson Å, Duan R-D (1999) Alkaline sphingomyelinases and ceramidases of the gastrointestinal tract. *Chem Phys Lipids* 102:97–105
- Duan RD (2006) Alkaline sphingomyelinase: an old enzyme with novel implications. *Biochim Biophys Acta* 1761:281–291
- Spence MW, Callahan JW (1989) Sphingomyelin-cholesterol lipidoses: the Niemann–Pick group of diseases. In: Scriver CR, Beaudet AL, Sly WS, Valle D (eds) *The metabolic basis of inherited diseases*. McGraw-Hill, New York, pp 1655–1676
- Duan RD, Bergman T, Xu N, Wu J, Cheng Y, Duan J, Nelander S, Palmberg C, Nilsson A (2003) Identification of human intestinal alkaline sphingomyelinase as a novel ecto-enzyme related to the nucleotide phosphodiesterase family. *J Biol Chem* 278:38528–38536
- Lillienau J, Crombie DL, Munoz J, Longmire-Cook SJ, Hagey LR, Hofmann AF (1993) Negative feedback regulation of the ileal bile acid transport system in rodents. *Gastroenterology* 104:38–46
- Duan RD, Verkade HJ, Cheng Y, Havinga R, Nilsson A (2007) Effects of bile diversion in rats on intestinal sphingomyelinases and ceramidase. *Biochim Biophys Acta* 1771:196–201
- Heider JG, Boyett RL (1978) The picomole determination of free and total cholesterol in cells in culture. *J Lipid Res* 19:514–518
- Duan RD, Nilsson A (2000) Sphingolipid hydrolyzing enzymes in the gastrointestinal tract. *Methods Enzymol* 311:276–286
- Cheng Y, Tauschel HT, Nilsson Å, Duan RD (1999) Administration of ursodeoxycholic acid increases the activities of alkaline sphingomyelinase and caspase-3 in rat colon. *Scand J Gastroenterol* 34:915–920
- Bligh EH, Dyer WJ (1959) A rapid method for total lipid extraction and purification. *Can J Biochem Physiol* 37:911–918
- Ezzet F, Krishna G, Wexler DB, Statkevich P, Kosoglou T, Batra VK (2001) A population pharmacokinetic model that describes multiple peaks due to enterohepatic recirculation of ezetimibe. *Clin Ther* 23:871–885
- Jenkins RW, Canals D, Hannun YA (2009) Roles and regulation of secretory and lysosomal acid sphingomyelinase. *Cell Signal* 21:836–846
- Davis HR, Veltri EP (2007) Zetia: inhibition of Niemann–Pick C1 like 1 (NPC1L1) to reduce intestinal cholesterol absorption and treat hyperlipidemia. *J Atheroscler Thromb* 14:99–108
- Yu L (2008) The structure and function of Niemann–Pick C1-like 1 protein. *Curr Opin Lipidol* 19:263–269
- Reagan J W Jr, Hubbert ML, Shelness GS (2000) Posttranslational regulation of acid sphingomyelinase in Niemann–Pick type C1 fibroblasts and free cholesterol-enriched Chinese hamster ovary cells. *J Biol Chem* 275:38104–38110
- Repa JJ, Turley SD, Quan G, Dietschy JM (2005) Delineation of molecular changes in intrahepatic cholesterol metabolism resulting from diminished cholesterol absorption. *J Lipid Res* 46:779–789
- Gatt S, Bierman EL (1980) Sphingomyelin suppresses the binding and utilization of low density lipoproteins by skin fibroblasts. *J Biol Chem* 255:3371–3376
- Nilsson A, Duan RD (2006) Absorption and lipoprotein transport of sphingomyelin. *J Lipid Res* 47:154–171
- Tani M, Ito M, Igarashi Y (2007) Ceramide/sphingosine/sphingosine 1-phosphate metabolism on the cell surface and in the extracellular space. *Cell Signal* 19:229–237
- Mari M, Fernandez-Checa JC (2007) Sphingolipid signalling and liver diseases. *Liver Int* 27:440–450
- Mari M, Colell A, Morales A, Paneda C, Varela-Nieto I, Garcia-Ruiz C, Fernandez-Checa JC (2004) Acidic sphingomyelinase

- downregulates the liver-specific methionine adenosyltransferase 1A, contributing to tumor necrosis factor-induced lethal hepatitis. *J Clin Invest* 113:895–904
33. Kirschnek S, Paris F, Weller M, Grassme H, Ferlinz K, Riehle A, Fuks Z, Kolesnick R, Gulbins E (2000) CD95-mediated apoptosis in vivo involves acid sphingomyelinase. *J Biol Chem* 275:27316–27323
 34. Arundel C, Lewis JH (2007) Drug-induced liver disease in 2006. *Curr Opin Gastroenterol* 23:244–254
 35. Stolk MF, Bex MC, Kuypers KC, Seldenrijk CA (2006) Severe hepatic side effects of ezetimibe. *Clin Gastroenterol Hepatol* 4:908–911
 36. van Heyningen C (2005) Drug-induced acute autoimmune hepatitis during combination therapy with atorvastatin and ezetimibe. *Ann Clin Biochem* 42:402–404
 37. Florentin M, Liberopoulos EN, Elisaf MS (2008) Ezetimibe-associated adverse effects: what the clinician needs to know. *Int J Clin Pract* 62:88–96
 38. Devlin CM, Leventhal AR, Kuriakose G, Schuchman EH, Williams KJ, Tabas I (2008) Acid sphingomyelinase promotes lipoprotein retention within early atheromata and accelerates lesion progression. *Arterioscler Thromb Vasc Biol* 28:1723–1730

Regulation of HMGCoA Reductase Activity by Policosanol and Octacosadienol, a New Synthetic Analogue of Octacosanol

Simonetta Oliaro-Bosso · Emanuela Calcio Gaudino · Stefano Mantegna · Enrico Giraudo · Claudia Meda · Franca Viola · Giancarlo Cravotto

Received: 30 June 2009 / Accepted: 12 August 2009 / Published online: 11 September 2009
© AOCs 2009

Abstract Octacosano-10,19-dien-1-ol is a newly synthesized long-chain alcohol, an unsaturated analogue of 1-octacosanol, the major component of policosanol, the purified natural mixture of different higher aliphatic alcohols obtained from sugarcane wax. Our efficient synthetic protocol (five steps with 50% overall yield) is well suited for gram scale preparations and a rapid generation of analogues with different degrees of unsaturation. Beneficial effects of policosanol in the prevention of atherosclerosis and thromboembolic disorders have been reported and related to the inhibition of sterol biosynthesis possibly by the regulation of the activity of HMGCoA reductase mediated by AMP-dependent kinase AMPK. We have compared the effect of octacosadienol and policosanol on the regulation of HMGCoA reductase in HUVEC and HepG2 human hepatoma cells. Octacosadienol was as effective as policosanol in inhibiting the upregulation of HMGCoA reductase, in inducing the phosphorylation of AMPK and in downregulating the HMGCoA reductase mRNA.

Keywords Long-chain alcohols synthesis · Octacosadienol · Octacosanol · HMGCoA reductase · Policosanol · AMPK phosphorylation

Abbreviations

AMPK	AMP-activated protein kinase
DMEM	Dulbecco-modified Eagle medium
EDTA	Ethylenediaminetetraacetic acid
EGTA	Ethylene glycol tetraacetic acid
HMGR	HydroxyMethylGlutaryl-Coenzyme A reductase
HUVEC	Human endothelial cells from umbilical cord veins
LDL	Low density lipoproteins
LDM	Lipid-depleted medium
PBS	Phosphate-buffered saline
RT-PCR	Real time-polymerase chain reaction
SDS	Sodium dodecyl sulfate
THF	Tetrahydrofurane

Introduction

For many years, higher aliphatic primary alcohols have been a subject of research. Early works were mainly focused on the biological activities of 1-triacontanol ($C_{30}H_{61}OH$) and 1-octacosanol ($C_{28}H_{57}OH$) [1–7]. The former was mainly isolated from beeswax [8], whereas 1-octacosanol from germ oils, wax sources (sugarcane, rice bran) and *Euphorbiaceae* [8–10]. 1-Triacontanol was highlighted as a plant growth promoter and an anti-inflammatory substance [1–3], while 1-octacosanol showed ergogenic, neurological and antioxidant properties [4, 5]. The C_{28} linear aliphatic

S. Oliaro-Bosso · E. Calcio Gaudino · S. Mantegna · F. Viola (✉) · G. Cravotto (✉)
Dipartimento di Scienza e Tecnologia del Farmaco,
University of Torino, Via Giuria 9, 10125 Torino, Italy
e-mail: franca.viola@unito.it

G. Cravotto
e-mail: giancarlo.cravotto@unito.it

E. Giraudo · C. Meda
Department of Oncological Sciences,
Institute for Cancer Research and Treatment,
University of Torino School of Medicine,
Str. Provinciale 142, 10060 Candiolo, Italy

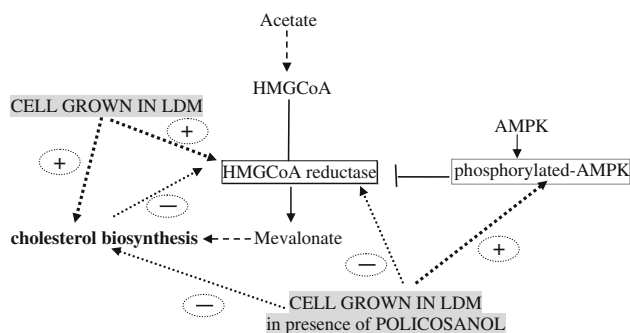
primary alcohol is the major component (60–70%) of policosanol, the purified natural product, was first described by Cuban researchers [11], and consists of a mixture of eight higher aliphatic alcohols obtained from the wax of sugarcane (*Saccharum officinarum* L.). Policosanol was found to inhibit cholesterol biosynthesis by indirect regulation of the activity of HydroxyMethylGlutaryl-Coenzyme A reductase (EC: 1.1.1.34) (HMGR) and by an enhancement of receptor-dependent LDL processing [12–15]. The relevant literature dealing with cholesterol and serum lipids lowering, antiplatelets and antioxidant properties of policosanol has been extensively reviewed [16, 17]. More recently, several authors have raised doubts on the cholesterol and serum lipids lowering, as well on the antioxidant properties of policosanol, on the basis of clinical studies on hypercholesterolemic patients [18–21].

In spite of the recent negative results as a cholesterol and lipid-lowering drug in clinical practice, policosanol seems able to affect some interesting cellular targets. The most important biochemical effect observed is the downregulation of HMGR activity, the regulatory enzyme of cholesterol biosynthesis, in homogenates of Vero fibroblasts grown for 24 h in lipid-depleted medium (LDM) in the presence of policosanol [13]. The decrease of HMGCoA reductase activity parallels the decrease of incorporation of labeled acetate in cholesterol (Scheme 1). Similar results have been observed in rat hepatoma cells grown in the presence of policosanol [22]. In a recent metabolic study, the possibility of a reduced cholesterol synthesis in the liver has been suggested to explain the observed decrease of fecal cholesterol end products after treatment with policosanol [23]. In neither Vero fibroblasts nor hepatoma cells could a direct inhibition of HMGR be found. Therefore the suppression of the upregulation of HMGR that occurs when the cells are grown in LDM [24] could be caused by the interference

of policosanol with the regulation of HMGR. One of the mechanisms of negative regulation of HMGR is the phosphorylation by the AMP kinase (AMPK) [25]. In rat hepatoma cells grown in the presence of policosanol, the decrease of sterol biosynthesis and HMGR activity was accompanied by a significant increase in phosphorylated AMPK, detected by immunoblot [22] (Scheme 1). The increase in phosphorylated AMPK is very close to the one obtained in the presence of metformin, a glucose-lowering drug which activates AMPK phosphorylation. Phosphorylation by AMP kinase also inactivates acetylCoA carboxylase, the enzyme catalyzing the first and regulatory step in fatty acid synthesis, suggesting the possibility of a coordinated regulation of cholesterol and fatty acid biosynthesis [25]. As a more general function, AMPK is involved in the control of the energy balance within the cell, acting as a metabolic sensor of the cellular AMP/ATP ratio [25, 26].

Owing to the involvement in the regulation of important signalling cascades controlling the cell proliferation and differentiation, AMPK has been suggested as a therapeutic target for atherosclerosis and cancer [27, 28]. An effect of policosanol on the activity of AMPK could interfere with the complex regulatory net of this kinase and explain the controversial results obtained in different experimental models or clinical trials. Moreover an effect on the regulation of sterol or fatty acid biosynthesis can open very important therapeutic opportunities in different fields, such as angiogenesis control. The antiangiogenic activity of the HMGR inhibitors statins is known [27, 29] and recently some common inhibitors of enzymes of the late steps of sterol biosynthesis such as itraconazole, an inhibitor of sterol C-14 demethylase, and naftifine, an inhibitor of squalene epoxidase, were shown to inhibit both the growth of HUVEC cells and angiogenesis [30, 31]. More recently octacosanol purified from the medicinal plant *Tinospora cordifolia*, showed antiangiogenic and antitumoral activity both in vitro and in vivo [32].

In an attempt to study a possible effect of analogues of policosanol mixture on the angiogenic process, we synthesized octacosano-10,19-dien-1-ol, a new unsaturated derivative of octacosanol. The effect on HMGR activity and expression of this synthetic compound was studied in HUVEC cells and, for comparison, in hepatoma cells and compared to the effect, in the same experimental condition, of a commercial mixture of policosanol (Source Naturals, Inc., Scotts Valley, CA). Our results showed that, in both cell types, in the presence of octacosadienol the upregulation of HMGR is decreased and the phosphorylation of AMP kinase increased. In HUVEC cells we could also observe by RT-PCR a decrease in HMGR mRNA. Octacosano-10,19-dien-1-ol showed almost the same activity as the natural policosanol mixture.



Scheme 1 Sterol biosynthesis and HMGCoA reductase activity are upregulated in cells grown in a delipidated medium (LDM). In the presence of policosanol the upregulation of HMGCoA reductase and the incorporation of acetate into sterols is decreased [13] and the phosphorylated form of AMPK is increased [22]

Experimental Procedures

Chemistry

Chemicals were purchased from Carlo Erba Reagenti and Acros Organics.

Buffers and cultural media were obtained from Sigma–Aldrich (Milan, Italy) unless otherwise specified.

3-Hydroxy-3-methyl[3-¹⁴C]glutaryl-coenzyme A (57 mCi/mmol) were obtained from Amersham Biosciences (UK). Policosanol 10-mg tablets were manufactured by Source Naturals, Inc. (Scotts Valley, CA) and purchased from a local health food store. Two 10-mg policosanol tablets were dissolved in 10 ml of absolute ethanol with the aid of a mortar and pestle. The insoluble excipients were removed by low-speed centrifugation (5000×g for 5 min), and the supernatant was aliquoted and stored at –20 °C or added directly to media upon use. Extracts were analysed by GC/MS using an Agilent 6850 gas chromatograph equipped with a 5973 MS detector and fitted with an HP-5 MS fused silica column (length 30 m; i.d. 0.25 mm; film thickness 0.25 mm).

Reactions were monitored by TLC on Fluka F₂₅₄ (0.25 mm) plates, which were visualized by spraying with a molybdic acid and heating.

Silica gel Merck 60 was used for column chromatography (CC). IR: Shimadzu FT-IR 8001 spectrophotometer. NMR: Bruker 300 Avance spectrometer (for ¹H NMR CDCl₃ was used as solvent, CHCl₃ at δ = 7.27 as reference. Low-resolution mass spectra: Finnigan-MAT TSQ70 in chemical ionization (CI-MS) with isobutane as reactant gas; ESI-MS were recorded on a Waters Micromass ZQ.

Methyl undec-10-enoate (**1**)

A solution of undecylenic acid (1.5 g, 8.14 mmol), anhydrous methanol (8 ml) and *p*-toluenesulfonic acid (50 mg, 0.29 mmol) in anhydrous toluene, placed in a 100-ml, two-neck, round-bottomed flask was heated under reflux for 5 h using a Dean-Stark apparatus and a condenser to remove esterification water. All glassware had been previously dried in an oven at 120 °C. The reaction progress was monitored by TLC on silica gel plates with hexane/ethyl acetate 7:3 as eluent (*R*_f ester = 0.64). Work-up: the product was diluted with ethyl acetate, washed twice with a 1:1 NaHCO₃/H₂O mixture, then with H₂O and brine; finally dried over Na₂SO₄. **1** was isolated as a transparent oil (1.5 g, 7.57 mmol, 93% yield). Residual traces of undecylenic acid were able to be removed by filtration on a pad of basic alumina. FT-IR (neat, cm⁻¹): ν = 2926, 1740, 1466, 1180, 1037, 742, 721, 669. ¹H NMR (300 MHz, CDCl₃): δ = 1.30 (m, 10 H, H-4-8), 1.68 (m, 2 H, H-3), 1.96 (m, 2 H, H-9), 2.31 (t, 2 H, *J* = 7.5 Hz, H-2), 3.6 (s, 3

H, -COOCH₃), 4.99 (m, 2 H, H-11), 5.70 ppm (m, 1 H, H-10). CI-MS *m/z* 199 [M + H]⁺ C₁₂H₂₂O₂.

Methyl 10-oxodecanoate (**2**)

A two-neck 250-ml round-bottomed flask containing methyl undec-10-enoate (2.43 g, 12.27 mmol) and H₂O/acetone 1:1 (50 ml) was placed in a high-power ultrasound bath (with ice-water) with an emitting titanium surface fixed to two sonotrodes (19.0 kHz). A 0.2-M solution of OsO₄ in toluene (305 μl; 0.061 mmol) and *N*-methylmorpholine-*N*-oxide (1.44 g, 12.27 mmol) were added to the mixture under sonication (70 W). After 5 min NaIO₄ (7.59 g, 35.46 mmol) was added in small portions over a time of 20 min at 20 °C. The reaction course was monitored by TLC on silica gel plates with hexane/ethyl acetate 7:3 as eluent (*R*_f of **2** = 0.5). After 3 h sonication the conversion was complete. Work-up: the reaction mixture was filtered on a porous sintered glass funnel, washing the residue with ethyl acetate. The filtrate was washed with brine, dried over Na₂SO₄ and evaporated under vacuum. The product was purified by column chromatography using hexane/ethyl acetate 9:1 as eluent. **2** was obtained as a pale yellow oil (2.11 g, 10.55 mmol, yield 86%). FT-IR (neat, cm⁻¹): ν = 2928, 2675, 1745, 1464, 1242, 1047, 943, 725. ¹H NMR (300 MHz, CDCl₃): δ = 1.29 (m, 8 H, H-3, 4, 5, 6), 1.56 (m, 2 H, H-8), 1.42 (m, 2 H, H-7), 2.31 (t, *J* = 7.5 Hz, 2 H, H-2), 2.4 (td, *J*_t = 8.1 Hz, *J*_d = 1.8 Hz, 2 H, H-9), 3.60 (s, 3 H, -OCH₃), 9.74 ppm (t, *J* = 1.8 Hz, 1 H, -CHO). CI-MS *m/z* 201 [M + H]⁺ C₁₁H₂₀O₃.

(*E*) Octadec-9-en triphenylphosphonium bromide (**3**)

The phosphonium salt was prepared from (*E*)-1-bromooc-tadec-9-ene (1.3 g, 3.9 mmol) heated under reflux overnight (N₂ atmosphere) in a toluene (30 ml) solution with triphenylphosphine (1.02 g, 3.9 mmol). After cooling down to 0 °C and addition of diethyl ether (30 ml), the precipitate of phosphonium salt was collected on a paper filter. **3** was obtained as a whitish-pink powder (1.87 g, 3.16 mmol, 81% yield). ¹H NMR (300 MHz, CDCl₃): δ = 0.87 (t, *J* = 6.4 Hz, 3H, H-18), 1.24 (m, 30 H, H-3-17), 1.65 (m, 4 H, H-1, 2), 7.85 ppm (m, 15 H, -ArH). CI-MS (*m/z*): 593 [M + H]⁺ C₃₆H₅₀BrP.

Methyl octacos-10,19-dienoate (**4**)

Glassware was previously dried at 120 °C for 2 h. The phosphonium bromide (**3**) (3.32 g, 5.6 mmol) was dissolved in 30 ml of anhydrous THF in a 100-ml, two-neck, round-bottomed flask. To the stirred solution under N₂ atmosphere 1.6 N BuLi (3.4 ml; 1.05 equiv) in hexane was

added dropwise. Due to the formation of phosphorus ylide the mixture turned orange-red. After 20 min, 5 ml of a solution of **2** (1.07 g, 5.35 mmol) were added dropwise and the solution turned yellow-orange. After the addition was complete, the mixture was allowed to stir overnight. TLC with hexane/ethyl acetate 9:1 as eluent (R_f **4** = 0.69). The crude product (**4**) was diluted with a 0.1 N solution of HCl, extracted with ethyl acetate, washed with brine and dried over sodium sulfate. Methyl octacosadienoate (**4**) was obtained in good yield as an oil (90%) (2.09 g, 4.82 mmol, 90% yield). FT-IR (neat cm^{-1}): 3005, 2926, 1709, 1288, 1120, 964, 721. ^1H NMR (300 MHz, CDCl_3): δ = 0.87 (t, J = 6.0 Hz, 3 H, H-28), 1.31 (m, 34 H, H-3-8, 13-17, 22-27), 2.01 (m, 8 H, H-9, 12, 18, 21), 2.36 (t, J = 6.5 Hz, 2 H, H-2), 3.5 (s, 3 H, $-\text{COOCH}_3$), 5.35 ppm (m, 4 H, H-10, 11, 19, 20). ^{13}C NMR (300 MHz, CDCl_3): δ = 13.77 (C-28), 22.48 (C-27), 27.14 (C-9,11,18, 21), 29.05 ($(\text{CH}_2)_n$), 31.50 (C-26), 34.17 (C-2), 51.4 ($-\text{OCH}_3$), 130.03 (C-10, 11, 19, 20), 174.3 ppm (C-1). CI-MS m/z 435 $[\text{M} + \text{H}]^+$ $\text{C}_{29}\text{H}_{54}\text{O}_2$. ESI-HRMS (m/z): 435.4117 ($\text{M} + \text{H}^+$), (calcd. 435.4124).

Octacosadienol (**5**)

To a suspension of LiAlH_4 (0.51 g, 13.4 mmol, 3eq) in anhydrous THF (30 ml) under N_2 , a solution of **4** (2.0 g, 4.6 mmol) in THF (10 ml) was added at 0 °C. The reaction was stirred at room temperature for 3 h and monitored by TLC with hexane/ethyl acetate 80:20 (R_f **5** = 0.4). Work-up: 1 N H_2SO_4 (15 ml) was added and the organic phase extracted with CH_2Cl_2 washed with brine and dried over sodium sulfate. The solvent was removed under vacuum and a white powder was obtained (1.59 g, 3.91 mmol, yield 85%). FT-IR (neat cm^{-1}): 3510, 2926, 1464, 1290, 1174, 1034, 965, 731. ^1H NMR (300 MHz, CDCl_3): δ = 0.88 (t, J = 6.0 Hz, 3 H, H-28), 1.28 (m, 34 H, H-3-8, 13-17, 22-27), 1.61 (m, 2 H, H-2), 2.02 (m, 8 H, H-9, 12, 18, 21), 3.64 (t, J = 6.0 Hz, 2 H, H-1), 4.45 (br, 1 H, OH), 5.35 ppm (m, 4 H, H-10, 11, 19, 20). ^{13}C NMR (300 MHz, CDCl_3): δ = 13.77 (C-28), 22.48 (C-27), 27.14 (C-9,11,18, 21), 29.05 ($(\text{CH}_2)_n$), 31.50 (C-26), 32.64 (C-2), 63.02 (C-1) 130.03 ppm (C-10, 11, 19, 20). CI-MS m/z 407 $[\text{M} + \text{H}]^+$ $\text{C}_{28}\text{H}_{54}\text{O}$. ESI-HRMS (m/z): 407.4160 ($\text{M} + \text{H}^+$), (calcd. 407.4175).

Cell Culture

Human hepatoma HepG2 cells (ATCC HB-8065, HepG2) were routinely maintained as monolayers in Dulbecco-modified Eagle medium (DMEM) supplemented with 10% v/v adult bovine serum, 0.03% of glutamine, penicillin 100 U/mL and streptomycin 0.1 mg/mL. Human endothelial cells from umbilical cord veins (HUVEC) were

prepared, characterized and grown as previously described [33]. HUVEC were routinely maintained as monolayers in M199 medium supplemented with 20% v/v adult bovine serum, 0.03% of glutamine, penicillin 100 U/mL, streptomycin 0.1 mg/mL and heparin 8.5 USP unit/mL. Cells were grown at 37 °C in a humidified atmosphere (air 95%/CO₂ 5%).

HMGR Assay

The HMGR activity was determined in HepG2 and HUVEC cells seeded in 24-well plastic clusters. Each well received 25,000 cells suspended in 1,000 μL of complete medium. After 24 h, cells were rinsed twice with phosphate-buffered saline (PBS) and the medium was replaced with 987.5 μL of fresh growth medium containing lipid-depleted serum [34] to induce the upregulation of HMGR. Cells were divided into three experimental groups and grown 24 h after addition of 12.5 μL of absolute ethanol (control wells) or 12.5 μL of an ethanolic solution of octacosadienol or policosanol (final concentration 50 $\mu\text{g}/\text{mL}$). In this range of concentration octacosadienol, policosanol and absolute ethanol had no effect on cell viability. As a control of the upregulation obtained in the above conditions, the HMGR activity was determined also in cells grown in parallel but in a medium supplemented with normal serum plus absolute ethanol. Cells were then washed with ice-cold PBS and lysed in ice for 20 min with 100 $\mu\text{L}/\text{well}$ of ice-cold phosphate buffer, pH 7.4, containing 0.1 M sucrose, 40 mM KH_2PO_4 , 30 mM EDTA, 50 mM KCl, 5 mM dithiothreitol, 0.25% (v/v) Brij 96. Cell debris was removed by centrifugation at 12,000 $\times g$ for 3 min and the protein concentration of the supernatant was determined with a SIGMA Protein assay Kit based on the method of Lowry modified by Peterson [35]. In order to measure the HMGR activity 80 μL of supernatant were added with 10 μL of NADPH-generating system and 10 μL of labeled substrate hydroxy-3-methyl[3- ^{14}C]glutaryl-coenzyme A. The final mixture assay (100 μL) contained 2.5 mM NADP, 20 mM glucose 6-phosphate, 1.5 units of glucose 6-phosphate dehydrogenase and 0.01 μCi of hydroxy-3-methyl[3- ^{14}C]glutaryl-coenzyme A. The enzymatic reaction was stopped after 60 min at 37 °C by addition of 10 μL of 5 M HCl. After an additional incubation for 30 min at 37 °C to allow for complete lactonisation of the product, the mixture was centrifuged at 12,000 $\times g$ for 2 min. The aqueous supernatant was applied to a silica column that was primed with 2 ml of eluting solvent mixture toluene/acetone (3:1, v/v). The mevalonolactone was eluted from the column with 6 ml of the eluting solvent mixture and the eluate collected in a scintillation vial for measuring ^{14}C radioactivity (2500 TR Liquid Scintillation Analyzer—Packard BioScience, Waltham,

MA—USA). TLC analysis (toluene/acetone, 1:1 as eluent) of the eluate with a System 200 Imaging Scanner (Canberra Packard, USA) showed that all the recovered radioactivity was in correspondence of the reference of mevalonolactone. The HMGR activity was expressed as dpm of [^{14}C]mevalonate formed per milligram of protein incubated.

RT-PCR

HepG2 and HUVEC cells were seeded in 100-mm diameter dishes and incubated in 5 ml of complete medium. At 70% confluence, cells were rinsed twice with phosphate-buffered saline (PBS) and the medium was replaced with fresh growth medium containing lipid-depleted serum [34]. At this point, cells were divided into three experimental groups and a further 24 h treatment was carried out in the presence of 62.5 μl of absolute ethanol (control wells) or 62.5 μl of an ethanolic solution of octacosadienol or policosanol (50 $\mu\text{g}/\text{mL}$). A further group of cells was grown in a medium supplemented with normal serum plus absolute ethanol to check the upregulation of HMGR after incubation with lipid-depleted serum. After 24 h cells were washed twice with phosphate-buffered saline, and total RNA was extracted using NucleoSpin[®] RNA II Kit (Machery-Nagel). The cDNA was synthesized with the RevertAid TM H Minus First Strand cDNA synthesis Kit (Fermentas). TaqMan[®] RT-PCR reactions (25 μl) were set up in 96-well reaction plates using a TaqMan[®] Gene Expression Assay Mix specific for human HMGR or a TaqMan[®] Endogenous Control TBP (TATA-box binding protein) Mix and a TaqMan[®] Universal Master Mix (Applied Biosystems). Real-time PCR was performed using an ABI Prism 7900 Sequence Detection System (Applied Biosystems), using generic cycling conditions.

Immunoquantitation of AMP-Kinase

HepG2 and HUVEC cells were seeded in 100-mm diameter dishes and incubated in 5 ml of complete medium. Cells were grown to 70% confluence and then maintained overnight in serum-free medium containing 1.5% bovine serum albumin. Cells were then divided into three experimental groups for a further 6 h culture in the presence of 62.5 μl of absolute ethanol (control wells) or 62.5 μl of an ethanolic solution of octacosadienol or policosanol (50 $\mu\text{g}/\text{mL}$). As a positive control cells were cultured as described above in the presence of metformin (360 $\mu\text{g}/\text{mL}$) and 62.5 μl of absolute ethanol. The treatment of HepG2 and HUVEC cells with metformin did not show any detectable cell toxicity. After 6 h cells were washed twice with phosphate-buffered saline, and lysed in ice-cold buffer (20 mM Tris-HCl, pH 8.0, 1% Nonidet P-40, 1 mM EDTA, 1 mM EGTA, 1 mM sodium orthovanadate, 1 mM

dithiothreitol, 1 mM phenylmethyl sulfonyl fluoride and 1 mM protease inhibitor cocktails (Sigma-Aldrich) [36]. Cells were scraped from the plates and collected in a micro-centrifuge tube. Cells debris was removed by centrifugation at 12,000 $\times g$ for 10 min and the resulting supernatant was used for Western Blotting. Protein concentration in cell lysate was measured using a BCA protein assay kit (Pierce). For Western Blotting, 20–50 μg of protein was separated by 10% SDS-polyacrylamide gel electrophoresis and electroblotted to a nylon membrane in a transfer buffer containing 125 mM Tris-HCl, 960 mM glycine, 0.5% SDS and 20% methanol. The membrane was blocked with 10% nonfat dry milk in PBS buffer and then incubated in the same buffer containing 0.1% Tween 20 with rabbit antibody to total AMP-kinase (anti-AMPK α -pan, 1:2,000; Upstate Biotechnology) or to phosphorylated AMP-kinase (anti-phospho-AMPK α , 1:1,000; Upstate Biotechnology). The immunoblot was developed with a secondary antibody conjugated to horseradish peroxidase and visualized and quantified by chemiluminescence (Western LightningTM Plus-ECL, Medical Imaging, PerkinElmer Life Sciences) on Molecular Imager Chemidoc XRS System, Quantity One software (Biorad).

Statistical Analysis

Data of HMGR activity (% of delipidated controls) were compared by the Kruskal–Wallis rank test [37], while RT-PCR data ($2^{\Delta\Delta\text{Ct}}$) were analyzed by ANOVA.

Results

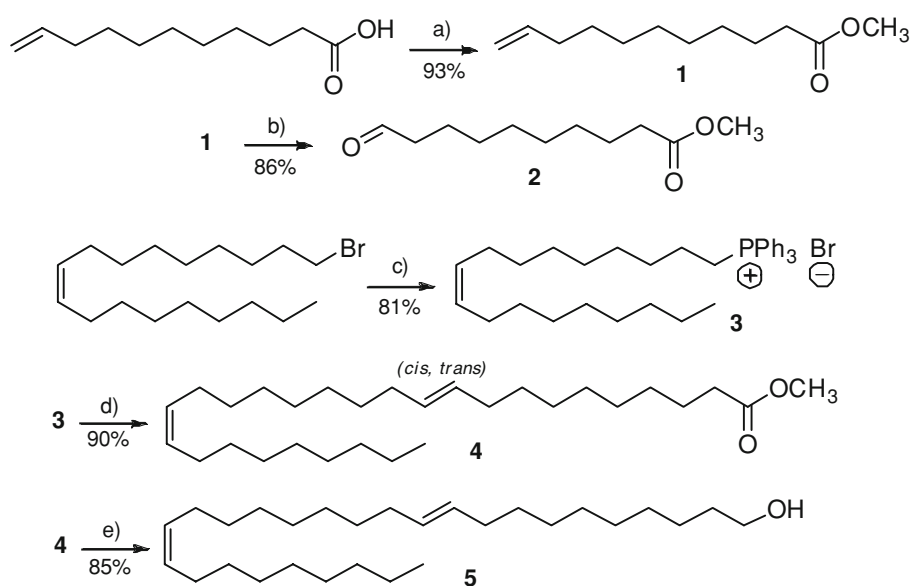
Synthesis of Octacosadienol

In the search of a more active synthetic analogue of policosanol and with the aim to study the effect of unsaturations on C-28 fatty alcohol, we planned the synthesis of octacosadienol. Our synthetic approach was studied for gram-scale production of long chain unsaturated fatty alcohols [38]. The key step was a Wittig olefination to bind two relatively cheap building blocks: the methyl ester of the 10-oxodecanoic acid and the phosphorus ylide obtained from oleyl bromide. The whole synthetic procedure is depicted in Scheme 2.

HMGR Activity Regulation

The effect on HMGR of the octacosadienol, the synthetic unsaturated derivative of octacosanol, was studied in HUVEC and hepatoma cells and compared with the effect of the natural policosanol mixture extracted from commercial tablets. The composition of ethanolic extracts of

Scheme 2 a MeOH, PTSA_{cat}, toluene, rfx. 5h. b H₂O/acetone, OsO₄, NMMO, NaIO₄, US 19 kHz. c toluene rfx., PPh₃ d **2**, BuLi, THF; e LiAlH₄, THF



tablets, analysed by GC/MS after extraction and purification [39] was the same found by Singh, Li and Porter [22]. Octacosanol content was about 60%.

In agreement with previous results from different authors [13, 22], we could not observe a direct inhibition of the enzyme after the addition of octacosadienol or policosanol to cell lysates from both cell lines.

However after a 24-h incubation of the cells grown in a delipidated medium with either octacosadienol or the commercial policosanol, the activity of HMGR measured in cell lysates was significantly reduced with respect to the controls grown in the same conditions in the absence of octacosadienol or policosanol. Figure 1 shows the HMGR activity measured in lysates of cells grown in a complete medium, compared to cells grown in a delipidated medium, in the absence or in the presence of octacosadienol or policosanol. As shown in the figure, the HMGR activity of cells grown in a delipidated medium was significantly increased by 50% in hepatoma and by 80% in HUVEC cells ($P < 0.01$), compared with cells grown in a normal medium. In hepatoma the addition of 50 $\mu\text{g/ml}$ of octacosadienol to the delipidated medium caused a 30% decrease in HMGR activity. In HUVEC cells the effect of octacosadienol was even higher and the enzymatic activity dropped by 50%. In both cell types octacosadienol was almost as effective as policosanol. The enzymatic activity did not drop to the level found in the not induced cells grown in a complete medium, but in both cell types the presence of policosanol or octacosadienol significantly reduced ($P < 0.01$) the induction of the enzymatic activity caused by the absence of uptake of sterols from the medium.

In order to find out if the decrease of the activity of HMGR in the presence octacosadienol or policosanol in

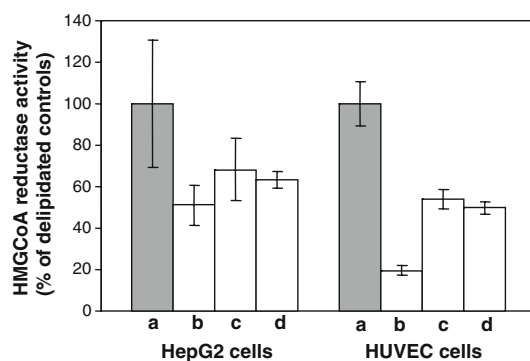
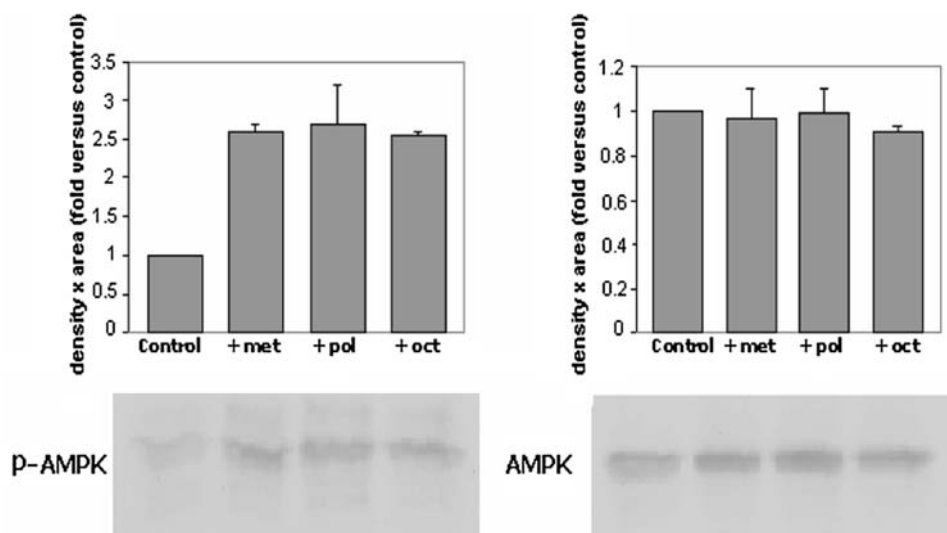


Fig. 1 Effect of octacosadienol and policosanol on the activity of HMGR of HUVEC and HepG2 hepatoma cells grown in a delipidated medium. The HMGR activity was measured in lysates prepared from HepG2 or HUVEC cells grown either in a delipidated or in a complete medium and compared with the activity of lysates of cells incubated with 50 $\mu\text{g/ml}$ of octacosadienol or policosanol in LDM. The HMGR activity is expressed as % of the activity found in control cells grown in LDM. Each value represents the mean and SE of at least two separate experiments in duplicate. **a** Control cells grown in LDM. **b** Control cells grown in a complete medium. **c** Cells grown in LDM with 50 $\mu\text{g/ml}$ octacosadienol. **d** Cells grown in LDM with 50 $\mu\text{g/ml}$ policosanol

HUVEC cells could be explained with an inactivation of the enzyme induced by AMPK we analyzed HUVEC cell lysates in western blot to evidence the phosphorylated form of AMPK by a specific antibody. As shown in Fig. 2 the increase of 2.5–3.5 fold of the phosphorylated form of AMPK in lysates of HUVEC cells grown in a delipidated medium in the presence of the same amount of octacosadienol or policosanol used to measure the activity of HMGR, is comparable to that obtained in the presence of metformin, a well known activator of the phosphorylation of AMPK [40]. A comparable increase of phosphorylated

Fig. 2 Immunoblot of total and phosphorylated AMPK in HUVEC cell lysates. Cell lysates untreated (controls) or incubated with 360 $\mu\text{g}/\text{mL}$ of metformin (+met) or 50 $\mu\text{g}/\text{mL}$ of policosanol (+pol) or octacosadienol (+oct) were fractionated by electrophoresis and transferred to nylon membranes for immunodetection with an antibody specific for total AMPK or for phosphorylated AMPK (P-AMPK). The band density determined as arbitrary units are expressed as ratio versus the untreated control. Bars represents SE of duplicate experiments



AMPK was observed in hepatoma cells treated with policosanol and octacosadienol in the same conditions. From these experiments the efficacy of octacosadienol is comparable to that of the natural mixture of policosanol.

Furthermore, in order to study the occurrence of an alternative or additional mechanism based on a decrease of the expression of the enzyme, we determined by quantitative RT-PCR the relative amount of the HMGR mRNA present in HUVEC cells grown in a delipidated medium in absence or in presence of octacosadienol. RNA was extracted from both cells grown in a complete medium and cells grown in a delipidated medium with or without the addition of 50 $\mu\text{g}/\text{mL}$ of octacosadienol. The cDNA from all the samples was obtained by RT-PCR using the same starting amount of RNA. The relative amount of cDNA was determined in real time PCR with the $2^{-\Delta\Delta\text{Ct}}$ method [41], using as housekeeping gene the TBP gene cDNA and as a calibrator the HMGR mRNA of HUVEC cells grown in a complete medium. By using this method the value of $2^{-\Delta\Delta\text{Ct}}$ of the calibrator (cells grown in a complete medium) is 1 and the $2^{-\Delta\Delta\text{Ct}}$ value of the cells grown in a delipidated medium in the presence or in the absence of octacosadienol or policosanol represents the fold change in mRNA in a delipidated medium. As shown in the histogram of Fig. 3, the increase of HMGR mRNA in HUVEC cells grown in a delipidated medium is almost six fold. The addition of octacosadienol reduces this increase by 50%, ($P < 0.05$). By comparing in the same experiment the $2^{-\Delta\Delta\text{Ct}}$ obtained in the presence of octacosadienol and of the mixture of policosanol we have shown that octacosadienol alone has the same activity of the mixture of policosanol, as can be seen in Fig. 4. A degree of variability among the experiments was observed mainly in the amount of the induction of the expression of HMGR in a delipidated medium. The higher the induction in the control cells, the more evident was the reduction effect of the octacosadienol. In hepatoma

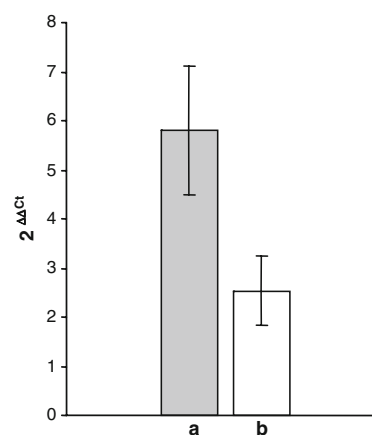


Fig. 3 Effect of octacosadienol on the HUVEC cells expression of HMGR. The cDNA obtained after extraction of total RNA from cell lysates was amplified in the presence of a TaqMan probe specific for HMGR in real-time PCR and quantified relatively to untreated controls grown in a complete medium. **a** Lysates from cells grown in LDM. **b** Lysates from cells grown in LDM with octacosadienol. Each value represents the mean and SE of six separate experiments

cells, we could not observe a significant effect of octacosadienol. In two different experiments we obtained no or very little (18%) reduction in the HMGR mRNA with respect to the control cells grown in a delipidated medium.

Discussion

The present paper describes an efficient synthetic procedure to obtain octacosadienol on a gram scale, starting from commercially available cheap building blocks, namely oleyl bromide and undecylenic acid. The method is extremely versatile because by varying the chain length of the alkenyl halide as well as the number/position of the double bonds, a wide number of analogues can be

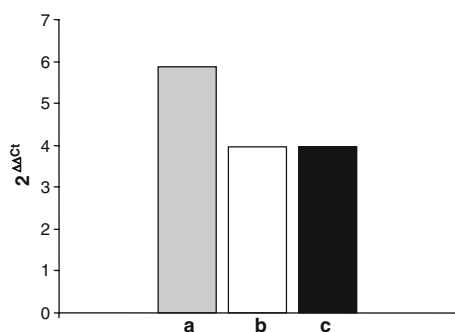


Fig. 4 Effect of octacosadienol and policosanol on the HUVEC cells expression of HMGR. The cDNA obtained after extraction of total RNA from cell lysates was amplified in the presence of a TaqMan probe specific for HMGR in real-time PCR and quantified relatively to untreated controls grown in a complete medium. **a** Lysates from cells grown in LDM. **b** Lysates from cells grown in LDM with octacosadienol. **c** Lysates from cells grown in LDM with policosanol

prepared. The simplicity of this protocol and the excellent overall yield (about 50%) are worthy of mention.

Our results show that the naturally occurring policosanol is able to downregulate the HMGR activation that occurs when the cells are grown in a delipidated medium also in cell types different from the previously studied fibroblasts and hepatoma cells [13, 22], i.e. the angiogenic HUVEC cells. Moreover, the synthetic unsaturated long-chain alcohol octacosadienol has the same activity as the natural product in both hepatoma and HUVEC cells. Both policosanol and octacosadienol increased the phosphorylation of AMPK, a kinase that phosphorylates several downstream substrates including HMGR, having the overall effect of switching off ATP-consuming pathways such as fatty acid and cholesterol synthesis and switching on ATP-generating pathways [25]. An increased phosphorylation of HMGR by AMPK could explain the downregulation of HMGR observed in hepatoma and HUVEC cells, since the phosphorylated HMGR is inactive [25]. The increased phosphorylation of AMPK can affect the activity of HMGR either by the direct phosphorylation and consequent inactivation of the enzyme, or by an indirect downregulation, mediated by transcription factors. SREBP-1, a transcription factor involved in the regulation of several lipogenic enzymes, included HMGR [27], has been recently shown to be downregulated following the activation of AMPK [26, 40]. Our quantification of HMGR mRNA by RT-PCR shows that in HUVEC cells both policosanol and octacosadienol affect the regulation of HMGR activity also at the transcription level, causing a decrease of mRNA. In hepatoma cells we could not detect a significant decrease of the level of the HMGR mRNA, and the observed downregulation of the enzyme could be mainly explained with the phosphorylation by AMPK and consequent inactivation.

Therefore, the induction of the phosphorylation of AMPK seems to be a general mechanism by which

policosanol, and also synthetic analogues of these natural compounds, contrast the upregulation of HMGR by activating different cell-specific mechanisms of regulation. The downregulation of HMGR, besides affecting cholesterol biosynthesis, could influence cell cycle progression as a consequence of the decreased synthesis of nonsterol mevalonate derivatives as farnesyl, geranyl and geranylgeranyl intermediates which are necessary for the prenylation of proteins as Ras and Rho, involved in the signal transduction cascades controlling cell proliferation and differentiation. Antitumor properties such as induction of growth arrest and apoptosis, inhibition of metastasis and inhibition of angiogenesis, have been observed in various cell lines and in experimental animals after treatment with statins, the most known inhibitors of HMGR. The mechanism that mediates the antitumoral effects of statins, originally related to the inhibition of Ras farnesylation, is still being discussed and possibly dissimilar in different cell lines [42]. Recently, the involvement of a long chain aliphatic alcohol in the control of cell proliferation has been described in a paper studying the effect of octacosanol purified from *Tinospora cordifolia*, on the proliferation of HUVEC and tumor cells. In this study, octacosanol has been shown to inhibit the proliferation of HUVEC and Ehrlich ascites tumor cells (EAT) [32]. Moreover, angiogenesis decreased in the peritoneum of EAT-bearing mice treated with octacosanol. The antiangiogenic activity was accompanied by a decrease in the secretion of VEGF in ascites fluid, a decreased activity in the collagenase MMP2, and the inhibition of nuclear translocation of NFκB, a transcription factor involved in the control of the inflammatory response and apoptosis and controlled by different, complex activation pathways [43, 44].

The regulation of the HMGR activity and AMPK phosphorylation in HUVEC cells by a synthetic long-chain alcohol such as octacosadienol opens promising perspectives for the design of new antiangiogenic compounds. Pathological angiogenesis is a hallmark of cancer and various ischemic and inflammatory diseases and anti-angiogenic therapy is one of the most promising approaches to cancer treatment, making the discovery of new anti-angiogenic molecules very attractive.

Acknowledgments The University of Turin and the regional government (Regione Piemonte: SINAPSI and Ricerca Sanitaria Finalizzata 2007–2008) are warmly acknowledged for the financial support.

References

- Houtz RL, Ries SK, Tolbert NE (1985) Effect of triacontanol on *Chlamydomonas*. II. Specific activity of ribulose-bisphosphate carboxylase/oxygenase, ribulose-bisphosphate concentration, and characteristics of photorespiration. *Plant Physiol* 79:365–370

2. Lesniak AP, Haug A, Ries SK (1986) Stimulation of ATPase activity in barley (*Hordeum vulgare*) root plasma membrane after treatment of intact tissues and cell free extracts with triacontanol. *Physiol Plant* 68:20–26
3. Mc Bride PT, Clark I, Krueger GG (1987) Evaluation of triacontanol-containing compounds as anti-inflammatory agents using guinea pig models. *J Invest Dermatol* 89:380–383
4. Saint-John M, McNaughton L (1986) Octacosanol ingestion and its effects on metabolic responses to submaximal cycle ergometry, reaction time and chest and grip strength. *Int Clin Nutr Rev* 6:81–87
5. Ohia Y, Ohashi K, Matsura T, Tokunaga K, Kitagawa A, Yamada K (2008) Octacosanol attenuates disrupted hepatic reactive oxygen species metabolism associated with acute liver injury progression in rats intoxicated with carbon tetrachloride. *J Clin Biochem Nutr* 42:118–125
6. Sho H, Chinen I, Fukuda N (1984) Effect of Okinawan sugar cane wax and fatty alcohol on serum and liver lipids in the rat. *J Nutr Sci Vitaminol* 30:539–553
7. Shimura S, Hasegawa T, Takano S, Suzuki T (1987) Studies on the effect of octacosanol on motor endurance in mice. *Nutr Rep Int* 36:1029–1038
8. Irmak S, Dunford NT, Milligan J (2005) Policosanol contents of beeswax, sugar cane and wheat extracts. *Food Chem* 95:312–318
9. Kazuko K, Kumlko A, Yohel H (1991) Free primary alcohols in oils and waxes from germs, kernels and other components of nuts, seeds, fruits and cereals. *J Am Oil Chem Soc* 68:869–872
10. Piatak DM, Reimann KA (1970) Isolation of 1-octacosanol from *Euphorbia corollata*. *Phytochemistry* 9:2585–2586
11. Hernandez F, Illnait J, Mas R, Castano G, Fernandez L, Gonzalez M, Cordovi N, Fernandez J (1992) Effect of policosanol on serum lipids and lipoproteins in healthy volunteers. *Curr Ther Res* 51:568–575
12. Menéndez R, Fernández I, Del Río A, González RM, Fraga V, Amor AM, Más R (1994) Policosanol inhibits cholesterol biosynthesis and enhances low-density lipoprotein processing in cultured human fibroblasts. *Biol Res* 27:199–203
13. Menéndez R, Amor A, Rodeiro I, Gonzalez RM, Gonzalez PC, Alfonso JL, Mas R (2001) Policosanol modulates HMG-CoA reductase activity in cultured fibroblasts. *Arch Med Res* 32:8–12
14. Menéndez R, Arruzazabala L, Mas R, Del Rio A, Amor AM, Gonzalez RM, Carbajal D, Fraga V, Molina V, Illnait J (1997) Cholesterol-lowering effect of policosanol on rabbits with hypercholesterolemia induced by a wheat starch–casein diet. *Br J Nutr* 77:923–932
15. Menéndez R, Amor AM, González RM, Fraga V, Mas R (1996) Effect of policosanol on the hepatic cholesterol biosynthesis of normocholesterolemic rats. *Biol Res* 29:253–257
16. Berthold IG, Berthold HK (2002) Policosanol: clinical pharmacology and therapeutic significance of a new lipid-lowering agent. *Am Heart J* 143:356–365
17. Viola F, Oliaro S, Binello A, Cravotto G (2008) Policosanol: updating and perspectives. *Mediterr J Nutr Metab* 1:77–83
18. Kassis A, Jones PJH (2006) Lack of cholesterol-lowering efficacy of Cuban sugar cane policosanol in hypercholesterolemic persons. *Am J Clin Nutr* 84:1003–1008
19. Dulin MF, Hatcher LF, Sasser HC, Barringer T (2006) Policosanol is ineffective in the treatment of hypercholesterolemia: a randomized controlled trial. *Am J Clin Nutr* 84:1543–1548
20. Berthold HK, Unverdorben S, Degenhardt R, Gouni-Berthold I (2006) Effect of policosanol on lipid levels among patients with hypercholesterolemia or combined hyperlipidemia. *J Am Med Assoc* 295:2262–2269
21. Kassis AN, Kubow S, Jones PJH (2009) Sugar cane policosanols do not reduce LDL oxidation in hypercholesterolemic individuals. *Lipids* 44:391–396
22. Singh DK, Li L, Porter TD (2006) Policosanol inhibits cholesterol synthesis in hepatoma cells by activation of AMP-kinase. *J Pharmacol Exp Ther* 318:1020–1026
23. Keller S, Gimmler F, Jahreis G (2008) Octacosanol administration to humans decreases neutral sterol and bile acid concentration in feces. *Lipids* 43:109–115
24. Goldstein JL, Brown MS (1990) Regulation of the mevalonate pathway. *Nature* 343:425–430
25. Hardie DG, Carling D, Carlson M (1998) The AMP-activated/SNF1 protein kinase subfamily: metabolic sensors of the eukaryotic cell? *Annu Rev Biochem* 67:821–855
26. Hardie DG (2004) The AMP-activated protein kinase pathway—new players upstream and downstream. *J Cell Sci* 117:5479–5487
27. Motoshima H, Goldstein BJ, Igata M, Araki E (2006) AMPK and cell proliferation—AMPK as a therapeutic target for atherosclerosis and cancer. *J Physiol* 574:63–71
28. Hadad SM, Fleming S, Thompson AM (2008) Targeting AMPK: a new therapeutic opportunity in breast cancer. *Crit Rev Oncol Hematol* 67:1–7
29. Takahashi HK, Nishibori M (2007) The antitumour activities of statins. *Curr Oncol* 14:246–247
30. Ho PL, Liang YC, Ho HS, Chen CT, Lee WS (2004) Inhibition of human vascular endothelial cells proliferation by terbinafine. *Int J Cancer* 111:51–59
31. Curtis R, Chong CR, Xu J, Lu J, Bhat S, Sullivan DJ Jr, Liu JO (2007) Inhibition of angiogenesis by the antifungal drug itraconazole. *ACS Chem Biol* 2:263–270
32. Thippeswamy G, Sheela MI, Salimath BP (2008) Octacosanol isolated from *Tinospora cordifolia* downregulates VEGF gene expression by inhibiting nuclear translocation of NF-kappaB and its DNA binding activity. *Eur J Pharmacol* 588:141–150
33. Bussolino F, Di Renzo MF, Ziche M, Bocchietto E, Olivero M, Naldini L, Gaudino G, Tamagnone L, Coffer A, Comoglio PM (1992) Hepatocyte growth factor is a potent angiogenic factor which stimulates endothelial cell motility and growth. *J Cell Biol* 119:629–641
34. Chan BE, Knowles BR (1976) A solvent system for delipidation of plasma or serum without protein precipitation. *J Lipid Res* 17:176–181
35. Peterson GL (1977) A simplification of the protein assay method of Lowry et al. which is more generally applicable. *Anal Biochem* 83:346–356
36. Zang M, Zuccollo A, Hou X, Nagata D, Walsh K, Herscovitz H, Brecher P, Ruderman NB, Cohen RA (2004) AMP-activated protein kinase is required for the lipid-lowering effect of metformin in insulin-resistant human HepG2 cells. *J Biol Chem* 279:47898–47905
37. Aviva P, Sabin C (2000) *Medical statistics at a glance*, Blackwell Science Ltd., Padstow, UK
38. Cravotto G (2003) A process for preparing long chain saturated or unsaturated oxygenated compounds. Patent WO/2003/106397; Long chain unsaturated oxygenated compounds and their use in the therapeutic, cosmetic and nutraceutical field. Patent WO/2003/105822
39. Cravotto G, Binello A, Merizzi G, Avogadro M (2004) Improving solvent-free extraction of policosanol from rice bran by high-intensity ultrasound treatment. *Eur J Lipid Sci Technol* 106:147–151
40. Zhou G, Myers R, Li Y, Chen Y, Shen X, Fenyk-Melody J, Wu M, Ventre J, Doebber T, Fujii N, Musi N, Hirshman MF, Goodyear LJ, Moller DE (2001) Role of AMP-activated protein kinase in mechanism of metformin action. *J Clin Invest* 108:1167–1174
41. Livak KJ, Schmittgen TD (2001) Analysis of relative gene expression data using real time quantitative PCR and the $2^{-\Delta\Delta C_t}$ method. *Methods* 25:402–408

42. Graaf MR, Richel DJ, van Noorden CJF, Guchelaar HJ (2004) Effects of statins and farnesyltransferase inhibitors on the development and progression of cancer. *Cancer Treat Rev* 30:609–641
43. Tang CH, Chiu YC, Tan TW, Yang RS, Fu WM (2007) Adiponectin enhances IL-6 production in human synovial fibroblast via an adipoR1 receptor, AMPK, p38, and NF- κ B pathway. *J Immunol* 179:5483–5492
44. Escarcega RO, Fuentes-Alexandro S, Garcia-Carrasco M, Gatica A, Zamora A (2007) The transcription factor nuclear factor-kappa B and cancer. *Clin Oncol* 19:154–161

In Vitro Simultaneous Transfer of Lipids to HDL in Coronary Artery Disease and in Statin Treatment

Ana C. Lo Prete · Clederson H. Dina · Carolina H. Azevedo ·
Camila G. Puk · Neuza H. M. Lopes · Whady A. Hueb ·
Raul Cavalcante Maranhão

Received: 17 June 2008 / Accepted: 1 September 2009 / Published online: 16 September 2009
© AOCs 2009

Abstract The exchange of lipids with cells and other lipoproteins is a crucial process in HDL metabolism and for HDL antiatherogenic function. Here, we tested a practical method to quantify the simultaneous transfer to HDL of phospholipids, free-cholesterol, esterified cholesterol and triacylglycerols and to verify the lipid transfer in patients with coronary artery disease (CAD) or undergoing statin treatment. Twenty-eight control subjects without CAD, 27 with CAD and 25 CAD patients under simvastatin treatment were studied. Plasma samples were incubated with a donor nanoemulsion prepared by ultrasonication of the constituent lipids and labeled with radioactive lipids; % lipids transferred to HDL were quantified in the HDL-containing supernatant after chemical precipitation of non-HDL fractions and the nanoemulsion. The assay was precise and reproducible. Increase of temperature (4–37 °C), of incubation period (5 min to 2 h), of HDL-cholesterol concentration (33–244 mg/dL) and of mass of nanoemulsion lipids (0.075–0.3 mg/ μ L) resulted in increased lipid transfer from the nanoemulsion to HDL. In contrast, increasing pH (6.5–8.5) and albumin concentration (3.5–7.0 g/dL) did not affect lipid transfer. There was no difference between CAD and control non-CAD with regard to the lipid transfer, but statin treatment

reduced the transfer to HDL of all four lipids. The test herein described is a valid and practical tool for exploring an important aspect of HDL metabolism.

Keywords High-density lipoprotein · Nanoemulsions · Coronary artery disease · Statins · Nanoparticles · Transfer proteins · Cholesterol · Triacylglycerols · Cholesteryl ester transfer protein (CETP) · Phospholipid transfer protein (PLTP)

Abbreviations

CETP Cholesteryl ester transfer protein
PLTP Phospholipid transfer protein
Apo Apolipoprotein
CAD Coronary artery disease
BMI Body mass index

Introduction

Plasma lipoproteins constantly exchange lipids, both those that make-up the lipoprotein surface monolayer, namely phospholipids and free cholesterol and the core lipids, triacylglycerols and cholesteryl esters. This process is facilitated by transfer proteins, namely cholesteryl ester transfer protein (CETP) [1] and phospholipid transfer protein (PLTP) [2]. In addition to the action of transfer proteins, other factors such as the composition and concentration of the lipoproteins and of some plasma constituents may affect the ability of the lipoprotein particles to receive and donate lipids [3–6].

Different from the other lipoprotein classes that are synthesized into the liver or intestinal cells, high-density

A. C. Lo Prete · C. H. Azevedo · R. C. Maranhão
Faculty of Pharmaceutical Sciences,
University of São Paulo, São Paulo, Brazil

C. H. Dina · C. G. Puk · N. H. M. Lopes ·
W. A. Hueb · R. C. Maranhão (✉)
Laboratório de Metabolismo de Lípidos, Instituto do Coração
(INCOR) do Hospital das Clínicas FMUSP,
Av. Dr. Enéas de Carvalho Aguiar, 44, 1° subsolo,
São Paulo, SP 05403-000, Brazil
e-mail: ramarans@usp.br

lipoprotein (HDL) is formed in the intravascular compartment. In the plasma, apolipoprotein A-I (apo A-I), which is synthesized by the liver or by the small intestine, receives phospholipids and cholesterol from cell membranes and from apoB-containing lipoproteins. This results in the formation of discoidal HDL that is converted to larger, spherical HDL by esterification of free cholesterol by lecithin:cholesterol acyltransferase (LCAT), using apo A1 as co-factor. The interaction of spherical HDL with CETP transfers HDL cholesteryl ester to apoB-containing lipoproteins. Cholesterol transported in HDL is taken-up by the liver, either via the selective uptake of HDL cholesteryl ester by scavenger receptor class B type I (SR-BI) or via the uptake of whole low-density lipoprotein (LDL) by the LDL receptor in the liver [7, 8]. HDL is thus constantly being remodeled by lipid transfers which are essential for the role of the lipoprotein in cholesterol esterification and in reverse cholesterol transport, whereby cholesterol from peripheral tissues is shuttled to the liver and excreted in bile, as described above. Because the lipid transfer process is determinant for HDL composition and thereby for the adhesion of proteins to the lipoprotein surface, it is possible that other atheroprotective functions of the lipoprotein, such as antioxidative, anti-inflammatory, antiapoptotic, vasodilatory, antithrombotic and anti-infectious may also be affected by this process.

Because the transfer of lipids to HDL is conceivably important for the maintenance of HDL structure, stability and function, the current study was designed to establish a practical method to evaluate the ability of the lipoprotein to simultaneously receive its main constituent lipid classes, namely phospholipids, free cholesterol, esterified cholesterol and triacylglycerols. This approach had not been previously explored. The studies in the literature have been focused on the transfer of isolated lipids to estimate the action of the transfer proteins. The novel method consists of the incubation of whole plasma with a cholesterol-rich artificial nanoemulsion as the donor of the four radioactive lipids. After chemical precipitation of the apo B-containing lipoproteins and the artificial nanoemulsion, the % of lipids that transferred to HDL is determined by radioactive counting of the supernatant. Lipid transfer to HDL was studied in subjects with or without coronary artery disease (CAD) and under simvastatin treatment.

Experimental Procedure

Study Subjects

Three groups of subjects grouped for age, body mass index (BMI) and HDL-cholesterol were studied: 28 control subjects without CAD, 27 with CAD and 25 CAD patients under simvastatin treatment (20 mg/day for at least 1 year).

Table 1 Clinical characteristics and blood biochemistry analyses of the three groups of participant subjects: non-CAD, CAD and CAD under simvastatin treatment

Parameters	Non-CAD (n = 28)	CAD (n = 27)	CAD + simvastatin (n = 25)
Age (years)	58 ± 5	57 ± 6	58 ± 7
BMI (kg/m ²)	29 ± 6	26 ± 3	28 ± 4
Glucose (mg/dL)	98 ± 10	98 ± 8	98 ± 10
Triacylglycerols (mg/dL)	145 ± 63	164 ± 34	146 ± 50
Cholesterol (mg/dL)			
Total	182 ± 42	212 ± 23*	180 ± 56
LDL	108 ± 35	145 ± 25*	108 ± 53
HDL	45 ± 11	46 ± 11	45 ± 13

Data are expressed as means ± SD

BMI body mass index, HDL high density lipoprotein, LDL low density lipoprotein

* $p < 0.001$ when compared to non-CAD and CAD under simvastatin treatment groups

The participants were of both genders and the presence or absence of CAD was confirmed by cineangiocoronariography performed over the last 6 months before they were studied. Exclusion criteria were diabetes, alcoholism, liver, renal, metabolic, inflammatory or neoplastic diseases. Their physical characteristics and plasma laboratorial profile are shown in Table 1. The Ethics Committee of the Medical School Hospital of the University of São Paulo approved the study and a written informed consent was obtained from all subjects after a complete description of the study.

Plasma Lipids

Total cholesterol (CHOD-PAP; Roche, Basel, Swiss) and triacylglycerols (Triglyceride Rapid; Roche) were determined by enzymatic methods on a Cobas Bio analyzer from plasma samples collected after a 12-h fast. HDL-cholesterol was measured by the same method used for total cholesterol after lipoprotein precipitation with magnesium phosphotungstate. LDL-cholesterol was estimated by the Friedewald formula [9].

HDL Particle Size Determination

The diameter of the HDL fraction particles was measured in fresh plasma collected after a 12-h fast as described by Lima and Maranhão [10], using a ZetaPALS Zeta Potential Analyzer (Brookhaven Instruments, Holtsville, NY).

Preparation of the Nanoemulsion

The lipid donor nanoemulsion was prepared from a lipid mixture composed of 40 mg cholesteryl oleate, 20 mg egg

phosphatidylcholine, 1 mg triolein and 0.5 mg cholesterol purchased from Sigma Chemical Company (St. Louis, MO). Emulsification of lipids by prolonged ultrasonic irradiation in aqueous media and under N₂ stream, and the procedure of two-step ultracentrifugation of the crude emulsion with density adjustment by addition of KBr to obtain the nanoemulsion was carried out by the method described previously by Ginsburg et al. [11] and modified by Maranhão et al. [12]. The fraction containing the nanoemulsion was dialyzed against 0.9% NaCl solution. Trace amounts of cholesteryl [1-¹⁴C] oleate and glycerol tri [9, 10(n)-³H] oleate or [7(n)-³H] cholesterol and L-3-phosphatidylcholine, 1-stearoyl-2-[1-¹⁴C] arachidonyl (Amersham, Little Chalfont, Buckinghamshire, UK) were added to the initial solution. The approximate specific activities of the isotopes (in cpm/mg of lipid) in the nanoemulsions were 10,000 for ¹⁴C-phospholipids, 20,000 for ³H-cholesteryl esters, 800,000 for ³H-cholesterol and 400,000 for ¹⁴C-triglycerides.

The lipid mixtures that originated the nanoemulsion and the final nanoemulsion preparation were tested in duplicate samples for lipid peroxidation by the TBARs method [13]. The malonaldehyde concentration was 9.5 in the lipid mixture and 7.3 nmol/mL in the resulting nanoemulsion, which implies that the emulsification procedure by prolonged ultrasonication does not increase the content of peroxides. The average diameter of the nanoemulsion particles, as measured by laser light scattering (Zeta Pals Analyser 90Plus, Brookhaven Instruments) was 43 nm.

Lipid Transfer from the Nanoemulsion to HDL

The assay consisted of the incubation of the radioactively labeled nanoemulsion with whole plasma followed by chemical precipitation of the apo B-containing lipoproteins and the nanoemulsion and radioactive counting of the supernatant for the lipids that shifted from the nanoemulsion to HDL. Plasma with EDTA that was stored at -80 °C in a 200 µL volume was incubated with 50 µL of the nanoemulsion labeled with ¹⁴C-cholesterol and ³H-triacylglycerols or with ³H-cholesteryl esters and ¹⁴C-phospholipids. After 1 h in a shaking bath at 37 °C, 250 µL of dextran sulfate/MgCl₂ was added as precipitation reagent. The mixture was mixed for 30 s, centrifuged for 10 min (3,000g) and 250 µL of the supernatant were immediately transferred to counting vials containing 5 mL scintillation solution (Packard BioScience, Groenigen, Netherlands). Radioactivity was then measured with a Packard 1600 TR model Liquid Scintillation Analyzer (Palo Alto, CA). The blank samples consisted of 200 µL TRIS solution with added labeled nanoemulsion with addition of the precipitation reagent after the incubation as described above. The results of radioactive transfer from the nanoemulsion to

plasma HDL were expressed as % of the total incubated radioactivity, determined in a plasma sample without the addition of precipitation reagent. One percent of ¹⁴C-phospholipids corresponded to a 0.217 µM transfer of this lipid from the nanoemulsion to HDL, 1% ³H-cholesteryl esters to 0.149 µM, 1% ³H-cholesterol to 0.006 µM and 1% ¹⁴C-triglycerides to 0.006 µM.

To demonstrate that chemical precipitation stops the lipid transfer to HDL, the supernatant radioactivity was measured 30 min after the addition of dextran and subsequent centrifugation, in a quadruplicate experiment. No further increase in the supernatant radioactivity counting was observed, which confirms that the lipid transfer was indeed interrupted.

Lipid Transfer under Different Conditions

The lipid transfer was analyzed under different conditions of temperature, pH, incubation time and albumin concentration. To evaluate the influence of temperature, the lipid transfer assay was performed at temperature range of 4–50 °C. The pH effect was evaluated at plasma pH 6.5–8.5 that was obtained by addition to the assay of Tris HCl or Tris NaOH buffer. To test the influence of incubation time, the assays were carried out at different incubation periods, ranging from 5 min to 6 h. The effect of the concentration of albumin in the plasma was tested at the range of 3.6–7.2 g/dL. It was also tested the effect on the lipid transfer of increasing the mass of nanoemulsion lipids (0.075–1.50 mg/µL) and HDL-cholesterol (33–244 mg/dL) in the plasma.

Lipid Transfer and Storage of Plasma and Nanoemulsion

The effect of the period of storage of the nanoemulsion and of the plasma samples on the lipid transfer to the HDL plasma fraction was tested. The transfer assay was performed using aliquots of the same labeled nanoemulsion or the same plasma sample in predetermined intervals over a 30-day or 1-year period, respectively.

Intra- and Inter-Assay Validation Parameters

The transfer assay method was validated for precision according to the FDA guidelines [14] in which the upper limit is 5%. Intra-assay precision studies included ten replicates of samples. Inter-assay precision was calculated based on three assays of ten replicates, run on three different days.

Statistical Analysis

Results are expressed as means and standard deviations (means ± SD). Differences of $p < 0.05$ were considered

significant. The Student's *t* test was used for normally distributed data and the Mann–Whitney test for those with non Gaussian distribution. The correlation between lipids transfer ratio with the other parameters was made by using analysis of variance and the Pearson's test.

Results

Figure 1 shows the effects of several variables on the results of the assay of the transfer of the four lipids from the nanoemulsion to HDL. In this respect, temperature, pH, incubation time, mass of the donor nanoemulsion, concentration of the recipient HDL and concentration of albumin in the incubate were tested. Increasing the temperature of the incubate resulted in progressive increase in the transfer of all lipids from 4 to 37 °C, when a plateau was reached until the last observation point, at 50 °C (Fig. 1a). Between 4 and 37 °C, the transfer values of phospholipids, free cholesterol, esterified cholesterol and triacylglycerols positively correlated with temperature ($r = 0.9212, 0.8709, 0.8656$ and 0.7983 , respectively, $p < 0.0001$). However, the correlation did not continue beyond the 37 °C temperature point.

The variation of the pH in the incubation from 6.5 to 8.5 did not affect the transfer of all lipids (Fig. 1b).

With respect to the effect of incubation time on lipid transfer, as shown in Fig. 1c the transfer of all lipids significantly increased ($p < 0.001$) up to 15 min incubation time. After this time, from 30 to 360 min, the apparent increase observed mainly in phospholipid transfer was not statistically significant. It can be stated that, between 2 and 4 h incubation time, a plateau of all lipid transfer was reached (Fig. 1c).

As shown in Fig. 1d, when the mass of nanoemulsion was increased in the assay, the transfer of phospholipids and free cholesterol pronouncedly increased from 0.075 to 0.3 mg/μL ($p < 0.001$). Regarding the transfer of the core lipids, the increase of both was statistically significant ($p < 0.001$) at increase from 0.075 to 0.1 mg/μL.

The variation of the recipient HDL mass in the assay resulted in increase of the transfer of all lipids in almost all tested HDL-cholesterol concentration intervals, from 33 to 244 mg/dL (Fig. 1e). Exceptions were free cholesterol transfer in HDL cholesterol concentration from 33 to 47 mg/dL and the esterified cholesterol transfer from 185 to 244 mg/dL HDL cholesterol concentration interval. Interestingly, the surface lipid transfer curves seem to show a linear shape while the transfer of core lipids looks like a sigmoidal curve. In addition, a positive correlation between HDL-cholesterol and transfer of the four lipids was found (phospholipids $r = 0.9508$,

free cholesterol $r = 0.9530$, esterified cholesterol $r = 0.8822$ and triacylglycerols $r = 0.8995$, $p < 0.002$ for all comparisons).

Finally, the transfer of the lipids to HDL was not affected by the albumin concentration in the assay (Fig. 1f).

The storage of nanoemulsion up to 15 days before the performance of the assay did not affect the results of the transfer of the four lipids to HDL. By day 30, however, there was a difference between the transfer values when compared to day 0 or day 1 ($p < 0.05$ for all four lipid transfer). The storage of the plasma sample for up to 1-year had no effect on the lipid transfer results ($p > 0.05$).

The coefficient of variation (C.V.) from intra-assay (phospholipids = 0.83; free cholesterol = 0.56; esterified cholesterol = 1.49; triacylglycerols = 0.51%) and inter-assay (phospholipids = 0.78; free cholesterol = 0.59; esterified cholesterol = 1.32; triacylglycerols = 0.58%) indicated that the method is reproducible.

Table 1 shows the physical characteristics and data of laboratorial analysis of 28 non-CAD controls, 27 CAD and 25 CAD patients under simvastatin treatment. As established in the inclusion criteria, the three groups did not differ regarding their age, BMI and HDL-cholesterol, but LDL-cholesterol was higher in the CAD group compared with the non-CAD controls. In Table 2, it is shown that the HDL particle size was equal in the three study groups. Transfer of phospholipids, free cholesterol, esterified cholesterol and triacylglycerols did not differ between CAD and non-CAD subjects. However, simvastatin treatment administered to CAD patients diminished the transfer of all four lipids.

A correlation analysis was performed between the transfer of the four lipids and the different clinical and laboratorial parameters of the three study groups. The only correlation found in this analysis was a positive correlation between free cholesterol transfer and HDL-cholesterol concentration observed in the non-CAD group. The HDL size did not correlate with any of the lipid transfers.

Discussion

Although it is well established that HDL-cholesterol levels inversely correlate with the incidence of CAD, it has been increasingly perceived that HDL-cholesterol does not necessarily reflect the qualitative and functional aspects of the lipoprotein that are important for its anti-atherogenic actions [15–17]. In this regard, subjects with apo A1 Milano mutation are protected from cardiovascular events [18, 19] despite their low HDL cholesterol levels. On the other hand, high HDL levels consequent to CETP or hepatic lipase mutations are not necessarily protective against CAD [4]. In a rather unexpected

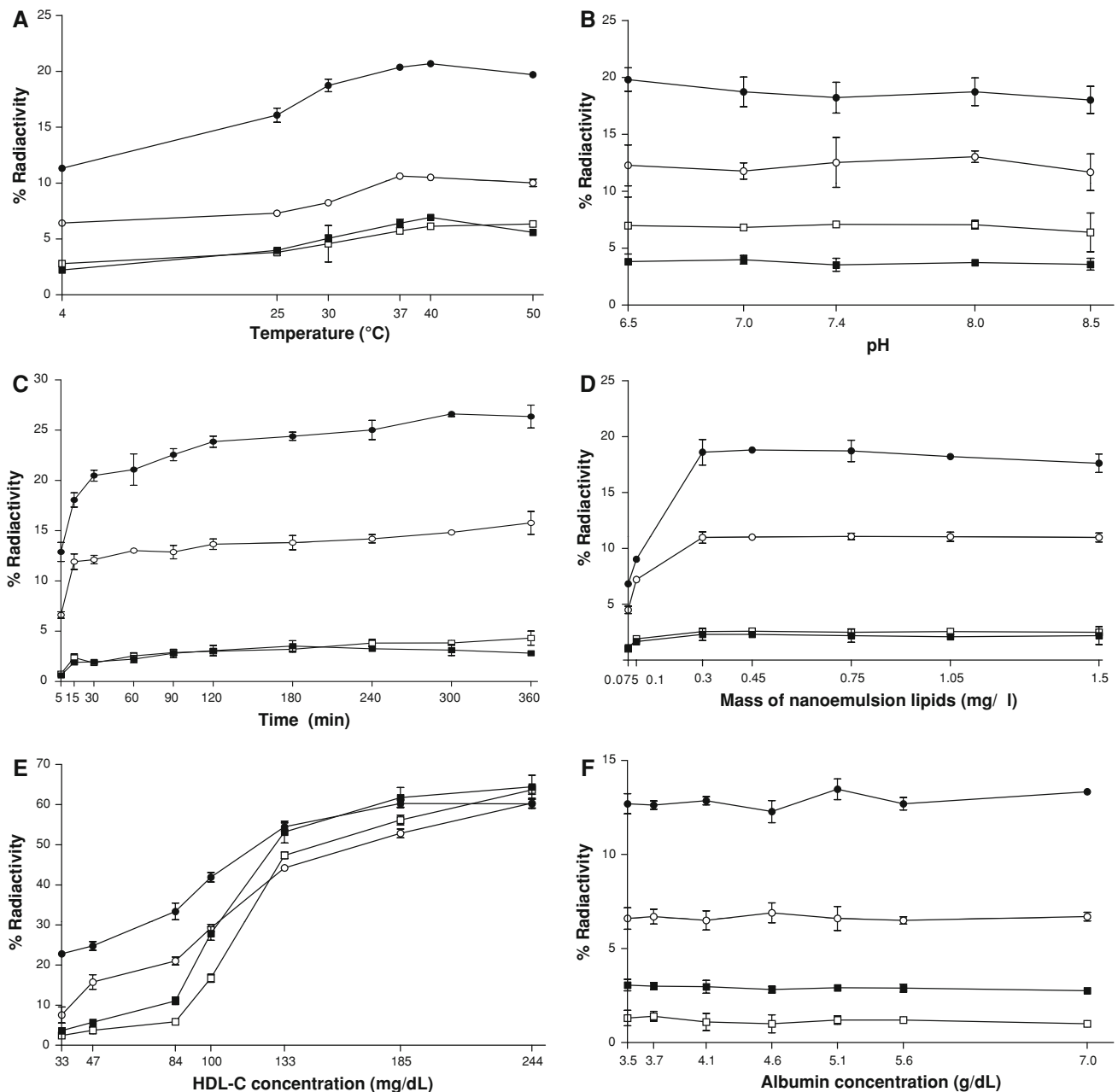


Fig. 1 **a** Effect of temperature variation on the lipids transfer from the nanoemulsion to HDL (*filled circles* phospholipids, *open circle* free cholesterol, *filled square* esterified cholesterol and *open square* triacylglycerols). Data are expressed as means \pm SD. **b** Effect of pH variation on the lipids transfer from the nanoemulsion to HDL (*filled circle* phospholipids, *open circles* free cholesterol, *filled squares* esterified cholesterol and *open squares* triacylglycerols). The experiment was performed at 37 °C. Data are expressed as means \pm SD. **c** Effect of incubation period on the lipids transfer from the nanoemulsion to HDL (*filled circles* phospholipids, *open circles* free cholesterol, *filled squares* esterified cholesterol and *open squares* triacylglycerols). The experiment was performed at 37 °C. Data are expressed as means \pm SD. **d** Effect of mass of nanoemulsion lipids

on the lipids transfer from the nanoemulsion to HDL (*filled circles* phospholipids, *open circles* free cholesterol, *filled squares* esterified cholesterol and *open squares* triacylglycerols). The experiment was performed at 37 °C. Data are expressed as means \pm SD. **e** Effect of HDL-cholesterol concentration on the lipids transfer from the nanoemulsion to HDL (*filled circles* phospholipids, *open circles* free cholesterol, *filled squares* esterified cholesterol and *open squares* triacylglycerols). The experiment was performed at 37 °C. Data are expressed as means \pm SD. **f** Effect of albumin concentration on the lipids transfer from the nanoemulsion to HDL (*filled circles* phospholipids, *open circles* free cholesterol, *filled squares* esterified cholesterol and *open squares* triacylglycerols). The experiment was performed at 37 °C. Data are expressed as means \pm SD

Table 2 HDL particle size and percentage of lipids transferred from a nanoemulsion to the HDL fraction in non-CAD control subjects and in patients with CAD without and with simvastatin treatment

Variables	Non-CAD (n = 28)	CAD (n = 27)	CAD + simvastatin (n = 25)
HDL diameter (nm)	9.1 ± 0.8	9.2 ± 0.5	9.0 ± 0.9
Lipid transfer %			
Esterified cholesterol	3.1 ± 0.6	3.2 ± 0.8	1.9 ± 0.8**†
Phospholipids	20.8 ± 1.6	21.4 ± 1.3	19.4 ± 1.6*†
Triacylglycerols	5.2 ± 1.0	5.3 ± 0.9	3.1 ± 0.7**†
Free cholesterol	5.8 ± 0.9	6.5 ± 1.2	5.0 ± 1.1†

Data are expressed as means ± SD

* $p < 0.05$ and ** $p < 0.001$ when compared to non-CAD group;

† $p < 0.001$ when compared to the CAD group

outcome, when HDL levels were increased by use of the CETP inhibitor Torcetrapib, there were excessive deaths and increases in CAD events, leading to discontinuation of the clinical trial [20].

The ability to receive lipids is a fundamental feature of HDL metabolism [4]. HDL function in cholesterol esterification is essential for the stabilization of this compound in the organism, and in reverse cholesterol transport, by which cholesterol from peripheral tissues is transported to the liver and excreted in bile [4], depends on lipid exchanges [21]. Hypertriglyceridemia is a typical condition in which lipid transfers are determinants of HDL metabolism. Accumulation in the plasma of very low-density lipoprotein (VLDL) leads to an increased transfer of cholesteryl esters from HDL to VLDL and HDL enrichment with triacylglycerols, as a result of combined mass action and CETP. This destabilizes HDL particles that tend to disappear faster from the plasma leading to decreased HDL-cholesterol [6].

By determining the composition of HDL, lipid exchanges are conceivably influential on the array of proteins that can be accommodated on the lipoprotein particle and that trigger the series of anti-inflammatory, antioxidant and anticoagulation properties of the lipoprotein. The *in vitro* assay described in this study was shown to be reproducible and precise. Among the tested factors, duration of the incubation period, temperature, and HDL concentration can affect the results and should be carefully monitored in the performance of the assay. In contrast, plasma pH, concentration of albumin and of the donor nanoemulsion were not determinants of the results.

The set-up of the assay described here permits a comparative analysis, not yet explored in the literature, of the transfer of the four main lipid constituents of the lipoproteins, as performed simultaneously, with the same lipid

donor particle and under identical experimental conditions. As expected [22, 23], lipid transfers increased as function of the incubation time and subsequently tended to reach a plateau indicative of the equilibrium state. Nonetheless, two distinct time-course behaviors clearly appeared: the transfer curve of core lipids—esterified cholesterol and triacylglycerols—were nearly identical and with much smaller perceptual transfer rates than those of surface lipids, namely phospholipids and free cholesterol. This can be ascribed to the location of surface lipid molecules that facilitates their dissociation from the donor nanoparticles and the incorporation into the surface monolayer of the recipient HDL. In addition, phospholipids are transferred not only by PLTP action but also by CETP, differently to esterified cholesterol and triacylglycerols [24], and free cholesterol may at least in part be transferred without the action of transfer proteins. In this respect, about half the phospholipids and free cholesterol had already transferred to HDL within the first 5 min of incubation, whereas the transfer of core lipids occurred pronouncedly slower. This is conceivably due to the fact that transfer of surface lipids depends on mechanisms that are different from those of the transfer of core lipids.

Variation in temperature of the incubation from 4 to 37 °C may have affected the lipid transfer by changing the fluidity of the lipoprotein structure and the rate of collisions among lipoprotein particles [3]. It is noteworthy, however, that between 37 and 50 °C increasing the temperature no longer increased the lipid transfer.

The positive correlation found in this study between the transfer of the four lipids and the HDL-cholesterol concentration in the incubation (Fig. 1e) was expected because the rate of collisions between donor and recipient particles increase with the concentration of the latter. Likewise, a positive correlation between lipid transfers and the concentration of the donor nanoemulsion in the assay would also be expected. Indeed there was an initial increase in lipid transfers, notably in the transfer of surface lipids (Fig. 1d), but a plateau was reached already at the third tested point (0.3 mg/μL nanoemulsion concentration). This indicates that the transfer assay was largely performed at saturation range of the donor nanoemulsion. By taking this finding into account, in all subsequent experiments, a saturating concentration of the nanoemulsion (1.5 mg/μL) was standardized to avoid interference of this variable on the results [25].

The fact that the variation of pH in the assay did not affect the lipid transfer to HDL was expected in view of data in the literature showing that CETP and PLTP are not affected by pH variation at a similar range [26–28]. In respect to albumin, other authors also observed that the concentration of this protein does not influence lipid transfer, regardless transfer proteins were present or not in

the assays [29–31]. In contrast, Sammet et al. [26] found that albumin could affect CETP action, depending on the amount of fatty acids associated with HDL in the mixtures and Lagrost et al. [30] found that albumin influenced the transfer of cholesteryl esters from HDL to VLDL.

Plasma samples can be stored for at least 1 year, when we last tested, without change in the lipid transfer results. Storage of plasma samples for a long period of time offers a great advantage for planning long-term clinical trials. Under the conditions when it was prepared, the donor nanoemulsion can be stored for 2 weeks only but this is not a drawback for the design of clinical trials of long duration. At any rate, the storage period of the nanoemulsion can eventually be prolonged with the use of antioxidants and stabilizers, but this procedure was not attempted in the current study.

The *in vitro* transfer of the four lipids to HDL was not different in CAD and non-CAD subjects. Many factors could have been influential in the results of this clinical study. One of the most important, HDL cholesterol levels, that is usually found to have decreased in CAD patients, was excluded by our pairing of CAD with non-CAD subjects by HDL cholesterol. LDL was increased in the CAD group; as LDL competes with HDL to receive lipids from the nanoemulsion, the higher levels of LDL-cholesterol would favor diminution of lipid transfer in the CAD group, which was ultimately not observed. CETP and PLTP action would also be major factors intervening in the process; however, it has been reported that mass and activity of CETP were not altered in CAD patients [32, 33]. Furthermore, as shown in the prospective study by Boekholdt et al. [34], CETP did not predict CAD development, unless triglyceride concentrations were increased, which is not the case of the study subjects. Data from the literature on the status of PLTP action in CAD patients are contradictory [35, 36]. Therefore, this overview on CETP and PLTP status in CAD is in agreement with the similar lipid transfer rates between CAD and non-CAD observed in our study subjects.

The diminished transfer of the four lipids to HDL by simvastatin treatment of the CAD patients may be ascribed to the diminished action and mass of CETP elicited by this hypocholesterolemic drug [37–40]. It can be hypothesized that a decrease in lipid transfer to HDL could also be observed with treatment with other statins, since atorvastatin also induces reduction in total CETP-dependent cholesterol ester transfer [41]. In contrast, the hypolipidemic resin cholestyramine did not change CETP action in hypercholesterolemic individuals [38]. In normolipidemic subjects, simvastatin administration also decreased the transfer of esterified cholesterol [37]. By increasing the clearance of LDL from the plasma and eliciting secondary changes in HDL metabolism, statins may change the

composition of those lipoprotein classes that could affect the lipid exchange that were reflected here by the decrease in lipid transfer to HDL.

Although not tested in this study, the concentration of free fatty acids has been documented as modifying CETP action [26] and may eventually change the transfer of lipids to HDL. This and other factors that influence the action of CETP or PLTP should be considered to interpret future results of studies using the currently described assay in disease states.

In conclusion, this practical *in vitro* assay designed to evaluate the lipid transfer to HDL described and validated here can be a useful tool for exploring the HDL metabolism in large populations and in several clinical conditions. The issue of how these transfer rates relate with the several HDL specific functions and HDL subclasses should be addressed in future studies.

Acknowledgments This study was supported by the Fundação do Amparo à Pesquisa do Estado de São Paulo (FAPESP), São Paulo, Brazil (Grant 0408048-3). Dr. Maranhão has a Research Award from the Conselho Nacional de Desenvolvimento Científico e Tecnológico (CNPq), Brasília, Brazil. The authors are grateful to Débora Deus for help with the experiments and to Dr. Fatima R. Freitas for her help in revising the manuscript.

References

1. Tall AR (1993) Plasma cholesteryl ester transfer protein. *J Lipid Res* 34:1255–1274
2. Tollefson JH, Ravnik S, Albers JJ (1988) Isolation and characterization of a phospholipid transfer protein (LTP-II) from human plasma. *J Lipid Res* 29:1593–1602
3. Ferretti G, Bacchetti T, Nègre-Salvayre A, Salvayre R, Dousset N, Curatola G (2006) Structural modifications of HDL and functional consequences. *Atherosclerosis* 184:1–7
4. Norata GD, Pirillo A, Catapano AL (2006) Modified HDL: biological and physiopathological consequences. *Nutr Metab Cardiovasc Dis* 16:371–386
5. Lamarche B, Rashid S, Lewis GF (1999) HDL metabolism in hypertriglyceridemic states: an overview. *Clin Chim Acta* 286:145–149
6. Rashid S, Watanabe T, Sakaue T, Lewis GF (2003) Mechanisms of HDL lowering in insulin resistant, hypertriglyceridemic states: the combined effect of HDL triglyceride enrichment and elevated hepatic lipase activity. *Clin Biochem* 36:421–429
7. Assmann G, Gotto AM Jr (2004) HDL cholesterol and protective factors in atherosclerosis. *Circulation* 109(23 Suppl 1):III8–14
8. Kontush A, Chapman MJ (2006) Antiatherogenic small, dense HDL—guardian angel of the arterial wall? *Nat Clin Pract Cardiovasc Med* 3:144–153
9. Friedewald WT, Levy RI, Fredrickson DS (1972) Estimation of the concentration of low-density lipoprotein cholesterol in plasma, without the use of the preparative ultracentrifuge. *Clin Chem* 18:499–502
10. Lima E, Maranhão RC (2004) Rapid, simple laser-light scattering method for HDL particle size in whole plasma. *Clin Chem* 50:1086–1091
11. Ginsburg GS, Small DM, Atkinson D (1982) Microemulsions of phospholipids and cholesterol ethers protein-free models of low-density lipoprotein. *J Biol Chem* 257:8216–8221

12. Maranhão RC, Cesar TB, Pedrosa-Mariani SR (1993) Metabolic behavior in rats of a nonprotein microemulsion resembling LDL. *Lipids* 28:691–696
13. Ohkawa H, Ohishi N, Yagi K (1979) Assay for lipid peroxides in animal tissues by thiobarbituric acid reaction. *Anal Biochem* 95:351–358
14. Guidance for Industry (2001) Bioanalytical method validation. US Department of Health and Human Services, Food and Drug Administration, Center for Drug Evaluation and Research (CDER) and Center for Veterinary Medicine (CVM)
15. Cutri BA, Hime NJ, Nicholls SJ (2006) High-density lipoproteins: an emerging target in the prevention of cardiovascular disease. *Cell Res* 16:799–804
16. Barter PJ, Rye KA (2006) Relationship between the concentration and antiatherogenic activity of high-density lipoproteins. *Curr Opin Lipid* 17:399–403
17. Lewis GF (2006) Determinants of plasma HDL concentrations and reverse cholesterol transport. *Curr Opin Cardiol* 21:345–352
18. Futterman LG, Lemberg L (2005) Apo a-I Milano. *Am J Crit Care* 14:244–247
19. Dullens SP, Plat J, Mensink RP (2007) Increasing apoA-I production as a target for CHD risk reduction. *Nutr Metab Cardiovasc Dis* 17:616–628
20. Tall AR, Yvan-Charvet L, Wang N (2007) The failure of torcetrapib: was it the molecule or the mechanism? *Arterioscler Thromb Vasc Biol* 27:257–260
21. Cheung MC, Wolfbauer G, Brown BG, Albers JJ (1999) Relationship between plasma phospholipid transfer protein activity and HDL subclasses among patients with low HDL and cardiovascular disease. *Atherosclerosis* 142:201–205
22. Tall AR, Forester LR, Bongiovanni GL (1983) Facilitation of phosphatidylcholine transfer into high density lipoproteins by an apolipoprotein in the density 1.20–1.26 g/mL fraction of plasma. *J Lipid Res* 24:277–289
23. Lassel TS, Guerin M, Auboiron S, Guy-Grand B, Chapman MJ (1999) Evidence for a cholesteryl ester donor activity of LDL particles during alimentary lipemia in normolipidemic subjects. *Atherosclerosis* 147:41–48
24. Clark RW, Ruggeri RB, Cunningham D, Bamberger MJ (2006) Description of the torcetrapib series of cholesteryl ester transfer protein inhibitors, including mechanism of action. *J Lipid Res* 47:537–552
25. Terpstra AH, Nicolosi RJ, Herbert PN (1989) In vitro incorporation of radiolabeled cholesteryl esters into high and low density lipoproteins. *J Lipid Res* 30:1663–1671
26. Sammett D, Tall AR (1985) Mechanisms of enhancement of cholesteryl ester transfer protein activity by lipolysis. *J Biol Chem* 260:6687–6697
27. Desrumaux C, Athias A, Masson D, Gambert P, Lallemand C, Lagrost L (1998) Influence of the electrostatic charge of lipoprotein particles on the activity of the human plasma phospholipid transfer protein. *J Lipid Res* 39:131–142
28. Soares TA, Ferreira R (2004) Aplicação da equação de Poisson-Boltzmann ao cálculo de propriedades dependentes do pH em proteínas. *Quim Nova* 27:640–647
29. Sparks DL, Pritchard PH (1989) Transfer of cholesteryl ester into high density lipoprotein by cholesteryl ester transfer protein: effect of HDL lipid and apoprotein content. *J Lipid Res* 30:1491–1498
30. Lagrost L, Florentin E, Guyard-Dangremont V, Athias A, Gandjini H, Lallemand C, Gambert P (1995) Evidence for non-esterified fatty acids as modulators of neutral lipid transfers in normolipidemic human plasma. *Arterioscler Thromb Vasc Biol* 15:1388–1396
31. Estronca LM, Moreno MJ, Laranjinha JA, Almeida LM, Vaz WL (2005) Kinetics and thermodynamics of lipid amphiphile exchange between lipoproteins and albumin in serum. *Biophys J* 88:557–565
32. Blankenberg S, Rupprecht HJ, Bickel C, Jiang XC, Poirier O, Lackner KJ, Meyer J, Cambien F, Tiret L (2003) Common genetic variation of the cholesteryl ester transfer protein gene strongly predicts future cardiovascular death in patients with coronary artery disease. *J Am Coll Cardiol* 41:1983–1989
33. Goto A, Sasai K, Suzuki S, Fukutomi T, Ito S, Matsushita T, Okamoto M, Suzuki T, Itoh M, Okumura-Noji K, Yokoyama S (2001) Cholesteryl ester transfer protein and atherosclerosis in Japanese subjects: a study based on coronary angiography. *Atherosclerosis* 159:153–163
34. Boekholdt SM, Kuivenhoven JA, Wareham NJ, Peters RJG, Jukema JW, Luben R, Bingham SA, Day NE, Kastelein JJ, Khaw KT (2004) Plasma levels of cholesteryl ester transfer protein and the risk of future coronary artery disease in apparently healthy men and women. *Circulation* 110:1418–1423
35. Schlitt A, Bickel C, Thumma P, Blankenberg S, Rupprecht HJ, Meyer J, Jiang XC (2003) High plasma phospholipid transfer protein levels as a risk factor for coronary artery disease. *Arterioscler Thromb Vasc Biol* 23:1857–1862
36. Schgoer W, Mueller T, Jauhiainen M, Wehinger A, Gander R, Tancevski I, Salzmann K, Eller P, Ritsch A, Haltmayer M, Ehnholm C, Patsch JR, Foeger B (2008) Low phospholipid transfer protein (PLTP) is a risk factor for peripheral atherosclerosis. *Atherosclerosis* 196:219–226
37. Ahnadi CE, Berthezène F, Ponsin G (1993) Simvastatin-induced decrease in the transfer of cholesterol esters from high density lipoproteins to very low and low density lipoproteins in normolipidemic subjects. *Atherosclerosis* 99:219–228
38. McPherson R (1999) Comparative effects of simvastatin and cholestyramine on plasma lipoproteins and CETP in humans. *Can J Clin Pharmacol* 6:85–90
39. de Vries R, Kerstens MN, Sluiter WJ, Groen AK, van Tol A, Dullaart RP (2005) Cellular cholesterol efflux to plasma from moderately hypercholesterolaemic type 1 diabetic patients is enhanced, and is unaffected by simvastatin treatment. *Diabetologia* 48:1105–1113
40. Sviridov D, Nestel P, Watts G (2007) Statins and metabolism of high density lipoprotein. *Cardiovasc Hematol Agents Med Chem* 5:215–221
41. Guerin M, Lassel TS, Le Goff W, Farnier M, Chapman MJ (2000) Action of atorvastatin in combined hyperlipidemia: preferential reduction of cholesteryl ester transfer from HDL to VLDL 1 particles. *Arterioscler Thromb Vasc Biol* 20(1):189–197

Suppression in Mevalonate Synthesis Mediates Antitumor Effects of Combined Statin and γ -Tocotrienol Treatment

Vikram B. Wali · Sunitha V. Bachawal ·
Paul W. Sylvester

Received: 21 July 2009 / Accepted: 3 September 2009 / Published online: 24 September 2009
© AOCs 2009

Abstract Statins directly inhibit 3-hydroxy-3-methylglutaryl-coenzyme A reductase (HMGR) activity, while γ -tocotrienol, an isoform of vitamin E, enhances the degradation and reduces cellular levels of HMGR in various tumor cell lines. Since treatment with statins or γ -tocotrienol alone induced a dose-responsive inhibition, whereas combined treatment with subeffective doses of these agents resulted in a synergistic inhibition in +SA mammary tumor cell growth, studies were conducted to investigate the role of the HMGR pathway in mediating the antiproliferative effects of combined low dose statin and γ -tocotrienol. Treatment with 8 μ M simvastatin inhibited cell growth and isoprenylation of Rap1A and Rab6, and supplementation with 2 μ M mevalonate reversed these effects. However, the growth inhibitory effects of 4 μ M γ -tocotrienol were not dependent upon suppression in mevalonate synthesis. Treatment with subeffective doses of simvastatin (0.25 μ M), lovastatin (0.25 μ M), mevastatin (0.25 μ M), pravastatin (10 μ M), or γ -tocotrienol (2 μ M) alone had no effect on protein prenylation or mitogenic signaling, whereas combined treatment with these agents resulted in a significant inhibition in +SA cell growth, and a corresponding decrease in total HMGR, Rap1A and Rab6 prenylation, and MAPK signaling, and mevalonate supplementation reversed these effects. These findings demonstrate that the synergistic antiproliferative effects of combined low dose statin and γ -tocotrienol treatment are directly related to an inhibition in HMGR activity and subsequent suppression in mevalonate synthesis.

Keywords Statins · γ -Tocotrienol · Breast cancer · Vitamin E · HMGR · Rab6 · Rap1A · Mevalonate · MAPK · p38

Abbreviations

HMGR	3-Hydroxy-3-methylglutaryl-coenzyme A reductase
MAPK	Mitogen-activated protein kinase
FPP	Farnesyl pyrophosphate
GGPP	Geranylgeranyl pyrophosphate
ERK	Extracellular signal-regulated kinase
BSA	Bovine serum albumin
DMEM	Dulbecco's modified Eagle's medium
PBS	Phosphate buffered saline
MTT	3-(4,5-Dimethylthiazol-2yl)-2,5-diphenyl tetrazolium bromide
SDS	Sodium dodecyl sulfate
PVDF	Polyvinylidene fluoride
TBST	10 mM Tris-HCl containing 50 mM NaCl and 0.1% Tween 20, pH 7.4
TBS	0.05 M Tris-buffered saline (TBS) pH 7.6
PI3K	Phosphatidylinositol 3-kinase

Introduction

3-Hydroxy-3-methylglutaryl-coenzyme A reductase (HMGR) is the rate limiting enzyme in the mevalonate biosynthetic pathway and is involved in the synthesis of sterol and non-sterol intermediates essential for cell survival and growth [1]. Specifically, HMGR catalyzes the conversion of 3-hydroxy-3-methylglutaryl-coenzyme A to mevalonate, which subsequently produces isoprenoid intermediates

V. B. Wali · S. V. Bachawal · P. W. Sylvester (✉)
College of Pharmacy, University of Louisiana at Monroe,
700 University Avenue, Monroe, LA 71209-470, USA
e-mail: sylvester@ulm.edu

such as farnesyl pyrophosphate (FPP) and geranylgeranyl pyrophosphate (GGPP) that are required for posttranslational modification (isoprenylation) of various small GTP-binding proteins including Ras, Rap, Rab, Rho, nuclear lamins, and heterotrimeric G-protein γ -subunit [1–3]. Isoprenylation is needed for anchoring these signaling proteins to the cell membrane in close proximity to growth factor receptors so that these signaling proteins can be activated following receptor activation, and subsequently participate in turning on downstream mitogenic signaling pathways such as MAPK and Akt [2–4].

HMGR activity is characteristically elevated and/or unregulated in many forms of cancer and thereby acts to promote cancer cell survival and proliferation by providing an abundance of non-sterol intermediates [5]. As a result, a great deal of attention has been focused on the development of agents that target and inhibit HMGR activity for use in cancer chemotherapy. Statins represent a class of such agents that act as competitive inhibitors of HMGR and display potent anticancer activity in a variety of cell culture and animal tumor models [6, 7]. However, clinical use of statins in the treatment of cancer has been greatly limited by their high-dose toxicity that includes severe myotoxicity, liver toxicity, gastrointestinal dysfunction, and even death [8, 9].

γ -Tocotrienol, a naturally occurring isoform within the vitamin E family of compounds, displays potent anticancer activity [10] and has been shown to reduce HMGR activity through the post-transcriptional down-regulation of this enzyme [11]. The vitamin E family of compounds is divided into two subgroups called tocopherols and tocotrienols. Tocopherols are commonly found in high concentrations in a wide variety of foods, whereas tocotrienols are relatively rare and found in appreciable levels only in a few specific vegetable fats, such as palm oil [10]. Although chemically very similar, tocopherols have a saturated, whereas tocotrienols have an unsaturated phytyl chain attached to a chroman ring structure. It is now clearly established that tocotrienols, but not tocopherols, display potent antiproliferative and apoptotic activity against mammary tumor cells at treatment doses that have little or no effect on normal cell growth and viability [10].

Previous studies demonstrated that combined treatment of subeffective doses of statins with subeffective doses of γ -tocotrienol, synergistically inhibited the growth of highly malignant +SA mammary epithelial cells in culture, and these effects were associated with a suppression in MAPK and Akt mitogenic signaling [12]. Other studies showed that similar combination therapy induced G1 cell cycle arrest in +SA mammary tumor cells and these effects were associated with an increase in p27 expression, decreased cyclin D1 expression, and hypophosphorylation of Rb [13]. However, the specific intracellular target responsible for

mediating the antiproliferative effects of combined statins and γ -tocotrienol treatment remains unclear. Since statins and γ -tocotrienol have both been shown to suppress HMGR activity, it was hypothesized that inhibition of mevalonate synthesis may be ultimately responsible for mediating the growth inhibiting effects of combined therapy with these agents. Therefore, studies were conducted to characterize the growth inhibitory effects of combined low dose statins and γ -tocotrienol treatment on mevalonate synthesis, isoprenylation of small G-proteins Rap1A and Rab6, and mitogenic signaling in +SA mammary tumor cells.

Experimental Procedures

Chemicals and Antibodies

All materials were purchased from Sigma Chemical Company (St. Louis, MO, USA), unless otherwise stated. Isolated γ -tocotrienol (>98% purity) was generously provided as a gift by First Tech International Ltd. (Hong Kong). Antibodies for cyclin D1, phospho-p44/42 ERK, phospho-p38, total p44/42 ERK, and total p38 were purchased from Cell Signaling Technology (Beverly, MA, USA). Antibodies for Ki-67 antigen, unprenylated Rap 1A and isoprenylated Rab 6 were purchased from Santa Cruz Biotechnology (Santa Cruz, CA, USA). Antibodies for HMGR and Ras were obtained from Upstate Biotechnology (Lake Placid, NY, USA) and BD Biosciences (San Jose, CA, USA), respectively. Anti- α -tubulin antibody was obtained from EMD Biosciences (La Jolla, CA, USA). Horseradish peroxidase-labeled goat anti-rabbit and anti-mouse secondary antibodies were purchased from PerkinElmer Biosciences (Boston, MA, USA) and donkey anti-goat secondary antibody was purchased from Santa Cruz Biotechnology (Santa Cruz, CA, USA). Alexa Fluor 594 donkey anti-goat secondary antibody was obtained from Molecular Probes (Eugene, Oregon, USA).

Cell Line and Culture Conditions

Experiments conducted in the present study represent a logical continuation of previous studies that have extensively characterized the antiproliferative and apoptotic effects of γ -tocotrienol in the highly malignant +SA mammary epithelial cell line [10]. The +SA mammary tumor cell line was derived from an adenocarcinoma that developed spontaneously in a BALB/c female mouse [14, 15]. +SA cells display anchorage-independent growth when cultured in soft agarose gels, and when injected back into the mammary gland fat pad of syngeneic female mice, +SA cells form anaplastic adenocarcinomas that

metastasize to the lung [15]. Cell culture conditions have been previously described in detail [12, 16, 17]. Briefly, +SA cells were maintained in serum-free defined medium consisting of Dulbecco's modified Eagle's medium (DMEM)/F12 containing 5 mg/mL bovine serum albumin (BSA), 10 $\mu\text{g}/\text{mL}$ transferrin, 100 U/mL soybean trypsin inhibitor, 100 U/mL penicillin, 0.1 mg/mL streptomycin, 10 $\mu\text{g}/\text{mL}$ insulin, and 10 ng/mL epidermal growth factor. For subculturing, cells were rinsed twice with sterile Ca^{2+} and Mg^{2+} -free phosphate buffered saline (PBS) and incubated in 0.05% trypsin containing 0.025% EDTA in PBS for 5 min at 37°C. The released cells were centrifuged, resuspended in serum-free media and counted using hemocytometer.

Experimental Treatments

To dissolve highly lipophilic γ -tocotrienol in aqueous culture media, a stock solution of γ -tocotrienol was first prepared by binding it to bovine serum albumin (BSA) as described previously [12, 13, 16, 17]. Simvastatin, lovastatin or mevastatin exist in their inactive lactone forms that do not inhibit HMGR, but are active as their corresponding open-ring hydroxy-derivatives [18, 19]. Hence,

these statins were activated prior to addition to treatment media as described previously [12, 13]. Briefly, statins were dissolved in a 70% ethanol solution containing 0.1 N NaOH and then incubated at 50°C for 1 h. The alkaline statin solution was then neutralized by the addition of 70% ethanol solution containing 0.1 N HCl to form a stock solution that was then used to prepare treatment media. Pravastatin has an active open ring structure and was therefore, directly dissolved in 70% ethanol to form a stock solution. All media was adjusted so that the final ethanol concentration was same in all the groups within a given experiment and never exceeded 0.05%, and all cells were fed fresh control or treatment media every day.

Growth Studies and Viable Cell Number

In growth studies (Figs. 1, 4), +SA cells were initially seeded at a density of 5×10^4 cells/well (6 wells/group) in 24-well culture plates in serum-free defined control media and allowed to attach overnight. Cells were then, exposed to respective experimental treatments containing simvastatin, lovastatin, mevastatin, pravastatin, γ -tocotrienol, mevalonate alone or in various combinations for 4 days. During this period, cells were fed fresh treatment or control

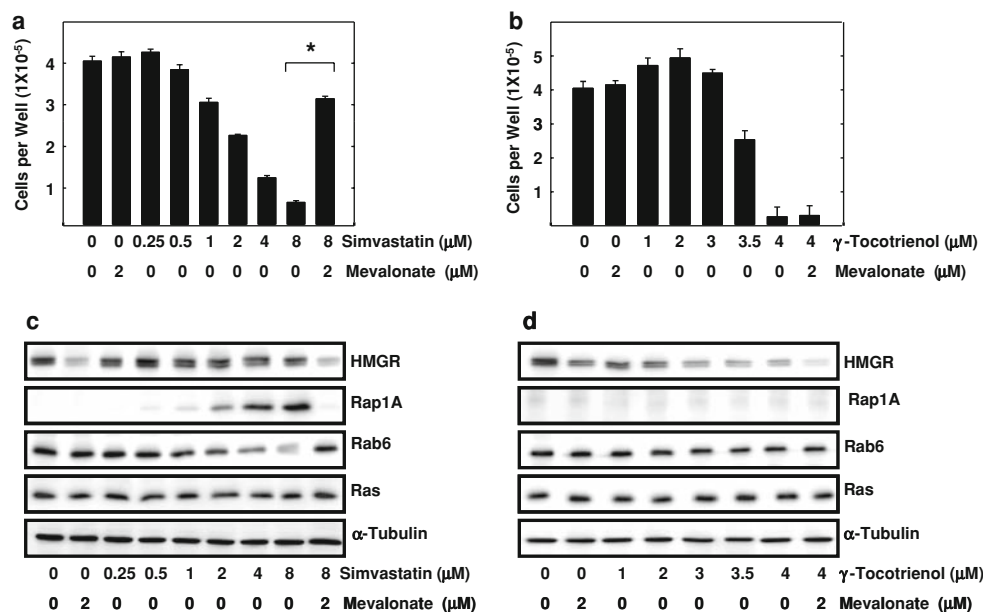


Fig. 1 Effects of simvastatin and γ -tocotrienol treatment on +SA cell growth, HMGR and Ras levels, and Rap1A and Rab6 isoprenylation. Cells were plated at a density of 5×10^4 cells/well (6 wells/group) in 24-well culture plates and exposed to 0–8 μM simvastatin treatment alone or the combined treatment of 8 μM simvastatin with 2 μM mevalonate (a), 0–4 μM γ -tocotrienol treatment alone or the combined treatment of 4 μM γ -tocotrienol with 2 μM mevalonate (b) for 4 days in culture. Afterwards, viable cell count was determined using MTT assay. Vertical bars indicate the mean cell count \pm SEM in each treatment group. * $P < 0.05$ as compared with

8 μM simvastatin-treated group. For Western blot studies (c, d), cells were plated at a density of 1×10^6 cells/100-mm culture dishes and treated with the above doses of simvastatin and mevalonate (c), or γ -tocotrienol and mevalonate (d) for a 4-day culture period. Afterwards, whole cell lysates were prepared for subsequent separation by polyacrylamide gel electrophoresis, followed by Western blot analysis to measure total HMGR, Rap1A (unprenylated), Rab6 (isoprenylated), total Ras and α -tubulin levels. α -Tubulin was visualized to ensure equal sample loading in each lane

media every day. At the end of the treatment exposure period, the viable cell number was determined by using the 3-(4,5-dimethylthiazol-2-yl)-2,5-diphenyl tetrazolium bromide (MTT) colorimetric assay as described previously [16, 17]. Briefly, cells in 24-well plates were incubated at 37°C with fresh defined control media containing 0.42 mg/mL MTT. After a 4-h incubation period, the media was removed and MTT crystals were dissolved in isopropanol (1 mL/well), and the optical density of each sample was measured at 570 nm on a microplate reader (SpectraCount, Packard BioScience Company). The number of cells/well was calculated against a standard curve prepared by plating various concentrations of cells, as determined by hemocytometry, at the beginning of each experiment.

Western Blot Analysis

For Western blot analysis, +SA cells were plated at a density of 1×10^6 cells/100-mm culture dish and grown in serum-free defined control or treatment media. After a 4-day treatment period, cells were isolated with trypsin, washed with PBS, and the whole cell lysates were then prepared as previously described [13, 16, 20]. Protein concentration in each sample was determined using the Bio-Rad protein assay kit (Bio-Rad, Hercules, CA, USA). Equal amounts (25 µg/lane) of each sample were subjected to electrophoresis through 7.5 to 15% SDS–polyacrylamide minigels. Minigels within a given experiment were run simultaneously using a AccuPower model 500 power supply unit (VWR, Suwanee, GA). Proteins separated on minigels were transblotted at 30 V for 12–16 h at 4°C onto a polyvinylidene fluoride (PVDF) membrane (PerkinElmer Lifesciences, Wellesley, MA, USA) in a Trans-Blot Cell (Bio-Rad Laboratories, Hercules, CA, USA) according to the methods of Towbin and these PVDF membranes were used for subsequent Western blot analyses as previously described [13, 16, 20, 21]. Briefly, membranes were then blocked with 2% BSA in 10 mM Tris–HCl containing 50 mM NaCl and 0.1% Tween 20, pH 7.4 (TBST) and then, incubated with specific primary antibodies against HMGR, Rap1A, Rab6, Ras, phospho-p44/42 ERK, phospho-p38, total p44/42 ERK, total p38, cyclin D1, and α -tubulin, diluted 1:2,000–1:10,000 in TBST/2% BSA for 2 h. Membranes were washed five times with TBST and then incubated with respective horseradish peroxidase-conjugated secondary antibodies diluted 1:5,000 in TBST/2% BSA for 1 h followed by rinsing with TBST. Chemiluminescence (Pierce, Rockford, IL, USA) was used to visualize the antibody bound proteins. Images of protein bands from all treatment groups within an experiment were acquired using Kodak Gel Logic 1500 Imaging System (Carestream Health Inc, New Haven, CT, USA). The visualization of α -tubulin was used to ensure equal sample

loading in each lane. All experiments were repeated at least three times and a representative Western Blot image from each experiment is shown in Figs. 1, 3 and 5.

Ki-67 Immunofluorescence

+SA cells were initially plated at a density of 2×10^5 cells/chamber in single chamber slides (Nalge Nunc International, Rochester, NY, USA) and allowed to attach overnight. Afterwards, cells were divided into different groups that fed their respective treatment media. After 4 days of treatment exposure, cells were rinsed with 0.05 M Tris-buffered saline (TBS) pH 7.6, and fixed with methanol previously cooled to -20°C . Fixed cells were blocked with 2% donkey serum in TBS for 1 h, followed by overnight incubation with Ki-67 primary antibody at 4°C. Cells were washed five times with TBS followed by 45 min incubation with fluorescent labeled anti-goat secondary antibody at room temperature in dark. After washing the cells five times with TBS, cells were embedded with Vectashield Mounting Medium (Vector Laboratories Inc., Burlingame, CA, USA) containing DAPI as the counterstain, followed by imaging by confocal microscopy (LSM Pascal confocal microscope, Carl Zeiss Microimaging Inc., Thornwood, NY, USA). Quantification of Ki-67 labeling was achieved by counting the number of +SA cells displaying positive staining versus the total number of cells within five randomly selected 80,000- μm^2 areas of each slide in each treatment group using LSM software ZEN 2007 (Carl Zeiss Microimaging Inc., Thornwood, NY).

Statistical Analysis

Differences among the various treatment groups in +SA cell growth studies were determined by analysis of variance (ANOVA) followed by Dunnett's *t* test. A difference of $P < 0.05$ was considered to be statistically significant as compared with vehicle-treated controls or as defined in the figure legends.

Results

Effects of Simvastatin and γ -Tocotrienol on +SA Cell Proliferation, HMGR Levels and Protein Prenylation

Treatment with 0–0.5 μM simvastatin or 2 μM mevalonate had no effect, whereas treatment with 1–8 μM simvastatin significantly inhibited +SA mammary tumor cell growth in a dose-dependent manner as compared with vehicle-treated controls (Fig. 1a). Simvastatin-induced growth inhibition was reversed in cells given 2 μM mevalonate

supplementation (Fig. 1a). Treatment with 1–8 μM simvastatin had little or no effect on the relative levels of HMGR, while treatment with 2 μM mevalonate decreased HMGR levels as compared with vehicle-treated controls (Fig. 1c). The anti-HMGR antibody used in these Western blots specifically detects two adjacent protein bands in +SA cell lysates and this doublet possibly indicates two isozymes of HMGR that have been reported previously [22]. Treatment with 1–8 μM simvastatin was also found to reduce the level of protein prenylation as evidenced by a marked increase in unprenylated Rap1A and a marked decrease in isoprenylated Rab6 as compared with their respective vehicle-treated controls (Fig. 1b). Simvastatin-induced inhibition of Rap1A and Rab6 prenylation was blocked by 2 μM mevalonate supplementation (Fig. 1c). Total Ras levels were similar in all treatments groups (Fig. 1c).

Treatment with 0–3 μM of γ -tocotrienol had no effect, whereas treatment with 3.5–4 μM γ -tocotrienol treatment significantly inhibited +SA cell growth in a dose-responsive manner (Fig. 1b). However, simultaneous administration of 4 μM γ -tocotrienol and 2 μM mevalonate did not reverse the growth inhibitory effects of γ -tocotrienol treatment (Fig. 1b). Treatment with 1–4 μM γ -tocotrienol or 2 μM mevalonate alone decreased HMGR levels, and combined treatment of these agents further decreased HMGR levels as compared with vehicle-treated controls (Fig. 1d). Treatment with 4 μM γ -tocotrienol or 2 μM mevalonate alone or in combination had no effect on Rap1A and Rab6 prenylation or total Ras levels as compared to vehicle-treated controls (Fig. 1d).

Combined Treatment Effects of Individual Statins and γ -Tocotrienol on +SA Cell Proliferation

It has been established that combined treatment with low dose statins and γ -tocotrienol results in a synergistic inhibition in +SA mammary tumor cell growth [12, 13]. Figure 2a shows the effects of statins and γ -tocotrienol alone or in combination on the ratio of +SA cells demonstrating positive Ki-67 immunofluorescent staining versus the total number of cells within each treatment group. The Ki-67 protein is specifically expressed and localized in the nucleus of proliferating cells and can be used as a marker for cell proliferation. More than 88% of cells displayed positive Ki-67 staining (pink) in the vehicle-treated control group (C) and groups treated with subeffective doses of simvastatin (S; 0.25 μM), lovastatin (L; 0.25 μM), mevastatin (M; 0.25 μM), pravastatin (P; 10 μM) or γ -tocotrienol (T; 2 μM) alone (Fig. 2a). However, combined treatment with subeffective doses of individual statins with a subeffective dose of γ -tocotrienol displayed <26% positive Ki-67 staining (Fig. 2a). Fluorescent

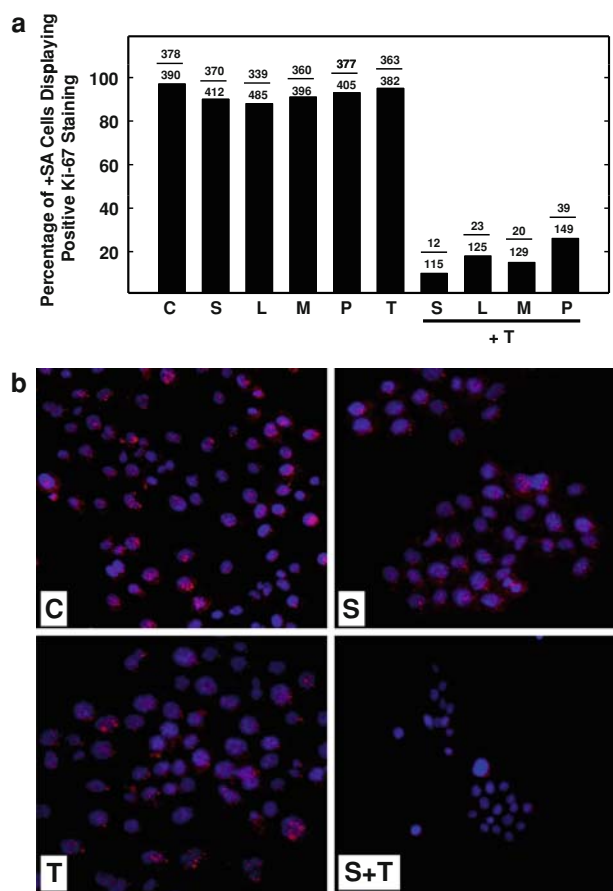


Fig. 2 Effects of low dose statin and γ -tocotrienol treatment on Ki-67 expression in +SA mammary tumor cells. +SA cells were initially plated at a density of 2×10^5 cells/chamber in single-well chamber slides and exposed to media containing vehicle (C), 0.25 μM simvastatin (S), 0.25 μM lovastatin (L), 0.25 μM mevastatin (M), 10 μM pravastatin (P), 2 μM γ -tocotrienol (T) or the combination of individual statins (S, L, M, or P) with 2 μM γ -tocotrienol (T) for a 4-day culture period. Afterwards, cells were fixed with methanol and stained with fluorescent Ki-67 antibody and counterstained with DAPI, and images were visualized by confocal microscopy. **a** Vertical bar graph shows percent of malignant +SA mammary epithelial cells displaying positive Ki-67 fluorescent staining in each treatment group. Numbers presented over each vertical bar represent the number of cells displaying positive Ki-67 staining over the total number of cells counted in each treatment group. Cells were counted in five squares of area equivalent to 80,000 μm^2 . **b** Confocal fluorescent images of positive Ki-67 staining in +SA mammary tumor cells. The pink color indicates positive Ki-67 staining in individual nuclei of +SA cells. Magnification of each image is $200\times$

confocal images of +SA cells in the vehicle-treated control (C), 0.25 μM simvastatin (S), 2 μM γ -tocotrienol (T), and combined 0.25 μM simvastatin and 2 μM γ -tocotrienol (S + T) treatment groups are shown in Fig. 2b. The majority of +SA cells in control (C), simvastatin alone (S) or γ -tocotrienol alone (T) treated groups showed abundant positive (pink) Ki-67 staining in their nuclei. In contrast, Ki-67 positive staining was greatly reduced in the +SA cell nuclei treated with the combination of simvastatin and

γ -tocotrienol (S + T; Fig. 2b). Similar results were obtained when +SA cells were exposed to 0.25 μ M lovastatin, 0.25 μ M mevastatin, or 10 μ M pravastatin alone or in combination with 2 μ M γ -tocotrienol (images not shown).

Effects of Combined Statin and γ -Tocotrienol Treatment on HMGR Levels, Protein Prenylation and Mitogenic Signaling

Figure 3 shows that treatment with 0.25 μ M simvastatin (S), 0.25 μ M lovastatin (L), 0.25 μ M mevastatin (M) or 10 μ M pravastatin (P) alone did not alter the relative levels of HMGR. However, treatment with 2 μ M tocotrienol (T) alone or in combination with the various statins caused a relatively large decrease in HMGR levels as compared to vehicle-treated controls (Fig. 3). Similar treatment with

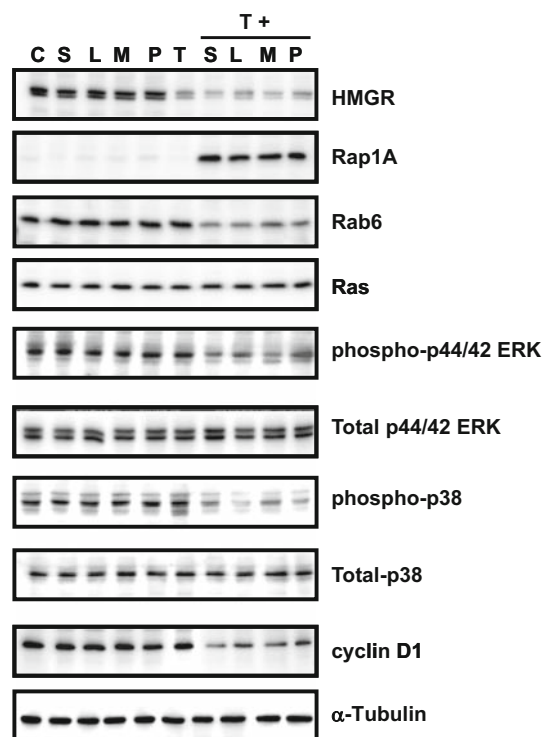


Fig. 3 Effects of statin and γ -tocotrienol treatment on the intracellular levels of HMGR, isoprenylated small G-proteins, MAPKs and cyclin D1 in +SA mammary tumor cells after a 4-day culture period. +SA cells were plated at a density of 1×10^6 cells/100 mm culture dishes and exposed to control (C) simvastatin (S), 0.25 μ M lovastatin (L), 0.25 μ M mevastatin (M), 10 μ M pravastatin (P), or 2 μ M γ -tocotrienol (T) alone, or the combination of individual statins (S, L, M or P) with 2 μ M γ -tocotrienol (T). Afterwards, cells in all treatment groups were isolated and whole cell lysates were prepared and electrophoresed through polyacrylamide minigels, transblotted to PVDF membrane, followed by Western blot analysis to measure relative levels of total HMGR, Rap1A (unprenylated), Rab6 (isoprenylated), total Ras, phospho-p44/42 ERK, phospho-p38 levels, total p44/42 ERK, total p38, cyclin D1 and α -tubulin levels. α -Tubulin was visualized to ensure equal sample loading in each lane

simvastatin, lovastatin, mevastatin, pravastatin, or γ -tocotrienol alone had no effect on the relative levels of unprenylated Rap1A, but combined treatment of γ -tocotrienol with individual statins dramatically increased unprenylated Rap1A levels as compared with vehicle-treated controls (Fig. 3). Likewise, the relative intracellular levels of isoprenylated Rab6, total Ras, phospho-p44/42 ERK, total ERK, phospho-p38, total p38 and cyclin D1 were unaffected by treatment with individual statins or γ -tocotrienol alone, whereas combined treatment of γ -tocotrienol with individual statins resulted in a reduction in the levels of isoprenylated Rab6, phospho-p44/42 ERK, phospho-p38 and cyclin D1, as compared with vehicle-treated controls (Fig. 3). These same combination treatments did not alter the relative levels of total Ras, total ERK, and total p38 (Fig. 3). The antibodies used to detect total and phosphorylated p44/42 ERK detect two bands at 44 and 42 kDa corresponding to the two protein kinases ERK1 and ERK2, respectively.

Effects of Mevalonate Supplementation on +SA Cell Growth

Treatment with 0.25 μ M simvastatin (S), 0.25 μ M lovastatin (L), 0.25 μ M mevastatin (M), 10 μ M pravastatin (P), 2 μ M γ -tocotrienol (T), 1 μ M (m1) mevalonate, or 2 μ M (m2) mevalonate alone had no effect on +SA mammary tumor cell growth as compared with vehicle-treated controls (C) following a 4-day culture period (Fig. 4). Combined treatment with similar doses of individual statins with γ -tocotrienol markedly suppressed growth of +SA cells. However, these growth inhibitory effects of combined statin and γ -tocotrienol treatment were partially reversed with 1 μ M mevalonate supplementation and completely reversed with 2 μ M mevalonate supplementation (Fig. 4). Interestingly, supplementation with 0–50 μ M FPP or GGPP was unable to reverse the inhibitory effect of combined statin and γ -tocotrienol treatment on the +SA mammary tumor cell growth (data not shown).

Effects of Statins, γ -Tocotrienol, and Mevalonate Supplementation on HMGR, Protein Prenylation and Mitogenic Signaling

Figure 5 shows that combined treatment of 0.25 μ M simvastatin (S), 0.25 μ M lovastatin (L), 0.25 μ M mevastatin (M) or 10 μ M pravastatin (P) with 2 μ M γ -tocotrienol (T) resulted in a large increase in unprenylated Rap1A levels and a corresponding decrease in the levels of HMGR, isoprenylated Rab6, phospho-p44/42 ERK, phospho-p38 and cyclin D1, as compared with vehicle-treated controls (C). In contrast, +SA cells receiving 2 μ M mevalonate supplementation (m) alone or together with combined

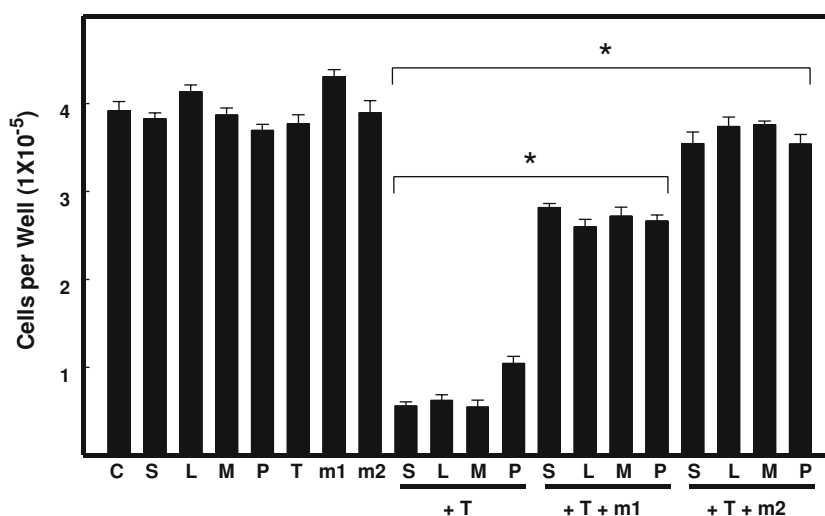


Fig. 4 Effects of mevalonate supplementation on the growth of +SA mammary tumor cells. Cells were plated at a density of 5×10^4 cells/well (6 wells/group) in 24-well culture plates and exposed to control (C), 0.25 μ M simvastatin (S), 0.25 μ M lovastatin (L), 0.25 μ M mevastatin (M), 10 μ M pravastatin (P), 2 μ M γ -tocotrienol (T), 1 μ M mevalonate (m1) or 2 μ M mevalonate (m2) alone, or combination

with individual statins (S, L, M or P) and/or γ -tocotrienol (T) for a 4-day culture period. Afterwards, viable cell count was determined using the MTT assay. Vertical bars indicate the mean cell count \pm SEM in each treatment group. * $P < 0.05$ as compared with respective combination statin and γ -tocotrienol treatment groups not exposed mevalonate supplementation

statins and γ -tocotrienol treatment showed no change in the relative levels of unprenylated Rap1A, isoprenylated Rab6, phospho-p44/42 ERK, phospho-p38 and cyclin D1 levels, as compared with vehicle-treated controls (Fig. 5). However, all groups receiving mevalonate supplementation displayed a decrease in HMGR levels as compared with vehicle-treated controls. The relative levels of total Ras, total ERK, and total p38 did not differ among any of the treatment groups (Fig. 5).

Discussion

Results in this study demonstrate that the growth inhibitory effects of statins on +SA mammary tumor cells are directly related to suppression in HMGR activity, mevalonate synthesis, small G-protein prenylation and mitogenic signaling. In contrast, the antiproliferative effects of γ -tocotrienol are not dependent on a reduction in HMGR activity, as evidenced by the finding that treatment with growth inhibiting doses of γ -tocotrienol has little effect on protein prenylation, and mevalonate supplementation does not reverse the antiproliferative effects of this form of vitamin E. However, the synergistic suppression of +SA mammary tumor cell growth that occurs with combined treatment of subeffective doses of individual statins with subeffective doses of γ -tocotrienol appears to result from the action of γ -tocotrienol to potentiate statin-dependent inhibition of HMGR activity. This suggestion is supported by the finding that mevalonate supplementation was able to reverse

the inhibitory effects of combined low dose statin and γ -tocotrienol treatment on +SA cell growth, protein prenylation and mitogenic signaling. These findings demonstrate that the synergistic antiproliferative effects of combined low dose statin and γ -tocotrienol treatment result directly from an inhibition in HMGR activity and subsequent suppression in mevalonate synthesis.

Previous investigations have indicated that the anticancer effects of statins are mediated by both HMGR-dependent and -independent mechanisms [18, 23]. However, the growth inhibitory effects of statins were reversed by mevalonate supplementation and indicate that inhibition of HMGR activity is the primary mechanism mediating the antiproliferative effects of statins in +SA mammary tumor cells. It was also found that mevalonate supplementation alone and in combination with individual statins decreased HMGR levels in +SA cells. This observation agrees with earlier findings that showed mevalonate supplementation induces a down-regulation in HMGR through both transcriptional and post-transcriptional mechanisms [1, 24].

The HMGR pathway plays an essential role in the synthesis of isoprenoids which are required for the isoprenylation of key signaling proteins such as Rap1A and Rab6. Rap and Rab family members are small G proteins similar to Ras that are involved with activating signal transduction pathways important in regulating cellular proliferation, differentiation, adhesion and cancer progression [25–27]. Rap1 activates the MAPK pathways through the interaction with B-Raf [28]. Rab proteins are characteristically elevated in prostate, bladder, ovarian and

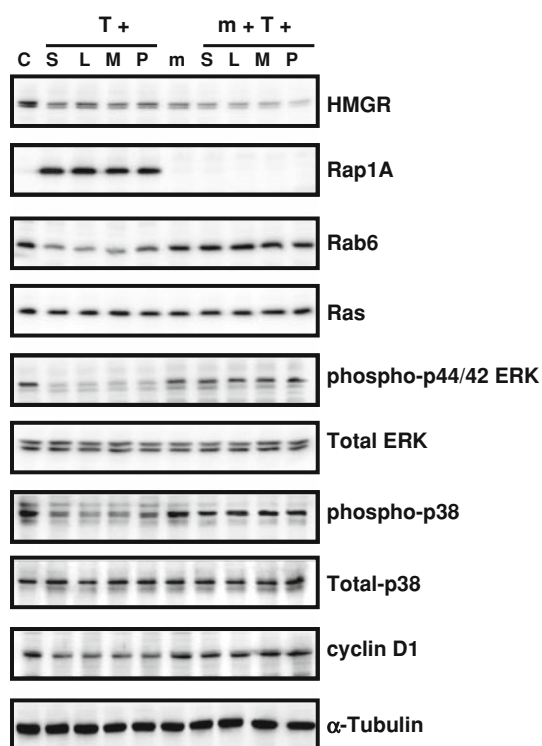


Fig. 5 Effects of mevalonate supplementation on intracellular levels of HMGR, isoprenylation of small G-proteins, MAPKs and cyclin D1. +SA cells were plated at a density of 1×10^6 cells/100 mm culture dishes and exposed to control media (C) or 2 μ M mevalonate (m) containing media, or treatment media containing the combination of 0.25 μ M simvastatin (S), 0.25 μ M lovastatin (L), 0.25 μ M mevastatin (M), or 10 μ M pravastatin (P), with 2 μ M γ -tocotrienol (T) alone or in combination with 2 μ M mevalonate (m) for a 4-day culture period. Afterwards, whole cell lysates were prepared and electrophoresed through polyacrylamide minigels, transblotted to PVDF membrane, followed by Western blot analysis to measure relative levels of total HMGR, unprenylated Rap1A, isoprenylated Rab6, total Ras, phospho-p44/42 ERK, phospho-p38, total p44/42 ERK, total p38, cyclin D1 and α -tubulin. α -Tubulin was visualized to ensure equal sample loading in each lane

breast cancers, and suppression of Rab6 prenylation can initiate apoptosis in many types of cancer cells [29, 30]. In contrast to statins, the growth inhibitory effects of γ -tocotrienol treatment alone occurs independently of HMGR activity and is not associated with a reduction in small G-protein prenylation. The reduction in HMGR levels observed following γ -tocotrienol treatment alone is apparently insufficient to decrease HMGR activity enough to block the prenylation of Rap1A and Rab6. However, combined low dose treatment of statins and γ -tocotrienol greatly reduced prenylation of Rap1A and Rab6, and this effect was reversed by mevalonate supplementation. Studies also found that unlike mevalonate, supplementation of FPP or GGPP did not reverse the inhibitory effects of combined low dose statin and γ -tocotrienol treatment (data not shown). It is possible that non-sterol products synthesized downstream of mevalonate, but upstream of FPP and

GGPP, such as isopentenyl pyrophosphate (IPP) and geranyl pyrophosphate (GPP), play an important role in the prenylation of Rap1A and Rab6 in +SA cells. Additional studies are required to determine the exact enzymatic step downstream of mevalonate that is targeted by combined statin and γ -tocotrienol treatment to prevent the prenylation of Rap1A and Rab6.

Previous studies have established that γ -tocotrienol decreases cellular levels of HMGR by accelerating the degradation of this enzyme [11]. However, the present findings clearly indicate that when given alone, the growth inhibitory effects of γ -tocotrienol are not dependent on its action to down regulate HMGR levels. The antiproliferative effects of γ -tocotrienol have been previously reported to be associated with a suppression in ErbB3/PI3K/Akt mitogenic signaling [31, 32]. ErbB/PI3K/Akt signaling pathway is important for cell survival and growth, and plays a pivotal role in tumorigenesis. Since Akt phosphorylates and stimulates the function of many intracellular proteins involved in proliferation and survival, enhanced Akt signaling has been shown to be associated with the development of breast cancer in humans [33]. The ability of subeffective doses of γ -tocotrienol to synergistically enhance the growth inhibitory effects of individual statins can be explained, at least in part, by the finding that statin inhibition of HMGR activity is associated in triggering a compensatory feedback mechanism that results in an up-regulation in HMGR expression [34, 35], and this self-limiting effect of statins is blocked when given in combination with γ -tocotrienol.

Mitogenic activation of small G-proteins like Ras, Rap and Rab stimulates MAPK pathways and promotes cell cycle progression [36–38]. MAPK signaling cascades such as Erk, p38, and JNK control the fundamental cellular processes of growth, proliferation, differentiation, migration and apoptosis, and elevated or unregulated MAPK signaling can play a critical role in the development and progression of cancer [39]. Over expression or enhanced Ras activation and MAPK signaling can result in enhanced expression of cyclin D1 and stimulate unregulated cell cycle progression in many types of human cancers [40]. Combined treatment of γ -tocotrienol with individual statins caused a reduction in Rap1A and Rab6 prenylation, decreased phosphorylation (activation) of p44/42-ERK and p38, and decreased expression of cyclin D1 which regulates cell cycle transition from G1 to S phase, and these effects were reversed by mevalonate supplementation. Although this same treatment was found to have no effect on total Ras levels, it is very likely that prenylated Ras levels were also reduced and contributed to the reduction in phosphorylated-MAPKs that was observed in these +SA mammary tumor cells. Further studies are necessary to determine the effects on combined low dose statin and γ -tocotrienol treatment on Ras prenylation.

HMGR activity and expression is characteristically elevated and often resistant to feedback regulation by sterols in many types of cancer cells [1, 41, 42]. Fortunately, HMGR activity has also been found to be highly sensitive to the feedback inhibition by non-sterol isoprenoids, and exogenous administration of plant derived isoprenoids such as α -limonene, perillyl alcohol, and β -ionone has been shown to induce a down-regulation of HMGR in various types of cancer cells [5, 22, 43]. Chemically, γ -tocotrienol is also classified as an isoprenoid and this property might explain the mechanism involved in mediating γ -tocotrienol-induced down-regulation of HMGR levels in +SA mammary tumor cells [11, 22].

In conclusion, the present findings demonstrate that suppression in HMGR activity and mevalonate synthesis is primarily responsible for mediating the antiproliferative effect of combined low-dose statin and γ -tocotrienol treatment in +SA mammary tumor cells. The synergistic antiproliferative activity of these agents appears to be due to the cooperative action of γ -tocotrienol to cause a down-regulation in HMGR levels and statins to directly inhibit HMGR activity. These findings also suggest that combined low-dose statin and γ -tocotrienol treatment may greatly improve therapeutic responsiveness in the treatment of breast cancer, while at the same time greatly reduce or eliminate the severe myotoxicity and other adverse side effects associated with high-dose statin monotherapy.

Acknowledgments This work was performed at the College of Pharmacy, University of Louisiana at Monroe, Monroe, LA and supported in part by grants from the National Institutes of Health (Grant CA 86833) and First Tech International Ltd.

References

- Goldstein JL, Brown MS (1990) Regulation of the mevalonate pathway. *Nature* 343:425–430
- Kato K, Cox AD, Hisaka MM, Graham SM, Buss JE, Der CJ (1992) Isoprenoid addition to Ras protein is the critical modification for its membrane association and transforming activity. *Proc Natl Acad Sci USA* 89:6403–6407
- Khosravi-Far R, Cox AD, Kato K, Der CJ (1992) Protein prenylation: key to Ras function and cancer intervention? *Cell Growth Differ* 3:461–469
- Maltese WA (1990) Posttranslational modification of proteins by isoprenoids in mammalian cells. *FASEB J* 4:3319–3328
- Mo H, Elson CE (2004) Studies of the isoprenoid-mediated inhibition of mevalonate synthesis applied to cancer chemotherapy and chemoprevention. *Exp Biol Med (Maywood)* 229:567–585
- Shibata MA, Ito Y, Morimoto J, Otsuki Y (2004) Lovastatin inhibits tumor growth and lung metastasis in mouse mammary carcinoma model: a p53-independent mitochondrial-mediated apoptotic mechanism. *Carcinogenesis* 25:1887–1898
- Campbell MJ, Esserman LJ, Zhou Y, Shoemaker M, Lobo M, Borman E, Baehner F, Kumar AS, Adduci K, Marx C, Petricoin EF, Liotta LA, Winters M, Benz S, Benz CC (2006) Breast cancer growth prevention by statins. *Cancer Res* 66:8707–8714
- Thibault A, Samid D, Tompkins AC, Figg WD, Cooper MR, Hohl RJ, Trepel J, Liang B, Patronas N, Venzon DJ, Reed E, Myers CE (1996) Phase I study of lovastatin, an inhibitor of the mevalonate pathway, in patients with cancer. *Clin Cancer Res* 2:483–491
- Staffa JA, Chang J, Green L (2002) Cerivastatin and reports of fatal rhabdomyolysis. *N Engl J Med* 346:539–540
- Sylvester PW, Shah SJ (2005) Mechanisms mediating the anti-proliferative and apoptotic effects of vitamin E in mammary cancer cells. *Front Biosci* 10:699–709
- Parker RA, Pearce BC, Clark RW, Gordon DA, Wright JJ (1993) Tocotrienols regulate cholesterol production in mammalian cells by post-transcriptional suppression of 3-hydroxy-3-methylglutaryl-coenzyme A reductase. *J Biol Chem* 268:11230–11238
- Wali VB, Sylvester PW (2007) Synergistic antiproliferative effects of gamma-tocotrienol and statin treatment on mammary tumor cells. *Lipids* 42:1113–1123
- Wali VB, Bachawal SV, Sylvester PW (2009) Combined treatment of gamma-tocotrienol with statins induce mammary tumor cell cycle arrest in G1. *Exp Biol Med (Maywood)* 234:639–650
- Danielson KG, Anderson LW, Hosick HL (1980) Selection and characterization in culture of mammary tumor cells with distinctive growth properties in vivo. *Cancer Res* 40:1812–1819
- Anderson LW, Danielson KG, Hosick HL (1981) Metastatic potential of hyperplastic alveolar nodule derived mouse mammary tumor cells following intravenous inoculation. *Eur J Cancer Clin Oncol* 17:1001–1008
- Shah S, Gapor A, Sylvester PW (2003) Role of caspase-8 activation in mediating vitamin E-induced apoptosis in murine mammary cancer cells. *Nutr Cancer* 45:236–246
- McIntyre BS, Briski KP, Gapor A, Sylvester PW (2000) Antiproliferative and apoptotic effects of tocopherols and tocotrienols on preneoplastic and neoplastic mouse mammary epithelial cells. *Proc Soc Exp Biol Med* 224:292–301
- Rao S, Porter DC, Chen X, Herliczek T, Lowe M, Keyomarsi K (1999) Lovastatin-mediated G1 arrest is through inhibition of the proteasome, independent of hydroxymethyl glutaryl-CoA reductase. *Proc Natl Acad Sci USA* 96:7797–7802
- Rodwell VW, Nordstrom JL, Mitschelen JJ (1976) Regulation of HMG-CoA reductase. *Adv Lipid Res* 14:1–74
- Sylvester PW, Birkenfeld HP, Hosick HL, Briski KP (1994) Fatty acid modulation of epidermal growth factor-induced mouse mammary epithelial cell proliferation in vitro. *Exp Cell Res* 214:145–153
- Towbin H, Staehelin T, Gordon J (1979) Electrophoretic transfer of proteins from polyacrylamide gels to nitrocellulose sheets: procedure and some applications. *Proc Natl Acad Sci USA* 76:4350–4354
- Elson CE, Peffley DM, Hentosh P, Mo H (1999) Isoprenoid-mediated inhibition of mevalonate synthesis: potential application to cancer. *Proc Soc Exp Biol Med* 221:294–311
- Graaf MR, Richel DJ, van Noorden CJ, Guchelaar HJ (2004) Effects of statins and farnesyltransferase inhibitors on the development and progression of cancer. *Cancer Treat Rev* 30:609–641
- Correll CC, Edwards PA (1994) Mevalonic acid-dependent degradation of 3-hydroxy-3-methylglutaryl-coenzyme A reductase in vivo and in vitro. *J Biol Chem* 269:633–638
- Cheng KW, Lahad JP, Gray JW, Mills GB (2005) Emerging role of RAB GTPases in cancer and human disease. *Cancer Res* 65:2516–2519
- Caron E (2003) Cellular functions of the Rap1 GTP-binding protein: a pattern emerges. *J Cell Sci* 116:435–440
- Wang Z, Dillon TJ, Pokala V, Mishra S, Labudda K, Hunter B, Stork PJ (2006) Rap1-mediated activation of extracellular signal-regulated kinases by cyclic AMP is dependent on the mode of Rap1 activation. *Mol Cell Biol* 26:2130–2145

28. Stork PJ, Schmitt JM (2002) Crosstalk between cAMP and MAP kinase signaling in the regulation of cell proliferation. *Trends Cell Biol* 12:258–266
29. Roelofs AJ, Hulley PA, Meijer A, Ebetino FH, Russell RG, Shipman CM (2006) Selective inhibition of Rab prenylation by a phosphonocarboxylate analogue of risedronate induces apoptosis, but not S-phase arrest, in human myeloma cells. *Int J Cancer* 119:1254–1261
30. Merrell MA, Wakchoure S, Lehenkari PP, Harris KW, Selander KS (2007) Inhibition of the mevalonate pathway and activation of p38 MAP kinase are independently regulated by nitrogen-containing bisphosphonates in breast cancer cells. *Eur J Pharmacol* 570:27–37
31. Shah SJ, Sylvester PW (2005) Gamma-tocotrienol inhibits neoplastic mammary epithelial cell proliferation by decreasing Akt and nuclear factor kappaB activity. *Exp Biol Med* (Maywood) 230:235–241
32. Samant GV, Sylvester PW (2006) gamma-Tocotrienol inhibits ErbB3-dependent PI3K/Akt mitogenic signalling in neoplastic mammary epithelial cells. *Cell Prolif* 39:563–574
33. Downward J (1998) Mechanisms and consequences of activation of protein kinase B/Akt. *Curr Opin Cell Biol* 10:262–267
34. Brown MS, Faust JR, Goldstein JL, Kaneko I, Endo A (1978) Induction of 3-hydroxy-3-methylglutaryl coenzyme A reductase activity in human fibroblasts incubated with compactin (ML-236B), a competitive inhibitor of the reductase. *J Biol Chem* 253:1121–1128
35. Nakanishi M, Goldstein JL, Brown MS (1988) Multivalent control of 3-hydroxy-3-methylglutaryl coenzyme A reductase. Mevalonate-derived product inhibits translation of mRNA and accelerates degradation of enzyme. *J Biol Chem* 263:8929–8937
36. Adjei AA (2001) Blocking oncogenic Ras signaling for cancer therapy. *J Natl Cancer Inst* 93:1062–1074
37. Norbury C, Nurse P (1992) Animal cell cycles and their control. *Annu Rev Biochem* 61:441–470
38. Sebolt-Leopold JS, Herrera R (2004) Targeting the mitogen-activated protein kinase cascade to treat cancer. *Nat Rev Cancer* 4:937–947
39. Dhillon AS, Hagan S, Rath O, Kolch W (2007) MAP kinase signalling pathways in cancer. *Oncogene* 26:3279–3290
40. Coleman ML, Marshall CJ, Olson MF (2004) RAS and RHO GTPases in G1-phase cell-cycle regulation. *Nat Rev Mol Cell Biol* 5:355–366
41. Siperstein MD, Fagan VM (1964) Deletion of the cholesterol-negative feedback system in liver tumors. *Cancer Res* 24:1108–1115
42. Siperstein MD, Fagan VM (1964) Studies on the feed-back regulation of cholesterol synthesis. *Adv Enzyme Regul* 2:249–264
43. Elson CE, Yu SG (1994) The chemoprevention of cancer by mevalonate-derived constituents of fruits and vegetables. *J Nutr* 124:607–614

Kinetic Study of the Prooxidant Effect of α -Tocopherol. Hydrogen Abstraction from Lipids by α -Tocoperoxyl Radical

Aya Ouchi · Masaharu Ishikura · Kensuke Konishi ·
Shin-ichi Nagaoka · Kazuo Mukai

Received: 26 June 2009 / Accepted: 26 August 2009 / Published online: 16 September 2009
© AOCS 2009

Abstract A kinetic study of the prooxidant effect of α -tocopherol was performed. The rates of allylic hydrogen abstraction from various unsaturated fatty acid esters (ethyl stearate **1**, ethyl oleate **2**, ethyl linoleate **3**, ethyl linolenate **4**, and ethyl arachidonate **5**) by α -tocoperoxyl radical in toluene were determined, using a double-mixing stopped-flow spectrophotometer. The second-order rate constants (k_p) obtained are $<1 \times 10^{-2} \text{ M}^{-1} \text{ s}^{-1}$ for **1**, $1.90 \times 10^{-2} \text{ M}^{-1} \text{ s}^{-1}$ for **2**, $8.33 \times 10^{-2} \text{ M}^{-1} \text{ s}^{-1}$ for **3**, $1.92 \times 10^{-1} \text{ M}^{-1} \text{ s}^{-1}$ for **4**, and $2.43 \times 10^{-1} \text{ M}^{-1} \text{ s}^{-1}$ for **5** at 25.0 °C. Fatty acid esters **3**, **4**, and **5** contain two, four, and six $-\text{CH}_2-$ hydrogen atoms activated by two π -electron systems ($-\text{C}=\text{C}-\text{CH}_2-\text{C}=\text{C}-$). On the other hand, fatty acid ester **2** has four $-\text{CH}_2-$ hydrogen atoms activated by a single π -electron system ($-\text{CH}_2-\text{C}=\text{C}-\text{CH}_2-$). Thus, the rate constants, $k_{\text{abstr}}/\text{H}$, given on an available hydrogen basis are $k_p/4 = 4.75 \times 10^{-3} \text{ M}^{-1} \text{ s}^{-1}$ for **2**, $k_p/2 = 4.16 \times 10^{-2} \text{ M}^{-1} \text{ s}^{-1}$ for **3**, $k_p/4 = 4.79 \times 10^{-2} \text{ M}^{-1} \text{ s}^{-1}$ for **4**, and $k_p/6 = 4.05 \times 10^{-2} \text{ M}^{-1} \text{ s}^{-1}$ for **5**. The $k_{\text{abstr}}/\text{H}$ values obtained for **3**, **4**, and **5** are similar to each other, and are by about one order of magnitude higher than that for **2**. From

these results, it is suggested that the prooxidant effect of α -tocopherol in edible oils, fats, and low-density lipoproteins may be induced by the above hydrogen abstraction reaction.

Keywords α -Tocopherol · α -Tocoperoxyl radical · Prooxidant effect · Kinetic study · Reaction rate constant · Stopped-flow spectrophotometer · Unsaturated lipids · Fatty acids · Vitamin E

Abbreviations

ArOH	2,6-Di- <i>tert</i> -butyl-4(4'-methoxyphenyl)phenol
ArO·	2,6-Di- <i>tert</i> -butyl-4(4'-methoxyphenyl)phenoxy (aroxyl)
AsH ⁻	Ascorbate mono anion
As· ⁻	Ascorbate mono anion radical
5,7-Di- <i>i</i> Pr-Toc·	5,7-Di-isopropyl-tocoperoxyl
ESR	Electron spin resonance
LDL	Low-density lipoprotein
LH	Lipid (or fatty acid ethyl ester)
LOOH	Lipid hydroperoxide (or methyl linoleate hydroperoxide)
LOO·	Lipid peroxy radical
LO·	Lipid alkoxy radical
NRP	Non-radical products
α -TocH	α -Tocopherol
α -Toc·	α -Tocoperoxyl

A. Ouchi · S. Nagaoka · K. Mukai (✉)
Department of Chemistry, Faculty of Science, Ehime University,
Matsuyama 790-8577, Japan
e-mail: mukai@chem.sci.ehime-u.ac.jp

A. Ouchi
e-mail: oouchi@chem.sci.ehime-u.ac.jp

M. Ishikura
Life Science Business Division, Research and Development
Operations, Yamaha Motor Co. Ltd., Shizuoka 437-0061, Japan

K. Konishi
Department of Physics, Faculty of Science, Ehime University,
Matsuyama 790-8577, Japan

Introduction

It is well known that vitamin E (α -tocopherol, α -TocH) is localized in biomembranes and functions as an antioxidant

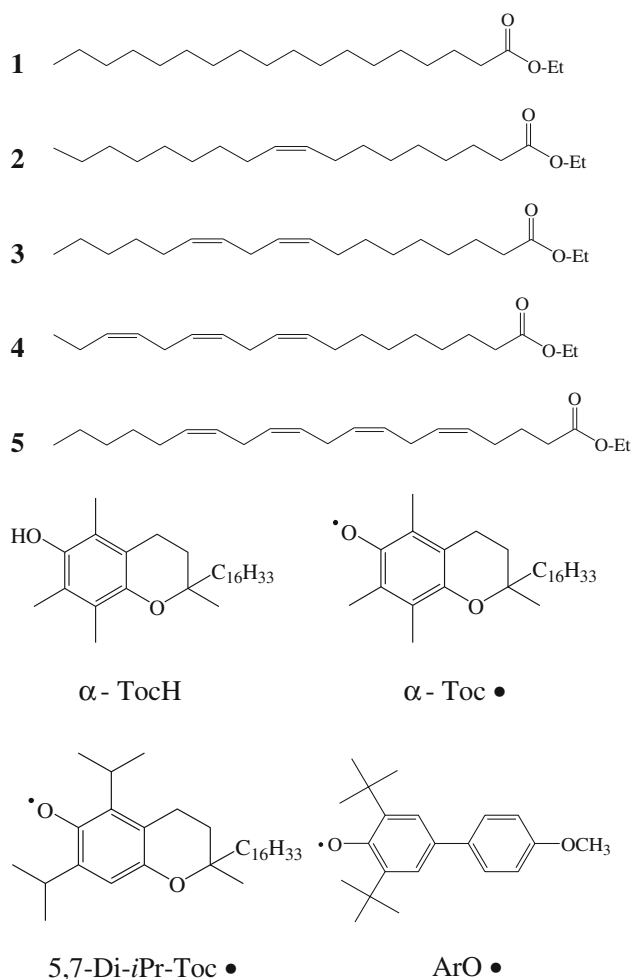
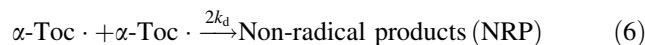
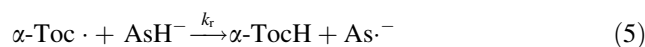
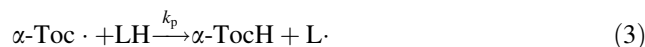
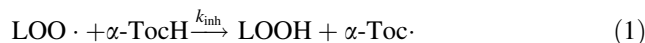


Fig. 1 Molecular structures of fatty acid ethyl esters (LH) (ethyl stearate **1**, ethyl oleate **2**, ethyl linoleate **3**, ethyl linolenate **4**, and ethyl arachidonate **5**), α -tocopherol (α -TocH), α -tocopheroxyl (α -Toc•), 5,7-di-isopropyl-tocopheroxyl (5,7-Di-iPr-Toc•), and aroxy (ArO•) radical

by protecting unsaturated lipids from peroxidation [1–4]. The antioxidant actions of the α -tocopherol have been ascribed to the scavenging reaction of active free radicals (LOO• and LO•), producing corresponding α -tocopheroxyl (α -Toc•) radicals (see Fig. 1 and reaction 1) [5, 6]. The α -Toc• radicals produced may combine with another peroxy (LOO•) radical (reaction 2) [6]. If α -tocopherols exist in biomembranes and oils, the α -Toc• radicals may react with unsaturated lipids (LH) (reaction 3) and lipid hydroperoxides (LOOH) (reaction 4). These reactions 3 and 4 are known as prooxidant reactions, which induce the degradation of unsaturated lipids [7–10]. α -Toc• radicals may be regenerated by vitamin C (ascorbate anion, AsH⁻) (reaction 5) [1] and/or ubiquinol-10 [11] in biomembranes, to protect the above prooxidant effects. Further, α -Toc• radicals disappear by bimolecular reaction with another α -Toc• to give non-radical products (NRP) (reaction 6) [6].



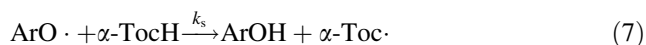
As described above, α -Toc• radical is an important key radical, which appears in the process of the antioxidant and prooxidant actions of α -TocH. Detailed kinetic studies have been performed for the reactions 1 [2, 6], 4 [12, 13], 5 [14–17] and 6 [6, 18–20], and the mechanisms involved have been studied extensively. However, the examples of the measurements of the rate constants (k_2 and k_p) for the reactions 2 [21] and (3) [21, 22] are limited, because of the instability of α -Toc• radicals. The reaction of LOO• with α -Toc• radical (reaction 2) is very fast with a rate constant (k_2) of $3 \times 10^8 \text{ M}^{-1} \text{ s}^{-1}$ [21]. The reaction rates (k_p) were measured by using more stable 5,7-di-isopropyl-tocopheroxyl (5,7-Di-iPr-Toc•) radical (see Fig. 1), and the structure–activity relationship was discussed for the reaction 3 [23, 24].

In the present work, in order to clarify the mechanism of prooxidant action of vitamin E (α -TocH) in biological systems, a kinetic study of the reaction of α -Toc• radical with saturated and unsaturated fatty acid esters (LH) (ethyl stearate **1**, ethyl oleate **2**, ethyl linoleate **3**, ethyl linolenate **4**, and ethyl arachidonate **5**) (Fig. 1) has been performed in toluene, using a double-mixing stopped-flow spectrophotometer.

Experimental Procedure

α -TocH was obtained from Calbiochem. Ethyl stearate **1** (>99%) was obtained from the Tokyo Chemical Industry Co. Ltd. Ethyl oleate **2** (>98%) was obtained from Aldrich. Ethyl linoleate **3** (>99%), ethyl linolenate **4** (>98%), and ethyl arachidonate **5** (>99%) were purchased from the Sigma Chemical Co. Aroxy radical (ArO•, 2,6-di-*t*-butyl-4-(4'-methoxyphenyl)phenoxyl) (see Fig. 1) was prepared according to the method of Rieker et al [26].

The measurement of the second-order rate constant (k_s) for the reaction of ArO• with α -TocH (reaction 7) was performed with a Unisoku single-mixing stopped-flow spectrophotometer (Model RSP-1000) by mixing equal volumes of toluene solutions of ArO• and α -TocH under a nitrogen atmosphere [25].

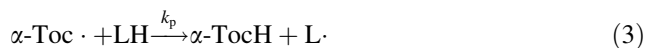
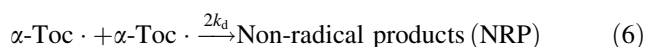
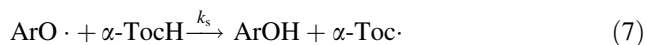


The measurement of the k_p value (reaction 3) was performed with a Unisoku double-mixing stopped-flow spectrophotometer (Model RSP-1000-03F). By mixing first equal volumes of toluene solutions of α -TocH with $\text{ArO}\cdot$, $\alpha\text{-Toc}\cdot$ radical was prepared (reaction 7), and after 2 s the second-mixing of equal volumes of $\alpha\text{-Toc}\cdot$ solution and LH 1–5 solutions (reaction 3) was performed, using double-mixing unit of the RSP-1000. The rate constants (k_p) were determined by analyzing the decay curve of $\alpha\text{-Toc}\cdot$ as described later. The time between mixing two solutions and recording the first data point (that is, dead time) was 10–20 ms. The reaction was monitored with either single wavelength detection or photo-diode array detector attached to the stopped-flow spectrophotometer. All measurements were performed at 25.0 ± 0.5 °C.

Results

Rate Constant (k_s) for the Reaction of α -Tocopherol with Aroxyl Radical in Toluene

The reactions studied in the present work are the following ones:



In order to determine the rate constant (k_p) for the reaction 3 of LH with $\alpha\text{-Toc}\cdot$, the measurements of the rate constants (k_s and $2k_d$) for the reactions 7 and 6 are necessary, as described later [20, 22].

The $\text{ArO}\cdot$ radical is stable in the absence of $\alpha\text{-TocH}$, and shows absorption peaks at $\lambda_{\text{max}} = 377$ nm ($\epsilon = 15,700$ M⁻¹ cm⁻¹), 528 nm ($\epsilon = 3,030$ M⁻¹ cm⁻¹), and 573 nm ($\epsilon = 3,450$ M⁻¹ cm⁻¹) in toluene solution, as shown in Fig. 2a. By adding the toluene solution of $\alpha\text{-TocH}$ (1.10×10^{-3} M) to the solution of $\text{ArO}\cdot$ (9.20×10^{-5} M) (1:1 in volume) at 25.0 °C, the absorption peak of $\text{ArO}\cdot$ disappeared quickly, and the spectrum was changed to that of $\alpha\text{-Toc}\cdot$ with four absorption peaks at $\lambda_{\text{max}} = 423$, 403, 382sh, and 341 nm (see Fig. 2a, b) [20, 25]. $\alpha\text{-Toc}\cdot$ is unstable at 25.0 °C, and its absorption peaks decreased gradually, after passing through the maximum (see Fig. 2b).

The decay rate of $\text{ArO}\cdot$ radical was determined by following the decrease in absorbance at 377 and/or 573 nm of

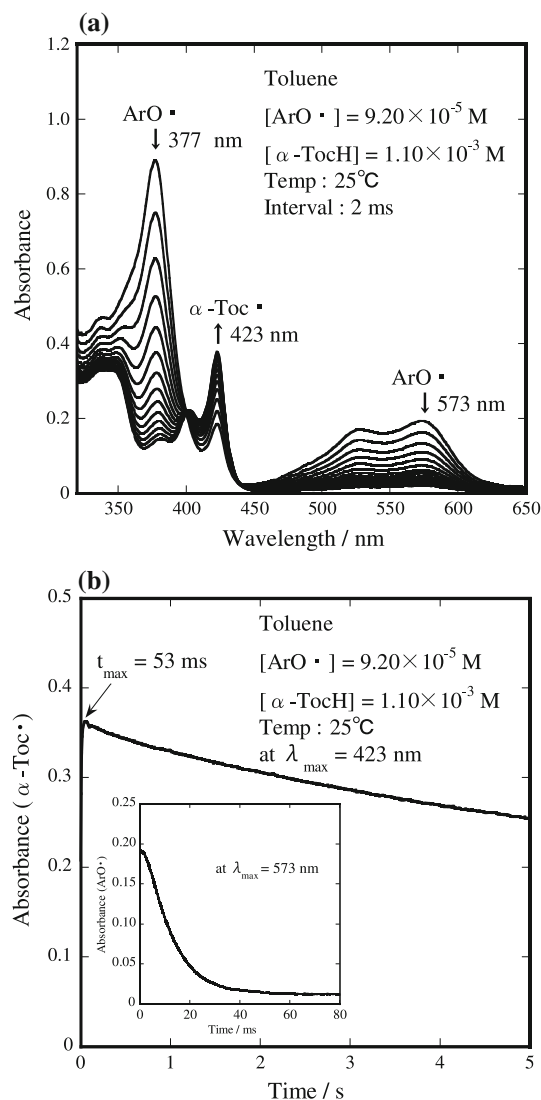


Fig. 2 **a** Change in electronic absorption spectrum of aroxyl ($\text{ArO}\cdot$) and $\alpha\text{-Toc}\cdot$ radical during the reaction of $\text{ArO}\cdot$ with $\alpha\text{-TocH}$ in toluene at 25.0 °C. $[\alpha\text{-TocH}]_{t=0} = 1.10 \times 10^{-3}$ M and $[\text{ArO}\cdot]_{t=0} = 9.20 \times 10^{-5}$ M. The spectra were recorded at 2-ms intervals. The arrow indicates a decrease ($\text{ArO}\cdot$) and an increase ($\alpha\text{-Toc}\cdot$) in an absorbance with time. **b** Time dependence of the absorbance of $\text{ArO}\cdot$ (at 573 nm) (inset) and $\alpha\text{-Toc}\cdot$ (at 423 nm) radicals produced by the reaction of $\text{ArO}\cdot$ with $\alpha\text{-TocH}$ in toluene at 25.0 °C. The values of $[\text{ArO}\cdot]_{t=0}$ and $[\alpha\text{-TocH}]_{t=0}$ are shown in Fig. 2b

the $\text{ArO}\cdot$ (see Fig. 2) [20, 25]. The pseudo-first-order rate constants (k_{obsd}) at 377 and/or 573 nm were linearly dependent on the concentration of $\alpha\text{-TocH}$ ($[\alpha\text{-TocH}]$), and thus the rate equation is expressed as

$$-d[\text{ArO}\cdot]/dt = k_{\text{obsd}}[\text{ArO}\cdot] = k_s[\alpha\text{-TocH}][\text{ArO}\cdot] \quad (8)$$

The rate constants (k_s) were obtained by plotting k_{obsd} against $[\alpha\text{-TocH}]$ (data are not shown). The k_s value obtained is 7.10×10^4 M⁻¹ s⁻¹.

Rate Constant ($2k_d$) for the Self-Bimolecular Reaction of α -Tocopheroxyl Radical in Toluene

By reacting $\text{ArO}\cdot$ with α -TocH in toluene (reaction 7), α -Toc \cdot radical is produced rapidly, and disappears by the bimolecular reaction (reaction 6) [6, 18–20], as shown in Fig. 2b. Independent reaction equations included in the reactions 7 and 6 are as follows:

$$-d[\text{ArO}\cdot]/dt = k_s[\alpha\text{-TocH}][\text{ArO}\cdot] \quad (9)$$

$$d[\alpha\text{-Toc}\cdot]/dt = k_s[\alpha\text{-TocH}][\text{ArO}\cdot] - 2k_d[\alpha\text{-Toc}\cdot]^2 \quad (10)$$

Recently, Eqs. 9 and 10 were solved numerically using the fourth-order Runge–Kutta method [18], and the $2k_d$ value was determined for several solvents [20]. Similar analysis was performed in the present work. The simulation of the formation and decay curves of α -Toc \cdot at $\lambda_{\text{max}} = 423$ nm in toluene was performed by varying the rate ($2k_d$) of bimolecular reaction and the molar extinction coefficient (ε) at 423 nm, where the concentration of α -Toc radical, $[\alpha\text{-Toc}\cdot]_t$, was calculated from the absorbance, by using Lambert–Beer's equation (absorbance (A_t) = $\varepsilon[\alpha\text{-Toc}\cdot]_t$). The value of k_s ($=7.10 \times 10^4 \text{ M}^{-1} \text{ s}^{-1}$) in toluene was used for the calculation. The results of the analysis performed for α -Toc \cdot are shown in Fig. 3.

The good agreement between the observed and simulation curves was obtained for the concentration of α -TocH ($[\alpha\text{-TocH}] = 1.10 \times 10^{-3} \text{ M}$) at $t = 0$ –10 s, when we used the values of k_s ($=7.10 \times 10^4 \text{ M}^{-1} \text{ s}^{-1}$), $2k_d$ ($=8.00 \times 10^2 \text{ M}^{-1} \text{ s}^{-1}$), and ε ($=3,820 \text{ M}^{-1} \text{ cm}^{-1}$ at $\lambda_{\text{max}} = 423$ nm) (see Fig. 3). As shown in Fig. 3, the concentration of α -Toc \cdot ($[\alpha\text{-Toc}\cdot]_t = 9.49 \times 10^{-5} \text{ M}$) at $t_{\text{max}} = 53$ ms is similar to

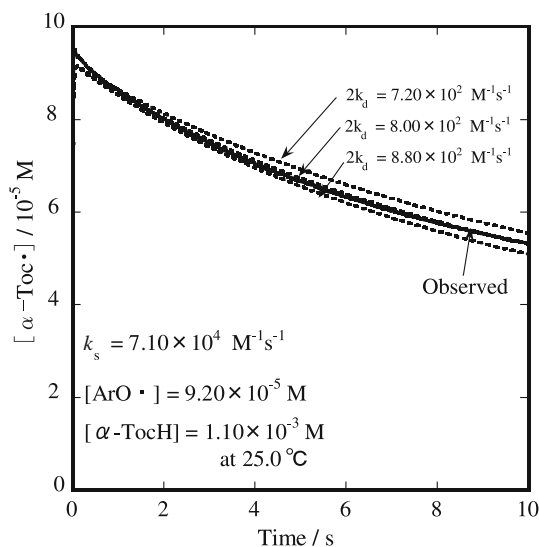


Fig. 3 Time dependence of the concentrations of α -Toc \cdot radical observed at λ_{max} (at 423 nm) during reaction of $\text{ArO}\cdot$ with α -TocH in toluene at 25.0 °C (solid line). The dotted line is a simulation curve. The values of $[\text{ArO}\cdot]_{t=0}$ and $[\alpha\text{-TocH}]_{t=0}$ are shown in Fig. 3

the initial concentration of $\text{ArO}\cdot$ ($[\text{ArO}\cdot]_{t=0} = 9.20 \times 10^{-5} \text{ M}$), if the concentration of α -TocH is high ($[\alpha\text{-TocH}] = 1.10 \times 10^{-3} \text{ M}$) and, thus, $\text{ArO}\cdot$ and α -Toc \cdot rapidly disappears and appears, respectively.

Rate Constants (k_p) for the Hydrogen Atom Abstraction by α -Tocopheroxyl Radical from Fatty Acid Ethyl Esters 1–5

As described above, measurements of the rate constant (k_p) for the reaction of α -Toc \cdot radical with LH 1–5 (reaction 3) were performed in toluene solution, using a double-mixing stopped-flow spectrophotometer. For example, the α -Toc radical was prepared by first-mixing of equal volumes of $\text{ArO}\cdot$ ($9.20 \times 10^{-5} \text{ M}$) and α -TocH ($1.10 \times 10^{-3} \text{ M}$) solutions (reaction 7), and after 2 s, the second-mixing of equal volumes of α -Toc \cdot solution and ethyl linolenate 4 solutions ($0, 1.81 \times 10^{-2}, 3.61 \times 10^{-2}, 5.42 \times 10^{-2}, 9.03 \times 10^{-2} \text{ M}$) (reaction 3) was performed. The decay curves of the absorbance of α -Toc \cdot at 423 nm in toluene were shown in Fig. 4b, indicating that the decay rates increase with increasing the concentration of 4. The decay of the absorbance of α -Toc \cdot at 423 nm without 4 is due to a bimolecular reaction 6 of α -Toc \cdot radicals. The rate constants (k_p) were determined by analyzing the decay curve of α -Toc \cdot as described later.

Similar measurements were performed for ethyl stearate 1, ethyl oleate 2, ethyl linoleate 3, and ethyl arachidonate 5. As shown in Fig. 4a, c and d, the reactions of α -Toc radical with ethyl oleate 2, ethyl linoleate 3 and ethyl arachidonate 5 in toluene were observed, respectively. On the other hand, the reaction of α -Toc \cdot with ethyl stearate 1 was negligible (data are not shown).

In the presence of LH 1–5, the rate of decay of α -Toc radical is given by Eq. 11, where k_p and $2k_d$ are the rate constants for reactions 3 and 6, respectively.

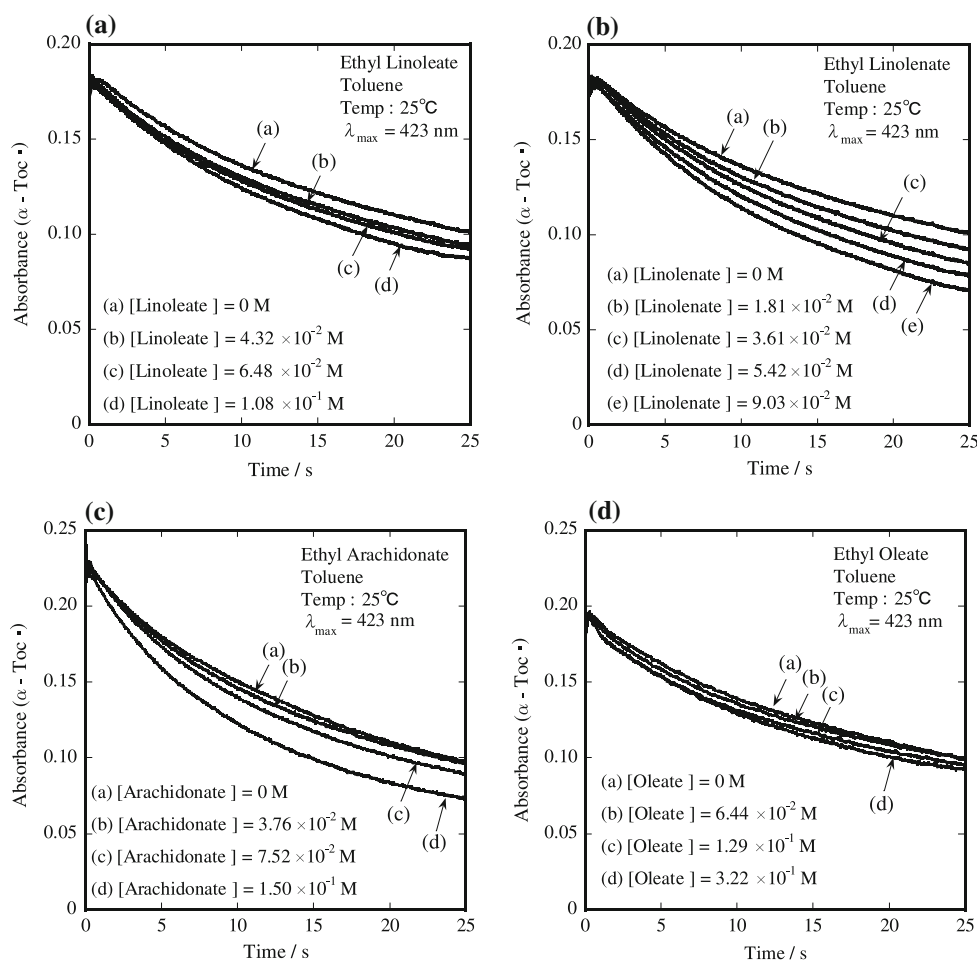
$$-d[\alpha\text{-Toc}\cdot]/dt = k_p[\text{LH}][\alpha\text{-Toc}\cdot] + 2k_d[\alpha\text{-Toc}\cdot]^2 \quad (11)$$

$$[\alpha\text{-Toc}\cdot]_{t=t} = \frac{\frac{k_p[\text{LH}][\alpha\text{-Toc}\cdot]_{t=0}}{2k_d[\alpha\text{-Toc}\cdot]_{t=0} + k_p[\text{LH}]} \exp(-k_p[\text{LH}]t)}{1 - \frac{2k_d[\alpha\text{-Toc}\cdot]_{t=0}}{2k_d[\alpha\text{-Toc}\cdot]_{t=0} + k_p[\text{LH}]} \exp(-k_p[\text{LH}]t)} \quad (12)$$

Equation (12) is obtained by an integration of Eq. 11, where $[\alpha\text{-Toc}\cdot]_{t=0}$ and $[\alpha\text{-Toc}\cdot]_{t=t}$ denote the concentrations of $[\alpha\text{-Toc}\cdot]$ at time $t = 0$ and $t = t$, respectively, [22]. The concentration of α -Toc radical, $[\alpha\text{-Toc}\cdot]_t$, (see Fig. 4) was calculated from the absorbance, by using Lambert–Beer's equation (absorbance (A_t) = $\varepsilon[\alpha\text{-Toc}\cdot]_t$). The values of ε ($=3,820 \text{ M}^{-1} \text{ cm}^{-1}$ at 423 nm) and $2k_d$ ($=8.00 \times 10^2 \text{ M}^{-1} \text{ s}^{-1}$) [20] obtained in toluene were used for the calculation.

The experimental decay curve for α -Toc radical in the presence of ethyl linolenate 4 ($[\text{LH } 4] = 9.03 \times 10^{-2} \text{ M}$)

Fig. 4 The decay of α -Toc· radical for the reaction of α -Toc· with fatty acid ethyl esters (a) LH 3, (b) LH 4, (c) LH 5, and (d) LH 2 observed at 423 nm in toluene at 25.0 °C. The values of $[\text{LH } 2\text{--}5]_{t=0}$ are shown in Fig. 4



is shown in Fig. 5b, as an example. The simulation of the decay curve of α -Toc· at $\lambda_{\text{max}} = 423 \text{ nm}$ in toluene was performed by varying the value of k_p . The calculated curves obtained by assuming various values for the rate constant k_p are also included in Fig. 5b. The good agreement between the observed and simulation curves was obtained for the four kinds of concentrations of **4** ([LH **4**] = 1.81×10^{-2} , 3.61×10^{-2} , 5.42×10^{-2} , and $9.03 \times 10^{-2} \text{ M}$) at $t = 0\text{--}15 \text{ s}$, when we used the values of k_p ($=1.82 \times 10^{-1}$, 2.03×10^{-1} , 1.98×10^{-1} , $1.84 \times 10^{-1} \text{ M}^{-1} \text{ s}^{-1}$), respectively. The four k_p values obtained and the average value ($k_p^{\text{av}} = 1.92 \times 10^{-1} \text{ M}^{-1} \text{ s}^{-1}$) of k_p are listed in Table 1. Experimental errors are estimated to be less than 10%.

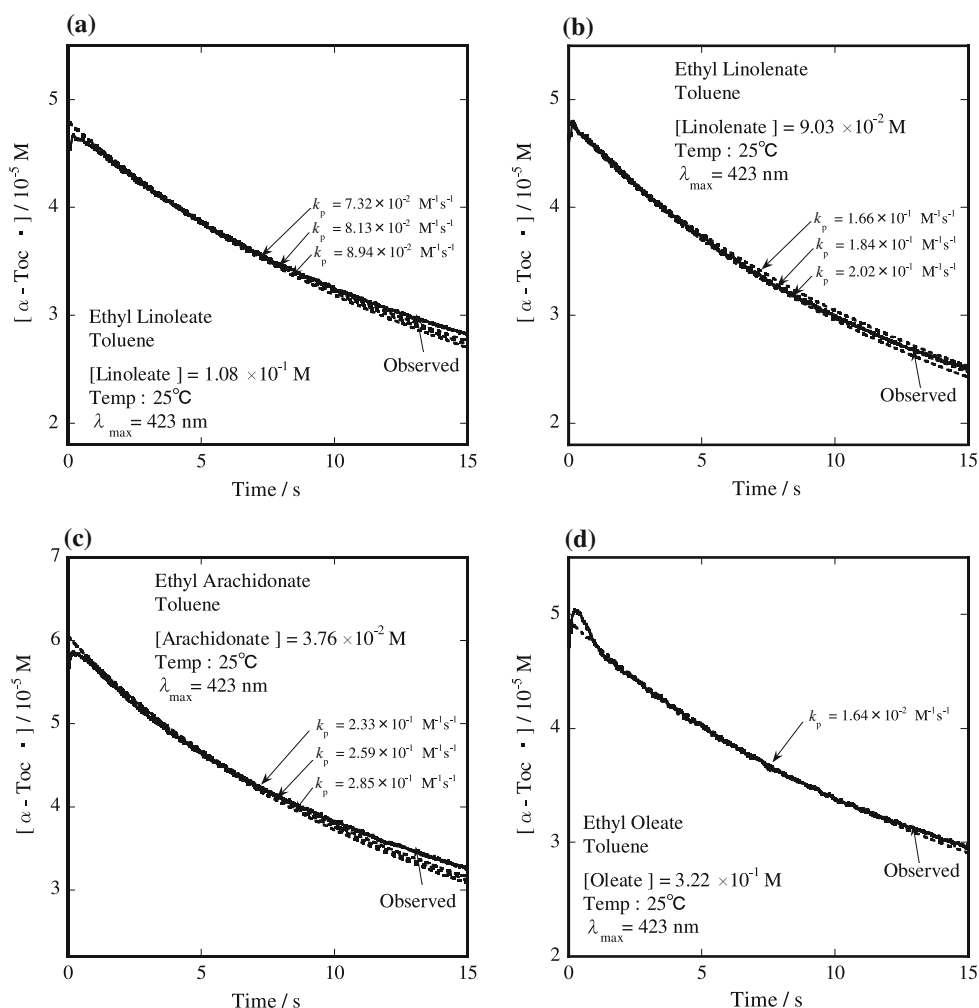
Similar analyses were performed for **2**, **3** and **5**, using the values of $2k_d$ ($=8.00 \times 10^2 \text{ M}^{-1} \text{ s}^{-1}$), and ε ($=3,820 \text{ M}^{-1} \text{ cm}^{-1}$ at $\lambda_{\text{max}} = 423 \text{ nm}$). As shown in Fig. 5, the good agreement between the observed and simulation curves was obtained for the four kinds of concentrations of LH (see Table 1) at $t = 0\text{--}15 \text{ s}$. On the other hand, in the case of ethyl stearate **1** containing no double bond, we could not determine the rate constant, because the hydrogen-atom abstraction reaction between α -Toc· and ethyl stearate **1** is

very slow and negligible. The k_p and k_p^{av} values obtained are summarized in Table 1. The rate constants (k_p^{av}) of hydrogen atom abstraction from the five kinds of **1**–**5** by α -Toc· radical decreased in the order of ethyl arachidonate **5** > ethyl linolenate **4** > ethyl linoleate **3** > ethyl oleate **2** > ethyl stearate **1**.

Discussion

In a previous work, we measured the reaction rate constants (k_p) for the hydrogen abstraction reaction of fatty acid ethyl esters **1**–**5** by 5,7-Di-*i*Pr-Toc· radical, because this radical is stable and we can easily obtain correct second-order rate constants without considering the decay of the radical, using usual UV-Vis spectrophotometer [23]. The values are $\ll 10^{-5} \text{ M}^{-1} \text{ s}^{-1}$ for **1**, $1.04 \times 10^{-5} \text{ M}^{-1} \text{ s}^{-1}$ for **2**, $1.82 \times 10^{-2} \text{ M}^{-1} \text{ s}^{-1}$ for **3**, $3.84 \times 10^{-2} \text{ M}^{-1} \text{ s}^{-1}$ for **4**, and $4.83 \times 10^{-2} \text{ M}^{-1} \text{ s}^{-1}$ for **5** in benzene solution at 25.0 °C. In order to interpret the observed features of the rate constants, ab initio molecular orbital calculations of models for the fatty acid esters were carried out [23]. From the calculation results, it was shown that the observed

Fig. 5 Time dependence of the concentrations of α -Toc \cdot radical observed at $\lambda_{\max} = 423$ nm during reaction of α -Toc \cdot with (a) LH 3, (b) LH 4, (c) LH 5, and (d) LH 2 in toluene at 25.0 °C (solid line). The Dotted line is a simulation curve. The values of $[\text{LH } 2\text{--}5]_t=0$ are shown in Fig. 5



features of the rate constant can be explained in terms of the pseudo- π -conjugation between the --C=C-- double bond and the active hydrogen-carbon bond of $\text{--CH}_2\text{--}$ group bound with --C=C-- double bond ($\text{--C=C--CH}_2\text{--C=C--}$).

The k_p value for the reaction of linoleic acid with α -Toc \cdot radical in benzene was also determined by using UV-Vis spectrophotometer; the k_p value tentatively obtained is $\sim 5 \times 10^{-2} \text{ M}^{-1} \text{ s}^{-1}$ [24]. The measurement of the k_p values for the reaction of fatty acid methyl esters with α -Toc \cdot was performed by Remorova and Roginskii, using a ESR technique [21]. The k_p values reported are $7.5 (\pm 0.6) \times 10^{-2} \text{ M}^{-1} \text{ s}^{-1}$ for methyl linoleate, $8.2 (\pm 0.3) \times 10^{-2} \text{ M}^{-1} \text{ s}^{-1}$ for methyl linolenate, and $< 3 \times 10^{-3} \text{ M}^{-1} \text{ s}^{-1}$ for methyl oleate in benzene at 50 °C. The measurement of the k_p value for the reaction of methyl linoleate with α -Toc \cdot in ethanol at 37 °C was performed by Watanabe et al., using a stopped-flow ESR technique [22]. The k_p value ($2.7 (\pm 0.4) \times 10^{-2} \text{ M}^{-1} \text{ s}^{-1}$) was determined by the simulation of the decay curve of α -Toc \cdot using Eq. (12). These values are summarized in Table 1. When ESR technique is used for the measurement, the estimation of the initial concentration of

α -Toc \cdot ($[\alpha\text{-Toc}\cdot]_t=0$) in Eq. (12) will be accompanied by a large experimental error, because α -Toc \cdot radical is unstable. In the present work, the concentration (that is, the value of ε_1) and decay rate ($2k_d$) of α -Toc \cdot in toluene were determined exactly, using a stopped-flow spectrophotometer and by the simulation of a kinetic model (see Fig. 3).

As listed in Table 1, the rate constants (k_p) in toluene decrease as the number of the double bond in fatty acid ethyl esters decreases in the order of $5 > 4 > 3 > 2 > 1$. The k_p values obtained for the reaction of 3, 4, and 5 with α -Toc \cdot radical in the present work are 4.6, 5.0, and 5.0 times as large as the corresponding those with 5,7-Di-*i*-Pr-Toc \cdot reported in a previous work, respectively. These ratios (4.6, 5.0, and 5.0) are similar to each other, suggesting that the values obtained by a simulation of the decay curve of α -Toc \cdot are correct ones. This substitution effect is likely due to the steric hindrance by the substituent groups at the 5- and 7-positions of the tocopheroxyl radical [24]. The bulkier the substituent groups at the 5- and 7-positions, the smaller the rate constant of the hydrogen abstraction. The reaction rate for 1 without --C=C-- double bond

Table 1 Rate constants for the reaction of fatty acid ethyl esters **1–5** and methyl linoleate hydroperoxide with α -tocopheroxyl radical in toluene at 25.0 °C

LH	[LH] (mM)	k_p ($M^{-1} s^{-1}$)	k_p (average) ^a ($M^{-1} s^{-1}$)	k_{abstr}/H ($M^{-1} s^{-1}$)
Ethyl stearate 1	1.28×10^{-2}		Very slow	
	2.55×10^{-2}			
	3.83×10^{-2}			
	6.39×10^{-2}			
Ethyl oleate 2	6.44×10^{-2}	1.60×10^{-2}	1.90×10^{-2}	4.75×10^{-3}
	1.29×10^{-1}	2.04×10^{-2}		
	1.93×10^{-1}	2.33×10^{-2}		
	3.22×10^{-1}	1.64×10^{-2}		
Ethyl linoleate 3	2.16×10^{-2}	8.80×10^{-2}	8.33×10^{-2}	4.16×10^{-2}
	4.32×10^{-2}	8.02×10^{-2}		
	6.48×10^{-2}	8.35×10^{-2}		
	1.08×10^{-1}	8.13×10^{-2}		
Ethyl linolenate 4	1.81×10^{-2}	1.82×10^{-1}	1.92×10^{-1}	4.79×10^{-2}
	3.61×10^{-2}	2.03×10^{-1}		
	5.42×10^{-2}	1.98×10^{-1}		
	9.03×10^{-2}	1.84×10^{-1}		
Ethyl arachidonate 5	1.88×10^{-2}	2.54×10^{-1}	2.43×10^{-1}	4.05×10^{-2}
	3.76×10^{-2}	2.59×10^{-1}		
	7.52×10^{-2}	2.32×10^{-1}		
	1.50×10^{-1}	2.27×10^{-1}		
Methyl linoleate hydroperoxide (LOOH)			5.0×10^{-1d}	

^a Experimental errors are estimated to be about 10% for LH **2–5** (see text)

^b See Ref. [21]. The value for methyl linoleate in benzene at 50 °C

^c See Ref. [22]. The value in ethanol at 37 °C

^d See Ref. [12]. The value in benzene at 25 °C

(without π -electron system) is negligibly small for both the radicals (α -Toc \cdot and 5,7-Di-*i*Pr-Toc \cdot). On the other hand, the k_p value of **2** for α -Toc \cdot is still 1/4.4 of that of **3**, although the k_p value of **2** for 5,7-Di-*i*Pr-Toc \cdot is by about three orders of magnitude smaller than that of **3**. Recently, we measured the second-order rate constants (k_s) for the reaction of **2** and **3** with ArO \cdot in toluene solution, in order to compare with those for carotenoids. The k_p value ($2.86 \times 10^{-4} M^{-1} s^{-1}$) of **2** for ArO \cdot is also still 1/4.4 of that ($1.25 \times 10^{-3} M^{-1} s^{-1}$) of **3**. The reason is not clear at present why the ratio of the rate constants for **2** and **3** changes drastically, depending on the kinds of free radicals.

By comparing the k_p values obtained for ethyl oleate **2** and ethyl linoleate **3**, it was found that the k_p value ($1.90 \times 10^{-2} M^{-1} s^{-1}$) of the former is 1/4.4 of that ($8.33 \times 10^{-2} M^{-1} s^{-1}$) of the latter, as described above. The ethyl oleate **2** has four $-CH_2-$ hydrogen atoms activated by a single π -electron system ($-CH_2-C=C-CH_2-$). Therefore, the rate constant, k_{abstr}/H , given on an available hydrogen basis, are $k_p/4 = 4.75 \times 10^{-3} M^{-1} s^{-1}$ for **2**. On the other hand, the ethyl linoleate **3** has two $-CH_2-$ hydrogen atoms activated by two π -electron systems ($-C=C-CH_2-C=C-$).

Consequently, these two hydrogen atoms will contribute to the high reactivity of ethyl linoleate **3** [23]. In fact, the polyunsaturated fatty acid esters **3**, **4**, and **5** show the same order of reactivity with α -Toc \cdot (k_{abstr}/H), as listed in Table 1. These fatty acid esters **3**, **4**, and **5** have two, four, and six hydrogen atoms activated by two π -electron systems, respectively, and thus the rate constants, k_{abstr}/H , given on an available hydrogen basis, are $k_p/2 = 4.16 \times 10^{-2} M^{-1} s^{-1}$ for **3**, $k_p/4 = 4.79 \times 10^{-2} M^{-1} s^{-1}$ for **4**, $k_p/6 = 4.05 \times 10^{-2} M^{-1} s^{-1}$ for **5**, if we neglect the contribution from the oleate-type four $-CH_2-$ hydrogen atoms activated by a single π -electron system in **3**, **4**, and **5**. These values are similar to each other, and by one order of magnitude larger than that ($4.75 \times 10^{-3} M^{-1} s^{-1}$) of ethyl oleate **2**. Since ethyl stearate **1**, which does not contain allylic hydrogens, negligibly react with α -Toc \cdot radical, we estimated that k_p of ethyl stearate **1** will be $\lesssim 1 \times 10^{-2} M^{-1} s^{-1}$. The results suggest that α -Toc \cdot radicals produced in edible oils and biomembranes mainly react with polyunsaturated lipids by abstracting hydrogen atoms activated by two π -electron systems, and induce the peroxidation of lipids.

As described in Introduction, the rate constant (k_4) for the reaction of methyl linoleate hydroperoxide (LOOH)

with α -Toc \cdot radical (reaction 4), i.e., the reverse of reaction 1 was reported [12]. The k_4 value was $5.0 \times 10^{-1} \text{ M}^{-1} \text{ s}^{-1}$ in benzene at 25.0 °C. On the other hand, the k_p values obtained for the reaction of LH 3, 4, and 5 with α -Toc \cdot radical are 0.833×10^{-1} , 1.92×10^{-1} , and $2.43 \times 10^{-1} \text{ M}^{-1} \text{ s}^{-1}$ in toluene at 25.0 °C, respectively, as listed in Table 1. The value of k_4 is 6.0, 2.6, and 2.1 times larger than those of k_p for 3, 4, and 5, respectively. However, the concentration of LOOH is much lower than that of LH in the initial stage of LH peroxidation. Consequently, the contribution of the reaction 4 is considered to be small and negligible. The initial prooxidant effect of α -TocH is induced by the hydrogen abstraction from LH by α -Toc \cdot (reaction 3). When the autoxidation proceeds and the concentration of LOOH increases, reaction 4 will contribute to the prooxidant effect of α -TocH.

It is well known that α -TocH is the major endogenous lipid-soluble antioxidant in human plasma [27], low-density lipoprotein (LDL) [24, 28] and edible oils, and acts as an antioxidant by protecting polyunsaturated fatty acids and lipids from peroxidation. However, for instance, if “antioxidant” α -TocH in high concentrations exists in edible oils, lipid peroxidations are accelerated, and further, the rate of lipid peroxidation increases by increasing the concentration of α -TocH [7, 8, 10]. Similarly, α -TocH acts as a prooxidant to oxidize polyunsaturated lipids in LDL in the absence of other endogenous antioxidants such as vitamin C and ubiquinol-10, as reported by Bowry et al. [9, 29]. They proposed that this prooxidant activity of α -TocH is caused by reaction of the α -Toc \cdot with active LH groups in LDL. It has been reported that, not only vitamin C and ubiquinol-10, but also many polyphenols (such as flavonoids [30], catechins [31], and caffeic acids [32]) function as antioxidants by regenerating α -Toc \cdot to α -TocH in LDL system. Similar tocopherol-mediated peroxidation and α -tocopherol regeneration reactions might take place in other biological systems.

The rate constants (k_r) for the regeneration reaction 5 from α -Toc \cdot to α -TocH have been reported for many natural antioxidants. For instance, the values are $2.73 \times 10^6 \text{ M}^{-1} \text{ s}^{-1}$ for vitamin C (sodium ascorbate) in ethanol:water (=5:1, v/v) solution [17], $3.74 \times 10^5 \text{ M}^{-1} \text{ s}^{-1}$ for ubiquinol-10 in benzene [15], and $2.39 \times 10^4 \text{ M}^{-1} \text{ s}^{-1}$ for epigallocatechin gallate (EGCG) in ethanol:water (=5:1, v/v) solution [33]. These values are ca. 10^5 – 10^7 times larger than those ($k_p = 8.33 \times 10^{-2}$ – $2.43 \times 10^{-1} \text{ M}^{-1} \text{ s}^{-1}$) for 3, 4, and 5 in toluene. The k_r value for caffeic acid is $2.31 \times 10^2 \text{ M}^{-1} \text{ s}^{-1}$ in ethanol [33], and by two to four orders of magnitude smaller than those for vitamin C, ubiquinol-10, and EGCG. However, it is by three orders of magnitude larger than those (k_p) for 3, 4, and 5. The results suggest that these antioxidants may contribute to the prevention of the prooxidant effect of α -TocH in many biological systems.

Summary

The hydrogen abstraction reaction of α -Toc \cdot radical from lipids is considered to be a key reaction for the prooxidant effect of α -TocH. However, a detailed kinetic study for the reaction between α -Toc \cdot radical and lipids (unsaturated fatty acids) (reaction 3) has not been performed so far, because α -Toc \cdot radical is unstable, showing the large self-bimolecular reaction rate constant ($2k_d = 8.00 \times 10^2 \text{ M}^{-1} \text{ s}^{-1}$) (reaction 6). In the present work, we have succeeded in determining the second-order rate constants (k_p) for the reaction of five kinds of saturated and unsaturated fatty acid ethyl esters (ethyl stearate 1, ethyl oleate 2, ethyl linoleate 3, ethyl linolenate 4, ethyl arachidonate 5) with α -Toc \cdot radical (reaction 3), using a double-mixing stopped-flow spectrophotometer. The k_p values obtained are $< \sim 1 \times 10^{-2} \text{ M}^{-1} \text{ s}^{-1}$ for 1, 1.90×10^{-2} for 2, 8.33×10^{-2} for 3, 1.92×10^{-1} for 4, and 2.39×10^{-1} for 5 in toluene, indicating that the rate constants decrease as the number of the double bond in fatty acid ethyl esters decreases in the order of $5 > 4 > 3 > 2 > 1$. The rate constants (k_p) for 2–5 were compared with the rate constants for the regeneration reaction (k_r) of α -Toc \cdot radical to α -TocH by natural antioxidants (such as vitamin C, ubiquinol-10, polyphenols), suggesting that the prooxidant effect of α -tocopherol may be prevented by these antioxidants.

References

- Niki E (1987) Antioxidants in relation to lipid peroxidation. *Chem Phys Lipids* 44:227–253
- Barclay LRC (1993) Model biomembranes: quantitative studies of peroxidation, antioxidant action, partitioning, and oxidative stress. *Can J Chem* 71:1–16
- Jiang Q, Christen S, Shigenaga MK, Ames BN (2001) γ -Tocopherol, the major form of vitamin E in the US diet, deserves more attention. *Am J Clin Nutr* 74:714–722
- Traber MG, Atkinson J (2007) Vitamin E, antioxidant and nothing more. *Free Radic Biol Med* 43:4–15
- Mukai K, Tsuzuki N, Ouchi S, Fukuzawa K (1982) Electron spin resonance studies of chromanoxyl radicals derived from tocopherols. *Chem Phys Lipids* 30:337–345
- Burton GW, Doba T, Gabe EJ, Hughes L, Lee FL, Prasad L, Ingold KU (1985) Autoxidation of biological molecules. 4. Maximizing the antioxidant activity of phenols. *J Am Chem Soc* 107:7053–7065
- Cillard J, Cillard P, Cormier M, Girre L (1980) α -Tocopherol prooxidant effect in aqueous media: increased autoxidation rate of linoleic acid. *J Am Oil Chem Soc* 57:252–255
- Terao J, Matsushita S (1986) The peroxidizing effect of α -tocopherol on autoxidation of methyl linoleate in bulk phase. *Lipids* 21:255–260
- Bowry VW, Stocker R (1993) Tocopherol-mediated peroxidation. The prooxidant effect of vitamin E on the radical-initiated oxidation of human low-density lipoprotein. *J Am Chem Soc* 115:6029–6044

10. Mukai K, Noborio S, Nagaoka S (2005) Why is the order reversed? Peroxyl-scavenging activity and fats-and-oils protecting activity of vitamin E. *Int J Chem Kinet* 37:605–610 and references are cited therein
11. Kagan VE, Quinn PJ (eds) (2001) *Coenzyme Q: molecular mechanisms in health and disease*. CRC Press, USA
12. Mukai K, Sawada K, Kohno Y, Terao J (1993) Kinetic study of the prooxidant effect of tocopherol. Hydrogen abstraction from lipid hydroperoxides by tocopheroxyls in solution. *Lipids* 28:747–752
13. Nagaoka S, Sawada K, Fukumoto Y, Nagashima U, Katsumata S, Mukai K (1992) Mechanism of prooxidant reaction of vitamin E. Kinetic, spectroscopic, and ab initio study of proton-transfer reaction. *J Phys Chem* 96:6663–6668
14. Packer JE, Slater TF, Willson RL (1979) Direct observation of a free radical interaction between vitamin E and vitamin C. *Nature* 278:737–738
15. Mukai K, Itoh S, Morimoto H (1992) Stopped-flow kinetic study of vitamin E regeneration reaction with biological hydroquinones (reduced forms of ubiquinone, vitamin K, and tocopherolquinone) in solution. *J Biol Chem* 267:22277–22281
16. Bisby RH, Parker AW (1995) Reaction of ascorbate with the α -tocopheroxyl radical in micellar and bilayer membrane systems. *Arch Biochem Biophys* 317:170–178
17. Nagaoka S, Kakiuchi T, Ohara K, Mukai K (2007) Kinetics of the reaction by which natural vitamin E is regenerated by vitamin C. *Chem Phys Lipids* 146:26–32
18. Lucarini M, Pedulli GF, Cipollone M (1994) Bond dissociation enthalpy of α -tocopherol and other phenolic antioxidants. *J Org Chem* 59:5063–5070
19. Gregor W, Grabner G, Adelwhrer C, Rosenau T, Gille L (2005) Antioxidant properties of natural and synthetic chromanol derivatives: study by fast kinetics and electron spin resonance spectroscopy. *J Org Chem* 70:3472–3483
20. Mukai K, Ouchi A, Mitarai A, Ohara K, Matsuoka C (2009) Formation and decay dynamics of vitamin E radical in the antioxidant reaction of vitamin E. *Bull Chem Soc Jpn* 82:494–503 and references are cited therein
21. Remorova AA, Roginsky VA (1991) Rate constants for the reaction of α -tocopherol phenoxy radicals with unsaturated fatty acid esters, and the contribution of this reaction to the kinetics of inhibition of lipid oxidation. *Kinet Catal* 32:726–731
22. Watanabe A, Noguchi N, Fujisawa A, Kodama T, Tamura K, Cynshi O, Niki E (2000) Stability and reactivity of aroxyl radicals derived from a novel antioxidant BO-653 and related compounds. Effects of substituent and side chain in solution and membranes. *J Am Chem Soc* 122:5438–5442
23. Nagaoka S, Okauchi Y, Urano S, Nagashima U, Mukai K (1990) Kinetic and ab initio study of the prooxidant effect of vitamin E. Hydrogen abstraction from fatty acid esters and egg yolk lecithin. *J Am Chem Soc* 112:8921–8924
24. Mukai K, Morimoto H, Okauchi Y, Nagaoka S (1993) Kinetic study of reactions between tocopheroxyl radicals and fatty acids. *Lipids* 28:753–756
25. Mukai K, Watanabe Y, Uemoto Y, Ishizu K (1986) Stopped-flow investigation of antioxidant activity of tocopherol. *Bull Chem Soc Jpn* 59:3113–3116
26. Rieker A, Scheffler K (1965) Die Beteiligung von Phenylresten an der Aroxylmesomerie. *Liebigs Ann Chem* 689:78–92
27. Burton GW, Ingold KU (1986) Vitamin E: applications of the principles of physical organic chemistry to the exploration of its structure and function. *Acc Chem Res* 19:194–201
28. Esterbauer H, Ramos P (1995) Chemistry and pathophysiology of oxidation of LDL. *Rev Physiol Biochem Pharmacol* 127:31–64
29. Bowry VW, Ingold KU, Stocker R (1992) Vitamin E in human low-density lipoprotein. *Biochem J* 288:341–344
30. Vinson JA, Jang J, Yang J, Dabbagh Y, Liang X, Serry M, Proch J, Cai S (1999) Vitamins and especially flavonoids in common beverages are powerful in vitro antioxidants which enrich lower density lipoproteins and increase their oxidative resistance after ex vivo spiking in human plasma. *J Agric Food Chem* 47:2502–2504
31. Liu Z-Q, Ma L-P, Zhou B, Yang L, Liu Z-L (2000) Antioxidative effects of green tea polyphenols on free radical initiated and photosensitized peroxidation of human low density lipoprotein. *Chem Phys Lipids* 106:53–63
32. Laranjinha J, Cadenas E (1999) Redox cycles of caffeic acid, α -tocopherol, and ascorbate: implications for protection of low-density lipoproteins against oxidation. *IUBMB Life* 48:57–65
33. Ohara K, Ichimura Y, Tsukamoto K, Ogata M, Nagaoka S, Mukai K (2006) Kinetic study on the free radical-scavenging and vitamin E-regenerating actions of caffeic acid and its related compounds. *Bull Chem Soc Jpn* 79:1501–1508

Changes in Oil Content of Transgenic Soybeans Expressing the Yeast *SLC1* Gene

Suryadevara S. Rao · David Hildebrand

Received: 12 September 2008 / Accepted: 26 July 2009 / Published online: 19 September 2009
© AOCs 2009

Abstract The wild type (Wt) and mutant form of yeast (sphingolipid compensation) genes, *SLC1* and *SLC1-1*, have been shown to have lysophosphatidic acid acyltransferase (LPAT) activities (Nageic et al. in *J Biol Chem* 269:22156–22163, 1993). Expression of these LPAT genes was reported to increase oil content in transgenic *Arabidopsis* and *Brassica napus*. It is of interest to determine if the TAG content increase would also be seen in soybeans. Therefore, the wild type *SLC1* was expressed in soybean somatic embryos under the control of seed specific phaseolin promoter. Some transgenic somatic embryos and in both T2 and T3 transgenic seeds showed higher oil contents. Compared to controls, the average increase in triglyceride values went up by 1.5% in transgenic somatic embryos. A maximum of 3.2% increase in seed oil content was observed in a T3 line. Expression of the yeast Wt LPAT gene did not alter the fatty acid composition of the seed oil.

Keywords Fatty acid analysis · Analytical techniques · Plant lipid biochemistry · Neutral lipid biosynthetic enzymes · Metabolism

Abbreviations

ACC Acetyl CoA carboxylase
DGAT Diacylglycerol acyltransferase
GPAT Glycerol-3-phosphate acyltransferase

LPAT The lyso-phosphatidic acid acyltransferase
ACS Long-chain-acyl CoA synthetase
QTL Quantitative trait loci
TAG Triacylglycerol
Wt Wild type

Introduction

Different plant species vary greatly in seed storage reserves with some grain seeds having >85% starch, while 50–70% oil in oil seeds, and legumes such as soybeans with 40% protein and 20% oil of the seed dry weight [2]. Soybeans are the largest oil seed crop in the world followed by Brassica, peanut, sunflower and cotton seeds [3, 4]. There is a significant amount of vegetable oil that is used for industrial purposes. For example, of the ~380 million tons of oilseeds produced in 2005, about 85% of the extracted oil is used for food and cooking applications, while nearly 15% is put to use in industry for, among others, lubricants, inks, coatings, plasticizers and biodiesel [5]. Since oil production has such tremendous importance, conventional and genetic engineering strategies are being applied to improve oil quantity and quality in oil seed crops [6].

The Kennedy pathway is the major TAG pathway of plants [7, 8] with the three acyltransferases the glycerol-3-phosphate acyltransferase (GPAT, EC 2.3.1.15), the lyso-phosphatidic acid acyltransferase (LPAT, EC 2.3.1.51) and the diacylglycerol acyltransferase (DGAT, EC 2.3.1.20) operating in a sequential manner. The other enzymes that directly participate in the DAG to TAG conversion are DAG transacylase and phospholipid-DAGAT [9]. Over-expression of Kennedy pathway enzymes, GPAT [10]; yeast LPAT [11, 12]; DAGAT [13, 14] have reportedly

Electronic supplementary material The online version of this article (doi:10.1007/s11745-009-3337-z) contains supplementary material, which is available to authorized users.

S. S. Rao · D. Hildebrand (✉)
Plant and Soil Sciences, University of Kentucky,
Lexington, KY 40546, USA
e-mail: dhild@uky.edu

increased oil content in plants and yeast. Maize high oil QTL (Qho6) encodes a mutated DAGAT1-2 allele [15]. Besides the Kennedy pathway, other pathway enzymes like glucose metabolism enzymes like glycerol-3-phosphate dehydrogenase (GPDH, EC 1.1.1.8) [16] and Dof-type transcription factors [17] were also implicated in the seed oil increase. *Arabidopsis* transcriptional factor FUSCA3 (FUS3) was implicated in the increased oil content in *Arabidopsis* seeds [18].

Saccharomyces cerevisiae sphingolipid suppressor gene, *SLC1-1* and the wild type *SLC1* gene proved to be acyltransferases with LPAT activity [1, 11]. Transforming plants with wild type (*SLC1*) and mutated (*SLC1-1*) forms of yeast genes resulted in increased triglyceride levels [11, 12, 19]. So far there are no reports on soybean seed oil enhancement except the high oil cultivar N88–480 developed by [20] through conventional breeding though several strategies were successfully reported for seed oil increase in plants [10, 14–16, 21]. Soybean seed expressing a diacylglycerol acyltransferase 2A from the soil fungus *Umbelopsis* (formerly *Mortierella*) *ramanniana* showed a 1.5% increase in oil levels [22].

An important method of soybean regeneration is somatic embryogenesis. Embryogenic tissues can be proliferated by subculture on a solid proliferation (MSD20) medium or a liquid suspension culture medium [23, 24]. Through somatic embryogenesis, genetic engineering of soybean has proved to be a powerful technique for improving seed compositions including the oil for enhanced edible and industrial purposes [25–27]. Furthermore, somatic embryo proliferation can result in a higher number of somatic embryos [24] thus probably increasing the rate of recovery. Another potential advantage of the somatic embryos system is that they are good targets in many cases of seed specific traits since they can be analyzed at the mature soybean somatic embryo stage prior to the zygotic embryonic stage, thus saving labor and time [28–33].

Here in this paper we report the generation of transgenic soybean somatic embryos (SS embryos) expressing the yeast *SLC1* gene with increased total lipids. We also report the generation of fertile transgenic soybean plants with seeds showing increased oil content.

Materials and Methods

Plant Material

Soybeans [*Glycine max* (L.) Merrill cv. ‘Jack’] were grown in a greenhouse at the University of Kentucky, Lexington under a 16 h photoperiod at 35 °C day and 25 °C night temperature. Pods with immature seeds were surface sterilized by immersing for 30 s in 70% 2-isopropyl alcohol

followed by a 10 min immersion in 25% bleach solution (with 1.5% final hypochlorite concentration) with a few drops of Liquinox (detergent). The pods were then rinsed three times in sterile water for 5 min each time. Immature seeds 3–6 mm in length were removed from the pods. The end containing the embryonic axis was cut off and discarded. Then the two cotyledons were pushed out from the seed coat, separated and placed with abaxial side (round side) down on MSD40 (Murashige and Skoog salts, 40 mg/l 2,4-dichlorophenoxyacetic acid, B5 vitamins, sucrose (3% wt/vol) with 0.2% gelrite) medium [34]. Cultures were then incubated at 25 °C at a 23 h photoperiod (low light intensity, 5–10 μE). Globular staged somatic embryo clusters were harvested from the explant tissues 4–6 weeks after induction and then placed on MSD20 (MS salts, B5 vitamins, sucrose (3% wt/vol), 20 mg/l 2,4-D with 0.2% gelrite) solid medium for a period of 1 month for proliferation. Embryogenic tissues were then transferred from MSD20 to FNL (Finer and Nagasawa “lite”) “liquid medium” [24] for further proliferation. Suspension cultures were agitated at 100 rpm and maintained with a 2 week subculture period at 25 °C with a 23 h photoperiod. The T1 and T2 generation transgenic plants were grown in the green house under the same conditions as described above for the Jack control plants.

Vector Construction

The amplified *SLC1* gene product was cloned into the PGEM T-vector. The product was sequenced using T7 and SP6 vector sequencing primers to confirm the sequence of the ligated product. A 0.9-kbp *NcoI/HpaI* T-Vector digested *SLC1* fragment was cloned into a pPHI472 vector [29] digested with the same enzymes to put the *SLC1* gene under the seed specific phaseolin promoter and phaseolin terminator. The whole cassette was digested with *EcoRI/PstI* and ligated to a pCAMBIA 1201 (Genbank accession number AF234293) plant transformation vector digested with the same restriction enzymes. The pCAMBIA 1201 binary vector has a chloramphenicol resistance gene for bacterial selection and a hygromycin resistance gene for plant selection. The GUS reporter gene was driven by the constitutive CaMV 35S promoter.

Microprojectile Bombardment

Green embryo clumps were slightly pressed with a spatula to partially separate them and were placed in the center of a moist filter paper in sterile petri plates (approximately 100–150 mg of somatic embryos per plate) and partially desiccated in a laminar flow hood for 15 min prior to bombardment. Transformation was carried out via particle bombardment with a gene gun (Dupont PDS1000; Bio-Rad Laboratories, Hercules, and CA) by gold/DNA

microprojectile preparations as described by [34]. Briefly, for 9 shots, 25 µg of plasmid DNA was used to coat 7.5 mg of 0.6 µm gold particles. Cultures were bombarded at 10,687 kPa (1,550 psi) helium gas pressure under 91 kPa (27 in) of Hg vacuum, at a shooting distance of 11 cm from the rupture disk to the target tissue. Immediately after bombardment, embryogenic cultures were placed on D20 proliferation media without any selective agent for 7 days.

Selection and Regeneration of Transformants

Bombarded globular SS embryos that were cultured on D20 were transferred (approximately 100 clumps of 0.3–0.4 cm diameter per plate) to FN Lite medium Samoylov et al. [35] containing 25 mg/l hygromycin. After 3–4 weeks, visibly growing clumps were moved to fresh selection medium. After approximately 12 weeks, green looking hygromycin resistant SS embryo clumps were transferred from FN Lite into 500-ml Erlenmeyer flasks containing 100 ml of liquid MS0 (MS salts, B5 vitamins and 3% sucrose) medium as described by Samoylov et al. [24]. Prior to transfer into flasks, each embryogenic cluster was gently pressed with a spatula to partially separate the individual globular-stage embryos. At 4 weeks, the resulting cotyledon-stage embryos were analyzed for GUS staining (β -glucuronidase) and RNA isolation. Some of the embryos were desiccated as described in [24]. Ten to twelve matured embryos were placed in a 100 × 15 mm Petri dish and sealed with Nescofilm. To allow gradual desiccation of embryos over a period of 5–7 days, a small piece (approximately 1 cm³) of solid MS0 medium (MSO medium with 0.2% Gelrite) was placed in the middle of the plate away from the embryos. Desiccated embryos were germinated on 1/5th MS medium (1/5th concentration of MS salts, B5 vitamins, 0.4% Gelrite without sucrose).

Yeast DNA Isolation and *SLC1* Gene Amplification

A pellet from a 10-ml culture of Yeast strain *InVsc1* (Invitrogen, Carlsbad, CA) was homogenized with mortar and pestle. Total DNA was isolated from the homogenized yeast following the procedure described by [36]. The *SLC1* gene [1] was directly amplified from yeast genomic DNA since no introns sequences were found. With 100 ng of yeast genomic DNA as template, PCR was done to amplify the *SLC1* gene using the primers 5'-CCATGGATGAGTG TGATAGGTAGGTTTC-3' and 5'-GTTAACAATGCATCT TTTTACAGATGA-3' for the sense and antisense strand, respectively. *NcoI* restriction site was added to the forward primer while the reverse primer was designed with a *HpaI* site. The PCR conditions were 94 °C for 2 min; 30 cycles at 94 °C, 30 s; 55 °C, 30 s; 72 °C, 1 min and a final extension at 72 °C for 8 min.

Plant DNA Isolation

Genomic DNA was isolated from soybean leaves and embryos as described by Reddy et al. [36]. Screening of transgenic soybean lines was done by PCR of the *SLC1* gene using 200 ng of the genomic DNA in 50-µl reactions. The primers and the PCR conditions for *SLC1* gene amplification were as described above.

Southern Blotting

Five micrograms of DNA was digested overnight with *EcoRI*, fractionated on a 0.8% agarose gel, and blotted onto a Zetaprobe membrane (Bio-Rad). Hybridization was done overnight at 42 °C in a hybridization solution containing 50% formamide, 0.12 M Na₂HPO₄, 0.25 M NaCl, and 1 mM EDTA with a *SLC1* gene-specific fragment random prime labeled with [α ³²P]-dCTP (Prime-It II Random Primer Labeling Kit; Stratagene, La Jolla, CA) as a probe. The membrane was washed three times at room temperature in 0.1 × SSC (1 × SSC is 0.15 M NaCl plus 0.015 M sodium citrate) and 0.1% SDS and exposed in a phosphorImager cassette (Molecular Dynamics, Sunnyvale, CA). The intensity of hybridized DNA bands was estimated using the ImageQuant software program (Molecular Dynamics).

RT-PCR

Total RNA was extracted from the hygromycin resistant matured soybean somatic embryos using the Trizol reagent as advised by the manufacturer (Invitrogen Corporation, Carlsbad, USA). Using the isolated total RNA as a template, reverse transcription was performed for the synthesis of the first-strand cDNA using oligo dT as prescribed by manufacturers of the Kit (Sigma-Aldrich Corporation, St. Louis, MO, USA) in a 20-µl reaction at 48 °C for 45 min. A 2-µl aliquot of the RT reaction was used in a 50-µl PCR reaction with the following profile: 94 °C for 2 min; 30 cycles at 94 °C, 30 s; 55 °C, 30 s; 72 °C, 1 min and a final extension at 72 °C for 8 min. The primers used were the same as in the PCR reaction described for *SLC1* gene amplification.

Lipid Analysis

Lipids were isolated as described in [37]. Total lipids were extracted independently from seed chips (~2 mg) cut from ten different matured seeds for each line. For fatty acid analysis of matured somatic embryos ten individual 5 week old (matured on 6% maltose containing MS medium plates) somatic embryos of a clone were used. The somatic embryos were desiccated before lyophilization. To allow

gradual desiccation of embryos over a period of 5 days a small piece (approximately 1 cm³) of solid MS0 medium was placed in the middle of the plate away from the embryos. The desiccated embryos were freeze dried and weighed. TAG (triacylglycerol) contents were calculated from the addition of known amounts of tri -17:0 (1,2,3-Triheptadecanoylglycerol, Sigma-Aldrich Corporation, St. Louis, MO, USA) internal standard added to the somatic embryos and seed chips before lipids were extracted. The lipids were methylated with 0.5 ml of sodium methoxide (4.2%, wt/vol) with shaking at 800 rpm for 45 min. The fatty acid methyl esters were extracted with 1 ml of hexane twice. The hexane extracts were combined and then washed with 1 ml of 0.9% KCl. The fatty acid methyl esters in hexane were analyzed by gas chromatography (Hewlett Packard 5890 with a flame ionization detector) on FFAP column of 14 m × 0.25 mm, 0.33 μm film thickness. The temperature program started from 140 °C for 1 min, then increased to 235 °C at a rate of 10 °C/min and held at this temperature for 20 min.

Additionally oil and protein content of the zygotic seeds were analyzed using a near infrared (NIR) analyzer as described by [38]. NIR analyses were performed in triplicate compared to the known oil and protein content of control soybean cultivar Jack [39] and high oil seeds, N88–480 [20].

Results

PCR, GUS staining and Southern blot hybridization techniques were used to identify the transgenic nature of the embryos and plants obtained by hygromycin selection. Thirteen transgenic lines were PCR positive for the introduced *SLC1* gene [S1 (supplementary SFig. 1)] when analyzed at the embryo stage. Only nine of those lines were further regenerated. The expected fragment size of 0.9 kbp was amplified in the transgenic samples but not in the negative control embryos. As a positive control, a *SLC1* expression cassette containing pCAMBIA 1201 vector DNA was used. Genomic DNA from empty pCAMBIA 1201 vector transformed embryos and the untransformed Jack embryos were used as negative controls. A strong PCR band was observed in the positive controls. No *SLC1* amplification was seen in the negative controls.

Southern blot hybridization was done for the first five independent transgenic lines (SFig. 1) for the presence of the *SLC1* gene. Southern blot hybridization (Fig. 1) analysis of these transgenic plants indicated the integration of the *SLC1* gene into the soybean genome. As expected, Southern blot hybridization bands from the transgenic plants were much larger than the size of the *SLC1* fragment. Southern blot analysis also revealed that the

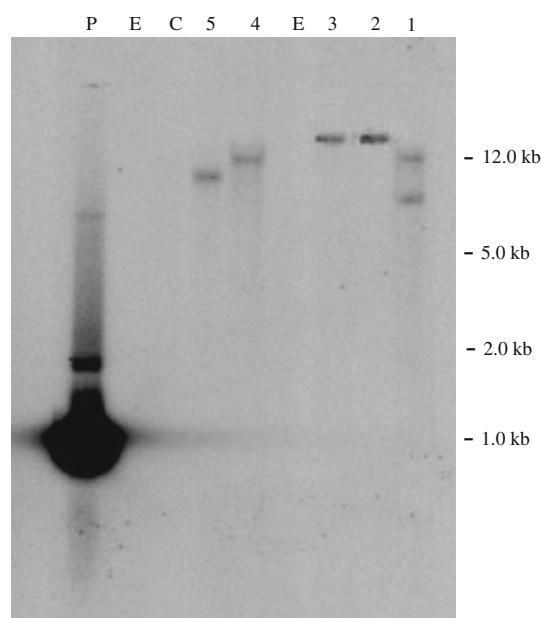


Fig. 1 Southern blot hybridization of yeast *LPAT* (*SLC1*) transgenic plants. Each lane represents a different transgenic line. Genomic DNA was digested with *EcoRI*. Since the yeast *SLC1* gene has no internal *EcoRI* restriction sites total DNA was digested with *EcoRI* restriction enzyme. As a positive control the PCR amplified 0.9 kb *SLC1* fragment was used. Lane 1 has two hybridization bands while other transgenic lines have single copy insertions of the transgene. The bands representing the *SLC1* transgenic lines are larger in size than the positive control. Molecular weights are given on the sides. Letters “P” and “C” represents positive and negative controls. “E” indicates an empty lane

introduced gene copy number varied from one to two. Four of the five transgenic plants analyzed have varying sized single insertions of the introduced *SLC1* cassette. A single transgenic plant (Plant 1) had two copies of the introduced gene. All the transgenic plants regenerated grew normal and set flowers and pods (SFig. 2). Except plant 3 all other southern positive plants are turned out to be GUS positive (SFig. 3). GUS expression among different transgenics lines varied with the blue GUS stain was visible in the leaves and flowers of some lines while it was visible only in the flowers in others (SFig. 3). The reasons for such variation are not clear since the GUS gene was expressed under a constitutive CaMV 35S promoter. GUS staining was also visible in the cotyledons and in the axis of matured somatic embryos (SFig. 4).

Total lipid content was analyzed in matured *SLC1* transgenic and vector control transformed soybean somatic embryos (Fig. 3). On average the total lipid content of the *SLC1* transgenic embryos was found to be 1.5% higher than the transgenic vector controls and Jack control embryos. In addition to GUS analysis (SFig. 4) RT-PCR was done to determine the expression of the introduced *SLC1* gene in matured somatic embryos (SFig. 5). Transgenic plant line 8 was established from the somatic

Table 1 Percentage oil content in T2 seeds of transgenic plants

Plant line	% oil
Control	20.7 ± 0.5
1	21.0 ± 1.8
2	22.7 ± 1.3
3	23.3 ± 0.9
4	22.4 ± 0.9
5	23.2 ± 1.5
6	21.6 ± 0.8
7	21.3 ± 0.9
8	21.8 ± 2.2
9	18.8 ± 1.7

embryos analyzed for total lipid content. As shown in Table 1 the seeds of transgenic line 8 also had a similar increase in total lipid content.

The total seed lipid content was analyzed from the seeds of greenhouse grown T1 and T2 plants. PCR was done to identify the presence of the *SLC1* gene in the T2 generation transgenic plants. The TAG content of vector transformed Jack control seeds was ~20% on a dry weight basis (Table 1) while some of the T2 transgenic seeds had increased total lipid contents that varied from 0.6 to 2.5% (Table 1). The average total lipid content of T2 generation *SLC1* transgenic line 9 were found to be lower than the vector-transformed Jack controls while transgenic line 1 had similar values (Table 1). TAG analysis of T3 seeds have shown that lines 1–11, 3–4, 3–9 and 6–20 have oil content increases of 1.6–3.2% compared to the vector control (Fig. 2). The T3 seeds of plants 1–11, 3–4, 3–9 and 6–20 represents the progeny of T1 transgenic lines 1, 3, and 6, respectively. The high oil cultivar N88–480 [20] showed TAG content of 22.5% by seed dry weight and the untransformed Jack plant 20.2%. The increase in lipid

content of these *SLC1* transgenics was accompanied by a decrease in protein content (Fig. 2).

Discussion

Some *Brassica* and *Arabidopsis* seeds that expressed the *SLC1* and its mutant form, *SLC1-1* genes with LPAT activity in yeast [1, 11, 19] showed increased oil levels. The present investigation examined the impact of the wild type *SLC1* gene on total fatty acid levels in soybean somatic embryos and seeds. Some transgenic soybeans thus developed showed high oil in the T2 and T3 seeds. The initial aim behind transforming *Brassica* with yeast *SLC1-1* gene was to increase erucic acid content though the transgenics also showed higher oil content [11]. As explained by Zou et al. [11] for *Brassica* and *Arabidopsis*, endogenous LPAT regulation might be one of the controlling steps in the TAG accumulation in soybeans also. Yeast LPAT with no significant homology to plant LPATs is likely not recognized by regulatory systems in plants thus creating a sink towards TAG accumulation in soybean seeds. Currently, there are at least 53 QTLs (quantitative trait loci) associated with oil content in different soybean cultivars, however, most of the QTLs are not confirmed [40]. As the accumulation of different storage components needs the coordination of several genes that encode the enzymes of the respective pathways [2] it will be interesting to know if any of the high oil QTLs encode for LPATs or for that matter any of the three Kennedy pathway acyltransferases. Besides yeast LPAT, safflower GPAT (glycerol-3-phosphate acyltransferase,) [10], *Mortierella* GPAT [41] and DGAT (Diacylglycerol acyltransferase) from *Arabidopsis* [21] have been reported to increase oil content in plants and yeast. A maize high oil QTL (Qho6) was recently analyzed [15] and known to encode DGAT.

Although larger seed sizes and ~40% increase in seed oil content have been reported for *Brassica* and *Arabidopsis* that expressed the yeast *SLC1* gene [11, 19] no such dramatic results were noticed in the case of soybean seeds by us. The highest increases observed were similar in values reported for high oil line N88–480 [20]. Maybe the smaller increase in seed oil might be a reason for regular seed sizes in case of *SLC1* transgenic soybean. To date the only soybean gene reported to have increased seed oil content when over-expressed are the two Dof-type transcription factor genes *GmDof4* and *GmDof11* [17]. When over-expressed in *Arabidopsis* these genes increased oil content. Over-expression of these genes activated the acetyl CoA carboxylase (ACC, EC 3.1.3.44) and long-chain-acyl CoA synthetase (ACS, EC 6.2.1.3). So one of the 58 reported QTLs of soybean oil enhancement might include these transcription factors also.

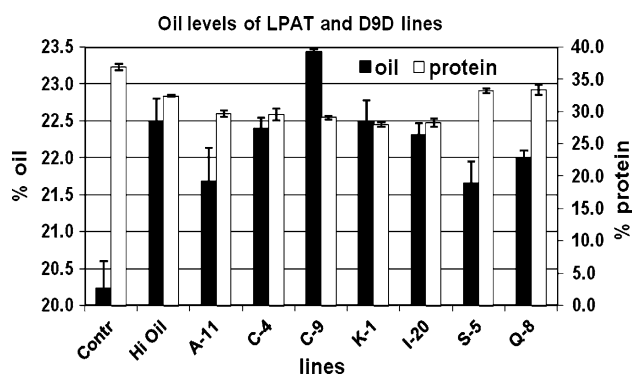


Fig. 2 Mean percentages oil and protein ± standard errors (SE) in T3 seed of some of the high oil transgenic plant lines, vector controls and high oil line N88–480 (*Hi*). Compared to the vector controls all the other lines had higher oil and lower protein levels. Line 3–9 showed the highest oil content

There is typically a negative correlation between protein and oil concentration in soybean seed [42]. Wilcox [43] showed that increased protein amounts led to a decrease in oil content in soybeans. Interestingly the two soybean transcription factors *GmDof4* and *GmDof11* that elevated the activity of lipid biosynthesis enzymes also down regulated the seed storage protein gene *CRA1* in *Arabidopsis* [17]. In the case of *SLC1* transgenics also we have noticed that an increase in oil content was associated with reduced protein amounts (Fig. 2). Our results also indicate that the oil increase in soybean seeds expressing this yeast gene with LPAT activity was at the expense of protein content [44].

Somatic embryos mimic zygotic embryos in developmental and physiological aspects [45, 46]. Confirming the expected transgenic trait at the somatic embryo stage itself saves time and effort in soybean transgenic research. If a desired trait is observed in somatic embryos different clones can be screened for better producers of the end product and further taken to germination. Transgenic soybean somatic embryos were screened for fatty acid modification traits. Liu et al. [29] were the first to show palmitoleic acid in the soybean somatic embryos by over-expressing a mammalian Δ^9 desaturase (SCD, EC 1.14.19.1). Cahoon et al. [32] produced vernolic acid and 12-epoxy-octadeca-9,15-dienoic acid; Δ^5 -eicosenoic acid and Δ^5 -hexadecenoic acid [31]; α -eleostearic acid and α -parinaric acids [30] in soybean somatic embryos by over-expressing the transgenes responsible for the synthesis of these compounds. As mentioned in the introduction several embryos can be generated and proliferated from a single clone of transgenic embryo. On an average when 10 embryo clones were analyzed the *SLC1* expressing embryo line has 1.5% increase in oil content compared to the vector control and untransformed Jack embryos (Fig. 3). In the T2 seeds of the transgenic line 8 produced from these embryos the TAG content increase was found to be similar

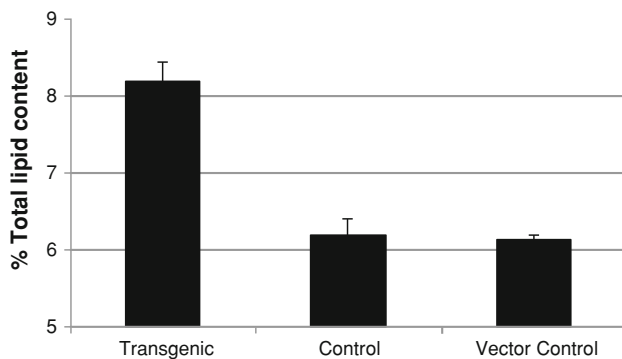


Fig. 3 Total lipid content of freeze dried *SLC1* transgenic soybean somatic embryos, Jack control and vector control embryos. The data represents three independent experiments. The bars represent standard errors

(Table 1). Besides the hygromycin resistance we have confirmed the transgenic status of the embryo line by RT-PCR by amplifying the introduced the *SLC1* gene and GUS analysis. This is the report on the total fatty acid content of transgenic somatic embryos being correlated with an increase in oil content of transgenic soybean seeds.

In conclusion, expression of the yeast *SLC1* gene that codes for a yeast lyso-phosphatidic acid acyltransferase led to an increase in soybean seed oil content. The increase in seed oil was accompanied by a reduction in seed protein content.

Analysis of soybean somatic embryos over-expressing the yeast *SLC1* gene led to an increase in total fatty acid content. Soybean somatic embryos can be used for analyzing quantitative changes in oil content before germinating and growing plants thus saving time and effort.

Acknowledgments The authors acknowledge the technical help provided by Wei Chen. The authors also acknowledge the financial support of the United Soybean Board and the support of the Kentucky Agricultural Experiment Station.

References

- Nageic M, Wells GB, Lester RL, Dickson RC (1993) A suppressor gene that enables *Saccharomyces cerevisiae* to grow without making sphingolipids encodes a protein that resembles and *Escherichia coli* fatty acyltransferase. *J Biol Chem* 269:22156–22163
- Ruuska S, Girke T, Benning C, Ohlrogge J (2002) Contrapuntal networks of gene expression during *Arabidopsis* seed filling. *Plant Cell* 14:1191–1206
- Scarth R, Tang J (2006) Modification of brassica oil using conventional and transgenic approaches. *Crop Sci* 46:1225–1236
- FAO (2005) Agricultural Data, FAOSTAT. <http://faostat.fao.org/faostat/collections?subset=agriculture>
- Dyer J, Mullen RT (2008) Engineering plant oils as high-value industrial feedstocks for biorefining: the need for underpinning cell biology research. *Physiol Plant* 132:11–22
- Lung S, Weselake RJ (2006) Diacylglycerol acyltransferase: a key mediator of plant triacylglycerol synthesis. *Lipids* 41:1073–1088
- Ohlrogge J, Browse J, Somerville CR (1991) The genetics of plant lipids. *Biochim Biophys Acta* 1082:1–26
- Perry H, Bligny R, Gout E, Harwood JL (1999) Changes in Kennedy pathway intermediates associated with increased triacylglycerol synthesis in oil-seed rape. *Phytochemistry* 52:799–804
- Saha S, Enugutti B, Rajakumari S, Rajasekharan R (2006) Cytosolic triacylglycerol biosynthetic pathway in oilseeds molecular cloning and expression of peanut cytosolic diacylglycerol acyltransferase. *Plant Physiol* 141:1533–1543
- Jain R, Coffey M, Lai K, Kumar A, MacKenzie SL (2000) Enhancement of seed oil content by expression of glycerol-3-phosphate acyltransferase genes. *Biochem Soc Trans* 28:958–961
- Zou J, Katavic V, Giblin EM, Barton DL, MacKenzie SL, Keller WA, Hu X, Taylor DC (1997) Modification of seed oil content and acyl composition in the Brassicaceae by expression of a yeast *sn-2* acyltransferase gene. *Plant Cell* 9:909–923
- Taylor DC, Katavic V, Zou J, MacKenzie SL, Keller WA, An J, Friesen W, Barton DL, Pedersen KK, Giblin EM, Ge Y, Dauk M,

- Sonntag C, Luciw T, Males D (2002) Field testing of transgenic rapeseed cv. Hero transformed with a yeast *sn-2* acyltransferase results in increased oil content, erucic acid content and seed yield. *Mol Breed* 8:317–322
13. Jako C, Kumar A, Wei YD, Zou JT, Barton DL, Giblin EM, Covello PS, Taylor DC (2001) Seed-specific over-expression of an *Arabidopsis* cDNA encoding a diacylglycerol acyltransferase enhances seed oil content and seed weight. *Plant Physiol* 126:861–874
 14. Bouvier-Navé P, Benveniste P, Oelkers P, Sturley SL, Schaller H (2000) Expression in yeast and tobacco of plant cDNAs encoding acyl CoA:diacylglycerol acyltransferase. *Eur J Biochem* 267:85–96
 15. Zheng P, Allen WB, Roesler K, Williams ME, Zhang S, Li J, Glassman K, Ranch J, Nubel D, Solawetz W, Bhatramakki D, Llaca V, Deschamps S, Zhong GY, Tarczynski MC, Shen B (2008) A phenylalanine in DGAT is a key determinant of oil content and composition in maize. *Nat Genet* 40:269–270
 16. Vigeolas H, Waldeck P, Zank T, Geigenberger P (2007) Increasing seed oil content in oil-seed rape (*Brassica napus* L.) by over-expression of a yeast glycerol-3-phosphate dehydrogenase under the control of a seed-specific promoter. *Plant Biotechnol J* 5:431–441
 17. Wang H, Zhang B, Hao YJ, Huang J, Tian AG, Liao Y, Zhang JS, Chen SY (2007) The soybean Dof-type transcription factor genes, GmDof4 and GmDof11, enhance lipid content in the seeds of transgenic *Arabidopsis* plants. *Plant J* 52:716–729
 18. Wang H, Guo J, Lambert KN, Li Y (2007) Developmental control of *Arabidopsis* seed oil biosynthesis. *Planta* 226:773–783
 19. Zou J, Taylor DC, Katavic V, MacKenzie SL, Keller WA (2000) Modification of plant lipids and seed oils utilizing yeast SLC genes. US Patent no. 6051755
 20. Burton JW, Wilson RF (1994) Registration of N88–480, a soybean germplasm line with a high concentration of oil in seeds. *Crop Sci* 34:313–314
 21. Jako C, Kumar A, Wei Y, Zou J, Barton DL, Giblin EM, Covello PS, Taylor D (2001) Seed-specific over-expression of an *Arabidopsis* cDNA encoding a diacylglycerol acyltransferase enhances seed oil content and seed weight. *Plant Physiol* 126:861–874
 22. Lardizabal K, Effertz R, Levering C, Mai J, Pedroso MC, Jury T, Aasen E, Gruys K, Bennett K (2008) Expression of *Umbelopsis ramanniana* DGAT2A in seed increases oil in soybean. *Plant Physiol* 148:89–96
 23. Finer JJ, Nagasawa A (1988) Development of an embryogenic suspension culture of soybean (*Glycine max* Merrill.). *Plant Cell Tissue Organ Cult* 15:125–136
 24. Samoylov VM, Tucker DM, Parrott WA (1998) A liquid medium-based protocol for rapid regeneration from embryogenic soybean cultures. *Plant Cell Rep* 18:49–54
 25. Kinney AJ (1994) Genetic modification of the storage lipids of plants. *Curr Opin Biotechnol* 5:144–151
 26. Kinney AJ (1997) Development of genetically engineered oilseeds from molecular biology to agronomics. In: Williams JP, Khan MU, Lem NW (eds) *Physiology biochemistry and molecular biology of plant lipids*. Kluwer, Dordrecht, pp 298–300
 27. Kinney AJ (2001) Perspectives on the production of industrial oils in genetically engineered oilseeds. In: Kuo TM, Gardner HW (eds) *Lipid biotechnology*. Marcel Dekker Inc., New York
 28. Perez-Grau L, Goldberg RB (1989) Soybean seed protein genes are regulated spatially during embryogenesis. *Plant Cell* 1:1095–1109
 29. Liu W, Torisky RS, McAllister KP, Avdiushko S, Hildebrand D, Collins GB (1997) Somatic embryo cycling: evaluation of a novel transformation and assay system for seed-specific gene expression in soybean. *Plant Cell Tissue Organ Cult* 47:33–42
 30. Cahoon EB, Carlson TJ, Ripp KG, Schweiger BJ, Cook GA, Hall SE, Kinney AJ (1999) Biosynthetic origin of conjugated double bonds: production of fatty acid components of high-value drying oils in transgenic soybean embryos. *Proc Natl Acad Sci USA* 96:12935–12940
 31. Cahoon EB, Marillia EF, Stecca KL, Hall SE, Taylor DC, Kinney AJ (2000) Production of fatty acid components of meadowfoam oil in somatic soybean embryos. *Plant Physiol* 124:243–251
 32. Cahoon EB, Ripp KG, Hall SE, McGonigle B (2002) Transgenic production of epoxy fatty acids by expression of a cytochrome P450 enzyme from *Euphorbia lagascae* seed. *Plant Physiol* 128:615–624
 33. Cahoon E, Kinney AJ (2004) Dimorphecolic acid is synthesized by the coordinate activities of two divergent 12-oleic acid desaturases. *J Biol Chem* 279:12495–12502
 34. Trick HN, Dinkins RD, Santarem ER, Di R, Samoylov VM, Meurer C, Walker D, Parrott WA, Finer JJ, Collins GB (1997) Recent advances in soybean transformation. *Plant Tissue Cult Biotechnol* 3:9–26
 35. Samoylov VM, Tucker DM, Parrott WA (1998) Soybean [*Glycine max* (L.) Merrill] embryogenic cultures: the role of sucrose and total nitrogen content on proliferation. *In Vitro Cell Dev Biol Plant* 34:8–13
 36. Reddy MSS, Dinkins RD, Redmond CT, Ghabrial SA, Collins GB (2001) Expression of bean pod mottle virus (BPMV) coat protein precursor results in resistance to (BPMV) in transgenic soybeans. *Phytopathology* 91:831–838
 37. Bligh EG, Dyer WJ (1959) A rapid method of total lipid extraction and purification. *Can J Biochem Physiol* 37:911–917
 38. McNeill S, Montross MD, Shearer SA (2005) Spatial variation of protein, oil, and starch in corn. *Appl Eng Agric* 21:619–625
 39. Nguyen M, Nickell CD, Widholm JM (2001) Selection for high seed oil content in soybean families derived from plants regenerated from protoplasts and tissue cultures. *Theor Appl Genet* 102:1072–1075
 40. Hyten D, Pantalone VR, Sams CE, Saxton AM, Landau-Ellis D, Stefaniak TR, Schmidt ME (2004) Quantitative trait loci for seed protein and oil concentration, and seed size in soybean. *Theor Appl Genet* 109:552–561
 41. Macool DJ, Xue Z (2007) A mortierella alpina glycerol-3-phosphate o-acyltransferase for alteration of polyunsaturated fatty acids and oil content in oleaginous organisms. US Patent no. 7192762
 42. Burton JW (1987) Quantitative genetics: results relevant to soybean breeding. In: Wilcox JR (ed) *Soybeans: improvement, production and uses*, 2nd edn. ASA, Madison, pp 211–247
 43. Wilcox J (1998) Increasing seed protein in soybean with eight cycles of recurrent selection. *Crop Sci* 38:1536–1540
 44. Wilcox J, Shibles RM (2001) Interrelationships among seed quality attributes in soybean. *Crop Sci* 41:11–14
 45. Mathew M, Philip VJ (2003) Somatic embryogenesis versus zygotic embryogenesis in *Ensete superbum*. *Plant Cell Tissue Organ Cult* 72:267–275
 46. Schmidt MA, Tucker DM, Cahoon EB, Parrott WA (2005) Towards normalization of soybean somatic embryo maturation. *Plant Cell Rep* 24:383–391
 47. Jefferson RA (1987) Assaying chimeric genes in plants: the GUS gene fusion system. *Plant Mol Biol Rep* 5:387–405

Total Synthesis and Antileishmanial Activity of the Natural Occurring Acetylenic Fatty Acids 6-Heptadecynoic Acid and 6-Icosynoic Acid

Néstor M. Carballeira · Michelle M. Cartagena ·
Christopher Fernández Prada · Celia Fernández Rubio ·
Rafael Balaña-Fouce

Received: 5 August 2009 / Accepted: 8 September 2009 / Published online: 30 September 2009
© AOCs 2009

Abstract The first total syntheses of the naturally occurring acetylenic fatty acids—6-heptadecynoic acid (59% overall yield) and 6-icosynoic acid (34% overall yield)—was accomplished in four steps. Using the same synthetic sequence the naturally occurring fatty acids (6*Z*)-heptadecenoic acid (46% overall yield) and (6*Z*)-icosenoic acid (27% overall yield) were also synthesized. The Δ^6 acetylenic fatty acids displayed good antiprotozoal activity towards *Leishmania donovani* promastigotes (EC_{50} = 1–6 $\mu\text{g/mL}$), but the 6-icosynoic acid was the most effective in the series. In addition, the (6*Z*)-icosenoic acid was a much better antiprotozoal compound (EC_{50} = 5–6 $\mu\text{g/mL}$) than the (6*Z*)-heptadecenoic acid (EC_{50} > 25 $\mu\text{g/mL}$). The saturated fatty acids *n*-heptadecanoic acid and *n*-eicosanoic acid were not effective towards *L. donovani*, indicating that the Δ^6 unsaturation in these fatty acids is necessary for leishmanicidal activity. In addition, both the 6-icosynoic acid and the (6*Z*)-icosenoic acid were inhibitors of the *Leishmania* DNA topoisomerase IB enzyme (EC_{50} 's = 36–49 μM), a possible intracellular target for these compounds. This is the first study assessing fatty acids as inhibitors of the *Leishmania* DNA topoisomerase IB enzyme.

Keywords Acetylenic fatty acids · Antiprotozoal activity · *Leishmania donovani* · Synthesis · Topoisomerase IB

Abbreviations

DNA	Deoxyribonucleic acid
EC_{50}	Effective concentration 50%
GC–MS	Gas chromatography–mass spectrometry
HRMS	High resolution mass spectrometry
IC_{50}	Inhibitory concentration 50%
IR	Infrared spectroscopy
LdTOPIB	<i>Leishmania</i> DNA topoisomerase IB
MIC	Minimum inhibitory concentration
NMR	Nuclear magnetic resonance
PDC	Pyridinium dichromate

Introduction

Many acetylenic fatty acids are natural plant constituents, but those with a C-6 triple bond, such as the 6-nonadecynoic acid, have displayed strong antifungal activity [1]. Recently, the novel 6-heptadecynoic acid (**1a**) and 6-icosynoic acid (**1b**) were isolated from the plant *Sommeria sabiceoides* [1]. While **1a** is a new natural product, **1b** has been known for sometime as a trace constituent of *Alvaradoa amorphoides* seed oil [2]. Neither of these two acetylenic fatty acids **1a** and **1b** have been explored for antiprotozoal activity nor their olefinic analogs (6*Z*)-heptadecenoic acid (**6a**) and (6*Z*)-icosenoic acid (**6b**), which are also natural products. The (6*Z*)-heptadecenoic acid (**6a**) was identified in the opisthobranch *Haminaea templadoi* as well as in a marine *Micrococcus* bacterium [3, 4], while **6b** is also a minor constituent of some seed oils [2].

Some fatty acids display antiprotozoal activity, in particular against *Leishmania donovani*, the causative agent of leishmaniasis [5]. Visceral leishmaniasis is a very serious

N. M. Carballeira (✉) · M. M. Cartagena
Department of Chemistry, University of Puerto Rico,
P.O. Box 23346, San Juan, PR 00931-3346, USA
e-mail: nmcarballeira@uprrp.edu

C. F. Prada · C. F. Rubio · R. Balaña-Fouce
Department of Biomedical Sciences (INTOXCAL),
University of León, Campus de Vegazana s/n,
24071 León, Spain

disease characterized by the invasion of spleen and liver macrophages, anaemia, fever and ultimately death if not diagnosed in time and left untreated. Visceral leishmaniasis is mostly found in India, Bangladesh, Indonesia [6] and Sudan [7] and in many cases is associated with an opportunistic infection in immunocompromised AIDS patients [8]. Pentavalent antimonials (meglumine antimoniate and sodium stibogluconate) have been used as first-line drugs despite the early reported resistances [9]. An emerging alternative to these compounds are the oral chemotherapy drugs, such as the alkylphosphocholine derivatives (miltefosine and edelfosine) and the antibiotic paromomycin [10, 11]. Miltefosine—originally developed as an anticancer drug—was confirmed as a major advance against visceral leishmaniasis since it was the first oral drug with high healing rates in phase IV studies, including pentavalent antimonials relapsing cases [12]. However, reproductive toxicity, its arbitrary use and its serious tendency to select resistant strains in the laboratory [13], suppose a high risk of emerging resistances during treatment with this drug, making it necessary to continue the search of new drugs for the treatment of this disease.

The toxicity of fatty acids towards *L. donovani* promastigotes is known, but it has not been thoroughly studied. Probably, the most representative work is that of Chaudhuri et al. [5] where the growth inhibition of a series of C₄–C₁₈ fatty acids towards *L. donovani* promastigotes was investigated. It was found that the longest fatty acids (up to 18 carbon atoms) were the most inhibitory and that unsaturated fatty acids were more toxic than their corresponding saturated analogs. For example, oleic acid displayed a MIC of 0.09 μmol/mL against *L. donovani* promastigotes, while octadecanoic acid resulted in a MIC of 0.18 μmol/mL [5]. *n*-Decanoic acid was less effective against *L. donovani* with a MIC of 1.39 μmol/mL. No conclusions regarding the inhibitory mechanism of these fatty acids could be drawn, but the Chaudhuri group found that growth inhibition was not due to leakage of metabolites from the protozoan cells or from the potential ability of these molecules to affect the surface tension of the growth medium. However, it was found that the studied fatty acids inhibited the uptake of glucose and leucine by *L. donovani*. An earlier work by Kuwahara et al. [14] reported that *n*-decanoic, *n*-dodecanoic, and *n*-hexadecanoic acids, at levels of 100 μg/mL, inhibited the motility of *L. donovani* promastigotes, but oleic acid had no effect.

The aim of the present study was to synthesize, for the first time, the naturally occurring 6-heptadecynoic acid (**1a**) and 6-icosynoic acid (**1b**), as well as the (6*Z*)-heptadecynoic acid (**6a**) and (6*Z*)-icosenoic acid (**6b**), and assess their antileishmanial activity against *L. donovani* promastigotes. The objective of the investigation was to determine, by keeping the chain length fixed, if a higher degree of

unsaturation favors a better antileishmanial activity. In addition, we also studied the inhibition of the Leishmania DNA topoisomerase IB enzyme by these fatty acids as a possible intracellular target.

Materials and Methods

General Experimental Procedures

¹H NMR (300 or 500 MHz) and ¹³C NMR (75 or 125 MHz) were either recorded on a Bruker DPX-300 or a Bruker DRX-500 spectrometer. ¹H-NMR chemical shifts are reported with respect to internal (CH₃)₄Si, ¹³C-NMR chemical shifts are reported in parts per million relative to CDCl₃ (77.0 ppm). GC/MS analyses were recorded at 70 eV using either a Hewlett Packard 5972A MS ChemStation or an Agilent 5975C MS ChemStation coupled to an Agilent 7890A GC where both instruments were equipped with a 30 m × 0.25 mm special performance capillary column (HP-5MS) of polymethyl siloxane crosslinked with 5% phenyl methylpolysiloxane. IR spectra were recorded on a Nicolet Magna 750 FT-IR spectrophotometer (Thermo-Nicolet, Madison, WI, USA). High resolution mass spectral data was performed at the Emory University Mass Spectrometry Center on a thermo LTQ-FTMS using APCI as the probe.

5-Bromo-1-[(tetrahydropyran-2-yl)oxy]pentane (**2**)

To 5-bromo-1-pentanol (4.0 g, 23.9 mmol) in 20 mL of CHCl₃ was added dropwise 2,3-dihydro-2*H*-pyran (DHP) (4.4 mL, 47.9 mmol) and catalytic amounts of *p*-toluenesulfonic acid (*p*-TSA). The reaction mixture was stirred for 90 min at room temperature. The organic layer was washed with water (1 × 50 mL), NaHCO₃ (1 × 50 mL), water (1 × 75 mL) and dried over Na₂SO₄. The crude product was purified using silica gel column chromatography eluting with hexane:ether (9:1) affording 5.93 g of **2** as a colorless oil for a 99% yield.

General Procedure for the Acetylide Coupling Reaction

Into a 100 mL round-bottomed flask at 0 °C containing dry THF (5.0–7.0 mL) was added the terminal alkyne (6.0–7.2 mmol) followed by the dropwise addition of 2.5 M *n*-BuLi (12.0–14.4 mmol). The mixture was stirred at 0 °C for 80 min. The temperature was then lowered to –60 °C and HMPA (10.0–14.0 mL) was added followed by the addition of **2** (6.0–7.2 mmol). The mixture was stirred for 24 h and then washed with brine (2 × 15 mL), extracted with hexane (2 × 15 mL) and the organic phase dried over Na₂SO₄ and evaporated in vacuo affording **3a**

(1.47 g, 54% yield) or **3b** (1.60 g, 79% yield) after purification by Kugelrohr distillation at 170 °C/3 mm Hg.

2-(Heptadec-6-ynyloxy)-tetrahydro-2H-pyran (**3a**)

This was obtained as a pale yellow oil in a 79% yield from the reaction of 1-dodecyne (1.3 mL, 6.0 mmol) with *n*-BuLi in dry THF (5.0 mL) and **2** (1.510 g, 6.0 mmol) according to the general procedure described above; IR (neat) ν_{\max} : 2,923, 2,853, 1,455, 1,440, 1,351, 1,136, 1,120, 1,077 cm^{-1} ; ^1H NMR (CDCl_3 , 300 MHz) δ 4.56 (1H, m), 3.85–3.73 (2H, m), 3.48–3.37 (2H, m, H-1), 2.12 (4H, m), 1.69–1.35 (6H, m), 1.26 (22H, brs, $-\text{CH}_2-$), 0.87 (3H, t, $J = 6.8$ Hz, $-\text{CH}_3$); ^{13}C NMR (CDCl_3 , 75 MHz) δ 98.8, 80.4 (C-7), 79.9 (C-6), 67.5, 62.3, 31.9, 30.7, 29.6, 29.5, 29.3, 29.3, 29.2, 29.0, 28.9, 26.9, 25.5, 22.7, 19.6, 18.7, 18.7, 14.1; GC–MS (70 eV) m/z (relative intensity) 336 (M^+ , 4), 265 (3), 264 (3), 263 (12), 252 (2), 251 (2), 195 (5), 181 (6), 167 (4), 135 (2), 125 (2), 95 (17), 93 (11), 86 (6), 85 (100), 81 (17), 79 (19), 69 (9), 67 (25), 57 (14), 55 (25); HRMS calcd for $\text{C}_{22}\text{H}_{40}\text{O}$ [$M + \text{H}$] $^+$ 337.3101, found 337.3102.

2-(Icos-6-ynyloxy)-tetrahydro-2H-pyran (**3b**)

This was obtained as a pale yellow oil in a 54% yield from the reaction of 1-pentadecyne (1.9 mL, 7.2 mmol) with *n*-BuLi in dry THF (7.0 mL) and **2** (1.82 g, 7.2 mmol) according to the general procedure described above; IR (neat) ν_{\max} : 2,922, 2,853, 1,464, 1,351, 1,322, 1,136, 1,120, 1,077 cm^{-1} ; ^1H NMR (CDCl_3 , 300 MHz) δ 4.57 (1H, m), 3.91–3.68 (2H, m), 3.55–3.34 (2H, m, H-1), 2.14 (4H, m), 1.90–1.40 (6H, m), 1.25 (28H, brs, $-\text{CH}_2-$), 0.87 (3H, t, $J = 6.8$ Hz, $-\text{CH}_3$); ^{13}C NMR (CDCl_3 , 75 MHz) δ 98.8, 80.4 (C-7), 79.9 (C-6), 67.5, 62.3, 31.9, 30.7, 29.7, 29.7, 29.6, 29.5, 29.4, 29.3, 29.2, 29.0, 28.9, 26.9, 25.5, 22.7, 19.7, 18.7, 18.7, 14.1; GC–MS (70 eV) m/z (relative intensity) 378 (M^+ , 1), 305 (4), 293 (2), 195 (6), 125 (2), 101 (10), 97 (4), 95 (11), 93 (6), 86 (5), 85 (100), 83 (7), 67 (19), 57 (12), 55 (18); HRMS calcd for $\text{C}_{25}\text{H}_{46}\text{O}_2$ [$M + \text{H}$] $^+$ 379.3571, found 379.3573.

General Procedure for the Tetrahydropyranyl Deprotection

To a mixture of methanol (10 mL) and either **3a** or **3b** (0.91–1.46 g, 2.7–3.9 mmol) was added catalytic amounts of *p*-toluenesulfonic acid (*p*-TSA) and the reaction mixture was stirred at 60 °C for 24 h. After this time the solvent was evaporated and then the organic extract was washed with a saturated solution of sodium bicarbonate (3 \times 25 mL), dried over Na_2SO_4 , filtered, and evaporated in vacuo, affording 0.68–0.95 g (83–99% yield) of the

alkynols **4a** and **4b**. The products were deemed sufficiently pure so as to be used as such for the next steps without further purification.

6-Heptadecynol (**4a**)

This was obtained as a pale yellow oil in a 99% yield from the reaction of **3a** (0.91 g, 2.7 mmol) with catalytic amounts of *p*-TSA in methanol (10 mL) according to the general procedure described above; IR (neat) ν_{\max} : 3,355, 2,923, 2,853, 1,460, 1,377, 1,333, 1,119, 1,047, 1,010, 724 cm^{-1} ; ^1H NMR (CDCl_3 , 300 MHz) δ 3.63 (2H, t, $J = 6.5$ Hz, H-1), 2.13 (4H, m), 1.40–1.61 (6H, m), 1.24 (16H, brs, $-\text{CH}_2-$), 0.87 (3H, t, $J = 6.8$ Hz, $-\text{CH}_3$); ^{13}C NMR (CDCl_3 , 75 MHz) δ 80.5 (C-7), 79.8 (C-6), 62.9 (C-1), 32.3, 31.9, 29.7, 29.6, 29.6, 29.3, 29.2, 29.1, 28.9, 24.9, 22.7, 18.7, 18.7, 14.1; GC–MS (70 eV) m/z (relative intensity) 252 (M^+ , 1), 152 (2), 135 (5), 124 (6), 108 (30), 98 (45), 97 (32), 95 (37), 93 (62), 91 (22), 84 (22), 83 (37), 82 (100), 81 (62), 80 (62), 79 (85), 70 (36), 69 (38), 67 (91), 65 (13), 57 (31), 55 (86); HRMS calcd for $\text{C}_{17}\text{H}_{32}\text{O}$ [$M + \text{H}$] $^+$ 253.2526, found 253.2527.

6-Icosynol (**4b**)

This was obtained as a semi solid in a 83% yield from the reaction of **3b** (1.46 g, 3.9 mmol) with catalytic amounts of *p*-TSA in methanol (10 mL) according to the general procedure described above; IR (neat) ν_{\max} : 3,321, 2,922, 2,852, 1,461, 1,376, 1,350, 1,120, 1,055, 721 cm^{-1} ; ^1H NMR (CDCl_3 , 300 MHz) δ 3.63 (2H, t, $J = 6.5$ Hz, H-1), 2.12 (4H, m), 1.51 (4H, m), 1.24 (24H, brs, $-\text{CH}_2-$), 0.86 (3H, t, $J = 7.0$ Hz, $-\text{CH}_3$); ^{13}C NMR (CDCl_3 , 75 MHz) δ 80.5 (C-7), 79.8 (C-6), 62.9 (C-1), 32.3, 31.9, 29.6, 29.6, 29.4, 29.2, 28.9, 24.9, 22.7, 19.7, 18.7, 14.1; GC–MS (70 eV) m/z (relative intensity) 292 (M^+ , 1), 194 (2), 135 (9), 126 (5), 111 (26), 108 (47), 98 (60), 97 (39), 95 (43), 93 (74), 91 (27), 82 (100), 81 (67), 80 (69), 79 (95), 69 (37), 68 (33), 67 (96), 57 (43), 55 (98); HRMS calcd for $\text{C}_{20}\text{H}_{38}\text{O}$ [$M + \text{H}$] $^+$ 295.2995, found 295.2998.

General Procedure for the Oxidation of the Alcohols

To a solution of pyridinium dichromate (PDC) (5.6–11.9 mmol) and 2 mL of dimethylformamide (DMF) was added under argon a solution of the alcohol (1.11–2.38 mmol) in 6.6 mL of DMF and the reaction mixture was left being stirred at room temperature for 48 h. The mixture was washed with water (3 \times 25 mL), extracted with hexane (1 \times 25 mL), the organic phase was dried over Na_2SO_4 , and the solvent removed in vacuo affording the corresponding carboxylic acids **1a** (0.26 g) and **1b** (0.48 g) in 76% yields.

6-Heptadecyanoic acid (**1a**)

This was obtained as a white solid (mp 38–40 °C, lit [1] mp 39 °C) in a 76% yield from the reaction of **4a** (0.6 g, 2.38 mmol) and PDC (4.5 g, 11.9 mmol) in DMF according to the general procedure described above. Compound **1a** presented spectral data similar to the one reported in the literature [1].

6-Icosynoic acid (**1b**)

This was obtained as a white solid (mp 52–54 °C, lit [1] mp 53 °C) in a 76% yield from the reaction of **4b** (0.3 g, 1.11 mmol) and PDC (2.1 g, 5.6 mmol) in DMF according to the general procedure described above. Compound **1b** also presented spectral data similar to the one reported in the literature [1].

General Procedure for the Catalytic Hydrogenation of the Alkynes

Into a 25-mL two-neck round-bottom flask were placed dry hexane, the alkynes **4a** (0.056 g) or **4b** (0.295 g), quinoline (0.18–0.8 mL), and 10% palladium on activated carbon (Pd/C). One of the necks was capped with a rubber septum and the other was connected via tygon tubing to a 25-mL graduated pipet ending in a 150-mL beaker with distilled water. While stirring at room temperature a 20-mL syringe with needle was used to withdraw air from the system and to draw water up into the graduated pipet to the 0.0 mL mark. Hydrogen was then introduced into the system using a balloon filled with hydrogen attached to a hose barb-to-luer-lock adapter with a stopcock and a needle. The reaction mixture consumed 5.4–24.6 mL of hydrogen in 1 h. The mixture was filtered and the solvent removed in vacuo obtaining the desired alkenols **5a** (0.046 g, 70% yield) and **5b** 0.208 g (82% yield) after purification by Kugelrohr distillation at 110 °C/3 mm Hg.

(6Z)-Heptadecenol (**5a**)

This was obtained as a colorless oil (0.046 g, 0.18 mmol) in a 82% yield from the catalytic hydrogenation described in the general procedure above; IR (neat) ν_{\max} : 3,328, 3,004, 2,922, 2,853, 1,658, 1,461, 1,377, 1,074, 1,053, 720 cm^{-1} ; ^1H NMR (CDCl_3 , 300 MHz) δ 5.32 (2H, m, H-6, H-7), 3.61 (2H, t, $J = 6.6$ Hz, H-1), 2.00 (4H, m), 1.55 (3H, m, $-\text{CH}_2-$, $-\text{OH}$), 1.24 (20H, brs, $-\text{CH}_2-$), 0.87 (3H, t, $J = 6.8$ Hz, $-\text{CH}_3$); ^{13}C NMR (CDCl_3 , 75 MHz) δ 130.2 (C-7), 129.5 (C-6), 63.0 (C-1), 32.7, 31.9, 29.8, 29.7, 29.6, 29.5, 29.4, 29.3, 27.2, 27.1, 25.4, 22.7, 14.1; GC–MS (70 eV) m/z (relative intensity) 254 (M^+ , 1), 236 (6), 208 (2), 180 (2), 123 (13), 97 (25), 96 (65), 95 (61), 82 (100),

81 (64), 69 (40), 68 (54), 67 (92), 57 (32), 55 (69); HRMS calcd for $\text{C}_{17}\text{H}_{34}\text{O}$ [$M + \text{H}$] $^+$ 255.2682, found 255.2684.

(6Z)-Icosenol (**5b**)

This was obtained as a semi solid (0.21 g, 0.71 mmol) in a 70% yield from the catalytic hydrogenation described in the general procedure above; IR (neat) ν_{\max} : 3,346, 3,002, 2,919, 2,850, 1,460, 1,363, 1,062, 724 cm^{-1} ; ^1H NMR (CDCl_3 , 500 MHz) δ 5.35 (2H, m, H-6, H-7), 3.63 (2H, m, $J = 6.6$ Hz, H-1), 2.02 (4H, m), 1.57 (2H, m), 1.25 (26H, brs, $-\text{CH}_2-$), 0.88 (3H, t, $J = 6.5$ Hz, $-\text{CH}_3$); ^{13}C NMR (CDCl_3 , 125 MHz) δ 130.2 (C-7), 129.5 (C-6), 63.0 (C-1), 32.7, 31.9, 29.8, 29.70, 29.67, 29.6, 29.5, 29.4, 29.3, 27.3, 27.2, 25.4, 22.7, 14.1; GC–MS (70 eV) m/z (relative intensity) 296 (M^+ , 1), 279 (2), 278 (9), 250 (2), 222 (2), 138 (6), 124 (10), 123 (11), 97 (26), 96 (61), 95 (52), 82 (100), 81 (59), 69 (41), 68 (55), 67 (89), 57 (41), 55 (77); HRMS calcd for $\text{C}_{20}\text{H}_{40}\text{O}$ [$M + \text{H}$] $^+$ 297.3152, found 297.3154.

General Procedure for the Oxidation of the Alkenols

To a solution of pyridinium dichromate (PDC) (1.27–1.77 mmol) and 2 mL of dimethylformamide (DMF) was added under argon a solution of the alcohol (0.25–0.35 mmol) in 5.0 mL of DMF and the reaction mixture was left being stirred at room temperature for 48 h. The mixture was washed with water (3 \times 25 mL), extracted with hexane (1 \times 25 mL), the organic phase was dried over Na_2SO_4 , and the solvent was removed in vacuo affording the carboxylic acids **6a** (0.067 g, 73% yield) and **6b** (0.069 g, 86% yield).

(6Z)-Heptadecenoic acid (**6a**)

This was obtained as a viscous oil in a 73% yield from the reaction of **5a** (0.09 g, 0.35 mmol) and PDC (0.69 g, 1.77 mmol) in DMF according to the general procedure described above; IR (neat) ν_{\max} 3,264, 3,005, 2,922, 2,853, 1,708 (C = O), 1,459, 1,412, 1,378, 1,342, 1,201, 1,119, 935, 720 cm^{-1} ; ^1H NMR (CDCl_3 , 500 MHz) δ 5.37 (2H, m, H-6, H-7), 2.37 (2H, t, $J = 7.6$ Hz, H-2), 2.14 (4H, m), 1.67 (2H, m), 1.27 (18H, brs, $-\text{CH}_2-$), 0.89 (3H, t, $J = 7.0$ Hz, $-\text{CH}_3$); ^{13}C NMR (CDCl_3 , 125 MHz) δ 179.6 (C-1), 130.5 (C-7), 128.9 (C-6), 33.9, 31.9, 29.7, 29.6, 29.5, 29.32, 29.29, 29.2, 29.1, 27.2, 26.7, 24.3, 22.7, 14.1; GC–MS (70 eV) m/z (relative intensity) 268 (M^+ , 4), 250 (15), 208 (7), 206 (6), 166 (6), 165 (3), 152 (5), 151 (5), 138 (6), 137 (7), 123 (11), 111 (17), 110 (15), 97 (35), 96 (27), 95 (29), 81 (47), 69 (45), 67 (59), 57 (36), 55 (100); HRMS calcd for $\text{C}_{17}\text{H}_{32}\text{O}_2$ [$M - \text{H}$] $^-$ 267.2330, found 267.2334.

(6Z)-Icosenoic acid (6b)

This was obtained as a white solid in a 86% yield from the reaction of **5b** (0.075 g, 0.25 mmol) and PDC (0.48 g, 1.27 mmol) in DMF according to the general procedure described above; mp 31–34 °C; IR (neat) ν_{\max} 3,200–3,095, 3,002, 2,922, 2,852, 1,709 (C = O), 1,462, 1,411, 1,377, 1,348, 1,120, 1,075, 936, 797, 719 cm^{-1} ; ^1H NMR (CDCl_3 , 500 MHz) δ 5.33 (2H, m, H-6, H-7), 2.34 (2H, m, $J = 7.2$ Hz, H-2), 2.10 (4H, m), 1.63 (2H, m), 1.38 (4H, m), 1.24 (20H, brs, $-\text{CH}_2-$), 0.86 (3H, t, $J = 7.1$ Hz, $-\text{CH}_3$); ^{13}C NMR (CDCl_3 , 125 MHz) δ 179.5 (C-1), 130.8 (C-7), 129.2 (C-6), 34.0, 32.2, 29.94, 29.91, 29.88, 29.8, 29.6, 29.5, 29.4, 29.3, 29.2, 27.5, 27.0, 24.5, 22.9, 14.3; GC–MS (70 eV) m/z (relative intensity) 310 (M^+ , 4), 292 (25), 211 (7), 208 (4), 250 (5), 249 (4), 248 (4), 194 (3), 165 (4), 164 (4), 152 (4), 151 (5), 123 (11), 122 (8), 111 (18), 110 (14), 109 (12), 97 (34), 95 (27), 85 (17), 81 (46), 67 (51), 55 (100); HRMS calcd for $\text{C}_{20}\text{H}_{36}\text{O}_2$ [$M - \text{H}$] $^-$ 309.2799, found 309.2802.

Cell Cultures

L. donovani (MHOM/ET67/L82 strain) promastigotes were propagated in a completely defined medium 199, supplemented with 10% heat inactivated fetal calf serum (FCS) and penicillin/streptomycin cocktail (containing 50 U/ml penicillin, 50 $\mu\text{g}/\text{ml}$ streptomycin). The IC_{50} values were determined after 48 h incubation with different concentrations of the fatty acids dissolved in DMSO (ranging from 0.6 to 25 $\mu\text{g}/\text{ml}$) added to cultures and cell population assessed by Coulter.

Murine macrophages (RAW 264.7) were grown at 37 °C in RPMI 1640 medium, supplemented with 10% FCS antibiotics (containing 50 U/ml penicillin, 50 $\mu\text{g}/\text{ml}$ streptomycin). Toxicity IC_{50} values were determined after 48 h incubation with different concentrations of the compounds dissolved in DMSO (0.3 to 100 $\mu\text{g}/\text{ml}$) using vital alamar-Blue[®] dye (Invitrogen, Carlsbad, CA, USA), according manufacturer recommendations.

Purification of Recombinant Leishmanial TopIB

Expression of a recombinant topoisomerase IB from *Leishmania donovani* (LdTopIB) in a topoisomerase IB-deficient *Saccharomyces cerevisiae* strain has been described elsewhere [15]. Purification of recombinant LdTopIB was done according to Diaz-González and coworkers [16]. Briefly, LdTopIB overexpressing yeasts were disrupted with one freeze/thaw cycle at -80 °C, with the purpose of weakening the yeast wall; after lysis with 425–600 μm acid-washed glass beads, the extracts were cleared by centrifugation at 15,000 $\times g$ for 30 min at 4 °C. The protein suspension was

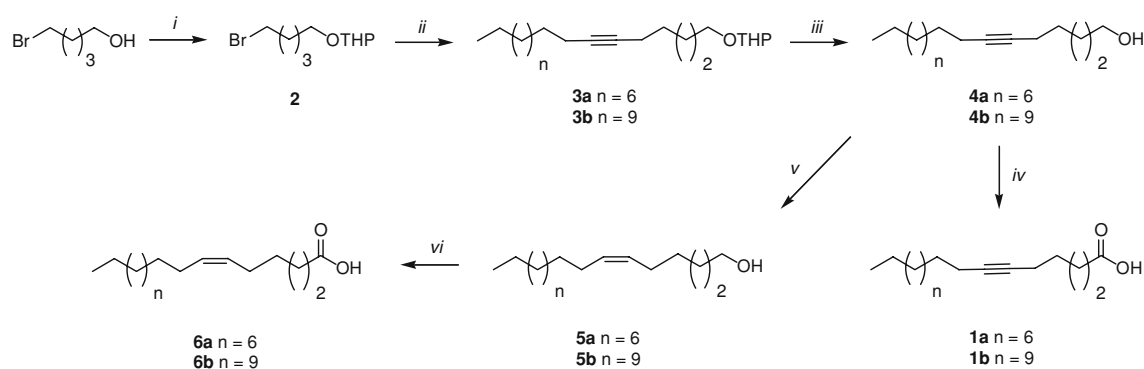
loaded onto a phosphocellulose (P-11) column, previously equilibrated as manufacturer indications. LdTopIB was eluted at 4 °C with a discontinuous gradient of KCl (0.2, 0.4, 0.6, 0.8 and 1 M) in TEEG buffer, supplemented with 0.1 mg/ml sodium bisulphite, 0.8 mg/ml NaF and the protease inhibitors cocktail. Active fractions were further loaded onto a phenyl-sepharose column (Sigma-Aldrich, St Louis, USA), eluted with a discontinuous inverse gradient of ammonium sulphate (1, 0.8, 0.6, 0.4 and 0.2 M) and then concentrated by Microcon YM-30 (Millipore) before use.

DNA Relaxation Assays

DNA topoisomerase I activity was assayed by the relaxation of negatively supercoiled plasmid DNA. The reaction mixture in a total volume of 20 μl contained 0.2 μg of supercoiled pHOT plasmid, 10 mM Tris–HCl buffer pH 7.5, 5 mM MgCl_2 , 0.1 mM EDTA, 15 $\mu\text{g}/\text{ml}$ bovine serum albumin, 50 mM KCl and various extracts containing altered proteins or wild type enzyme, starting with 1 unit LdTopIB. The reaction mixtures were incubated for 30 min at 37 °C. The enzyme reactions were stopped by the addition of up to 1% SDS—final concentration—and digested by 2 mg/mL proteinase K with 1 h incubation to remove protein bonded to the DNA fragment. The extent of plasmid DNA relaxation was assessed by electrophoresis in a 1% agarose gel in 0.1 M Tris acetate EDTA (TAE) buffer pH 8.0 at 2 V/cm for 14 h. The gels were visualized under UV illumination after being stained with ethidium bromide (0.5 mg/ml) and a posterior electrophoresis in the presence of 0.1 mg/ml ethidium bromide, in order to separate the nicked DNA from the relaxed topoisomers. One unit of LdTopIB is defined as the amount of purified protein able to relax 0.2 μg of pHOT supercoiled DNA per 30 min at 37 °C.

Results and Discussion

Our approach towards the total synthesis of either 6-heptadecynoic acid (**1a**) or 6-icosynoic acid (**1b**) started with commercially available 1-dodecyne or 1-pentadecyne which were successfully alkylated with 2-(5-bromopentyloxy)tetrahydropyran (**2**) in the presence of *n*-BuLi in THF–HMPA at 0 °C affording the tetrahydropyranyl protected alkynes **3a** (79% yield) and **3b** (54% yield) (Scheme 1). Deprotection of either **3a** or **3b** was achieved with *p*-toluenesulfonic acid (PTSA) in methanol at 60 °C, which yielded the desired 6-heptadecynol (**4a**) (99% yield) or 6-icosynol (**4b**) (83% yield). Final oxidation of either **4a** or **4b** with pyridinium dichromate (PDC) in DMF afforded the desired 6-heptadecynoic acid (**1a**) or 6-icosynoic acid (**1b**) in 76% yields. The overall yields for the last three steps of the syntheses of **1a**



i) DHP, p-TSA, CHCl_3 , rt, 90 min; ii) 1-dodecyne or 1-pentadecyne, *n*-BuLi, THF-HMPA, 0 °C, 80 min; iii) p-TSA, MeOH, 60 °C, 24h; iv) PDC, DMF, 48 h; v) H_2 , Pd/C (10%), quinoline, hexane; vi) PDC, DMF, 48 h.

Scheme 1 Synthesis of the acetylenic acids **1a** and **1b** and the olefinic acids **6a** and **6b**

Table 1 Antileishmanial activities (in $\mu\text{g/mL}$) of the studied fatty acids

Fatty acids	<i>L. donovani</i> promastigotes EC_{50}	Murine macrophages IC_{50}	Therapeutic index $\text{IC}_{50}/\text{EC}_{50}$
6-Heptadecynoic (1a)	6.67 ± 1.42	5.66 ± 0.92	0.85
(6 <i>Z</i>)-Heptadecenoic (6a)	>25	11.86 ± 1.63	n/a
Heptadecanoic (17:0)	>25	14.18 ± 7.48	n/a
6-Icosynoic (1b)	1.11 ± 0.28	5.35 ± 2.14	4.82
(6 <i>Z</i>)-Icosenoic (6b)	5.67 ± 1.07	28.20 ± 7.54	4.97
Icosanoic (20:0)	>25	21.93 ± 2.61	n/a

As a positive control we determined that miltefosine displays an IC_{50} of $0.79 \pm 0.14 \mu\text{M}$ against *L. donovani* and an EC_{50} of $1.95 \pm 0.37 \mu\text{M}$ against murine macrophages

n/a not assessed

(59% yield) and **1b** (34% yield) favored the shorter chain acid **1a**. The syntheses shown in Scheme 1 represent the first synthesis for both **1a** and **1b**.

Taking advantage of the same synthetic methodology (Scheme 1) we synthesized the naturally occurring fatty acids (6*Z*)-heptadecenoic acid (**6a**) and (6*Z*)-icosenoic acid (**6b**). For example, diverting the alkyne intermediates **4a** or **4b** to a catalytic hydrogenation under Lindlar's conditions resulted in the (6*Z*)-heptadecenol (**5a**) (82% yield) or the (6*Z*)-icosenol (**5b**) (70% yield) with a 100% *cis* stereochemistry for the double bonds. Oxidation of either **5a** or **5b** with pyridinium dichromate (PDC) in DMF afforded the desired (6*Z*)-heptadecenoic acid (**6a**) (73% isolated yield) and (6*Z*)-icosenoic acid (**6b**) (86% isolated yield). The overall yields for the four-step synthesis of **6a** (36%) and **6b** (21%) from **2** again favored the shorter chain acid **6a**. Surprisingly, this is also the first reported synthesis for either the alkenoic acids **6a** or **6b**.

Aiming at exploring the antiprotozoal activity of the acetylenic fatty acids **1a** and **1b** as well as that of the olefinic fatty acids **6a** and **6b** we studied their toxicity

towards *L. donovani* promastigotes. The results of our investigation are shown in Table 1. As the table shows, the acetylenic fatty acids **1a** and **1b** as well as the olefinic fatty acid **6b** displayed good antileishmanial activities towards *L. donovani* promastigotes ($\text{EC}_{50} = 1\text{--}7 \mu\text{g/mL}$). Surprisingly, the (6*Z*)-heptadecenoic acid (**6a**) was not effective against *L. donovani* ($\text{EC}_{50} > 25 \mu\text{g/mL}$). The saturated fatty acids *n*-heptadecanoic acid and *n*-icosanoic acid were tested as a control and they were also not effective towards *L. donovani* promastigotes ($\text{EC}_{50} > 25 \mu\text{g/mL}$), thus corroborating the previous literature report that unsaturation is an important factor for the antileishmanial activity of fatty acids [5]. From the results with the *L. donovani* promastigotes we can conclude that the C_{20} fatty acids were the more effective antileishmanial compounds since both acids **1b** and **6b** displayed a better therapeutic index ($\text{IC}_{50}/\text{EC}_{50} \approx 5$) over either **1a** or **6a**. Among the C_{17} fatty acids the acetylenic acid **1a** was the most efficient antiprotozoal compound, thus corroborating the importance of the C-6 triple bond in the antileishmanial activity of these compounds. Therefore, these results tend to indicate that

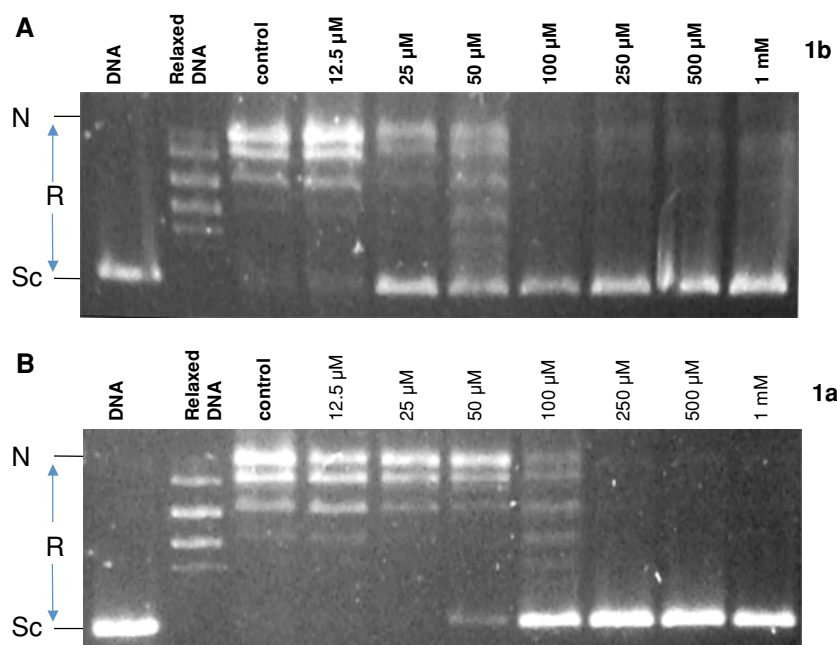


Fig. 1 Inhibition of the relaxation activity of recombinant LdTopIB by the 6-icosynoic acid (**1b**) (top) and the 6-heptadecynoic acid (**1a**) (bottom). One unit of recombinant LdTop1 was assayed in a plasmid DNA relaxation assay for 30 min at 37 °C (as described under “Materials and Methods”) in the presence of 12.5–1,000 μM compounds **1a** and **1b**. Reaction products were resolved in agarose

gel and subsequently visualized by ethidium bromide staining. The relative position of the negatively supercoiled DNA substrate is indicated by Sc, N is the nicked DNA, whereas the ladder of relaxed DNA topoisomer bands is labeled R. Reactions were stopped with a mixture of 1% SDS and 6.1 μg of proteinase K. Lane 1 contains 0.2 μg of pHOT plasmid DNA and lane 2 is a relaxed marker

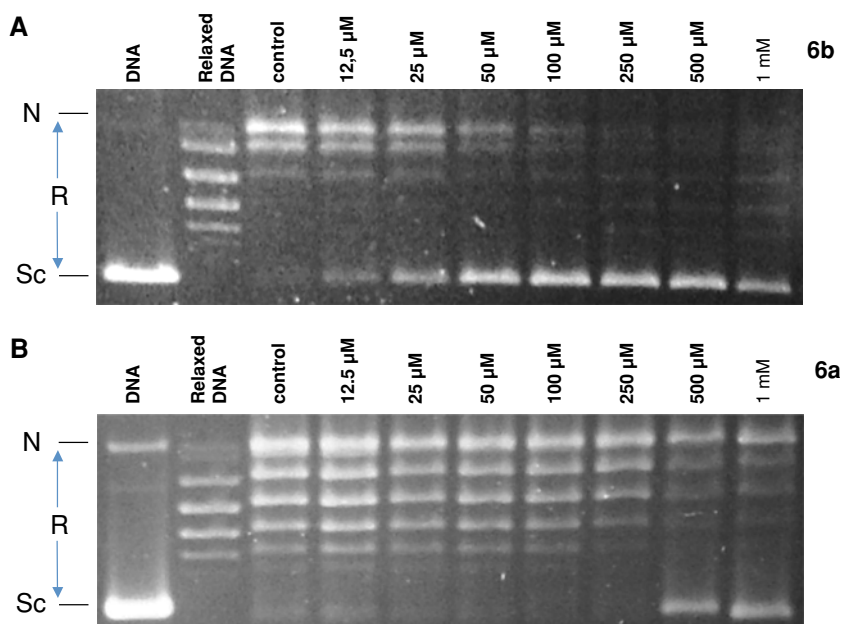
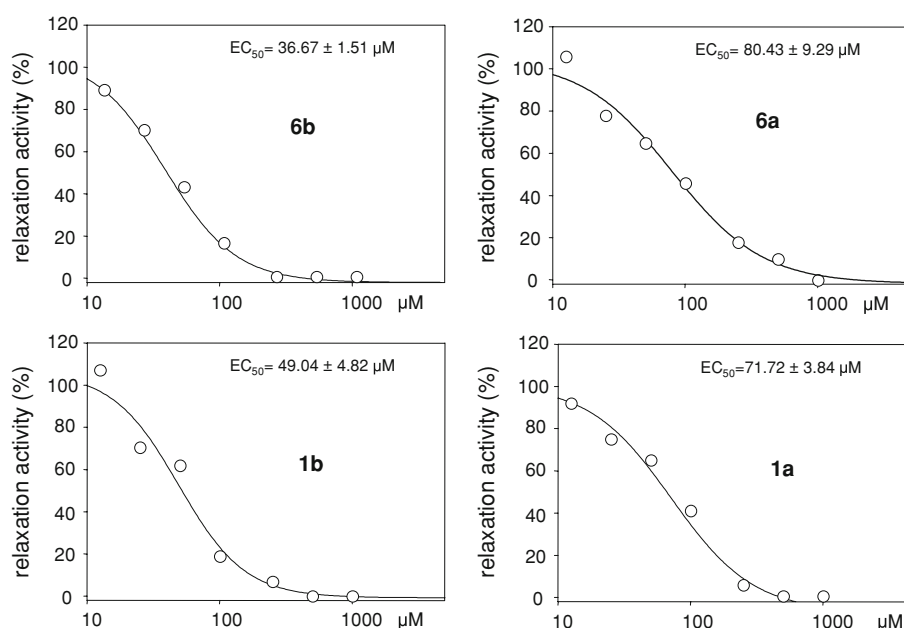


Fig. 2 Inhibition of the relaxation activity of recombinant LdTopIB by the (6Z)-icosenoic acid (**6b**) (top) and the (6Z)-heptadecenoic acid (**6a**) (bottom). One unit of recombinant LdTop1 was assayed in a plasmid DNA relaxation assay for 30 min at 37 °C (as described under “Materials and Methods”) in the presence of 12.5–1,000 μM compounds **6a** and **6b**. Reaction products were resolved in agarose

gel and subsequently visualized by ethidium bromide staining. The relative position of the negatively supercoiled DNA substrate is indicated by Sc, N is the nicked DNA, whereas the ladder of relaxed DNA topoisomer bands is labeled R. Reactions were stopped with a mixture of 1% SDS and 6.1 μg of proteinase K. Lane 1 contains 0.2 μg of pHOT plasmid DNA and lane 2 is a relaxed marker

Fig. 3 Plots of relaxation activities (%) of the LdTOPIB enzyme versus concentration (μM) of the acetylenic fatty acids **1a** and **1b**, and the olefinic fatty acids **6a** and **6b**. The EC_{50} values are shown at the top of each graph



naturally occurring Δ^6 acetylenic fatty acids could be valuable fatty acids that can be optimized for developing more potent antileishmanial agents and thus merit further scrutiny in the search for better analogs.

As a possible mechanism of toxicity we also studied the inhibition of these Δ^6 fatty acids towards the Leishmania DNA topoisomerase IB (LdTOPIB) enzyme since nothing is known in the literature as to the interaction of fatty acids with this particular enzyme. One aim here was to determine a possible selectivity of the studied fatty acids towards the LdTOPIB enzyme as a function of the level of unsaturation. The LdTOPIB enzyme is substantially different from the human topoisomerase I enzyme since the LdTOPIB enzyme is a heterodimer resulting from two separate genes encoding for the core and catalytic domains of the enzyme [9]. Our results with the acetylenic acids **1a** and **1b** are shown in Fig. 1 and with the alkenoic acids **6a** and **6b** in Fig. 2, while the corresponding inhibition plots are shown in Fig. 3. As can be seen from Figs. 1 and 3 the 6-icosynoic acid (**1b**) was more efficient ($\text{EC}_{50} = 49.04 \pm 4.82 \mu\text{M}$) than the 6-heptadecynoic acid (**1a**) ($\text{EC}_{50} = 71.72 \pm 3.84 \mu\text{M}$) in inhibiting the LdTOPIB enzyme. On the other hand, the (6Z)-icosenoic acid (**6b**) also displayed reasonably good inhibition of the enzyme ($\text{EC}_{50} = 36.67 \pm 1.51 \mu\text{M}$) (Figs. 2, 3), but the (6Z)-heptadecenoic acid (**6a**) displayed a weak inhibition of the enzyme ($\text{EC}_{50} = 80.43 \pm 9.29 \mu\text{M}$), which seems to explain its lack of toxicity towards the *L. donovani* promastigotes. The saturated fatty acids *n*-heptadecanoic acid and *n*-icosanoic acid did not inhibit the enzyme, even at concentrations as high as 1 mM (gel not shown). Therefore, the 6-icosynoic acid (**1b**) and the (6Z)-icosenoic acid (**6b**) were among the best inhibitors in the series of the LdTOPIB enzyme indicating that both

unsaturation and chain length are important factors when considering inhibition of the LdTOPIB enzyme by fatty acids. Therefore, the LdTOPIB enzyme seems to be a likely intracellular target for these C_{20} unsaturated fatty acids. We believe that our results should pave the way for the development of more potent antileishmanial fatty acids towards *L. donovani* and similar protozoa such as the trypanosomes, who share a similar topoisomerase IB enzyme.

Acknowledgments The project described was supported by Award Number SC1GM084708 from the National Institutes of General Medical Sciences of the NIH. M. Cartagena thanks the UPR RISE program for a graduate fellowship. We thank Dr. Fred Strobel (Emory University) for the high resolution mass spectral data. This research was also partially supported by a grant (Gr238) from Junta de Castilla y León and the Tropical Diseases Network (RICET) from Ministerio de Salud y Consumo (SPAIN).

References

- Li X-C, Jacob MR, Khan SI, Ashfaq MK, Babu KS, Agarwal AK, ElSohly HN, Manly SP, Clark AM (2008) Potent in vitro antifungal activities of naturally occurring acetylenic acids. *Antimicrob Agents Chemother* 52:2442–2448
- Pearl MB, Kleiman R, Earle FR (1973) Acetylenic acids of *Alvaradoa amorphoides* seed oil. *Lipids* 8:627–630
- Carballeira NM, Anastacio E, Salvá J, Ortega MJ (1992) Identification of the new 10, 15-eicosadienoic acid and related acids in the opisthobranch *Haminaea templadoi*. *J Nat Prod* 55:1783–1786
- Carballeira NM, Pagán M, Shalabi F, Nechev JT, Lahtchev K, Ivanova A, Stefanov K (2000) Two novel iso-branched octadecenoic acids from a *Micrococcus* species. *J Nat Prod* 63:1573–1575
- Chaudhuri G, Ghoshal K, Banerjee AB (1986) Toxic effects of fatty acids on *Leishmania donovani* promastigotes. *Indian J Med Res* 84:361–365

6. Desjeux P (2004) Leishmaniasis: current situation and new perspectives. *Comp Immunol Microbiol Infect Dis* 27:305–318
7. Berman J (2006) Visceral leishmaniasis in the New World & Africa. *Indian J Med Res* 123:289–294
8. Cruz I, Nieto J, Moreno J, Cañavate C, Desjeux P, Alvar J (2006) Leishmania/HIV co-infections in the second decade. *Indian J Med Res* 123:357–388
9. Balaña-Fouce R, Cubría JC, Reguera RM, Ordóñez D (1998) The pharmacology of leishmaniasis. *Gen Pharmacol* 30:435–443
10. Marty P, Rosenthal E (2002) Treatment of visceral leishmaniasis: a review of current treatment practices. *Expert Opin Pharmacother* 3:1101–1108
11. Berman J (2005) Miltefosine to treat leishmaniasis. *Expert Opin Pharmacol* 6:1381–1388
12. Sundar S, Chakravarty J (2008) Paromomycin in the treatment of leishmaniasis. *Expert Opin Investig Drugs* 17:787–794
13. Bhattacharya S, Sinha PK, Sundar S, Thakur CP, Jha TK, Pandey K, Das VR, Kumar N, Lal C, Verma N, Singh VP, Ranjan A, Verma RB, Anders G, Sindermann H, Ganguly NK (2007) Phase 4 trial of miltefosine for the treatment of Indian visceral leishmaniasis. *J Infect Dis* 196:591–598
14. Cunningham LV, Kazan BH, Kuwahara SS (1972) Effect of long-chain fatty acids on some trypanosomatid flagellates. *J Gen Microbiol* 70:491–496
15. Villa H, Otero Marcos AR, Reguera RM, Balaña-Fouce R, García-Estrada C, Pérez-Pertejo Y, Tekwani BL, Tyler PJ, Stuart KD, Bjornsti MA, Ordóñez DA (2003) A novel active DNA topoisomerase I in *Leishmania donovani*. *J Biol Chem* 278:3521–3526
16. Diaz-González R, Pérez-Pertejo Y, Pommier Y, Balaña-Fouce R, Reguera RM (2008) Mutational study of the “catalytic tetrad” of DNA topoisomerase IB from the hemoflagellate *Leishmania donovani*: role of Asp-353 and Asn-221 in camptothecin resistance. *Biochem Pharmacol* 76:608–619

oils, several strategies to increase TAG production in plants have been explored [4–6].

The two major pathways leading to TAG production in humans, proposed many years ago, converge in the last step catalyzed by acyl-CoA:diacylglycerol acyltransferase (DGAT, EC 2.3.1.20) [7]. DGAT utilizes *sn*-1,2-diacylglycerol (DAG) and acyl-CoA as substrates to form TAG [8, 9] and at least two distinct membrane-bound polypeptides, referred to as DGAT1 [10, 11] and DGAT2 [12–14] have been identified. In yeast TAG can be also formed through the catalytic action of phospholipid:diacylglycerol acyltransferase (PDAT, EC 2.3.1.158) which is encoded by the *LRO1* gene and uses a phospholipid as the acyl donor and DAG as the acceptor [15]. Orthologues of PDAT have been found in plant genomes, but their contribution to overall TAG biosynthesis remains unclear [16, 17]. In addition yeast possesses two other enzymes with minor DGAT activity. These enzymes, encoded by *ARE1* and *ARE2* genes, are mainly responsible for the biosynthesis of sterol esters [18].

Standard methods to measure the enzyme activity of DGAT and PDAT, here referred to as TAG synthesizing enzymes (TAG-SE), require a sensitive but rather laborious assay with radio-labeled substrates [19]. Due to the hydrophobic nature of TAG, their analysis entails time-consuming techniques such as solvent extraction and/or thin layer chromatography (TLC). In addition, TAG synthesizing enzymes are usually associated with membranes and therefore, enzyme assays typically use microsomal fractions obtained through ultracentrifugation, further decreasing the throughput of the assay. These factors contribute to the delay of fundamental and applied research involving TAG-SE. Moreover, a relatively small number of known genes, mostly identified by homology-based cloning, limit our understanding of this group of enzymes.

In the present work, we developed an activity-based screening method capable of identifying yeast clones expressing a functional DGAT. The method uses a eukaryotic heterologous expression system and a modified baker's yeast (*Saccharomyces cerevisiae*) strain H1246. This strain is particularly suitable for heterologous expression of *DGAT*, as it is free of TAG and sterol esters as a result of knockouts in four genes (*DGA1*, *LRO1*, *ARE1* and *ARE2*) [18]. To further evaluate the DGAT clones and quantitatively measure the enzyme activity we applied an additional method to determine the amounts of TAG accumulated in intact living cells using Nile red, a fluorescent dye commonly used to stain neutral lipids [20]. The changes in fluorescence caused by the interaction of the dye with TAG correlate with DGAT activity as demonstrated for several *DGAT1* mutants. The simple nature of the assay makes it amenable to higher throughput experimental designs. We discuss several applications for these

two methods applied independently or in combination. Siloto et al. [21] have presented a preliminary account of some of this work.

Experimental Procedures

Yeast Cell Culture and Reagents

Yeast nitrogen base without amino acids (YNB), glucose, raffinose, galactose and amino acid drop-out supplement were obtained from BD Difco (Oakville, Canada). Oleic acid and tergitol were purchased from Sigma–Aldrich (Oakville, Canada) and other FAs were from Nu-Chek Prep (Elysian, USA). Nile red (7-diethylamino-3,4-benzophenoxazine-2-one) was obtained from Molecular Probes (Invitrogen, Carlsbad, USA). Oligonucleotides were synthesized by Integrated DNA Technologies (Coralville, USA).

The *S. cerevisiae* strain H1246 (*MAT α are1- Δ ::HIS3, are2- Δ ::LEU2, dga1- Δ ::KanMX4, lro1- Δ ::TRP1 ADE2*) containing knockouts of the *DGA1*, *LRO1*, *ARE1* and *ARE2* genes, was kindly donated by Drs. S. Stymne and U. Ståhl. The strain 12501 (*MAT α dga1- Δ ::KanMX4*) was obtained from Open Biosystems (Thermo Fisher Scientific, Huntsville, USA). Yeast transformation was performed according to Gietz and Schiestl [22] using heat-shock at 42 °C for 12 min. After transformation, the yeast culture was cultivated in minimal medium with dextrose (YNBD) containing 0.67% (w/v) of YNB, 2% (w/v) dextrose, 20 mg/L of adenine, arginine, tryptophan, methionine, histidine, and tyrosine, 30 mg/L of lysine and 100 mg/L of leucine. The cultures were grown at 30 °C, 250 rpm.

Cloning and Expression of DGAT in Yeast

For expression of *Brassica napus DGAT1* (*BnDGAT1*) in yeast, the coding region of *BnDGAT1* was amplified using a cDNA clone previously isolated in our laboratory (unpublished) using forward primer 5'-gaccatggggattttggattctg gagg-3' and reverse primer 5'-ctgatgaccggaaaggggtccatgt cc-3'. The amplified DNA was cloned into the yeast expression vector pYES DEST52 (Invitrogen) under the control of GAL1 promoter to yield pYESBnDGAT1. Flax (*Linum usitatissimum*) and castor bean (*Ricinus communis*) *DGAT1* (*LuDGAT1* and *RcDGAT1*, respectively) were similarly cloned to generate pYESLuDGAT1 and pYESRcDGAT1. The *LuDGAT1* coding region was amplified using forward primer 5'-gaccatggggcgtgctgcacactcctgacaatc-3', reverse primer 5'-caggaatgggaaagatggaatcaagcttaaa-3', and a cDNA template previously isolated in our laboratory (Siloto et al., unpublished data). The *RcDGAT1* coding region was amplified using forward primer 5'-gaatcgcca

tggaacaagcttaa-3', reverse primer 5'-caggaatgggaaagatggaatcaagctt-3', and a cDNA clone template [23]. pYES-LacZ, used as a negative control, was obtained from Invitrogen. The variants of *RcDGAT1* were similarly obtained by PCR. N1, N2 and N3, are N-terminus truncations while C1 and C2 are C-terminus truncations. Y302F, Y199F, S226A and S168A are point mutants of *RcDGAT1* obtained by site-directed mutagenesis.

Expression of the recombinant genes in yeast was induced using minimal medium containing 2% (w/v) galactose and 1% (w/v) raffinose (YNBG). Prior to induction, cultures were centrifuged for 5 min at 3,000g at room temperature and washed twice with water.

FA Supplementation

FAs were dissolved in ethanol at 0.5 M with the exception of palmitic and stearic acids that were dissolved at 0.25 M in hot ethanol. FA solutions were diluted in a warm medium containing 0.01% (v/v) tergitol immediately before yeast inoculation. Tergitol is a nonionic surfactant that was used to assist the dispersion of the FA in the medium. Control experiments without FAs contained the same volume of ethanol and 0.01% (v/v) of tergitol.

Yeast Lipid Analysis

Induced yeast cultures at the stationary growth stage, cultivated in 50 mL medium, were washed twice with water and resuspended in 2 mL of methanol. Glass beads (0.5 mm) were added and the suspension was vigorously vortexed. Lipids were extracted by adding 4 mL of chloroform and 1 mL of 0.9% (w/v) of sodium chloride. The sample was vortexed and centrifuged at 2,000g for 2 min. The lower phase was recovered and the remaining lipids were re-extracted twice with an additional 4 mL of chloroform. Chloroform fractions were pooled, dried under nitrogen, resuspended in 20 μ L of chloroform, and spotted on a TLC plate (SIL G25, 0.25 mm, Macherey–Nagel, Germany). The plate was developed with hexane/diethyl ether/acetic acid (80:20:1, v/v/v) and lipids visualized with 8% (w/v) copper sulfate and 5% (v/v) phosphoric acid followed by charring at 350 °C for 1 h.

In Vitro Measurement of Microsomal DGAT Activity in Yeast

Induced yeast cultures were collected at 3,000g for 5 min and washed twice with 1 mL of buffer containing 20 mM Tris–HCl pH 7.5, 10 mM MgCl₂, 1 mM EDTA, 5% (v/v) glycerol, 300 mM ammonium sulfate and 2 mM dithiothreitol. Yeast cells were resuspended in 1 mL of the same buffer and homogenized with a bead beater (Biospec,

Bartlesville, USA) using 0.5 mm glass beads. The homogenate was centrifuged at 10,000g, at 4 °C for 10 min and the supernatant was recovered. The microsomal fraction was recovered through centrifugation at 100,000g, at 4 °C for 1 h. The pellet was resuspended in 50 μ L of 3 mM imidazole buffer (pH 7.4) containing 125 mM sucrose. The crude protein concentration in the microsomal fraction was normalized using the BCA assay (Pierce, Rockford, USA) with a BSA standard curve. DGAT assays were conducted with 15 μ g of microsomal protein in the presence of 25 mM sucrose, 0.1 mM EDTA, 15 mM Tris–HCl pH 7.4, 125 μ g/mL BSA (FA-free), 320 μ M *sn*-1,2-diolein and 15 μ M [¹⁴C] oleoyl-CoA in a total volume of 60 μ L in a similar fashion to a previously described method [24]. The reaction was allowed to proceed at 30 °C for 15 min and quenched with 10 μ L of sodium dodecyl sulfate 10% (w/v). The reaction was spotted on a TLC plate (SIL G25, 0.25 mm, Macherey–Nagel), along with 100 μ g of triolein standard. The plate was developed with hexane/diethyl ether/acetic acid (80:20:1, v/v/v). TAG spots were detected with iodine, scraped, and measured in a Beckman-Coulter LS6500 liquid scintillation counter. The assays were performed in three technical replicates.

Nile Red Assay

Nile red assay and optical density determination were performed in 96-well polystyrene flat-bottom microplates (UNIPLATE, Whatman, UK). The Nile red fluorescence assay was performed by placing 95 μ L of yeast culture in a 96-well dark plate. The background fluorescence was measured using a multi-well plate fluorimeter (Fluoroscan Ascent, Thermo, Milford, USA) for 100 ms with excitation and emission filters of 485 and 538 nm, respectively. Five microliters of freshly prepared methanolic Nile red solution were added to the culture using a built-in automatic dispenser. Different concentrations of Nile red in methanol were used as described in the “Results” section and the optimal concentration was determined as 0.8 mg/mL. The mixture was then briefly mixed and incubated for 5 min at room temperature. A second fluorescence measurement was performed using the same conditions. The assays were performed with four technical replicates. Nile red was protected from light to avoid photo-bleaching.

Results

Positive Selection of Yeast Cells Expressing DGAT

Most yeast expression systems use the galactokinase (GAL1) promoter to control the expression of the heterologous gene [25]. The induction of the heterologous

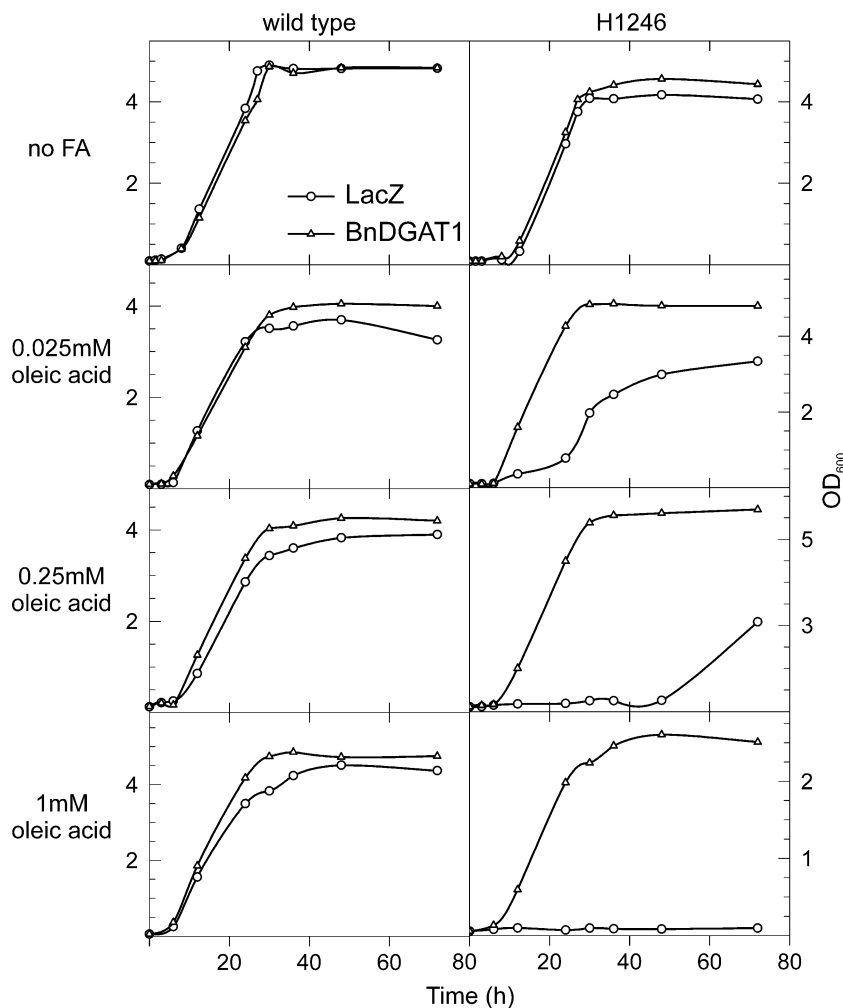
expression is achieved by changing the carbon source in the medium from glucose (medium YNBD) to galactose (YNBG) which activates the GAL1 promoter [26]. The quadruple knockout yeast strain H1246 is suitable for expression and characterization of DGAT genes as it is devoid of DGAT activity and does not accumulate storage lipids [18]. Since yeast is able to import exogenous FAs and convert them to respective acyl-CoA derivatives, supplementation of the medium with FA can further enhance the TAG accumulation conferred by the recombinant DGAT gene.

In our experiments we routinely use the pYES vector coding for the bacterial protein LacZ as a negative control. We noticed that H1246 cultures transformed with pYES-LacZ grew normally in YNBD, but displayed a reduced growth rate in the FA-containing induction medium when compared to *DGAT*-expressing cells. Growth curve experiments confirmed this observation and revealed dependence of this phenotype on the FA concentration (Fig. 1). Interestingly, expression of *BnDGAT1* in the H1246 background was able to reverse the effect of FA and the growth curve of

the *BnDGAT1*-expressing culture was similar to that of the *wild type* yeast even at the highest tested FA concentration that entirely inhibited the growth of *LacZ*-expressing strain. In fact, expression of *BnDGAT1* in *wild type* host slightly favored yeast growth. To eliminate the possibility that growth was adversely affected by the *LacZ* expression, we repeated the experiments with yeast harboring an empty pYES vector with results similar to those of *LacZ* control strain (Fig. 2a). Additionally we observed only a partial FA-induced growth inhibition using the *S. cerevisiae* mutant 12501 which contains a single knockout in *DGAI1* gene that encodes yeast DGAT (Fig. 2a).

In another experiment we inoculated H1246 cultures expressing *LacZ* and *BnDGAT1* on YNBG solid medium with and without FA supplement. Similarly to the liquid medium, the plates containing 1 mM oleic acid distinguished the two cultures (Fig. 3a). To investigate the nature of the growth effect and assess broader applicability of the selection system, we inoculated both *LacZ*- and *BnDGAT1*-expressing cultures on YNBG plates supplemented with a range of FA differing in the carbon-chain length as

Fig. 1 Exogenous FAs inhibit growth of yeast cells devoid of TAG synthesizing enzyme activity. Cultures of *S. cerevisiae* strain H1246 (right column) and the corresponding parental strain (left column) transformed with pYESLacZ or pYESBnDGAT1 were inoculated in YNBG at a final OD₆₀₀ of 0.1. Oleic acid, dissolved in ethanol at 0.5 M, was supplemented to the cultures at the final concentrations indicated. The cultures were incubated at 30 °C, 250 rpm and the growth was monitored for 72 h. Cultures expressing *LacZ* or *BnDGAT1* are denoted by circles or triangles, respectively



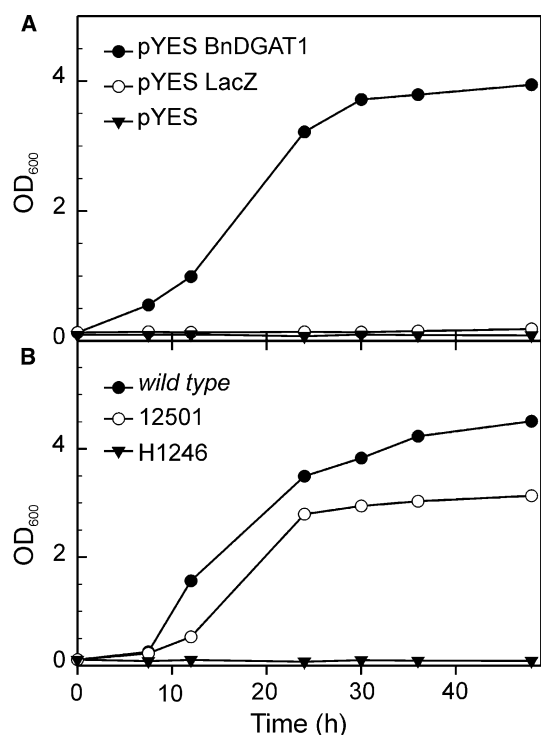


Fig. 2 Effect of yeast genetic background in FA-growth inhibition. **a** *S. cerevisiae* strain H1246 transformed with pYESBnDGAT1, pYESLacZ or pYES were inoculated in YNBG at a final OD₆₀₀ of 0.1 and oleic acid was supplemented to the cultures at a final concentration of 1 mM. The cultures were incubated at 30 °C, 250 rpm and the cell growth was monitored for 48 h. **b** *S. cerevisiae* wild type, 12501 (*DGA1* knockout) or H1246 (*DGA1*, *LROI*, *ARE1* and *ARE2* knockout) were transformed with pYESLacZ. The recombinant yeast strains were inoculated in YNBG at final OD₆₀₀ of 0.1 and oleic acid was supplemented to the cultures at a final concentration of 1 mM. The cultures were incubated at 30 °C, 250 rpm and the cell growth was monitored for 48 h

well as in the degree of saturation (Fig. 3b). The growth of the control strain was inhibited in most cases except when palmitic, stearic and erucic acids were supplemented, most likely due to their lower dispersion in the aqueous medium. Lowering the concentration of these FAs to 0.5 mM seemed to help their dispersion in the medium, but it did not substantially improve the selectivity of the media. Media containing 1 mM linoleic, α -linolenic or docosahexaenoic acids, on the other hand, inhibited the growth of both cultures. In view of the results obtained with liquid media supplemented with different amounts of oleic acid, we tested a range of lower concentrations and found that plates with 0.5 mM concentrations of α -linolenic or docosahexaenoic acids were suitable for selection (Fig. 3c).

Taken together, these results suggested that the growth inhibition of the H1246 yeast strain in the presence of FA could provide a basis for a functional complementation assay capable of identifying recombinant genes encoding a

functional DGAT. To test this hypothesis we transformed H1246 with a mixture of plasmids consisting of 0.9 μ g of pYESLacZ and 0.1 μ g of pYESBnDGAT1 along with controls consisting of 1 μ g of each vector. The transformed cells were spread on YNBG plates with or without 1 mM oleic acid. In the presence of FA, the number of colonies growing on the plates with mixed vectors represented 10.1% of those formed by the pYESBnDGAT1 transformation. As expected, pYESLacZ did not produce any colonies on plates containing oleic acid (Fig. 3d).

In Situ Quantification of TAG Synthesizing Enzyme Activity in Yeast Cells

The functional complementation assay allowed for easy identification and isolation of yeast cells expressing a functional TAG-SE or other free FA-detoxifying enzymes. Since H1246 yeast strain is essentially devoid of neutral lipids, the TAG produced and accumulated is directly attributable to the activity of the expressed heterologous DGAT. We used this relationship to extend the previously described system of qualitative selection, adding a quantitative dimension in a simple in situ fluorescent assay. To quantify the amount of TAG that accumulated in transformed yeast cells, we used Nile red, a fluorescent dye commonly applied in microscopy to stain lipid particles [20]. The emission maximum of Nile red conjugated with neutral lipids differs from that of the dye-polar lipid complex. Moreover, the intensity of fluorescence caused by the interaction of the dye with neutral lipids is much higher than it is with polar lipids, making Nile red suitable for our purpose. Nile red dye moves freely across cellular membrane and thus makes it possible to perform the quantitative neutral lipid assay in living cells, eliminating the need for sample preparation.

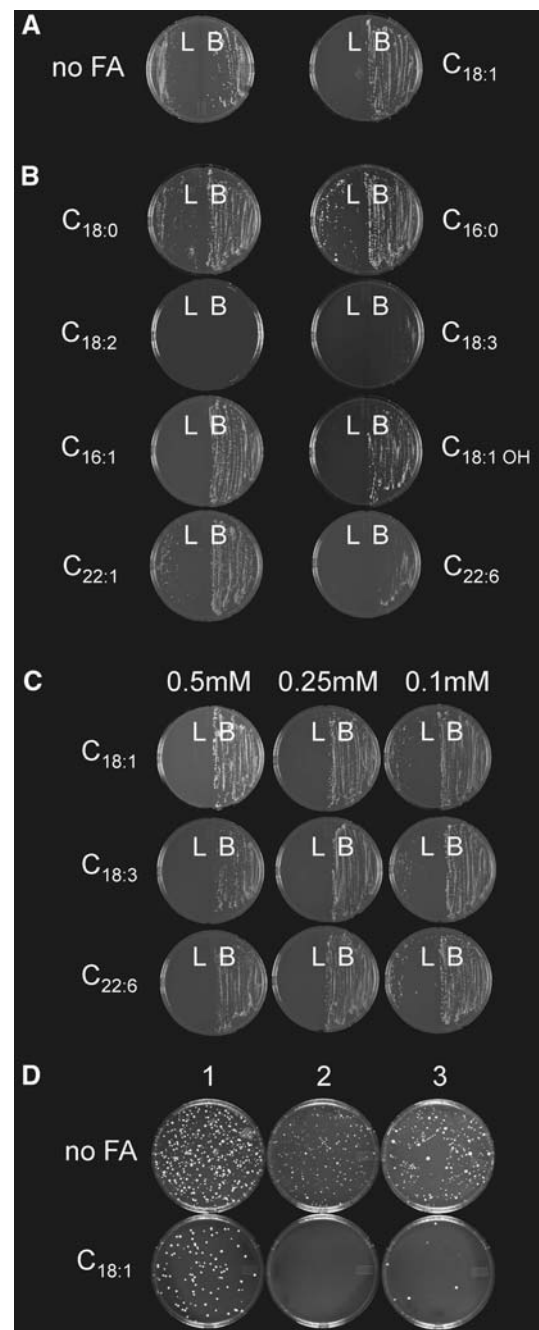
An example of NRA is illustrated in Fig. 4. The fluorescence increase (ΔF) is significantly higher in yeast cultures expressing *BnDGAT1* and *LuDGAT1* than in the culture deficient in the biosynthesis of neutral lipids (expressing *LacZ*) (Fig. 4a). The results of NRA correlated well with DGAT activity quantified by a standard in vitro radioactive assay. Thin layer chromatography of neutral lipids extracted from the three cultures confirmed the presence of TAG only in cultures expressing heterologous DGATs (Fig. 4b). We therefore concluded that the fluorescent NRA can be used to rapidly estimate the activity of the recombinant DGAT in living yeast cells without the need for extensive sample preparation.

Optimization of the Fluorescent NRA

To optimize NRA and investigate factors influencing fluorescence values, we conducted several experiments

Fig. 3 Growth phenotype is observed on solid medium supplemented with FAs. H1246 yeast strain expressing *LacZ* (L) or *BnDGAT1* (B) were inoculated on the corresponding YNBG solid medium and incubated at 30 °C for 6 days. **a** Plates of YNBG with and without supplement of 1 mM oleic acid (18:1^{*cis*Δ9}) dissolved in ethanol. The plate without FA contained the same volume of ethanol only. **b** Plates of YNBG supplemented with 1 mM palmitoleic (16:1^{*cis*Δ9}), linoleic (18:2^{*cis*Δ9,12}), α-linolenic (18:3^{*cis*Δ9,12,15}), docosahexaenoic (22:6^{*cis*Δ4,7,10,13,16,19}), ricinoleic (18:1^{12-OH *cis*Δ9}), erucic (22:1^{*cis*Δ13}) and 0.5 mM palmitic (16:0) and stearic (18:0) acids. The FAs were dissolved in ethanol at 0.5 or 0.25 M and added to the YNBG prior to plating. **c** Plates supplemented with oleic, α-linolenic and docosahexaenoic acids at the final concentrations indicated. **d** Selection of yeast cells in medium with FA after transformation. H1246 cells were transformed with 1 μg of pYESBnDGAT1 (column 1), 1 μg of pYESLacZ (column 2) and 0.1 μg of pYESBnDGAT1 mixed with 0.9 μg of pYESLacZ (column 3). After transformation, yeast cells were recovered in liquid YNBD medium for 6 h, inoculated in YNBG plates with or without supplement of 1 mM oleic acid and incubated at 30 °C for 6 days

using *BnDGAT1*- or *LacZ*-expressing cultures cultivated to stationary growth phase in YNBG. Initially, we prepared Nile red solution in methanol at different concentrations and conducted the NRA by mixing 5% of the dye in the yeast cultures, normalized to a range of cell densities (OD₆₀₀). The highest Δ*F* values were obtained using Nile red at final concentration of 0.04 mg/mL of yeast culture (Fig. 5a). The difference between Δ*F* values obtained for *LacZ*- and *BnDGAT1*-expressing cultures was clearly observed with concentrations up to 0.2 mg/mL. Although the cell density did not affect the concentrations at which maximal Δ*F* values were observed, it did alter the measured fluorescence values. In order to investigate the effect of cell density on Δ*F* values, NRA was performed with *BnDGAT1*- or *LacZ*-expressing cultures adjusted to a range of OD₆₀₀ values using plain YNBG medium as a diluent. As illustrated in Fig. 5b, there was a clear distinction between the fluorescence increases due to the cell density in the culture accumulating TAG (*BnDGAT1*-expressing cultures) and the increase of background fluorescence in the control (*LacZ*-expressing cultures). The results further indicated that Δ*F* values are not affected by the medium itself and correlate linearly with the cell density within the studied OD₆₀₀ range. Consequently, it is possible to normalize Δ*F* values by calculating the Δ*F*/OD ratio rather than trying to achieve the same cell density across samples, which can be impractical. To test the reliability of the assay over a range of possible amounts of TAG produced by the yeast culture, we performed NRA with mixtures of *BnDGAT1*- and *LacZ*-expressing cultures, both adjusted to the same cell density (Fig. 5c). As expected, the observed Δ*F* increased with the proportion of the *BnDGAT1*-expressing culture in the mixture in a linear fashion, indicating that NRA provides a good estimate of TAG accumulated in yeast cells and, in conjunction with the quadruple knockout



strain H1246, also an estimate of the heterologous DGAT activity.

Validation of the Methods with DGAT Mutants

To evaluate the efficacy of the DGAT screening system we tested the selection by functional complementation and the NRA with mutants of a castor bean *DGAT1* (*RcDGAT1*) prepared and characterized in our laboratory. Several mutants of *RcDGAT1* were constructed by truncation of the N-terminus (N1, N2 and N3), C-terminus (C1 and C2) as

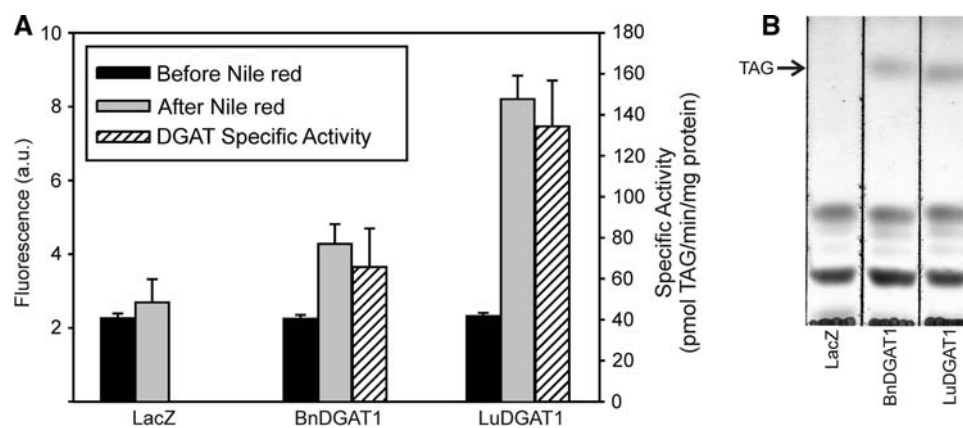


Fig. 4 NRA correlates with DGAT activity and TAG accumulation in yeast. **a** NRA and DGAT enzyme assays performed with H1246 yeast cultures expressing *LacZ*, *BnDGAT1* or *LuDGAT1*. Fluorescence was measured with 95 μ L of cultures in YNBG at the stationary phase using 485 (excitation) and 538 nm (emission) before and after the addition of Nile red, and expressed in arbitrary units (a.u.). DGAT activity was measured with the microsomal fraction extracted from

the same cultures induced for 16 h in YNBG. DGAT activity in the H1246 yeast culture expressing *LacZ* was not detected. **b** Lipid profile of the same cultures in YNBG at the stationary growth phase. Total yeast lipids were extracted with methanol/chloroform, resolved by TLC and visualized by charring in the presence of copper acetate. The position of TAG is indicated

well as by the substitution of single residues (Y302F, Y199F, S226A and S168A) through site-directed mutagenesis (unpublished). These mutants display a wide range of DGAT activity, providing us with a useful model for validation of the novel methods. Briefly, the mutation Y302F produced no significant effect on the enzyme activity while other mutations resulted in lower degrees of activity compared to the *wild type RcdGAT1*. We used the selection on FA-containing plates to verify the phenotype of each mutant (Fig. 6a). As expected, *RcdGAT1*-expressing cells displayed normal growth on YNBG with FA. The mutants Y302F, Y199F, S226A and S168A also grew normally while no growth could be detected for N1, N2, N3, C1 and C2 over the same period of incubation. We also performed NRA and the radioactive *in vitro* assay with liquid cultures expressing *RcdGAT1* variants. Briefly, the relative comparison of DGAT activity of the *wild type* and the modified *RcdGAT1* variants measured by NRA resembled the results of the *in vitro* enzyme assay for most of the mutants analyzed here (Fig. 6a). Positive correlation between the fluorescent *in situ* and the conventional *in vitro* enzyme assay (Fig. 6b) suggests that NRA can be used to measure recombinant DGAT activity in yeast, especially in large-scale experiments.

Discussion

DGAT plays a pivotal role in TAG accumulation and homeostasis in eukaryotes [8, 9]. It had been suggested that in plants DGAT activity may be the rate-limiting step for TAG biosynthesis in developing seeds [27], a hypothesis confirmed by several independent genetic studies [28–30].

The growing demand for vegetable oil worldwide has stimulated research in the area of TAG synthesis and DGAT is at the center of multiple genetic engineering efforts to modify the amount and quality of oil accumulated in seeds [6, 31]. In mammals, a fat-rich diet combined with a sedentary lifestyle results in an excessive accumulation of TAG associated with obesity and other metabolic disorders. One of the possible strategies for the treatment of obesity is to restrict TAG synthesis and DGAT has been considered a potential target [32]. In spite of the continuing advances in our understanding of TAG biosynthesis, many questions related to the roles of enzymes involved and their regulation remain to be addressed.

Most DGAT studies rely on some type of heterologous expression followed by an enzyme assay. The conventional DGAT activity assay is laborious and requires radio-labeled substrates. Commonly, phase separation and/or TLC are employed to isolate the reaction product before liquid scintillation [19]. The low throughput of such assays considerably limits the choice of applicable experimental designs. Here we describe the NRA method that can be used to rapidly estimate accumulated TAG and hence DGAT activity in genetically altered yeast cultures. This live-cell-based assay is versatile and particularly suitable for high-throughput applications. Similar methods to estimate neutral lipid content in oleaginous microorganisms such as *Umbelopsis ramanniana* [33] or mammalian cultured cells [34] have been previously devised. By combining a Nile red-based fluorescent assay with the *S. cerevisiae* H1246 strain, the NRA method described here estimates the activity of a single recombinant DGAT in live yeast cells. Such estimates are biologically relevant, even though some of the tested *RcdGAT1* mutants appear to

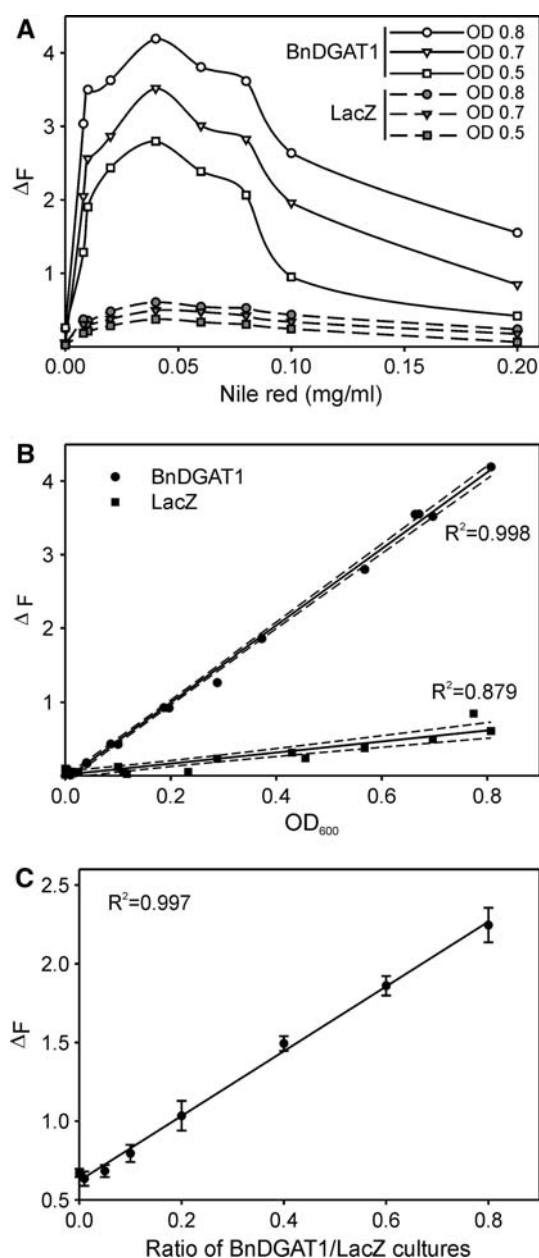


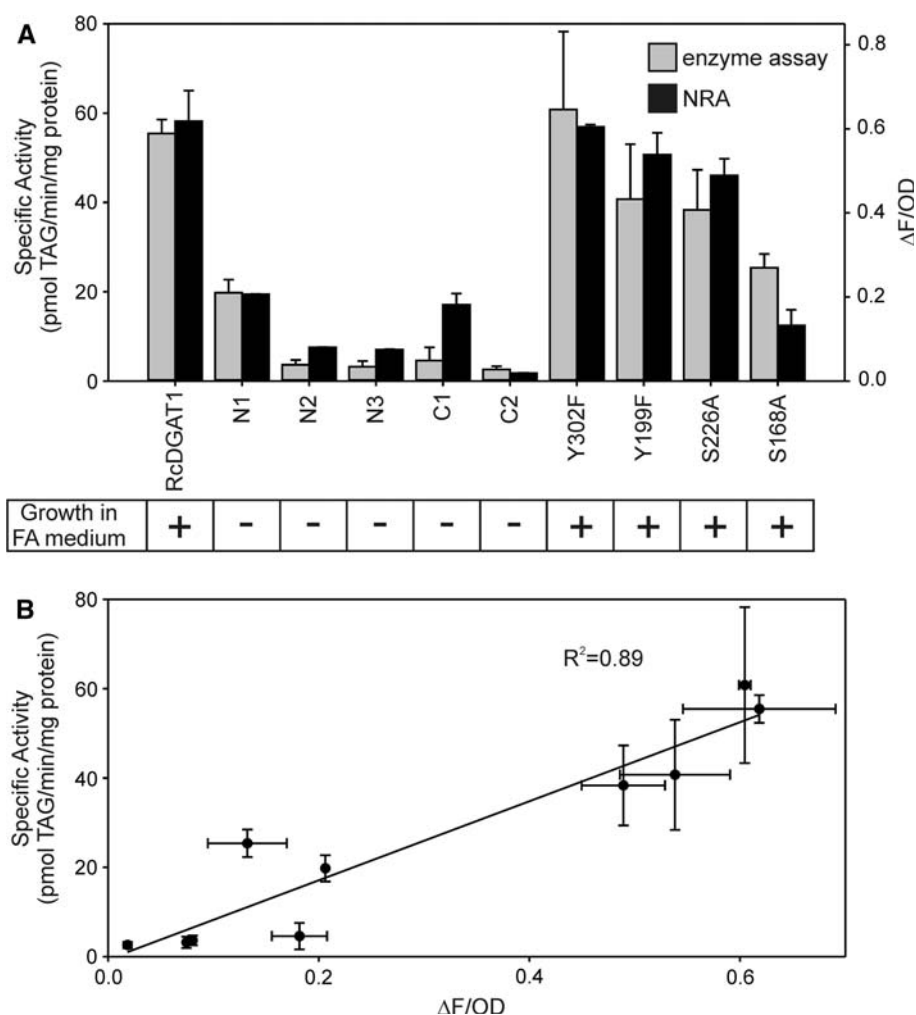
Fig. 5 Characterization of factors influencing NRA. **a** Optimization of Nile red concentration. NRA was performed with 95 μ L of H1246 cultures expressing *LacZ* (dashed lines) or *BnDGAT1* (full lines) at stationary phase and diluted at different cell densities as described. After measuring the background fluorescence, 5 μ L of methanolic solution of Nile red at different concentrations were added and followed by the second measurement with 5-min interval from the first measurement. The difference between the first and second measurement is denoted in *Y* axis as ΔF in arbitrary units (a.u.) and the final concentration of Nile red in the culture is denoted in the *X* axis as ΔF in arbitrary units (a.u.). **b** NRA of the same cultures at stationary phase plotted as a function of cell density (OD_{600}). Full lines denote linear regression with dashes corresponding to intervals of 99% confidence. **c** NRA performed with mixtures of *BnDGAT1*- and *LacZ*-expressing cultures normalized to the same cell density. The full line represents the linear regression with the error bars representing standard deviation

deviate from the linear relationship between the two assays. One of the possible reasons for such deviation is that the radio-active assay is performed *in vitro* in a controlled environment, typically with relatively high substrate content in the reaction mixture under linear initial reaction velocity conditions, while NRA is subject to a limited availability of substrates controlled by multiple endogenous cellular mechanisms. The protein stability can affect the read-out since the *in vitro* assay reflects the conversion of labeled substrates into TAG during a relatively short time period. NRA, however, quantifies the accumulation of storage lipids over the course of individual cell lives. Consequently, while standard assays provide an accurate quantification of the enzyme activity in the controlled environment, NRA might better reflect the performance of a DGAT under study in the live cell context.

Motivated by the pharmaceutical importance of DGAT inhibitors, Seethala et al. [35] recently developed an improved radioactive method based on scintillation proximity assay. The method uses DAG and tritium-labeled acyl-CoA substrates with the resulting TAG being bound by scintillant-containing microsphere beads. The proximity of a radioactive atom causes the bead to emit signal detected by a fluorescent imaging system or a microplate scintillation counter. The assay uses a microsomal fraction as a source of DGAT and is therefore amenable for high throughput experiments which evaluate interactions of an array of chemical compounds with TAG-SE from a single biological source. In contrast, the methods described here are suitable for experimental designs studying a large number of individual gene products. Since NRA does not require sample preparation, it is possible to assess the activity of an array of enzymes, for instance, an expressed cDNA library or a mutagenized population of a single gene. NRA could equally well serve in specific DGAT inhibitor screens, providing additional information regarding the cytotoxicity and ability of compounds to move across the cellular membrane.

The combination of the functional complementation assay and NRA can be used as a unique high throughput screening system, an essential element for optimizing directed evolution of proteins [36]. Such an approach might produce DGATs with enhanced catalytic efficiency or modified substrate selectivity [21]. In addition, information obtained from large mutagenized cDNA populations would advance our understanding of the structure–function relationship in DGAT. Few studies investigating the influence of specific amino acid residues on DGAT enzyme activity have been conducted [37, 38] and most of the information available on the structure and function of DGATs has been derived from comparisons of homologous enzymes. Application of the methods described here could enhance

Fig. 6 Validation of the selection system and NRA with mutants of *RcDGAT1*. **a** NRA and DGAT microsomal activity. Enzyme activity was determined by radioactive assay for each *RcDGAT1* variant and NRA results were expressed as ΔF (a.u.) divided by OD_{600} . The table below indicates the selection system results for H1246 cultures expressing *RcDGAT1* and the respective variants. *Negative* (–) and *positive* (+) indicate the ability to produce colonies in solid YNBG supplemented with 1 mM oleic acid. **b** Relationship between $\Delta F/OD$ and the specific activity measured by radioactive assay. The line denotes linear regression; error bars represent standard deviation



our knowledge of the molecular mechanisms involved in DGAT activity.

Yeast cultures are routinely analyzed at a single-cell level by flow cytometry [39]. The nature of NRA, based on the detection of fluorescent signal in individual cells, offers an exciting possibility to significantly bolster the throughput of the technique by employing fluorescence-activated cell sorting (FACS). This method has been used, for instance, in yeast viability assessment [40] and Muller and Losche [41] have used Nile red staining of neutral lipids as one of the parameters in their characterization of brewing yeast subpopulations.

There is substantial data showing that yeast internalizes FAs via a process known as vectorial acylation, where an acyl-CoA is formed upon crossing the plasma membrane. Genetic studies have identified the key elements of the protein complex that involve acyl-CoA synthetases [42, 43]. The import of FAs by yeast is tightly coupled to their utilization, and the size of the internal sink is limited under glucose repression [44]. Harnessing the natural capability of yeast to import FA and to convert them to their

acyl-CoA equivalents constitutes one of the main advantages of the described cell-based methods. Any FA that can be made available to yeast cells in the medium and undergoes efficient vectorial acylation can be used for selection and activity evaluation. In contrast to conventional in vitro assays, where substrates have to be presented in an acyl-CoA form, supplementing growth medium with FA is simple, inexpensive and more flexible. The spectrum of FAs that can be used in such experiments extends far beyond the typical yeast lipid profile. Different FA, however, displayed varying efficacy for triggering the restricted growth phenotype. The most efficient were oleic, palmitoleic and the polyunsaturated α -linolenic and docosahexaenoic acids, probably due to their relatively good dispersion in the medium and consequently their availability for yeast internalization. In contrast, saturated FAs (palmitic and stearic) were much more difficult to disperse in the solid medium. Lowering their concentration to 0.5 mM prevented the formation of visible aggregates on the surface of the solid medium. Such plates, however, were not effective in FA-induced selection. Similarly, the selection was more

efficient with long-chain (16–18 carbons) than with very-long-chain monounsaturated FAs (22 carbons). Finally, docosahexaenoic acid at 1 mM concentration prevented even the growth of *DGAT*-expressing cultures, suggesting that Bn*DGAT1* might not efficiently utilize very-long-chain and/or polyunsaturated substrates (Fig. 3).

Although we did not investigate the biochemical mechanism of growth inhibition on FA-containing media, Zhang et al. [45] have demonstrated the inhibitory role of cellular DAG accumulation in a fission yeast strain (*Schizosaccharomyces pombe*) lacking the main TAG-synthesizing enzymes. Unlike *S. cerevisiae*, where FA exposure apparently led to a prolonged lag phase in a concentration-dependent manner, similar treatment in *S. pombe* caused apoptosis of cells in their stationary phase. We did not observe an FA-induced growth inhibition in the *S. cerevisiae* mutant 12501 where PDAT, another enzyme using DAG as acyl-acceptor encoded by *LROI*, was intact (Fig. 2b). It is therefore likely that the FA-induced growth inhibition in baker's yeast is also a result of the accumulation of DAG which is indeed considered an important regulator of many metabolic networks [46].

In summary the methods described here have broad applicability for studies involving *DGAT* and possibly other TAG-SE. Most genes encoding these enzymes have been isolated by usual DNA or polypeptide homology-based cloning. The functional complementation assay on FA-containing media could accelerate the identification of novel genes involved in TAG synthesis from genomes or tissues that have not been yet explored. Moreover, the combination of FACS with heterologous expression of target cDNAs in the H1246 background could also provide efficient tools for identifying enzymes involved in the biosynthesis of other neutral lipids, directed evolution of such enzymes and identification of their potential modulators. Experiments exploring these possibilities have been initiated in our laboratory.

Acknowledgments We thank S. Szymne and U. Ståhl for providing the yeast strain H1246 and the corresponding parental line and C. Snyder for reviewing the manuscript. This research was supported by AVAC Ltd., the Natural Science and Engineering Research Council of Canada and the Canada Research Chairs Program.

References

1. Farese RV, Cases S, Smith SJ (2000) Triglyceride synthesis: insights from the cloning of diacylglycerol acyltransferase. *Curr Opin Lipidol* 11:229–234
2. Metzger JO, Bornscheuer U (2006) Lipids as renewable resources: current state of chemical and biotechnological conversion and diversification. *Appl Microbiol Biotechnol* 71:13–22
3. Vasudevan PT, Briggs M (2008) Biodiesel production—current state of the art and challenges. *J Ind Microbiol Biotechnol* 35:421–430
4. Lardizabal K, Effertz R, Levering C, Mai J, Pedroso MC, Jury T, Aasen E, Gruys K, Bennett K (2008) Expression of *Umbelopsis ramanniana* *DGAT2A* in seed increases oil in soybean. *Plant Physiol* 148:89–96
5. Weselake R (2002) Biochemistry and biotechnology of TAG accumulation in plants. In: Gardner HW, Kuo TM (eds) *Lipid biotechnology*. Marcel Dekker, Peoria
6. Weselake RJ, Taylor DC, Shah S, Laroche A, Harwood J (2009) Molecular strategies for increasing seed oil content. In: Hou CT, Shaw JF (eds) *Biocatalysis and agricultural biotechnology*. Taylor and Francis-CRC Press, Boca Raton
7. Lehner R, Kuksis A (1996) Biosynthesis of triacylglycerols. *Prog Lipid Res* 35:169–201
8. Yen CL, Stone SJ, Koliwad S, Harris C, Farese RV (2008) *DGAT* enzymes and triacylglycerol biosynthesis. *J Lipid Res* 49:2283–2301
9. Lung SC, Weselake RJ (2006) Diacylglycerol acyltransferase: a key mediator of plant triacylglycerol synthesis. *Lipids* 41:1073–1088
10. Cases S, Smith SJ, Zheng YW, Myers HM, Lear SR, Sande E, Novak S, Collins C, Welch CB, Lusis AJ, Erickson SK, Farese RV (1998) Identification of a gene encoding an acyl CoA:diacylglycerol acyltransferase, a key enzyme in triacylglycerol synthesis. *Proc Natl Acad Sci USA* 95:13018–13023
11. Hobbs DH, Lu CF, Hills MJ (1999) Cloning of a cDNA encoding diacylglycerol acyltransferase from *Arabidopsis thaliana* and its functional expression. *FEBS Lett* 452:145–149
12. Lardizabal KD, Mai JT, Wagner NW, Wyrick A, Voelker T, Hawkins DJ (2001) *DGAT2* is a new diacylglycerol acyltransferase gene family. *J Biol Chem* 276:38862–38869
13. Cases S, Stone SJ, Zhou P, Yen E, Tow B, Lardizabal KD, Voelker T, Farese RV (2001) Cloning of *DGAT2*, a second mammalian diacylglycerol acyltransferase, and related family members. *J Biol Chem* 276:38870–38876
14. Shockey JM, Gidda SK, Chapital DC, Kuan JC, Dhanoa PK, Bland JM, Rothstein SJ, Mullen RT, Dyer JM (2006) Tung tree *DGAT1* and *DGAT2* have nonredundant functions in triacylglycerol biosynthesis and are localized to different subdomains of the endoplasmic reticulum. *Plant Cell* 18:2294–2313
15. Dahlqvist A, Stahl U, Lenman M, Banas A, Lee M, Sandager L, Ronne H, Szymne S (2000) Phospholipid:diacylglycerol acyltransferase: an enzyme that catalyzes the acyl-CoA-independent formation of triacylglycerol in yeast and plants. *Proc Natl Acad Sci USA* 97:6487–6492
16. Stahl U, Carlsson AS, Lenman M, Dahlqvist A, Huang BQ, Banas W, Banas A, Szymne S (2004) Cloning and functional characterization of a phospholipid:diacylglycerol acyltransferase from *Arabidopsis*. *Plant Physiol* 135:1324–1335
17. Mhaske V, Beldjilali K, Ohlrogge J, Pollard M (2005) Isolation and characterization of an *Arabidopsis thaliana* knockout line for phospholipid: diacylglycerol transacylase gene (*At5g13640*). *Plant Physiol Biochem* 43:413–417
18. Sandager L, Gustavsson MH, Stahl U, Dahlqvist A, Wiberg E, Banas A, Lenman M, Ronne H, Szymne S (2002) Storage lipid synthesis is non-essential in yeast. *J Biol Chem* 277:6478–6482
19. Coleman RA (1992) Diacylglycerol acyltransferase and monoacylglycerol acyltransferase from liver and intestine. *Meth Enzymol* 209:98–104
20. Greenspan P, Mayer EP, Fowler SD (1985) Nile red: a selective fluorescent stain for intracellular lipid droplets. *J Cell Biol* 100:965–973
21. Siloto RMP, Truksa M, Brownfield D, Good AG, Weselake RJ (2009) Directed evolution of acyl-CoA:diacylglycerol acyltransferase: development and characterization of *Brassica napus* *DGAT1* mutagenized libraries. *Plant Physiol Biochem* 47:456–461

22. Gietz RD, Schiestl RH (2007) High-efficiency yeast transformation using the LiAc/SS carrier DNA/PEG method. *Nat Protoc* 2:31–34
23. He XH, Turner C, Chen GQ, Lin JT, Mckee TA (2004) Cloning and characterization of a cDNA encoding diacylglycerol acyltransferase from castor bean. *Lipids* 39:311–318
24. Byers SD, Laroche A, Smith KC, Weselake RJ (1999) Factors enhancing diacylglycerol acyltransferase activity in microsomes from cell-suspension cultures of oilseed rape. *Lipids* 34:1143–1149
25. West RW, Yocum RR, Ptashne M (1984) *Saccharomyces cerevisiae* GAL1-GAL10 divergent promoter region: location and function of the upstream activating sequence UASG. *Mol Cell Biol* 4:2467–2478
26. Johnston M (1987) A model fungal gene regulatory mechanism: the GAL genes of *Saccharomyces cerevisiae*. *Microbiol Rev* 51:458–476
27. Perry HJ, Harwood JL (1993) Changes in the lipid-content of developing seeds of *Brassica napus*. *Phytochemistry* 32:1411–1415
28. Katavic V, Reed DW, Taylor DC, Giblin EM, Barton DL, Zou JT, Mackenzie SL, Covello PS, Kunst L (1995) Alteration of seed fatty-acid composition by an ethyl methanesulfonate-induced mutation in *Arabidopsis thaliana* affecting diacylglycerol acyltransferase activity. *Plant Physiol* 108:399–409
29. Zou JT, Wei YD, Jako C, Kumar A, Selvaraj G, Taylor DC (1999) The *Arabidopsis thaliana* TAG1 mutant has a mutation in a diacylglycerol acyltransferase gene. *Plant J* 19:645–653
30. Zheng P, Allen WB, Roesler K, Williams ME, Zhang S, Li J, Glassman K, Ranch J, Nubel D, Solawetz W, Bhatramakki D, Llaca V, Deschamps S, Zhong GY, Tarczynski MC, Shen B (2008) A phenylalanine in DGAT is a key determinant of oil content and composition in maize. *Nat Genet* 40:367–372
31. Cahoon EB, Shockey JM, Dietrich CR, Gidda SK, Mullen RT, Dyer JM (2007) Engineering oilseeds for sustainable production of industrial and nutritional feedstocks: solving bottlenecks in fatty acid flux. *Curr Opin Plant Biol* 10:236–244
32. Tomoda H, Omura S (2007) Potential therapeutics for obesity and atherosclerosis: inhibitors of neutral lipid metabolism from microorganisms. *Pharmacol Ther* 115:375–389
33. Kimura K, Yamaoka M, Kamisaka Y (2004) Rapid estimation of lipids in oleaginous fungi and yeasts using Nile red fluorescence. *J Microbiol Methods* 56:331–338
34. Cadigan KM, Chang CCY, Chang TY (1989) Isolation of Chinese-hamster ovary cell-lines expressing human acyl-coenzyme-a cholesterol acyltransferase activity. *J Cell Biol* 108:2201–2210
35. Seethala R, Peterson T, Dong J, Chu CH, Chen L, Golla R, Ma Z, Panemangalore R, Lawrence RM, Cheng D (2008) A simple homogeneous scintillation proximity assay for acyl-coenzyme A:diacylglycerol acyltransferase. *Anal Biochem* 383:144–150
36. Tao HY, Cornish VW (2002) Milestones in directed enzyme evolution. *Curr Opin Chem Biol* 6:858–864
37. Stone SJ, Levin MC, Farese RV (2006) Membrane topology and identification of key functional amino acid residues of murine Acyl-CoA:diacylglycerol acyltransferase-2. *J Biol Chem* 281:40273–40282
38. Xu JY, Francis T, Mietkiewska E, Giblin EM, Barton DL, Zhang Y, Zhang M, Taylor DC (2008) Cloning and characterization of an acyl-CoA-dependent diacylglycerol acyltransferase 1 (DGAT1) gene from *Tropaeolum majus*, and a study of the functional motifs of the DGAT protein using site-directed mutagenesis to modify enzyme activity and oil content. *Plant Biotech J* 6:799–818
39. Edwards C, Porter J, West M (1997) Fluorescent probes for measuring physiological fitness of yeast. *Ferment* 9:288–293
40. Deere D, Shen J, Vesey G, Bell P, Bissinger P, Veal D (1998) Flow cytometry and cell sorting for yeast viability assessment and cell selection. *Yeast* 14:147–160
41. Muller S, Losche A (2004) Population profiles of a commercial yeast strain in the course of brewing. *J Food Eng* 63:375–381
42. Faergeman NJ, DiRusso CC, Elberger A, Knudsen J, Black PN (1997) Disruption of the *Saccharomyces cerevisiae* homologue to the murine fatty acid transport protein impairs uptake and growth on long-chain fatty acids. *J Biol Chem* 272:8531–8538
43. Faergeman NJ, Black PN, Zhao XD, Knudsen J, DiRusso CC (2001) The acyl-CoA synthetases encoded within *FAA1* and *FAA4* in *Saccharomyces cerevisiae* function as components of the fatty acid transport system linking import, activation, and intracellular utilization. *J Biol Chem* 276:37051–37059
44. Carlson M (1999) Glucose repression in yeast. *Curr Opin Microbiol* 2:202–207
45. Zhang Q, Chieu HK, Low CP, Zhang SC, Heng CK, Yang HY (2003) *Schizosaccharomyces pombe* cells deficient in triacylglycerols synthesis undergo apoptosis upon entry into the stationary phase. *J Biol Chem* 278:47145–47155
46. Carrasco S, Merida I (2008) Diacylglycerol, when simplicity becomes complex. *Trends Biochem Sci* 32:27–36

Conjugated Linoleic Acid Induces Uncoupling Protein 1 in White Adipose Tissue of *ob/ob* Mice

Angela A. Wendel · Aparna Purushotham ·
Li-Fen Liu · Martha A. Belury

Received: 18 February 2009 / Accepted: 8 September 2009 / Published online: 25 September 2009
© AOCs 2009

Abstract Conjugated linoleic acid (CLA) reduces body weight and adipose mass in a variety of species. The mechanisms by which CLA depletes adipose mass are unclear, but two independent microarray analyses indicate that in white adipose tissue (WAT), uncoupling protein 1 (UCP1) was among genes most changed by CLA. The objective of this study was to determine whether CLA induces ectopic expression of UCP1 in WAT, which may contribute to increased energy expenditure and weight loss. Six-week old, male *ob/ob* mice were fed either a control diet (CON) or a diet supplemented with 1.5% mixed isomer CLA (CLA) for 4 weeks. A third group of mice (LEPTIN) was fed the control diet and received daily injections of recombinant leptin as a positive control for adipose depletion in *ob/ob* mice. CLA did not alter several mRNA markers of lipid oxidation in epididymal white adipose

tissue (eWAT), but significantly increased carnitine palmitoyltransferase-1b (CPT1b) and PPAR gamma coactivator-1 α (PGC1 α) expression. Notably, CLA increased both mRNA and protein expression of uncoupling protein-1 (UCP1). β 3-adrenoceptor mRNA and phosphorylated-p38 mitogen activated protein kinase (MAPK) protein levels were not affected by CLA, but were upregulated by LEPTIN. These data suggest the increased CPT1b, PGC1 α , and UCP1, in WAT of CLA-fed mice may contribute to the depletion of adipose, and CLA does not appear to increase UCP1 through β 3-adrenergic signaling. Future studies will focus on understanding how CLA increases mitochondrial oxidation and energy dissipation in white adipose tissue.

Keywords Conjugated linoleic acid · Adipose · White adipose tissue · Brown adipose tissue · Inflammation · Uncoupling protein-1

A. A. Wendel · A. Purushotham · L.-F. Liu · M. A. Belury (✉)
Department of Human Nutrition, The Ohio State University,
1787 Neil Avenue, Columbus, OH 43210, USA
e-mail: belury.1@osu.edu

Present Address:

A. A. Wendel
Department of Nutrition, University of North Carolina,
Chapel Hill, NC 27599, USA

Present Address:

A. Purushotham
Laboratory of Signal Transduction,
National Institute of Environmental Health Sciences,
Research Triangle Park, NC, USA

Present Address:

L.-F. Liu
Division of Endocrinology, Stanford University,
Palo Alto, CA, USA

Abbreviations

ACOX1	Acyl-coA oxidase-1
ATGL	Adipose triglyceride lipase
BAT	Brown adipose tissue
CPT1b	Carnitine palmitoyltransferase-1b
CLA	Conjugated linoleic acid
CON	Control diet
FAS	Fatty acid synthase
HSL	Hormone sensitive lipase
LPL	Lipoprotein lipase
NEFA	Non-esterified fatty acids
PPAR γ	Peroxisome proliferator activated receptor- γ
PGC1 α	PPAR gamma coactivator 1 α
SREBP-1	Sterol receptor element binding protein-1
UCP	Uncoupling protein
WAT	White adipose tissue

Introduction

Conjugated linoleic acid (CLA) is a group of dietary fatty acids that has received considerable attention due to its ability to significantly reduce adipose mass in a variety of species [1–4]. While these dienoic isomers of linoleic acid are naturally found in products derived from ruminants, such as dairy and beef, CLA is also commercially available as a mixed isomer, weight loss supplement. CLA, specifically the *trans*-10, *cis*-12 isomer, probably reduces adipose through a combination of mechanisms including apoptosis, decreased preadipocyte differentiation and lipogenesis, and increased fatty acid oxidation and energy expenditure [5]. However, the data are conflicting, and therefore, the mechanisms by which CLA depletes adipose remain unclear. Several studies report CLA decreases adipose mass concomitant with increased energy expenditure [6–10], but the results are inconsistent as to whether CLA increases energy expenditure through increased fatty acid oxidation or by another mechanism. Several groups have postulated that increased energy expenditure by CLA may be due to increased thermogenesis, yet CLA does not change, or in some reports, decreases uncoupling protein 1 (UCP1) expression in brown adipose tissue (BAT) [7, 8, 11–13].

UCP1 mediates adaptive thermogenesis in brown adipose tissue (BAT) by uncoupling respiration, generating heat instead of ATP. Under normal physiological conditions, UCP1 is expressed almost exclusively in BAT, which, unlike white adipose tissue (WAT), is rich in mitochondria and has a high oxidative capacity, thereby contributing to energy expenditure [14, 15]. In addition to thermogenesis, the roles of UCP1 and BAT have expanded to include preventing or reducing adiposity. Mice with genetic ablation of BAT become hyperphagic and obese [16]. Mouse strain differences in susceptibility to diet-induced metabolic syndrome can be partly attributed to increased ectopic expression of UCP1 [17]. Notably, treating rodents with a β 3-adrenergic receptor agonist [18–23] or leptin [24, 25] stimulates ectopic expression of UCP1 in WAT and prevents or reduces adiposity. Two independent microarray analyses of WAT from mice fed CLA report that UCP1 was among genes most differentially expressed [26, 27]. An increase in ectopic UCP1 in WAT by CLA may have a significant role in the CLA-mediated reduction of adiposity. Therefore, the objective of this study was to determine whether CLA induces ectopic expression of UCP1 in WAT.

Research Design and Methods

Experimental Design

In this study, we continued our analyses of mice described previously [28]. Six-week old, male B6.V-*Lepob/OlaHsd*

(*ob/ob*) mice (Harlan, Indianapolis, IN) were housed 4/cage at 22 ± 0.5 °C on a 12-h light/dark cycle. Diets were isocaloric, modified AIN-93G diets (Bio-Serv, Frenchtown, NJ) containing 6.5% fat by weight. Mice received either a control diet that contained 6.5% soybean oil (CON; $n = 8$) or a CLA-supplemented diet containing 5% soybean oil and 1.5% CLA mixed triglycerides (CLA; $n = 8$). CLA mixed triglycerides (Tonalin TG 80, Cognis Corp., Cincinnati, OH) were ~80% CLA composed of 39.2% *c9t11*- and 38.5% *t10c12*-CLA isomers. Leptin increases energy expenditure through induction of UCP1 expression in WAT via a β -3 adrenoceptor mediated pathway [25], therefore, a third group of mice received the control diet and an intraperitoneal injection of 1 mg/kg BW recombinant mouse leptin (R&D Systems, Minneapolis, MN) (LEPTIN; $n = 8$). CON and CLA mice received injections of similar volumes of the vehicle (PBS). Mice were injected daily, 2 h before the onset of the dark cycle. Food intake between mice treated with LEPTIN or CLA was similar (13.5 vs. 12.4 g/day per 4 mice, respectively; $P = 0.56$). At 4 weeks, after an overnight (12 h) fast, mice were anesthetized with isoflurane and blood was collected via cardiac puncture. Epididymal adipose was quickly harvested, weighed, snap-frozen with liquid nitrogen, and stored at -80 °C until analyses. All procedures were in accordance with institution guidelines and approved by the Institutional Animal Care and Use Committee of The Ohio State University.

Analysis of Serum Lipids

Serum free fatty acids, glycerol, and triglyceride were determined using colorimetric kits (NEFA C, Wako Chemicals, Richmond, VA and Free-Glycerol and triglyceride reagents, Sigma, St. Louis, MO, respectively).

Real-time RT-PCR

RNA was extracted from epididymal adipose tissue using the RNeasy® Lipid Tissue Mini kit (Qiagen, Valencia, CA) according to manufacturers' protocols. RNA was reverse transcribed with High Capacity cDNA Archive Kit (ABI, Foster City, CA) according to directions and then amplified by real-time PCR using pre-designed and validated primers (FAM probes) under universal cycling conditions defined by ABI (TaqMan Gene Expression Assays, ABI, Foster City, CA). Target gene expression was normalized to the endogenous control 18S (VIC probe) amplified in the same reaction and expressed as $2^{-\Delta\Delta Ct}$ relative to the CON group [29] for each gene.

Western Blot Analyses

Epididymal adipose tissue was homogenized in 3 volumes of ice cold lysis buffer (20 mM Trizma base, 50 mM NaCl,

250 mM sucrose, 50 mM NaF, 5 mM $\text{Na}_4\text{P}_2\text{O}_7 \cdot 10\text{H}_2\text{O}$, 1% Triton-X100, and protease inhibitors). Protein concentrations were measured by the bicinchoninic acid (BCA) method (Pierce, Rockford, IL). Either 40 (AMPK and p38 MAPK) or 80 μg (UCP1) of protein was mixed and boiled for 5 min with 4 \times loading buffer (125 mM Tris HCl at pH 6.8, 50% glycerol, 4% SDS, 0.02% Bromophenol Blue) and β -mercaptoethanol and subjected to SDS-PAGE using 10% gels for 1 h. Protein was then transferred to 0.45 μm nitrocellulose membranes for 1 h at 120 V on ice. Membranes were probed for P-AMPK, P-p38 (Cell Signaling Technology, Inc., Danvers, MA), or UCP1 (AbCam Inc., Cambridge, MA) according to manufacturer's protocol. Membranes were incubated in SuperSignal West Femto Maximum Sensitivity Substrate (Pierce, Rockford, IL) for 5 min. Densities of bands were detected and measured by Kodak ImageStation 2000RT using 1D Kodak software. Membranes were stripped with RestoreTM Western Blot Stripping Buffer (Pierce, Rockford, IL) for 30 min at RT and reprobed with total-AMPK, -p38, or β -actin (Cell Signaling).

Statistical Analyses

Data are expressed as least square means (LSM) \pm standard error (SE). Data were analyzed by one-way ANOVA using the GLM procedure of Statistical Analysis System (SAS v9.1; SAS Institute Inc., Cary, NC) with Dunnett's adjustment for post hoc analysis using CON as the control. Differences of $P < 0.05$ were considered significant.

Results

CLA Did Not Induce Markers of Lipolysis

As we previously reported [28], mice from both LEPTIN (34.79 g \pm 0.99) and CLA (28.98 g \pm 0.99) treatments had significantly lower final body weights compared to CON mice (42.20 g \pm 0.9). LEPTIN (2.16 g \pm 0.14) and CLA (1.71 g \pm 0.14) treatments also significantly decreased epididymal adipose masses compared to CON (2.96 g \pm 0.14). Elevated serum non-esterified fatty acids (NEFA) and glycerol concentrations may indicate increased adipose lipolysis. After 4 weeks of treatments, neither CLA nor LEPTIN altered serum NEFA or glycerol concentrations (Table 1). Expression of adipose triglyceride lipase (ATGL) and hormone sensitive lipase (HSL), two prominent lipases involved in lipolysis in adipose tissue, was measured in eWAT. CLA did not change ATGL but decreased HSL mRNA expression (Table 1). LEPTIN did not change HSL but increased ATGL mRNA expression.

Table 1 Effects of CLA on markers of lipolysis

	CON	LEPTIN	CLA
Serum triacylglycerol (mg/dl)	88.1 \pm 16.2	122.9 \pm 14.0	131.4 \pm 16.2
Serum NEFA (mequiv/L)	0.90 \pm 0.09	0.83 \pm 0.09	1.03 \pm 0.09
Serum glycerol (mg/dl)	5.9 \pm 0.9	5.8 \pm 0.8	3.8 \pm 1.1
eWAT ATGL mRNA ^a	1.05 \pm 0.09	1.39 \pm 0.09*	1.03 \pm 0.09
eWAT HSL mRNA ^a	1.07 \pm 0.09	1.18 \pm 0.09	0.6 \pm 0.09*

Values represent LSM \pm SE ($n = 7-8$) with significant differences ($P < 0.05$) from CON denoted by *

^a mRNA was measured from eWAT of fasted mice by real time RT-PCR. Data are expressed as $2^{-\Delta\Delta\text{Ct}}$ relative to the 18S endogenous control and the CON group

CLA Increased mRNA Expression of Markers of Fatty Acid Uptake and β -Oxidation in eWAT

Figure 1a shows that both CLA and LEPTIN decreased lipoprotein lipase (LPL), whereas, CLA and LEPTIN increased fatty acid transporter (FAT/CD36) mRNA, a marker of fatty acid uptake. Both CLA and LEPTIN decreased mRNA of sterol receptor element binding protein-1 (SREBP-1), a marker of lipogenesis, but only LEPTIN decreased mRNA of its downstream target, fatty acid synthase (FAS). Both CLA and LEPTIN also reduced expression of peroxisome proliferator activated receptor- γ (PPAR γ) by approximately 60%. CLA and LEPTIN did not alter mRNA levels of several markers of fatty acid oxidation: PPAR α , acyl-coA oxidase-1 (ACOX1), and carnitine palmitoyltransferase-1a (CPT1a) (Fig. 1a). However, CLA significantly increased CPT1b mRNA by nearly 25-fold (Fig. 1b).

To determine the involvement of signaling upstream of β -oxidation, we examined levels of phosphorylated (P-) and total-AMPK in eWAT. CLA, but not LEPTIN, significantly increased the ratio of P-AMPK relative to total-AMPK (Fig. 2) in eWAT. However, neither CLA nor LEPTIN increased P-ACC/total ACC, the downstream target of AMPK (data not shown).

CLA Increased Ectopic Expression of UCP1 mRNA and Protein in eWAT

After 4 weeks of treatments, CLA significantly increased ectopic expression of UCP1 mRNA by 89-fold (Fig. 3a) and protein by approximately 7.8-fold (Fig. 3b) in eWAT. As expected, LEPTIN increased UCP1 mRNA expression \sim 57-fold over CON (Fig. 3a; $P = 0.055$). However, LEPTIN did not alter protein levels of UCP1 in eWAT (Fig. 3b). CLA also significantly increased UCP2, but not UCP3 mRNA expression (Fig. 3c, d, respectively).

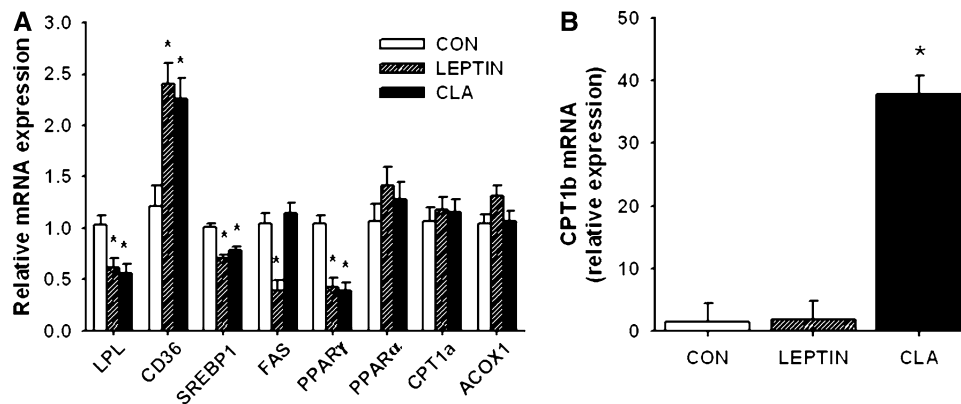


Fig. 1 Effects of CLA on markers of lipid metabolism in eWAT. **a** mRNA expression of markers of lipid uptake (*LPL* and *CD36*), lipogenesis (*SREBP1* and *FAS*), and lipid oxidation (*PPARα*, *CPT1a*, and *ACOX1*). **b** *CPT1b* mRNA expression. Mice were fed a control diet and treated with vehicle (*CON*) or leptin (*LEPTIN*) or fed a CLA-supplemented diet and treated with vehicle (*CLA*). After 4 weeks,

mRNA was measured from eWAT of fasted mice by real-time RT-PCR. Data are expressed as $2^{-\Delta\Delta Ct}$ relative to the 18S endogenous control and the *CON* group for each gene. Values represent LSM \pm SE ($n = 8$) with significant differences ($P < 0.05$) from *CON* denoted by asterisks

Conversely, *LEPTIN* did not change *UCP2* expression, but significantly increased *UCP3* mRNA expression in eWAT (Fig. 3c, d, respectively).

Effects of CLA on the Regulation of *UCP1*

Increased *UCP1* transcription may be mediated through induction of *PGC1α* and β_3 adrenergic signaling [30]. We, therefore, measured transcript levels of *PGC1α* and β_3 adrenoceptor (β_3AR). Both *CLA* and *LEPTIN* significantly increased expression of *PGC1α* in eWAT (Fig. 4a). Unlike *LEPTIN*, which increased β_3AR mRNA expression 4.3-fold, *CLA* did not alter levels of β_3AR (Fig. 4b). Phosphorylation of p38 mitogen activated protein kinase (*MAPK*) is a critical signaling step in β_3 adrenergic induction of *PGC1α* and *UCP1* [30]. Similar to the trend in β_3AR expression, *LEPTIN*, but not *CLA*, increased P-p38/total-p38 *MAPK* protein expression (Fig. 4c). *CLA*, but not *LEPTIN*, decreased mRNA expression of *RIP140*, a repressor of *UCP1* transcription [31]; however, the decrease was not statistically significant (Fig. 4d). Because *UCP1* is highly expressed in *BAT*, but was induced by *CLA* in eWAT, we measured mRNA expression of *Cidea* (cell-death-inducing DFF45-like effector), which is expressed in several tissues at low levels but at high levels in *BAT* and is therefore considered a *BAT*-specific marker [32]. While *LEPTIN* did not affect levels of *Cidea*, *CLA* significantly increased *Cidea* mRNA expression by 2.5-fold (Fig. 4e).

Discussion

The ability of *CLA* to reduce adipose mass dramatically in a variety of species has received considerable attention.

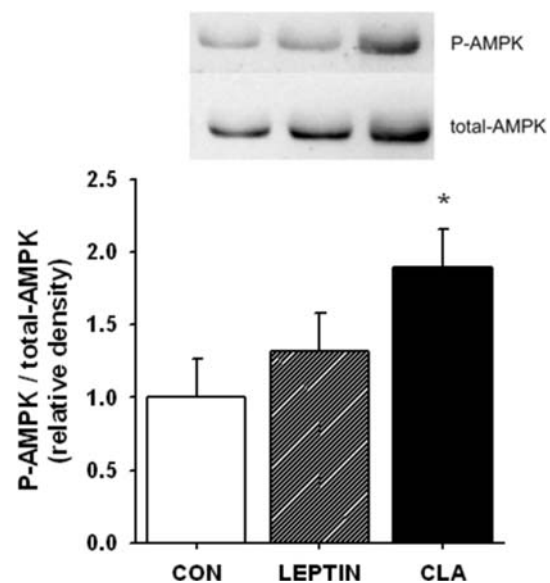
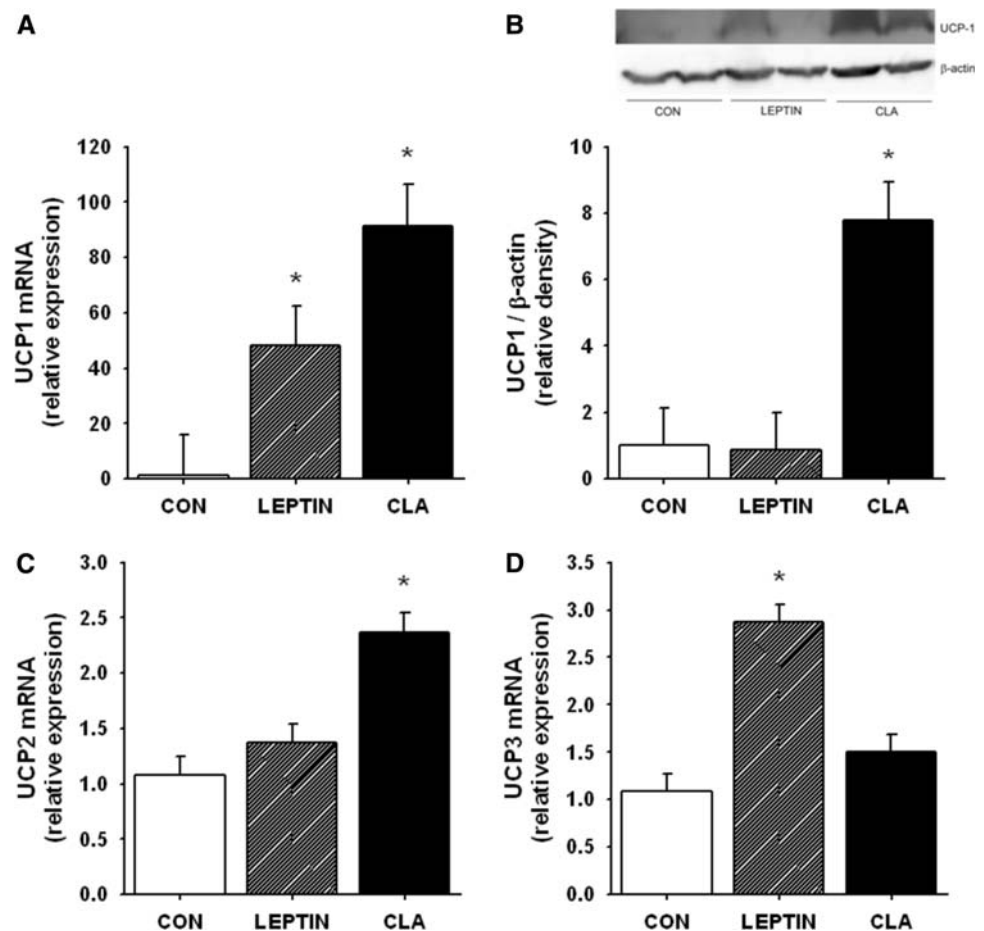


Fig. 2 Effect of *CLA* on activation of *AMPK* in eWAT. Mice were fed a control diet and treated with vehicle (*CON*) or leptin (*LEPTIN*) or fed a *CLA*-supplemented diet and treated with vehicle (*CLA*). After 4 weeks, expression of P-*AMPK* and total-*AMPK* were measured from eWAT of fasted mice by Western blot analysis. A representative blot is shown. Values represent LSM \pm SE ($n = 8$) with significant differences ($P < 0.05$) from *CON* denoted by asterisks

However, the mechanisms by which *CLA* induces *WAT* loss remain unclear. Previously, we reported that in *ob/ob* mice, *CLA* decreases body weight and adipose mass [28]. In the present study, we report that in these same mice, *CLA* increased both *UCP1* mRNA by 89-fold and protein expression by over 7-fold in eWAT. These observations suggest that *CLA* depletes adipose mass by inducing ectopic uncoupled oxidation in *WAT*.

Fig. 3 Effect of CLA on UCP expression in eWAT. **a** UCP1 mRNA; **b** Analysis of UCP1 protein expression in eWAT of fasted mice by Western blot with β -actin to show equal loading. A representative blot is shown; **c** UCP2; and **d** UCP3 mRNA expression. mRNA was measured from eWAT of fasted mice by real time RT-PCR. Data are expressed as $2^{-\Delta\Delta Ct}$ relative to the 18S endogenous control and the CON group for each gene. Values represent LSM \pm SE ($n = 7-8$) with significant differences ($P < 0.05$) from CON denoted by asterisks



CLA rapidly and significantly reduces body weight and adipose mass in as little as 6 days in C57Bl/6J mice [33, 34]. However, hepatomegaly and hepatic lipid accumulation [13, 35, 36] also occurs with CLA-induced weight loss, resulting in lipodystrophy. The redistribution of lipid, coupled with increased lipolysis, as observed in several in vitro studies [3, 37, 38] may partially account for the loss of WAT mass. We previously reported that compared to CON, both CLA and LEPTIN reduce body weight by 33 and 18%, respectively. Additionally, CLA and LEPTIN decrease epididymal adipose mass by 54 and 27%, respectively [28]. However, as opposed to LEPTIN, the changes in body weight and adipose mass induced by CLA were not accompanied by decreased lipid accumulation in other tissues or altered molecular markers of lipogenesis and fatty acid oxidation in liver or skeletal muscle. LEPTIN decreased both hepatic [28] and muscle (unpublished data) TAG, whereas, CLA did not change TAG contents of either liver [28] or gastrocnemius muscle (unpublished data). In this study, we report that CLA did not increase HSL and ATGL expression in eWAT or serum NEFA or glycerol concentrations, supporting previous in vivo data [39, 40]. These data suggest that lipids were not being mobilized from adipose and accumulating or being

oxidized in non-adipose tissues. However, CLA increased FAT/CD36 mRNA expression, suggesting fatty acid uptake was increased into eWAT. The fate of this assumed increase in lipid uptake in eWAT was unclear, as it was obviously not being stored. While others have shown CLA generally reduces markers of lipogenesis, [13, 26, 27, 41, 42], the slight changes in markers of lipogenesis in eWAT of this study suggests decreased lipogenesis in adipose does not play a significant role in CLA depletion of adipose, especially in a system which ectopic lipid accumulation does not seem to occur.

Previous studies have demonstrated that CLA increases fatty acid oxidation in adipose in both in vitro and in vivo models, but the results are somewhat contradictory. McIntosh's group reported that CLA increased fatty acid oxidation in 3T3-L1 preadipocytes [38] but later showed CLA decreased fatty acid oxidation in human adipocytes derived from primary stromal vascular cells [43]. Others [44, 45] have reported increased CPT activity in rats fed CLA, and analyses of differential gene expression in WAT of CLA-fed mice show a general increase in mRNA expression of genes involved in fatty acid oxidation, most notably, CPT1a and CPT1b [26, 27]. We did not find significant differences in either PPAR α or downstream targets,

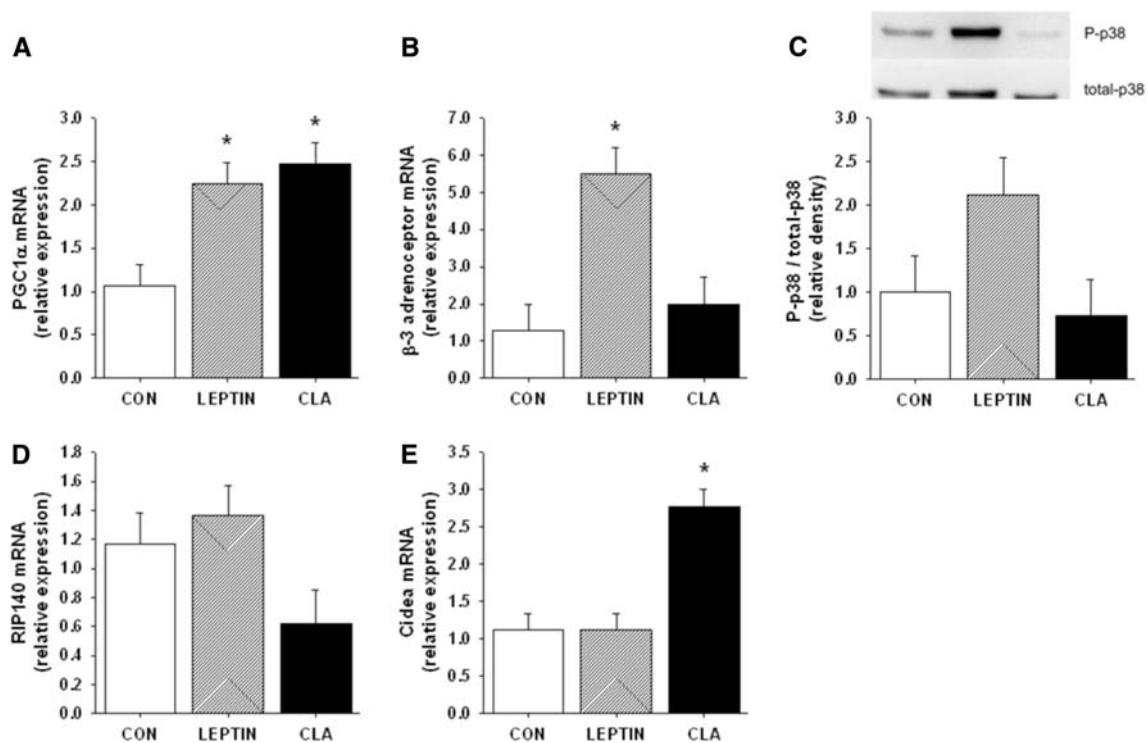


Fig. 4 Effects of CLA on the regulation of UCP1. **a** PGC1 α mRNA; **b** β -3 adrenoceptor mRNA; **c** Analysis of p38 MAPK protein activation. P-p38 and total-p38 MAPK were measured by Western blotting. A representative blot is shown; **d** RIP140 mRNA; and **e** Cidea mRNA. mRNA was measured from eWAT of fasted mice by

real time RT-PCR. Data are expressed as $2^{-\Delta\Delta Ct}$ relative to the 18S endogenous control and the CON group for each gene. Values represent LSM \pm SE ($n = 7-8$) with significant differences ($P < 0.05$) from CON denoted by asterisks

CPT1a and ACOX1, genes involved with mitochondrial and peroxisomal fatty acid oxidation, respectively, in eWAT. However, CLA greatly increased CPT1b, which is highly expressed in muscle and BAT [46]. The combined increases in FAT/CD36 and CPT1b expression implied that fatty acids were being taken up into adipocytes and mitochondria for oxidation.

The protons created from the influx and subsequent oxidation of fatty acids in the mitochondria usually drive ATP generation, as in normal oxidative phosphorylation. Alternatively, uncoupling proteins can dissipate the proton gradient, producing heat instead of ATP and increasing energy expenditure [14]. While UCP1 clearly mediates adaptive thermogenesis and increases energy expenditure [47], the contributions of UCP2 and UCP3 to thermogenesis and energy expenditure is controversial. Rather, UCP2 seems to have a role in preventing reactive oxygen species generation and inflammation [48]. In this study, CLA increased eWAT UCP2 expression over twofold and was associated with increased eWAT macrophage infiltration (previously reported [28]). This is consistent with other reports that CLA increases UCP2 in WAT [11–13, 49]. The increased UCP2 and associated WAT inflammation and apoptosis [13] likely contribute to the mechanism by which CLA induces insulin resistance.

While uncoupled energy expenditure is generally used for non-shivering thermogenesis, the role of ectopic UCP1 in WAT depletion is strengthening. Both overexpressing UCP1 in WAT [23] and stimulation with β_3 -adrenergic agonists [18–22] prevents or reverses obesity in rodents. Furthermore, upon stimulation with β_3 AR agonists or with leptin, WAT adopts brown adipose-like characteristics, including increased UCP1 expression [18–20, 50], increased mitochondrial biogenesis [50, 51], and a multilocular morphology [18–20, 50, 51]. Additionally, transgenic expression of UCP1 in white adipose has been associated with activation of AMPK and increased fatty acid oxidation [52]. Previous studies report that CLA does not change or decreases UCP1 expression in BAT [7, 8, 11–13], suggesting CLA does not increase energy expenditure through thermogenesis in BAT. Nevertheless, two independent microarray analyses of WAT from mice fed CLA report that UCP1 was among genes most differentially expressed [26, 27]. Peters et al. [49] has also reported that UCP1 mRNA expression is increased in gonadal WAT. In the present study, CLA robustly increased both UCP1 mRNA and protein expression in eWAT. This was accompanied by increased eWAT expression of genes associated with an oxidative phenotype, CPT1b and PGC1 α . These data suggest that CLA increases energy expenditure by increasing uncoupled oxidation in WAT.

UCP1 transcription is mediated through β_3 adrenergic signaling and PGC1 α , a cofactor for PPAR- α and - γ that target the enhancer region of UCP1 [53]. The β_3 AR-mediated stimulation of UCP1 is dependent on a cascade of events, notably activation of p38 MAPK [30, 54] and subsequent phosphorylation of transcription factors that act directly at the UCP1 promoter region as well as indirectly by regulating PGC1 α . Stimulation of the sympathetic nervous system by leptin increases transcription of UCP1 through β_3 AR signaling [55]. Appropriately, LEPTIN increased both β_3 AR mRNA expression and P-p38 MAPK protein expression. CLA, conversely, did not alter expression of either of these markers, suggesting CLA did not increase UCP1 expression through β_3 AR signaling. However, CLA increases serum noradrenaline and adrenaline levels 2 h after administration concomitant with increased oxygen consumption and fat oxidation, possibly by stimulating sympathetic nervous activity via β_3 AR signaling [56]. The lack of effect after 4 weeks of CLA-supplementation, therefore, does not rule out possible β_3 AR stimulation in earlier events.

In summary, this study demonstrates that, in *ob/ob* mice, CLA-induced depletion of adipose is accompanied by increased WAT expression of markers of uncoupled energy dissipation, CPT1b, PGC1 α , and UCP1. Furthermore, CLA does not appear to increase UCP1 through β_3 AR signaling, but perhaps by some other mechanisms. Understanding the mechanisms by which unique fatty acids, such as CLA, enhance energy expenditure in WAT will contribute to the development of therapeutic prevention and treatment of obesity and type 2 diabetes.

Acknowledgments We thank all of the members of the Belury lab for their assistance with care and feeding of mice and discussions of the work in this manuscript. This work was supported by funds from the Carol S. Kennedy professorship, the Ohio Agriculture Research and Development Center (OARDC), and the USDA.

References

- Houseknecht KL, Vanden Heuvel JP, Moya-Camarena SY, Portocarrero CP, Peck LW, Nickel KP, Belury MA (1998) Dietary conjugated linoleic acid normalizes impaired glucose tolerance in the Zucker diabetic fatty fa/fa rat. *Biochem Biophys Res Commun* 244:678–682
- Ostrowska E, Muralitharan M, Cross RF, Bauman DE, Dunshea FR (1999) Dietary conjugated linoleic acids increase lean tissue and decrease fat deposition in growing pigs. *J Nutr* 129:2037–2042
- Park Y, Albright KJ, Liu W, Storkson JM, Cook ME, Pariza MW (1997) Effect of conjugated linoleic acid on body composition in mice. *Lipids* 32:853–858
- Park Y, Storkson JM, Albright KJ, Liu W, Pariza MW (1999) Evidence that the *trans*-10, *cis*-12 isomer of conjugated linoleic acid induces body composition changes in mice. *Lipids* 34:235–241
- House RL, Cassady JP, Eisen EJ, McIntosh MK, Odle J (2005) Conjugated linoleic acid evokes de-lipidation through the regulation of genes controlling lipid metabolism in adipose and liver tissue. *Obes Rev* 6:247–258
- Terpstra AH, Beynen AC, Everts H, Kocsis S, Katan MB, Zock PL (2002) The decrease in body fat in mice fed conjugated linoleic acid is due to increases in energy expenditure and energy loss in the excreta. *J Nutr* 132:940–945
- Takahashi Y, Kushiro M, Shinohara K, Ide T (2002) Dietary conjugated linoleic acid reduces body fat mass and affects gene expression of proteins regulating energy metabolism in mice. *Comp Biochem Physiol B Biochem Mol Biol* 133:395–404
- West DB, Blohm FY, Truett AA, Delany JP (2000) Conjugated linoleic acid persistently increases total energy expenditure in AKR/J mice without increasing uncoupling protein gene expression. *J Nutr* 130:2471–2477
- Delany JP, West DB (2000) Changes in body composition with conjugated linoleic acid. *J Am Coll Nutr* 19:487S–493S
- West DB, Delany JP, Camet PM, Blohm F, Truett AA, Scimeca J (1998) Effects of conjugated linoleic acid on body fat and energy metabolism in the mouse. *Am J Physiol* 275:R667–R672
- Ealey KN, El Sohemy A, Archer MC (2002) Effects of dietary conjugated linoleic acid on the expression of uncoupling proteins in mice and rats. *Lipids* 37:853–861
- Ryder JW, Portocarrero CP, Song XM, Cui L, Yu M, Combatsiaris T, Galuska D, Bauman DE, Barbano DM, Charron MJ, Zierath JR, Houseknecht KL (2001) Isomer-specific antidiabetic properties of conjugated linoleic acid. Improved glucose tolerance, skeletal muscle insulin action, and UCP-2 gene expression. *Diabetes* 50:1149–1157
- Tsuboyama-Kasaoka N, Takahashi M, Tanemura K, Kim HJ, Tange T, Okuyama H, Kasai M, Ikemoto S, Ezaki O (2000) Conjugated linoleic acid supplementation reduces adipose tissue by apoptosis and develops lipodystrophy in mice. *Diabetes* 49:1534–1542
- Nicholls DG, Locke RM (1984) Thermogenic mechanisms in brown fat. *Physiol Rev* 64:1–64
- Lowell BB, Spiegelman BM (2000) Towards a molecular understanding of adaptive thermogenesis. *Nature* 404:652–660
- Lowell BB, Susulic V, Hamann A, Lawitts JA, Himms-Hagen J, Boyer BB, Kozak LP, Flier JS (1993) Development of obesity in transgenic mice after genetic ablation of brown adipose tissue. *Nature* 366:740–742
- Almind K, Manieri M, Sivitz WI, Cinti S, Kahn CR (2007) Ectopic brown adipose tissue in muscle provides a mechanism for differences in risk of metabolic syndrome in mice. *Proc Natl Acad Sci USA* 104:2366–2371
- Ghorbani M, Claus TH, Himms-Hagen J (1997) Hypertrophy of brown adipocytes in brown and white adipose tissues and reversal of diet-induced obesity in rats treated with a beta3-adrenoceptor agonist. *Biochem Pharmacol* 54:121–131
- Himms-Hagen J, Cui J, Danforth E Jr, Taatjes DJ, Lang SS, Waters BL, Claus TH (1994) Effect of CL-316, 243, a thermogenic beta 3-agonist, on energy balance and brown and white adipose tissues in rats. *Am J Physiol* 266:R1371–R1382
- Guerra C, Koza RA, Yamashita H, Walsh K, Kozak LP (1998) Emergence of brown adipocytes in white fat in mice is under genetic control. Effects on body weight and adiposity. *J Clin Invest* 102:412–420
- Inokuma K, Okamatsu-Ogura Y, Omachi A, Matsushita Y, Kimura K, Yamashita H, Saito M (2006) Indispensable role of mitochondrial UCP1 for antiobesity effect of beta3-adrenergic stimulation. *Am J Physiol Endocrinol Metab* 290:E1014–E1021
- Nagase I, Yoshida T, Kumamoto K, Umekawa T, Sakane N, Nikami H, Kawada T, Saito M (1996) Expression of uncoupling protein in skeletal muscle and white fat of obese mice treated with thermogenic beta 3-adrenergic agonist. *J Clin Invest* 97:2898–2904

23. Kopecky J, Clarke G, Enerback S, Spiegelman B, Kozak LP (1995) Expression of the mitochondrial uncoupling protein gene from the *aP2* gene promoter prevents genetic obesity. *J Clin Invest* 96:2914–2923
24. Commins SP, Watson PM, Padgett MA, Dudley A, Argyropoulos G, Gettys TW (1999) Induction of uncoupling protein expression in brown and white adipose tissue by leptin. *Endocrinology* 140:292–300
25. Orzi L, Cook WS, Ravazzola M, Wang MY, Park BH, Montesano R, Unger RH (2004) Rapid transformation of white adipocytes into fat-oxidizing machines. *Proc Natl Acad Sci USA* 101:2058–2063
26. House RL, Cassady JP, Eisen EJ, Eling TE, Collins JB, Grissom SF, Odle J (2005) Functional genomic characterization of delipidation elicited by *trans*-10, *cis*-12-conjugated linoleic acid (t10c12-CLA) in a polygenic obese line of mice. *Physiol Genomics* 21:351–361
27. Larosa PC, Miner J, Xia Y, Zhou Y, Kachman S, Fromm ME (2006) *Trans*-10, *cis*-12 conjugated linoleic acid causes inflammation and delipidation of white adipose tissue in mice: a microarray and histological analysis. *Physiol Genomics* 27:282–294
28. Wendel AA, Purushotham A, Liu LF, Belury MA (2008) Conjugated linoleic acid fails to worsen insulin resistance but induces hepatic steatosis in the presence of leptin in ob/ob mice. *J Lipid Res* 49:98–106
29. Livak KJ, Schmittgen TD (2001) Analysis of relative gene expression data using real-time quantitative PCR and the $2^{-\Delta\Delta C(T)}$ method. *Methods* 25:402–408
30. Cao W, Daniel KW, Robidoux J, Puigserver P, Medvedev AV, Bai X, Floering LM, Spiegelman BM, Collins S (2004) p38 Mitogen-activated protein kinase is the central regulator of cyclic AMP-dependent transcription of the brown fat uncoupling protein 1 gene. *Mol Cell Biol* 24:3057–3067
31. Christian M, Kiskinis E, Debevec D, Leonardsson G, White R, Parker MG (2005) RIP140-targeted repression of gene expression in adipocytes. *Mol Cell Biol* 25:9383–9391
32. Zhou Z, Yon TS, Chen Z, Guo K, Ng CP, Ponniah S, Lin SC, Hong W, Li P (2003) Cidea-deficient mice have lean phenotype and are resistant to obesity. *Nat Genet* 35:49–56
33. Poirier H, Rouault C, Clement L, Niot I, Monnot MC, Guerre-Millo M, Besnard P (2005) Hyperinsulinaemia triggered by dietary conjugated linoleic acid is associated with a decrease in leptin and adiponectin plasma levels and pancreatic beta cell hyperplasia in the mouse. *Diabetologia* 48:1059–1065
34. Poirier H, Shapiro JS, Kim RJ, Lazar MA (2006) Nutritional supplementation with *trans*-10, *cis*-12-conjugated linoleic acid induces inflammation of white adipose tissue. *Diabetes* 55:1634–1641
35. Belury MA, Kempa-Steczko A (1997) Conjugated linoleic acid modulates hepatic lipid composition in mice. *Lipids* 32:199–204
36. Clement L, Poirier H, Niot I, Bocher V, Guerre-Millo M, Krief S, Staels B, Besnard P (2002) Dietary *trans*-10, *cis*-12 conjugated linoleic acid induces hyperinsulinemia and fatty liver in the mouse. *J Lipid Res* 43:1400–1409
37. Brown JM, Halvorsen YD, Lea-Currie YR, Geigerman C, McIntosh M (2001) *Trans*-10, *cis*-12, but not *cis*-9, *trans*-11, conjugated linoleic acid attenuates lipogenesis in primary cultures of stromal vascular cells from human adipose tissue. *J Nutr* 131:2316–2321
38. Evans M, Lin X, Odle J, McIntosh M (2002) *Trans*-10, *cis*-12 conjugated linoleic acid increases fatty acid oxidation in 3T3-L1 preadipocytes. *J Nutr* 132:450–455
39. Xu X, Storkson J, Kim S, Sugimoto K, Park Y, Pariza MW (2003) Short-term intake of conjugated linoleic acid inhibits lipoprotein lipase and glucose metabolism but does not enhance lipolysis in mouse adipose tissue. *J Nutr* 133:663–667
40. Simon E, Macarulla MT, Fernandez-Quintela A, Rodriguez VM, Portillo MP (2005) Body fat-lowering effect of conjugated linoleic acid is not due to increased lipolysis. *J Physiol Biochem* 61:363–369
41. Kang K, Liu W, Albright KJ, Park Y, Pariza MW (2003) *Trans*-10, *cis*-12 CLA inhibits differentiation of 3T3-L1 adipocytes and decreases PPAR gamma expression. *Biochem Biophys Res Commun* 303:795–799
42. Brown JM, Boysen MS, Jensen SS, Morrison RF, Storkson J, Lea-Currie R, Pariza M, Mandrup S, McIntosh MK (2003) Isomer-specific regulation of metabolism and PPARgamma signaling by CLA in human preadipocytes. *J Lipid Res* 44:1287–1300
43. Brown JM, Boysen MS, Chung S, Fabyi O, Morrison RF, Mandrup S, McIntosh MK (2004) Conjugated linoleic acid induces human adipocyte delipidation: autocrine/paracrine regulation of MEK/ERK signaling by adipocytokines. *J Biol Chem* 279:26735–26747
44. Martin JC, Gregoire S, Siess MH, Genty M, Chardigny JM, Berdeaux O, Juaneda P, Sebedio JL (2000) Effects of conjugated linoleic acid isomers on lipid-metabolizing enzymes in male rats. *Lipids* 35:91–98
45. Rahman SM, Wang Y, Yotsumoto H, Cha J, Han S, Inoue S, Yanagita T (2001) Effects of conjugated linoleic acid on serum leptin concentration, body-fat accumulation, and beta-oxidation of fatty acid in OLETF rats. *Nutrition* 17:385–390
46. Esser V, Brown NF, Cowan AT, Foster DW, McGarry JD (1996) Expression of a cDNA isolated from rat brown adipose tissue and heart identifies the product as the muscle isoform of carnitine palmitoyltransferase I (M-CPT I). M-CPT I is the predominant CPT I isoform expressed in both white (epididymal) and brown adipocytes. *J Biol Chem* 271:6972–6977
47. Golozoubova V, Cannon B, Nedergaard J (2006) UCP1 is essential for adaptive adrenergic nonshivering thermogenesis. *Am J Physiol Endocrinol Metab* 291:E350–E357
48. Brand MD, Esteves TC (2005) Physiological functions of the mitochondrial uncoupling proteins UCP2 and UCP3. *Cell Metab* 2:85–93
49. Peters JM, Park Y, Gonzalez FJ, Pariza MW (2001) Influence of conjugated linoleic acid on body composition and target gene expression in peroxisome proliferator-activated receptor alpha-null mice. *Biochim Biophys Acta* 1533:233–242
50. Himms-Hagen J, Melnyk A, Zingaretti MC, Ceresi E, Barbatelli G, Cinti S (2000) Multilocular fat cells in WAT of CL-316243-treated rats derive directly from white adipocytes. *Am J Physiol Cell Physiol* 279:C670–C681
51. Granneman JG, Li P, Zhu Z, Lu Y (2005) Metabolic and cellular plasticity in white adipose tissue I: effects of beta3-adrenergic receptor activation. *Am J Physiol Endocrinol Metab* 289:E608–E616
52. Matejkova O, Mustard KJ, Sponarova J, Flachs P, Rossmeisl M, Miksik I, Thomason-Hughes M, Grahame HD, Kopecky J (2004) Possible involvement of AMP-activated protein kinase in obesity resistance induced by respiratory uncoupling in white fat. *FEBS Lett* 569:245–248
53. Oberkofler H, Esterbauer H, Linnemayr V, Strosberg AD, Krempler F, Patsch W (2002) Peroxisome proliferator-activated receptor (PPAR) gamma coactivator-1 recruitment regulates PPAR subtype specificity. *J Biol Chem* 277:16750–16757
54. Robidoux J, Cao W, Quan H, Daniel KW, Moukdar F, Bai X, Floering LM, Collins S (2005) Selective activation of mitogen-activated protein (MAP) kinase kinase 3 and p38alpha MAP kinase is essential for cyclic AMP-dependent UCP1 expression in adipocytes. *Mol Cell Biol* 25:5466–5479
55. Scarpace PJ, Matheny M (1998) Leptin induction of UCP1 gene expression is dependent on sympathetic innervation. *Am J Physiol Endocrinol Metab* 275:E259–E264
56. Ohnuki K, Haramizu S, Oki K, Ishihara K, Fushiki T (2001) A single oral administration of conjugated linoleic acid enhanced energy metabolism in mice. *Lipids* 36:583–587

Conjugated Linoleic Acid Isomers, *t10c12* and *c9t11*, are Differentially Incorporated into Adipose Tissue and Skeletal Muscle in Humans

Julia H. Goedecke · Dale E. Rae · Cornelius M. Smuts · Estelle V. Lambert · Marianne O'Shea

Received: 18 March 2009 / Accepted: 2 October 2009 / Published online: 23 October 2009
© AOCS 2009

Abstract Conjugated linoleic acid (CLA) is a popular supplement believed to enhance immune function, body composition and insulin sensitivity, but results of scientific studies investigating its effects are conflicting. The isomer- and tissue-specific effects of CLA may explain these conflicting results. Therefore, this study quantified the incorporation of the *c9t11* and *t10c12* CLA isomers into adipose tissue and skeletal muscle in response to supplementation in healthy, regularly-exercising, non-obese persons. The CLA group ($n = 14$) ingested 3.9 g per day CLA (50:50 *t9c11*:*c10t12*) and the placebo group ($n = 11$) 3.9 g per day high-oleic-acid sunflower oil for 12 weeks. Following supplementation, the *t10c12* isomer was incorporated into adipose tissue triacylglycerol ($P < 0.001$), and the *c9t11* isomer tended to increase in skeletal muscle phospholipids ($P = 0.056$). Therefore, human adipose tissue and skeletal muscle are enriched with CLA in an isomer-specific manner.

Keywords CLA supplementation · Isomer-specific fatty acid incorporation · Adipose tissue triacylglycerol · Skeletal muscle phospholipids

Abbreviations

CLA Conjugated linoleic acid
TAG Triacylglycerol

Introduction

Conjugated linoleic acid (CLA) is the generic name for the mixture of isomers of linoleic acid, an 18-carbon polyunsaturated fatty acid. The most common CLA isomers contain double bonds in the 9 and 11, 10 and 12 and 11 and 13 positions, in either the *cis* or *trans* positions. This fatty acid, which is primarily obtained from the food products of ruminant animals, but can also be manufactured, is a popular supplement believed to enhance immune function [1, 2], body composition [3–6] and insulin sensitivity. However, the numerous clinical trials conducted in humans to investigate the effects of CLA supplementation have produced varying, and sometimes conflicting results [4, 5, 7–13].

Each CLA isomer is thought to have a distinct mode of action [14–17], and in some instances these actions are antagonistic. For example, cell culture studies have shown that the *c9t11* CLA isomer appears to be more effectively incorporated in tissue membranes and lipid droplets, and may in fact increase triglyceride content in humans; while the *t10c12* CLA isomer may be better metabolised in the β -oxidation pathway and is thought to be anti-adipogenic in nature [11, 18–20]. Since most of the studies to date

J. H. Goedecke (✉) · D. E. Rae · E. V. Lambert
UCT/MRC Research Unit for Exercise Science and Sports
Medicine, Department of Human Biology,
Faculty of Health Sciences, University of Cape Town,
115, Newlands, 7725 Cape Town, South Africa
e-mail: Julia.Goedecke@uct.ac.za

D. E. Rae
e-mail: dale.rae@uct.ac.za

J. H. Goedecke · C. M. Smuts
South African Medical Research Council,
Cape Town, South Africa

M. O'Shea
Loders Croklaan Lipid Nutrition, Wormerveer,
The Netherlands

have used CLA preparations containing varying amounts and ratios of up to four isomers, the unique and sometimes opposing actions of the isomers may, in part, explain the inconsistent results.

A first step towards understanding the clinical effects of CLA supplementation in humans is to determine which tissues may be enriched with CLA in response to supplementation. We propose that incorporation of CLA isomers into human tissue is both tissue and isomer-specific. Therefore the result of any given trial might be a reflection of the quantity of a specific isomer present in the supplement as well as its site of incorporation and subsequent effect within the target tissue. Adipose tissue and skeletal muscle are regarded as important tissues with respect to adipogenesis and insulin sensitivity, two factors believed to be altered by CLA supplementation. Therefore, changes in their fatty acid profile, specifically the CLA isomers, may provide the basis for understanding the clinical effects of CLA supplementation. Accordingly, the aim of this study was to measure the incorporation of the *c9t11* and *t10c12* CLA isomers into adipose tissue and skeletal muscle in apparently healthy, non-obese, exercising individuals supplementing with a commercially available 50:50 *c9t11:t10c12* CLA preparation.

Experimental Procedures

This experiment formed part of a larger study, the detailed design of which has been reported previously [21], and was approved by the Research and Ethics Committee of the Faculty of Health Sciences, University of Cape Town. All volunteers signed consent forms agreeing to participate in the trial. Briefly, in this double-blind study, 25 non-obese, regularly exercising, apparently healthy white male and female volunteers, aged 21–45 years, were randomly assigned to either the experimental (CLA, $n = 11$) or control (placebo, $n = 14$) groups. Only individuals who were exercising at least three times per week at the time of the study and had been doing so for the past six months, were not obese ($\text{BMI} < 30 \text{ kg m}^{-2}$), had maintained a stable weight ($\pm 2\text{--}3 \text{ kg}$) for the three months preceding the trial, did not suffer from any chronic illness, and were not taking any medication or nutritional supplements (other than a general multi-vitamin) were included in this study. Lactating women, or those planning on becoming pregnant, were excluded.

All volunteers underwent a two week placebo ‘run-in’ period, followed by baseline testing, 12 weeks of supplementation and follow-up testing, as described previously [21]. They were asked to keep their training and diet constant throughout the trial and met with registered dietitians every two weeks who monitored any adverse

responses to supplementation, changes in training, lifestyle or eating patterns, and pill compliance.

The 3.9 g daily CLA supplement, taken each morning in the form of four capsules, consisted primarily of the *c9t11* (29.7%) and *t10c12* (30.9%) isomers, as well as other CLA isomers (2.9%) and oleic (18:1 *n*-9; 24.7%), palmitic (16:0; 3.5%), linoleic (18:2 *n*-6; 1.9%) and stearic (18:0; 1.3%) acid (Formule Naturelle Ltd., France, containing Clarinol™ from Lodders Croklaan, Lipid Nutrition, The Netherlands). The placebo capsules contained 3.9 g of high oleic acid sunflower oil.

Fasting (10–12 h) gluteal adipose tissue biopsies were obtained prior to and after the 12-week supplementation period. Biopsies of the vastus lateralis muscle [22] were also obtained from a sub-sample of participants (6 CLA, 6 Placebo). The samples were stored at $-80 \text{ }^{\circ}\text{C}$ and subsequently used to determine the fatty acid composition of the adipose tissue and muscle triacylglycerols (TAG), and the muscle membrane phospholipids.

The frozen muscle samples were thawed and homogenised using a mortar and pestle [23]. Total lipids were extracted from approximately 20 mg (wet weight) portions of the muscle tissue and from 10 mg of the frozen adipose tissue using chloroform:methanol (2:1 v/v) according to a modified method of Folch et al. [24]. All the extraction solvents contained 0.01% butylated hydroxytoluene (BHT) as an antioxidant. Heptadecanoic acid (C17:0) was used as an internal standard to quantify the individual fatty acids. TAG were separated from total phospholipids by thin-layer-chromatography (TLC) on pre-coated silica gel 60 plates (10 × 10 cm) without a fluorescent indicator (Art. 1.05721; Merck, Darmstadt, Germany) using the solvent system petroleum benzene (bp 40–60 °C):diethyl ether (peroxide free):acetic acid (90:30:1 v/v/v). The lipid bands were visualised with long wave ultraviolet light after spraying the plates with chloroform:methanol (1:1 v/v) containing 2,5-bis-(5'-*tert*-butylbenzoxazolyl-[2'])thiophene BBOT (10 mg/100 ml) (Sigma Chemical Co.).

The TAG and the total phospholipid bands from muscle tissue and the TAG band from adipose tissue were scraped off and analysed for fatty acid composition. The different lipid classes were transmethylated using 5% H_2SO_4 /methanol at 70 °C for 2 h. After cooling, the resulting fatty acid methyl esters (FAMES) were extracted with 1 ml of water and 2 ml of *n*-hexane. The FAME were purified by TLC and analysed by gas liquid chromatography (Varian Model 3300 equipped with flame ionisation detection) using 60 m BPX70 capillary columns of 0.25 mm internal diameter (SGE, Australia). The gas flow rate for hydrogen was 25 ml min^{-1} and $2\text{--}4 \text{ ml min}^{-1}$ for the hydrogen carrier gas. The initial column temperature was held at 150 °C for 18 min, followed by a linear programming at $3 \text{ }^{\circ}\text{C min}^{-1}$ with a final temperature of 220 °C, an injector temperature

of 240 °C and a detector temperature of 250 °C. The FAME were identified by comparison of the retention times to those of a standard FAME mixture (Nu-Chek-Prep Inc., Elysian, MN, USA). The fatty acid composition of the different lipid classes was expressed as a percentage of the total fatty acids identified.

Baseline characteristics of the CLA and placebo groups were compared using an independent *t* test. Two-way repeated measures ANOVA was used to examine the effects of supplementation on all measured variables. Correlations were performed using a Pearson product moment test. Statistical significance was accepted at $P < 0.05$. All results are presented as mean \pm SD.

Results

The groups had similar baseline body composition, fasting glucose and insulin levels, and insulin resistance [as estimated by the Homeostasis Assessment Model (HOMA) and the Insulin Sensitivity Index (ISI)] prior to supplementation (Table 1). All participants completed this trial, pill compliance was above 90% for both groups, and of the few adverse events reported both groups tolerated the supplements equally [21]. Following 12 weeks of supplementation, significantly higher levels of the *t10c12* isomer ($P < 0.001$) and oleic acid ($P = 0.019$) were present in adipose tissue TAG in the CLA group than in the Placebo group (Table 2). The *c9t11* isomer, linoleic acid, total saturated, monounsaturated and polyunsaturated fatty acid (Table 2) and all other fatty acid (data not shown) levels measured did not change over the supplementation period.

There was a trend for the *c9t11* isomer ($P = 0.056$) and oleic acid ($P = 0.055$) to be incorporated into the skeletal muscle phospholipids of the CLA group, however, there was no evidence of incorporation of CLA isomers into skeletal muscle TAG (Table 2). The *t10c12* isomer was not present in the phospholipids and supplementation did not change the levels of linoleic acid, total saturated, mono-unsaturated or polyunsaturated fatty acids (Table 2) or any of the other fatty acids (data not shown) measured.

Twelve weeks of CLA supplementation did not alter body composition, glucose or insulin parameters (Table 1), or the serum lipid profiles (data not shown) of the two groups. Dietary analysis indicated that the contributions of saturated (CLA: $13.4 \pm 9.1\%$, placebo: $11.4 \pm 5.7\%$, $P = 0.570$), monounsaturated (CLA: $9.4 \pm 3.5\%$, placebo: $7.4 \pm 2.5\%$, $P = 0.094$) and polyunsaturated (CLA: $6.5 \pm 3.0\%$, placebo: $6.4 \pm 2.7\%$, $P = 0.900$) fats to the diet were similar in both groups prior to the trial and remained constant during the trial (data not shown). Lastly, reported physical activity energy expenditure remained constant throughout the trial for all subjects ($P = 0.433$).

Discussion

Few studies have investigated the in vivo effects of CLA supplementation in humans on tissue-specific CLA isomer incorporation. This is the first study, to the best of our knowledge, to show that 12 weeks of supplementation with a 50:50 *c9t11*:*t10c12* CLA preparation results in incorporation of the *t10c12* isomer into adipose tissue TAG in humans.

Table 1 Baseline characteristics (pre) and subsequent changes (post) in response to 12 weeks of supplementation

	CLA ($n = 11$)		Placebo ($n = 14$)		<i>P</i> value	
	Pre	Post	Pre	Post	^a	^b
Gender (male/female)	5/6	–	5/9	–	–	–
Body mass (kg)	71.0 ± 13.2	71.1 ± 13.9	68.9 ± 11.9	68.2 ± 11.7	0.684	0.302
BMI (kg m^{-2})	24.2 ± 2.2	23.9 ± 2.1	24.5 ± 2.4	24.0 ± 2.0	0.512	0.456
Body fat (%)	24.4 ± 7.9	24.0 ± 7.6	26.4 ± 9.6	26.5 ± 9.4	0.583	0.485
Fasting serum insulin ($\mu\text{U ml}^{-1}$)	5.39 ± 2.52	5.00 ± 2.56	4.83 ± 2.56	6.04 ± 2.67	0.596	0.197
Fasting plasma glucose (mmol L^{-1})	4.88 ± 0.43	4.23 ± 0.62	4.88 ± 0.38	4.19 ± 0.38	0.966	0.859
HOMA	1.17 ± 0.54	0.97 ± 0.58	1.06 ± 0.61	1.13 ± 0.52	0.657	0.312
ISI	10.82 ± 4.71	14.11 ± 7.65	13.47 ± 8.92	13.20 ± 8.27	0.381	0.211

Values are expressed as means \pm SD

CLA conjugated linoleic acid supplementation group, BMI body mass index, HOMA homeostasis assessment model, ISI insulin sensitivity index

^a These *P* values compare the baseline values of each group before CLA supplementation

^b These *P* values represent the repeated measures ANOVA time-by-treatment interaction effect and compare the differences by which the variables change between the groups with supplementation

Table 2 Changes in the fatty acid composition of adipose tissue and skeletal muscle in response to 12 weeks of supplementation

Fatty acid (%)	CLA (<i>n</i> = 11)		Placebo (<i>n</i> = 14)		<i>P</i> value ^a
	Pre	Post	Pre	Post	
Adipose tissue TAG					
<i>c9t11</i>	0.58 ± 0.13	0.56 ± 0.16	0.52 ± 0.16	0.51 ± 0.11	0.908
<i>t10c12</i>	0.00 ± 0.01	0.08 ± 0.05	0.01 ± 0.03	0.02 ± 0.03	<0.001*
Oleic acid (18:1)	44.58 ± 1.31	45.29 ± 1.51	43.82 ± 1.52	43.81 ± 1.46	0.019*
Linoleic acid (18:2)	20.64 ± 2.64	20.67 ± 2.21	20.10 ± 2.88	20.31 ± 2.80	0.523
Saturated ^b	24.22 ± 2.81	24.04 ± 3.18	25.45 ± 2.04	24.55 ± 2.35	0.139
Monounsaturated ^b	52.15 ± 2.26	52.26 ± 2.57	51.41 ± 2.41	52.00 ± 2.53	0.445
Polyunsaturated ^b	23.63 ± 2.68	23.70 ± 2.10	23.14 ± 2.95	23.44 ± 2.87	0.524
Skeletal muscle TAG					
<i>c9t11</i>	0.35 ± 0.10	0.40 ± 0.14	0.47 ± 0.10	0.46 ± 0.03	0.167
<i>t10c12</i>	0.01 ± 0.01	0.06 ± 0.04	0.03 ± 0.03	0.05 ± 0.09	0.418
Oleic acid (18:1)	40.81 ± 2.43	41.98 ± 5.12	36.16 ± 2.27	37.57 ± 3.63	0.927
Linoleic acid (18:2)	15.76 ± 2.38	15.46 ± 3.39	15.95 ± 1.73	13.89 ± 2.39	0.246
Saturated ^b	36.18 ± 3.34	35.34 ± 2.44	38.20 ± 1.74	41.06 ± 6.18	0.207
Monounsaturated ^b	44.45 ± 3.49	45.46 ± 5.21	40.60 ± 3.06	40.63 ± 4.32	0.712
Polyunsaturated ^b	19.37 ± 2.97	19.17 ± 4.72	21.21 ± 3.17	18.31 ± 3.12	0.137
Skeletal muscle phospholipids					
<i>c9t11</i>	0.19 ± 0.03	0.23 ± 0.04	0.18 ± 0.05	0.17 ± 0.01	0.056
<i>t10c12</i>	Not present				–
Oleic acid (18:1)	8.81 ± 1.34	8.12 ± 0.83	7.42 ± 0.86	8.02 ± 0.97	0.055
Linoleic acid (18:2)	34.66 ± 3.23	36.16 ± 1.49	33.89 ± 2.10	34.88 ± 1.74	0.704
Saturated ^b	34.29 ± 0.98	34.53 ± 0.91	35.26 ± 2.26	34.27 ± 0.79	0.289
Monounsaturated ^b	9.71 ± 1.57	9.01 ± 0.91	8.21 ± 0.93	8.85 ± 1.13	0.075
Polyunsaturated ^b	56.00 ± 1.57	56.46 ± 1.16	56.52 ± 2.35	56.88 ± 1.35	0.906

Values are expressed as means ± SD. The amount of each fatty acid presented is expressed as a percentage of the total amount of all fatty acids measured

CLA conjugated linoleic acid supplementation group, TAG triacylglycerol

*Significant difference between the CLA and placebo group

^a The *P* value represents the repeated measures ANOVA time-by-treatment interaction effect and compares the differences by which the variables change between the groups with supplementation

^b The combined amounts of all fatty acids in either the saturated, monounsaturated or polyunsaturated lipid classes are expressed as a percentage of all fatty acids identified

The significance of this finding may lie in adipose tissue's role in lipid storage and/or insulin resistance. The *t10c12* isomer of CLA is believed to inhibit the actions of lipoprotein lipase and stearoyl-CoA-desaturase, which would inhibit the uptake of lipids into adipocytes (reviewed in Pariza 2001) [25]. The *t10c12* CLA isomer has also been proposed to increase insulin resistance in human adipocytes, possibly by antagonising peroxisome proliferator-activated receptor γ signalling, which in turn may indirectly reduce the expression of insulin-stimulated glucose transporter 4 and insulin-stimulated glucose uptake in adipocytes ([14] and reviewed in [19]).

Whether there is an association between the incorporation of the *t10c12* isomer into adipose tissue and its

subsequent effect on lipid uptake or insulin sensitivity in humans supplementing with CLA remains to be determined, since we did not see any change in insulin sensitivity in this group of individuals. Thrush et al. [26] have, however, shown that 12 weeks of supplementation with CLA (50:50, *t10c12:c9t11*) increases the content of the *t10c12* and *c9t11* isomers in skeletal muscle and this is accompanied by a decrease in insulin sensitivity in overweight, but non-diabetic individuals. Furthermore, the extent of the increase in the *t10c12* isomer was similar to that which we found in adipose tissue TAG (~0.01%) [26]. Therefore, it is possible that a very small enrichment of a tissue with the *t10c12* isomer may be sufficient to result in a functional change in the tissue.

In contrast to our results, Benito et al. [27], failed to detect the *t10c12* isomer in the adipose tissue of healthy females following 63 days of supplementation with a 4-isomer mixture of CLA (*c9t11*, *t8c10*, *c11t12* and *t10c12*) [27]. One explanation for this discrepancy might be that the supplement used in our study contained more than twice of the *t10c12* isomer (30.9%, 1.885 g) than that used by Benito et al. [27] (14.7%, 0.882 g).

There was also a trend towards significant incorporation of the *c9t11* isomer into the skeletal muscle phospholipids. While this study could not determine the functional implications of this, it warrants further investigation as fatty acid incorporation into the muscle phospholipids has been shown to result in various sequelae including changes in muscle cell membrane permeability, an increase in the number of insulin receptors [28, 29], insulin resistance and excessive accumulation of body fat (reviewed in [30]), depending on the proportions of the fatty acids. Indeed, Thrush et al. [26] showed that incorporation of both the *c9t11* and *t10c12* isomers in skeletal muscle lipids (TAG, diacylglycerol and ceramide) following 12 weeks of supplementation with CLA (50:50 *c9t11*:*t10c12*) was associated with a reduction in insulin sensitivity in nine overweight, non-diabetic individuals.

We also found that CLA supplementation was associated with increased oleic acid content of adipose tissue TAG and a trend for increased incorporation in skeletal muscle phospholipids. The CLA supplement contained 24.7% oleic acid and the placebo supplement was made up purely from high oleic sunflower oil. Therefore, one would expect oleic acid levels to increase in both groups. While oleic acid has been shown to be absorbed into plasma lipids following supplementation with CLA and a sunflower oil placebo [31], the location and extent of oleic acid incorporation into either adipose tissue or skeletal muscle following supplementation is not clear, making these observations difficult to explain. From a functional perspective, however, these changes in oleic acid levels were not differentially associated with any changes in body composition or insulin sensitivity.

The tissue-specific incorporation of the CLA isomers and oleic acid observed in this study were not accompanied by changes in variables such as body composition or insulin sensitivity. One explanation may be related to the antagonistic actions of the *c9t11* and *t10c12* CLA isomers. Given that our CLA supplement contained equal amounts of the two isomers, it is possible that any anti-adipogenic effect of the *t10c12* isomer was negated by the *c9t11* isomer, which appears to increase adipocyte triglyceride content in humans [19]. Alternatively, the relatively small sample size used in this study may not have been sensitive enough to detect physiological changes which typically have a large degree of inter-individual

variance. Another explanation may be that a longer supplementation period may be required for the observed fatty acid changes to be translated into physiological changes. Finally, the gender, body composition, activity level or health status of the individuals studied might have influenced such changes.

In conclusion, the fatty acid composition of adipose tissue TAG and skeletal muscle phospholipids may be altered in an isomer-specific manner with CLA supplementation in healthy, non-obese, regularly exercising individuals. The functional significance of these findings has yet to be elucidated.

Acknowledgments We thank the participants who gave of their time to participate in this study; Ryan Jankelowitz for his expert medical assistance; Jack Bergman and Debbie Steele of Symington Radiology, and Tobie de Villiers for performing the CT and DXA scans, respectively. We are also grateful to Judy Bolojne for her expert technical assistance and Jenny Ann Smuts for her assistance in dietary analysis. This study was funded in part by Loders Crokiaan, The Netherlands; RP Schere, UK; Aspen Pharmacare, South Africa; and Technology and Human Resources for Industry Programme, South Africa.

References

- O'Shea M, Bassaganya-Riera J, Mohede IC (2004) Immunomodulatory properties of conjugated linoleic acid. *Am J Clin Nutr* 79:1199S–1206S
- Albers R, van der Wielen RP, Brink EJ, Hendriks HF, Dorovskata-Taran VN, Mohede IC (2003) Effects of *cis*-9, *trans*-11 and *trans*-10, *cis*-12 conjugated linoleic acid (CLA) isomers on immune function in healthy men. *Eur J Clin Nutr* 57:595–603
- Blankson H, Stakkestad JA, Fagertun H, Thom E, Wadstein J, Gudmundsen O (2000) Conjugated linoleic acid reduces body fat mass in overweight and obese humans. *J Nutr* 130:2943–2948
- Gaullier JM, Halse J, Høye K, Kristiansen K, Fagertun H, Vik H, Gudmundsen O (2004) Conjugated linoleic acid supplementation for 1 year reduces body fat mass in healthy overweight humans. *Am J Clin Nutr* 79:1118–1125
- Smedman A, Vessby B (2001) Conjugated linoleic acid supplementation in humans—metabolic effects. *Lipids* 36:773–781
- Thom E, Wadstein J, Gudmundsen O (2001) Conjugated linoleic acid reduces body fat in healthy exercising humans. *J Int Med Res* 29:392–396
- Berven G, Bye A, Hals O, Blankson H, Fagertun H, Thom E, Wadstein J, Gudmundsen O (2000) Safety of conjugated linoleic acid (CLA) in overweight or obese human volunteers. *Eur J Lipid Sci Technol* 102:455–462
- Malpuech-Brugere C, Verboeket-van de Venne WP, Mensink RP, Arnal MA, Morio B, Brandolini M, Saebø A, Lassel TS, Char-digny JM, Sebedio JL, Beaufre B (2004) Effects of two conjugated linoleic acid isomers on body fat mass in overweight humans. *Obes Res* 12:591–598
- Riserus U, Berglund L, Vessby B (2001) Conjugated linoleic acid (CLA) reduced abdominal adipose tissue in obese middle-aged men with signs of the metabolic syndrome: a randomised controlled trial. *Int J Obes Relat Metab Disord* 25:1129–1135
- Whigham LD, O'Shea M, Mohede IC, Walaski HP, Atkinson RL (2004) Safety profile of conjugated linoleic acid in a 12-month trial in obese humans. *Food Chem Toxicol* 42:1701–1709

11. Noone EJ, Roche HM, Nugent AP, Gibney MJ (2002) The effect of dietary supplementation using isomeric blends of conjugated linoleic acid on lipid metabolism in healthy human subjects. *Br J Nutr* 88:243–251
12. Tricon S, Burdge GC, Kew S, Banerjee T, Russell JJ, Jones EL, Grimble RF, Williams CM, Yaqoob P, Calder PC (2004) Opposing effects of *cis*-9, *trans*-11 and *trans*-10, *cis*-12 conjugated linoleic acid on blood lipids in healthy humans. *Am J Clin Nutr* 80:614–620
13. Syvertsen C, Halse J, Hoivik HO, Gaullier JM, Nurminiemi M, Kristiansen K, Einerhand A, O'Shea M, Gudmundsen O (2007) The effect of 6 months supplementation with conjugated linoleic acid on insulin resistance in overweight and obese. *Int J Obes* 31:1148–1154
14. Brown JM, Boysen MS, Jensen SS, Morrison RF, Storkson J, Lea-Currie R, Pariza M, Mandrup S, McIntosh MK (2003) Isomer-specific regulation of metabolism and PPAR γ signaling by CLA in human preadipocytes. *J Lipid Res* 44:1287–1300
15. Ecker J, Langmann T, Moehle C, Schmitz G (2007) Isomer specific effects of Conjugated Linoleic Acid on macrophage ABCG1 transcription by a SREBP-1c dependent mechanism. *Biochem Biophys Res Commun* 352:805–811
16. Ma DW, Field CJ, Clandinin MT (2002) An enriched mixture of *trans*-10, *cis*-12-CLA inhibits linoleic acid metabolism and PGE2 synthesis in MDA-MB-231 cells. *Nutr Cancer* 44:203–212
17. Smedman A, Vessby B, Basu S (2004) Isomer-specific effects of conjugated linoleic acid on lipid peroxidation in humans: regulation by alpha-tocopherol and cyclo-oxygenase-2 inhibitor. *Clin Sci (Lond)* 106:67–73
18. Belury MA (2002) Dietary conjugated linoleic acid in health: physiological effects and mechanisms of action. *Annu Rev Nutr* 22:505–531
19. Brown JM, McIntosh MK (2003) Conjugated linoleic acid in humans: regulation of adiposity and insulin sensitivity. *J Nutr* 133:3041–3046
20. Martin JC, Gregoire S, Siess MH, Genty M, Chardigny JM, Berdeaux O, Juaneda P, Sebedio JL (2000) Effects of conjugated linoleic acid isomers on lipid-metabolizing enzymes in male rats. *Lipids* 35:91–98
21. Lambert EV, Goedecke JH, Bluett K, Heggie K, Claassen A, Rae DE, West S, Dugas J, Dugas L, Meltzer S, Charlton K, Mohede I (2007) Conjugated linoleic acid versus high-oleic acid sunflower oil: effects on energy metabolism, glucose tolerance, blood lipids, appetite and body composition in regularly exercising individuals. *Br J Nutr* 97:1001–1011
22. Bergström J (1962) Muscle electrolytes in man. *Scand J Clin Lab Med* 14:511–513
23. Smuts CM, Kruger M, Jaarsveld PJ, Fincham JE, Schall R, van der Merwe KJ, Benadé AJS (1992) The influence of fish supplementation on plasma lipoproteins and arterial lipids in vervet monkeys with established atherosclerosis. *Prostaglandins Leukot Essent Fatty Acids* 47:129–138
24. Folch J, Lees M, Sloane-Stanley GH (1957) A simple method for the isolation and purification of total lipids from animal tissues. *J Biol Chem* 226:497–509
25. Pariza MW, Park Y, Cook ME (2001) The biologically active isomers of conjugated linoleic acid. *Prog Lipid Res* 40:283–298
26. Thrush AB, Chabowski A, Heigenhauser GJ, McBride BW, Or-Rashid M, Dyck DJ (2007) Conjugated linoleic acid increases skeletal muscle ceramide content and decreases insulin sensitivity in overweight, non-diabetic humans. *Appl Physiol Nutr Metab* 32:372–382
27. Benito P, Nelson GJ, Kelley DS, Bartolini G, Schmidt PC, Simon V (2001) The effect of conjugated linoleic acid on plasma lipoproteins and tissue fatty acid composition in humans. *Lipids* 36:229–236
28. Ginsberg BH, Jabour J, Spector AA (1982) Effect of alterations in membrane lipid unsaturation on the properties of the insulin receptor of Ehrlich ascites cells. *Biochim Biophys Acta* 690:157–164
29. Ginsberg BH, Brown TJ, Simon I, Spector AA (1981) Effect of the membrane lipid environment on the properties of insulin receptors. *Diabetes* 30:773–780
30. Storlien LH, Pan DA, Kriketos AD, O'Connor J, Caterson ID, Cooney GJ, Jenkins AB, Baur LA (1996) Skeletal muscle membrane lipids and insulin resistance. *Lipids* 31:S261–S265
31. Emken EA, Adlof RO, Duval S, Nelson G, Benito P (2002) Effect of dietary conjugated linoleic acid (CLA) on metabolism of isotope-labeled oleic, linoleic, and CLA isomers in women. *Lipids* 37:741–750

activate fatty acids of C12–C20 in chain lengths [1]. Since the rat ACSL1 cDNA was first cloned in 1990, to date, five distinct isoforms of ACSL that share a common structure have been identified and characterized in mammals [2–6]. Based on amino acid identity, these isoforms can be further divided into two subfamilies. The first subfamily consists of ACSL1, 5 and 6, which share about 60% amino acid sequence homology with each other and ~30% with the second subfamily made up by ACSL3 and ACSL4 that have 68% identity to each other [2–6]. In addition, all five ACSL isoforms differ in tissue distribution [2–7] and subcellular organelle location (reviewed in [1]). For instance, rat ACSL3 and ACSL6 mRNA expression is most abundant in brain followed by testis [3, 6, 7]. Recent studies also found ACSL3 protein, together with ACSL4, in a lipid droplet-enriched fraction isolated from the human hepatoma-derived Huh7 cell line [8, 9] as well as in lipid droplets from lipolytically stimulated 3T3-L1 adipocytes [10].

Despite the fact that our knowledge of the ACSL family has advanced greatly in recent years, the functional role of the individual isoforms in lipid metabolism is yet to be fully understood. It has been hypothesized that individual ACSL isoforms could channel fatty acids into different metabolic pathways. Evidence supporting this idea initially came from *in vitro* studies using ACSL inhibitors particularly triacsin C, a specific inhibitor of ACSL1, 3 and 4 [11–13]. For example, triacsin C was shown to block *de novo* synthesis of glycerolipids while had very little inhibition on the incorporation of oleate or arachidonate into phospholipids in human fibroblasts [14]. Subsequent studies in which some isoforms of ACSL were overexpressed through adenoviral-mediated gene delivery provided direct evidence for the role of ACSL in fatty acid partitioning within the cell [15–17]. Overexpression of ACSL1 in HepG2 cells, for instance, increased both cellular long-chain acyl-CoAs and oleate incorporation into extractable lipids without altering fatty acid oxidation, and caused a TG level increase in mouse liver [17]. It was also shown that ACSL1 directed fatty acids into diacylglycerol and phospholipids synthesis and away from cholesterol esterification and β -oxidation in primary rat hepatocytes [15].

To date, only limited information regarding the regulation of ACSL isoforms under hyperlipidemic conditions is available. For instance, one report investigating the regulation of ACSL isoforms and cytosolic thioesterase 1 (CTE1) in rodent heart has shown that while streptozotocin-induced diabetes and fasting both induced CTE1 and repressed ACSL6 mRNA, high-fat feeding only induced CTE1 expression without affecting all five ACSL isoforms [18].

We previously identified ACSL3 and ACSL5 as novel genes regulated by oncostatin M (OM), a lipid-lowering

cytokine, in liver cells [19]. We showed that OM upregulated mRNA expression of both ACSL3 and ACSL5 in HepG2 cells through ERK signaling pathways. More importantly, we demonstrated that overexpression either ACSL3 or ACSL5 led to fatty acid partitioning into β -oxidation. These *in vitro* data suggest that ACSL3 might regulate hepatic fatty acids metabolism under normal physiological or pathological conditions. In this report, we extend our initial *in vitro* study to *in vivo* investigation by examining ACSL3 expression and regulation under both physiological and disease conditions, particularly hyperlipidemia.

It is well established that the hamster is an attractive animal model for the study of lipid metabolism [20, 21]. With regard to their lipid metabolism profiles, hamsters share more characteristic features of those found in humans than do other rodents such as mouse and rat. In addition, hamsters quickly develop hyperlipidemia when fed high-fat diets. Therefore, in the present studies, we utilized hyperlipidemic hamsters as our *in vivo* model to investigate the effects of HFHC feeding as well as changes in nutritional status on ACSL3 expression in various tissues. Our study revealed that expression of ACSL3 was upregulated specifically in liver of HFHC-fed hamsters. Furthermore, the abundance of ACSL3 mRNA was differentially affected by fasting and refeeding in livers of hamsters fed normal chow or HFHC diet. These new findings suggest that ACSL3 may have an important role in hepatic FFA metabolism.

Experimental Procedure

Cloning of Hamster ACSL3 Complete Coding Sequence

To clone the hamster ACSL3 complete coding sequence (cds), we first compared mRNA sequences from human, mouse and rat ACSL3 genes and selected regions that are highly conserved across these species for primer sets design. Using primers identified by this approach, hamster ACSL3 cds was amplified from a cDNA pool generated from hamster liver samples and TA cloned into pCR2.1-Topo (Invitrogen, Carlsbad, CA, USA) and sequenced. Primers were 5'-ATGAATAACCACACACCTTC-3' (forward) and 5'-TTACTTCCTCCCATACATCCGCTC-3' (reverse).

Animal Diet Study

Six-week old male Golden Syrian hamsters were purchased from Harlan Sprague–Dawley and caged (3 animals/cage) under controlled temperature (22 °C) and lighting

(12 h light/dark cycle). Animals had free access to autoclaved water and food. The hamsters were randomly allocated to receive either a standard rodent diet (SD group, $n = 15$) or a high-fat and high-cholesterol rodent diet containing 35% calories from fat and 1.25% cholesterol (#D12336, Research Diets, Inc., New Brunswick, NJ, USA) (HFHC group, $n = 15$) for 2 weeks before the experiments. For the fasting and refeeding experiments, animals within each diet group were further randomly divided into three subgroups of five animals each: fed, fasted and refed. The fed subgroup remained on chow diet and were sacrificed at 7:00 am. The fasted subgroup was fasted for 24 h (from 7:00 am to 7:00 am next day), and the refed subgroup was fasted for 24 h and then refed for 10 h before sacrifice. At the time of dissection, the liver was removed, rinsed in $1 \times$ PBS buffer, weighed, cut into small pieces, immediately frozen in liquid nitrogen and stored at -80°C . All other tissues were collected at the same time. Serum was isolated by low speed centrifugation and aliquots were stored at -80°C . All animal procedures were approved by the Institutional Animal Care and Use Committee of the VA Palo Alto Health Care System.

Serum Lipid Measurement

Serum total cholesterol (TC), triglyceride (TG), free fatty acid (FFA), low-density lipoprotein-cholesterol (LDL-C), and high-density lipoprotein-cholesterol (HDL-C) levels were determined using kits obtained from Stanbio Laboratory (Boerne, TX, USA) and Wako Chemical GmbH (Neuss, Germany).

RNA Isolation and Real-Time RT-PCR

Total RNA was isolated from flash-frozen hamster tissues using an RNeasy kit (Qiagen, CA, USA). RNA integrity was confirmed by agarose gel electrophoresis and ethidium bromide staining. Two microgram of total RNA was reverse transcribed with a high-capacity cDNA reverse transcription kit (Applied Biosystems, Foster City, CA, USA) using random primers according to the manufacturer's instructions. Real-time PCR was performed on the ABI PRISM[®] 7900HT Sequence Detection System (Foster City, CA, USA) with SYBR PCR master mix (Applied Biosystems, Foster City, CA). Each cDNA sample was run in duplicate. Primer sequences used were: ham-ACSL3: forward: GGGCACCATTAGTTTGCTGT, reverse: CCGC TGTCATTTTCATCTT; ham-GAPDH: forward: ACCC AGAAGACTGTGGATGG, reverse: CGACATGTGAGA TCCACGAC; ham-18S rRNA: forward: TTCCGATA ACGAACGAGACTCT, reverse: TGGCTGAACGCCACT TGTC [22].

Generation of ACSL3-Specific Antibodies and Immunoblotting

Rabbit polyclonal antibodies against ACSL3 were raised commercially by GenScript Corporation (Piscataway, NJ, USA). Briefly, a peptide corresponding to the C-terminal end of hamster ACSL3 that is 100% identical to human, mouse and rat ACSL3 (THYQADIERMYGRK) was synthesized, purified and conjugated to keyhole limpet hemocyanin (KLH). Rabbit antiserum against ACSL3 peptide antigen was obtained using a standard immunization protocol and subject to affinity-purification. For immunoblotting experiments, an equal amount of protein (unless otherwise indicated) was separated on 10% SDS-PAGE, transferred to a PVDF membrane and probed with the anti-ACSL3 antibody (1:5,000), an anti-FLAG M2 antibody (Sigma, St Louis, MO, USA), an anti- β -Actin AC-15 antibody (Sigma, St Louis, MO), or an anti- γ -tubulin DQ-19 antibody (Sigma, St Louis, MO). Immunoreactive bands were visualized using an ECL plus kit (GE Healthcare life Sciences, Piscataway, NJ, USA) and quantified with the KODAK Molecular Imaging Software (Kodak, New Haven, CT, USA).

Statistical Analysis

Data were analyzed by two-way ANOVA (diet and feeding status) followed by post hoc LSD tests and by Student's two-tailed t test. A p value less than 0.05 is considered statistically significant.

Results

Cloning of the Hamster ACSL3 Coding Region

It is well known that hamsters are a very useful species for studying lipid metabolism because the hamster responds to dietary lipids in a fashion that is comparable to humans [20, 21]. The ACSL3 gene has been identified and characterized in mammals including human, mouse and rat. However, to date, no sequence data are available for the hamster ACSL3 gene. In order to study the role of ACSL3 in lipid metabolism of hyperlipidemic hamsters, we cloned the ACSL3 entire coding region from a hamster liver cDNA pool. The hamster ACSL3 cDNA coding sequence is 2,060 base pairs in length that is 88, 92 and 91% identical to human, mouse and rat sequences, respectively (Fig. 1a). It encodes the hamster ACSL3 protein of 720 amino acids with a calculated molecular weight of 80.57 kDa. The overall homology of hamster ACSL3 amino acids to human, mouse and rat is 91, 95 and 93%, respectively (Fig. 1b). Moreover, protein sequence analysis

Fig. 1 Comparison of hamster, human, mouse and rat ACSL3 cDNA coding regions and protein sequences. **a** The hamster ACSL3 cDNA complete coding sequence (cnds) was cloned and shows an open reading frame of 2,163 nucleotides. It was aligned with the human, mouse or rat cnds by using the DNASTAR software (DNASTAR, Inc., Madison, WI, USA). Boxes indicate nucleotides of the human, mouse or rat ACSL3 cnds that differ from those of the hamster sequence. **b** Alignment of hamster, human, mouse and rat ACSL3 protein sequence. Amino acid residues of the human, mouse or rat ACSL3 that differ from those of the hamster sequence are boxed. The *open box* at the end indicates stop codon. Two luciferase-like regions (LR) 1 (133–389) and 2 (434–686) are shown as *underlined*

A

Hamster	ATGAATAACCGACACCTTCAAACCATCTACCATGAAGCTAAAACAGACCTCAACCCCTATCTTTTATATTTGATAAATTTGTAATATATCTCTATA	100
Human	ATGAATAACCGACACCTTCAAACCATCTACCATGAAGCTAAAACAGACCTCAACCCCTATCTTTTATATTTGATAAATTTGTAATATATCTCTATA	100
Mouse	ATGAATAACCGACACCTTCAAACCATCTACCATGAAGCTAAAACAGACCTCAACCCCTATCTTTTATATTTGATAAATTTGTAATATATCTCTATA	100
Rat	ATGAATAACCGACACCTTCAAACCATCTACCATGAAGCTAAAACAGACCTCAACCCCTATCTTTTATATTTGATAAATTTGTAATATATCTCTATA	100
Hamster	CTATTTAAACATACATTCATTTTACTTTTTGTCTGAGTCACGACAAAGAAAATCAAAACAAATTAAGGAAAACCTGCAATTCAAACCGGATCTCTGC	200
Human	CTATTTAAACATACATTCATTTTACTTTTTGTCTGAGTCACGACAAAGAAAATCAAAACAAATTAAGGAAAACCTGCAATTCAAACCGGATCTCTGC	200
Mouse	CTATTTAAACATACATTCATTTTACTTTTTGTCTGAGTCACGACAAAGAAAATCAAAACAAATTAAGGAAAACCTGCAATTCAAACCGGATCTCTGC	200
Rat	CTATTTAAACATACATTCATTTTACTTTTTGTCTGAGTCACGACAAAGAAAATCAAAACAAATTAAGGAAAACCTGCAATTCAAACCGGATCTCTGC	200
Hamster	ATTCAAGATCTATAAAGAGCTGGACAGCTGGCTCATATTGTATCCGGCTGTGATACCTTGATAAAAGCTTTTATGATGATGCAAAAATAAATTTAAAG	300
Human	ATTCAAGATCTATAAAGAGCTGGACAGCTGGCTCATATTGTATCCGGCTGTGATACCTTGATAAAAGCTTTTATGATGATGCAAAAATAAATTTAAAG	300
Mouse	ATTCAAGATCTATAAAGAGCTGGACAGCTGGCTCATATTGTATCCGGCTGTGATACCTTGATAAAAGCTTTTATGATGATGCAAAAATAAATTTAAAG	300
Rat	ATTCAAGATCTATAAAGAGCTGGACAGCTGGCTCATATTGTATCCGGCTGTGATACCTTGATAAAAGCTTTTATGATGATGCAAAAATAAATTTAAAG	300
Hamster	GACAAAAGCCTACTGGGAACCGTGAATTTTGAATGAGGAAGATGAAATCAACCAAAATGAAAATTTTAAAGAGGTTATCTGGGACAGTGTAAAT	400
Human	GACAAAAGCCTACTGGGAACCGTGAATTTTGAATGAGGAAGATGAAATCAACCAAAATGAAAATTTTAAAGAGGTTATCTGGGACAGTGTAAAT	400
Mouse	GACAAAAGCCTACTGGGAACCGTGAATTTTGAATGAGGAAGATGAAATCAACCAAAATGAAAATTTTAAAGAGGTTATCTGGGACAGTGTAAAT	400
Rat	GACAAAAGCCTACTGGGAACCGTGAATTTTGAATGAGGAAGATGAAATCAACCAAAATGAAAATTTTAAAGAGGTTATCTGGGACAGTGTAAAT	400
Hamster	GGCTTTCCATGAAAGTGTCTTCACTCGACGCTTGAATTTGGAAATGGGTTGCAATGTTGGGCCAGAAACCGAAACCAATGATCTCTCTGTG	500
Human	GGCTTTCCATGAAAGTGTCTTCACTCGACGCTTGAATTTGGAAATGGGTTGCAATGTTGGGCCAGAAACCGAAACCAATGATCTCTCTGTG	500
Mouse	GGCTTTCCATGAAAGTGTCTTCACTCGACGCTTGAATTTGGAAATGGGTTGCAATGTTGGGCCAGAAACCGAAACCAATGATCTCTCTGTG	500
Rat	GGCTTTCCATGAAAGTGTCTTCACTCGACGCTTGAATTTGGAAATGGGTTGCAATGTTGGGCCAGAAACCGAAACCAATGATCTCTCTGTG	500
Hamster	GACCCGGCCGAGTGGATGATCCGGCAGACGGCTGCTTCATGTATAACTCCAGCTGTGTACCTGTGTGCCACCTGGAGGTCAACCCGCTGTTGAT	600
Human	GACCCGGCCGAGTGGATGATCCGGCAGACGGCTGCTTCATGTATAACTCCAGCTGTGTACCTGTGTGCCACCTGGAGGTCAACCCGCTGTTGAT	600
Mouse	GACCCGGCCGAGTGGATGATCCGGCAGACGGCTGCTTCATGTATAACTCCAGCTGTGTACCTGTGTGCCACCTGGAGGTCAACCCGCTGTTGAT	600
Rat	GACCCGGCCGAGTGGATGATCCGGCAGACGGCTGCTTCATGTATAACTCCAGCTGTGTACCTGTGTGCCACCTGGAGGTCAACCCGCTGTTGAT	600
Hamster	GGACTAATGAGACAGAGGTGACCAACATCATTACTAGTAAAGACGCTTGCACAAAAGCTGAAAGATATACTCGTGGTCCACGCTGCGCCAT	700
Human	GGACTAATGAGACAGAGGTGACCAACATCATTACTAGTAAAGACGCTTGCACAAAAGCTGAAAGATATACTCGTGGTCCACGCTGCGCCAT	700
Mouse	GGACTAATGAGACAGAGGTGACCAACATCATTACTAGTAAAGACGCTTGCACAAAAGCTGAAAGATATACTCGTGGTCCACGCTGCGCCAT	700
Rat	GGACTAATGAGACAGAGGTGACCAACATCATTACTAGTAAAGACGCTTGCACAAAAGCTGAAAGATATACTCGTGGTCCACGCTGCGCCAT	700
Hamster	TCAATGCTGTGATGGAAGCCTCCAACTGGTGTGATGTCGCCAACGGGTGTCTTGTACAACCATGGCTGCATGGAGGCTTGGAGTGAAGGCCAA	800
Human	TCAATGCTGTGATGGAAGCCTCCAACTGGTGTGATGTCGCCAACGGGTGTCTTGTACAACCATGGCTGCATGGAGGCTTGGAGTGAAGGCCAA	800
Mouse	TCAATGCTGTGATGGAAGCCTCCAACTGGTGTGATGTCGCCAACGGGTGTCTTGTACAACCATGGCTGCATGGAGGCTTGGAGTGAAGGCCAA	800
Rat	TCAATGCTGTGATGGAAGCCTCCAACTGGTGTGATGTCGCCAACGGGTGTCTTGTACAACCATGGCTGCATGGAGGCTTGGAGTGAAGGCCAA	800
Hamster	CGTGGAAAATAAGCTCAGGCAAAACCGTGGCCCTCAGACATGCAATGATGATACAAGTGGTCCACAGGAATCCAAAAGGAGTCAATGATCTCC	900
Human	CGTGGAAAATAAGCTCAGGCAAAACCGTGGCCCTCAGACATGCAATGATGATACAAGTGGTCCACAGGAATCCAAAAGGAGTCAATGATCTCC	900
Mouse	CGTGGAAAATAAGCTCAGGCAAAACCGTGGCCCTCAGACATGCAATGATGATACAAGTGGTCCACAGGAATCCAAAAGGAGTCAATGATCTCC	900
Rat	CGTGGAAAATAAGCTCAGGCAAAACCGTGGCCCTCAGACATGCAATGATGATACAAGTGGTCCACAGGAATCCAAAAGGAGTCAATGATCTCC	900
Hamster	CACAGCAACATCATTGCTGCTATAACTGGATGGCAGGAAGGATCCAAAGCTGGGAGGAGGATGATGATACATGGATATTTCCCTCGGCCATGTTG	1000
Human	CACAGCAACATCATTGCTGCTATAACTGGATGGCAGGAAGGATCCAAAGCTGGGAGGAGGATGATGATACATGGATATTTCCCTCGGCCATGTTG	1000
Mouse	CACAGCAACATCATTGCTGCTATAACTGGATGGCAGGAAGGATCCAAAGCTGGGAGGAGGATGATGATACATGGATATTTCCCTCGGCCATGTTG	1000
Rat	CACAGCAACATCATTGCTGCTATAACTGGATGGCAGGAAGGATCCAAAGCTGGGAGGAGGATGATGATACATGGATATTTCCCTCGGCCATGTTG	1000
Hamster	TAGAATTAAGTCCCAACTGTGTGTTTCTCATGATGCCGAATGGCTACTCTTACCACAGACTTTAGCAATCAAGTCTTCAAAAATAAAAAAGG	1100
Human	TAGAATTAAGTCCCAACTGTGTGTTTCTCATGATGCCGAATGGCTACTCTTACCACAGACTTTAGCAATCAAGTCTTCAAAAATAAAAAAGG	1100
Mouse	TAGAATTAAGTCCCAACTGTGTGTTTCTCATGATGCCGAATGGCTACTCTTACCACAGACTTTAGCAATCAAGTCTTCAAAAATAAAAAAGG	1100
Rat	TAGAATTAAGTCCCAACTGTGTGTTTCTCATGATGCCGAATGGCTACTCTTACCACAGACTTTAGCAATCAAGTCTTCAAAAATAAAAAAGG	1100
Hamster	AAGCAAAAGGACACATCATGATGGAAGCAACATGATGGACGCTGTCGGGAAATCATGGATTCGGATCTAATAAATGATCATGAATAAGTGAATGAA	1200
Human	AAGCAAAAGGACACATCATGATGGAAGCAACATGATGGACGCTGTCGGGAAATCATGGATTCGGATCTAATAAATGATCATGAATAAGTGAATGAA	1200
Mouse	AAGCAAAAGGACACATCATGATGGAAGCAACATGATGGACGCTGTCGGGAAATCATGGATTCGGATCTAATAAATGATCATGAATAAGTGAATGAA	1200
Rat	AAGCAAAAGGACACATCATGATGGAAGCAACATGATGGACGCTGTCGGGAAATCATGGATTCGGATCTAATAAATGATCATGAATAAGTGAATGAA	1200
Hamster	ATGAGAAAGTTTCAAGGAACTGTGTTATTTGGCCATAAATACAAGATGGAAGGATTTCAAAAAGGTTGATGATCTCCGCTGTGTGACCGTTTGTGT	1300
Human	ATGAGAAAGTTTCAAGGAACTGTGTTATTTGGCCATAAATACAAGATGGAAGGATTTCAAAAAGGTTGATGATCTCCGCTGTGTGACCGTTTGTGT	1300
Mouse	ATGAGAAAGTTTCAAGGAACTGTGTTATTTGGCCATAAATACAAGATGGAAGGATTTCAAAAAGGTTGATGATCTCCGCTGTGTGACCGTTTGTGT	1300
Rat	ATGAGAAAGTTTCAAGGAACTGTGTTATTTGGCCATAAATACAAGATGGAAGGATTTCAAAAAGGTTGATGATCTCCGCTGTGTGACCGTTTGTGT	1300
Hamster	TCCGGAATGTCCGAAGCTGCTGGGTGAAATATTCCGCTTTTGTGTGTGGTGGTCTCCACTTTCTGCAACAACAGAGATTCATGAATATCTGTTT	1400
Human	TCCGGAATGTCCGAAGCTGCTGGGTGAAATATTCCGCTTTTGTGTGTGGTGGTCTCCACTTTCTGCAACAACAGAGATTCATGAATATCTGTTT	1400
Mouse	TCCGGAATGTCCGAAGCTGCTGGGTGAAATATTCCGCTTTTGTGTGTGGTGGTCTCCACTTTCTGCAACAACAGAGATTCATGAATATCTGTTT	1400
Rat	TCCGGAATGTCCGAAGCTGCTGGGTGAAATATTCCGCTTTTGTGTGTGGTGGTCTCCACTTTCTGCAACAACAGAGATTCATGAATATCTGTTT	1400
Hamster	CTGCTGTTGGTGGTCAAGGGTATGGACTCAGGAAATCAACTGGGGCTGGAACAATACAAGATGGAAGTACAACTGCGCAACTGGCAAGTGGGGGCCA	1500
Human	CTGCTGTTGGTGGTCAAGGGTATGGACTCAGGAAATCAACTGGGGCTGGAACAATACAAGATGGAAGTACAACTGCGCAACTGGCAAGTGGGGGCCA	1500
Mouse	CTGCTGTTGGTGGTCAAGGGTATGGACTCAGGAAATCAACTGGGGCTGGAACAATACAAGATGGAAGTACAACTGCGCAACTGGCAAGTGGGGGCCA	1500
Rat	CTGCTGTTGGTGGTCAAGGGTATGGACTCAGGAAATCAACTGGGGCTGGAACAATACAAGATGGAAGTACAACTGCGCAACTGGCAAGTGGGGGCCA	1500
Hamster	TTAGTTTGCTGTGAAATCAAATTAAGAACTGGGAGGAAGTGGCTATTTTAATACTGACAAACCAATCCCAAGGTGAAATCTTATTGGTGGCCAAA	1600
Human	TTAGTTTGCTGTGAAATCAAATTAAGAACTGGGAGGAAGTGGCTATTTTAATACTGACAAACCAATCCCAAGGTGAAATCTTATTGGTGGCCAAA	1600
Mouse	TTAGTTTGCTGTGAAATCAAATTAAGAACTGGGAGGAAGTGGCTATTTTAATACTGACAAACCAATCCCAAGGTGAAATCTTATTGGTGGCCAAA	1600
Rat	TTAGTTTGCTGTGAAATCAAATTAAGAACTGGGAGGAAGTGGCTATTTTAATACTGACAAACCAATCCCAAGGTGAAATCTTATTGGTGGCCAAA	1600
Hamster	ATGTGCAATGGGTAATATAAATGAAGCAAAACAAATACTGATTTCTTTGAAGATGAAATGGACAGCGTGGCTCTGCAAGGATGATTGGAGA	1700
Human	ATGTGCAATGGGTAATATAAATGAAGCAAAACAAATACTGATTTCTTTGAAGATGAAATGGACAGCGTGGCTCTGCAAGGATGATTGGAGA	1700
Mouse	ATGTGCAATGGGTAATATAAATGAAGCAAAACAAATACTGATTTCTTTGAAGATGAAATGGACAGCGTGGCTCTGCAAGGATGATTGGAGA	1700
Rat	ATGTGCAATGGGTAATATAAATGAAGCAAAACAAATACTGATTTCTTTGAAGATGAAATGGACAGCGTGGCTCTGCAAGGATGATTGGAGA	1700
Hamster	ATTTGACCCGTGATGGTGTCTGAGGATATTGATCGTAGAAGAACCTGTGAAACTGCAAGGCAGGAGTATGTTTCTCTGGGAAAATGAGGACGCT	1800
Human	ATTTGACCCGTGATGGTGTCTGAGGATATTGATCGTAGAAGAACCTGTGAAACTGCAAGGCAGGAGTATGTTTCTCTGGGAAAATGAGGACGCT	1800
Mouse	ATTTGACCCGTGATGGTGTCTGAGGATATTGATCGTAGAAGAACCTGTGAAACTGCAAGGCAGGAGTATGTTTCTCTGGGAAAATGAGGACGCT	1800
Rat	ATTTGACCCGTGATGGTGTCTGAGGATATTGATCGTAGAAGAACCTGTGAAACTGCAAGGCAGGAGTATGTTTCTCTGGGAAAATGAGGACGCT	1800
Hamster	TTGAAAGCCTCCCACTGATAGTAACATCTGTGGCTAGCAAAAGCTTACCATCTTACGTAATGGATTTGTTGTGCAAAATCAAAGGAACTCAAG	1900
Human	TTGAAAGCCTCCCACTGATAGTAACATCTGTGGCTAGCAAAAGCTTACCATCTTACGTAATGGATTTGTTGTGCAAAATCAAAGGAACTCAAG	1900
Mouse	TTGAAAGCCTCCCACTGATAGTAACATCTGTGGCTAGCAAAAGCTTACCATCTTACGTAATGGATTTGTTGTGCAAAATCAAAGGAACTCAAG	1900
Rat	TTGAAAGCCTCCCACTGATAGTAACATCTGTGGCTAGCAAAAGCTTACCATCTTACGTAATGGATTTGTTGTGCAAAATCAAAGGAACTCAAG	1900
Hamster	AGCTAGCTGAAATGAAAGGATTTAAGGGGACTTGGGAGAGCTGTGTAACAGCTGGTAAATGAAATGAGTGTCTTAAAGCTCTTCAAGGCTGCTAT	2000
Human	AGCTAGCTGAAATGAAAGGATTTAAGGGGACTTGGGAGAGCTGTGTAACAGCTGGTAAATGAAATGAGTGTCTTAAAGCTCTTCAAGGCTGCTAT	2000
Mouse	AGCTAGCTGAAATGAAAGGATTTAAGGGGACTTGGGAGAGCTGTGTAACAGCTGGTAAATGAAATGAGTGTCTTAAAGCTCTTCAAGGCTGCTAT	2000
Rat	AGCTAGCTGAAATGAAAGGATTTAAGGGGACTTGGGAGAGCTGTGTAACAGCTGGTAAATGAAATGAGTGTCTTAAAGCTCTTCAAGGCTGCTAT	2000
Hamster	TTCAAGGAGCTGGAAGGTTGAAATCCAGTGAATCCGTTTGAAGCTGACCCATGGACTCTGAACTGGTCTGGTGGACGATGCTTCAAAGTTG	2100
Human	TTCAAGGAGCTGGAAGGTTGAAATCCAGTGAATCCGTTTGAAGCTGACCCATGGACTCTGAACTGGTCTGGTGGACGATGCTTCAAAGTTG	2100
Mouse	TTCAAGGAGCTGGAAGGTTGAAATCCAGTGAATCCGTTTGAAGCTGACCCATGGACTCTGAACTGGTCTGGTGGACGATGCTTCAAAGTTG	2100
Rat	TTCAAGGAGCTGGAAGGTTGAAATCCAGTGAATCCGTTTGAAGCTGACCCATGGACTCTGAACTGGTCTGGTGGACGATGCTTCAAAGTTG	2100
Hamster	AAAAGTAAAAGGCTTAAACAATACCAAGGCAATGAGCGGATGATGGGAGGAAATAA	2163
Human	AAAAGTAAAAGGCTTAAACAATACCAAGGCAATGAGCGGATGATGGGAGGAAATAA	2163
Mouse	AAAAGTAAAAGGCTTAAACAATACCAAGGCAATGAGCGGATGATGGGAGGAAATAA	2163
Rat	AAAAGTAAAAGGCTTAAACAATACCAAGGCAATGAGCGGATGATGGGAGGAAATAA	2163

Fig. 1 continued

B

Hamster	MNNHTPSKPSMMLKQTI NPI LL YFI NFVI YL YTI LTYI PF YFL SESROEKSNOI KAKPVNSKPDASFRSI NSLDSLASLL YPGCDTLDKVFMYAKNKF K 100
Human	MNNHTPSKPSMMLKQTI NPI LL YFI NFVI YL YTI LTYI PF YFL SESROEKSNOI KAKPVNSKPDASFRSI NSLDSLASLL YPGCDTLDKVFMYAKNKF K 100
Mouse	MNNHTPSKPSMMLKQTI NPI LL YFI NFVI YL YTI LTYI PF YFL SESROEKSNOI KAKPVNSKPDASFRSI NSLDSLASLL YPGCDTLDKVFMYAKNKF K 100
Rat	MNNHTPSKPSMMLKQTI NPI LL YFI NFVI YL YTI LTYI PF YFL SESROEKSNOI KAKPVNSKPDASFRSI NSLDSLASLL YPGCDTLDKVFMYAKNKF K 100
Hamster	DKRLLGTREI LNEEDEI OPNGKI FKKVI LGGCNWLSYEDVFI RALDFGNGLQMLGOKPKTNI AI FCTRAEAWI AAOACFMYNFQLVTLVATLGGPAVYH 200
Human	DKRLLGTREI LNEEDEI OPNGKI FKKVI LGGCNWLSYEDVFI RALDFGNGLQMLGOKPKTNI AI FCTRAEAWI AAOACFMYNFQLVTLVATLGGPAVYH 200
Mouse	DKRLLGTREI LNEEDEI OPNGKI FKKVI LGGCNWLSYEDVFI RALDFGNGLQMLGOKPKTNI AI FCTRAEAWI AAOACFMYNFQLVTLVATLGGPAVYH 200
Rat	DKRLLGTREI LNEEDEI OPNGKI FKKVI LGGCNWLSYEDVFI RALDFGNGLQMLGOKPKTNI AI FCTRAEAWI AAOACFMYNFQLVTLVATLGGPAVYH 200
Hamster	GLNETEVTNI I TSKERLQTKL KDI VSLVPLRHHI I AVDGKPTVSEFPKGI VHTMAAVQALGVKANVENKAHSHKPLPSDI AVI MTSGSTGI PKGVMI S 300
Human	GLNETEVTNI I TSKERLQTKL KDI VSLVPLRHHI I AVDGKPTVSEFPKGI VHTMAAVQALGVKANVENKAHSHKPLPSDI AVI MTSGSTGI PKGVMI S 300
Mouse	GLNETEVTNI I TSKERLQTKL KDI VSLVPLRHHI I AVDGKPTVSEFPKGI VHTMAAVQALGVKANVENKAHSHKPLPSDI AVI MTSGSTGI PKGVMI S 300
Rat	GLNETEVTNI I TSKERLQTKL KDI VSLVPLRHHI I AVDGKPTVSEFPKGI VHTMAAVQALGVKANVENKAHSHKPLPSDI AVI MTSGSTGI PKGVMI S 300
Hamster	HSNI I AAI TGMARRI PSLGEDDVYI GYLPLAHVLEL SAELVGVSHGRCI GYSSPOTLADGSSKI KKGSKGDT SMLKPTLMAAVPEI MORI YKNVMNKVNE 400
Human	HSNI I AAI TGMARRI PSLGEDDVYI GYLPLAHVLEL SAELVGVSHGRCI GYSSPOTLADGSSKI KKGSKGDT SMLKPTLMAAVPEI MORI YKNVMNKVNE 400
Mouse	HSNI I AAI TGMARRI PSLGEDDVYI GYLPLAHVLEL SAELVGVSHGRCI GYSSPOTLADGSSKI KKGSKGDT SMLKPTLMAAVPEI MORI YKNVMNKVNE 400
Rat	HSNI I AAI TGMARRI PSLGEDDVYI GYLPLAHVLEL SAELVGVSHGRCI GYSSPOTLADGSSKI KKGSKGDT SMLKPTLMAAVPEI MORI YKNVMNKVNE 400
Hamster	MRSFORNLF I LAINYKMEQI SKGCSSTPLCDRFVFRNVRRL LGGNI RLL LCGGAPLSATTORFMNI CFCCSVGGVGLTESTGAGTI TEMVDYNTGRVGAP 500
Human	MRSFORNLF I LAINYKMEQI SKGCSSTPLCDRFVFRNVRRL LGGNI RLL LCGGAPLSATTORFMNI CFCCSVGGVGLTESTGAGTI TEMVDYNTGRVGAP 500
Mouse	MRSFORNLF I LAINYKMEQI SKGCSSTPLCDRFVFRNVRRL LGGNI RLL LCGGAPLSATTORFMNI CFCCSVGGVGLTESTGAGTI TEMVDYNTGRVGAP 500
Rat	MRSFORNLF I LAINYKMEQI SKGCSSTPLCDRFVFRNVRRL LGGNI RLL LCGGAPLSATTORFMNI CFCCSVGGVGLTESTGAGTI TEMVDYNTGRVGAP 500
Hamster	LVCCIEI KLNWEEGGYF NTDKPHRPEI LI GGNVNTMSYKNEAKTNT OFF EDENGORWL CT GDI GEFDPDGCCLKI DRKKDLVKLOAGEYVSLGKVEAA 600
Human	LVCCIEI KLNWEEGGYF NTDKPHRPEI LI GGNVNTMSYKNEAKTNT OFF EDENGORWL CT GDI GEFDPDGCCLKI DRKKDLVKLOAGEYVSLGKVEAA 600
Mouse	LVCCIEI KLNWEEGGYF NTDKPHRPEI LI GGNVNTMSYKNEAKTNT OFF EDENGORWL CT GDI GEFDPDGCCLKI DRKKDLVKLOAGEYVSLGKVEAA 600
Rat	LVCCIEI KLNWEEGGYF NTDKPHRPEI LI GGNVNTMSYKNEAKTNT OFF EDENGORWL CT GDI GEFDPDGCCLKI DRKKDLVKLOAGEYVSLGKVEAA 600
Hamster	LKNLPLI DNI CAYANSYHSYVI GFVVPNOKELTELARMKGFKGTWEELCNSSEMENEVLKVLSEAAI SASLEKFEI PVKI RLSADPW PETGLVTDFAFKL 700
Human	LKNLPLI DNI CAYANSYHSYVI GFVVPNOKELTELARMKGFKGTWEELCNSSEMENEVLKVLSEAAI SASLEKFEI PVKI RLSADPW PETGLVTDFAFKL 700
Mouse	LKNLPLI DNI CAYANSYHSYVI GFVVPNOKELTELARMKGFKGTWEELCNSSEMENEVLKVLSEAAI SASLEKFEI PVKI RLSADPW PETGLVTDFAFKL 700
Rat	LKNLPLI DNI CAYANSYHSYVI GFVVPNOKELTELARMKGFKGTWEELCNSSEMENEVLKVLSEAAI SASLEKFEI PVKI RLSADPW PETGLVTDFAFKL 700
Hamster	KRKELKTHYQADI ERMVGRK 721
Human	KRKELKTHYQADI ERMVGRK 721
Mouse	KRKELKTHYQADI ERMVGRK 721
Rat	KRKELKTHYQADI ERMVGRK 721

showed that hamster ACSL3 protein also contained two similar putative conserved luciferase-like regions (LS) (Fig. 1b) as found in human, mouse and rat ACSL3 [3, 23].

Generation and Characterization of Anti-ACSL3 Antibody

To facilitate current and future studies on ACSL3, we generated a rabbit polyclonal antibody against hamster ACSL3 residues 707–720 at the C-terminus, a peptide sequence that is identical to that in human, mouse and rat, but not conserved in other ACSL isoforms. To test whether the antibody can specifically recognize the ACSL3 protein, we performed western blot analysis on protein extracts prepared from HepG2 cells and HepG2 cells overexpressing a C-terminal Flag-tagged hamster ACSL3 recombinant protein (Ad-hams-Acs13-Flag) or a control GFP (Ad-GFP). A single band with an approximate molecular weight of 80 kDa was observed in HepG2 (Fig. 2a, lane 1). In addition, the antibody also detected a higher molecular weight band around 83 kDa in HepG2 overexpressing the hamster ACSL3 recombinant protein (Fig. 2a, lane 3) but not in the cells expressing the plasmid control protein GFP (Fig. 2a, lane 2). Immunoblotting on the same extracts with an anti-FLAG M2 antibody showed a single band at the same position as the higher band detected by the ACSL3 antibody (Fig. 2b, left panel), confirming that the higher band found in transduced HepG2 cells is indeed correspondent to the overexpressed recombinant hamster ACSL3 protein with a Flag tag. Furthermore, co-incubation of the ACSL3 antibody with the immunizing peptides completely eliminated the ACSL3 signal (Fig. 2a, lanes 4–6). Additionally, a single band was also observed in

human Huh7 and rat McA-RH777 cells in a dose-dependent manner (Fig. 2c). Together, these data demonstrate that the anti-ACSL3 antibody can specifically recognize the ACSL3 protein from various species. With both the coding sequence and specific antibody on hand, we next investigated the effects of HFHC diet and food consumption on ACSL3 mRNA and protein expression in hamsters.

Upregulation of Hepatic ACSL3 Expression by a Fat and Cholesterol-Enriched Diet

We first examined tissue expression of ACSL3 mRNA in standard diet (SD)-fed hamsters. As shown in Fig. 3a by black bars, ACSL3 mRNA is highly expressed in brain and testis, with moderate expression in white adipose tissue, liver and heart. In addition, muscle also expresses low levels of ACSL3 mRNA. Detection of ACSL3 protein in these tissues using the specific ACSL3 polyclonal antibody confirmed this tissue-specific expression pattern of the ACSL3 gene at the protein level (Fig. 3b).

Next, we examined the ACSL3 mRNA levels in tissues of hamsters fed the HFHC diet. Two weeks of feeding with a HFHC diet induced hyperlipidemia in hamsters as evidenced by a marked increase in plasma levels of triglycerides (TG), cholesterol (TC) and free fatty acids (FFA) (Table 1). Strikingly, compared to the mRNA levels in SD-fed hamsters, HFHC feeding specifically increased ACSL3 mRNA abundance 2.3-fold ($p < 0.001$) in liver and 1.8-fold ($p < 0.05$) in muscle without an effect on other tissues including white adipose tissue, brain, heart, and testis. Moreover, the ACSL3 protein levels in livers of SD-fed and HFHC-fed hamsters, as determined by Western blot analysis, were firmly correlated with the results seen at

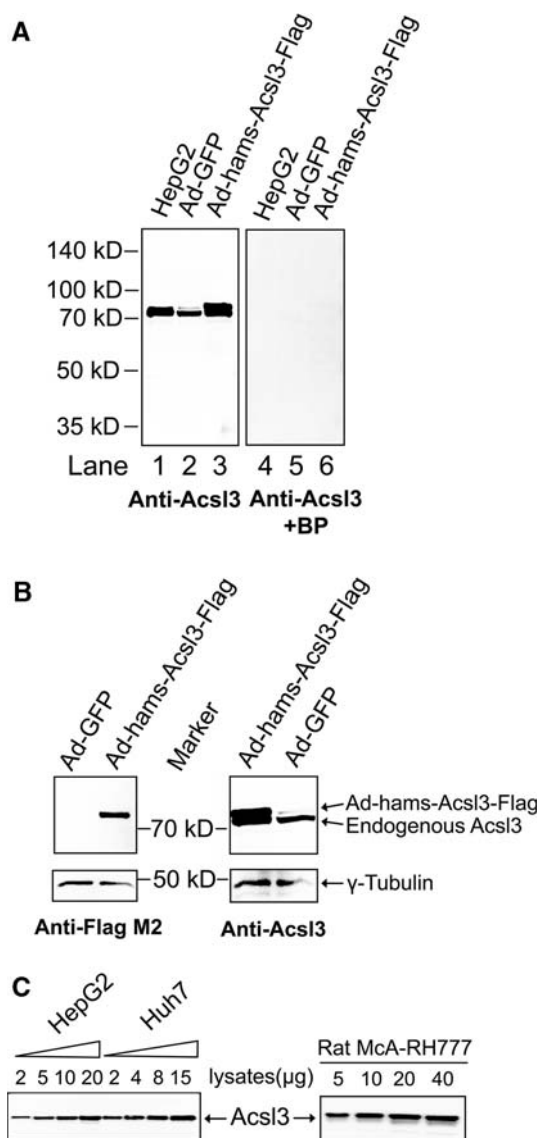


Fig. 2 Characterization of anti-ACSL3 polyclonal antibody. **a** Extracts from regular HepG2 cells and HepG2 cells infected with recombinant adenoviruses expressing either a GFP control or a C-terminal Flag-tagged hamster ACSL3 recombinant protein were separated on 10% SDS-PAGE gel, transferred to PVDF membranes and immunoblotted using a rabbit polyclonal anti-ACSL3 antibody or the antibody plus the immunizing blocking peptides (BP, THY-QADIERMYGRK) at a final concentration of 100 μ g/mL. Protein markers are shown on the left to indicate the protein molecular weights. **b** Western blot analysis of the overexpressed recombinant hamster ACSL3 and endogenous ACSL3 protein in HepG2 cells using either an anti-Flag M2 antibody or the anti-ACSL3 antibody. γ -tubulin was used as a loading control. **c** Western blot analysis using anti-ACSL3 antibody in HepG2, Huh7 and rat McA-RH777 cells

the mRNA level (Fig. 3c). We could not verify the HFHC diet-induced increase in ACSL3 protein expression in muscle due to the extremely low level of expression.

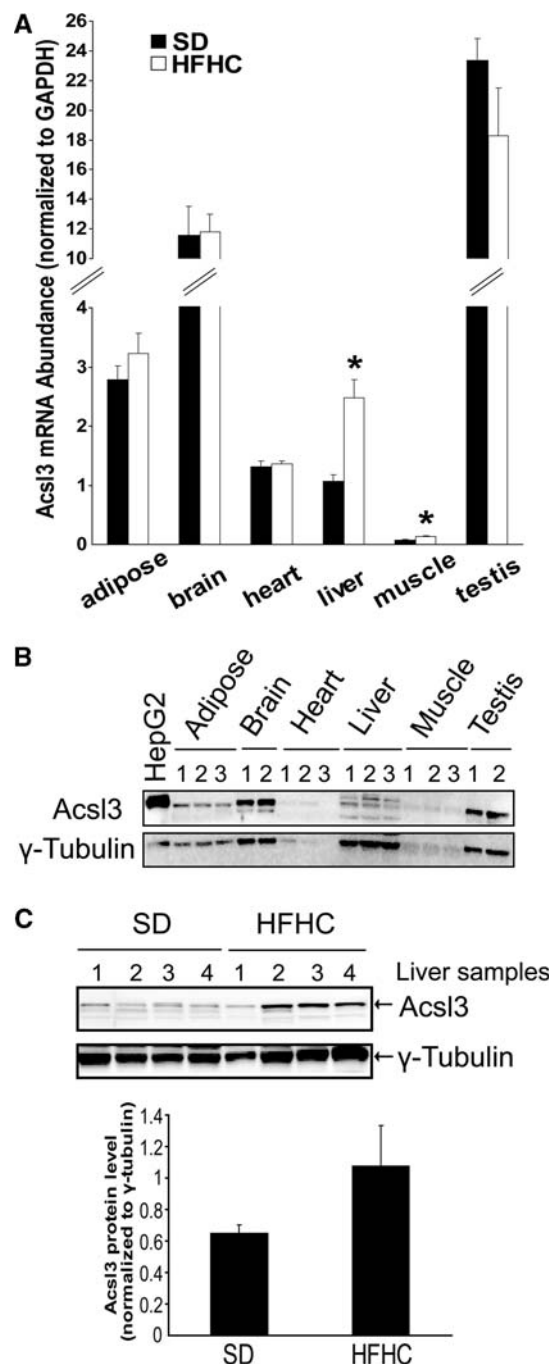


Fig. 3 ACSL3 expression in SD- and HFHC-fed hamster tissues. **a** ACSL3 mRNA expression in various tissues from SD-fed (black bars) and HFHC-fed (white bars) hamsters. Abundance of mRNA was determined by real-time RT-PCR and normalized to GAPDH. Data represent means \pm SEM ($n = 5$). * $p < 0.05$ versus SD. **b** Western blot analysis of ACSL3 protein in representative tissue samples from SD-fed hamsters. HepG2 extracts were included as a control to indicate the position of the ACSL3 protein. γ -Tubulin was used as a loading control. **c** Comparison of ACSL3 protein levels in liver samples from hamsters fed SD and HFHC diets. Expression levels were quantified with the KODAK Molecular Imaging Software and normalized to γ -tubulin

Table 1 Serum lipid profile of normal and hyperlipidemic hamsters

Diet	SD			HFHC		
	Fed	Fasted	Refed	Fed	Fasted	Refed
Triglyceride (mg/dL)	139 (13)	55 (7)*	105 (12)	317 (37)*	76 (17) [§]	132 (33)
Cholesterol (mg/dL)	94 (11)	81 (12)	67 (6)	387 (35)*	274 (27) [§]	337 (18)
Free fatty acids (mequiv/ml)	0.54 (0.03)	0.65 (0.11)	0.42 (0.04)	0.95 (0.06)*	0.92 (0.1)	0.56 (0.05) ^{§§}
LDL-C (mg/dL)	63 (10)	47 (8)	43 (5)	125 (6)*	174 (14) [§]	190 (13)
HDL-C (mg/dL)	86 (12)	68 (9)	55 (6)	168 (8)*	142 (6)	154 (8)

Values shown are means (\pm SEM)

* $p < 0.05$ versus SD fed

[§] $p < 0.05$ versus HFHC fed

^{§§} $p < 0.05$ versus HFHC fasted as determined by ANOVA and post hoc LSD tests

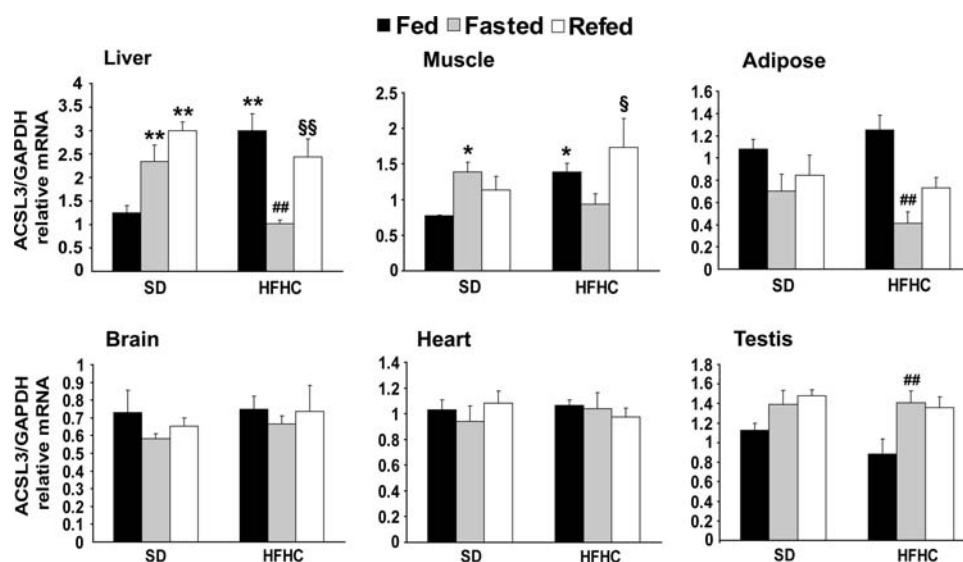


Fig. 4 Regulation of ACSL3 mRNA expression by food consumption in healthy and hyperlipidemic hamsters. ACSL3 mRNA expression, as quantified by real-time RT-PCR and normalized to GAPDH, in various tissues from fed hamsters, hamsters fasted for 24 h, and hamsters fasted for 24 h and refed for 10 h under healthy (SD) and

hyperlipidemic (HFHC) conditions. Data show as means + SEM. ($n = 5$ or 4). * $p < 0.05$ versus SD fed, ** $p < 0.01$ versus SD fed, ## $p < 0.01$ versus HFHC fed, [§] $p < 0.05$ versus HFHC fasted, and ^{§§} $p < 0.05$ versus HFHC fasted by two-way ANOVA and post hoc LSD tests

Changes in Nutritional Status Differentially Affected ACSL3 mRNA Expression in SD- and HFHC-Fed Hamsters

To further investigate the influence of HFHC diet on ACSL3 expression, we examined ACSL3 mRNA abundance in tissues of fed, fasted, and refed hamsters from both SD and HFHC groups. As shown in Fig. 4, the most significant changes of ACSL3 mRNA expression caused by different nutritional status were again observed in liver. In SD-fed hamster livers, fasting significantly increased the level of ACSL3 mRNA by 88% ($p < 0.01$), and refeeding led to a further 28% elevation ($p < 0.01$). Interestingly, in contrast to the change seen in the SD group, in livers of HFHC-fed hamsters, the mRNA for ACSL3 declined by

almost 70% upon fasting ($p < 0.01$) and returned to slightly reduced levels after refeeding ($p < 0.01$). We further validated these results by normalizing ACSL3 mRNA expression to another reference gene 18S rRNA and obtained similar results (data not shown).

In addition to liver, we observed a similar pattern in muscles but to a lesser extent. In white adipose tissue, fasting caused ACSL3 mRNA expression to decline by 35% ($p > 0.05$) in SD group and 67% ($p < 0.01$) in HFHC group. In both dietary groups, ACSL3 mRNAs showed only minor or insignificant changes in brain, heart and testis after fasting and refeeding.

To determine whether ACSL3 protein expression correlated with changes in ACSL3 mRNA abundance caused by the fasting and refeeding regimen, we measured ACSL3

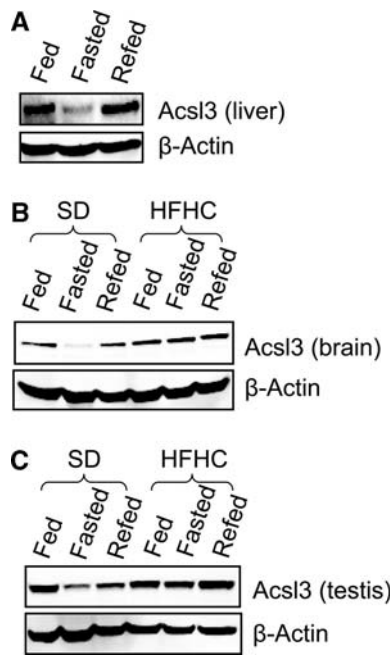


Fig. 5 Regulation of ACSL3 protein expression by food consumption in hamster liver, brain and testis tissues. **a** Western blot analysis of ACSL3 protein expression in tissue extracts from pooled livers of HFHC-fed hamsters (four to five hamster livers per feeding group). β -actin was used as a loading control. Western blot analysis of ACSL3 protein expression in tissue extracts from pooled brains (**b**) and testis (**c**) of both SD and HFHC-fed hamsters (four to five samples per group were pooled). β -actin was used as a loading control

protein in all tissues (pooled samples) in which mRNA levels were quantified. Due to the low protein expression, we were unable to measure ACSL3 protein abundance using our ACSL3 polyclonal antibody in muscle, adipose and heart tissues of both diet groups, and liver samples of SD group. In HFHC-fed hamster livers, fasting resulted in a decline in ACSL3 protein and refeeding increased ACSL3 protein abundance (Fig. 5a), which was consistent with the changes seen at the mRNA levels. Interestingly, fasting notably decreased ACSL3 protein levels in brain and testis of SD-fed animals but not in brain or testis of HFHC-fed hamsters (Fig. 5b, c). These data suggest that ACSL3 protein expression might be regulated at the level of translation in brain and testis of healthy but not hyperlipidemic animals.

Discussion

We previously reported the identification of two members of the ACSL family, ACSL3 and ACSL5, as OM-regulated genes in HepG2 cells and suggested that the TG-lowering effect of OM observed in hamsters could be mediated through the stimulation of the transcription of ACSL specific isoforms in the liver [19]. To further understand the

role of ACSL in fatty acids metabolism in vivo, in the current study we investigated the nutritional regulation of ACSL3, one of the least characterized members of the ACSL family with only few known functions [9, 19, 24], in normolipidemic and hyperlipidemic hamsters.

Through the cloning of coding region, we demonstrate that hamster ACSL3 has a high degree of sequence homology to human, mouse and rat ACSL3 at both nucleotide and amino acid levels, which is in line with the notion that this enzyme is highly conserved among different species. We show that hamster ACSL3 mRNA, consistent with rat ACSL3 data previously reported [3, 7], is predominantly expressed in both brain and testis, suggesting physiological importance of this ACSL isoform in the regulation of lipid metabolism during the development of the central nervous and reproductive systems. In addition, it's also been shown that the mRNA abundance of ACSL3 changes during the development of mouse heart, suggesting that ACSL3 may play a critical role during the development of the fetal heart [25]. However, the detailed mechanism by which ACSL3 functions in these specific tissues still remains to be elicited. With the specific antibody developed in this current study, for the first time, the tissue expression of ACSL3 protein was determined and the results mirror the data from mRNA detection.

One of the important findings of this study is the demonstration of the distinct elevation of hepatic ACSL3 expression by a HFHC feeding at both mRNA (2.3-fold increase) and protein (1.7-fold increase) levels compared to those in livers of SD-fed hamsters. These data suggest that, at least in hamsters, ACSL3 is actively involved in hepatic fatty acid metabolism and its increased expression in HFHC-fed hamster livers might reflect the demand of body to metabolize excessive FFAs in a feed-forward regulatory mechanism.

In addition to the HFHC-induced upregulation, a functional role of ACSL3 in liver fatty acid metabolism can be further inferred from the fact that the most significant alteration of ACSL3 mRNA levels caused by changes in food consumption was in the liver, and the different patterns between SD-fed and HFHC-fed hamsters. Fasting increased ACSL3 mRNA level by 88% and refeeding led to a further 28% elevation in SD-fed hamster liver, whereas in hyperlipidemic hamster liver the mRNA level declined by almost 70% upon fasting and returned to slightly reduced levels after refeeding. It is also worth noting that the same pattern of changes under two different diets was recaptured in muscle but not in other tissues. Liver and muscle are recognized as major organs of FFA utilization for energy production or for lipid synthesis. Thus, it is plausible to speculate that these two organs might share similar regulatory mechanisms for ACSL3 gene transcription.

Previous studies in rodent models have shown that the expression of some isoforms of the ACSL family is regulated by food consumption under both physiological and pathological conditions [2, 4, 7, 18]. Our results here also indicate that ACSL3 expression is differentially regulated in normal chow-fed versus HFHC diet-fed hamsters in a tissue-specific manner. This warrants further studies to examine the expression and regulation of other ACSL isoforms under pathological conditions, which may help to better understand the causes of dyslipidemia and its related diseases, especially in the liver, such as NASH.

Currently, the transcriptional network involving in ACSL3 gene expression in liver tissue is largely uncharacterized. Possible candidates might include members of the PPAR transcription factor family, since it's been shown that both ACSL1 and ACSL4 expression increased after the treatment with PPAR α agonist GW9578 in rat liver [26]. Indeed, a PPAR responsive element (PPRE) has been identified on the ACSL1 gene promoter [27, 28]. In addition, ACSL1 and ACSL5 mRNA increase in adipose tissue upon PPAR γ agonists stimulation [29]. Moreover, a recent report investigating the regulation of ACSL isoform gene expression in rat heart concluded that ACSL1 is a PPAR α -regulated gene whereas ACSL6 is an insulin-regulated gene [18]. In the same study, it has also been shown that insulin significantly increased the expression of ACSL3, as well as ACSL1 and ACSL6, in adult rat cardiomyocytes. Therefore, further work is needed to determine whether the PPAR and/or insulin are involved in the regulation of ACSL3 in the liver under different diet conditions.

Acknowledgments This study was supported by the Department of Veterans Affairs (Office of Research and Development, Medical Research Service) and by grants (1R01 AT002543-01A1, 1R21AT003195-01A2) from the National Center for Complementary and Alternative Medicine.

References

- Soupe E, Kuypers FA (2008) Mammalian long-chain acyl-CoA synthetases. *Exp Biol Med* 233:507–521
- Oikawa E, Iijima H, Suzuki T, Sasano H, Sato H, Kamataki A, Nagura H, Kang MJ, Fujino T, Suzuki H, Yamamoto TT (1998) A novel acyl-CoA synthetase, ACS5, expressed in intestinal epithelial cells and proliferating preadipocytes. *J Biochem* 124:679–685
- Fujino T, Kang MJ, Suzuki H, Iijima H, Yamamoto T (1996) Molecular characterization and expression of rat acyl-CoA synthetase 3. *J Biol Chem* 271:16748–16752
- Suzuki H, Kawarabayasi Y, Kondo J, Abe T, Nishikawa K, Kimura S, Hashimoto T, Yamamoto T (1990) Structure and regulation of rat long-chain acyl-CoA synthetase. *J Biol Chem* 265:8681–8685
- Kang MJ, Fujino T, Sasano H, Minekura H, Yabuki N, Nagura H, Iijima H, Yamamoto TT (1997) A novel arachidonate-preferring acyl-CoA synthetase is present in steroidogenic cells of the rat adrenal, ovary, and testis. *Proc Natl Acad Sci USA* 94:2880–2884
- Fujino T, Yamamoto T (1992) Cloning and functional expression of a novel long-chain acyl-CoA synthetase expressed in brain. *J Biochem* 111:197–203
- Mashek DG, Li LO, Coleman RA (2006) Rat long-chain acyl-CoA synthetase mRNA, protein, and activity vary in tissue distribution and in response to diet. *J Lipid Res* 47:2004–2010
- Fujimoto Y, Itabe H, Sakai J, Makita M, Noda J, Mori M, Higashi Y, Kojima S, Takano T (2004) Identification of major proteins in the lipid droplet-enriched fraction isolated from the human hepatocyte cell line HuH7. *Biochim Biophys Acta* 1644:47–59
- Fujimoto Y, Itabe H, Kinoshita T, Homma KJ, Onoduka J, Mori M, Yamaguchi S, Makita M, Higashi Y, Yamashita A, Takano T (2007) Involvement of ACSL in local synthesis of neutral lipids in cytoplasmic lipid droplets in human hepatocyte HuH7. *J Lipid Res* 48:1280–1292
- Brasaemle DL, Dolios G, Shapiro L, Wang R (2004) Proteomic analysis of proteins associated with lipid droplets of basal and lipolytically stimulated 3T3-L1 adipocytes. *J Biol Chem* 279:46835–46842
- Van Horn CG, Caviglia JM, Li LO, Wang S, Granger DA, Coleman RA (2005) Characterization of recombinant long-chain rat acyl-CoA synthetase isoforms 3 and 6: identification of a novel variant of isoform 6. *Biochemistry* 44:1635–1642
- Lewin TM, Kim JH, Granger DA, Vance JE, Coleman RA (2001) Acyl-CoA synthetase isoforms 1, 4, and 5 are present in different subcellular membranes in rat liver and can be inhibited independently. *J Biol Chem* 276:24674–24679
- Kim JH, Lewin TM, Coleman RA (2001) Expression and characterization of recombinant rat Acyl-CoA synthetases 1, 4, and 5. Selective inhibition by triacsin C and thiazolidinediones. *J Biol Chem* 276:24667–24673
- Igal RA, Wang P, Coleman RA (1997) Triacsin C blocks de novo synthesis of glycerolipids and cholesterol esters but not recycling of fatty acid into phospholipid: evidence for functionally separate pools of acyl-CoA. *Biochem J* 324:529–534
- Li LO, Mashek DG, An J, Doughman SD, Newgard CB, Coleman RA (2006) Overexpression of rat long chain acyl-CoA synthetase 1 alters fatty acid metabolism in rat primary hepatocytes. *J Biol Chem* 281:37246–37255
- Mashek DG, McKenzie MA, Van Horn CG, Coleman RA (2006) Rat long chain acyl-CoA synthetase 5 increases fatty acid uptake and partitioning to cellular triacylglycerol in McArdle-RH777 cells. *J Biol Chem* 281:945–950
- Parkes HA, Preston E, Wilks D, Ballesteros M, Carpenter L, Wood L, Kraegen EW, Furler SM, Cooney GJ (2006) Overexpression of acyl-CoA synthetase-I increases lipid deposition in hepatic (HepG2) cells and rodent liver in vivo. *Am J Physiol Endocrinol Metab* 291:E737–E744
- Durgan DJ, Smith JK, Hotze MA, Egbejimi O, Cuthbert KD, Zaha VG, Dyck JR, Abel ED, Young ME (2006) Distinct transcriptional regulation of long-chain acyl-CoA synthetase isoforms and cytosolic thioesterase 1 in the rodent heart by fatty acids and insulin. *Am J Physiol Heart Circ Physiol* 290:H2480–H2497
- Zhou Y, Abidi P, Kim A, Chen W, Huang TT, Kraemer FB, Liu J (2007) Transcriptional activation of hepatic ACSL3 and ACSL5 by oncostatin m reduces hypertriglyceridemia through enhanced beta-oxidation. *Arterioscler Thromb Vasc Biol* 27:2198–2205
- Ohtani H, Hayashi K, Hirata Y, Dojo S, Nakashima K, Nishio E, Kurushima H, Saeki M, Kajiyama G (1990) Effects of dietary cholesterol and fatty acids on plasma cholesterol level and hepatic lipoprotein metabolism. *J Lipid Res* 31:1413–1422
- Sullivan MP, Cerda JJ, Robbins FL, Burgin CW, Beatty RJ (1993) The gerbil, hamster, and guinea pig as rodent models for hyperlipidemia. *Lab Anim Sci* 43:575–578

22. Bilz S, Samuel V, Morino K, Savage D, Choi CS, Shulman GI (2006) Activation of the farnesoid X receptor improves lipid metabolism in combined hyperlipidemic hamsters. *Am J Physiol Endocrinol Metab* 290:E716–E722
23. Minekura H, Fujino T, Kang MJ, Fujita T, Endo Y, Yamamoto TT (1997) Human acyl-coenzyme A synthetase 3 cDNA and localization of its gene (ACS3) to chromosome band 2q34–q35. *Genomics* 42:180–181
24. Yao H, Ye J (2008) Long chain acyl-CoA synthetase 3-mediated phosphatidylcholine synthesis is required for assembly of very low density lipoproteins in human hepatoma Huh7 cells. *J Biol Chem* 283:849–854
25. de Jong H, Neal AC, Coleman RA, Lewin TM (2007) Ontogeny of mRNA expression and activity of long-chain acyl-CoA synthetase (ACSL) isoforms in *Mus musculus* heart. *Biochim Biophys Acta* 1771:75–82
26. Lewin TM, Van Horn CG, Krisans SK, Coleman RA (2002) Rat liver acyl-CoA synthetase 4 is a peripheral-membrane protein located in two distinct subcellular organelles, peroxisomes, and mitochondrial-associated membrane. *Arch Biochem Biophys* 404:263–270
27. Schoonjans K, Watanabe M, Suzuki H, Mahfoudi A, Krey G, Wahli W, Grimaldi P, Staels B, Yamamoto T, Auwerx J (1995) Induction of the acyl-coenzyme A synthetase gene by fibrates and fatty acids is mediated by a peroxisome proliferator response element in the C promoter. *J Biol Chem* 270:19269–19276
28. Martin G, Schoonjans K, Lefebvre AM, Staels B, Auwerx J (1997) Coordinate regulation of the expression of the fatty acid transport protein and acyl-CoA synthetase genes by PPARalpha and PPARgamma activators. *J Biol Chem* 272:28210–28217
29. Coleman RA, Lewin TM, Van Horn CG, Gonzalez-Baró MR (2002) Do long-chain acyl-CoA synthetases regulate fatty acid entry into synthetic versus degradative pathways. *J Nutr* 132:2123–2126

such as meat tenderness, juiciness and taste [1]. IMF tissue which is present in connective tissue surrounding muscle fibers and muscle fiber bundles, is composed of adipocytes interspersed between fiber fascicule (intramuscular adipocytes) [2].

In general, adipocytes arise from preadipose cells recruited from a population of mesodermal origin stem cells [3]. And the increase of adipose tissue mass is due to a combination of an increase in adipocyte number (hyperplasia) and in size (hypertrophy) [4], but the ratio between both processes varies among tissues [5]. The hyperplasia of intramuscular adipocytes may play a more important role in the deposition of IMF than other adipose tissues [6].

Adipogenesis is the process by which mesodermal precursor cells (preadipocytes or stem cells) differentiate into adipocytes, which store lipid and serve as central regulators of metabolism [7]. The adipogenesis process is documented as being controlled by both positive and negative regulators [7]. Transcription factor peroxisome proliferator-activated receptor γ (PPAR γ) is the chief positive and central regulator of adipogenesis to trigger hyperplasia of adipocytes, and is both necessary and sufficient for preadipocytes and stem cells differentiation [8–10]. On the other hand, Wnt/ β -Catenin signaling is considered as the main negative regulator of adipogenesis [11]. Wnts are an evolutionarily conserved family of secreted lipidated glycoproteins and Wnt/ β -Catenin signaling functions as an adipogenic switch, when it is on, adipogenesis is repressed [11, 12].

It is worth mentioning that another transcription factor PPAR δ is also involved in adipogenesis but playing different roles from PPAR γ [13]. PPAR δ is demonstrated to be not directly involved in the regulation of adipose terminal differentiation, but to be implicated in the initial steps of the adipogenic program by inducing PPAR γ gene expression in response to various adipogenic nutrients which are ligands of PPAR δ , especially long chain fatty acids [13–15].

The n-3 polyunsaturated fatty acids (n-3 PUFA) which belong to one of the major classes of long chain fatty acids are potential activators of PPAR δ [16]. Activating PPAR δ by n-3 PUFA may in turn induce PPAR γ to stimulate adipogenesis. There was also evidence by which n-3 PUFA exerted inhibition on Wnt/ β -Catenin signaling pathway in cell cultures [17]. So it is likely that n-3 PUFA could induce adipogenesis through affecting both positive and negative regulators.

Hsu et al. [18] pointed out that effective regulation of the expression of a certain gene such as adipocyte determination and differentiation-dependent factor 1 (ADD1) in adipose tissue may need much n-3 PUFA enrichment, so it is reasonable to assume that the same case may also exist in skeletal muscle. The n-3 PUFA level can be increased in pork by feeding linseed, which contains about one-third oil,

of which more than 50% is α -linolenic acid (18:3n-3, ALA), and duration of linseed feeding could increase n-3 PUFA enrichment in tissues [19]. In the current study, experiments were designed by feeding pigs with a diet containing 10% linseed for 0, 30, 60 and 90 days before slaughter to test the hypothesis that increasing the n-3 PUFA enrichment in the skeletal muscle of growing-finishing pigs by feeding linseed, could activate PPAR δ , which may subsequently upregulate the expression of PPAR γ to promote adipogenesis. Meanwhile, n-3 PUFA enriched in the skeletal muscle could also decrease Wnt/ β -Catenin signaling to release the inhibition of adipogenesis, consequently to increase IMF deposition.

Experimental Procedures

Animals and Diets

The study was carried out according to Huazhong Agriculture University Animal Care and Use Committee guidelines. Two isoenergetic, isonitrogenous and isolipidic diets were formulated: a basal diet containing saturated fat powder and a linseed diet containing 10% (wt%) linseed. Diet composition is presented in Table 1. The fatty acid composition of the diets was analyzed and listed in Table 2. Twenty-four Landrace \times NewDamLine barrows weighing 35 ± 3.7 kg were randomly assigned to four treatment groups with six pigs per group. The NewDamLine is a cross-bred pig bred at Huazhong Agriculture University containing 25% blood of a Chinese breed “Taihu pig”. Throughout the experimental period of 90 days, pigs in treatment group 1 (T1), T2, T3 and T4 were respectively fed first the control diet for 90, 60, 30 and 0 days and then the linseed diet for 0, 30, 60 and 90 days, respectively. Pigs were housed individually and fed ad libitum. At the end of the trial the pigs were humanely slaughtered at the age of 170 days by electrical stunning coupled with exsanguinations. Tissue samples were rapidly removed, wrapped in foil, and frozen in liquid nitrogen to be stored at -70 °C. Skeletal muscle samples (separated from adhering adipose tissue) were removed from longissimus muscle between the 10th and the last rib, and then collected for subsequent RNA extraction. Another set of longissimus muscle samples were also collected from each pig and stored at -20 °C for fatty acid analysis. And the longissimus muscle samples used for meat quality evaluation were also collected.

Meat Quality Evaluation

Drip loss (wt%) was calculated as fluid loss after storage of longissimus muscle in plastic bags at 4 °C for 24 h. Water

Table 1 Composition and calculated analysis (as-fed basis) of diets (wt%)

Item	Growing phase (30–60 kg)		Finishing phase (60–115 kg)	
	Control diet	Linseed diet	Control diet	Linseed diet
Ingredients (wt%)				
Corn	48.70	60.50	52.90	65.00
Wheat middling	18.00	–	20.00	1.00
Soybean meal	27.00	26.50	21.00	21.00
Fat powder ^a	3.30	–	3.10	–
Linseed	–	10.00	–	10.00
Premix ^b	3.00	3.00	3.00	3.00
Analyzed composition				
CP (wt%)	18.07	18.01	16.05	16.08
Ether extract (wt%)	4.60	4.50	5.05	5.10
Calcium (wt%)	0.69	0.66	0.65	0.70
Phosphorus (wt%)	0.50	0.51	0.49	0.55
Calculated value				
DE (MJ/kg)	14.30	14.28	14.23	14.23
Lysine (wt%)	1.07	1.05	0.93	0.95

CP crude protein, DE digestible energy

^a The fat powder is commercially available (BERGAFAT HTL-306 from Berg & Schmidt Co.) with a main composition of a palm oil fraction and phospholipid and the ether extract content is more than 99.50%. Fatty acid profile of the fat powder: palmitic acid (16:0), 70–80%; stearic acid (18:0), 5–10%; oleic acid (18:1), 8–15%

^b Provided per kg of premix: retinyl acetate, 3,870 µg; cholecalciferol, 62.5 µg; DL- α -tocopheryl acetate, 200 mg; menadione, 2.5 mg; thiamin, 2.5 mg; riboflavin, 6.0 mg; nicotinamide, 25 mg; D-pantothenic acid, 8 mg; pyridoxine hydrochloride, 3.0 mg; cyanocobalamin, 0.08 mg; D-biotin, 0.1 mg; pteroyl glutamic acid, 12.5 mg; copper, 20 mg; iron, 50 mg; manganese, 30 mg; zinc, 80 mg; iodine, 0.8 mg

Table 2 Fatty acid composition (%)^a of diets

Item	Growing phase (30–60 kg)		Finishing phase (60–115 kg)	
	Control diet	Linseed diet	Control diet	Linseed diet
14:0	1.09	0.11	1.10	0.11
16:0	69.50	11.40	69.60	10.54
16:1	0.10	0.38	0.11	0.39
18:0	4.00	4.76	4.09	4.25
18:1n-9	11.73	24.81	10.74	24.18
18:2n-6	12.49	24.17	11.96	25.90
18:3n-3	0.97	30.34	1.08	32.59
20:0	0.19	0.21	0.18	0.21
20:1	0.06	0.06	0.04	0.23
22:0	0.04	0.12	0.05	0.11
SFA ^b	74.82	16.60	75.02	15.22
PUFA	13.46	54.50	13.05	58.49

^a The fatty acid results were presented as g/100 g fatty acids (wt%)

^b Saturated fatty acids (SFA) percentage is the sum of 14:0, 16:0, 18:0, 20:0, and 22:0; polyunsaturated fatty acids (PUFA) percentage is the sum of 18:2n-6, 18:3n-3 (α -linolenic acid)

holding capacity (wt%) was measured by the press technique [20] using a 2.523 cm diameter 1 cm high columnar meat sample pressed for 5 min between 36 medium-speed

filter papers (Xinhua Paper Industry Co. Ltd., China) using a swelling press (Qinchuan Electric Apparatus Factory, China) and an applied force of 35 kg [21]. The pH₄₅ (portable pH meter, model 3071, Jenway, England) of the longissimus muscle was directly measured 45 min after slaughter at the level of the first lumbar vertebra using a combined glass electrode (P19/BNC). Water moisture content (wt%) was measured in a drying oven at 102 °C for 18 h [22]. The intramuscular fat content (wt%) of the last thoracic vertebral longissimus muscle was determined by chloroform-methanol extraction and expressed as the weight percentage of wet muscle tissue [23].

Fatty Acid Analysis

Lipids were extracted from the diet and longissimus muscle samples by the chloroform:methanol procedure as described by Folch et al. [24]. Fatty acid methyl esters (FAME) were prepared for gas chromatography determination using KOH/methanol [25].

The CP-3800 gas chromatography (Varian Inc., USA) equipped with a 1177 injector, a flame ionization detector and a capillary chromatographic column CPSi188 (Varian, Inc. USA) for FAME (50 m × 0.25 mm id × 0.20 µm) was used in this experiment. The injector and detector

temperature were kept at 250 and 270 °C, respectively. Nitrogen was used as carrier gas with a flow rate of 1.0 ml/min, split ratio was 1:100. The column was programmed as follows: 100 °C at first, increase to 200 °C (5 °C/min) and held constant for 5 min. Subsequently, the temperature was increased to 225 °C (2 °C/min) and kept constant for 2 min. The total analysis time was 39.5 min. The fatty acids were identified by comparing the retention times of the peaks with those of known standards (Sigam Chemical Co., St. Louis, MO, USA). Response factors for the fatty acids were calculated using the same standard mixtures plus an internal standard [26]. Peaks were identified using standards where available (Sigma Chemical Co. Ltd, Poole).

RNA Isolation

Total RNA was extracted from skeletal muscle samples using the TRIzol reagent (Invitrogen, Carlsbad, CA, USA) according to the manufacturer's specifications. RNA samples were then treated with a DNA-free kit (Applied Biosystems, Foster City, CA, USA) to remove any contamination with genomic DNA. The RNA samples were quantified spectrophotometrically at 260 and 280 nm. The ratio of light absorbance at 260 nm to that at 280 nm was between 1.8 and 2.0, indicating that they were pure and clean. The quality of RNA was also checked by 1.0% agarose gel electrophoresis and staining with 1 µg/mL ethidium bromide.

Reverse Transcription and Real-Time PCR Analysis

Oligo-(dT)_{20n} (Toyobo, Japan) was used as the primer in cDNA synthesis. The reverse transcription reaction solution (20 µL) consisted of 4 µL of total RNA (1 µg/µL),

100 U of Moloney Murine Leukemia Virus reverse transcriptase (Toyobo, Japan), 20 U of an RNase inhibitor (Toyobo, Japan), 0.5 mmol/L of deoxyribonucleotide triphosphate, and 2.5 µL oligo-(dT)_{20n} primers. The reverse transcription reaction parameters were as follows: reverse transcription at 42 °C for 60 min followed by denaturation at 99 °C for 5 min. The cDNA stock was stored at -20 °C.

Relative mRNA levels of *PPAR*δ, *PPAR*γ, *adipocyte fatty acid-binding protein (aP2)*, *lipoprotein lipase (LPL)*, *wingless related MMTV integration site 10b (Wnt10b)*, *myogenic differentiation 1 (MyoD)* and *α-actin* were quantified using real-time PCR with an iQTM5 Real Time PCR Detection System (BioRad). The *β-actin* mRNA levels were similarly measured and served as the reference gene. Of each cDNA, 0.1 µg were added to PCR reagent mixture, SYBR[®] Green Master Mix (Applied Biosystems), with the sense and antisense primers (500 nM each) (Table 3). Specific primers were synthesized commercially (Shanghai Sangon Biological Engineering Technology & Services Co, Ltd., Shanghai, China).

The PCR parameters were as follows: denaturation at 95 °C for 3 min followed by 40 cycles of denaturation at 94 °C for 20 s, annealing for 20 s (annealing temperatures in Table 3), extension at 72 °C for 20 s and reading plate for 10 s. All sample mRNA levels were normalized to the values of *β-actin* and the results expressed as fold changes of threshold cycle (Ct) value relative to controls using the 2^{-ΔΔCt} method [27]. All samples were measured in triplicate.

Statistical Analysis

Experimental animals were assigned to different treatments in a completely randomized design. Statistical analysis was

Table 3 Oligonucleotide polymerase chain reaction primers

Gene	Primers sense/antisense	Product length (bp)	Ta ^a (°C)
<i>PPAR</i> δ	5'-TGGCTGGGCTGACGGCAAAC-3'	181	60
	5'-TCGATGTCGTGGATCACAAAGG-3'		
<i>PPAR</i> γ	5'-AGCCCTTTGGTGACTT-3'	213	56
	5'-AGGACTCTGGGTGGTT-3'		
<i>aP2</i>	5'-CCTGGTACAGGTGCAGAA-3'	190	58
	5'-TGTCGGGACAATACATCC-3'		
<i>LPL</i>	5'-CACATTCACCAGAGGGTC-3'	177	58
	5'-TCATGGGAGCACTTCACG-3'		
<i>Wnt10b</i>	5'-TTCTCTCGGGATTTCTTGATTCC-3'	118	59
	5'-TGCATTTCCGCTTCAGATTTTC-3'		
<i>MyoD</i>	5'-GGTGACTCAGACGCATCCA-3'	157	57
	5'-ACACCGCAGCATTCTTCC-3'		
<i>α-actin</i>	5'-CGTGGCTACTCCTTCGTGAC-3'	147	58
	5'-GTCTGGCAGCTCGTAGCTCT-3'		
<i>β-actin</i>	5'-CCAGGTCATCACCATCGG-3'	158	-
	5'-CCGTGTTGGCGTAGAGGT-3'		

*PPAR*δ peroxisome proliferator-activated receptor δ, *PPAR*γ peroxisome proliferator-activated receptor γ, *aP2* adipocyte fatty acid-binding protein, *LPL* lipoprotein lipase, *Wnt10b* wingless related MMTV integration site 10b, *MyoD* myogenic differentiation 1

^a Ta optimal PCR annealing temperature

Table 4 Effect of different linseed inclusion period on meat quality in growing-finishing pigs

Item	Addition of linseed before slaughter (days)				SEM	T
	0 (T1) ^a	30 (T2)	60 (T3)	90 (T4)		
Drip loss (wt%)	5.19	5.01	4.83	3.63	0.48	NS
Water holding capacity (wt%)	92.70	92.76	92.64	92.89	0.51	NS
pH ₄₅ ^b	6.47	6.37	6.57	6.58	0.08	NS
Moisture (wt%)	73.73	70.44	73.17	72.77	0.61	NS
Intramuscular fat (wt%)	2.49 ^c	3.64 ^{c,d}	4.26 ^d	4.42 ^d	0.35	L*

T time effect, NS not significant, L significant linear effect to days of linseed diet; * $P < 0.05$

^a The four treatment groups had 6 pigs each, including a control diet group (T1) and three 10% linseed supplementation diet groups (T2, T3 and T4) which differed in diet duration

^b pH₄₅ refer to the pH measured 45 min after slaughter

^{c,d} Means in the same row without common superscripts differ ($P < 0.05$)

performed using SAS software package (version 8.2; SAS Institute, Cary, NC, USA). The basic variable was linseed addition time (days). Linear and quadratic relationships were determined for parameters collected from treatment groups. The data variances were analyzed using a general linear model (PROC GLM, SAS, 1985). The equations which describe quadratic relations were generated by iterative nonlinear least-squares regression. And the equations which describe linear relations were generated by linear regression. The correlations between enrichment of fatty acids and IMF content were also assessed. Data are presented as least squares means. Means were considered statistically different at $P < 0.05$.

Results

Meat Quality

The effects of linseed supplementation in the diets on meat quality in growing-finishing pigs are presented in Table 4. The content of IMF increased linearly ($P < 0.05$) as the time of feeding linseed diet prolonged, whereas no significant difference ($P > 0.05$) was observed for drip loss, water holding capacity, pH₄₅ and moisture in longissimus muscle among treatment groups. In addition, the significant difference ($P < 0.05$) compared with group T1 (0 days) was observed in group T3 (60 days) and group T4 (90 days), but not in group T2 (30 days).

Tissue Fatty Acid Composition

Fatty acids profile of total fat in longissimus muscle was shown in Table 5. Fatty acid analysis of longissimus muscle showed a linear increase ($P < 0.01$) in PUFA and n-3 PUFA content. 18:3n-3, 20:5n-3 and 22:5n-3 content

Table 5 Fatty acid composition (%) of longissimus muscle

Item	Addition of linseed before slaughter (days)				SEM	T
	0 (T1) ^a	30 (T2)	60 (T3)	90 (T4)		
14:0	1.30	1.36	1.26	1.06	0.09	L*
16:0	25.34	24.85	24.06	23.84	0.55	L*
18:0	13.00	12.57	12.23	12.07	0.39	NS
20:0	0.19	0.17	0.18	0.16	0.02	NS
18:1	37.83	36.52	35.78	31.79	1.15	L**
18:2n-6	11.65	12.09	13.03	15.98	0.94	L**
20:4n-6	2.99	2.82	2.30	2.19	0.24	L**
18:3n-3	0.49	2.46	3.32	4.15	0.16	L**
20:5n-3	0.13	0.46	0.61	1.13	0.10	L**
22:5n-3	0.34	0.56	0.65	0.96	0.06	L**
22:6n-3	0.15	0.15	0.16	0.40	0.02	Q**
n-6 PUFA ^b	15.43	15.53	15.82	18.68	1.07	L*
n-3 PUFA	1.11	3.93	5.16	7.13	0.19	L**
SFA	40.17	39.22	38.02	37.42	0.75	L**
PUFA	16.80	19.73	21.27	26.12	1.13	L**

The fatty acid results were presented as g/100 g fatty acids (wt%)

T time effect, NS not significant, L significant linear effect to days of linseed diet, Q significant quadratic effect to days of linseed diet; * $P < 0.05$; ** $P < 0.01$

^a The four treatment groups had 6 pigs each, including a control diet group (T1) and three 10% linseed supplementation diet groups (T2, T3 and T4) which differed in diet duration

^b n-6 polyunsaturated fatty acids (n-6 PUFA) percentage is the sum of 18:2n-6 and 20:4n-6; n-3 polyunsaturated fatty acids (n-3 PUFA) percentage is the sum of 18:3n-3, 20:5n-3, 22:5n-3 and 22:6n-3; saturated fatty acids (SFA) percentage is the sum of 14:0, 16:0, 18:0 and 20:0; polyunsaturated fatty acids (PUFA) percentage was calculated as the sum of n-3 PUFA and n-6 PUFA

increased linearly ($P < 0.01$) in longissimus muscle too, whereas 22:6n-3 content in longissimus muscle increased quadratically ($P < 0.01$) as linseed diet feeding time increased.

Table 6 Effects of different linseed inclusion period on relative expression of genes in longissimus muscle

Item	Addition of linseed before slaughter (days)				SEM	T
	0 (T1) ^a	30 (T2)	60 (T3)	90 (T4)		
<i>PPAR</i> δ	1.35 ^b	1.43 ^{b,c}	1.65 ^{c,d}	1.78 ^d	0.086	L**
<i>PPAR</i> γ	1.15 ^b	1.32 ^{b,c}	1.50 ^{c,d}	1.71 ^d	0.070	L**
<i>aP2</i>	1.20 ^b	1.38 ^b	1.79 ^c	2.03 ^c	0.109	L**
<i>LPL</i>	1.20 ^b	1.56 ^c	1.64 ^c	1.70 ^c	0.092	L**
<i>Wnt10b</i>	1.40 ^b	1.42 ^b	0.92 ^c	0.84 ^c	0.103	L**
<i>MyoD</i>	0.99	1.16	1.07	1.17	0.105	NS
<i>α-actin</i>	1.03 ^b	0.63 ^c	0.40 ^d	0.55 ^{c,d}	0.070	Q**

Values of real-time PCR are presented as a ratio of the specified gene signal normalized to the *β-actin* signal using the $2^{-\Delta\Delta Ct}$ method

*PPAR*δ peroxisome proliferator-activated receptor δ, *PPAR*γ peroxisome proliferator-activated receptor γ, *aP2* adipocyte fatty acid-binding protein, *LPL* lipoprotein lipase, *Wnt10b* wingless related MMTV integration site 10b, *MyoD* myogenic differentiation 1

T time effect, NS not significant, L significant linear effect to days of linseed diet, Q significant quadratic effect to days of linseed diet; ***P* < 0.01

^a The four treatment groups had 6 pigs each, included a control diet group (T1) and three 10% linseed supplementation diet groups (T2, T3 and T4) which differed in diet duration

^{b,c,d} Means in the same row without common superscripts differ significantly (*P* < 0.05)

Gene Expression in Longissimus Muscle

The genes having a positive effect (*PPAR*δ, *PPAR*γ, *aP2* and *LPL*) and a negative effect (*Wnt10b*) on adipogenesis were determined using real-time PCR. The genes involved in myogenesis (*MyoD* and *α-actin*) were determined as well. Relative mRNA levels of the genes were all normalized to *β-actin* signals. The results are presented in Table 6 and show that relative expression levels of *PPAR*δ, *PPAR*γ, *aP2* and *LPL* were all increased (*P* < 0.01) linearly with increasing duration of feeding linseed diet. And the relative expression level of *Wnt10b* linearly decreased (*P* < 0.01), while the relative expression level of *α-actin* quadratically decreased (*P* < 0.01) with the increasing time on linseed diet. No significant difference (*P* > 0.05) was observed for the relative expression level of *MyoD* among groups. In addition, the significant changes (*P* < 0.05) in expression levels of *PPAR*δ, *PPAR*γ, *aP2* and *Wnt10b* occurred after 60 days of feeding a 10% linseed diet, while those of *LPL* and *α-actin* occurred after 30 days of treatment (Table 6).

Correlations between Enrichment of Fatty Acids and Intramuscular Fat Content

The simple correlation analysis was conducted to evaluate the correlations between enrichment of fatty acids in longissimus muscle and intramuscular fat content. As shown in

Table 7 Correlations between enrichment of fatty acids and intramuscular fat content

Item	IMF content	
	<i>r</i>	<i>P</i>
14:0 enrichment	−0.347 ^a	0.097
16:0 enrichment	−0.439	0.032
18:0 enrichment	−0.398	0.054
20:0 enrichment	−0.357	0.087
18:1 enrichment	−0.522	0.009
18:2n-6 enrichment	0.457	0.025
20:4n-6 enrichment	−0.431	0.035
18:3n-3 enrichment	0.832	<0.001
20:5n-3 enrichment	0.787	<0.001
22:5n-3 enrichment	0.722	<0.001
22:6n-3 enrichment	0.691	<0.001
n-6 PUFA enrichment	0.312	0.138
n-3 PUFA enrichment	0.870	<0.001
SFA enrichment	−0.538	0.007
PUFA enrichment	0.666	<0.001

IMF intramuscular fat, n-3 PUFA n-3 polyunsaturated fatty acids, n-6 PUFA n-6 polyunsaturated fatty acids, PUFA sum of n-3 PUFA and n-6 PUFA

^a Correlation coefficient between two items

Table 7, 18:2n-6, 18:3n-3, 20:5n-3, 22:5n-3, 22:6n-3, n-3 PUFA and PUFA enrichment were all positively correlated with IMF content (*P* < 0.01), and the greatest correlation coefficient was observed between n-3 PUFA enrichment and IMF content, whereas no significant correlation of n-6 PUFA to IMF content was found (*P* = 0.138).

Regressions between n-3 PUFA Enrichment and Intramuscular Fat Content or Gene Expressions

The results of regressions between n-3 PUFA enrichment and IMF content or gene expressions are presented in Table 8. A significant (*P* < 0.01) quadratic relation was found between n-3 PUFA enrichment and IMF content (Table 8; Fig. 1). There was a statistically significant (*P* < 0.01) linear relation between n-3 PUFA enrichment and the expression of *PPAR*δ or *LPL*, while significant (*P* < 0.01) quadratic relation was found between n-3 PUFA enrichment and the expression of *PPAR*γ, *aP2*, *Wnt10b* or *α-actin* (Table 8).

Regressions between Gene Expressions and Intramuscular Fat Content

The results of regressions between gene expressions and IMF content were presented in Table 9. There was

Table 8 Regressions between n-3 PUFA enrichment and intramuscular fat content or gene expressions

Item ^a	n-3 PUFA enrichment (X)		
	Regressive equations	R ²	E ^b
IMF content (Y)	$Y = 0.0320 X^2 + 0.0753 X + 2.5344$	0.79	Q**
<i>PPAR</i> δ	$Y = 0.0802 X + 1.1828$	0.44	L**
<i>PPAR</i> γ	$Y = 0.0111 X^2 + 1.1580$	0.62	Q**
<i>aP2</i>	$Y = 0.0187 X^2 + 1.1560$	0.73	Q**
<i>LPL</i>	$Y = 0.0849 X + 1.1550$	0.44	L**
<i>Wnt10b</i>	$Y = -0.0129 X^2 + 1.4501$	0.49	Q**
<i>α-actin</i>	$Y = 0.0250 X^2 - 0.2923 X + 1.3267$	0.63	Q**

IMF intramuscular fat, n-3 PUFA total n-3 polyunsaturated fatty acids, *PPAR*δ peroxisome proliferator-activated receptor δ, *PPAR*γ peroxisome proliferator-activated receptor γ, *aP2* adipocyte fatty acid-binding protein, *LPL* lipoprotein lipase, *Wnt10b* wingless related MMTV integration site 10b

^a In the regression analysis, n-3 PUFA enrichment was used as independent variable (X), while IMF content and the expression of *PPAR*δ, *PPAR*γ, *aP2*, *LPL*, *Wnt10b* and *α-actin* were used as dependent variables (Y)

^b E effect of two items; L and Q are significant linear and quadratic effect of two items, respectively; ** $P < 0.01$

statistically significant ($P < 0.01$) quadratic or linear relation between the expression of *PPAR*γ, *aP2*, *Wnt10b* or *α-actin* and IMF content in longissimus muscle (Table 9; Figs. 2, 3, 4 and 5), whereas no significant linear or quadratic relation was found between the expression of *PPAR*δ or *LPL* and IMF content in longissimus muscle (Table 9).

Discussion

Intramuscular adipose site is a later developing tissue [6, 28]. The major increase in IMF begins after 16 weeks of age in pigs and the number of intramuscular adipocytes does not reach a plateau even at 24 weeks but continues to increase [6]. It is well known that traits of animals are developed in a specific growth and development period and the traits are more likely to be influenced during this period. Based on these facts, the trial period (from 80 to 170 days of age) of pigs was designed in the current study. The result of the present study showed that IMF content increased linearly ($P < 0.05$) along with the increasing time on a linseed diet without affecting drip loss, water holding capacity, pH₄₅ and moisture in longissimus muscle among treatment groups (Table 4). In addition, average daily feed intake was also not affected by the treatment [29]. Noteworthy, the significant difference ($P < 0.05$) in IMF content compared with group T1 (0 days) was observed in group T3 (60 days) and T4 (90 days), but not in group T2 (30 days), suggesting that a certain length of duration of feeding linseed diet has to be reached in order

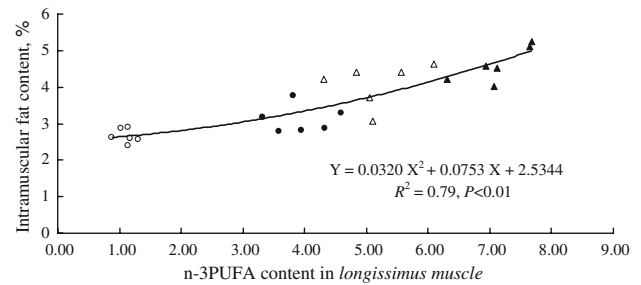


Fig. 1 The quadratic relation between n-3 PUFA content and intramuscular fat content in longissimus muscle. The inclusion of linseed in diets was initiated at the last 0 days (open circles), 30 days (filled circles), 60 days (open triangles) and 90 days (filled triangles) before slaughter, respectively. These data were represented in Table 4 (for the intramuscular fat content), Table 5 (for the n-3 PUFA content). The fatty acid results were presented as g/100 g fatty acids (wt%)

Table 9 Regressions between gene expressions and intramuscular fat content

Item ^a	IMF content (Y)		
	Regressive equations	R ²	E ^b
<i>PPAR</i> δ (X)			NS
<i>PPAR</i> γ	$Y = 0.9945 X^2 + 1.5422$	0.72	Q**
<i>aP2</i>	$Y = 1.8201 X + 0.7074$	0.75	L**
<i>LPL</i>			NS
<i>Wnt10b</i>	$Y = -2.0931 X + 6.0119$	0.71	L**
<i>α-actin</i>	$Y = -2.0237 X + 4.9392$	0.44	L**

IMF intramuscular fat, *PPAR*δ peroxisome proliferator-activated receptor δ, *PPAR*γ peroxisome proliferator-activated receptor γ, *aP2* adipocyte fatty acid-binding protein, *LPL* lipoprotein lipase, *Wnt10b* wingless related MMTV integration site 10b

E effect of two items; L and Q are significant linear and quadratic effect of two items, respectively, NS not significant, ** $P < 0.01$

^a In the regression analysis, the expression of *PPAR*δ, *PPAR*γ, *aP2*, *LPL*, *Wnt10b* and *α-actin* were used as independent variables (X), while IMF content was used as dependent variable (Y)

to influence the IMF content. However, the current result of intramuscular fat was inconsistent with other studies where no significant change was found by feeding a linseed diet [30–37]. As Zhan et al. [29] pointed out, the stimulatory effect of linseed on growth may not be significant when the level added is less than 5% or the feeding duration is shorter than 60 days in growing-finishing pigs, the effect of linseed on IMF content may exhibit a similar pattern. The inconsistent results of those studies might be due to differences in trial designs, such as: lower dietary linseed or ALA level [30–34]; short linseed feeding duration [33, 35] and not adopting isoenergetic, isonitrogenous and isolipidic diets [36, 37].

In the present study, n-3 PUFA content in longissimus muscle of pig was raised linearly by feeding linseed diet

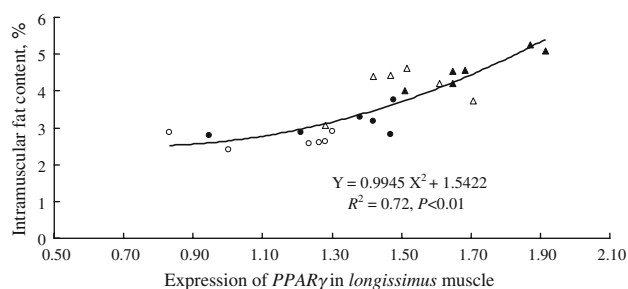


Fig. 2 The quadratic relation between expression of *peroxisome proliferator-activated receptor γ* (*PPAR γ*) and intramuscular fat content in longissimus muscle. The inclusion of linseed in diets was initiated at the last 0 days (*open circles*), 30 days (*filled circles*), 60 days (*open triangles*) and 90 days (*filled triangles*) before slaughter, respectively. These data are presented in Table 4 (for the intramuscular fat content), Table 6 (for the expression of *PPAR γ*)

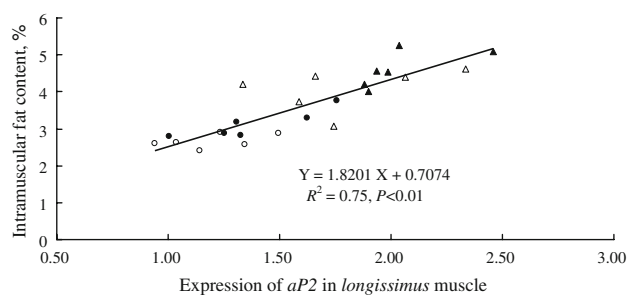


Fig. 3 The linear relation between expression of *adipocyte fatty acid-binding protein* (*aP2*) and intramuscular fat content in longissimus muscle. The inclusion of linseed in diets was initiated at the last 0 days (*open circles*), 30 days (*filled circles*), 60 days (*open triangles*) and 90 days (*filled triangles*) before slaughter, respectively. These data are presented in Table 4 (for the intramuscular fat content), Table 6 (for the expression of *aP2*)

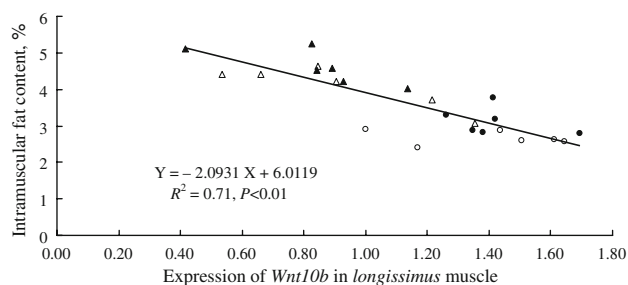


Fig. 4 The linear relation between expression of *wingless related MMTV integration site 10b* (*Wnt10b*) and intramuscular fat content in longissimus muscle. The inclusion of linseed in diets was initiated at the last 0 days (*open circles*), 30 days (*filled circles*), 60 days (*open triangles*) and 90 days (*filled triangles*) before slaughter, respectively. These data are presented in Table 4 (for the intramuscular fat content), Table 6 (for the expression of *Wnt10b*)

(Table 5), which was in general agreement with other studies [35]. Among 18:2n-6, 18:3n-3, 20:5n-3, 22:5n-3, 22:6n-3, n-3 PUFA and PUFA enrichment which were all positively correlated with IMF content, the greatest

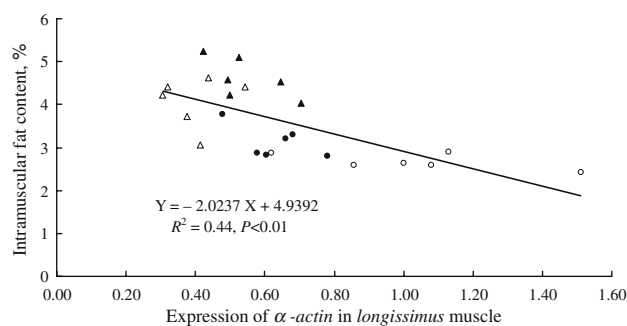


Fig. 5 The linear relation between expression of α -actin and intramuscular fat content in longissimus muscle. The inclusion of linseed in diets was initiated at the last 0 days (*open circles*), 30 days (*filled circles*), 60 days (*open triangles*) and 90 days (*filled triangles*) before slaughter, respectively. These data are presented in Table 4 (for the intramuscular fat content), Table 6 (for the expression of α -actin)

correlation coefficient with IMF content was observed in n-3 PUFA enrichment, implying the highest correlation between n-3 PUFA enrichment and IMF content (Table 7). Moreover, regression analysis showed that enhancement of the IMF content was quadratically related to n-3 PUFA enrichment and n-3 PUFA enrichment could explain 79% of IMF content variation through the regressive equation (Table 8; Fig. 1). These results suggested that, of all the fatty acids, n-3 PUFA enrichment in muscle may play the most important role for IMF deposition extent in the context of our trial, coinciding with its dramatic fold change (from 1.11 to 7.13%, 6.42 times) in longissimus muscle. Moreover, the significant difference ($P < 0.05$) in IMF content was first found in group T3 (60 days) with an n-3 PUFA enrichment of 5.16%, implying certain n-3 PUFA enrichment may be required for efficiently affecting IMF deposition. It seems confusing that the present result was inconsistent with other studies where a negative correlation was found between PUFA enrichment and IMF content [34, 38]. However, in those studies, the PUFA enrichment especially n-3 PUFA enrichment in muscle was much lower than that of present study. And the low level of the n-3 PUFA enrichment in muscle may not be sufficient to affect IMF deposition. And the increase of IMF content in those studies is probably due to the increase of neutral lipids in the intramuscular adipocytes which lead to a dilution of phospholipids rich in PUFA and result in the decrease in PUFA content [39]. In contrast, the increase of IMF content in present study might be caused by the stimulatory effect of high enrichment of PUFA, especially n-3 PUFA.

Dietary n-3 PUFA has been demonstrated to affect diverse physiological processes such as the regulation of plasma lipid levels, cardiovascular and immune function, insulin action, neuronal development and visual function

[40]. However, the influence of IMF deposition by n-3 PUFA is seldom documented.

PUFA including n-3 PUFA or its derivatives can directly act at the level of nucleus to influence the transcription activity of transcription factors and in turn the transcription of their target genes responding to diverse cellular processes including adipogenesis [41]. Therefore, the expression levels of the genes involved in adipogenesis were assessed and the result showed that the expression of *PPAR δ* , *PPAR γ* , *aP2*, *LPL* and *Wnt10b* all exhibited a significant ($P < 0.01$) linear response to the duration of feeding linseed diet (Table 6), implying a time-dependent manner. Meanwhile, a significant ($P < 0.01$) quadratic or linear relation was observed between the n-3 PUFA enrichment and the expression of these genes (Table 8), suggesting that the expression of these genes were influenced by the n-3 PUFA enrichment in longissimus muscle in a dose-dependent manner. In addition, the significant changes in expression levels of *PPAR δ* , *PPAR γ* , *aP2* and *Wnt10b* occurred after 60 days of feeding 10% linseed diet, while that of *LPL* occurred after 30 days (Table 6), suggesting that affecting certain genes expression may need certain duration of feeding linseed diet and certain enrichment of n-3 PUFA as well.

Peroxisome proliferator-activated receptors (PPARs) belong to the steroid hormone nuclear receptor superfamily of ligand-activated transcription factors [42]. Two isoforms of PPARs, *PPAR δ* and *PPAR γ* are documented as positive regulators involved in adipogenesis [13]. *PPAR δ* is a widely expressed in all tissues and is the main PPAR isoform expressed in skeletal muscle [43, 44]. Although *PPAR δ* was described for its role in fatty acid oxidation in several tissues [45], gain-of-function experiments suggested that both *PPAR δ* and *PPAR γ* isoforms are required to facilitate maximal lipid accumulation and differentiation during adipogenesis [14]. Furthermore, *PPAR δ* is demonstrated not directly involved in the regulation of adipose terminal differentiation, but is implicated in control by long chain fatty acids of *PPAR γ* gene expression [13]. In the current study, a linear relation between n-3 PUFA enrichment and *PPAR δ* mRNA abundance suggested that *PPAR δ* was directly upregulated by n-3 PUFA which may be good ligands of *PPAR δ* , which corresponded with other studies [46, 47]. A quadratic relation was also observed between n-3 PUFA enrichment and the expression of *PPAR γ* (Table 8). However, fatty acids including n-3 PUFA are proved to be poor activators of *PPAR γ* [47–49], thus, the inducing expression of *PPAR γ* seemed not to be direct action by n-3 PUFA. Instead, it could be due to the effect of *PPAR δ* which was directly activated by n-3 PUFA. Similar result was reported by Kronberg et al. [50] that feeding linseed diet to increase n-3 PUFA enrichment in bovine muscle upregulated *PPAR γ* expression in muscle tissue.

PPAR γ which is predominantly expressed in adipose tissues, is a central regulator during adipogenesis [9], and activation of *PPAR γ* can promote stem cells or preadipocytes to differentiate into adipocytes [51]. A relative high expression of *PPAR γ* was detected in the current study, revealing high adipogenesis in the skeletal muscle, which was consistent with the high amount of IMF content. However, the expression of *PPAR γ* in skeletal muscle failed to be detected in pigs of 30 kg weight [52]. This may be due to the fact that development of IMF was not predominant in the 30-kg weight stage, coinciding with the result that the major increase in IMF begins after 16 weeks of age in pigs [6]. Moreover, a statistically significant ($P < 0.01$) quadratic relation was observed between the expression of *PPAR γ* and IMF content in longissimus muscle (Table 9; Fig. 2), suggesting that the increasing of IMF content was directly related to the enhancement of adipogenesis and the expression of *PPAR γ* in skeletal muscle would be an important determinant of the extent of the IMF deposition. However, no significant ($P > 0.05$) linear or quadratic relation was found between the expression of *PPAR δ* and IMF content (Table 9), which implies that *PPAR δ* may act as an activator of *PPAR γ* , rather than directly affecting adipocytes differentiation, and the action of *PPAR δ* was different from that of *PPAR γ* which is the direct factor that determines the differentiation of adipocytes from preadipocytes or stem cells [51].

Due to the increasing expression of *PPAR γ* , the expression of two target genes of *PPAR γ* , *aP2* and *LPL* were also linearly increased ($P < 0.01$) along with increasing time on linseed diet. *aP2* is adipocyte specific fatty acid binding protein, directly participates in fatty acid uptake and transport process of intramuscular adipocytes [53]. And the *LPL* can hydrolyze the lipoprotein triacylglycerols from cycling and release free fatty acid for skeletal muscle uptake [54], so *LPL* directly participates in IMF deposition. The increasing expression of the two genes indicated that the ability to uptake exogenous fatty acid and afterward synthesize triacylglycerols could be increased, which could increase IMF deposition. Furthermore, statistically significant ($P < 0.01$) linear relation was observed between the expression of *aP2* and IMF content in longissimus muscle (Table 9; Fig. 3), corresponding with other results [55], but no significant ($P > 0.05$) linear or quadratic relation was observed between the expression of *LPL* and IMF content (Table 9). This may be because *aP2* is an adipocyte-specific gene which is known to be a later marker of adipogenesis, whereas *LPL* is widely expressed in most cell types not only functioning in adipocytes [53, 54].

Wnt/ β -Catenin signaling is demonstrated as the main negative regulator to repress adipogenesis and maintain the undifferentiated state of preadipocytes [11, 56]. Activation

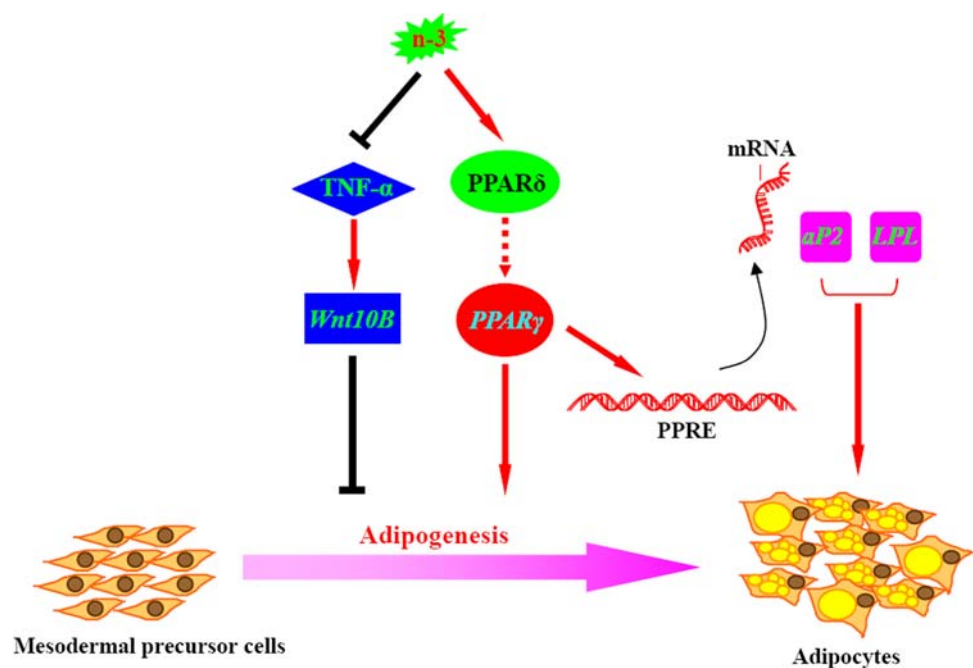
of Wnt/ β -Catenin signaling is mediated by paracrine and/or autocrine production of members of Wnt family of secreted polypeptides [56]. Wnt10b is one of the main endogenous Wnt signaling molecules, and is highly expressed in stromal vascular cells, which are enriched in preadipocytes, but not in mature adipocytes [12]. Suppressing the expression of Wnt10b is needed for adipogenesis [11]. It has been demonstrated that skeletal muscle is an endocrine tissue, capable of expressing a wide range of molecules with endocrine actions [57]. Wnt10b mRNA was detected in the present study, suggesting that Wnt10b may serve as an endogenous inhibitor of adipogenesis in skeletal muscle, i.e. as the inhibitor of the IMF deposition. The Wnt10b expression level was quadratically decreased with the enhancement of n-3 PUFA enrichment in the present study (Table 8), implying that the transcription of Wnt10b was inhibited by n-3 PUFA. Similar result was reported that n-3 PUFA could inhibit Wnt/ β -Catenin signaling in cell cultures, but without mention about Wnt10b [17]. It is not surprising that Wnt10b could be inhibited by n-3 PUFA. It was demonstrated that Wnt10b expression can be upregulated by proinflammatory cytokine tumor necrosis factor- α (TNF- α) [58]. Meanwhile, dietary n-3 PUFA was reported to decrease the production of TNF- α in different animal species [59–61]. Previous work of our research team also revealed that the serum concentration of TNF- α as well as the expression level of TNF- α in skeletal muscle both linearly decreased with duration of linseed diet [29], therefore, the downregulation of Wnt10b expression may be due to the inhibition on production of TNF- α by dietary n-3 PUFA. Interestingly, a linear relation was observed

between expression of Wnt10b and IMF content (Table 9; Fig. 4), suggesting that extent of inhibition of Wnt10b expression was another determinant of the extent of the IMF deposition.

Two genes involved in myogenesis were also assessed in the present study. The expression of MyoD which is expressed in the early stages of myogenesis [62] was not affected by the treatment (Table 6), implying that n-3 PUFA might not influence the early myogenesis processes. However, it was interesting that the relative expression level of α -actin which is a late marker of myogenesis quadratically decreased ($P < 0.01$) with the increasing of n-3 PUFA enrichment (Table 8), suggesting that myogenesis might be inhibited by n-3 PUFA during the late growing-finishing period of pigs. In addition, the linear relation between expression level of α -actin and IMF content suggested that the enhancement of adipogenesis might be accompanied by decrease in myogenesis (Table 9; Fig. 5). Similar result was observed that the expression of α -actin decreased with the IMF content increasing in cattle between early and late fattening stages [63]. Several studies also reported that inhibition myogenesis could induce adipogenic process in myogenic cell lines [64–66], which implicated that the decrease in myogenesis might to some extent be involved in the enhancing of adipogenesis by n-3 PUFA enriched in skeletal muscle in the present study.

In conclusion, increasing the n-3 PUFA enrichment in the skeletal muscle of growing-finishing pigs by feeding linseed could activate PPAR δ , which may subsequently upregulate the expression of PPAR γ to promote

Fig. 6 The pathways of adipogenesis potential to be affected by n-3 PUFA in skeletal muscle. n-3 PUFA enrichment in the skeletal muscle could activate peroxisome proliferator-activated receptor δ (PPAR δ), which may subsequently upregulate the expression of PPAR γ and then the target genes of PPAR γ (such as adipocyte fatty acid-binding protein (aP2) and lipoprotein lipase (LPL)) to promote adipogenesis; n-3 PUFA could also inhibit the producing of tumor necrosis factor- α (TNF α) and then decrease the expression of wingless related MMTV integration site 10b (Wnt10b), so as to release the inhibition of adipogenesis by Wnt signaling



adipogenesis. Meanwhile, n-3 PUFA enriched in the skeletal muscle could also decrease the expression of *Wnt10b* and *Wnt/β-Catenin* signaling to release the inhibition of adipogenesis, consequently increasing IMF deposition (Fig. 6). Sufficient n-3 PUFA enrichment (5.16% in the present study) in skeletal muscle may be required for efficiently affecting the expression of genes involved in adipogenesis, and further influencing IMF deposition.

Implication

IMF content is an important determinant of meat eating quality. In the present study, we revealed that including linseed (rich in n-3 PUFA) in the diet could increase the IMF content of pigs, which might then enhance the eating quality of pork. The result indicates that IMF content could be manipulated by dietary nutrients. Dietary nutrients can regulate metabolism and genes expression in tissues, the investigation of nutritional regulation pathways and mechanisms of IMF deposition would provide a basis for nutritional manipulation of IMF, and also facilitate successful regulation of improving IMF content and meat eating quality.

Acknowledgments This research was supported by the National High Technology R & D Program of China (No. 2006AA10Z140), National Natural Science Foundation of China (No. 30871779) and Major Science & Technology Industrialization Projects in Wuhan City of China (No. 200720112026). All authors contributed to the preparation of the paper and agreed with the submitted manuscript content.

Conflict of interest statement None.

References

- Verbeke W, Van Oeckel MJ, Warnants N, Viaene J, Boucque CV (1999) Consumer perception, facts and possibilities to improve acceptability of health and sensory characteristics of pork. *Meat Sci* 53:77–99
- Poulos SP, Hausman GJ (2005) Intramuscular adipocytes-potential to prevent lipotoxicity in skeletal muscle. *Adipocytes* 1:79–94
- Young HE, Mancini ML, Wright RP, Smith JC, Black AC Jr, Reagan CR, Lucas PA (1995) Mesenchymal stem cells reside within the connective tissues of many organs. *Dev Dyn* 202:137–144
- Shepherd PR, Gnudi L, Tozzo E, Yang H, Leach F, Kahn BB (1993) Adipose cell hyperplasia and enhanced glucose disposal in transgenic mice overexpressing GLUT4 selectively in adipose tissue. *J Biol Chem* 268:22243–22246
- Gerbens F (2004) Genetic control of intramuscular fat accretion. In: MFW te Pas, Everts ME, Haagsman HP (ed) *Muscle development of livestock animals: physiology, genetics and meat quality*. CABI Publishing, London
- Lee YB, Kauffman RG (1974) Cellular and enzymatic changes with animal growth in porcine intramuscular adipose tissue. *J Anim Sci* 38:532–537
- Farmer SR (2006) Transcriptional control of adipocyte formation. *Cell Metab* 4:263–273
- Rosen ED, Walkey CJ, Puigserver P, Spiegelman BM (2000) Transcriptional regulation of adipogenesis. *Genes Dev* 14:1293–1307
- Otto TC, Lane MD (2005) Adipose development: from stem cell to adipocyte. *Crit Rev Biochem Mol Biol* 40:229–242
- Rosen ED, MacDougald OA (2006) Adipocyte differentiation from the inside out. *Nat Rev Mol Cell Biol* 7:885–896
- Ross SE, Hemati N, Longo KA, Bennett CN, Lucas PC, Erickson RL, MacDougald OA (2000) Inhibition of adipogenesis by Wnt signaling. *Science* 289:950–953
- Prestwich TC, Macdougald OA (2007) Wnt/beta-catenin signaling in adipogenesis and metabolism. *Curr Opin Cell Biol* 19:612–617
- Grimaldi PA (2001) The roles of PPARs in adipocyte differentiation. *Prog Lipid Res* 40:269–281
- Matsusue K, Peters JM, Gonzalez FJ (2004) PPARbeta/delta potentiates PPARgamma-stimulated adipocyte differentiation. *FASEB J* 18:1477–1479
- Grimaldi PA (2007) Peroxisome proliferator-activated receptors as sensors of fatty acids and derivatives. *Cell Mol Life Sci* 64:2459–2464
- MacLaren LA, Guzeloglu A, Michel F, Thatcher WW (2006) Peroxisome proliferator-activated receptor (PPAR) expression in cultured bovine endometrial cells and response to omega-3 fatty acid, growth hormone and agonist stimulation in relation to series 2 prostaglandin production. *Domest Anim Endocrinol* 30:155–169
- Lim K, Han C, Xu L, Isse K, Demetris AJ, Wu T (2008) Cyclooxygenase-2-derived prostaglandin E2 activates beta-catenin in human cholangiocarcinoma cells: evidence for inhibition of these signaling pathways by omega 3 polyunsaturated fatty acids. *Cancer Res* 68:553–560
- Hsu JM, Wang PH, Liu BH, Ding ST (2004) The effect of dietary docosahexaenoic acid on the expression of porcine lipid metabolism-related genes. *J Anim Sci* 82:683–689
- Wood JD, Richardson RI, Nute GR, Fisher AV, Campo MM, Kasapidou E, Sheard PR, Enser M (2004) Effects of fatty acids on meat quality: a review. *Meat Sci* 66:21–32
- Wierbicki E, Deatherage FE (1958) Water content of meats, determination of water-holding capacity of fresh meats. *J Agric Food Chem* 6:387–392
- Xiong YZ, Deng CY (1999) *Principle and method of swine testing*. Chinese Agriculture Press, Beijing
- Bourke RS, Nelson KM, Naumann RA, Young OM (1970) Studies of the production and subsequent reduction swelling in primate: cerebral cortex under isosmotic conditions in vivo. *Exp Brain Res* 10:427–446
- Bligh EG, Dyer WJ (1959) A rapid method of total lipid extraction and purification. *Can J Biochem Physiol* 37:911–917
- Folch J, Lees M, Sloane Stanley GH (1957) A simple method for the isolation and purification of total lipids from animal tissues. *J Biol Chem* 226:497–509
- Demirel G, Wachira AM, Sinclair LA, Wilkinson RG, Wood JD, Enser M (2004) Effects of dietary n-3 polyunsaturated fatty acids, breed and dietary vitamin E on the fatty acids of lamb muscle, liver and adipose tissue. *Br J Nutr* 91:551–565
- Enser M, Hallett KG, Hewett B, Fursey GAJ, Wood JD, Harrington G (1998) The polyunsaturated fatty acid composition of beef and lamb liver. *Meat Sci* 49:321–327
- Livak K, Schmittgen T (2001) Analysis of relative gene expression data using real-time quantitative PCR and the $2^{-\Delta\Delta Ct}$ method. *Methods* 25:402–408
- Harper GS, Pethick DW (2004) How might marbling begin? *Aust J Exp Agr* 44:653–662

29. Zhan ZP, Huang FR, Luo J, Dai JJ, Yan XH, Peng J (2009) Duration of feeding linseed diet influences expression of inflammation-related genes and growth performance of growing-finishing barrows. *J Anim Sci* 87:603–611
30. Warnants N, Van Oeckel MJ, Boucqué CHV (1996) Incorporation of dietary polyunsaturated fatty acids in pork tissues and its implications for the quality of the end products. *Meat Sci* 44:125–144
31. Enser M, Richardson RI, Wood JD, Gill BP, Sheard PR (2000) Feeding linseed to increase the n-3 PUFA of pork: fatty acid composition of muscle, adipose tissue, liver and sausages. *Meat Sci* 55:201–212
32. Leskanich CO, Matthews KR, Warkup CC, Noble RC, Hazzledine M (1997) The effect of dietary oil containing (n-3) fatty acids on the fatty acid, physicochemical, and organoleptic characteristics of pig meat and fat. *J Anim Sci* 75:673–683
33. Riley PA, Enser M, Nute GR, Wood JD (2000) Effects of dietary linseed on nutritional value and other quality aspects of pig muscle and adipose tissue. *Anim Sci* 71:483–500
34. Van Oeckel MJ, Casteels M, Warnants N, Van Damme L, Boucqué ChV (1996) Omega-3 fatty acids in pig nutrition: Implications for the intrinsic and sensory quality of the meat. *Meat Sci* 44:55–63
35. Romans JR, Johnson RC, Wulf DM, Libal GW, Costello WJ (1995) Effects of ground flaxseed in swine diets on pig performance and on physical and sensory characteristics and omega-3 fatty acid content of pork: I. Dietary level of flaxseed. *J Anim Sci* 73:1982–1986
36. Kouba M, Enser M, Whittington FM, Nute GR, Wood JD (2003) Effect of a high-linolenic acid diet on lipogenic enzyme activities, fatty acid composition, and meat quality in the growing pig. *J Anim Sci* 81:1967–1979
37. Specht-Overholt S, Romans JR, Marchello MJ, Izard RS, Crews MG, Simon DM, Costello WJ, Evenson PD (1997) Fatty acid composition of commercially manufactured omega-3 enriched pork products, haddock, and mackerel. *J Anim Sci* 75:2335–2343
38. Högberg A, Pickova J, Andersson K, Lundström K (2003) Fatty acid composition and tocopherol content of muscle in pigs fed organic and conventional feed with different n6/n3 ratios, respectively. *Food Chem* 80:177–186
39. Cameron ND, Enser MB (1991) Fatty acid composition of lipid in Longissimus dorsi muscle of Duroc and British Landrace pigs and its relationship with eating quality. *Meat Sci* 29:295–307
40. Jump DB (2002) The biochemistry of n-3 polyunsaturated fatty acids. *J Biol Chem* 277:8755–8758
41. Sampath H, Ntambi JM (2005) Polyunsaturated fatty acid regulation of genes of lipid metabolism. *Annu Rev Nutr* 25:317–340
42. Lee C-H, Olson P, Vans RM (2003) Minireview: lipid metabolism, metabolic diseases, and peroxisome proliferator-activated receptors. *Endocrinology* 144:2201–2207
43. Escher P, Braissant O, Basu-Modak S, Michalik L, Wahli W, Desvergne B (2001) Rat PPARs: quantitative analysis in adult rat tissues and regulation in fasting and refeeding. *Endocrinology* 142:4195–4202
44. Tanaka T, Yamamoto J, Iwasaki S et al (2003) Activation of peroxisome proliferator-activated receptor delta induces fatty acid beta-oxidation in skeletal muscle and attenuates metabolic syndrome. *Proc Natl Acad Sci USA* 100:15924–15929
45. Fredenrich A, Grimaldi PA (2005) PPAR delta: an incompletely known nuclear receptor. *Diabetes Metab* 31:23–27
46. Amri EZ, Bonino F, Ailhaud G, Abumrad NA, Grimaldi PA (1995) Cloning of a protein that mediates transcriptional effects of fatty acids in preadipocytes: homology to peroxisome proliferator-activated receptors. *J Biol Chem* 270:2367–2371
47. Forman BM, Chen J, Evans RM (1997) Hypolipidemic drugs, polyunsaturated fatty acids, and eicosanoids are ligands for peroxisome proliferator-activated receptors alpha and delta. *Proc Natl Acad Sci USA* 94:4312–4317
48. Kliewer SA, Forman BM, Blumberg B, Ong ES, Borgmeyer U, Mangelsdorf DJ, Umesono K, Evans RM (1994) Differential expression and activation of a family of murine peroxisome proliferator-activated receptors. *Proc Natl Acad Sci USA* 91:7355–7359
49. Tontonoz P, Nagy L, Alvarez JG, Thomazy VA, Evans RM (1998) PPARgamma promotes monocyte/macrophage differentiation and uptake of oxidized LDL. *Cell* 93:241–252
50. Kronberg SL, Barcelo-Coblijn G, Shin J, Lee K, Murphy EJ (2006) Bovine muscle n-3 fatty acid content is increased with flaxseed feeding. *Lipids* 41:1059–1068
51. Valet P, Tavernier G, Castan-Laurell I, Saulnier-Blache JS, Langin D (2002) Understanding adipose tissue development from transgenic animal models. *J Lipid Res* 43:835–860
52. Ding ST, Schinckel AP, Weber TE, Mersmann HJ (2000) Expression of porcine transcription factors and genes related to fatty acid metabolism in different tissues and genetic populations. *J Anim Sci* 78:2127–2134
53. Haunerland NH, Spener F (2004) Fatty acid-binding proteins—insights from genetic manipulations. *Prog Lipid Res* 43:328–349
54. Goldberg IJ (1996) Lipoprotein lipase and lipolysis: central roles in lipoprotein metabolism and atherogenesis. *J Lipid Res* 37:693–707
55. Wang YH, Byrne KA, Reverter A, Harper GS, Taniguchi M, McWilliam SM, Mannen H, Oyama K, Lehnert SA (2005) Transcriptional profiling of skeletal muscle tissue from two breeds of cattle. *Mamm Genome* 16:201–210
56. Moldes M, Zuo Y, Morrison RF, Silva D, Park BH, Liu J, Farmer SR (2003) Peroxisome-proliferator-activated receptor gamma suppresses Wnt/beta-catenin signalling during adipogenesis. *Biochem J* 376:607–613
57. Argiles JM, Lopez-Soriano J, Almendro V, Busquets S, Lopez-Soriano FJ (2005) Cross-talk between skeletal muscle and adipose tissue: a link with obesity? *Med Res Rev* 25:49–65
58. Katoh M, Katoh M (2007) AP1- and NF-kappaB-binding sites conserved among mammalian WNT10B orthologs elucidate the TNFalpha-WNT10B signaling loop implicated in carcinogenesis and adipogenesis. *Int J Mol Med* 19:699–703
59. Korver DR, Klasing KC (1997) Dietary fish oil alters specific and inflammatory immune responses in chicks. *J Nutr* 127:2039–2046
60. Xi S, Cohen D, Barve S, Chen LH (2001) Fish oil suppressed cytokines and nuclear factor-kappaB induced by murine AIDS virus infection. *Nutr Res* 21:865–878
61. Gaines AM, Carroll JA, Yi GF, Allee GL, Zannelli ME (2003) Effect of menhaden fish oil supplementation and lipopolysaccharide exposure on nursery pigs. II: effects on the immune axis when fed simple or complex diets containing no spray-dried plasma. *Domest Anim Endocrinol* 24:353–365
62. Dias P, Dilling M, Houghton P (1994) The molecular basis of skeletal muscle differentiation. *Semin Diagn Pathol* 11:3–14
63. Lee SH, Park EW, Cho YM, Kim SK, Lee JH, Jeon JT, Lee CS, Im SK, Oh SJ, Thompson JM, Yoon D (2007) Identification of differentially expressed genes related to intramuscular fat development in the early and late fattening stages of hanwoo steers. *J Biochem Mol Biol* 40:757–764
64. Teboul L, Gaillard D, Staccini L, Inadera H, Amri E-Z, Grimaldi PA (1995) Thiazolidinediones and fatty acids convert myogenic cells into adipose-like cells. *J Biol Chem* 270:28183–28187
65. Grimaldi PA, Teboul L, Inadera H, Gaillard D, Amri EZ (1997) Trans-differentiation of myoblasts to adipoblasts: triggering effects of fatty acids and thiazolidinediones. *Prostaglandin Leuk Essent Fatty* 57:71–75
66. Yeow K, Phillips B, Dani C, Cabane C, Amri EZ, Derijard B (2001) Inhibition of myogenesis enables adipogenic trans-differentiation in the C2C12 myogenic cell line. *FEBS Lett* 506:157–162

FXR	Farnesoid X receptor
PPAR α	Peroxisome proliferator-activated receptor α
SREBP	Sterol regulatory element binding proteins
IRS	Insulin receptor substrate
GSK3 β	Glycogen synthase kinase 3 β
STAT	Signal transducer and activator of transcription
SOCS2	Suppressor of cytokine signaling 2
EGR1	Early growth response 1
AMPK	AMP-activated protein kinase
CPT	Carnitine palmitoyl transferase
ACC	Acetyl-CoA carboxylase
SCD	Stearoyl-CoA desaturase
IGFBP-1	Insulin-like growth factor-binding protein 1
CYP7A1	Cytochrome P450, family 7, subfamily A
ABCG5	ATP-binding cassette, sub-family G, member 5
3-PGDH	3-Phosphoglycerate dehydrogenase
PSAT1	Phosphoserine aminotransferase 1
RPLP	Ribosomal protein long-chain protein P0

Introduction

Numerous studies have been performed on the effects of dark chocolate or cocoa in relation to public health [1, 2]. Improved immune function [3, 4], cardiovascular status [5] and insulin sensitivity [6, 7] are among the reported positive health effects of cocoa. Cocoa contains flavonoids, which are believed to mediate the beneficial effects of dark chocolate. Flavan-3-ol has recently received much attention due to its cardioprotective properties [1]. However, the lipid content of chocolate and cocoa is relatively high, and with a high percentage of saturated fatty acids (SFA).

Epidemiological studies have shown that intake of excess SFA is the principal lifestyle-related cause of insulin resistance and obesity-related diseases in humans [8]. Carbohydrate tolerance and whole-body insulin sensitivity have been shown to be impaired with consumption of diets enriched with SFA in healthy human subjects [9, 10] and experimental animals [11–13]. The concept that dietary SFA produces hypercholesterolemia is also widely accepted. However, cocoa butter has been shown to have little or no effect on plasma cholesterol levels and the development of atherosclerosis when fed to animals [14–16] and humans [17, 18]. It has been suggested that this neutral effect of cocoa butter might be related to its relatively low digestibility [19] and lymphatic absorption [20]. Furthermore, stearic acid, which is the main saturated fatty acid in cocoa butter, has been shown to have a neutral effect on the plasma lipid profile [21]. Ingested cocoa has also been shown to reduce de novo lipid synthesis in rat liver [22], which might explain some of the positive health

effects of cocoa. Whether cocoa butter would exert similar effects on the liver is not known.

It is well accepted that hepatic fat accumulation is linked to insulin resistance [23], and that fatty liver is an independent predictor of type 2 diabetes, the metabolic syndrome and cardiovascular disease [24, 25]. Since fatty liver leads to failure of insulin to suppress hepatic glucose production, subjects with a fatty liver have an increased risk of developing hyperglycemia, glucose intolerance and peripheral insulin resistance. Furthermore, hepatic insulin resistance includes the decreased ability of insulin to suppress triglyceride-rich VLDL particle production in the liver [26], leading to hypertriglyceridemia and low HDL cholesterol concentration [27]. Hepatic insulin resistance is thus likely to be an important factor of the metabolic syndrome.

Short term (3 days) high-fat feeding in rats results specifically in hepatic fat accumulation and has been used as a model to study the mechanisms underlying hepatic insulin resistance [28, 29]. Three days of high-fat feeding, using safflower oil as lipid source, is sufficient to cause a threefold increase in hepatic lipid content and to suppress insulin sensitivity [29]. Safflower oil is rich in linoleic acid (18:2n-6) and has been shown to increase oxidative and inflammatory stresses [30–32], which are thought to be involved in the development of e.g. hepatic insulin resistance. Since hepatic insulin signaling results in increased de novo lipogenesis, suppressed hepatic insulin sensitivity might be protective for the liver during situations of increased dietary fat. Short-term oxidative stress, in the absence of lipotoxicity and inflammation, might thus be part of a cellular defense system where reduced insulin signaling protects the liver from further lipid loading. It has been proposed that insulin resistance is good when viewed in its original evolutionary context, but becomes pathological upon persistent stimulation by oxidative stress [33].

In contrast to the neutral effect of cocoa butter on plasma cholesterol levels, linoleic acid-enriched diets have beneficial effects on circulating cholesterol levels [34–36]. The aim of this study was to get clues as to whether this difference can be attributed to differences at the level of hepatic metabolism. The lipid content of chocolate and cocoa is relatively high, but the effects of ingested cocoa butter on markers for hepatic lipid metabolism and insulin signaling have to our knowledge not been addressed before. In the present study we sought (1) to answer whether short-term cocoa butter feeding is neutral, beneficial or detrimental regarding hepatic lipid metabolism, and (2) to identify similarities as well as differences between cocoa butter and safflower oil regarding effects on plasma lipoproteins, hepatic gene expression, lipid metabolism and insulin sensitivity using short-term high-fat feeding in rats.

Experimental Procedure

Animal Experiments

Seven week old male Sprague–Dawley rats (Scanbur BK AB) were maintained on standard chow (R36, Lactamin, Sweden) for a week before start of the experiment. Rats were thereafter fed for 3 days with either standard, cocoa butter- or safflower oil-enriched R36 diets. The compositions of these diets are shown in Table 1. The fatty acid compositions of the high-fat diets were the following; the safflower-enriched diet contained 77% linoleic, 15% oleic, 6% palmitic and 2% stearic acid; whereas the cocoa butter-enriched diet contained 36% stearic, 33% oleic, 25% palmitic and 3% linoleic acid. Food was removed late in the evening (11 p.m.), so that the animals were without food for 12 h before they were sacrificed.

Four rats from each group were injected intraperitoneally with insulin (Actrapid, Novo Nordisk), at a dose of 5 mU/g body weight, and four with saline only. Immediately before and 40 min after the injection, a drop of blood was collected from the tip of the tail and analyzed for blood glucose, using a Precision Xtra glucometer and test strips (Abbot Scandinavia AB). The rats were sacrificed and tissues removed and frozen in liquid nitrogen. The animal experiments were approved by the regional Ethics Committee on Animal Experiments.

Plasma Analysis

Blood was collected from the vena cava in 10-ml tubes containing 17.5 mg EDTA (B&D). Plasma was obtained by centrifugation at 3,000 g for 10 min. The resulting supernatants were removed and analyzed for insulin (RIA kits from Millipore) and lipids. Lipoprotein separation, by size-exclusion chromatography on individual samples from each animal, and lipid content calculations

were performed as described previously [37]. Plasma levels of cytokines (IL-1 β , IL-6, IL-17 and TNF α) were determined using Rat Cytokine/Chemokine Milliplex Kit (Millipore) and a Luminex instrument (LABScan 100, Luminex), according to the manufacturer's instructions.

Hepatic Lipid Content

Cellular lipids were extracted from the rat liver using chloroform and methanol (2:1 v/v), using the Folch method [38]. The extracts were dried, dissolved and analyzed for triacylglycerides and total (free and esterified) cholesterol, using kits from Roche and Calbiochem, respectively. Samples were analyzed in triplicate and the results expressed as microgram lipid per milligram liver weight.

Fatty Acid Oxidation

Hepatic β -oxidation was assayed by monitoring the palmitoyl-CoA-dependent reduction of NAD to NADH in sub-fractionated liver homogenates, as described previously [39]. Liver tissues (300 mg) were homogenized in 3 ml ice-cold sucrose-solution (0.25 M sucrose, 10 mM HEPES, 1 mM EDTA) using a Potter–Elvehjem glass-Teflon homogenizer. The homogenates (1 ml) were centrifuged for 10 min at 500 g, the supernatants withdrawn and centrifuged for 10 min at 10,000 g, and the resulting pellet re-suspended in sucrose-solution. The samples were added to the reaction buffer to a final concentration of 30 mM phosphate buffer pH 7.5, 0.2 mM NAD, 0.1 mM coenzyme A, 12 mM DTT, 0.15 mg/ml BSA (fatty acid free) and 0.01% triton X-100 (Sigma–Aldrich, Inc). The initial rate of NADH production was determined upon addition of palmitoyl-CoA (Sigma–Aldrich, Inc) (10 μ g/ml) at 37 °C. The absorbance at 340 nm was measured spectrophotometrically.

Table 1 Diet compositions

	R36 standard		Safflower oil-enriched		Cocoa butter-enriched	
	Component (g/100 g diet)	Energy (%)	Component (g/100 g diet)	Energy (%)	Component (g/100 g diet)	Energy (%)
Moisture	10	–	10	–	10	–
Ash	6	–	6	–	6	–
Fiber	3.5	0.8	2.7	0.5	2.7	0.5
Carbohydrate	58	67.8	40.1	36.3	40.1	36.3
Protein	18.5	22.2	12.2	11.4	12.2	11.4
Fat	4	9.2	29.5	51.8	29	51.8
Total calories (kJ/100 g)	128.8		166.1		166.1	

Analysis of Gene Expression by Quantitative Real-Time PCR

Total RNA was isolated by homogenization of frozen rat livers using a polytrone PT-2000 (Kinematica AG) and TRIzol[®] Reagent (Invitrogen Life Technologies) according to the protocol supplied by the manufacturer. The RNA concentration was determined spectrophotometrically at 260 and 280 nm. The quality of the RNA samples was examined using a RNA 6000 Nano Bioanalyzer according to the manufacturer's instructions (Agilent Technologies).

5 µg total RNA was treated with DNase (RQ1) and reverse transcribed using iScript[™] reverse transcriptase and 5× buffer for a First Strand cDNA synthesis (Bio-Rad Laboratories AB). The purity of the synthesized cDNA was checked by agarose gel electrophoresis. Subsequently, 2 µl of each first strand cDNA served as a template in a 20 µl PCR reaction mix containing the primers for the gene of interest (see Table 2) and iQ SYBR Green Supermix (Bio-Rad Laboratories AB). Quantification of gene expression was performed according to the manufacturer's protocol using DNA Engine Opticon[™]2 real-time PCR detection system (MJ Research). A relative standard curve was constructed with serial dilutions (1:1, 1:5 and 1:25) using a pool of the cDNA generated from all animals used in the study. The amplification program consisted of 1 cycle of 95 °C for 10 min, followed by 45 cycles of 95 °C for 15 s, annealing temperature for 10 s, 72 °C for 30 s; fluorescent intensity was measured at a specific acquisition temperature for each gene. The protocol was validated for each gene of interest by checking melting curves for the absence of primer-dimers or other unwanted amplicons. The level of individual mRNAs was normalized with the level of the housekeeping gene ribosomal protein long-chain protein P0 (RPLP). Results are expressed in arbitrary units.

Immunoblotting

Whole liver cell lysates were obtained by homogenizing 100 mg of liver in 1 ml RIPA buffer (50 mM Tris-HCl, pH 7.4, 1% Triton X-100, 150 mM NaCl, 5 mM EDTA,

1 mM PMSF, 1 mM Na₃VO₄, 10 mM NaF, 1 µg/ml of aprotinin, leupeptin, and pepstatin), using a polytrone PT-2000 (Kinematica AG), followed by 20 min of centrifugation (12,000g). The resulting supernatants were collected and proteins resolved by SDS-PAGE and transferred to PVDF membranes. The membranes were blocked for 1 h in Tris-buffered saline (TBS; 10 mM Tris pH 8.0, 150 mM NaCl) containing 0.1% (v/v) Tween-20 and 5% (w/v) milk powder or 5% (w/v) bovine serum albumin, incubated overnight at 4 °C with the antibody of interest diluted in TBS-T with 1% milk or bovine serum albumin. Antibodies for detecting IGFBP1 (1:500) were from Abcam; p-STAT3-Tyr705, STAT3, p-STAT5-Tyr694 (1:500), SOCS2, STAT5, p-AMPK-Thr172 and AMPK (1:1,000) were from Cell signaling; SCD-1 (1:500), SREBP-1, IRS (1:2,000), p-IRS1-Ser307 (1:1,000) and β-actin (1:50,000) were from SantaCruz. The membranes were washed and incubated with secondary antibody for 1 h in room temperature according to the data sheet provided by the company. After additional washing steps antibody binding was visualized using an ECL detection system (Pierce Biotechnology, Inc). Densitometry analysis was performed using the software Quantity One 4.6.5 Basic (Bio-Rad) to compare the amount of the antibody of interest to β-actin.

Akt Phosphorylation

Whole liver cell lysates were obtained by homogenizing 1 g of liver in 3 ml RIPA buffer, as described above). The resulting supernatants were collected and the degree of insulin signaling was analyzed by measuring the degree of insulin-dependent phosphorylation of Akt and GSK3β. Akt activation was determined by analyzing the amount of phosphorylated Akt (p-Akt-Ser473) in relation to total Akt, using commercially available ELISA kits (Biosource). Samples were analyzed in triplicate and the results determined as unit p-Akt per ng total Akt.

Expression Profiling Using Microarrays

Microarrays containing 70-mer oligonucleotide probes for 27,649 rat protein-coding genes were fabricated and used

Table 2 Primers

Accession no.	Gene		Forward primer (5'–3')	Reverse primer (5'–3')
NM_013144	IGFBP-1	Insulin-like growth factor-binding protein 1	GTGGAATGCCATTAGCACCT	CAGCAAACAGTGCGAGACAT
NM_130752	FGF21	Fibroblast growth factor 21	ACACCGCAGTCCAGAAAGTC	TCACTTTGATCCTGAGGCCT
NM_139192	SCD-1	Stearoyl-coenzyme A desaturase1	GATATCCACGACCCAGCTC	TACCTTATCAGTGCCCTGGG
NM_058208	SOCS2	Suppressor of cytokine signaling 2	GACGGGAAATTCAGATTGG	ACTTCTGCCGACTCAGCATT
NM_022402	RPLP	Ribosomal protein long-chain protein P0	CAGCAGGTGTTGACAATGG	AAAGGGTCTGGCTTTGCTC

to obtain transcript profiles, essentially as described previously [40]. A 40- μg amount of the total RNA from each sample were DNase-treated using RNeasy MiniElute Cleanup kit (QIAGEN) according to the supplied protocol and RNA concentrations measured using a NanoDrop ND-1000 Spectrophotometer (NanoDrop Technologies Inc.). The microarray experiments were performed using the Pronto!TM Plus Direct Systems (Corning Incorporated and Promega Corporation, NY), according to the manufacturer's instructions using 5 μg total RNA from each sample. In the first set of experiments, each hybridization compared Cy3-labeled cDNA reverse transcribed from RNA isolated from rats fed the standard diet with Cy5-labeled cDNA isolated from rats fed the high-fat diets. Each experiment was analyzed using individual samples and dye-swapping. The Cy3-labelled cDNA was mixed with Cy5-labelled cDNA and purified using the Chip-ShotTM Membrane Clean-Up System. The probes were next mixed with 45 μl hybridization solution, added to the arrays and placed in sealed hybridization chambers at 42 °C. After an overnight incubation (18–19 h), arrays were washed, dried and scanned to create images, using a Genepix 4200A laser scanner (Axon Instruments, Union City, CA, USA). For each array, the photomultiplier tubes and power of the laser were adjusted so that the overall count ratio of Cy5 to Cy3 signal was approximately 1. Image analysis was performed using the GenePix 6.0 software (Axon Instruments). Automatic flagging was used to localize absent or very weak spots, which were excluded from further analysis.

The analyzed image files were filtered for spots showing signals at least two times above background. The fluorescence ratios of the spots were further normalized with the Lowess (Locally Weighted Scatter Plot Smoother) method using the statistical language R (R 1.3.1 software). Identification of differentially expressed genes (due to high-fat feeding) was performed using the SAM 1.21 (Significance Analysis for Microarray) software incorporated in Microsoft office Excel program. A 5% false discovery rate was used as a first cut-off. Genes with a greater than 1.5-fold increase or decrease were considered as being regulated, even though smaller changes in gene expression may also have important biological consequences. The results are represented as the mean of at least three independent determinations. All data are available from the NCBI Gene Expression Omnibus database (GEO; <http://www.ncbi.nlm.nih.gov/geo/>) using the series entry GSE13936.

Statistical Analysis

All data were subjected to analysis of variance (one-way ANOVA) followed by Fisher's post-hoc analysis and expressed as means \pm SE. Differences between groups

were considered statistically significant when the probability that they occurred by chance was <0.05 .

Results

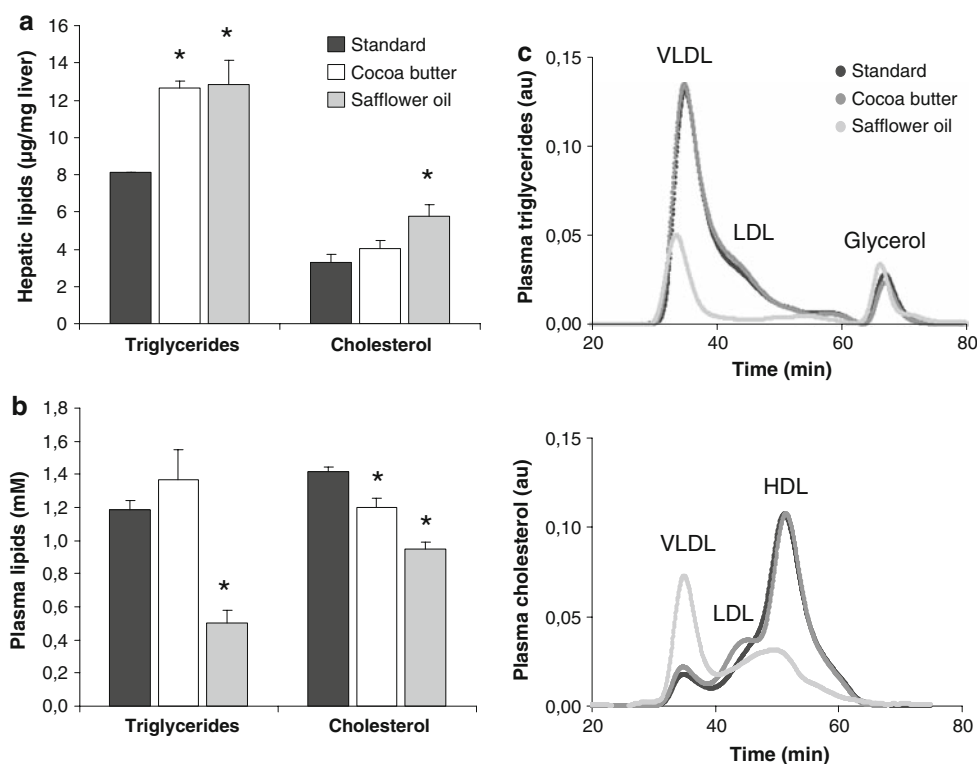
High-Fat Diet-Mediated Effects on Lipid Profiles and Hepatic Gene Expression

Rats fed a cocoa butter-enriched diet (CBD; 52% of the energy from cocoa butter) for 3 days were compared to rats fed safflower oil-enriched diet (SOD; 52% of the energy from safflower oil) or standard diet (StD; 9% of the energy from cocoa butter). Hepatic triglyceride (TG) content was increased in animals fed high-fat diets, as compared to those fed StD (Fig. 1a). No difference in TG content was observed between the two different high-fat diets. In contrast, only SOD-fed rats had increased levels of hepatic cholesterol. Safflower oil exerted the biggest effects on plasma lipids. As illustrated in Fig. 1b, the SOD-fed rats had the lowest plasma levels of TG and cholesterol. CBD-fed rats had similar plasma TG content as the rats on StD, but lower levels of plasma cholesterol.

To determine the effects of the different high-fat diets on lipoproteins, plasma lipid profiles were generated from the three diet groups. Again, SOD had the greatest impact on plasma lipids. As shown in Fig. 1c, ingested safflower oil decreased TG-rich VLDL particles and increased cholesterol-rich VLDL particles. At the same time, HDL cholesterol was reduced. No difference was observed between the rats fed CBD and StD. Thus, in spite of similar hepatic lipid content, the two different high-fat diets elicited different effects on plasma lipoprotein particles. The results are in line with previous publications [34], and indicate lipid-specific effects (i.e. dependent on lipid source) on hepatic lipid and lipoprotein metabolism.

To get an overview of high-fat diet-mediated alterations within the liver, whole-genome rat oligo microarrays were used to generate hepatic transcript profiles (using livers from StD-fed animals as control). Surprisingly, the CBD had a much greater impact on gene expression than the SOD. With a 5% false discovery rate and a cut-off at 1.5-fold difference, 822 transcripts were significantly different between CBD- and StD-fed animals, whereas only 151 transcripts were altered in response to SOD-feeding. Most effects were lipid-specific (i.e. dependent on lipid source), but 73 transcripts were similarly altered in the two high-fat groups (Fig. 2a). The high-fat-regulated transcripts were grouped according to cellular functions and some interesting results are listed in Table 3. All data are available from the NCBI Gene Expression Omnibus database (GEO; <http://www.ncbi.nlm.nih.gov/geo/>) using the series entry GSE13936.

Fig. 1 Effects of short-term high-fat feeding on lipid levels in liver and plasma. Triglyceride and cholesterol levels were measured in **a** hepatic lipid extracts or **b** plasma and **c** lipoprotein profiles were generated from rats fed a standard diet or either cocoa butter- or safflower oil-enriched diets. Data are represented as means \pm SE, and * indicates significant differences compared to standard diet ($n = 4$). The chromatograms represent the average from determinations performed on individual samples



High-Fat Diet-Mediated Changes in Gene Expression Independent on Lipid Source

As mentioned above, hepatic TG content was increased to the same extent in the two high-fat groups, which might elicit a similar response on certain genes. Among the gene products similarly altered in the two high-fat groups, the biggest changes (more than 2.5-fold) were observed for stearoyl-CoA desaturase 1 (SCD-1) and 2 (SCD-2), fibroblast growth factor 21 (FGF21), nuclear protein 1 (p8) and serine dehydratase (Table 3). Reduced levels of serine dehydratase might indicate reduced amino acid catabolism. Similarly, increased levels of glucokinase (Table 3) indicate enhanced capacity for hepatic glucose uptake and enhanced activity through anabolic pathways.

The p8 protein is a transcription factor that regulates the expression of genes involved in cell defense against adverse effects of stress [41]. Such stress-mediated survival mechanisms within the liver involve protein kinase C delta binding protein (DIG-1) and insulin-like growth factor-binding protein 1 (IGFBP-1) [42]. Both DIG-1 and IGFBP-1 mRNA were increased in our high-fat fed animals (Table 3). Based on microarray data IGFBP-1 mRNA levels were only increased in CBD-fed rats, but quantitative RT-PCR showed increased IGFBP-1 mRNA levels in both fat-fed groups (Fig. 2b). However, IGFBP-1 protein was increased in CBD-fed rats only (Fig. 3a).

As shown in Fig. 2b, the high-fat-mediated induction of FGF21 mRNA was confirmed using RT-PCR. Since FGF21-treatment in animals has been shown to increase fat utilization and to reduce hepatosteatosis [43], the rate of β -oxidation was compared between the groups. As shown in Fig. 4a, the SOD-fed rats had a 2.7-fold increase in fatty acid (FA) turnover rate. A trend ($p = 0.07$) towards increased β -oxidation was also observed in the CBD-fed rats.

Among the lipid-induced effects on gene products from metabolic pathways, the biggest changes were observed for SCD-1 and 2. The high-fat-mediated reduction of SCD-1 mRNAs was confirmed using RT-PCR (Fig. 2b) and reduced SCD-1 protein levels were demonstrated using immunoblotting (Fig. 3b). This is an interesting finding since SCD-1 deficiency leads to activation of lipid oxidation, reduced TG synthesis and storage within the liver [44]. The lowest levels of both mRNA and protein were observed in the SOD-fed rats. Increased AMP-activated protein kinase (AMPK) activity has been shown to mediate SCD-1 dependent effects on hepatic β -oxidation [45]. We analyzed the degree of AMPK activation, i.e. the degree of phosphorylation, but the higher rate of β -oxidation in the SOD group was not paralleled by increased AMPK phosphorylation (Fig. 4b).

Both PUFA and monounsaturated fatty acids (MUFA) activate farnesoid X receptor (FXR), and thereby decrease the mature form of sterol regulatory element binding

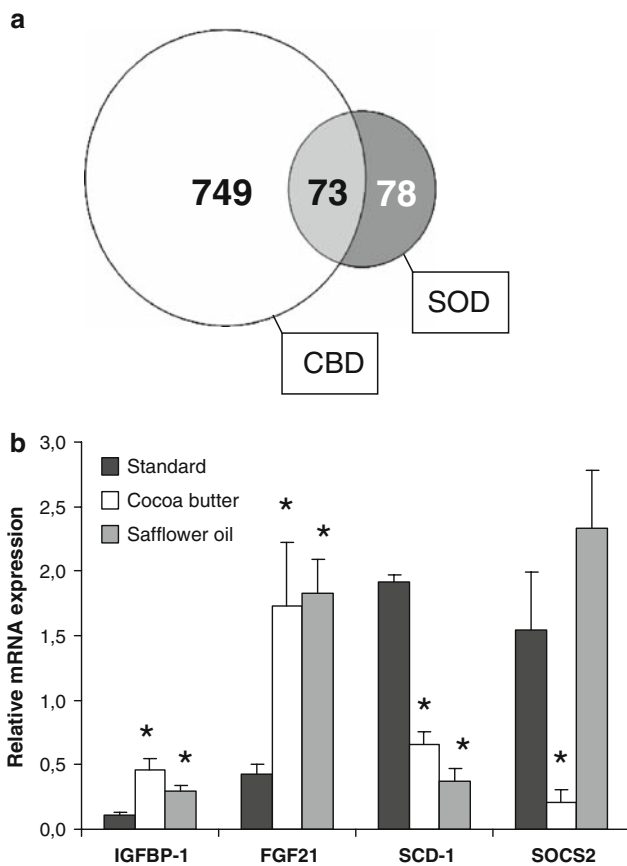


Fig. 2 Effects of short-term high-fat feeding on hepatic gene expression. **a** Overview of results obtained from microarray analysis comparing the effects of cocoa butter and safflower oil on hepatic gene expression. Whole-genome rat oligo microarrays were used to generate transcript profiles from rats fed a standard diet (StD) or either cocoa butter- (CBD) or safflower oil- (SOD) enriched diets ($n = 4$). StD-fed animals were used as control. A 5% false discovery rate was used and transcripts with a greater value than 1.5-fold increase or decrease (compared to StD) were considered differentially expressed. The total number of hepatic gene products affected by CBD (no fill), SOD (black fill), or both (gray fill) are indicated. **b** Effects of short-term high-fat feeding on selected hepatic transcript levels. Hepatic mRNA was isolated from rats fed standard or high-fat diets. Expression levels were quantified by real-time PCR and normalized to the housekeeping gene RPLP. Data are represented as means \pm SE, and * indicates significant differences compared to standard diet ($n = 4$)

protein-1c (SREBP-1c), as well as the expression of its target lipogenic genes such as SCD-1 in liver [46]. We therefore compared the content of hepatic SREBP-1 between the three diet groups. Surprisingly, the mature form of SREBP-1 (68 kDa) was elevated at the expense of unprocessed SREBP-1 (125 kDa) in both CBD- and SOD-fed rats (Fig. 4c). This observation suggests that SCD-1 expression can be repressed upon high-fat feeding through a mechanism that does not depend on reduced SREBP-1 maturation.

Taken together, these results indicate that a lipid-induced program for hepatic lipid disposal and cell survival might be operating upon 3 days of high-fat feeding. The former might involve increased levels of FGF21 and reduced levels of SCD-1 and SCD-2, whereas the latter includes increased levels of p8, DIG-1 and IGFBP-1.

Cocoa Butter Diet-Mediated Changes in Gene Expression

As summarized in Table 3, cocoa butter had a greater impact on hepatic genes from all functional groups listed, as compared to safflower oil. Rats fed CBD had increased levels of gene products from anabolic pathways, including biosynthesis of amino acids and lipids with cholesterologenesis being represented by the largest number of transcripts (Table 3). Several genes from the glycolytic pathway and de novo lipid synthesis were increased about twofold, including transketolase, pyruvate kinase, malic enzyme 1, ATP citrate lyase and spot 14. ATP citrate lyase catalyzes the formation of acetyl-CoA and oxaloacetate, and acetyl-CoA serves several important biosynthetic pathways such as fatty acid, cholesterol and bile acid synthesis. However, the biggest changes in expression levels (more than fivefold) were observed for 3-phosphoglycerate dehydrogenase (3-PGDH), phosphoserine aminotransferase 1 (PSAT1), asparagine synthase and early growth response 1 (EGR1). Higher levels of 3-PGDH and PSAT1 indicate a greater capacity for serine synthesis and serine-dependent pathways, such as the biosynthesis of phosphatidylserine and glutathione.

The effect on EGR1 might be related to a CBD-specific effect on inflammatory mediators, including the observed increase in expression of macrophage migration inhibitory factor and interleukin 17 receptor B (Table 3). This is in line with previous reports on EGR1 as a master switch to trigger the expression of inflammatory genes involved in e.g. atherosclerosis [47]. Since EGR1-negative mice have been shown to exhibit decreased expression of hepatic IL-6 mRNA [48], this and other cytokines (IL-1 β , IL-17, and TNF α) were measured in plasma from the different rats. However, only one animal (from the SOD group) had detectable levels of inflammatory cytokines (IL-6, 945 pg/ml; IL-1 β , 168 pg/ml). We further measured the degree of activation (phosphorylation) of the transcription factor STAT3, which is known to be activated in response to IL-6 and other cytokines [49]. There was no indication of enhanced STAT3 signaling in these rats, as determined by immunoblotting (data not shown).

Within the group of transcripts for signaling molecules, suppressor of cytokine signaling 2 (SOCS2) showed the greatest response to CBD-feeding. Reduced expression of SOCS2 mRNA was confirmed using RT-PCR (Fig. 2b),

Table 3 High-fat diet-induced changes in hepatic gene expression

Accession no.	Gene name	Effect of diet (high-fat vs. standard)	
		Cocoa butter	Safflower oil
Signaling molecules			
Endocrine, paracrine and autocrine factors			
NM_013144	Insulin-like growth factor binding protein 1	4.61	
NM_130752	Fibroblast growth factor 21	3.30	3.91
NM_031051	Macrophage migration inhibitory factor	1.79	
XM_343169	Adipsin	1.67	
NM_199115	Angiopoietin-like protein 4	0.64	
NM_001004274	Insulin-like growth factor binding protein 4	0.63	
NM_053329	Insulin-like growth factor binding protein, acid labile subunit	0.58	
NM_012549	Endothelin 2	0.42	
NM_031351	Attractin	0.60	0.60
Membrane-bound receptors			
NM_053019	Arginine vasopressin receptor 1A	2.21	
XM_224604	Interleukin 17 receptor B	1.88	
NM_199114	Fibroblast growth factor receptor-like 1	1.67	
NM_013123	Interleukin 1 receptor, type I	0.63	
NM_013036	Somatostatin receptor 4	0.62	
NM_012704	Prostaglandin E receptor 3	0.61	
NM_017183	Interleukin 8 receptor, beta	0.60	
NM_012630	Prolactin receptor	0.50	
NM_017018	Histamine receptor H 1	0.47	
NM_012550	Endothelin receptor type A	0.44	
Intracellular signaling mediators			
NM_199405	Leucine carboxyl methyltransferase 1	2.52	1.74
NM_053857	Eukaryotic translation initiation factor 4E binding protein 1	2.43	2.31
NM_134449	PKC delta binding protein (DIG-1)	2.12	2.11
NM_013055	Mitogen activated protein kinase kinase kinase 12	0.51	
XM_343472	Cytokine inducible SH2-containing protein	0.46	
NM_058208	Suppressor of cytokine signaling 2	0.27	
Transcription factors			
NM_012551	Early growth response 1	6.76	
NM_053611	Nuclear protein 1 (p8)	4.26	3.40
NM_013149	Aryl hydrocarbon receptor	1.74	
XM_217192	RAR-related orphan receptor alpha	1.68	
NM_001100966	SREBP cleavage activating protein	1.54	
NM_031668	MYB binding protein (P160) 1a	1.53	
NM_175582	Inhibitor of DNA binding 4	1.52	
NM_013086	cAMP responsive element modulator	0.65	
NM_012805	Retinoid X receptor alpha	0.60	0.58
NM_012524	CCAAT/enhancer binding protein (C/EBP) alpha	0.57	
NM_012543	D site albumin promoter binding protein	0.54	
NM_138875	Jun D proto-oncogene	0.54	
NM_022671	One cut domain, family member 1 (HNF6 alpha)	0.35	
Cellular metabolism			
Amino acid turnover			
NM_031620	3-phosphoglycerate dehydrogenase	8.42	
NM_198738	Phosphoserine aminotransferase 1	6.21	
NM_013079	Asparagine synthetase	5.50	

Table 3 continued

Accession no.	Gene name	Effect of diet (high-fat vs. standard)	
		Cocoa butter	Safflower oil
NM_012571	Glutamate oxaloacetate transaminase 1	0.55	0.54
NM_017159	Histidine ammonia lyase	0.53	
NM_022619	Solute carrier family 7, member 2	0.46	0.52
NM_053962	Serine dehydratase	0.09	0.38
Carbohydrate turnover			
NM_012565	Glucokinase	4.00	2.44
NM_016987	ATP citrate lyase	2.22	
NM_022592	Transketolase	2.22	
NM_012600	Malic enzyme 1	1.81	
NM_022268	Liver glycogen phosphorylase	1.80	
NM_012624	Pyruvate kinase	1.59	
NM_031151	Malate dehydrogenase, mitochondrial	1.54	
NM_012621	6-phosphofructo-2-kinase/fructose-2,6-biphosphatase 1	1.53	
NM_022215	Glycerol-3-phosphate dehydrogenase 1	0.63	
Cholesterol and bile acid turnover			
NM_019238	Farnesyl diphosphate farnesyl transferase 1	2.69	
NM_031062	Mevalonate (diphospho) decarboxylase	2.12	
NM_053607	Cholate-CoA ligase	2.01	
NM_017268	3-hydroxy-3-methylglutaryl-Coenzyme A synthase 1	1.89	
NM_017136	Squalene epoxidase	1.87	
NM_022389	7-dehydrocholesterol reductase	1.72	
NM_031049	Lanosterol synthase	1.72	
NM_031840	Farnesyl diphosphate synthase	1.66	
NM_024143	Bile acid-CoA ligase	1.63	
NM_173307	ATP-binding cassette, subfamily A, member 5	0.46	
NM_053754	ATP-binding cassette, subfamily G, member 5		2.34
NM_012942	CYP7A1		3.64
Fatty acid turnover			
NM_001006995	Acetyl-CoA acetyltransferase 2	2.00	
NM_017075	Acetyl-CoA acetyltransferase 1	1.63	
NM_012703	Thyroid hormone responsive protein, SPOT14	1.59	
NM_053445	Fatty acid desaturase 1	1.71	
NM_031344	Fatty acid desaturase 2	1.57	
NM_173137	Fatty acid desaturase 3	1.69	
NM_053365	Fatty acid binding protein 4	0.64	
NM_138907	Mitochondrial acyl-CoA thioesterase 1	0.63	0.42
XM_234398	Peroxisomal acyl-CoA thioesterase 2B	0.63	
NM_012597	Lipase, hepatic	0.62	
NM_144750	Lysophospholipase	0.50	0.44
NM_173151	CTP:phosphocholine cytidyltransferase	0.48	
NM_031841	Stearoyl-CoA desaturase 2	0.27	0.08
NM_139192	Stearoyl-CoA desaturase 1	0.22	0.10
Retinol metabolism			
NM_022407	Aldehyde dehydrogenase family 1, member A1	2.40	
NM_017158	CYP2C7	0.50	

Total hepatic RNA was extracted from rats fed different diets ($n = 4$) and the effect of cocoa butter or safflower oil on gene expression was studied using rat whole-genome oligo arrays. The data were obtained using SAM at a false discovery rate of 5% and are represented as mean fold changes. All data are available from the NCBI Gene Expression Omnibus database (GEO; <http://www.ncbi.nlm.nih.gov/geo/>) using the series entry GSE13936

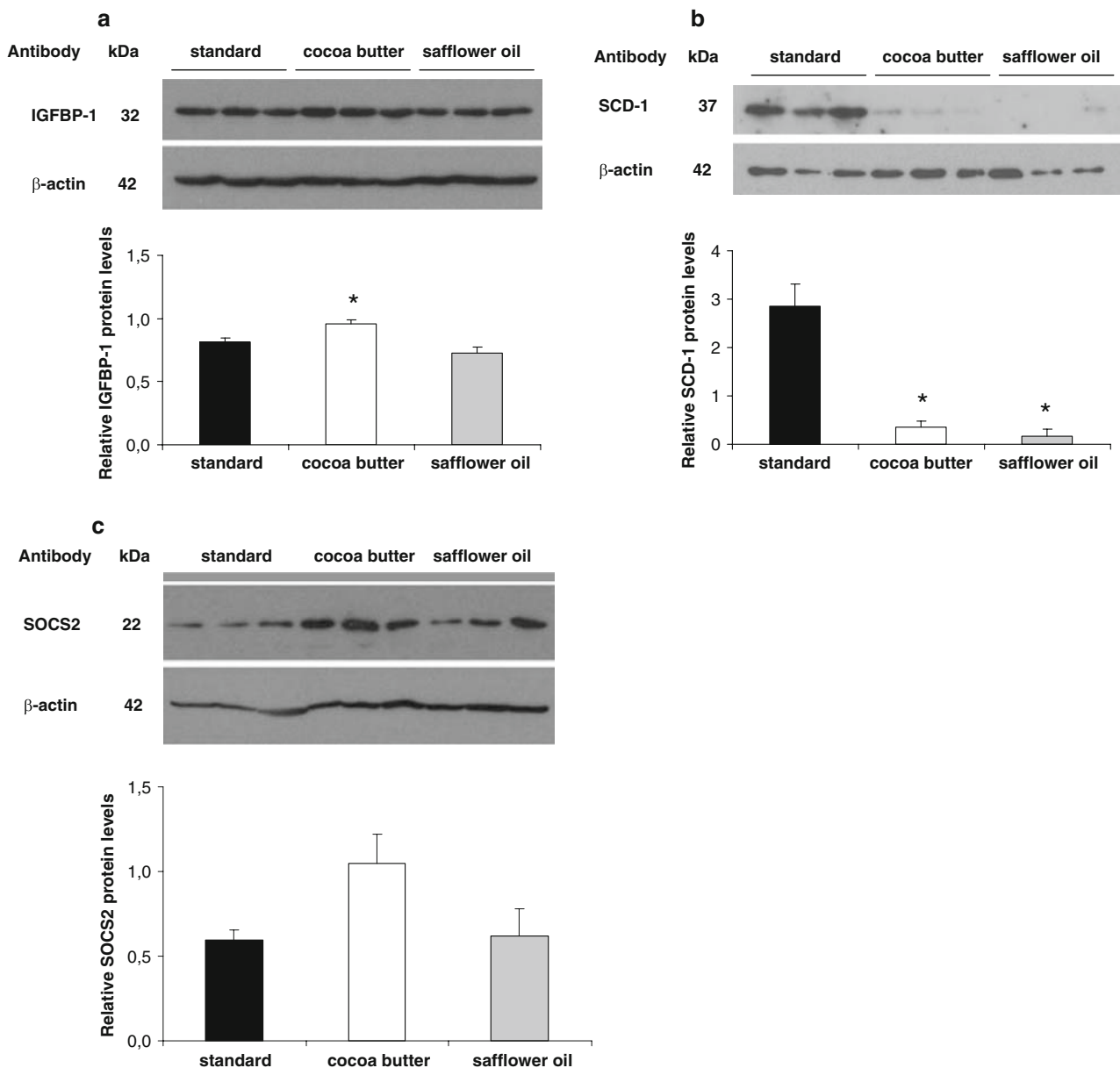


Fig. 3 Effects of short-term high-fat feeding on selected hepatic protein levels. Livers from rats fed standard or high-fat diets were used to extract whole-cell lysates. Protein levels of **a** IGFBP-1, **b** SCD-1 and **c** SOCS2 were analyzed by immunoblotting (*upper*

section) and quantified by densitometry analysis in relation to β -actin (*lower section*). Data are represented as means \pm SE, and * indicates significant differences compared to standard diet ($n = 3$)

but a trend ($p = 0,112$) towards increased SOCS2 protein levels were demonstrated using immunoblotting (Fig. 3c). SOCS2 is a negative regulator of growth hormone (GH)-mediated signaling and gene regulation, which includes down-regulation of its own GH-dependent expression [50, 51]. Reduced GH signaling, supposedly due to increased SOCS2 protein in the CBD group, might thus explain the reduced expression of SOCS2 mRNA as well as the observed effects on other GH-regulated transcripts in these animals (Table 3). Those include IGFBP1 [52], insulin-like

growth factor binding protein acid labile subunit [53], prolactin receptor [54], CYP2C7 [55], SCD-1 [40, 56] and SCD-2 [51].

Taken together, the results described above suggest that rats fed a cocoa butter-enriched diet for 3 days might have a higher capacity to synthesize fatty acids, phospholipids, cholesterol and bile acids, as compared to rats fed safflower oil. Altered GH-signaling and expression of GH-regulated genes in the CBD-fed rats might lead to further perturbations in hepatic lipid metabolism.

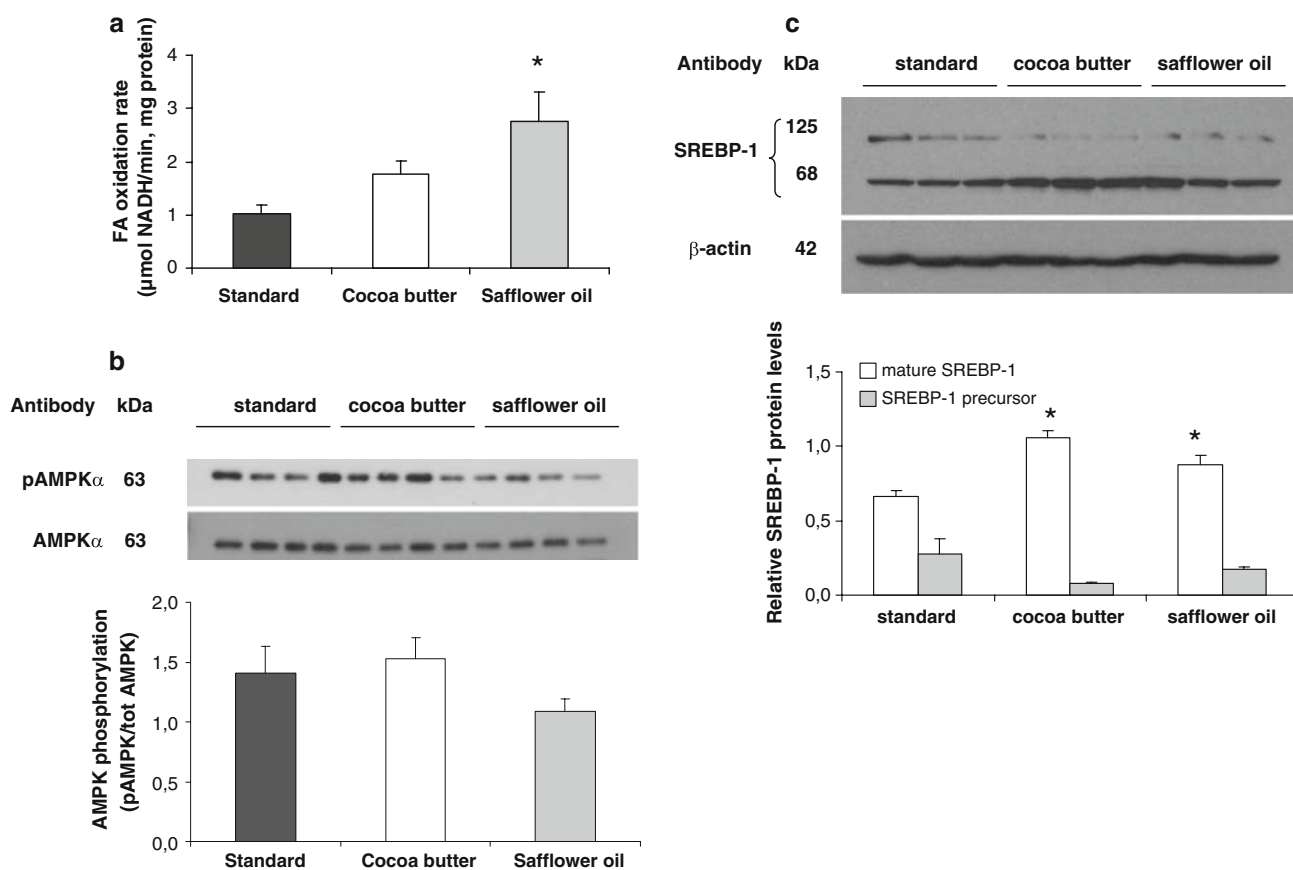


Fig. 4 Effects of short-term high-fat feeding on hepatic fatty acid oxidation rates and SREBP-1 protein levels. **a** Fatty acid oxidation rates were determined in liver homogenates ($n = 4$), whereas **b** AMPK phosphorylation ($n = 4$) and **c** SREBP-1 maturation ($n = 3$) were

determined in whole-cell lysates by immunoblotting (*upper section*) and quantified by densitometry analysis in relation to total AMPK or β -actin (*lower section*). Data are represented as means \pm SE, and * indicates significant differences compared to standard diet

High-Fat Diet-Mediated Effects on Hepatic Insulin Sensitivity

Finally, hepatic insulin sensitivity was compared between the three diet groups. The effect of insulin treatment (i.p. injection) was investigated using the degree of Akt-activation (phosphorylation at Ser473) as a measure of insulin receptor signaling [57]. All rats responded to insulin through increased Akt-phosphorylation, but the safflower oil-fed rats were only half as sensitive as the other animals (Fig. 5a). This indicates that, in spite of a similar degree of hepatic lipid content, hepatic insulin signaling was more efficient in the CBD-fed rats as compared to those fed with safflower oil. Cellular stress and free fatty acids (among other things) are known to induce insulin resistance through the activation of several serine/threonine kinases that phosphorylate and inactivate IRS1. In the liver, phosphorylation of IRS1 at Ser307 has been suggested to play a role in the development of high-fat feeding-induced insulin resistance [58]. To find an explanation for the lipid-dependent differences in Akt-phosphorylation we next compared the degree of IRS1-phosphorylation. There was

no indication of enhanced phosphorylation of IRS1 at Ser307 in the SOD-fed rats, as determined by immunoblotting (data not shown).

One important function of hepatic insulin signaling is to suppress TG-rich VLDL particle production [24]. Comparing rats on StD with those on CBD, a similar reduction in both plasma TG levels (Fig. 5c) and TG-rich VLDL particles (Fig. 5d) were observed. The SOD-fed rats did not respond, which might reflect reduced hepatic insulin sensitivity or alternatively be due to the already low levels of TG-rich VLDL in these rats. All rats responded equally well to insulin at the level of blood glucose lowering, and their basal glucose levels were the same (Fig. 5b). Basal insulin levels were also similar between the groups (StD 1.57 ± 0.15 ng/ml; CBD 1.10 ± 0.07 ng/ml; SOD 1.62 ± 0.23 ng/ml).

Discussion

In the present study, short-term cocoa butter feeding in healthy rats was neutral regarding serum lipids and hepatic

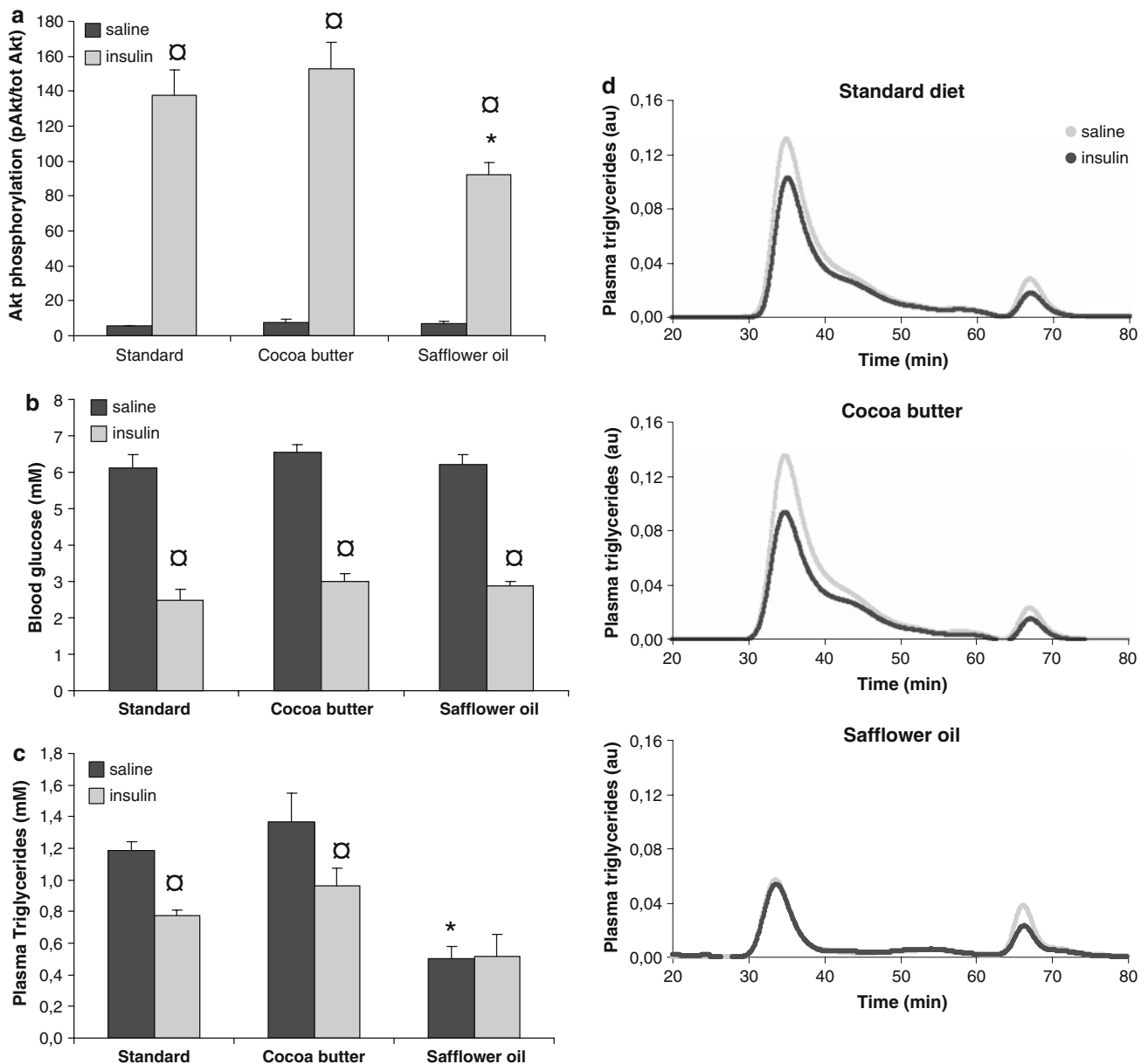


Fig. 5 Effects of short-term high-fat feeding on effects of insulin treatment. Rats fed standard or high-fat diets were subjected to 40 min of saline or insulin treatment. **a** The ratio between phosphorylated and unphosphorylated Akt was determined in whole liver cell lysates using ELISA. Levels of **b** glucose in blood and **c** TG in plasma were

determined, and **d** plasma lipoprotein profiles were generated. Data are represented as means \pm SE, * indicates significant differences compared to standard diet, and \square indicates significant differences compared to saline treatment ($n = 4$). The chromatograms represent the average from determinations performed in individual samples

insulin sensitivity, but changes in hepatic gene expression were induced that might lead to increased lipid synthesis, lipotoxicity, inflammation and insulin resistance if maintained. Safflower oil increased hepatic β -oxidation, was beneficial in terms of circulating TG-rich VLDL particles, but led to reduced hepatic insulin receptor signaling. The effects of safflower oil on hepatic gene expression were partly overlapping with those exerted by cocoa butter, but fewer transcripts from anabolic pathways were altered.

Increased hepatic cholesterol levels and increased expression of hepatic CYP7A1 and ABCG5 mRNA, important gene products in bile acid production and cholesterol excretion, were specific effects elicited by safflower oil only. Common effects on gene expression included increased levels of p8, DIG-1, IGF1BP-1 and FGF21, as well as reduced levels of SCD-1 and SCD-2. This indicates that a lipid-dependent program for hepatic lipid disposal and cell survival was induced by 3 days of high-fat

feeding, independently of the lipid source. The observation that cocoa butter exerted a similar degree of SCD-1 reduction as did safflower oil has to our knowledge not been described before. The mechanism behind this effect is as yet unknown, but data presented herein suggest that it is independent of reduced SREBP-1 maturation.

The diet-specific effects on plasma lipids are in agreement with previous studies [34], and might partly be explained by differences in hepatic FA oxidation rates. The level of TG in plasma is most often related to VLDL production in the liver, and this in turn is dependent on whether FA are being used for FA oxidation or re-esterification [27]. The enhanced FA oxidation rate in the SOD-fed rats indicates that both de novo FA synthesis [45] and lipoprotein formation was reduced [59], leading to lowered levels of plasma TG. Another explanation might be provided by diet-specific FA compositions in combination with reduced hepatic expression of SCD-1.

SCD-1 is a microsomal enzyme required for the biosynthesis of oleate and palmitoleate, which are the major MUFA of membrane phospholipids, TG, and cholesteryl esters (CE). SCD-1 gene expression is highly regulated by dietary factors; induced by carbohydrates or cholesterol but repressed by PUFA to maintain lipid homeostasis [60, 61]. Cholesterol has been shown to override PUFA-mediated repression of the SCD-1 gene [62], which might redistribute FA from FA oxidation to esterification, CE formation and VLDL production. SCD-1 deficiency has been linked to reduced plasma VLDL secretion [63], lending further support to the notion that oleoyl-CoA and palmitoleyl-CoA produced by SCD-1 are necessary to synthesize CE targeted to hepatic VLDL secretion. In the present study, low expression of SCD-1 might thus contribute to the reduced plasma levels of TG-rich VLDL particles observed in the SOD-fed rats. Cocoa butter has a higher content of MUFA compared to safflower oil (33 vs. 15%). Since MUFA (mainly oleate) are supplied to a greater extent by the CBD, reduced synthesis of oleoyl-CoA and palmitoleyl-CoA might not affect VLDL secretion to the same extent as in the SOD-fed rats. Supposedly, the higher rate of β -oxidation upon SOD-feeding might in part be a consequence of reduced VLDL secretion and re-esterification of FA into CE.

Hepatic cholesterol was increased, VLDL cholesterol increased and HDL cholesterol reduced after 3 days SOD-feeding, whereas there were no such changes due to CBD-feeding. Since reduced reverse cholesterol transport is well-known to promote atherosclerosis, this indicates a potential proatherogenic effect of the former dietary regimen. The SOD-mediated increase in hepatic cholesterol might lead to liver X receptor (LXR) stimulation and thus explain the increased expression of CYP7A1 [64] and the sterol transporter ABCG5 [65]. This effect of safflower oil

on gene products involved in hepatic cholesterol turnover has to our knowledge not been described before but might be related to the reduced expression of SCD-1 and capacity to export CE in VLDL particles in the SOD-fed rats.

Although it is well accepted that inhibition of SCD-1 prevents many aspects of the metabolic syndrome (diet-induced obesity, hepatic steatosis, insulin resistance, hypertriglyceridemia), it was recently shown that low levels of SCD-1 might promote aortic atherosclerosis in a mouse model of hyperlipidemia and atherosclerosis [66]. It was suggested that inhibition of SCD-1 in the liver results in secretion of VLDL particles that are highly enriched in SFA-rich CE, giving rise to SFA-CE-rich LDL particles. Increased delivery of SFA to macrophages leads to accumulation of SFA, enhanced inflammatory cytokine secretion and a proinflammatory phenotype. In the present study, reduced expression of SCD-1, in the absence of sufficient levels of dietary MUFA (i.e. in the SOD group only), was paralleled by increased hepatic cholesterol, increased VLDL cholesterol and reduced HDL-cholesterol. Whether this effect would persist upon longer periods of high dietary intake of safflower oil is not known and should be addressed.

The finding that SOD exerted a greater effect on FA oxidation as compared to CBD is in accordance with previous studies and might be related to its higher content of PUFA, which are known to be potent activators of PPAR α and modulators of lipid metabolism [67]. Upon PPAR α activation, CPT-I and II, peroxisomal and mitochondrial β -oxidation enzymes, enzymes of ketogenesis, and omega-oxidation enzymes are induced and create an increased capacity for FA oxidation [59]. However, none of these gene products were induced in the SOD-fed rats in this study (see GEO; <http://www.ncbi.nlm.nih.gov/geo/>). Increased β -oxidation has also been shown to be an effect of SCD-1 deficiency [44], but the CBD-fed rats had almost equally reduced SCD-1 expression without the same increase in FA oxidation. Increased AMPK activity has been shown to mediate the SCD-1 dependent effects on hepatic β -oxidation [45]. This pathway involves AMPK-dependent repression of acetyl-CoA carboxylase (ACC), reduced ACC-mediated formation of malonyl-CoA, and thereby de-repression of CPT-Ia enzymatic activity, leading to enhanced transfer of FA into the mitochondria [45, 68]. However, a higher rate of β -oxidation was not paralleled by an increased degree of AMPK phosphorylation in the SOD-fed rats.

The high-fat diet-mediated increase in FGF21 mRNA is interesting in this regard, since FGF21 has been shown to increase β -oxidation. FGF21, a hormone induced by fasting, is predominantly expressed in the liver and has beneficial effects on glucose homeostasis and insulin sensitivity both in rodents [69], monkeys [70] and man [71]. Furthermore, FGF21-treatment in animals was recently

shown to mediate increased energy expenditure, fat utilization and lipid excretion, to reduce hepatosteatosis and improve glycemia [43]. The mechanisms behind these effects were recently shown to include peroxisome proliferator-activated receptor gamma coactivator protein-1 α [72]. Whether there is any link between increased FGF21 levels and reduced SCD-1 expression has to await further studies.

It has also been shown that FGF21 induces SOCS2, blocks GH-dependent STAT5b signaling and alters the expression of GH-regulated genes during starvation [73]. Among other GH-suppressed gene products [74, 75], hepatic IGFBP-1 expression was found to be induced by FGF21 [73]. Our finding that FGF21 was induced by high-fat feeding in parallel with increased IGFBP-1 and increased FA oxidation is in line with the reports cited above, and adds to the picture of FGF21 as a sensor of FA availability, during starvation as well as during hepatic fatty infiltration. In the present study, 3 days of cocoa butter feeding seemed to induce the level of hepatic SOCS2 protein and altered the expression of genes previously shown to be under the regulation of GH, such as IGFBP1, insulin-like growth factor binding protein acid labile subunit, prolactin receptor, CYP2C7, SCD-1, SCD-2 as well as SOCS2. A down-regulation of SOCS2 mRNA in the CBD-fed rats indicates that GH sensitivity might become normalized with time and, since GH has lipogenic effects in the liver [76–78], lead to enhanced fatty infiltration if the high-fat feeding is maintained.

Circulating fasting levels of IGFBP-1 were recently shown to reflect hepatic lipid content and insulin sensitivity in non-diabetic humans, with IGFBP-1 levels being positively correlated with hepatic insulin sensitivity and inversely related to liver fat content [79]. Furthermore, low circulating IGFBP-1 concentrations have been linked with increased risk of macrovascular disease in humans [80]. Although the cause and effect relationship has not been proven, increased hepatic lipid content might lead to elevated levels of hepatic and circulating IGFBP-1, beneficial for metabolic health. Furthermore, stress-mediated survival mechanisms within the liver of rodents have been shown to involve IGFBP-1 [42]. In this study, we have shown that the p8 protein, DIG-1 and IGFBP-1 were induced by short-term high-fat feeding. The p8 protein is a transcription factor that regulates the expression of genes involved in cell defense, whereas DIG-1 is a protein kinase C delta binding protein that increases the protein stability of p53. When the expression of p53 target genes such as IGFBP-1 is increased, a survival pathway is initiated, which is thought to give the cell an opportunity to repair low-level damage. Since high levels of lipids within the hepatocyte are toxic to the cell, this high-fat response might include ways to reduce the hepatic lipid content. Another

interesting gene product of importance during situations of nutrient overload, and induced by high-fat feeding in the present study, is the eukaryotic translation initiation factor 4E-binding (eIF4E-binding) protein 1 (4E-BP1). The combined disruption of 4E-BP1 and 4E-BP2 in mice has been shown to increase their sensitivity to diet-induced obesity and insulin resistance [81]. It was suggested that 4E-BP1 and 2 play important roles as metabolic brakes in the development of obesity and type 2 diabetes. 4E-BP1 was induced to the same extent (more than twofold) in both CBD- and SOD-fed rats (Table 3).

The notion that SOD-feeding reduces hepatic insulin sensitivity has been described before [28, 29]. Our finding that 3 days on SOD reduces insulin-mediated phosphorylation of Akt in the absence of any detectable change in p-IRS1-Ser307 verifies the results presented by Samuel et al. [29]. In the same study, reduced activation of Akt was paralleled by blunted insulin-mediated suppression of hepatic glucose output (HGO). This important measure of hepatic insulin sensitivity was not investigated in the present study, and it can not be ruled out that cocoa butter feeding would lead to the same detrimental effect. The possibility that short-term HGO regulation is independent of Akt-phosphorylation should be investigated, but it would also be interesting to compare the impact of different high-fat feeding protocols on other hepatic effects of insulin, such as lipid and glycogen synthesis. Furthermore, there are Akt-independent signaling pathways that might have been differently affected by the high-fat diets. Further studies are required to address this and to find the SOD-mediated mechanism that blocks insulin receptor signaling up-stream of Akt. Specifically, the hypothesis that a greater FA oxidation rate, as a consequence of high dietary intake of safflower oil or similar fat sources, might lead to enhanced oxidative stress and insulin resistance should be tested.

As indicated above, the difference in insulin sensitivity at the level of Akt and GSK3 β between CBD- and SOD-fed rats does not exclude that hepatic insulin resistance might develop upon excess intake of cocoa butter. On the contrary, our transcript profiles could be interpreted as an increased capacity for lipid synthesis within the liver of CBD-fed rats, which might increase the risk of developing steatosis and insulin resistance. This is in contrast to the effects of cocoa ingestion, which was reported to suppress the expression of genes for enzymes involved in fatty acid synthesis in rat liver [22]. This beneficial effect of cocoa might therefore depend on lipophobic molecules absent in the butter fraction of cocoa.

Taken together, we have described short-term effects of high-fat feeding on hepatic gene expression in relation to lipid profiles and insulin signaling. Three days of a high dietary intake of cocoa butter led to changes within the

liver that might be part of a defense program triggered by the increase in hepatic TG. This included reduced expression of SCD-1, which could result in reduced synthesis of oleoyl-CoA and palmitoleyl-CoA of importance for VLDL secretion. However, the high content of oleate in cocoa butter (i.e. provided by the diet) might explain why there were no changes in plasma lipoproteins or hepatic cholesterol levels, in spite of reduced SCD-1. Thus, 3 days on this diet might not be a metabolic problem, but since there were other changes in transcript levels indicative of increased activity through anabolic pathways, it might be speculated that longer treatment duration would lead to steatosis and insulin resistance. In comparison, 3 days on a safflower oil-enriched diet resulted in similar defense-related changes, but this was paralleled by reduced TG-rich VLDL and HDL cholesterol in plasma, increased hepatic cholesterol, increased FA oxidation and reduced insulin signaling. The low expression of SCD-1 in the absence of sufficient MUFA supplied by the diet might result in a reduced ability to produce CE and VLDL, leading to reduced TG-rich VLDL in the circulation, increased cholesterol and fatty acids in the liver, and as a consequence of the latter, increased FA oxidation, ROS formation and insulin resistance. In summary, we speculate that increased hepatic TG leads to reduced expression of SCD-1, which might mediate either neutral, beneficial or unfavorable effects on hepatic metabolism upon high-fat feeding, depending on which fatty acids were provided by the diet.

Acknowledgments This work was supported by grants from the Swedish Medical Research Council, the Swedish Society of Medical Research, the Family Erling-Persson Foundation, the Swedish Diabetes Association and Barry-Callebaut. We are grateful to Peter Nilsson at the KTH Microarray Center for the kind gift of the microarrays.

References

- Mehrinfar R, Frishman W (2008) Flavanol-rich cocoa: a cardio-protective nutraceutical. *Cardiol Rev* 16:109–115
- Erdman JW Jr, Carson L, Kwik-Urbe C, Evans EM, Allen RR (2008) Effects of cocoa flavanols on risk factors for cardiovascular disease. *Asia Pac J Clin Nutr* 17:284–287
- Ramiro-Puig E, Pérez-Cano F, Ramírez-Santana C, Castellote C, Izquierdo-Pulido M, Permanyer J, Franch A, Castell M (2007) Spleen lymphocyte function modulated by a cocoa-enriched diet. *Clin Exp Immunol* 149:535–542
- Sanbongi C, Suzukia N, Sakane T (1997) Polyphenols in chocolate, which have antioxidant activity, modulate immune functions in humans in vitro. *Cell Immunol* 177:129–136
- Vinson JA, Proch J, Bose P, Muchler S, Taffera P, Shuta D, Samman N, Agbor GA (2006) Chocolate is a powerful ex vivo in vivo antioxidant, an antiatherosclerotic agent in an animal model, and a significant contributor to antioxidants in the European and American diets. *J Agric Food Chem* 54:8071–8076
- Grassi D, Necozione S, Lippi C, Croce G, Valeri L, Pasqualetti P, Desideri G, Blumberg JB, Ferri C (2005) Cocoa reduces blood pressure and insulin resistance and improves endothelium-dependent vasodilation in hypertensives. *Hypertension* 46:398–405
- Grassi D, Desideri G, Necozione S, Lippi C, Casale R, Properzi G, Blumberg JB, Ferri C (2008) Blood pressure is reduced and insulin sensitivity increased in glucose-intolerant, hypertensive subjects after 15 days of consuming high-polyphenol dark chocolate. *J Nutr* 138:1671–1676
- Riccardi G, Giacobbe R, Rivellese A (2004) Dietary fat, insulin sensitivity and the metabolic syndrome. *Clin Nutr* 23:447–456
- Stettler R, Ith M, Acheson KJ, Decombaz J, Boesch C, Tappy L, Binnert C (2005) Interaction between dietary lipids and physical inactivity on insulin sensitivity and on intramyocellular lipids in healthy men. *Diabetes Care* 28:1404–1409
- Vessby B, Unsitupa M, Hermansen K, Riccardi G, Rivellese A, Tapsell L, Näslén C, Berglund L, Louheranta A et al (2001) Substituting dietary saturated for monounsaturated fat impairs insulin sensitivity in healthy men and women: The KANWU study. *Diabetologia* 44:312–319
- Lardinois C, Starich G (1991) Polyunsaturated fats enhance peripheral glucose utilization in rats. *J Am Coll Nutr* 10:340–345
- Storlien L, Jenkins A, Chisholm D, Pascoe W, Khouri S, Kraegen E (1991) Influence of dietary fat composition on development of insulin resistance in rats. Relationship to muscle triglyceride and omega-3 fatty acids in muscle phospholipid. *Diabetes* 40:280–289
- van Amelsvoort J, van der Beek A, Stam J, Houtsmuller U (1988) Dietary influence on the insulin function in the epididymal fat cell of the Wistar rat. I. Effect of type of fat. *Ann Nutr Metab* 32:138–148
- Farnworth E, Kramer J, Thompson B, Corner A (1982) Role of dietary saturated fatty acids on lowering the incidence of heart lesions in male rats. *J Nutr* 112:231–240
- Kritchevsky D, Tepper S, Bises G, Klurfeld D (1982) Experimental atherosclerosis in rabbits fed cholesterol-free diets. *Atherosclerosis* 41:279–284
- Anonymous (1982) Influence of cocoa butter on cholesterol metabolism in rats: comparison with corn oil, coconut oil and palm kernel oil. *Nutr Res* 3: 229–236
- Erickson B, Coots R, Mattson F, Kligman A (1964) The effect of partial hydrogenation of dietary fats, of the ratio of polyunsaturated to saturated fatty acids, and of dietary cholesterol upon plasma lipids in man. *J Clin Invest* 43:2017–2025
- Reiser R (1973) Saturated fat in the diet and serum cholesterol concentration: a critical examination of the literature. *Am J Clin Nutr* 26:524–555
- Apgar JL, Shively CA, Tarka SM Jr (1987) Digestibility of cocoa butter and corn oil and their influence on fatty acid distribution in rats. *J Nutr* 117:660–665
- Porsgaard T, Hoy C-E (2000) Lymphatic transport in rats of several dietary fats differing in fatty acid profile and triacylglycerol structure. *J Nutr* 130:1619–1624
- Hegsted D, McGandy R, Myers M, Stare F (1965) Quantitative effects of dietary fat on serum cholesterol in man. *Am J Clin Nutr* 17:281–295
- Matsui N, Ito R, Nishimura E, Yoshikawa M, Kato M, Kamei M, Shibata H, Matsumoto I, Abe K, Hashizume S (2005) Ingested cocoa can prevent high-fat diet-induced obesity by regulating the expression of genes for fatty acid metabolism. *Nutrition* 21:594–601
- Marchesini G, Brizi M, Morselli-Labate AM, Bianchi G, Bugianesi E, McCullough AJ, Forlani G, Melchionda N (1999) Association of nonalcoholic fatty liver disease with insulin resistance. *Am J Med* 107:450–455
- Kotronen A, Yki-Jarvinen H (2008) Fatty liver: a novel component of the metabolic syndrome. *Arterioscler Thromb Vasc Biol* 28:27–38

25. Norbert S, Kantartzis K, Haring H-U (2008) Causes and metabolic consequences of fatty liver. *Endocr Rev* 29:939–960
26. Malmstrom R, Packard CJ, Watson TDG, Rannikko S, Caslake M, Bedford D, Stewart P, Yki-Jarvinen H, Shepherd J, Taskinen M-R (1997) Metabolic basis of hypotriglyceridemic effects of insulin in normal men. *Arterioscler Thromb Vasc Biol* 17:1454–1464
27. Julius U (2003) Influence of plasma free fatty acids on lipoprotein synthesis and diabetic dyslipidemia. *Exp Clin Endocrinol Diabetes* 111:246–250
28. Kraegen EW, Clark PW, Jenkins AB, Daley EA, Chisholm DJ, Storlien LH (1991) Development of muscle insulin resistance after liver insulin resistance in high-fat-fed rats. *Diabetes* 40:1397–1403
29. Samuel VT, Liu Z-X, Qu X, Elder BD, Bilz S, Befroy D, Romanelli AJ, Shulman GI (2004) Mechanism of hepatic insulin resistance in non-alcoholic fatty liver disease. *J Biol Chem* 279:32345–32353
30. Eder E, Wacker M, Lutz U, Nair J, Fang X, Bartsch H, Beland FA, Schlatter J, Lutz WK (2006) Oxidative stress related DNA adducts in the liver of female rats fed with sunflower-, rapeseed-, olive- or coconut oil supplemented diets. *Chem Biol Interact* 159:81–89
31. Greene J, Hammock B (1999) Toxicity of linoleic acid metabolites. *Adv Exp Med Biol* 469:471–477
32. Moran JH, Mitchell LA, Bradbury JA, Qu W, Zeldin DC, Schnellmann RG, Grant DF (2000) Analysis of the Cytotoxic Properties of Linoleic Acid Metabolites Produced by Renal and Hepatic P450s. *Toxicol Appl Pharmacol* 168:268–279
33. Erol A (2007) Insulin resistance is an evolutionarily conserved physiological mechanism at the cellular level for protection against increased oxidative stress. *Bioessays* 29:811–818
34. Degirolamo C, Shelness GS, Rudel LL (2008) LDL cholesteryl oleate as a predictor for atherosclerosis: evidence from human and animal studies on dietary fat. *J Lipid Res* 50(Suppl):S434–S439
35. Rudel L, Parks J, Sawyer J (1995) Compared with dietary monounsaturated and saturated fat, polyunsaturated fat protects African green monkeys from coronary artery atherosclerosis. *Arterioscler Thromb Vasc Biol* 15:2101–2110
36. Sato M, Shibata K, Nomura R, Kawamoto D, Nagamine R, Imaizumi K (2005) Linoleic acid-rich fats reduce atherosclerosis development beyond its oxidative and inflammatory stress-increasing effect in apolipoprotein E-deficient mice in comparison with saturated fatty acid-rich fats. *Br J Nutr* 94:896–901
37. Parini P, Johansson L, Bröijersén A, Angelin B, Rudling M (2006) Lipoprotein profiles in plasma and interstitial fluid analyzed with an automated gel-filtration system. *Eur J Clin Invest* 36:98–104
38. Folch J, Lees M, Stanley GHS (1957) A simple method for the isolation and purification of total lipids from animal tissues. *J Biol Chem* 226:497–509
39. Ganning A, Olsson M, Peterson E, Dallner G (1989) Fatty acid oxidation in hepatic peroxisomes and mitochondria after treatment of rats with di(2-ethylhexyl)phthalate. *Pharmacol Toxicol* 65:265–268
40. Tollet-Egnell P, Flores-Morales A, Stahlberg N, Malek RL, Lee N, Norstedt G (2001) Gene expression profile of the aging process in rat liver: normalizing effects of growth hormone replacement. *Mol Endocrinol* 15:308–318
41. Iovanna J (2002) Expression of the stress-associated protein p8 is a requisite for tumor development. *Int J Gastrointest Cancer* 31:89–98
42. Leu J, George D (2007) Hepatic IGFBP1 is a prosurvival factor that binds to BAK, protects the liver from apoptosis, and antagonizes the proapoptotic actions of p53 at mitochondria. *Genes Dev* 21:3095–3109
43. Coskun T, Bina HA, Schneider MA, Dunbar JD, Hu CC, Chen Y, Moller DE, Kharitonov A (2008) FGF21 corrects obesity in mice. *Endocrinology* 149:6018–6027
44. Ntambi JM, Miyazaki M, Stoehr JP, Lan H, Kendzierski CM, Yandell BS, Song Y, Cohen P, Friedman JM, Attie AD (2002) Loss of stearoyl-CoA desaturase-1 function protects mice against adiposity. *Proc Natl Acad Sci USA* 99:11482–11486
45. Dobrzyn P, Dobrzyn A, Miyazaki M, Cohen P, Asilmaz E, Hardie DG, Friedman JM, Ntambi JM (2004) Stearoyl-CoA desaturase 1 deficiency increases fatty acid oxidation by activating AMP-activated protein kinase in liver. *Proc Natl Acad Sci USA* 101:6409–6414
46. Sekiya M, Yahagi N, Matsuzaka T, Najima Y, Nakakuki M, Nagai R, Ishibashi S, Osuga J-I, Yamada N, Shimano H (2003) Polyunsaturated fatty acids ameliorate hepatic steatosis in obese mice by SREBP-1 suppression. *Hepatology* 38:1529–1539
47. McCaffrey T, Fu C, Du B, Eksinar S, Kent K, Bush HJ, Kreiger K, Rosengart T, Cybulsky M et al (2000) High-level expression of Egr-1 and Egr-1-inducible genes in mouse and human atherosclerosis. *J Clin Invest* 105:653–662
48. Harja E, Bucciarelli LG, Lu Y, Stern DM, Zou YS, Schmidt AM, Yan S-F (2004) Early growth response-1 promotes atherogenesis: mice deficient in early growth response-1 and apolipoprotein E display decreased atherosclerosis and vascular inflammation. *Circ Res* 94:333–339
49. Stepkowski S, Chen W, Ross J, Nagy Z, Kirken R (2008) STAT3: an important regulator of multiple cytokine functions. *Transplantation* 85:1372–1377
50. Rico-Bautista E, Flores-Morales A, Fernández-Pérez L (2006) Suppressor of cytokine signaling (SOCS) 2, a protein with multiple functions. *Cytokine Growth Factor Rev* 17:431–439
51. Vidal OM, Merino R, Rico-Bautista E, Fernandez-Perez L, Chia DJ, Woelfle J, Ono M, Lenhard B, Norstedt G et al (2007) In vivo transcript profiling and phylogenetic analysis identifies suppressor of cytokine signaling 2 as a direct signal transducer and activator of transcription 5b target in liver. *Mol Endocrinol* 21:293–311
52. Ono M, Chia DJ, Merino-Martinez R, Flores-Morales A, Unterman TG, Rotwein P (2007) Signal transducer and activator of transcription (Stat) 5b-mediated inhibition of insulin-like growth factor binding protein-1 gene transcription: a mechanism for repression of gene expression by growth hormone. *Mol Endocrinol* 21:1443–1457
53. Ooi GT, Cohen FJ, Tseng LYH, Rechler MM, Boisclair YR (1997) Growth hormone stimulates transcription of the gene encoding the acid-labile subunit (ALS) of the circulating insulin-like growth factor-binding protein complex and als promoter activity in rat liver. *Mol Endocrinol* 11:997–1007
54. Norstedt G (1984) Effect of growth hormone on prolactin receptors and on estrogen receptors in the liver of prepubertal rats. *Mol Cell Endocrinol* 36:195–200
55. Westin S, Mode A, Murray M, Chen R, Gustafsson JA (1993) Growth hormone and vitamin A induce P450C7 mRNA expression in primary rat hepatocytes. *Mol Pharmacol* 44:997–1002
56. Flores-Morales A, Stahlberg N, Tollet-Egnell P, Lundeberg J, Malek RL, Quackenbush J, Lee NH, Norstedt G (2001) Microarray analysis of the in vivo effects of hypophysectomy and growth hormone treatment on gene expression in the rat. *Endocrinology* 142:3163–3176
57. Burgering B, Coffer P (1995) Protein kinase B (c-Akt) in phosphatidylinositol-3-OH kinase signal transduction. *Nature* 376:599–602

58. Gual P, Le Marchand-Brustel Y, Tanti J-F (2005) Positive and negative regulation of insulin signaling through IRS-1 phosphorylation. *Biochimie* 87:99–109
59. Bremer J (2001) The biochemistry of hypo- and hyperlipidemic fatty acid derivatives: metabolism and metabolic effects. *Prog Lipid Res* 40:231–268
60. Ntambi JM (1992) Dietary regulation of stearoyl-CoA desaturase 1 gene expression in mouse liver. *J Biol Chem* 267:10925–10930
61. Landau J, Sekowski A, Hamm M (1997) Dietary cholesterol and the activity of stearoyl CoA desaturase in rats: evidence for an indirect regulatory effect. *Biochim Biophys Acta* 1345:349–357
62. Kim H-J, Miyazaki M, Ntambi JM (2002) Dietary cholesterol opposes PUFA-mediated repression of the stearoyl-CoA desaturase-1 gene by SREBP-1 independent mechanism. *J Lipid Res* 43:1750–1757
63. Miyazaki M, Kim Y-C, Gray-Keller MP, Attie AD, Ntambi JM (2000) The biosynthesis of hepatic cholesterol esters and triglycerides is impaired in mice with a disruption of the gene for stearoyl-CoA desaturase 1. *J Biol Chem* 275:30132–30138
64. Chiang JYL, Kimmel R, Stroup D (2001) Regulation of cholesterol 7[alpha]-hydroxylase gene (CYP7A1) transcription by the liver orphan receptor (LXR[alpha]). *Gene* 262:257–265
65. Repa JJ, Berge KE, Pomajzl C, Richardson JA, Hobbs H, Mangelsdorf DJ (2002) Regulation of ATP-binding cassette sterol transporters ABCG5 and ABCG8 by the liver X receptors alpha and beta. *J Biol Chem* 277:18793–18800
66. Brown JM, Chung S, Sawyer JK, Degirolamo C, Alger HM, Nguyen T, Zhu X, Duong M-N, Wibley AL et al (2008) Inhibition of stearoyl-coenzyme a desaturase 1 dissociates insulin resistance and obesity from atherosclerosis. *Circulation* 118:1467–1475
67. Bordoni A, Di Nunzio M, Danesi F, Biagi P (2006) Polyunsaturated fatty acids: from diet to binding to PPARS and other nuclear receptors. *Genes Nutr* 1:95–106
68. Dobrzyń A, Dobrzyń P (2006) Stearoyl-CoA desaturase—a new player in skeletal muscle metabolism regulation. *J Physiol Pharmacol* 57:31–42
69. Badman M, Pissios P, Kennedy A, Koukos G, Flier J, Maratos-Flier E (2007) Hepatic fibroblast growth factor 21 is regulated by PPARalpha and is a key mediator of hepatic lipid metabolism in ketotic states. *Cell Metab* 5:426–437
70. Kharitonkov A, Wroblewski VJ, Koester A, Chen Y-F, Clutinger CK, Tigno XT, Hansen BC, Shanafelt AB, Etgen GJ (2007) The metabolic state of diabetic monkeys is regulated by fibroblast growth factor-21. *Endocrinology* 148:774–781
71. Gälman C, Lundåsen T, Kharitonkov A, Bina HA, Eriksson M, Hafström I, Dahlin M, Åmark P, Angelin B, Rudling M (2008) The circulating metabolic regulator FGF21 is induced by prolonged fasting and PPARalpha activation in man. *Cell Metab* 8:169–174
72. Potthoff MJ, Inagaki T, Satapati S, Ding X, He T, Goetz R, Mohammadi M, Finck BN, Mangelsdorf DJ et al (2009) FGF21 induces PGC-1alpha and regulates carbohydrate and fatty acid metabolism during the adaptive starvation response. *Proc Natl Acad Sci USA* 106:10853–10858
73. Inagaki T, Lin V, Goetz R, Mohammadi M, Mangelsdorf D, Kliewer S (2008) Inhibition of growth hormone signaling by the fasting-induced hormone FGF21. *Cell Metab* 8:77–83
74. Ono M, Chia D, Merino-Martinez R, Flores-Morales A, Unterman T, Rotwein P (2007) Signal transducer and activator of transcription (Stat) 5b-mediated inhibition of insulin-like growth factor binding protein-1 gene transcription: a mechanism for repression of gene expression by growth hormone. *Mol Endocrinol* 21:1443–1457
75. Woelfle J, Chia DJ, Rotwein P (2003) Mechanisms of growth hormone (GH) action: identification of conserved Stat5 binding sites that mediate GH-induced insulin-like growth factor-I gene activation. *J Biol Chem* 278:51261–51266
76. Stahlberg N, Rico-Bautista E, Fisher RM, Wu X, Cheung L, Flores-Morales A, Tybring G, Norstedt G, Tollet-Egnell P (2004) Female-predominant expression of fatty acid translocase/CD36 in rat and human liver. *Endocrinology* 145:1972–1979
77. Elam MB, Simkevich CP, Solomon SS, Wilcox HG, Heimberg M (1988) Stimulation of in vitro triglyceride synthesis in the rat hepatocyte by growth hormone treatment in vivo. *Endocrinology* 122:1397–1402
78. Sjöberg A, Oscarsson J, Borén J, Edén S, Olofsson S (1996) Mode of growth hormone administration influences triacylglycerol synthesis and assembly of apolipoprotein B-containing lipoproteins in cultured rat hepatocytes. *J Lipid Res* 37:275–289
79. Kotronen A, Lewitt M, Hall K, Brismar K, Yki-Jarvinen H (2008) Insulin-like growth factor binding protein 1 as a novel specific marker of hepatic insulin sensitivity. *J Clin Endocrinol Metab* 93:4867–4872
80. Ezzat V, Duncan E, Wheatcroft S, Kearney M (2008) The role of IGF-I and its binding proteins in the development of type 2 diabetes and cardiovascular disease. *Diabetes Obes Metab* 10:198–211
81. Le Bacquer O, Petroulakis E, Pagliarlunga S, Poulin F, Richard D, Cianflone K, Sonenberg N (2007) Elevated sensitivity to diet-induced obesity and insulin resistance in mice lacking 4E-BP1 and 4E-BP2. *J Clin Invest* 117:387–396

local pigs than in other commercial pigs [3–5]. The Wujin pig is one of the Chinese local pigs, which is regarded as fatty genotype [6, 7]. The Landrace pig is considered a lean breed. Therefore, the underlying mechanism of fat deposition in fatty and lean pigs could be elucidated using these two pig models.

Triacylglycerol (TAG), the major component of IMF in muscles, is stored within the myofibers and mostly within the intramuscular adipocytes [8]. From a physiological perspective, lipid metabolism could theoretically contribute to the variation of fat deposition content [9–11]. Previous studies have investigated the difference of muscle lipid metabolism between fat and lean pig lines. However, these studies were mainly limited to lipogenesis and did not consider other aspects of lipid metabolism [12]. The extent of fat deposition in skeletal muscles depends on the balance of synthesis and degradation of TAG, which includes TAG synthesis, fat mobilization, fatty acid transport as well as fatty acid oxidation [13]. This fact implies that not only lipogenesis, but also lipolysis and fatty acid transport are involved in IMF deposition. Thus, the hypothesis is that higher IMF deposition may be attributed to increasing fat catabolism or diminishing endogenous fatty acid synthesis or both processes.

Therefore, the objective of this study is to investigate the expression of genes involved in lipogenesis, lipolysis and fatty acid transport in muscle, to compare the expression pattern of lipid metabolism associated genes in pigs with different fat deposition capacity, and then to elucidate the mechanism of IMF deposition between fatty and lean pigs.

Materials and Methods

All experiment procedures were performed according to the Guide for Animal Care and Use of Laboratory Animals in the Institutional Animal Care and Use Committee of Yunnan Agricultural University. The experimental protocol was approved by the Department Animal Ethics Committee of Yunnan Agricultural University.

Animals and Samples

Twelve Wujin and 12 Landrace pigs were used. All pigs had free access to water from nipple drinkers. The diets were not isonitrogenous or isoenergetic because the growth rate of the two breeds was so divergent (Table 1) and were provided ad libitum. Pigs were weighed individually for the calculation of average daily gain. When the pigs reached 100 kg body weight, they were transported to Yunnan Agricultural Center Meats Laboratory and slaughtered after electrical stunning. Longissimus muscle samples from the last ribs were collected from every animal.

Table 1 Composition of diets (% , as fed basis)

	Wujin pigs	Landrace pigs
Corn	68.90	75.70
Wheat bran	22.40	7.30
Soybean meal	5.60	11.80
Fish meal	0.50	1.20
Limestone	0.97	0.40
Monocalcium phosphate	0.10	0.70
Salt	0.30	0.30
Premix ^a	1.00	1.00
Calculated nutritional composition		
Crude protein	11.42	13.20
Total lysine	0.69	0.60
Digestive energy (MJ/kg)	13.11	13.56
Calcium	0.46	0.45
Total phosphorus	0.37	0.40
Available phosphorus	0.14	0.15

^a A vitamin premix provided the following per kilogram of diet: vitamin A, 8,267 IU; vitamin D2, 2,480 IU; vitamin E, 66 IU; menadione (as menadione pyrimidyl bisulfite complex), 6.2 mg; riboflavin, 10 mg; Ca D-pantothenic acid, 37 mg; niacin, 66 mg; vitamin B12, 45 µg; D-biotin, 331 µg; folic acid, 2.5 mg; pyridoxine, 3.31 mg; thiamine, 3.31 mg; vitamin C, 83 µg; Trace mineral premix provided the following per kilogram of diet: Zn, 127 mg; Fe, 127 mg; Mn, 20 mg; Cu, 12.7 mg; I, 0.80 mg, as zinc sulfate, ferrous sulfate, manganese sulfate, copper sulfate, ethylenediamine dihydride, respectively, with calcium carbonate as the carrier. Provided 0.3 mg Se per kilogram of diet

Determination of Adipocyte Diameter

Adipocytes were obtained by collagenase treatment. Adipocyte diameters were determined in five serial cross sections (10 µm thick at 40 µm intervals) of frozen tissues cut with a cryostat (2800 Frigocut Reichert-Jung, Francheville, France). Results corresponded to the mean of determinations performed on the five sections of each sample and were expressed as the diameter (µm) of visible adipocytes [14].

Measurement of IMF Content

Muscles were sampled for IMF content evaluation 24 h after slaughtering by following the Soxhlet petroleum-ether extraction method.

Determination of Fatty Acid Composition

Lyophilized muscle samples were methylated using methyl sulfate solution. Briefly, 0.5 g muscle was added in 5 ml methyl sulfate solution and backed on the 70 °C water bath pan for 1 h, then cooled and extracted using 10 ml extraction solution. After centrifugation, supernatant was dehydrated

Table 2 Specific primers used for real-time quantitative PCR

Gene name	Sequence	Product size	Accession number	Cycle profile
<i>β-actin</i>	F:5'-ACT GCC GCA TCC TCT TCC TC-3' R:5'-CTC CTG CTT GCT GAT CCA CAT C-3'	399 bp (766–1164)	DQ845171	95 °C/30 s, 56.5 °C/30 s, 72 °C/90 s
<i>FAS</i>	F:5'-AGC CTA ACT CCT CGC TGC AAT-3' R:5'-TCC TTG GAA CCG TCT GTG TTC-3'	196 bp (504–699)	AY183428	95 °C/40 s, 58 °C/40 s, 72 °C/55 s
<i>SREBP-1c</i>	F:5'-GCG ACG GTG CCT CTG GTA GT-3' R:5'-CGC AAG ACG GCG GAT TTA-3'	218 bp (194–411)	AF102873	95 °C/35 s, 60 °C/45 s, 72 °C/70 s
<i>H-FABP</i>	F:5'-CAG GAA AGT CAA GAG CAC CA-3' R:5'-TCG GGA CAA TAC ATC CAA CA-3'	227 bp (234–460)	AJ416020	95 °C/40 s, 61 °C/50 s, 72 °C/65 s
<i>A-FABP</i>	F:5'-CAG GAA AGT CAA GAG CAC CA-3' R:5'-TCG GGA CAA TAC ATC CAA CA-3'	227 bp (234–460)	AJ416020	95 °C/35 s, 60 °C/40 s, 72 °C/90 s
<i>HSL</i>	F:5'-GCT CCC ATC GTC AAG AAT C-3' R:5'-TAA AGC GAA TGC GGT CC-3'	262 bp (2407–2668)	AJ000482	95 °C/40 s, 60.5 °C/40 s, 72 °C/90 s
<i>CPT-1B</i>	F:5'-ATG GTG GGC GAC TAA CT-3' R:5'-TGC CTG CTG TCT GTG AG-3'	321 bp (681–1001)	AY181062	95 °C/30 s, 59 °C/45 s, 72 °C/60 s
<i>SCD</i>	F:5'-TCT GGG CGT TTG CCT ACT ATC T-3' R:5'-TCT TTG ACG GCT GGG TGT TT-3'	280 bp (481–760)	AY487829	95 °C/40 s, 60.5 °C/45 s, 72 °C/60 s
<i>ATGL</i>	F: 5'-AGT TCA GCC TGC GCA ACC TC-3' R: 5'-AGG GCA CCA TCA TGG CTG-3'	220 bp (1060–841)	EF583921	95 °C/45 s, 61.5 °C/45 s, 72 °C/80 s

over film and measured on the machine. Fatty acid profile was determined on an HP 1100 gas chromatograph (GC, USA), with a flame ionization detector (FID), and an automatic sample injection operating a septum-equipped programmable injector operating. Inlet temperature was 240 °C and detector temperature was 250 °C. Programmed temperature start at 195 °C for 2 min, 195 °C for 6 min, 215 °C for 5 min, 225 °C for 10 min and ended at 235 °C. Fatty acid methyl esters were identified according to peak retention times using standards (Sigma–Aldrich). C21:0 was used as the internal standard. The response factors of the individual FA were previously calculated. Selected abbreviations are saturated fatty acid (SFA) = C14:0 + C16:0 + C18:0 + C20:0; monounsaturated fatty acid (MUFA) = C16:1 + C18:1; and polyunsaturated fatty acid (PUFA) = C18:2 + C18:3 + C20:4 + C20:5 + C22:5. Results are expressed as weight percentages of total fatty acid.

Muscle Tissue Enzyme Activity Analyses

Approximately 1 g muscle tissue was homogenized using an Ultra-Turrax T8 (IKA Laboratory Technics; Vienna, Austria) in 3 mL of 10 mmol/L HEPES buffer containing 0.25 mol/L sucrose, 1 mol/L EDTA, and 1 mmol/L dithiothreitol, and then centrifuged at 100,000g for 30 min at 4 °C. Supernatants were collected and used for enzyme activity assays. Spectrophotometric assays were used for FAS [15]. The assay for HSL activity was based on a cholesterol esterase assay described by Osterlund et al.

[16]. The whole mitochondrial was isolated using the method of Beiber et al. [17]. The CPT-1B activity was assayed directly using whole mitochondrial isolates which were resuspended in 0.3 mmol/L sucrose containing 10 mmol/L Tris–HCl (pH 7.4 at 0 °C) and 1 mmol/L EDTA and sonicated to obtain a mitochondrial supernatant after centrifugation at 20,000g for 40 min at 4 °C [17]. Microsome was extracted from muscle tissue and SCD enzyme activity was determined as described by Archibeque et al. [18]. All assays were conducted in the range of linearity with respect to the amount of enzyme and time. Soluble protein concentration in the tissue supernatants was measured according to the method of Bradford [19], using bovine serum albumin as the standard. Except otherwise mentioned, all reagents were obtained from Sigma Chemical.

Real-Time PCR Analysis

Total RNA was isolated from muscle tissues using Trizol reagent according to the manufacturer's protocol (Invitrogen, USA). RNA was stored at –80 °C prior to use. Two micrograms of total RNA was used for RT in a final volume of 25 µL according to the manufacturer's instructions (Promega, America). Each primer (Table 2) was designed according to porcine nucleotide sequences in GenBank using Primes Premier 5, and synthesized by Shanghai Shengong Biological Company (Shanghai, China).

Real-time PCR was performed to quantitate mRNA expression of *A-FABP*, *H-FABP*, *FAS*, *SREBP-1*, *HSL*, *CPT-1B*, *SCD* and *ATGL* genes. Each 25 μ L PCR mixture contained 12.5 μ L of 2 \times iQTM SYBR Green Supermix, 0.5 μ L (10 mmol/L) of each primer and 1 L of cDNA. As an internal control, the same reverse transcription products were also subjected to PCR in the presence of a second pair of primers specific to pig β -actin RNA. Mixtures were incubated in an iCycler iQ Real-time Detection system (Bio-Rad, USA). Optimal PCR conditions for 40 cycles were shown in Table 2. Quantitation of the transcripts was performed using a standard curve with 10-fold serial dilutions of cDNA. A melting curve was constructed to ensure that only a single PCR product was amplified. Samples were assayed in triplicate, and each experiment was repeated at least twice. Negative and positive control reactions (without template or Taq enzyme) were performed for each sample.

Western Blotting

Whole frozen muscle samples (0.5 g) were homogenized on ice in 700 μ L buffer A [50 mmol/L Tris-HCl (pH 7.5), 50 mmol/L NaF, 5 mmol/L sodium pyrophosphate, 1 mmol/L EDTA, 1 mmol/L DTT, 0.1 mmol/L phenylmethyl sulfonyl fluoride, 10% glycerol] containing 1% Triton X-100, 5 μ mol/L aprotinin, leupeptin and pepstatin. The lysates were centrifuged at 6,000g for 20 min at 4 $^{\circ}$ C to remove insoluble material. Thereafter, the supernatant extracts were collected and protein concentration was determined using the method of Bradford [19]. The extracts were frozen at -80 $^{\circ}$ C until the western blot analyses were performed.

A-FABP, H-FABP, SREBP-1c and ATGL protein expression was measured according to the method described by Doran et al. [20]. Briefly, 50 μ g of total whole cell protein extract were separated by sodium dodecyl sulfate-polyacrylamide gel electrophoresis (12% resolving gel), transferred to a nitrocellulose membrane and probed respectively (1:500, 1:800, 1:1,000 and 1:2,000 dilution) with a rabbit polyclonal anti-A-FABP (HPA002188), H-FABP(AV33823) (Sigma, USA), SREBP-1c (SC-367) and ATGL (SC-67355) (Santa Cruz, USA) antibody overnight. The membranes were then probed with a goat anti-rabbit IgG-horseradish peroxidase conjugate (1:20,000) (Sigma, USA) for 1 h at room temperature. Blots were developed using the SuperSignal West Pico Chemiluminescent Substrate system (Bio-Rad, Hercules, CA, USA) and imaged onto microfilm for image analysis and densitometry. Signal intensity was quantified using Quantity One 1-D analysis software (Bio-Rad, Hercules, CA, USA).

Statistical Analysis

The results were expressed as means \pm SE and differences were considered significant when $P < 0.05$ tested by one

Table 3 Growth performance

	Wujin pigs	Landrace pigs
Daily gain (g/day)	0.59 \pm 0.02	0.77 \pm 0.01*
Feed intake (g/day)	1.86 \pm 0.14	1.87 \pm 0.14
Gain: feed (g/g)	0.32 \pm 0.01	0.41 \pm 0.01*

Values are expressed as means \pm SE and values in the same row with asterisks differ significantly ($P < 0.05$)

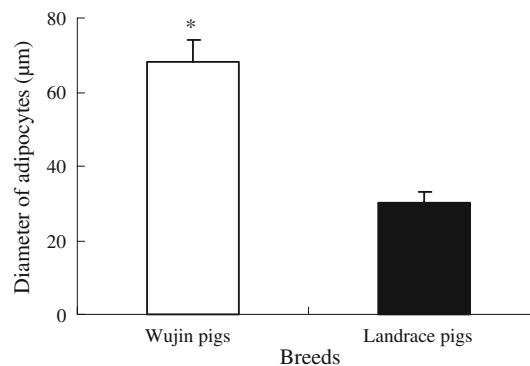


Fig. 1 Diameter of adipocytes in Wujin and Landrace pigs. Data are expressed as means \pm SE. Asterisks signify differences between two pigs of the same breed ($P < 0.05$)

way analysis of variance (ANOVA) with Statistical Packages for Social Science 12.0 and Excel 2003 in Microsoft.

Results

Growth Performance

Table 3 showed growth performance of Wujin and Landrace pigs. Average daily gains for Wujin and Landrace pigs were 0.59 and 0.77 kg, respectively ($P < 0.05$). There was no significant difference of daily feed intake between both pigs. The feed conversion ratio for Wujin and Landrace pigs was 0.32 and 0.41 ($P < 0.05$), respectively.

Adipocyte Diameter, IMF Content and Fatty Acid Composition

Figure 1 showed adipocyte diameters in Wujin and Landrace pigs. The results showed that adipocyte diameter in Wujin pigs was significantly higher than in Landrace pigs ($P < 0.05$). IMF content and fatty acid composition of muscle tissue in Wujin and Landrace pigs are shown in Table 4. IMF content in Wujin pigs (6.58%) was significantly higher than in Landrace pigs (3.90%) ($P < 0.05$). Wujin pigs possessed higher contents of C16:1, C18:2, C18:3, C20:4 and C20:5 than Landrace pigs ($P < 0.05$).

Table 4 Fatty acid composition and IMF content

	Wujin pigs	Landrace pigs
C14:0	2.06 ± 0.09	1.99 ± 0.08
C16:0	27.11 ± 0.72	27.22 ± 0.57
C16:1	4.99 ± 0.09*	4.06 ± 0.08
C18:0	10.11 ± 0.24	14.43 ± 0.28*
C18:1	40.81 ± 0.73	40.98 ± 0.96
C18:2	12.16 ± 0.28	9.39 ± 0.13*
C18:3	0.94 ± 0.03	0.62 ± 0.05*
C20:0	0.92 ± 0.03	0.80 ± 0.05
C20:4	0.38 ± 0.03	0.20 ± 0.04*
C20:5	0.28 ± 0.03	0.11 ± 0.01*
C22:5	0.24 ± 0.02	0.20 ± 0.03
SFA	40.20 ± 0.68	44.44 ± 0.73*
MUFA	45.80 ± 0.74	45.04 ± 0.96
PUFA	14.00 ± 0.30	10.52 ± 0.12*
IMF	6.58 ± 0.13*	3.90 ± 0.10

Data are expressed as means ± SE and values in the same row with asterisks differ significantly ($P < 0.05$)

Table 5 Enzyme activities

Items	Wujin pigs	Landrace pigs
FAS ^a	8.23 ± 3.45 ^{e*}	4.41 ± 2.84
HSL ^b	0.21 ± 0.04	0.73 ± 0.02*
CPT-1B ^c	10.94 ± 0.62	16.12 ± 0.04*
SCD ^d	9.21 ± 0.02*	4.43 ± 0.06

Units are:

^a nmol reduced nicotinamide adenine dinucleotide phosphate (NADPH) min⁻¹ mg protein⁻¹

^b mU mg protein⁻¹

^c nmol palmitate min⁻¹ mg protein⁻¹

^d nmol/(7 min⁻¹ mg of tissue)

^e Values are expressed as means ± SE and values in the same row with asterisks differ significantly ($P < 0.05$)

However, the percentage of C18:0 in Wujin pigs was significantly lower than in Landrace pigs ($P < 0.05$). In addition, Wujin pigs had a higher percentage of total PUFA ($P < 0.05$). However, the UFA percentage in Wujin pigs was significantly higher compared with Landrace pigs ($P < 0.05$).

Enzyme Activity

The activities of FAS, SCD, HSL and CPT-1B enzymes were shown in Table 5. The enzyme activities of FAS and SCD were significantly higher ($P < 0.05$) in Wujin pigs than in Landrace pigs. However, the activities of HSL and

CPT-1B enzymes in Wujin pigs were significantly lower ($P < 0.05$) compared with Landrace pigs.

Gene Expression

Results are presented as numerical relative gene expression values (using β -actin as a housekeeping calibrator) (Fig. 2). The expression of lipogenetic genes, *SREBP-1c* and *FAS*, were significantly higher in Wujin pigs than in Landrace pigs ($P < 0.05$). Wujin pigs exhibited significantly higher mRNA abundance of fatty acid transportation genes, *H-FABP* and *A-FABP*, than Landrace pigs ($P < 0.05$). However, the expression intensity of genes involved in fatty acid oxidation and fat mobilization, *ATGL*, *CPT-1B* and *HSL*, was lower in Wujin pigs than in Landrace pigs ($P < 0.05$). Wujin pigs have a significantly higher mRNA abundance of the desaturase gene, *SCD*, compared with Landrace pigs ($P < 0.05$).

Protein Expression

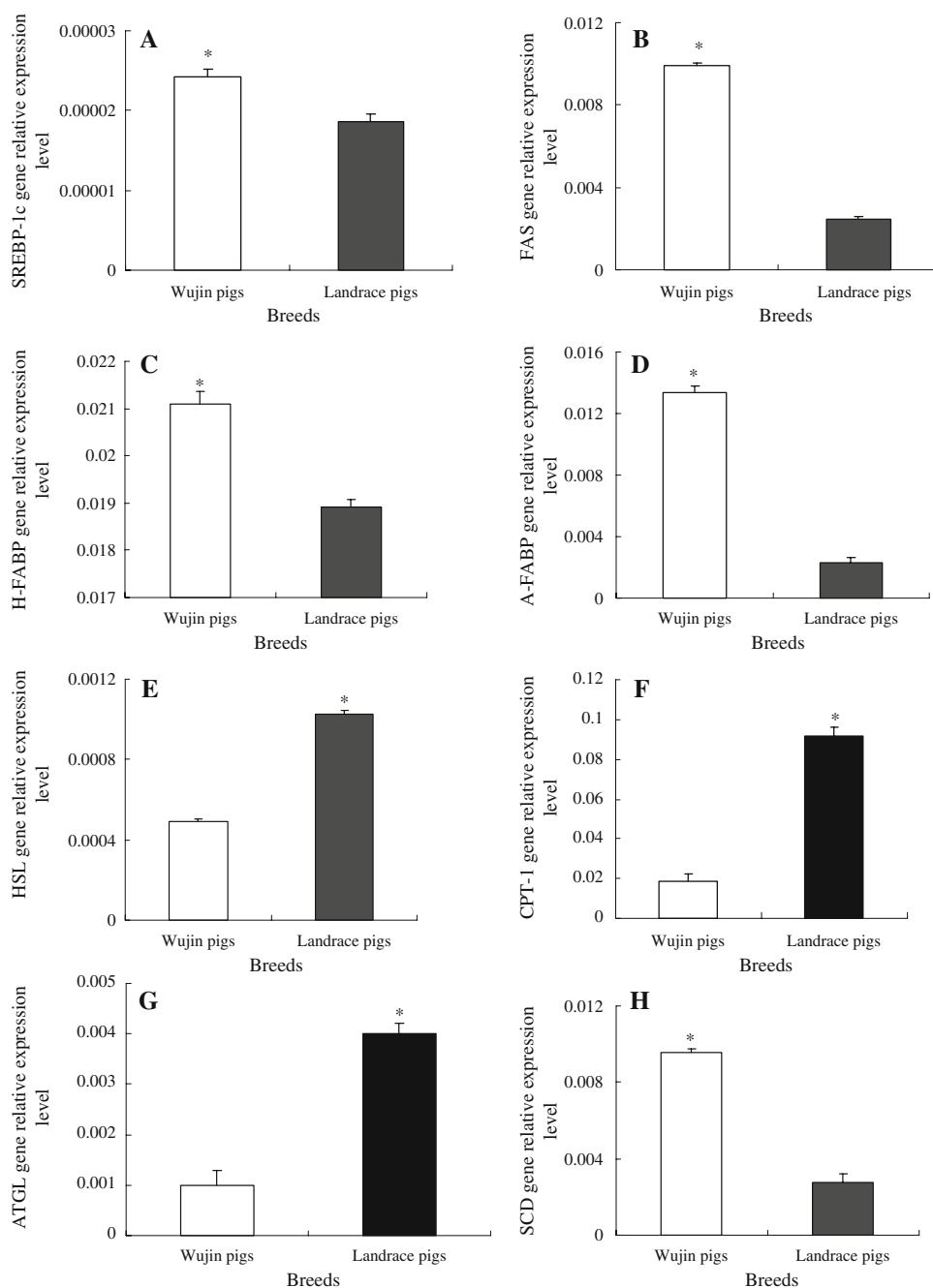
Figure 3 showed the expression of H-FABP, A-FABP, SREBP-1c and ATGL proteins in Wujin and Landrace pigs. Wujin pigs exhibited the higher expression of A-FABP compared with Landrace pigs, but the difference was not significant. The expression of H-FABP and SREBP-1c proteins in Wujin pigs was significantly higher ($P < 0.05$) than in Landrace pigs. The expression of ATGL protein in Wujin pigs was lower ($P < 0.05$) compared with Landrace pigs.

Discussion

Previous data indicated that local Chinese pigs deposit more fat than other commercial pigs, especially higher IMF content which can reach up to 6–7% [3–5]. Mersmann et al. [21] and Campion et al. [22] reported that the plasma and muscle of obese pigs had a greater triglycerides percentage than the lean pigs. TAG, the major component of IMF in muscles, is stored within the intramuscular adipocytes [8]. Hauser et al. [23] indicated that intramuscular adipocytes appeared to be larger in Meishan than Pietrain pigs. In this study, IMF content (6.58%) in Wujin pigs was significantly greater than in Landrace pigs (3.90%). Moreover, the average adipocyte diameter in Wujin pigs was higher than that in Landrace pigs. This suggested that the fatty Wujin pigs possessed the higher capacity to deposit TAG in muscle tissue compared with the lean Landrace pigs.

Additionally, not only the amount of IMF has to be considered, but also the composition of fatty acid is of great interest because of its association with human health [24–26]. This study showed that contents of C16:1, C18:2,

Fig. 2 Relative mRNA abundance of muscle tissue in Wujin and Landrace pigs. Data are expressed as means \pm SE of specific mRNA: β -actin for 12 pigs. Asterisks show significant differences between two pig breeds ($P < 0.05$). A, B, C, D, E, F, G and H represented *SREBP-1c*, *FAS*, *H-FABP*, *A-FABP*, *HSL*, *CPT-1B*, *ATGL* and *SCD* genes, respectively

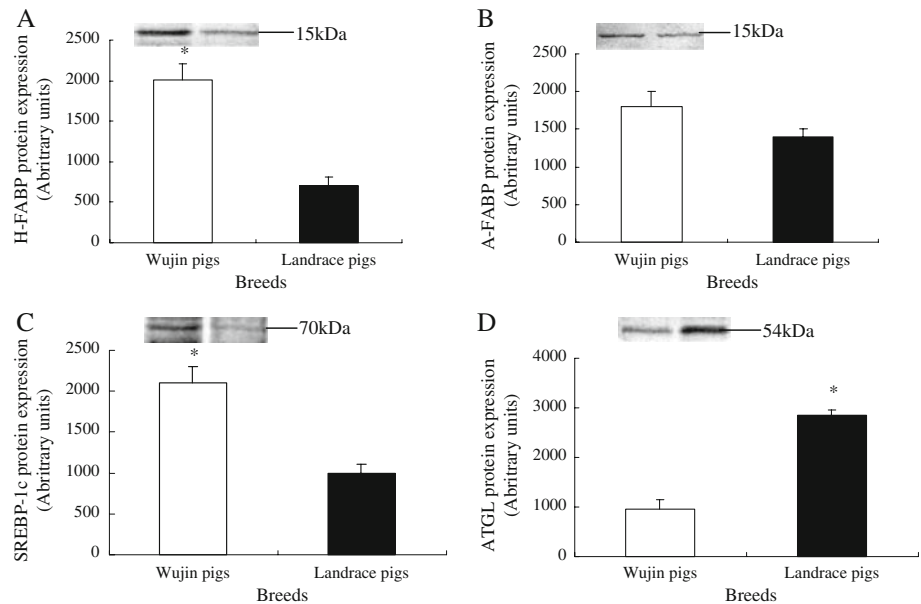


C18:3, C20:4 and C20:5 were higher in Wujin pigs than in Landrace pigs. Wujin pigs possessed a higher UFA concentration compared with Landrace pigs, which means that muscle UFA percentage was higher in fatty pigs than in lean pigs. This result indicated that the fatty acid composition in muscle tissue was different in fatty and lean pigs. The difference of fatty acid composition between both genotypes may be due to the variance of SCD, because SCD is a rate-limiting enzyme in the biosynthesis of unsaturated fatty acid [20]. SCD or Δ^9 -desaturase catalyzes the conversion of C16:0 and C18:0 to C16:1 and C18:1, the

2 major MUFA of muscle lipids [26]. Smith et al. [27] indicated that *SCD* gene expression would be greater in obese pigs than in crossbred, contemporary pigs. The present study showed that mRNA abundance of *SCD* gene and enzyme activity in Wujin pigs was higher compared with Landrace pigs. Therefore, the results suggested that the different expression of SCD between Wujin and Landrace pigs may result in the variation of muscle fatty acid composition.

The intramuscular adipose tissue possesses adequate levels of lipogenic enzymes [12] and was markedly

Fig. 3 Protein expressions of muscle tissues in Wujin pigs and Landrace pigs. Data are expressed as means \pm SE. Letters with asterisks differ significantly between the two pig breeds ($P < 0.05$). A, B, C and D represent A-FABP, H-FABP, SREBP-1c and ATGL



influenced by the animal breed [28, 29]. FAS is transcriptionally regulated and a key enzyme in fatty acid synthesis [30]. SREBP-1c has been shown to be the principal regulatory transcription factor for fatty acid synthesis in animals [31]. Thus FAS and SREBP-1 have been shown to be critical to lipogenesis. Our results showed that the fatty Wujin pigs showed higher mRNA abundance and enzyme activity of FAS and higher expression of *SREBP-1c* gene and protein compared with the lean Landrace pigs. Muscle lipogenic enzyme activities were generally higher in fatty pigs than in lean pigs [12]. This suggested that the muscle lipid synthesis in fatty Wujin pigs was higher compared with the lean Landrace pigs.

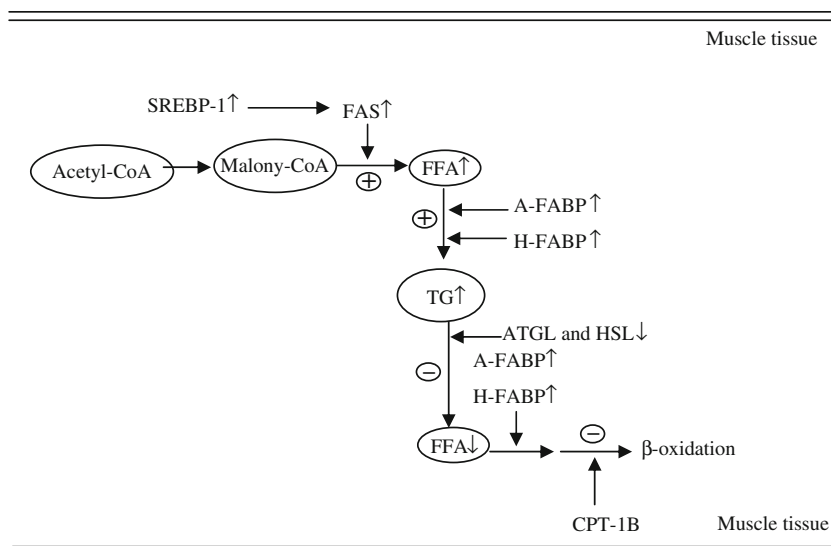
Although lipogenesis appears to be more important than lipolysis in regulating backfat thickness in the breeds of swine [11] and adipose tissue lipolysis does not appear to be a major metabolic factor leading to the excessive fat accretion in the obese pigs [32]. Fat deposition is determined by a complex balance between lipogenic and lipolytic enzymes [9–11]. Adipose tissue of obese pigs had lipolytic rates expressed on a cellular basis or per 100 mg adipose tissue in vitro that were greater than those from lean pigs [33–35]. The present study compared the expression of muscle lipolysis related gene and protein as well as enzyme activities between the fatty Wujin pigs and the lean Landrace pigs. ATGL is a newly identified lipase and its expression reacts to hormonal stimuli and plays a role in catecholamine-induced lipolysis in porcine adipose tissue [36]. HSL cleaves fatty acid from intracellular triacylglycerol for oxidation and exportation [37]. CPT-1B is involved in regulating mitochondrial fatty acid oxidation [13]. Our results showed that the fatty Wujin pigs exhibited lower mRNA abundance, enzyme activities or protein

expression for ATGL, CPT-1B and HSL compared with the lean Landrace pigs. For our knowledge, this is the first report to compare porcine muscle lipid catabolism between the fatty and lean pigs. Previous reports focused on the muscle lipogenes independent of the muscle lipolysis [12]. This data suggested that the mRNA and protein expression of genes related to oxidative metabolism and fat mobilization were lower in Wujin pigs contrasted with Landrace pigs.

Previous studies revealed the role of FABPs. Of them, A-FABP and H-FABP play a critical role in intracellular trafficking of fatty acid and have been elucidated as candidate genes related to fat deposition in pigs [38–42]. Additionally, H-FABP is critical for fatty acid uptake as well as trafficking in heart and in brain in *H-FABP* gene-ablated mice [43]. Furthermore, L-FABP facilitates fatty acid uptake and disposition into L-cell phospholipids whereas I-FABP did not facilitate uptake and targeted the fatty acids to TAG [44–47]. However, Damon et al. [48] indicated that there was no difference of A-FABP mRNA or protein levels between low fat and high fat groups, but H-FABP content may be a valuable marker of lipid accretion [49]. In our study, mRNA abundance and protein expression level of A-FABP and H-FABP in Wujin pigs was higher than in Landrace pigs. This data suggested Wujin pigs could transport more fatty acid into intracellular trafficking compared with Landrace pigs.

In conclusion, this study demonstrated the different expression patterns of muscle lipid anabolic and catabolic genes and fatty acid transporting genes in the pigs with different IMF deposition. The cause underlying higher IMF content in Wujin pigs appear to be that Wujin pigs possessed a higher capacity of lipogenesis and fatty acid

Fig. 4 The causes of higher IMF content in Wujin pigs comparing with Landrace pigs. ↑ Represents up-regulated gene expression. ↓ Represents down-regulated gene expression. ⊕ Represents the metabolism pathways being strengthened. ⊖ Represents the metabolism pathways being weakened



transport, lower potential of fat mobilization and fatty acid oxidation (Fig. 4).

Acknowledgments This work was supported by National Key Foundation Research Development Project of China (973 Project, No. 2007CB116201) and Natural Science Foundation Key Project of Yunnan Province (No. 2005C0008Z).

References

- Fernandez X, Monin G, Talmant A, Mouro J, Lebre B (1999) Influence of intramuscular fat content on the quality of pig meat—1. Composition of the lipid fraction and sensory characteristics of m. longissimus lumborum. *Meat Sci* 53:59–65
- Sellier P (1998) Genetics of meat and carcass traits. In: The genetics of the pig. Rothschild MF, Ruvinsky A (eds) CAB International, Wallingford, UK p 463
- Kinyamu HK, Ewan RC (1994) Energy and protein metabolism of the Chinese pig. *J Anim Sci* 72:2068–2074
- Yen JT, Nienaber JA, Klindt J, Crouse JD (1991) Effect of racotamine on growth, carcass traits, and fasting heat production of US contemporary crossbred and Chinese Meishan pure- and crossbred pigs. *J Anim Sci* 69:4810–4817
- Young LD (1992) Comparison of Meishan, Fengjing, Minzhu and Duroc swine: effects on postweaning growth, feed efficiency, and carcass traits. *J Anim Sci* 70:2020–2029
- Zhang X, Ge CR, Zhao SM, Lai H, Li CQ, Gao SZ (2008) Effects of dietary composition and digestive energy levels on meat quality in Wujin Pigs. *Chin J Anim Nutri* 20:58–65
- Ge CR, Zhao SM, Zhang X, Lai H, Li CQ, Gao SZ (2008) Effects of dietary protein levels on meat quality in Wujin Pigs. *Acta Veter Zoote Sini* 39:1692–1700
- Pethick DW, Harper GS, Oddy VH (2004) Growth, development and nutritional manipulation of marbling in cattle: a review. *Aust J Exp Agric* 44:705–715
- Ding ST, Schinkel AP, Weber TE, Mersmann HJ (2000) Expression of porcine transcription factors and genes related to fatty acid metabolism in different tissues and genetic populations. *J Anim Sci* 78:2127–2134
- Reiter SS, Halsey CHC, Stronach BM, Bartosh JL, Owsley WF, Bergen WG (2007) Lipid metabolism related gene-expression profiling in liver, skeletal muscle and adipose tissue in crossbred Duroc and Pietrain pigs. *Comp Biochem Phys D* 2:200–206
- Scott RA, Cornelius SG, Mersmann HJ (1981) Effects of age on lipogenesis and lipolysis in lean and obese swine. *J Anim Sci* 52:505–511
- Mouro J, Kouba M (1998) Lipogenic enzyme activities in muscles of growing Large White and Meishan pigs. *Livest Prod Sci* 55:127–133
- Bernlohr DA, Jenkins AE, Bennaars AA (2002) Adipose tissue and lipid metabolism. In: Vance DE, Vance JE (eds) *Biochemistry of lipids, lipoproteins and membranes*, 4th edn. Elsevier, Amsterdam, pp 263–289
- Etherton TD, Chung CS (1981) Preparation, characterization, and insulin sensitivity of isolated swine adipocytes: comparison with adipose tissue slices. *J Lipid Res* 22:1053–1059
- Ingle DL, Bauman DE, Mellenberger RW, Johnson DE (1973) Lipogenesis in the ruminant: effect of fasting and refeeding on fatty acid synthesis and enzymatic activity of sheep adipose tissue. *J Nutr* 103:1479–1488
- Osterlund TB, Danielsson ED, Contreras JA, Edren G, Davis RC, Schotz MC, Holm C (1996) Domain-structure analysis of recombinant rat hormone-sensitive lipase. *Biochem J* 319:411–420
- Bieber LL, Abraham T, Helmuth T (1972) A rapid spectrophotometric assay for carnitine palmitoyltransferase. *Anal Biochem* 50:509–518
- Archibeque SL, Lunt DK, Tume RK, Smith SB (2005) Fatty acid indices of stearoyl CoA desaturase activity do not reflect actual stearoyl Co-A desaturase enzyme activity in adipose tissues of beef steers finished with corn-, flaxseed-, or sorghum- based diets. *J Anim Sci* 83:1153–1166
- Bradford MM (1976) A rapid and sensitive method for the quantitation of microgram quantities of protein utilizing the principle of protein-dye binding. *Anal Biochem* 72:248–254
- Doran O, Moule SK, Teye GA, Whittington FM, Hallett KG, Wood JD (2006) A reduced protein diet induces stearoyl-CoA desaturase protein expression in pig muscle but not in subcutaneous adipose tissue: relationship with intramuscular lipid formation. *Brit J Nutr* 95:609–617
- Mersmann HJ, Pond WG, Yen JT (1982) Plasma glucose, insulin and lipids during growth of genetically lean and obese swine. *Growth* 46:189–198
- Campion DR, Hausman GJ, Meredith FI (1983) Skeletal muscle metabolism in neonatal lean and obese pigs. *J Anim Sci* 57:26–33

23. Hauser N, Mourot J, De Clercq L, Genart C, Remacle C (1997) The cellularity of developing adipose tissues in Pietrain and Meishan pigs. *Reprod Nutr Dev* 37:617–625
24. Fernandez X, Monin G, Talmant A, Mourot J, Lebreton B (1999) Influence of intramuscular fat content on the quality of pig meat—2. Consumer acceptability of *m. longissimus lumborum*. *Meat Sci* 53:67–72
25. Woollett LA, Spady DK, Dietschy JM (1992) Saturated and unsaturated fatty acid independently regulate low density lipoprotein receptor activity and production rate. *J Lipid Res* 33:77–88
26. Rudel LL, Park JS, Sawyer JK (1995) Compared with dietary monounsaturated and saturated fat, polyunsaturated fat protects African green monkeys from coronary artery atherosclerosis. *Arterioscler Thromb Vasc Biol* 15:2101–2110
27. Smith SB, Mersmann HJ, Smith EO, Britain KG (1999) Stearoyl-coenzyme A desaturase gene expression during growth in adipose tissue from obese and crossbred pigs. *J Anim Sci* 77:1710–1716
28. Morales J, Perez JF, Baucells MD, Mourot J, Gasa J (2002) Comparative digestibility and lipogenic activity in Landrace and Iberian finishing pigs fed ad libitum corn- and corn-sorghum-acorn-based diets. *Livest Prod Sci* 77:195–205
29. Martin RJ, Herbein JH (1976) A comparison of the enzyme levels and the in vitro utilization of various substrates for lipogenesis in pair-fed lean and obese pigs. *Proc Soc Exp Bio Med* 151:231–235
30. Sul HS, Wang D (1998) Nutritional and hormonal regulation of enzymes in fat synthesis: studies of fatty acid synthase and mitochondrial glycerol-3-phosphate acyltransferase gene transcription. *Annu Rev Nutr* 18:331–351
31. Horton JD, Goldstein JL, Brown MS (2002) SREBPs: activators of the complete program of cholesterol and fatty acid synthesis in the liver. *J Clin Invest* 109:1125–1131
32. Mersmann HJ (1985) Adipose tissue lipolytic rate in genetically obese and lean swine. *J Anim Sci* 60:131–135
33. Mersmann HJ, MacNeil MD (1985) Relationship of plasma lipid concentrations to fat deposition in pigs. *J Anim Sci* 61:122–128
34. Mersmann HJ (1986) Postnatal expression of adipose tissue metabolic activity associated with a porcine genetic obesity. *J Anim Sci* 63:741–746
35. Buhlinger CA, Wangsness PJ, Martin RJ, Ziegler JH (1978) Body composition, in vitro lipid metabolism and skeletal muscle characteristics in fast-growing, lean and in slow-growing, obese pigs at equal age and weight. *Growth* 42:225–236
36. Deulius JA, Shin J, Bae D, Azain MJ, Barb R, Lee K (2008) Developmental, hormonal, and nutritional regulation of porcine adipose triglyceride lipase (ATGL). *Lipids* 43:215–225
37. Mersmann HJ (1998) Lipoprotein and hormone-sensitive lipases in porcine adipose tissue. *J Anim Sci* 76:1396–1404
38. Gerbens F, de Koning DJ, Harders FL, Meuwissen THE, Janss LLG, Groenen MA, Veerkamp JH, Van Arendonk JA, te Pas MF (2000) The effect of adipocyte and heart fatty acid-binding protein genes on intramuscular fat and backfat content in Meishan cross bred pigs. *J Anim Sci* 78:552–559
39. Gerbens F, Jansen A, van Erp AJM, Harders F, Meuwissen THE, Rettenberger G, Veerkamp JH, te Pas MFW (1998) The adipocyte fatty acid-binding protein locus: characterization and association with intramuscular fat content in pigs. *Mamm Genome* 9:1022–1026
40. Gerbens F, Rettenberger G, Lenstra JA, Veerkamp JH, te Pas MFW (1997) Characterization, chromosomal localization, and genetic variation of the porcine heart fatty acid-binding protein. *Mamm Genome* 8:328–331
41. Gerbens F, van Erp AJM, Harders FL, Verburg FJ, Meuwissen THE, Veerkamp JH, te Pas MFW (1999) Effect of genetic variants of the heart fatty acid-binding protein gene on intramuscular fat and performance traits in pigs. *J Anim Sci* 77:846–852
42. Chmurzynska A (2006) The multigene family of fatty acid-binding proteins (FABPs): function, structure and polymorphism. *J Appl Genet* 47:39–48
43. Murphy Eric J, Barcelo-Coblijn Gwendolyn, Binias Bert, Glatz Jan FC (2004) Heart fatty acid uptake is decreased in heart fatty acid-binding protein gene-ablated mice. *J Biol Chem* 279:34481–34488
44. Prows DR, Murphy EJ, Schroeder F (1995) Lipids. Intestinal and liver fatty acid binding proteins differentially affect fatty acid uptake and esterification in L-cells 30:907–910
45. Murphy EJ, Prows D, Stiles T, Schroeder F (2000) Liver and intestinal fatty acid-binding protein expression increases phospholipid content and alters phospholipid fatty acid composition in L-cell fibroblasts. *Lipids* 35:729–738
46. Prows DR, Murphy EJ, Moncecchi D, Schroeder F (1996) Intestinal fatty acid-binding protein expression stimulates fibroblast fatty acid esterification. *Chem Phys Lipids* 84:47–56
47. Murphy EJ, Prows DR, Jefferson JR, Schroeder F (1996) Liver fatty acid-binding protein expression in transfected fibroblasts stimulates fatty acid uptake and metabolism. *Biochim Biophys Acta-Lipids Lipid Metab* 1301:191–198
48. Damon M, Louveau I, Lefaucheur L, Lebreton B, Vincent A, Leroy P, Sanchez MP, Herpin P, Gondret F (2006) Number of intramuscular adipocytes and fatty acid binding protein-4 content are significant indicators of intramuscular fat level in crossbred Large White Duroc pigs. *J Anim Sci* 84:1083–1092
49. Li B, Zerby HN, Lee K (2007) Heart fatty acid binding protein is upregulated during porcine adipocyte development. *J Anim Sci* 85:1651–1659

Remarkably, studies performed on various cell systems have shown that administration of short-chain ceramides may also induce accumulation of the long-chain forms of this molecule [4–7]. Although the latter phenomenon has been appreciated for a long time, only recently have its metabolic bases and biological implications started being investigated [8–10]. In the above-reported setting, a previous study from this laboratory showed that administration of *N*-hexanoylsphingosine (C6-Cer) to CHP-100 human neuroepithelioma cells induces both apoptosis and LC-Cer accumulation [7]. In the present study, we experimentally addressed the issue of whether, in the above-mentioned cell system, LC-Cer generation is relevant to the apoptotic response evoked by administration of its short-chain analogue.

Experimental Procedures

Materials

Material for cell culture, phosphatidylcholine, natural ceramide from bovine brain, *D*-erythro-C6-Cer, *D*-erythro-sphingosine, *L*-cycloserine (L-CS) and fumonisins B1 (FB1) were from Sigma-Aldrich Chemical Co. The anti-poly-(ADP)ribose polymerase (PARP) mouse monoclonal antibody was from Biomol. Res. Lab. The mouse monoclonal anti-cytochrome *c* antibody was from Pharmingen. The DNA fluorescent dye Hoechst 33342, the fluorescein isothiocyanate (FITC)-conjugated anti-mouse antibody and Mitotracker Red were from Invitrogen. The caspase-9 fluorogenic peptide substrate *acetyl*-Leu-Glu-His-Asp-amido-4-trifluoromethyl-coumarin (*Ac*-LEHD-AFC) was from Calbiochem. Silica gel 60 high-performance thin layer chromatography (HPTLC) plates were from Merck. The chemiluminescence ECL detection system was from Amersham Corp.

Cell Culture and Treatments

CHP-100 cells were grown at 37 °C in RPMI 1640 medium, supplemented with 10% (v/v) heat-inactivated foetal calf serum, 2 mM glutamine, 100 i.u./ml penicillin and 100 µg/ml streptomycin, in a humidified atmosphere with 5% CO₂. C6-Cer, sphingosine and FB1 were administered to cells from dimethylsulfoxide stock solutions (30, 10 and 50 mM, respectively); L-CS was administered from a 1 M aqueous stock solution. After treatments, adherent cells were mechanically removed from the substrate directly in the culture medium, containing already detached cells; total cells were then washed three times with phosphate-buffered saline (PBS, pH 7.4) prior to further processing.

Lipid Analysis

Lipids were extracted by the method of Folch et al. [11]. For ceramide analysis, the Folch lower phase was dried under vacuum, lipids resuspended in 0.1 M methanolic KOH, subjected to mild alkaline hydrolysis for 1 h at 37 °C and re-extracted by Folch's method. Ceramide was resolved by HPTLC in chloroform/acetic acid (9:1, by vol) and visualized after charring with 3% cupric acetate in 8% phosphoric acid [12, 13]. Bands were quantitated by densitometric analysis, referring to known amounts of lipid standards (C6-Cer and natural ceramide from bovine brain) developed along with samples, using a computerized image processing system (Gel-Pro Analyzer). Phosphatidylcholine was resolved from the Folch lower phase by two-dimensional HPTLC, using chloroform/methanol/25% ammonia/water (6.4:9.8:1:1, by vol) and chloroform/methanol/acetone/acetic acid/water (15:5:6:3:1.5, by vol) as solvent systems. Phosphatidylcholine spots were identified by co-migration with authentic standards, visualized by plate exposure to iodine vapour and scraped off. Phosphate content was measured according to Marinetti [14].

Immunofluorescence Microscopy

Cells were grown on coverslips and incubated in a medium containing 30 µM C6-Cer for 24 h. Mitotracker Red (40 nM) was added overnight to the cell medium before washing and fixing in 4% paraformaldehyde. Cells were then subjected to immunocytochemistry by using an anti-cytochrome *c* antibody, followed by incubation with a FITC-conjugated anti-mouse antibody. Cellular nuclei were stained with Hoechst dye (0.5 µg/ml) and the samples analyzed by confocal microscopy. Confocal microscopy images were acquired using a laser scanning microscope (model LSM 510 Combi; Carl Zeiss MicroImaging, Inc.) equipped with a visible and infrared Ti-Sa pulsed laser (Tsunami/Millenia Spectra-Physics). Post-acquisition processing was performed with Adobe Photoshop software.

Apoptosis Evaluation and PARP Cleavage Analysis

Cells were fixed in 4% paraformaldehyde in PBS and incubated for 15 min with a solution of 0.5 µg/ml Hoechst 33342 in PBS. Nuclei were visualized with a Zeiss fluorescence microscope; condensed or fragmented elements were scored as apoptotic. In parallel, apoptosis was monitored by flow cytometric analysis, after evaluation of the fluorescence of propidium iodide-stained nuclei, as reported in detail elsewhere [15]. The two methods gave similar results. For Western blot analysis of PARP, cells were lysed in 62 mM Tris-HCl, pH 6.8, containing 2% SDS, 2 mM EDTA, 20 µg/ml aprotinin, 10 µg/ml leupeptin,

1 mM phenylmethylsulfonyl fluoride and 1 mM sodium vanadate. After sonication, aliquots of the lysates were saved for protein determination [16] and, after addition of 0.05% β -mercaptoethanol, samples were boiled for 10 min. Proteins from cell lysates (40 μ g) were resolved by 10% SDS-PAGE, transferred onto nitrocellulose paper and probed by Western blot, as previously described [15]. Immunoreactivity was revealed by an ECL detection kit, according to the manufacturer's instructions.

Evaluation of Caspase-9 Activity

Caspase-9 activity was monitored by a fluorogenic assay, using *Ac-LEHD-AFC* as a substrate [17]. Briefly, CHP-100 cells, either left untreated or treated for 24 h with 30 μ M C6-Cer, were harvested directly in the culture medium and washed three times in PBS. The final pellets were resuspended in lysis buffer (150 mM NaCl, 50 mM Tris-HCl, pH 8.0, 0.1% SDS, 1% Nonidet P-40, 0.5% sodium deoxycholate) and incubated for 30 min at 4 °C. Aliquots of the lysates corresponding to 50 μ g or 100 μ g of protein were incubated in an assay buffer (100 mM HEPES, pH 7.0, 1 mM EDTA, 0.1% CHAPS, 10% glycerol, 20 mM dithiothreitol), in the presence of 75 μ M *Ac-LEHD-AFC*, for 1 or 2 h, at 37 °C. Substrate cleavage by caspase-9 resulted in the release of the free fluorochrome (AFC), producing a yellow–green fluorescence that was monitored using a Perkin-Elmer LS-5 luminescence spectrometer, by setting λ_{ex} at 400 nm and λ_{em} at 505 nm. Under the above-reported conditions, enzymatic activity assays were linear with respect to time and protein content. Fluorescence intensity values were normalized to protein amount and to incubation time, and used to estimate the relative changes in caspase-9 activity.

Statistical Analysis

Statistical significance was determined by unpaired Student's *t* test. Differences were considered significant at $P < 0.05$.

Results

CHP-100 Cells Rapidly Accumulate LC-Cer in Response to C6-Cer: Evidence that the Phenomenon is Inhibited by FB1, but not by L-CS

Accumulation of LC-Cer in response to C6-Cer administration has been previously demonstrated in CHP-100 cells after equilibrium labeling with radioactive palmitic acid [7]. In this study, cells were exposed to 30 μ M C6-Cer for different periods and changes in LC-Cer and C6-Cer mass

simultaneously estimated by densitometric analysis, after lipid separation by HPTLC and staining by charring [12, 13]. As shown in Fig. 1, C6-Cer was rapidly incorporated by CHP-100 cells and its levels were already sub-maximal after 2 h of incubation, maintaining at steady-state throughout the remaining period examined. Remarkably, a rapid increase of LC-Cer levels was also observed, albeit with slower kinetics than those occurring for the short-chain counterpart: as shown in Fig. 1, LC-Cer accumulation was already evident after 2 h from the beginning of cell treatment with C6-Cer, reaching, by 8 h, a 5-fold elevation over the basal level and remaining at this steady-state at later times. As expected, LC-Cer migrated as a doublet, reflecting the heterogeneous length of the fatty acids linked to the sphingosine backbone.

To get insight into the mechanism driving C6-Cer-evoked LC-Cer accumulation, we investigated the sensitivity of the phenomenon to L-CS (1 mM), a serine-palmitoyltransferase inhibitor [18], or to FB1 (50 μ M), an inhibitor of CoA-dependent dihydroceramide/ceramide synthase [18, 19]. As shown in Fig. 2(a, b), neither basal LC-Cer levels nor C6-Cer-evoked LC-Cer accumulation were significantly affected by L-CS; on the other hand, Fig. 2(c, d) shows that FB1, beside attenuating basal LC-Cer levels, potently inhibited LC-Cer accumulation in response to C6-Cer. Altogether, the above-reported results strongly suggested that LC-Cer might be predominantly produced via the salvage pathway, namely by C6-Cer deacylation and sphingosine reacylation with a long-chain fatty acid [20].

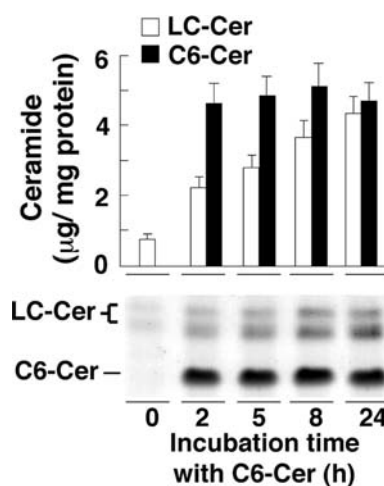


Fig. 1 Time-course of intracellular ceramide accumulation in cells exposed to C6-Cer. CHP-100 cells were incubated with 30 μ M C6-Cer for the indicated times; thereafter, aliquots of the lower phase of the Folch extracts from the different samples, corresponding to equal amounts of protein, were resolved by HPTLC and LC-Cer and C6-Cer levels analysed as reported in the text. The *upper panel* shows data obtained from four different experiments, expressed as means and SD. A representative HPTLC analysis is shown in the *lower panel*

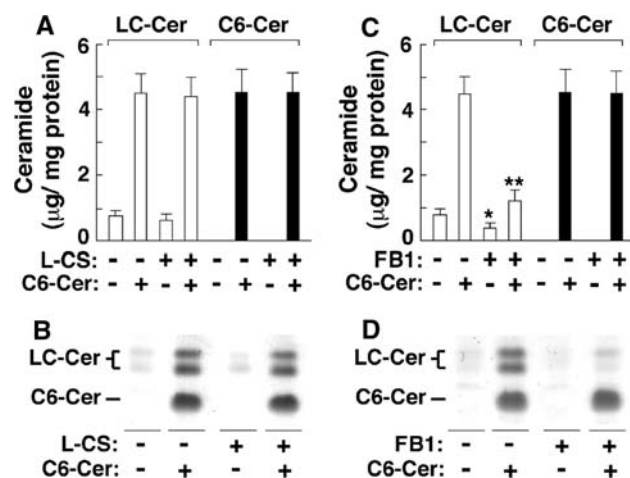


Fig. 2 FB1, but not L-CS, inhibits LC-Cer generation in response to C6-Cer. **a** Cells were incubated for 24 h either in the presence (+) or absence (–) of 30 μM C6-Cer in media enriched (+) or devoid (–) of 1 mM L-CS. Aliquots of the Folch lower phase from the different samples, corresponding to equal amounts of cell protein, were then resolved by HPTLC and LC-Cer and C6-Cer levels analysed as reported in the text. Data are from four different experiments and are expressed as means and SD. **b** Representative HPTLC analysis from the experiment reported in **a**. **c** Cells were incubated for 24 h either in the presence (+) or absence (–) of 30 μM C6-Cer, in media enriched (+) or devoid (–) of 50 μM FB1. Aliquots of the Folch lower phase from the different samples, corresponding to equal amounts of cell protein, were then resolved by HPTLC and LC-Cer and C6-Cer levels analysed as reported in the text. Data are from four different experiments and are expressed as means and SD. Statistical significance: * $P < 0.05$ and ** $P < 0.0001$, as compared to the counterparts incubated in the absence of Fum B1, after Student's *t* test. **d** Representative HPTLC analysis from the experiment reported in **c**

Apoptosis Induced by C6-Cer Administration Associates with Cytochrome *c* Release from Mitochondria and Caspase-9 Activation and is not Inhibited by FB1

It has been reported that exposure of CHP-100 cells to 30 μM C6-Cer also evokes caspase-dependent apoptosis [7, 21]. Notably, Fig. 3 now shows that apoptotic nuclear condensation and fragmentation associate with cytochrome *c* release into the cytosol. Moreover, in line with the possibility that mitochondrial permeabilization might provide a relevant mechanism for the apoptotic response evoked by C6-Cer administration, Fig. 4 shows that caspase-9 was also activated [22]. To test whether C6-Cer-evoked LC-Cer accumulation was instrumental to apoptosis induction, we investigated whether apoptosis was attenuated by impairing LC-Cer accumulation by co-treatment with FB1. In this respect, we observed that 50 μM FB1 was neither toxic by itself to CHP-100 cells, nor did it affect the apoptotic response induced by cell exposure to 30 μM C6-Cer over a 24 h-period, as monitored by evaluation of apoptotic nuclei (Fig. 5a) and cleavage of the caspase substrate PARP (Fig. 5b).

Exogenously Administered Sphingosine Evokes Elevation of LC-Cer Levels Without Inducing Apoptosis

As mentioned above, the differential inhibitory effect displayed by FB1 and L-CS on C6-Cer-evoked LC-Cer

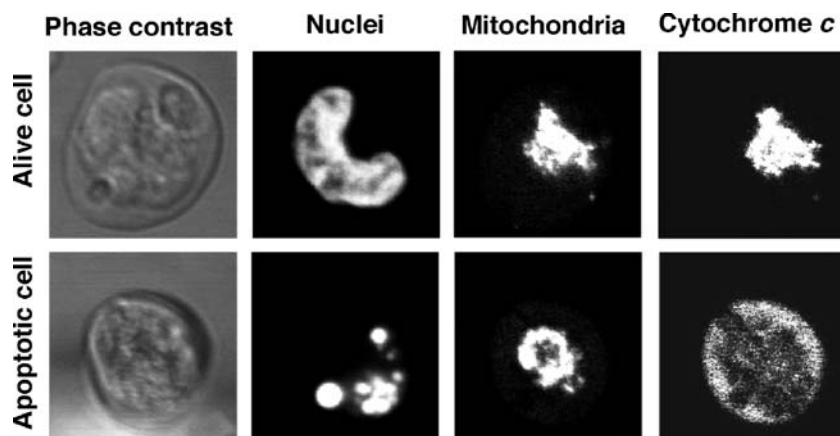


Fig. 3 Apoptosis induced by C6-Cer in CHP-100 cells associates with cytochrome *c* release from mitochondria. CHP-100 cells were grown on coverslips and incubated in medium containing 30 μM C6-Cer for 24 h. Nuclei were stained with Hoechst, mitochondria with Mitotracker Red, and cytochrome *c* with a specific antibody, followed by treatment with a FITC-conjugated secondary antibody, as reported

in the text. Cells were then analyzed by phase contrast and confocal microscopy. The *upper* and *lower* rows, respectively, show typical alive and apoptotic cells. Note the fragmented nucleus and condensed chromatin, as well as the different localization of mitochondria and cytochrome *c*, in the apoptotic cell

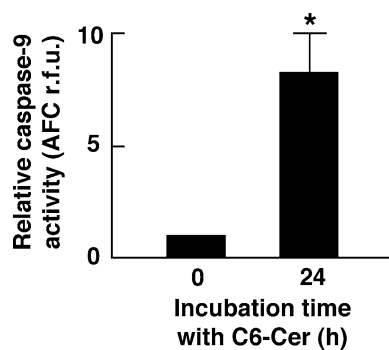


Fig. 4 C6-Cer administration induces caspase-9 activation in CHP-100 cells. Cells were either left untreated or treated for 24 h with 30 μ M C6-Cer. Thereafter, aliquots of cell lysates corresponding to equal amounts of protein were probed for caspase-9 activity, by measuring release of the free fluorochrome AFC, after hydrolysis of the enzyme fluorogenic substrate Ac-LEHD-AFC, as described in the text. Data are expressed as relative fluorescence units (r.f.u.) and are means and SD from four independent experiments. Statistical significance: * $P = 0.0001$, as compared to untreated cells, after Student's t test

accumulation strongly suggested that the latter phenomenon might occur along the sphingosine salvage pathway [20]. To study whether CHP-100 cells efficiently acylate free

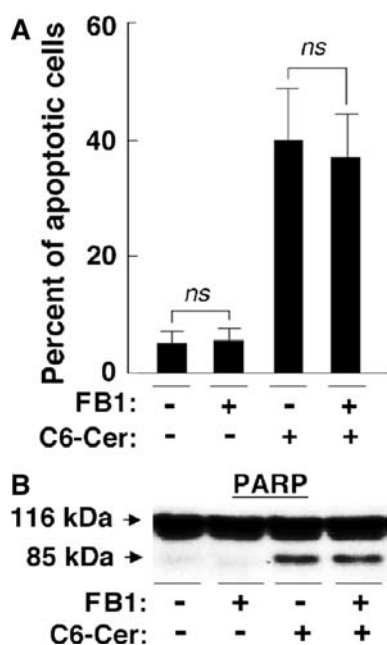


Fig. 5 FB1 does not affect the apoptotic response evoked by C6-Cer administration. **a** Cells were incubated for 24 h either in the presence (+) or absence (-) of 30 μ M C6-Cer, in media enriched (+) or devoid (-) of 50 μ M FB1. Cells were then collected and the percentage of apoptotic elements determined as described in the text. Data are from four different experiments and are expressed as means and SD; *ns* difference not statistically significant, as by Student's t test. **b** Cells were incubated for 24 h either in the presence (+) or absence (-) of 30 μ M C6-Cer, in media enriched (+) or devoid (-) of 50 μ M FB1. Equal amounts of protein from total lysates were then resolved by SDS-PAGE and probed for the native (116 kDa) and the cleaved form (85 kDa) of PARP

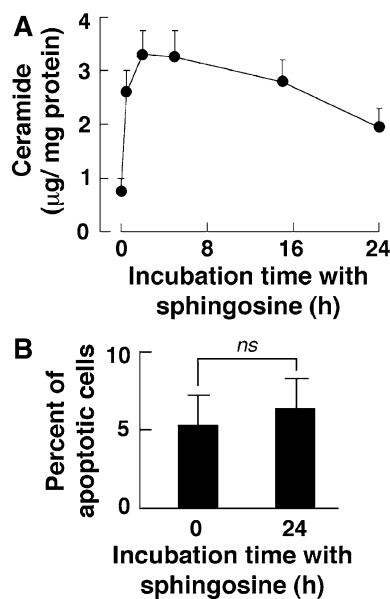


Fig. 6 Exogenously administered sphingosine evokes elevation of LC-Cer levels but not apoptosis. **a** CHP-100 cells were incubated with 10 μ M sphingosine for the indicated times; aliquots of the lower phase of the Folch extracts corresponding to equal amounts of cell protein were then analyzed for LC-Cer content, by HPTLC separation and densitometric analysis, as reported in the text. Data are from four different experiments and are expressed as means and SD. **b** Cells were either left untreated or incubated for 24 h in the presence of 10 μ M sphingosine and apoptosis determined as described in the text. Data are from four different experiments and are expressed as means and SD; *ns* difference not statistically significant, as by Student's t test

sphingosine, this lipid was administered in the medium at a 10 μ M concentration and intracellular LC-Cer levels monitored. As shown in Fig. 6a, LC-Cer levels promptly increased in response to sphingosine administration, reaching by 2 h a more than 4-fold increase over the basal level. On prolonging the incubation period, LC-Cer levels maintained initially at this high steady-state, to slowly decrease thereafter: however, by 24 h, LC-Cer levels were still two to three times the basal level (Fig. 6a). On the basis of this result we monitored whether LC-Cer accumulation, as evoked by sphingosine administration, associated with apoptosis induction. We observed that sphingosine, administered at a 10 μ M concentration for 24 h, caused cell rounding, associated with detachment of a minor fraction of the total cell population from the substrate (not shown); however, as reported in Fig. 6b, cell viability was not significantly affected.

Discussion

The above-reported results support the notion that LC-Cer accumulation, as observed in CHP-100 neuroepithelioma cells exposed to C6-Cer, is dispensable for apoptosis

induction. In this respect, the first key evidence is provided by the finding that LC-Cer synthesis can be severely impaired by the ceramide synthase inhibitor FB1, with no effect on the apoptotic response. We also observed that LC-Cer produced in response to C6-Cer, albeit potently inhibited by FB1, was insensitive to the palmitoyl-transferase inhibitor L-CS, a result strongly suggesting that LC-Cer is synthesized through the sphingosine salvage pathway [20]. In line with this possibility we have shown that CHP-100 cells markedly accumulate LC-Cer after administration of exogenous sphingosine: however, LC-Cer accumulation did not induce an apoptotic response. It can be argued that exogenously administered free sphingosine might not be functionally equivalent to sphingosine derived from C6-Cer deacylation, due to the fact that the two pools of the sphingoid base are expected to follow different intracellular traffic and processing, prior to be acylated [8, 23]. However, we observe that, in any case, the latter reaction is expected to occur in the endoplasmic reticulum, where the members of the ceramide synthase family reside [24]. It cannot be excluded that LC-Cer synthesis after administration of either C6-Cer or sphingosine is operated by ceramide synthase isoforms with a different sub-location within the endoplasmic reticulum and/or different fatty acid specificity. Nevertheless, it is evident from our results that, in the cell system presently employed, LC-Cer produced via the sphingosine salvage pathway displays no apoptotic potential.

The reasons as to why, in CHP-100 cells, apoptosis appears to be selectively triggered by C6-Cer over LC-Cer remain to be elucidated; nevertheless, an important clue may be provided by the evidence that apoptosis associates with cytochrome *c* release into the cytosol and caspase-9 activation, thus lending support to the notion that the phenomenon might occur, at least partly, via the mitochondrial pathway [22]. Indeed, studies on isolated mitochondria have shown that both short- and long-chain ceramides can induce organelle permeabilization and cytochrome *c* release [25]: however, in intact cells, the picture is made more complex by the fact that ceramide must efficiently accumulate in mitochondria to exert its cytotoxic activity. On the one hand, internalized C6-Cer, due to its property to form water-soluble micellar aggregates [3], may be expected to freely diffuse to mitochondria, possibly via the cytosolic milieu; in this respect, a study performed with a fluorescent C6-Cer analogue demonstrated that this exogenous sphingolipid rapidly labels mitochondria over other membrane compartments, prior to accumulation in the Golgi complex [26]. On the other hand, there is evidence that LC-Cer, due to its high hydrophobic characteristics, must be produced at the mitochondrial level to be cytotoxic [27, 28] or therein efficiently transported from its site of production [29]. On this basis, an issue deserving further investigation is

whether, in CHP-100 cells, LC-Cer produced via the sphingosine salvage pathway remains compartmentalized outside mitochondria. With respect to this point, it is also worth mentioning that studies on neural systems have shown that ceramide synthase activity localized in the endoplasmic reticulum is FB1-sensitive, whereas mitochondria harbor a reverse ceramidase activity able to acylate sphingosine that, however, is not inhibited by FB1 [30]. Of course it remains to be elucidated whether loss of mitochondrial integrity is the sole mechanisms through which C6-Cer induces apoptosis in the cell system presently investigated: in fact, short-chain ceramide ability to target various membrane compartments and to affect their physical and biological properties, leaves open the possibility that it might exert its cytotoxic effect through pleiotropic mechanisms.

Remarkably, it has been shown that short-chain ceramides may inhibit enzymes involved in phosphatidylcholine biosynthesis [31, 32]. Based on the notion that severe downregulation of phosphatidylcholine levels may induce apoptosis [33], this might provide a further mechanism through which short-chain ceramides exert their apoptotic effect [31, 32]. However, in an additional set of experiments, we observed that the phosphatidylcholine mass was 68 ± 12 nmol/mg protein ($n = 4$) in untreated CHP-100 cells and 62 ± 10 nmol/mg protein ($n = 4$) in cells exposed for 24 h to 30 μ M C6-Cer ($n = 4$) (not statistically significant, as shown by Student's *t* test). On the one hand, this result indicates that, in the system presently investigated, and under the experimental conditions employed, apoptosis is not accounted for by a general and dramatic downregulation of phosphatidylcholine levels. On the other hand, the possibility that the apoptotic effect of C6-Cer might also impact on reduction of phosphatidylcholine synthesis cannot be presently ruled out: in fact, it remains to be elucidated whether the rate of phosphatidylcholine turnover is reduced by C6-Cer treatment and/or whether a reduction of phosphatidylcholine mass locally occurs at the level of particular membrane compartments.

As our results are consistent with the notion that C6-Cer, but not LC-Cer synthesized via the salvage pathway, has pro-apoptotic properties, a study performed on human keratinocytes showed that C6-Cer efficiently induces apoptosis through LC-Cer production [10]; in addition, a study performed on HeLa cells demonstrated that apoptosis observed after C6-Cer administration was indeed due to elevation of the intracellular levels of sphingosine produced through the salvage pathway, that caused Golgi fragmentation [34]. Altogether, these observations underscore the important notion that short-chain ceramides may cause apoptosis through multiple mechanisms, depending on the cell system and, possibly, on the specific apoptotic pathway(s) involved.

Indeed, in line with the notion the LC-Cer produced through the salvage pathway may be dispensable for apoptosis induction, it has been shown that both *D-erythro-* and *L-erythro-C6-Cer* are equally effective in inducing apoptosis in leukemia HL-60 cells [8]. In the same study, it was shown that neither *D-erythro-* nor *L-erythro-C6-Cer* induced apoptosis in A549 lung adenocarcinoma cells; on the other hand, *D-erythro-*, but not *L-erythro-C6-Cer*, was able to modulate telomerase activity and to suppress cell growth, in a FB1-sensitive fashion. Intriguingly, we previously demonstrated that C6-Cer also causes growth inhibition and retinoblastoma protein dephosphorylation in CHP-100 cells [35]: thus it will be interesting to investigate whether, different to apoptosis, these phenomena are dependent on LC-Cer production through the salvage pathway.

As it is widely recognized that endogenous ceramide plays important roles in the control of a variety of cell functions, the present study lends support to the notion that caution must be exercised when investigating its biological effects by use of exogenously administered short-chain analogues. Indeed, short-chain ceramides may still provide useful research tools, provided the awareness that their peculiar chemico-physical properties might not invariably mimic the behavior of the endogenous counterparts.

Acknowledgments This work was partly supported by MIUR (Ministero dell'Istruzione dell'Università e della Ricerca) funds (60%) to Angelo Spinedi.

References

- Perry DK, Hannun YA (1998) The role of ceramide in cell signalling. *Biochim Biophys Acta* 1436:233–243
- Posse de Chaves EI (2006) Sphingolipids in apoptosis, survival and regeneration in the nervous system. *Biochim Biophys Acta* 1758:1995–2015
- van Blitterswijk WJ, van der Luit AH, Veldman RJ, Verheij M, Borst J (2003) Ceramide: second messenger or modulator of membrane structure and dynamics? *Biochem J* 369:199–211
- Abe A, Wu D, Shayman JA, Radin NS (1992) Metabolic effects of short-chain ceramide and glucosylceramide on sphingolipids and protein kinase C. *Eur J Biochem* 210:765–773
- Ridgway ND, Merriam DL (1995) Metabolism of short-chain ceramide and dihydroceramide analogues in Chinese hamster ovary (CHO) cells. *Biochim Biophys Acta* 1256:57–70
- Jaffrézou JP, Maestre N, de Mas-Mansat V, Bezombes C, Levade T, Laurent G (1998) Positive feedback control of neutral sphingomyelinase activity by ceramide. *FASEB J* 12:999–1006
- Spinedi A, Di Bartolomeo S, Piacentini M (1998) Apoptosis induced by *N*-hexanoylsphingosine in CHP-100 cells associates with accumulation of endogenous ceramide and is potentiated by inhibition of glucocerebroside synthesis. *Cell Death Differ* 5:785–791
- Ogretmen B, Pettus BJ, Rossi MJ, Wood R, Usta J, Szulc Z, Bielawska A, Obeid LM, Hannun YA (2002) Biochemical mechanisms of the generation of endogenous long chain ceramide in response to exogenous short chain ceramide in the A549 human lung adenocarcinoma cell line: role for endogenous ceramide in mediating the action of exogenous ceramide. *J Biol Chem* 277:12960–12969
- Sultan I, Senkal CE, Ponnusamy S, Bielawski J, Szulc Z, Bielawska A, Hannun YA, Ogretmen B (2006) Regulation of the sphingosine-recycling pathway for ceramide generation by oxidative stress, and its role in controlling c-Myc/Max function. *Biochem J* 393:513–521
- Takeda S, Mitsutake S, Tsuji K, Igarashi Y (2006) Apoptosis occurs via the ceramide recycling pathway in human HaCaT keratinocytes. *J Biochem* 139:255–262
- Folch J, Lees M, Sloane-Stanley GH (1957) A simple method for the isolation and purification of total lipides from animal tissues. *J Biol Chem* 266:497–509
- Macala LJ, Yu RK, Ando S (1983) Analysis of brain lipids by high performance thin layer chromatography and densitometry. *J Lipid Res* 24:1243–1250
- Herget T, Esdar C, Oehrlein SA, Heinrich M, Schütze S, Maelicke A, van Echten-Deckert G (2000) Production of ceramides causes apoptosis during early neural differentiation in vitro. *J Biol Chem* 275:30344–30354
- Marinetti GV (1962) Chromatographic separation, identification, and analysis of phosphatides. *J Lipid Res* 3:1–20
- Di Bartolomeo S, Di Sano F, Piacentini M, Spinedi A (2000) Apoptosis induced by doxorubicin in neurotumor cells is divorced from drug effects on ceramide accumulation and may involve cell cycle-specific caspase activation. *J Neurochem* 75:532–539
- Lowry OH, Rosebrough NJ, Farr AL, Randall RJ (1951) Protein measurement with the Folin phenol reagent. *J Biol Chem* 193:265–275
- Mohan J, Gandhi AA, Bhavya BC, Rashmi R, Karunakaran D, Indu R, Santhoshkumar TR (2006) Caspase-2 triggers Bax-Bak-dependent and -independent cell death in colon cancer cells treated with resveratrol. *J Biol Chem* 281:17599–17611
- Hinkovska-Galcheva V, Boxer L, Mansfield PJ, Schreiber AD, Shayman JA (2003) Enhanced phagocytosis through inhibition of de novo ceramide synthesis. *J Biol Chem* 278:974–982
- Wang E, Norred WP, Bacon CW, Riley RT, Merrill AH Jr (1991) Inhibition of sphingolipid biosynthesis by fumonisins. *J Biol Chem* 266:14486–14490
- Kitatani K, Idkowiak-Baldys J, Hannun YA (2008) The sphingolipid salvage pathway in ceramide metabolism and signalling. *Cell Signal* 20:1010–1018
- Di Bartolomeo S, Spinedi A (2002) Ordering ceramide-induced cell detachment and apoptosis in human neuroepithelioma. *Neurosci Lett* 334:149–152
- Slee EA, Harte MT, Kluck RM, Wolf BB, Casiano CA, Newmeyer DD, Wang HG, Reed JC, Nicholson DW, Alnemri ES, Green DR, Martin SJ (1999) Ordering the cytochrome c-initiated caspase cascade: hierarchical activation of caspases-2, -3, -6, -7, -8, and -10 in a caspase-9-dependent manner. *J Cell Biol* 144:281–292
- Le Stunff H, Giussani P, Maceyka M, Lépine S, Milstien S, Spiegel S (2007) Recycling of sphingosine is regulated by the concerted actions of sphingosine-1-phosphate phosphohydrolase 1 and sphingosine kinase 2. *J Biol Chem* 282:34372–34380
- Pewzner-Jung Y, Ben-Dor S, Futerman AH (2006) When do Lasses (longevity assurance genes) become CerS (ceramide synthases)? Insights into the regulation of ceramide synthesis. *J Biol Chem* 281:25001–25005
- Siskind LJ (2005) Mitochondrial ceramide and the induction of apoptosis. *J Bioenerg Biomembr* 37:143–153
- Lipsky NG, Pagano RE (1983) Sphingolipid metabolism in cultured fibroblasts: microscopic and biochemical studies employing a fluorescent ceramide analogue. *Proc Natl Acad Sci USA* 80:2608–2612

27. Birbes H, El Bawab S, Hannun YA, Obeid LM (2001) Selective hydrolysis of a mitochondrial pool of sphingomyelin induces apoptosis. *FASEB J* 15:2669–2679
28. Dai Q, Liu J, Chen J, Durrant D, McIntyre TM, Lee RM (2004) Mitochondrial ceramide increases in UV-irradiated HeLa cells and is mainly derived from hydrolysis of sphingomyelin. *Oncogene* 23:3650–3658
29. Stiban J, Caputo L, Colombini M (2008) Ceramide synthesis in the endoplasmic reticulum can permeabilize mitochondria to proapoptotic proteins. *J Lipid Res* 49:625–634
30. van Echten-Deckert G, Herget T (2006) Sphingolipid metabolism in neural cells. *Biochim Biophys Acta* 1758:1978–1994
31. Bladergroen BA, Bussière M, Klein W, Geelen MJ, Van Golde LM, Houweling M (1999) Inhibition of phosphatidylcholine and phosphatidylethanolamine biosynthesis in rat-2 fibroblasts by cell-permeable ceramides. *Eur J Biochem* 264:152–160
32. Ramos B, El Mouedden M, Claro E, Jackowski S (2002) Inhibition of CTP:phosphocholine cytidyltransferase by C(2)-ceramide and its relationship to apoptosis. *Mol Pharmacol* 62:1068–1075
33. Cui Z, Houweling M (2002) Phosphatidylcholine and cell death. *Biochim Biophys Acta* 1585:87–96
34. Hu W, Xu R, Zhang G, Jin J, Szulc ZM, Bielawski J, Hannun YA, Obeid LM, Mao C (2005) Golgi fragmentation is associated with ceramide-induced cellular effects. *Mol Biol Cell* 16:1555–1567
35. Spinedi A, Amendola A, Di Bartolomeo S, Piacentini M (1998) Ceramide-induced apoptosis is mediated by caspase activation independently from retinoblastoma protein post-translational modification. *Biochem Biophys Res Commun* 243:852–857

Traditionally, thin layer chromatography (TLC) and high performance liquid chromatography (HPLC) with evaporative light scattering or ultraviolet detection [4–7] methods have been used to quantitatively profile PL levels in tissues. However, these identification techniques are limited in their ability to identify PL species within each class.

Electrospray ionization-mass spectrometry (ESI-MS) offers sensitivity and selectivity over these more traditional TLC and HPLC methods for PL detection, identification, and quantification [8–13]. Chromatographic separation of PLs prior to MS can help to avoid the ion suppression effects that are often observed in the analysis of complex PL mixtures by MS, and also simplifies the analysis of very complex samples by separation of the components to be measured [14, 15]. HPLC-ESI-MS is now widely used for lipid analysis and has been used for the analysis of selected PL classes, qualitatively by comparing peak intensities without a calibration curve [16] and quantitatively using peak areas obtained from the total ion current (TIC) with an external standard curve [14–17].

In this study, we describe the development of an LC-MS/MS method that utilizes PL-class-specific fragmentations to measure changes in the relative concentration of five prominent classes of PLs in the brain tissues of 80-day-old Wistar rats [Choline glycerophospholipid ((ChoGpl) consists of phosphatidyl choline (PtdCho) and plasmeyl choline (PlsCho)), Ethanolamine glycerophospholipid ((EtnGpl) consist of phosphatidyl ethanolamine (PtdEtn) and plasmeyl ethanolamine (PlsEtn)), phosphatidyl serine (PtdSer), phosphatidyl inositol (PtdIns), and sphingomyelin (CerPCho)]. Neutral loss or precursor ion scanning was used to generate, in the extracted ion chromatogram, a discrete peak for each PL class analysed based on head group identification. The advantage of a headgroup detection system is that the complexity within the PL class is able to be accommodated. This complexity is due to the large combination of fatty acids present which means a large range of molecular masses which must be quantified. Calibration curves were generated based on these peak areas. This approach, as opposed to using the TIC peak areas obtained from the LC-MS methods discussed above, allows much improved specificity, has a shortened analysis time, and relies less heavily on the efficiency of chromatographic separation for the effective analysis of the PLs.

Materials and Methods

Standards and Chemicals

PL standards were obtained from Avanti Polar Lipids, (Alabaster, AL, USA). All solvents used were of liquid

chromatography grade (Merck, Darmstadt, Germany), except for chloroform which was analytical grade (ethanol stabilized).

Sample Preparation

At 80 days of age, the Wistar rats were sacrificed and the brain lipids were extracted using the Svennerholm and Fredman extraction protocol [18].

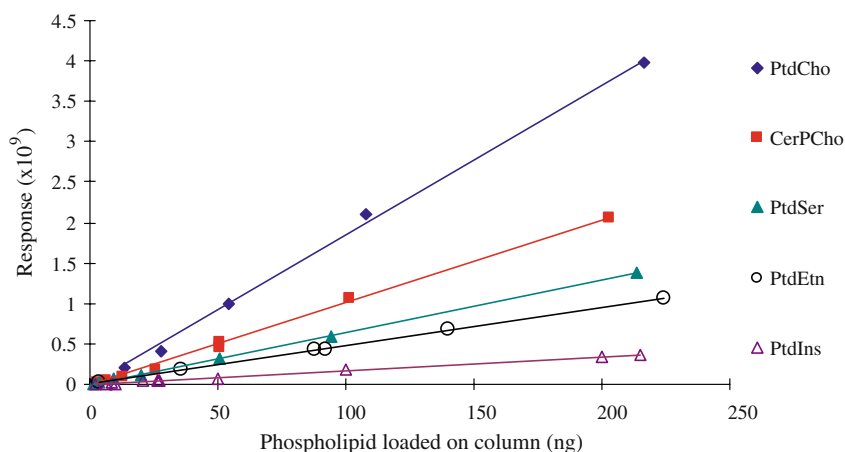
Briefly, the left hemisphere of rat brain was homogenized in 3 mL of water for 1–2 min in an ice bath using an ultrasonicator probe (5 Watts, Misonic Incorporated, Farmingdale, NY, USA). A portion of the rat brain homogenate (0.5 mL) was weighed into a 10 mL Kimax tube. Water (0.5 mL) was added to the homogenate, followed by methanol (2.7 mL) and chloroform (1.35 mL) at room temperature. The mixture was allowed to rock gently for 30 min on a rocker before centrifugation at 2,000g for 30 min. The supernatant was transferred to a 15 mL Kimax tube and the pellet was re-extracted using water (0.5 mL) and chloroform/methanol (1:2, 2 mL). After mixing and centrifugation (30 min at 2,000g), the supernatants were pooled and the pellet was discarded. Solvent partition of the supernatant was achieved by the addition of water (1.3 mL) and gentle inversion 3–4 times, followed by centrifugation (2,000g for 30 min). The upper phase was removed. KCl (0.01 M, 0.5 mL) was added to the remaining lower phase and any interfacial fluff (minimal) and was centrifuged (2,000g, 20 min).

The lower phase was used for PL analysis. Samples were aliquoted into HPLC vials and stored under nitrogen at -80°C prior to analysis. Sample analysis was completed within 2 weeks of extraction and samples were analyzed immediately upon thawing to reduce any degradation of the PLs.

Standard Preparation

PL standards [PtdCho (porcine brain), PtdEtn (bovine heart), PtdSer (porcine brain), PtdIns (bovine liver), and CerPCho (bovine brain)] were purchased from Avanti Polar Lipids (Alabaster, AL, USA). Stock solutions were prepared at 1 mg/mL in chloroform/methanol (1:2) and stored at -80°C under nitrogen, for no longer than 2 months. An intermediate mixed standard solution was prepared from each stock solution into a 10 mL volumetric flask, and was serially diluted further in chloroform/methanol (1:2) to give a six-point calibration curve for each PL class (Fig. 1). Standards were selected based on availability and similarity of fatty acid distribution to the phospholipids identified in the samples.

Fig. 1 Typical phospholipid calibration curve. The regression coefficient (r^2) is typically >0.9 . *PtdCho* phosphatidyl choline, *CerPCho* sphingomyelin, *PtdSer* phosphatidyl serine, *PtdEtn* phosphatidyl ethanolamine, *PtdIns* phosphatidyl inositol



High Performance Liquid Chromatography

An Alliance HPLC (Model 2690, Waters, Milford, MA, USA) system, consisting of an ultraviolet–visible detector and a refrigerated auto-sampler (set to 5 °C), was used for this work. The samples were loaded on to an APS-2 Hypersil (aminopropyl group stationary phase) column (150 mm × 2.1 mm, 3 μm, Thermo Scientific, Waltham, MA, USA) protected by a guard column containing the same column packing (10 mm × 2.1 mm inner diameter). The column temperature was set to 50 °C. Ten microliters of sample or standard was loaded on to the column. The PLs were separated with an acetonitrile/ammonium acetate buffer gradient, as described in Table 1. The flow rate was set at 0.5 mL/min.

Mass Spectrometry

The eluate from the HPLC system was introduced into a Thermo Scientific TSQ Quantum triple quadrupole mass spectrometer using a heated electrospray ionization (HESI) probe, except for the first 4 min and the last 6 min of the run, which were diverted to waste. Ions were generated and focused using an ESI voltage of 3,750 V, a sheath gas flow of 30 L/min, an auxiliary gas flow of 10 L/min, and a capillary temperature of 300 °C.

Common ions (precursor ions) or neutral losses that occur when each PL class [11, 19, 20] is fragmented in the collision cell were detected with the appropriate mass range selected, as outlined in Table 2. The mass distribution of the PL species within a class determined the mass window range used and to some extent the mass spectrometer tube lens voltage.

The excellent specificity of the method also allowed us to use it confidently to quantify phospholipids in rat serum samples (extracted using the modified Svennerholm and Fredman extraction protocol where the serum samples were treated the same as homogenised brains), which have

Table 1 HPLC mobile phase solvent gradient for separation of the phospholipids

Time (min)	Divert valve	Flow rate (mL/min)	%A	%B
0	To waste	0.5	100	0
4	To detector			
7.5		0.5	50	50
8.5		0.5	50	50
9		0.5	50	50
11		0.5	0	100
12		0.5	0	100
14	To waste	0.5	0	100
15			100	0
20			100	0

Solvent A: 95:5 acetonitrile/50 mM ammonium acetate buffer, pH 5.6. Solvent B: 50:50 acetonitrile/50 mM ammonium acetate buffer, pH 5.6

proportionally much lower levels of some phospholipids than brain extracts (Fig. 2).

Accuracy and Precision

The accuracy of the method was evaluated by performing recovery studies. The between-day precision and the within-day precision were assessed by repeated analysis of a quality control sample.

Results and Discussion

HPLC–MS

A typical separation of PLs on the aminopropyl HPLC column is shown in Fig. 2. We used a hydrophilic HPLC column because of its ability to separate PLs largely by their polar head group or class, as opposed to reversed-phase

Table 2 Summary of the phospholipid-class-specific scan events in positive ion mode

Scan event	Phospholipid specificity	Scan mode	Phospholipid fragment detected	Mass window (m/z)	Tube lens (volts)	Collision energy (volts)
1	Lyso-PtdCho	Precursor 184	Phosphoryl choline	470–550	125	26
2	Lyso-PtdEtn	Neutral loss 141	Phosphoryl ethanolamine	450–550	110	18
	EtnGpl	Neutral loss 141	Phosphoryl ethanolamine	730–830	150	18
3	PtdSer	Neutral loss 185	Phosphoryl serine	650–750	150	20
		Neutral loss 185	Phosphoryl serine	750–850	165	20
4	PtdIns	Neutral loss 277	Phosphoryl inositol (+NH ₄)	800–900	130	20
		Neutral loss 277	Phosphoryl inositol (+NH ₄)	900–1000	130	20
5	CerPCho,ChoGpl	Precursor 184	Phosphoryl choline	650–850	125	26

ChoGpl choline glycerophospholipid, *EtnGpl* ethanolamine glycerophospholipid, *PtdSer* phosphatidyl serine, *PtdIns* phosphatidyl inositol, *CerPCho* sphingomyelin

columns, which separate PLs largely by carbon number, leading to multiple peaks for each class of PL [10, 21–23]. Our method, based on the head group characteristics of each PL, could not resolve PtdEtn from PlsEtn, both of which are present in approximately equal amounts in adult rat brain, and could not resolve PtdCho from PlsCho, which is present in negligible amounts in rat brain [24–26]. Consequently, both ethanolamine and choline species present in the rat brain were quantified as EtnGpl and ChoGpl, respectively (the sum of the two components) using PtdEtn and PtdCho standards. In contrast to the other PL classes measured, it was important to keep PtdCho and CerPCho baseline resolved because they were detected using the same head group (phosphoryl choline) and the scan mode, in the same scan event. In order to keep this baseline resolution, the guard column was changed frequently (50–75 sample injections as prepared in this study). In general, the peaks were of reasonable resolution, with peak widths at base between 0.5 and 0.7 min, except for the PtdSer peak, which was significantly wider (1.8 min) due to the acidic nature of this PL. The extracted ion chromatograms shown in Fig. 2d, e and f demonstrate the selectivity and sensitivity of this technique compared to using the TIC peak areas (Fig. 2a, b and c) for quantification, allowing this method to be extended to other tissue samples such as serum (Fig. 2).

The parent ion spectra under each extracted PL peak could be viewed. PtdSer, ChoGpl, CerPCho, and EtnGpl were detected as $[M + H]^+$ ions in the spectra whereas PtdIns, negatively charged at pH 5.6, was detected as the ammonium adduct $[M + NH_4]^+$ ions in the spectra.

Positive ion mode ESI-MS/MS was chosen as the research focus was on the quantification of CerPCho and PtdCho in rat brains.

Calibration Curve

The HPLC-MS method used an external standard to quantify the relative amounts of PLs present in 80-day-old

rat brains. The linear calibration range used routinely in this study was up to 100 ng on-column but could be extended to twice that magnitude if required. The variation in response observed between the PL classes (Fig. 1) was not unexpected because, in positive ion mode, PtdCho and CerPCho ionize the most effectively and PtdIns ionizes the least effectively [10, 27]. PtdIns would be more effectively detected in negative ion mode. Unfortunately, it was not possible to switch between positive ion mode and negative ion mode during analysis on the mass spectrometer used in this study.

The current method was used to compare samples derived from the same sample matrix, i.e., 80-day-old rat brains. As the results were not corrected for variation of the ionization and/or fragmentation efficiencies within a given PL class, [11, 22, 28], they may not be absolute. However, as was the case in this study, the selection of standards with a fatty acid profile similar to the fatty acid profiles of the PLs in rat brain should eliminate some of these variations.

Precision and Accuracy

Matrix Effects

Matrix effects are a potential problem with most analytical methods. The components in the sample matrix may either suppress or enhance the analytical signal, leading to an under- or over-estimation of the analytical results.

In this study, the samples were evaluated for matrix effects. The brain extracts were serially diluted and compared with their respective standard curve. This resulted in close to parallel lines between the standard and the sample for EtnGpl, PtdSer, CerPCho, and ChoGpl indicating the effect of matrix on the analysis was minimal. However, considerable matrix effects were observed for PtdIns at all concentrations studied. It is unclear what components in the matrix were affecting the PtdIns response, but the low sensitivity of the PtdIns response would mean that it would

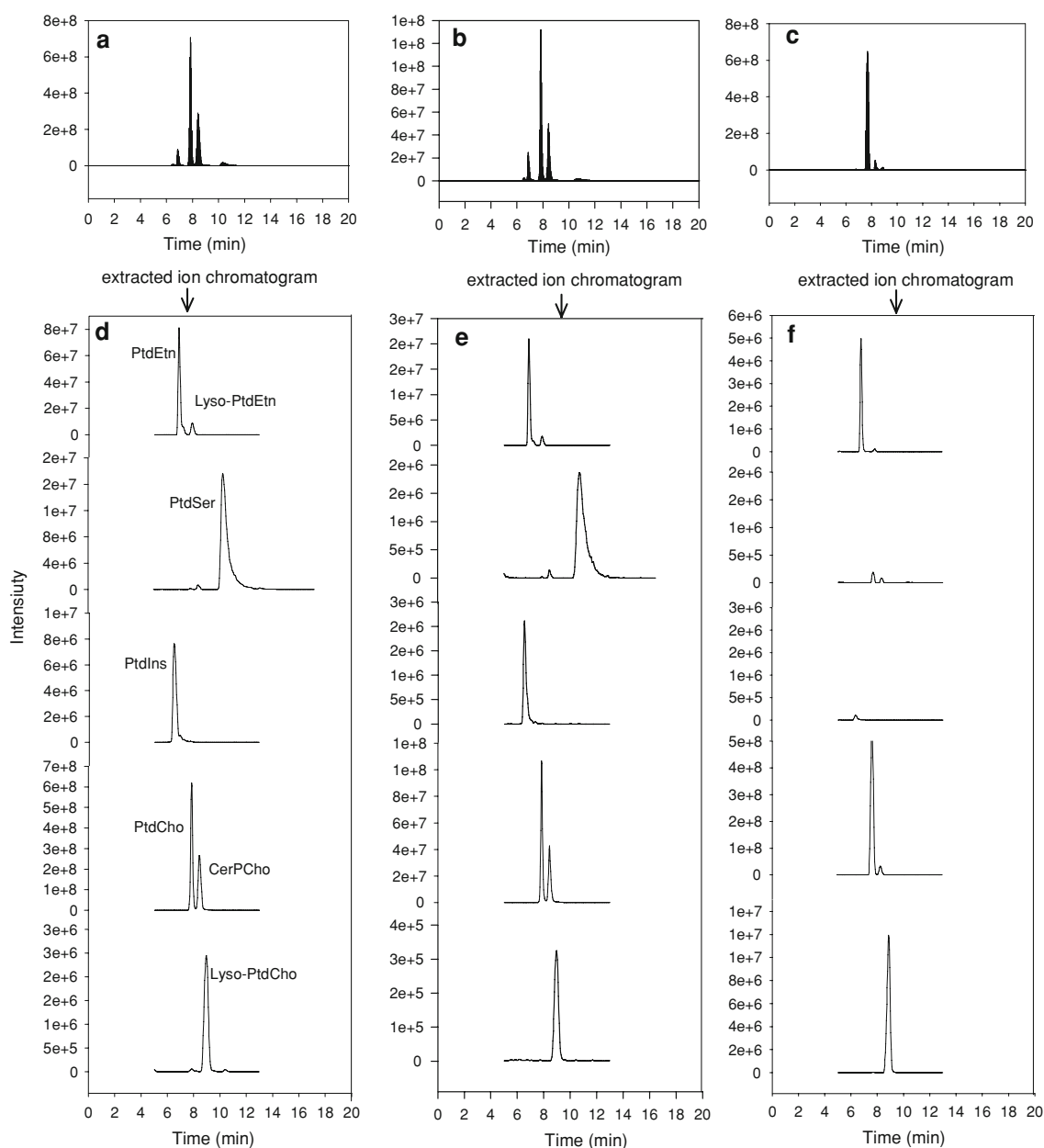


Fig. 2 TSQ Quantum triple quadrupole mass spectrometer total ion current trace of phospholipid standard mixture (10 ng load, **a**) and 80-day-old rat brain extract (**b**) and rat serum (**c**). The lower traces are their respective extracted ion chromatograms for each phospholipid

class—phospholipid standard (**d**), 80-day-old rat brain extract (**e**) and rat serum (**f**). The phospholipid classes are *PtdCho* phosphatidyl choline, *CerPCho* sphingomyelin, *PtdSer* phosphatidyl serine, *PtdEtn* phosphatidyl ethanolamine, *PtdIns* phosphatidyl inositol

be more affected by the matrix. This may explain the high variations observed for *PtdIns* (Table 3).

Spiked Recovery

Recovery experiments were conducted using homogenized rat brains spiked with a mixed phospholipid standard. Given the nature of the method, solvent/solvent extraction, the recoveries, ranging from 87 to 107% (Table 4) gave a good indication that the extraction protocol recovered

almost all of the PLs. Higher than 100% recovery can be explained by the coefficients of variance of the method measuring the endogenous phospholipids.

Repeatability and Reproducibility

The repeatability standard deviation was determined by analyzing the same sample over several days, whereas reproducibility was established over a longer period, over several months, by pooling the standard deviation of 48

Table 3 Repeatability and reproducibility coefficient of variation (CV) for the HPLC–MS phospholipid method

	ChoGpl	EtnGpl	PtdSer	PtdIns	CerPCho
Repeatability CV (%)	3	7	8	32	9
Reproducibility CV (%)	11	10	11	14	12

Repeatability was determined from analysis of the quality control sample between days whereas reproducibility was determined from duplicate extractions of 48 samples over several months using pooled standard deviation calculations

ChoGpl choline glycerophospholipid, *EtnGpl* ethanolamine glycerophospholipid, *PtdSer* phosphatidyl serine, *PtdIns* phosphatidyl inositol, *CerPCho* sphingomyelin

Table 4 Recovery of phospholipids spiked into rat brain

Phospholipid	Recovery (%)
PtdCho	107, 101
PtdEtn	97, 99
PtdSer	101, 103
PtdIns	102, 87
CerPCho	98, 104

ChoGpl choline glycerophospholipid, *EtnGpl* ethanolamine glycerophospholipid, *PtdSer* phosphatidyl serine, *PtdIns* phosphatidyl inositol, *CerPCho* sphingomyelin

samples analyzed in duplicate. Upon thawing, samples were analyzed immediately to reduce degradation of the PLs, which would have contributed to the assay variation. Degradation of the PLs in the sample was able to be monitored in part by observation of an increase in the lyso-PtdCho and lyso-PtdEtn peak areas (Fig. 2).

The repeatabilities and reproducibilities for EtnGpl, PtdSer, ChoGpl, and CerPCho (repeatability CV of 3–9%

and reproducibility CV of 10–12%, Table 3) were acceptable for such LC–MS/MS analyses. However, the PtdIns data had higher variation than expected. This may have been because PtdIns is not as effectively or reproducibly ionized under positive ion mode as discussed above. It could also have been related to the low response of PtdIns and the matrix effect issues observed as discussed above.

PLs in the Brains of 80-day-Old Rats

The total amount of PL in the 80-day-old rat brain (42 ± 1.3 mg/g brain, wet weight, $n = 9$) was derived from the sum of the individual PLs measured in this study (EtnGpl, ChoGpl, PtdIns, PtdSer, and CerPCho). This result was expected to account for greater than 95% of the total PL present in rat brain (minor PLs, e.g., lysophospholipid, phosphoglycerols, phosphatidic acid were not measured) [29] and showed excellent comparison with the PL results (44 ± 1.7 mg/g brain, wet weight mg, $n = 4$) converted from the total amount of phosphorus (54 ± 2.2 μ mol/g brain, wet weight) measured from the same rat brains. Total phosphorus determined as described by Vogel [30] provides an estimate of the amount of PL present in a sample based on multiplying the measured phosphorus value by a factor of 25, which is derived by dividing the average PL molecular weight of 754 by the phosphorus molecular weight of 31 [31].

The distributions of the individual PL classes were also consistent with literature data (Fig. 3), with ChoGpl and EtnGpl making up approximately 80% of the total PL in the rat brains. The results from Wells and Dittmer [25], Metz and Dunphy [24], and this study measured EtnGpl as the sum of PtdEtn and PlsEtn present in the samples

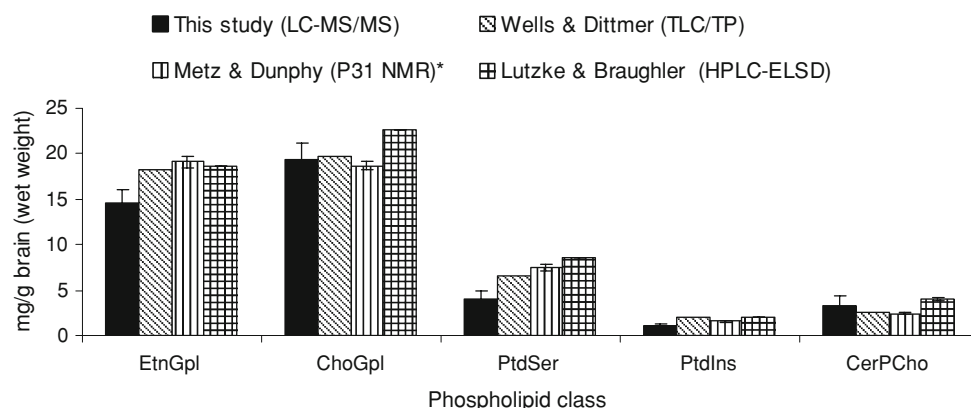


Fig. 3 Phospholipid distribution in 80-day-old rat brain (this study) compared with literature data. The rat strain and the rat age were Sprague–Dawley (42 days) for Wells and Dittmer [25], ACI/Seg-Hsd (70–84 days) for Metz and Dunphy [23], and Sprague–Dawley (no age given) for Lutzke and Braugler [30]. Standard deviation error bars are given where available. In this figure, PtdEtn and PlsEtn were

combined as a single EtnGpl value for the results presented for Wells and Dittmer [25], Metz and Dunphy [24], and this study. * Converted from total phosphorus results using a factor of 25 [29]. *EtnGpl* ethanolamine Glycerophospholipid, *ChoGpl* choline glycerophospholipid, *PtdSer* phosphatidyl serine, *PtdIns* phosphatidyl inositol, *CerPCho* sphingomyelin

(Fig. 3). It was assumed that this was also the case for the Lutzke and Braughler [32] results, as the values compared well, although the authors did not specifically define this. The differences in the amounts observed (Fig. 3) may in part be explained by differences in the rat strain and the age of the rat brain [29], and differences in the analytical methods used, i.e., both Wells and Dittmer [25] and Metz and Dunphy [24] used phosphorus as an indirect measure of PL amount, in comparison with the Lutzke and Braughler [32] study and this study, which quantified PLs directly using HPLC-ELSD and HPLC-MS/MS, respectively. It is also possible that the amount of EtnGpl has been underestimated in our analysis. Berry et al. [33] identified a reduced efficiency for the neutral loss of the ethanolamine head group (141 Da) from PlsEtn compared to PtdEtn. This potential problem could be rectified by using a EthGpl standard from a brain source (which contain around 50% PlsEtn). Furthermore, the lower PtdIns results obtained in this study may have been caused by the inefficiency of PtdIns ionization in positive ion mode as discussed earlier.

In summary, a rapid, selective and sensitive LC-MS/MS method, using an external calibration curve, has been developed to provide quantitative or comparative data for five PL classes in rat brain. The use of headgroup detection in this method overcame the complexities of the wide range of molecular masses within a class of phospholipids. This method could be extended to samples other than brain as illustrated by the serum sample in Fig. 2.

Acknowledgments The authors would like to thank Kathleen Schoeman for technical support, Charles Yang (Thermo Fisher Scientific, San Jose, CA, USA) for LC-MS discussions, Claire Woodhall for editing, and Mark Vickers (Liggins Institute, Auckland University, New Zealand) for providing the rat brain samples.

References

- Rösner H (1994) Gangliosides and brain development. In: Nicolini M, Zatta PF (eds) *Glycobiology and the brain*. Pergamon Press, New York, pp 19–36
- Prinetti A, Loberto N, Chigorno V, Sonnino S (2009) Glycosphingolipid behaviour in complex membranes. *Biochim Biophys Acta* 1788:184–193
- Michel V, Bakovic M (2007) Lipid rafts in health and disease. *Bio Cell* 99:129–140
- Nakabayashi H, Iwamori M, Nagai Y (1984) Analysis and quantitation of gangliosides as para-bromophenacyl derivatives by high-performance liquid-chromatography. *J Biochem* 96:977–984
- Ullman MD, McCluer RH (1985) Quantitative-analysis of brain gangliosides by high-performance liquid-chromatography of their perbenzoyl derivatives. *J Lipid Res* 26:501–506
- Miyazaki K, Okamura N, Kishimoto Y, Lee YC (1986) Determination of gangliosides as 2,4-dinitrophenylhydrazides by high-performance liquid-chromatography. *Biochem J* 235:755–761
- Traylor TD, Koontz DA, Hogan EL (1983) High-performance liquid-chromatographic resolution of para-nitrobenzyloxyamine derivatives of brain gangliosides. *J Chromatogr* 272:9–20
- Han XL, Gross RW (1995) Structural determination of picomole amounts of phospholipids via electrospray ionization tandem mass spectrometry. *J Am Soc Mass Spectrom* 6:1202–1210
- Kerwin JL, Tuininga AR, Ericsson LH (1994) Identification of molecular-species of glycerophospholipids and sphingomyelin using electrospray mass-spectrometry. *J Lipid Res* 35:1102–1114
- Kim HY, Wang TCL, Ma YC (1994) Liquid-chromatography mass-spectrometry of phospholipids using electrospray-ionization. *Anal Chem* 66:3977–3982
- Brugger B, Erben G, Sandhoff R, Wieland FT, Lehmann WD (1997) Quantitative analysis of biological membrane lipids at the low picomole level by nano-electrospray ionization tandem mass spectrometry. *Pro Natl Acad Sci USA* 94:2339–2344
- Fridriksson EK, Shipkova PA, Sheets ED, Holowka D, Baird B, McLafferty FW (1999) Quantitative analysis of phospholipids in functionally important membrane domains from RBL-2H3 mast cells using tandem high-resolution mass spectrometry. *Biochemistry* 38:8056–8063
- Sweetman G, Trinei M, Modha J, Kusel J, Freestone P, Fishov I, JoseleauPetit D, Redman C, Farmer P, Norris V (1996) Electrospray ionization mass spectrometric analysis of phospholipids of *Escherichia coli*. *Mol Microbiol* 20:233–234
- Bang DY, Kang DJ, Moon MH (2006) Nanoflow liquid chromatography-tandem mass spectrometry for the characterization of intact phosphatidylcholines from soybean, bovine brain, and liver. *J Chromatogr A* 1104:222–229
- Oursel D, Loutelier-Bourhis C, Orange N, Chevalier S, Norris V, Lange CM (2007) Lipid composition of membranes of *Escherichia coli* by liquid chromatography/tandem mass spectrometry using negative electrospray ionization. *Rapid Commun Mass Spectrom* 21:1721–1728
- Uran S, Larsen A, Jacobsen PB, Skotland T (2001) Analysis of phospholipid species in human blood using normal-phase liquid chromatography coupled with electrospray ionization ion-trap tandem mass spectrometry. *J Chromatogr B* 758:265–275
- Pang LQ, Liang QL, Wang YM, Ping L, Luo GA (2008) Simultaneous determination and quantification of seven major phospholipid classes in human blood using normal-phase liquid chromatography coupled with electrospray mass spectrometry and the application in diabetes nephropathy. *J Chromatogr B Analyt Techno Biomed Life Sci* 869:118–125
- Svennerholm L, Fredman P (1980) A procedure for the quantitative isolation of brain gangliosides. *Biochim Biophys Acta* 617:97–109
- Taguchi R, Houjou T, Nakanishi H, Yamazaki T, Ishida M, Imagawa M, Shimizu T (2005) Focused lipidomics by tandem mass spectrometry. *J Chromatogr B Analyt Techno Biomed Life Sci* 823:26–36
- Cole MJ, Enke CG (1991) Direct determination of phospholipid structures in microorganisms by fast-atom-bombardment triple quadrupole mass-spectrometry. *Anal Chem* 63:1032–1038
- Kim H, Ahn E, Moon MH (2008) Profiling of human urinary phospholipids by nanoflow liquid chromatography/tandem mass spectrometry. *Analyst* 133:1656–1663
- Ahn EJ, Kim H, Chung BC, Moon MH (2007) Quantitative analysis of phosphatidylcholine in rat liver tissue by nanoflow liquid chromatography/tandem mass spectrometry. *J Sep Sci* 30:2598–2604
- Buyukpamukcu E, Hau J, Fay LB, Dionisi F (2007) Analysis of phospholipids using electrospray ionisation tandem mass spectrometry. *Lipid Technol* 19(16):136–138

24. Metz KR, Dunphy LK (1996) Absolute quantitation of tissue phospholipids using P-31 NMR spectroscopy. *J Lipid Res* 37:2251–2265
25. Wells MA, Dittmer JC (1967) A comprehensive study of post-natal changes in concentration of lipids of developing rat brain. *Biochemistry* 6:3169
26. Andre A, Juaneda P, Sebedio JL, Chardigny JM (2005) Effects of aging and dietary n-3 fatty acids on rat brain phospholipids: Focus on plasmalogens. *Lipids* 40:799–806
27. Ivanova PT, Cerda BA, Horn DM, Cohen JS, McLafferty FW, Brown HA (2001) Electrospray ionization mass spectrometry analysis of changes in phospholipids in RBL-2H3 mastocytoma cells during degranulation. *Proc Natl Acad Sci USA* 98:7152–7157
28. Koivusalo M, Haimi P, Heikinheimo L, Kostianen R, Somerharju P (2001) Quantitative determination of phospholipid compositions by ESI-MS: effects of acyl chain length, unsaturation, and lipid concentration on instrument response. *J Lipid Res* 42:663–672
29. Yorek MA (1993) Part III: biological aspects. Chapter 21: biological distribution. In: Cevc G (ed) *Phospholipids handbook*. CRC Press, New York, pp 745–776
30. Vogel AI (1962) *A text book of quantitative inorganic analysis, including elementary instrumental analysis*. Longmans, London
31. Hanahan DJ (1997) *A guide to phospholipid chemistry*. Oxford University Press, New York
32. Lutzke BS, Braughler JM (1990) An improved method for the identification and quantitation of biological lipids by HPLC using laser light-scattering detection. *J Lipid Res* 31:2127–2130
33. Berry KAZ, Murphy RC (2004) Electrospray ionization tandem mass spectrometry of glycerophosphoethanolamine plasmalogen phospholipids. *J Am Soc Mass Spectrom* 15:1499–1508

intermediates in the isoprenoid biosynthetic pathway (Fig. 1). This pathway is responsible for the production of a vast array of products which have very diverse cellular activities [1]. Both FPP and GGPP are positioned at branch-points leading to the synthesis of longer-chain isoprenoids. Head-to-head condensation of two FPP units, catalyzed by squalene synthase (SQS), leads to the first precursor in the sterol pathway [2]. In addition, FPP is used for the synthesis of dolichols, ubiquinone and heme A. FPP and GGPP also serve substrates for protein isoprenylation reactions [3]. Farnesylation and geranylgeranylation, catalyzed by farnesyl transferase (FTase) and geranylgeranyl transferase (GGTase) I and II respectively, ensure proper membrane localization and function of a number of key proteins including members of the Ras small GTPase superfamily [4].

In plants, GPP is a direct precursor for monoterpenes, which represent a large family of natural products. Monoterpenes play roles in repelling or attracting animals or insects, resisting microbial attack, and interfering with the growth of other plants [1]. In addition, monoterpenes are utilized in a diverse array of commercial products, including insecticides, cosmetics, and flavorings. In plants, GPP is produced by geranyl diphosphate synthase via the condensation of isopentenyl diphosphate (IPP) with dimethylallyl diphosphate (DMAPP) [5]. In animal cells however, farnesyl diphosphate synthase (FDPS) catalyzes the synthesis of both GPP and FPP via sequential addition reactions (Fig. 1) [6]. First, GPP is produced via condensation of IPP and DMAPP. GPP then reacts with IPP to yield FPP. Little is known about the role of GPP in mammalian cells, aside from serving as an intermediate in the synthesis of FPP.

The isoprenoid biosynthetic pathway has been targeted extensively by numerous therapeutic agents [7]. The statins, widely used to manage hyperlipidemia, inhibit

HMG-CoA reductase (HMGR), the rate-limiting enzyme in the pathway, and thus deplete cells of all downstream isoprenoid products including cholesterol [8]. The nitrogenous bisphosphonates (NBS), used to treat osteoporosis and metastatic bone disease, inhibit FDPS [9–11] and likewise deplete downstream products [12]. We have developed a series of GGPP synthase (GDPS) inhibitors which deplete cells of GGPP [13]. Inhibitors of SQS [14], FTase [15], and GGTase I [16] are currently at varying stages of clinical development.

In general, the effects of inhibitors of the isoprenoid biosynthetic pathway have been considered to be a consequence of depletion of key isoprenoid-derived species. However, there is increasing evidence to suggest that accumulation of upstream products may also be of importance. Accumulation of IPP/DMAPP in human peripheral blood monocytes following zoledronic acid administration has been shown to activate $V\gamma 9V\delta 2$ T cells, which in turn, have been linked to anti-tumoral activity as well as a flu-like acute-phase reaction [17]. Treatment of mice with inhibitors of SQS leads to large increases in urinary excretion of FPP derivatives [18]. Additionally, we have shown that SQS inhibitors dramatically increase intracellular levels of FPP [19]. This is relevant because farnesol, a derivative of FPP, can induce apoptosis [20, 21]. Therefore, as more drugs that target downstream isoprenoid biosynthesis become available it will be necessary to understand their concomitant effects on the upstream species.

Several methods for measuring FPP and GGPP in biological samples have been reported [22–25]. Unfortunately, issues such as limited sensitivity, heavy instrument requirement (e.g., LC–MS–MS), or complex procedures (e.g., column switching) have limited their routine application. Recently, we reported an analytical method to quantify FPP or GGPP in biological samples by HPLC [19]. This method is based on the ability of FPP or GGPP to be incorporated into fluorescent peptides by FTase or GGTase I, respectively. Using this method, cellular levels of FPP and GGPP have been determined in cultured cells and in animal tissues [19, 26]. Importantly, this method is sensitive enough to measure the changes of FPP and GGPP in cultured cells upon treatment with isoprenoid pathway inhibitors [27, 28].

Previously published GPP quantification methods have relied on radioactive tracing or HPLC–MS/MS [25, 29]. The major challenges in developing a method for GPP quantification in biological samples have been the low basal concentrations of GPP as well as its instability [25, 30]. We have developed a non-radioactive and sensitive method for measuring GPP levels in mammalian cells which is based on the ability of GPP to serve as a substrate for FTase *in vitro* [31]. This methodology allows for the

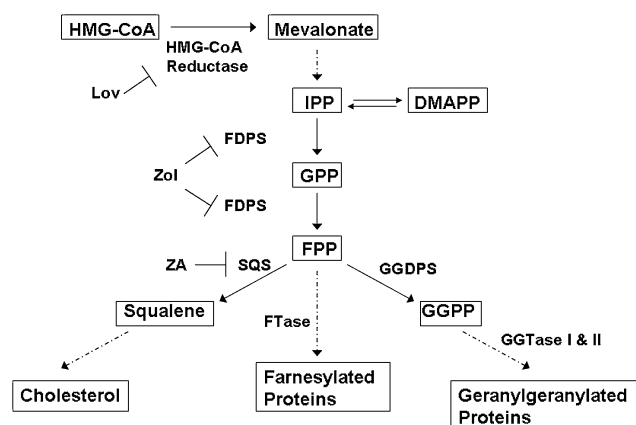


Fig. 1 The isoprenoid biosynthetic pathway. Key substrates, products, enzymes, and pharmacological inhibitors [lovastatin (*Lov*), zaragozic acid (*ZA*), and zoledronic acid (*Zol*)] are shown

measurement of basal levels of GPP as well as induced changes following treatment with isoprenoid biosynthetic pathway inhibitors. Furthermore, this methodology allows for the simultaneous measurement of GPP, FPP and GGPP levels.

Experimental Procedure

Cell Culture and Reagents

RPMI-8226, U266, H929 and K562 cells were obtained from the American Type Culture Collection (Manassas, VA). RPMI-8226, U266, H929 cell lines are human myeloma lines while the K562 cell line is a human erythroleukemia line that was established from a patient with chronic myelogenous leukemia [32]. Cells were grown in RPMI-1640 medium supplemented with fetal bovine serum, penicillin/streptomycin, and glutamine. GPP, FPP, GGPP, *n*-octyl β -glucopyranoside, and lovastatin were purchased from Sigma (St. Louis, MO). Zoledronate was purchased from Novartis (East Hanover, NJ). D*-GCVLS and D*-GCVLL (dansyl-labeled peptides) were obtained from Bio-Synthesis (Lewisville, TX). Rat recombinant FTase and GGTase-1 were purchased from EMD Biosciences (La Jolla, CA) or Jena Biosciences (Jena, Germany). HPLC-grade water was prepared with a Milli-Q system (Millipore, Bedford, MA). All solvents were optima or HPLC grade.

Extraction of GPP from Cultured Cells

RPMI-8226, U266 and H929 cells ($5\text{--}10 \times 10^6$) were incubated in the absence or presence of lovastatin or zoledronic acid for 24 h. Cells were collected and counted using a hemocytometer and Trypan blue staining. Cells were pelleted by centrifugation at 4 °C for 10 min at 2,800 rpm. The cell pellet was resuspended in 1 ml ice-cooled $1 \times$ PBS and then centrifuged at 20,000 $\times g$ 4 °C for 2 min. The PBS was aspirated and the cell pellet was again washed with 1 ml of ice-cold $1 \times$ PBS. Extraction solvent (isopropanol/75 mM ammonium hydroxide/acetone 1:1.5:5) (1.2 mL) was added to the cell pellet and vortexed for 1 min. The mixture was then centrifuged at 20,000 $\times g$ at 15 °C for 2 min. The supernatant was saved and the protein pellet was re-extracted in 1.2 ml of extraction solvent. After repeating the centrifugation step (20,000 $\times g$ at 15 °C for 5 min), the supernatants were combined and the volume was reduced to approximately 150 μ l via a stream of nitrogen at 30 °C. The samples were then dried using a speed vacuum (Savant SpeedVac Concentrator). The residue was dissolved in 50 mM Tris–HCl assay buffer (40 μ l, pH 7.5) containing 5 mM DTT,

5 mM MgCl₂, 10 μ M ZnCl₂, and 1.0% octyl- β -D-glucopyranoside.

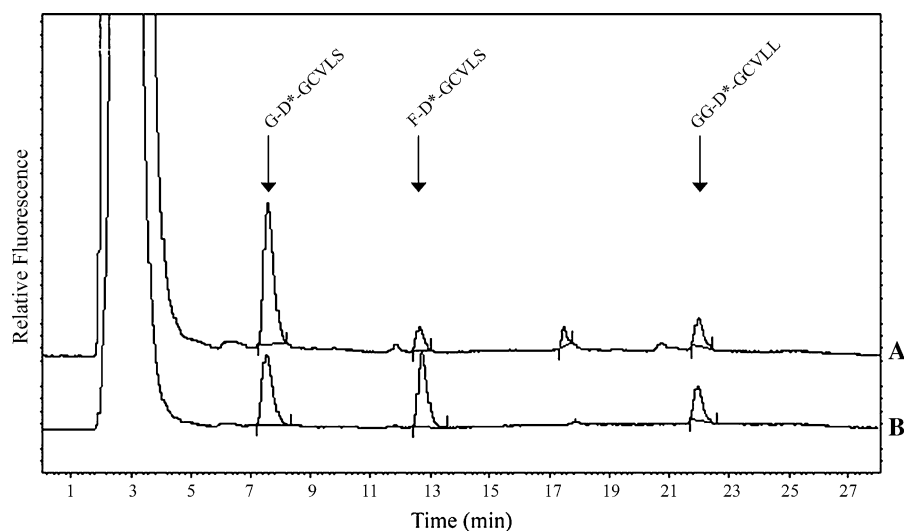
Enzymatic Reaction

An appropriate amount of GPP (or FPP), D*-GCVLS (0.25 nmol), and FTase (1 μ l, 61 μ g/ml protein) were added to 50 mM Tris–HCl assay buffer (40 μ l). For GGPP, the reaction mixture contained GGPP, D*-GCVLL (0.25 nmol), and GGTase-1 (1 μ l). The assay mixture was incubated at 38 °C for up to 120 min. The reaction was terminated by addition of acetonitrile (60 μ l). The reaction products are stable over 24 h at 4 °C. Denatured proteins were removed by centrifugation at 20,000 $\times g$ at 15 °C for 5 min and the supernatant was analyzed by HPLC. For cross-reactivity studies, enzyme reactions were performed in which GPP (0.2 or 0.5 ng) was added to the FTase assay mixture containing tenfold FPP (2 or 5 ng) and D*-GCVLS (0.25 nmol). Likewise, FPP (0.2 or 0.5 ng) was added to the FTase assay mixture containing tenfold GPP (2 or 5 ng) and D*-GCVLS (0.25 nmol). For simultaneous measurement of GPP, FPP, and GGPP, the reaction mixture contained 0.25 nmol of each dansylated peptide (D*-GCVLS and D*-GCVLL) and 1 μ l of each enzyme (FTase and GGTase-1).

Quantification of GPP in Cell Extracts

HPLC analysis was carried out on a Beckman Gold system (126 solvent module, 168 detector, and 508 autosampler from Beckman Coulter, Inc., Ontario, CA) connected to a FP-920 intelligent fluorescence detector (Jasco Co., Tokyo, Japan). The sample analysis was performed on a C18 reverse phase analytical column (250 \times 3.0 mm, 5 μ m, Luna, C18 (2), Phenomenex) protected by a guard cartridge system (4 \times 3.0 mm, 5 μ m, Phenomenex). To separate prenylated peptides (G-D*-GCVLS, F-D*-GCVLS and GG-D*-GCVLL), two solvent systems were used: solvent A, 20 mM ammonium acetate in 40% acetonitrile and solvent B, 20 mM ammonium acetate in 90% acetonitrile. The program was initiated at 26% B for 0.8 min, and then solvent was brought to 60% B by a linear gradient in 3 min. At 9 min, the solvent was raised to 100% in 1 min. An isocratic 100% solvent B was run at 19 min, then the solvent was brought back to 26% B by a linear gradient in 4 min. The total run time was 28 min. The flow rate of 0.5 ml/min was kept throughout the analysis. The peptide and geranyl- and farnesyl- (or geranylgeranyl-) adducts were monitored by a fluorescence detector at the excitation wavelength of 335 nm and the emission wavelength of 528 nm. The entire procedure was performed at ambient temperature. The retention time for the G-D*-GCVLS, F-D*-GCVLS and the GG-D*-GCVLL peaks were 7.5, 12.8 and 21.8 min, respectively.

Fig. 2 Fluorescence chromatogram of G-D*-GCVLS, F-D*-GCVLS and GG-D*-GCVLL products from FTase/GGTase I reactions. **a** Extracts from RPMI-8226 cells treated with zoledronic acid for 24 h. **b** Standards from FTase/GGTase I reactions utilizing GPP, FPP, and GGPP



Determination of Extraction Efficiency

The assay mixture was incubated at 38 °C for 2 h. A modified external calibration curve was constructed for the calculation of GPP in cultured cell extracts using the previously described method [19]. In brief, 0, 100, 250, 500, 1,000, 1500 or 2,000 pg of standard GPP was added to K562 cells pellets (5×10^6) which had been depleted of GPP via incubation at 4 °C for 24 h. The standard was extracted, incorporated and analyzed as described above.

Results

Sample Preparation

Measurement of intracellular GPP has historically been limited by low levels and poor stability. GPP hydrolysis has previously been demonstrated to rapidly occur in the presence of Mn^{2+} and/or at high temperatures [30]. In particular, at pH 7.0 in the absence of Mn^{2+} , the rate of GPP hydrolysis increases 13-fold as the temperature increases from 25 to 46.5 °C [30]. We observed that GPP rapidly disappears from samples even at 4 °C and that GPP is much less stable than FPP and GGPP during sample processing (data not shown). Our preliminary studies showed that the overall recovery of GPP from GPP-spiked cell samples is approximately 20% when using the previously published solvent system (butanol/75 mM ammonium hydroxide/ethanol 1:1.25:2.75) and sample processing procedure [19]. We found that sample processing at relatively low temperatures, as compared with the 70 °C utilized in the previously published methodology, allows for a better recovery and more accurate determination of GPP in cell samples.

The newly developed method includes a different solvent system (isopropanol/75 mM ammonium hydroxide/acetone 1:1.5:5), low temperature (4 °C) sample processing and drying, as well as a new HPLC program which allows for complete resolution of geranyl-conjugated dansyl peptide (G-D*-GCVLS) from farnesylated (F-D*-GCVLS) or geranylgeranylated (GG-D*-GCVLL) peptide peaks on a C18 column in less than 30 min (Fig. 2).

Conjugation of GPP to Dansylated Peptide by Enzymatic Reaction

Pompliano et al. [31] previously demonstrated that GPP may be utilized as a substrate by FTase to prenylate Ras-CVLS in vitro. To determine whether GPP is incorporated into D*-GCVLS as quickly as FPP, a reaction time study was performed using a fixed concentration of GPP with D*-GCVLS and FTase via our previously established methodology [19]. Figure 3a demonstrates that the incorporation of GPP into D*-GCVLS occurs within 2 h. As shown in Fig. 3b, GPP and FPP can be simultaneously incorporated into D*-GCVLS in the same reaction mixture within 2 h. Interestingly, although the initial reaction rate of FPP incorporation is faster than that of GPP, the GPP reaction rate was not decreased in the presence of FPP. In this selected reaction system, we chose to use an excess of peptides, relatively large amounts of FTase (or GGTase I), and a long incubation time (2 h) to ensure complete conversion of GPP, FPP and GGPP to the fluorescent derivatives. The potential mutual interference between GPP and FPP on FTase-mediated reactions was further investigated under conditions in which tenfold of the assumed interfering isoprenyl diphosphate (GPP or FPP) was added to the FTase reaction mixture. As shown in Table 1, excess

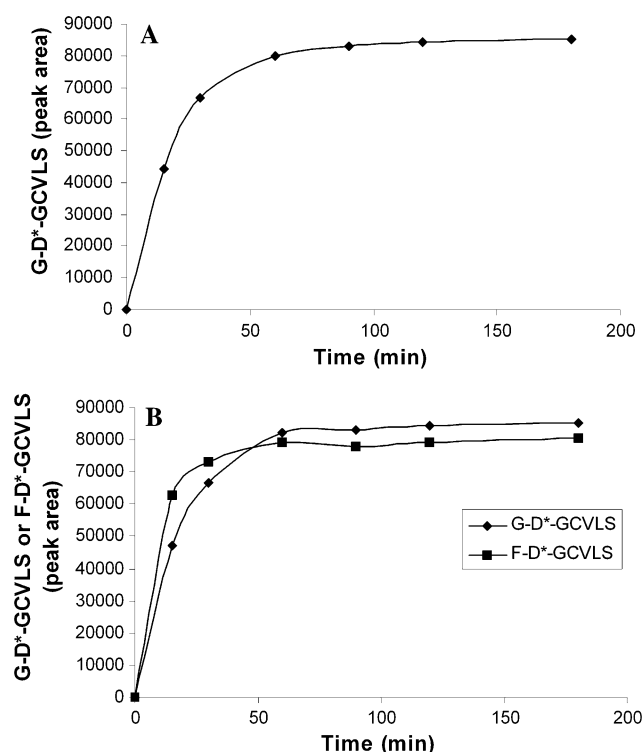


Fig. 3 Effects of reaction time on FTase-mediated product formation. The enzymatic reaction was performed as described in “[Experimental Procedure](#)” using 1 ng of GPP alone **a** or in the presence of 1 ng FPP **b**

Table 1 GPP (or FPP) recovery in the presence of tenfold excess FPP (or GPP)

Measured isoprenoid	Quantity of spiked isoprenoid	
	0.2 ng (% Recovered)	0.5 ng (% Recovered)
GPP (with tenfold FPP) ($n = 5$)	105 ± 10	98 ± 8
FPP (with tenfold GPP) ($n = 5$)	100 ± 15	102 ± 2

levels of FPP or GPP did not interfere with the measurement of either GPP or FPP, respectively. Additional experiments demonstrated that FTase does not transfer GPP to D*-GCVLL and that GGTase I cannot use GPP as a substrate (data not shown).

Calibration Curves and Method Validation

An external calibration curve was constructed for the determination of GPP levels in cell samples (Fig. 4). To mimic the condition of tissue samples, K562 cells were used as a carrier for the analytical procedure. In brief, K562 cell pellets were incubated at 4 °C for 24 h to deplete endogenous GPP. Different amounts of GPP were then

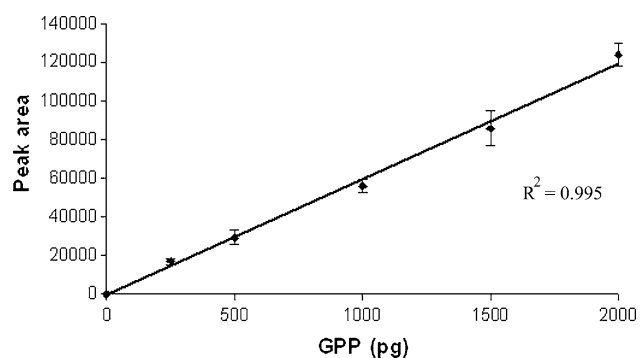


Fig. 4 GPP calibration curve. Known quantities of GPP were extracted from K562 cells as described in the text and a calibration curve was determined. Data are shown as mean ± SEM ($n = 3$)

added to the washed cell pellets and isolated and analyzed following the procedure described in “[Experimental Procedure](#)”. Under these conditions, a linear response was established over a range of 0–2,000 pg (Fig. 4). The lower limit of detection was approximately 5 pg. To fully validate the method, GPP-spiked K562 cells were used to determine the overall recovery for the procedure. The average recoveries of GPP at the 250, 500, and 1,000 pg levels were 92.5 ± 5.1%, 95.0 ± 8.2% and 95.8 ± 4.1%, respectively ($n = 3$).

This method also allows for simultaneous measurement of FPP and GGPP levels. To determine whether this method is as sensitive as our previously established method [19], FPP and GGPP levels were measured in various cell lines using both methods. In all cases, the measured levels of FPP and GGPP were slightly higher (by 5–10%) using the previously established method (Table 2).

Determination of GPP Levels in Cultured Cells

Using the method described above, levels of GPP in RPMI-8226, H929 and U266 cells were determined (Table 3). Detectable basal GPP levels were found in all tested cell lines, with a range of 0.029–0.101 pmol/million cells. To determine whether this methodology could be used to measure changes in GPP levels following treatment of cells with drugs known to inhibit the isoprenoid biosynthetic pathway, experiments were performed in which cells were treated with either lovastatin or zoledronic acid. Lovastatin, an HMGCR inhibitor, prevents mevalonate synthesis and thus depletes cells of downstream isoprenoid intermediates, including GPP. As shown in Table 3, treatment of cells for 24 h with lovastatin resulted in a decrease in GPP levels by over 50% in all tested cell lines. In contrast, when cells were treated with zoledronic acid, an FDPS inhibitor, it was found that GPP levels markedly increased (16 to 107-fold) in all tested cell lines.

Table 2 FPP and GGPP levels in human cell lines, as determined by the newly developed method and the previously established method

Cell line ($n = 3$)	FPP (pmol/10 ⁶ cells)		GGPP (pmol/10 ⁶ cells)	
	New method ^a	Established method ^b	New method	Established method
K562	0.087 ± 0.020	0.097 ± 0.021	0.182 ± 0.005	0.188 ± 0.023
RPMI-8226	0.145 ± 0.010	0.165 ± 0.010	0.271 ± 0.041	0.299 ± 0.001
U266	0.751 ± 0.054	0.802 ± 0.017	0.320 ± 0.011	0.333 ± 0.030
H929	0.143 ± 0.016	0.148 ± 0.013	0.154 ± 0.030	0.154 ± 0.014

^a New method: as described in “[Experimental Procedure](#)”

^b Established method: as previously reported by Tong et al. [19]

Discussion

In these studies we present a simple and sensitive method for the determination of GPP levels in cultured mammalian cells. This method involves the extraction of GPP from cells followed by incorporation into a dansyl-labeled peptide via enzymatic reaction. The fluorescent product is then analyzed by HPLC (Fig. 2). This method is significantly more sensitive than a previously published method [25] and is the first to allow for detection of basal levels of GPP (Table 3). In addition, this method allows for concomitant measurement of GPP, FPP, and GGPP. Although FPP and GGPP levels measured with this methodology are slightly lower (by 5–10%) than those obtained from our established method, the results may likely be acceptable for some studies. In particular, simultaneous determination of GPP, FPP, and GGPP in the setting of limited sample size (e.g., patient samples) is advantageous and allows for conservation of time and resources.

This methodology relies on the ability of GPP to serve as a substrate for FTase in an *in vitro* enzyme reaction [31]. We have demonstrated that the presence of FPP does not interfere with the utilization of GPP (Fig. 3b; Table 1), thereby

allowing for the determination of both GPP and FPP levels in one enzymatic system. GPP has not previously been demonstrated to serve as a substrate for prenylation reactions *in vivo* under standard conditions, although geranyl-cysteine has been detected in radiolabeling experiments involving mevalonate starvation [33]. This is presumably due to low basal levels of GPP and to FTase preferring FPP as a substrate; the K_M is 6,200 nM for GPP versus 390 nM for FPP when using Ras-CVLS as the peptide acceptor [31]. However, we have demonstrated that GPP levels markedly increase following zoledronic acid treatment (Table 3). It is interesting to speculate that in this setting, the induced changes in GPP and FPP levels may allow for FTase utilization of GPP. Further studies will be necessary to determine whether geranylation of proteins occurs in this setting. Protein geranylation, as compared with farnesylation or geranylgeranylation, could have significant impact on prenylated protein localization and/or function.

These studies represent the first time that basal GPP levels have been determined in mammalian cells. To our knowledge, the male bark beetle is the only animal which has been shown to synthesize GPP for monoterpene-derived pheromones [34, 35]. Otherwise, it has been assumed that in animals, GPP exists only as a transient intermediate in the FDPS-catalyzed synthesis of FPP. That we have been able to measure basal levels of GPP raises the hypothesis that there are mechanisms in place which regulate GPP pool size and that GPP may have additional functions within the cell. The consequences of markedly increasing GPP levels, as seen when cells were treated with zoledronic acid, are unknown. Geraniol, the alcohol version of GPP, has been demonstrated to inhibit colon cancer cell growth [36] and to have chemopreventative properties in a rat model [37]. A GPP pyrophosphatase activity has been described in cockerels [38]. Thus excess levels of GPP may result in geraniol production. Aminobisphosphonates have been recognized to have anti-neoplastic properties which have been largely attributed to the inhibition of protein prenylation [39]. Our results raise the hypothesis that intracellular accumulation of GPP may also contribute to these cytotoxic effects.

Table 3 GPP levels in human myeloma cell lines following 24 h incubation in the presence or absence of lovastatin or zoledronic acid

Cell line ($n = 5$)	GPP (pmol/10 ⁶ cells)
RPMI-8226	
Control	0.101 ± 0.016
Lovastatin (10 μM)	0.033 ± 0.018
Zoledronic acid (50 μM)	10.846 ± 1.519
H929	
Control	0.073 ± 0.029
Lovastatin (10 μM)	0.035 ± 0.017
Zoledronic acid (50 μM)	1.915 ± 0.391
U266	
Control	0.029 ± 0.011
Lovastatin (10 μM)	0.014 ± 0.011
Zoledronic acid (50 μM)	0.473 ± 0.121

It has been well-documented that aminobisphosphonates induce an increase in IPP levels and lead to the production of the ATP analog ApppI (triphosphoric acid 1-adenosin-5'-yl ester 3-(3-methyl-but-3-enyl) ester) [40–42]. However, an induced increase in GPP has not been previously demonstrated following alendronate treatment [9, 25]. Whether this is secondary to the loss of GPP during the analytical procedures or is due to differences between alendronate- and zoledronic acid-FDPS interactions remains to be determined. The aminobisphosphonates have been shown to bind to the allylic (i.e., DMAPP or GPP) substrate site, leading to the partial closure of the active site [43, 44]. Subsequent binding of IPP further stabilizes the inhibitor-enzyme complex in the fully closed position [44]. Thus it would be predicted that both GPP and FPP synthesis would be inhibited. However, our findings reveal that zoledronic acid treatment leads to an increase in GPP levels in all tested cell lines (Table 3). This suggests a complex relationship between IPP/DMAPP/GPP levels and flux through the pathway, regulation of FDPS activity, and inhibitor. Further studies will be needed to delineate the mechanism underlying the observed increase in GPP levels.

In summary, we have established a sensitive nonradioactive method for the measurement of GPP in mammalian cells. We have reported the first basal measurements of GPP in mammalian cells and have demonstrated that this method can be used to quantify the effects of isoprenoid pathway inhibitors on GPP levels. There is still much to be learned with regard to the role of GPP, the flux of isoprenoid intermediates through the biosynthetic pathway, regulation of isoprenoid concentration, and hierarchy of utilization under conditions of isoprenoid precursor deprivation. Furthermore, given the interest in isoprenoid biosynthetic pathway inhibitors [45, 46] and isoprenyl transferase inhibitors [47] for the treatment of cancer and other diseases, as well as the emerging role of isoprenoids as regulators of protein expression [48, 49], there are a wide variety of applications for which measurement of GPP, FPP and GGPP levels will be important.

Acknowledgments This project was supported by the Roy J. Carver Charitable Trust as a Research Program of Excellence and the Roland W. Holden Family Program for Experimental Cancer Therapeutics. S.A.H. was supported through a NIH T32 training grant.

References

- Holstein SA, Hohl RJ (2004) Isoprenoids: remarkable diversity of form and function. *Lipids* 39:293–309
- Popjak G, Agnew WS (1979) Squalene synthetase. *Mol Cell Biochem* 27:97–116
- Zhang FL, Casey PJ (1996) Protein prenylation: molecular mechanisms and functional consequences. *Annu Rev Biochem* 65:241–269
- Hori Y, Kikuchi A, Isomura M, Katayama M, Miura Y, Fujioka H, Kaibuchi K, Takai Y (1991) Post-translational modifications of the C-terminal region of the rho protein are important for its interaction with membranes and the stimulatory and inhibitory GDP/GTP exchange proteins. *Oncogene* 6:515–522
- Banthorpe DV, Charlwood BV, Francis MJ (1972) The biosynthesis of monoterpenes. *Chem Rev* 72:115–155
- Poulter CD, Argyle JC, Mash EA (1978) Farnesyl pyrophosphate synthetase. Mechanistic studies of the 1'-4 coupling reaction with 2-fluorogeranyl pyrophosphate. *J Biol Chem* 253:7227–7233
- Swanson KM, Hohl RJ (2006) Anti-cancer therapy: targeting the mevalonate pathway. *Curr Cancer Drug Targets* 6:15–37
- Grundy SM (1988) HMG-CoA reductase inhibitors for treatment of hypercholesterolemia. *N Engl J Med* 319:24–33
- Keller RK, Fliesler SJ (1999) Mechanism of aminobisphosphonate action: characterization of alendronate inhibition of the isoprenoid pathway. *Biochem Biophys Res Commun* 266:560–563
- Bergstrom JD, Bostedor RG, Masarachia PJ, Reszka AA, Rodan G (2000) Alendronate is a specific, nanomolar inhibitor of farnesyl diphosphate synthase. *Arch Biochem Biophys* 373:231–241
- Dunford JE, Thompson K, Coxon FP, Luckman SP, Hahn FM, Poulter CD, Ebetino FH, Rogers MJ (2001) Structure-activity relationships for inhibition of farnesyl diphosphate synthase in vitro and inhibition of bone resorption in vivo by nitrogen-containing bisphosphonates. *J Pharmacol Exp Ther* 296:235–242
- Reszka AA, Rodan GA (2004) Nitrogen-containing bisphosphonate mechanism of action. *Mini Rev Med Chem* 4:711–719
- Wiemer AJ, Yu JS, Lamb KM, Hohl RJ, Wiemer DF (2008) Mono- and dialkyl isoprenoid bisphosphonates as geranylgeranyl diphosphate synthase inhibitors. *Bioorg Med Chem* 16:390–399
- Charlton-Menys V, Durrington PN (2007) Squalene synthase inhibitors: clinical pharmacology and cholesterol-lowering potential. *Drugs* 67:11–16
- Basso AD, Kirschmeier P, Bishop WR (2006) Lipid posttranslational modifications. Farnesyl transferase inhibitors. *J Lipid Res* 47:15–31
- El Oualid F, Cohen LH, van der Marel GA, Overhand M (2006) Inhibitors of protein: geranylgeranyl transferases. *Curr Med Chem* 13:2385–2427
- Roelofs AJ, Jauhiainen M, Monkkonen H, Rogers MJ, Monkkonen J, Thompson K (2009) Peripheral blood monocytes are responsible for gamma delta T cell activation induced by zoledronic acid through accumulation of IPP/DMAPP. *Br J Haematol* 144:245–250
- Bergstrom JD, Kurtz MM, Rew DJ, Amend AM, Karkas JD, Bostedor RG, Bansal VS, Dufresne C, VanMiddlesworth FL, Hensens OD et al (1993) Zaragozic acids: a family of fungal metabolites that are picomolar competitive inhibitors of squalene synthase. *Proc Natl Acad Sci USA* 90:80–84
- Tong H, Holstein SA, Hohl RJ (2005) Simultaneous determination of farnesyl and geranylgeranyl pyrophosphate levels in cultured cells. *Anal Biochem* 336:51–59
- Voziyan PA, Haug JS, Melnykovich G (1995) Mechanism of farnesol cytotoxicity: further evidence for the role of PKC-dependent signal transduction in farnesol-induced apoptotic cell death. *Biochem Biophys Res Commun* 212:479–486
- Haug JS, Goldner CM, Yazlovitskaya EM, Voziyan PA, Melnykovich G (1994) Directed cell killing (apoptosis) in human lymphoblastoid cells incubated in the presence of farnesol: effect of phosphatidylcholine. *Biochim Biophys Acta* 1223:133–140
- Bruenger E, Rilling HC (1988) Determination of isopentenyl diphosphate and farnesyl diphosphate in tissue samples with a comment on secondary regulation of polyisoprenoid biosynthesis. *Anal Biochem* 173:321–327
- Keller RK (1996) Squalene synthase inhibition alters metabolism of nonsterols in rat liver. *Biochim Biophys Acta* 1303:169–179

24. Saisho Y, Morimoto A, Umeda T (1997) Determination of farnesyl pyrophosphate in dog and human plasma by high-performance liquid chromatography with fluorescence detection. *Anal Biochem* 252:89–95
25. Henneman L, van Cruchten AG, Denis SW, Amolins MW, Placzek AT, Gibbs RA, Kulik W, Waterham HR (2008) Detection of nonsterol isoprenoids by HPLC–MS/MS. *Anal Biochem* 383:18–24
26. Tong H, Wiemer AJ, Neighbors JD, Hohl RJ (2008) Quantitative determination of farnesyl and geranylgeranyl diphosphate levels in mammalian tissue. *Anal Biochem* 378:138–143
27. Wiemer AJ, Tong H, Swanson KM, Hohl RJ (2007) Digeranyl bisphosphonate inhibits geranylgeranyl pyrophosphate synthase. *Biochem Biophys Res Commun* 353:921–925
28. Murthy S, Tong H, Hohl RJ (2005) Regulation of fatty acid synthesis by farnesyl pyrophosphate. *J Biol Chem* 280:41793–41804
29. McCaskill D, Croteau R (1993) Procedures for the isolation and quantification of the intermediates of the mevalonic acid pathway. *Anal Biochem* 215:142–149
30. Vial MV, Rojas C, Portilla G, Chayet L, Perez LM, Cori O, Bunton B (1981) Enhancement of the hydrolysis of geranyl pyrophosphate by bivalent metal ions. A model for enzymic biosynthesis of cyclic monoterpenes. *Tetrahedron* 37:2351–2357
31. Pompiano DL, Schaber MD, Mosser SD, Omer CA, Shafer JA, Gibbs JB (1993) Isoprenoid diphosphate utilization by recombinant human farnesyl:protein transferase: interactive binding between substrates and a preferred kinetic pathway. *Biochemistry* 32:8341–8347
32. Koeffler HP, Golde DW (1980) Human myeloid leukemia cell lines: a review. *Blood* 56:344–350
33. Rilling HC, Bruenger E, Leining LM, Buss JE, Epstein WW (1993) Differential prenylation of proteins as a function of mevalonate concentration in CHO cells. *Arch Biochem Biophys* 301:210–215
34. Seybold SJ, Quilici DR, Tillman JA, Vanderwel D, Wood DL, Blomquist GJ (1995) De novo biosynthesis of the aggregation pheromone components ipsenol and ipsdienol by the pine bark beetles *Ips paraconfusus* Lanier and *Ips pini* (Say) (Coleoptera: Scolytidae). *Proc Natl Acad Sci USA* 92:8393–8397
35. Gilg AB, Bearfield JC, Tittiger C, Welch WH, Blomquist GJ (2005) Isolation and functional expression of an animal geranyl diphosphate synthase and its role in bark beetle pheromone biosynthesis. *Proc Natl Acad Sci USA* 102:9760–9765
36. Carnesecchi S, Schneider Y, Ceraline J, Duranton B, Gosse F, Seiler N, Raul F (2001) Geraniol, a component of plant essential oils, inhibits growth and polyamine biosynthesis in human colon cancer cells. *J Pharmacol Exp Ther* 298:197–200
37. Ong TP, Heidor R, de Conti A, Dagli ML, Moreno FS (2006) Farnesol and geraniol chemopreventive activities during the initial phases of hepatocarcinogenesis involve similar actions on cell proliferation and DNA damage, but distinct actions on apoptosis, plasma cholesterol and HMGCoA reductase. *Carcinogenesis* 27:1194–1203
38. Case GL, He L, Mo H, Elson CE (1995) Induction of geranyl pyrophosphate pyrophosphatase activity by cholesterol-suppressive isoprenoids. *Lipids* 30:357–359
39. Stresing V, Daubine F, Benzaid I, Monkkonen H, Clezardin P (2007) Bisphosphonates in cancer therapy. *Cancer Lett* 257:16–35
40. Monkkonen H, Auriola S, Lehenkari P, Kellinsalmi M, Hassinen IE, Vepsalainen J, Monkkonen J (2006) A new endogenous ATP analog (ApppI) inhibits the mitochondrial adenine nucleotide translocase (ANT) and is responsible for the apoptosis induced by nitrogen-containing bisphosphonates. *Br J Pharmacol* 147:437–445
41. Monkkonen H, Ottewell PD, Kuokkanen J, Monkkonen J, Auriola S, Holen I (2007) Zoledronic acid-induced IPP/ApppI production in vivo. *Life Sci* 81:1066–1070
42. Jauhainen M, Monkkonen H, Raikkonen J, Monkkonen J, Auriola S (2009) Analysis of endogenous ATP analogs and mevalonate pathway metabolites in cancer cell cultures using liquid chromatography–electrospray ionization mass spectrometry. *J Chromatogr B Analyt Technol Biomed Life Sci* 877:2967–2975
43. Kavanagh KL, Guo K, Dunford JE, Wu X, Knapp S, Ebetino FH, Rogers MJ, Russell RG, Oppermann U (2006) The molecular mechanism of nitrogen-containing bisphosphonates as antiosteoporosis drugs. *Proc Natl Acad Sci USA* 103:7829–7834
44. Rondeau JM, Bitsch F, Bourgier E, Geiser M, Hemmig R, Kroemer M, Lehmann S, Ramage P, Rieffel S, Strauss A, Green JR, Jahnke W (2006) Structural basis for the exceptional in vivo efficacy of bisphosphonate drugs. *ChemMedChem* 1:267–273
45. Chan KK, Oza AM, Siu LL (2003) The statins as anticancer agents. *Clin Cancer Res* 9:10–19
46. Fleisch H (2002) Development of bisphosphonates. *Breast Cancer Res* 4:30–34
47. Baum C, Kirschmeier P (2003) Preclinical and clinical evaluation of farnesyltransferase inhibitors. *Curr Oncol Rep* 5:99–107
48. Holstein SA, Wohlford-Lenane CL, Hohl RJ (2002) Consequences of mevalonate depletion. Differential transcriptional, translational, and post-translational up-regulation of Ras, Rap1a, RhoA, AND RhoB. *J Biol Chem* 277:10678–10682
49. Holstein SA, Wohlford-Lenane CL, Wiemer DF, Hohl RJ (2003) Isoprenoid pyrophosphate analogues regulate expression of Ras-related proteins. *Biochemistry* 42:4384–4391

minor constituent in human bile [6] and is used as a drug to dissolve cholesterol gallstones, to treat biliary cirrhosis, bile reflux gastritis, treatment of colorectal cancer and a range of other adult cholestatic conditions [7, 8]. Several instrumental approaches have been described for the analysis of bile acids in bulk or in pharmaceutical preparations, including potentiometry, voltammetry, micellar electrokinetic chromatography (MEKC), supercritical fluid chromatography (SFC), gas chromatography and HPLC. However, the procedures are generally quite onerous and involve difficult or time-consuming extraction procedures [9, 10]. The extensive use of bile acids in the pharmaceutical formulations for aesthetics clinics and pharmacies shows the need for biotechnological studies to develop alternative methods for fast analysis of these products, making it easier to implement the government health policy (ANVISA and FDA) to control the illegal commerce of these products.

In this context, cyclodextrins (CDs) are a group of naturally occurring cyclic oligosaccharides with six (α -), seven (β -) or eight (γ -) glucose residues linked by α -(1–4) glycosidic bonds [11, 12]. In aqueous solution, they possess a truncated cone shaped structure with a hydrophilic exterior and a hydrophobic interior [13] capable of forming inclusion complexes with a wide variety of substrates such as dyes, drugs, small anions, carboxylic acids and alcohols [14]. The inclusion complexes formed are often able to promote enhancements or perturbations of the photophysical and photochemical properties of included guest molecules [15]. Hence, investigation of the inclusion mechanisms can be accomplished using a great variety of methods including molecular absorption spectrophotometry and fluorometry, HPLC, surface tension, electrochemistry and calorimetry [16]. However, reports of the use of CDs as analytical reagents in UV–Vis spectrophotometry are scarce. Xie et al. [17] used the absorption spectra of the dibenzoyl peroxide- β -cyclodextrin complex in the analysis of benzoic acid concentrations. Yanez et al. [18] proposed the use of β -CD to directly quantify the furnidipine through of the inclusion complex formed and Yuexian et al. [15] resorted to the methyl orange- α -cyclodextrin inclusion complex to determine aromatic amino acids. More commonly, CDs have been used in UV–Vis spectrophotometry mainly to improve the solubility and stability of colored compounds and to increase the sensitivity and selectivity of colorimetric reactions [19].

Phenolphthalein (PHP) is a typical acid/base indicator that forms a colorless 1:1 inclusion complex with β -CD and can be used for the determination of colorless compounds through competitive complexation reaction [20, 21]. In this context, the objective of this work is the proposal of the colorimetric determination of deoxycholic and ursodeoxycholic acid based on competitive complexation reaction

with phenolphthalein- β -cyclodextrin inclusion complexes. Two factorial designs were developed to identify the constraints and study the experimental conditions to accomplish optimized determination procedures. Good figures achieved for the proposed procedures enable one to envisage low costs and simple application in large scale monitoring and control tasks.

Experimental

Materials

Absorption spectra and data were collected by means of a Pharmacia Ultraspec 3000pro UV–Vis spectrophotometer using 1-cm path length quartz cells. Statistical evaluations were carried out by means of the Statistica software (StatSoft Inc., Tulsa, OK, USA).

Double deionized water and analytical grade chemicals were used without further purification. β -cyclodextrin was obtained from Fluka (Steinheim, Germany). Phenolphthalein, deoxycholic (sodium salt) and ursodeoxycholic acids were obtained from Sigma (St. Louis, MO, USA). Under acidic conditions, the measurements were performed using a 150 mM KCl–HCl buffer solution, pH 2.0. A 150 mM carbonate buffer solution was prepared to provide measurements at basic conditions [20].

Methods

The co-precipitation technique [22] was used to prepare the inclusion complexes. Therefore, solutions were mixed in the following order: 1.0 mL of the indicator solution, 1.0 mL of buffer, 1.0 mL of β -CD solution. The mixture was stirred vigorously after the addition of each solution (the order did not interfere in the results). After, this the initial mixture was homogenized with 1.0 mL of the bile acid sample. The blank solution was composed of 1.0 mL of buffer and 3.0 mL of water.

The ratio between the concentrations of β -CD and indicator (6:1) was recorded to find the best indicator inclusion complex to accomplish the bile acids determinations. Thus, the following concentrations of indicators were tested: bromophenol blue (4×10^{-5} M), bromocresol blue (1.85×10^{-5} M), methyl orange (5.1×10^{-5} M at pH 2.0 and 4.0×10^{-4} M at pH 9.5), methyl red (3.1×10^{-4} M), phenol red (7.5×10^{-5} M), phenolphthalein (3.1×10^{-4} M, only in basic conditions) and thymol blue (1.3×10^{-4} M). All the concentrations referred were in the linear range of spectrophotometric response for the respective indicator.

The equilibrium constants of the β -CD-PHP inclusion complex was measured using solutions of 3.1×10^{-4} M

phenolphthalein in different amounts of β -CD (5.17×10^{-5} – 1.86×10^{-3} M) at pH 9.5 or of 1.55×10^{-4} M phenolphthalein in the 2.58×10^{-5} – 9.3×10^{-4} M β -CD range at pH 10.5, were respectively prepared. The equilibrium constants of the β -CD-DCA inclusion complex was determined mixing DCA to final concentrations between 1.56×10^{-5} and 6.25×10^{-3} M to the β -CD-PHP (1.24×10^{-3} : 3.1×10^{-4} M) solution. The same experimental conditions were performed for measuring the β -CD-UDCA equilibrium constant, utilizing UDCA concentrations in the interval of 4.84×10^{-5} – 3.1×10^{-3} M prepared with a constant ratio of β -CD-PHP (6.2×10^{-4} : 1.55×10^{-4} M).

Applications

The study was performed by the addition of known amounts of the DCA and UDCA standards to a sample with a known amount of pharmaceutical formulations such as, injectable phosphatidylcholine formula [23] (phosphatidylcholine 5% w/v, deoxycholic acid sodium salt 4.75% w/v, benzyl alcohol 0.9% v/v, and water up to a volume of 100 mL) and injectable deoxycholate formula [24] (Deoxycholic acid 2.5% w/v, Benzyl alcohol 1% v/v, propylene glycol 10% v/v, Water 100 mL) for the DCA and Ursacol (labeled with 300 mg of ursodeoxycholic acid per pill) for the UDCA.

Results

Evaluation of the Inclusion Complexes Between β -Cyclodextrin and Different Indicators

Figure 1 shows the spectral changes of different common pH indicators after addition of β -CD up to a concentration ratio of 6:1 at pH 2.0 and 9.5 media. For bromocresol blue, bromophenol blue, thymol blue and phenol red, no significant changes were observed in the respective spectra when β -CD was added. However, the phenolphthalein (PHP) showed a strong interaction with the β -CD in alkaline pH since there was a decrease in the absorption peak (at a wavelength of 553 nm) (Fig. 1a) of more than 95%. Inclusion complexes between methyl orange and the β -CD were observed on both pH conditions tested (Fig. 1b). At pH 2.0, the absorption peak at 506 nm decreased slightly, whereas at pH 9.5 the formation of two isobestic points at 400 and 456 nm and a blue shift of the absorption band of about 6 nm were registered. Methyl red also formed inclusion complexes with β -CD at the two pH values (Fig. 1c), evidenced by the appearance of two isobestic points in acid (484 nm and 579 nm), basic pH (335 nm and 433 nm) and a blue shift of 8 nm in the wavelength corresponding to the absorption maxima.

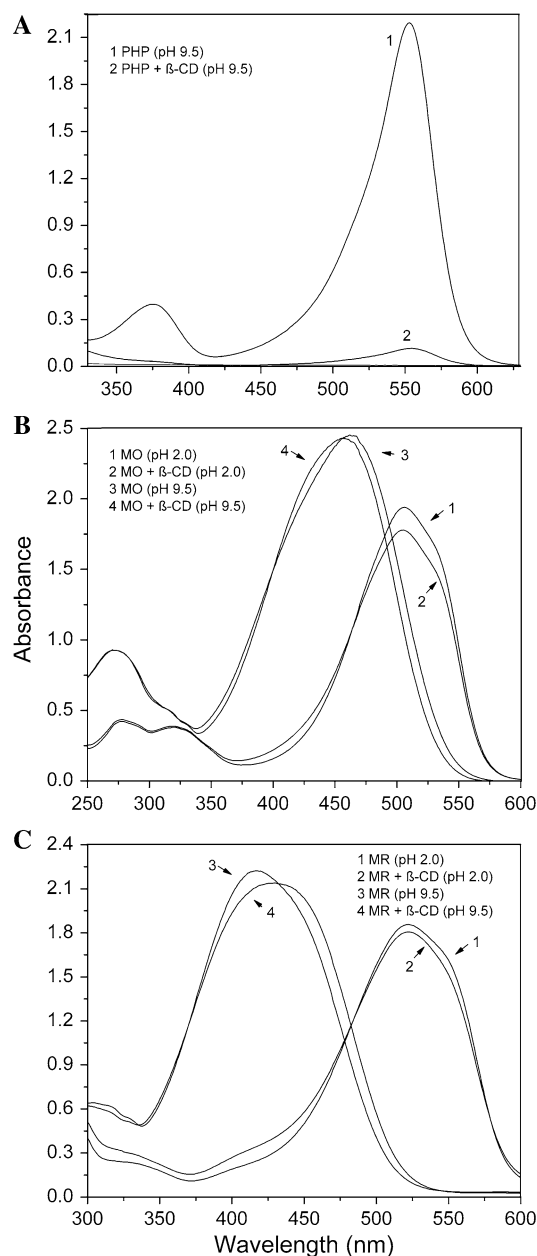


Fig. 1 Absorption spectra at acid (2.0) and alkaline pH (9.5) of **a** phenolphthalein (3.1×10^{-4} M, only in basic solution), **b** methyl orange (5.1×10^{-5} M at pH 2.0 and 4.0×10^{-4} M at pH 9.5), **c** methyl red (3.1×10^{-4} M), at a ratio of 1:6 with β -CD

Based on previous observations, it is clear that inclusion complexes are formed with particular forms of the indicators, but the spectral changes are more pronounced in the case of the β -CD-PHP complex. When the PHP is forced to leave the cavity of β -CD by a competitive colorless guest which it will again confer the red color to the solution. Thus, the extent of the solution color change can then be easily determined against a calibration curve of the free indicator and the corresponding amount related with the amount of the host substance. The absorption spectra of

PHP solutions with concentrations of β -CD ranging from 5.17×10^{-5} – 1.86×10^{-3} M revealed a proportional decrease in the free PHP up to a concentration of 1.24×10^{-3} M at pH 9.5 and up to 6.2×10^{-4} M at pH 10.5, showing a concentration ratio of 4:1 (β -CD:PHP). Higher concentrations of β -CD did not cause an additional observable decrease in absorption under both pH values. Some reports have been established the premise that under the assay conditions, phenolphthalein is only capable of forming 1:1 inclusion complexes with β -cyclodextrin as in Eq. 1 [20, 22, 25], a double reciprocal plot shows a linear relationship corresponding to the equilibrium constant (K_c), which can be obtained from Eq. 2. The equilibrium constant (K_c) for the formation of the inclusion complex was determined from the ratio of the intercept to the slope in the linear Benesi–Hildbrand plot [26, 27]:



$$\frac{1}{A - A_0} = \frac{1}{a} + \frac{1}{aK_c[\beta\text{-CD}_0]} \quad (2)$$

where A and A_0 are the absorbance of PHP in the presence and absence of β -CD, respectively, K_c is the equilibrium constant for the formation of a 1:1 inclusion complex, a is a constant related to the molar absorption coefficients changes, and $[\beta\text{-CD}_0]$ is the initial concentration of β -CD. The equilibrium constants (K_c) were then determined both at pH 9.5 and pH 10.5 from the linear plots experimentally obtained. The respective values of $1.65 (\pm 0.98) \times 10^4$ and $5.10 (\pm 0.37) \times 10^4 \text{ M}^{-1}$ demonstrated that the smaller amount of free PHP found at the higher pH is congruent with the higher value of the complex equilibrium constant.

Determination of Deoxycholic Acid and Ursodeoxycholic Acid by Their Competitive Complexation Reaction with β -Cyclodextrin-Phenolphthalein inclusion complex

The inclusion complex formation was instantaneous and could be seen without any equipment. Figure 2 shows the absorption spectra of the β -CD-PHP inclusion complex under different concentrations of DCA (Fig. 2a) and the UDCA (Fig. 2b). It is clear that with the addition of DCA or UDCA, an increase in the monitored absorbances occurred. This behavior indicates competition of the DCA or of the UDCA with PHP to form the inclusion complex with the β -CD. However, at pH 9.5 the spectral changes of the solution with the increasing amounts of UDCA were absent. For the studies of the conditions for the determinations of both acids and simultaneous evaluation of the robustness of the experimental conditions, two independent factorial designs were developed considering the pH

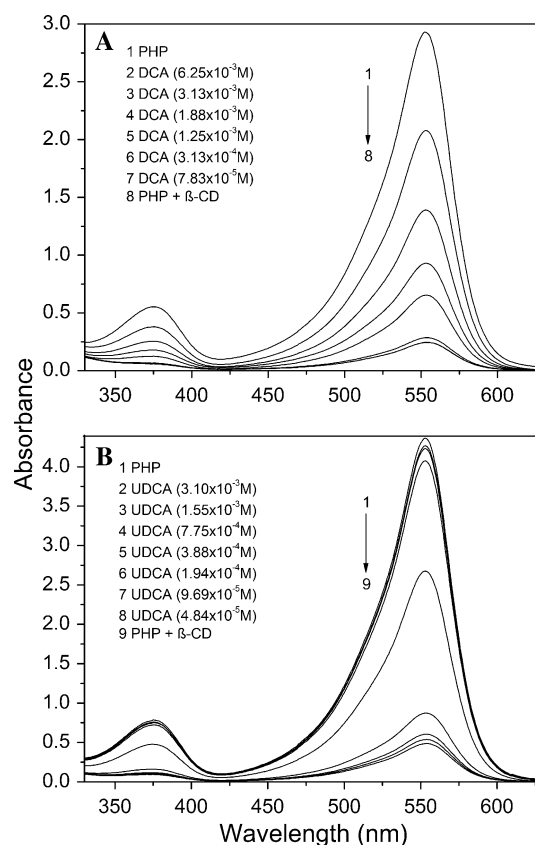


Fig. 2 Determination of various concentrations of DCA (a) by the β -CD-PHP inclusion complex at pH 9.5 (β -CD-PHP: 1.24×10^{-3} ; 3.1×10^{-4} M) and UDCA (b) at pH 10.5 (β -CD-PHP: 6.2×10^{-4} ; 1.55×10^{-4} M)

changes, the temperature, the concentration of the inclusion complex and the buffer concentration (Table 1). The central points of both designs were also assayed in quadruplicate for determination of the pure error.

The results obtained through a 2^3 full factorial design for the study of the variables that influence the determination of DCA demonstrated that the pH had the main statistically significant positive effect ($p < 0.05$). In fact, there was an increase of about 73.2% in the result for DCA (1.88×10^{-3} M) for the pH values 9.2 and 10.7 (Fig. 3), and only of 2.85% between the pH values 10.5 and 10.7 (increase not significant according to the Tukey test ($p < 0.05$)). Thus, the adoption of the higher pH conditions provided the larger variation in the absorbance of the sample under the conditions studied. The second order interactions between the pH and β -CD-PHP concentration values and between temperature and β -CD-PHP concentration values also presented positive effects, meaning that the main pH effect was slightly enhanced by raising the levels of the other two variables. The other main effects and third order interactions were not statistically significant ($p < 0.05$). To calculate the equilibrium constants of the β -CD-DCA inclusion

Table 1 Experimental parameters using a full factorial design to determinate DCA (2^3 factorial design) and UDCA (2^4 factorial design)

Factors	−1	Central point	+1
pH	9.2 ^a ; 10.3 ^b	9.5 ^a ; 10.5 ^b	9.8 ^a ; 10.7 ^b
Temperature (°C)	20	25	30
Concentration β -CD-PHP (M)	A ^a : 6.2×10^{-4} : 1.55×10^{-4} A ^b : 3.1×10^{-4} : 7.75×10^{-5}	B ^a : 1.24×10^{-3} : 3.1×10^{-4} B ^b : 6.2×10^{-4} : 1.55×10^{-4}	C ^a : 1.9×10^{-3} : 4.65×10^{-4} C ^b : 9.3×10^{-4} : 2.33×10^{-4}
Concentration buffer (mM)	50 ^b	200 ^b	350 ^b

Factors	Effect	<i>p</i>
Results of the 2^3 full factorial design:		
Mean/interaction	0.638500	0.0000021
(1) pH	0.430500	0.00001001
(2) Temperature	0.013500	0.15462335
(3) [B-CD:PHP]	0.003000	0.70224584
1 by 2	−0.011000	0.22055080
1 by 3	0.050500	0.00578764
2 by 3	0.028500	0.02805735
1 × 2 × 3	0.003000	0.70224584
Results of the 2^4 factorial design		
Mean/Interaction	1.26055	0.000001
(1) pH	0.11525	0.007339
(2) Temperature	−0.03975	0.110165
(3) [BCD-PHP]	−1.01550	0.000012
(4) Buffer	−0.05900	0.044509
1 by 2	0.03175	0.170465
1 by 3	0.05150	0.061885
1 by 4	0.02700	0.224251
2 by 3	0.10700	0.009056
2 by 4	−0.01350	0.500771
3 by 4	−0.01075	0.586191
1 × 2 × 3	0.04150	0.100604
1 × 2 × 4	0.00000	1.000000
1 × 3 × 4	0.03125	0.175374

Factors in bold were statistically significant ($p < 0.05$) and the pure error was 1.017×10^{-4} and 1.25×10^{-3} for DCA and UDCA, respectively
^a 2^3 factorial design to determinate DCA, ^b 2^4 factorial design to determinate UDCA

complexes with a 1:1 stoichiometry, the modified Benesi–Hildbrand [26, 27] equation (Eq. 3) can be resorted to, since the β -CD-PHP complex is colorless at the monitoring wavelength and any absorbance of the solution is due to the free PHP₀ displaced from the complex and thus proportional to the bile acid concentration.

$$\frac{1}{A - A_0} = \frac{1}{a} + \frac{1}{aK_c[\text{PHP}_0]} \quad (3)$$

The values of K_c of 8.65×10^3 and $2.58 \times 10^4 \text{ M}^{-1}$ were found at the pH values of 9.5 and 10.5, respectively.

The results obtained through the 2^4 full factorial design for the study of the variables with significant influence in the determination of UDCA are presented in the Table 1.

The concentration of the β -CD-PHP complex had a negative and highly significant effect ($p < 0.05$), indicating that smaller inclusion complex concentrations lead to larger absorbance values under the studied conditions. The pH (positive effect) and buffer concentration (negative effect) variables used in the solution of UDCA presented low statistically significant effects. Only a second-order interaction was significant, namely the interaction between temperature and β -CD-PHP concentration, indicating a positive effect of those variables on the absorbance. As can be seen on Fig. 4, and settling a constant 4:1 ratio between β -CD and PHP concentrations, the absorbance of the complex remained stable above 7.75×10^{-5} : $1.94 \times 10^{-5} \text{ M}$. However, the studies of these

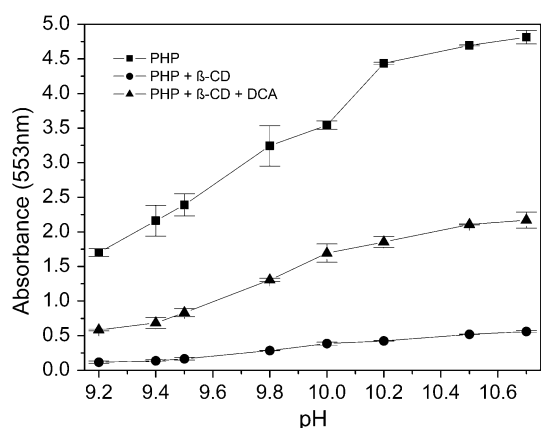


Fig. 3 pH effect in the β -CD-PHP inclusion complex (6.2×10^{-4} : 1.55×10^{-4} M) formation and your interaction with DCA (1.88×10^{-3} M)

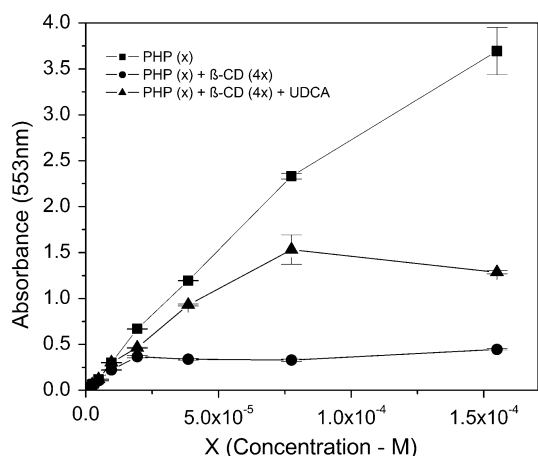


Fig. 4 Concentration effects of PHP, β -CD-PHP inclusion complex without UDCA and with UDCA (3.88×10^{-4} M) in the absorbance values

inclusion complexes in the presence of 3.88×10^{-4} M of UDCA, showed an increase in the response of 43.2% (difference statistically significant according to the Tukey test, $p \leq 0.05$) at the concentration of β -CD-PHP complex, 3.1×10^{-4} : 7.75×10^{-5} M, compared to that previously used (6.2×10^{-4} : 1.55×10^{-4} M).

Under these conditions, the straight line obtained from the Benesi–Hildbrand plot enabled us to obtain the value of $2.22 \times 10^4 \text{ M}^{-1}$ for K_c .

Analytical Parameters

From the measurements performed under the optimum conditions described above, the calibration graph was linear in the range 6.1×10^{-6} – 3.13×10^{-3} M of DCA allowing the establishment of a regression line of equation: $A = 698(\pm 10)\text{DCA}_M - 0.005(\pm 0.012)$ with a correlation coefficient of 0.9995. For UDCA a quadratic relationship

was found in the range 6.05×10^{-6} – 3.88×10^{-4} M, but translated in a linear regression line if this is established in the form of $A^{0.5} = 3,814(\pm 133)\text{UDCA}_M + 0.03(\pm 0.01)$ with a correlation coefficient of 0.9991. The limits of detection were of 3.94×10^{-5} M for DCA and of 4.08×10^{-5} M for UDCA. The corresponding limits of quantification were respectively of 1.31×10^{-4} and 1.36×10^{-4} M.

Based on Tukey's test there were no significant differences between the standards and the pharmaceutical formulations (three replicates, $p < 0.05$), according to the method described in the experimental section (variation: injectable phosphatidylcholine 4% and injectable deoxycholate 2.6% for DCA and 1% for UDCA). Table 2 shows a summary of the analytical parameters for the determination of DCA and UDCA.

Discussion

CDs are the most important and widely studied examples of host molecular receptors due to their high affinity for hydrophobic molecules in aqueous media. In particular, herein we report the preparation, characterization and application of the inclusion complexes with β -cyclodextrin and indicators to determine bile acids spectrophotometrically in pharmaceutical formulations.

In this work, we tested β -CD with nine different indicators, in which it was not possible to detect spectral changes for six of them, obtaining the best inclusion complexes with phenolphthalein (PHP), methyl orange, and methyl red.

The strong interaction between phenolphthalein (PHP) and β -CD at alkaline pH values shown in the Fig. 1a can be explained because under this pH condition, the ionized red form of PHP becomes enclosed in the β -CD cage, where it is forced into its colorless lactone structure without, however, protonating the phenolic groups [20]. However, the results obtained with the inclusion complexes between methyl orange and the β -CD observed on Fig. 1b, showed that the decrease in absorbance values, according to the literature, can be justified due to the lack of coplanarity of methyl orange caused by the constrained conformation of methyl orange in the cyclodextrin cavity [15, 28]. The same authors reported a similar behavior between the methyl orange and α -CD. In the basic pH, the formation of an isosbestic point was also noted by Sueishi and Miyakawa [29]. While the inclusion complexes obtained with methyl red and β -CD at the two pH values (Fig. 1c) showed two isosbestic points (acidic and basic pH). The isosbestic point's appearance characterizes the formation of the azonium tautomer inclusion complex, one of the cationic protonated forms of methyl red. Similar findings were previously described by Tawarah and Khouri [30] and

Table 2 Summary of the best analytical parameters for the determination of deoxycholic and ursodeoxycholic acids using an inclusion complex

Analytical parameters	Deoxycholic acid	Ursodeoxycholic acid
β -CD-PHP inclusion complex (M)	6.2×10^{-4} : 1.55×10^{-4}	3.1×10^{-4} : 7.75×10^{-5}
Temperature (°C)	20–30	20–30
pH	10.5	10.5
Solubility	Water	Carbonate buffer 50 mM
Reaction time	Instantaneous	Instantaneous
Wavelength (nm)	553	553
Linearity range (M)	6.1×10^{-6} – 3.13×10^{-3}	6.05×10^{-6} – 3.88×10^{-4}
Limit of detection (M)	3.94×10^{-5}	4.08×10^{-5}
Limit of quantification (M)	1.31×10^{-4}	1.36×10^{-4}

Kuwabara et al. [31] concerning the inclusion complexes with γ -CD and β -CD, respectively.

According to Del Valle [22], the measurements of stability or equilibrium constants (K_c) or the dissociation constants (K_d) of the guest–cyclodextrin complexes are important since this is an index of changes in the physicochemical properties of a compound upon inclusion. Then, if the K -value is high, it means that the inclusion complex is stable, as is the case of the β -CD-PHP, a colorless 1:1 inclusion complex [20, 21] at pH 10.5 and 25 °C, obtained in this work which is the method reagent proposed. In this way, only hydrophobic molecules with high affinity to the cyclodextrin cavity will be able to replace the PHP in the β -CD cavity, causing spectral changes in the visible spectrum. In addition, in the concentrations studied, the excipients used in the formulations and water type did not interfere with the results using the reagent complex (β -CD-PHP) (data not shown).

Based on the results reported here, it is clear that inclusion complexes were formed with particular forms of the indicators, but the spectral changes were more pronounced in the case of the β -CD-PHP complex at a concentrations ratio of 4:1 β -CD-PHP for determination of the DCA and UDCA. The proposed method is capable of determining the bile acid concentration using the visible spectrum, eliminating the sample preparation steps of the methods using UV detectors such as HPLC that can exhibit problems due to bile acids absorbing weakly at about 200 nm, where it is possible to function only after oxygen removal, otherwise a derivatization must be performed [32].

The other advantages of the procedure proposed herein are the short time for the analysis completion, qualitative analysis in commercial facilities, use of low cost reagents and the low concentrations which can be used for determinations. The best pH condition found for determining DCA was 10.5 and similar to that proposed for fluoxetine and tetrahydrofuran by Afkhami et al. [20] and Zarzycki and Lamparczyk [33], respectively. The development of low cost methods for determining DCA is important in quality control of pharmaceutical formulations, for

example, in deoxycholate-hydrogels [34] to prevent misuse when considering aesthetic usage purposes. The limit of detection of 3.94×10^{-5} M and a linearity varying the order of 6.1×10^{-6} – 3.13×10^{-3} M makes possible the determination of its content in samples of phosphatidylcholine injections (50 mg/mL) indiscriminately used in injection lipolysis [5, 23]. The limit of detection for the UDCA determinations is more than ten times lower than the concentrations found in liver $5\text{--}6 \times 10^{-4}$ M [35] and the typical pattern provided by the European Pharmacopoeia for tablets is 60 mg.

DCA and UDCA were satisfactorily determined in the pharmaceutical formulations by a competitive complexation reaction with a color indicator to form β -cyclodextrin-inclusion complexes. The proposed method can be used for qualitative and fast pre-examination at commercial facilities (aesthetics clinics and pharmacies), which would be useful for health policies in testing pharmaceutical formulations containing DCA and UDCA. Furthermore, the products can be submitted to quantitative analysis by this technique we have developed which is characterized by simplicity, high stability over a large temperature range, instantaneous reaction, high sample throughput and low cost for reagents and instrumentation.

Acknowledgments The authors would like to thank FACEPE, CAPES-GRICES, LIKA/UFPE, CNPq. Dr. Benício B. Neto provided assistance in the statistical analysis of the manuscript.

References

1. Yoo SH (2007) Preparation of aqueous clear solution dosage forms with bile acids. US Patent 7,303,768
2. Fernandez-Leyes MD, Messina PV, Schulz PC (2007) Aqueous sodium dehydrocholate-sodium deoxycholate mixtures at low concentration. *J Colloid Interface Sci* 314:659–664
3. Rodriguez VG, Lucangioli SE, Fernandez Otero GC, Carducci CN (2000) Determination of bile acids in pharmaceutical formulations using micellar electrokinetic chromatography. *J Pharm Biomed Anal* 23:375–381
4. Matarasso A, Pfeifer TM (2009) Mesotherapy and injection lipolysis. *Clin Plast Surg* 36:181–192

5. Rotunda AM, Kolodney MS (2006) Mesotherapy and phosphatidylcholine injections: historical clarification and review. *Dermatol Surg* 32:465–480
6. Orienti I, Cerchiara T, Zecchi V, Arias Blanco MJ, Gines JM, Moyano JR, Rabasco Alvarez AM (1999) Complexation of ursodeoxycholic acid with β -cyclodextrin-choline dichloride coprecipitate. *Int J Pharm* 190:139–153
7. Tay J, Timmouth A, Fergusson D, Huebsch L, Allan DS (2007) Systematic review of controlled clinical trials on the use of ursodeoxycholic acid for the prevention of hepatic veno-occlusive disease in hematopoietic stem cell transplantation. *Biol Blood Marrow Transplant* 13:206–217
8. Setchell KDR, Galzigna L, O'Connell N, Brunetti G, Tauschel HD (2005) Bioequivalence of a new liquid formulation of ursodeoxycholic acid (Ursofalk suspension) and Ursosalk capsules measured by plasma pharmacokinetics and biliary enrichment. *Aliment Pharmacol Ther* 21:709–721
9. Lin M-C, Wu H-L, Kou H-S, Wu S-M, Chen S-H (2003) Simple and sensitive fluorimetric liquid chromatography for simultaneous analysis of chenodiol and ursodiol in pharmaceutical formulations. *Anal Chim Acta* 493:159–166
10. Momose T, Mure M, Iida T, Goto J, Nambara T (1998) Method for the separation of the unconjugates and conjugates of chenodeoxycholic acid and deoxycholic acid by two-dimensional reversed-phase thin-layer chromatography with methyl β -cyclodextrin. *J Chromatogr A* 811:171–180
11. Jh Wang, Cai Z (2008) Investigation of inclusion complex of miconazole nitrate with β -cyclodextrin. *Carbohydr Polym* 72:255–260
12. Teranishi K, Nishiguchi T (2004) Cyclodextrin-bound 6-(4-methoxyphenyl)imidazo[1, 2- α]pyrazin-3(7H)-ones with fluorescein as green chemiluminescent probes for superoxide anions. *Anal Biochem* 325:185–195
13. Jh Wang, Cai Z (2008) Incorporation of the antibacterial agent, miconazole nitrate into a cellulosic fabric grafted with β -cyclodextrin. *Carbohydr Polym* 72:695–700
14. Gunaratne A, Corke H (2008) Effect of hydroxypropyl β -cyclodextrin on physical properties and transition parameters of amylose–lipid complexes of native and acetylated starches. *Food Chem* 108:14–22
15. Yuexian F, Yu Y, Shaomin S, Chuan D (2005) Molecular recognition of α -cyclodextrin (CD) to choral amino acids based on methyl orange as a molecular probe. *Spectrochim Acta A* 61:953–959
16. Zhu X, Sun J, Wu J (2007) Study on the inclusion interactions of β -cyclodextrin and its derivative with dyes by spectrofluorimetry and its analytical application. *Talanta* 72:237–242
17. Xie H, Wang HY, Ma LY, Xiao Y, Han J (2005) Spectrophotometric study of the inclusion complex between β -cyclodextrin and dibenzoyl peroxide and its analytical application. *Spectrochim Acta A* 62:197–202
18. Yanez C, Salazar R, Nunez-Vergara LJ, Squella JA (2004) Spectrophotometric and electrochemical study of the inclusion complex between β -cyclodextrin and fumidipine. *J Pharm Biomed Anal* 35:51–56
19. De Leon-Rodriguez LM, Basuil-Tobias DA (2005) Testing the possibility of using UV–vis spectrophotometric techniques to determine non-absorbing analytes by inclusion complex competition in cyclodextrins. *Anal Chim Acta* 543:282–290
20. Afkhami A, Madrakian T, Khalafi L (2006) Spectrophotometric determination of fluoxetine by batch and flow injection methods. *Chem Pharm Bull* 54:1642–1646
21. Glazyrin AE, Grachev MK, Kurochkina GI, Nifant'ev EE (2004) Inclusion compounds of some water-soluble β -cyclodextrin derivatives with phenolphthalein. *Russ J Gen Chem* 74:1922–1925
22. Del Valle EMM (2004) Cyclodextrins and their uses: a review. *Process Biochem* 39:1033–1046
23. Rotunda AM, Suzuki H, Moy RL, Kolodney MS (2004) Detergent effects of sodium deoxycholate are a major feature of an injectable phosphatidylcholine formulation used for localized fat dissolution. *Dermatol Surg* 30:1001–1008
24. Yagima Odo ME, Cuce LC, Odo LM, Natrielli A (2007) Action of sodium deoxycholate on subcutaneous human tissue: Local and systemic effects. *Dermatol Surg* 33:178–188
25. Brewster ME, Loftsson T (2007) Cyclodextrins as pharmaceutical solubilizers. *Adv Drug Deliv Rev* 59:645–666
26. Abdel-Shafi AA (2007) Spectroscopic studies on the inclusion complex of 2-naphthol-6-sulfonate with β -cyclodextrin. *Spectrochim Acta A* 66:732–738
27. Benesi HA, Hildebrand JH (1949) A spectrophotometric investigation of the interaction of iodine with aromatic hydrocarbons. *J Am Chem Soc* 71:2703–2707
28. Zhang H, Chen G, Wang L, Ding L, Tian Y, Jin W, Zhang H (2006) Study on the inclusion complexes of cyclodextrin and sulphonated azo dyes by electrospray ionization mass spectrometry. *Int J Mass Spectrom* 252:1–10
29. Sueishi Y, Miyakawa T (1999) Complexation of phenols with β - and γ -cyclodextrins: Determination of the association constants by using the isomerization of spiropyran. *J Phys Org Chem* 12:541–546
30. Tawarah KM, Khouri SiJ (2000) Determination of the stability and stoichiometry of p-methyl red inclusion complexes with γ -cyclodextrin. *Dyes Pigm* 45:229–233
31. Kuwabara T, Nakamura A, Ueno A, Toda F (1994) Inclusion complexes and guest-induced color changes of pH-indicator-modified β -cyclodextrins. *J Phys Chem* 98:6297–6303
32. Arias De Fuentes O, Campanella L, Crescentini G, Falcioni A, Sammartino MP, Tomassetti M (2000) Flow injection analysis of cholic acids in pharmaceutical preparations using a polymeric membrane ISE as detector. *J Pharm Biomed Anal* 23:89–98
33. Zarzycki PK, Lamparczyk H (1998) The equilibrium constant of β -cyclodextrin-phenolphthalein complex; influence of temperature and tetrahydrofuran addition. *J Pharm Biomed Anal* 18:165–170
34. Valenta C, Nowack E, Bernkop-Schnurch A (1999) Deoxycholate-hydrogels: novel drug carrier systems for topical use. *Int J Pharm* 185:103–111
35. Poupon R, Poupon RE (1995) Ursodeoxycholic acid therapy of chronic cholestatic conditions in adults and children. *Pharmacol Ther* 66:1–15

Introduction

The role of nutrition in the management of diseases has often centered on correcting apparent nutrient deficiencies or meeting estimated nutritional requirements of patients. Recently, further understanding of the underlying mechanisms of various disease processes and how certain nutrients possess pharmacological properties have fueled an interest in exploring how nutritional therapies themselves could modify the behavior of various conditions. Nutrients such as n-3 PUFA have been demonstrated to have at least the potential to modulate diseases. Eicosapentaenoic (C20:5n-3, EPA) and docosahexaenoic acid (C22:6n-3, DHA), the n-3 PUFA present in marine foods, have an important role in the prevention of many diseases, particularly cardiovascular diseases (CVD) [1, 2] and the American Heart Association and the European Society of Cardiology recommend a higher fish consumption and/or the daily intake of 1 g n-3 PUFA for primary and especially for secondary prevention [3].

n-3 PUFA preventive activity is related to their hypocholesterolemic, hypotriglyceridemic and anti-inflammatory effect, to the reduction of platelet aggregation and blood viscosity, to the antithrombotic and fibrinolytic activities [4, 5] and to the protection from ischemia/reperfusion-induced cellular damage and arrhythmias [6]. Among the different mechanisms considered at the basis of PUFA effects, the modulation of gene expression [7] is of particular interest. Actually, in a recent work [8] we demonstrated that EPA and DHA supplementation to cultured neonatal rat cardiomyocytes is able to modulate the expression of more than 100 genes, many of them related to cardiac hypertrophy.

The fatty acids regulate gene expression binding directly to nuclear receptors or affecting SREBP, ChREBP and NF kappa B protein content. PPAR are considered important effectors of fatty acid regulation of gene transcription, and recent studies have identified that PPAR have some new effects in CVD [9]. PPAR belong to a ligand-activated nuclear receptor super-family that includes three members (α , β/δ , and γ) encoded by distinct genes, which bind to sequence-specific target elements as an hetero-dimer with the retinoid X receptor (RXR) in the promoter region of target genes [10].

The first aim of the present study was to elucidate if EPA and DHA act simply by increasing PPAR/RXR DNA binding or if they can also increase the biosynthesis of PPAR themselves, so regulating the nuclear abundance of these nuclear factors.

The second aim of this work was to establish a new link between the modification of fatty acid composition induced by n-3 PUFA and their molecular effects.

Experimental Procedure

Material

Fatty acids, Ham F10 medium, fetal calf serum (FCS), horse serum (HS), gentamicin, amphotericin B, BSA, pentadecanoic acid, CelLytic™ M, protease inhibitor cocktail, DTNB, palmitoyl coenzyme A lithium salt, anti-rat β -actin IgG were from Sigma (Milan, Italy). Anti-rat α , β/δ , γ PPAR, nucleophosmin and HRP-conjugated goat anti-rabbit IgG were from Santa Cruz Biotechnology (Milan, Italy). All other chemicals and solvents were of the highest analytical grade.

Methods

Cell Cultures

Primary cultures of neonatal cardiomyocytes were obtained from the ventricles of 2–4 day old Wistar rats according to Yagev et al. [11]. The research was conducted in conformity with the Public Health Service Policy on Human Care and Use of Laboratory Animals, and the study protocol was approved by The Animal Care Committee of the University of Bologna (Italy). Cells were seeded at a density of 1.5×10^6 cells/ml in 100-mm i.d. Petri dishes in Ham F10 nutrient mixture supplemented with 10% v/v FCS, 10% v/v HS, gentamicin (1%), amphotericin B (1%), and grown at 37°C, 5% CO₂ and 95% humidity. Forty-eight hours from seeding, cardiomyocytes were randomly divided into control and fatty acid supplemented groups. EPA and DHA were dissolved in ethanol and supplemented at 60 μ M concentration. Control medium was added with the same volume of ethanol ($\leq 0.1\%$ v/v), to avoid interference due to the vehicle. Media were changed every 48 h and on day 8 from seeding, after a 6-day exposure to fatty acids and at complete confluence, cardiomyocytes were washed three times with 0.9% NaCl and the cells scraped off. Whole cell lysate (WCL) was obtained using CelLytic™ M plus protease inhibitor cocktail (1 μ M AEBSF, 0.8 μ M aprotinin, 20 μ M leupeptin, 40 μ M bestatin, 15 μ M pepstatin A and 14 μ M E-64) while the nuclear (NF) and cytoplasmic fraction (CF) were obtained by differential centrifugations as previously reported by Wright et al. [12].

PPAR DNA Binding

The degree of DNA binding of the three PPAR isoforms was determined by an immunosorbent assay (ELISA) utilizing PPAR α , β/δ and γ transcription factor assay kits (Cayman Chemicals, USA) following the manufacturer's instructions. Briefly, a specific double stranded DNA sequence containing the peroxisome proliferator responsive

element (PPRE) was immobilized onto the bottom of the wells of 96-well plates. Aliquots of NF diluted to obtain 50 μg protein in each assay were added to each well, so that PPAR contained in the extract bind specifically to the PPRE. Different PPAR isoforms were detected by the addition of specific primary antibodies directed against PPAR α , β/δ , or γ . A secondary antibody conjugated to HRP was added to provide a sensitive colorimetric readout at 450 nm. DNA binding of all the three isoforms was evaluated in each NF.

Western Blot Analysis

Western blotting was performed on WCL, CF and NF. Aliquots corresponding to 30 μg of proteins were analyzed by SDS-PAGE (12% gel). Proteins were transferred onto a nitrocellulose membrane and probed at room temperature for 60 min with the specific primary antibody anti- α , anti- β/δ , anti- γ PPAR, anti-nucleophosmin (B23) (1:1,000) or anti- β -actin (1:20,000). After further washing, the membrane was incubated with HRP-conjugated goat anti-rabbit IgG for 30 min. Final detection was performed with an enhanced chemiluminescence (ECL AdvanceTM) Western blotting detection kit (Amersham Biosciences, UK). β -Actin was used in WCL and CF [13, 14], and B23 in NF [15] as loading control.

Fatty Acid Composition

Total lipids were extracted from CF and NF according to Folch et al. [16] and methyl esterified according to Stoffel et al. [17]. Prior to methyl esterification, pentadecanoic acid (C15:0) was added as the internal standard. Fatty acid composition (as methyl esters) was determined by gas chromatography (GC 8000, Fisons, Milan, Italy) using a capillary column (SP 2340, 0.2 μm film thickness) at a programmed temperature gradient (160–210 $^{\circ}\text{C}$, 8 $^{\circ}\text{C}/\text{min}$) as previously reported [18]. The gas chromatographic peaks were identified on the basis of their retention time ratio relative to methyl stearate and predetermined on authentic samples. Gas chromatographic traces and quantitative evaluations were obtained using a Chrom Card Software (Thermo Electron Scientific, Milan, Italy) computing integrator.

Acyl-CoA Thioesterase Activity

Acyl-CoA thioesterase (EC 3.1.2.2, ACOT) activity was determined spectrophotometrically according to Ofman et al. [19] by measuring the cleavage of the free thiol group of palmitoyl coenzyme A, used as the substrate. The reaction mixture contained 50 mM HEPES, 50 mM KCl, 1 mg/ml BSA and 100 μM palmitoyl coenzyme A lithium

salt. Reactions started with the addition of 100 μl of WCL, and after 15 min at 37 $^{\circ}\text{C}$ were stopped by the addition of DTNB at a final concentration of 0.5 mM. DTNB reacted with CoA-SH, and the TNB formed was measured at 412 nm using a spectrophotometer (Beckman Coulter DU730, Milan, Italy). Substrate blanks were run in order to correct for aspecific TNB formation. ACOT activity was calculated from the TNB molar extinction coefficient ($\epsilon = 13,600 \text{ M}^{-1} \text{ cm}^{-1}$) and normalized for protein content in the same sample.

Protein Content

The protein content in the samples was determined according to Bradford [20] using BSA as standard.

Statistical Analysis

Data are reported as means \pm SD of results obtained in at least three independent cell cultures. Differences were tested for statistical significance by one way ANOVA using Tukey's test.

Results

The evaluation of DNA binding of the three PPAR isoforms revealed a significant increase in EPA and DHA supplemented cardiomyocytes for the β/δ isoform only (Fig. 1).

As evidenced by western blotting analysis, all three PPAR isoforms appeared expressed in WCL (Fig. 2a), and PUFA supplementation did not apparently modify protein

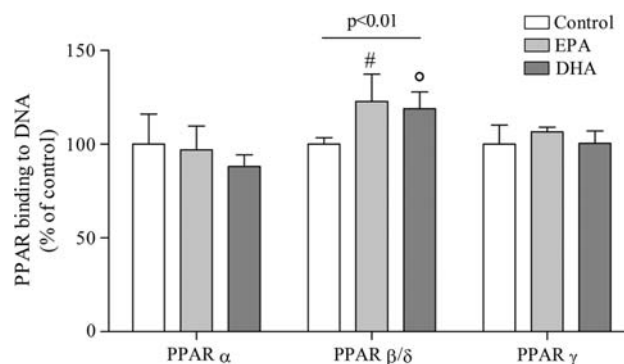


Fig. 1 PPAR binding to DNA in control and EPA or DHA supplemented cardiomyocytes. PPAR binding was measured using aliquots of NF as described in “Methods”, and is expressed as percentage of control cells, assigned as 100%. Data are mean \pm SD of five samples obtained in independent cell cultures. Statistical analysis was by one way ANOVA (PPAR β/δ $P < 0.01$) with Tukey as post-test ($\#P < 0.05$ and $^{\circ}P < 0.01$ vs. control)

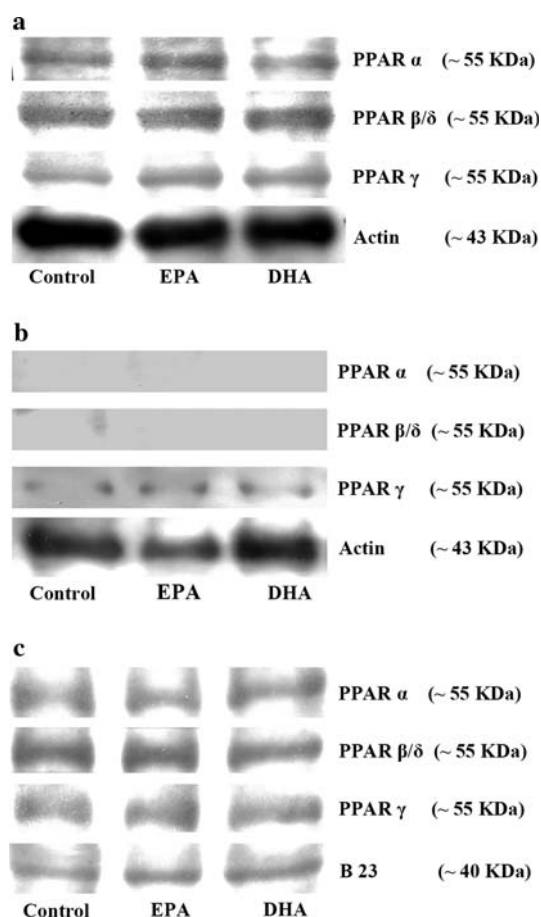


Fig. 2 PPAR α , β/δ and γ protein expression and subcellular localization in control, EPA and DHA supplemented cardiomyocytes. PPAR protein expression was analyzed in whole cell lysate (a), cytosolic fraction (b), and nuclear fraction (c) using SDS-PAGE as described in “Methods”. Pictures are representative of three different western blotting experiments

expression, regardless of the isoform considered. Western blotting analysis in CF (Fig. 2b) and NF (Fig. 2c) clearly showed that all PPAR isoforms were present almost exclusively in the nucleus, while at the cytoplasmic level, a very mild appearance was noted only for the γ subtype. Differences due to PUFA supplementation were not apparent either in WCL nor in NF.

The fatty acid composition of CF is reported in Fig. 3a. EPA supplementation led to an enhanced EPA and n-3 docosapentaenoic (C22:5n-3, DPA) relative molar content, without any increase in DHA content. DHA relative molar content increased in CF of DHA supplemented cardiomyocytes. In both cases, incorporation of n-3 PUFA was paralleled by a reduction in C18:1, C18:2n-6, and C20:4n-6 relative molar content. Total concentration of fatty acids in CF was unaffected by PUFA supplementation (Fig. 3b).

Even in NF, supplementation with EPA led to an enhanced EPA and n-3 DPA relative molar content, without any increase in DHA content, while supplemented

DHA was significantly incorporated without any appreciable retro conversion to n-3 DPA and EPA (Fig. 4a). Supplementation with both PUFA caused a reduction in C16:0, C18:0, C18:1, and C20:4n-6 relative molar content, more evident in EPA supplemented cells. Furthermore, both n-3 PUFA supplementations increased fatty acid concentration in NF (Fig. 4b).

As shown in Fig. 5 n-3 PUFA supplementation, particularly DHA one, significantly increased ACOT activity.

Discussion

The evaluation of PPAR α , β/δ and γ protein mass confirmed that all PPAR isoforms are expressed in neonatal rat cardiomyocytes, according to Takano et al. [21] and Planavila et al. [22], and that they are almost exclusively localized at the nuclear level, as reported by Takano et al. [21] and Cheng et al. [23] in neonatal and adult rat cardiomyocytes, respectively. The mild expression of γ isoform in CF is in agreement with Burgermeister and Seger [24], who reported the export to and retention in cytosol of this isoform due to its interaction with mitogen-activated protein kinase/extracellular signal-regulated kinase (MEK1) [25]. The enhanced PPAR β/δ DNA binding observed in n-3 PUFA supplemented cells could be due to both a PPAR enhanced activity state or to a higher PPAR concentration. Although immunoblotting did not reveal any modification in PPAR protein mass it is difficult to exclude it, since ELISA assays are most sensitive.

EPA and DHA supplementation deeply changed the acyl composition of both CF and NF. In the NF the increase in n-3 PUFA relative content occurred at the expense of saturated C16:0 and C18:0, indicating that supplementation had a stronger effect on the PUFA/SFA ratio in the nucleus than in the cytosol. The high content of total FA, and in particular of EPA and DHA, and its increase following supplementation suggests a selective accumulation of n-3 PUFAs in the nucleus. This is in agreement with Brochot et al. [26], who observed a particularly high incorporation of n-3 PUFAs in the nuclear membrane of cardiac cells after feeding rats an α -linolenic supplemented diet, and supports a direct interaction of EPA and DHA with PPAR, since, in order to act as a bona fide ligand, a compound has to be present within the nucleus in sufficient amounts.

Obviously, for acting within the nucleus, EPA and DHA have to get into the nucleus. In this study, EPA and DHA were delivered as non-esterified fatty acids (NEFA) to the cell from extracellular sources, and CF composition clearly show that they were taken up from media. Once within the cell, free EPA and DHA may continue to diffuse into the nucleus, but more likely they are modified by enzymes for acylation into membrane phospholipids, or they are bound

Fig. 3 Fatty acid percent composition and concentration of cytoplasmic fraction in control, EPA and DHA supplemented cardiomyocytes. Cytosolic fraction was separated by centrifugation, lipids were extracted, methylesterified and analyzed by gas chromatography as described in “Methods”. Data are expressed as mol/100 mol (a) and $\mu\text{g}/\text{plate}$ (b), and are mean \pm SD of at least six samples obtained in three independent cell cultures. Statistical analysis was by one way ANOVA (18:1 $P < 0.001$; 18:2n-6 $P < 0.05$; 20:4n-6 $P < 0.001$; 20:5n-3 $P < 0.001$; 22:5n-3 $P < 0.001$; 22:6n-3 $P < 0.001$) with Tukey as post-test ($^{\circ}P < 0.01$ and $*P < 0.001$ vs. control)

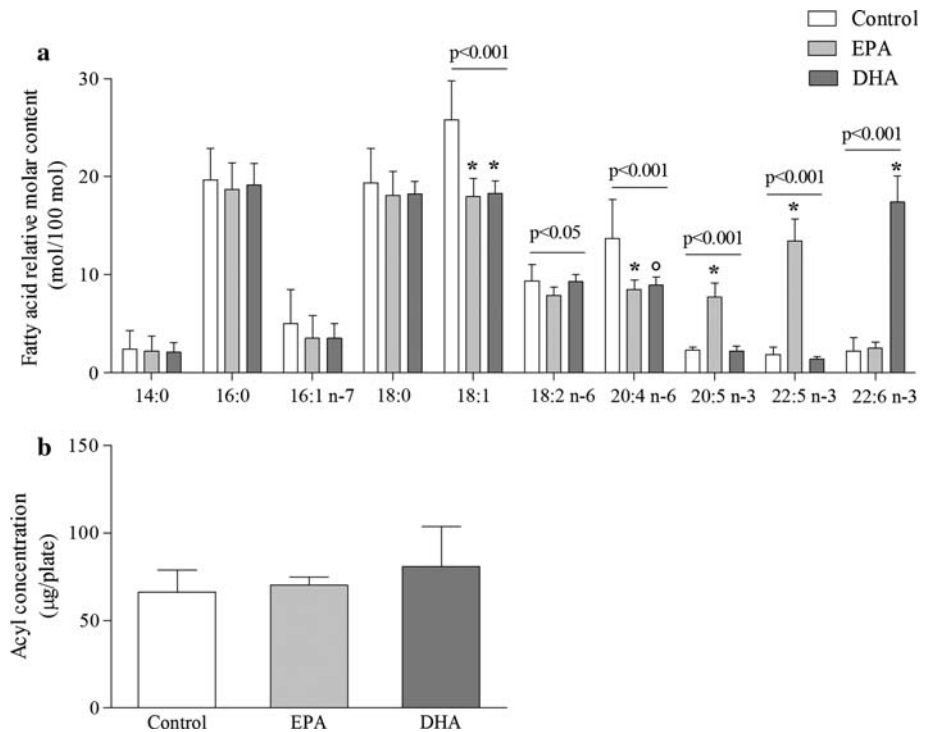
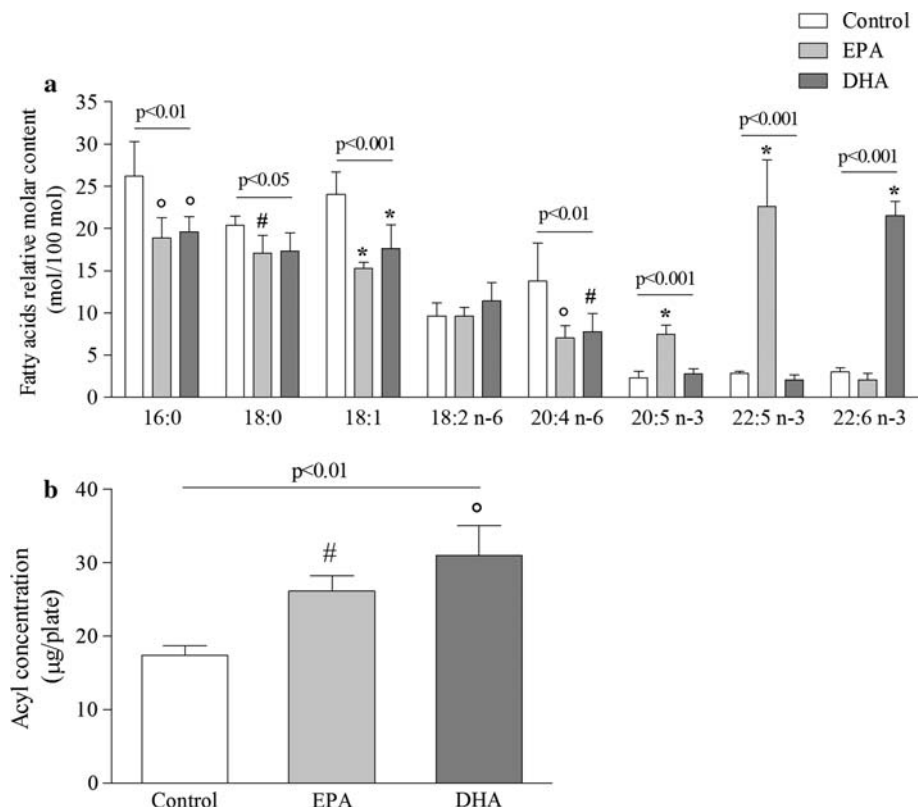


Fig. 4 Fatty acid percent composition and concentration of nuclear fraction in control, EPA and DHA supplemented cardiomyocytes. Nuclear fraction was separated by centrifugation, lipids were extracted, methylesterified and analyzed by gas chromatography as described in Methods. Data are expressed as mol/100 mol (a) and $\mu\text{g}/\text{plate}$ (b), and are mean \pm SD of at least six samples obtained in three independent cell cultures. Statistical analysis was by one way ANOVA (16:0 $P < 0.01$; 18:0 $P < 0.05$; 18:1 $P < 0.001$; 20:4n-6 $P < 0.01$; 20:5n-3 $P < 0.001$; 22:5n-3 $P < 0.001$; 22:6n-3 $P < 0.001$) with Tukey as post-test ($\#P < 0.05$; $^{\circ}P < 0.01$ and $*P < 0.001$ vs. control)



by fatty acid binding proteins (FABP). FABP have been shown to strongly bind medium- and long-chain FA [27, 28]. Binding of FA to FABP within the cytoplasm results in the rapid movement of the lipid-protein complex through

the nuclear pores into the nucleus [29, 30]. Since FABP bind NEFA with higher affinity than acyl-CoAs [31, 32], and long-chain acyl-CoA esters act as antagonists while long-chain NEFA as agonists for the PPAR [32, 33],

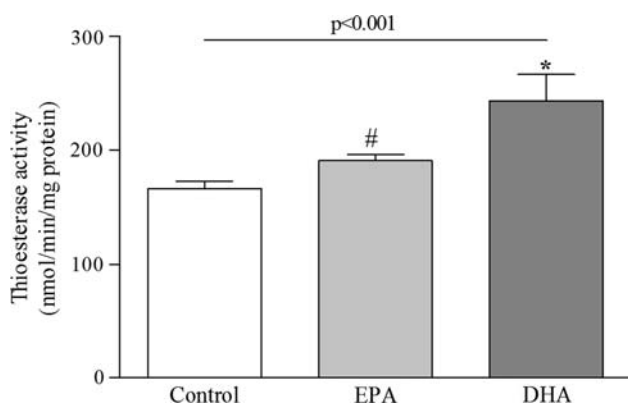


Fig. 5 Acyl-CoA thioesterase (ACOT) activity in control, EPA and DHA supplemented cardiomyocytes. ACOT activity was measured in whole cell extract as described in “Methods”. Data are expressed as nmol/min/mg protein, and are mean \pm SD of at least six samples obtained in three independent cell cultures. Statistical analysis was by one way ANOVA ($P < 0.001$) with Tukey as post-test (# $P < 0.05$; * $P < 0.001$ vs. control)

the NEFA/acyl-CoA ratio is an important determinant in fatty acid transport to the nucleus and in the regulation of gene transcription. The activity of ACOT, catalyzing the reaction leading to NEFA from acyl-CoA, increased in n-3 PUFA supplemented cells, in agreement with Ramos and Colquhoun [34]. Although ACOT activity is not the only parameter for NEFA/acyl-CoA ratio, it is conceivable that it is important for the control of the NEFA pool composition, as also suggested by Pawar and Jump [35] and Mandard et al. [36]. Recently, Dongol et al. [37] reported the presence of a functional PPRE in the promoter region of ACOT gene. Since EPA and DHA are PPAR ligands, they could upregulate ACOT gene transcription, creating a self-maintaining loop that guarantees a high cytosolic NEFA concentration. NEFA are then transferred to the nucleus by FABP, where they can exert their activity as PPAR ligands.

The selective activation of PPAR β/δ is difficult to explain. Tentatively, we can suggest the intervention of FABP. Within the nucleus, FABP may interact with PPAR [28] and apparently donate the fatty acid to activate the PPAR [38]. Tan et al. [38] provided evidence that in adipocytes some FABP act in concert with PPAR and that this activity is highly selective for particular FABP-PPAR pairs: A-FABP specifically enhances the activity of PPAR γ , while K-FABP activates PPAR β/δ . Although further studies are needed to verify if similar pairs are also present in cardiomyocytes, and eventually if they have preferential ligands, this hypothesis could explain the preferential PPAR β/δ activation.

Although the original concept that ligand availability is the sole and primary factor controlling the activity of PPAR has been replaced in recent years, due to the

recognition of different control mechanisms of PPAR activity (competition for the dimerization partner RXR and for PPRE sites, recruitment of co-activators and repressors, degree of phosphorylation), it remains the sine qua non of the event. Our data further clarify what happens in cardiomyocytes following n-3 PUFA supplementation, linking the modification of acyl composition to ACOT activity and PPAR activation. This may contribute to the understanding of the protective mechanisms of n-3 PUFA in CVD.

Acknowledgments This work was partially supported by Granarolo S.p.A. (Bologna, Italy) and by Italian MIUR (RFO 2007). The authors thank Mrs. Fabiana Missiroli for her skillful technical assistance.

References

- Xue H, Wan M, Song D, Li Y, Li J (2006) Eicosapentaenoic acid and docosahexaenoic acid modulate mitogen-activated protein kinase activity in endothelium. *Vascul Pharmacol* 44:434–439
- Harris WS, Miller M, Tighe AP, Davidson MH, Schaefer EJ (2008) Omega-3 fatty acids and coronary heart disease risk: clinical and mechanistic perspectives. *Atherosclerosis* 197:12–24
- Weber HS, Selimi D, Huber G (2006) Prevention of cardiovascular diseases and highly concentrated n-3 polyunsaturated fatty acids (PUFAs). *Herz* 31(Suppl 3):24–30
- Calder PC (2004) n-3 Fatty acids and cardiovascular disease: evidence explained and mechanisms explored. *Clin Sci* 107:1–11
- Benatti P, Peluso G, Nicolai R, Calvani M (2004) Polyunsaturated fatty acids: biochemical, nutritional and epigenetic properties. *J Am Coll Nutr* 23:281–302
- Demaison L, Moreau D (2002) Dietary n-3 polyunsaturated fatty acids and coronary heart disease-related mortality: a possible mechanism of action. *Cell Mol Life Sci* 59:463–477
- Jump DB, Botolin D, Wang Y, Xu J, Demeure O, Christian B (2008) Docosahexaenoic acid (DHA) and hepatic gene transcription. *Chem Phys Lipids* 153:3–13
- Bordoni A, Astolfi A, Morandi L, Pession A, Danesi F, Di Nunzio M, Franzoni M, Biagi P (2007) n-3 PUFAs modulate global gene expression profile in cultured rat cardiomyocytes. Implications in cardiac hypertrophy and heart failure. *FEBS Lett* 581:923–929
- Chen R, Liang F, Moriya J, Yamakawa J, Takahashi T, Shen L, Kanda T (2008) Peroxisome proliferator-activated receptors (PPARs) and their agonists for hypertension and heart failure: are the reagents beneficial or harmful? *Int J Cardiol* 130:131–139
- Feige JN, Gelman L, Michalik L, Desvergne B, Wahli W (2006) From molecular action to physiological outputs: peroxisome proliferator-activated receptors are nuclear receptors at the crossroads of key cellular functions. *Prog Lipid Res* 45:120–159
- Yagev S, Heller M, Pinson A (1984) Changes in cytoplasmic and lysosomal enzyme activities in cultured rat heart cells: the relationship to cell differentiation and cell population in culture. *In Vitro* 20:893–898
- Wright G, Singh IS, Hasday JD, Farrance IK, Hall G, Cross AS, Rogers TB (2002) Endotoxin stress-response in cardiomyocytes: NF-kappaB activation and tumor necrosis factor-alpha expression. *Am J Physiol Heart Circ Physiol* 282:H872–H879
- Gilde AJ, Van Bilsen M (2003) Peroxisome proliferator-activated receptors (PPARs): regulators of gene expression in heart and skeletal muscle. *Acta Physiol Scand* 178:425–434

14. Xu M, McCarrey JR, Hecht NB (2008) A cytoplasmic variant of the KH-type splicing regulatory protein serves as a decay-promoting factor for phosphoglycerate kinase 2 mRNA in murine male germ cells. *Nucleic Acids Res* 36:7157–7167
15. van Deursen D, Jansen H, Verhoeven AJ (2008) Glucose increases hepatic lipase expression in HepG2 liver cells through upregulation of upstream stimulatory factors 1 and 2. *Diabetologia* 51:2078–2087
16. Folch J, Lees M, Sloane Stanley GH (1957) A simple method for the isolation and purification of total lipides from animal tissues. *J Biol Chem* 226:497–509
17. Stoffel W, Chu F, Ahrens EH (1959) Analysis of long-chain fatty acids by gas–liquid chromatography. Micromethod for the preparation of methyl esters. *Anal Chem* 31:307–308
18. Bordoni A, Angeloni C, Leoncini E, Danesi F, Maranesi M, Biagi PL, Hrelia S (2005) Hypoxia/reoxygenation alters essential fatty acids metabolism in cultured rat cardiomyocytes: protection by antioxidants. *Nutr Metab Cardiovasc Dis* 15:166–173
19. Ofman R, el Mrabet L, Dacremont G, Spijker D, Wanders RJ (2002) Demonstration of dimethylnonanoyl-CoA thioesterase activity in rat liver peroxisomes followed by purification and molecular cloning of the thioesterase involved. *Biochem Biophys Res Commun* 290:629–634
20. Bradford MM (1976) A rapid and sensitive method for the quantitation of microgram quantities of protein utilizing the principle of protein–dye binding. *Anal Biochem* 72:248–254
21. Takano H, Nagai T, Asakawa M, Toyozaki T, Oka T, Komuro I, Saito T, Masuda Y (2000) Peroxisome proliferator-activated receptor activators inhibit lipopolysaccharide-induced tumor necrosis factor- α expression in neonatal rat cardiac myocytes. *Circ Res* 87:596–602
22. Planavila A, Rodriguez-Calvo R, Jove M, Michalik L, Wahli W, Laguna JC, Vazquez-Carrera M (2005) Peroxisome proliferator-activated receptor beta/delta activation inhibits hypertrophy in neonatal rat cardiomyocytes. *Cardiovasc Res* 65:832–841
23. Cheng L, Ding G, Qin Q, Xiao Y, Woods D, Chen YE, Yang Q (2004) Peroxisome proliferator-activated receptor delta activates fatty acid oxidation in cultured neonatal and adult cardiomyocytes. *Biochem Biophys Res Commun* 313:277–286
24. Burgermeister E, Seger R (2007) MAPK kinases as nucleocytoplasmic shuttles for PPAR γ . *Cell Cycle* 6:1539–1548
25. Burgermeister E, Chuderland D, Hanoch T, Meyer M, Liscovitch M, Seger R (2007) Interaction with MEK causes nuclear export and downregulation of peroxisome proliferator-activated receptor gamma. *Mol Cell Biol* 27:803–817
26. Brochot A, Guinot M, Auchere D, Macaire JP, Weill P, Grynberg A, Rousseau-Ralliard D (2009) Effects of alpha-linolenic acid vs. docosahexaenoic acid supply on the distribution of fatty acids among the rat cardiac subcellular membranes after a short- or long-term dietary exposure. *Nutr Metab* 6:14
27. Ek-Von Mentzer BA, Zhang F, Hamilton JA (2001) Binding of 13-HODE and 15-HETE to phospholipid bilayers, albumin, and intracellular fatty acid binding proteins. Implications for transmembrane and intracellular transport and for protection from lipid peroxidation. *J Biol Chem* 276:15575–15580
28. Wolfrum C, Borchers T, Sacchetti JC, Spener F (2000) Binding of fatty acids and peroxisome proliferators to orthologous fatty acid binding proteins from human, murine, and bovine liver. *Biochemistry* 39:1469–1474
29. Lawrence JW, Kroll DJ, Eacho PI (2000) Ligand-dependent interaction of hepatic fatty acid-binding protein with the nucleus. *J Lipid Res* 41:1390–1401
30. Huang H, Starodub O, McIntosh A, Kier AB, Schroeder F (2002) Liver fatty acid-binding protein targets fatty acids to the nucleus. Real time confocal and multiphoton fluorescence imaging in living cells. *J Biol Chem* 277:29139–29151
31. Huhtinen K, O’Byrne J, Lindquist PJ, Contreras JA, Alexson SE (2002) The peroxisome proliferator-induced cytosolic type I acyl-CoA thioesterase (CTE-I) is a serine–histidine–aspartic acid alpha/beta hydrolase. *J Biol Chem* 277:3424–3432
32. Murakami K, Ide T, Nakazawa T, Okazaki T, Mochizuki T, Kadowaki T (2001) Fatty-acyl-CoA thioesters inhibit recruitment of steroid receptor co-activator 1 to alpha and gamma isoforms of peroxisome-proliferator-activated receptors by competing with agonists. *Biochem J* 353:231–238
33. Elholm M, Dam I, Jorgensen C, Krogsdam AM, Holst D, Kratchmarova I, Gottlicher M, Gustafsson JA, Berge R, Flatmark T, Knudsen J, Mandrup S, Kristiansen K (2001) Acyl-CoA esters antagonize the effects of ligands on peroxisome proliferator-activated receptor alpha conformation, DNA binding, and interaction with Co-factors. *J Biol Chem* 276:21410–21416
34. Ramos KL, Colquhoun A (2001) Evidence for the involvement of polyunsaturated fatty acids in the regulation of long-chain acyl CoA thioesterases and peroxisome proliferation in rat carcinosarcoma. *Cell Biochem Funct* 19:1–9
35. Pawar A, Jump DB (2003) Unsaturated fatty acid regulation of peroxisome proliferator-activated receptor alpha activity in rat primary hepatocytes. *J Biol Chem* 278:35931–35939
36. Mandard S, Muller M, Kersten S (2004) Peroxisome proliferator-activated receptor alpha target genes. *Cell Mol Life Sci* 61:393–416
37. Dongol B, Shah Y, Kim I, Gonzalez FJ, Hunt MC (2007) The acyl-CoA thioesterase I is regulated by PPAR α and HNF4 α via a distal response element in the promoter. *J Lipid Res* 48:1781–1791
38. Tan NS, Shaw NS, Vinckenbosch N, Liu P, Yasmin R, Desvergne B, Wahli W, Noy N (2002) Selective cooperation between fatty acid binding proteins and peroxisome proliferator-activated receptors in regulating transcription. *Mol Cell Biol* 22:5114–5127

involved in the absorption of dietary fats and subsequent postprandial metabolism of the dietary-derived TRLs [3]. Studies in humans, examining the short-term effects of dietary fatty acids on postprandial lipaemia, have suggested that the fatty acid composition of the test meal may influence the absorption, synthesis and secretion of dietary TAG, as well as chylomicron (CM) particle size. However, mechanisms responsible for the qualitative and quantitative differences in postprandial TRLs following meals of different fatty acids are limited. We have previously shown marked differences in the composition of TRLs within the Svedberg flotation rate (S_f) > 400 fraction, in response to meals of differing fatty acid composition in middle-aged men. Although greater numbers of apolipoprotein (apo) B-48 containing lipoproteins were present in the circulation following the monounsaturated fatty acid (MUFA)-rich meal, there was a greater TAG to apoB ratio and enrichment of the TRLs with apos C-III and E following a single meal containing predominately saturated fatty acids (SFAs) [4]. These unexpected findings raise questions as to the origin of these compositional differences, in particular whether differences in TRL composition originate in the enterocyte or result from differences in their metabolic processing in the circulation.

Whilst the majority of *in vitro* studies have examined the impact of single fatty acids on CM synthesis and secretion by enterocytes [5–10], very few studies have used mixtures of fatty acids similar to those found in the diet. van Greevenbroek et al. [11] incubated Caco-2 cells for 24 h with mixtures of palmitic acid (PA), oleic acid (OA) and linoleic acid (LA) to represent: (a) western type dietary fat, (b) olive oil, (c) corn oil and (d) cream fat. Even though the fatty acid composition of the incubates did not influence cellular TAG levels, secreted apoB or TAG levels, the secreted TAG to apoB ratio and the incorporation of newly synthesised lipids into lipoproteins was shown to be increased after incubation with the ‘olive oil’ compared with ‘corn oil’ mixture. Interestingly, incubation of cells with all of the dietary fatty acids, including the SFA-rich mixture led to the secretion of TRL-sized lipoproteins similar to CM/very low density lipoprotein (VLDL), a finding which contrasts with experiments using single SFAs, where intermediate density lipoprotein (IDL)/low density lipoprotein (LDL) density particles are found to be secreted [10, 11].

In the present study, we examined the effects of mixtures of PA, stearic acid (SA), OA and LA resembling the SFA-, polyunsaturated fatty acid (PUFA)- and MUFA-rich meals used in our human postprandial study [4], on lipoprotein synthesis and secretion using the Caco-2 cell line. Our findings reveal there was some concordance between our cell studies and the composition of TRLs isolated in our previous postprandial study, and indicate that some of

the differences in the postprandial response to meal fatty acids could originate in the enterocyte.

Methods

Cell Culture

Caco-2 cells (European Collection of Cell Culture, Centre for Applied Microbiology and Research, UK), passage 39–58, were seeded at 5×10^5 cell/ml on Transwell (Corning Inc., USA) permeable polyester filters (0.4 μ m pore size and 4.7 cm² surface area) and grown to confluence in complete medium as previously described [10]. Prior to the start of the fatty acid treatments, Caco-2 cells were incubated for 24 h with serum-free complete medium. In the apical compartment, monolayers were incubated with 1.5 ml of complete medium containing 20% lipid-depleted serum (First Link (UK) Ltd.) and the 0.5 mM fatty acid mixtures for a period of 4 days. The fatty acid mixtures were formulated to be as close as possible to the composition of the SFA-, PUFA- and MUFA-rich meals from our previously reported human study [4]. The composition of the mixtures was as follows: (1) SFA-rich mixture contained 0.2 mM PA, 0.1 mM SA and 0.2 mM OA, (2) the PUFA-rich mixture 0.325 mM LA, 0.1 mM OA, 0.05 mM PA and 0.025 mM SA and (3) the MUFA-rich mixture 0.35 mM OA, 0.075 mM PA and 0.075 mM LA. All of the fatty acid mixtures were emulsified with taurocholate to form micelles as previously described [10]. The basolateral compartment contained 2.6 ml of serum-free complete medium. The media in the apical compartment were changed and refreshed every 24 h for a period of 4 days while the basolateral media were collected, aliquoted and stored at -20°C with the addition of a preservative to prevent the proteolytic degradation of apoB [12] for subsequent analysis of secreted lipoproteins. Transepithelial electrical resistance (TER) measurements, an index of tight junction formation and Caco-2 cell growth, were taken daily during the post-confluent experimental period.

Experiments were conducted in Caco-2 cells to determine effects of SFA-, PUFA- and MUFA-rich mixtures on Caco-2 cell: (1) integrity, by measurements of cytotoxicity and TER, (2) functional capacity for lipid and lipoprotein synthesis and secretion, by measurement of cellular and basolateral accumulation of lipids, apos B-100 and B-48, TRL ($d < 1.016$ g/ml) and IDL/LDL-density ($d = 1.016$ – 1.049 g/ml) lipoproteins, (3) fatty acid profile of the cellular and secreted (basolateral) lipids and (4) cellular morphology by electron microscopy.

Cytotoxicity of Fatty Acid Mixtures

The release of lactate dehydrogenase (LDH; a sensitive indicator of cell-membrane damage) in the apical medium was determined after each 24 h incubation with the 0.5 mM concentrations of the fatty acid mixtures using a colorimetric cytotoxicity assay (Biogeneis, UK).

Transepithelial Electrical Resistance Measurements

TER was determined with a Millicell-ERS apparatus (Millipore Corp., USA). Measurements of two Transwells without a cell monolayer, but containing media, were used as blanks. Data are expressed as $\Omega \times \text{cm}^2$.

Total Lipid Extraction from the Basolateral Medium and Cell Monolayers

Basolateral medium samples from 4 successive 24-h incubations from each monolayer were pooled and concentrated in Vivaspin tubes (Sartorius Ltd., UK) for the analysis of secreted lipid as previously described [10]. TAG and cholesterol concentrations were measured with an ILAB 600 (Instrumentation Laboratory (IL), UK) using enzyme-based colorimetric kits supplied by IL. Cellular lipids were extracted as previously described [10] and analysed as above.

Fatty Acid Profile of the Cell Monolayers and Basolateral Medium

Gas chromatography was used for the determination of the fatty acid profile of the cellular and secreted lipids. Cell monolayers were trypsinised and centrifuged at $100 \times g$ for 5 min. Lipids in the cell pellets and concentrated basolateral medium were extracted using chloroform:methanol (2:1, by v/v) containing butylated hydroxytoluene (50 mg/ml) and saponified and methylated in methanol containing 2% (v/v) H_2SO_4 at 70 °C for 1 h. Fatty acid methyl esters (FAME) were recovered by extraction into hexane and analysed in a gas chromatograph as previously described [13]. FAME were identified by comparison of retention times against known standards, Supelco 37 component FAME mix and PUFA-3 menhaden oil (Supelco, Dorset, UK).

Isolation of Lipoprotein Particles

Lipoproteins of different densities secreted by Caco-2 cell monolayers were isolated from self-generating gradients of iodixanol [14, 15] as previously described [10]. Each tube was fractionated based on density of the lipoprotein fractions, where the top 0.8 ml corresponded to TRL-density

fraction ($d < 1.016 \text{ g/ml}$) while the next 2.08 ml corresponded to the IDL/LDL-density fraction ($d = 1.016\text{--}1.049 \text{ g/ml}$). The fractions were assayed for TAG concentration as before.

Apolipoprotein B-100 and B-48 Determination

Basolateral medium samples from four successive 24-h incubations from each monolayer were pooled and concentrated in Vivaspin tubes for the analysis of apoB-100 and B-48 using specific ELISAs, adapted from methods developed to assay human TRL samples [4].

Electron Microscopy

Caco-2 cells, grown on Transwell membranes, were incubated for 24-h periods over 3 days with 0.5 mM fatty acid mixtures before being fixed and prepared for electron microscopy according to Curry et al. [16] as previously described [10]. Sections were examined with a Phillips CM10 transmission electron microscope and magnifications are stated in the individual figure legends.

Statistical Analysis

Data were analysed using SPSS version 14 (SPSS Inc., Chicago, USA) and presented in the tables and figures as means \pm SD. Two-way ANOVA was used to determine the effects of the fatty acid treatments over time on TER measurements and LDH release. The effects of the SFA-, PUFA- and MUFA-rich mixtures on lipid and lipoprotein parameters were analysed using one-way ANOVA. A Tukey post hoc test was used to determine significant pairwise differences. The apoB-100 and fatty acid profile data which could not be normalised was analysed using the Kruskal–Wallis test and Mann–Whitney test. $P < 0.05$ was taken as being significant.

Results

TER Measurements and Cytotoxicity Data

On day 0, prior to the cell monolayers being supplemented with specific fatty acid mixtures, TER measurements were not significantly different between wells. Incubation with the SFA-rich mixture lowered TER measurements compared to the PUFA- and MUFA-rich mixtures (Fig. 1a). Monolayers supplemented with the PUFA- and MUFA-rich mixtures released significantly lower amounts of LDH into the cell culture media compared with the SFA-rich mixture during the experiment ($P < 0.05$; Fig. 1b).

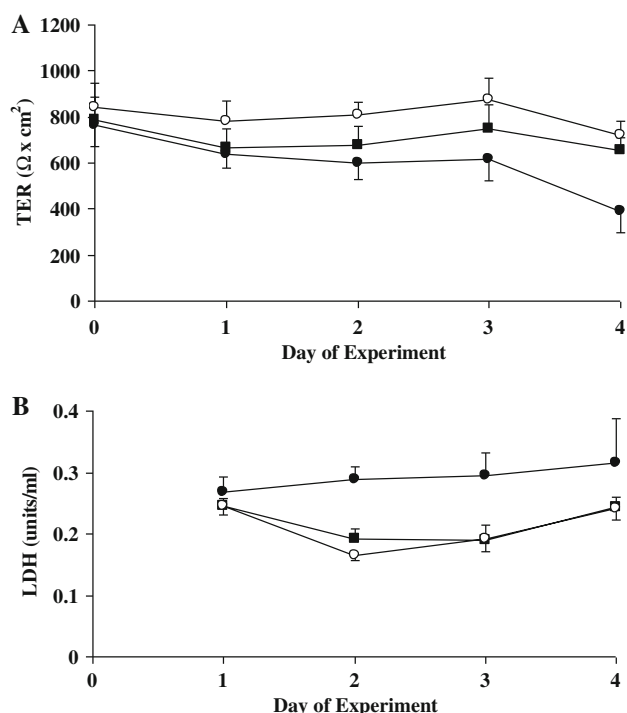


Fig. 1 **a** TER measurements across Caco-2 cells and **b** LDH release from cells during incubation with the SFA- (closed circles), PUFA- (open circles) and MUFA-rich (closed squares) mixtures for 4 days. Data are mean \pm SD for $n = 12$ experiments. LDH release was determined in the apical medium samples collected on days 1–4 and calculated relative to a standard curve of the LDH enzyme standard. For the TER measurements and LDH release, there was a significant effect of treatment ($P < 0.02$), time ($P < 0.001$) and a time \times treatment interaction ($P < 0.05$)

Cellular and Secreted Lipids

Monolayers exposed to the SFA-rich mixture had the lowest cellular TAG content compared with the PUFA- or MUFA-rich mixtures over the 4-day treatment period ($P < 0.001$). Cellular cholesterol contents were significantly greater in monolayers exposed to the MUFA compared with the PUFA-rich mixture, but not the SFA mixture ($P < 0.05$; Table 1). There were no differences in the cellular cholesterol content of monolayers treated with either the SFA- or PUFA-rich incubates.

TAG secretion from cells exposed to the MUFA-rich mixture was greater than from cells exposed to the SFA- or PUFA-rich mixtures ($P < 0.005$) whereas cholesterol secretion was greater compared with the SFA-rich mixture only ($P < 0.05$; Table 1). Lipid secretion from monolayers supplemented with the SFA- and PUFA-rich mixtures was similar.

The fatty acid profiles of the cellular and secreted lipids are shown in Table 2. As expected, the proportions of PA and SA were greater in the monolayers treated with the SFA-rich mixture ($P < 0.004$), LA greater in the monolayers exposed to the PUFA-rich mixture ($P = 0.005$) and OA greater in the cells treated with the MUFA-rich mixture ($P < 0.0001$). The proportions of arachidonic acid, eicosapentaenoic acid (EPA), docosahexaenoic acid (DHA) and docosapentaenoic acid (DPA) were greater in the cells treated with the SFA-rich compared with the unsaturated fatty acid-rich mixtures.

Table 1 Effects of SFA-, PUFA- and MUFA-rich mixtures on cellular and secreted lipids, apoB concentrations and TAG to apoB ratio of lipoproteins secreted by Caco-2 cells

Parameter	Fatty acid mixtures						ANOVA
	SFA		PUFA		MUFA		
	Mean	SD	Mean	SD	Mean	SD	
Cellular							
TAG	0.32 ^a	0.06	0.60	0.12	0.54	0.09	$P < 0.0001$
Cholesterol	0.12	0.02	0.12 [*]	0.02	0.15	0.02	$P = 0.021$
Secreted							
TAG	25.28 ^{**}	2.2	26.60 ^{**}	2.0	36.60	1.0	$P = 0.003$
Cholesterol	4.62 [*]	0.5	4.70	0.4	5.26	0.2	$P = 0.025$
ApoB-48	1.76	0.7	1.99	0.6	2.14	0.7	NS
ApoB-100	5.19	1.4	5.33 [*]	0.3	6.09	0.7	$P = 0.046$
TAG to apoB ratio	3704.5	688	3807.5	226	4469.7	531	NS

Values represent mean SD for $n = 6$ –11 experiments. The cellular lipids (TAG and cholesterol) are expressed as $\mu\text{mol}/\text{mg}$ cell protein, secreted lipids (TAG and cholesterol) as nmol/ml basolateral medium and secreted apolipoprotein (apo) B (B-48 and B-100) as pmol/ml basolateral medium. The TAG to apoB ratio is expressed as molecules of TAG per apoB particle (apoB-48 and B-100 concentrations combined)

^{*} $P < 0.05$, ^{**} $P < 0.005$, significantly different to MUFA-rich mixture

^a $P < 0.05$, significantly different to PUFA- and MUFA-rich mixtures

Table 2 Effects of the SFA, PUFA and MUFA-rich mixtures on the fatty acid profile of the cellular and secreted lipids

Fatty acid	Cellular lipid						ANOVA	Secreted lipid						ANOVA
	SFA		PUFA		MUFA			SFA		PUFA		MUFA		
	Mean	SD	Mean	SD	Mean	SD		Mean	SD	Mean	SD	Mean	SD	
	<i>% weight of total fatty acid</i>							<i>% weight of total fatty acid</i>						
Palmitic acid	27.9 ^c	1.1	11.0 ^{**}	0.5	13.4	0.3	$P < 0.0001$	24.9 ^c	1.6	15.0 [*]	1.4	16.8	0.6	$P = 0.001$
Palmitoleic acid	1.7 ^c	0.2	1.0 [*]	0.1	1.3	0.1	$P = 0.002$	2.3 ^b	0.1	1.8	0.2	2.0	0.2	$P = 0.026$
Stearic acid	16.4 ^c	0.3	7.5 ^{**}	0.4	5.2	0.1	$P < 0.0001$	15.8 ^c	0.7	10.2	1.5	9.1	0.5	$P = 0.001$
Oleic acid	42.2 ^c	1.0	20.7 ^{**}	0.5	57.6	0.9	$P < 0.0001$	33.2 ^c	1.1	18.2 ^{**}	1.7	41.2	2.1	$P = 0.001$
Elaidic acid	3.0	0.1	2.7	0.3	3.1	0.3	NS	5.3	0.7	5.6	2.1	5.1	0.3	NS
Linoleic acid	1.2 ^c	0.1	49.6 ^{**}	1.5	12.2	0.4	$P < 0.0001$	2.2 ^c	0.1	31.8 ^{**}	4.1	10.6	0.7	$P < 0.0001$
Arachidic acid	0.5	0.2	0.5	0.3	0.5	0.3	NS	1.6	0.6	2.3	1.9	1.6	0.5	NS
γ -Linolenic acid	0.6	0.1	0.5	0.2	0.5	0.3	NS	1.5	0.7	1.6	1.2	1.7	0.7	NS
α -Linolenic acid	1.0	0.7	1.0	0.9	1.8	0.9	NS	3.0	0.7	3.9	2.3	3.2	1.1	NS
Eicosenoic acid	0.5	0.3	0.6	0.3	0.6	0.4	NS	0.8	0.5	1.2	0.9	0.9	0.3	NS
Arachidonic acid	1.6 ^c	0.1	1.1	0.2	1.2	0.1	$P = 0.002$	2.5 ^c	0.2	2.0	0.2	2.1	0.1	$P = 0.002$
EPA	0.4 ^c	0.1	0.1 [*]	0.1	0.2	0.0	$P = 0.001$	0.4	0.1	0.3 ^a	0.1	0.4	0.0	$P = 0.019$
DPA	0.5 ^c	0.0	0.3	0.0	0.2	0.0	$P = 0.002$	1.3	0.1	1.1	0.2	1.0	0.1	NS
DHA	0.8 ^c	0.1	0.4	0.1	0.5	0.1	$P = 0.002$	2.0 ^c	0.2	1.6	0.2	1.6	0.1	$P = 0.009$

Values represent means SD for $n = 6$ experiments. *DHA*, docosahexaenoic acid; *DPA*, docosapentaenoic acid; *EPA*, eicosapentaenoic acid

* $P < 0.05$, ** $P < 0.005$, significantly different to MUFA-rich mixture

^a $P < 0.03$, significantly different to the SFA and MUFA-rich mixtures

^b $P < 0.03$, ^c $P < 0.005$, significantly different to PUFA- and MUFA-rich mixtures

A similar fatty acid profile was observed in the lipids secreted into the basolateral medium from the cells treated with the different fatty acid mixtures (Table 2).

Lipoprotein Secretion from Caco-2 Cells

The MUFA-rich mixture led to a greater apoB-100 secretion by Caco-2 cells than the PUFA-rich mixture ($P < 0.05$) whereas apoB-100 secretion from cells exposed to the SFA-rich mixture did not differ significantly from cells exposed to either the MUFA- or PUFA-rich mixtures (Table 1). Although the secretion of apoB-48 by Caco-2 cells followed a similar trend to that of apoB-100, there was no significant effect of the fatty acid composition of the mixtures. The ratio of TAG to apoB has been previously used as an indicator of particle size [11]. There was a tendency for the MUFA-rich mixture to lead to a greater TAG to apoB ratio (apoB-48 and B-100 data combined) in secreted lipoproteins than the SFA- and PUFA-rich mixtures (Table 1).

As expected, TAG concentrations were greater in the TRL ($d < 1.016$ g/ml) compared with the IDL/LDL ($d = 1.016$ – 1.049 g/ml) fraction in cells exposed to the fatty acid treatments ($P < 0.005$; Fig. 2). Incubation of the cell monolayers with the MUFA-rich mixture led to significantly greater TAG concentrations in both the TRL- and

IDL/LDL-density fractions compared with the SFA- and PUFA-rich mixtures ($P < 0.05$; Fig. 2).

Caco-2 Cellular Morphology

Treatment of cells with the SFA-rich mixture led to detrimental effects on cellular morphology compared with the PUFA- and MUFA-rich mixtures. The microvilli at the apical membrane were numerous and relatively mature in cells exposed to the unsaturated fatty acid-rich mixtures (Fig. 3a, b) and to a lesser extent, in cells exposed to the SFA-rich mixture (Fig. 3c; Table 3). The tight junctions of cells exposed to the MUFA- and PUFA-rich mixtures were also relatively mature and showed interdigitation and desmosomes (Fig. 3a, b) whilst the junctions of cells exposed to the SFA-rich mixture were disrupted, immature and lacking desmosomes (Fig. 3c). Ribosomes and mitochondria were numerous in cells exposed to the MUFA- and PUFA-rich mixtures indicating a high level of metabolic activity and the nuclei showed no sign of chromatin degradation. Glycogen-rich areas were also observed in these cells but not in those exposed to the SFA-rich mixture. Lipid-dense organelles were present in all cells but whereas these organelles were often surrounded by mitochondria, multivesicular bodies and other membrane-bound organelles in the MUFA- and PUFA-treated cells, in the cells

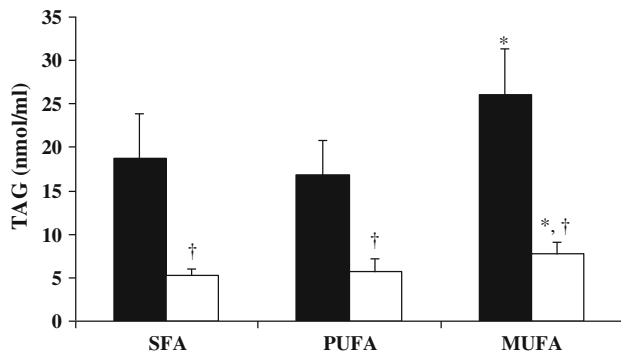


Fig. 2 Effects of SFA-, PUFA- and MUFA-rich mixtures on the secretion of TRL (black bars) and IDL/LDL (white bars) density lipoproteins by Caco-2 cells. Data are mean \pm SD for $n = 6$ experiments. * $P < 0.05$, compared with the SFA- and PUFA-rich mixtures, † $P < 0.005$, compared with the TRL density TAG concentration

exposed to the SFA-rich mixture, they appeared to be crystallised and surrounded by white degraded areas. Mitochondria and endoplasmic reticulum membranes surrounded these lipid-dense organelles, suggesting some metabolic activity in these SFA-treated cells (Fig. 3c).

Figure 4 indicates the endocytosis of a lipid-rich particle, probably a MUFA-rich mixture micelle at the apical membrane of the MUFA-treated Caco-2 cells.

Discussion

In a recent human study, we reported marked differences in both the number and lipid composition of $S_f > 400$ fraction

TRL particles (predominantly CMs) following meals enriched in SFA (a mixture of palm oil and cocoa butter), PUFA (safflower oil) and MUFA (olive oil). In order to determine if these meal fatty acid-induced differences in TRL number and composition could originate in the enterocyte, we incubated Caco-2 cells with mixtures of fatty acids representative of the test meals used in our human study to determine their effects on lipoprotein synthesis and secretion.

The fatty acid profile of the cells and secreted lipids reflected the quantities of PA, SA, LA and OA used to prepare the SFA, PUFA and MUFA-rich mixtures. The proportions of arachidonic acid, EPA and DHA were also different between the fatty acid treatments, with higher amounts in the cells exposed to the SFA-rich mixture. However, the changes in these fatty acids were less dramatic compared with those of PA, SA, OA and LA and most likely secondary effects of the overall fatty acid composition and a result of expressing the data as percentage weight of total fatty acids.

The MUFA-rich mixture promoted greater TAG and apoB-100 secretion and a tendency for increased apoB-48 secretion. Previous findings in the literature, including our own, have shown lipoprotein secretion to vary in the order OA > LA > PA = SA [5, 8, 10, 11], yet our current data indicates similar levels of TAG secretion after the SFA- and PUFA-rich mixtures, even though the PUFA-rich mixture promoted greater intracellular TAG accumulation than did the SFA-rich mixture. These findings are consistent with our hypothesis that MUFA increase the number of intestinally derived lipoproteins, rather than that MUFA-

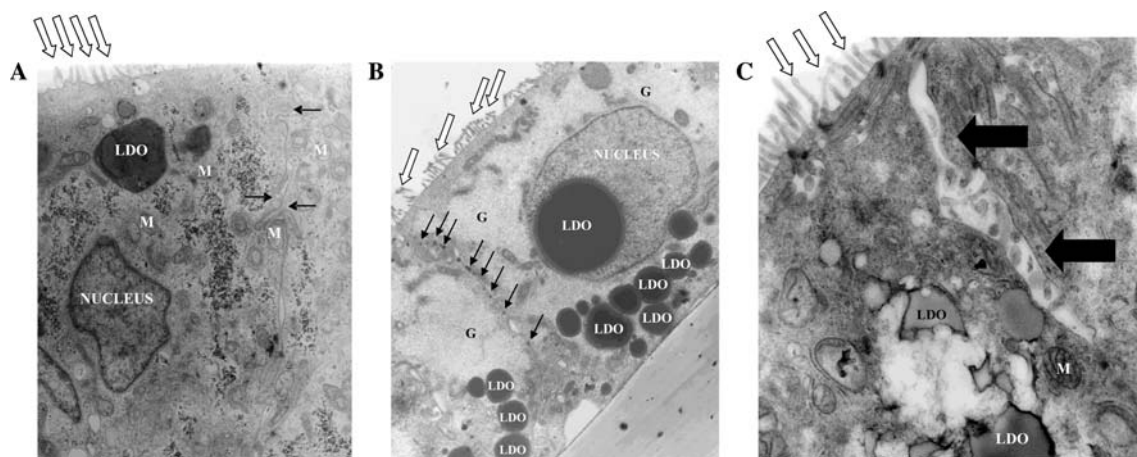


Fig. 3 Electron micrographs of Caco-2 cells after supplementation with **a** the MUFA-rich mixture (magnification 15,300 \times), **b** the PUFA-rich mixture (magnification 8,750 \times) and **c** the SFA-rich mixture (magnification 29,500 \times) for three successive 24 h periods. Microvilli are numerous and mature (white arrows) after all treatments. With the MUFA- and PUFA-rich mixtures, tight junctions between cells are mature, well formed and desmosomes are present

(small black arrows). There are large lipid dense organelles (LDO) which are surrounded by mitochondria (M) and rough endoplasmic reticulum. There are also areas rich in glycogen (G). With the SFA-rich mixture, the junctions are disrupted and immature (large black arrows). There are crystallised lipid dense organelles (LDO) present associated with mitochondria (M) and endoplasmic reticulum

Table 3 Effects of SFA-, PUFA- and MUFA-rich mixtures on Caco-2 cellular morphology

Fatty acid mixture	Microvilli length (nm)		Number of microvilli per μm of apical membrane	
	Mean	SD	Mean	SD
SFA	726	81	6.2	1.2
PUFA	836	230	7.4	1.5
MUFA	892	327	5.2	1.2

Values represent means SD for $n = 5$ – 10 micrographs from a representative experiment

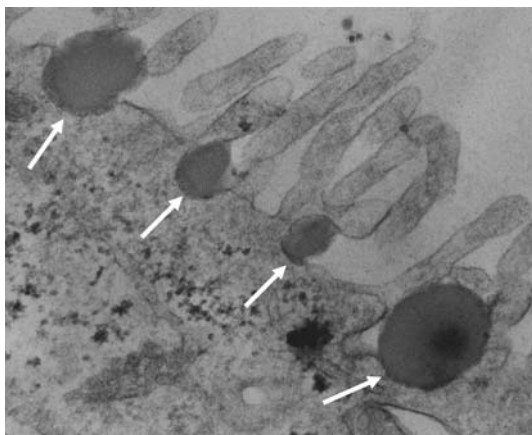


Fig. 4 Electron micrograph of the endocytosis of MUFA-taurocholate micelles at the apical membrane of a Caco-2 cell (magnification 71,250 \times). The micrograph clearly shows the formation of membranes around the endocytosed micelles (white arrows)

containing TRL particles are less effectively cleared from the circulation.

As well as greater numbers of secreted apoB-containing particles, we also observed incubation of the Caco-2 cell monolayers with fatty acid mixtures to lead to increased secretion of lipoprotein particles of TRL-density compared with IDL/LDL-density. There was also a tendency for the ratio of secreted TAG to apoB to be increased when Caco-2 cells were exposed to MUFA compared with PUFA-rich mixtures. Van Greevenbroek et al. [11] proposed that olive oil promoted the production and secretion of larger lipoproteins and hypothesised that TAG synthesised during incubation with the ‘olive oil’ mixture was more efficiently translocated to the preformed lipoprotein particle. In the present study, incubation with the MUFA-rich mixture led to significantly greater TAG concentrations within both the TRL- and IDL/LDL-density fractions compared with the PUFA-rich mixtures. Although van Greevenbroek and co-workers hypothesised that unsaturated fatty acids were required in the mixtures for the secretion of lipoproteins of TRL-density [17], our present findings are suggestive that OA is the key fatty acid involved in the ‘core expansion’ stage of CM synthesis, at least in Caco-2 cells.

The electron micrographs obtained from cells exposed to the different fatty acid mixtures may also shed further

light on possible mechanisms underlying the promotion of TRL secretion by the MUFA-rich mixture. In the case of both the MUFA- and PUFA-rich mixtures, the electron micrographs demonstrate appearance of many lipid-dense bodies, termed ‘secondary TAG-rich particles’ [18]. The presence of ‘secondary TAG-rich particles’ is consistent with the proposal of a two-step mechanism of CM formation [19] in which a ‘first-step’ primordial lipid-poor apoB-48-containing particle is synthesised before fusing with a large TAG-rich ‘second-step’ particle to produce a CM particle. Hamilton et al. [18] observed that secondary TAG-rich particles would increase in size if they did not fuse with ‘first-step’ particles to produce large viable lipoproteins that can be secreted, suggesting that the capacity for production of primordial lipid-poor apoB-containing particles is rate limiting in the secretory pathway. Our previous study [10] showed OA (major fatty acid in the MUFA mixture) to upregulate the gene expression of apoB together with proteins involved in the recruitment of apoB for TRL synthesis and secretion, suggesting greater capacity for primordial particle formation with OA than other fatty acids.

One interesting, unexpected and novel feature of the cells treated with MUFA-rich mixture, is the observation from the electron micrographs of evidence for endocytosis of lipid micelles at the apical membrane. How this mechanism occurs in the Caco-2 cells cannot be determined from these electron micrographs. It has been proposed that fatty acid uptake by enterocytes is a carrier mediated process, possibly involving caveolin, a protein involved in the endocytosis of LDL. Baba et al. [20] reported that in the middle segment of the small intestine in suckling rats, the absorptive cells had apical coated pits, apical invaginations, coated vesicles, tubules, early endosomes, late endosomes and a large homogeneous electron dense lysosome at the supranuclear region. It was suggested that the endocytic membrane system in the absorptive cells were specialised for quick and active intracellular digestion. However, Baba et al. [20] did not observe the actual endocytosis of lipid. In the present study, coupled with the apparent endocytosis of fatty acid micelles, there are numerous multivesicular bodies and other membrane-bound organelles consistent with the findings of Baba and

co-workers. This novel and unexpected finding warrants further investigation as the mechanisms by which the absorption of dietary fatty acids occur remain controversial.

The Caco-2 cell line is generally regarded as an acceptable model for the study of lipoprotein production. However, we have recently highlighted the cytotoxic effects of SFAs, in particular PA when incubated as a single fatty acid, and proposed that mixtures of fatty acids may provide a more physiological model for studying impact of dietary fatty acids on lipoprotein synthesis and secretion [10]. However, the inclusion of 0.2 mM OA in the SFA-rich mixture used in the present study failed to prevent cytotoxicity or detrimental effects on cellular morphology. Our data indicate that within 3 days of supplementing cells with the SFA-rich mixture, fully differentiated cells apparently regress to a less polarised state (reflected by the lower TER measurements) which may partially explain why there is a lower capacity for lipid synthesis compared with the predominately unsaturated fatty acid mixtures. The novel observation of crystalline lipid-dense organelles in the cells suggests that solidified tripalmitoylglycerol may actually be formed in the cells, resulting in failure to translocate TAG from lipid droplets to primordial particles and thereby failure in CM secretion. In addition, recent evidence in liver and pancreatic cell lines has suggested that incubation with single SFAs may induce endoplasmic reticulum stress and apoptosis independently of the formation of ceramide [21, 22], a finding yet to be confirmed in Caco-2 cells. However, it is not as yet clear to what extent the effects of SFA on (a) the structural integrity of the cells and (b) CM synthesis and secretion resemble those which occur *in vivo*.

In conclusion, our cell studies have shown the MUFA mixture (rich in OA) to stimulate a greater secretion of TRLs, of larger particle size than the PUFA-rich mixture. Furthermore, the MUFA- and PUFA-rich mixtures were shown to be able to maintain cell membrane integrity and cellular morphology over the period of incubation, whereas the SFA-rich mixture was not. In both Caco-2 cells and our human study, MUFA stimulated greater TRL secretion, highlighting the importance of OA in the formation and secretion of viable CMs by the enterocyte. The electron micrographs provide evidence that, in Caco-2 cells at least, there appears to be some endocytotic uptake of large lipid-containing micelles which we suggest may increase lipoprotein formation by promoting recruitment of a greater number of primordial apoB-containing particles.

Acknowledgments The authors thank Dr. Esti Olano-Martin and Dr. Paul Sharpe for advice on the Caco-2 cell line and Dr. Ian Davies and Dr. John Graham for helpful discussions regarding iodixanol gradient ultracentrifugation. We are grateful to Dr. Alan Curry for his expertise in providing the electron microscopy images and Dr. Caroline Childs for her time and advice on the GC analysis. This

work was supported by the Biotechnology and Biological Sciences Research Council (BBSRC, UK; Project No: 45/D15215).

References

- Karpe F, Steiner G, Uffelman K, Olivecrona T, Hamsten A (1994) Postprandial lipoproteins and progression of coronary atherosclerosis. *Atherosclerosis* 106:83–97
- Patsch JR (1994) Triglyceride-rich lipoproteins and atherosclerosis. *Atherosclerosis* 110:S23–S26
- Williams CM (1999) Dietary interventions affecting chylomicron and chylomicron remnants. *Atherosclerosis* 141:S87–S92
- Jackson KG, Wolstencroft EJ, Bateman PA, Yaqoob P, Williams CM (2005) Greater enrichment of triacylglycerol-rich lipoproteins with apolipoproteins E and C-III after meals rich in saturated fatty acids than after meals rich in unsaturated fatty acids. *Am J Clin Nutr* 81:25–34
- Field FJ, Albright E, Mathur SN (1988) Regulation of triglyceride-rich lipoprotein secretion by fatty acids in Caco-2 cells. *J Lipid Res* 29:1427–1437
- Dashti N, Smith EA, Alaupovic P (1990) Increased production of apolipoprotein B and its lipoproteins by oleic acid in Caco-2 cells. *J Lipid Res* 31:113–123
- Ranheim T, Gedde-Dahl A, Rustan AC, Drevon CA (1994) Fatty acid uptake and metabolism in Caco-2 cells: eicosapentaenoic acid (20:5(n-3)) and oleic acid (18:1(n-9)) presented in association with micelles or albumin. *Biochim Biophys Acta* 1212:295–304
- van Greevenbroek MMJ, Voorhout WF, Erkelens DW, van Meer G, de Bruin TWA (1995) Palmitic acid and linoleic acid metabolism in Caco-2 cells: different triglyceride synthesis and lipoprotein secretion. *J Lipid Res* 36:13–24
- van Greevenbroek MMJ, Robertus-Teunissen MG, Erkelens DW, de Bruin TWA (1998) Lipoprotein secretion by intestinal Caco-2 cells is affected differently by *trans* and *cis* unsaturated fatty acids: effect of carbon chain length and position of the double bond. *Am J Clin Nutr* 68:561–567
- Bateman PA, Jackson KG, Maitin V, Yaqoob P, Williams CM (2007) Differences in the cell morphology, lipid and apo B secretory capacity in Caco-2 cells following long-term treatment with saturated and monounsaturated fatty acids. *Biochim Biophys Acta* 1771:475–485
- van Greevenbroek MMJ, van Meer G, Erkelens DW, de Bruin TWA (1996) Effects of saturated, mono-, and poly-unsaturated fatty acids on the secretion of apo B containing lipoproteins by Caco-2 cells. *Atherosclerosis* 121:139–150
- Edelstein C, Scanu M (1986) Precautionary measures for collecting blood destined for lipoprotein isolation. *Methods Enzymol* 128:151–155
- Kew S, Mesa MD, Tricon S, Buckley R, Minihane AM, Yaqoob P (2004) Effects of oils rich in eicosapentaenoic and docosahexaenoic acids on immune cell composition and function in healthy humans. *Am J Clin Nutr* 79:674–681
- Graham JM, Higgins JA, Gillott T, Taylor T, Wilkinson J, Ford T, Billington D (1996) A novel method for the rapid separation of plasma lipoproteins using self-generating gradients of Iodixanol. *Atherosclerosis* 124:125–134
- Higgins JA, Graham JM, Davies IG (1996) Separation of plasma lipoproteins in self-generated gradients of Iodixanol. In: Drew AF (ed) *Methods in molecular medicine, atherosclerosis: experimental methods and protocols*. Humana Press., New Jersey, pp 37–49
- Curry A, Jones DM, Skelton-Stroud P (1989) Novel ultrastructural findings in helical bacterium in the baboon (*Papio anubis*) stomach. *J Gen Microbiol* 135:2223–2231

17. van Greevenbroek MMJ, Robertus-Teunissen MG, Erkelens DW, de Bruin TWA (1998) Participation of the microsomal triglyceride transfer protein in lipoprotein assembly in Caco-2 cells: interactions with saturated and unsaturated fatty acids. *J Lipid Res* 39:173–185
18. Hamilton RL, Wong JS, Cham VM, Nielson LB, Young SG (1998) Chylomicron-sized lipid particles are formed in the setting of apolipoprotein deficiency. *J Lipid Res* 39:1543–1557
19. Hussain MM (2000) A proposed model for the assembly of chylomicrons. *Atherosclerosis* 148:1–15
20. Baba R, Fujita M, Tein CE, Miyoshi M (2002) Endocytosis by absorptive cells in the middle segment of the suckling rat small intestine. *Anat Sci Int* 77:117–123
21. Wei Y, Wang D, Topczewski F, Pagliassotti MJ (2006) Saturated fatty acids induce endoplasmic reticulum stress and apoptosis independently of ceramide in liver cells. *Am J Physiol Endocrinol Metab* 291:E275–281
22. Diakogiannaki E, Morgan NG (2008) Differential regulation of the ER stress response by long-chain fatty acids in the pancreatic β -cell. *Biochem Soc Trans* 36:959–962

IBW Initial body weight
HPLC High performance liquid chromatography

Introduction

Highly unsaturated fatty acids (HUFAs) have a well-known, essential role as components of structural phospholipids of cell membranes in animals. HUFAs are crucial to the nutritional health, physiology and reproductivity of higher vertebrates [1]. Diseases arising from HUFAs deficiency are well documented in many species [2, 3]. Freshwater fish, such as salmonids, can generally synthesize HUFAs from C18 precursors, 18:3n-3 and 18:2n-6. However, marine fish, which lack or have a very low activity of Δ 5-desaturase and Δ 6-desaturase, cannot convert 18:3n-3 and 18:2n-6 to their corresponding HUFAs at a rate of permitting their normal growth and development. Therefore, marine fish require dietary HUFAs for normal growth, reproduction and health [4, 5]. Of HUFAs, EPA and DHA are the most important [6–9] and must be supplied in the diet of marine fish, especially in larvae and juveniles [10–12].

DHA and EPA function completely differently in their metabolism in marine fish juveniles [13–15]. Thus, on the one hand, DHA and EPA should be simultaneously supplied in the diet of marine fish juvenile [14, 16–18]; on the other hand, their suitable quantity and ratio should be investigated at the same time since increasing dietary DHA/EPA ratios enhanced growth [15]. Sargent et al. [19] suggested that the optimal DHA and EPA ratio was 2:1 in the diet of sea bass larvae. However, the requirement of DHA and EPA varies in different stages and species attributable to differences in their environments and metabolisms [20].

The optimal amount and ratio of DHA and EPA is one of the hottest topics for fish studies, especially in new species [8, 21, 22]. Cobia is a new cultured species and a fast developing marine fish which is important in industrial fishery. Although the amount of DHA and EPA was reported from 0.8 to 1.2% of the dried diet in cobia [23], little is known about the optimal amount and ratio of DHA and EPA in cobia juveniles.

The present paper reports on the effect of different ratios of DHA and EPA on the growth, nucleic acid and fatty acids of cobia juveniles fed for 8 weeks in the laboratory.

Materials and Methods

Main Feed Materials

Mixed fish-meal containing protein 65% was bought from Gaolong Feed Ltd. Co. of Shunde City, Guangdong

Province, China. Three kinds of fish oils were from Yuwang Company in Shandong Province, China and their contents were as follows: (1) DHA 62.40%, EPA 14.11%; (2) EPA 33.86%, DHA 30.93%; (3) DHA 14.51%, EPA 25.85%, respectively. Vitamin mixtures, mineral mixtures and taste attractant were bought from Biotechnological Ltd. Co. of Chengyi, Guangzhou City, China.

Fish and Diets

Two thousand cobia juveniles, 30 days old with around 5-g body weight, were from a fish breeding farm in Shanyia City, Hainan Province, China, in July 2005. The juveniles were reared in floating sea net cages at Shen Ao Bay, near the Nan Ao Marine Biology Station of Shantou University, China. The water temperature was 26.0–30.0 °C, salinity 25.35–33.00‰ and pH 7.82–7.99. The cobia juveniles were fed a fish-diet for 2 weeks and a control diet (D-0) for one more week. Then the juveniles were moved and kept in glass-steel tanks (200-l volume) in the Laboratory of the Seashore at Shen Ao Bay and fed D-0 for 7 days. Through the tanks flowed filtered-seawater of Shen Ao Bay at a rate of 2–2.5 L min⁻¹ and compressed air. The laboratory was lit from 6 a.m. to 6 p.m. every day during the experiment.

After acclimatizing to the glass-steel tank, 380 cobia juveniles (age 56-day, body weight 6.86 ± 0.03 g, body length 9.23 ± 0.06 cm) were selected and 20 of them were randomly selected and their initial body weight, length, and the biochemical analysis of their livers, muscle and blood in the week 0 were measured. A further 360 cobia juveniles were randomly assigned into eight groups in triplicate, in total 24 tanks with 15 fish in each. The juveniles were reared in glass-steel tanks using the same climatic conditions and fed D-0–D-7 for 8 weeks from August to October 2005. D-1–D-7 contained the same amount of DHA and EPA (1.5 ± 0.1% of dried diet) but varying DHA/EPA ratios (0.90, 1.10, 1.30, 1.50, 1.70, 1.90, 2.10, respectively) differing from those of D-0 (DHA + EPA = 0.8% of dried diet, DHA/EPA = 1.30) (Tables 1, 2). The juveniles were fed twice a day at 8:00–9:00 a.m. and 4:00–5:00 p.m. using different diets at around 5% (dried diet) of body weight. The diets delivered were completely ingested aided by mixing an additive, namely, 0.1% of taste attractant and controlling the feeding amount. The juveniles were weighed every other week and washed with freshwater once a week to prevent parasites.

Sampling

Five (5) fish per tank were randomly selected, their body weight and length measured, then the biochemical analysis of their livers, muscle and blood at the end of weeks 4 and 8, respectively was carried out. Before sampling, the juveniles

Table 1 Ingredient and proximate composition (% dried diet except DHA/EPA ratio) of experimental diets for cobia juveniles

Ingredient	Diet							
	D-0	D-1	D-2	D-3	D-4	D-5	D-6	D-7
Mixed-fish meal	67.00	67.00	67.00	67.00	67.00	67.00	67.00	67.00
Cellulose	2.00	2.00	2.00	2.00	2.00	2.00	2.00	2.00
α -Starch	15.00	15.00	15.00	15.00	15.00	15.00	15.00	15.00
Vitamin mixture ^a	2.00	2.00	2.00	2.00	2.00	2.00	2.00	2.00
Mineral mixture ^b	2.00	2.00	2.00	2.00	2.00	2.00	2.00	2.00
Soybean meal	1.00	1.00	1.00	1.00	1.00	1.00	1.00	1.00
Taste attractant	0.10	0.10	0.10	0.10	0.10	0.10	0.10	0.10
Corn oil	9.29	7.95	9.10	9.20	9.26	9.30	9.33	9.38
Fish oil a ^c				0.58	0.90	1.13	1.30	1.54
Fish oil b ^d			1.90	1.22	0.84	0.57	0.37	0.08
Fish oil c ^e		3.05						
Olive oil	1.71							
Proximate composition								
Moisture	7.36	6.98	7.29	7.08	7.43	7.16	7.15	7.61
Ash	15.09	14.87	14.97	14.62	14.62	14.97	15.07	15.16
Crude protein	43.28	42.93	43.00	43.20	43.02	43.32	42.99	43.36
Crude lipid	17.03	17.08	16.91	16.94	16.98	16.98	16.98	17.07
DHA	0.45	0.71	0.84	0.88	0.91	0.95	0.96	1.10
EPA	0.35	0.79	0.78	0.67	0.60	0.56	0.50	0.52
DHA + EPA	0.80	1.50	1.62	1.56	1.52	1.51	1.46	1.62
DHA/EPA	1.30	0.90	1.10	1.30	1.50	1.70	1.90	2.10

^a *Vitamin mixture*: vitamin A 4,000,000 IU; vitamin D 32,000,000 IU; vitamin E 60 g; vitamin K 36 g; vitamin B 17.5 g; vitamin B₂ 16 g; vitamin B₆ 12 g; vitamin B₁₂ 100 mg; niacin nicotinic acid 88 g; potassium pantothenic 36 g; folic acid 2 g; biotin 100 mg; inositol 100 g; vitamin C 200 g

^b *Mineral mixture*: iron 8 g; zinc 30 g; manganese 2 g; cobalt 1 g; iodine 500 g; selenium 40 mg, etc

^c Fish oil a contained DHA 62.40 and EPA 14.11%

^d Fish oil b contained DHA 30.93 and EPA 33.86%

^e Fish oil c contained DHA 14.51 and EPA 25.85%

were starved for 1 day and then anaesthetized one by one using MS-222 (1/10,000–15,000). The fish body weight was measured immediately after being anaesthetized. Blood was sampled from the anaesthetized fish and kept for 4 h at room temperature. Then the blood was centrifuged for 10 min at 3,000×g and the serum was taken for freezing in liquid nitrogen and then stored at –80 °C for analyzing later. The anaesthetized fish was then killed by being struck on the head and the liver and muscle dissected out. The liver and muscle were immediately frozen in liquid nitrogen and then stored at –80 °C for analyzing later.

Reagents and Determination of Samples

Reagents

A DNA-extracting kit was purchased from Shanghai Biotechnological Company, Shanghai, China and TaKaRa RNAiso reagent from the Bao Biotechnological Company,

Dalian, Liaoning, China. Standard fatty acids (>98% purity) were bought from the Sigma Chemical Company, USA. Ethanol, methanol, hexane, acetone and isopropanol were high performance liquid chromatography (HPLC) grade and bought from Fair Lawn New Jersey, USA. Potassium permanganate, BFCI₃, sodium citric acid, sodium chloride, potassium hydroxide, sodium hydroxide and ether were of analytic grade and bought from Qanyi Trade Ltd. Co. of Shantou City, Guangdong Province, China. H₂SO₄ was of analytic grade and bought from Guanghua Chemical Factory of Shantou City, Guangdong Province, China.

Extraction and Determination of DNA

DNA was extracted from the tissues of the cobia juveniles using a DNA-extracting kit. A tissue sample (30 mg) of the cobia juvenile was ground into powder after immersion in liquid nitrogen (DNA extraction from serum without this

Table 2 Composition (%) of fatty acids in the formulated diets of cobia juveniles

Fatty acid	Diet							
	D-0	D-1	D-2	D-3	D-4	D-5	D-6	D-7
12:00	0.08	0.12	0.08	0.07	0.08	0.07	0.08	0.07
14:00	1.14	1.9	1.17	1.17	1.16	1.18	1.17	1.15
15:00	0.08	0.19	0.08	0.08	0.08	0.08	0.08	0.08
16:00	12.23	12.18	11.05	11.11	11.08	11.04	11.1	11.04
17:00	0.11	0.15	0.12	0.11	0.11	0.11	0.1	0.09
18:00	2.26	2.14	2.11	2.09	2.07	2.05	2.15	2.12
20:00	0.35	0.32	0.34	0.33	0.33	0.33	0.33	0.33
22:00	0.13	0.12	0.13	0.14	0.15	0.15	0.15	0.16
24:00:00	0.14	0.11	0.12	0.12	tr	tr	tr	tr
∑SFAs	16.52	17.23	15.2	15.22	15.06	15.01	15.16	15.04
16:1n-7	1.6	2.2	1.51	1.49	1.46	1.48	1.47	1.45
17:1n-8	tr	tr	tr	tr	0.1	0.1	0.09	0.08
18:1n-9	27.3	20.53	21.52	21.65	21.67	21.49	21.83	21.95
20:1n-9	4.06	4.43	4.42	4.34	4.22	4.23	4.28	4.21
22:1n-11	2.83	3.08	3.12	3.14	3.12	3.16	3.21	3.24
24:1n-11	0.24	0.23	0.23	0.23	0.22	0.24	0.24	0.21
∑MUFAs	36.03	30.47	30.8	30.85	30.79	30.7	31.12	31.14
18:2n-6	34.95	30.54	33.81	34.29	34.59	34.56	34.64	35.05
18:3n-6	0.21	0.22	0.2	0.2	0.19	0.19	0.2	0.2
20:2n-6	tr*	0.31	0.21	0.17	0.15	0.14	0.11	0.1
20:4n-6	0.28	0.64	0.53	0.46	0.42	0.4	0.37	0.33
22:2n-6	tr	0.18	0.22	0.28	0.34	0.37	0.36	0.4
∑n-6 PUFAs	35.44	31.89	34.97	35.4	35.69	35.66	35.68	36.08
18:3n-3	2.05	2.04	1.96	1.93	1.89	1.86	1.83	1.81
18:4n-3	0.65	1.51	0.93	0.82	0.76	0.73	0.69	0.65
20:3n-3	0.23	0.66	0.57	0.48	0.44	0.42	0.37	0.33
20:5n-3	2.72	6.67	6.06	5.38	4.72	4.54	4.15	3.86
22:3n-3	tr	0.17	0.19	0.25	0.3	0.32	0.3	0.33
22:5n-3	0.34	0.58	0.65	0.73	0.81	0.85	0.82	0.86
22:6n-3	3.61	5.87	6.63	7.17	7.29	7.8	7.83	8.13
∑n-3PUFAs	9.6	17.5	16.99	16.56	16.41	16.42	15.99	15.87
∑PUFAs	45.04	49.39	51.96	51.96	52.1	52.08	51.67	51.95
∑HUFAs	7.18	14.59	14.63	14.27	14.18	14.23	13.84	13.74
n-3/n-6	0.27	0.55	0.49	0.47	0.46	0.46	0.45	0.44
DHA + EPA	6.33	12.54	12.69	12.55	12.01	12.34	11.98	11.99
DHA/EPA	1.33	0.88	1.09	1.33	1.54	1.72	1.89	2.11

All data are mean \pm SD ($n = 3$)

tr Trace (peak area <0.05%)

* $P < 0.0001$

step) and then placed in a 1.5-mL centrifuge tube. Twenty μ L of proteinase K after having been pre-activated for 1 h at 37 °C and 300 μ L of antimicrobial catheter lock (ACL) solution were added to the above-mentioned centrifuge tube and mixed with the tissue powder to extract DNA for 1–3 h at 55 °C and stirred at intervals. The mixed tissue sample was cooled to room temperature and centrifuged for

5 min at 12,000 \times g. A volume of 300 μ L of supernatant with DNA were applied to a UNIQ-10 column (from Shanghai Biotechnological Company, Shanghai, China) to be absorbed. Then, 300 μ L of AB solution was placed in the column, shaken two to three times inversely and allowed to stand for 3 min. The column-supernatant-AB solution (with UNIQ-10 column) mixture was centrifuged

for 3 min at 2,500–3,000×g and the solution in the column-collecting tube was discarded. A wash solution (500 µL) (with UNIQ-10 column) was added to the above-mentioned column and centrifuged for 0.5 min at 8,000×g at room temperature. The step was repeated again and the solution in the column-collecting tube was discarded. The UNIQ-10 column was centrifuged for 0.5 min at 10,000×g to remove the superfluous wash solution. The contents of the column were placed in a newly cleaned 1.5-mL centrifuge tube and DNA eluted for 2 min by the addition of 50 µL of elution buffer (with UNIQ-10 column) at 55 °C. The column was centrifuged for 1 min at 10,000×g at room temperature and the DNA in the elution buffer was immediately tested on a NanoDrop 1000 instrument (NanoDrop Technologies Co., USA) according to the User's Manual or stored at –20 °C for determination later.

Extraction and Determination of RNA

RNA was extracted from the tissues of the cobia juvenile using a TaKaRa RNAiso reagent (from Bao Biotechnological Company, Dalian, Liaoning, China). About 100 mg of a tissue from the cobia juvenile was ground into powder after immersion in liquid nitrogen (RNA extraction from serum without this step) and then placed in a 5-mL of centrifuge tube. One milliliter of RNAiso reagent was added to the centrifuge tube, mixed and allowed to stand for 5 min. The mixed sample in the centrifuge tube was centrifuged for 5 min at 12,000×g at 4 °C. The upper supernatant layer was carefully moved to a new centrifuge tube and centrifuged for 15 min at 12,000×g at 4 °C. The upper supernatant that had a white color was carefully moved to another new centrifuge tube. The same volume of iso-propanol was added to the supernatant in the centrifuge tube, mixed by inversion and allowed to stand for 10 min at 15–30 °C. The mixture of supernatant and iso-propanol was centrifuged for 10 min at 12,000×g at 4 °C and the upper supernatant layer was carefully removed. One milliliter of 75% ethanol was slowly added to the centrifuge tube down the tube wall and the deposit was gently washed by inversion. The washed deposit was centrifuged for 5 min at 12,000×g at 4 °C. The ethanol was removed and the deposit (RNA) in the centrifuge tube was allowed to evaporate naturally for 2–5 min at room temperature. The deposit (RNA) was dissolved in a volume of RNase-free water and immediately tested on a NanoDrop 1000 instrument (NanoDrop Technologies Co., USA) according to the User's Manual or stored at –80 °C for determination later.

Determination of Lipids

Crude lipids were extracted with chloroform and methanol 2:1 (v/v) and then estimated gravimetrically [24].

Determination of Fatty Acids

The composition of fatty acids in the samples was analyzed by comparing with standard fatty acids using a gas chromatograph (GC, Agilent 6890 N, Agilent Company, USA) with a hydrogen flame ionization detector (FID) and an HP-5 column (30 m × 0.32 mm). A sample was injected at 1 µL and analyzed at a speed of 40 mL min⁻¹ for hydrogen, which was used as the carrier. The column temperature was initially held at 140 °C for 5 min, then 200 °C for 5 min, 240 °C for 15 min and 260 °C for 15 min with all the temperature ramps increasing at a rate of 4 °C min⁻¹.

Determination of Protein

Crude protein was determined by the Kjeldahl method (Association of Official Analytical Chemists 1980) [25]. Put simply, nitrogen contained in the sample was extracted and determined. And then the protein was calculated according to the amount of nitrogen using the following formula:

$$\text{Protein (\%)} = \text{Nitrogen (\%)} \times 6.25$$

Data Analysis and Statistics

Data were analyzed by analysis of variance with Fisher's Protected l.s.d. Post hoc Test (Super ANOVA V1.11 Folder) (Abacus Concepts, Inc., 1984 Bonita Avenue, Berkeley, CA, USA) followed by Tukey's multiple comparison test. The effects of diets on all of the data were determined by two-way ANOVA and differences were regarded as significant when $P < 0.05$.

Results

The body weight (BW) of juveniles fed D-0–D-7 increased significantly by the end of experiment (from 6.86 ± 1.64 in week 0 to 58.52 ± 16.45 g at the end of week 8 on average, $P < 0.05$) (Table 3).

The RNA levels and RNA/DNA ratios in the muscle (Table 4) and liver (Table 5) of cobia juveniles were much higher than those of the serum (Table 6) although all of them were markedly higher at the end of experiment than at the beginning ($P < 0.05$). The ratio of RNA to DNA in the muscle and liver of cobia juveniles increased with their growth and this demonstrates an obvious positive relationship, especially in the muscle of the cobia juveniles, based on regression analysis (Fig. 1).

The RNA level was the highest in the muscle of cobia juveniles fed D-0 (297.41 ± 11.84 µg mg⁻¹) and the lowest in those fed D-5 (232.26 ± 26.30 µg mg⁻¹)

Table 3 Effect of different ratios of DHA and EPA on the average body weight (g) of cobia juveniles fed for 8 weeks

	D-0	D-1	D-2	D-3	D-4	D-5	D-6	D-7	Mean
Week 0	6.83 ± 1.65 ^a	6.85 ± 1.84 ^a	6.90 ± 1.27 ^a	6.91 ± 1.77 ^a	6.81 ± 1.21 ^a	6.84 ± 1.65 ^a	6.86 ± 1.75 ^a	6.86 ± 2.00 ^a	6.86 ± 1.64 ^a
Week 8	73.28 ± 17.09 ^c	60.99 ± 15.57 ^b	60.15 ± 17.09 ^b	54.76 ± 12.29 ^b	56.81 ± 18.08 ^b	51.32 ± 14.07 ^b	55.88 ± 16.47 ^b	54.94 ± 20.94 ^b	58.52 ± 16.45 ^b

All data are means ± SE ($n = 3 \times 3$), different superscript letters in the same row denote a significant difference between groups

Table 4 Effect of different ratios of DHA and EPA on the ratio and amount ($\mu\text{g mg}^{-1}$) of RNA and DNA in the muscle of cobia juveniles fed for 8 weeks

	Initial	D-0	D-1	D-2	D-3	D-4	D-5	D-6	D-7	Mean (D-0 to D-7)
RNA	39.62 ± 1.30 ^a	297.41 ± 11.84 ^d	280.24 ± 11.31 ^{bcd}	290.54 ± 4.84 ^{bcd}	297.13 ± 6.62 ^d	296.37 ± 4.25 ^{cd}	232.26 ± 26.30 ^b	237.68 ± 7.73 ^{bc}	240.73 ± 12.70 ^{bcd}	272.55 ± 10.70 ^{bcd}
DNA	17.34 ± 0.41	20.46 ± 2.82	19.22 ± 1.46	20.05 ± 1.33	20.62 ± 0.80	20.98 ± 0.98	17.01 ± 1.19	16.77 ± 1.77	15.47 ± 2.43	18.75 ± 1.60
RNA/DNA	2.29 ± 0.11 ^a	15.14 ± 2.22 ^b	14.84 ± 1.66 ^b	14.63 ± 1.04 ^b	14.45 ± 0.61 ^b	14.18 ± 0.63 ^b	13.85 ± 2.14 ^b	14.54 ± 1.79 ^b	14.72 ± 3.09 ^b	14.54 ± 1.75 ^b

All data are means ± SE ($n = 3 \times 3$), the data with different superscript letters in the same row denote a significant difference between groups

Table 5 Effect of different ratios of DHA and EPA on the ratio and amount ($\mu\text{g mg}^{-1}$) of RNA and DNA in the liver of cobia juveniles fed for 8 weeks

Initial	D-0	D-1	D-2	D-3	D-4	D-5	D-6	D-7	Mean (D-0 to D-7)	
RNA	117.70 \pm 11.15 ^a	800.42 \pm 9.45 ^b	839.70 \pm 13.93 ^b	870.07 \pm 24.97 ^b	870.07 \pm 7.29 ^b	717.78 \pm 7.47 ^b	820.91 \pm 22.19 ^b	783.78 \pm 20.00 ^b	800.11 \pm 10.12 ^b	793.07 \pm 13.38 ^b
DNA	37.44 \pm 0.62 ^a	61.05 \pm 3.96 ^{bc}	65.13 \pm 1.52 ^{bc}	58.23 \pm 7.92 ^{bc}	58.23 \pm 1.06 ^{bc}	48.71 \pm 2.56 ^{ab}	67.15 \pm 2.37 ^c	59.20 \pm 4.98 ^{bc}	64.47 \pm 1.75 ^{bc}	61.10 \pm 327 ^{bc}
RNA/DNA	3.14 \pm 0.25	11.76 \pm 0.76	12.36 \pm 0.47	13.29 \pm 1.75	14.96 \pm 0.39	14.83 \pm 0.87	12.28 \pm 0.73	13.39 \pm 0.91	12.42 \pm 0.19	13.16 \pm 0.76

All data are means \pm SE ($n = 3 \times 3$), different superscript letters in the same row denote a significant difference between groups

Table 6 Effect of different ratios of DHA and EPA on ratio and amount ($\mu\text{g mg}^{-1}$) of RNA and DNA in the serum of cobia juveniles fed for 8 weeks

Initial	D-0	D-1	D-2	D-3	D-4	D-5	D-6	D-7	Mean (D-0–D-7)	
RNA	15.73 \pm 1.18 ^a	100.92 \pm 0.82 ^b	108.07 \pm 1.63 ^{bc}	113.02 \pm 2.55 ^{cd}	116.72 \pm 1.18 ^d	101.41 \pm 0.34 ^b	105.32 \pm 2.39 ^{bc}	102.15 \pm 2.59 ^b	104.08 \pm 1.36 ^b	106.46 \pm 1.61 ^{bc}
DNA	5.48 \pm 0.02 ^a	8.15 \pm 0.36 ^b	8.41 \pm 0.13 ^b	8.52 \pm 0.71 ^b	7.89 \pm 0.06 ^b	6.97 \pm 0.22 ^{ab}	8.42 \pm 0.16 ^b	7.60 \pm 0.50 ^b	7.99 \pm 0.30 ^b	7.99 \pm 0.31 ^b
RNA/DNA	2.87 \pm 0.20 ^a	12.44 \pm 0.63 ^b	12.86 \pm 0.38 ^b	13.44 \pm 1.09 ^b	14.81 \pm 0.26 ^b	14.58 \pm 0.50 ^b	12.52 \pm 0.28 ^b	13.53 \pm 0.65 ^b	13.07 \pm 0.62 ^b	13.41 \pm 0.55 ^b

All data are means \pm SE ($n = 3 \times 3$), different superscript letters in the same row denote a significant difference between groups

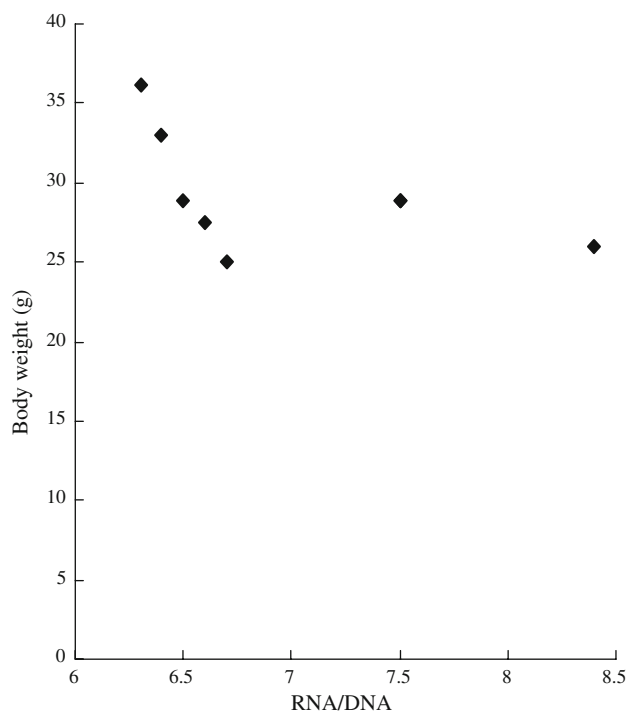


Fig. 1 Regression relationship between body weight and RNA/DNA ratio in the muscle of cobia juveniles fed for 8 weeks (total average, $n = 3 \times 3$). $Y = -12.04 \times 3 + 264.84 \times 2 - 1932.1x + 4703.5$, $R^2 = 0.8839$

(Table 4); however, there were no significant differences between those fed D-0 and D-1–D-7 ($P > 0.05$). The amounts of DNA in the muscles of cobia juveniles fed D-0 were higher than in the muscles of those fed D-1–D-2 and D-5–D-7; however, there was no significant difference among each of these others ($P > 0.05$) (Table 4). The amounts of RNA and the RNA/DNA ratios in the liver of cobia juveniles fed D-0 were lower than those fed D-1–D-7, but there was no significant differences among the others ($P > 0.05$) (Table 5).

Compared to the beginning, lipid content increased significantly in the liver (from 29.82 ± 0.99 to $37.47 \pm 3.25\%$) and in muscle (from 6.74 ± 0.25 to $10.63 \pm 0.23\%$) of cobia juveniles at the end of week 8 ($P < 0.05$). However, no significant differences were found in the lipid contents of juveniles fed different diets for 8 weeks ($P > 0.05$) (Table 7).

The effect of different ratios and amounts of DHA and EPA on the fatty acid composition of the muscle, liver and serum in cobia juveniles at the end of week 8 is shown in Tables 8, 9 and 10. Generally, in the muscle and liver of juveniles, the EPA decreased with its reduction in the diet; DHA, DHA/EPA ratios and PUFAs usually increased with their increment in the diet; while these parameters varied in the serum. The amounts of DHA were higher in the tested tissues of the cobia juvenile than in the corresponding diet and those of EPA were lower ($P > 0.05$).

Table 7 Comparison of lipid contents (%) in the muscle and liver of cobia juveniles fed different ratios of DHA and EPA for 8 weeks

Diet	Muscle	Liver	N
Initial*	6.74 ± 0.25^e	29.82 ± 0.99^b	$N = 8 \times 3$
0	10.23 ± 0.04^c	39.77 ± 4.96^a	$N = 3 \times 3$
1	9.19 ± 0.19^d	36.62 ± 2.88^{ab}	$N = 3 \times 3$
2	12.13 ± 0.02^b	34.04 ± 1.49^{ab}	$N = 3 \times 3$
3	10.17 ± 0.08^{cd}	35.96 ± 3.86^{ab}	$N = 3 \times 3$
4	9.63 ± 0.84^{cd}	40.95 ± 1.74^a	$N = 3 \times 3$
5	9.69 ± 0.15^{cd}	38.65 ± 3.10^{ab}	$N = 3 \times 3$
6	10.62 ± 0.46^c	35.47 ± 4.61^{ab}	$N = 3 \times 3$
7	13.38 ± 0.04^a	38.26 ± 3.36^{ab}	$N = 3 \times 3$
Total mean**	10.63 ± 0.23	37.47 ± 3.25	$N = 8 \times 3$

All above data are means \pm SD. Different superscript letters in the same column indicate significant differences ($P < 0.05$)

*Initial means in the week 0 ($n = 8 \times 3$)

**Total mean is an average datum of eight diets ($n = 8 \times 3$)

Discussion

With our experimental diets consisting of 67% mixed fish-meal and 17% lipids (Table 1), the amount (0.8%) and ratio (1.30) of DHA and EPA in D-0 met with the requirement of cobia juveniles, resulting in our obtaining the highest growth (Table 3). The content, 0.8% of DHA and EPA, is in the range of 0.8–1.2% of DHA and EPA required by cobia [23]. The amount ($1.50 \pm 0.1\%$ of dried diet) of DHA and EPA as well as their ratios (0.90, 1.10, 1.30, 1.50, 1.70, 1.90, 2.10) in the treatment diets did not benefit the growth of cobia juveniles, actually resulting in less growth. The result is consistent with previous reports in that a negative effect of HUFAs excess can be encountered for higher HUFAs levels or at low lipid levels in some species [26–28]. Higher n-3 HUFAs were reported to be unavailable in the growth of *Platichthys flesus* larvae [29, 30] since higher n-3 HUFAs influenced the balance of the membrane phospholipids, resulting in dysfunction of the cell membrane [29, 31]. In our experiment, the ratio of DHA to EPA in D-3 and D-0 was the same, 1.30, however, the amounts of DHA and EPA in D-3 were almost twofold that in D-0, resulting in poor growth in cobia juveniles fed D-3 (Tables 1, 3). This is consistent with the report by Rodriguez et al. [28] in that a suitable ratio of DHA to EPA was 1.3:1 in the diet of gilt-head bream (*Sparus aurata*) larvae; over EPA or lack of DHA could result in lower effectiveness of the diet and slowing down of the growth of the larvae.

Nucleic acid analysis has provided a useful tool for studying recent growth and mortality of young fishes and their responses to environmental variability. The ratio of RNA–DNA (R/D) has been shown to respond to changes in feeding conditions and growth after periods as short as

Table 8 Effect of different ratios of DHA and EPA on the fatty acid composition (%) of muscle in cobia juveniles fed for 8 weeks

Fatty acid	Diet								
	Initially	0	1	2	3	4	5	6	7
14:00	1.84 ± 0.14 ^a	1.09 ± 0.05 ^c	1.59 ± 0.12 ^b	1.19 ± 0.01 ^c	1.16 ± 0.06 ^c	1.20 ± 0.00 ^c	1.22 ± 0.02 ^c	1.19 ± 0.03 ^c	1.20 ± 0.02 ^c
15:00	0.32 ± 0.04 ^a	0.12 ± 0.01 ^b	0.24 ± 0.03 ^{ab}	0.17 ± 0.05 ^{ab}	0.29 ± 0.22 ^{ab}	0.14 ± 0.01 ^{ab}	0.13 ± 0.01 ^{ab}	0.16 ± 0.02 ^{ab}	0.15 ± 0.02 ^{ab}
16:00	16.50 ± 0.07 ^a	15.08 ± 0.64 ^b	14.96 ± 0.58 ^{bc}	14.23 ± 0.39 ^{bc}	14.48 ± 0.32 ^{bc}	14.35 ± 0.22 ^{bc}	13.81 ± 0.04 ^c	14.15 ± 0.55 ^{bc}	14.06 ± 0.28 ^{bc}
17:00	0.44 ± 0.02 ^a	0.13 ± 0.01 ^d	0.20 ± 0.01 ^b	0.15 ± 0.00 ^{cd}	0.16 ± 0.00 ^{bc}	0.16 ± 0.01 ^{cd}	0.14 ± 0.01 ^{cd}	0.15 ± 0.01 ^{cd}	0.15 ± 0.01 ^{cd}
18:00	6.31 ± 0.09 ^a	4.84 ± 0.65 ^b	4.05 ± 0.67 ^b	4.27 ± 0.58 ^b	4.75 ± 0.05 ^b	4.12 ± 0.13 ^b	3.70 ± 0.15 ^b	4.23 ± 0.33 ^b	4.14 ± 0.20 ^b
19:00	0.11 ± 0.00	0.05 ± 0.09	0.08 ± 0.02	tr	0.11 ± 0.04	0.06 ± 0.05	0.09 ± 0.03	0.08 ± 0.02	0.07 ± 0.01
20:00	0.31 ± 0.00	0.30 ± 0.03	0.30 ± 0.04	0.32 ± 0.02	0.34 ± 0.04	0.31 ± 0.02	0.31 ± 0.02	0.31 ± 0.03	0.31 ± 0.02
∑SFAs	25.83 ± 0.22 ^a	21.61 ± 1.21 ^b	21.43 ± 1.11 ^{bc}	20.35 ± 0.91 ^{bc}	21.30 ± 0.18 ^{bc}	20.34 ± 0.39 ^{bc}	19.40 ± 0.17 ^c	20.26 ± 0.84 ^{bc}	20.07 ± 0.28 ^{bc}
16:1n-7	3.16 ± 0.37 ^a	1.56 ± 0.07 ^c	2.15 ± 0.16 ^b	1.54 ± 0.10 ^c	1.47 ± 0.00 ^c	1.55 ± 0.04 ^c	1.58 ± 0.02 ^c	1.48 ± 0.02 ^c	1.49 ± 0.05 ^c
17:1n-8	0.22 ± 0.00 ^a	0.17 ± 0.00 ^{ab}	0.19 ± 0.02 ^{ab}	0.16 ± 0.03 ^{ab}	0.17 ± 0.03 ^{ab}	0.18 ± 0.03 ^{ab}	0.14 ± 0.04 ^b	0.14 ± 0.02 ^b	0.14 ± 0.02 ^b
18:1n-9	15.91 ± 0.47 ^d	25.25 ± 0.49 ^a	20.04 ± 0.40 ^{bc}	20.18 ± 0.14 ^{bc}	19.47 ± 0.56 ^c	21.15 ± 0.61 ^b	20.71 ± 0.41 ^{bc}	20.11 ± 0.51 ^{bc}	20.29 ± 0.33 ^{bc}
20:1n-9	3.26 ± 0.03 ^c	3.97 ± 0.02 ^b	4.38 ± 0.13 ^{ab}	4.42 ± 0.13 ^{ab}	4.08 ± 0.23 ^{ab}	4.42 ± 0.23 ^a	4.34 ± 0.07 ^{ab}	4.16 ± 0.14 ^{ab}	4.31 ± 0.23 ^{ab}
22:1n-11	nd	tr	0.14 ± 0.02 ^a	0.12 ± 0.00 ^a	0.13 ± 0.04 ^a	0.14 ± 0.05 ^a	0.11 ± 0.00 ^{ab}	0.13 ± 0.01 ^a	0.12 ± 0.01 ^a
22:1n-11	2.29 ± 0.03 ^a	1.79 ± 0.03 ^b	2.08 ± 0.22 ^{ab}	2.08 ± 0.12 ^{ab}	1.91 ± 0.03 ^{ab}	2.07 ± 0.24 ^{ab}	2.24 ± 0.14 ^a	2.17 ± 0.17 ^{ab}	2.20 ± 0.10 ^{ab}
24:1n-15	0.32 ± 0.06 ^b	0.49 ± 0.13 ^{ab}	0.56 ± 0.06 ^{ab}	0.49 ± 0.14 ^{ab}	0.54 ± 0.13 ^{ab}	0.61 ± 0.03 ^{ab}	0.64 ± 0.02 ^a	0.47 ± 0.06 ^{ab}	0.68 ± 0.09 ^a
∑MUFAs	25.17 ± 0.11 ^d	33.27 ± 0.65 ^a	29.54 ± 0.73 ^{bc}	28.98 ± 0.25 ^{bc}	27.77 ± 1.02 ^c	30.11 ± 1.08 ^b	29.75 ± 0.51 ^{bc}	28.66 ± 0.67 ^{bc}	29.24 ± 0.52 ^{bc}
18:2n-6	12.31 ± 1.00 ^d	27.93 ± 0.74 ^{abc}	25.55 ± 0.90 ^c	27.25 ± 0.52 ^{abc}	25.67 ± 0.68 ^{bc}	29.01 ± 1.32 ^a	28.94 ± 0.65 ^a	27.46 ± 0.88 ^{abc}	28.36 ± 0.61 ^{ab}
18:3n-6	0.17 ± 0.02	0.18 ± 0.00	0.20 ± 0.01	0.18 ± 0.02	0.17 ± 0.01	0.18 ± 0.03	0.21 ± 0.02	0.20 ± 0.01	0.19 ± 0.01
20:2n-6	0.39 ± 0.02 ^{abc}	0.19 ± 0.03 ^c	0.52 ± 0.04 ^a	0.43 ± 0.02 ^a	0.32 ± 0.05 ^{abc}	0.40 ± 0.15 ^{ab}	0.30 ± 0.01 ^{bc}	0.31 ± 0.06 ^{bc}	0.26 ± 0.00 ^{bc}
20:4n-6	1.07 ± 0.02 ^a	0.48 ± 0.08 ^b	0.72 ± 0.15 ^b	0.77 ± 0.19 ^{ab}	0.82 ± 0.06 ^{ab}	0.56 ± 0.05 ^b	0.48 ± 0.04 ^b	0.55 ± 0.04 ^b	0.65 ± 0.14 ^b
22:2n-6	0.18 ± 0.02 ^c	0.03 ± 0.05 ^d	0.21 ± 0.03 ^c	0.24 ± 0.07 ^{bc}	0.33 ± 0.08 ^{abc}	0.32 ± 0.05 ^{abc}	0.34 ± 0.02 ^{ab}	0.36 ± 0.01 ^{ab}	0.41 ± 0.03 ^a
∑n-6PUFAs	14.12 ± 0.95 ^d	28.81 ± 0.70 ^{abc}	27.20 ± 0.84 ^c	28.87 ± 0.35 ^{abc}	27.31 ± 0.70 ^{bc}	30.47 ± 1.32 ^a	30.27 ± 0.66 ^a	28.89 ± 0.88 ^{abc}	29.86 ± 0.58 ^{ab}
16:3n-3	0.14 ± 0.01 ^a	0.09 ± 0.01 ^b	0.12 ± 0.02 ^{ab}	0.11 ± 0.01 ^{ab}	0.12 ± 0.00 ^{ab}	0.09 ± 0.00 ^b	0.10 ± 0.02 ^b	0.09 ± 0.01 ^b	0.09 ± 0.00 ^b
16:4n-3	nd	0.12 ± 0.02 ^c	0.18 ± 0.02 ^{ab}	0.17 ± 0.02 ^{abc}	0.21 ± 0.03 ^{abc}	0.17 ± 0.02 ^{ab}	0.14 ± 0.02 ^{bc}	0.17 ± 0.01 ^{abc}	0.16 ± 0.01 ^{abc}
18:3n-3	3.44 ± 0.06 ^a	2.63 ± 0.04 ^b	2.54 ± 0.09 ^b	2.36 ± 0.05 ^c	2.33 ± 0.02 ^c	2.37 ± 0.07 ^c	2.31 ± 0.03 ^c	2.27 ± 0.07 ^c	2.22 ± 0.04 ^c
18:4n-3	1.08 ± 0.15 ^a	0.42 ± 0.05 ^c	1.06 ± 0.13 ^b	0.62 ± 0.07 ^c	0.52 ± 0.06 ^c	0.55 ± 0.09 ^c	0.59 ± 0.06 ^c	0.55 ± 0.02 ^c	0.49 ± 0.02 ^c
20:5n-3	5.45 ± 0.38 ^a	2.36 ± 0.19 ^d	4.99 ± 0.29 ^{ab}	4.48 ± 0.24 ^b	3.60 ± 0.27 ^c	3.62 ± 0.51 ^c	3.45 ± 0.06 ^c	3.36 ± 0.05 ^c	3.25 ± 0.08 ^c
22:3n-3	nd	nd	nd	nd	0.20 ± 0.04	0.21 ± 0.06	0.22 ± 0.03	0.25 ± 0.02	0.27 ± 0.02
22:5n-3	1.49 ± 0.14 ^a	0.62 ± 0.03 ^d	0.86 ± 0.01 ^c	0.84 ± 0.10 ^c	1.00 ± 0.05 ^{bc}	0.99 ± 0.09 ^{bc}	0.98 ± 0.01 ^{bc}	1.01 ± 0.03 ^{bc}	1.06 ± 0.03 ^b
22:6n-3	18.42 ± 0.29 ^a	7.19 ± 0.80 ^d	8.11 ± 1.37 ^{cd}	8.86 ± 0.75 ^{bcd}	10.95 ± 0.66 ^b	9.94 ± 1.22 ^{bc}	9.05 ± 0.29 ^{bcd}	10.09 ± 0.67 ^{bc}	9.96 ± 0.43 ^{bc}
∑n-3PUFAs	29.88 ± 1.03 ^a	13.22 ± 0.64 ^c	17.55 ± 1.04 ^b	17.17 ± 0.58 ^b	18.60 ± 0.56 ^b	17.68 ± 0.73 ^b	16.60 ± 0.22 ^b	17.53 ± 0.71 ^b	17.25 ± 0.36 ^b
∑PUFAs	44.00 ± 0.07 ^{de}	42.03 ± 0.58 ^e	44.76 ± 0.70 ^d	46.04 ± 0.75 ^{bcd}	45.90 ± 0.13 ^{bcd}	48.15 ± 1.18 ^a	46.87 ± 0.58 ^{ab}	46.41 ± 0.68 ^{abc}	47.12 ± 0.48 ^{ab}
∑n-3HUFAs	25.36 ± 0.81 ^a	10.17 ± 0.65 ^c	13.95 ± 1.09 ^b	14.19 ± 0.56 ^b	15.55 ± 0.45 ^b	14.54 ± 0.81 ^b	13.48 ± 0.32 ^b	14.46 ± 0.65 ^b	14.27 ± 0.36 ^b
n-3/n-6	2.12 ± 0.22 ^a	0.46 ± 0.03 ^c	0.65 ± 0.05 ^b	0.59 ± 0.02 ^b	0.68 ± 0.04 ^b	0.59 ± 0.04 ^{bc}	0.55 ± 0.02 ^{bc}	0.61 ± 0.04 ^{bc}	0.58 ± 0.02 ^{bc}
DHA + EPA	23.88 ± 0.67 ^a	9.55 ± 0.61 ^c	13.10 ± 1.09 ^b	13.35 ± 0.53 ^b	14.55 ± 0.39 ^b	13.56 ± 0.73 ^b	12.50 ± 0.33 ^b	13.45 ± 0.63 ^b	13.21 ± 0.35 ^b
DHA/EPA	3.38 ± 0.18 ^a	3.08 ± 0.58 ^{ab}	1.64 ± 0.38 ^c	1.99 ± 0.27 ^{bc}	3.06 ± 0.41 ^{ab}	2.82 ± 0.80 ^{abc}	2.62 ± 0.07 ^{abc}	3.00 ± 0.24 ^{ab}	3.07 ± 0.20 ^{ab}

All above data are means ± SD ($n = 3 \times 3$). Different superscript letters in the same row indicate a significant difference among the data ($P < 0.05$)

N-6 PUFAs include 18:2n-6, 20:2n-6, 20:4n-6, 22:2n-6 here. N-3 PUFAs include 18:3n-3, 18:4n-3, 20:3n-3, 20:5n-3, 22:3n-3, 22:5n-3, 22:6n-3 here. N-3 HUFAs include 20:5n-3, 22:5n-3, 22:6n-3 here

tr Trace (peak area <0.05%); nd not detected; Initially means in week 0

Table 9 Effect of different ratios of DHA and EPA on the fatty acid composition (%) of liver in cobia juveniles fed for 8 weeks

Fatty acid	Diet								
	Initially	0	1	2	3	4	5	6	7
14:00	1.48 ± 0.01 ^a	0.67 ± 0.05 ^b	0.97 ± 0.18 ^b	0.70 ± 0.13 ^b	0.88 ± 0.11 ^b	0.75 ± 0.05 ^b	0.77 ± 0.09 ^b	0.80 ± 0.07 ^b	0.74 ± 0.13 ^b
15:00	0.36 ± 0.03 ^a	0.14 ± 0.01 ^c	0.21 ± 0.05 ^b	0.15 ± 0.01 ^{bc}	0.18 ± 0.02 ^{bc}	0.15 ± 0.05 ^b	0.14 ± 0.01 ^{bc}	0.16 ± 0.01 ^{bc}	0.17 ± 0.00 ^{bc}
16:00	17.31 ± 0.32 ^a	13.56 ± 0.45 ^b	13.10 ± 0.78 ^{bc}	12.88 ± 0.59 ^{bc}	12.47 ± 0.47 ^{bc}	11.90 ± 0.16 ^c	12.50 ± 0.28 ^{bc}	12.14 ± 0.28 ^{bc}	12.54 ± 0.77 ^{bc}
17:00	0.58 ± 0.00 ^a	0.16 ± 0.00 ^b	0.20 ± 0.03 ^b	0.17 ± 0.01 ^b	0.16 ± 0.01 ^b	0.15 ± 0.00 ^b	0.16 ± 0.01 ^b	0.16 ± 0.03 ^b	0.17 ± 0.03 ^b
18:00	5.97 ± 0.13 ^a	3.19 ± 0.22 ^b	2.63 ± 0.44 ^{bc}	2.52 ± 0.34 ^{bc}	2.34 ± 0.12 ^{bc}	2.37 ± 0.29 ^{bc}	2.62 ± 0.11 ^{bc}	2.43 ± 0.45 ^{bc}	2.27 ± 0.41 ^c
19:00	nd	0.07 ± 0.00 ^a	0.08 ± 0.01 ^a	0.07 ± 0.01 ^{ab}	0.08 ± 0.01 ^a	0.08 ± 0.01 ^a	0.07 ± 0.00 ^a	tr ^b	0.07 ± 0.00 ^{ab}
20:00	0.17 ± 0.00	0.17 ± 0.01	0.17 ± 0.05	0.18 ± 0.02	0.16 ± 0.02	0.15 ± 0.01	0.17 ± 0.01	0.15 ± 0.01	0.15 ± 0.01
∑SFAs	25.88 ± 0.42 ^a	17.95 ± 0.57 ^b	17.37 ± 1.26 ^{bc}	16.67 ± 0.74 ^{bc}	16.27 ± 0.72 ^{bc}	15.55 ± 0.17 ^c	16.43 ± 0.28 ^{bc}	15.86 ± 0.67 ^{bc}	16.10 ± 1.12 ^{bc}
16:1n-7	4.11 ± 0.26 ^a	1.72 ± 0.08 ^{bc}	2.00 ± 0.29 ^b	1.66 ± 0.08 ^{bc}	1.68 ± 0.01 ^{bc}	1.58 ± 0.03 ^c	1.61 ± 0.02 ^c	1.62 ± 0.07 ^c	1.59 ± 0.05 ^c
17:1n-8	0.39 ± 0.03 ^a	0.24 ± 0.01 ^b	0.32 ± 0.07 ^{ab}	0.26 ± 0.03 ^b	0.24 ± 0.03 ^b	0.24 ± 0.02 ^b	0.23 ± 0.00 ^b	0.24 ± 0.03 ^b	0.28 ± 0.03 ^b
18:1n-9	18.45 ± 0.16 ^c	27.61 ± 0.25 ^d	20.80 ± 0.73 ^b	21.55 ± 0.46 ^b	20.94 ± 0.58 ^b	20.46 ± 0.16 ^b	20.76 ± 0.26 ^b	21.02 ± 0.56 ^b	21.38 ± 0.72 ^b
20:1n-9	3.40 ± 0.01 ^c	4.71 ± 0.08 ^a	4.26 ± 0.14 ^{ab}	4.22 ± 0.33 ^{ab}	3.94 ± 0.19 ^{bc}	3.96 ± 0.22 ^{bc}	4.25 ± 0.13 ^{ab}	3.87 ± 0.14 ^{bc}	3.93 ± 0.22 ^{bc}
20:1n-11	0.23 ± 0.01 ^a	0.13 ± 0.00 ^b	0.14 ± 0.04 ^b	0.13 ± 0.01 ^b	0.11 ± 0.02 ^b	0.11 ± 0.01 ^b	0.11 ± 0.01 ^b	0.10 ± 0.01 ^b	0.11 ± 0.02 ^b
22:1n-11	1.70 ± 0.02	1.65 ± 0.05	1.67 ± 0.01	1.58 ± 0.19	1.60 ± 0.23	1.58 ± 0.09	1.80 ± 0.09	1.61 ± 0.02	1.60 ± 0.07
24:1n-15	0.19 ± 0.03 ^b	0.29 ± 0.03 ^{ab}	0.27 ± 0.04 ^{ab}	0.32 ± 0.05 ^{ab}	0.36 ± 0.06 ^a	0.26 ± 0.03 ^{ab}	0.36 ± 0.03 ^a	0.32 ± 0.05 ^{ab}	0.32 ± 0.05 ^{ab}
∑MUFAs	28.46 ± 0.10 ^b	36.34 ± 0.21 ^a	29.46 ± 0.33 ^b	29.73 ± 0.78 ^b	28.87 ± 0.68 ^b	28.18 ± 0.45 ^b	29.13 ± 0.41 ^b	28.78 ± 0.66 ^b	29.20 ± 0.92 ^b
16:2n-4	0.45 ± 0.03	0.38 ± 0.03	0.41 ± 0.04	0.43 ± 0.09	0.43 ± 0.08	0.37 ± 0.02	0.35 ± 0.01	0.41 ± 0.05	0.47 ± 0.05
18:2n-6	13.04 ± 0.10 ^b	31.69 ± 0.16 ^a	28.74 ± 4.00 ^a	31.17 ± 2.08 ^a	32.11 ± 0.54 ^a	32.26 ± 0.62 ^a	30.36 ± 0.95 ^a	31.68 ± 0.92 ^a	32.12 ± 0.37 ^a
18:3n-6	0.26 ± 0.01 ^a	0.21 ± 0.01 ^b	0.25 ± 0.04 ^{ab}	0.22 ± 0.01 ^{ab}	0.22 ± 0.01 ^{ab}	0.22 ± 0.01 ^{ab}	0.21 ± 0.00 ^b	0.21 ± 0.00 ^b	0.21 ± 0.01 ^b
20:2n-6	nd	0.17 ± 0.01 ^d	0.43 ± 0.08 ^a	0.38 ± 0.04 ^{ab}	0.33 ± 0.03 ^{ab}	0.32 ± 0.01 ^{bc}	0.30 ± 0.02 ^{bc}	0.29 ± 0.01 ^{bc}	0.25 ± 0.01 ^{cd}
20:4n-6	1.07 ± 0.05 ^a	0.44 ± 0.02 ^e	0.85 ± 0.09 ^b	0.74 ± 0.04 ^{bc}	0.69 ± 0.04 ^{cd}	0.65 ± 0.02 ^{cd}	0.65 ± 0.03 ^{cd}	0.63 ± 0.00 ^{cd}	0.58 ± 0.03 ^d
22:2n-6	0.34 ± 0.03 ^{de}	0.26 ± 0.03 ^e	0.42 ± 0.04 ^{bcd}	0.40 ± 0.03 ^{cde}	0.54 ± 0.09 ^{abc}	0.55 ± 0.00 ^{abc}	0.56 ± 0.02 ^{ab}	0.58 ± 0.03 ^{ab}	0.59 ± 0.11 ^a
22:4n-6	nd	nd	0.21 ± 0.02 ^b	0.22 ± 0.01 ^b	0.27 ± 0.03 ^b	0.34 ± 0.02 ^a	0.34 ± 0.01 ^a	0.37 ± 0.01 ^a	0.38 ± 0.04 ^a
∑n-6PUFAs	14.72 ± 0.11 ^b	32.76 ± 0.19 ^a	30.90 ± 3.83 ^a	33.11 ± 2.09 ^a	34.17 ± 0.43 ^a	34.33 ± 0.61 ^a	32.43 ± 0.95 ^a	33.76 ± 0.93 ^a	34.13 ± 0.51 ^a
16:3n-3	0.12 ± 0.01 ^a	0.07 ± 0.00 ^e	0.09 ± 0.01 ^{bc}	0.08 ± 0.00 ^{bc}	0.09 ± 0.00 ^{bc}	0.08 ± 0.00 ^{bc}	0.08 ± 0.00 ^{bc}	0.08 ± 0.00 ^{bc}	0.09 ± 0.00 ^b
16:4n-3	0.21 ± 0.01 ^d	0.27 ± 0.02 ^{cd}	0.35 ± 0.08 ^{abcd}	0.37 ± 0.08 ^{abc}	0.44 ± 0.06 ^{ab}	0.36 ± 0.04 ^{abcd}	0.30 ± 0.03 ^{bcd}	0.38 ± 0.03 ^{abc}	0.45 ± 0.03 ^a
18:3n-3	4.53 ± 0.21 ^a	2.44 ± 0.08 ^{bc}	2.50 ± 0.04 ^b	2.38 ± 0.04 ^{bcd}	2.34 ± 0.06 ^{bcd}	2.17 ± 0.01 ^d	2.22 ± 0.06 ^{cd}	2.22 ± 0.04 ^{cd}	2.25 ± 0.13 ^{cd}
18:4n-3	1.04 ± 0.03 ^a	0.29 ± 0.01 ^d	0.77 ± 0.16 ^b	0.52 ± 0.03 ^c	0.54 ± 0.02 ^c	0.49 ± 0.01 ^c	0.46 ± 0.02 ^{cd}	0.45 ± 0.04 ^{cd}	0.39 ± 0.04 ^{cd}
20:3n-3	0.58 ± 0.01 ^a	nd	0.08 ± 0.03 ^b	0.07 ± 0.00 ^b	0.06 ± 0.01 ^{bc}	0.05 ± 0.00 ^{bc}	0.05 ± 0.00 ^{bc}	tr ^c	0.05 ± 0.01 ^{bc}
20:5n-3	5.63 ± 0.10 ^a	1.88 ± 0.18 ^d	5.03 ± 0.62 ^a	4.37 ± 0.37 ^a	4.24 ± 0.61 ^{bc}	4.25 ± 0.24 ^{bc}	4.13 ± 0.26 ^{bc}	3.91 ± 0.31 ^{bc}	3.16 ± 0.56 ^c
22:5n-3	1.60 ± 0.02 ^a	0.85 ± 0.02 ^c	1.13 ± 0.13 ^{bc}	1.16 ± 0.14 ^b	1.06 ± 0.12 ^{bc}	1.23 ± 0.09 ^b	1.32 ± 0.10 ^{ab}	1.24 ± 0.07 ^b	1.13 ± 0.09 ^{bc}
22:6n-3	14.82 ± 0.09 ^a	5.73 ± 0.23 ^e	9.26 ± 0.46 ^d	9.81 ± 0.67 ^{cd}	10.20 ± 0.76 ^{bcd}	11.56 ± 0.57 ^{bc}	11.63 ± 0.45 ^{bc}	11.88 ± 0.19 ^b	10.78 ± 1.44 ^{bcd}
∑n-3PUFAs	28.36 ± 0.00 ^a	12.37 ± 0.84 ^c	18.89 ± 1.70 ^b	18.86 ± 0.26 ^b	18.63 ± 0.32 ^b	17.73 ± 1.68 ^b	18.95 ± 1.46 ^b	18.90 ± 0.76 ^b	18.69 ± 0.74 ^b
∑PUFAs	43.53 ± 0.11 ^b	45.51 ± 0.39 ^b	50.20 ± 1.15 ^a	52.40 ± 1.71 ^a	53.23 ± 0.72 ^a	52.43 ± 2.86 ^a	51.73 ± 0.95 ^a	53.07 ± 0.42 ^a	53.29 ± 0.72 ^a

Table 9 continued

Fatty acid	Diet								
	Initially	0	1	2	3	4	5	6	7
∑n-3HUFAs	22.04 ± 0.01 ^a	8.46 ± 0.34 ^c	15.63 ± 1.19 ^b	15.56 ± 0.90 ^b	15.77 ± 1.51 ^b	17.38 ± 0.89 ^b	17.42 ± 0.78 ^b	17.40 ± 0.42 ^b	15.45 ± 2.13 ^b
n-3/n-6	1.93 ± 0.01 ^a	0.39 ± 0.03 ^c	0.61 ± 0.08 ^b	0.61 ± 0.02 ^b	0.60 ± 0.02 ^b	0.56 ± 0.04 ^b	0.58 ± 0.07 ^b	0.58 ± 0.03 ^b	0.55 ± 0.03 ^b
DHA + EPA	20.44 ± 0.01 ^a	7.61 ± 0.33 ^c	14.29 ± 1.07 ^b	14.18 ± 0.76 ^b	14.44 ± 1.37 ^b	15.81 ± 0.80 ^b	15.76 ± 0.67 ^b	15.79 ± 0.48 ^b	13.94 ± 2.01 ^b
DHA/EPA	2.63 ± 0.06 ^{bcd}	3.07 ± 0.29 ^{ab}	1.85 ± 0.15 ^e	2.26 ± 0.26 ^{de}	2.42 ± 0.17 ^{cd}	2.72 ± 0.03 ^{bcd}	2.82 ± 0.11 ^{bc}	3.05 ± 0.19 ^{ab}	3.43 ± 0.17 ^a

All above data are mean ± SD ($n = 3 \times 3$). Different superscript letters in the same row indicate significant differences ($P < 0.05$)

N-6 PUFAs include 18:2n-6, 20:2n-6, 20:4n-6, 22:2n-6 here; N-3 PUFAs include 18:3n-3, 18:4n-3, 20:3n-3, 20:5n-3, 22:3n-3, 22:5n-3, 22:6n-3 here; N-3 HUFAs include 20:5n-3, 22:5n-3, 22:6n-3 here

tr Trace (peak area <0.05%); nd not detected; Initially means in the week 0

1–3 days in a variety of fish species [32, 33]. RNA:DNA, a surrogate measure of growth and feeding condition, corroborated somatic growth trends [34]. The ratio of tissue RNA to DNA (R/D) has proven to provide a reliable indicator of recent growth and nutritional conditions of larvae and juvenile fish [35–39]. Therefore, the ratio of tissue RNA to DNA (R/D) is a widely used index of recent growth and nutritional conditions in larvae and juvenile fish [40, 41].

In experiments, the RNA levels and RNA/DNA ratios in the muscle and liver of cobia juveniles fed D-0–D-7 were significantly higher at the end of the 8-week period than at the beginning ($P < 0.05$, Tables 4, 5) The RNA/DNA ratio in the muscle and liver of cobia juveniles increased with their growth and appeared to be an obvious positive relationship, especially in the muscle, based on regression analysis (Fig. 1). Fish growth is mainly performed by synthesizing proteins, while proteins are translated by rRNA. In other word, the amount of proteins is determined by the level of RNA, therefore, the synthesis of proteins and fish growth can be predicted by determining the quantity of RNA [42]. Speed of growth of a fish can be calculated by the ratio of RNA to DNA in the fish even though the fish is in its initial growth stage. The amount of DNA is fixed in a cell of a fish and the total amount of DNA in a fish is related to the number of cells in the fish [43]; whereas the ratio of RNA to DNA is determined by the RNA concentration in the cell of the fish [44]. Therefore, the ratio of RNA to DNA is a better indicator of RNA concentration in a fish and can exactly indicate the metabolism of the growing-fish.

Fish grow by a change in the RNA/DNA ratio and/or rapid synthesis of proteins. Compared to the liver of the cobia juvenile, the RNA/DNA ratio in the muscle appeared a better positive indicator of its growth based on regression analysis (Fig. 1), therefore, the RNA/DNA ratio in the muscle can more exactly indicate the growth of the cobia juvenile. The results are consistent with a previous report [45] in that an obvious positive relationship existed in the ratio of RNA to DNA in the muscle of shrimps based on regression analysis.

The RNA/DNA ratio in the liver and serum of cobia juveniles fed D-0 was lower than that in juveniles fed D-1–D-7. While the RNA level was the highest in the muscle of cobia juveniles fed D-0 from among the experimental groups (Tables 4, 5, 6). However, no significant differences were found in the RNA/DNA ratio and/or RNA level between juveniles fed D-0 and D-1–D-7 ($P > 0.05$). These results imply that there was no significant effect of different ratios and the amounts of DHA and EPA on the RNA/DNA ratios as well as the RNA levels of cobia juveniles under our experimental conditions.

The lipid contents, amounts of DHA, DHA/EPA ratios and amounts of PUFAs generally increased in the liver and muscle of cobia juveniles with increasing amounts and

Table 10 Effect of different ratios of DHA and EPA on the fatty acid composition (%) of serum in cobia juveniles fed for 8 weeks

Fatty acid	Diet								
	Initially	0	1	2	3	4	5	6	7
14:00	1.32 ± 0.14 ^a	0.66 ± 0.10 ^b	1.05 ± 0.23 ^{ab}	0.85 ± 0.48 ^{ab}	0.91 ± 0.26 ^{ab}	0.73 ± 0.08 ^{ab}	0.76 ± 0.16 ^{ab}	0.71 ± 0.13 ^{ab}	0.76 ± 0.20 ^{ab}
16:00	27.99 ± 1.09 ^a	21.85 ± 0.32 ^b	21.53 ± 0.74 ^b	20.67 ± 2.13 ^b	20.39 ± 0.87 ^b	20.97 ± 0.42 ^b	21.12 ± 0.77 ^b	19.21 ± 3.09 ^b	19.09 ± 2.04 ^b
18:00	18.98 ± 1.69 ^a	11.29 ± 0.55 ^b	10.58 ± 1.27 ^b	10.01 ± 1.44 ^b	9.87 ± 0.49 ^b	10.49 ± 0.77 ^b	10.72 ± 1.19 ^b	8.84 ± 2.64 ^b	8.90 ± 0.86 ^b
20:00	nd	nd	nd	nd	nd	nd	nd	0.21 ± 0.18	0.10 ± 0.17
22:00	2.11 ± 0.26 ^a	0.54 ± 0.47 ^b	0.81 ± 0.15 ^b	0.72 ± 0.18 ^b	0.78 ± 0.08 ^b	0.75 ± 0.05 ^b	0.89 ± 0.21 ^b	0.69 ± 0.37 ^b	0.72 ± 0.23 ^b
∑SFA	50.39 ± 2.62 ^a	34.34 ± 0.89 ^b	33.97 ± 2.36 ^b	32.25 ± 3.95 ^b	31.94 ± 1.66 ^b	32.94 ± 1.12 ^b	33.49 ± 2.26 ^b	29.66 ± 6.02 ^b	29.57 ± 3.17 ^b
14:1	nd	0.31 ± 0.28	0.15 ± 0.27	0.42 ± 0.45	0.47 ± 0.17	0.47 ± 0.46	0.29 ± 0.25	0.17 ± 0.15	0.41 ± 0.48
16:1n-7	0.33 ± 0.57	0.85 ± 0.13	0.81 ± 0.09	0.40 ± 0.35	0.68 ± 0.10	0.53 ± 0.01	0.67 ± 0.12	0.55 ± 0.48	0.70 ± 0.14
20:1n-9	nd	2.18 ± 0.25	1.87 ± 0.16	1.78 ± 0.11	1.97 ± 0.26	1.73 ± 0.04	1.94 ± 0.17	2.09 ± 0.39	2.13 ± 0.46
18:1n-9	9.60 ± 0.48 ^b	15.59 ± 0.89 ^a	14.14 ± 2.36 ^a	13.25 ± 1.13 ^{ab}	14.23 ± 1.33 ^a	13.35 ± 0.08 ^{ab}	13.46 ± 0.53 ^{ab}	14.99 ± 1.68 ^a	14.72 ± 2.34 ^a
22:1n-11	nd	0.70 ± 0.05	0.86 ± 0.06	0.41 ± 0.36	0.82 ± 0.09	0.65 ± 0.15	0.80 ± 0.09	0.57 ± 0.49	0.46 ± 0.41
∑MUFA	9.93 ± 0.48 ^b	19.62 ± 1.39 ^a	17.83 ± 2.16 ^a	16.25 ± 1.40 ^a	18.16 ± 1.53 ^a	16.73 ± 0.68 ^a	17.17 ± 0.67 ^a	18.37 ± 3.18 ^a	18.42 ± 2.89 ^a
16:2n-4	nd	nd	nd	0.14 ± 0.24	0.16 ± 0.27	nd	0.14 ± 0.25	0.26 ± 0.26	0.28 ± 0.25
18:2n-6	7.50 ± 0.65 ^b	16.80 ± 0.82 ^{ab}	12.97 ± 0.52 ^a	14.97 ± 2.28 ^a	16.13 ± 2.00 ^a	14.95 ± 0.85 ^a	15.28 ± 1.26 ^a	18.12 ± 4.27 ^a	17.86 ± 3.85 ^a
20:4n-6	1.21 ± 0.25 ^{ab}	0.82 ± 0.01 ^c	1.37 ± 0.04 ^a	1.04 ± 0.10 ^{abc}	1.20 ± 0.04 ^{ab}	1.07 ± 0.18 ^{abc}	1.03 ± 0.10 ^{abc}	0.80 ± 0.09 ^c	0.86 ± 0.17 ^{bc}
22:2n-6	nd	0.57 ± 0.53	0.91 ± 0.12	1.17 ± 0.31	0.96 ± 0.28	1.22 ± 0.22	1.08 ± 0.26	1.08 ± 0.16	1.25 ± 0.44
∑n-6PUFA	8.71 ± 0.48 ^b	18.19 ± 0.35 ^a	15.25 ± 0.41 ^a	17.19 ± 1.89 ^a	18.29 ± 1.68 ^a	17.25 ± 0.51 ^a	17.39 ± 1.22 ^a	19.99 ± 4.09 ^a	19.97 ± 3.36 ^a
18:3n-3	1.41 ± 0.10	1.64 ± 0.08	1.62 ± 0.10	1.66 ± 0.21	1.57 ± 0.11	1.62 ± 0.11	1.61 ± 0.13	1.80 ± 0.23	1.71 ± 0.25
22:5n-3	0.43 ± 0.75	0.73 ± 0.11	0.70 ± 0.12	0.73 ± 0.05	0.70 ± 0.00	0.66 ± 0.06	0.66 ± 0.06	0.68 ± 0.06	0.74 ± 0.10
22:6n-3	18.81 ± 1.72 ^b	19.63 ± 3.00 ^{ab}	22.08 ± 0.71 ^{ab}	24.62 ± 1.34 ^a	22.35 ± 1.45 ^{ab}	24.06 ± 1.27 ^{ab}	22.97 ± 1.73 ^{ab}	23.35 ± 1.63 ^{ab}	23.84 ± 2.79 ^{ab}
20:5n-3	3.35 ± 0.67 ^{bc}	2.38 ± 0.53 ^c	4.77 ± 0.13 ^a	3.72 ± 0.30 ^{ab}	3.87 ± 0.18 ^{ab}	3.56 ± 0.27 ^b	3.52 ± 0.10 ^b	3.05 ± 0.28 ^{bc}	3.03 ± 0.58 ^{bc}
∑n-3PUFA	24.00 ± 2.18 ^b	24.38 ± 3.21 ^b	29.19 ± 0.98 ^{ab}	30.73 ± 1.28 ^a	28.49 ± 1.32 ^{ab}	29.90 ± 1.10 ^{ab}	28.77 ± 1.59 ^{ab}	28.88 ± 1.19 ^{ab}	29.33 ± 2.91 ^a
∑PUFA	32.71 ± 3.05 ^c	42.57 ± 2.92 ^b	44.44 ± 1.30 ^a	47.92 ± 3.16 ^{ab}	46.78 ± 0.46 ^{ab}	47.15 ± 1.57 ^{ab}	46.16 ± 1.63 ^{ab}	48.88 ± 2.92 ^{ab}	49.29 ± 0.82 ^a
∑n-3HUFA	22.60 ± 3.10 ^b	22.74 ± 3.17 ^b	27.56 ± 0.93 ^{ab}	29.07 ± 1.12 ^a	26.92 ± 1.43 ^{ab}	28.29 ± 1.06 ^{ab}	27.16 ± 1.71 ^{ab}	27.08 ± 1.34 ^{ab}	27.61 ± 3.16 ^{ab}
n-3/n-6	2.77 ± 0.45 ^a	1.34 ± 0.20 ^b	1.91 ± 0.05 ^b	1.80 ± 0.13 ^b	1.57 ± 0.23 ^b	1.73 ± 0.03 ^b	1.66 ± 0.17 ^b	1.50 ± 0.41 ^b	1.51 ± 0.41 ^b
DHA + EPA	22.16 ± 2.39 ^b	22.01 ± 3.25 ^b	26.86 ± 0.83 ^{ab}	28.34 ± 1.10 ^a	26.22 ± 1.43 ^{ab}	27.62 ± 1.07 ^{ab}	26.50 ± 1.74 ^{ab}	26.40 ± 1.41 ^{ab}	26.87 ± 3.26 ^{ab}
DHA/EPA	5.70 ± 0.65 ^{ab}	8.50 ± 2.38 ^a	4.63 ± 0.05 ^b	6.67 ± 0.88 ^{ab}	5.78 ± 0.50 ^{ab}	6.80 ± 0.87 ^{ab}	6.52 ± 0.50 ^{ab}	7.73 ± 1.23 ^a	7.98 ± 0.99 ^a

All above data are mean ± SD (n = 3 × 3). Different superscript letters in the same row indicate significant differences (P < 0.05)

N-6 PUFAs include 18:2n-6, 20:2n-6, 20:4n-6, 22:2n-6 here; N-3 PUFAs include 18:3n-3, 18:4n-3, 20:3n-3, 20:5n-3, 22:3n-3, 22:5n-3, 22:6n-3 here; N-3 HUFA include 20:5n-3, 22:5n-3, 22:6n-3 here

tr Trace (peak area <0.05%); nd not detected; Initially means in the week 0

higher ratios of DHA and EPA in their diets, while EPA decreased in the experiment (Tables 7, 8, 9).

Different ratios and amounts of DHA and EPA could directly influence the composition of fatty acids in the tissues of cobia juvenile. In the muscle and liver of cobia juveniles, the amount and ratio of DHA and EPA increased with their increase in the diet since cobia juveniles absorbed n-3 HUFAs in the diet to increase the contents in their tissues. Dietary nutrients have been proved to be effectively incorporated into the tissues of fish, resulting in the change of biochemical composition and growth performance of the fish [19, 46–49]. HUFAs, especially DHA and EPA, have effects not only on biological and physiological conditions, but also on fatty acid profiles of the fish tissues [50, 51]. Fatty acid composition of fish muscle lipids usually reflects that of the lipids in their feed [19, 52–55]. Our results are in agreement with previous reports that dietary EPA and DHA concentrations show good correlations with tissue concentrations of DHA and EPA [56].

In addition, the DHA/EPA ratio could be increased by conversion of EPA to DHA, by a greater reduction of EPA relative to DHA in the effects of selective HUFA deposition in the tissues or higher oxidation of EPA relative to DHA. These changes resulted in no significant differences being found among the lipid contents in the same organ of cobia juveniles fed different diets ($P > 0.05$).

The fact that PUFAs, including the amount and the ratio of DHA to EPA, varied in the serum implied that the composition of fatty acids was unstable in the serum and was sensitively influenced by diets and free endogenesis fatty acids. This might relate to the difference in the functions and enzymes in the serum in comparison to those of the muscle and liver in cobia juveniles [15, 57].

Acknowledgments Authors would like to give thanks for the help given by the staff of the institutes involved. This research was financially supported by a grant from the National Natural Science Foundation of China (30571448), a NSFA-RSE international grant fund (30711130272), a Ph.D. station fund from the Education Ministry (20060560001), natural science funds of Guangxi (Gui-ke-zi 0728014, 0728011) and key funds of Guangxi University (CC 150008, 150009).

References

1. Simopoulos AP (2000) Human requirements for n-3 polyunsaturated fatty acids. *Poult Sci* 79:961–970
2. Nugent AP (2004) The metabolic syndrome. *Food Nutr Bull* 29:36–43
3. Graham IA, Cirpus P, Rein D, Napier JA (2004) The use of very long chain polyunsaturated fatty acids to ameliorate metabolic syndrome: transgenic plants as an alternative sustainable source to fish oils. *Food Nutr Bull* 29:228–233
4. Sargent JR, Tocher DR, Bell JG (2002) The lipid. In: Halver JE, Hardy RW (eds) *Fish nutrition*, 3rd edn. Elsevier, USA, pp 181–257
5. Li YY, Chen WZ, Sun ZW, Chen JH, Wu KG (2005) Effects of n-3 HUFA content in broodstock diet on spawning performance and fatty acid composition of eggs and larvae in *Plectorhynchus cinctus*. *Aquaculture* 245:263–272
6. Rodríguez C, Acosta C, Badia P, Cejas JR, Santamaria FJ, Lorenzo A (2004) Assessment of lipid and essential fatty acids requirements of black seabream (*Spondyliosoma cantharus*) by comparison of lipid composition in muscle and liver of wild and captive adult fish. *Comp Biochem Physiol B Biochem Mol Biol* 139:619–629
7. Xu Y, Ding Z (2005) Studies on metabolism of astaxanthin in fish. In: Wang QY (ed) *Theory and techniques for ecological aquaculture in sea water*. Sea Publisher, Beijing, pp 203–205
8. Xu Y, Zheng Z, Ding Z (2006) Studies on the culture and assorted feed of cobia (*Rachycentron canadum*). *Fish Sci* 25(1):34–36
9. Hong J, Om AD, Umino T, Yoshimatsu T, Nakagawa H, Asano M, Nakagawa A (2007) Effect of dietary laurate on lipid metabolism and vitality in juvenile red sea bream (*Pagrus major*). *Acta Oceanol Sin* 26(1):112–121
10. Tocher DR, Leaver MJ, Hodgson P (1998) A recent advances in the biochemistry and molecular biology of fatty acyl desaturases. *Lipid Res* 37:73–117
11. Johnson GH (2001) A fish story-essential fatty acid requirements during infancy. *InTouch* 18(3):1–2
12. Masuda R, Ziemann DA, Ostrowski AC (2001) Patchiness formation and development of schooling behavior in Pacific threadling, *Polydactylus sexfilis* reared with different dietary highly unsaturated fatty acids contents. *J World Aquac Soc* 32:309–316
13. Ibeas JJ, Lozano I, Perdignes F, Jimenez J (1997) Dynamics of flor yeast populations during the biological aging of sherry wines. *Am J Enol Vitic* 48:75–79
14. Lee SM (2001) Review of the lipid and essential fatty acids requirements of rockfish (*Sebastes schlegeli*). *Aquac Res* 32(Suppl L):8–17
15. Wu FC, Ting YY, Chen HY (2002) Docosahexaenoic acid is superior to Eicosapentaenoic acid as the essential fatty acid for growth of grouper, *Epinephelus malabaricus*. *J Nutr* 132:72–79
16. Furuita H, Konishi K, Takeuchi T (1999) Effect of different levels of eicosapentaenoic acid and docosahexaenoic acid in *Artemia nauplii* on growth, survival and salinity tolerance of larvae of the Japanese flounder, *Paralichthys olivaceus*. *Aquaculture* 170:59–69
17. Sargent J, McEvoy L, Estevez A, Bell G, Bell M, Henderson J, Tocher D (1999) Lipid nutrition of marine fish during early development: current status and future directions. *Aquaculture* 179:217–229
18. Lee SM, Lee JH, Kim KD (2003) Effect of dietary essential fatty acids on growth, body composition and blood chemistry of juvenile starry flounder (*Platichthys stellatus*). *Aquaculture* 225:269–281
19. Sargent JR, Bell JG, McEvoy LA, Tocher DR, Estevez A (1999) Recent developments in the essential fatty acid nutrition of fish. *Aquaculture* 177:191–199
20. Takeuchi T (1997) Essential fatty acid requirements of aquatic animals with emphasis on fish larvae and fingerlings. *Rev Fish Sci* 5:1–25
21. Brown-Peterson NJ, Overstreet RM, Lotz JM, Franks JS, Burns KM (2001) Reproductive biology of cobia, *Rachycentron canadum*, from coastal waters of the southern United States. *Fish Bull* 99:15–28
22. Cynthia K, Faulk A, Joan HG (2003) Lipid nutrition and feeding of cobia (*Rachycentron canadum*) larvae. *J World Aquac Soc* 34(3):368–378
23. Chou RL, Su MS, Chen HY (2001) Optimal dietary protein and lipid levels for juvenile cobia (*Rachycentron canadum*). *Aquaculture* 193:81–89

24. Folch J, Less M, Sloane SGH (1957) A simple method for the isolation for and purification of total lipids from animal tissues. *J Biol Chem* 226:497–509
25. Association of Official Analytical Chemists (1980) Official methods of analysis, 13th edn. AOAC, Washington
26. Takeuchi T, Shiina Y, Watanabe T (1992) Suitable levels of n-3 highly unsaturated fatty acids in diet for fingerlings of red sea bream. *Nippon Suisan Gakkaishi (Bull Jpn Soc Sci Fish)* 58(3):509–514
27. Takeuchi T, Shiina Y, Watanabe T, Sekiya S, Imaizumi K (1992) Suitable levels of n-3 highly unsaturated fatty acids in diet for fingerlings of yellowtail. *Nippon Suisan Gakkaishi (Bull Jpn Soc Sci Fish)* 58(7):1341–1346
28. Rodríguez C, Pérez JA, Diaz M, Izquierdo MS, Fernandez-Palacios H, Lorenzo A (1997) Influence of EPA/DHA ratio in rotifers on gilthead sea bream (*Sparus aurata*) larval development. *Aquaculture* 150:77–89
29. Lochman RT, Gatlin DM (1993) Essential fatty acid requirement of juvenile red drum (*Sciaenops ocellatus*). *Fish Physiol Biochem* 12:221–235
30. Furuita H, Tanaka H, Yamamoto Y, Suzuki N, Takeuchi T (2002) Effects of high levels of n-3 HUFA in brood stock diet on egg quality and egg fatty acid composition of Japanese flounder (*Paralichthys olivaceus*). *Aquaculture* 210:323–333
31. Ibeas C, Rodríguez C, Badia P, Cejas JR, Santamaría FJ, Lorenzo A (2000) Efficacy of dietary methyl esters of n-3 HUFA vs. triacylglycerols of n-3 HUFA by gilthead bream (*Sparus aurata* L.) juveniles. *Aquaculture* 190:273–287
32. Wagner M, Durbin E, Buckley L (1998) RNA:DNA ratios as indicators of nutritional condition in the copepod *Calanus finmarchicus*. *Mar Ecol Prog Ser* 162:173–181
33. Buckley L, Caldarone E, Ong TL (1999) RNA–DNA ratio and other nucleic acid-based indicators for growth and condition of marine fishes. *Hydrobiologia* 401:265–277
34. Meng L, Taylor DL, Serbst J, Powell JC (2008) Assessing habitat quality of Mount Hope Bay and Narragansett Bay using growth, RNA:DNA, and feeding habits of caged juvenile winter flounder (*Pseudopleuronectes americanus* Walbaum). *North East Nat* 15(1):35–56
35. Rooker JR, Holt GJ (1996) Application of RNA:DNA ratios to evaluate the condition and growth of larval and juvenile red drum (*Sciaenops ocellatus*). *Mar Freshw Res* 47:283–290
36. Chicharro MA (1998) Nutritional condition and starvation in *Sardina pilchardus* (L.) larvae off southern Portugal compared with some environmental factors. *J Exp Mar Biol Ecol* 225:123–137
37. Peck MA, Buckley LJ, Caldarone EM, Bengtson DA (2003) Effects of food consumption and temperature on growth rate and biochemical-based indicators of growth in early juvenile Atlantic cod *Gadus morhua* and haddock *Melanogrammus aeglefinus*. *Mar Ecol Prog Ser* 251:233–243
38. Tanaka Y, Satoh K, Yamada H, Takebe T, Nikaido H, Shiozawa S (2008) Assessment of the nutritional status of field-caught larval Pacific bluefin tuna by RNA/DNA ratio based on a starvation experiment of hatchery-reared fish. *J Exp Mar Biol Ecol* 354(1):56–64
39. Glémet H, Rodríguez MA (2007) Short-term growth (RNA/DNA ratio) of yellow perch (*Perca flavescens*) in relation to environmental influences and spatio-temporal variation in a shallow fluvial lake. *Can J Fish Aquat Sci* 64(12):1646–1655(10)
40. Vinagre C, Fonseca V, Maia A, Amara R, Cabral H (2008) Habitat specific growth rates and condition indices for the sympatric soles *Solea solea* (Linnaeus, 1758) and *Solea senegalensis* Kaup 1858, in the Tagus estuary, Portugal, based on otolith daily increments and RNA–DNA ratio. *Zeitschrift fur Angewandte Ichthyologie* 24(2):163–169
41. Masuda Y, Oku H, Okumura T, Nomura K, Kurokawa T (2009) Feeding restriction alters expression of some ATP related genes more sensitively than the RNA/DNA ratio in zebrafish, *Danio rerio*. *Comp Biochem Physiol B Biochem Mol Biol* 152(3):287–291
42. Tomas OH, Gorokhova E, Hansson S (2008) RNA:DNA ratios of Baltic herring larvae and copepods in embayment and open sea habitats. *Estuar Coast Shelf Sci* 76:29–35
43. Cavalier-Smith T (1978) Nuclear volume control by nucleoskeletal DNA, selection for cell volume and cell growth rate and the solution of the DNA-c value paradox. *J Cell Sci* 34:247–278
44. Mustafa S (1977) Influence of maturation on the concentrations of RNA and DNA in the fish of the catfish *Clarius batrachus*. *Trans Am Fish Soc* 106:449–455
45. Liu CQ (2006) Study on the relationship between RNA/DNA ratio and the growth of Japanese shrimp. *J Hebei Univ* 26(5):524–528
46. Bell JG, Henderson RJ, Tocher DR, Mcghee F, Dick JR, Porter A, Smullen RP, Sargent JR (2002) Substituting fish oil with crude palm oil in the diet of Atlantic salmon (*Salmo salar*) affects muscle fatty acid composition and hepatic fatty acid metabolism. *J Nutr* 132:222–230
47. Tocher DR, Bell JG, Dick JR, Crampton VO (2003) Effect of dietary vegetable oil on Atlantic salmon hepatocyte fatty acid desaturation and liver fatty acid compositions. *Lipids* 38:723–732
48. Figueiredo-Silva A, Rocha E, Dias J, Silva P, Rema P, Gomes E, Valente LMP (2005) Partial replacement of fish oil by soybean oil on lipid distribution and liver histology in European sea bass (*Dicentrarchus labrax*) and rainbow trout (*Oncorhynchus mykiss*) juveniles. *Aquac Nutr* 11:147–155
49. Schulz C, Knaus U, Wirth M, Rennert B (2005) Effects of varying dietary fatty acid profile on growth performance, fatty acid, body and tissue composition of juvenile pike perch (*Sander lucioperca*). *Aquac Nutr* 11:403–413
50. Ishizaki Y, Uematsu K, Takeuchi T (2000) Preliminary study of the effect of dietary docosahexaenoic acid on the volumetric growth of the brain in larval yellowtail. *Fish Sci* 66:611–613
51. Montero D, Robaina LE, Socorro J, Vergara JM, Tort L, Izquierdo MS (2001) Alternation of liver and muscle fatty acid composition in gilthead sea bream (*Sparus aurata*) juveniles held at high stocking density and fed an essential fatty acid deficient diet. *Fish Physiol Biochem* 24:63–72
52. Kamler E, Krasicka B, Rakusa-Suszczewski S (2001) Comparison of lipid content and fatty acid composition in muscle and liver of two notothenioid fishes from Admiralty Bay (Antarctica): an eco-physiological perspective. *Polar Biol* 24:735–743
53. Glencross BD, Hawkins W, Curnow J (2003) Evaluation of canola oils as alternative lipid resources in diets for juvenile red sea bream, *Pagrus auratus*. *Aquac Nutr* 9:305–315
54. Glencross BD, Hawkins W, Curnow J (2003) Restoration of the fatty acid composition of red sea bream (*Pagrus auratus*) using a fish oil finishing diet after grow-out on plant oil based diets. *Aquac Nutr* 9:409–418
55. Martínez-Lioren S, Vidal AT, Monino AV, Torres MP, Cerda MJ (2007) Effects of dietary soybean oil concentration on growth, nutrient utilization and muscle fatty acid composition of gilthead sea bream (*Sparus aurata* L.). *Aquac Res* 38:76–81
56. Wu FC, Ting YY, Chen HY (2003) Dietary docosahexaenoic acid is more optimal than eicosapentaenoic acid affecting the level of cellular defence responses of the juvenile grouper *Epinephelus malabaricus*. *Fish Shellfish Immunol* 14:223–238
57. Ding Z, Xu Y (2004) Traced studies on metabolism of astaxanthin in Atlantic salmon (*Salmo salar*). *J Exp Zool* 301A:317–323

The intention in this work is to study the chemical changes taking place in glycerides containing 18:2 fatty acids, namely trilinolein and trilinoelaidin during thermal induction in inert atmosphere. This study would give understanding of the quantities of the isomers formed, the chemistry of isomerization and the relative stability of the fatty acid molecules towards isomerization. Reports involving the analysis of products formed from the glycerides containing 18:2 fatty acids during thermal induction are scarce in the literature. Furthermore, there are no reports in the literature regarding thermal induction of 18:2 fatty acids with *trans*, *trans* configuration. The published literature only deals with the chemical analysis of the mixture formed during heating of edible fats in the temperature range 240–265 °C [15–17]. The analysis in one of the reports [15] was carried out for the purpose of determining kinetic parameters for the *cis*–*trans* isomerization of linoleic acid. The acids analyzed were only 9t12t, 9c12t and 9t12c. There was no mention about the other products formed during heating. Here, the assumption was that the formation of 9t12t, 9c12t and 9t12c were purely from 9c12c fatty acid. The second paper [16] reports the appearance of the individual isomers during heat induced isomerization of α -linolenic acid. The effect of temperature and heating time were study parameters in this report. In both reports, the identification of isomers was carried out from the total chromatogram of the fatty acid methyl esters (FAME) of the fatty acids in the samples. The third report [17] deals with the quantification of *cis*/*trans* isomerization in triolein, trilinolein, trilinolenin during heat induction. The maximum heating time was 8 h and the *trans* isomer formation in trilinolein was not significant. Furthermore, there was no attempt to look at the chemistry of the formation of the *trans* isomers in the heated mixture.

When the fatty acids in the glyceride molecules are identical, then analysis of the glyceride for products after heating becomes comparatively easy. Trilinolein and trilinoelaidin are glycerides of 18:2 (9, 12) fatty acids with *cis*, *cis* and *trans*, *trans* configurations respectively. The acid molecules in the glyceride backbone are of definitive structure and the products formed should originate from these acid molecules. This will give understanding of the changes taking place and how the molecules behave under thermal stress.

The major products formed during thermal induction of the triglyceride samples were mixtures of isomers with *cis* or *trans* hydrogens on the double bonds in trilinolein and trilinoelaidin. These were analysed by two different techniques namely gas chromatography and infrared spectroscopy. The use of infrared spectroscopy and gas chromatography to determine the *trans* content in edible oils and fats have been extensively investigated and they are standardized by The American Oil Chemists Society

(AOCS) [18]. The quantitative determination of *trans* fatty acid concentration in fats and oils is based on the fact that the *trans* isomers of monounsaturated fatty acids and *trans* isomers of the polyunsaturated fatty acids containing isolated *cis*–*trans*, *trans*–*cis* and *trans*–*trans* double bonds give rise to one specific absorption at 969 cm^{-1} [19–22]. Conjugated linoleic acids (CLAs) with *cis*, *trans* and *trans*, *cis* configurations give rise to two specific absorptions around 986 and 946 cm^{-1} . These absorptions arise due to the =CH out of plane deformation vibration [23]. The =CH out of plane deformation vibration of the *tt* (*trans*, *trans*) isomers absorb around 982 cm^{-1} and, *cis*–*cis* isomers do not absorb in this region. This characteristic difference in the absorptions makes it possible to quantify methylene interrupted *trans* isomers and CLA isomers with *cis*, *trans* and *trans*, *cis* configurations using infrared spectroscopy. Christy et al. [24] have utilized this fact in simultaneous quantification of isolated *trans*, and CLAs in oils and fats. Furthermore, the presence of absorption peaks at 986 and 946 cm^{-1} of the fatty acids formed during the isomerization is a clear indication of the formation of CLA isomers containing *cis*, *trans* and *trans*, *cis* configurations.

Gas chromatography involves saponification and derivatization of the oil or fat involved and the separation of the methyl esters using a high resolution capillary column that is suitable for the separation of isomers. Quantification of different isomer components is carried out using Standards of fatty acids methyl esters and literature references [25].

Experimental

Samples and Methods

The triglycerides of 9t12t and 9c12c fatty acids and the methyl esters of the same fatty acids were purchased from Sigma-Aldrich. The methyl esters containing the 9c11t and 10t12c (99%) fatty acids were purchased from Larodan Chemicals, Sweden.

The heating experiments were carried out in micro glass ampules with a length of 4 cm. These were made from glass tubes of 1.5 mm internal diameter and a wall thickness of 1 mm. The triglyceride samples containing the 9c12c fatty acid were injected in the tubes using a plastic syringe and each sample was flushed by a weak nitrogen flow. The open end of the glass tubes were melted and sealed. In the presence of air, the samples undergo oxidation and polymerization. The ampules containing the samples were then placed in a short glass vial and placed in a chromatographic oven set at 250 °C. Thermally induced samples were removed from the oven at regular intervals, cut open, their infrared spectrum recorded, sealed again by paraffin film and stored in darkness for the analysis by gas

chromatography at the end of the thermal induction experiment. The experiments were repeated with the triglyceride of the 9t12t fatty acid.

Infrared Spectroscopic Measurements

Each of the samples removed from the oven was subjected to infrared measurements. A Perkin Elmer Spectrum One FT-IR spectrometer equipped with a Harrick single reflectance attenuated total internal reflectance (ATR) accessory and lead glycine sulfate detector was used in measuring the infrared spectra. Each sample was spread on the ATR crystal using a capillary glass tube. The blunt side of the capillary tube was used to pick up a small amount of the sample and spread on the ATR plate. A background spectrum was scanned in the range of 4,000–600 cm^{-1} before the application of a sample. A total of 30 scans at a resolution of 4 cm^{-1} were then measured on each sample. The ATR crystal was washed with dichloromethane and acetone after each measurement. The same procedure was repeated for the thermally induced 9t12t LA samples. All the infrared spectra were saved in absorbance format. The spectra were then doubly derived and used in the quantitative analysis.

Gas Chromatographic Analysis

The remaining glyceride samples containing 9c12c and 9t12t fatty acids after the infrared analysis were subjected to derivatization. Each glass tube containing the sample was cut just above the liquid mark and crushed inside a 15-ml test tube. To each test tube was then added 2 ml of 0.5 M sodium methanolic sodium hydroxide and placed in a water bath at 60 °C for 15 min. After cooling, 2-ml portions of BF_3 /methanol were added to the solutions in the test tubes and placed in the water bath again for 10 min. To the solutions in each test tube was then added a 2-ml portion of a saturated solution of NaCl followed by a 1-ml portion of heptane and the resultant mixture well shaken to aid separation and dissolution of the FAMES in the heptane layer. After a few minutes standing, anhydrous magnesium sulphate powder was added to the top heptane layers in the test tubes. The heptane layers from the test tubes were extracted, placed in small brown vials and stored in dark for gas chromatographic analysis.

The GC analysis of the methyl esters of the fatty acids resulting from the thermal induction was carried out by using a Hewlett Packard 5890 gas chromatograph equipped with a 100-m capillary column with 0.25 mm internal diameter coated with a 0.20- μm thick 90%-bis-(cyano-propyl)-methyl polysiloxane stationary phase (HP 88). A temperature program involving two step gradients was used. The program started with 1 min at an initial

temperature of 150 °C and followed by a temperature gradient of 5 °C min^{-1} to reach a temperature of 180 °C. After 50 min at 180 °C another temperature gradient of 5 °C min^{-1} was used to bring the final temperature to 220 °C. The temperature was held at 220 °C for 30 min giving a total running time of 95 min for each sample.

Results and Discussion

Infrared Spectroscopy

The thermal induction of 9c12c fatty acid is expected to give 9c12t, 9t12c and 9t12t isomers. In addition to these, decomposition and formation of CLA isomers can also be expected [26, 27]. The positional isomers containing *trans* configurations are expected to absorb at 969 cm^{-1} in the infrared because of the =CH *trans* bending vibrations. The infrared spectra measured on the thermally induced samples of trilinolein and trilinoelaidin are given in Fig. 1. The figures clearly show that the peak at 969 cm^{-1} increases with time in the case of trilinolein samples and decreases with time in the case of trilinoelaidin samples. The transformation of fatty acid chains is clearly evident in both cases. The trilinolein has a weak absorption around 3,004 cm^{-1} because of the =CH stretching modes. This absorption decreases as the fatty acid moieties in the trilinolein molecules isomerize.

The formation of CLAs in the heated samples of 9c12c fatty acid has been demonstrated by Destailats and Angers [26]. There is also evidence in the infrared spectra of the

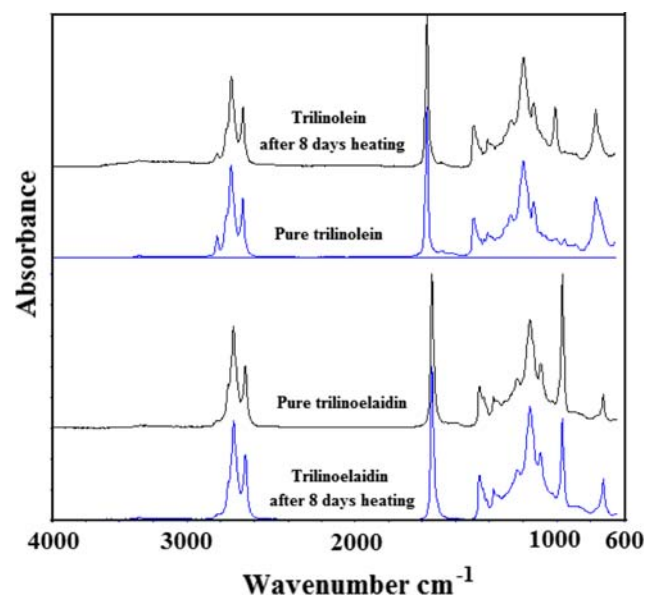


Fig. 1 Infrared spectra of heated samples of trilinolein and trilinoelaidin. The spectra are scale adjusted for clarity

heated samples for the formation of CLAs. There are humps on both sides of the peak at 969 cm^{-1} which become clearly evident in the fourth derivative spectra of the heated samples of trilinolein (Fig. 2). The peaks at 987 and 946 cm^{-1} are characteristic to CLAs. The formation of CLAs in the heated samples of trilinoelaidin has been shown by Christy [8] in a recent report. The fourth derivative spectrum of the heated sample of trilinoelaidin shows absorptions at 989 , 969 and 946 cm^{-1} . The peaks at 989 and 946 cm^{-1} indicate the presence of CLAs in the heated sample. The slight shift in the peak at 989 cm^{-1} indicates the presence *trans, trans* isomers in the mixture of the CLAs formed. The CLAs in the heated sample are a mixture of *c,tt,c* and *t,t* isomers of CLAs with a high percentage of *t, t* isomers. The peak at 969 cm^{-1} indicates the presence of *t, c* or *c, t* or *t, t* LAs or mixture of these isomers.

Gas Chromatography

The gas chromatograms of the FAME of the heat-treated trilinolein and trilinoelaidin are shown in Figs. 3 and 4, respectively. The concentrations of the isomers from both trilinolein and trilinoelaidin are presented in Fig. 5. The FAME profiles are very different for these samples. The 9c12c fatty acid readily isomerizes to 9c12t and 9t12c isomers. Furthermore, isomerization into 9t12t isomer seems to be very slow. In contrast to this, the isomerization of 9t12t fatty acid into the 9c12t, 9t12c and 9c12c isomers is much slower.

The 9c12t and 9t12c isomers in heat-treated trilinolein are equal in concentration. This fact proves that the isomerization of the 9,12 double bonds in 9c12c fatty acids are equally probable. However, heat-treated trilinoelaidin gives different concentration profiles for 9c12t and 9t12c isomers with relatively higher concentrations of 9t12c

compared to 9c12t isomers in all the heated samples of trilinoelaidin. Formation of different concentrations of 9t12c and 9c12t isomers imply that the double bonds in the 9t12t molecules are perturbed by the neighboring molecules or groups. The absolute lower concentrations of 9t12c, 9c12t and 9c12c isomers in the heated samples of trilinoelaidin show the stability of 9t12t double bonds towards isomerization.

These results enable the depiction of an energy diagram for the isomerization (Fig. 6). The isomerization of 9t12t fatty acid into 9c12t and 9t12c isomers requires higher activation energy. Furthermore, the isomerization of 9t12t fatty acid into 9t12c requires relatively lower activation energy compared to the isomerization into 9c12t. It is not clear why the isomerization of 9t12c requires lower activation energy. A theoretical approach is necessary to resolve this question.

Apart from positional isomerization, heat induction of trilinolein and trilinoelaidin also forms CLAs [8, 26, 27]. The CLA profiles produced in these thermal induction reactions are identical [8]. The top parts of the Figs. 3 and 4 show the CLA isomers produced in trilinolein and trilinoelaidin during thermal induction. The concentrations of total CLAs and the concentration of *trans, trans* CLAs within the total CLAs are shown in Fig. 7. The bar diagrams show the increase in concentration of CLAs during thermal induction of trilinolein and trilinoelaidin. The relative total concentration of CLAs in the heated samples approaches a maximum of around 5%. When the degradation of the trilinoelaidin (Fig. 8) is taken into account, the concentration of the total CLA in the heated trilinoelaidin amounts to around 2.2%. At the same time when the degradation of trilinolein (Fig. 8) is taken into account, the concentration of CLAs in the heated glyceride samples of 9c12c fatty acids amounts to around 3.3%. The relative concentration of *t, t* CLA isomers which elute together amounts to around 60% in all the heated samples.

The mechanism of formation of CLAs from heat induced 9c12c fatty acids has been described in detail elsewhere [26]. The same mechanisms can also be applied to the formation of CLAs from heat induced isomerization of 9t12t fatty acids [8]. Conjugated 9t11t and 10t12t fatty acids are formed as primary products through either (1) A free radical chain reaction mechanism or (2) An intramolecular [1, 3] sigmatropic rearrangement mechanism. All the other isomers of the CLAs are formed from these primary products through a series of positional isomerization and [1, 5] sigmatropic rearrangements [8].

Gas Chromatography and Infrared Spectrometry

As mentioned earlier, the acid molecules in the trilinolein and trilinoelaidin undergo degradation and a part of the

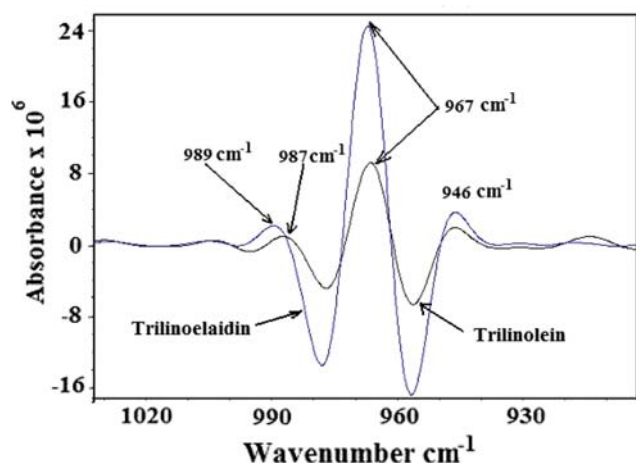


Fig. 2 Fourth derivative spectra of trilinoelaidin and trilinolein

Fig. 3 Gas chromatograms of FAMES of the heated trilinolein samples. The *top window* shows the elution order of CLAs formed during heating (Reprinted from Christy [8] with permission from Elsevier)

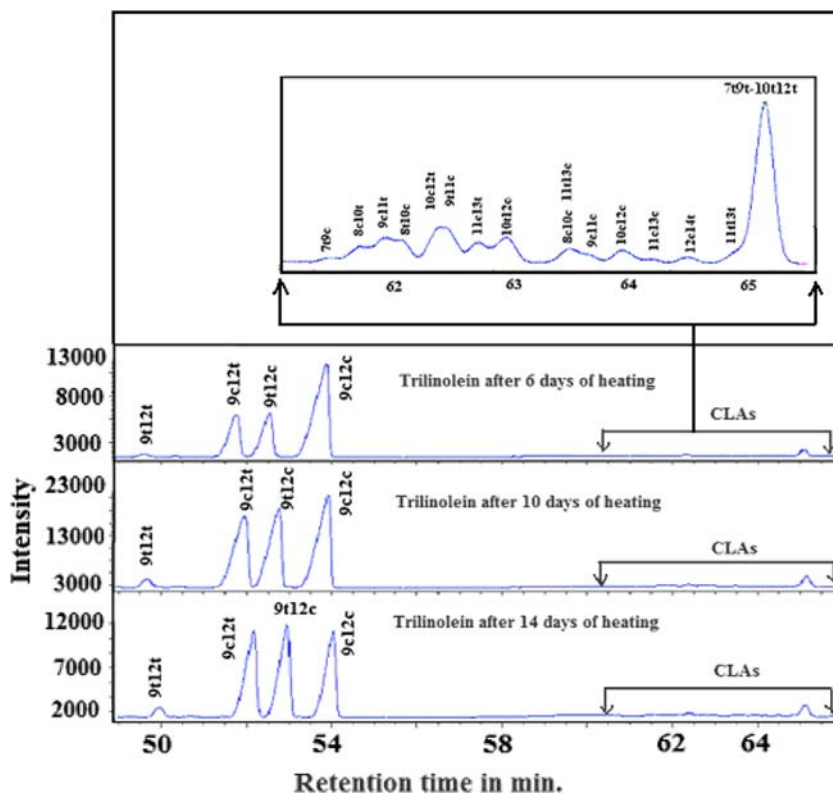
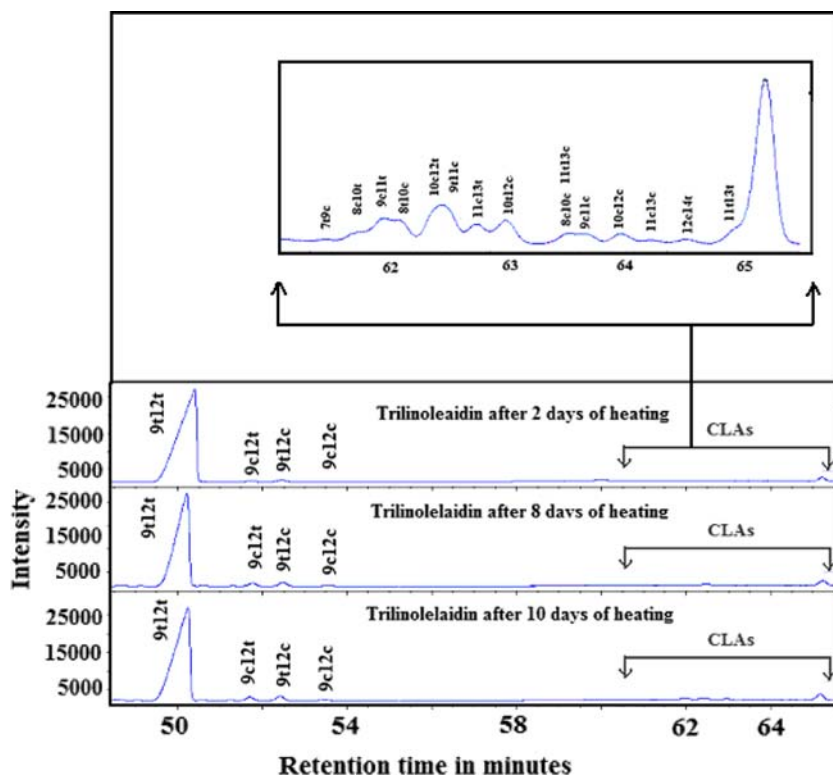


Fig. 4 Gas chromatograms of FAMES of the heated trilinoelaidin samples. The *top window* shows the elution order of CLAs formed during heating (Reprinted from Christy [8] with permission from Elsevier)



molecules will not be available for the isomerization reaction. The remaining trilinoelaidin can be quantitatively determined by using a pure trilinoelaidin standard. The use

of peak at 969 cm^{-1} in quantifying the concentrations of rest trilinoelaidin in the mixtures is reasonable. Heat-treated trilinoelaidin yields around 6–7% 9c12t and 9t12c

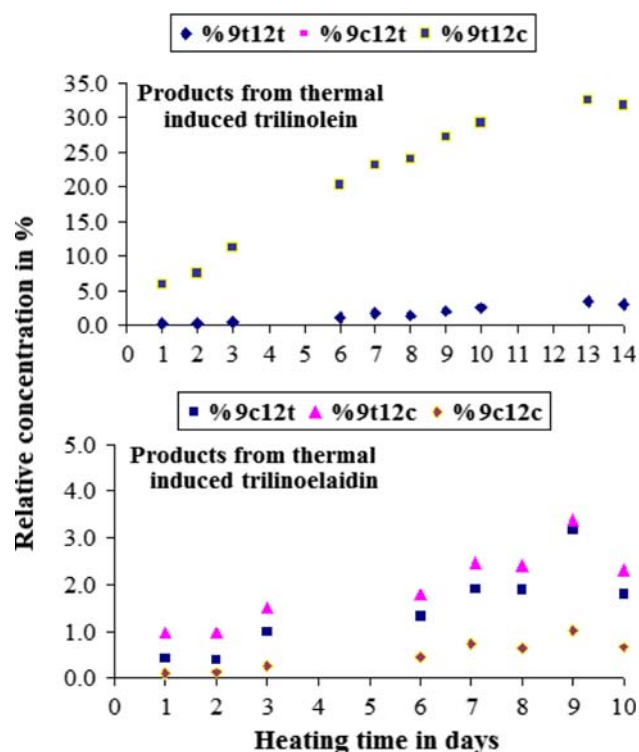


Fig. 5 Concentration profiles of the isomers formed during heating. The concentrations of 9t12c and 9c12t are identical in the heat induced trilinolein

isomers and therefore the error in the determination of rest trilinoelaidin will be in that range. In the case of trilinolein, the formation of 9t12t is around 3% and therefore the total concentration of 9c12t and 9t12c in each sample can be determined by comparing the peak height at 969 cm^{-1} with trielaidin peak height at the same wavenumber. Rest trilinolein can then be calculated by relative comparison of the percentages.

Fig. 6 Energy level diagram for the isomerization into mono *trans* isomers following a diradical mechanism

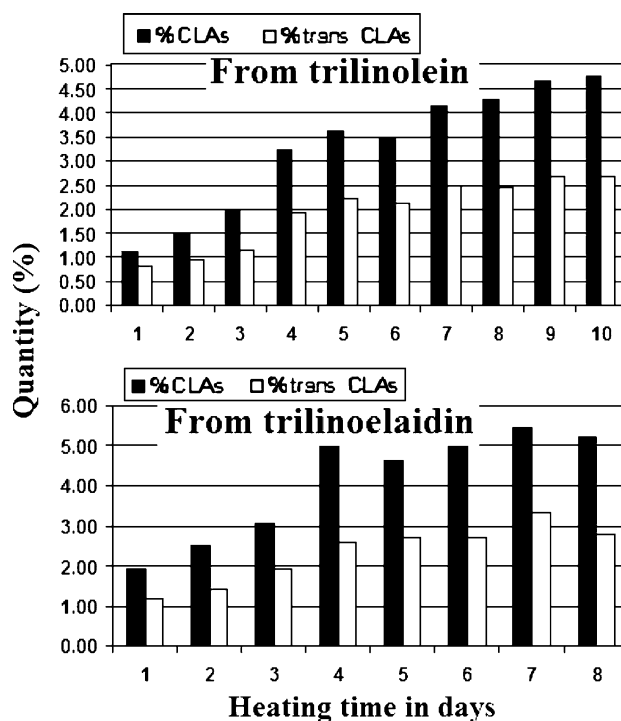
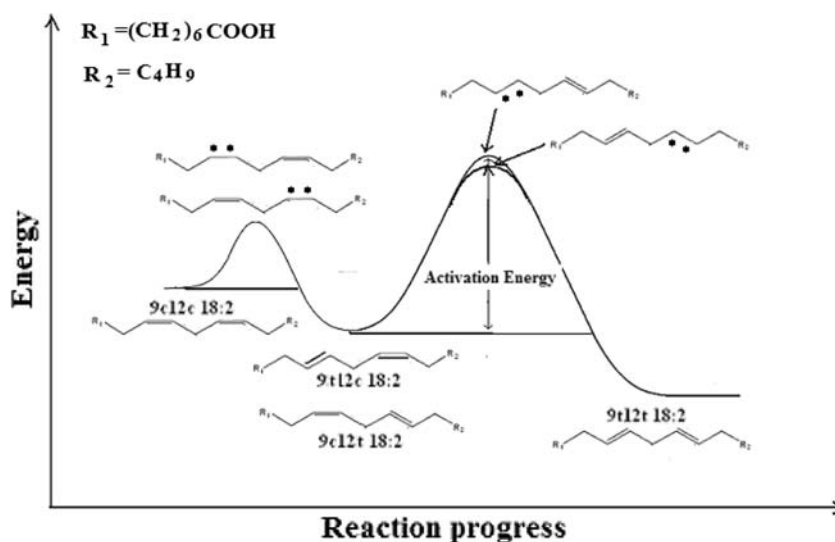


Fig. 7 Concentration profiles of conjugated linoleic acids in the heated trilinolein and trilinoelaidin

The concentration of rest trilinoelaidin and trilinolein in the heat-treated samples determined by infrared spectrometry and gas chromatography are given in Fig. 8. The plots clearly show the difference between the concentrations determined by GC and infrared spectroscopy. The analysis of fatty acids in the thermally induced mixtures was carried out after derivatization into FAMES. This derivatization reaction involves only the acidic components formed during thermal induction in the mixture and excludes all the other organic components formed from the

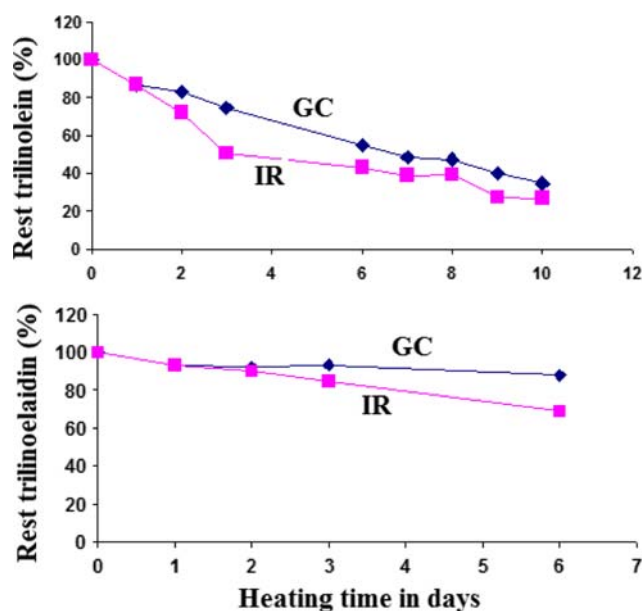


Fig. 8 Concentration of remaining trilinolein and trilinoelaidin in the heated samples as estimated by gas chromatography and infrared spectroscopy

thermal degradation. That is the concentrations of fatty acids determined as FAME profiles by gas chromatography are overestimated. The calculations show that both trilinolein and trilinoelaidin decompose during heating in addition to isomerization. Around 50% of trilinoelaidin decomposed after 10 days of heating and at the same time around 30% trilinolein decomposed after 10 days of heating. Differences in the decomposition characteristics are not difficult to understand. The concentration profiles of the products formed during the heat induction of trilinolein suggest that the activation energy for the isomerization is low and most of the fatty acid molecules in the molecule isomerize before decomposition into various products. In the case of trilinoelaidin, the molecule is very stable and the activation energy for the isomerization is very high and decomposition of trilinoelaidin may take place under thermal stress. These characteristics support the energy diagram shown in Fig. 6.

The decomposition products are mostly saturated and unsaturated aldehydes and shorter fatty acids [7]. Some of these aldehydes are carcinogenic [28]. These products were not analyzed for their chemical composition. However, there is evidence in the infrared spectra of the trilinolein and trilinoelaidin for oxidation during thermal induction. Infrared spectra of the heated sample of trilinolein and trilinoelaidin are given in Fig. 9. The absorption at $3,470\text{ cm}^{-1}$ is due to the overtone of the -C-O stretching in the glyceride molecules [29]. As the sample is being heated, some molecules are oxidised and hydroperoxide molecules formed. These hydroperoxide groups give a

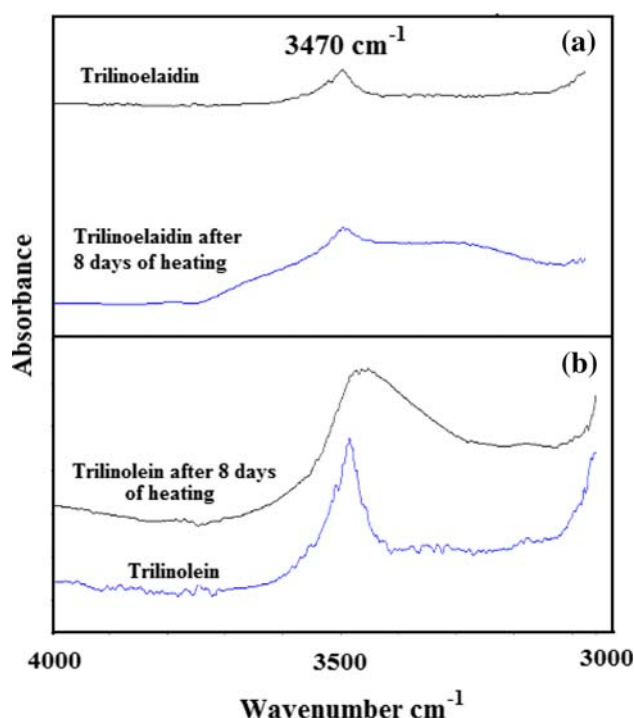


Fig. 9 Infrared spectra of heat-treated trilinolein and trilinoelaidin samples in the region $4,000\text{--}3,000\text{ cm}^{-1}$

broad band which overlaps with the -C-O overtone. Several aldehydes are formed depending on the position of the peroxide group in the molecules [30, 31]. A detailed mechanism for the formation of different aldehydes during the oxidation process can be found in Ref. 31.

Conclusion

In this paper, I have shown the transformation of trilinolein and trilinoelaidin under thermal stress. The fatty acids in the triglyceride molecules undergo decomposition and isomerization. The concentration profiles of the positional isomers and CLAs have been acquired. These profiles give clear indications of the behavior of the molecules under thermal stress. The 9c12c fatty acids lead to isomerization easily compared to the 9t12t fatty acids. These findings confirm the stability of the 9t12t isomer compared to 9c12c.

The thermal decomposition of 9c12c and 9t12t also follow different patterns. Because of the molecular stability of the 9t12t fatty acid, the molecule undergoes decomposition easily instead of isomerization. Almost 50% of the trilinoelaidin decomposes in 10 days and at the same time 30% of trilinolein decomposes in 10 days. The products of the decomposition include peroxides and aldehydes.

The 9c12c and 9t12t fatty acids isomerize also into CLAs. The maximum concentration of CLAs in the heated

samples reaches around 5% both in trilinolein and trilinolein. All the *trans*, *trans* isomers except 11t13t co-elute under a large peak which comprises about 60% of the total CLAs in the sample. The concentration of CLAs formed from the 9t12t fatty acid is almost 66% of that yielded by 9c12c fatty acid. This again reaffirms the stability of 9t12t fatty acid toward transformations.

These findings suggest that linoleic acids in oils and fats transform into other products in the same way as the mono-unsaturated fatty acids. Because of these changes, oils and fats turn into a mixture of complex organic molecules that may have implications for human health.

References

- Mensink RP, Katan MB (1990) Effect of dietary *trans* fatty acids on high-density and low density lipoprotein cholesterol levels in healthy subjects. *New Engl J Med* 323:439–445
- Zock PL, Katan MB (1992) Hydrogenation alternatives: effects of *trans* fatty acids and stearic acid versus linoleic on serum lipids and lipoproteins in humans. *J Lipid Res* 33:399–410
- Daush JG (2002) *Trans*-fatty acids: a regulatory update. *J Am Diet Assoc* 102:18–20
- Stender S, Dyerberg J (2004) Influence of *trans*-fatty acids on health. *Ann Nutr Metab* 48:61–66
- Judd JT, Clevidence BA, Muesing RA, Wittes J, Sunkin ME, Podczasy JJ (1994) Dietary *trans* fatty acids: effects on plasma lipids and lipoproteins of healthy men and women. *Am J Clin Nutr* 59:861–888
- Dutton HJ (1979) Hydrogenation of fats and its significance. In: Emken EA, Dutton HJ (eds) *Geometrical and positional fatty acids isomers*. American Oil Chemists' Society Press, Champaign, pp 1–16
- Christy AA, Xu Z, Harrington PB (2009) Thermal degradation and isomerisation kinetics of triolein studied by infrared spectrometry and GC–MS combined with chemometrics. *Chem Phys Lipids* 158:22–31
- Christy AA (2009) Evidence in the formation of conjugated linoleic acids from thermally induced 9t12t linoleic acid: a study by gas chromatography and infrared spectroscopy. *Chem Phys Lipids* 161:86–94
- Beatriz M, Oliveira PP, Ferreira MA (1996) Capillary gas chromatographic evaluation of *trans*-fatty acid content of food produced under the traditional conditions of semi-industrial frying. *J High Resol Chromatogr* 19:180–182
- Moreira RG, Castel-Perez ME, Barufet MA (1999) Deep-fat frying: fundamentals and applications. Aspen Publishers, Gaithersburg
- Rojo JA, Perkins EG (1987) Cyclic and fatty acid monomer formation in frying fats. *J Am Oil Chem Soc* 64:414–421
- Fullana A, Carbonell-Barrachina AA, Sidhu S (2004) Volatile aldehyde emissions from heated cooking oils. *J Sci Food Agric* 84:2015–2021
- Umamo K, Shibamoto T (2001) Analysis of cooking oil fumes by ultraviolet spectroscopy and gas chromatography-mass spectrometry. *J Sci Food Agric* 49:4790–4794
- Fujisaki M, Endo Y, Fujimoto K (2002) Retardation of volatile aldehyde formation in the exhaust of frying oil by heating under low oxygen atmospheres. *J Am Oil Chem Soc* 79:909–914
- Leon-Camacho M, Ruiz-Mendez MV, Gaciani-Constante M, Gaciani-Constante E (2001) Kinetics of the *cis-trans* isomerization of linoleic acid in the deodorization and/or physical refining of edible fats. *Eur J Lipid Sci Technol* 103:85–92
- Wolff RL (1993) Heat-Induced geometrical isomerization of α -linoleic acid: effect of temperature and heating time on the appearance of individual isomers. *JAOCS* 70:425–430
- Tsuzuki W, Nagata R, Yunoki R, Nakajima M, Nagata T (2007) *cis/trans*-Isomerisation of triolein, trilinolein and trilinolenin induced by heat treatment. *Food Chem* 108:75–80
- Official Methods and Recommended Practices of the American Oil Chemists' Society (1989) In: D. Firestone (ed), 4th edn. American Oil Chemists' Society Press, Champaign
- Mossoba MM, Yurawecz MP, McDonald RE (1996) Rapid determination of total *trans* content of neat hydrogenated oils by attenuated total reflection spectroscopy. *JOACS* 73:1003–1009
- Belton PS, Wilson RH, Sadehgi-Jorabegi H, Peers KE (1988) A rapid method for the estimation of isolated *trans* double bonds in oils and fats using FTIR combined with ATR. *Lebensm Wiss Technol* 21:153–157
- Dutton HJ (1974) Analysis and monitoring of *Trans*-isomerization by IR ATR spectrometry. *JAOCS* 51:406–409
- Lancer AC, Emken EA (1988) Comparison of FTIR and capillary gas chromatographic methods for quantitation of *trans* unsaturation in fatty acid methyl esters. *JAOCS* 65:1483–1487
- Mossoba MM, McDonald RE, Armstrong DJ, Page SW (1991) Identification of minor C₁₈ triene and conjugated diene isomers in hydrogenated soybean oil and margarine by GC-MI-FT-IR spectroscopy. *J Chromatogr Sci* 29:324–330
- Christy AA, Egeberg PK, Østensen ET (2003) Simultaneous quantitative determination of isolated *trans* fatty acids and conjugated linoleic acids in oils and fats by chemometric analysis of the infrared profiles. *Vib Spectrosc* 33:37–48
- Eulitz K, Yurawecz MP, Sehat N, Fritsche J, Roach JAG, Mossoba MM, Kramer, JKG, Adlof RO, Ku Y (1999) Preparation, separation, and confirmation of the eight geometrical *cis/trans* conjugated linoleic acid isomers 8,10-through 11,13-18:2. *Lipids* 34:873–877
- Destailats F, Angers P (2002) Evidence for [1, 5] sigmatropic rearrangements of CLA in heated oils. *Lipids* 30:435–438
- Destailats F, Angers P (2005) Thermally induced formation of conjugated isomers of linoleic acid. *Eur J Lipid Sci Technol* 107:167–172
- Schauenstein EH, Esterbauer H, Jaag G, Taufer M (1964) The effect of aldehydes on normal and malignant cells. 1st report: hydroxyoctenal, a new fat aldehyde. *Monatsh Chem* 95:180–183
- Hamed SF, Allam MA (2006) Application of FTIR spectroscopy in the determination of antioxidant efficiency in sunflower oil. *J Appl Sci Res* 2:27–33
- Han IH, Csallany AS (2009) Formation of toxic α , β -unsaturated 4-hydroxy-aldehydes in thermally oxidized fatty acid methyl esters. *JAOCS* 86:253–260
- Cyberlipid Center, Secondary peroxidation products from fatty acids or more complex lipids. <http://www.cyberlipid.org/perox/oxid0009.htm>

Introduction

In marine environments, heterotrophic bacteria play a predominant role in particulate and dissolved organic matter (OM) transformations [1–4]. They control most OM fluxes since they are the main trophic level able to use dissolved OM efficiently. However, OM is made up of diverse chemicals, including proteins, peptides, polysaccharides, lipids, nucleic acids and other organic acids, phosphoric esters and humic substances [5]. Moreover, although bacterial abundance is regulated around a relatively constant value (10^5 to 10^6 cell ml^{-1}) [6], the bacterial species making up the pool of marine bacteria, are very diverse and have structures/functions/physiological conditions that may vary considerably, depending on the substrate and environmental conditions. One important bacterial function is hydrolysis that enables them to cleave the biopolymers into monomers before assimilation. Thus, protease, lipase and carbohydrase activity are fundamental to the carbon cycle. Understanding the specific and functional diversity of bacteria required to transform these targeted chemical substances is an important challenge in environmental research.

Lipids represent 3 to 55% of the OM in aquatic environments [7, 8]. They are natural substances derived from biological production, and are good tracers of the carbon cycle. Lipid hydrolysis, by lipases produced by heterotrophic bacteria, is essential for lipid assimilation by the bacteria. Studies regarding the specific relationships between lipids and lipase positive bacteria are uncommon [9] and lipid hydrolysis rates are poorly documented. Current methods used to measure lipase activity are the use of analog fluorogenic substrates as 4-methylumbelliferyl (MUF) fatty acyl esters [10], or radiolabelled triglycerides [11]. Lipase activities have been reported in the range 0.9–5.8 nM h^{-1} (using 12.5 nM MUF-oleate as the substrate), in a New-Caledonia lagoon [11] and Goutx et al. (unpublished results) measured lipase activities in the range of 5–7 nM h^{-1} (using 30 μM saturating MUF-oleate concentration) in the 0–60 m layer at the DYFAMED site (north-western Mediterranean Sea).

Using also MUF-oleate analog substrate (20 μM), specific lipase activity ranged over 3 orders of magnitude on pure cultures (0.2–584 $\text{amol cell}^{-1} \text{h}^{-1}$) and 20–70 $\text{amol cell}^{-1} \text{h}^{-1}$ in Coastal Californian waters [12], i.e. higher values than obtained at DYFAMED site (mean sd 3.3 ± 2.7 $\text{amol cell}^{-1} \text{h}^{-1}$).

Although lipid hydrolysis rates can be obtained by measuring lipase activities, it is still not known which organisms are responsible for the activities measured. To date, the potential capacity of the various bacterial communities to process a substrate have been estimated by comparing specific activities (activities per cell), based on

the misplaced assumption that all cells i) express the targeted enzyme and ii) exhibit the same activities. However, in order to focus on relationships between the targeted chemical substances (such as lipids) and the bacterial species able to process these substrates (named lipase + throughout the text), it is necessary to identify the bacteria responsible for the measured lipase activities.

Current methods used to measure lipase activity cannot detect the source of the activity measured. However, another analog fluorescent substrate, ELF-palmitate, may be used as a probe to target lipase + bacteria. Unlike MUF, which is soluble in water, ELF Alcohol (ELFA), the fluorescent product of the substrate hydrolysis, is insoluble in water and precipitates at the enzymatic site responsible for its hydrolysis. Thus, the walls of the bacteria having lipase activity are marked by ELF fluorescent crystals, enabling them to be detected by microscopy.

This method has been developed using ELF-phosphate substrate for detecting alkaline phosphatase and was first used on natural populations of marine and lake plankton [13–16]. The method was then adapted to marine heterotrophic bacteria [17]. ELF-palmitate has also been used for lipase detection on filamentous bacteria in wastewater treatment [18–21] and in rotifers digestive tracts in lakes [22]. However, no specific methodological developments have been reported in the literature on the use of ELF-palmitate, or its use in detecting lipase activities in free marine heterotrophic bacteria. The kinetics of ELF-palmitate hydrolysis and the mechanisms leading to the formation of fluorescent precipitates at the enzymatic sites are still poorly understood.

In this study, we used diverse techniques for measuring lipase activities of marine bacteria. Lipid substrate consumption and lipase activities were measured using both a chemical and an enzymatic approach (using the fluorogenic analogs MUF-palmitate and ELF-palmitate). Finally, we observed the accumulation of ELFA fluorescence over time but no precipitates were clearly associated with bacteria on prepared slides, neither for pure cultures of *Alteromonas macleodii* nor for natural samples from the Bay of Marseille, France. Possible factors controlling ELFA precipitation are discussed.

Experimental Procedure

Control of the Lipase + Properties of *Alteromonas macleodii*

The Gram-negative marine strain was obtained from the collection of the Observatoire Océanologique de Banyuls-sur-mer, in France, isolated from Mediterranean coastal

waters. This strain, named *Alteromonas infernus* in previous studies [17, 23] was recently reclassified as *Alteromonas macleodii*. On thawing, the strain was incubated at 25 °C on nutrient agar. The lipase + property was tested using a medium containing Tween 80, which is easily hydrolyzed by lipases, and calcium which reacts with the products of the Tween 80 hydrolysis. The reaction was characterized by an opaque halo around the colonies. The strain was then cultured in a triglyceride (TG) enriched medium in which lipase activities were measured.

Culture Media

Experiments were conducted in artificial sea water, based on f/2 Lyman & Fleming composition [24], in which we added excess NH_4Cl (6.7 mM N) and KH_2PO_4 (165 μM P) as sources of N and P, as well as traces of iron and vitamins. In the PYR medium, pyruvate was the single carbon source, supplied at low concentration (330 μM C) to obtain less dense cultures. The TG medium was a triglyceride-enriched medium (i.e. PYR medium + 1.2 μM tripalmitate, corresponding to 63 μM C of tripalmitate) which can theoretically induce lipase activity.

Bacterial Culture

Different experiments were performed. Whatever the final objectives of the experiments (synthesized in Table 1), all cultures were conducted in a reproducible manner as follows: prior to each culture, 48 h-colonies were inoculated into 100 ml pre-cultures of the PYR medium, allowing the bacteria to adapt to their new growth conditions. Following

24 h incubations at 25 °C, an inoculum was provided so that bacterial abundance was around 1×10^6 cell ml^{-1} in the cultures. The 300-ml cultures were continuously shaken, left growing in an incubated chamber at 25 °C in the dark until the stationary phase had been reached (generally lasting 50 h or more). PYR cultures and TG cultures are the cultures grown in PYR and TG media, respectively.

First, a series of three successive experiments were conducted to define the most propitious growth phase for ELFA labelling (experiments 1, 2, 3, Table 1). Bacterial abundance and lipase activities measured with the MUF-palmitate substrate were monitored over a period of 50 h in PYR and TG cultures. As these successive experiments showed reproducible patterns (see results), we thus felt confident enough to compare data acquired during experiments that were not run simultaneously (Table 1). Secondly, a duplicate experiment was performed on TG cultures (experiment 4, Table 1) to follow the tripalmitate decay over 144 h during bacterial growth. Then, experiments were performed on TG cultures, during the exponential phase (20 h) to verify the ectoenzymatic property of lipases (experiment 5, Table 1), test the effect of the ELF-palmitate solvent on lipase activities (experiment 6, Table 1), the competitive inhibition between MUF-palmitate and ELF-palmitate (experiment 7, Table 1) and ELF-palmitate labelling (experiment 8, Table 1).

Bacterial Counts

Bacterial abundance was estimated using epifluorescence microscopy counts following 4',6-diamidino-2-phénylindole (DAPI) staining. Samples (1 ml for pure cultures and

Table 1 Aims of the different experiments performed during this study

Experiments		PYR culture	TG culture	Cell count	MUF-based activity	ELF-based activity	Tripalmitate decay	ELF labelling	Time of the experiment (h)	Aim of the experiment
1	Successive experiments	×	×	×	×			0–50	Determine the most propitious growth phase for ELF-labelling	
2		×	×	×	×					
3		×	×	×	×					
4	Duplicate experiment		×	×			×	0–144	Follow tripalmitate decay over time	
5	Triplicate experiment		×		×			20	Verify the ectoenzymatic property of lipases	
6	Duplicate experiment		×		×			20	Verify the effect of the ELF-palmitate solvent on MUF-based activities	
7	Duplicate experiment		×		×	×		20	Inhibition kinetic experiment	
8	Triplicate experiment		×		×	×		×	20	ELF labelling, measurements of MUF- and ELF-based activities in parallel

10 ml for the natural environment) were fixed with 2% final concentration of buffered formaldehyde (pre-filtered through 0.2 μm membrane). Then, bacteria were incubated with a DAPI solution ($\sim 2.5 \mu\text{g ml}^{-1}$ final concentration) for 10–15 min in the dark and at room temperature. Samples were then filtered onto black polycarbonate membranes (0.2 μm) and mounted onto glass slides using an Olympus immersion oil for fluorescence (nd 1.404). DAPI stained cells were counted with an Olympus BH2 microscope equipped with a long pass cube type U (dichroic mirror DM 400, barrier filter L420). Bacterial abundance was calculated from thirty fields with a minimum of thirty cells counted per field.

MUF-Palmitate Lipase Activity Measurement

Lipase activity was measured fluorometrically using 4-methylumbelliferyl-palmitate (MUF-palmitate) analog substrate [25]. The hydrolysis of MUF-palmitate releases a fluorochrome (MUF) that is soluble in the aqueous phase and can be detected spectrofluorometrically. Samples of pure culture (20 ml) were incubated with MUF-palmitate (50 μM final concentration), in the dark (25 °C). The linear increase in sample fluorescence was followed over an appropriate time period, with a spectrofluorometer Kontron SFM 25 calibrated with standard solutions of MUF (in the range 0.05–10 μM , excitation 365 nm, emission 450 nm). The MUF-palmitate concentration was chosen in order to reach saturating conditions as verified in previous concentration kinetic experiments (data not shown). Briefly, the parameters V_{max} (maximum hydrolysis rate) and K_m (Michaelis constant which reflects enzyme affinity for the substrate) were determined by fitting the data using a non-linear regression on the Michaelis–Menten equation.

Controls were performed in a sterile medium. Lipid hydrolysis rates were determined from the regression slope of the MUF fluorescence and calibration factors. Specific lipase activity was calculated by the ratio rates to abundances.

Chemical Monitoring of the TG Substrate Degradation

The decrease in tripalmitate concentration was estimated over time in duplicate experiments in the TG medium, using chemical analysis (experiment 4, Table 1).

Samples were collected regularly, over the 144 h of culture monitoring, to measure the concentration of dissolved lipids and bacterial abundance. A control was carried out in sterile TG medium to evaluate the abiotic decomposition of the substrate.

Lipids were extracted by liquid–liquid extraction, using dichloromethane: two extractions at natural pH followed by one extraction following acidification at pH <2 using HCl.

An internal standard (hexadecanone) was used to take into account the loss of lipid material during the analytical protocol.

Lipid extracts were analyzed by thin layer chromatography–flame ionization detection (TLC–FID). Depending on their polarity, lipids were separated into classes of compounds, on chromarods SIII (0.9 mm diameter, 150 mm length, 75 μm thick silica) and quantified using an Iatrosan TH10 apparatus model MK-IV (Iatron, Japan; hydrogen flow, 160 ml min^{-1} ; air flow, 2,000 ml min^{-1}) coupled to a Borwin integration system (Bionis, Paris). The complete elution scheme has been described previously [26]. It allows reliable separation and quantification of twelve classes of compounds, including triglycerides and their hydrolysis products, the free fatty acids (FFA) [27]. In this study, we reported on TG and FFA patterns only.

Verification of the Ectoenzymatic Property of Lipases

Experiments were conducted in triplicate in TG enriched cultures (experiment 5, Table 1). The control was performed in a sterile TG medium. The MUF-palmitate hydrolysis rate was measured in TG cultures and in the 0.2 μm filtrate of TG cultures in order to measure activity in the dissolved phase.

Lipase + Bacteria Labelling by the ELF-Palmitate Fluorescent Probe, Principle of Reaction

The ELF-palmitate substrate is a lipid analog substrate, as is MUF-palmitate. It consists of a lipid residue (palmitate) bound by an ester bond to the fluorochrome ELF. The product of ELF-palmitate hydrolysis, a brightly fluorescent ELF97 alcohol (ELFA), is water insoluble and precipitates theoretically at the site of its origin, labelling the cells that develop lipase activity with a more or less bright yellow staining that is detected under UV light by using epifluorescence microscopy.

The ELF-palmitate was purchased from Molecular Probes, in powder form (5 mg) and was solubilized in dimethylsulfoxide (DMSO). The solubility limit was reached at a concentration of 2.5 mM. Aliquots of stock solutions (150 μl) were kept at $-18 \text{ }^\circ\text{C}$. After thawing, one aliquot was filtered through 0.2- μm spin-filters before being used for bacteria labelling.

Effect of the Solvent of ELF-Palmitate (DMSO) on Bacterial Activity

The influence of DMSO on bacterial activity was tested by measuring the MUF-palmitate hydrolysis rate in the presence of increasing concentrations of DMSO (0.5, 1, 2, 5, 7 and 10% of the final volume) (experiment 6, Table 1).

Inhibition Kinetics Experiments

The ability of ELF-palmitate to saturate the sites of the enzymes responsible for the cleavage of MUF-palmitate was tested (experiment 7, Table 1). The effect of ELF-palmitate, added in a series of concentrations (0.1–184 μM), on the hydrolysis rate of MUF-palmitate, applied at a single low concentration (0.5 μM) was examined. The concentration of MUF-palmitate was close to K_m , the Michaelis constant for MUF-palmitate hydrolysis by extracellular lipases present in the sample examined, determined in previous saturation experiments, using a concentration range of 0.05–100 μM .

The MUF-palmitate hydrolysis rate in presence of ELF-palmitate was expressed as a percentage of the control value (occurring in the absence of ELF-palmitate), and plotted on a semilogarithmic graph, as a function of ELF-palmitate concentrations. The IC_{50} , which corresponds to the ELF-palmitate concentration giving a 50% inhibition of MUF-palmitate hydrolysis, was calculated using nonlinear regression by fitting data with a decelerating 3-parameter sigmoid function (displacement curve), assuming competitive inhibition (as in previous study, [28]):

$$v = \text{Min} + (\text{Max} - \text{Min}) / (1 + I/\text{IC}_{50}),$$

where v is the substrate (MUF-palmitate) hydrolysis rate (% of control), Max and Min are the upper and lower plateaus of displacement curve, respectively (% of control), and I is inhibitor concentration (i.e. final ELF-palmitate concentration). The Prism 4 (GraphPad Software, San Diego, USA) statistical package was used to perform nonlinear regressions.

Standard Protocol for ELF-Labeling in a Liquid Medium

Labelling tests were conducted in triplicate on TG cultures, based on existing protocols used for alkaline phosphatase labelling [16] (experiment 8, Table 1).

Samples (2,640 μl) were incubated with 60 μl of a 2.5 mM stock solution of ELF-palmitate in DMSO for a final substrate concentration of 50 μM for 1–5 h. 300 μl of a 100 mM Tris-HCl (pH 7.5) was added in order to provide pH stability during incubation. Indeed, a high pH would lead to the formation of a non-fluorescent and soluble form of ELF [29].

During the incubations, hydrolysis of ELF-palmitate was measured using spectrofluorimetry in order to compare with the activity measured using MUF-palmitate. The increase in fluorescence of ELFA was measured as a function of time (excitation 365 nm, emission 530 nm). As for MUF, the spectrofluorometer was calibrated using a concentration range of ELFA from 0.05 to 2 μM to

determine the conversion factor of fluorescence units to nmol of ELFA product released.

Aliquots were also taken at different incubation times for microscopy observation. The reaction was stopped by formalin tetraborate (2% final concentration). The samples were then stained with DAPI before being filtered onto a black polycarbonate membrane (0.2 μm). Then the filter was mounted on a glass slide for epifluorescence microscopy observation. Dual staining (combining ELFA and DAPI) enables us to discriminate between the total bacterial abundance and ELFA labelled cells [17, 30, 31].

Tests in the Natural Environment

Sea water was sampled from April to July 2007 at two stations in the Bay of Marseille, France: Riou (43°09'N, 5°24'E) and Cortiou (43°12'N, 5°24'E). Lipase activity was measured using MUF-palmitate (kinetic concentrations 0.05–50 μM), along with the measurement of bacterial abundance. The proportion of ELFA-labelled cells was investigated in the natural bacterial community, following the same protocol as for pure cultures, except that we tested different concentrations of ELF-palmitate (12–50 μM).

Results

Growth of *Alteromonas macleodii*

In cultures, bacterial growths (Fig. 1) were initiated with an average concentration of $1.6 (\pm 0.2) \times 10^6$ cell ml^{-1} in PYR cultures and $1.5 (\pm 0.4) \times 10^6$ cell ml^{-1} in TG cultures. During bacterial growth, a lag phase of approximately 6 h was systematically observed, followed by a log phase, the time period of which depended on the substrate. The stationary phase was reached after 30–40 h of culture with final concentrations of $2.5 (\pm 0.5) \times 10^8$ cell ml^{-1} and $3.0 (\pm 0.4) \times 10^8$ cell ml^{-1} in PYR and TG cultures, respectively. There were no significant differences between PYR and TG cultures, shown by non-significant differences between growth rates (test t , $p > 0.05$, slopes compared with data from log phase) and between abundances reached at stationary phase (ANOVA, $p > 0.05$). Although the four experiments were successive, there were no statistical differences between each other (test t and ANOVA, $p > 0.05$). We thus considered that they were comparable and that following experiments were also comparable.

Lipase Activity in *Alteromonas macleodii* Cultures: The Enzymatic Approach

During experiments 1, 2 and 3, bacterial counts were associated with MUF-palmitate hydrolysis rates measurements

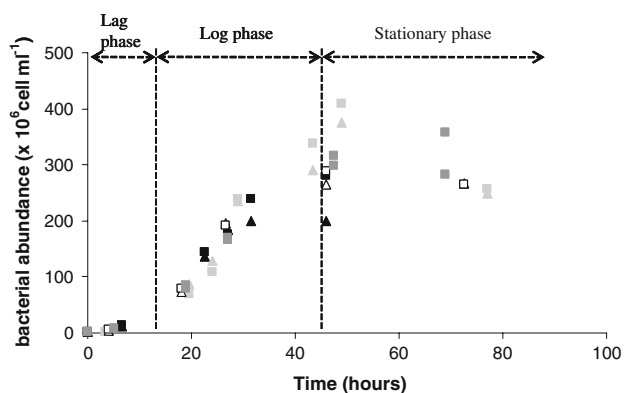


Fig. 1 Evolution of bacterial abundances (cell ml^{-1}) in four successive experiments. *Triangle*: PYR cultures, *square*: TG cultures. Experiment 1: *black*, experiment 2: *light grey*, experiment 3: *white*, experiment 4: *dark grey*

(Table 1). The latter varied in a larger range than abundances between the three successive experiments. Potential MUF-palmitate hydrolysis rates ($50 \mu\text{M}$ additions) ranged between $2.8\text{--}9.3 \mu\text{M h}^{-1}$ after 20 h of culture and $4.3\text{--}21.4 \mu\text{M h}^{-1}$ at the stationary phase (47 h) in the PYR cultures (Fig. 2). In the TG cultures, lipase activities ranged between $4.6\text{--}9.4 \mu\text{M h}^{-1}$ at 20 h and $5.5\text{--}18.2 \mu\text{M h}^{-1}$ at the stationary phase. In a given experiment, MUF-palmitate hydrolysis rates measured in a PYR culture were always close to and occasionally higher than those measured in a TG culture. The same was observed for specific potential activities ranging between $2.0\text{--}11 \times 10^{-2} \text{fmol cell}^{-1} \text{h}^{-1}$ at 20 h and $2.1\text{--}8.0 \times 10^{-2} \text{fmol cell}^{-1} \text{h}^{-1}$ at the stationary phase in PYR cultures. In TG cultures specific activities were $3.2\text{--}14.0 \times 10^{-2} \text{fmol cell}^{-1} \text{h}^{-1}$ at 20 h and $2.0\text{--}6.9 \times 10^{-2} \text{fmol cell}^{-1} \text{h}^{-1}$ at the stationary phase. The growth phase where specific potential activities were the highest was difficult to determine using the enzymatic approach. Specific activities were clearly highest during the

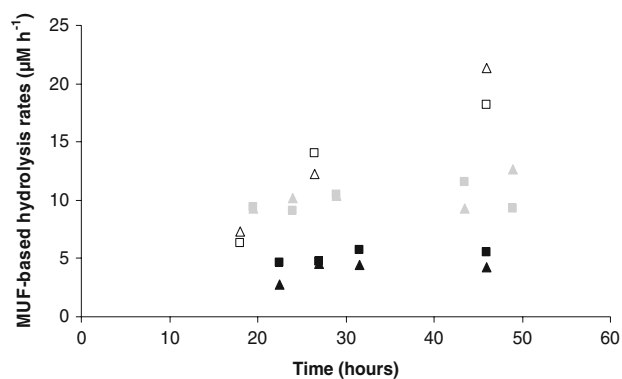


Fig. 2 Evolution of MUF-palmitate hydrolysis rates measured with $50 \mu\text{M}$ MUF-palmitate final concentration ($\mu\text{M h}^{-1}$) in the successive experiments 1, 2, 3. *triangles*: PYR cultures, *squares*: TG cultures. Experiment 1: *black*, experiment 2: *grey*, experiment 3: *white*

Table 2 Specific activity during bacterial growth

Experiments	Log phase		Stationary phase	
	PYR	TG	PYR	TG
1	2.0	3.2	2.1	2.0
2	11.0	14.0	3.4	2.3
3	9.9	8.0	8.0	6.9

Specific activities ($\times 10^{-2} \text{fmol cell}^{-1} \text{h}^{-1}$) measured at the log and stationary phases with MUF-palmitate ($50 \mu\text{M}$ final concentration) in PYR and TG cultures, during three successive experiments

early log phase in both PYR and TG cultures in only two of the three experiments performed (Table 2).

Lipase Activity in *Alteromonas macleodii* Cultures: the Chemical Degradation of the TG Substrate

Tripalmitate concentrations decreased (Fig. 3), from $1.2 (\pm 0.3) \mu\text{M}$ at the beginning of the experiments to $0.1 (\pm 0.02) \mu\text{M}$ after 144 h of culture. About 90% of the tripalmitate was degraded during the experiment. There were no free fatty acids (FFA) at the beginning of the cultures in either of the 2 experiments. They appeared after 19 h of culture with a concentration of $0.4 (\pm 0.04) \mu\text{M}$. Their concentration increased to $0.9 (\pm 0.6) \mu\text{M}$ after 27 h of growth then fell to $0.5 (\pm 0.03) \mu\text{M}$ after 144 h of culture. Two phases of tripalmitate decay can be distinguished: a short first phase, from 0 to 19 h, and a longer second phase, between 19 and 144 h, that fitted into linear regressions. Between 0 and 19 h, $0.6 \mu\text{M}$ of the triglycerides were consumed. Using these chemical data, we calculated a tripalmitate hydrolysis rate that we considered to be the real lipase activity (Table 3). It was 30nM h^{-1} during the first phase. During the second phase, between 19 and 144 h, the same substrate quantity was consumed, $0.6 \mu\text{M}$, which was equivalent to a lipase activity of 5nM h^{-1} . During these two phases, a range of specific activities was estimated, based on the smaller and highest values of bacterial abundance during each phase. Values were $0.4\text{--}2.1 \times 10^{-2} \text{fmol cell}^{-1} \text{h}^{-1}$ for the first phase and $1.2\text{--}5.7 \times 10^{-5} \text{fmol cell}^{-1} \text{h}^{-1}$ for the second one.

Verification of the Ecto enzymatic Property of Lipases

In the fifth experiment, the average MUF-palmitate hydrolysis rate was $2.5 (\pm 0.2) \mu\text{M h}^{-1}$ in the unfiltered culture, while no activity was detected in the dissolved phase of the culture or in the sterile medium. Lipases were thus firmly attached to bacteria, which was a prerequisite condition for labelling the membrane enzymatic sites with the ELF-palmitate.

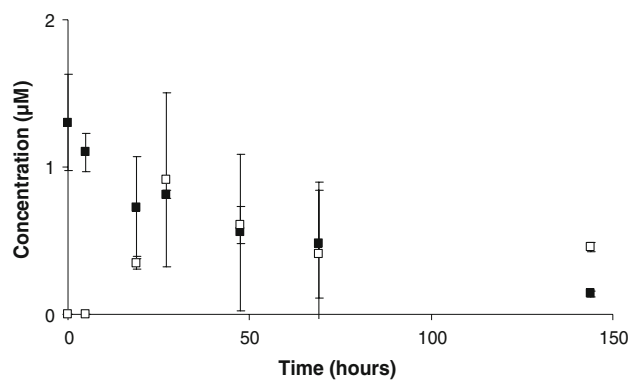


Fig. 3 Evolution of tripalmitate (*black squares*) and fatty acids (*white squares*) concentrations (μM) during bacterial growth in TG cultures. *Error bars* represent the standard deviation between duplicates. Note that one molecule of tripalmitate contains three fatty acids chains (experiment 4)

Table 3 Real lipase activity

Growth phase	Lipase activity ($\mu\text{M h}^{-1}$)	Specific activity ($\text{fmol cell}^{-1} \text{h}^{-1}$)
Phase 1	0.03	$0.4\text{--}2.1 \times 10^{-2}$
Phase 2	0.005	$1.2\text{--}5.7 \times 10^{-5}$

Tripalmitate decay rates ($\mu\text{M h}^{-1}$) and specific activity ($\text{fmol cell}^{-1} \text{h}^{-1}$) during phase 1 (phase where triglycerides decay was high) and phase 2 (phase where triglycerides decay was low), during bacterial growth in TG cultures

Solvent of ELF-Palmitate Effect

MUF-palmitate hydrolysis rates were measured with different DMSO proportions. Without DMSO, the measured activity was considered to be 100%. With up to 2% DMSO of the final volume, lipase activity did not decrease by more than 6%. Lipase activity decreased from 35 to 72% when DMSO represented 5% or more of the final volume. Hence, we considered that lipase activity was not influenced by the presence of DMSO as long as its proportion was less than 2% of the final volume.

Inhibition Kinetics Experiments

Measured data on the inhibition of MUF-palmitate hydrolysis by ELF-palmitate fitted well with the competitive inhibition model ($R^2 = 0.91$). The IC_{50} value obtained with the model was $44.7 \mu\text{M}$. So, the maximum ELF-palmitate concentration ($184 \mu\text{M}$) was only 4 times the IC_{50} . Inhibition of MUF-palmitate hydrolysis reached 80% (Fig. 4).

Although 100% inhibition of MUF-palmitate hydrolysis was not reached, the competitive inhibition experiment showed that more than 80% of enzymatic sites that

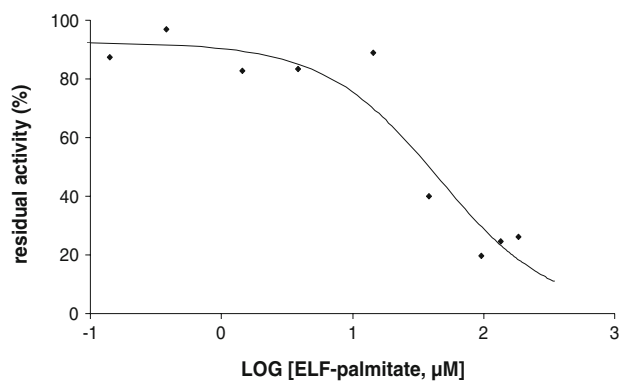


Fig. 4 Inhibition of MUF-palmitate hydrolysis by ELF-palmitate applied at different concentrations, in samples from TG cultures. MUF-based activity is given as a percentage of MUF-based activity measured without ELF-palmitate

hydrolyzed the MUF-palmitate also hydrolyzed the ELF-palmitate.

ELF-Labeling Tests

Prior to any labelling, the presence of both MUF-based and ELF-based activities was checked by spectrofluorometry in TG cultures, with a $50\text{-}\mu\text{M}$ final concentration for both substrates. The experiment was performed in triplicate (experiment 8, Table 1). The average MUF-based activity was $2 (\pm 0.2) \mu\text{M h}^{-1}$. The average ELF-based activity was about 5 times greater $10 (\pm 1) \mu\text{M h}^{-1}$. There was no MUF-based or ELF-based activity in the abiotic control. The ELFA fluorescence increased linearly as a function of time up to 5 h, after a lag time of about 1 h (result not shown). Specific ELF-based activities were in the range of $7\text{--}10 \times 10^{-2} \text{fmol cell}^{-1} \text{h}^{-1}$.

In the natural environment, MUF-based activities ranged from 1.5 to 7.5nM h^{-1} corresponding to $1.8\text{--}8.6 \times 10^{-3} \text{fmol cell}^{-1} \text{h}^{-1}$. ELF-based activities ranged from 30.4 to 88.1nM h^{-1} and corresponded to $2.4\text{--}9 \times 10^{-2} \text{fmol cell}^{-1} \text{h}^{-1}$. Comparing MUF- and ELF-based activities with the same substrate concentrations, no correlation was found between the two substrates in the natural environment.

During incubation in the presence of the ELF-palmitate substrate, samples from pure cultures and sea water were periodically taken to observe under the microscope, to look for any ELFA stained cells. For most replicates and at most incubation times, the labelling was not conclusive. Only yellow-green halos were spread on filters, not clearly associated with bacteria (Fig. 5).

However, at only one occasion in the pure cultures, for one of the replicates, we observed ELFA spots associated with bacteria. In this case, about 3% and 7% of bacteria were labelled with the ELFA, after 1 and 2 h of incubation,

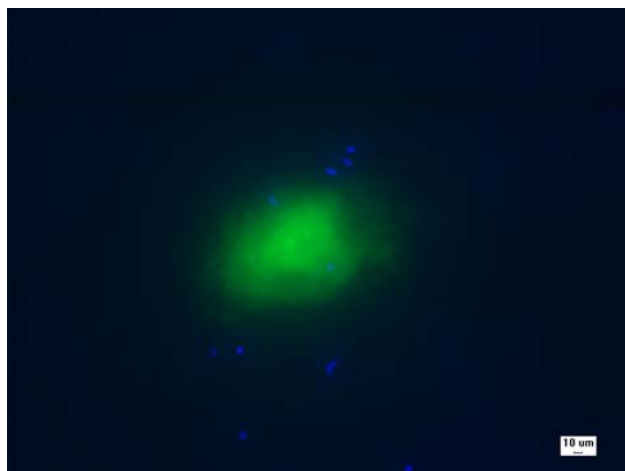


Fig. 5 Heterotrophic bacteria from the natural community of the Bay of Marseille stained with DAPI. ELFA halos (yellow-green) are observed but no ELFA grains are associated with bacteria. Composite image obtained from two digitalized images: one with a narrow DAPI-filter (for blue, total bacteria) and one with a large DAPI filter combined with a low level of intensity of excitation (for yellow-green, ELFA halos)

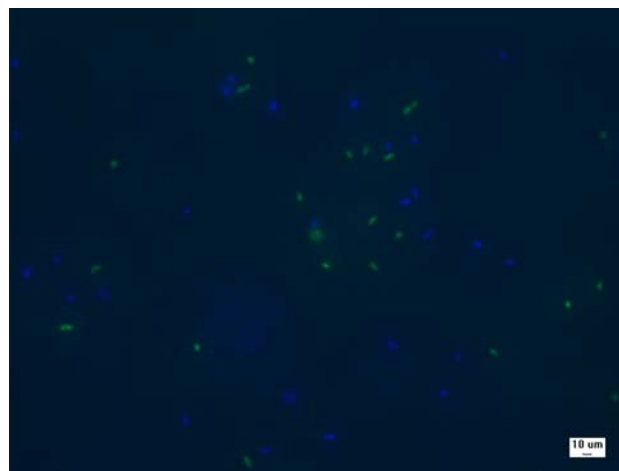


Fig. 6 *Alteromonas macleodii*. ELFA labelled cells (yellow-green) counterstained with DAPI (blue) in TG cultures. Composite image obtained from two digitalized images: one with a narrow DAPI-filter (for blue, total bacteria) and one with a large DAPI filter combined with a low level of intensity of excitation (for yellow-green, ELFA-labeled bacteria)

respectively (Fig. 6). After 3 h of incubation, the staining was no longer visible and this result was never reproduced in other tests.

In the natural bacterial community, in order to verify that lipase activity was responsible for the appearance of such halos, we determined when possible the surface of these halos on the filters, over time (Fig. 7). At station Riou, there was no clear trend over time. At station Cortiou, the area occupied by the ELFA halos did not change during the first hour, but there were a sharp increase after about 2 h of incubation, particularly in June. In filtered samples (0.2 µm), there were only few halos and no trend over time.

Discussion

Reports in the literature state that lipases are mostly inducible enzymes [32]. Their production is greatly influenced by environmental parameters such as carbon and nitrogen sources, inorganic nutrients, temperature, dissolved oxygen concentration, pH [33] and the presence of lipids generally enhance their production [34–37].

As lipase synthesis represents an energetic cost for cells, we expected an enhancement of lipase activity in TG cultures at the stationary phase, when the most available substrate (pyruvate) should be limiting. However, in TG cultures, differences in specific MUF-based activities were not significant between the exponential growth phase and the stationary phase. Based on a bacterial yield of $2\text{--}3.4 \times 10^8$ cell ml⁻¹ and assuming a bacterial carbon

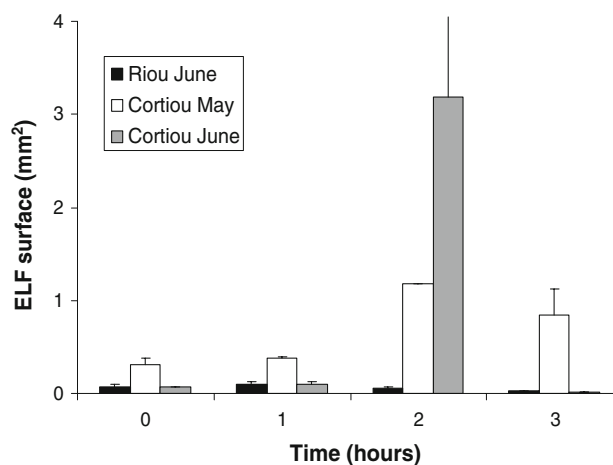


Fig. 7 Effect of incubation time on the surface area of filters occupied by ELFA halos (mm²), with 25 µM of ELF-palmitate added. Tests made in natural samples from the Bay of Marseille

content between 12.4 and 20 fg C cell⁻¹ [38, 39] and a bacterial growth efficiency between 0.14 and 0.38 for *Alteromonas macleodii* growing on pyruvate [40], the bacterial carbon demand would range between 540 and 4,000 µM C. This theoretical value is higher than the available carbon in our cultures (330 and 393 µM C in PYR and TG cultures, respectively). However, while the cell number increased, microscopic observations showed a decrease of the cell size over time. This “fragmentation phenomenon” [41] reflects a situation of carbon starvation which seems to take place very quickly in our cultures (approximately 20 h). Because of carbon limitation, the

rapid utilization of lipids (see Fig. 3) would explain why no difference was observed between the exponential growth phase and the stationary phase.

Finally, our results did not show the expected contrast “no lipase activity in PYR cultures/induced lipase activity in TG cultures”.

All these results suggest that lipases were constitutive for this *Alteromonas macleodii* strain. Phosphatases were reported to be in part constitutive for the same strain [17]. Other studies show that lipid enrichment does not systematically induce the enzyme synthesis [42] in natural microbial assemblages of deep marine sediments. Constitutive lipases were also reported for psychrotrophic bacteria [43].

The chemical measurement of lipid concentrations in TG cultures showed the disappearance of tripalmitate and the appearance of its hydrolysis products (free fatty acids) over time, thus ensuring the use of the lipidic substrate by bacteria. Another result concerned the lipolytic capacity of *Alteromonas macleodii* that was found in the range of previously reported real lipid hydrolysis rates. The tripalmitate hydrolysis rate that we obtained by the chemical approach corresponded to 2.0×10^{-5} to 2.1×10^{-2} fmol cell⁻¹ h⁻¹. Using trace concentrations of a radiolabelled triglyceride substrate, which (as for the chemical approach) was assumed to measure real rates, hydrolysis rates were measured in the Mediterranean Sea, ranging from 1.1×10^{-5} to 1.8×10^{-3} fmol cell⁻¹ h⁻¹ (with 0.13 to 0.26 nM of [³H]-triolein, at seawater temperature between 13 and 26 °C) [9]. Consequently, these rates obtained in lipid enriched cultures were on the same order of magnitude than in natural samples, suggesting efficient potentialities for lipid hydrolysis in the marine environment.

Comparison between MUF-based and ELF-based activities measured fluorometrically suggest that ELF-palmitate may be used to measure the potential hydrolysis rate of lipids: the increase in the ELFA fluorescence as a function of time was linear. However, ELF-based activities were four times greater than MUF-based activities with the same concentration of substrate added (50 μM) in pure cultures and no correlation was found with MUF-based activities in the natural environment. In a study of the ELF-phosphate kinetics on phytoplankton populations in freshwater lakes, similar results were found with 2–4 times more activity measured with the ELF-phosphate than with the MUF-phosphate [16]. In our experiment, the ELFA fluorescence appeared to increase linearly from the beginning of the ELF-palmitate incubation. However, the first two fluorescence measurements were separated by an important time step (1 h) that did not necessarily allow the observation of a possible shorter lag time. Indeed, other tests (data not shown) showed that the ELFA fluorescence increase may occur after a lag time of 30 min to 1 h. This

observation was well consistent with previous work [16] where a lag time ranging from a few minutes to more than 4 h was obtained in samples from lakes incubated at 25 °C.

The study of the ELF-palmitate kinetics required using varying and high substrate concentrations. However, we were limited by the proportion of DMSO, which we observed, should not exceed 2% of the final volume. Through inhibition experiments, this problem could be partly resolved. The maximum ELF-palmitate concentration used in this experiment was determined by the maximum amount of DMSO usable without modification of the lipase activity. To achieve it, we have however exceeded 2% of DMSO and reached a maximum of 4% of DMSO. Thus, the maximum concentration in ELF-palmitate (184 μM) represented only 4 times IC₅₀ (ELF-palmitate concentration causing 50% inhibition of the MUF-based activity). However, the inhibitor concentration is expected to exceed IC₅₀ by at least two orders of magnitude to observe 100% inhibition. This explains why only 80% of the maximum inhibition was reached. The experiment using ELF-palmitate as the inhibitor of MUF-palmitate showed that at least 80% of the enzymes interacting with ELF-palmitate hydrolyzed MUF-palmitate as well. We assumed that both substrates were in competition for the same enzymatic sites.

Finally, three substrates were used for measuring lipase potential and real activity. It was therefore interesting to compare them. Although bacterial abundances showed a very stable pattern, lipase activities measured with MUF-palmitate and tripalmitate showed a high variability between the successive experiments performed (see Figs. 2, 3). It may be due to the insoluble property of lipids and their capacity to form micelles that are not always homogeneously spread in culture media. Nevertheless, potential activity measurements, obtained with MUF-palmitate added at saturating concentrations were in the range of 3–25 μM h⁻¹ and thus far exceeded the real activities (5–30 nM h⁻¹), measured by following the tripalmitate decay chemically. The initial MUF-palmitate concentration was at saturating concentration (50 μM) while the TG concentration was approximately 1.2 μM, about 40 times less, which may partly explain the observed differences. We calculated MUF-palmitate hydrolysis rate based on a substrate addition of 1.2 μM and using the terms of Michaelis-Menten equation (based on MUF-palmitate kinetics) as described previously [44]. These “apparent real rates” were still much higher (7–57 times) than tripalmitate hydrolysis rate. The difference in structure between MUF-palmitate and tripalmitate, used to measure hydrolysis rates may be partly responsible for the differences found in our study. Indeed the quantity of esters bonds is different for the two molecules: the MUF-palmitate contains only one while the tripalmitate contains three bonds. At the same

substrate concentrations, and assuming that the two substrates are recognized in the same way by lipase, there should be a difference of a factor of three between the measured activities. As far as we know, there is no other comparison between MUF-palmitate and the natural corresponding triglyceride (tripalmitate). However, other studies reported comparison between MUF-oleate and triolein. Oleate is a long unsaturated fatty acid (18:1) compared to palmitate (16:0) and probably behaves somewhat differently (when combined to MUF-or p-nitrophenyl fluorogenic derivatives) in tests on pure enzymes [45] and environment [46]. Lipases do not behave the same way with the MUF-oleate analog and their natural substrate: triglycerides [47, 48]. The fluorogenic analog, whose structure differs from that of the natural substrate, is not necessarily recognized by the targeted enzyme [49] and may undergo a non-specific hydrolysis by various carboxylesterases [47, 48], for example. In addition, a comparison of two methods for enzymatic activity measurements showed that the MUF-oleate was probably more labile and more easily hydrolyzed by lipases than the radiolabelled ^3H -triolein [11]. Although MUF- and ELF-palmitate were hydrolyzed by the same enzymes, these substrates were probably not hydrolyzed specifically by lipases (defined as triacylglycerol acylhydrolase, E.C. 3.1.1.3) but rather by “lipolytic enzymes”.

Before testing ELFA labelling on bacteria, we checked that the enzymes responsible for the measured potential enzymatic activities were attached to bacteria. This verification ensured that ELFA insoluble crystals could precipitate at the enzymatic site responsible for the substrate hydrolysis. The early log phase of *Alteromonas macleodii* growth (between 5 and 20 h) exhibited the highest specific activity (measured chemically) and was most suitable for the ELFA staining of *Alteromonas macleodii* cells. Therefore we carried out the labelling tests at this growth phase. Theoretically, all conditions were met to observe the ELFA labelling of bacteria under microscopy.

Yet, in most cases only a yellow-green halo was spread over the filter's surface (absent at the beginning of incubation). In only one case spots of ELFA, as those observed in previous study ([17], see their Fig. 1) were obtained, and only in that case we were able to associate ELFA spots with bacteria. But this result was not reproducible in both cultures and in situ samples.

Many factors control ELFA precipitation. The non-fluorescent water-soluble phenol form of ELFA converts into its fluorescent water-insoluble form due to the spontaneous formation of an intramolecular hydrogen bond, and only subsequently precipitates. A pH > 10 would lead to inhibit the formation of this intramolecular hydrogen bond of the ELFA molecule [50]. An increase in local ELFA concentration over a certain level is also required to initiate

its precipitation [16]. Adding ELFA in certain conditions has been found to promote fine structure resolution [51]. The undissolved alcohol could promote precise crystallization of the reaction product at the site of enzymatic activity (serving as crystal nucleation sites) but also maintain its localized precipitation. We did not add ELFA in samples during incubation with ELF-palmitate. We ensured that the level of specific activities was sufficient for observing ELFA precipitation. A $0.17 \text{ fmol cell}^{-1} \text{ h}^{-1}$ minimum phosphatase activity was recommended to observe ELFA spots formation in bacterial samples from acidified mountain lakes [31]. However, 30% ELFA labelled cells were reported in pure cultures of *Alteromonas macleodii* with an alkaline phosphatase activity of $0.01\text{--}0.16 \text{ fmol cell}^{-1} \text{ h}^{-1}$ [17]. In our cultures, specific activities varied in a similar range ($0.07\text{--}0.10 \text{ fmol cell}^{-1} \text{ h}^{-1}$ measured with ELF-palmitate). Thus, the low percentage of labelled bacteria that we obtained in our samples cannot be inferred onto the level of specific activities. Salt concentrations can also be involved in the formation of fine precipitates [51]. To detect alkaline phosphatase, the use of a salt-rich reactive (B reactive of the ELF-97 Endogenous Phosphatase Detection kit E6601) with ELF-phosphate is proposed by Molecular Probes. However, alkaline phosphatase was stained by ELF on marine bacteria without the use of this component [16].

It has been previously suggested that a kind of nucleation (e.g. on hydrophobic structures) may trigger ELFA precipitation [16]. Lipid-enriched target sites were found to form large crystals [51].

The specificity of hydrophilic/hydrophobic interactions and the complex mechanisms underlying the precipitates formation might explain the difficulty in obtaining ELFA spots in lipid-enriched media. Instead, we obtained a rather diffuse staining in our preparations. ELFA spots attached to filaments of filamentous bacteria were observed in studies of wastewaters from different treatment plants after incubation with ELF-palmitate [19, 20]. Another study [21] also reported ELFA spots attached to the filaments of filamentous bacteria. In these studies, the signal was never observed on free cells. However, filamentous bacteria in wastewater often have a hydrophobic surface, whereas free cells have rather a hydrophilic surface [19, 52, 53]. ELFA labelling was also observed on *Alteromonas macleodii* strain in pure cultures [17, 23]. In these cultures, the strain formed aggregates, which could characterize cells with hydrophobic surface. The ELF-phosphate substrate dissolved in milli-Q water could behave differently than ELF-palmitate dissolved in DMSO. In our study, the strain never formed aggregates and no clear ELFA signal was observed. The growing conditions in these previous experiments may promote the increase of the hydrophobicity degree on the site of ectoenzymatic activities of *Alteromonas macleodii*,

while the growing conditions of our experiments may have tended to favor its decline. Indeed, the degree of hydrophobicity of the cell surface may change depending on environmental conditions (degree of starvation, [54]) and a strong correlation between the adhesion of cells to sludge flocs and cell surface hydrophobicity was demonstrated [53].

In highly eutrophicated aquatic environments (wastewater treatment plants), free cells are rather hydrophilic [52]. This may explain the lack of significant bacterial labelling in an eutrophicated marine environment in this study. Among the three stations, Cortiou is the nearest station to the Marseille wastewater discharge outflow. Our hypothesis was that the presence of enhanced concentrations of glycerides, previously recorded in wastewater [55], would trigger bacterial lipolytic activity and, thus, the number of ELFA labelled cells, capable of developing lipase activity, among the natural bacterial community. Activities were measured with the MUF-palmitate substrate and were enhanced at the different stations, depending on the season (Duflos et al. in prep). Although we observed an increase in ELFA halos spread on filters at Cortiou, suggesting a biological origin for the ELF-palmitate hydrolysis, we never observed any ELFA labelled cells on the filters, for natural communities. This problem has also been encountered for the detection of alkaline phosphatase of heterotrophic bacteria in the Mediterranean Sea [17].

In conclusion, this study uses the first assay of ELF-palmitate for marine bacteria staining. We saw clear evidence that ELF-palmitate was cleaved by bacterial enzymatic activity but that cell labelling cannot be obtained routinely, even on a small percentage of cells. Although several conditions for the assay were set up (growth phase, solvent solubilization), it is likely that assay conditions have to be optimized before routine use.

However, other alternatives should be sought to identify the organisms which are responsible for the measured lipase activity in the marine environment. Indeed, this method seems selective and ELFA labelling of lipolytic bacteria seems influenced by the degree of hydrophobicity of the cell surfaces. This study therefore suggests that prior to proving that the ELFA can precipitate indiscriminately on hydrophobic and hydrophilic surfaces, this substrate must be used with extreme caution.

Acknowledgments We acknowledge the anonymous reviewers for their helpful comments. We also thank Tracy Bentley and Rose Campbell for improving the English. This study was supported by a graduate research fellowship from the Conseil Régional Provence-Alpes-Côte d'Azur. Funding was obtained from the "Agence de l'eau" de Marseille in the framework of the IBISCUS project (Indicateurs Biologiques et chimiques de Contaminations Urbaines).

This work is a CNRS-INSU and Université d'Aix-Marseille II research contribution.

References

1. Billen G, Joiris C, Wijnant J, Gillain G (1980) Concentration and microbial utilization of small organic molecules in the Scheldt estuary, the Belgian coastal zone of the North Sea and the English Channel. *Estuar Coast Mar Sci* 11:279–294
2. Ducklow HW, Purdie DA, Williams PJJ, Davies JM (1986) Bacterioplankton: a sink for a carbon in a coastal marine plankton community. *Science* 232:865–867
3. Joint IR, Morris RJ (1982) The role of bacteria in the turnover of organic matter in the sea. *Oceanogr Mar Biol A Rev* 20:65–118
4. Pomeroy L, Wiebe W (1988) Energetics of microbial food webs. *Hydrobiologia* 159:7–18
5. Münster U, Albrecht D (1994) Analysis of composition and function by a molecular–biochemical approach. In: Overbeck J, Chrost RJ (eds) *Microbial ecology of lake Plußsee*. Springer, NY
6. Bianchi M (1998) Nouvelles approches d'étude des réseaux microbiens. *Ann Limnol* 34(4):465–473
7. Jeffrey LM (1966) Lipids in sea water. *J Am Oil Chem Soc* 43:211–214
8. Ogura N, Ambe Y, Ogura K, Ishiwatari R, Mizutani T, Satoh Y, Matsushima H, Katase T, Ochiai M, Tadokoro K, Takada T, Sugihara K, Matsumoto G, Nakamoto N, Funakoshi M, Hanya T (1975) Chemical composition of organic compounds present in water of the Tamagawa River. *Jpn J Limnol* 36:23–30
9. Bourguet N, Goutx M, Ghiglione JF, Pujo-Pay M, Mével G, Momzikoff A, Mousseau L, Guigue C, Garcia N, Raimbault P, Pete R, Oriol L, Lefèvre D (2009) Lipid biomarkers and bacterial lipase activities as indicators of organic matter and bacterial dynamics in contrasted regimes at the dyfamed site, NW Mediterranean. *Deep Sea Res Part II*. doi:10.1016/j.dsr2.2008.11.034
10. Hoppe HG (1993) Use of fluorogenic model substrates for extracellular enzyme activity (EEA) measurement of bacteria. In: Kemp PF, Sherr BF, Sherr EB, Cole JJ (eds) *Handbook of methods in aquatic microbial ecology*. Lewis, Boca Raton
11. Bourguet N, Torretton JP, Galy O, Arondel V, Goutx M (2003) Application of a specific and sensitive radiometric assay for microbial lipase activities in marine water samples from the Lagoon of Noumea. *Appl Environ Microbiol* 69:7395–7400
12. Martinez J, Smith DC, Steward GF, Azam F (1996) Variability in ectohydrolytic enzyme activities of pelagic marine bacteria and its significance for substrate processing in the sea. *Aquat Microb Ecol* 10:223–230
13. Gonzalez-Gil S, Keafer BA, Jovine RVM, Aguilera A, Lu S, Anderson DM (1998) Detection and quantification of alkaline phosphatase in single cells of phosphorus-starved marine phytoplankton. *Mar Ecol Prog Ser* 164:21–35
14. Rengefors K, Pettersson K, Blenckner T, Anderson DM (2001) Species-specific alkaline phosphatase activity in freshwater spring phytoplankton: application of a novel method. *J Plankton Res* 23:435–443
15. Strojsova A, Vrba J, Nedoma J, Komrkova J, Znachor P (2003) Seasonal study of extracellular phosphatase expression in the phytoplankton of a eutrophic reservoir. *Eur J Phycol* 38:295–306
16. Nedoma J, Strojsova A, Vrba J, Komarkova J, Simek K (2003) Extracellular phosphatase activity of natural plankton studied with ELF97 phosphate: fluorescence quantification and labelling kinetics. *Environ Microbiol* 5:462–472
17. Van Wambeke F, Nedoma J, Duhamel S, Lebaron P (2008) Alkaline phosphatase activity of marine bacteria studied with

- ELF 97 substrate: success and limits in the P-limited Mediterranean Sea. *Aquat Microb Ecol* 52:245–251
18. Kragelund C, Remesova Z, Nielsen JL, Thomsen TR, Eales K, Seviour R, Wanner J, Nielsen PH (2007) Ecophysiology of mycolic acid-containing actinobacteria (mycolata) in activated sludge foams. *FEMS Microbiol Ecol* 61:174–184
 19. Kragelund C, Kong Y, van der Waarde J, Thelen K, Eikelboom D, Tandoi V, Thomsen TR, Nielsen PH (2006) Ecophysiology of different filamentous Alphaproteobacteria in industrial wastewater treatment plants. *Microbiology* 152:3003–3012
 20. Kragelund C, Nielsen JL, Thomsen TR, Nielsen PH (2005) Ecophysiology of the filamentous Alphaproteobacterium *Meganema perideroedes* in activated sludge. *FEMS Microbiol Ecol* 54:111–122
 21. Schade M, Lemmer H (2005) Lipase Activities in Activated Sludge and Scum - Comparison of New and Conventional Techniques. *Acta hydrochimica et hydrobiologica* 33:210–215
 22. Strojsova A, Vrba J (2005) Direct detection of digestive enzymes in planktonic rotifers using enzyme-labelled fluorescence (ELF). *Mar Freshw Res* 56:189–195
 23. Duhamel S, Gregori G, Van Wambeke F, Mauriac R, Nedoma J (2008) A method for analysing phosphatase activity in aquatic bacteria at the single cell level using flow cytometry. *J Microbiol Meth* 75:269–278
 24. Lyman J, Fleming RH (1940) Composition of seawater. *J Mar Res* 3:134–146
 25. Hoppe HG (1983) Significance of exoenzymatic activities in the ecology of brackish water: measurements by means of methylumbelliferyl-substrates. *Mar Ecol Prog Ser* 11:299–308
 26. Striby L, Lafont R, Goutx M (1999) Improvement in the Iatroskan thin-layer chromatographic-flame ionisation detection analysis of marine lipids. Separation and quantitation of monoacylglycerols and diacylglycerols in standards and natural samples. *J Chromatogr A* 849:371–380
 27. Goutx M, Guigue C, Striby L (2003) Triacylglycerol biodegradation experiment in marine environmental conditions: definition of a new lipolysis index. *Org Geochem* 34:1465–1473
 28. Nedoma J, Van Wambeke F, Strojsova A, Strojsova M, Duhamel S (2007) An alternative way to determine the affinity of extracellular phosphatases for ELF97 phosphate in aquatic environments. *Mar Freshw Res* 58:454–460
 29. Strojsova A, Vrba J (2006) Phytoplankton extracellular phosphatases: investigation using the ELF (enzyme Labelled Fluorescence) technique. *Pol J Ecol* 54:715–723
 30. Carlsson P, Caron DA (2001) Seasonal variation of phosphorus limitation of bacterial growth in a small lake. *Limnol Oceanogr* 46:108–120
 31. Nedoma J, Vrba J (2006) Specific activity of cell-surface acid phosphatase in different bacterioplankton morphotypes in an acidified mountain lake. *Environ Microbiol* 8:1271–1279
 32. Lotti M, Monticelli S, Luis Montesinos J, Brocca S, Valero F, Lafuente J (1998) Physiological control on the expression and secretion of *Candida rugosa* lipase. *Chem Phys Lipids* 93:143–148
 33. Brune AK, Gotz F (1992) Degradation of lipids by bacterial lipases. In: Winkelmann G (ed) *Microbial degradation of natural products*. VCH, Weinheim
 34. Chróst RJ, Gajewski AJ (1995) Microbial utilization of lipids in lake water. *FEMS Microbiol Ecol* 18:45–50
 35. Gupta R, Gupta N, Rathi P (2004) Bacterial lipases: an overview of production, purification and biochemical properties. *Appl Microbiol Biotechnol* 64:763–781
 36. Kosugi Y, Kamibayashi A (1971) Thermostable lipase from *Pseudomonas* sp.: cultural conditions and properties of the crude enzyme. *J Ferment Technol* 49:968–980
 37. Sztajer H, Maliszewska I, Wieczorek J (1988) Production of exogenous lipases by bacteria, fungi, and actinomycetes. *Enzyme Microb Technol* 10:492–497
 38. Lee S, Fuhrman JA (1987) Relationships between biovolume and biomass of naturally derived marine bacterioplankton. *Appl Environ Microbiol* 53:1298–1303
 39. Fukuda R, Ogawa H, Nagata T, Koike I (1998) Direct determination of carbon and nitrogen contents of natural bacterial assemblages in marine environments. *Appl Environ Microbiol* 64:3352–3358
 40. Eichinger M (2007) Bacterial degradation of dissolved organic carbon in the water column: an experimental and modelling approach. Thesis Vrije Universiteit Amsterdam, The Netherlands/University of Aix-Marseille II, France, p 163
 41. Novitsky JA, Morita RY (1977) Survival of a psychrophilic marine *vibrio* under long-term nutrient starvation. *Appl Environ Microbiol* 33:635–641
 42. Boetius A, Lochte K (1996) Effect of organic enrichments on hydrolytic potentials and growth of bacteria in deep-sea sediments. *Mar Ecol Prog Ser* 140:239–250
 43. McKellar RC (1989) Regulation and control of synthesis. In: McKellar RC (ed) *Enzymes of psychrotrophs in raw food*. CRC Press, Boca Raton
 44. Crottereau C, Delmas D (1998) Exoproteolytic activity in an Atlantic pond (France): estimates of in situ activity. *Aquat Microb Ecol* 15:217–224
 45. Lee MH, Lee CH, Oh TK, Song JK, Yoon JH (2006) Isolation and characterization of a novel lipase from a metagenomic library of tidal flat sediments: evidence for a new family of bacterial lipases. *Appl Environ Microbiol* 72:7406–7409
 46. Taylor GT, Way J, Yu Y, Scranton MI (2003) Ecto-hydrolyase activity in surface waters of the Hudson River and western Long Island Sound estuaries. *Mar Ecol Prog Ser* 263:1–15
 47. Beisson F, Ferte N, Nari J, Noat G, Arondel V, Verger R (1999) Use of naturally fluorescent triacylglycerols from *Parinari glaberrimum* to detect low lipase activities from *Arabidopsis thaliana* seedlings. *J Lipid Res* 40:2313–2321
 48. Hendrickson HS (1994) Fluorescence-based assays of lipases, phospholipases, and other lipolytic enzymes. *Anal Biochem* 219:1–8
 49. Beisson F, Tiss A, Rivière C, Verger R (2000) Methods for lipase detection and assay: a critical review. *Eur J Lipid Sci Technol* 102:33–153
 50. Huang Z, Terpetschnig E, You W, Haugland RP (1992) 2-(2'-phosphoryloxyphenyl)-4-(3H)-quinazolinone derivatives as fluorogenic precipitating substrates of phosphatases. *Anal Biochem* 207:32–39
 51. Paragas VB, Kramer JA, Fox C, Haugland RP, Singer VL (2002) The ELF®-97 phosphatase substrate provides a sensitive, photostable method for labelling cytological targets. *J Microsc* 206:106–119
 52. Zita A, Hermansson M (1997) Determination of bacterial cell surface hydrophobicity of single cells in cultures and in wastewater in situ. *FEMS Microbiol Lett* 152:299–306
 53. Zita A, Hermansson M (1997) Effects of bacterial cell surface structures and hydrophobicity on attachment to activated sludge flocs. *Appl Environ Microbiol* 63:1168–1170
 54. Kjelleberg S, Hermansson M (1984) Starvation-induced effects on bacterial surface characteristics. *Appl Environ Microbiol* 48:497–503
 55. Hita C, Parlanti E, Jambu P, Joffre J, Ambès A (1996) Triglyceride degradation in soil. *Org Geochem* 25:19–28

high density lipoprotein (HDL) cholesterol levels and small, dense low-density lipoprotein (LDL) particles. These alterations in plasma lipoprotein-lipid metabolism have been shown to increase the risk for cardiovascular disease in both men and women [2].

The state of dyslipidemia is influenced by the body fat distribution with central obesity leading to a higher risk for cardiovascular disease [3]. Both, transfer proteins such as cholesteryl ester transfer protein (CETP) and phospholipid transfer protein (PLTP), and lipases such as lipoprotein lipase (LPL) and hepatic lipase (HL) are candidates to mediate the higher risk for cardiovascular disease [4].

Adipose tissue is a prominent source of CETP and obesity is associated with elevated plasma CETP concentrations [5, 6]. CETP is an important determinant of lipoprotein composition due to its capacity to mediate the transfer of cholesteryl esters (CE) from CE-rich lipoproteins to TG-rich lipoproteins in exchange for triglycerides. It has been suggested that CETP plays a key role in the reversibility of the atherogenic lipoprotein profile seen in obese subjects [7]. During marked reduction in fat mass the serum levels of both CETP-mass and CETP-activity are reduced in parallel [8, 9].

PLTP circulates bound to HDL and mediates the transfer of phospholipids from apo B-containing lipoproteins into HDL, thus modulating HDL size and lipid composition. PLTP activity generates pre-beta HDL, the major acceptor of cholesterol in the reverse-cholesterol transport route [10]. Liver, adipose tissue and lung are presumably the major sources of circulating PLTP [11]. PLTP-knockout mice have been shown to have markedly reduced HDL levels due to defective transfer of phospholipids from triglyceride-rich lipoproteins into HDL [12]. In a cross-sectional study elevated PLTP levels were associated with an increased risk for coronary artery disease [13]. Furthermore, it has been hypothesized that reduction of PLTP activity and increase of HDL particle size are important component factors in converting the atherogenic lipoprotein profile of obese subjects into a less atherogenic profile with weight loss [14].

The HL plays a role in the metabolism of chylomicrons and very low-density lipoprotein (VLDL) remnants, LDL, and high-density lipoproteins (HDL), which are all implicated in atherosclerosis [15–17]. A decrease in the activity of postheparin HL was found in 21 obese older men after weight loss, suggesting that the reduced HL concentrations might mediate the improvement in the lipoprotein profile [18].

LPL is a rate-limiting enzyme that hydrolyzes circulating triglyceride (TG)-rich lipoproteins, such as VLDL and chylomicrons [19]. A decrease in LPL activity is associated with an increase in plasma TG levels and a decrease in HDL-cholesterol [19].

As compared to previous weight loss studies, which evaluated either lipid transfer proteins or lipolytic enzymes, we determined—to our knowledge for the first time—the influence of weight reduction on both the lipid transfer proteins CETP and PLTP and the lipolytic enzymes LPL and HL in parallel and in a prospective study design.

Subjects and Methods

Subjects

Nineteen morbidly obese women defined by a BMI of more than 40 kg/m² participated in this prospective study. Subjects desiring surgical intervention for the treatment of obesity were referred from the surgical department to the outpatient clinic for metabolism, where they were consecutively screened for eligibility. Exclusion criteria were secondary causes of adiposity, diabetes mellitus, pregnancy, intake of lipid lowering drugs or other medically significant illness. Examinations of the study subjects were undertaken within 2 months prior to Laparoscopic Adjustable Gastric Banding (LAGB) and 1 year post LAGB. Informed consent was obtained from each participant before entering the study, and all procedures were performed in accordance with institutional guidelines at the Internal Department of the medical faculty of the University of Innsbruck. The study protocol was approved by the Ethical Committee of the Medical University Innsbruck.

Surgical Procedure

The surgical procedure was performed as described by Forsell [20] at the Department of Surgery, University of Innsbruck [21]. The Swedish Adjustable Gastric Band was used in all of the study patients (SAGB Obtech Medical AG, Zug, Switzerland).

Analysis of Body Composition

BMI was calculated as body weight in kilograms divided by height in meters squared. Body composition was determined by impedance analysis using InBody 3.0 Body Composition Analyzer from Biospace Europe (Dietzenbach, Germany). Measurements were taken in the morning in the fasted state.

Glucose Metabolism, Leptin and Lipoprotein Analysis

Blood was collected after an overnight fast. Plasma was separated from erythrocytes by centrifugation at 3,000 rpm for 10 min at 4 °C immediately after collection. Plasma samples were stored frozen at –80 °C until assayed. Plasma

TG, cholesterol, apo-AI and apo-B concentrations were quantified using a commercially available enzymatic kit (Roche Diagnostic Systems, Basel, Switzerland) on a Cobas Mira analyzer. HDL-cholesterol and HDL₃-C concentrations were determined using precipitation procedures with polyethylene glycol (Immuno, Vienna, Austria) [22]. HDL₂-C concentrations were calculated by subtracting HDL₃-C from HDL-C. LDL-C was calculated according to the formula of Friedewald et al. [23]. Plasma glucose was measured by the hexokinase method on a Cobas MIRA analyzer. Plasma insulin was determined by a micro particle enzyme immunoassay from Abbott (Wiesbaden, Germany). The homeostasis model of assessment of insulin resistance (HOMA-IR) was calculated by the following formula: fasting serum insulin concentration ($\mu\text{IU mL}^{-1}$) \times blood glucose concentration (mmol L^{-1})/22.5. Leptin concentrations were measured using an ELISA (R&D Systems, Wiesbaden, Germany).

CETP Mass

CETP concentrations were determined by capture enzyme-linked immunosorbent assay. Wells were coated with recombinant single-chain antibody fragments 1CL8 [24]. CETP was detected using a polyclonal anti-CETP antibody conjugated directly to alkaline phosphatase [25, 26].

PLTP Activity

The ability of plasma PLTP to transfer [³H]-dipalmitoyl-phosphatidylcholine (NEN Life science Products, Boston, MA, USA) from phosphatidylcholine vesicles to HDL₃ was measured as described previously [27].

LPL- and HL-Activity

LPL activity and HL activity were measured as described previously [28, 29]. Briefly, postheparin plasma was collected 15 min after an intravenous heparin dose of 50 Units per kg body weight into cold tubes to maintain the enzyme activity. For HL activity, we used a gum arabic emulsion of [³H]-glycerol-trioleate, under these conditions LPL is inactivated. To measure LPL activity we used an emulsion of Intralipid[®] into which [³H]-glycerol-trioleate was incorporated by sonication. HL activity was inhibited by goat immunoglobulins to human HL, that was a kindly provided by Thomas Olivecrona, University of Umea, Sweden.

Statistical Analysis

Descriptive data are expressed as mean values \pm SD. Normal distribution was estimated using a Shapiro–Wilk

Table 1 Anthropomorphic measures of the study participants at baseline and after weight loss induced by LAGB

	Pre LAGB	Post LAGB	Test probability
Age (years)	37.2 \pm 11.6	38.5 \pm 11.7	
Height (cm)	167 \pm 6		
Weight (kg)	116.8 \pm 12.2	94.6 \pm 14.4	<0.001
BMI (kg/m^2)	41.7 \pm 2.9	33.7 \pm 4.3	<0.001
Fat mass (kg)	57.5 \pm 8.1	37.0 \pm 8.4	<0.001

Data are expressed as means \pm SD. Statistical significance was estimated by paired-samples *t* test

test. Normally distributed data from the pre- and post-gastric banding group were compared using a paired-samples *t* test. Not normally distributed data from the pre- and post-gastric banding group were compared using a Wilcoxon test for paired samples. Associations between PLTP activity and CETP mass were assessed using the Spearman *r* correlation coefficient. Statistical significance was inferred at a two-tailed *P* value of less than 0.05. Statistical analyses were calculated using SPSS release 11.5 for Windows (SPSS, Chicago, USA).

Results

Clinical Characteristics

Anthropomorphic measures of the study subjects are shown in Table 1. The mean age was 37.2 \pm 11.6 years in pre-gastric banding subjects. In this group the mean body weight was 116.8 \pm 12.2 kg and the BMI was 41.7 \pm 2.9 kg/m^2 . Mean body weight loss after the surgical procedure was 22.2 kg ($P < 0.001$), respectively. Mean BMI decreased in parallel by 8 kg/m^2 after 1 year ($P < 0.001$). The body fat mass was 57.5 \pm 8.1 kg in the subjects undergoing surgical intervention. After bariatric surgery body fat mass decreased to 37.0 \pm 8.4 kg, corresponding to a loss of 20.5 kg fat mass ($P < 0.001$). Thus, in these study subjects weight loss mainly due to loss of fat mass.

Lipids and Apolipoproteins

Lipid parameters at baseline and after LAGB are shown in Table 2. Mean triglyceride levels decreased by 0.45 mmol L^{-1} after weight loss ($P = 0.027$). HDL-cholesterol tended to increase from 1.37 \pm 0.31 mmol L^{-1} in the pre-gastric banding group to 1.43 \pm 0.28 mmol L^{-1} in the post-gastric banding group. Mean HDL₂-C concentrations increased significantly by 0.02 mmol L^{-1} ($P = 0.009$). Further mean Apo-B levels decreased 4 mg dL^{-1} from baseline concentrations 1 year after LAGB, respectively.

Table 2 Lipid parameters and apolipoproteins at baseline and after weight loss induced by LAGB

	Pre LAGB	Post LAGB	Test probability
Glucose (mmol L ⁻¹) ^a	5.28 ± 1.07	5.23 ± 0.62	ns
Insulin (pmol L ⁻¹) ^a	122.7 ± 113.4	61.3 ± 38.1	0.006
HOMA-IR ^a	4.40 ± 4.79	2.06 ± 1.26	0.007
Leptin	44.4 ± 17.0	18.5 ± 11.9	<0.001
Total cholesterol (mmol L ⁻¹)	5.22 ± 0.72	4.86 ± 0.91	ns
Triglyceride (mmol L ⁻¹)	1.52 ± 0.97	1.07 ± 0.47	0.027
LDL-C (mmol L ⁻¹)	3.12 ± 0.57	2.88 ± 0.75	ns
HDL-C (mmol L ⁻¹)	1.37 ± 0.31	1.43 ± 0.28	ns
HDL ₂ -C (mmol L ⁻¹)	0.26 ± 0.13	0.28 ± 0.10	0.009
HDL ₃ -C (mmol L ⁻¹)	1.14 ± 0.20	1.14 ± 0.20	ns
apo-AI (mg dL ⁻¹)	159 ± 22	157 ± 24	ns
apo-B (mg dL ⁻¹)	89 ± 18	85 ± 17	ns

Data are expressed as means ± SD

ns not significant

Statistical significance was estimated by paired-samples *t* test or ^aWilcoxon-signed-ranks test

Table 3 Lipoprotein transfer proteins and lipases at baseline and after weight loss induced by LAGB

	Pre LAGB	Post LAGB	Test probability
CETP (μg mL ⁻¹)	1.81 ± 0.50	1.66 ± 0.44	0.043
PLTP activity (μmol mL ⁻¹ h ⁻¹)	7.15 ± 1.00	6.12 ± 1.07	0.002
LPL activity (nmol mL ⁻¹ h ⁻¹)	297 ± 96	248 ± 74	0.139
HL activity (nmol mL ⁻¹ h ⁻¹)	371 ± 148	319 ± 151	0.170

Data are expressed as means ± SD. Statistical significance was estimated by paired-samples *t* test

Lipid Transfer Proteins and Lipolytic Enzymes

The CETP mass was 1.81 ± 0.5 μg mL⁻¹ at baseline. After a weight loss of 20.5 kg in fat mass, CETP mass decreased by 8.3% ($P = 0.043$; Table 3). Baseline PLTP activity of 7.15 ± 1.0 (μmol mL⁻¹ h⁻¹) decreased by 14.4% ($P = 0.002$; Table 3). In univariate analysis CETP mass and PLTP activity were significantly associated at baseline ($r = .539$, $P = 0.026$), but not after weight loss ($r = .248$, $P = 0.338$). The correlation coefficient for Δ CETP and Δ PLTP was not significant ($r = .074$, $P = 0.787$). LPL activity tended to decrease from baseline levels of 297 ± 96 to 248 ± 74 nmol mL⁻¹ h⁻¹ ($P = 0.139$) and, also, the HL activity tended to decrease from 371 ± 148 to 319 ± 151 nmol mL⁻¹ h⁻¹ ($P = 0.170$).

Discussion

Obesity is associated with a higher risk for morbidity and mortality from atherosclerotic disease [1]. Bariatric surgery is an efficient method for reducing body weight and thereby reducing mortality and morbidity [30]. Weight loss leads to beneficial metabolic effects such as lowering serum triglycerides, improving the insulin sensitivity and increasing HDL-cholesterol. The Swedish Obese Subjects Study represents the first prospective controlled intervention study

on overall mortality after bariatric surgery [31]. After an observation period of 10 years several lipid parameters ameliorated in the bariatric surgery group: triglycerides decreased by 16%, HDL-cholesterol increased by 24% and total cholesterol decreased by 5.4% [31]. Changes in lipid transfer proteins and lipolytic enzymes could account for these improvements.

Consequently, we evaluated the influence of weight reduction by bariatric surgery on the lipid transfer proteins CETP and PLTP and the lipolytic enzymes LPL and HL in parallel in a prospective study. The study cohort comprised healthy obese women to minimize potential confounding factors.

One year post gastric banding fat mass decreased by 35.7% and, in parallel, CETP mass and PLTP activity decreased significantly by 8.3% and by 14.4%, respectively. We previously reported that CETP mass and activity decreased in subjects undergoing weight loss after bariatric surgery leading to a more favorable lipoprotein profile. After the bariatric procedure a consistent increase in LDL particle diameters was found in parallel to the plasma CETP diminution [8]. PLTP is another lipid transfer protein that plays a crucial role in improving the atherogenic lipoprotein profile of obese subjects during weight loss. In a previous study we found a significant reduction of PLTP activity and a concomitant increase in HDL₂ particle size during weight loss, whereas no

alteration of HDL₃ particle size was observed [14]. We hypothesized that a reduction in PLTP activity and an increase in HDL particle size are important component factors in converting the atherogenic lipoprotein profile of obese subjects into a less atherogenic profile with weight loss [14]. Furthermore, decreased PLTP activity was positively correlated with the change in subcutaneous fat after weight loss, but there was no significant relationship between the change in PLTP activity and the change in intraabdominal fat and insulin sensitivity [32]. Parallel CETP and PLTP plasma level reduction has already been found after slight weight loss induced by caloric restriction in obese women [33]. CETP and PLTP showed to correlate positively in obese females before weight reduction [33]. After weight loss the positive relationship between CETP and PLTP disappeared [33]. Both lipid transfer proteins seem to play a favorable role in the variances of lipids after weight reduction.

In contrast, postheparin HL activity and LPL activity did not change significantly after LAGB induced weight loss in the present study. However, we noted a tendency to decrease in both lipolytic enzymes. The role of HL and LPL in weight loss associated improvements of the lipid profile has been explored in previous studies. Pardina et al. [34] recently reported a significant reduction of plasma and liver HL activity after gastric bypass surgery. Purnell et al. [18] observed a reduction in postheparin HL activity after weight loss which contributed to the observed increase in LDL size and HDL₂-C, especially in those subjects with pattern B LDL particles before weight loss. A recently published study postulated that the lowering of plasma lipids following a weight reduction program was due to increased expression of both LPL and LDL receptor mRNA [35]. However, in another study by Berman et al. [36] regional adipose tissue LPL did not change after weight loss. The different weight loss inducing interventions investigated in the above-mentioned trials may be responsible for the conflicting results. In our study, HL and LPL activity seem to be unaffected by LAGB, a caloric intake restricting procedure.

A major limitation of this study is the restriction to women and the limited number of subjects. The latter could explain that, although we found a decrease in both LPL and HL activity, these differences were not significant in the respective statistical analysis.

In conclusion weight loss induced by bariatric surgery results in amelioration of TG and HDL-2 concentrations in normolipidemic obese women. These improvements may be attributable to decreased mass and action of the adipocyte tissue derived lipid transfer proteins CETP and PLTP, while the modest increase in HDL-2 could be the consequence of the change in TG independent of, or in combination with, the changes in the transfer proteins.

Acknowledgments The expert technical assistance of Ursula Stanzl and Karin Salzmann is gratefully acknowledged.

References

1. Stevens J, Cai J, Pamuk ER, Williamson DF, Thun MJ, Wood JL (1998) The effect of age on the association between body-mass index and mortality. *N Engl J Med* 338:1–7
2. Lamon-Fava S, Wilson PW, Schaefer EJ (1996) Impact of body mass index on coronary heart disease risk factors in men and women. The Framingham Offspring Study. *Arterioscler Thromb Vasc Biol* 16:1509–1515
3. Kannel WB, Cupples LA, Ramaswami R, Stokes J, Kreger BE, Higgins M (1991) Regional obesity and risk of cardiovascular disease; the Framingham Study. *J Clin Epidemiol* 44:183–190
4. Dusserre E, Moulin P, Vidal H (2000) Differences in mRNA expression of the proteins secreted by the adipocytes in human subcutaneous and visceral adipose tissues. *Biochim Biophys Acta* 1500:88–96
5. Arai T, Yamashita S, Hirano K, Sakai N, Kotani K, Fujioka S, Nozaki S, Keno Y, Yamane M, Shinohara E et al (1994) Increased plasma cholesteryl ester transfer protein in obese subjects. A possible mechanism for the reduction of serum HDL cholesterol levels in obesity. *Arterioscler Thromb* 14:1129–1136
6. Dullaart RP, Sluiter WJ, Dikkeschei LD, Hoogenberg K, Van Tol A (1994) Effect of adiposity on plasma lipid transfer protein activities: a possible link between insulin resistance and high density lipoprotein metabolism. *Eur J Clin Invest* 24:188–194
7. Ebenbichler C, Kirchmair R, Egger C, Patsch JR (1995) Postprandial lipemia and atherosclerosis. *Curr Opin Lipidol* 6:286–290
8. Ebenbichler CF, Laimer M, Kaser S, Ritsch A, Sandhofer A, Weiss H, Aigner F, Patsch JR (2002) Relationship between cholesteryl ester transfer protein and the atherogenic lipoprotein profile in morbidly obese women. *Arterioscler Thromb Vasc Biol* 22:1465–1469
9. Ritsch A, Patsch JR (2003) Cholesteryl ester transfer protein: gathering momentum as a genetic marker and as drug target. *Curr Opin Lipidol* 14:173–179
10. Jauhiainen M, Metso J, Pahlman R, Blomqvist S, Tol A, Ehnholm C (1993) Human plasma phospholipid transfer protein causes high density lipoprotein conversion. *J Biol Chem* 268:4032–4036
11. Jiang XC, Moulin P, Quinet E, Goldberg IJ, Yacoub LK, Agellon LB, Compton D, Schnitzer-Polokoff R, Tall AR (1991) Mammalian adipose tissue and muscle are the major source of lipid transfer protein mRNA. *J Biol Chem* 266:4631–4639
12. Jiang XC, Bruce C, Mar J, Lin M, Ji Y, Francone OL, Tall AR (1999) Targeted mutation of plasma phospholipid transfer protein gene markedly reduces high-density lipoprotein levels. *J Clin Invest* 103:907–914
13. Schlitt A, Bickel C, Thumma P, Blankenberg S, Rupprecht HJ, Meyer J, Jiang XC (2003) High plasma phospholipid transfer protein levels as a risk factor for coronary artery disease. *Arterioscler Thromb Vasc Biol* 23:1857–1862
14. Kaser S, Laimer M, Sandhofer A, Salzmann K, Ebenbichler CF, Patsch JR (2004) Effects of weight loss on PLTP activity and HDL particle size. *Int J Obes Relat Metab Disord* 28:1280–1282
15. Zambon A, Bertocco S, Vitturi N, Polentarutti V, Vianello D, Crepaldi G (2003) Relevance of hepatic lipase to the metabolism of triacylglycerol-rich lipoproteins. *Biochem Soc Trans* 31:1070–1074
16. Deeb SS, Zambon A, Carr MC, Ayyobi AF, Brunzell JD (2003) Hepatic lipase and dyslipidemia: interactions among genetic variants, obesity, gender, and diet. *J Lipid Res* 44:1279–1286

17. Cohen JC, Vega GL, Grundy SM (1999) Hepatic lipase: new insights from genetic and metabolic studies. *Curr Opin Lipidol* 10:259–267
18. Purnell JQ, Kahn SE, Albers JJ, Nevin DN, Brunzell JD, Schwartz RS (2000) Effect of weight loss with reduction of intra-abdominal fat on lipid metabolism in older men. *J Clin Endocrinol Metab* 85:977–982
19. Preiss-Landl K, Zimmermann R, Hammerle G, Zechner R (2002) Lipoprotein lipase: the regulation of tissue specific expression and its role in lipid and energy metabolism. *Curr Opin Lipidol* 13:471–481
20. Forsell P, Hallberg D, Hellers G (1993) Gastric banding for morbid obesity: initial experience with a new adjustable band. *Obes Surg* 3:369–374
21. Mittermair RP, Weiss H, Nehoda H, Kirchmayr W, Aigner F (2003) Laparoscopic Swedish adjustable gastric banding: 6-year follow-up and comparison to other laparoscopic bariatric procedures. *Obes Surg* 13:412–417
22. Patsch W, Brown SA, Morrisett JD, Gotto AM Jr, Patsch JR (1989) A dual-precipitation method evaluated for measurement of cholesterol in high-density lipoprotein subfractions HDL2 and HDL3 in human plasma. *Clin Chem* 35:265–270
23. Friedewald WT, Levy RI, Fredrickson DS (1972) Estimation of the concentration of low-density lipoprotein cholesterol in plasma, without use of the preparative ultracentrifuge. *Clin Chem* 18:499–502
24. Ritsch A, Ebenbichler C, Naschberger E, Schgoer W, Stanzl U, Dietrich H, Heinrich PC, Saito K, Patsch JR (2004) Phage-displayed recombinant single-chain antibody fragments with high affinity for cholesteryl ester transfer protein (CETP): cDNA cloning, characterization and CETP quantification. *Clin Chem Lab Med* 42:247–255
25. Ritsch A, Auer B, Föger B, Schwarz S, Patsch JR (1993) Polyclonal antibody-based immunoradiometric assay for quantification of cholesteryl ester transfer protein. *J Lipid Res* 34:673–679
26. Kaser S, Ebenbichler CF, Wolf HJ, Sandhofer A, Stanzl U, Ritsch A, Patsch JR (2001) Lipoprotein profile and cholesteryl ester transfer protein in neonates. *Metabolism* 50:723–728
27. Kaser S, Sandhofer A, Foger B, Ebenbichler CF, Igelseder B, Malaimare L, Paulweber B, Patsch JR (2001) Influence of obesity and insulin sensitivity on phospholipid transfer protein activity. *Diabetologia* 44:1111–1117
28. Deckelbaum RJ, Hamilton JA, Moser A, Bengtsson-Olivecrona G, Butbul E, Carpentier YA, Gutman A, Olivecrona T (1990) Medium-chain versus long-chain triacylglycerol emulsion hydrolysis by lipoprotein lipase and hepatic lipase: implications for the mechanisms of lipase action. *Biochemistry* 29:1136–1142
29. Eriksson JW, Buren J, Svensson M, Olivecrona T, Olivecrona G (2003) Postprandial regulation of blood lipids and adipose tissue lipoprotein lipase in type 2 diabetes patients and healthy control subjects. *Atherosclerosis* 166:359–367
30. Sampalis JS, Liberman M, Auger S, Christou NV (2004) The impact of weight reduction surgery on health-care costs in morbidly obese patients. *Obes Surg* 14:939–947
31. Sjostrom L, Lindroos AK, Peltonen M, Torgerson J, Bouchard C, Carlsson B, Dahlgren S, Larsson B, Narbro K, Sjostrom CD, Sullivan M, Wedel H (2004) Lifestyle, diabetes, and cardiovascular risk factors 10 years after bariatric surgery. *N Engl J Med* 351:2683–2693
32. Murdoch SJ, Kahn SE, Albers JJ, Brunzell JD, Purnell JQ (2003) PLTP activity decreases with weight loss: changes in PLTP are associated with changes in subcutaneous fat and FFA but not IAF or insulin sensitivity. *J Lipid Res* 44:1705–1712
33. Tzotzas T, Dumont L, Triantos A, Karamouzis M, Constantinidis T, Lagrost L (2006) Early decreases in plasma lipid transfer proteins during weight reduction. *Obesity (Silver Spring)* 14:1038–1045
34. Pardina E, Baena-Fustegueras JA, Catalan R, Galard R, Lecube A, Fort JM, Allende H, Vargas V, Peinado-Onsurbe J (2009) Increased expression and activity of hepatic lipase in the liver of morbidly obese adult patients in relation to lipid content. *Obes Surg* 19:894–904
35. Patalay M, Lofgren IE, Freake HC, Koo SI, Fernandez ML (2005) The lowering of plasma lipids following a weight reduction program is related to increased expression of the LDL receptor and lipoprotein lipase. *J Nutr* 135:735–739
36. Berman DM, Nicklas BJ, Ryan AS, Rogus EM, Dennis KE, Goldberg AP (2004) Regulation of lipolysis and lipoprotein lipase after weight loss in obese, postmenopausal women. *Obes Res* 12:32–39

Introduction

The link between high serum low-density lipoprotein (LDL) cholesterol concentrations and cardiovascular disease (CVD) has been clearly established [1]. However, evidence is accumulating that high serum concentrations of triacylglycerols (TAG)—also known as hypertriglyceridemia—and low serum concentrations of high-density lipoprotein (HDL) cholesterol are also causally related to CVD [1]. TAG are major lipids in chylomicrons and very-low-density lipoprotein (VLDL) particles. These particles are closely related to the metabolism of other lipoproteins, including HDL. High TAG and low HDL often occur together, frequently with normal concentrations of LDL cholesterol, increased concentrations of small dense (sd) LDL and apoB, and insulin resistance [1]. This lipid abnormality is a fundamental characteristic of patients with the metabolic syndrome, a condition strongly associated with the risk to develop type II diabetes (DM2) and CVD [1].

Interestingly, a recent meta-analysis has indicated that consumption of plant stanol esters (PSE) not only lowers serum LDL cholesterol, but also serum TAG concentrations, in particular in subjects with high baseline TAG concentrations [2]. This meta-analysis was based on five trials carried out in our department and included almost 400 subjects. The reason that these effects have not been observed in individual studies may have been due to a lack of statistical power, as effects were only marginal in subjects with normal serum TAG concentrations. We therefore decided to design for the first time a study to specifically evaluate the effects of PSE on the serum lipoprotein profile in a population with elevated fasting serum TAG concentrations.

Subjects and methods

Subjects

Subjects, aged between 18 and 70 years, were recruited among an already existing cohort of patients diagnosed with familial combined hyperlipidemia (FCHL) at the Academic Hospital Maastricht (AZM). Patients were characterized by a specific phenotype, i.e. serum total cholesterol concentrations >6.5 mmol/L and/or elevated serum TAG concentrations (>2.3 mmol/L) at different visits before taking medication. Also subjects, who had serum TAG concentrations between 1.7 and 4.0 mmol/L, as indicated in earlier studies at our department, were approached. A fasting serum TAG concentration >1.7 mmol/L was chosen as lower boundary as this concentrations is considered to be elevated [3], while subjects with concentrations >4.0 mmol/L frequently need to be treated with medication [4].

Participants were further selected for the study according to the following inclusion criteria: no history of CVD such as congestive heart failure or recent (<6 months) event (acute myocardial infarction, CVA), type I and II diabetes mellitus, epilepsy, asthma, COPD (chronic obstructive pulmonary disease), inflammatory bowel diseases, cancer, or rheumatoid arthritis; no use of diuretics; no abuse of drugs and/or alcohol; willing to abstain from alcohol 3 days before blood sampling; no pregnant or breast-feeding women; and no use of an investigational product 30 days before the study. The Medical Ethical Committee of the University of Maastricht had approved the study. Participants were given a detailed description of the experimental protocol and purpose of the study before they gave their written informed consent. Twenty-nine volunteers were selected for the study. One subject withdrew in the third week of the study because of difficulty in performing venipuncture. All other 28 volunteers, 16 men and 12 women, completed the study. Baseline characteristics did not differ between the treatment groups, except for the number of smokers (Table 1).

Experimental design

The study had a randomized, double-blind, placebo-controlled, parallel design. Two weeks before the start of the actual study and during the 4 weeks of the study, subjects had to stop [in consultation with their general practitioner (GP)] the intake of their regular cholesterol-lowering medication (statins or cholesterol-absorption inhibitors) when appropriate. No other classes of cholesterol-lowering drugs were used. Besides serum LDL and HDL cholesterol concentrations, this medication can also lower serum TAG concentrations. During the first 2 weeks of the study (before the run-in period), subjects were given a control margarine containing 60% absorbable fats. After these 2 weeks, the volunteers returned for blood sampling to the university. Further participation (and thus continuation of the medication-free period) was allowed only if serum total cholesterol concentrations were <8.0 mmol/L and TAG concentrations <4.0 mmol/L. Otherwise, subjects were sent back to their GP and were advised to (re)start lipid-lowering medication according to the Dutch Cholesterol Consensus [4]. When serum cholesterol concentrations were <8.0 mmol/L and TAG concentrations between 1.7 and 4.0 mmol/L, subjects continued to consume daily 20 g of the control margarine for one more week. At the end of this run-in period, subjects were randomly divided over two groups, stratified for gender. The following 3 weeks (experimental period), one group continued to consume the control margarine, while the other group consumed daily 20 g of the experimental margarine, which had a similar fat content and fatty acid composition as the control

Table 1 Baseline characteristics

	All	Control diet	PSE diet	<i>P</i> value ^a
Number (M/F)	28 (16/12)	14 (8/6)	14 (8/6)	–
Age (years)	54 ± 8	55 ± 9	53 ± 8	0.598
BMI (kg/m ²)	28 ± 3	28 ± 3	29 ± 4	0.208
Systolic blood pressure (mmHg)	131 ± 13	132 ± 12	131 ± 14	0.808
Diastolic blood pressure (mmHg)	87 ± 8	89 ± 9	86 ± 6	0.321
Total cholesterol (mmol/L)	7.17 ± 0.96	7.02 ± 1.14	7.32 ± 0.76	0.425
LDL cholesterol (mmol/L)	4.75 ± 1.01	4.67 ± 1.00	5.03 ± 0.77	0.272
HDL cholesterol (mmol/L)	1.27 ± 0.33	1.32 ± 0.43	1.21 ± 0.17	0.375
Triacylglycerol (mmol/L)	2.62 ± 0.68	2.61 ± 0.59	2.63 ± 0.77	0.947
Smokers	4	0	4	0.031
Lipid-lowering medication ^b	5	2	3	0.637

Values are means ± SD

PSE plant stanol esters

^a Data were analyzed by the independent Student's *t* test. Differences were considered statistically significant at *P* < 0.05

^b Subjects had to stop the intake of their lipid-lowering medication 2 weeks before the actual start of the study and during the 4 weeks of the study

margarine, but provided 2.5 g plant stanols. Plant stanols were made by saturation of plant sterols from tall oil, with a distribution of sitostanol (77.7%), campestanol (16.7%), sitosterol (2.2%), campesterol (1.8%), brassicasterol (0.1%), stigmaterol (0.1%), and other phytosterols (1.4%) (Raisio Group, Finland). The free plant stanols were esterified with fatty acids derived from sunflower oil before incorporation into the margarine. The margarine was packed in tubs of 140 g, equivalent to margarine for 7 days. Subjects had to divide the content of one tub into seven equal pieces of 20 g of margarine. One piece of 20 g had to be used on bread/crackers each day. All products were coded with a color label to blind the subjects and the investigators. All margarine leftovers had to be returned to the department and were weighed for the calculation of average daily margarine intake.

Participants recorded in diaries any signs of illness, medication used, menstrual phase, alcohol consumption, any deviations of the study protocol, and any of the following experienced complaints: headache, stomach complaints, nausea, bloated feeling, flatulence, diarrhea, constipation, itching, eruptions/rashes, fatigue and dizziness. Other possible side effects were monitored at the end of the run-in (day 21) and experimental period (day 42) by assessing parameters reflecting liver function.

Subjects also recorded their food intake for the previous 3 weeks at days 21 and 42 by completing food-frequency questionnaires (FFQ) to estimate their energy and nutrient intakes (Table 2). FFQ were checked by a registered dietician in the presence of the subjects. Body weight without shoes or heavy clothes was recorded at each visit.

Blood sampling

Five fasting blood samples were drawn during the study. All venipunctures were generally carried out by the same person, at the same location, and at the same time of the day (between 07:45 and 11:00 a.m.) on days 14, 21, 32, 37, and 42. Blood samples were taken from a forearm vein using vacutainers under minimal stasis with the subject in a supine position. On the morning of sampling, subjects were not allowed to smoke, to eat or to drink (except water). Volunteers had been fasting since 10 p.m. on the day preceding blood sampling. In addition, subjects were not allowed to drink alcohol 3 days before sampling.

Blood was collected in a 10-mL serum tube (Becton–Dickinson Vacutainer Systems, Breda, The Netherlands) for analysis of lipids (total cholesterol, HDL cholesterol, TAG), apolipoproteins (apoA-I, apoB-100), plant sterols and stanols, insulin, hs-CRP, and indices of liver function. Serum tubes were kept at room temperature after blood sampling. At least 1 h after venipuncture, serum was obtained by centrifuging at 2,000×*g* for 30 min at 4 °C. Serum was aliquoted and thereafter stored at –80 °C. At the same time, 4 mL of blood was also collected in a NaF tube (Becton–Dickinson Vacutainer Systems, Breda, The Netherlands) for analysis of glucose. Plasma was obtained immediately by centrifugation at 2,000×*g* for 30 min at 4 °C. Plasma was then divided into aliquots, snap-frozen, and stored at –80 °C. At days 21 and 42, blood was also collected in a 10-mL EDTA tube (Becton–Dickinson Vacutainer Systems, Breda, The Netherlands) for analysis of the plasma lipoprotein profile (lipoprotein particles).

Table 2 Nutrient composition of the two diets according to food frequency questionnaires

	Run-in period	Test period	<i>P</i> value ^a
Energy (MJ/day)			
Control diet	10.0 ± 2.0	10.3 ± 2.9	0.167
PSE diet	8.9 ± 2.3	8.6 ± 2.1	
Protein (en%)			
Control diet	17.5 ± 2.5	17.1 ± 2.3	0.697
PSE diet	17.3 ± 2.3	17.2 ± 2.2	
Total fat (en%)			
Control diet	35.7 ± 4.6	35.8 ± 1.3	0.583
PSE diet	35.5 ± 4.1	36.0 ± 3.6	
SFA (en%)			
Control diet	12.5 ± 2.5	12.5 ± 2.6	0.656
PSE diet	11.9 ± 1.5	12.2 ± 1.1	
MUFA (en%)			
Control diet	11.7 ± 1.6	11.7 ± 1.6	0.865
PSE diet	11.6 ± 2.0	11.6 ± 2.0	
PUFA (en%)			
Control diet	8.0 ± 1.5	8.0 ± 1.8	0.560
PSE diet	9.1 ± 1.8	9.3 ± 1.7	
Carbohydrates (en%)			
Control diet	44.7 ± 4.0	44.5 ± 4.5	0.975
PSE diet	45.0 ± 5.8	44.9 ± 6.0	
Fiber (g/MJ)			
Control diet	3.0 ± 0.8	2.9 ± 0.9	0.603
PSE diet	3.0 ± 0.5	2.9 ± 0.6	
Alcohol (en%)			
Control diet	1.7 ± 2.3	2.2 ± 2.4	0.373
PSE diet	1.9 ± 3.0	1.8 ± 3.5	
Cholesterol (mg/MJ)			
Control diet	22.2 ± 5.2	21.0 ± 5.4	0.446
PSE diet	22.0 ± 4.3	21.7 ± 5.4	

Values are means ± SD

PSE plant stanol esters

^a The difference between the change in the control versus the change in the PSE group was considered statistically significant at *P* < 0.05. Data were analyzed by the independent Student's *t* test

EDTA plasma was obtained directly by centrifugation of the EDTA tube at 2,000×*g* for 30 min at 4 °C. Plasma was then divided into aliquots, snap-frozen, and subsequently stored at −80 °C until analysis.

Side effects

Serum samples from days 21 and 42 were analyzed to determine parameters of liver function (alanine transaminase, aspartate aminotransferase, γ -glutamyl transpeptidase, alkaline phosphatase, and total bilirubin). Measurements were carried out on a Beckman Coulter Synchron LX20 PRO Clinical System (Beckman Coulter Inc., Fullerton, CA, USA). All samples from one subject were analyzed in the same analytical run.

Inflammation

Serum samples from days 21 and 42 were analyzed to determine hs-CRP with a highly sensitive immunoturbidimetric assay (Kamiya Biomedical Company, Seattle, WA, USA). All samples from one subject were analyzed in the same analytical run.

Lipid metabolism

Concentrations of total cholesterol (ABX Diagnostics, Montpellier, France), HDL cholesterol (precipitation method; Roche Diagnostics Corporation, Indianapolis, IN, USA), and TAG corrected for free glycerol (Sigma–Aldrich Chemie, Steinheim, Germany) were analyzed enzymatically in all serum samples. Apolipoprotein concentrations (apoA-I, apoB-100) were analyzed in serum samples from days 14, 21, 37, and 42 using an immunoturbidimetric method (ABX Diagnostics, Montpellier, France). Serum LDL cholesterol concentrations were calculated by the formula of Friedewald et al. [5]. The plasma lipoprotein profile (lipoprotein particles) was analyzed with NMR by Liposcience (NMR LipoProfile test, Liposcience Inc., Raleigh, NC, USA). All samples from one subject were analyzed in the same analytical run.

Glucose metabolism

Plasma samples from days 14, 21, 37, and 42 were analyzed enzymatically to determine glucose concentrations by using the hexokinase method (Roche Diagnostic Systems, Hoffmann-La Roche Ltd., Basel, Switzerland). Insulin was measured using an ELISA method (DRG Instruments GmbH, Germany). The HOMA index, a measure of insulin sensitivity, was calculated [6]. All samples from one subject were analyzed in the same analytical run.

Serum plant sterols and stanols

Plant sterols and stanols (campestanol, sitostanol, campesterol, sitosterol, lathosterol) were determined in serum samples from days 21 and 42 as described [7]. All samples from one subject were analyzed in the same analytical run.

Statistics

The sample size was calculated at 14 subjects per group to provide 80% statistical power to detect a true difference in fasting serum TAG concentrations equal or greater than 0.50 mmol/L between both groups.

Before the statistical analyses were carried out, serum lipid and lipoprotein concentrations from days 14 and 21 and days 37 and 42 were averaged for each subject. Plasma glucose and insulin concentrations from days 14 and 21 and days 37 and 42 were averaged as well. Normality was tested by the Shapiro–Wilk test. Hs-CRP concentrations and indices of liver function were not normally distributed and analyzed accordingly by the non-parametric Mann–Whitney test. Differences in baseline characteristics between the control and intervention groups, and differences in changes in dietary intakes were analyzed by the independent Student's *t* test. Metabolic parameters were analyzed by ANCOVA. To answer the question whether baseline subject characteristics influenced response-to-treatment, the baseline value of that variable was included (as a covariate) into the model together with an interaction term (baseline value \times treatment). The interaction term was only included in the final statistical model if statistically significant. Values are presented as means \pm SD. Pearson correlation coefficients were determined for the relationship between the PSE-induced changes in TAG and the changes in the different lipoprotein particles. Differences were considered statistically significant at a $P < 0.05$. Statistical analyses were performed using SPSS 11.0 (version 11.0.3) for Macintosh OS X (version 10.3.9).

Inspection of the diaries revealed that five subjects had consumed alcohol during the 3-day period before blood sampling. For this reason, their corresponding TAG values for that particular day were omitted from the analyses. In addition, one subject had to be excluded from the statistical analyses, because of alcohol consumption on days 14, 37, and 42. Another subject was excluded, because he confirmed that he had continued his use of lipid-lowering medication during a part of the study, as indicated by a questionnaire filled out at the end of the study. Therefore in the final statistical analyses, the data of 26 subjects were used.

Results

Side effects

Liver function was assessed to monitor side effects. Throughout the study, all variables remained within the normal range for all subjects and no treatment effects were present (data not shown).

Dietary intake and body weight

As calculated from the returned tubs, average daily consumption of margarine on the control and PSE diets was 19.3 ± 1.9 and 19.3 ± 1.8 g, respectively. Average daily plant stanol intake was therefore 2.41 ± 0.23 g. Changes in daily energy intake and nutrient composition of the diets did not differ among the treatment groups (Table 2). Changes in body weight were similar for the control and PSE groups ($P = 0.579$), and were -0.10 ± 0.92 and 0.11 ± 0.74 kg, respectively.

Inflammation

Concentrations of hs-CRP, a marker for inflammation, also did not change during the study. Five subjects had, unrelated to the dietary treatments, on one or more occasion hs-CRP concentrations >9 mg/L [8]. When these subjects were excluded from the analysis, conclusions did not change (data not shown).

Lipid metabolism

Compared to the control diet, consumption of PSE significantly decreased serum total and LDL cholesterol concentrations by 6.7% ($P = 0.015$) and 9.5% ($P = 0.041$), respectively. In addition, serum apoB-100 concentrations were significantly lowered by 7.1% ($P = 0.007$). Changes in serum HDL cholesterol and apoA-1 concentrations did not differ among the diet groups (Table 3). A significant interaction between baseline TAG value and PSE intake was found ($P = 0.009$). PSE consumption lowered TAG concentrations by 11% in subjects with high baseline TAG concentrations (>2.3 mmol/L). For subjects with lower baseline serum TAG concentrations (<2.3 mmol/L), PSE consumption did not affect serum TAG concentrations.

Further, a significant interaction between the baseline number of the total LDL particles (LDL-P) and PSE intake was found ($P = 0.020$; Table 4). Supplementation of PSE lowered the total number of LDL-P, primarily in subjects with elevated baseline values. This decrease was reflected by a reduction of similar magnitude in the number of sdLDL particles, but this decline did not reach statistical significance ($P = 0.150$).

Serum sterols and stanols

Cholesterol-standardized serum sterol and stanol concentrations are presented in Table 5. A significant interaction between baseline concentrations of cholesterol-standardized sitostanol and response-to-treatment was found ($P = 0.011$). Consumption of PSE increased cholesterol-standardized sitostanol concentrations, in particular in subjects

Table 3 Effects of PSE consumption on serum lipids and lipoproteins

	Run-in period	Test period	<i>P</i> value ^a		
			Baseline	Diet	Baseline × diet
Total cholesterol					
Control diet	7.14 ± 0.89	7.13 ± 1.03	0.866	0.015	–
PSE diet	7.35 ± 0.67	6.85 ± 0.73			
LDL cholesterol					
Control diet	4.63 ± 0.89	4.62 ± 0.97	0.265	0.041	–
PSE diet	4.96 ± 0.70	4.48 ± 0.66			
HDL cholesterol					
Control diet	1.30 ± 0.41	1.19 ± 0.40	0.271	0.586	–
PSE diet	1.20 ± 0.18	1.18 ± 0.17			
Triacylglycerols					
Control diet	2.63 ± 0.58	2.71 ± 0.71	n.a.	n.a.	0.009
PSE diet	2.52 ± 0.66	2.50 ± 0.47			
ApoB-100					
Control diet	1.28 ± 0.23	1.30 ± 0.22	0.322	0.007	–
PSE diet	1.36 ± 0.16	1.28 ± 0.16			
ApoA-1					
Control diet	1.46 ± 0.34	1.46 ± 0.35	0.746	0.666	–
PSE diet	1.42 ± 0.19	1.41 ± 0.19			

Values are means ± SD and are expressed in mmol/L, except for apoB-100 and apoA-1 which are expressed in mg/L. Days 14 and 21 were averaged for the end of the run-in period. Days 37 and 42 were averaged for the end of the experimental period

n.a. not applicable, PSE plant stanol esters

^a The difference between the change in the control versus the change in the PSE group was considered statistically significant at $P < 0.05$. Data were analyzed by ANCOVA. To answer the question whether baseline subject characteristics influenced response-to- treatment, the baseline value of the variable of interest was included (as a covariate) into the model together with an interaction term (baseline value × diet). The interaction term was only included in the statistical model if statistically significant. For the control group, diet was coded with a “0” and for the intervention group with a “1”

with elevated baseline values. Additionally, eating the PSE-enriched margarine significantly increased cholesterol-standardized serum campestanol concentrations ($P < 0.001$). Plant stanol concentrations increased in every subject receiving the PSE-enriched margarines, which demonstrates good compliance with the study protocol.

Compared to the control diet, cholesterol-standardized serum sitosterol ($P = 0.008$) and campesterol ($P = 0.020$) concentrations significantly decreased after PSE consumption, indicating decreased intestinal cholesterol absorption [9]. A significant interaction between baseline cholesterol-standardized lathosterol concentrations and plant stanol intake was found ($P = 0.043$). Daily intake of PSE increased this marker for endogenous cholesterol synthesis, especially in subjects with elevated baseline values.

Glucose metabolism

Changes in plasma glucose and insulin concentrations, and HOMA index did not differ among the diet groups (data not shown).

Correlations

Significant correlations were found between PSE-induced changes in concentrations of TAG and large VLDL particles ($r = 0.713$, $P < 0.001$), large LDL-P ($r = -0.575$, $P = 0.002$), and sdLDL particles ($r = 0.438$, $P = 0.025$). Further, PSE-induced changes in TAG significantly correlated with medium HDL particle concentrations ($r = 0.394$, $P = 0.047$). Regarding the remaining lipoprotein particles, no significant correlations were found with the PSE-induced changes in TAG (data not shown).

Discussion

This study was specifically designed to examine the effects of PSE on serum TAG concentrations in subjects with elevated serum concentrations of TAG. In line with our recent meta-analysis [2], a significant interaction between baseline TAG concentrations and PSE intake was found. Also, we have recently shown that plant stanols lowered

Table 4 Effects of PSE consumption on the plasma NMR lipoprofile

	Run-in period	Test period	<i>P</i> value ^a		
			Baseline	Diet	Baseline × diet
Total VLDL					
Control diet	107 ± 29	106 ± 28	0.040	0.643	–
PSE diet	117 ± 29	116 ± 29			
Large VLDL					
Control diet	13 ± 6	12 ± 5	0.028	0.897	–
PSE diet	11 ± 7	13 ± 10			
Medium VLDL					
Control diet	46 ± 20	53 ± 20	0.007	0.322	–
PSE diet	54 ± 22	51 ± 16			
Small VLDL					
Control diet	48 ± 18	41 ± 17	0.052	0.148	–
PSE diet	52 ± 19	52 ± 26			
Total LDL					
Control diet	1784 ± 413	1791 ± 519	n.a.	n.a.	0.020
PSE diet	1901 ± 337	1688 ± 306			
IDL					
Control diet	78 ± 57	99 ± 55	0.015	0.368	–
PSE diet	105 ± 44	82 ± 58			
Large LDL					
Control diet	240 ± 197	224 ± 189	0.009	0.600	–
PSE diet	175 ± 158	168 ± 137			
sdLDL					
Control diet	1466 ± 471	1468 ± 531	0.277	0.150	–
PSE diet	1621 ± 364	1438 ± 320			
Total HDL					
Control diet	30 ± 7	31 ± 8	0.873	0.268	–
PSE diet	31 ± 4	31 ± 3			
Large HDL					
Control diet	4.7 ± 3.6	4.7 ± 3.7	0.341	0.728	–
PSE diet	3.6 ± 2.1	3.8 ± 2.0			
Medium HDL					
Control diet	5.6 ± 4.8	5.3 ± 2.9	0.004	0.992	–
PSE diet	4.2 ± 3.3	5.0 ± 4.7			
Small HDL					
Control diet	20 ± 6	21 ± 6	0.052	0.748	–
PSE diet	24 ± 3	23 ± 4			

Values are means ± SD and are expressed in nmol/L, except for HDL particles which are expressed in μmol/L

n.a. not applicable, *PSE* plant stanol esters

^a The difference between the change in the control versus the change in the PSE group was considered statistically significant at $P < 0.05$. Data were analyzed by ANCOVA. To answer the question whether baseline subject characteristics influenced response-to-treatment, the baseline value of the variable of interest was included (as a covariate) into the model together with an interaction term (baseline value × diet). The interaction term was only included in the statistical model if statistically significant. For the control group, diet was coded with a “0” and for the intervention group with a “1”

serum TAG concentrations in subjects with the metabolic syndrome [10]. Based on the meta-analysis [2], the expected decrease in serum TAG concentrations was on average 0.09 mmol/L for “borderline high” baseline TAG

concentrations (1.7–2.2 mmol/L; [3]) and a daily plant stanol intake of 2.5 g. At a similar intake, the expected decline in serum TAG concentrations at “high” baseline TAG values (2.3–4.0 mmol/L; [3]), was on average

Table 5 Serum phytosterols (corrected for serum cholesterol as measured by GC)

	Run-in period	Test period	<i>P</i> value ^a		
			Baseline	Diet	Baseline × diet
Campestanol					
Control diet	1.12 ± 0.49	1.12 ± 0.42	0.270	<0.001	–
PSE diet	1.20 ± 0.56	10.06 ± 3.58			
Sitostanol					
Control diet	2.58 ± 0.70	2.41 ± 0.62	n.a.	n.a.	0.011
PSE diet	2.51 ± 0.69	22.97 ± 7.60			
Campesterol					
Control diet	159 ± 41	154 ± 42	0.021	0.020	–
PSE diet	183 ± 73	152 ± 61			
Sitosterol					
Control diet	129 ± 31	123 ± 27	0.007	0.008	–
PSE diet	141 ± 47	114 ± 39			
Lathosterol					
Control diet	188 ± 64	195 ± 46	n.a.	n.a.	0.043
PSE diet	184 ± 54	210 ± 65			

Values are means ± SD and are expressed in (μmol/mmol cholesterol) × 100

n.a. not applicable, PSE plant stanol esters

^a The difference between the change in the control versus the change in the PSE group was considered statistically significant at $P < 0.05$. Data were analyzed by ANCOVA. To answer the question to whether baseline subject characteristics influenced response-to-treatment, the baseline value of the variable of interest was included (as a covariate) into the model together with an interaction term (baseline value × diet). The interaction term was only included in the statistical model if statistically significant. For the control group, diet was coded with a “0” and for the intervention group with a “1”

0.19 mmol/L. Compared to these predicted effects, our results are slightly different since a reduction in serum TAG concentrations was hardly present at baseline TAG values <2.3 mmol/L. In contrast, at “high” baseline TAG concentration, the average decrease was larger than anticipated, i.e. 0.35 mmol/L. It is possible that the estimates from the meta-analysis for subjects selected on disturbances in TAG metabolism are less precise, because most of the subjects in the meta-analysis had serum TAG concentrations <2.0 mmol/L.

As TAG in the fasted state are mainly transported by VLDL particles, it can be suggested that VLDL metabolism is changed after consumption of PSE. However, plasma concentrations of VLDL particles (large, medium, small) were not significantly altered after the PSE diet. TAG-rich lipoproteins (TRL), such as chylomicrons, VLDL (small, large), and TRL remnants play a significant role in the pathogenesis of atherosclerosis, the main cause of CVD [1]. It has been proposed that the potential atherogenicity of the large VLDL particles resides in their susceptibility to oxidation, which promotes foam cell formation by a mechanism analogous to that of oxidized LDL [11]. In support, however, of an effect on VLDL metabolism, a significant correlation was found between the PSE-induced changes in TAG and large VLDL particle

concentrations. Regarding medium and small VLDL particles, no significant correlations were found between the change in these particle numbers and the change in TAG concentrations. Possibly, the variation in response of the different VLDL particles was too large to reach statistically significant dietary effects.

Daily consumption of 2.4 g plant stanols also significantly decreased serum LDL cholesterol concentrations by 9.5%. This change is consistent with the estimated mean change in LDL cholesterol concentrations of –8.9% for daily intakes of 2.0 to 2.4 g plant sterols or stanols [12]. Serum apoB-100 concentrations were lowered by 7.1%, which is in the same range as the reductions for total and LDL cholesterol. As expected, no effects on serum HDL cholesterol and apoA-1 concentrations were found. Plant sterols and stanols lower serum LDL cholesterol by interfering with the absorption of cholesterol in the intestine [13]. As a consequence, endogenous cholesterol synthesis and LDL receptor-mediated cholesterol uptake will increase, which will lead to decreased serum LDL cholesterol [14]. In support of this working mechanism and in agreement with previous studies [15, 16], consumption of PSE significantly lowered concentrations of markers reflecting cholesterol absorption and increased concentrations of a marker reflecting endogenous cholesterol

synthesis. In our study, the serum LDL cholesterol-lowering effect was mainly related to a decrease (−11.2%) in the atherogenic sdLDL particles, but this effect was not statistically significant. A significant positive correlation however was found between the plant stanol-induced changes in TAG and sdLDL particle concentrations. sdLDL particles are particularly considered to be atherogenic, since these particles are retained preferentially by the artery wall and are readily oxidized [1, 17]. Generation of small, dense LDL occurs by intravascular lipoprotein remodeling as a result of metabolic disturbances, which are frequently present in patients with DM2 and the metabolic syndrome [17]. The common underlying predisposing factor may be the development of a fatty liver resulting in hypertriglyceridemia, due to in particular large VLDL particles. Large VLDL particles are a precursor for the synthesis of sdLDL by LPL mediated processes [18].

Hypertriglyceridemia is also associated with an overproduction of other cardiovascular risk factors, such as glucose, hs-CRP, plasminogen activator inhibitor-1 (PAI-1), fibrinogen, and coagulation factors [1]. We therefore looked into the effects of the PSE diet on glucose metabolism in our hypertriglyceridemic study population. However, consumption of PSE did not favorably alter glucose and insulin concentrations, and consequently the HOMA index (insulin resistance measurement) was also unchanged. These effects are in line with earlier findings in healthy subjects, where glucose concentrations were not changed after supplementation of a reduced-calorie orange juice beverage enriched with plant sterols (2 g/day) [19]. In addition, daily consumption of plant sterol ester (1.9 g plant sterols) and PSE (2.0 g plant stanols)-enriched spreads for 10 weeks did not change plasma glucose and serum insulin concentrations in hypercholesterolemic subjects [20].

There are some limitations of this study. First, we did not measure effects on postprandial TAG concentrations. As PSE consumption interferes with intestinal cholesterol absorption, it can be suggested that effects on postprandial lipid metabolism are even more pronounced. Studies on the postprandial effects of phytosterols are however scarce. In healthy subjects, 2-week PSE consumption (3 g/day plant stanols) only tended to diminish postprandial TAG concentrations [21]. In addition, the use of PSE (3 g/day plant stanols)-enriched margarine did not decrease postprandial triglyceridemia in statin patients [22]. Another limitation is the generalization of our findings to different etiologies of hypertriglyceridemia. Like hypercholesterolemia, hypertriglyceridemia has a broad genetic base and cannot be extrapolated depending on the mechanism.

To summarize, consumption of PSE significantly lowered serum LDL cholesterol in subjects with elevated TAG concentrations, primarily by a decrease in the atherogenic

sdLDL particles. The PSE-induced TAG-lowering in these subjects was related to their baseline TAG concentrations, and was particularly evident in subjects with high serum TAG concentrations. Taken together, these findings show that functional foods enriched with PSE are not only of benefit to lower increased serum LDL cholesterol concentrations, but also those of TAG in subjects with overt hypertriglyceridemia.

Acknowledgements We thank the study participants for their cooperation and enthusiasm. We also thank the technical and dietary staff from our department for their support. The study was supported financially by the Raisio Group Finland.

References

1. Malloy MJ, Kane JP (2001) A risk factor for atherosclerosis: triglyceride-rich lipoproteins. *Adv Intern Med* 47:111–136
2. Naumann E, Plat J, Kester AD, Mensink RP (2008) The baseline serum lipoprotein profile is related to plant stanol induced changes in serum lipoprotein cholesterol and triacylglycerol concentrations. *J Am Coll Nutr* 27:117–126
3. Haymore BR, Parks JR, Oliver TG, Gliester BC (2005) Hypertriglyceridemia. *Hospital Physician*, 17–24
4. Syllabus behandeling en preventie van coronaire hartziekten door verlaging van de plasmaconcentratie. Utrecht: Centraal Begeleidingsorgaan voor de Intercollegiale Toetsing, 1998
5. Friedewald WT, Levy RI, Fredrickson DS (1972) Estimation of the concentration of low-density lipoprotein cholesterol in plasma, without use of the preparative ultracentrifuge. *Clin Chem* 18:499–502
6. Matthews DR, Hosker JP, Rudenski AS, Naylor BA, Treacher DF, Turner RC (1985) Homeostasis model assessment: insulin resistance and beta-cell function from fasting plasma glucose and insulin concentrations in man. *Diabetologia* 28:412–419
7. Plat J, Mensink RP (2001) Effects of diets enriched with two different plant stanol ester mixtures on plasma ubiquinol-10 and fat-soluble antioxidant concentrations. *Metabolism* 50:520–529
8. Shine B, de Beer FC, Pepys MB (1981) Solid phase radioimmunoassays for human C-reactive protein. *Clin Chim Acta* 117:13–23
9. Nissinen MJ, Gylling H, Miettinen TA (2008) Responses of surrogate markers of cholesterol absorption and synthesis to changes in cholesterol metabolism during various amounts of fat and cholesterol feeding among healthy men. *Br J Nutr* 99:370–378
10. Plat J, Brufau G, Dallinga-Thie GM, Dasselaar M, Mensink RP (2009) A plant stanol yogurt drink alone or combined with a low-dose statin lowers serum triacylglycerol and non-HDL cholesterol in metabolic syndrome patients. *J Nutr* 139:1143–1149
11. Havel RJ (2000) Remnant lipoproteins as therapeutic targets. *Curr Opin Lipidol* 11:615–620
12. Katan MB, Grundy SM, Jones P, Law M, Miettinen T, Paoletti R (2003) Efficacy and safety of plant stanols and sterols in the management of blood cholesterol levels. *Mayo Clin Proc* 78:965–978
13. Plat J, Nichols JA, Mensink RP (2005) Plant sterols and stanols: effects on mixed micellar composition and LXR (target gene) activation. *J Lipid Res* 46:2468–2476
14. Plat J, Mensink RP (2002) Effects of plant stanol esters on LDL receptor protein expression and on LDL receptor and HMG-CoA reductase mRNA expression in mononuclear blood cells of healthy men and women. *Faseb J* 16:258–260

15. Vuorio AF, Gylling H, Turtola H, Kontula K, Ketonen P, Miettinen TA (2000) Stanol ester margarine alone and with simvastatin lowers serum cholesterol in families with familial hypercholesterolemia caused by the FH-North Karelia mutation. *Arterioscler Thromb Vasc Biol* 20:500–506
16. Theuwissen E, Mensink RP (2007) Simultaneous intake of β -glucan and plant stanol esters affects lipid metabolism in slightly hypercholesterolemic subjects. *J Nutr* 137:583–588
17. Packard CJ (2003) Triacylglycerol-rich lipoproteins and the generation of small, dense low-density lipoprotein. *Biochem Soc Trans* 31:1066–1069
18. Cohn JS, Marcoux C, Davignon J (1999) Detection, quantification, and characterization of potentially atherogenic triglyceride-rich remnant lipoproteins. *Arterioscler Thromb Vasc Biol* 19:2474–2486
19. Devaraj S, Autret BC, Jialal I (2006) Reduced-calorie orange juice beverage with plant sterols lowers C-reactive protein concentrations and improves the lipid profile in human volunteers. *Am J Clin Nutr* 84:756–761
20. Hallikainen M, Lyyra-Laitinen T, Laitinen T et al (2006) Endothelial function in hypercholesterolemic subjects: effects of plant stanol and sterol esters. *Atherosclerosis* 188:425–432
21. Relas H, Gylling H, Miettinen TA (2000) Effect of stanol ester on postabsorptive squalene and retinyl palmitate. *Metabolism* 49:473–478
22. Castro Cabezas M, de Vries JH, Van Oostrom AJ, Iestra J, van Staveren WA (2006) Effects of a stanol-enriched diet on plasma cholesterol and triglycerides in patients treated with statins. *J Am Diet Assoc* 106:1564–1569

makes it possible to transform such molecules into alcohol. MP is used in China in the treatment of lipid disorders. In Western countries, the use is mainly limited to the pigmentation of meat, fish, cheese, alcoholic drinks and cured meats [1–4]. The hypocholesterolemic efficacy of MP was evaluated through experimental [5–8] and clinical [9–13] trials. By acting through the direct inhibition of 3-hydroxy-3-methylglutaryl coenzymeA reductase, MP could partially have the same effect as statins [14]. In order to enhance agent safety by giving the lowest dose without losing its hypocholesterolemic effect, MP was combined with Linear aliphatic alcohols (LAAs). LAAs show a synergic effect with MP as they induce the down-regulation of 3-hydroxy-3-methylglutaryl coenzymeA reductase [15]. MP and LAAs seem to have lowering effect on cholesterol, but not on TG. Niacin (N) was added because of its well-known hypotriglyceridemic effect. If given in high doses, N also induces an increase in HDLC [16, 17]. In this study Dif1stat[®] effects have been evaluated on a long-term basis in patients with primary moderate hypercholesterolemia.

Aim of the Study

Experimental Design

The target of this randomized trial for parallel groups was to evaluate the efficacy of adding MP–LAAs–N (Dif1stat[®]), 1 capsule/day [Composition: MP, dry extract, 200 mg (corresponding to 3 mg of mevinolin) + LAAs, 10 mg + N, 27 mg] to the treatment of patients with primary moderate hypercholesterolemia (lipoprotein phenotype IIa). One group (A) was treated with hypolipidemic diet according to adult treatment panel III (ATPIII) criteria [18]. In the second group (B) diet was supplemented with Dif1stat[®]. The study lasted 8 months.

Patients

The trial included 240 patients randomly assigned into two groups. The first group (group A # 130) was treated with diet only. In the second group (group B # 110) a capsule of Dif1stat[®] a day was added to the diet (Fig. 1). The average patient age was 56.5 ± 9 years. The average BMI was 22.3 ± 8.5 kg/cm² (Table 1). All the patients were under primary prevention with an overall coronary risk lower than 20% according to the Framingham algorithm [19]. All the patients were given an hypocholesterolemic diet in accordance with ATPIII guidelines (30% of total calories represented by lipids, less than 10% of them being saturated fats, 19% of proteins, 52% of carbohydrates for a

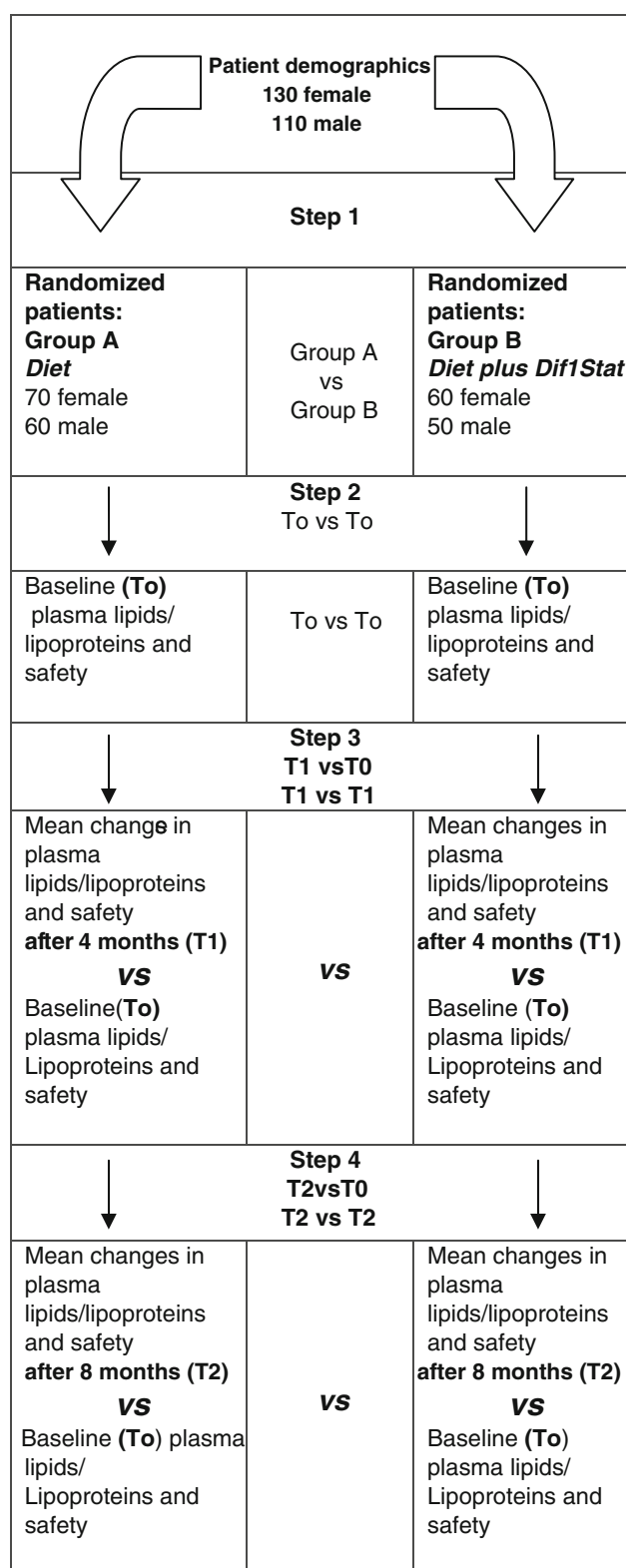


Fig. 1 Study design and schedule

total amount of 1,500/1,800 Kcal a day). The compliance to the diet was assessed every 2 months by two dieticians by way of 24-h dietary recall.

Table 1 Patient demographics

Study groups	No. of patients 240 (female/male)	Age (years \pm SD) 56.5 \pm 9	BMI T0 (kg/m ² \pm SD) 22.3 \pm 8.5	BMI T1 (kg/m ² \pm SD)	BMI T2 (kg/m ² \pm SD)
Diet (group A)	70/60	57 \pm 8	21.3 \pm 10	21.0 \pm 10	20.9 \pm 7.9
Diet plus Dif1Stat (group B)	60/50	56 \pm 10	23.3 \pm 7	23.0 \pm 6.8	22.8 \pm 7.1
<i>P</i> value		NS	NS	NS	NS

NS not significant

Exclusion Criteria

The subjects involved in the trial did not show clinical and hematological evidence of hepatic, kidney or thyroid disorders. There was no clinical evidence of cardiovascular disease, hypertension, diabetes or obesity. The patients were not taking lipid-lowering agents or drugs affecting lipid metabolism such as: β -blockers, diuretics, and corticosteroids.

Laboratory Methods

Clinical laboratory measurements were performed in a certified central university hospital laboratory. Blood samples for lipid measurements were taken from peripheral veins after overnight fasting (12 h). Plasma TC and TG levels were determined by enzyme assay (Cholesterol and Triglycerides Tests TM Instrumentation Laboratory Company-Lexington, MA, USA). The plasma HDLC level was determined with a combined immune and enzymatic assay (HDL Cholesterol Test TM Instrumentation Laboratory Company-Lexington, MA, USA). The plasma LDLC level was calculated according to the formula of Friedewald: $LDLC = TC - (HDLC + TG/5)$ [20]. The plasma non-HDLC level was calculated according to the following formula: $non-HDLC = TC - HDLC$. Laboratory safety parameters were determined by usual enzymatic and chemical methods. The blood cell count was determined with a Beckman Coulter ACT Diff. (Beckman Coulter, S.p.A, Milan, Italy-EU).

Ethics

Informed consent was obtained from all patients, according to the recommendations of the declaration of Helsinki guiding physicians in biomedical research involving human subjects. Adopted by the 18th World Medical Assembly, Helsinki, Finland, June 1964, amended by the 29th World Medical Assembly, Tokyo, Japan, October 1975, the 35th World Medical Assembly, Venice, Italy,

October 1983, and the 41st World Medical Assembly, Hong Kong, September 1989. The work was approved by the ethical panel of our institution.

Statistical Analysis

Statistical analysis was performed according to parametric tests, depending on parameters under evaluation. All results are expressed as means \pm SD. Within group and between groups differences were tested for statistical significance using Student's *t* test for paired data. The percent variation ($\Delta\%$) of mean lipid and lipoprotein levels in plasma was also estimated. Patients were randomized according to a list created by a random number generator included in the statistical package (SPSS version 15.0—Statistical Product and Services Solutions, SPSS Inc., Chicago, IL, USA).

Results

Plasma TC, LDLC, HDLC, TG, non-HDLC, ALT, AST, γ GT, CK, creatinine, urea and the fibrinogen profile at T0, are shown in Table 2. Between groups, statistically significant differences at baseline were not observed. Neither significant changes in lipid nor lipoprotein levels in plasma were observed after 4 months (T1) in group A. After 8 months (T2), significant reductions in plasma TC ($\Delta\%$: -22), LDLC ($\Delta\%$: -30) and non-HDLC ($\Delta\%$: -27) ($P \leq 0.001$) levels were observed in the same group; TG ($\Delta\%$: -8.4) and HDLC ($\Delta\%$: -5.5) were only slightly lower (Table 3; Fig. 2). Table 3 and Fig. 3 show the results obtained after Dif1stat[®] addition to the diet in group B. After 4 months (T1), the addition of Dif1stat[®] to the diet had induced a significant reduction in TC ($\Delta\%$: -21.3), LDLC ($\Delta\%$: -29) and non-HDLC ($\Delta\%$: -26) ($P \leq 0.001$). Significant differences in TG ($\Delta\%$: -6) and HDLC ($\Delta\%$: -2) were not observed. After 8 months (T2), the change of TC ($\Delta\%$: -29.4), LDLC ($\Delta\%$: -38), non-HDLC ($\Delta\%$: -37%) and TG ($\Delta\%$: -33%) in plasma showed a further increase ($P \leq 0.001$). HDLC was only slightly increased

Table 2 Baseline (T0) plasma lipids/lipoproteins, ALT, AST, γ -glutamyl transferase (γ -GT), creatine kinase (CK), creatinine, nitrogen, and fibrinogen concentrations in patients with mild hypercholesterolemia, randomized to treatment with Diet only and Diet plus Dif1Stat

Lipid/lipoproteins (mg/dL \pm SD)	Diet (group A) T0	Diet + Dif 1Stat T0 (group B)	P value
TC	262 \pm 12	272 \pm 10	NS
TG	142 \pm 9	146 \pm 6	NS
HDLC	54 \pm 14	53 \pm 13	NS
LDLC	179.6 \pm 45	190 \pm 51	NS
Non-HDLC	208 \pm 15	219 \pm 21	NS
ALT (UL \pm SD)	22 \pm 5	23 \pm 8	NS
AST (UL \pm SD)	27 \pm 10	28 \pm 9	NS
γ -GT (UL \pm SD)	12 \pm 4	11 \pm 7	NS
CK (UL \pm SD)	116 \pm 11	103 \pm 15	NS
Creatinine (mg/dL \pm SD)	0.78 \pm 6	0.8 \pm 8	NS
Nitrogen (mg/dL \pm SD)	35 \pm 3	37 \pm 5	NS
Fibrinogen (mg/dL \pm SD)	292 \pm 15	290 \pm 14	NS

HDLC high density lipoprotein-cholesterol, LDLC low-density lipoprotein-cholesterol, TC total cholesterol, non-HDLC non high density lipoprotein-cholesterol, TG triglycerides, NS not significant

Differences are calculated as follows: T0 versus T0

Table 3 Mean changes in plasma lipid and lipoproteins profile after 4 and 8 months treatment with Diet and Diet plus Dif1Stat

Lipid/lipoproteins (mg/dL \pm SD)	Baseline (T0)	4 months (T1)	Mean change (%)	P value	8 months (T2)	Mean change (%)	P value
Diet (group A)							
TC	262 \pm 12	242 \pm 15	-7.6	NS	203 \pm 50	-22	<0.001
TG	142 \pm 9	140 \pm 20	-1.4	NS	130 \pm 35	-8.4	NS
HDLC	54 \pm 14	53 \pm 21	-2	NS	51 \pm 18	-5.5	NS
LDLC	179.6 \pm 45	161 \pm 38	-10.3	NS	126 \pm 37	-30	<0.001
Non-HDLC	208 \pm 15	189 \pm 13	-9.13	NS	152 \pm 22	-27	<0.001
Diet plus Dif 1Stat (group B)							
TC	272 \pm 10	214 \pm 30	-21.3	<0.001	192 \pm 23	-29.4	<0.001
TG	146 \pm 6	137 \pm 24	-6	NS	98 \pm 12	-33	<0.001
HDLC	53 \pm 13	52 \pm 12	-2	NS	54 \pm 15	2	NS
LDLC	190 \pm 51	134.6 \pm 48	-29	<0.001	118.4 \pm 21	-38	<0.001
Non-HDLC	219 \pm 21	162 \pm 19	-26	<0.001	138 \pm 11	-37	<0.001

HDLC high density lipoprotein-cholesterol, LDLC low-density lipoprotein-cholesterol, TC Total cholesterol, non-HDLC non high density lipoprotein-cholesterol, TG triglycerides, NS not significant

Differences are calculated as follows diet (group A): T0 versus T1; T0 versus T2. Diet plus Dif 1Stat (group B): T0 versus T1; T0 versus T2

($\Delta\%$: +2) when compared to T0. The variation of safety parameters in plasma in both groups is shown in Table 4. A change in plasma profile of AST ($\Delta\%$: -29.6; $\Delta\%$: -59) and γ GT ($\Delta\%$: 25; $\Delta\%$: 33) was observed in group A after 4 (T1), and 8 (T2) months of treatment, respectively. The above mentioned variations were statistically significant when compared to the basal values ($P \leq 0.001$). Statistically significant reductions of ALT ($\Delta\%$: -21), AST ($\Delta\%$: 43) and γ GT ($\Delta\%$: -33%) ($P \leq 0.001$) levels were observed also in group B, but only after 8 months of treatment (T2). The change of lipid and lipoprotein profile between groups (A vs. B) after 4 (T1) and 8 (T2) months,

is shown in Table 5, and Fig. 4. After 8 months (T2), the addition of Dif1stat[®] to the diet in group B had induced a significant reduction in TG: (B) $\Delta\%$ -33 versus (A) $\Delta\%$ -8.4 ($P \leq 0.001$). Side effects were not observed in either of the groups.

Discussion

Available studies have highlighted that statins have a good lowering effect on C-reactive protein but not on lipoprotein (a) [Lp(a)] [21–24]. The extract of MP seems to be able to

Fig. 2 Plasma concentrations of total cholesterol (TC), triglycerides (TG), low-density lipoprotein-cholesterol (LDLC), high-density lipoprotein-cholesterol (HDLC) and non-HDLC in patients with mild hypercholesterolemic, baseline (T0), after 4 (T1) and 8 (T2) months treatment with Diet. * $P \leq 0.001$

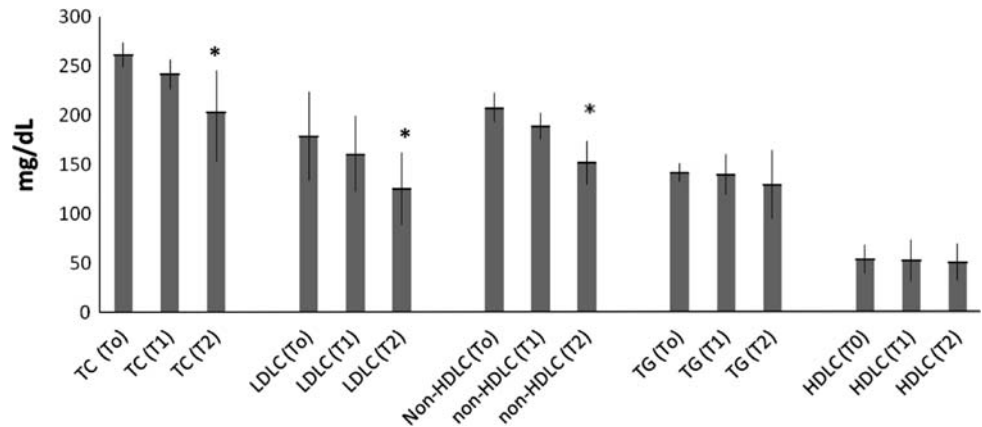


Fig. 3 Plasma concentrations of total cholesterol (TC), triglycerides (TG), low-density lipoprotein-cholesterol (LDLC), high-density lipoprotein-cholesterol (HDLC) and non-HDLC in patients with mild hypercholesterolemia values at baseline (T0), after 4 (T1) and 8 (T2) months treatment with Diet plus Dif1Stat. * $P \leq 0.001$

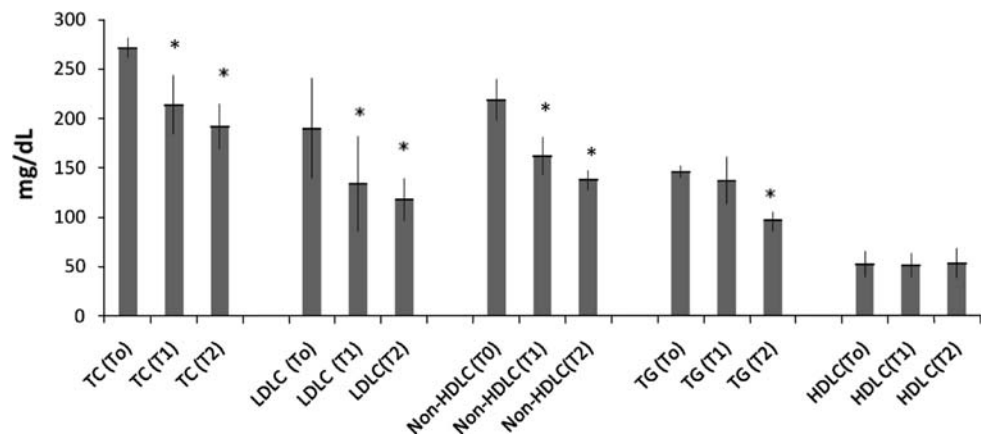


Table 4 Mean changes in plasma ALT, AST, γ -glutamyl transferase (γ -GT), creatine kinase (CK), creatinine, nitrogen, and fibrinogen levels after 4 and 8 months of treatment with Diet and Diet plus Dif1Stat

Enzyme/metabolite	Baseline (T0)	4 months (T1)	Mean change (%)	<i>P</i> value	8 months (T2)	Mean change (%)	<i>P</i> value
Diet (group A)							
ALT (UL \pm SD)	22 \pm 5	24 \pm 8	9	NS	23 \pm 14	4.4	NS
AST (UL \pm SD)	27 \pm 10	19 \pm 15	-29.6	<0.001	11 \pm 9	-59	<0.001
γ -GT (UL \pm SD)	12 \pm 6	15 \pm 7	25	<0.001	16 \pm 12	33	<0.001
CK (UL \pm SD)	116 \pm 11	122 \pm 21	5.1	NS	108 \pm 32	-7	NS
Creatinine (mg/dL \pm SD)	0.78 \pm 6	0.70 \pm 18	-10.2	NS	0.75 \pm 16	-3.8	NS
Nitrogen (mg/dL \pm SD)	35 \pm 13	32 \pm 21	-8.5	NS	34 \pm 18	-3	NS
Fibrinogen (mg/dL \pm SD)	292 \pm 15	287 \pm 25	-1.7	NS	294 \pm 36	0.68	NS
Diet plus Dif1Stat (group B)							
ALT (UL \pm SD)	23 \pm 8	21 \pm 15	-8.6	NS	18 \pm 22	-21	<0.001
AST (UL \pm SD)	28 \pm 9	26 \pm 19	-7	NS	16 \pm 6	-43	<0.001
γ -GT (UL \pm SD)	15 \pm 7	13 \pm 12	-13	NS	10 \pm 16	-33	<0.001
CK (UL \pm SD)	123 \pm 15	110 \pm 27	-10	NS	124 \pm 32	0.8	NS
Creatinine (mg/dL \pm SD)	0.8 \pm 18	0.92 \pm 11	15	NS	0.71 \pm 13	-11	NS
Nitrogen (mg/dL \pm SD)	37 \pm 5	31 \pm 12	-16	NS	34 \pm 24	-8	NS
Fibrinogen (mg/dL \pm SD)	290 \pm 14	294 \pm 29	1.3	NS	287 \pm 37	-1	NS

NS not significant

Table 5 Mean changes in lipid and lipoproteins profile after 4 and 8 months of treatment

Lipid/lipoproteins	Mean change (%) in group A 4 months (T1)	Mean change (%) in group B 4 months (T1)	<i>P</i> value	Mean change (%) in group A 8 months (T2)	Mean change (%) in group B 8 months (T2)	<i>P</i> value
TC	-7.6	-21.3	NS	-22	-29.4	NS
TG	-1.4	-6	NS	-8.4	-33	<0.001
HDLC	-2	-2	NS	-5.5	2	NS
LDLC	-10.3	-29	NS	-30	-38	NS
Non-HDLC	-9.13	-26	NS	-27	-37	NS

HDLC high density lipoprotein-cholesterol, *LDLC* low-density lipoprotein-cholesterol, *TC* Total cholesterol, *non-HDLC* non high density lipoprotein-cholesterol, *TG* triglycerides, *NS* not significant

Comparison between groups (Diet vs. Diet + Dif 1Stat)

Differences are calculated as follows Diet (group A) versus Diet plus Dif 1Stat (group B): T1 versus T1; T2 versus T2



Fig. 4 Mean change in plasma (*TC*), triglycerides (*TG*), low-density lipoprotein-cholesterol (*LDLC*), high-density lipoprotein-cholesterol (*HDLC*) and non-HDLC levels, in patients with mild hypercholesterolemia after 8 months (*T2*) of treatment with Diet and Diet plus Dif 1Stat

reduce the level of Lp(a) [25]. However, the effects of Dif1stat® on the above mentioned inflammatory and lipid parameters were not taken into account in our study. A trial with 60 patients affected by coronary heart disease assigned to two groups (extract of MP 1,200 mg/day vs. placebo for 6 weeks) showed that the extract of MP can significantly inhibit the postprandial increase of TG in blood [26]. The effect of MP on postprandial TG is more evident than the presence of LAAs could suggest. MP seems to be able to reduce TG by 32, 38, and 43%, after 2, 4, and 6 h, respectively. Some authors suggested that the effect of MP is not related only to the presence of LAAs but probably to a synergy between the various therapeutic agents. Some studies have demonstrated that the combination of MP, LAAs and N induces a significant decrease of TC, LDLC and TG. Castaño et al. [10] have carried out a randomized, double blind, controlled trial on patients affected by hypercholesterolemia with lipoprotein phenotype IIa. Two different doses of policosanol were given: 20 mg/day (# 29 patients) and 40 mg/day (# 30 patients). After 24 weeks, the two groups showed a reduction in LDLC of 27.1 and 28.1%, respectively. HDLC showed a

statistically significant increase of 17.6 and 17.0%, respectively. The LDLC/HDLC ratio changed by 37.2 and 36.5%. Lastly, TG decreased by 12.7 and 15.6%, respectively. The authors concluded that their trial failed to highlight any difference possibly related to the dosages, at least for the cholesterol-lowering effect of policosanol. In other words, the 40 mg/day dose given, did not demonstrate any further significant cholesterol-lowering effect. In the trial carried out by Cicero et al. [12] 111 patients with low cardiovascular risk profile (<20% acc. to the Framingham algorithm) treated with Dif1stat, were compared to 20 patients taking pravastatin at low doses. The first group showed a significant reduction in TC, LDLC and TG, without side effects. In particular, the reduction of LDLC was 20%; the same observed in the group with moderate hypercholesterolemia treated with pravastatin. An interesting meta-analysis by Chen JT highlighted the efficacy and safety of vegetable sterols and stanols versus policosanol in terms of taking advantage of both lipid-lowering and anti-atherogenic effects [11]. The impact on LDLC was evaluated as a primary endpoint in 4,596 patients belonging to 52 randomized and controlled trials. The weighed average of the percentage differences underlined the following variations: -11% for the vegetable sterols and stanols given at a dosage of 3.4 g/day (range 2–9 g/day; # 893 patients) in 23 trials, versus -23.7% for policosanol given at a dosage of 12 mg/day (range 5–40 mg/day; # 1,528 patients). The differences in both groups versus the placebo group were statistically significant. The absolute decrease in LDLC was higher in the group treated with policosanol: -24 versus -10% ($P \leq 0.0001$). The activity of policosanol was also more pronounced on TC, HDLC and TG, inducing a significant improvement in the LDL/HDL ratio. The authors concluded that not only policosanol, but also vegetable sterols and stanols were effective and safe. However, policosanol showed a greater LDLC-lowering effect. A multicenter, randomized, double-blind controlled trial versus placebo

carried out by Berthold HK on 143 patients with hypercholesterolemia, was reported in 2006 [13]. The patients had levels of LDLC \geq 150 mg/dL with no one or only 1 cardiovascular risk factor, or with a documented coronary heart disease, or with baseline levels of LDLC between 150 and 189 mg/dL and two or more cardiovascular risk factors. The patients were treated with policosanol at dosages of up to 80 mg/day. They were assigned to five groups, and the figures analyzed according to the intention-to-treat statistical model. The study failed to demonstrate a decrease of LDLC greater than 10% compared to the values at the baseline. Moreover, TC, HDLC, TG, Lp(a) and the LDLC/HDLC ratio did not demonstrate statistically significant change. The authors concluded that policosanol given at a usual or higher dose, failed to show any substantial effect in terms of reduction of lipids and lipoproteins in plasma compared to the patients on placebo. In our study, the administration of Diflstat[®] with a controlled diet induced a significant decrease in plasma of TC, LDLC, non-HDL and TG, in patients with moderate hypercholesterolemia compared to those treated only with the diet. Interestingly, the diet had positive effects on both groups (A and B). The result regarding the reduction in cholesterolemia in group A after 4 months, goes beyond every possible expectation considering that the control group underwent only dietetic treatment. Nevertheless, it is necessary to observe that the patients were extremely motivated by the investigators and the dieticians who administered the 24-h dietary recall, strongly stimulating the connection with diet. There was much insistence on the modification of life-style and dietary habits. A preventive operation on the consumption of alcoholic beverages was also carried out. The above mentioned recommendations and a hypocaloric diet—1,500/1,800 kcal/day—containing cholesterol equal to 200 mg/day, achieved not only the reduction in the plasmatic concentration of cholesterolemia, but also a discreet ponderal reduction, although not statistically significant. The reduction in weight also contributed to the hypolipidemic effects of the diet. The patients did not have any input concerning the consumption of functional foods, neither from doctors nor dieticians. Moreover, the good result obtained is likely attributed to the detailed operation put into direct action to modify life-style and above all, dietary habits. As reasonably expected, Diflstat[®] had better results in terms of reduction of lipids and lipoproteins, and particularly of TG, when both groups were compared after 8 months of treatment. Diflstat[®], in association with a suitable diet, was well tolerated in the long-term and induced an anti-atherogenic plasma profile of lipids and lipoproteins in patients with moderate hyperlipidemia.

It is to be emphasized that up to now, only one patient treated with cyclosporine after a kidney transplantation

developed a modest asymptomatic rhabdomyolysis while taking MP [27]. However, it is well known that cyclosporine enhances the cytotoxicity of many drugs by strongly inhibiting the liver CYP3A4 enzymatic system. It will be interesting to study the effect of Diflstat[®] with a longer administration (>1–2 years) to definitely assess if it may be considered as a valuable lipid-lowering agent for primary prevention of cardiovascular risk, or if it may be preferably used as a therapeutic alternative for statin-intolerant patients with moderate hypercholesterolemia, [28], or not.

Conflict of interest statement The author(s) certify that they have no affiliation with or financial involvement in any organization or entity with a direct financial interest in the subject matter or materials discussed in this manuscript.

References

1. Wang TH, Lin TF (2007) Monascus rice products. *Adv Food Nutr Res* 53:123–159 Review
2. Juzlova P, Rezanka T, Martinova L, Kren V (1996) Long-chain fatty acids from *Monascus purpureus*. *Phytochemistry* 43(1): 151–153
3. Heber D, Yip I, Ashley JM, Elashoff DA, Elashoff RM, Go VL (1999) Cholesterol-lowering effects of a proprietary Chinese red-yeast-rice dietary supplement. *Am J Clin Nutr* 69(2):231–236
4. Caron MF, White CM (2001) Evaluation of the antihyperlipidemic properties of dietary supplements. *Pharmacotherapy* 21:481–487 2
5. Li C, Zhu Y, Wang Y, Zhu JS, Chang J, Kritchevsky D (1997) *Monascus purpureus*-fermented rice (red yeast): a natural food product that lowers blood cholesterol in animal models of hypercholesterolemia. *Nutr Res* 18:71–81
6. Wang IK, Lin-Shiau SY, Chen PC, Lin JK (2000) Hypotriglyceridemic effect of anka (a fermented rice product of *Monascus* sp.) in rats. *J Agric Food Chem* 48:3183–3189
7. Wei W, Li C, Wang Y, Su H, Zhu J, Kritchevsky D (2003) Hypolipidemic and anti-atherogenic effects of long-term Cholestin (*Monascus purpureus*-fermented rice, red yeast rice) in cholesterol fed rabbits. *J Nutr Biochem* 14(6):314–318
8. Lee CL, Tsai TY, Wang JJ, Pan TM (2006) In vivo hypolipidemic effects and safety of low dosage *Monascus* powder in a hamster model of hyperlipidemia. *Appl Microbiol Biotechnol* 70(5):533–540
9. Wang J, Lu Z, Chi J, Wang W, Su M, Kou W, Yu P, Yu L, Chen L, Zhu JS, Chang J (1997) Multicenter clinical trial of the serum lipid-lowering effects of a *Monascus purpureus* (red yeast) rice preparation from traditional Chinese medicine. *Curr Ther Res* 58(12):964–978
10. Castaño, Mas R, Fernández L, Illnait J, Gámez R, Alvarez E (2001) Effects of policosanol 20 versus 40 mg/day in the treatment of patients with type II hypercholesterolemia: a 6-month double-blind study. *Int J Clin Pharmacol Res* 21(1):43–57
11. Chen JT, Wesley R, Shamburek RD, Pucino F, Csako G (2005) Meta-analysis of natural therapies for hyperlipidemia: plant sterols and stanols versus policosanol. *Pharmacotherapy* 25(2):171–183
12. Cicero AF, Brancaleoni M, Laghi L, Donati F, Mino M (2005) Antihyperlipidaemic effect of a *Monascus purpureus* brand dietary supplement on a large sample of subjects at low risk for

- cardiovascular disease: a pilot study. *Complement Ther Med* 13(4):273–278
13. Berthold HK, Unverdorben S, Degenhardt R et al (2006) Effect of policosanol on lipid levels among patients with hypercholesterolemia or combined hyperlipidemia: a randomized controlled trial *JAMA* 295(19):2262–2269
 14. Endo A, Monakolin K (1980) A new hypocholesterolemic agent that specifically inhibits 3-hydroxy-3-methylglutaryl coenzyme A reductase. *J Antibiot* 33(3):334–336
 15. McCarthy MF, Hung M, Sikorska M, Borowy-Borowski H (2002) Policosanol safely down-regulates HMG-CoA reductase—potential as a component of the Esselstyn regimen. *Med Hypotheses* 59:268–279
 16. Malik S, Kashyap ML (2003) Niacin, lipids, and heart disease. *Curr Cardiol Rep* 5:470–476
 17. Ganji SH, Kamanna VS, Kashyap ML (2003) Niacin and cholesterol: role in cardiovascular disease. *J Nutr Biochem* 6:298–305
 18. (2001) Executive Summary of the Third report of the National Cholesterol Education Program (NCEP) expert panel on detection, evaluation, and treatment of high blood cholesterol in adults (Adult Treatment Panel III). *JAMA* 285(19):2486–2497
 19. Anderson KM, Wilson PWF, Odell PM, Kannel WB (1991) An updated coronary risk profile. A statement for health professionals. *Circulation* 83:356–362
 20. Friedewald WT, Levy RI, Fredrickson DS (1972) Estimation of the concentration of low-density lipoprotein cholesterol in plasma, without use of the preparative ultracentrifuge. *Clin Chem* 18:499–502
 21. Plenge JK, Hernandez TL, Weil KM, Poirier P, Grunwald GK, Marcovina SM, Eckel RH (2002) Simvastatin lowers C-reactive protein within 14 days: an effect independent of low-density lipoprotein cholesterol reduction. *Circulation* 106(12):1447–1452
 22. Cobbaert C, Jukema JW, Zwinderman AH, Withagen AJ, Lindemans J, Bruschke AV (1997) Modulation of lipoprotein(a) atherogenicity by high density lipoprotein cholesterol levels in middle-aged men with symptomatic coronary artery disease and normal to moderately elevated serum cholesterol. Regression Growth Evaluation Statin Study (REGRESS) Study Group. *J Am Coll Cardiol* 30:1491–1499
 23. Gonbert S, Malinsky S, Sposito AC, Laouenan H, Doucet C, Chapman MJ et al (2002) Atorvastatin lowers lipoprotein(a) but not apolipoprotein(a) fragment levels in hypercholesterolemic subjects at high cardiovascular risk. *Atherosclerosis* 48:1454–1459
 24. Marcovina SM, Koschinsky ML, Albers JJ, Skarlatos S (2003) Report of the National Heart, Lung, and Blood Institute Workshop on Lipoprotein (a) and Cardiovascular Disease: recent advances and future directions. *Clin Chem* 49(11):1785–1796
 25. Liu L, Zhao SP, Cheng YC, Li YL (2003) Xuezhikang decreases serum Lipoprotein(a) and C-Reactive Protein concentrations in patients with coronary heart disease. *Clin Chem* 49(8):1347–1352
 26. Zhao SP, Liu L, Cheng YC, Li YL (2003) Effect of Xuezhikang, a cholestin extract, on reflecting postprandial triglyceridemia after a high-fat meal in patients with coronary heart disease. *Atherosclerosis* 168:375–380
 27. Prasad GV, Wong T, Meliton G, Bhaloo S (2002) Rhabdomyolysis due to red yeast rice (*Monascus purpureus*) in a renal transplant recipient *Transplantation* 74(8):1200–1201
 28. Becker DJ, Gordon RY, Steven C, Halbert SC, French B, Patti B, Morris PB, Daniel J, Rader DJ (2009) Red yeast rice for dyslipidemia in statin-intolerant patients. *Ann Intern Med* 150(12):830–839

double-blind placebo-controlled intervention study in normolipidemic subjects in which no effects of plant stanol esters consumption on serum TAG concentrations were found [6].

Methods

Study 1: Metabolic Syndrome Subjects, Diets and Design

Subject characteristics of this study have been reported before [5]. In short, we included 18 subjects, who had the metabolic syndrome according to the ATP III criteria [7]. All subjects gave their written informed consent before the start of the study. The study was approved by the medical ethical committee of Maastricht University. During a 3-week run-in period, all subjects were instructed to consume with the meals (lunch or diner, but not breakfast) a low-fat yogurt drink (Emmi, Lucerne, Swiss) containing no plant stanol esters. At the beginning of the experimental period, subjects were randomly allocated to one of the two treatment groups, stratified for gender and age. Baseline characteristics of the groups are listed in Table 1. The control group continued to use the placebo yogurt drink for another 8 weeks, while a second group used the same low-fat yogurt drink to which a vegetable oil based stanol ester mixture was added. Daily intake of plant stanols was 2 g provided as a one-shot yogurt drink. All products were coded with a coloured label to blind the subjects and the investigators.

Study 2: Normolipidemic Subjects, Diets and Design

As described earlier [6], 112 non-hypercholesterolemic apparently healthy subjects participated in a double-blind placebo-controlled trial in which we compared the effects of vegetable oil based and pine-wood based plant stanol esters versus placebo. In brief, during a 4-week run-in period subjects were instructed to use margarines and shortenings with breakfast, lunch and for the preparation of dinner. At the beginning of the experimental period, subjects were randomly allocated to one of the three treatment groups, stratified for gender and age. Since there were no differences between the two plant stanol ester sources in their effects on cholesterol metabolism [6, 8, 9], the vegetable-oil based and pine-wood based groups were combined into one plant stanol ester group for further analysis. For the current analysis, we randomly selected 25 subjects from the control and 25 subjects from each plant stanol ester group, hereby taking gender distributions into account. Baseline characteristics of the control versus the intervention groups are listed in Table 1. The control group continued to use the placebo margarines and shortenings for another 8 weeks, while a second group used the same margarines and shortenings to which the plant stanol ester mixtures were added. Total daily plant stanol intake was 3.8–4.1 g/day, which is higher than the currently recommended intake. All products were coded with a coloured label to blind the subjects and the investigators. As in study 1, all subjects gave their written informed consent before the start of the study, and the study was approved by the medical ethical committee of Maastricht University.

Table 1 Baseline population characteristics of metabolic syndrome (study 1) and normolipidemic (study 2) subjects

	Metabolic syndrome subjects		Normolipidemic subjects	
	Controls (<i>N</i> = 9)	Plant stanols (<i>N</i> = 9)	Controls (<i>N</i> = 25)	Plant stanols (<i>N</i> = 50)
Age (years)	60 ± 7	60 ± 4	35 ± 17	34 ± 15
BMI (kg/m ²)	30.2 ± 1.9	28.1 ± 2.6	23.0 ± 3.2	22.9 ± 3.0
Blood pressure (mm Hg)				
Systolic BP	142 ± 14	138 ± 11	119 ± 12	123 ± 12
Diastolic BP	92 ± 10	94 ± 8	74 ± 8	75 ± 8
Serum lipid (mmol/L)				
Total cholesterol	6.50 ± 1.59	6.29 ± 1.19	4.81 ± 0.79	5.02 ± 0.69
Non-HDL cholesterol	5.47 ± 1.29	5.32 ± 1.29	–	–
LDL cholesterol	–	–	2.82 ± 0.73	2.89 ± 0.71
HDL cholesterol	1.03 ± 0.26	0.97 ± 0.15	1.61 ± 0.32	1.58 ± 0.39
Triacylglycerol	2.24 ± 1.26	2.21 ± 0.98	0.83 ± 0.34	1.02 ± 0.61

Values are means ± SD. To convert values for total, HDL and LDL cholesterol to mg/dL × 38.67. To convert values for triacylglycerols to mg/dL × 88.54

Blood Sampling and Analyses

Blood Sampling

In both studies, blood samples obtained at the end of the run-in period and at the end of the 8 weeks experimental periods, were used for further analysis. All blood samples were taken after an overnight fast; i.e., subjects were not allowed to eat and drink (except water) after 10 p.m. in the evening preceding blood sampling, to drink alcohol the day preceding blood sampling, or to smoke on the morning of blood sampling. Blood was sampled into clotting tubes (CORVAC, integrated serum separator tube, Sherwood Medical Company, St. Louis, USA). Serum was obtained by centrifugation of the clotting tubes at $2,000\times g$ for 30 min at 4 °C, minimally 1 h after venipuncture. All serum samples were immediately stored in small portions, snap-frozen, and stored at -80 °C until further analysis.

Lipids, Lipoproteins and Lipoprotein Profiles

Serum lipids and lipoproteins were analysed as described [5]. All samples from one subject were analysed within the same run at the end of the study. In study 1, we reported serum non-HDL cholesterol concentrations instead of serum LDL cholesterol concentrations because we could not use the Friedewald equation to calculate serum LDL cholesterol, because of the increased serum TAG concentrations of our population. Lipoprotein profiles at the end of the run-in period and at the end of the 8 week intervention period were evaluated by NMR (Liposcience, Raleigh, USA). Before NMR analysis, two blood samples at the end of the run-in period and at the end of the experimental period (at least three and maximally 7 days between both blood sampling moments) were pooled to minimise the noise due to normal day-to-day variation in lipoprotein particle concentrations. Although the two intervention studies were performed 8 years apart, all NMR analysis were performed in samples stored at -80 °C in retrospect for both studies at the same time.

Statistics

Changes for all parameters were calculated for each subject as the difference between values of the intervention period and run-in periods and reported as means \pm SD. The differences in changes between the groups were tested with an unpaired *t* test in which a $P < 0.05$ was considered significant. All statistical analyses were performed with Statview 4.5.

Results and Discussion

Serum Lipid and Lipoproteins

In both studies, plant stanol ester consumption improved serum lipoprotein profiles. Compared with the control group, consumption of plant stanol esters for 8 weeks lowered serum non-HDL cholesterol concentrations by 0.73 ± 0.52 mmol/L or 13.8% ($P = 0.012$) in the metabolic syndrome subjects. In addition, plant stanol esters lowered TAG concentrations by 0.23 ± 0.36 mmol/L or 27.5% ($P = 0.044$). No effects on serum HDL cholesterol concentrations were found.

In normolipidemic subjects, plant stanol esters also significantly lowered serum LDL cholesterol concentrations. Compared with the control group, this decrease was 0.44 ± 0.29 mmol/L or 13.7% ($P < 0.001$) for the plant stanol ester group. There were no effects on serum TAG and HDL cholesterol concentrations. The finding that serum TAG concentrations were unchanged in this study is in line with all other studies in normolipidemic subjects [1].

We now aim to find an explanation for the observed effects on serum TAG concentrations and here postulate the hypothesis that the TAG lowering effect of plant stanol esters originates from a reduced hepatic production of large TAG-rich VLDL-1 particles. We had earlier excluded that the effects of plant stanol ester consumption on serum TAG concentrations could be explained by changes in serum apoCII and apoCIII concentrations, which are both determinants of lipoprotein lipase (LPL) activity [5]. In line with the unaffected HDL cholesterol concentrations, we have also shown that CETP activity was not changed [5]. The hypothesis postulating effects on hepatic VLDL-1 production is based on the present finding that in metabolic syndrome subjects plant stanol esters significantly reduced concentrations of large (>60 nm) and medium (35–60 nm) VLDL particles, as compared to the control group. We are aware of the fact that we did not measure hepatic VLDL particle production and VLDL kinetics (i.e., referring to LPL activity) by using stable isotope approaches. Therefore it remains speculative whether the suggested hypothetical mechanism is correct. No effects were found on small (27–35 nm) VLDL particles or any of the other lipoprotein fractions (Table 2). The fact that there was no change in the number of small sized LDL particles was somewhat unexpected, since the large VLDL-1 particles—of which the numbers were strongly reduced after plant stanol ester consumption—are precursors for the smaller denser LDL particles. This might also imply that the effects on VLDL-1 concentrations are not caused by a reduced hepatic VLDL-1 production.

Table 2 Effects of plant stanol esters on lipoprotein particle concentrations in metabolic syndrome (study 1) and normolipidemic (study 2) subjects

	Metabolic syndrome subjects		Normolipidemic subjects	
	Controls (<i>N</i> = 9)	Plant stanols (<i>N</i> = 9)	Controls (<i>N</i> = 25)	Plant stanols (<i>N</i> = 50)
Large VLDL particles, >60 nm (nmol/L)				
Run-in	5.9 ± 7.1	6.7 ± 8.2	1.9 ± 1.6	2.5 ± 4.1
Test period	8.1 ± 6.8	2.9 ± 3.2	2.0 ± 2.1	1.8 ± 2.8
Change	2.2 ± 5.1	−3.8 ± 6.7 ^a	0.1 ± 2.7	−0.7 ± 3.1 ^a
Medium VLDL particles, 35–60 nm (nmol/L)				
Run-in	33.4 ± 21.5	36.6 ± 20.9	21.8 ± 10.6	22.7 ± 10.6
Test period	39.2 ± 20.8	27.5 ± 17.8	20.3 ± 12.1	22.0 ± 14.7
Change	5.8 ± 17.5	−9.1 ± 17.7 ^a	−1.5 ± 15.5	−0.7 ± 17.3
Small VLDL particles, 27–35 nm (nmol/L)				
Run-in	54.3 ± 14.8	53.6 ± 13.8	41.4 ± 11.6	44.9 ± 17.4
Test period	51.9 ± 17.1	55.5 ± 20.7	35.3 ± 11.9	38.1 ± 19.2
Change	−2.5 ± 9.9	1.9 ± 17.6	−6.1 ± 13.7	−6.8 ± 23.1
IDL particles, 23–27 nm (nmol/L)				
Run-in	107.9 ± 68.4	76.3 ± 72.4	27.0 ± 25.9	49.4 ± 48.5
Test period	107.7 ± 80.1	84.0 ± 54.0	35.8 ± 35.1	36.3 ± 35.5
Change	−0.2 ± 45.1	7.6 ± 54.3	8.7 ± 50.5	−13.1 ± 48.9 ^a
Large LDL particles, 21.2–23 nm (nmol/L)				
Run-in	358 ± 154	416 ± 285	378 ± 115	388 ± 131
Test period	248 ± 210	348 ± 167	351 ± 87	372 ± 116
Change	−110 ± 192	−69 ± 213	−26 ± 133	−16 ± 155
Small LDL particles, 18–21.2 nm (nmol/L)				
Run-in	1,303 ± 633	1,319 ± 456	521 ± 195	589 ± 328
Test period	1,449 ± 652	1,388 ± 363	548 ± 214	567 ± 326
Change	146 ± 315	68 ± 338	27 ± 279	−22 ± 411
Large HDL particles, 8.8–13 nm (μmol/L)				
Run-in	3.7 ± 2.0	5.0 ± 2.3	7.7 ± 2.6	8.3 ± 3.9
Test period	3.6 ± 2.0	5.2 ± 1.7	7.8 ± 2.9	8.2 ± 3.5
Change	−0.1 ± 1.2	0.3 ± 2.7	0.1 ± 3.9	−0.2 ± 3.7
Medium HDL particles 8.2–8.8 nm (μmol/L)				
Run-in	4.1 ± 3.3	2.8 ± 3.0	3.2 ± 2.4	3.7 ± 3.0
Test period	3.9 ± 3.4	2.7 ± 3.3	3.2 ± 2.4	4.4 ± 3.5
Change	−0.2 ± 1.8	−0.1 ± 3.7	−0.0 ± 3.9	0.6 ± 3.7
Small HDL particles, 7.3–8.2 nm (μmol/L)				
Run-in	23.6 ± 2.4	21.8 ± 2.7	21.3 ± 3.8	19.5 ± 4.8
Test period	23.8 ± 2.7	22.6 ± 3.4	20.6 ± 5.5	20.2 ± 4.7
Change	0.2 ± 2.0	0.8 ± 2.6	−0.7 ± 6.6	0.6 ± 5.0

Values are means ± SD

^a *P* < 0.05 versus control

In the normolipidemic subjects we also found a reduction in the number of large VLDL-1 particles (Table 2) in serum from the plant stanol ester group, as compared to controls. The reduction was however, smaller as compared to the reduction observed in subjects with the metabolic syndrome, which is in line with the lack of effects on serum TAG concentrations. There are however, substantial differences between both studies (i.e., plant stanol intake, age,

etc.) not allowing a direct comparison between the outcomes from both studies.

Assuming that plant stanol esters lower hepatic VLDL-1 production in humans, the mechanism underlying this effect is still open. In this respect, Ikeda et al. [11] have recently shown that campest-5-en-3-one (campestenone), an oxidised derivative of campesterol, was a potent hepatic PPARα activator in mice. Consumption of this plant

sterol derivative resulted in a lower concentration of TAG in serum and liver. These changes in mice fit very well with our suggestion of a lowered hepatic large TAG-rich VLDL particle production after plant stanol ester consumption. However, in our studies we provided plant stanol esters and not plant sterol esters. This introduces the question whether intermediates with similar effects can be formed from plant stanol esters *in vivo* in humans.

In apoE*3-Leiden mice, Volger et al. [10] have shown that plant stanol ester consumption lowered hepatic TAG (−38%), free cholesterol (−31%), and cholesterol ester (−62%) content. Since hepatic TAG concentrations are thought to be a driving force behind large sized VLDL particle production—at least in humans—[12], the observed reduction in hepatic TAG in these mice suggest that the number of larger sized VLDL particles was probably lowered. However, only cholesterol incorporation into nascent VLDL particles was lowered, while total VLDL-TAG and total VLDL-apoB production rates were surprisingly unchanged. Unfortunately, VLDL production rates of the different VLDL-particle subpopulations were not measured.

This data also introduces a final discussion point: the functional consequences of a lowered VLDL-1 production. In humans, it is generally recognised that the amount of fat in the liver is an important factor determining hepatic VLDL-1 production [12]. Therefore, the lowered hepatic VLDL-1 production may indicate a reduced ectopic fat accumulation in the liver. If this is indeed true, plant stanol ester consumption may be even more beneficial than currently anticipated. This latter assumption warrants, however, further study.

In conclusion, we have earlier reported that plant stanol esters not only lower serum LDL cholesterol concentrations, but also serum TAG concentrations in subjects with elevated TAG concentrations at baseline. We here present data supporting the hypothesis that the effect is caused by a reduction in the hepatic production of large TAG-rich VLDL-1 particles. Effects are most pronounced in metabolic syndrome subjects, resulting in subsequent reductions in serum TAG concentrations.

Acknowledgments We are indebted to the members of our dietary and technical staff, and to all volunteers for their cooperation and interest. The studies were sponsored by RAISIO Life Sciences, Raisio, Finland (study 2), and McNeil, UK (study 1).

Open Access This article is distributed under the terms of the Creative Commons Attribution Noncommercial License which

permits any noncommercial use, distribution, and reproduction in any medium, provided the original author(s) and source are credited.

References

- Demonty I, Ras RT, van der Knaap HCM, Duchateau GSMJE, Meijer L, Zock PL, Geliñse JM, Trautwein EA (2009) Continuous dose–response relationship of the LDL cholesterol lowering effect of phytosterol intake. *J Nutr* 139:271–284
- Katan MB, Grundy SM, Jones P, Law M, Miettinen T, Paoletti R (2003) Efficacy and safety of plant stanols and sterols in the management of blood cholesterol levels. *Mayo Clin Proc* 78:965–978
- Chan YM, Varady KA, Lin Y, Trautwein E, Mensink RP, Plat J, Jones PJ (2006) Plasma concentrations of plant sterols: physiology and relationship with coronary heart disease. *Nutr Rev* 64:385–402
- Naumann E, Plat J, Kester ADM, Mensink RP (2008) The baseline serum lipoprotein profile is related to plant stanol induced changes in serum lipids and lipoproteins. *J Am Coll Nutr* 27:117–126
- Plat J, Brufau G, Dallingha-Thie GM, Dasselaar M, Mensink RP (2009) A plant stanol yogurt drink alone or combined with a low-dose statin lowers serum triacylglycerol and non-HDL cholesterol in metabolic syndrome patients. *J Nutr* 139:1143–1149
- Plat J, Mensink RP (2000) Vegetable oil based versus wood based stanol ester mixtures: effects on serum lipids and hemostatic factors in non hypercholesterolemic subjects. *Atherosclerosis* 148:101–112
- Grundy SM (2001) United States cholesterol guidelines 2001: expanded scope of intensive low-density lipoprotein-lowering therapy. *Am J Cardiol* 88:23J–27J
- Plat J, Mensink RP (2001) Effects of diets enriched with two different plant stanol ester mixtures on plasma ubiquinol-10 and fat-soluble antioxidant concentrations. *Metabolism* 50:520–529
- Plat J, Mensink RP (2001) Effects of plant stanol esters on LDL receptor protein expression and on LDL receptor and HMG-CoA reductase mRNA expression in mononuclear blood cells of healthy men and women. *FASEB J* 16:258–260
- Volger OL, van der Boom J, de Wit ECM, van Duyvenvoorde W, Hornstra G, Plat J, Havekes LM, Mensink RP, Princen HMG (2001) Dietary plant stanol esters reduce VLDL-cholesterol secretion and bile saturation in apoE*3-Leiden transgenic mice. *Arterioscler Thromb Vasc Biol* 21:1046–1052
- Ikeda I, Konno R, Shimizu T, Ide T, Takahashi N, Kawada T, Nagao K, Inoue N, Yanagita T, Hamada T, Morinaga Y, Tomoyori H, Imaizumi K, Suzuki K (2006) Campesterol, an oxidized derivative of campesterol, activates PPAR α , promotes energy consumption and reduces visceral fat deposition in rats. *Biochim Biophys Acta* 1760:800–807
- Adiels M, Taskinen MR, Packard C, Caslake MJ, Soro-Paavonen A, Westerbacka J, Vehkavaara S, Häkkinen A, Olofsson SO, Yki-Järvinen H, Borén J (2006) Overproduction of large VLDL particles is driven by increased liver fat content in man. *Diabetologia* 49:755–765

As part of a program aimed at the search for new marine natural products [14], including minor ones, we have continued to study the ethanol extract of lyophilized sponge *Rhizochalina incrustata*, collected near the northern point of the island of Madagascar [1, 3, 4] in the hope of finding new trace bipolar metabolites whose structures may be of interest for illuminating biogenetic aspects of this intriguing group of lipids.

Herein, we wish to report isorhizochalin (**1**), a new two-headed sphingolipid from *R. incrustata*, which is a minor C-2 epimer of rhizochalin, the major component of the sponge. The structure elucidation of isorhizochalin including absolute configuration is the subject of this paper.

Experimental Procedure

General Experimental Procedures

Optical rotations were measured using a Perkin–Elmer 343 polarimeter. CD spectra were recorded on a Jasco J810 spectrometer using quartz cells (0.2-mm pathlength) at a scan rate of 50 nm/s. The ^1H - and ^{13}C -NMR spectra were recorded on a Bruker DPX-500 spectrometer at 500 and 125 MHz, respectively, with Me_4Si as an internal standard. ESI mass spectra were obtained on an Agilent 6510 Q-TOF LC–MS spectrometer by direct infusion in MeOH containing HCOOH (0.1%). MALDI-TOF mass spectra were obtained on a Bruker Biflex III laser desorption spectrometer coupled with delayed extraction using an N_2 laser (λ 337 nm) on 2,5-dihydroxybenzoic acid (DHB) and α -cyano-4-hydroxycinnamic acid (CCA) as matrix. Low-pressure column liquid chromatography was performed using Polichrome I (powder Teflon[®], Biolar, Latvia). Low-pressure column liquid chromatography was performed using silica gel L (50/160 μm ; Sorbopolymer, Russia). Silica gel plates, 4.5 \times 6.0 cm (5–17 μm ; Sorbfil, Russia), were used for thin layer chromatography. HPLC was performed using an Agilent Series 1100 Instrument equipped with the differential refractometer RID-DE14901810.

Animal Material

The sponge *Rhizochalina incrustata* (phylum Porifera, class Demospongiae, subclass Ceratinomorpha, order Haplosclerida, family Phloeodictyidiidae) was collected using SCUBA (depth 3–5 m) during the 3-d scientific cruise on-board R/V “Akademik Oparin”. A voucher specimen is kept under the registration number PIBOC #03-98 in the marine invertebrate collection of the Pacific Institute of Bioorganic Chemistry (Vladivostok, Russia).

Extraction and Isolation

The fresh collection of the sponge *R. incrustata* was immediately lyophilized and kept at -20°C . The lyophilized material (300 g) was extracted with EtOH (200 ml \times 3). The combined EtOH extract was concentrated under reduced pressure and redissolved in EtOH– H_2O (9:1). This solution was partitioned three times with equal volumes of *n*-hexane. The aqueous EtOH layer was evaporated in vacuo at 50°C to give brown oil (44.2 g) which was separated over a Polichrome I by elution with gradient of $\text{H}_2\text{O} \rightarrow \text{EtOH}$. The two-headed sphingolipid fraction (ninhydrin positive) was eluted with 40% EtOH.

Peracetylation

A portion of the two-headed sphingolipid fraction, obtained by chromatographic separation over Polichrome I (182.0 mg) was dissolved in pyridine (1.0 ml) and acetic anhydride (1.0 ml) and allowed to stand at 25°C for 18 h. Removal of the volatile materials give a residue with peracetates of rhizochalin and isorhizochalin (**1**) (191.0 mg). The latter was separated by preparative HPLC (YMC-Pack ODS-A column, 80% aqueous EtOH) followed by rechromatography on an YMC-Pack ODS-A HPLC column (75% aqueous EtOH) to yield rhizochalin peracetate (90 mg, 0.02% dry weight) and isorhizochalin peracetate (**1a**) (2.0 mg, 0.0005% dry weight).

Isorhizochalin Peracetate

Colorless solid; $[\alpha]_{\text{D}} +6.7$ (c 0.33, CHCl_3); HRMS-ESI: m/z $[\text{M} + \text{H}^+]$ calcd for $\text{C}_{48}\text{H}_{83}\text{N}_2\text{O}_{15}$: 927.5788; found: 927.5779; $[\text{M} + \text{Na}^+]$ calcd for $\text{C}_{48}\text{H}_{82}\text{N}_2\text{O}_{15}\text{Na}$: 949.5607; found: 949.5614. MALDI-TOF m/z 949 $[\text{M} + \text{Na}^+]$; NMR (CDCl_3 , see Table 1).

Methanolysis of Isorhizochalin Peracetate

A solution of **1a** (1.8 mg) in mixture of 5% HCl in MeOH (0.5 ml) was heated in a sealed vial at 75°C for 24 h. The mixture was cooled, concentrated, and subjected to chromatography on silica gel column to provide two fractions.

Fraction 1, eluted with CHCl_3 –MeOH (4:1) and gave an anomeric mixture of D-1-*O*-methyl galactopyranosides (0.4 mg) HRMS-ESI: m/z $[\text{M} + \text{H}^+]$ calcd for $\text{C}_7\text{H}_{15}\text{O}_6$: 195.0863; found: 195.0987; calcd for $\text{C}_7\text{H}_{14}\text{O}_7\text{Na}$: 217.0683; found: 217.0683.

Fraction 2, eluted with CHCl_3 –MeOH– NH_4OH (16:4:1) gave a heterogeneous mixture of amino lipid and partially deacetylated analogs (0.5 mg). The mixture was dissolved

Table 1 NMR data for isorhizochalin peracetate (**1a**, CDCl₃, TMS)

Atom No.	1a			
	δ_C	δ_H (mult, <i>J</i> Hz)	COSY	HMBC (10 Hz)
1	13.4	1.07 (<i>d</i> , 6.8)	H2	C2, C3
2	47.1	3.99 (<i>m</i>)	H1, H3	
3	83.4	3.60 (<i>m</i>)	H2, H4a	
4a	32.8	1.39 (<i>m</i>)	H3	
4b		1.49 (<i>m</i>)		
5–15	29.1–29.7	1.27–1.29 (<i>bs</i>)		
16	25.2	1.56 (<i>m</i>)	H17	C18, C15
17	42.8	2.369 (<i>t</i> , 7.0)	H16	C15, C16, C18
18	211.6			
19	42.9	2.374 (<i>t</i> , 7.0)	H20	C18, C20, C21
20	25.6	1.56 (<i>m</i>)	H19	C18, C21
21–24	29.1–29.7	1.27–1.29		
25	31.6	1.52 (<i>m</i>)	H26	
26	76.5	4.85 (<i>m</i>)	H25, H27	
27	47.2	4.20 (<i>m</i>)	H26, H28	
28	18.5	1.10 (<i>d</i> , 6.8)	H27	C26, C27
2-NH	6.41 (<i>d</i> , 8.5)			
27-NH	5.51 (<i>d</i> , 9.0)			
1'	101.5	4.46, <i>d</i> , 7.8	H2'	C3
2'	69.0	5.20, <i>dd</i> , 7.8 10.5	H3', H1'	
3'	70.8	5.03, <i>dd</i> , 3.4, 10.5		
4'	67.2	5.40, <i>dd</i> , 1.1, 3.4		
5'	71.0	3.91, <i>dt</i> , 1.11, 6.6, 6.6		
6'	61.7	4.10, <i>dd</i> , 6.6, 11.2; 4.19, <i>dd</i> , 6.6, 11.2		
Ac		2.19, <i>s</i> ; 2.09, <i>s</i> ; 2.06, <i>s</i> ; 2.05, <i>s</i> ; 1.99, <i>s</i> ; 1.987, <i>s</i> ; 1.94, <i>s</i>		

in pyridine (0.2 ml) and acetic anhydride (0.2 ml) and allowed to stand at 25 °C for 18 h. Removal of the volatile materials gave isorhizochalinin peracetate **2** (0.6 mg); $[\alpha]_D^{25}$: +7.0 (*c* 0.06, MeOH); HRMS-ESI: m/z [$M + Na^+$] calcd for C₃₆H₆₆N₂O₇Na: 661.4762; found: 661.4731; [$M + Na^+$]; NMR (CDCl₃, see Table 2).

Isorhizochalinin

Isorhizochalinin peracetate (**2**) (0.6 mg) in 5% HCl in MeOH (500 μ l) was heated at 80 °C for 48 h in a sealed vial. The solution was cooled, concentrated under reduced pressure, and the residue subjected to microcolumn silica gel chromatography with successive elution by 9:4:1 CHCl₃/MeOH/NH₄OH to provide a mixture of aglycone and aglycone acetates (0.5 mg).

Preparative HPLC of the mixture (80:20:0.1% MeOH–H₂O–TFA) gave **2a** (0.4 mg). HRMS-ESI: m/z [$M + Na^+$] calcd for C₂₈H₅₉N₂O₃: 471.4520; found: 471.4591; [$M + Na^+$]; NMR (CD₃OD, see Table 2).

Isorhizochalinin Perbenzoate

A mixture of isorhizochalinin **2a** (0.1 mg, 0.2 μ mol), DMAP (dimethylaminopyridine, 1 mg), benzoic acid (9.2 mg, 0.075 mmol), and EDC (1-ethyl-3 [3-dimethylaminopropyl] carbodiimide hydrochloride, 12.2 mg, 0.067 mmol) in CH₂Cl₂ (1 ml) was stirred at room temperature for 6 days. The product was purified by silica gel column chromatography (20:1 CHCl₃/EtOAc) followed by preparative HPLC (93:7 EtOH–H₂O) to obtain isorhizochalinin perbenzoate (**2b**, 0.1 mg): CD (MeOH) λ 221 ($\Delta\epsilon$ + 4.4), 239 (–5.8). HRMS-ESI: m/z [$M + H^+$] calcd for C₅₆H₇₃N₂O₇: 887.5569; found: 887.5570; [$M + Na^+$] calcd for C₅₆H₇₂N₂O₇Na: 909.5388; found: 909.5385. ¹H NMR (500 MHz, CDCl₃): 8.09 (2 H, *d*, *J* = 7.6, *O*-PhCOO for *erythro* terminus); 8.03 (2 H, *d*, *J* = 7.6, *O*-PhCOO for *threo* terminus); 7.77 (2 H, *d*, *J* = 7.6, *ortho*-PhCONH for *erythro* terminus); 7.72 (2 H, *d*, *J* = 7.6, *ortho*-PhCONH for *threo* terminus); 7.39–7.61 (*m*, 12H; aryl H); 2.355 (2H, *t*, *J* = 7.0, 17-H); 2.349 (2H, *t*, *J* = 7.0, 19-H); 1.26 (*bs*, 38H, 4–16H);

Table 2 NMR data for isorhizochalinin (**2a**) and isorhizochalinin peracetate (**2**)

Atom no.	2a (CD ₃ OD)		2 (CDCl ₃)		
	δ_{H} (mult, <i>J</i> Hz)	COSY	δ_{H} (mult, <i>J</i> Hz)	δ_{C}	HMBC
1	1.21 (<i>d</i> , 6.8)	H2	1.09 (<i>d</i> , 6.8)	14.8	C2, C3
2	3.27 (<i>m</i>)	H1, H3	4.16 (<i>m</i>)	47.6	
3	3.69 (<i>m</i>)	H2, H4	4.83 (<i>m</i>)	76.9	
4	1.44 (<i>m</i>)	H3	1.55 (<i>m</i>)	31.3	
5–15	1.31 (<i>bs</i>)		1.25–1.29 (<i>bs</i>)	29.1–29.7	
16	1.56 (<i>m</i>)	H17	1.55 (<i>m</i>)	25.2	C18, C15
17	2.43 (<i>t</i> , 7.0)	H16	2.368 (<i>t</i> , 7.0)	42.8	C15, C16, C18
18				211.6	
19	2.44 (<i>t</i> , 7.0)	H20	2.37 (<i>t</i> , 7.0)	42.9	C18, C20, C21
20	1.56 (<i>m</i>)	H19	1.55 (<i>m</i>)	25.6	C18, C21
21–24	1.31 (<i>bs</i>)		1.25–1.29	29.1–29.7	
25	1.42 (<i>m</i>)	H26	1.52 (<i>m</i>)	31.6	
26	3.44 (<i>m</i>)	H25, H27	4.85 (<i>m</i>)	76.5	
27	3.08 (<i>sept.</i> , 7.0)	H26, H28	4.20 (<i>m</i>)	47.2	
28	1.26 (<i>d</i> , 6.8)	H27	1.10 (<i>d</i> , 6.8)	18.5	C26, C27
2-NH			5.78 (<i>d</i> , 8.3)		
27-NH			5.51 (<i>d</i> , 8.8)		
Ac			2.09, <i>s</i> ; 2.086, <i>s</i> ; 1.98, <i>s</i> ; 1.95, <i>s</i>		

20–25H); 1.289 (3H, *d*, *J* = 6.8, 1-H); 1.296 (3H, *d*, *J* = 6.8, 28-H); (other signals see Table 3 and 4).

Baeyer–Villiger Oxidation of Isorhizochalin Peracetate

A mixture of TFA (>99%) and H₂O₂ (30% v/v aq.) [TFA/H₂O₂, 3:1 (60 μ l)] was added to a solution of **1a** (0.2 mg) in MeOH (50 μ l). The mixture was heated at 60 °C for 2 h, left for 72 h at room temperature. The volatiles were removed under reduced pressure and the residue acetylated with Ac₂O/pyridine (1:1, 100 μ l). The resulting mixture of peracetates, **3a** and **3b**, was analyzed by MALDI-TOF-MS: *m/z* 724 [M + Na]⁺.

Cytotoxicity Assay

Cell culture: HL-60 (human promyelocytic leukemia) and THP-1 (human monocytic leukemia) cell lines were

cultured in monolayers at 37 °C and 5% CO₂ in RPMI containing 10% FBS, 2 mmol/l L-glutamine, 100 units/ml penicillin, and 100 μ g/ml streptomycin.

The effect of the compounds on HL-60 or THP-1 cells viability was evaluated using MTS reduction into its formazan product [15]. The cells were cultured for 12 h in 96-well plates (6,000 cells/well) in RPMI medium (50 μ l/well) containing 10% FBS. Then 50 μ l of the fresh RPMI/FBS medium containing the indicated concentrations of the compounds was added into each well and the cells were incubated for 22 h. Next, 20 μ l of the MTS reagent was added into each well, and MTS reduction was measured 2 h later spectrophotometrically at 492 and 690 nm as background using the μ Quant microplate reader (Bio-Tek Instruments, Inc.). Data were obtained as the mean \pm SD from six samples of two independent experiments. The statistical computer program Statistica 6.0 for

Table 3 Partial ¹H-NMR chemical shift data of the **2b**, **4a**, **4b** perbenzoates, and *erythro*-leucettamol A perbenzoate

α -Terminus [reference]	δ (ppm)			<i>J</i> values (Hz)
	$\delta_{\text{C2-NH}}$	$\delta_{\text{3-H}}$	$\delta_{\text{2-H}}$	<i>J</i> _{NH-H-2}
<i>erythro</i> - 2b	6.95	5.23	4.46	8.3
<i>erythro</i> - 4b [17]	6.97	5.24	4.46	7.8
<i>threo</i> - 4a [17]	6.39	5.22	4.54	9.0
<i>erythro</i> -Leucettamol A perbenzoate [19]	6.99	5.22	4.46	7.8

Table 4 Partial ¹H-NMR chemical shift data of isorhizochalinin (**2b**), rhizochalinin, rhizochalinin D, and **4a** perbenzoates

ω -Terminus [reference]	δ (ppm)			<i>J</i> values (Hz)
	$\delta_{\text{C27-NH}}$	$\delta_{\text{26-H}}$	$\delta_{\text{27-H}}$	<i>J</i> _{NH-H-27}
<i>threo</i> - 4a [17]	6.38	5.21	4.53	8.9
<i>threo</i> -Rhizochalinin perbenzoate [18]	6.38	5.21	4.53	8.9
<i>threo</i> -Rhizochalinin D perbenzoate [3]	6.39	5.22	4.54	9.0
<i>threo</i> - 2b	6.37	5.21	4.53	9.0

Windows (StatSoft, Inc., 2001) was used to compute SD and IC₅₀ in corresponding experiments.

Results and Discussion

The EtOH extract of *R. incrustata* was concentrated and partitioned between *n*-hexane and aqueous EtOH. The aqueous EtOH-soluble materials were further separated by column chromatography on Polychrome-1 to obtain a crude mixture of two-headed sphingolipids. Part of the mixture was acetylated, and the products of the reaction were separated by preparative HPLC to give rhizochalin peracetate and the minor compound, isorhizochalin peracetate (**1a**, 0.0005%, based on dry weight of the sponge). The molecular formula of **1a**, C₄₈H₈₂N₂O₁₅, was derived from HRMS-ESI (*m/z* 927.5779 [M + H⁺], calculated 927.5788). The ¹H and ¹³C NMR data of **1a** were similar to those of rhizochalin peracetate [1]. These included signals of two secondary methyl groups (δ_{H} 1.07; 1.10; δ_{C} 13.4; 18.5), two *N*-substituted CH carbons (δ_{H} 3.99, m; 4.20, m; δ_{C} 47.1, CH; 47.2, CH), two hydroxymethines (δ_{H} 3.60, m; 4.85, m; δ_{C} 83.4, CH; 76.5, CH), and a ketone carbonyl group (δ_{C} 211.6), flanked by two α -CH₂ groups (δ_{H} 2.369, t, 2.374, t; δ_{C} 42.8, 42.9). The remainder of the signals was assigned to long CH₂ chains (δ_{H} 1.27–1.29; δ_{C} 29.1–29.7) and a sugar moiety. In contrast with the NMR data of rhizochalin peracetate, the amide doublet (C₂-NH) and hydroxymethine multiplet were shifted down-field from δ_{H} 5.87 to 6.41 ppm and from δ_{H} 3.49 to 3.60 ppm, respectively. The signal of one of two secondary methyl groups was shifted up-field from δ_{H} 1.17 to 1.07 ppm. Consequently, the structure of **1a** was suggested as an analogue of rhizochalin with a stereochemical modification from *threo* to *erythro* at the α -terminus (defined as the glycosylated end group) that was revealed by analyses of ¹³C

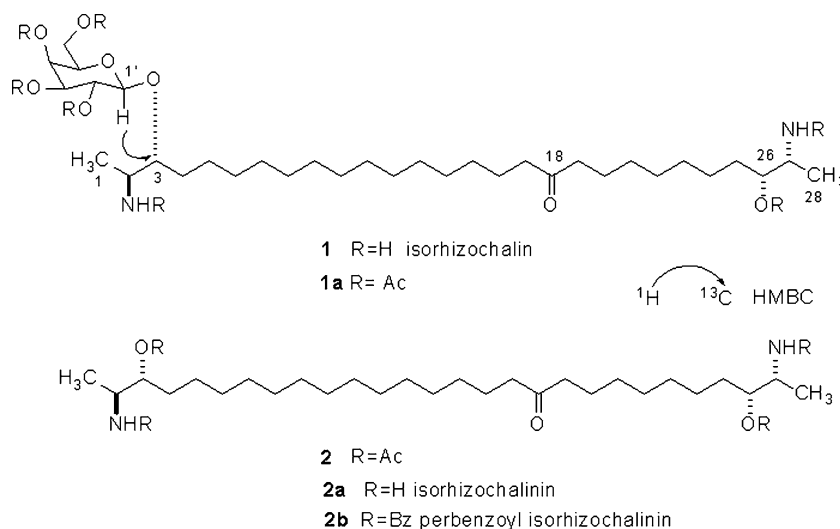
NMR, COSY and HMBC data. In fact, the down field shift of the amide NH is a characteristic difference in the NMR spectra of *N*-acyl *erythro*-sphingosines compared to the corresponding *threo*-derivatives [16, 17] (Fig. 1).

The HMBC spectrum of **1a** showed a cross peak from H-1' (δ_{H} 4.46) to C-3 (δ 83.4), confirming the attachment of the *O*-galactopyranosyl residue at C-3. The ³*J*-coupling constant of the anomeric proton H-1' (d, *J* = 7.8 Hz) and other NMR data indicated that isorhizochalin is a β -galactoside.

Methanolysis of **1a** (5% HCl in MeOH, 75°C, 24 h) gave two fractions that were separated by silica gel column chromatography, the first-eluting fraction was a mixture of anomeric *O*-methyl *D*-galactosides (C₇H₁₅O₅, *m/z* 195.0987, M + H⁺), confirmed by the positive specific rotation. The second fraction, eluted from the column with NH₃-MeOH-CHCl₃ represented a mixture of aglycone and aglycone acetates that was re-acetylated (Ac₂O/pyr) to provide the peracetylated aglycone, isorhizochalinin peracetate (**2**). A molecular formula for **2**, C₃₆H₆₆N₂O₇, was derived from HRMS-ESI (*m/z* 661.4731 [M + Na⁺], $\Delta m\mu$ 3.1). The ¹H and ¹³C NMR data of **2** were similar to those of rhizochalinin peracetate [1], with the exception of the amide doublet (C-2-NH) which was shifted downfield from δ_{H} 5.51 to 5.78 ppm and the C-3 hydroxymethine multiplet that was shifted upfield from δ_{H} 4.20 to 4.16 ppm. The signal of one secondary methyl group was shifted upfield from δ_{H} 1.10 to 1.09 ppm. Consequently, the structure of **2** was formulated as an analogue of rhizochalinin peracetate with a stereochemical modification at one terminus.

Methanolysis of **2** (5% HCl in MeOH, 80 °C, 48 h) gave a mixture of aglycone and aglycone peracetates which were purified by preparative HPLC to provide the pure isorhizochalinin (**2a**). The molecular formula C₂₈H₅₈N₂O₃ of **2a** was derived from HRMS-ESI (*m/z* 471.4491 [M + H⁺], $\Delta m\mu$ = 3). The ¹H NMR data of **2a** were similar to those

Fig. 1 Structures of isorhizochalin and its derivatives



of rhizochalinin. In contrast with the NMR data of rhizochalinin, one hydroxymethine multiplet was shifted downfield from δ_{H} 3.08 to 3.27 ppm. The signal of one secondary methyl group was shifted upfield from δ_{H} 1.26 to 1.21 ppm. The foregoing evidence confirmed the structure of isorhizochalin as a glycosylated two-headed sphingolipid, having a ketone group embedded at C-18 in a long-chain but with a C-2,3 *erythro* configuration at the α -terminus instead of *threo* found in rhizochalin.

Interpretation of spectroscopic data could not establish the position of the carbonyl group of these natural products. As in our previous studies of ketosphingolipids, we applied a procedure for localization of the C=O group based on in situ MS analysis of Baeyer–Villiger oxidation products obtained from the ketone [3]. Treatment of peracetate **1a** with TFA-H₂O₂ in MeOH, followed by acetylation (Ac₂O, pyridine) of the oxidation-solvolysis products gave **3a,b** as shown by MALDI-TOF-MS (principal ion at m/z 724 [M + Na⁺]), and permitted placement of the C=O group at the C-18 position in **1a** (Fig. 2).

The foregoing ¹H-NMR analysis failed to distinguish *S,R* or *R,R* stereoisomers from their antipodes at either terminus. Consequently, the absolute configuration of isorhizochalin was assigned from deconvolution of the CD spectrum of the corresponding perbenzoyl aglycone **2b** following a procedure we developed specifically for two headed-sphingolipids, including rhizochalin [18] and oceanapaside [17]. The method has been applied recently by Kingston and coworkers to calyxoside [9], and by Molinski and co-workers to leucettamol A [19].

Perbenzoyl compound **2b** was prepared using a conventional procedure (benzoic acid, EDC, CH₂Cl₂) and purified by HPLC. When the CD spectrum of the natural product-derived perbenzoyl aglycone was compared with ‘hybrid CD spectra’ generated from all eight possible linear combinations of terminal group configurations [17] a unique solution to the absolute configurations at the four stereocenters emerged, but only when interpreted in combination with NMR data as follows. The CD spectrum of **2b** (Fig. 3) shows a split Cotton effect with negative signal

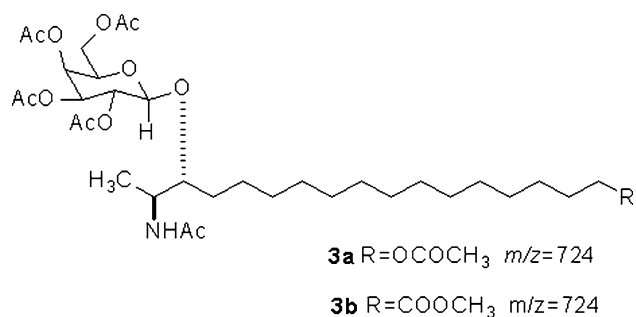


Fig. 2 Structures of degradation products from isorhizochalin

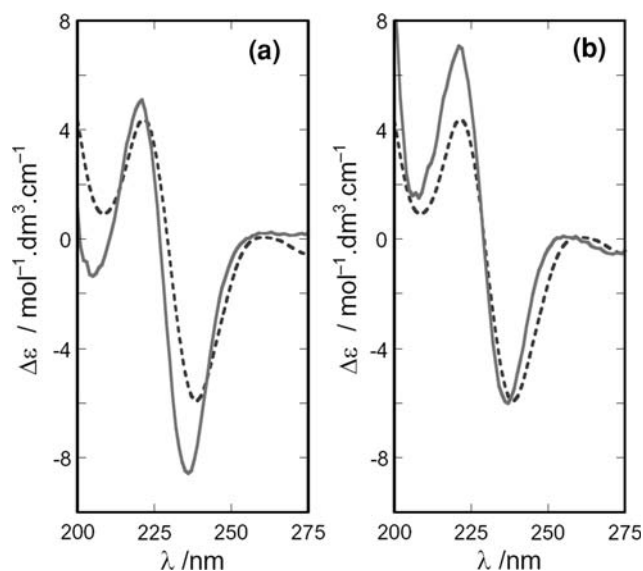


Fig. 3 CD spectrum of isorhizochalin perbenzoate (**2b**, dashed line) (MeOH, 23 °C, $c = 2.8 \times 10^{-5}$ M) overlaid with ‘hybrid’ CD spectra generated from linear combinations of **a** *ent-threo-4a* + *erythro-4b* and **b** *ent-threo-4a* + *ent-threo-4a*

at $\sim \lambda$ 239 ($\Delta\epsilon - 5.8$) and a positive signal at λ 221 ($\Delta\epsilon + 4.4$) that corresponds closely to two ‘hybrid’ spectra that are similar and consistent with either *2S,3R,26R,27R* (Fig. 3a) or *2R,3R,26R,27R* (Fig. 3b). Since the latter configuration had already been assigned to the *pseudo-C*₂ symmetric epimer, perbenzoyl rhizochalinin [18], the non-symmetrical *C*₁ epimer **2b** must have the *2S,3R,26R,27R* configuration,¹ however, we independently corroborated this assignment as follows. Comparative analysis of the ¹H-NMR spectrum of **2b** with those of the perbenzoyl rhizochalinin and *N,O*-dibenzoyl model compounds (**4a**, **4b**) [17] (Fig. 4), as shown in Tables 3 and 4 revealed similar chemical shifts and coupling constants for the α -terminus of isorhizochalinin perbenzoate (**2b**) to those of the *erythro*- model compound **4b**. Therefore, isorhizochalinin perbenzoate (**2b**) and isorhizochalin (**1**) share the *erythro* configurations at C-2, C-3 of the α -terminus (Table 3) and isorhizochalin (**1**) is the C-2 epimer of rhizochalin [1] (Fig. 1).

Compound **1** differs from earlier reported rhizochalins A, B and D [2, 3, 5], and oceanalin A [10] which possess the *threo* configuration at each α -terminus. The ¹H-NMR chemical shifts and coupling constants for the ω -terminus

¹ Of all 16 possible diastereomers of ‘two-headed’ sphingolipids, the two most difficult to discriminate by the CD deconvolution method are those represented by rhizochalinin and isorhizochalinin (*ent-threo/ent-threo* and *erythro/ent-threo* end groups). The differences in the hybrid CD spectra constructed from CD spectra of models **4a** and **4b** measured in MeOH are small, but somewhat differentiated when measured in CH₃CN.

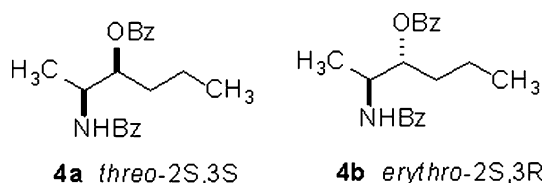


Fig. 4 Structures of *N,O*-dibenzoyl model compounds

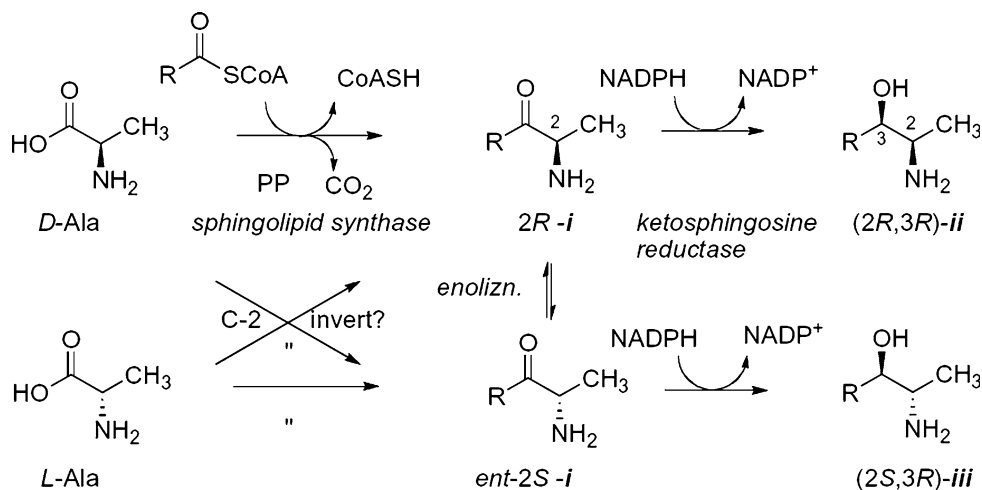
of isorhizochalinin perbenzoate (**2b**) and ω -termini of rhizochalinin, rhizochalinins C, D perbenzoates [3], oceanin perbenzoate [8] and calyxinin perbenzoate [9], and model compound (**4a**) are identical (Tables 3 and 4).

Taking into consideration that biosynthesis of the both termini in **1** and related metabolites most likely proceeds by pyridoxal phosphate-dependent, sphingolipid synthase catalyzed condensation of alanine (or serine in the case of oceanapiside and other C-1 hydroxylated analogs) with fatty acyl CoA ester followed by NADPH-dependent reduction of the incipient ‘ketosphingosine-like’ intermediate. The biosynthesis of the mycotoxin fumonisin B₁-like B₂, a (2*S*,3*S*)-sphingolipid [20], has been shown by ²H- and ¹³C-labeling studies to involve incorporation of L-alanine [21] with loss of CO₂ and retention of the C-2 configuration at the condensation step, similar to sphingosine biosynthesis. The absolute stereochemistry of **1** and its C-2 epimer rhizochalin, both found in the same sponge, now suggests two possible pathways that may explain their stereochemical heterogeneity. The α -terminus of **1** may be biosynthesized from L-alanine, while the ω -terminus derives from D-alanine, each with C-2 retention and the same ketoreductase stereospecificity for C-3 and C-26. D-alanine may derive from a host-derived epimerase, or a symbiotic bacterium in the sponge. Alternatively, both head group configurations, *ii*, and *iii*, could originate from L-alanine, with *inversion* of C-2 at the condensation step, and high 3*R* stereospecificity of the ketoreductase for both

termini. The *erythro* terminus *iii* could arise from a second C-2 inversion (not retention) in the 3-ketosphingosine-like intermediate 2*R-i* to *ent*-2*S-i* through enolization-reprotonation (Fig. 5). Since the all-*R*-configured rhizochalin is the predominant metabolite in the sponge and (2*S*,3*R*)-**1** is a very minor epimer, the latter compound may represent ‘leakage’ of C-2 stereofidelity in the canonical pathway. The second pathway has a certain appeal since it explains the plasticity of the C-2 configuration throughout the family of sponge-derived two-headed sphingolipids, but conservation of C-3. It is of special interest that so far only one similar *erythro*-, *threo*- bipolar metabolite has been described: oceanapiside, the major two-headed sphingolipid from the sponge *Oceanapia phillipensis* [17]: with termini that formally derive from D-alanine and L-serine configurations, respectively.

Both isorhizochalinin (**2a**) and rhizochalinin show same prominent cytotoxicities against human leukemia HL-60 cells with IC₅₀ values of 2.90 and 2.57 μ M as well as against human leukemia THP-1 cells with IC₅₀ values of 2.20 and 1.70 μ M, respectively. Thus, it appeared that the stereochemistry at position C-2 was not important structural requirement for cytotoxic activities of these two-headed sphingolipids. In addition, isorhizochalin is the first representative of essentially constitutionally symmetric two-headed sphingolipid natural product that lacks *pseudo*-C₂ symmetry. Structure identification of isorhizochalin reveals that the position of the keto group is conserved at C-18 in all known two-headed ketosphingolipids, but the stereochemistry for the α -termini can be *threo* (the majority of lipids in this group) or *erythro* (less common). It is possible, that a unified biosynthetic pathway may yet link these natural compounds to a common, but as-yet unidentified biosynthetic C₂₈ lipid intermediate, however the details of two-headed sphingolipid metabolism remain to be elucidated.

Fig. 5 Alternative biosynthetic hypotheses for stereochemical heterogeneity of long-chain base head groups of **1** and rhizochalin [1, 2]



Acknowledgments This investigation was supported by the Fogarty International Center and NIH (TWO06301-01) and the NIH (AI039987 and CA122256 to T.F.M.). The research described here was made possible in part by Program of Presidium of RAS “Molecular and Cell Biology”, Grant N SS-2813.2008.4 from the President of RF., Grant 09-04-00015-a from RFBR, and Grant 09-III-A-139 from FEB RAS.

References

- Makarieva TN, Denisenko VA, Stonik VA, Milgrom YM, Rashkes YV (1989) Rhizochalin, a novel secondary metabolite of mixed biosynthesis from the sponge *Rhizochalina incrustata*. *Tetrahedron Lett* 30:6581–6584
- Makarieva TN, Guzii AG, Denisenko VA, Dmitrenok PS, Santalova EA, Pokanevich EV, Molinski TF, Stonik VA (2005) Rhizochalin A, a novel two-headed sphingolipid from the sponge *Rhizochalina incrustata*. *J Nat Prod* 68:255–257
- Makarieva TN, Dmitrenok PS, Zakharenko AM, Denisenko VA, Guzii AG, Li R, Skepper CK, Molinski TF, Stonik VA (2007) Rhizochalins C and D from the sponge *Rhizochalina incrustata*. A rare *threo*-sphingolipid and a facile method for determination of the carbonyl position in α , ω -bifunctionalized ketosphingolipids. *J Nat Prod* 70:1991–1998
- Makarieva TN, Zakharenko AM, Denisenko VA, Dmitrenok PS, Guzii AG, Shubina LK, Kapustina II, Fedorov SN (2007) Rhizochalinin A, a new antileukemic two-headed sphingolipid from the sponge *Rhizochalina incrustata*. *Chem Nat Comp* 43:468–469
- Makarieva TN, Guzii AG, Denisenko VA, Dmitrenok PS, Stonik VA (2008) New two-headed sphingolipid-like compounds from the marine sponge *Oceanapia* sp. *Rus Chem Bull* 57:669–673
- Kong F, Faulkner DJ (1993) Leucettamols A and B, two antimicrobial lipids from the calcareous sponge *Leucetta microrhaphis*. *J Org Chem* 58:970–971
- Willis RH, De Vries DJ (1997) BRS1, a C30 bis-amino, bis-hydroxy polyunsaturated lipid from an Australian calcareous sponge that inhibits protein kinase C. *Toxicon* 35:1125–1129
- Nicholas GM, Hong TW, Molinski TF, Lerch ML, Cancilla MT, Lebrilla CB (1999) Oceanapiside, an antifungal bis- α , ω -amino alcohol glycoside from the marine sponge *Oceanapia phillipensis*. *J Nat Prod* 62:1678–1681
- Zhou BN, Mattern MP, Johnson RK, Kingston DG (2001) Structure and stereochemistry of a novel bioactive sphingolipid from a *Calyx* sp. *Tetrahedron* 57:9549–9554
- Makarieva TN, Denisenko VA, Dmitrenok PS, Guzii AG, Santalova EA, Stonik VA, MacMillan JB, Molinski TF (2005) Oceanalin A, a hybrid α , ω -bifunctionalized sphingoid tetrahydroisoquinoline β -glycoside from the marine sponge *Oceanapia* sp. *Org Lett* 7:2897–2900
- Fedorov SN, Makarieva TN, Guzii AG, Shubina LK, Kwak JY, Stonik VA (2009) Marine two-headed sphingolipid-like compound rhizochalin inhibits EGF-induced transformation of JB6 P⁺ Cl41 cells. *Lipids* 44:777–785
- Jin JO, Shastina VV, Park JI, Han JY, Makarieva TN, Fedorov SN, Rasskazov VA, Stonik VA, Kwak JY (2009) Differential induction of apoptosis of leukemic cells by rhizochalin two headed sphingolipids from sponge and its derivatives. *Biol Pharm Bull* 32:956–962
- Tsukamoto S, Takeuchi T, Rotinsulu H, Mangindaan REP, Van Soest RWM, Ukai K, Kobayashi H, Namikoshi M, Ohta T, Yokosawa H (2008) Leucettamol A: a new inhibitor of Ubc13–Uev1A interaction isolated from a marine sponge, *Leucetta aff. microrhaphis*. *Bioorg Med Chem Lett* 18:6319–6320
- Guzii AG, Makarieva TN, Denisenko VA, Dmitrenok PS, Burtseva YV, Krasokhin VB, Stonik VA (2008) Topsentasterol sulfates with novel iodinated and chlorinated side chains from the marine sponge *Topsentia* sp. *Tetrahedron Lett* 49:7191–7193
- Baltrop JA, Owen TC, Cory AH, Cory JG (1991) 5-(3-Carboxymethoxyphenyl)-2-(4,5-dimethylthiazolyl)-3-(4-sulfophenyl) tetrazolium, inner salt (MTS) and related analogs of 3-(4,5-dimethylthiazolyl)-2,5-diphenyltetrazolium bromide (MTT) reducing to purple water-soluble formazans as cell-viability indicators. *Bioorg Med Chem Lett* 1:611–614
- Makarieva TN, Denisenko VA, Svetashev VI, Vysotsky MV, Stonik VA (1989) Cerebrosides from the Far-Eastern sponge *Hymenyacionon assimilis*. *Chem Nat Comp* 634–638 (in Russian)
- Nicholas GM, Molinski TF (2000) Enantiodivergent biosynthesis of the dimeric sphingolipid oceanapiside from the marine sponge *Oceanapia phillipensis*. Determination of remote stereochemistry. *J Am Chem Soc* 122:4011–4019
- Molinski TF, Makarieva TN, Stonik VA (2000) (–)Rhizochalin is a dimeric enantiomeric (2R)-sphingolipid: absolute configuration of pseudo-C_{2v}-symmetric bis-2-amino-3-alkanols by CD. *Angew Chem Int Ed Engl* 39:4076–4079
- Dalisay DS, Tsukamoto S, Molinski TF (2009) Absolute configuration of the α , ω -bifunctionalized sphingolipid Leucettamol A from *Leucetta microrhaphis* by deconvoluted exciton coupled CD. *J Nat Prod* 72:353–359
- Harmange J-C, Boyle CD, Kishi Y (1994) Relative and absolute stereochemistry of the fumonisin B₂ backbone. *Tetrahedron Lett* 35:6819–6822
- Branham BE, Plattner RD (1993) Alanine is a precursor in the biosynthesis of fumonisin B-1 by *Fusarium moniliforme*. *Mycopathologia* 124:99–104